Appendix A: Technical Reports for the Rhode Island Ocean Special Area Management Plan

August 1, 2010

Appendix A Table of Contents

1.

The Planning and Policy Context for the Rhode Island Ocean Special Area Management Plan

By Ken Payne

June 23, 2010

Plans have their life in their creation, in their use, and their relationship with other plans and policies.[1] This document examines how the *Ocean Special Area Management Plan* relates to other Rhode Island plans—in other words it looks at the planning context of the *Ocean SAMP* beyond the use the Coastal Resources Management Council may make of it. The document focuses on plans that are authorized in Rhode Island law and, for reasons that are set forth below, that are part of the state guide plan system.

A key driver in the preparation of the *Ocean SAMP* has been the proposal to develop an off-shore wind farm to help meet Rhode Island's electrical needs from renewable energy. Obtaining electricity from renewable resources is both a requirement of law and a priority of the Carcieri administration.[2] A project of the magnitude of the proposed wind farm, if it is subject to State permitting comes under the jurisdiction of the Energy Facility Siting Board[3] as well as the Coastal Resources Management Council.[4] A procedure for review of projects by the Energy Facility Siting Board is an investigation by the statewide planning program, specifically: "The statewide planning program within the department of administration shall conduct an

[1] Hopkins, Lewis D. and E.R. Alexander. 2009. Introduction to Symposium: Panning in Complex Multiorganizational Systems. *Journal of Planning Education and Research* 28: 470-475.

[2] RIGL chapter 39-26, which was enacted in 2004 and sets the statutory goal of acquiring fifteen percent of Rhode Island's electrical demand from renewable resources by 2020, and Executive Order 06-02 of Governor Donald L. Carcieri, the accompanying press release of January 12, 2006,, and the Governor's Five Point Energy Agenda, which includes the goal that fifteen percent of "Rhode Island's electricity demand will be supplied by environmentally progressive wind power".

[3] RIGL chapter 42-98. The definition of "Major energy facility" in section 42-98-3 includes "facilities for the generation of electricity designed or capable of operating at a gross capacity of forty (40) megawatts or more; transmission lines of sixty-nine (69) Kv or over;" and the Energy Facility Siting Board is given jurisdiction, although exclusive jurisdiction over major energy facilities by section 42-98-4, which states **"**No person shall site, construct, or alter a major energy facility within the state without first obtaining a license from the siting board pursuant to this chapter."

investigation and render an advisory opinion as to the socio-economic impact of the proposed facility and its construction and consistency with the state guide plan".[5]

The establishment of the statewide planning program proceeds from the following finding: "The general assembly finds that the people of this state have a fundamental interest in the orderly development of the state; the state has a positive interest and demonstrated need for establishment of a comprehensive strategic state planning process and the preparation, maintenance, and implementation of plans for the physical, economic, and social development of the state; the continued growth and development of the state presents problems that cannot be met by the cities and towns individually and that require effective planning by the state; and state and local plans and programs must be properly coordinated with the planning requirements and programs of the federal government."[6] The statute sets forth matters to be covered in and the broad functions of the state guide plan as follows: the state guide plan, "shall be comprised of functional elements or plans dealing with land use; physical development and environmental concerns; economic development; housing production; energy supply, including the development of renewable energy resources in Rhode Island, and energy access, use, and conservation; human services; and other factors necessary to accomplish the objective of this section. The state guide plan shall be a means for centralizing, integrating, and monitoring long-range goals, policies, plans, and implementation activities related thereto. State agencies concerned with specific subject areas, local governments, and the public shall participate in the state guide planning process, which shall be closely coordinated with the budgeting process."[7]

The state guide plan currently has some 30 elements, two of which highly pertinent to the *Ocean SAMP*, the *Rhode Island Energy Plan* and the *Economic Development Policies and Plan*, are currently being updated.

The state guide plan also has life in the context of Federal environmental law. The National Environmental Policy Act requires the preparation of environmental impact statements (EIS)

[4] RIGL chapter 46-23.
[5] RIGL subsection 42-98-9(e).

[6] RIGL 42-11-10 (a).
[7] RIGL section 42-11-10 (d), emphasis added.

when Federal actions might have adverse environmental consequences. If an EIS is required then, social, cultural, and economic effects must be addressed as well.[8] State and local plans are recognized as important in determining these impacts.[9]

How does the *Ocean SAMP* relate to the state guide plan and to other state and local plans?

In *Land Use 2025*, the core element of the state guide plan, summarizes the uses of the state guide plan as follows:

The State Guide Plan promotes planning coordination in several ways, being used as both a resource and review mechanism for projects and implementation measures, such as:

- Proposals requesting federal funds.
- Applications for U.S. Army Corps of Engineers permits.
- Environmental Impact Statements.
- R.I. Economic Development Corporation projects.
- Projects being reviewed by the Energy Facility Siting Board.
- Applications for various loans, grants, or other federal or State financing.
- Rules and regulations promulgated by State agencies.
- Property leases and conveyances proposed before the State Properties Committee.

Besides these, one of the most important roles the State Guide Plan plays in coordinating planning is in the review of local comprehensive plans. This determines whether the State will certify a local plan so that State projects are bound to be consistent with it in the same way that local projects are consistent with the State Guide Plan.[10]

Since the offshore wind project receives support from the renewable energy development fund[11] administered by the RI Economic Development Corporation, RIGL 42-64-13.2, it can be

[8] Council on Environmental Quality describes effects as follows: "Effects and impacts as used in these regulations are synonymous. Effects includes ecological (such as the effects on natural resources and on the components, structures, and functioning of affected ecosystems), aesthetic, historic, cultural, economic, social, or health, whether direct, indirect, or cumulative." 40 CFR 1508.8

[9] See 40 CFR 1506.2 with regard to the affirmative interest of the CEQ in cooperation with planning efforts of states.

[10] 2006, p. 5.1.

[11] RIGL section 42-64-13.2.

considered an a project of the Corporation.[12] For projects including renewable energy projects of the Corporation, the Corporation is required to make a finding that the project is in conformity with the state guide plan.[13]

Land Use 2025: State Land Use Policies and Plan is "the State of Rhode Island's plan for conservation and development in the 21st century" and as such is "the major connective State Guide Plan element in Rhode Island's planning and development system. The Plan articulates the State's over-arching goals, objectives, and strategies to guide and coordinate the land use plans and regulations of municipalities and State agencies and to direct good, strategic projects at both the State and municipal level."[14]

While *Land Use 2025* is concerned with terrestrial issues, including "where land meets water, the waterfront edge,"[15] and this *Ocean Special Area Management Plan* is concerned with offshore marine issues, the two plans are conceptually congruent. First, each plan is essentially geospatial; second, each plan proceeds from a consideration of natural resource conditions; third, each plan is centrally concerned with current and potential future uses, and fourth, each plan is guided by how strongly things, such as historical resources, are valued. If the two plans were not conceptually congruent their use in an integrated or complementary manner would be problematic. However since they are, broadly, conceptually congruent, their potential integrated and complementary use depends on their specific content. Does, for example, *Land Use 2025* contain goals for a course of action that is at odds with the underlying principles embedded in the *Ocean SAMP*? Basic conflicts in content do not appear to be the case, rather the two seem to be

[12] RIGL 42-64-3 (20): "Project" or "port project" means (20) "Project" or "port project" means the acquisition, ownership, operation, construction, reconstruction, rehabilitation, improvement, development, sale, lease, or other disposition of, or the provision of financing for, any real or personal property (by whomever owned) or any interests in real or personal property, including without limiting the generality of the foregoing, any port facility, recreational facility, industrial facility, airport facility, pollution control facility, utility facility, solid waste disposal facility, civic facility, residential facility, water supply facility, energy facility or renewable energy facility, or any other facility, or any combination of two (2) or more of the foregoing, or any other activity undertaken by the corporation.

[13] RIGL 42-64-10 (a)(1)(v).

[14] Land Use 2025, p. v.

[15] Land Use 2025, p. 2.1.

of a piece. The vision of *Land Use 2025* is that "Rhode Island in 2025. . . will be green and blue." [16]

Land Use 2025 has as matters of policy to "promote holistic systems planning at the watershed level" and to "preserve and enhance wildlife, fish, and plant species diversity and stability through habitat protection, restoration, enhancement and prevention or mitigation of adverse impacts due to human activities."[17]

An important goal of *Land Use 2025* is "First class infrastructure that protects the public's health, safety and welfare, fosters economic well-being, preserves and enhances environmental quality," and a land use objective is to "Locate new infrastructure in appropriate areas."[18] The *Ocean SAMP* endeavors to accomplish precisely this in a broad area, the offshore environment that is not covered by *Land Use 2025*.

Other *Land Use 2025* objectives include: "2A. Permanently protect critical natural resources" and "3B. Preserve and enhance special districts and special places, supporting particular uses and resources."[19] The second of these two objectives would logically apply to the port and waterfront areas used by the commercial and recreational fishing industries.

Local comprehensive plans are required to be brought into conformity with the State Guide Plan.[20] *Land Use 2025* has the final objective, "5F. Achieve greater integration of State and municipal planning systems and support regional efforts." The *Ocean SAMP* is on a Rhode Island scale a form of regional effort, and the conceptual congruity of *Land Use 2025* and this *Ocean SAMP* should facilitate appropriate use of the *Ocean SAMP* in relevant areas of municipal. A meeting on January 30, 2009, among state and municipal planners and *Ocean SAMP* team members concluded that this fit was present and making the *Ocean SAMP* binding on municipal plans through its adoption as an element of the State Guide Plan was unnecessary:

[16] Op cit.

[17] Ibid., p. 2-9, 2-10; see also pp. 5-6, 5.7.
[18] Ibid,, pp 2-8, 2-9; see also pp. 5-14, 5-16.

[19] Ibid., pp. 5-8, 5-10.

[20] RIGL 45-22.2-9.

if there were no conflicts between the *Ocean SAMP* and local comprehensive plans, requiring local governments to review their comprehensive plans would be a paper exercise without any significant value.

As has been noted, the State Guide Plan has some thirty elements, of which *Land Use 2025* is but one, albeit it is "the major connective State Guide Plan element…." Other State Guide Plan elements merit consideration as well because they might contain provisions with a direct bearing on matters under consideration in the *Ocean SAMP*.

The *Rhode Island Energy Plan 2002*[21], which predates the State's renewable energy standard[22] and current efforts to develop renewable energy, contains nothing that conflicts with the pursuit of off-shore wind energy development in the Ocean SAMP area. It contains the goals of "Goal 3. Setting and achieving objectives that preserve or enhance environmental quality while ensuring adequate energy supplies," "Goal 4. The attainment of a fuel mix that is reasonably reliable and that satisfies economic need," and "Goal 8. The development of permanently sustainable energy resources that are environmentally and economically feasible."[23] Presciently, the Plan includes as a justification for the goal of preserving and enhancing environmental quality, "reducing greenhouse gas emissions and their contribution to climate change by promoting energy efficiency, energy conservation, and alternative energy use."[24] An Objective under Goal 8 is "To take advantage of indigenous resources and to decrease our dependence on fossil fuels."[25] With regard to wind energy specifically, the *Plan* while acknowledging that wind energy may become one of the "cheapest sources of power within the decade" finds that "wind resources in the state are not exceptional…."[26] The *Plan* was, however, taking into account only on-shore wind resources, not the off-shore wind resources of the *Ocean*

[21] State Guide Plan Element 781, August 8, 2002.

[22] RIGL chapter 39-26.

[23] *Rhode Island Energy Plan* 2002, pp. 1.1, 1.2, 1.3.

[24] Ibid., p. 1.1.

[25] Ibid., p. 3.27.

[26] Ibid., p. 3.30.

SAMP area. While reasonable for its time, the *Plan* is dated in many respects, and at the time of the *Ocean SAMP's* being prepared, it is being rewritten. The outline and initial versions of the revised *Energy Plan* include appropriate references to the *Ocean SAMP*.

The adopted *Economic Development Policies and Plan*[27] is similarly dated and currently being rewritten. Nevertheless, it too contains provisions that have a constructive bearing on topics covered by the *Ocean SAMP*. The *Economic Development Policies and Plan* holds that "Sustainable development is a process whose goal is to mitigate or eliminate the environmental problems facing society while simultaneously creating economic opportunities; it is a process to enhance the quality of life and save the environment. It recognizes that economic development and environmental quality are not mutually exclusive."[28] The *Plan* recognizes the value of renewable energy:

> To ensure that future generations are not left a legacy of vanished or depleted resources, *The Rhode Island Energy Plan* (Element 781 of the State Guide Plan) recommends the development of permanently sustainable energy resources that are environmentally benign and economically feasible. Even from a purely economic standpoint, this policy is key. Failure to exploit even modest opportunities for indigenous and renewable sources of energy that fit these criteria increases reliance on costly alternatives that could be avoided, postponed, or replaced – such as the construction of a new power plant, or continued dependence on fossil fuels produced outside the region that are subject to pricing policies beyond our control….
>
> Wider use of renewable energy can improve the business climate. It can help satisfy environmental objectives while addressing what has always been a disincentive to business location in New England – high energy costs owing to our position, literally, at the end of the pipeline. The phase-in of renewables can be complemented by a re- dedication to energy conservation, in recognition and appreciation of the fact that energy is too valuable a resource to waste or squander. [29]

[27] *Economic Development Policies and Plan*, Report Number 99, State Guide Plan Element 211, April 2000.

[28] Ibid., p. 2.32.

[29] Ibid., p. 2.33-2.34.

The Plan also addresses as economically important other activities that take place in the *Ocean SAMP* area, including commercial shipping[30], commercial and recreational fishing[31], recreation[32], and defense--the Navy[33]. And it has as facilities objectives to:

> 12. Encourage development of sport and commercial fisheries both inshore and offshore up to levels of maximum sustainable yield by supporting the provision of appropriate infrastructure, research and training facilities, aquaculture, management activities, and enforcement of water quality standards. Reserve suitable port access areas for commercial fishing vessels.
>
> 13. Encourage new industrial development in the coastal zone that places a priority on the maximum efficient and appropriate utilization of existing marine infrastructure, such as the Port of Providence and Quonset Davisville.
>
> 15. Promote tourism as a major industry, and encourage and support the use of the wide range of facilities that make up the industry's infrastructure.[34]

In December 2002, the statewide planning program issued the *Rhode Island Comprehensive Economic Development Strategy 5 Year Update*, which builds upon the objectives and policies of the 2000 *Economic Development Policies and Plan*.[35] The *5 Year Update* too recognizes the importance of sustainable development as a "process whose goal is to mitigate or eliminate environmental problems facing society while simultaneously creating economic opportunities."[36] The *5 Year Update* considers marine sectors, including shipping, the Navy, marine fisheries, and marine trades such as boat building and repairs and marinas. A major challenge identified in the *5 Year Update* is the long-term loss of manufacturing jobs, which peaked at 136,200 jobs in

[30] Ibid., p. 236.

[31] Ibid., p. 237.

[32] Ibid., p. 2.38.
[33] Ibid., pp. 2.22-2.24, 2.36.

[34] Ibid., p. 3.4

.

[35] Statewide planning Program, 2002. *Rhode Island Comprehensive Economic Development Strategy 5 Year Update,* p. v.

[36] Ibid., p. 19.

1978. The *5 Year Update* recommends a diversification of the state's industrial base,[37] which is something the development of offshore wind energy facilities could contribute to, especially in concert a facilities objective "to encourage sustainable industrial and commercial development that advance the long-term economic and environmental well-being of the state…."[38] In sum, while the *5 Year Update* is concerned with economic development on land, it contains broad principles that can be applied to development in the *Ocean SAMP* area.

While the *Economic Development Policies and Plan* treatment of recreation and tourism is brief, the Guide Plan element for recreation, *Ocean State Outdoors*[39], is extensive and up-to-date. It was amended in 2009 and gives attention to issues and matters related to the *Ocean SAMP*. First, it calls for maintaining "natural diversity by preserving habitat"[40]; second, it urges the preservation of "significant historic, architectural and archeological sites"[41], and third, it recognizes the significance of climate change.[42] Among its policies is the preservation and expansion of recreational boating.[43]

The *State Historical Preservation Plan*[44] states the following principle: "For archaeological sites Rhode Island's preferred treatment is avoidance; data recovery is sometimes used as a last resort when avoidance is not possible. In general, however, the cost of data recovery and the irreversible damage to historical resources that recovery necessarily entails suggest that avoidance should be preferred. Further, in some property types such as burial places ethical and legal considerations require avoidance."[45] The *Historical Preservation Plan* contains the strategy

[37] Ibid., p. 80.

[38] Ibid., p. 85.

[39] *State Historical Preservation Plan,* State Guide Plan Element 152, adopted 2003. Amended 2009.

[40] Ibid., p. ES.4

[41] Ibid., p. ES.5.

[42] Ibid., pp. 2.5-2.6.

[43] Ibid., p. 4.29.

[44] State Guide Plan Element 140, revised June 1996.

[45] Ibid., p. 140.2.

to "Work toward the development of a context for understanding archaeological resources, which are underwater."[46] The *Ocean SAMP* is contributing to this.

The *Rivers Policy and Classification Plan*[47] is a "guide for action to protect the quality and use of Rhode Island's watersheds." The *Policy and Classification Plan* is notable because it looks at rivers and watershed in three ways: first, their ecological and natural value, second, their current and potential uses[48], including economic uses, and third, the values communities place on the rivers and watersheds.[49] While the Rivers Council's responsibilities are for watershed planning for fresh water bodies, and thus do not overlap with the *Ocean SAMP*, the planning approaches underlying the *Rivers Policy and Classification Plan* and the *Ocean SAMP* are in concert.

The Bays, Rivers and Watersheds Coordination Team[50] endeavors to provide integrated plan for fresh and marine waters. Its membership includes representatives from the Coastal Resources Management Council, the Rhode Island Rivers Council, the Department of Environmental Management, the Water Resources Board, the Narragansett Bay Commission, the RI Economic Development Corporation, and the Division of Planning in the Department of Administration. The Coordination Team is charged with developing and overseeing the implementation of a system-level plan which "establish overall goals and priorities for the management, preservation, and restoration of the state's bays, rivers, and watersheds, and the promotion of sustainable economic development of the water cluster." The Coordination Team

[46] Ibid., p. 140.6.

[47] Rivers Policy and Classification Plan, State Guide Plan Element 162, adopted 1998, amended 2004.

[48] RIGL section 46-28-7 (4): "The classifications shall identify characteristics of water bodies beyond their quality to reflect their current or potential uses for drinking water sources, agricultural irrigation, industrial processes, including cooling water sources, water-based recreation, aquatic habitat, aesthetic enhancement, and others. The classification plan shall be consistent with current water quality classifications adopted by the department of environmental management."

[49] RIGL section 46-8-7, the RI Rivers Council has the power and the duty "(7) To formally recognize and to provide grants to local watershed councils;" and "(8) To foster public involvement in river planning and decision-making processes…."

[50] RIGL chapter 46-31.

may recommend "adoption of all or portions of said plan by the state planning council as elements of the state guide plan."[51]

A systems integration plan[52] was adopted by the Coordination Team in July 2008. The *Systems Integration Plan* proceeds from a vision that:

> In the future, Rhode Island's waters and coasts are fishable, swimmable, prosperous, and resilient, and state and local environmental and economic development policies are well-managed, integrated, and cost-effective.
> Numerous socio-economic uses and values are thriving, including commercial and recreational fishing, recreational boating, renewable energy generation, ocean and bay monitoring, water-dependent transport and industry, maritime technologies, recreation and tourism.
> State and regional governance of Rhode Island's waters and watersheds fully incorporates systems perspectives, particularly the principles of ecosystem-based management, and is based upon world-class programs in monitoring, research, education and outreach, and strategic planning and evaluation.[53]

The *Systems Integration Plan* squarely recognizes climate change as a major challenge facing marine systems[54] and points to development of "ocean renewable energy resources in a balanced manner that accommodates and promotes existing uses of Rhode Island's marine waters and submerged lands such as fisheries and recreation."[55]

The *Systems Integration Plan* looks at four existing "water-reliant" industries: recreation and tourism; boatbuilding, shipbuilding and boating-related businesses; water-based transportation, and commercial fisheries and aquaculture.[56] Regarding commercial fisheries the *Systems Integration Plan* observes, "Commercial fishing has been a mainstay of Rhode Island's economy since the state's inception and continues to play an important role in Rhode Island's

[51] RIGL section 46-31-5.

[52] The Rhode Island Bays, Rivers, and Watersheds Bays, Rivers, and Watersheds Coordination Team, July 2008. *Bays, Rivers, and Watersheds Systems-Level Plan: 2009-2013.*

[53] Ibid., p. iii.

[54] Ibid., pp. 4-7.

[55] Ibid., p. 3.

[56] Ibid., pp. 38-50.

economy"[57] and "The development of the commercial fishing industry [in Rhode Island] and the constraints of distribution capabilities early in the development of the industry led to close association of the downstream processing activities with fishing ports. This clustering of production and processing activities created significant economic value and wealth for local fishing communities. The remnants of this clustering continue to exist in part due to the capital intensity of the industry."[58]

Significantly, the Coordination team is concerned with economic and ecological issues and embraces the principles of eco-system based management. Thus there is a conceptual congruence between the *Systems-Level Plan* and the *Ocean SAMP*.

Conclusion

Rhode Island has a highly developed system of planning, with the state guide plan as the primary means of inter-plan coordination and harmonization. While the currently adopted elements of the state guide plan do not plan for the area covered by the *Ocean SAMP*, there is conceptual congruence between the relevant state guide plan elements and the *Ocean SAMP*; thus basic conflicts between the state guide plan and the *Ocean SAMP* would seem unlikely. More probably the two could be understood as mutually reinforcing. Indeed the *Ocean SAMP* can be appreciated as major extension of state planning principles into an area not previously covered by state plans.

What is also significant is that state guide plan elements do address activities, such as shipping, commercial and recreational fishing, recreational boating, and defense—the Navy, that take place in the *Ocean SAMP* area. This both shows that Rhode Island has long-established and well-recognized interests in the *Ocean SAMP* area and gives additional justification for the preparation and adoption of the *Ocean SAMP*.

It is also noteworthy that Rhode Island over the last decade has been moving demonstratively toward eco-system based planning and management. The *Ocean SAMP* is the

[57] Ibid., p. 102.

[58] Ibid., p. 104.

fullest expression to-date of this trend. This commitment of Rhode Island to planning holistically is critically important to addressing climate change and its effects.

2.

Characterizing the Physical Oceanography of Coastal Waters Off Rhode Island, Part 1: Literature Review, Available Observations, and A Representative Model Simulation

Prepared for the Rhode Island Ocean Special Area Management Plan 2010

By

Daniel L. Codiga and David S. Ullman

University of Rhode Island, March 24, 2010

Executive Summary

In support of the Rhode Island Ocean Special Area Management Plan development process, the physical oceanography of coastal waters off Rhode Island is reviewed and summarized. The OSAMP area includes central and eastern Block Island Sound (BIS), all of Rhode Island Sound (RIS) except state waters along its northern and eastern boundaries, and an area of the continental shelf extending about 25 km offshore southward from each. A literature review, updated analyses of key observations, and results of a hydrodynamic simulation are used to provide an updated, integrated view of the physical oceanography of the system. The focus is on the geographic and vertical spatial structure, and seasonal evolution, of hydrographic (temperature, salinity, and density) and circulation (seasonal-mean and weather-band) features, and on characterizing tidal variations. Conditions are shaped by a complex interplay among wind-driven variability, tidal processes, and density gradients that arise from combined effects of interaction with adjacent estuaries, solar heating, and heat flux through the air-sea interface. BIS is mostly estuarine in character, with the lowest salinities, the strongest tidal currents, relatively constant density stratification year-round dominantly due to salinity, and strong and persistent seasonal-mean currents including bidirectional exchange flow at each of its three openings and a prominent estuarine outflow bounded by a front on the shelf to the south. In RIS and the offshore area, the seasonal cycle is more pronounced: in winter and fall the stratification is minimal and circulation is a weak upwelling pattern directed offshore at shallow depths and onshore near the seafloor; in spring and summer strong stratification develops due to an important temperature contribution, and a system of more distinct currents occurs. These include the southern New England shelf flow westward along the offshore area, which bifurcates in the east where a portion moves northward as the RIS Current, a narrow flow that proceeds counterclockwise around the perimeter of RIS likely in association with a tidal mixing front. In southwestern RIS the southward RIS Current strengthens, in association with sharpened density gradients of the outflow front, then merges south of Block Island with the estuarine outflow and joins the southern New England shelf flow to leave the area westward. Tidal currents are stronger than or comparable to these seasonal-mean flow patterns, as are weather-band current variations driven by the wind. The baseline knowledge of physical oceanography presented here forms a component of the ecological characterization of the area needed to support assessments of potential impacts of policy decisions regarding development and protection of ocean-based resources.

Table of Contents

List of Figures

List of Tables

List of Appendices

Abstract

An integrated view has been developed for the physical oceanography of coastal waters off Rhode Island, including central and eastern Block Island Sound (BIS), Rhode Island Sound (RIS), and an offshore area extending about 25 km to the south from them. Results are based on a comprehensive literature review of observational and modeling studies; updated observational analyses of (i) satellite sea surface temperatures, (ii) a hydrographic climatology constructed from archived conductivity-temperature-depth (CTD) casts, and (iii) HF radar surface currents; and output from a realistically configured and forced data-assimilative hydrodynamic model spanning a larger regional domain. Emphasis is on the geographic and vertical spatial structure, and seasonal evolution, of hydrographic (temperature, salinity, and density) and circulation (seasonal-mean and weather-band) features, and on characterizing tidal variations. The seasonal cycle in temperatures spans from about 3 ^{o}C to about 21 ^{o}C, as shaped mainly by heat fluxes across the air-sea interface and solar radiative heating, and hence is relatively uniform geographically except for a tendency for shallow inshore waters to be up to a few degrees colder due to enhanced tidal mixing there. In deeper areas surface temperatures exceed deep temperatures by about 5-6 ^{o}C in spring and up to 10-12 ^{o}C in summer, but only by about 1 ^{o}C or less in fall, and in winter the deep water can be warmer by up to a degree due to surface cooling. Salinity variations reflect the influence of interactions with surrounding estuarine systems, and range from about 31 to 33 PSU with the freshest water in and near BIS due to strong influence of Long Island Sound (LIS) exchange flow, and surface values persistently about 0.1 to 0.9 PSS fresher than at depth. Density stratification has pronounced seasonality in deeper areas, with a pycnocline in winter and fall that is about 30-40 m deep and weak (surface to seafloor difference $\Delta\sigma_t$ of about 0.1 kg m^{-3}; peak buoyancy frequency N^2 about 2-3x10^{-4} s^{-2}) due to surface cooling and strong winds, then about 10-20 m deep and stronger in spring ($\Delta\sigma_t$ about 1 kg m^{-3}; peak N^2 about 5-6 x10^{-4} s^{-2}) and summer ($\Delta\sigma_t$ about 2-2.5 kg m^{-3}; peak N^2 about 10-12 s^{-2}), when the temperature influence dominates. Stratification is strongest in BIS during the winter, due to LIS exchange flow, and weakest there in summer due to strong tidal currents. BIS has relatively strong (5-15 cm s^{-1}) seasonal-mean currents including bidirectional exchange flow at each of its three openings, and a prominent geostrophic estuarine outflow bounded by a hydrographic front that spans the water column on the shelf to the south. In RIS and the offshore area, seasonal-mean currents undergo a stronger seasonal cycle: in winter and fall there is a weak (~1-2 cm s^{-1}) upwelling pattern, and in spring and summer a system of more distinct currents. These include

the southern New England shelf flow (up to 10 cm s^{-1}) westward along the offshore area, which bifurcates in the east where a portion moves northward as the RIS Current, a narrow flow moving counterclockwise around the perimeter of the stratified interior of RIS at about 5 cm s^{-1} likely in association with geostrophic adjustment of the horizontal density gradient due to a tidal mixing front. In southwestern RIS the southward RIS Current strengthens to about 15-20 cm s^{-1}, in association with sharpened warm-season inshore-offshore density gradients, then merges south of Block Island with the estuarine outflow and joins the southern New England shelf flow to leave the area westward. The strengths of these seasonal-mean flow patterns are, at most, comparable to tidal and weather-band current fluctuations and generally much weaker than them. Tidal currents are dominantly semi-diurnal and sharply enhanced (up to 100 cm s^{-1}) in and near BIS due to the resonant response of LIS. Weather-band current variations are driven predominantly by the wind, decay modestly with depth except in summer when they are isolated in the upper layer by the strong pycnocline, and peak in winter at about 20-30 cm s^{-1} when they are dominantly parallel to the nearly east-west orientation of the larger regional coastline.

1 Purpose and Scope

The purpose of this report is to summarize the current state of understanding of the physical oceanography of coastal waters off Rhode Island. The region of interest is the Rhode Island Ocean Special Area Management Plan (OSAMP) domain (Figure 1), which can be broken in to three areas: (a) approximately the eastern half of Block Island Sound (BIS), (b) all of Rhode Island Sound (RIS) with the exception of an area extending up to several kilometers south from the entrances to the Narragansett Bay and Mount Hope Bay estuarine system, and excluding the Massachusetts state waters at its eastern end, and (c) an offshore region extending about 25-30 km southward from these two areas. Water depths are typically 10-35 m and reach up to about 70 m in the offshore area; a companion OSAMP report discusses the bathymetric features and terminal-moraine geologic history of the region in detail.

The focus here is primarily on gross attributes of hydrographic fields (temperature, salinity, density, and density stratification) and circulation characteristics (seasonal-mean flow, weather band variations, and tidal fluctuations), including their geographic variations and water column vertical structure. Companion OSAMP reports cover waves, sediment transport, and other water properties such as oxygen concentration, none of which are addressed here. Our three main aims are to (a) review relevant literature, (b) use available observations to characterize the area, and (c) describe the output from a representative regional numerical hydrodynamic simulation configured to model the system realistically using up-to-date techniques including data assimilation. In the companion Part 2 report, the findings of a new observational campaign will be presented.

2 Introduction

2.1 Regional Setting

The RI OSAMP region is an inshore temperate shelf sea on the inner portion of the southern New England continental shelf (Figure 1). The southern New England shelf lies south of Massachusetts, Rhode Island, and Long Island, New York, extending nominally from the Hudson Shelf Canyon in the west to Nantucket Shoals in the east; it is the northern half of the region between Cape Hatteras and Cape Cod known as the Middle Atlantic Bight. The physical oceanography of the broader southern New England shelf, which bounds the RI OSAMP region to the south (Figure 2), has received considerable attention and a solid baseline understanding has therefore been built up (see, e.g., reviews by Beardsley and Boicourt (1981), Ingham (1982),

Mountain (2003), and (Lentz 2008a, b)). The OSAMP area, in sharp contrast, been the focus of relatively little research; for example, in a recent review of Mid-Atlantic Bight observed mean circulation using all available archived moored current meter records, the OSAMP area forms a somewhat conspicuous gap in coverage (see Figure 1 of Lentz (2008a)).

Water on the southern New England shelf originates primarily from the Scotian Shelf to the north (Chapman and Beardsley 1989), and passes across Nantucket Shoals (adjacent the RI OSAMP region to the southeast), generally after having passed through the Gulf of Maine and around or across Georges Bank. The polar origins, together with the effects of river and estuarine contributions, lead to shelf waters that are generally cooler and fresher on the inshore side of the shelf break front than the adjacent deep ocean slope water conditions to the south. Shelf waters undergo a pronounced seasonal cycle in temperature, influenced largely by air-sea interaction. Seasonality in salinity, associated mainly with spring freshening due to episodic coastal runoff, is less regular than that of temperature, and commonly weaker than inter-annual variability. Stratification, the vertical gradient in density associated with horizontal layering of water such that less dense layers overlie denser layers, results from comparably important influences of river freshening and surface heating, and peaks in summer. Cold bottom water formed in the winter, referred to as a "cold pool", can persist in some areas throughout the summer heating period and subsequent fall overturning when winds increase.

The regional-scale long-term mean vertical-average general circulation of the southern New England shelf is alongshore to the southwest, increasing in strength with distance offshore to reach 10-15 cm/s in a jet centered near the shelf break (e.g., Lentz 2008a); it is typically strongest at the surface and weakens toward the seafloor without reversing direction. Spatial and temporal variability of non-tidal flow superposed on this broad mean circulation pattern is significant (typically 10 to 40 cm/s, but up to 80 cm/s) and results largely from wind fluctuations, coastal-origin flows emanating from rivers and estuaries, and, in some years to a limited extent, interactions with Gulf Stream rings or the influence of hurricanes.

Regional surface winds (described in detail in a companion OSAMP report) in winter average about 4-12 m/s East-Southeastward, and due to storms are highly variable with peak speeds up to about 25 m/s. Summer winds are much less variable and weaker, averaging 2.5-7.5 m/s, and oriented in the East-Northeastward direction. Although wind fluctuations drive much of the variability of the circulation, wind is of secondary importance to mean currents, which are driven primarily by a large-scale alongshore pressure gradient and oriented largely in the upwind

direction. In the across-shelf direction, deep flow on the shelf is weakly onshore throughout the region (Bumpus et al. 1973); this is consistent with both the upwelling-favorable sense of mean winds driving shallow water offshore by Ekman transport, and also with the influence of deep onshore limbs of bidirectional exchange flows at the mouths of numerous estuaries in the area. Regional tidal conditions (Moody et al. 1984) over the main shelf include dominance of semi-diurnal constituents, typical sea level amplitudes of about 0.5 to 1 m, and tidal currents of up to 5 cm/s. In inshore areas, these attributes can be modified by near resonance of estuaries, for example Long Island Sound, which can amplify currents to as much as 100 cm/s.

2.2 Influences of Immediately Adjacent Waters

In addition to the deeper shelf area to its south, numerous bodies of water bound the OSAMP domain (Figure 2). Moving clockwise from the west, these include (a) western BIS and the Long Island Sound (LIS); (b) the West Passage, East Passage, and Sakonnet Passage entrances to the Narragansett Bay (NB) and Mount Hope Bay (MHB) estuarine system; (c) the semi-enclosed embayment Buzzards Bay (BB); and (d) Vineyard Sound (VS), a tidal strait that connects at its eastern end to Nantucket Sound. Exchanges of water and water properties with the OSAMP domain occur at each of these boundaries. Estimates of long-term mean volume transport exhanges based on sparse available observations (Table 1) were compiled by Codiga (2009),

Table 1. Estimated long-term mean volume transport exchanges with adjacent waters.

Body of water	Transport ($1000\ m^3\ s^{-1}$)	Source of observations used
Long Island Sound	23 +/- 5	Codiga and Aurin (2007)
Narragansett Bay	1-3 +/- 2	Kincaid et al. (2003)
Buzzards Bay	1-2 +/- 2	Signell (1987), Butman et al. (1988)
Vineyard Sound	4 +/- 4	Geyer & Signell (1990), Beardsley et al. (2007)

who emphasized that interaction with LIS has the most important influence on the OSAMP region. This conclusion holds despite the large uncertainties in the transport estimates, including the possibility that the sampling on which the LIS estimate is based significantly overestimates the net exchange because it lies within a local recirculation. The dominance of LIS can be anticipated based on river inputs to each system; the long-term mean river runoff to LIS

(approximately 500 m^3/s, the large majority of which is from the Connecticut River, see Figure 2) is about 10 times as high as that entering NB/MHB, with even smaller amounts entering BB and VS; the bi-directional estuarine exchange flows for the LIS and NB/MHB estuarine systems are amplified relative to these river inputs by a factor of about 15-25.

3 Characterization Based on Observations

In this section, available observations from the OSAMP region are summarized. Previously analyzed field studies are described, and new analyses are presented for sea surface temperature (SST), archived historical conductivity-temperature-depth (CTD) casts, and surface currents measured by high-frequency (HF) radar. Hydrographic fields are taken up first, then currents, with a literature review at the start of each subsection; in these literature reviews and those that follow in later sections, an important resource is the comprehensive catalogue of publications gathered and described by Battelle (USACE 2002) as part of an Army Corps of Engineers dredged material disposal site assessment. Appendix A includes a complete listing (Table A1) of observation-oriented publications and Appendix B includes a complete listing (Table B1) of modeling-oriented publications.

3.1 Hydrographic Fields

3.1.1 Literature Review

Some of the earliest and still very pertinent scientific analyses of OSAMP waters consist of a series of 1950s publications by Gordon A. Riley and colleagues that focused primarily on LIS but encompassed BIS and, to a lesser extent, RIS as well. A view of the geographic patterns and seasonal cycle of temperatures and salinities was laid out in an analysis of a series of vessel-based CTD surveys completed in the late 1940s (Riley 1952) that included a small number of bathythermograph transects across BIS and RIS. For OSAMP area surface temperatures, they documented the seasonal range of surface temperatures from about 2-4 ^oC in winter to about 20 ^oC in summer. The tendency was noted for inshore temperatures to be a few degrees cooler during winter, and to a lesser extent warmer during summer, relative the offshore OSAMP area. Surface salinities were in the range of 29.5 to 32.5 parts per thousand (PPT), with a prominent gradient of increasingly lower values from western RIS through BIS towards LIS. Together with freshening towards BB and eastward in to VS, this was considered evidence of dilution of saltier ocean waters by river inputs, which was concluded to be the dominant process determining hydrographic conditions along with air-sea heating/cooling. In late fall and winter, temperature

increases with depth of up to about 1 ^{o}C were commonly observed, indicative of a lag between cooling of shallow and deeper waters. In other seasons, typical surface temperatures were about 1-2 ^{o}C higher than at the bottom in shallow areas, reaching 5 ^{o}C higher in deeper areas, and offshore of Block Island in summer there were decreases of about 10 ^{o}C across a distinct thermocline about 15 m deep. Vertical salinity gradients were reported as typically no more than 1 ppt. Results of a similar survey in 1951-1952 presented by Powers (1953), which included more complete measurements of the vertical structure of the water column and seafloor conditions, demonstrated very similar features. In these early surveys complex spatial structure of water properties on scales of about 1 to 10 km were prominent, and recognized to be transient features that varied in response to river flow, wind, and tidal conditions, but further diagnosis of related processes was not possible due to the short sampling duration.

In 1963-1964, a US Navy field program obtained CTD casts repeated about each 2-3 months along two onshore-offshore transects in western-central and eastern-central RIS (Shonting et al. 1966; Shonting and Cook 1970). The seasonal temperature ranges noted above were confirmed and a mid-depth thermocline, with temperature differences of about 5-6 ^{o}C in spring increasing to at least 10 ^{o}C in late summer, was noted to span most of the area and be replaced by nearly homogenous temperatures in fall and winter as a consequence of wind mixing. Salinity patterns included persistent freshening in the upper several meters within 10-20 km of the northern shore, which was attributed to outflow from NB, and vertical gradients over most of the area that sharpened to about 1 PPT in late spring and early summer but were essentially absent during the late fall and winter. The density anomaly sigma-t was shown to take values in the range of about 23.8 to 25.2 kg m^{-3}, with peak vertical differences of 1-1.5 kg m^{-3} in early summer when near-surface freshening contributed in the same sense of, and with comparable importance to, higher surface temperatures. As in earlier surveys, transient small-scale variability in both temperature and salinity, including large fluctuations in the thermocline depth within a single survey and from survey to survey, were prominent and could not be addressed by the short-term nature of the nearly synoptic sampling.

CTD casts along transects across BIS were sampled in the late 1960s and early 1970s (Ichiye 1967; Williams 1969; Hardy 1972; Hollman 1974). These studies revealed similarities of BIS hydrography to that of RIS, including comparable vertical gradients. There were also notable geographic variations, with water in the south and west of BIS generally the most fresh, by up to 1 PPT, and the least strongly stratified. This feature was interpreted as the signature of fresh

outflow from LIS that spans the entire water column and is concentrated along the coast of Long Island and rounds Montauk Point to exit BIS southward. The saltiest water in BIS was near the bottom toward the north. Tidal fluctuations in water properties were also resolved and quantified, and attributed to advection by strong BIS tidal currents oriented largely east-west along the large-scale salinity gradient.

In the early 1970s an intensive field campaign was undertaken by Raytheon (1975) to characterize waters of northeastern BIS, as motivated by their potential capability to accommodate heat from cooling towers of a proposed nuclear power facility near Ninigret Pond. CTD casts were collected nominally each 2 weeks from July 1975 through September 1976 at a rectangular 3 by 4 array of stations spanning an area about 4 km by 6 km in the northeastern portion of BIS. Analysis by Snooks et al. (1977) confirmed in greater detail many of the features described in previous studies: seasonal formation (April) and breakdown (September) of a mid-depth thermocline, across which temperatures decrease in depth by up to 8-12 ^{o}C; temperature increases of about 1 ^{o}C with depth during fall and winter; salinities with a weak annual cycle but strong and irregular variability on timescales of weeks to months in association with river runoff, and typical surface to bottom differences of about 0.5 PPT; and variations in density and stratification controlled both by temperature and salinity. Photographic-method thermographs were also mounted on moorings at shallow and deep depths and recorded temperatures each 15 minutes at two sites for more than a year (Raytheon 1975). These records showed that temperature changes occur primarily on several-day timescales in association with weather events, and how the spring and summer warming process is slow and gradual while the fall breakdown in the resulting stratification occurs abruptly over a few days or less.

Bowman and Esaias (1981) reported results of a one-week CTD survey in September 1978 that included several casts in BIS. Their analysis emphasized the geographic variations in stratification, using top to bottom density differences, and as in previous studies showed it is substantially stronger over most of BIS than in the southwestern portion along the northern shores of Long Island and near Montauk Point. They compared measured stratification to the theoretical h/U^3 index (water depth h over cube of tidal current U) developed by Simpson and Hunter (1974) for a one-dimensional balance between surface heating and turbulent mixing driven by tidal flow across seafloor roughness. Observed stratification was generally strongest in regions of high h/U^3 and vice-versa, in agreement with the theory, despite that it does not incorporate salinity stratification and horizontal advection which are both known to be important.

A comprehensive compilation of temperature observations in RIS is provided by Armstrong (1998), which depicts results of a 10-year campaign of monthly expendable bathythermograph sampling along a shore to shelf-break north-south oriented band of water centered on RIS and spanning most of its width. The 10-year mean seasonal cycle is characterized, much as described above but depicted in greater detail, and deviations from it in individual years are shown to reach up to several ^{o}C. Emphasis was on bottom temperatures, and the faster spring/summer warming and higher resulting temperatures at inshore sites was quantified.

Frontal boundaries, while generally not detectable by CTD surveys, are prominent in the 12 years of ~1 km resolution satellite SST observations analyzed by Ullman and Cornillon (1999; 2001). The fronts are dynamical features commonly exhibiting sharp gradients in both salinity and temperature, and typically separate fresher inshore water from saltier offshore water. As detected in SST, the seasons when they are most common are winter, then summer, then spring, and they are relatively uncommon during fall. Frontal probabilities are highest in the area south of Block Island and also high along a band that stretches roughly from there northward and eastward, east of Block Island, to west-central RIS. As discussed in the next section below, this distribution can be understood to mark the edge of the LIS outflow, which during low river flow may extend eastward only to mid-BIS but during high river flow can extend to central RIS. Satellite sea surface temperature (SST) observations were also analyzed by Fox et al. (2000), who examined vernal warming using 1997 data from areas of BIS, central RIS, and the portion of RIS that enters VS. They identified LIS outflow water by its cool temperature, and quantified its spatial extent and aspects of its pronounced weather-band temporal variability. They also noted that areas of BIS and VS tended to be cooler than central RIS, which they attributed to more efficient mixing of colder deep water to the surface.

CTD surveys were repeated several times in 1998-1999, mostly during the summer and winter months, at 5 stations near and north of the OSAMP domain boundary in the vicinity of the mouth of NB (Kincaid et al. 2003). The vertical structure and seasonal variations of temperature and salinity were consistent with those described above for northern RIS, and an east-west gradient, with salinity increasing eastward across the mouths of the West and East Passages, was noted. This was interpreted as evidence that the NB/MHB estuarine exchange circulation consists mostly of northward inflow of salty RIS waters through the eastern side of East Passage together with a southward outflow of fresher water through the western side of East Passage, and to a lesser extent the West Passage.

A number of analyses resulted from an intensive field program during 2000-2002 focused on investigating the dynamics of the frontal boundary of LIS outflow on the inner shelf south of Montauk Point and Block Island in the southwestern corner of the OSAMP region. Kirincich and Hebert (2005), based on vessel-based surveys using a CTD mounted on a towed undulator, described the vertical and across-shelf structure of the temperature, salinity, and density of the front in spring 2002. The front shoals in the offshore direction, consistent with thermal wind shear of the southward and westward moving outflow jet observed in concurrent velocity measurements. During their survey the front intersected the seafloor at about 30 m deep, where they noted the near-bottom tidal variability was substantial. O'Donnell and Houk (2009) presented results of two 48-hour CTD surveys of BIS, western RIS, and the southwestern SAMP inner shelf, collected under different wind conditions, demonstrating the substantial range of weather-band variability in the geographic extent and vertical structure of the LIS outflow. Moored CTD profiler sampling of vertical casts hourly for multi-week intervals showed evidence of a mid-depth pycnocline in fall, in contrast to stratification throughout the upper water column in spring (Codiga and Rear 2004). An analysis of historical archived CTD casts by Ullman and Codiga (2004) contrasted the timing and intensity of the seasonal cycle of stratification in areas inshore and offshore of the front, quantifying the across-front density difference and demonstrating that its temperature contribution opposes its salinity contribution in winter and spring, then reinforces it during summer and fall. They showed that the strengthening of the along-front current in summer was linked to the stronger density gradient through geostrophic dynamics. Levine et al. (2009) identified smaller-scale fronts in the vicinity of the gap between Montauk Point and Block Island, with sharp gradients in salinity and temperature on scales of 10s of m, and interpreted them as boundaries of tidally-driven headland eddies associated with swift tidal currents there. Significantly, they also reported the only direct measurements of small-scale turbulent kinetic energy dissipation rate within the OSAMP domain, demonstrating elevated levels of up to 10^{-5}-10^{-4} W/kg near these fronts and linking them to shear instabilities.

Finally, CTD casts were collected during a few days of April and September 2004 at a proposed dredge disposal site about 38 m deep in west-central RIS (SAIC 2005). Measured conditions fit well within the expected range based on previous studies, but vividly demonstrated that temperatures and salinities in the upper water column, and hence stratification, vary substantially on timescales of hours to days. Advection of inhomogeneous water properties by small-scale eddying motions, tidal currents, and wind-driven movements are clearly a strong influence on hydrographic fields on short timescales.

3.1.2 Satellite Sea Surface Temperature Observations

An analysis of sea surface temperature (SST) observations was performed with the aim of describing the seasonal and spatial variability of SST across the OSAMP region. Satellite-derived SST data provide a high-resolution (~1 km) view of surface ocean conditions multiple times per day. We used all available observations from the moderate resolution imaging spectroradiometer (MODIS) sensors aboard the NASA Terra and Aqua satellite platforms during the period 2002-2007. Level 2 SST data (in satellite coordinates) from the 11 μm channel and the corresponding data quality flag were obtained from NASA's Ocean Color website (http://oceancolor.gsfc.nasa.gov/). To facilitate subsequent statistical analyses, the satellite passes from this dataset were remapped into a standard equirectangular projection.

We present maps showing the mean and standard deviation of SST averaged over all seasons and years as well as these same statistics computed on a seasonal basis. For the purpose of this report, seasons are defined as follows: Winter: January-March; Spring: April-June; Summer: July-September; Autumn: October-December. Seasonal averages are calculated using data from all years during that particular season. To avoid contamination by clouds (which generally appear colder than the sea surface), the statistical measures of SST presented here were computed using only those data values passing the most stringent data quality tests (quality flag = 0). The mean and standard deviation estimates at a given pixel (location) are displayed only if at least 50 SST values passing this test are included in the average.

Figure 3 shows the mean SST field and its standard deviation averaged over all seasons and all years. Warmest temperatures (11-13 °C) occur in central RIS in a region that extends to the south into the open ocean and also in northeastern Buzzards Bay. BIS and the eastern margin of RIS are generally a degree or two colder, likely a result of stronger tidal mixing in these regions, which reduces summertime SST. The boundary between the cooler BIS and warmer RIS surface waters is located slightly to the east of Block Island and then extends southwestward in the area to the south of BIS. As noted above, this front, which is seen more clearly in the seasonal maps to be described below, is the surface temperature manifestation of the low salinity LIS outflow (Ullman and Codiga 2004). The SST standard deviation indicates the range of SST encountered during the averaging period. In this case, the variability is a combination of seasonal variability and year-to-year variability, with the latter presumably showing little spatial structure. Highest standard deviations (7-9 °C) occur in regions near the coasts and in the relatively shallow Buzzards Bay indicating the strong seasonal SST swings in these areas. BIS is characterized by

lower standard deviations (5-7 °C), consistent with a reduction in the amplitude of the seasonal cycle of SST due to enhanced vertical mixing, which tends to distribute seasonal heat gain in summer over a deeper water column, associated with stronger tidal currents.

Winter SST (Figure 4) in RIS and BIS ranges from 1 to 5 °C with highest temperatures in southern RIS over the western portion of Cox Ledge (Figure 2) and the deep channel to the west of the Ledge. Lowest temperatures occur in the relatively shallow waters on the periphery of the Sounds, where winter surface cooling distributed over a shallower water column results in lower surface temperatures than in deeper areas. It is notable that in the eastern part of RIS the strong temperature gradient region along the outer edge of the cold band (occurring at a temperature of about 3.5 °C) does not appear to follow the isobaths as it does in northwestern RIS and in BIS. This suggests that the heat balance in this region may be significantly influenced by the advection of cold water northwestward into RIS from Nantucket Shoals, where extremely low winter SST is observed (Ullman and Cornillon 1999). SST standard deviation in winter is generally low (less than 2.5 °C) with highest and lowest values in central RIS and western BIS respectively.

In spring (Figure 5), highest SST (10-11 °C) occurs in northern and central RIS, while BIS, the area around Block Island, and the nearshore regions in eastern RIS are relatively cooler (8-10 °C). A sharp gradient is apparent around the periphery of the cooler BIS waters. This SST front is coincident with a co-occurring front in surface salinity that delineates the region influenced by the low salinity surface outflow from LIS. Strong vertical mixing caused by intense tidal currents in eastern LIS and western BIS distributes the springtime surface heat flux over a large portion of the water column in the LIS outflow region. This results in a smaller increase in surface temperature during spring than in regions with weaker tidal currents (e.g. central RIS) where the effects of surface heating tend to be trapped in a shallow surface mixed layer. The presence of cool water in the shallow eastern parts of RIS is likely a result of this mechanism as well. SST standard deviations are largest in central RIS (4-5 °C) and lowest in BIS and along the eastern margin of RIS (3.5-4.5 °C). This reflects the fact that the latter regions exhibit a smaller springtime increase in SST from their winter values. It also likely results from the fact that inter-annual variation in surface heat flux produces larger temperature variations in areas where the surface flux is trapped in a thin surface layer (central RIS) rather than being mixed throughout the water column.

Summer SST patterns (Figure 6) are similar to those in spring. A strong contrast is evident between cool SST in BIS (less than 20 °C) and relatively warmer values in central RIS (greater than 20 °C) arising from the same mechanism discussed above. As in spring, surface waters in eastern RIS are relatively cool (less than 20 °C), and the boundary between these waters and the warmer central RIS waters is more pronounced than in spring. Summer SST standard deviations tend to be low (less than 2 °C) partly reflecting the fact that summer (like winter) is the period when seasonal SST changes are at a minimum due to the change in sign of the surface heat flux from net heating to net cooling.

In autumn (Figure 7), waters in the region cool from the summer peak, with mean SST during autumn between 10.5-13.5 °C. Central RIS remains about 1 °C warmer than BIS and the coastal areas in eastern RIS. Coastal areas in northern RIS near the mouth of NB, and around eastern Long Island, exhibit warmer temperatures (SST values of 13-14 °C) than those observed in deeper areas. It is not clear what causes this; further investigation is needed to determine if this is a real signal or an artifact of the averaging procedure performed. SST standard deviation during autumn tends to be lowest in central and southern RIS due to slower cooling of the deeper water column there.

3.1.3 Hydrographic Climatology: Temperature

In this subsection and the three that follow we describe the temperature, salinity, density, and density stratification across the OSAMP domain with emphasis on seasonal variations of large-scale geographic patterns and water column vertical structure. The analysis is based on a "hydrographic climatology" computed from a compilation of historical archived CTD casts from 1980 to 2007, including those of Hydrobase (e.g., Curry 2001) and many casts from the National Marine Fisheries Service (NMFS) Marine Resources Monitoring Assessment and Prediction (MARMAP) program (e.g., Mountain 2003) of the National Oceanographic and Atmospheric Administration (NOAA). Casts from January through March, April through June, July through September, and October through December are treated as the winter, spring, summer and fall seasons respectively. During each of the four seasons there are about 150-300 casts, collectively over the 27-year period, distributed non-uniformly across the OSAMP domain (Figure 8, upper). Taken as a whole these casts are adequate to characterize the seasonal cycle but too sparse in time and space to yield meaningful information regarding inter-annual variability, which will therefore not be considered. Furthermore, it should be noted that in BIS there are no casts except

in the southernmost and easternmost areas, where the seasonal distribution of casts is highly non-uniform. In the following descriptions, BIS conditions are therefore the least certain.

Values were assigned by objective analysis (Hendry and He 1996) to a grid (not shown) having an unstructured horizontal mesh with node spacing from about 3 to 8 km across the OSAMP domain, and 22 evenly spaced fractional-depth levels relative to a suitably smoothed bathymetry (in Figure 8 the bathymetry in the lower panel is the smoothed version; compare to the upper panel). Surfaces were then computed at constant-depth levels with 10 m vertical spacing, and at the seafloor. The resulting fields presented here cannot capture sharp horizontal or vertical gradients, such as the frontal boundaries and detailed pycnocline characteristics described above. However, they provide valuable insight because unlike nearly all previous studies they illuminate large-scale gradients spanning nearly the entire OSAMP domain. As importantly, for large expanses of central and eastern RIS this climatology represents the best available characterization of vertical structure, for example density stratification, and its seasonal cycle.

For each of the four water properties (temperature, salinity, density, and stratification), seven figures are presented that collectively convey seasonal changes, geographic patterns, and vertical structure. The first three figures are maps showing the seasonal progression at several depths. They are followed by the seasonal cycle of vertical structure, presented in two figures along a series of east-west oriented vertical sections, and in two figures along a series of north-south oriented vertical sections (Figure 8, lower, is a map showing the section locations).

The dominant characteristic of temperatures (Figures 9 to 15) consists of the seasonal shifts from minima of about 3-6 ^{o}C in winter to maxima of about 9-21 ^{o}C in summer. In winter, temperature gradients overall are modest. The coldest temperatures are in the northeastern portion of the domain. Relative to the offshore OSAMP region, inshore areas are cooler by about 1.5-2.0 ^{o}C with the gradient strengthening toward the west. The likely causes for this are more effective cooling of shallower waters by loss of heat through the air-sea interface, and cold temperatures of river runoff. The winter temperature pattern is also characterized by warming with depth, from surface to seafloor, by typically about 0.5-1 ^{o}C. This feature is evidence that cooling by loss of heat to the atmosphere lags at depth relative to near the surface. It intensifies toward the south and central west, where increased water depths and vertical salinity gradients allow such temperature differences to be more persistent. The destabilizing influence of temperature on density stratification is overcome by salinity increases with depth (described in

the next subsection). The warm deep temperatures are characteristic of shelf waters to the south of the OSAMP region.

Spring warming brings higher mean temperatures as well as a larger range, about 6 to 12 ^{o}C. The warmest values are found in the upper water column, where geographic variations are modest and consist mainly of increases by about 1 ^{o}C from east to west across the domain. Throughout the domain the temperatures decrease sharply with depth, with surface to seafloor differences of about 4-6 ^{o}C and the sharpest vertical gradients concentrated in the upper water column. Near the seafloor, the geographic pattern includes increases by up to 4 ^{o}C in shallower areas relative to deeper areas, opposite the winter pattern, a signature of more efficient penetration of vernal warming with depth where water is shallower. Spring temperatures are generally uniform across the domain geographically and decrease primarily with distance from the surface, a pattern consistent with the relatively homogenous distribution of solar heating that drives warming.

Summer mean temperatures span about 9-21 ^{o}C, with sharp decreases in depth similar to those in spring except that surface to bottom differences increase to 6-10 ^{o}C or more. At the surface and 10 m deep there is a slight increase in temperature in the offshore direction but throughout the water column below the gradient is reversed and the seafloor temperature pattern, much like that in spring, is characterized by values several degrees higher in shallow inshore areas. Coldest temperatures occur at depth offshore, particularly to the south and west of the domain where surface warming penetrates less deep as a result of stratification due to salinity (discussed below).

The fall mean temperatures are relatively uniform in the range from about 12-13.5 ^{o}C. The main geographic pattern is a weak gradient from cold to warm in the offshore direction, which can be interpreted in terms of the influence of surface cooling penetrating fastest in shallower areas. The warmest water occurs at about mid-depth in the southern portion of the domain, where upper water-column temperatures increase with depth, as in winter (as described above). The mid-depth temperature maximum can be understood as a remnant of the summer waters that were coldest at depth with near-surface layers now cooled by surface heat loss.

3.1.4 Hydrographic Climatology: Salinity

Seasonal-mean salinity values (Figures 16 to 22) range from about 29.75 to 33.50 practical salinity scale (PSS) units. The seasonal cycle is dominated by overall freshening of about 0.5-1.0

PSS during spring and summer, which is concentrated in the west and to a lesser extent in the north. The primary geographic patterns in salinity are an upper water column east-west gradient toward values up to 1 PSS lower in the west, and slightly weaker increases in the offshore direction deeper in the water column. This reflects the fact that the main process influencing salinities is river runoff, with the Connecticut River in LIS the main source of fresh water reaching the OSAMP domain, as discussed in the Introduction. Compared to that of temperature, the seasonal progression of salinity is far less pronounced; geographic variations of seasonal-mean values for a single season are generally comparable to changes between seasons.

Salinities increase in the offshore direction nearly everywhere throughout the OSAMP domain, and always increase with depth. The surface to bottom difference ranges from about 0.5 to 2 PSS, peaks in spring and remains strong in summer. It is largest in the western half of the domain, in particular in BIS and to the south and west of Block Island, where the persistent influence of the relatively fresh LIS outflow is felt. As will be described below, tidal currents are stronger in BIS than in RIS, so the more persistent salinity stratification in BIS relative to RIS is an indication of the extent to which the freshening influence of LIS outflow reduces tidally driven turbulent mixing there.

3.1.5 Hydrographic Climatology: Density

The density anomaly sigma-t (σ_t) (Figures 23 to 29) ranges from about 21.75 to 26.00 kg m^{-3}, with geographic, vertical, and seasonal changes that reflect the underlying temperature and salinity patterns, each of which make important contributions. Overall seasonal variations in sigma-t are modest, intermediate between that of temperature and salinity when compared to geographic variations in each. The least dense water occurs in BIS, and to a lesser extent other inshore areas, near the surface during spring and summer. The densest water occurs in RIS and offshore, at the bottom during fall and winter. Hence the upper water column geographic pattern is dominantly an east-west gradient, with eastward decrease across the domain toward BIS that peaks at about 1 kg m^{-3} during spring, while at depth it consists of increases in the offshore direction that peak at about 1.5 kg m^{-3} during summer. For most of the year, variations in salinity make the primary contribution to variations in density, with temperature becoming comparably important during summer. The season with the most uniform density is winter, under the homogenizing influence of wind-driven mixing, when the increase in temperature with depth has a destabilizing influence that counteracts the stabilizing increase of salinity with depth. Similarly, during winter the influence on density of the onshore-offshore gradient in temperature

counteracts that of salinity, weakening the lateral gradient of density, as shown by Ullman and Codiga (2004). In contrast, the vertical and onshore-offshore gradients in density peak when contributions from temperature and salinity are in the same sense during summer, and to a lesser extent spring. Vertical variations in sigma-t are hence distinctly seasonal, reaching peak surface to seafloor differences of about 3 kg m^{-3} in summer, intermediate values of about 1-1.5 kg m^{-3} in spring, and about 0.5 kg m^{-3} or less in winter and fall.

3.1.6 Hydrographic Climatology: Stratification

Density stratification (Figures 30 to 36) is quantified using the buoyancy frequency squared, $N^2 = -(g/\rho_o)d(\sigma_t)/dz$ where g is gravitational acceleration, ρ_o is a constant reference density, and z is the vertical coordinate positive upward. The vertical differences are calculated over 10 m distances and are thus likely lower limits for stratification at smaller vertical scales. In units of 10^{-4} s^{-2}, peak values range from 2-3 in winter and fall, to 5-6 in spring, to 10-12 in summer.

Geographic variations undergo a distinct seasonal cycle. In winter stratification is strongest in BIS, where wind and tidal mixing influences are counteracted most effectively by the freshening influence of LIS outflow, as described above. In spring, stratification is enhanced throughout eastern BIS and portions of western RIS as well as the southwestern offshore portion of the OSAMP domain, in association with LIS outflow which has a broader influence due to peak river runoff. In summer and fall, the influence of surface warming causes stratification more broadly across the OSAMP domain but peak values remain in the west, particularly south of Block Island.

The strongest stratification occurs at middle depths within the water column, corresponding to a pycnocline, which is consistent with the freshening influence of estuarine waters being homogenized across the upper water column by wind mixing. During fall the pycnocline is about 30-40 m deep south of Block Island where it is strongest, and during other seasons it is generally about 10-20 m deep.

3.2 Currents

3.2.1 Literature Review

The earliest efforts to analyze current observations from waters within the OSAMP domain focused mainly on tidal motions in BIS (LeLacheur and Sammons 1932), and at one station at the mouth of VS (Haight 1938). BIS tidal currents were shown to be mostly rectilinear and east-

west oriented by LeLacheur and Sammons, who deduced amplitudes of about 50 cm/s in eastern BIS that increase to about 75 cm/s or more in western BIS. They also noted "ebb dominance", which can now be recognized as the presence of a residual (persistent, non-tidal) flow westward out of LIS, was prevalent throughout southern BIS including the area just north of Block Island, with "flood dominance" in northern BIS and near Point Judith. Finally, they documented a distinct phase lead of the tidal current reversal near the seafloor, by up to about an hour earlier, compared to near the surface. Haight (1938) showed that in far eastern RIS, tidal currents rotate clockwise in time with speeds of about 10-25 cm/s.

That the tidal motions are shaped strongly by near resonance of the semidiurnal components with LIS was recognized by Riley. However, for some three decades after the 1930s compilations, progress understanding the non-tidal flow was mainly limited to qualitative inferences based on water properties due to the lack of direct current measurements in BIS and RIS. Early views of surface salinity distributions (discussed above) were interpreted (e.g., Riley 1952) as indicative of a residual drift that originates in LIS and moves through BIS eastward and then southward through the gap between Montauk Point and Block Island. By differencing flood and ebb tidal currents, Riley (1952) also concluded near-surface residual drift in BIS was southeastward and estimated its strength to be in the range of 2 to 7 cm/s. It wasn't until the mid 1960s that additional current observations were collected (Williams 1969; Meguire 1971; Long 1978), which showed a more detailed view of vertical structure of currents in BIS, and were used to estimate volume transport there.

In the 1960s and 1970s an improved view of the direction of non-tidal circulation patterns also emerged from a series of field campaigns using surface floats and seabed drifters. Seabed drifters were weakly negatively buoyant, with weighted plastic stems to help maintain suspension above the bottom. The drifters were released offshore, marked with offers of 50¢ rewards to those who return them along with the date and place where they were retrieved along the coastline, and statistics were compiled of the recovery sites and the number recovered relative to the number released. Interpretation of the results of such studies can be problematic due to the ambiguity between unrecovered drifters that were carried offshore and those which happened not to be recovered for other reasons. A seabed drifter study by Bumpus (1965) spanning the broader New England shelf, including a few releases in and near RIS and BIS, concluded that near-seafloor flow was onshore over the inner half of the shelf including all of the OSAMP domain.

Cook (1966) presented results of a study using both surface and seabed drifters that were deployed at an array of stations spanning most of RIS during a short series of cruises in each of the four seasons. Pronounced variability of the results in response to weather-band shifts in the winds prior to and during the cruises reinforced awareness of the strong wind influence on the circulation. The range of current speeds was crudely estimated to be 2 to 16 cm/s at the surface and about 0.1 to 3.5 cm/s near the bottom. Surface flow directions were variable but generally northward during the spring and summer sampling, commonly eastward between Point Judith and Block Island during most seasons, and interpreted to be southward during the winter and fall (largely based on the low drifter return rate). The most persistent attributes of near-bottom flow included motion westward in western RIS, westward through the gap between Point Judith and Block Island, and northward in central and northern RIS. These features were noted to be consistent with the influence of the surrounding estuaries, particularly LIS and NB. In later years, similar drifter methods were applied by Hollman and Sandberg (1972) along a north-south transect in east-central BIS and by Collins (1974) and Snooks and Jacobsen (1979) along north-south oriented transects from the southern RI coast to Block Island. At these BIS sites the surface flow directions were most commonly eastward and southward, with high variability that was attributed to wind forcing, while deep flow was quite persistently westward toward LIS.

The interpretation by Cook (1966) of drifter results, as well as the small number of other studies available from surrounding waters, included an argument that a cyclonic (counterclockwise) surface flow gyre occupies RIS during typical spring and summer conditions, but is broken up by river runoff events and by winds in fall and winter. The gyre consisted of flow entering RIS primarily from Nantucket Shoals but also from BIS, NB, and BB, moving around the periphery of RIS cyclonically, while exiting RIS mainly from its southwest corner but also towards VS. Along the southern boundary of RIS the gyre included eastward flow. Currents were also depicted exiting BIS southward through the gap between Montauk Point and Block Island. Despite the lack of support in modern measurements for the eastward current that closes the gyre in southern RIS, many aspects of this early conceptualization of the spring and summer residual circulation remain pertinent today, as will be seen below.

Moored current meter deployments that enabled current strengths and directions to be quantified on short timescales, unlike drifter studies, became more common starting in the late 1960s. Shonting (1969) reported on a 13-day summer 1967 deployment of four moorings in a 1 km square in central RIS, each with current sensors recording each 20 minutes at two depths

shallower than and deeper than the strong seasonal pycnocline at about 8-12 m deep. Measured speeds ranged from about 15-40 cm/s and 5-20 cm/s at the shallower and deeper depths respectively, reflecting the isolation by the pycnocline of the deep water from wind-forced variability of the surface layer. Surface residual drift was about 10-12 cm/s westward in the upper layer, and about 2 cm/s at depth with a northward component. Semidiurnal currents with amplitudes of up to several cm/s were apparent, as well as intermittent near-inertial (period 18.3 hours) rotary motions with amplitudes of up to 5-6 cm/s.

In the early 1970s moored current meters were deployed within a few m of the bottom near a 35 m deep dredge disposal site in eastern central RIS (Saila et al. 1972; Pratt et al. 1975; Griscom 1977). The range of current speeds was 0 to 5 cm/s more than half the time, with semidiurnal tidal currents of a few cm/s, and occasional increases associated with storms reaching about 20 cm/s. Long-term mean flow was mostly eastward, which was interpreted as movement towards VS, and noted to be in agreement with the Cook schematic described above.

Year-long moored current meter deployments were part of the mid-1970s fieldwork in northern and eastern BIS (Raytheon 1975; Snooks and Jacobsen 1979). Current speeds were mostly in the range of 20-45 cm/s, with an east-west oriented semidiurnal tidal component of magnitude 20-30 cm/s, and marked wind-driven variability that was enhanced modestly during winter and fall compared to spring and summer. Nearest the northern coast, flow was oriented mostly east-west parallel to the shore, with frequent reversals; long-term means were about 5 - 10 cm/s with variable directions near the surface but a westward component at nearly all sites and all seasons at depth. Drogued drifter deployments at this site (Raytheon 1975) lasting about a tidal cycle also confirmed the importance of tidal motions in the overall flow. Moving southward approaching Block Island the tidal, wind-driven and mean flow magnitudes were similar with increasingly larger ranges of directions occurring, though the east-west orientation was still most prominent, and both shallow and deep mean flow became increasingly eastward-directed. A related experiment (Krabach and Snooks 1977) measured currents and dye concentrations within about 5 km of the northern shore of BIS in order to estimate flushing times.

The next relevant current measurement program was nearly two decades later, when Geyer and Signell (1990) used new acoustic Doppler current profiler (ADCP) technology in a vessel-based survey to examine flow in VS at the eastern boundary of the OSAMP domain. They quantified the tidal current strengths at 50 to 70 cm/s, in association with swift water exchanges through VS. They also identified a non-tidal residual flow structure that included persistent

eddies several km in size, with flow up to 25 cm/s, on either side of a headland. Some 10 years later Kincaid et al. (2003; 2008) carried out a similar series of vessel-based ADCP surveys, and deployments of a bottom-mounted ADCP, near the mouth of NB at the northern boundary of the OSAMP domain. Based on the surveys, non-tidal currents were stronger at the East Passage opening to NB than at the West Passage opening, and there were pronounced horizontal and vertical gradients in the speed and direction of both tidal and non-tidal flow. Residual flow moved northward in to NB in the eastern side of East Passage but southward on its western side. A westward current in northern RIS, in proximity to the northern boundary of the OSAMP domain, was also identified in summer, with speeds of 5 to 15 cm/s; it was not present in winter observations. The moored instrument showed 10-15 cm/s weather-band variability related to wind and river runoff events, with surface and deep flow decoupled from each other most strongly during summer in a manner consistent with the findings of Shonting (1969).

Significant advances in understanding of several aspects of OSAMP domain currents were made during the early 2000s in association with intensive observational campaigns focused on the frontal boundary in hydrographic properties south of Block Island. An array of bottom-mounted ADCPs was deployed there for numerous season-length intervals; vessel-based ADCP and towed undulating CTD surveys were carried out; and a high-frequency (HF) radar system (described below, with most recent analysis; see section 3.2.2) was installed and began continuous operations that remain active. The HF radar measures surface currents hourly with ~2 km resolution over nearly all of BIS, an area extending about 20 km south of Montauk Point and Block Island, and a small portion of western RIS. In addition, surface drifters released in BIS (Ullman et al. 2006) gave a detailed view of east-west tidal motions in northern BIS and rapid southward flow out the gap between Montauk Point and Block Island.

Seasonal-mean patterns in surface flow were examined using the HF radar by Ullman and Codiga (2004) and Mau et al. (2007b). Southern and western BIS surface currents are dominated year-round by LIS outflow moving at about 15-30 cm/s towards and through the opening between Montauk Point and Block Island. Northern and eastern BIS surface currents are weaker and more variable. South of Montauk Point the LIS outflow continues, now directed southwestward. During summer, a 25 – 30 cm/s southwestward surface jet originating east of Block Island with mainly geostrophic dynamics joins the LIS outflow south of Block Island, where together they feed a westward coastal current along the southern shore of Long Island. During winter, flow south of Block Island shifts in direction to be nearly directly offshore, and

the jet east of Block Island is weak or absent. Together with the summer-only westward flow in northern RIS noted by Kincaid et al. (2003), the summer jet is consistent with the Cook (1966) schematic for counterclockwise flow in northern and western RIS during spring/summer.

Codiga (2005) used moored ADCP records to investigate the vertical structure of the seasonal-mean flow south of Montauk Point and Block Island, identifying a sharp frontal boundary in velocity that extends upward and offshore from the seafloor at about 25-40 m deep. Flow shallower than and inshore of the front is southwestward and strongest in spring, while motion deeper than and offshore of the front is weak in spring but in winter reaches 5-10 cm/s northeastward, opposite the shallow flow. Currents measured by vessel-based surveys during spring 2002 (Kirincich and Hebert 2005) had vertical-offshore structure consistent with this picture and were shown to be in geostrophic balance with the concurrently measured density field. Substantial temporal changes were observed to occur in response to weather band variations in wind and river inputs; a number of specific patterns in surface currents were identified by Mau et al. (2007b) using the HF radar data, and subtidal principal axes ellipses at both near-surface and near-bottom depths based on the moored ADCP array are about 15-25 cm/s (Mau et al. 2008).

Tidal currents are dominated by the M_2 constituent and have pronounced spatial structure across BIS and the area south of Montauk Point and Block Island, as demonstrated by Ullman and Codiga (2004) and Mau et al. (2007a) using HF radar and by Codiga and Rear (2004) using moored ADCP records. Tidal current ellipses are elongated toward LIS, owing to its near-resonance at semidiurnal frequencies, with major axes of about 80 cm/s, 30 cm/s, and 100 cm/s in western, northeastern, and southern BIS respectively. Decay of tidal currents offshore southward from Block Island is swift, from 55 to 20 cm/s across a 10 km moored array (Codiga and Rear 2004). As the seafloor is approached, in agreement with theory for frictional effects, tidal ellipses become smaller and more rectilinear, with an enhanced counterclockwise in time rotary component. South of Block Island, substantial reduction in the size of tidal current ellipses in the upper water column during spring was attributed by Codiga and Rear (2004) to interaction with the background lateral shear of the strong LIS outflow.

On timescales shorter than tidal, vessel-based ADCP current measurements with high vertical resolution at frontal locations by Levine et al. (2009) revealed very strong local shears, indicating shear instability is active and supports enhanced turbulence in these locations. Several-hour long bottom-mounted ADCP records with 1-minute resolution (SAIC 2005) revealed fluctuations of

up to several cm/s on timescales of 5-20 minutes, with substantial nonuniformity in depth, superposed on the ambient 10-12 cm/s tidal current.

3.2.2 Analysis of HF Radar Surface Current Observations

Observations of surface currents from shore-based HF radar were obtained from the University of Rhode Island's standard-range CODAR system. This system provides maps of surface currents, at hourly intervals with spatial resolution of approximately 2 km, over most of BIS and the inner shelf south of BIS. The system is comprised of three radar sites, located at Southeast Lighthouse on Block Island, Misquamicut State Beach on Rhode Island's south coast, and Montauk Point Lighthouse on the eastern tip of Long Island. Each site provides maps of the radial component (the component towards or away from the site) of the surface current field, and the measurements from 2 or more sites, in regions of overlapping coverage, are combined to provide estimates of the surface current vector field. Further details on the operation of this system can be found in Ullman and Codiga (2004). The radial combination step was performed using the least-squares methodology of Lipa and Barrick (1983) with an averaging radius of 2 km. The least squares estimation of the vector velocity components also provides scaled estimates of the uncertainty in the velocity components (e_x, e_y). These were used to form a mapping error, $e_{map} = \sqrt{e_x^2 + e_y^2}$, which is related to the Geometric Dilution of Precision (Gurgel 1994). Current vectors with mapping error greater than 1.25 were deemed highly uncertain and excluded from the analysis.

For the analysis presented here, surface current data from June 2000 through September 2008 were used. Over this time interval, there were a number of relatively short periods during which data were not available because of equipment problems at one or more of the radar sites. However, for this report, where we present long-term or seasonal averages, this was not considered to be a problem and is ignored. Variability in the effective range of an individual CODAR site arises due to changes in the local surface wave field and the level of external radio frequency noise, which results in corresponding variability in the region covered by the vector current map. We limit the subsequent analysis to those areas in the coverage region where valid current vectors (passing the mapping error criterion) are available at least 50% of the time.

In order to focus on the non-tidal surface currents, the tidal component of the current field was removed by application of a low-pass filter (4^{th} order Butterworth filter with cutoff period of 36 hours) to the multi-year time series at each CODAR gridpoint. The resulting timeseries are

composed of a mean component plus variability at timescales ranging from several days to seasonal and interannual periods. Figure 37 displays the overall mean surface current field as well as a measure of the variability at all subtidal frequencies, while Figures 38 to 41 show the same quantities averaged by season. The ellipses centered on the mean vector tips in the figures represent 1 standard deviation of variability. This means that 66% of the time, the tip of the non-tidal velocity vector will lie within the ellipse. If the ellipse encloses the vector origin (the diamonds), this indicates that the variability is large enough such that the non-tidal current flows in a direction opposite to the mean at a significant number of observation times.

The overall mean current vectors (Figure 37) show generally southeastward flow in BIS consistent with the mean surface outflow from LIS. Between Montauk and Block Island, surface currents veer southward and over the inner shelf currents are southwestward. This southwestward flow appears to originate to the east of Block Island, where the flow is southward. The overall pattern thus appears to be the merging of the LIS estuarine outflow, which exits BIS between Montauk and Block Island, with a southwestward current on the inner shelf. Subtidal variability, which in the case of the overall mean contains seasonal variability, is generally large relative to the mean over most of BIS and in the southeast part of the coverage region over the inner shelf. Western BIS and the inner shelf just south of the Montauk-Block Island line are the only places where the mean flow is large compared to the variability.

The seasonal cycle of the non-tidal surface currents is shown in Figures 38 to 41 which present averages over the winter (Jan.-Mar.), spring (Apr.-Jun.), summer (Jul.-Sep.), and autumn (Oct.-Dec.) periods of the entire 2000-2008 time series respectively. During all seasons, the general pattern of LIS outflow through BIS, exiting southward between Montauk and Block Island is present. This outflow is strongest in spring and summer and weakest in winter. The southwestward inner shelf flow is strong in spring and summer and weak during autumn and winter. During winter, and to a lesser extent in autumn, the flow over the inner shelf has a significant offshore (southeastward) component that is driven by strong westward winds in winter (Ullman and Codiga 2004). Subtidal variability is stronger over the inner shelf than within BIS and the variability increases in autumn and winter in response to increased wind variability during those seasons. The subtidal ellipses are generally elongated in the east-west direction, which is roughly the alongshelf direction along this portion of the coast.

A harmonic tidal analysis, using the T_TIDE MATLAB package (Pawlowicz et al. 2002), was performed on CODAR-derived surface currents over the entire 2005 year, a period when

data return was excellent. The five most energetic constituents are the principal lunar M_2, the larger lunar elliptic N_2, the principal solar S_2, the luni-solar diurnal K_1, and the principal lunar diurnal O_1. The M_2 (Figure 42) is by far the most important (note the different scales for the ellipses in Figures 42 to 46) with maximum amplitude of approximately 1 m/s. Tidal ellipses are highly elongated with the major axis generally oriented north-south on the inner shelf, rotating to be roughly east-west within BIS. Amplitudes increase from the inner shelf to BIS consistent with amplification associated with tidal resonance of Long Island Sound at the semi-diurnal period (see, e.g., Codiga and Rear 2004). Some increase in amplitude is also seen in the area between Montauk Point and Block Island, presumably caused by the presence of a relatively shallow sill there. M_2 tidal currents generally rotate clockwise in time (the few counterclockwise-rotation ellipses in Figure 42 are very elongated, indicating nearly rectilinear motion). The other semidiurnal tidal constituents, N_2 (Figure 43) and S_2 (Figure 44) have amplitudes of less than 20 cm/s throughout the coverage region and approximately rectilinear currents. As with M_2, a similar increase in amplitude moving from the inner shelf towards BIS is observed for these constituents. The K_1 (Figure 45) is the most energetic of the diurnal tidal constituents with maximum amplitude of approximately 10 cm/s, while O_1 amplitudes are generally less than 5 cm/s (Figure 46). Little amplification towards BIS and LIS is observed for the diurnal constituents, consistent with the fact that LIS is far from resonance at diurnal frequencies. Currents at the diurnal frequencies generally are clockwise rotating.

4 Characterization Based on Hydrodynamic Simulation

As is abundantly clear from the previous section there are large areas of the OSAMP domain, particularly in central and eastern RIS, in which very few if any observations have ever been collected. This is particularly true with respect to the circulation, to processes that occur at frequencies higher than tidal, and to mixing and dispersion. Hydrodynamic model simulations can therefore play an important role, not only in providing a view of what water properties and circulation characteristics may be in the most poorly sampled areas, but also in enhancing temporal and spatial resolution of processes in locales where there may be adequate measurements. This section begins with a literature review focused on hydrodynamic modeling studies that have addressed portions of the OSAMP domain. Next, the configuration and forcing functions of a representative model simulation are described in detail. Finally, the hydrographic and circulation fields of the model output are presented and discussed.

4.1 Literature Review

Modern methods of hydrodynamic modeling developed in the late 1970s and focused initially on tidal elevations and tidal currents (e.g., URI 1979). Spaulding and Gordon (1982) reviewed all earlier modeling and observational studies, then presented results of a barotropic simulation of tidal flow that incorporated realistic coastline and bathymetry spanning the OSAMP domain and surrounding estuaries. Horizontal resolution was 1.8 km and an offshore area of the shelf was included to improve handling of the open boundary condition. The amplification of the semidiurnal component towards and within LIS due to its near-resonance was captured, and good agreement was found with sea level observations. Tidal currents were noted to be mostly rectilinear in LIS, BIS, BB, and VS while more rotary in RIS. Although modeling techniques advanced substantially in the years that followed, and were applied to nearby systems (e.g. Signell (1987) in BB, Spaulding et al. (1996) in NB, Signell et al. (2000) in LIS), it was more than two decades later when the next modeling simulations were published that included analysis focused on a sizable portion of the OSAMP area.

An investigation of LIS outflow dynamics was carried out by Edwards et al. (2004a; 2004b) using the MIT general circulation model MITgcm (Marshall et al. 1997), a finite-volume c-grid Navier-Stokes solver, in hydrostatic mode with a length-scale turbulence closure scheme and a linear equation of state. The model was configured to include eastern LIS, BIS, RIS, and the surrounding shelf areas with horizontal resolution ranging from 0.5 km near BIS to 2-3 km along the open boundary; z-level grid spacing was 2 to 5 m in the vertical. Realistic tidal forcing was applied along the open boundary and estuarine buoyancy inputs were incorporated through relaxation toward climatological temperature and salinity observations. In Edwards et al. (2004a), wind forcing was omitted and the focus was on understanding dynamics of the front south of Block Island during the springtime 2000 period. A front having characteristics in agreement with available measurements occurred in the model at the location where it is observed, and a diagnosis of its dynamics demonstrated that tidal mixing in BIS, advection by the LIS outflow and inner shelf currents, and a tidally-driven residual flow headland eddy each played important roles. The h/U^3 theoretical boundary of tidally-mixed waters (Simpson and Hunter 1974) was shown to run approximately north-south through eastern central BIS then eastward to Block Island, and from there along an arc leading to the south shore of Montauk Point and extending southward by up to about 10 km. In Edwards et al. (2004b) the focus was on capturing the subtidal weather-band variability in currents that are prominent in observations.

Wind forcing and, more importantly, a barotropic inverse method using local moored ADCP records, were applied and shown to improve the model skill due to their representation of offshore processes otherwise not captured by the tide-only open boundary condition forcing.

Eastern RIS, though not addressed in any detail by Edwards et al., was within the area of interest in model simulations by He and Wilkin (2006) and Wilkin (2006) using the Regional Ocean Modeling System ROMS (e.g., Shchepetkin and McWilliams 2005). ROMS is a free-surface, finite difference, hydrostatic c-grid primitive equation solver with a terrain-following vertical coordinate, and the turbulence closure of Mellor and Yamada (1982) level 2.5 (MY2.5) was applied. Their domain was centered on Nantucket shoals and extended to eastern RIS, Cape Cod, and mid-shelf, with 1 km horizontal resolution. Data assimilation methods were applied by He and Wilkin (2006) and the focus was limited to barotropic tidal dynamics, which were shown to be shaped by interactions with the complicated coastlines and bathymetry of the area and consist of a complex response that has significant propagating and standing wave components. In eastern RIS, the dominant M_2 constituent had northwest-southeast oriented rotary ellipses with major and minor axes of up to 15-25 cm/s; magnitudes were similar in BB but amplified to 50 cm/s or more in VS. The theoretical h/U^3 tidal mixing front boundary was shown to lie east of the OSAMP domain boundaries. Tidally-induced residual circulation of about 5 cm/s flowed northwestward in to the eastern half of RIS from south of Martha's Vineyard. In Wilkin (2006), fine vertical resolution was included and realistic atmospheric, tidal, and open boundary forcing was applied in order to investigate the heat budget during summer 2002. Different dynamical balances controlled the heat budget in Nantucket Sound, Nantucket Shoals, and the area south of Martha's Vineyard. The eastern RIS area is most similar to the latter, where surface waters warm steadily through July and August because advection and tidally-driven mixing are relatively weak.

Mau et al. (2007a; 2008) investigated the circulation and hydrography of BIS and the LIS outflow using the Princeton Ocean Model (POM: e.g., Blumberg and Mellor 1987) configured to include LIS, the OSAMP domain, and portions of the surrounding shelf. POM is a c-grid primitive equation model with terrain-following vertical coordinate and it was run using MY2.5 turbulence closure with 1-2 km horizontal resolution and 16 equally-spaced vertical layers, for a year-long period. In Mau et al. (2007a) the focus was tidal currents and detailed comparisons of model output with HF radar and moored ADCP observations showed the model captured aspects of the horizontal and vertical structure of tidal ellipses (described above) well. In contrast, Mau

et al. (2008) examined dynamics of LIS outflow in year-long model simulations with realistic tidal forcing, observed winds applied uniformly over the domain, relaxation to a seasonal hydrographic climatology, and an open boundary condition that incorporated the ambient coastal current. Comparisons to a number of observational datasets were very favorable, with one main exception being a more pronounced Montauk Point headland eddy than seen in the HF radar measurements. From a series of runs suppressing individual processes, it was concluded that the surface plume strength is limited by tidal and wind mixing and enhanced by the presence of the ambient coastal current.

Finally, Cowles et al. (2008) investigated the low-frequency circulation and hydrography of the entire Gulf of Maine and New England shelf region using data-assimilative simulations with the Finite Volume Coastal Ocean Model (FVCOM). FVCOM (described in the next section) was forced with spatially-resolved meteorological model output for winds and air-sea fluxes, realistic tides, and freshwater inflows from major rivers, and used the MY2.5 turbulence closure. Across the OSAMP domain the horizontal resolution was about 8-10 km, substantially lower than in the simulations described above. Dynamics of the OSAMP region were not investigated in detail, since most of the analysis was centered on demonstrating that model skill was high with respect to a comprehensive set of observations from a 70 m deep mid-shelf site south of Martha's Vineyard. A discrepancy between model and observations was mid-shelf near-surface salinities that were not as fresh in the model as observed during May 1997. It was concluded that the LIS outflow plume in the model did not extend as far offshore as observed due to advection by a westward model current near that location which was stronger than the actual flow.

4.2 A Representative Simulation: FVCOM During 2006

In keeping with the scope of this report, output from a model simulation was sought in order to facilitate an investigation of hydrographic and circulation attributes across the OSAMP domain, with emphasis on geographic, vertical, and seasonal variations. The simulation needed to be representative of current modeling practices, including assimilation of observations (see previous section); have adequate horizontal and vertical resolution across the entire OSAMP domain; incorporate realistic bathymetry and coastline; be driven by realistic meteorological, river runoff, tidal, and open boundary forcing; have duration of at least a full year; and be available to us for purposes of this analysis. The model output selected is a simulation of the year 2006 using FVCOM (Chen et al. 2006) for a similar Gulf of Maine and southern New England shelf regional domain and model configuration as that of Cowles et al. (2008), but with a higher

grid resolution (about 0.25 – 2.5 km) across the OSAMP domain. Different models have differing strengths and weaknesses with respect to various analysis objectives; use of this model output is not intended as endorsement of it as the best-performing, rather it was selected because it met the requirements listed above in the most complete way.

FVCOM is a prognostic, unstructured-grid, finite-volume, free-surface, 3-D primitive equation model consisting of momentum, continuity, temperature, salinity and density equations with parameterization of turbulence closure. The grid used ("Gulf of Maine generation two") extends from Nova Scotia to New Jersey and offshore past the shelf break. The horizontal grid is unstructured triangular cells with increased resolution near the coastline and the shelf break, and the vertical coordinate is terrain-following with 30 layers. The numerical solver uses a second-order accurate discrete flux calculation in the integral form of the governing equations. Wind stress and air-sea flux forcing were from the fifth-generation mesoscale meteorological model (MM5, Grell et al. 1994). The MY2.5 turbulence closure scheme and quadratic bottom friction were applied. The largest 7 rivers, including the Connecticut River, were forced (in contrast to the 29 rivers in Cowles et al. (2008)) using United States Geological Survey data uncorrected for ungauged areas. Along the open boundary, tidal elevations were forced and temperature and salinity were nudged toward hydrographic climatology observations. Inner shelf sea level setup near the northern limits of the domain, far from the OSAMP area, was handled following Pringle (2006). Sea surface temperatures were nudged to post-processed satellite SST.

The model bathymetry in the OSAMP area (smoothed relative to upper frame of Figure 8), the horizontal model grid, and the vertical sections along which model fields are plotted (the same as for the hydrographic climatology in sections 3.1.3 to 3.1.6 above) are shown in Figure 47. Simulation fields were analyzed at the free surface, constant-depth levels spaced 5 m apart, and a seafloor layer. Tidal elevation and current constituents were computed using the t-tide package (Pawlowicz et al. 2002) using the entire simulation year. Subtidal currents were computed using a low pass 5th order Butterworth filter with 30-hour cutoff. Seasonal-averaged quantities were computed using the same seasonal intervals as used in prior sections (Jan.-Mar, Apr.-Jun., Jul.-Sep., and Nov.-Dec. for winter, spring, summer, and fall respectively). Model outputs, referred to as "the simulation" from here forward, are described in detail in the next section.

The simulation period is the year 2006 only, so the fields presented are not representative of long-term average conditions, nor can the analysis address inter-annual variability. This should

be borne in mind when comparisons are made to measurements taken in years other than 2006, and to multi-year mean fields such as the hydrographic climatology presented above. The year 2006 had an anomalously wet late spring period and a summer with relatively weak winds. In surrounding estuaries such as NB, this led to stronger than average stratification during the spring and summer periods, and similar conditions could be expected to have occurred in the OSAMP domain. On the other hand, influences of estuarine freshwater delivery on the model hydrography and circulation in the OSAMP area may be underestimated because the simulation was forced by only the 7 largest rivers, among many more that exist across the Nova Scotia to New Jersey domain, and river flows were uncorrected for ungauged area. Despite the potential difficulties of interpretation that these aspects of the analysis may cause, the insight gained through the model analysis is a constructive complement to the spatially and temporally sparse observational analyses presented earlier.

4.3 Simulation Seasonal Means and Subtidal Variability

4.3.1 Hydrography: Seasonal Means and Standard Deviations

The spatial structures and seasonal cycles of temperature (Figures 48 to 54), salinity (Figures 55 to 61), density anomaly (Figures 62 to 68), and stratification (Figures 69 to 74) in the simulation share most of the gross features of satellite SST (described in section 3.1.2) and the hydrographic climatology from archived CTD casts (described in sections 3.1.3 to 3.1.6). The simulation differs from the hydrographic climatology in its finer spatial detail due to its higher horizontal and vertical resolution, and in its span of the entire OSAMP domain and surrounding areas, including, importantly, all of BIS. In the following discussion, the emphasis is on differences from, and extensions relative to, the results from earlier analyses of satellite SST and the hydrographic climatology.

Simulation surface temperatures agree well with the range of values and geographic patterns in the multi-year mean satellite SST observations on scales of 10s of km. On smaller scales there are differences, notably within a several km of the shoreline, where the satellite data shows more substantial spring/summer cooling in areas such as the western end of VS. Given that the simulation assimilates satellite SST, this is most likely due to real differences between 2006 SST and the multiyear mean of the climatology, but it may reflect an inaccurate balance in the simulation between vertical mixing and arrival of estuarine water.

With few exceptions the simulation temperatures agree with the seasonal evolution in the range of values, the geographic patterns, and the sense of the inshore-offshore gradients of the hydrographic climatology. The primary difference is that the simulation does not have warmer temperatures at depth during the winter, as in the climatology. The reason for this is not clear but potential explanations include: the model portrays 2006 conditions well but warm water did not occur at depth that year; warm water at depth occurred in the simulation but persisted for a short enough duration that it is not apparent in the season-length means; or that in the simulation the balance between vertical mixing and fall/winter surface cooling does not result in the needed surface water temperature reduction.

The fine temporal resolution of the simulation supports calculation of subtidal standard deviations, as were computed for satellite SST but not for the hydrographic climatology due to its sparse underlying sampling. Standard deviations (shown for surface and seafloor depths) are based on 30-hour low-pass timeseries and thus are an indication of both weather-band variability and the trend of the seasonal cycle that occurs during a given season (most pronounced for spring and fall). Comparison between simulation surface temperature standard deviation (lower, Figure 48) and that of satellite observations (section 3.1.2) shows substantial differences in geographic patterns and magnitudes. As noted above, this is probably due to real differences between 2006 conditions and the multi-year climatology. At the seafloor, simulation temperature standard deviations (lower, Figure 50) are smallest during winter, when they decrease across the OSAMP domain towards the north and east where the coldest temperatures occur. Temperature standard deviations are largest in spring and fall, when they peak in western BIS and BB, due to seasonal warming/cooling, and decrease towards the central south OSAMP area. In summer, there is a region of western RIS, oriented roughly north-south, where maximum seafloor temperature standard deviations occur. Given the weak overall warming/cooling during this season, a likely cause for it is weather-band variability. The summer region of high seafloor temperature standard deviation occurs near where a strong southward summer current flows (e.g., section 3.2.1, and upper frame of Figure 6) and may be the signature of weather-band meandering of the current and an associated hydrographic front that intersects the seafloor. There summer seafloor salinity standard deviation (Figure 57, lower) is also enhanced in this region, which is consistent with this interpretation since such fronts are typically characterized by both salinity and temperature gradients.

Simulation BIS temperatures are warmer in summer and colder in winter, compared to central RIS. Temperature gradients across BIS are not as extreme as in RIS; in the horizontal this may be because its shallow sills mean that deeper shelf water affect it more weakly, while in the vertical it is likely due at least in part to the enhanced influence of tidal mixing in BIS associated with shallower water depths and stronger tidal currents.

While the general sense and magnitude of horizontal gradients in simulation salinities (Figures 55 to 61) agree with those of the hydrographic climatology, there are more substantial differences between them, particularly as regards salinity magnitudes, than for temperatures. The most prominent example is that in the simulation the freshest waters (about 29.6 PSS) are seen in western BIS in fall, and to a lesser extent summer; in the climatology they occur in spring and summer, though also at the most western locales (eastern BIS for the climatology). Simulation vertical salinity gradients are substantially weaker than in the hydrographic climatology. It is possible these differences reflect real differences between 2006 conditions and the multi-year climatology; this would be consistent with the fact that many observations suggest the seasonal cycle in salinity is not strongly more pronounced than inter-annual variability. Alternatively, the budget for fresh water in the simulation may be inaccurate, due to the way river forcing has been implemented (mentioned in the previous section), given that 2006 had more spring river runoff than a typical year. Simulation salinity standard deviations (lower frames, Figures 55 and 57) are most pronounced near the surface, as expected given the strong influence buoyant estuarine outflow have on them; during spring and summer they are strongest and peak in offshore areas, during winter they peak in western BIS, and during fall they are weakest. At the seafloor the pattern of standard deviations is similar to that at the surface in winter, but weaker in spring and summer, and there is pronounced peak during fall in the offshore area south of Block Island, and including the area west of Block Island where seafloor temperature standard deviations also peak as discussed earlier in this section.

The simulation density anomaly field (sigma-t; Figures 62 to 68) reflects the combined contributions of temperatures and salinities just described, and differs from the hydrographic climatology in corresponding ways. As in the climatology, the overall seasonal cycle in simulated densities reflects mainly the influence of temperature. However, salinity makes an important contribution to density stratification in all seasons, while that of temperature is becomes important mainly in spring and summer. As expected given its higher vertical resolution, in the simulation the stratification (Figures 69 to 74; note different scale for each

season) tends to be concentrated in a pycnocline that spans a narrower range of depths than in the climatology. Simulation buoyancy frequency squared is lowest in winter, when there is a weak pycnocline only in deeper RIS and the offshore area, centered at about 30 m deep and strengthening offshore. In fall the pattern is similar to winter but with higher buoyancy frequencies, and also a thin strongly stratified layer very near the surface in the northern half of BIS occurs. In spring and summer a sharp pycnocline occurs in central RIS and the offshore areas, at about 10 m deep or less, and strengthens considerably in the offshore direction. Relative to the hydrographic climatology, the simulation stratification does not occur as uniformly across the OSAMP region; this is probably due to the limited ability of the spatially coarse climatology to capture geographic variations. In the simulation, BIS remains unstratified or very weakly stratified in all seasons; the stratification seen in the portions of BIS included in the climatology clearly differs, but is based on very few data so may be more representative of the individual years they were collected than it is of long-term average conditions.

4.3.2 Sea Level: Seasonal Means and Standard Deviations

Results of this subsection are based on analysis of the non-tidal low-passed filtered simulation sea level. The seasonal-mean sea level takes maximum overall values in spring, and minima in fall (Figure 75, upper). The main spatial features consist of a peak offshore gradient of up to several cm across the OSAMP domain, due to high values in inshore areas, during spring and summer, but a weaker oppositely-directed gradient in winter and fall. The spring/summer offshore gradient is associated with the strongest alongshore southwestward currents in the offshore area, as discussed by Ullman and Codiga (2004) in interpreting sea level observations. They concluded that the steric effect of freshwater outflow is likely responsible for peak values in inshore areas during spring, and the inshore set-down during winter is consistent with the influence of upwelling-favorable winds and weakening of the alongshore flow. The simulation sea level in the vicinity of Montauk Point is persistly low year-round, which could be associated with tidally-driven headland eddy dynamics there, as discussed by Edwards et al. (2004a) and Mau et al. (2008); the latter analysis concluded a headland eddy was more pronounced in their model than in HF radar observations, which may also be true for this simulation. The standard deviation of simulation sea level (Figure 75, lower) is minimal in summer, modest in spring, and strongest in fall and winter with values increasing across the domain from about 5-6 cm towards their peaks of about 10-12 cm in BIS. This is consistent with the seasonality of wind fluctuations and probably represents wind-driven variability in the circulation. Tidal sea level variations are

generally substantially larger than these seasonal and subtidal fluctuations, and are discussed in detail in section 4.4.1.

4.3.3 Currents: Seasonal Means and Subtidal Principal Component Ellipses

Seasonal means, and principal axes components of subtidal flow, were calculated (Figures 76 to 87) from simulation horizontal currents as for HF radar currents (section 3.2.2), using the non-tidal low-passed model output for each season at several depths. The ellipses thus primarily reflect weather-band variability. The results are presented as vectors (seasonal-means) and ellipses (subtidal principal axes) on maps (Figures 76 to 79), east-west vertical sections (Figures 80 to 83), and north-south vertical sections (Figures 84 to 87). In all figures, including the vertical sections, the vectors and ellipses appear in plan view showing eastward and northward flow upward and rightward on the page, respectively; no vertical velocities are shown. Only Eulerian means are considered and no particle-tracking nor Lagrangian-mean analysis in included. In this section, the seasonal-mean vectors (red arrows in figures) are described first, followed by the subtidal ellipses.

In southern and central BIS, including the area just north of Block Island, changes in flow from season to season are modest. Seasonal-mean currents near the surface range from about 5-15 cm/s, with a persistently eastward component and peak values during the summer. This can be identified as the outward component of the LIS estuarine exchange flow, which Codiga and Aurin (2007) observed to peak during summer in eastern LIS. With increasing depth the eastward flow weakens in magnitude, and becomes directed more northward in the east near Block Island. In northern BIS, currents are generally weaker (about 1-5 cm/s) and have a westward component except in winter when flow is mostly southeast as driven by strong southeastward winds; an exception is the very shallow, northwest-most location, adjacent to shore in BIS, where flow is strongly westward. These westward movements are likely part of the inward return component of the exchange with LIS. In the north-south oriented gap between Point Judith and Block Island, flow in the northern half is westward and weaker than the eastward flow just described in the southern half. The two-way nature of flow in this gap is likely influenced by the LIS estuarine exchange flow (see Table 1).

In the vicinity of the east-west oriented southern opening of BIS, there is eastward flow of about 10-15 cm/s that persists in all seasons along the shoal immediately south and east of Montauk Point. Together with southward and southwestward flow to the east and south of there, this is likely a portion of a tidally-driven headland eddy (discussed by Edwards et al. (2004a) and

Mau et al. (2008)). The southward/southwestward current over the canyon outside southern BIS strengthens sharply in spring and summer, reaching speeds of 20 cm/s or more, the strongest anywhere across the domain. It is a combination of LIS outflow and a southward current to the east of Block Island that also intensifies strongly in spring/summer, reaching up to 20 cm/s while typically 5 cm/s or less in fall and winter. The western RIS spring/summer intensified southward current in the simulation, identified as a jet by Ullman and Codiga (2004) in HF radar observations and described in section 3.2.2 above, flows westward along the southern edge of Block Island, and together with the eastward flow off Montauk causes a strongly convergent pattern on the inner shelf just outside the southern opening of BIS. Some of this water moves through the jet then northward along the western side of Block Island, particularly at depth, so that in all seasons the flow between Montauk Point and Block Island has both a southward and northward component, another signature likely associated with the LIS estuarine exchange flow. There is evidence that mean flow very near to Block Island circulates around all of its sides in the clockwise sense.

There are pronounced season-to-season changes in the offshore portion of the OSAMP domain. In winter and fall this offshore region, as well as most of RIS, are characterized by weak mean flow, a few cm/s, in the south and east direction offshore in the upper water column, and onshore north and east at depth. This is consistent with an upwelling circulation driven by the strong winds in those seasons, which are southeastward and hence have an offshore component as well as a component in the upwelling alongshore direction. In spring and summer this flow pattern changes, in the offshore areas, to a stronger (about 10 cm/s) east-southeastward directed current along the southern boundary of RIS. This current is strongest at the surface in spring and just beneath the surface in summer, and weakens modestly with depth but extends throughout the water column with only minor changes in orientation. This current likely originates on Nantucket Shoals and only a fraction of it enters RIS, most instead moving from south of Martha's Vineyard directly along the southern boundary of RIS to the area south of Block Island.

Within RIS, where seasonal mean currents are generally the weakest, the near-surface offshore winter flow becomes westward and northward in spring, apparently driven by the inflow from Nantucket Shoals. Summer mean flow is very weak, except for the far eastern and northern portions of RIS where a narrow current of up to 5-10 cm/s moves counterclockwise around its edges and ultimately feeds the southward jet in western RIS. This system of flow is similar to the "cyclonic eddy" described by Cook (1966), except that in the simulation it does not close on

itself because flow at the southern edge of RIS is westward not eastward. It seems likely that the counterclockwise flow along the western, northern, and eastern edges of RIS is associated with the hydrographic boundary between stratified and unstratified waters, marked by the tidal mixing front. In fall and winter the stratification in RIS is diminished, hence the hydrographic front weakened, as is the current along it.

A prominent attribute of simulation subtidal currents (blue ellipses in figures) is that, over most of the OSAMP domain and during much of the year, they have semi-major and semi-minor axes of about 5-15 cm/s, and are thus stronger than the seasonal mean flow. This is evidenced by vectors for which the head and tail both lie within the ellipse. It is most pronounced near the surface, the most directly responsive to wind forcing. This feature underscores the strong relationship between the currents at a given time, which are commonly oriented toward a substantially different direction than they were a few days earlier, and the strength and direction of the wind over the past several days. Subtidal ellipses larger than seasonal-mean flow vectors are seen in all four seasons over all of central RIS and most of eastern RIS, as well as in the central and eastern offshore region in winter and fall. Areas where seasonal-mean current vectors are larger than subtidal ellipses, indicative that changes in direction of flow are much less common, include the system of stronger currents just described, and BIS, which is not as exposed to wind influences and hence generally has slightly weaker weather-band variability.

Subtidal ellipses are larger in winter and fall than in spring and summer, which is consistent with fluctuations that are predominantly wind-driven, given that the strongest wind stress variability occurs in fall and winter. In the open areas outside BIS that are less constrained by bathymetry and coastline geometry, the increased ellipse size in winter and fall is mostly in the east-west component; nearly round spring/summer ellipses become elongated in the east-west direction during winter and spring. This is indicative that a major component of variability is upwelling/downwelling circulation oriented along the larger-scale east-souteastward/west-northwestward regional coastline orientation.

Subtidal ellipses diminish with depth in all seasons, to half of their surface amplitudes or less at the seafloor. In winter and fall, the decay in depth is quite uniform over the water column. In summer and spring, in locations where stratification is strong such as in central RIS, the ellipse amplitudes diminish sharply just deeper than the pycnocline, and are weak everywhere deeper, relative to the 10-20 m deep surface layer. This characteristic of the simulation is in very good agreement with the early observations of Shonting (1969).

4.4 Simulation Tidal Processes

4.4.1 Tidal heights

The most energetic constituents in harmonic fits to simulation sea level are M_2, N_2, S_2, K_1, and O_1, the same five included in the above HF radar currents analysis (section 3.2.2). The amplitude and Greenwich phase lag of each constituent is presented (Figures 88 to 92). The tidal response in the area is complicated, as discussed by He and Wilkin (2006) for eastern RIS, by reflection and refraction by the complex coastline and bathymetry, in addition to the influence of resonances in nearby semi-enclosed water bodies.

Collectively, the resultant of the five constituents leads to tidal height amplitudes of about 1 m, with pronounced spring-neap variability, across much of the OSAMP domain. The M_2 constituent (Figure 88) amplitude is in the range of 35-65 cm across the OSAMP domain, while the amplitudes of N_2 (Figure 89) and S_2 (Figure 90) are in the range of about 8-13 cm each. These three semidiurnal constituents have very similar spatial patterns in amplitude and Greenwich phase lag. Amplitudes are maximal in northern RIS and towards BB and decrease from there offshore and towards BIS, where they take their minima in central southwestern BIS near Montauk Point. Modest Greenwich phase lag variations of about 30-40^o occur across the domain, with maxima in western BIS, decreases eastward across BIS from there, and relatively uniform values across the rest of the domain. The nearly quarter-wave resonance response of LIS to semidiurnal frequencies plays a large role in these patterns, since eastern LIS has characteristics of a node.

The two diurnal constituents K_1 (Figure 91) and O_1 (Figure 92) each have amplitudes in the range of about 5-7 cm, and similar spatial patterns of amplitude and Greenwich phase lag to each other. Amplitudes are maximal in western BIS and decay across BIS eastward. For K_1, amplitudes decrease relatively uniformly toward BB, and for O_1 they are relatively uniform across the rest of the domain. Greenwich phase lags only vary by about 15^o, with peak values near Montauk Point and decreases across the domain toward minima along the eastern and northern edges of RIS. Unlike the semidiurnal constituents, these diurnal constituents are not near the resonance frequency of LIS, which therefore influences their spatial patterns much less strongly.

4.4.2 Tidal currents

In harmonic analysis of simulation currents, in addition to the above five constituents the currents of the main quarter-diurnal non-linear M_4 and the smaller solar elliptic L_2 are energetic. While the M_4 and L_2 components of sea level variability were not significant, their currents were stronger than the diurnal constituents over much of the region, so are included in this analysis. It is likely their generation is through nonlinear interactions. HF radar in BIS and surroundings, as well as moored ADCP records on the inner shelf south of BIS, do not show a level of M_4 and L_2 energy as high as in the model output. Additional measurements are needed from areas further east, including RIS, to assess whether this aspect of the simulation agrees with observations there.

The relative importance of tidal currents to the total (tidal and non-tidal) flow field can be quantified as the ratio (expressed as a percentage, Figure 93) between the variances of the tidal currents and the total currents. This percentage is very high (> 90%) throughout BIS, except in a small area adjacent the western shore of Block Island, as well as areas extending about 5-10 km outside of BIS southward on the inner shelf and eastward in western RIS. It is also very high (>80%) within 5-10 km of the mouths of NB, BB, and VS. These areas are associated with amplification due to coastline constrictions and/or resonant responses of adjacent water bodies. In contrast, the percentage is lower (40-60%), in northern RIS very near to Sakonnet passage, in the open-water area extending from southeast of Block Island toward south-central RIS, and over the western offshore area. This results from relatively weak tidal currents or stronger weather-band variability (discussed above). Over most of central eastern RIS and the offshore area to its south, tidal current variance is about 60-80% of total current variance.

Spatial structure of tidal flow for each constituent is revealed by maps of tidal current ellipses, with instantaneous flow vectors, at the surface and seafloor (Figures 94 to 100). For the most energetic M_2 constituent (Figure 94), the ellipses are presented with a scale such that their size corresponds to the distance a passive particle would be advected during one tidal period by that constituent alone, in order to emphasize the tidal advection length and how it varies across the domain. Surface M_2 ellipses are elongated towards LIS throughout BIS and the areas southeast and northeast of Block Island; generally rotate clockwise in time; and reach maximum semi-major axes of up to 80-90 cm/s in southern BIS then decay over 10-20 km southward to about 10-20 cm/s. These features are consistent with the HF radar observations described above. In offshore areas and most of RIS, simulation ellipses also rotate clockwise in time and are more

round; semi-major axes over much of this area are 5-10 cm/s and increase gradually eastward to more than 50 cm/s within a few km of BB and VS. Similar amplification is not seen at the mouth of NB, where, in the area east of Point Judith, currents rotate counterclockwise in time. The M_2 ellipses at the seafloor are about half as large as those at the surface but share most of their general characteristics, with the exception of an amplified counterclockwise-in-time component; over most of the domain, this results in more narrow ellipses that still rotate clockwise in time, while in contrast across much of BIS and an expanded area east of Point Judith they become counterclockwise in time. The amplification of the counterclockwise component as the seafloor is approached is a fundamental feature of frictional tidal boundary layers (e.g., Soulsby 1990) and has been observed on the inner shelf south of BIS (Codiga and Rear 2004); an alternative explanation could be superposition of incident and reflected/refracted waves causes by interaction with the complex coastal boundaries, although it is not obvious how this would lead to enhancement of counterclockwise-in-time rotation near the seafloor. For the N_2 (Figure 95) and S_2 (Figure 96) constituents, ellipse amplitudes are lower (see scale in figures; amplification factor relative to advection is also noted in captions), but all the ellipse characteristics just described for M_2 are very similar.

The diurnal constituents K_1 and O_1 (Figures 97 and 98) have very similar amplitudes and geographic patterns to each other. They are much weaker than the semi-diurnal constituents (note different scales in figures) and much more uniform spatially across the region, with relatively round ellipses and rotation in time clockwise. Moderate amplification occurs in eastern RIS, and in BIS where there is a tendency for deep ellipses to rotate counterclockwise in time.

The M_4 constituent is relatively uniform across the domain, with nearly round ellipses and rotation counterclockwise in time. Amplification occurs in the mouth of VS, and in BIS where ellipses are amplified and rotate clockwise in time. Variations with depth are modest.

For the L2 constituent over areas outside of BIS, ellipses are elongated northeast-southwest and rotate clockwise in time at the surface but counterclockwise in time at the seafloor. In BIS amplitudes are amplified and rotation is clockwise in time at both the surface and seafloor.

Additional information about the vertical variation of tidal current amplitudes within the water column is seen in vertical section plots of the RMS semi-major and semi-minor axes of the tidal current ellipses along the transects in Figure 47. The pattern for semi-diurnal constituents is represented by that of M_2 (Figure 101 upper; Figure 102 left) and consists of modest decreases uniformly from surface to seafloor across most of the domain, but sharper decay in the vertical

within BIS where enhanced frictional influences due to bed-driven turbulence are expected due to the amplified currents there. In contrast, the pattern for diurnal constituents, represented by K_1 (Figure 101 lower; Figure 102 right), consists of moderate vertical gradients that are more uniform over the domain, since amplification in BIS and eastern RIS is so much more modest. For M_4 and L_2 the vertical amplitude variations (Figures 103 and 104) over most the domain are relatively weak, with sharp vertical decay occurring only in small areas of BIS, and to a lesser extent eastern RIS, where amplification is significant.

5 Summary

A stylized schematic depiction of prominent seasonal-mean hydrographic and circulation features of the OSAMP domain and immediate surroundings has been constructed (Figure 105) in order to concisely summarize the main aspects of geographic variations, vertical structure, and the seasonal cycle. This section gives a detailed explanation of the schematic, which was prepared based on all aspects of the above analysis including the literature review, observations, and hydrodynamic model output. It is important to note that the schematic does not include wind-driven or tidal currents, which are both typically stronger than the seasonal-mean currents that appear in it. However, most of the important features of wind-driven and tidal current variations are seen in Figure 80 and Figure 94 respectively; thus a reasonably complete view of the characteristics of OSAMP domain hydrography and circulation can be ascertained using three key graphics (Figures 80, 94, and 105).

The schematic (Figure 105) includes gray bathymetric contours at 10 m intervals (starting from 20 m) and depicts hydrographic properties at five representative sites (BIS, south of Block Island, central RIS, south of RIS, and northeastern RIS) using a set of three colored bars for temperature, salinity, and density anomaly (see legend, upper right frame). The height of the colored bars represents the water depth at each site. Each colored bar includes shallow and deep portions, divided by the pycnocline, which varies in depth from site to site and season to season as shown. The scales for temperature, salinity, and density anomaly are presented in the color legends in the lower right frame. Density stratification is depicted using the difference $\Delta\sigma_t$ between deep and shallow density anomaly (sigma-t) values, and shown in a bar plot immediately above each set of three color bars; in the bar plot, the left-most and middle bars (white) are $\Delta\sigma_t$ due to temperature and salinity respectively, and the right-most (black) bar is the total $\Delta\sigma_t$.

The key features of the hydrographic fields, as described in detail in prior sections, are apparent in the schematic:

- Temperature changes from season to season that far exceed geographic variations during a given season: the dominant influences are the combined effects of air-sea heat exchange and solar radiative forcing, which have modest spatial variations
- Geographic variations in salinity during a given season that have magnitude comparable to that of the seasonal cycle; inshore areas are generally fresher, by an extent determined through mixing between estuarine waters and saltier shelf waters
- BIS salinities generally freshest relative to other areas, owing to the dominance of volume transports to and from OSAMP waters by LIS exchange flow which carries outflow from the Connecticut River, the largest river in the region
- Temperatures that are slightly cooler in shallow inshore areas in winter, and warmer in summer, reflecting interplay there between enhanced tidal mixing and stronger influence of temperature extremes associated with estuarine waters
- Minimal temperature differences between shallow and deep layers during winter and fall, owing to cooling of surface waters and enhanced wind mixing
- Shallow temperatures higher than deep temperatures by about 4-6 ^{o}C in spring and up to 11 ^{o}C in summer due to surface solar heating
- Salinity differences between shallow and deep layers of about 0.2 to 0.9 PSS year-round, maintained by arrival of freshened estuarine waters from surrounding water bodies
- Density stratification that is minimal in winter and fall, when temperature contributes little to stratification (or, in some areas, is destabilizing due to cooling of the shallow layer), and the weak pycnocline is about 30-40 m deep due to effective wind mixing at shallower depths
- Density stratification, in terms of $\Delta\sigma_t$, reaching about 1.5 kg m^{-3} in spring, when the temperature influence is comparable to that of salinity, and about 2.5 kg m^{-3} in summer when the temperature influence is more important than salinity; a sharp pycnocline about 10-20 m deep during these seasons

- Seasonal cycle of density stratification that is more pronounced in RIS than in BIS, with BIS more weakly stratified than RIS in summer as limited by tidal mixing, but more strongly stratified in winter due to LIS exchange flow
- An estuarine outflow front (sharp horizontal gradient) to the south of Block Island that bounds fresher inshore water from saltier offshore water, and lies farther from land in spring and summer, when it extends northward to the east of Block Island
- In summer and to a lesser extent spring, a tidal mixing front that divides the more homogenous inshore water column from more strongly stratified deeper water: along the northern and eastern boundaries of RIS, and along an arc between the southern sides of Montauk Point and Block Island

Seasonal-mean velocities of the shallow and deep layers are depicted using green and blue arrows respectively. Some key circulation features, which for clarity are only labeled in a single frame of the figure, are nonetheless present year-round:

- LIS exchange flow, in western BIS: eastward flow in the southern portion, most strongly in the shallow layer, and westward flow in the northern portion in both deep and shallow layers
- Eastern BIS exchange flow, in the gap between Point Judith and Block Island: eastward flow nearest Block Island and strongest in the shallow layer, with westward flow in both layers near Point Judith
- Southern BIS exchange flow, in the gap between Montauk Point and Block Island: southward flow in the shallow layer, strongest toward the west, and northward flow at depth in the eastern portion
- Weak westward and southward flow outside the mouth of NB
- LIS outflow, east and south of Montauk Point, that is directed southward then westward with increasing distance offshore, is bounded on its offshore edge by the outflow front, and is likely bounded on its inshore edge by a tidally-driven clockwise headland eddy
- A southward current in western RIS along the eastern side of Block Island
- A coastal current westward along the southern Long Island shore to the south and west of Montauk Point

Seasonal shifts in the seasonal-mean flow in and near BIS are modest compared to the rest of the domain, and consist of a strengthening in spring and summer of the exchange circulations, LIS outflow, southward flow east of Block Island. The latter three currents are most closely associated with a horizontal gradient in density, from less dense to more dense in the offshore direction, with a dominantly geostrophic dynamical balance such that the current is stronger when the gradient is sharper. The gradient sharpens in summer because, while the salinity distribution maintains the density gradient year-round due to the continual freshening influence of estuaries on inshore areas, inshore-offshore temperature differences act to weaken the density gradient in the winter and strengthen it in summer.

Across RIS and the offshore portion of the OSAMP domain, there are substantial changes in the direction and strength of seasonal-mean currents, as follows:

- In winter and fall, flow shows only weak geographic variations and is consistent with a wind-driven upwelling circulation: shallow flow is weakly offshore toward the southeast, while deep flow is slightly slower in essentially in the opposite direction
- In spring the inshore edge of the southern New England shelf flow, a strong current in both shallow and deep layers, flows along the offshore OSAMP area directed just south of westward; in RIS, flow is weak and generally westward in both layers
- In summer the southern New England shelf flow is slightly weaker than in spring and bifurcates at the eastern end of the domain, with a significant component moving northward as the RIS current, a narrow flow likely linked to the horizontal density gradient associated with the tidal mixing front and moving counterclockwise around the strongly stratified interior of RIS in both shallow and deep layers
- In spring and summer the southward-flowing western RIS portion of the RIS current strengthens considerably and occupies both shallow and deep layers; south of Block Island it merges with the southern New England shelf flow and the LIS outflow, all of which ultimately feed in to the coastal current along the southern shore of Long Island

6 Knowledge Gaps

It is apparent that there are numerous important gaps in knowledge of physical oceanography of the OSAMP waters. First and foremost is probably the lack of measurements, using modern instrumentation, of even baseline conditions over most of central and eastern RIS. However, even in the better-sampled areas where enough measurements are available to piece together the

seasonal patterns that have been described above, there is a pronounced need for more observations with dense spatial coverage in the horizontal and vertical and finer temporal sampling. This applies to both hydrographic and circulation fields. The need arises due to the sampling demands of the highly variable conditions, which result from complex interactions of wind, tidal, and buoyancy forcing on timescales as short as hours to days and as long as the seasonal cycle and inter-annual variability. For example, our ability to estimate transports of water and water properties between the OSAMP domain and surrounding areas, and transports passing through key constrictions such as the gaps from Block Island to Point Judith and Montauk Point, is severely constrained by the lack of measurements with sufficient coverage and resolution in the space and time. Two topic areas seem worthy of designation as having had the most inadequate attention to date. The first is turbulence characteristics and processes, including horizontal and vertical rates of mixing and dispersion. The second is the potential importance of processes occurring on timescales shorter than tidal, such as the nonlinear internal waves that are known to be energetic in other inshore shelf seas.

Acknowledgements

We thank Carlton Hunt (Battelle) for providing an excellent starting point for the literature reviews of observations; Charles Law (Oregon Health and Science University) and Kevin Ruddock (Nature Conservancy) for providing the objectively analyzed archived hydrographic measurements; and Changsheng Chen (UMass Dartmouth) for providing FVCOM model output.

References

Armstrong, R.S. 1998. Water Temperatures and Climatological Conditions South of New England, 1974-83. *NOAA Technical Report NMFS 134, U.S. Department of Commerce*.

Beardsley, R.C., W.C. Boicourt. 1981. On estuarine and continental shelf circulation in the Middle Atlantic Bight. In: Anonymous (Ed.), MIT Press, Cambridge, MA, USA, pp. 198-233.

Beardsley, R.C., R. Limeburner, C. Chen. 2007. Nantucket Sound Circulation - Observations, Analysis and Model Development. *Sea Grant Project Report Website*, http://www.whoi.edu/science/PO/Nobska_Mooring/index.html.

Blumberg, A.F., G.L. Mellor. 1987. A description of a three-dimensional coastal ocean circulation model. . *Three-Dimensional Coastal ocean Models, edited by N. Heaps. American Geophysical Union.*, 208 pp.

Bowman, M.J., W.E. Esaias. 1981. Fronts, stratification, and mixing in Long Island and Block Island Sounds. *J. Geophys. Res.* 86, 4260-4264.

Bumpus, D.F. 1965. Residual drift along the bottom on the continental shelf in the middle Atlantic bight area. *Limnology and Oceanography* 10(Supplement), R50-53.

Bumpus, D.F., R.E. Lynde, D.M. Shaw. 1973. Coastal and offshore environmental inventory - Cape Hatteras to Nantucket Shoals: Physical Oceanography. In: Anonymous (Ed.), Univ. Rhode Island., Kingston, RI (USA). pp. 1-72.

Butman, B., R.P. Signell, P. Shoukimas, R.C. Beardsley. 1988. Current observations in Buzzards Bay, Massachusetts, 1982-1986. *United States Geological Survey, Open File Report 88-5*, 211pp.

Chapman, D.C., R.C. Beardsley. 1989. On the origin of shelf water in the Middle Atlantic Bight. *J. Phys. Oceanogr.* 19(3), 384-391.

Chen, C., R.C. Beardsley, G. Cowles. 2006. An unstructured grid, finite-volume coastal ocean model (FVCOM) system. *Oceanography: Special Issue "Advance in Computational Oceanography"* 19(1), 78-89.

Codiga, D.L., L.V. Rear. 2004. Observed tidal currents outside Block Island Sound: Offshore decay and effects of estuarine outflow. *J. Geophys. Res.* 109, doi:10.1029/2003JC001804.

Codiga, D.L. 2005. Interplay of wind forcing and buoyant discharge off Montauk Point: seasonal changes to velocity structure and a coastal front. *J. Phys. Oceanogr.* 35, 1068-1085.

Codiga, D.L., D.A. Aurin. 2007. Residual circulation in eastern Long Island Sound: Observed transverse-vertical structure and exchange transport. *Continental Shelf Research* 27, 103-116.

Codiga, D.L. 2009. Circulation in Block Island Sound, Rhode Island Sound, and adjacent waters, with emphasis on subsurface flows. In: Schwartz, M.L., A. Desbonnet,B.A. Costa-Pierce (Eds.), Sound Connections: The Science of Rhode Island and Block Island Sounds. Proceedings of the 7th Annual Ronald C. Baird Sea Grant Science Symposium, Block Island, Rhode Island. [http://seagrantadm.gso.uri.edu/Baird_08/Abstracts/codiga.pdf].

Collins, B.P. 1974. Suspended material transport in lower Narragansett Bay and western Rhode Island Sound. *MS Dissertation, University of Rhode Island. Kingston, RI.*, 85pp.

Cook, G.S. 1966. Non-tidal circulation in Rhode Island Sound-- drift bottle and sea bed drifter experiments (1962-1963). *Technical Memorandum 369, Naval Underwater Weapons Research Engineering Station*, Newport, RI, 37pp.

Cowles, G., S. Lentz, C. Chen, Q. Xu, R.C. Beardsely. 2008. Comparison of observed and model-computed low frequency circulation and hydrography on the New England shelf. 113(C09015), doi:10.1029/2007JC004394.

Curry, R. 2001. HydroBase 2: A Database of Hydrographic Profiles and Tools for Climatological Analysis. *Woods Hole Oceanographic Institution, Draft Technical Reference*, ftp://flotsam.whoi.edu/HydroBase2/DOC/TechRef_draft.pdf.

Edwards, C.A., T.A. Fake, P.S. Bogden. 2004a. A numerical model investigation of spring-summer frontogenesis at the mouth of Block Island Sound. *J. Geophys. Res.* 109 C12021, doi:12010.11029/12003JC002132.

Edwards, C.E., T.A. Fake, D.L. Codiga, P.S. Bogden. 2004b. Combining ADCP records with a GCM using a linear depth-averaged inverse model: the effect of low frequency motions on fronts near Block Island Sound. *J. Geophys. Res.* 109(C12022), doi:10.1029/2003JC002133.

Fox, M.F., D.R. Kester, J.E. Andrews, A. Magnuson, C.G. Zoski. 2000. Seasonal warming of Narragansett Bay and Rhode Island Sound in 1997: Advanced very high resolution radiometer sea surface temperature and in situ measurements. *Journal of Geophysical Research* 105(C9).

Geyer, W.R., R.P. Signell. 1990. Measurements of Tidal Flow Around a Headland With a Shipboard Acoustic Doppler Current Profiler. *J. Geophys. Res.* 95, 3189-3197.

Grell, G.A., J. Dudhia, D.R. Stauffer. 1994. A description of the fifth generation Penn State/NCAR Mesoscale Model (MM5). *National Center for Atmospheric Research, Tech. Note 398+STR*.

Griscom, C.A. 1977. Near Bottom Currents and their potential for sediment resuspension as measured by an EM Current Meter. *In: A study and report on oceanographic conditions in the vicinity of Browns Ledge. RIS Report 2, Division of Marine Resources, University of Rhode Island, Kingston, RI.*

Gurgel, K.W. 1994. Shipborne measurement of surface current fields by HF radar. *L'Onde Electr.* 74, 54-59.

Haight, F.J. 1938. Currents in Narragansett bay, Buzzards bay, and Nantucket and Vineyard sounds. *U.S. Coast and Geodetic Survey, Washington DC*, 103pp.

Hardy, C.D. 1972. Hydrographic data report : Long Island Sound, 1970, Part II. . *Marine Sciences Research Center, State University of New York, Stony Brook, with support from Nassau-Suffolk Regional Planning Board*.

He, R., J.L. Wilkin. 2006. Barotropic tides on the southeast New England shelf: A view from a hybrid data assimilative modeling approach. *Journal of Geophysical Research* 111, C08002, doi:08010.01029/02005JC003254.

Hendry, R., I. He. 1996. Technical Report on Objective Analysis Project. *Prepared for Bedford Institute of Oceanography*, http://www.mar.dfo-mpo.gc.ca/science/ocean/coastal_hydrodynamics/Oax/download/techrep.

Hollman, R., G.R. Sandberg. 1972. The residual drift in eastern Long Island Sound and Block Island Sound; a preliminary report. N.p.

Hollman, R. 1974. An interdisciplinary study of the estuarine and coastal oceanography of Block Island Sound and adjacent New York coastal waters: ground truth, final report. *New York Ocean Science Laboratory, Montauk, NY*, Technical Report 27.

Ichiye, T. 1967. Tidal variation of hydrography of Block Island Sound observed in August 1965. *Lamont Geological Observatory, Palisades, NY.* Technical Report No CU-15-67, Office Of Naval Research Contract Nonr 266-48

Ingham, M.C. 1982. Summary of the physical oceanographic processes and features pertinent to pollution distribution in the coastal and offshore waters of the northeastern United States, Virginia to Maine. In, NOAA, Woods Hole, MA.; Woods Hole, MA, pp. 1-166.

Kincaid, C., R.A. Pockalny, L.M. Huzzey. 2003. Spatial and temporal variability in flow at the mouth of Narragansett Bay. *J. Geophys. Res.-Oceans* 108.

Kincaid, C., D.L. Bergondo, K. Rosenberger. 2008. The dynamics of water exchange between Narragansett Bay and Rhode Island Sound. In: Desbonnet, A.,B.A. Costa-Pierce (Eds.), Science for ecosystem-based management: Narragansett Bay in the 21st Century, Springer Series on Environmental Management, New York, pp. 301-324.

Kirincich, A., D. Hebert. 2005. The structure of the coastal density front at the outflow of Long Island Sound in spring 2002. *Continental Shelf Research* 25, 1097-1114.

Krabach, M.H., J.H. Snooks. 1977. Coastal zone flushing characteristics, NEP 1 & 2, Charlestown, RI. *Yankee Atomic Electric Company, Nuclear Services Division, Westborough, MA.*

LeLacheur, E.A., J.C. Sammons. 1932. Tides and currents in Long Island and Block Island sounds. *U.S. Coast and Geodetic Survey, Special Publication 174*, 181pp.

Lentz, S.J. 2008a. Observations and a model of the mean circulation over the Middle Atlantic Bight continental shelf. *J. Phys. Ocean.* 38, 1203-1221.

Lentz, S.J. 2008b. Seasonal variations in the circulation over the Middle Atlantic Bight continental shelf. *J. Phys. Ocean.* 38, 1486-1500.

Levine, E.R., L.R. Goodman, J. O'Donnell. 2009. Turbulence in coastal fronts near the mouths of Block Island and Long Island Sounds *Journal of Marine Systems* 78(3), 476-488.

Lipa, B.J., and D. E. Barrick. 1983. Least-squares methods for the extraction of surface currents from CODAR crossed-loop data: Application at ARSLOE. *IEEE J. Oceanic Eng.* 8, 226-253.

Long, E.E. 1978. Tide and tidal current observations from 1965 through 1967 in Long Island Sound, Block Island Sound, and tributaries. Dept. of Commerce, National Oceanic and Atmospheric Administration, National Ocean Survey, Rockville, Md.

Marshall, J.C., A. Adcroft, C. Hill, L. Perelman, C. Heisey. 1997. A finite-volume, incompressible navier stokes model for studies of the

ocean on parallel computers. *J. Geophys. Res.* 102, 5753– 5766.

Mau, J.-C., D.-P. Wang, D.S. Ullman, D.L. Codiga. 2007a. Comparison of observed (HF radar, ADCP) and model barotropic tidal currents in the New York Bight and Block Island Sound. *Est. Coast. Shelf. Sci.* 72, 129-137.

Mau, J.-C., D.-P. Wang, D.S. Ullman, D.L. Codiga. 2007b. Characterizing Long Island Sound outflows from HF radar using self-organizing maps. *Est. Coast. Shelf. Sci.* 74, 155-165.

Mau, J.-C., D.-P. Wang, D.S. Ullman, D.L. Codiga. 2008. Model of the Long Island Sound outflow: Comparison with year-long HF radar and Doppler current observations. *Cont. Shelf Res.* 28, 1791-1799.

Meguire, R.E. 1971. Tidal currents and water exchanges in western Block Island Sound. *M.S. Thesis, Long Island University*, 83pp.

Mellor, G.L., T. Yamada. 1982. Development of a turbulence closure model for geophysical fluid problems. *Rev. Geophys. Space Phys.* 20, 851-875.

Moody, J.A., B. Butman, R.C. Beardsley, W.S. Brown, P. Daifuku, J.D. Irish, D.A. Mayer, H.O. Mofjeld, B. Petrie, S. Ramp, P. Smith, W.R. Wright. 1984. Atlas of tidal elevation and current observations on the Northeast American continental shelf and slope. In, U. S. Geological Survey, Reston, VA, United States (USA), pp. 1-122.

Mountain, D.G. 2003. Variability in the properties of Shelf Water in the Middle Atlantic Bight, 1977-1999. *Journal of Geophysical Research-Oceans* 108, 3014-3014.

O'Donnell, J., A.E. Houk. 2009. The structure and variability of the hydrography of the Block Island Sound. In: Schwartz, M.L., A. Desbonnet,B.A. Costa-Pierce (Eds.), Sound Connections: The Science of Rhode Island and Block Island Sounds. Proceedings of the 7th Annual Ronald C. Baird Sea Grant Science Symposium, Block Island, Rhode Island. [http://seagrantadm.gso.uri.edu/Baird_08/Abstracts/codiga.pdf].

Pawlowicz, R., B. Beardsley, S. Lentz. 2002. Classical tidal harmonic analysis including error estimates in MATLAB using T-TIDE. *Computers & Geosciences* 28, 929-937.

Powers, C.F. 1953. Circulation in the Newport Bight - Block Island Sound - New York Bight Area. *Status Report No. 25, Contract N6, Office of Naval Research 264, Task 15 NR #083-033.* Cornell University.

Pratt, S.D., C.A. Griscom, R.A. Heavers. 1975. Survey of currents, water turbidity, and benthic biology in the vicinity of Browns Ledge, Rhode Island Sound. *Marine Experiment Station, Graduate School of Oceanography, University of Rhode Island. Kingston, RI.*, 114pp.

Pringle, J.M. 2006. Sources of variability in Gulf of Maine circulation, and the observations needed to model it *Deep-Sea Research-II* 53(23-24)

2457-2476.

Raytheon. 1975. Charlestown Hydrographic Study, April 1974 to April 1975. *Final Technical Report, Prepared for Yankee Atomic Electric Company, Westborough, Massachusetts.*

Riley, G.A. 1952. Hydrography of the Long Island and Block Island Sounds. *Bulletin of the Bingham Oceanographic Collection* 3, Article 3.

SAIC. 2005. Disposal Plume Tracking and Assessment at the Rhode Island Sound Disposal Site, Spring 2004. *US Army Corps of Engineers, New England District, Concord, MA.* DAMOS Contribution No. 166., 184pp.

Saila, S.B., S.D. Pratt, T.T. Polgar. 1972. Dredge spoil disposal in Rhode Island Sound *University of Rhode Island, Kingston, RI.*, 48pp.

Shchepetkin, A.F., J.C. McWilliams. 2005. The Regional Ocean Modeling System (ROMS): A split-explicit, free-surface, topography-following coordinates ocean model. *Ocean Modelling* 9(4), 347-404.

Shonting, D., D. Cook. 1970. On the seasonal distribution of temperature and salinity in Rhode Island Sound. *Limnol. & Oceanogr.* 15, 100-112.

Shonting, D.H., D. Cook, F.G. Wyatt. 1966. Seasonal distribution of oceanographic variables in Rhode Island Sound during 1963-1964, A data report. . *CONSEC No. 423, Naval Underwater Weapons Research Engineering Station, Newport, R.I.*, 121pp.

Shonting, D.H. 1969. Rhode Island Sound Square Kilometer Study 1967 - Flow Patterns and Kinetic Energy Distribution. *Journal of Geophysical Research* 74, 3386-&.

Signell, R., J. List, A. Farris. 2000. Bottom Currents and Sediment Transport in Long Island Sound: A Modeling Study. *Journal of Coastal Research* 16, 551-566.

Signell, R.P. 1987. Tide- and Wind-Forced Currents in Buzzards Bay, Massachusetts. *M.S. Thesis.* Massachusetts Institute of Technology, 86 pp.

Simpson, J.H., J.R. Hunter. 1974. Fronts in the Irish Sea. *Nature* 250, 404-406.

Snooks, J.H., J.P. Jacobson, W.P. Kramer. 1977. Summary of temperature and salinity observations in Block Island Sound during July 1975 through September 1976. *Prepared for New England Power Company / Yankee Atomic Electric Company, Westborough, Mass.*

Snooks, J.H., J.P. Jacobsen. 1979. Currents and Residual Drift in Block Island Sound during the Period February through December 1977. *Yankee Atomic Electric Company, Environmental Sciences Group. Westborough, MA.*

Soulsby, R.L. 1990. Tidal-current boundary layers. In: Le Mehaute, B., Hanes, D.M (Ed.), The Sea; Ocean Engineering Science Vol. 9A, Wiley-Interscience, New York, pp. 523-566.

Spaulding, M.L., R.B. Gordon. 1982. A nested numerical tidal model of the southern New England bight. *Ocean Engineering* 9(2), 107-126.

Spaulding, M.L., T. Opishinksi, S. Haynes. 1996. COASTMAP: an integrated monitoring and modeling system to support oil spill response. *Spill Science and Technology Bulletin* 3(3), 149-169.

Ullman, D.S., P.C. Cornillon. 1999. Satellite-derived sea surface temperature fronts on the continental shelf off the northeast US coast. *J. Geophys. Res.-Oceans* 104, 23459-23478.

Ullman, D.S., P.C. Cornillon. 2001. Continental shelf surface thermal fronts in winter off the northeast US coast. *Continental Shelf Research* 21, 1139-1156.

Ullman, D.S., D.L. Codiga. 2004. Seasonal variation of a coastal jet in the Long Island Sound outflow region based on HF radar and Doppler current observations. *J. Geophys. Res.* 109, doi:10.1029/2002JC001660.

Ullman, D.S., J. O'Donnell, J. Kohut, T.A. Fake, A. Allen. 2006. Trajectory prediction using HF radar surface currents: Monte Carlo simulations of prediction uncertainties. *Journal of Geophysical Research* 111 (C12005), doi:10.1029/2006JC003715.

URI. 1979. Model-predicted tidal current charts, Long Island Sound to Buzzards Bay. *Marine bulletin (University of Rhode Island)* Kingston, RI. No. 30, 27pp.

USACE. 2002. Final Report: Results of Literature Review and Data Gaps Assessment. US Army Corps of Engineers, Rhode Island Region Long Term Dredge Material Disposal Site Evaluation Project. Contract No. DACW33-01-D-0004, 222pp.

Wilkin, J. 2006. The summertime heat budget and circulation of southeast New England shelf waters. *J. Phys. Oceanogr.* 36, 1997-2011.

Williams, R.G. 1969. The physical oceanography of Block Island Sound. U. S. Navy Underwater Sound Laboratory, New London, Conn.

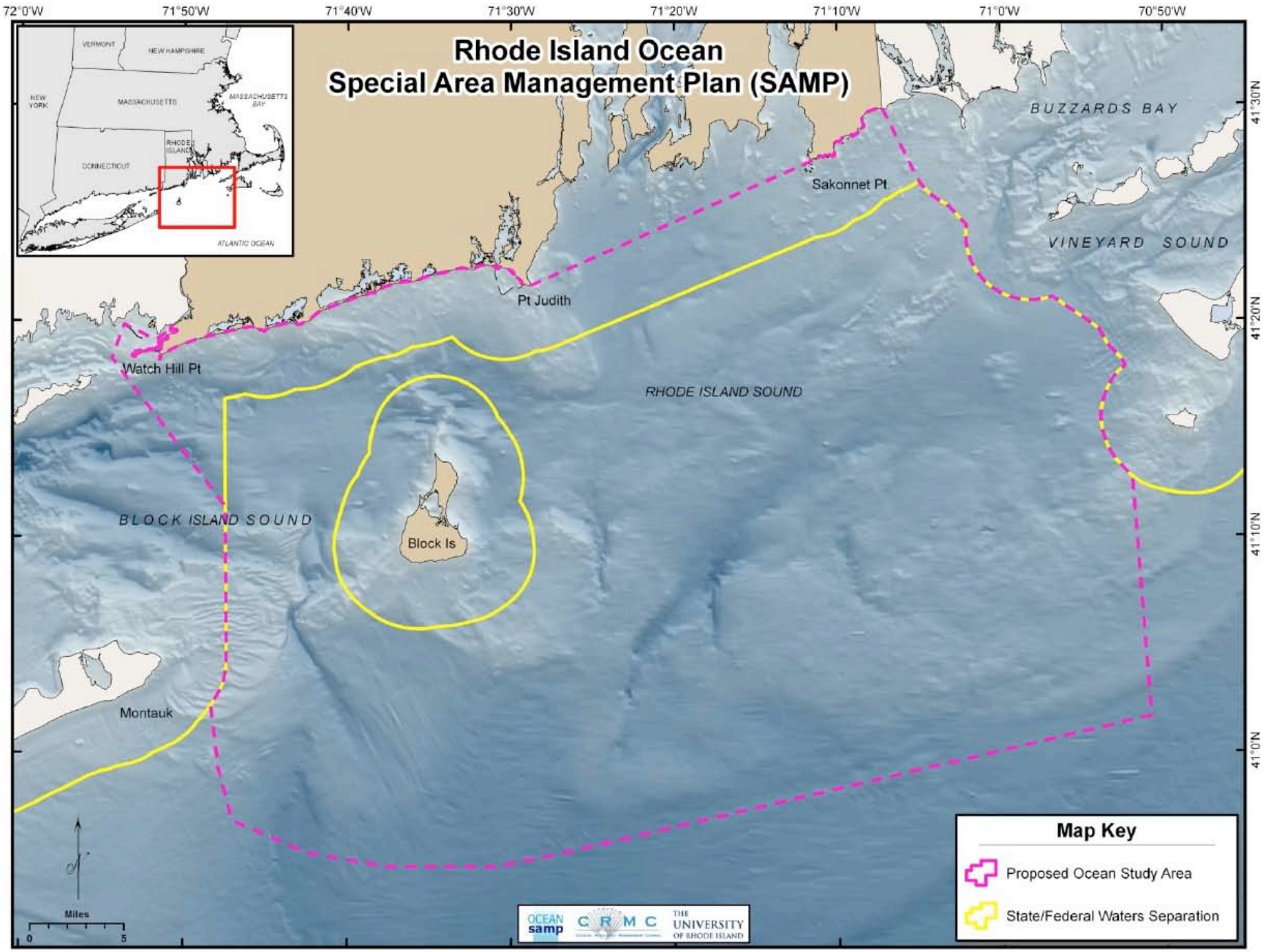

Figure 1. Map of OSAMP domain, boundary marked by dashed magenta line.

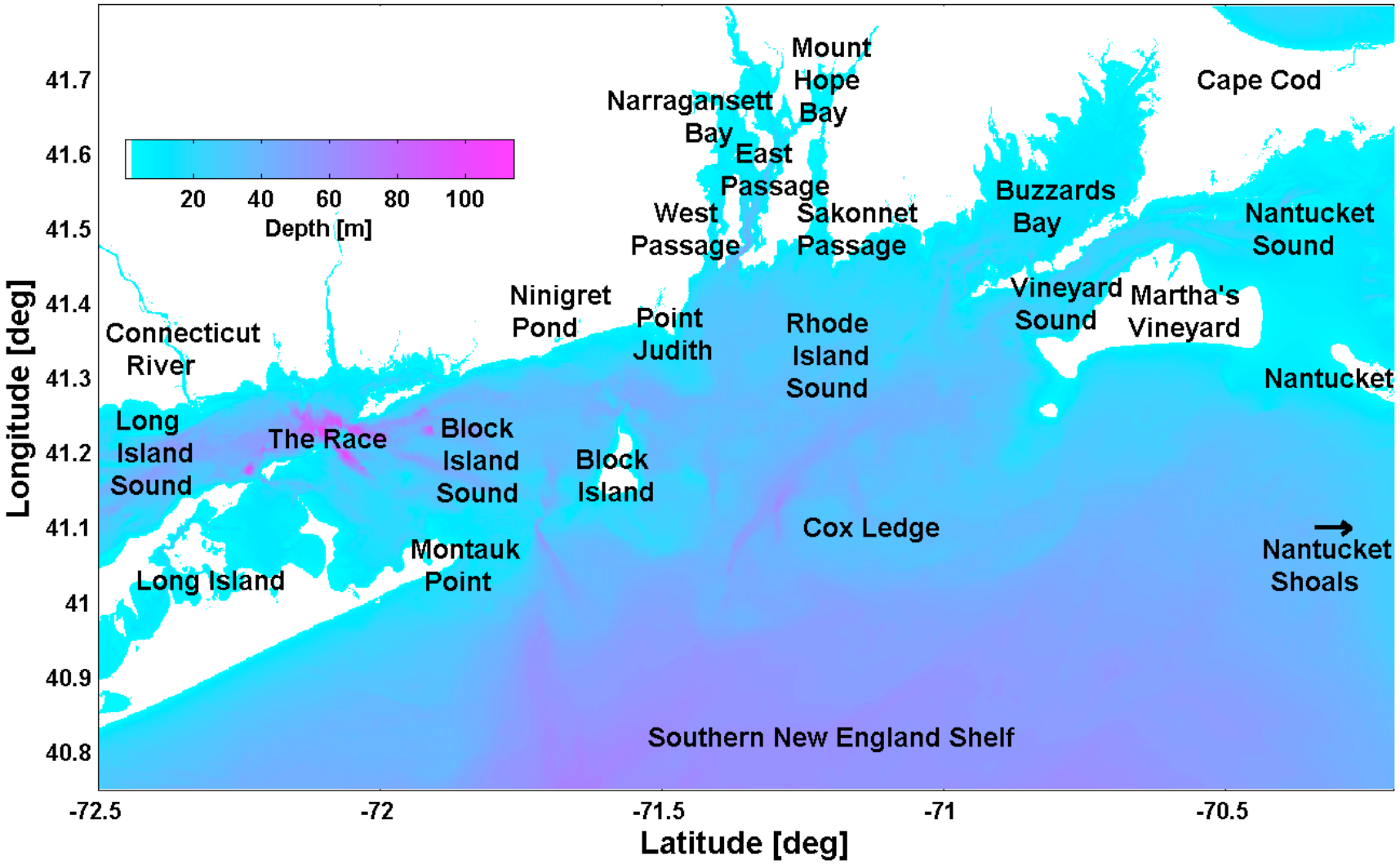

Figure 2. Bathymetry and geographic features of regional setting surrounding OSAMP domain..

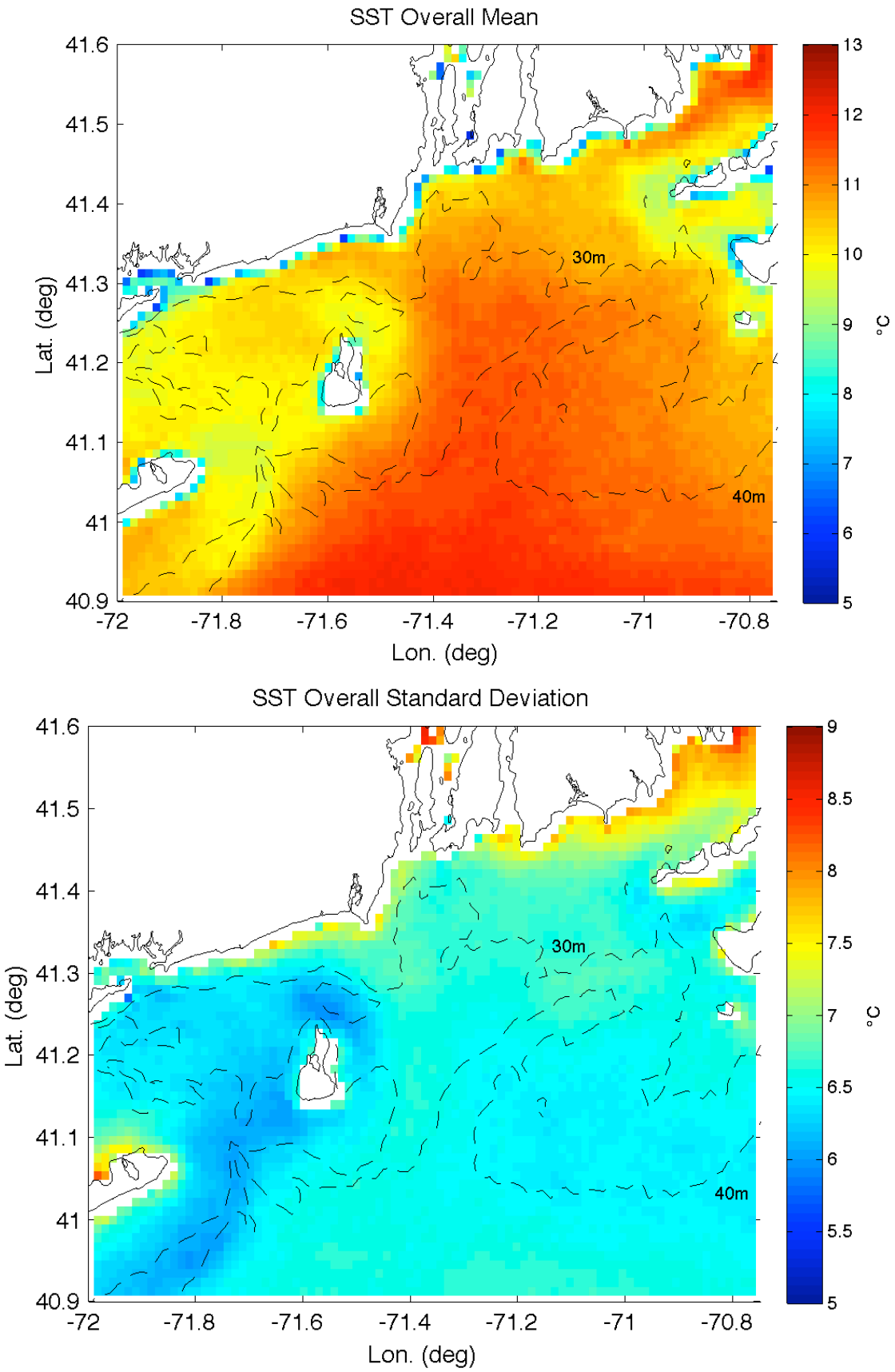

Figure 3. SST: All seasons 2002-2007. (upper) Mean. (lower) Standard deviation.

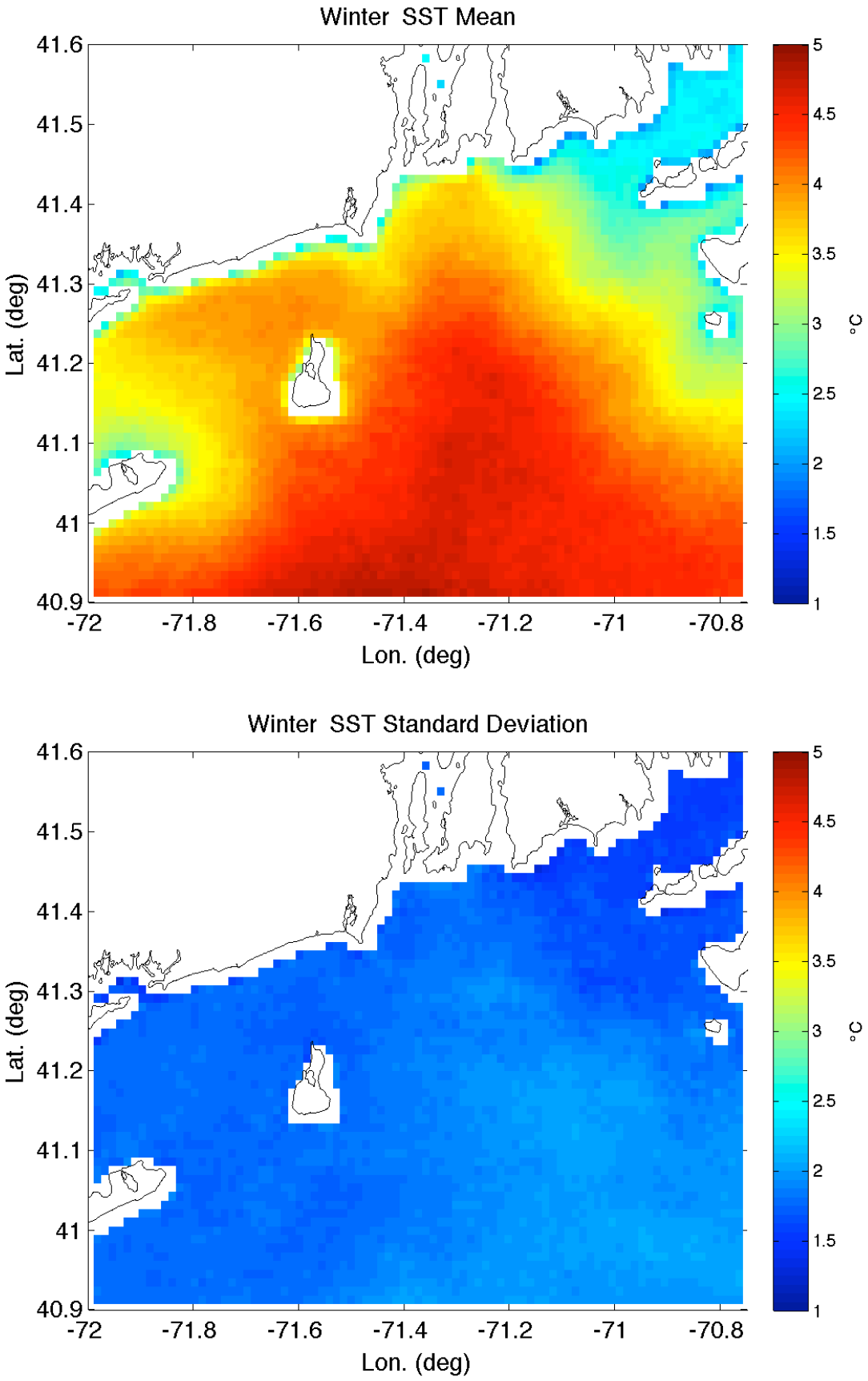

Figure 4. SST: Winter 2002-2007. (upper) Mean. (lower) Standard deviation.

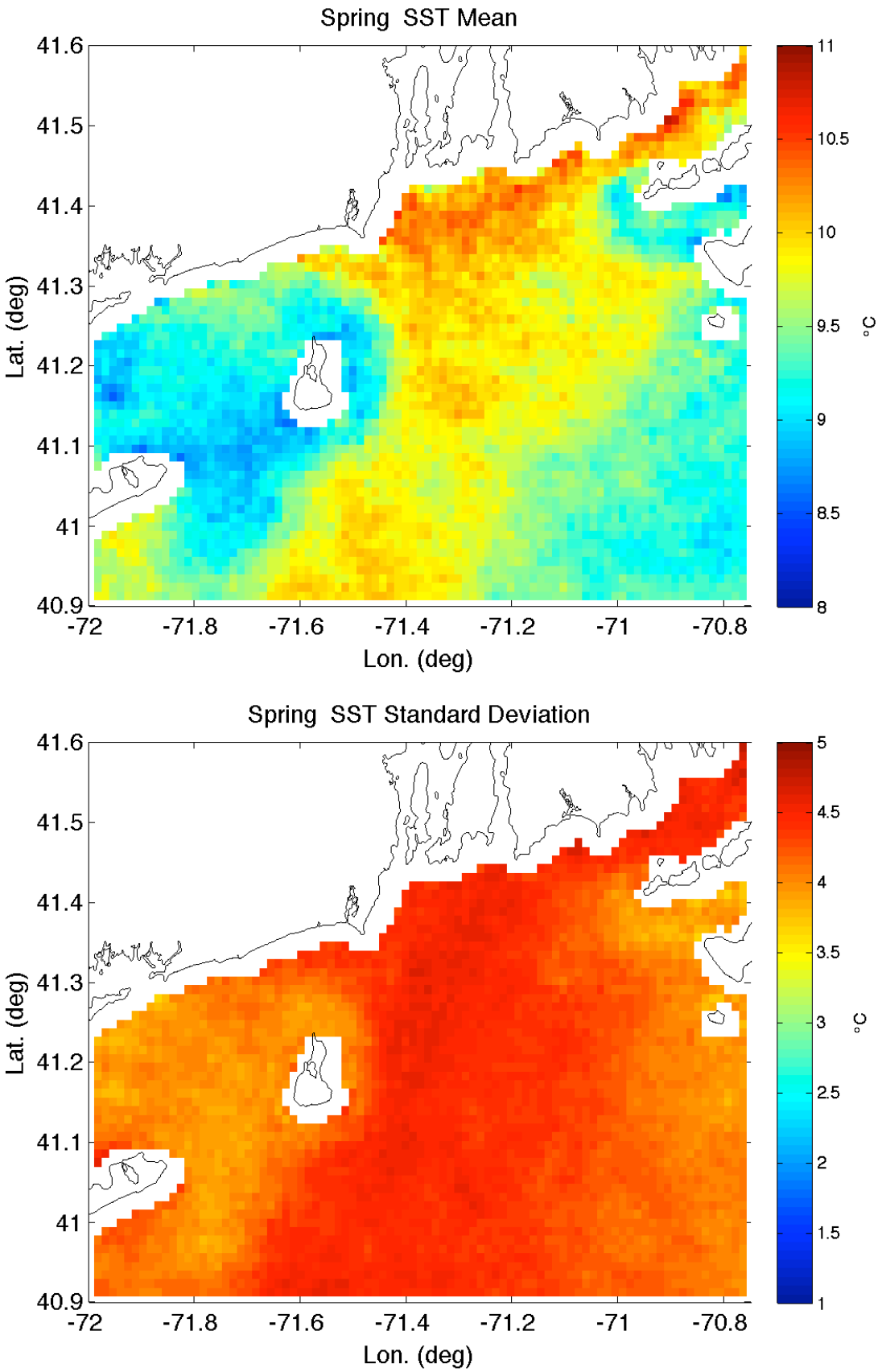

Figure 5. SST: Spring 2002-2007. (upper) Mean. (lower) Standard deviation.

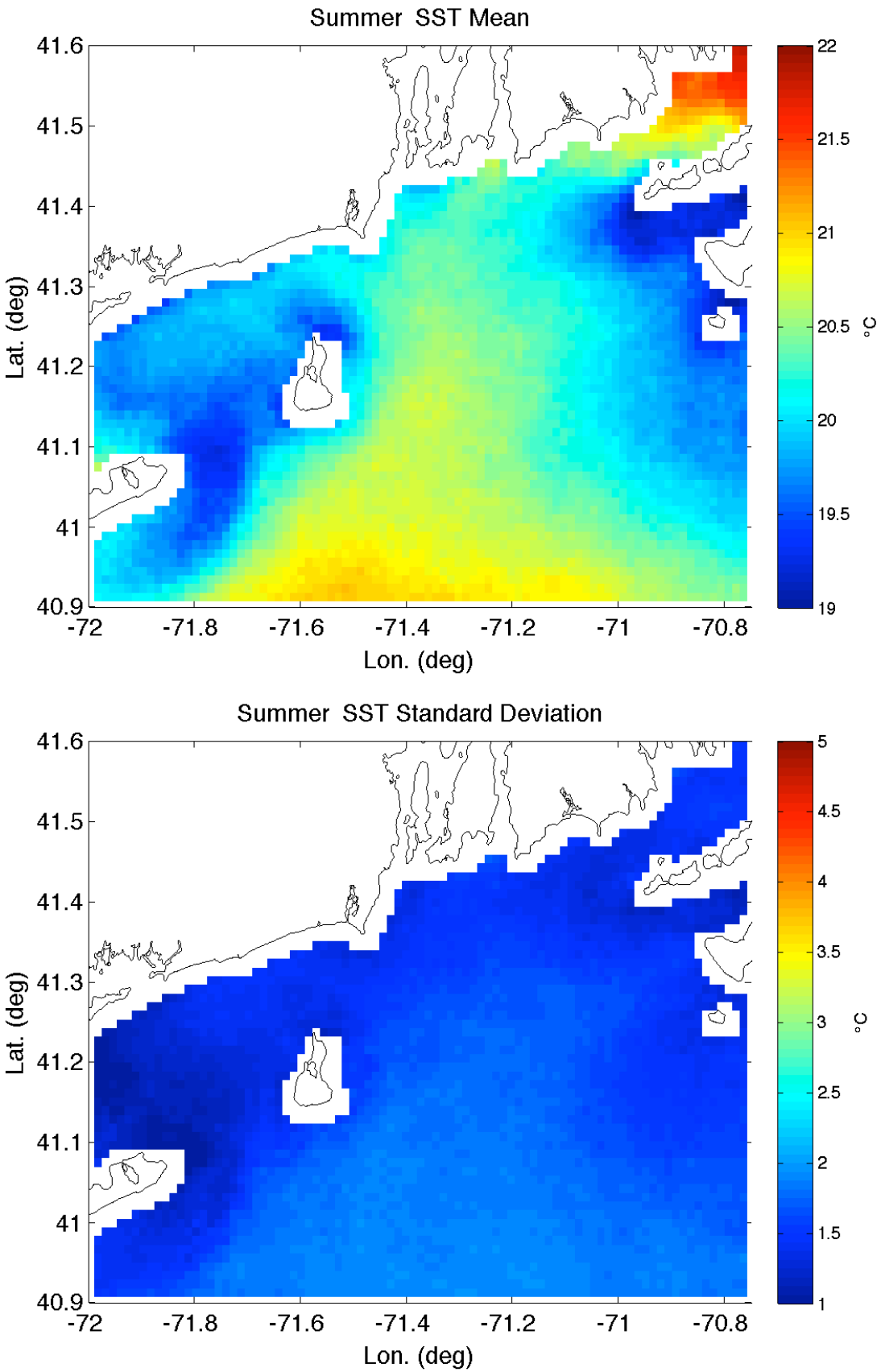

Figure 6. SST: Summer 2002-2007. (upper) Mean. (lower) Standard deviation.

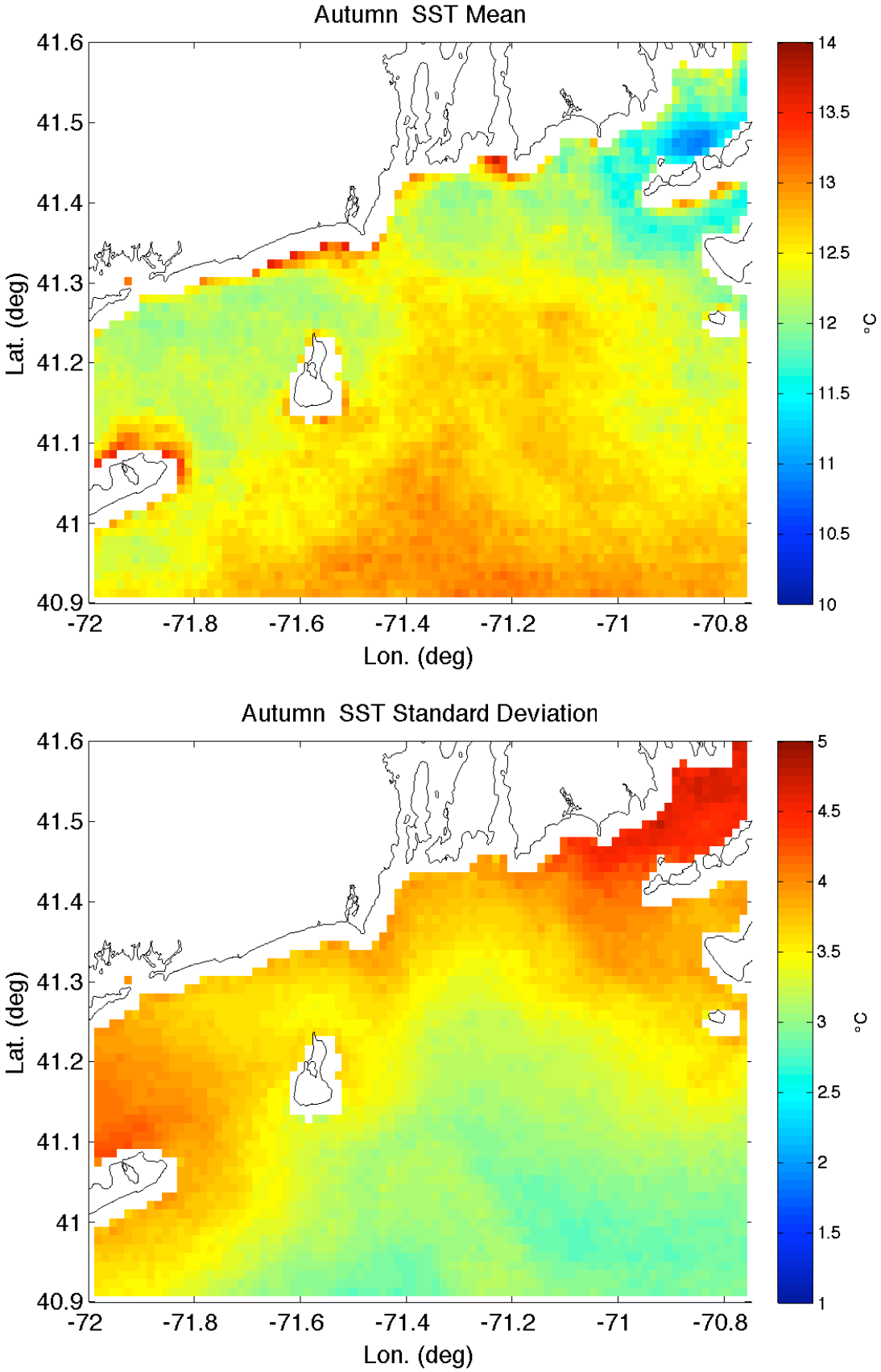

Figure 7. SST: Fall 2002-2007. (upper) Mean. (lower) Standard deviation.

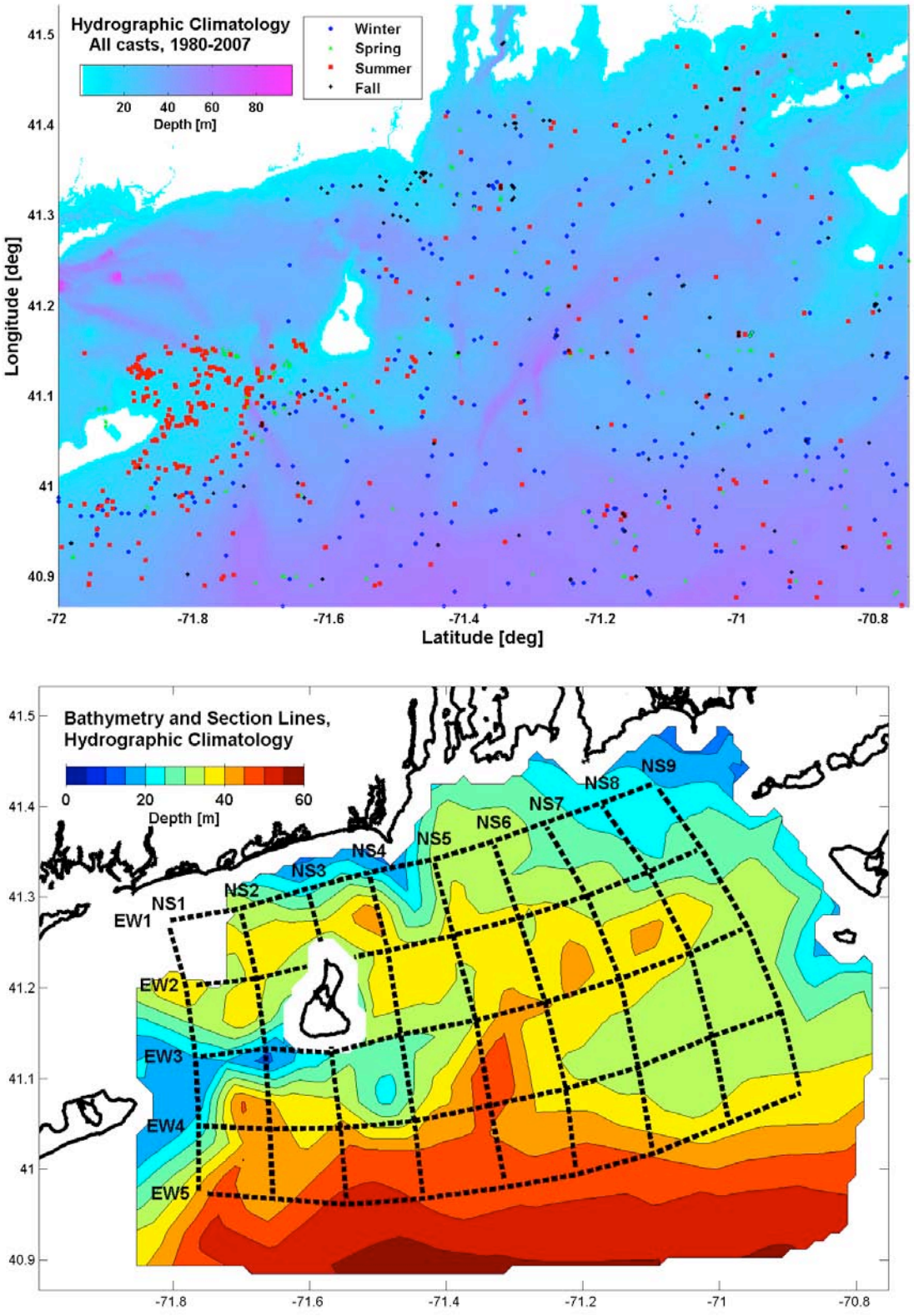

Figure 8. Hydrographic climatology. (upper) Cast locations. (lower) Section lines.

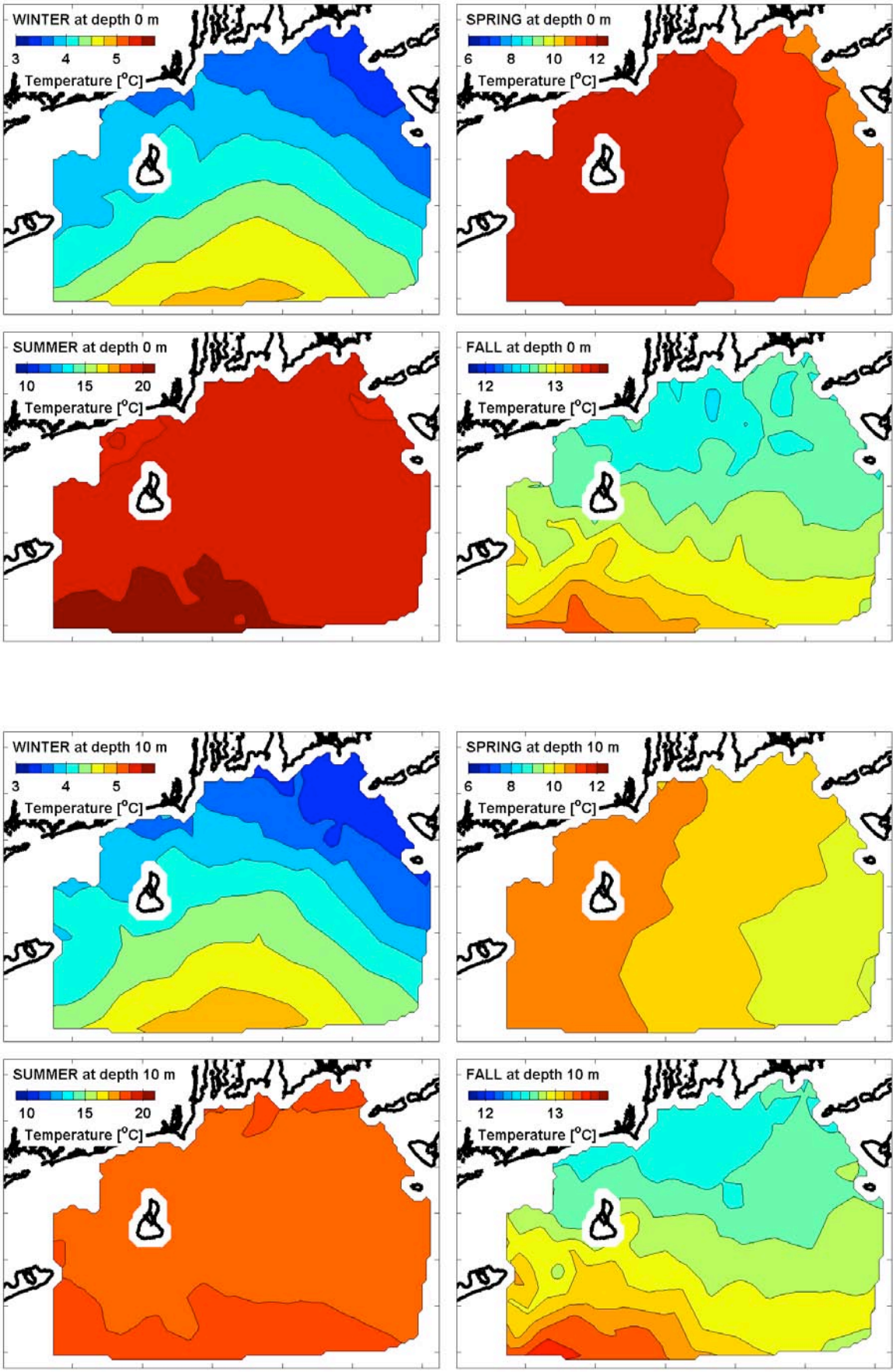

Figure 9. Hydrographic climatology. Temperature. (upper) Surface. (lower) Depth 10 m.

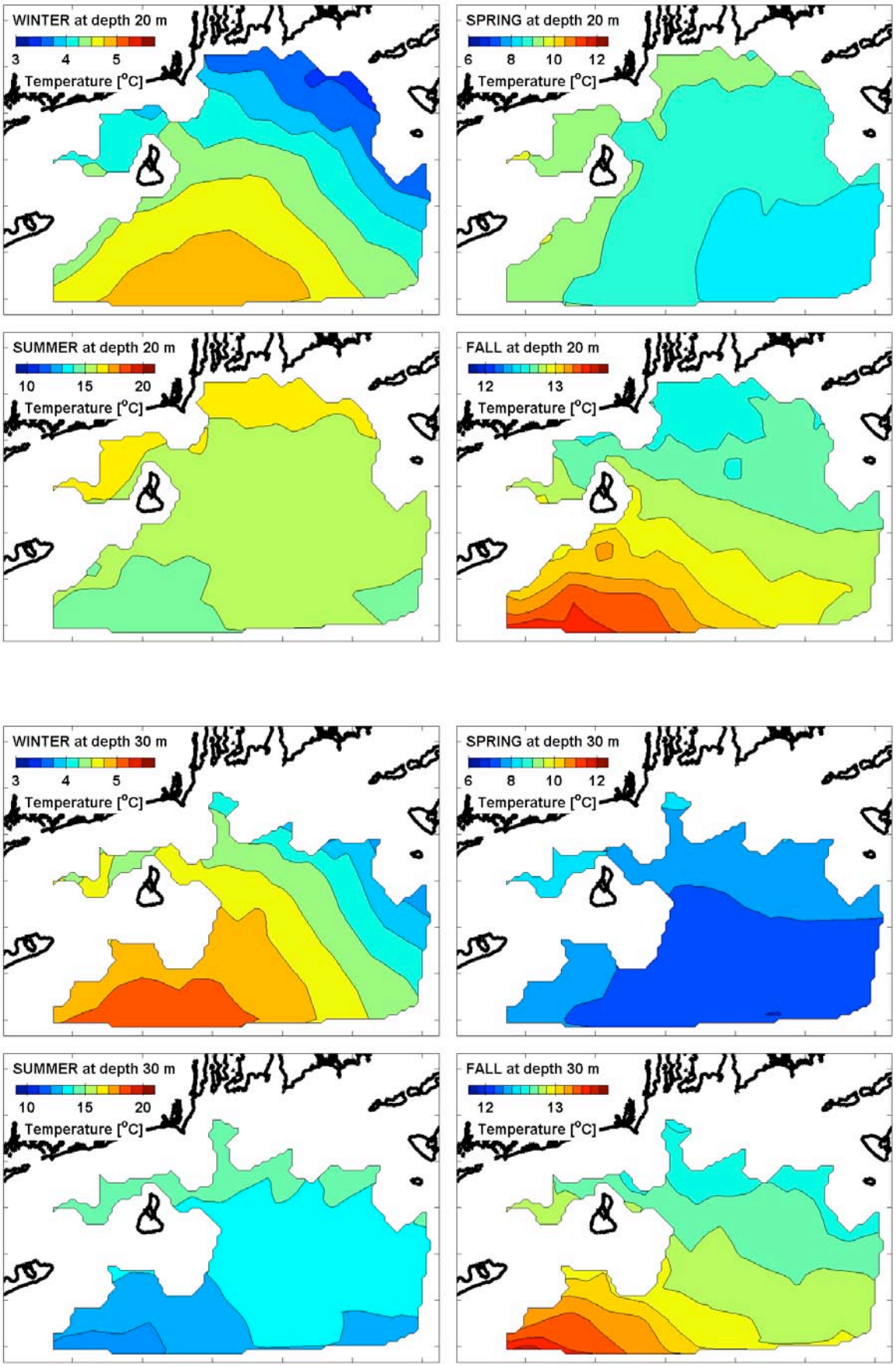

Figure 10. Hydrographic climatology. Temperature. (upper) Depth 20 m. (lower) Depth 30 m.

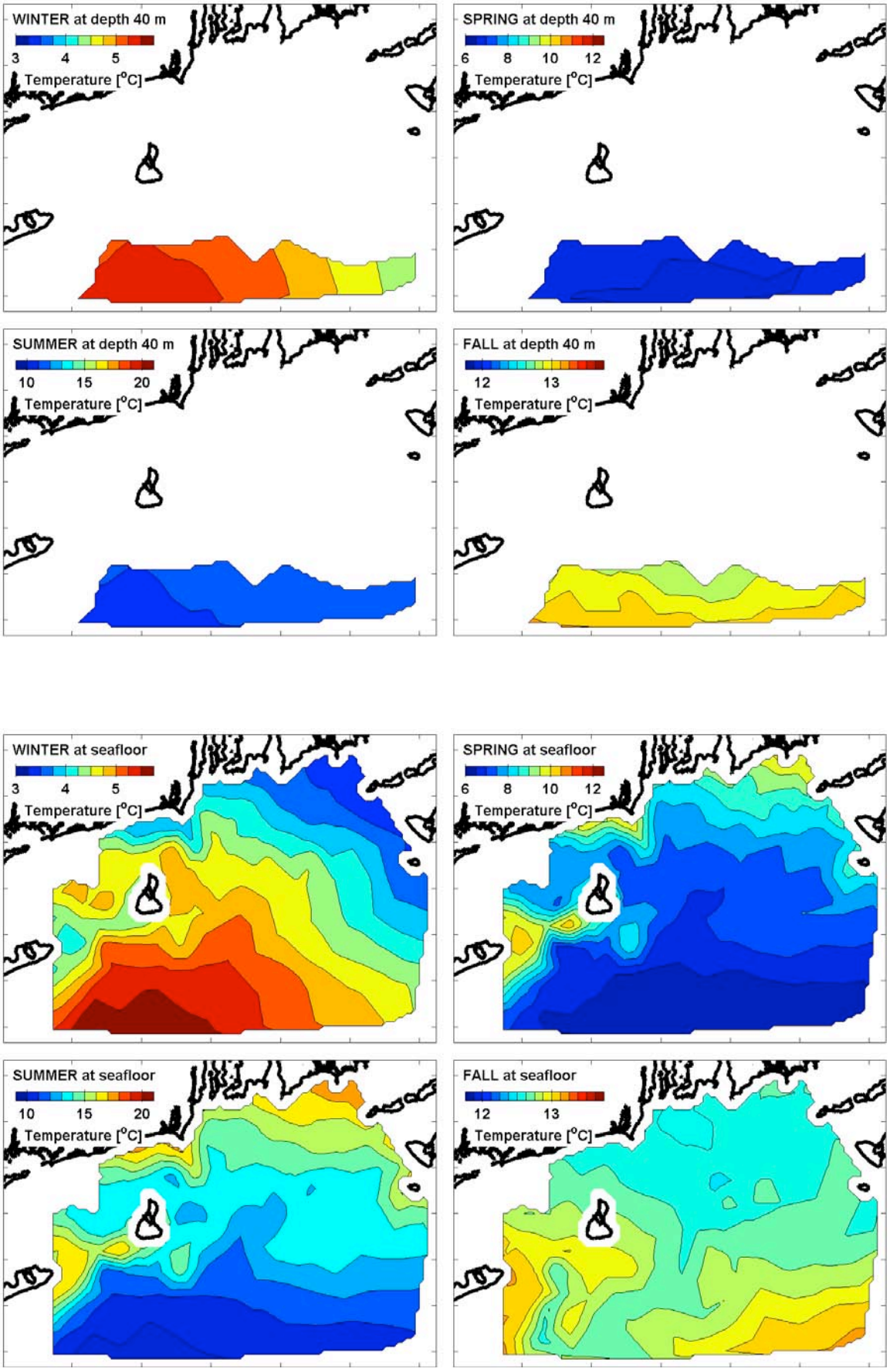

Figure 11. Hydrographic climatology. Temperature. (upper) Depth 40 m. (lower) Seafloor.

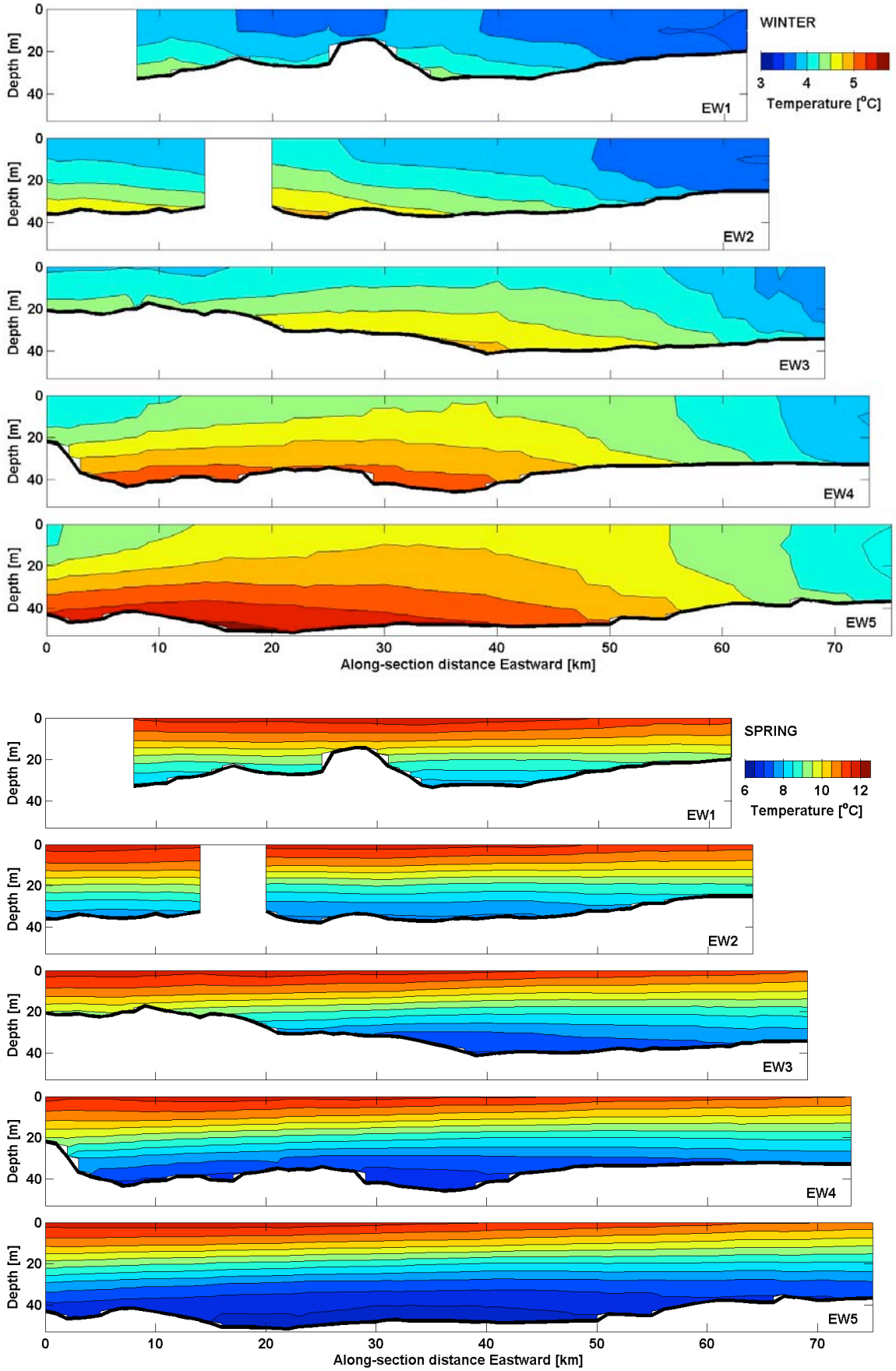

Figure 12. Hydrographic climatology. Temperature. EW. (upper) Winter. (lower) Spring.

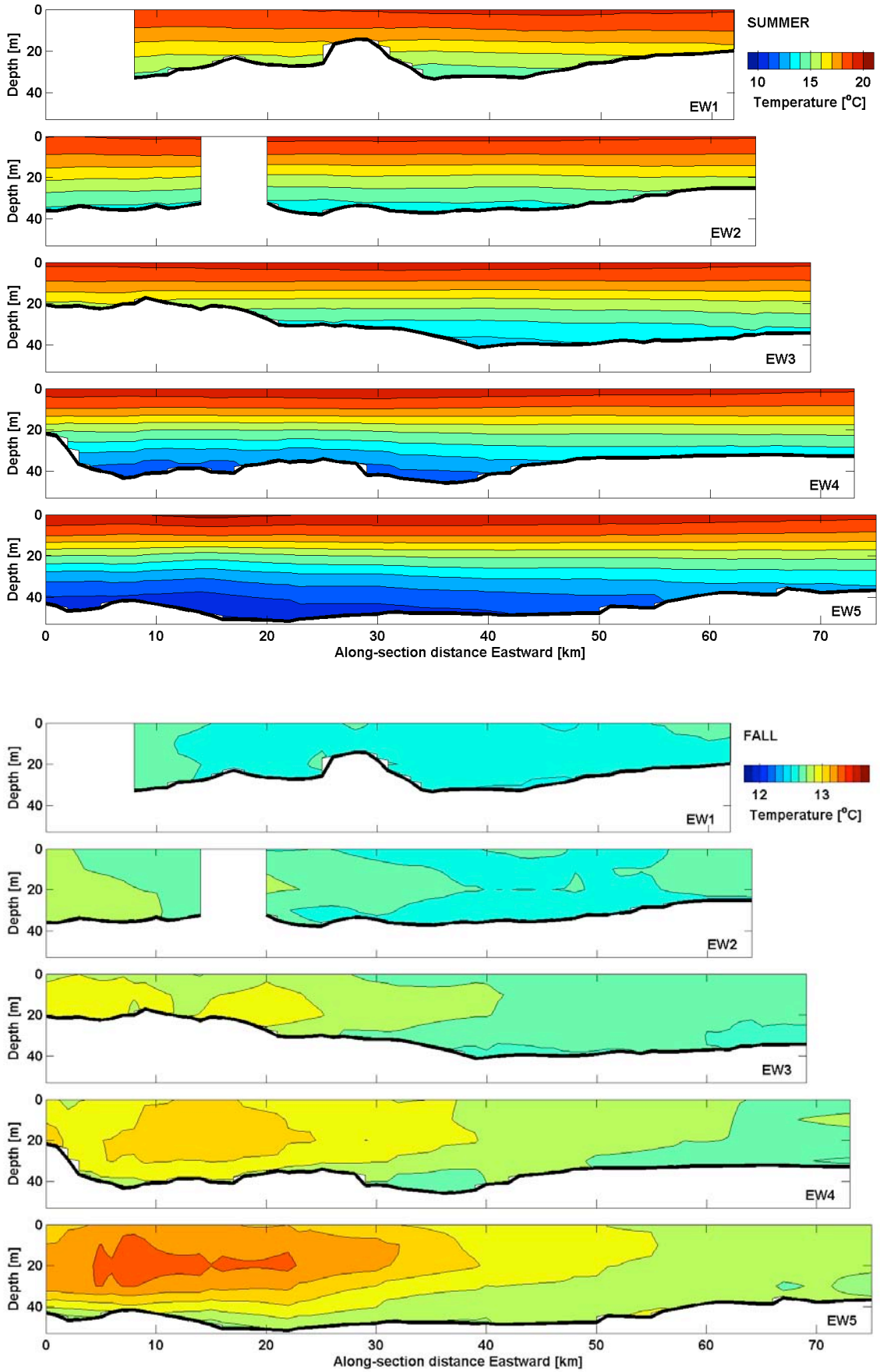

Figure 13. Hydrographic climatology. Temperature. EW. (upper) Summer. (lower) Fall.

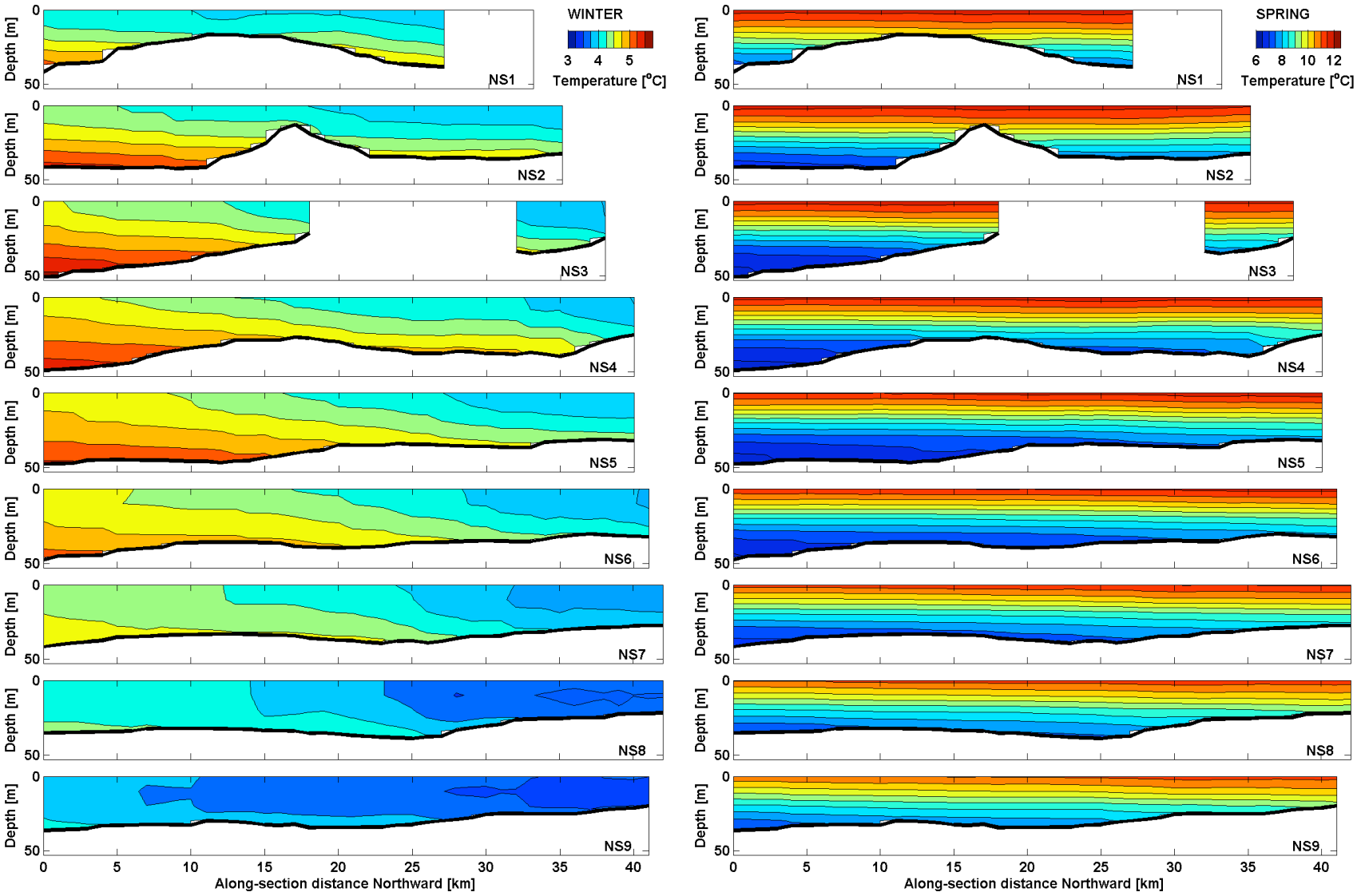

Figure 14. Hydrographic climatology. Temperature. NS. (left) Winter. (right) Spring.

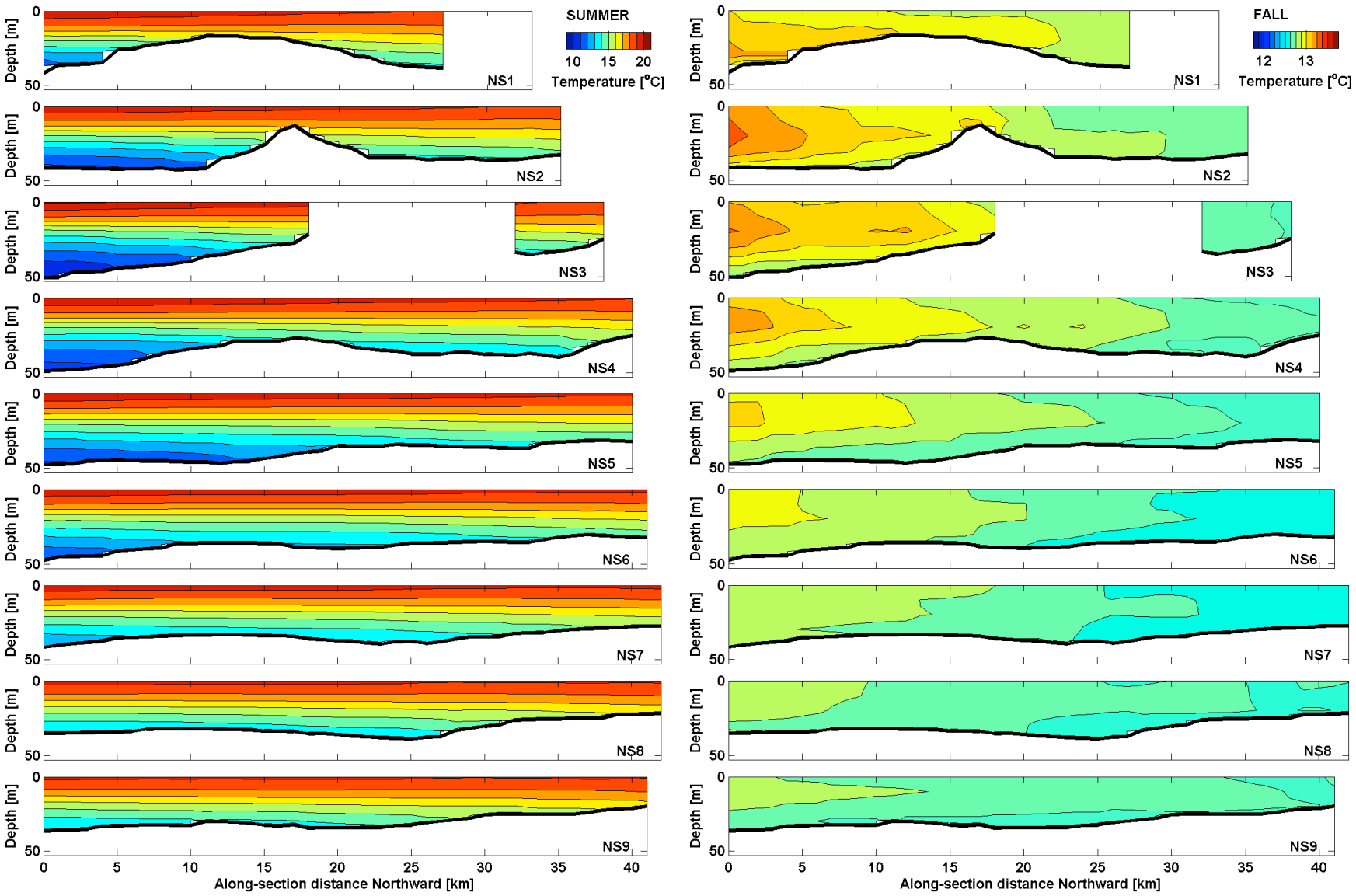

Figure 15. Hydrographic climatology. Temperature. NS. (left) Summer. (right) Fall.

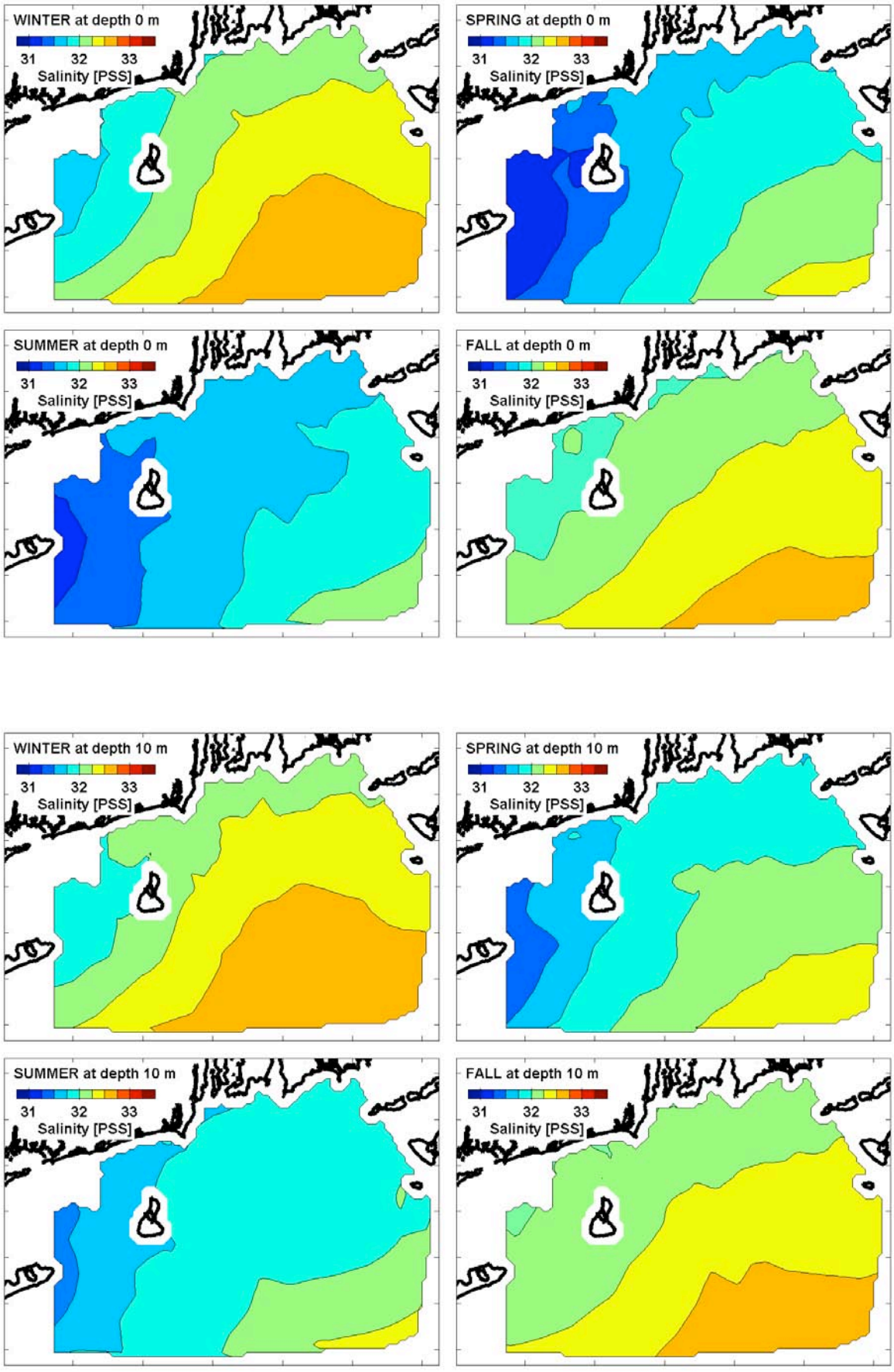

Figure 16. Hydrographic climatology. Salinity. (upper) Surface. (lower) Depth 10 m.

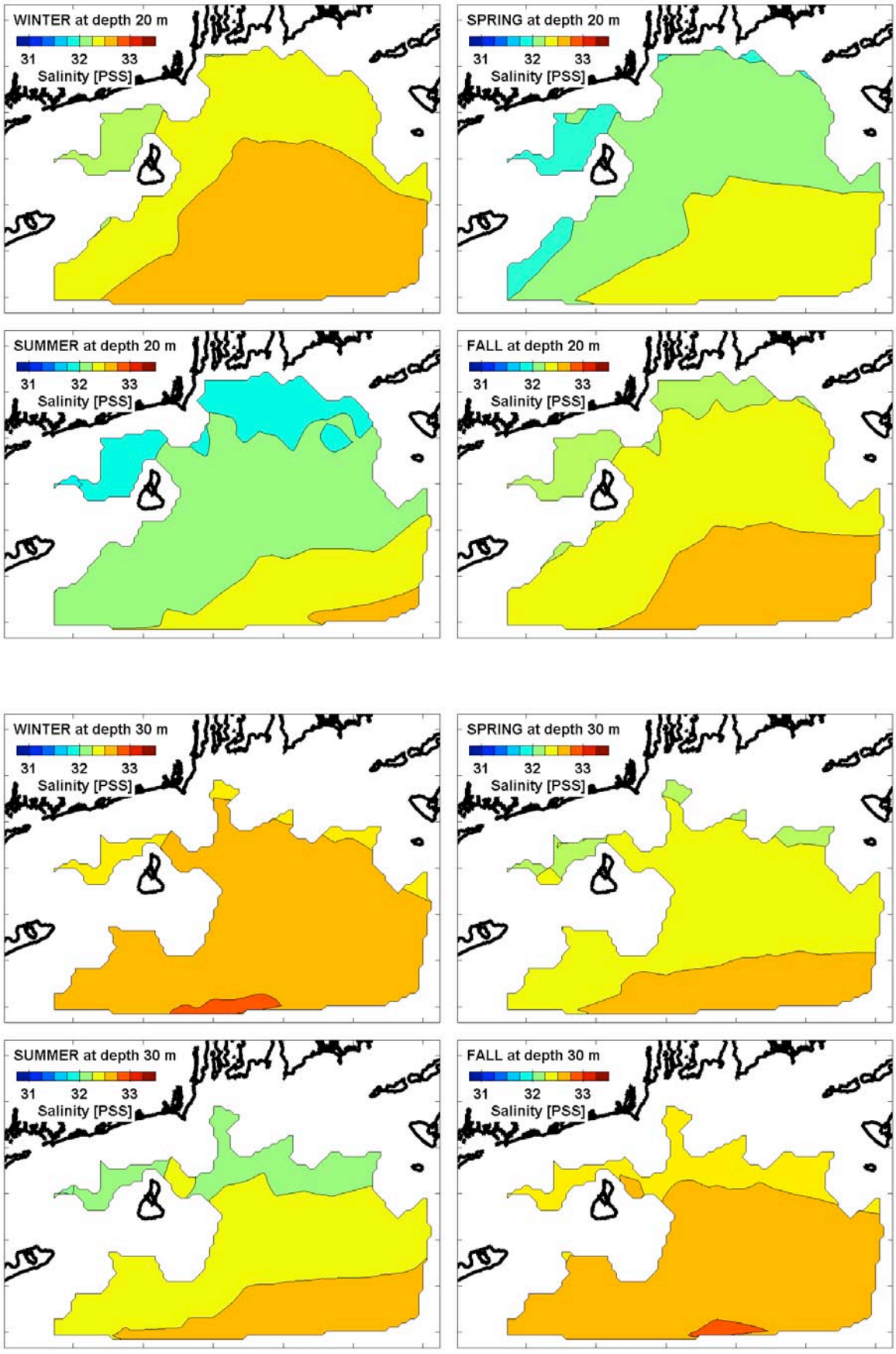

Figure 17. Hydrographic climatology. Salinity. (upper) Depth 20 m. (lower) Depth 30 m.

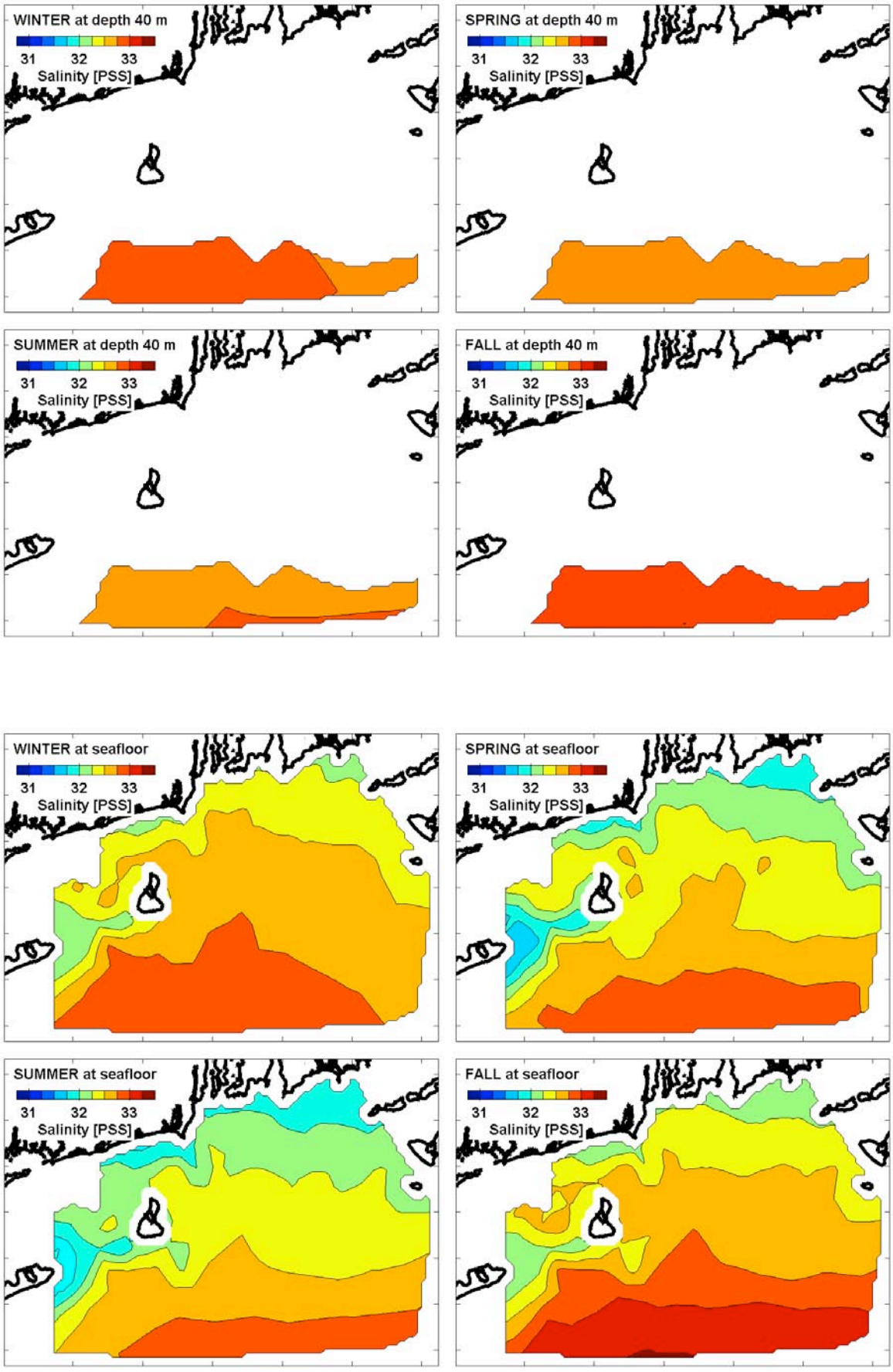

Figure 18. Hydrographic climatology. Salinity. (upper) Depth 40 m. (lower) Seafloor.

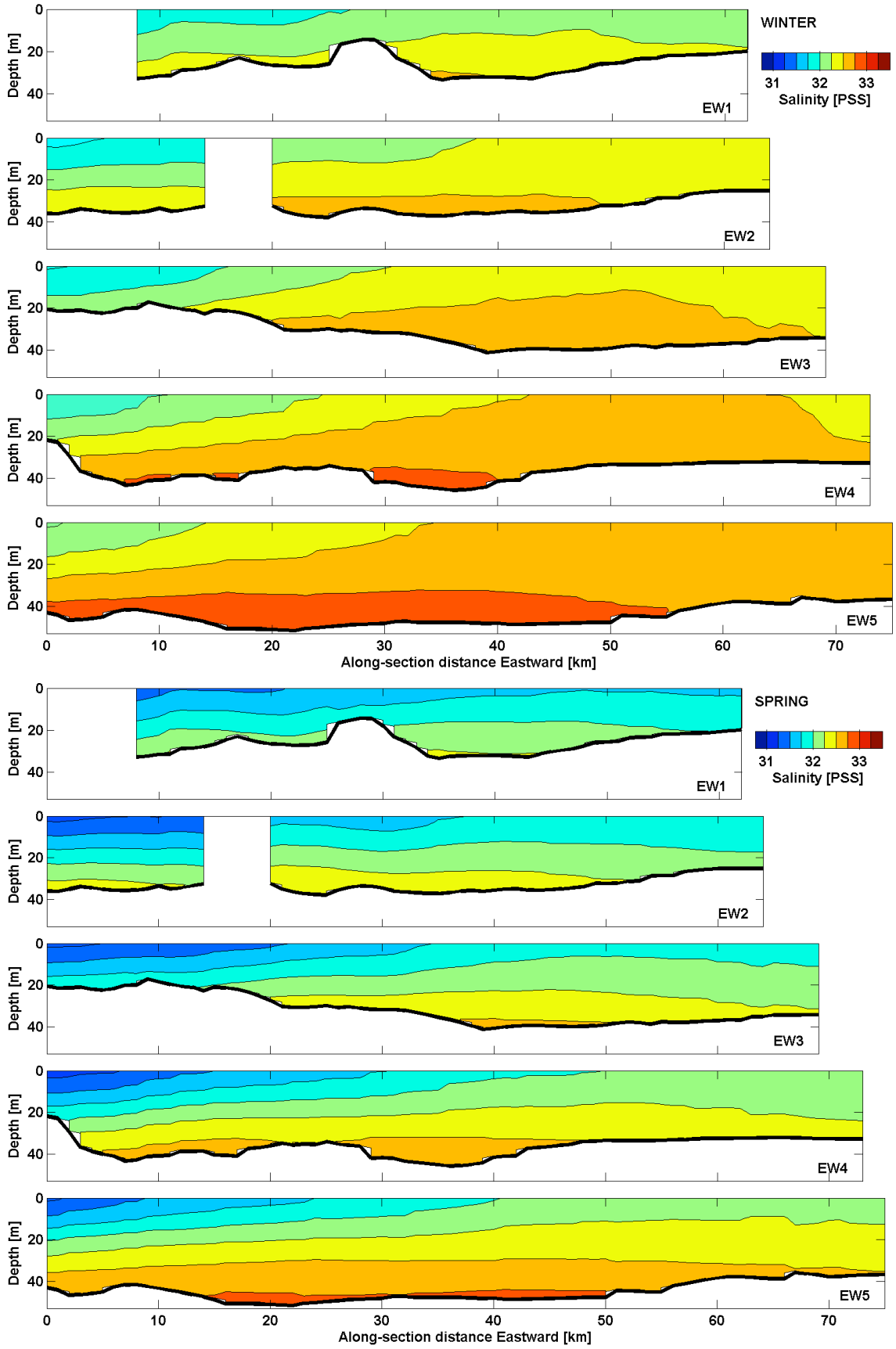

Figure 19. Hydrographic climatology. Salinity. EW. (upper) Winter. (lower) Spring.

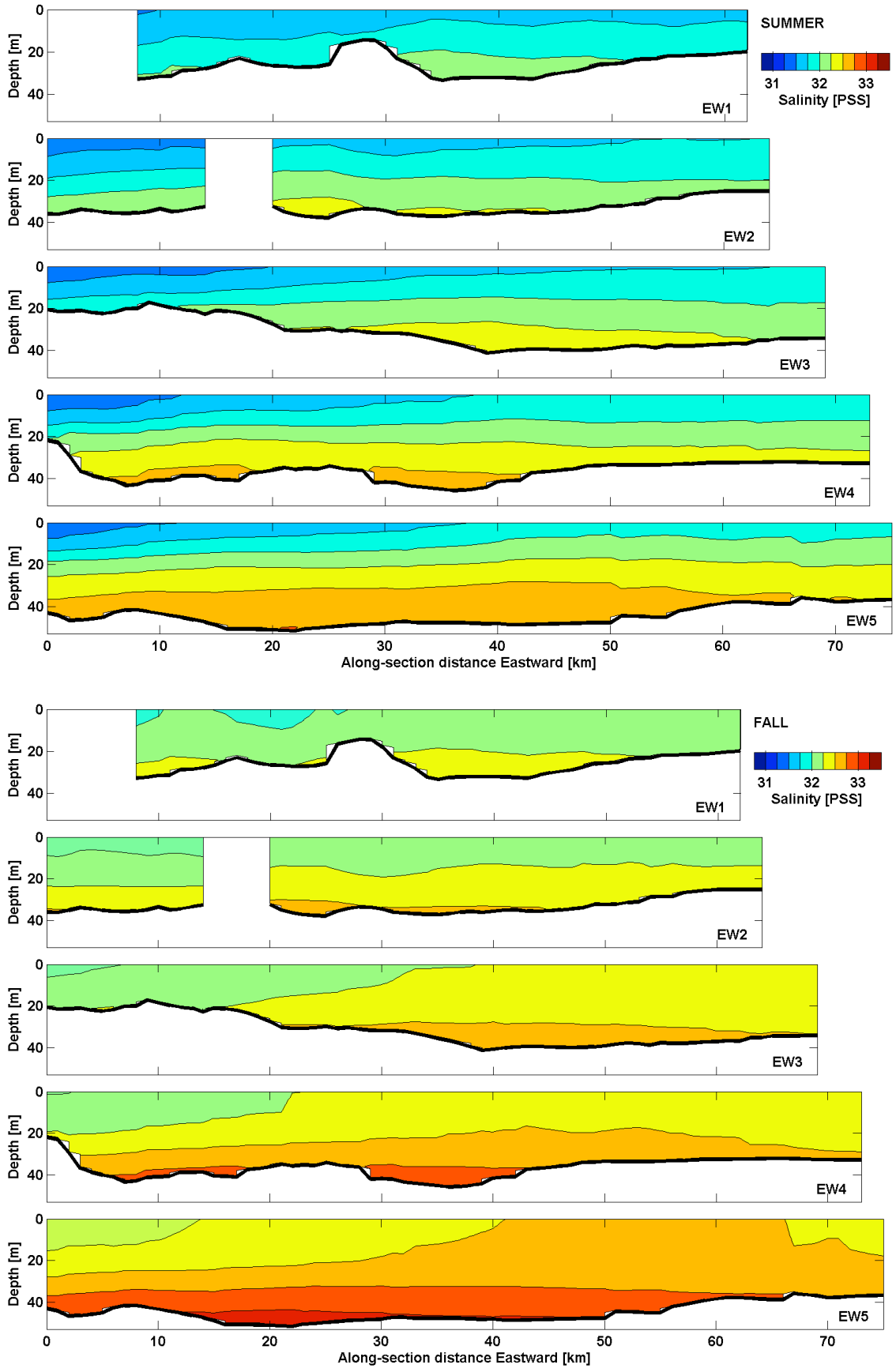

Figure 20. Hydrographic climatology. Salinity. EW. (upper) Summer. (lower) Fall.

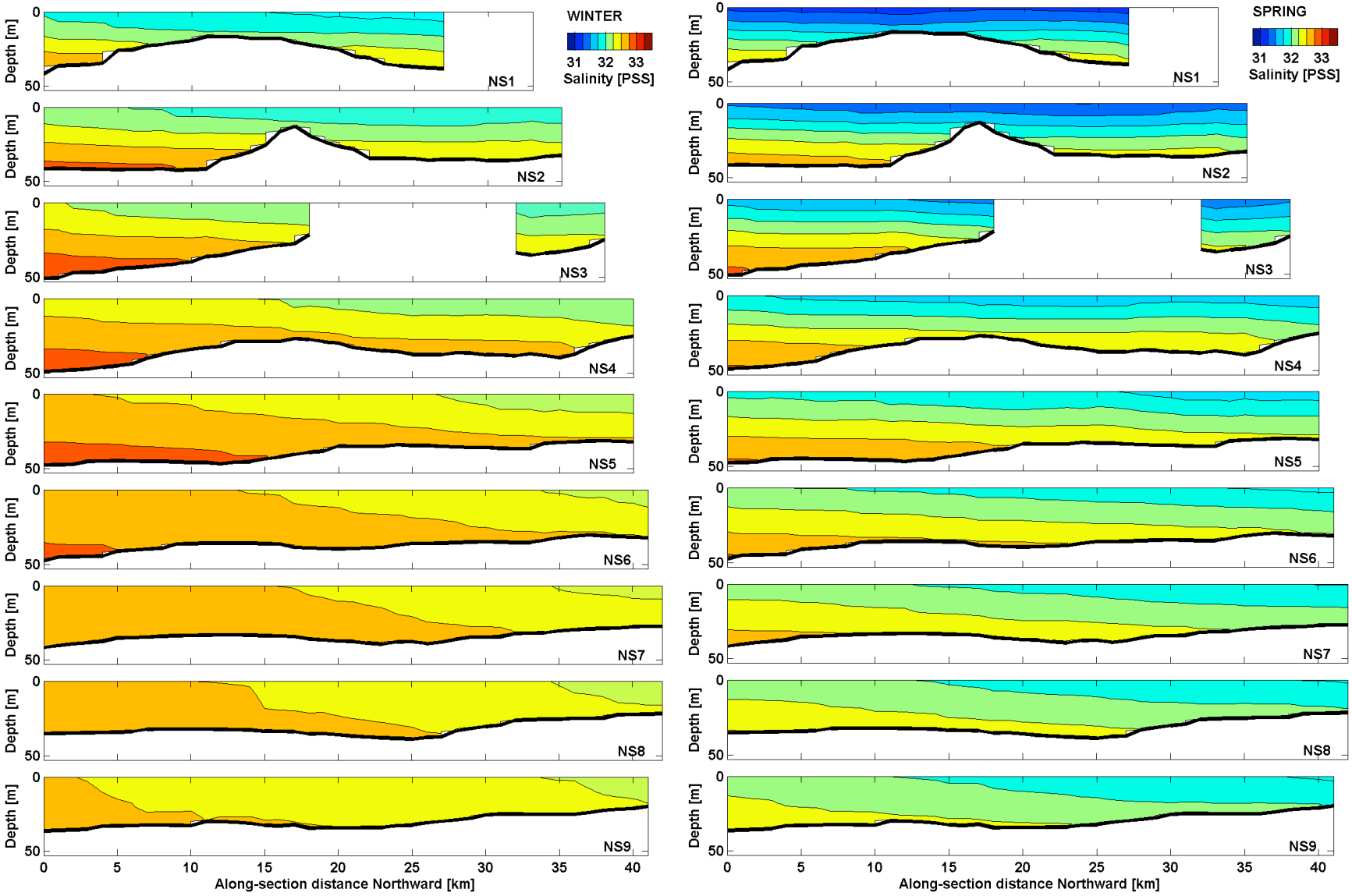

Figure 21. Hydrographic climatology. Salinity. NS. (left) Winter. (right) Spring.

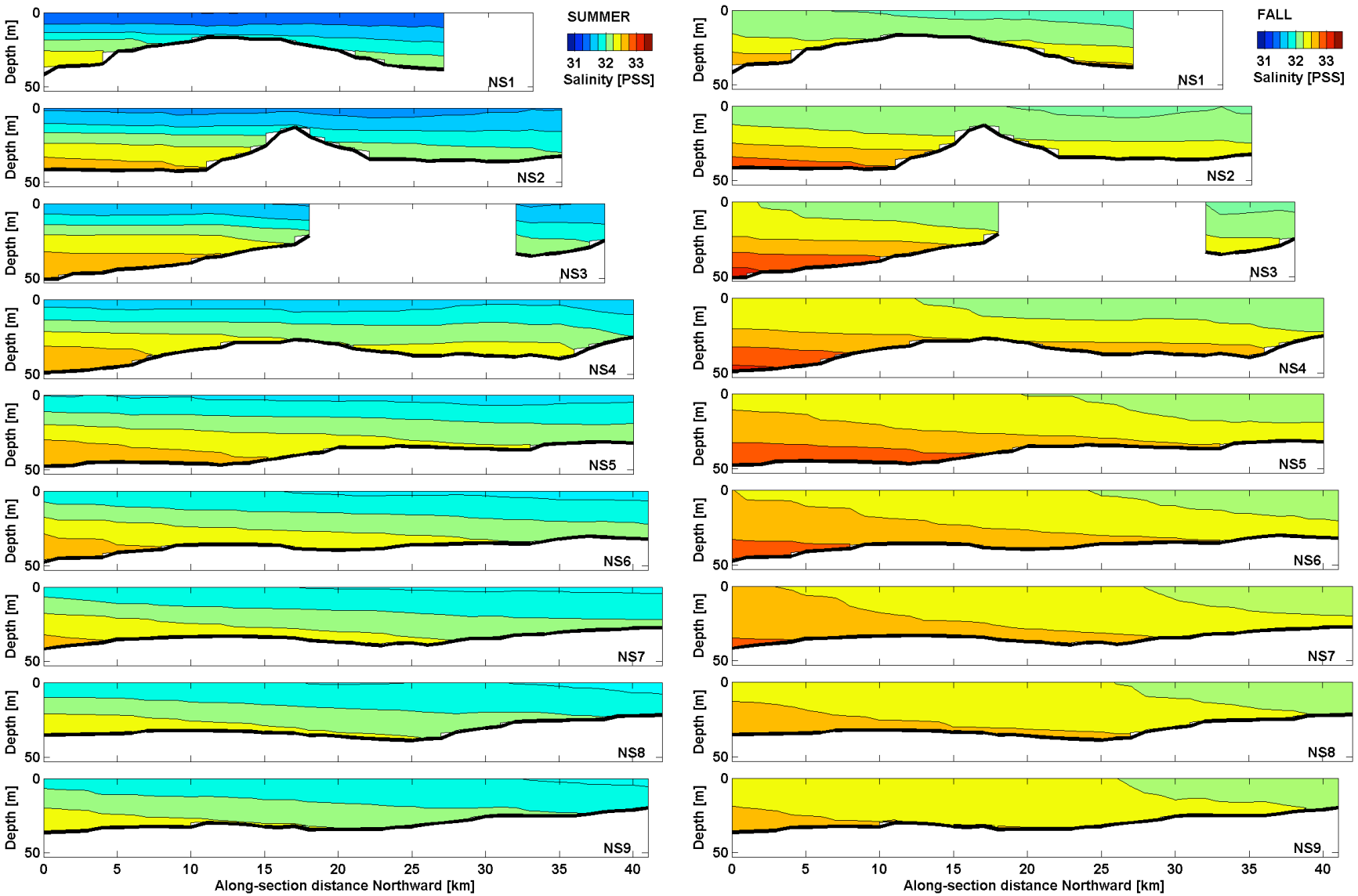

Figure 22. Hydrographic climatology. Salinity. NS. (left) Summer. (right) Fall.

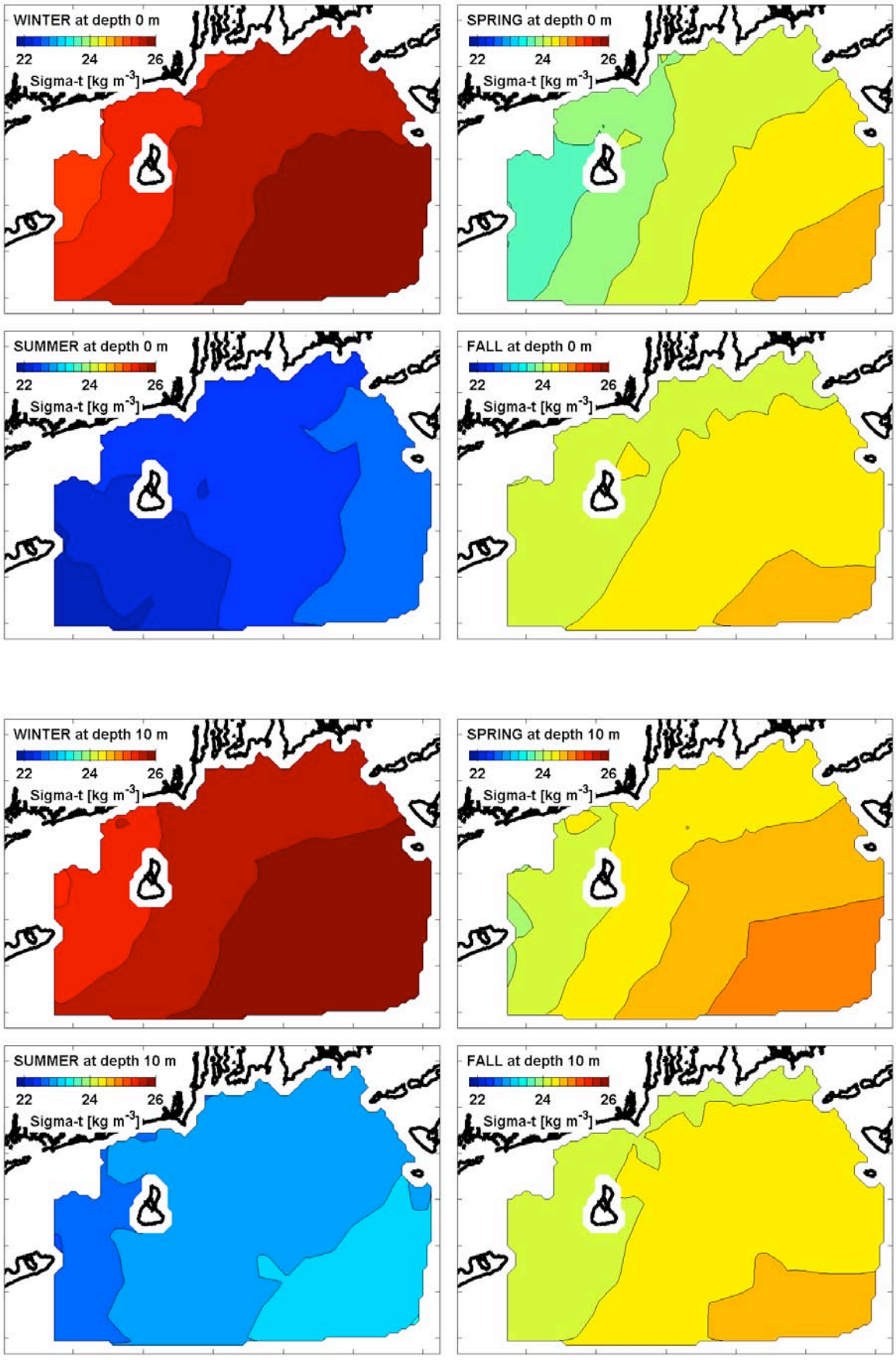

Figure 23. Hydrographic climatology. Density anomaly. (upper) Surface. (lower) Depth 10 m.

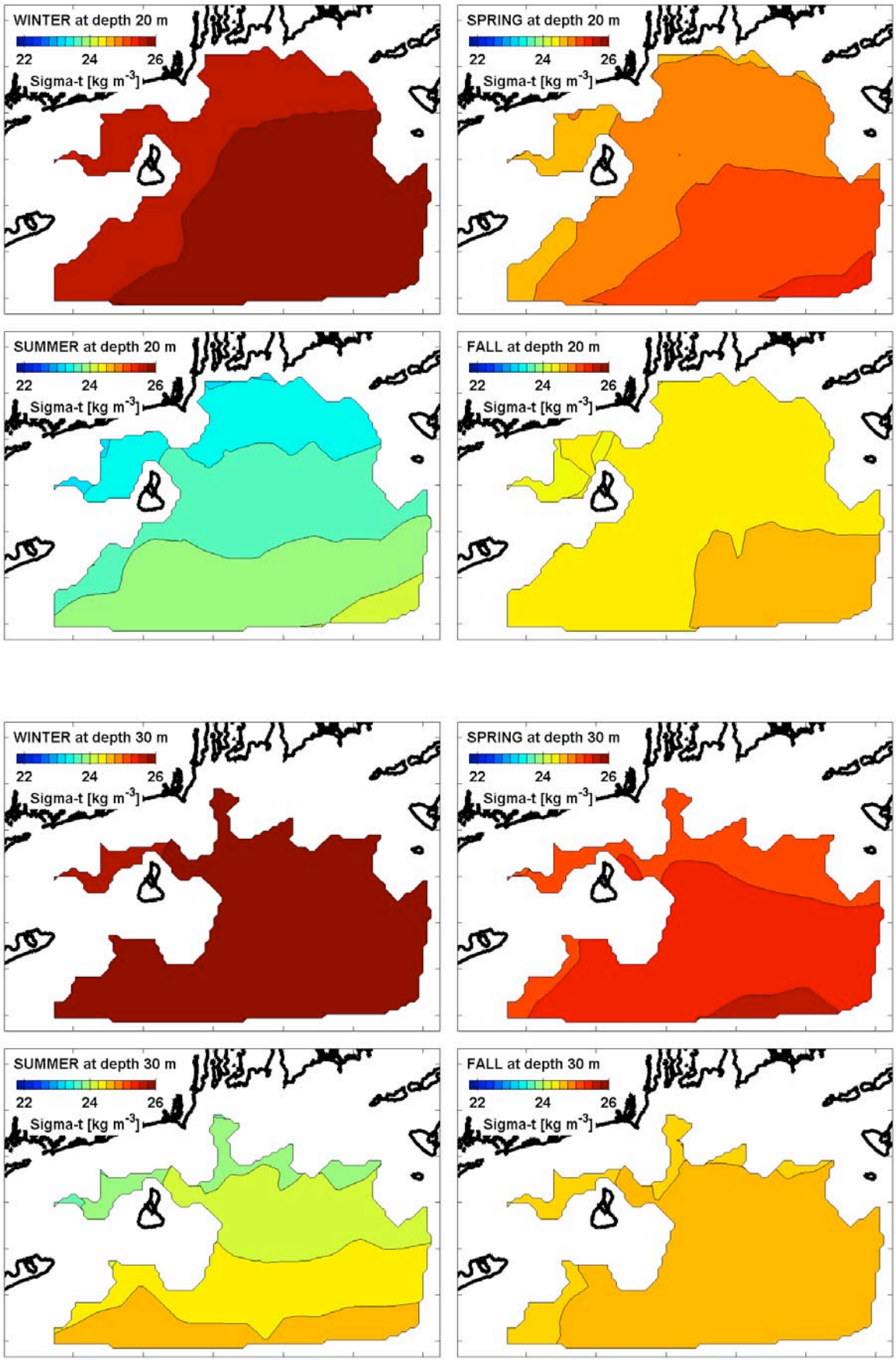

Figure 24. Hydrographic climatology. Density anomaly. (upper) Depth 20 m. (lower) Depth 30 m.

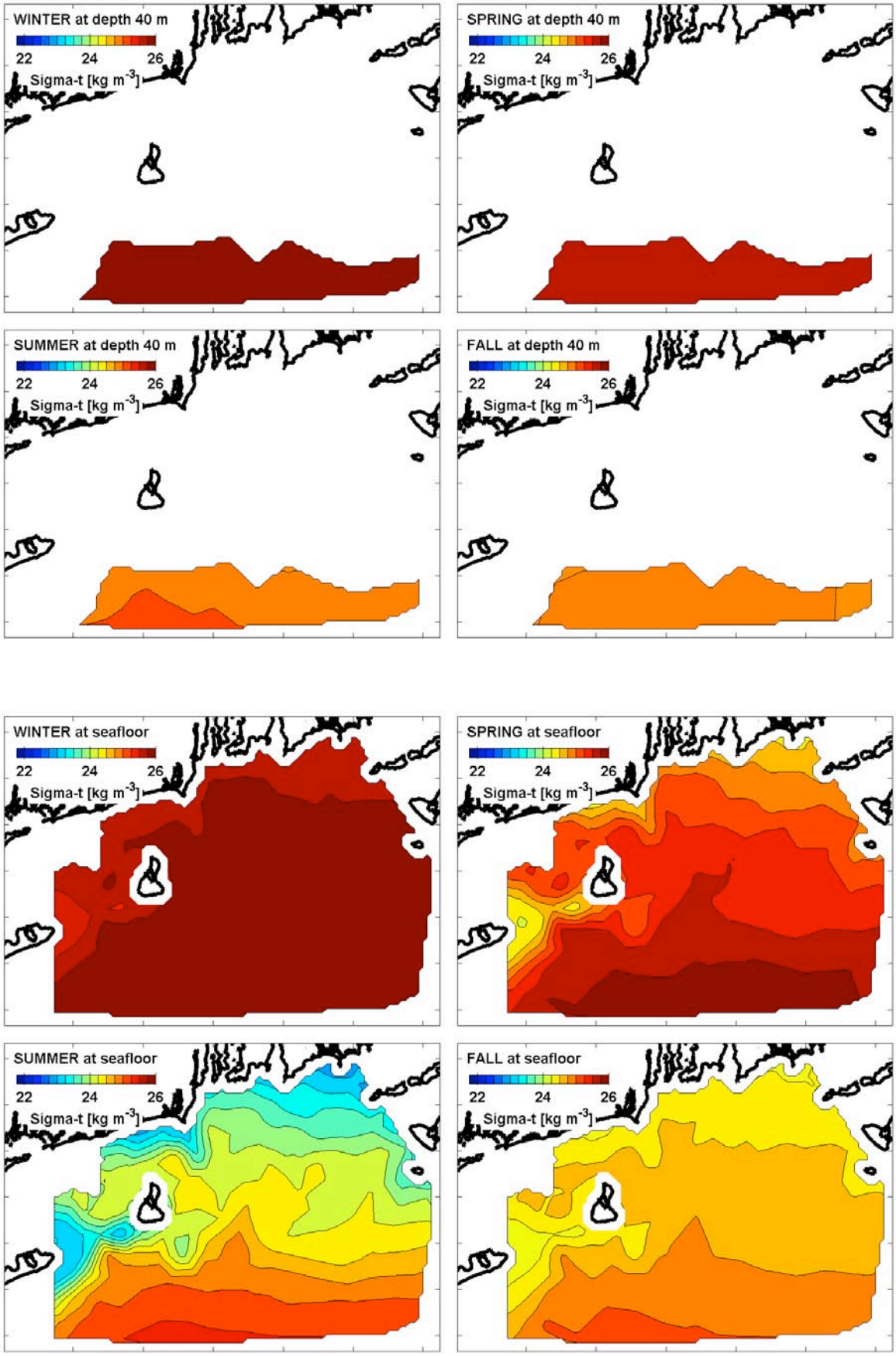

Figure 25. Hydrographic climatology. Density anomaly. (upper) Depth 40 m. (lower) Seafloor.

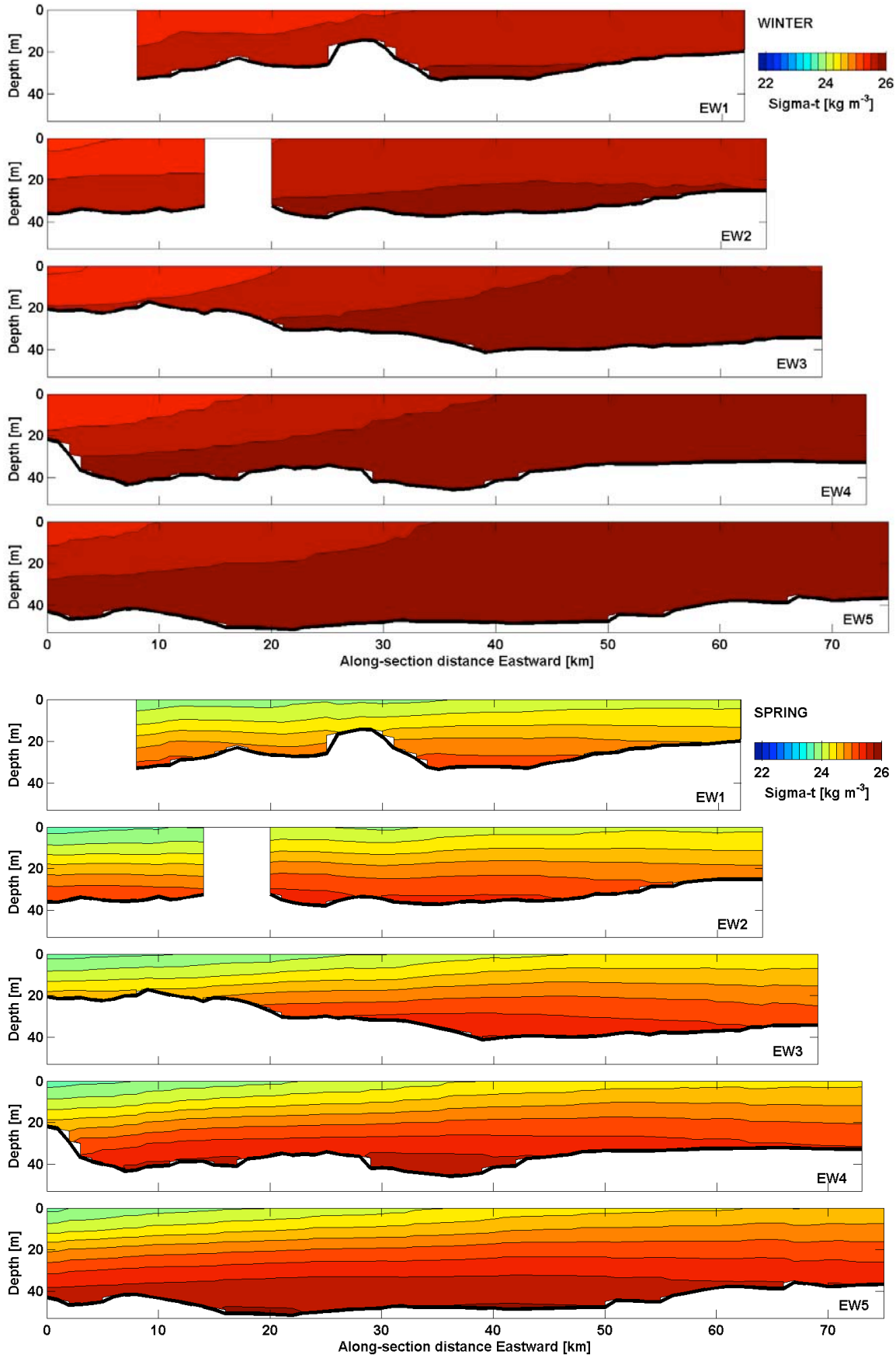

Figure 26. Hydrographic climatology. Density anomaly. EW. (upper) Winter. (lower) Spring.

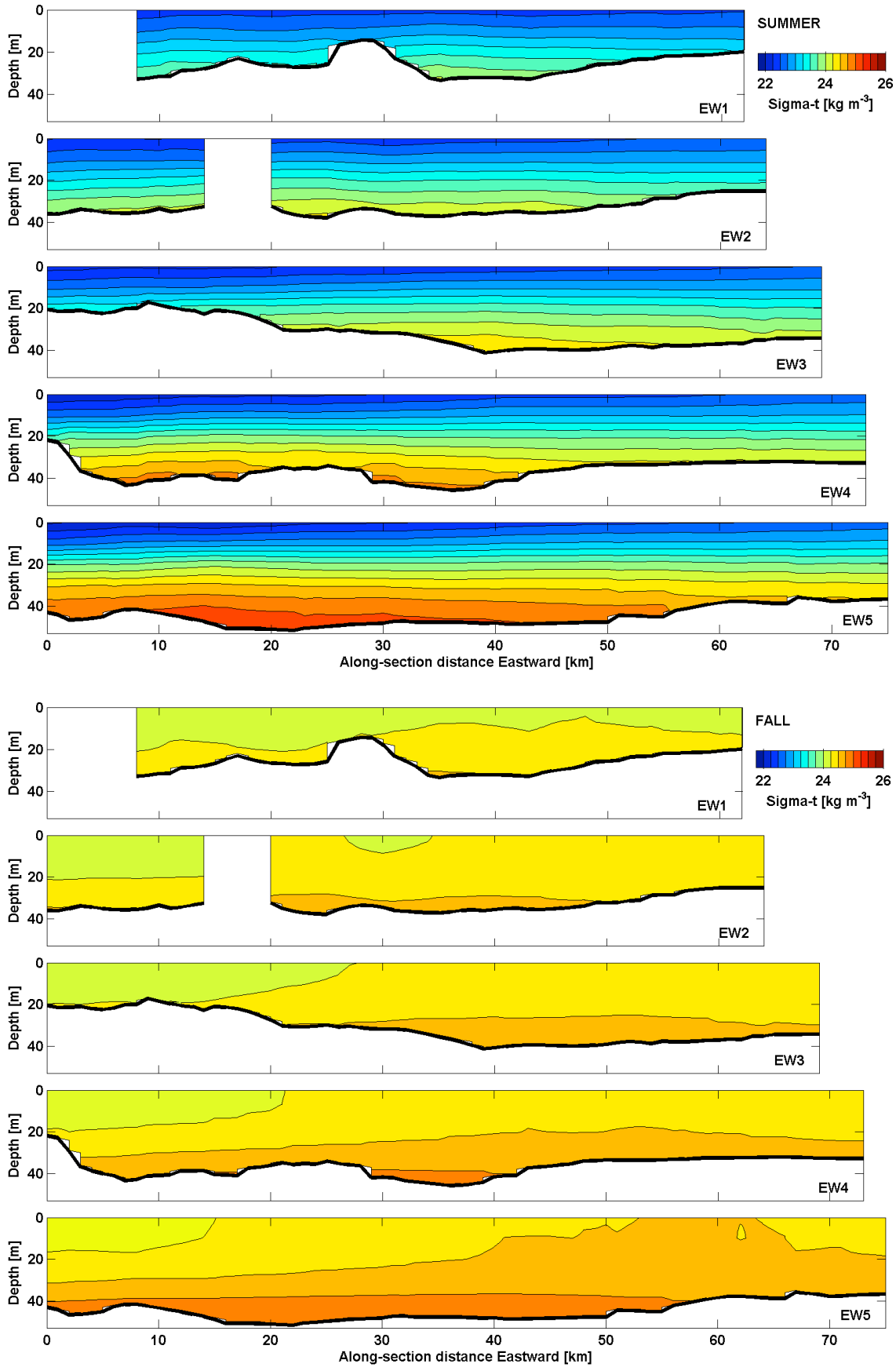

Figure 27. Hydrographic climatology. Density anomaly. EW. (upper) Summer. (lower) Fall.

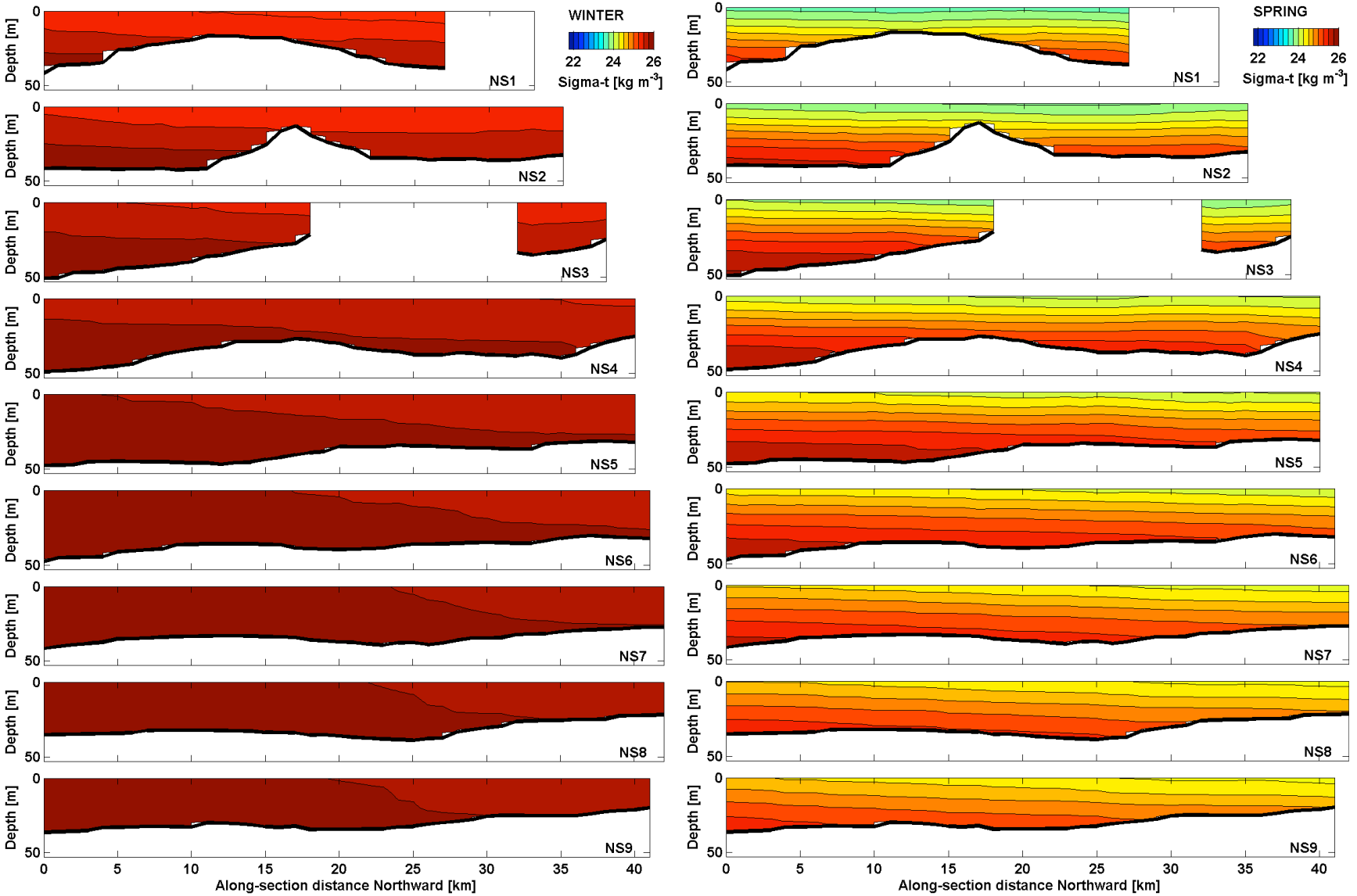

Figure 28. Hydrographic climatology. Density anomaly. NS. (left) Winter. (right) Spring.

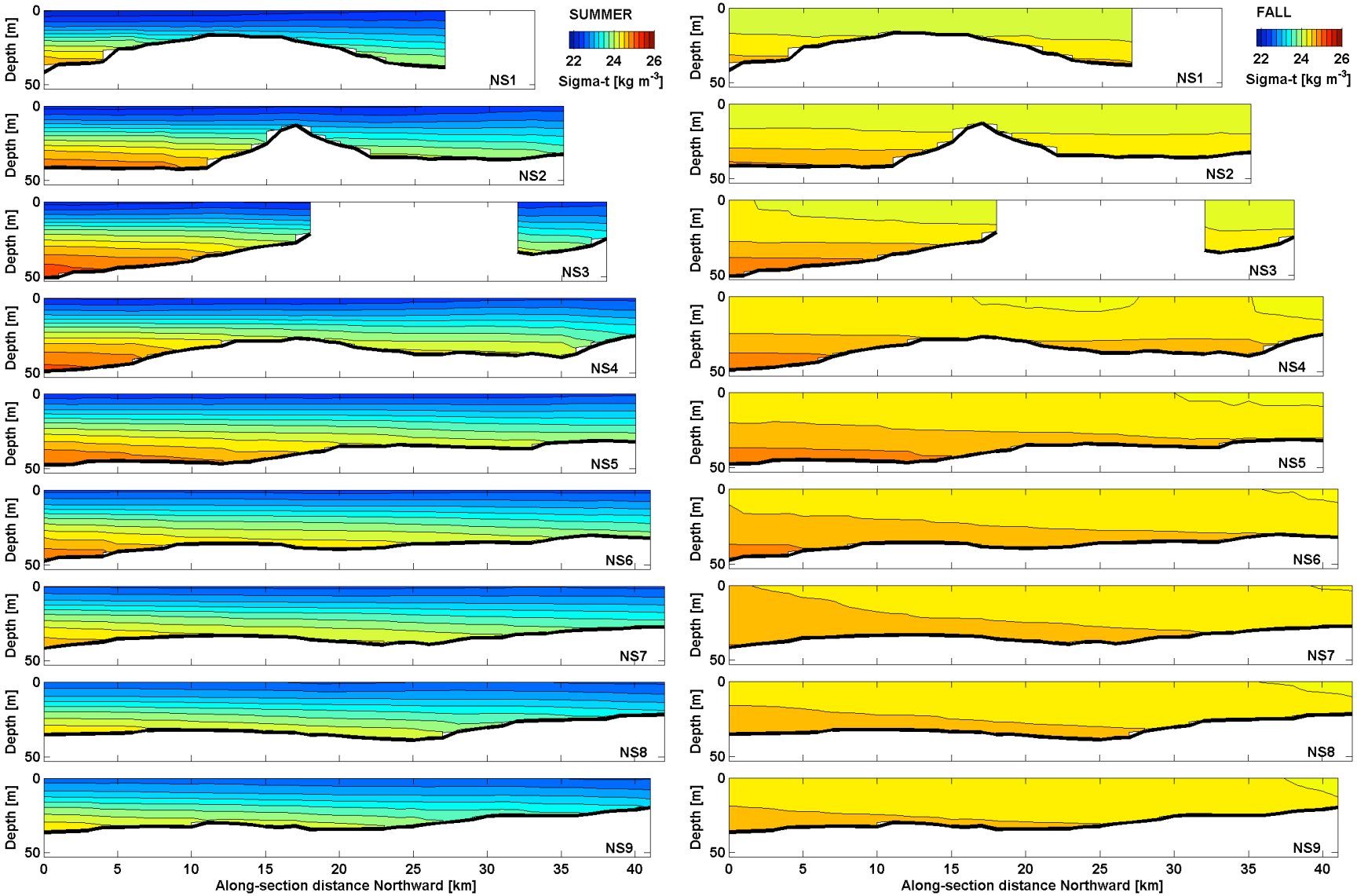

Figure 29. Hydrographic climatology. Density anomaly. NS. (left) Summer. (right) Fall.

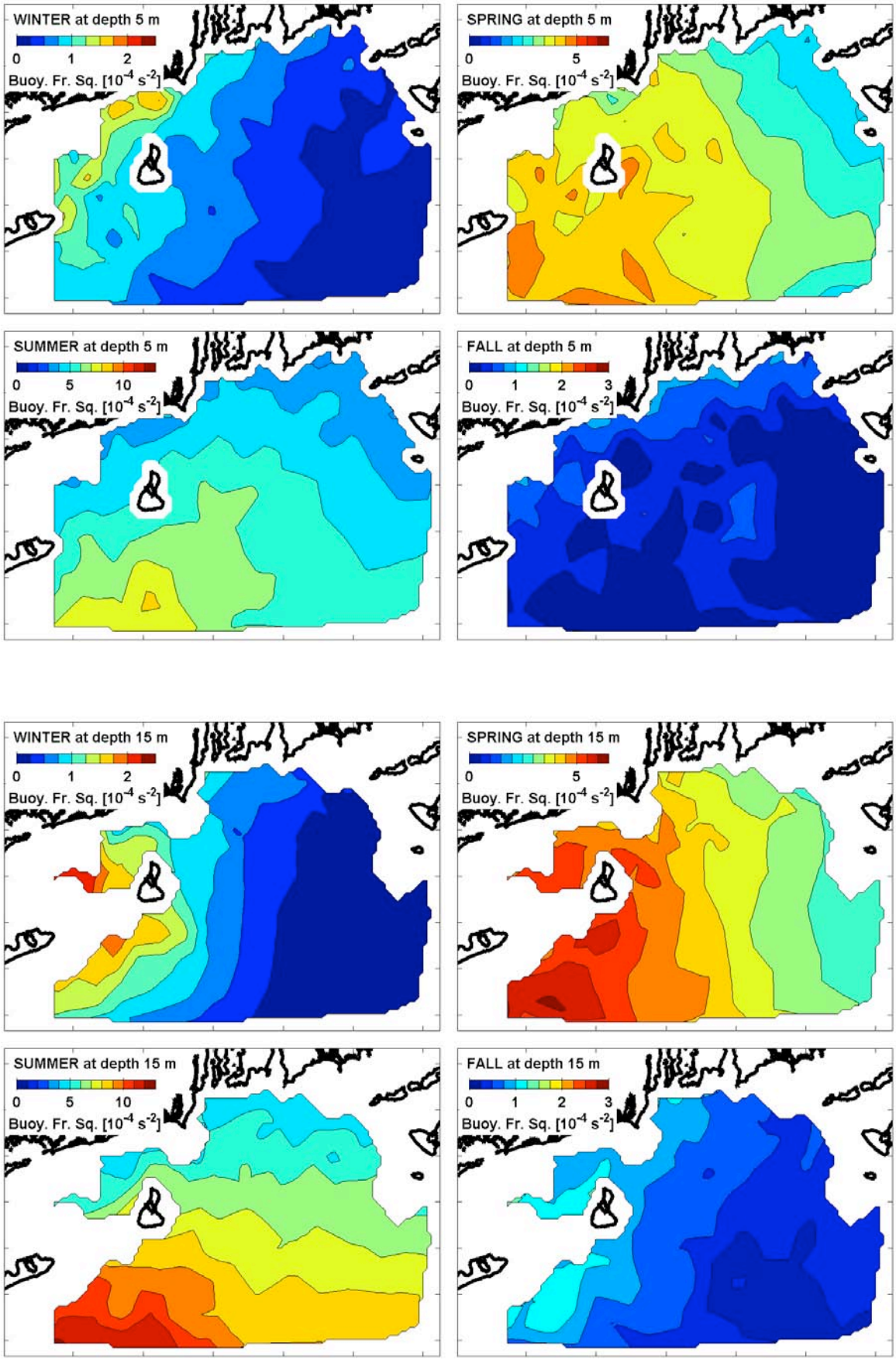

Figure 30. Hydrographic climatology. Stratification. (upper) Depth 5 m. (lower) Depth 15 m.

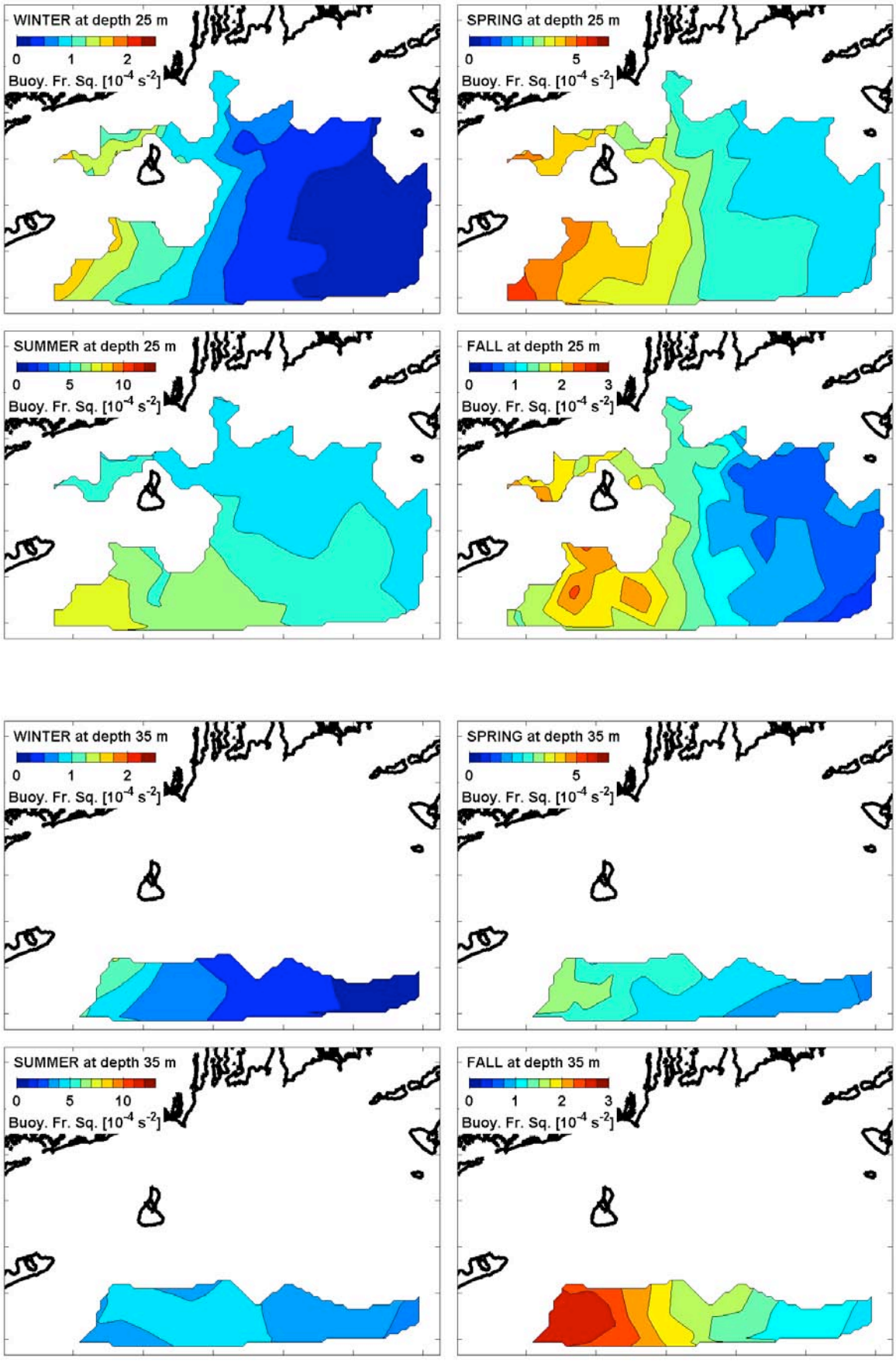

Figure 31. Hydrographic climatology. Stratification. (upper) Depth 25 m. (lower) Depth 35 m.

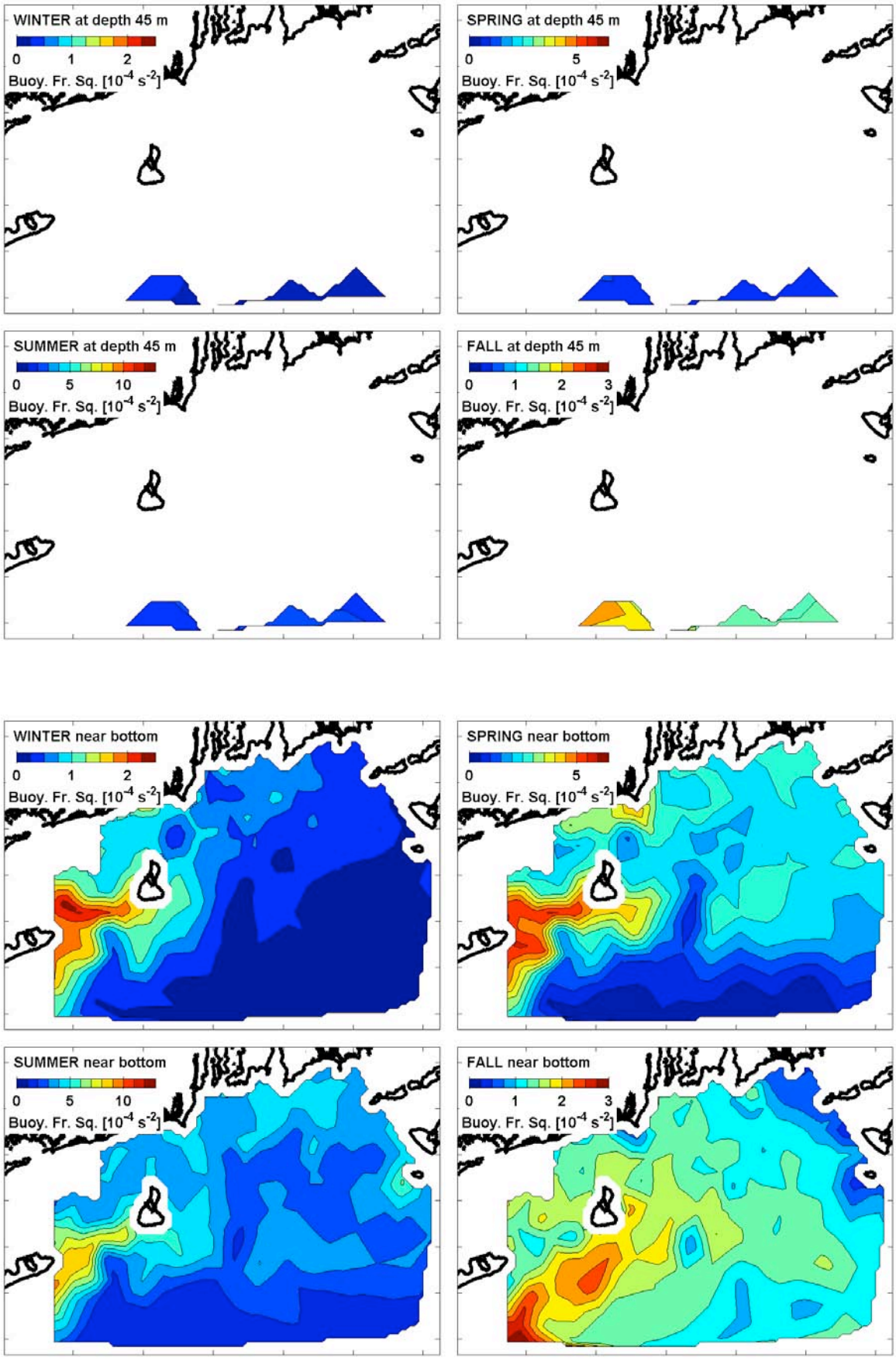

Figure 32. Hydrographic climatology. Stratification. (upper) Depth 45 m. (lower) Near seafloor.

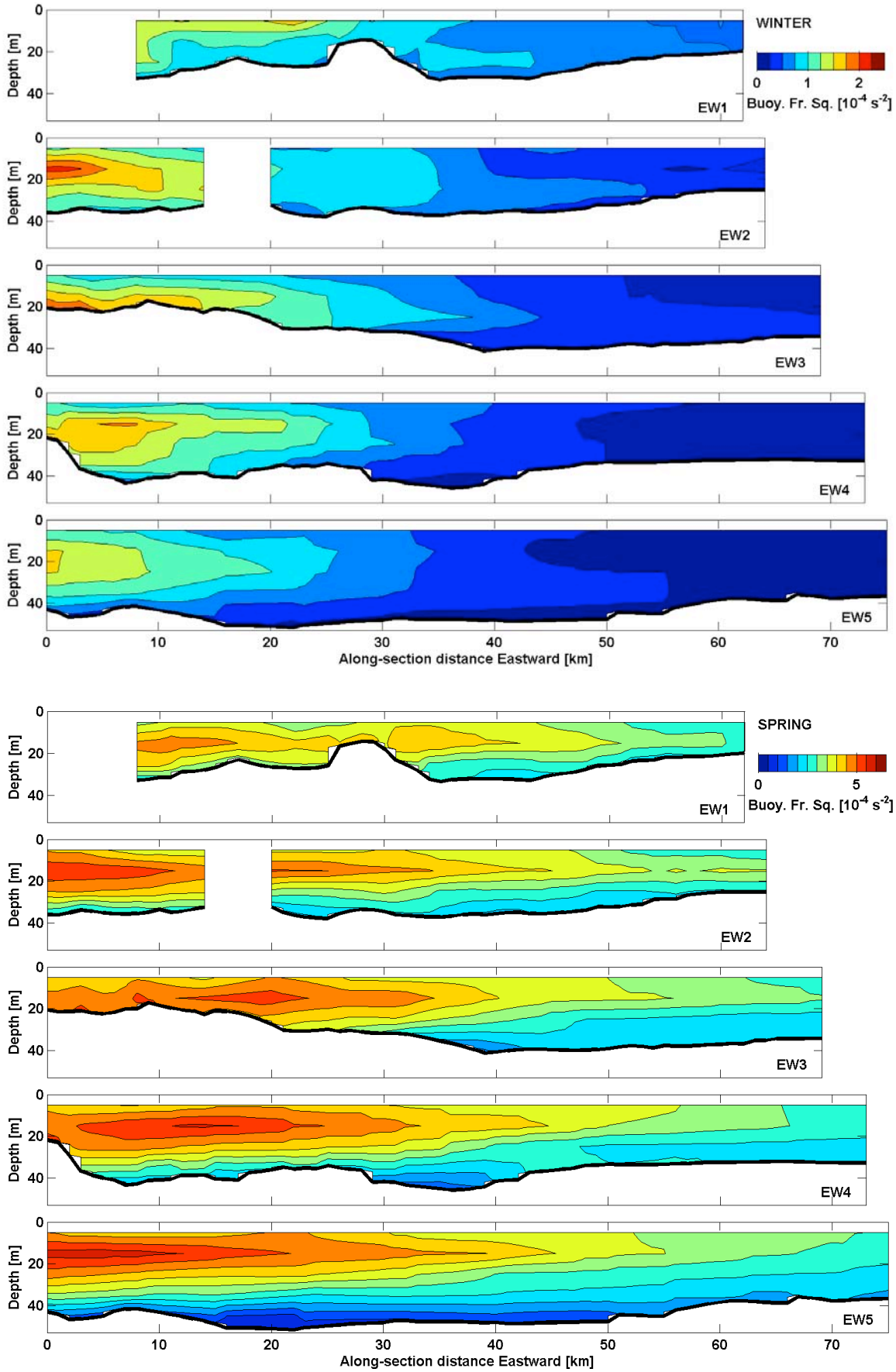

Figure 33. Hydrographic climatology. Stratification. EW. (upper) Winter. (lower) Spring.

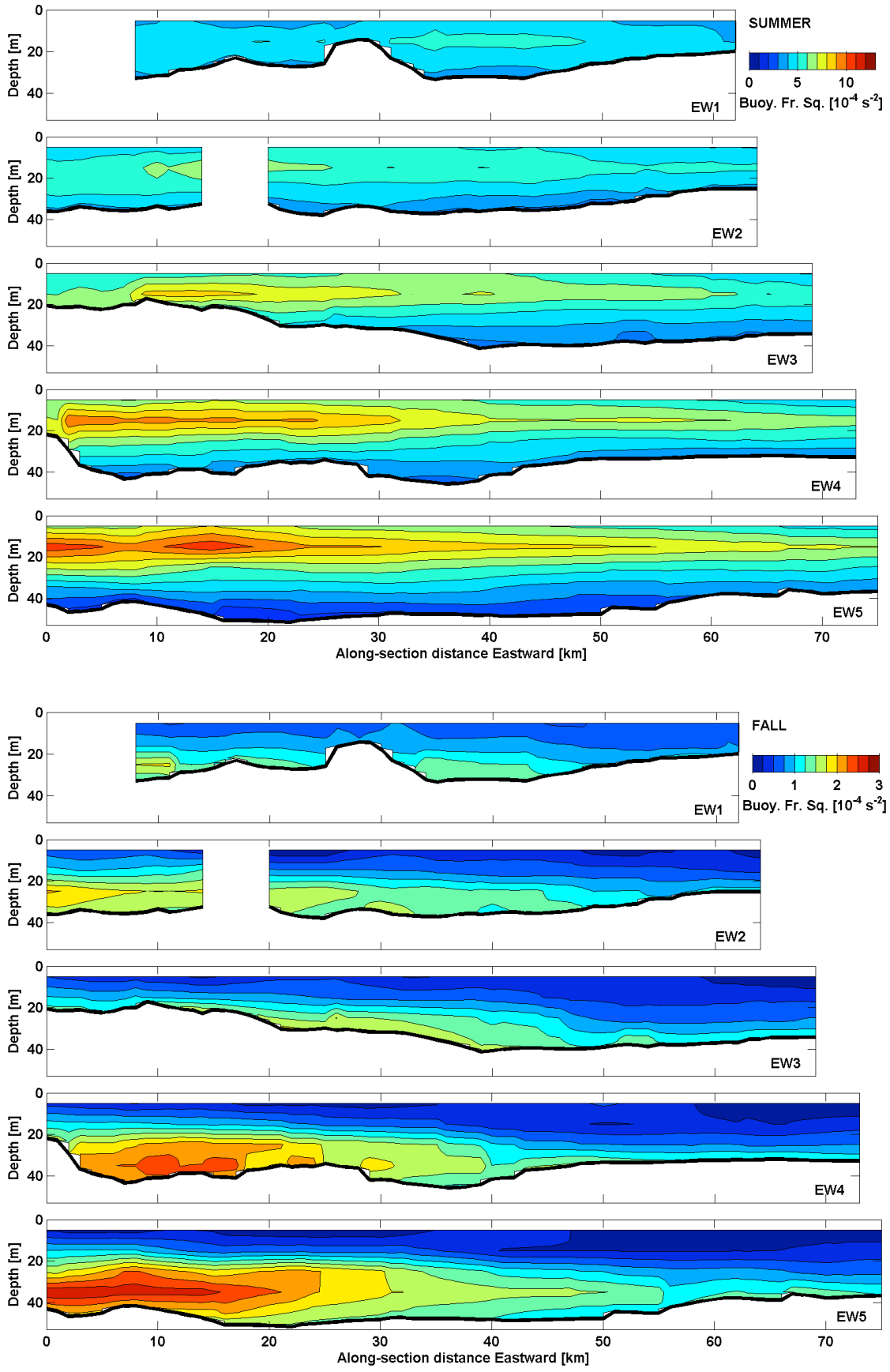

Figure 34. Hydrographic climatology. Stratification. EW. (upper) Summer. (lower) Fall.

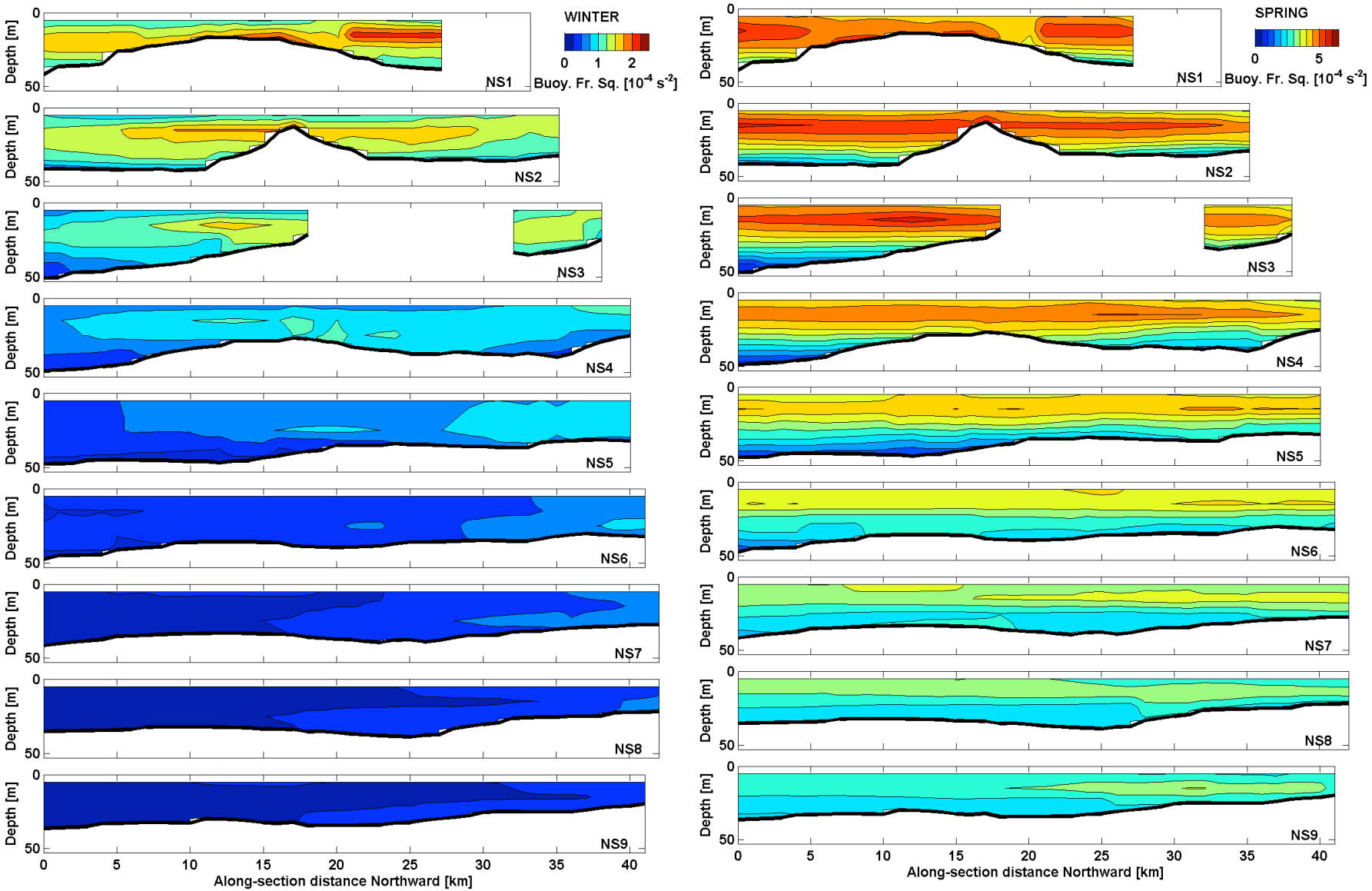

Figure 35. Hydrographic climatology. Stratification. NS. (left) Winter. (right) Spring.

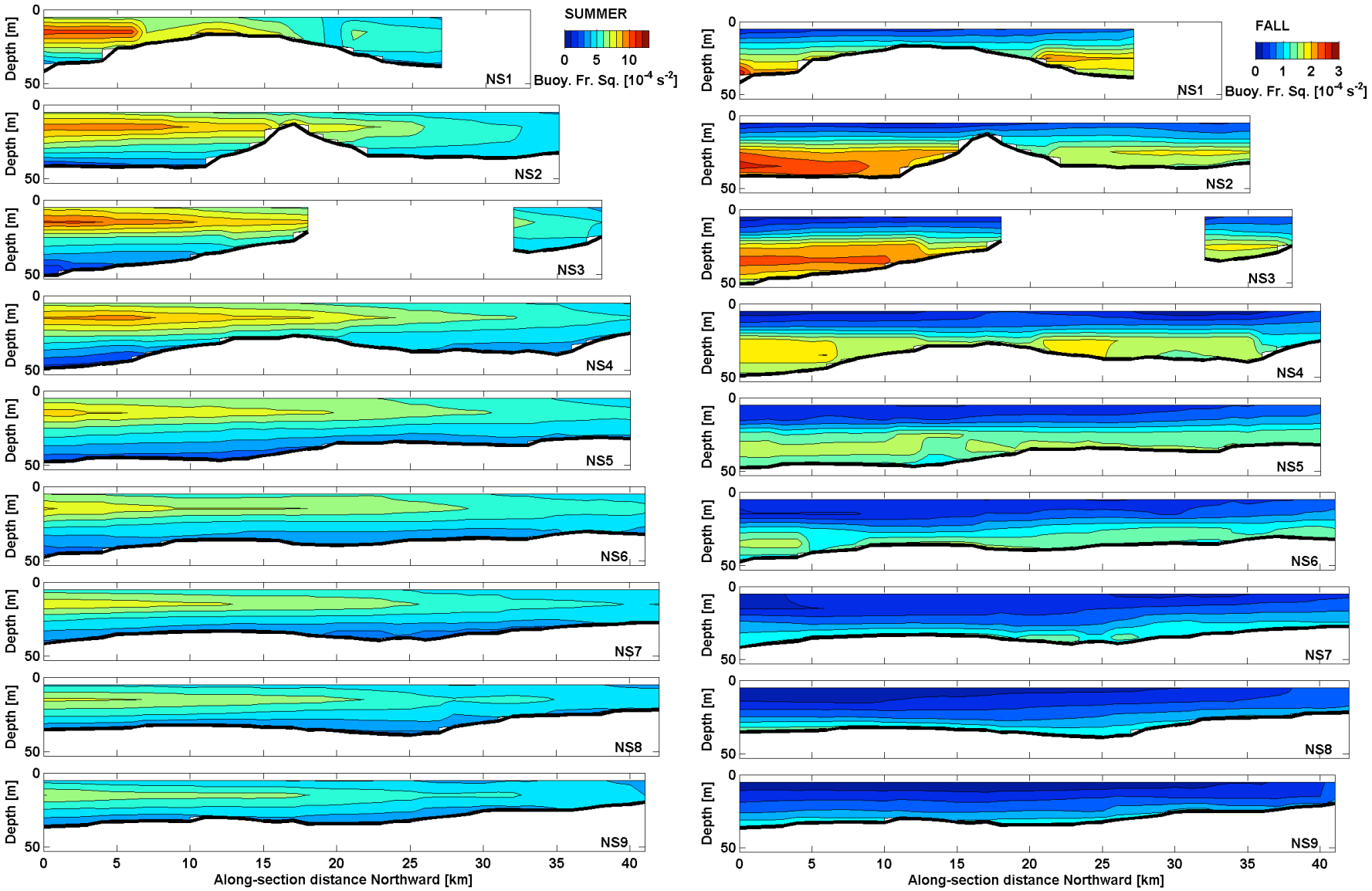

Figure 36. Hydrographic climatology. Stratification. NS. (left) Summer. (right) Fall.

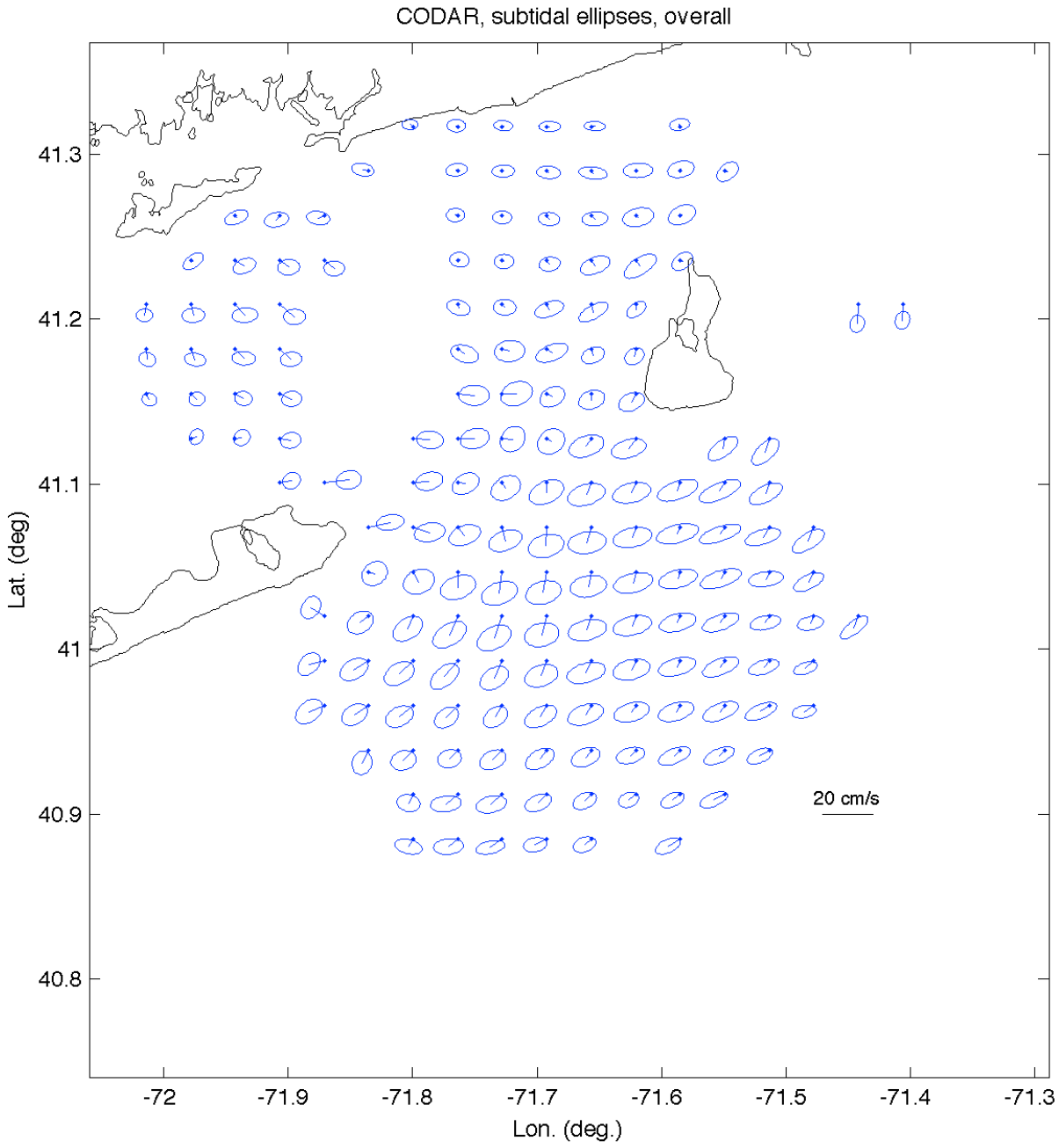

Figure 37. HF radar currents. All seasons mean flow and subtidal principal component ellipses.

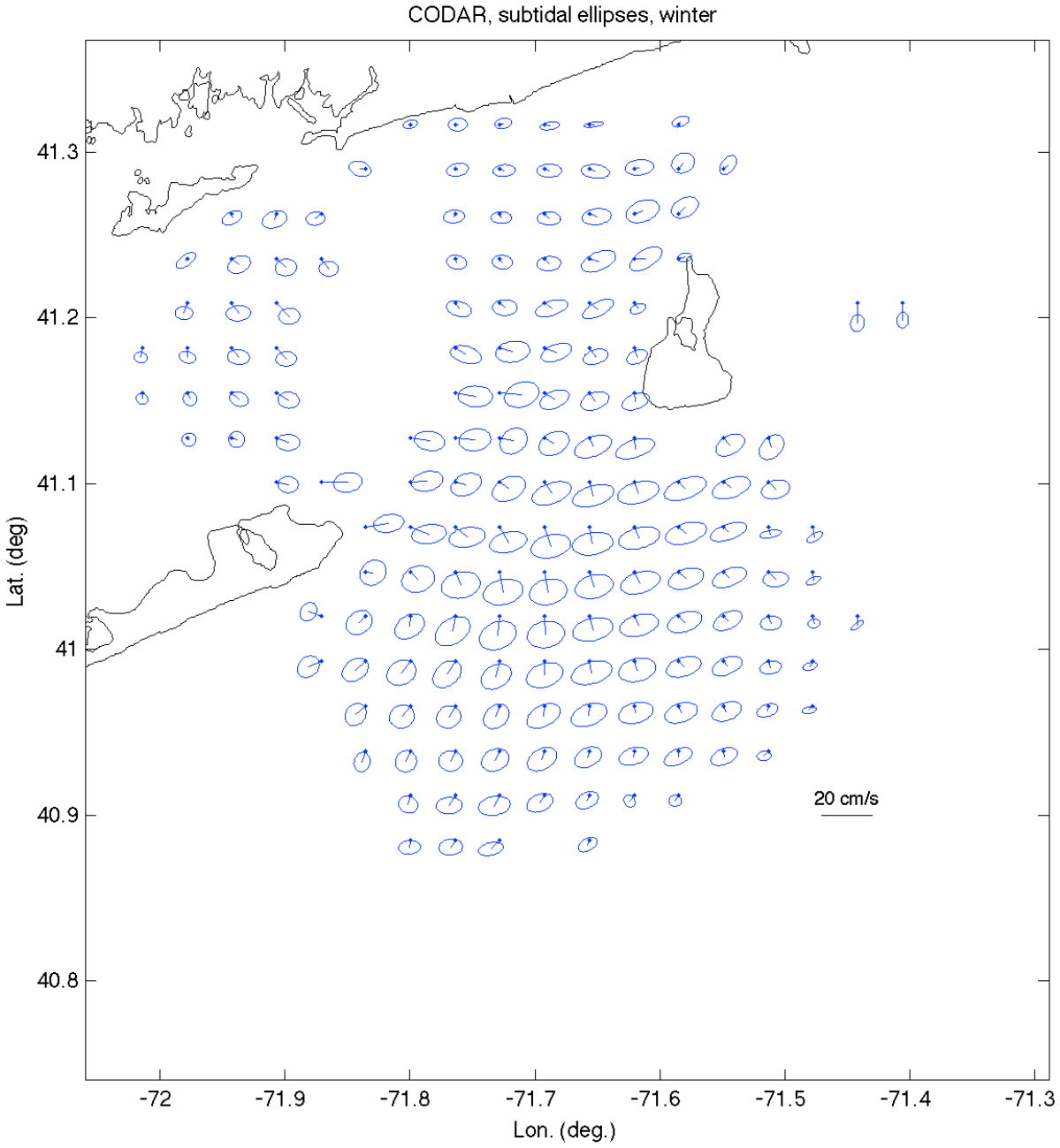

Figure 38. HF radar currents. Winter mean flow and subtidal principal axes ellipses.

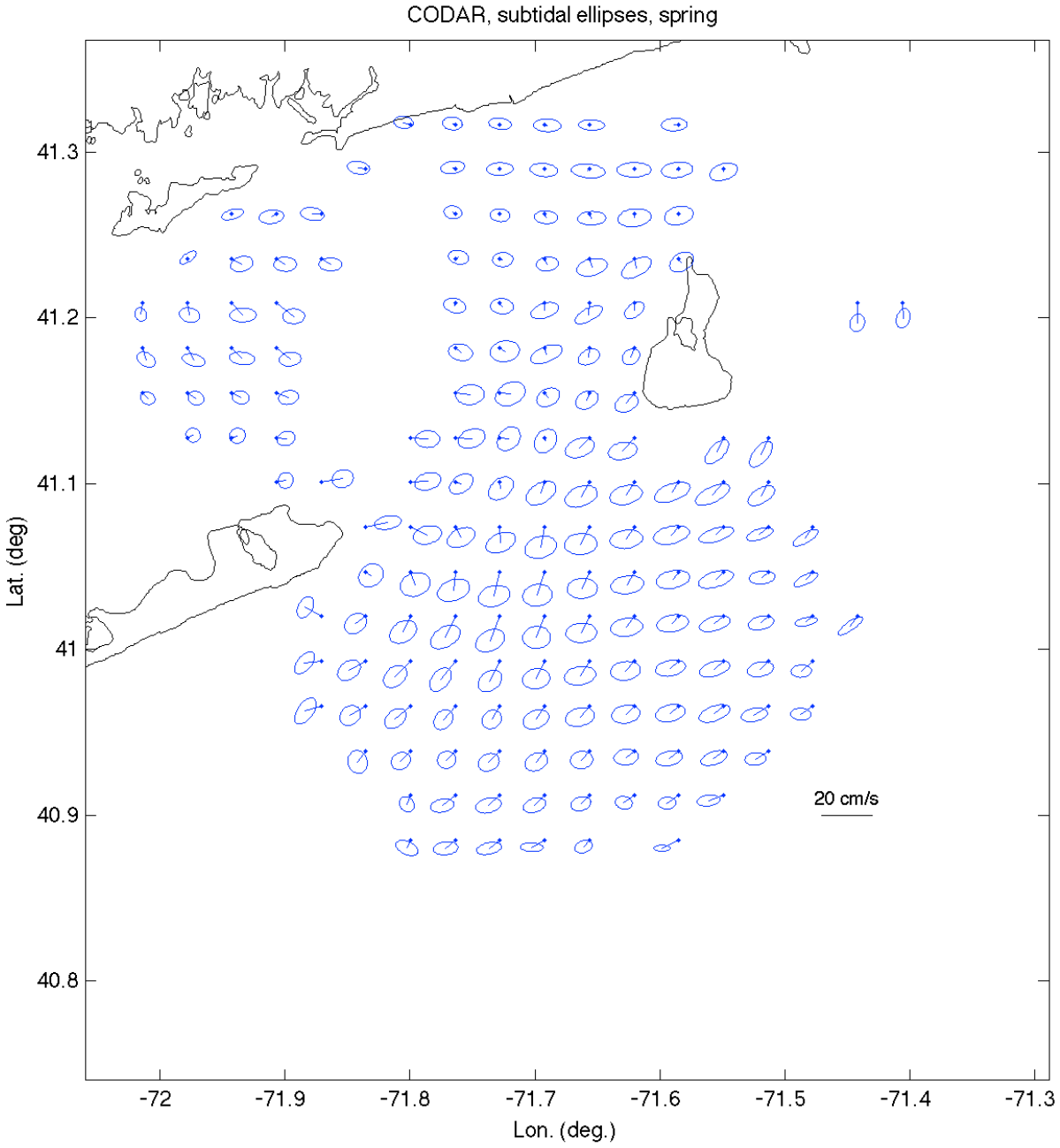

Figure 39. HF radar currents. Spring mean flow and subtidal principal axes ellipses.

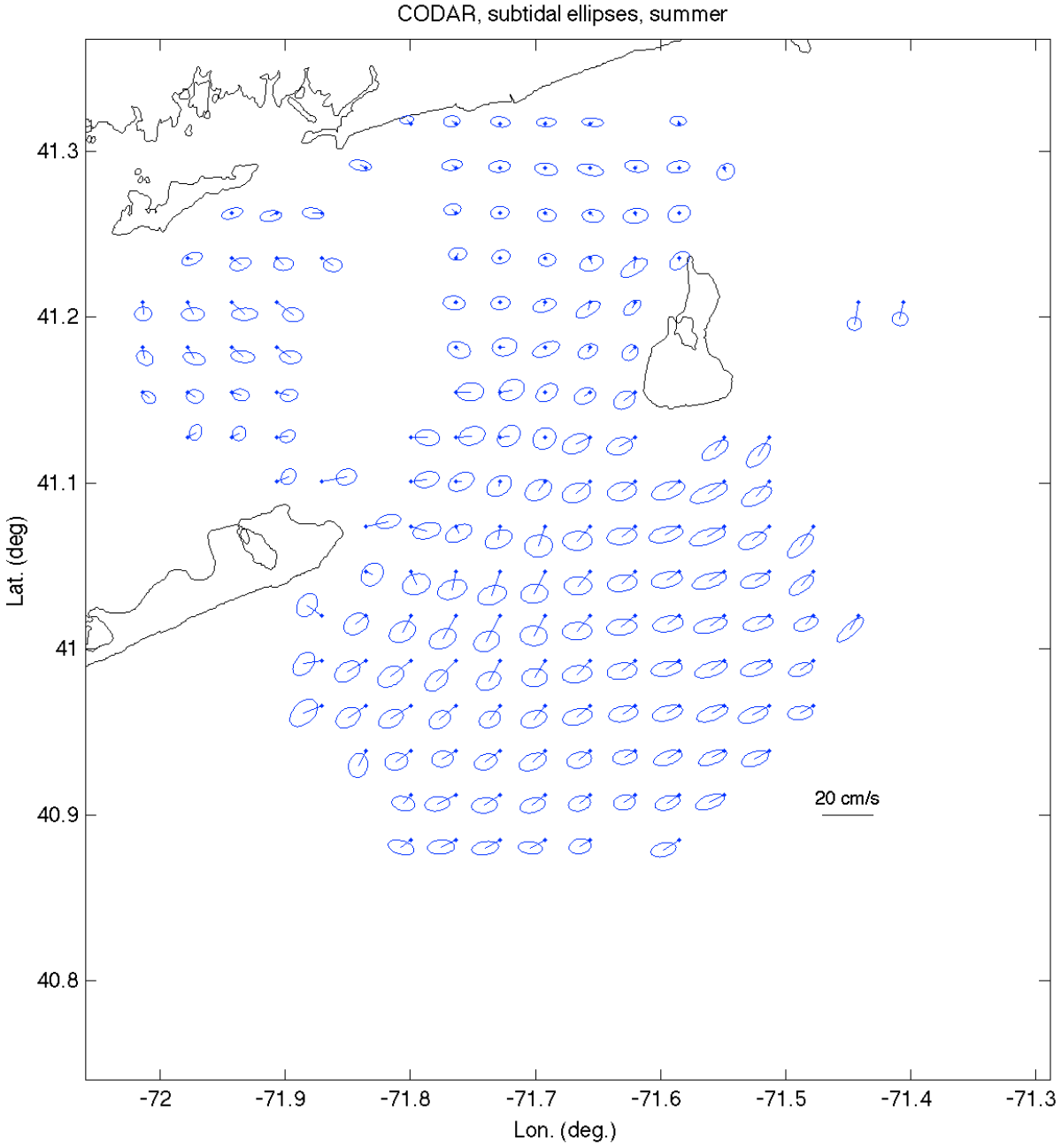

Figure 40. HF radar currents. Summer mean flow and subtidal principal axes ellipses.

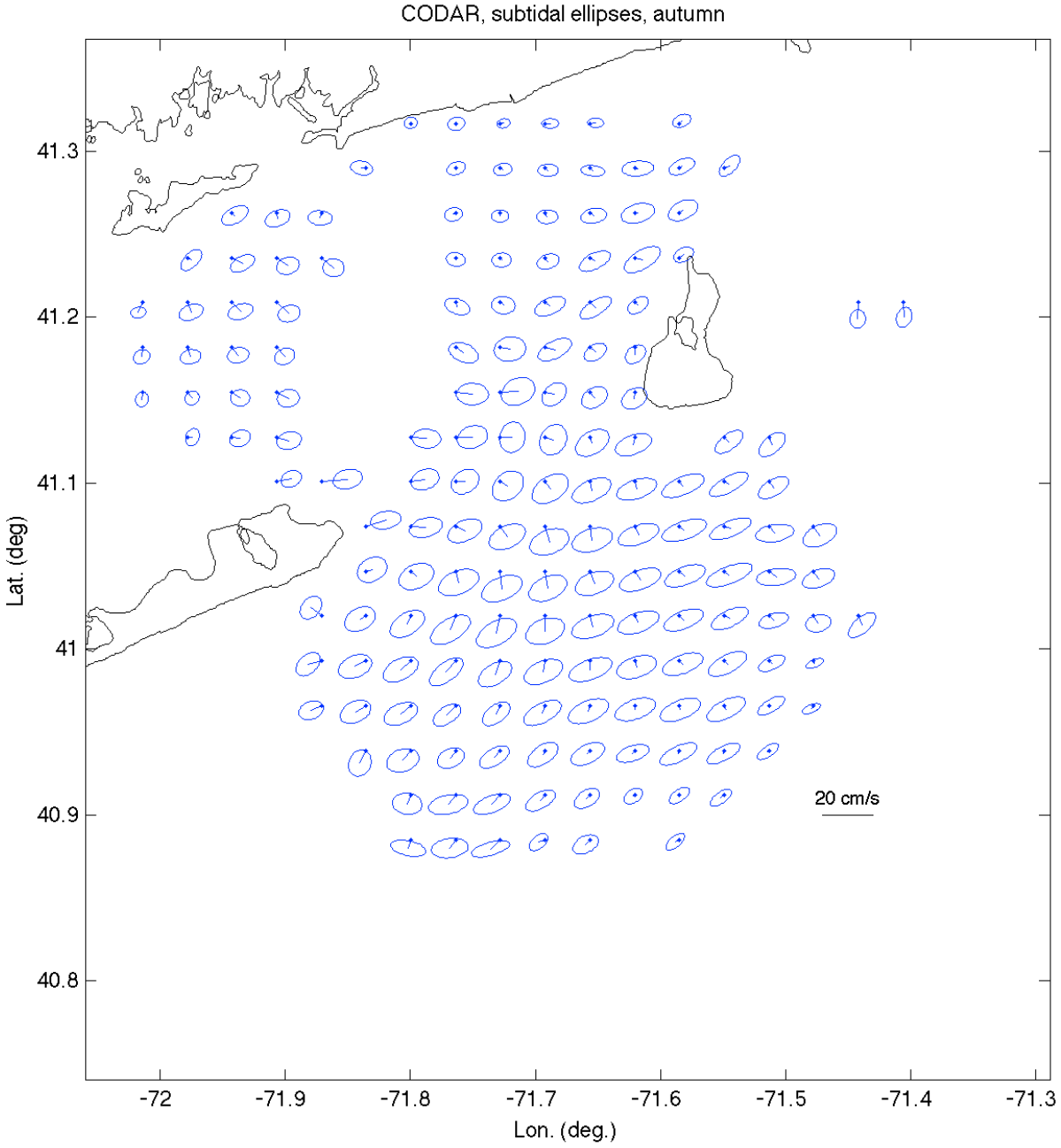

Figure 41. HF radar currents. Fall mean flow and subtidal principal axes ellipses.

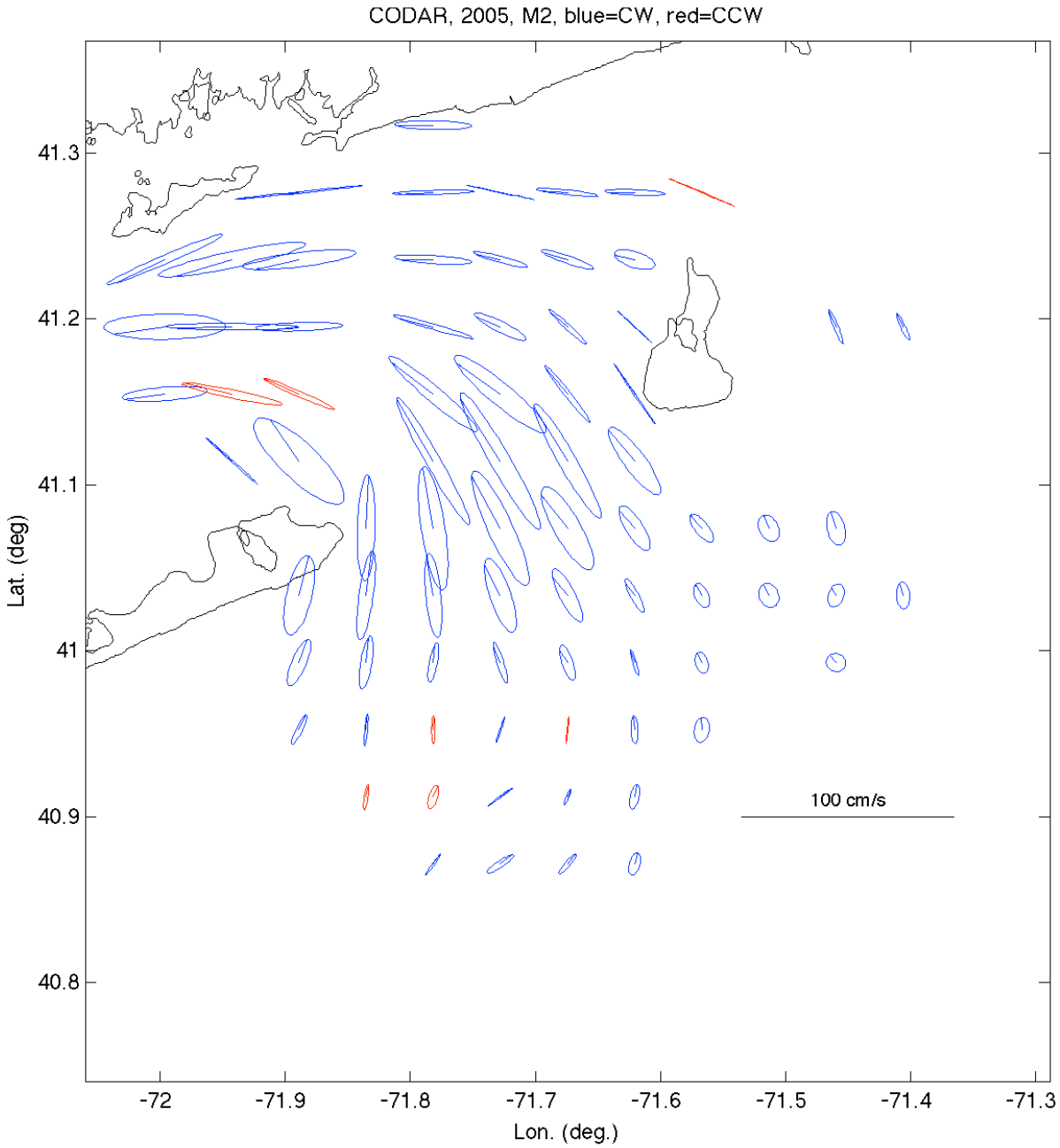

Figure 42. HF radar currents: M_2 tidal ellipses.

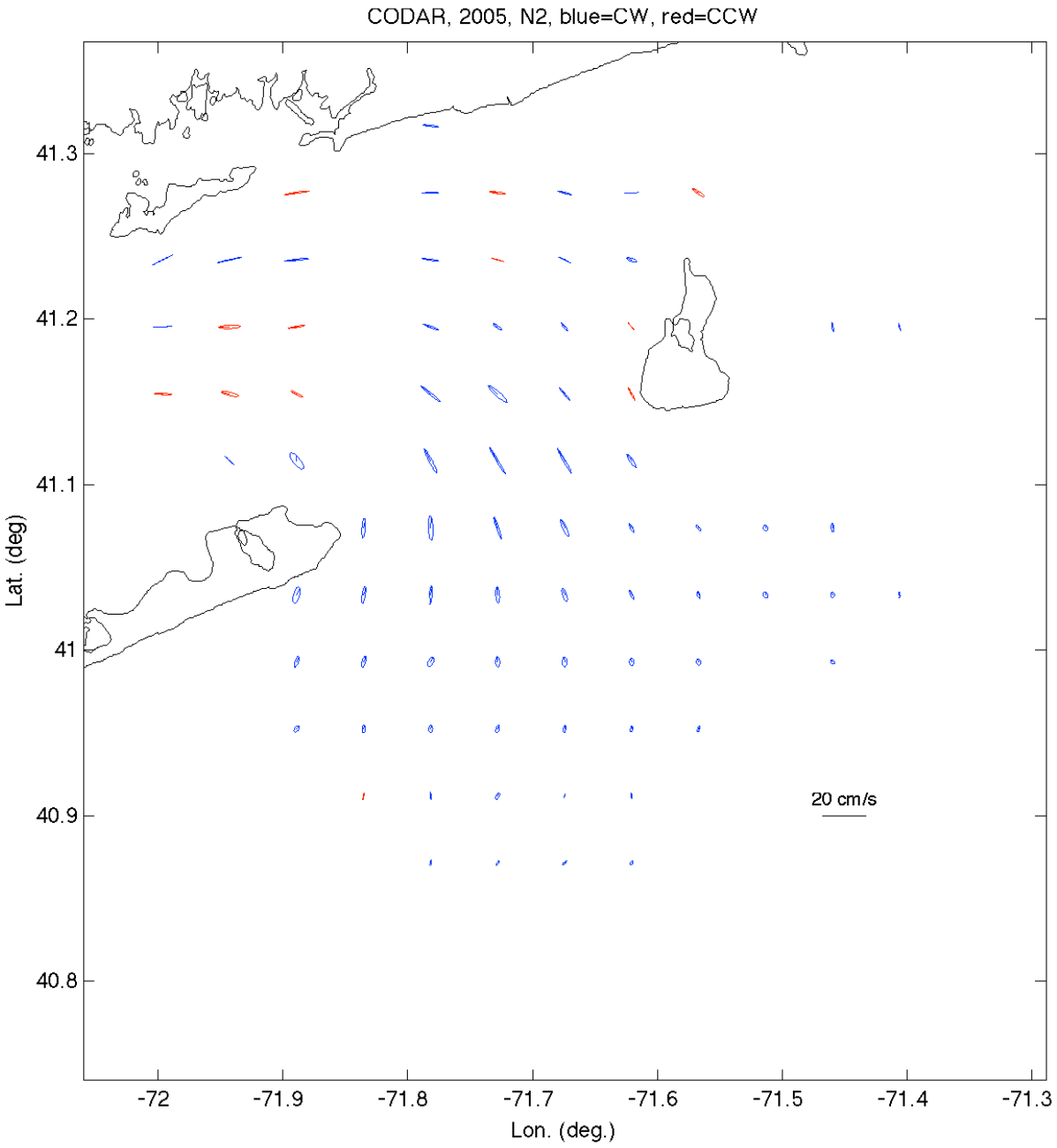

Figure 43. HF radar currents. N_2 tidal ellipses.

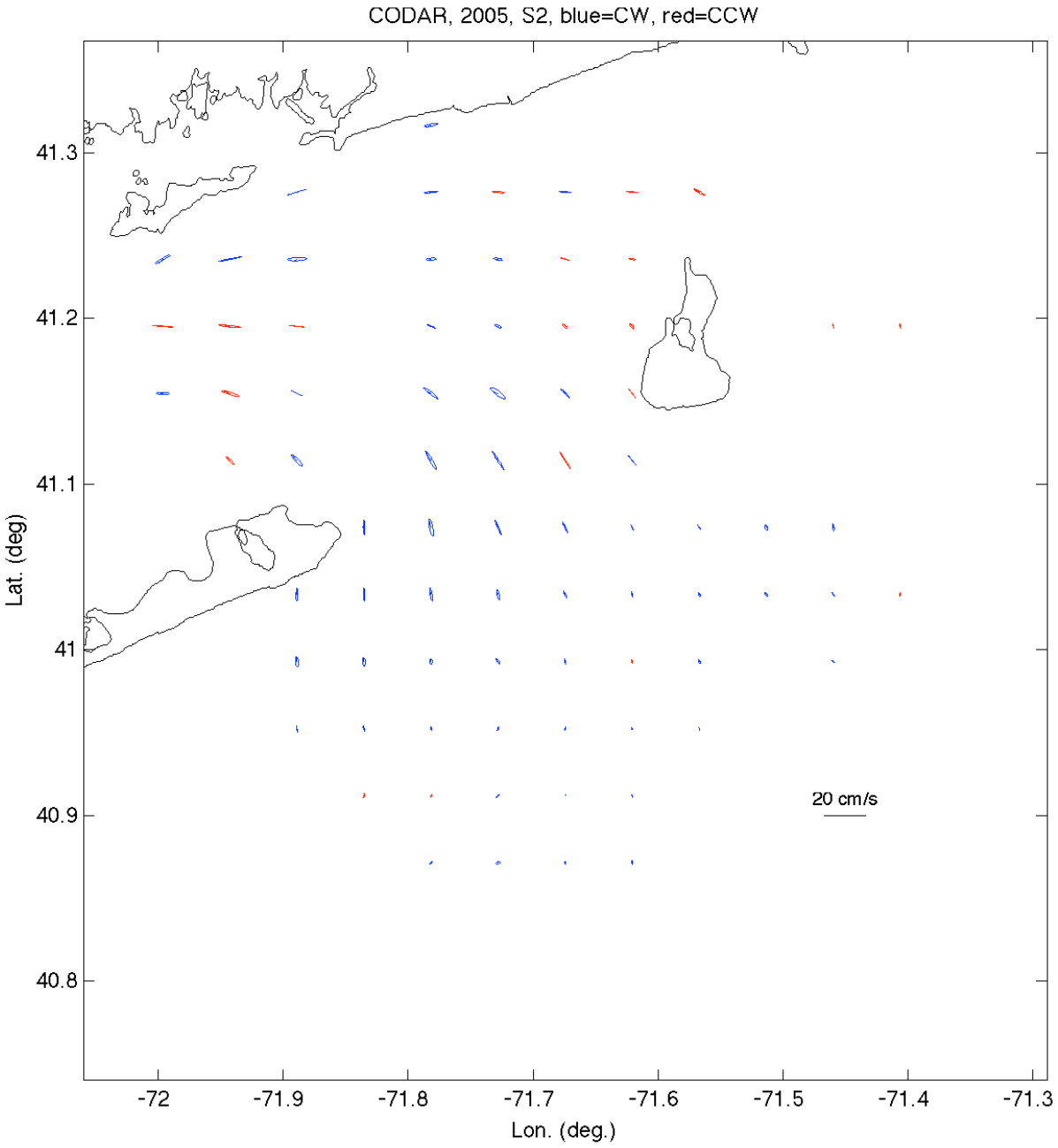

Figure 44. HF radar currents. S_2 tidal ellipses.

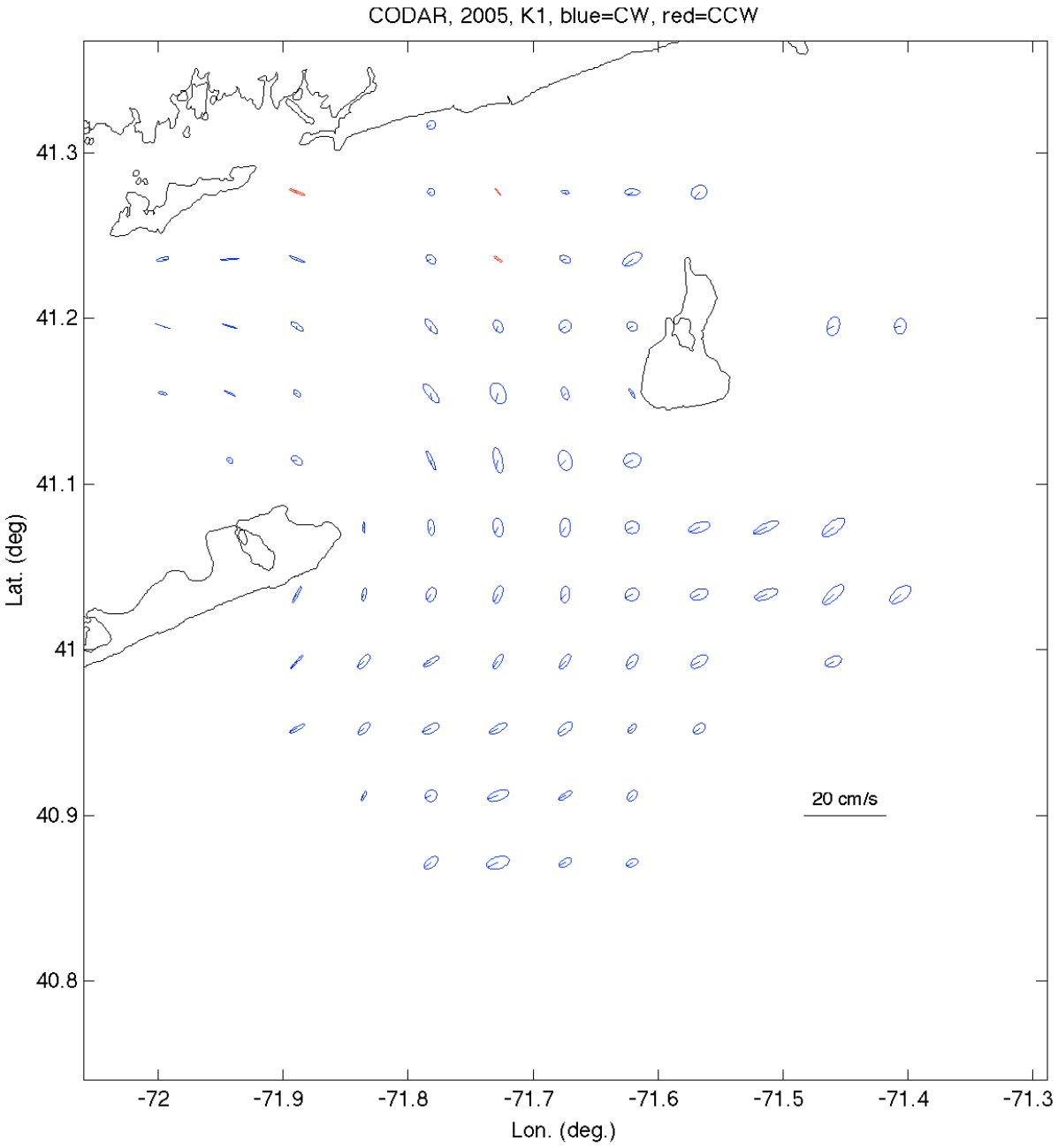

Figure 45. HF radar currents. K_1 tidal ellipses.

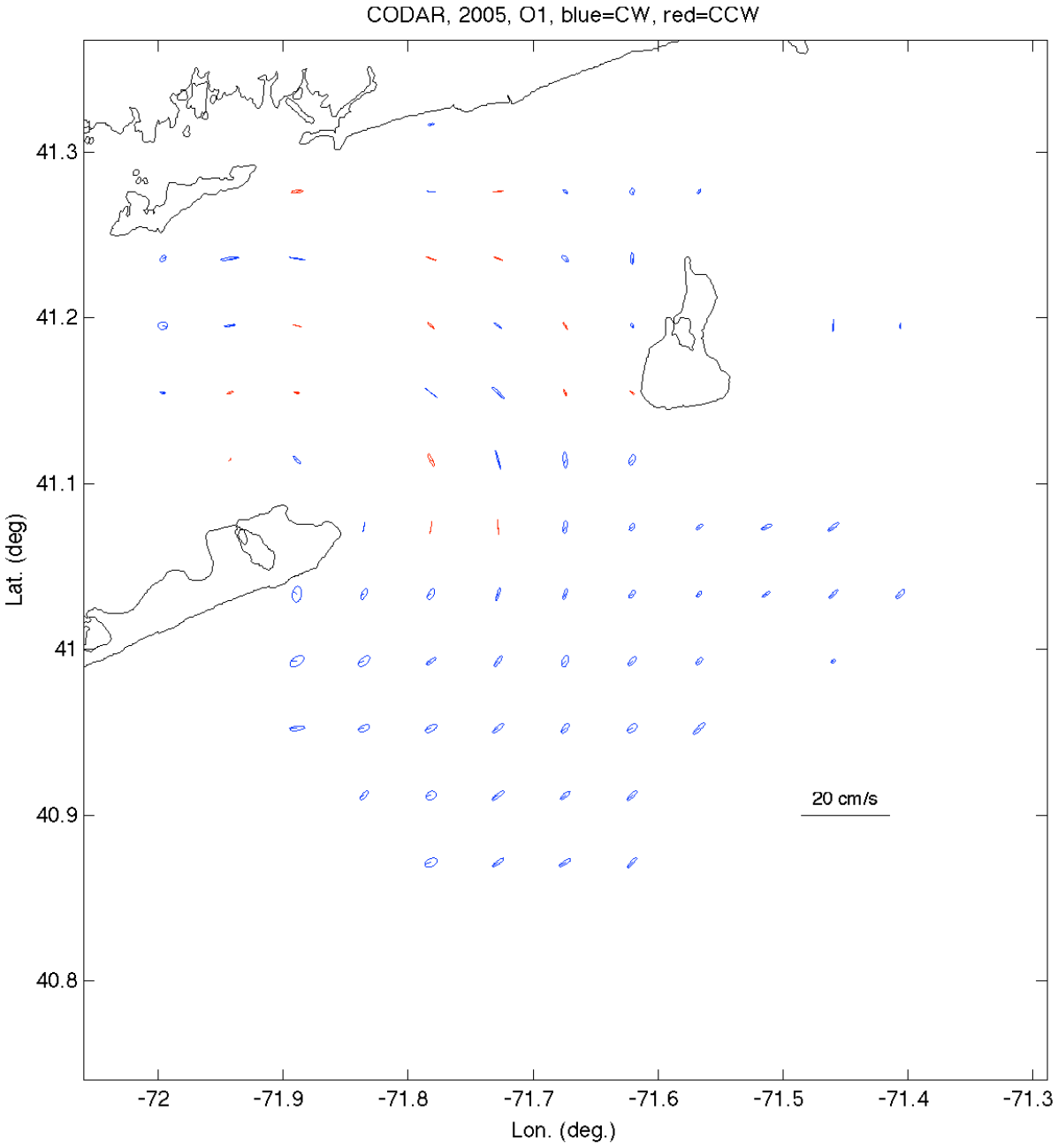

Figure 46. HF radar currents. O_1 tidal ellipses.

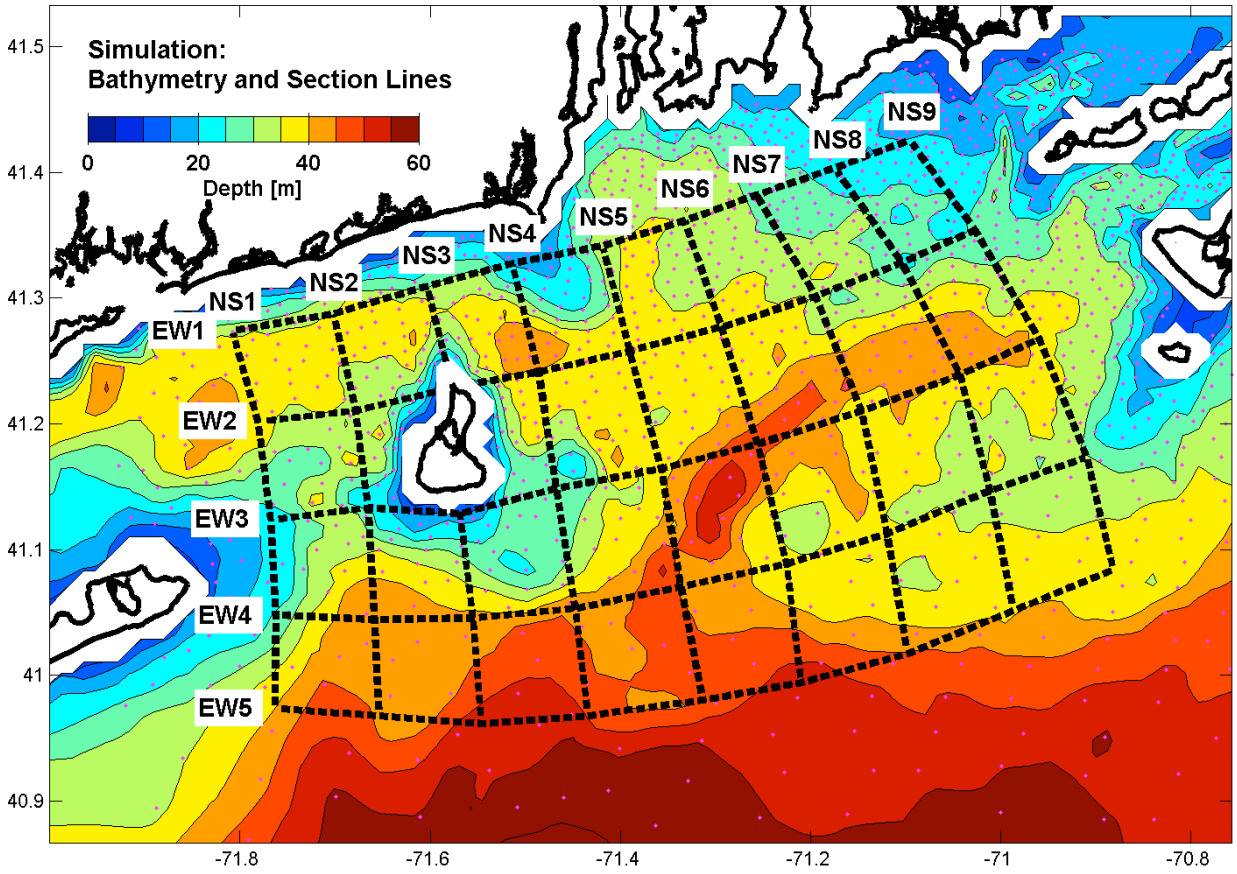

Figure 47. Simulation: Bathymetry, section lines, and grid nodes (sparsified by 3 for clarity).

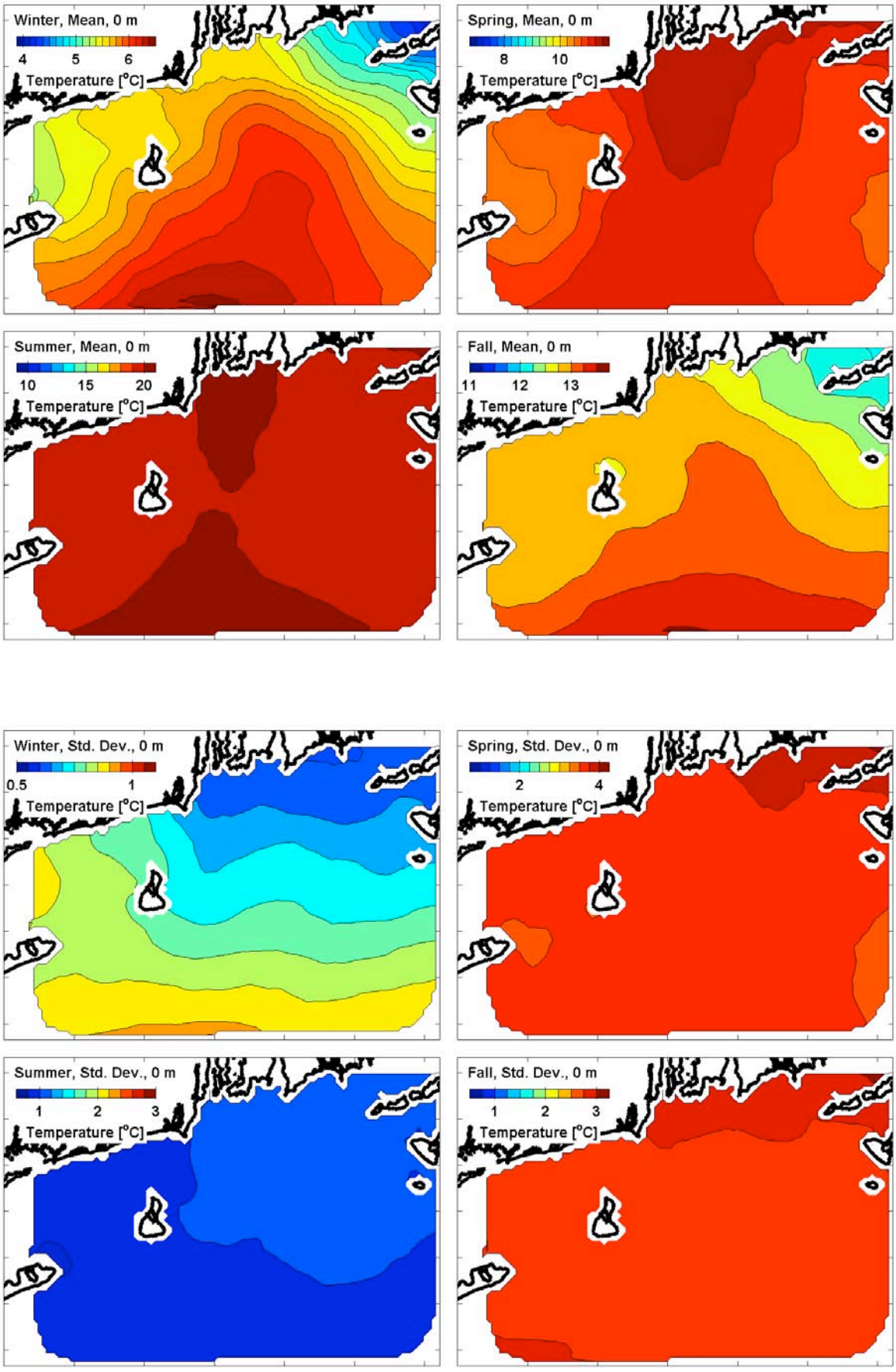

Figure 48. Simulation: Temperature, four seasons, surface. (upper) Mean. (lower) Std. dev.

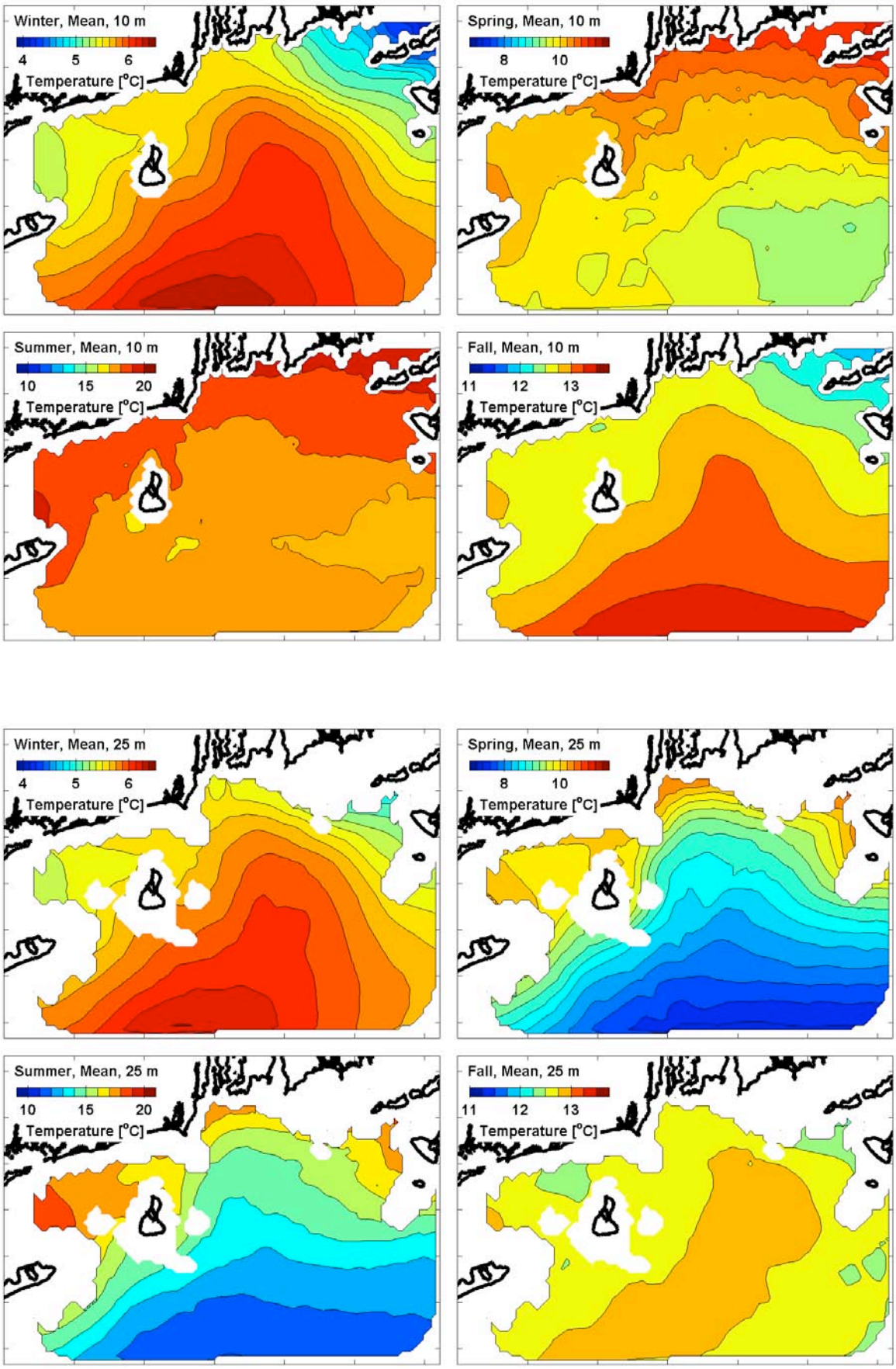

Figure 49. Simulation: Temperature, seasonal-mean. (upper) 10 m deep. (lower) 25 m deep.

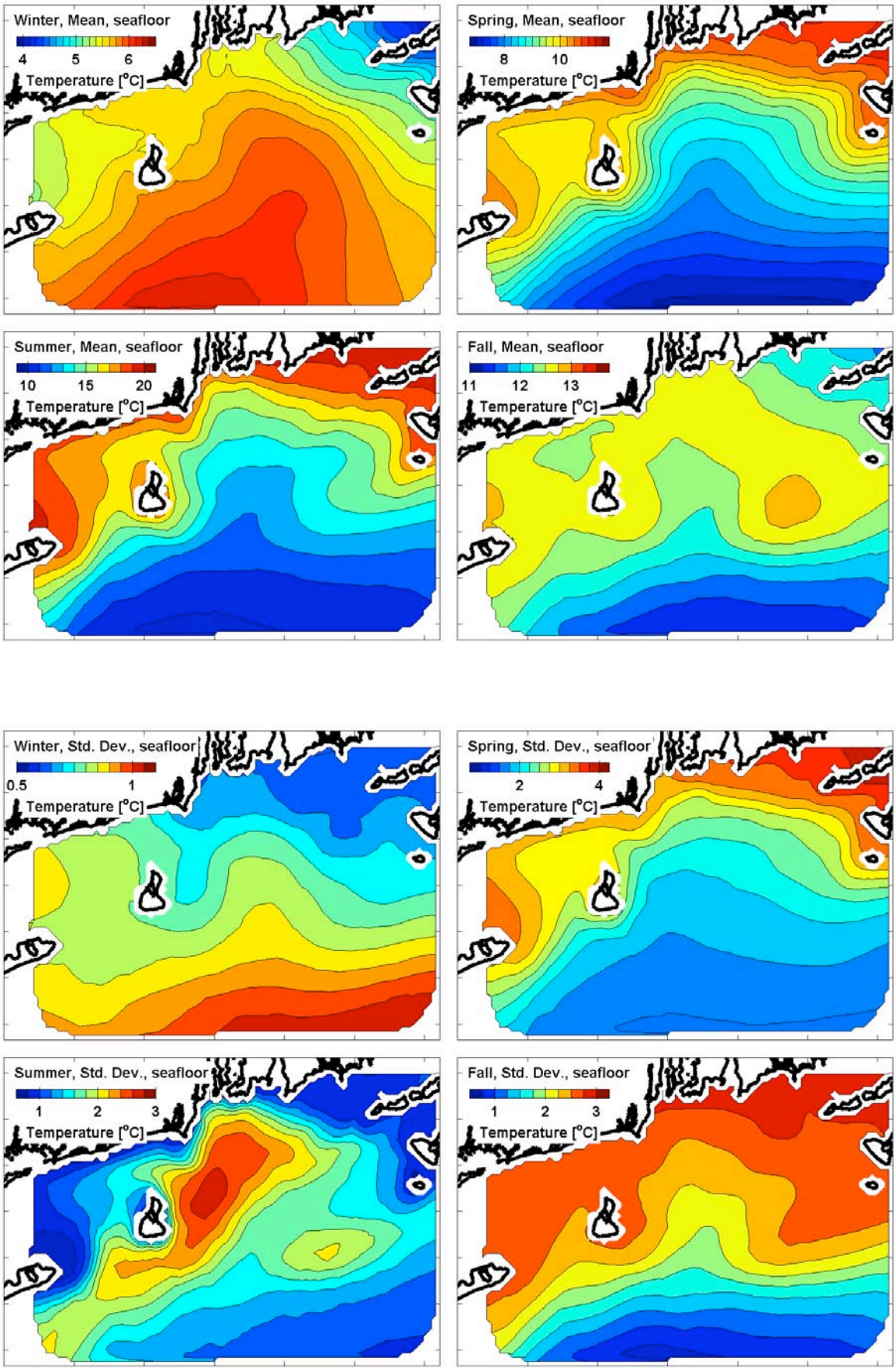

Figure 50. Simulation: Temperature, four seasons, seafloor. (upper) Mean. (lower) Std. dev.

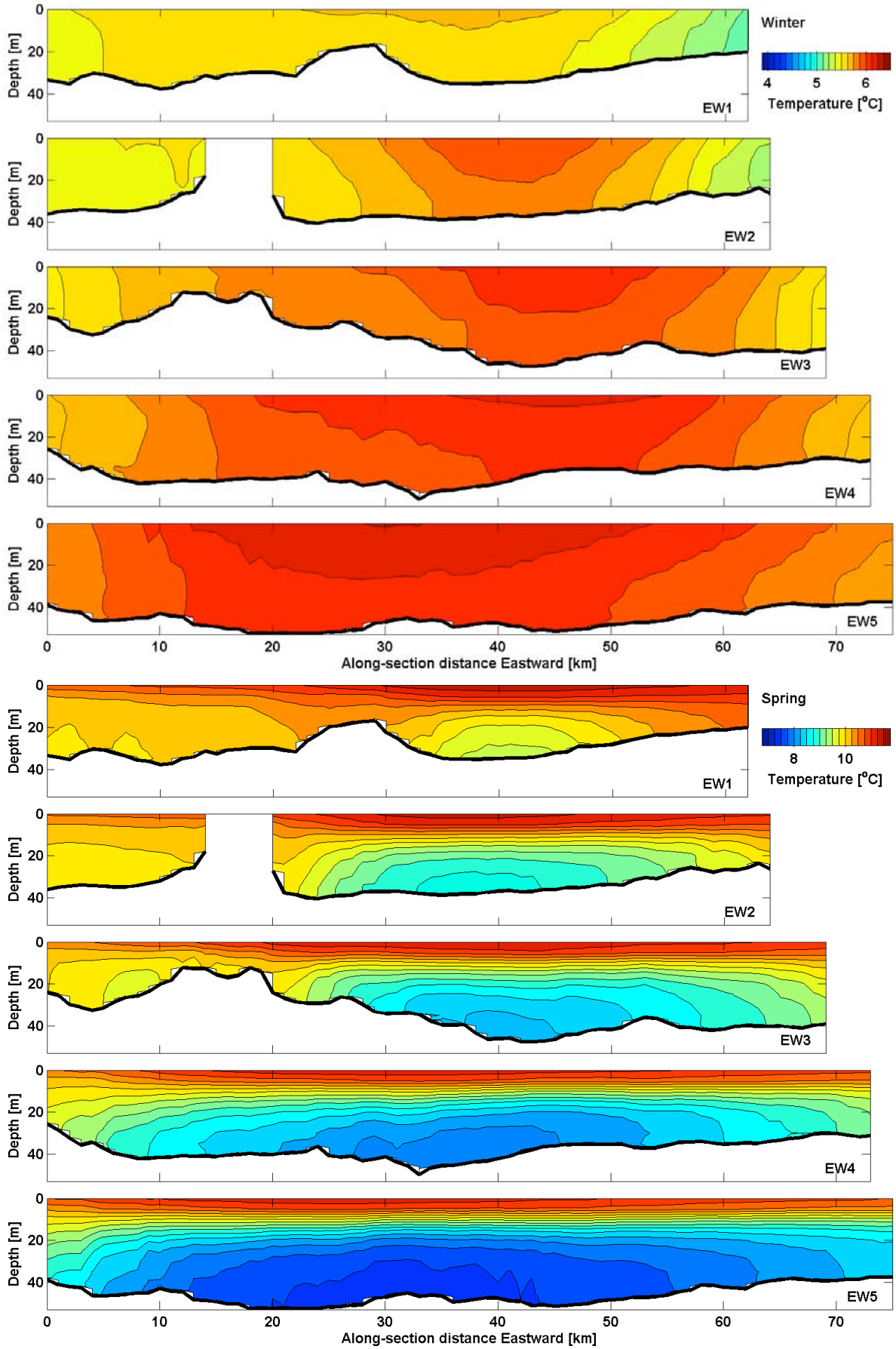

Figure 51. Simulation: Temperature, seasonal-mean, EW. (upper) Winter. (lower) Spring.

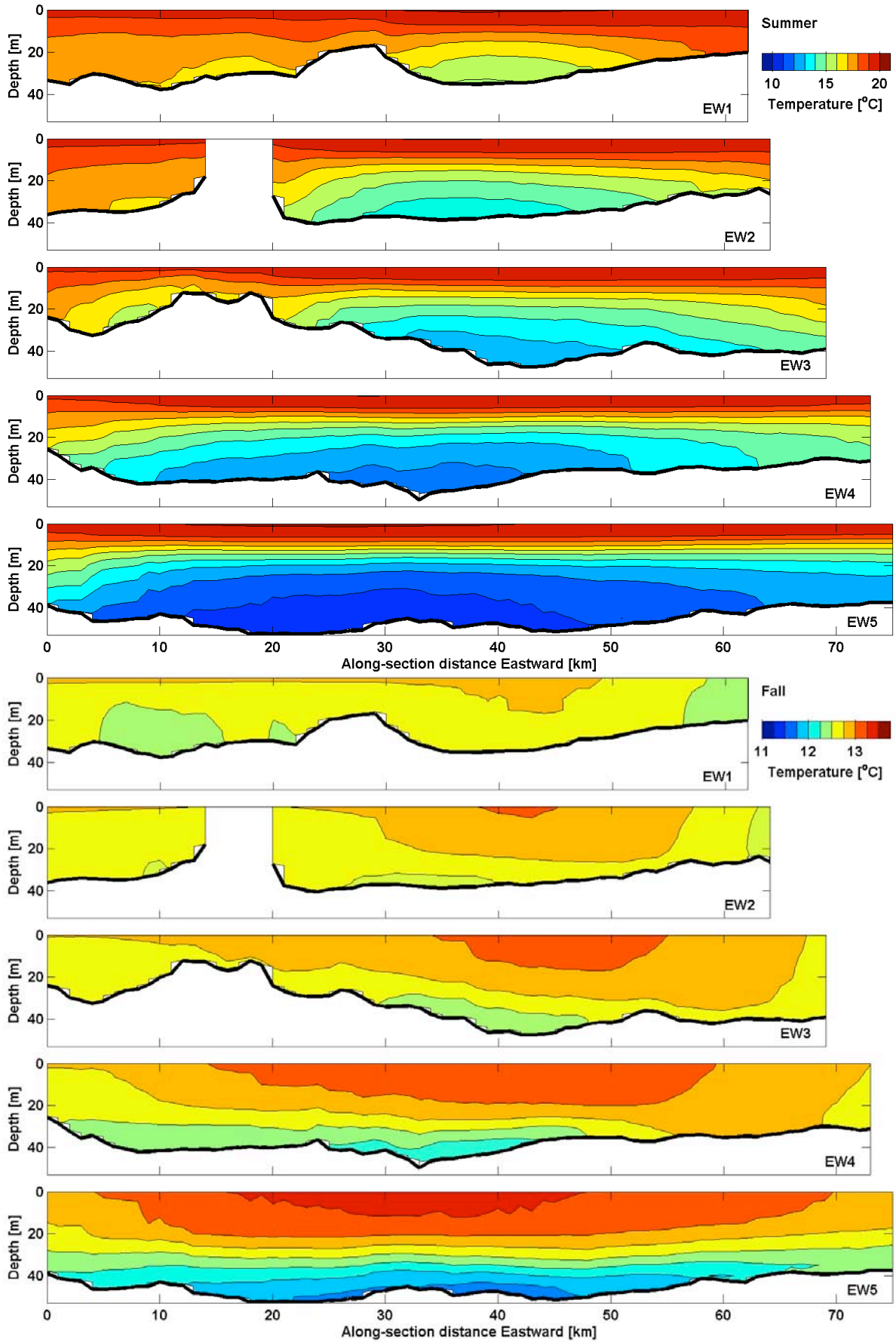

Figure 52. Simulation: Temperature, seasonal-mean, EW. (upper) Summer. (lower) Fall.

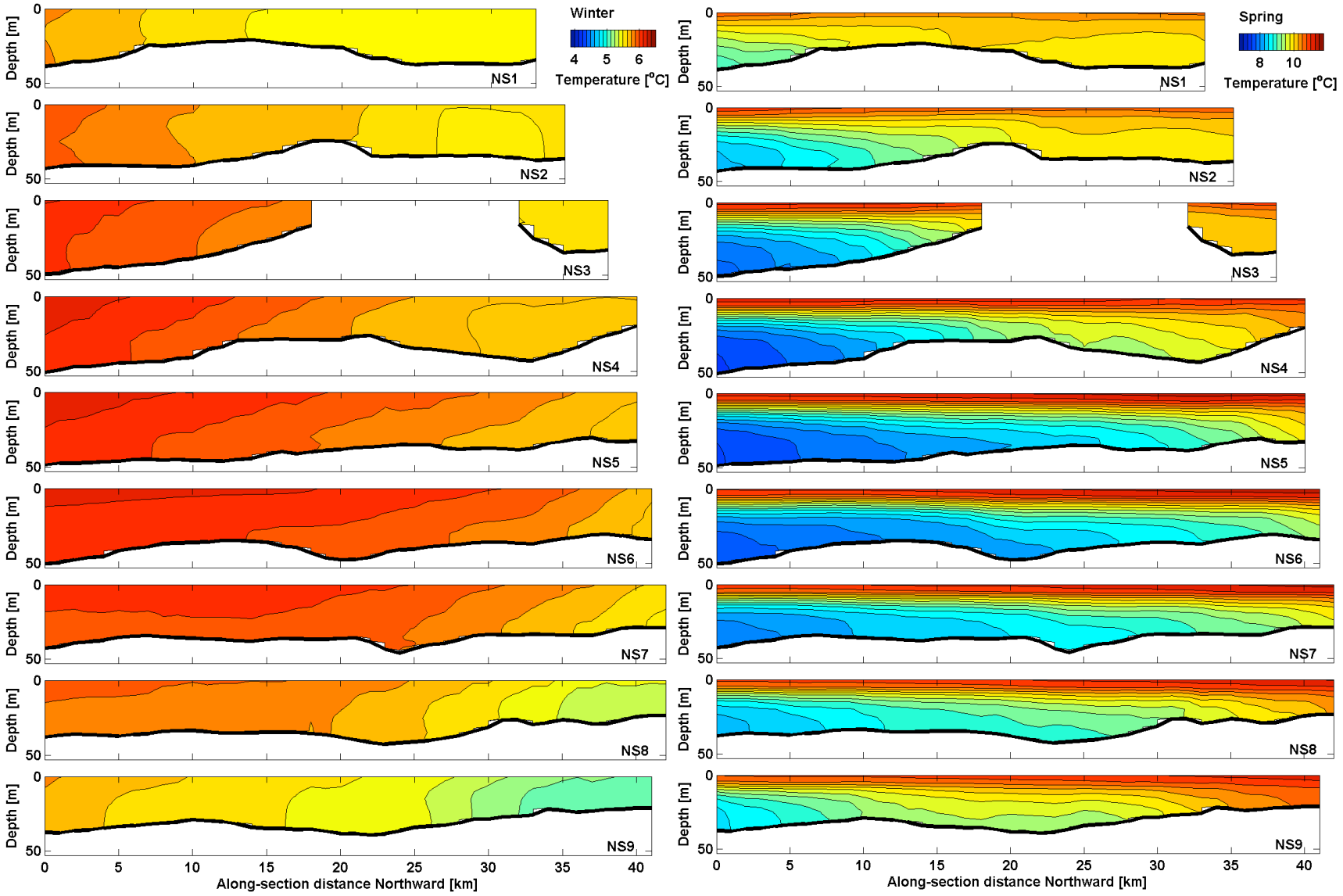

Figure 53. Simulation: Temperature, seasonal-mean, NS. (left) Winter. (right) Spring.

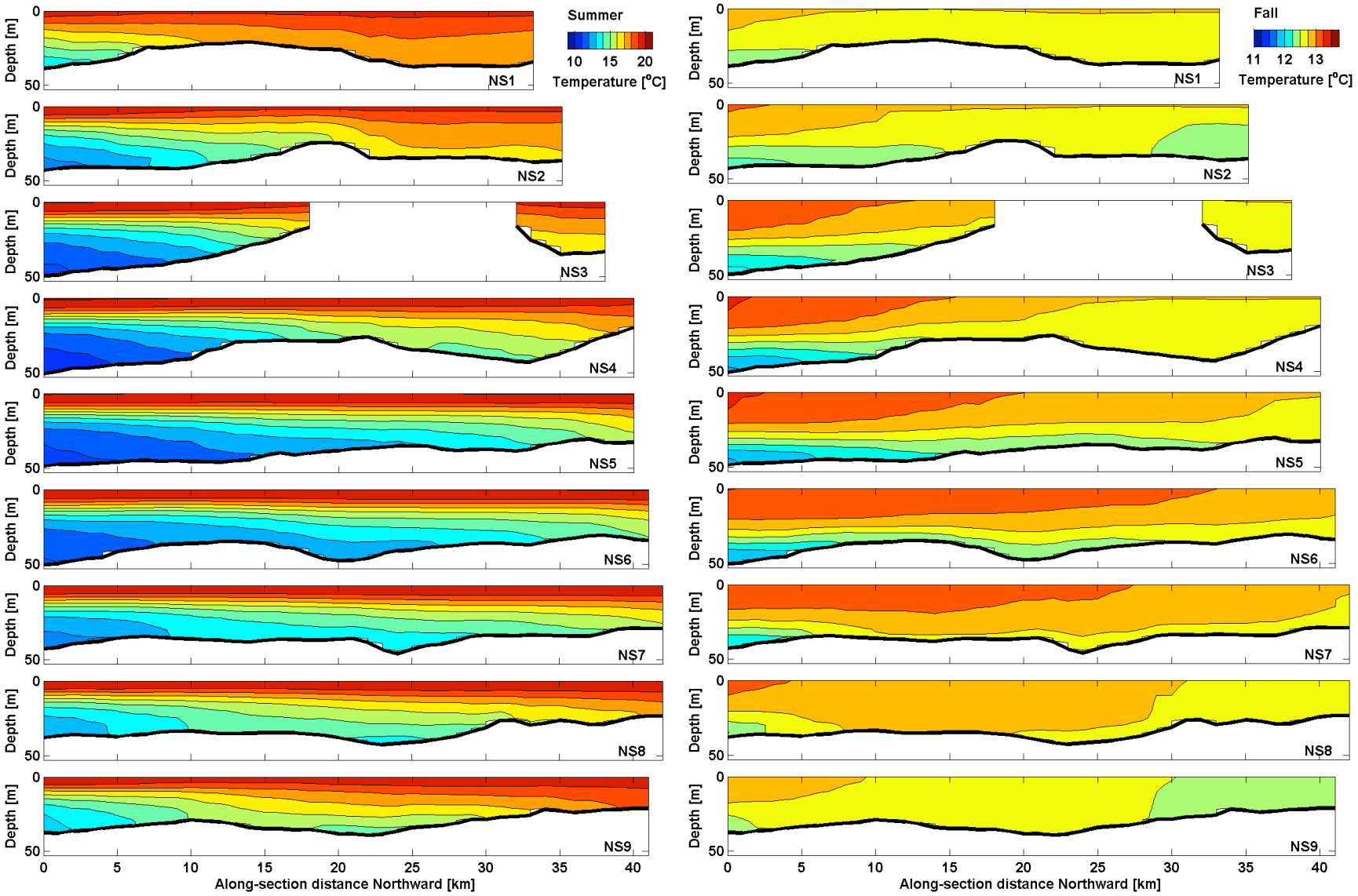

Figure 54. Simulation: Temperature, seasonal-mean, NS. (left) Summer. (right) Fall.

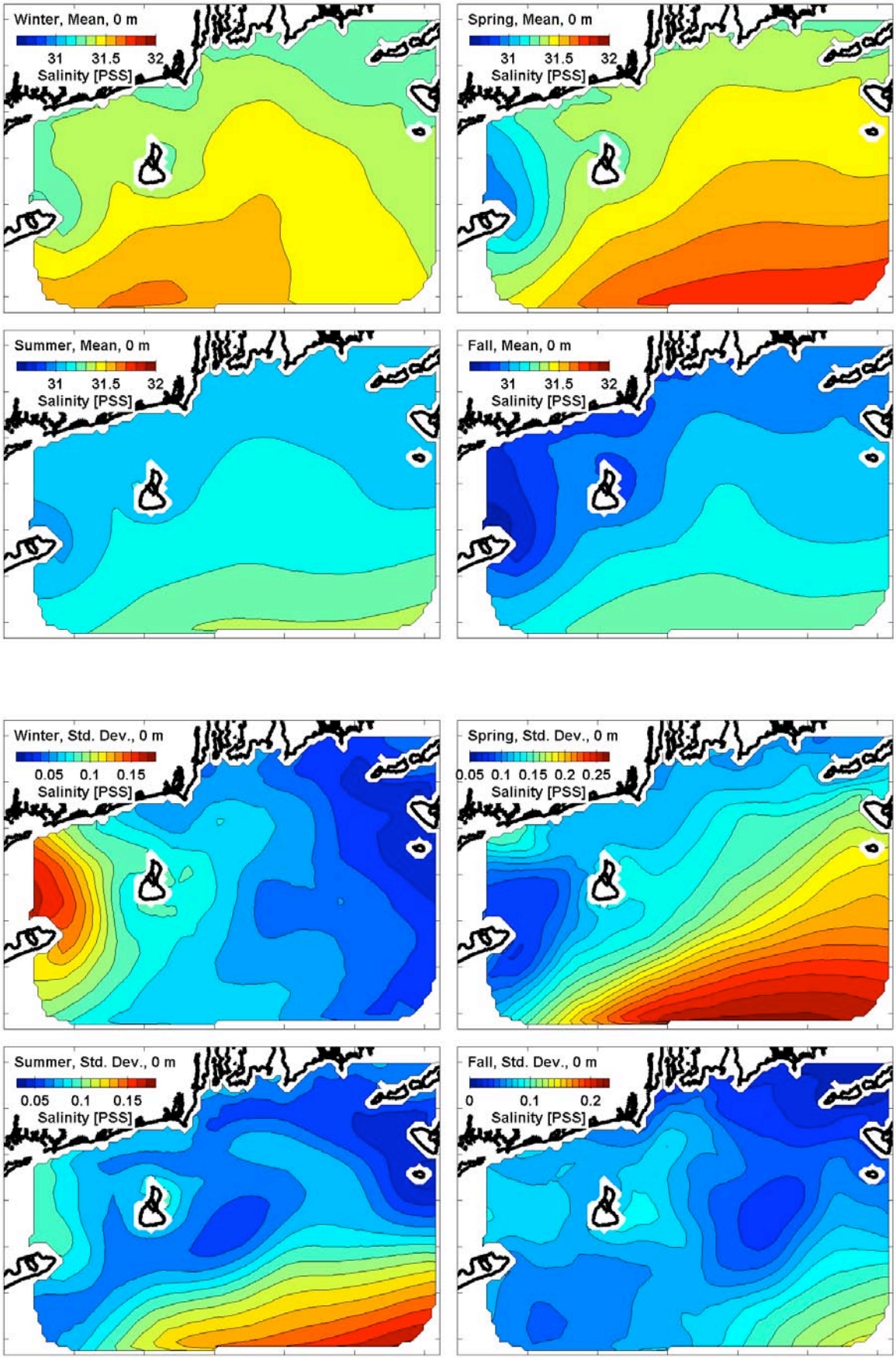

Figure 55. Simulation: Salinity, four seasons, surface. (upper) Mean. (lower) Std. dev.

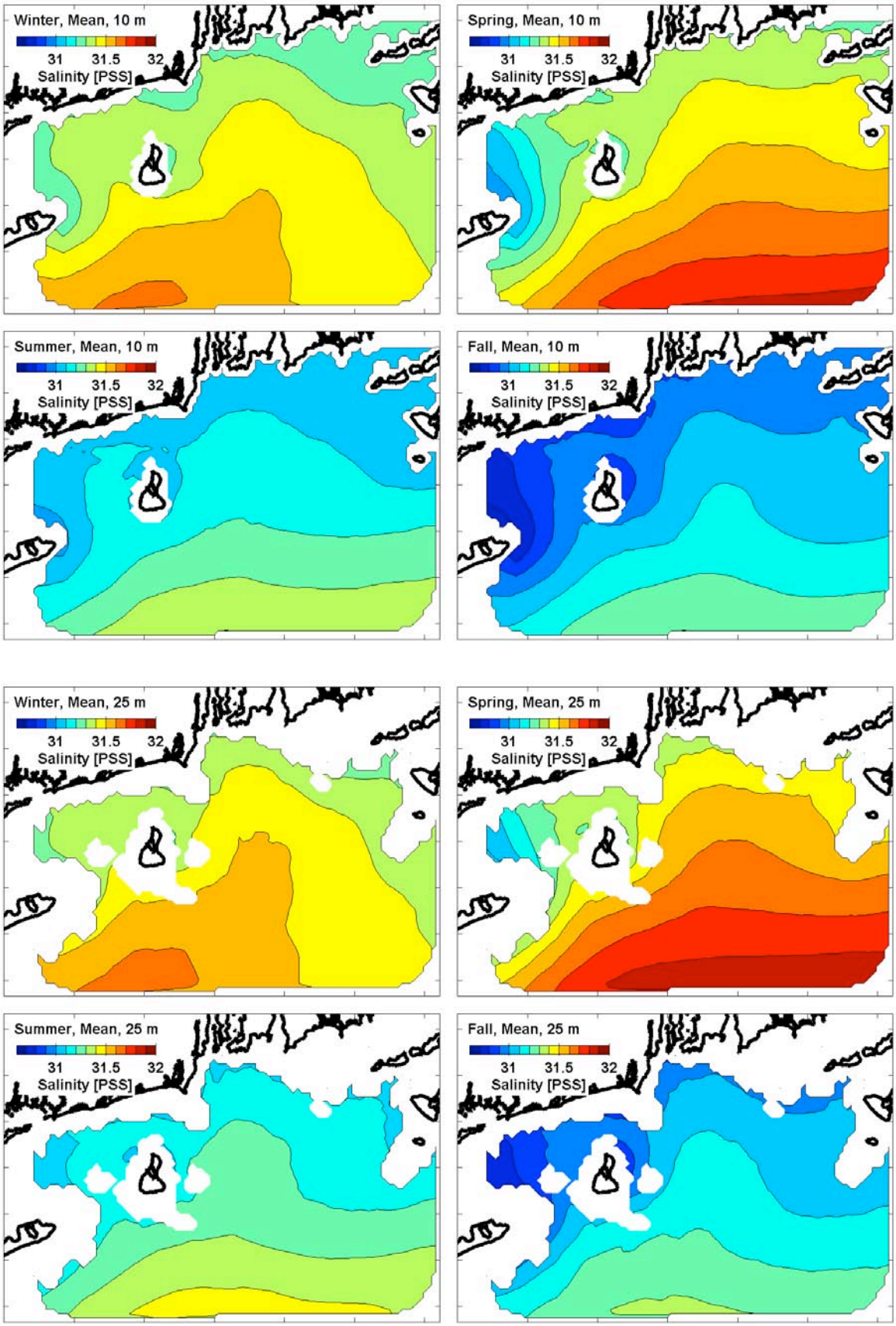

Figure 56. Simulation: Salinity, seasonal-mean. (upper) 10 m deep. (lower) 25 m deep.

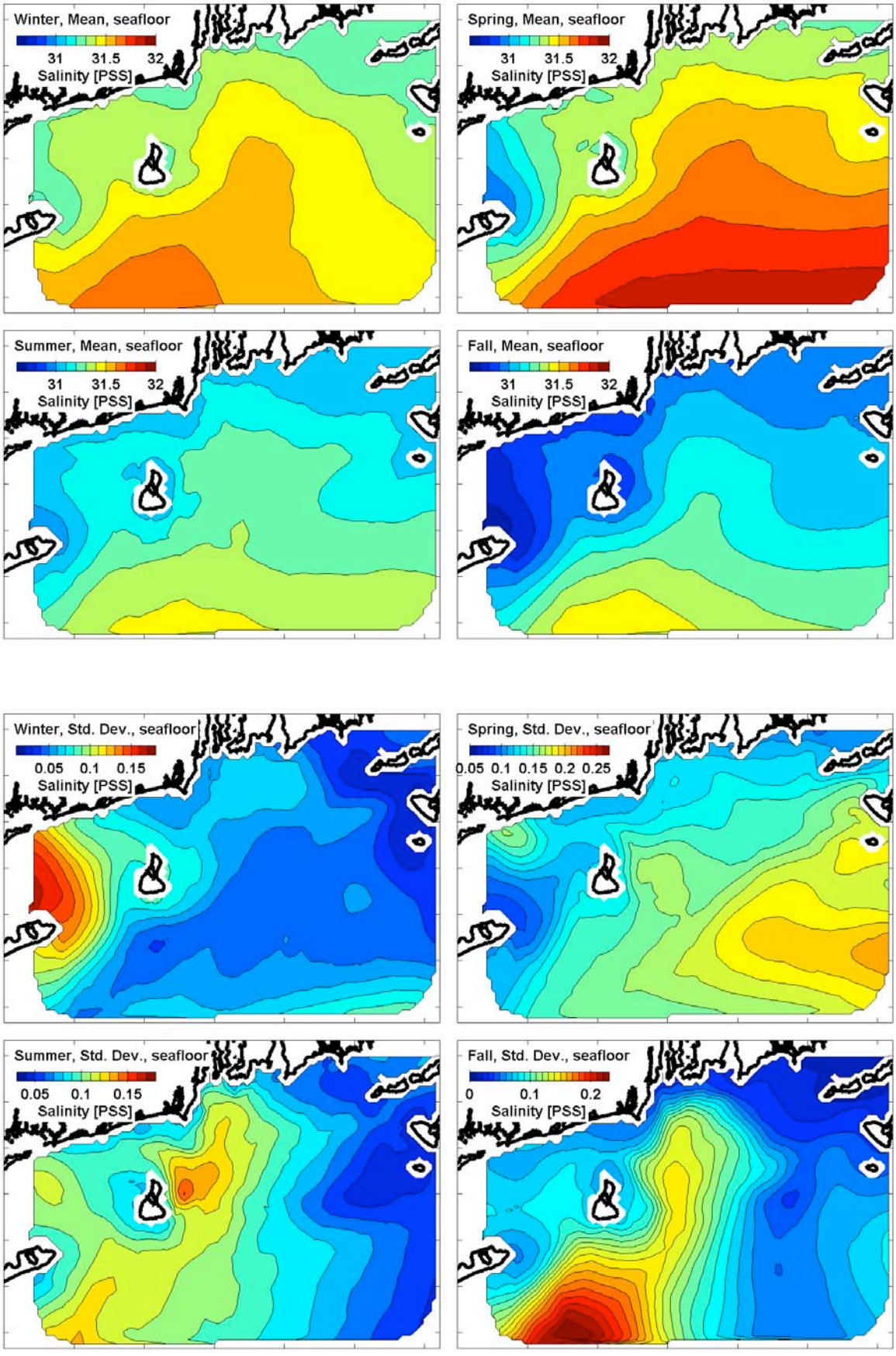

Figure 57. Simulation: Salinity, four seasons, seafloor. (upper) Mean. (lower) Std. dev.

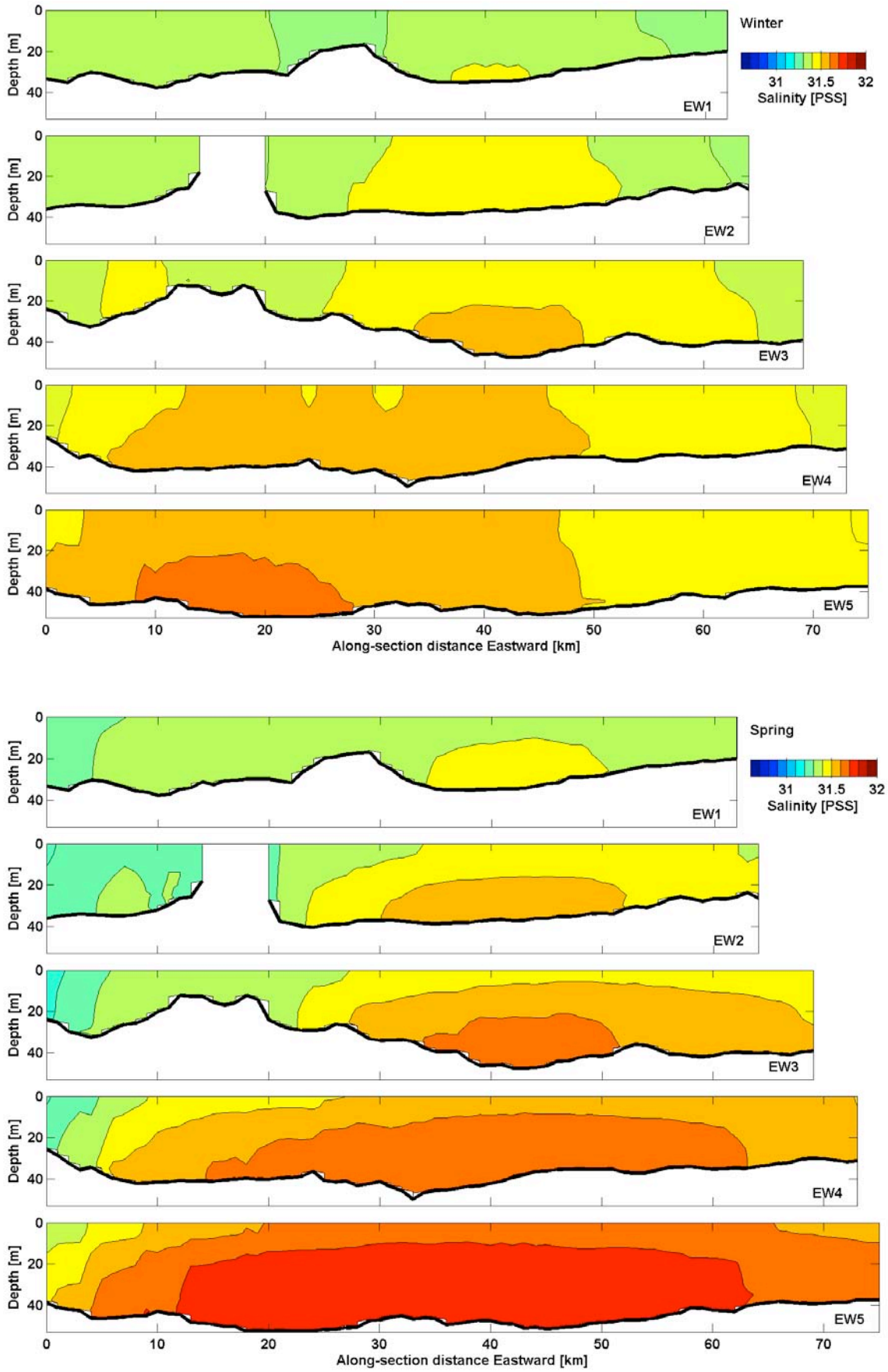

Figure 58. Simulation: Salinity, seasonal-mean, EW. (upper) Winter. (lower) Spring.

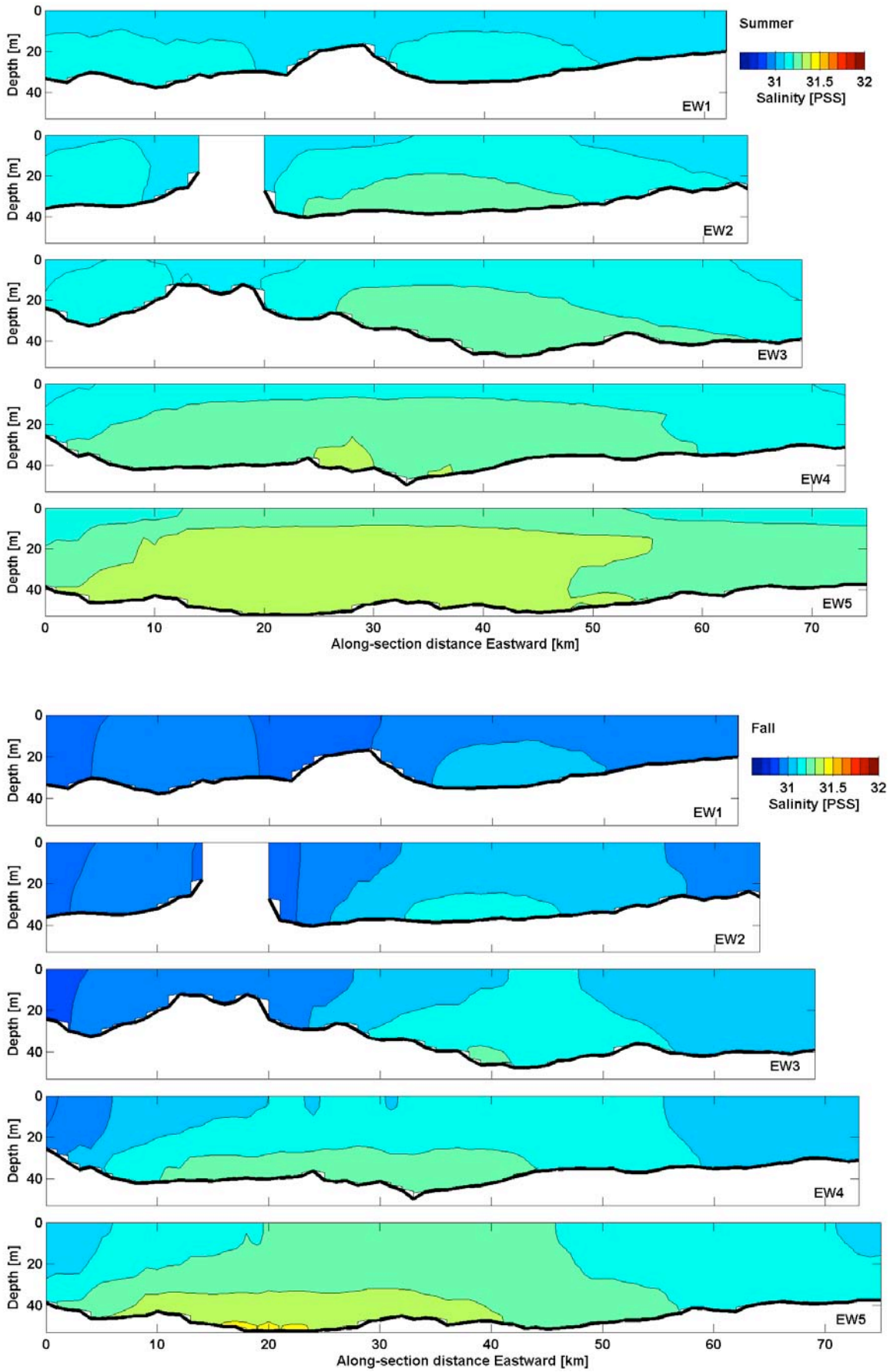

Figure 59. Simulation: Salinity, seasonal-mean, EW. (upper) Summer. (lower) Fall.

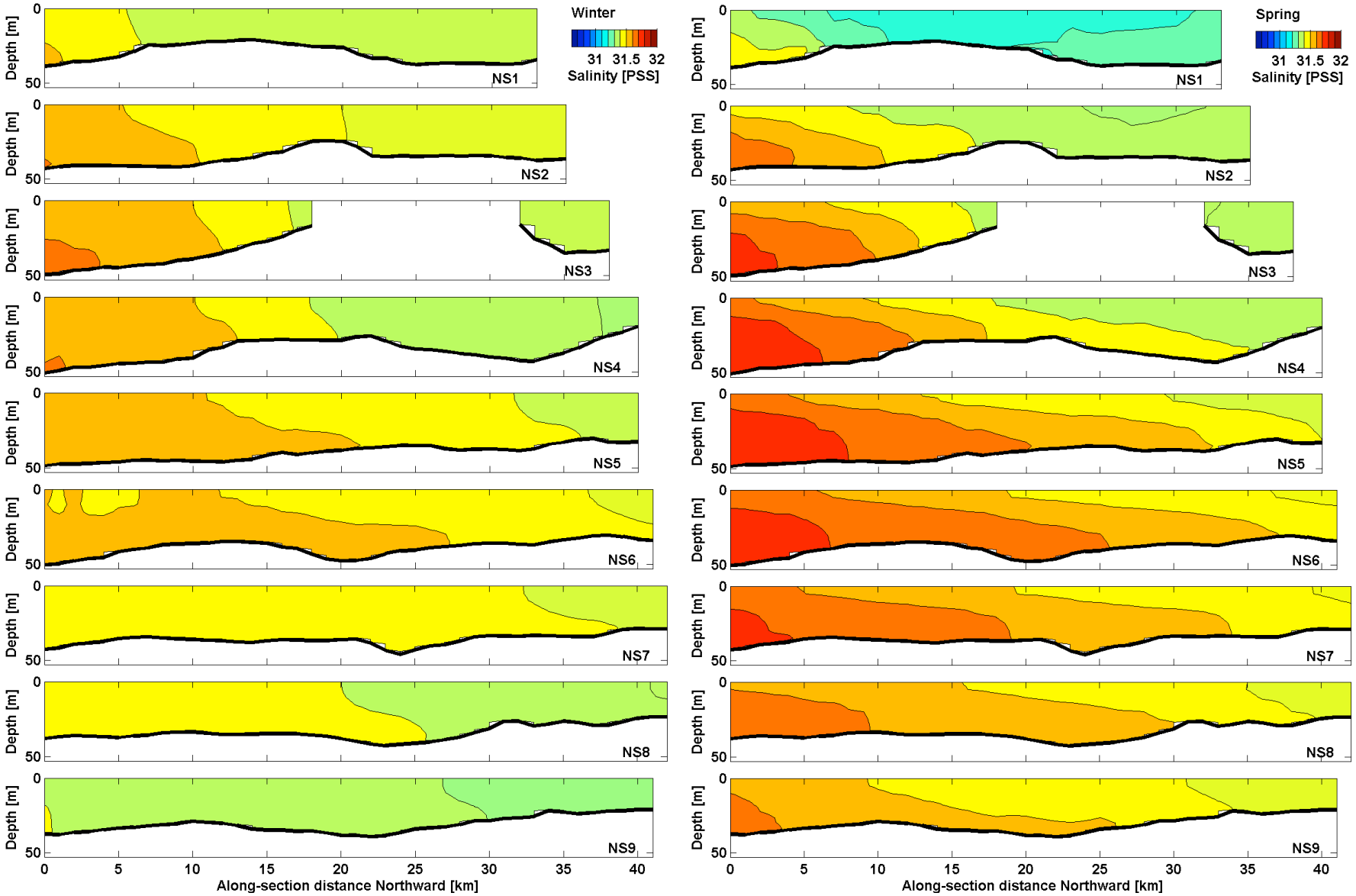

Figure 60. Simulation: Salinity, seasonal-mean, NS. (left) Winter. (right) Spring.

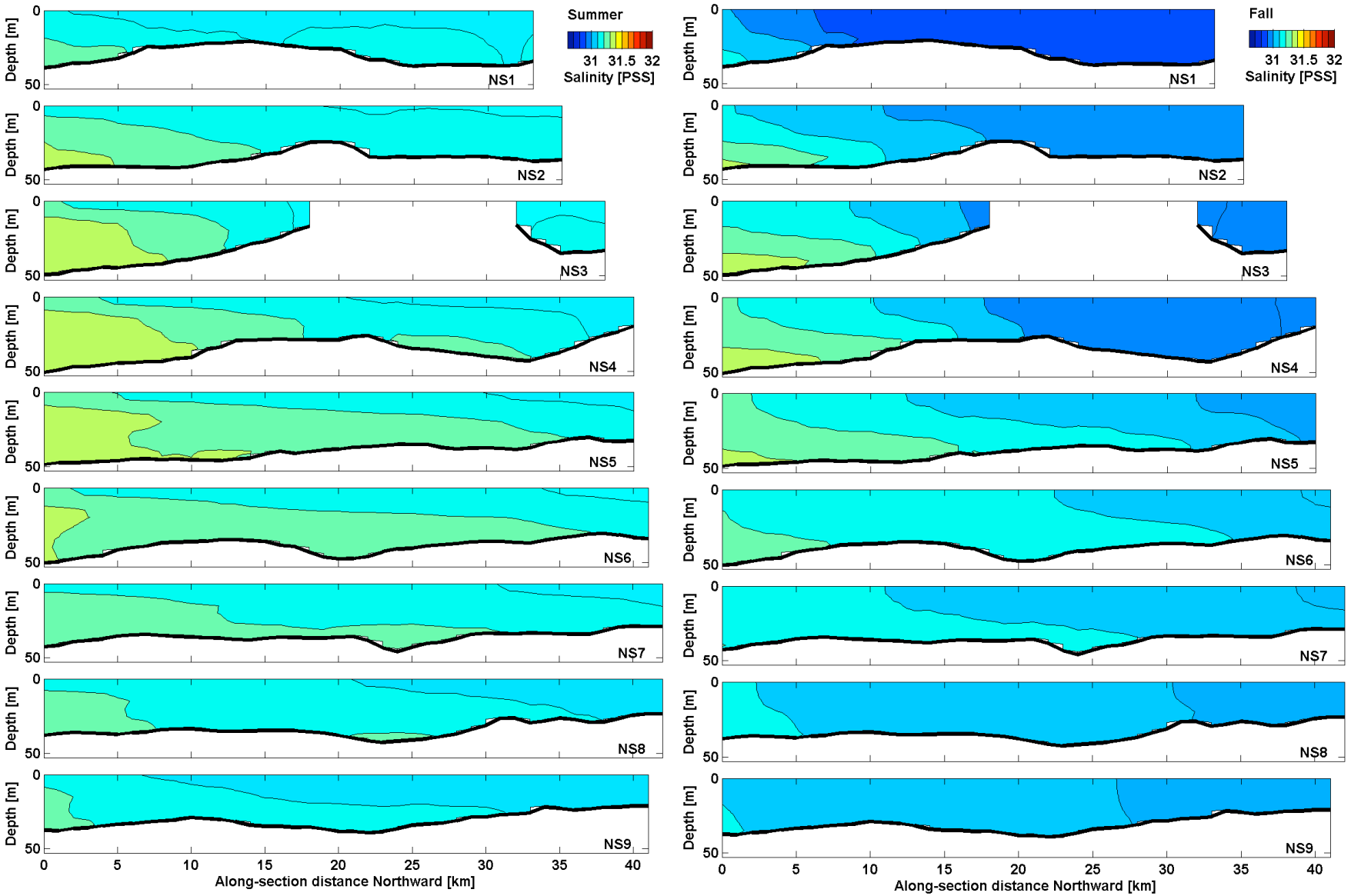

Figure 61. Simulation: Salinity, seasonal-mean, NS. (left) Summer. (right) Fall.

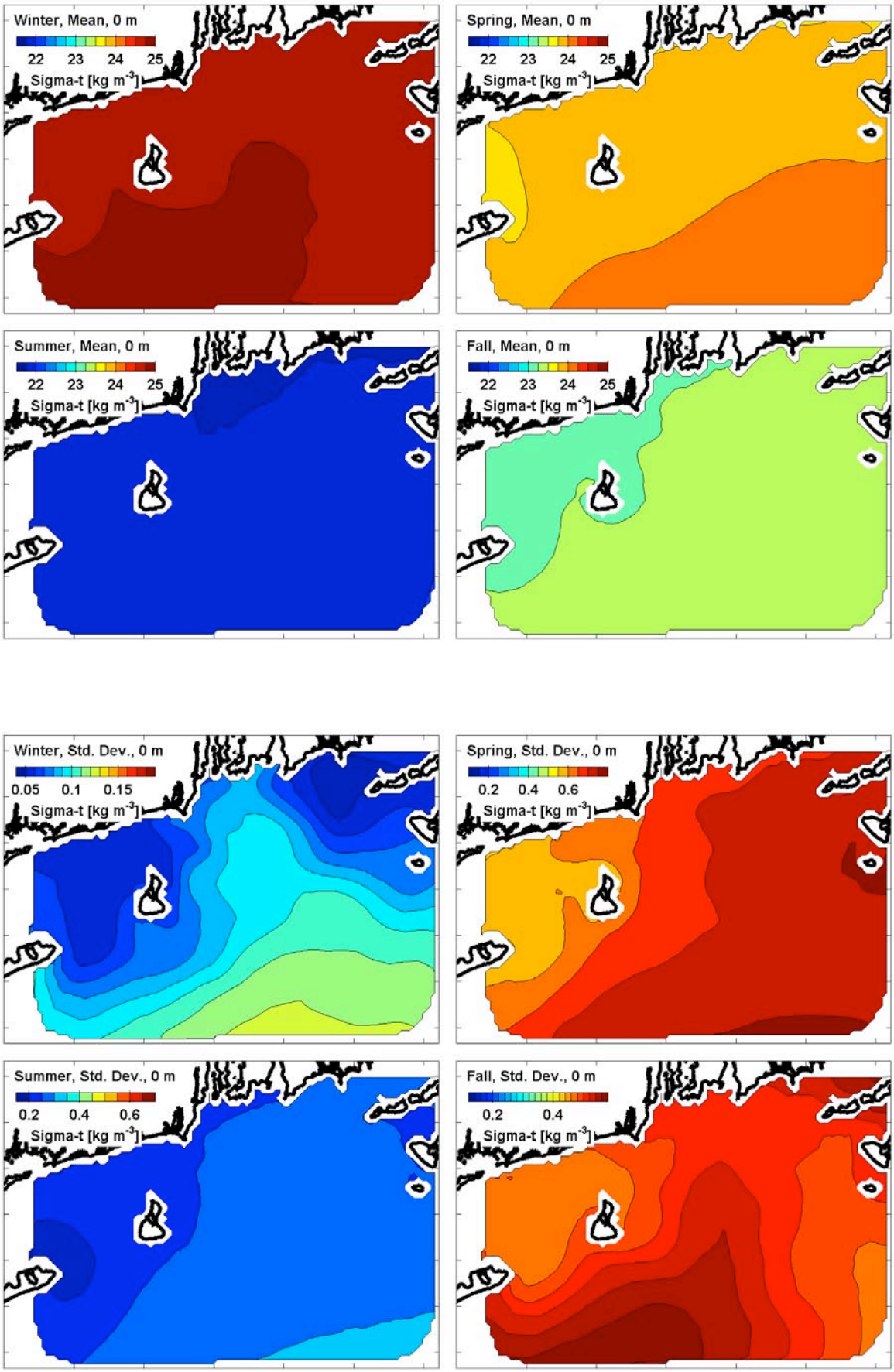

Figure 62. Simulation: Density anomaly, four seasons, surface. (upper) Mean. (lower) Std. dev.

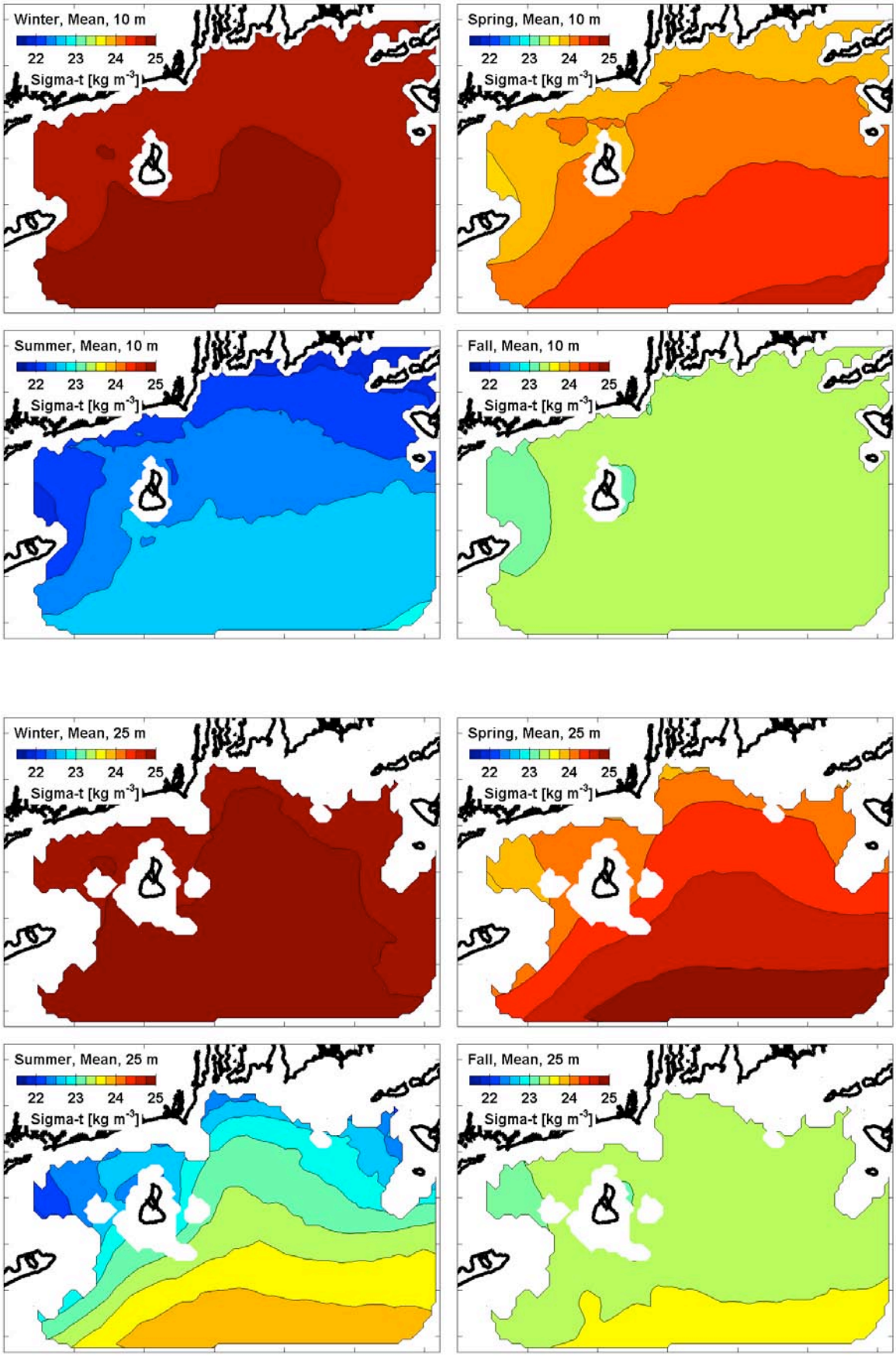

Figure 63. Simulation: Density anomaly, seasonal mean. (upper) 10 m deep. (lower) 25 m deep.

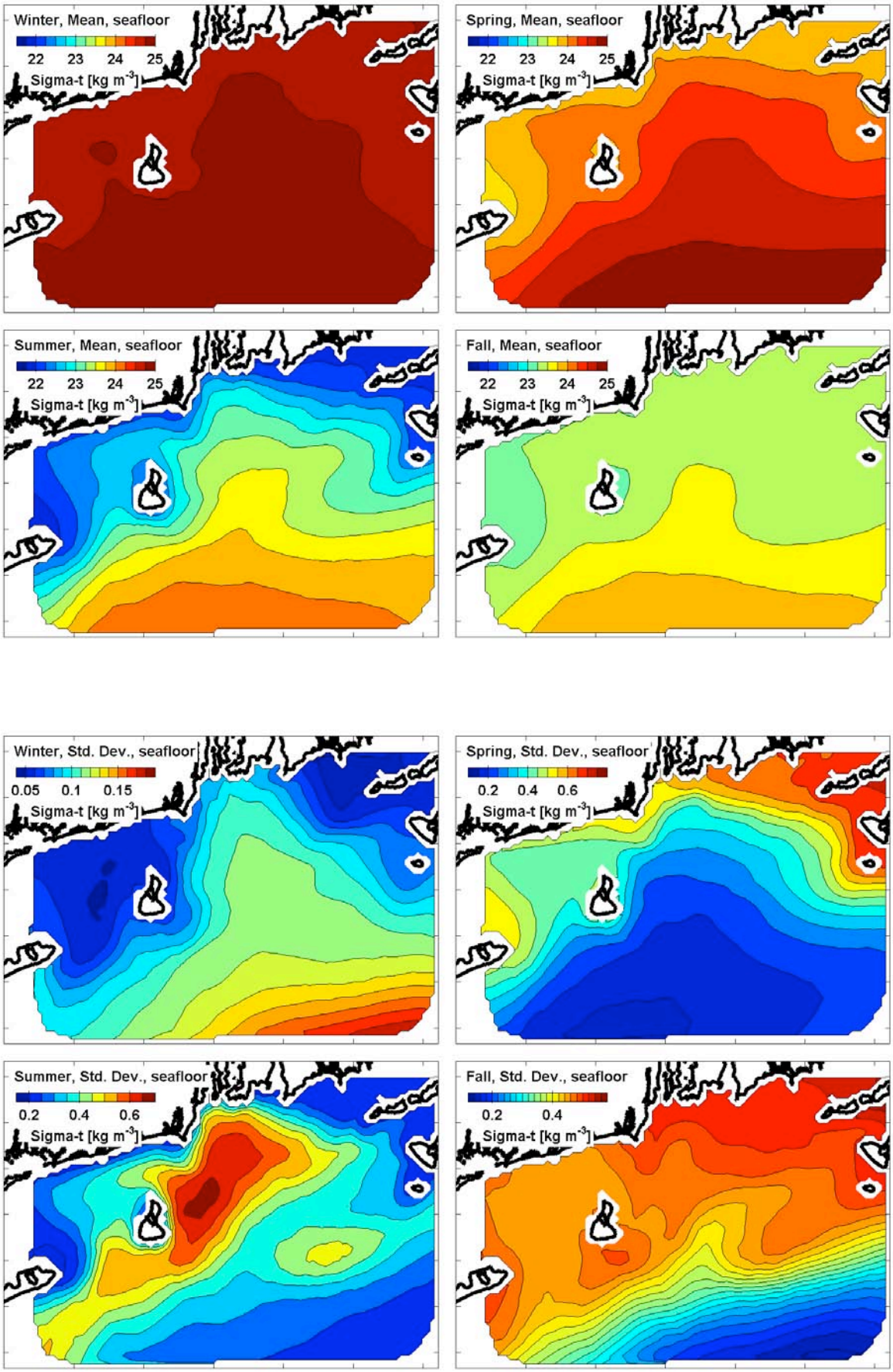

Figure 64. Simulation: Density anomaly, four seasons, seafloor. (upper) Mean. (lower) Std. dev.

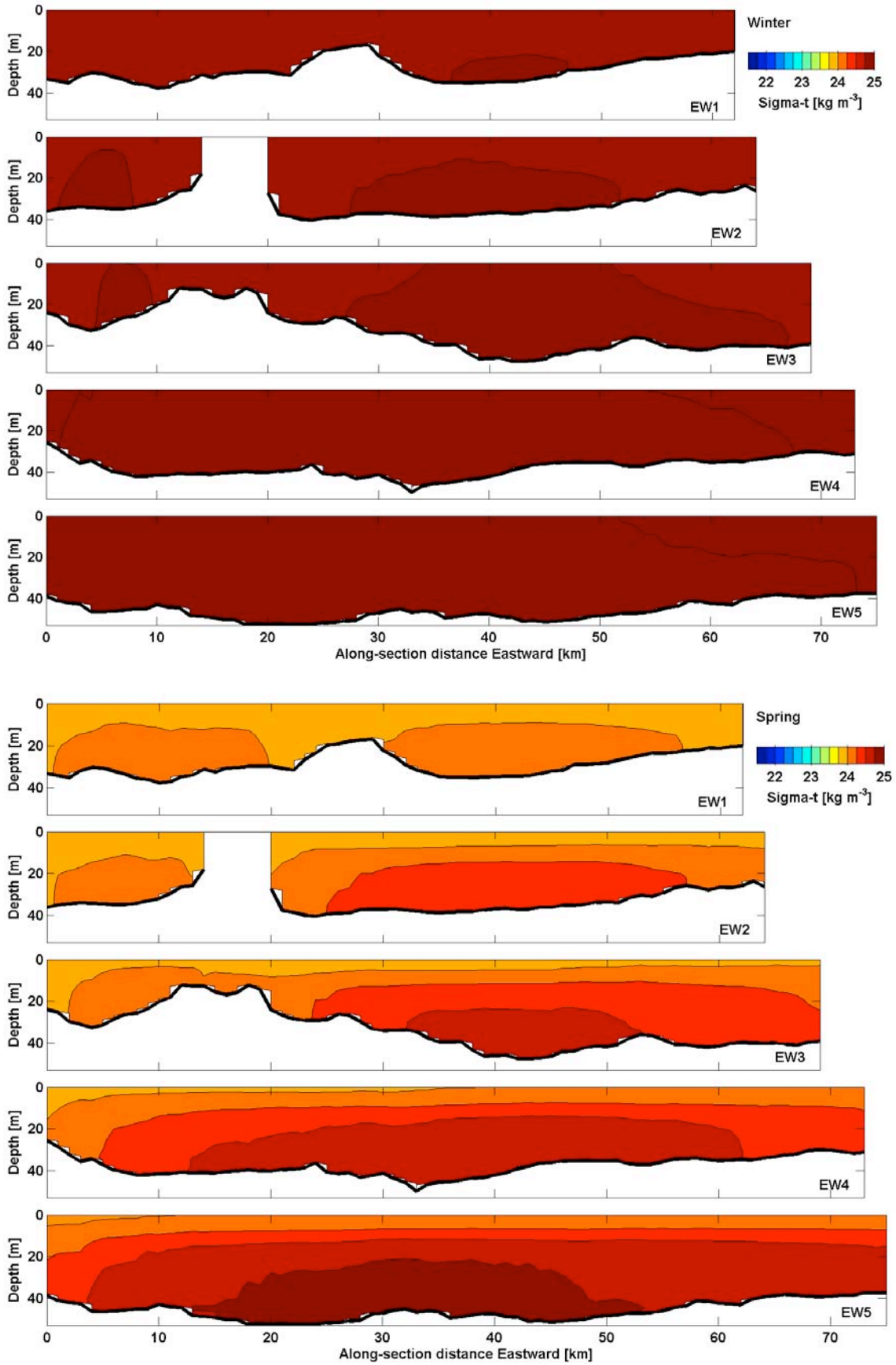

Figure 65. Simulation: Density anomaly, seasonal-mean, EW. (upper) Winter. (lower) Spring.

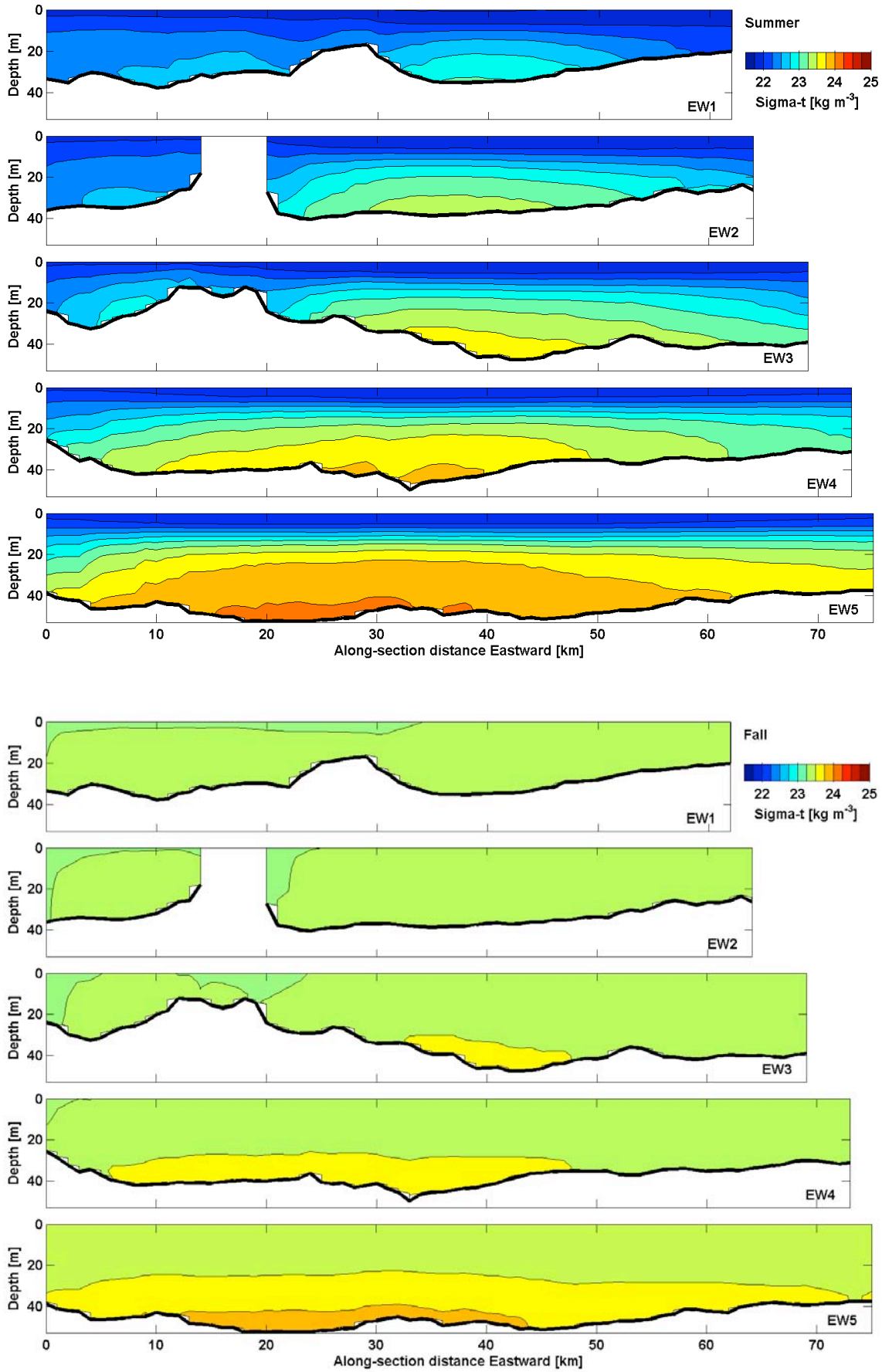

Figure 66. Simulation: Density anomaly, seasonal-mean, EW. (upper) Summer. (Lower) Fall.

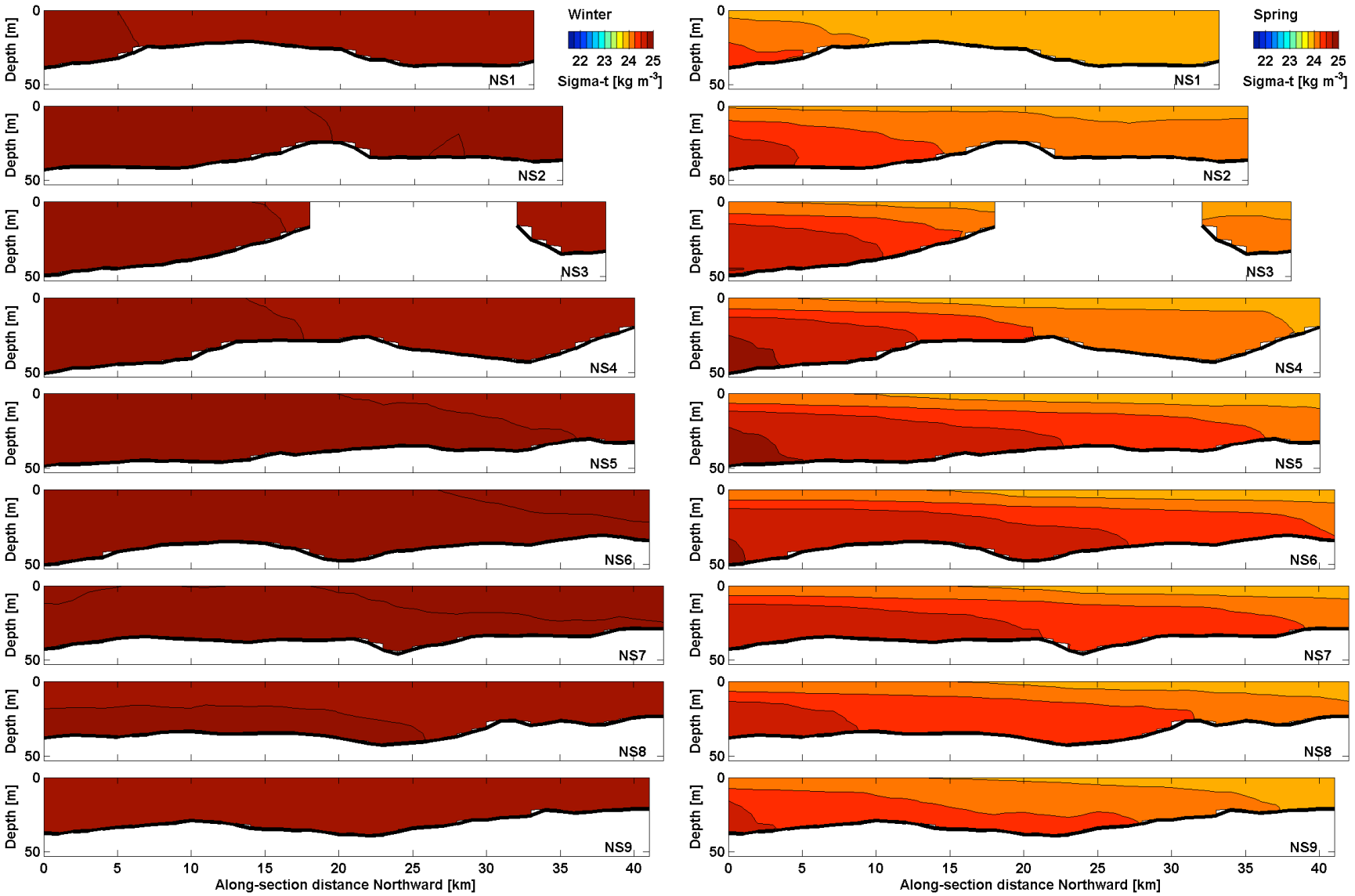

Figure 67. Simulation: Density anomaly, seasonal-mean, NS. (left) Winter. (right) Spring.

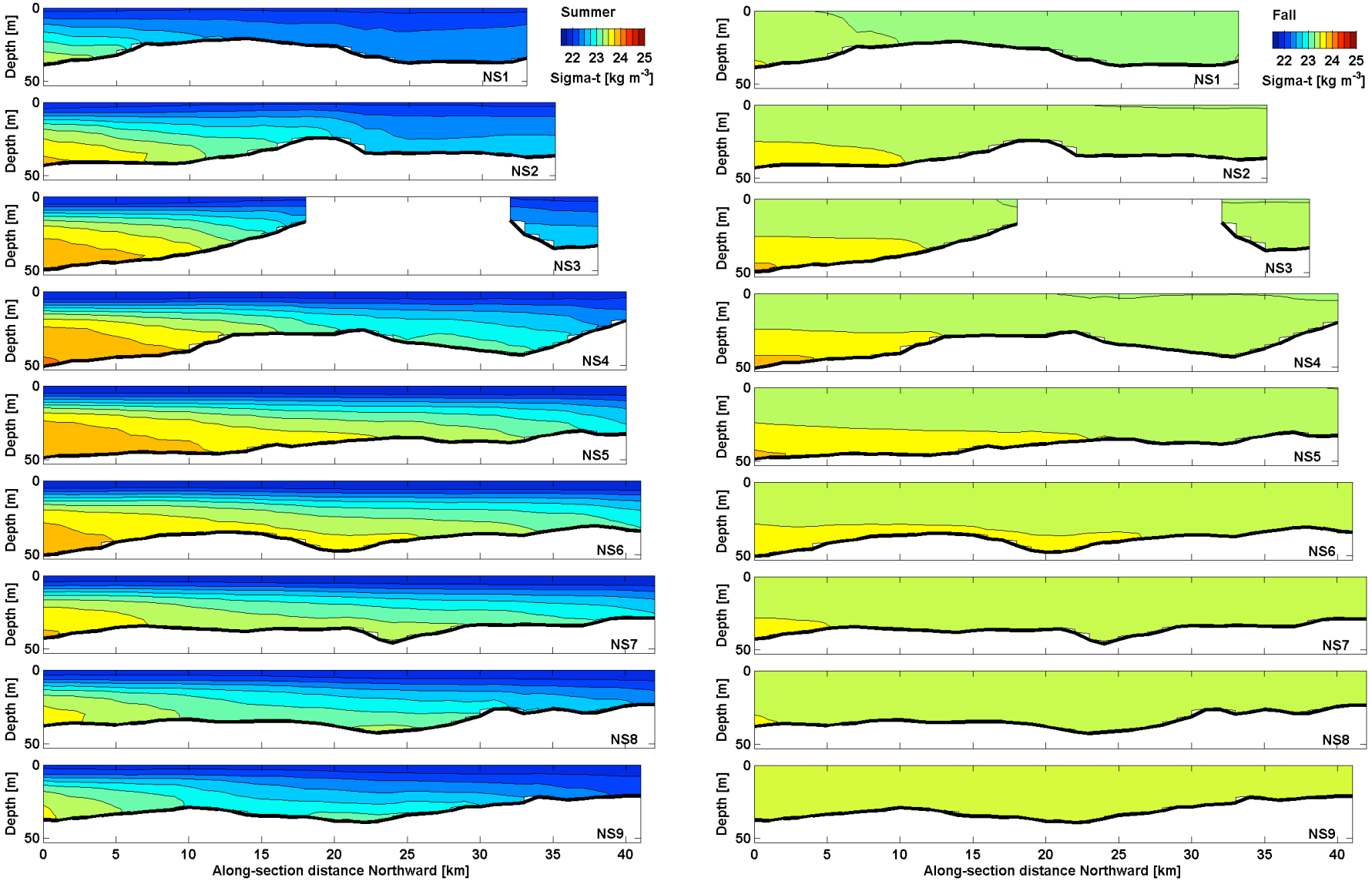

Figure 68. Simulation: Density anomaly, seasonal-mean, NS. (left) Summer. (right) Fall.

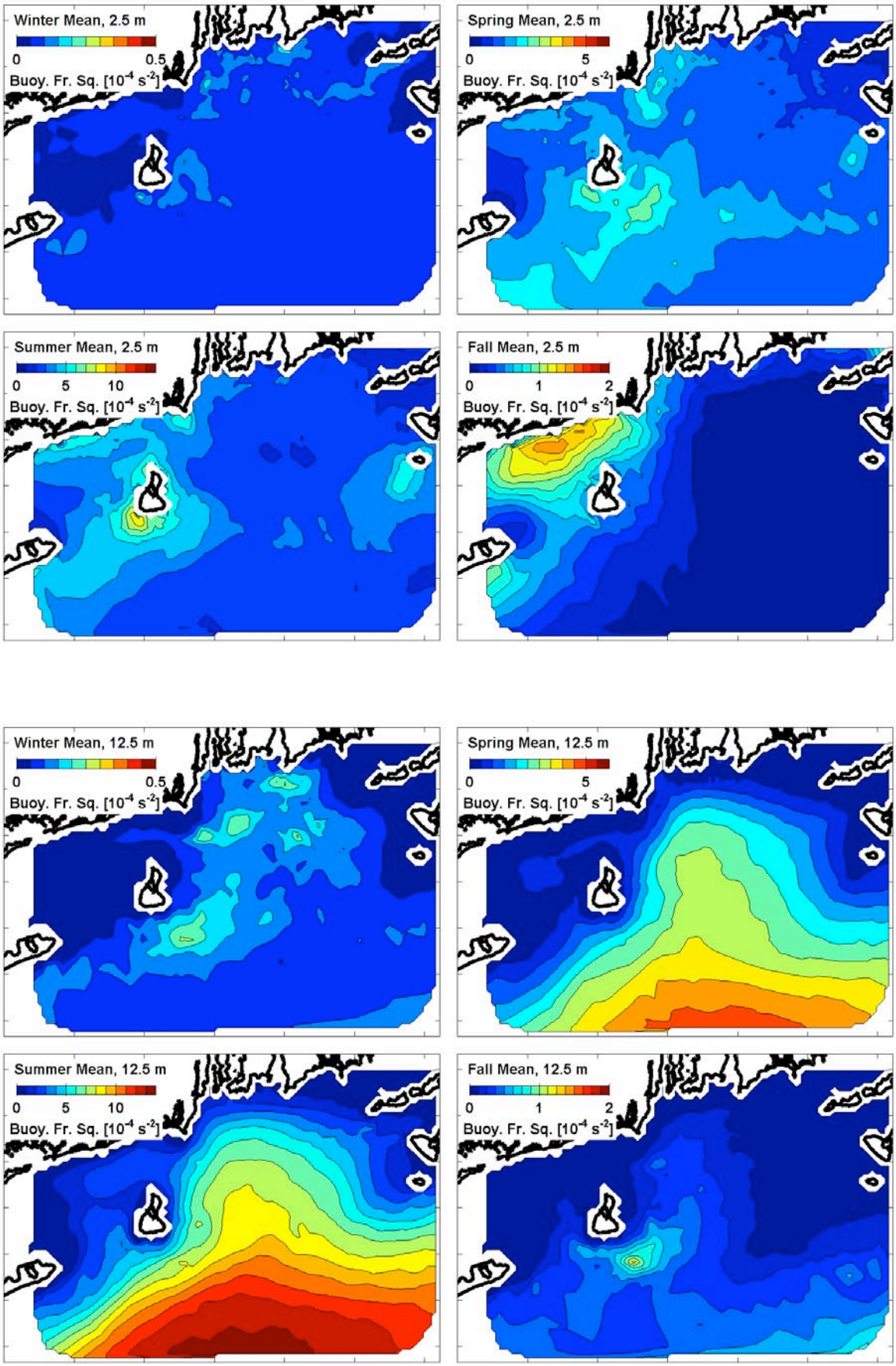

Figure 69. Simulation: Stratification, seasonal-mean. (upper) 2.5 m deep. (lower) 12.5 m deep.

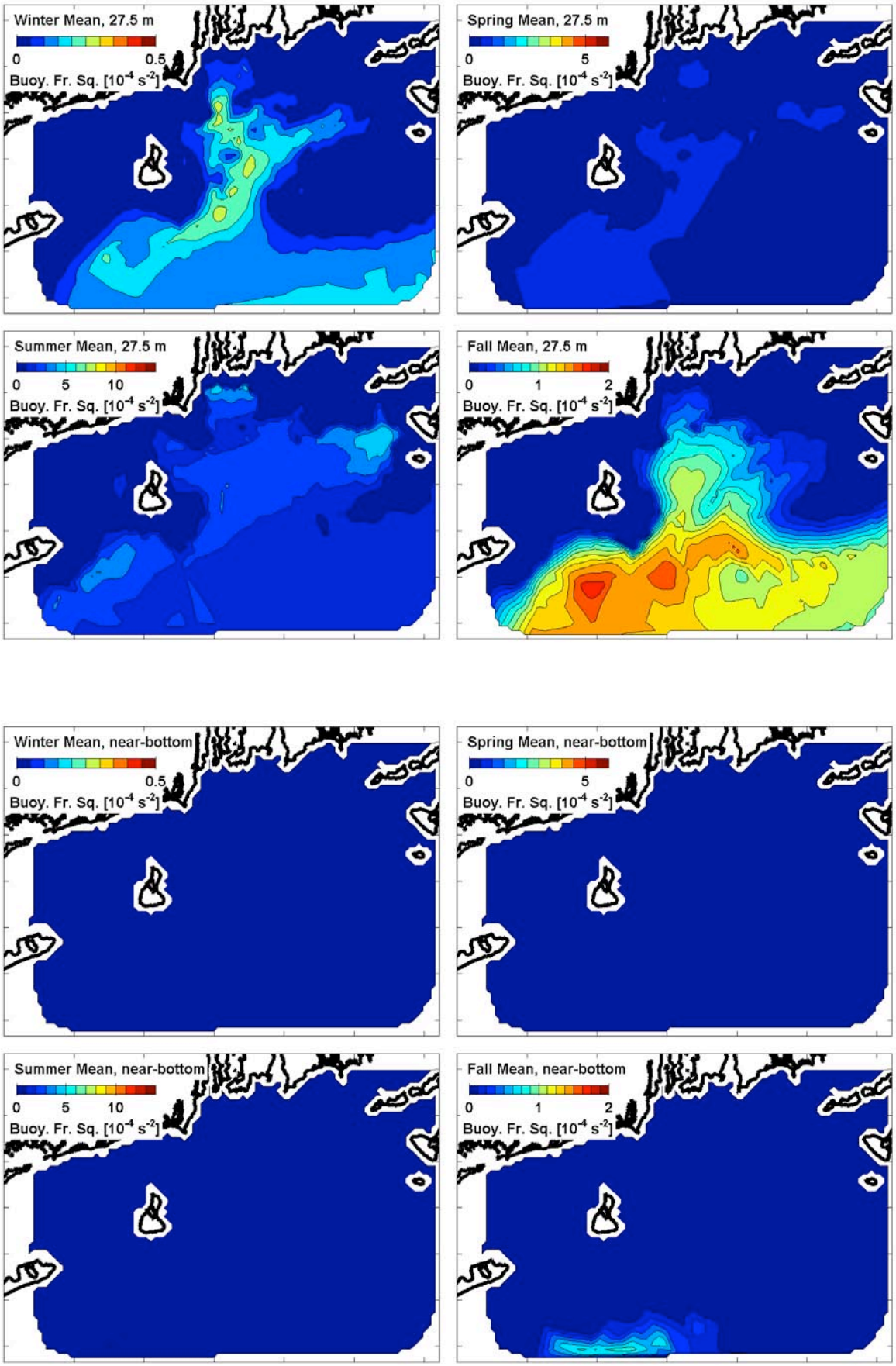

Figure 70. Simulation: Stratification, seasonal-mean. (upper) 27.5 m deep. (lower) near seafloor.

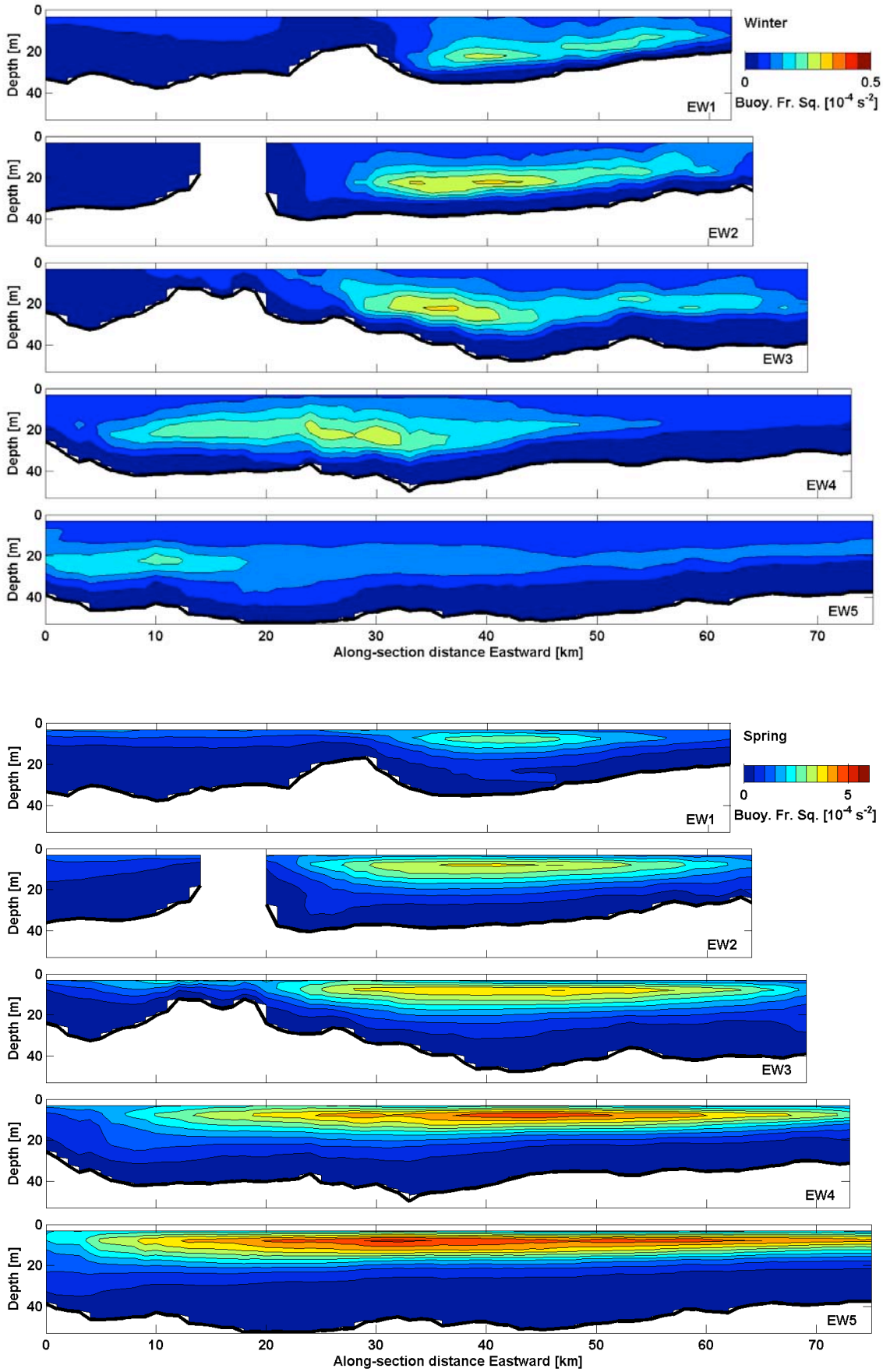

Figure 71. Simulation: Stratification, seasonal-mean, EW. (upper) Winter. (lower) Spring.

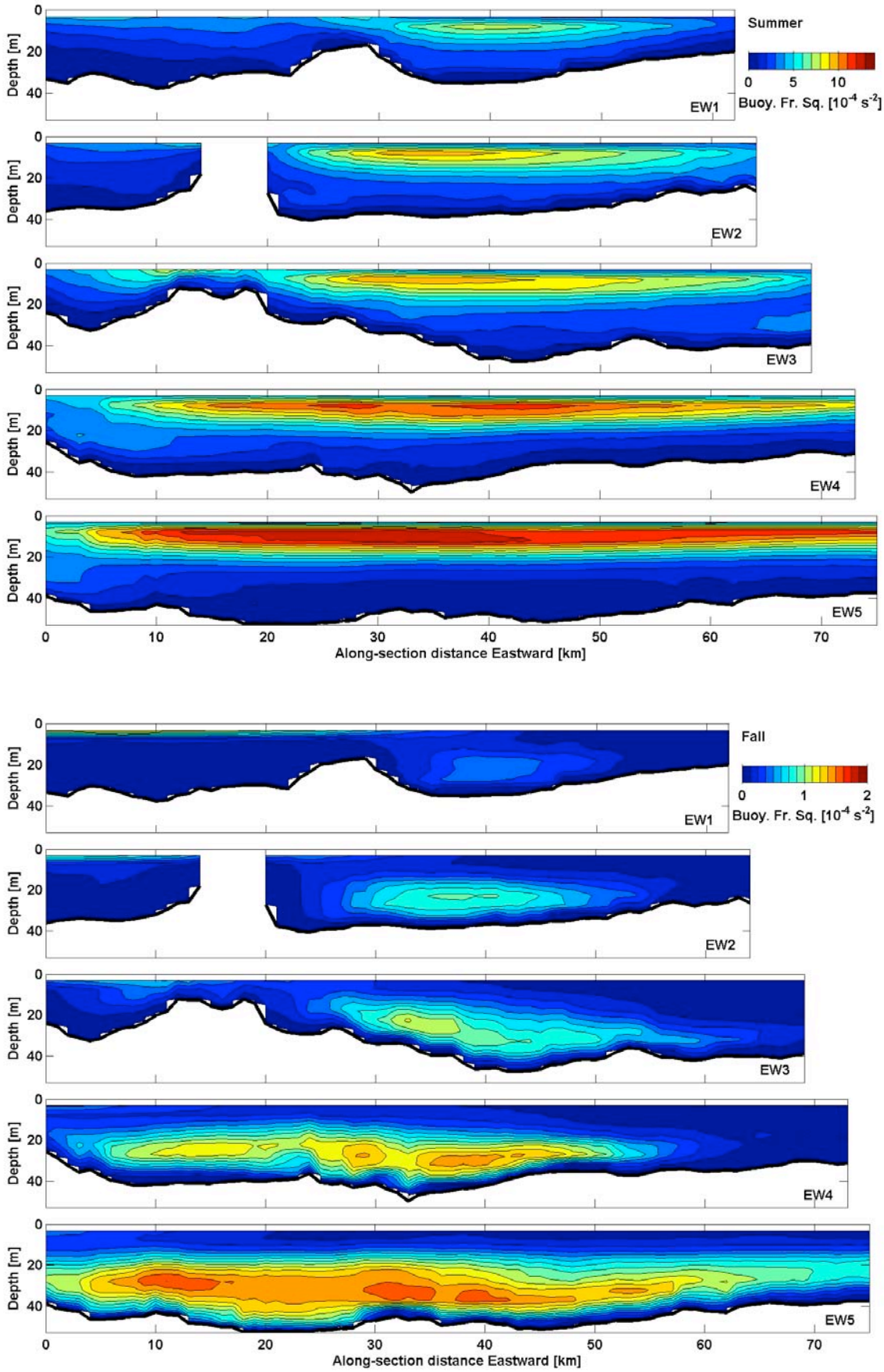

Figure 72. Simulation: Stratification, seasonal-mean, EW. (upper) Summer. (lower) Fall.

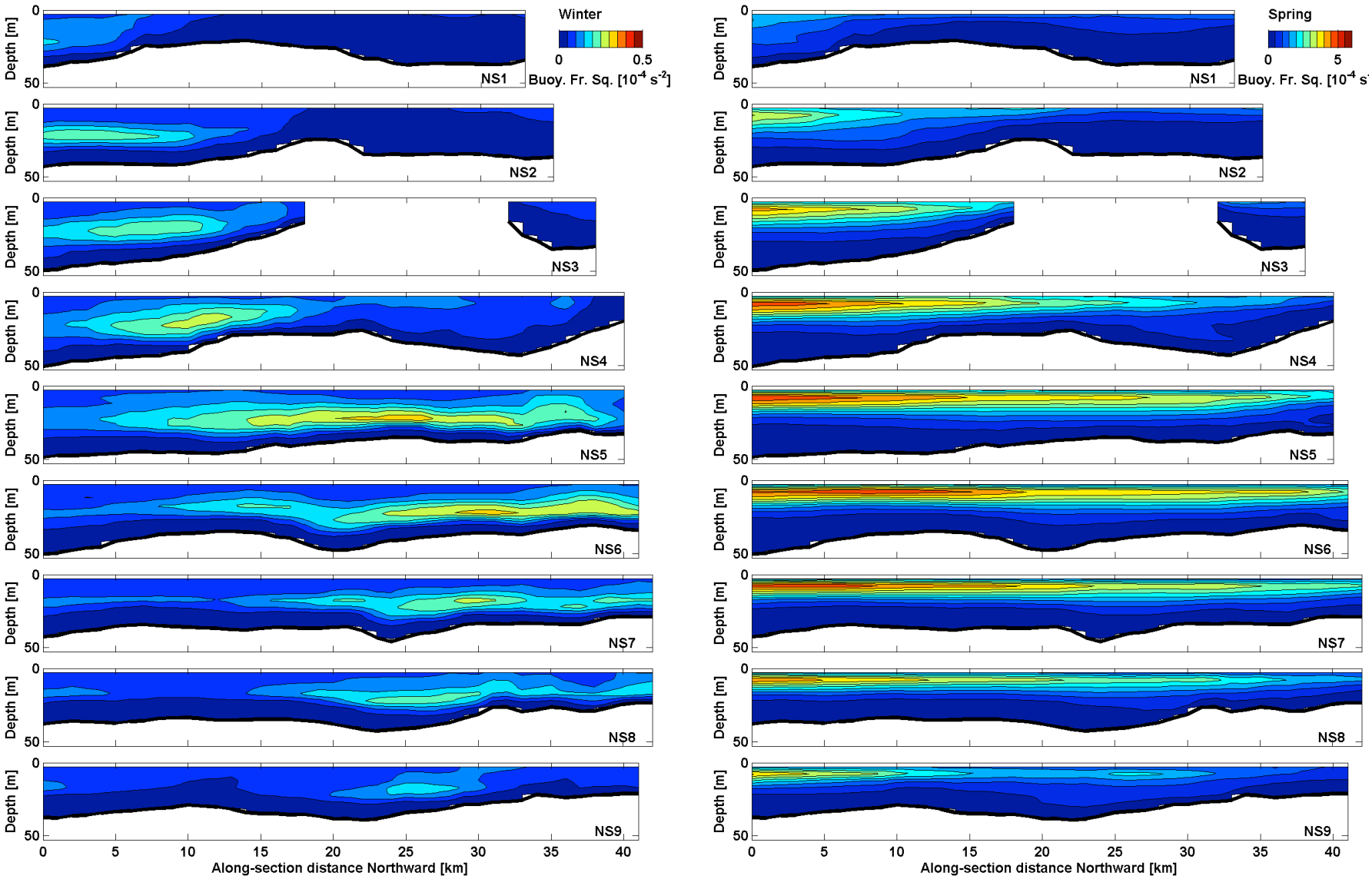

Figure 73. Simulation: Stratification, seasonal-mean, NS. (left) Winter. (right) Spring.

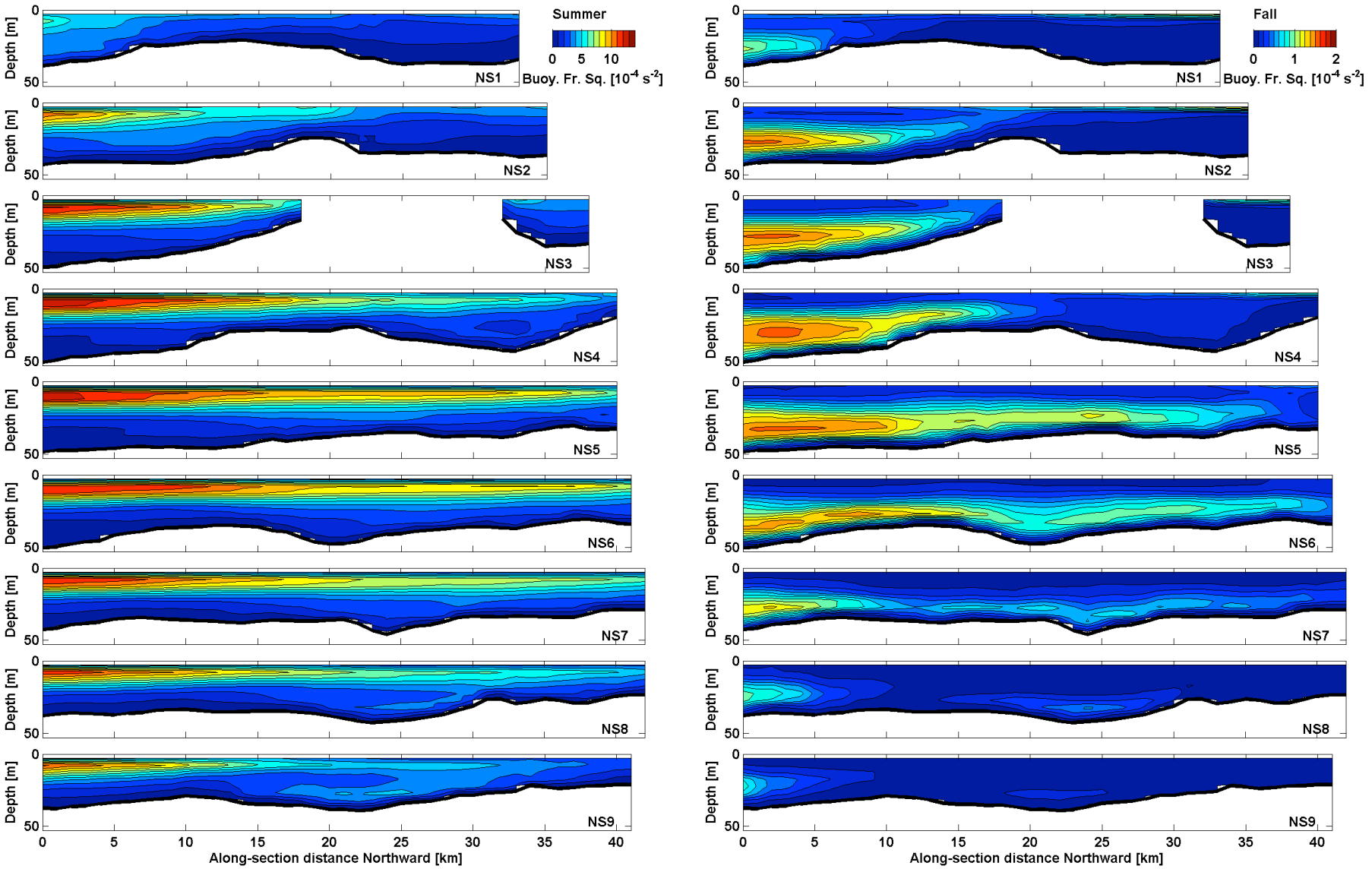

Figure 74. Simulation: Stratification, seasonal-mean, NS. (left) Summer. (right) Fall.

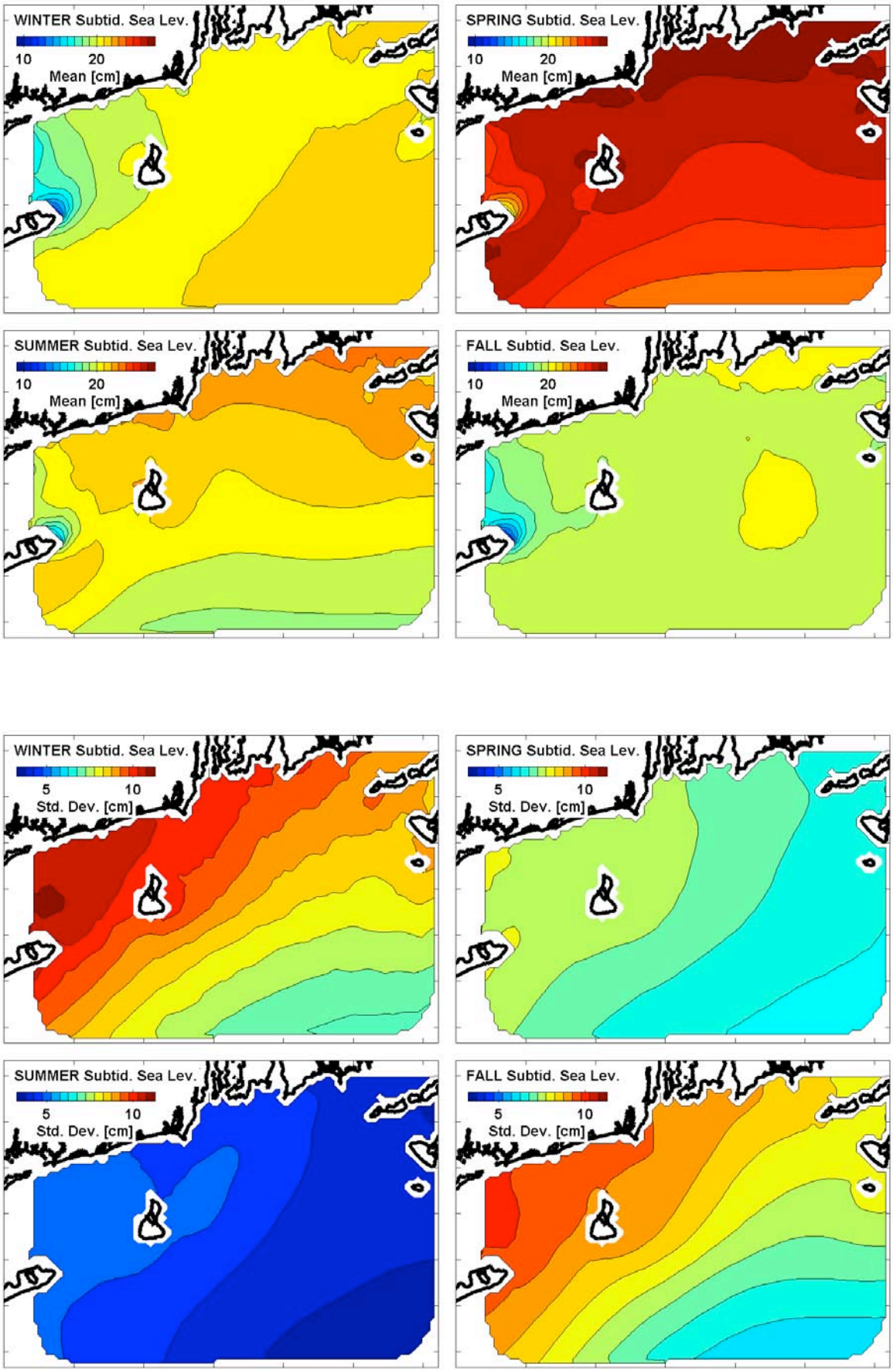

Figure 75. Simulation: Subtidal sea level, four seasons. (upper) Mean. (lower) Std. dev.

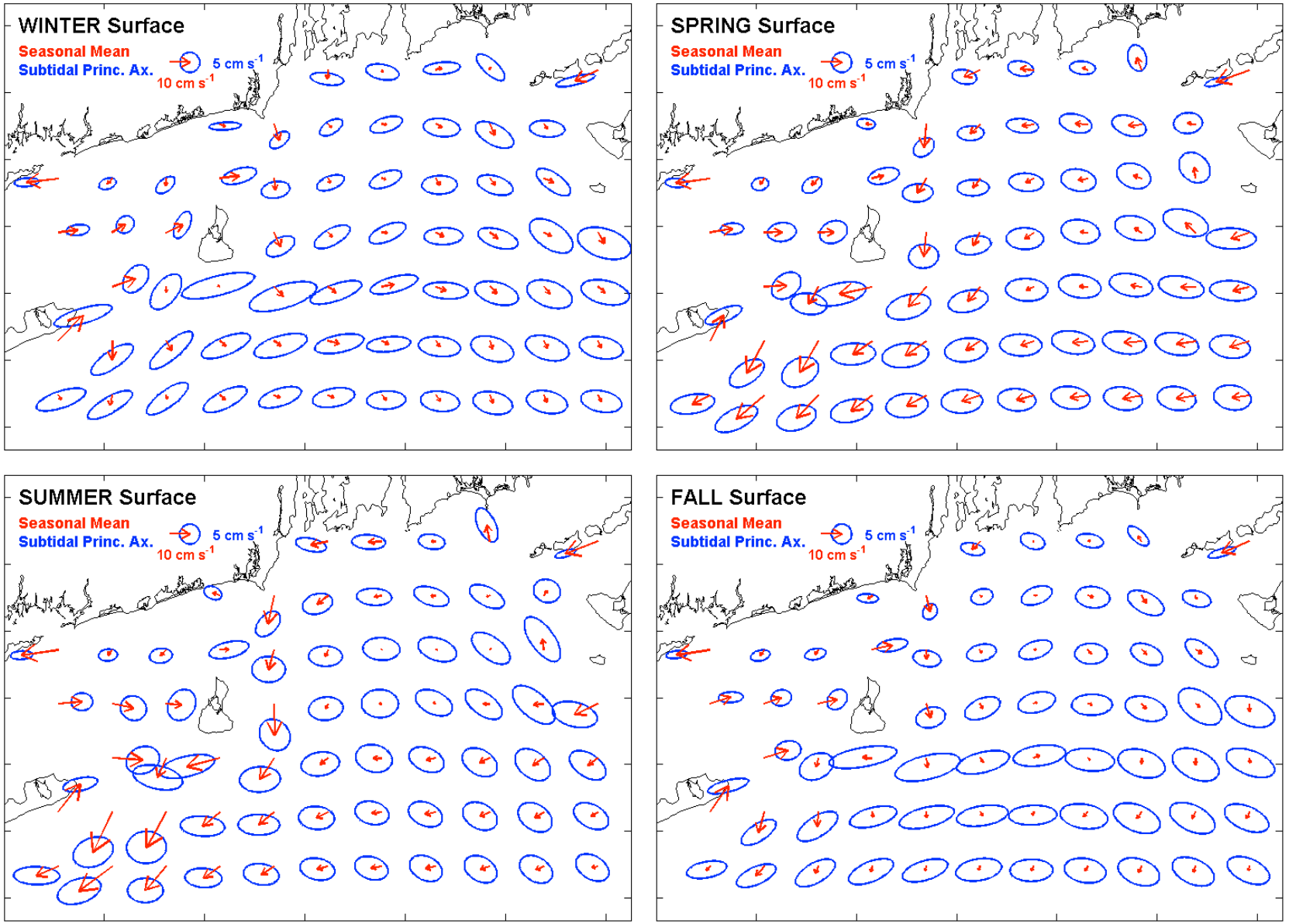

Figure 76. Simulation: Currents, seasonal-mean & subtidal ellipses. Surface.

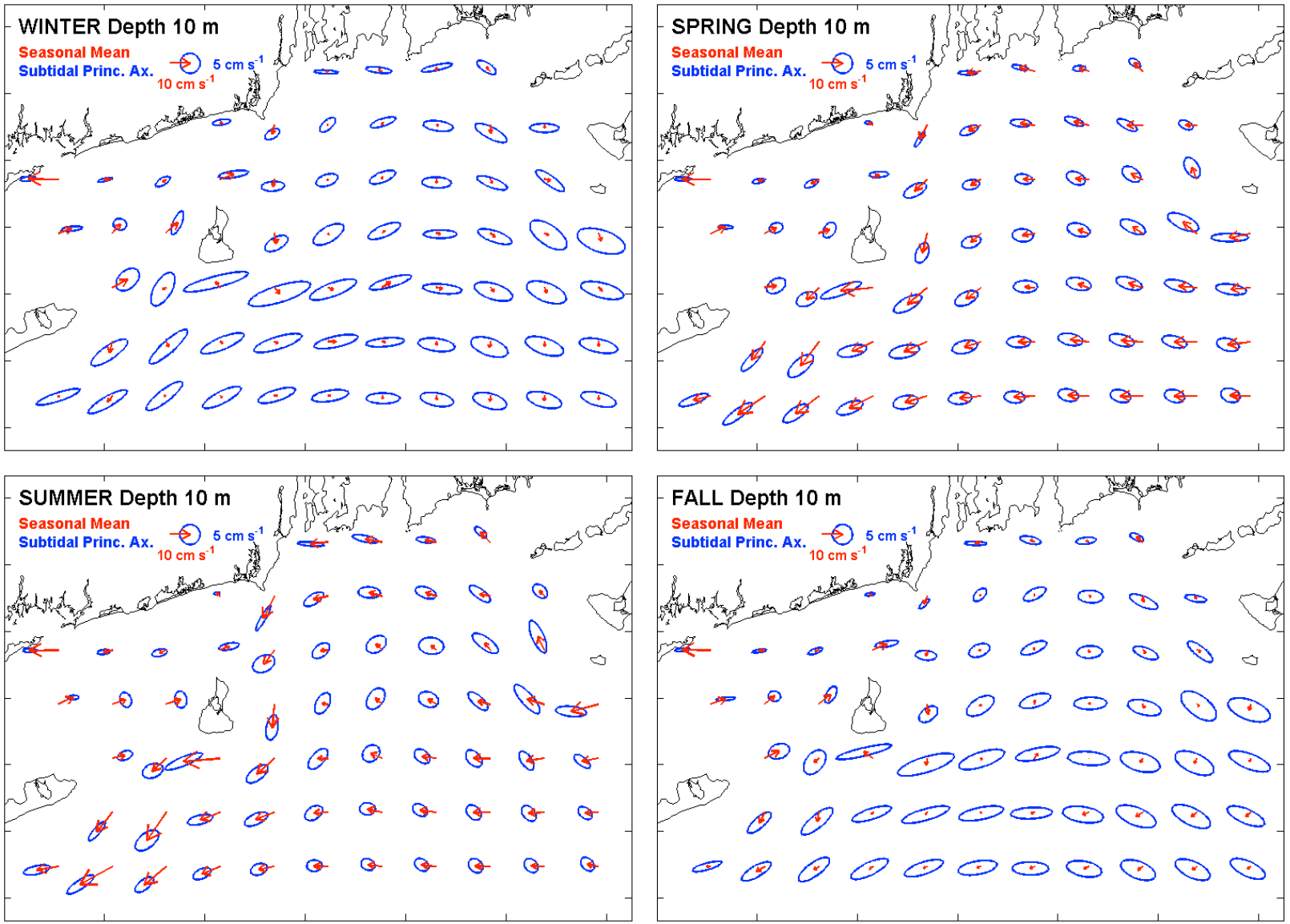

Figure 77. Simulation: Currents, seasonal-mean & subtidal ellipses. Depth 10 m.

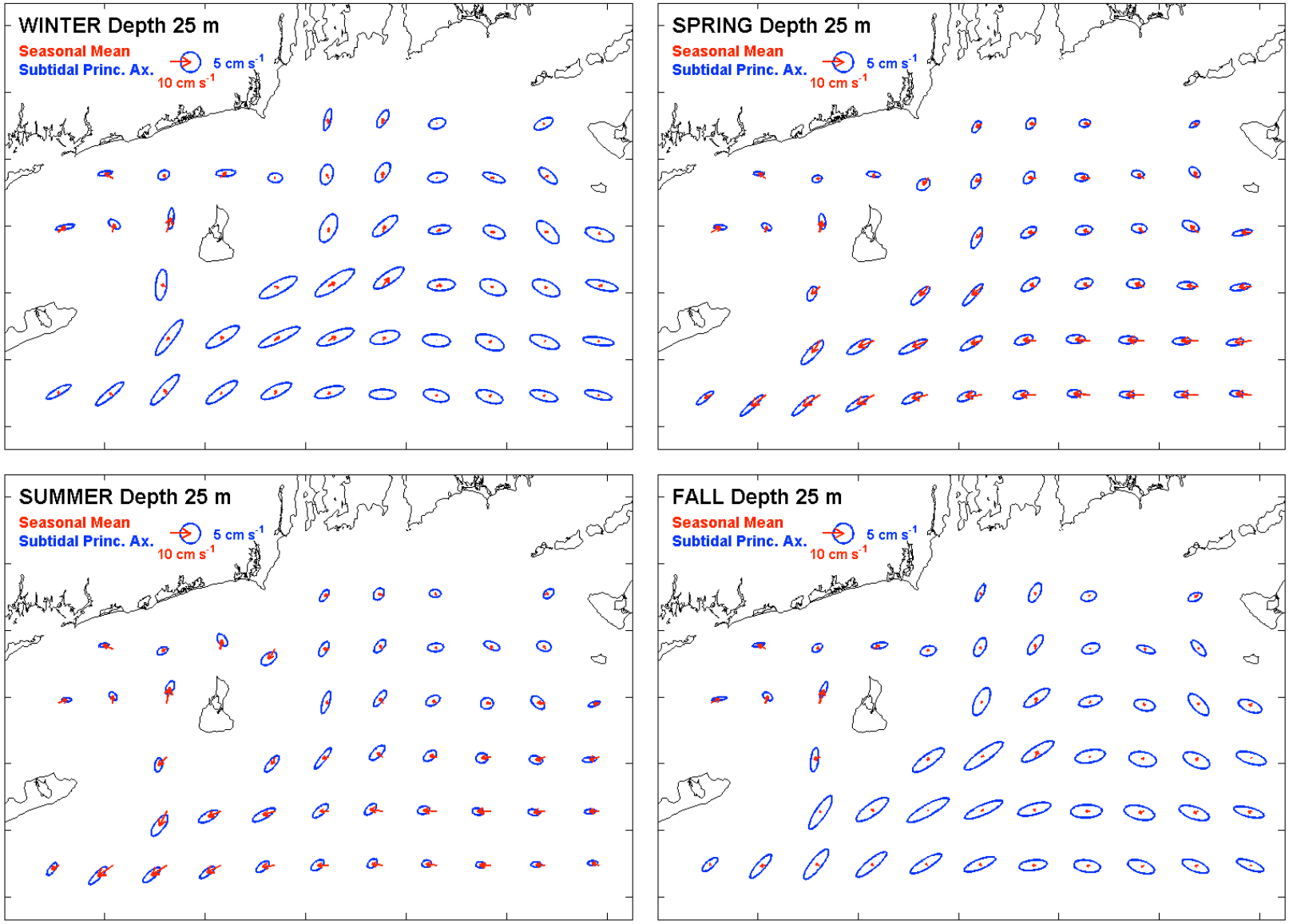

Figure 78. Simulation: Currents, seasonal-mean & subtidal ellipses. Depth 25 m.

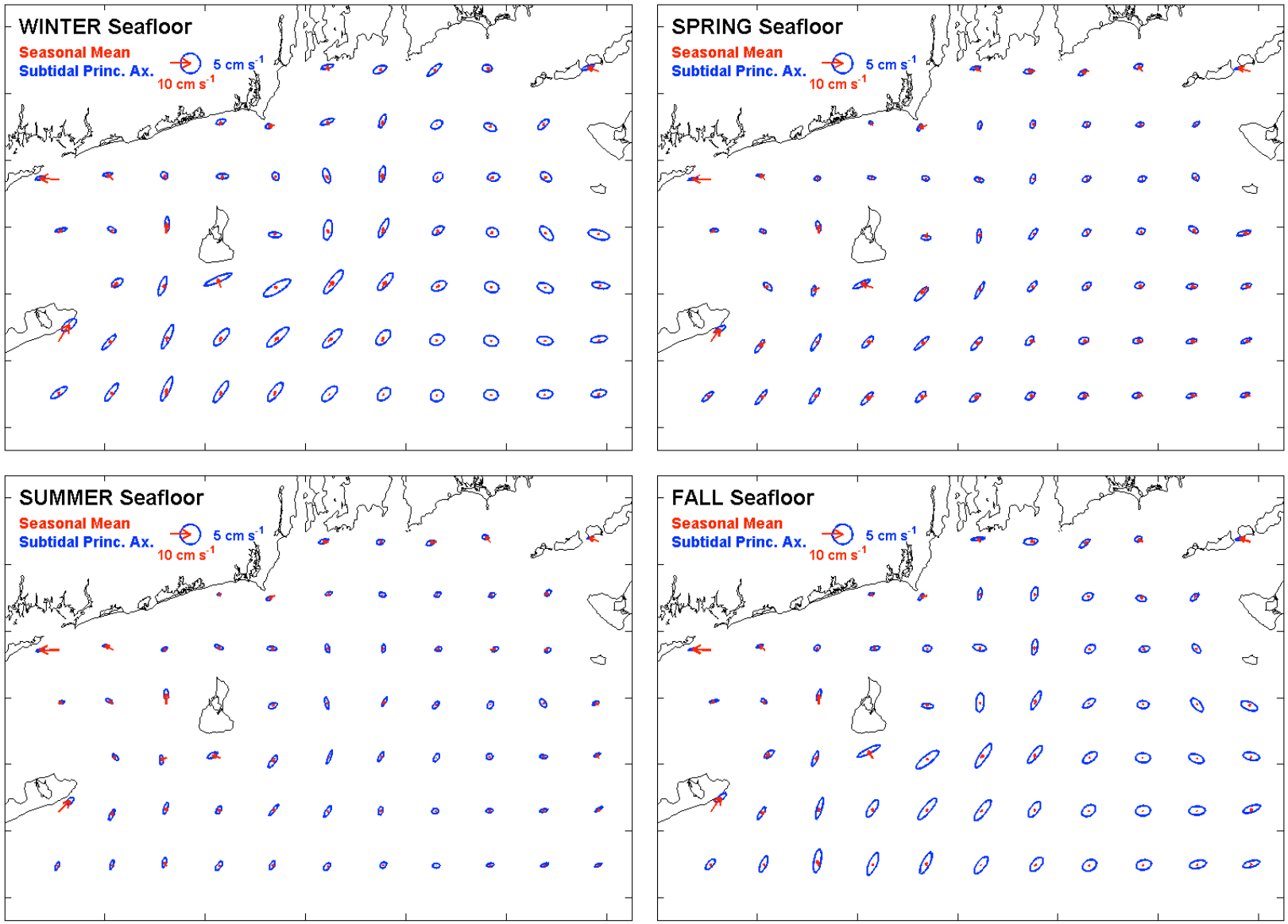

Figure 79. Simulation: Currents, seasonal-mean & subtidal ellipses. Seafloor.

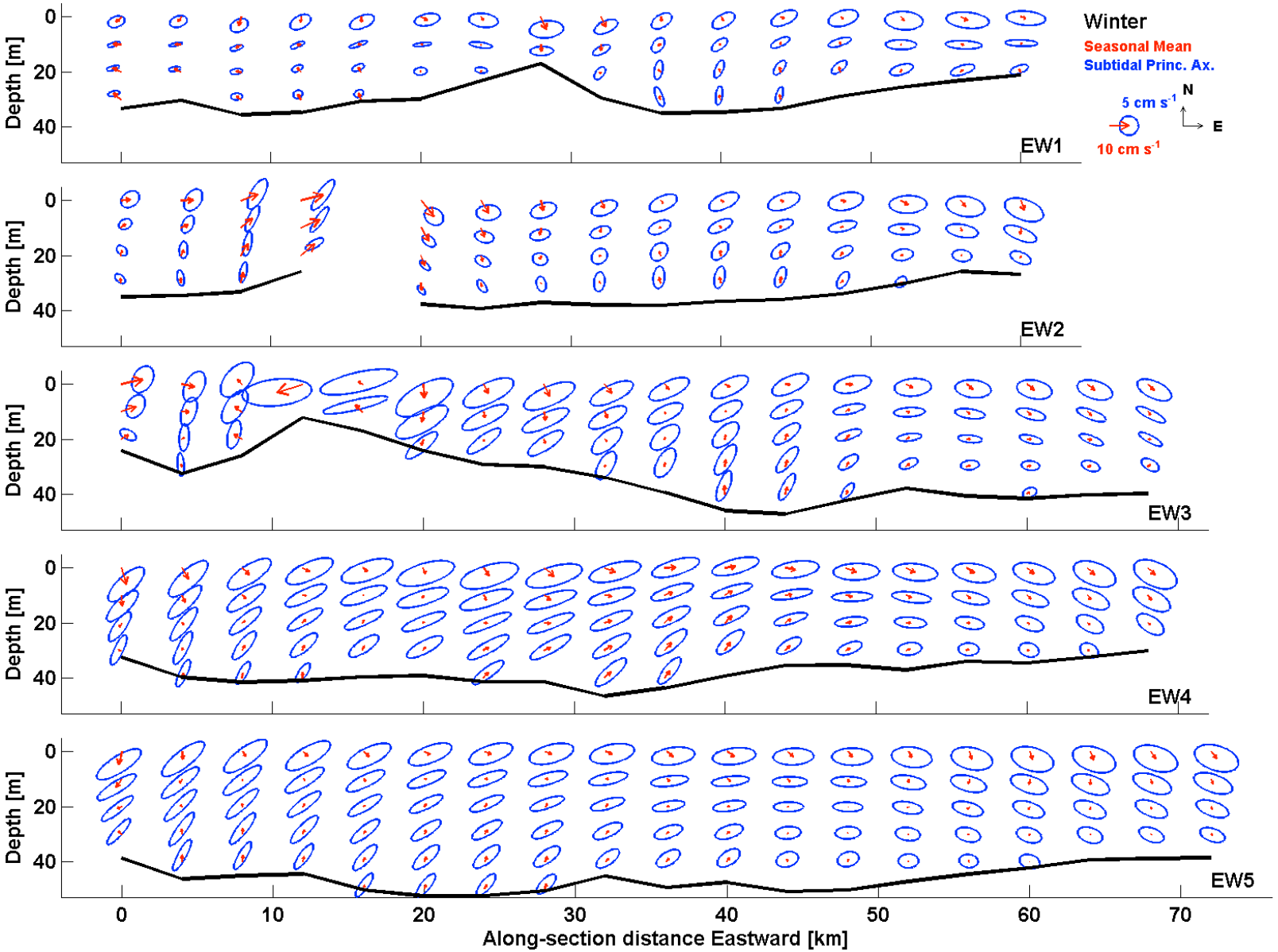

Figure 80. Simulation: Currents, plan view seas. mean & subtid. ellipses. EW sections, winter.

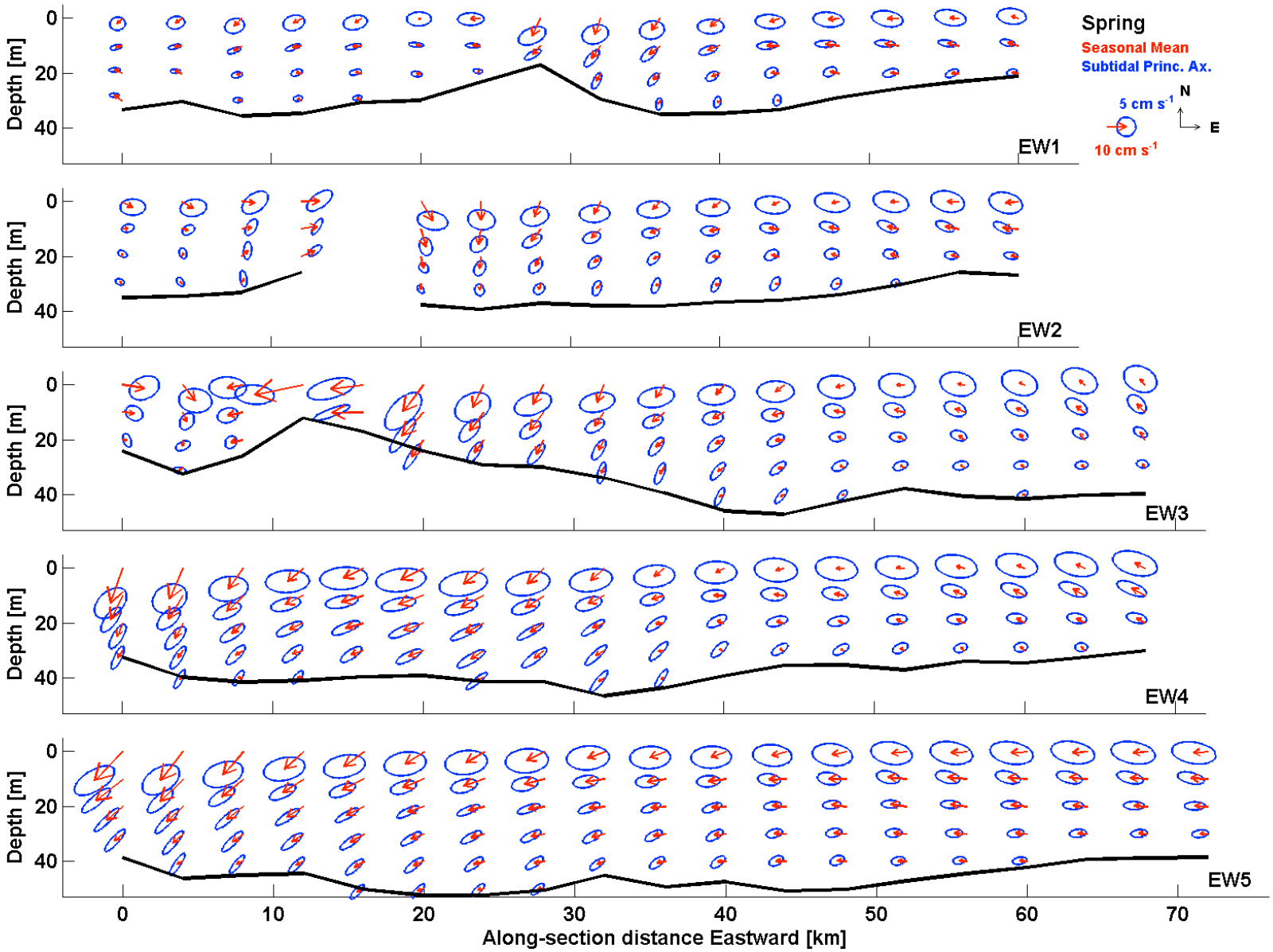

Figure 81. Simulation: Currents, plan view seas. mean & subtid. ellipses. EW sections, spring.

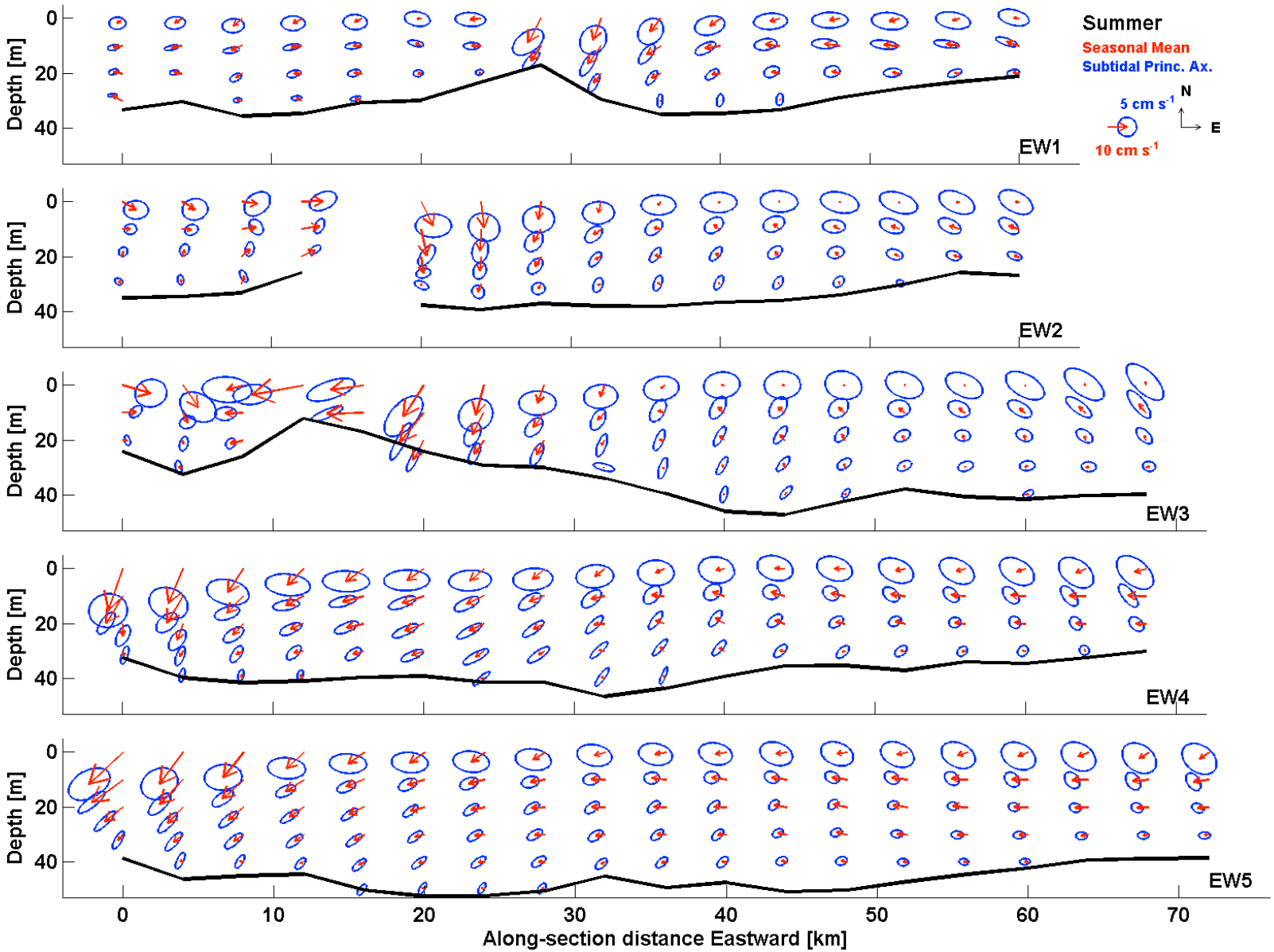

Figure 82. Simulation: Currents, plan view seas. mean & subtid. ellipses. EW sections, summer.

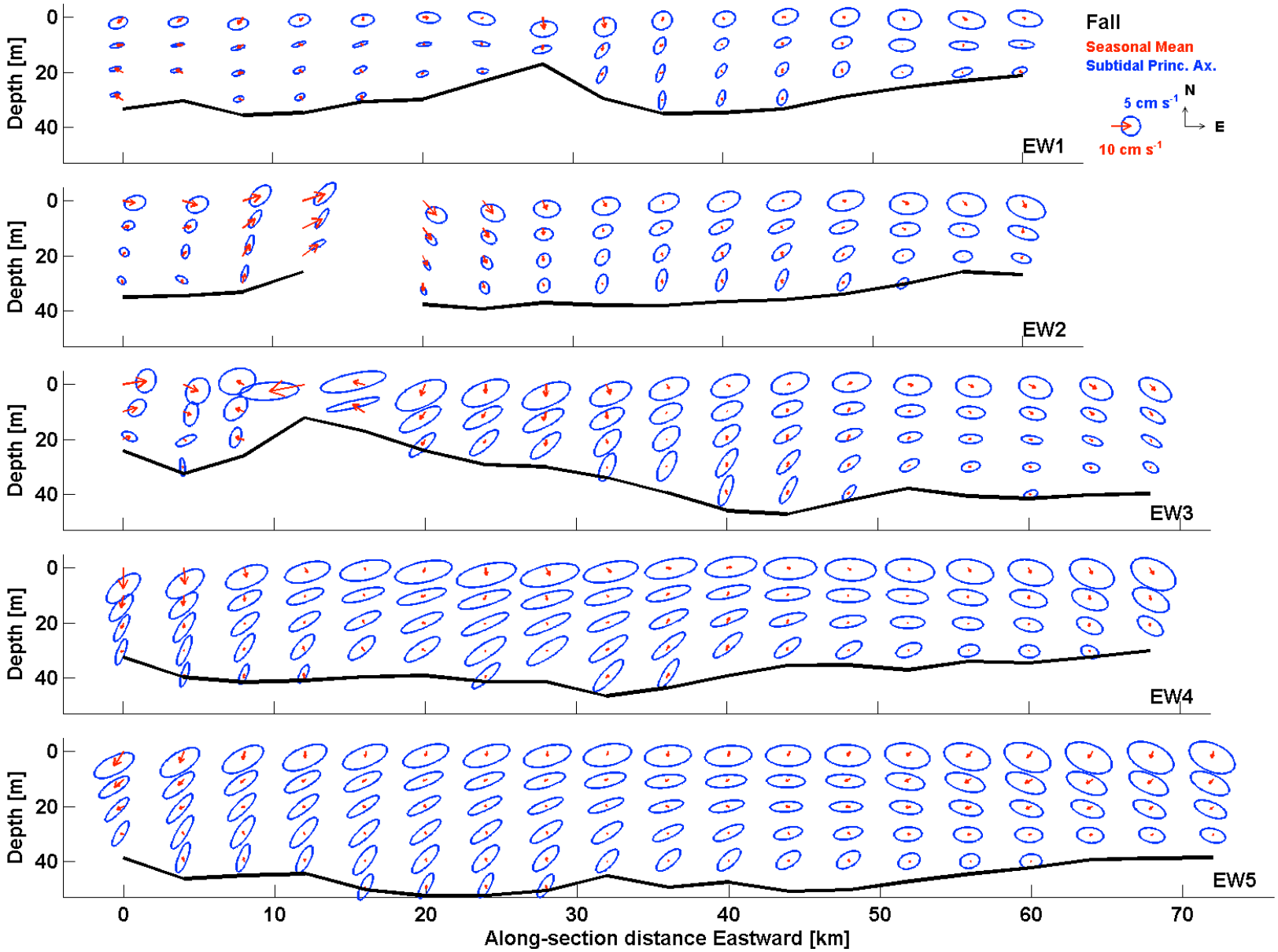

Figure 83. Simulation: Currents, plan view seas. mean & subtid. ellipses. EW sections, fall.

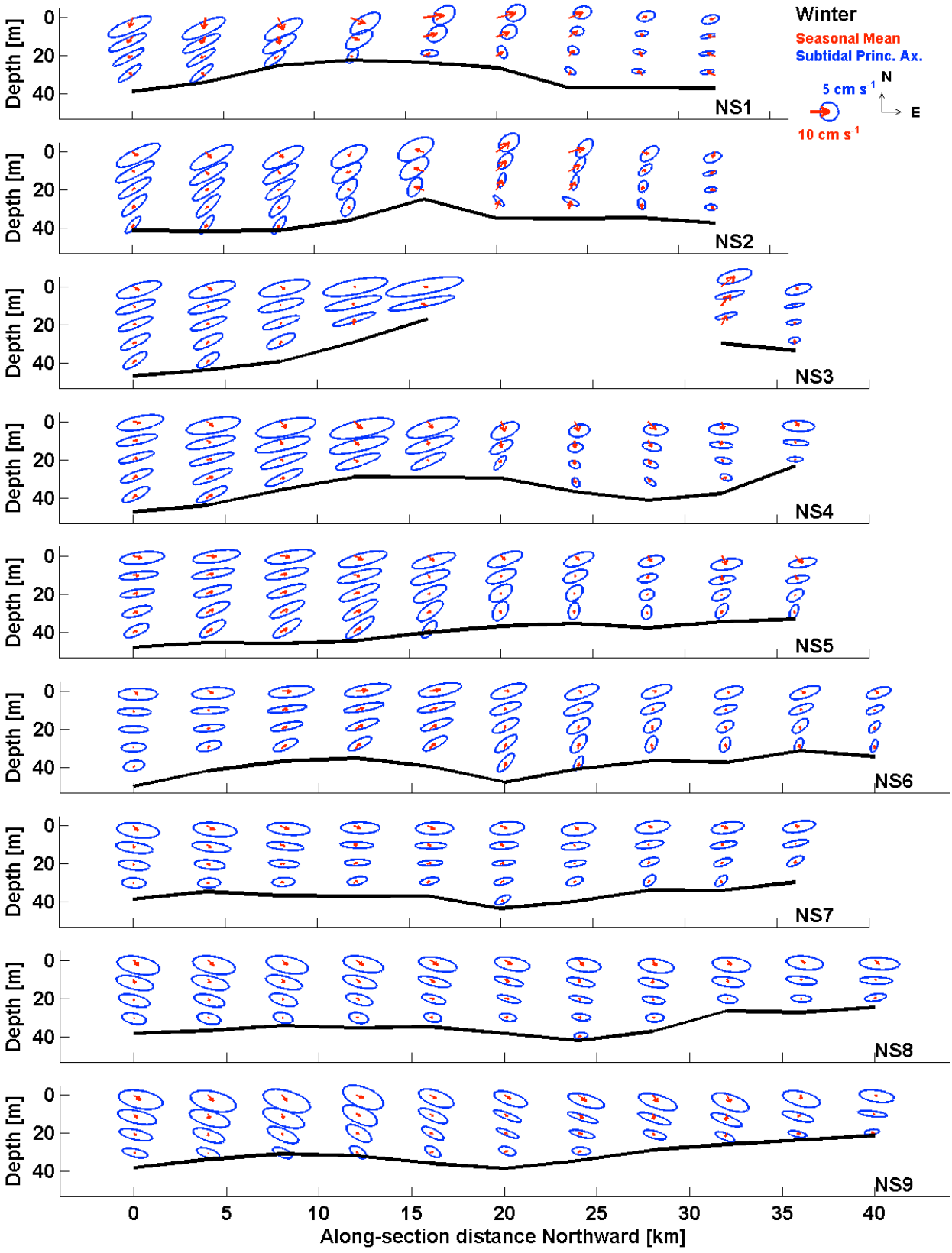

Figure 84. Simulation: Currents, plan view seas. mean & subtid. ellipses. NS sections, winter.

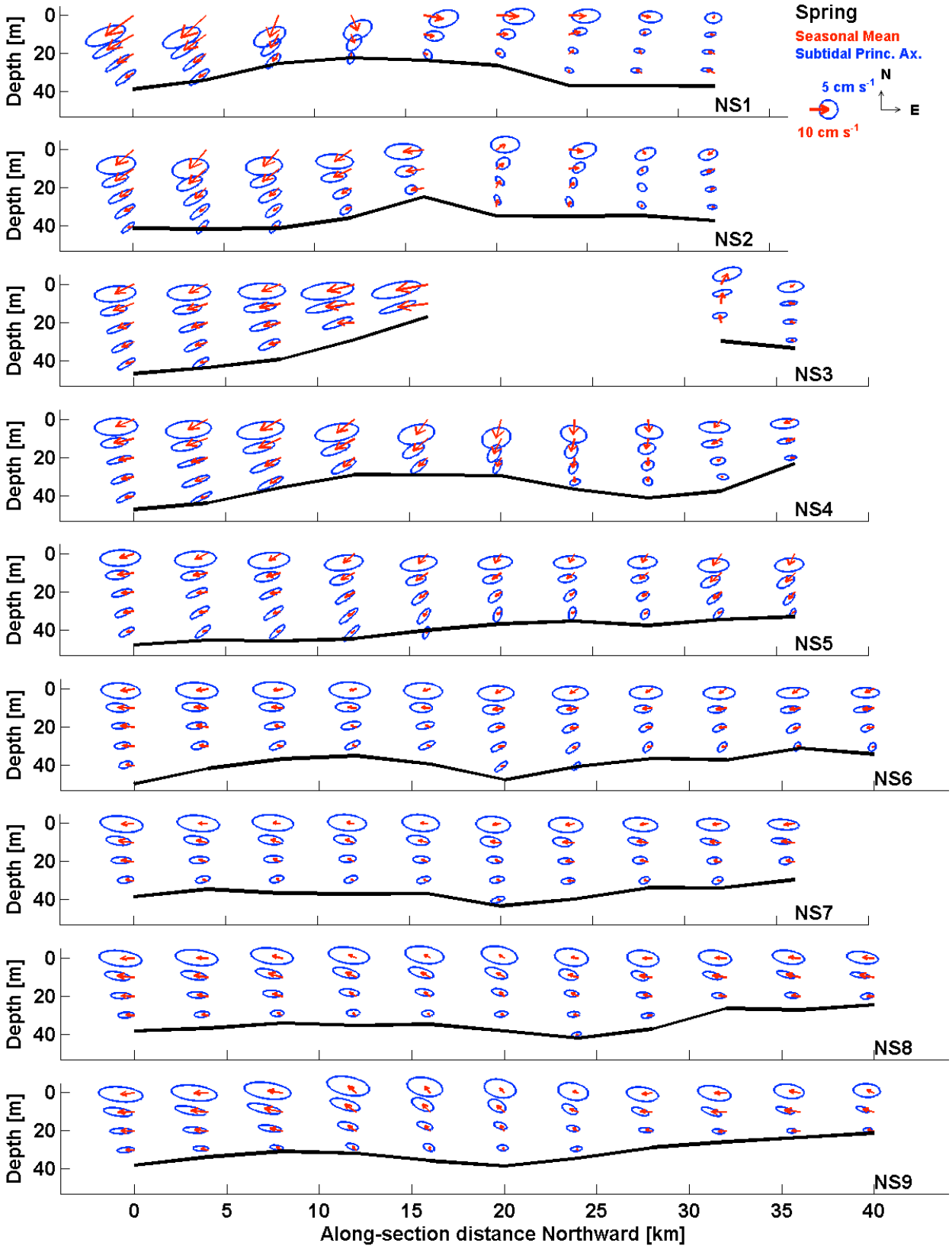

Figure 85. Simulation: Currents, plan view seas. mean & subtid. ellipses. NS sections, spring.

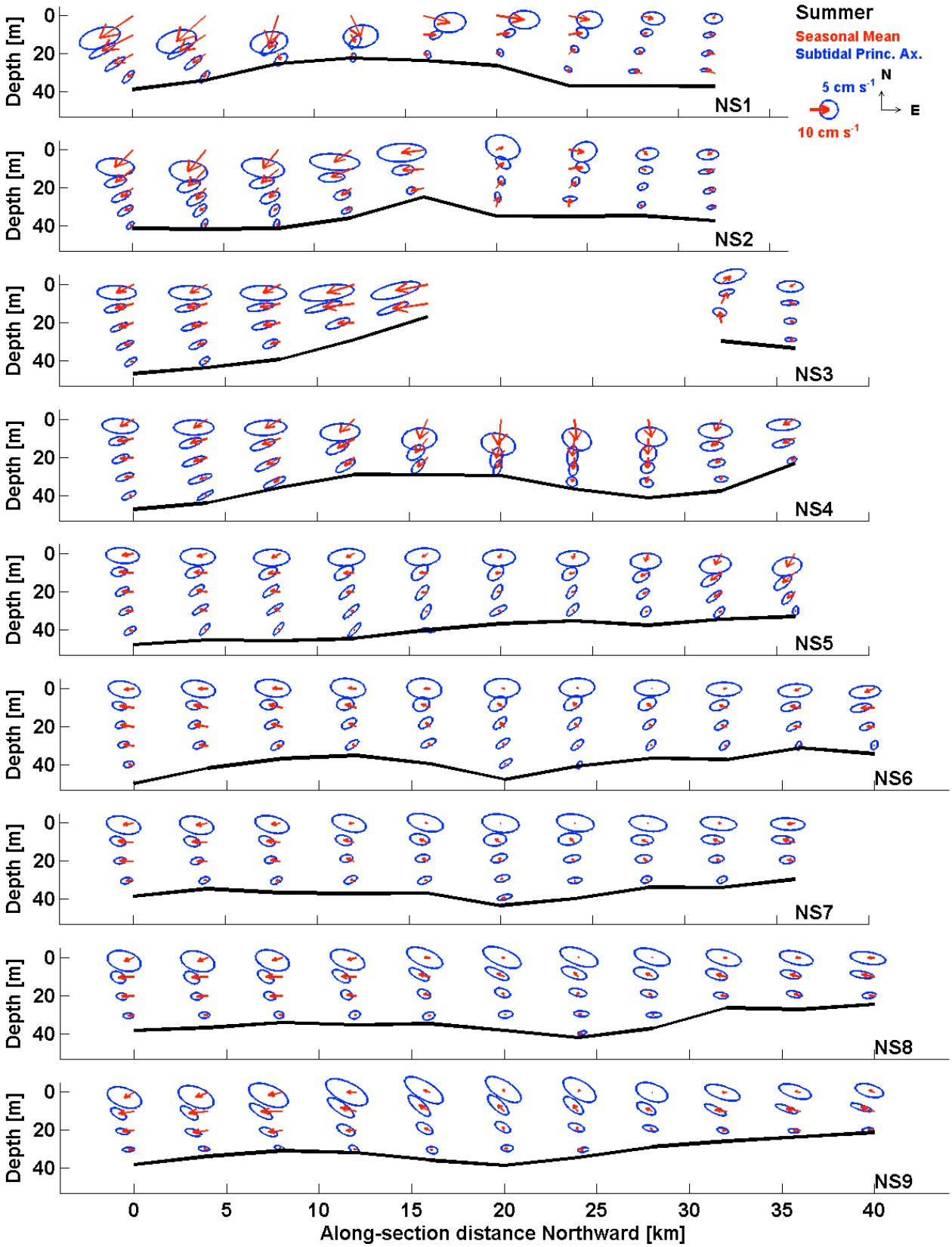

Figure 86. Simulation: Currents, plan view seas. mean & subtid. ellipses. NS sections, summer.

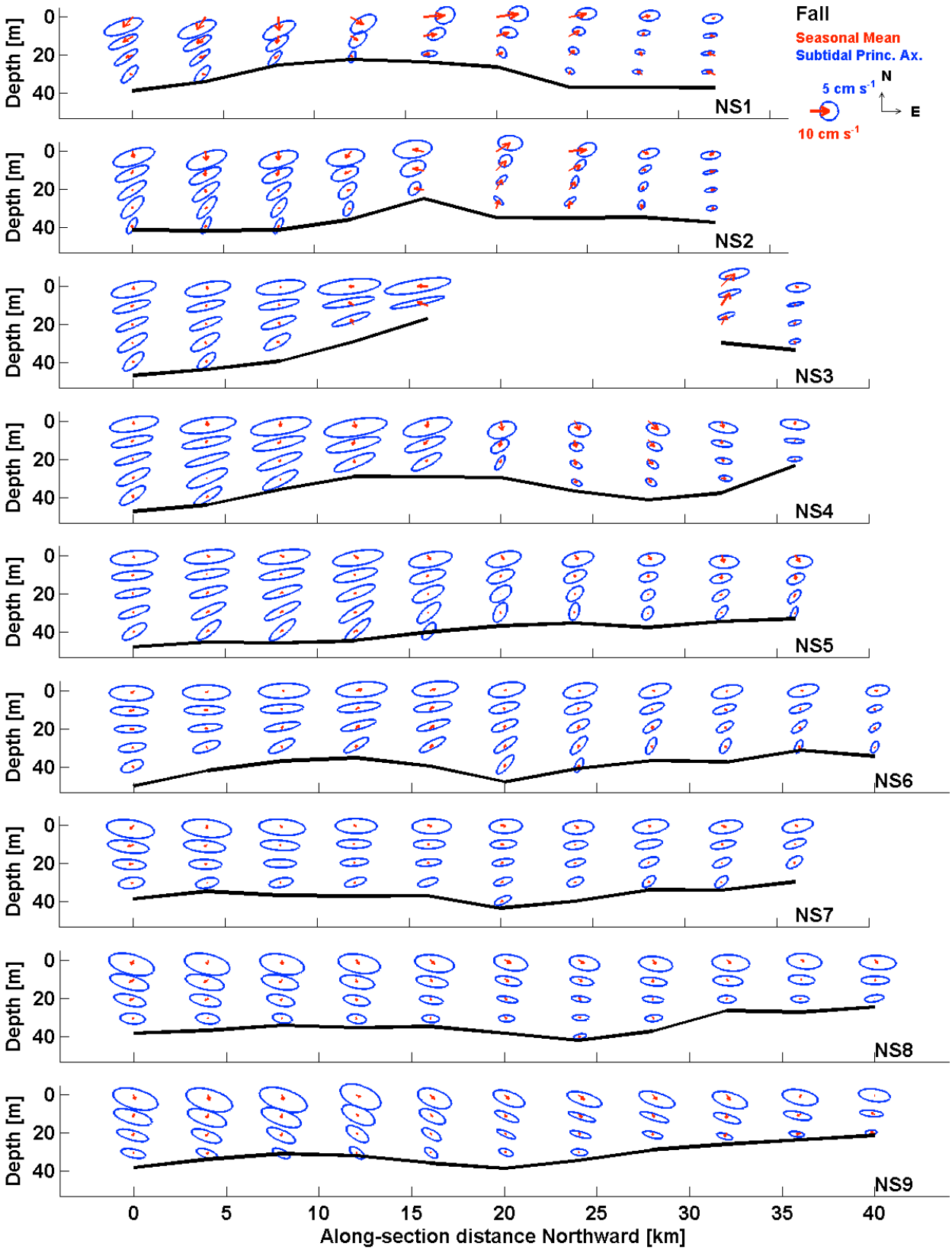

Figure 87. Simulation: Currents, plan view seas. mean & subtid. ellipses. NS sections, fall.

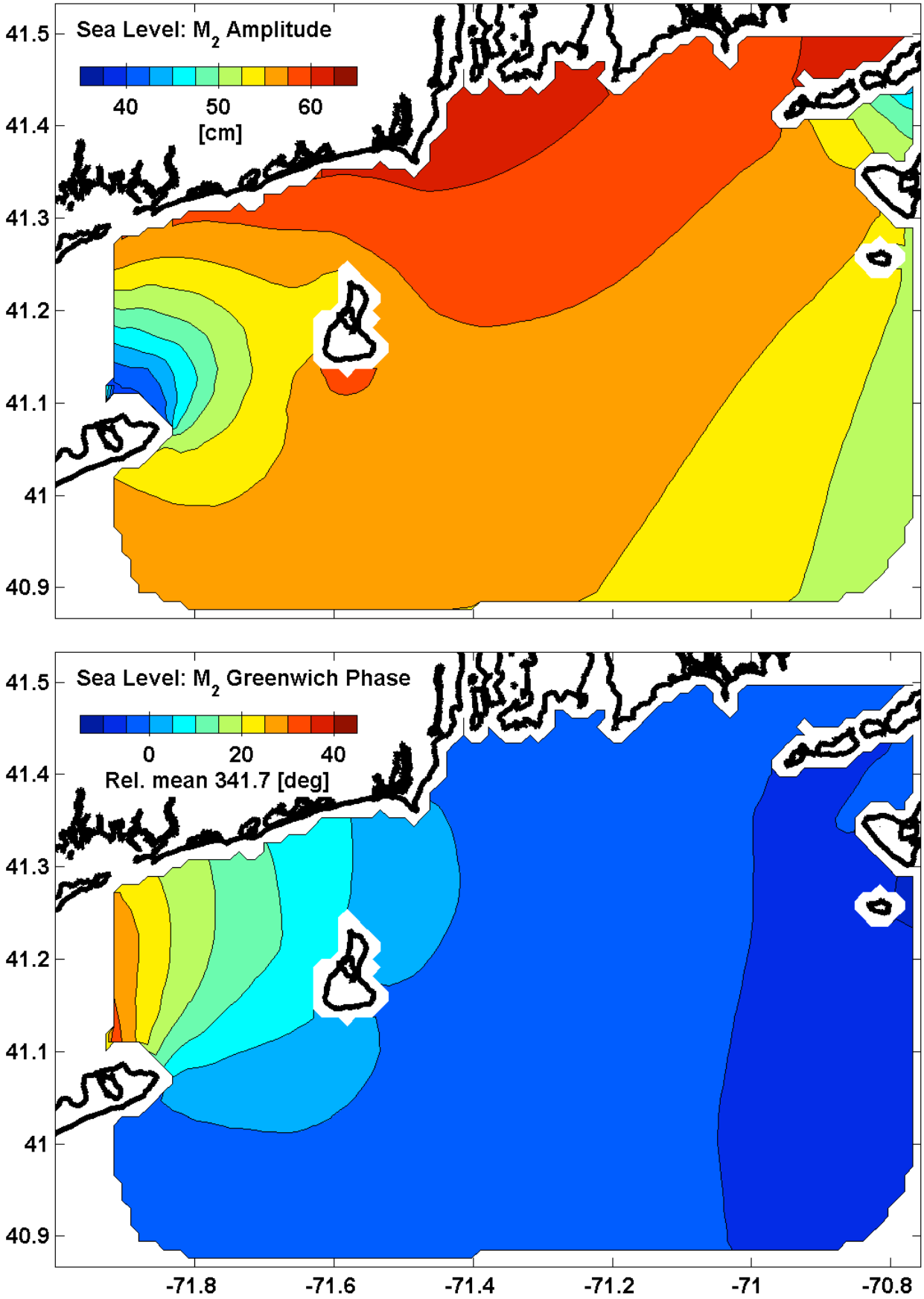

Figure 88. Simulation: Tidal height, M_2 constituent. (upper) Amplitude. (lower) Phase.

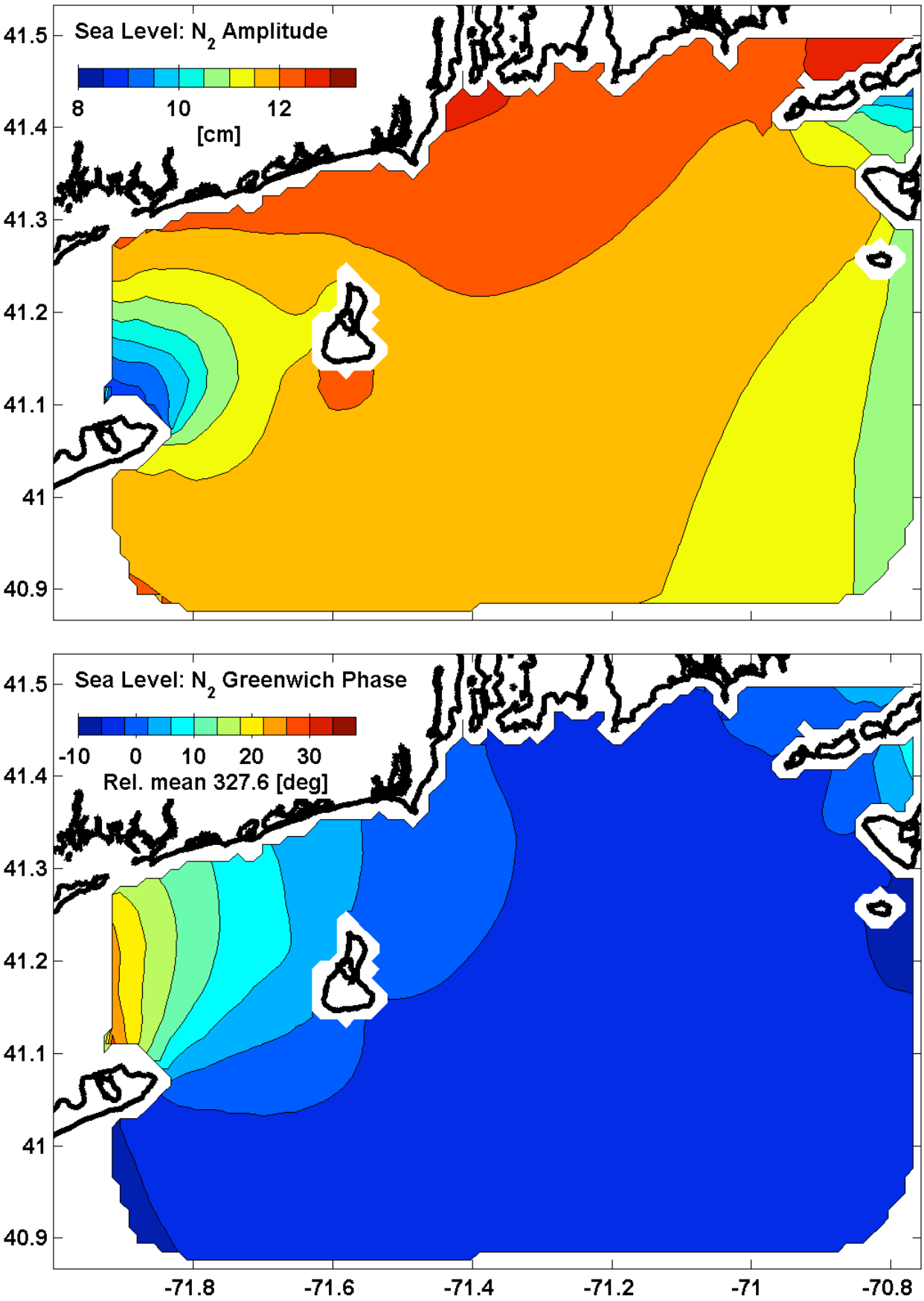

Figure 89. Simulation: Tidal height, N_2 constituent. (upper) Amplitude. (lower) Phase.

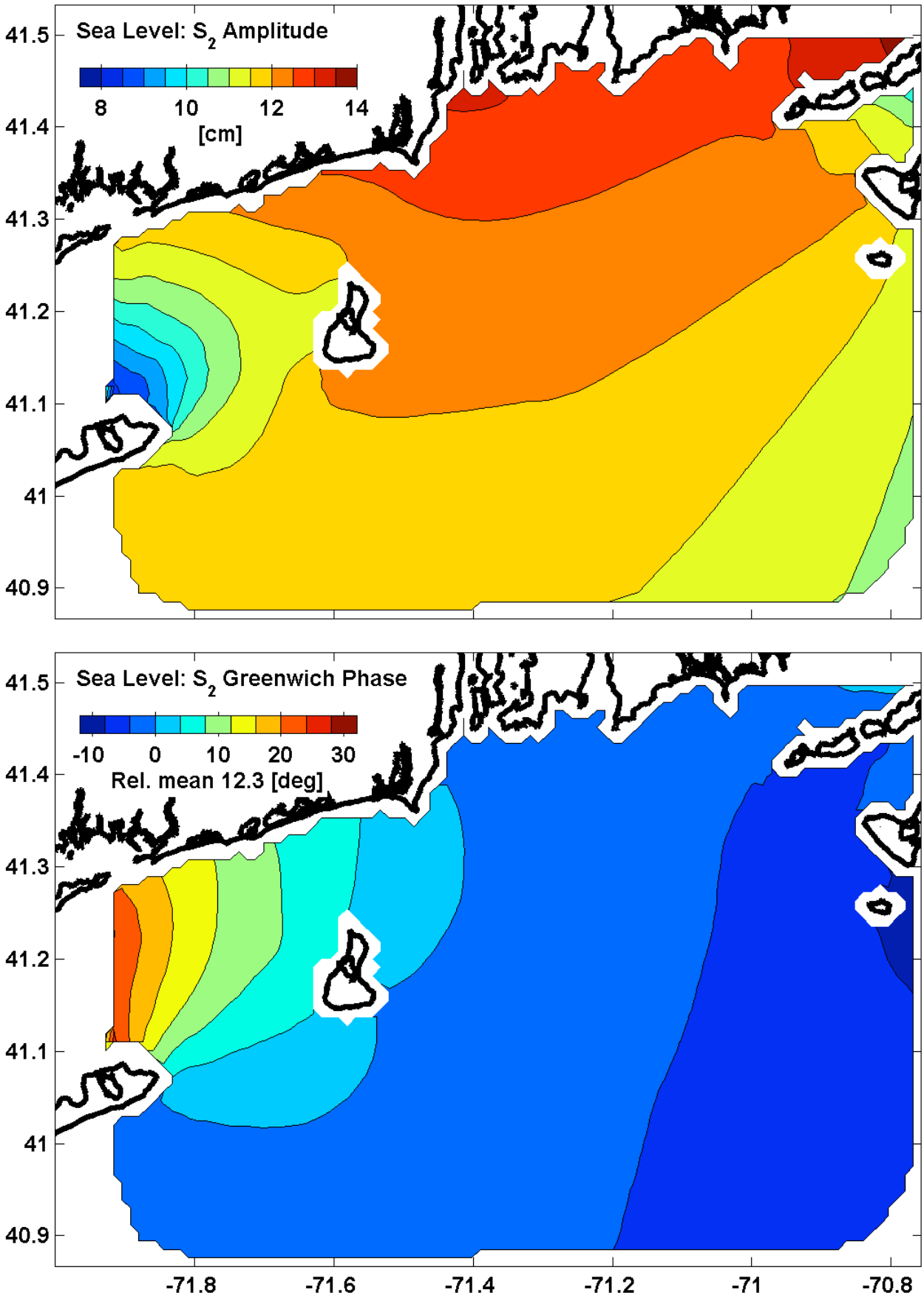

Figure 90. Simulation: Tidal height, S_2 constituent. (upper) Amplitude. (lower) Phase.

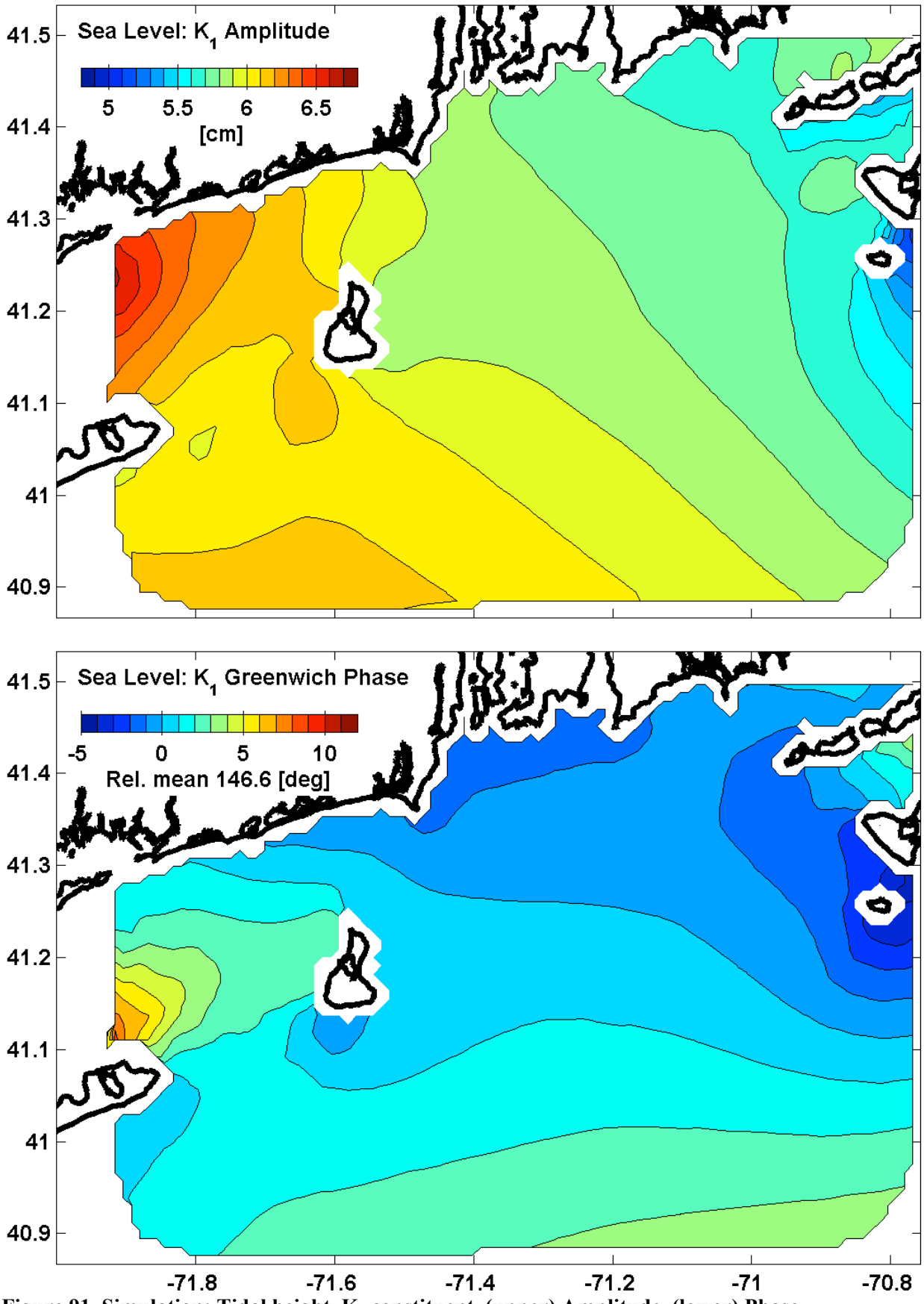

Figure 91. Simulation: Tidal height, K_1 constituent. (upper) Amplitude. (lower) Phase.

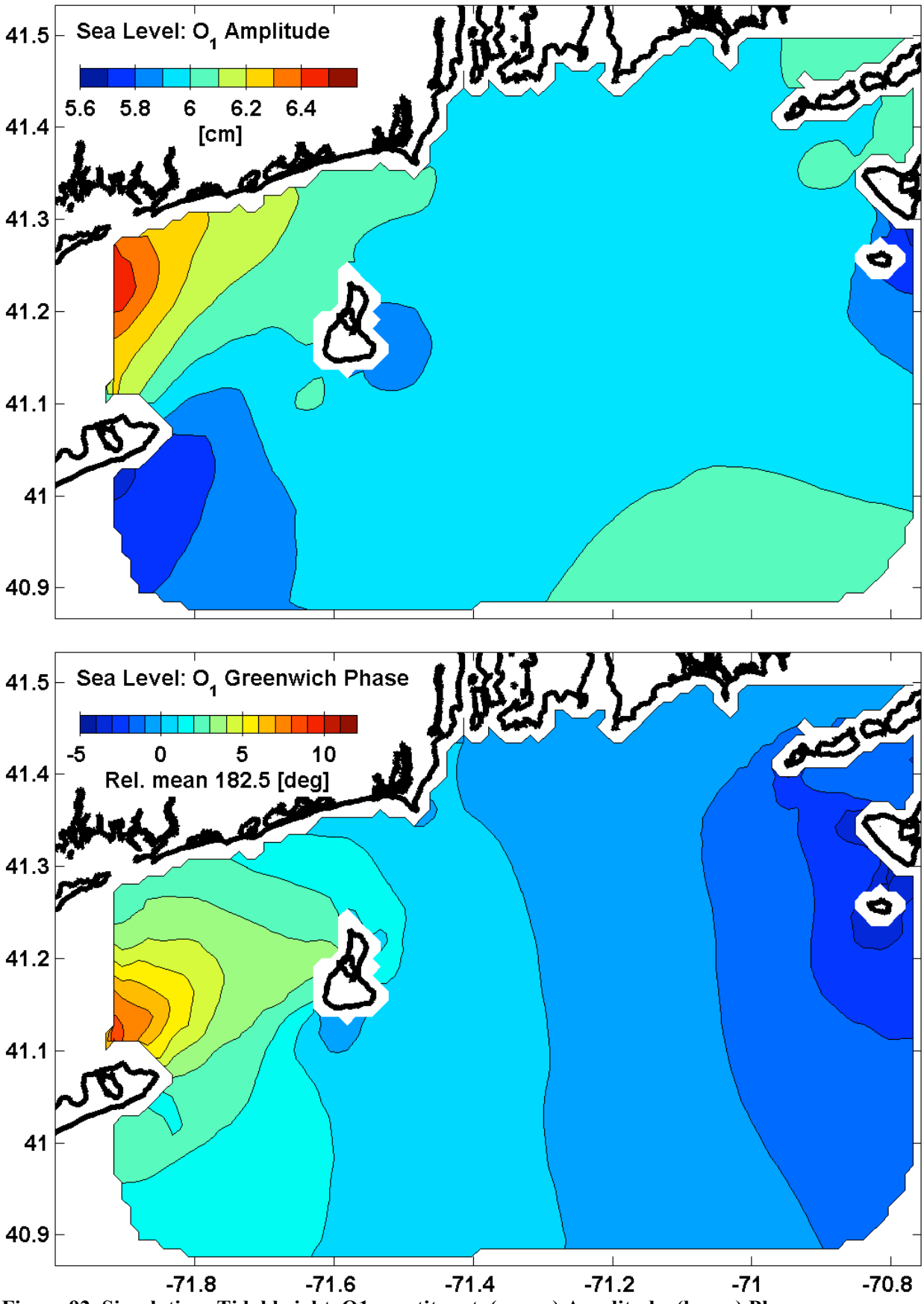

Figure 92. Simulation: Tidal height, O1 constituent. (upper) Amplitude. (lower) Phase.

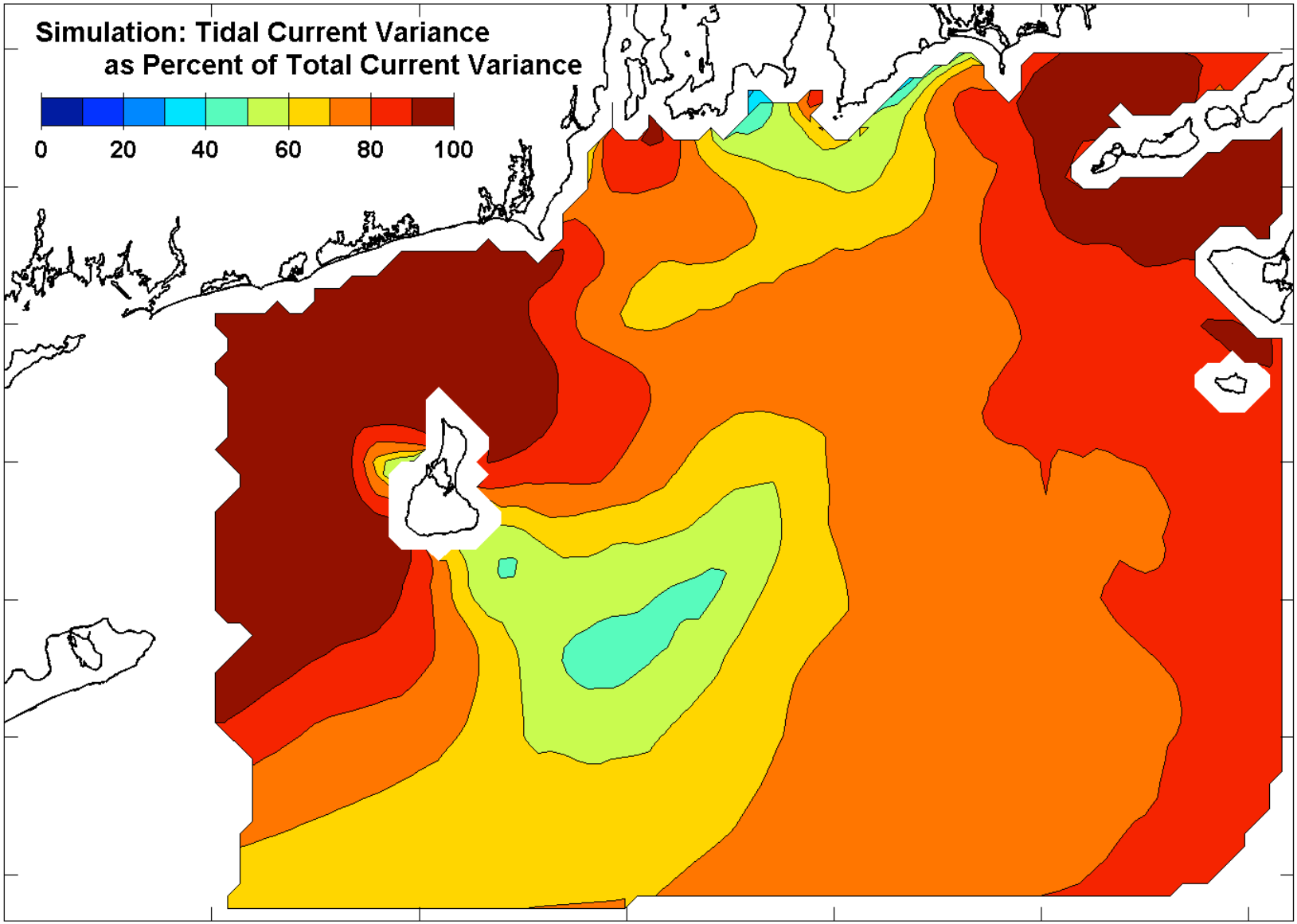

Figure 93. Simulation: Tidal current KE variance, pct. of summed tidal/non-tidal KE variances.

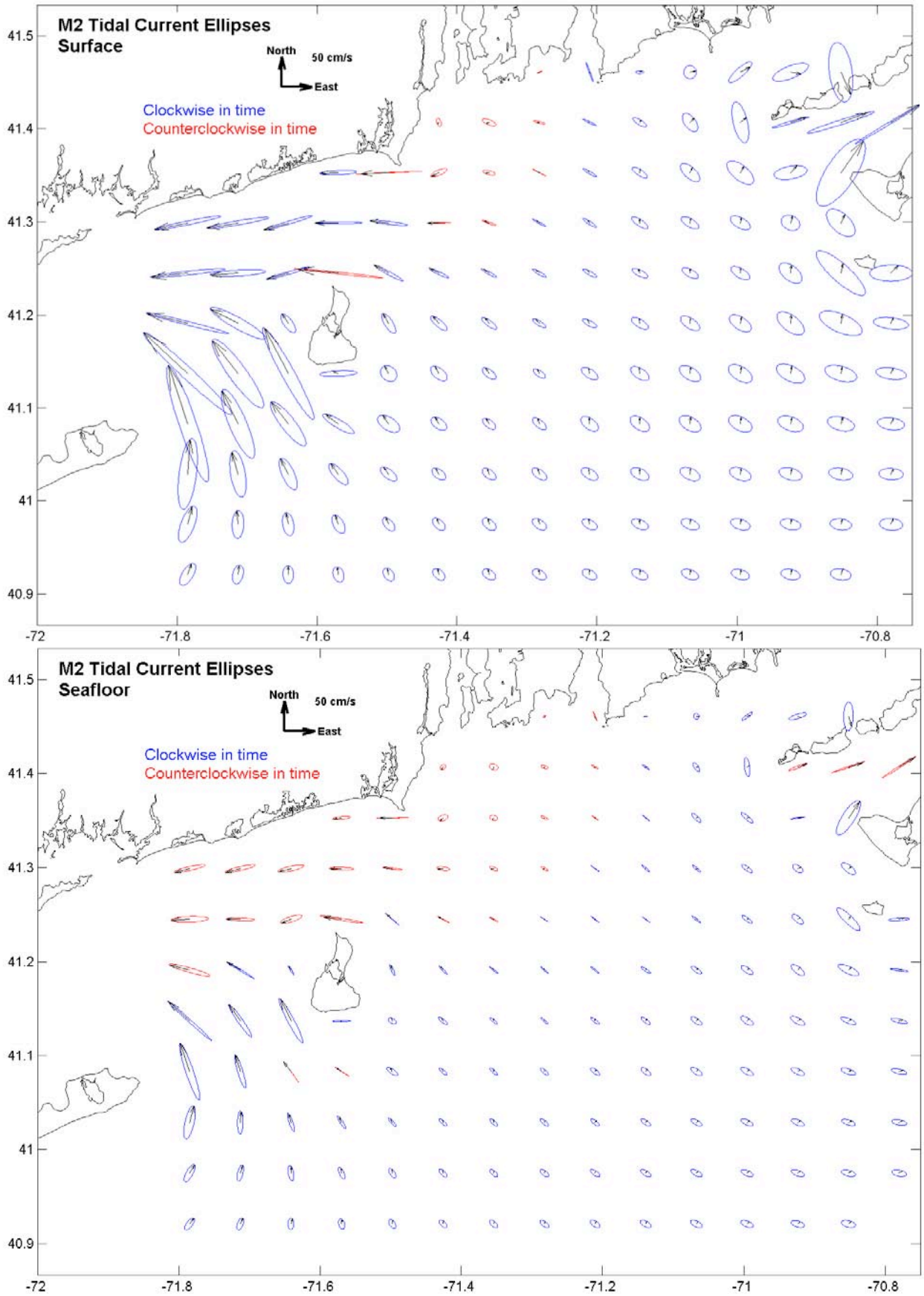

Figure 94. Simulation: Tidal currents, M_2, size 1X advection. (upper) Surface. (lower) Bottom.

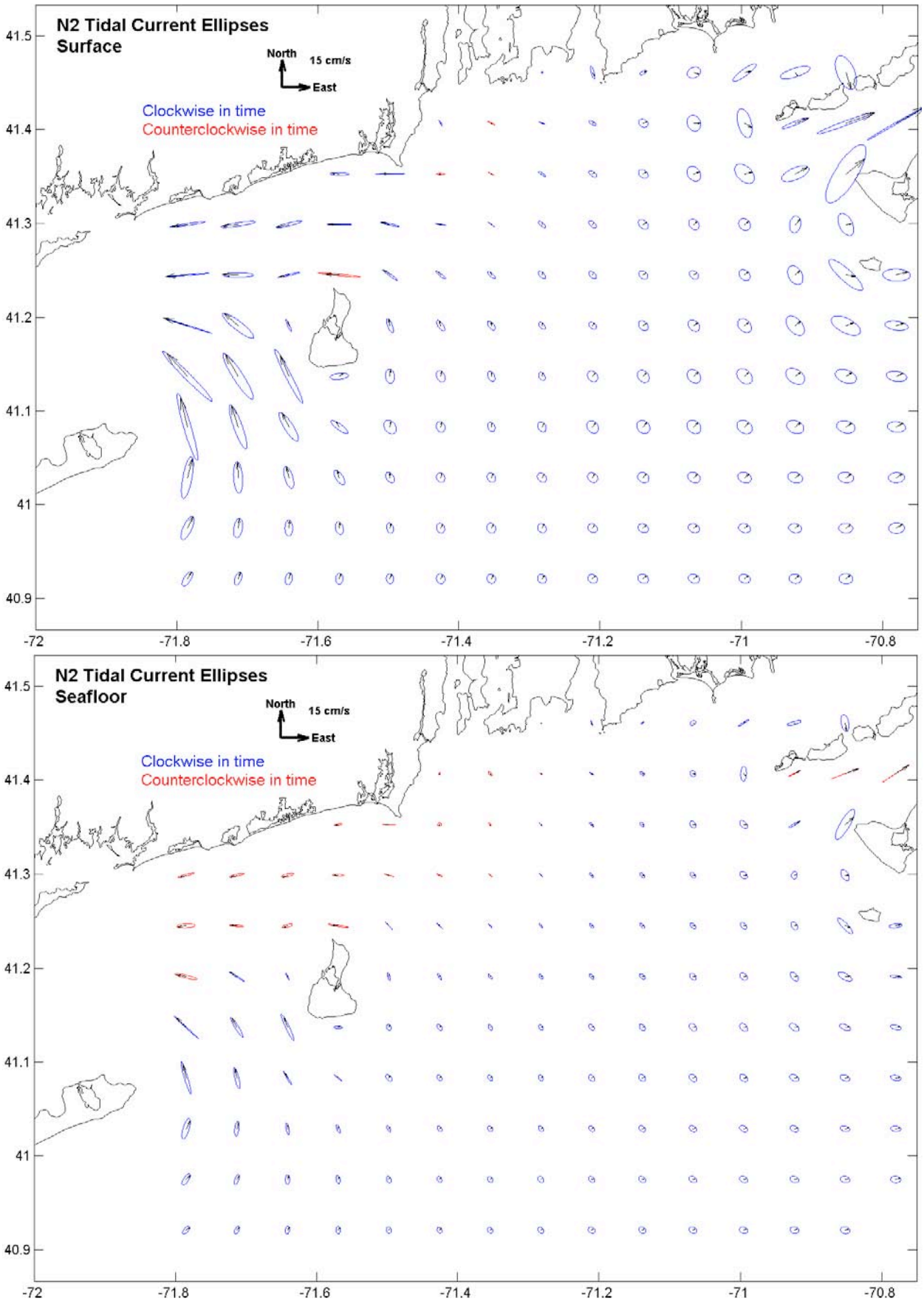

Figure 95. Simulation: Tidal currents, N_2, size 3X advection. (upper) Surface. (lower) Bottom.

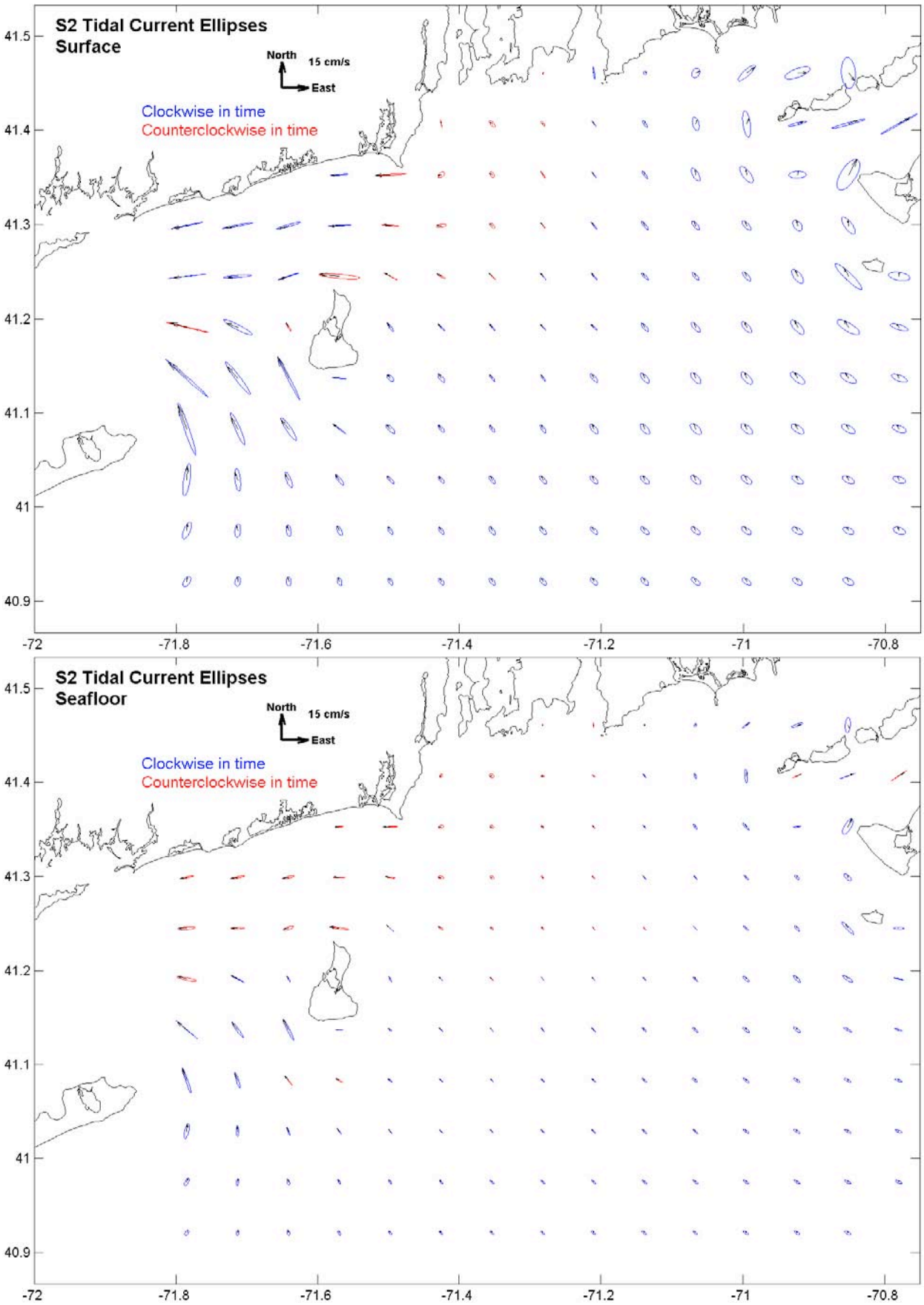

Figure 96. Simulation: Tidal currents, S_2, size 3X advection. (upper) Surface. (lower) Bottom.

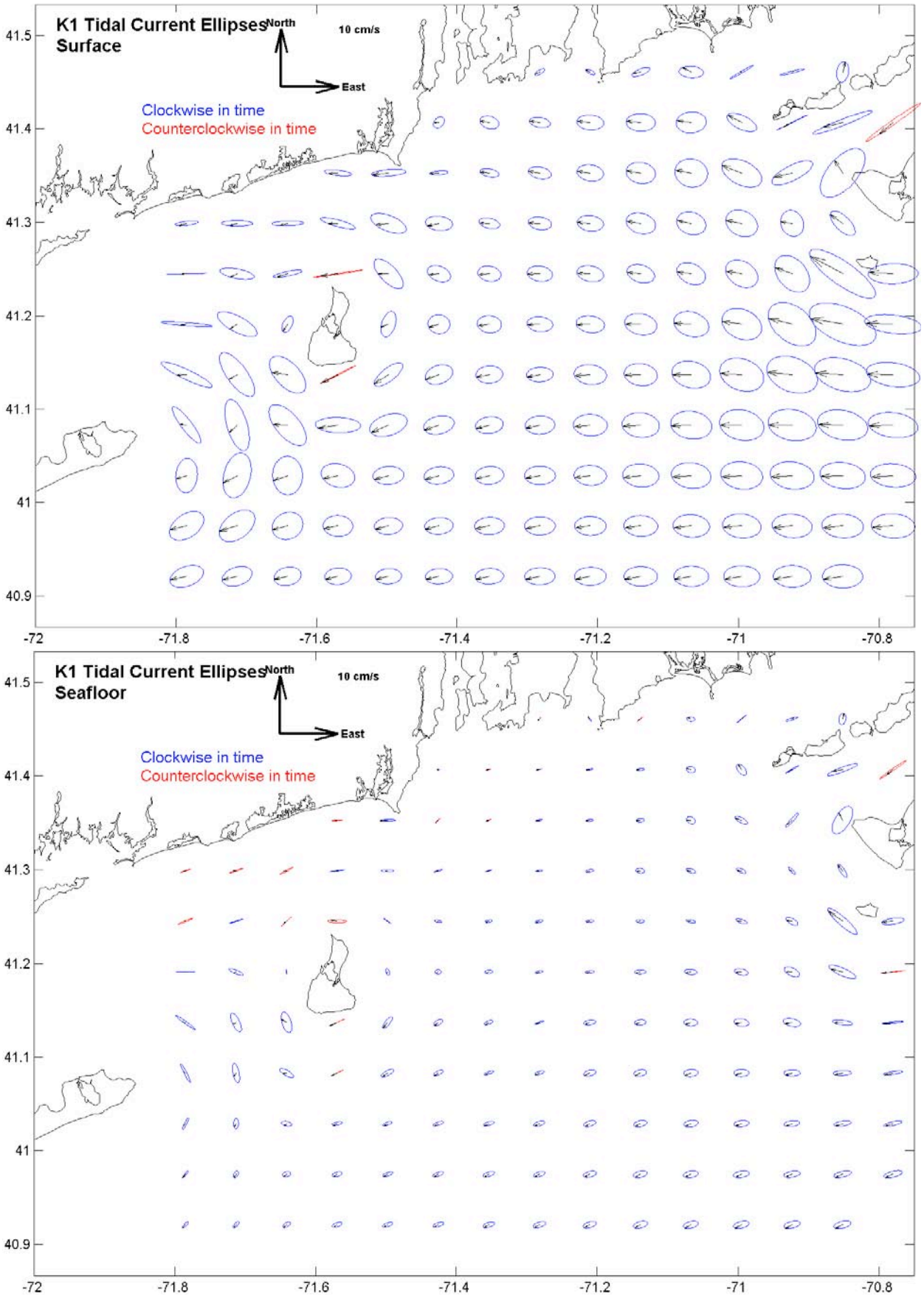

Figure 97. Simulation: Tidal currents, K_1, size 5X advection. (upper) Surface. (lower) Bottom.

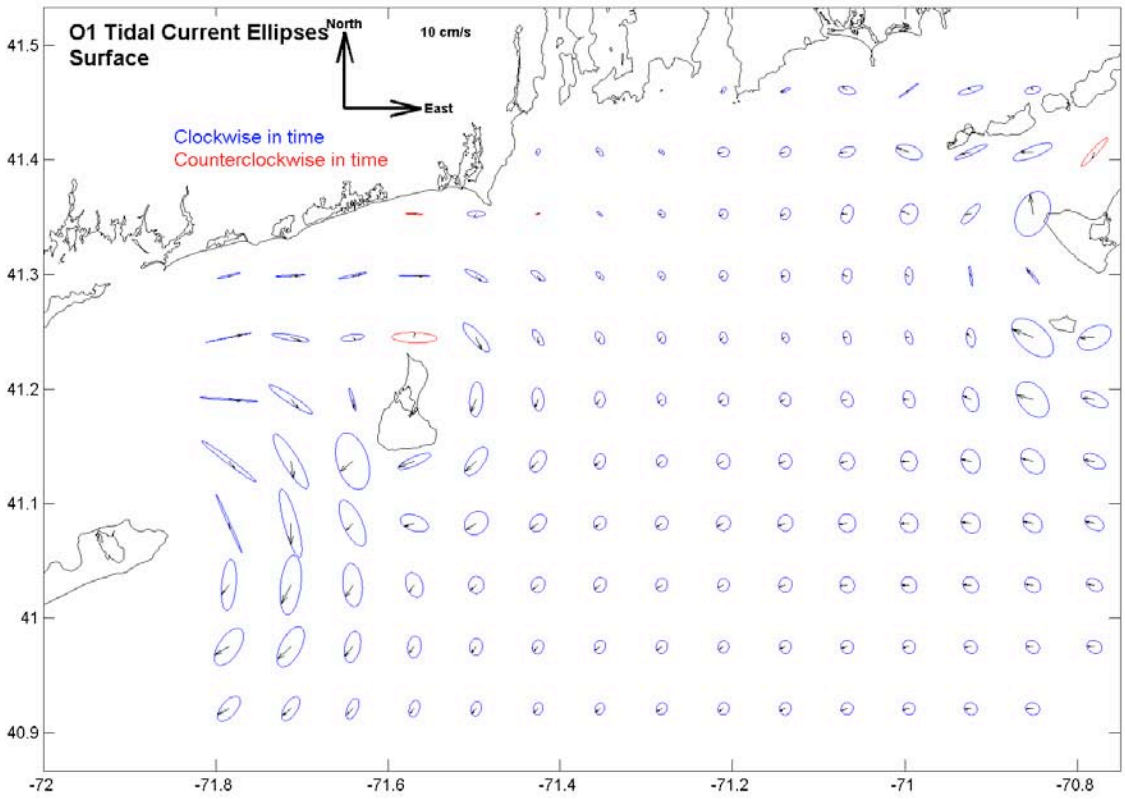

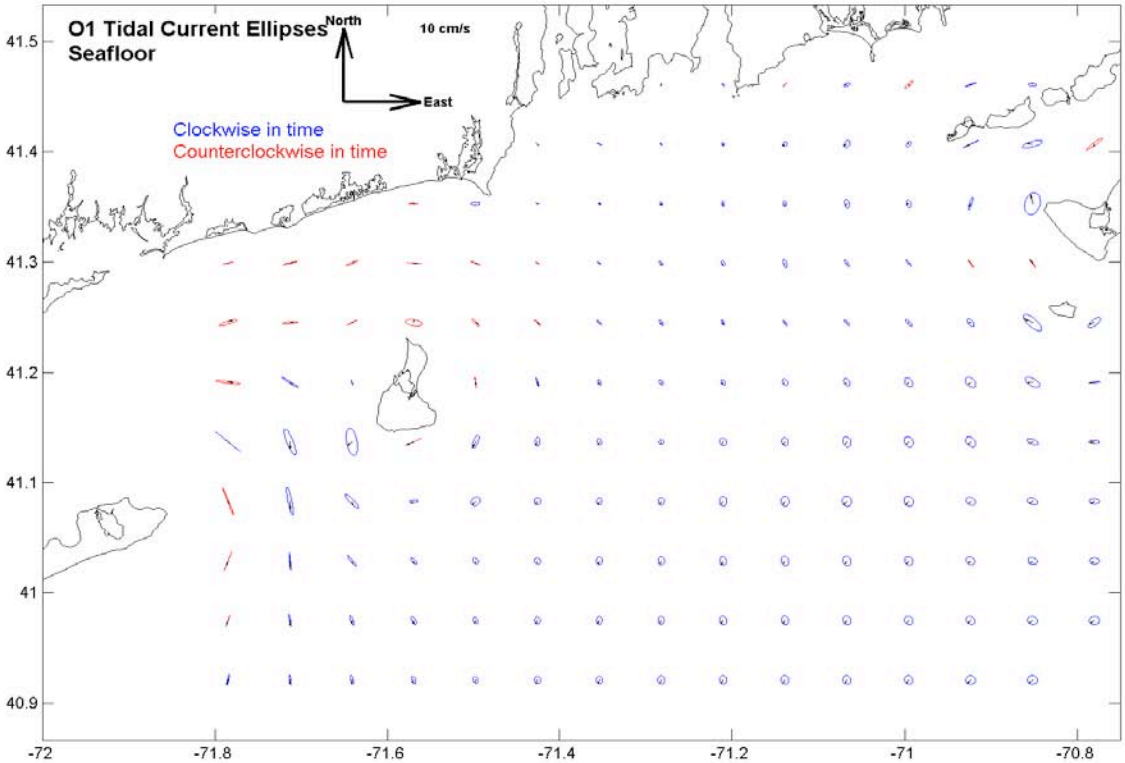

Figure 98. Simulation: Tidal currents, O_1, size 5X advection. (upper) Surface. (lower) Bottom.

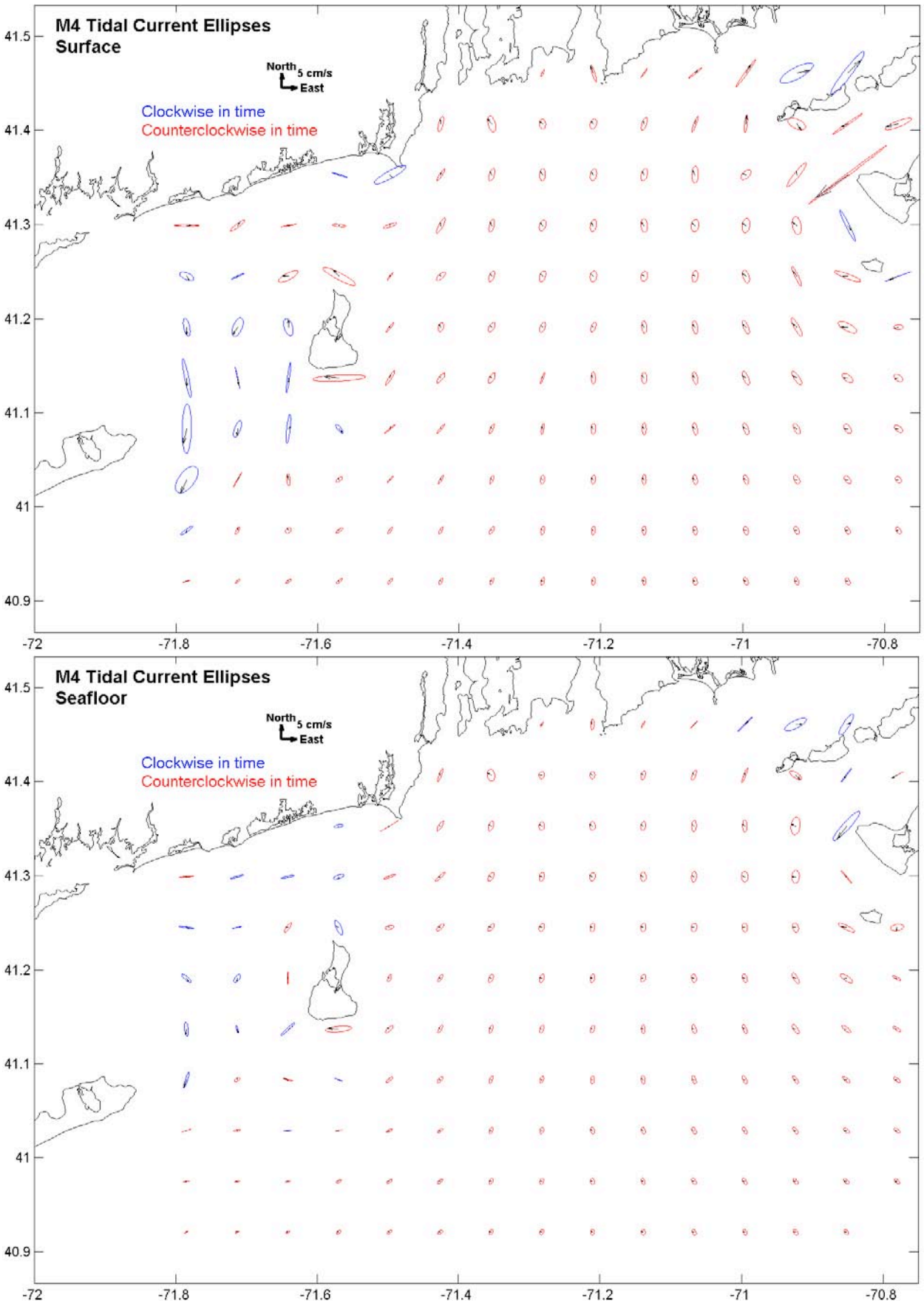

Figure 99. Simulation: Tidal currents, M_4, size 10X advection. (upper) Surface. (lower) Bottom.

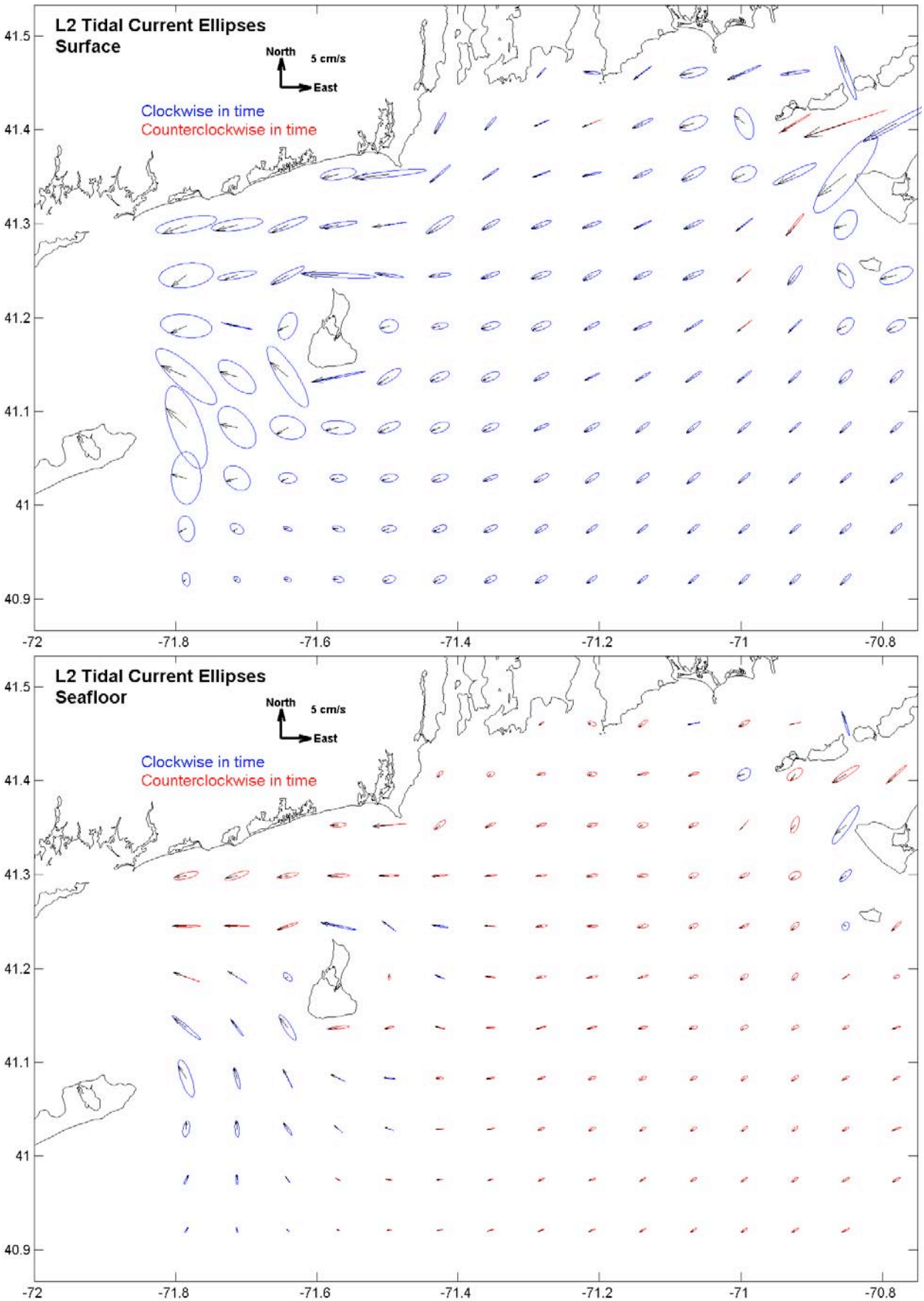

Figure 100. Simulation: Tidal currents, L_2, size 10X advection. (upper) Surface. (lower) Bottom.

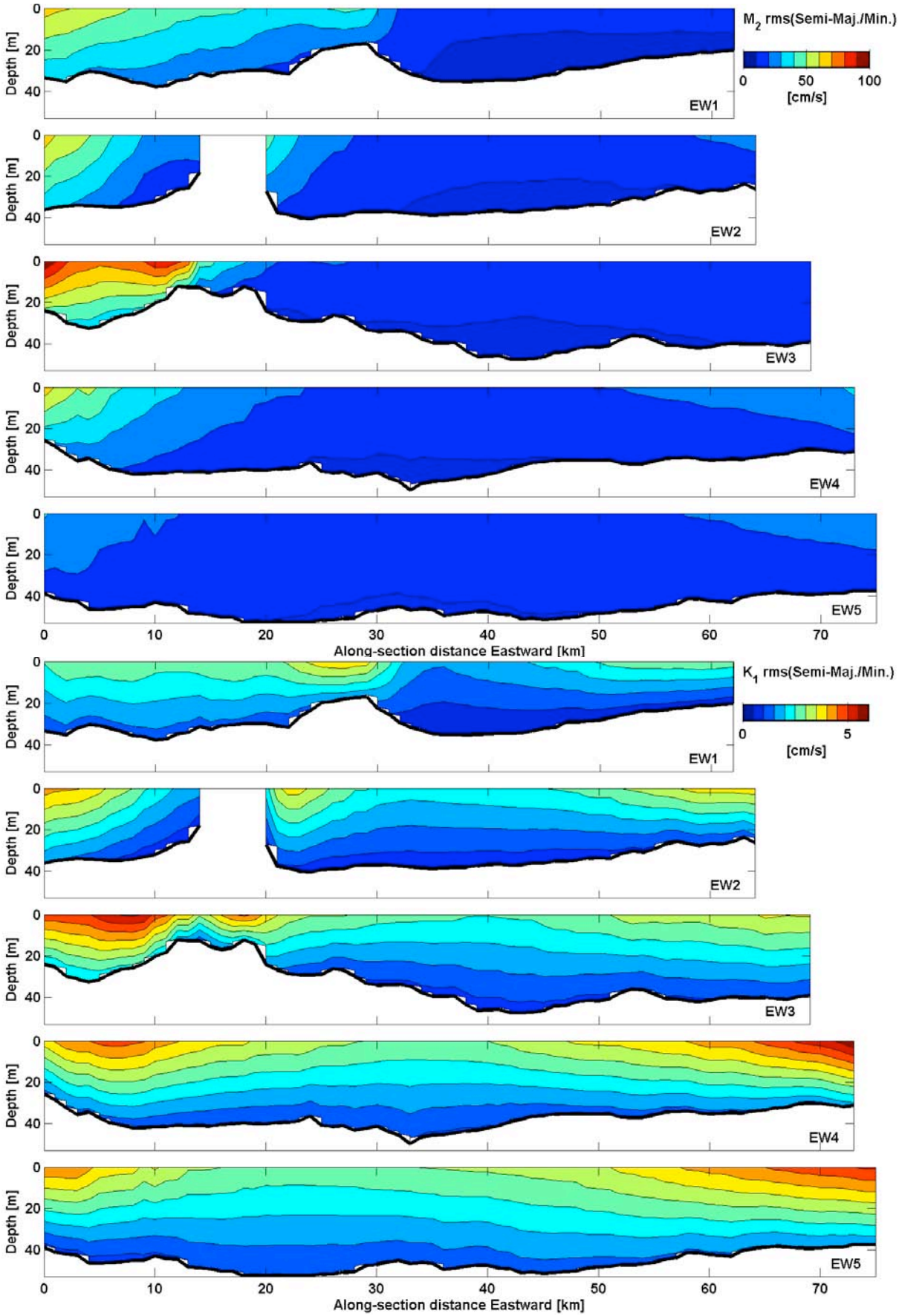

Figure 101. Simulation: Tidal currents, RMS ellipse semi-axes, EW. (upper) M_2. (lower) K_1.

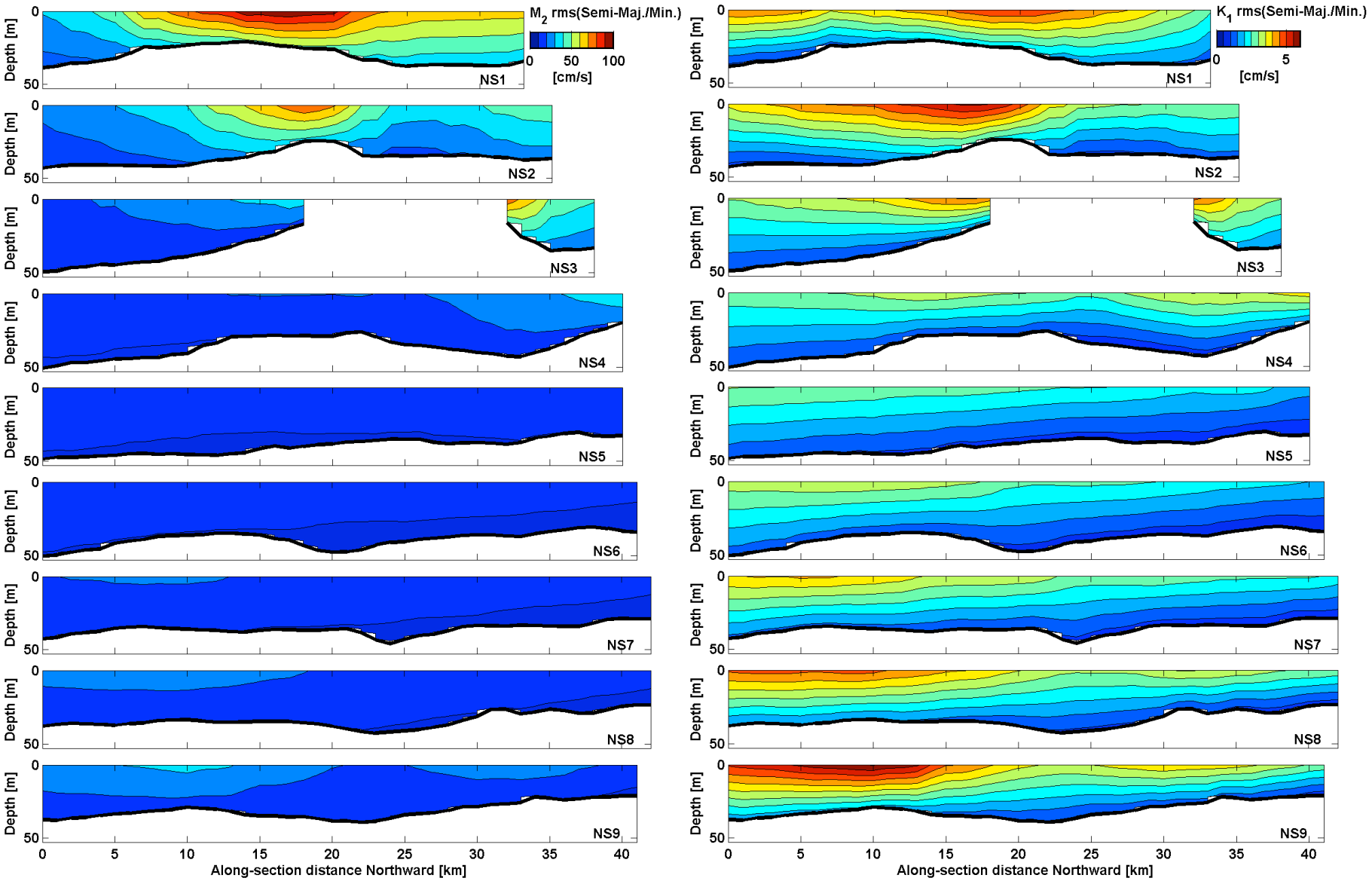

Figure 102. Simulation: Tidal currents, RMS ellipse semi-axes, NS. (left) M_2. (right) K_1.

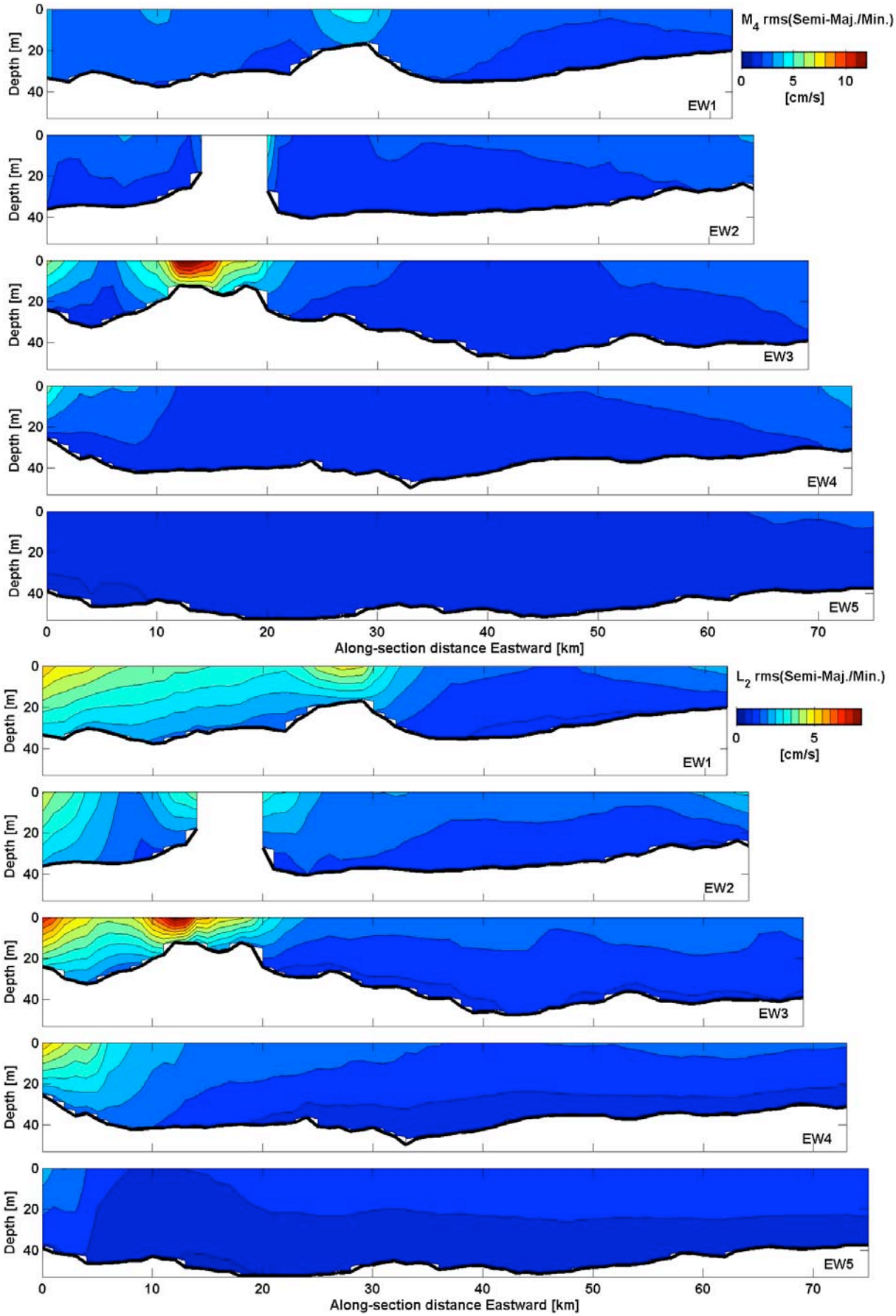

Figure 103. Simulation: Tidal currents, RMS ellipse semi-axes, EW. (upper) M_4. (lower) L_2.

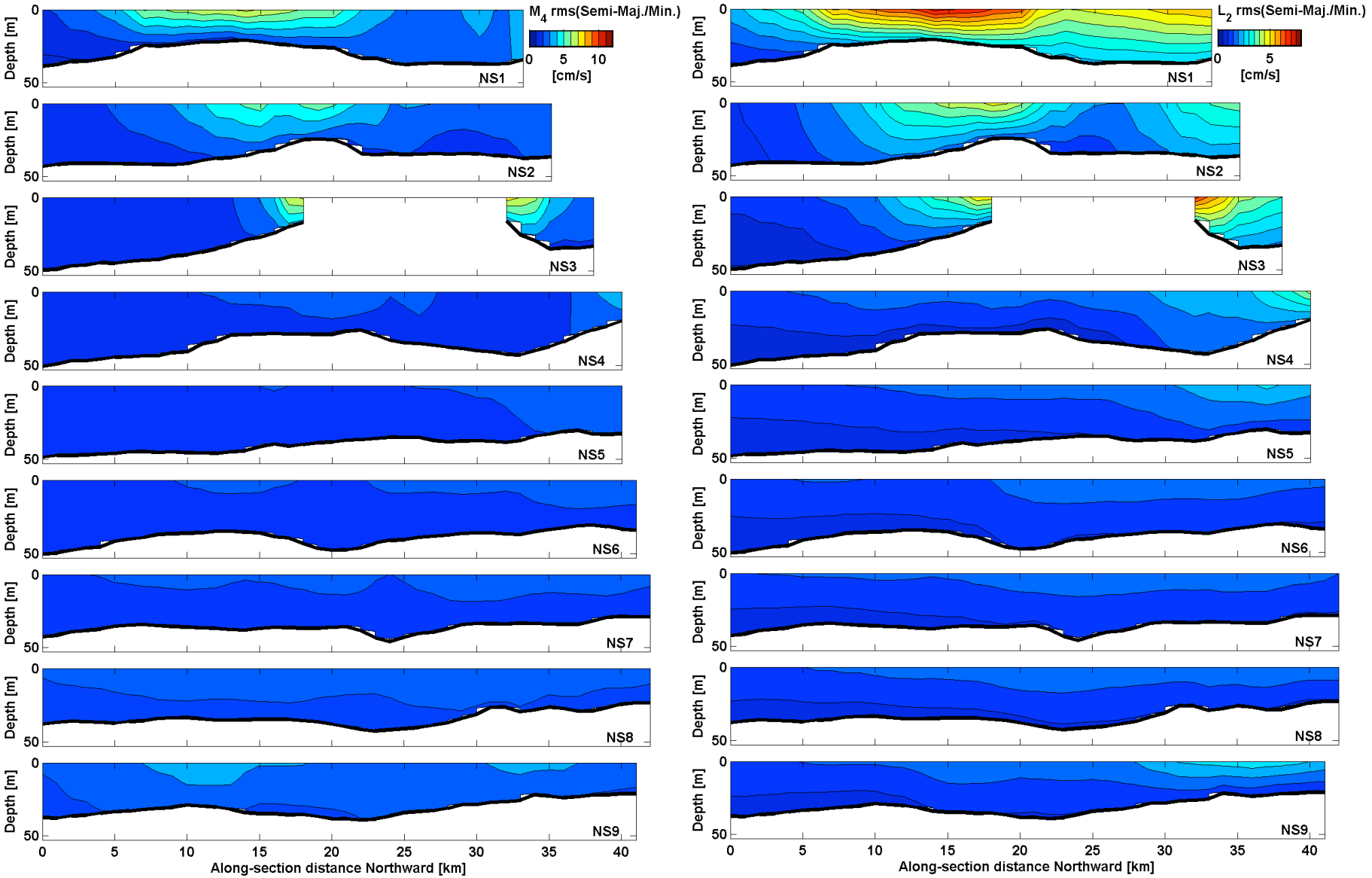

Figure 104. Simulation: Tidal currents, RMS ellipse semi-axes, NS. (left) M_4. (right) L_2.

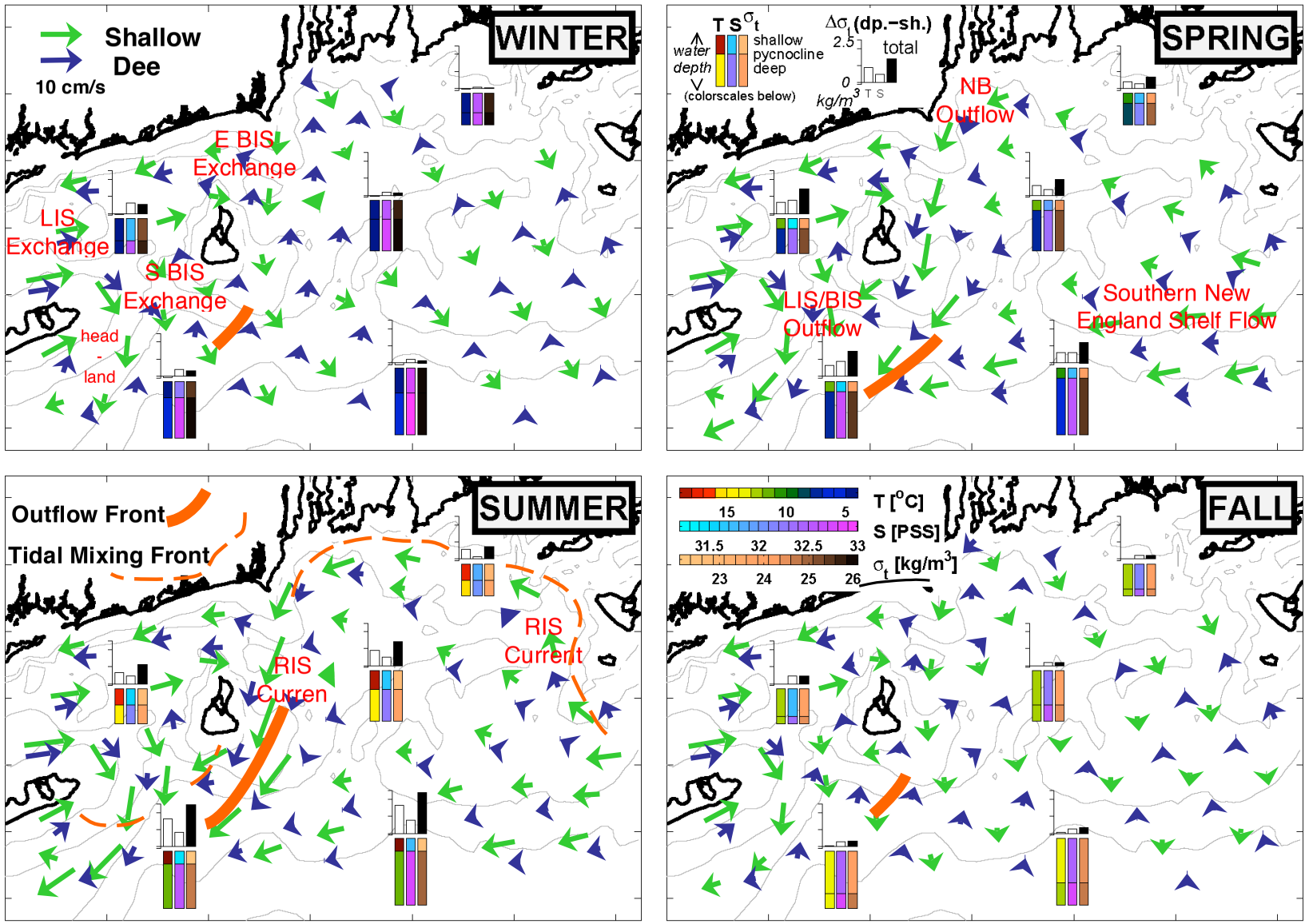

Figure 105. Summary schematic, seasonal-mean hydrography & circulation (explained in text).

Appendix A. Catalogue of Observational Studies

Below is a compilation of published studies that report on observations of hydrographic fields (temperature, salinity) or currents from locations within Rhode Island Sound and Block Island Sound, listed in chronological order by publication year. While this listing may not be absolutely comprehensive, to the best of our knowledge the primary content of any references that do not appear is represented well by one of the references listed.

The following is a key to abbreviations in the table:

Measurements: U = currents; T = temperature; S= salinity; FR = flushing rates; KED = kinetic energy dissipation

Where: sh = shallow or near-surface; dp = deep or near-bottom; N/S/E/W = North/South/East/West; BIS = Block Island Sound; RIS = Rhode Island Sound; MP = Shelf off Montauk Point

Method: CTD = vessel-based hydrographic casts or bathythermograph; MT/MS = moored thermistor/salinity sensor; CM = moored current meters; SD = surface drifters; BD = seabed drifters; VC = vessel-based current sampling; TB = towed-body sampling; SAT = satellite radiometer; HFR = high-frequency radar; AUV = autonomous underwater vehicle

Table A1. Catalogue of published observational studies.

Citation	Msmt	Where	When	Method
LeLacheur & Sammons 1932	U	BIS	Pre-1930s	VC
Haight, 1938	U	E RIS	1930s & before	VC
Riley 1952	TS, U	BIS, RIS	1946-47	CTD, CM
Powers, 1953	TS	BIS, RIS	1951	CTD
Bumpus 1965	U	RIS, BIS	1961-64	BD
Cook 1966	U	RIS	1962-63	SD, BD
Shonting et al 1966	TS	RIS	1963-64	CTD
Ichiye 1967	TS	BIS	Aug 1965	CTD
Shonting 1969	U	RIS	Aug 1967, 13 d	CM
Williams 1969	U	BIS	May 1965	CM
Hardy 1970	TS	BIS	Jan-Apr 1970	CTD
Shonting and Cook, 1970	TS	RIS	1963-64	CTD
Meguire 1971	U	BIS, sh	1965-67	VC
Hollman & Sandberg 1972	U	BIS	1970-71	SD, BD
Saila et al 1972	U	E RIS, dp	Jul 1970, 4 d	CM
Collins 1974	U	N/W RIS	Feb 1973	BD
Hollman 1974	TS	BIS	1972-73	CTD
Pratt et al 1975	U	E RIS, dp	May/Jun 1974	CM

Citation	Msmt	Where	When	Method
Raytheon, 1975	TS, U	BIS	1974-75	CTD, CM, MT/MS, SD
Griscom 1977	U	E RIS, dp	Sep-Oct 1976	CM
Krabach & Snooks 1977	FR	NE BIS	Aug 1974	Dye
Snooks et al 1977	TS	NE BIS	1975-76	CTD
Long, 1978	U	BIS	1965-67	VC, CM
Snooks and Jacobsen 1979	U	NE BIS	Feb-Dec 1977	CM, SD, BD
Bowman and Esais, 1981	TS	BIS	1978	CTD
Armstrong 1998	T	RIS	1974-83	CTD
Fox et al 2000	T	RIS, BIS	1997	SAT
Ullman & Cornillon, 1999, 2001	TS	RIS, BIS	1985-96	SAT
Kincaid et al 2003	U, TS	N RIS	1998-99	VC, CTD
Codiga and Rear 2004	U, TS	MP	2001-02	CM, MT/MS
Ullman and Codiga 2004	U, TS	BIS, WRIS, MP	2000-01	HFR, CM
Codiga 2005	U	MP	1999-2002	CM
Kirincich & Hebert 2005	U, TS	MP	Apr 2002, 2 d	TB-CTD, VC
SAIC 2005	U, TS	RIS	2004	VC, CTD
Ullman et al. 2006	U	BIS	2002 & 03; 3 d	SD
Mau et al. 2006, 2007	U	BIS, W RIS	2001	HFR
Kincaid et al 2008	U	N RIS	2000-01	CM
O'Donnell & Houk, 2009	TS	BIS, MP	2000-2001	CTD
Levine et al 2009	TS,U, KED	MP	2000-01	CTD, VC, AUV

Appendix B. Catalogue of Modeling Studies

This is a compilation of published, modern numerical/computational hydrodynamic model studies that focus on hydrodynamic fields (temperature, salinity) and/or currents and are configured with the aim of realistic simulation of at least some of the RI Ocean SAMP region, presented in chronological order. Spaulding and Gordon (1982) includes a table listing previous (1970s) modeling studies. The site abbreviations are the same as in Appendix A.

Table B1. Catalogue of published modeling studies.

Citation	*Where*	*Period modeled*	*Emphasis*
URI, 1979	BIS, RIS	--	Barotropic tidal flow
Spaulding and Gordon, 1982	BIS, RIS	--	Barotropic tidal flow
Edwards et al 2004a,b	BIS, W RIS, MP	2000	Frontogenesis, MP area
He and Wilkin 2006	E RIS	--	Barotropic tidal flow
Wilkin 2006	E RIS	2001-2003	Summer heat budget
Mau et al, 2007, 2008	BIS, RIS, MP	2001	Tidal flow (2007), MP outflow (2008)
Cowles et al, 2008	BIS, RIS, MP	1996-1997	Low-frequency flow and hydrography

Appendix C. List of GIS Layers

The following is a list of GIS layers that have been produced for the RI Ocean SAMP project. Each is listed with the number of the figure which it appears as in this report.

See the RI Ocean SAMP Supplement for these figures.

3.

Characterizing the Physical Oceanography of Coastal Waters Off Rhode Island, Part 2: New Observations of Water Properties, Currents, and Waves

Prepared for the Rhode Island Ocean Special Area Management Plan 2010

By

David S. Ullman and Daniel L. Codiga

University of Rhode Island, June 30, 2010

PARTIALLY COMPLETE DRAFT
NOT READY FOR DISTRIBUTION OR EXTERNAL REVIEW

Executive Summary

Part 2 of the Rhode Island Ocean Special Area Management Plan physical oceanography characterization study complemented the review of archival observations and model runs carried out in Part 1 by focusing on the collection and analysis of new observations that can help provide a more complete description of the seasonal mean and variability of the water column structure, circulation, and waves. The physical oceanography of Rhode Island coastal waters is investigated using a combination of wide-area vessel-based surveys of water properties at 3-month intervals and long-term moorings at 5 sites to collect observations of hydrography, waves, and currents. The results improve our understanding of the seasonal cycle in the OSAMP region and also demonstrate the marked inter-annual variability that is manifest in the region.

The surveys and moored observations of hydrography during the period from September 2009 to July 2010 generally agree with the hydrographic climatology analyzed in Part 1. However, during late autumn/early winter of 2009, the observational program observed a previously undocumented intrusion of warm salty water, normally found near the shelf break, into the OSAMP region. The properties of this water, which floods the deep areas of the region during December 2009, are far different from our best prior estimate of the mean regional properties.

Currents measured by moored instruments at four locations are broken in to tidal and subtidal components. Tidal currents are dominated by semidiurnal components and tidal current ellipses reflect geographic amplification associated with nearby estuaries, and vertical structure of frictional bottom boundary layer, in very good agreement with previous observations and modeling. Subtidal currents have energetic weather band variability, which is strongly shaped by wind variations and dominates the longer-term residual circulation.

Waves have typical significant heights of 2-4 m and typical dominant periods of several seconds, both tending toward the lower/higher end of these ranges in summer/winter. During storm events the significant wave height reaches up to 7m and the dominant wave period reaches 14 s. The direction of peak wave energy is most commonly northward and slightly eastward, and variability in the direction is more pronounced at offshore sites.

Table of Contents

List of Figures

List of Tables

Abstract

(PREPARATION UNDERWAY)

1 Purpose and Scope

The purpose of this report, which is Part 2 in a two-part series and complements the review of previously gathered information in Part 1 (Codiga and Ullman 2010), is to present new observations collected to characterize water properties, currents, and waves in the Rhode Island Special Area Management Plan (OSAMP) region. These observations expand on prior investigations through use of modern measurement techniques and by exploring geographic areas that have, as described in Part 1, received almost no previous attention. For water properties, the emphasis is on geographic and vertical structure, and seasonal changes. For currents, the emphasis is on descriptions of tidal fluctuations, weather-band variability (changes on timescales of about 1 to 10 days), and longer-term means at four specific locations, including comparisons among the sites. Surface wave parameters from five locations are described. The reader is referred to Part 1 for overall context, including descriptions of the geographic and bathymetric setting (see Figures 1 and 2 of Codiga and Ullman 2010).

In addition to temperature and salinity, the water properties analysis includes measurements of dissolved oxygen, Chlorophyll fluorescence, photosynthetically active radiation, and turbidity; while the latter four quantities are described briefly here, for more complete discussion of their implications to biological and sediment transport processes the relevant companion OSAMP reports should be consulted. Similarly, while our analysis presents wind measurements, it does so solely for context in interpreting currents; for a comprehensive description of winds reference should be made to the dedicated OSAMP report. Tidal and weather-band fluctuations in sea level are addressed here but the durations of the observations do not permit us to address climatic change in sea level, which is taken up in a separate OSAMP report. Finally, the treatment of wave observations here is cursory because a companion OSAMP report includes a thorough investigation of wave processes based on both these observations and an intensive modeling effort.

2 Introduction

Temperature and salinity characteristics across sizable portions of the OSAMP domain, particularly eastern Rhode Island Sound (RIS), are historically severely under-sampled. This was made clear by the review of available temperature and salinity observations in Part 1, and was a primary motivation for the seasonal series of vessel-based conductivity-temperature-depth (CTD) surveys completed and described here. In order to capture vertical structure and

geographic patterns, the surveys include profiles spanning the water column at stations covering the entire OSAMP domain with nominal spacing of 8-12 km (Figure 1). The station grid is nearly identical to that used in Part 1 for explorations of historical observations and model outputs, so facilitates direct comparisons. The goal of the surveys was to characterize the seasonal cycle, so one 2-3 day survey was completed in each of September 2009, December 2009, March 2010, and June 2010. In addition to temperature and salinity the surveys measured water properties relevant to biological and sediment transport processes (straightforward using modern instrumentation): dissolved oxygen, Chlorophyll fluorescence, photosynthetically active radiation, and turbidity. The maps and sections of these quantities presented here are a considerable advance over previously available observations of them.

A series of deployments of moored instrumentation captured temporal variability of temperature, salinity, currents and waves on timescales from hours to seasons in order to complement the broad geographic coverage but minimal temporal resolution and of the vessel-based water property surveys. Moored instruments sampled a total of five sites (Figure 2, Table 1).

At two sites, moorings instrumented with a suite of water-column sensors (temperature, salinity, currents), accelerometers to measure wave properties, and meteorological sensors (winds, temperature, pressure) were maintained continuously year-round starting in October 2009. The deployments were carried out by University of Maine under subcontract, as part of the Northeastern Regional Association of Coastal Ocean Observing Systems (NERACOOS), and data was delivered and distributed in real time. These two moorings are denoted MD-S and MD-F; MD indicates Multi-Disciplinary (both meteorological and physical oceanographic parameters were sampled), S indicates the site is in RI state waters south of Block Island, and F indicates the site is in federal waters in southeastern Rhode Island Sound.

To provide improved understanding of geographic variations in water column properties (temperature, salinity, and currents) and wave attributes, moored instruments were deployed at two additional sites that complement MD-S and MD-F. One was located about 10 km SE of MD-S, to help characterize the transition toward deeper water, and the second was located about 15 km NNW of MD-F, to help understand how properties change inshore of MDF towards central RIS. At these complementary sites, only physical oceanographic parameters were sampled, hence they are referred to a PO-S and PO-F respectively. Note that, despite its name, the PO-S site is not in state waters. The PO-S and PO-F moorings were maintained for two deployments,

one in late Fall 2009 (denoted FA09) and one in late Spring 2010 (denoted SP10), as year-round sampling was not possible given budgetary and logistical constraints. As these instruments were not intended for real time sampling they recorded and stored data internally.

At a fifth site the Army Corps of Engineers established a Datawell directional wave buoy, denoted the Block Island Wave Buoy (BIWB) although it is located offshore from central RIS. It has operated continuously since October 2009 and its real-time data stream is managed by the Coastal Data Information Program (CDIP) at Scripps Institution of Oceanography.

3 Methods

3.1 Vessel-Based Water Properties Surveys

Four vessel-based surveys, at approximately 3-month intervals covering the seasonal cycle, were carried out from the University of Rhode Island's research vessel Hope Hudner. The station grid (Figure 1) extends across eastern Block Island Sound (BIS), Rhode Island Sound (RIS), and the offshore area to the south. Surveys took 2-3 days to complete (see Table 2 for the survey dates) and were made without regard to tidal phase. During the December 2009 survey, not all stations were occupied (the omitted stations are obvious in the maps presented below) due to weather conditions.

At each station, vertical profiles of electrical conductivity (C), temperature (T), pressure (P), oxygen concentration (O_2), chlorophyll fluorescence, turbidity, and photosynthetic active radiation (PAR) were obtained using a hand-lowered package. The sensors included a SeaBird Electronics SBE 19plus CTD, with T, C, and O_2 (SBE 43) sensors located within a pumped duct; a Turner Designs SCUFA 2000-007 Fluorometer; and a BioSpherical QSP2300 PAR sensor.

The data were processed using SeaBird's data processing software (SBE Data Processing), including corrections for sensor alignment, conductivity cell thermal mass, and the response time of the O_2 sensor. Salinity was computed from the measured C, T, and P data, and all variables were averaged into 1 dbar (~1m) vertical bins. Chlorophyll fluorescence measurements were converted to chlorophyll concentrations using a generic calibration. The vertical profiles of PAR were used to estimate the light extinction coefficient by fitting the observed data to an exponential function: $I(z) = I_0 e^{-kz}$, where *I(z)* is light intensity at depth z, I_0 is the intensity at the surface (z=0), and k is the extinction coefficient (units m^{-1}). For profiles where the CTD was not shaded by the survey vessel at the surface, the fits were performed using observations from the surface down to a depth at which the sensor response was observed to roll off. When the CTD

was shaded at the surface, the upper 5-10 m of the profile was omitted from the fit. The depth of the euphotic zone was estimated as the depth at which the light intensity was 1% of the surface value (I_0).

3.2 MD-S and MD-F Moored Instrumentation

On the MD-S and MD-F moorings the subsurface instrumentation (Table 1) included three CTDs, a 2m-deep Aanderaa 3429 current/temperature sensor recording once per hour, and a downward-looking Teledyne RD Instruments 600 kHz acoustic Doppler current profiler (ADCP) that sampled each meter from 5 m deep to within 3-4 m of the seafloor using 6-second ping interval for 8 minutes once an hour. The CTDs were SeaBird Electronics 37 Series; one mounted on the buoy sampling each 30 minutes, one on the mooring wire in the upper water column, and one on the wire nearest the seafloor, the latter two sampling each 60 minutes and sending their data inductively to a coupler at the top of the wire rope. Wave parameters were measured by a Summit 34103A accelerometer package on the buoy operating at 2 Hz for a 17-minute interval each 30 minutes. The meteorological package included redundant Gill WindSonic wind sensors at 4m above sea level, and a Campbell 107L temperature sensor and Setra 270 barometric pressure sensor both at 3m above sea level.

3.3 PO-S and PO-F Moored Instrumentation

During each period (FA09 and SP10), a mooring instrumented with 7 CTD sensors distributed through the water column, and an upward-looking acoustic Doppler current profiler (ADCP) in a bottom frame very close nearby, were both deployed. The CTDs, measuring pressure as well as temperature and conductivity, consisted of a Falmouth Scientific Instruments NXIC bracketed to the buoy, sampling at 6 Hz for about 10 seconds each 90 seconds, and six SBE-37SM Microcats on the wire rope below sampling once each 16 seconds. After passing the data through a 3 point running median filter to remove spurious values, the CTD data were averaged into 4-minute ensembles.

The ADCP was a Teledyne RD Instruments 600 kHz deployed and recovered in a Mooring Systems Incorporated bottom frame. It measured currents each meter from about 2-3 m off the seafloor to about 3-4 m below the surface, with pings each 6 seconds and 20-minute ensemble averaging interval. The ADCP also measured wave orbital motions and computed directional wave parameters, using a 20-minute burst of 1 Hz sampling each 2 hours.

3.4 BIWB Moored Instrumentation

The BIWB is a Datawell directional buoy measuring significant wave height, peak wave period, and peak wave direction, based on 17-minute bursts of sampling each 30 minutes. Details of the processing are provided at the CDIP website, cdip.ucsd.edu.

3.5 Analysis techniques

Tidal analysis was carried out using the t-tide software package (Pawlowicz et al. 2002). Sub-tidal quantities were calculated using a 25-hour halfwidth triangle-weight low-pass filter and subsampled to 12-hourly values.

4 Water Properties

4.1 Maps & Sections of Hydrographic Parameters from Vessel-Based Surveys

We present the observations in two forms: (1) maps showing variables at a given depth below the water surface or height above the bottom, and (2) vertical sections along the approximately north-south and east-west lines shown in Figure 1. Although the data are treated as if the stations were sampled synoptically, it should be borne in mind that 2-3 days were required to complete the surveys. Therefore some smearing of features is expected due to advection of features by tidal and subtidal currents as well as by temporal evolution of the fields. Should note the times of spring and neap tides relative to the survey dates.

4.1.1 Temperature

During the late summer hydrographic survey in September 2009 (Figure 3, Figure 4, Figure 6), near-surface temperature gradients are generally small. This is in contrast to the observation, in satellite-derived sea surface temperature (SST) climatologies (e.g. Codiga and Ullman, 2010), of a moderately strong temperature front ($\Delta T \sim$ 1-2 °C) separating cooler BIS waters from warmer RIS and offshore waters. Strong near-bottom gradients occur along the 40 m isobath on the south side of Coxes Ledge (southern end of lines NS6 and NS7) and between the 30 m and 40 m isobaths south of Block Island. A deep thermocline (~30 m or deeper) is observed in central RIS and in the areas offshore of RIS and BIS, whereas in BIS and north-central RIS there is little vertical temperature structure. Vertical temperature differences range from less than 1.5 °C along the northern edge of the survey region to around 7 °C in the offshore region south of RIS. At the offshore end of line NS7, a thin layer of warm (18-19 °C) water is observed just above the thermocline (~30 m depth). Examination of the corresponding salinity section (Figure

9) shows that this water is saltier than the water above and below, suggesting that this feature is an intrusion of outer shelf water similar to those observed in earlier surveys.

Whereas the late summer survey observed warmer surface water temperatures than deep temperatures, during the early winter survey in December 2009 (Figure 3, Figure 4, Figure 6), the temperature gradient is reversed with coolest water near the surface and warmest water at depth. Vertical temperature differences range from near zero in BIS and the shallower northern and eastern parts of RIS to 4-5 °C at the offshore end of line NS3 south of Block Island. Near-surface temperatures generally decrease towards the north and east where the shallow water column tends to cool most rapidly in late fall. However, as during summer, near-surface temperature gradients are weaker than those at depth. Near the bottom, highest gradients occur in the region south of Block Island and in central RIS associated with the edges of a warm patch centered on the deep channel extending northeast into central RIS. Water temperatures at depth in this patch, which appears to be contiguous with offshore deep waters south of Block Island , are greater than 15 °C. Temperatures in this region are anomalously high compared to temperatures during fall (≤13 °C) and winter (≤6 °C) at the seafloor in the climatology and the model output examined by Codiga and Ullman (2010). As will be discussed in the next section, this water is also anomalously salty, suggesting outer shelf origin.

During the late winter survey in March 2010 (Figure 3, Figure 5, Figure 7), the range of observed temperature over the whole region is quite small (range of 2-4 °C over the entire region at all depths) reflecting the homogenization of temperature due to strong surface cooling in winter (and possibly the offshore retreat of the anomalously warm deep water observed in late autumn). Coldest water during this survey was located near the bottom in northeast RIS while warmest temperatures were observed near the surface in the western half of the survey region. The relatively warm surface layer in BIS and western RIS was less than 10 m thick.

The late spring hydrographic survey in June 2010 (Figure 3, Figure 5, Figure 7) shows the re-emergence of strong thermal stratification in the region. Vertical surface to bottom temperature differences range from 2-3 °C in BIS and northeastern RIS to ~10 °C at the offshore edge of the survey region. Surface temperatures in BIS are ~2 °C cooler than surface waters offshore and in RIS, consistent with the SST climatology of Codiga and Ullman (2010). As was seen in the September survey, large gradients in near-bottom temperature occur, but during this survey the high-gradient region is shifted to shallower areas (roughly the 30 m isobath). This shift is probably explained by the shallower temperature surface mixed layer during the June survey

compared to September. In this interpretation, the high near-bottom gradients are found where the thermocline intersects the bottom.

4.1.2 Salinity

The salinity field during the September 2009 survey (Figure 8, Figure 9, Figure 11) is dominated by the low-salinity outflow from LIS. Near surface salinities increase from less than 31 psu in central/western BIS to greater than 31.5 psu in central RIS to greater than 32 psu in offshore areas. Near-bottom salinities increase by roughly the same amount (~1.5 psu) over the same areas with some indication that the horizontal gradient steepens in the southwest corner of the survey region where the coastal current associated with the LIS outflow onto the continental shelf is known to lie (Ullman and Codiga, 2004). Vertical salinity stratification is strongest in BIS where surface to bottom differences of up to 2 psu occur, and weakest to the east and offshore (except for the westernmost portion of the offshore zone which is influenced by the aforementioned coastal outflow). Although salinity generally increases with depth (and distance eastward), the highest salinities in the entire region occur in the thin intrusive feature identified in the temperature data (see section 4.1.1) at about 30 m depth at the offshore end of line NS7. The maximum observed salinity in this intrusion (which is also warmer than water above and below) is approximately 33.5 psu, which according to the shelfbreak front climatology of Linder and Gawarkiewicz (1998) is outer shelf water found on average on the inshore side of the shelfbreak front.

In the December survey (Figure 8, Figure 9, Figure 11), observed near-bottom salinities in areas of the survey region with water depth greater than about 35 m are extremely high. Salinity in the deep channel north and west of Coxes Ledge is greater than 34 psu and the peak salinity of greater than 34.5 is observed at the offshore end of line NS3. Note that the offshore station of line NS4 was not sampled during this survey and it is possible that the high salinity core is larger than it appears in Figure 8. Nonetheless, the deep water observed in the December survey is clearly anomalous (compare with peak near-bottom salinities of 33.25 psu in the fall and winter SAMP region climatology (Codiga and Ullman, 2010)). In fact the shelfbreak front climatology of Linder and Gawarkiewicz (1998) puts the 34.5 isohaline in the center of the front, intersecting the bottom on average at approximately the 100 m isobath. Minimum surface salinity of less than 31 psu was observed in the December 2009 survey in west/central BIS. This value is approximately the same as the minimum value observed in the September survey, although the areal extent of the low salinity region appears to be somewhat reduced. Examination of the

SAMP climatological surface salinity in west/central BIS, shows that the observed December values are approximately equal to the fall climatological values and are fresher (by several tenths of a psu) than the winter means.

Strongest near-surface horizontal salinity gradients in the December survey are observed on the shelf southwest of Block Island (as in September) and also in northeastern RIS. In northeast RIS, on lines NS7 and NS8, a surface-layer front with cross-frontal salinity difference of approximately 0.5 psu over 10 km is observed (Figure 9). The front weakens slightly in the RIS sections to the west (NS4 – NS6) and appears to become more surface-trapped there. Vertical surface-bottom salinity differences during the December survey ranges from several tenths of a psu in BIS to ~ 3 psu in the offshore regions influenced by the high salinity intrusion discussed above.

The March 2010 survey found the deep salinity in the deep central RIS and offshore regions to be greatly reduced from the December values (Figure 8, Figure 10, Figure 12) indicating offshore retreat of the presumed outer shelf water (or alongshore advection out of the OSAMP survey region). Maximum salinity during the March survey was ~32.5 psu, while the freshest water, at the surface in west/central BIS, was less than 29.5 psu. Near-surface salinities increase rapidly towards eastern BIS and the front between the freshest water and RIS and shelf surface water extends from eastern BIS southwest onto the shelf to the southwest of Block Island. The sloping front on the shelf south of BIS intersects the bottom roughly between the 30 m and 40 m isobaths. Vertical salinity stratification in BIS is much stronger during March 2010 than during the previous surveys, with surface-bottom salinity differences of ~2 psu there. Salinity stratification weakens towards the east, with surface-bottom differences of less than 1 psu in eastern RIS. However, even in eastern RIS, there is evidence of a slightly freshened (S ~ 31 psu) lens of relatively low salinity water at the northern edge of the survey region.

During the June 2010 survey period (Figure 8, Figure 10, Figure 12), the observed salinity range is slightly reduced from that encountered in the March survey. Minimum observed salinity in west/central BIS was about 0.5 psu saltier (~30 psu), while maximum salinity at depth offshore is approximately the same (32-32.5 psu). Eastern BIS and central RIS are fresher (by ~0.5 psu) in June as compared with March, suggesting an expansion of the region influenced by the outflow from LIS. Horizontal as well as vertical gradients of salinity are somewhat reduced in June compared to March. There is a weak signal of freshening along the edge of the survey region in northeast RIS.

4.1.3 Dissolved Oxygen

Dissolved oxygen levels during the September 2009 survey (Figure 13, Figure 14, Figure 16) generally decrease with depth. The near surface concentration in west/central BIS is in the range 7-8 mg/l and increases towards the east, reaching 8-9 mg/l in surface waters of eastern RIS. Near-bottom oxygen concentration is generally 6-7 mg/l except for a portion of north/central RIS (northern part of lines NS5 and NS6) where concentrations fall to around 5 mg/l.

In December oxygen concentrations in the bottom water of north/central RIS are increased above the levels observed in September (Figure 13, Figure 14, Figure 16). Concentrations during December are above 6 mg/l. Lowest concentrations during the December survey occur near the bottom in the deep channel of central RIS, the area of apparent deep intrusion of outer shelf water. Surface oxygen levels in December are everywhere above 8 mg/l. During the March 2010 survey when water temperatures are at a minimum, oxygen concentrations are uniformly high throughout the water column with values above 10 mg/l everywhere (Figure 13, Figure 15, Figure 17).

The June 2010 survey found dissolved oxygen concentrations (Figure 13, Figure 15, Figure 17) reduced significantly over the March values, presumably in part due to the increase in water temperatures. The region of low concentration in north/central RIS appears to be redeveloping, with concentrations of 6-7 mg/l observed at the north end of line NS5. A significant feature during the June survey is a subsurface oxygen maximum with concentrations above 9 mg/l occurring in bands of order 10 m thick in the southern, offshore region of the survey. The location of the most intense of these maxima is typically at depths of 20-30 m, although there are places where the maximum is found at depths of 10-20 m. As will be discussed in Section 4.1.4, subsurface maxima in Chlorophyll concentration were detected in the June survey and it is likely that the oxygen maxima observed here are a result of phytoplankton photosynthesis.

4.1.4 Chlorophyll

Near-surface chlorophyll concentrations (derived from fluorometric measurements) during the September 2009 survey are below 4 μg/l throughout the survey region (Figure 18, Figure 19, Figure 21). Highest values occur around Block Island and lowest concentrations (less than 1 μg/l) are found in the southern and eastern portions of the survey region. The vertical sections (Figure 19, Figure 21) show that chlorophyll concentrations are often elevated at mid-water depths. These subsurface maxima, with concentrations reaching ~10 μg/l in places but usually 5-

6 μg/l, are detected at various depths, ranging from near the bottom on lines NS8 and NS9 to approximately 10 m depth along lines NS1 – NS3. In general, phytoplankton biomass as measured by chlorophyll concentration tends to be highest in northwestern RIS and BIS and also in eastern RIS.

Chlorophyll levels in December 2009 (Figure 18, Figure 19, Figure 21) are somewhat lower than were found during the September survey. Near-surface levels are below 3 μg/l, but the region of highest concentration has shifted to central and eastern RIS. In most parts of the survey region, chlorophyll is low throughout the water column in December, although a weak subsurface maximum (3-4 μg/l) was detected at several stations in central RIS.

In March 2010, very low chlorophyll concentrations were observed throughout the OSAMP survey region (Figure 18, Figure 20, Figure 22). Surface values are less than 1 μg/l, and concentrations at depth are generally lower than 2 μg/l, except in northeast RIS. In that region, near bottom chlorophyll levels of 3-4 μg/l are observed.

Surface chlorophyll concentrations during the June 2010 survey (Figure 18, Figure 20, Figure 22) remained at low levels, less than 1 μg/l over most of the region and only 1-2 μg/l around Block Island and in isolated areas along the northern and western periphery of the survey region. In much of the region, especially central and southern RIS and BIS, a subsurface chlorophyll maximum was observed, with concentrations of up to approximately 5 μg/l at depths of 20-30 m.

4.1.5 Turbidity

Estimates of water turbidity from the fluorometer were below 1 nephelometric turbidity units (NTU) during the September 2009 survey (Figure 23, Figure 24, Figure 26). Highest values (0.75-1.0 NTU) were detected in BIS and near the bottom in the shallowest areas along the northern edge of the survey region. Values in the middle of the water column in central RIS are lower (~0.5 NTU). High near surface turbidity approaching 1 NTU was detected at station 47 near the offshore end of line NS7. Adjacent stations did not exhibit a similar elevation suggesting either an instrument malfunction or the presence of a very small scale feature. The lack of a corresponding signal in either the Chlorophyll concentration (Figure 19) or the depth of the euphotic zone (Figure 28, to be discussed in Section 4.1.6) suggests the former explanation.

Turbidity values during the December 2009 survey (Figure 23, Figure 24, Figure 26) appear to have been significantly higher than during September. Highest values (1.25-1.5 NTU) were

detected in northeastern RIS. Moderately high turbidity (0.75-1.0 NTU) was observed in west/central BIS with decreasing turbidity towards the east.

During the March 2010 survey, turbidity was low throughout the survey region, with values below 0.75 NTU everywhere (Figure 23, Figure 25, Figure 27). Highest turbidity (above 0.5 NTU) was detected in northern RIS and in BIS, with offshore values generally low.

Near-surface turbidity in June 2010 was generally very low, with values in the range of 0.25 – 0.5 NTU (Figure 23, Figure 25, Figure 27). Near bottom turbidity was elevated to 0.5-0.75 NTU in west/central BIS and in the far northeast corner of the survey region.

4.1.6 Euphotic Zone Depth

The estimated depth of the euphotic zone during the September survey was quite variable, ranging from ~10 m to 40 m (Figure 28). Highest values occur in central RIS and in the offshore areas and lowest values in BIS and in the far eastern portion of the survey region. The boundary between the BIS region of shallow euphotic zone depth and the region of deeper light penetration to the south and east is quite sharp and extends continuously from Pt. Judith southwest past Block Island to the southwest corner of the survey region. During the December survey, the euphotic zone depth is generally less than 20 m, with a general increase in the offshore direction, although without the sharp frontal boundary observed in September. In March 2010, the depth of the euphotic zone is everywhere greater than 20 m with some increase offshore. During June, the map of the euphotic zone depth resembles the September map, with low values (less than 20 m) in BIS and around the periphery of RIS and higher values offshore (30-40 m).

4.2 Temperature and Salinity Time Series from Moored Instruments

4.2.1 Fall 2009 Deployment

The PO-F and PO-S CTD moorings were deployed in mid-September 2009 with planned recovery in mid-December 2009. However, adverse weather conditions prevented us from carrying out this operation until mid January (see Table 1 for details on the mooring deployments). The Microcats filled their onboard memory in late December (28 Dec., 17:00 UTC) and no data were recorded after this time. Upon recovery (at a location 1 km to the southwest of its deployment location), the PO-S CTD mooring showed clear signs that it had been dragged by a trawler. Two instruments (nominally at depths of 12 and 20 m) were severely damaged and no data were recovered. Other instruments, although damaged, provided useful data for various lengths of time. One instrument (nominally at a depth of 7 m) was moved on the

mooring wire to a final depth of ~3 m below the surface. The lengths of the data records from the various instruments can be deduced from the instrument pressure records shown in Figure 29.

The pressure records from the CTDs at moorings PO-F and PO-S (Figure 29) provide information on the vertical motion of the instruments in response to waves and currents. The instruments are seen to experience correlated upward excursions of up to 2-3 m on time scales of days. The magnitude of the depth excursions appears to increase with the nominal depth of the instruments. In the analysis that follows, no attempt has been made to correct for the vertical motion of the sensors. The CTDs on moorings MD-F and MD-S were not equipped with pressure sensors, so no such analysis could be performed for these records.

In mid-September 2009 when the PO-F and PO-S moorings were deployed, the water column at both sites was stratified, with warm, lower salinity water overlying cooler, saltier water. At both sites, the upper portion of the water column (down to at least 20 m at site PO-F) was fairly well mixed, with clear differences apparent between the deepest instruments (35 m) and the near surface units (Figure 30 and Figure 31). This indicates that the seasonal pycnocline was quite deep at this time. At both moorings, the period of vertical stratification abruptly ends in mid-October when the water column becomes well-mixed (see Figure 32 and Figure 33). This event coincides with the occurrence of a strong northeasterly wind event (Figure XX), which has been shown by Lentz et al. (20??) to be much more effective at achieving vertical mixing than similar strength wind events from other directions. The MD-S and MD-F moorings were deployed in early October 2009 and were located in shallower water than the corresponding PO moorings. The vertical stratification at these moorings is much less intense than at the deeper PO moorings, nonetheless the stratification abruptly disappears at the time of the northeaster.

After the destratratification event in mid-October, the water column continues to cool and remains essentially isothermal until late November. During this period, the deeper moorings (PO-F and PO-S) as well as the MD-S mooring experience moderately large fluctuations (~1 psu) in salinity. The largest signal is observed at the deeper sensors where salinity is observed to increase for several days to a two weeks only to decrease again. The near-surface response is weaker but is generally in the opposite sense; that is a decrease in near-surface salinity occurs at the same time as an increase in deep salinity.

A dramatic hydrographic transistion occurs in late November at all mooring sites. At this time, the deep salinity abruptly increases by approximately 2 psu at PO-S (Figure 31) with lesser increases observed at the other moorings (Figure 30, Figure 34, Figure 35). Contrary to what was

observed in the previous events, in this case, the increase in deep salinity is accompanied by an increase in deep temperature as well. There is also a small decrease in near-surface salinity at this time at all locations except for MD-F. The duration of this event is 3-4 weeks at PO-S and somewhat less at the other locations. At PO-S, there is a brief period, about 2 weeks after the onset of the event, during which time the deep salinity decreases and the near-surface salinity increases. This is quickly followed by the return of the deep saline water. At station PO-S, the peak salinity during this event is nearly 35 psu, whereas the peak at PO-F is approximately 34 psu. This is clearly the same outer shelf/slope water seen during the December 2009 CTD survey.

4.2.2 Winter/Spring 2010 Deployment

UNDER PREPARATION

5 Currents and Sea Level

5.1 Tidal Motions

Characteristics of tidal heights and tidal currents across the OSAMP region were described in some detail using hydrodynamic model output and previously available observations by Codiga and Ullman (2010); the reader is referred to Part 1 for background information on which constituents are most energetic, and the role of surrounding waterbodies such as LIS in shaping the response. This section presents new measurements from moored instrumentation. For the MD-S and MD-F sites (Figure 2), data from October 2010 through June 2010 are used. For the PO-S and PO-F sites the FA09 records are used and not the SP10 records; FA09 records are 4 months long and so better suited for the harmonic analysis than the 3 month SP10 records, which, for tidal quantities, give very similar results in any case. The seven tidal constituents (M2, K1, N2, O1, S2, M4, and L2) that are dominant in the new observations are, as expected, the same as those seen in previous analyses.

Sea level observations were collected only by the PO-S and PO-F moorings. The superposition of the seven main constituents (Figure 42) at these two locations reveals several important features. At both sites there is a distinct spring-neap cycle characterized by neap periods which alternate in their amplitudes, such that every second neap period is typically significantly weaker. During spring conditions, peak-to-peak amplitudes are typically 1.1-1.3 m at PO-S and 1.2-1.4 m at PO-F; during neap conditions they are about 0.5-0.6 m. The daily inequality changes as the spring-neap cycle progresses, and is maximal during spring conditions.

In addition to the minor differences in overall amplitudes between the two sites, small differences in the relative importance of diurnal and semidiurnal constituents, as expected due to their geographic variations (Codiga and Ullman 2010), are apparent.

Tidal current ellipses for each of the seven constituents (Figure 43), based on observed vertical-mean currents, reveal distinct patterns at the MD-S, MD-F, PO-S, and PO-F sites. The relative importance of the constituents, including dominance by M_2, is similar at all four sites. Except for the M_4 constituent at three of the sites, currents rotate clockwise in time. The magnitudes and orientations of the ellipses vary from site to site; for example, M2 ellipses are largest at MD-S, where the major axis is oriented in a NW-SE direction, and at PO-F, where the ellipse is more round. Overall, the geographic variations and many other detailed aspects of the observed current ellipse characteristics from these four sites are in very good agreement with those of the simulation described by Codiga and Ullman (2010).

The vertical variations of tidal ellipse characteristics across the water column, for the dominant M_2 constituent, are clear from plots of the four current ellipse parameters at each of the four sites (Figure 44). In general, as the seafloor is approached amplitudes decay, major axes turn slightly clockwise, and ellipses flatten; the vertical extent off the seafloor in which these changes occur varies from 5-10 m, where currents are most energetic, to less than 5 m. These features are characteristic of theory for frictional tidal boundary layers over a flat seafloor influenced by background rotation (e.g. Soulsby 1990); Codiga and Rear (2004) analyzed ADCP records from the inner shelf south of Block Island Sound, including one record from a site a few km ENE of PO-S where the vertical structure was very similar to that presented here, and demonstrated they compare favorably to the theory. Patterns that diverge from the theory occur in locations influenced by sharp topographic features the bathymetry alters the patterns, which is likely the explanation for why at PO-S, a site where the bottom slopes steeply offshore, the minor axis decreases over most of the water column instead of in a 5-10 m near-bottom layer as the theory would suggest. Owing to the lack of characteristic reversals of velocity in depth, it can be concluded that energetic internal tides are not occurring, unless they are at sufficiently higher frequencies and/or sufficiently intermittent to not be isolated by the harmonic analysis (as seen, for example, by Colosi et al. (2001) on the shelf to the south of Martha's Vineyard).

5.2 Subtidal Motions

TEXT UNDER PREPARATION – Descriptions of Figure 45, Figure 46, Figure 47, Figure 48, Figure 49, Figure 50, Figure 51, Figure 52

5.3 Monthly-Mean Flow and Principal Axes of Weather-Band Currents

TEXT AND FIGURES UNDER PREPARATION

6 Waves

6.1 Wave Parameters from Accelerometers on Multidisciplinary Buoys

TEXT UNDER PREPARATION – Descriptions of Figure 53 and Figure 54

6.2 Directional Wave Parameters from Bottom-Mounted Acoustic Sensors

TEXT UNDER PREPARATION – Descriptions of Figure 53 and Figure 54

6.3 Directional Wave Parameters from Waverider Buoy

TEXT UNDER PREPARATION – Descriptions of Figure 53 and Figure 54

7 Summary

UNDER PREPARATION.

Acknowledgements

Instrument design and preparation by Jim Fontaine was crucial to the success of the vessel-based surveys and PO mooring deployments. We thank Captain Tom Puckett for his superb work on the R/V Cap'n Bert for mooring deployments/recoveries and on the R/V Hope Hudner for the vessel-based surveys, for which Brian Oakley was also very helpful. Candace Oviatt generously provided us with the CTD package for the vessel-based surveys.

References (UNDER PREPARATION)

Codiga, D.L., L.V. Rear. 2004. Observed tidal currents outside Block Island Sound: Offshore decay and effects of estuarine outflow. *J. Geophys. Res.* 109, doi:10.1029/2003JC001804.

Codiga, D.L., D.S. Ullman. 2010. Characterizing the Physical Oceanography of Coastal Waters Off Rhode Island, Part 1: Literature Review, Available Observations, and A Representative Model Simulation. *Prepared for the Rhode Island Ocean Special Area Management Plan 2010*, (Draft March 2010) 2166 pp.

Colosi, J.A., R.C. Beardsley, J.F. Lynch, G. Gawarkiewicz, C.S. Chiu, A. Scotti. 2001. Observations of nonlinear internal waves on the outer New England continental shelf during the summer Shelfbreak Primer study. *J. Geophys. Res.-Oceans* 106, 9587-9601.

Pawlowicz, R., B. Beardsley, S. Lentz. 2002. Classical tidal harmonic analysis including error estimates in MATLAB using T-TIDE. *Computers & Geosciences* 28, 929-937.

Soulsby, R.L. 1990. Tidal-current boundary layers. In: Le Mehaute, B., Hanes, D.M (Ed.), The Sea; Ocean Engineering Science Vol. 9A, Wiley-Interscience, New York, pp. 523-566.

Table 1. Moored instrumentation locations, deployment dates, and sensors.

	MD-S	MD-F	PO-S	PO-F	BIWB
Latitude	41° 06.045'	41° 07.096'	41° 02.869'	41° 14.970'	40° 58.117'
Longitude	71° 34.174'	71° 01.703'	71° 29.972'	71° 05.297'	71° 07.565
Depth [m]	26	34	44.1	43.5	48.2
Dates	Since Oct 9, 2009		FA09: Sep 15, 2009 to Jan 14, 2010 SP10: Mar 19, 2010 to Jun 23, 2010		Since Oct 21, 2009
Sensors: CTD	1, 6, 18m	1, 6, 28m	1, 3, 7, 12, 20, 28, 35m		(none)
Sensors: Currents	Aanderaa 2m; ADCP 5, 6, 7, … 21, 22 m	Aanderaa 2m; ADCP 5, 6, 7, … 30, 31 m	ADCP 4, 5, 6, … 40, 41, 42m	ADCP 4, 5, 6, … 39, 40, 41m	(none)
Sensors: Waves	Accelerometers on discus buoy		Orbital currents from bottom-mounted ADCP		Datawell buoy
Sensors: Meteorology	Winds: 4m Temperature, Pressure: 3m	Winds: 4m Temperature, Pressure: 3m	(none)	(none)	(none)

Notes: See text for abbreviations. The PO-S and PO-F coordinates apply to the bottom-mounted ADCPs; the buoys were within a few hundred meters of them, PO-S buoy at 41° 02.893 71° 30.016 and PO-F buoy at 41° 15.000' 71° 05.500.

Table 2. Vessel-based hydrographic survey dates.

Survey	Dates	Number of Stations
1 – late summer	2009 Sep. 22, 23, 24	45
2 – late autumn	2009 Dec. 7, 8	38
3 – late winter	2010 Mar. 9, 10, 11	45
4 – late spring	2010 Jun. 16, 18	45

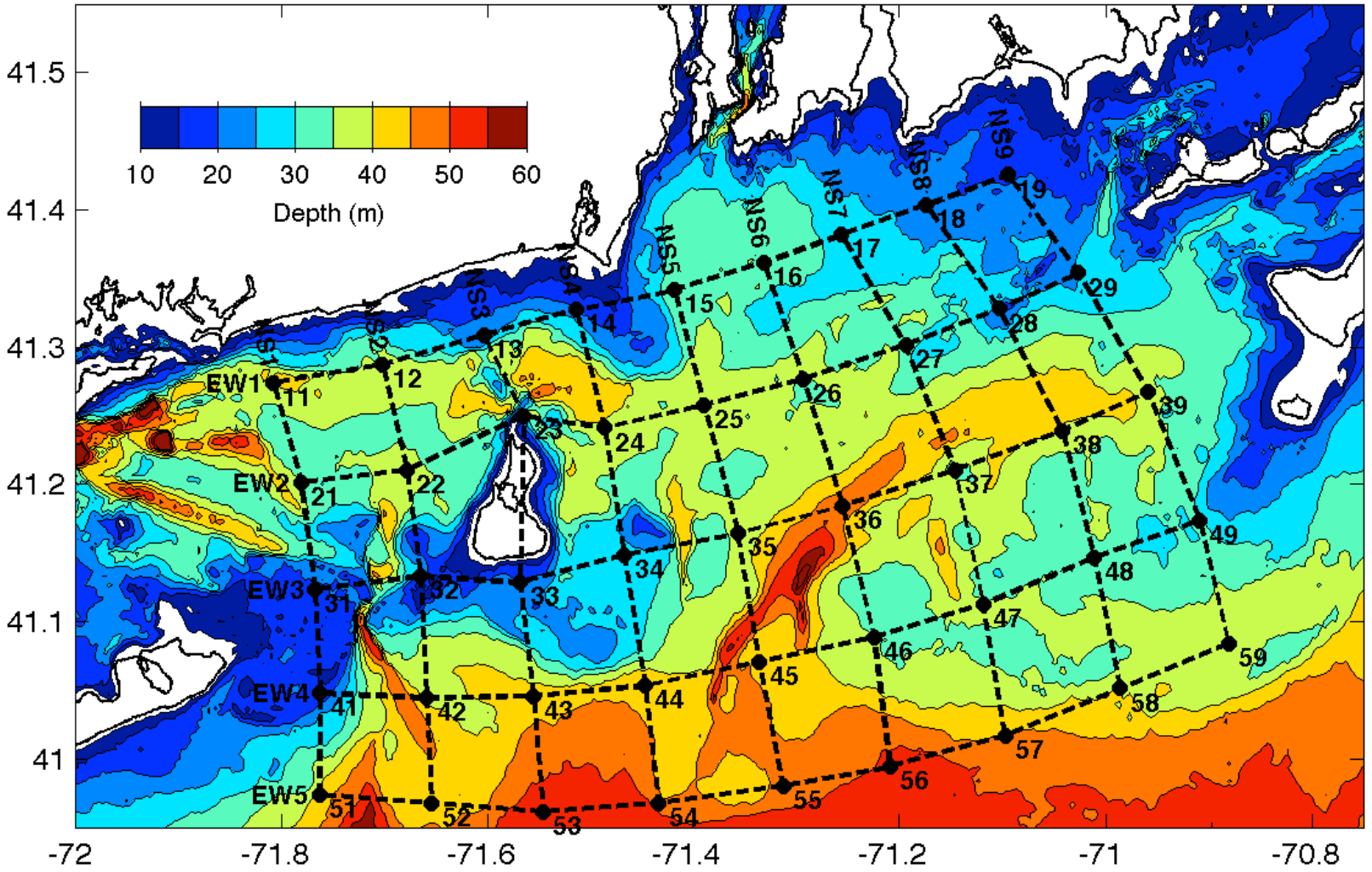

Figure 1. Vessel-based survey station grid superimposed on regional bathymetry.
The dashed lines denote the 9 north-south lines and 5 east-west lines along which vertical sections of hydrographic parameters are presented below.

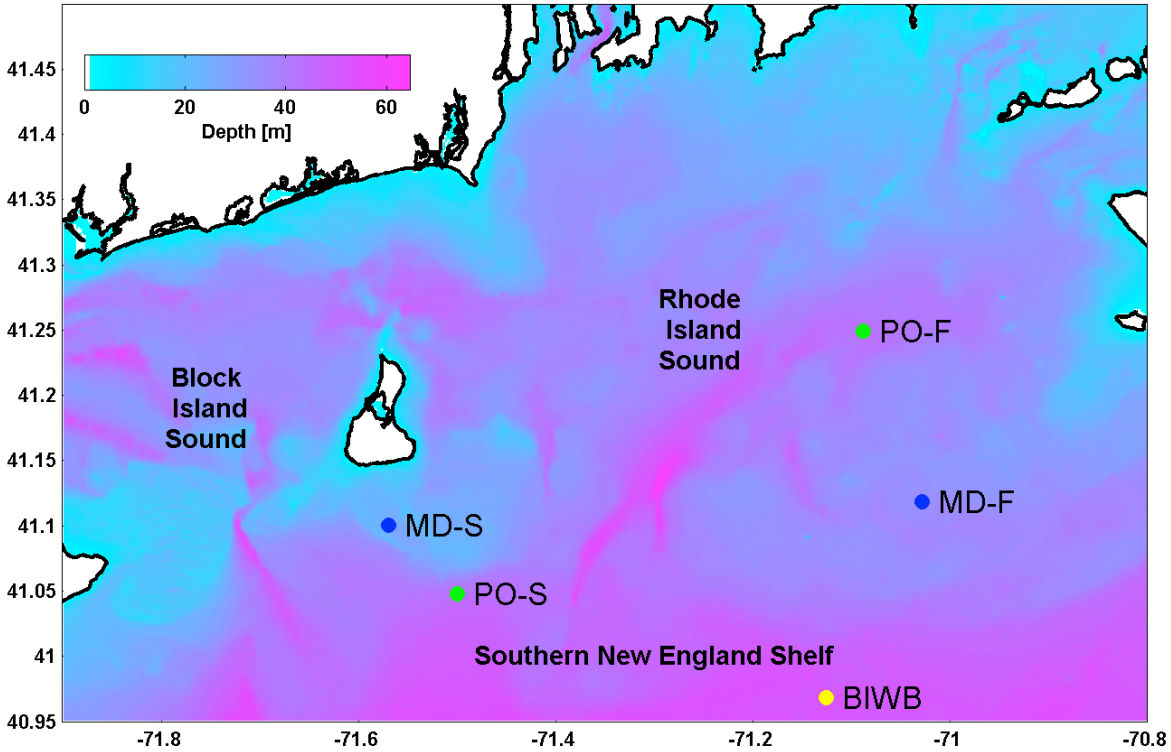

Figure 2. Moored instrumentation sites: MD-S, MD-F, PO-S, PO-F, and BIWB.

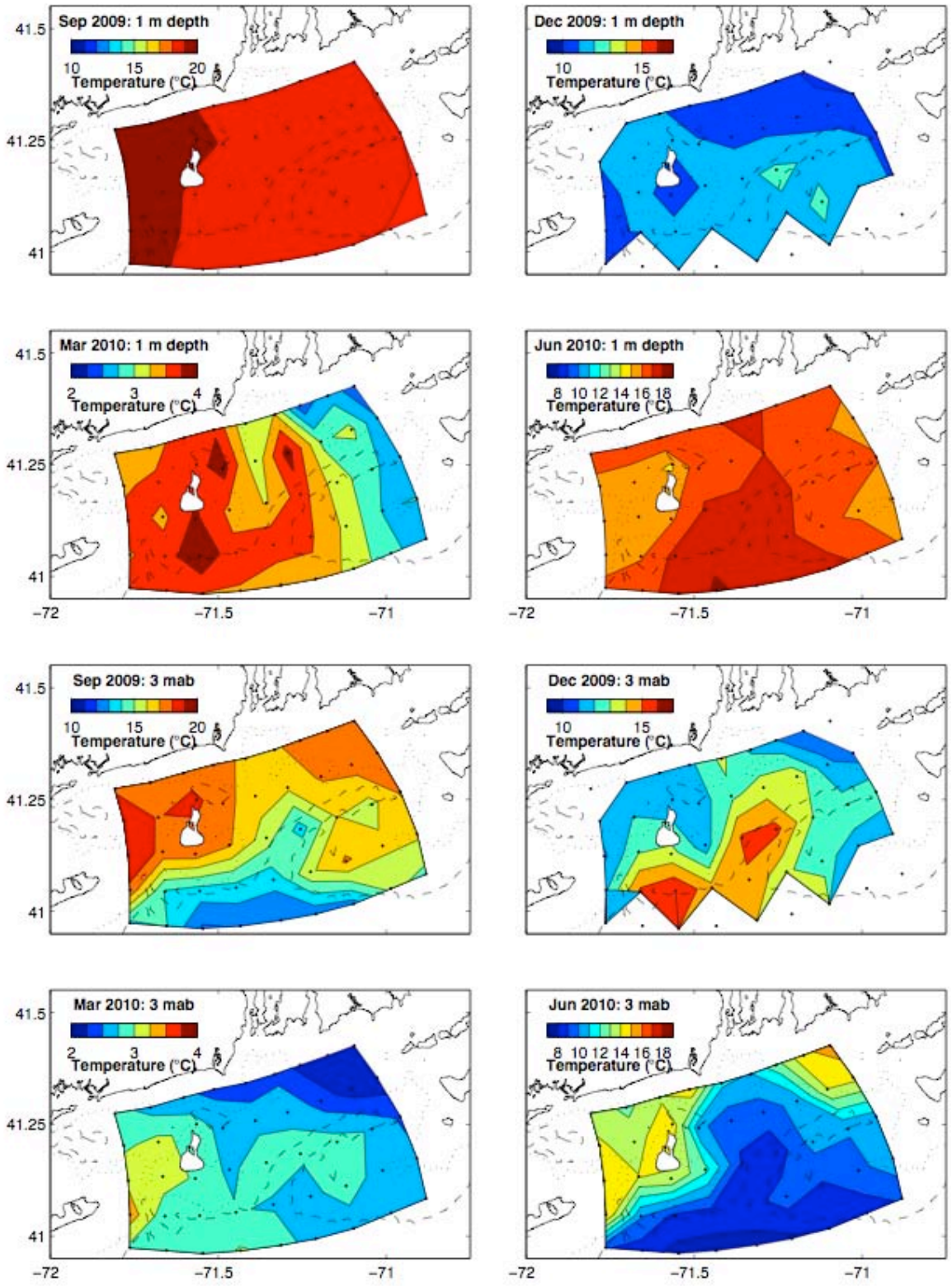

Figure 3. Maps of temperature at 1 m below the surface (top) and 3 m above the bottom (bottom) during all 4 surveys.
The CTD cast locations are denoted by the black dots. The dotted and dashed lines are the 30 m and 40 m isobaths, respectively.

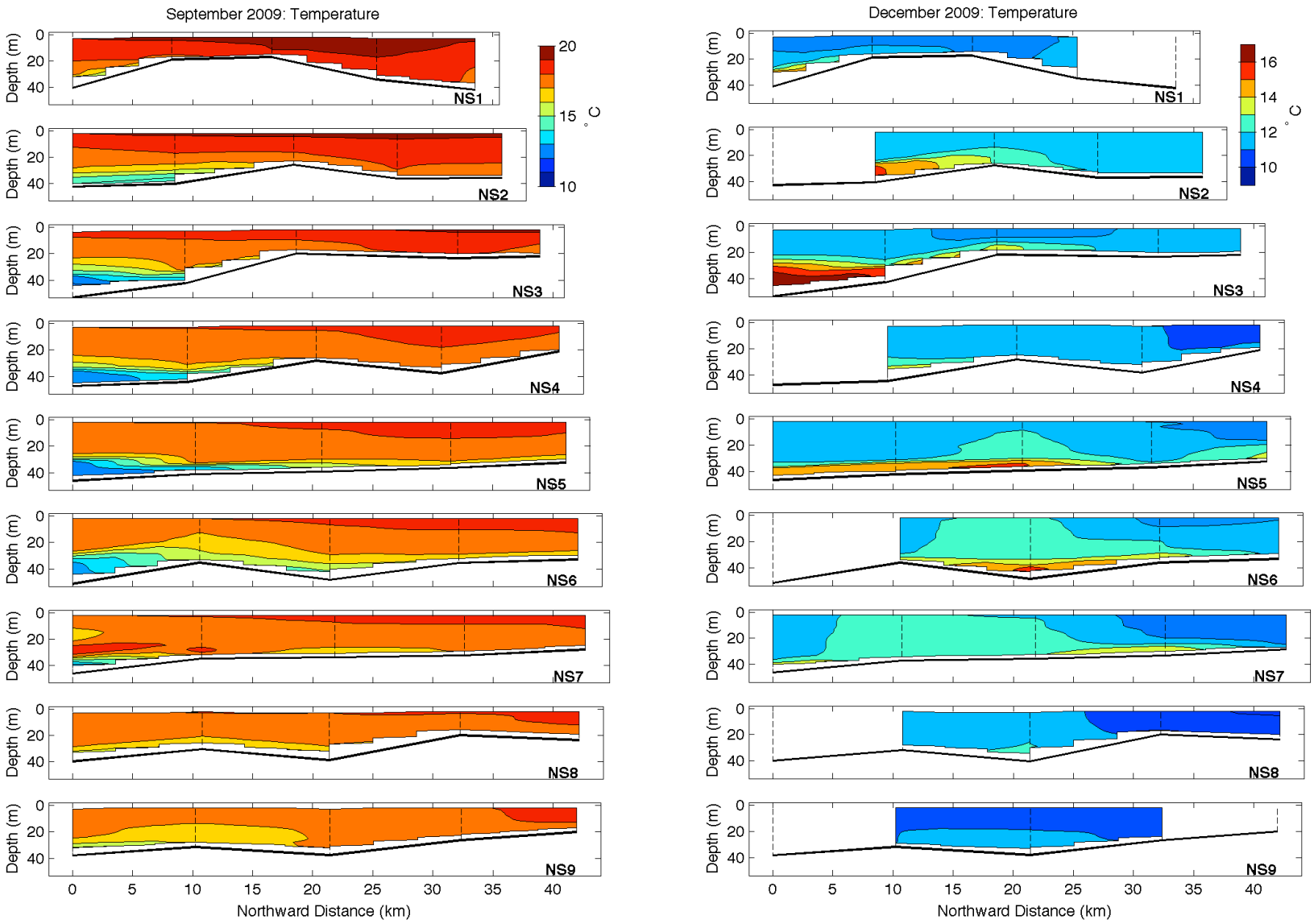

Figure 4. North-south sections of temperature during September 2009 (left) and December 2009 (right).
The section numbers are referenced to the map in Figure 1. The dashed lines denote the locations of the CTD casts.

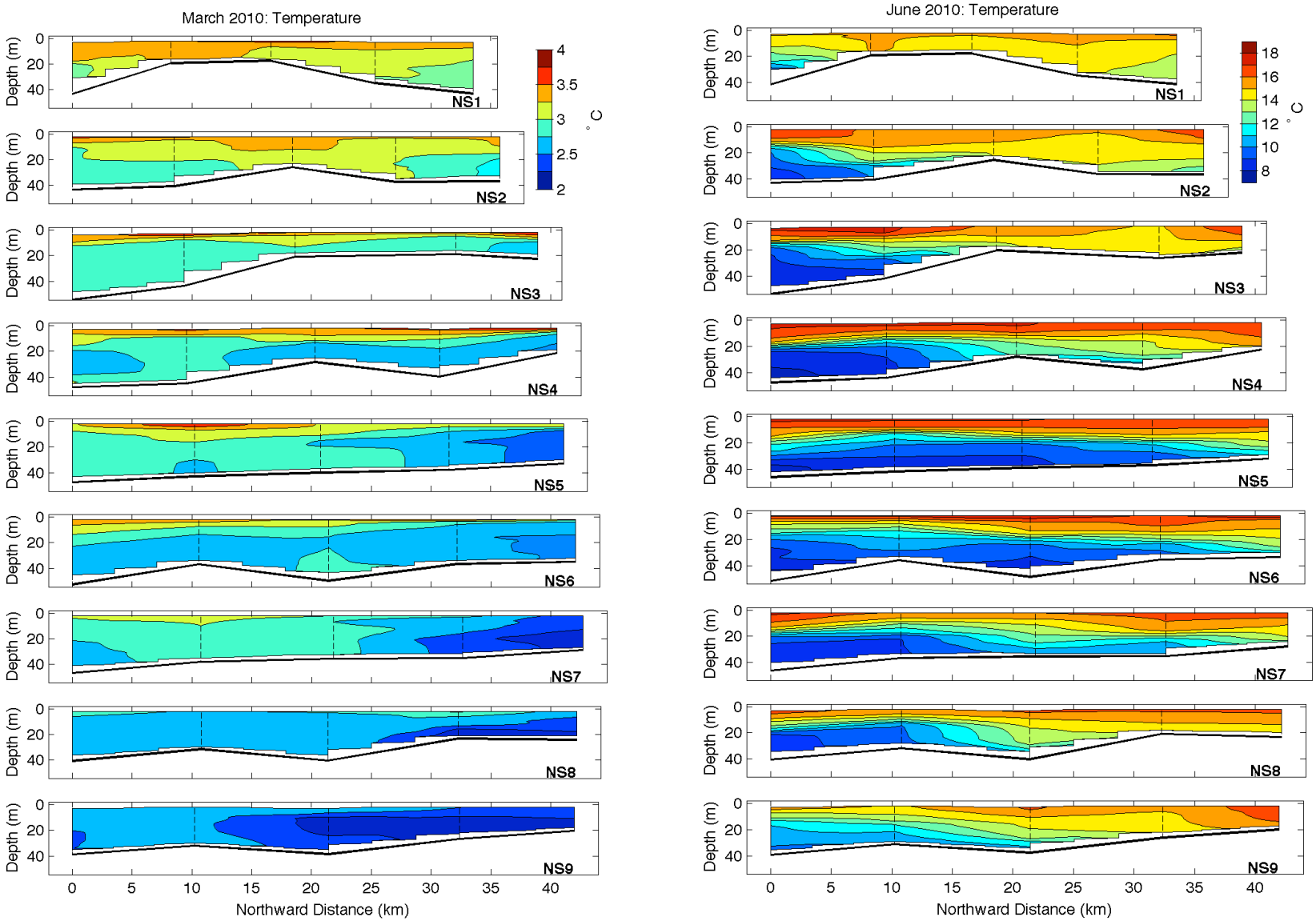

Figure 5. North-south sections of temperature during March 2010 (left) and June 2010 (right).
The section numbers are referenced to the map in Figure 1. The dashed lines denote the locations of the CTD casts.

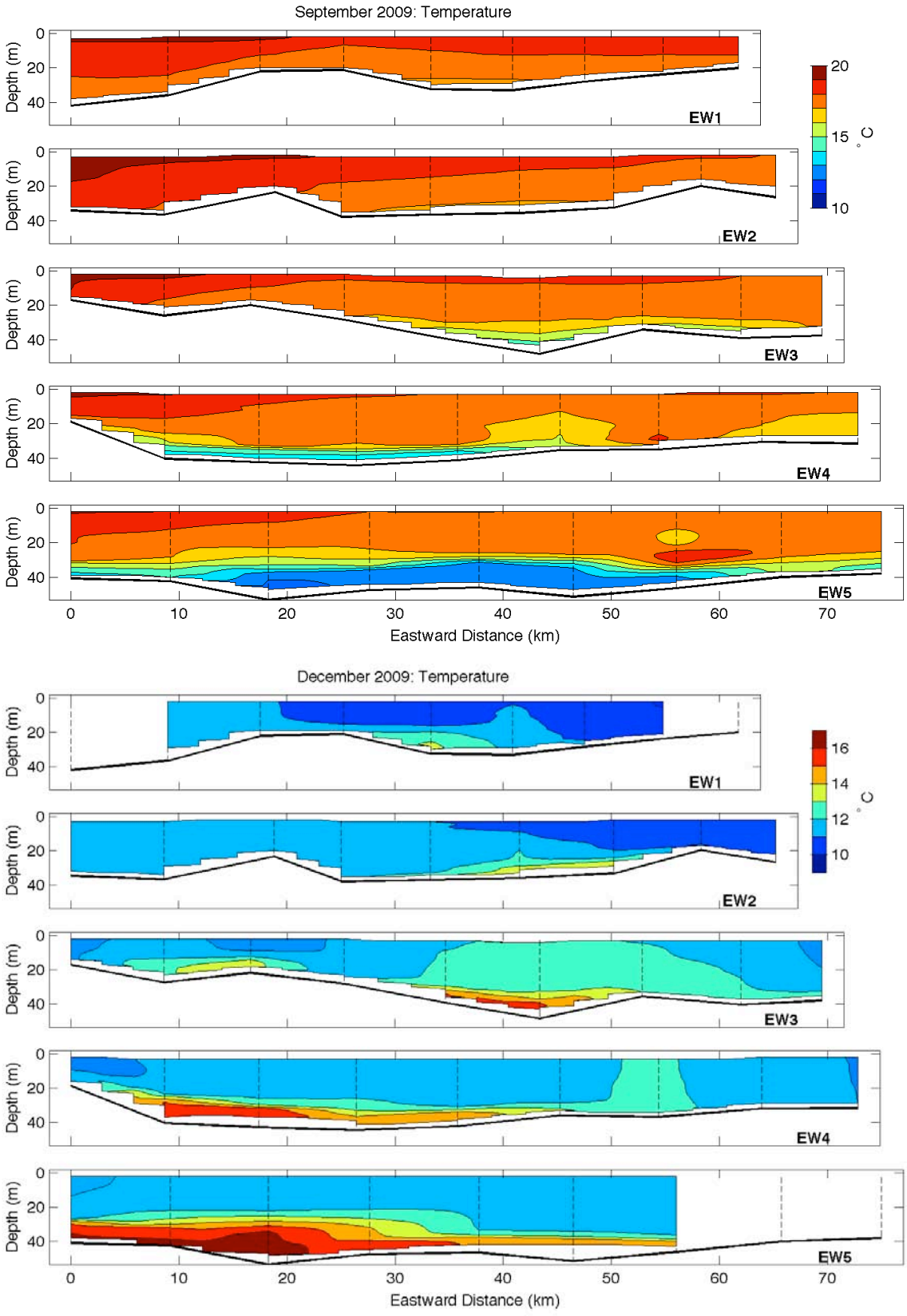

Figure 6. East-west sections of temperature during September 2009 (top) and December 2009 (bottom).
The section numbers are referenced to the map in Figure 1. The dashed lines denote the locations of the CTD casts.

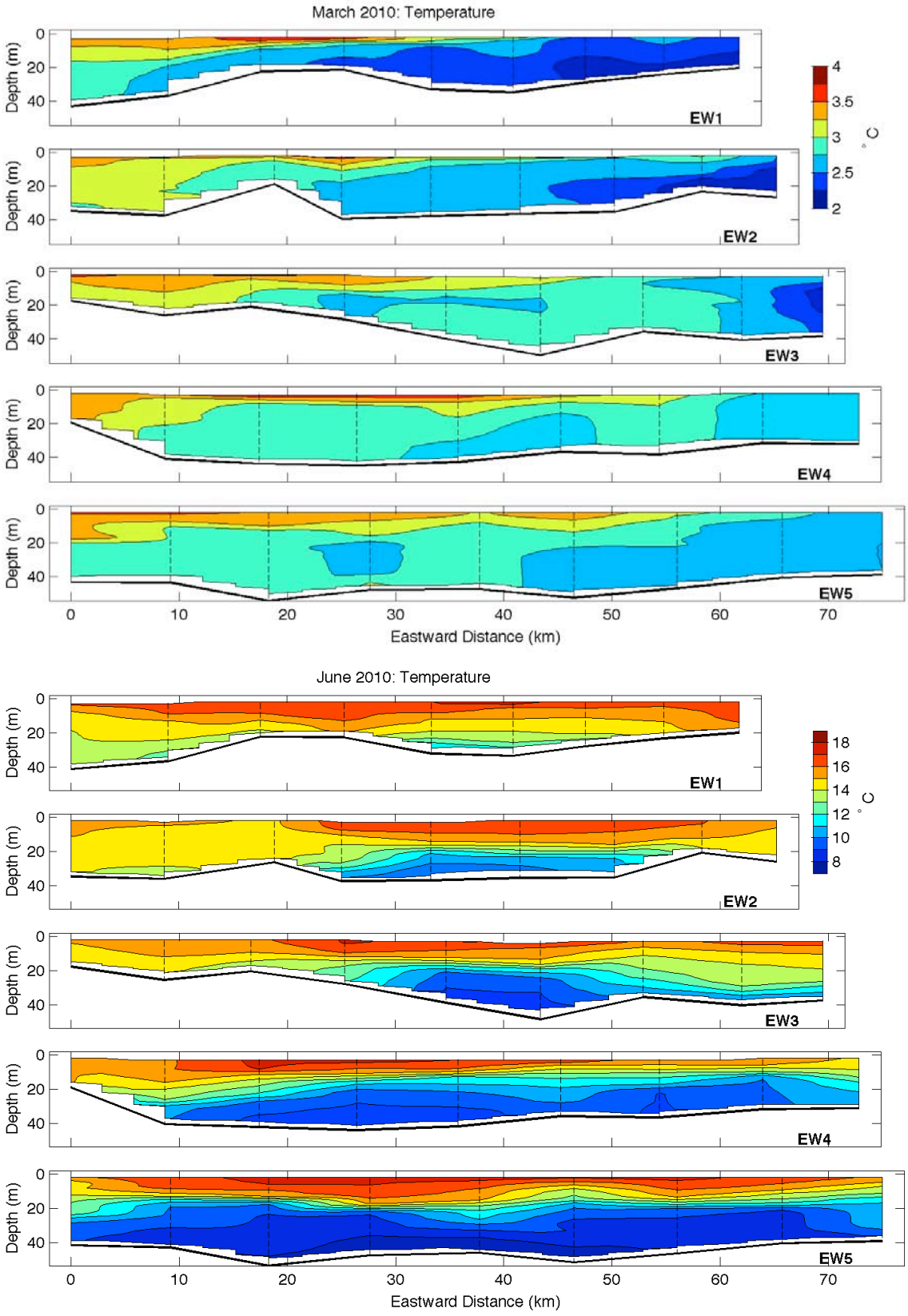

Figure 7. East-west sections of temperature during March 2010 (top) and June 2010 (bottom).

The section numbers are referenced to the map in Figure 1. The dashed lines denote the locations of the CTD casts.

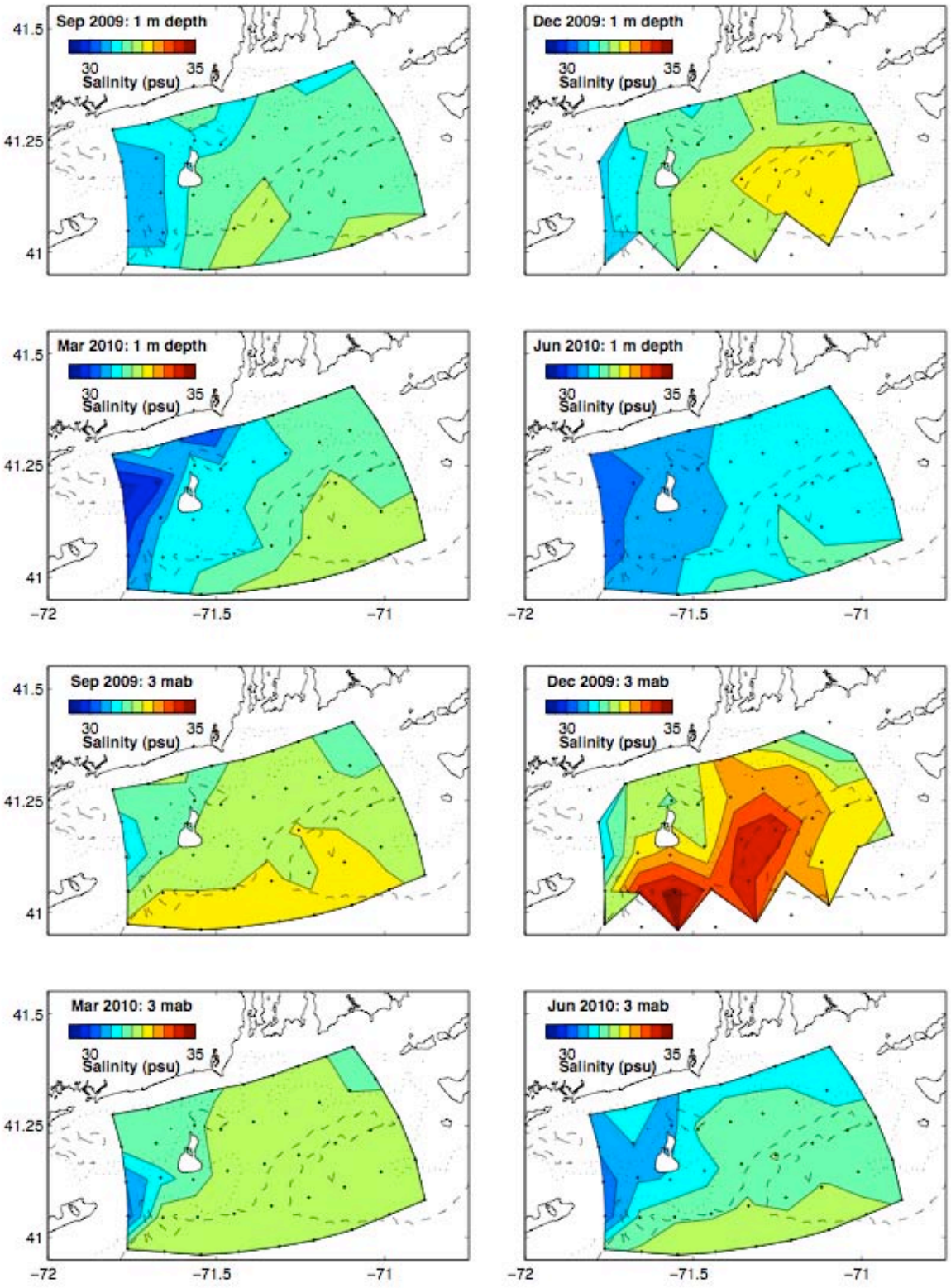

Figure 8. Maps of salinity at 1 m below the surface (top) and 3 m above the bottom (bottom) during all 4 surveys.
The CTD cast locations are denoted by the black dots. The dotted and dashed lines are the 30 m and 40 m isobaths, respectively.

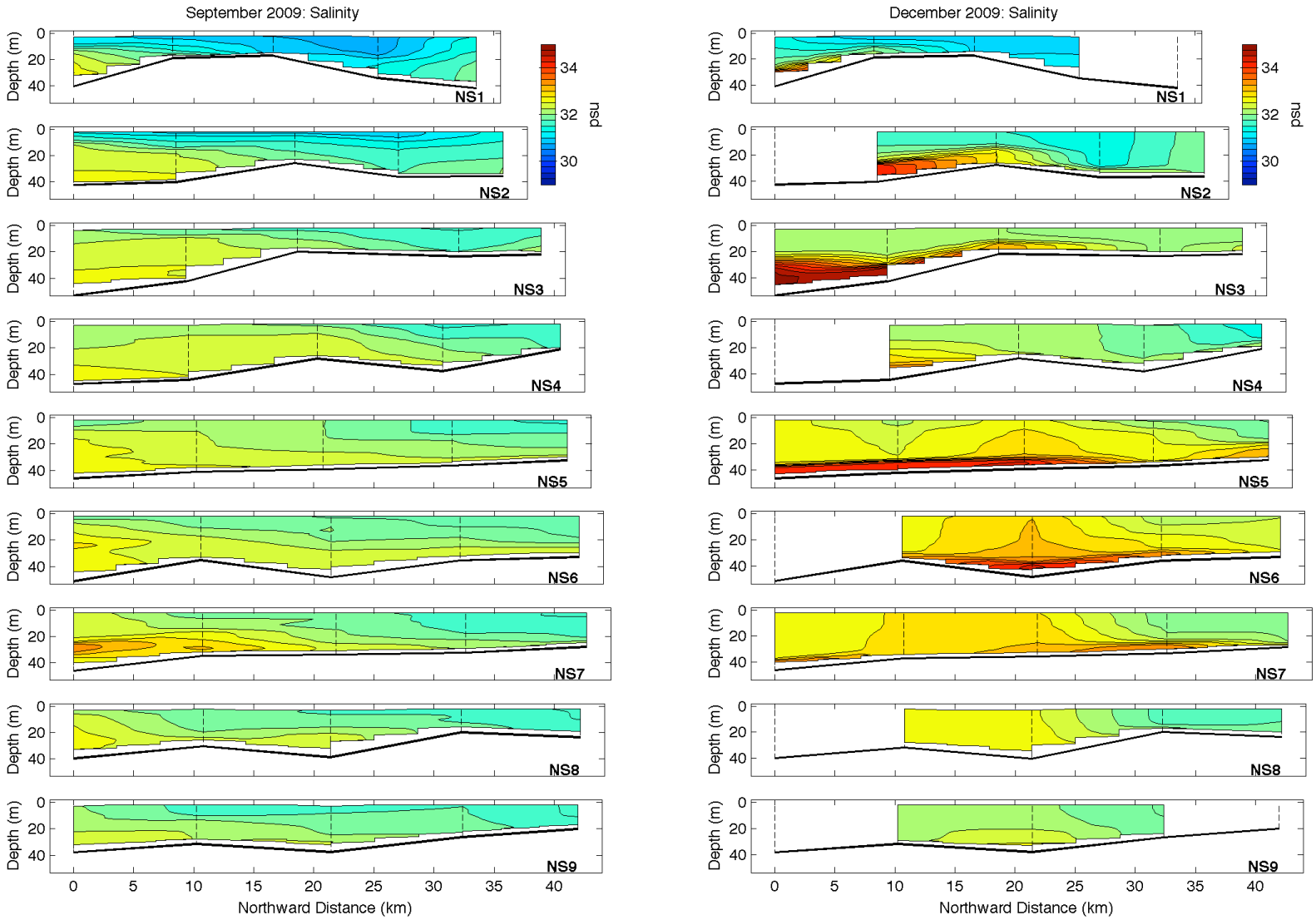

Figure 9. North-south sections of salinity during September 2009 (left) and December 2009 (right).
The section numbers are referenced to the map in Figure 1. The dashed lines denote the locations of the CTD casts.

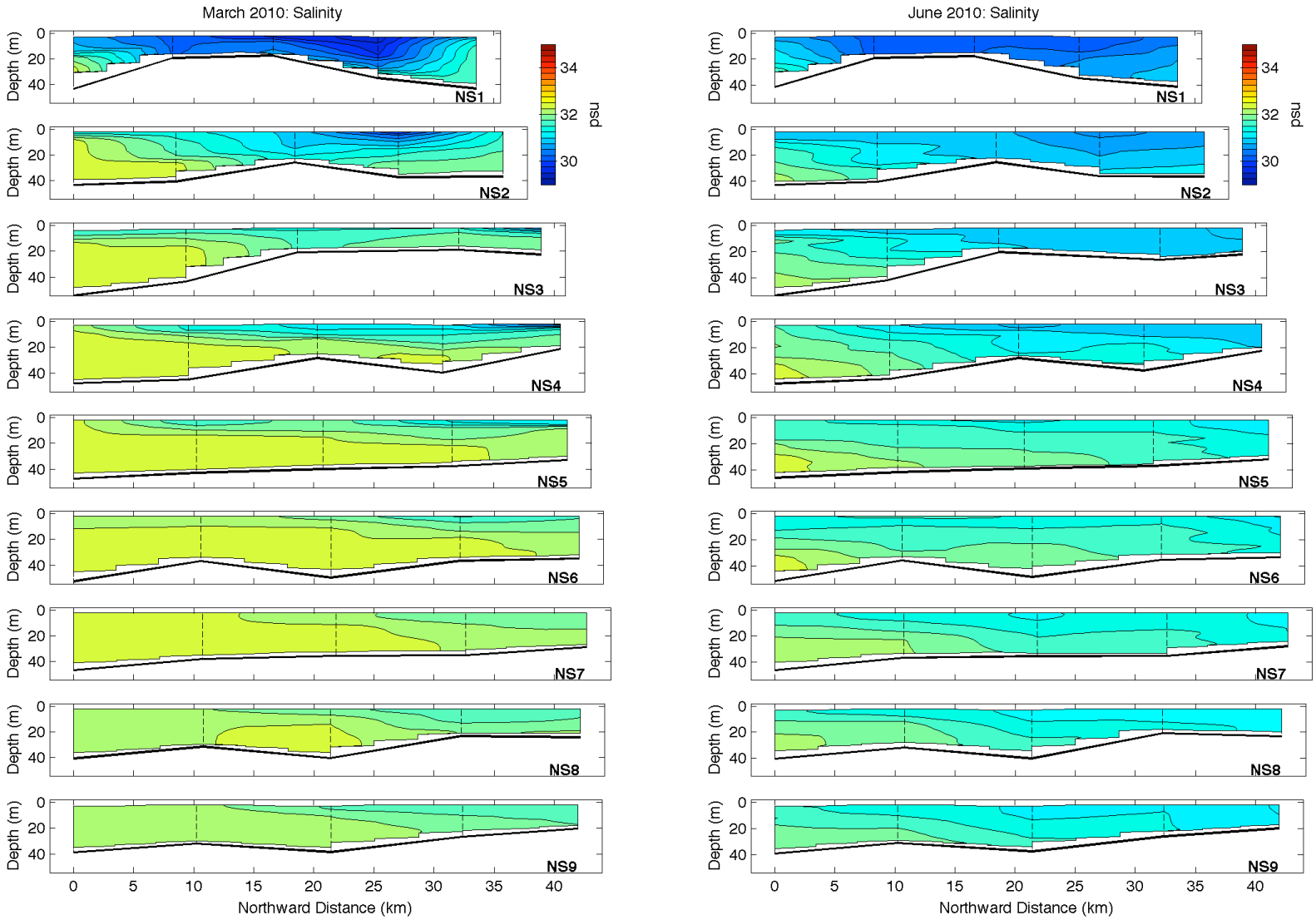

Figure 10. North-south sections of salinity during March 2010 (left) and June 2010 (right).
The section numbers are referenced to the map in Figure 1. The dashed lines denote the locations of the CTD casts.

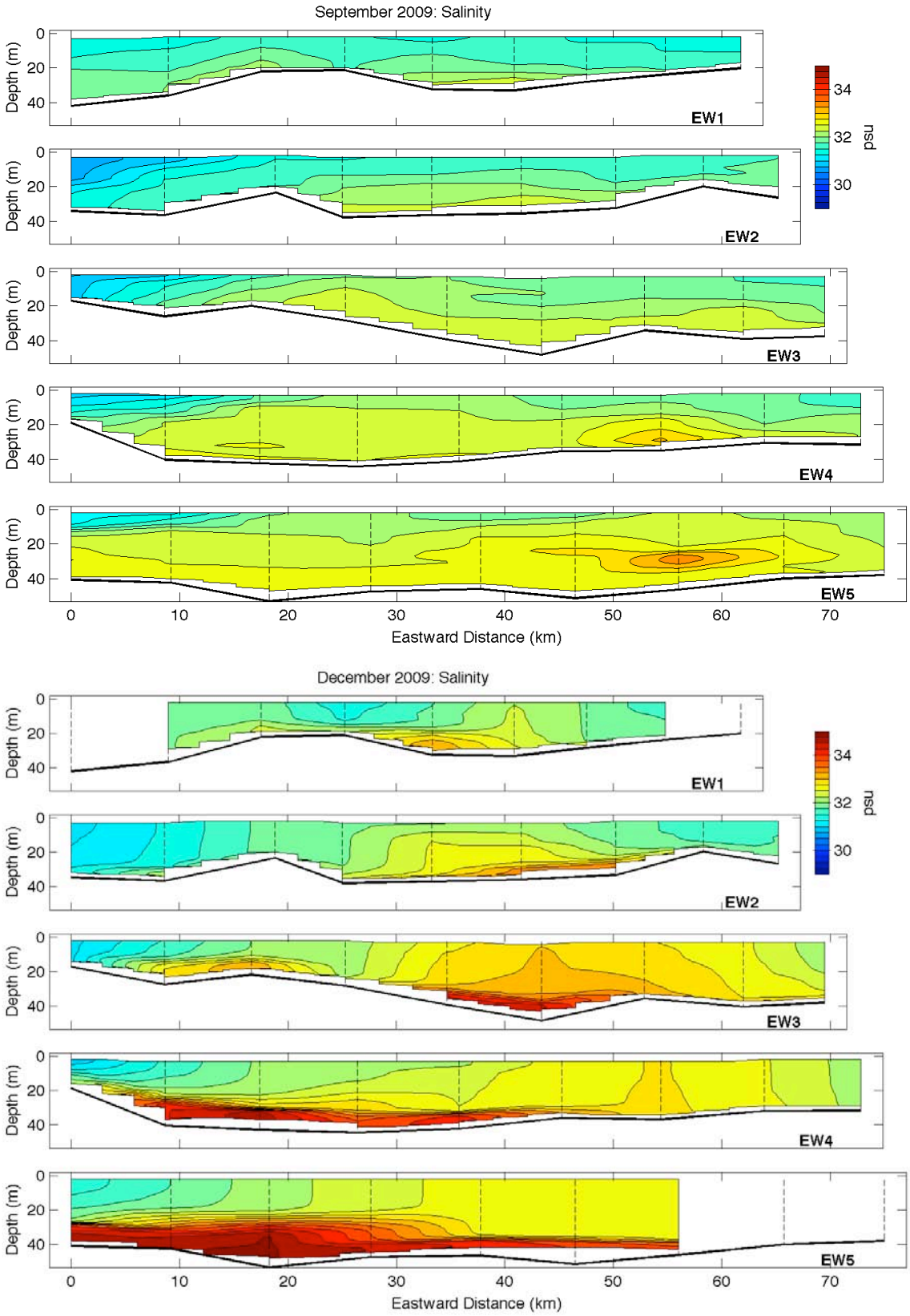

Figure 11. East-west sections of salinity during September 2009 (top) and December 2009 (bottom).

The section numbers are referenced to the map in Figure 1. The dashed lines denote the locations of the CTD casts.

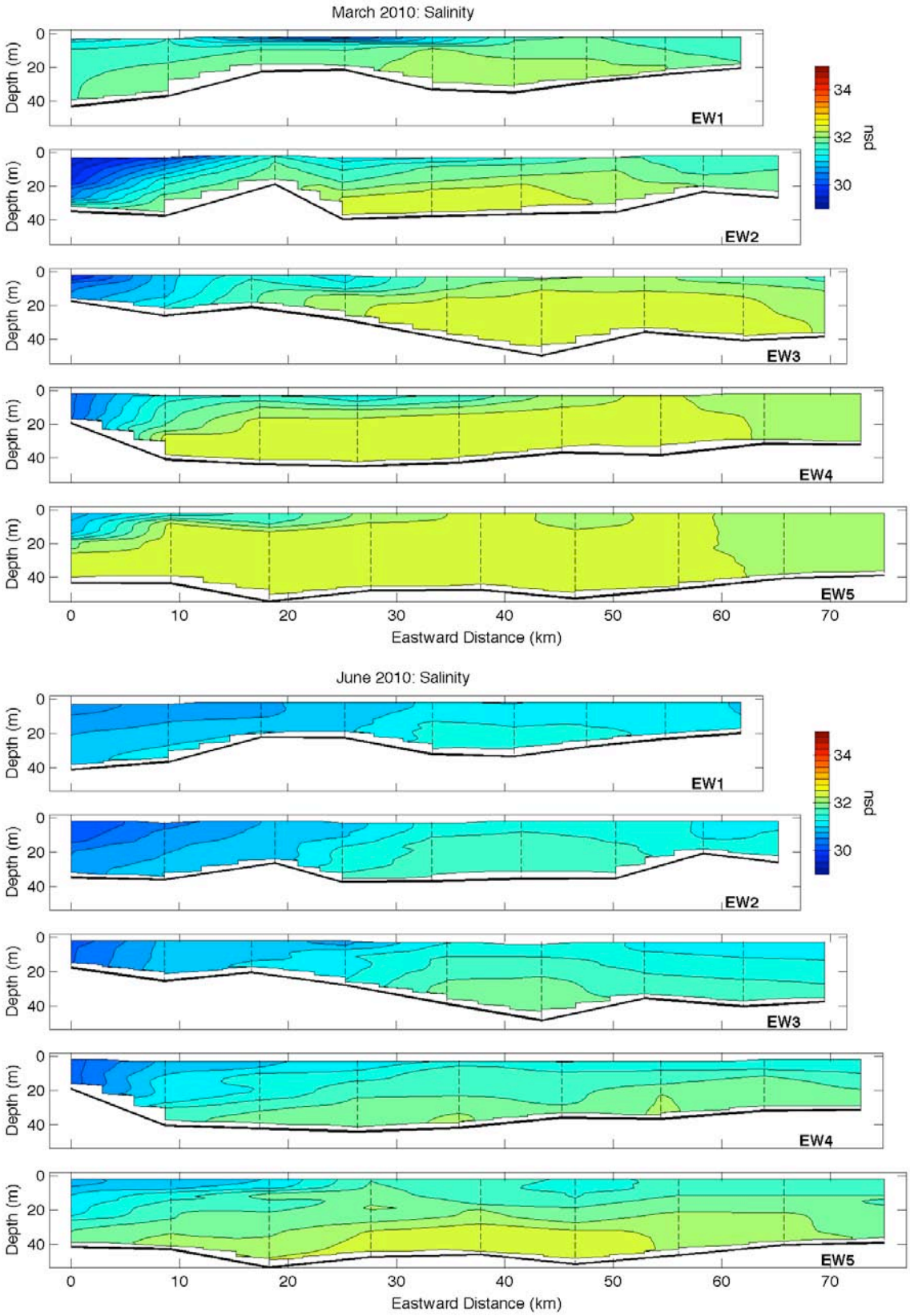

Figure 12. East-west sections of salinity during March 2010 (top) and June 2010 (bottom). The section numbers are referenced to the map in Figure 1. The dashed lines denote the locations of the CTD casts.

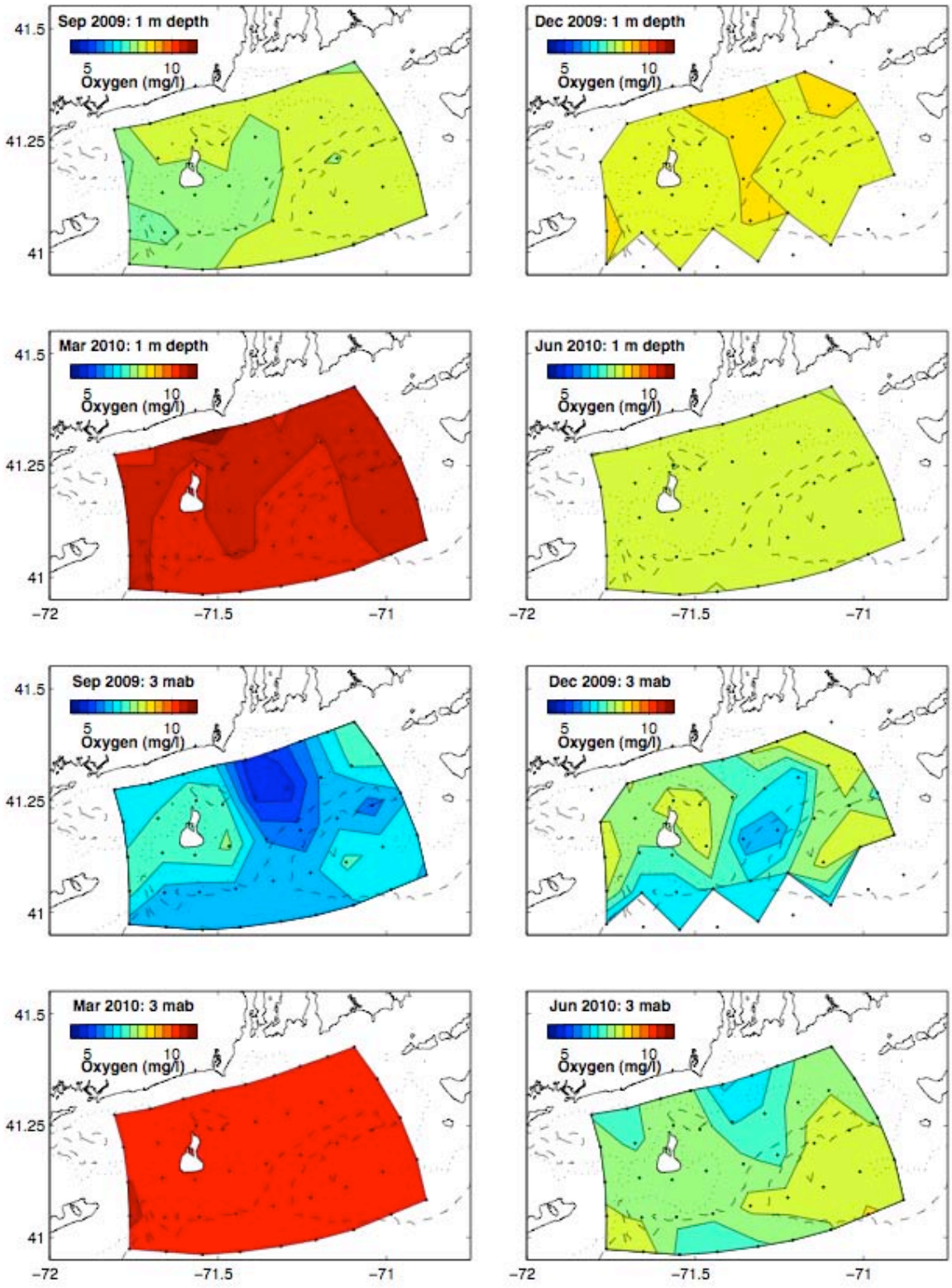

Figure 13. Maps of Oxygen concentration at 1 m below the surface (top) and 3 m above the bottom (bottom) during all 4 surveys.
The CTD cast locations are denoted by the black dots. The dotted and dashed lines are the 30 m and 40 m isobaths, respectively.

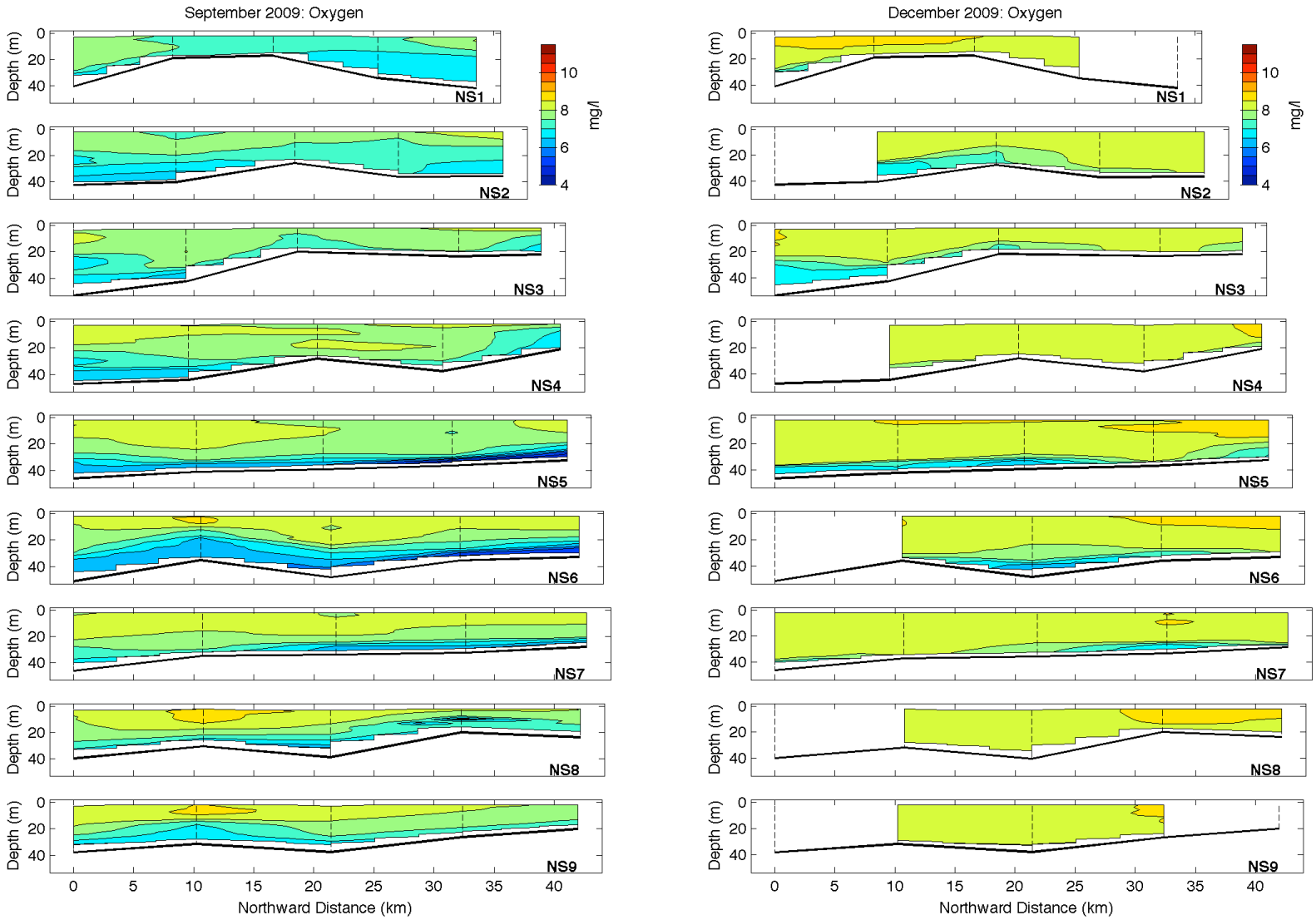

Figure 14. North-south sections of Oxygen concentration during September 2009 (left) and December 2009 (right). The section numbers are referenced to the map in Figure 1. The dashed lines denote the locations of the CTD casts.

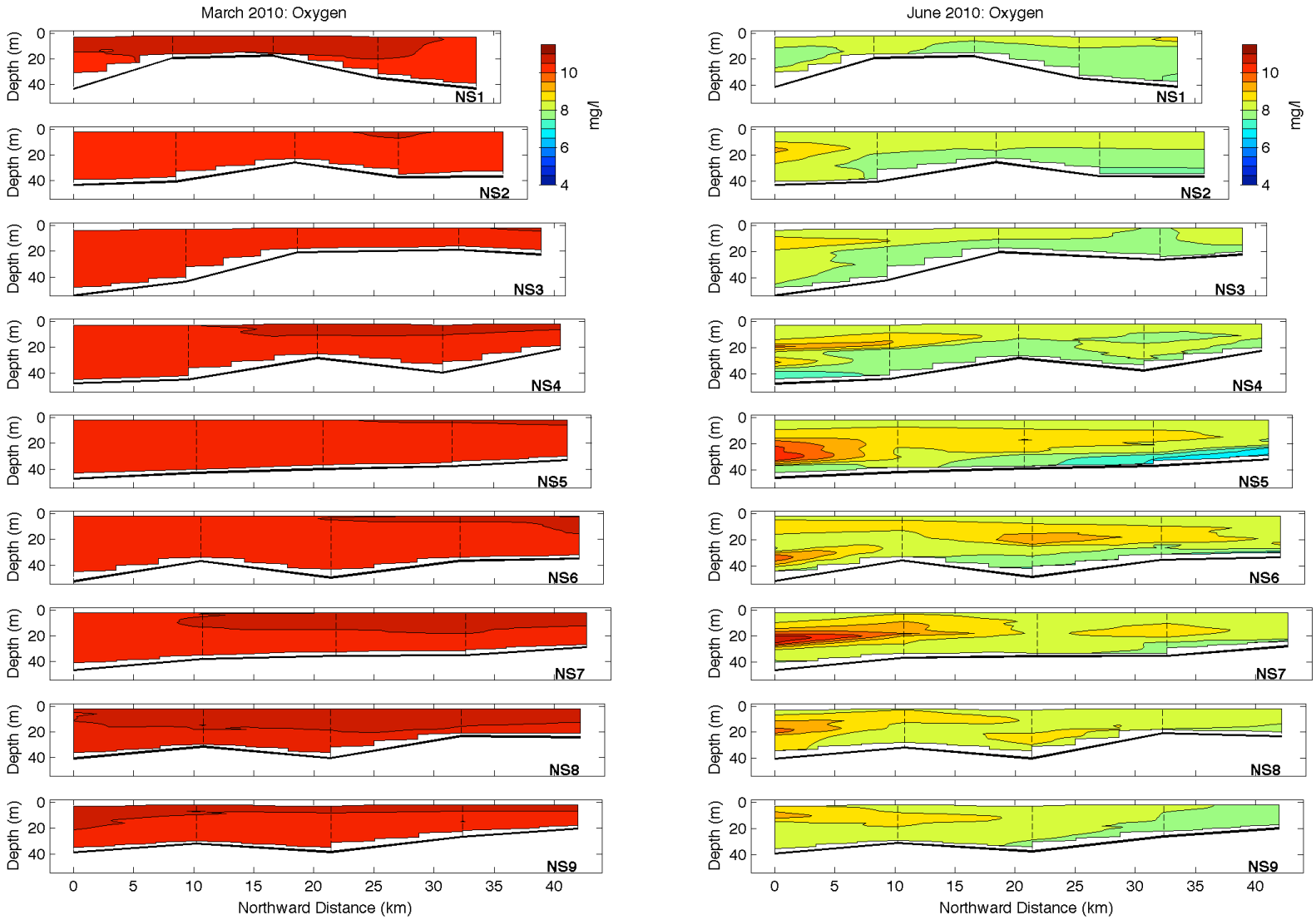

Figure 15. North-south sections of Oxygen concentration during March 2010 (left) and June 2010 (right).
The section numbers are referenced to the map in Figure 1. The dashed lines denote the locations of the CTD casts.

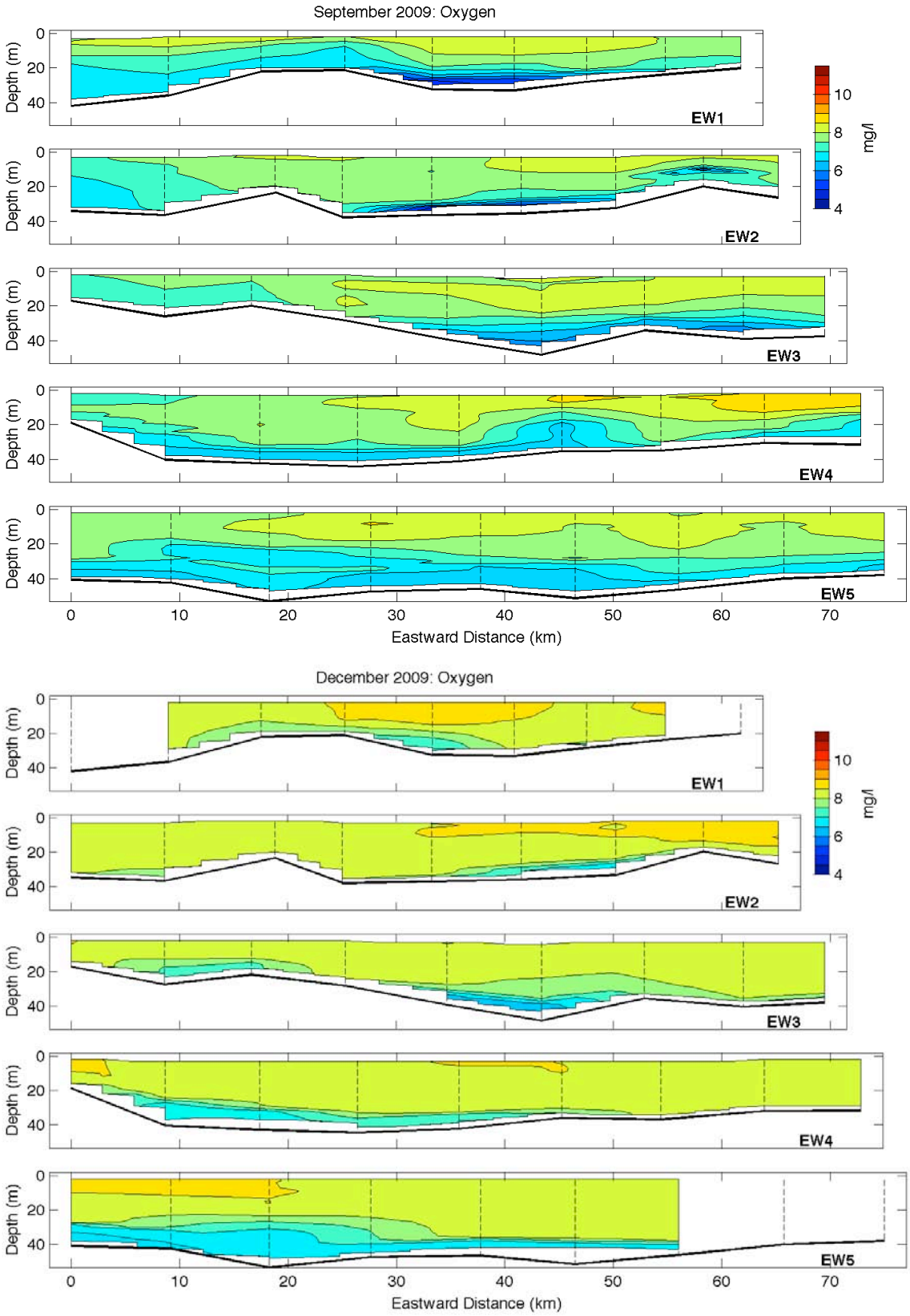

Figure 16. East-west sections of Oxygen concentration during September 2009 (top) and December 2009 (bottom).
The section numbers are referenced to the map in Figure 1. The dashed lines denote the locations of the CTD casts.

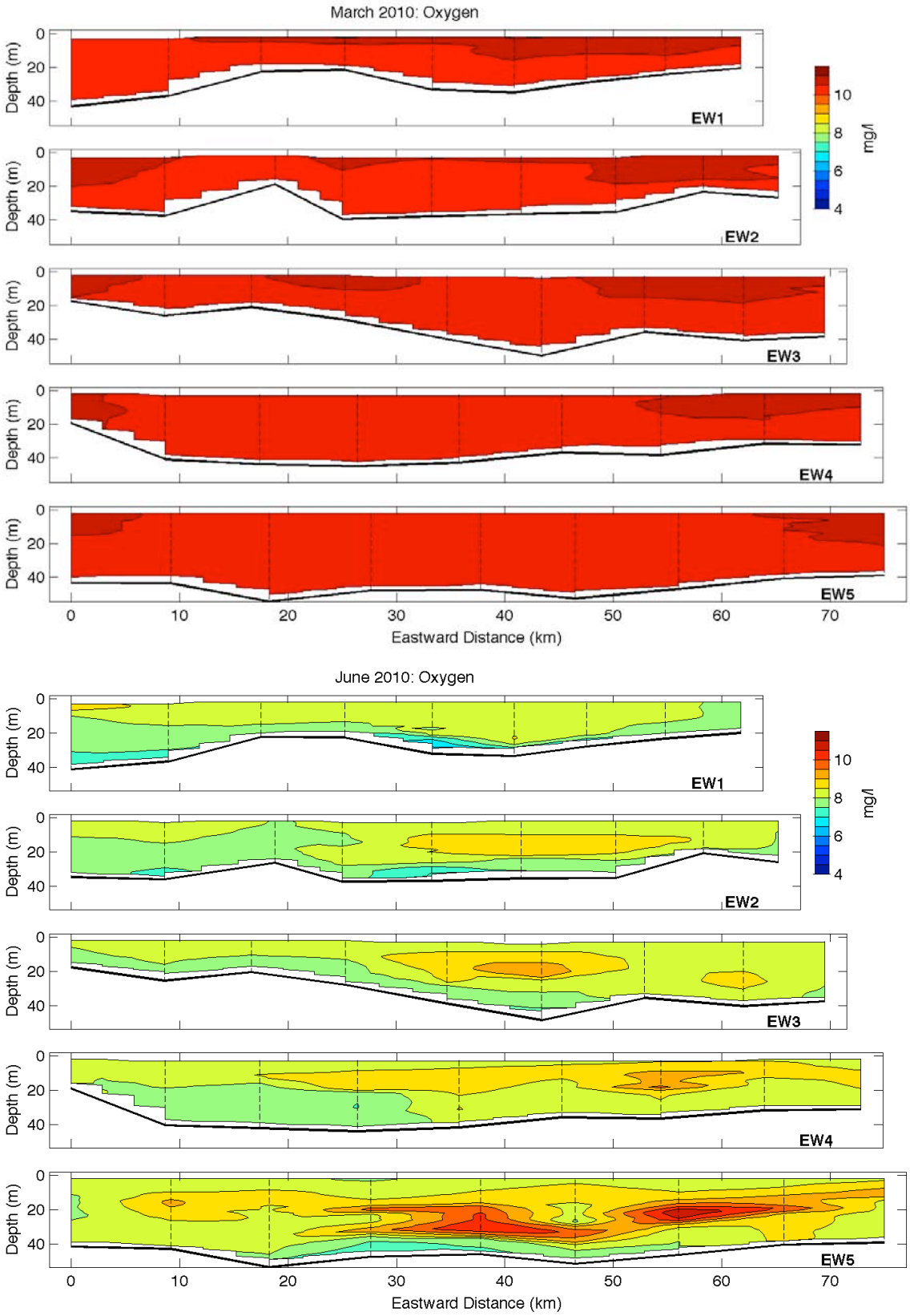

Figure 17. East-west sections of Oxygen concentration during March 2010 (top) and June 2010 (bottom).
The section numbers are referenced to the map in Figure 1. The dashed lines denote the locations of the CTD casts.

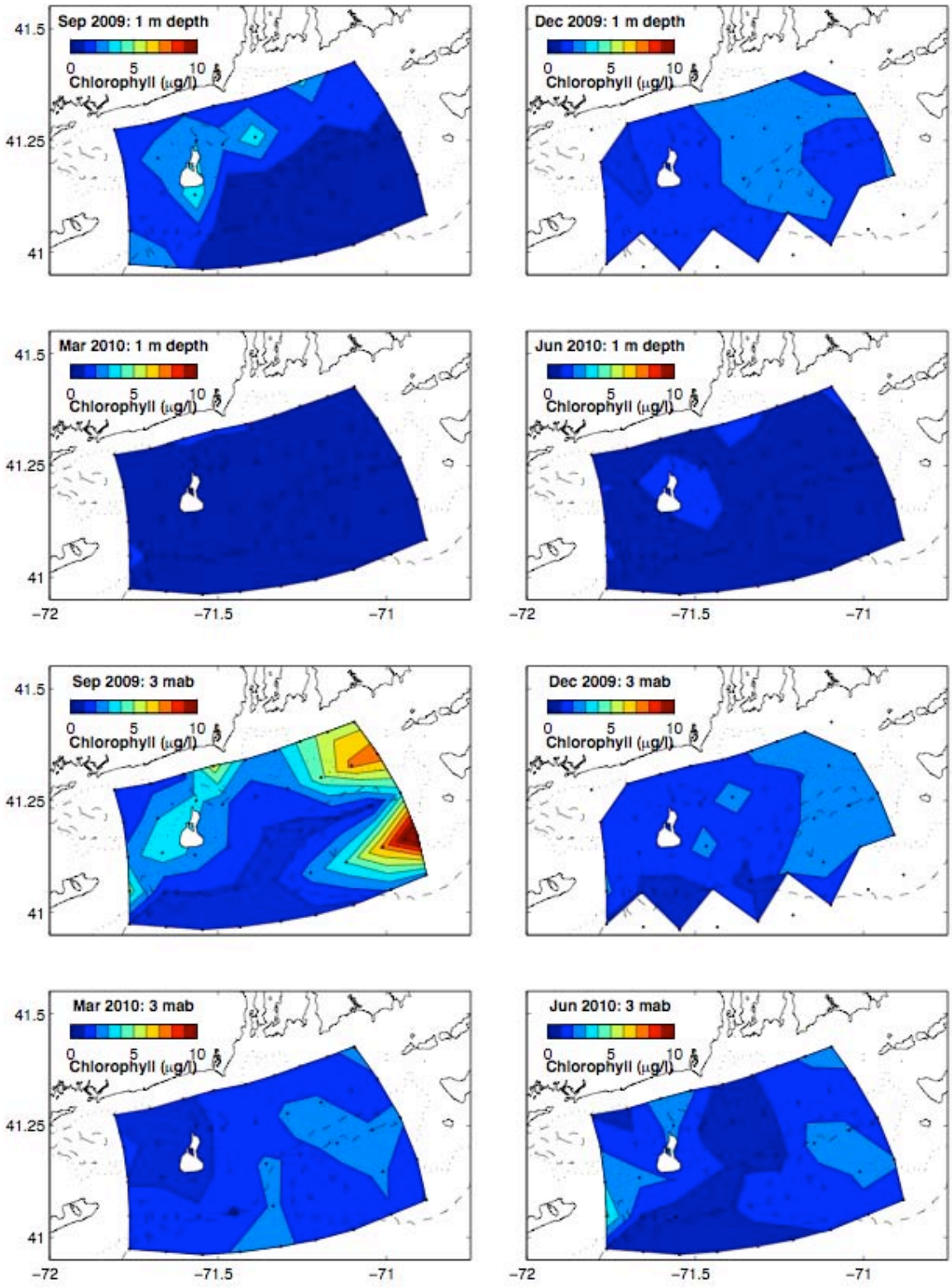

Figure 18. Maps of chlorophyll concentration at 1 m below the surface (top) and 3 m above the bottom (bottom) during all 4 surveys.
The CTD cast locations are denoted by the black dots. The dotted and dashed lines are the 30 m and 40 m isobaths, respectively.

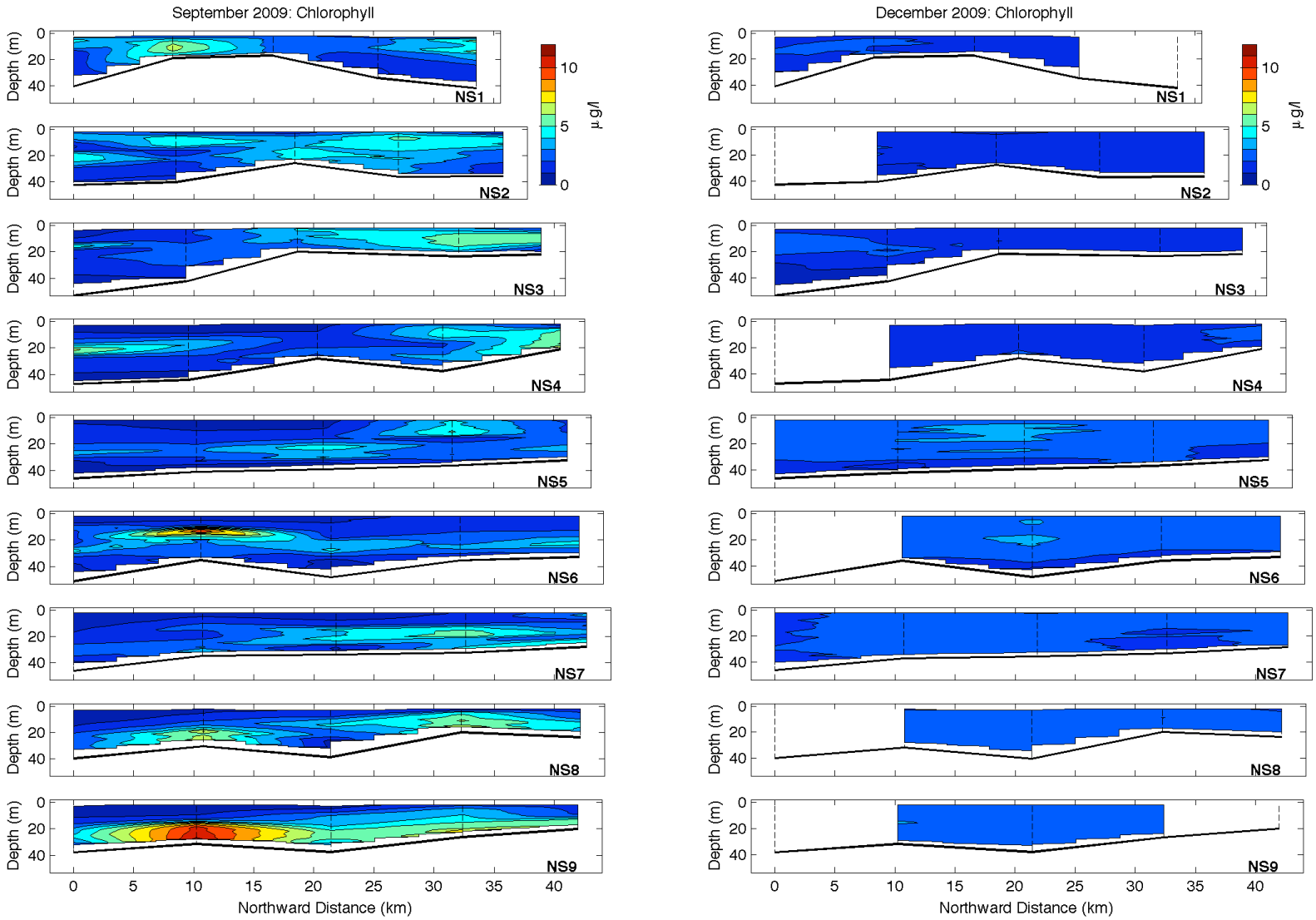

Figure 19. North-south sections of chlorophyll concentration during September 2009 (left) and December 2009 (right). The section numbers are referenced to the map in Figure 1. The dashed lines denote the locations of the CTD casts.

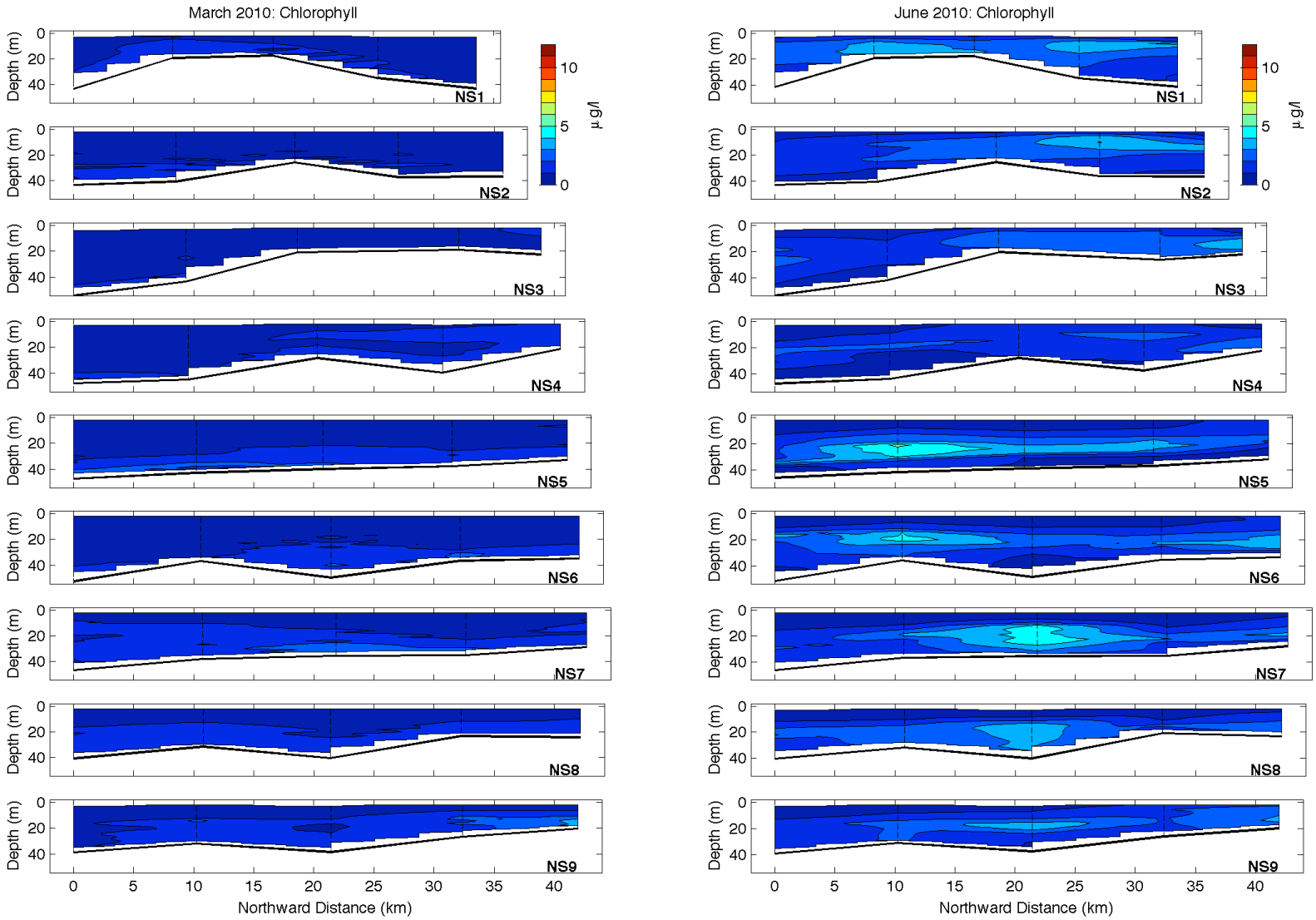

Figure 20. North-south sections of chlorophyll concentration during March 2010 (left) and June 2010 (right).
The section numbers are referenced to the map in **Figure 1**. The dashed lines denote the locations of the CTD casts.

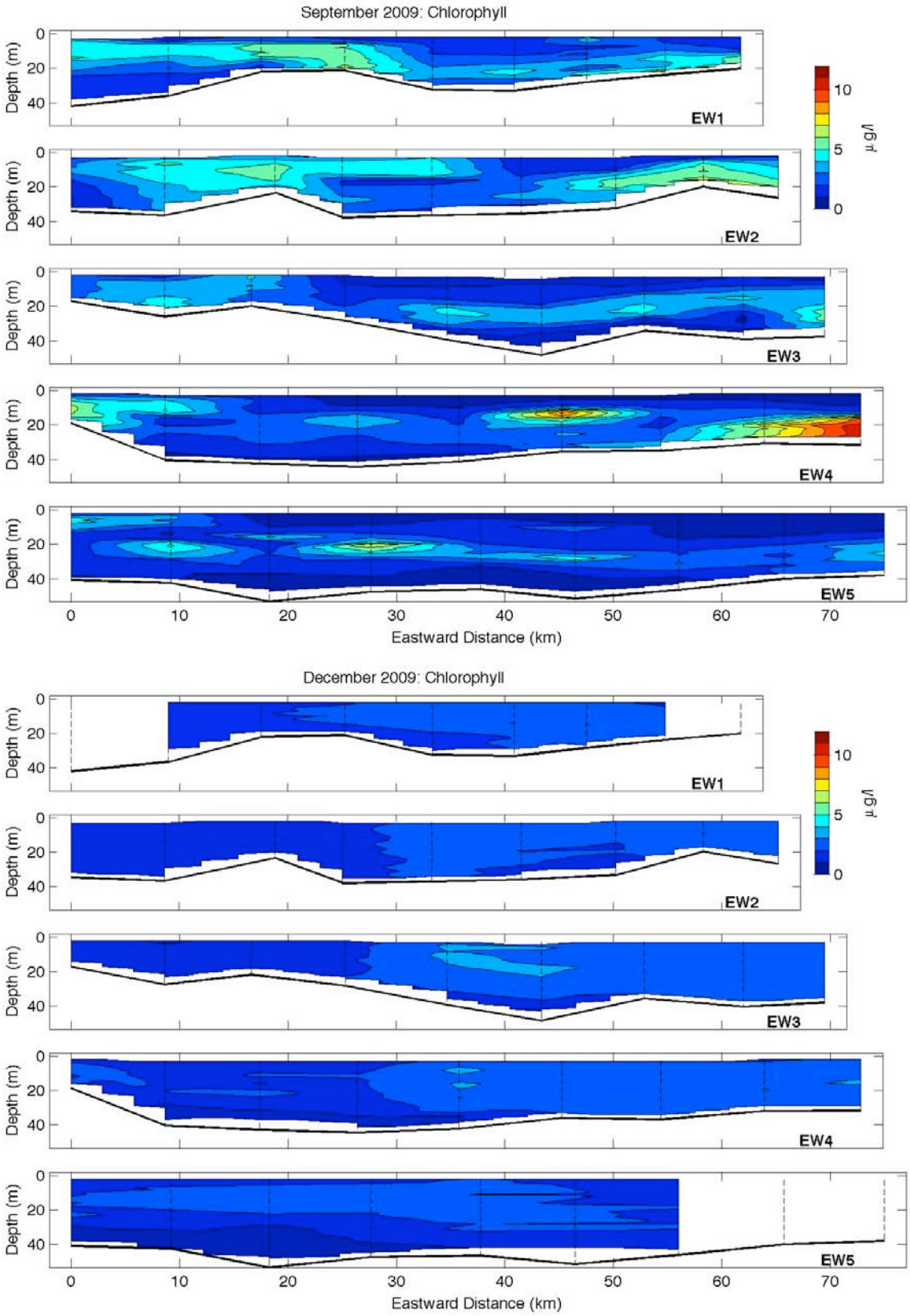

Figure 21. East-west sections of chlorophyll concentration during September 2009 (top) and December 2009 (bottom).
The section numbers are referenced to the map in Figure 1. The dashed lines denote the locations of the CTD casts.

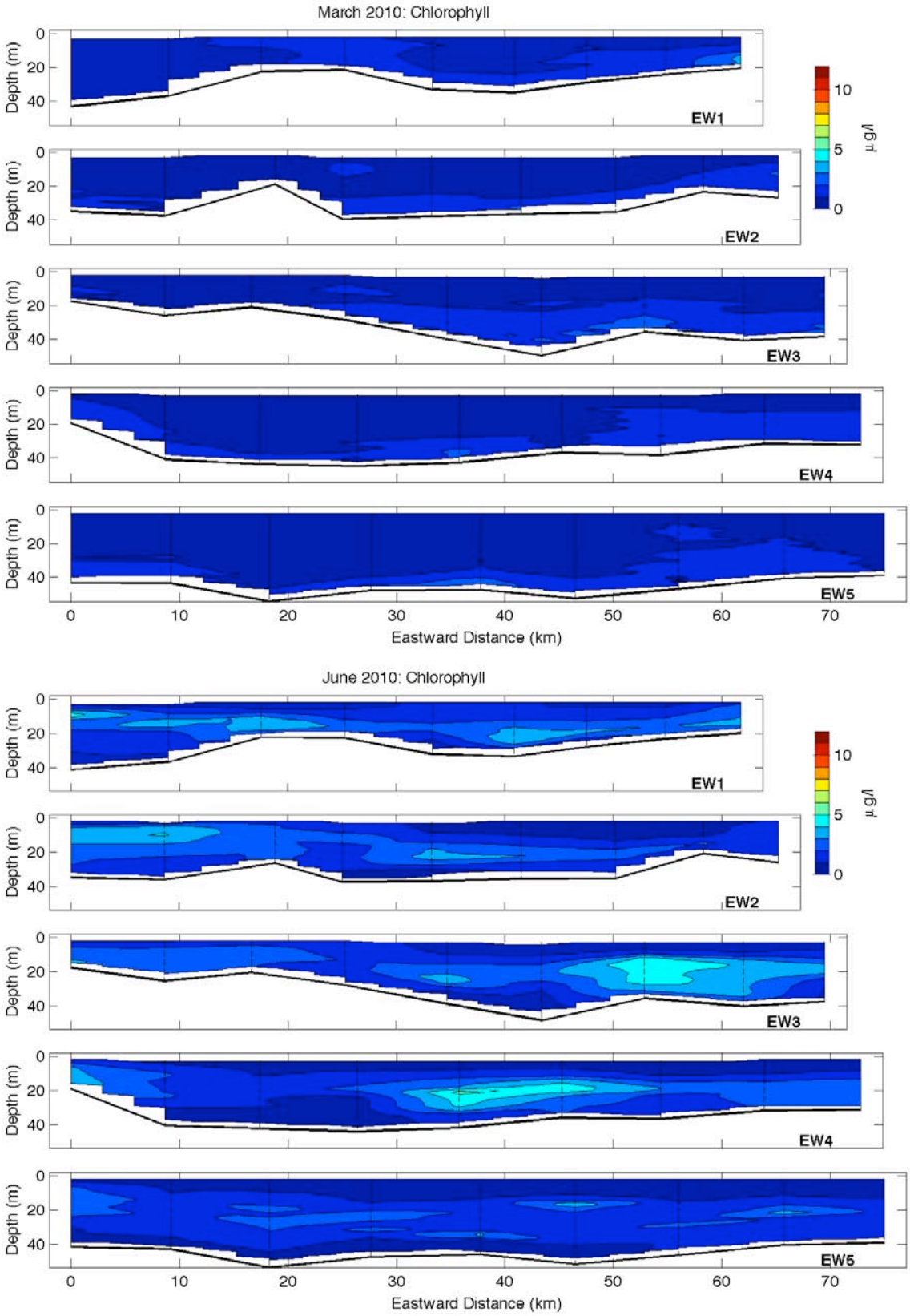

Figure 22. East-west sections of chlorophyll concentration during March 2010 (top) and June 2010 (bottom).
The section numbers are referenced to the map in Figure 1. The dashed lines denote the locations of the CTD casts.

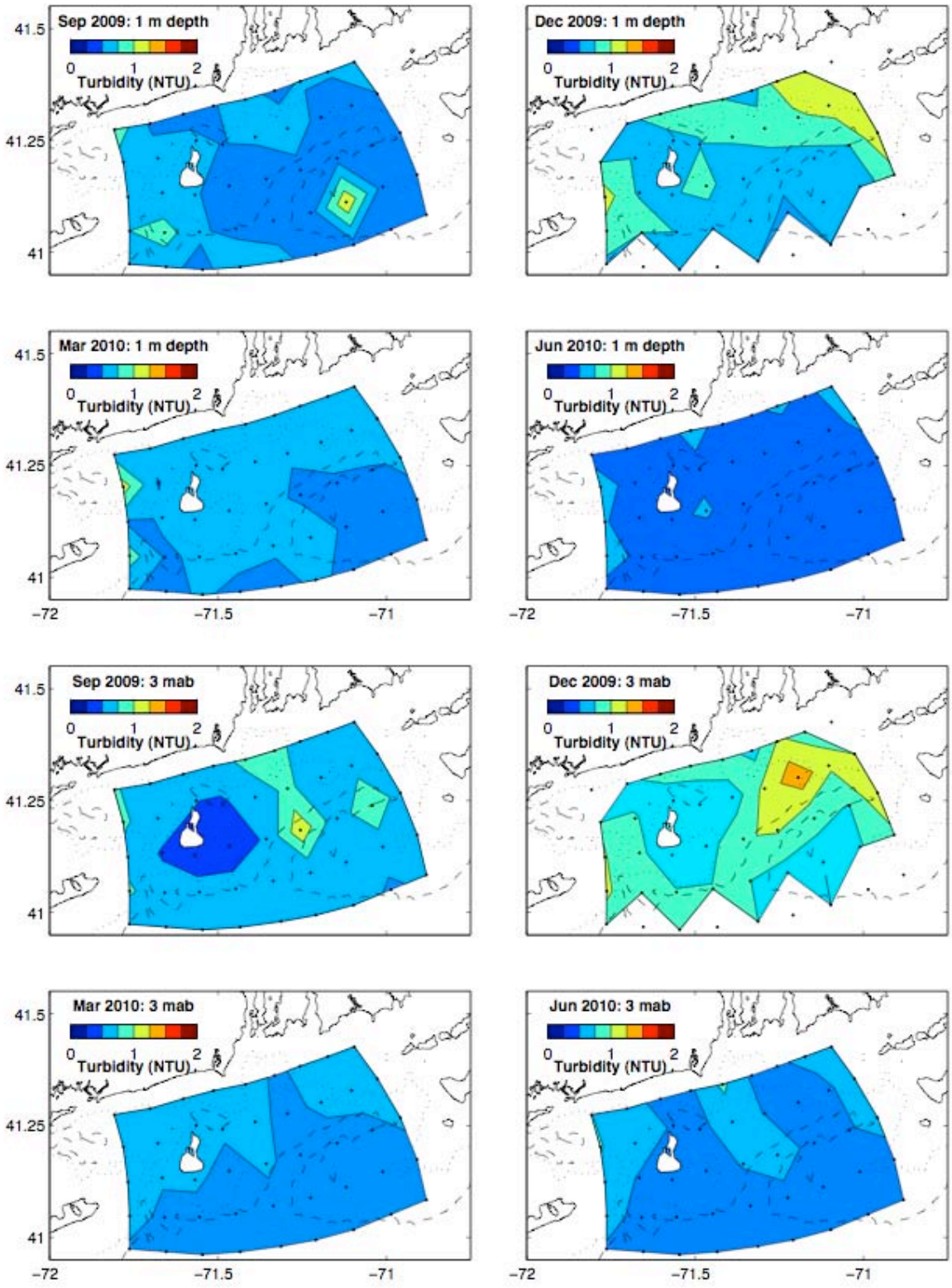

Figure 23. Maps of water turbidity at 1 m below the surface (top) and 3 m above the bottom (bottom) during all 4 surveys.
The CTD cast locations are denoted by the black dots. The dotted and dashed lines are the 30 m and 40 m isobaths, respectively.

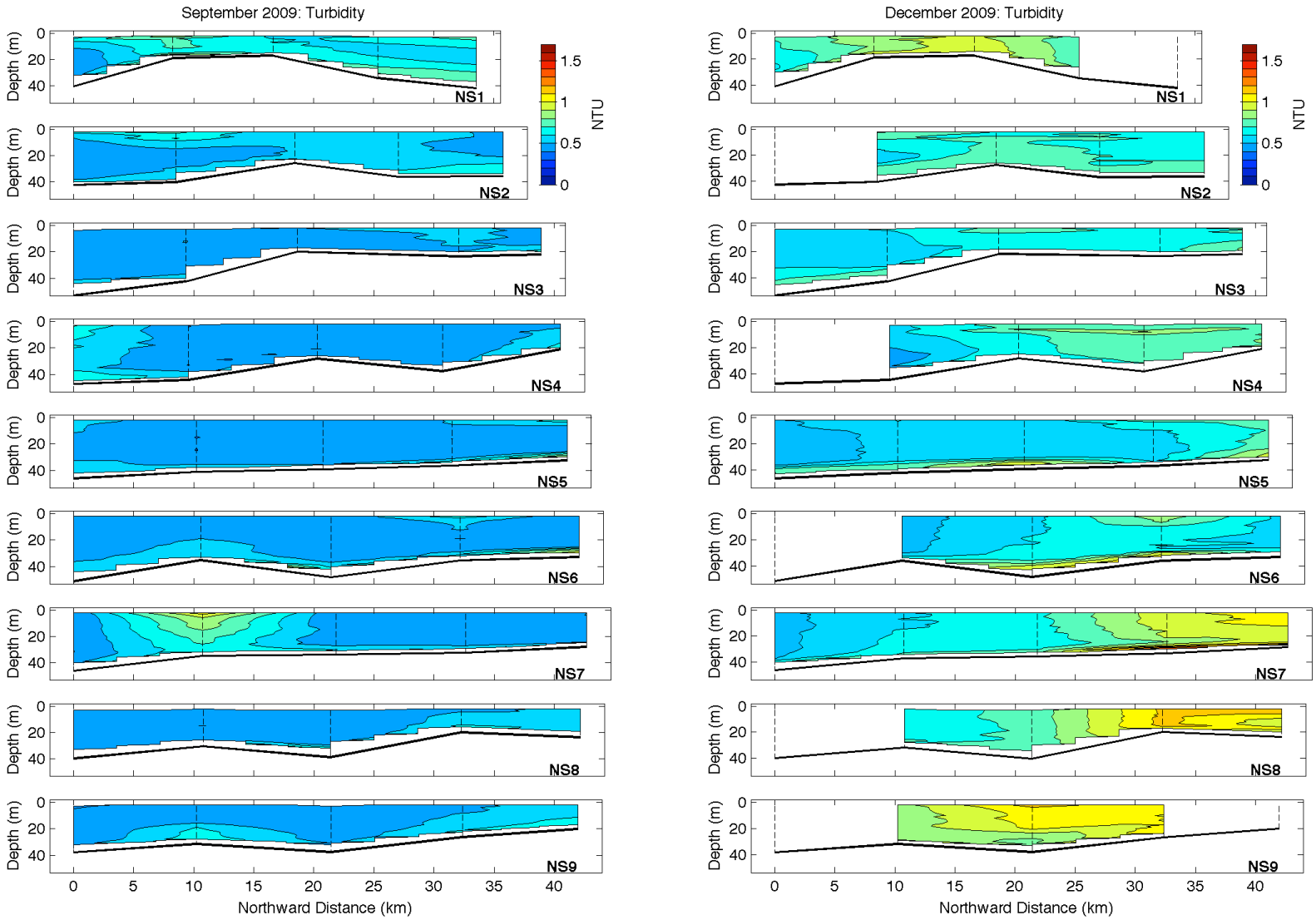

Figure 24. North-south sections of water turbidity during September 2009 (left) and December 2009 (right).
The section numbers are referenced to the map in Figure 1. The dashed lines denote the locations of the CTD casts.

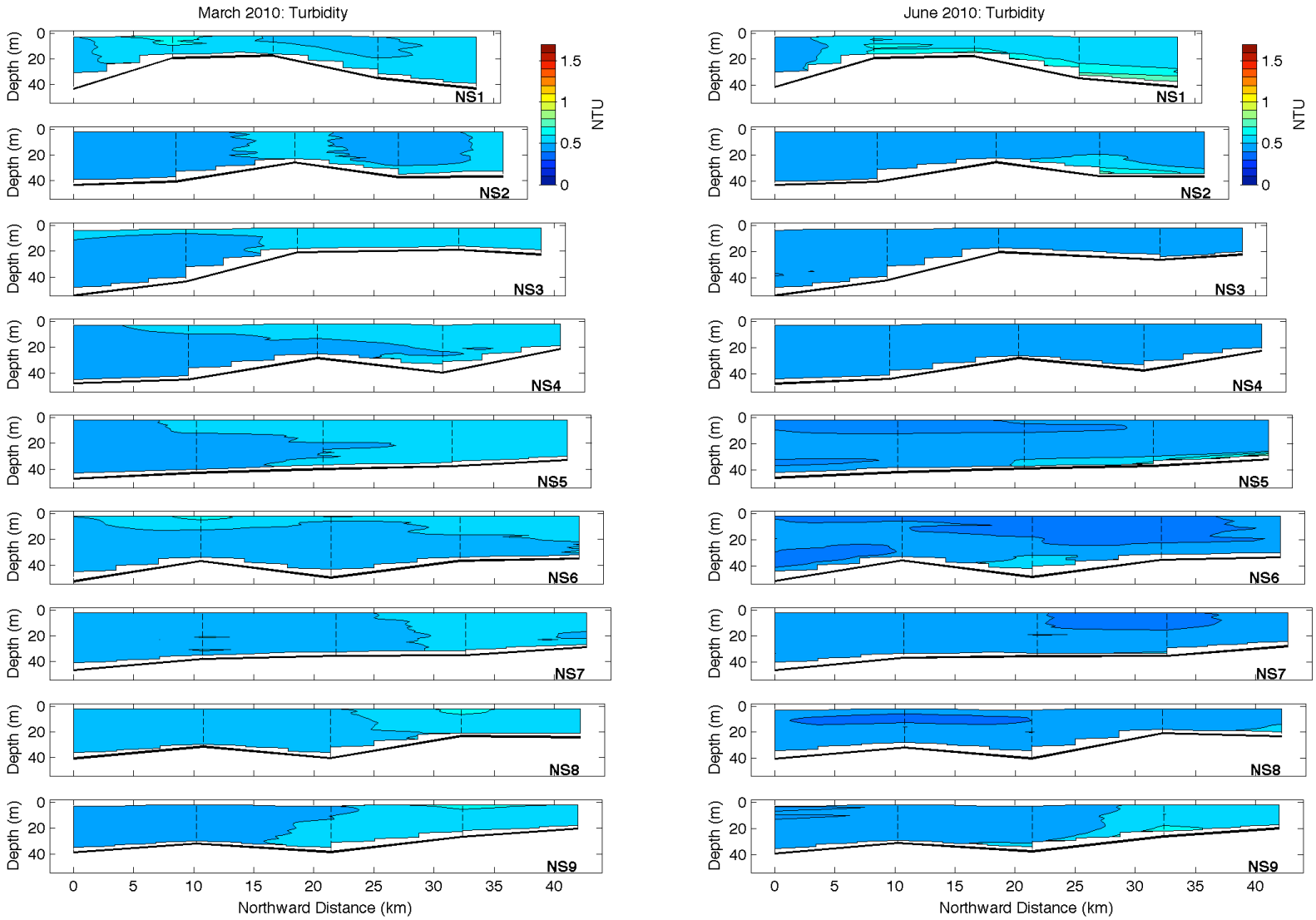

Figure 25. North-south sections of water turbidity during March 2010 (left) and June 2010 (right).
The section numbers are referenced to the map in Figure 1. The dashed lines denote the locations of the CTD casts.

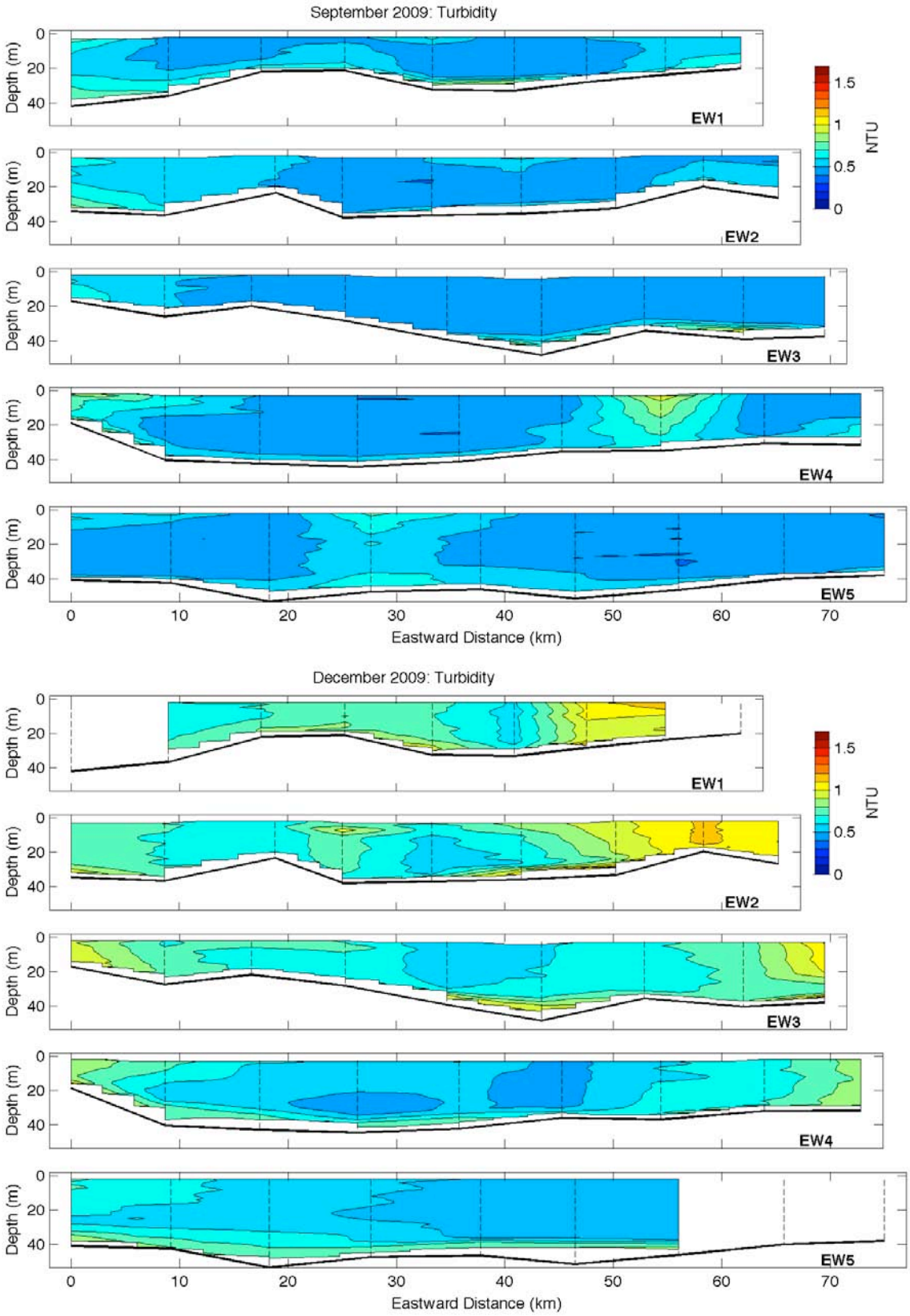

Figure 26. East-west sections of water turbidity during September 2009 (top) and December 2009 (bottom).
The section numbers are referenced to the map in Figure 1. The dashed lines denote the locations of the CTD casts.

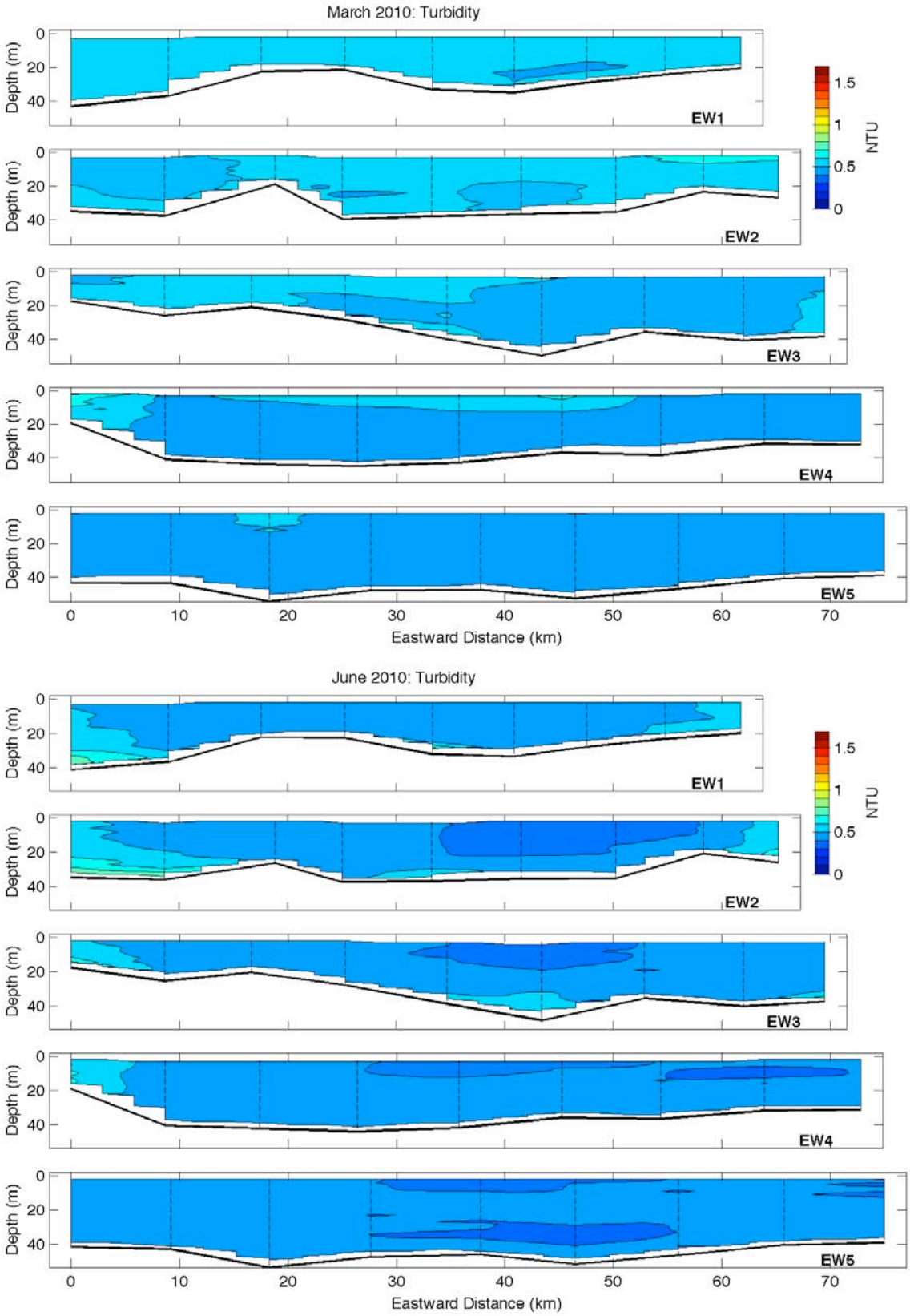

Figure 27. East-west sections of water turbidity during March 2010 (top) and June 2010 (bottom).

The section numbers are referenced to the map in Figure 1. The dashed lines denote the locations of the CTD casts.

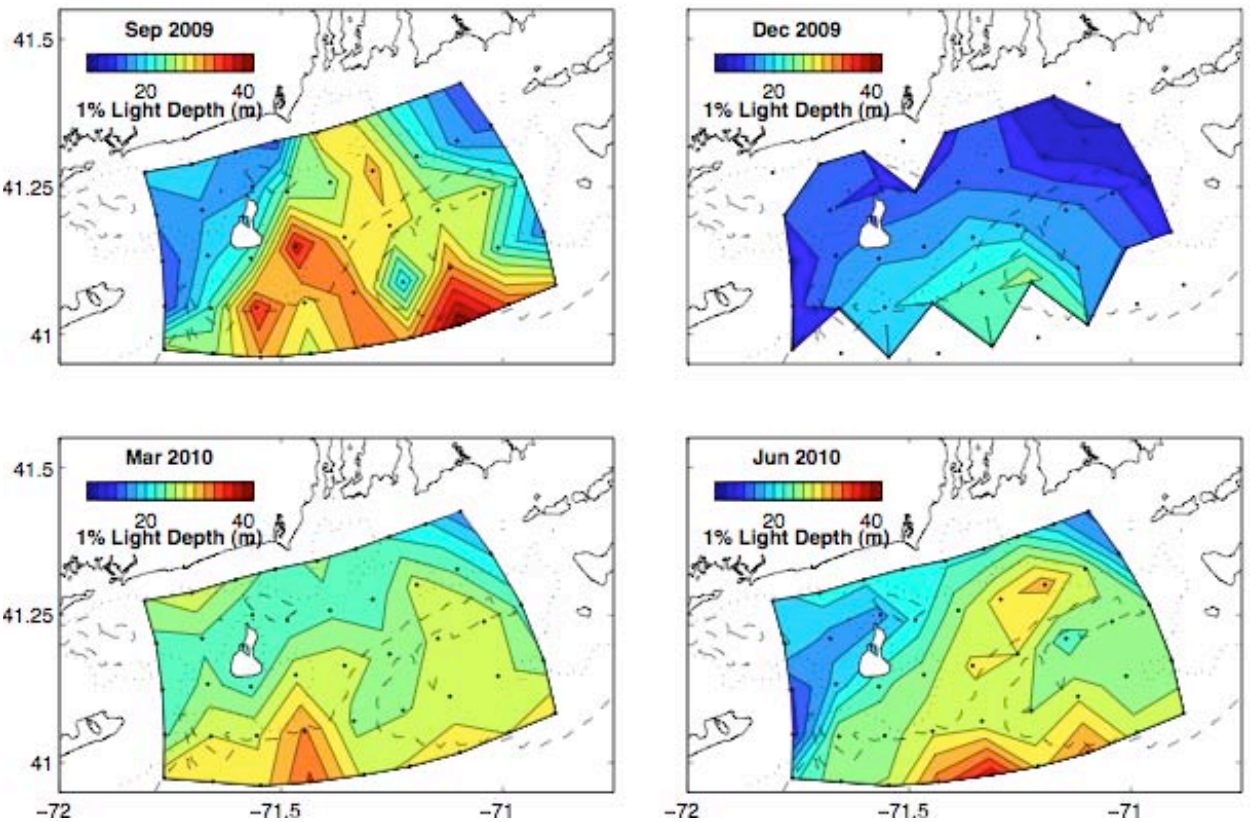

Figure 28. Maps of the depth of the euphotic zone during all 4 surveys.
The CTD cast locations are denoted by the black dots. The dotted and dashed lines are the 30 m and 40 m isobaths, respectively.

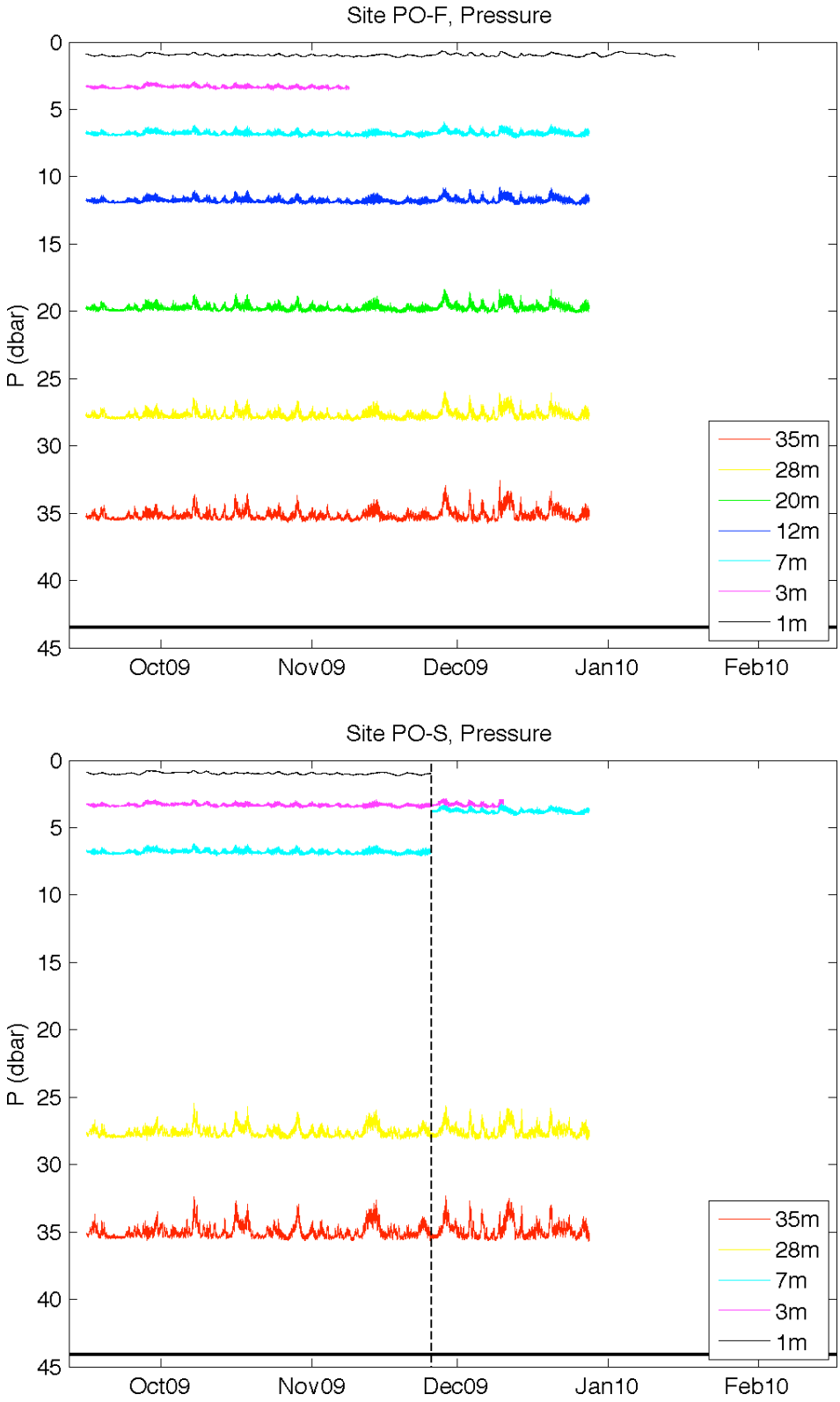

Figure 29. Moored CTD pressure records for mooring PO-F (top) and PO-S (bottom) for time period 1.
The legend lists the nominal depths of each instrument. The vertical dashed line in the bottom plot shows the time at which the mooring was dragged.

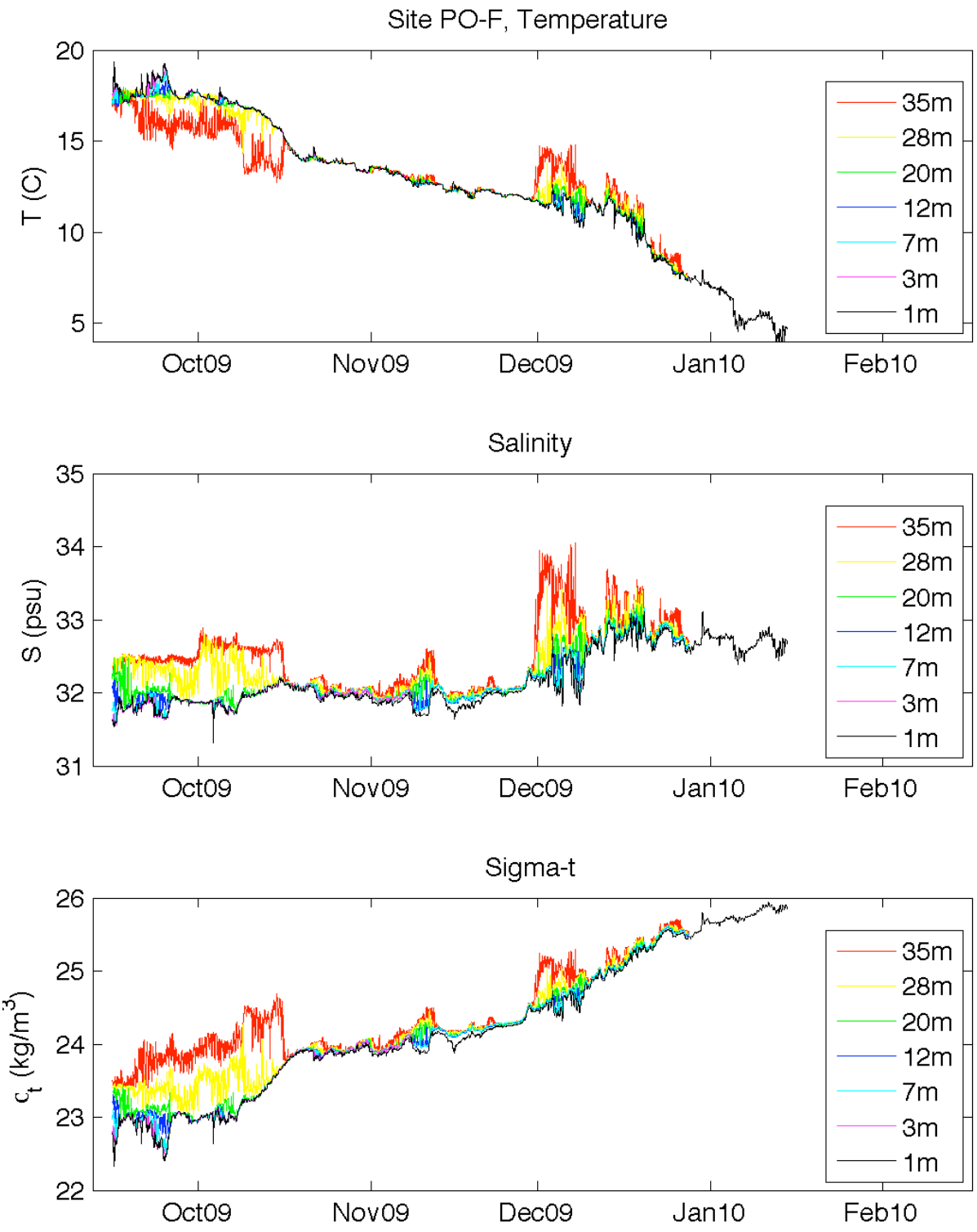

Figure 30. Time series of temperature (top), salinity (middle), and sigma-t (bottom) for mooring PO-F instruments during time period 1.
The legend gives the nominal depths of each CTD.

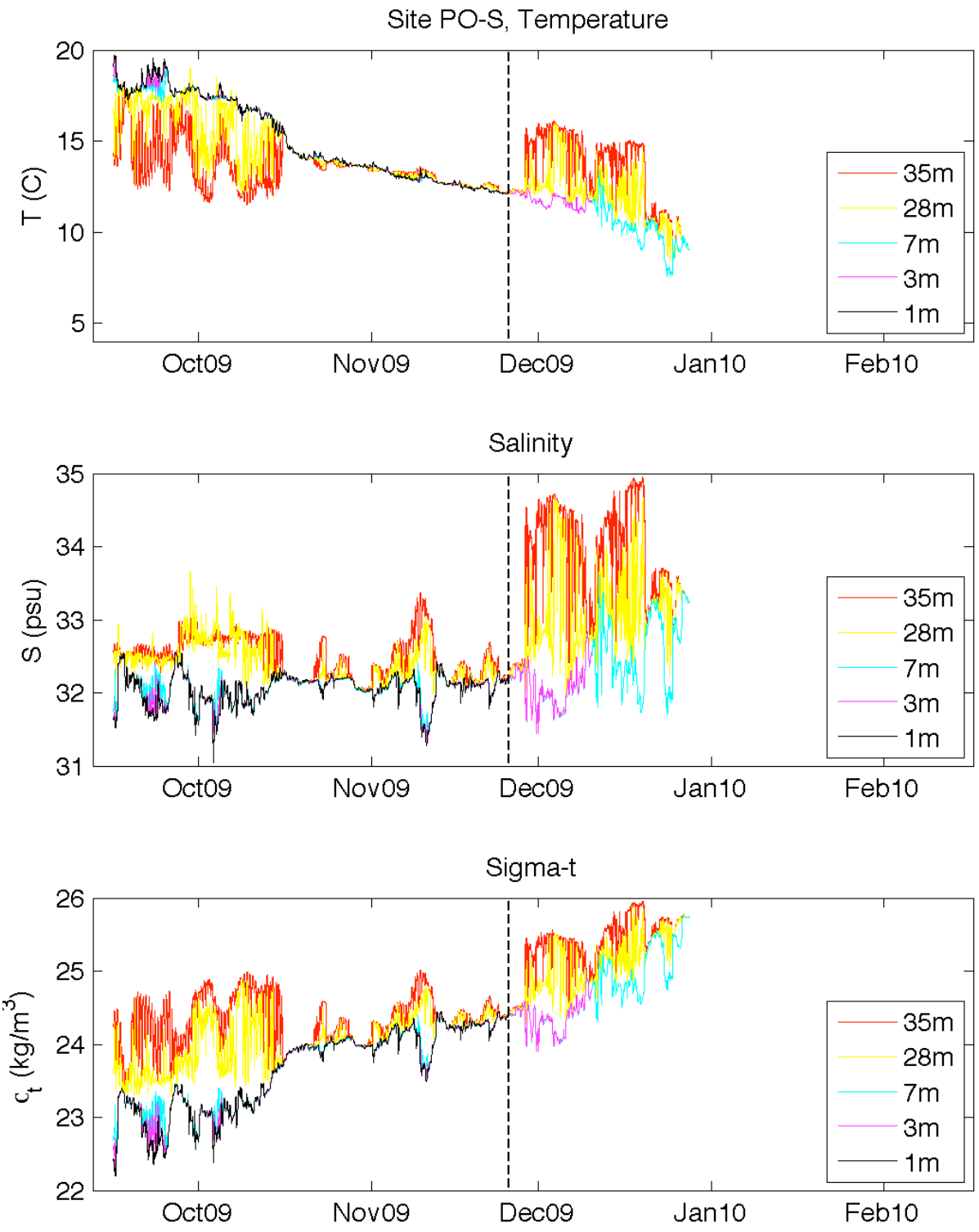

Figure 31. Time series of temperature (top), salinity (middle), and sigma-t (bottom) for mooring PO-S instruments during time period 1.
The legend gives the nominal depths of each CTD. The dashed vertical line is the time at which the mooring was dragged.

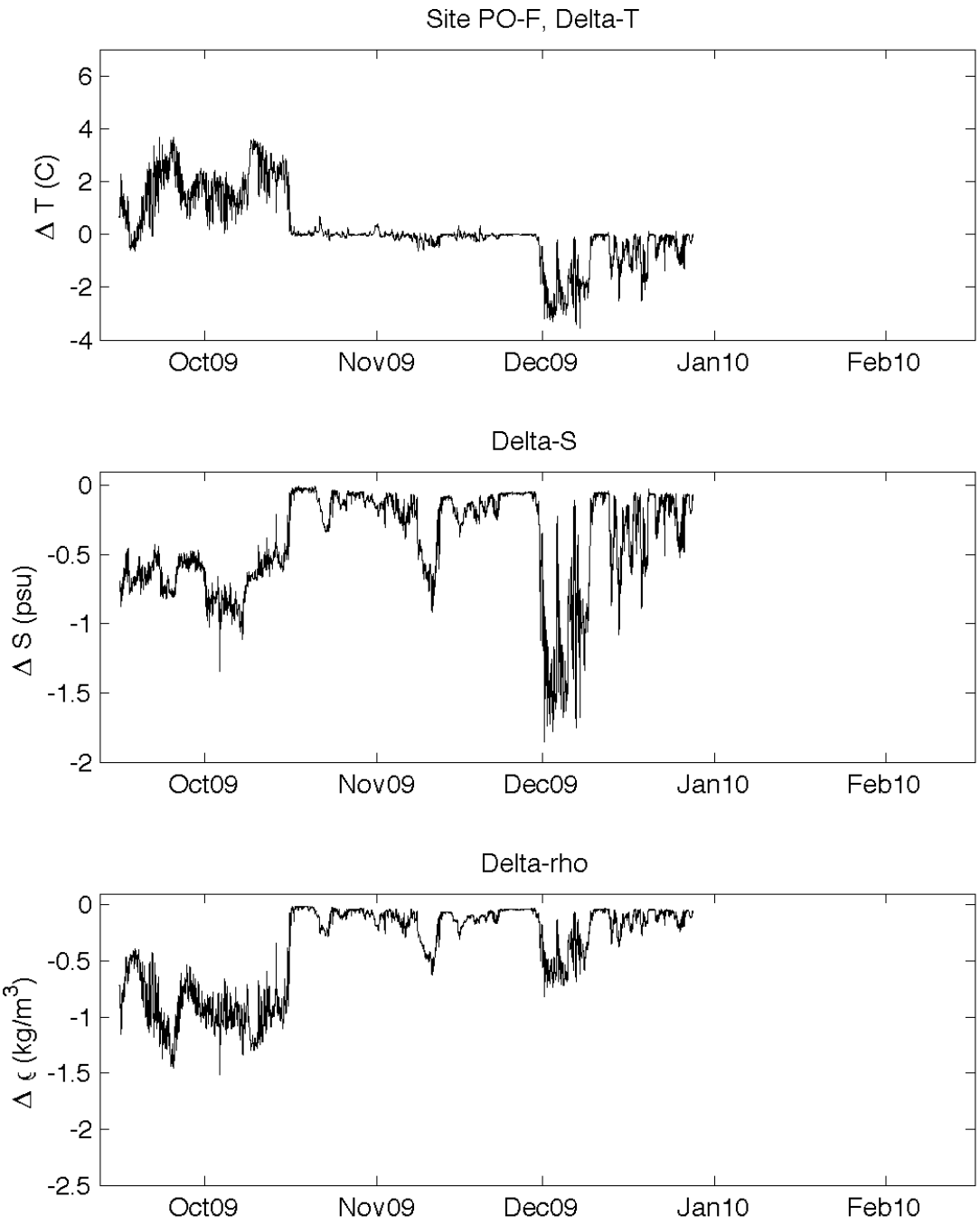

Figure 32. Time series of vertical differences in temperature (top), salinity (middle), and sigma-t (bottom) for mooring PO-F during time period 1.
Differences are computed as the value at 1 m (nominal) minus its value at 35 m (nominal).

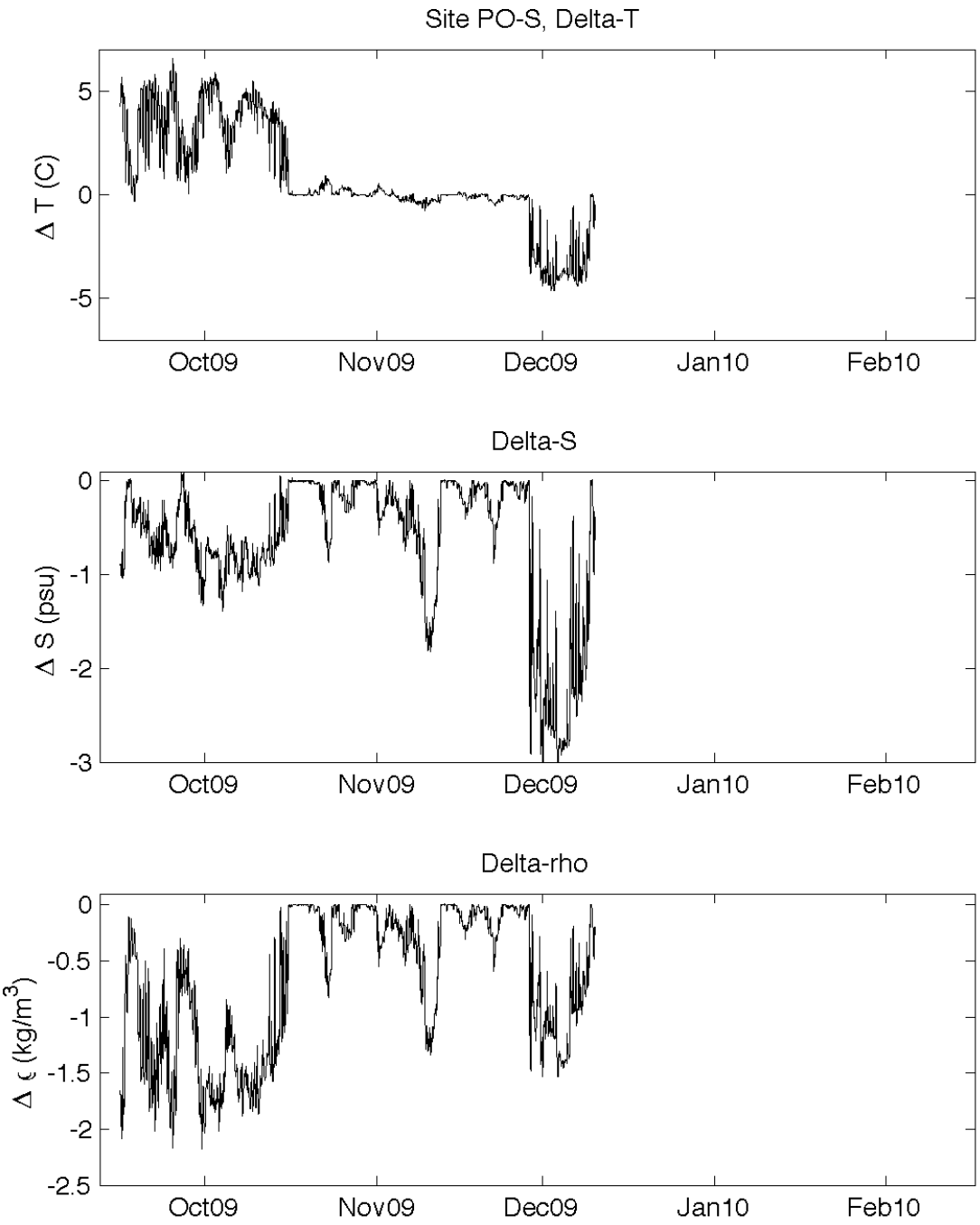

Figure 33. Time series of vertical differences in temperature (top), salinity (middle), and sigma-t (bottom) for mooring PO-S during time period 1.
Differences are computed as the value at 3 m (nominal) minus its value at 35 m (nominal).

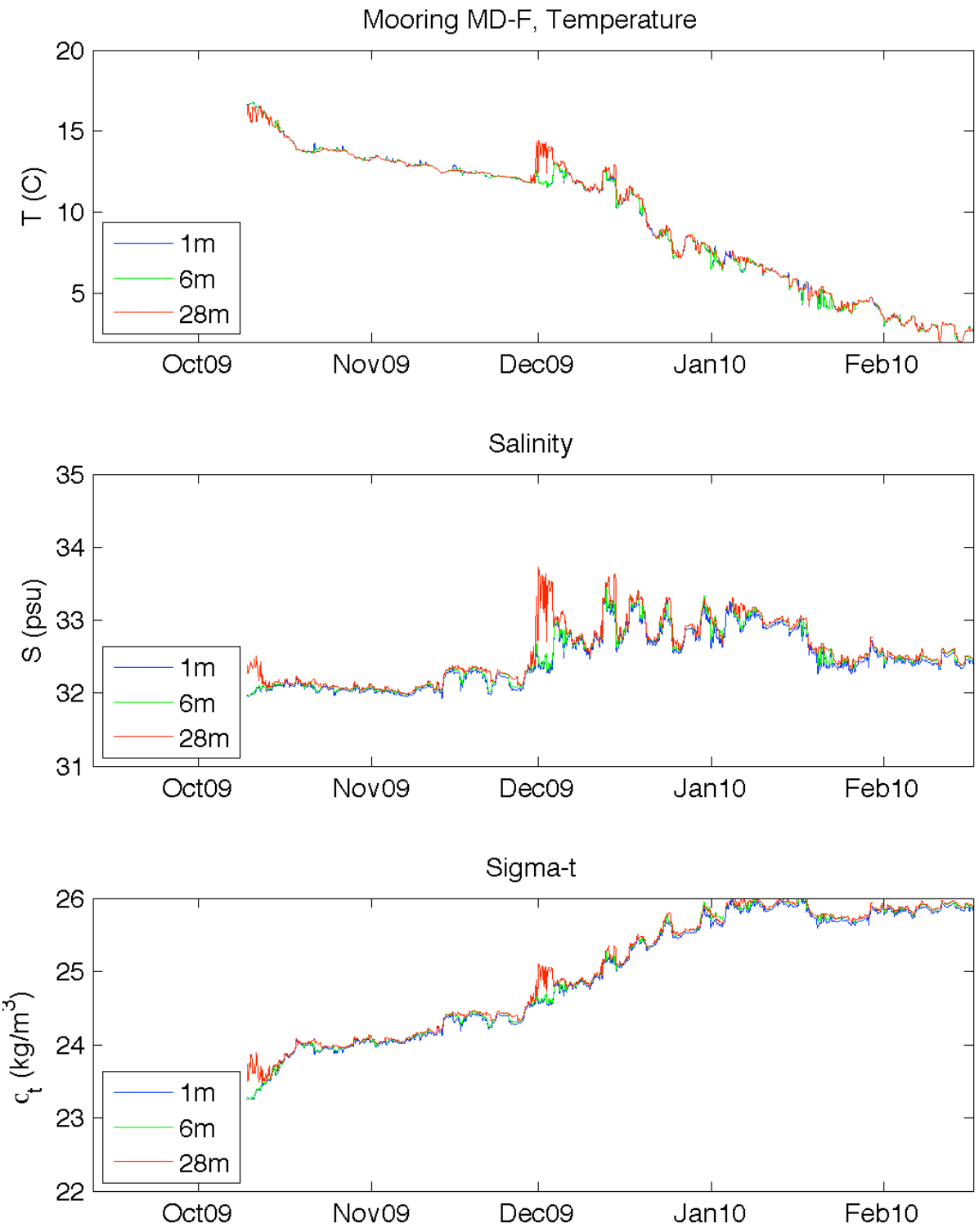

Figure 34. Time series of temperature (top), salinity (middle), and sigma-t (bottom) for mooring MD-F instruments during time period 1.
The legend gives the nominal depths of each CTD.

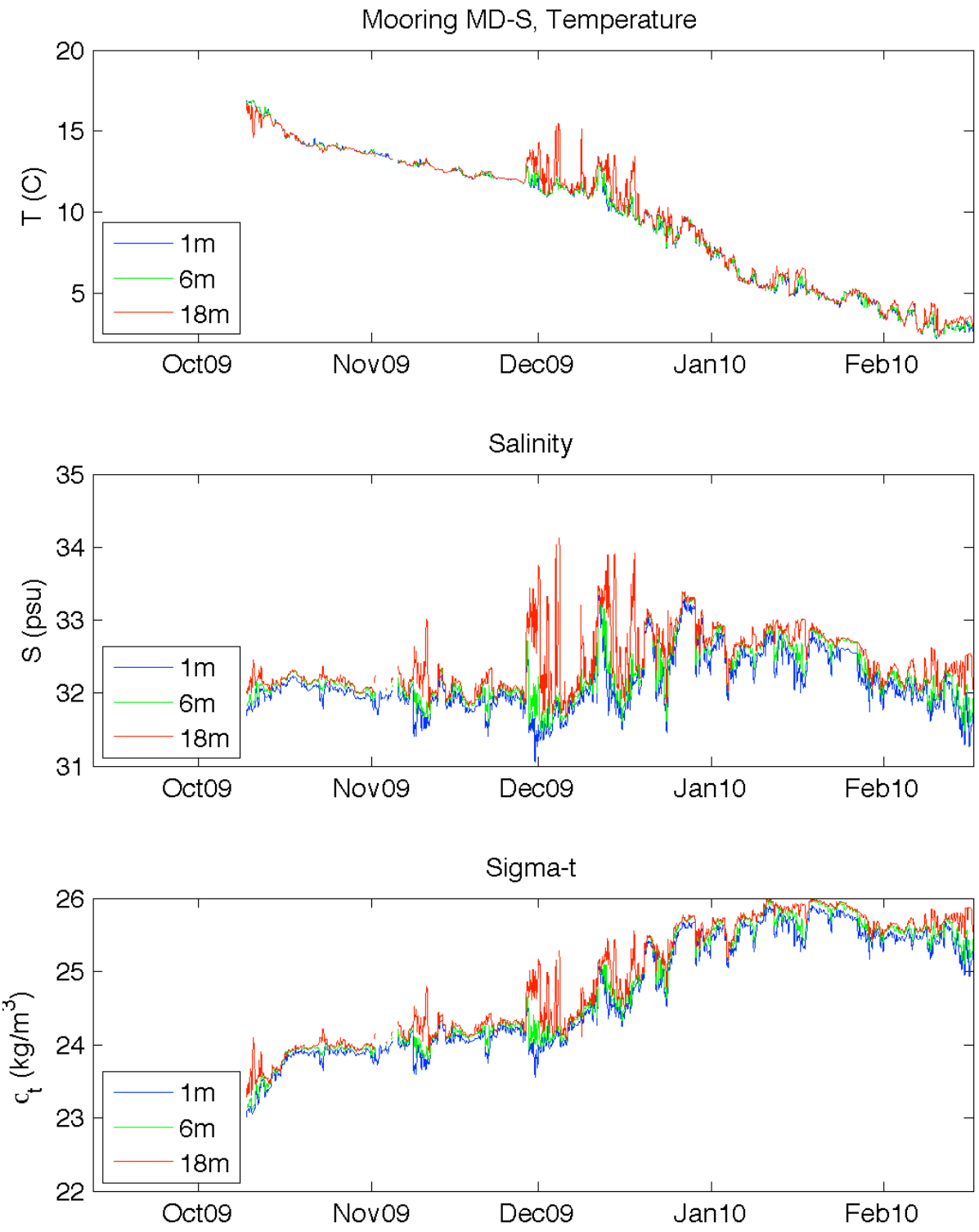

Figure 35. Time series of temperature (top), salinity (middle), and sigma-t (bottom) for mooring MD-S instruments during time period 1.
The legend gives the nominal depths of each CTD.

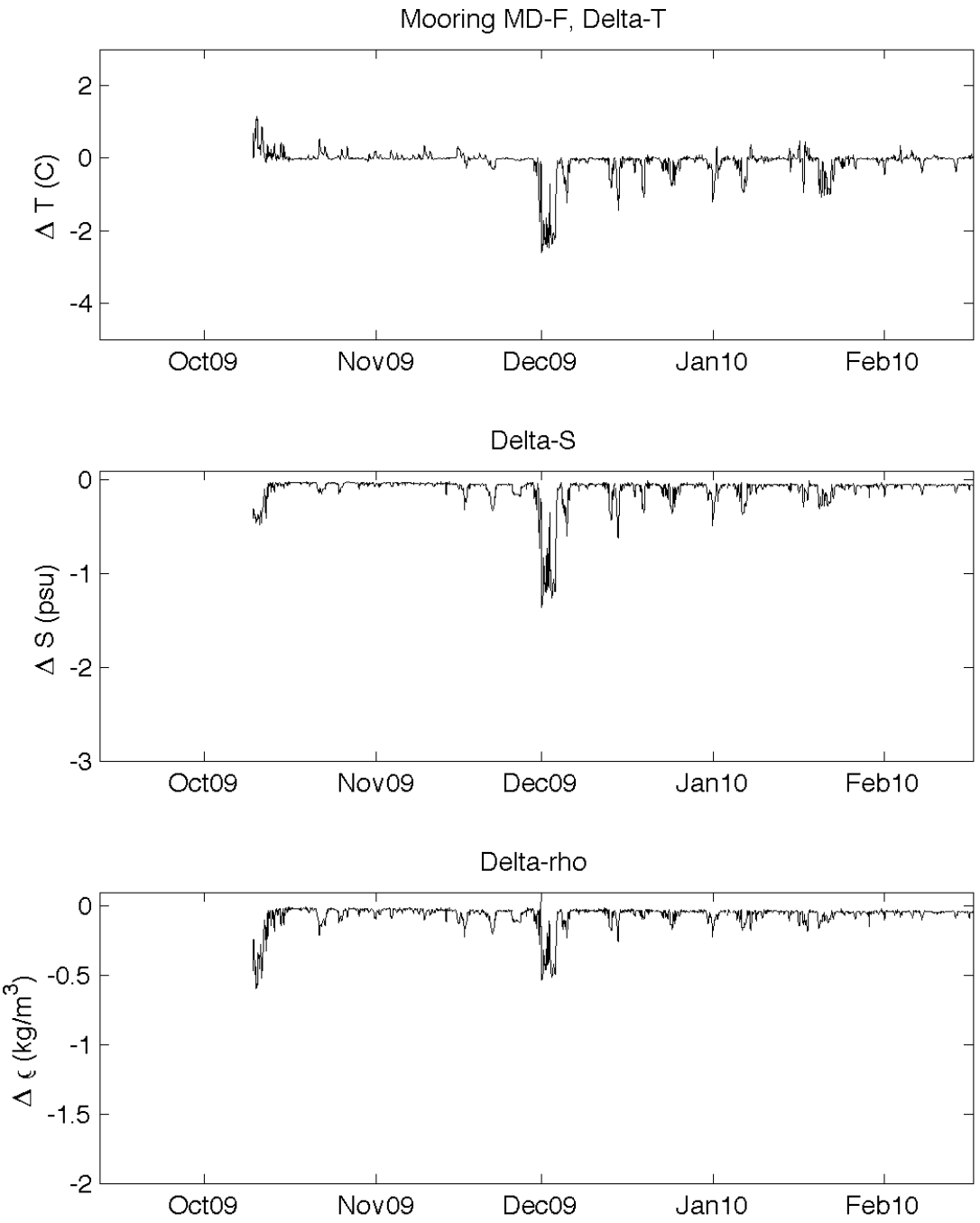

Figure 36. Time series of vertical differences in temperature (top), salinity (middle), and sigma-t (bottom) for mooring MD-F during time period 1.
Differences are computed as the value at 1 m (nominal) minus its value at 28 m (nominal).

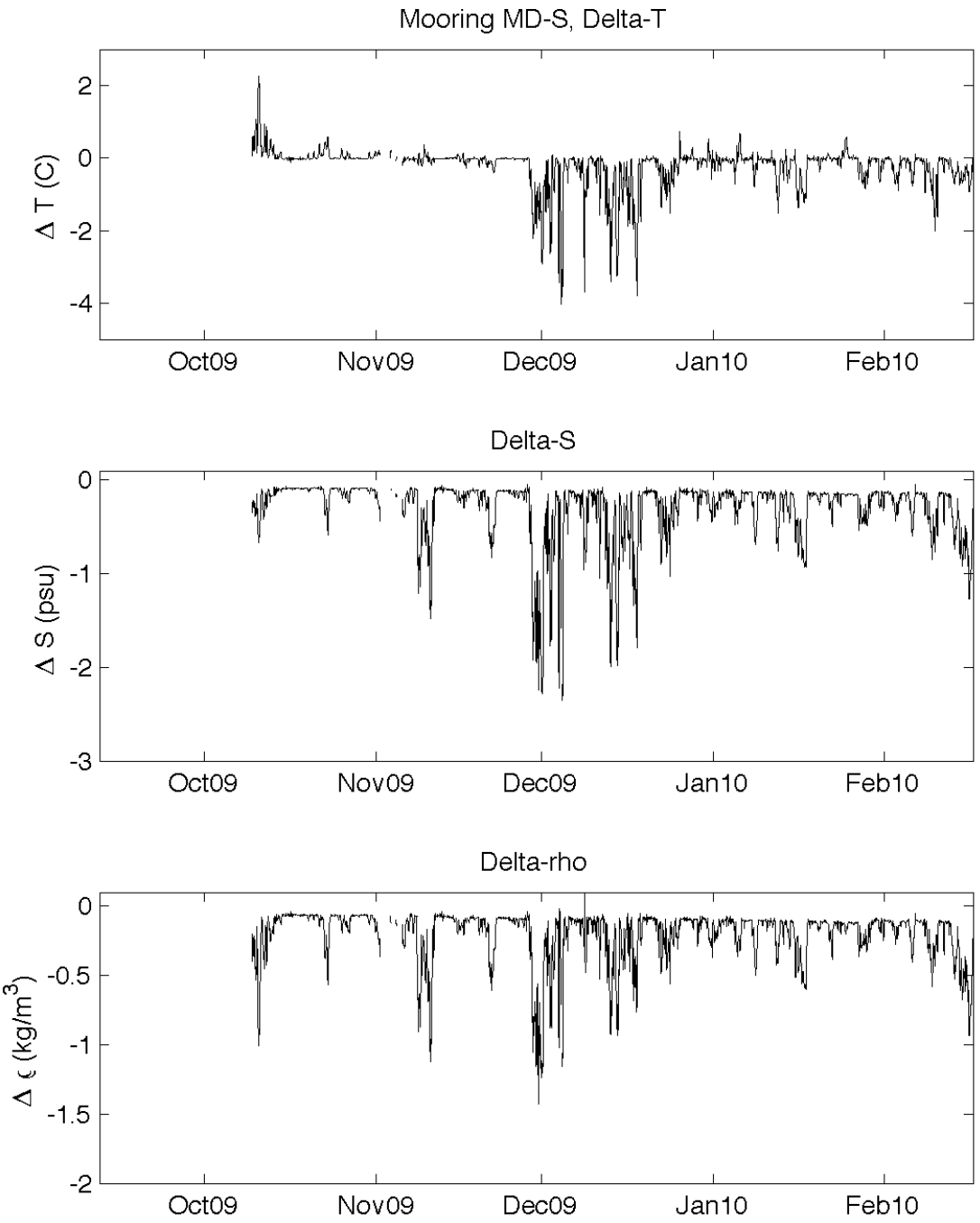

Figure 37. Time series of vertical differences in temperature (top), salinity (middle), and sigma-t (bottom) for mooring MD-S during time period 1.
Differences are computed as the value at 1 m (nominal) minus its value at 18 m (nominal).

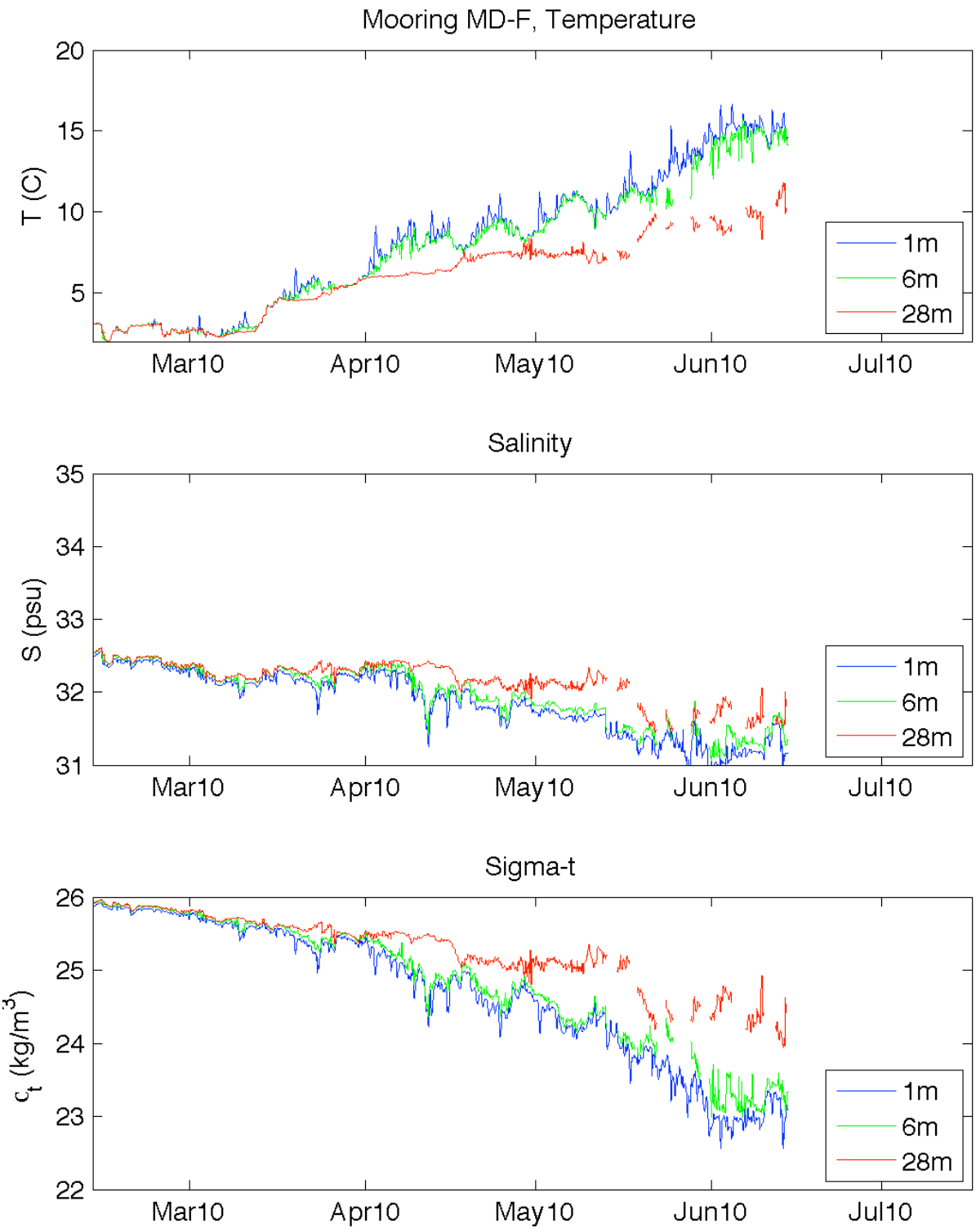

Figure 38. Time series of temperature (top), salinity (middle), and sigma-t (bottom) for mooring MD-F instruments during time period 2.
The legend gives the nominal depths of each CTD.

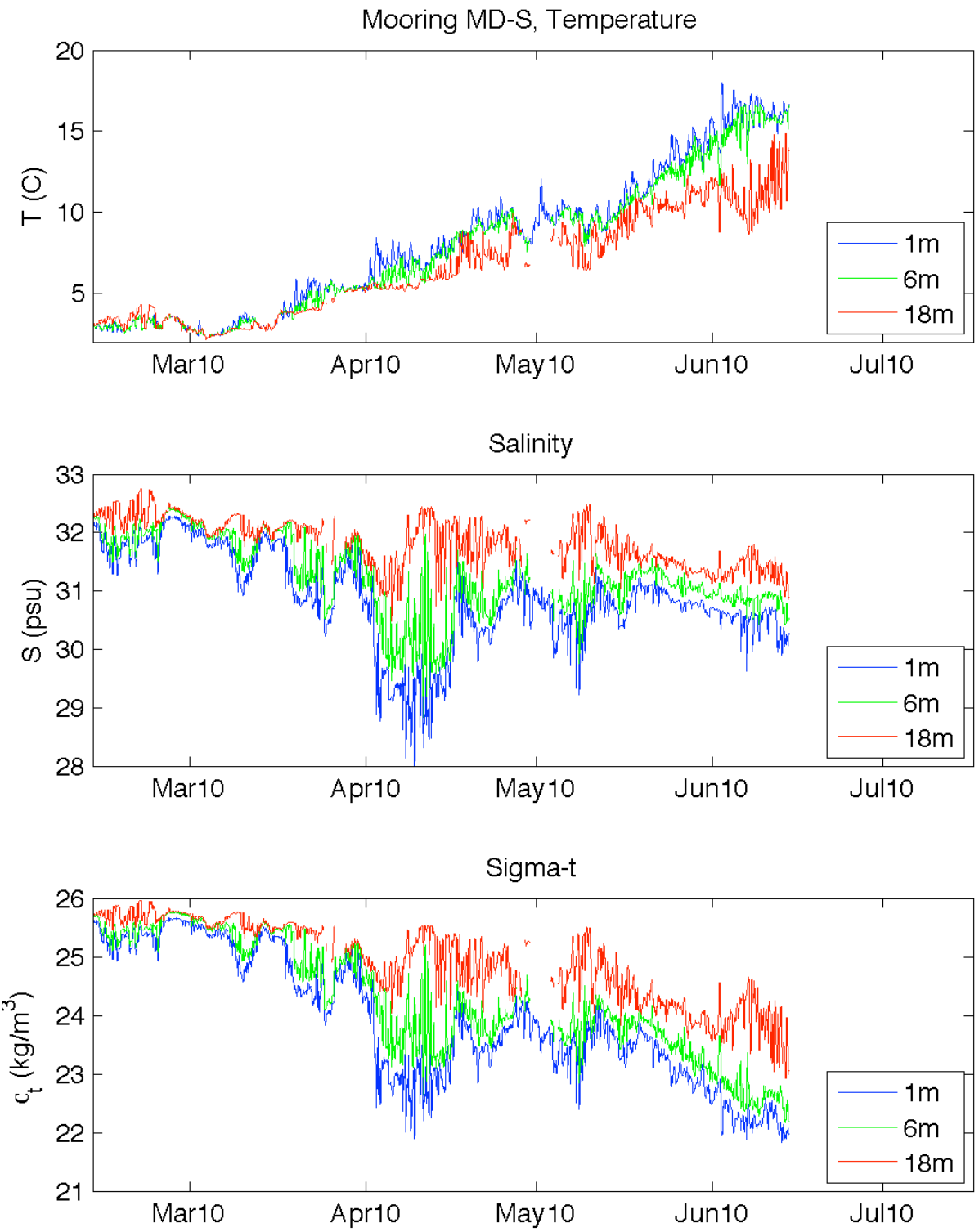

Figure 39. Time series of temperature (top), salinity (middle), and sigma-t (bottom) for mooring MD-S instruments during time period 2.
The legend gives the nominal depths of each CTD.

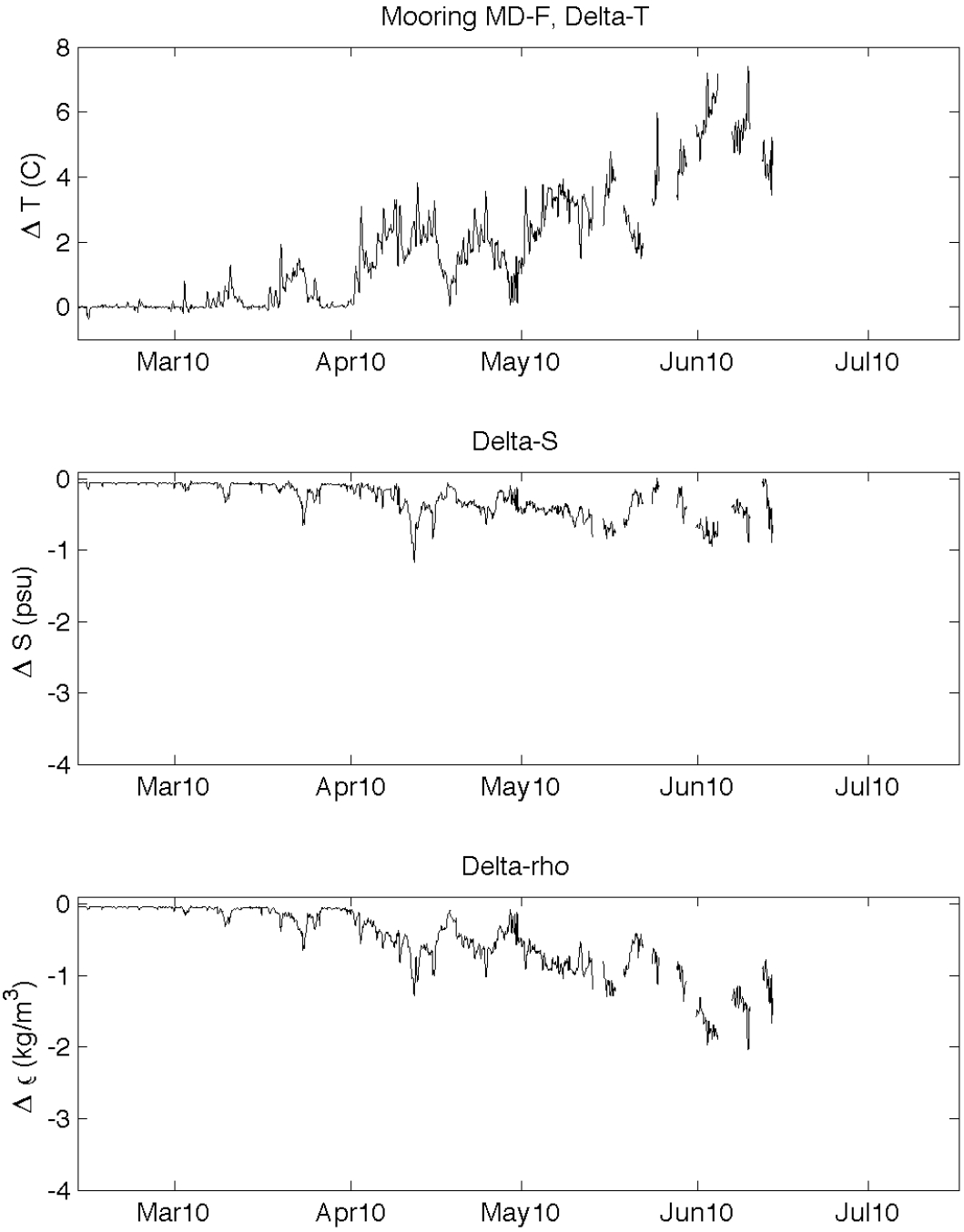

Figure 40. Time series of vertical differences in temperature (top), salinity (middle), and sigma-t (bottom) for mooring MD-F during time period 2.
Differences are computed as the value at 1 m (nominal) minus its value at 28 m (nominal).

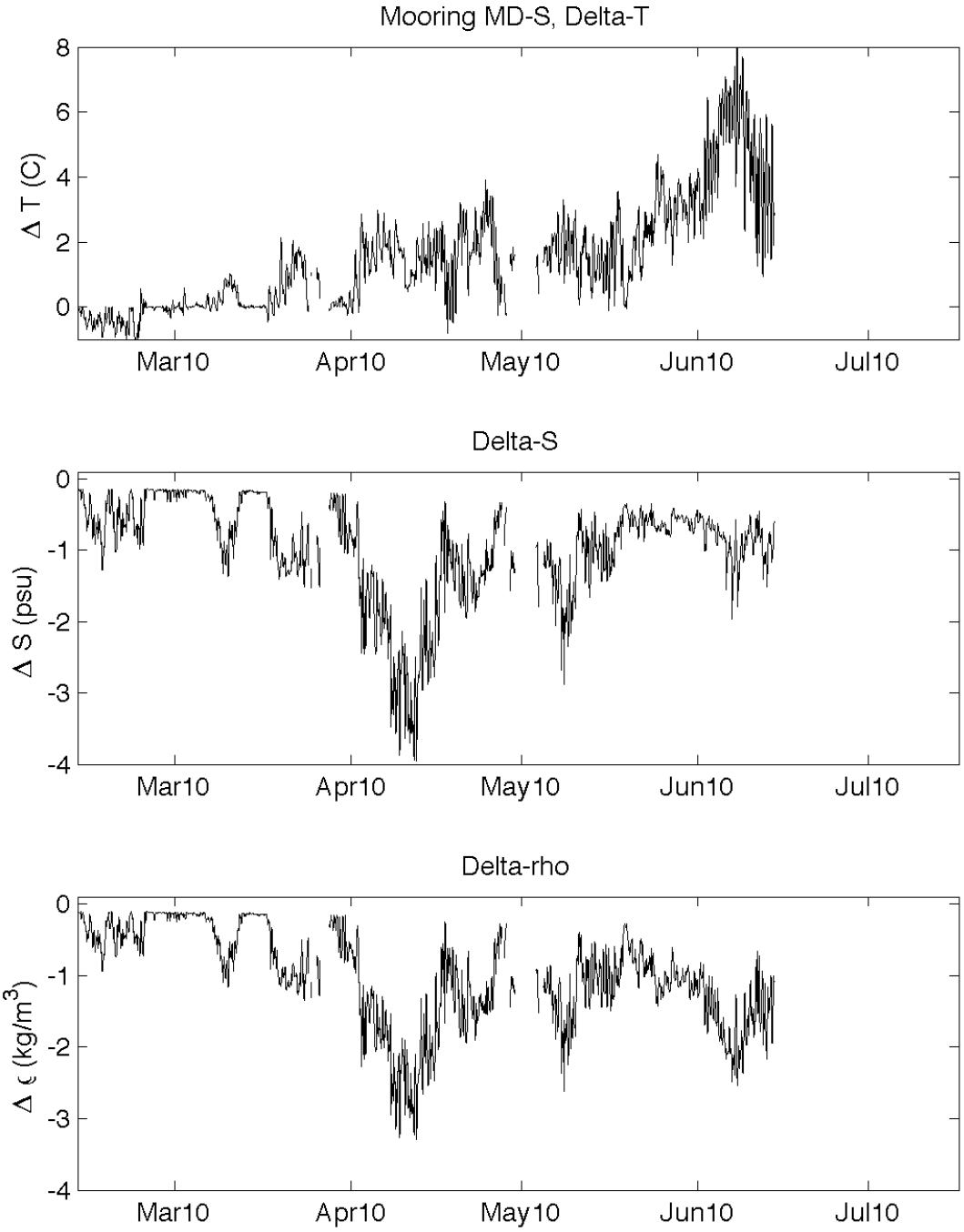

Figure 41. Time series of vertical differences in temperature (top), salinity (middle), and sigma-t (bottom) for mooring MD-S during time period 2.
Differences are computed as the value at 1 m (nominal) minus its value at 18 m (nominal).

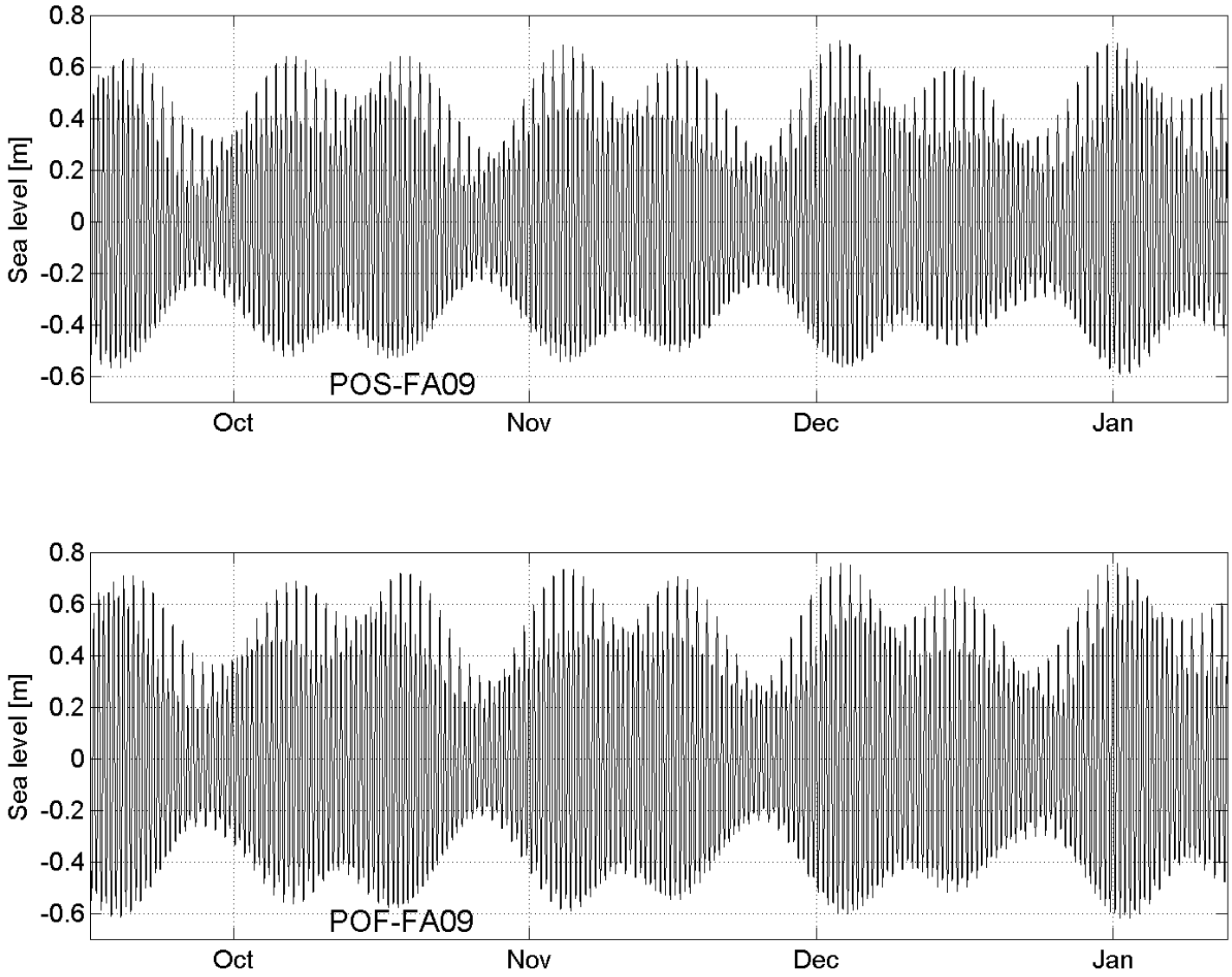

Figure 42. Tidal sea level variations: PO-S (upper) and PO-F (lower).

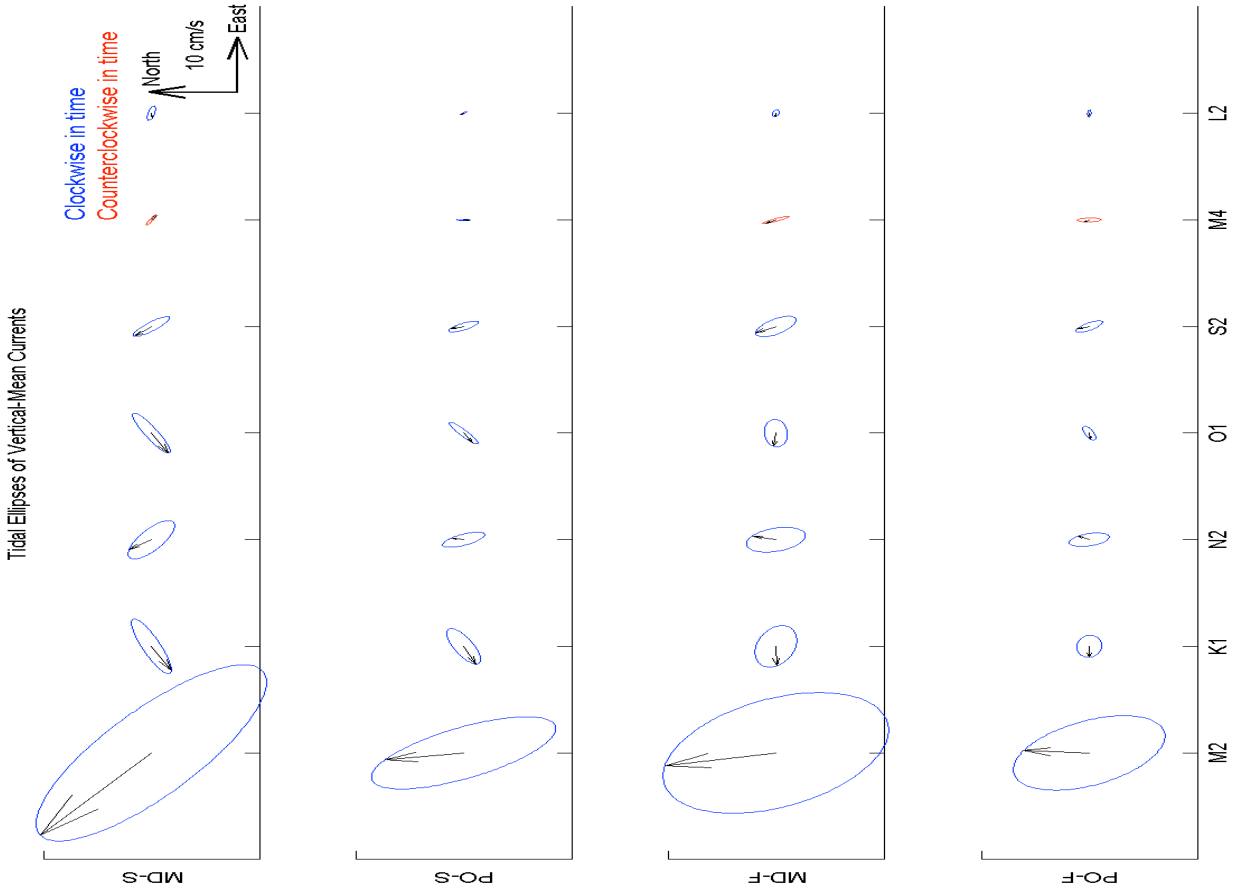

Figure 43. Tidal current ellipses, vertical-mean currents: seven dominant constituents, four sites.
Greenwich phase lag is indicated by the instantaneous velocity vector within each ellipse.

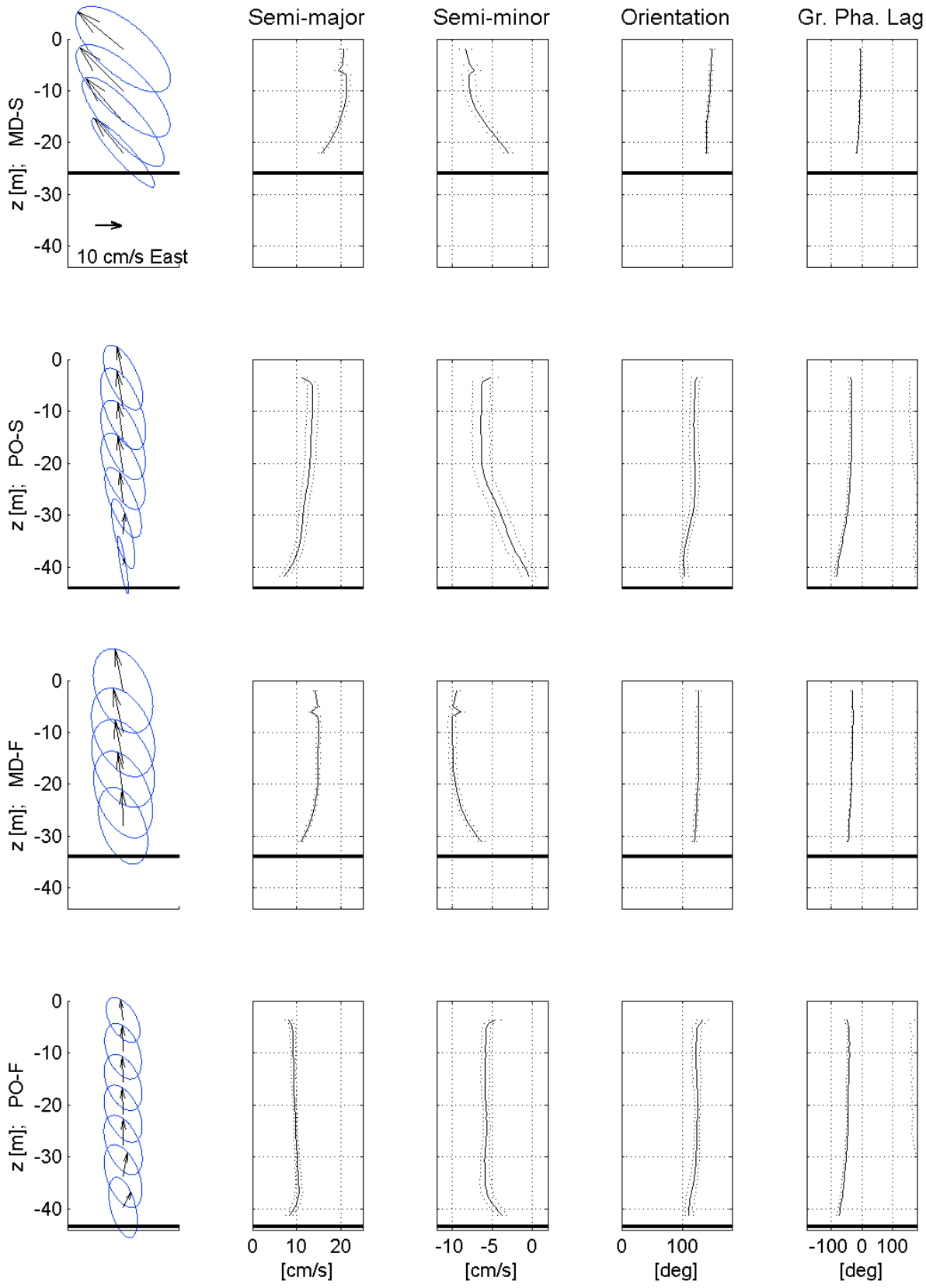

Figure 44. Tidal current ellipses, M_2 constituent, vertical profiles, four sites.

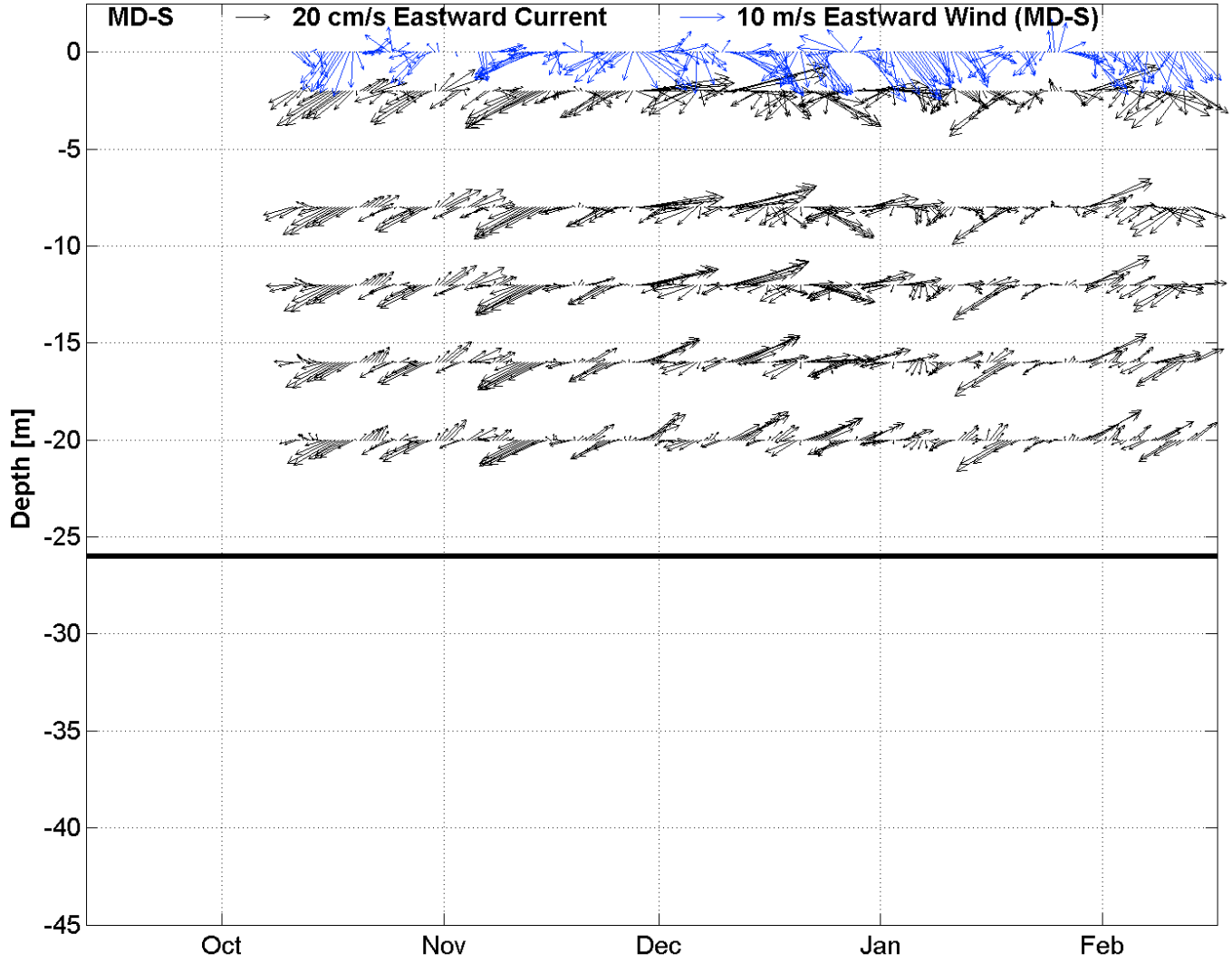

Figure 45. Subtidal currents and winds, MD-S, Sep 2009 to Feb 2010.

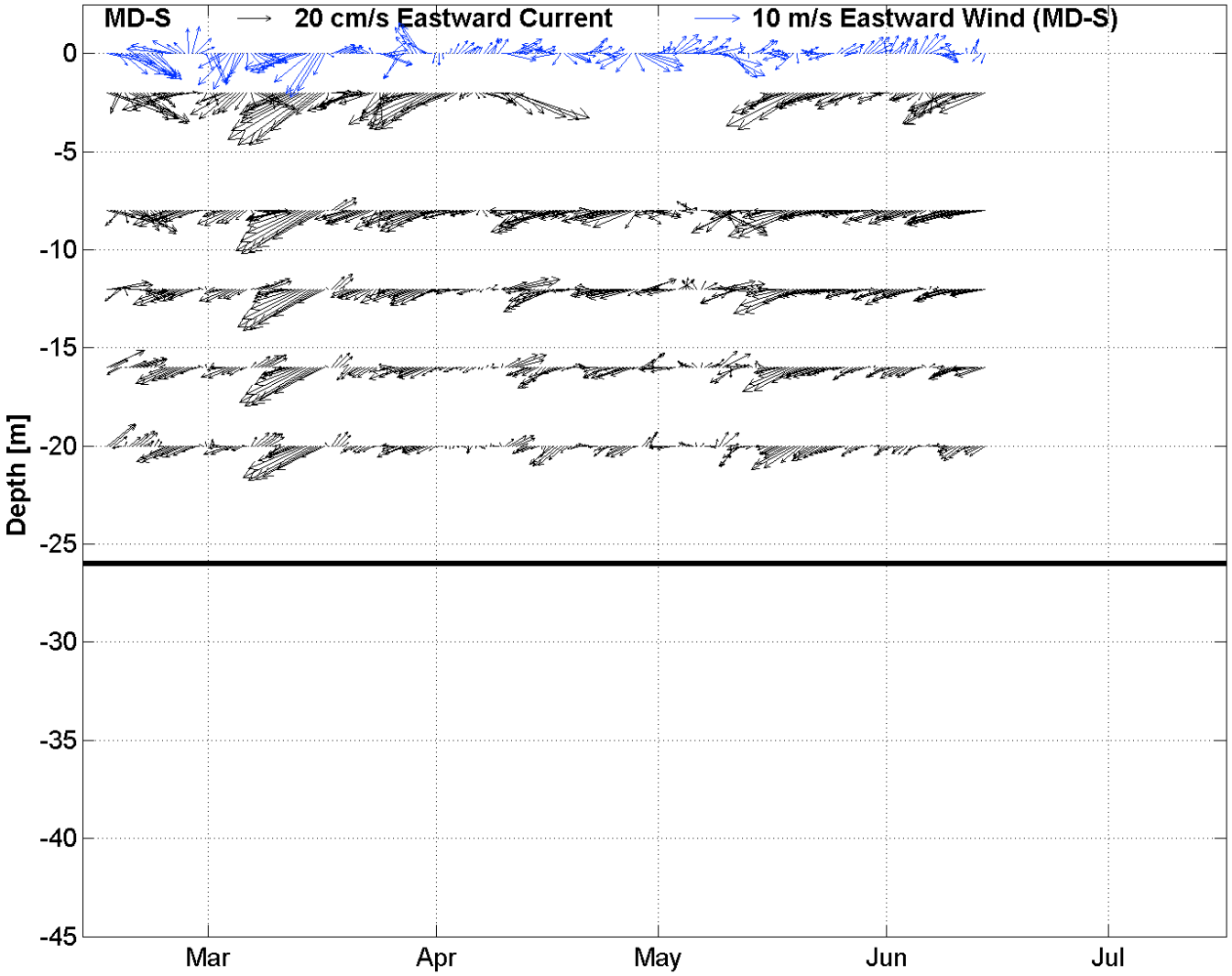

Figure 46. Subtidal currents and winds, MD-S, Feb to Jul 2010.

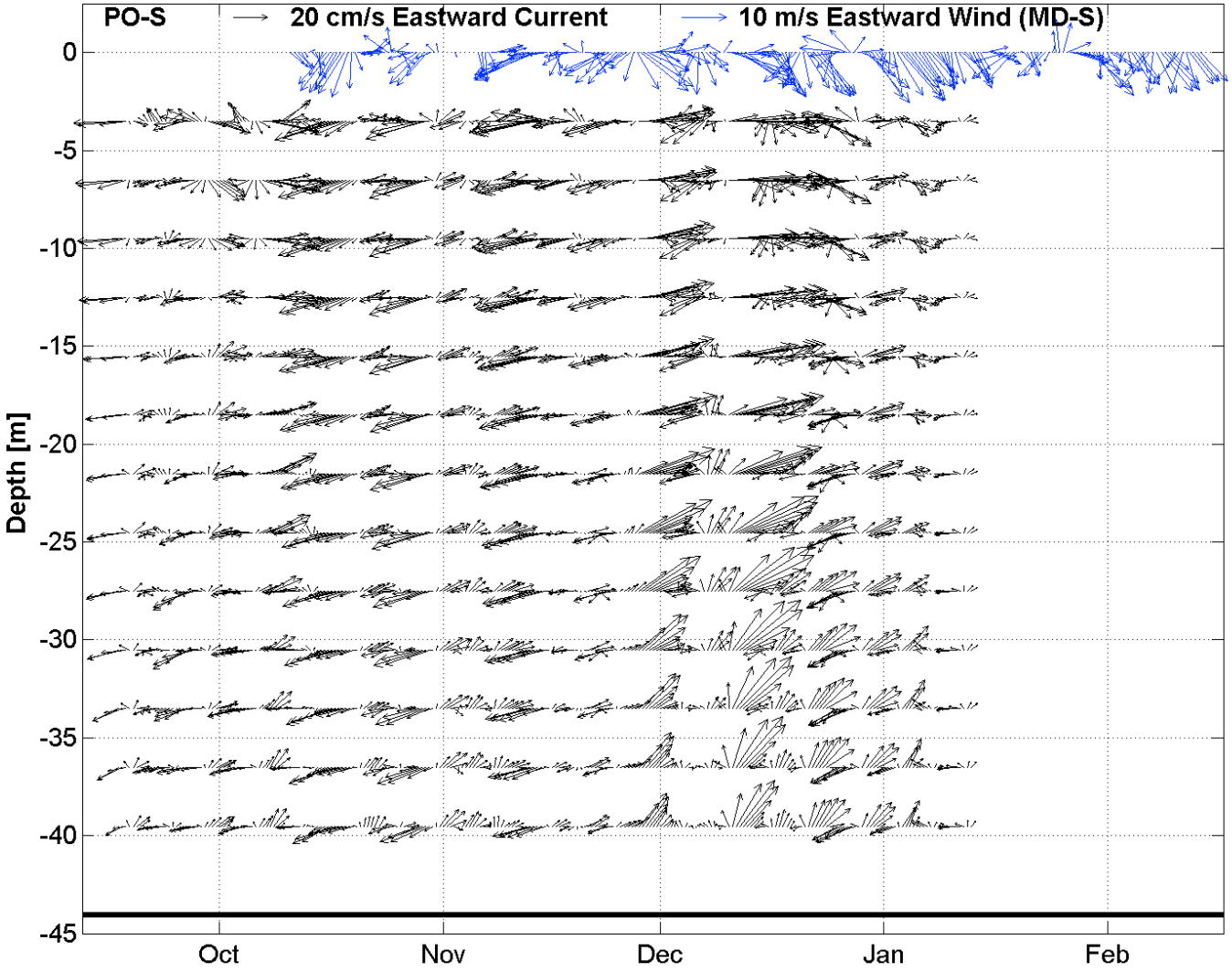

Figure 47. Subtidal currents and winds, PO-S, Sep 2009 to Feb 2010.

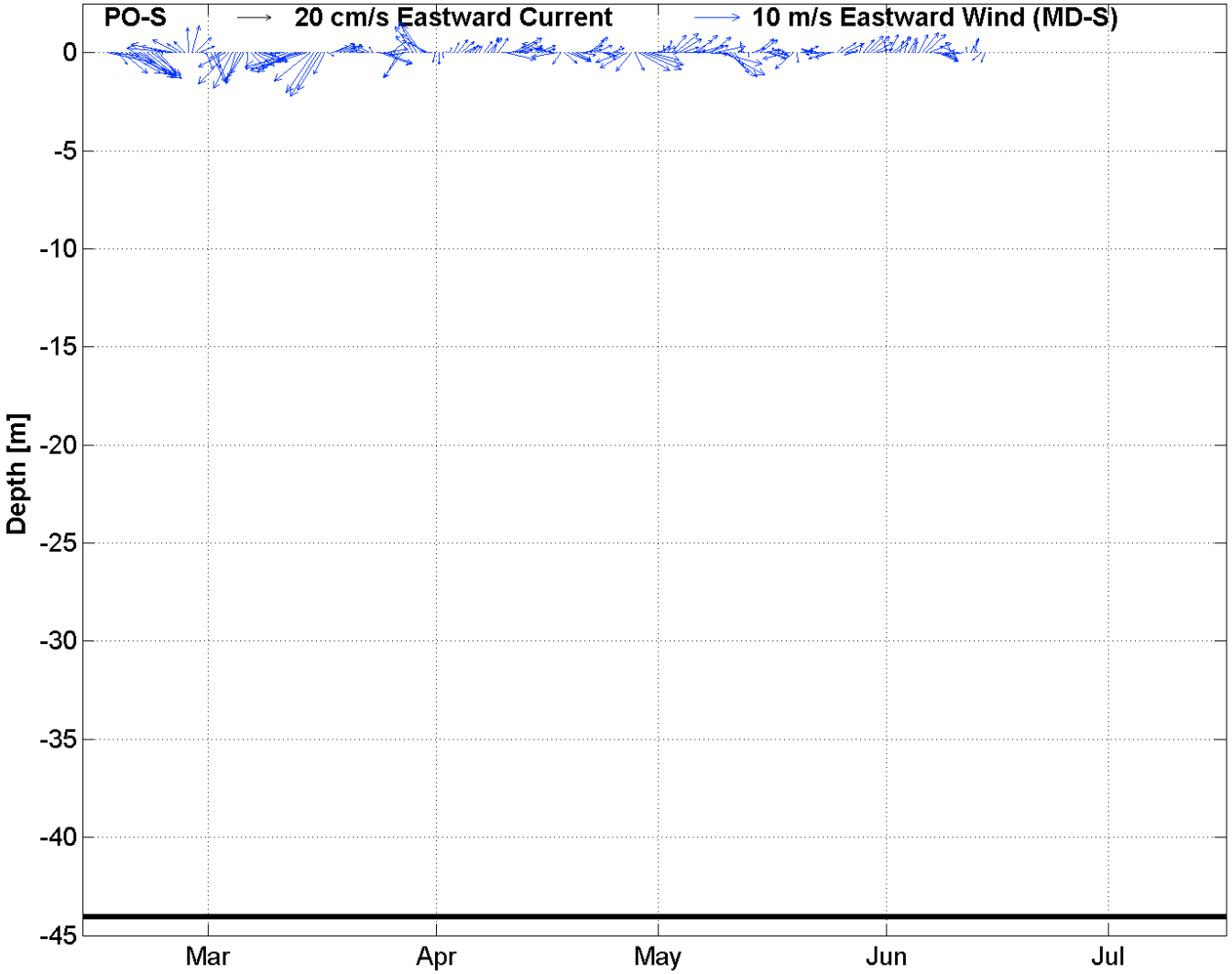

Figure 48. Subtidal currents and winds, PO-S, Feb to Jul 2010. (ANALYSIS UNDERWAY)

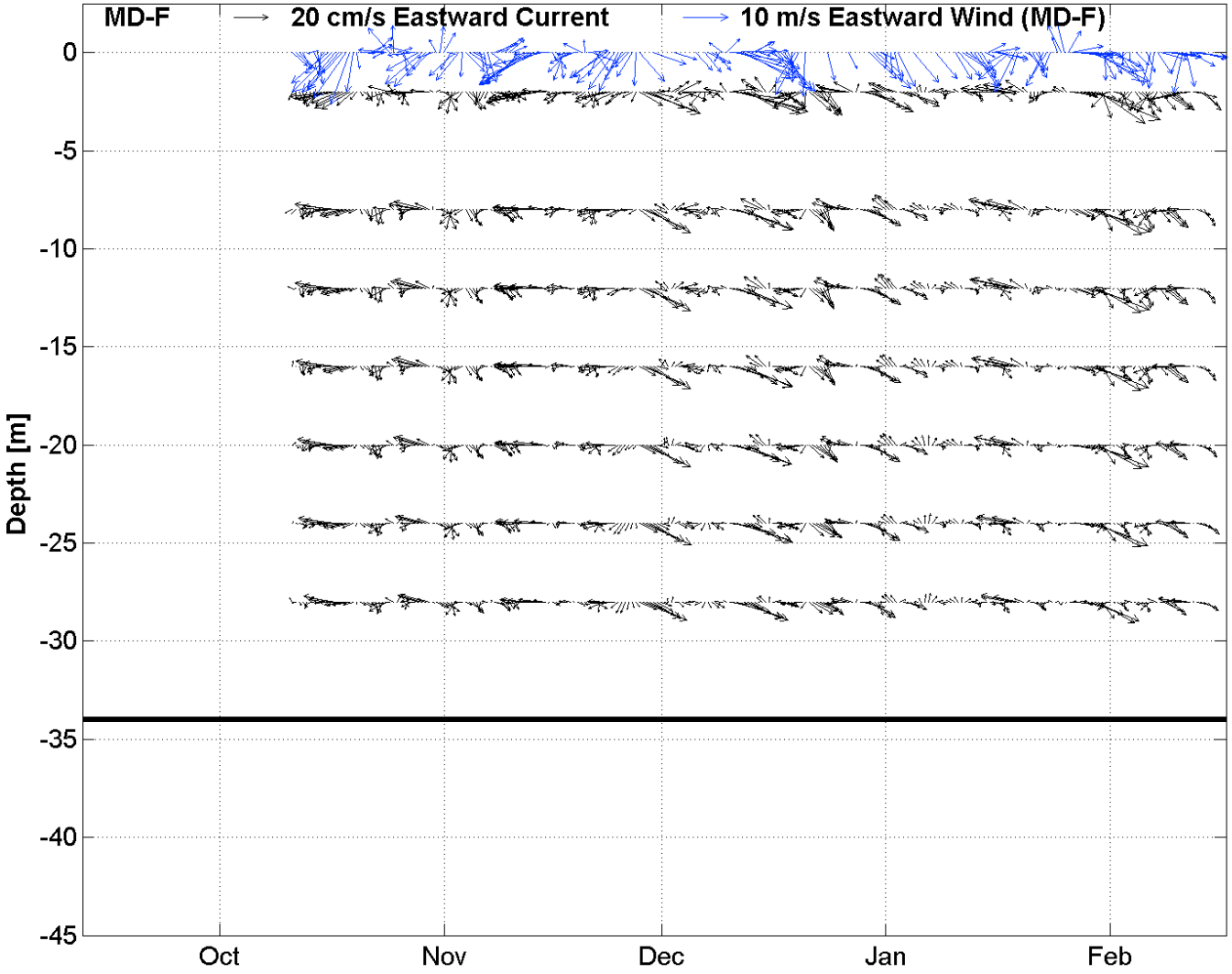

Figure 49. Subtidal currents and winds, MD-F, Sep 2009 to Feb 2010.

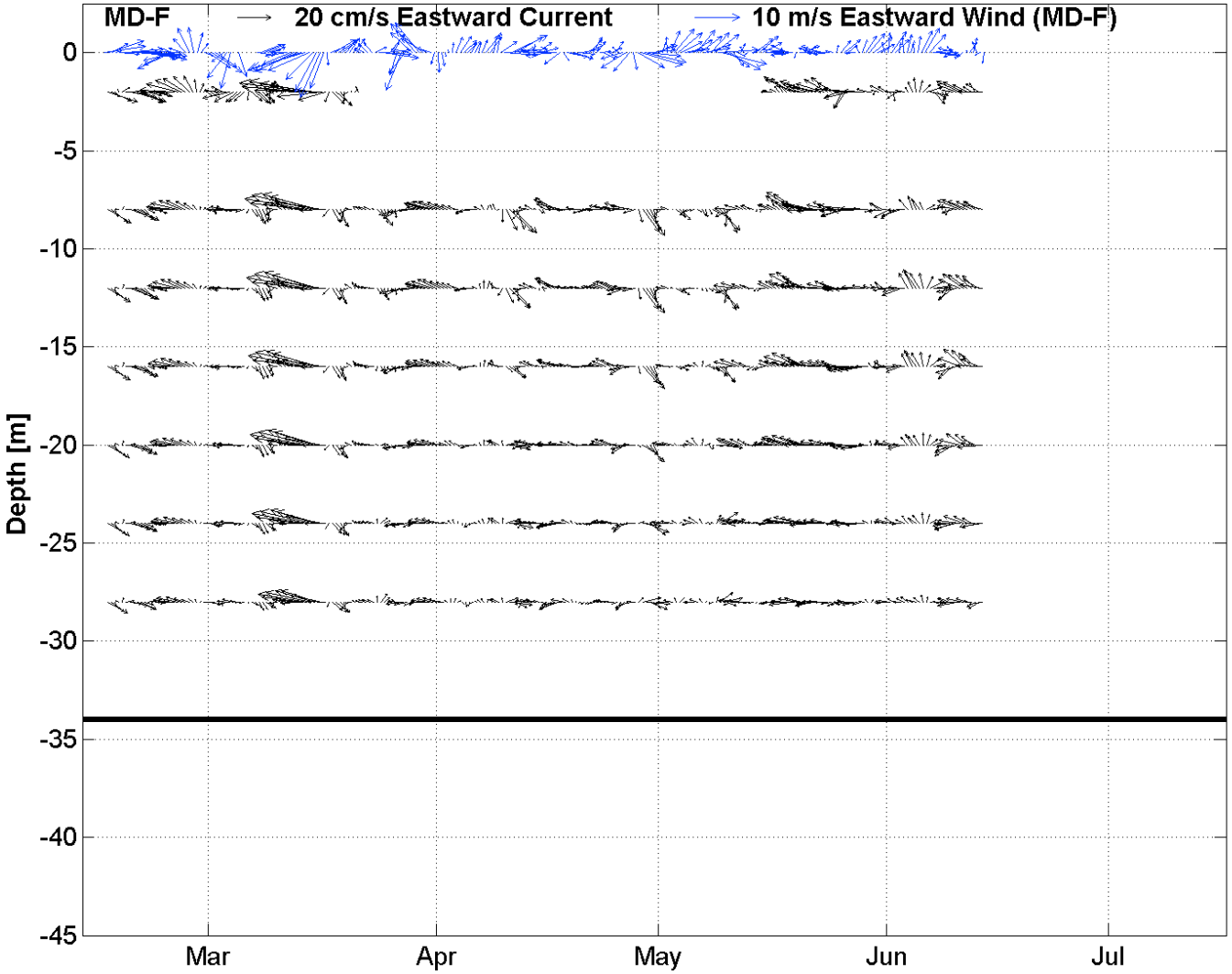

Figure 50. Subtidal currents and winds, MD-F, Feb to Jul 2010.

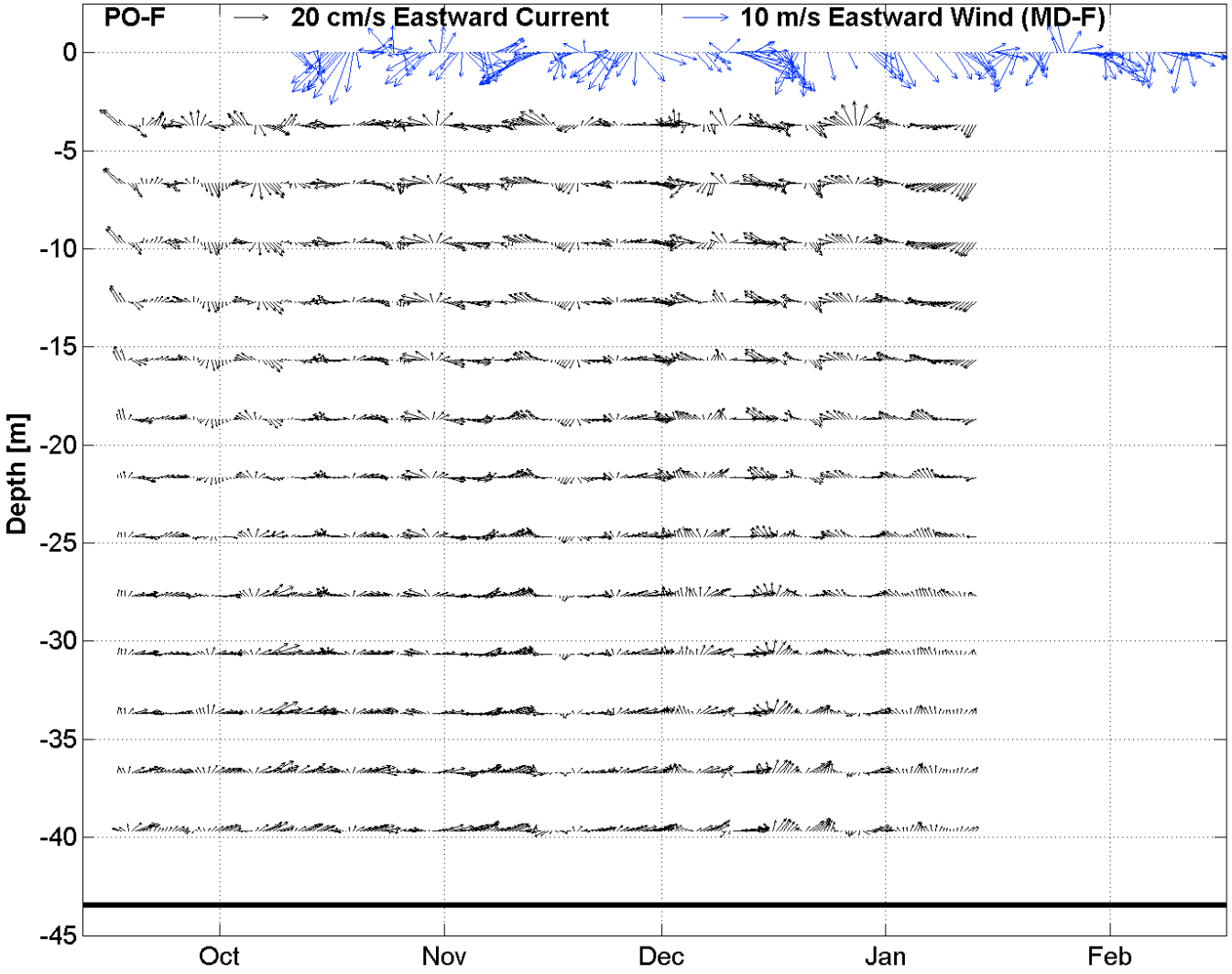

Figure 51. Subtidal currents and winds, PO-F, Sep 2009 to Feb 2010.

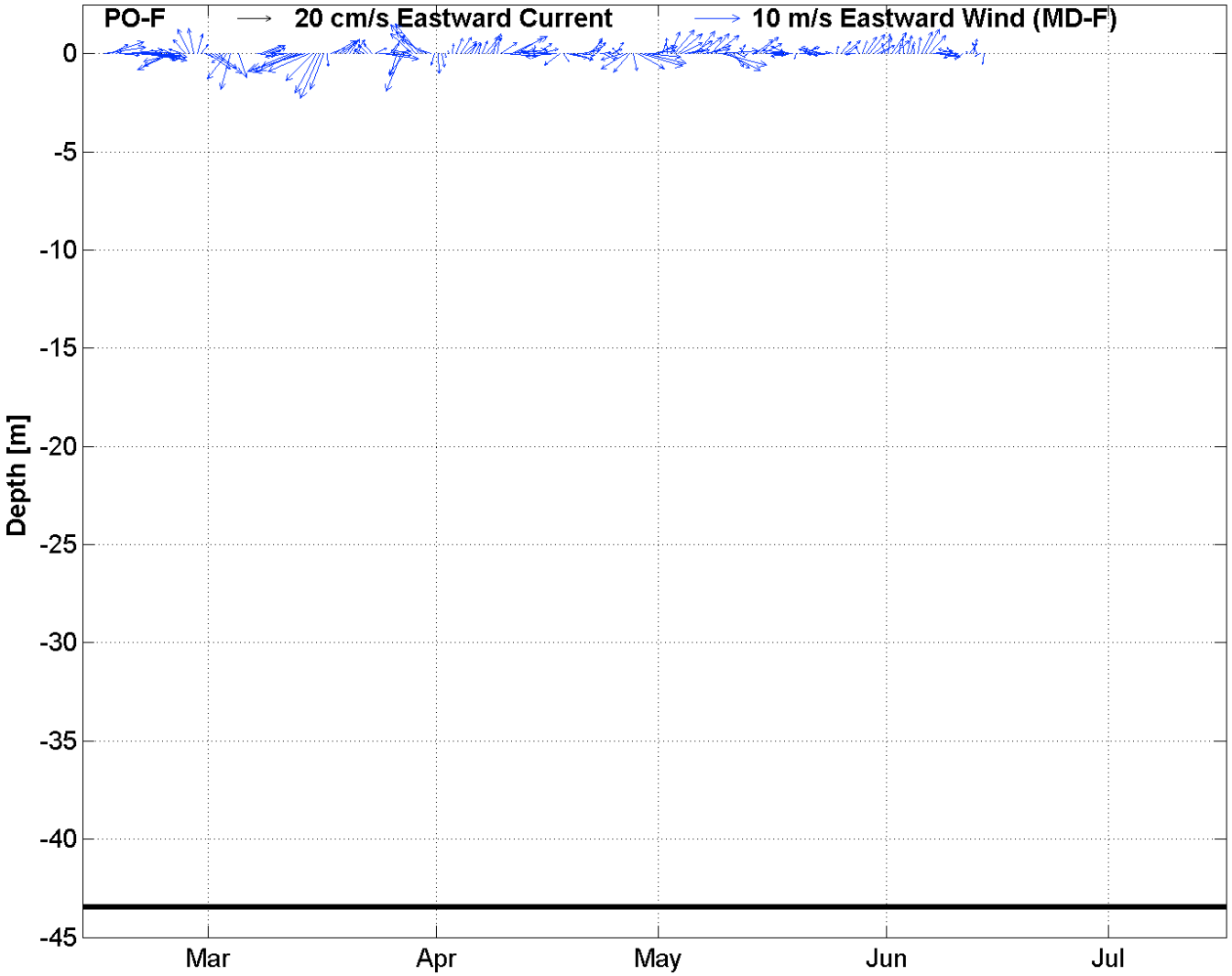

Figure 52. Subtidal currents and winds, PO-F, Feb to Jul 2010. (ANALYSIS UNDERWAY)

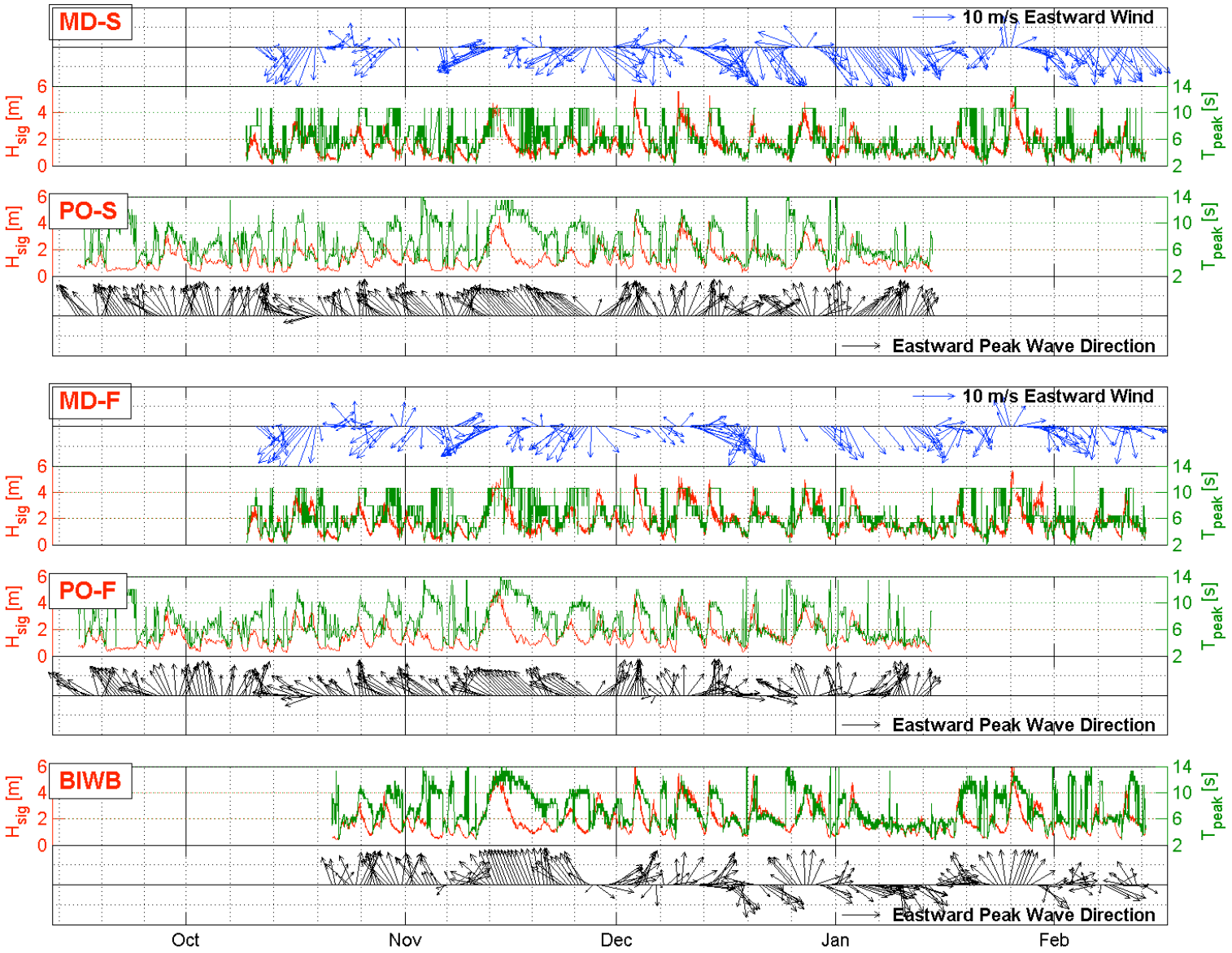

Figure 53. Wave parameters and winds, Sep 2009 to Feb 2010.

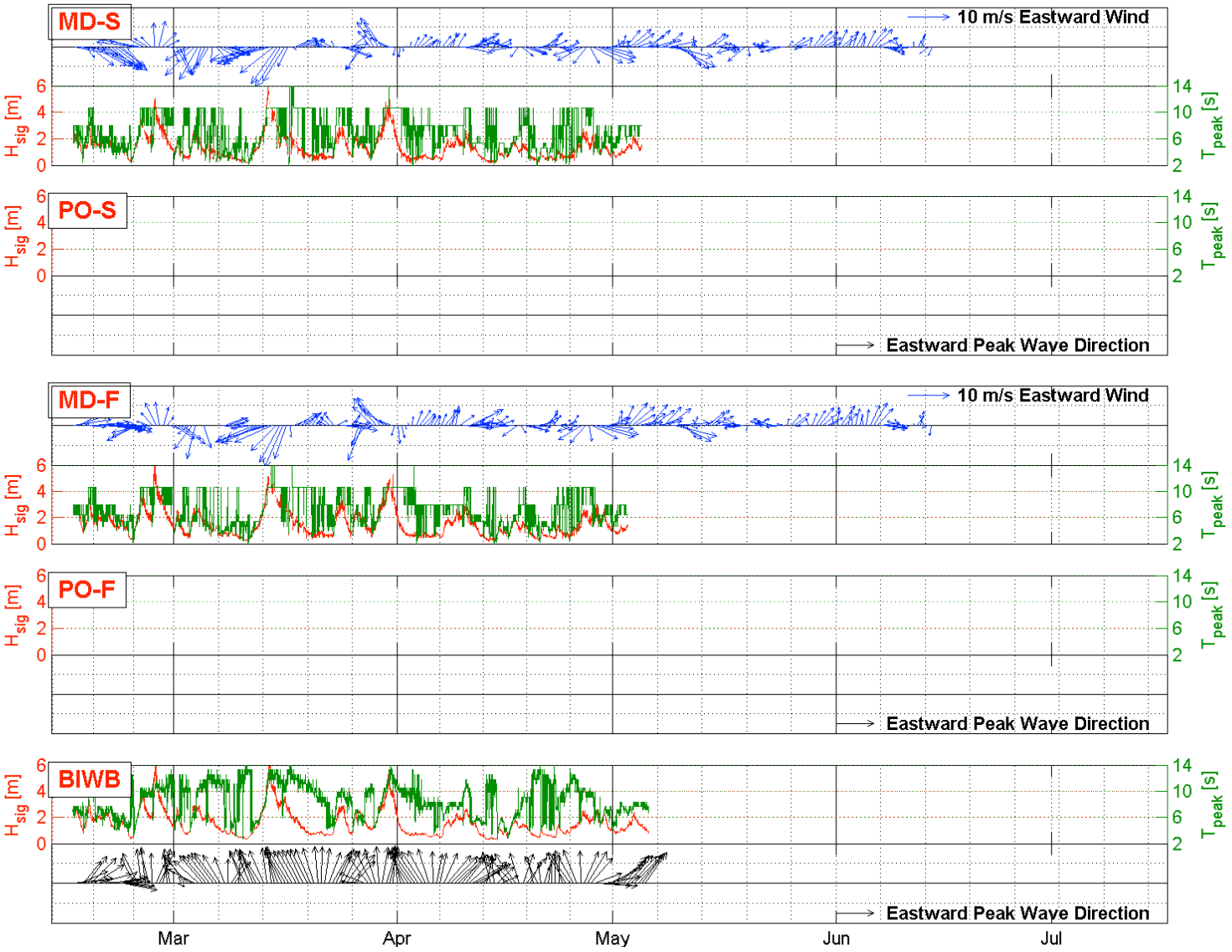

Figure 54. Wave parameters and winds, Mar to Jul 2010.

This page intentionally left blank.

4.

Benthic Habitat Distribution and Subsurface Geology Selected Sites from the Rhode Island Ocean Special Area Management Study Area

by

Monique LaFrance, Emily Shumchenia, John King, Robert Pockalny, Bryan Oakley, Sheldon Pratt, Jon Boothroyd

University of Rhode Island, June 28, 2010

Executive Summary

The goal of this study was to use acoustic surveys (swath bathymetry, side-scan and sub-bottom sonar) and ground-truth surveys to delineate the benthic habitat distribution, subsurface geology, and cultural resources for selected sites within the RI Ocean SAMP study area. Benthic habitat distribution and subsurface geology were examined for two large sites, one in state waters to the south of Block Island (BI) and one in federal waters (FED) in eastern RI Sound. Cultural resources were studied at BI only. A total of more than 150 square miles were surveyed and further characterized by ground-truth studies. Preliminary results of the benthic environment characterization suggest that in order to complete a bottom-up integration of the data, as has been completed for smaller-scale projects, a greater density in ground-truth samples would be necessary. The recommended approach, therefore, is to use the top-down method to describe the benthic biological assemblages found within each depositional environment type. This relationship was found to be statistically strong and significant in BI, but data are not yet available for FED. The top-down approach will produce full-coverage habitat maps for both BI and FED that describe general, broad-scale patterns in both geological and biological resources. The subsurface geology studies revealed that locations to the south of Block Island were large enough and had sufficient thicknesses of unconsolidated sediments to allow installation of foundation structures by pile driving thereby facilitating the construction of a small wind farm. In addition, the area of the buried valley structures in the central FED area and the general western FED area had a sufficient thickness of unconsolidated sediments to facilitate the installation of a larger wind farm. However further work is probably necessary to the west and to the south of The FED area to find sufficient space for a 100+ turbine wind farm.

Table of Contents

List of Figures

Figure I-12. Bubble plot of diversity within BI and FED. The size of the bubble is proportional to the diversity (measured at the genus level) at each station. The highest diversity is seen at BI stations 39, 37, and 16 and the lowest diversity exists at BI stations 3, 23, 24, 25, and 42. Note the scales are the same for both BI and FED to allow comparison between study areas.

Figure I-13. Bubble plot of abundance within BI and FED. The size of the bubble is proportional to the abundance at each station. Stations with the highest abundance are BI 39, 37, and 16. BI stations 3, 24, 25, and 42 exhibit the lowest abundances. Note the scales are the same for both BI and FED to allow comparison between study areas.

Figure I-14. Benthic geologic environment of BI. The environments were derived from side-scan imagery, sub-bottom profile imagery, sediment samples, and underwater video. The polygons are labeled by depositional environment units, reporting form (capital letters) followed by facies (lower case letters). The abbreviations are as follows: Form: DB = Depositional Basin; GAF = Alluvial Fan; GDP = Glacial Delta Plain; M = Moraine; MS = Moraine Shelf; LFDB = Lake Floor/Depositional Basin; Facies: sisa = silty sand; bgc = boulder gravel concentrations; cgp = cobble gravel pavement; csd = coarse sand with small dunes; pgcs = pebble gravel coarse sand; ss = sheet sand; sw = sand waves.

Figure I-15. Genus-defined benthic geologic environment of BI. The depositional environments were labeled by the most abundant genus, as determined from the bottom samples. An ANOSIM revealed the macrofaunal assemblages within each environment are significantly different (global R = 0.556, p = 0.001).

Figure I-16. LINKTREE output for BI and FED. The linkage tree identified 16 classes within BI and FED. Each class is defined by a quantitative threshold of one the five abiotic variables identified in the BIOENV procedure. Note that BI and FED share only 3 classes, while 11 classes contain only BI samples and two classes contain only FED samples. The thresholds and descriptions for each split is listed in Table I-9 and Table I-10, respectively.

Figure I-17. Spatial extent of classified benthic habitats within BI and FED. The habitat map is comprised on 64, 100 m resolution pixels. Full-coverage benthic habitat maps are not possible at this time because of unsuccessful interpolation attempts due to the fact that the grain size datasets (derived from sediment analysis of the point-coverage bottom samples) are not spatially auto-correlated.

Figure I-18. Benthic habitat classification map for BI and FED. The benthic habitats were classified by the most abundant genus and the associated abiotic threshold. For four classes two genera were used in the classification because both showed high abundances. A total of 16 habitat classes were identified from the analyses. There are 14 habitats present within BI and 5 within FED. Ten of the classes are identified (at least in part) by a genus of tube-building amphipod, with *Ampelisca* being responsible for 7 of these classes.

Figure II-1. Map showing locations of previous subbottom surveys within the SAMP area.

Figure II-2. Sub-bottom seismic tracklines (white lines) superimposed on bathymetry (http://www.ngdc.noaa.gov/mgg/coastal/crm.html) for the Block Island (top) and the Federal (bottom) survey areas. The yellow lines identify the location of seismic sections shown Figures 3 and 4.

Figure II-3. Processed seismic cross-sections of selected lines from Block Island survey area (see Fig 2, top) with sub-bottom interpretations. The yellow regions correspond to the sediment-water interface at the top and the deepest visible reflection at the bottom. The questions marks indicate sections of the seismic record where our identified deepest reflector extends below the resolvable depth limit. Multiple reflections of the sediment-water interface (white dashed lines) and internal reflectors (blue dashed lines) within the identified sediment package are indicated. The location of crossing lines are indicate with arrows and appropriate line number. The vertical axis of the section is plotted as two-way travel time (milliseconds) and thickness of the sediment section (MBSF, meters below seafloor), assuming a seismic velocity of 1500 m/s.

Figure II-4. Processed seismic cross-sections of selected lines from Federal survey area (see Fig 2, bottom) with sub-bottom interpretations. Axes labels and highlighted attributes are the same as in Figure 3.

Figure II-5. (top) Sediment isopach of the Federal survey area comparing our sediment thickness estimates (colored contours) with a previous study (gray shading) by O'Hara, [1980]. (bottom) Sediment thickness contours from the O'Hara study are overlain on side-scan reflectivity.

Figure II-6. Map showing ease of construction for wind turbines in the BI study area.

List of Tables

the most abundant genus, and the genus most responsible for the within-class similarity (as identified by the SIMPER procedure) is listed. Note there are seven classes for which the same genus is the most abundant and is the most responsible for the within-class similarity.

1. General Introduction for Benthic Habitat Distribution and Subsurface Geology

This report represents the current status of, and subsequent ground-truth and archaeology studies done for the Rhode Island Ocean SAMP (RI SAMP) between August, 2008 and the present. The RI SAMP study area is shown in Figure I-1. Some of the work is ongoing and additional data will be added to this report in the near future. The report is structured in three subsections: (1) subsurface geology and (2) benthic habitat distribution. The subsurface geology and benthic habitat sections are focused on a large survey area around the south end of Block Island, and a large survey area in Federal waters located in eastern Rhode Island Sound

2. General Background

The project team leadership consists of geologists, geophysicists, biologists, and archaeologists. The names, affiliations , and areas of expertise are summarized in Table 1, below.

Table 1: Project Science Team

NAME	AFFILIATION	EXPERTISE
John W. King	Professor, URI Graduate School of Oceanography	Geology, Geophysics, Habitat Mapping
Jon Boothroyd	Professor, URI Department of Geosciences; Rhode Island State Geologist	Geology, Geophysics, Habitat Mapping
Rob Pockalny	Marine Research Scientist, Graduate School of Oceanography, URI	Geophysics, Geology, Mapping
Sheldon Pratt	Research Associate, Graduate School of Oceanography, URI	Benthic Biology, Habitat Mapping
Sam Debow	Manager, Operations, Graduate School of Oceanography, Special Research	Ship operations, Bathymetry and Sidescan Sonar Mapping

The SAMP study area is too large (approximately 1500 square miles) to be surveyed in detail in this study. Therefore, the results of prior studies were compiled to determine the extent of existing coverage and to identify data gaps. Existing coverage was not extensive. In addition, areas that would be potential sites for development of offshore wind farms based on

multiple criteria (Spaulding, et al., 2010), including minimal user conflict, were identified. Two areas were examined in detail, one within Block Island Sound (BIS) and the other in eastern Rhode Island Sound (RIS). The BIS study area (referred to as BI hereafter) is located within state waters around the south end of Block Island (Figure I-2). The Rhode Island Sound study area (referred to as FED hereafter) is located in Federal waters to the west of Martha's Vineyard.

3. General Methods for Acoustic Data Acquisition and Processing

The data for the 53.5 square mile BI study area were obtained in September 2008 on the R/V Endeavor over a period of ten days and over ten days on the R/V Eastern Surveyor during July and August of 2009. For the 68 square mile FED study area, data was collected in part during an August, 2009 4-day cruise on the EPA R/V Bold, and in September 2009 on the R/V Endeavor during a nine day cruise. During the surveys, raw data was continuously recorded in digital XTF format using Triton Isis (BI 2008) or in digital OIC format using Ocean Imaging Consultants (OIC) GeoDas (BI 2009, FED) acquisition software and monitored in real-time with a topside processor. A differential GPS assured positional accuracy (submeter horizontal accuracy) of the data. A TSS Meridian Gyroscope corrected for vessel heading (+/- 0.60° secant latitude dynamic accuracy, 0.10° secant latitude static error). A TSS DMS-05 motion reference unit (MRU) offered real-time correction of the vessel's pitch, heave, and roll (+/- 0.05° dynamic accuracy). An Applanix POS-MV system was used for motion correction o the 2009 Endeavor cruise. All survey lines were planned and logged in real-time using Hypack (version 6.2a) navigation software. Each survey was composed of parallel track lines spaced such that 100% or greater cover was achieved. Survey speed was between 4 and 6 knots.

We use a pole-mounted custom composite system that consists of a Teledyne Benthos C3D-LPM interferometric sonar to acquire swath bathymetric and sidescan sonar data. In addition, a Teledyne Benthos CHIRP III/3.5 kHz subbottom sonar system is integrated into the pole-mounted body. The subbottom system can be switched from a high-resolution CHIRP mode to 3.5 kHz mode when deeper subbottom penetration is needed. The subbottom system has a simultaneous trigger that prevents acoustic interference with the C3D system. The composite system allows simultaneous acquisition of bathymetry, sidescan, and subbottom data. The range of the bathymetry data is 10X the water depth, whereas the sidescan range is approximately 20X the water depth. In order to achieve 100 % survey coverage, the line spacing is determined based on the 10X range of the bathymetry coverage. A 100m line spacing works well in depths of 10 -15 m. Bottom penetration using the CHIRP system was limited in areas of

hard bottom. In these areas we used a more powerful Datasonics Bubble Pulser system to obtain deeper penetration. The line spacing used for the Bubble Pulser was 500-1000 meters.

The raw XTF and OIC files were processed into side scan backscatter (2 m pixel resolution) and bathymetry (10 m) mosaics using Cleansweep (version 3.4.25551, 64-bit) software (Ocean Imaging Consultants, Inc., Honolulu, HI). For the side scan, bottom tracking, angle- varying gains (AVG) and look-up tables (LUT) were applied to the data as necessary to correct for water column returns, arrival angle, and to increase the signal-to-noise ratio of the backscatter returns. These corrections helped create a uniform image that most effectively displayed the features of the seafloor. The backscatter intensity mosaic is displayed on an inverse grey-scale, ranging from zero (black) to 255 (white). Backscatter intensity indicates the density, slope and roughness of the seafloor, where lighter pixels represent highly reflective (usually harder) surfaces, and dark backscatter pixels represent acoustically absorbent (usually softer) bottoms. The final side scan backscatter and bathymetry mosaics were exported as geo-referenced .tiff files and ArcGrid files, respectively.

SECTION 1: BENTHIC HABITAT DISTRIBUTION

1.1 Introduction

Maps of the benthic environment are important marine spatial planning tools for understanding the ecosystem services provided to humans (food, nutrient cycling, storm buffering, aesthetic) and for measuring the impacts of our past and future activities (resource extraction, recreation, dredging, construction) (McArthur 2010). The Interagency Ocean Policy Taskforce has identified "habitat maps" as foundational data for the management and planning of U.S. nearshore and offshore waters (IOPTF, 2009). Our operative definition of "habitat" is that of the National Oceanic and Atmospheric Administration (NOAA): "bottom environments with distinct physical, geochemical, and biological characteristics that may vary widely depending upon their location and depth; often characterized by dominant structural features and biological communities." (NOAA CSC, 2010). Further, the ICES stresses that benthic habitats consist of both abiotic (substrate, bathymetry and water energy) and biotic (flora and fauna) components (ICES 2006). The activity of "habitat mapping" has been defined as "plotting the distribution and extent of habitats to create a complete coverage map of the seabed with distinct boundaries separating adjacent habitats" representing the "best estimate of habitat distribution at a point in time, making best use of the knowledge…available at that time." (Foster-Smith et al., 2007).

A simplified list of steps to habitat mapping has been proposed by Van Lancker and Foster-Smith (2007): (1) Process coverage (side scan, bathymetry) data; (2) Process ground-truth data; (3) Integrate the coverage and ground-truth data; (4) Design and layout the habitat map. The most important step of the four outlined above is the integration step, which has been accomplished using different strategies and methods depending on the types of data available and the overall goals of the mapping project. Marine benthic habitat mapping has traditionally consisted of a "top-down" protocol where acoustic tools are used to delineate landscape-level features that are usually geological in origin, followed by the ground-truthing of these features and biological characteristics (Brown et al., 2002, Solan et al., 2003, Eastwood et al., 2006). The adoption of this approach implies that acoustic classes or geologic features contain distinct biological assemblages. As a result, the sampling scheme and subsequent data integration process, where habitats are defined, is often geology-centric (e.g., Greene et al., 1999), even when the reported purpose of the mapping is driven by management of biological resources (Kenny et al., 2003, Diaz, et al. 2004). The alternative to this "top-down" methodology is the "bottom-up" approach. The purpose of the "bottom up" protocol is to establish relationships between biological communities and environmental variables in order to delineate habitat map units. Habitat units are built based on biological similarity and are then given environmental context by establishing statistical (e.g., multivariate) relationships with associated abiotic variables (underlying geology and/or overlying oceanography). These relationships could then be used to interpolate between individual samples of fauna to create predictive biological assemblages maps (Hewitt et al., 2004, McBreen et al., 2008). Because the bottom up approach preserves organism-environment relationships, it has better potential to generate units that are ecologically meaningful (Hewitt et al., 2004, Rooper and Zimmerman, 2007, Verfaillie et al., 2009).

Integrating biotic and abiotic data presents significant challenges. One of the first challenges that arise when attempting to integrate data is in choosing which variables to include or exclude from the analyses. This choice is usually addressed by including all available variables, then statistically eliminating those that do not show relationships with the biology, for example. A second major challenge is the coverage extent and spatial resolution of the different datasets. Full coverage acoustic data can be collected rapidly over large scales and at high resolutions (2 m pixel resolution, for example). The resulting products are often used to interpret broad-scale seafloor features (several to hundreds of meters in size). Conversely, point-coverage ground-truth data are collected over coarser resolutions, and with samples typically

encompassing a seafloor area of < 1 m^2. The resulting data are examined at a fine scale (individual sediment grains and organisms are resolved). Describing patterns at scales of ecological importance amidst the varying scales of data acquisition is an issue that the mapping community continues to work to address (ICES 2007). A third challenge is that both coverage and ground-truth data represent single sampling events in time, and therefore cannot always provide information about the temporal dynamics of habitats. Clues to temporal dynamics and disturbance can be found in benthic community analysis (e.g., indicator species) and geologic facies mapping (e.g., mobile sand waves) so that some generalizations may be avoided. Many of these issues are now addressed by NOAA's draft habitat scheme, the Coastal and Marine Ecological Classification Standard (CMECS) (Madden et al., 2010). CMECS was created to document and describe ecologically meaningful units using a common terminology for science, management and conservation. The CMECS structure organizes habitat data hierarchically from geologic setting to biotope (Table I-1), and provides ample opportunity to describe temporal dynamics and/or relevance. CMECS is currently seeking approval and endorsement as the national marine habitat classification standard by the Federal Geographic Data Committee.

Predicting biological communities poses challenges, as well. Studies have shown that biological communities in physically rigorous environments are adapted to high environmental variability whereas communities in more stable environments are more influenced by biological interactions such as competition and symbioses (Pratt 1973). This observation would suggest that biological community composition is more readily predictable in physically rigorous environments than in stable quiescent environments. Both types of environments exist within the RI Ocean SAMP study area.

Strategy

Rhode Island Sound (RIS) and Block Island Sound (BIS) are transitional seas that separate the estuaries of Narragansett Bay and Long Island Sound from the outer continental shelf (refer to Figure I-1). Providing the link between near-shore and offshore processes as well as state and federal waters, these transitional seas are both important from an ecological and management perspective. The sounds are also valuable human-use areas, e.g. for alternative energy sites, commercial and recreational fishing, boating, shipping routes and ferry routes, and tourism. In order to appropriately zone for such uses, a sound understanding of the benthic ecosystem is essential. Characterizing benthic environments is important because the organisms living there reflect long-term environmental conditions (Elliot, 1994), serve as a trophic link

between primary producers and commercially and ecologically important species (e.g., fish) (Snelgrove, 1998), and affect local sedimentary processes (Gray, 1974, Rhoads, 1974).

Since it was not feasible to map benthic habitats covering the entire RI Ocean SAMP study area at a resolution (spatial or taxonomic) acceptable for marine spatial planning and management, our goal for the two study years was to describe and map relationships between the biology and abiotic (environmental) variables in two large target areas that are also prime potential sites for offshore wind development at a high overall resolution (spatial and taxonomic). We expect that many of the organism-sediment and community-environment relationships that we define will be generally applicable across the SAMP area. This information will be a valuable contribution in making scientifically valid, ecosystem-based management decisions for Rhode Island's coastal waters.

We will examine abiotic and biotic features of the benthic environment at fine scales (100 m, species-level). Using a step-wise multivariate approach, we will determine which abiotic variables best explain the pattern in benthic communities across the target study areas. We will then use a classification tree to identify habitats by grouping stations according to benthic community pattern and significant thresholds of the relevant abiotic variables. This approach has been used in estuarine habitat classification (Valesini et al., 2010) and estuarine habitat mapping (Shumchenia and King, in review), but never in offshore environments where data density tends to be much lower.

1.2 Background

Prior work

Two previous studies (McMaster, 1960, CONMAP, 2005) within the SAMP area have produced coarse resolution maps of surficial sediment type (Figure I-3 (upper panels). Two others (Figure I-3 ,lower panels) (Boothroyd and Oakley, this volume; McMullen et al., 2007-2009) have produced maps that begin to integrate depositional environment (Figure I-3, lower left panel), and transport process information (Figure I-3, lower right panel) with grain size information. All of these studies produce variations of geological "habitat" maps. The maps shown in Figure I-3 (upper panel) are produced by grain size analysis of bottom grab samples. The map in Figure I-3 (lower left panel) is produced by interpretation of bathymetry data and limited subbottom sonar and side scan data in terms of the major geoforms (e.g., moraine, lakefloor) within the study area. The map in Figure I-3 (lower right panel) is based on

interpretation of high-resolution swath bathymetry and side scan sonar data in terms of geological processes but with limited ground-truth studies. The map shown in Figure I-3 (lower right panel) is the only previous benthic habitat study within the SAMP area that is based on mapping data of comparable quality to that obtained by the RI Ocean SAMP project.

The current spatial distribution and availability of mapping data of comparable quality to the mapping data obtained by the RI Ocean SAMP project is shown in Figure I-4. Note that none of the data currently available is located in areas that are considered high priority sites for wind development.

A major goal of the RI Ocean SAMP project is to produce benthic habitat maps from high-quality, complete coverage seismic studies that are extensively ground-truthed. The SAMP project acquires both geological and biological ground-truth data. Acquisition of both types of data allows us to produce a multidimensional geological habitat map that includes geoform, grain size, and depositional environment information and a biological habitat map. The distribution of recent, high-quality ground-truth data of both geological and biological data obtained by previous studies is shown in Figure I-5. Again very little previous data is available from potential high-priority sites for offshore wind development.

1.3 Methods - Construction of RI Ocean SAMP benthic habitat distribution maps

Data resolution

Although both side scan backscatter and multibeam bathymetry datasets were collected at very high resolution (2 m and 10 m pixels, respectively), this level of detail would be prohibitive (computation time, file sizes) in the analyses and generation of broad-scale habitats. Therefore, data were imported into ArcInfo 9.2 and aggregated to 100 m pixels. Major geophysical changes and boundaries across both study areas were still visible in the side scan backscatter and bathymetry mosaics.

Acoustic analyses

The mean, minimum, maximum, and standard deviation of the side scan backscatter intensity were calculated from the side scan mosaics using Block Statistics in the Spatial Analyst Toolbox. From the bathymetry dataset, the Neighborhood Statistics feature within the Spatial Analyst extension was used to calculate the mean water depth, slope and aspect using a moving-window algorithm with window size of 100 m. In addition, Neighborhood Statistics was used to

derive surface roughness by calculating the standard deviation of the slope within a search radius of 1000 m (i.e. 10 pixels) (Damon, 2010). This procedure was performed on a dataset created from a set of 1.9 million National Ocean Service (NOS) soundings (Damon, 2010).

Bottom samples

Sampling sites were positioned within what appeared to be distinct geophysical bottom types based on visible boundaries in the side scan backscatter and bathymetry mosaics (Figure I-6). Sites were spread across the BI and FED study areas such that most major geophysical units contained at least one bottom sample. This approach resulted in approximately 1 grab sample per square mile within BI, with a total of 59 samples acquired over four occasions between October 2008 and August 2009 (see Figure I-6). About two grab samples per square mile (16 total) were taken within FED in December 2009. Surface samples were collected aboard the R/V McMaster using a Smith-McIntyre grab sampler (0.05 m^2 area).

Sediment samples

An ~ 25 ml sub-sample was taken from the surface of each Smith-McIntyre grab sample and analyzed using a Mastersizer 2000E particle size analyzer. The Mastersizer generated the weight percent of each Wentworth particle size fraction (e.g., very fine sand, fine sand, medium sand), along with the skewness, kurtosis, and standard deviation of the particle size distribution for the entire sample.

Macrofaunal samples

The remaining material from each Smith-McIntyre grab was sieved on 1 mm mesh and macrofauna were retained. All individuals were counted and identified to at least the genus level. A functional group designation (e.g. surface burrower, tube-builder, mobile) for each genus was made. The macrofauna abundances from the BI and FED study areas were pooled and only the species contributing to 95% of the total abundance between the two areas were included in further analyses. This eliminated genera with very low abundances.

Underwater video

Underwater video transects of roughly 200 m length were taken at 45 of the 59 sample locations within BI (stations 1-45). The data was collected over three consecutive days in June 2009 on the R/V McMaster using a video camera mounted to a sled and towed behind the vessel. A differential GPS and Hypack were used for navigation and to record the vessel tracks, which

were later imported into ArcInfo. Further work is being conducted to collect underwater video for the stations within FED.

Quantitative parameters were derived from visual analysis of the BI video. Specifically, the general sediment compositions and types of seafloor (bottom) present along the transect were recorded. These data were expressed as percentages of the total of each transect (i.e. bottom type is 50% boulder field, 25% flat sand, 25% tube mat). The number of habitat types that exist within each transect was also noted. In terms of biological information, the video for each station was qualitatively examined for the presence and approximate abundance of organisms (algae, fish, invertebrates).

Benthic geologic environments

Within the BI, the extent of the Quaternary depositional environments were interpreted from high resolution side-scan sonar and bathymetric images, sub-bottom seismic reflection profiles, as well as surface sediment grab samples and underwater video imagery. Environments interpreted with map units > 10 of square kilometers correspond to the Geoform level in CMECS, and include moraines, glacial lakefloor basins, deltas, alluvial fans and shelf valleys.

Refined Quarternary depositional environments are equivalent to the subform level in CMECS and represent the modern (Late Holocene) processes acting on the study area, and are known as benthic geologic habitats. Benthic geologic habitats are spatially recognizable areas of the seafloor with geologic characteristics different from adjacent units, and are mapped with units < 10 square kilometers (most polygons were < 1 square kilometers). These map units include information on the surface sediment characteristics, bed roughness, and includes depositional environments such as sand wave fields, low-energy depositional basins, and depositional cobble gravel pavement. The benthic geologic habitats are named based on a combination of Quaternary depositional environment, surface sediment grain size and a descriptor of the bed configuration or any other pertinent information. As an example, areas on the Quaternary moraine with coarse sand with small dunes would be mapped as (ISM csd), for an Inner Shelf Moraine, coarse sand with small dunes.

Integration of abiotic and biotic data

A suite of abiotic variables were generated from the multiple layers of data (side scan backscatter, bathymetry, sediment samples, underwater video) at each bottom sampling station (Table I-2). Of the 75 stations, two were excluded from the statistical analysis because they did not have accompanying acoustic data (BI 44 and 45). Another nine sites were removed due to

there being little or no sediment recovered by the Smith-McIntyre grab sampler (BI 4-6, 18, 30, 608, 1308, 1408, and FED 2). Typically, unsuccessful grabs are an indication the seafloor is comprised of coarse sediments not easily recoverable. Underwater video was taken at seven of the excluded sampling stations. For six of the stations, the video confirms the samples were located in areas of coarse sediments (gravels, cobbles, boulders). It is unclear why no grab was collected at the remaining station, as the video indicates it is located in fine-grained sand.

In PRIMER 6, a draftsman plot was created to assess the correlation between the variables. Variables that were highly correlated, and, therefore, redundant ($r > 0.85$) were eliminated from the analysis. The variables were then normalized to correct for differences in units, and a resemblance matrix was created based on the Euclidean distance metric.

The macrofauna abundance data were 4^{th} root transformed to reduce the influence of highly abundant genera and the Bray-Curtis similarity index was used to create a matrix of station-similarity.

Univariate analysis

The Pearson correlation coefficient, r, was used to investigate the relationship between surface roughness, macrofaunal diversity (total # genera per site) and abundance (total # individuals per site). It was hypothesized that surface roughness would be positively correlated ($r >> 0$) with both macrofauna diversity and abundance.

Multivariate analyses

An analysis of similarity (ANOSIM) was performed on the Bray-Curtis similarity matrix of the macrofaunal abundances using benthic geologic environment as a factor. ANOSIM tests the null hypothesis that there are no differences between groups of samples (the biotic Bray-Curtis similarity matrix) when examined in the context of an a-priori factor (benthic geologic environment) (Clarke and Gorley, 2006). An R value of 0 indicates there are no differences between groups (i.e. null hypothesis is accepted), while an R value greater than 0 (null hypothesis rejected) reflects the degree of the differences. The test is permuted 999 times to generate a significance level ($p < 0.05$ used here).

The macrofauna similarity matrix and abiotic variables were subject to the BIOENV procedure in PRIMER 6. The BIOENV approach identifies a subset of abiotic variables that best "explains" macrofaunal composition (Clarke and Gorley, 2006). The approach analyzes the extent to which the abiotic parameters match the biological data by searching for high rank correlations between variables in the two matrices (the abiotic Euclidean distance matrix and the

biotic Bray-Curtis similarity matrix). BIOENV outputs the highest Spearman rank correlation coefficient between a combination of abiotic variables and the biotic similarity matrix. The maximum number of variables permitted in the output was capped at five. This procedure was performed twice. The first BIOENV routine (BIOENV + video) included the underwater video variables in addition to the remaining abiotic parameters and was performed on only the 38 BI stations. All variables must be present at all stations in order to run BIOENV. Since no underwater video variables were available in FED, the second run of BIOENV (BIOENV + BI & FED) was conducted without underwater video variables in order to include all 64 stations between BI and FED.

The variables selected as important by the BIOENV were then entered into the LINKTREE procedure in PRIMER 6 to classify the macrofauna data according to patterns in these important abiotic variables. LINKTREE groups the macrofauna samples by successive binary division using the abiotic variables as drivers and maximizing the ANOSIM R value at each division (Clarke and Gorley, 2006). The ANOSIM R was constrained to be greater than 0.30 and the minimum group size was set at two. Each resulting class is defined by a suite of biological samples and quantitative thresholds of the abiotic variable(s). An ANOSIM was performed on the LINKTREE classes to test the hypothesis that there are no significant ($p < 0.05$) differences in the macrofaunal assemblages among LINKTREE classes. The similarity percentages (SIMPER) routine was then used to determine the within-class similarity of the resulting LINKTREE classes and to identify the genera contributing most to the similarity.

Mapping

Due to the lack of spatial auto-correlation (e.g. samples closer in space will be more similar than those further away) of the grain size point samples, traditional interpolation methods (e.g. Ordinary Kriging, Inverse Distance Weighting) could not be used to create full-coverage data layers. Instead, a conservative approach was taken to create the benthic habitat maps in order to preserve the accuracy of the maps. For this approach, the maps were created by classifying pixels (64, 100 m pixels) for which abiotic data were available in ArcInfo. The habitat classes follow the LINKTREE classification and are labeled according to the LINKTREE threshold defining each class and the dominant genus within each class.

1.4 Results

Acoustics

The side scan backscatter mosaics reveal both BI and FED have heterogeneous benthic environments (Figure I-7). Interpreted bottom types include sheet sands, sand waves, and boulder fields, along with flat sandy and muddy environments. The bathymetry, slope, and surface roughness of the two areas (Figures I-8, I-9, I-10) also reflect heterogeneity in varying degrees of smooth and rough bottom.

The mean side scan backscatter intensity (100 m resolution) within BI and FED ranged from 40.99 to 239.13 and the standard deviation varied from 7.35 to 98.61 (Table I-3). Bathymetry (100 m resolution) ranged from 13.8 m to 44.0 m. The slope was between 0.01˚ and 1.54˚ and the standard deviation of the slope (measure of surface roughness) was between 0.05˚ and 1.39˚. The aspect had a range of 9.36˚ to 354.21˚. BI appears to have a more variable benthic environment, as evidenced by wider ranges in the acoustic variables (backscatter, slope) and their standard deviations (refer to Table I-3).

Bottom Samples

Sediment samples

Between both study areas, medium grained sand is the dominant sediment (32.48%), followed by coarse sand (29.34%) and fine sand (15.32%) (Table I-4). Medium sand comprised as much as 76.34% of sediment samples, while coarse sand and fine sand comprised as much as 69.57% and 57.82% of sediment samples, respectively. Similar to the acoustics, BI seems to exhibit more heterogeneous sediment characteristics, as evidenced by a much larger standard deviation of the grain size (90.6 μm to 459.8 μm range for BI versus a range of 105.9 μm to 302.4 m for FED).

Macrofaunal samples

More than 20,500 individuals belonging to11 phyla and 173 genera were sampled across the 64 stations within the BI and FED study areas (Table I-5). Both areas were dominated by three phyla, Crustacean, Polychaete, and Mollusc (Figure I-11). In terms of spatial distribution, the most abundant genera were *Lumbrineris* (recovered at 68% of the stations sampled), small surface burrowing polycheates, *Unciola* (46%), small surface burrowing amphipod (crustaceans), and *Glycera* (42%), large deep burrowing polycheates. With regards to counts of individuals,

the most abundant genera were *Ampelisca* (comprised 33.0 % of the total individuals), *Byblis* (11.7%), and *Leptocheirus* (6.2%), all tube-building amphipods.

The average biodiversity (total number of genera per sample) between both study areas was 23, ranging from 6 to 40 genera (Table I-6). The average abundance (total number of individuals within each sample) within BI and FED was 324 and ranged between 12 and 2,333 individuals. The highest biodiversity was found within BI at stations 37 and 39, with both samples having 39 genera present, followed by BI station 16 (38 genera) (Figures I-12 and I-13). The highest abundance also occurred within BI at station 39 (# of individuals > 2,000), followed by BI stations 2, 1, 37, and 16 (# of individuals > 1,000). The stations with the lowest biodiversity are BI 24 (6 genera), BI 3 (7 genera), and BI 23 and 42 (9 genera each). The lowest abundance was found at BI stations 3 and 24 (each sample recovered 12 individuals) and BI 25 (25 individuals).

Overall, the BI stations were more diverse, with 11 phyla and 156 genera (versus 8 phyla and 75 genera within the FED stations). In addition, BI had a higher average abundance and wider ranges of both abundance and diversity.

Underwater video

The underwater video dataset currently does not include transects collected within FED or BI stations 108 through 1408. Therefore, the findings presented below are preliminary and may change as additional data is included into the analyses.

The underwater video transects showed that the majority of the stations (30 of 45 stations) within BI had bottom environments comprised of flat surfaces characterized by little relief (Table I-7). Sediment composition for these areas varied widely ranging from fine sand to cobble. Numerous stations (18) exhibited areas of fine or coarse grained sand ripples. Boulder fields were noted at ten stations. At four stations the seafloor was comprised of soft sediments and dominated by dense tube-mats. The number of bottom types along each station transect ranged from one to 11, with one bottom being the most common (27 of 45 stations).

The first BIOENV procedure, BIOENV + video, identified a subset of five variables as most influential to the macrofaunal assemblage composition (Rho = 0.641). The single variable having the highest correlation with the biology was percent coarse sand of the grain size analysis (correlation = 0.362). The five variables comprising the best correlation were percent fine sand from the grain size analysis, percent fine sand as identified from the video analysis, maximum backscatter intensity, water depth, and surface roughness.

Benthic geologic environment

The dataset for the benthic geologic environment currently does not include the FED study area. Therefore, the findings presented below are preliminary and may change as additional data is included into the analyses.

Four Quaternary (glacial) depositional environments were interpreted from the high-resolution bathymetry data, including; Moraines, delta plain, alluvial fan and lakefloor basins (Figure I-14). The depositional environments were arbitrarily separated into geographic regions: North of the moraine shoal southwest of Block Island is considered Block Island Sound, and north of the moraine shoal southeast of Block Island is Rhode Island Sound; south of the moraine shoals is the Inner Continental Shelf. The moraines were separated into to two categories; Moraine Shoal for the two segments of moraine continuous with Block Island, dominated by outcrops of boulder gravel, and sandy Inner Shelf Moraines south of the moraine shoals. The moraine shoal that forms Southwest Ledge is as shallow as 6 m below sea-level and waves break on it during storms. The formation of the Inner Shelf Moraine and the concentration of boulder gravel on the inner shelf south of the moraine remain enigmatic. The Inner Shelf Moraine may represent the maximum advance of the Laurentide Ice Sheet at Block Island, or ice tectonics as the ice margin fluctuated and deformed the stratified (Alluvial fan) deposited in front of the ice margin.

Map unit MS bgc (Moraine Shoal boulder gravel concentrations) is spatially the most extensive depositional environment, covering 30 square kilometers (11.6 square miles; 21.7% of study area) within BI. Portions of the inner shelf moraine, and extending onto the inner shelf south of the moraine is a large sand wave field, with orientations suggesting sediment transport in both an east to west and southeast to northwest directions, or towards Block Island Sound. Crest to crest spacing of the sand waves average 100 m, but range from 10 to 300 m, and are likely active only during storm events.

Extending south from the moraine shoals, two broad areas interpreted to represent alluvial fans that were deposited by braided rivers graded to either a glacial lake on the inner shelf south of the study area, or to the Late Wisconsinan low-stand marine shoreline. This area is dominated by sandy and gravelly depositional environments, and map unit GAF csd (Glacial Alluvial Fan coarse sand with small dunes encompasses 29 square kilometers (11.3 square miles, 21.3% of BI study area) and GAF pgcs (Glacial Alluvial Fan pebble gravel coarse sand, 13 square kilometers (5.1 square miles, 9.5%). The small dunes in map unit GAF csd represent wave orbital bedforms, and are ubiquitous in depositional environments with coarse sand

throughout the study area. Crest to crest spacing averages 1 m, and ranges from 0.75 to 2 m (Clifton, 1976). Based on the water depth and grainsize within this unit, the velocity needed to form these bedforms can be estimated at 0.75 – 1.5 m s^{-1}. At a depth of 25 m, these velocities are reached with a minimum wave height of 4 – 5 m, with a period of 10 seconds (Komar, 1976; Sherwood, 2007).

North of the moraine at Southwest Ledge, a relatively flat area at -30 m below present sea-level is interpreted as a glacial delta that formed when the ice front was at the small segment of Moraine in the northwest corner of the study area. This probably represents a small glacial lake that existed between the ice front and moraine that was filled by the prograding delta. The surface sediment characteristics of this unit are dominated by pebble gravel and coarse sand depositional environments.

Two deeper areas (30 – 40 m below present sea-level) on the western and northern end of the study areas were mapped as depositional basins, and are dominated by fine-grained (silt to silty sand sized) sediment. The northern basin was interpreted as a lakefloor basin, and underwater video and sub-bottom seismic reflection data suggests that the lakefloor may crop out in portions of this map unit. The depositional basin on the western edge of the study area extends into Block Channel and occupies a closed depression (> 40 m water depth). Lakefloor was not identified in video or seismic data from this map unit, so it was not further classified as a lakefloor depositional basin.

There were fifteen different depositional environment types in BI sampled for macrofauna (Table I-9). However, four of these contained only a single macrofauna sample, and therefore pairwise statistical comparisons were not possible for these types. This issue reduces the power of the ANOSIM test, but the global R value may still be indicative of general patterns. The results of the ANOSIM using BI depositional environment type as a factor indicate that there are significantly different macrofaunal assemblages among depositional environment types (global $R = 0.556$, $p = 0.001$). Each depositional environment was labeled for the most abundant genus within samples retrieved there (Figure I-15).

The depositional environments within FED have not yet been distinguished; the relationship between these environments and the biology will, however, be assessed in detail in the near-term. The data from both areas will be pooled to determine the influence of depositional environment type on macrofauna composition.

Integrating biotic and abiotic data

The Pearson correlation coefficient rejected the hypothesis that surface roughness (a measure of habitat complexity) has a positive correlation with macrofauna biodiversity and abundance (r = -0.001 and 0.087, respectively).

The second BIOENV procedure, BIOENV + BI & FED, again identified a subset of five abiotic variables as being the most correlated the macrofaunal composition (Rho = 0.544). The variables responsible were percent fine sand, percent medium sand, percent coarse sand, maximum backscatter intensity, and surface roughness. Percent coarse sand was the single variable best correlated (Rho = 0.453) with the macrofaunal assemblage.

The LINKTREE created using the subset of abiotic variables identified in the BIOENV + BI & FED procedure resulted in 16 classes (Figure I-16). Of the 16 classes, 11 classes were comprised of only BI samples, two of only FED samples, and three contained samples from both BI and FED. The BI area contained 14 LINKTREE classes, whereas five were found within FED. The number of samples in each class ranged from 2 to 11. Each class is defined by a quantitative threshold of one of the five input variables (Table I-9). Percent fine sand was responsible for three of the thresholds, maximum backscatter intensity, surface roughness, and percent medium sand were responsible for five, two, and five thresholds, respectively. A number of these thresholds are defined over a narrow range (refer to Table I-9); for example, split "K" divides to the left at percent medium sand greater than 44.89 and to the right at percent medium sand less than 43.32. The ANOSIM indicated there are strong differences (R = 0.646, p = 0.001) between the macrofaunal assemblage among LINKTREE classes.

Within each LINKTREE class, the most abundant genus was determined (Table I-10). For four classes, the two most abundant genera were noted because both genera showed very high abundances compared to other genera present. Most commonly, *Ampelisca* was the most abundant genus, being dominant or sharing dominance for seven classes. Two other genera were found to be most abundant for more than one class; *Byblis* was dominant or shared dominancy for three classes and *Polycirrus* did so for two classes.

SIMPER results showed that the genus most responsible for the within-class similarity of each LINKTREE class were either polychaetes, or crustaceans and contributed between 39.69% and 11.02% to the within-class similarity (refer to Table I-10). In total, SIMPER identified nine genera for the 16 classes. The genera indicated for multiple classes were *Lumbrineries,* which was responsible for the greatest similarity for four classes, *Ampelisca* for three, and *Byblis* and *Protohaustorius* for two. The same genus was the most abundant and the most responsible for

the within-group similarity for seven of the 16 classes, five of which were the tube-building amphipods *Byblis* or *Ampelisca* (refer to Table 10).

Mapping

The benthic habitat maps included 64 pixels of 100 m resolution (Figure I-17). The maps contained 16 benthic habitat classes, as identified in the LINKTREE procedure. The habitats were classified according to their LINKTREE threshold and the dominant genus in terms of abundance (Figure I-18). Four classes are classified by the two most abundant genera because both genera showed very high abundances relative to the other genera present. Ten of the 16 classes are classified by tube-building amphipods, with *Ampelisca* accounting for seven of these classes. The class defined by *Polycirrus-Lumbrineries* occurred most often, encompassing 11 pixels within BI, followed by the class *Leptocheirus*, having 6 pixels within BI. Classes identified by *Byblis* (shown in light pink), *Protohaustorius*, *Mytilus*, *Ampelisca-Byblis*, and *Ampelisca* (shown in light grey) were the least dominant, each with two occurrences. BI and FED only share three classes, all defined by amphipods: *Byblis* (shown in dark purple), *Ampelisca-Byblis*, and *Ampelisca* (shown in bright pink).

1.5 Discussion

Maps of the distribution of benthic habitats are valuable tools for numerous ecological and management reasons, including understanding ecosystem patterns and processes, determining environmental baselines, impact assessment, and conservation efforts. The purpose of this study was to construct benthic habitat maps for two areas, BI and FED, within the RI Ocean SAMP study area using methods not before applied to offshore environments. To generate the habitat maps, a bottom-up methodology was employed to integrate multiple types of data over various scales and establish relationships between macrofaunal communities and environmental parameters.

Macrofauna diversity and abundance were linked. Stations with the highest diversity also had the highest abundance (BI 39, 37, 16) and diversity was particularly high in samples containing tube-building organisms. This association between diversity and tube-builders suggests tube-mat structures provide valuable habitats. Ellingsen (2002) suggested polychaete tube-mat structures may increase sediment heterogeneity (i.e. habitat complexity), and, as a result, positively influence benthic ecosystems. It is also possible that tube-builders positively interact with other genera (predator, prey, competition), which results in increased diversity.

Pratt (1973) reported that suspension feeders (such as tube-building amphipods) physically dominate hard surfaces, but, despite this, a diverse range of fauna (deposit feeders, predators, browsers) reach high densities in mature epifaunal assemblages. Pratt (1973) also noted that within Rhode Island Sound there was a correlation between the presence of the amphipod, *Ampelisca agassizi*, and the abundances of several infaunal species including detritus feeding amphipods, isopods, cumaceans, and a polycheate, *Prionospio malmgreni*.

Environmental conditions may explain the reason for the stations with the lowest macrofauna diversity also having the lowest abundance (BI 24, 3, 25, 42). Comparison of stations BI 24 and BI 42 (both classified as *Protohaustorius*, defined by maximum backscatter intensity less than 123.16) and BI 25 (classified as *Byblis*, defined by medium sand greater than 65.76%) with the grain size analysis, underwater video, and benthic geologic environment indicate that these sampling stations occur within the inner shelf moraine on large-scale medium and coarse grained sand waves or sheets. Station BI 3 (classified as *Polycirrus*, defined by medium sand less than 13.77%) is located on the moraine shoal within an area of boulders and very coarse grained material. The existence of sand waves, sheets, and ripples suggest sediment mobility. Therefore, these dynamic environments may present conditions too stressful for many genera, as organisms living in these areas must be adapted for movement in sand and be able to recover from burial (Pratt 1973).

Station BI 23, is unique in the BI and FED study areas because it has low diversity (9 genera), but high abundance (680 individuals), with the genus *Byblis* accounting for 97% of this abundance. This station exhibits biologic characteristics contradictory to typical assemblages with tube-building amphipods, as described by Pratt (1973) and discussed above. The reason this environment can support *Byblis*, but few other genera (including other tube-builders) is not resolved. Data from the underwater video, benthic geologic environment and grain size analysis show that BI 23 is located within the glacial alluvial fan in a sandy, rippled environment, which may partly explain the low diversity. BI station 23 may have low diversity and high abundance if the area has underwent a recent disturbance event and is in the process of recovery. A study of disturbance from dredge spoil on a stable sand area found that amphipod species, including *Byblis*, were among the early colonizers of the spoil material (Pratt 1973).

There is a high degree of benthic habitat heterogeneity within BI and FED. This heterogeneity is evidenced by there being little to no spatial autocorrelation (e.g. samples closer in space are more similar than those further away) between percent fine, medium or coarse sand samples within BI or FED. Sediment samples were collected at a density of one (BI) or two

(FED) samples per square mile, suggesting habitat changes occur over spatial resolutions (i.e. scales) as small as one-half square mile. Additional evidence of habitat heterogeneity over small scales is found in the LINKTREE results, where the thresholds used to define benthic habitat classes occur over narrow ranges of the abiotic variables (refer to Table I-9).

The scale at which the environmental parameters and acoustic patterns are examined is important. This importance can be seen in the results of the BIOENV procedures (+ video and + BI & FED). For example, the macrofauna patterns within BI and FED are linked to sediment characteristics at both fine and broad spatial scales. The fine scale link is with the grain size from the analysis of the sediment sample (i.e. percent fine, medium, and coarse sand). Similar sediment-macrofauna relationships have been observed in a number of previous studies (Gray, 1974, Rhoads, 1974, Chang et al.,1992, Snelgrove and Butman,1994, Zajac et al., 2000, Ellingsen, 2002, Verfaillie et al., 2009). A broad-scale link between sediment and macrofauna is seen with the bottom type cover (i.e. percent fine sand bottom) of the underwater video. Other studies (Brown and Collier, 2008, Rooper and Zimmerman, 2007, Kendall et al., 2005), have also found underwater video metrics (such as sediment composition) to be valuable in constructing and classifying habitat maps. Recognizing this, our aim is to incorporate underwater video analyses in both BI and FED habitat maps when the full datasets are available.

The reason for the broad-scale link between macrofauna and the maximum backscatter intensity of the side scan sonar mosaic (100 m resolution) is unclear. Studies have shown positive correlations between backscatter intensity and grain size (Goff et al., 2000, Hewitt et al., 2004, Collier and Brown, 2005). Therefore, perhaps the maximum backscatter intensity represents a macrofauna-sediment link.

The relationship between macrofauna patterns and surface roughness (a measure of environmental heterogeneity) within BI and FED also occurs over a broad scale. This finding supports that of previous studies (Gray, 1974, Ellingsen, 2002), which reported positive relationships between habitat variety and species diversity, following the rationale that a greater degree of sediment heterogeneity offers more potential niches, and therefore, allows for higher diversity (Rosenzweig, 1995).

Scale is important also in assessing the relationship between surface roughness and macrofaunal diversity and abundance. The univariate analysis showed very little correlation between surface roughness and either diversity or abundance, while both multivariate BIOENV procedures (BIOENV + video and BIOENV + BI & FED) showed strong surface roughness-macrofaunal assemblage composition. We hypothesize the reason for this mismatch is related to

the statistical method and the scale at which the macrofaunal and abiotic data within BI and FED were examined. Multivariate analyses tend to be more sensitive than univariate methods to small changes in faunal composition (Gray et al., 1990, Warwick and Clarke, 1991, 1993). The BIOENV routine considers the composition of the macrofaunal assemblage for each station, while the Pearson correlation coefficient utilizes a summary statistic for the diversity and abundance at each station. Because of this difference, the BIOENV procedure may discern finer scale relationships between the biology and the abiotic variables. For example, one or more genera may be influencing the results of the BIOENV if a strong link exists with one or more abiotic parameters. Such links were found by Olsgard and Somerfield (2000) who reported polychaetes exhibited the strongest relationship to the environmental parameters. Similarly, in another study (Ellingsen, 2002), molluscs, followed by polychaetes, had stronger connections to the environmental variables than that of crustaceans and echinoderms.

The LINKTREE classes can be split into two categories – classes with tube-building amphipods (8 classes on left side of LINKTREE) and those with few to no amphipods (non-amphipod classes) (8 classes on right side of LINKTREE). This division begins at the first split of the LINKTREE (split "A", based on percent medium sand). Their prominence in structuring the linkage tree classes highlights the influence of tube-building amphipods on the composition of macrofaunal assemblages. Despite this influence, the macrofauna composition of all LINKTREE classes was significantly different (ANOSIM global $R = 0.646$, $p = 0.001$), suggesting that factors other than amphipod presence contribute to assemblage composition.

The majority of the benthic habitat classes (13) were contained solely within BI or FED, suggesting the macrofaunal assemblages vary between the two study areas and primarily have their own associations with the environment. If the goal of the mapping effort was to characterize the finest-scale abiotic-biotic relationships in both areas, the observed degree of separation between BI and FED classes makes the case for conducting separate analyses and generating separate maps for each study area. From a management perspective, overly-site-specific analyses and maps may not be as useful as a geographically-broad analysis that allows habitat comparisons between areas. Our approach addresses the latter point, and the results indicate that BI and FED may differ fundamentally in terms of how species utilize the benthic environment.

Temporal variability can present a challenge to benthic habitat mapping, both in data collection and in creating final products. In terms of data collection, it is possible seasonal differences in macrofaunal community composition are reflected in our results. However,

Steimle (1982) reported there were no clearly defined seasonal changes between biological communities examined in February and in September within BIS. He also presented evidence to suggest BIS is a relatively stable environment. In addition, a study by Vincx et al. (2007) pooled biological data spanning 10 years and all seasons.

With regards to temporal variability and creating final products, benthic habitat maps often do not reflect the temporal dynamics of mobile features since they are created using abiotic and biotic datasets representing single sampling/survey events in time. However qualitative descriptors of temporal patterns/variability may be inferred from the abiotic and biotic data. For example, stations BI 22-25 are unstable physical environments (mobile sheet sands, sand waves, sand ripples) and characteristics (abiotic and biotic) of the benthic habitats in these areas may change. Temporal variability may be indicated by the presence of opportunistic species that reflect recent habitat disturbance, or the presence of large, long-lived individuals that indicate a more stable environment and potentially lower temporal variability in macrofauna composition (Pearson 1978).

1.5.1 Future work

The narrow ranges of the LINKTREE thresholds indicates that our statistical methods were very sensitive to environmental and biological characteristics, and argues for including additional data types (e.g. sediment organic content, average annual surface chlorophyll concentration, rugosity, nutrient availability, and trophic interactions) in the future that may help refine abiotic-biotic relationships and habitat patterns.

The high degree of environmental heterogeneity within BI and FED impedes our ability to confidently interpolate the grain size point samples into full-coverage data layers using traditional methods (such as Ordinary Kriging and Inverse Distance Weighting). Our concern of retaining accuracy is echoed by Brown and Collier (2008), who remarked interpolation methods can often lead to erroneous assumptions in the resulting map, particularly if the degree of seafloor heterogeneity in terms of surficial geology and biota is high. Consequently, taking a conservative approach and constructing benthic habitat maps for BI and FED retaining the original extent of the available abiotic data was the most accurate approach. Future studies will examine the linear relationship between the grain size data (point-coverage) and acoustic data (full-coverage) to assess the possibility of interpolating the grain size data via linear regression.

1.6 Conclusion

In the BI and FED areas within the RI Ocean SAMP study area, we used data integration methods (e.g., bottom-up instead of top-down) not before applied to offshore environments. Although the bottom-up approach identified five abiotic variables that influenced macrofauna composition, spatial heterogeneity in these abiotic variables prevented broad-scale extrapolation of habitat units using this method. Given a higher spatial density of bottom samples, this problem could be rectified.

Absent further sampling, the most promising solution is to use the top-down approach to describe the benthic biological assemblages found within each depositional environment (geological habitat) type. This relationship was found to be statistically strong and significant in BI (although less than the relationship defined with the bottom-up method), but data are not yet available for FED. Given the greater degree of habitat heterogeneity in BI, it is likely that the top-down approach will be successful in FED as well. The top-down approach will produce full-coverage habitat maps for both BI and FED that describe general, broad-scale patterns in both benthic geological and biological resources.

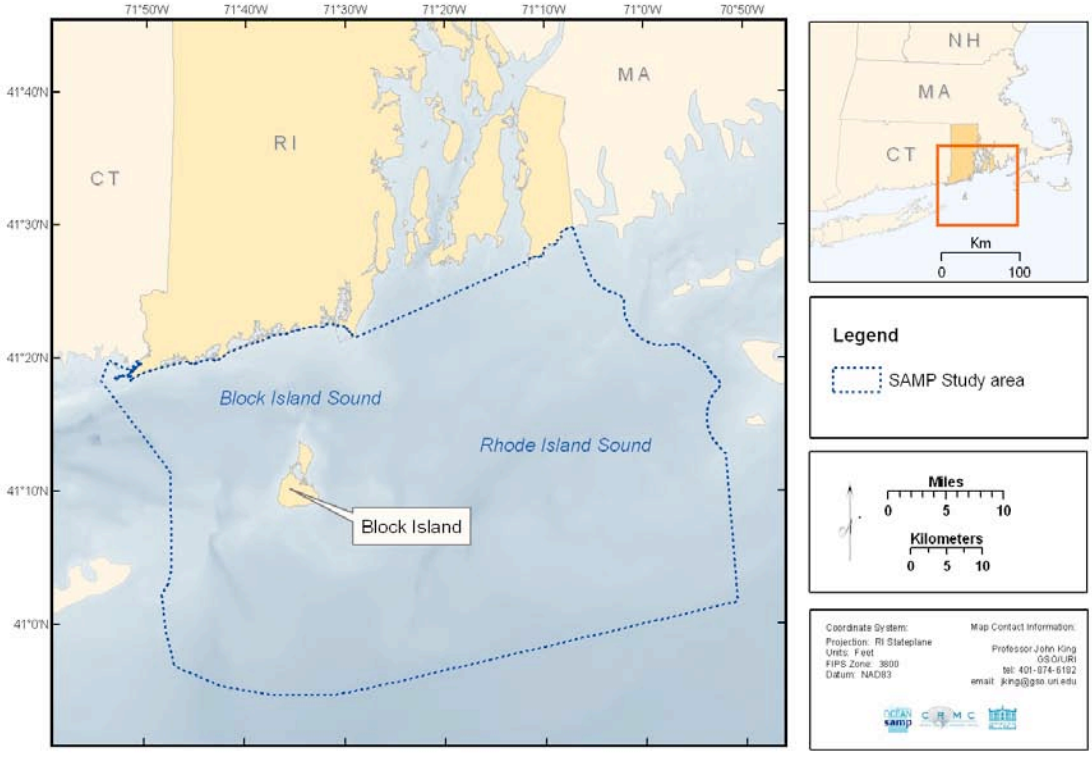

Figure I-1. RI Ocean SAMP study area.

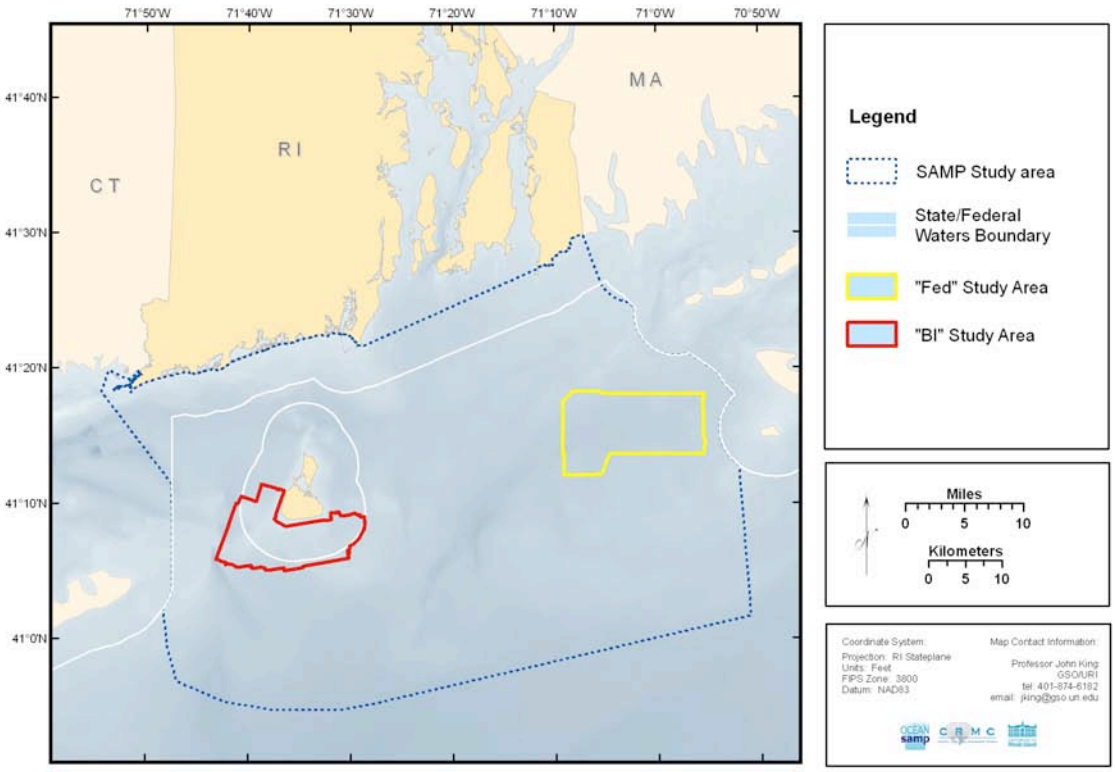

Figure I-2. Locations of BI and FED study areas within RI Ocean SAMP study area.

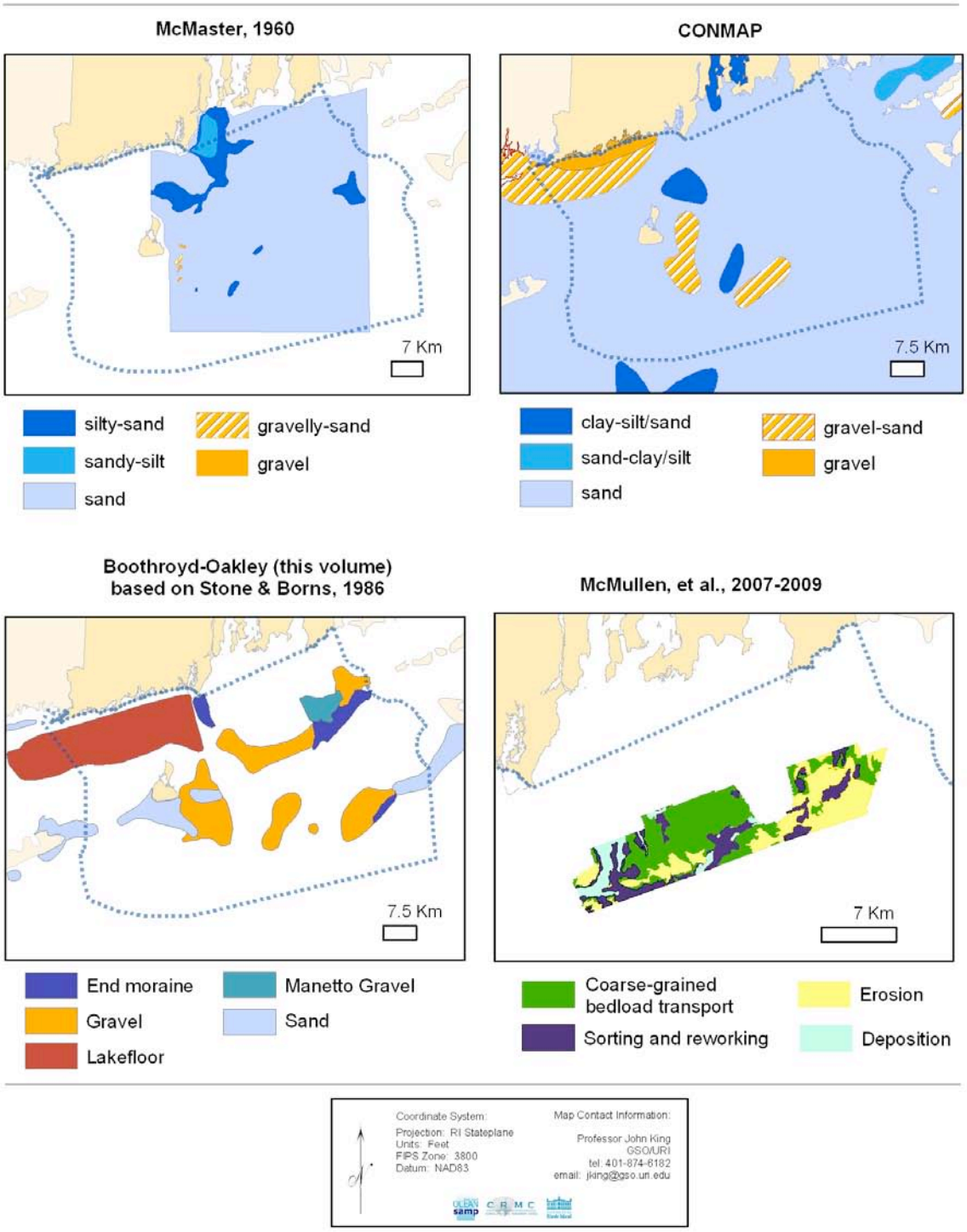

Figure I-3. Results of previous studies of surficial sediments in RI Ocean SAMP study area.

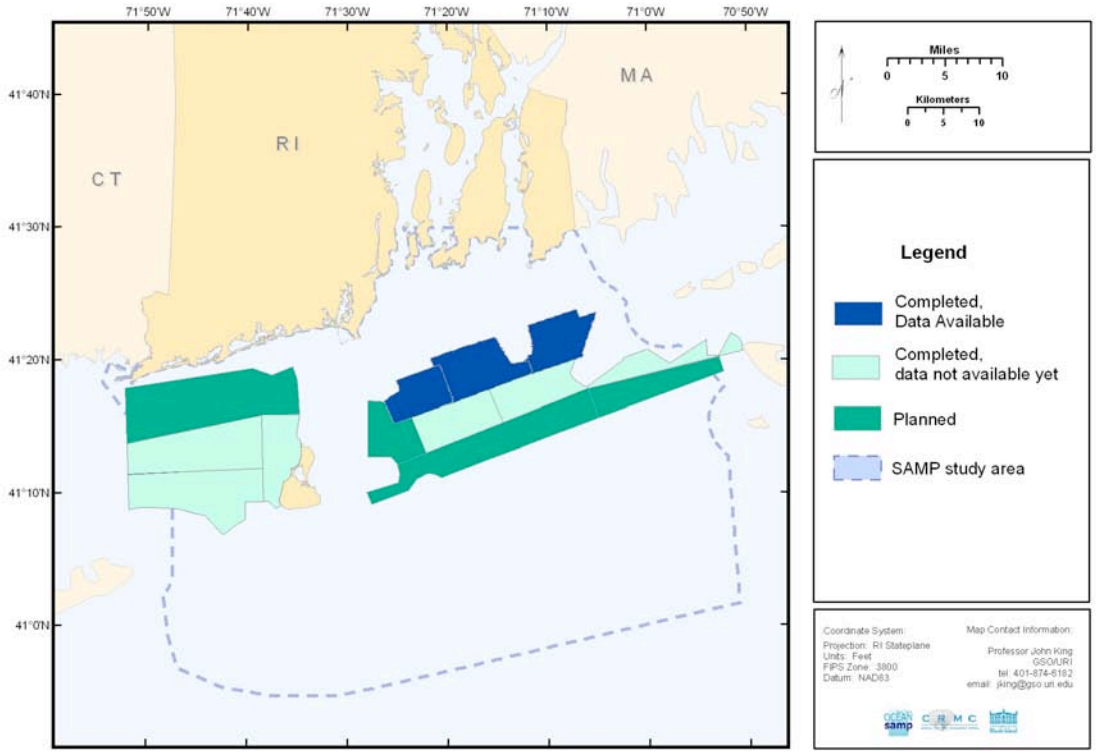

Figure I-4. High-resolution swath bathymetry and side-scan sonar surveys within RI Ocean SAMP study area by NOAA.

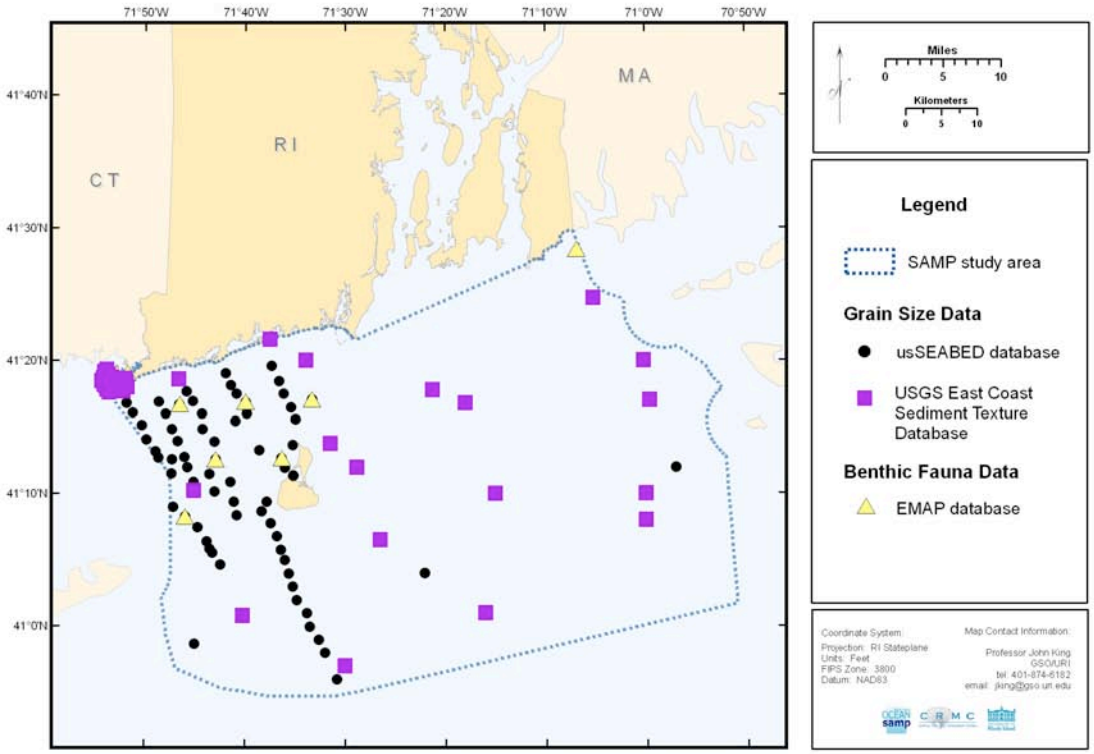

Figure I-5. Previous ground-truth studies within RI Ocean SAMP study area. EMAP 2002, U.S. Geological Survey 2005, usSEABED, 2005.

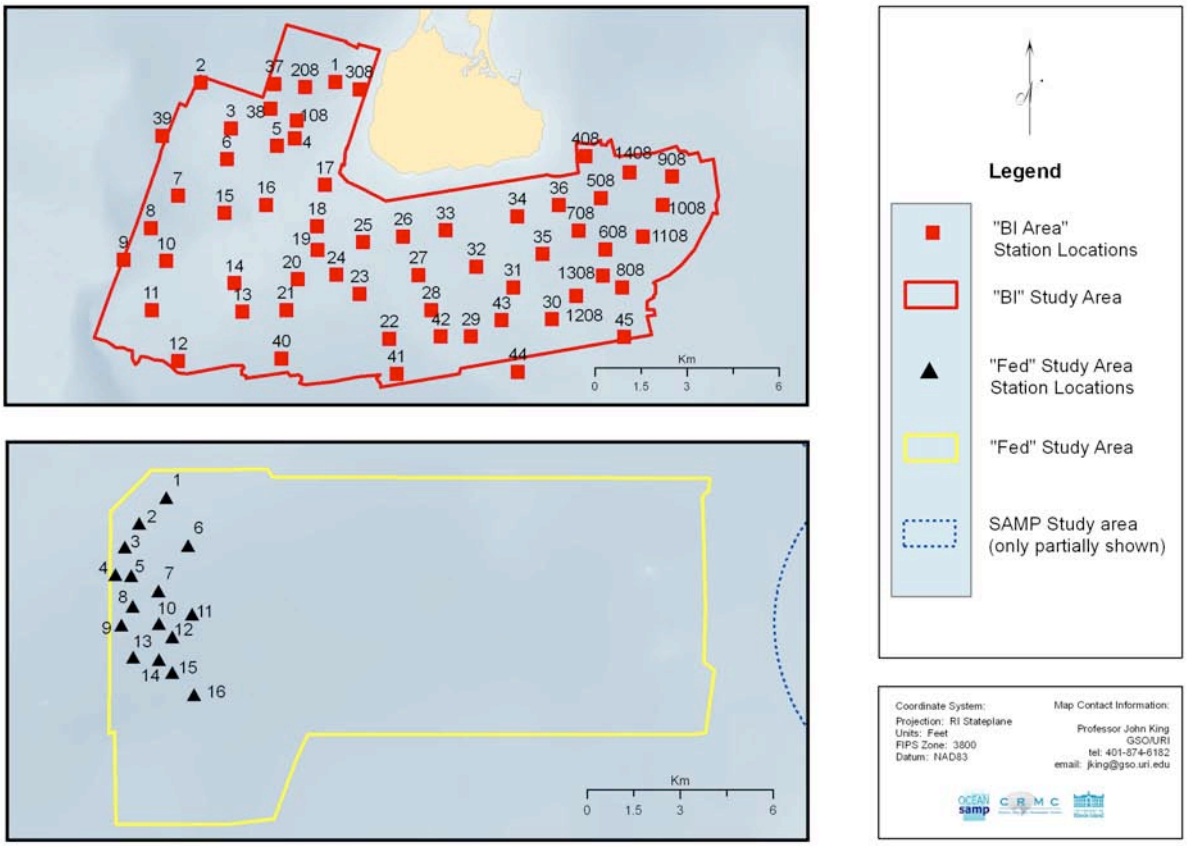

Figure I-6. Locations of the samples taken within BI and FED. Bottom samples were collected at all locations. Underwater video was collected for BI stations 1-45 only. BI samples 44 and 45 were removed from this study because they did not have accompanying acoustic data. In addition, BI samples 4, 5, 6, 18, 30, 608, 1308, 1408, and FED 2 were eliminated from the study because little to no material was recovered in the bottom sample.

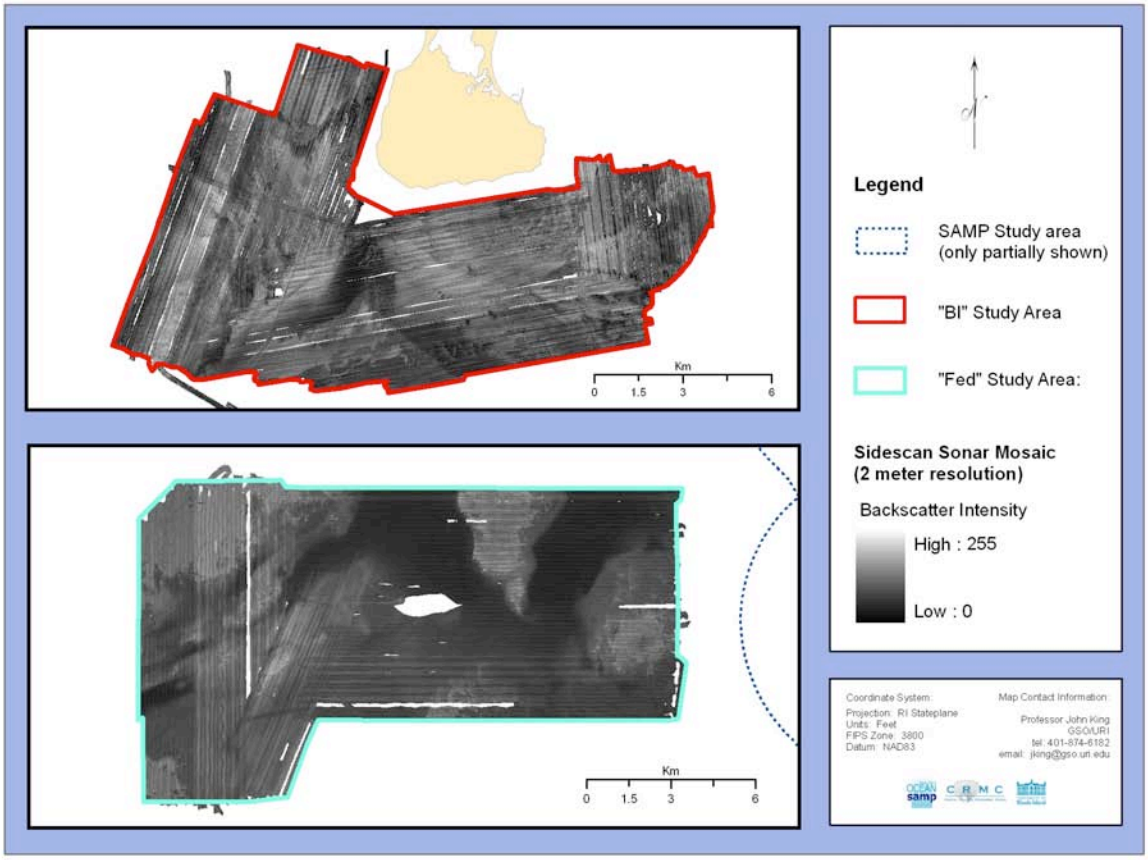

Figure I-7. Side-scan sonar mosaics of BI and FED. The mosaic is displayed on an inverse grey-scale. White (255) represents high backscatter intensity and black (0) represents low backscatter intensity, indicative of reflective (usually harder) surfaces and absorbent (usually softer) surfaces, respectively. The pixel resolution of the mosaics is 2 m. For the statistical analyses, the pixels were aggregated to 100 m resolution (not shown).

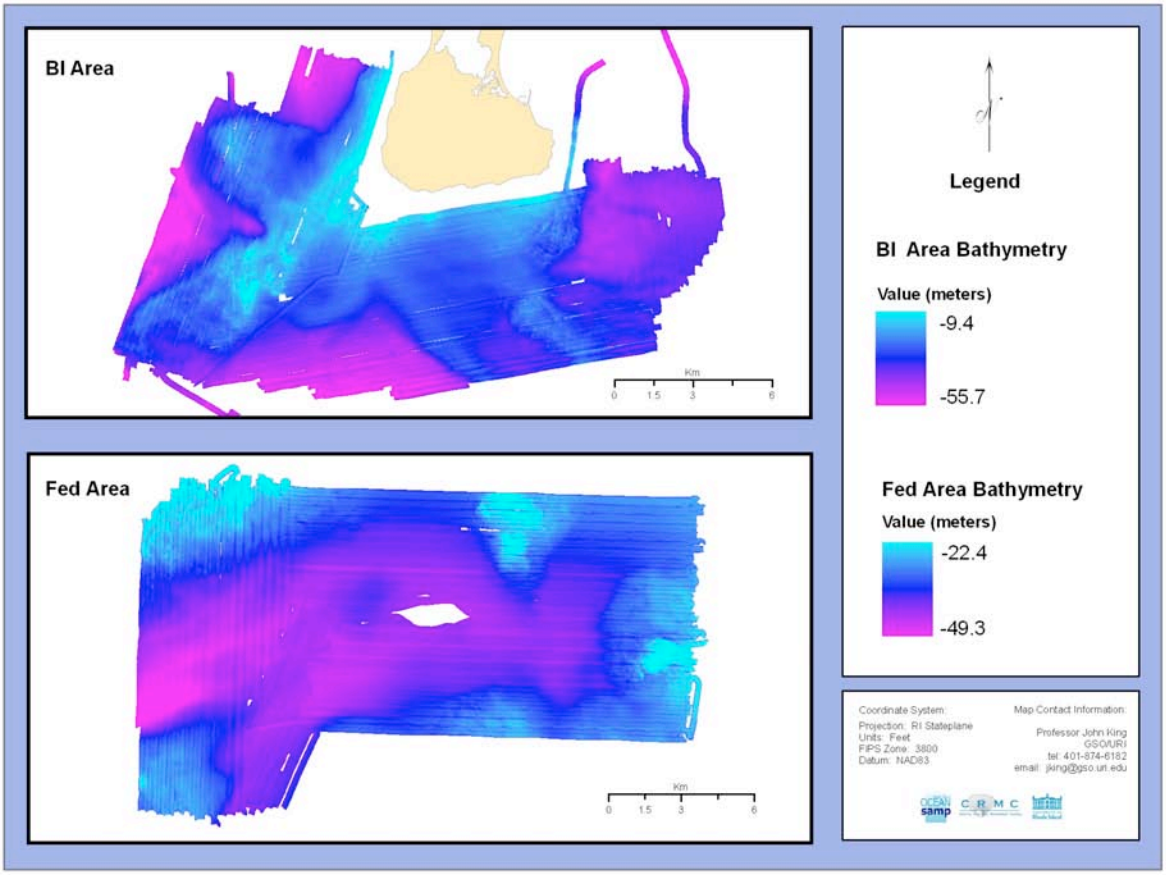

I-8. Bathymetry of BI and FED. Water depth ranges from 9.4 m to 55.7 m, with light blue signifying shallower depths and purple signifying deeper depths. Note the scales for BI and FED are different, so as to visually enhance the features within each area. The pixel resolution of the mosaics is 10 m. For statistical analyses, the pixel resolution was aggregated to 100 m (not shown).

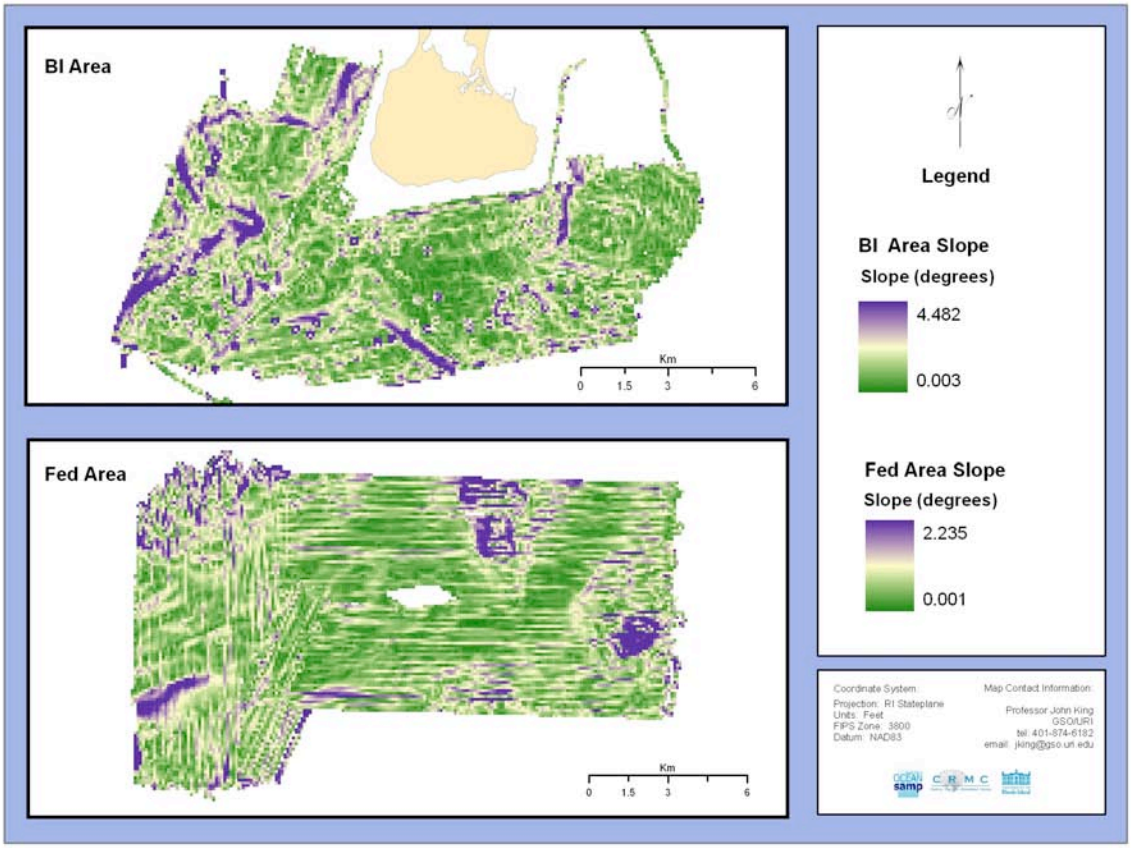

Figure I-9. Slope of BI and FED. The slope is measured in degrees, with purple indicating high slope values and green representing low slope values. Note the scales for BI and FED are different, so as to visually enhance the features within each area. The slope was calculated at 100 m pixel resolution.

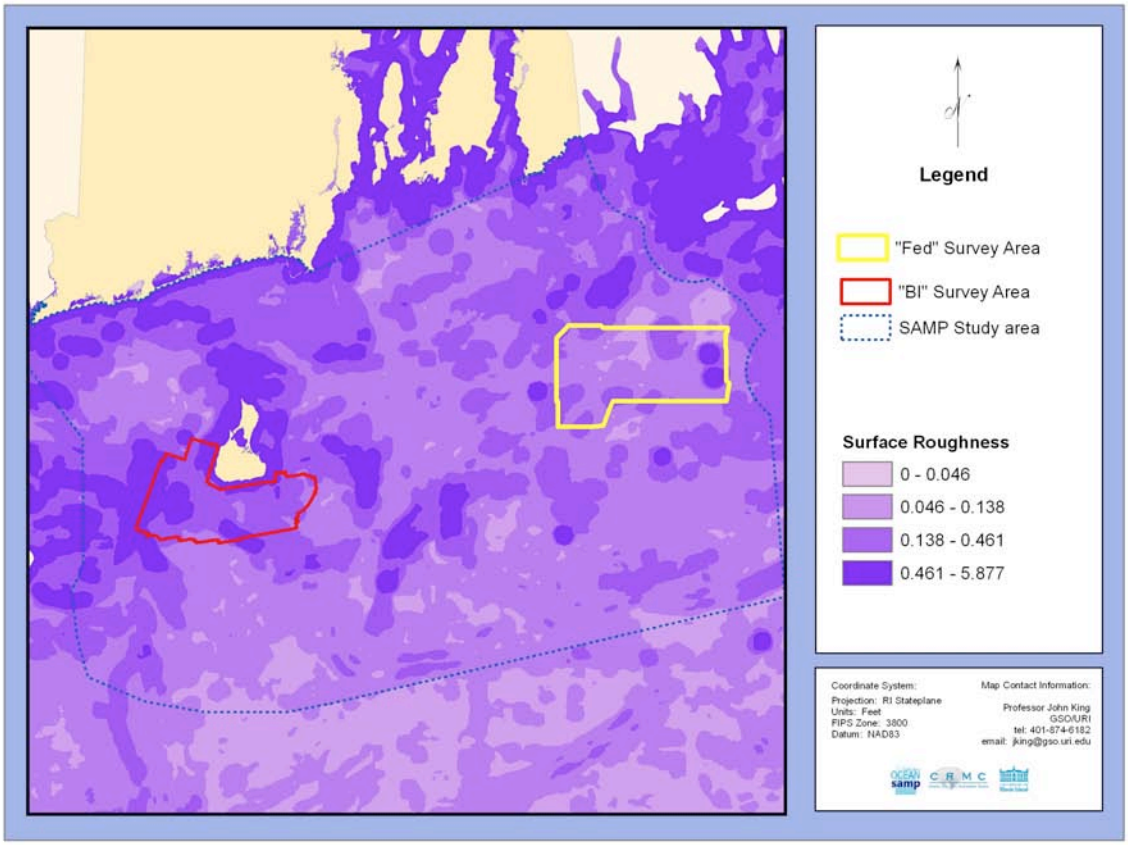

Figure I-10. Surface roughness of the RI Ocean SAMP study area. Surface roughness is reflects environmental heterogeneity. The dark purple is indicative of high heterogeneity and light purple signifies low heterogeneity. The red and yellow polygons represent the BI and FED study areas, respectively. The data layer is 100 m pixel resolution and is calculated by taking the standard deviation of the slope within a 1000 m radius.

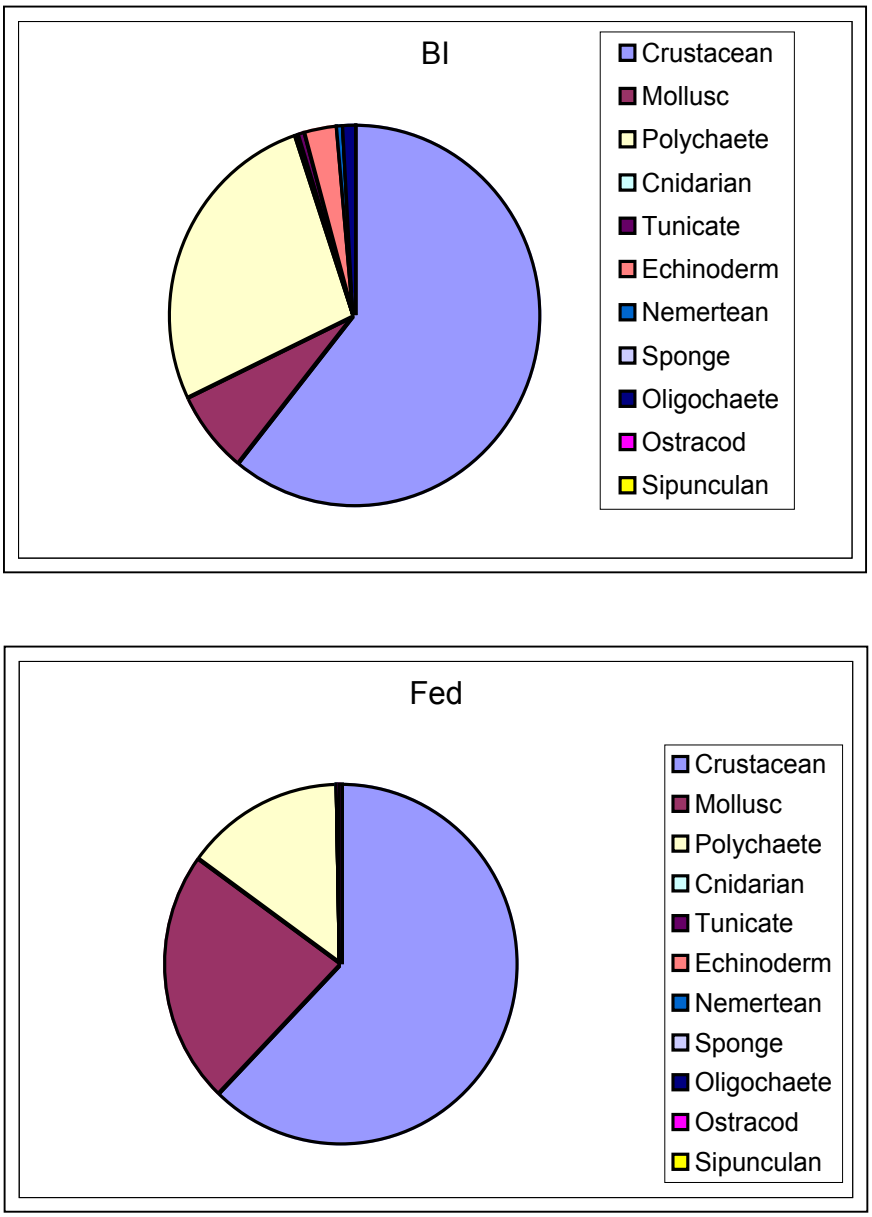

Figure I-11. Pie charts showing the Phyla composition of BI and FED. Crustaceans are the dominant phylum within both study areas. For BI, the second and third most prominent phyla are Polychaetes and Molluscs. This is reversed for FED, with Molluscs being more dominant than Polychaetes. A total of 11 phyla were recovered within BI and FED. All 11 phyla are seen within BI and 8 are present within FED.

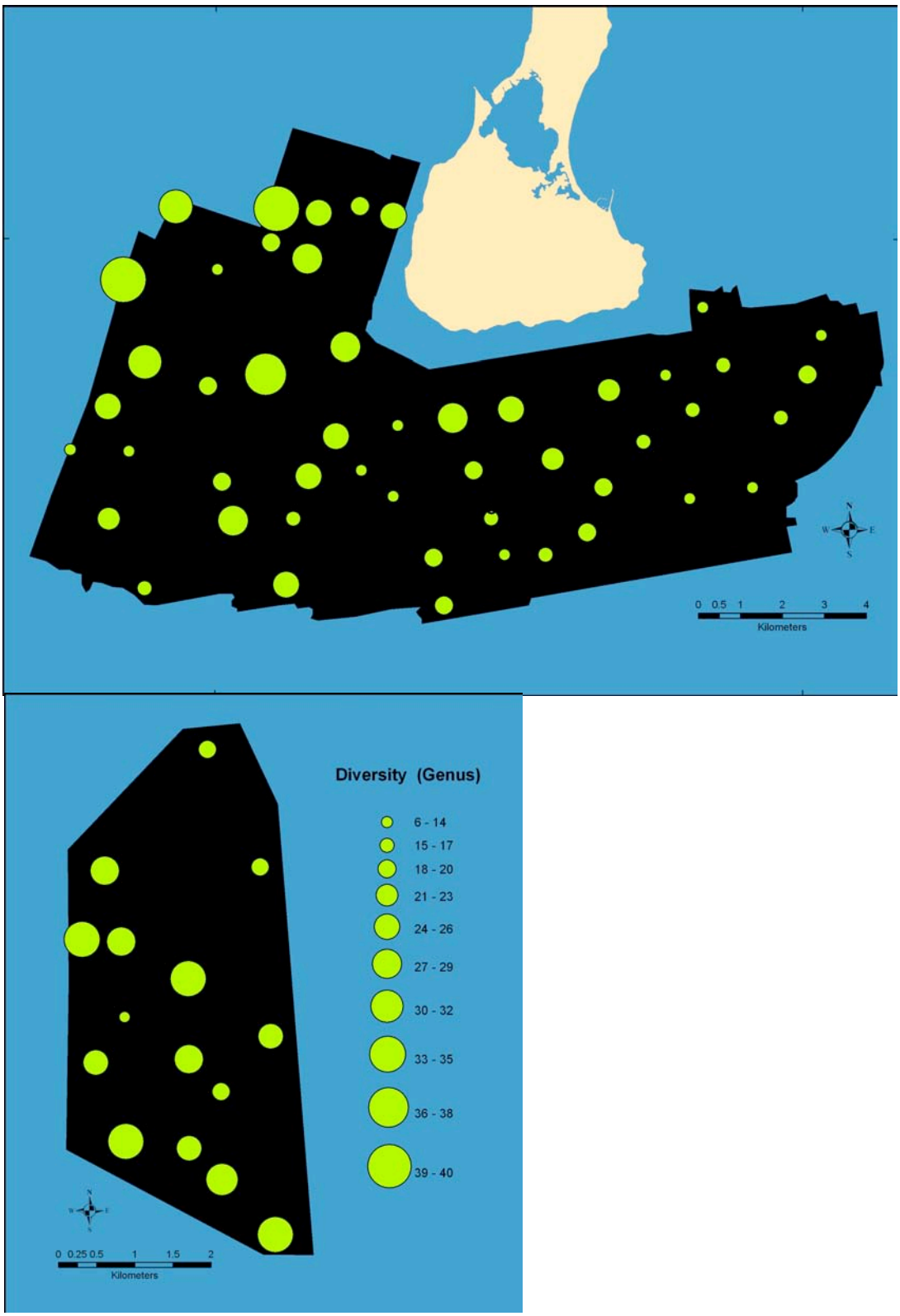

Figure I-12. Bubble plot of diversity within BI and FED. The size of the bubble is proportional to the diversity (measured at the genus level) at each station. Note the scales are the same for both BI and FED to allow comparison between study areas.

Figure I-13. Bubble plot of abundance within BI and FED. The size of the bubble is proportional to the diversity (measured at the genus level) at each station. Note the scales are the same for both BI and FED to allow comparison between study areas.

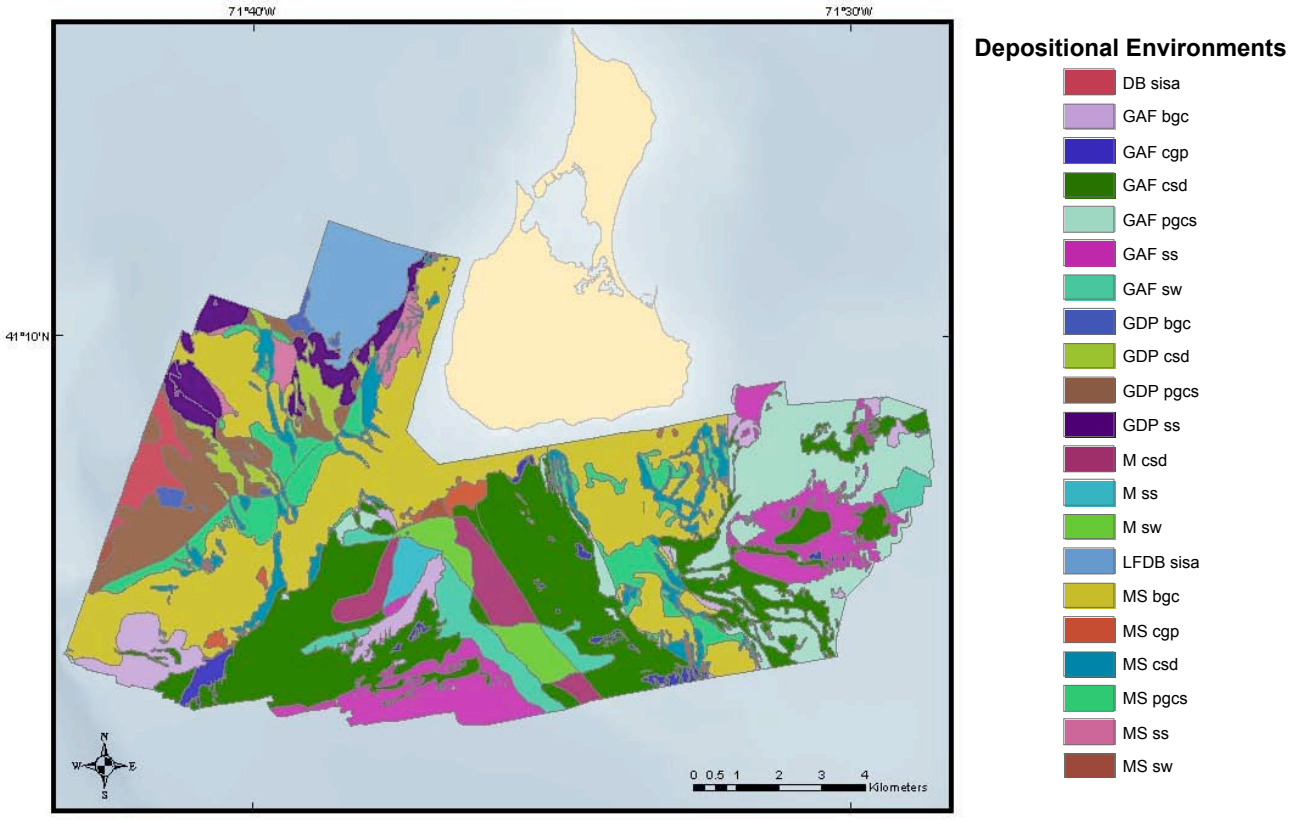

Figure I-14. Benthic geologic environment of BI. The environments were derived from side-scan imagery, sub-bottom profile imagery, sediment samples, and underwater video. The polygons are labeled by depositional environment units, reporting form (capital letters) followed by facies (lower case letters). The abbreviations are as follows: Form: DB = Depositional Basin; GAF = Alluvial Fan; GDP = Glacial Delta Plain; M = Moraine; MS = Moraine Shelf; LFDB = Lake Floor/Depositional Basin; Facies: sisa = silty sand; bgc = boulder gravel concentrations; cgp = cobble gravel pavement; csd = coarse sand with small dunes; pgcs = pebble gravel coarse sand; ss = sheet sand; sw = sand waves.

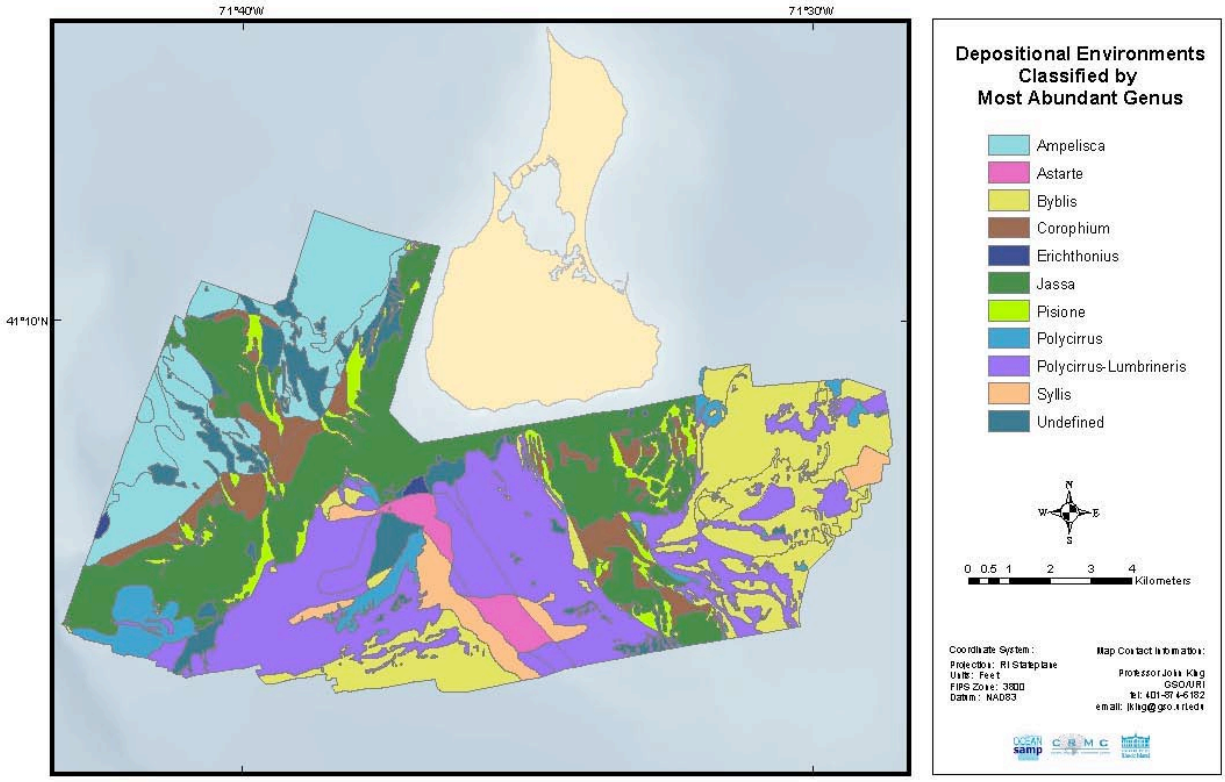

Figure I-15. Genus-defined benthic geologic environment of BI. The depositional environments were labeled by the most abundant genus, as determined from the bottom samples. An ANOSIM revealed the macrofaunal assemblages within each environment are significantly different (global R = 0.556, p = 0.001).

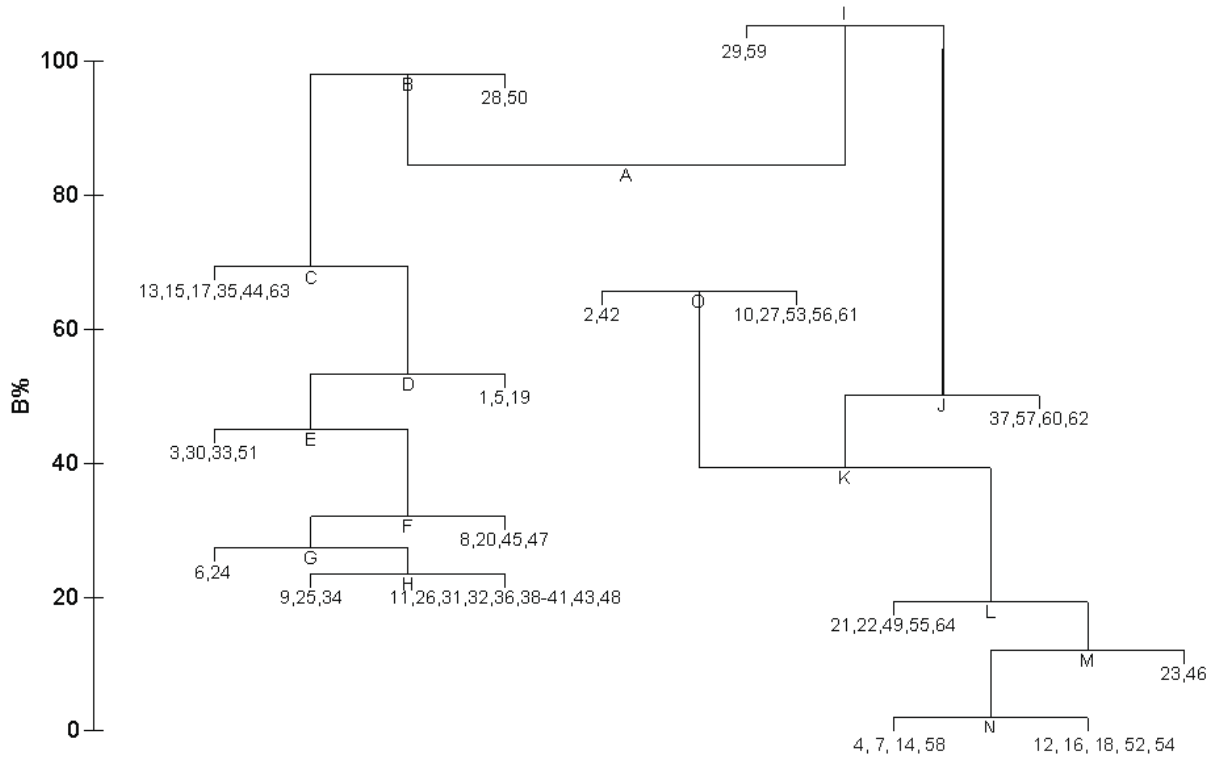

Figure I-16. LINKTREE output for BI and FED. The linkage tree identified 16 classes within BI and FED. Each class is defined by a quantitative threshold of one the five abiotic variables identified in the BIOENV procedure. Note that BI and FED share only 3 classes, while 11 classes contain only BI samples and two classes contain only FED samples. The threshold for each split is listed in Table I-9.

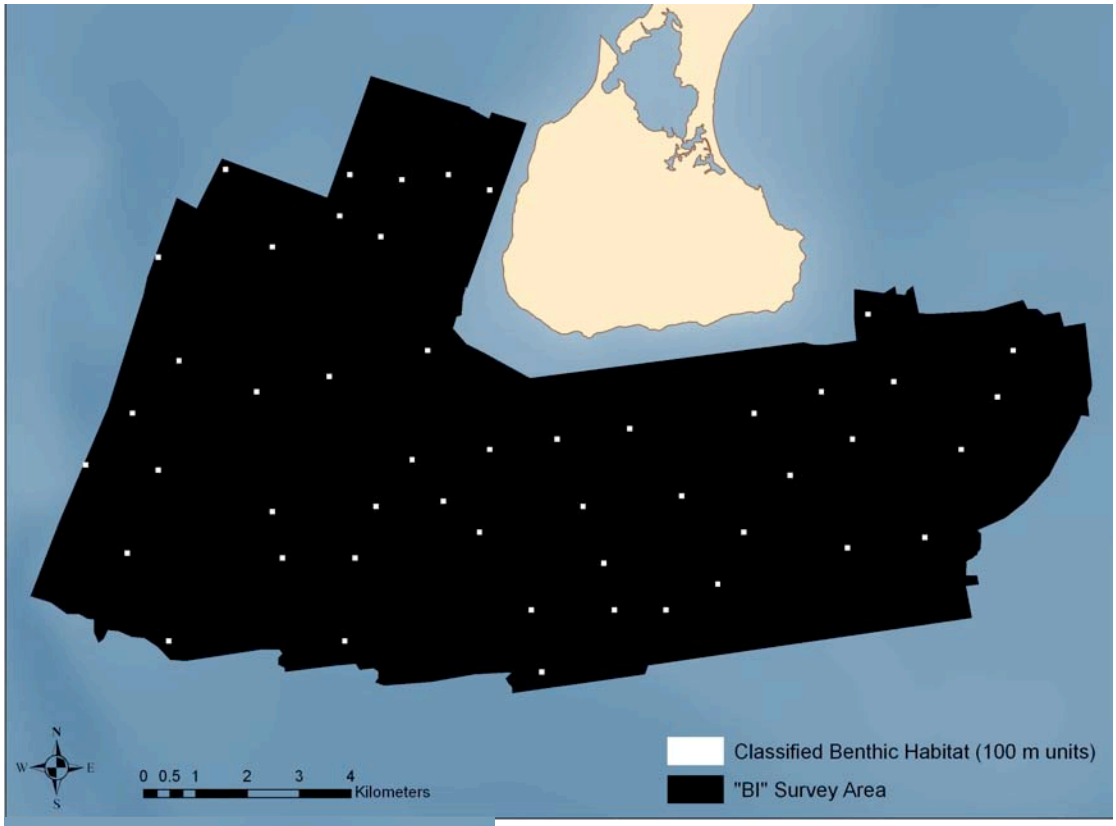

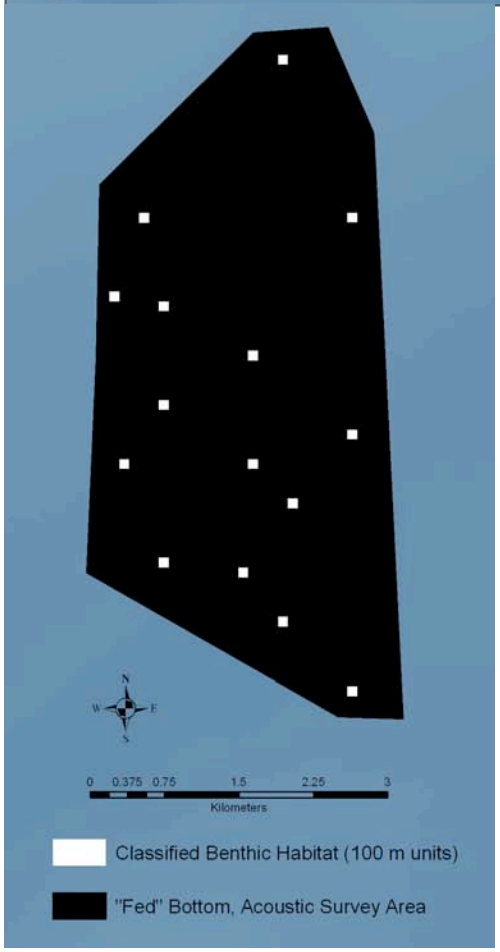

Figure I-17. Spatial extent of classified benthic habitats within BI and FED. The habitat map is comprised on 64, 100 m resolution pixels. Full-coverage benthic habitat maps are not possible at this time because of unsuccessful interpolation attempts due to the fact that the grain size datasets (derived from sediment analysis of the point-coverage bottom samples) are not spatially auto-correlated.

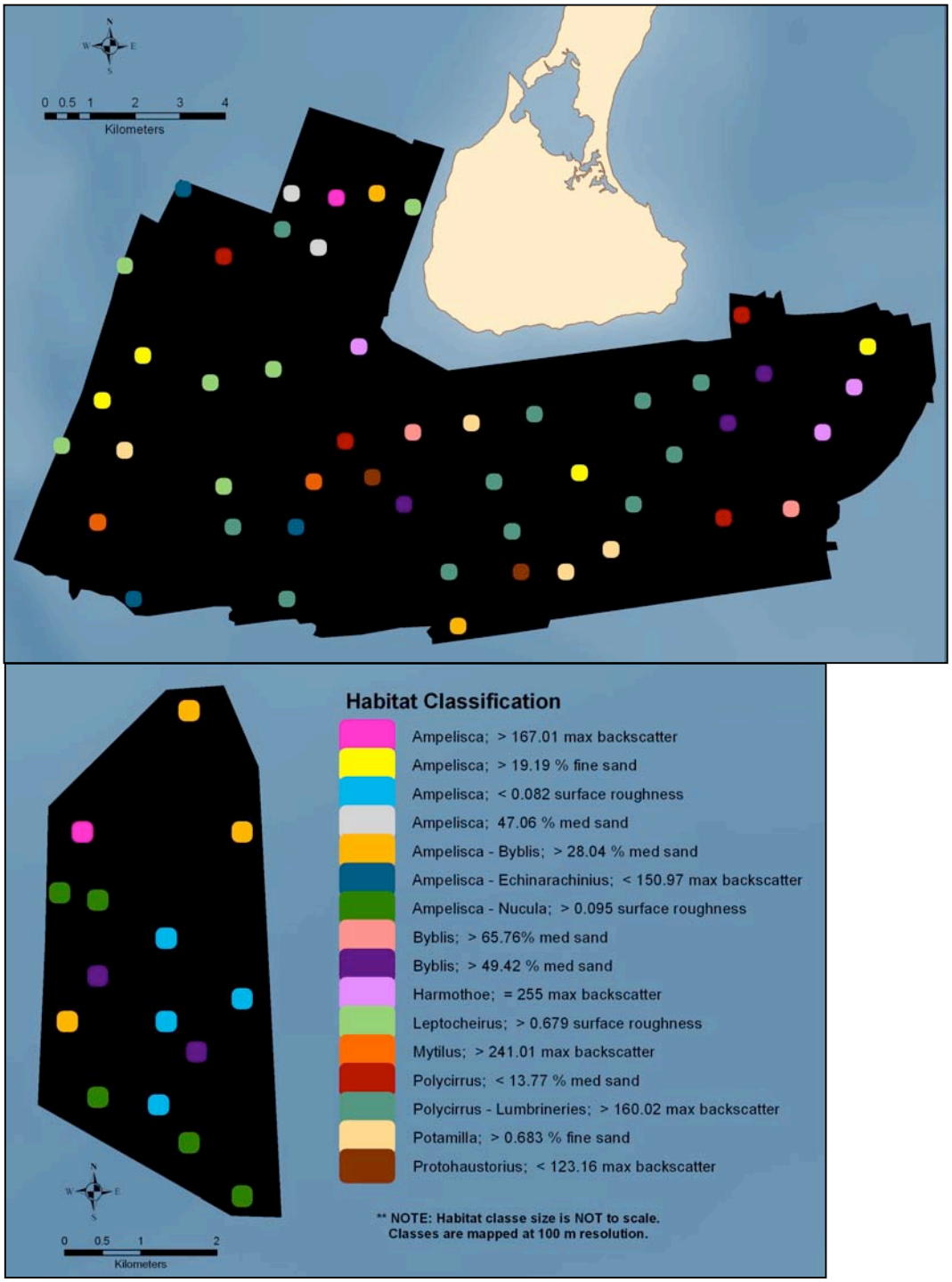

Figure I-18. Benthic habitat classification map for BI and FED. The benthic habitats were classified by the most abundant genus and the associated abiotic threshold. For four classes two genera were used in the classification because both showed high abundances. A total of 16 habitat classes were identified from the analyses. There are 14 habitats present within BI and 5 within FED. Note habitat class size is NOT to scale. Classes are mapped at 100 m pixel resolution (see Figure I-17)

Table I-1. Structure of the Geoform, Surface Geology, and Benthic Biotic Components with examples in NOAA's Coastal Marine Ecosystem Classification Standard (CMECS) (Madden, et al., 2010).

System	> Marine		
> Subsystem	> Nearshore subtidal		
	Geoform Component	**> Coastal Region**	> New England seaboard lowland
		> Physiographic Setting	> Coast
		> Geoform (coastal)	> Moraine
		> Subform	> Moraine top
		> Anthropogenic Geoform	> Jetty
	Surface Geology Component	**> Class**	> Unconsolidated Substrate
		> Subclass	> Sand
	Benthic Biotic Component	**> Class**	> Faunal Bed
		> Subclass	> Epifauna
		> Biotic Group	> Tube-building amphipods
		> Biotope	> *Ampelisca* community

Table I-2. List of abiotic and biotic variables used in the study. The source, type of coverage attained, and the resolution of each variable is also listed. In total, 19 abiotic variables were included in the statistical analyses and 2 biotic variables.

Source	Coverage	Resolution (m)	Variable
Backscatter	Continuous	100	Mean
			Maximum
			Minimum
			Standard Deviation
Bathymetry	Continuous	100	Water Depth (m)
			Aspect (degrees)
			Slope (degrees)
			Surface Roughness (Std Dev of Slope within 1000 m Radius)
Video	Transect	44 stations	Grain Size (%)
			Bottom Type (%)
			Number of Patches
Grain Size	Point	64 stations	% Clay
			% Fine Silt
			% Course Silt
			% Very Fine Sand
			% Fine Sand
			% Medium Sand
			% Coarse Sand
			% Very Coarse Sand
Biology	Point	64 stations	Identificantion (genus level)
			Counts (individuals)

Table I-3. Ranges of the acoustic variables within BI and FED. Note the wider ranges exhibited by BI for all of the acoustic variables.

Acoustic Variables (100m)	Range		
	BI	**FED**	**BI and FED**
Mean Backscatter Intensity	40.99 - 239.13	69.39 - 146.48	40.99 - 239.13
Max Backscatter Intensity	88 - 255	95 - 178	88 - 255
Min Backscatter Intensity	1 - 110	1 - 85	1 - 110
Standard Deviation of Backscatter	10.86 - 98.61	7.35 - 17.59	7.35 - 98.61
Water Depth (m)	13.82 - 38.63	31.89 - 44.01	13.82 - 44.01
Slope (degrees)	0.01 - 1.54	0.02 - 0.47	0.01 - 1.54
Surface Roughness (Std Dev of Slope w/in a 1000m Radius)	0.09 - 1.39	0.05 - 0.22	0.05 - 1.39
Aspect (degrees)	9.36 -352.27	89.68 - 354.21	9.36 - 354.21

Table I-4. Percent composition and ranges of the grain size from analysis of the sediment samples within BI and FED. BI is dominated by medium and coarse grained sands and fine and medium sands dominate FED. Within both study areas, the dominant sediment is medium and coarse grained sands. The stations within BI exhibit wider ranges for most of the sediment variables and for the standard deviation of the grain size (um).

Sediment Variables	**Percent Composition**		
	BI (%)	**FED (%)**	**BI and FED (%)**
% Clay	1.61	5.38	2.45
% Fine Silt	3.40	10.19	4.91
% Course Silt	0.84	2.53	1.22
% Very Fine Sand	1.45	11.97	3.79
% Fine Sand	9.91	34.24	15.32
% Medium Sand	33.41	29.25	32.48
% Coarse Sand	36.01	5.98	29.34
% Very Coarse Sand	13.36	0.46	10.50
Sediment Variables	**Range**		
	BI	**FED**	**BI and FED**
% Clay	0 - 20.12	1.84 - 9.22	0 - 20.12
% Fine Silt	0 - 36.79	2.04 - 23.40	0 - 36.79
% Course Silt	0 - 8.43	0.48 - 9.16	0 - 9.16
% Very Fine Sand	0 - 9.89	0.41 - 28.45	0 - 28.45
% Fine Sand	0 - 57.82	3.92 - 46.97	0 - 57.82
% Medium Sand	0.43 - 76.34	8.73 - 57.54	0.43 - 76.34
% Coarse Sand	0.27 - 69.57	0.27 - 32.00	0.27 - 69.57
% Very Coarse Sand	0 - 62.73	0 - 3.44	0 - 62.73
Standard Deviation of Grain Size, um	90.56 - 459.78	105.86 - 302.42	90.56 - 459.78

Table I-5. Number phyla, genera, and individuals recovered within BI and FED.

	BI	FED	Combined
Total Number of Phyla	11	8	11
Total Number of Genera	156	75	173
Total Number of Individuals	16,269	4,464	20,733

Table I-6. Diversity and Abundance within BI and FED. Diversity is defined as the number of genera per station. Abundance defined as is the number of individuals per station.

	BI	FED	Combined
Range of Diversity per Station	6 - 40	14 - 38	6 - 40
Mean Diversity per Station	21	28	23
Range of Abundance per Station	12 - 2,333	38 - 555	12 - 2,333
Mean Abundance per Station	332	298	324

Table I-7. General description of underwater video collected at BI stations. Video was only obtained for BI stations 1-45. The most common bottom type was flat surface, for which the sediment composition ranged from coarse sand to cobble. The most common sediment type was coarse sand. Over half of the stations exhibited one bottom type throughout the 200 m transect.

Underwater video parameters	# of Stations
Bottom Type	
Dense Tube-mat	4
Flat surface	21
Rippled surface (regular pattern)	9
Rippled surface (irregular pattern)	9
Boulder field	10
Sediment Type	
Fine sediment (silt, clay, fine sand)	6
Fine sand	4
Coarse sand	30
Gravel	13
Cobble	9
Boulders	11
# Bottom patches	
1	26
2	3
3	1
4	2
5	3
6	1
7	7
8	3
9	0
10	2
11	1

Table I-8. Description of the depositional environments. The environments in bold font are those with the greatest spatial extent within BI. The unit is labeled by form (capital letters) followed by facies (lower case letters). The abbreviations are as follows: Form: DB = Depositional Basin; GAF = Alluvial Fan; GDP = Glacial Delta Plain; M = Moraine; MS = Moraine Shelf; LFDB = Lake Floor/Depositional Basin; Facies: sisa = silty sand; bgc = boulder gravel concentrations; cgp = cobble gravel pavement; csd = coarse sand with small dunes; pgcs = pebble gravel coarse sand; ss = sheet sand; sw = sand waves.

Unit	Area (km sq)	Coverage (%)	# Biology Samples
AF bgc	5.01	3.63	2
AF cgp	1.44	1.04	0
AF csd	**29.39**	**21.30**	**14**
AF pgcs	**13.16**	**9.54**	**5**
AF ss	**10.26**	**7.44**	**2**
AF sw	4.49	3.25	2
DB sisa	1.84	1.34	0
GDP bgc	0.67	0.48	0
GDP csd	2.23	1.61	0
GDP pgcs	6.91	5.00	4
GDP ss	4.26	3.09	3
LFDB sisa	5.44	3.94	4
M csd	3.52	2.55	1
M ss	1.03	0.75	1
M sw	2.72	1.97	2
MS bgc	**29.97**	**21.72**	**5**
MS cgp	1.04	0.75	0
MS csd	5.67	4.11	1
MS pgcs	7.71	5.58	2
MS ss	1.59	1.15	0
MS sw	0.34	0.24	1

Table I-9. LINKTREE thresholds. The branch to the left side of the LINKTREE is listed first and the branch to the right side of the LINKTREE is listed second in brackets. For example, for Class A, the stations on the left side of the split have a threshold of < 8.55 % fine sand and the stations on the right side of the split have a threshold of > 9.39 % fine sand. Note that many of the thresholds are defined by narrow ranges of the abiotic variables.

Linktree Thresholds		
Class		
A	% fine sand	< 8.55 (> 9.39)
B	max backscatter	> 128.05 (< 123.16)
C	surface roughness	> 0.679 (< 0.609)
D	max backscatter	< 247.81 (> 255)
E	% fine sand	> 6.83 (< 6.23)
F	% medium sand	> 15.84 (< 13.77)
G	max backscatter	> 241.01 (< 226.01)
H	max backscatter	< 150.97 (> 160.02)
I	% medium sand	> 65.76 (< 57.59)
J	% fine sand	> 19.19 (< 16.18)
K	% medium sand	> 44.89 (< 43.32)
L	% medium sand	> 28.04 (< 27.79)
M	max backscatter	< 154.00 (> 167.01)
N	surface roughness	< 0.082 (> 0.095)
O	% medium sand	< 47.06 (> 49.42)

Table I-10. Description of LINKTREE classes. For each class, the comprising stations, the most abundant genus, and the genus most responsible for the within-class similarity (as identified by the SIMPER procedure) is listed. The classes marked with ** are the seven classes for which the same genus is the most abundant and is the most responsible for the within-class similarity.

Class	Comprising Stations	Most Abundant Genus	Genus Most Responsible for Within-Class Similarity
1	BI 25, 808	*Byblis*	*Protohaustorius* (39.69 %)
2**	BI 24, 42	*Protohaustorius*	*Protohaustorius* (30.49 %)
3	BI 9, 14, 15, 16, 39, 308	*Leptocheirus*	*Corophium* (11.15 %)
4	BI 17, 1008, 1108	*Harmothoe*	*Glycera* (15.19 %)
5	BI 10, 26, 29, 43	*Potamilla*	*Lumbrineries* (25.47 %)
6	BI 3, 19, 408, 1208	*Polycirrus*	*Polygordius* (22.47 %)
7	BI 11, 20	*Mytilus*	*Pisione* (16.83 %)
8	BI 2, 12, 21	*Ampelisca-Echinarachinius*	*Lumbrineries* (26.07 %)
9**	BI 13, 22, 27, 28, 31, 33, 34, 35, 36, 38, 40	*Polycirrus-Lumbrineries*	*Lumbrineries* (11.20 %)
10	BI 7, 8, 32, 908	*Ampelisca*	*Unciola* (16.27 %)
11**	BI 1, 41; FED 1, 6, 9	*Ampelisca-Byblis*	*Byblis* (17.46 %)
12	BI 208; FED 3	*Ampelisca*	*Lumbrineries* (16.5 %)
13**	FED 7, 10, 11, 14	*Ampelisca*	*Ampelisca* (13.93 %)
14**	FED 4, 5, 13, 15, 16	*Ampelisca-Nucula*	*Ampelisca* (11.02 %)
15**	BI 37, 108	*Ampelisca*	*Ampelisca* (12.95 %)
16**	BI 23, 508, 708; FED 8, 12	*Byblis*	*Byblis* (36.81 %)
** Same genus is most abundant and most responsible for within-class similarity			

References

Brown, C., Cooper, K., Meadows, W., Limpenny, D., Rees, H., 2002. Small scale mapping of sea-bed assemblages in the eastern English Channel using sidescan sonar and remote sampling techniques. Estuarine, Coastal and Shelf Science 54, 263-278.

Brown, C.J., Collier, J.S., 2008. Mapping benthic habitat in regions of gradational substrata: An automated approach utilizing geophysical, geological, and biological relationships. Estuarine, Coastal and Shelf Science 78, 203-214

Clarke, K.R., Gorley, R.N., 2006. PRIMER v6 User Manual/Tutorial. PRIMER-E: Plymouth

Clifton, H.E., 2006, A reexamination of facies models for clastic shorelines, in. Posamentier, H.W., and Walker, R.G., eds, Facies Models Revisited: Society of Economic Paleontologists and Mineralogists, Special publication 84, p. 293-337

CONMAP (Continental Margin Mapping) Sediment Grainsize Distribution for the United States East Coast Continental Margin. U.S. Geological Survey (USGS) Coastal and Marine Geology Program, 2005. Woods Hole Science Center. Open-File Report, 2005-1001. GIS data are available online at: http://woodshole.er.usgs.gov/openfile/of2005-1001/htmldocs/datacatalog.htm

Derous, S., Verfaillie, E., Van Lancker, V., Courtens, W., Stienen, E.W.M., Hostens K., Moulaert I., Hillewaert H., Mees J., Deneudt K., Deckers P., Cuvelier D., Vincx M., Degraer S., 2007. A biological valuation map for the Belgian part of the North Sea: BWZee, Final report, Research in the framework of the BELSPO programme "Global chance, ecosystems ans biodiversity" – SPSD II, March 2007, pp. 99

Diaz, R., Solan, M., Valente, R., 2004. A review of approaches for classifying benthic habitats and evaluating habitat quality. Journal of Environmental Management 73, 165-181.

Eastwood, P., Souissi, S., Rogers, S., Coggan, R., Brown, C., 2006. Mapping seabed assemblages using comparative top-down and bottom-up classification approaches. Canadian Journal of Fisheries and Aquatic Sciences 63, 1536-1548.

Ellingsen, K.E., 2002. Soft-sediment benthic biodiversity on the continental shelf in relation to environmental variability. Marine Ecology Progress Series 232, 15-27.

Elliot, M., 1994. The analysis of macrobenthic community data. Marine Pollution Bulletin 28, 62-64.

Environmental Monitoring and Assessment Program (EMAP), National Coastal Assessment Database, Northeast Region, 2000-2002. U.S. Environmental Protection Agency. Dataset names: Benthic Replicate Abundance, Benthic Grab Information by Replicate, Benthic Summary Data by Station. Data catalog authors: J. Kiddon and H. Buffman. Data available online at: http://www.epa.gov/emap/nca/html/data/

Foster-Smith, R., Connor, D., Davies, J. 2007. What is habitat mapping? In: MESH Guide to Habitat Mapping, MESH Project, 2007, JNCC, Peterborough. Available online at: (http://www.searchmesh.net/default.aspx?page=1900, Last accessed 6/1/10.

Goff, J.A., Olson, H.C., Duncan, C.S., 2000. Correlation of side-scan backscatter intensity with grain-size distribution of shelf sediments, New Jersey margin. Geo-Marine Letters 20, 43-49

Gray, J., 1974. Animal-sediment relationships. Oceanography and Marine Biology: An Annual Review 12, 223-262.

Gray, J.S., Clarke, K.R., Warwick, R.M., Hobbs, G., 1990. Detection of initial effects of pollution on marine benthos: an example from the Ekofisk and Eldfish oilfields, North Sea. Marine Ecology Press Series 66, 285-299

Greene, H., Yoklavich, M., Starr, R., O'Connell, V., Wakefield, W., Sullivan, D., McCrea, J., Cailliet, G., 1999. A classification scheme for deepwater habitats. Oceanologica acta 22, 663-678.

Hewitt, J., Thrush, S., Legendre, P., Funnell, G., Ellis, J., Morrison, M., 2004. Mapping of marine soft-sediment communities: Integrated sampling for ecological interpretation. Ecological Applications 14, 1203-1216.

ICES, 2006. Report on the working group on marine habitat mapping (WGMHM). April 4-7, 2006, Galway, Ireland. ICES CM 2006/MHC:05 Ref. FTC, ACE. 132 pp.

ICES, 2007. Acoustic seabed classificationof marine physical and biological landscapes. ICES Cooperative Research Report No. 286, 183 pp.

IOPTF (Interagency Ocean Policy Task Force), 2009. Draft interim framework for effective coastal and marine spatial planning. White House Council on Environmental Quality, Washington DC, 35 pp.

Kendall, M.S., Olaf, P.J., Alexander, C., Field, D., McFall, G., Bohne, R., Monaco, M.E., 2005. Benthic mapping using sonar, video transects, and an innovative approach to accuracy assessment: A characterization of bottom features in the Georgia Bight. Journal of Coastal Research 21(6), 1154-1165.

Kenny, A., Cato, I., Desprez, M., Fader, G., Schuttenhelm, R., Side, J., 2003. An overview of seabed-mapping technologies in the context of marine habitat classification. ICES Journal of Marine Science 60, 411-418.

Komar, P. D., 1976, Beach Processes and Sedimentation. Prentice-Hall, Inc., Englewood Cliffs. 429 p.

Kostylev, V., Todd, B., Fader, G., Courtney, R., Cameron, G., Pickrill, R. 2001. Benthic habitat mapping on the Scotian Shelf based on multibeam bathymetry, surficial geology and sea floor photographs. Marine Ecology Progress Series 219, 121-137.

Madden, C., Goodin, K., Allee, R., Cicchetti, G., Moses, C., Finkbeiner, M., Soule, J., King, J., Shumchenia, E., 2010. Coastal and marine ecological classification standard. NOAA and NatureServe, 149 pp.

McArthur, M., Brooke, B., Przeslawski, R., Ryan, D., Lucieer, V., Nichol, S., McCallum, A., Mellin, C., Cresswell, I., Radke, L., 2010. On the use of abiotic surrogates to describe marine benthic biodiversity. Estuarine, Coastal and Shelf Science 88, 21-32.

McBreen, F., Wilson, J., Mackie, A., Aonghusa, C., 2008. Seabed mapping in the southern Irish Sea: predicting benthic biological communities based on sediment characteristics. Hydrobiologia 606, 93-103.

McMaster, R. L., 1960. Sediments of the Narragansett Bay system and Rhode Island Sound, Rhode Island. Journal of Sedimentary Petrology, vol. 30., no 2., pp. 249-274.

McMaster, R. L., and Ashraf, A., 1973, Subbottom Basement Drainage System of Inner Continental Shelf off Southern New England: Geological Society of America Bulletin, v. 84, no. 1, p. 187-190.

McMullen, K. Y., L. J. Poppe, E. R. Twomey, W.W. Danforth, T. A. Haupt, and J. A. Crocker, 2007. Sidescan-sonar imagery and surficial geologic interpretations of the sea floor in Rhode Island Sound, off Sakonnet Point, Rhode Island, 2007. U.S. Geological Survey Open-File Report 2007-1150. Report and data available online at: http://woodshole.er.usgs.gov/pubs/of2007-1150/index.html

McMullen, K. Y., L. J. Poppe, T. A. Haupt, and J. M. Crocker, 2008. Sidescan-sonar imagery and surficial geologic interpretations of the sea floor in central Rhode Island Sound. U.S. Geological Survey Open-File Report 2007-1366. Report and data available online at: http://woodshole.er.usgs.gov/pubs/of2007-1366/

McMullen, K. Y., L. J. Poppe, T. A. Haupt, and J. M. Crocker, 2009. Sidescan-sonar imagery and surficial geologic interpretations of the sea floor in western Rhode Island Sound. U.S. Geological Survey Open-File Report 2008-1181. Report and data available online at: http://woodshole.er.usgs.gov/pubs/of2008-1181/index.html

Needell, S. W., O'Hara, C. J., and Knebel, H. J., 1983, Maps showing geology and shallow structure of western Rhode Island Sound, Rhode Island: U.S. Geological Survey Miscellaneous Field Studies Map MF-1537, scale 1:125,000.

Needell, S. W., and Lewis, R. S., 1984, Geology and structure of Block Island Sound, Rhode Island and New York: , Miscellaneous Field Studies Map - U. S. Geological Survey, MF-1621 (4 Sheets), scale 1:125,000.

NOAA CSC (National Oceanic and Atmospheric Administration Coastal Services Center), 2010. Benthic habitat mapping: What is benthic habitat? http://www.csc.noaa.gov/benthic/start/what.htm, Last accessed 6/1/10.

O'Hara, C. J., and Oldale, R. N., 1980, Maps showing geology and shallow structure of eastern Rhode Island Sound and Vineyard Sound, Massachusetts: Miscellaneous Field Studies Map- U.S. Geological Survey, Report: MF-1186, scale 1:125,000.

Pratt, S.D. 1973. Benthic Fauna. In: Coastal and offshore environmental inventory: Cape Hatteras to Nantucket Shoals. Marine Publication Series No. 2, University of Rhode Island, pp. 5.1-5.70.

Rhoads, D., 1974. Organism-sediment relations on the muddy sea floor. Oceanography and Marine Biology: An Annual Review 12, 200-263.

Rooper, C., Zimmermann, M., 2007. A bottom-up methodology for integrating underwater video and acoustic mapping for seafloor substrate classification. Continental Shelf Research 27, 947-957.

Rosenzweig, M.L., 1995. Species diversity in space and time. Cambridge University Press, Cambridge

Schafer, J. P., and Hartshorn, J., 1965, The Quaternary of New England, *in* Frey, J. W. a. D., ed., The quaternary of the United States: Princeton, N.J., Princeton University Press, p. 113-127.

Shumchenia, E., and King, J. In review. Comparison of methods for integrating biological and physical data for marine habitat mapping and classification. Continental Shelf Research.

Sirkin, L. A., 1982, Wisconsinan glaciation of Long Island, New York to Block Island, Rhode Island, *in* Larson, G. J., and Stone, B. D., eds., Late Wisconsinan glaciation of New England: Dubugue, IA, Kendall/Hunt, p. 35-60.

Snelgrove, P., Butman, C., 1994. Animal-sediment relationships revisited: cause versus effect. Oceanography and Marine Biology: An Annual Review 32, 111-177.

Snelgrove, P.V.R., 1998. The biodiversity of macrofaunal organisms in marine sediments. Biodiversity and Conservation 7, 1123-1132

Solan, M., Germano, J., Rhoads, D., Smith, C., Michaud, E., Parry, D., Wenzhafer, F., Kennedy, R., Henriques, C., Battle, E., Carey, D., Iocco, L., Valente, R., Watson, J., Rosenberg, R., 2003. Towards a greater understanding of pattern, scale and process in marine benthic systems: a picture is worth a thousand worms. Journal of Experimental Marine Biology and Ecology 285/286, 313-338.

Steimle, F.W., 1982. The benthic macroinvertebrates of the Block Island Sound. Estuarine, Coastal and Shelf Science 15, 1-16

Stone, B. D., and Borns jr., H., 1986, Pleistocene glacial and interglacial stratigraphy of New England, Long Island and adjacent Georges Bank and Gluf of Maine, *in* V. Sibrava, D. Q. B. a. G. M. R., ed., Quaternary glaciations in the Northern Hemispher: New York, Pergamon, p. 39-52.

Stone, B.D., and Sirkin, L.A., 1996, The Geology of Block Island, *in* Johnston, H.E. and Veeger, A., eds. The water resources of Block Island, Rhode Island: U.S. Geological Survey Water Resources Bulletin 94-4096

Valesini, F.J., Hourston, M., Wildsmith, M.D., Coen, N.J., Potter, I.C., 2010. New quantitative approaches for classifying and predicting local-scale habitats in estuaries. Estuarine, Coastal and Shelf Science 86, 645-664.

Van Lancker, V. and Foster-Smith, R. 2007. How do I make a map? In: MESH Guide to Habitat Mapping, MESH Project, 2007, JNCC, Peterborough. Available online at: (http://www.searchmesh.net/default.aspx?page=1900), Last accessed 6/1/10.

Verfaillie, E., Degraer, S., Schelfault, K., Willems, W., Van Lancker, V., 2009. A protocol for classifying ecologically relevant marine zones, a statistical approach. Estuarine, Coastal and Shelf Science 83, 175-185.

Warwick, R.M., Clarke, K.R., 1991. A comparison of some methods for analyzing changes in benthic community structure. Journal of the Marine Biological Association of the United Kingdom 71, 225-244

U.S. Geological Survey, (Poppe, L. J., S.J. Williams, V. F. Paskevich) , 2005. East Coast Sediment Texture Database: Procedures, Database, and GIS. . USGS Open-File report 2005-1001. U.S.G.S. Coastal and Marine Geology Program, Woods Hole Science Center, Woods Hole, MA. Data available online at: http://pubs.usgs.gov/of/2005/1001/htmldocs/datacatalog.htm

usSEABED (U.S. Geological Survey, University of Colorado), 2005. Data available online at: http://coastalmap.marine.usgs.gov/regional/contusa/eastcoast/atlanticcoast/data.html.

Warwick, R.M., Clarke, K.R., 1993. Comparing the severity of disturbance: a meta-analysis of marine macrobenthic community data. Marine Ecology Press Series 92, 221-231

SECTION II: SUBSURFACE GEOLOGY

II.1 Introduction

The goal of the subsurface geology studies as to determine if the subbottom sediments were unconsolidated and thick enough to readily install structures by pile-driving. We used a high resolution sonar to characterize the subsurface geology of the study area. We interpreted the depth to a hard subsurface lithology only, and did not examine the details of the overlying soft sediments.

II.2 Background

Prior studies by McMaster, *et al*., 1968, and a series of U.S. Geological Survey surveys (McMullen, *et al*., Needell and Lewis, 1984, Poppe, *et al*., 2002) provide good coarse-resolution coverage of the northern part of the SAMP area, and very limited coverage of the southern part of the SAMP area. The trackline coverage of the these surveys is shown in Figure II-1. Additional information and interpretation from the USGS surveys, as well as a significant number of GIS datalayers, are available online through a series of digital data releases and Open File reports. Online addresses are included with the references. The McMaster, *et. al.* (1968) data is not available in digital format

II.3 Methods

Sub-bottom seismic data were obtained with a 400-Hz bubble pulser towed profiling system along GPS-navigated survey lines. The target vessel speed was 4 kts with a shotpoint interval of 0.25 s, which resulted in an along-track shotpoint interval of 0.5 m with a maximum seismic penetration of 200 m (assuming 1600 m/s seismic velocity of sediments). A digital sampling interval of 100 ms along individual traces results in a 2 mm vertical sampling interval.

Seismic data were collected in two primary survey areas (Fig. 2): 1) Block Island, along the southern half of the island extending from the shoreline out to 5-10 km offshore, and 2) Federal Area, southwest of Martha's Vineyard in an 8 km x 18 km rectangular region surrounding the WHOI buoy field. The Block Island seismic data were collected on several cruises aboard the 28' R/V McMaster during July (14th, 15th and 29th) and August (6th) of 2009.

Typical spacing between adjacent lines was about 0.5-1 km with more widely spaced crossing tie lines. The seismic data from the Federal Area were collected aboard the R/V Endeavor during cruise EN468 from September 17 to September 25, 2009. Seismic operations were limited by daylight and weather conditions during the latter cruise; so seismic trackline spacing is more variable (0.5-3 km) in this region.

Post-processing of the sub-bottom seismic data involved two steps: band-pass filtering and time-dependant normalization. A band-pass filter was applied to each seismic line with a low-cut frequency of 300-400 Hz and a high-cut frequency of 1000-2000 Hz. The band-pass frequency ranges were chosen qualitatively from a matrix of seismic panels with incremental variations in frequencies. The time-dependant normalization was achieved with automatic gain control with a window length of 50-100 ms and a gain of 1-1.5 dB. As with the band-pass filtering, the automatic gain control parameters were chosen based on a matrix of varying window length and gain.

II.4 Results

Representative examples of interpreted processed seismic data from each region are shown in Figure 3 and 4. A sediment thickness map of the Federal Area was generated by digitizing the sediment-water interface and the deepest visible reflection in the processed seismic data (Figure 5). The along-track location of each reflector was digitized at least every 200 m and wherever significant changes in reflector depth occurred. Linearly interpolated and geo-referenced seismic horizons were then generated with SonarWeb software from which sediment thickness estimates at each shot-point were calculated. These geo-referenced sediment thickness estimates were used as input in contouring and two-dimensional surface-fitting algorithms from Generic Mapping Tool to create sediment isopach maps. It should be noted that these sediment thickness estimates and associated isopach maps represent minimum sediment thicknesses; there likely exists deeper sediment/sediment or sediment/basement interfaces.

II.5 Discussion

The comparison of sediment isopach maps from previous USGS surveys and our recent survey in the Federal Area provides several useful observations. First, in the eastern half of the survey area, the sediment thickness estimates from both surveys are very similar and indicate sediment thicknesses in excess of 100 m. These thicker sediments correlate to darker regions in

the sidescan data and appear to represent two southward-merging buried valleys. The brighter regions in the side-scan data are associated with thinner sediments (< 20 m). Second, in the central portion of the survey area, both sets of seismic data identify a NW-SE trending ridge buried by a thinner sediment layer (< 20 m). Finally, in the westernmost portion of the survey area, both surveys indicate increased sediment thickness; however, the sediment is significantly thicker in the USGS survey data. The most likely reason for the difference is the inability of our recent data to resolve the deeper seismic reflections; the closely spaced seismic lines in the recent data do not have crossing tie-lines and the sea state was significantly degraded during the collection of these survey lines. Therefore, the interpretation from the USGS study is likely to be more representative of the region. It is also interesting to note that a correlation between sediment thickness and side-scan reflectivity does not exist in the western half of the survey area, so side-scan reflectivity alone may not be appropriate to infer relative sediment thickness.

The subsurface geology can be interpreted in terms of effort required to install wind turbines. Ease of construction is based on the technology needed to install wind turbines in areas with specific subbottom types. Subbottom sediment types that are unconsolidated and thick enough to allow pile-driving as the installation technology are rated between 1 and 3, with 1 being the easiest. Any lithology that would require drilling for installation of piles would be rated greater than 3. For example, Figure II-6 shows interpreted construction efforts within the BI study area.

II.6 Conclusions

The subsurface geology studies allow us to identify areas that would be suitable for the installation of foundation structures by pile-driving. It is apparent from Figure II-6 that most areas located to the south of Block Island are suitable for installation of piles by pile-driving including the site proposed by DeepWater Wind shown by the yellow dots (representing borehole locations).

Our studies of the FED indicate that there are also suitable locations in the central to western part of the survey area for installation of piles by pile-driving.

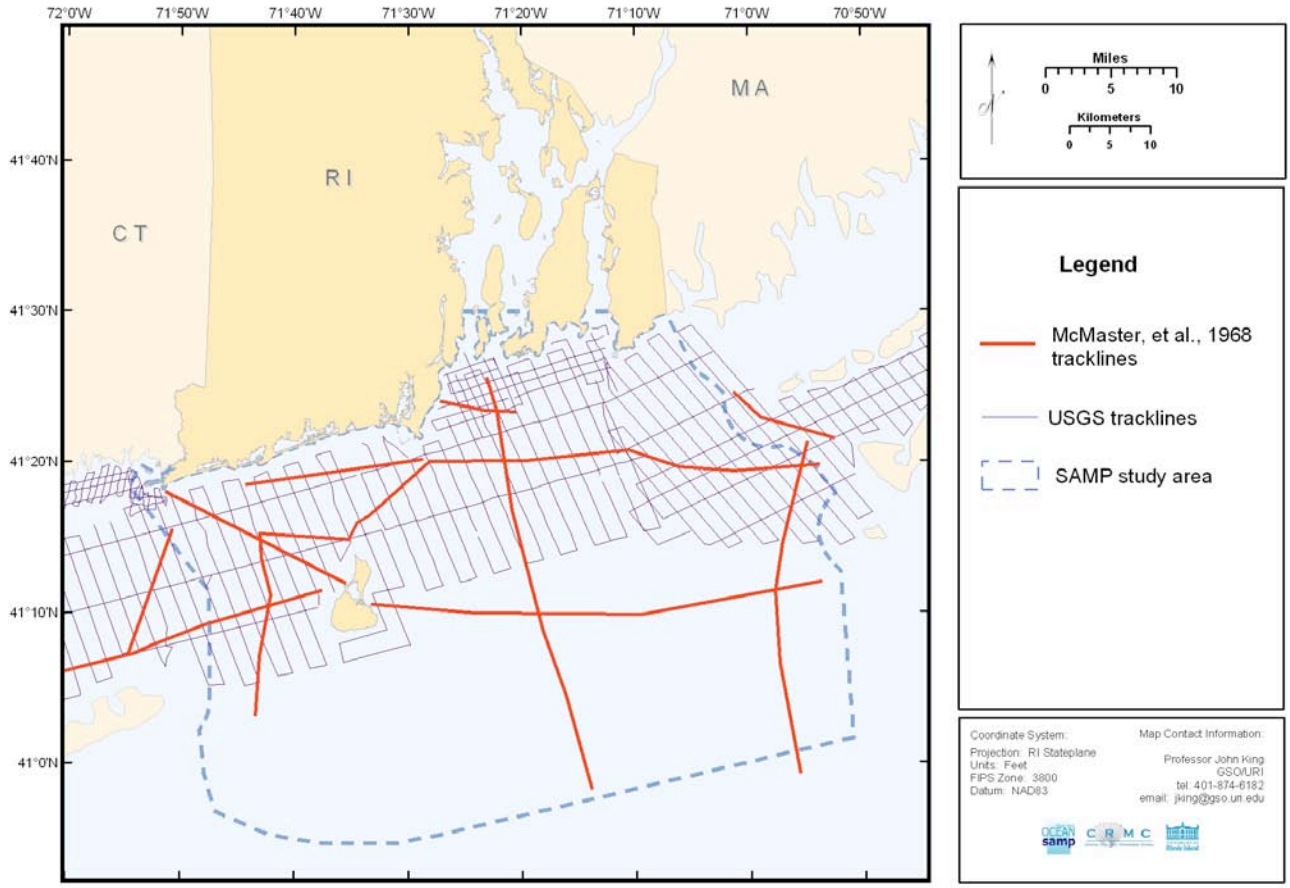

Figure II-1. Map showing locations of previous subbottom surveys within the SAMP area.

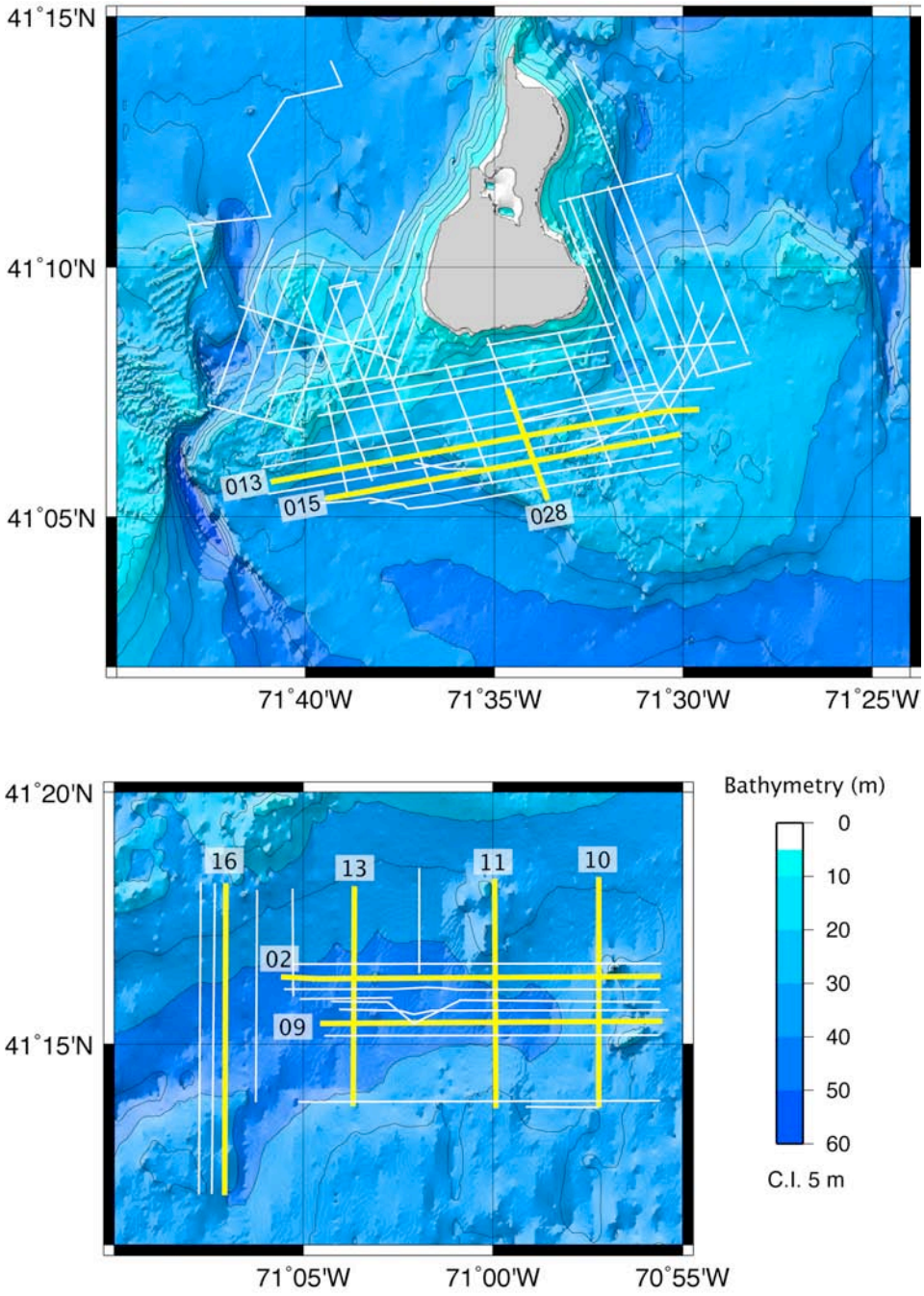

Figure II-2. Sub-bottom seismic tracklines (white lines) superimposed on bathymetry (http://www.ngdc.noaa.gov/mgg/coastal/crm.html) for the Block Island (top) and the Federal (bottom) survey areas. The yellow lines identify the location of seismic sections shown Figures 3 and 4.

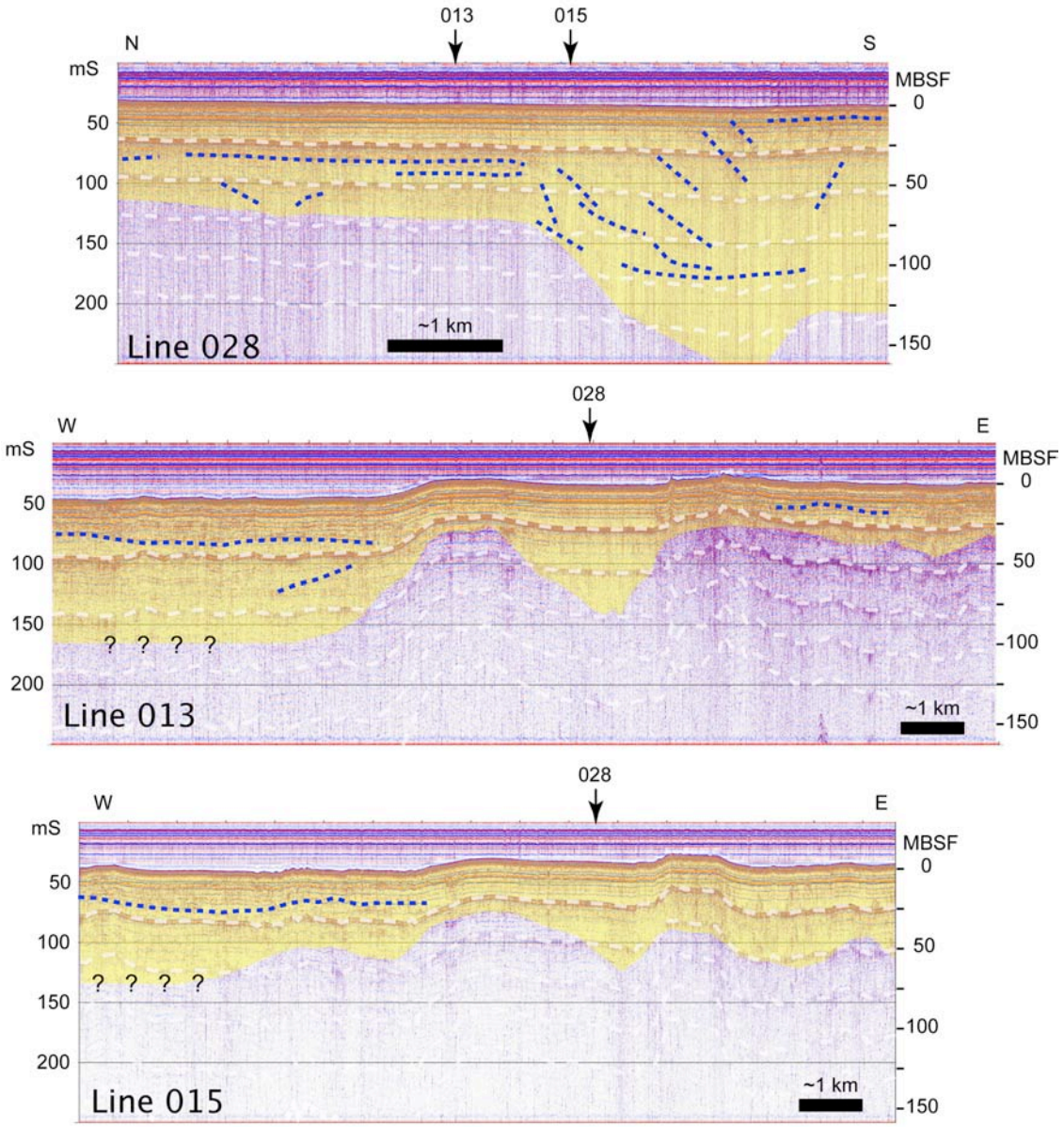

Figure II-3. Processed seismic cross-sections of selected lines from Block Island survey area (see Fig 2, top) with sub-bottom interpretations. The yellow regions correspond to the sediment-water interface at the top and the deepest visible reflection at the bottom. The questions marks indicate sections of the seismic record where our identified deepest reflector extends below the resolvable depth limit. Multiple reflections of the sediment-water interface (white dashed lines) and internal reflectors (blue dashed lines) within the identified sediment package are indicated. The location of crossing lines are indicate with arrows and appropriate line number. The vertical axis of the section is plotted as two-way travel time (milliseconds) and thickness of the sediment section (MBSF, meters below seafloor), assuming a seismic velocity of 1500 m/s.

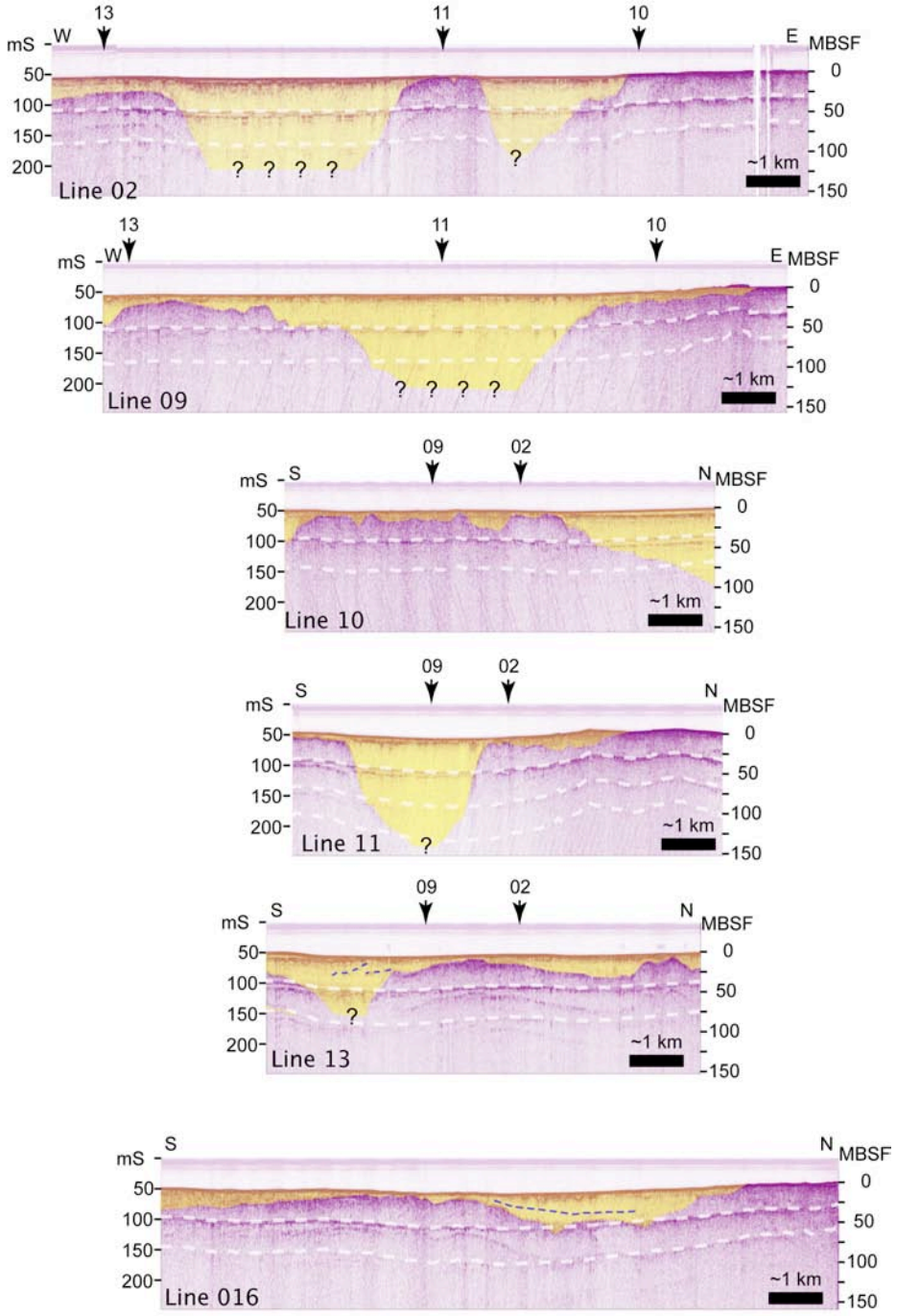

Figure II-4. Processed seismic cross-sections of selected lines from Federal survey area (see Fig 2, bottom) with sub-bottom interpretations. Axes labels and highlighted attributes are the same as in Figure 3.

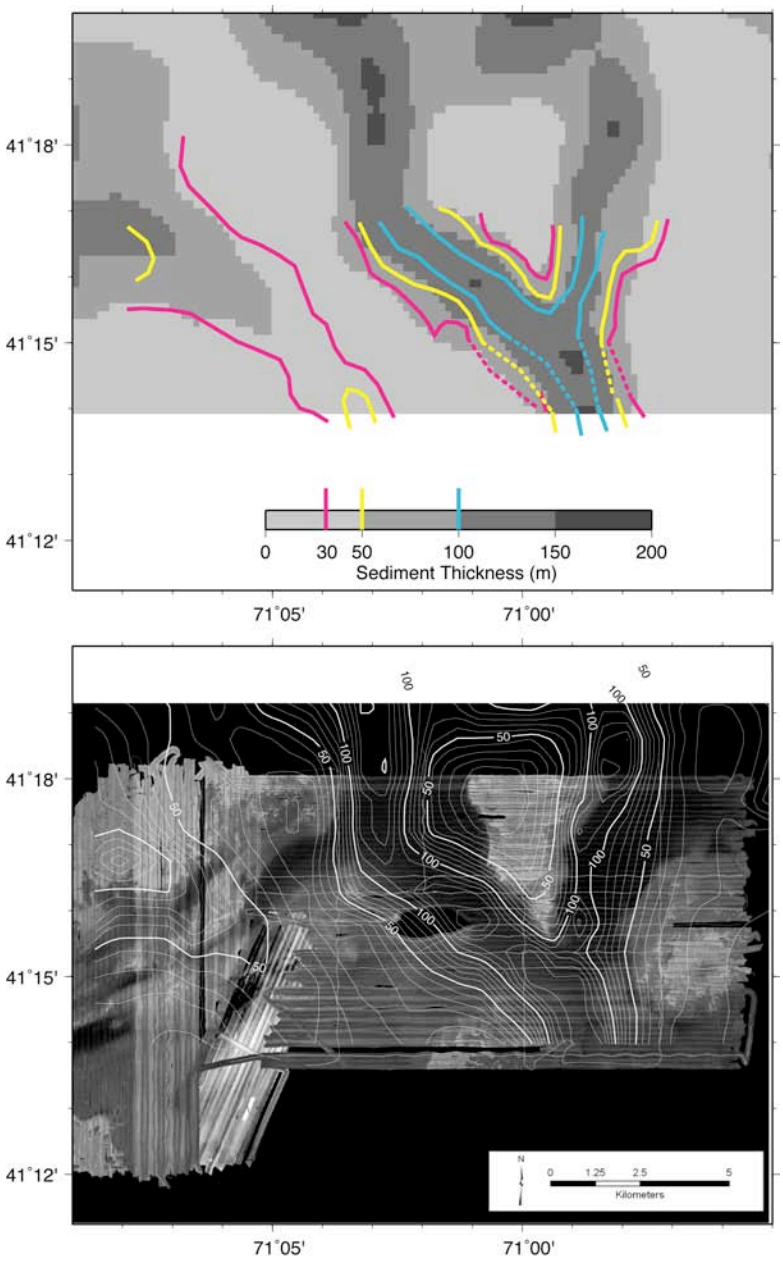

Figure II-5. (top) Sediment isopach of the Federal survey area comparing our sediment thickness estimates (colored contours) with a previous study (gray shading) by O'Hara, [1980]. (bottom) Sediment thickness contours from the O'Hara study are overlain on side-scan reflectivity.

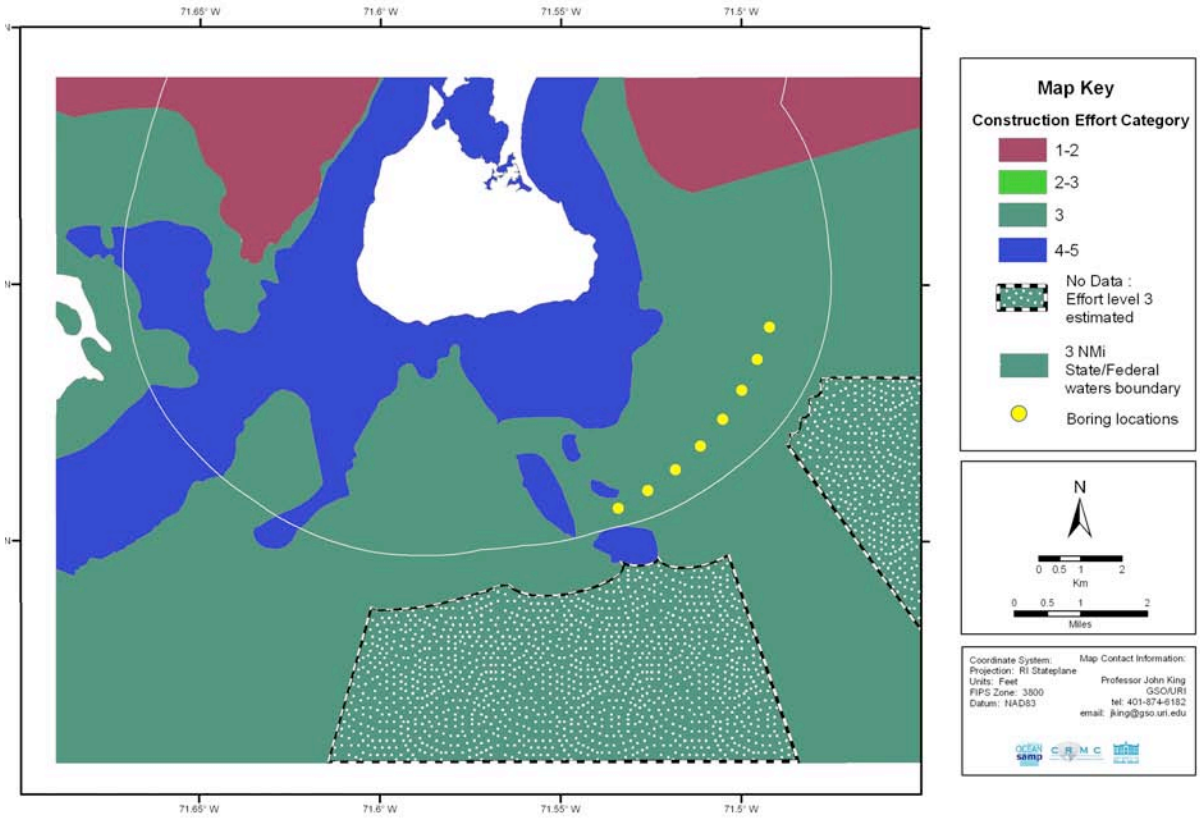

Figure II-6. Map showing ease of construction for wind turbines in the BI study area.

II.7 References

McMaster, R., L., R. P. Lachance, and L. E. Garrison, 1968. Seismic-reflection studies in Block Island and Rhode Island Sounds. *The American Association of Petroleum Geologists Bulletin*, 52:3, 465-474.

McMullen, K. Y., L. J. Poppe, and N. K. Soderberg, 2009. Digital seismic-reflection data from western Rhode Island Sound, 1980. *U.S. Geological Survey Open-File Report 2009-1002*. Report and data available online at: http://pubs.usgs.gov/of/2009/1002/index.html

Needell, S. W., and Lewis, R. S., 1984. Geology of Block Island sound, Rhode Island and New York. Geological framework data from Long Island Sound, 1981-1990 - A digital data release. *U.S. Geological Survey Open-File Report 02-002*

O'Hara, C.J., 1980, High-resolution seismic-reflection profiling data from the Inner Continental Shelf of southeastern Massachusetts: *U.S. Geological Survey Open-File Report 80-178.*

Poppe, L. J., V. F. Paskevich, R. S. Lewis, and M. L. DiGiacomo-Cohen, 2002. Geological Framework Data from Long Island Sound, 1981-1990: A Digital Data Release. *U.S. Geological Survey Open-File Report 02-002*. Report and data available online at: http://woodshole.er.usgs.gov/openfile/of02-002/index.htm

5.

Investigations into Block Island's Submerged Cultural Sites and Landscapes

for the Rhode Island Ocean Special Area Management Plan 2010

by

Rod Mather and John Jensen

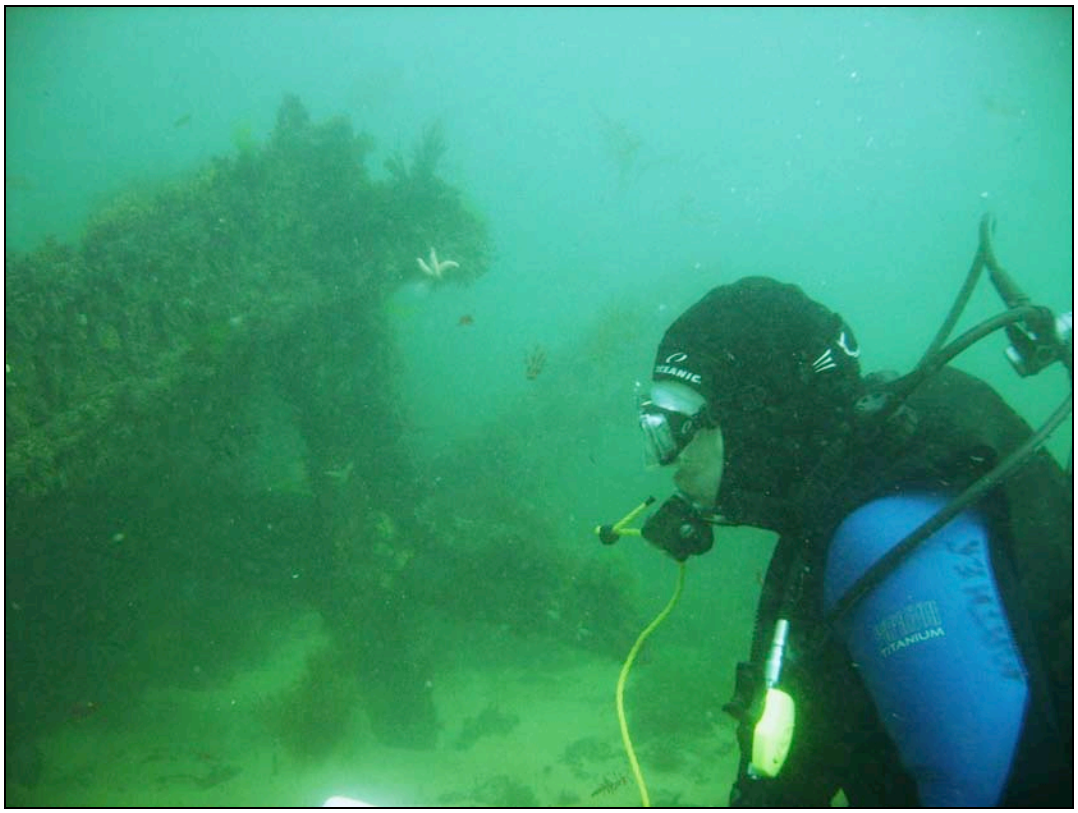

University of Rhode Island, June, 20, 2010

Executive Summary

This report describes the cultural heritage research conducted to support the development of the Rhode Island Ocean Special Area Management Plan. The principle focus in this report is the state waters surrounding the southern end of Block Island that include the likely sites for Rhode Island first off shore renewable energy wind towers. While the research presented here was conducted under the umbrella of geophysical survey and mapping, the research design also incorporated archaeological survey and reconnaissance, and historical research that included a substantial secondary literature review and selected investigations of published and digitally available primary sources and archival research.

The project represents Rhode Island's first application of cultural landscape-based approach to the study and management of its marine cultural heritage. The cultural landscape approach recognizes that places and cultural heritage resources can have different or multiple meanings and levels of significance based on how people from different cultures, times, or backgrounds have interacted with the landscape. Adopting this broader pluralistic approach increases the likelihood that significant cultural heritage resources will be found *and* recognized.

The larger Ocean SAMP cultural heritage project identified several potential cultural landscape contexts. Among these contexts, two-fisheries and energy-have special significance for the study area. Fishing has taken place for millennia in this area and has exercised considerable direct effects on marine ecosystems and more recently on the content and condition of marine archaeological resources in Rhode Island waters. This report underscores the historical and cultural significance of fishing and identifies this landscape and its associated properties as particularly vulnerable to human impacts.

The quest for safe, reliable, and economical energy supplies has driven the Ocean SAMP process. This project revealed that energy has exercised dramatic and long-term effects on the local environment and on the composition of its archaeological landscapes. Historic shipwrecks associated with energy dominate in these waters. The drive to supply energy in industrial quantities to New England after 1850, led to hundreds of thousands of voyages through Rhode Island's outer waters and to the wrecking of many vessels. The report concludes that while posing potential threats to specific underwater resources, offshore renewable energy does not represent a completely new cultural landscape; rather it should be understand a part of this longer-term process of supplying New England domestic and industrial power.

Table of Contents

List of Figures

List of Tables

Abstract

This report describes the cultural heritage research conducted by the University of Rhode Island in support of the Ocean Special Area Management Plan. This aspect of the project focused on the Rhode Island state waters adjacent to the Southern end of Block Island. The project revealed the presence of a rich and dynamic array of cultural heritage resources in the study area. This report highlights the cultural landscape approach, offers guidelines for applying federal historic preservation criteria to marine landscapes, and identifies specific landscape contexts and archaeological resources. The report also highlights the particular influence and resources associated with fisheries and energy as well as the long-term influence of military and conflict in shaping marine cultural heritage resources in Rhode Island.

1 Introduction

Rhode Island has an important maritime history inextricably linked to exploration, colonization, trade, shipbuilding, commerce, warfare, transportation, fishing and recreation. Almost four centuries of intense maritime activities in the region have left a rich repository shipwrecks and other cultural material in local waters. These resources contain vital and highly significant information about our nautical past, and are protected by a variety of state and federal laws and regulations. The presence of historically and archaeologically significant shipwrecks can affect development projects and is important to marine spatial planning.

Despite the undoubted abundance of cultural material in regional waters, the historical and archaeological significance of these resources, and the protection afforded to them by federal and state law, our understanding of the resources is limited. Historic property resource managers and marine spatial planners need a combination of survey work, historical research, on-site investigations and a theoretical approach that contributes in significant ways to our understanding of cultural resources in Rhode Island waters and facilitates planning, protection and development.

2 Background - Cultural Landscapes as an Approach to Analyzing Heritage Resources

In Rhode Island, thousands of years of use of the ocean and its resources have resulted in rich and diverse array range of cultural resources underwater and in the coastal zone. These resources provide cultural, educational, recreational, environmental, and economic services that humans want and need. They are among the broader package of ecosystem services provided by area encompassed within the Ocean SAMP. Submerged archaeological sites and landscapes are non renewable—once gone they cannot be restored. The significance, sensitivity, and non-renewable nature of cultural and historic resources and the special services they provide make them a challenging and important aspect of the Ocean SAMP process.

Throughout the United States federal and states agencies, tribes, and the private sector are working to integrate cultural and heritage resources into Marine Spatial Planning. This challenging task is required under federal and state laws and is consistent with the tenants of Ecosystem Based Management as practiced in Rhode Island. While appropriate historic preservation tools exist to support marine spatial planning, most were developed to address terrestrial scales, environments, and issues. The natural environment, property types, and the large geographic scale of ocean spaces require that some land-based tools and methods be adapted and new ones incorporated to achieve effective Marine Spatial Planning. Employing a cultural landscaping is one such method.

Whether characterized by historians, archaeologists, or cultural practitioners as districts, sites, buildings, objects, or landscapes, cultural heritage resources reflect millennia of human use of Block Island's marine and coastal environment. Submerged pre-contact tribal landscapes and historic shipwrecks, two of the most significant categories of cultural heritage, have no direct parallels on land and have the greatest untapped potential to add substantial knowledge about

human activity on Block Island and surrounding waters (Little Red Book Section 220 B1). Cultural heritage contains ecological as well as cultural and historical information, and many resources have become integrated into marine ecosystems as habitat or as parts of the benthic environment. The cultural landscape approach directly recognizes dynamic relationships between nature and culture and allows for the inclusion of ecological significance in study and management.

The integration or blending of submerged cultural heritage resources and the natural environment make identifying many of these resources challenging. Covered by sediments or disguised by the rocks and boulders many of archaeological resources in the Area are difficult to discern with or without specialized instrumentation. Their lack of visibility protects them from looting, but leaves them vulnerable to unintentional damage through human activities such as recreational boating, fishing, and construction. Larger modern shipwrecks are visible and many of them are important recreational and well as cultural heritage resources. Easily identified cultural heritage resources are vulnerable to looting by divers—a serious problem in the New England region.

Marine Spatial Planning for cultural resource requires a comprehensive understanding of the ocean landscape and its historic uses. The Rhode Island Historical Preservation and Heritage Commission employs a predictive model in evaluating the potential impact of projects on archaeological sites on land in the coastal zone. Unfortunately, this model applies only to Native American sites, and not the historic cultural heritage resources that represent the majority of underwater cultural heritage. A pressing need exists to develop comparable tools including a complete sensitivity analysis in order to protect underwater cultural heritage in Rhode Island. The intensive work undertaken to survey and evaluate cultural heritage resources using cultural landscapes off the southern end of Block Island by SAMP investigators represents an initial step in developing the necessary tools.

2.1 Understanding Cultural Landscapes

Shipwrecks and other cultural materials deposited on the bottomlands and along the shore can be mapped and evaluated as a series of cultural landscapes that reflect distinct (though often overlapping) historical contexts and cultural orientations (Anschuetz et. al., citing Binford, 1983, 380). Cultural landscapes contain both material and symbolic elements, but key for archaeologists, historians, and preservationists is that cultural landscapes reflect patterned human behavior that one can analyze, interpret and preserve. The study of maritime cultural landscapes has great potential for yielding archaeological, historical, and cultural information about the study area and the places adjacent to it. Depending upon the question or resource type being considered, applying the landscape framework can encompass and, when required transcend, political, ethnic, geographic, and cultural boundaries and contribute to a more holistic management regime (C. Cameron and M. Rossler, "Global Strategy: Canals and Cultural Routes," *World Heritage Newsletter* 8 (1995)). Applying the cultural landscape framework to the Area's submerged cultural resources leads to the asking of historical and anthropological questions that encompass and transcend state and local boundaries. This will allow the significance of cultural heritage resources of the study area to be evaluated in light of regional, national and international processes (C. Cameron and M. Rossler, "Global Strategy: Canals and Cultural Routes," *World Heritage Newsletter* 8 (1995).

Although tied to quantifiable material cultural such as shipwrecks, marine-related objects, and patterns of geographical dispersion, the cultural landscape framework encourages the asking of

broader theoretical questions. For example, how did the early Indian or European explorers "see" and experience these waters and surrounding landforms? How did their Block Islanders perceptions of the local marine environment influence the design of the watercraft they built and the ways in which they operated them? In what ways did the industrialization of New England during 19th century affect the natural environment and the composition of its maritime archaeological resources? In what ways did changes in the organization and technologies of fishing effect marine environments and local communities? Did specific ethnic or cultural identities affect maritime or environmental strategies or behaviors? Carefully designed archaeological projects examining Rhode Islands shipwrecks and associated cultural materials can help to answer these and other broad questions, but only when isolated events and individual sites are approached through an integrating paradigm such as the cultural landscape (G. Fry, "From Objects to Landscapes In Natural and Cultural Heritage Management: A Role for Landscape Interfaces," in H. Palang and G. Fry, eds., *Landscape Interfaces: Cultural Heritage in Changing Landscapes* (Boston: Kluwer Academic Publishers, 2001 240).

The southern Block Island sector of the SAMP area has known shipwrecks with associated with military, commercial shipping, energy, and fisheries landscapes, most dating from the nineteenth and twentieth centuries. Much older highly shipwrecks associated with exploration, early fishing, and commerce almost certainly exist, but have are not documented in historical records. In a similar vein, local builders produced uncounted numbers of small vernacular craft including fishing boats that escaped historical documentation. Further removed in time, pre-contact Indian landscapes existed and may still survive in some form and the area. With or without the presence of material culture these submerged landscapes retain meaning for Rhode Island's Indian people. Without careful evaluation at the landscape level, proposed and current economic activities in the SAMP Study Area pose serious threats to these important but often undocumented resources.

Defining an archaeological resource as part of a cultural landscape does not enforce a hegemonic, theoretical or cultural valuation. As Anschuetz et. al., note on the application of cultural landscapes to archaeology, "a landscape paradigm offers the potential to accommodate, if not integrate, different theoretical perspectives even while these constructs seemingly exist in tension with one another in their presentation of alternative constructions of the past"(Anschuetz, et. al., 20). Employing a cultural landscape framework allows for the documenting and preservation of historical and archaeological resources while leaving open the interpretation of significance to multiple cultural and theoretical perspectives (C. Howett, "Integrity as a Value in Cultural Landscape Preservation," in *Preserving Cultural Landscapes in America*. A.R. Alanen and R.Z. Melnick, eds., (Baltimore: The Johns Hopkins University Press, 2000, p. 206-7).

As the editors of the recent volume *Preserving Cultural Landscapes in America* noted "the vast majority of cultural landscapes . . . generally evolve unintentionally and represent multiple layers of time and cultural activity" (A.R. Alanen and R.Z. Melnick, "Why Cultural Landscape Preservation," in Alanen and Melnick, eds., 2000, 5). Cultural landscapes are discrete physical places, and a way of organizing and analyzing the relationship between culture and nature wherever the two intersect and leave a material or cultural imprint on the land. Off the southern end of Block Island as elsewhere, culture landscapes are largely unintentional products of human activity. Layered by time and shifts in human behavior, cultural landscapes represent changing relationships between humankind and the environment, as well as major historical or cultural events or processes.

2.2 The National Register of Historic Places and Maritime Cultural Landscapes

Beyond their usefulness in interpreting cultural heritage, cultural landscapes are a property type recognized by the National Register of Historic Places. The National Park Service sets the criteria for the Register and defines a cultural landscape as "a geographical area, including both natural and cultural resources, associated with a historic event, activity, or person" (D. Egan, "Defining Cultural and Ethnographic Landscapes: A Primer for Understanding National Park Service Cultural Resource Management Terminology," Ecological Restoration 21 (2003), 259). NPS recognizes four categories of cultural landscapes, among these are included." Historic vernacular landscapes that "evolved through use by people whose activities or occupancy shaped the landscape. Through social or cultural attitudes on an individual, family or a community, the landscape reflects the physical, biological, and cultural character of those every day lives" (C. Birnbaum, *Preservation Brief 36. Protecting Cultural Landscapes: Planning, Treatment, and Management of Historic Landscapes*, National Park Service (1994). Vernacular landscapes exist in rural, suburban, and urban areas; however, those mostly commonly recognized by the NPS are the rural historic landscapes (Egan 2003, 259).

National Register Bulletin 30, Guidelines for Evaluating Rural Historic Landscapes defines a rural historic landscape as: "a geographical area that historically has been used by people, or shaped or modified by human activity, occupancy, or intervention, and that possess a significant concentration, linkage or continuity of areas of land use, vegetation, buildings and structures, roads and waterways, and natural features" (L.F. McClelland, J.T. Keller, G.P. Keller, and R.Z. Melnick, *How to Identify, Evaluate, and Register Rural Historic Landscapes*, *National Register Bulletin 30.* National Park Service, 1990. Hereafter referred to as *NPS Bulletin 30*). Included among the normative types of rural landscape are those associated with "maritime activities such as fishing," "transportation systems," and "migration trails."

2.3 Applying National Register Historic Landscape Characteristics to the Southern Block Island Study Area.

National Register Bulletin 30, Guidelines for Evaluating and Documenting Rural Historic Landscapes evaluates the eligibility of rural historic landscapes for the National Register using eleven categories: four land shaping processes and seven physical components visible on the land. These categories and their maritime applications are treated individually in the paragraphs that follow. Those interested in a closer examination of these characteristics are directed to *NPS Bulletin 30*.

The discussions that follow below offers guidance in applying National Register criteria for landscapes to cultural and natural resources within the Study Area. They also bring into relief the broader composition of these landscapes and offer additional examples of the Study Area's potential archaeological and historical resources.

2.4 Rural Historic Landscape Characteristics

Processes:
Land Uses and Activities
Patterns of Spatial Organization

Response to the Natural Environment
Cultural Traditions
Components:
- Circulation Networks
- Boundary Demarcations
- Vegetation Related to Land Use
- Buildings, Structures, and Objects
- Clusters
- Archaeological Sites
- Small Scale Elements

2.4.1 Land Uses and Activities

"An examination of changing and continuing land uses may lead to a general understanding of how people have interacted with their environment and provide clues about the kinds of physical features and historic properties that should be present." (NPS Bulletin 30)

Landscapes are not static; they form spaces on which cultures imprint ideas, practices, and values through alterations in the land, symbolic or spiritual valuation, and by depositing material culture. The identification of discrete patterns of material culture visible on the land may reflect continuing and changing uses, the adoption of new technologies, the influence of ethnic traditions, and other natural and cultural factors. Over the centuries in maritime Rhode Island discrete economic and ecological niches opened and closed, sometimes quite rapidly, different political or cultural groups with differing values controlled allocations of natural resources, power, or space. These discrete cultural niches or processes have left distinct signatures on the landscape and in the historic record associated with Block Island.

Southern Block Island adjacent to high traffic zones characterized in places by dangerous rocks and shoals, unpredictable currents, and a tendency dense fog, squalls, and in the winter heavy snow. Exposed the fury of the Atlantic Ocean, this high-energy environment is characterized by intermittent high seas and ever-present dangerous shores. Shipwrecks and in associated terrestrial maritime landscape features such as lighthouses, lifesaving stations, aids to navigation, and harbors of refuge all record how people thought about, used, responded to, and altered the maritime and coastal environment on or near Block Island.

2.4.2 Patterns of Spatial Organization

"The organization of land on a large scale depends upon the relationship among major physical components, predominant landforms, and natural features. Politics, economics, and technology, as well as the natural environment, have influenced the organization of communities by determining settlement patterns, proximity to markets, and the availability of transportation." (NPS Bulletin 30)

The spatial organization of the settled land reflects a combination of social and natural factors. For example, politics, major landforms, and proximity to markets influence the locations and success of communities, the development of roads, and systems of property. This extends into the study area through maritime corridors, the placement of harbors at Block Island, Point Judith, and Newport, the locations of fishing grounds. The spatial organization of the cultural

landscape also reveals the study area's place and influence in regional, national, and international maritime transportation networks.

Economics influence the historical and geographical distributions of shipwrecks. Transportation economics and the small margins associated with industrial shipping forced shipping lines to search for the shortest or least expensive routes between places. The principal routes used by steam and sailing vessels approaching or passing southern Block Island are documented in contemporary published coast pilots, marked on navigation charts, miscellaneous transportation maps, in the placement of lighthouses and other aids to navigation, and in clusters of wrecked vessels on the edges of Block Island.

2.4.3 Response to the Natural Environment

"Major natural features . . . influenced both the location and organization of rural communities. Climate, similarly, influenced the siting of buildings, construction materials, and the location of clusters of buildings and structures. Traditions in land use, construction methods, and social customs commonly evolved as people responded to the physiography and ecological systems of the area where they settled."(NPS Bulletin 30)

While the NPS rural landscape guide focuses on *settlement* patterns in describing responses to the natural environment, in a maritime transportation corridor, the fundamental patterns and features reflect the *movement* of vessels as well as the siting of maritime buildings and structures.

Archaeological resources reveal complex human responses to the natural environment. Environmental factors such as water depth, prevailing wind patterns, and the availability of native building material influenced the designs of and construction methods used in building generations of local vessels such as the famed Block Island double ended fishing boats.

The density of and types of wrecks in the Study Area has the potential to reveal much about the influence of natural and market forces on the operation of ships and boats in Rhode Island. Evolving regional economic geography influenced physical parameters for vessels governing their size, influencing hull designs, and, where applicable, sailing rigs. This was true in the late nineteenth century when shippers turned to the schooner-barge (a cargo vessel with a simple auxiliary sailing rig tow by a steamer) to carry coals from Virginia, Delaware, and Pennsylvania to the New England's grown cities and mills. It has remained equally true in the later 20th and early 21st century and is expressed the types and wrecking patterns of the region's commercial fishing vessels. Politics, the economy, cultural traditions, and the availability of building materials affected the designs, quality, use, and loss of ships and boats in the Study Area. These broader issues, once again, call for an evaluation that includes the landscape along with the study of individual sites.

2.4.4 Cultural Traditions

"Cultural traditions affect the ways the land is used, occupied, and shaped." (NPS Bulletin 30).

Indian efforts to shape New England's ecosystems before European contact and settlement are well documented (Cronon 1982). The cultural traditions and practices of Atlantic mariners

and certainly of Rhode Island's native and non-native fishermen are also written into the cultural landscape. The choice of species hunted, methods employed, and systems for allocating of space and natural resources, are all cultural elements that shaped and continue to influence the ecology and cultural landscape of Block Island. The cultivation of oysters, the use and location of fish traps and weirs, are just two examples of this category. Perhaps even more important are the spiritual meaning and uses of the landscape by Indian people.

2.4.5 Circulation Networks

"Circulation networks are systems for transporting people, goods, and raw materials from one point to another. They range in scale from livestock trails and footpaths, to roads, canals, major highways, and even airstrips. Some, such as farm or lumbering roads, internally served a rural community, while others, such as railroads and waterways, connected it to the surrounding region."(NPS Bulletin 30).

The survey area includes corridor segments of a nationally significant circulation system that helped define the cultural and economic character of the Northeastern United States from the time of European exploration into the early 20th century. Corridors are distinct linear features within circulation systems that facilitate the movement of people, materials, energy, biota, and ideas between places. The waters adjacent to Block Island were part of a larger transportation network that facilitated the low cost and rapid transfer of people and natural resources including wood, food, and sources of energy in New England. As a recent scholar of archaeology and cultural landscapes noted, "an important research theme is the way transport infrastructure and modes of transport affect our concepts of place and space" (Fry, 2001, 241-242). Maritime cultural landscapes ioffer frameworks for understand place and space on Block and Rhode Island Sounds as they relates to culture and environment of rural and urban areas. The content and intensity of the maritime connections between places is documented in the copious surviving federal records, such as the lighthouse keepers who documented the daily passage of hundreds of tall ships. Shipwrecks and navigation system-related objects, sites, structures, and buildings provide physical evidence of this historically significant circulation system.

2.4.6 Boundary Demarcations

"Boundary demarcations delineate areas of ownership and land use . . . they also separate smaller areas having special functions. Fences, walls, tree lines, hedge rows, drainage or irrigation ditches, roadways, creeks, and rivers commonly marked historic boundaries."(NPS Bulletin 30).

Boundary demarcations offer one of the most challenging aspects of defining maritime landscapes to according to National Register standards. The lack of clearly established boundaries, however, failed to prevent the determination of Nantucket Sound as a cultural landscape eligible for the National Register of Historic Places. The physical boundary demarcations listed in *NPS Bulletin 30* were not developed for marine spatial planning or maritime preservation. However, the depth contours, marked navigation channels, lighthouses and buoys, and harbors of refuge can provide boundary demarcations that accurately reflect the patterned uses of the Rhode Islands' waterways.

2.4.7 Vegetation Related to Land Use

The characteristic "vegetation" may apply to the SAMP Areas maritime landscapes through patterned alteration to shoreline plant life such as include eelgrasses or other species effected by development. A different application of the vegetation characteristic involves the long-term use of peat for fuel by Block Islanders. The extensive extraction of peat left discernable physical signatures on the coastal and underwater landscape, the extent of which is currently unknown. This important but rarely recognized activity influenced the ecosystem, landscape, and life ways of people who lived in the Study Area. Vegetation patterns can be important markers within the archaeological record for connecting human uses of the Study Area with the condition and composition of the ecosystem. It may be possible to broaden vegetation category to also incorporate biology, such as the deliberate introduction of non-native species, or the introduction of invasive species by ocean going vessels passing through or wrecking in Rhode Island waters. The archaeological remains of shipwrecks and other cultural landscape features have a strong potential for adding significant ecological information about Block Island and surrounding waters.

2.4.8 Buildings, Structures, and Objects

"*Various types of buildings, structures, and objects serve human needs related to the occupation and use of the land. Their function, materials, date, condition, construction methods, and location reflect the historic activities, customs, tastes, and skills of the people who built and used them." (NPS Bulletin 30)*

According to National Park Service definitions ships, canals, bridges, docks, and breakwaters are structures. Many ships ply the survey area today and continue with the historic activities such as of carrying passengers or fuel in the form of coal and petrochemicals. Commercial fishing vessels from Rhode Island and beyond continue to work these historic grounds. Fishing vessels are working mobile structures that contribute to the cultural landscape's historical integrity by evoking the historic feeling and character of Rhode Island's maritime economy. Many of the fishing vessels working in Rhode Island today will someday be eligible for the National Register, and those older fifty years old are already potentially eligible. Even many of the newer vessels plying out of Point Judith and New England ports possess esthetic values consistent with ships built during late nineteenth and early decades of the 20th century. Given the current challenges facing Rhode Island commercial fishermen, attention to the structures associated with the fisheries cultural landscape seems both important and urgent.

Rhode Island's bottomlands are scattered with historic objects: anchors, jettisoned cargo, refuse, industrial and military equipment in the form of munitions, aircraft, and miscellaneous discarded goods. There are also a vast number of disarticulated architectural features from ships: rudders, major timbers, and parts of sides, bottoms, and decks. The cultural landscape framework facilitates the evaluation and management of these broad archaeological mosaics and offers ways through GIS mapping and reporting to monitor cumulative natural and human impacts on cultural and historic resources.

2.4.9 Clusters

"Groupings of building, fences, and other features, as seen in a farmstead, ranch, or mining complex, result from function, social tradition, climate, or other influences, cultural or natural.

The arrangement of clusters may reveal information about historical and continuing activities, as well as the impact of varying technologies and the preferences of particular generations. . . . Also, the location of clusters, such as the market towns that emerged at the crossroads of early highways, may reflect broad patterns of a region's cultural geography." (NPS Bulletin 30)

The landscape characteristic of "cluster" applies directly to maritime cultural landscapes. Determining the spatial patterns of archaeological resources requires carefully designed studies. The survey of the southern Block Island portions of the Study Area conduct by SAMP research revealed a patterned cluster of shipwrecks. The density of sites is greater where human and natural factors combine to create dangerous conditions. Dozens of sailing vessels were damaged or destroyed by going aground on Block Island. The locations of clusters of archaeological sites and objects and their association with ports and particular trades "reflect broad patterns of [the] region's cultural geography" (*NPS Bulletin 30*). Identifying such clusters is critical for preserving cultural landscapes while also encouraging the sustainable economic uses of the ocean. Clusters of abandoned and wrecked ships from the late nineteenth and early twentieth century similar to those on the edges of Block Island are on the National Register of Historic Places as individual sites and as part of archaeological districts.

2.4.10 Archaeological Sites and Small Scale Elements

[Archaeological sites] "may provide valuable information about the ways the land has been used, patterns of social history, or the methods and extent of activities such as shipping, milling, lumbering, or quarrying. The ruins of mills, charcoal kilns, canals, outbuildings, piers, quarries, and mines commonly indicate previous uses of the land . . . The spatial distribution of features, surface disturbances, subsurface remains, patterns of soil erosion and deposition, ands soil composition may also yield information about the evolution and past uses of the land."

"Small-scale elements . . . add to the historic setting of a rural landscape. These features may be characteristic of a region and may occur repeatedly throughout a region . . . . Collectively, they often form larger components, such as circulation networks or boundary demarcations. Small-scale elements also include minor remnants-such as canal stones, road traces, mill stones, individual fruit trees, abandoned machinery, or fence posts—that mark the location of historic activities, but lack significance or integrity as archaeological sites."(NPS Bulletin 30)

Archaeological sites and small-scale elements are the principle features marking Rhode Island's historic navigation corridors. Small-scale elements may include the only remaining physical trace remaining of cultural significant tribal cultural landscapes. Remnants of human activity can provide the most comprehensive material record of the evolving human use of Rhode Island's Ocean resources. The historic uses of local waterways included more than transportation or fishing. The waters served as a testing grounds for military equipment, a sink for sewage, a trash dump, a scientific laboratory, a recreational zone, and as an aesthetic vista and spiritual place. These activities affect ecosystems and cultures and yet management of marine resources tend to overlook their historical and cultural significance. By adopting the landscape paradigm, scholars and resource managers can create aggregates out of individual sites and small-scale elements and identify additional, perhaps yet unseen but significant patterns of use and cultural meaning. These fine grain approaches to cultural resources are not restricted to preservation. Managers can use them to identify past, current, and potential environmental threats to Rhode Island's marine ecosystems.

2.5 GIS and Marine Spatial Planning for Historical and Cultural Resources.

Modern methods of spatial analysis powered by GIS systems have the potential to revolutionize the management of Rhode Island's marine cultural resources. For decades archaeologists and cultural resource managers routinely dismiss single object are artifacts as isolated finds that lack archaeological context. Today this is not longer true. An isolated anchor from a historic schooner or a pre-contact stone tool trawled up by a commercial fisherman may seem to have little significance or historic integrity on its own, but as a quantifiable item in a cultural landscape map it will contribute to the broader understanding the human use of Rhode Island's marine environment. Similarly, the analysis of items once dismissed as isolated beach wreckage will, when tracked as part of a cultural landscape GIS, lead to a greater understanding of the physical dynamics governing the preservation of submerged resources. Furthermore, small durable sections of ship wreckage such as rudders, frames, pieces of bilges and sides, or machinery, while lacking sufficient individual integrity to qualify as a National Register eligible archaeological site take on new value when analyzed against the area's broader cultural landscape. Given the huge geographical spaces involved and the complexity and expense of marine archaeological surveys, a shift towards a GIS powered cultural landscape approach will support the development the model, sensitivity analysis, and practical plans needed to manage Rhode Islands submerged and marine cultural resources during an era of expanding economic opportunities of our shores.

3 Methods

3.1 Secondary Sources, Published Material and Literature Review

A wide variety of newspaper databases were consulted in the effort to expand our knowledge of vessel losses in the Ocean SAMP area. The Newspaper Archive (Newspaper Archive.com) allowed for a good if opportunistic examination of regional newspapers. The archive has a national cross-section of second tier papers that tend to catch any wrecks or incidents that had more than local coverage. Particularly useful in the archive was an incomplete but extensive run of the *Newport Daily News* (1846–1977).

Additional local coverage came from the card index and microfilm runs from the *Providence Journal* located at the Providence Public Library. Web-based databases and editions of the *New York Times* and the *Brooklyn Daily Eagle* provided a useful New York perspective.

Extensive use was made of the online U.S. Serial Set and Serial Set Map databases. They provided in depth coverage of congressional publications that provided comprehensive statistics, congressional hearings, and annual agency reports.

Further information about published sources and databases can be found in section 3.4 below.

3.2 Archival Research

Historians working for the Ocean SAMP study conducted archival research at the Regional National Archives in Waltham, Massachusetts. That research comprised three separate research trips. On each occasion, historians examined, copied and photographed records kept by federal

agencies. A major focus was to evaluate records at the local level in order to identify shipwrecks and other cultural elements that were not considered of sufficient importance to include in published reports.

3.2.1 Submarine Cable Research

The following record records were consulted for research on submarine cables in the Ocean SAMP area. This line of inquiry was triggered by questions and concerns over a cable area to the southwest of Block Island.

Submarine Communication Cables - Narragansett, RI - [Project #] D-RI-423*, 1956 - 1957*
ARC Identifier 1272264
Textual Records from the General Services Administration. Public Buildings Service. Region 1. (12/11/1949 -)
NARA's Northeast Region (Boston), Waltham, MA
File Unit from Record Group 121: Records of the Public Buildings Service, 1801 – 2000

Bonnett Shore - Subterranean cable easements - Narragansett, RI*, 1957 - 1957*
ARC Identifier 660245
Textual Records from the General Services Administration. Region 1. Real Property Division. (ca. 1949 -)
NARA's Northeast Region (Boston), Waltham, MA
File Unit from Record Group 269: General Records of the General Services Administration, 1922 – 1997

Real Property Disposal Case Files*, compiled ca. 1949 - ca. 1976, documenting the period ca. 1939 - ca. 1976*
ARC Identifier 1155019
Textual Records from the General Services Administration. Public Buildings Service. Region 1. (12/11/1949 -)
NARA's Northeast Region (Boston), Waltham, MA
Series from Record Group 121: Records of the Public Buildings Service, 1801 – 2000

Real Property Disposal Case Files*, compiled 1949 - ca. 1987, documenting the period 1946 - ca. 1987*
ARC Identifier 607931
Textual Records from the General Services Administration. Region 1. Real Property Division. (ca. 1949 -)
NARA's Northeast Region (Boston), Waltham, MA
Series from Record Group 269: General Records of the General Services Administration, 1922 – 1997

Subterranean Cable Easements - Block Island, RI*, 1956 - 1960*
ARC Identifier 1272266
Textual Records from the General Services Administration. Public Buildings Service. Region 1. (12/11/1949 -)
NARA's Northeast Region (Boston), Waltham, MA
File Unit from Record Group 121: Records of the Public Buildings Service, 1801 – 2000

Block Island (portion) - Subterranean cable easements - Narragansett, RI*, 1957 - 1958*
ARC Identifier 660246
Textual Records from the General Services Administration. Region 1. Real Property Division. (ca. 1949 -)
NARA's Northeast Region (Boston), Waltham, MA
File Unit from Record Group 269: General Records of the General Services Administration, 1922 - 1997

Green Hill Fire Control Station - subterranean cable - South Kingston, RI - [Project #] D-RI-415*, 1944 - 1958*
ARC Identifier 1272032
Textual Records from the General Services Administration. Public Buildings Service. Region 1. (12/11/1949 -)
NARA's Northeast Region (Boston), Waltham, MA
File Unit from Record Group 121: Records of the Public Buildings Service, 1801 – 2000

Naval Base - telephone cable system - Newport, RI - [Project #] N-RI-427*, 1957 - 1957*
ARC Identifier 1272137
Textual Records from the General Services Administration. Public Buildings Service. Region 1. (12/11/1949 -)
NARA's Northeast Region (Boston), Waltham, MA
File Unit from Record Group 121: Records of the Public Buildings Service, 1801 – 2000

Green Hill - Subterranean cable easements - South Kingston, RI*, 1958 - 1958*
ARC Identifier 660257
Textual Records from the General Services Administration. Region 1. Real Property Division. (ca. 1949 -)
NARA's Northeast Region (Boston), Waltham, MA
File Unit from Record Group 269: General Records of the General Services Administration, 1922 – 1997

3.2.2 Shipwreck Research

The following records were consulted in an attempt to expand our understanding of shipwreck losses in the Ocean SAMP area.

Wreck Reports for Sandy Point Lifesaving Station*, 1899 - 1916*
ARC Identifier 648090
Textual Records from the Department of the Treasury. U.S. Coast Guard. Eastern Division. (1915 - 1933)
NARA's Northeast Region (Boston), Waltham, MA
File Unit from Record Group 26: Records of the U.S. Coast Guard, 1785 - 2005

Fog Signal Logbooks*, compiled 1891 - 1945*
ARC Identifier 1256995
Textual Records from the Department of the Treasury. U.S. Coast Guard. Beavertail Light Station, Jamestown, Rhode Island. (07/01/1939 - 04/01/1967)
NARA's Northeast Region (Boston), Waltham, MA
Series from Record Group 26: Records of the U.S. Coast Guard, 1785 – 2005

Records of Passing Vessels*, compiled 1880 - 1894*
ARC Identifier 1257003
Textual Records from the Department of the Treasury. Lighthouse Board. Beavertail Light Station, Jamestown, Rhode Island. (10/09/1852 - 1903)
NARA's Northeast Region (Boston), Waltham, MA
Series from Record Group 26: Records of the U.S. Coast Guard, 1785 – 2005

Journals of Shipwrecks*, compiled 1856 - 1927*
ARC Identifier 645541
Textual Records from the Department of Commerce. Bureau of Lighthouses. (1913 - 07/01/1939)
NARA's Northeast Region (Boston), Waltham, MA
Series from Record Group 26: Records of the U.S. Coast Guard, 1785 – 2005

Lifesaving Station Logs*, compiled 1872 - 1942*
ARC Identifier 645099
Textual Records from the Department of the Treasury. U.S. Coast Guard. Boston Coast Guard District. (06/20/1939 - ca. 1944)
NARA's Northeast Region (Boston), Waltham, MA
Series from Record Group 26: Records of the U.S. Coast Guard, 1785 – 2005

Wreck Reports for Point Judith Lifesaving Station*, 1903 - 1919*
ARC Identifier 648089
Textual Records from the Department of the Treasury. U.S. Coast Guard. Eastern Division. (1915 - 1933)
NARA's Northeast Region (Boston), Waltham, MA
File Unit from Record Group 26: Records of the U.S. Coast Guard, 1785 – 2005

Wreck Reports for Watch Hill Lifesaving Station*, 1907 - 1907*
ARC Identifier 648091
Textual Records from the Department of the Treasury. U.S. Coast Guard. Eastern Division. (1915 - 1933)
NARA's Northeast Region (Boston), Waltham, MA
File Unit from Record Group 26: Records of the U.S. Coast Guard, 1785 – 2005

Wreck Reports for Narragansett Pier Lifesaving Station*, 1905 - 1918*
ARC Identifier 648088
Textual Records from the Department of the Treasury. U.S. Coast Guard. Eastern Division. (1915 - 1933)
NARA's Northeast Region (Boston), Waltham, MA
File Unit from Record Group 26: Records of the U.S. Coast Guard, 1785 – 2005

Wreck and Obstruction Files*, compiled 1942 - 1979*
ARC Identifier 1756157
Textual Records from the Department of Defense. Department of the Army. U.S. Army Corps of Engineers. North Atlantic Division. U.S. Army Engineer District, New England. (06/14/1979 -)
NARA's Northeast Region (Boston), Waltham, MA

Series from Record Group 77: Records of the Office of the Chief of Engineers, 1789 – 1999

Wreck Reports*, compiled 1877 - 1909*
ARC Identifier 645703
Textual Records from the Department of the Treasury. Customs Service. Collection District of Bristol and Warren, Rhode Island. Office of the Collector of Customs. (02/25/1801 - 1913)
NARA's Northeast Region (Boston), Waltham, MA
Series from Record Group 36: Records of the U.S. Customs Service, 1745 – 1997

Wreck Reports*, compiled 1911 - 1963*
ARC Identifier 645702
Textual Records from the Department of the Treasury. Bureau of Customs. Collection District of Rhode Island. Office of the Collector of Customs. (1927 - 1973)
NARA's Northeast Region (Boston), Waltham, MA
Series from Record Group 36: Records of the U.S. Customs Service, 1745 – 1997

Wreck Reports*, compiled 1873 - 1874*
ARC Identifier 645701
Textual Records from the Department of the Treasury. Customs Service. Collection District of Newport, Rhode Island. Office of the Collector of Customs. (06/14/1790 - 1913)
NARA's Northeast Region (Boston), Waltham, MA
Series from Record Group 36: Records of the U.S. Customs Service, 1745 – 1997

Wreck Reports*, compiled 1874 - 1954*
ARC Identifier 1105543
Textual Records from the Department of the Treasury. Bureau of Customs. Collection District of Rhode Island. Office of the Collector of Customs. (1927 - 1973)
NARA's Northeast Region (Boston), Waltham, MA
Series from Record Group 26: Records of the U.S. Coast Guard, 1785 – 2005

General Records Relating to Lighthouses*, compiled 06/1792 - 1870*
ARC Identifier 2022360
Textual Records from the Department of the Treasury. Customs Service. Collection District of Newport, Rhode Island. Office of the Collector of Customs. (06/14/1790 - 1913)
NARA's Northeast Region (Boston), Waltham, MA
Series from Record Group 26: Records of the U.S. Coast Guard, 1785 – 2005

3.3 Historic Cartographic Research

The historic cartographic research to support this study focused on geo-rectifying historic navigation charts for Block Island. The charts for 1914, 1934, 1957, 1966, 1968, 1970, 1971, 1972, 1973, 1975, 1977, 1978, 1985, 1996, 1997, 1999 were geo-referenced and laid on top of the modern navigation chart. A similar procedure with navigational charts for Block Island Sound was followed, although in this case the process was less exhaustive. It did, however, incorporate data from the 1901 navigation chart of Block Island Sound which in turn is based on survey data from 1848. URI researchers also geo-rectified 1934 and 1999 charts of the Block Island Sound. In the process of doing this work they identified what was almost certainly the first modern hydrographic survey of Block Island waters – completed by the US Coast Survey in 1839 (Figure 1). From these charts, researchers were able to map historic navigation corridors,

hazards to navigation, obstructions, shipwrecks, shoaling, shoreline changes and patterns of maritime commerce. That data is currently being incorporated into a GIS database.

Figure 1. First Hydrographic Survey of Block Island, 1839.

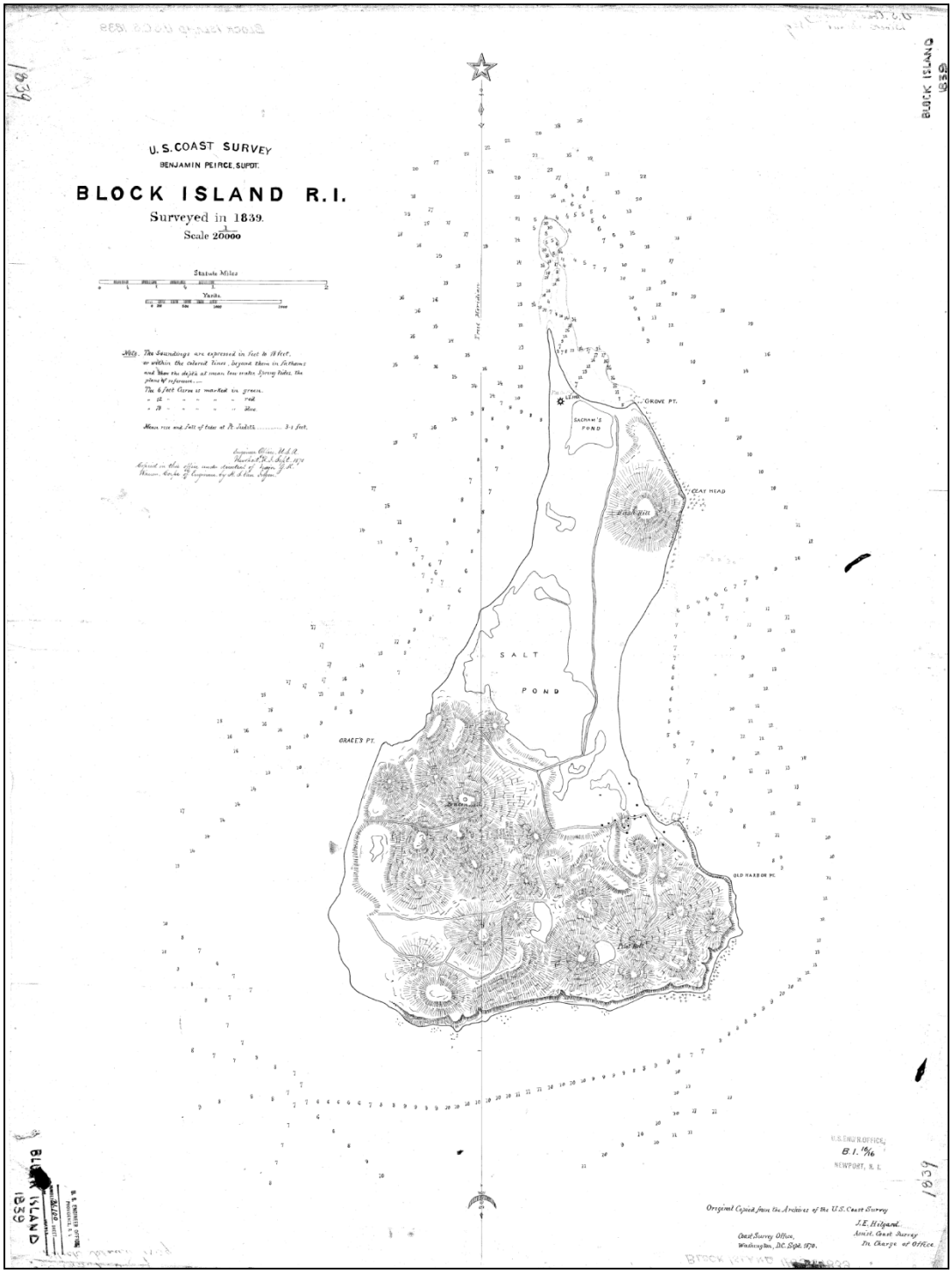

3.4 Database Development

Data about shipwreck losses in the Ocean SAMP area comes in multiple forms. Prior to this project, them most reliable database of shipwrecks was maintained by the Rhode Island State Historic Preservation and Heritage Commission (the Official State Database), which contained listings for 1041 shipwrecks in Rhode Island state waters. The Official State Database also includes significant information collected over many years by the Rhode Island Marine Archaeology Project (RIMAP) headed by Dr. Kathy Abbass. Two additional databases complement that held by the state. First, the Northern Shipwrecks Database, comprising in excess of 100,000 shipwrecks, has at least 1200 recorded in Rhode Island waters. Second, the National Oceanographic and Atmospheric Administration's Office of Coast Survey maintains the Automated Wreck and Obstruction Information System (AWOIS) that has 850 wrecks and obstructions for a region (Region 2) that extends from Long Island Sound to Cape Cod and includes Rhode Island waters.

The University of Rhode Island has developed three databases, all of which were augmented as a result of the Ocean SAMP study; a working archaeological database with 618 shipwrecks in Rhode Island waters (URI Working Database); a geophysical survey database containing acoustic images of at least 30 shipwrecks in Rhode Island (URI Geophysical Survey Database); and a supplementary historic database, built from various sources including historic charts, records of the US Life Saving Service, the US Coast Guard, the Navy and the Department of Commerce (URI Supplementary Historic Database). The URI Supplementary Historic Database currently contains listings for 584 wrecking events occurring in Rhode Island prior to 1908 as well as considerable information about non-shipwreck submerged cultural resources. Archival research conducted as part of the Ocean SAMP helped build and refine this database.

All databases described above can be augmented with published dive guides - the most important of which are Marlene and Don Snyder's books *Rhode Island Adventure Diving* and Rhode Island Adventure Diving II; and Henry Keatts and George Farr's book, *The Bell Tolls: Shipwrecks & Lighthouses, Volume 1, Block Island*.

Outside government agencies, organized avocational groups, and academic institutions many individual people including fishermen, divers, and amateur historians possess critical information about shipwrecks and other submerged archaeological sites in Rhode Island.

All of these databases and sources of information have strengths and weaknesses. While there is considerable overlap, there are also significant discrepancies between the datasets. As part of the SAMP process, researchers at the University of Rhode Island started to augment the Official State Database with extensive data from elsewhere. Although still not complete, the final rationalized product will be an improved estimate of the location and extent of submerged cultural resources in the Ocean SAMP area.

3.5 Geophysical Data Analysis

Funding limitations and budget reductions prevented comprehensive cultural resource analysis of geophysical data collected as part of the Ocean SAMP studies. As a result, URI archaeologists were only asked to completed analysis of data from the 2008 *Endeavor* cruise. This cruise covered approximately 25 square miles to the south and west of Block Island out to approximately the 3-mile demarcation of state waters.

Using CARIS acoustic data processing software, each line of side scan sonar data from the 2008 *Endeavor* cruise was examined for potential cultural resources. Researchers then classified each target in accordance with a 5-point scale.

1. Certain – the acoustic data alone made it possible to identify the target as a shipwreck or other cultural resource.
2. Probable – the acoustic data was highly suggestive of cultural resources, containing features such as linearity and regular patterning that are commonly associated with shipwrecks of other cultural resources.
3. Possible – the acoustic data has some features that have been reliably associated with cultural resources but might also be indicative of features in the natural world.
4. Unlikely – the acoustic data has features that are normally associated with the natural environment, but may have some features that show regularity and could be cultural in origin.
5. Conceivable – the acoustic data is almost certainly associated with features in the natural world, but could conceivably be cultural in origin.

Researchers then developed a table containing each target, its location, a description and classification. Through this process, targets with acoustic signatures that were indicative of submerged cultural resources were identified and prioritized for groundtruthing (on-site investigation and study).

Figure 2. Post Processing Endeavor Cruise Side Scan Sonar Data and Target Identification

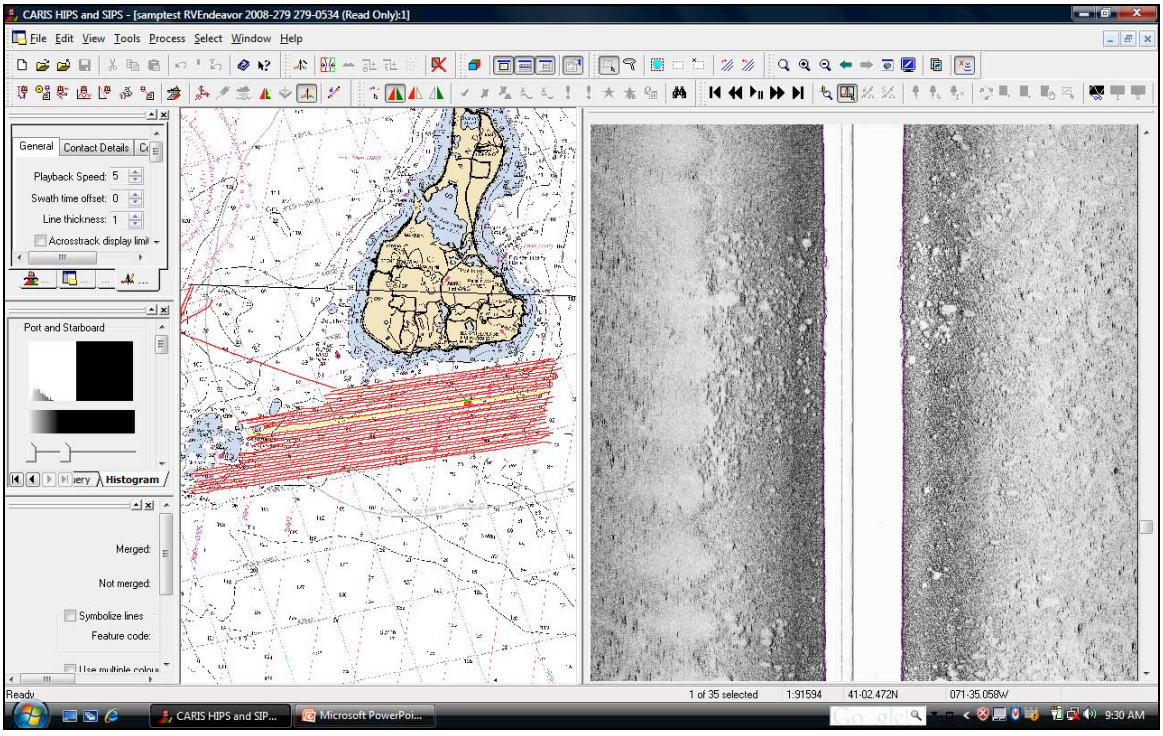

3.6 Site Specific Investigations

3.6.1 Coastal Pedestrian Survey

While coastal and onshore cultural resources were not the focus of this part of the Ocean SAMP studies, researchers did complete a preliminary cultural resources pedestrian survey of the southeastern coast of Block Island. At evenly spaced intervals (3 m), researchers walked the shore recording and photographing cultural material. The data was organized into an image library and is available upon request. The following points delineated the extents of the survey:

Eastern end of Pedestrian Archaeological Survey: 41 09.442N; 71 32.704W
Western end of Pedestrian Archaeological Survey: 41 09.095N; 71 33.405W

3.6.2 Underwater Site Studies

The investigation of underwater archaeological resources was the primary focus of on-site investigations for this part of the Ocean SAMP study. Fieldwork comprised two 4-day expeditions to Block Island, one from June 16-20, 2009 and the other from August 24-28, 2009. On each occasion, we used the R/V *Hope Hudner* – a 38-foot, fiberglass former lobster boat owned by the University of Rhode Island. The *Hudner* is well appointed for survey work and dive operations. For the second trip we also used a 26' inboard/outboard support boat – the RB-1. Personnel for the June 2009 expedition were Rod Mather, John Jensen, Mark Gustafson and Matt Horn. Personnel for the August 2009 expedition were Rod Mather, John Jensen, Mark Gustafson, Jamin Wells and Abigail Howe.

The potential scope of on-site archaeological investigations off Block Island was considerable and could have comprised many months of fieldwork. Since that was neither practical nor funded, the object of on-site investigations was to conduct archaeological assessments of 2-3 representative known sites and to groundtruth a similar number of side scan sonar targets from the 2008 *Endeavor* survey. In addition, we planned side scan sonar work including a survey close to the southern shore of Block Island up to the 10-foot contour. The waters between the 10 and 35-foot contours were too shallow to be surveyed by R/V *Endeavor*.

Overall, the purposes of side scan sonar work associated with this part of the Ocean SAMP study were:

1. To reacquire targets identified during post-processing of the *Endeavor* 2008 data. This was important both to confirm the target's presence and establish locations for dive operations.
2. To investigate reported locations of shipwreck sites close to but outside the coverage of *Endeavor*.
3. To complete side scan sonar survey work inside the coverage of the *Endeavor (*as described above). This was particularly important as multiple shipwrecks are known to have gone ashore along the southern coast of Block Island. Of these, five were particularly important; the *Meteor*, the *USS Leydon*, the *Essex*, and *Lightburne* and the *Spartan*.

The side scan sonar at our disposal was an Edgetech 272, 100 kHz towfish. The survey was controlled using a Furuno DGPS and HYPACK hydrographic survey software. The towfish was deployed by hand and towed at an altitude of 10% of the swath width. Sonar data was acquired using Chesapeake Technology SonarWiz software. Targets were identified during the survey and listed for potential groundtruthing.

During field operations in June and August, we conducted in-water archaeological inspections of the *Lightburne, Essex* and *Idene*, and 2 of the most promising side scan sonar targets from the *Endeavor* cruise. At each of the shipwrecks scuba-equipped archaeologists completed visual inspections of the structural remains, documented the site using video and still photography; assessed the stability of the site, and estimated the extent of anthropogenic impacts – including looting.

In addition to these in-water investigations, archaeologists also conducted on-the-surface reconnaissance operations at the sites of the *Montana*, *Meteor, USS Leyden* and *Spartan*.

Besides the known wrecks, no side scan sonar targets from the 2008 *Endeavor* cruise represented either "certain" or "probable" archaeological sites (classifications "1" and "2" as described in 3.5 above). As a result, we selected three side scan sonar targets as representative examples and completed in-water archaeological investigations designed to identify the source of the acoustic target and determine the presence or absence of cultural material. In all cases, the sites were documented using video and still photography. If cultural material was found we were prepared to delineate the extent of that material and provide, as far as possible, an assessment of its date, form and cultural affiliation.

4 Results

4.1 Block Island and Submerged Cultural Landscapes

Historical research and the analysis of historical shipwreck patterns, combined with archaeological survey resulted in the identification of multiple cultural landscape contexts for the Ocean SAMP area. The contexts provide narrative framework that describe the significance of known and potential cultural heritage resources. The segments that follow do not represent the totality of the heritage resources in or near the project area. They represent known landscapes and associated resources that coastal planners, managers, and prospective developers will most likely encounter in the study area. As such they represent some of the most important findings of this study.

The location of Block Island at the crossroads of local, regional, national, and international maritime navigation and economic systems make drawing deliberate lines around specific landscapes and describing their significance challenging, but rewarding. The depth of coverage in these contexts varies from a very limited recognition of pre-contact Native American landscapes to a detailed discussion of the "energy landscape." Future historical research and archaeological investigations will add significant additional information to the landscapes discussed here and may result in the identification of additional cultural landscapes.

4.1.1 Pre and Post-Contact Native American Landscapes

Chapter Four of the Ocean SAMP report includes a general history produced the Narragansett Indian tribe. Including written sources and oral traditions, the history goes back centuries and includes the period before sea level rise submerged significant areas between the mainland and Block Island. The URI archaeological team was neither tasked nor funded to conduct research into Indian history or prehistory. Geophysical survey and analysis have identified conditions that might have resulted in the survival of material culture from submerged lands. Those are reported elsewhere in these studies.

Cultural landscapes are not so much specific physical places as ways of identifying and organizing cultural and historical meaning. Indian people who used the lands before their submergence also hunted and gathered resources from the sea. Their descendants continue many of these traditional activities. While Indians have used these places in multiple ways and have the capacity to identify their own specific landscapes, that task is outside of the scope of this report and the expertise of the investigators. Indian practices and artifacts, however, are also elements in other cultural landscapes such as energy and fishing and are included in those contexts.

4.1.2 European Exploration and Settlement 1492-1776

There are no *known* shipwrecks in the survey area associated with early European exploration. However, ample written and circumstantial evidence indicate that significant European maritime traffic passed by Block Island during the exploration and early settlement eras. The cultural and environmental legacy of that early activity is apparent today in the name Block Island and in the radically transformed island ecology (see energy context). The paragraphs that follow provide a context for understanding the expansion of maritime activity near the study area in seventeenth and eighteenth centuries. Although outside of the known historical record, European vessels surely passed by Block Island in the sixteenth century as well (see 4.1.3 below).

The exploration and settlement of New England was a "vast maritime enterprise" in that conquerors and settlers traveled across the ocean and were sustained by it. Marine resources along with coastal and oceanic trade routes ensured the physical and economic survival of European colonies in New England, including Rhode Island (Bridenbaugh, 9-10). The Ocean SAMP area influenced and was influenced by these human processes. Some of these influences exist today as place names, archaeological sites (known and undiscovered), and altered marine and coastal ecosystems.

The recorded European exploration, contact, and settlement history of the Block Island area begins with the voyage of Giovanni da Verrazano in 1523. Under orders from the French crown, Verrazano explored the east coast of the present day United States from Cape Fear, North Carolina to Cape Cod, Massachusetts Searching for the fabled "North West Passage" to Asia, Verrazano also spent considerable time interacting and trading with Indians. In April 1524, he sighted Block Island describing it as 10 leagues from the mainland, similar size to the island of Rhodes, hilly, forested, and triangular shaped. Noticing the many fires on shore, Verrazano predicted that the island was heavily inhabited (Wroth 1970). Bad weather forced Verrazano to pass by Block Island. Sailing into Narragansett Bay, and anchoring in Newport Harbor he recorded his observations of the countryside, the plants and animals, and the local Indian people-- their leaders, homes, and their interactions with the coastal environment (Wroth 1970).

The Dutch East India Company sponsored explorations in New York region led to several voyages through the SAMP area. On his fourth voyage in 1614, explorer Adriaen Block lost his ship the *Tyger* in a fire at Manhattan. In response, he built the 42-foot coastal vessel *Onrust* that he used to explore the East River, Long Island Sound, and parts of what is now the Ocean SAMP area, charting Block Island for the first time. These early Dutch interests in New York continued to influence the history and patterns of maritime commerce through the SAMP area into the nineteenth century.

After European colonization, Rhode Island quickly developed aggressive and highly successful maritime enterprises. These rapid maritime successes reflect the unusual cultural and political history of Rhode Island's establishment, and its unique geography. For example, the circumstances of Roger Williams move to Rhode Island established conditions that contributed to Rhode Island's rapid rise as a maritime economy and colony. Williams, considered the father of organized colonization in Rhode Island, was a religious radical with close Indian ties. In 1636, he fled Massachusetts for Mount Hope Bay in 1636 where the sympathetic Indian chief Massasoit granted him land on east bank of the Seekonk River. Somewhat later Williams moved his expanding group, settling close to present day Fox Point where he reestablished the community he called Providence (McLoughlin 6-7).

Other dissenters followed Williams to Rhode Island resulting in a collection of scattered settlements lead by people with diverse and sometimes controversial religious beliefs. This diversity ultimately led to a social and religious openness that proved a critical asset to Rhode Island's maritime economy (McLoughlin 3-4, 15; Bridenbaugh 10).

Communication and commerce in Rhode Island depended on the water with most early households possessing one or more canoes (Vickers 14). Roger Williams used these native craft to travel the colony and to visit and trade with local Indian leaders. The dispersed coastal settlement pattern combined with religious toleration to multiply the natural significance of Rhode Island's waterways, especially in Narragansett Bay.

The Rhode Island colony was a maritime place, bounded by protected waters, gifted with good harbors, and access to coastal natural resources. Fish provided food, fertilizer, and saleable commodity. The islands including Hog, Patience, Prudence, Dyer, Gould, Goat, Conanicut, Dutch and Aquidneck, contributed in important ways to Rhode Island's colonial settlement, survival, and economic success. With natural water access, many islands had good land, trees and fertile soil. The islands in Narragansett Bay and Rhode Island Sound proved critical for agriculture and animal husbandry offering confinement, forage, and save havens from wolves for pigs and goats - and later cattle, sheep and horses. Indeed, the names of Hog and Goat Island reflect their early employment in Rhode Island animal husbandry (Bridenbaugh 12-16) In 1639 grazing potential also drew attention to Block Island when William Codrington of Newport dispatched a small coastal trading vessel to Block Island with livestock. In 1661, Dr. John Alcock and a group of Roxbury men built a barque and transported cattle from Braintree to Block Island (Bridenbaugh, 43). The quest for fish and for places to raise animals brought English settlement and increased vessel traffic to previously isolated areas within the Ocean SAMP boundaries.

Agricultural development proved critical to Rhode Island's survival as a colony and to its rapid maritime commercial expansion. As such, it directly influenced the Ocean SAMP area and surrounding landscapes. English settlers bought their own ideas about agriculture to Rhode

Island, but also copied Native American practices including cultivating corn, a crop the one could consume, trade, or feed to animals. Ultimately, animal husbandry proved easier and more lucrative than crop cultivation–and within a decade or two of settlement, Rhode Islanders, particularly on Aquidneck Island, generated surpluses in pigs, goats, cattle, sheep and horses (Bridenbaugh, 39). Pigs had a special connection to Rhode Island's early maritime economy and to the diet of New England mariners. The indiscriminately foraging pigs fattened quickly. Mature pigs traveled by sea to Boston's butcheries where they became salt pork, a staple food of North Atlantic mariners and fishermen. By 1649, cattle joined the commercial market.

Agricultural surpluses, protected harbors, economic freedom, religious toleration, and lax regulation from London ensured Rhode Island's early and aggressive economic development and reinforced its ties with the ocean (Bridenbaugh, 28-31). These developments brought English settlement and a new environmental regime to Block Island and increased vessel traffic through the SAMP area. Indian traditions and the observations of early explorers and settlers evidence the changes in the landscapes adjacent to the waters of the Ocean SAMP area.

The year 1776 brought war to Block Island waters. While the military landscape is addressed separately, the contemporary newspapers report the capture of numerous American merchant vessels by British Warships stationed off Block Island. These reports describe the trade routes of vessels and the commodities carried through or near the survey area. The *Leviathan* was seized carrying lumber from Milford Connecticut to St. Croix. The *William*, hailing from St. Eustatius for Salem, Massachusetts, carried a cargo of wine, rum, and linen. The whaleship *Mercury* was heading home to Nantucket from Brazil with a cargo of whale oil. The *Hawke* from Newburyport carried flower, beef, pork, and fish for Surinam (*Public Advertiser* 15 May 1777). Such cargos typified the New England maritime commerce during the colonial period.

Despite significant levels of traffic, there are few records of shipwrecks associated with Block Island during the colonial period. Three wrecks associated with Block Island occurred during the 1750s, the brig *Halifax* and ship *Palatine* in 1752, and the sloop *Martha and Hannah* in 1755. The *Palatine* wrecked on the Northeastern end of the island, well outside of the survey area. Many other wrecks certainly occurred, but have yet to come to light through historical research.

4.1.3 Fisheries Landscape

Located a few miles off mainland Rhode Island, Block Island is a natural fishing platform that has sustained commercial fisheries since the early days of English settlement. For thousands of years before the English commoditized local fish, Indians hunted and gathered marine resources on and around the island for subsistence use. In the second half of the nineteenth century, the island became the popular destination for sports fisherman that it remains today.

On Block Island and its surrounding waters, exists a cultural landscape defined by fishing. Whether commercial, subsistence, or recreational, fishing involves the application and adaptation of human technologies in harvesting living marine resources. Because of the direct effects fishing has on the marine environment, any change in technologies, markets, and cultural meaning associated with it—however innocuous it might first appear—has the potential to cause significant changes in the condition of marine ecosystems.

Because fishing has been central to maritime cultures using Block Island and its waters for

millennia, a high potential for encountering unknown but historically or culturally significant resources in some form. On and around Block Island exist many known and undiscovered or unrecognized components of a fisheries landscape, such as historic fishing vessels, fish traps, working and remnant piers, and the altered habitats of historic fishing groups represent untapped opportunities to gain important knowledge about human activities and their relationships with the marine environment. Despite the significance of commercial fisheries in history and culture, marine archaeologists have until recently paid little attention to its study. Many historic resources associated with commercial fishing in New England and Mid-Atlantic resources have been lost because their significance was not recognized.

Part of a continually unfolding story, many fisheries resources including unique or representative fishing vessels and the archeological remains of traps and piers that are fifty years old or older are likely candidates for the National Register of Historic Places. Fixed on shore, the presence of historic submerged piers or fish traps are easier to determine and locate. The locations of many fishing vessels, however, are unknown—indeed, the number of vessels lost in the area since the European contact remains unknown. Fishing includes brings with it important historical and archaeological research questions and has implications for the siting of new structures in the waters off the Block Island.

4.1.3.1 Fishing, Subsistence and Sustainability on Block Island

Significant living marine resource use and human habitation have been connected for thousands of years on Block Island. Modern archaeological investigations suggest that Indian people living on Block Island depended heavily marine plant and fish life as early as 3000 years ago (Tsekov 1997). There is historical evidence of significant Indian fishing during the late 17th century on Block Island. Two centuries later, beach walkers continued to find heavy grooved stone sinkers fashion by Indian fishers on Block Island (Livermore 1877).

Fish and marine vegetation directly and indirectly influenced diets and ecological conditions on Block Island, promoting sufficient nutrition and sustainable agriculture. Beginning in the late 18th century, possibly earlier, Block Island farmers (many of them also fishermen) used seaweed to protect crops from extreme weather and to nourish the heavily worked soil. Farmers also mixed seaweed with fish offal and soil to create compost. These marine resources and local agricultural practices maintained the soil's fertility despite centuries of intensive use. Livermore, the island's principal early historian, noted that Islanders gathered over 6,000 cords of seaweed valued at $10,000 in 1875. At that time, many Islanders maintained exclusive rights to collect weed from specific areas of the shore (Livermore 1877: 30 -32). A large area of public beach also remained opened to all islanders to gather seaweed. Such boundary divisions are important markers of a fisheries cultural landscape on the island.

Commercial fishing has long and important history in New England. Intimately tied to early exploration and settlement in the region during the first century, fish enticed thousands of ships and tens thousands of European mariners and fisherman to cross the North Atlantic to the Americas. They discovered and charted off shore banks and interacted with native people. In terms of economic value, the fish caught and processed by the French and English fishermen outstripped the more famous New World treasures of gold and silver extracted by the Spanish Empire (Fagin, Fish on Friday, Pope, Fish into Wine).

Cod was the most important species for the Atlantic markets. Great abundance combined with a low level of oil in the flesh made it possible to store dried salted cod for extended periods. Cod, caught in the fall and the spring of the year, was the most important commercial species for Block Island fishermen in the 19th century. In 1880, Block Island fisheries employed 263 people, producing in excess of one million pounds of fish, roughly three-quarters of this was dry cod. The waters also produced bountiful others species such as dogfish, mackerel. Fishermen from other Rhode Island ports as well as from other states also fished in the SAMP area in the 19th century (Goode).

Block Islander fishermen developed distinctive type of fishing craft. Double ended and highly seaworthy, Block Island fishing boats coped with the heavy seas that commonly lashed the island and could ride out the intermittent violent Atlantic squalls that claimed other small craft. Local lore proudly reports that none of the islands double-ended fishing boats ever sank. While strictly true or not, the Block Island boats engendered respect along the coast and demonstrate the close connection between island fishermen and the local marine environment.

Attached to entrenched methods and technologies, Block Islanders proved conservative in the face of the rapid changes occurring during the later nineteenth century, for example resisting the introduction of new fishing technologies to "their" waters in the 1880s (Goode). On important exception came in the late 1860s when fish traps or pound nets came into use around the island. Pound nets required the driven of many piling, remnants of which might exist in regularly spaced intervals near shore areas around the island (Livermore 1877; Goode 301). The rough Atlantic environment made maintaining traps challenging, but archaeological remnants may well remain.

4.1.3.2 Historic Harbor Features

Commercial fishing drove the development of harbor facilities in the SAMP area in the 17th through the 20th centuries. In 1670's, the first legislation supporting the construction of a pier at Block Island cited the encouragement of fishing as its principle justification. Subsequent successful and unsuccessful efforts to establish safe harbors on the island focus on fish. In 1816, Block Island fisherman constructed the "pole harbor" near present day old harbor. Consisting of pilings driven into the bottom and boulders, the pole harbor offered adequate shelter in normal conditions. If stormy weather threatened, fishermen pulled their boats on to the shore. By 1870s and the opening of the government pier, the pole harbor consisted of 750 piling (Goode; Mendum *New England Magazine*, Volume 16, 1897). For the next two centuries and beyond, all efforts to build harbor facilities at Block Island had strong ties to the fisheries (Livermore 1877: 33-34; Goode 299).

4.1.3.3 Historic Fishing Vessel Shipwrecks

The wrecking of ships, particularly of fishing vessels has occurred throughout the centuries in Rhode Island and remains a common occurrence in the SAMP area during the present day. How many wrecking in the survey area remains unknown as fishing is an elusive and often confusing subject in the historical record. Accounts of the transporting and selling of fish are available for some places and periods. In the later 19th century, government-generated statistics become more common. However, in the distant past and in more recent times, the records of individual fishing voyages remain rare and those that survive usually reveal little information about actual fishing activities, much less fishing life. Official documents between the 16th through the early 19th centuries rarely recorded (or at best under recorded) the losses of fishing vessels. Based on

examinations of archival sources, historic newspapers, and federal records the pattern of underreporting seems to continue in the late 19th and into 20th centuries.

The potential for unreported but historically significant commercial fishing vessel wrecks of historical significance in the SAMP area and surrounding waters is extremely high. The potential within the survey area is more difficult to assess. The most important individual wrecks would be the rare early vessels of 16th through the mid 19th centuries where historical documentation is sparse or non-existent. However, when considered as part of a larger fisheries landscape in Rhode Island and in the SAMP area, fishing vessels and associated technologies from the late 19th century through the 20th century have the potential to provide an unbroken, representative, and highly informative archaeological record. These types of cultural heritage have extraordinary potential to add significant new knowledge to our understanding of marine environments and cultures. Although too often overlooked because the unromantic uses and perceived commonality, it is essential to note that any commercial fishing vessel built 50 years ago or more may be eligible for the National Register of Historic Places. Research is clearly needed identify these resources and to develop standards to evaluate these wrecks for purposes of study, public use, and historic preservation.

Cultural heritage research relating to commercial fishing is in its early stages in neighboring Massachusetts, where archaeologists and biologists at Stellwagen Bank National Marine Sanctuary have located several sunken fishing vessels. Efforts are underway to evaluate and nominate some of these wrecks to the National Register of Historic Places. Many wrecks of similar vessels exist in the waters surround Block Island and in adjacent waters. While not all of the wrecks likely merit preservation, they require inventory and assessment—a level of study that will generate an improved understanding of the Block Island area's cultural and natural heritage.

4.1.4 Military Landscape

During the post-contact period, twenty or more wars and endless conflicts have affected the composition of marine cultural heritage on southern end of Block Island and a much larger impact on adjacent waters. Some of these wars such as the Revolutionary War, the Quasi War with France, the War of 1812, and World War II had clear effects on maritime transportation near Block Island. During these wars, control for of sea-lanes was contested by warring nations, and in the case of World War II resulted in historically significant shipwrecks off of Block Island.

Among the wars, the American Revolution and the two World Wars (especially World War II) proved especially influential on the region's marine cultural landscape. The Revolutionary War altered the trajectory of Rhode Island history, reshaped its economy played host to fighting on land and at sea resulting in at least 33 historically significant shipwrecks in Rhode Island waters. Likewise, the global conflicts of the first half of the 20th century, especially World War II strongly influenced Rhode Island history and the Ocean SAMP area's cultural landscape. Naval facilities, bases, warships, fuel depots, hospitals, gun emplacements, testing ground, and shipwrecks from WWII all contributed to the fabric of the SAMP area history and many elements remain as archaeological or historic sites.

The outbreak of the Pequot war is tied to the study area. In 1634, John Oldham, a trader from Massachusetts, was killed during his interactions with Indians on Block Island. In response, Massachusetts attacked, conquered and settled the island.

The three Anglo - Dutch Wars (1652-1654, 1665-1667, 1672-1674) affected in long-term ways patterns trade and traffic through the SAMP area. New York's extraordinary influence on the history of Rhode Island traces directly to the early Dutch colony of New Amsterdam and the conflicts it engendered. The regional Dutch - Rhode Island connections persisted after the English took control of New York in 1664, continuing to influence trading relationships and traffic patterns through the SAMP area for centuries.

During the period covering King William's War (1689-1698) and Queen Anne's War (1702-1713), the English government expended little effort to control or regulate Rhode Island. The religiously tolerant, independent-spirited, and economically motivated Rhode Islanders refused to supply soldiers or military support to New England colonial armies (McLoughlin 52-53).

In contrast with land war, Rhode Islanders enthusiastically embraced the for-profit warfare of privateering. During the many Anglo-French wars (1689-1754) Rhode Island and other colonies licensed large numbers of privateers that sailed through the waters of the SAMP area. Privateers were privately owned armed ships licensed by the government in times of conflict and granted permission to raid enemy shipping. Privateering could be highly profitable and provided some level of naval defense for the colony. In 1690, Thomas Paine, a privateer from Jamestown, help drive off French ships that landed on Block Island (McLoughlin 52-54, 80).

The late-17th and early-18th centuries blurred the distinctions between legal privateering and illegal piracy. Thomas Paine, the hero at Block Island, was suspected of piracy, and the colony produced the well-known pirates Thomas Tew and Captain Want. In the 1690s, Rhode Island reportedly welcomed the famed pirate William "Captain" Kidd (Hawkes). Pirate booty boosted the Rhode Island economy, fattening the purses of certain merchants and government officials who might overlook illicit cargos and questionable practices (Bridenbaugh, 25). After about 1720, piracy along the eastern seaboard of colonial America declined and the separation between illegal pirates and legal privateers became clearer.

During King George's War and the French and Indian War (1739 – 1749, 1754 – 1763), Rhode Island dispatched a large numbers of privateers during the eighteenth century wars. During King George's War (1739 – 1749) Rhode Island was home to 25 percent of all privateers in operating in America (Swanson, 185). During the French and Indian War (1754 – 1763), powerful Rhode Island merchant families such as the Browns and Bannisters dispatched fleets of privateers through the SAMP area waters.

The French and Indian War emptied the British government's coffers, leaving an immense war debt that threatened the national economy. The clumsy plans devised by Imperial authorities to raise revenues from the America colonies threatening the cherished semi-independence and finances of Rhode Island and sister colonies and ultimately led to the War for Independence.

A Maritime-based economy meant that the new heavy British hand was perhaps felt sooner and with more pain in Rhode Island than in the other British North American colonies. Rhode Island responded by becoming the first colony to take up arms against Britain, the first to

propose a Continental Congress, the first to formally sever ties with the British monarchy, and the first to create a navy.

Armed resistance to British rule in America began on Rhode Island waters and set the stage for the development of the United States navy. In December 1763, the HMS *Squirrel* sailed through the waters included in the SAMP area and into Narragansett Bay to enforce the new regulations. Seven months later in July 1764, at the orders of two members of governor's council, gunners fired eight shots at a tender from *Squirrel* after a British-sparked mobbing incident at Newport.

Attacking Royal Navy vessels became a pattern in Rhode Island. Major incidents occurred in 1765 when a Royal Navy ship *HMS Maidstone* attempted to impress local sailors at Newport, and in 1769 when a mob boarded the Royal Navy ship *Liberty*, running it ashore and setting it aflame (McLoughlin 86, Bartlett 6: 428-429; Carroll 239-255).

The most important incident of this kind was the burning of the HMS *Gaspee* in the Providence River by disgruntled colonists in 1772. The *Gaspee* affair ranks alongside the Boston Tea Party and the Stamp Act Crisis as a large step on the road to the American Revolution (Bartlett; McLoughlin, 90-91).

The colony's independent streak and eye for profits continued in the early 1770. When the other colonies banded together in refusing to accept imported British manufactures, Rhode Island claimed poverty and abstained. At expense of the other colonies, Rhode Island Sound and Narragansett Bay remained open to British commerce. At a direct cost to the other colonies, ships, goods, and money flowed through the SAMP area waters into Rhode Island's ports (McLoughlin, 90).

The 1773 Tea Act and the infamous Boston Tea Party fed Rhode Islanders appetite for rebellion. In 1774, Rhode Island called for a Continental Congress and became the first colony to elect delegates. During this period, British warships increased operations in Rhode Island Sound beginning to block traffic into and out of Narragansett Bay.

In June of 1775, the Rhode Island legislature established America's first navy, commissioning the *Washington* and the 12-gun sloop *Katy* (later renamed the sloop *Providence*). Within a few days, the *Katy* captured the Royal Navy's tender *Diana* (tender to the HMS *Rose*) off Jamestown, in some respects the first naval battle of the Revolution (Fowler).

In October 1775, the Continental Congress passed a Rhode Island proposed resolution to create a Continental Navy. Rhode Island supplied two of thirteen new ships, the 28-gun frigate *Providence* (a different vessel from the sloop *Katy/Providence)*, and the 32-gun frigate *Warren*. The following month, Rhode Island sea captain Esek Hopkins became the Continental Navy's first commander-in-chief (Fowler).

Some of the United States Navy's earliest actions took place in SAMP area waters. In April 1776, Commander-in-Chief Esek Hopkins, captaining the *Providence*, captured a British tender *Hawk* off Block Island and a brig (bomb vessel) *Bolton*. On April 6, Hopkins' squadron engaged but did not capture HMS *Glasgow* off Point Judith. The following month, John Paul Jones, often considered the father of the American Navy, became the captain of the sloop *Providence (*the former *Katy*) (McLoughlin 96).

In a dramatic prelude to the formal United States Declaration of Independence, on May 4, 1776, Rhode Island "abrogated its allegiance to the king." The waters around the Rhode Island, including the study area became state waters on July 22, 1776 when Rhode Island altered the identity on its charter from "colony" to "state" (McLoughlin 92-93, 94).

As with earlier imperial conflicts, Rhode Island embraced privateering during the Revolutionary War, commissioning 65 privateers between May and December 1776.

In December 1776, the British took Newport in an amphibious assault. The subsequent three-year British occupation had dire consequences for maritime Rhode Island, ending forever the glory days of Newport-owned ships transiting the SAMP area waters on their way to distant markets. Many colonial merchants fled, taking their trade and shipping with them. Rhode Island's center of political and economic influence shifted from Newport to Providence, where it would remain after the war ended.

Britain also responded by cutting off Rhode Island's customary access to the sea, and station vessels off Block Island to cut off access to Narragansett Bay. Dozens of ships were seized (see exploration and early settlement landscape) brought serious hardships for patriots in Providence.

The British occupation of Newport and control of the entrance to Narragansett Bay had trapped the new frigates *Providence* and *Warren* along with the sloop *Providence* at the head of the bay. In February 1778, the *Warren* slipped the blockade, followed a month later by the *Providence*. The Continental ship *Columbus* failed in its bid for the open sea, running aground and burning near Point Judith.

In March 1778, France recognized the United States of America and entered the war as an ally. This changed war's character from a colonial rebellion to a broader European and Atlantic conflict. The French king sent a fleet under French Admiral d'Estaing, to assist the Continental forces. One of its first actions involved supporting an unsuccessful American effort to liberate Newport in the summer of 1778.

The French fleet comprised 12 ship-of-the-line, 4 frigates and 2,800 marines, a force far more powerful than the British frigates and smaller vessels stationed in Rhode Island. Faced with certain capture, between July 29 and August 8, 1778 the British forces sunk, scuttled or burned all of their vessels. English losses including the sloops *Kingsfisher* and *Falcon*, the galleys *Alarm* and *Spitfire*, and the frigates *Lark*, *Cerberus*, *Orpheus*, *Juno* and *Flora* as well as 13 transport ships in Newport Harbor (Abbass). Today, all of these wrecks are almost undoubtedly eligible for the National Register of Historic Places.

Despite these successes, the American and French efforts to take Newport stalled. The British, however, finally withdrew from the Island and Newport on their own accord in October 1779.

In July 1780, a French fleet under Admiral Ternay and carrying carry troops commanded by the comte de Rochambeau arrived in Newport. French warships stayed through the following winter. In March 1781, General Washington and Rochambeau, who would become the architects of the British defeat at Yorktown, held a series of strategic meetings at Newport. Shortly thereafter, the French evacuated Rhode Island (McLoughlin 99).

Between 1798 and 1800, the United States fought the so-called Quasi-War with France. Rhode Islanders participated enthusiastically, sending out many privateers to stalk French merchant ships with significant skirmished occurring off Block Island

The War of 1812 brought a mixed reaction in Rhode Island. The state government opposed the war, however, the lucrative prospects of privateering enticed many Rhode Islanders into action. One Bristol privateer, the *Yankee* captured 40 vessels worth a total of $5,000,000 (Coleman 1963). No battles took place in Rhode Island; however, the heavy presence the British Navy's off the east coast including Long Island Sound and the Block Island area seriously hampered Rhode Island's maritime activities.

The Civil War (1861-1865) renewed a relationship between Rhode Island and the U.S. Navy that would continue for the next 150 years. At the beginning of the war, the Union government, concerned about the proximity of the Naval Academy at Annapolis the south, relocated it to Newport. Despite strong efforts to keep the Academy in Rhode Island, it returned to Annapolis after the war.

In 1869, underwater mines and explosive warfare were in their infancy and the Navy established of a torpedo experimentation and development facility on Goat Island. The Newport torpedo development, testing, training and manufacturing station is central to the history of the propeller-driven torpedo in America. The navy subsequently established testing ranges inside Narragansett Bay and in Rhode Island Sound.

The Navy expanded operations to include Rose (1883) and Gould (World War I) Islands. During World War I, the Newport Torpedo Station added depth charges and mines to its manufactures. During World War II, the station had 13,000 employees who manufactured 57,653 torpedoes, about a third of all torpedoes manufactured in the United States. In 1942, the Navy authorized the station to proof-fire 100 torpedoes a day. Through testing and actual warfare, unexploded torpedoes and other ordinance are historically significant, if potentially dangerous components of the military landscape of Narragansett Bay and Rhode Island and Block Island Sounds. In 1944, the Stonington, Connecticut fishing trawler *Nathanial B. Palmer* sank after a mine caught in a fish net exploded.

Narragansett Bay and Rhode Island Sound during the first half of the 20th century. On the eve of the Second World War, six battleships, eight cruisers, thirty destroyers, two submarines, two destroyer tenders and two supply ships along with many smaller vessels were based in Rhode Island.

Naval facilities developed to service this growing Navy presence. In 1900, the Navy created the Bradford Coaling Station near Melville, near the site of the Portsmouth Grove Civil War hospital. Again Stephen Luce, although now retired, was involved in this decision. By 1917, the coaling station had developed into a general fueling facility, with extensive oil storage capacity. By 1937, it could store 13 million gallons of fuel. More capacity was added during World War II.

Military naval and military activities in Rhode Island and its waters during the Second World War. Providence yards built Liberty ships and the famed Herreshoff shipyard built small boats for the Navy.

In 1940, the Navy broke ground on what would become the Quonset Naval Air Station, one of two naval air stations on the east coast. Used first a training facility it became a command center for the First Naval District. "Quonsett-based aircraft carriers and planes participated actively in antisubmarine warfare, convoy escort duties, and air and sea rescue missions, as well as in air patrol operations in coastal waters" (Schroder 86-88). In 1942, the Navy built the Naval Auxiliary Air Facility in Charlestown with an on the ground deck for carrier landing practice. The skies above the study area saw countless thousands of over-flights by military aircraft, several crashed in coastal waters.

Other naval facilities developed in Rhode Island during World War II included: a naval supply depot at Coddington Cove (1942); the naval net depot that built steel anti-submarine nets (1941); a marine Barracks at Coddington Cove (1943); a naval magazine on Prudence Island (April 1942); a communication station at Beavertail (1941); a small arms firing range at Sachuest Point (1942); a naval operating base in Newport (August 1941); an anti-aircraft training center at Price's Neck near Brenton Point (1942); an inshore patrol facility on Long Wharf in Newport; and a demagnetizing facility at Gould Island used counteract mines or torpedoes attracted to ships or detonated by magnetism. (Schroder)

In 1942, the Navy built a Motor Torpedo Boat (Patrol Torpedo Boat) Squadrons Training Center at Melville (February 1942). By 1944, the center's 28 PT boats worked extensively in the Rhode Island coastal waters and acted as listening posts farther out to sea (Schroder).

Between 1952 and 1973, the Cruiser-Destroyer Force Atlantic based out of Newport. In 1973, the Navy dramatically downsized its Rhode Island presence, cause serious economic damage. The War College remained open as did the Navy Undersea Warfare Center and smaller navy unit, known as Surface Group 4, comprising mostly frigates and minesweepers, (What a Difference a Bay Makes, 100-103)

The history described above influenced the Ocean SAMP study area in many ways over the past 300 years. Conflict and peacetime Navy operations have left a rich repository of submerged archaeological sites. By far the greatest numbers of potential and known sites are tied to World War II and/or the development of Naval facilities in Rhode Island during the later-19th and 20th centuries. These resources include vessels lost by accident, vessels deliberately sunk as part of weapons testing, derelicts, military aircraft, merchant marine vessels sunk during war, ordnance, and other lost or abandoned military equipment. The locations of these resources are known, many others certainly await discovery.

Shipwrecks and other submerged archaeological sites tied to the American Revolutionary War are central to understanding the importance of the military landscape of the Ocean SAMP area. Rhode Island's coastal waters have perhaps the largest number of known Revolutionary War shipwreck sites in the United States. The intensity of American, British and French military activity in Rhode Island from 1775-1778, makes probable that unidentified vessel losses occurred and that yet unknown Revolutionary War shipwrecks await discovery in or near the Ocean SAMP area.

Rhode Island was one of the great centers of American privateering during many of the Wars between the late 17th century and the end of the War of 1812 and numbers related shipwrecks

almost certainly occurred in the SAMP area. Two privateers are known to have been lost in Rhode Island waters with the more likely awaiting discovery.

Known and potential military-related shipwrecks from other periods of Rhode Island history also contribute to the submerged military landscape. While few in numbers and less characteristic of the overall landscape, some of these may be highly significant. Military vessels from the late-17th century or early-18th century, as yet unknown, if discovered they would contribute significantly to our understanding of Rhode Island history.

4.1.5 Energy Landscape

For nearly 300 years, the production and transfer of energy has shaped the cultural landscape of the SAMP area and adjacent coastal areas. The initial shaping took place on land, but during the nineteenth century, it encompassed the ocean.

For more than one thousand years before the European invasion of New England, Block Island supported large Indian populations. They met their energy needs by taking sustainable quantities of wood from the island's dense forests. When Europeans settled Block Island in 1662, they commenced altering an ecosystem and visual landscape created through centuries of deliberate Indian activity (Cronon 198E). The limited coverage of trees and miles of stone fences marking the island today resulted from a quest for energy that soon exhausted the Island's forests. In 1721, Simon Ray, a town elder warned that the wasteful consumption of trees could force the community to abandon the Island for lack of fuel and building material. Survival came not from rational conservation but the discovery of Block Island's vast beds of peat. Wet compressed decomposed organics; peat is the geological ancestor of coal. Using peat for fuel required Block Islanders to engage in the time consuming and laborious process of digging, flattening, stacking, and drying. Known as "tug" on Block Island, the fuel was carefully stored in purpose build "tug houses." Between about 1750 (possibly earlier) and 1860, peat provided the only reliable source of energy on Block Island (Livermore 1877). The work required to gather and process peat made it an expensive source of energy when measured in terms of human time and effort. In effect, Block Islanders have been paying a premium for energy for nearly three hundred years though hard work and high prices.

A 1846 shipwreck in Cow Cove brought some interest in a new fuel for Block Island, coal. However, it took some time for coal to be accepted on the Island with the shift from native peat to imported coal coming with the 1873 completion of federal protected harbor and landing (Old Harbor). Began in 1870, the harbor ushered in a new era on the Island. According Reverend Samuel Livermore, a Block Island historian writing in 1877, more construction had taken place on the island in the previous five years, than in the fifty that proceeded it. Livermore also described in the installation of the Island's first coal furnace, in the First Baptist Church in 1875. By that year, Islanders had gotten past their fears and had shifted to the coal for their household stove

In 2010, the transportation of energy dominated commercial shipping through the SAMP area, accounting for 80 percent of the volume of cargo entering Narragansett Bay. This figure will rise if the proposed Hess LNG terminal at Weaver's Cove is constructed. Transporting energy by sea brings risks. In 1996, the *North Cape*, a barge containing 3.9 million gallons of home heating oil, grounded at Moonstone Beach in Rhode Island. The ensuing spill of 828,000 gallons was the one of the worst environmental disaster to occur in Rhode Island's waters. In term of

human use and its cultural and environmental impacts, the *North Cape* grounding was but one of the latest in hundreds of energy transport related accidents that have occurred over the past 170 years in the SAMP area (http://www.fws.gov/Contaminants/restorationplans/NorthCape/NorthCape.cfm, Ocean SAMP Chapter 7).

New England's dependence on energy delivered by sea through the SAMP area resulted from major historical processes that transformed the United States into the world's leading industrial economy. Three processes directly associated with Rhode Island created unprecedented demands for fuel in New England: the introduction of stationary industrial steam engines, the expansion of heat intensive metal manufacturing processes, and the replacement of wood by coal for industrial energy. Just as industrialization shaped Rhode Island's historic landscapes on land, it exercised parallel effects in the SAMP area, leading or contributing substantially to hundreds of accidents and deaths through shipwrecks and to major alterations to environment through the construction or improvement harbors, dredging of shipping channels, construction or improvements to lighthouses, docks, and lifesaving stations.

Although the "Ocean State", Rhode Island 's history is more commonly associated with industry than the ocean. Many landmark moments in U.S., industrial history occurred in Rhode Island. In 1780, the Brown family installed the second industrial steam engine in the United States. Used to pump water, the engine kept an iron mine in service to supply a successful Brown blast furnace (Hunter 1985). Ten years later in a historic partnership, Moses Brown and the English millwright Samuel Slater constructed the first Arkwright-style textile mill in the United States (Coleman 1963). Like other American mills of the period, the motive power came from flowing water. However, in another Rhode Island first occurring in 1827, Slater established a steam-powered textile mill at Providence. Slater's steam mill also effectively inaugurated the New England energy lifeline. The anthracite coal used to fuel the mill originated Pennsylvania's Schuylkill region (Coleman 1963). Coal's several hundred-mile journey from mine to mill followed a freshwater path to Philadelphia where it embarked on an sea voyage that would passed by Block Island into Narragansett Bay and up to Providence.

The spread of the stationary steam engine such as the one used by Slater, facilitated the growth of industry in New England, and freed it from geographic dependence on waterpower. Stationary steam allowed industry to centralize in urban areas where mill, factory, and foundry operators could find readily available pools of skilled and unskilled labor, excellent sources of capital, and well developed ports and railway connections (Hunter 1985). Providence became the national capital for stationary steam with the 1849 patenting of the Corliss Engine, developed and manufactured in Providence. With improved fuel efficiency and operational consistency, the Corliss became the nation's most important steam engine with nearly 500 constructed in Providence before the Civil War (Hunter 1985).

The Corliss works was one of many energy intensive precious and base metal enterprises that transformed Rhode Island into America's most industrialized state. By 1880, Rhode Island's steam engines produced 38.1 horsepower per acre; nearly double Massachusetts (21.3), four times New Jersey (9.8), and nine times New York (4.9) (Hunter 1979). Rhode Island's concentrated style of industrialization was occurring across the urban areas of southern New England. Between 1850 when American's consumed an estimated .36 lbs of coal per capita and 1918, coal consumption grew 77-fold nationwide, with a sizable proportion of this increase occurring in New England. . By 1907 American were consuming nearly 5 tons of coal per

capita annually (Schurr 1960), In the industrialized areas of New England the per capita consumptions was much higher. That year over 10 millions tons of coal arrived at New England ports, 3.5 million in Providence alone. In 1918, perhaps the peak year for the coal trade, the regional figure of coal shipped by sea reached nearly twenty million tons (Gordon 1978; *Atlantic Deeper Waterways Commission* 1908).

Unlike America's other industrializing regions, New England lacked native coal in industrial quantities. For New England's industries to thrive, they relied on inexpensive coal mined in Virginia, West Virginia, Kentucky, Ohio, and Pennsylvania and transported as cheaply as possible. During the second half of the nineteenth century an add-hoc and grossly inefficient system of coal transportation by sea developed. Canals, rivers and railroads carried coal to the major Atlantic ports where it was loaded on a grimy armada of schooners, schooner-barges, and barges that sailed or steamed north to a bewildering array of destinations. Figure 3 below produced in 1929 depicts the general flow of coal from mine to New England. (It does not represent the several ports that shipped coal through much of the period when coal transportation to New England expanded. By the 1920s, coal shipping had centralized in Virginia). In 1903, midway through the expansion of the coal trade, the principal coal companies reported delivering product to 142 separate destinations, most of them in New England. The quantities sent were huge, but many of the vessels were not. In January of that year, Boston received 333,000 tons of coal and Providence 181,000 tons (57th Cong. 2nd Sess. H. Doc. 15 pts 7,8 & 9 *Monthly Summary of Commerce and Finance of the United States for the Fiscal Year 1903*).

Large quantities of coal combined with a decentralized fleet, many of them small vessels made the New England coal trade contribute to the highest levels of traffic and human activity in the recorded history of the SAMP area. During the peak decades of coal, maritime traffic dwarfed the contemporary levels described in the Ocean SAMP Chapter 7, exceeding it by orders of magnitude in term of the numbers of ships and transits. In 1893, more than 60,000 vessels passed by Point Judith. Most of these (34,000) were classified as schooners. Barges accounted for an addition 9000 transits. With current data, it is difficult to precisely estimate the proportion of these vessels engaged in the coal trade but it would include nearly all of the barges, and probably a significant majority of the schooners. The 60,000 figure does not include the sizable number of larger schooners and schooner-barges that passed through the SAMP area east of Block Island the same year (55th cong. 2d session House Document 60, *Harbors of Refuge at Point Judith, Block Island, and Great Salt Pond, etc.* 1903).

At the beginning of the twentieth century, coal carriers followed one of two main routes through the SAMP area. Many, probably the majority, steered a course past Point Judith, sailing closer to the mainland than Block Island. Larger vessels or those transiting to or from ports further north often passed east and south of Block Island. When threatened by heavy weather, these vessels sought protection on the lee sides of Block Island, a practice that contributed to many shipwrecks (55th cong. 2d session House Document 60, *Harbors of Refuge at Point Judith, Block Island, and Great Salt Pond, etc.* 1903).

Future research is required to provide estimates of the number of wrecks occurring in the SAMP area before the Civil War, or that relate to commercial fishing. Current data, however, suggests that the majority of shipwrecks in the SAMP area involved transportation of coal to New England during a fifty year of period between 1870 and 1920 when the United States developed into the world's largest industrial economy. The rapidly increasing demand for abundant AND inexpensive energy in New England led to the creation of an ad hoc system of

transportation that relied on many low-cost and vulnerable types of vessels operated by poorly paid mariners who represented the lowest strata on the maritime social scale (*Hearing Held Before the Committee on Merchant Marine and Fisheries on House Bill 11372*, December 14, 1911).

The study area's energy landscape is highly significant in the history of Rhode Island and greater New England. The coal vessels provided critical infrastructure without which the region would have languished economically after the Civil War. It has been a largely forgotten chapter in the states maritime or industrial history. Where merchant vessels such as the famous Brown family East Indiaman *Ann and Hope* that wrecked at Block Island in 1815 were highly visible in cultural terms and associated with the wealth and social status of their owners, the coal vessels brought few and fleeting profits and only rarely contributed to social status to their owners, officers, or crew. Indeed other merchant mariners often regarded the grimy armada of coaling vessels and their crews with mixture contempt and pity due to the low wages, harsh living conditions, mixed racial composition of the workforce, and the frequent accidents they endured (*Hearing Held Before the Committee on Merchant Marine and Fisheries on House Bill 11372*, December 14, 1911).

Figure 3. Tidewater Shipments of Bituminous Coal, 1929

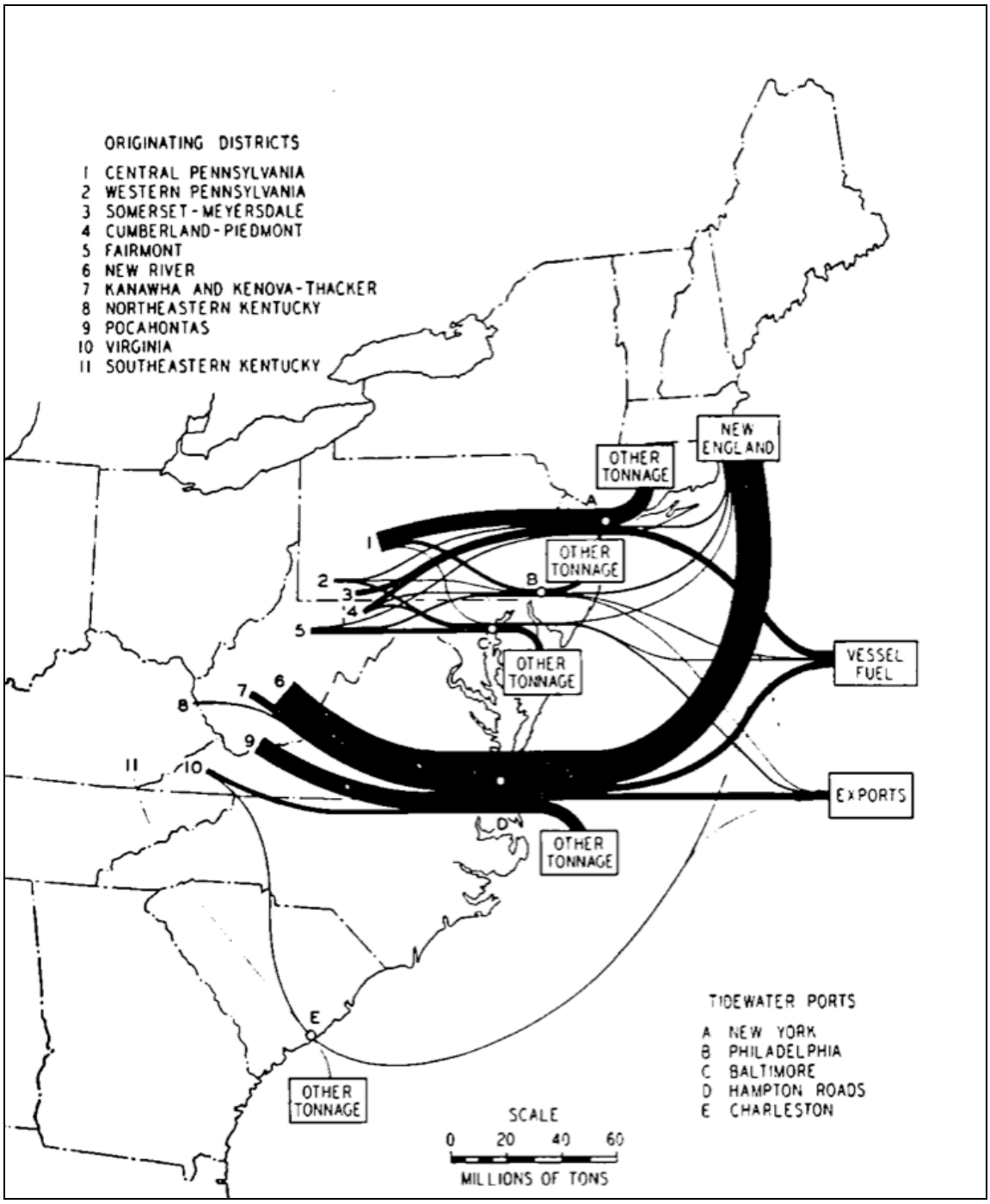

The rapidly growing New England coal trade operated within a unique context of obsolescence, innovation, and forced operational economy. It resulted in a complex and historically significant cultural landscape in the SAMP area consisting of shipwrecks, harbors, canals, lifesaving stations, and aids to navigation. Among the most common wrecks are those of merchant sailing vessels built in the 1850s, 1860s, and 1870s and repurposed to carry coals, towed in long lines behind steam tugs. As the demand for coal continued to grow and the supplies of older ships diminished, new classes of vessel evolved to fill the void, including some of the largest commercial sailing vessels ever built (Snow and Lee: 1999). Less majestic and

more common, shipyards turned out specially designed schooner-barges—sail-equipped vessels with some capacity for independent navigation. Over time, however, the relentless drive for economy led to an increasing emphasis on cheap, easy to construct barges –many with poor seagoing capacities

A full analysis of wrecking in or near Rhode Island's outer waters has not been completed, but preliminary research conducted by SAMP researchers suggest that number of serious wrecking events occurring per decade in the region may have increased as much as six-fold between 1870 and 1900, with disasters continuing to occur at high levels into the 1920s. The most serious accident, the sinking of the Joy Line Steamer *Larchmont* through collision with a coal schooner occurred in 1907. That one alone event resulted in the deaths of more than 100 people. In 1909, a collision between the *Merrill C. Hart* and *John S. Bennett* sunk both vessel and claimed 11 lives. The Bennett was heading to Halifax N.S. with a load of coal while the Hart was heading to New York probably to load coal (*New York Times* 11/10/1909; *Annual Report Chief of Engineers* 1910: 12). In 1911, destruction of the coal carrying schooner-barges *Vermont* and *Helen A. Wyman* near Block Island claimed six to eight lives, possibly including the wives of the two captains. The wreckage thoroughly covered the island's western beaches (*New York Times* 11/21/1911).

The shipwrecks of the SAMP area's energy landscape are important heritage resources associated with the industrialization of American seafaring. While not every wreck merits preservation, they all potentially can contribute a broader understanding of human activity within the SAMP area. At the very least, many of the energy related shipwrecks are almost surely eligible for the National Register of Historic Places. In addition, specific areas of the SAMP may be eligible as rural cultural landscapes. Other locations are beginning to study and preserve industrial vessels such as those found in the SAMPO. At the Stellwagen Bank National Marine Sanctuary in Massachusetts NOAA archaeologists recently documented three coal schooners, *Paul Palmer*, *Frank A. Palmer*, and *Louise B. Crary* and prepared a successful nominations to the National Register of Historic Places. Archaeologists working in the Great Lakes region have documented and nominated numerous industrial era steamers, schooner, schooner-barges and related craft. Determining which of wrecks in the SAMP area 's energy landscape should be included on the Register will require a broader scale regional study. At this point, any coal vessels built more than fifty years ago are potentially eligible for listing.

There is no clearly defined temporal end to the coal era in the energy landscape. In 2007, more than 4 million tons of coal entered Narragansett Bay and transited through the SAMP area. The context of industrial shipwrecks, however, can be more tightly defined. During the 1920s structural changes in the transportation of coal and advances in marine safety and navigation greatly reduced, although did not eliminate the wrecking of coal carrying vessels in the SAMP area. The centralization of coal shipping in Virginia and improvements in the receiving of coal at larger New England ports removed physical and economic roadblocks that prevented investments in safer large capacity coal barges and vessels. As long as waiting times to unload were irregular and often protracted, larger, safer, and more capital-intensive vessels could not compete with the inferior or less expensive vessel whose wrecks line the bottom and shorelines of the Atlantic Coast from Virginia through New England.

Coal dominates the energy landscape, but other fuels and technologies have an important presence also have an important presence. While the absolute volume of coal transported through the SAMP has continued high, its relative dominance in New England's energy lifeline

began to slowly diminish after 1918 and rapid increases in the use of oil for fuel. In 1918, the burning of fuel oils produced the equivalent of 8% energy of the total energy produced by coal in the United States. By 1922 that figure had doubled to 16% and by 1935 reached 21.5% (Schurr 1960). Although coal in vast quantities fueled New England's power plants, it was increasing amounts of petroleum in the form of fuel oil, kerosene, and gasoline that provided energy to heat homes and power the millions of new motor vehicles that were reshaping the country.

In 2007, more than 6 million short tons of petroleum products entered Narragansett Bay via the SAMP area (SAMP Chapter 7). As the 1996 *North Cape* grounding illustrated, the conveyance of petroleum products is an important and potentially dangerous component of the SAMP area's energy cultural landscape. Like coal, it the conveyance of petroleum has a unique history, one marked in the landscape by shipwrecks and shore facilities. The history of transporting petroleum products by sea differs greatly from coal. It developed quickly and took on a highly rationalized form that included efficient port infrastructures for loading and unloading (Schurr 1960).

Modern tankers first appeared in Europe in the 1880s, with the first American built tanker launched for Standard Oil in 1888. Tankers became more common with increased use of petroleum for fuel and this became increasingly true with the mass production of the automobile and the skyrocketing consumption of gasoline. In 1918 Americans consumed an estimated 74.5 million barrels of gasoline, a figure that grew 7-fold by 1939, the year that the tanker *Lightburne* ran aground and broke up on Block Island carrying a cargo of gasoline and kerosene (Schurr 1960; Snyder 2001). The *Lightburne* was not the first petroleum-carrying vessel to wreck in Rhode Island. A wreck the may be even more historically significant that the is the old iron tanker *Llewellyn Howland* that ran aground and broke up on Seal Ledge, dumping thousands of barrels of fuel oil into the SAMP area in 1924 (Snyder 2001). The *Howland'*s history is not well known; however, research by URI investigators suggests that it is a first generation oil tanker built in 1888, and a very likely candidate for the National Register of Historic Places.

The production and distribution of energy dramatically shaped in the cultural landscape of the Block Island and Point Judith areas. Some of the landscape features such as historic shipwrecks associated with the transportation of coal and petroleum are easy to identify in this historical record and to associate with the energy landscape. The cultural and historical significance of this is archaeological landscape is clearly high, but determining specific value of the individual wrecks that help to define the landscape will requires further research and analysis. At a minimum level, these wrecks connect with a time in history (1870 – 1920) when the human footprint on the ocean area seemed more pronounced and its visual characteristics markedly different from 2010. Crossing over to Block Island on a typical day would have presented passengers with an industrial maritime thoroughfare characterized by passage of hundreds of vessels and thousands of people. On land, modern harbors, industrial docks, deepwater navigation channels, and shipping lanes that developed during this period are just a few of the non-shipwreck landscape feature that connect in meaningful and *documentable* ways with the area's energy landscape.

Contemporary plans to develop renewable offshore energy in the Block Island area are a direct continuation of three centuries of energy history. The connection of the proposed wind turbines with Block Island's power grid would provide the community with a local source of energy that is at one reliable, renewable, and economical--the first since Indian people last controlled the island's forest resources in the 17th century. Implemented with care offshore

wind energy should pose little overall threat to the historical significance, meaning, and preservation of the energy landscape and its individual components. Distinctive and new, the proposed towers would become come the latest cultural signature on the area's historic energy landscape.

4.2 Submerged Telecommunications Cables

Modern telecommunication cables and corridors are well understood in the Ocean SAMP area. The southern coast of Rhode Island has been heavily utilized in a succession of transatlantic communication cables. Cables currently "in service" include Transatlantic No. 12/13 (TAT-12/13), part of which runs from Green Hill, Rhode Island to Lands End, England; Gemini, part of which runs from Charlestown, Rhode Island to Oxwich Bay, near Swansea, Wales; and FLAG Atlantic 1 which runs from New York to the UK intersecting Long Island Sound and Block Island Sound. "Out of service" cables include Transatlantic No. 5 (TAT-5), part of which runs from Green Hill, Rhode Island to Conil, Spain; Transatlantic No. 6 (TAT-6), part of which runs from Green Hill, Rhode Island St. Hilaire-de-Riez, France; and Transatlantic No. 10 (TAT-10), part of which runs from Green Hill, Rhode Island Norden, Germany. The majority of these cables whether in service or not, run out of Green Hill, RI to the southeast and then south, passing between 3 and 9 nautical miles east of Block Island. The exceptions are TAT-12/13 and FLAG Atlantic 1, which run west of Block Island.

Historic cables, however, are less well understood than their modern counterparts, and under certain circumstances might be considered historic resources. They also present problems for management of development projects. Of particular concern to marine planners in the Ocean SAMP region is the cable area off the southwest coast of Block Island, which runs across Blocks Island Sound to Montauk Point on the eastern end of Long Island. In an attempt to understand the origin of this area and its potential to house historic resources, we traced the cable laying history of Block Island Sound.

In 1880, Congress appropriated $15,000 for the US Army Signal Corps to lay the first telecommunications cable from Block Island to the mainland. The work was complete in 1884. Although justified for military communications and the transmittal of weather information, Rhode Islanders clearly saw this as a way to attract Federal dollars for communication infrastructure that would allow connections with the otherwise isolated communities on Block Island. Safety-at-sea was also an immediate concern. Throughout the state's history, shipwrecks and loss of life-at-sea in the SAMP area had never been higher.

The two-conductor cable ran from Sandy Point at the north end at the Block Island to Narragansett Pier (Annual reports of the War Department, 1899; An Act to Authorize the Laying of a Telegraph Cable from the Main Land in Rhode Island to Block Island, 14 Jan. 1880). Within two years, however, the cable was unserviceable and Congress appropriated an additional $18,350 to replace it. Lawmakers specifically recognized the importance of the Block Island cable and the role it played in connecting signal stations with life-saving stations and lighthouses. (Statutes of the United States of America, 1885-1886). In March 1888, the cable was rendered unserviceable for a second time. This time a vessel (possibly the schooner William Jordan), that had become stranded some time, broke apart in a springtime storm and severed the cable. By the turn of the century, the signal corps had repaired the cable, but now started to question its military utility and its value for transmitting weather information. Its utility, however, for general telegraph communication, life–saving, shipping, and commerce was still

acknowledged. According the Chief Signal Officer of the Army in 1889, the Block Island line, and a similar cable connecting Nantucket with the mainland, were "probably the most valuable of all the sea-coast lines, giving ….service to about 75,000 people during the hot summer months, and at the same time sending valuable vessel reports." (Annual Report of the Chief Signal Officer of the Army, 1889). He went on to question, however, the military utility of the cables and hinted at a transfer of ownership and responsibility.

In 1902, the Block Island cable, was transferred to the Weather Bureau, under the Department of Agriculture, on condition that the Bureau maintain it and allow military use of it during war. By this time, the salt-water environment and marine organisms (particularly teredo) had once again taken their toll on the communication infrastructure. The cable had become so badly deteriorated that the Department of Agriculture requested an appropriation of $40,000 for a complete replacement. This time guttapercha would be used instead of rubber. [Annual Reports of the Department of Agriculture, 1902; A Digest of Opinions of the Judge of the Advocates General of the Army, 1912]. The current cable corridors from the north end of Block Island to the mainland stem from these years.

Figure 4. Map Showing De-Accessioning of Communications Cables after WWII (NARA's Northeast Region (Boston), Waltham, MA)

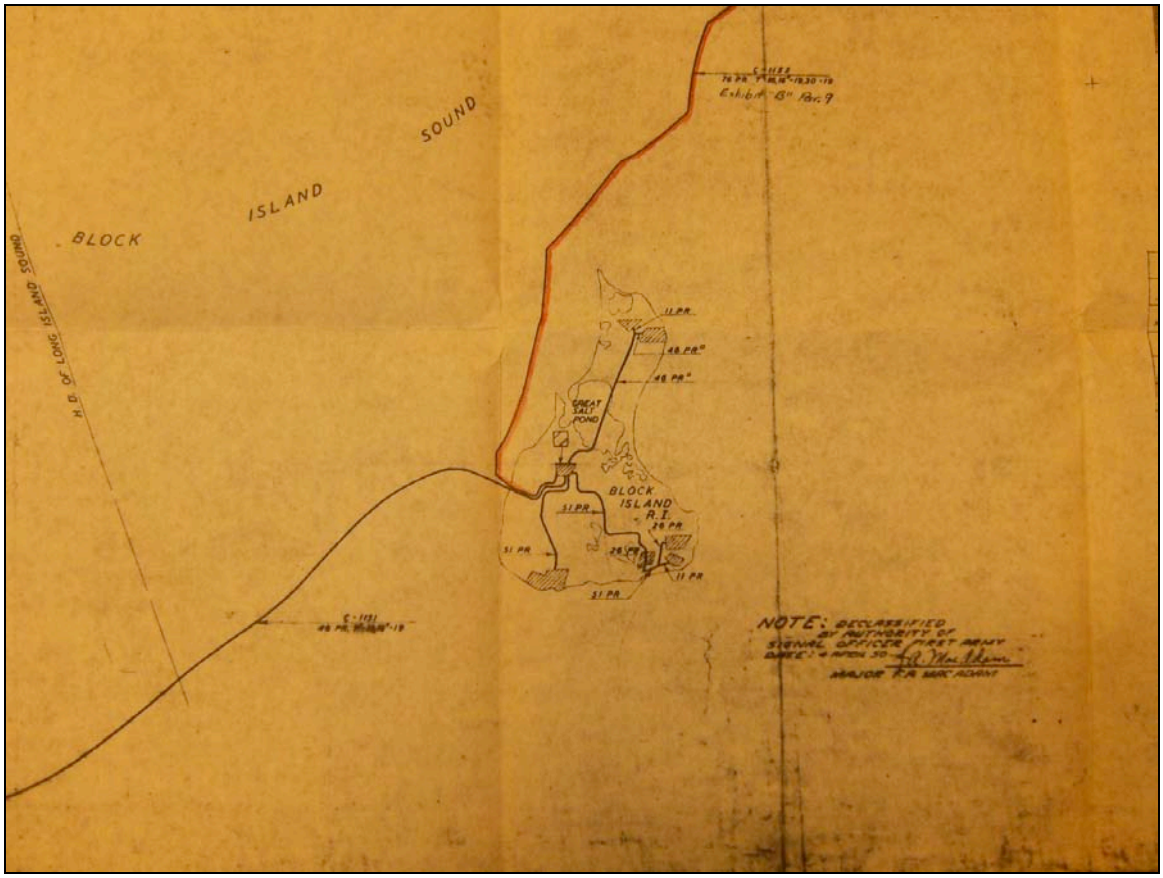

During WWII, as German submarines threatened the Atlantic coast of the United States, the US military renewed its interest in signal stations and communication cables. As a result, the army and navy initiated an extensive cable laying operation, requiring governmental easements over private property on land and the designation of new cable corridors in Rhode Island Sound,

Block Island Sound and Narragansett Bay. This cable infrastructure included cables that ran from Fort Greene (then near Point Judith) to Green Hill, and from there onto stations at Charlestown, Noyes Point and Watch Hill. It also included cables from Block Island to Fort Greene (near Point Judith) and Block Island to Montauk Point, Long Island. Block Island's southwest cable corridor originates from this time. Both the Block Island cables were de-accessioned between 1956 and 1957 (Submarine Cable Easements – Narragansett RI, 1957-1958, Record Group 269, GSA, 1922-1997; Submarine Cable Easements – Block Island, RI, 1956-1960, Record Group 121, Records of the Public Buildings Service, 1801-1976) (Figure 4)

4.3 Database Amalgamation and Archaeological Site Distribution Patterns

Attempts to create a master list of Rhode Island shipwrecks, by combining databases and adding geophysical and archival data are still ongoing. Analysis thus far, however, does enable some preliminary findings as to about site and temporal distribution patterns in the Ocean SAMP area.

During the last 300 years, there have been at least 1200 maritime accidents and disasters Rhode Island and Rhode Island Sound that probably resulted in vessel loss and/or deposition of cultural material. This number excludes many 17th and 18th century accidents that are much more difficult to track in the historical record. Of the 1200 or more vessels lost in RI waters, approximately half occurred in the SAMP area. Of these, more than half have some locational association with Block Island. Other places strongly represented are the waters off Point Judith, Watch Hill and Beavertail.

It is difficult to know how many of the recorded maritime accidents and disasters left a material record that can be found, studied, protected and analyzed – but it is certainly a significant number. We have good location information for approximately 50 shipwrecks in the SAMP area, but given the number of known wrecks, many others clearly await discovery and assessment. The complete results from all geophysical survey conducted as part of the Ocean SAMP study are not yet available, but when the archaeological processing of that data is complete the RIHPHC will have additional shipwrecks and/or better information in their database. Much of the Ocean SAMP area remains un-surveyed for archaeological sites and important historic resources certainly lie in those areas.

Figure 5 shows the preliminary spatial distribution of Reported Rhode Island Shipwrecks. This data was compiled from multiple database sources, but it is yet to be fully analyzed and consolidated. Not all the shipwrecks have been confirmed and in a few instances the map contains more than one point for an individual shipwreck. Nevertheless, and despite its weaknesses, the map shows identifiable spatial patterning from which some general conclusions might be drawn.

Figure 5. Potential Historic Shipwreck Locations

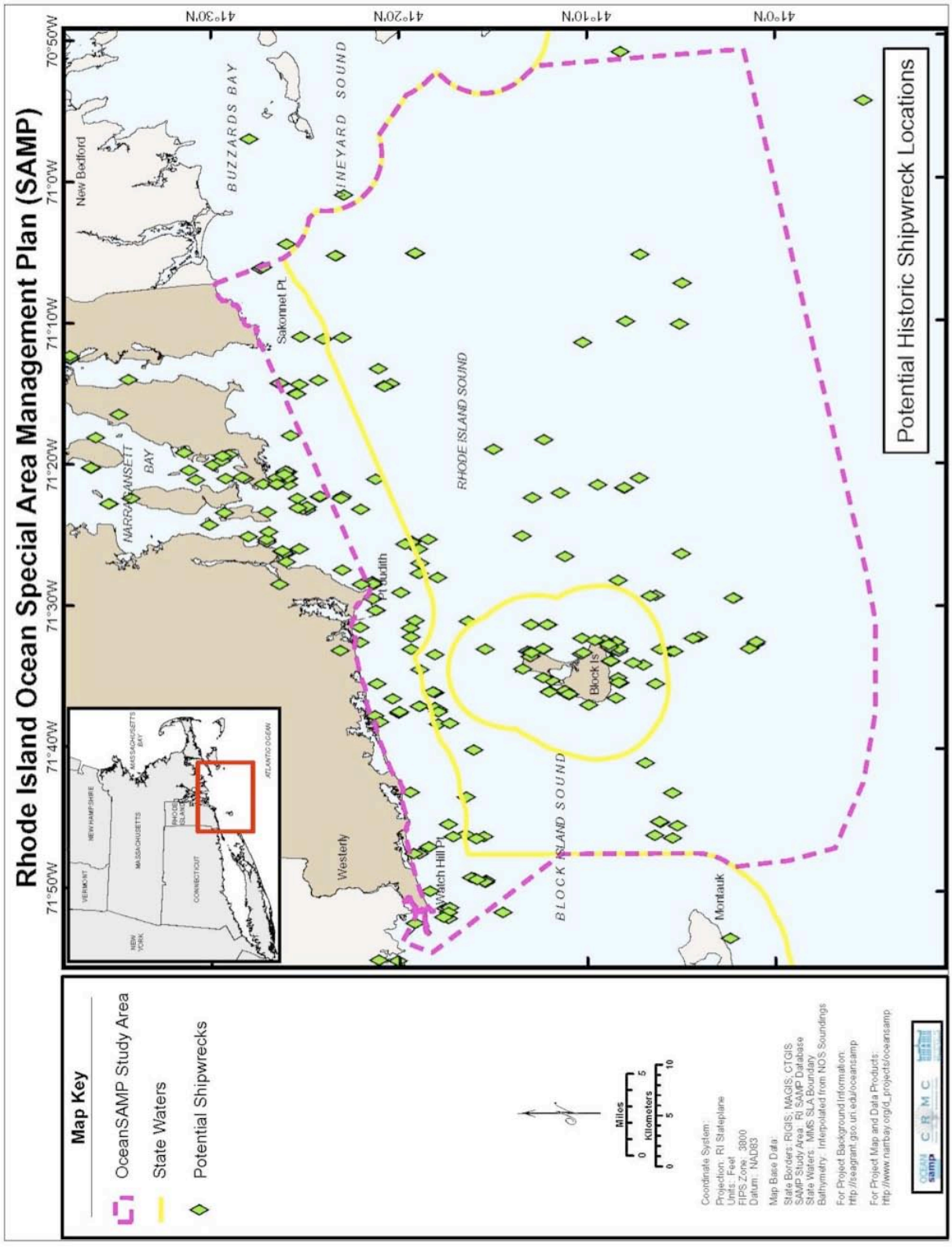

Block Island has been a focus of vessel loss in Rhode Island waters. Heavy levels of commercial traffic over the past three centuries combined with strong currents, storms and frequent periods of heavy fog created environment in which shipwrecks on shore and collisions at sea were relatively common. The Ocean SAMP area shows another concentration of shipwrecks in a corridor that runs along the southern edge of the Rhode Island coast from Watch Hill to Point Judith. The lee shore and heavy levels of commercial and passenger traffic during the nineteenth century out of New York and along the southern coast of Connecticut and Rhode Island are largely responsible for this concentration. This heavier concentration, along with dangers to navigation around Block Island, go a long way in explaining higher densities of shipwrecks in the northwestern part of the SAMP area. There is, however, an important caveat. The central-southern and southeastern parts of the SAMP area were further off shore and further away from land observation. Stricken vessels in these areas were less likely to be have been seen and less likely to have boasted survivors. In addition, there have been fewer modern attempts to map the ocean floor in the central and eastern parts of the SAMP area. As a result, our knowledge of these areas is less authoritative. They probably contain higher numbers of shipwrecks than are reflected current distribution patterns.

Figure 6. Temporal Distribution of Shipwrecks in the Ocean SAMP Area (Mather, 2010)

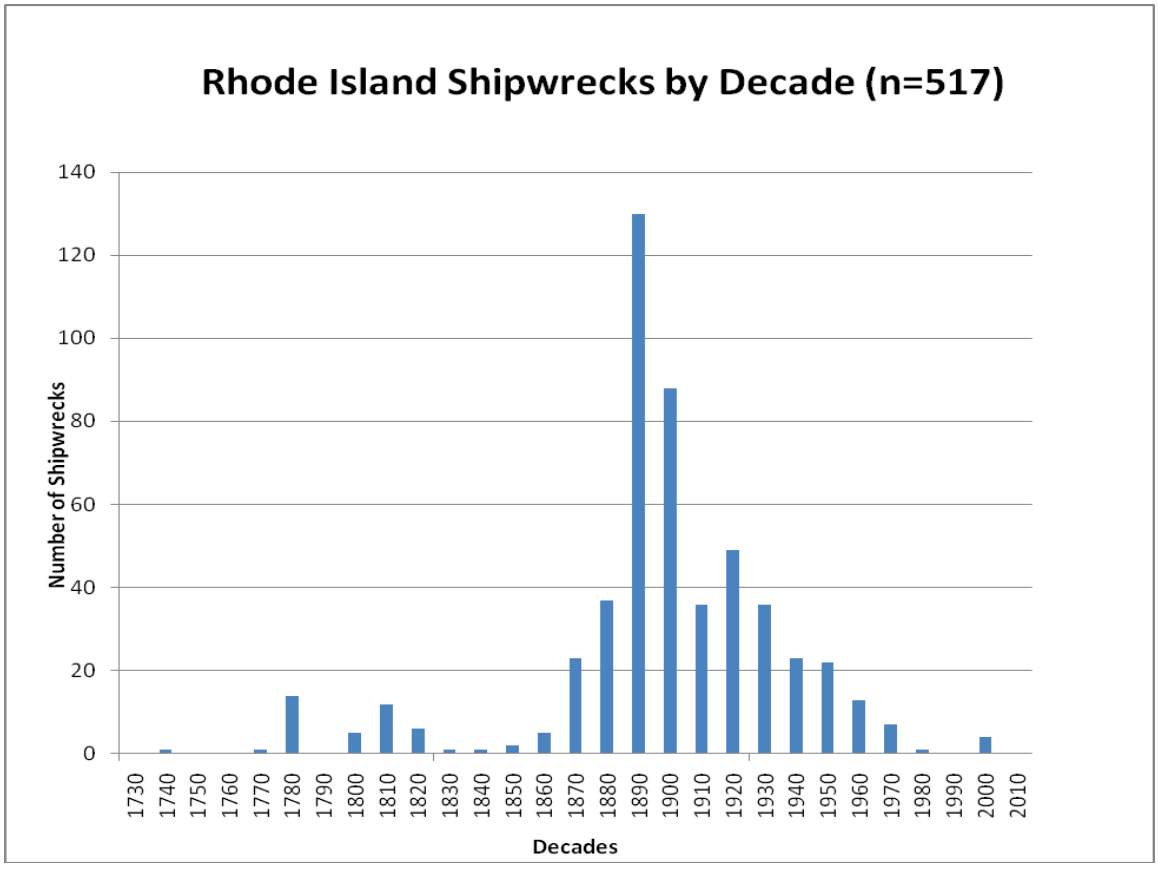

Figure 6 shows the temporal distribution of Rhode Island shipwrecks from the early 18th century to modern times, grouped by decade. The data comes from the URI Working Database, but analyses of other Rhode Island shipwreck databases mirror these results.

The graph shows a spike in the number of Rhode Island shipwrecks during the Revolutionary War and another during the first two decades of the nineteenth century. Starting in the 1860s, Rhode Island saw a sharp rise in the number of shipwrecks occurring in its waters. The numbers continued to rise, reaching their zenith during the 1880s. This certainly resulted from the rapid expansion of shipping activity across the Ocean SAMP area during America's most rapid period of industrial development. Demands for energy, particularly coal, in New England during the late 19th century caused hundreds of vessels a day to move through the Ocean SAMP area. Heavy traffic, hazardous waters and pre-electronic navigational instruments, provided a recipe for high losses of shipping and life. A decline in the number of shipwrecks per decade in the in the 20th century corresponded with improvements in navigational instruments and greater capitalization of US shipping.

4.4 Archival Research Shipwrecks

The following is a tabular listing of shipwrecks in Rhode Island identified through archival research, primarily at the Regional National Archives in Waltham, MA. There is still more of this work to be done.

Table 1. Shipwrecks in Rhode Island Waters Identified Through Archival Research

Year	Name	Type	Location	Detail
1752	Halifax	Brig	Block Island	Wrecked
1752	Palatine	Ship	Block Island	Wrecked
1755	Martha and Hannah	Sloop	Block Island	Wrecked
1780	Golden Grove	Brig	Block Island	Wrecked
1781	Mars	Ship	Block Island	Wrecked
1807	Brutus			
1815	Ann and Hope	Ship	Block Island	Wrecked
1827	Hannah		Block Island	Sunk
1829	Echo			
1831	Warrior	Schooner	Block Island	Wrecked
1838	J. Palmer	Brigantine	Beaver Tail	Lost
1841	Fortitute	Sloop	Pt. Judith/Block Island	Sunk
1841	Forrest	Schooner	Pt. Judith/Block Island	Sunk
1842	Fortitude	Sloop		Sunk
1846	Atlantic	Steamer	Fisher's Island	Wrecked
1849	Mary Elizabeth		EastSide Block Island	
1850		Schooner		
1852	Fellowship	Schooner	Hulls Cove	Lost
1853	unknown	Schooner	Mackeral Cove	Lost
1853/54	Lemontine	Brigantine	Beaver Tail	Lost
1855	Moluncus	Brigantine	Block Island	Wrecked
1855	Silas Wright	Schooner	Narragansett Pier	Wrecked
1855	Nelson Harvey	Schooner	Whale Rock	Run Down
1855	Joseph C. Baxter	Schooner	Fishing Rocks	Wrecked
1855	William H. Tierce	Schooner	Point Judith	Wrecked

1855 North State	Schooner	Point Judith	Wrecked
1855 Tyrall	Schooner	Point Judith	Wrecked
1855 Elizabeth	Sloop	Point Judith	Wrecked
1855 Mary E. McHale	Schooner	Quonochontaug	Wrecked
1855 Issac Webb	Schooner	Noyes Beach	Wrecked
1855 Ere	Schooner	Noyes Beach	Wrecked
1855 Alida	Schooner	Point Judith	Leak, Sunk
1855 unknown	propellor	Green Hill	Sunk
1860 Target	Schooner	Kettle Bottom	Lost
1864 Amelia	Schooner	Point Judith	Wrecked
1864 Normany	Brig	Point Judith	Wrecked
1864 Mary	Schooner	Lions Head	Lost
1866 C.B. Hamilton	Barkentine	Point Judith	Wrecked
1868 Henry Hubbard	Schooner	Block Island	
1869 Sarah L.	Schooner	Point Judith	Wrecked
1869 Spray	Schooner	Narragansett Pier	
1869 Meteor	Brig	Point Judith	Wrecked
1869 unidentified	Schooner	Kettle Bottom	Lost
1869 Chas. E. Raymond	Schooner	Beaver Tail	
1869 Ezra H. Day	Schooner	Whale Rock	Lost
1872 Metis	Steamer	Watch Hill	Sunk
1872 H.T. Hedges	Schooner	Block Island	Refloated
1874 Harriet Lewis	Schooner	Beaver Tail	Wrecked
1874 Express Tilton	Schooner	Beaver Tail	Wrecked
1874 John Morris	Schooner	Narragansett	Wreck
1875 Robin	Schooner	Whale Rock	wreck
1876 Caroline and Cornelia	Schooner	Beaver Tail	Lost
1876 McGee	Schooner	Block Island	Broke Up
1876 Mary Augusta	Schooner	Block Island	Went to pieces
1876 Alfred Hurdle	Schooner	Lion Head	Lost
1877 Caroline Meenaie	Schooner	Block Island	Wrecked
1877 L.M. Lamond	Schooner	Block Island	Wrecked
1877 William S. Scull	Schooner	Block Island	Wrecked
1877 Bayuduce	Schooner	Block Island	Wrecked
1877 Venus	Schooner	Point Judith	Wrecked
1878 unidentified	Schooner	Mackerel Cove	Lost
1878 J.H. Duncan	Schooner	Block Island	Loss
1879 A.E. Hooper	Schooner	Block Island	Wrecked
1879 Alexendra	Schooner	Block Island	Wrecked
1879 Open Sea	Brig	Napatree Point	Sunk
1880 Illinois	Schooner	Point Judith	Wrecked
1880 Joseph Fitch	Schooner	Sugar Reef	Wrecked
1880 Paul and Thomas	Schooner	Fisher's Island	Sunk
1880 Nellie	Brig	Fisher's Island	Sunk

1880 Franklin Treat			
1881 Paladium	Schooner	Point Judith	Wrecked
1881 Calvin F. Baker	Schooner	Block Island	Refloated
1881 Tillie E	Schooner	Point Judith	Wrecked
1881 Lillie	Schooner	Block Island	Loss
1881 John T. Manson	Schooner	Block Island	Refloated?
1881 E. Sinnickson	Schooner	Block Island	Refloated?
1881		Block Island	?
1881 Roda G.	Schooner	Block Island	Loss
1881 Etta M. Story	Schooner	Block Island	Refloated?
1882 Sarah W. Blake	Schooner	Point Judith	Sunk
1882 Manhattan	Barge	Watch Hill	Wrecked
1882 Smith	Schooner	Beaver Tail	Lost
1883 Warren Gates	Schooner	Point Judith	Sunk
1883 Annie Whiting	Schooner	Block Island	Wrecked
1883 Strickland	Schooner	Brenton Reef	Lost
1884 Adrianna	Schooner	Block Island	Loss
1884 S.C. Noyes	Schooner	Block Island	Sunk
1884 Victor	Schooner	Block Island	
1884 Augusta	Brig	Block Island	Refloated?
1884 Nellie B.	Schooner	Block Island	Loss
1884 Julia A. Tate	Schooner	Point Judith	Wrecked
1884 Guard	Brigantine	Watch Hill	Sunk
1884 Clarissa Allen	Schooner	Stonington Point	Sunk
1885 Vrale	Schooner	Watch Hill	Sunk
1885 Bucco	Schooner	Lions Head	Lost
1885 Lizzie D. Barker	Schooner	Block Island	Loss?
1885 Almon Bacon	Schooner	Point Judith	Sunk
1885 Peacedale Woods			
1885 Fred A. Carl	Schooner	Watch Hill	Sunk
1885 Mott Haven	Schooner	Point Judith	Sunk
1885 Willie DeWolf	Schooner	Block Island	Sunk
1886 Cleo Chilcot	Schooner	Watch Hill	Wrecked
1886 Lucy Blossom	Schooner	Watch Hill	Sunk
1886 Isabella Jewett	Schooner	West Quague Beach	Wrecked
1886 Wild Pidgeon	Schooner	Block Island	Wrecked
1886 Toronto	Brig	Watch Hill	Wrecked
1886 Mary Natt	Schooner	Point Judith	Sunk
1887 Harry A. Barry	Schooner	Point Judith	Wrecked
1887 Path Finder	Schooner	New Shoreham	Wrecked
1888 William Jordon	Schooner	Block Island	Wrecked
1888 John Welah jr.	Brig	Point Judith	Wrecked
1888 Henry H. Olds	Schooner	Whale Rock	Sunk
1888 Issac Borden	Schooner	Point Judith	Wrecked

1889 Alexander Campbell	Bark	Block Island	Sunk
1890 Pocahontas	Schooner	Block Island	Wrecked
1890 Pochohantas			
1890 Lady of the Lake	Bark	Block Island	Wrecked
1890 Avenger	Schooner	Watch Hill	Wrecked
1890 Bill Stowe	Schooner	Narragansett Pier	Wrecked
1890 A.H. Hurlburt	Schooner	Narragansett Pier	Wrecked
1890 Carrie A. Lane	Schooner	Napatree Point	Wrecked
1891 Lydia Skolfield	Ship	Newport	Wrecked
1891 A.T. Boardman	Schooner	Block Island	Wrecked
1891 Sunshine	Schooner	Watch Hill	Wrecked
1892 Harry White	Schooner	Quonochontaug	Sunk
1892 Falcon	Catboat	Point Judith	Sunk
1892 Fashion	Sloop	Fort Adams	Sunk
1893 John Paull	Schooner	Green Hill	Wrecked
1893 East Wind	Schooner	Point Judith	Wrecked
1893 Highlander	Brig	Fisher's Island	Lost
1893 Reliance	Barge	Block Island	Lost
1893 Menunctatuck	Schooner	Watch Hill	scuttled
1893 Oliver Chase	Schooner	Point Judith	Sunk
1893 Rapidan	Schooner	Narragansett	Wrecked
1893 Rapidan pontoon 1	Pontoon	Narragansett	Wrecked
1893 Rapidan pontoon 2	Pontoon	Narragansett	Wrecked
1893 Rapidan pontoon 3	Pontoon	Narragansett	Wrecked
1893 Rapidan pontoon 4	Pontoon	Narragansett	Wrecked
1893 Wm. G.R. Mowry	Schooner	Beaver Tail	Wrecked
1894 Leonessa	Schooner	Watson Pier	Wrecked
1894 L.C. Foster	Schooner	Block Island	Wrecked
1894 scow no. 15	Scow	Narragansett	Wrecked
1894 scow no. 17	Scow	Narragansett	Wrecked
1894 Megella	Steam Brigantine	Point Judith	Wrecked
1894 Agricola	Schooner	Napatree Point	Wrecked
1894 Allen	Schooner	Fisher's Island	Wrecked
1894 Red Rover	Sloop	Block Island	Sunk
1895 Olinda (spanish)	Steamer	Fisher's Island	Wrecked
1895 Muriel	Sloop	Watch Hill	Wrecked
1895 Brunhilde	Schooner	Watch Hill	Wrecked
1895 Cora Yacht	Sloop	Brenton Point	Wrecked
1895 Josie F.	Schooner	Napatree Point	Wrecked
1895 unidentified	Catboat	Newport	Wrecked
1895 Evelyn	Schooner	Block Island	Wrecked
1896 Belle R. Hull	Schooner	Watch Hill	Wrecked
1896 Clarissa Allen	Schooner	Point Judith	Wrecked
1896 Water Witch	Brig	Brenton Point	Wrecked

1896 unidentified	Skiff	Newport	Wrecked
1896 Warsteed	Schooner	Quonochontaug	Wrecked
1896 Lady of the Lake	Schooner	New Shoreham	Wrecked
1896 unidentified	Catboat	Point Judith	Sunk
1896 Helen	Schooner	Block Island	Sunk
1896 Zephyr	Schooner	Watch Hill	Wrecked
1896 S.R. Parker	Sloop	New Shoreham	Wrecked
1896 Four Brothers	Schooner	Block Island	Wrecked
1896 Lady of the Lake	Schooner	Block Island	Wrecked
1896 Sea Serpent	Sloop	Block Island	Wrecked
1896 Sharon	Sloop	New Shoreham	Wrecked
1897 Edward M. McLaughlin	Schooner	Point Judith	Sunk
1898 Mary Ellen	Schooner	Point Judith	Sunk
1898 Actress	Schooner	Brenton Point	Sunk
1898 crocodile	Sloop	Quonochontaug	Wrecked
1898 Rose Brothers	Schooner	New Shoreham	Wrecked
1898 Lexington	Schooner	Block Island	Wrecked
1898 Cassie	Sloop	Block Island	Wrecked
1898 Nellie B.	Sloop	Block Island	Wrecked
1898 Arabell	Schooner	Block Island	Wrecked
1898 Aloha	Sloop	New Shoreham	Sunk
1898 Anna Pitcher	Sloop	Block Island	Sunk
1898 Agnes	Schooner	Point Judith	Sunk
1898 Vamoose	Schooner	Block Island	Wrecked
1898 Jonathan Cone	Schooner	Watch Hill	Wrecked
1898 Agnes		Off of Pt. Judith	
1899 Percy	Schooner	Block Island	Wrecked
1899 Addie M. Anderson	Schooner	Whale Rock	Sunk
1899 New Hampshire	Barge	unkonwn	Sunk
1900 Gertrude	Schooner	Block Island	
1900 Hudson	Barge	Block Island	Foundered
1900 Robert I. Carter	Barge	Block Island	Foundered
1900 Percy	Schooner	Block Island	Foundered
1901 Polas Wave	Fishing Schooner	Block Island	Sunk
1901 J.G. Fell	Schooner	Point Judith	Sunk
1901 Rhode Island	Schooner	Brenton Reef	Sunk
1901 Percy	Fishing Smack	Disabled off BI	Wrecked
1902 no name	Fish boat	Point Judith	Lost
1902 Glance	Catboat	Quonochontaug	Lost
1902 Kate and Mary	Schooner	Quonochontaug	Wrecked
1903 John J. Burkee	Brigantine	Watch Hill	Wrecked
1903 USS Leyden	Tug	New Shoreham	Wrecked
1903 Opitsah	Sloop	Quonochontaug	Wrecked
1903 Due	Sloop	Block Island	Wrecked

1903 Jennie R. Dubois	Schooner	New Shoreham	Wrecked
1903 Curlew	Sloop	Point Judith	Wrecked
1904 Louella	Schooner Yacht	Block Island	Lost
1904 Posiedon	Catboat	Point Judith	Sunk
1904 Young American	Sloop	Brenton Point	Sunk
1904 Peggy	Catboat	Block Island	Sunk
1905 George and Albert	Schooner	Brenton Point	Sunk
1905 Moonbeam	Schooner	Point Judith	Sunk
1905 L.M. Eaton	Schooner	Point Judith	Sunk
1905 Maid of the Mist	Catboat	Block Island	Sunk
1906 Edward J. Berwind	Unrigged	Block Island	Sunk
1906 Bouquet	Brigantine	Quonochontaug	Sunk
1906 unnamed	Launch	Green Hill	Sunk
1906 Margie Todd	Schooner	Watch Hill	Sunk
1906 Ailva	Steam Launch	Block Island	Sunk
1906 Auxillary	Sloop	Brenton Point	Sunk
1906 Lugano	Schooner	Point Judith	Wrecked
1906 John Feeney	Schooner	Block Island	Wrecked
1907 Montana	Barge	Block Island	Sunk
1907 Harry Knowlton	Schooner	Quonochontaug	Sunk
1907 Larchmont	Steamer	Quonochontaug	Sunk
1907 Ida	Barge	Point Judith	Sunk
1907 jamie	Barge	Point Judith	Lost
1909 G.A. Hayden	Schooner	Point Judith	Lost
1909 Emily	Catboat	Matunick Beach	Lost
1909 Shawmont	Schooner Barge	Long Is Sound	?
1909 John S. Bennett	Barkentine	Block Island	Sunk
1909 Herril C. Hart	Schooner	Block Island	Sunk
1911 Sailor	Barge	Block Island Sound	Lost
1911 Armette	Sloop	Point Judith	Lost then saved
1911 Rye	Barge	Point Judith	Sunk
1911 Helen A. Wyman	Schooner Barge	Block Island	Loss?
1911 Vermont	Schooner Barge	Block Island	Loss?
1911 Mary Adelaide Randall	Schooner	Block Island	Loss
1912 Pioneer	Barge	Point Judith	Lost
1914 Helen	Gas Sloop	Narragansett Pier	
1914 J.H. Cooper	Schooner	Point Judith	Lost
1914 St. Daniels	Box Barge	Narragansett Pier	Lost
1914 Luella Nickerson	Schooner	Point Judith	Sunk
1915 Active	Auxilliary Schooner	Block Island	Lost
1916 Francis Mulqueen	Barge	Point Judith	Sunk
1916 St. Daniels	Barge	Point Judith	Sunk
1916 Number 12	Barge	Pt. Judith	Sunk
1916 Cora	Barge	Point Judith	Sunk

1917	Power Skiff	Point Judith	Lost
1917 Madison	Barge	Narragansett Pier	Total Loss
1917 Thomas Edison Mulqueen	Barge	Point Judith	Sunk
1917 Capital City	Barge	Brenton Point	Sunk
1917 Catherine Horan	Barge	Quonochontaug	beached
1917 Madison	Barge	Beaver Tail	Sunk
1917 Chippewa	Barge	Beaver Tail	Sunk
1917 Marion B	Barge	Beaver Tail	Sunk
1918 Henry Failing	Barge	Block Island	Sunk
1921 Barbara W	Schooner	Block Island	Refloated?
1922 Grace Clinton	Schooner	Block Island Sound	Loss
1922 Ino	Schooner	Block Island	Sunk
1945 Nathaniel B. Palmore	Fishing Trawler	Rhode Island	Sunk
1946 unknown poss. E & C	Fishing Boat	Block Island	
1961 Joshua B	Fishing Charter Boat	SW of Block Island	
1970 Julia DaCruz	Fishing Trawler	Block Island	Sunk

4.5 Analysis of Geophysical Data

The following table comprises the results of cultural resource target analysis for the 2008 Endeavor cruise. The ranking corresponds of targets corresponds with the 5-point scale outlined in section 3.5, namely:

1. Certain – the acoustic data alone made it possible to identify the target as a shipwreck or other cultural resource.
2. Probable – the acoustic data was highly suggestive of cultural resources, containing features such as linearity and regular patterning that are commonly associated with shipwrecks of other cultural resources.
3. Possible – the acoustic data has some features that have been reliably associated with cultural resources but might also be indicative of features in the natural world.
4. Unlikely – the acoustic data has features that are normally associated with the natural environment, but may have some features that show regularity and could be cultural in origin.
5. Conceivable – the acoustic data is almost certainly associated with features in the natural world, but could conceivably be cultural in origin.

There were no targets that could be classified as either "1 – Certain" or "2-Probable." Twelve targets were classified as "3," nineteen as "4" and twelve as "5." This is not to say, of course, that cultural resources are absent from the waters off Block Island. We know of, and investigated, shipwrecks sites inshore of the *Endeavor* cruise data, immediately to the east of it, and to the south.

The *Endeavor* data clearly shows a moraine feature to the southeast of Block Island, characterized by scatters and concentrations of rocks. It is often difficult to identify early historic shipwrecks, which typically consist of piles of ballast rock, from this kind of geological background. To date we have found no 17th or 18th century shipwrecks in Rhode Island waters

outside Narragansett Bay. Nevertheless, they almost certainly exist and are certainly historically and archaeologically important.

Table 2. Cultural Resource Target Analysis for Data from 2008 *Endeavor* Cruise

Line/Data	Ping	Lat.	Long.	Description	Ranking
278_1204	18947	41 08.393	71 34.328	Substantial target with some regularity	3
278_1907	16201	41 08.184	71 35.537	Series of regular shaped objects	3
278_2112	27039	41 07.697	71 37.816	Round object	5
278_2238	10282	41 07.721	71 37.525	Series of circles in linear fashion	4
279_0315	20443	41 07.508	71 37.492	Possibly linear	5
279_1415	10440	41 07.544	71 34.345	Substantial target with an associated linear object	3
279_1415	35832	41 06.785	71 39.764	Very long linear feature, but data collected on the turn	3
279_1659	12223	41 07.314	71 34.806	Linear feature	3
280_0545	14608	41 06.887	71 35.271	Small feature with some regularity	4
281_1041	24964	41 06.572	71 35.118	Probably lg rock, some regularity	4
281_1230	14884	41 06.641	71 33.922	Regular shaped rock scatter	5
281_1528	34840	41 06.644	71 33 033	Two regular rock scatters	4
281_1732	10583	41 06.635	71 33.012	Rock pile and bump on ocean floor	4
281_1732	38828	41 05.564	71 40.250	Small isolated distortion with some relief and linearity	4
281_1909	3600	41 05.622	71 40.277	Small isolated distortion with some relief	4
281_1909	28064	41 06.351	71 34.188	Probable rock scatter	5
281_2054	13840	41 06.437	71 33.429	Single object, some linearity and relief	4
281_2054	23664	41 06.096	71 35.600	single linear object	5
281_2240	46755	41 06.901	71 30.332	Small object, fairly hard return, some relief	5
282_0515	287	41 07.631	71 38.135	Small object, probably a rock, but with considerable relief	4
282_0539	4134	41 08.462	71 37.779	Pile of rocks, probably geological	5
282_0604	9987	41 09.276	71 37.436	Interesting scatter, possible scower marks, likely geological	5
282_0632	9993	41 07.828	71 38.184	Semi-circular and in parts linear	4
282_0703	669	41 07.709	71 38.414	3 objects, some relief, probably geological	5
282_0703	2635	41 08.039	71 38.221	Dark object, considerable relief, probably two rocks	5
282_0934	7783	41 05.757	71 37.748	Fairly substantial linear feature, with some relief	3
282_0934	22467	41 06.177	71 34.287	Rock scatter, probably geological	5
282_1108	28829	41 05.803	71 36.831	Small linear object	4

282_1756	4153 41 06.410	71 31.451	Possible linear feature, no relief, possibly cable	4
282_1756	31615 41 05.406	71 39.127	Possible linear feature in the sand waves	4
282_1913	7488 41 05.431	71 37.497	Possibly two linear features	4
282_1913	8569 41 05.468	71 37.183	Linear feature	4
282_1913	9901 41 05.525	71 36.792	Linear feature	4
282_2206	14901 41 05.913	71 34.045	Scatter of small dark regular features	4
282_2343	11250 41 06.039	71 32.549	Possible linear feature, in area of sand waves, some relief	3
282_0113	21778 41 05.910	71 32.819	Small linear feature	4
282_0113	27764 41 06.067	71 31.346	Isolated feature, probably geological	5
283_0230	9270 41 05.939	71 32.302	Feature with substantial regular edge	3
283_0230	13935 41 05.835	71 33.316	Small isolated linear feature	4
283_0729	13193 41 05.540	71 32.953	First in a series of three linear features	3
283_0729	13450 41 05.540	71 33.012	Second in a series of three linear features	3
283_0729	13689 41 05.532	71 33.065	Third in a series of three linear features	3
283_0729	20626 41 05.347	71 34.599	Two substantial linear parallel lines with some relief. In among sand waves	3

4.6 Site Specific Investigations

Site-specific investigations are discussed in the order that the fieldwork took place.

4.6.1 *Green Arrow*

On December 22, 1996, the Rhode Island fishing trawler *Green Arrow* ran aground near the Southeast Light on Block Island. Earlier that day, she had departed Point Judith on her way to fishing grounds south of Block Island. It is unclear whether the crewman on watch at the time had been asleep, or whether he had gone below to check the engine.

We encountered the remains of the *Green Arrow* during our pedestrian survey along the southern shore of Block Island (Figure 7). The most prominent feature of the site is part of the stern of the ship with the net reel and parts of the winches. A little further away is a smaller part of the ship's hull. Most of the Gre*en Arrow* washed away or scattered over the ocean floor.

Figure 7. Remains of the Trawler *Green Arrow*.

4.6.2 *Montana*

On January 20, 1907, a fierce storm with 50 mile-an-hour winds was brewing off the coast of southern New England. Out at sea, the steam tug *Buccaneer* passed Montauk Point headed to Providence, Rhode Island, with two schooner barges in tow: the 242' *Ash* followed by he165' *Montana*. The *Montana* had been a graceful sailing vessel built in Port Gilbert, Nova Scotia in 1870, but like many of her type, had been converted into a coal-carrying barge toward the end of the 19th century.

About 10 miles northeast of Montauk Point, the *Ash* took on so much water that she started to sink. The *Buccaneer* cut the tow cable and rescued, with great difficulty, the *Ash*'s captain, family and crew. Likewise, the *Montana* severed her tow cable with the *Ash* so as to avoid being taken down. The vessel drifted helplessly in the violent waters waiting for the tug to re-establish a tow. The *Montana*, however, was taking on so much water that her crew eventually anchored and abandoned ship, which sank off the western Block Island coast on 21 January 1907.

The reported site of the *Montana* is about ¼ mile outside the entrance to Old Harbor. Water depth is between 85'-90'. Reconnaissance operations at the site revealed a small echo-sounder feature the seafloor at her reported location. No dive operations were undertaken here. The site

is close to the navigation corridors into and out of Old Harbor, but the water depth makes it traffic impact on the wreck unlikely.

4.6.3 USS *Leyden*

The USS *Leyden* was a navy steam tug, 137' in length, built in 1865 and lost on the southern coast of Block Island on January 21, 1903. She had served first at Boston Navy Yard, then at Portsmouth (New Hampshire) Navy Yard and then finally at Newport Torpedo Station. During the Spanish American War she had been involved in operations off Cuba. In January 1903, she was on route from Puerto Rico to Newport. Off the coast of Block Island, her captain Lieutenant Chester Wells ran into a bank of think fog. Believing that he was further east than he was, Wells set course for Point Judith. This navigation error bought the *Leyden* onto the rocks approximately 1 mile west of the Southeast Light.

The reported location of the USS *Leyden* is about 200 yards off the southern coast of Block Island in about 10- 15 feet of water. The little articulated hull structure remaining includes some iron frames, wood deck, screw propeller and part of the machinery. Multiple large rocks surround the wreck.

Our side scan sonar survey of shallow waters along the southern coast of Block Island included the area in the vicinity of the USS *Leyden*. However, large rocks masked the site and prevented us from approaching it. As a result, the sonar survey did not detect an acoustic signature from the USS *Leyden*. We did not conduct dive operations on the wreck.

4.6.4 *Meteor*

In July 1926, the 3,500 ton, 254' long steam collier *Meteor* headed out of Norfolk, Virginia to Boston. Enjoying clear weather until passing Block Island where the vessel encountered dense fog. A navigation error brought the collier onto the shore near Cat Rock Cove, close to the southwest point of the island. A salvage company made a failed attempt to drag the ship off the rocks.

The remains of the *Meteor* are in very shallow water just to the north of southwest light, Block Island. All that remains of the site are some elements of her boiler and machinery. Our side scan sonar survey of the shallow waters along the southern coast of Block Island included the area in the vicinity of the *Meteor*. However, shallow water prevented us approaching wreck close enough to obtain an acoustic signature. We did not conduct dive operations on the wreck.

4.6.5 *Spartan*

In the afternoon of March 18, 1905, the steam freighter *Spartan*, owned by the Boston and Philadelphia Steamship Company, headed out of Providence and down Narragansett Bay for Philadelphia. She was 220' long, 1596 tons and carried a general cargo, including textiles. As she headed out to sea, dense fog set in and a navigational error bought her onto the shore between Old Harbor and Southeast point, Block Island. She was steaming due west when she ran into the island. A salvage company rescued some of the cargo, but could not save the vessel.

The remains of the *Spartan* are close to shore in very shallow water, about three quarters of a mile north of the Southeast Light, Block Island. Elements of the ships power plant and propulsion systems are present at the site. Our side scan sonar survey of the shallow waters along the southern coast of Block Island included the area in the vicinity of the *Spartan*. However, shallow water prevented us from getting close enough to obtain an acoustic signature. We did not conduct dive operations on the wreck.

4.6.6 *Lightburne*

The tanker *Lightburne*, built in Bath Maine in 1919, was a little over 431' long and 6,429 gross tons. While on route from Port Arthur, Texas to Providence on 10 February 1939 she encountered a dense fog and went aground right below the Southeast Light, Block Island. Several vessels came to the aid of the *Lightburne*, but poor visibility and heavy seas prevented them from coming along side. After several hours, a Coast Guard lifeboat evacuated the captain, crew and the ship's dog. The following day, some of the tanker's cargo of gasoline ignited and burned for several hours. The crew subsequently returned to the vessel to salvage personal possessions and a professional salvage company took off some of the remaining gasoline.

Figure 8. Examining the Structural Remains of the *Lightburne*

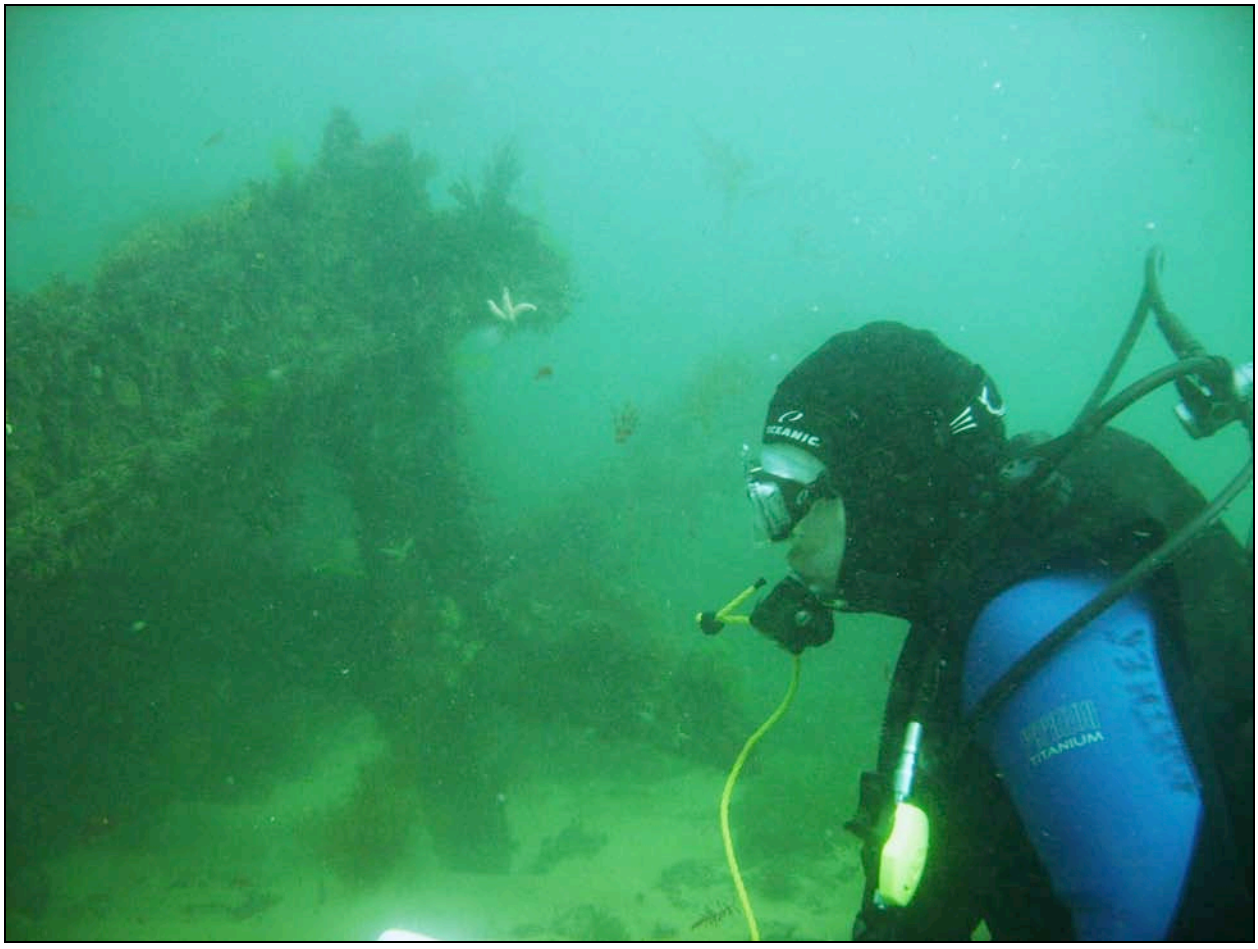

The remains of the *Lightburne* were readily identifiable in our side scan sonar survey of the shallow waters along the southern coast of Block Island. The wreck is located inside navigation

marker and close to the wreck of the *Essex*. We conducted an archaeological assessment of the site and recorded evidence of anthropogenic effects. We documented the site with both video footage and still imagery (Figure 8).

Figure 9. Evidence of Looting at the *Lightburne*.

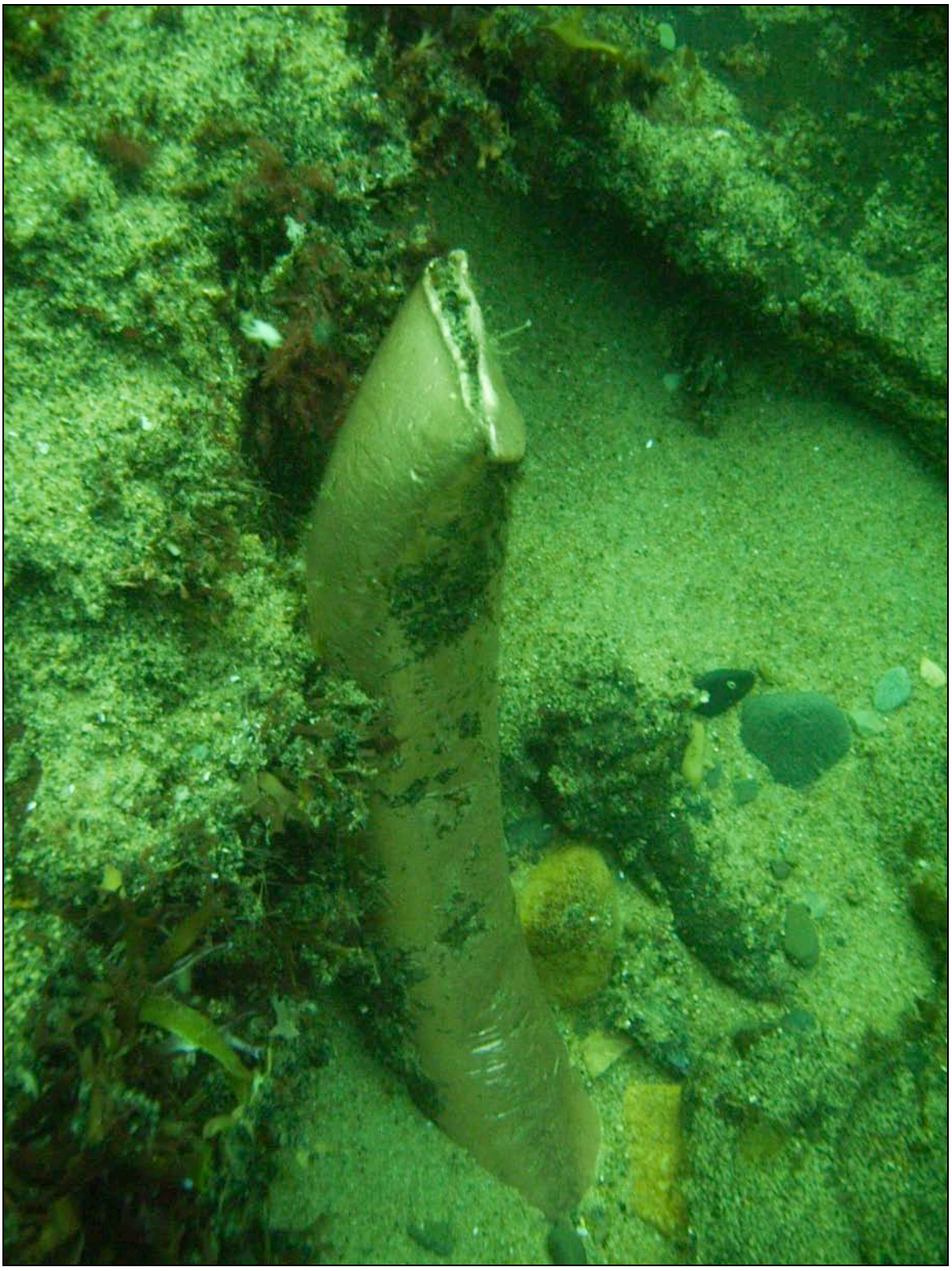

The *Lightburne* sits in approximately 25' of water off the Southeast Light. The wreckage is spread out over at least 400'. The most prominent features of the site are elements of the wreck's superstructure which including a series of transverse bulkheads that rise as much as 15' from the bottom. Much of the hull plating is gone. There are still some parts of the ship's machinery present at the site. Sports divers frequent the site, and while few artifacts remain on the surface, there is some evidence of looting. In at least two places, brass pipes and fittings have been removed using substantial hand held cutting tools (Figure 9). Some sports fishing gear is located at the site, but no commercial fishing gear of note. The *Lightburne* is located in a high-energy environment

4.6.7 *Essex*

Built by William Cramp & Sons in Philadelphia in 1890, the steel-hulled, passenger-freighter *Essex* was 272' long and 3,018 tons. In 1940, she was sold to the White Pearl Shipping Corporation for use almost exclusively as a freighter. On her first voyage under new ownership, a passage from Lisbon to New York, she ran aground on Block Island, very close to the *Lightburne*. The *Essex* ran aground during the evening of September 25, 1941 under peculiar circumstance of calm and clear weather. The vessel's captain claimed to have hit a floating object that caused the *Essex* to take on water. Rather than sink in open water, the captain claimed that he ran the vessel ashore. An alternative version of the accident suggests that the captain accidently ran the vessel ashore. After backing her off, the *Essex* started taking on water, forcing the captain to run her ashore a second time. Salvage efforts enjoyed partial success, before a subsequent storm broke up the ship and scattered her wreckage.

Figure 10. Iron Debris from the *Essex*

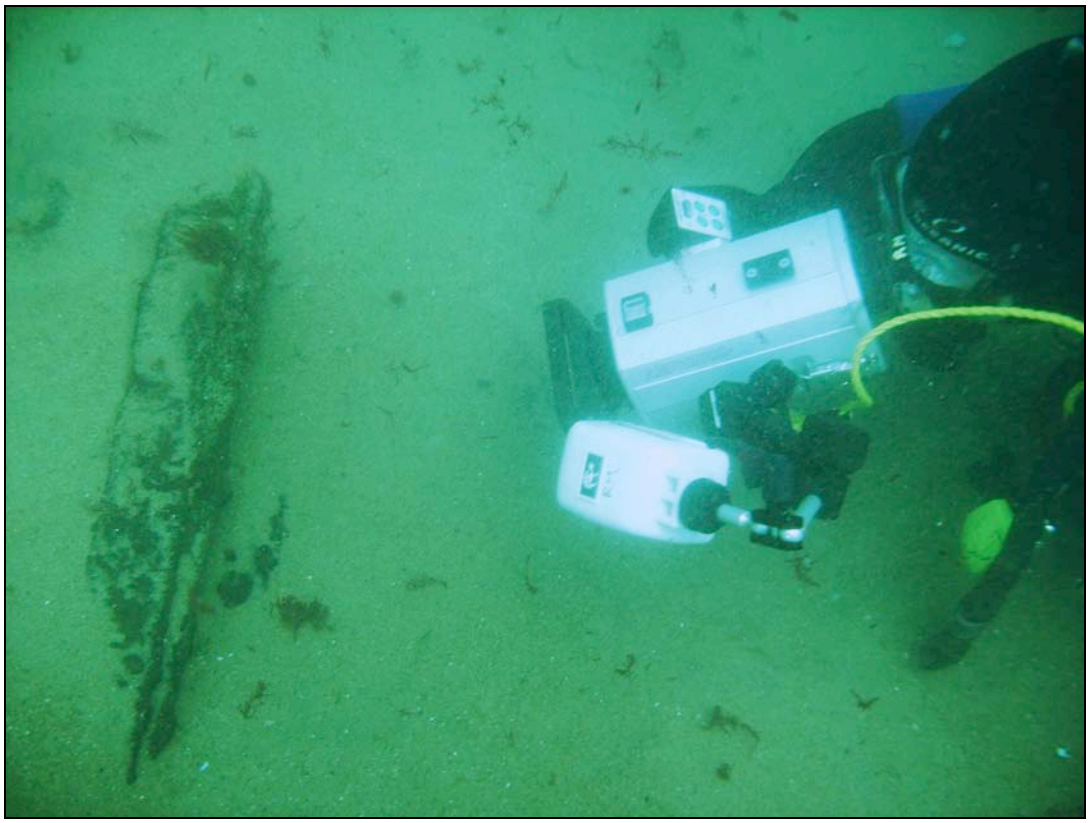

The remains of the *Essex* were readily identifiable in our side scan sonar survey of the shallow waters along the southern coast of Block Island. The wreck is located inside a navigation marker and close to the wreck of the *Lightburne*. We conducted an archaeological assessment of the site and recorded evidence of anthropogenic effects. We documented the site with both video footage and still imagery.

The *Essex* sits in approximately 25' of water off the Southeast Light. The wreckage comprises several large pieces of hull structure and an associated debris field. The large structural elements contain iron frames and wooden planking. At least one section appears to include part of the ship's deck, within which there is evidence of a hatch and companionway. Some of the hull structure is flush with the sand, while other elements rise at least 7' from the bottom. The wreckage is dispersed out over at least 250'. Surrounding the main structural elements is a debris field that contains pieces of iron, including iron plating (Figure 10). The *Essex* is located in a high-energy environment. We did not observe evidence of looting. Neither was there evidence of commercial fishing gear.

4.6.8 *Idene*

The *Idene* was a 120' Rhode Island eastern-rigged fishing trawler deliberately sunk approximately 4 miles south of Block Island in 1991. Declared obsolete by her owners some years earlier, the *Idene* was scuttled after rusting at a Snug Harbor dock for several years.

The *Idene's* proximity to possible locations for off shore wind turbines rendered her of particular interest in these site-specific studies. We used side scan sonar to establish good coordinates for the wreck. We then conducted an archaeological assessment of the site and recorded evidence of anthropogenic impacts. We documented the site with both video footage and still imagery.

The *Idene* sits in approximately 85' of water, 4 miles south of Block Island. In water visibility was not good during our dives. The site supports a rich variety of sea life including anemones, tautog, bluefish, Pollock and blue sharks. Although intact, a crack runs through the hull just aft of the forward mast. The mast is still standing, the bow is virtually complete and the deck has at least two open hatches each with ladders leading down to cargo holds. Toward the stern, the sport divers who regularly visit the site easily penetrate the intact pilothouse. The *Idene* site houses few artifacts or structural element that would attract serious looting. We observed some sports fishing gear on the site but no commercial nets.

4.6.9 Endeavor Cruise Targets

While the Endeavor cruise produced no targets that could be identified as "1-Certain" or "2-Probable" cultural resources, 12 targets were ranked as "3-Possible." After careful review, SAMP researchers selected two of these for groundtruthing by scuba-equipped archaeologists.

Target 278_1204_18947 was identified in the *Endeavor* acoustic data as a substantial target, fairly close to the Block Island shore, with some regularity. The target was re-acquired using the Edgetech 272 tow fish, marked and investigated. Water depth at the site was approximately 25 feet. The source of the signature was a substantial rock pile.

Target 282_0934_7783 was identified in the *Endeavor* acoustic data as fairly long linear feature with some relief, located toward the shoal water southwest of Block Island. The target was re-acquired using the Edgetech 272 tow fish, marked and investigated. The source of the signature was a series of linear arrangements of rock. Water depth at the site was approximately 45-50 feet.

With additional field time, the archaeological team would have investigated at least three other targets, all of which had some features that could have been associated with cultural resources.

5 Conclusions

Field investigations conducted as part of this study have provided insight into Rhode Island's rich cultural heritage. The shallow hazardous waters along Block Island's southern coast have been the loci for numerous wrecks over the past 300 years. As such they are particularly archaeologically sensitive. Clay Head, Old Harbor and Black Rock are similarly sensitive. Shipwrecks certainly exist further off shore, and some are close to areas of potential wind farm development. The earliest, and in some cases archaeologically most sensitive shipwrecks, are also the most difficult to find. Wrecks from the 17th and 18th century undoubtedly exist in Rhode Island Sound, but to date none have been found.

The Ocean SAMP project has potentially opened a new door in the study and management of Rhode Island maritime and coastal cultural heritage. The study of Block Island and the surrounding region's marine archaeology has begun to reveal the richness and complexity of the state's cultural heritage. Although far from comprehensive, the project looked at cultural heritage from the cultural landscape perspective. Looking the ways different people and different cultures have interacted with marine environments underscored heritage elements common to all Rhode Islanders while recognizing the special and unique connections that Indians, fishermen, military personal, and sailors among others depended on and used the ocean landscape and its resources.

From a policy standpoint, cultural heritage remains an uneasy fit with many professionals involved in marine spatial planning. This is not unique to Rhode Island. In some respects, the Ocean SAMP has brought real improvement. However, gaps in our knowledge and understanding threaten cultural heritage resources. While the destruction of archaeological resources may be avoided by applying the data collected in this study—real progress will come with the embrasure of perspectives that integrate Rhode Islands cultural and natural heritage. The cultural signatures, material resources, recorded and oral history offer underused or untapped sources for understanding the condition of marine and coastal ecosystems and how it relates to culture and human behavior.

In our view, adopting a cultural landscape approach to the study, management, and public interpretation of coastal and marine heritage resources offers the best chance to take Rhode Island to the forefront of effective marine spatial planning and pubic marine archaeology. This report and the historical research and survey work were informed by cultural landscape theory. Fully developing the contexts to understand Rhode Island's marine cultural landscapes will require far more time and effort that could be marshaled here. Despite resource limitations, the project revealed important new insights about Rhode Island maritime history and marine archaeology.

By taking a cultural landscape approach, we identified an archaeologically rich and historically very significant set of resources—the shipwrecks and landscapes associated with the gathering and movement of energy. The connections between early use and exhaustion of wood resources on Block Island and current efforts to construct renewable energy wind towers near by are neither coincidence nor forced. The quest for reliable energy transformed the Block Island landscape. A century later, this same quest when undertaken at the regional and national scale provided tens of thousands of seafaring jobs and, as the historical and archaeological record reveals, to innumerable tragedies—many in Rhode Island. The density of maritime traffic support this trade created a rich archaeological record that the coast planner will have to take into careful account.

Far from fully developed, but of more contemporary significance, the region's fisheries history has resulted in a connected archaeological and cultural legacy that spans millennia. The economic and technological transformations in commercial fishing during the nineteenth and twentieth centuries dramatically changed local ecosystems. They have also supported generations of fishing families. As present conditions cloud the futures of fish and fishermen in Rhode Island, it seems essential to recognize, study, and where appropriate preserve the material culture and living memories of the a crucial and historic group of harvesters. For many, the loss of vessels and lives out of ports such as Pt. Judith seem contemporary and immediate—yet what is going one now represents the last chapters in the lives of many potentially historic vessels. Local shipwrecks of fishing boats, many of them unfound, are also memorial sites to the living relatives of many of the states lost mariners. Fishing, we suggest, is one of most at risk and important cultural landscapes in Coastal Rhode Island.

Another overwhelming and perhaps less surprising conclusion involved the extraordinary effects of military activity in shaping cultural landscapes. From countless shore properties to warships ranging from the Revolutionary War to World War II, conflict has created intensive activity and left profound cultural marks. As with any historic landscape, not everything reflects glory or is worth preserving. State bottomlands are covered in places with ordinance and varying kinds of military refuse.

The cultural landscape approach to management we advocate does not call for the preservation of every historic structure or object. It requires looking closely at all of the material culture found in or along the ocean floor. These materials are a record of human interaction with the environment and not simply memorials to human achievement. The place-based contexts prescribed by Marine Spatial Planning off an appropriate geographic scale for studying and applying the knowledge derived from our cultural heritage.

References

A Digest of Opinions of the Judge Advocates General of the Army, 1912. 1917. Washington: Government Printing Office.

Abbass, D. K. 2000. Naval History and the Submerged Cultural Resources of Rhode Island, Volume I. Newport, RI: Rhode Island Marine Archaeology Project.

Albion, R. G., Labaree, B. W. and Baker, W. A. 1970. New England and the Sea. Mystic, CT: Mystic Seaport Press.

Annual Reports of the War Department for the Fiscal Year Ended June 30, 1899. 1899. Washington: Government Printing Office.

Annual Report of the Auditor of the Railroad Accounts made to the Secretary of the Interior for the Year Ending June 30, 1880. 1880. Washington: Government Printing Office.

Annual Report of the Chief Signal Officer of the Army to the Secretary of War for the Year 1888. 1889. Washington: Government Printing Office.

Annual Reports of the Department of Agriculture for the Fiscal Year Ended June 30, 1902. 1902. Washington: Government Printing Office.

Atlantic Deeper Waterways Association. 1908. First Annual Convention Held at Baltimore November 17, 18, 19 1908: Report of the Proceedings. Philadelphia: Atlantic Deeper Waterways Commission.

Bartlett, John Russell, 1858. Records of the Colony of Rhode Island and Providence Plantations in New England. Providence: Knowles, Anthony & Co.

Bridenbaugh, Carl. Fat Mutton and Liberty of Conscience, Society in Rhode Island, 1636-1690. Providence, RI: Brown University Press.

Carroll, Charles. 1932. Rhode Island: Three Centuries of Democracy. New York: Lewis Historical Publishing Company.

Coleman, Peter J. 1963. The Transformation of Rhode Island 1790 – 1860. Providence: Brown University Press.

Cooper, David J. and John O. Jensen. 1995. Davidson's Goliaths: Underwater Archaeological Investigations of the Steamer Frank O'Connor and the Schooner-Barge Pretoria. Madison: State Historical Society of Wisconsin.

Cronon, William. 1983. Changes in the Land: Indians, Colonists and the Ecology of New England. Hill and Wang.

DeAlteris, J.T.; Gibson, M.; Skrobe, L.G. 2000. Fisheries of Rhode Island (Working Draft). Narragansett Bay Summit 2000: White Paper.

Fagan, Brian. 2006. Fish on Friday: Feasting, Fasting and the Discovery of the New World. New York: Basic Books.

Fowler, William M. 1976. Rebels Under Sail: The American Navy during the Revolution. New York: Charles Scribner's Sons.

Gasner, Pamela. 2008. "Structures and Sites from 1680 – 1948 on Block Island/Town of New Shoreham" Block Island Historical Society.

Goode, G. Brown. 1884. The Fisheries and Fishing Industries of the United States, Section II. Washington, DC: Government Printing Office.

Gordon, Richard L. 1978. Coal in the U.S. Energy Market: History and Prospects. Lexington: D.C. Heath.

Graaebner, William. 1974. "Great Expectations: The Search for Order in Bituminous Coal. 1890 – 1917. " The Business History Review. Vol. 48: 49 – 72.

Hale, Stuart O. 1998 (updated ed.). Narragansett Bay: A Friend's Perspective. University of Rhode Island Marine Advisory Service NOAA/Sea Grant Marine Bulletin 42.

Harbors of Refuge at Point Judith, Block Island, and Great Salt Pond, etc. 1903. 55th Cong. 2nd Sess. H. Doc 60.

Hearings before the Committee on Expenditures in the Department of Agriculture, House of Representatives. 1907. Washington: Government Printing Office.

Hawes, Alexander Boyd. 1999. Off Soundings: Aspects of the Maritime History of Rhode Island. Chevy Chase, MD: Posterity Press.

Hunter, Louis C. 1979. A History of Industrial Power in America. Volume One: Water Power in the Century of the Steam Engine. Charlottesville: University of Virginia Press.

Hunter, Louis C. 1985. A History of Industrial Power in America. Volume Two: Steam Power. Charlottesville: University of Virginia Press.

Hall-Arber M, Dyer C, Poggie J, McNally J, Gagne R. 2001. New England's Fishing Communities. Cambridge (MA): MIT Sea Grant 01-15. Available from: http://seagrant.mit.edu/cmss/

Jones, Daniel P. The Economic and Social Transformation of Rural Rhode Island, 1780-1850. Boston MA: Northeastern University Press.

Keatts, Henry and George Farr. 2002. The Bell Tolls: Shipwrecks and Lighthouses, Volume 1, Block Island. Laurel, NY: Main Road Books.

Kellner, G. H. and Lemons, J. S. 2004. Rhode Island the Ocean State: An Illustrated History. Sun Valley, CA: American Historical Press.

Labaree, B. W., Fowler, W. M. Jr., Sloan, E. W., Hattendorf, J. B., Safford, J. J., and German, A. W. 1998. America and the Sea: A Maritime History. Mystic, CT: Mystic Seaport Press.

Livermore, Samuel. 1877. A History of Block Island from its Discovery, in 1514 to the Present Time, 1876. Hartford, CT: Case, Lockwood & Brainard.

Marx, Deborah and Mathew Lawrence. 2006. "Nomination of Frank A. Palmer and Louise B. Crary – Shipwreck Remains to the National Register of Historic Places."

McLoughlin, William G. Rhode Island, A History. New York, NY: W. W. Norton & Co.

Mendum, Samuel W. 1897. New England Magazine. Vol. 16: 738–751

Monthly Summary of Commerce and Finance of the United States for the Fiscal Year 1903. 57th Cong. 2nd Sess. H. Doc. 15 parts 7, 8 & 9.

National Park Service. 2010. Web site, "National Historic Landmarks Program." http://www.nps.gov/history/nhl/QA.htm#1

Ocean SAMP Chapter 7. "Marine Transportation, Navigation, and Infrastructure."

Olsen, S.; Stevenson, D. 1975. Commercial Marine Fish and Fisheries of Rhode Island. Coastal Resources Center, University of Rhode Island: Marine Technical Report 34.

Pope, Peter E. 2004. Fish into Wine: The Newfoundland Plantation in the Seventeenth Century. Chapel Hill, NC: University of North Carolina Press.

Rhode Island Historical Preservation and Heritage Commission (RIHPHC). 2007. Performance Standards and Guidelines for Archaeological Survey: Standards for Archaeological Survey" RIHPHC, Providence, RI.

Rhode Island Historical Preservation and Heritage Commission (RIHPHC). 2010. Web site, "National Register." RIHPHC, Providence, RI. http://www.preservation.ri.gov/register/

Rhode Island Historical Society, 1993. What a Difference a Bay Makes. Providence, RI: Rhode Island Department of State Library Services.

Ritchie, Ethel Colt. 1980. Block Island, Lore and Legends. Block Island, RI: Francis M. Nugent.

Schroder, Walter K. Defenses of Narragansett Bay in World War II, 1980 repr. 1996. Chapel Hill, NC: Professional Press.

St. Martin, Kevin and Madeleine Hall-Arber. 2008. "The missing layer: Geo-technologies, communities, and implications for marine spatial planning. Marine Policy, 32: 779-786.

Schurr, Sam H. and Bruce C. Netschert. 1960. Energy in the American Economy, 1850 - 1975: An Economic Study of its History and its Prospects. Baltimore: The Johns Hopkins Press.

The Seaman's Bill: Hearings Held Before the Committee on Merchant Marine and Fisheries on House Bill 11372, December 14, 1911. 1911. Washington: GPO.

Snow, Ralph Linwood and Douglas K. Lee. 1999. A Small Shipyard in Maine: Percy & Small and the Great Schooners. Bath: Maine Maritime Museum.

Snyder, Marlene and Don Snyder. 1998. Rhode Island Adventure Diving. Westfield: Marlene and Don Snyder.

Snyder, Marlene and Don Snyder. 1999. Rhode Island Adventure Diving II. Westfield: Marlene and Don Snyder.

Statutes of the United States of America passed at the First Session of the Forty-Ninth Congress, 1885-1886. 1886. Washington: Government Printing Office.

Swanson, Carl E., 1991. Predators and Prizes: American Privateering and Imperial Warfare, 1739-1748. Columbia, SC: University of South Carolina Press.

Tveskov, Mark. 1997. Maritime Settlement and Subsistence Along the Southern New England Coast: Evidence from Block Island, Rhode Island. North American Archaeologist, 18: 4, pp. 343-361.

U.S. Fish and Wildlife Service. North Cape Oil Spill Restoration. Available on line at http://www.fws.gov/Contaminants/restorationplans/NorthCape/NorthCape.cfm Last accessed March 27, 2010.

Vickers, Daniel. 1994. Farmers and Fishermen: Two Centuries of Work in Essex County. Chapel Hill: University of North Carolina Press.

Wroth, Lawrence C., ed. 1970. The Voyages of Giovanni da Verrazzano, 1524-1528. New Haven: Yale University Press.

6.

High resolution modeling of meteorological, hydrodynamic, wave and sediment processes in SAMP study area

by

Stephan Grilli[1], Jeffrey Harris[1], Ravi Sharma[1], Lauren Decker[2], David Stuebe[2], Danny Mendelsohn[2], Deborah Crowley[2] and Steve Decker[3]

1. Department of Ocean Engineering, University of Rhode Island
2. Applied Sciences Associates, Inc., Wakefield, RI
3. Rutgers University

University of Rhode Island, July 13, 2010

Executive Summary

This work was performed as a part of the Rhode Island Ocean Special Area Management Plan (SAMP), to acquire insight into local meteorological, hydrodynamic, wave, and sediment processes. The approach followed consists in first performing an exhaustive literature review of relevant work to date in the area, and then in light of this, to develop and apply numerical models of wind, wave, current, and sediment suspension and transport processes. Several models were considered and used, including two for simualting wind fields over Block Island (WRF and RAMS), and a coupled hydrodynamic, wave, and sediment model of the waters of southern New England (ROMS/SWAN). Additionally since tides are the key and ever present forcing for sediment processes in local shelf waters, an additional and independent tidal model was applied (HYDROMAP), whose results were compared to ROMS to provide cross-validation.

Atmospheric modeling with WRF was performed in collaboration with Applied Sciences Associates (ASA) to show effects of Block Island on wind velocity and shear in the wake of the island. Detailed two-dimensional (2D) simulations in vertical planes were performed across the island, for 8 main wind directions and a variety of atmospheric shear (i.e., neutral, stable, unstable) related to air-sea temperature differences. A limited number of three-dimensional (3D) simulations were then performed with WRF, but due to computational limitations, work was shifted to using the less computationally intensive "Regional Atmospheric Model System" (RAMS), for 3D simulations, as part of a collaboration with Weatherflow Inc. (this part of the work is only summarized in this report and reported on in detailed elsewhere). RAMS was used to create a five-month (10/09-2/10) high-resolution hindcast of the wind fields over Block Island, using a 4 level nesting model, with increasing resolution, whose finer encompassed the entire SAMP study area. These fields were then used to force the hydrodynamic model ROMS.

The "Regional Ocean Modeling System" (ROMS) was used to simulate currents due to various environmental forcing, in a computational domain extending from Long Island Sound to the Nantucket Shoals at a grid resolution of 600 m. Various configurations were considered: (i) only tidal forcing; (ii) tidal and wind forcing; and (iii) tidal, wind, and wave forcings (the latter using the wave model SWAN coupled to ROMS, with boundary conditions obtained form the larger scale operational wave model WAVEWATCH III). In addition, all ROMS simulations included an embedded sediment suspension and transport model, which was used to study sediment suspension in the SAMP study area.

HYDROMAP simulations were performed using tidal and wind forcing (although only spatially uniform wind forcing given from a point-measurement were used), and compared to ROMS results for the same forcing cases. HYDROMAP results generally supported similar ROMS results and at higher spatial resolution, although HYDROMAP was not used to study the effects of sediment suspension.

All results are compared against available data. RAMS simulations results for wind speed and direction were extensively compared to and validated with field data (this is reported on in detail elsewhere). Wave and current data recorded at five buoys in and near the SAMP study area, for the period from October 2009 to January 2010, was favorably compared to ROMS simulation results for the same period. Surficial sediment processes simulated with ROMS/SWAN were also qualitatively compared to measurements at the field buoys (using backscattering level in ADCP measurements as an indicator of sediment suspension concentration).

Overall simulation results indicate that some level of sediment suspension occurs in limited locations of the SAMP area, due to tidal forcing, and additional suspension occurs in shallower waters, as a result of episodes of strong long swells. None of this sediment activity, however, should pose a problem for wind turbine foundation.

Table of Contents

List of Figures

List of Tables

List of Attachments and Appendices

Appendix A : HYDROMAP tidal simulations.

Abstract

As a part of the Rhode Island Ocean Special Area Management Plan (SAMP) work, local meteorological, hydrodynamic, wave, and sediment processes are studied through numerical simulation, analyzed and summarized in this report. The work consists in both a literature review and the application of numerical models. Several models were considered, including two of the wind over Block Island (WRF and RAMS), a coupled hydrodynamic, wave, and sediment model of the waters of southern New England (ROMS/SWAN), and an additional tidal model (HYDROMAP). Results are compared against available data, including surficial sediment properties and processes, and wave and current data recorded at five buoys in and near the SAMP study area for the period from October 2009 to January 2010.

Overall simulation results indicate that some level of sediment suspension occurs in limited locations of the SAMP area, due to tidal forcing, and additional suspension occurs in shallower waters, as a result of episodes of strong long swells. None of this sediment activity, however, should pose a problem for wind turbine foundation.

1 Background

It has been proposed that a wind turbine farm be developed off the southeastern coast of Block Island, south of the Rhode Island mainland. The development of an offshore wind farm will necessarily require a great deal of underwater construction including drilling and setting the piles for the turbine foundations, burying electrical transmission cables and other infrastructure construction tasks. During this period additional water column suspended sediments may impact the construction areas and it is therefore of interest to understand what the current speeds and circulation patterns are in the development area, as a result of environmental forcing from tides, waves and wind. Additionally, it is important to characterize the seafloor sediment properties and their distribution, as well as to quantify sediment suspension and transport, as a result of the bottom currents.

To this end, in this work, we perform a hydrodynamic modeling study using the coupled ROMS/SWAN model, to estimate currents and circulation in the tentative wind farm siting area, thereby referred to as the SAMP study area, with a focus on bottom stress and currents, as well as sediment processes (characteristics and suspension). We do not model the specific effects of individual wind turbine sites, or the collective effects of a wind farm, as the models used have not been developed for that purpose and are applied on meshes with grid cell sizes adequate to capture salient environmental processes, but too large to resolve wind turbine support structures.

While tidal forcing along the SAMP study area boundary can be (and is being) obtained at a reasonable resolution from tidal databases (either based directly on assimilated satellite altimetry, or from the results of a hydrodynamic model such as ADCIRC on a larger domain), and wave forcing is obtained from operational wind-wave models such as NOAA's WAVEWATCH-III, high-resolution winds are not readily available in the SAMP area, particularly in and around Block Island (Fig. 1), around which tentative wind farm sites have been selected. Such wind fields can only be obtained through atmospheric modeling at sufficient resolution. The latter is done using two different atmospheric models: (1) WRF at a very high resolution in a series of vertical (two-dimensional; 2D) sections through Block Island (Fig. 1), in order to gain insight into the key wind processes in the lee of the island where tentative sites were selected; (2) in a coarser resolution three-dimensional (3D) implementation of the RAMS model.

Hence, in section 2, we present results of the 2D-WRF wind modeling (performed in collaboration with Applied Science Associates, Inc., as part of a sub-contract), in Section 3, we summarize results of the 3D-RAMS modeling (performed as part of a subcontract to Weatherflow Inc. and analyzed and reported on in another SAMP sub-project; Spaulding et al., 2010a,b), and in Section 4, we detail the hydrodynamic ROMS/SWAN simulations (including HDROMAP tidal simulations, used for validation, and performed as part of a subcontract to Applied Science Associates, Inc., whose full report is attached in Appendix A). Finally, Section 5 provides some conclusions.

2 Fine Scale Meteorological Modeling around Block Island using WRF

2.1 Overview

This part of the work was performed in collaboration with David Stuebe and Lauren Decker at Applied Sciences Associates (ASA), who via a subcontract were tasked to perform "High Resolution Ocean Metrological Modeling in the RI SAMP Study Area" using the atmospheric: "Weather Research and Forecasting" (WRF) model, which is a Large Eddy Simulation (LES) numerical weather prediction and atmospheric simulation system designed for both research and operational applications (WRF, 2008).

At ASA, this part of the work was led by David Stuebe, who managed the project, with help from Lauren Decker, who run the majority of the model test cases (Fig. 1a) and developed the analysis methods for the results. Additionally, Prof. Steve Decker from Rutgers University, who was hired as a consultant by ASA, provided key insight on the dynamics of coastal meteorology and the application of the WRF model. Prof. Decker also did much of the research on the existing literature about compressible flow over topography.

(a) (b)

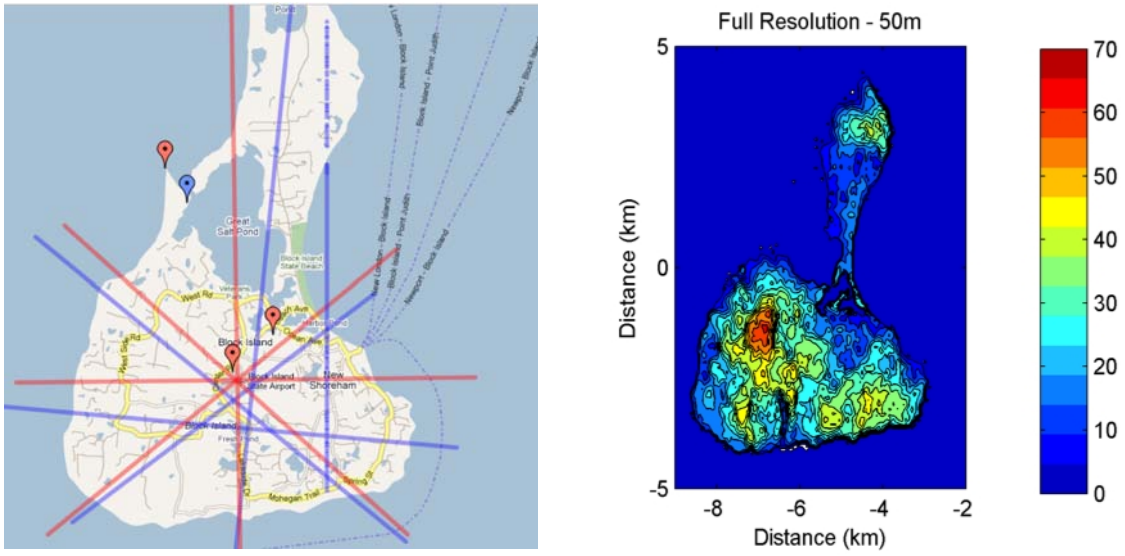

Figure 1: (a) Block Island, RI and various cross section traces where the 2D-WRF model was run; (b) Block Island topography as represented in a 50m by 50m numerical model grid.

This work initially included two main tasks:

- Implement and run the high resolution, atmospheric model WRF to answer critical questions about topographic relief effects (Fig. 1b) on the wind patterns in the lee of Block Island, where windfarm sites are being considering.
- Develop hindcast of meteorological conditions in the dynamically relevant regions of the SAMP study area, to drive a hydrodynamic circulation model and a wave model covering the region.

As work progressed, it became increasingly apparent that the computational cost of running high resolution three-dimensional (3D) simulations using WRF, to address the second task, was prohibitive. Hence, an alternative strategy was selected, which consisted in only addressing the first task using WRF, and to instead use the less demanding "Regional Atmospheric Model System" (RAMS 2010; which is also a LES model, but at more amenable coarser resolution), to address task one. To perform the latter work, ASA subcontracted Weatherflow Inc., who have an operational version of RAMS. The freed resources at ASA were re-allocated for performing an independent set of tidal simulations (since tide-induced currents represent the main forcing for sediment suspension and transport in the SAMP area), in support of the hydrodynamic studies that are also part of this SAMP sub-project.

Accordingly, the following subsections detail WRF results for task 1. Section 3 then briefly summarizes results of task 2, which has been the object of separate reports (Spaulding et al., 2010a,b). Results of ASA's tidal simulations are summarized as part of Section 4, and a full report prepared by ASA is provided in Appendix A.

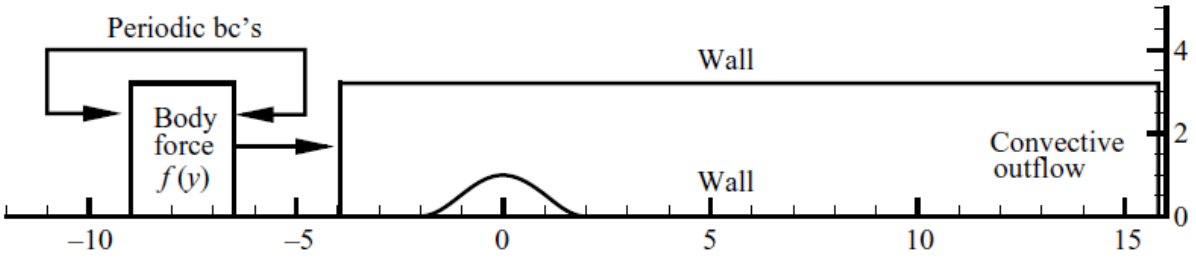

Figure 2: The numerical model WRF setup is similar to that shown in this figure from Garcia-Villalba et.al. The figure sketches the model domain and the inflow and outflow boundary conditions, as well as an idealized topographic hill. Axes are arbitrarily graduated in kilometers.

2.2 Literature Review

The bibliography relevant to the study was reviewed and findings are summarized in the following. Topographic relief affects wind flow over islands the most when:

- The hill/island is taller
- The wind speed is faster
- The ground slope is steeper (i.e., higher aspect ratio), and
- The atmospheric stability is higher (i.e., colder ocean and warmer or stratified atmosphere).

2.2.1 Large Island Wake

Previous studies have employed theory, observations, and modeling to study the effects of 3D obstacles on low-level atmospheric flow. Some of the earliest work focused on vortex streets observed in the lee of large islands. These could be monitored via satellite and are considered to be atmospheric analogues to two-dimensional (2D) (horizontal) laboratory flows around cylinders. Thomson and Gower (1977) exemplify this approach to studying wind perturbations induced by large islands. In their case, they used satellite observations of cloud patterns in the wake of the Aleutian Islands to calculate fluid dynamical quantities such as Reynolds and Strouhal numbers. The emphasis is on explaining the cloud patterns in terms of what is observed in the laboratory. Note that the islands studied here have elevations in excess of 1,000 m (as opposed to Block Island, which is 64 m high). Smith and Grubišic (1993) study a similar wake in the lee of the island of Hawaii (elevation over 4,000 m) using a research aircraft. They found counter-rotating vortices and associated shear lines in Hawaii's wake. Due to Hawaii's position in the trade wind regime, these flows are quasi-steady. Incidentally, it was Captain Cook's encounter with the wake of Hawaii that likely damaged his ship, forcing him to return to the island, where he was subsequently killed by the natives. As later studies make it explicit, the large size of Hawaii and the Aleutians forces the air to go primarily around the island, producing notable vortices in their wake. Smaller obstructions behave differently.

A smaller island (St. Vincent, maximum height around 1,000 m) was studied by Smith et al. (1997) to examine the effects of relatively small islands on the flow. St. Vincent generates what is called a “weak wake” (in contrast to Hawaii or the Aleutians) because, although vorticity is generated by the interaction with the island, the wind does not “close off” into eddies (i.e., vortices). In other words, vorticity is present in the wake, but not a closed circulation. This study summarizes previous theoretical work with a discussion of four different types of wakes, depending on the parameter regime. The key parameter is h/h_c (the ratio of maximum obstruction height to the critical height for (atmospheric) wave breaking). If that quantity is less than one, no

wake should be observed. A value between one and two represents a weak wake, and larger values produce strong wakes (e.g., Hawaii). The critical height for wave breaking, h_c, is highly dependent on the shape of the obstruction, the wind speed, and the stability of the atmosphere. If the obstruction has a *Witch of Agnesi* shape (sort of like a Gaussian bump; Fig. 2), wave breaking (and thus a wake) would occur if the non-dimensional terrain height: hN/U is greater than 0.85, where N is the Brunt-Vaisala frequency, and U is wind speed. Thus, the higher the wind speed, the more stable the atmosphere, and the higher the height of the obstruction, the more likely a wake will be produced. For the case of St. Vincent, wakes were observed to extend over 300 km in the lee. To see if these long wakes could be modeled, a highly idealized (inviscid, no surface fluxes, no surface friction, smoothed topography) 3D atmospheric model (not all that different from the WRF Model in its overall construction) was run on a grid with 2 km mesh spacing and 60 vertical levels extending from the surface to 6 km. Their model reached a steady state after about 12 hours of simulation. After varying a host of parameters, they concluded that the effect of the turbulence parameterization was nontrivial, suggesting much finer resolution may be necessary to generate a simulation of high fidelity (since more of the turbulence can be explicitly resolved).

Lane et al. (2006) performed a similar study to model the wake of Kauai, where the non-dimensional height on the day of interest was about 1.67. Once again, a classic wake was successfully simulated using mesh sizes: Δx = 167 m and Δz = 50 m. Kauai is 1,600 m tall.

2.2.2 Small Hills

Much smaller obstacles to the flow (primarily hills), similar to the situation in Block Island, where the maximum elevation is about 70 m (Fig. 1b), have been modeled in a variety of ways. Apsley and Castro (1997) took a highly idealized approach, using an incompressible model (known as the SWIFT model) to simulate flow around Cinder Cone Butte, a 100 m high hill rising above flat terrain. In their run, the atmosphere was set to be highly stable, and as a result, streamlines flowed around the hill below about 20 m, but over the hill at heights above that. [Thus, 20 m is the height of the theoretical *dividing streamline* for this case.] The SWIFT model solves for the steady-state flow only, but because of the computational cost of even this highly simplified model, they did not attempt to demonstrate grid convergence (i.e., that the results are insensitive to grid spacing) for their Cinder Cone Butte run.

In an idealized Large-Eddy Simulation (LES) study, Ding and Street (2003) simulated the flow in the wake of a 3D hill that had a shape similar to a Gaussian bump. Again, the factor

U/Nh was deemed important. When that number is much less than one, then flow around the hill is expected (just like 2D laboratory flow around cylinders). Values closer to one are expected to result in more flow over the hill. However, in either case, counter-rotating vortices are expected in the wake. Additionally, the wake is expected to approach steady state when *Ut/h* is around 25. Because running LES on the real-world scale is so computationally expensive, the domain size used in Ding and Street's work was laboratory scale: 2 m x 1.5 m x 0.8 m, with a hill height of 10 cm, using 194 x 98 x 130 grid points. They found the width of the wake decreased as *U/Nh* increased.

Relating the latter work to Block Island, we should expect to see flow around the island produce a wide wake when the flow is slow and stable. Flow over the island producing a narrow wake is expected during fast-moving neutral flow (most likely in fall/early winter).

Garcia-Villalba et al. (2009) also use LES models to simulate flows on laboratory scales, although their results may have more relevance to designers of wind turbines rather than those trying to determine where to put the turbines.

2.2.3 Askervein Hill

A number of studies have used observations from a field campaign at Askervein Hill (~150 m tall and 1 km wide; in Scotland) to improve their model simulations of flows in complex terrain. These models tend to be one of two types: (1) Reynolds-averaged Navier-Stokes (RANS) solvers; or (2) LES. RANS models solve for the steady-state flow, while LES models attempt to capture the time-dependent turbulent nature of the flow; thus LES model solutions are inherently unsteady. Additionally, the LES approach does not rely on an assumed eddy viscosity. Walmsley and Taylor (1996) provide an early review of this work. It is important to note that most studies involving Askervein Hill examine the flow on the hill and perhaps up to a kilometer or two in the lee. This is closer to the obstruction than the proposed Block Island wind farm.

Eidsvik (2005) notes that the wind power available to windmills varies by a factor of one over flat topography (owing to variations in surface roughness), but by a factor of five in mountainous terrain, and then uses the RANS approach to see how well the flow around Askervein Hill can be modeled in this wind energy context. Their model (SIMRA) matches the observations within 50%, considered to be within the range of the observational errors, showing that confidence can be placed in models to generate fields of wind energy availability on small scales. The SIMRA model used 100 m grid spacing in the horizontal, with 1 m grid spacing in the vertical near the surface. The Coriolis force was ignored, and the flow was assumed to be adiabatic (including no surface heat flux). Eidsvik (2005) mentions that slopes (*H/L*) greater than 0.5 can lead to

separated flow in the lee (i.e., the wind in the direction of the large-scale flow becomes negative) for neutral stratification. Additionally, the following scaling are provided:

$$\frac{l_z}{z_0}\ln^2\left(\frac{l_z}{z_0}\right) \approx 2\kappa^2\frac{L}{z_0} \quad ; \quad \frac{\Delta u(l_z)}{u_0(l_z)} \approx 1.8\frac{H}{L} \quad ; \quad \frac{\Delta K}{K_0} \approx 2\frac{\Delta u}{u_0} \tag{1}$$

Despite the apparent success, Eidsvik (2005) concludes with the following caution: "...any estimation of actual stratified flows in mountainous terrain will probably be associated with significant uncertainty."

Prospathopoulos and Voutsinas (2006) provide an overview of the RANS approach and use it to model the Askervein Hill flow. They perform a number of sensitivity tests (varying vertical and horizontal resolution, the size of the grid, the surface roughness, etc.) to assess the impact the various "tuning knobs" have on their steady-state solution. With appropriate settings, they generate reasonable results. It is interesting to note that they mention problems getting the flow in the lee of the hill correct, but then state that it is an inappropriate location for wind energy applications, so it is irrelevant. [For the Askervein Hill case, it is the speedup region at the top of the hill that is most important for wind energy.] The Askervein Hill is only a few kilometers wide, though, so the "lee of the hill" in their paper just means within a kilometer or two of the summit. Any wake extending further downstream is ignored.

Silva Lopes et al. (2007) used an LES model to simulate the flow over Askervein Hill, and found an improvement relative to the RANS approach on the upwind side, but continued difficulty on the downwind side, including the lack of grid convergence.

Chow and Street (2009) also used the LES approach, describing the situation thusly: "The development of accurate wind energy prediction models for flow over complex terrain has been notoriously difficult as a result of the representation of steep topography, unsteadiness in the flow, poor performance of turbulence models, and lack of adequate field data for validation, among other factors." In their study, Chow and Street focus on improving the modeling of turbulence, using the ARPS model. [ARPS, RAMS, and WRF are the three "standard" Numerical Weather Prediction models in use, at least in this country, and broadly speaking they all are constructed in a similar fashion.] Their run uses 35 m grid spacing in the horizontal and 5 m grid spacing in the vertical at the lowest layer, stretching above that to give 59 layers in their 700-m-deep model domain. They note, this is a coarser vertical resolution than other Askervein Hill studies have used, but state that "finer resolution is not practical for real atmospheric flows over complex terrain." They also emphasize the need to have a suitable aspect ratio between Δx

and Δz in LES modeling. No surface heat or moisture fluxes are allowed, and their run encompassed a day with neutral stability. To force their model, they first ran an identical simulation over a domain with no topography to allow a fully turbulent flow to spin up. The outflow from this run then served as the inflow to their run with topography. An attempted run with uniform inflow did not produce adequate results. Their runs matched the observations well, with a slight reduction in the wind speed on the windward side of the hill, a significant speedup at the summit, and a significant slowdown (about 70% slower) in the lee at 10 m above the ground.

2.2.4 Other Relevant Work

Perhaps the island closest to Block Island in size that has been studied is Nauru, in the tropical Pacific. Nauru is about 5 km x 5 km in size, with a maximum elevation of 71 m, situated in the trade winds where easterlies of 5 to 10 m/s are common. In an observational study, Matthews et al. (2007) attempt to understand how the island generates a plume of cumulus clouds extending up to 200 km in its lee. [Malkus and Bunker (1952) report a less extensive wake (30 km) in the lee of Nantucket.] The physical process producing these plumes is the strong surface flux of sensible heat, which generates a warm plume that results in cumulus clouds at altitudes around 750 m to 1 km. The length of the cloud plume was likely maintained by horizontal convective rolls formed in part by the topographic obstruction. It was found that this warm plume detached from the surface about 20 km in the lee of the island. To the extent that Block Island is similar, we could expect impacts to be felt that far in the lee near the surface in our case as well.

Removing topography from consideration, the understanding and modeling of flows in the boundary layer depends on knowledge of the surface roughness, and the ways in which these flows evolve can be dependent on the wind profile. Fedorovich et al. (2001) present an LES modeling study that examines the effect these two factors have on the flow. They show that rougher surfaces and negative shear (wind speed decrease with height above the boundary layer) increases the depth of the boundary layer when stratified flow is heated from below. This could have applications to understanding flow patterns around Block Island during the fall season, with the added complications of topography of course.

Moeng et al. (2007) document the first use of the WRF model as a LES. After making a few modifications (included in the latest versions of the WRF 2008 model), they obtained good results with their idealized experiments. Their validation consisted of comparing their results to observations, laboratory studies, and other LES results.

Shaw et al. (2009) briefly review the state of the science, highlighting the problems that exist with modeling the turbulent mixing that leads to the actual winds and shears experienced by the turbines. The surface and boundary layers, according to Shaw et al., are still poorly understood, with limited observations being one of the problems. They suggest the LES approach may be a way to bridge the gap.

2.3 Numerical Modeling Approach

2.3.1 Overview

In task 1 of the fine scale meteorological modeling work, reported here, we simulate at high resolution the effects Block Island (BI) has on the turbulent atmospheric flow, under a variety of conditions (e.g., atmospheric stability, wind speed and direction). We focus the analysis of results, particularly on the island's lee side.

For performing high-resolution atmospheric simulations, we use the WRF model in Large Eddy Simulation (LES) mode (WRF 2008). A schematic of the model setup around BI is shown in Fig. 2. In three-dimensions (3D), this approach was found very computationally demanding, so to generate more runs in a given amount of time, 2D runs were first carried out for a series of vertical cross-sections through BI (Fig. 1a). These were followed by a small number of 3D WRF simulations. Although it is expected that the 2D runs may miss critical aspects of the flow, these were deemed good enough for identifying parameters yielding important patterns and phenomena. In the end, comparing the 2D and 3D WRF runs will determine how useful the 2D runs might be. [Note, as explained in the introduction, in view of the demands of running high resolutions 3D WRF simulations, an alternate strategy was selected, consisting in switching to the less computationally demanding RAMS model for performing most of the subsequent 3D simulations in and around BI.]

The LES approach generates inherently unsteady flows (i.e., no steady state is or can be reached in simulations), but this should allow for important quantities for the wind turbines, such as variance in vertical wind shear, to be assessed. LES of a steady turbulent boundary layer, for instance, will only result in a steady state result from a statistical point of view, similar to an actual experiment.

2.3.2 The WRF Model

The Advanced Research WRF (Weather Research Forecast) model is a collaborative effort between multiple federal agencies and universities, to develop a new generation of numerical

weather prediction tools. The model solves the fully compressible Euler equations for non-hydrostatic fluid motion with conservation of all scalar quantities using a 4th order Runge-Kutta integration scheme. The model prognostic variables include momentum and fluid density due to temperature and water vapor. The model uses a sigma, terrain following, pressure coordinate in the vertical. The top of the model is a constant pressure surface, which has no friction and no flux. There is a damping term for vertically propagating gravity waves to prevent artificial reflection. In the horizontal direction, the model uses an Arakawa C-grid discretization. The lateral boundaries used in the model are open (gravity wave radiating), periodic, or specified.

The bottom boundary of the 2D simulations (Fig. 2) uses physical parameterization of surface roughness to estimate shear stress at the no flux boundary. All of the subgrid scale physics options for the surface boundary layer are turned off (i.e., we are attempting to perform direct Navier-Stokes simulations). Unlike a true direct numerical simulation of the Navier-Stokes equations, the smallest turbulent length scales are not resolved, but often at very high Reynolds numbers (where the flow is nearly Reynolds number independent), the subgrid scale physics are not overly dependent on the eddy viscosity. The models run for this project are LESs, which directly resolve the unsteady turbulent flow over the topography of BI. This differentiates this model from other high resolution models, which may use a Reynolds Average or other parameterizations for the turbulent flow (e.g., as will be the case for RAMS simulations).

2.3.3 Development of the Block Island 2D Cross Section Atmospheric Modeling

The WRF model has been adapted from existing idealized 2D simulations for use in studying the flow over BI, in a series of 2D cross-sections (Fig. 1a). Based on an idealized test case of flow over a hill (e.g., Fig. 2), the model setup and initial conditions have been adapted to use the real topography of Block Island (Fig. 1b). Similar to the hill case in Fig. 2, the boundary condition normal to the flow is periodic. The most difficult aspect of this semi-idealized 2D implementation of the model has been the correct expression of the upstream boundary condition. To do so, we experimented with various options for open, periodic and specified boundary conditions, using a range of techniques to relax model results to the desired value, such as nudging and sponge layers. Our experiments showed that the open boundary does not react in a dynamically consistent way when using a specified condition for only velocity and temperature. It is thus critical to specify all of the prognostic variables inside the domain so that the model will adjust in a dynamically consistent way.

2.4 Two-dimensional Idealized WRF Simulations

The idealized 2D simulations in vertical cross-sections (Fig. 1a) use a 25 m horizontal grid resolution. To meet the assumptions of the numerical methods and the physical dynamics of the model, the vertical to horizontal aspect ratio $\Delta z/\Delta x$ must be nearly 1 to 1, so the vertical grid resolution is selected here at 20 m. Figure 3 shows the horizontal grid resolution over Block Island (the vertical grid is omitted for readability). A sensitivity analysis to the grid resolution does suggest, however, that the model is not fully resolved. Selected model runs at 10 m resolution have a more developed boundary layer, but preliminary results suggest that there is little difference in the overall wind profile or the effect of the island when using such a small grid. Hence, simulations are performed using the 25 x 20 m grid.

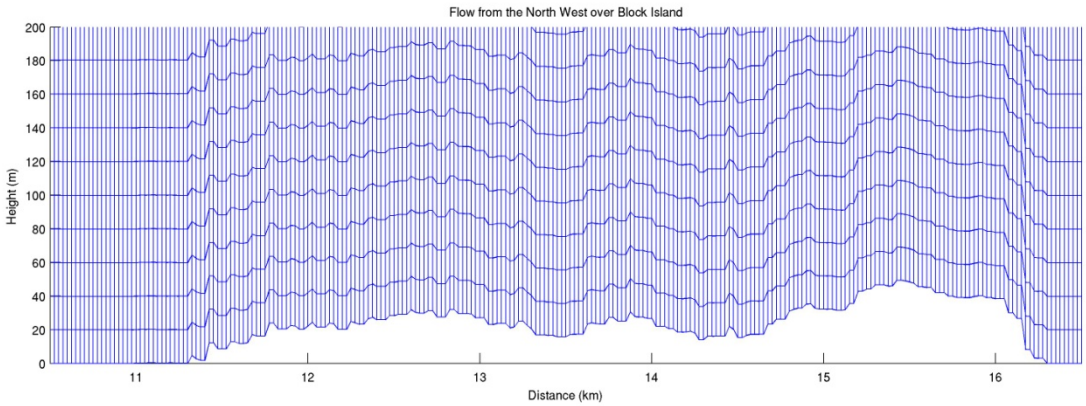

Figure 3: The region of the model grid over Block Island showing the vertical and horizontal resolution.

2.4.1 Ocean Boundary Layer Experiments

Initial experiments have run the 2D micro-scale model, with no topography, to determine the boundary layer thickness in the absence of the island, under the following conditions:

*Wind Speed***:** 5, 10 m/s

*Atmospheric Stability***:** stable, neutral, unstable as determined by the air-sea temperature difference (a colder ocean than the atmosphere yields a more stable atmosphere than a warmer ocean).

Results from these initial experiments, which are aimed at assessing model parameterization and setting open ocean boundary conditions, are not reported here in details. Results of these experiments are then used to specify the inflow boundary condition for the simulation cases examining flow over the BI topography.

Figure 4, for instance, shows the simulated wind speed (horizontal component) in a typical model run for a NW wind of free stream velocity of 10 m/s in a neutral atmosphere. The figure shows instantaneous contours of constant velocity along the length of the model domain, for 166 and 496 min into the simulation, which illustrate the convergence of the (mean) wind speed. We observe that the velocity increases with height and the atmospheric shear increases over the island. These results are characteristic of our initial work, though the issues with the inflow boundary condition make comparison between the upstream and downstream of the flow impossible. These issues have later been resolved as discussed above.

To aid in comparing the flow across the BI topography shown in Fig. 4, we created profiles at different points in the domain as shown in Fig. 5 (from results of Fig. 4b). Such an analysis is critical in determining the effects of the island, once the upstream boundary conditions are properly set, for a specified atmospheric stability. [Note, results shown in Fig. 5 are for a case with a slightly lower resolution of 50 m, used in developing the boundary condition.]

2.4.2 Island Cross Section Experiments

Based on the steady state approximation of the Ocean Boundary Layer experiments reported above, the upstream boundary is set to force an idealized wind field approaching BI from various different directions, wind speeds, and stabilities. For these cases, the island topography and surface roughness have been extracted from the USGS land surface model. Below are the various cases that were simulated using WRF in 2D vertical cross-sections through BI (Fig. 1a):

Direction: 4 compass points (SW,W,NW, N)

Wind Speed: 5, 10 m/s

Atmospheric Stability: Stable, Neutral, Unstable

(a)

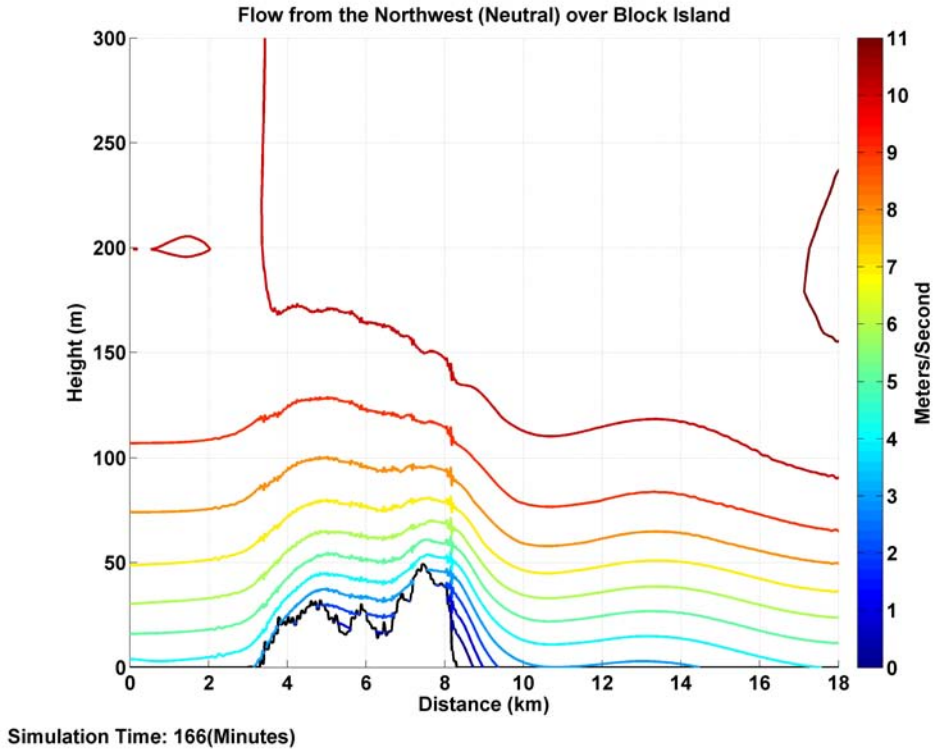

(b)

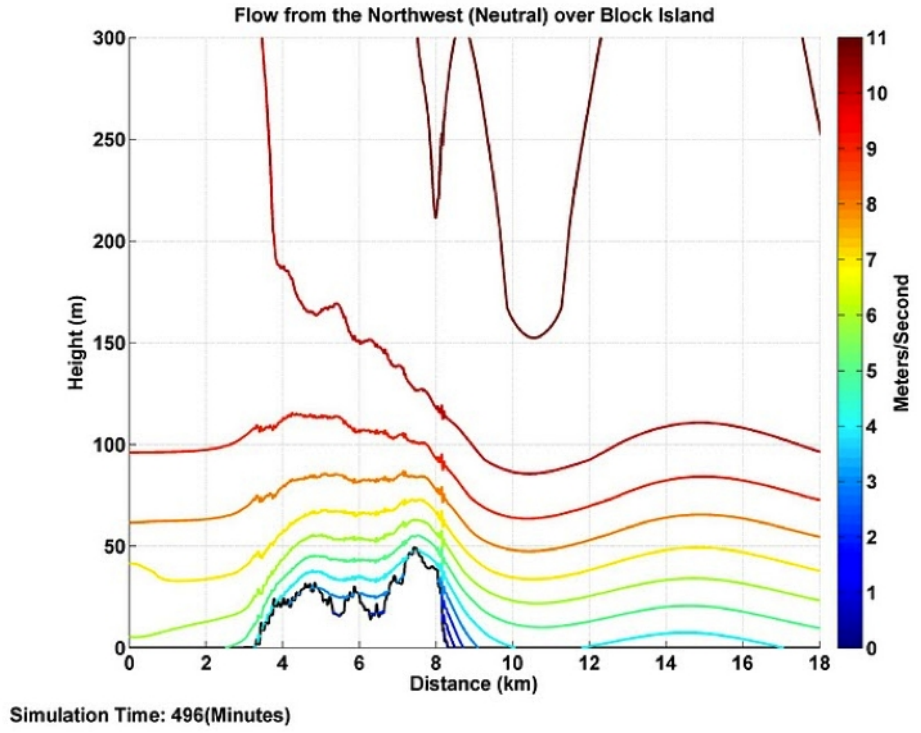

Figure 4: Instantaneous velocity contours for typical neutral NW flow (10 m/s in free stream) over Block Island, at two different simulation times: (a) 166 min; (b) 496 min.

All these results are plotted into figures such as Fig. 4, for velocity components, pressure and temperature (not shown here but available on demand). Based on such simulations, meaningful results for windfarm siting are extracted in the form of horizontal velocity for various stability conditions, as a function of the distance from BI, at selected heights (e.g., 80 and 130 m for approximate extension of windmill airfoils). Figure 6 shows an example of such results obtained from three different simulations. Clearly the marked difference in speed between 80 and 130 m would induce significant shear in the windmill airfoils.

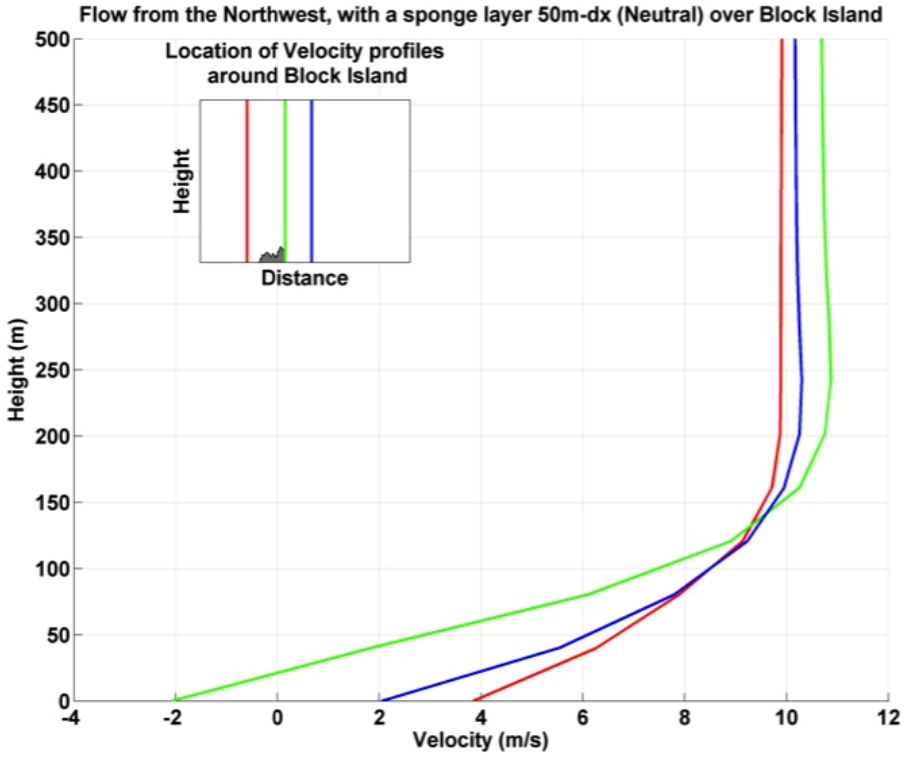

Figure 5: Profiles of horizontal velocity from Fig. 4b results, at different location along the length of the model domain shown in inserted figure.

Figures such as Fig. 6 are available for all tested wind directions and speed, and allow for direct comparison of the impact of air-sea stability on the dynamics of the model and wind speed as a function of distance and height in the lee of the island.

2.4.3 Validation and Verification

To validate the 2D simulation approach illustrated above, a limited number of 3D model experiments were performed, using the same physical parameters as for 2D simulations (e.g., Figs. 4-6). It was initially planned to perform a systematic comparison of 2D and 3D results, by

(a)

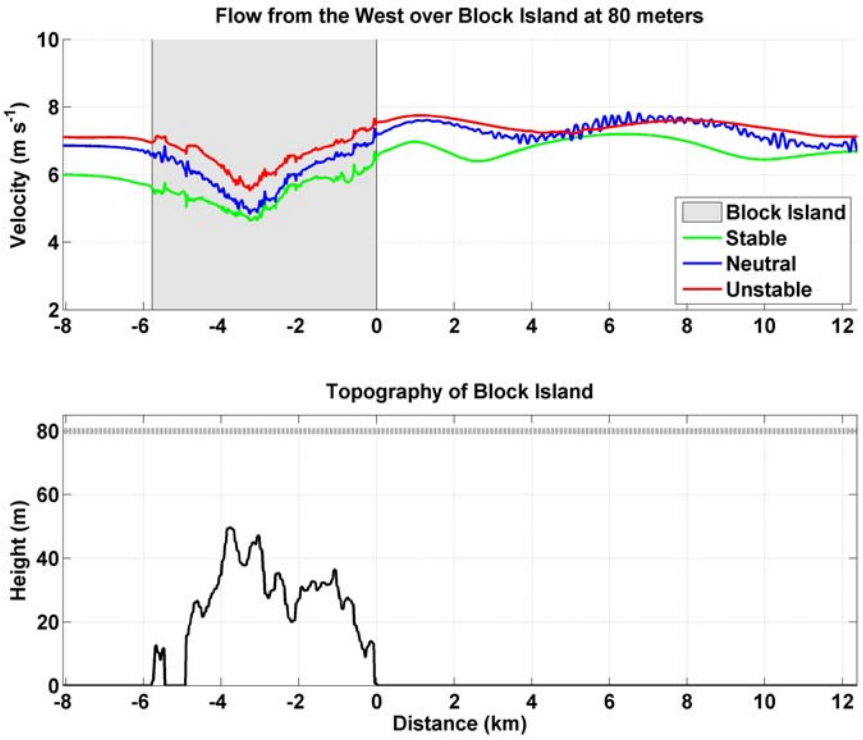

(b)

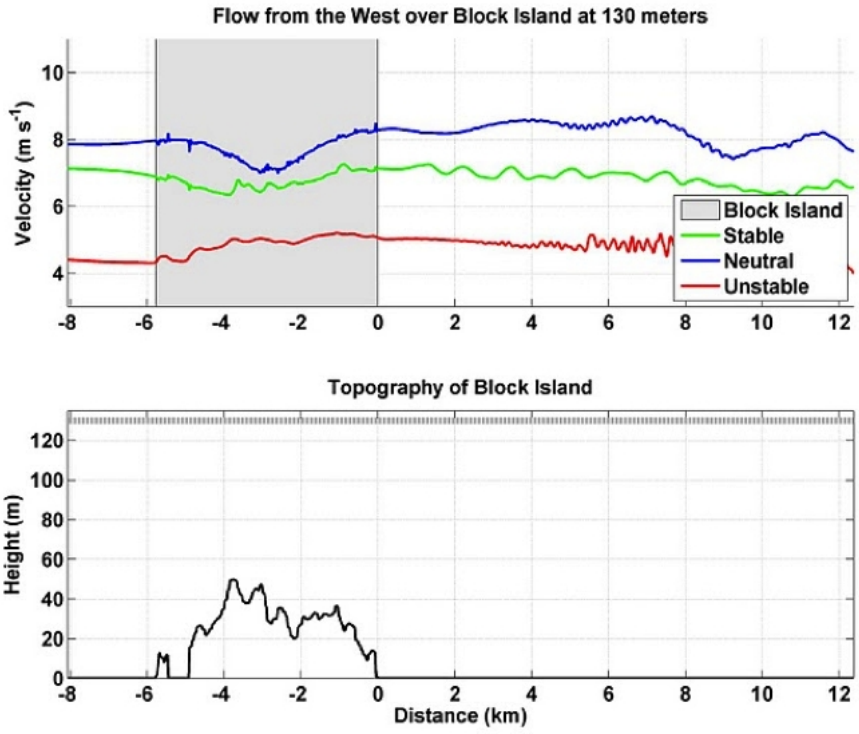

Figure 6: Comparison of horizontal wind speed at two heights : (a) 80 m; (b) 130 m, due to Westerly wind flows (10 m/s free stream velocity), and different atmospheric stability conditions.

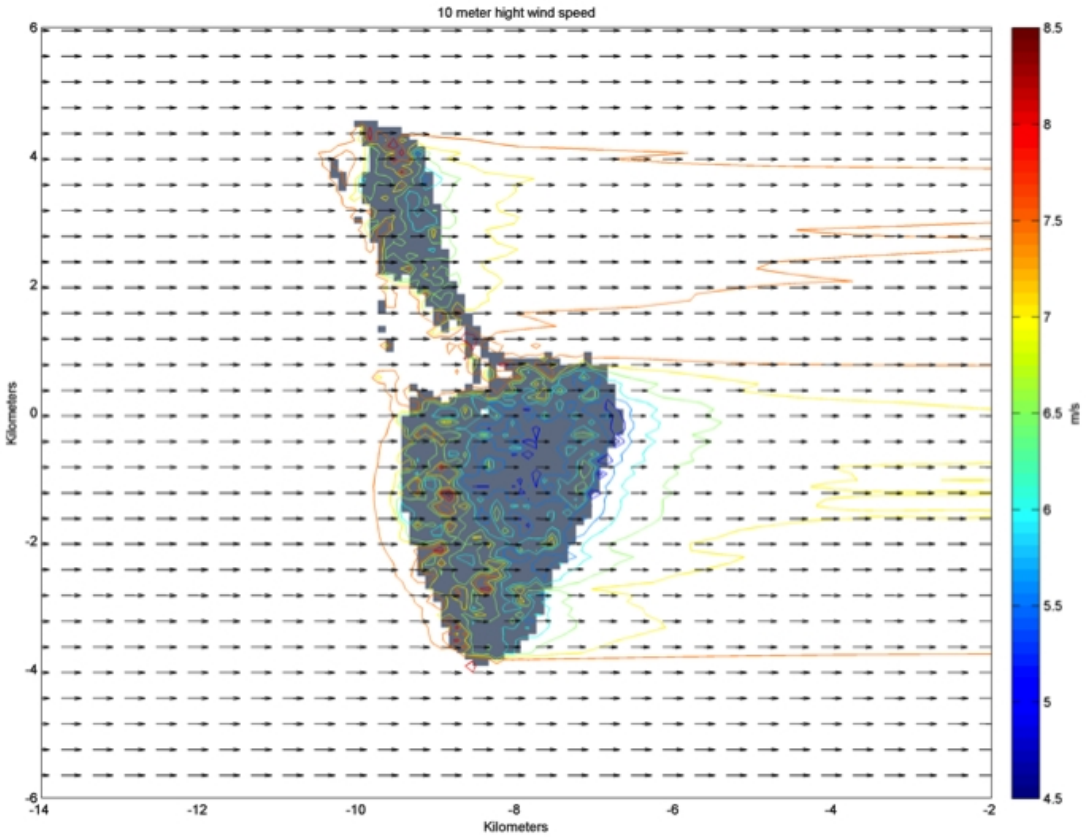

Figure 7: Wind Speed at 10 m high over Block Island, from 3D WRF model simulations for an idealized flow from the West.

extracting 2D section data from 3D results, for comparison with the 2D simulations. Additionally, it was planned to examine the overall magnitude of the turbulent cross-stream flow.

A typical result of 3D WRF simulations is shown in Fig. 7, for a westerly flow (10 m/s free stream velocity) at 10 m elevation over BI. Such results show there is little cross-stream flow, which is consistent with the assumptions of the 2D model approach.

At this stage in view of the high computational cost of running sufficiently resolved 3D WRF simulations, it was decided to change strategy and instead use the regional model RAMS, to perform the 3D simulations of wind over BI on a series of 4 nested grids, the finer and smaller one having a 500 m horizontal resolution (which is to be contrasted with the 25-50 m horizontal and vertical resolution used in the WRF simulations discussed above), and a 20 m vertical resolution in the lower layers (geometrically increased with elevation). This work was performed by another subcontractor, Weatherflow Inc. and results are reported on and analyzed in separate reports by Spaulding et al., 2010a,b. Section 3 of this report gives a brief summary of this work.

3. Regional Meteorological Modeling around Block Island using RAMS

Below is a summary of this work, which is separately reported on in Spaulding et al., 2010a,b. Results of RAMS, in the form of wind field and induced surface shear, are used to force the ROMS/SWAN simulations reported on in Section 4 of this report, over the period 10/1/09 to 2/28/10. On example of 3D RAMS's results obtained in the fourth and finest nested grid is given in Fig. 8, hindcast for the actual situation on 8/5/09; the figure shows wind velocity (magnitude and direction; contour lines) in and around BI at 84 m elevation. Due to BI's topographic relief effects (Fig. 1b), to large size vortex-like structures in wind speed can be seen on the NE and S sides of the island.

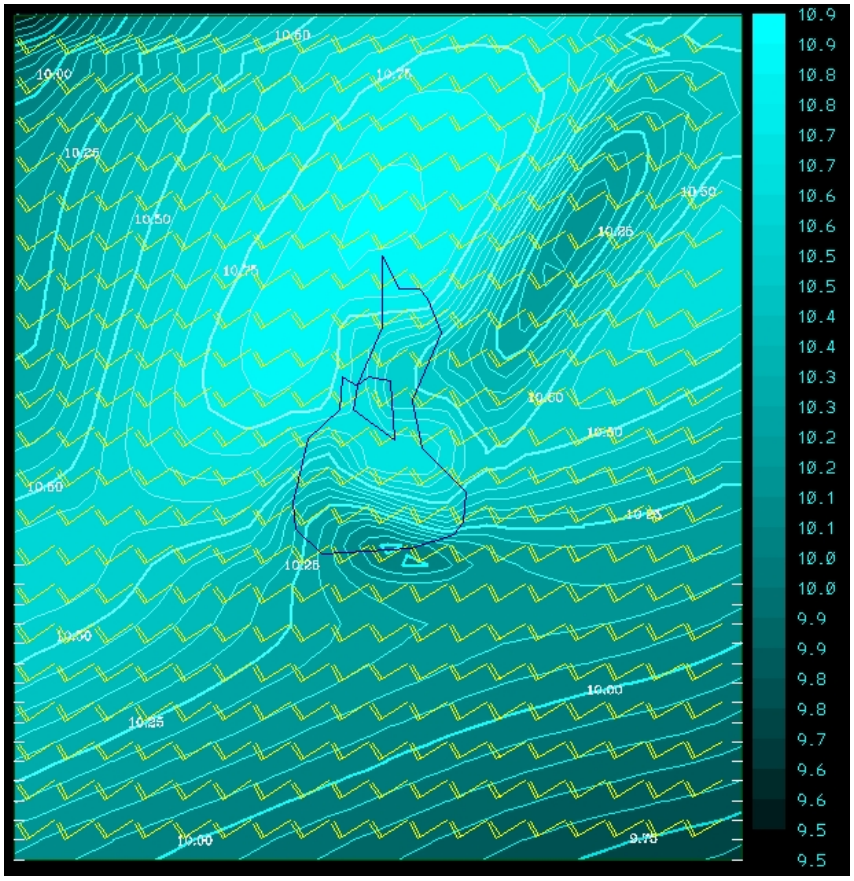

Figure 8: Wind at 84 m high over Block Island, from 3D RAMS model simulations for the hindcast flow on 8/5/09 (speed in m/s, directional symbols). BI is marked by a thin blue line.

3.1. Abstract of Spaulding et al., 2010a

Hindcast simulations of the winds in the vicinity of Block Island were performed using the Regional Atmospheric Modeling System, RAMS, V6, from October 1, 2009 to February 28, 2010 to assist in evaluating various sites south of Block Island for a small wind farm. This period

was selected since wind and air temperature observations were available from an offshore buoy (4 m elevation) immediately south (4.5 km) of the island and from a meteorological tower (9.9, 32, 47.6 and 57.4 m elevations) near the center, west coast of the island. The model was implemented in a four level nested system with grid resolutions of 12, 6, 2, and 0.5 km. The model was driven by NAM 12 km analyses. The model employed a 20 m vertical grid resolution at the surface, that geometrically increased with elevation. Island land cover and topography and sea surface temperature were provided by national digital data bases.

The winds during this period were predominantly from the NW, with the next most frequent direction from the NE. The wind distribution is typical of winter winds in the area, but with enhanced winds from the NE. The meteorological tower observations showed very low shear coefficients, 0.7 to 0.9, during the simulation period, typical of neutral to unstable, winter winds.

Model simulations were compared to meteorological tower observations at 57 m on shore of Block Island and showed good agreement with the data, with similar trends for passing weather events. The observed mean speed was 9.73 m/sec and the RAMS predicted was 9.3 m/sec (5.1% difference). The wind power followed a similar trend, 1000 kW/m^2 observed and 838 kW/m^2 RAMS (16.2% difference). The model predicted shear was higher than meteorological tower observations. The predicted shear coefficients increased dramatically over the island, reaching values as high as 0.45 over the southern end of the island where vegetative cover is dense. Model predictions also show lee effects from the topography/land cover at the southern end of the island (mean elevation of 35 m) for the two predominant wind directions. Lee effects were clearly noted 8 km from the island. Model predictions were also compared to winds (10 m elevation) from an offshore buoy and again showed good agreement (observed - 8.54 m/sec vs RAMS- 8.32 m/sec).

Simulations were performed for the dominant NW wind case to assess the sensitivity of the model to how the island was represented: by both its topography and land cover, or by each separately. The model predictions showed that either topography or land cover contributed substantially to lee effects.

Model predictions were integrated over the simulation period to estimate mean wind speeds and average power at 80 m. The mean wind speed and power contour lines are parallel to the BI shoreline. Wind speeds decrease from 10.2 m/sec south of Block Island to 9.7 m/sec at the northern end of the island. Power decreases from 1150 kW/m^2 to 965 kW/m^2 over the same distance. Power estimates were made at three potential locations for a small wind farm (5 to 8

turbines), SE, S and SW of the island following the state water boundary line (5 km) from the island. Mean powers were predicted to be SE—1,097 kW/m^2, S—1139 kW/m^2, and SW—1,076 kW/m^2. The S site has the highest power production potential; 3.6 to 5.4 % higher than the other two sites. The difference between the sites is due to lee effects from the island for NW winds at the SE site and for NE winds at the SW site. The SW site, in addition, is the lee of eastern end of Long Island (Montauk Point) for westerly winds. Lee effects at the S site are minimal since winds from the N are rare. Simulations have not been performed for spring and summer months where SW winds dominant. Winds from this direction are likely to be comparable at all three sites, since there is no lee effect and the locations are quite close. There is some degradation of winds from the W due however to lee effects from Long Island and an increase to the SW of the island due to channel enhancements for southerly winds.

Simulations, using a template based method, were performed using the observed wind rose at the AWS Met site and model predicted wind fields for eight compass directions. Predicted mean wind speeds and power densities were in generally good agreement with the hindcasts. The differences could be explained in part by the model predicting lower frequency for the NW winds and higher frequency for W winds than observed. When the model predicted wind rose at the AWS Met was used the predictive performance improved measurably.

3.2. Abstract of Spaulding et al., 2010b

The focus of the paper is to assess the wind resources for the area in state waters (4.5 km from land) immediately south of Block Island, a small, 9 km by 6 km, low relief (35 m elevation) pear shaped island located 15 km off the coast of RI, for the siting of a small (5 to 8 turbine) wind farm. The area is being considered for designation as the potential site for offshore wind development. A review of existing wind observations was performed and showed that the wind speed and power density roses were dominated by westerly winds with NW dominant in the winter and SW in the summer. Wind shear measurements from meteorological tower observations on the island showed low shears in the winter during unstable atmospheric conditions and higher values during the stable summer winds. The shears were also strongly impacted by the Block Island land cover and the positioning of the observation tower relative to these features.

A template based scaling method was used to estimate the annual mean wind speed and power density distribution in the vicinity of the southern end of the island. Hindcast simulations were performed using a four level nested version of RAMS for eight points of the compass for selected time periods over the last two years. These model predictions were compared to observations at two locations on the island and showed good agreement for direction and temporal trends of the speed but consistently under predicted the speed. The results of the simulations were used in conjunction with a wind speed frequency rose in the study area and, assuming linear speed scaling, estimates were made for the annual mean values. The large scale patterns showed wind speeds and power increasing with distance offshore. This pattern was modified in the vicinity of the island by lee effects from the predominant and strong NW winds. The impacted area extended at least 8 km to the SE of the island. Areas to the W-WSW of the island were impacted by lee effects from NE winds and roughness effects from Long Island, immediately to the west. Predictions showed the highest annual mean wind speeds and power densities to the S of the island with sites to the SW and SE having lower values. Power production potential was estimated for three sites: SE, S and SW of island. Wind power at the S site was 4.9 % and 6.9 % greater than the SW and SE sites, respectively.

Three separate wake models were applied to the SE and S sites to assess the impact of turbine layout. The SW site was not viable for a farm because of seabed geology making installation of pile foundations challenging. The turbines were nominally spaced 1 km apart. Simulations were performed for each wind direction and showed wake losses as high as 14 %, when the wind was in alignment with the field. When weighted by data from a nearby wind rose, the annual losses were shown to be several percent at the SE site and about half of that at the S site. The difference is due to the fact that SW winds are dominant in the summer while W winds are less frequent.

Considering both lee effects from the island and wake effects, the S site is the preferred location for a small wind farm.

4. Hydrodynamic, Wave, and Sediment Process Modeling using ROMS/SWAN

4.1 Introduction

The goal of this task is to characterize hydrodynamic flows in the ocean in the SAMP area (Fig. 9), due to general circulation currents, tides, waves and wind-driven circulation. Based on these and a data-basis of seafloor sediment characteristics, one also aims at characterizing near bottom sediment processes (namely suspension and transport). Understanding sediment suspension induced by currents resulting from combined environmental processes is important to the ocean SAMP ecological work, because a significant change in suspended sediment can have a detrimental effect on benthic life. Such a study should be conducted prior to any large-scale wind farm installation, in order to characterize suspended sediment processes in the areas envisioned for wind farm development.

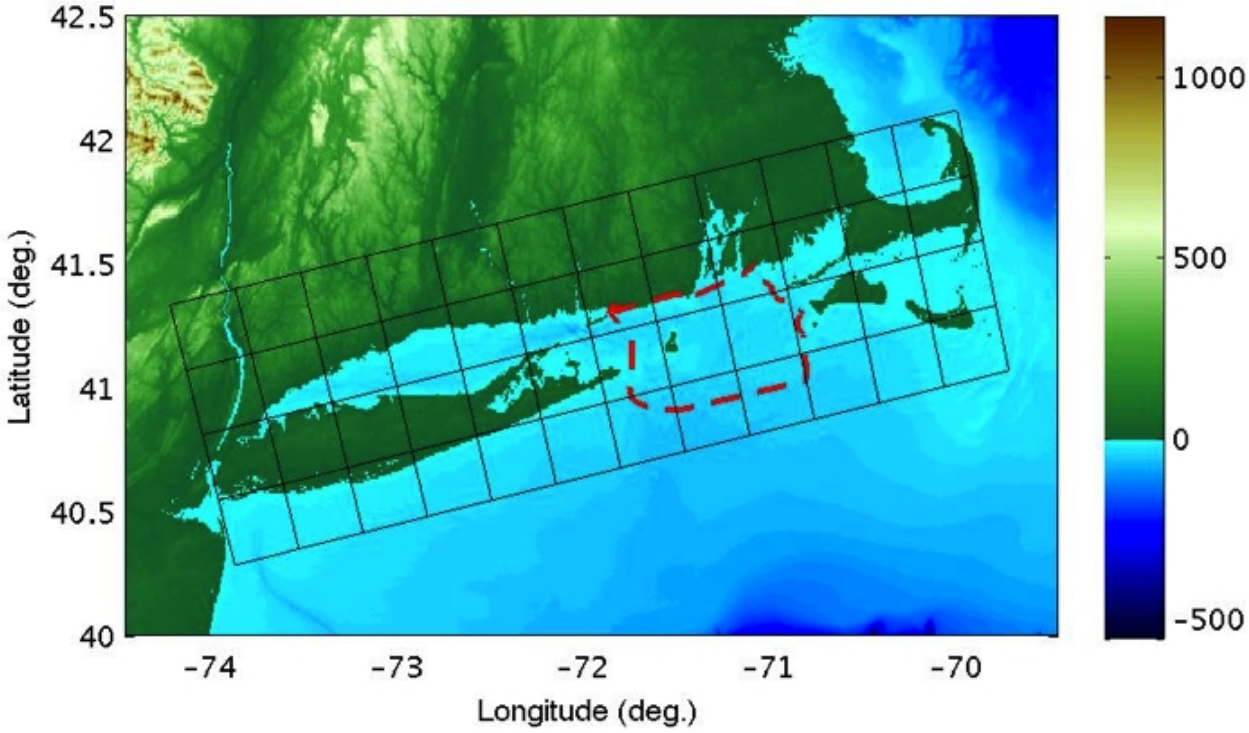

Figure 9: Overview map of bathymetry and topography around the SAMP study area, showing the ROMS model domain (black grid; each square is 30 km across, corresponding to 50x50 gridpoints in the high resolution simulations) and the SAMP study area (dashed; red).

Accordingly, this task included:

- Applying high resolution hydrodynamic and wave models to SAMP study area (Fig. 9) to investigate details of spatial and temporal structures of current and wave fields.

- Developing a characterization of the spatial and temporal variability of the current (tide-, wind-, and wave-driven).
- Estimating the potential for sediment suspension under wave and current forcing in the SAMP study area.

Note that this work does not investigate changes to overall sediment transport around Block Island due to wind farm support structures, since these are at much smaller scales than that of the model grids used in this work. Hence, we do not attempt to characterize scour around the windmill support structures; besides scour around coastal structure is a complex, specific, and still active area of research (see e.g., Sumer et al. 2001), which is outside the scope of the SAMP work. What is known is that wind turbine installations usually consist of several vertical piles, the presence of which can increase suspended sediment by eroding sediment around the pile circumference (Laursen 1963). This process is initiated by the formation of a horseshoe vortex and the contraction of streamlines (Sumer and Fredsoe 2001).

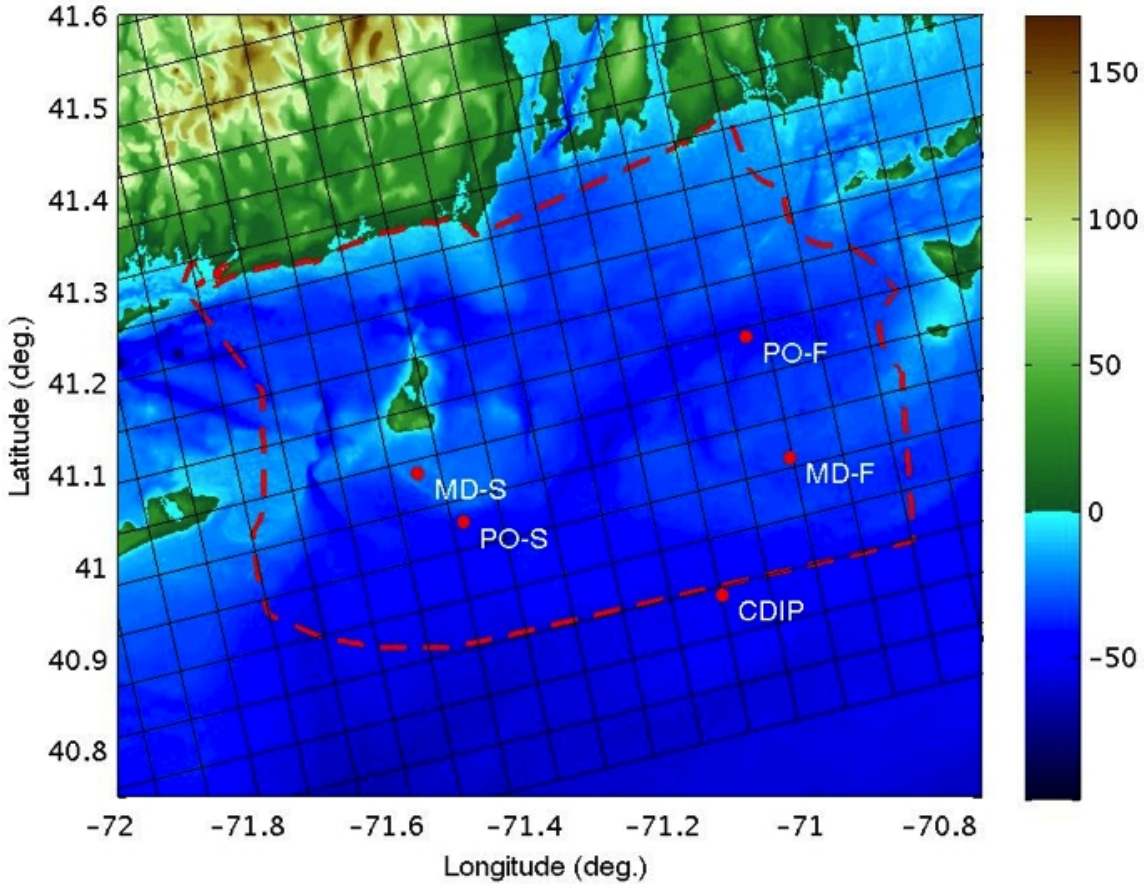

Figure 10: Overview map of bathymetry and topography around the bounds of the SAMP study area (marked by dashed red contour) and domain (black grid; each square is 6 km across, corresponding to 10x10 grid points in the high resolution ROMS/SWAN simulations). White labels show locations where wave and current data was recorded (Table 1).

There are little to no pre-existing measurements of suspended sediments in the SAMP area, but meaningful predictions can be made based on a properly validated regional hydrodynamic model of the area, which is the goal of this work. Sediment suspension is dependent on near-bottom currents, which in the SAMP study area are primarily tidally driven, except during episodes of storm waves (characterized by long, long-crested swells whose induced particle velocity may cause significantly shear on the seafloor). Except during those episodes, subsurface currents generated by winds and waves in the area, and density-driven circulation are relatively weak in comparison to tides, although observations of tidal currents have noted significant seasonal changes in tidal current ellipses (Codiga and Rear 2004).

4.2 Literature Review

A variety of ocean models have recently been used to study hydrodynamics in the area around our SAMP study area (Fig. 1), although none have focused on the waters immediately around Block Island as we seek (e.g., Oey et al., 1995; Edwards et al., 2004; He and Wilkin, 2006; and Mau et al., 2006). In each case, a spin-up time of 15-30 days is used to achieve quasi-periodic model results, which are then compared to observational data. Emery and Thompson (2001) showed that 30 days is sufficient to resolve the 5 major tidal constituents.

Edwards et al. (2004) used the MIT general circulation model (Marshall et al., 1997) to study front generation in BI Sound (BIS). Importantly, although they focused their attention on BIS, their domain extended over the entire length of Long Island Sound, which can experience tidal velocities of over 1 m/s because of a resonance with the period of the M2 component of the tides. Edwards et al. favorably compared their results against ADCP data from the FRONT project (Codiga and Houk, 2002).

He and Wilkin (2006) used the Regional Ocean Modeling System (ROMS; see Shchepetkin and McWilliams, 2005), as we are doing in the present work, to study the tidal dynamics south of Cape Cod, Massachusetts, to the east of our study area (Fig. 1). They specifically focused on tidal gage and bottom pressure measurements, because their domain of interest extended over the New England Shelf where Shearman and Lentz (2004) had previously found that internal waves can have a strong effect on velocity measurements. He and Wilkin were able to find good agreement with measurements. Note that they used a hybrid data assimilation modeling system

that used TRUXTON (see Lynch et al., 1998) as an inverse model to correct the tidal open boundary conditions.

Mau et al. (2006) used the Princeton Ocean Model (Blumberg, 1987) to simulate the semidiurnal tidal currents slightly to the west of our study area. They compared their results against an atlas of tidal current and bottom pressure (Moody et al., 1984), HF radar measurements of surface currents (Ullman and Codiga, 2004), as well as ADCP profiles (Codiga and Houk, 2002), of the New York Bight and BIS. Mau et al. found that the model reproduces the correct flow patterns and vertical structure, which earlier one-dimensional models of the tides in the area could not (see Codiga and Aurin 2007). They claim that such model results for the barotropic tidal currents are as accurate as observations.

Readers are referred to Codiga and Ullman (2010) for a more complete review of the physical oceanography of the SAMP study area. They review satellite measurements, recorded CTD casts, surface currents measured by HF radar, and output from a hydrodynamic model of the region on a large scale. Some of these results are discussed below, particularly regarding the stratification noted in a climatology of the area and numerical simulations of a larger domain.

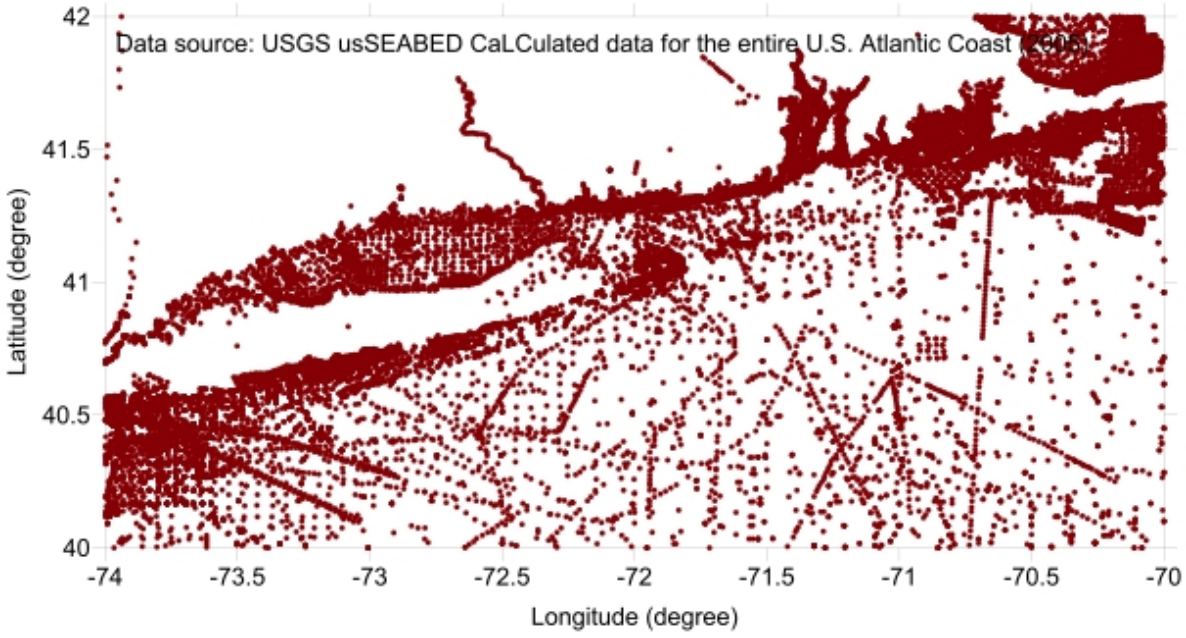

Figure 11: Locations where data was collected for USGS sediment texture database (Reid et al., 2005).

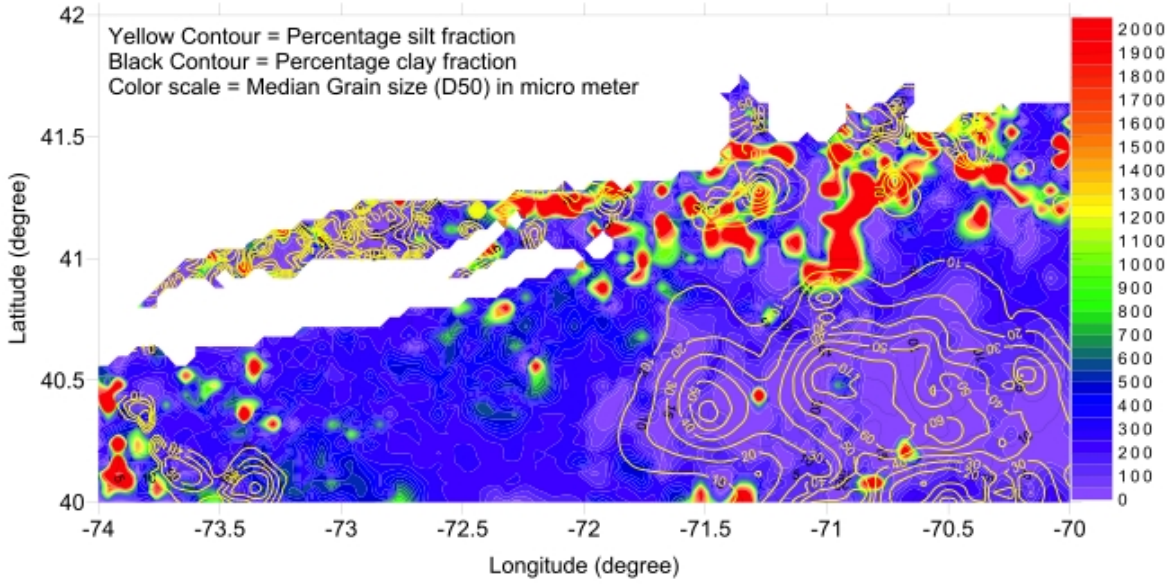

Figure 12: Map of median grain size, silt fraction, and clay fraction from the USGS sediment texture database (Reid et al., 2005).

4.3 Data for Model Validation

4.3.1 Buoy Data

Only a small number of observational studies have looked at currents in the area, and we discuss these below in the context of other modeling studies as well as the observational field program that is part of SAMP. Most data is obtained from tidal gage and bottom pressure measurements, although there is also surface data from radars, and vertical profiles of velocity at a few locations, from moorings or acoustic Doppler current profiler (ADCP) results. For this report, we will limit our discussion to measurements obtained from five locations listed in Table 1 and marked on Fig. 10, which include two buoys with surface-mounted ADCPs (at multi-disciplinary measurement sites in both state and federal waters; MD-S; MD-F), two bottom-mounted ADCPs (at a physical oceanography measurement site at nearby locations; PO-S; PO-F), and at a CDIP buoy station number 44097, which only measures wave parameters. The five locations are positioned in representative locations throughout the ocean SAMP study area (Fig. 10). Details regarding the exact variables measured are given below.

Table 1. Locations and data type for field buoys deployed in SAMP study area

Buoy	Latitude	Longitude	Deployed	Recorded variables
PO-S	41.0482° N	71.5003° W	9-15-2009—1-15-2010	$H_s, T_{peak}, \theta_{mean}, u, v$
PO-F	41.2500° N	71.0917° W	9-15-2009—1-15-2010	$H_s, T_{peak}, \theta_{mean}, u, v$
MD-S	41.1012° N	71.5672° W	9-Oct-2009 —	$H_s, T_{peak}, \theta_{mean}, u, v$
MD-F	41.1183° N	71.0284° W	9-Oct-2009 —	$H_s, T_{peak}, \theta_{mean}, u, v$
CDIP	40.9686° N	71.1261° W	Continuously	$H_s, T_{peak}, \theta_{mean}$

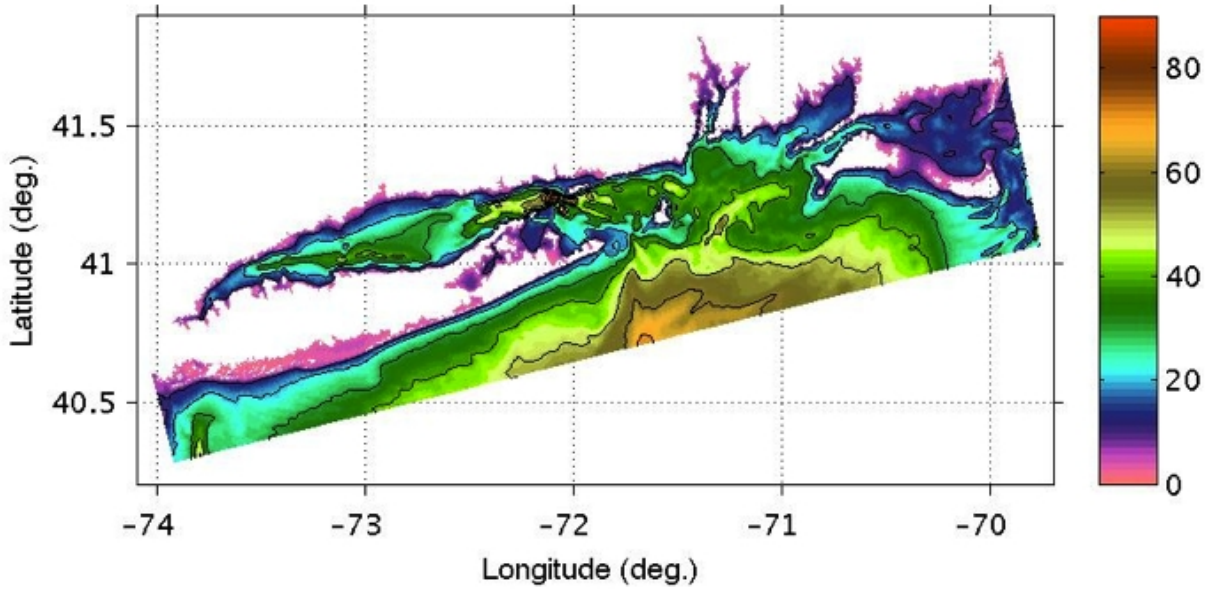

Figure 13. Bathymetry (m) for computational domain. Note that Massachusetts Bay and small rivers have been blanked out, since they do not connect with the computational domain in the area of interest.

4.3.2 Surficial Sediment Data

In order to understand sediment suspension due to bottom current velocity, it is first important to understand the present seafloor surficial sediment properties. A number of surveys have been conducted, of the surficial sediments in the area surrounding the SAMP study area (see e.g. Battelle, 2003). The most comprehensive summary of these studies is the USGS sediment texture database (Reid et al., 2005). By applying kriging to this dataset (Fig. 10), it is possible to

develop a surface map of the sediment properties (Fig. 11). Most of the surface sediment in the SAMP study area is coarse sand, but there is a wide range of variability.

Note that the USGS database only lists median grain size and not the grain size distribution, such as would be required for an initial condition of a sediment transport model. [Earlier results of Hastings et al. (2000) did include grain size distributions, but did not have as many samples in the area of interest.]

Model results mentioned earlier primarily focus on currents and other hydrographic fields, and there is very little information available concerning suspended sediment. Warner et al. (2008a) described a coupling of ROMS, mentioned above, with the wave model "Simulating Waves in the Nearshore" (SWAN) and a sediment transport model. This coupling has been successfully used by Blaas et al. (2007) for modeling sediment transport off of California, and by Warner et al. (2008b) for modeling sediment transport off of Massachusetts. Blaas et al. used a simple relationship between depth and grain size to initialize the seabed characteristics over their domain. One can see comparing Figs. 12 and 13, however, that this would not be an accurate reflection of the SAMP study area. Instead, to model sediment transport here, one would have to follow a methodology more similar to that of Warner et al., who started with an even distribution of many grain sizes, which over the spin-up time of the simulation, evolved into something approximating the actual seabed distribution.

4.4 Hydrodynamic Model ROMS/SWAN Overview and Setup

4.4.1 Bathymetry and Gridding

The Regional Ocean Modeling System (ROMS) is a high-resolution, free-surface, terrain-following coordinate oceanic model (Shchepetkin and McWilliams, 2005), which has been applied extensively to basin-scale and coastal circulation. Here we apply ROMS to study the hydrodynamics of the SAMP study area.

The computational domain, which extends over all of Long Island Sound, Block Island Sound, and Rhode Island Sound (Fig. 9) is discretized horizontally with an orthogonal curvilinear Arakawa-C grid, and vertically with a terrain-following sigma-coordinate formulation. To set-up the grid, detailed bathymetry was obtained from the 3" (about 90 m) resolution Coastal Relief Model data (Divins, 2003; Fig. 11). [In order to prevent numerical instabilities, the bathymetry was smoothed with three iterations of a second-order Shapiro (1975)

filter.] The southwestern-most point of the grid is at 40.8° N 73.92° W, and the grid is rotated 14 degrees counterclockwise with respect to a meridian. The horizontal grid used here for all of the ROMS simulations is 200 x 600, with a uniform 600 m resolution (Figs. 9, 10, 13).

In the vertical direction, the grid consists of 10 terrain-following levels. The vertical coordinate transformation is determined by the stretching function of Song and Haivogel (1994):

$$z(x,y,\sigma,t) = S(x,y,\sigma) + \zeta(x,y,t)\left[1 + \frac{S(x,y,\sigma)}{h(x,y)}\right]$$
$$S(x,y,\sigma) = h_c\sigma + [h(x,y) - h_c]C(\sigma)$$
$$C(\sigma) = (1-\theta_B)\frac{\sinh(\theta_S\sigma)}{\sinh\theta_S} + \theta_B\left[\frac{\tanh[\theta_S(\sigma+\frac{1}{2})]}{2\tanh(\frac{1}{2}\theta_S)} - \frac{1}{2}\right] \quad (2)$$

where σ varies from -1 (at the seabed) to 0 (at the surface). For the simulations in this report, θ_S is 1.0, θ_B is 0.8, and h_c is 0.0.

Unconnected sections of the ocean (e.g., unresolved rivers; Massachusetts Bay) were masked from the computational domain, since their results would be anomalous and have no effect on the region of interest.

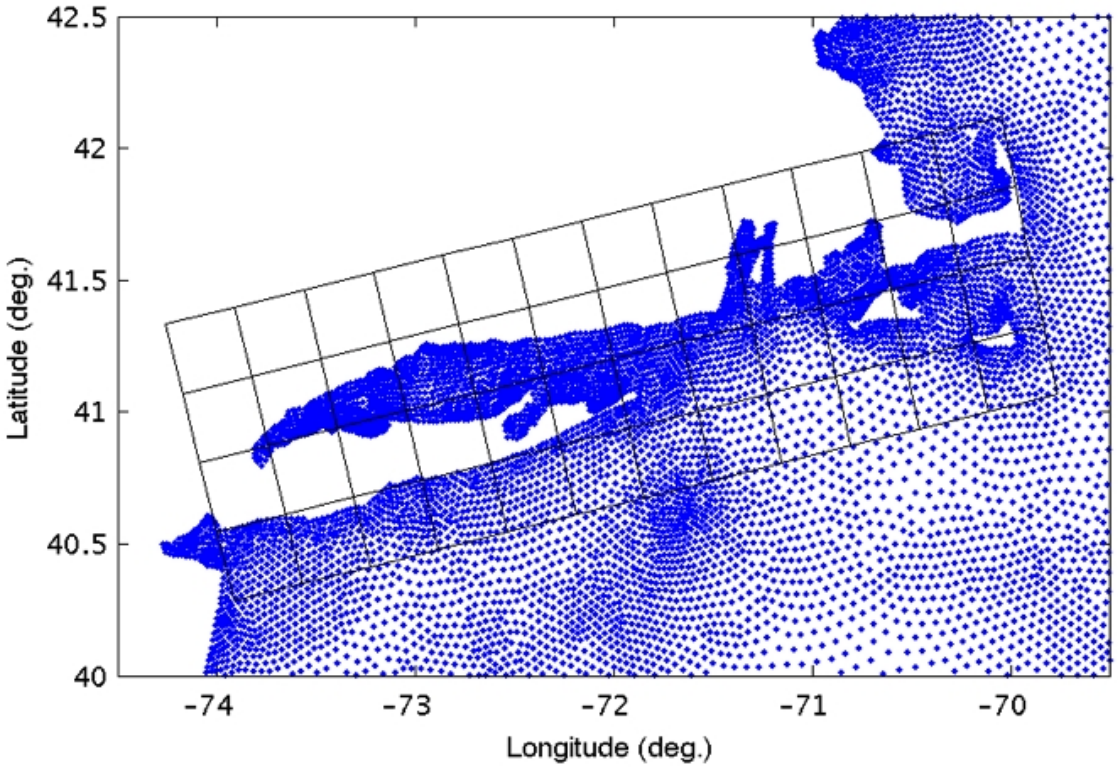

Figure 14. The black grid indicates part of the ROMS/SWAN grid (each square is 30 km across, corresponding to 50x50 gridpoints in the high resolution simulations). Blue points mark the unstructured grid used in the ADCIRC regional model of tides.

4.4.2 Tidal forcing

One of the most important forcing for bottom currents over the SAMP study area is from tides. Hence, two separate modeling investigations were conducted for this important aspect of coastal hydrodynamics in the SAMP area. This allowed for cross-validation between those independent approaches, with the additional experimental validation (discussed later) using data from SAMP's field program. The first modeling of tides was performed as part of ASA's subcontract, using their in-house code HYDROMAP. A detailed report of this work is provided in Appendix A. The second modeling of tides was done as part of ROMS simulations, first only using tidal forcing, then using all the other environmental forcing (waves and wind) together with tides.

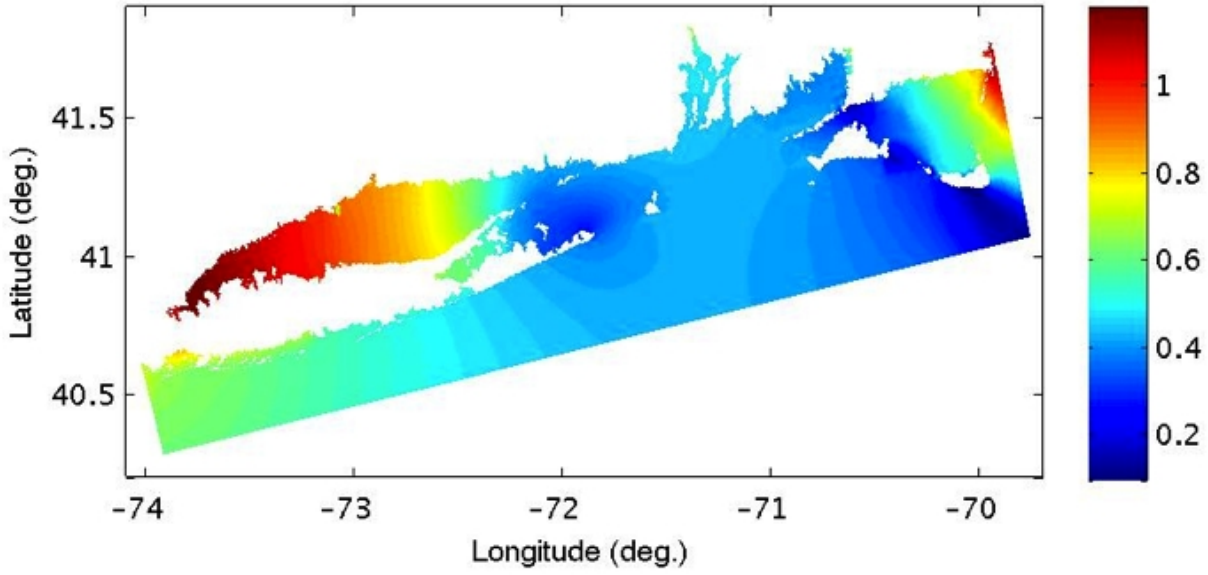

Figure 15. M_2 tidal amplitude (m) from ADCIRC tidal database as interpolated onto the ROMS grid.

To force tides in the ROMS model, we use the Western North Atlantic, Caribbean and Gulf of Mexico Tidal Database (Mukai et al. 2002), which includes the M_2, S_2, N_2, K_2, O_1, K_1, Q_1, M_4, M_6, and steady tidal constituents. This database is based on simulation results from the coastal circulation model ADCIRC (Fig. 14), which itself is forced along the open boundary with the Le Provost et al. (1998) tidal database FES95.2, formed from satellite altimetry. This ADCIRC tidal forcing was independently validated against measured tidal amplitudes and phases for 7 different components, at several stations close to the SAMP area (i.e., at Woods Hole, MA, Nantucket Island, MA, Block Island, RI, and Montauk, NY; for details see Mukai et al., 2002). Note that

the M_2 tidal constituent (Figs. 15, 16) is most significant around BI. For all the stations used for validation by Mukai et al. along the Atlantic Coast, an error of 2.7% for the amplitude and 2.5 deg for the phase was found for the M_2 component.

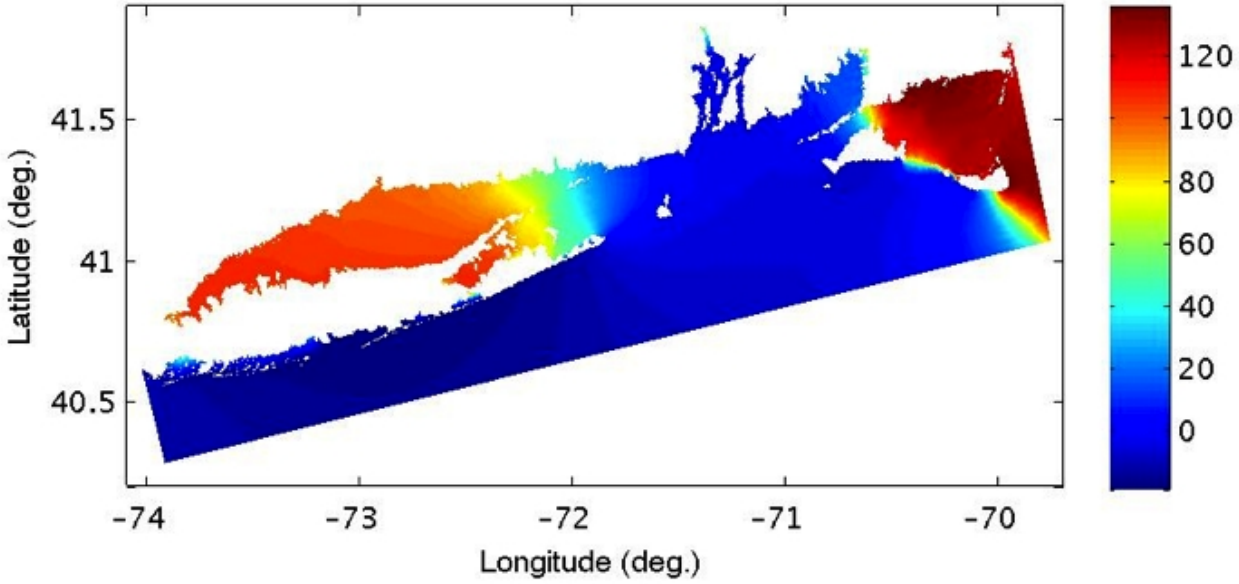

Figure 16. M_2 tidal phase (degrees from GMT) from ADCIRC tidal database as interpolated onto the ROMS grid.

For tidal simulations using ROMS, velocity and sea surface height from the ADCIRC tidal database are applied as numerical forcing along the boundary of our ROMS grid, using both the Flather (1976) radiation condition as well as the Chapman (1985) boundary condition. Nudging is also applied to the grid points closest to the boundary, to force the ROMS's solution at the boundary to tend towards that of the tidal boundary condition. In order to use the ADCIRC results to initialize simulations in the ROMS/SWAN grid, the tidal amplitude and phase of each constituent were linearly interpolated onto the new grid (Figs. 15, 16). For points of the ROMS grid that are outside the ADCIRC grid, values were filled in with the average of the nearest grid points that did fall within the tidal database.

4.4.3 Wave Forcing

For the complete ROMS runs, wave forcing is applied together with tidal and other forcing, by coupling ROMS to the SWAN model (Simulating Waves Nearshore; Booij et al., 1999). SWAN is a third-generation, non-stationary (time-varying), phase-averaged model that solves for the wave action density conservation (including wind forcing terms, wave breaking and bottom friction dissipation, and nonlinear quadruplet wave-wave interactions). SWAN simulations were

performed in a grid identical to that used for ROMS (Fig. 9). Information exchanged between SWAN and ROMS includes wave direction, significant wave height, average wavelength, wave period, bathymetry, free-surface height, vertically integrated momentum, and bottom roughness.

The boundary conditions for SWAN is set using a similar but larger scale operational ocean wave prediction model, NOAA's WAVEWATCH III. NOAA keeps records of significant wave height, peak period, and peak wave direction. To apply these as both initial and boundary conditions in SWAN, a JONSWAP wave energy spectrum $S(\omega)$ (Hasselmann et al., 1973) is assumed at each grid point, based on the WAVEWATCH III parameters defined as the significant wave height H_s, the peak wave period, $T_p = 2\pi/\omega_p$, and the peak wave direction, θ_p:

$$S(\omega,\theta) = S(\omega)D(\theta)$$
$$D(\theta) = \frac{2}{\pi}\cos^2(\theta - \theta_p) \tag{3}$$

where:

$$S(\omega) = \frac{\alpha g^2}{\omega^5}\exp\left[-\frac{5}{4}\left(\frac{\omega_p}{\omega}\right)^4\right]\gamma^r$$
$$r = \exp\left[-\frac{(\omega-\omega_p)^2}{2\sigma_0^2\omega_p^2}\right] \tag{4}$$

and

$$\sigma_0 = \begin{cases} 0.07 & \omega < \omega_p \\ 0.09 & \omega \geq \omega_p \end{cases}$$
$$\gamma = 3.3 \tag{5}$$

the average peakedness factor, and α is the equilibrium-range (or Phillips) parameter. Note, a coarser resolution (4 minute or about 5.6 km east-west and 7.4 km north-south) grid is used for WAVEWATCH III (Fig. 17). A process similar to that used for tides is used to fill-in data for points on the ROMS grid that fall outside the WAVEWATCH III grid. In order to verify whether WAVEWATCH III data represents a good boundary condition to the SWAN simulations, the WAVEWATCH III data is compared to the wave data recorded at the five stations mentioned

earlier (Table 1, Fig. 10). This is done in Figs. 18—22 and we see that, at least qualitatively, the agreement is quite good.

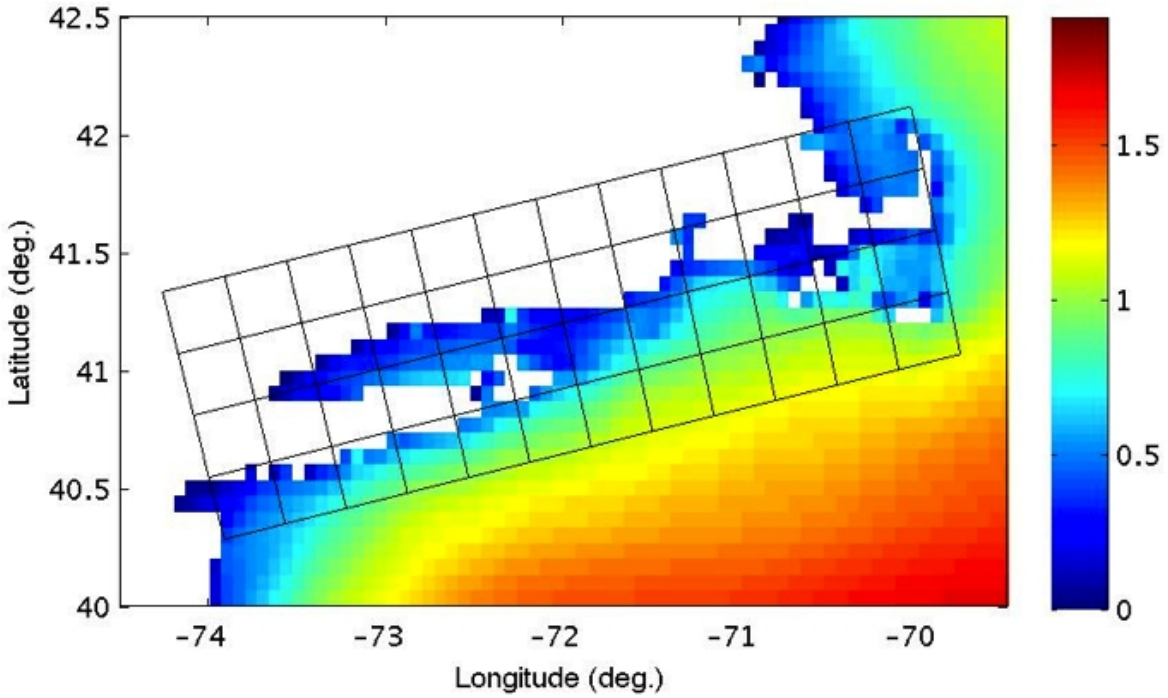

Figure 17: Significant wave height (m) predicted by WAVEWATCH III on Oct. 1st, 2009 at 000 GMT, and ROMS/SWAN domain (black grid; each square is 30 km across, corresponding to 50x50 grid points in the 600 m resolution simulations, in comparison to the 4 min. or about 5.6 km east-west and 7.4 km north-south resolution of the WAVEWATCH III results).

4.4.4 Wind Forcing

For the complete ROMS runs, wind forcing was applied as well, using results of a 5 month hindcast (October 2009 — February 2010) conducted by WeatherFlow on a SAMP subcontract. These wind simulations were performed with version 6.1 of the Regional Atmospheric Modeling System (RAMS), using 4 levels of nested grids (varying in horizontal resolution from 500 m to 12 km), the finer one being centered around Block Island. The vertical resolution was 20 m at the surface, with a stretching ratio of 1.15. The RAMS model was initialized and bounded by the North American Mesoscale (NAM) results, produced by the National Center for Environmental Prediction (NCEP), which is presently generated by the Weather Research and Forecasting Non-hydrostatic Mesoscale Model (WRF-NMM).

The time varying wind speed at 10 m computed by RAMS is used to force ROMS and SWAN (Figs. 23 and 24). Because of project time limitations, it was not possible to have RAMS output the wind stress at each point, but instead the 10 m wind is applied to SWAN, and a surface stress

is applied to the ROMS domain, assuming a neutrally stable atmosphere. Specifically, given the wind at 10 m, the surface stress is computed assuming that near the surface the velocity profile can be approximated by:

$$u = \frac{u_*}{\kappa} \log \frac{z}{z_0}$$
$$z_0 = 0.016 \frac{u_*^2}{g} \qquad (6)$$

where u is the wind velocity, u_* is the friction velocity, z is the height (e.g., 10 m), κ is the Von Karman constant (0.40), g is the acceleration due to gravity (9.81 m/s^2), and z_0 is the surface roughness, given by a Charnock's relationship as shown above.

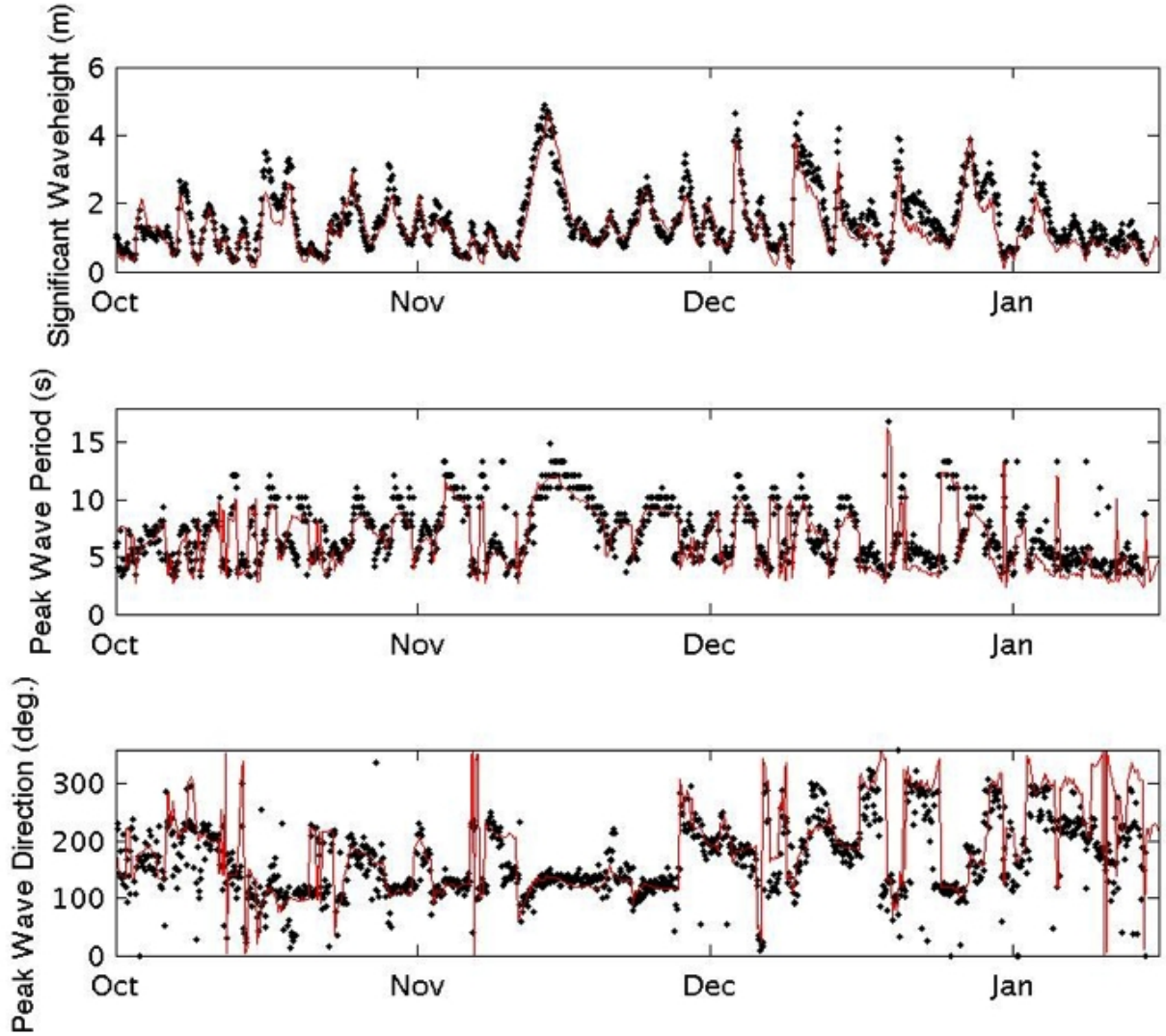

Figure 18: Significant wave height, peak period and direction measured at the PO-S buoy (41.0482° N 71.5003° W) (black dots), compared to WAVEWATCH III simulations (solid red line).

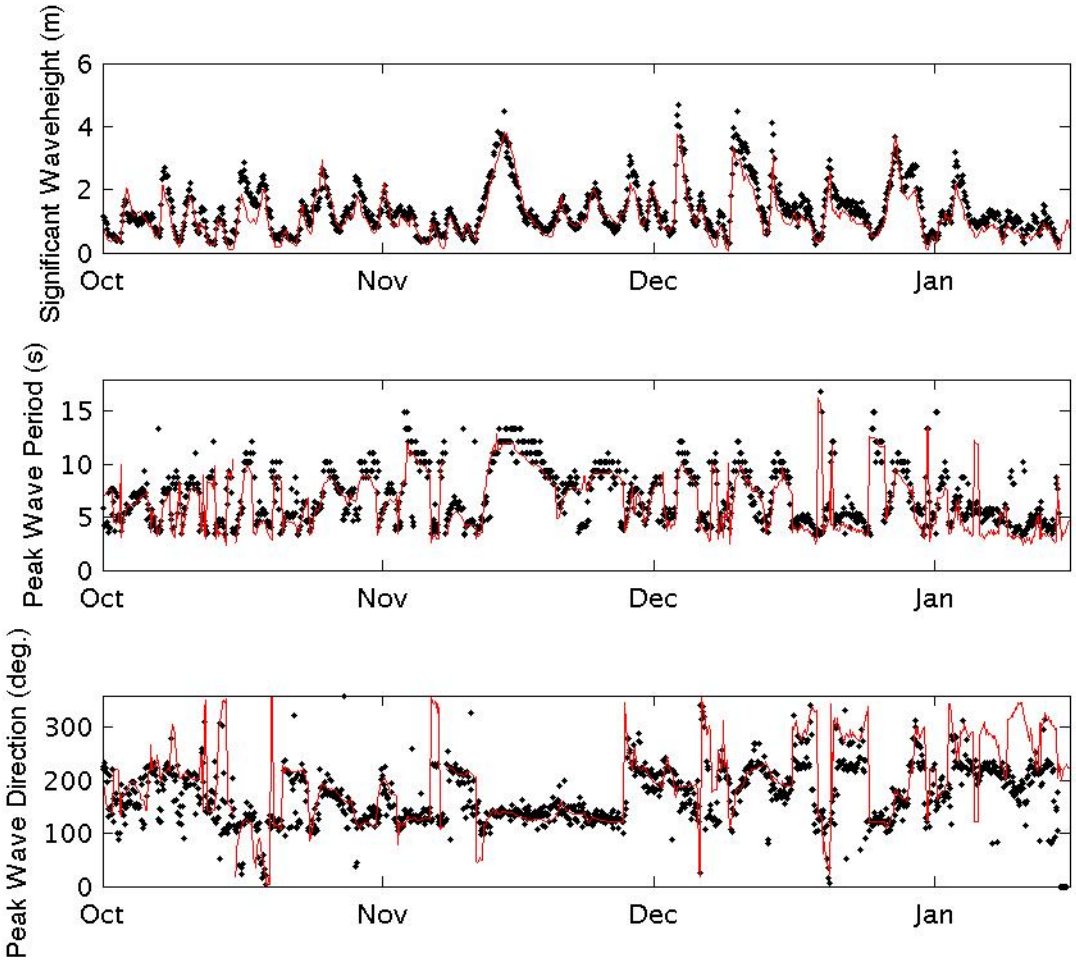

Figure 19. Same as Fig. 18 at the PO-F buoy (41.2500^{o} N 71.0917^{o} W).

The coefficient 0.016 is consistent with that used in the RAMS hindcast. Note that this ignores wind gustiness.

Since all three simulations use different parameterizations of the ocean-atmospheric boundary layer, a slight inconsistency is unavoidable. For instance, RAMS simulations include the effect of atmospheric stability (resulting from the air-sea temperature difference) in determining the surface wind stress. ROMS is able to do the same, but here we force ROMS assuming an essentially neutrally-stable atmosphere. SWAN assumes a logarithmic profile for the wind over the ocean, but accounts for the wave height, which the other two models do not.

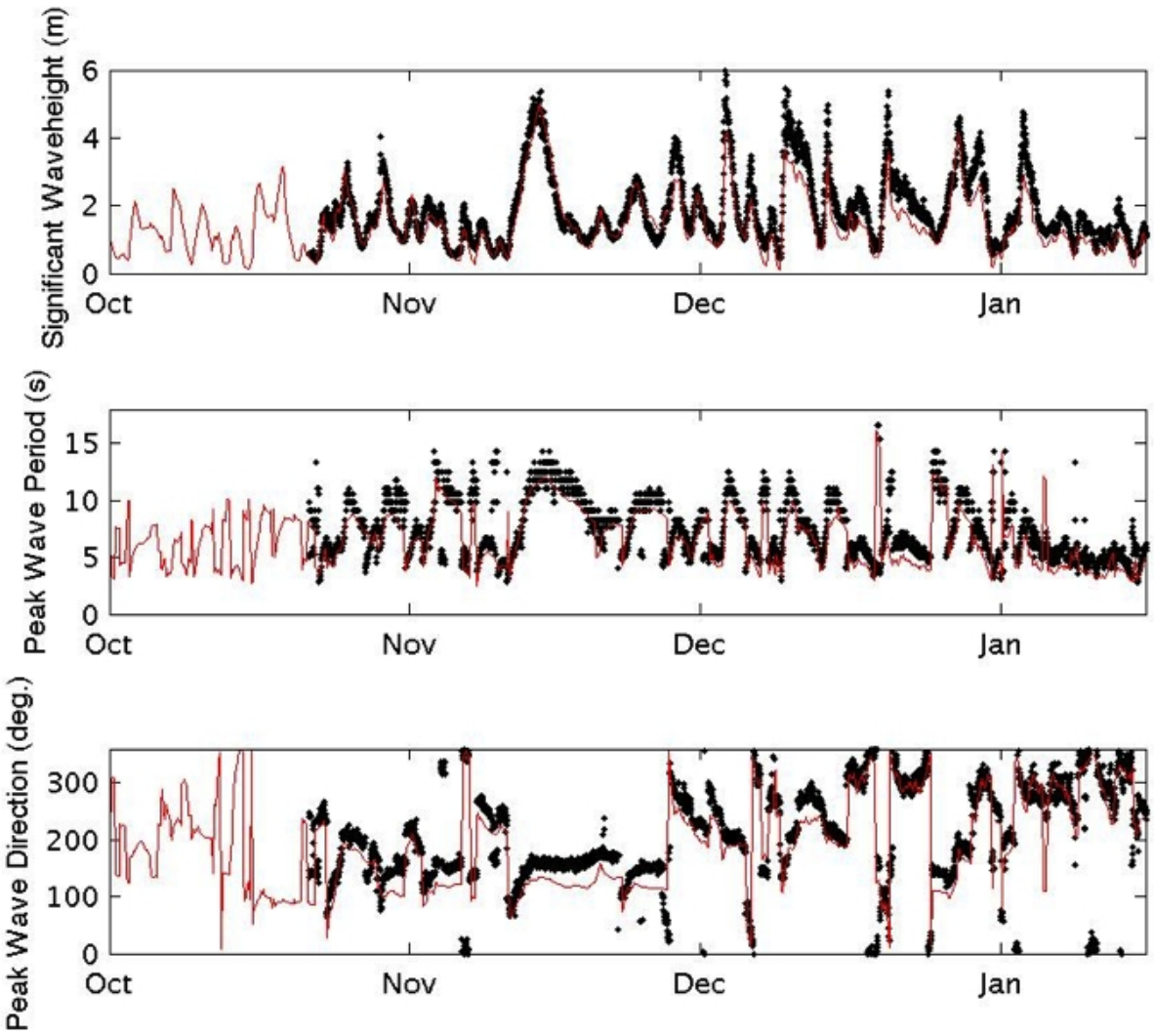

Figure 20. Same as Fig. 18 at the CDIP buoy (40.9686^{o} N 71.1261^{o} W)

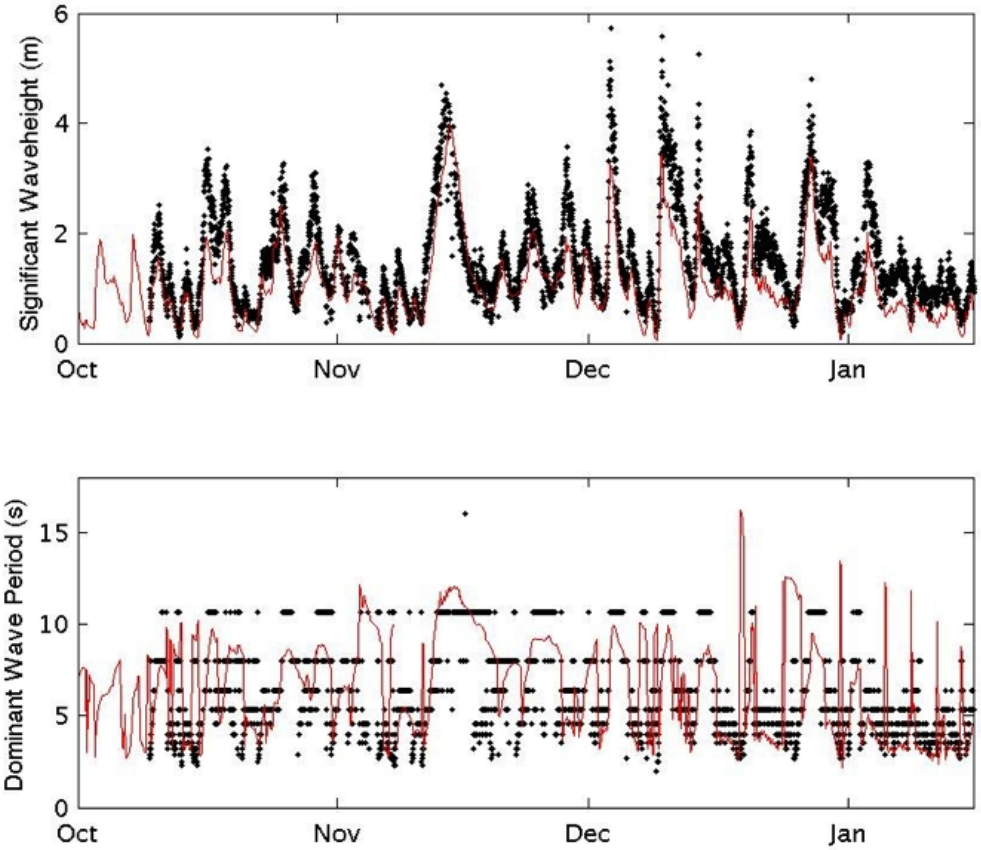

Figure 21. Same as Fig 18 at the MD-S buoy (41.1012° N 71.5672° W).

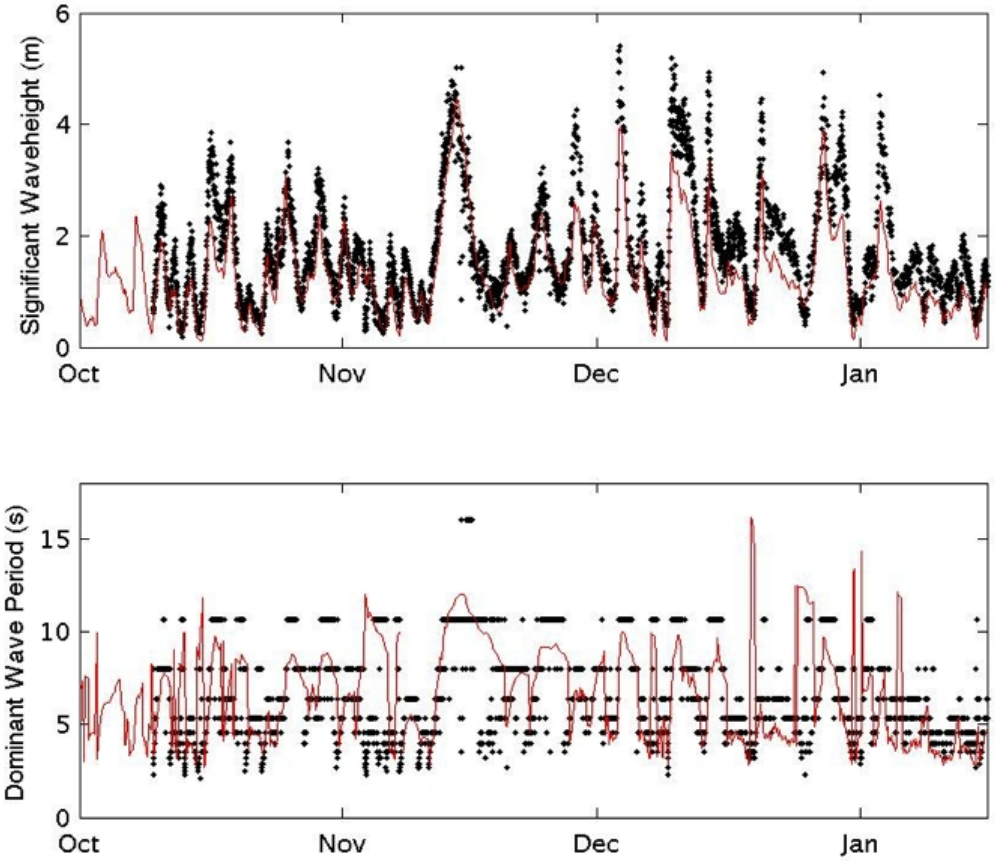

Figure 22. Same as Fig. 18 at the MD-F buoy (41.1183° N 71.0284° W).

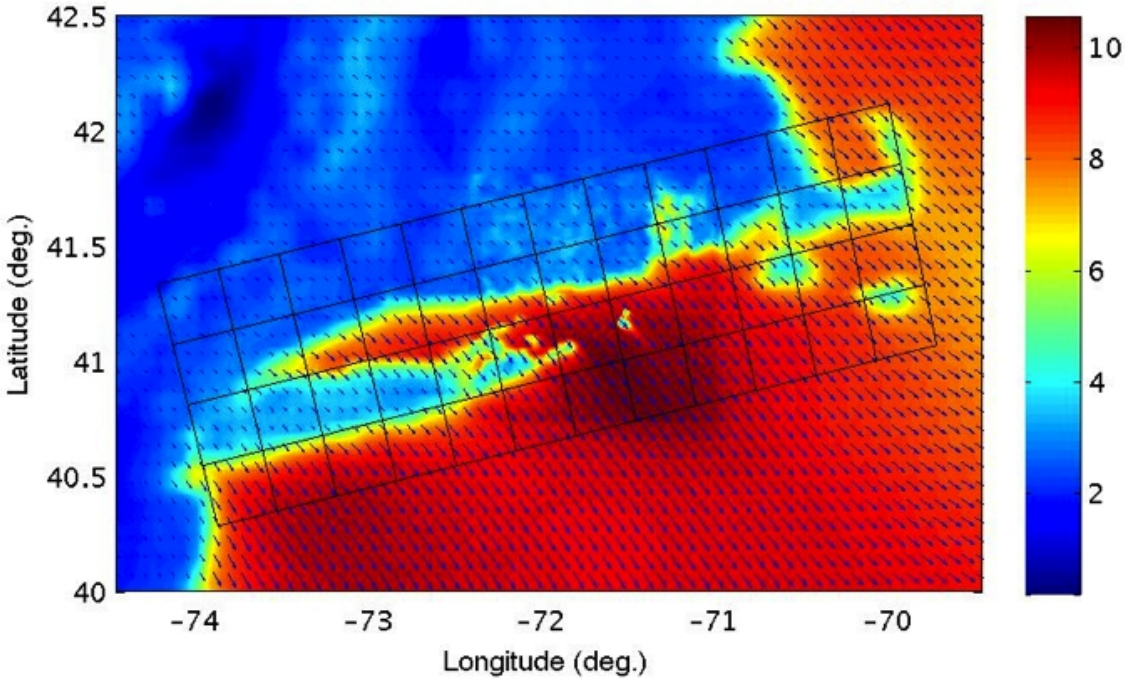

Figure 23. Wind speed at 10 m as simulated by RAMS on Oct. 26th, 2009 at 000 GMT (color in m/s). Vectors indicate wind direction, and the black grid indicates the ROMS/SWAN domain (each square is 30 km across, corresponding to 50x50 grid points in the high resolution 600 m simulations).

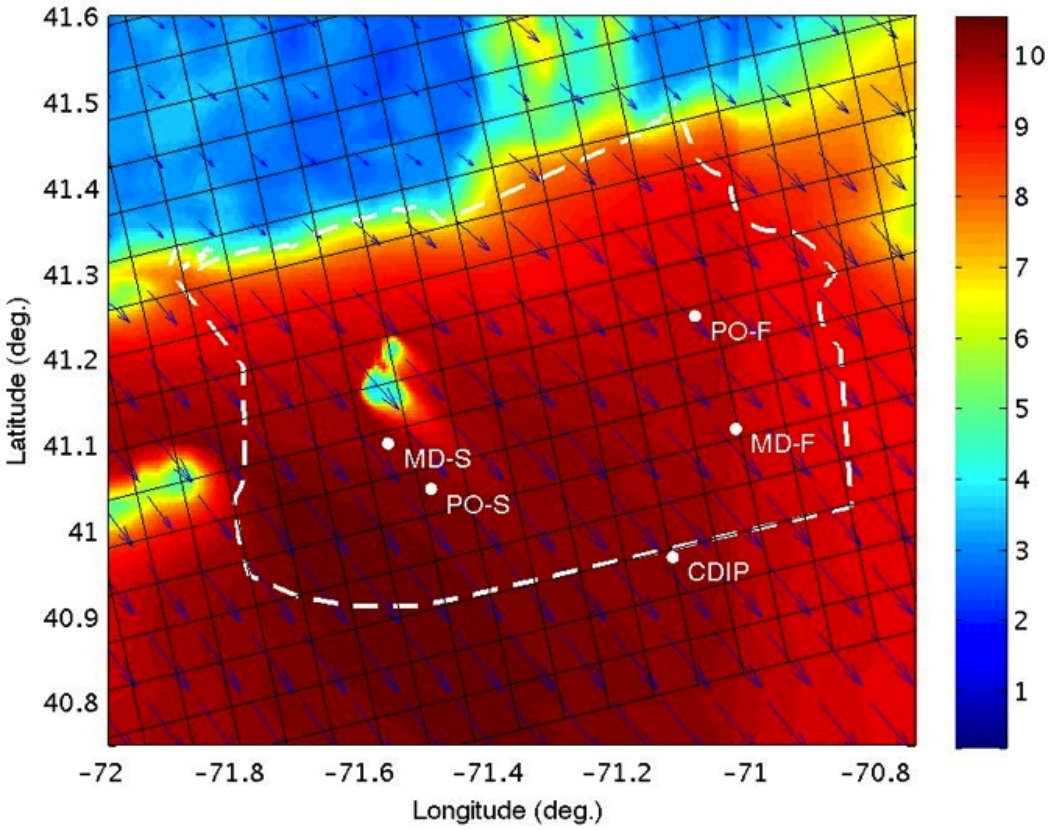

Figure 24. Zoom of Fig. 23 on SAMP area (black grid is ROMS/SWAN dimain; each square is 6 km across, corresponding to 10x10 grid points in the high resolution simulations).

4.4.5 Bottom Boundary Layer and Turbulence Closure

The bottom boundary layer stress can be significantly affected by surface waves. When considering only tides, and not waves as well, a quadratic form of seabed drag is used. In order to remain consistent with the ADCIRC tidal simulation data, we use a drag coefficient C_f = 0.0025. Because of this, we expect that the tidal velocities simulated in ROMS should be approximately as accurate as those obtained by the ADCIRC model itself, simply on a finer grid.

When a coupled ROMS/SWAN simulation is conducted, a wave-current bottom boundary layer model is applied instead, using the *ssw_bbl* formulation as described by Warner et al. (2008a). The seabed is assumed to have ripples of height and wavelength estimated using the method of Wiberg and Harris (1994): the bottom boundary layer roughness is estimated as a combination of that from grain roughness, sediment transport, and bedform roughness length; the seabed stress is predicted as a sum of that from both waves and currents, and the mean bottom stress is determined iteratively from an assumed eddy viscosity profile.

In each case, the Mellor-Yamada 2.5 closure is used for the vertical mixing scheme (1982).

Table 2. Characteristics used in ROMS sediment suspension and transport simulations (8 classes).

Sediment (phi)	Diameter (mm)	Density (kg m^{-3})	Settling vel. (mm s^{-1})	Erosion rt. (kg m^{-2} s^{-1})	Crit. shear (N m^{-2})
-2	4.0	2650	276.2	$5.0 \cdot 10^{-6}$	2.913
-1	2.0	2650	189.2	$5.0 \cdot 10^{-6}$	1.457
0	1.0	2650	122.8	$5.0 \cdot 10^{-6}$	0.612
1	0.5	2650	70.6	$5.0 \cdot 10^{-6}$	0.249
2	0.25	2650	32.7	$5.0 \cdot 10^{-6}$	0.178
3	0.125	2650	11.7	$5.0 \cdot 10^{-6}$	0.173
4	0.0625	2650	3.4	$5.0 \cdot 10^{-6}$	0.116
5	0.03125	2650	0.92	$5.0 \cdot 10^{-6}$	0.073

4.5 Sediment Modeling

Suspended sediment is modeled by ROMS, as a conservative tracer using an advection-diffusion equation with a constant vertical settling velocity term. See Warner et al. (2008a) for full details of the coupled ROMS, SWAN, and sediment transport model. In order to model a distribution of sediment diameters, 8 different sediment classes are considered, from 4 mm to 0.03125 mm.

Sediment modeling depends on a number of parameters, including settling velocity, density, critical shear strength, and many others (Table 2). Settling velocity was determined using the empirical relation of Jimenez and Madsen (2003), and the critical shear stress is set by the explicit formulation of the Shields curve as formulated by Cao et al. (2006). Because the sediment characteristics are not well-known, the erosion rate and porosity of the bed is chosen to match the study of Warner et al. (2008b), of sediment transport in Massachusetts Bay.

Although not a primary goal of this work, bedload transport is also modeled as part of ROMS simulations. When waves are not simulated, the Meyer-Peter Mueller (1948) formulation of bedload transport is used, relating the bedload transport to the excess shear stress. When SWAN is coupled to ROMS, the model of Soulsby and Damgaard (2005) is applied, which takes into account the combined wave and current effects.

In order to test the validity of the ROMS results, simulations are conducted for the period from Oct. 1, 2009 to Jan. 16, 2010. This starts at the beginning of the available RAMS hindcast data, and ends at the end of the available ADCP data. The ROMS time step for each simulation is 2 minutes, and the SWAN time step for those involving wave-coupling is 4 minutes.

4.6 Results and Applications

4.6.1 Available Buoy Data

In addition to wave parameter measurements shown earlier (Fig. 18—22), the measurements at PO-S and PO-F include the current profiles and the surface elevation. We observe significant variation in the currents at these two stations (Fig. 25, 26) at both tidal and subtidal frequencies, although the currents at PO-S are noticeably stronger than those at PO-F.

Another use of the data measured at PO-S and PO-F is to verify the simulated tidal elevation at these locations (Fig. 27, 28), using the data from the pressure sensor attached to the bottom-mounted ADCP. While numerical limitations can affect the tidal elevations from ROMS near shore (e.g., within one or two grid cells of the shoreline), both the tidal elevation and amplitudes at an offshore location such as those two stations (i.e., PO-S; PO-F) should be correct if the hydrodynamics is correctly modeled. An analysis of the results, using T_TIDE (Pawlowicz et al., 2002) provides the harmonic constituents for future comparison (Tables 3, 4). For PO-S, 84.9% of the variance measured can be attributed to the tidal predictions, and for PO-F, 82.4% of the variance measured can be attributed to the tides.

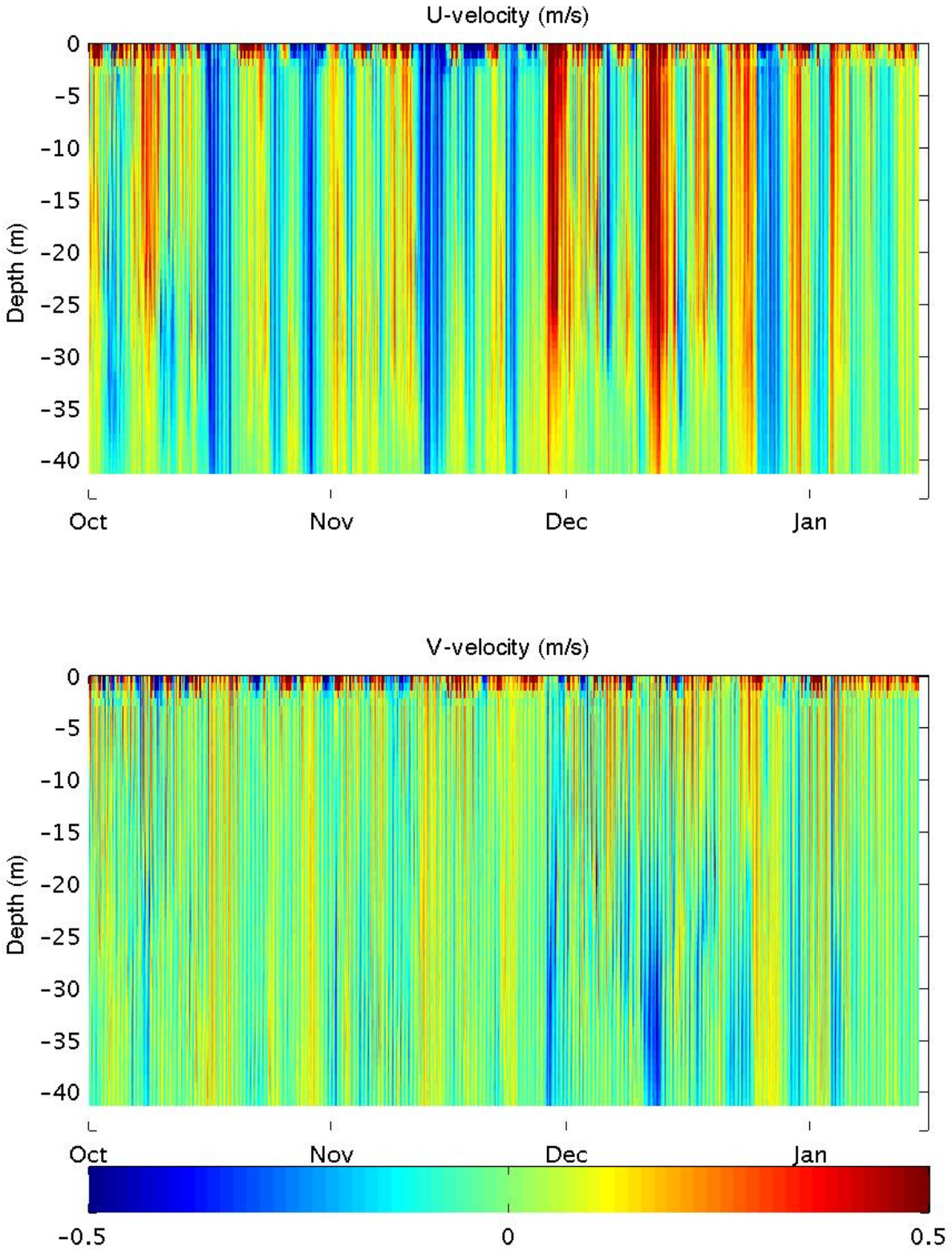

Figure 25. Current profiles for PO-S (41.0482° N 71.5003° W) measured by bottom-mounted ADCP. Note the strong diurnal signal throughout most of the water column, and that any strong vertical gradients of currents occurs near the surface.

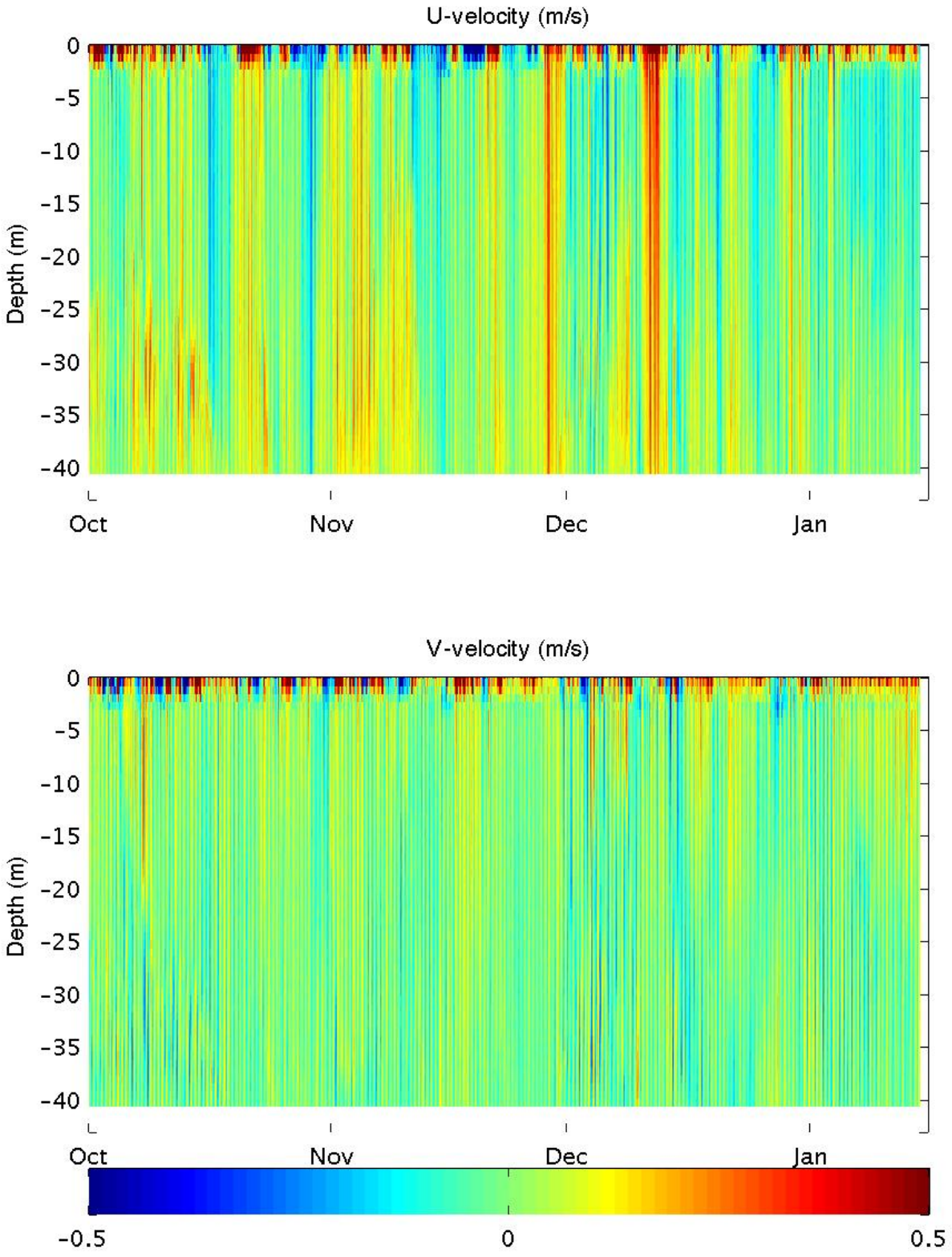

Figure 26. Current profiles for PO-F (41.2500° N 71.0917° W) measured by bottom-mounted ADCP. Note the strong diurnal signal throughout most of the water column, and that any strong vertical gradients of currents occurs near the surface.

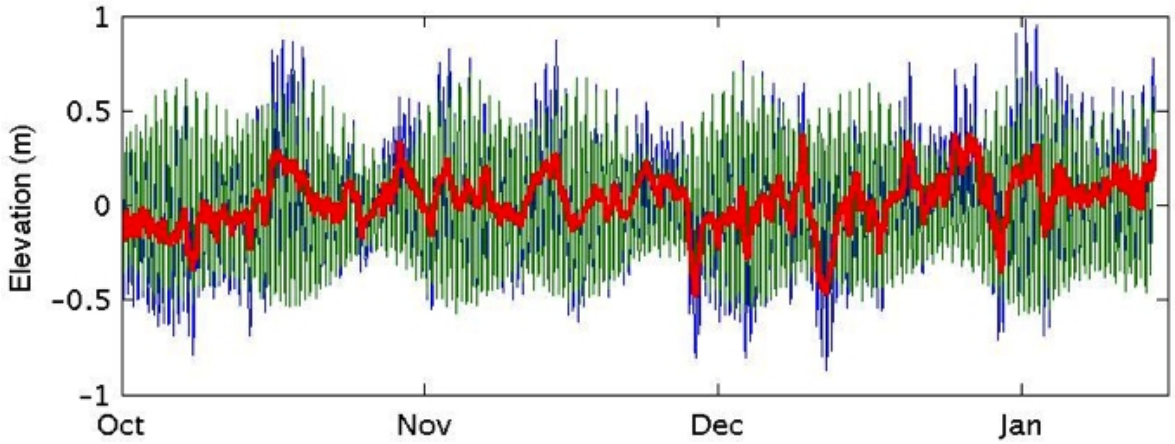

Figure 27. Surface elevation derived from pressure measured at a bottom-mounted ADCP, at the PO-S buoy (41.0482° N 71.5003° W), including original time-series (blue), tidal prediction from ROMS analysis (green), and difference between measurements and prediction (red).

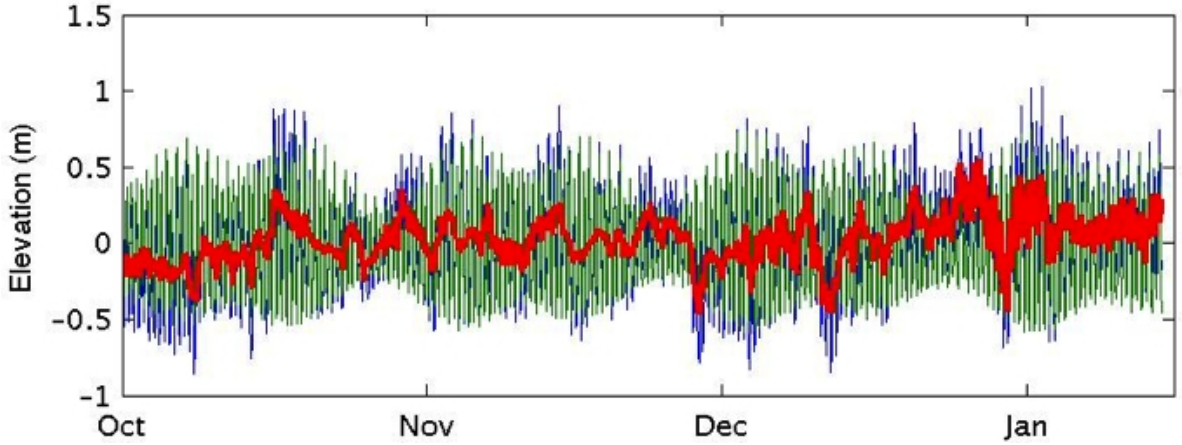

Figure 28. Same as Fig. 27 for the PO-F buoy (41.2500° N 71.0917° W).

Table 3. Amplitude and phase angle measurements for the seven most significant harmonic constituents at PO-S (41.0482° N 71.5003° W) (Fig. 26).

Constituent	Amp. (m)	Amp. Err. (m)	Phase (deg.)	Phase Err. (deg.)
O1	0.0466	0.009	193.33	10.30
K1	0.0725	0.009	166.82	6.85
N2	0.1035	0.008	350.54	4.63
M2	0.4427	0.007	3.92	0.98
S2	0.0945	0.008	18.70	4.83
M4	0.0218	0.002	16.31	6.08
M6	0.0107	0.002	201.29	11.78

Table 4. Amplitude and phase angle measurements for the seven most significant harmonic constituents at PO-F (41.2500° N 71.0917° W) (Fig. 27).

Constituent	Amp. (m)	Amp. Err. (m)	Phase (deg.)	Phase Err. (deg.)
O1	0.0478	0.010	194.82	11.92
K1	0.0684	0.010	167.20	8.77
N2	0.1114	0.013	344.74	7.52
M2	0.4517	0.013	0.92	1.70
S2	0.0976	0.012	18.23	6.82
M4	0.0335	0.004	7.41	7.35
M6	0.0057	0.002	180.12	23.10

While no measurements of the suspended sediment were made at any of the buoy locations, it is possible to apply a heuristic approach. Indeed, the ADCP backscattering data can be related to suspended sediment concentration, by assuming that near-bottom backscattering would be significantly higher when sediment is suspended. Because the ADCP deployments at PO-S and PO-F were not setup to intentionally measure suspended sediment concentration, no calibrations of the sensors were conducted. ADCP backscatter is recorded as a received signal strength indicator count, which is proportional to the backscatter intensity in decibels. The constant of proportionality can vary as much as 20% even among the different transducers of the same ADCP (Deines 1999). This, in combination with not knowing the exact grain size distribution or other details of potential suspended matter, means that it is not possible to exactly compute a suspended sediment concentration from ADCP counts, although it is an area of recent research (see e.g., Gostiaux and van Haren 2010). In general, though, a higher ADCP count corresponds to a greater amount of backscatter. Acoustic backscatter can be caused by any material suspended in the water column, including bubbles, fish, plankton, and sediment. For the three month period of interest, high ADCP counts seem to roughly correspond to periods of large wave height (Fig. 28), but there is not a similar agreement with wind speed or other measured parameters. The strong (qualitative) correlation between ADCP counts and significant wave height thus suggests that backscattering may primarily not be biological in nature but likely related to sediment suspension induced by wave bottom currents (and at over 40 m of depth, bubbles are unlikely to contribute significantly).

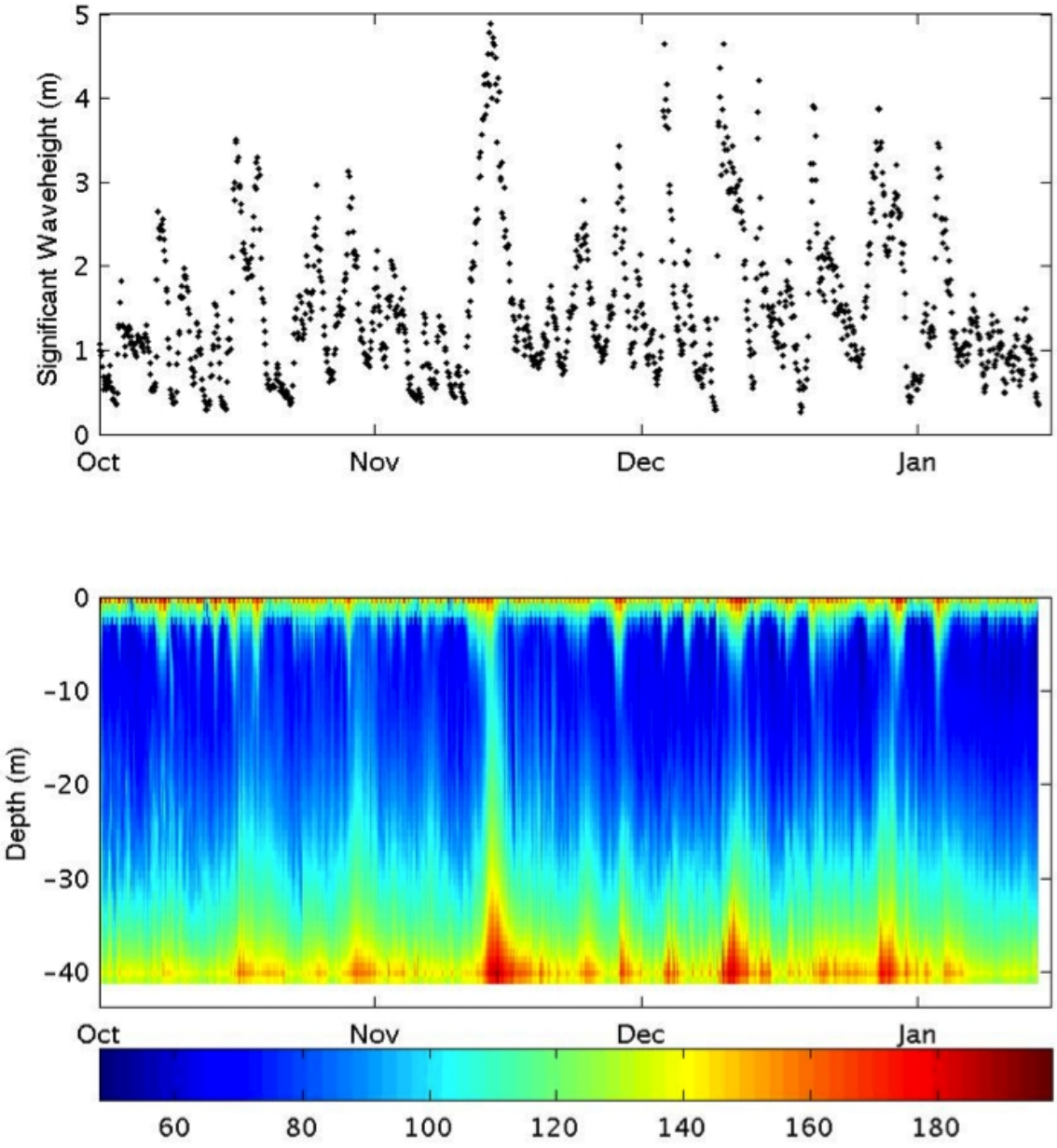

Figure 29. Comparison of the significant waveheight measured at PO-S (41.0482° N 71.5003° W; top) and the ADCP counts at the same location, indicative of backscatter intensity (bottom) for October 2009 through mid-January 2010. Note that ADCP counts near the seabed (potentially indicative of suspended sediment) is qualitatively related to the local waveheight.

4.6.2 ROMS Simulation: Forced by Tides

The most important forcing is due to tides, as it is persistent even in calm conditions, and tidal velocities can be sufficient to suspend sediment in the area. Other forcing, such as from winds, waves, primarily acts on surface velocities, except under storm conditions, and density-driven circulation is generally very weak in the area.

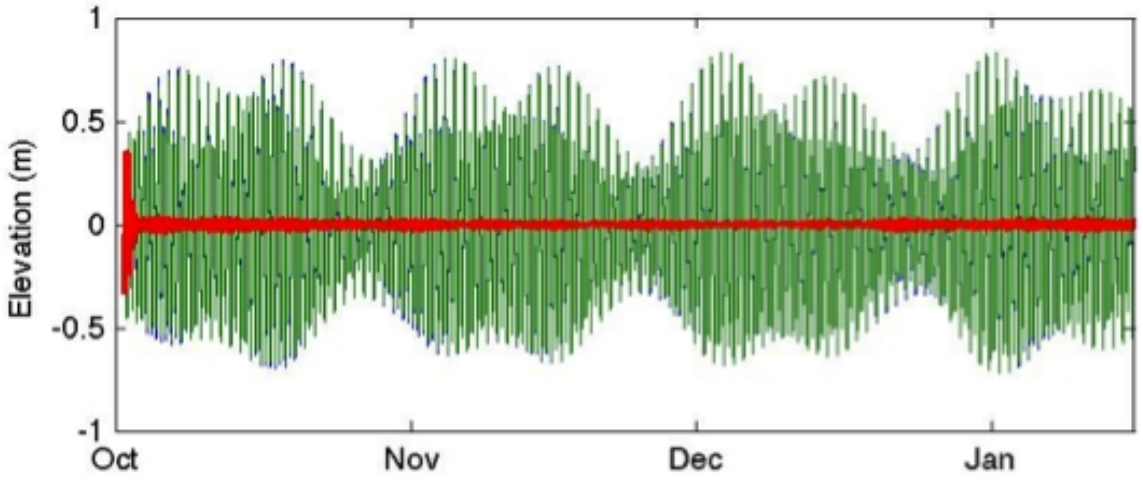

Figure 30. Surface elevation predicted by ROMS with only tidal forcing, at PO-S (41.0482° N 71.5003° W): modeled time-series (blue); predicted oscillations corresponding to tidal frequencies (e.g., M2, N2, K1, S2, etc.) (green); and differences between time-series and prediction (red). Note that the non-tidal transient of model spin-up subsides within a few days and quickly achieves a quasi-steady result.

Table 5. Amplitude and phase angle predictions for ROMS simulations with only ADCIRC tidal forcing (Fig. 29), for the 8 most significant harmonic constituents at PO-S (41.0482° N 71.5003° W).

Constituent	Amp. (m)	Amp. Err. (m)	Phase (deg.)	Phase Err. (deg.)
Q1	0.0109	0.001	181.71	4.06
O1	0.0607	0.001	183.73	0.71
K1	0.0958	0.001	169.11	0.49
N2	0.1305	0.005	0.19	2.32
M2	0.4939	0.005	21.97	0.55
S2	0.0876	0.005	28.97	2.65
M4	0.0264	0.000	324.80	0.72
M6	0.0071	0.000	199.87	3.94

In order to evaluate the performance of ROMS for predicting tides, we first consider the tidal elevation record simulated at PO-S (Fig. 29), comparing the modeled elevation record to the modeled elevation record that matches the frequency of tidal constituents. We find that the differences between the two are negligible for most of the simulation time. At the very beginning of the simulation, during model spin-up, there is a significant transient, but this subsides within a few days. By doing a similar tidal analysis as in the prior section, we find that the modeled harmonic constituents (Table 5) match the measured data (Table 3) well, for nearly all constituents. The agreement is not as good as that found between tidal measurements in the same area and the original ADCIRC database (Mukai et al. 2002), but e.g., the M2 amplitude only has an 11% error at the PO-S station.

In terms of velocity profiles, the results are relatively straightforward: with only tidal forcing at the boundaries of ROMS, and drag at the seabed, the vertical variation in velocities is minimal, with smaller tidal amplitudes at depth than at the surface (Fig. 31, 32).

While, overall, these results do not appear to be close to the measurements at PO-S and PO-F (Fig. 25, 26), if one considers only a time-series at, e.g., 20 m (Fig. 33), one obtains a different view. One can clearly see on Fig. 33 that the measured velocity has a time variability similar to that of the tidally-induced velocity, but at times the velocity can differ or be shifted significantly from the tidal velocities. Examining a shorter time period in Fig. 34, however, it seems that the north-south (*v*-component) velocity does show a better agreement between the ROMS results and the ADCP measurements, including the phase of the tidal component, but this agreement is not as good in the east-west direction (*u*-component). This suggests that the missing forcing terms in the tidal only ROMS simulations (i.e., waves and winds) should be acting most significantly along the east-west direction. This will be further discussed for the complete ROMS simulations, including all forcing terms, which are presented later in this report.

The other substantial result from this ROMS simulation, that only considers tides, is with respect to sediment processes. One can start by considering simulated suspended sediment concentrations at the PO-S buoy site (Fig. 35). Rather than considering each class of sediment independently, the sum of all suspended sediment concentrations is plotted on the figure. Most of the suspended sediment, however, is from the finer grains, and the coarsest sediment classes contribute little or none. Note that, sediment suspension seems to primarily occur at spring tides, and even then the amount of sediment suspended into the water column is not particularly large (with a maximum suspended sediment concentration of 0.0126 kg/m^3, or a volume fraction of only 4.75×10^{-6}).

After the initial model spin-up period, the pattern of mean grain diameter on the seabed achieves a quasi-steady state (Figs. 36 and 37). Note that, while little can be said quantitatively with respect to comparing these results to measured surficial sediment properties (Fig. 12), the general pattern appears to be the same. Also note that only the finest sands show any suspension in the SAMP study area, when only tidal forcing is applied, even though the sediment is disturbed with respect to its initial condition (Fig. 36, 37). The most substantial difference is east of Block Island, near PO-F and MD-F, where the measured median grain size is substantially coarser than that predicted. This region also corresponds to a shallower area (Cox Ledge; Figs. 9, 10, 13), however, suggesting that wave forcing may be the driving force in suspending

sediment in that area, whereas, in much of the rest of the ROMS domain, tidal forcing is sufficient to suspend the finer sediments.

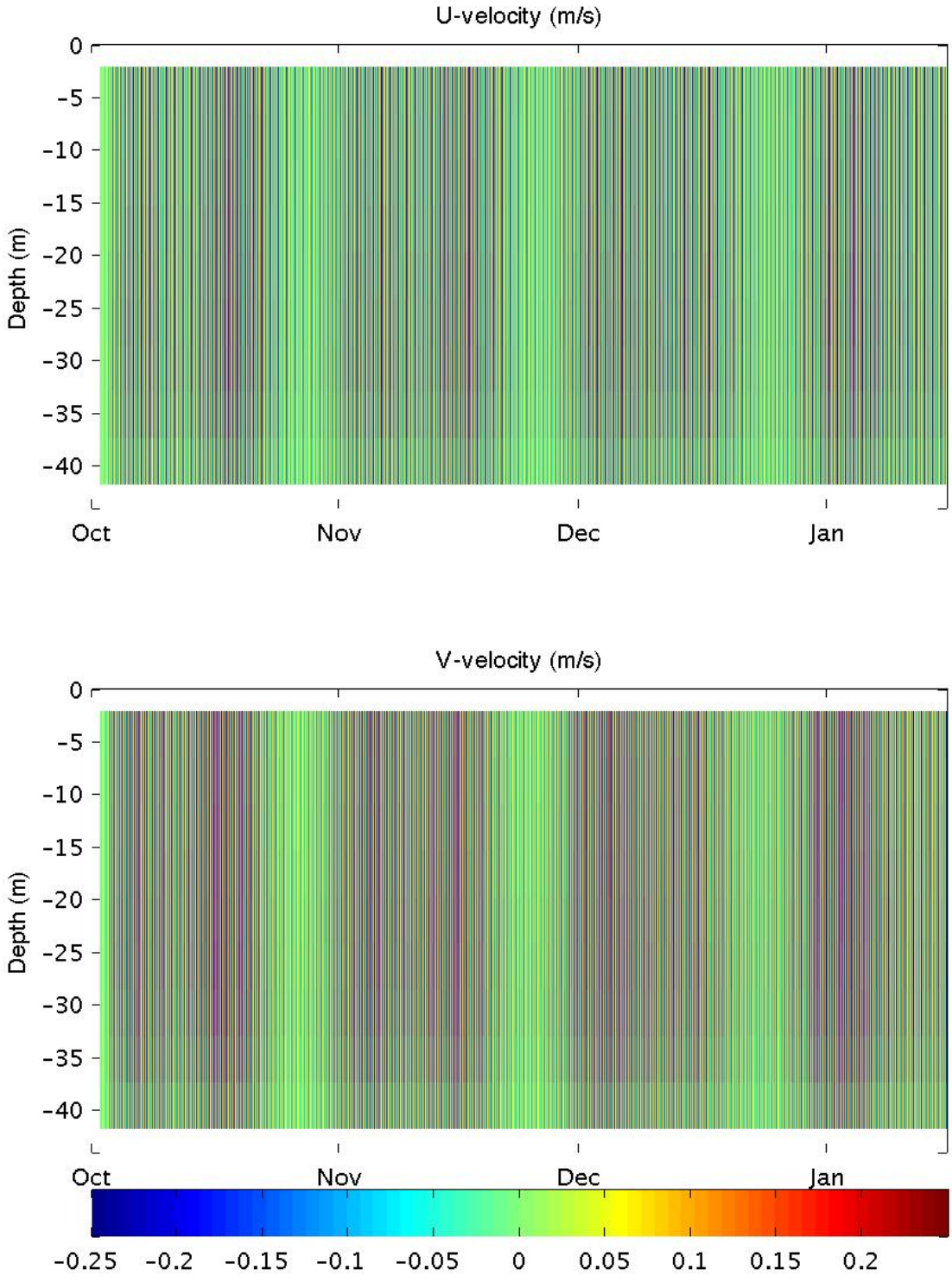

Figure 31. Current profiles (color in m/s) predicted by ROMS using only tidal forcing for PO-S (41.0482° N 71.5003° W). Note the lack of significant vertical gradients.

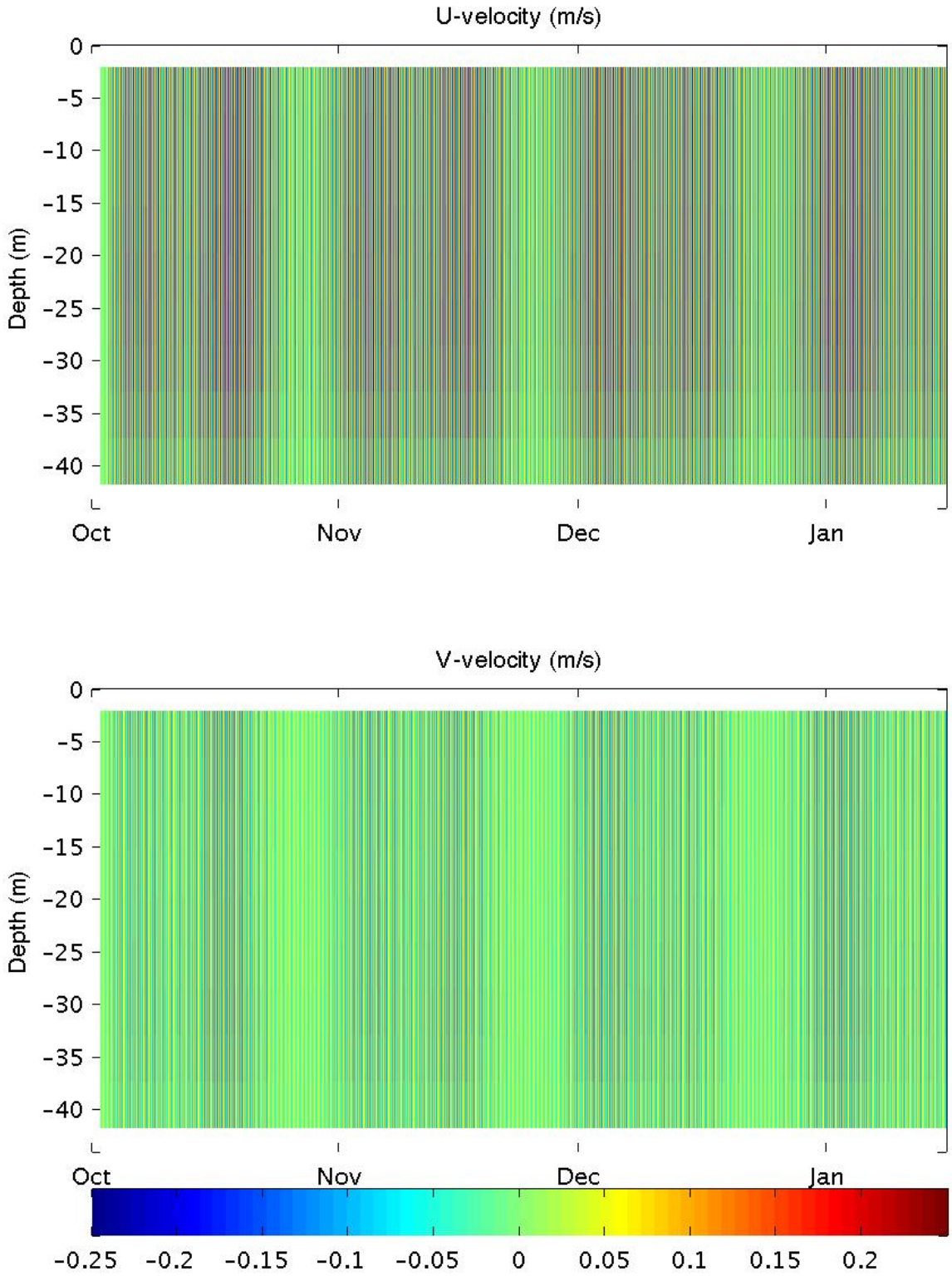

Figure 32. Current profiles (color in m/s) predicted by ROMS using only tidal forcing for PO-F (41.2500° N 71.0917° W). Note the lack of significant vertical gradients.

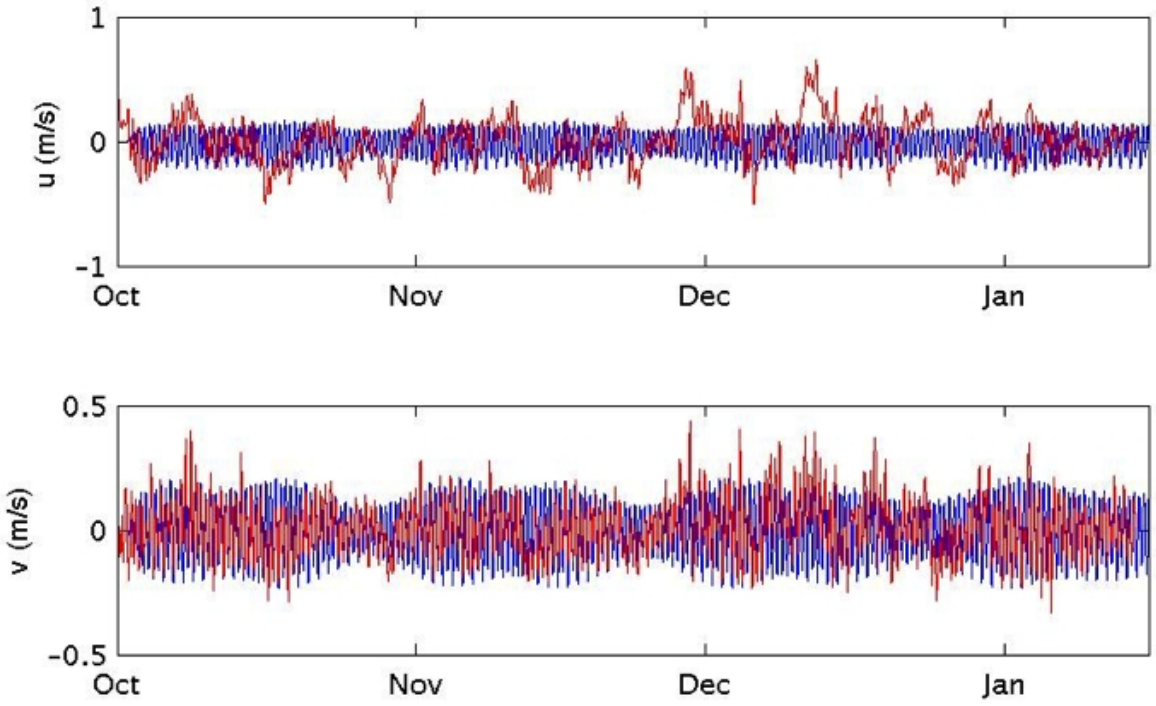

Figure 33. Time-series of current predicted by ROMS (blue) at 20 m depth, using only ADCIRC tidal forcing, for PO-S (41.0482° N 71.5003° W), and currents measured by ADCP (red) at the same location.

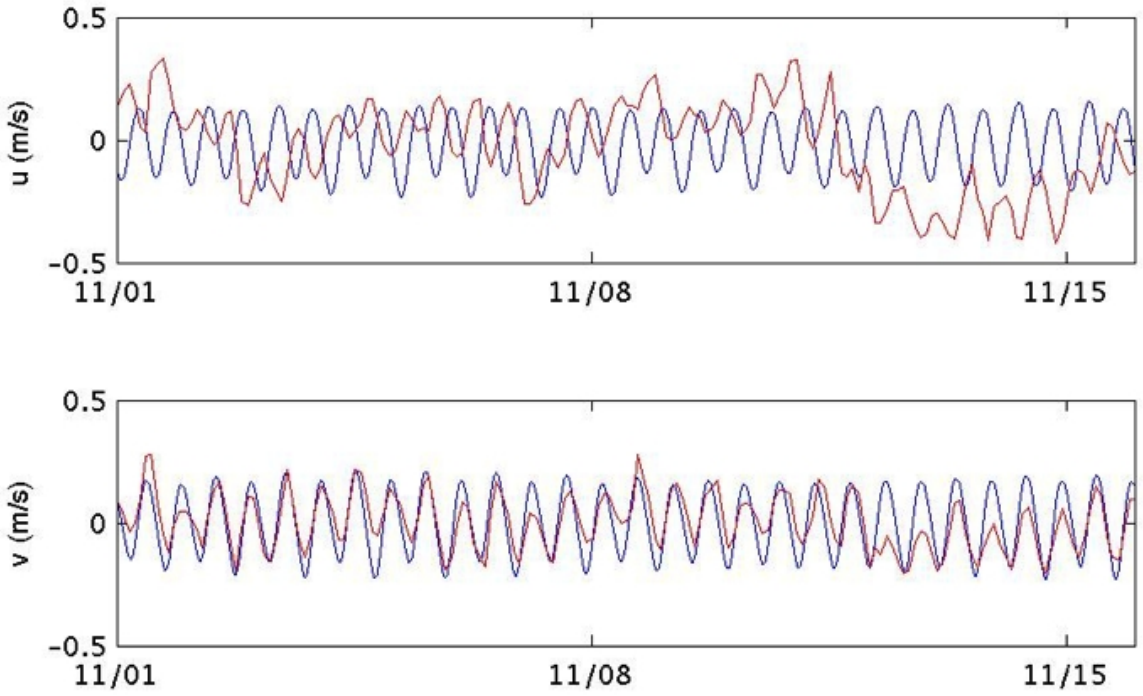

Figure 34. Zoom from Fig. 33.

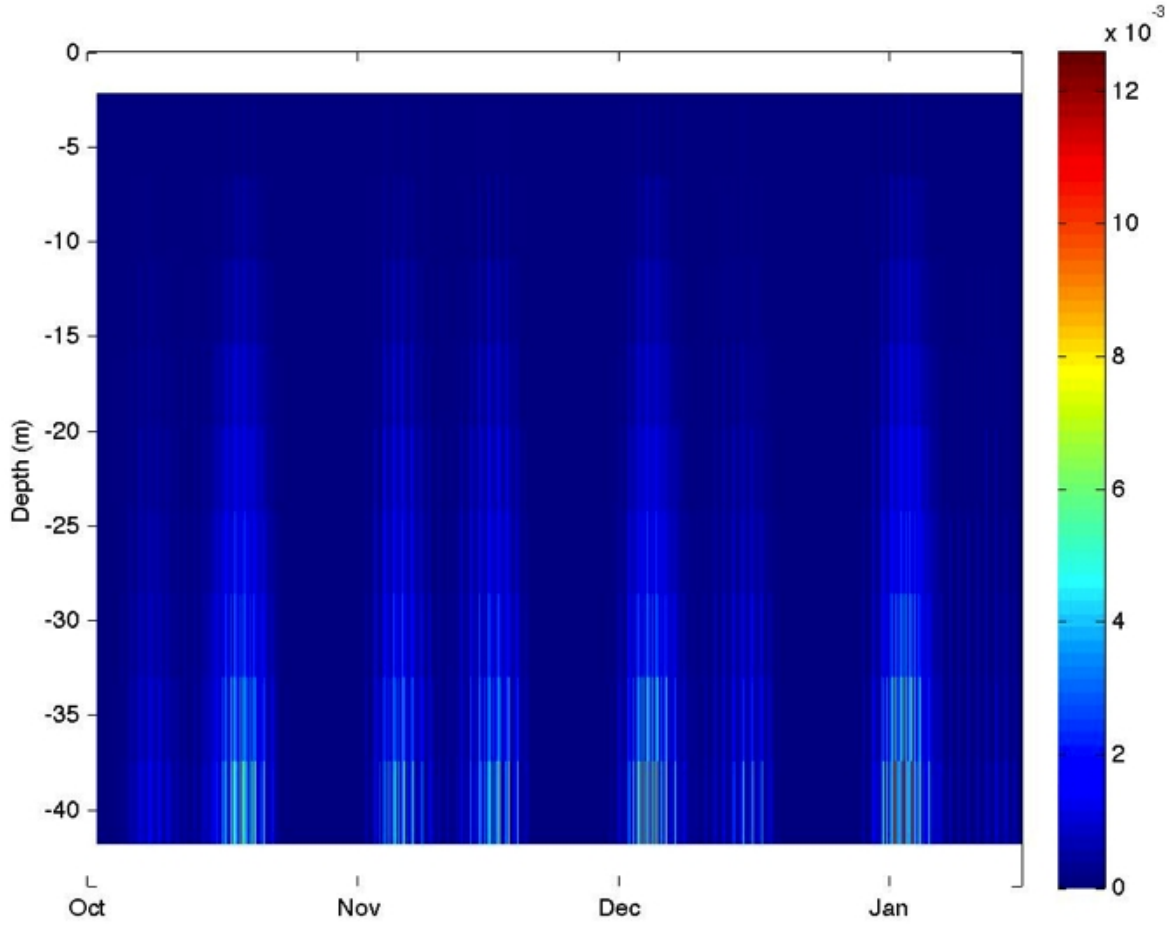

Figure 35. Suspended sediment concentration (color scale in kg/m^3; sum of all modeled grainsizes) over time, predicted by ROMS using only tidal forcing, at the PO-S station (41.0482^o N 71.5003^o W).

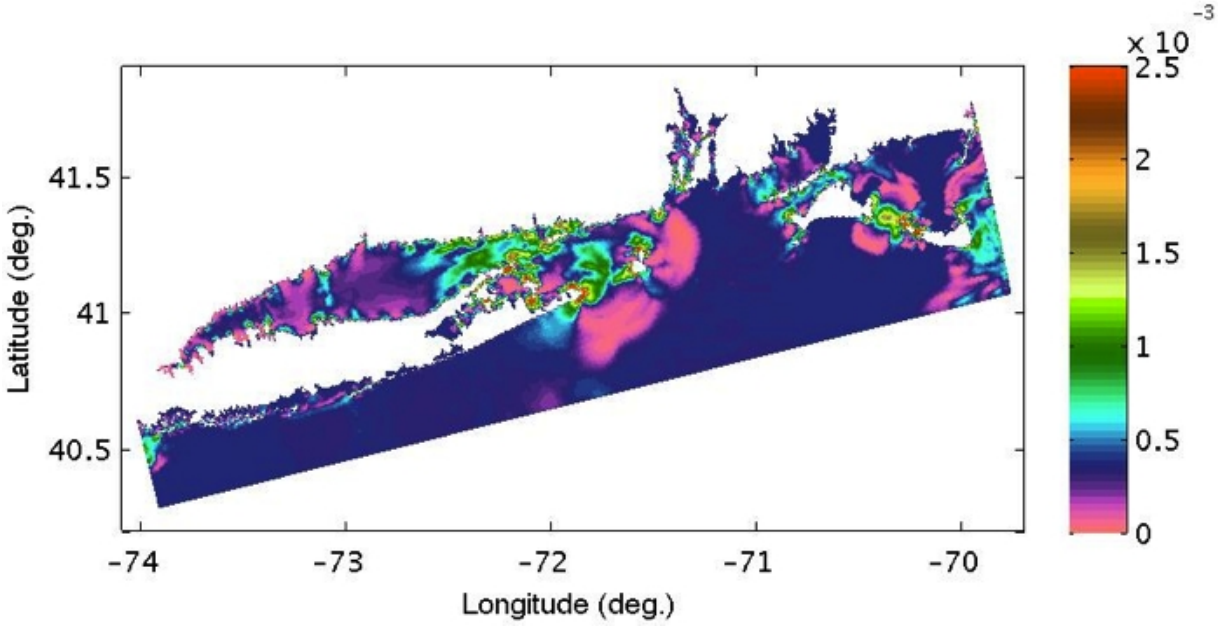

Figure 36. Median grain diameter (m) at the seabed after 107 days of simulated time with only tidal forcing.

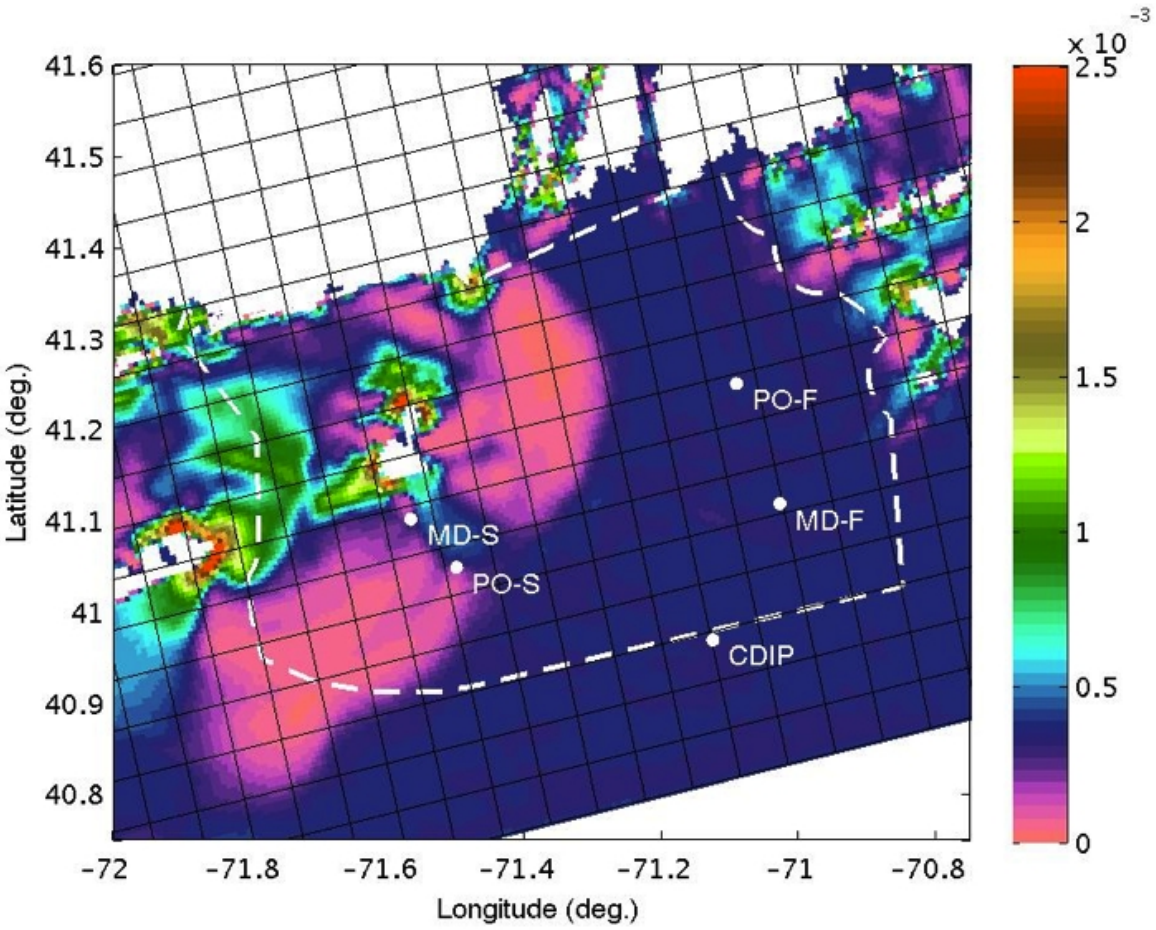

Figure 37. Median grain diameter (d_{50} in m) at the seabed after 107 days of ROMS simulations with only tidal forcing, including station locations, SAMP boundary (dashed), and model grid (black grid; each square is 6 km across, corresponding to 10x10 grid points in the high resolution simulations).

4.6.3 ROMS Simulation: Forced by Tides and Winds

After considering tidal forcing, it is instructive to consider adding in each forcing individually, next considering tidal and wind forcing.

Similar to the tidal elevation analysis for the tidally-forced simulation (Fig. 29), we can again show the model spin-up by again comparing the modeled elevation record to the modeled elevation record that matches the frequency of tidal constituents (Fig. 38). We again find that the difference between the two is small for most of the simulation time, although not as negligible as the tidally forced simulation. We can also note that the local elevation does not have as much subtidal variation as the actual observations (Fig. 27, 28).

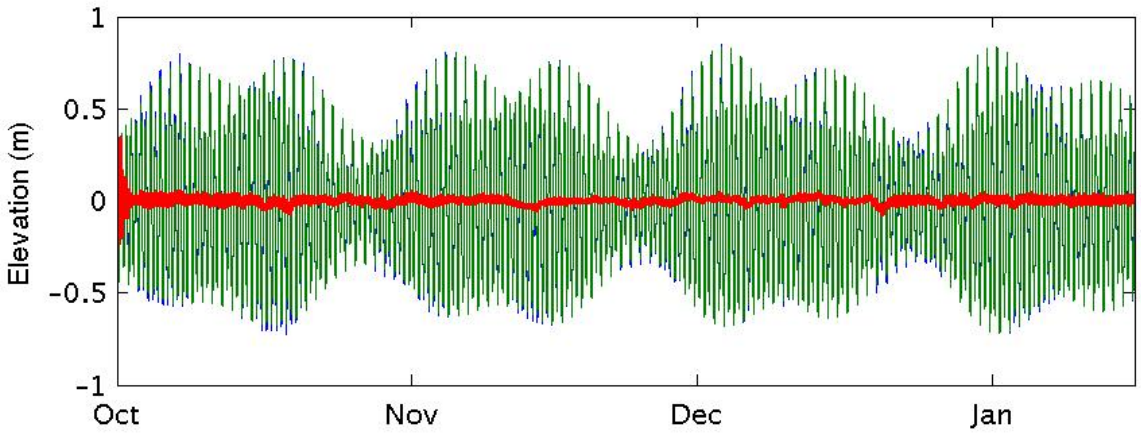

Figure 38. Surface elevation predicted by ROMS with tidal and wind forcing, at PO-S (41.0482° N 71.5003° W): modeled time-series (blue); predicted oscillations corresponding to tidal frequencies (e.g., M2, N2, K1, S2, etc.) (green); and differences between time-series and prediction (red). Note that the non-tidal transient of model spin-up subsides within a few days and quickly achieves a quasi-steady result.

In terms of velocity profiles, the results (Fig. 39, 40) qualitatively approximate the observed velocities better than before, as an additional important forcing term is included. Particularly note the strong eastward velocity mid-November at PO-S that is captured with the tidal and wind forcing and the observations, but not the only tidally-forced ROMS simulation. Again a time-series at 20 m depth can be considered at PO-S (Fig. 41, 42). Here the general variation is captured by the ROMS simulation.

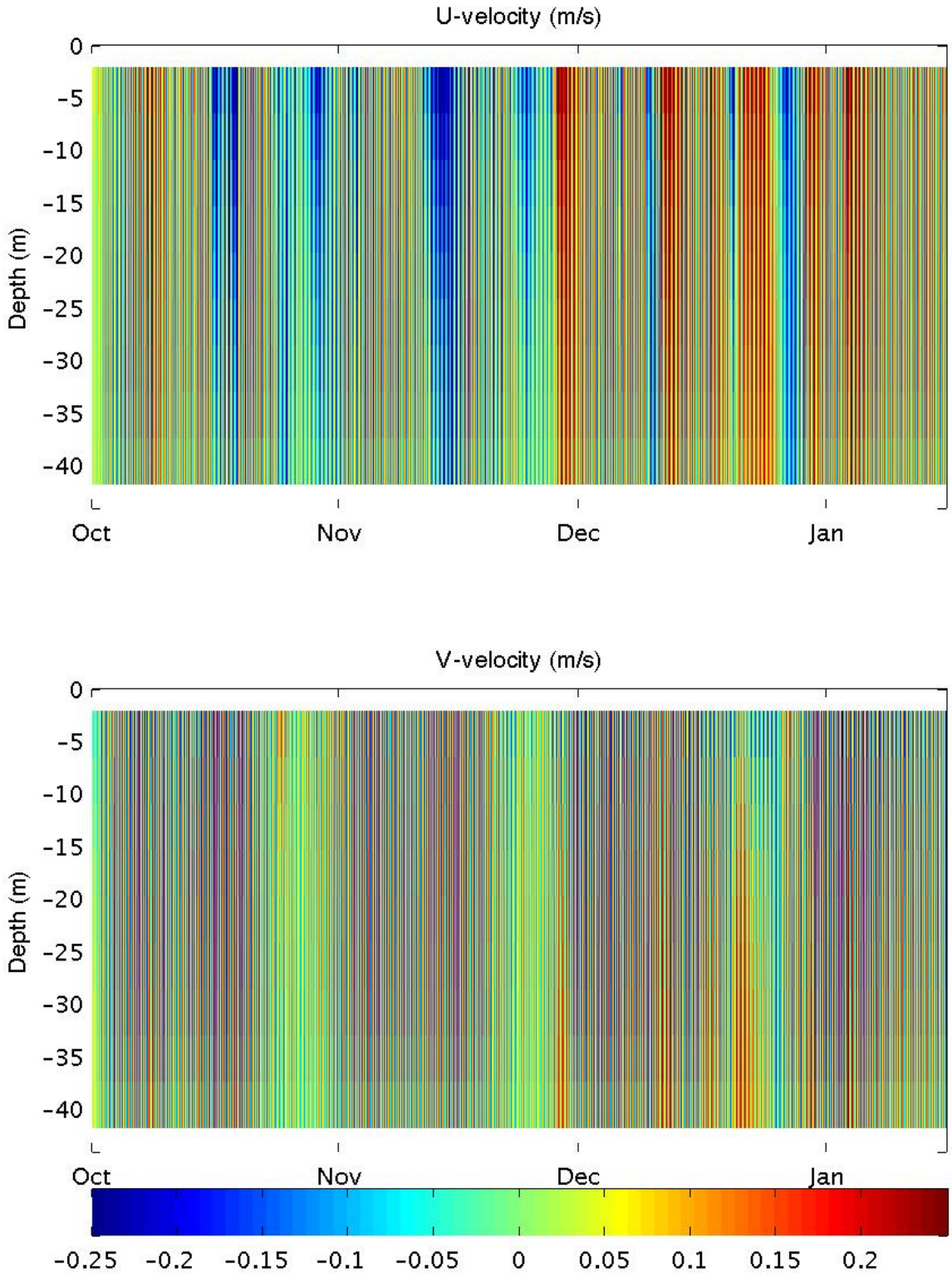

Figure 39. Current profiles (color in m/s) predicted by ROMS using tidal and wind forcing for PO-S (41.0482° N 71.5003° W).

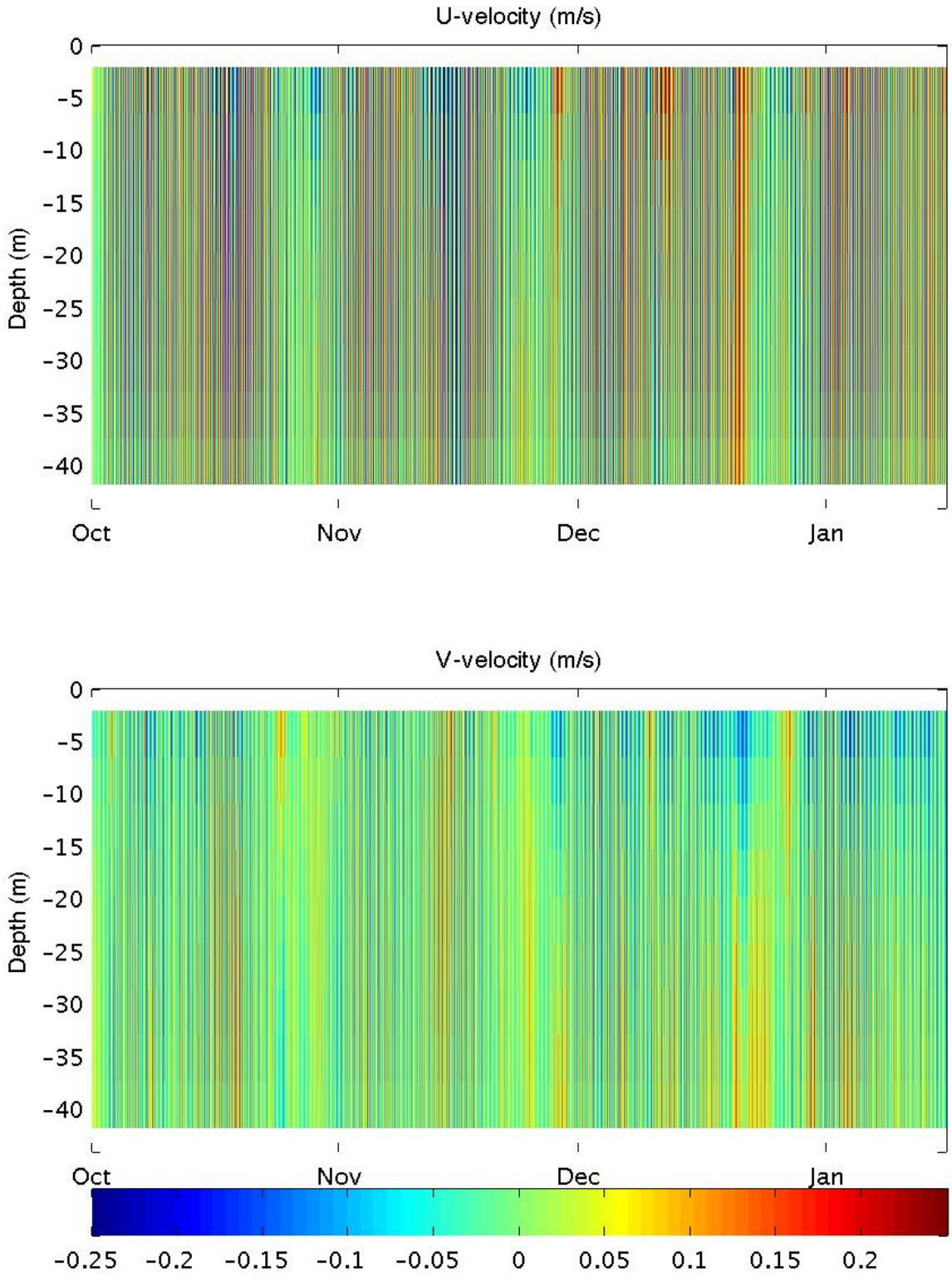

Figure 40. Current profiles (color in m/s) predicted by ROMS using tidal and wind forcing for PO-F (41.2500° N 71.0917° W.

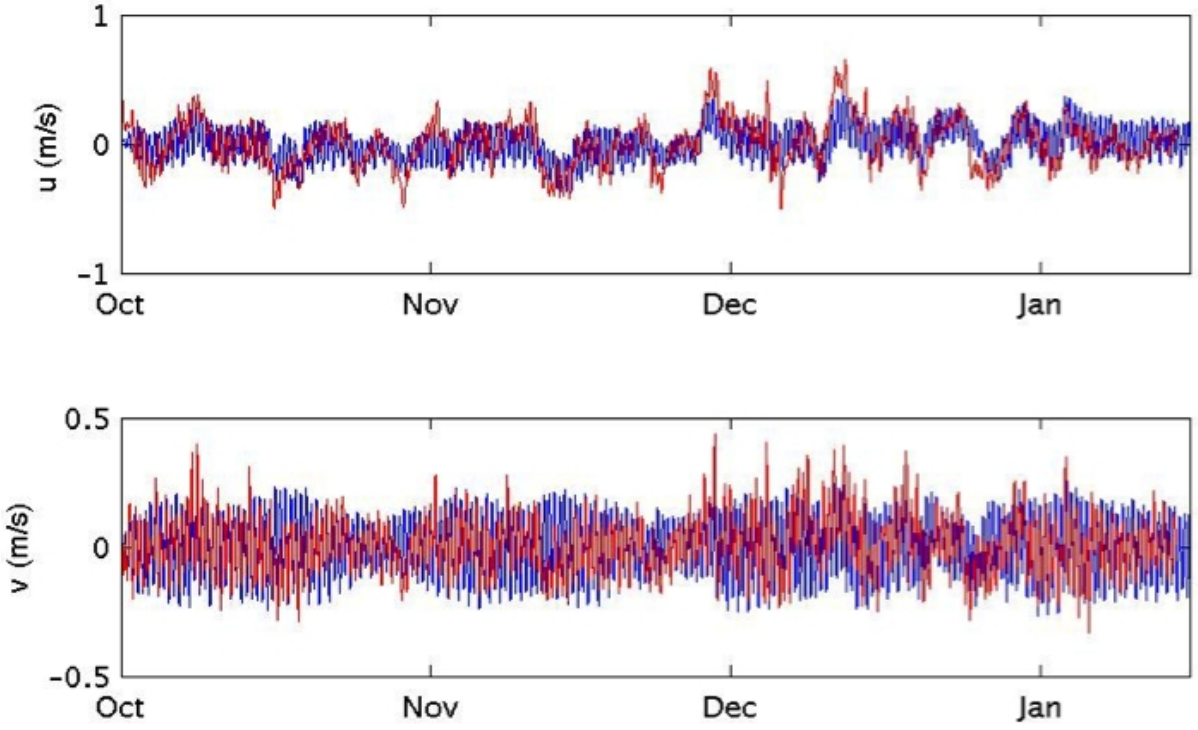

Figure 41. Time-series of current predicted by ROMS (blue) at 20 m depth, using tidal and wind forcing, for PO-S (41.0482° N 71.5003° W), and currents measured by ADCP (red) at the same location.

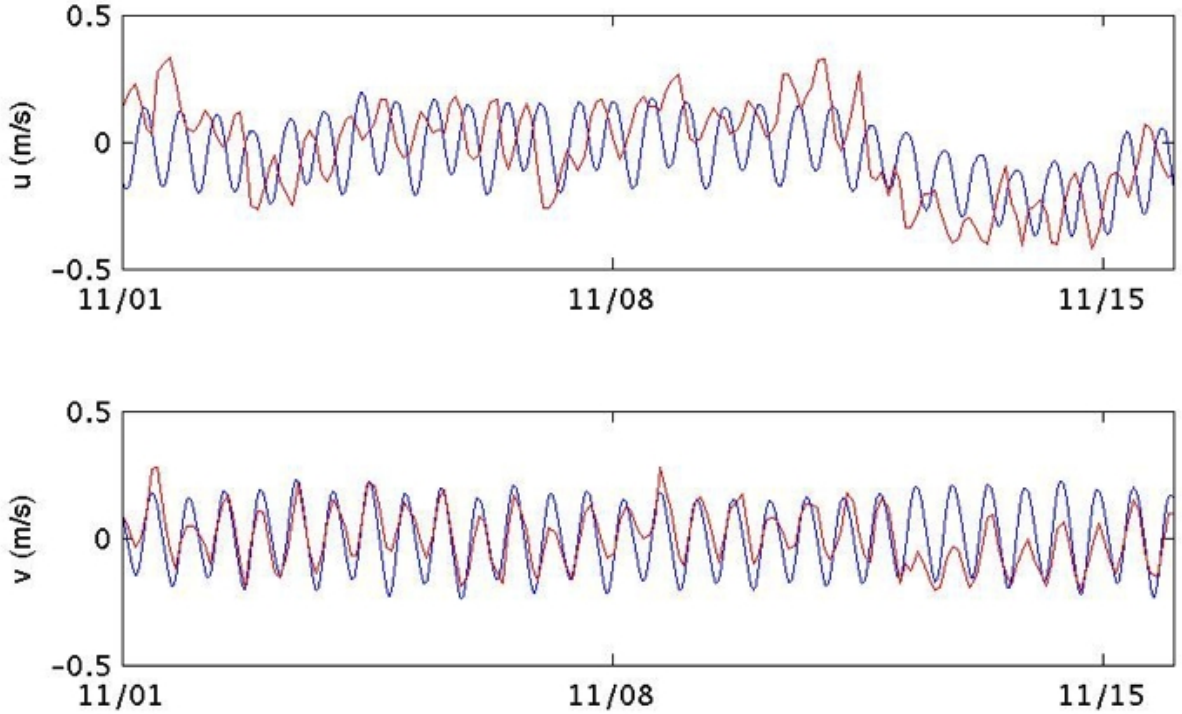

Figure 42. Zoom from Fig. 33.

Regarding suspended sediment, we find that the suspended sediment concentration at the PO-S buoy site (Fig. 43) better matches the observations than the only tidal simulation. Note that, sediment suspension seems to primarily occur at spring tides, and even then the amount of sediment suspended into the water column is not particularly large (with a maximum suspended sediment concentration of 0.0351 kg/m^3, or a volume fraction of only 1.32x10^{-5}). The largest discrepancy between the ADCP counts and the modeled SSC occurred during the mid-November storm.

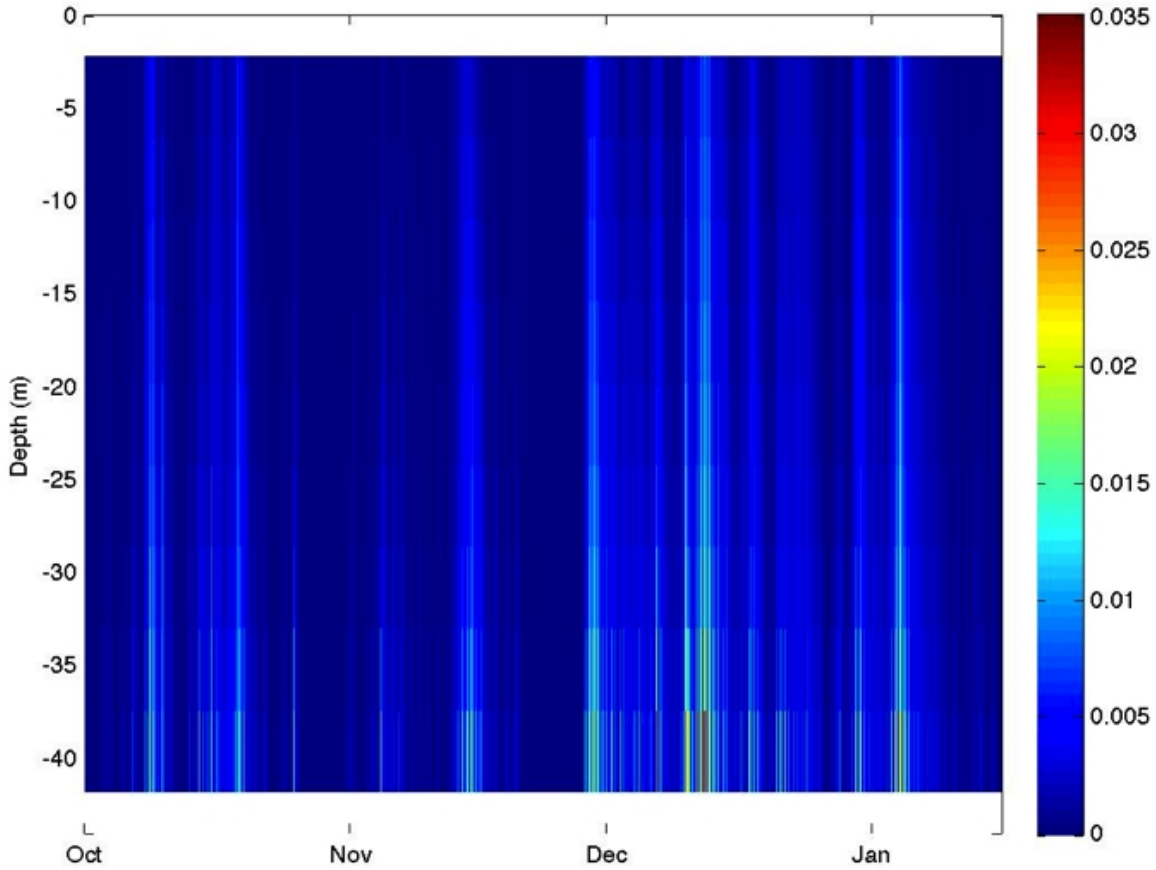

Figure 43. Suspended sediment concentration (color scale in kg/m^3; sum of all modeled grainsizes) over time, predicted by ROMS using tidal and wind forcing, at the PO-S station (41.0482^o N 71.5003^o W).

After the initial model spin-up period, the pattern of mean grain diameter on the seabed achieves a quasi-steady state (Figs. 44 and 45). Note that while little can be said quantitatively with respect to comparing these results to measured surficial sediment properties (Fig. 12), the general patterns appears to be the same, and a better agreement is found than with only tidal forcing, particularly around the shallow Cox Ledge (Figs. 9, 10, 13).

4.6.4 HYDROMAP Simulations: Forced by Tides and Winds

Appendix A provides the full report on this work, prepared by ASA, as part of their subcontract. Below is a summary of findings and then a comparison with ROMS tidal simulation results, for purpose of validation.

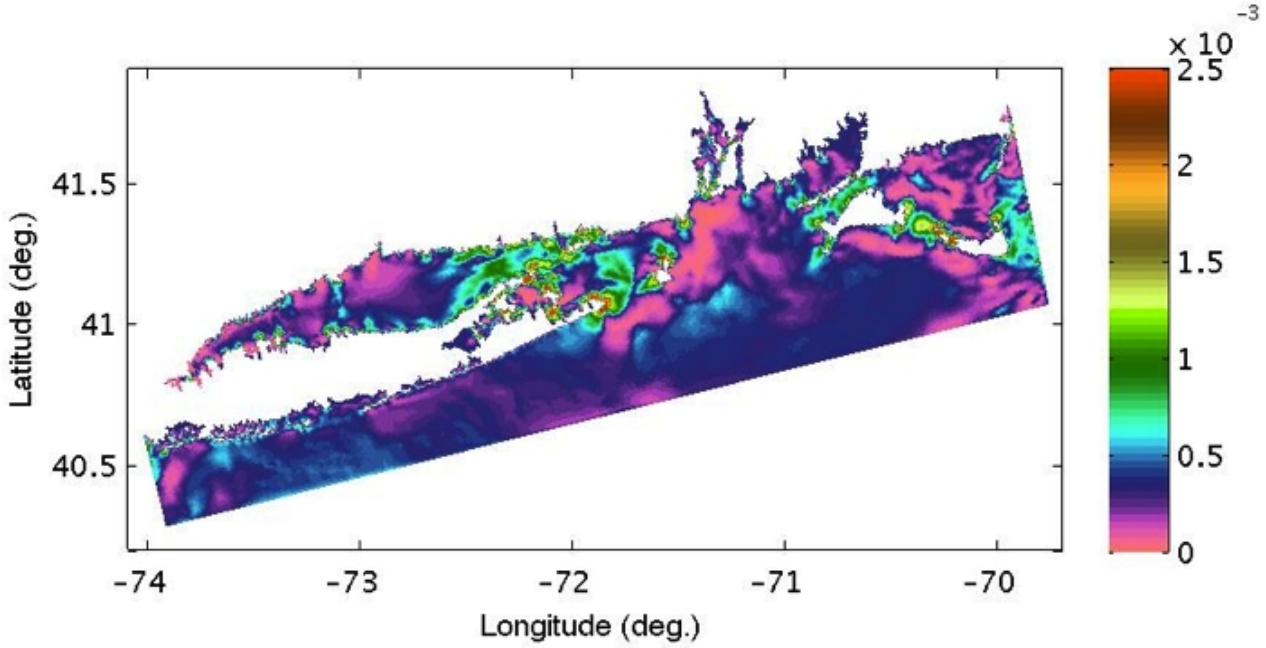

Figure 44. Median grain diameter (m) at the seabed after 107 days of simulated time with tidal and wind forcing.

Applied Science Associates, Inc. (ASA) performed a hydrodynamic modeling study focused on estimating the (mostly tide-induced) currents and circulation in the renewable energy (RE) development area with a focus on bottom stress and currents. ASA used the HYDROMAP model system, which calculates velocity vectors on a stepwise continuous variable rectangular grid system. A benefit of the model is that it allows coarse grid resolution in the areas offshore the coast of Rhode Island and finer resolution in the Block Island Sound area and renewable energy zone area of interest. The model was driven by tidal harmonic data along the open boundaries and constant wind stress at the surface. The model predictions were compared to observations collected as part of the SAMP field program, including four ADCP current meter locations and NOAA tidal elevation data at Montauk and Newport. The comparisons showed that the model not only adequately predicted the tidal forcing response in the study area, but also the longer period episodic wind driven events that are characterized by passing weather systems. The model appeared to be able to reproduce both the horizontal spatial variability in the system as well as

the vertical profile of the currents, as represented by the ADCP observations at the surface, mid and bottom of the water column.

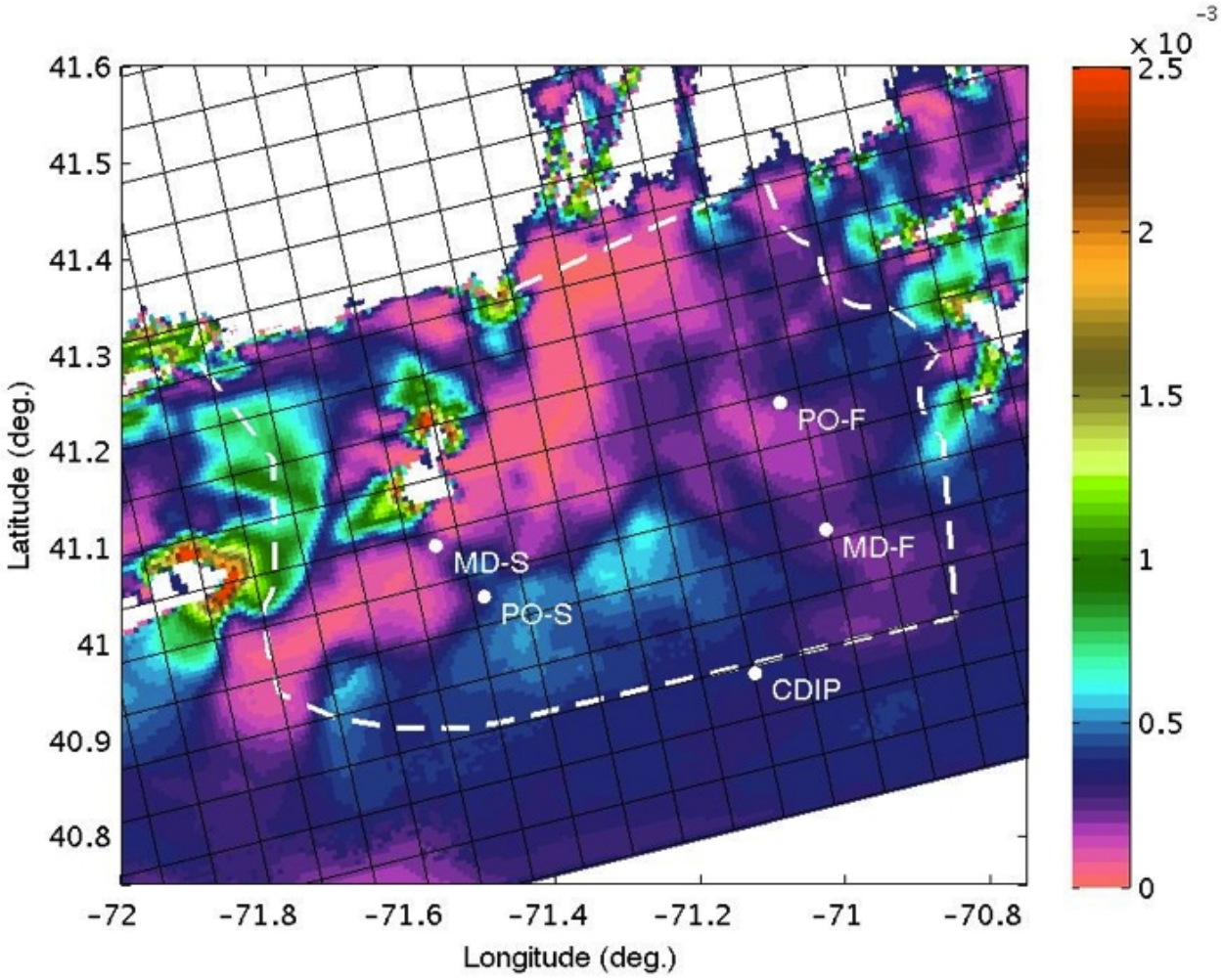

Figure 45. Median grain diameter (d_{50} in m) at the seabed after 107 days of ROMS simulations with tidal and wind forcing, including station locations, SAMP boundary (dashed), and model grid (black grid; each square is 6 km across, corresponding to 10x10 grid points in the high resolution simulations).

Both observations and model predictions confirm that the dominating tidal constituent is the M2 constituent, which represents between 50-60% of the total tidal amplitude at all stations. The amplitude predictions for all constituents tend to be higher than the observed but are generally within 20% of the observed with the exception of Montauk. The Montauk station is located in the shallows of an embayment that the mode grid does not resolve in fine detail, this may contribute to the over prediction of tidal amplitude.

Review of the current analysis indicates that the differences between model predicted and observed M2 constituent major axes are generally less than 0.02 m/s, with a maximum deviation

of 0.05 m/s in the MDF bottom current ellipse. The difference in the remaining constituents is variable, remaining less than 0.01 m/s for the majority. The M2 phase comparison between the model predictions and observations is similarly close, with the difference angle remaining less than about 10 degrees with an exception in the bottom currents at both the POS and POF stations. In general, the model predicted tidal current ellipses, driven predominantly by the M2 tidal component, show a close agreement with the observations indicating that the model captures the magnitude and the circulation patterns in the study area.

The bottom currents were further reviewed and an understanding of the bottom speed developed. The renewable energy zone follows the edge of the 3 mile state waters limit along the southern portion of the line, from the straights between Long Island and Block Island to the west, to the shipping channel exclusion zone on the east. The zone is approximately 2 km wide, and has a bulge on the east side representing the shipping channel exclusion zone. Bathymetry in the RE zone is quite variable ranging from less than 10 m, in the western portion to greater than 35 m to the east. This bathymetric range and the straights to the west produce a significant variability in the bottom current speeds as well, ranging from a high in the shallow western portions of 0.25 m/s down to a high in the eastern portions of 0.15 m/s.

4.6.5 ROMS Simulations: Forced by Tides, Winds, and Waves

Because of the limitations in modeling the observed hydrodynamics of the SAMP study area when only using a tidal forcing, as described above, additional forcing terms need to be included. When wave and realistic wind forcing terms are included, a number of significant differences are noted.

The first distinction is in the current profiles (Fig. 46), which are not nearly as vertically homogeneous as the earlier tidal simulations. One can then see that (unlike Fig. 31), and more similar to the observed data (Fig. 25), there is at times significant vertical variation in the velocity field. The addition of the wave forcing, in combination with a bottom boundary layer model (*ssw_bbl*), which takes into account the added seabed stress induced by surface waves, results in more sediment being suspended (Fig. 47).

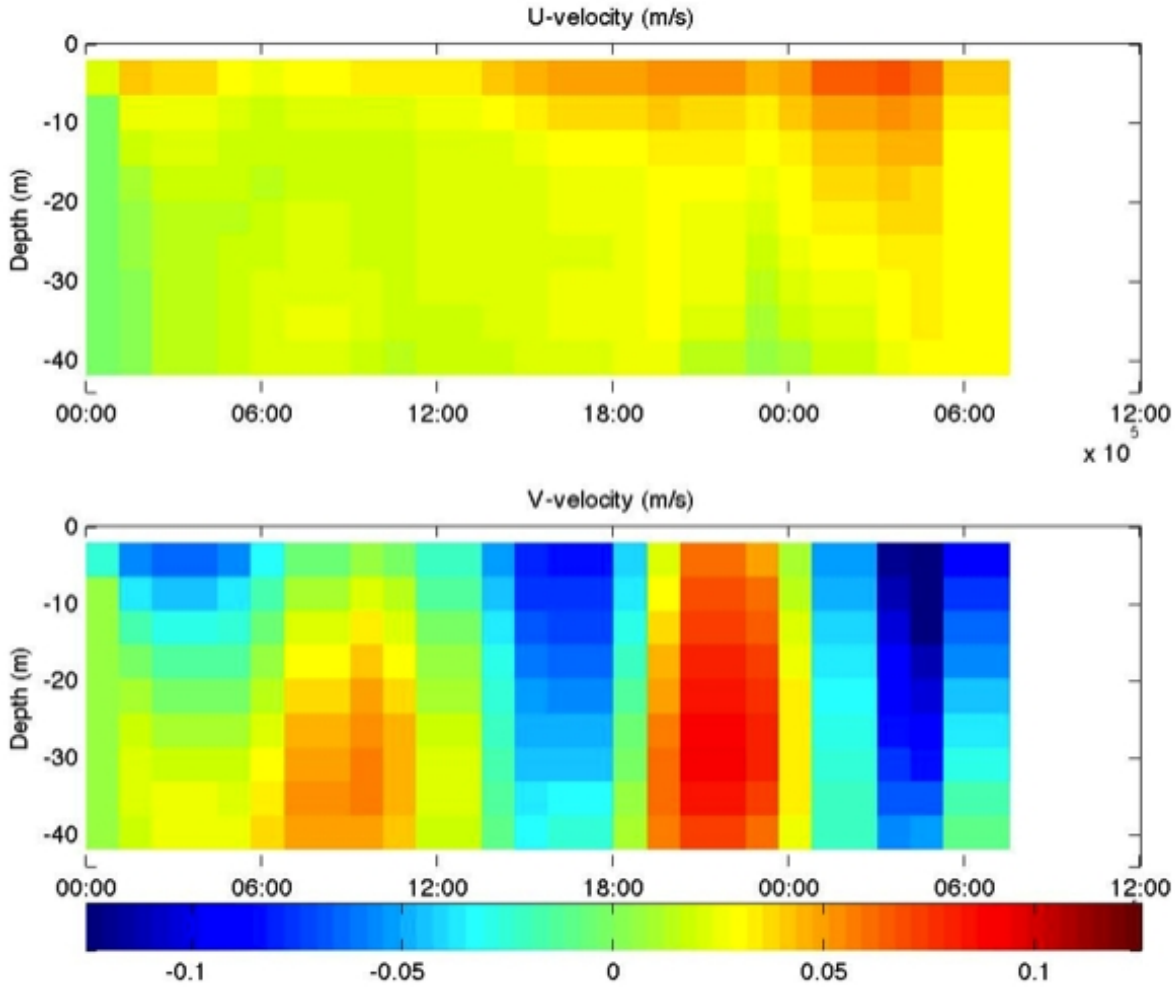

Figure 46. Current profiles (color in m/s) predicted at the start of a coupled ROMS/SWAN simulation using tidal, wave, and wind forcing for PO-S (41.0482° N 71.5003° W). Note, the vertical structure of the currents, in contrast to the ROMS simulations, which only considered tides.

One of the best records of the sediment characteristics in the SAMP area is the map of median grain size (Fig. 12). The tidal ROMS simulations mentioned earlier (Figs. 34, 35) qualitatively show many, but not all, of the same features as the observed map. In general, however, the coupled ROMS/SWAN simulations are able to obtain a better agreement (Figs. 48, 49). One of the most substantial differences is that the coupled ROMS/SWAN simulations show coarser sediment in the eastern half of the SAMP area (around PO-F and MD-F). This is likely caused by the added seabed stress due to waves in the shallower waters in that area (see Fig. 13).

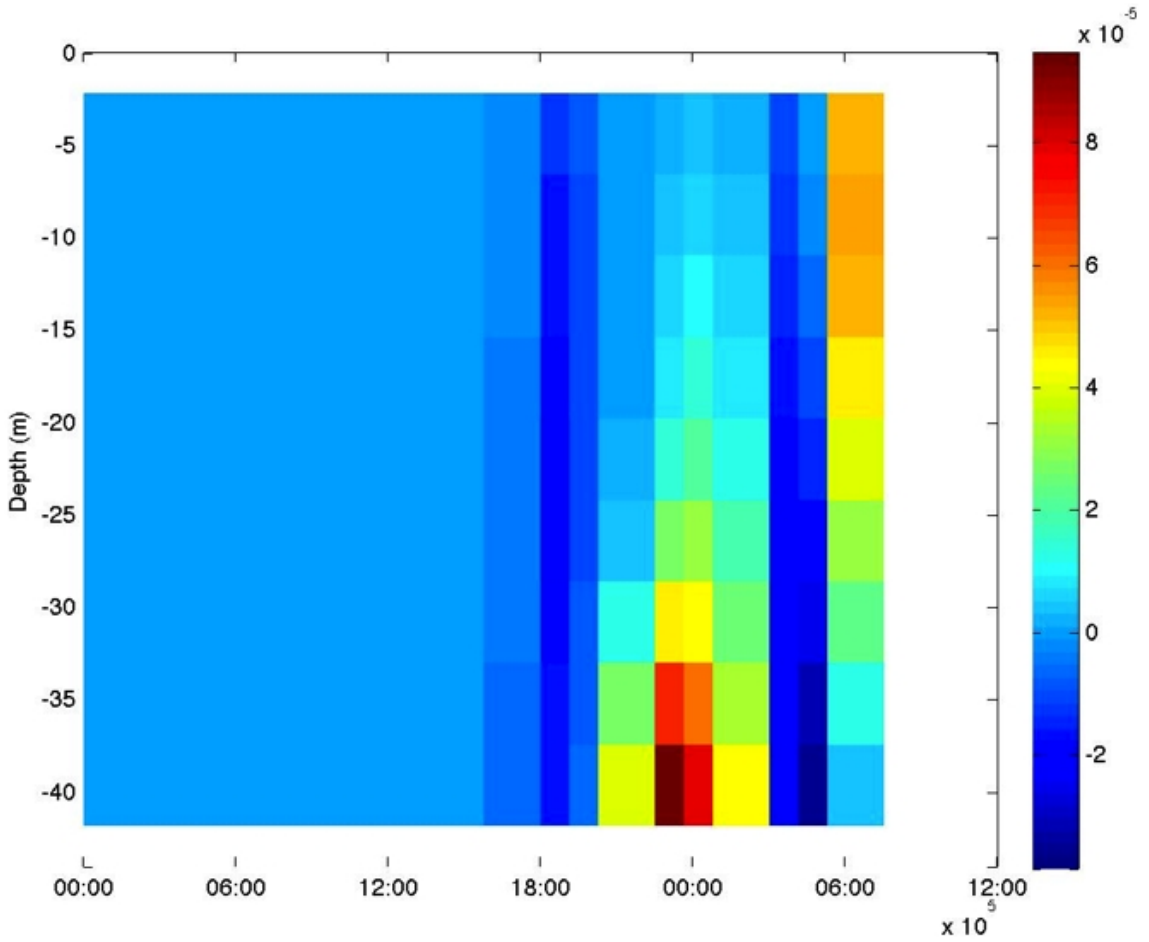

Figure 47. Suspended sediment concentration (color scale in kg/m^3; sum of all modeled grain sizes) over time, predicted at the start of a coupled ROMS/SWAN simulation using tidal, wave, and wind forcing at the PO-S station (41.0482^o N 71.5003^o W).

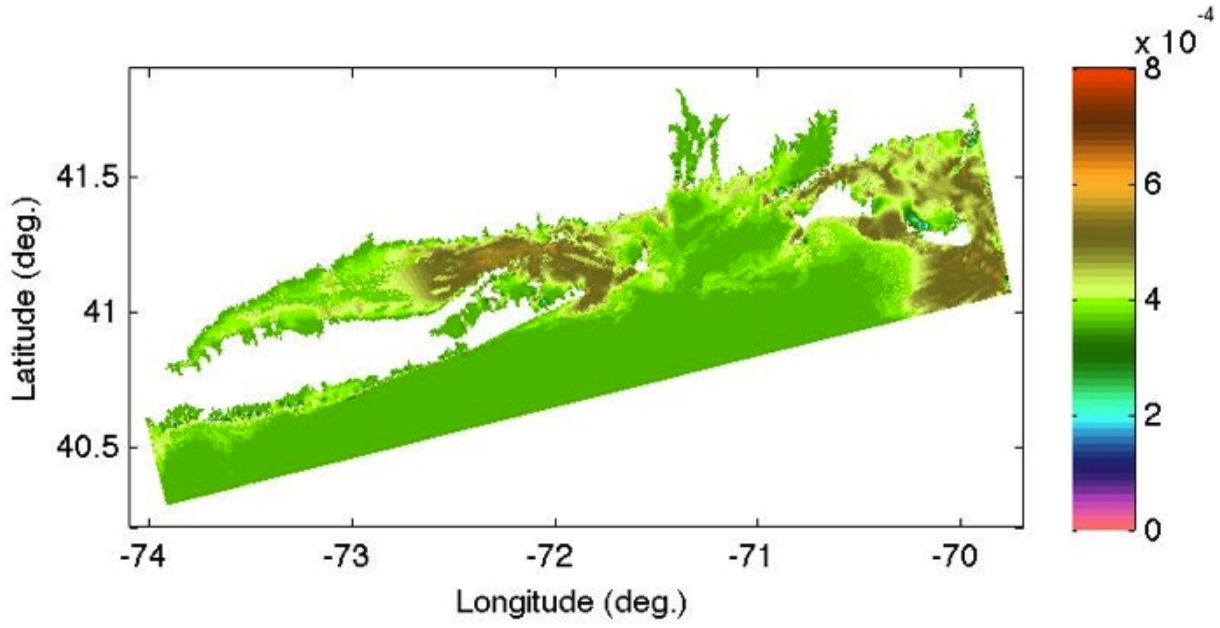

Figure 48. Median grain diameter (m) at the seabed after 1 day of simulated time with tide, wave, and wind forcing.

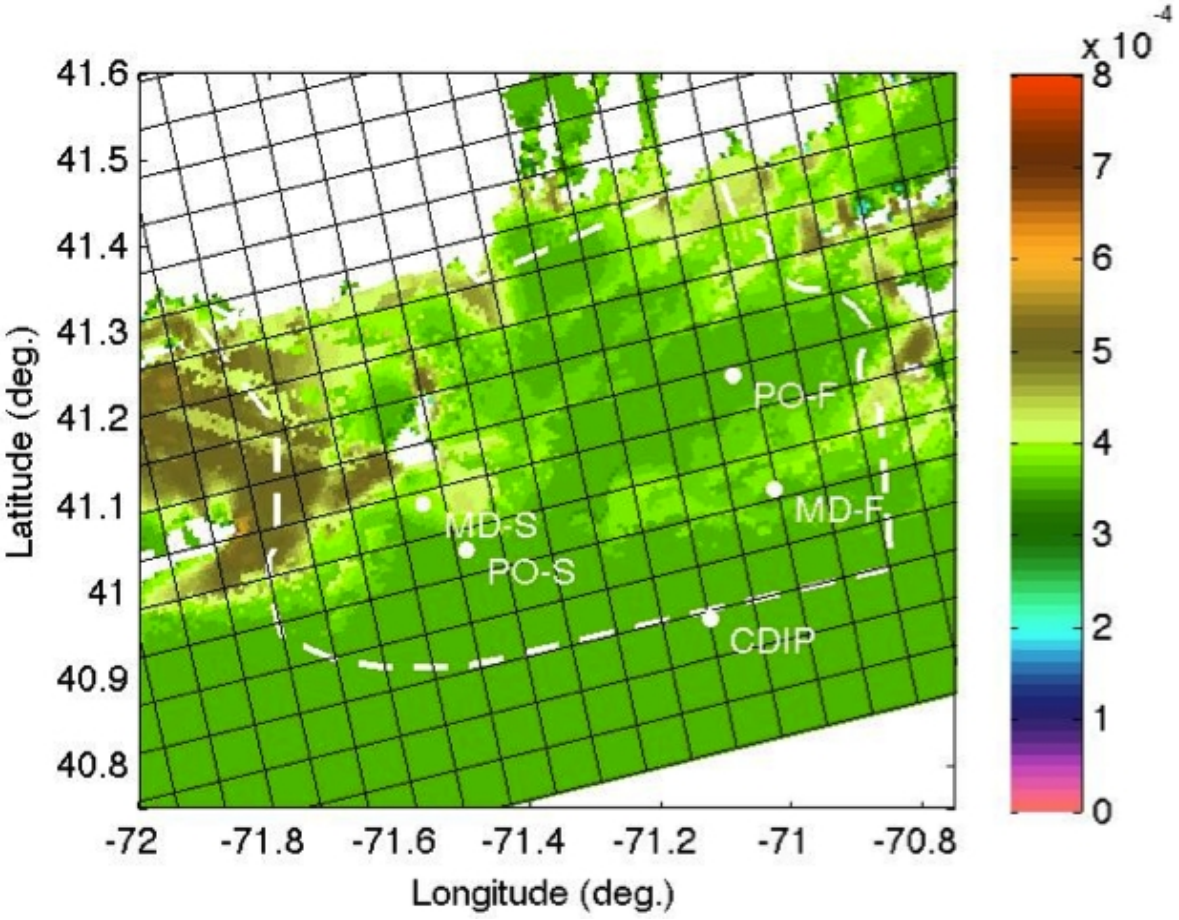

Figure 49. Median grain diameter (d_{50} in m) at the seabed, after 1 day of coupled ROMS/SWAN simulations with tidal, wave, and wind forcing, including station locations, SAMP boundary (dashed), and model grid (black grid; each square is 6 km across, corresponding to 10x10 grid points in the high resolution simulations).

5 Discussion

5.1 Implications of buoy measurements

The vertical profiles in Figs. 25 and 26 clearly show that there is a distinct layer in the upper 5 m. While the large measured surface layer velocities may be in error due to side lobe reflection of the ADCP signal off of the surface, note that there is minimal vertical variation for much of the time over the rest of the water column. One suggestion might be that this is a layer, which is distinct due to density differences, and while the current ROMS simulations do not include density-driven circulation, Codiga and Ullman (2010) analyzed FVCOM simulations of the southern New England shelf for 2006 in the fall, and found stratification was most significant deeper (i.e., at 20 m). Neglecting inter-annual variations in stratification, this suggests that density is not a fundamental driving force of the currents in the area in the autumn.

Overall, the buoy data suggests several things about the hydrodynamics of the area. On time-scales of weeks, at least in the fall, density-driven circulation is not critical to the understanding of the SAMP study area hydrodynamics. The ever-present tidal currents are of the same magnitude as the instantaneous currents, and their effects can be seen throughout the water column, but they are likely not the dominant force for suspending sediment. The latter appears to result from episodes of large (and long) storm waves.

5.2 Velocity profiles in ROMS simulations and ADCP data

In general, the observed ADCP velocity profiles (Fig. 25, 26) can be described as lacking significant vertical variation (except perhaps at the very surface or bottom of the water column, where noise interferes with quality measurements), and seemingly being tidally dominated except at various storm events.

All of the ROMS simulations show similar velocity magnitudes, although clearly tidal forcing alone is not sufficient to capture the variations in velocity (Fig. 34). When additional forcings are included, however, qualitatively the simulated velocity variation matches observations well (e.g., Fig. 41).

5.3 Comparison of ROMS and HYDROMAP tidal simulations

In general, the results of ROMS and HYDROMAP are found to be in good agreement. For example, the M2 amplitude (the dominant tidal forcing component) at station PO-S was predicted by ROMS to be 0.494 m, and HYDROMAP predicting 0.478 m. Similar errors were found in both magnitude and phase angle of the tidal constituents.

A number of significant differences, however, exist between how ROMS and HYDROMAP were set-up, beyond the differences in numerical methods, including the forcing terms, the grid, and the focus, which explains why those two sets of tidal simulations may differ in some details. For ROMS, simulations discussed above only considered a tidal forcing from the ADCIRC data base of tidal constituent data along the east coast of North America, whereas the HYDROMAP set-up used the TPXO global tidal model data. The HYDROMAP set-up also included the effects of winds and was thus able to show better agreement with the current profiles – this deficiency in the ROMS setup is alleviated in simulations reported in the next section, where wave and wind forcing is applied to ROMS in addition to tidal forcing, but as well it is difficult

to separate the effects of waves and wind from the available data, because of the correlation between high waves and strong winds. One limitation of the HYDROMAP wind forcing was that it involved using a spatially uniform, albeit time-varying, wind field, obtained from measurements made at a single buoy. It is not clear how significant the spatial variation of the wind field is, but it is worth noting nevertheless, because the computational domains are large enough (e.g., the ROMS domain is 360 km across), that significant variations in the wind field are present. In ROMS simulations reported in the next section, by contrast, we use the full wind field hindcast using RAMS, varying over both space and time.

In terms of gridding, HYDROMAP used a nested grid, which increased in resolution around Block Island, down to 125 x 125 m cells. This is nearly 5 times higher a resolution than in the ROMS simulations. It would require significant computational resources to conduct multiple ROMS simulations over such time periods, using a uniform 125 m grid, so the nested approach is advantageous here. [Although it is possible to use nested grids with ROMS, that approach was not implemented here.] Some results not mentioned in this report show possible advantages of using HYDROMAP for tides: the ROMS results for coastal tidal stations (e.g., Newport, Montauk) were substantially different from observed data, yet HYDROMAP results were closer to the observed results. This is most likely because HYDROMAP uses a nested grid and so was able to resolve the important features of nearshore bathymetry, whereas the ROMS grid had a resolution of 600 m everywhere. However, ROMS results for tidal forcing should be sufficiently accurate in the deeper waters around the tentative wind farm sites in the SAMP areas.

Although the HYDROMAP simulation was able to more easily capture the behavior of the observed velocity structure, it did not consider the effect of surface waves or compute what sediment suspension would be, which both are important effects. In addition to the importance of modeling surface waves and sediment transport, in order to obtain meaningful information about sediment suspension, both can significantly affect seabed drag.

In closing, it appears that the independent HYDROMAP simulations have served their purpose well in showing that the more complete and comprehensive, but less resolved, ROMS simulations provide sufficiently accurate results for the key component of tidal forcing (M2) in the SAMP area.

5.4 Sediment suspension in the ROMS and ROMS/SWAN simulations

There are two sets of observed data that relate directly to sediment suspension in the SAMP study area: the map of median grain size (Fig. 12) of the surficial sediments which shows the seabed conditions, and the recording of ADCP backscatter at PO-S (Fig. 29) which may relate to the suspended sediment concentration.

For the seabed grain size diameter (Fig. 12), we note that in general offshore of the SAMP study area sediments are very fine with little variation. Around the SAMP study area, there are areas of coarser sediment (in excess of 2 mm diameter) at the mouth of Long Island Sound to the west, near Martha's Vineyard to the east, and around Block Island there are large variations between very fine and very coarse sediments. As well, there are very coarse sediments on Cox's Ledge, which is east of Block Island, where the water is shallow.

In the ROMS simulations with only tidal forcing, we observe many of these features around Block Island and Long Island Sound. [The lack of a quantitative match is not necessarily detrimental to the simulations, but rather the initial conditions, whereby using a uniform distribution of sediment classes with exponentially varying grain size will result in an abnormally low median value.] In order to get significant sediment transport in the eastern half of the SAMP study area, the wind forcing is required (Fig. 45), although with only tides and wind forcing, the region of coarser grain size is much smaller than in the observed (Fig. 12). In the ROMS/SWAN simulation with all three forcings (tides, waves and winds), the median grain size is most realistic, with coarser sand at the mouth of Long Island Sound, as well as on Cox's Ledge, with significant variation around all of the SAMP study area.

Regarding suspended sediment, ADCP backscatter suggests that sediment is suspended the most when the local waveheight is highest, most notably at events in mid-November, and in several smaller storms in December. When only tidal forcing is considered (Fig. 35), sediment suspension occurs primarily at the spring tides, not lining up very well with the ADCP backscatter measurements. When winds are included (Fig. 43), higher suspended sediment concentrations are predicted, although the large storm event in mid-November is does not result is as much sediment suspension as that in December, since the distinguishing feature between the two is the significant wave height, so a wave model coupling is required to better match the observations.

6 Conclusions

Results are presented for simulations of the hydrodynamics and sediment suspension in the ocean SAMP study area. In order to validate the models against observations, a period of three and a half months (October 2009 to mid-January 2010) was selected. A selection of tidal, wind, and wave forcings were considered, ignoring density-driven circulation. The Regional Ocean Modeling System (ROMS) was the primary modeling tool for conducting these simulations, but ROMS results were also compared to HYDROMAP simulations conducted by ASA for tidal and space-uniform wind forcing, and coupled ROMS/SWAN simulations were used to model coupled ocean-wave processes. Data was primarily compared against ADCP measurements of the currents obtained at four different buoys as part of the SAMP field program, as well as significant wave height.

Improvements to the numerical modeling could be made by increasing horizontal resolution, as well as tuning the vertical stretching parameters to better capture the surface and bottom boundary layer processes. Future work could better test result sensitivity to boundary conditions and the turbulence closure scheme, ensuring that the amount of suspended sediment is approximately correct. It may be possible to include effects of density-driven circulation, but as this work shows, at least for the Fall season, density-driven circulation does not appear necessary to explain many aspects of sediment suspension. Improvements could also be made on the measurement side, in particular by attempting to make a meaningful estimate of suspended sediment concentrations, from records of ADCP counts.

ROMS simulations with only tidal forcing were able to predict the tide elevation and currents in the SAMP study area, with good agreement with observations (and with higher-resolution HYDROMAP simulations). These simulations, forced only by tides, were also able to model sediment transport over the computational domain, and an initially uniform grain size distribution was shown to evolve to one qualitatively approximating the observed grain size distribution on the seabed. Comparing model results with observations, however, highlighted the importance of non-tidal currents in the area and of adding the other forcing terms from waves and wind.

HYDROMAP simulations of the area, for tidal and (uniform) wind forcing, using nested grids with a much higher resolution in some areas (down to 125 m), were used for comparison with ROMS tidal simulations. HYDROMAP results showed similar agreement with observed tidal elevations. In addition, obtained current profiles matched the ADCP observations better than the

initial ROMS simulations, which only considered tides, stressing the importance of wind forcing. The HYDROMAP results had several significant limitations, though, most significantly in neglecting waves and all sediment transport, and using a spatially uniform wind. They however served their purpose well in validating the coarser resolution (uniform 600 m grid) ROMS simulations of the key tidal components (e.g., M2) in the SAMP area.

Coupled ROMS/SWAN simulations in the SAMP area were conducted with tidal, wave, and wind forcing. The main difference seen between the ROMS/SWAN results and the earlier ROMS and HYDROMAP simulations is the improved agreement with available data regarding sediment grain size at the seabed. Although the 600 m resolution of the ROMS/SWAN grid does not show details as well as the HYDROMAP results, these coupled results show good agreement with available data regarding the hydrodynamics and seabed properties for the area.

7. References

Apsley, D.D. and I.P. Castro 1997. Flow and dispersion over hills: Comparison between numerical predictions and experimental data. *J. Wind Eng. Ind. Aerodyn.* 67: 375-386.

Asher, T.G., A.R. Grilli, S.T. Grilli and M.L. Spaulding 2010. Analysis of extreme wave climates in Rhode Island waters south of Block Island, Ocean Engineering, University of Rhode Island, Narragansett, RI, 37 pp.

Battelle 2003. *Alternative site screening report: Rhode Island region long-term dredged material disposal site evaluation project*. Tech. Report.

Blass, M., C. Dong, P. Marchesiello, J.C. McWilliams, and K.D. Stolzenbach 2007. Sediment-transport modeling on Southern California shelves: A ROMS case study. *Continental Shelf Res.* 27: 832-853.

Blumberg, A.F. and G.L. Mellor 1987. Three-dimensional Coastal Ocean Models, chapter A. Description of a three-dimensional coastal ocean circulation model. American Geophysical Union, pps. 1-16.

Booij, N., R.C. Ris, L.H. Holthuijsen 1999. A third-generation wave model for coastal regions. Part I – Model description and validation. *J. Geophys. Res.* 104: 7649-7666.

Cao, Z., G. Pender, and J. Meng 2006. Explicit formulation of the Shields diagram for incipient motion of sediment. *J. Hydr. Engng.* 132(10): 1097-1099.

Chapman, D.C. 1985. Numerical treatment of cross-shelf open boundaries in a barotropic coastal ocean model. *J. Phys. Oceanogr.* 15: 1060—1075.

Chow, F.K. and R.L. Street 2009. Evaluation of turbulence closure models for large-eddy simulation over complex terrain: Flow over Askervein Hill. *J. Appl. Meteor. Clim.* 48: 1050-1065.

Codiga, D.L. and D.A. Aurin 2007. Residual circulation in eastern Long Island Sound: Observed transverse-vertical structure and exchange transport. *Continental Shelf Res.* 27:103-116.

Codiga, D.L. and A.E. Houk 2002. *Current profile time series from the FRONT moored array, technique report*. Technical report, Department of Marine Science, University of Connecticut.

Codiga, D.L. and D.S. Ullman 2010. *Characterizing the physical oceanography of coastal waters off Rhode Island, Part I: Literature review, available observations, and a representative model simulation*. University of Rhode Island. Prepared for the Rhode Island Ocean Special Area Management Plan 2010.

Deines, K.L. 1999. Backscatter estimation using broadband acoustic Doppler current profilers. *Proc. Sixth Working Conf. on Current Measurement.* San Diego, CA, *IEEE*: 249-253.

Ding, L. and R.L. Street 2003. Numerical study of the wake structure behind a three-dimensional hill. *J. Atmos. Sci.* 60: 1678-1690.

Divins, D.L. and D. Metzger 2003. *National Geophysical Data Center coastal relief model*.

Edwards, C.A., T.A. Fake, and P.S. Bogden 2004. Spring-summer frontogenesis at the mouth of Block Island Sound: 1. A numerical investigation into tidal and buoyancy-forced motion. *J. Geophys. Res.* 109: C12021.

Eidsvik, K.J. 2005. A system for wind power estimation in mountainous terrain. Prediction of Askervein Hill data. *Wind Energy* 8: 237-249.

Emery, W.J. and R.E. Thompson 2001. *Data Analysis Methods in Oceanography.* Elsevier.

Fedorovich, E., E.T.M. Nieuwstadth, and R. Kaiser 2001. Numerical and laboratory study of a horizontally evolving convective boundary layer. Part I: Transition regimes and development of the mixed layer. *J. Atmos. Sci.* 58: 70-86.

Flather, R.A. 1976. A tidal model of the northwest European continental shelf. *Memoire de la Société Royale des Sciences de Liège 6ème série.* 10: 141-164.

Gostiaux, L. and H. van Haren 2010. Extracting meaningful information from uncalibrated backscattered echo intensity data. *J. Atmos. Oceanic Tech.* 27:943-949.

Hasselmann, K. and D. Olbers 1973. Measurements of wind-wave growth and swell decay during the Joint North Sea Wave Project (JONSWAP). *Erganzung zur Deut. Hydrog. Z. Reihe A* (8) 12: 1-95.

Hastings, M.E., L.J. Poppe, and J.C. Hathaway 2000. *USGS east-coast sediment analysis: procedures, database, and georeferenced displays*. Chapter 2: surficial sediment database. USGS open-file report 00-358.

He, R. and J.L. Wilkin 2006. Barotropic tides on the southeast New England shelf: A view from a hybrid data assimilative modeling approach. *J. Geophys. Res.* 111:C08002.

Jimenez, J.A. and O.S. Madsen 2003. A simple formula to estimate settling velocity of natural sediments. *J. Waterway, Port, Coastal and Ocean Engng.* 129(2): 70-78.

Lane, T.P., R.D. Sharman, R.G. Frehlich and J.M. Brown 2006. Numerical simulations of the wake of Kauai. *J. Appl. Meteor. Clim.* 45: 1313-1331.

Le Provost, C., F. Lyard, J.M. Molines, M.L. Genco, and F. Rabilloud 1998. A hydrodynamic ocean tide model improved by assimilating a satellite altimeter-derived data set. *J. Geophys. Res.* 103(C3): 5513-5529.

Lynch, D.R., C.E. Naimie, and C.G. Hannah 1998. Hindcasting the Georges Bank circulation, Part I: detiding. *Continental Shelf Res.* 18: 607-639.

Malkus, J.S., and A. E. Bunker 1952. Observational studies of the air flow over Nantucket island during the summer of 1950. *Papers in Physical Oceanography and Meteorology*, XII, No. 2, Massachusetts Institute of Technology and Woods Hole Oceanographic Institution, 50 pp.

Marshall, J.C., A. Adcroft, C. Hill, L. Perelman, and C. Heisey 1997. A finite-volume, incompressible Navier Stokes model for studies of the ocean on parallel computers. *J. Geophys. Res.* 102: 5753-5766.

Matthews, S., J. M. Hacker, J. Colle, J. Hare, C. N. Long, and R. M. Reynolds 2007. Modification of the atmospheric boundary layer by a small island: Observations from Nauru. *Mon. Wea. Rev.* 135: 891–905, doi:10.1175/MWR3319.1.

Mau, J.-C., D.-P. Wang, D.S. Ullman, and D.L. Codiga 2006. Comparisons of observed (HF radar, ADCP) and model barotropic tidal currents in the New York Bight and Block Island Sound. *Estuarine Coastal and Shelf Sci.* 72: 129-137.

Mellor, G.L. and T. Yamada 1982. Development of a turbulence closure model for geophysical fluid problems. *Rev. Geophys. Space Phys.* 20: 851-875.

Meyer-Peter, E. and R. Mueller 1948. Formulas for bedload transport. In: *Report on the second meeting of the International Association Hydraulic Structure Research.* Stockholm, Sweden: 39—64.

Moeng, C.-H., J. Dudhia, J. Klemp, and P. Sullivan 2007. Examining two-way grid nesting for large eddy simulation of the PBL using the WRF model. *Mon. Weather Rev.* 135: 2295-2311.

Moody, J.A., B. Butman, R.C. Beardsley, W.S. Brown, P. Daifuku, J.D. Irish, D.A. Mayer, H.O. Mofield, B. Petrie, S. Ramp, P. Smith, and W.R. Wright 1984. *Atlas of tidal elevation and current observations on the Northeast*. American Continental Shelf and Slope. United States Geological Survey.

Mukai, A.Y., J.J. Westerink, R.A. Luettich, Jr., and D. Mark 2002. *Eastcoast 2001, a tidal constituent database for western North Atlantic, Gulf of Mexico, and Caribbean Sea*. Tech. Report. ERDC/CHL TR-02-24. Coastal and Hydraulics Laboratory, US Army Corps of Engineers.

Oey, L.-Y., H.T. Manning, and K.W. Young 1995. *Quantitative Skill 1 Assessment for Coastal Ocean Models, chapter A*. A plume and wind driven circulation model of the New York Bight. American Geophysics Union, pps. 329-347.

Pawlowicz, R., B. Beardsley, and S. Lentz 2002. Classical tidal harmonic analysis including error estimates in MATLAB using T_TIDE. *Computers and Geosci.* 28: 929-937.

Prospathopoulos, J., and S.G. Voutsinas 2006. Implementation issues in 3D wind flow predictions over complex terrain. *J. Sol. Energy Eng.* 128: 539-553.

RAMS 2010. Regional Atmospheric Modeling System Technical Manual, Weather Flow.

Reid, J.M., J.A. Reid, C.J. Jenkins, M.E. Hastings, S.J. Williams, and L.J. Poppe 2005. *usSEABED: Atlantic coast offshore surficial sediment data release*. US Geological Survey Data Series 118, version 1.0.

Shchepetkin, A.F. and J.C. McWilliams 2005. Regional Ocean Model System: a split-explicit ocean model with a free-surface and topography-following vertical coordinate. *Ocean Modelling* 9: 347-404.

Shapiro, R. 1975. Linear filtering. *Mathematics of Comput.* 29: 1094-1097.

Shaw, W.J., J.K. Lundquist and S.J. Schreck 2009. Research needs for wind resource characterization. *Bull. Amer. Meteor. Soc.* 90: 535-538, doi:10.1175/2008BAMS2729.1.

Shearman, R.K. and S. J. Lentz 2004. Observatinos of tidal variability on the New England Shelf. *J. Geophys. Res.* 109: C06010.

Silva Lopes, A., J.M.L.M. Palma, and F.A. Castro 2007. Simulation of the Askervein flow. Part 2: Large-eddy simulations. *Bound.-Layer Meteor*. 125: 85-108.

Smith, R.B., and V. Grubišic 1993. Aerial observations of Hawaii's wake. *J. Atmos. Sci.* 50: 3728-3750.

Smith, R.B., A. C. Gleason, P.A. Gluhosky, and V. Grubišic 1997. The wake of St. Vincent. *J. Atmos. Sci.* 54: 606–623.

Song, Y. and D.B. Haidvogel 1994. A semi-implicit ocean circulation model using a generalized topography-following coordinate system. *J. Comp. Phys.* 115(1): 228-244.

Soulsby, R.L. and J.S. Damgaard 2005. Bedload sediment transport in coastal waters. *Coastal Engng.* 52: 673-689.

Spaulding, M.L., M. Bell, J. Titlow, L. Decker , A.R. Grilli, R. Sharma and D. Mendelsohn 2010a. Meteorological Model based Wind Resource Assessment in the Vicinity of Block Island. *SAMP Report.* Ocean Engineering, University of Rhode Island, Narragansett, RI, 34 pp.

Spaulding, M.L., M. Bell, Jay Titlow, R. Sharma, A.R. Grilli, A. Crosby and L. Decker and Daniel Mendelsohn 2010b. Wind Resource Assessment in the Vicinity of a Small, Low Relief Coastal Island. *SAMP Report.* Ocean Engineering, University of Rhode Island, Narragansett, RI, 45 pp.

Thomson, R.E., J.F.R. Gower, and N.W. Bowker 1977. Vortex streets in the wake of the Aleutian Islands. *Mon. Wea. Rev*. 105: 873-884.

Ullman, D.S. and D.L. Codiga 2004. Seasonal variation of a coastal jet in the Long Island Sound outflow region based on HF radar and Doppler current observations. *J. Geophys. Res.* 109: C07S06.

Walmsley, J.L. and P.A. Taylor 1996. Boundary-layer flow over topography: Impacts of the Askervein study. *Bound.-Layer Meteor*. 78: 291-320.

Warner, J.C., C.R. Sherwood, R.P. Signell, C.K. Harris, and H.G. Arango 2008a. Development of a three-dimensional, regional, coupled wave, current, and sediment-transport model. *Computers and Geosc.* 34:1284-1306.

Warner, J.C., B. Butman, and P.S. Dalyander 2008b. Storm-driven sediment transport in Massachusetts Bay. *Continental Shelf Res.* 28: 257-282.

Wiberg, P.L. and C.K. Harris 1994. Ripple geometry in wave-dominated environments. *J. Geophys. Res.* 99(C1): 775-789.

WRF 2008. *A description of the Advanced Research WRF Version 3.* NCAR Technical Note TN-475+STR, 125 pp.

Appendix A:

Hydrodynamics of Block Island Sound (HYDROMAP tidal simulations) for the Rhode Island Ocean Special Area Management Plan

by

Deborah Crowley and Daniel Mendelsohn

Applied Science Asociates, Inc.

55 Village Square Drive

South Kingstown, RI 02879

June 16, 2010

Executive Summary

It has been proposed that a wind turbine farm be developed off the southeastern coast of Block Island, south of the Rhode Island mainland. The development of an offshore wind farm will necessarily require a great deal of underwater construction including drilling and setting the piles for the turbine foundations, burying electrical transmission cables and other infrastructure construction tasks. During this period additional water column suspended sediments may impact the construction areas and it is therefore of interest to understand what the current speeds and circulation patterns are in the development area. To that end, Applied Science Associates, Inc. (ASA) has performed a hydrodynamic modeling study to estimate the currents and circulation in the renewable energy (RE) development area with a focus on bottom stress and currents. The results of the study will be used by URI scientists to determine the potential for sediment re-suspension and transport of suspended sediment that might results from the construction and operation of the small wind farm.

ASA used the HYDROMAP model system, which calculates velocity vectors on a stepwise continuous variable rectangular grid system. A benefit of the model is that it allows coarse grid resolution in the areas offshore the coast of Rhode Island and finer resolution in the Block Island Sound area and renewable energy zone area of interest. The model was driven by tidal harmonic data along the open boundaries and wind stress at the surface. The model predictions were compared to observations collected as part of the OSAMP, including four ADCP current meter locations and NOAA tidal elevation data at Montauk and Newport. The comparisons showed that the model not only adequately predicted the tidal forcing response in the study area, but also the longer period episodic wind driven events that are characterized by passing weather systems. The model appeared to be able to reproduce both the horizontal spatial variability in the system as well as the vertical profile of the currents, as represented by the ADCP observations at the surface, mid and bottom of the water column.

Both observations and the model predictions confirm that the dominating tidal constituent is the M2 constituent which represents between 50-60% of the total tidal amplitude at all stations. The amplitude predictions for all constituents tend to be higher than the observed but are generally within 20% of the observed with the exception of Montauk. The Montauk station is located in the shallows of an embayment that the mode grid does not resolve in fine detail, this may contribute to the over prediction of tidal amplitude.

Review of the current analysis indicates that the differences between the model predicted and observed M2 constituent major axes are generally less than 0.02 m/s with a maximum deviation of 0.05 m/s in the MDF bottom current ellipse. The difference in the remaining constituents is variable, remaining less than 0.01 m/s for the majority. The M2 phase comparison between the model predictions and observations is similarly close, with the difference angle remaining less than about 10 degrees with an exception in the bottom currents at both the POS and POF stations. In general, the model predicted tidal current ellipses, driven predominantly by the M2 tidal component, show a close agreement with the observations indicating that the model captures the magnitude and the circulation patterns in the study area.

The bottom currents were further reviewed and an understanding of the bottom speed developed. The renewable energy zone follows the edge of the 3 mile state waters limit along the southern portion of the line, from the straights between Long Island and Block Island to the west, to the shipping channel exclusion zone on the east. The zone is approximately 2 km wide, and has a bulge on the east side representing the shipping channel exclusion zone. Bathymetry in the RE zone is quite variable ranging from less than 10m, in the western portion to greater than 35m to the east. This bathymetric range and the straights to the west produce a significant variability in the bottom speeds as well, ranging from a high in the shallow western portions of 0.25 m/s down to a high in the eastern portions of 0.15 m/s.

Tabel of Contents

List of Figures

List of Tables

1 Introduction

Deepwater Wind Associates LLC has proposed to build a wind turbine farm off the southeastern coast of Block Island, south of the Rhode Island mainland. The pilot project will consist of 8-10 wind turbine generators (WTG), located in a line inside of the 3-nautical mile state waters limit and roughly following the 3-nautical mile boundary. As a part of the state of Rhode Island's evaluation of the project, the RI Coastal Resources Management Council (CRMC) is developing an Ocean Special Area Management Plan (OSAMP) for the area to evaluate and weight competing uses for the area. The result will be a final renewable energy area set aside for offshore wind development projects.

The University of Rhode Island has contracted with Applied Science Associates, Inc. to perform an analysis to estimate the currents and circulation in the renewable energy development area with a focus on bottom stress and currents. The results will be evaluated by URI scientists to determine the potential for sediment re-suspension and transport of suspended sediment that might result from the construction and operation of the small wind farm.

Currents were simulated by the ASA model, HYDROMAP, which calculates velocity vectors on a stepwise continuous variable rectangular grid system. The model allows coarse grid resolution in the areas offshore the coast of Rhode Island and finer resolution in the Block Island Sound area. The model predicts water surface elevation and currents that can be used directly in other ASA transport and distribution models for sediment and pollutant transport modeling.

This report documents the model application and predictions of the HYDROMAP model application to Block Island Sound. Section 2 describes the study area and project. Section 3 presents the HYDROMAP model used to simulate currents and its application and results. Section 4 provides a discussion and conclusions from the study and Section 6 lists references.

2 Description of the Study Area

The proposed wind energy project is to be located just less than 3 miles from the southeast coast of Block Island in an area where Block Island Sound Rhode Island Sound and the Atlantic Ocean meet (Figure 2-1). Also shown in the figure is the OSMAP proposed study area which encompasses both RI state and federal waters and the 3 nautical mile limit of the RI state waters. The SAMP area lies south of the southern coast of Rhode Island and lies west of Martha's Vineyard and east of Long Island. It is approximately 2300 km^2 (880 mi^2) in area with depths

ranging from less than 20 m (65 ft) below Mean Sea Level (MSL) to greater than 80 m (260 ft) MSL.

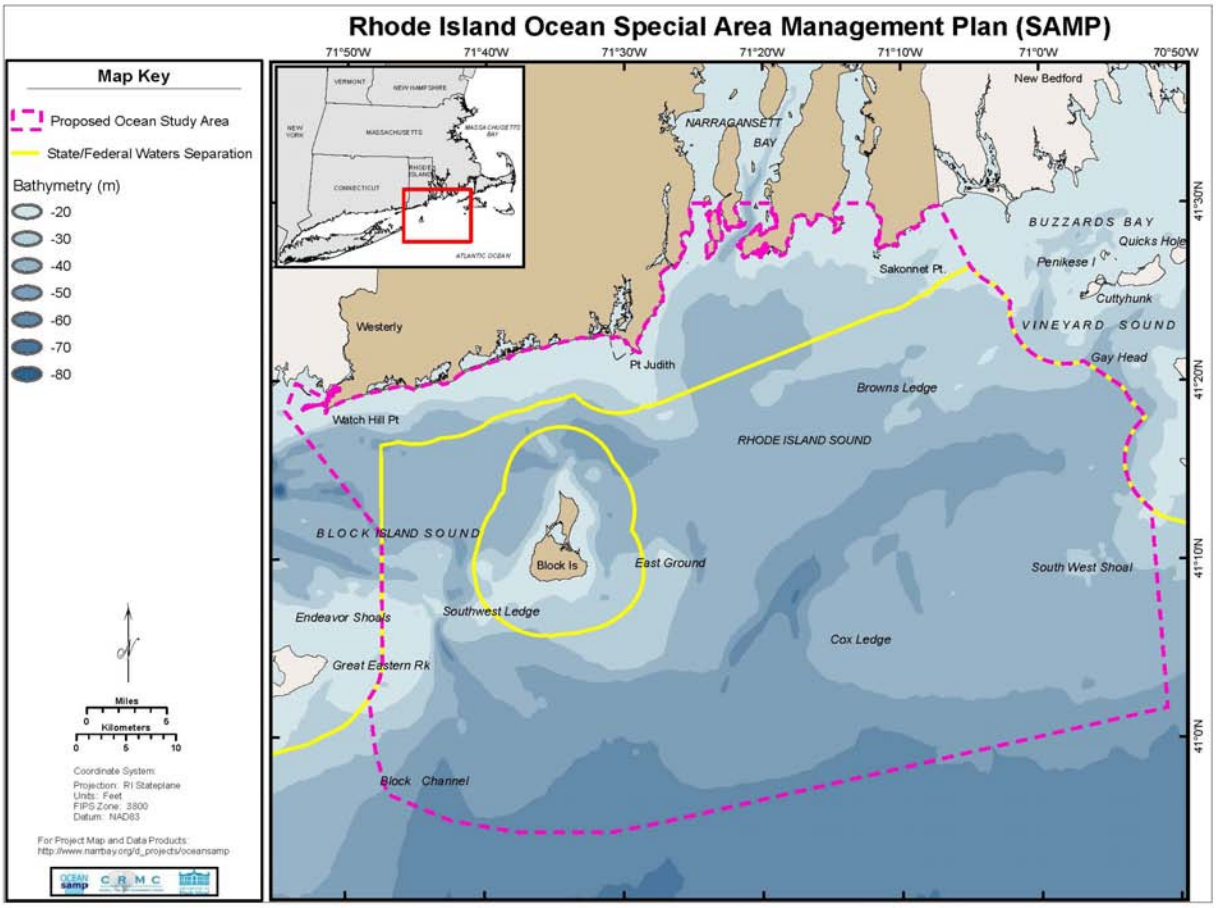

Figure 2-1 Block Island Sound study area showing the OSAMP designated area and the modeled domain between Buzzards Bay and Long Island Sound.

The proposed Renewable Energy (RE) Zone lies along the southern arc of the limit of state waters around Block Island, in a 2 kilometer wide band (Figure 2-2). The eastern edge of the RE zone is cut out to allow for the shipping lane exclusion area. The proposed pilot project wind park will consist of 8-10 wind turbine generators (WTG), in a line curving along the eastern part of the RE zone. Each WTG is to be mounted on a jacket structure with 4 piles, each of which will be driven into the seabed.

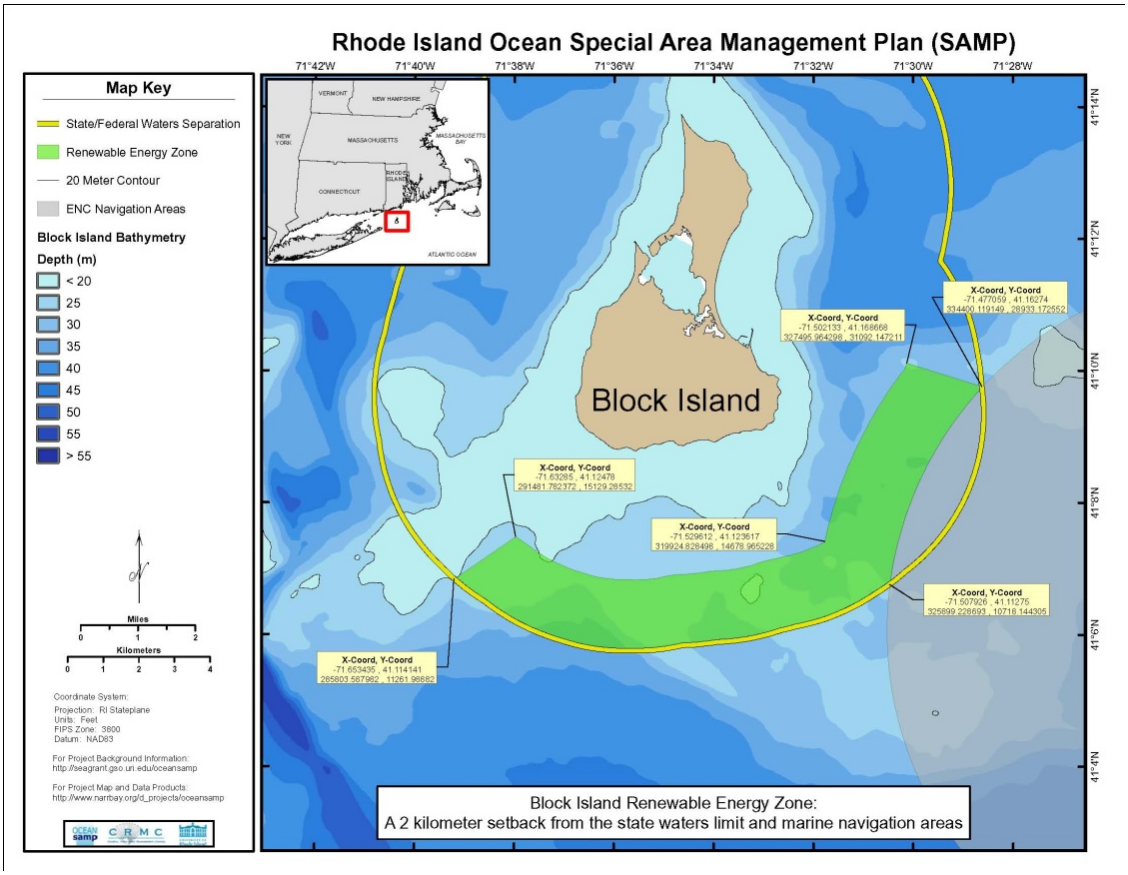

Figure 2-2 Proposed renewable energy zone in Rhode Island State waters, south of Block Island

2.1 Hydrographic Observations in the Area

As a part of the OSAMP a large field program was developed and implemented through which four offshore stations were deployed; the locations of these stations are illustrated in Figure 2 3. The offshore stations include two buoys that are fitted with both a surface current meter and a downward looking Acoustic Doppler Current Profiler (ADCP), both measuring current magnitude and direction, as well as meteorological observation equipment recording wind speed and direction. One of these buoy stations (Station MDS) is located south of Block Island on the 3 nautical mile state boundary limit and the other is located east of Block Island in federal waters (Station MDF). The remaining two offshore stations have deployed bottom mounted ADCPs measuring water pressure (surface elevation) and current magnitude and direction. These stations are located in close proximity to the buoy stations; one farther south of MDS (Station POS) and the other inshore of MDF (Station POF); these locations are also

illustrated in Figure 2-3. In addition to OSAMP deployed instrumentation there are a number of fixed stations in the study area maintained by NOAA; of these stations two were queried for surface elevation data: Montauk, NY (Station 8510560) and Newport, RI (Station 8452660), these stations are also illustrated in Figure 2-3.

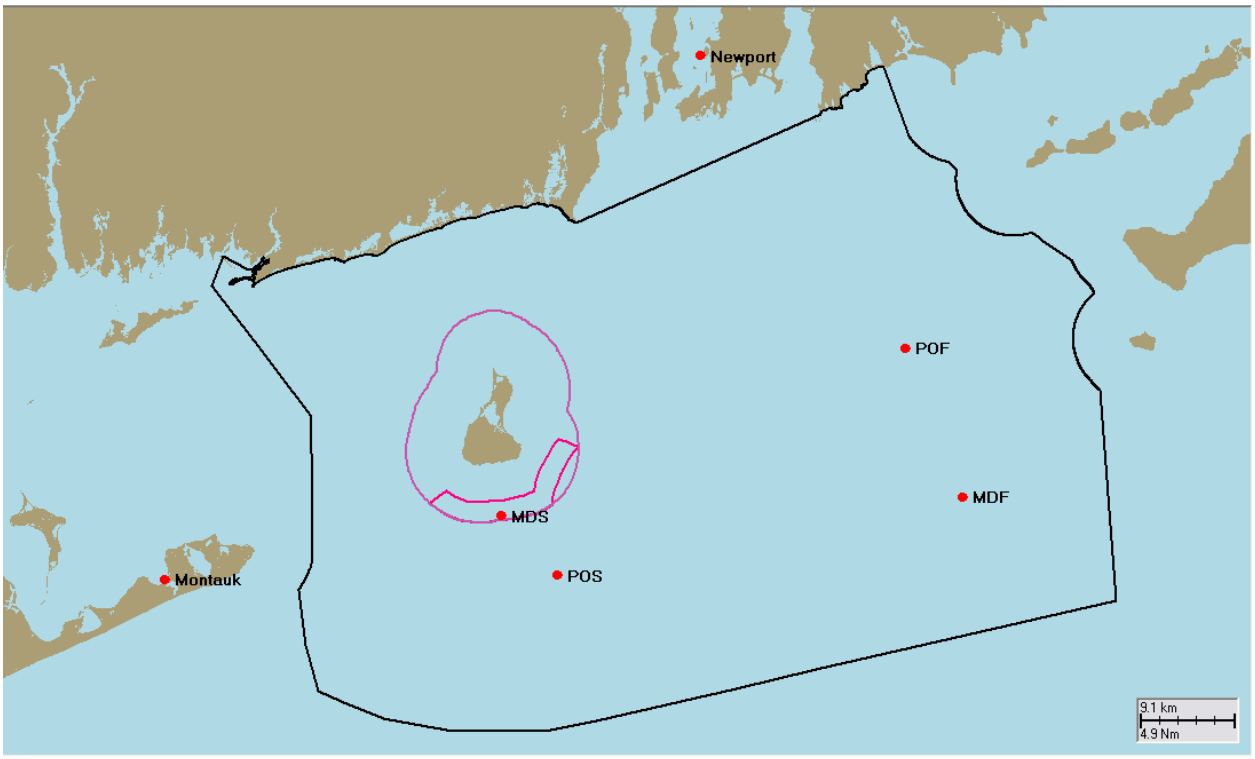

Figure 2-3 Offshore monitoring station locations for the OSMAP field program. Figure also shows the NOAA tide station locations at Newport, RI and Montauk, NY on Long Island.

2.1.1 Tidal Elevation Observations

Water surface elevation data was available from stations POS and POF as well as from NOAA observations stations at Montauk, NY (Station 8510560) and Newport, RI (Station 8452660); all locations are illustrated in Figure 2-3. Observations at stations POS and POF were recorded at two hour intervals and observations at Montauk and Newport were recorded at six minute intervals.

2.1.2 Current Observations

The previously mentioned MDS, MDF, POS and POF stations recorded ocean water currents. The MDS and MDF stations are identical in set up and instrumentation however differ from the

setup and instrumentation at POS and POF which are set up identical to each other; all station locations are illustrated in Figure 2-3.

Stations MDS and MDF included both top mounted ADCPs located 5m below the water surface and a surface current meter located 3m below the water surface. The top mounted ADCPs record the current vector components (U and V) at 1m depth intervals from 5m below the water surface to the bottom; these observations are recorded at an hourly interval. The surface current meter records the speed and direction at a depth of 3m below the water surface; these observations are recorded at an hourly interval. Observations at these stations were available from October 2009 through present (June 2010).

Stations POS and POF include bottom mounted ADCPs which record current speed and direction at 0.75m intervals from the bottom (1st bin centered at approximately 1.8m above the sea floor) to the surface; these observations are recorded on a two hour interval and observations were available from September 2009 through January 2010.

2.1.3 Wind Observations

Both MDS and MDF stations record wind speed and direction at a height of 5m above the water surface. These observations are recorded hourly and were available from October 2000 through present (June 2010).

3 HYDROMAP Hydrodynamic Model

3.1 Model Description

HYDROMAP is a globally re-locatable hydrodynamic model (Isaji, et al., 2001) capable of simulating complex circulation patterns due to tidal forcing, wind stress and fresh water flows quickly and efficiently anywhere on the globe. HYDROMAP employs a novel step-wise-continuous-variable-rectangular (SCVR) gridding strategy with up to six levels of resolution. The term step-wise continuous implies that the boundaries between successively smaller and larger grids are managed in a consistent integer step. The advantage of this approach is that large areas of widely differing spatial scales can be addressed within one consistent model application. Grids constructed by the SCVR are still "structured," so that arbitrary locations can be easily located to corresponding computational cells. This mapping facility is particularly advantageous

when outputs of the hydrodynamics model propagate to subsequent application programs (e.g. Lagrangian particle transport model [SSFATE, OILMAP]) that use another grid or grid structure.

The hydrodynamic model solves the time dependent, three-dimensional conservation equations for water mass, density, and momentum in spherical coordinates with the Boussinesq and hydrostatic assumptions applied. Model output consists of surface elevation and the three dimensional field of horizontal current velocities. The numerical solution methodology follows that of Davies (1977) and Owen (1980). The interested reader is directed to Isaji, et al. (2001), and Isaji and Spaulding (1984) for a detailed description of the model.

3.2 Model Application to the Ocean SAMP Area

3.2.1 Model Grid

The Ocean SAMP area is located in a complex topographic and bathymetric area which results in a complex current velocity structure. In order to account for this complexity the hydrodynamic model domain was extended to deep waters (~200 m [660 ft]) in the south and east directions off of Cape Cod and Nantucket, to the terminus of Long Island Sound and the New York Bight in the west direction and approximately 45 miles south, offshore of the OSAMP study area and the coasts of New York, Rhode Island and Massachusetts.

Figure 3-1 shows the computational model grid cells for the entire domain, consisting of 27,569 active water cells. At the open boundary and in the outer regions, a maximum cell size of ~2.0 km (~1.25 mi) was assigned. Cell resolution was gradually increased toward OSAMP area (Figure 3 2) with the finest resolution of ~125 m (~410 ft) applied in the Renewable Energy zone south of Block Island (Figure 3-3). The model set up allows for three dimensional model simulations, which was utilized for this study. The vertical grid is represented by Legendre polynomials, in this instance six polynomials were used to represent the vertical variability in the currents.

The bathymetry data used in the model grid was assembled from various sources: NOAA NGDC Coastal Relief Model (2010), and ETOPO2 (NGDC 2001). Figure 3-4 through Figure 3-6 show the bathymetry used in the model for the three grid views shown in Figure 3-1 through Figure 3-3).

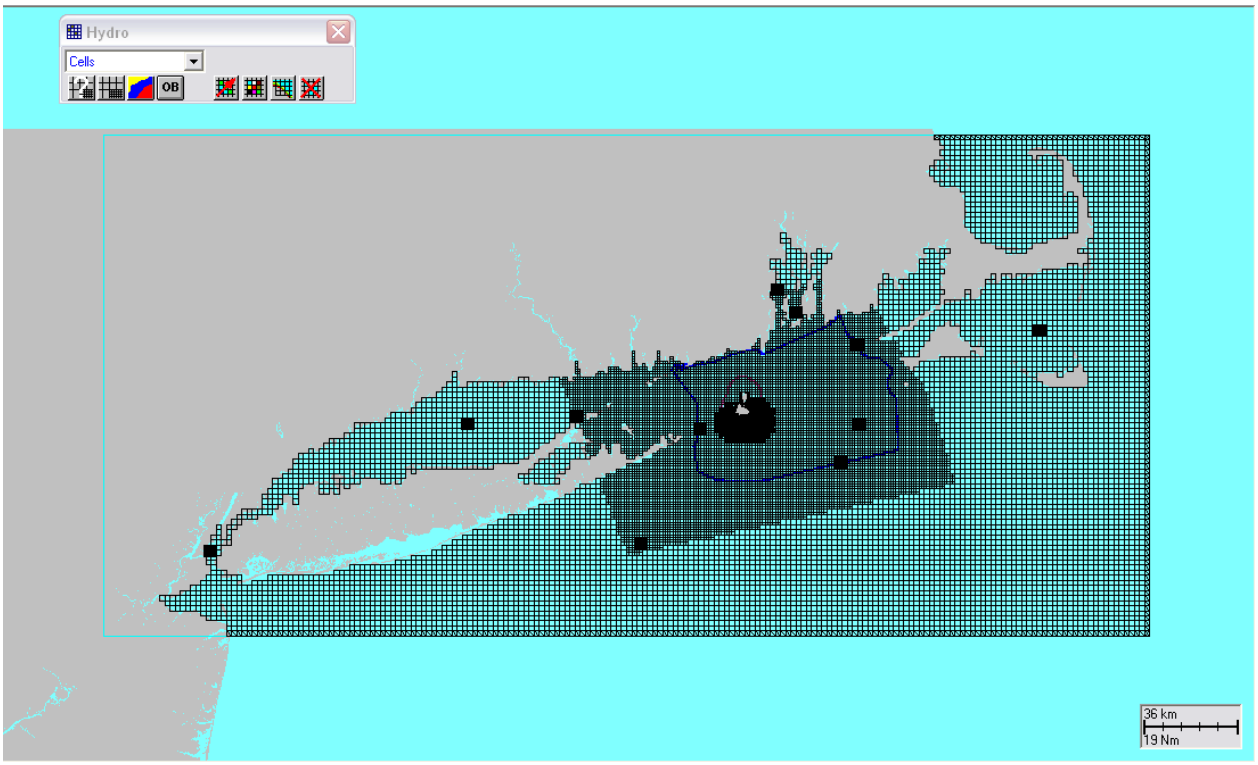

Figure 3-1 Hydrodynamic model grid cells for the entire HYDROMAP area.

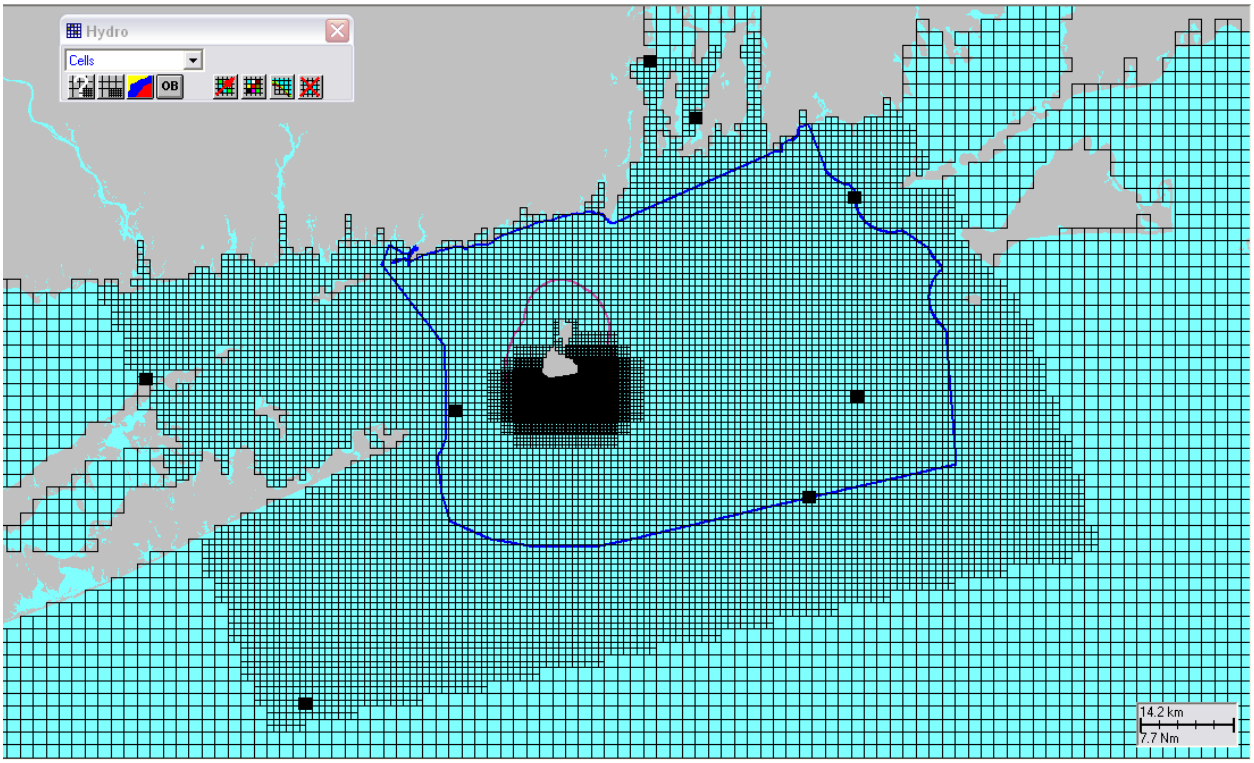

Figure 3-2 Hydrodynamic model grid cells for the OSAMP area.

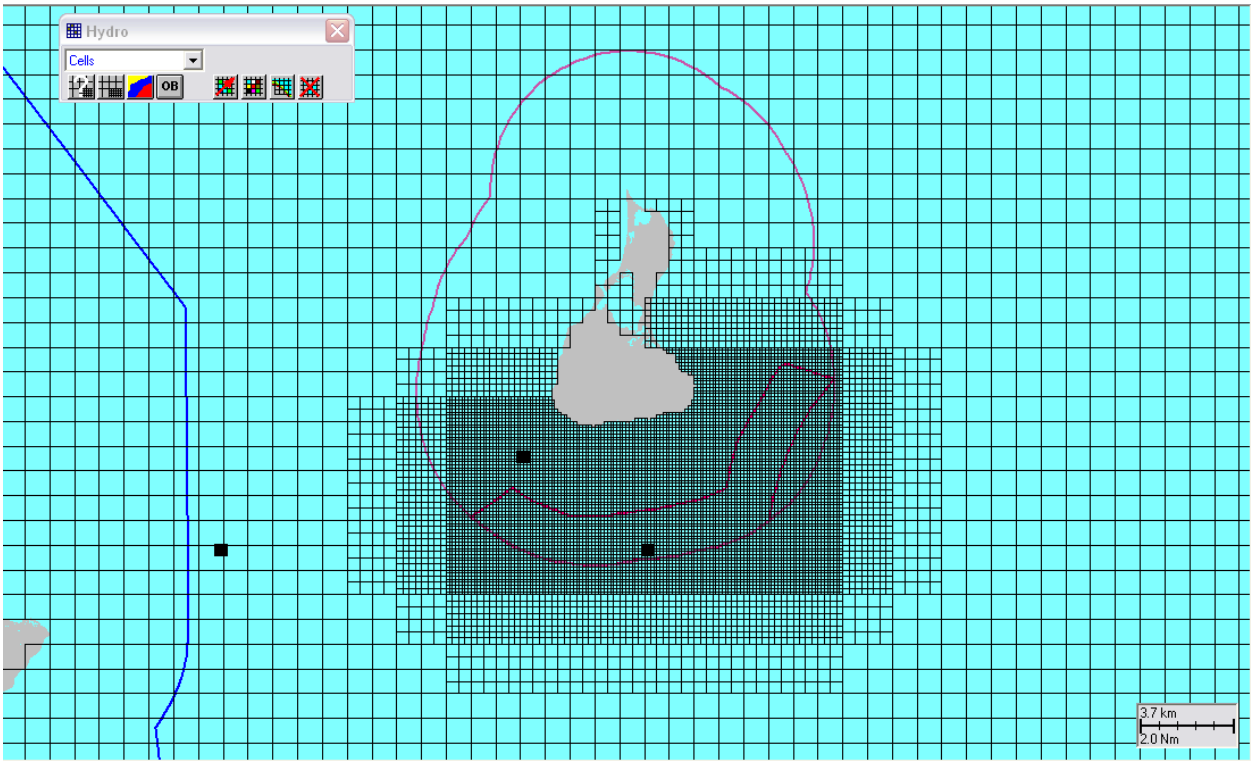

Figure 3-3 Hydrodynamic model grid cells for the Block Island Sound area.

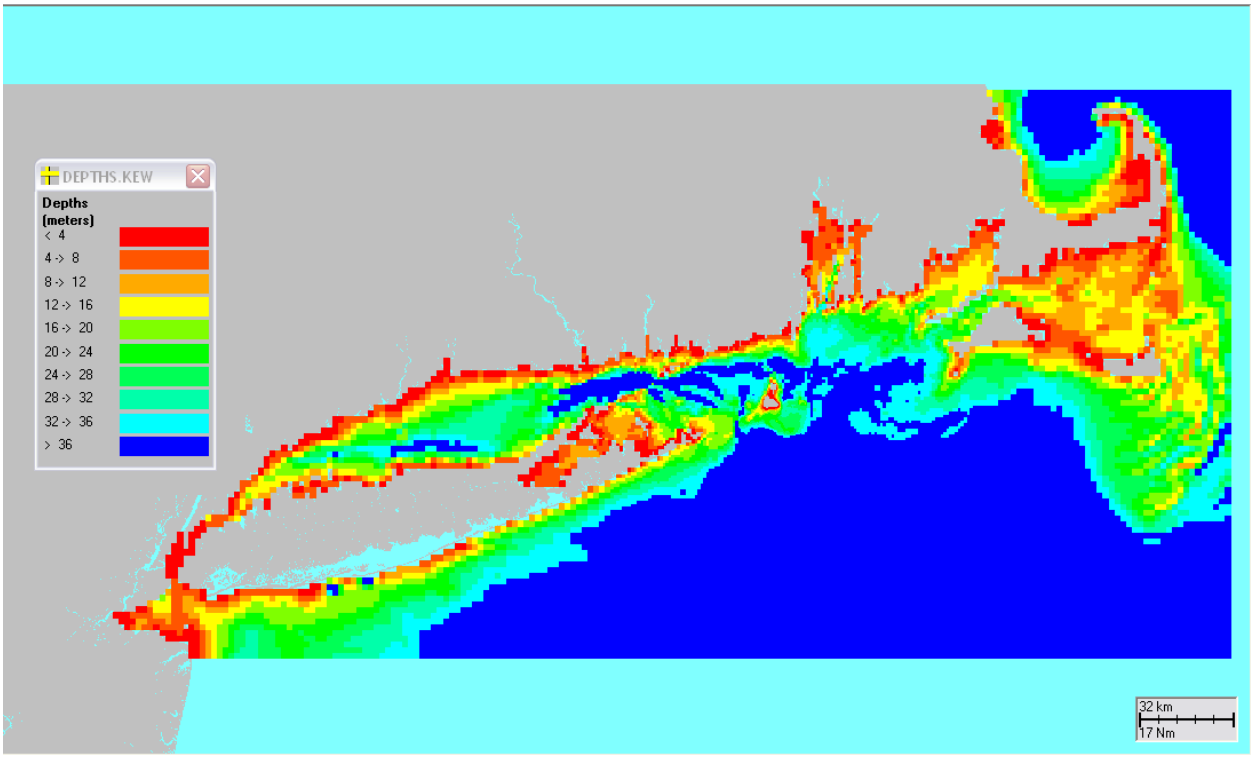

Figure 3-4 Hydrodynamic model grid depths for the entire HYDROMAP grid area.

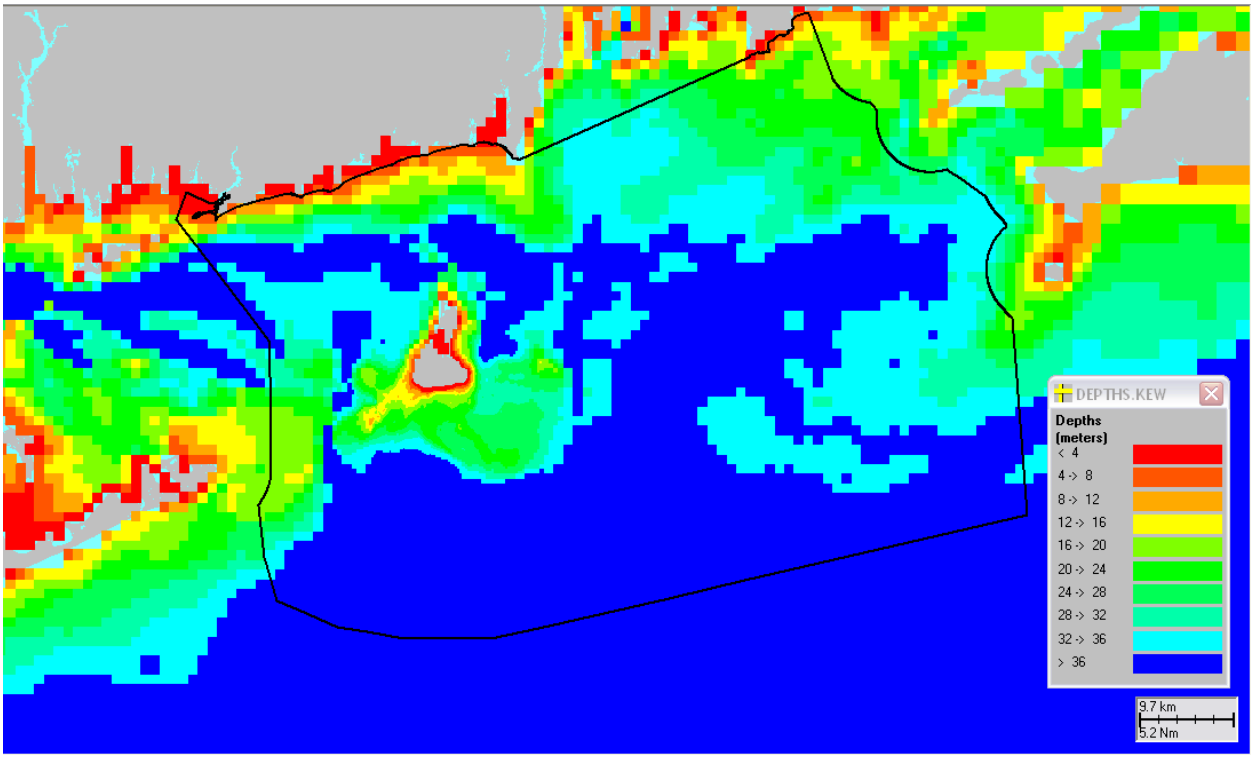

Figure 3-5 Hydrodynamic model grid depths for the OSAMP area.

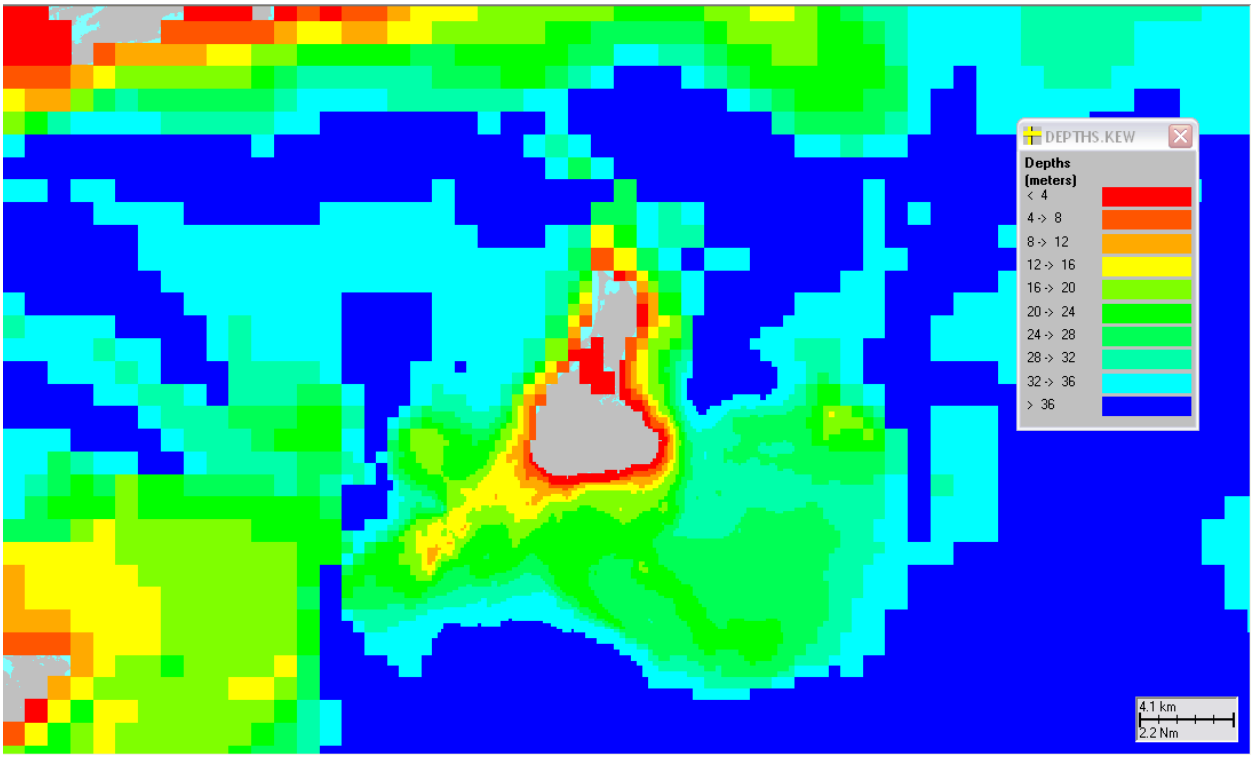

Figure 3-6 Hydrodynamic model grid depths for the Block Island Sound area.

3.2.2 Model Forcing

3.2.2.1 Tides

The water circulation in Block Island Sound is mostly tidally driven (Gordon and Spaulding, 1979). Harmonic constituent data extracted from the TPXO global tidal model was used at the model open boundaries. Each boundary cell was assigned a unique set of the harmonic constituent amplitudes and phases. An example of the M2 constituent amplitude is presented in Figure 3-7. In total, the open boundary was specified for the predominant 5 tidal constituents in the area: three semi-diurnals (M2, N2, and S2) and two diurnals (K1 and O1). HYDROMAP (Isaji et al 2001), employs a strategy that uses the harmonic construction of astronomic tidal currents where each harmonic (constituent) is simulated individually and then the real time tide is assembled using the harmonic summation of these simulated constituents.

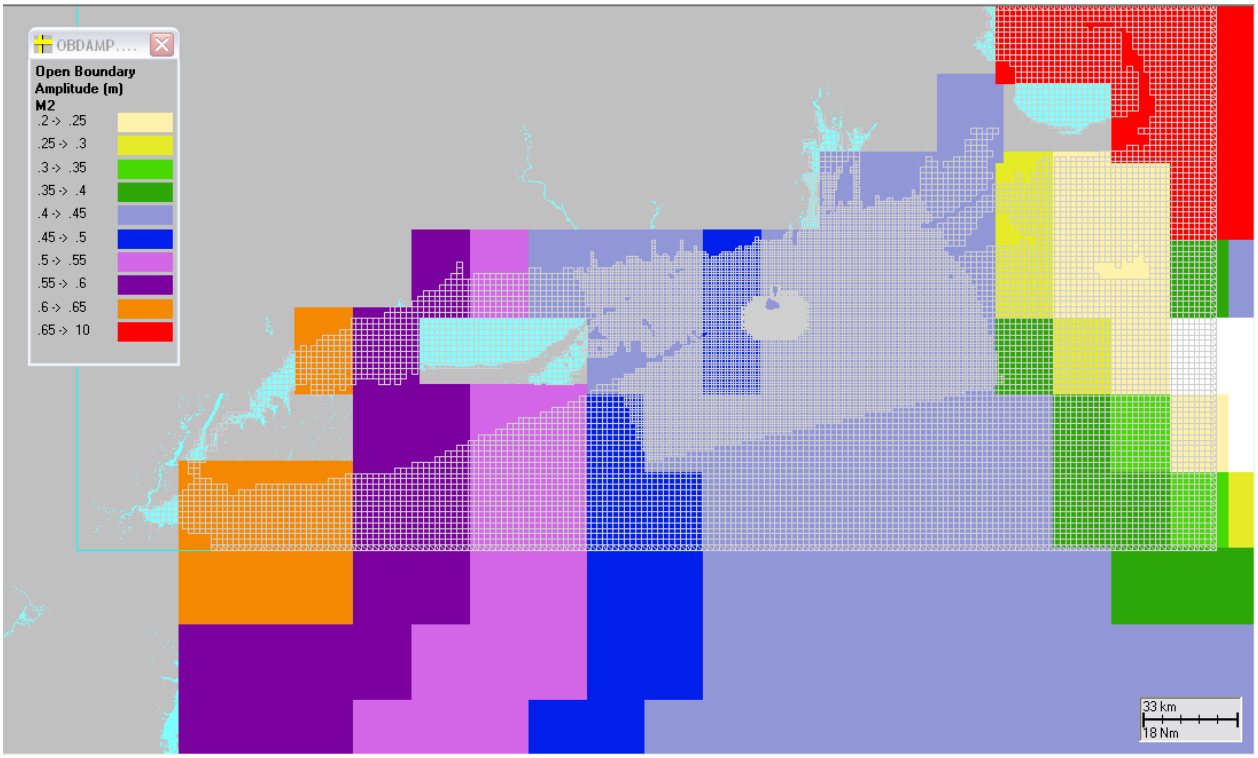

Figure 3-7 Example hydrodynamic model M2 harmonic constituent amplitudes covering the HYDROMAP grid domain.

Once calculated, this harmonic set can be used for any future time or for any simulation length. The bottom currents and shear stress can also be calculated for any future time or past time for use in hindcast assessments where the wind and wave environment and associated sediment concentrations might be known. In addition, application models that use this

hydrodynamic output, such as SSFATE for suspended sediments, can be run for any specific date or period without extra effort.

3.2.2.2 Wind Forcing

After the tides the wind on the water surface is the most important forcing in the study domain. Wind observations recorded at the MDS station were used as input for the wind forcing in the model. A time series plot of the wind vectors is presented in Figure 3-8 for the study time period.

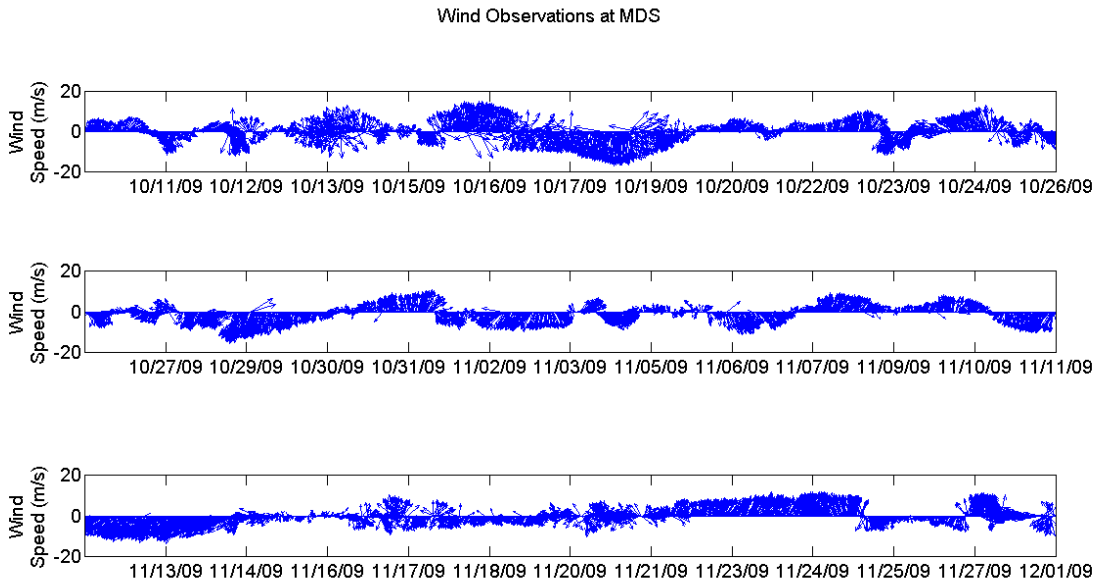

Figure 3-8 Wind time series stick plot of observations at station MDS, located south of Block Island.

3.3 HYDROMAP Model Results

The hydrodynamic model was set up and run for a time period within the field program, running from October 15, 2009 through December 3, 2009. Model predictions of surface elevation and currents were compared to observations during this time period and the following sections present both qualitative and quantitative comparisons.

3.3.1 Tides

The model predicted surface elevations were compared to observation to evaluate the model performance. Both time series comparisons and comparisons of the results of harmonic

decomposition were performed. Figure 3-9 illustrates the time series of observed and predicted surface elevations at Newport, Montauk, POS and POF. This figure shows that the model does well predicting the tidal amplitude and phase over time; the tidal amplitude at all stations is less than 1m. There are periods of time in which the observed surface elevation mean deviates from zero that the model does not capture; these events are likely due to meteorological or large scale ocean currents that are not included in the model forcing.

Table 3-1 and Table 3-3 compare the observed with the simulated harmonic constituent amplitudes and phase respectively. Both observations and the model confirm that the dominating tidal constituent is the M2 constituent which represents between 50-60% of the total tidal amplitude at all stations for both model and observed. The amplitude predictions for all constituents tend to be higher than the observed. The model predictions for the M2 tide are within 20% of the observed with the exception of Montauk. The Montauk station is located in the shallows of an embayment that the mode grid does not resolve in fine detail, this may contribute to the over prediction of tidal amplitude. The predicted amplitudes of the remaining constituents differ in higher percentages, however their contribution to the tidal signal is much smaller than the M2 and therefore even small amplitude differences result in large percentages. The phase predictions for the M2 are also good, with all but Montauk predictions within 16 degrees (33 minutes) of those observed. The remaining constituent phase predictions are all within 37 degrees of those observed.

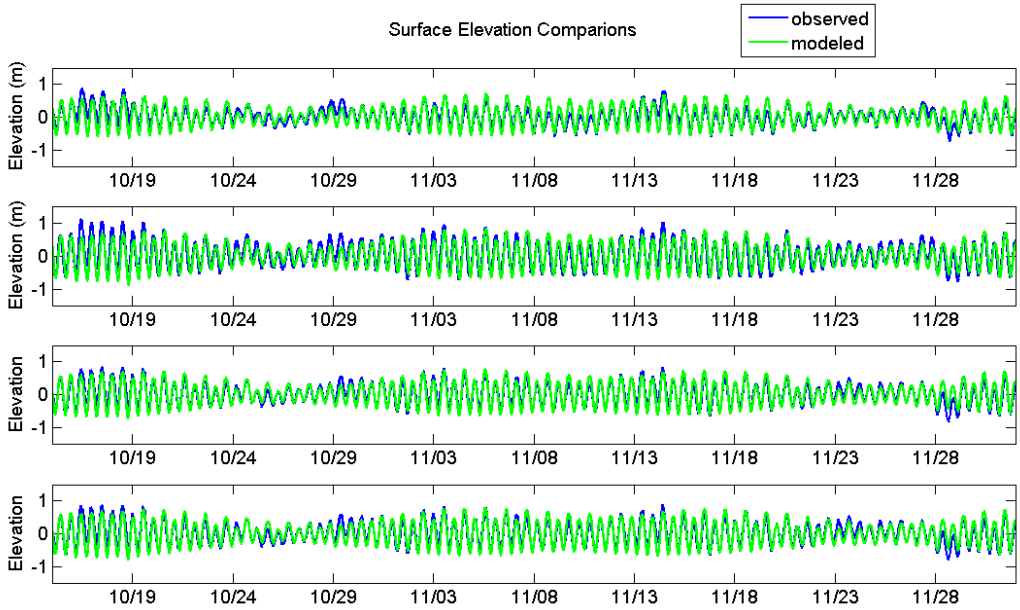

Figure 3-9 Time series comparison of tidal elevations at 4 stations in the study area including stations Montauk, Newport, POS and POF.

Table 3-1 Tidal amplitude comparison between model predictions and observations for the most significant harmonic constants at Newport, Montauk, POS and POF.

Station	Const	Amplitude (m) modeled	Amplitude (m) observed	Difference (Model - Obs)
Newport	M2	0.514	0.505	0.009
Montauk	M2	0.413	0.289	0.124
POS	M2	0.478	0.402	0.077
POF	M2	0.494	0.420	0.075
Newport	N2	0.156	0.107	0.049
Montauk	N2	0.129	0.067	0.062
POS	N2	0.147	0.085	0.061
POF	N2	0.152	0.091	0.061
Newport	S2	0.096	0.106	-0.010
Montauk	S2	0.075	0.048	0.027
POS	S2	0.092	0.085	0.007
POF	S2	0.093	0.090	0.004
Newport	K1	0.093	0.065	0.028
Montauk	K1	0.102	0.074	0.029
POS	K1	0.090	0.073	0.018
POF	K1	0.092	0.068	0.024
Newport	O1	0.063	0.048	0.015
Montauk	O1	0.069	0.047	0.021
POS	O1	0.062	0.046	0.015
POF	O1	0.063	0.049	0.014

Table 3-2 Tidal phase comparison between model predictions and observations for the most significant harmonic constants at Newport, Montauk, POS and POF.

Station	Const	Phase (deg) modeled	Phase (deg) observed	Difference (Model - Obs)	Difference (Model - Obs) minutes
Newport	M2	7	3	4	9
Montauk	M2	25	50	-25	-52
POS	M2	347	4	16	33
POF	M2	351	4	14	29
Newport	N2	353	353	-1	-1
Montauk	N2	8	31	-23	-48
POS	N2	333	351	-18	-38
POF	N2	335	353	-18	-37
Newport	S2	181	156	24	50
Montauk	S2	33	41	-8	-16
POS	S2	360	9	9	19
POF	S2	2	10	-8	-16
Newport	K1	181	156	24	50
Montauk	K1	181	166	15	32
POS	K1	171	158	13	27
POF	K1	172	159	13	26
Newport	O1	176	207	-31	-64
Montauk	O1	176	213	-37	-76
POS	O1	168	200	-32	-67
POF	O1	168	205	-37	-77

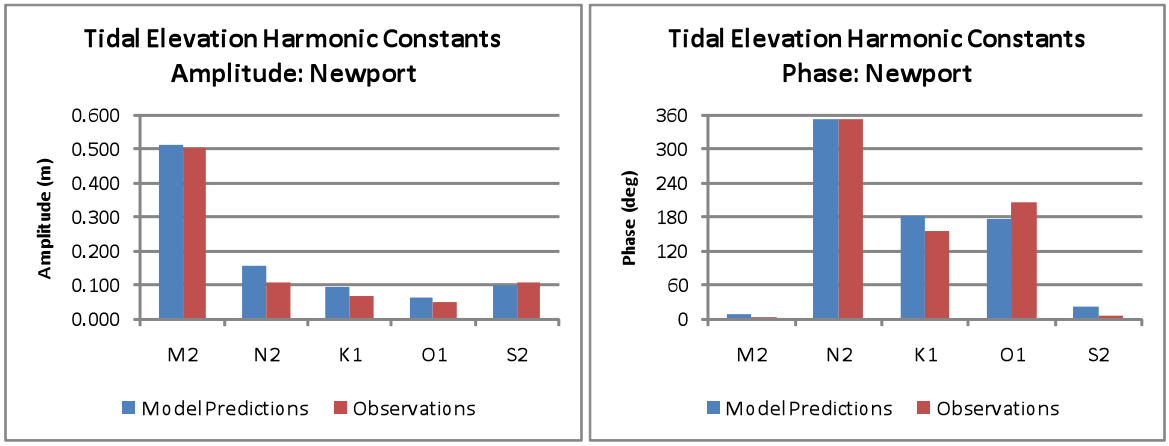

Figure 3-10 Comparison of model predicted and observed tidal harmonic constituent amplitudes and phases for Newport.

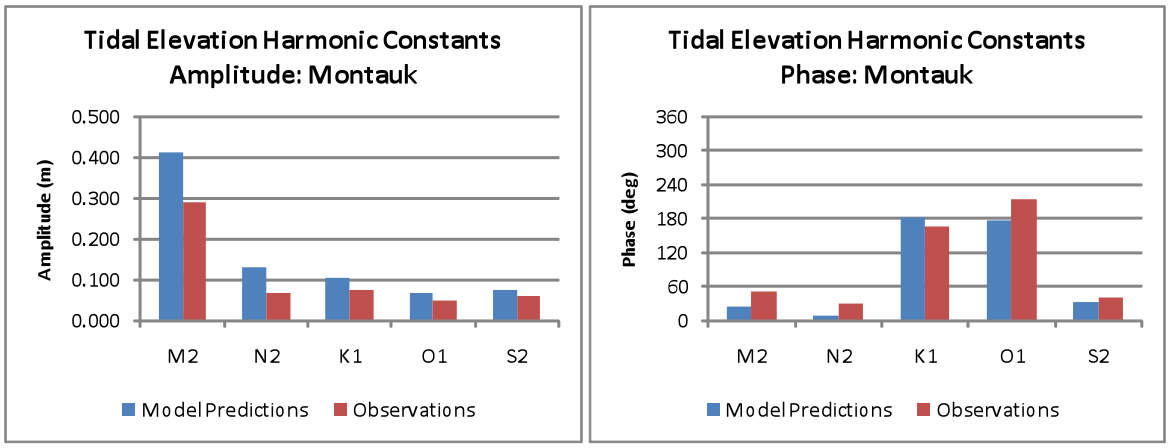

Figure 3-11 Comparison of model predicted and observed tidal harmonic constituent amplitudes and phases for Montauk.

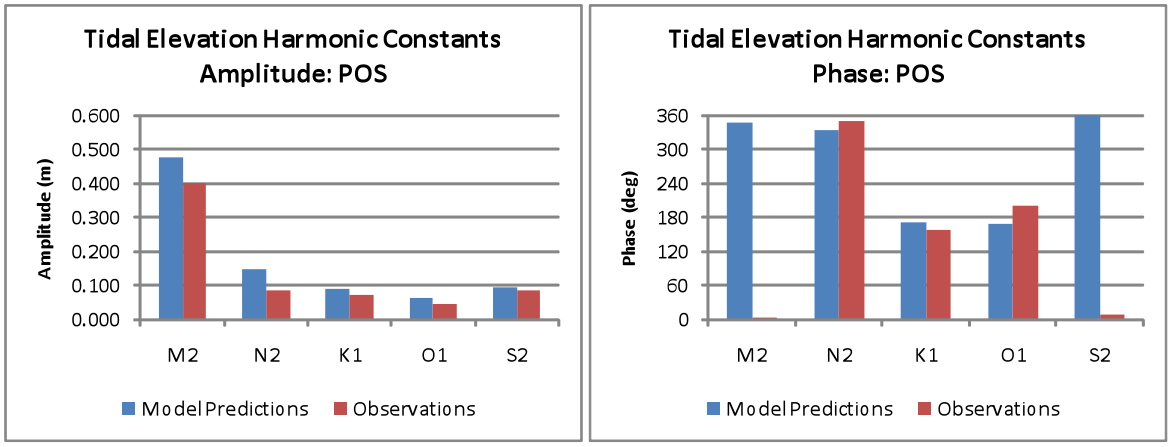

Figure 3-12 Comparison of model predicted and observed tidal harmonic constituent amplitudes and phases for Station POS.

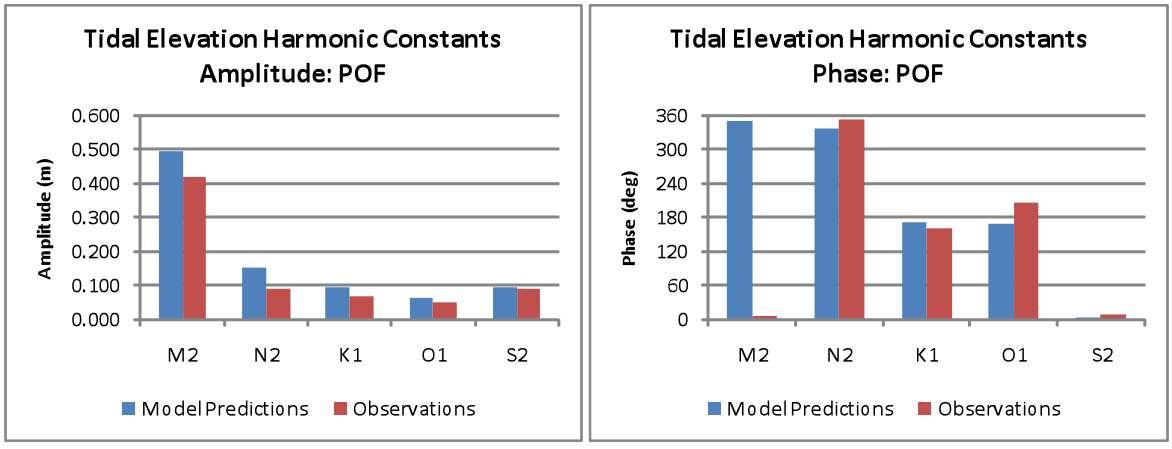

Figure 3-13 Comparison of model predicted and observed tidal harmonic constituent amplitudes and phases for Station POF.

3.2.2 Currents

The model predicted currents were compared to observation to evaluate the model performance. Time series comparisons and comparison of harmonic constituents and tidal ellipses sizes were performed for the study period.

Comparisons of observed vs. predicted currents were made at stations MDS, MDF, POS and POF; Figure 3-14 a & b through Figure 3-16 a & b show the comparison of east/west (U) and north/south (V) velocity components where blue lines represent the observations and green lines the model predictions. Reviewing the time series plots, several major features are apparent at all of the stations. In addition to the presence of the semi-diurnal component of the currents, attributable to the M2 tidal harmonic component as will be discussed below, there is a significant variability in the mean currents, clearly attributable to wind forcing. This response to the atmospheric forcing is most apparent in the U-component of the surface currents, and in the area south of Block Island (MDS and POS) where the currents may be forced to align somewhat in the east/west direction due to the presence of the island itself for wind driven events. It is also clear the model is reproducing both the regularity of the tidal forcing as well as the irregular, event driven response. These plots show that the model captured the trend of the mean current component magnitude as well as the amplitude and phase of each components signal. In addition a comparison of the three time series plots per page (representing the top, middle and bottom currents) shows that the model also represented the vertical profile well.

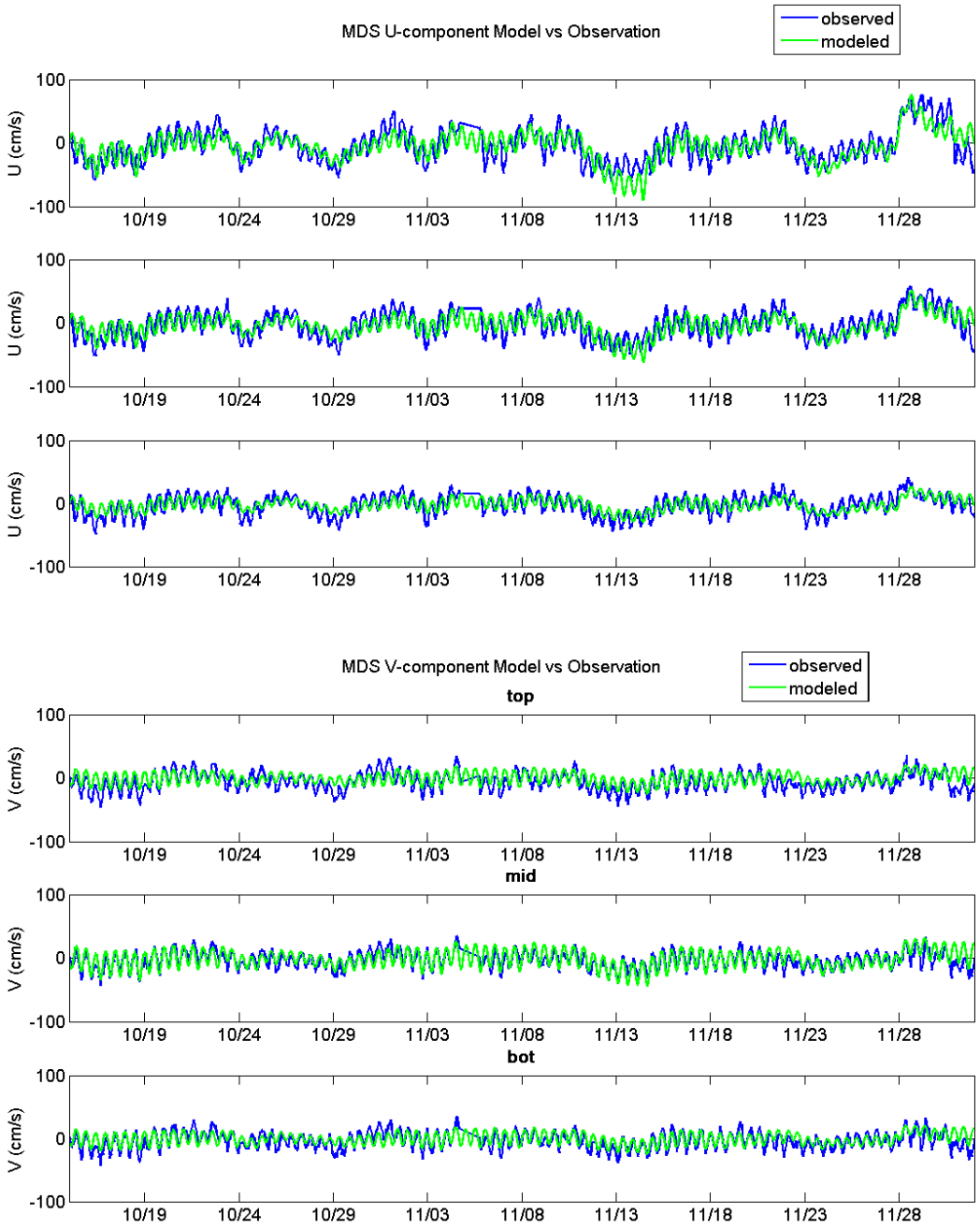

Figure 3-14 Time series comparison of model predicted and observed currents at MDS in the top, middle and bottom layers, for the: a) u-component and b) v-component.

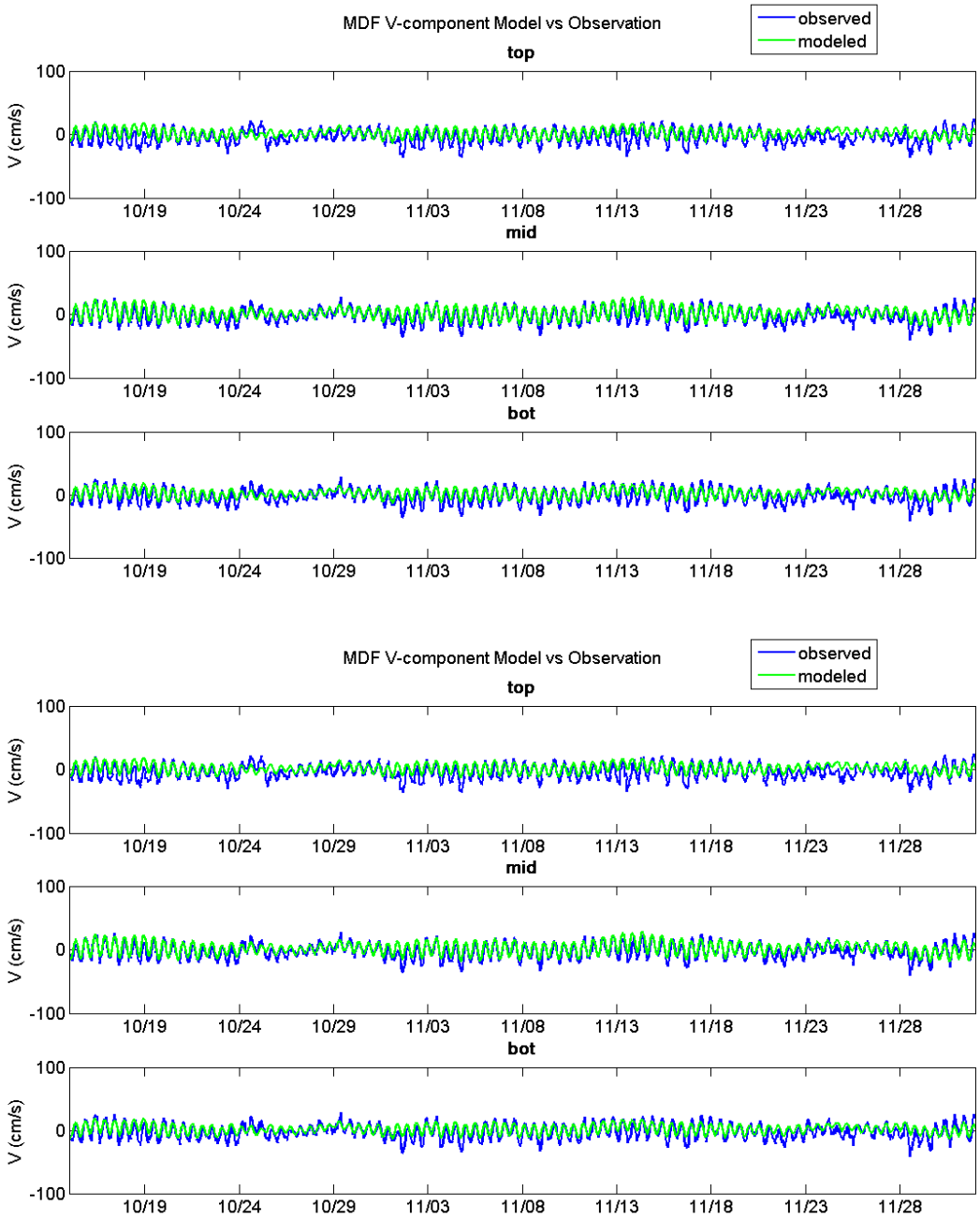

Figure 3-15 Time series comparison of model predicted and observed currents at MDF in the top, middle and bottom layers, for the: a) u-component and b) v-component.

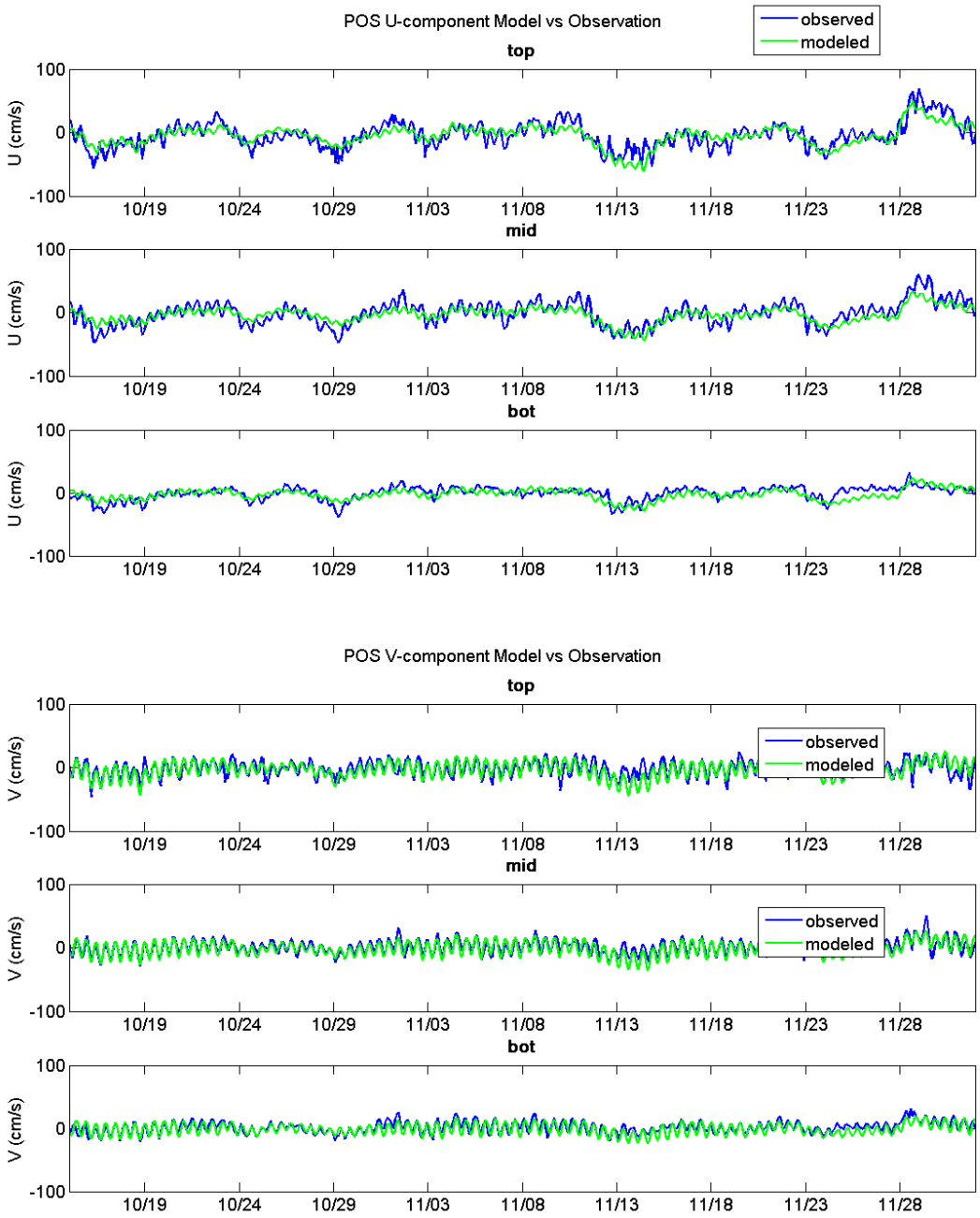

Figure 3-16 Time series comparison of model predicted and observed currents at POS in the top, middle and bottom layers, for the: a) u-component and b) v-component.

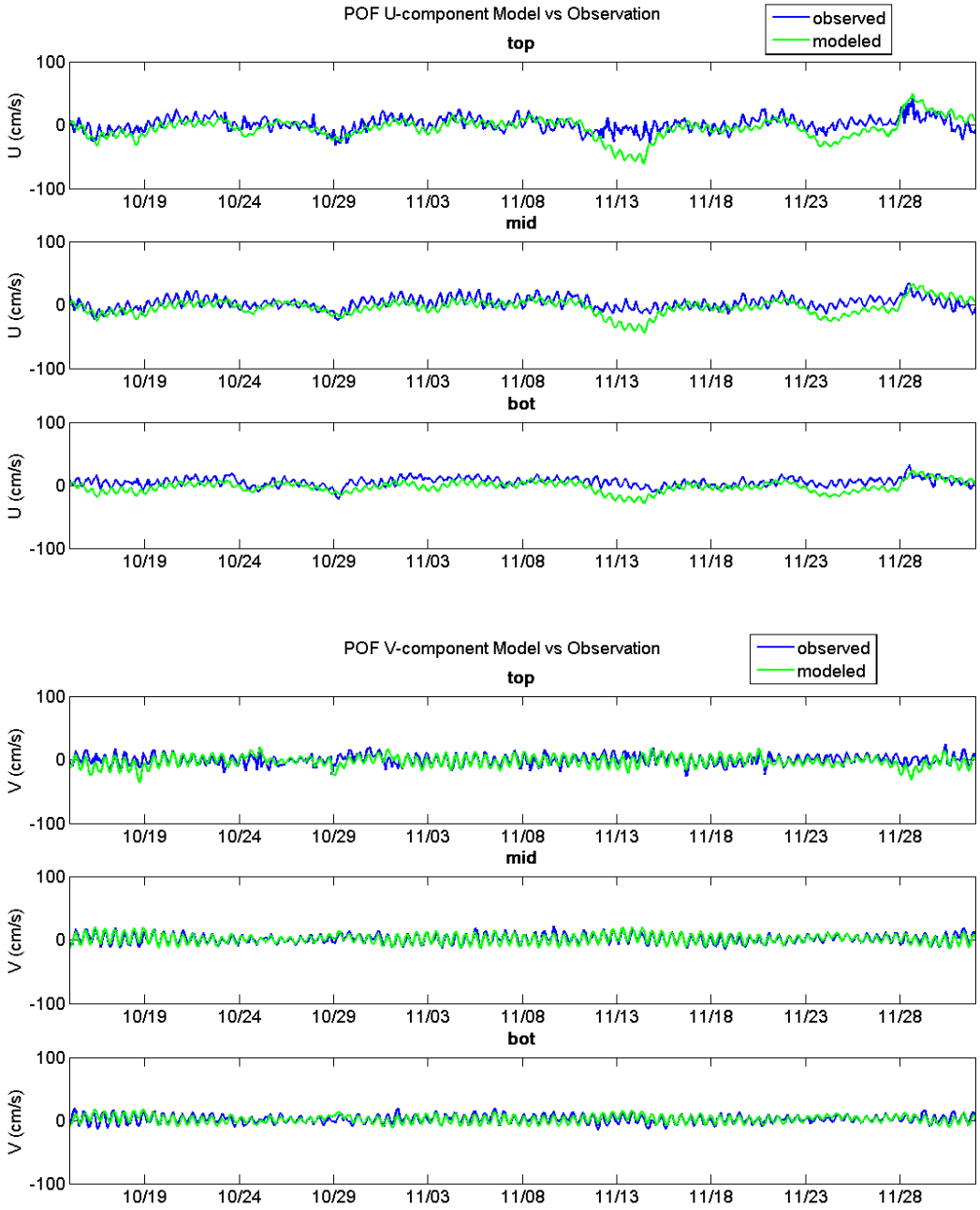

Figure 3-17 Time series comparison of model predicted and observed currents at POF in the top, middle and bottom layers, for the: a) u-component and b) v-component.

To further evaluate the model predictions, harmonic decomposition was performed on both the observed and predicted records of current velocity components for the surface, middle and bottom of the water column. This analysis yielded the major and minor axes of the current ellipses and phases of the contributing harmonic constituents for both observed and predicted current components. For each of the 4 stations the current ellipses were determined and based on

these results a summary of the comparisons is provided in Table 3-3 through Table 3-6 for stations MDS, MDF, POS, and POF respectively. Both observations and model predictions showed that the M2 frequency was the predominant current frequency, containing the majority of the tidal energy. The model predicted the M2 current amplitude best at surface and mid layers and had more variance at the bottom layer, furthermore predictions were better at stations closer to Block Island (MDS and POS) than those further away (at MDF, although the POF comparisons were remarkably good). At the farther stations this could be due to the reduced grid resolution and therefore resolution of bathymetric features in those areas.

Referring to the tables is can be seen that the differences between the model predicted and observed M2 constituent major axes are generally less than 0.02 m/s with a maximum deviation of 0.05 m/s in the MDF bottom current ellipse. The difference in the remaining constituents is variable, remaining less than 0.01 m/s for the majority. The M2 phase comparison between the model predictions and observations is similarly close, with the difference angle remaining less than about 10 degrees with an exception in the bottom currents at both the POS and POF stations. In general, the model predicted tidal current ellipses, driven predominantly by the M2 tidal component, show a close agreement with the observations indicating that the model captures the magnitude and the circulation patterns in the study area.

Table 3-3 Comparison of tidal current ellipses for significant harmonic constants at MDS.

Layer	Constituent	Frequency	Current Ellipse Major Axis (m/s) modeled	Current Ellipse Minor Axis (m/s) modeled	Current Ellipse Phase Angle (deg) modeled	Current Ellipse Major Axis (m/s) observed	Current Ellipse Minor Axis (m/s) observed	Current Ellipse Phase Angle (deg) observed	Major Axis Difference (Model - Obs)	Minor Axis Difference (Model - Obs)
top	O1	0.038731	0.02	0.01	104	0.04	0.01	192	-0.022	-0.003
top	K1	0.041781	0.02	0.01	112	0.04	0.01	178	-0.015	0.002
top	N2	0.078999	0.06	0.02	341	0.02	0.00	338	0.035	0.013
top	M2	0.080511	0.21	0.07	4	0.20	0.07	356	0.014	-0.004
top	S2	0.083333	0.04	0.01	9	0.02	0.01	341	0.012	-0.007
mid	O1	0.038731	0.02	0.01	103	0.03	0.00	173	-0.019	0.005
mid	K1	0.041781	0.02	0.01	105	0.04	0.01	178	-0.015	0.001
mid	N2	0.078999	0.05	0.02	335	0.02	0.01	6	0.030	0.001
mid	M2	0.080511	0.20	0.06	1	0.20	0.07	354	-0.001	-0.009
mid	S2	0.083333	0.03	0.01	6	0.02	0.01	318	0.009	0.000
bot	O1	0.038731	0.01	0.00	98	0.03	0.00	175	-0.015	0.000
bot	K1	0.041781	0.02	0.01	102	0.03	0.00	172	-0.018	0.004
bot	N2	0.078999	0.03	0.01	329	0.03	0.01	5	0.005	-0.003
bot	M2	0.080511	0.14	0.04	357	0.16	0.04	346	-0.022	0.005
bot	S2	0.083333	0.02	0.01	7	0.02	0.01	316	0.004	0.000

Table 3-4 Comparison of tidal current ellipses for significant harmonic constants at MDF.

Layer	Constituent	Frequency	Current Ellipse Major Axis (m/s) modeled	Current Ellipse Minor Axis (m/s) modeled	Current Ellipse Phase Angle (deg) modeled	Current Ellipse Major Axis (m/s) observed	Current Ellipse Minor Axis (m/s) observed	Current Ellipse Phase Angle (deg) observed	Major Axis Difference (Model - Obs)	Minor Axis Difference (Model - Obs)
top	O1	0.038731	0.01	0.00	107	0.03	0.01	157	-0.016	-0.009
top	K1	0.041781	0.01	0.01	127	0.04	0.02	6	-0.022	-0.016
top	N2	0.078999	0.03	0.00	295	0.04	0.02	303	-0.003	-0.015
top	M2	0.080511	0.13	0.04	322	0.15	0.10	310	-0.018	-0.058
top	S2	0.083333	0.03	0.01	314	0.03	0.02	302	0.000	-0.008
mid	O1	0.038731	0.01	0.00	112	0.02	0.01	150	-0.013	-0.009
mid	K1	0.041781	0.02	0.00	115	0.03	0.02	5	-0.018	-0.019
mid	N2	0.078999	0.04	0.01	293	0.04	0.02	301	-0.002	-0.011
mid	M2	0.080511	0.13	0.04	318	0.15	0.10	311	-0.022	-0.059
mid	S2	0.083333	0.03	0.01	315	0.03	0.02	299	-0.003	-0.008
bot	O1	0.038731	0.01	0.00	110	0.02	0.01	147	-0.013	-0.004
bot	K1	0.041781	0.01	0.00	112	0.03	0.02	359	-0.021	-0.018
bot	N2	0.078999	0.02	0.00	288	0.03	0.01	304	-0.009	-0.008
bot	M2	0.080511	0.09	0.03	313	0.14	0.10	311	-0.051	-0.063
bot	S2	0.083333	0.02	0.00	320	0.03	0.01	301	-0.010	-0.010

Table 3-5 Comparison of tidal current ellipses for significant harmonic constants at POS.

Layer	Constituent	Frequency	Current Ellipse Major Axis (m/s) modeled	Current Ellipse Minor Axis (m/s) modeled	Current Ellipse Phase Angle (deg) modeled	Current Ellipse Major Axis (m/s) observed	Current Ellipse Minor Axis (m/s) observed	Current Ellipse Phase Angle (deg) observed	Major Axis Difference (Model - Obs)	Minor Axis Difference (Model - Obs)
top	O1	0.038731	0.01	0.01	103	0.02	0.00	160	-0.014	0.003
top	K1	0.041781	0.02	0.01	108	0.03	0.01	199	-0.018	-0.004
top	N2	0.078999	0.03	0.01	328	0.02	0.01	323	0.011	-0.003
top	M2	0.080511	0.13	0.03	352	0.12	0.05	354	0.007	-0.027
top	S2	0.083333	0.02	0.00	358	0.01	0.01	325	0.007	-0.006
mid	O1	0.038731	0.01	0.01	105	0.03	0.00	160	-0.017	0.001
mid	K1	0.041781	0.02	0.01	107	0.04	0.01	181	-0.020	-0.005
mid	N2	0.078999	0.03	0.01	325	0.01	0.01	320	0.020	-0.004
mid	M2	0.080511	0.13	0.03	350	0.12	0.06	350	0.010	-0.034
mid	S2	0.083333	0.02	0.00	357	0.02	0.01	344	0.003	-0.007
bot	O1	0.038731	0.01	0.00	103	0.02	0.00	164	-0.007	0.003
bot	K1	0.041781	0.01	0.01	106	0.02	0.00	189	-0.008	0.006
bot	N2	0.078999	0.03	0.00	323	0.02	0.01	298	0.004	-0.002
bot	M2	0.080511	0.11	0.02	348	0.08	0.01	316	0.031	0.011
bot	S2	0.083333	0.02	0.00	0	0.02	0.01	9	0.001	-0.011

Table 3-6 Comparison of tidal current ellipses for significant harmonic constants at POF.

Laye	Constituen	Frequenc	Ellipse Axis modele	Ellipse Axis modele	Ellipse Angle modele	Ellipse Axis observe	Ellipse Axis observe	Ellipse Angle observe	Major Differenc (Model -	Minor Differenc (Model -
to	O	0.03873	0.0	0.0	10	0.0	0.0	10	-	0.00
to	K	0.04178	0.0	0.0	15	0.0	0.0	1	-	-
to	N	0.07899	0.0	0.0	29	0.0	0.0	32	0.00	-
to	M	0.08051	0.0	0.0	32	0.0	0.0	30	0.00	-
to	S	0.08333	0.0	0.0	31	0.0	0.0	31	0.00	-
mi	O	0.03873	0.0	0.0	11	0.0	0.0	12	-	0.00
mi	K	0.04178	0.0	0.0	11	0.0	0.0	16	-	-
mi	N	0.07899	0.0	0.0	29	0.0	0.0	30	0.00	-
mi	M	0.08051	0.0	0.0	31	0.0	0.0	31	0.00	-
mi	S	0.08333	0.0	0.0	31	0.0	0.0	31	0.00	0.00
bo	O	0.03873	0.0	0.0	11	0.0	0.0	13	-	0.00
bo	K	0.04178	0.0	0.0	11	0.0	0.0	7	-	-
bo	N	0.07899	0.0	0.0	28	0.0	0.0	26	-	-
bo	M	0.08051	0.0	0.0	31	0.0	0.0	28	-	-
bo	S	0.08333	0.0	0.0	32	0.0	0.0	27	0.00	0.00

Figure 3-18 and Figure 3-19 show examples of model predicted flood and ebb tidal surface currents in the OSAMP and RE zone area, respectively. The OSAMP area, covering the area between the entrance to Long Island Sound on the west, to the entrance to Buzzards Bay to the east and Narragansett Bay to the north is clearly a complicated domain. During the flood tide, the currents essentially bifurcate near the center of the OSAMP area (Rhode Island Sound), heading west into Long Island Sounds at the western edge, east into Buzzards Bay on the eastern edge and north into Narragansett Bay to the north. The currents exhibit the opposite pattern on the ebb tide. An acceleration of current speeds is clearly seen in the narrow straights between the eastern end of Long Island and Block Island during both the flood and ebb stages. This partly due to the narrowing of the area feeding Long Island Sound and partly due to the shallow areas on both sides of the central channel through the straights (see Figure 3-5).

The complicated flood and ebb patterns seen in the larger OSAMP domain, affect the circulation patterns in the RE zone south of Block Island as well. There is often a split in the flow to either side of the island during both flood and ebb stages, where the current speeds are considerably larger on the west side of the zone as a function of the narrowing and swallowing of the straights area between Block Island and Long Island (Figure 3-19). Model predicted surface current speeds in the RE zone range from a high of 0.5 (m/s) in the western portion to 0.25 (m/s) to the area southeast of Block Island.

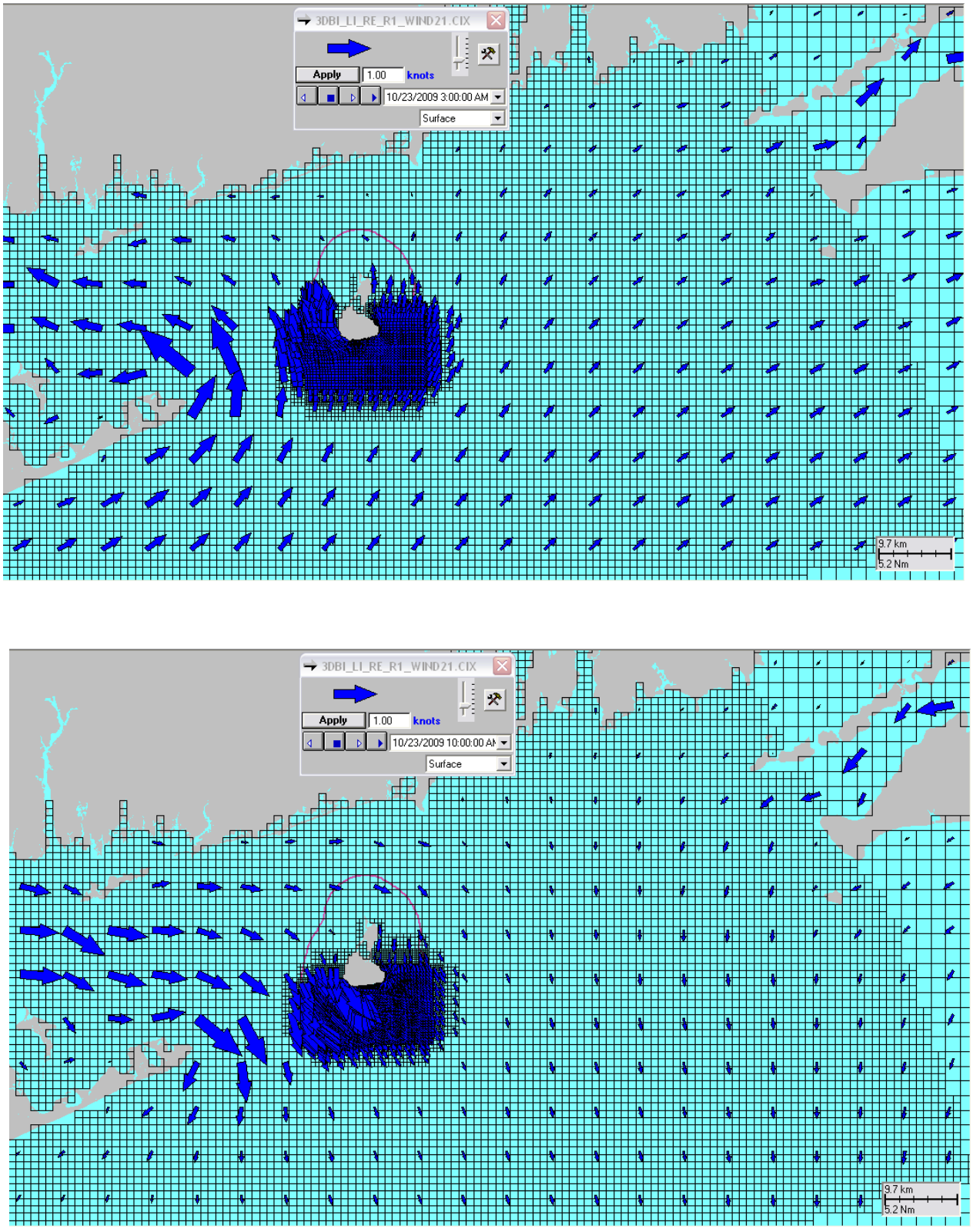

Figure 3-18 Example model predicted surface current vector map for the OSMAP area, showing every third current vector for: a) flood tide and b) ebb tide.

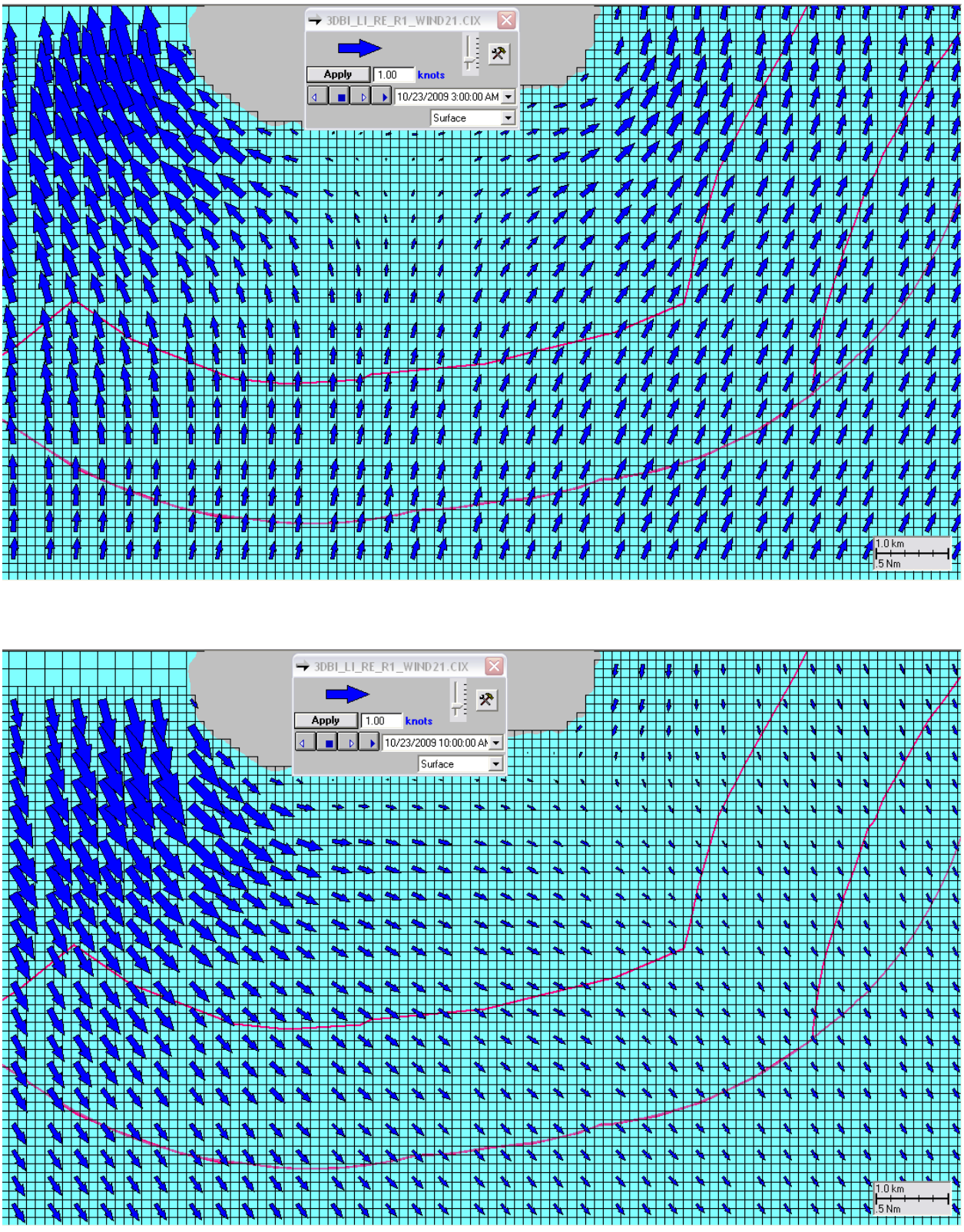

Figure 3-19 Example model predicted surface current vector map in the RE zone for: a) flood tide and b) ebb tide.

The model predicted bottom currents in the RE zone are presented in Figure 3-20(a) and (b) for the flood and ebb tidal stages respectively. Again, the currents show a large variability ranging from the largest currents, 0.25 (ms/) in the western portion of the RE zone near the straights to the smallest currents 0.15 (m/s) in the deeper eastern section near the shipping channel. Figure 3-21(a) and (b) show the contours of bottom current speed for these examples of flood and ebb.

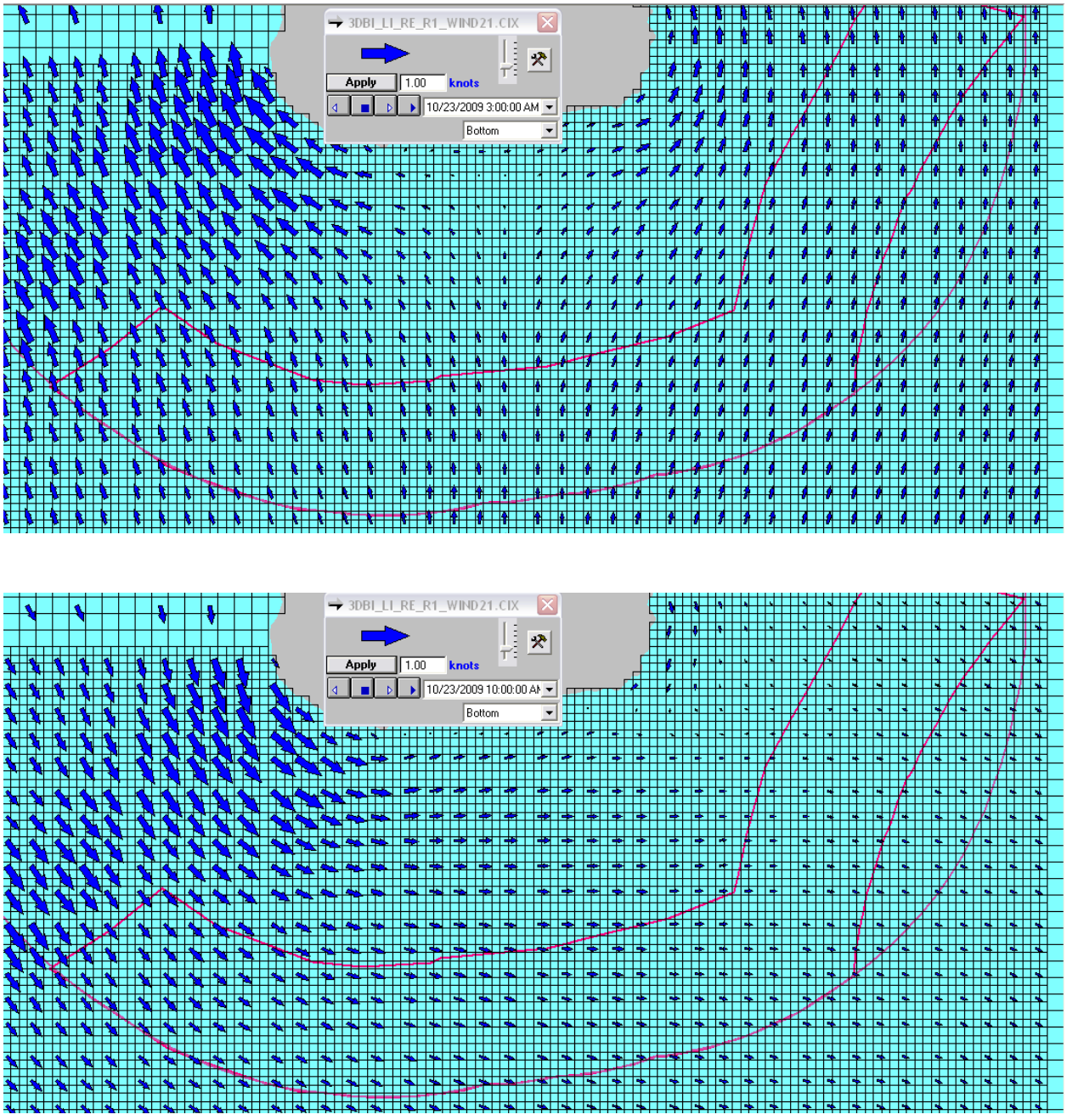

Figure 3-20 Example model predicted bottom current vector map in the RE zone for: a) flood tide and b) ebb tide.

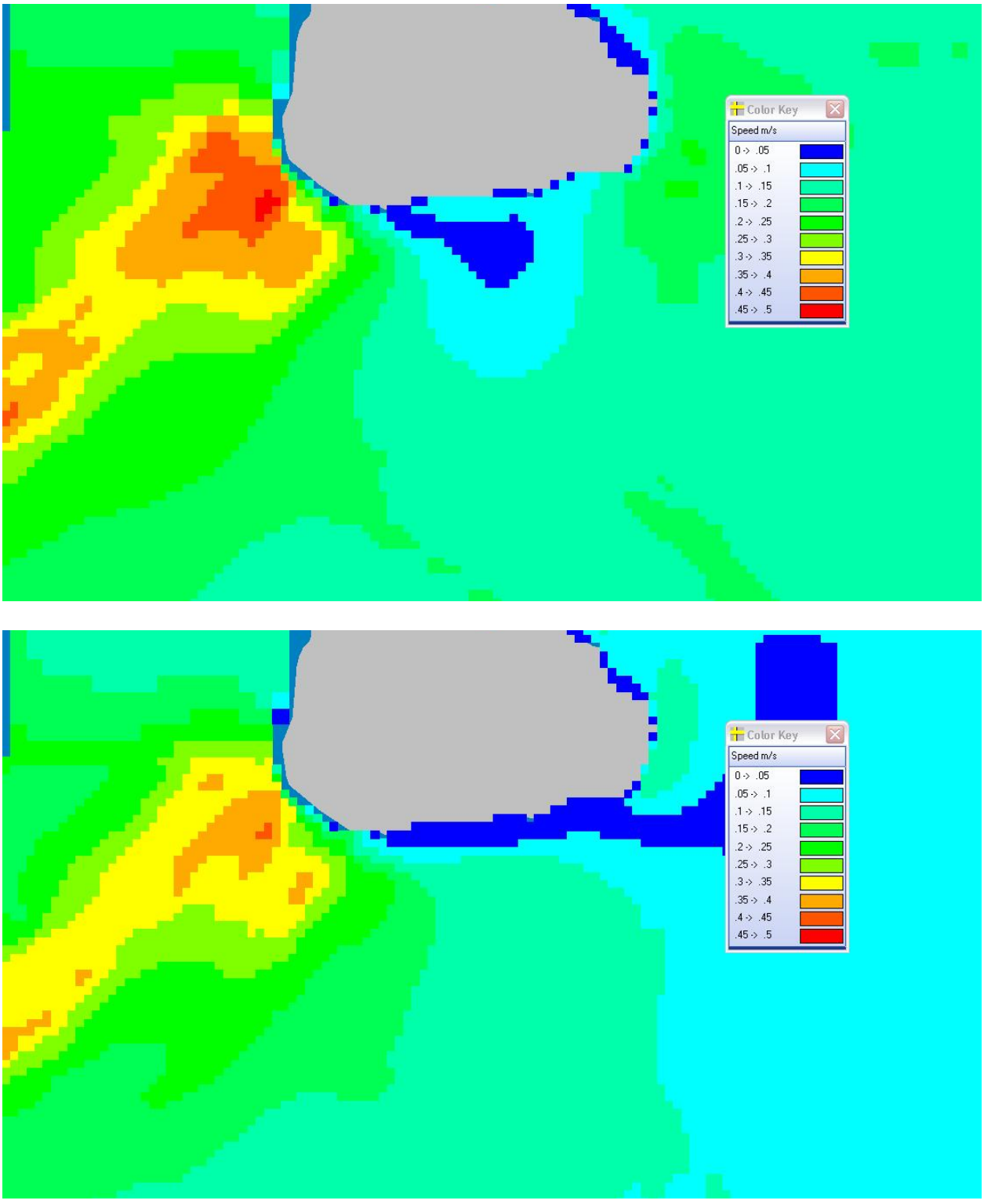

Figure 3-21 Example model predicted bottom current speed map in the RE zone for: a) maximum flood tide and b) maximum ebb tide.

4 Discussion and Conclusions

It has been proposed that a wind turbine farm be developed off the southeastern coast of Block Island, south of the Rhode Island mainland. The development of an offshore wind farm will necessarily require a great deal of underwater construction including drilling and setting the piles for the turbine foundations, burying electrical transmission cables and other infrastructure construction tasks. During this period additional water column suspended sediments may impact the construction areas and it is therefore of interest to understand what the current speeds and circulation patterns are in the development area. To that end, Applied Science Associates, Inc. (ASA) has performed a hydrodynamic modeling study to estimate the currents and circulation in the renewable energy (RE) development area with a focus on bottom stress and currents. The results of the study will be used by URI scientists to determine the potential for sediment re-suspension and transport of suspended sediment that might results from the construction and operation of the small wind farm.

ASA used the HYDROMAP model system, which calculates velocity vectors on a stepwise continuous variable rectangular grid system. A benefit of the model is that it allows coarse grid resolution in the areas offshore the coast of Rhode Island and finer resolution in the Block Island Sound area and renewable energy zone area of interest. The model was driven by tidal harmonic data along the open boundaries and wind stress at the surface. The model predictions were compared to observations collected as part of the OSAMP, including four ADCP current meter locations and NOAA tidal elevation data at Montauk and Newport. The comparisons showed that the model not only adequately predicted the tidal forcing response in the study area, but also the longer period episodic wind driven events that are characterized by passing weather systems. The model appeared to be able to reproduce both the horizontal spatial variability in the system as well as the vertical profile of the currents, as represented by the ADCP observations at the surface, mid and bottom of the water column.

Both observations and the model predictions confirm that the dominating tidal constituent is the M2 constituent which represents between 50-60% of the total tidal amplitude at all stations. The amplitude predictions for all constituents tend to be higher than the observed but are generally within 20% of the observed with the exception of Montauk. The Montauk station is located in the shallows of an embayment that the mode grid does not resolve in fine detail, this may contribute to the over prediction of tidal amplitude.

Review of the current analysis indicates that the differences between the model predicted and observed M2 constituent major axes are generally less than 0.02 m/s with a maximum deviation of 0.05 m/s in the MDF bottom current ellipse. The difference in the remaining constituents is variable, remaining less than 0.01 m/s for the majority. The M2 phase comparison between the model predictions and observations is similarly close, with the difference angle remaining less than about 10 degrees with an exception in the bottom currents at both the POS and POF stations. In general, the model predicted tidal current ellipses, driven predominantly by the M2 tidal component, show a close agreement with the observations indicating that the model captures the magnitude and the circulation patterns in the study area.

The bottom currents were further reviewed and an understanding of the bottom speed developed. The renewable energy zone follows the edge of the 3 mile state waters limit along the southern portion of the line, from the straights between Long Island and Block Island to the west, to the shipping channel exclusion zone on the east. The zone is approximately 2 km wide, and has a bulge on the east side representing the shipping channel exclusion zone. Bathymetry in the RE zone is quite variable ranging from less than 10m, in the western portion to greater than 35m to the east. This bathymetric range and the straights to the west produce a significant variability in the bottom speeds as well, ranging from a high in the shallow western portions of 0.25 m/s down to a high in the eastern portions of 0.15 m/s.

5 References

Davies, A.M. 1977: The numerical solutions of the three-dimensional hydrodynamical equations using a B-spline representation of the vertical current profile. Bottom Turbulence. Proc. 8th liege colloquium on Ocean hydrodynamics. J. C. J. Nihoul. Ed.. Elsevier. 27-48.

Gordon, R.B. and M.L. Spaulding, 1979. A nested numerical tidal model of the Southern New England Bight. Report to NOAA, Hampton, VA, From Univ. of Rhode Island, Kingston RI.

Isaji, T.E., Howlett, C. Dalton and E. Anderson, 2001. Stepwise- continuous-variable-rectangular grid, in Proceedings of the 7th International Conference on Estuarine and Coastal Modeling, St. Pete Beach, FL, November 5-7, 2001.

Isaji, T. and M. Spaulding, 1984. Notes and Correspondence. A model of the tidally induced residual circulation in the Gulf of Maine and Georges Bank, *Journal of Phys. Ocean.,* June. pp. 1119-1126.

Mukai, A.M., Westerink, J.J., and Luettich, R.A., 2001. Guidelines for using the Eastcoast 2001 database of tidal constituents within the western North Atlantic Ocean, Gulf of Mexico

and Caribbean Sea, Coastal and Hydraulics Technical Note CERD/CHL CHTEN-IV-40, U.S. Army Engineer Research and Development Center, Vicksburg, MS.

National Geophysical Data Center, 1998. GEOphysical Data System for Hydrographic Survey Data, National Ocean Service, Ver. 4.

National Geophysical Data Center, 2001. 2-Minute gridded global relief data, (October 2001) CD-ROM.

Owen, A., 1980. A three-dimensional model of the Bristol Channel. J. Phys. Oceanog. 1987. 10, 1290-1302.

7.

Fog and Icing Occurrence, and Air Quality Factors

for the Rhode Island Ocean Special Area Management Plan 2010

by

John Merrill

University of Rhode Island, June 28, 2010

Executive Summary

An analysis of three focused environmental concerns for the Rhode Island Ocean SAMP area is presented here. The occurrence of fog and the potential for accumulation of ice on moving vessels, both potentially significant hazards to navigation and marine operations, are estimated based on meteorological and oceanographic data from nearby offshore towers. Also, the annual variation of surface ozone mixing ratios observed at Narragansett, RI, adjacent to the Ocean SAMP domain, is presented and analyzed. Rhode Island (and other New England states) does not meet current ambient air quality standards. Extensive marine operations in the offshore area would lead to additional emissions of pollutants, including ozone precursors. An analysis of the impact of extensive offshore marine operations is beyond the scope of this work.

Table of Contents

List of Figures

Abstract

An analysis of three focused environmental concerns for the Rhode Island Ocean SAMP area is presented here. The occurrence of fog and the potential for accumulation of ice on moving vessels, both potentially significant hazards to navigation and marine operations, are estimated based on meteorological and oceanographic data from nearby offshore towers. Also, the annual variation of surface ozone mixing ratios observed at Narragansett, RI, adjacent to the Ocean SAMP domain, is presented and analyzed. Rhode Island (and other New England states) does not meet current ambient air quality standards. Extensive marine operations in the offshore area would lead to additional emissions of pollutants, including ozone precursors. An analysis of the impact of extensive offshore marine operations is beyond the scope of this work.

1 Introduction

This report summarizes work and results on study of three focused environmental concerns for the Rhode Island Ocean SAMP area. These are the occurrence of fog, the occurrence of icing conditions, and the mixing ratio of ozone in the context of air quality standards. These topics would fall naturally into a comprehensive analysis of the meteorology of the area, but have been studied separately given the organizational approach selected for the overall study.

2 Background

The occurrence of fog, and of vessel icing, present distinct hazards to marine operations in many areas, and the Ocean SAMP domain is among them. While these hazards are well known to experienced mariners, particularly those who have worked in New England coastal waters, it is deemed important to describe and document the nature and extent of their occurrence. The ozone air quality information provided here is less directly tied to marine operations. Rather it relates to the interplay of ambient air quality regulations, impacts of local emissions and downstream effects.

Fog forms in various circumstances in different places, and these varying conditions lead to its characterizations as radiation fog, advection fog, arctic steam smoke, or inversion fog. These and other types are described with specific reference to the marine environment by Kotsch (1983). The most common type in coastal marine environments, and the type most often observed by far in the Ocean SAMP area, is advection fog. When warmer air blows over cold water, the air gives up heat, and if it cools to the dew point, condensation takes place and fog forms. Because of the relatively low drag in the marine environment (relative to wind flow over a land surface), little mixing occurs even when near-surface wind speed approaches 15 m s^{-1}, and fog persists. In contrast, when winds are stronger or the drag greater, mixing through a deep layer reduces the likelihood of fog formation in favor of a stratiform cloud deck.

A concise but informative discussion is in Hsu (1988), Section 7.3. This includes figures from Kotsch (1983) illustrating areas where fog formation is common in US coastal areas. The broad estimates of the frequency of fog formation in New England shown there provide a useful point of comparison for the frequencies calculated here, as discussed in Section 5, below.

Ice accretion is a significant safety hazard in cold waters, especially for small vessels with limited freeboard, and in circumstances where wave-generated spray is common. An extended discussion is in Kotsch (1983), Chapter 10. As detailed below, however, in the work presented here a more recent formulation is used. Overland *et al*. (1986) presented a method for estimating icing potential dependent upon ambient environmental variables. The method is based on numerous observations of icing events, but by design is not specific to a particular vessel type or a specific location. The target application was operational forecasting by the weather service, using data fields for sea surface temperature and forecast wind and air temperature fields. In Overland (1990) additional analysis led to a slightly revised formulation. The careful statistical analysis of Overland *et al*. (1986) and the discussion of operational forecasting and verification in Overland (1990) constitute a convincing case for the usefulness of this approach.

The analysis of air quality data presented here is limited to near-surface ozone mixing ratio data. Ozone is one of the 6 "criteria pollutants" regulated by the Environmental Protection Agency. Attainment of compliance with clean air requirements is based on the National Ambient Air Quality Standards (NAAQS). The focus on ozone here is based on its being the substance for which compliance is most often not attained in onshore areas adjacent to the Ocean SAMP domain, and on the availability of routine air quality monitoring data for ozone at a site in Narragansett. The NAAQS 8 hour standard for O_3 is met if the 3 year average of the fourth-highest daily maximum mixing ratio at each monitoring site does not exceed 0.075 ppm (parts per million) by volume. At each site the three highest 8-hour values are noted, but do not constitute a violation. It is worth noting that peak 1-hour values and longer-term averages are not regulated directly.

Surface ozone mixing ratios have been declining in recent years in the US in response to regulatory measures. Nevertheless, Rhode Island remains a moderate non-attainment area, and the standard is not met at any of the three monitoring sites in Rhode Island. The ozone mixing ratio varies in time in a way that differs among the monitoring sites. This variation is informative in the context of on-shore/off-shore variations. Also, the EPA has proposed strengthening the standard for ozone to make it consistent with the recommendations of its panel of advisors. This change will make meeting the standard more challenging.

3 Methods

Data acquired at two offshore towers have been analyzed for the occurrence of fog, and at one of them of icing conditions. Surface ozone data acquired for air quality monitoring have been used to prepare a composite view of the ozone distribution and variation. In this section the sources of the data and the methods used in the analysis are described.

The first set of offshore meteorological data are from sensors mounted on the Buzzard's Bay Tower, BUZM3, which is owned and maintained by the National Data Buoy Center. The observations are distributed and archived under WMO Station ID 44070. The tower is at 41.397˚N, 71.033˚W, in Buzzard's Bay, west of the Elizabeth Islands (and Martha's Vineyard), and SSW of New Bedford, MA. The relevant meteorological sensors are located between 24 and 25 meters above mean sea level. Sea surface temperature measurements, needed for the analysis of icing conditions, are from 1 m below the water surface.

The estimates presented here are based on data from BUZM3 for the period 1997-2009. Data are recorded continuously, but there are gaps in the availability of some data owing to equipment failures. In the case of the meteorological instruments at BUZM3 the outages typically extend over weeks or months, and short-lived outages are uncommon. This patterns has implications for dealing with the missing data, as discussed further below.

The second site with offshore meteorological data is the Martha's Vineyard Coastal Observatory, MVCO, which is owned and maintained by the Woods Hole Oceanographic Institution. The Air-Sea Interaction Tower at the MVCO is 3 km offshore of South Beach, Martha's Vineyard, MA, in 15 m deep water in the Atlantic Ocean at 41.325˚N, 70.567˚W. Air temperature and relative humidity data from the offshore tower are used here. Outages in the data from the ASIT instruments are infrequent and brief during the period analyzed here. The available data are for the years 2007-2009.

The ozone mixing ratio data used here are in an archive maintained for the US EPA. The data are acquired by the Rhode Island Department of Health using instrumentation at the Narragansett Laboratory of the EPA, at the northern edge of the Bay Campus of the University of Rhode Island. Hourly average ozone mixing ratio values are available; periodic calibration procedures lead to missing data points every other day or so.

3.1 Analysis of meteorological data for fog

Air temperature and dew point values were used for fog occurrence estimation at the BUZM3 tower. Here a day is considered foggy when the air and dew point temperatures are equal at some point. It is important to note that fog can persist when the indicated relative humidity is less than 100%, and that non-foggy conditions can prevail for some time at 100% relative humidity At the BUZM3 tower the aggregate data availability for the suite of sensors needed here for the period used is close to 60%, so that in most months there are the equivalent of approximately 8 years of data for the years 1997-2009. Fog occurrence frequency estimates have been averaged over the heterogeneous, temporally discontinuous periods of data availability. The assumption that the absence of data is uncorrelated with the presence or absence of fog is well justified.

3.2 Analysis of meteorological data for icing

The icing potential was evaluated using a formulation based on data analyzed by Overland *et al*., 1986, as revised and discussed by Overland (1990). The underlying analysis is for a categorical prediction of potential icing rate: light, moderate or heavy. In Overland (1990) a fourth category, extreme, was added. Data (or forecast estimates) for the wind speed and the air and water temperature are used to calculate a predictor, and the potential icing rate categories correspond to specified ranges of the predictor value. The predictor value is proportional to $V_a(T_f - T_a)$, that is, to the product of the wind speed V_a and the difference between T_f, -1.8˚C, the freezing temperature of sea water, and the air temperature, T_a. The predictor value decreases with increasing values of $(T_w - T_f)$, the difference between the freezing temperature of seawater and the ambient sea surface temperature. Heavy and extreme ice accretion potentials are not expected in the Ocean SAMP area, as these are present only when the ambient water temperature is below 0˚C. Icing is generally not observed when the water temperature is greater than 6˚C, so in most months of the year, and on many days during the winter months there is no potential for ice accretion. In the analysis presented below we converted the ice accumulation predictor from a categorical variable to a continuous variable using a polynomial formulation from Overland (1990). In the results presented in the following we used directly observed values of these environmental parameters, not the forecast or analysis data type for which the underlying analysis was designed. This difference is not expected to weaken the analysis to any significant extent, as the categories cover a range of ice accumulation rates, and the accuracy of the observations is high. It is important to note that the analysis presented here relates to vessels underway in marine operations. It is not suited to vessels that are stationary, nor to stationary

structures of any kind. The estimates presented and discussed below can, however, be considered as very conservative upper limits for icing potential for stationary vessels and structures. In these situations the reduced occurrence and intensity of wave breaking because the hull or structure is stationary lessens the volume of water raised above the sea surface, reducing the icing potential dramatically.

3.3 Analysis of air quality data

The ozone data have simply been plotted in a way that makes clear the multiple forms of variation present in the data themselves. Hourly average data for each day are juxtaposed in a vertical column, with data for each day adjacent to that for the next. The result is a time of day vs. day of year display of the data, with color-fill values indicating the hourly-average ozone mixing ratio for each day and time.

4 Results

The annual distribution of the **occurrence of fog** estimated using thermodynamic data at the BUZM3 tower is shown in the upper panel of Fig. 1, while the lower panel shows the quantity of data available in each month. During the months of March-May and October-December there are typically between 3 and 4 foggy days per month at this site. As expected, there is a significantly higher occurrence of fog during the months of June, July and August. In these months the flow of warm, moist air over water that has not yet reached its maximum temperature is particularly favorable for the formation of fog. The occurrence of foggy days in these months is between 6 and 10 days per month, on average. Given the assumptions needed to complete this analysis and the variability in the formation and persistence of fog, a judicious interpretation of these results would be simply that during these three months the occurrence of fog is more likely than at other times, and that fog may be present 20-30% of the time.

As noted above, these are aggregate results for periods when data from both the air temperature and dew point instruments are available, for the period 1997-2009. As indicated in the bottom panel of Fig. 1, the joint availability of the two data types varies around 60%.

Related results for the occurrence of fog using thermodynamic data from the offshore Air-Sea Interaction Tower near the Martha's Vineyard Coastal Observatory are shown in Fig. 2. Both the overall frequency of occurrence and the variation through the year differ from the BUZM3 site data shown in Fig. 1. The highest rate of occurrence at the MVCO site is somewhat lower than at the BUZM3 location, and elevated frequencies extend into September and October at MVCO,

later in the year than at BUZM3. However, the differences may have limited significance. The peak frequencies are in the same range, and the occurrence of persistent, widespread fog may not differ significantly between these sites.

The annual variation of the **occurrence of icing days** at the BUZM3 site and the corresponding days of data availability are shown in the upper and lower panels, respectively, of Fig. 3. The count of days when light and moderate accumulation of ice could be expected on vessels underway is shown by the light and dark bars in the upper panel of Fig. 3, respectively. As expected, the threat of icing conditions is greatest during the winter months, when air temperatures are low and wind speeds are relatively high. The number of days when the icing potential could be expected to fall in the moderate category is less than 1 per month at all times, and approaches this value only in January. The corresponding estimate for the light accumulation category is higher than 5 days per month in December, January and February.

The uncertainty in the peak values as estimated here may be significant because of the limitation in the availability of data. Because icing is not especially common in this area, missing data periods may happen to include the very conditions we seek to document. In this context it is worth noting that some of the months with the least days of data availability fall in the winter, when icing conditions are most common. Thus the values shown in Fig. 3 should be taken as a lower limit. However, as discussed in the following paragraph, the majority of the icing predictor estimates suggest only very light accumulation rates.

As noted in Section 3, above, the icing rate estimation algorithm yields values in three or four categories. The distribution of the occurrence of (days of) icing *vs*. expected rate of icing is shown in Fig. 4, using the parameterized characterization for the icing potential as a continuous variable discussed by Overland (1990). The upper limit of the low and moderate categories are indicated by the red, vertical lines. Note that the vast majority of cases in the low category fall are at the low end of the accumulation rate scale. The relatively few cases in the moderate category, similarly, fall at the low rate side of the category domain. There are no cases that fall in the high accumulation potential category.

Time of day vs. day of year displays of the surface ozone mixing ratio measured onshore at Narragansett, RI, are shown in Fig. 5; panels a) through g) show data for 2003 through 2009. The filled colors indicated mixing ratio values in 5 ppbv (parts per billion by volume) increments, as indicated by the color bar at the right, and the intervals in black include values exceeding 125 ppbv. The green/yellow transition is at 75 ppbv, a limit in current regulations; periods of 8 hours

at or above this mixing ratio are counted toward non-compliance with EPA ambient air quality standards. Periods exceeding this value occur irregularly each year. Ozone decreases at night, in the absence of light to drive photochemical production, and low values are observed to extend well after sunrise on many days at this site.

In 2004 there were unusually few occurrences of high ozone at Narragansett. In 2006 there was a highly polluted period in July. In 2007 there were frequent pollution outbreaks in June, July and August, and an event extending over several days occurred in July, 2008. The structure and variability of the ambient ozone concentration as observed adjacent to the Ocean SAMP area is a reminder of the role of anthropogenic emissions of precursors, leading to significant pollution events.

5 Discussion

The conditions conducive to the formation of fog indicated at the two offshore tower sites are believed to be representative of the Rhode Island Ocean SAMP area, given their similar environments and relative proximity. Additional analysis of the distribution of the depression of the dew point temperature below the ambient air temperature at BUZM3 (not shown) indicates that the lower quartile of the distribution of this difference exhibits especially low values indicating saturation and the potential for fog formation or persistence, during the summer months. In particular, the difference falls at 0˚C during June, July and August, consistent with the counts of days when fog is expected, as shown in Fig. 1. Similarly, analysis of the air/water temperature difference (not shown) indicates warm air flowing over cooler water in the months March-September, and most commonly in June, July and August, again consistent with the analysis shown in Fig. 1. Kotsch (1983) presents a figure (also shown in Hsu, 1988) mapping areas of common occurrence of fog during the summer months along the northeast coast of the US and Canada. The broad characterization of "20 to 30 days" of foggy conditions during June-August shown there is consistent with the results presented here.

Observations of fog at onshore and island sites also corroborate the analysis presented here. Estimates of the frequency of occurrence of fog at the airport at Block Island were tabulated in the Annual Summary of Local Climatological Data. For example, in 1982 a summary for a 14-year period ending in 1982 indicated that heavy fog, with visibility restricted to 0.25 miles or less, occurred most commonly in May – August. The average number of days of heavy fog during these months was reported as 11, 11, 12 and 11 over this period. In contrast, fewer than 5

days per month of fog were reported for the months October – February. Conditions favorable for fog formation differ between the airport location and the open waters of the Ocean SAMP domain, but the widespread distribution of fog observed in these coastal environments is evident in the correspondence between these fog frequency estimates.

The estimates of the occurrence of conditions favorable to the accumulation of ice on vessels underway discussed above are based on data from the BUZM3 site, but these, too, are believed to be representative of conditions likely to be encountered in the Ocean SAMP area. The infrequent occurrence of water temperatures lower than 6˚C is a primary determinant of icing potential, and the Ocean SAMP area has similar characteristics to Buzzards Bay in this regard.

6 Conclusions

The analysis of the occurrence of foggy conditions presented here is based on meteorological data from two instrumented towers. The towers are the BUZM3 facility in Buzzards Bay, MA and the Coastal Observatory, offshore of Martha's Vineyard, MA. The data records are relatively short by the standards of climatological analysis, but the consistency with generally accepted knowledge supports a sanguine view of this limitation. Based on a data record corresponding to about 8 years of observations at BUZM3 and 3 years of data at MVCO, the annual variation of foggy days has its peak values during the months of June, July and August, with peak frequencies in the range of 6-11 days per month of fog. In the winter months fog is much less common in this area, with fewer than 3 days expected in each of these months.

The analysis of conditions favorable for the accretion of ice on moving vessels requires joint availability of wind, air temperature and water temperature observations. The ice accumulation analysis was limited to the BUZM3 site here. The results indicate that light accumulation conditions can be expected to occur on 5 or more days per month in the offshore area during the months of December, January and February. The frequency of moderate ice accumulation conditions is much lower, with less than one day per month of such conditions expected during the coldest weeks of winter. It is important to note that the majority of cases of icing conditions correspond to very low rates of accumulation predicted.

The analysis of ambient ozone mixing ratios presented here is based on surface observations made for air quality monitoring in the regulatory context at Narragansett, Rhode Island, onshore and adjacent to the Ocean SAMP area. Frequent occurrences of ozone exceeding the current

regulatory value of 75 ppbv (parts per billion by volume) are evident in the data. Pollution outbreaks tend to occur in the sunny, warm summer months, and can extend over periods of hours to days. These occurrences could be extended by emissions of ozone precursors from offshore marine operations, for example.

7 Acknowledgments

The Rhode Island Ocean SAMP program provided support for part of the work presented here. Alexander Lataille carried out some of the data acquisition and analysis while working here as a summer intern, and GSO graduate student Michael St. Laurent helped put some of the results in graphical form. Ruth Platner assisted and enabled this work with advanced computer programming skills. The ozone profile data were acquired with support from the NOAA Environmental Sciences Research Laboratory. I am pleased to acknowledge these agencies and people for their assistance.

References

Hsu, S. A. 1988. *Coastal Meteorology*. Academic Press, Inc., San Diego, CA.

Kotsch, W. J. 1983. *Weather for Mariners*. Naval Institute Press, Annapolis, MD.

Overland, J. E. 1990. Prediction of vessel icing for near-freezing sea temperatures. *Weather and Forecasting,* 5:62-77.

Overland, J. E., Pease, C. H., Priesendorfer, R. W. and Comiskey, A. L. 1986. Prediction of vessel icing. *J. Climate and Applied Meteor.,* 25:1793-1806.

US Department of Commerce, NOAA, Local Climatological Data, Block Island, Rhode Island, 1982. National Climatic Data Center, Asheville, NC.

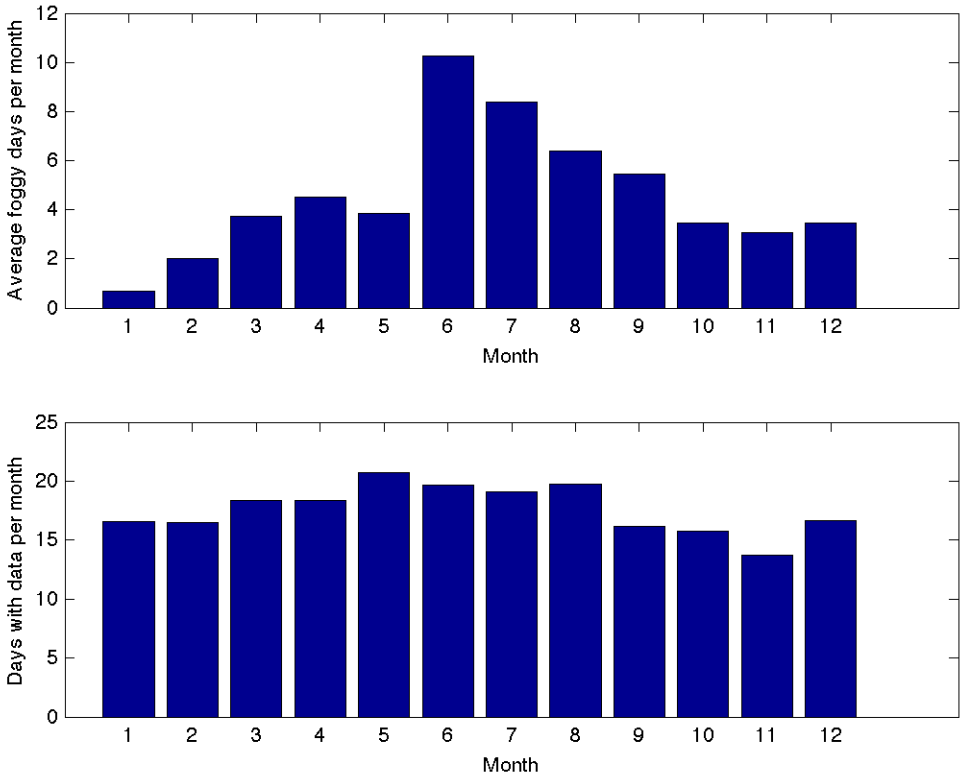

Figure 1. Annual distribution of days of fog at BUZM3 (upper panel) and days of available data (lower panel).

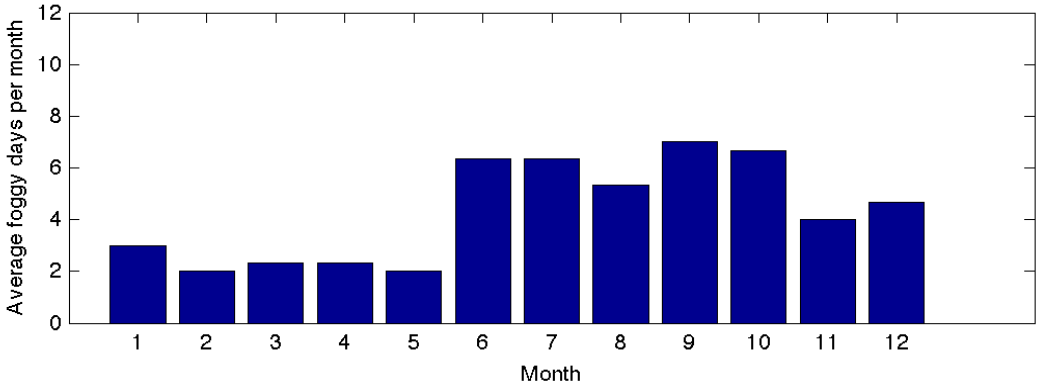

Figure 2. Annual distribution of days of fog at MVCO.

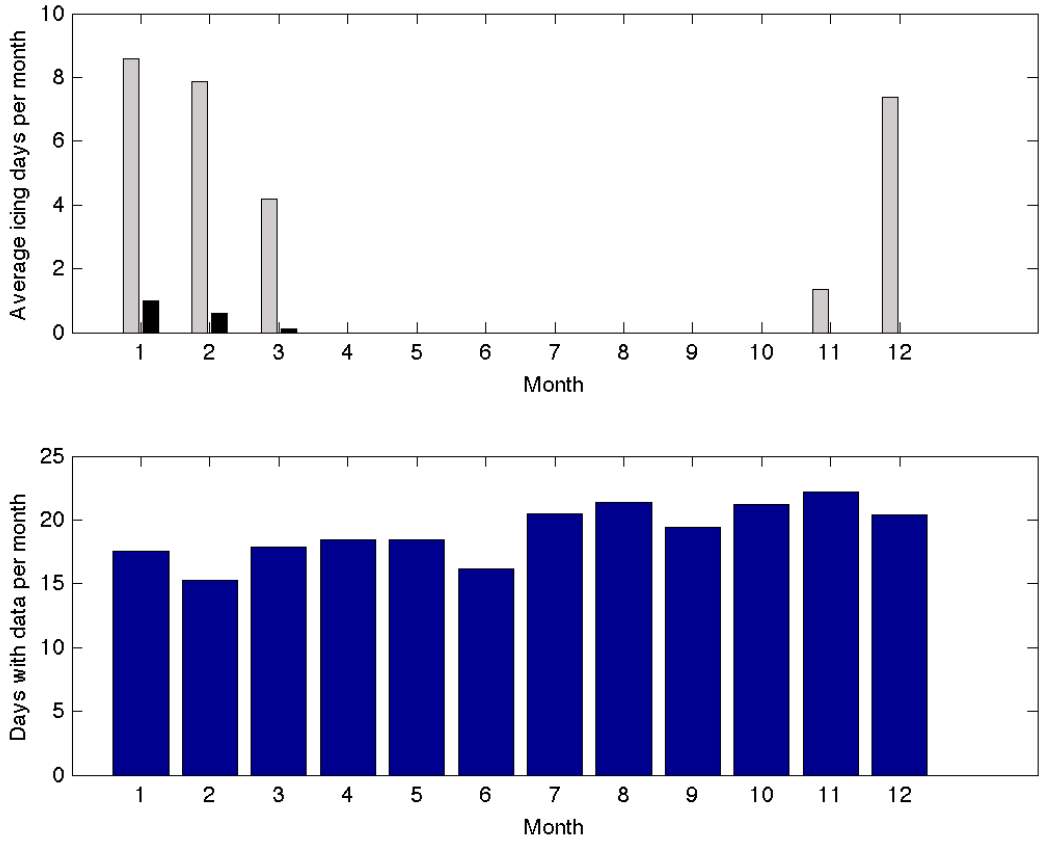

Figure 3. Annual distribution of icing days at BUZM3, in the light and moderate categories, in light and dark bars, respectively, (upper panel) and days of available data (lower panel).

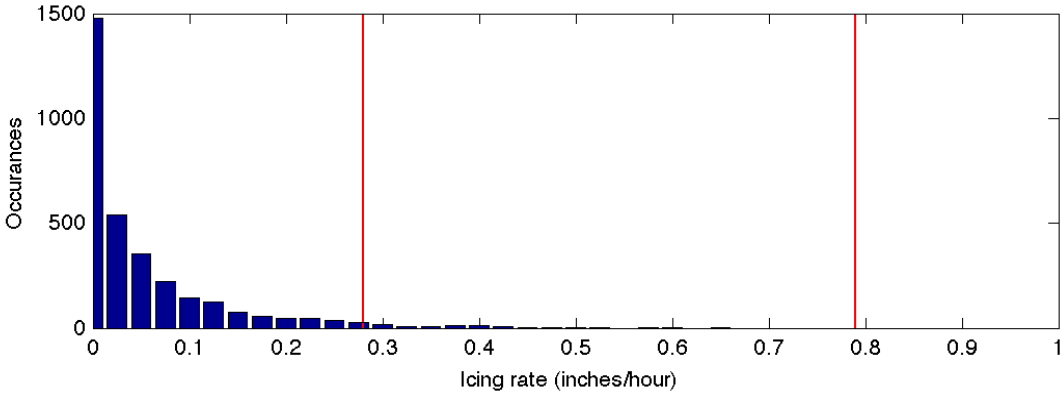

Figure 4. Occurrences vs. rate of icing, summed over available data periods at station BUZM3. The limits of the light and moderate accumulation categories are shown by the vertical bars.

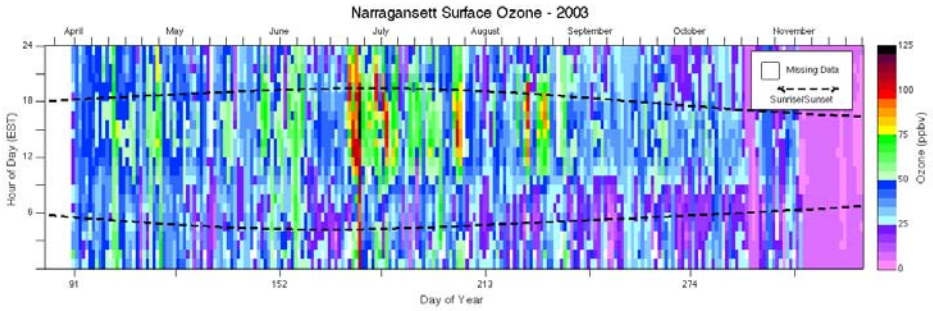

Figure 5a. Surface ozone mixing ratio, parts per billion by volume, displayed in hour of the day vs. day of the year form. Data for the Narragansett EPA laboratory site for the ozone season of 2003. Sunrise and sunset times are indicated, and blank areas represent missing data periods.

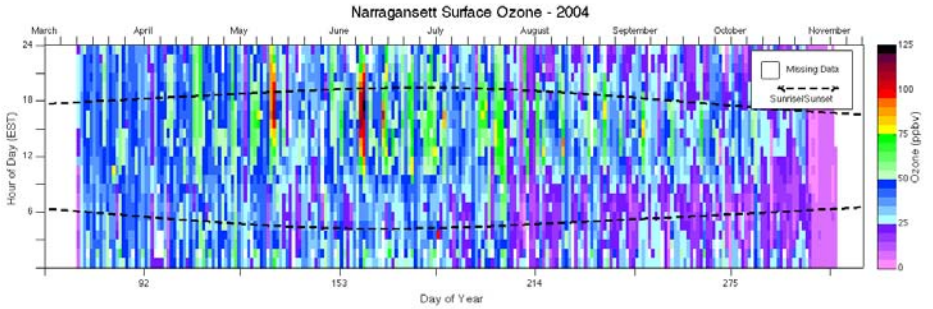

Figure 5b. Surface ozone mixing ratio data for Narragansett, 2004.

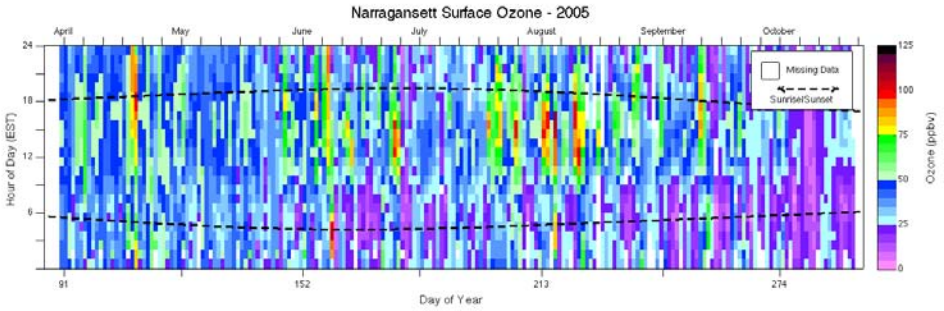

Figure 5c. Surface ozone mixing ratio data for Narragansett, 2005.

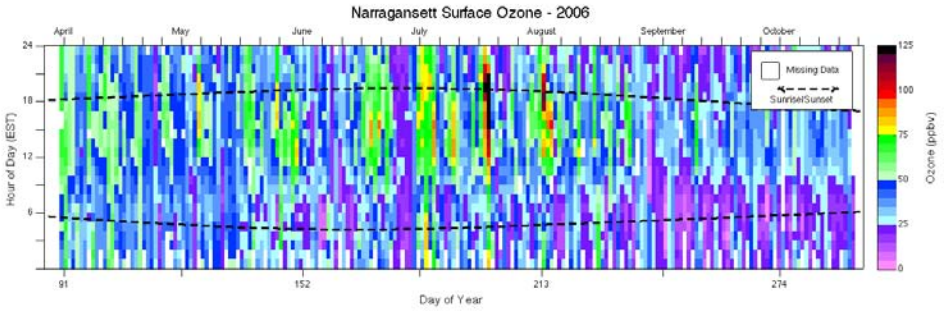

Figure 5d. Surface ozone mixing ratio data for Narragansett, 2006.

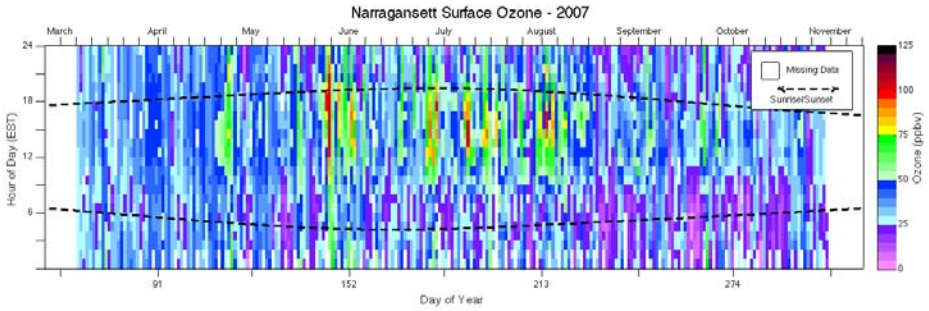

Figure 5e. Surface ozone mixing ratio data for Narragansett, 2007.

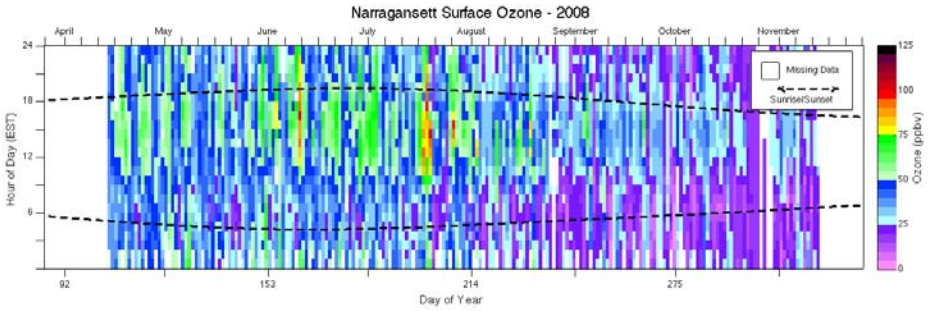

Figure 5f. Surface ozone mixing ratio data for Narragansett, 2008.

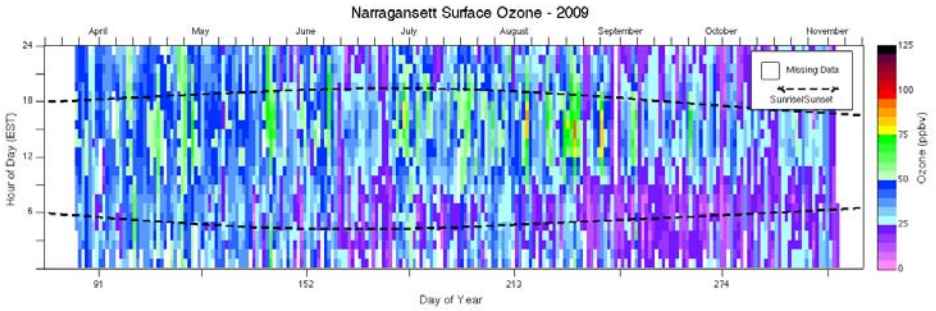

Figure 5g. Surface ozone mixing ratio data for Narragansett, 2009.

8.

Analysis of Extreme Wave Climates in Rhode Island Waters South of Block Island

for the Rhode Island Ocean Special Area Management Plan 2010

by

T.G. Asher, A.R. Grilli, S.T. Grilli and M.L. Spaulding

Ocean Engineering, University of Rhode Island

August 12, 2009

Executive Summary

This project is one component of comprehensive multidisciplinary studies performed at the University of Rhode Island 2008 to 2010, to develop a Special Area Management Plan (SAMP) for siting offshore wind farms in Rhode Island waters.

A characterization of extreme wave climates is required when considering such ocean structures, e.g. for designing wind turbine support structures and foundations or for verifying the long-term stability of their foundations against scour.

An analysis of the extreme wave climate off the southern coast of Block Island was performed, from which significant wave heights and peak spectral periods were derived, for sea states corresponding to long return period events (i.e., 20, 50, 75 and 100 years) from a variety of directions. Wave propagation simulation analyses using STWAVE, a steady-state spectral wave model and forced by wave hindcast data from the US Army Corp of Engineers, Wave Information Studies (WIS) were performed to estimate these extreme events. Various model grids were used, which represented rectangular areas, from 616 to 978 km^2, surrounding Block Island and the regions where potential wind farms might be sited to the southwest, south, and southeast of the island.

Simulation results predicted the occurrence, south and southeast of the island, of significant wave heights of at least 8 m for all return periods (upper 95% confidence limit), with wave heights exceeding 10 m in the 100 year case. Southwest and west of Block Island, significant wave heights were significantly reduced in all cases, by about 2 meters, due to intense breaking and dissipation over the shallower waters (15 m deep) between Block Island and Montauk Point (eastern end of Long Island) associated with large boulders and quaternary glacial deposits.

Table of Contents

List of Figures

List of Tables

List of Appendices

Appendix A: Overview of STWAVE equations and implementation.

1 Introduction

1.1 Background

The RI WINDS program was established by the State of Rhode Island, in January 2006, to develop wind energy as a cost-effective means to provide 15% of the state's 1,000 MW energy demand. A Phase I Siting study performed by Applied Technology and Management (ATM) under this program showed that most significant wind resources in state were in offshore waters and identified potential wind farm sites in RI and adjacent federal waters..

The University of Rhode Island was subsequently tasked by the State of RI with developing a more comprehensive and multidisciplinary Ocean Special Area Management Plan (SAMP) (2008-2010) aimed at updating the initial RI WINDS siting study and identifying areas suitable for offshore wind energy development.

A preliminary evaluation currently in progress as part of the Ocean SAMP, identified two areas in state waters southeast and south southwest of Block Island (Fig 1.1) that might be viable as sites for a wind farm. Identification of additional sites in federal waters is also underway. The focus of the present study is to characterize the extreme wave environment in the vicinity of these two sites

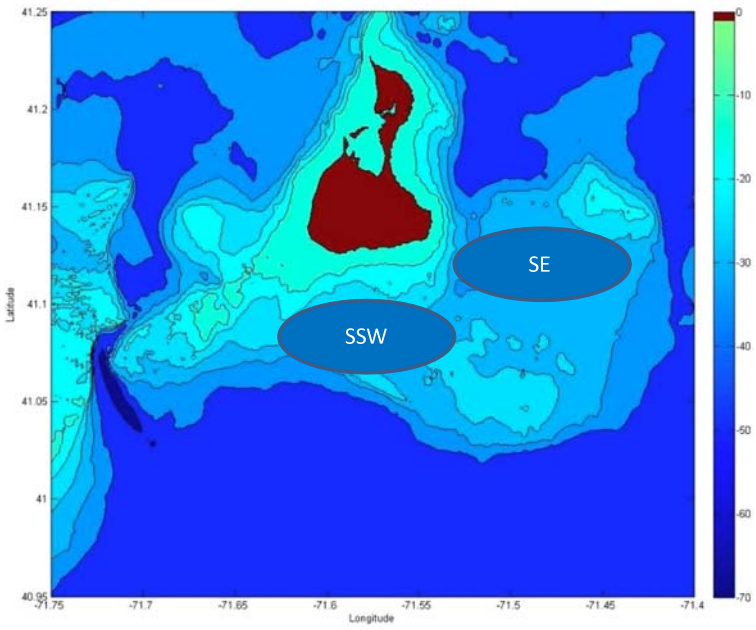

Figure 1.1 : Location of two sites, SSW and SE of Block Island under consideration for siting of a wind farm. The map background is the bathymetry of the area from the NOAA ENC (axis in m).

1.2 Study objectives

The main objective of this study is the preliminary characterization of extreme wave climates near potential wind farm sites, in state waters south of Block Island, This information is essential

in designing the foundations and support structures for the wind turbines and also useful in screening sites to locate the farm We chose to characterize proposed sites based on extreme wave conditions only, as this constitutes the limiting (i.e., structural survival), or excluding, factor. If an area is not appropriate for extreme conditions, there is no point to consider it further for development.

In view of the bathymetry in the considered areas of Fig. 1.1 and the expected height and period of extreme waves (order 10 m and 15 s period), for instance, it can be inferred a priori that intense breaking will occur west of both the island and the SSW area identified in Fig. 1.1. Hence such sites would be very undesirable for wind farm construction.

By contrast, directly south or east of these critical areas, due to larger water depth, the wave climate should be more appropriate for a wind farm. Accordingly, siting areas shown in Fig. 1.1 also roughly overlap with the primary and alternate wind farm project sites proposed by DeepWater Wind Inc. in their recent proposal to the State of RI.

Extreme wave conditions were analyzed in and around the sites of Fig. 1.1, by performing spectral wave propagation modeling studies. In those, incident wave values (in the form of a directional wave spectrum) were specified based on the upper 95 % confidence limit of wave parameters obtained from a statistical analysis of 20 years worth of hindcast wave data available at the nearby US Army Corp, Wave Information Study (WIS) station 101.

More specifically, this study had two main parts :

- Estimation of extreme conditions for selected storm return periods (20, 50, 75, and 100 years) in terms of wind and wave climate characteristics, using WIS data at station 101. Key parameters are:
    1. Wind speed and direction
    2. Significant wave height
    3. Peak wave period and direction
    4. Spectral shape
    5. Storm surge

- Prediction of wave climate in an area encompassing the selected sites, by performing simulations with STWAVE (spectral wave propagation program), over a model grid representing the relevant area. Simulations were performed using the various extreme wave and wind conditions as inputs.

2 Estimates of Extreme Conditions

2.1 Wind and wave conditions

Estimation of wind and wave parameters was made using hindcast data available from station 101 (41^{o} latitude North, 71.67^{o} longitude West) of the U.S. Army Corps of Engineers, Wave Information Studies (WIS) (U.S. ACE, 2004). This source provided 20 years (1980-1999) of hourly data for wind speed and direction and wave height and period.

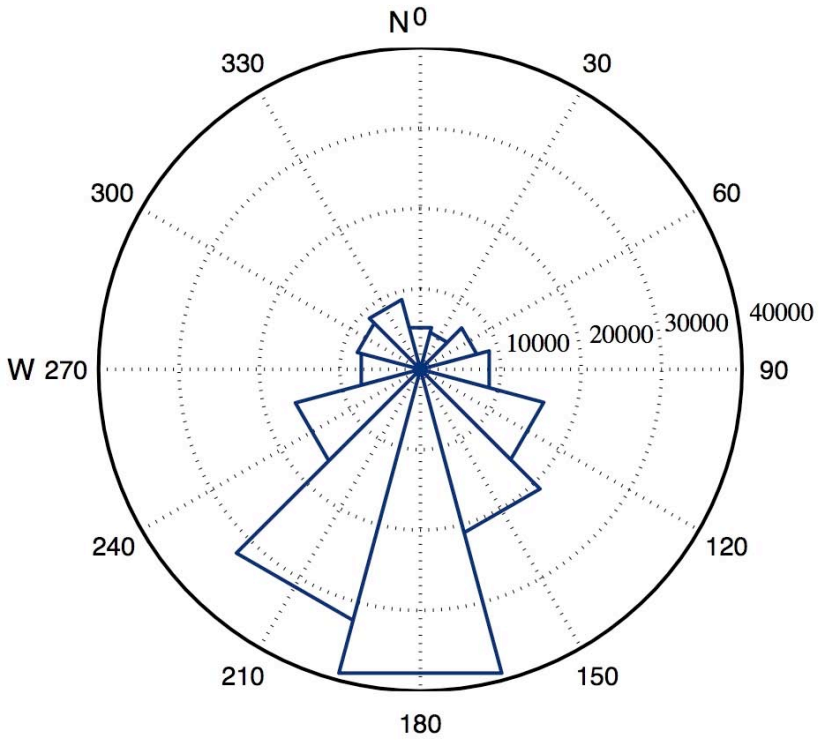

Figure 2.1 : Frequency of wave direction hindcast at WIS station 101, over 1980-1999.

A statistical analysis of waves by direction at station 101 shows the highest frequency of waves from the South (Fig. 2.1) (independent from their height). A histogram of the significant wave heights at station 101 (Fig. 2.2; all directions included) shows a mean H_s of about 1.2 m over 20 years, while extreme values range up to 8.4 m.

In nature, wind speed and wave height populations closely follow Weibull and Rayleigh probability distributions, respectively (see, e.g., Fig. 2.2 for the wave heights). Individual extreme wind and wave height values, however, are usually distributed according to a Gumbel distribution, also known as Fisher-Tippet type 1 distribution. In the present case, since we are only interested in extreme values, a time series of such values is first extracted from the 20 year hourly time series, in the form of N = 240 monthly extreme values. Then, a Gumbel distribution is fit to these monthly maxima and used to predict (extrapolate) longer-term return period values.

The Gumbel (Goda, 2000) cumulative probability distribution $F(x)$ of a variable x (e.g., extreme wind speed W (m/s) or significant wave height H_s) is defined as,

$$F(x) = \exp\left[-\exp\left(-\frac{x-B}{A}\right)\right] \qquad (0.1)$$

where, A is a scale parameter and B is a location parameter corresponding to the mode of the distribution. Standard deviation estimate, s_x, and mean values, $\bar{x}$, of the extreme value sample are related to these parameters by: $\bar{x} = B + A\gamma$; $s_x = 1.28255A$, with $\gamma = 0.5272$ being the Euler constant. Note these are (average) theoretical values assuming an ideal Gumbel distribution.

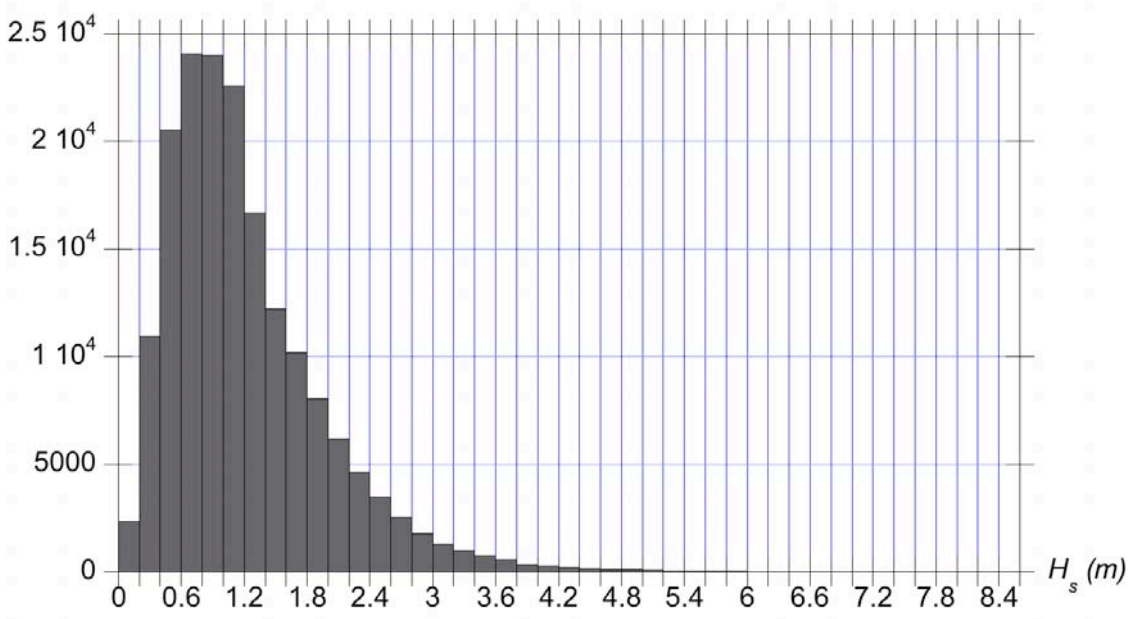

Figure 2.1 : Histogram (in count) of significant wave height at WIS station 101 over 1980-1999.

The return period, T_r (in years), of extreme events exceeding a certain threshold x_r is defined as,

$$T_r = \frac{1}{1 - F(x_r)} \tag{0.2}$$

where the denominator is the probability of exceedance, or the probability that the extreme variable $x > x_r$.

In the sample of observed extreme values x_i, with $i = 1,\ldots, N$, ordered by decreasing magnitude, the probability that $x \leq x_m$, the m^{th} ordered variable is,

$$\widehat{F}(x_m) = 1 - \frac{m}{N+1} \tag{0.3}$$

Using Eq. (0.3), one can plot events x_m versus their probability of occurrence expressed as $y_m = \ln(\ln \widehat{F}(x_m))$, or using the return period formula Eq. (2.1.2), versus their return period expressed as $y_r = \ln(\ln(1 - 1/T_r))$.

(a)

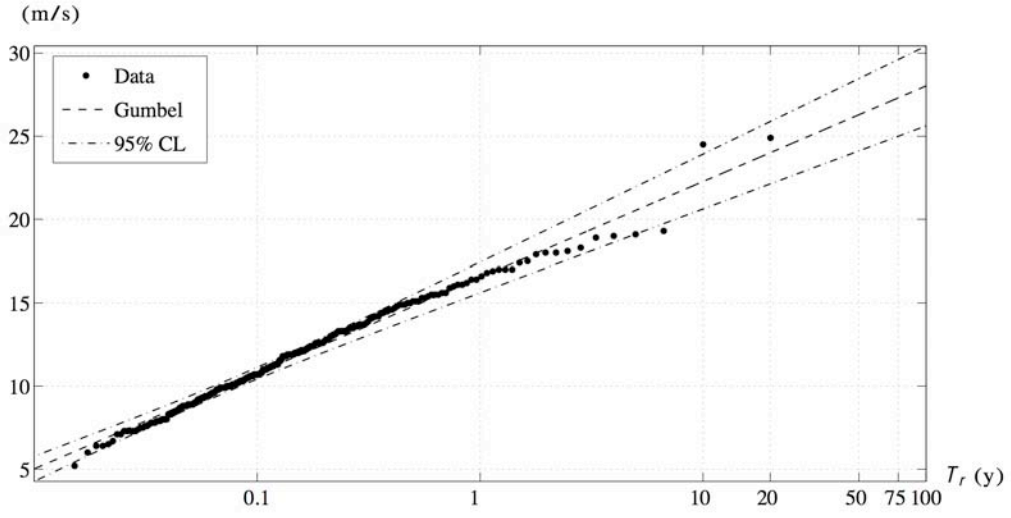

(b)

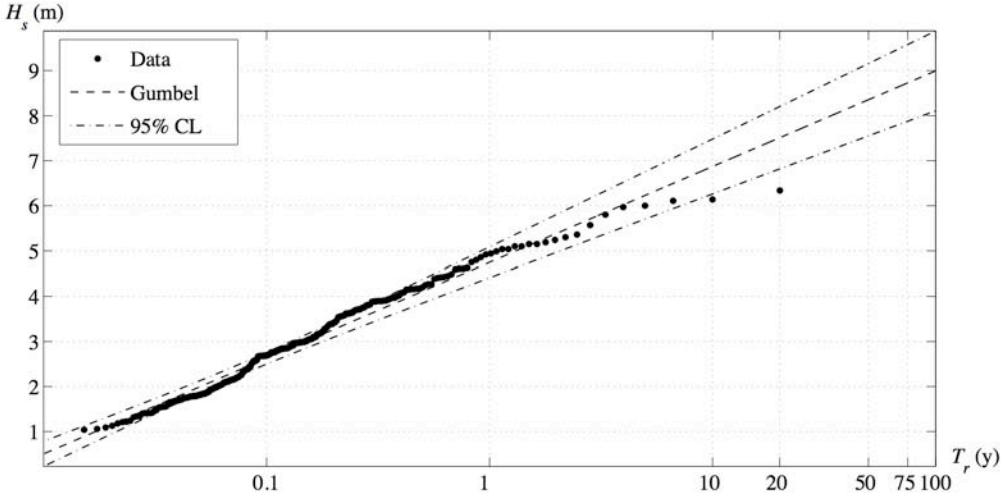

Figure 2.2 : Gumbel probability plot and curve fit, for extreme: (a) wind speed; and (b) significant wave height, as a function of return period T_r, based on monthly extrema hindcast at WIS station 101 over 1980-1999, in the 30 deg. sector centered on the Southern direction (i.e., 180 deg. from North).

A linear curve fit of the form, $x = Ay + B$, then allows one to find the most representative values of Gumbel coefficients *(A, B)* for the given sample of extreme values. Once this is done, the Gumbel distribution is used to predict the x value corresponding to a specified return period longer than 20 years. As is customary in statistical inference, a 95 % confidence interval for extrapolated values is calculated and, in the present case, the upper limit is used as a conservative extreme estimate.

Samples of N = 240 monthly extreme significant wave height and wind values were thus constituted based on the 20 year time series of hindcast WIS data, for a series of 30 degree directional sectors centered on 90, 120, 150, 180, 210, and 240 degrees clockwise from North. Curve fits were performed for each of those directional bins, as explained above, providing six pairs of Gumbel coefficients. These allow extrapolation of extreme wind and wave directional

data to 50, 75, and 100 year return periods, and their upper 95% confidence limit. Figure 2.3 illustrates our methodology and results for extreme winds and significant wave heights, in the southern sector 180 deg. from North. The confidence limits appear in the figure in the form of extended hyperbola, due to the logarithmic scale. We see most of the data falls within the confidence limits, with only a few *outliers* in each case.

Extreme peak spectral wave periods, $T_{p,}$ are estimated from predicted extreme significant wave height, H_s, by assuming these correspond to fully developed sea conditions, according to the following formula (U.S. ACE, 2002),

$$T_p = 15.66\sqrt{\frac{H_s}{g}} \qquad (0.4)$$

Tables 2.1 and 2.2 give results of analyses for the wave and wind parameters, respectively, as a function of storm return period and direction.

Extreme wind speeds and wave heights (and the limits of the 95% confidence interval for each return period) are used to formulate input wave spectra for STWAVE simulations presented in Section 3.

Direction from North	Return Period (yr)	H_s mean (m)	T_p mean (s)	H_s lower 95% (m)	T_p lower 95% (s)	H_s upper 95% (m)	T_p upper 95% (s)
90.0	100	8.8	14.8	7.8	14.0	9.8	15.7
	75	8.5	14.6	7.6	13.7	9.5	15.4
	50	8.1	14.2	7.2	13.4	9.0	15.0
	20	7.2	13.4	6.4	12.7	8.0	14.1
120.0	100	8.6	14.7	7.7	13.9	9.6	15.5
	75	8.4	14.5	7.5	13.7	9.3	15.2
	50	8.0	14.1	7.1	13.3	8.8	14.8
	20	7.1	13.3	6.4	12.6	7.8	14.0
150.0	100	8.9	14.9	7.9	14.1	9.8	15.6
	75	8.6	14.6	7.7	13.9	9.5	15.4
	50	8.2	14.3	7.4	13.6	9.0	15.0
	20	7.3	13.5	6.6	12.8	8.0	14.2
180.0	100	9.0	15.0	8.1	14.2	9.9	15.7
	75	8.7	14.8	7.9	14.0	9.6	15.5
	50	8.4	14.5	7.6	13.7	9.2	15.1
	20	7.5	13.7	6.8	13.1	8.2	14.3
210.0	100	8.8	14.8	7.9	14.1	9.7	15.6
	75	8.6	14.6	7.7	13.9	9.4	15.3
	50	8.2	14.3	7.4	13.6	9.0	15.0
	20	7.3	13.5	6.6	12.9	8.0	14.2
240.0	100	8.3	14.4	7.4	13.6	9.1	15.1
	75	8.0	14.1	7.2	13.4	8.8	14.9
	50	7.6	13.8	6.9	13.1	8.4	14.5
	20	6.8	13.1	6.1	12.4	7.5	13.7

Table 2.1: Extreme wave parameters (with upper and lower 95% confidence intervals), as a function of storm return period and direction, based on analyzing 20 years of data (1980-1999) at WIS station 101.

Direction	Return Period (yr)	U mean (m/s)	U lower 95% (m/s)	U upper 95 % (m/s)
90	100	31.0	28.0	34.0
	75	30.1	27.2	33.0
	50	28.9	26.1	31.6
	20	26.1	23.7	28.4
120	100	29.7	26.8	32.5
	75	28.8	26.1	31.5
	50	27.6	25.1	30.2
	20	25.0	22.8	27.1
150	100	27.8	25.3	30.3
	75	27.0	24.6	29.4
	50	26.0	23.7	28.2
	20	23.6	21.7	25.6
180	100	28.0	25.6	30.4
	75	27.3	25.0	29.6
	50	26.3	24.1	28.5
	20	24.0	22.1	25.9
210	100	29.2	26.8	31.7
	75	28.5	26.1	30.9
	50	27.5	25.2	29.7
	20	25.1	23.2	27.0
240	100	31.3	28.5	34.0
	75	30.5	27.8	33.1
	50	29.3	26.8	31.8
	20	26.7	24.5	28.9

Table 2.2: Extreme wind parameters (with upper and lower 95% confidence intervals), as a function of storm return period and direction, based on analyzing 20 years of data (1980-1999) at WIS station 101.

Return Period (yr)	Water level (m) at MHHW
20	3.706
50	4.376
75	4.416
100	4.446

Table 2.3: Extreme storm surge events in study area, from U.S. ACE, 1988.

2.2 Storm Surge

Storm surge values in the study area were found from U.S. Army Corps of Engineers tidal flood profiles (U.S. ACE, 1988), and are reported in Table 2.3. These values are also used as input for STWAVE simulations. Note, the interest here is to determine the impact of storm surge on the wave field and specifically how increases in water depths alter wave heights in this study area.

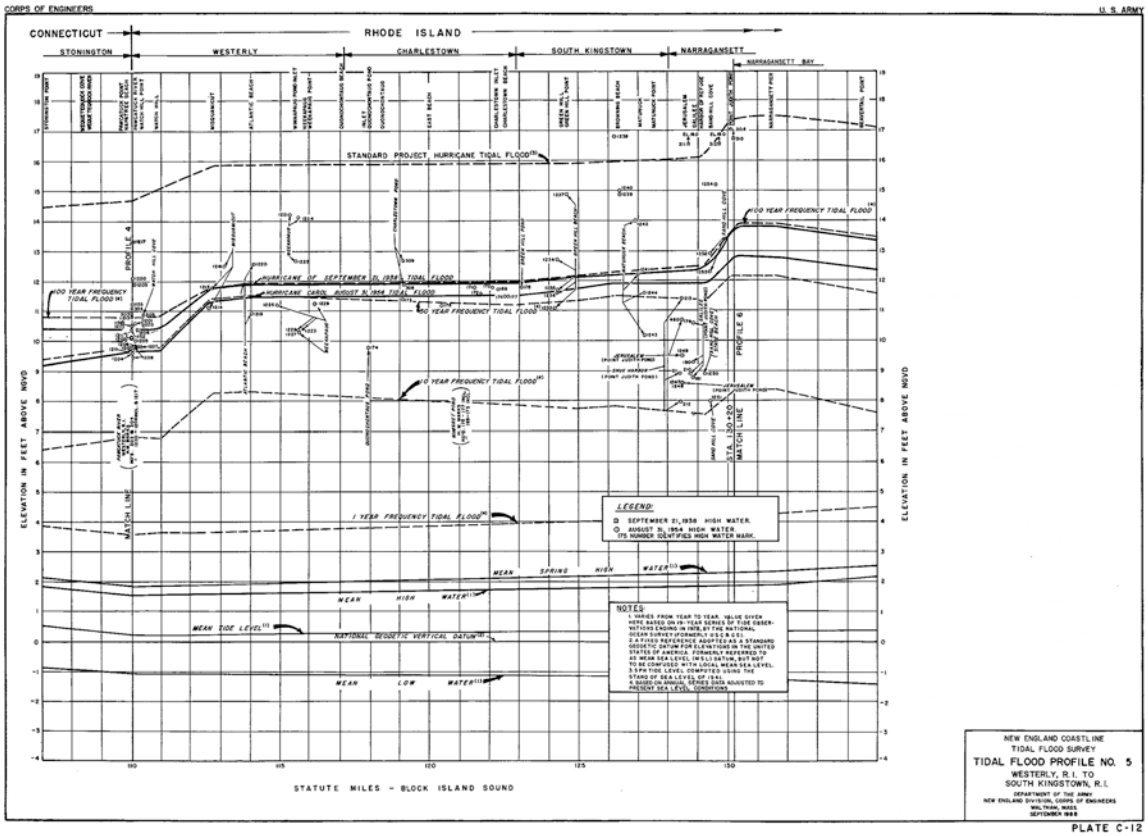

Figure 2.3 : Tidal flood profile; matchline #123 was used for storm surge values.

Using matchline #123 on Fig. 2.4, predictions for storm surge at certain return intervals are provided. By linearly interpolating, storm surge values for the 25- and 75-year return period cases were found.

3 Wave Modeling

3.1 Model governing equations and numerical methods

Propagation of incident wave climates for various return periods and directions, obtained from WIS station 101 data as detailed in Section 2, combined with corresponding storm surges, is simulated in the wave model STWAVE (version 4.0), developed and maintained by the US Army Corps of Engineers (Smith, et al., 2001). STWAVE is a steady-state spectral model, based on the wave action balance. The model is capable of simulating wind forcing (fetch growth), wave-current interactions, and breaking dissipation (both surf zone and white capping). Details on STWAVE are provided in Appendix A.

3.2 Input directional wave spectrum

A standard frequency vector ranging linearly from 0.04 to 0.2 Hz was used in most STWAVE simulations to define both input and calculated spectra over the model grid. 50 equally-spaced frequency bins were used, along with 35 directional bins (5 degree spacing).

The wave directional frequency spectrum is formulated here as a two-dimensional Bretschneider-Mitsuyasu frequency spectrum, multiplied by a standard cosine-squared directional spreading (Smith, et al., 2001),

$$S(f,\theta) = 0.257 \frac{H_{1/3}^2}{T_{1/3}^4} f^{-5} \exp\left\{-1.03\left(T_{1/3} f\right)^{-4}\right\} G(f,\theta)$$

$$T_{1/3} = \frac{T_p}{1.05} \qquad (0.1)$$

where, T_p is peak spectral period (s), $H_{1/3}$ and $T_{1/3}$ are significant wave height (m) and period (s), respectively, and f is frequency (Hz), with

$$G(f,\theta) = G_0 \cos^{2s}\left\{\frac{\theta - \theta_p}{2}\right\} \qquad (0.2)$$

and,

$$s = \begin{cases} s_{\max}\left(\frac{f}{f_p}\right)^5 & f \le f_p \\ s_{\max}\left(\frac{f}{f_p}\right)^{-2.5} & f > f_p \end{cases} \quad \text{with} \quad s_{\max} = 11.5\left(\frac{g}{2\pi W f_p}\right)^{2.5} \qquad (0.3)$$

where θ is wave component direction, θ_p is the spectral peak direction, and W is the wind speed (m/s) at 10 m above sea level, and coefficient G_0 is such that the definite integral of the spreading function over its entire angular domain is equal to 1.

The input values for specific spectra, T_p, $H_{1/3}$, θ_p, and W, were obtained from the various earlier estimates of extreme wave conditions (see Section 0).

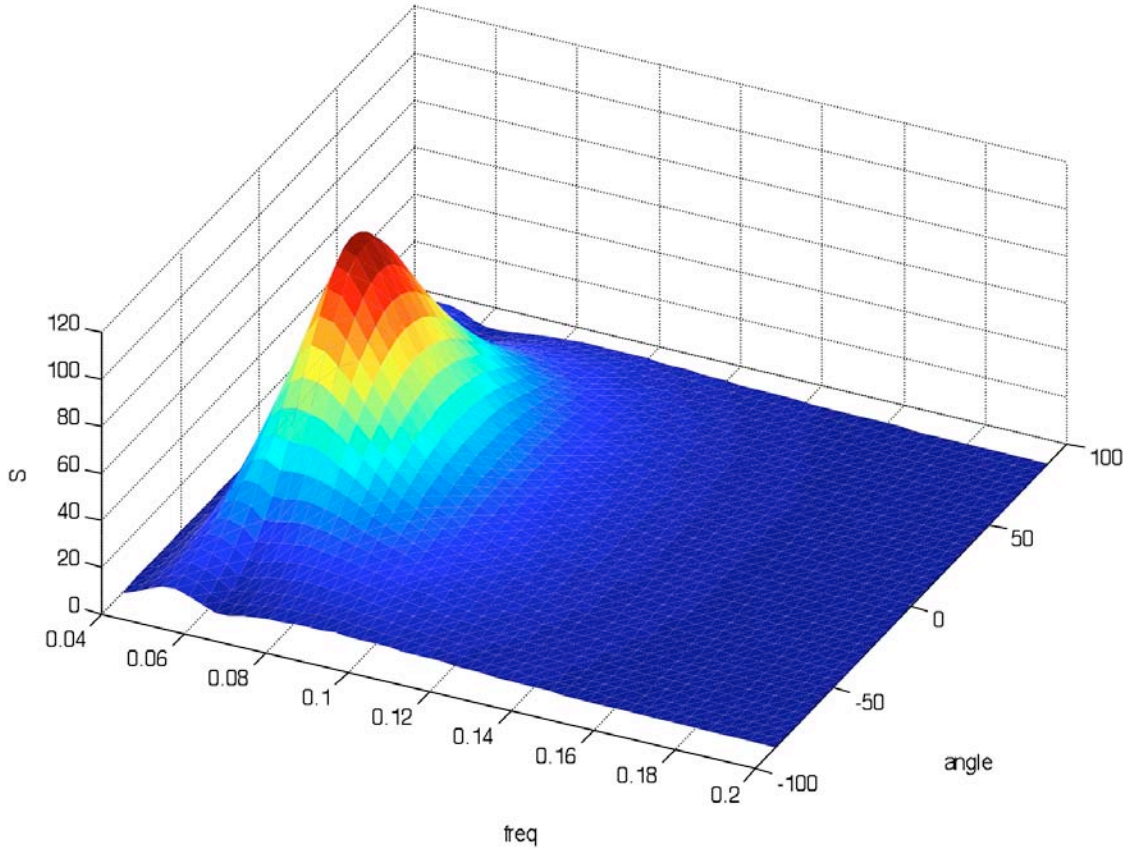

Figure 3.1 : Example of Bretschneider-Mitsuyasu directional frequency spectrum used as input to STWAVE, for T_p = 15.7 s, $H_{1/3}$ = H_s = 9.9 m, θ_p = 30 deg., and W = 30 m/s.

4 Results of Wave Simulations for Block Island Sites

4.1 Computational domains for Block Island sites

STWAVE computational domains are designed to maximize their size and resolution relative to the region of interest, while keeping computational costs reasonable.

Domain	Western Boundary Long. W	Eastern Boundary Long. W	Southern Boundary Lat. N	Northern Boundary Lat. N	Grid size (m)	Cells W->E	Cells S->N	Offshore boundary
1	-71.75	-71.40	40.95	41.25	50	588	665	east
2	-71.75	-71.50	41.00	41.25	50	419	588	south
3	-71.85	-71.50	41.00	41.25	50	555	588	south

Table 3.1: Parameters for three main computational domains used in STWAVE.

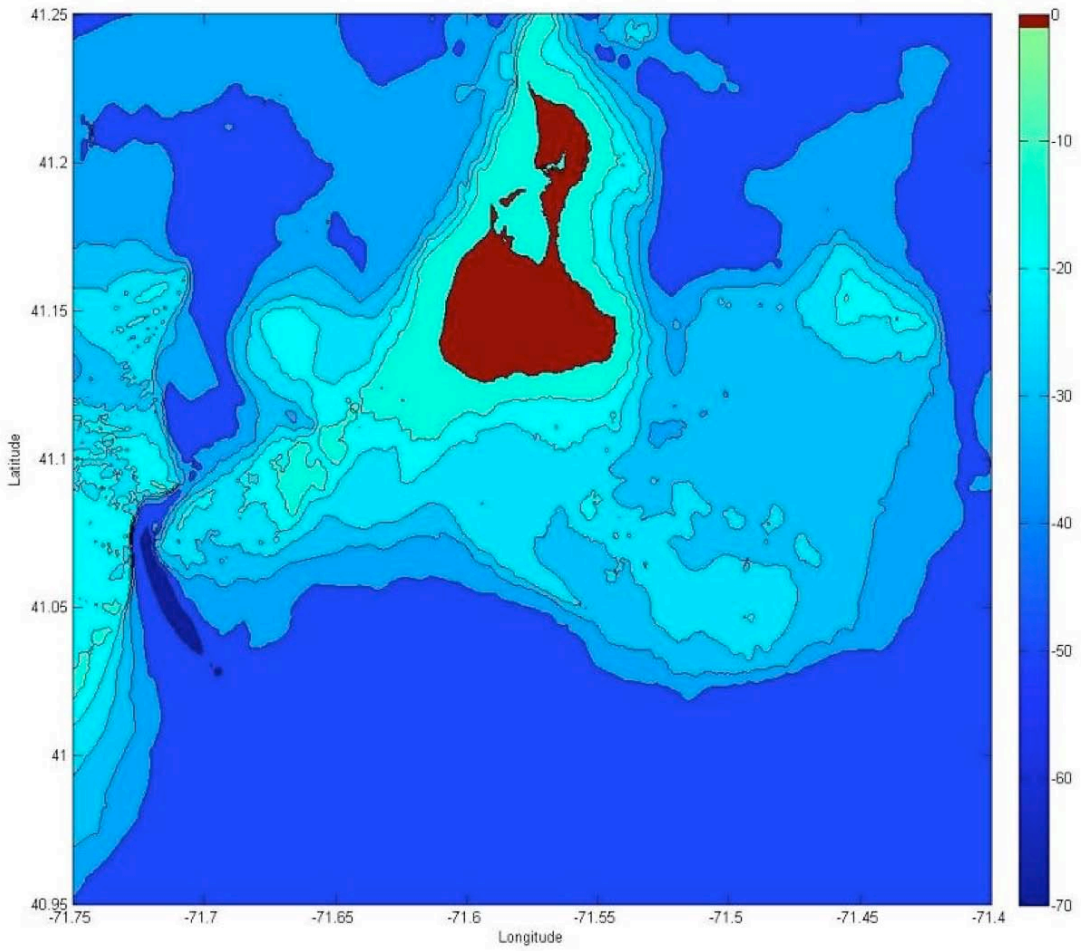

Figure 4.1 : Bathymetry (m) near and around Block Island used in STWAVE, and extent of first computational domain.

Considering the sites under consideration, adjacent to Block Island (Fig. 1.1), and the comuting size/cost limitations in STWAVE, three separate model domains were generated for the purpose of this study. Bathymetric features (NOAA Electronic Navigation Charts (ENC)), which might

have a significant effect on wave transformation in the considered region, have been included in each computational domain. Table 3.1 gives main model parameters (grid size and number of grids in each direction) for these domains. The domains are shown in Figs. 4.1, 4.2, and 4.3. These cover areas from 616 to 978 km^2.

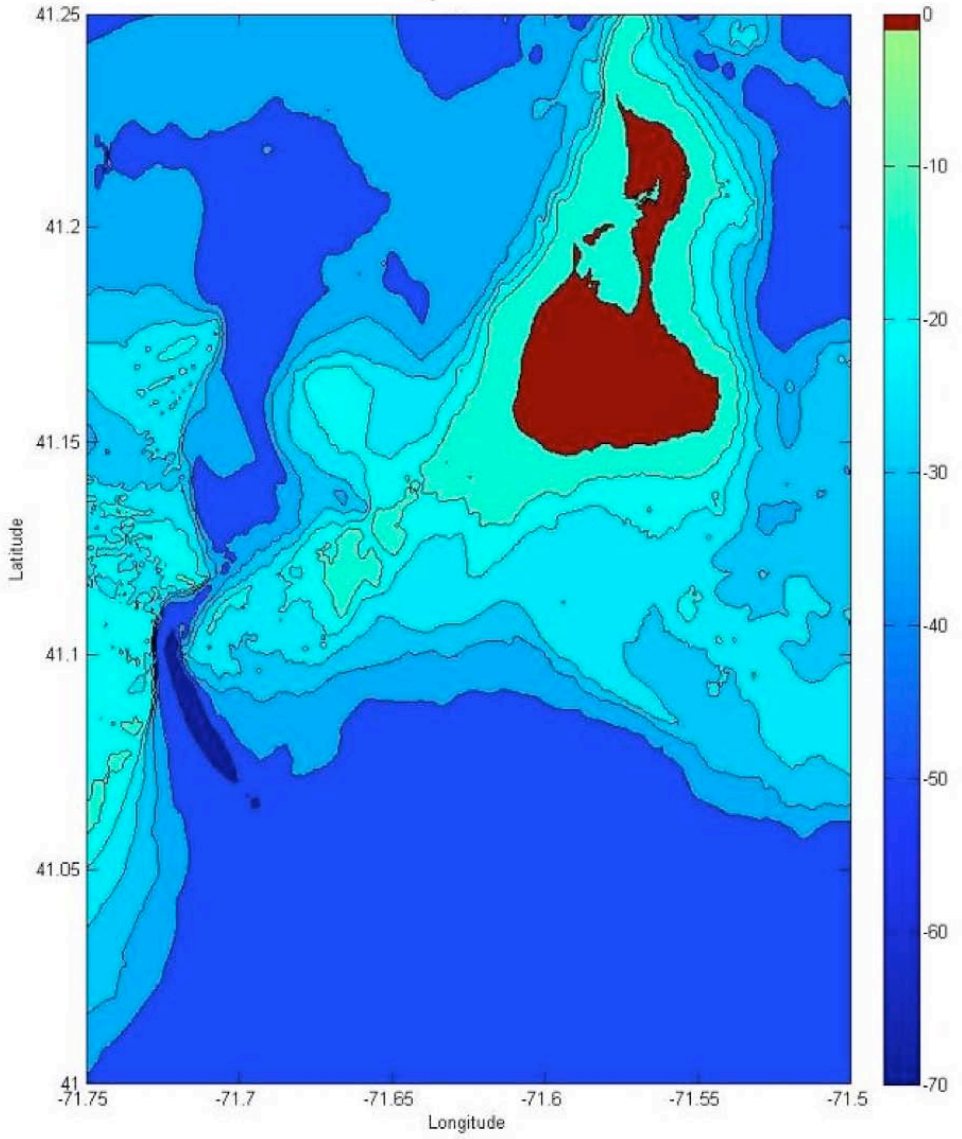

Figure 4.2 : Bathymetry (m) near and around Block Island used in STWAVE, and extent of second computational domain.

The first computational domain (Fig. 4.1) is used for simulating spectra for waves from 90^o and 120^o. The domain encompasses an area of 978 km^2 (29.4 km (W-E) x 33.25 km (S-N)), with the offshore boundary in STWAVE defined as the eastern boundary of the domain. The grid size is 50 m. It should be noted that while WIS station 101 is not spatially near the eastern boundary of this domain, analysis of other WIS stations closer to this boundary showed little variation in extreme wave parameters.

The second computational domain (Fig. 4.2) is used for simulating spectra for waves from 210°-150°. It encompasses an area of 616 km^2 (20.95 km (W-E) x 29.4 km (S-N)), with the offshore boundary in STWAVE defined as the southern boundary of the domain. The grid size is 50 m. This boundary is chosen to match the latitude of WIS station 101. Since incident wave climates are estimated from the hindcast data at this WIS station, this selection typically ensures that the wave climate at the start of the simulation is accurate. This domain, the smallest of the three, is used for the majority of simulations.

The third computational domain (Fig. 4.3) is used for simulating spectra for waves from 240°. It encompasses an area of 816 km^2 (27.75 km (W-E) x 29.4 km (S-N)), with the offshore boundary in STWAVE defined again as the southern boundary of the domain. The grid size is 50 m. Because of the direction of this simulation, it was deemed necessary to include more of the bathymetry west of Block Island. Accordingly, domain two was extended westward.

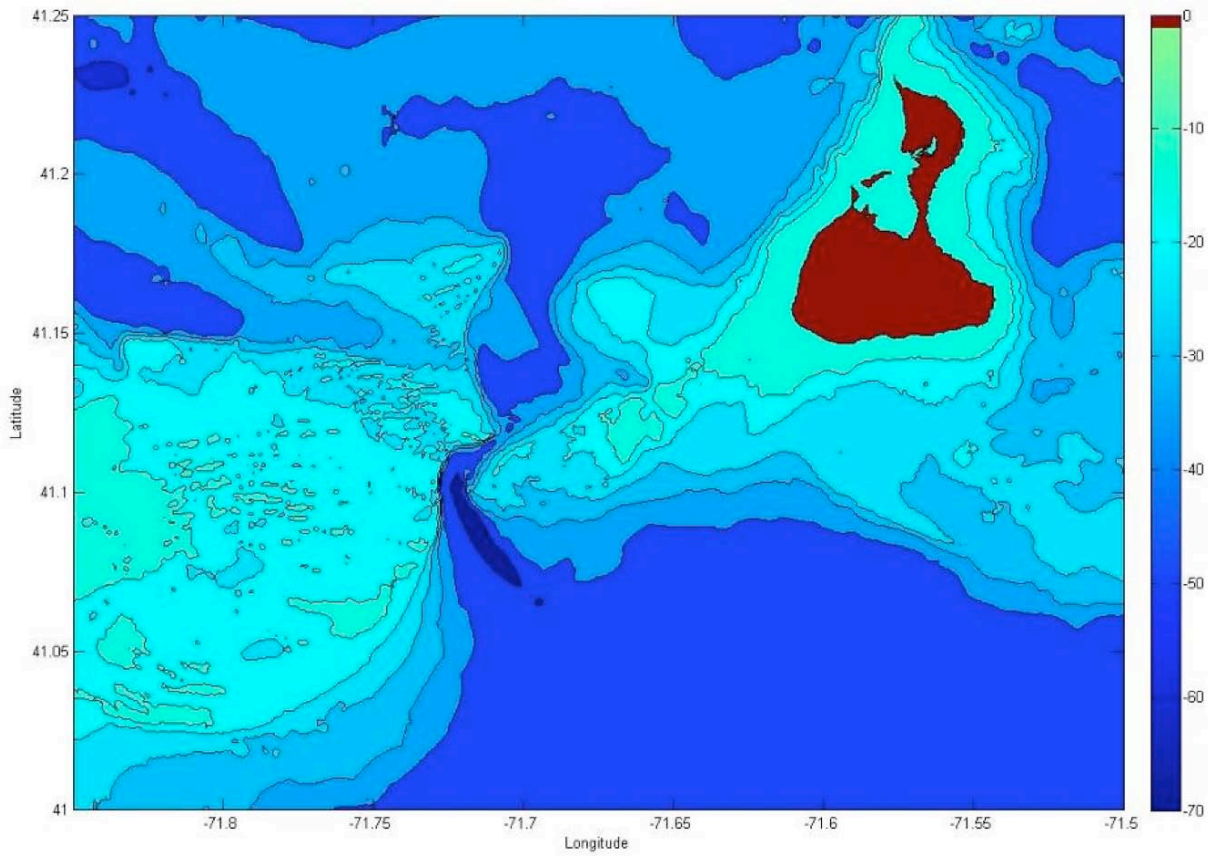

Figure 4.3 : Bathymetry (m) near and around Block Island used in STWAVE, and extent of third computational domain.

4.2 Simulation results

Although simulations were done for multiple wave directions, a leading angle of incidence of 180° (waves arriving from the south), and to a lesser extent 90°, consistently provided the worst-case scenarios in the region of interest.

The worst-case scenario (waves from the south) significant wave heights are plotted in Figs. 4.4, 4.5, 4.6, and 4.7, for the 20, 50, 75, and 100 year storms, respectively. The plots show colored renditions of the significant wave height within the study domain. Note the same height scale is used on each of the figures.

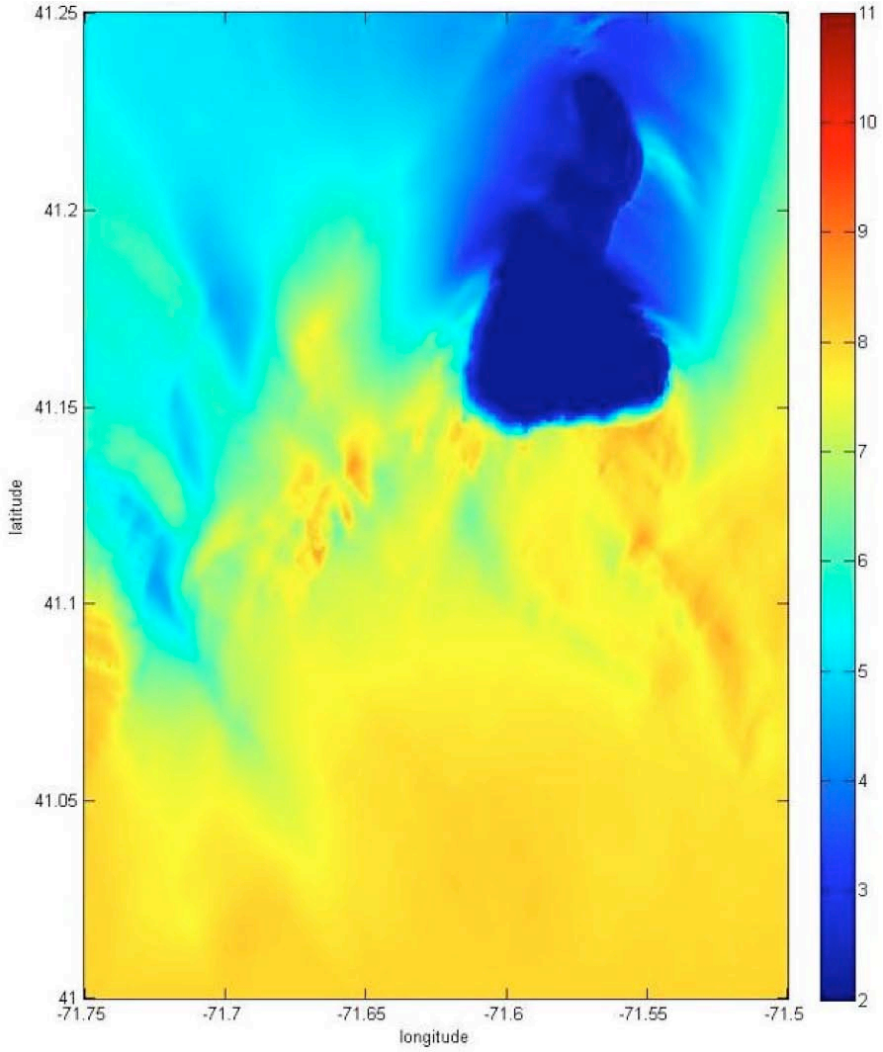

Figure 4.4 : Worst-case scenario significant wave height for 20 year storm (axis in m). Incident conditions : H_s = 8.2 m, T_p = 14.3 s, W = 25.9 m/s, and 180^o direction.

Qualitatively, the canyon (approximately 71.71^{o}W, 41.05^{o}N) in the southwestern section of the study area and the shoal (approximately 71.66^{o}W, 41.08^{o}N) northeast of it, appear to provide some sheltering for the area west of Block Island, yielding significant wave heights of 6-8 m across most of the region for the 100 year storm (Figs. 4.7). South and east of the island, however, no such protection occurs and large significant waves prevail, some in excess of 10 m for the 100 year storm. For the shorter return period waves (Figs. 4.4, 4.5, and 4.6) the wave amplitudes are reduced but the pattern remains the same as for the 100 yr case.

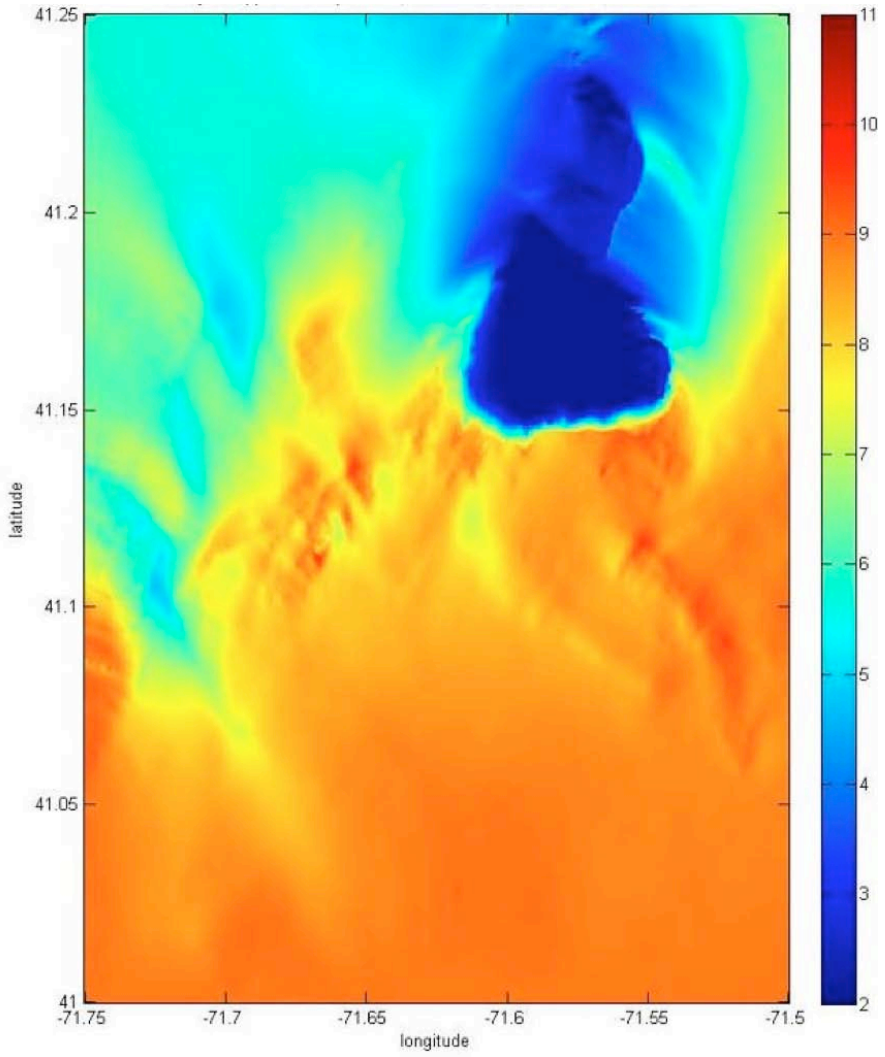

Figure 4.5 : Worst-case scenario significant wave height for 50 year storm (axis in m). Incident conditions : H_s = 9.2 m, T_p = 15.1 s, W = 28.5 m/s, and 180^o direction.

Comparing simulated variations in significant wave height across different return periods reveals that the above sheltering effects also limit wave heights west of Block Island to some degree. South of the island, the 20 year return period significant waves (Fig. 4.4) are about 2.5 m smaller than those in the 100 year scenario (Fig. 4.7). North of the canyon and shoal, however, the disparity in wave height among various return periods is generally less than 1 m. This can be explained through the depth-limitation of a given wave height, i.e. shallow depth induces wave breaking, dissipating energy continually until wave height has reduced below the breaking limit. This explanation is also confirmed by the fact that, beyond a transition zone, wave height is approximately the same for each return period.

The above results are consistent with expectations and confirm that wave climate should be considered as a determining factor for the siting of a wind farm off of Block Island. In particular, the reduced wave height west of the island marks this area as a much more desirable option than south or south-east of the island, based on the extreme wave height aspect only.

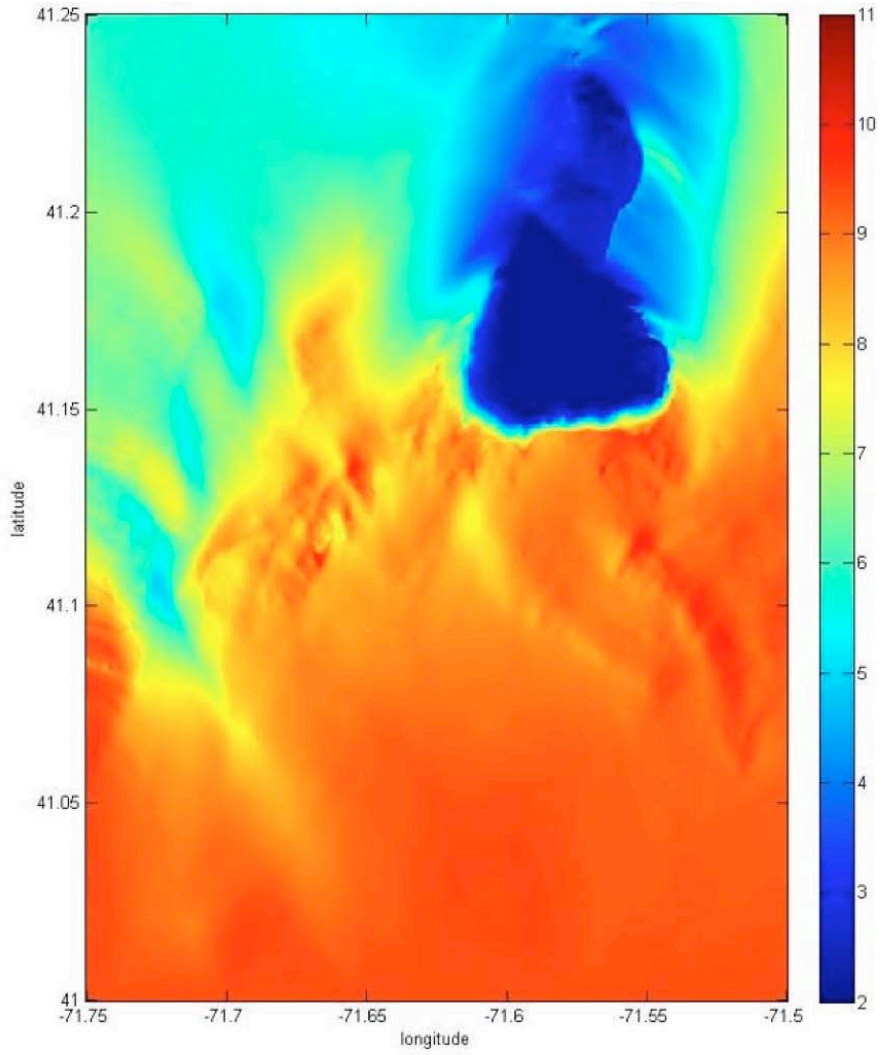

Figure 4.6 : Worst-case scenario significant wave height for 75 year storm (axis in m). Incident conditions : H_s = 9.6 m, T_p = 15.5 s, W = 29.6 m/s, and 180^o direction.

Figure 4.8 shows simulation results for the worst-case scenario for waves from the east. We note that large amplitude waves propagate to the shoreline with some evidence of a small amplification to the south and southeast of Block Island. Wave heights are dramatically lower in the lee of the island and landward of the shoal area to the SW of the island.

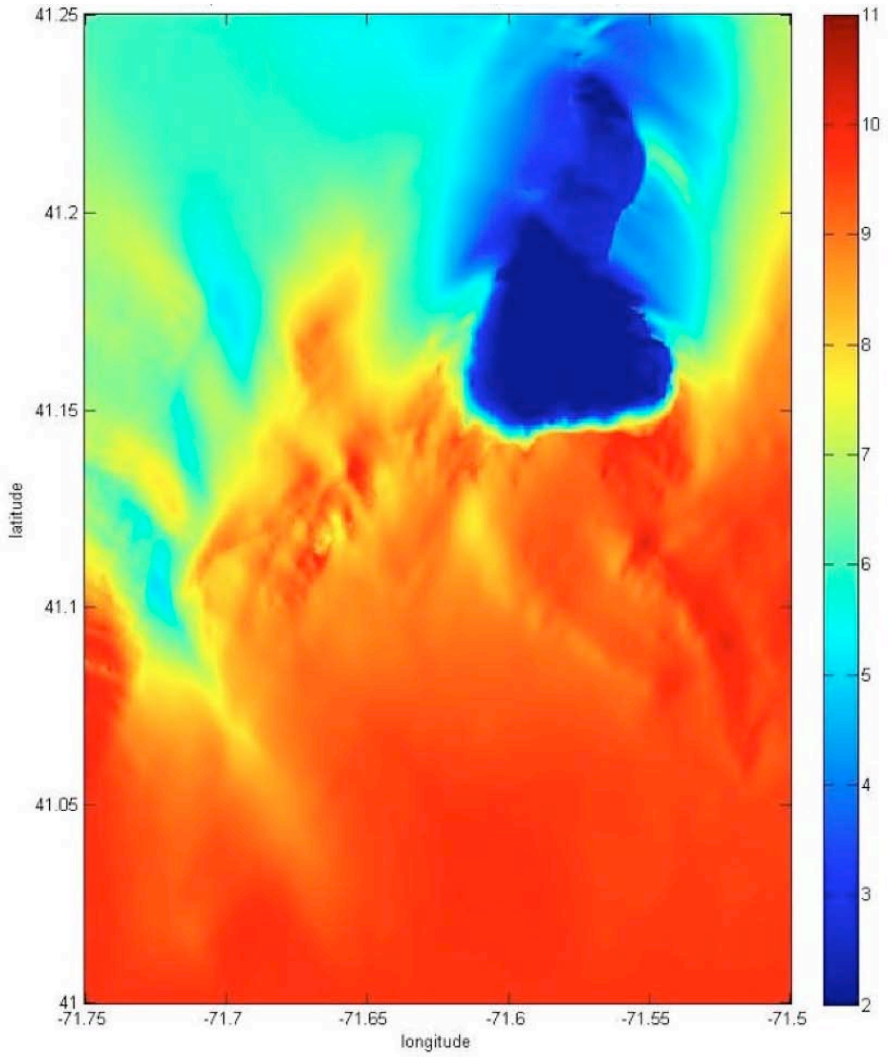

Figure 4.7 : Worst-case scenario wave height for 100 year storm (axis in m), 180 deg. incidence. Incident conditions : H_s = 9.9 m, T_p = 15.7 s, W = 30 m/s, and 180^o direction.

4.3 Sensitivity to bathymetric resolution

In this section, we verify the accuracy of STWAVE simulations with respect to the bathymetric resolution, defined as the size of grid cells in the computational domain. Three cases have been tested, with different grid cell sizes: 30 m for the highest resolution; 50 m for the intermediate case (default value used in standard extreme analysis simulations presented above); and 70 m for the lowest resolution case.

Figures 4.9 (30 m), 4.10 (50 m) , and 4.11 (70 m) show results for the three bathymetric resolutions for 9 m, 15 s waves from the south with winds of 30 m/s. We see negligible differences in significant wave height across the domain for all three cases. It can therefore be concluded that the 50 m bathymetric resolution used in earlier simulations adequately represents the study area and does not represent a significant source of error for the wave predictions.

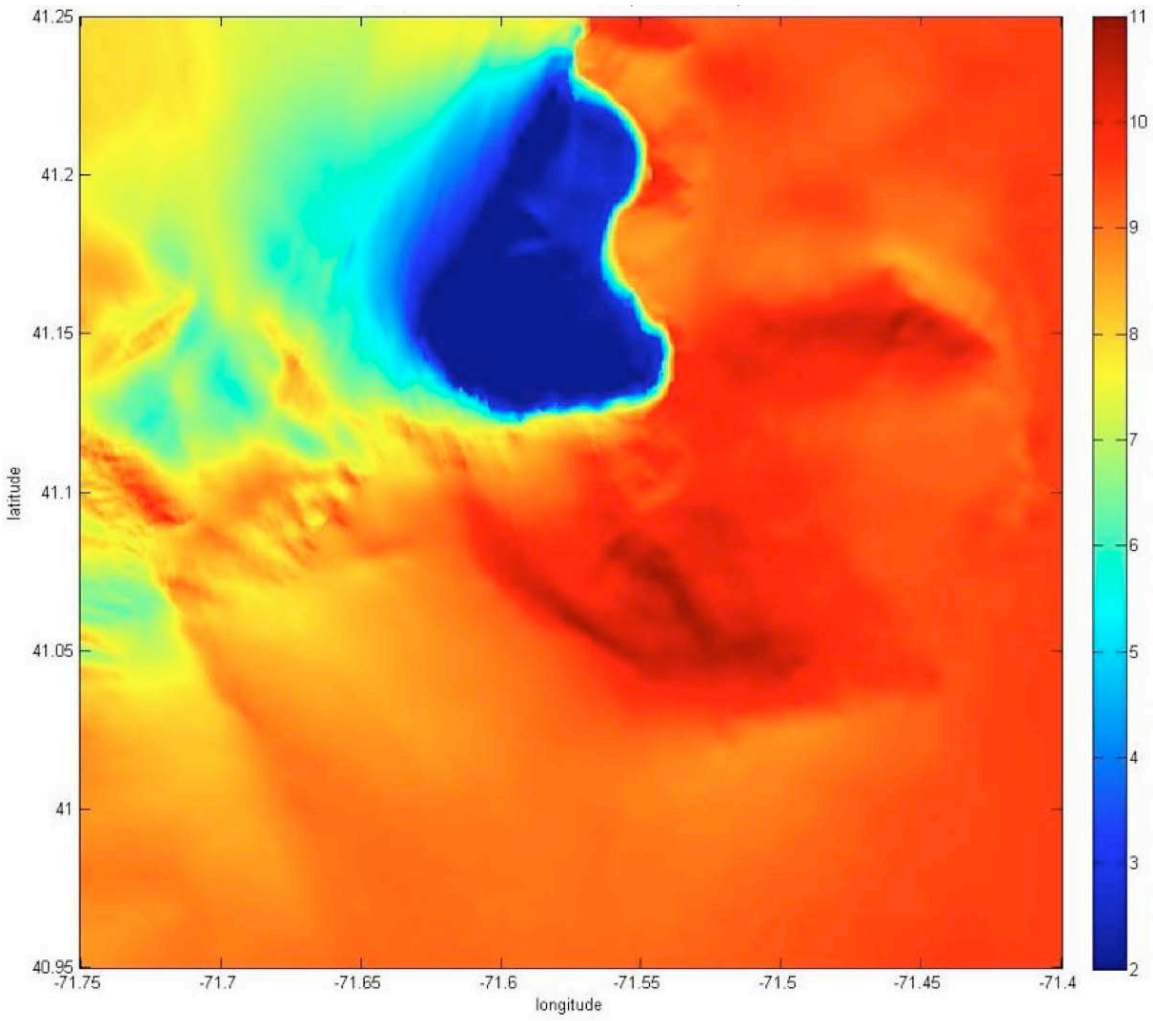

Figure 4.8 : Worst-case scenario wave height for 100 year storm (axis in m), 90 deg. incidence. Incident conditions : H_s = 9.8 m, T_p = 15.7 s, W = 34 m/s, and 90^o direction.

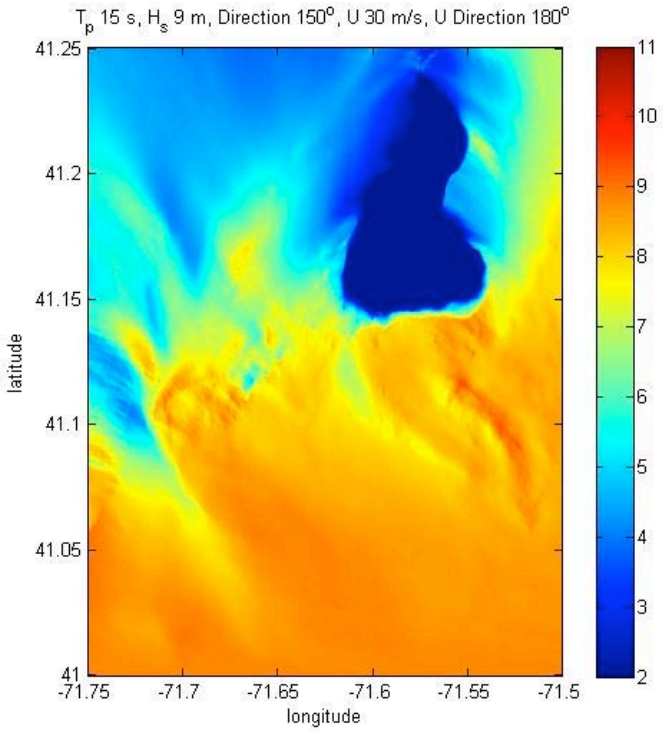

Figure 4.9 : Significant wave height (axis in m), for 30 m bathymetric resolution.

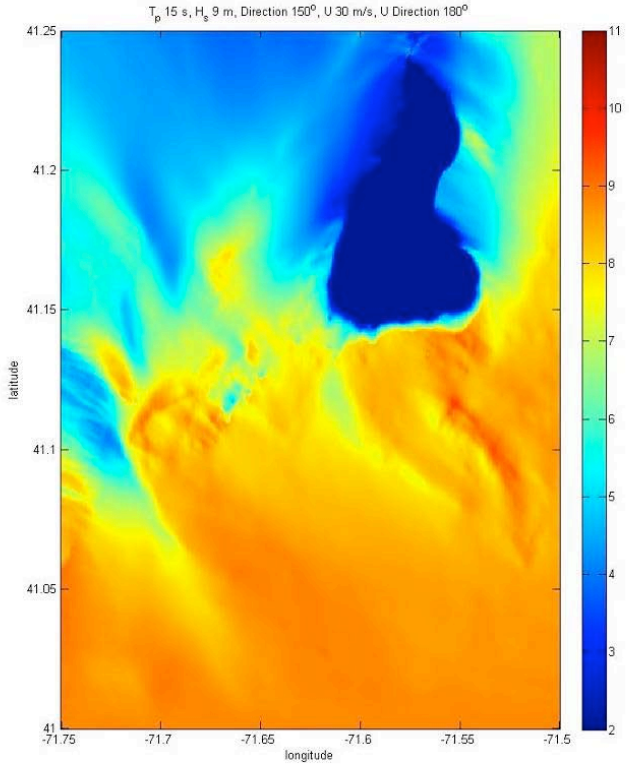

Figure 4.10 : Significant wave height (axis in m), for 50 m bathymetric resolution.

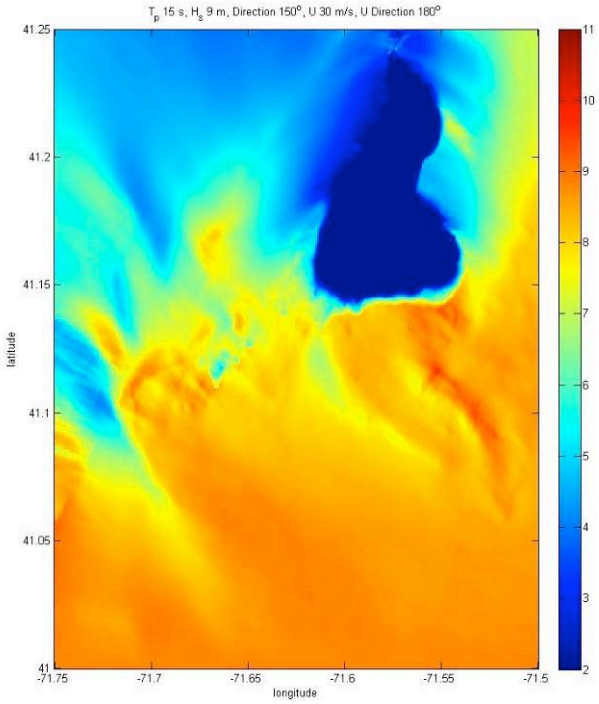

Figure 4.11 : Significant wave height (axis in m), for 70 m bathymetric resolution.

4.4 Sensitivity to domain size

In this section, we verify the accuracy of STWAVE simulations with respect to the extent of the computational domain. The latter can have an effect if salient aspects of the bathymetry that might otherwise influence wave transformation processes, such as refraction, are not included in the domain.

In these tests, the southern boundary of the computational domain is kept at around the location of the WIS station 101 (i.e., 41^o lat.), and the longitudinal extent of the domain is gradually increased. Three cases were tested, 71.85-71.40^o W (wide domain), 71.75-71.50^o W (standard used in simulations), and 71.72-71.53^{o}W (narrow domain). Simulations were performed for a 9 m, 15 s wave from 150 deg with a 30 m/s wind from the south.

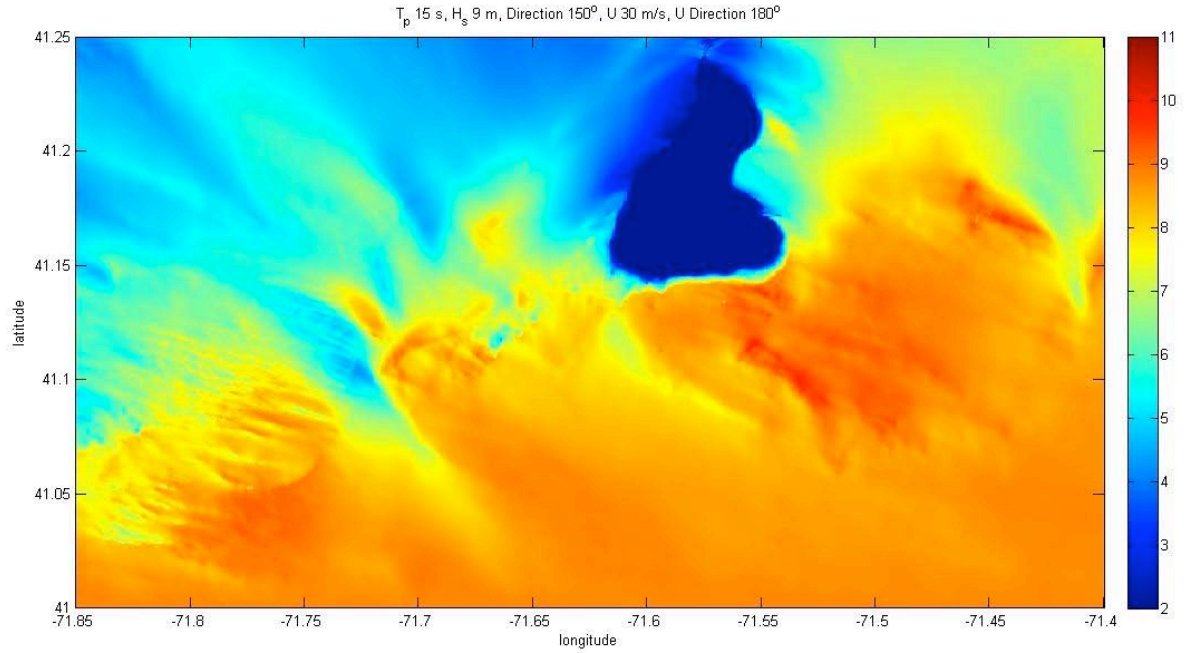

Figure 4.12 : Significant wave height (axis in m) for wide domain.

Results for the two wider domains in Figs. 4.12 (wide) and 4.13 (mid) show small variations in simulated significant wave height. Results for the narrower domain in Fig. 4.14 (narrow), however, show significant differences, particularly in the region far west of Block Island, where wave heights are larger. This is likely due to the absence of effects of the complex bathymetry around the canyon mentioned earlier. These simulations show results are independent of domain size as long as the domain is larger than the medium case (Fig. 4.13), but are significantly impacted for the narrow case (Fig. 4.14). The simulation cases presented in Section 3 used the medium domain case and hence should give reliable estimates.

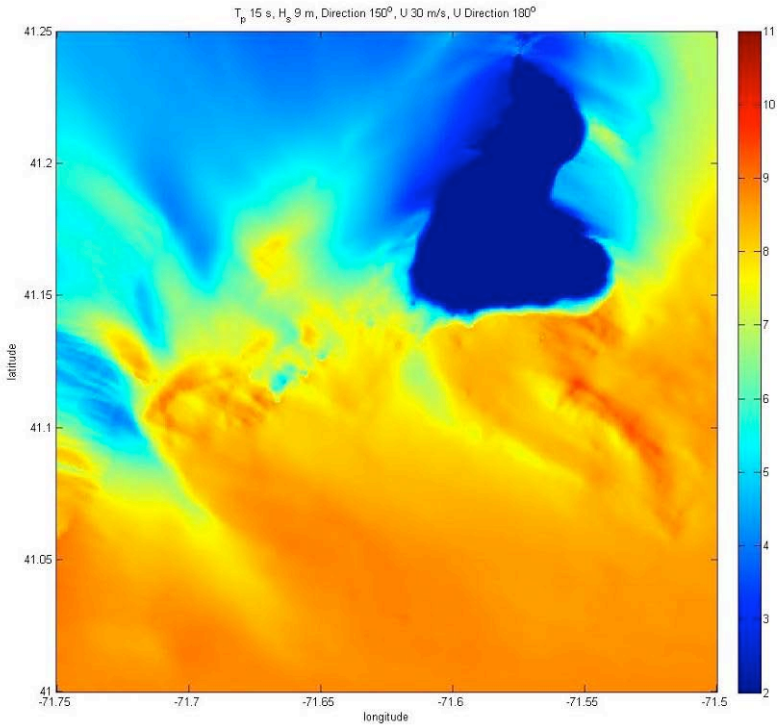

Figure 4.13 : Significant wave height (axis in m) for medium (standard) domain.

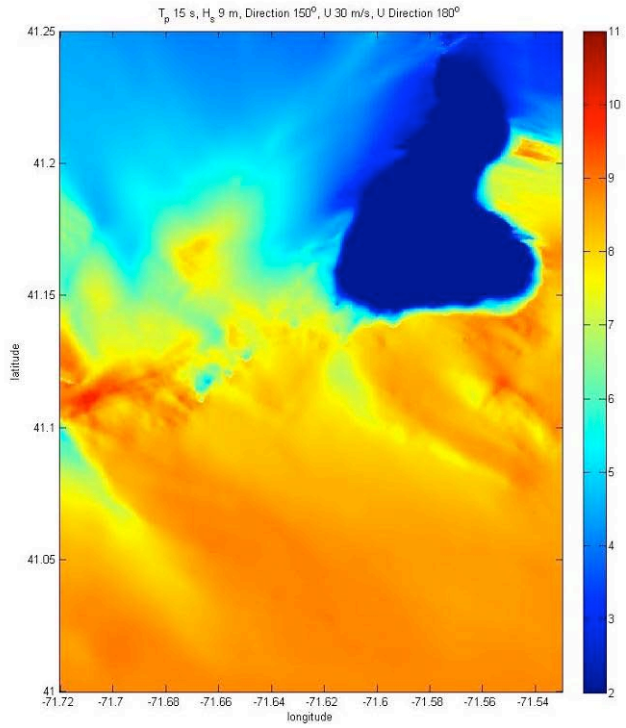

Figure 4.14a : Significant wave height (axis in m) for narrow domain.

4.5 Sensitivity to spectral resolution

In this section, we verify the accuracy of STWAVE simulations with respect to the frequency resolution of the wave spectrum used as input to the model.

The latter must accurately represent the shape of the incident wave spectrum, as well as the effects of subsequent wave transformations, as these are both related to frequency. As before, three cases were evaluated: 20 frequency bins (low resolution), 50 frequency bins (medium resolution; the standard value used in extreme simulations), and 80 frequency bins (high resolution). Simulations were performed for a 9 m, 15 s wave from 150 deg with 30 m/s winds from the south.

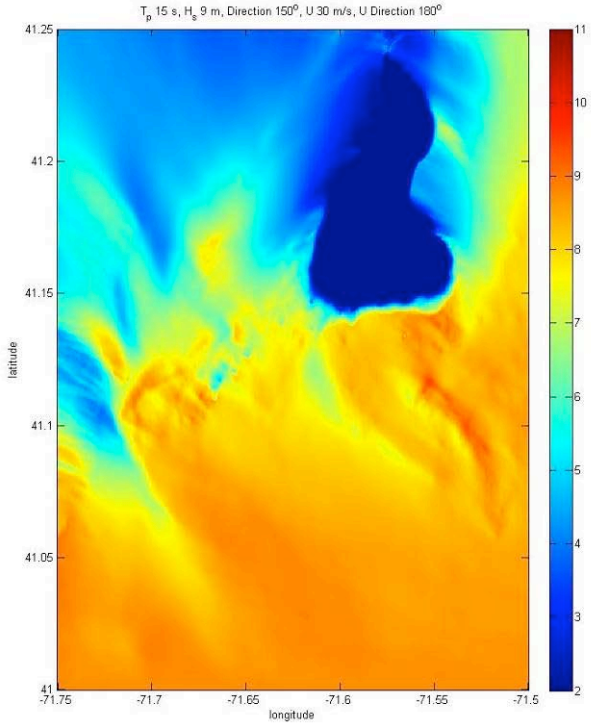

Figure 4.14b : Significant wave height (axis in m) for low frequency resolution.

The difference in results, shown in Figs. 4.14, 4.15 and 4.16, for low, medium, and high frequency cases, respectively is negligible. While the low resolution case shows larger wave heights in the region southeast of Block Island, it is also very similar to results of the 80 frequency bin case.

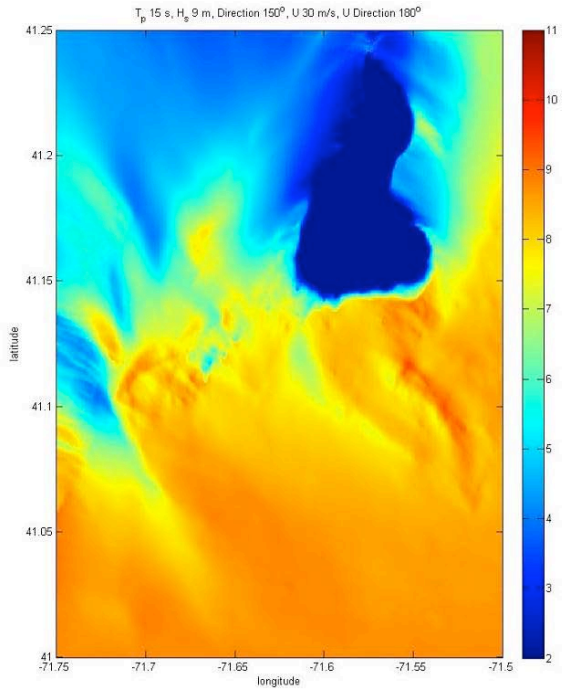

Figure 4.15 : Significant wave height (axis in m) for medium (standard) frequency resolution.

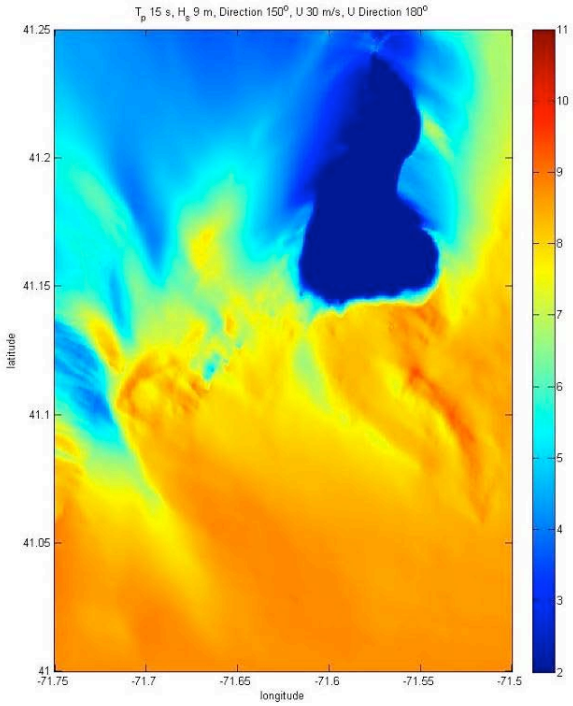

Figure 4.16 : Significant wave height (axis in m) for high frequency resolution.

5 Conclusions

The objectives of this study were first to obtain estimates of conditions associated with extreme storm events, for return periods of 20, 50, 75, and 100 years in the coastal region immediately to south of Block Island, and then to use these estimates as inputs into a numerical simulation that could provide estimates of the extreme wave climate for the region.

The wave estimates were calculated based on a statistical analysis of 20 years of hindcast wave (and wind) data available from the nearby WIS station 101. These were converted into standard directional wave frequency spectra and used as input to STWAVE, a steady-state spectral wave model. The outputs of such simulations were significant wave height, peak spectral period, and directional spread, as well as locations of actively breaking waves.

Wave climates were found to vary strongly geographically, with the significant wave heights west of Block Island typically being 2-3 m less than that south of Block Island (9 m). Similarly, the difference in wave height for each return period is smaller in the region west of the island due to depth-limiting shallow shoals that cause breaking and dissipation (i.e., bathymetric filtering).

Thus, as far as exposure of wind turbine structures to extreme waves, the waters surrounding Block Island cannot be considered homogeneous in terms of potential for development of offshore wind farms. The difference in wave climates west and south of the island represents a key distinguishing factor, with the more desirable area in this respect being southwest and west of the island.

A sensitivity analysis of simulation results to grid size and frequency showed negligible effects. Results only show a small sensitivity to the lateral extent of the computational domain and showed that the width must be sufficient to capture effects of salient bathymetric features. This was the case for the standard domains used in these simulations.

The STWAVE simulations, within the assumptions of the model (see Appendix A) may therefore be considered representative of actual extreme storm wave conditions that can be expected at the site, during the typical life time of wind farm.

6 References

Goda Y, 2000. Random seas and design of maritime structures, in Advanced series of Ocean Engineering, Vol. 15. Published by World Scientific, 443p.

Smith, Jane McKee, Sherlock, Ann R., & Resio, Donald T. *STWAVE: Steady-State Spectral Wave Model User's Manual for STWAVE, Version 3.0*. Coastal and Hydraulic Laboratory, U.S. Army Engineer Research and Development Center. February, 2001.

U.S. Army Corps of Engineers, 2004. Coastal and Hydraulics Laboratory Wave Information Studies, ERDC Waterways Experiment Station, Vicksburg, MS.

U.S. Army Corps of Engineers. 2002. Coastal Engineering Manual. Engineer Manual 1110-2-1100, U.S. Army Corps of Engineers, Washington, D.C. (in 6 volumes).

U.S. Army Corps of Engineers, Hydraulics and Water Quality Section, New England Division, September, 1988. *Tidal Flood Profiles New England Coastline*.

Dean R.R. and Dalrymple, R.A. 1991. *Water Wave Mechanics for Engineers and Scientists*. World Sc. Pub.

Mei, C.C., 1989. *The Applied Dynamics of Ocean Surface Waves.* World Sc. Pub.

A Appendix: Overview of STWAVE equations and implementation

STWAVE is a steady state, finite difference, spectral wave model developed by the US Corps of Engineers (Smith, et al., 2001), based on the conservation of wave action balance equation. STWAVE simulates depth-induced wave refraction and shoaling, current-induced refraction and shoaling, depth- and steepness-induced wave breaking, diffraction, wind-wave growth, and wave-wave interaction and white-capping that redistribute and dissipate energy in a growing wave field. STWAVE is based on the assumption that the relative phases of the spectral components are random, and thus phase information is not tracked (i.e., it is a phase-averaged model). In practical applications, wave phase information throughout a model domain is rarely known accurately enough to initiate a phase-resolving model. Typically, wave phase information is only required to resolve wave-height variations near coastal structures for detailed, near-field reflection and diffraction patterns. Thus, for these situations, a phase-resolving model should be applied.

A.1 STWAVE assumptions

a. Mild bottom slope and negligible wave reflection. STWAVE is a half-plane model. Waves reflected from the shoreline thus are neglected. Forward-scattered waves, e.g., waves reflected off a structure but traveling in the +x-direction, are also neglected. The half-plane model also means that wind directions greater than 60^o relative to the x-axis will result in under-prediction.

b. Spatially homogeneous offshore wave conditions. The input spectrum in STWAVE is constant along the offshore boundary.

c. Steady-state waves, currents, and winds. STWAVE is formulated as a steady-state appropriate for wave conditions that vary more slowly than the time it takes for waves to transit the computational grid. Wind waves are in fetch-limited or fully developed conditions.

d. Linear refraction and shoaling, *depth-uniform current*, and n*egligible bottom friction*.

A.2 Equations

Interactions of waves with a space-varying current *U(x,y)* are simulated in depth *D(x,y),* in a reference frame moving with the current. Wave parameters in this frame are denoted with the subscript *r*, for being "relative" to the current, and parameters in the non-moving reference frame have subscript *a*, for "absolute."

The (linear) wave dispersion relationship is given in the moving and absolute reference frames as (Dean and Dalrymple, 1991),

$$\omega_r^2 = gk\tanh kD \quad ; \quad \omega_a = \omega_r + kU\cos(\delta - \alpha) \tag{A.1}$$

with ω and k the wave angular frequency and wavenumber, respectively, δ the local angle of the current and α the local angle of the wave orthogonal direction (i.e., normal to the wave crest) both with respect to the x-axis.

Similarly, one defines the local wave celerity C and group velocity C_g in both frames as,

$$\begin{aligned} C_r &= \frac{\omega_r}{k} \quad ; \quad C_a = C_r + U\cos(\delta - \alpha) \\ C_{gr} &= \frac{C_r}{2}\left(1 + \frac{2kD}{\sinh 2kD}\right) \quad ; \quad C_{ga_i} = C_{gr_i} + U_i \end{aligned} \tag{A.2}$$

where subscript i =1,2, denotes both horizontal components in tensor notation.

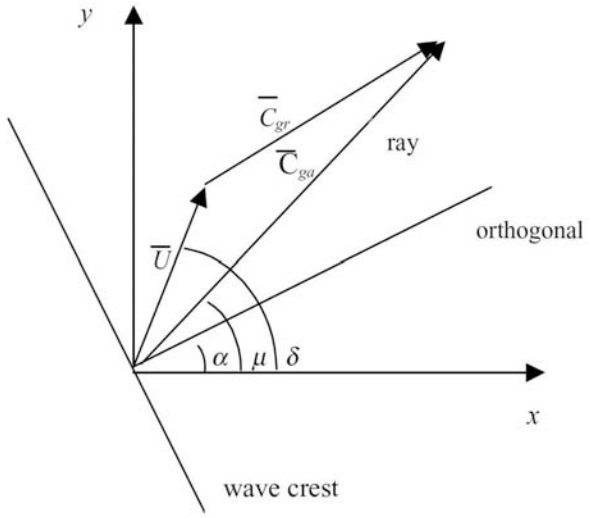

Figure A.1 : Definition sketch of wave and current vectors in STWAVE [2].

The direction vector of the wave orthogonal, also defined as k_i/k = (cos α, sin α), is also that of local wave celerity C_a. The direction vector of the wave ray, which indicates the direction of energy propagation, is defined as (cos μ, sin μ), and is also that of the absolute group velocity C_{ga}. From Eq. (A.2), we thus find,

$$\mu = \arctan\left(\frac{C_{gr}\sin\alpha + U\sin\delta}{C_{gr}\cos\alpha + U\cos\delta}\right) gk\tanh kD \tag{A.3}$$

Note, without current, the wave rays and orthogonals are identical.

In steady-state conditions, the wave orthogonal direction is given by Mei (1989), in a curvilinear coordinate system *(r,n)* as,

$$C_{ga}\frac{d\alpha}{dr} = -\frac{C_r k}{\sinh 2kD}\frac{dD}{dn} - \frac{k_i}{k}\frac{dU_i}{dn} \tag{A.4}$$

where *r* is coordinate in the direction of the wave ray and *n* is the coordinate normal to the direction of the wave ray.

The governing equation for steady-state conservation of spectral wave action along a wave ray is given as,

$$C_{ga_i}\frac{\partial}{\partial x_i}\left(\frac{C_a C_{ga}\cos(\mu-\alpha)E(\omega_a,\alpha)}{\omega_r}\right)=\sum\frac{S}{\omega_r} \qquad \text{(A.5)}$$

where *E is* wave energy density (divided by $\rho_w g$, with ρ_w the water density) and *S* is energy source/sink terms (e.g., due to wind energy input and wave breaking dissipation).

Note that no current was used in the simulations in this work, thus all terms in the current frame of reference are equal to those in the absolute frame of reference. However, these equations were presented for completeness as they are used in STWAVE.

A.3 Source/sink terms

Surf-zone wave breaking. The maximum limit on the zero-moment wave height in STWAVE is,

$$H_{m0}^{\max}=0.1L\tanh kD \qquad \text{(A.6)}$$

The energy in the spectrum is reduced at each frequency and direction in proportion to the amount of pre-breaking energy in each frequency and direction band. Nonlinear transfers of energy to high frequencies that occur during breaking are not represented in the model. Model grid cells where wave height is limited by Eq. (A.6) are flagged as actively breaking cells.

Wind input. Waves grow through the transfer of momentum from the wind field to the wave field. The flux of energy F_{in}, into the wave field in STWAVE is given by,

$$F_{in}=0.85\lambda\frac{\rho_a}{\rho_w}C_m\frac{u_*^2}{g} \qquad \text{(A.7)}$$

where λ is a partitioning coefficient that represents the percentage of total atmosphere to water momentum transfer that goes directly into the wave field (typically 0.75) ρ_a is air density, C_m is mean wave celerity, and $u^* = W(C_D)^{1/2}$ is friction velocity with the wind speed *W*, and the surface drag coefficient, $C_D = .0012 + .000025W$.

The energy gain to the spectrum is calculated by multiplying the energy flux F_{in} by the equivalent time Δt for the wave to travel across a grid cell of length Δx,

$$\Delta t=\frac{\Delta x}{\beta C_{gm}\cos\alpha_m} \qquad \text{(A.8)}$$

with β a factor equal to 0.9 for the wind sea portion of the spectrum, and C_{gm} and α_m average group celerity and mean direction relative to the grid of waves in the spectrum. Note, because STWAVE is a half-plane model, only winds blowing toward shore (+*x* direction) are included.

Wave-wave interaction and white-capping. As energy is fed into the waves from the wind, it is redistributed through nonlinear wave-wave interaction. Energy is transferred from the peak of the spectrum to lower frequencies (decreasing the peak frequency or increasing the peak period) and to high frequencies (where it is dissipated). In STWAVE, the frequency of the spectral peak is allowed to increase with fetch (or equivalently propagation time across a fetch).

Wave energy is dissipated (most notably in an actively growing wave field) through energy transferred to high frequencies and dissipated through wave breaking (white-capping) and turbulent/viscous effects. There is a dynamic balance between energy entering the wave field because of wind input and energy leaving the wave field because of nonlinear fluxes to higher frequencies. These effects are parameterized in STWAVE.

A.4 Numerical implementation

STWAVE is a finite-difference numerical model, formulated on a Cartesian grid with square cells (Fig. A.1). The orientation of the grid is such that the input wave spectrum starts at the offshore boundary, defined by the *y*-axis, and waves are propagated in the cross-shore (positive *x*-direction). Wave angles are also defined in a typical Cartesian sense, i.e., measured counterclockwise from the positive *x*-axis. Wave refraction and shoaling are simulated in STWAVE by applying the conservation of wave action Eq. (A.5), with Eqs. (A.1-4), along backward traced wave rays. Rays are traced in a piecewise manner, from one model grid column to the next. A two-dimensional (i.e, in frequency and direction) wave spectra is set as input along the first grid column (the offshore boundary). For a point on the second grid column, the spectrum is calculated by back tracing a ray for each frequency and direction component of the spectrum. The ray direction, , is determined by Eq. (A.3). Only ray directions propagating toward the shore (-87.5 to +87.5 deg) are included. Energy propagating toward the offshore is neglected.

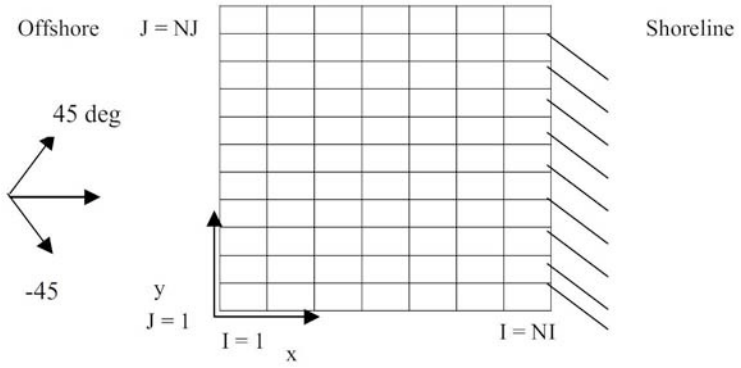

Figure A.2: STWAVE coordinate system and grid definition [2].

More specifically, each wave ray is traced back to the previous grid column, and the length of the ray segment is calculated. Derivatives of depth and current components normal to the wave orthogonal are estimated (based on the orthogonal direction at column at the current column) and

substituted into Eq. (A.4), to calculate the wave orthogonal direction at the previous column. Then, the wave number, wave and group celerities, and ray angle in the previous column are calculated. The energy is calculated as a weighted average of energy between the two adjacent grid points in the column and the direction bins. The energy density is corrected by a factor that is the ratio of the 5-degree standard angle bandwidth to the width of the back-traced band to account for the different angle increment in the back-traced ray. The shoaled and refracted wave energy in the current column is then calculated from the conservation of wave action along a ray (A.5).

A.5 Input/output files

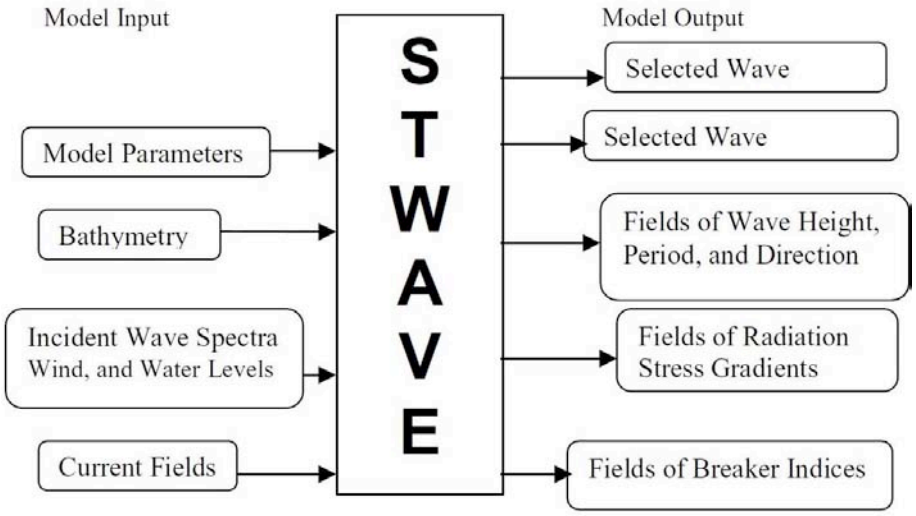

Figure A.3: STWAVE input and output files [2].

STWAVE takes up to four input files, with the current field being optional (and not used in this study). For brevity, aspects of the input and output files not used in this simulation will not be discussed within this document. Full discussion of input and output files, as well as their contents and examples are available in the software user manual [2].

A.5.1 Model Parameters

The model parameters file contains switches for various options:

- IPRP: Switch for propagation only (1), or propagation and source/sink (0) terms. These terms include wind-wave generation, wave-wave interactions, and whitecapping. These terms were included for simulations in this study.
- IBREAK: Switch for printing (1) or not (0) the field of breaker indices. Breaker indices were printed in this study, as active wave breaking has an effect on wave growth and forcing estimates.

A.5.2 Bathymetry

The bathymetry file determines the simulation domain size and shape, as well as provides the bathymetry for each cell in the domain:

- NI, NJ: The number of cross-shore (x-axis) and long-shore (y-axis) grid cells, respectively.
- DXINC: The grid spacing (meters). This, along with NI and NJ determine the actual spatial size of the simulation domain.
- Depths: The depths are listed starting at (1,NJ) and read in the cross-shore direction. Positive values indicate depth and negative values indicate altitude.

A.5.3 Incident Wave Spectra

The incident wave spectra file contains information on the spectral resolution and extent, as well as various other parameters. Multiple input spectra may be placed in the same file, such that multiple simulations may be run in succession. The parameters *W*, UDIR, and DADD (discussed below) are uniquely defined for each simulation.

- NF: The number of frequency bins in the spectra. 50 bins was the default value, also used for simulations in this study.
- NA: The number of directional bins in the spectra. This value must be 35, yielding a 5 degree bin width across STWAVE's ±87.5 degrees domain.
- *W*: Wind speed (meters/second), considered constant across the simulation domain.
- UDIR: Wind direction (degrees) relative to the STWAVE coordinate system.
- DADD: Water elevation correction (meters), used for water level changes due to storm surge, tidal changes, etc. This value is also considered constant across the simulation domain.
- Frequencies: A NF-length series of frequencies (Hz). This frequency vector is the same for all simulations in the same file. Accordingly, a standard frequency vector ranging linearly from 0.04 to 0.2 Hz was used in most simulations.
- Spectrum: The energy densities (meters^2/Hz/radian) of the input wave spectrum are listed starting with the lowest frequency and direction and continuing to the highest direction. This process is then repeated for the second-lowest frequency and so on. The number of points in the spectrum must be NF*NA.

A.5.4 Wave Parameter Fields

The wave parameters (significant wave height H_{m0}, peak period T_p, and mean direction α) are printed for each grid cell in the simulation. The values are written in the same order as the bathymetry values, starting at (1,NJ) and proceeding in the cross-shore direction to (NI,NJ), then moving over one row to begin again at (1,NJ-1). This process is performed for wave height, then period, then direction.

A.5.5 Breaker Index Field

The breaker indices are printed as binary indices, with 1 signaling breaking and 0, no breaking. The values are written in the same order as the wave parameter fields and bathymetries.

9.

Spatial and Temporal Variability of Surface Chlorophyll, Primary Production, and Benthic Metabolism in Rhode Island and Block Island Sounds

for the Rhode Island Ocean Special Area Management Plan 2010

by

Scott Nixon, Stephen Granger, Candace Oviatt, Lindsey Fields, and Jeff Mercer

University of Rhode Island, June 15, 2010

Executive Summary

The ecosystems of Rhode Island Sound (RIS) and Block Island Sound (BIS) are dependent on the growth of phytoplankton – single celled microscopic plants. It is the phytoplankton that ultimately support the growth of all of the animals in the sounds. Because of their importance, managing the sounds should include a consideration of where and when the phytoplankton are found and the rates at which they are growing in different areas throughout the annual cycle. Prior to the work described in this report, surprisingly little was known about the phytoplankton in RIS or BIS. In this study we were very fortunate to be able to work with local fishermen who agreed to collaborate with us and other members of the OSAMP science team to collect surface water samples from all over the OSAMP study area in both sounds over a full year. These water samples were retrieved and brought to our laboratories at the Graduate School of Oceanography (GSO) where they were filtered. The phytoplankton were collected on the filter and the photosynthetic pigment they contain (chlorophyll) was extracted and measured. This is a standard way of quantifying the amount of phytoplankton present in marine waters and is much less time consuming that counting the individual cells. Our results showed that during most of the year phytoplankton are significantly more abundant in the surface water of RIS then in BIS. The exception is during summer, when the weaker tidal currents in RIS allow the water column to become thermally stratified – that is, the surface waters are sufficiently warmer than the bottom water that the water column does not mix vertically. When the water column is not well mixed, the inorganic nutrients the phytoplankton need to grow become depleted in the sunlit surface water while they accumulate in the dark bottom waters where light limitation prevents phytoplankton from growing. The nutrients (nitrogen and phosphorus and silica) accumulate in the bottom water because the phytoplankton sink out of the surface waters when they die or they sink as fecal pellets if they are eaten by small animals in the surface water. Much of the nitrogen and phosphorus and silica that the sinking organic mater contains is regenerated on the bottom by animals and bacteria living on and in the sediments.

The chlorophyll measurements also showed that there was a strong bloom or period of rapid growth in abundance of the phytoplankton in the sounds during fall. This fall bloom was not seen in similar measurements made by the GSO plankton monitoring program in mid Narragansett Bay. Aside from the fall bloom period, the concentrations of phytoplankton in the sounds are significantly lower than found in the mid bay. This does not necessarily mean that the total abundance of phytoplankton beneath a given area of water in the sounds is lower than in the bay

because the sounds are much deeper and the water there is clearer than in the bay. Thus, phytoplankton may be able to live and grow at greater depths in the sounds. We began making measurements of how fast the phytoplankton were growing about six months after the chlorophyll measurements began when some extra funding became available. These measurements are much more technically challenging and we are still analyzing the measurements that have been made. It seems likely at this point that rates of growth will be similar to those measured by others in the lower West Passage on Narragansett Bay (100-200 g Carbon per square meter per year).

We also measured the rates at which organic matter was being consumed and nutrients were being regenerated on the bottom at stations in each sound where organic matter accumulated (areas with fine grained sediments relatively high in organic matter in contrast to the coarser sandy sediments that cover a larger part of the sounds). These measurements were made by dropping a large (0.25 m^2) box corer to the bottom and collecting sediments that were then brought up to the surface and put on the deck of a fishing boat. Smaller cores of this sediment were collected with plastic pipes and returned to the laboratory where they were kept in the dark at constant temperature (the same as measured in the bottom water in the sounds) in large walk-in environmental chambers. Filtered bottom water was carefully placed over the sediments in each core and changes in the concentrations of dissolved oxygen, ammonium, nitrite, nitrate, phosphate, and silicate were measured over many hours. These gave us a measure of how fast organic matter was being respired by the bottom and how fast nutrients were being regenerated. The rates appear similar in both sounds and appear to be significantly higher that similar rates in Narragansett Bay. This is probably due to the fact that the fine grained silt-clay sediment areas we were sampling in the sounds concentrate organic matter sinking to the bottom. All of these studies will be continued with support from RI Sea Grant and the National Science Foundation even though the OSAMP research program has concluded.

Table of Contents

List of Figures

concentrations also indicate dates upon which samples were collected and incubated for primary production estimates.

Fig 13. Daily Areal Production (blue lines) estimates and measured chlorophyll a concentrations (red dots) from BIS utiizing niskin sampling method. The dates corresponding to the chl a concentrations also indicate dates upon which samples were collected and incubated for primary production estimates.

Fig 14. Mean sediment oxygen uptake measured through sediment core incubations at different temperatures (17°C, 7°C , and 4°C) for 2 stations in RIS and 1 station in BIS. Station RIS 2 is the easternmost RIS station, and RIS 1 is the western Rhode Island Sound station. Bars represent standard deviation.

Fig 15. Sediment oxygen uptake for mid-Narragnsett Bay over an annual temperature cycle. Opaque circles are historical values (Nixon et al. 1976, 1980, and unpublished data), open circles are from more recent measurements taken in 2005-2006 (Fulweiler 2007). Red and yellow circles show mean sediment oxygen uptake for Rhode Island Sound (RIS) and Block Island Sound (BIS), respectively. Adapted from Fulweiler and Nixon (2009).

List of Tables

Abstract

The goal of this project was to obtain the first measurements of phytoplankton biomass (standing crop) measured as chlorophyll over an annual cycle throughout Rhode Island and Block Island Sounds as well as the first measurements over an annual cycle of carbon fixation by the phytoplankton using modern ^{14}C uptake techniques. We also sought to obtain the first measurements of benthic-pelagic coupling in the sounds by incubating fine grained silt-clay sediment cores collected from two stations in Rhode Island Sound (RIS) and one in Block Island Sound (BIS). During these incubations we measured the sediment-water flux of dissolved oxygen and major inorganic nutrients (ammonium, nitrite, nitrate, phosphate, silicate). The first goal was achieved through collaboration with commercial fishermen and fellow OMSAP scientists who collected surface water samples many times at dozens of locations for our analyses. The seasonal cycle throughout both sounds was marked by a strong fall bloom that was not observed at a long-term monitoring station in mid Narragansett Bay. The bloom appeared to be synchronous throughout inner and outer reaches of both sounds. Chlorophyll concentrations in the surface water were lower than found in the mid bay. While surface chlorophyll was lower in RIS when it was thermally stratified during summer (1.3 $\mu g\ L^{-1}$ in RIS vs 2.0 $\mu g\ L^{-1}$ in BIS), the mean annual concentration was higher in RIS (2.7 $\mu g\ L^{-1}$ in RIS vs 1.8 $\mu g\ L^{-1}$ in BIS). It is possible that the higher mean annual chlorophyll in RIS reflects a higher annual carbon fixation that contributes to the higher biomass of fish and lobsters per unit area that was found in RIS by the National Marine Fisheries Service/Virginia Institute of Marine Science Northeast Area Monitoring and Assessment Program (NEAMAP) Near-Shore Trawl Survey. ^{14}C measurements of primary production by the phytoplankton became possible when additional funding became available, so only seven months of data have been acquired at this writing. Additional sampling is planned to complete the annual cycle. Based on the measurements in hand, we anticipate that annual production may be in the 100 to 200 g C $m^{-2}\ y^{-1}$ range in both sounds. This is similar to values measured previously by others in the lower West Passage of Narragansett Bay. While nutrient exchanges between the sediments and the overlying water are still being analyzed, the oxygen uptake data show little difference between the sounds. The oxygen uptake rates are significantly higher than measured in Narragansett Bay during the 1970s and 1980s, and are much higher than recent measurements in the mid bay. It is probable that these higher rates reflect the focusing of organic deposition in the fine-grained sediment areas where cores from the sounds were collected.

1 Introduction and Background

Marine ecology became a quantitative science in the late 1800s and early 1900s in order to answer a basic and very practical question, "why do some lakes or areas of the sea consistently yield greater catches than others?" For marine fisheries, the pursuit of this question led to the formation of the Kiel Commission for the Scientific Study of the German Seas, precursor to the current International Council for the Exploration of the Sea or ICES (Nixon et al. 1986, Mills 1989). Advances in analytical chemistry made it possible to begin to obtain measurements of the low concentrations of primary plant nutrients dissolved in sea water and the development of metered nets and coring devices made it possible to take quantitative samples of plants and animals in the water column and in sediments. The application of these tools led early researchers to see links between nutrient levels, phytoplankton (or, in shallower systems, macrophytes like eelgrass), zooplankton, and fisheries yields. As Karl Brandt, one of the leading marine scientists of the time, put it in 1901:

> The animals which inhabit the sea are developed in proportion to the quantity of their food. Now, since all this food comes directly or indirectly from plants, it follows that we can just as well estimate the real production of animal life in water by means of the annual yield of vegetation as we can estimate the product of a farm by the quantity of grass and fodder that it affords.

This view predominated for many decades and supported what the great fisheries ecologist D. H. Cushing (1975) called the "agricultural model" of marine productivity. But, of course, agriculture is necessary precisely because unmanaged nature does not often provide simple, low–diversity ecosystems with short, linear food chains that support high yields.

The development and application of radioactive (e.g. ^{14}C, ^{32}P, ^{3}H) and stable (e.g. $\delta^{13}C$, $\delta^{15}N$) isotopic techniques following the Second World War, as well as greatly enhanced optical and electron microscope capabilities, allowed us to see that measurements of standing crops of larger organisms missed a great deal of microbial complexity and a very dynamic cycling of nutrients in marine systems. The ways in which traditional grazing food chains leading to the production of relatively large and long-lived animals interact with the diverse microbial parts of the

ecosystem that turn over very rapidly remains a key question in marine ecology. And, of course, these interactions must respond in complex ways to changes over virtually all time scales in the physical environment.

In spite of all this complexity, it is still possible to see some first order correlations between primary production by phytoplankton and marine fish production (Iverson 1990) and harvest (Nixon 1988), at least in systems where hypoxia and over harvesting are not important stresses (e.g. Breitburg et al. 2009). Because there is a correlation between phytoplankton standing crop (measured as chlorophyll) and carbon fixation measured using ^{14}C uptake (e.g. various BZI models, Cloern et al. 1995, Brush et al. 2002), it is also possible in some cases to find correlations between phytoplankton chlorophyll and marine fishery yields (e.g. Ware and Thomson 2005). Because of these cross system correlations there is reason to believe that factors which influence the standing crop of phytoplankton may also influence the production of the phytoplankton and thus the productivity of fish, shell fish, and decapods (e.g. Nixon et al. 2009). Gaining some basic understanding of phytoplankton standing crop and productivity and the nutrient cycling that support this primary production is a first step in understanding and managing coastal marine fisheries ecosystems like Rhode Island and Block Island Sounds. The purpose of this project was to take this first step for the longer term Ocean Special Area Management Planning in Rhode Island.

In southern New England coastal waters there is strong stoichiometric as well as experimental evidence that the supply of dissolved inorganic nitrogen (DIN) is one of the most important factors that limits the standing crop and productivity of phytoplankton, especially during summer (e.g. Kremer and Nixon 1976, Oviatt et al. 1995, Smayda and Borkman 2008). And in inner shelf systems like Rhode Island Sound (RIS) and Block Island Sound (BIS), Rhode Island's major fishery ecosystems and the setting for the work described here (Fig. 1), the supply of DIN in the surface water is believed to be strongly regulated by the degree of vertical density stratification. This, in turn, is influenced by fresh water runoff, solar heating, wind mixing, and tidal stirring. The overall interplay of these factors appears to result in Rhode Island Sound being stratified during the warmer months and the more energetic Block Island Sound remaining generally well-mixed vertically year around (Shonting and Cook 1970, Edwards et al. 2004, Granger and Nixon unpublished survey data, Fig. 1). The transition in stratification between the two adjacent Sounds appears to be largely due to tidal mixing which can be seen in context using contours of the mean

Vertical Stratification Index (Simpson and Hunter 1974) calculated by C. Chen (U. Mass. Dartmouth, personal communication) using the FVCOM model (Fig. 2) (Chen et al. 2003).

Based on this difference in the physics of the two Sounds, we hypothesized that phytoplankton chlorophyll (and primary production per unit area) in smaller, well– mixed BIS (~ 635 km2, mean depth of 28 m) would be higher than in the much larger and seasonally stratified RIS (~ 1420 km^2, mean depth of 29 m). The reason being that deep DIN–rich shelf water coming into the Sounds will be more rapidly mixed up into the euphotic surface water in BIS as will DIN released from the bottom sediments as organic matter sinking out of the water column is decomposed. In other words, the productive pelagic part of the ecosystem is more tightly coupled with the heterotrophic regenerative bottom part in BIS than in RIS. On the other hand, RIS lies immediately off Narragansett Bay which receives large amounts of nitrogen from land drainage and direct sewage discharges (Nixon et al.2008). The importance of this for productivity in RIS is unknown. The concentrations of DIN in lower Narragansett Bay are about 2-4μM during the warmer months (Pilson 1985), but the volume of RIS is about 20 times that of the bay. BIS lies between RIS and Long Island Sound, and the latter also receives large amounts of land drainage. But water from Long Island Sound largely leaves the sound around Montauk Pt. at the tip of Long Island and may not mix much with BIS water (Edwards et al. 2004, D. Ullman, URI, personal communication). Hypoxia does not appear to be a significant factor in RIS or BIS.

It may seem surprising that we could not make a definitive statement about the comparative standing crop of phytoplankton and primary production in RIS and BIS prior to this study, especially given the wealth of marine research institutions surrounding them and their importance as fishery ecosystems. But these inner shelf coastal systems appear to have previously "slipped through the crack," perhaps because they are too small for blue water oceanographic research ships and too large and exposed for small inshore research vessels. In any case, we began the first systematic sampling program for chlorophyll (and light attenuation in the water column) in both sounds in December, 2008 and the sampling is on-going. Prior to this very few observations of water column ecology had been made in the systems (or at least published) since the pioneering studies by Gordon Riley in BIS over half a century ago (Riley 1952 a, b). At that time Riley (1952b) concluded, "… there seems to be little doubt that B.I.S. has a higher concentration of phytoplankton than the adjacent waters to the east and south…" An ongoing analysis of SeaWiFS sea surface color imagery by K. Hyde and J. O'Reilly at the National Marine Fisheries Service (NMFS) laboratory in Narragansett (personal communication)

suggests that the surface chlorophyll between 1998 and 2007 may have averaged about 2.1 mg m^{-3} in BIS compared with 1.4 mg m^{-3} in RIS. But this is based on an algorithm that has not been calibrated with local measurements of chlorophyll and primary production in the sounds. We are working with the NMFS scientists to develop a seasonally adjusted (if necessary) field verified algorithm for each sound so that we can make spatially explicit estimates of chlorophyll and productivity from satellite color imagery (SeaWiFS and MODIS). When additional OSAMP funding became available, C. Oviatt and J. Mercer began measurements of ^{14}C uptake by the phytoplankton at one station in RIS and the BIS station (along with supporting measurements of vertical light attenuation, temperature, and salinity) beginning in October 2009. Their work is also on-going. Methods for all of this analytical work are described in more detail in the methods sections below.

Strong benthic-pelagic coupling is characteristic of coastal systems. To document this connection, wanted to obtain the first measurements of the benthic metabolism in the sounds as measured by oxygen uptake and inorganic nutrient regeneration. Measuring the benthic metabolism would have the added benefit of providing a rough check on our estimates of primary production since cross-system comparisons have shown correlations between the primary production in the water and respiration on the bottom. As described above, our hypothesis was that nutrients regenerated on the bottom and in bottom waters would be more rapidly mixed up into the euphotic zone in RIS than in BIS and help to support higher primary production there.

2 Methods

2.1 Surface Chlorophyll and Vertical Light Attenuation

Surface water samples were collected in two ways. In the great majority of cases, bucket samples were collected, placed in opaque plastic bottles and kept cool in the dark until returned to the laboratory for processing. In a relatively few cases when primary production was also being measured, water was collected using a long tube as described below in the primary production methods section. The chlorophyll concentrations measured in the tube samples are not co-mingled with the concentrations from bucket samples. The largest number of samples were collected by two collaborating commercial fishermen during voyages of opportunity (Capt. Michael Marchetti and Capt. Rodman Sykes). While the time between water collection and

processing in the laboratory necessarily varied by station and circumstance, it was usually about five hours. Samples were also collected by collaborating OSAMP scientists and/or their students (D. Ullman, D. Codiga, J. King, P. Payton, S. McWilliams) in addition to our own laboratory personnel. Because voyages of opportunity were used as the only practical way in which to sample the large areas involved, surface chlorophyll samples were not collected on a fixed time scale or at fixed locations. In all cases, sample locations were taken using GPS.

Vertical light attenuation coefficients (-k m^{-1}) were calculated from profiles of light at various depths as described below. These measurements were made by our laboratory personnel or by collaborating scientists noted above. The commercial fishermen took Secchi disk readings (on a downcast) using a calibrated line and a 20 cm dia black and white disk. These were converted to approximate –k values using 1.7/D (Idso and Gilbert 1974). When available, -k values were also calculated from measurements of light attenuation with depth taken with a SeaCat 19 SeaBird Electronic equipped with a LiCor 4π light sensor.

From each sample bottle, three 100 ml aliquots of sample were filtered onto 0.7 μm GF/F filters (Whatman, 2.5 cm dia; Aminot and Rey 2000). Chlorophyll was extracted by placing each filter in 10 mL of 90% buffered acetone (20 ml for tube samples) for 24 hours (Cohen 1995). Following extraction, each sample was centrifuged for 5 minutes. Each extract was transferred to a clean 50 mL glass tube where it was well mixed before approximately 8 mL were transferred to a clean glass tube that was inserted into the fluorometer. Fluorescence readings were measured with a Turner Designs 10AU Laboratory Fluorometer.

Chlorophyll and phaeophytin concentrations (μgL^{-1}) were calculated using the EPA Method 445.0 by Arar and Collins (1997). After the initial fluorescence reading (f_o), two drops of 10% HCl were added and a second reading was taken (f_a).

$$\text{Chlorophyll } a \text{ (g/L)} = Fs * [r/(r-1)] * (fo-fa) * (V_e/V_f)$$

$$\text{Phaeophytin (g/L)} = Fs * [r/(r-1)] * (r*fa-fo) * (V_e / V_f)$$

Where:

Fs = known chlorophyll concentration / fluorometer reading
r = fo of pure chlorophyll standard / fa of pure chlorophyll standard
fo = fluorescence of sample, before acidification

fa = fluorescence of sample, after acidification
V_e = Volume of extracted chlorophyll *a*
V_f = Volume filtered

Mean chlorophyll and phaeophytin values were calculated from triplicate sub samples. Chlorophyll a concentrations were plotted versus daily areal productivity measured at the same time to determine if chlorophyll a concentrations could be used as a reliable indicator of primary production.

2.2 Primary Production

2.2.1 Sample Collection

In order to obtain estimates of primary production in the offshore waters of Rhode Island two sites were sampled; one in Block Island Sound and one in Rhode Island Sound (Fig 3). The Rhode Island Sound sampling site was approximately 15.5 kilometers northeast of the northern tip of Block Island at 71° 23.825' W and 41° 16.361' N. The depth at this station was approximately 40 meters. The Rhode Island sampling site was 7.0 kilometers southwest of the northern tip of Block Island at 71° 39.652' W and 41° 13.007' N. The depth at this station was approximately 36 meters.

When possible, water samples were collected by two different methods. The first method was to collect water using a Niskin bottle 1 meter below the surface. The second method involved using a 17 meter long by 3/4 inch diameter hose to obtain a depth integrated water sample. A hose with an open valve at the top end was lowered to 17 meters (~ avg. euphotic depth) at which point the valve was closed. The hose was then brought to the surface at which point the valve was again opened and the water drained into a large bucket and homogenized. This procedure is analogous to putting your thumb over the top of a straw in a glass of water and then removing the straw and the water it contains from the glass. With both sampling methods the water was filtered through a 300 µm-mesh screen (to remove large zooplankton) into opaque 1-L polyethylene bottles. The samples were then placed in a cooler filled with ambient seawater (to maintain ambient temperature) and transferred to the URI MERL laboratory. In addition, vertical profiles of temperature, salinity, PAR, and in situ fluorescence measurements were collected using a SeaBird CTD equipped with a Turner SCUFA submersible fluorometer and a Biospherical Scalar PAR sensor.

In order to obtain as many samples as possible, water was collected by two volunteer fishermen who collected samples when a University chartered boat was not available. These fishermen collected water samples using a Niskin bottle as noted above and also recorded Secchi depth measurements to be used in primary production calculations.

2.2.2 Primary Productivity by ^{14}C

Primary production was measured using a small volume/short incubation time method (Lewis and Smith, 1983) using standard ^{14}C procedures from Strickland and Parsons (1972). 20 mL borosilicate vials were spiked with 100 µL of 10 µCi/mL (1µCi for 5 mL of water) carbon-14 (^{14}C) stock solution. Individual water samples were gently mixed and 5 mL of sample was pipetted into the spiked 20 mL borosilicate vials. A total of 18 vials (16 light and 2 dark) were filled for each water sample, capped, and two vials were immediately placed into opaque covers. Each vial was placed into a specified location in an incubation tray.

Incubation trays were placed into a light and temperature controlled incubator and were incubated within 2°C of the *in situ* temperature for two hours. Each location in the tray had a specified light intensity (range 0-2000 $\mu Em^{-2}s^{-1}$) which was achieved by applying neutral-density screening to the underside of the tray. The light intensity at each vial location within the incubator was measured with a LiCor 192SA cosine irradiance sensor before the incubation period. The cosine values were converted to 4π readings using an empirically determined equation:

$$4\pi = 19.2 + 1.098 (\cos) - 0.00011 (\cos)^2$$

with both 4π and cosine light intensity in units of $\mu E\ m^{-2}\ sec^{-1}$. The light data measured in the incubator were converted prior to fitting P-I curves.

Upon removal from the incubator, 200 µL of 0.10N HCl was added to each vial, capped and mixed, and then uncapped again. Vials remain uncapped while gently agitated in the dark for approximately 40 hours to allow all of the unincorporated ^{14}C to be converted to CO_2 gas and removed from the sample. After this time period, 17 mL of MP Biomedicals Universol Scintillation Cocktail was added and the tightly capped vials were shaken vigorously. Measurements of ^{14}C converted into organic carbon are made on a Packard TriCarb Liquid

Scintillation Counter (Model 2900). The scintillation counter was configured to measure single labeled ^{14}C samples as disintegrations per minute (DPM) for five minutes.

To calculate the specific activity added on each incubation date, 100 µL of 10 µCi/mL ^{14}C stock was added to each of three vials containing 3 mL of β-phenylethylamine. After the stock was added, 17 mL of scintillation cocktail was added. The three specific activity vials, along with one blank containing 17 mL of scintillation cocktail, were counted with each set of samples.

2.2.3 Calculation of Primary Production

Volume specific primary production was calculated using equations similar to that of Strickland and Parsons (1972) as follows:

$$P(i) = \frac{(1.05DPM(i))DIC}{A_{sp}T}$$

$$P(d) = \frac{(1.05DPM(d))DIC}{A_{sp}T}$$

$$A_{sp} = DPM(sa)-DPM(back)$$

$$P(I) = P(i) – P(d)$$

Where:

P(*i*) = primary production rate at light intensity I (µgC L^{-1} h^{-1} or mgC m^{-3} h^{-1})
P(d) = dark production, (µgC L^{-1} h^{-1} or mgC m^{-3} h^{-1})
DPM(*i*) = dpm of sample incubated at light intensity I
DPM(d) = dpm of dark incubated sample
DPM(back) = background dpm in vial containing only scintillation cocktail
DPM(sa) = specific activity added to incubation samples (DPM)
T = incubation time (h)
DIC=concentration of dissolved inorganic carbon (µg/mL) (methods below)

For each of the water samples, a P – I curve (P(I) vs. the irradiance (I, µE m^{-2} s^{-1}) to which the incubating sample was exposed) was calculated from the data. The P – I curves were fit via one of two possible models, depending on whether significant photoinhibition occurred. In cases where photoinhibition was evident, the model of Platt *et al*. (1980) was fit to obtain the theoretical maximum production and terms for light-dependent rise in production and degree of photoinhibition.

$$P(I) = P_{sb}(1-e^{-a})e^{-b}$$

Where:

P(I) = primary production at irradiance I, corrected for dark fixation (P(i)-P(d))
P_{sb} = theoretical maximum production without photoinhibition
a = αI/ P_{sb} where α is the initial slope the light dependent rise in production
b = βI/ P_{sb}, where β is a term relaying the degree of photoinhibition.

If it was not possible to converge upon a solution, an alternative model of Webb *et al.* (1974) was similarly fit to obtain the maximum production and the term for light-dependent rise in production.

$$P(I) = P_{max}(1-e^{a'})$$

Where:

P(*I*) = primary production at irradiance I corrected for dark fixation (P(i)-P(d))
P_{max} = light saturated maximum production
a' = αI/ P_{max}, where α is the initial slope the light-dependent rise in production

P_{max} and P_{sb} are not equivalent but they are mathematically related using the equation:

$$P_{max} = P_{sb}\ [a/(a+b)][b/(a+b)]b/a$$

2.2.4 Light vs. depth profiles

To obtain a numerical representation of the light field throughout the water column averaged CTD light profiles (0.25 m intervals) were fit to the standard irradiance vs. depth equation:

$$I_z=I_o e^{-kz}$$

Where:

I_z=light irradiance at depth Z
I_o=incident irradiance (Z=0)
k=extinction coefficient

For each station profile, an extinction coefficient (k) was determined by regressing $\ln(I_z/I_0)$ *vs.* depth. The slope of the regression line estimates k (m^{-1}). When no CTD light profiles were available Secchi depth (Z_{sd}) measurements were made and k was calculated using the relationship determined by Holmes (1970) where $k = 1.44 / Z_{sd}$

Incident light data

Incident light data were collected and recorded at 15 min intervals using a Kipp & Zonen, Pyranometer Model SP Lite located at the nearby National Climatic Data Center (NOAA-NESDIS) Observatory in Kingston, RI. The total incident light data were converted to PAR using an empirically determined equation:

PAR = 0.4363 (Total Irradiance)

These data are used as the photoperiod incident light (I_o) time series in the following calculations.

2.2.5 Calculation of Daily and Areal Primary Production

Given the best fit parameters (P_{sb} or P_{max}, a, b) of the P – I curves obtained for each of the water samples, the photoperiod incident light (I_o) time series, and the extinction coefficient, it is possible to compute daily volumetric and areal production for each sample. Daily production ($\mu gC\ L^{-1}\ d^{-1}$) is obtained by integration of the determined activity throughout the photoperiod. The primary assumption of the approach is that the P – I relationship obtained at the time of sample procurement (towards the middle of the photoperiod) will be representative of the majority of production occurring during the photoperiod, which should be the case. Areal production ($mgC\ m^{-2}\ d^{-1}$) is obtained by integration of daily volumetric production vs. depth down to the depth of the euphotic zone. P – I parameters and extinction coefficients from the nearest sampling date and the actual photoperiod incident light series were used in order to obtain estimates for daily areal production on days that samples were not taken.

2.2.6 Dissolved Inorganic Carbon (DIC)

Inorganic carbon was determined by the measurement of carbon dioxide released by acidification of a sample. The sample was siphoned with a small bore tube into a 40 mL glass vial so as to not introduce any gas bubbles then 2 drops (0.1 mL) of sodium azide were added for preservation. The vial was capped with a Teflon/silica septa, making sure no bubbles were present, and stored at 4°C until analysis. Duplicate samples were collected, from which three replicates were measured. The sample was automatically injected into the instrument, which was fitted with a 0.343 mL sample loop, followed by the addition of 0.5 mL of 5% phosphoric acid.

As the pH of the sample is lowered, carbonate and bicarbonate ions are converted to dissolved carbon dioxide. High purity nitrogen purges any carbon dioxide and carries it to the molecular seive trap where it is held at 25°C, trapped, and concentrated. When this is complete, the trap is rapidly heated to 200°C. A stream of gas desorbs the carbon dioxide from the trap and carries it into a non-dispersive infrared analyzer (NDIR) which was calibrated to directly display the mass of carbon dioxide detected. Concentration of DIC was calculated by dividing this mass by the sample volume.

2.2.7 Adjustment for Rhode Island Sound Fall Bloom

When productivity measurements were compared to a time series of chlorophyll measurements from Rhode Island Sound it became obvious that our sampling dates missed a significant fall bloom. Over a 23 day time period between 10/20/2009 – 11/11/2009 (during which [Chl*a*] exceeded 4.5 μgL^{-1}) productivity values were adjusted to attempt to correct for this sampling bias. The first correction method utilized the chlorophyll *a* vs. production relationship described above. Nine chlorophyll measurements were obtained during the 23 day time period and were used to adjust daily areal production values over the time period by using chlorophyll concentration values from the closest possible date. This method however does not take into account differences in light intensity during the 23 day period. The second method followed the procedures described in the "Calculation of Daily and Areal Primary Production" section above but utilized P_{sb}, a, b, and k parameters from the January 19, 2010 sampling date as the average chlorophyll concentration over the 23 day time period was nearly identical to chlorophyll values from the January sampling date. This method allowed for the incorporation of variations in light intensity.

2.3 Benthic Metabolism

2.3.1 Field Collection

Triplicate sediment cores were collected on three occasions (fall, winter, and spring) from two stations in Rhode Island Sound and one station in Block Island Sound (Fig 3). Collections occurred when bottom water temperatures were 17˚C (October 2009), 4˚C (January 2010), and 7˚C (May 2010). The stations are located in depositional areas with fine-grain sediments that were found by ground truthing available sediment type data (McMaster 1960; U.S. Geological

Survey) and using suggestions made by J. Boothroyd (URI Geology, pers. comm.) and local fishermen. Intact sediment cores were collected using a 0.25 m^2 box corer. Three PVC subcores (30.5 cm long with a 10 cm inner diameter) were pre-mounted in the box corer (Hopkinson et al. 2001) to minimize disturbance of the surface layer during the coring operation. Cores were capped, dug out of the box corer, and maintained on deck in a dark cooler filled with water and held at ambient temperature during transportation back to the laboratory. Near-bottom water used during incubations (Hopkinson et al 2001; Fulweiler 2007; Fulweiler and Nixon 2009) was collected using a hose and pump and then filtered on deck down to 0.2 μm (A. Giblin, pers. comm.).

2.3.2 Analytical Methods

Upon returning to the laboratory, the cores were placed in a water bath in a dark temperature-controlled (at mean *in situ* field temperature) walk-in environmental chamber at the URI Graduate School of Oceanography. Cores were left uncapped with air stones gently bubbling oxygen through the overlying water in each core overnight (Hopkinson et al. 2001, Fulweiler 2007) to maintain the cores at saturation level. Before incubations, the overlying water in each core was gently siphoned off and replaced with 0.2 μm filtered *in situ* water (Hopkinson and Smith 2005) to reduce the effect of water column respiration during incubations.

During incubations cores are fitted with gas-tight covers with attached magnetic stir bars that slowly and continuously stirred the overlying water throughout the incubation (Fulweiler 2007; Fulweiler and Nixon 2009) to prevent stratification (Hopkinson et al. 2001) while avoiding sediment resuspension (Renaud et al 2008). Dissolved oxygen concentrations were monitored in the overlying water throughout the incubations using a Hach HQ30 LDO probe. Dissolved oxygen levels were allowed to drop by at least 2 ppm, but incubations were stopped before the overlying water reached hypoxia (a drop below 3 ppm; Fulweiler 2007; Hopkinson et al. 2001).

2.3.3 Data Analysis

Sediment oxygen consumption was determined from a linear regression of oxygen concentration over incubation time (Clough et al. 2005; Renaud et al. 2008). Values were adjusted for the volume and area of the core to obtain net fluxes (m^{-2} h^{-1}; Nixon et al. 1980). The differences in sediment oxygen consumption between seasons (temperatures) and locations were

examined using ANOVA. Statistical analyses were done using JMP software (version 5.1, SAS Institute, Inc.).

3 Results

3.1 Surface Chlorophyll

At the time of this writing we have analyzed over 825 samples of bucket collected surface water from the almost 3500 km^2 OSAMP area (Fig 3). Because of its large size, we broke the area into four sub areas consisting of inner and outer RIS and BIS. During the annual cycle sampled there was a clear seasonal cycle in all four areas, the most remarkable feature of which was a strong fall phytoplankton bloom (Fig 4). This bloom was not seen in mid Narragansett Bay by the GSO plankton monitoring program. On the other hand, a strong winter-spring bloom was observed in the bay during 2009-2010 that was not observed offshore and summer chlorophyll levels were considerably higher in the mid bay than offshore (Fig 5). Mean ± SD surface chlorophyll by region and by season is given in Table 1. Because the data were not normally distributed (and were not made so by any simple manipulation), we analyzed the differences between the sounds and between seasons using non-parametric statistics in JMP. Since there were no statistically significant differences between the inner and outer RIS or BIS, we pooled the inner and outer data. The pooled data for RIS showed significant differences between mean fall, winter, and summer or spring (which were not significantly different from one another) (Kruskal-Wallis test, $p < 0.001$). The same analysis of BIS seasonal means showed that each season differed significantly from all the others ($p< 0.001$). Differences between the two sounds were significant during winter ($p < 0.0179$) and summer ($p < 0.001$), but not during spring or fall. Comparison of the annual means also showed that RIS was significantly higher than BIS ($p < 0.001$). Analysis of the frequency distribution of surface chlorophyll in the two sounds showed that values above 4.5 $\mu g\ L^{-1}$ were unusual, but much more common in RIS than in BIS (Fig 6). The most common concentration observed in either sound fell between 0.5 and 1 $\mu g\ L^{-1}$.

3.2 Vertical Light Attenuation

Estimates of $-k\ m^{-1}$ based on the Secchi disk observations were consistent with the less frequent measurements of light attenuation taken with the SeaCat CTD (Fig 7). Water clarity was generally more variable in RIS than in BIS and there was no evidence of a clear seasonal cycle in

either area (Fig 7). The latter suggests that chlorophyll contributes relatively little to the absorption of light in the water column compared with other suspended solids and colored dissolved organic matter. There is the suggestion of increasing water clarity in both sounds over the period of study. A linear regression of k over time revealed a significant slope ($p<0.0001$) of the regression in BIS, but not in RIS.

Before proceeding with statistical analyses of the data, we excluded the one very high spring value from BIS and the two outlying high values during fall in RIS. These points fell outside an ellipse encompassing 99% of the data. While the data from RIS were normally distributed, those for BIS were not, so we again compared systems and seasons using non parametric analyses. In both sounds, the mean light attenuation was lowest during spring (Kruskal-Wallis test, BIS $p=0.0002$, RIS $p=0.0111$), and the summer mean attenuation was significantly ($p < 0.001$) higher in BIS than in the other seasons (Table 2).

3.3 Primary Production

3.3.1 Rhode Island Sound Productivity

Utilizing the Niskin bottle sampling technique, total productivity over the 7 month period from October 1, 2009 – April 30, 2010 was estimated at 79 gCm^{-2} (Fig 8). The integrated hose sampling yielded lower estimates for this time period at 39 gCm^{-2} (Fig 9). Measured Daily Areal Productivity in Rhode Island Sound (RIS) ranged from 70 $mgCm^{-2}\ d^{-1}$ to 1116 $mgCm^{-2}\ d^{-1}$ (Table 3).

Measured productivity in RIS was lowest on the January 19, 2010 sampling. However, this was mainly due to the low amount of incident light on the date the samples were collected. When the parameters estimated from the incubations on this date were modeled with incident light from preceding and following days, the estimated production was relatively high (avg. Niskin 469 mgC $m^{-2}\ d^{-1}$, hose 373 mgC $m^{-2}\ d^{-1}$) compared to estimates throughout the rest of the winter months. This sampling date also corresponds to the highest chlorophyll a concentrations measured on productivity sampling dates (6.1µg l^{-1}). During this time period an intense winter/spring bloom occurred in Narragansett Bay (Oviatt, Monitoring Network data).

Niskin sampling of surface waters resulted in highest productivity estimates (1116 mgC $m^{-2}\ d^{-1}$) for Rhode Island Sound on April 6, 2010. This sampling date was just after large amounts of rain and record flooding in Rhode Island which lasted from March 30 – April 1. A

chlorophyll concentration spike in Narragansett Bay was also observed immediately following the flooding (MERL data). One possible reason why the total estimated production over 7 months of samples collected with the hose method were lower than the Niskin method was that samples utilizing the hose method were not available for this date. This sharp spike in production was short lived, with both Niskin and hose sample estimates decreasing to 324 and 233, respectively, by April 14, 2010.

When additional RIS chlorophyll measurements (Fields, Codiga, Ullman, SAMP data) were incorporated into the analysis it became clear that a fall bloom occurred in RIS and was slightly later than the one in BIS, beginning at the end of October and therefore missed by our sampling. We have used two corrections to account for this bloom. The first utilized the chlorophyll to production relationship obtained from all of the Niskin bottle samples (Fig 10). The second involved modeling using parameters from the January 19, 2010 sampling date when similar chlorophyll values were observed. When the corrections were made to the Niskin measurement and the productivity was summed over the 7 month period total productivity values of 86 gCm^{-2} from the modeled correction (Fig 11) and 91 gCm^{-2} from the chlorophyll relationship were obtained. This range is similar to the Niskin productivity measurements of 87 gCm^{-2} from BIS (see below).

3.3.2 Block Island Sound Productivity

Utilizing the Niskin bottle sampling technique, total productivity over the 7 month period from October 1, 2009 – April 30, 2010 was estimated at 87 gCm^{-2} (Fig 12). The integrated hose sampling yielded lower estimates for this time period at 78 gCm^{-2} (Fig 13). Measured Daily Areal Productivity in Block Island Sound (BIS) ranged from 59 mgC m^{-2} d^{-1} to 1738 mgC m^{-2} d^{-1} (Table 3). As for RIS the lowest measured productivity in BIS was observed on the January 19, 2010 sampling date due to the low incident light on that specific date. When parameters were applied to incident light values from preceding and following days the average productivity values obtained from the Niskin sampling suggested that productivity was highest for the winter months at this time. The hose sampling method indicated that productivity was slightly higher in February than January. Chlorophyll values supported these observations.

In BIS chlorophyll a concentrations were highest on the October sampling date with values of 8.3 μgl^{-1} obtained from Niskin sampling and 7.7 μgl^{-1} from integrated hose sampling. The productivity measurements obtained from this date reflected these high chlorophyll values

with measured values of 1738 mgC m^{-2} d^{-1}, much higher than values observed during the rest of the 7 month study period. The measured productivity from the hose sample was 563 mgC m^{-2} d^{-1} which was relatively high, yet when the parameters were applied to the incident light for the 36 closest days the average productivity over this time period was less than the productivity from January and February.

3.3.3 Niskin versus Hose Estimations of Primary Production

Except for two occasions surface Niskin samples resulted in higher estimates of primary production than integrated depth or hose samples (Table 3). Most of the active chlorophyll was likely present in surface waters of the Niskin sampling procedure. Samples recovered from over the euphotic depth resulted in lower concentrations of active chlorophyll and reduced primary production estimations. In January and February when higher productivities were measured over the euphotic depth than from surface samples sub surface chlorophyll concentrations from winter blooms may have been present. Surface samples produced the highest potential estimations of primary production and integrated depth samples produced lowest potential estimations of primary production.

3.4 Benthic Metabolism

Sediment cores were collected and incubated at three different *in situ* bottom water temperatures (17°C, 7°C, and 4°C) from three stations (1 in BIS, and 2 in RIS, Fig 3). Data were normally distributed, so all comparisons were made using ANOVA in JMP. Data from the RIS 2 station were logarithmically transformed to obtain a normal distribution for statistical analysis across incubation temperatures.

At all three stations, mean sediment oxygen uptake decreased with decreasing temperature (Fig 14). This difference was most dramatic in BIS, where the mean O_2 uptake values were significantly different for all three incubation temperatures ($p=0.0058$). In RIS 2 (the easternmost RIS station, Fig 3), only the O_2 uptake at the warmest temperature (17°C) was significantly different than the rest ($p=0.0006$). At the other RIS station (RIS 1, the westernmost RIS station), the differences in sediment oxygen uptake between temperatures was not statistically significant.

There was no clear trend in rates of sediment oxygen uptake between stations at different incubation temperatures (Fig 14). At the two cooler bottom water temperatures (7°C and 4°C), the RIS 1 station exhibited the highest rate of benthic metabolism ($p=0.0175$ for 7°C, and $p=0.005$ for 4°C). During the warmest incubation (17°C), the BIS station had the highest rate of O_2 uptake, although none of the differences between stations was statistically significant. Table 4 summarizes the statistically significant differences in mean benthic metabolism across temperatures and stations.

To compare benthic metabolism in BIS and RIS overall, we pooled the data from both RIS stations. Sediment core incubations for Block Island and Rhode Island Sound revealed no significant differences in overall mean benthic metabolism between the sounds over the 13°C temperature range. However, there was a significant difference in mean sediment oxygen uptake (mg m^{-2} h^{-1}) for both sounds between each of the three incubation temperatures (one-way ANOVA, $p=0.0001$). For the two warmer bottom-water temperatures (17°C and 7°C), mean oxygen uptake in BIS was greater than in RIS although the differences were not statistically significant (Table 5).

4 Discussion

It is, of course, inappropriate to generalize too widely based on the relatively short sampling reported here (one year for chlorophyll and light attenuation, seven months for primary production, and three benthic flux measurements, albeit it across a wide temperature range). Based on the results so far, it appears that the seasonal pattern in phytoplankton abundance in the sounds is consistent in terms of timing across both RIS and BIS and in both inner and outer sound areas. The seasonal cycle in the sounds was quite different from that observed over the same time period in Narragansett Bay. Surface chlorophyll concentrations in the sounds were, as expected, considerably lower than found in mid Narragansett Bay. Our initial hypothesis that standing crops of phytoplankton would be higher in relatively well-mixed BIS than in RIS does not appear to be correct, except during summer when RIS is thermally stratified. On an annual basis, the opposite appears to be the case. This also contrasts with Riley's (1952b) belief based on cell count data from over half a century ago and the preliminary satellite sea surface color analysis of decadal annual mean chlorophyll (Hyde and O'Reilly,NMFS Narragansett, personal communication). The absolute values of annual means estimated from the satellite data (for years

prior to the sampling reported here) are not very different from our measured annual means (RIS 2.7 ± 2.2 our data vs 1.4 μg L^{-1} satellite; BIS 1.8 ± 1.4 our data vs 2.1 μg L^{-1} satellite). It was also surprising to us that the vertical light attenuation in both systems showed so little evidence of a seasonal cycle and the differences between the sounds were not statistically significant except during summer. Clearly, the thermal stratification in RIS results in significant differences in the base of the food chain in the two sounds during summer.

While the higher mean annual surface chlorophyll in RIS may well mean that annual primary production is higher there as well, we are not yet able to assess that directly with the measurements in hand. For the measurements made so far, there was little difference between integrated seven month production of RIS (79 g C m^{-2}) and BIS (87 g C m^{-2}) based on surface water only. As noted in results, tube samples of the euphotic zone yielded much lower values in RIS (39 g C m^{-2}) and slightly lower values in BIS (78 g C m^{-2}). We are still working to reconcile the apparent differences and to acquire a full annual cycle of sampling so that we do not have to make numerous assumptions about how to handle the production during the large fall bloom that occurred before the present sampling program began.

We began the introduction to this report by noting the cross system studies showing correlations between phytoplankton standing crops, primary production, and the yields of fish. While fisheries landings data are not reported separately for the sounds, a great benefit of the OSAMP process was that it stimulated interactions between the local research community and the recently completed Northeast Area Monitoring and Assessment Program (NEAMAP) Near-Shore Trawl Survey (Bonzek et al. 2009). This NMFS funded program carried out by the Virginia Institute of Marine Science (VIMS) sampled 17 stations in RIS and 10 stations in BIS using standard trawls during spring and fall. The principal investigator of that project was kind enough to provide us with average numbers and biomass for each species per standard trawl in RIS and BIS between fall 2007 and spring 2009 (C. Bonzak, personal communication, Table 6). The result was that the total number and biomass of organisms captured per unit effort was greater during both spring and fall sampling in RIS than in BIS. This was true for pelagic as well as demersal species and almost always the case for all of the most abundant and commercially important species (Table 6). Since fishing pressure appears to be similar in both systems and both are subject to the same fisheries management regulations, this difference may reflect a great productivity in RIS, consistent with the surface chlorophyll data.

The benthic respiration data collected thus far did not indicate large differences between oxygen uptake by the fine grained sediments in the two sounds. However, benthic flux data are notoriously variable and additional sampling will be carried out with support from other sources to make measurements throughout an annual cycle. Since most of the bottom in both sounds is composed of coarser grained sediments than the depositional areas sampled here, we will also be sampling those areas, though we anticipate that the metabolic rates will be significantly lower. For both BIS and RIS at all incubation temperatures, mean oxygen uptake was much higher than recent measurements made in nearby Narragansett Bay (Fig 15, Fulweiler 2007). In every case, measurements in BIS and RIS were higher than historic Narragansett Bay values of benthic metabolism from Nixon et al (1976, 1980, unpublished data). Since the primary production data collected thus far do not suggest that depth integrated primary production in the sounds is higher than it was historically in the bay (Nixon et al. 2009), the higher rates of benthic metabolism in the fine grained sediments in the sounds probably reflect the fact that they are depositional areas in which sinking organic matter accumulates.

5 Conclusions

• Both Rhode Island Sound (RIS) and Block Island Sound (BIS) appear to be productive inner shelf systems where primary production may ultimately be found to fall between 100 and 200 g C m-2 y-1, though this must await the completion of an annual cycle of measurements now underway.

• The concentration of phytoplankton in the sounds (measured as chlorophyll) was substantially lower than in mid Narragansett Bay except during fall, when the sounds experienced a marked bloom not seen in the bay.

• The concentration of phytoplankton in surface waters was higher in RIS than in BIS except during summer, when the thermally stratified RIS was less turbid and contained lower phytoplankton concentrations.

• Based on spring and fall sampling carried out by the Northeast Area Monitoring and Assessment Program (NEAMAP) Near-Shore Trawl Survey (Bonzek et al. 2009), it appears that the abundance and biomass of fish and lobsters per unit area is greater in RIS than BIS, consistent with the higher mean annual chlorophyll concentrations found in the surface water.

• Rate of oxygen uptake by the fine grained sediments in both sounds are higher than measured historically (1970s and 1980s) and recently in Narragansett Bay, perhaps reflecting the depositional nature of the areas where these sediments accumulate.

References

Aminot, A. and Rey, F. 2000. Standard procedure for the determination of chlorophyll *a* by spectroscopic methods. International Council for the Exploration of the Sea, Copenhagen, Denmark, March 2000.

Arar, E.J. and Collins, G.B. 1997. Method 445.0, *In Vitro* Determination of Chlorophyll *a* and Pheophytin *a* in Marine and Freshwater Algae by Fluorescence. In: *Methods for the Determination of Chemical Substances in Marine and Estuarine Environmental Matrices, 2nd Edition*. National Exposure Research Laboratory, Office of research and development, USEPA., Cincinnati, Ohio (EPA/600/R-97/072, Sept. 1997).

Bonzek, C., Gartland, J., Lange, J., and Latour, R. 2009. *Northeast Area Monitoring and Assessment Program (NEAMAP) Near-Shore Trawl Survey: Data Collection and Analysis in Support of Single and Multispecies Stock Assessments in the Mid-Atlantic and Southern New England, Final Report 2005-2009*. Submitted to the Atlantic States Marine Fisheries Commission, Washington, D.C. Virginia Institute of Marine Science, Gloucester Point, Va.

Brandt, K. 1901. Life in the Ocean. *Annual Report, Smithsonian Inst*. 1900:493-506.

Breitburg, D., and 17 coauthors. 2009. Nutrient enrichment and fisheries exploitation: interactive effects on estuarine living resources and their management. *Hydrobiologia* 629:31-47.

Brush, M., Brawley, J., Nixon, S.W., and Kremer, J. 2002. Modeling phytoplankton production: Problems with the Eppley curve and an empirical alternative. *Marine Ecology Progress Series* 238:31-45.

Chen, C., Liu, H., and Beardsley, R. 2003. An unstructured, finite volume, three-dimensional, primitive equation model: application to coastal ocean and estuaries. *Journal of Atmospheric and Ocean Technology* 20:159-186.

Cloern, J., Grenz, C., and Vidergar-Lucas, L. 1995. An empirical model of the phytoplankton chlorophyll:carbon ratio – the conversion factor between productivity and growth rate. *Limnology and Oceanography* 40:1313-1321.

Clough, L.M., Renaud, P.E., and Ambrose, W.G. 2005. Impacts of water depth, sediment pigment concentration, and benthic macfofaunal biomass on sediment oxygen demand in the western Arctic Ocean. *Canadian Journal of Fisheries and Aquatic Science* 62:1756-1765.

Cohen, K. 1995. A comparison of three chlorophyll *a* extraction methods. Unpublished manuscript, Graduate School of Oceanography, University of Rhode Island, Kingston, RI.

Cushing, D. 1975. *Marine Ecology and Fisheries.* Cambridge University Press, NY.

Edwards, C., Fake, T., and Bogden, P. 2004. Spring-summer frontogenesis at the mouth of Block

Island Sound: 1. A numerical investigation into tidal and buoyancy-forced motion. *Journal of Geophysical Research* 109:C12021.

Fulweiler, R.W. 2007. The impact of climate change on benthic-pelagic coupling and the biogeochemical cycling of Narragansett Bay, R.I. Ph.D. Thesis, Graduate School of Oceanography, University of Rhode Island, Narragansett, RI.

Fulweiler, R.W., and Nixon, S.W. 2009. Responses of benthic-pelagic coupling to climate change in a temperate estuary. *Hydrobiologia* 629:147-156.

Hopkinson, C. Jr, Giblin, A.E., and Tucker, J. 2001. Benthic metabolism and nutrient regeneration on the continental shelf of eastern Massachusetts, USA. *Marine Ecology Progress Series* 224:1-19.

Hopkinson, C. Jr, and Smith, E. 2005. Estuarine respiration: An overview of benthic, pelagic, and whole system respiration. In: *Respiration in Aquatic Systems*, pp. 122-146. Del Giorgio, P. and Williams, P. (eds.), Oxford University Press, New York.

Idso, S.B., and Gilbert, R.G. 1974. On the universality of the poole and atkins secchi disk-light extinction equation. *Journal of Applied Ecology* 11:399-401.

Iverson, R. 1990. Control of marine fish production. *Limnology and Oceanography* 35:1593-1504.

Kremer, J. and Nixon, S. 1978. *A Coastal Marine Ecosystem – Simulation and Analysis.* Ecological Studies 24, Springer Verlag, NY.

Lewis, M. R., and Smith, J. C. 1983. A small volume, short-incubation-time method for measurement of photosynthesis as a function of incident irradiance. *Marine Ecology Progress Series* 13:99-102.

McMaster, R. 1960. Sediments of Narragansett Bay system and Rhode Island Sound, Rhode Island. *Journal of Sediment Petrology* 30:249-274.

Mills, E. 1989. *Biological Oceanography: An Early History, 1870-1960*. Cornell University Press, NY.

Nixon, S.W., Oviatt, C.A., and Hale, S.S. 1976. Nitrogen regeneration and the metabolism of coastal marine bottom communities. In: *The role of terrestrial and aquatic organisms in decomposition processes*, pp. 269-283. Anderson, J.M. and Macfadyen, A., (eds.), Blackwell Science Publications, London.

Nixon, S.W., Kelly, J.R., Fumas, B.N., Oviatt, C.A., and Hale, S.S. 1980. Phosphorus regeneration and the metabolism of coastal marine bottom communities. In: *Marine Benthic Dynamics*, pp. 219-242. Tenore, K.R. and Coull, B.C (eds.), University of South Carolina Press, South Carolina. pp.

Nixon S.W., Oviatt C., Frithsen, J., and Sullivan, B. 1986. Nutrients and the productivity of estuarine and coastal marine ecosystems. *Journal of the Limnological Society of South Africa* 12:43-71.

Nixon, S.W. 1988. Physical energy inputs and the ecology of lake and marine ecosystems. *Limnology and Oceanography* 33:1005-1025.

Nixon, S.W., Buckley, B., Granger, S., Harris, L., Oczkowski, A., Fulweiler, R., and Cole, L. 2008. Nitrogen and phosphorus inputs to Narragansett Bay: past, present, and future. In: *Science for Ecosystem-Based Management, Narragansett Bay in the 21st Century*, pp. 101-175. Desbonnet, A., and Costa-Pierce, B., (eds.), Springer, NY.

Nixon, S.W., Fulweiler, R., Buckley, B., Granger, S., Nowicki, B., and Henry, K. 2009. The impact of changing climate on phenology, productivity, and benthic-pelagic coupling in Narragansett Bay. *Estuarine, Coastal, and Shelf Science* 82:1-18.

Oviatt, C., Doering, P., Nowicki, B., Reed, L., Cole, J., and Frithsen, J. 1995. An ecosystem level experiment on nutrient limitation in temperate coastal marine environments. *Marine Ecology Progress Series* 116:171-179.

Pilson, M.E.Q. 1985. Annual cycles of nutrients and chlorophyll in Narragansett Bay, Rhode Island. *Journal of Marine Research* 43:849-873.

Platt, T., C. L. Gallegos, and W. G. Harrison, 1980. Photoinhibition of photosynthesis and light for natural assemblages of coastal marine phytoplankton. *Journal of Marine Research* 28:687-701.

Renaud, P., Morata, N., Carroll, M.L., Denisenko, S.G., and Reigstad, M. 2008. Pelagic-benthic coupling in the western Barents Sea: Processes and time scales. *Deep Sea Research (II Topographical Studies Oceanography)* 55: 2372-2380.

Riley, G. 1952a. Hydrography of Long Island and Block Island Sounds. *Bulletin of the Bingham Oceanographic Collection* 13:40-64.

Riley, G. 1952b. Phytoplankton of Block Island Sound 1949. *Bulletin of the Bingham Oceanographic Collection* 13:40-64.

Smayda T, Borkman D 2008. Nutrient and plankton dynamics in Narragansett Bay. In: *Science for Ecosystem-Based Management, Narragansett Bay in the 21st Century,* pp 431-484. A. Desbonnet, Costa-Pierce, B., (eds.),. Springer, NY.

Shonting, D., and Cook, G. 1970. On the seasonal distribution of temperature and salinity in Rhode Island Sound. *Limnology and Oceanography* 15:100-112.

Simpson, J. and Hunter, J. 1974. Fronts in the Irish Sea. *Nature* 250:404-406.

Strickland, J.D.H., and Parson, T.R. 1968. *A Practical Handbook of Seawater Analysis*. Fisheries Research Board of Canada, Bulletin 167. 293pp.

Ware D., and Thomson, R. 2005. Bottom-up ecosystem trophic dynamics determine fish production in the northeast Pacific. Sciencexpress 21 April 2005; 10.1126/science.1109049

Webb, W.L., Newton, N., and D. Starr. 1974. Carbon dioxide exchange of *Alnus rubra*: a mathematical model. *Oecologia* 17: 281-291.

Table 1. Overall and seasonal mean (± SD) surface chlorophyll listed by region.

Location	Area* (km^2)	n	Overall Mean Surface Chlorophyll ± SD ($\mu g\ L^{-1}$)	Seasonal Mean Surface Chlorophyll ± SD ($\mu g\ L^{-1}$)			
				Summer (Jun-Aug)	Fall (Sept – Nov)	Winter (Dec – Feb)	Spring (Mar – May)
Inner BIS	728	353	1.82 ±1.42	2.15 ±0.57	3.8 ±1.48	2.73 ±1.44	0.98 ±0.73
Inner RIS	784	213	2.78 ±1.83	1.72 ±0.80	4.41 ±1.92	2.86 ±1.23	1.12 ±0.87
Outer BIS	337	40	1.80 ±1.14	1.29 ±.38	3.81 ±1.23	2.30 ±0.97	0.85 ±0.37
Outer RIS	1,570	233	2.57 ±2.42	0.90 ±0.22	4.65 ±3.3	3.0 ±0.95	0.92 ±0.53
Total BIS	1,065	393	1.81 ±1.39	2.04 ±0.62	3.80 ±1.46	2.64 ±1.36	0.98 ±0.70
Total RIS	2,354	446	2.67 ±2.16	1.30 ±0.71	4.53 ±2.70	2.93 ±1.10	1.00 ±0.70

*Areas given here have been adjusted to include the ocean SAMP study area (McCann 2009), and are not the traditional literature values used when referencing these regions.

Table 2. Mean extinction coefficient (-k) values for Block Island and Rhode Island Sound overall and by season. Letters show statistically significant differences ($p<0.05$) based on Kruskal-Wallis test (values not connected by the same letter are significantly different).

Region	n	Overall Mean –k (m^{-1})	Seasonal Mean –k (m^{-1})			
			Summer (Jun-Aug)	Fall (Sept -Nov)	Winter (Dec – Feb)	Spring (Mar – May)
Block Island Sound	51	0.3 ± 0.06	0.35 ± 0.03 a	0.29 ± 0.04 c	0.31 ± 0.03 d	0.25 ± 0.06 cd
Rhode Island Sound	60	0.29 ± 0.08	0.31 ± 0.06 b	0.27 ± 0.07 bc	0.33 ± 0.1 d	0.21 ± 0.04 cd

Table 3. Results from primary production sampling and CTD water column profiles. k is the calculated extinction coefficient from which Zeu (euphotic depth) was calculated. Pmax/Psb, a, and b were determined by fitting either the Platt (Psb, a, b) or Webb model (Pmax, a) to the P vs. I relationship obtained from each productivity incubation. Model start and end dates are the period over which the parameters were applied when total productivity calculations were made using a daily time series of total incident light.

Cruise	Site	Method	Date	Model Start Date	Model End Date	Model Period (Days)	k	Zeu	P_{max} / P_{sb}	a	b	[Chl a] (μgL^{-1})	Measured Daily Areal Productivity ($mgCm^{-2}d^{-1}$)	Avg Daily Areal Productivity Over Period ($mgCm^{-2}d^{-1}$)	Stratified	Depth of pycnocline (m)
SP1002	RIS	Niskin	10/2/2009	10/1/2009	11/1/2009	33	0.155	29.8	2.263	0.019	0.0012	0.844	235.16	160.97	Y	24
SP1002	RIS	Hose	10/2/2009	10/1/2009	11/4/2009	35	0.155	29.8	0.494	0.007		0.913	70.27	49.52	Y	24
SP1002	BIS	Niskin	10/2/2009	10/1/2009	10/25/2009	26	0.341	13.5	37.289	0.308	0.0180	8.323	1737.92	1279.60	Y	21
SP1002	BIS	Hose	10/2/2009	10/1/2009	11/4/2009	36	0.341	13.5	11.213	0.110	0.0064	7.653	563.36	390.88	Y	21
SP1118	BIS	Niskin	11/18/2009	10/26/2009	12/19/2009	54	0.288	16	1.950E+08	0.040	3.397E+05	2.675	200.02	185.39		
SP1202	RIS	Niskin	12/2/2009	11/2/2009	12/26/2009	54	0.320	14.4	16.453	0.098	0.0106	3.901	386.88	340.43		
SP1207	RIS	Hose	12/7/2009	11/5/2009	12/28/2009	55	0.404	11.4	15.663	0.050	0.0131	3.948	132.85	149.39	N	
SP1208	BIS	Hose	12/8/2009	11/5/2009	12/29/2009	54	0.320	14.4	7.324	0.026	0.0062	1.821	132.67	95.63	Y	28
SP0119	RIS	Niskin	1/19/2010	12/27/2009	1/27/2010	33	0.320	14.4	14.828	0.149	0.0018	6.069	79.49	469.44	N	
SP0119	RIS	Hose	1/19/2010	12/29/2009	1/27/2010	30	0.320	14.4	2.460E+08	0.083	4.264E+05	6.075	46.77	373.05	N	
SP0119	BIS	Niskin	1/19/2010	12/20/2009	1/27/2010	40	0.314	14.7	29.594	0.104	0.0225	5.974	58.99	421.21	N	
SP0119	BIS	Hose	1/19/2010	12/30/2009	1/27/2010	30	0.314	14.7	13.208	0.163	0.0075	4.549	86.58	464.77	N	
SP0205	RIS	Niskin	2/5/2010	1/28/2010	2/21/2010	25	0.290	15.9	12.203	0.071	0.0009	4.301	454.27	446.65	N	
SP0205	RIS	Hose	2/5/2010	1/28/2010	3/11/2010	42	0.290	15.9	2.035E+05	0.023	278.447	3.771	185.16	175.26	N	
SP0205	BIS	Niskin	2/5/2010	1/28/2010	2/21/2010	25	0.355	13	14.513	0.097	0.0075	5.026	452.29	442.89	WEAK	
SP0205	BIS	Hose	2/5/2010	1/28/2010	3/11/2010	42	0.355	13	18.511	0.235	0.0041	4.802	857.82	813.53	WEAK	
SP0310	RIS	Niskin	3/10/2010	2/22/2010	3/23/2010	30	0.241	19.13	2.561	0.023		1.308	207.06	141.15	WEAK	
SP0310	BIS	Niskin	3/10/2010	2/22/2010	3/27/2010	34	0.239	19.32	3.816	0.011	0.0026	1.402	130.89	89.70	WEAK	
SP0406	RIS	Niskin	4/6/2010	3/24/2010	4/10/2010	17	0.206	22.4	17.633	0.099	0.0030	2.864	1115.60	1089.67		
SP0414	RIS	Niskin	4/14/2010	4/11/2010	4/22/2010	12	0.156	29.5	2.729	0.020	0.0002	0.884	392.43	324.27	Y	15
SP0414	RIS	Hose	4/14/2010	3/12/2010	4/22/2010	42	0.156	29.5	2.107	0.021	0.0006	2.486	334.64	232.89	Y	15
SP0414	BIS	Niskin	4/14/2010	3/28/2010	4/22/2010	25	0.216	21.3	5.577	0.024		1.332	448.73	322.33	WEAK	
SP0414	BIS	Hose	4/14/2010	3/12/2010	4/22/2010	42	0.216	21.3	9.596	0.015	0.0140	1.449	257.59	172.61	WEAK	
SP0430	RIS	Niskin	4/30/2010	4/23/2010	4/30/2010	8	0.227	20.3	2.864	0.025	0.0002	0.937	320.49	232.88	Y	24
SP0430	RIS	Hose	4/30/2010	4/23/2010	4/30/2010	8	0.227	20.3	3.609	0.020	0.0018	1.049	286.20	204.60	Y	24
SP0430	BIS	Niskin	4/30/2010	4/23/2010	4/30/2010	8	0.214	21.5	22.539	0.039	0.0157	2.103	826.74	555.52	WEAK	
SP0430	BIS	Hose	4/30/2010	4/23/2010	4/30/2010	8	0.214	21.5	9.880	0.030	0.0025	2.198	622.04	419.20	WEAK	

Table 4. Statistically significant differences in benthic metabolism across temperatures and core collection stations. Each letter represents a significant difference (stations and temperatures with the same letter are not significantly different from each other).

Temperature	Station		
	RIS 1	RIS 2	BIS
17°C	a	a	a
7°C	a	b	b
4°C	a	b	c

Table 5. Mean ± SD sediment oxygen uptake for Block Island and Rhode Island Sounds determined from three sediment core incubations at mean *in situ* bottom water temperatures of 17°C (Oct 2009), 7°C (May 2010), and 4°C (Jan 2010).

Sound	n	Mean O_2 uptake (mg m^{-2} h^{-1})			
		Overall	17°C	7°C	4°C
Block Island Sound	9	54.91 ±30.79	86.61 ±13.26	55.88 ±22.11	22.25 ±4.21
Rhode Island Sound	18	44.54 ±25.38	66.25 ±13.97	39.93 ±27.61	27.45 ±17.05

Table 6. Comparison of mean biomass (kg live weight per trawl) found in Rhode Island Sound (RIS) and Block Island Sound (BIS) during standard seasonal surveys carried out by the Virginia Institute of Marine Science (VIMS) for the NMFS. Data courtesy of Dr. Chris Bonzek, VIMS. Sampling details are given in Bonzek et al. (2009).

	Fall '07	Spring '08	Fall '08	Spring '09
		TOTAL BIOMASS		
RIS	271	262	431	292
BIS	161	129	190	200
		SCUP		
RIS	34	20	84	90
BIS	24	14	41	24
		DOGFISH		
RIS	4	20	104	58
BIS	6	7	4	24
		SQUID		
RIS	51	5	33	1
BIS	31	4	28	5
		WINTER FLOUNDER		
RIS	6	20	8	12
BIS	0.3	9	2	16
		TOTAL FOUNDER		
RIS	13	30	14	18
BIS	5	16	7	22
		TOTAL SKATES		
RIS	90	113	119	71
BIS	40	65	75	113
		LOBSTER		
RIS	3.2	4.4	4.7	4.9
BIS	0.4	0.9	0.2	1.1

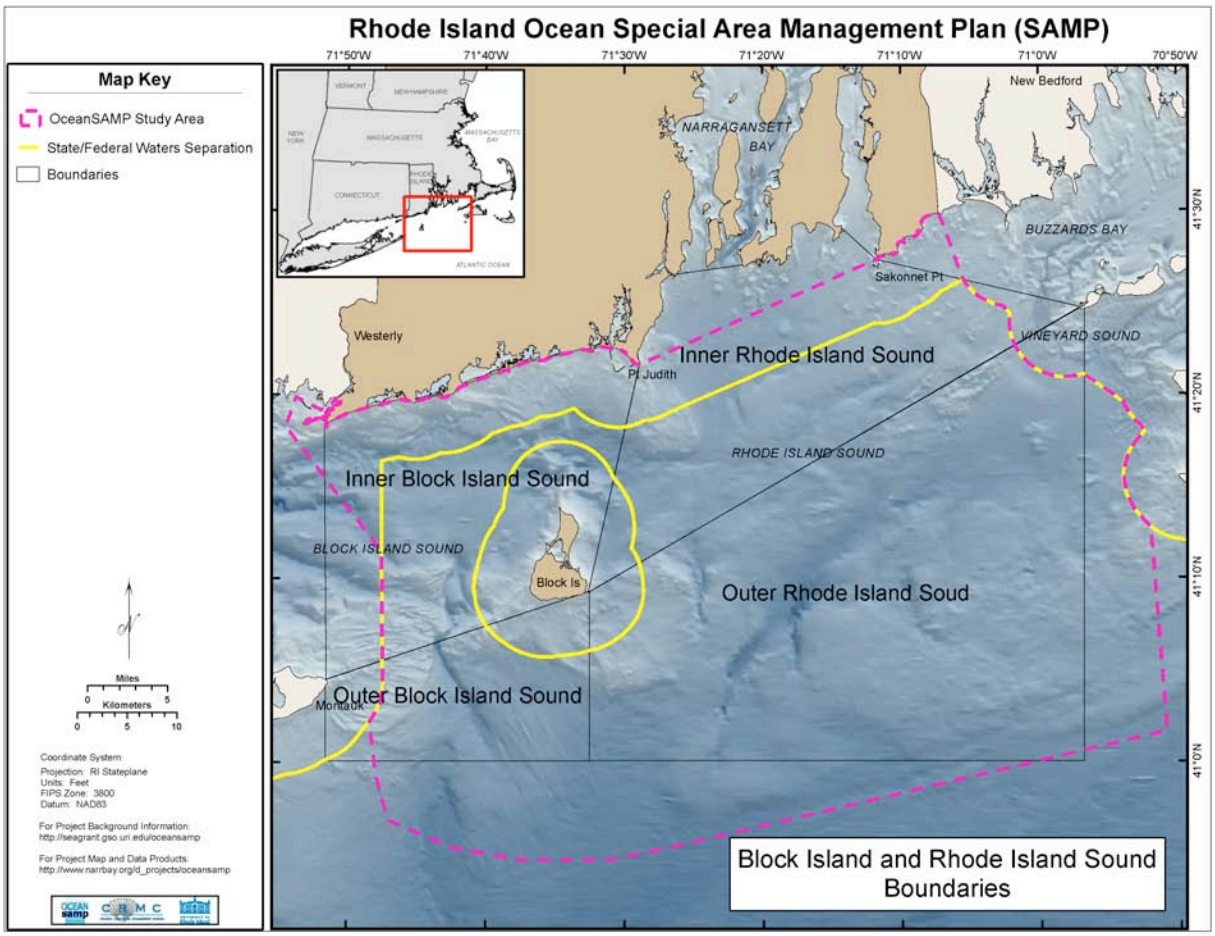

Fig 1. Ocean SAMP study area (McCann 2009) and delineations of inner and outer Block Island and Rhode Island Sound used in this study.

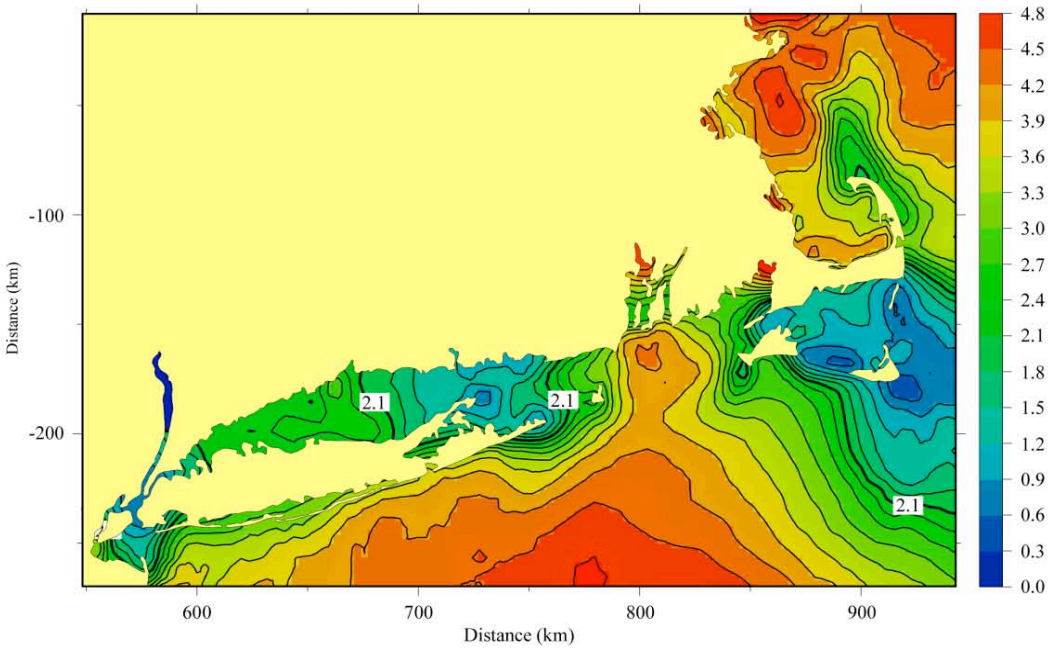

Fig 2. Contours of Simpson and Hunter's (1974) "Vertical Stratification Index" (log h/v^3) for southern New England coastal areas calculated by C. Chen (U. Mass. Dartmouth) using FVCOM model (Chen et al. 2003). Red-brown is strongly stratified while blue is well mixed.

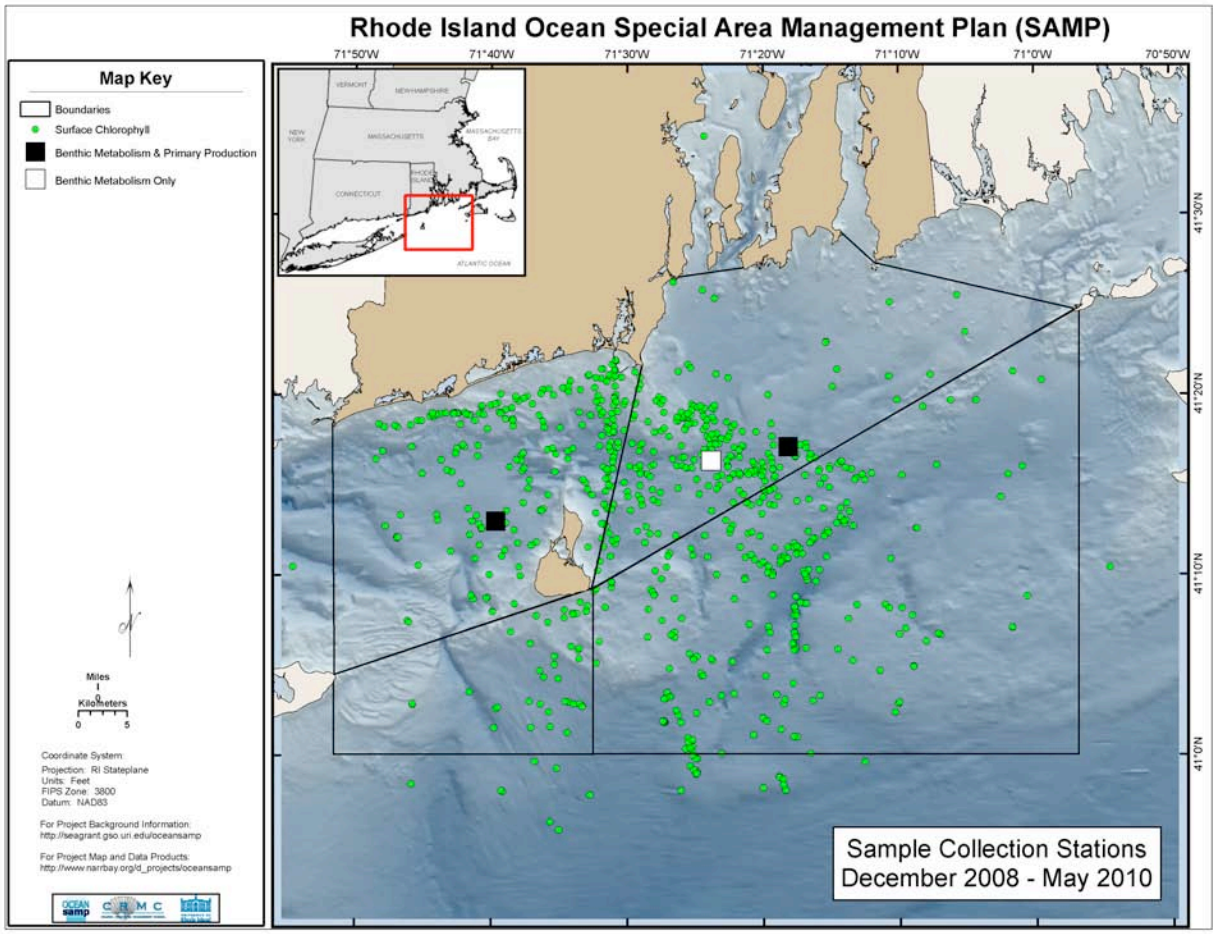

Fig 3. Surface chlorophyll, primary production, and benthic metabolism sampling stations in Block Island and Rhode Island Sound. Benthic metabolism stations are referred to as BIS (Block Island Sound station), RIS 1 (western Rhode Island Sound station), and RIS 2 (eastern Rhode Island Sound station).

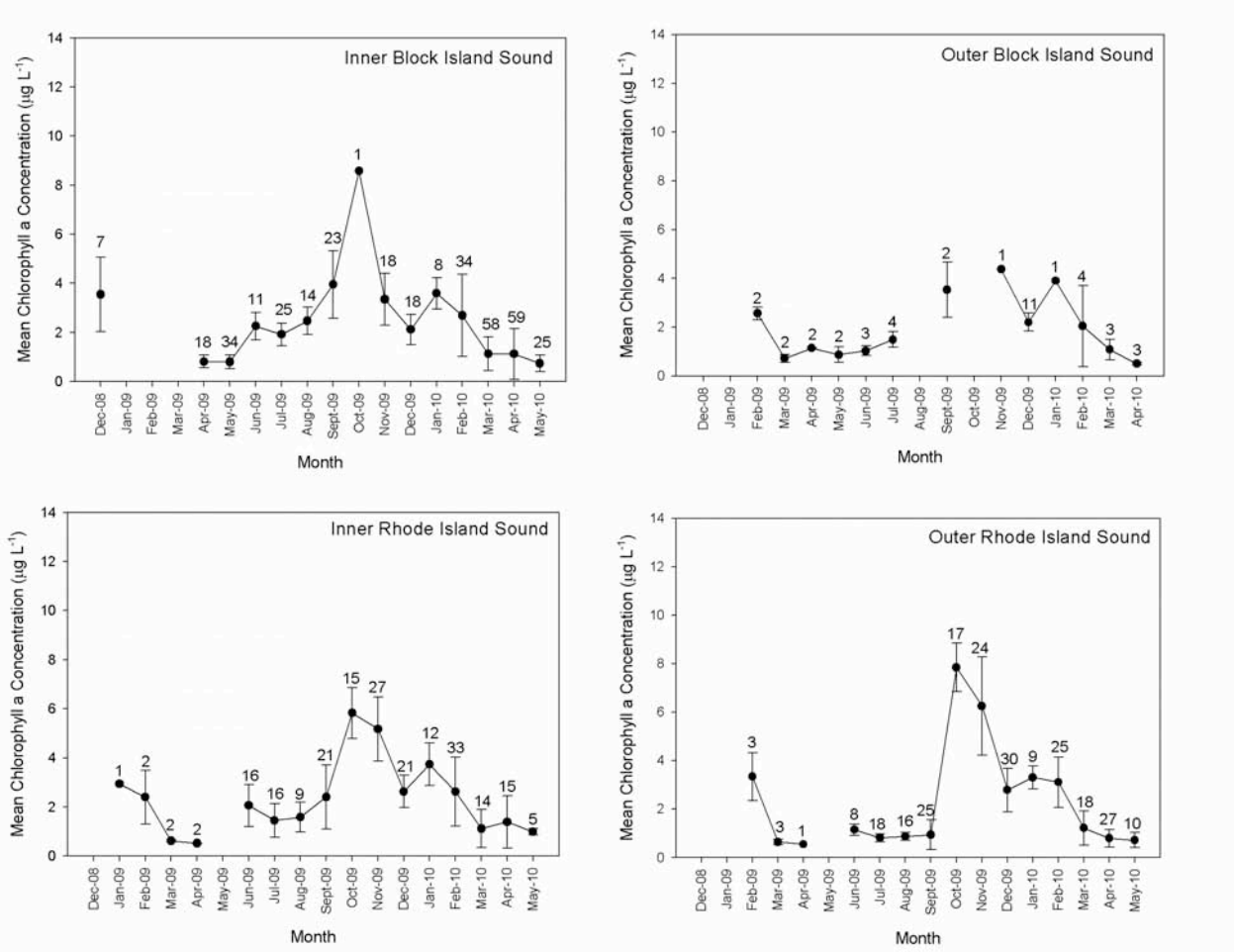

Fig 4. Monthly mean surface chlorophyll concentrations in (top left) inner BIS, (top right) outer BIS, (bottom left) inner RIS, and (bottom right) outer RIS. Error bars represent standard deviation, numbers above bars represent sample size.

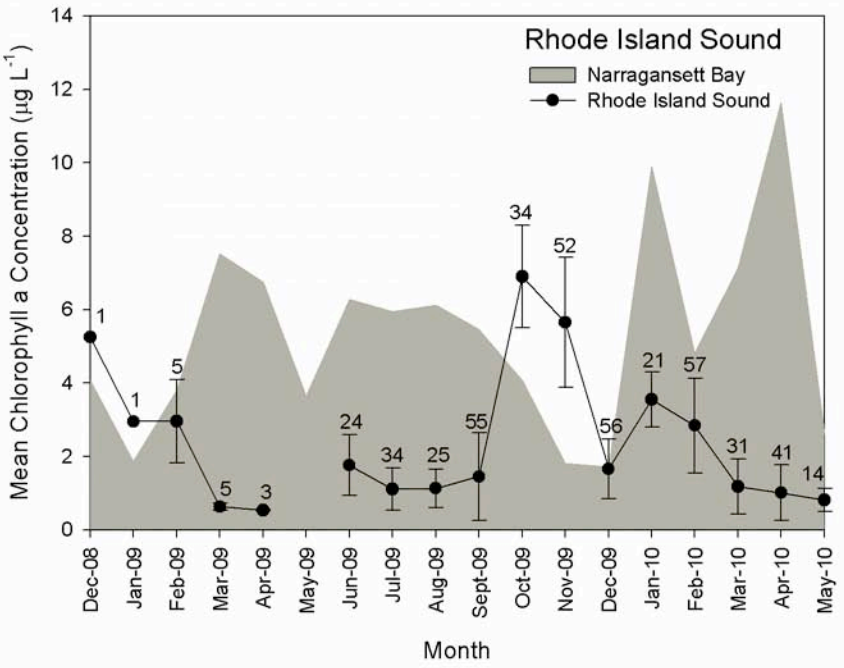

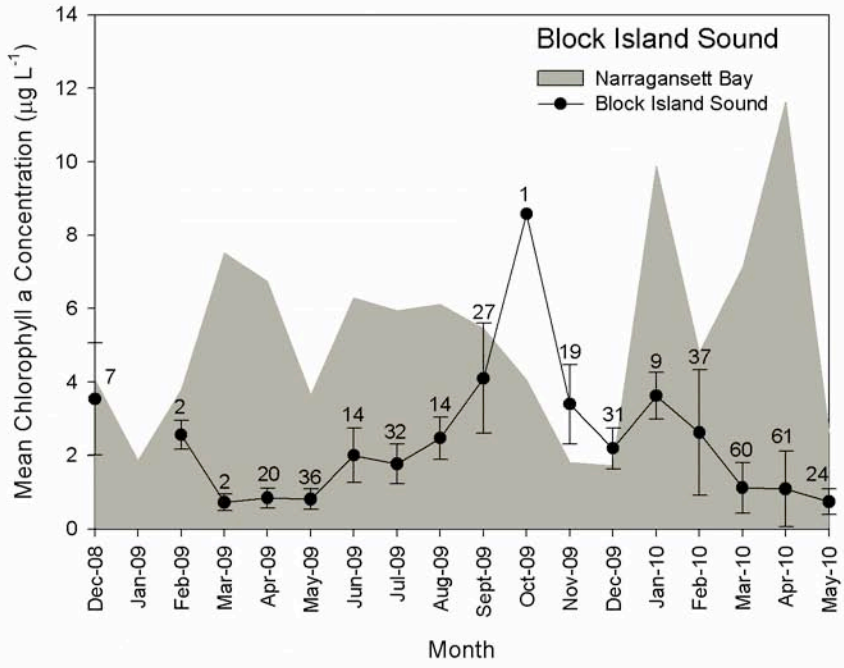

Fig 5. Monthly mean surface chlorophyll concentrations in (top) Rhode Island Sound and (bottom) Block Island Sound. Error bars represent standard deviation, numbers above bars represent sample size. Shaded areas are monthly mean chlorophyll concentrations calculated from the weekly sampling of the URI Graduate School of Oceanography long-term monitoring program (www.gso.uri.edu/phytoplankton).

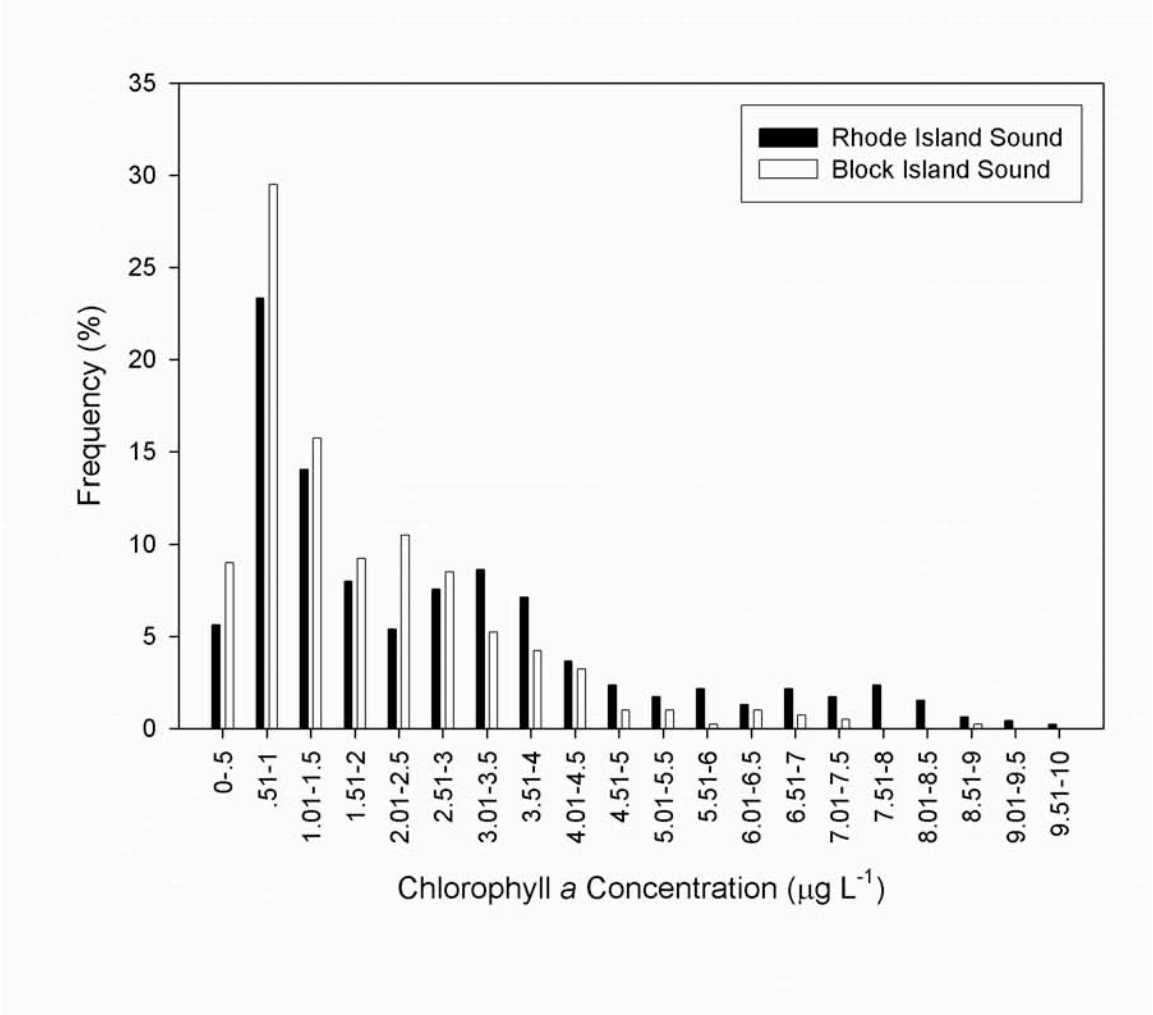

Fig 6. Frequency of surface chlorophyll values measured in Block Island and Rhode Island Sounds, binned in 0.5 μg L^{-1} increments.

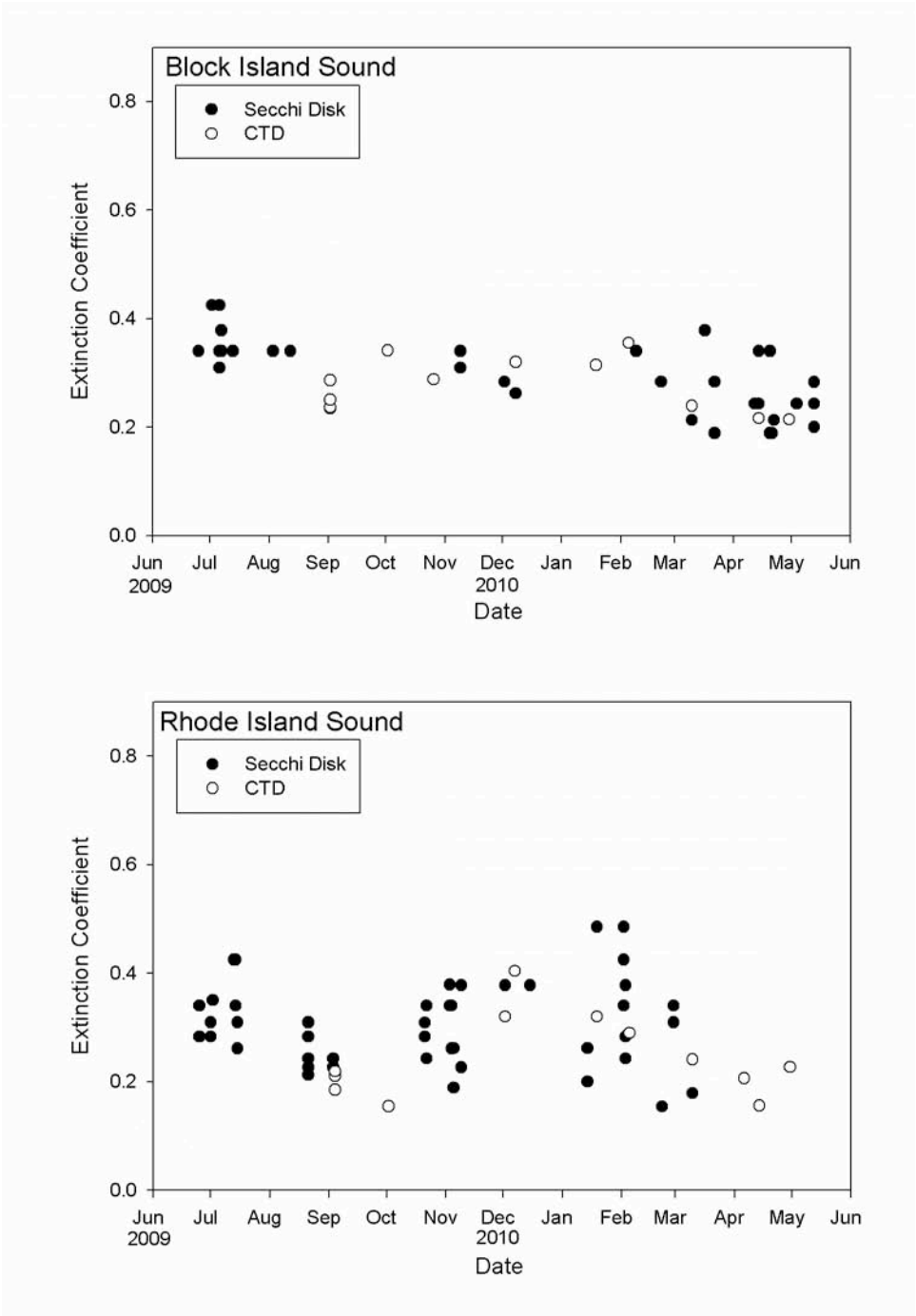

Fig 7. Extinction coefficients (k, in m^{-1}) plotted over time for (top) Block Island and (bottom) Rhode Island Sounds. K values were calculated from Secchi disk (opaque circles; Idso and Gilbert 1974) and CTD light profiles (open circles).

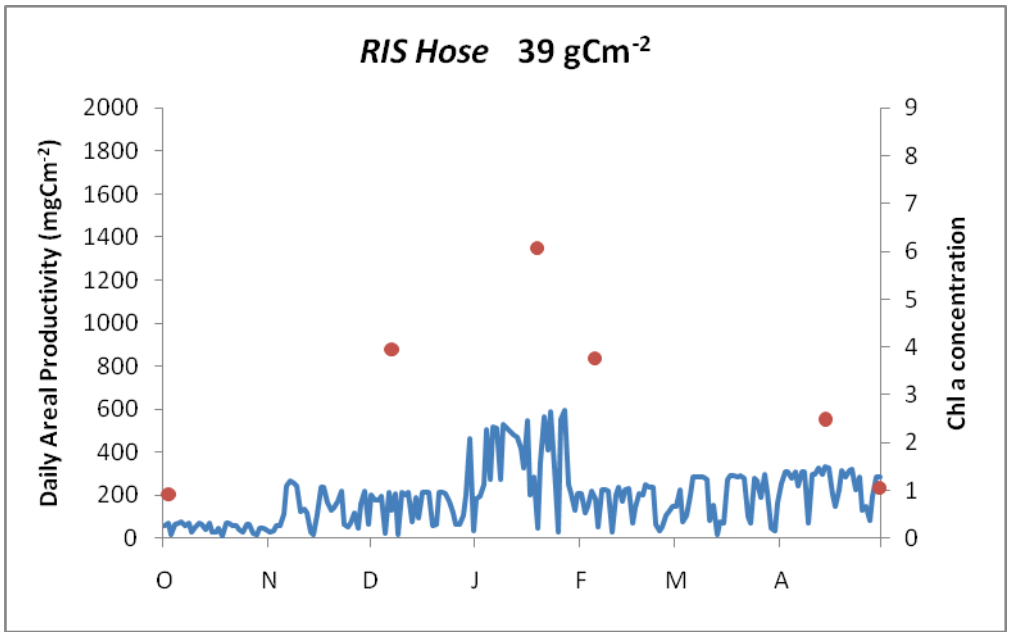

Fig 8. Daily Areal Production (blue lines) estimates and measured chlorophyll a concentrations (red dots) from RIS utiizing hose sampling method. The dates corresponding to the chl a concentrations also indicate dates upon which samples were collected and incubated for primary production estimates.

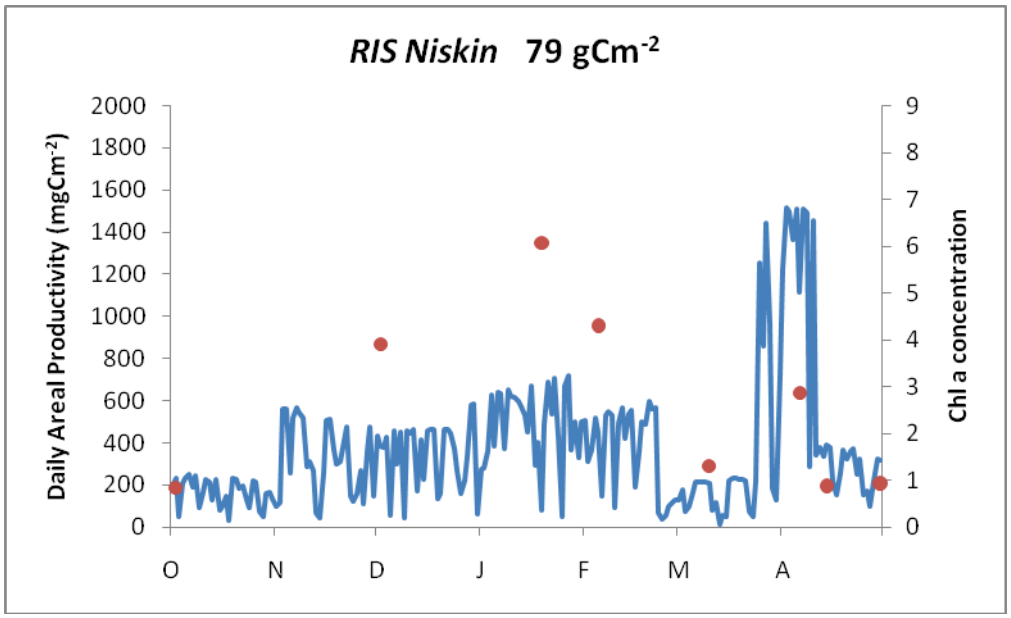

Fig 9. Daily Areal Production (blue lines) estimates and measured chlorophyll a concentrations (red dots) from RIS utiizing niskin sampling method. The dates corresponding to the chl a concentrations also indicate dates upon which samples were collected and incubated for primary production estimates.

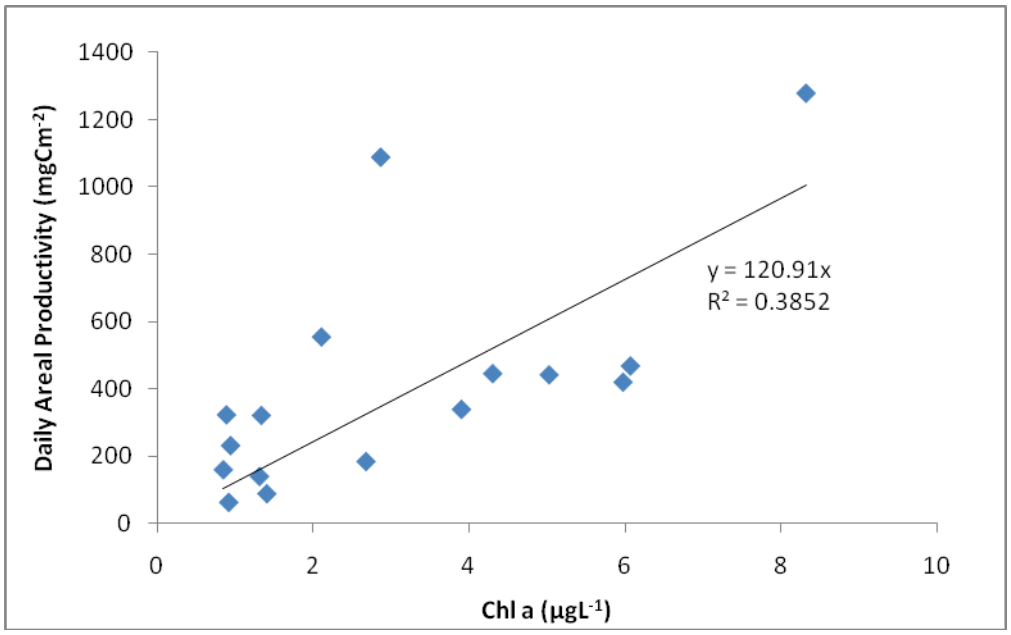

Fig 10. Production vs. Chlorophyll a concentration for samples from both sites collected with a Niskin water sampler.

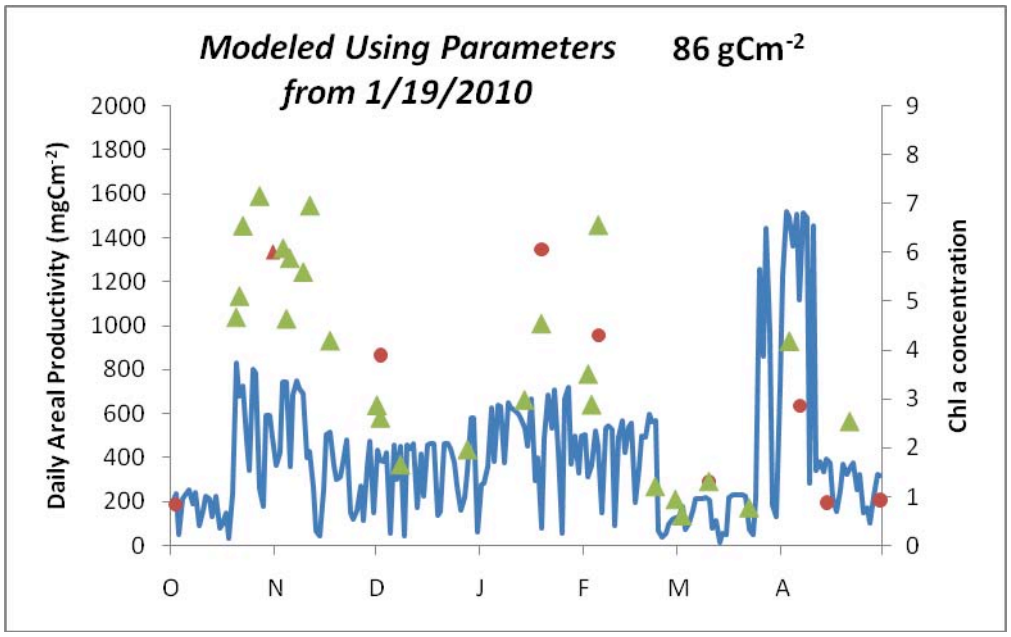

Fig 11. Daily Areal Production (blue lines) estimates for RIS using parameters from 1/19/2010 for the time period between 10/20/2009 – 11/11/2009 to attempt to correct for the missed phytoplankton bloom. Measured chlorophyll a concentrations on when production estimates were made are indicated by red dots and chlorophyll a concentrations on days that primary production incubations were not completed are indicated by green triangles.

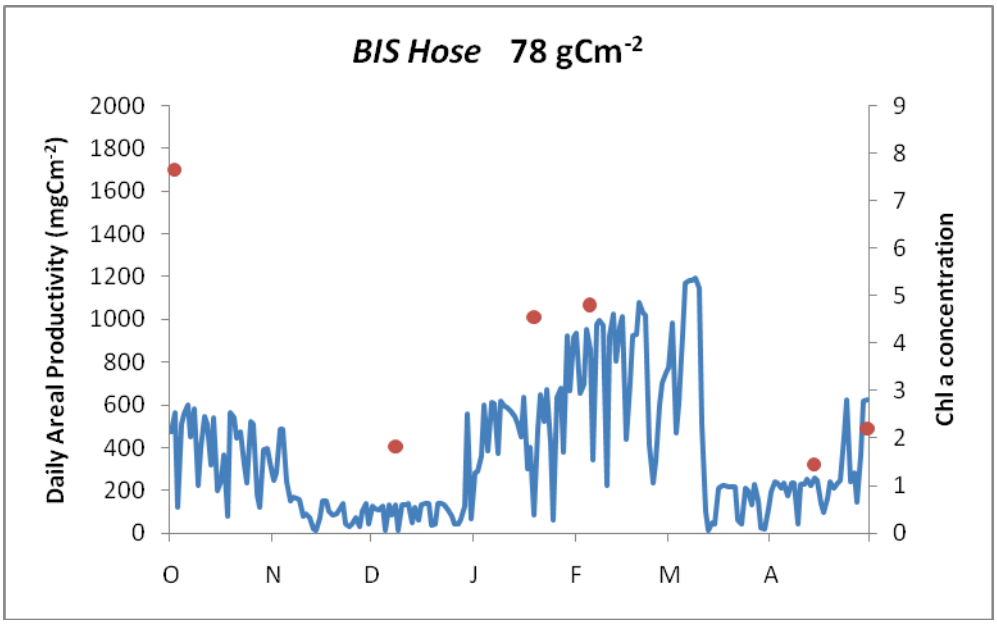

Fig 12. Daily Areal Production (blue lines) estimates and measured chlorophyll a concentrations (red dots) from BIS utiizing hose sampling method. The dates corresponding to the chl a concentrations also indicate dates upon which samples were collected and incubated for primary production estimates.

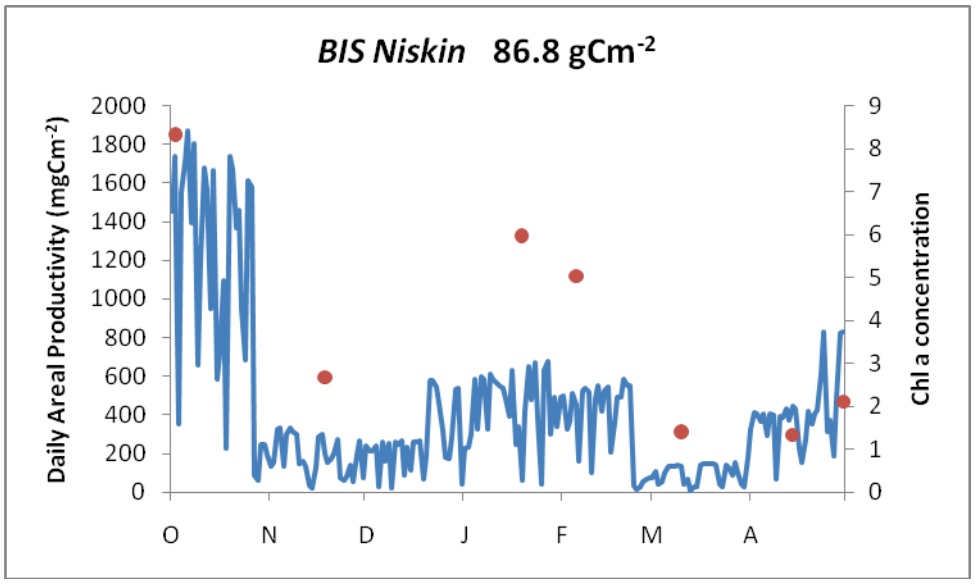

Fig 13. Daily Areal Production (blue lines) estimates and measured chlorophyll a concentrations (red dots) from BIS utiizing niskin sampling method. The dates corresponding to the chl a concentrations also indicate dates upon which samples were collected and incubated for primary production estimates.

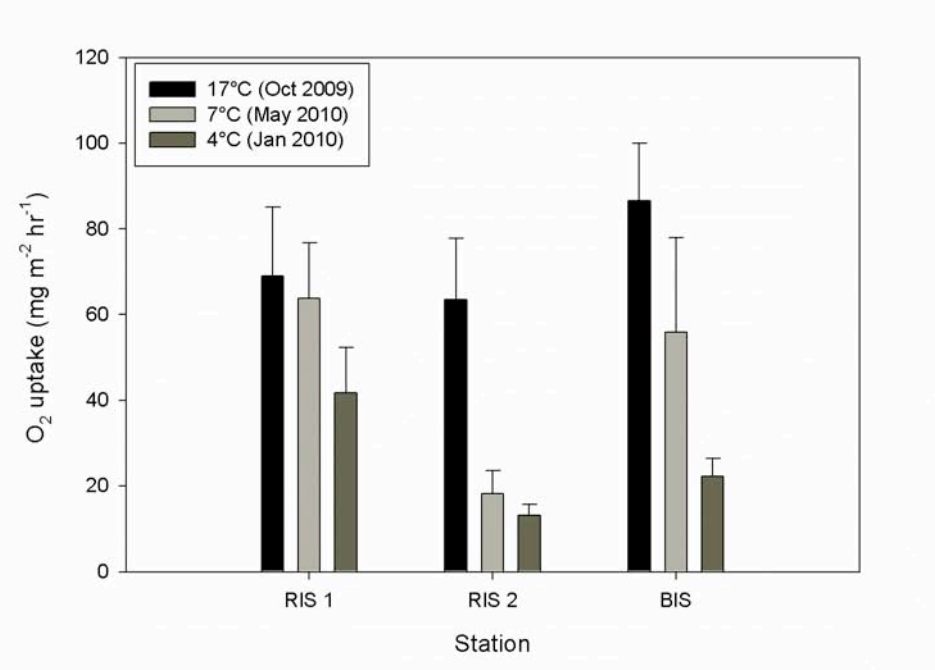

Fig 14. Mean sediment oxygen uptake measured through sediment core incubations at different temperatures (17°C, 7°C , and 4°C) for 2 stations in RIS and 1 station in BIS. Station RIS 2 is the easternmost RIS station, and RIS 1 is the western Rhode Island Sound station. Bars represent standard deviation.

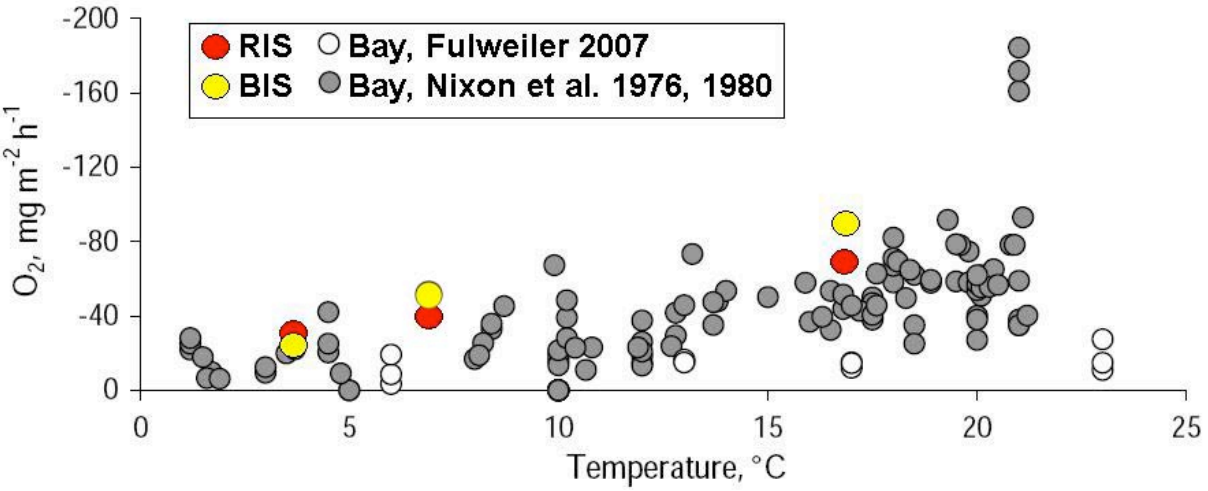

Fig 15. Sediment oxygen uptake for mid-Narragnsett Bay over an annual temperature cycle. Opaque circles are historical values (Nixon et al. 1976, 1980, and unpublished data), open circles are from more recent measurements taken in 2005-2006 (Fulweiler 2007). Red and yellow circles show mean sediment oxygen uptake for Rhode Island Sound (RIS) and Block Island Sound (BIS), respectively. Adapted from Fulweiler and Nixon (2009).

10.

Marine Mammals and Sea Turtles of Narragansett Bay, Block Island Sound, Rhode Island Sound, and Nearby Waters: An Analysis of Existing Data for the Rhode Island Ocean Special Area Management Plan

by

Robert D. Kenney and Kathleen J. Vigness-Raposa

University of Rhode Island, June 22, 2010

Executive Summary

All available sources of information on the occurrence of marine mammals and sea turtles in the waters of the Rhode Island study area—encompassing Narragansett Bay, Block Island Sound, Rhode Island Sound, and nearby coastal and continental shelf areas—were combined to assess the distribution and relative abundance of those species with respect to the Rhode Island Special Area Management Plan. Thirty-six species of marine mammals (30 cetaceans, 5 seals, 1 manatee) and four species of sea turtles are known to occur in the area. Sixteen were categorized as common to abundant (>100 total records from all sources combined), six as regular (10–100 records), and eighteen as rare to accidental (<10 records). Eleven of those species—six whales, the manatee, and four sea turtles—are listed as Endangered or Threatened under the U.S. Endangered Species Act. One other species was present historically but is now extinct in the North Atlantic—the gray whale. Eight additional species, including one Endangered sea turtle, are considered to be hypothetical in the study area—with one or more records nearby. The forty marine mammal and sea turtle species that occur in the study area have been ranked into five levels of conservation priority relative to the SAMP, taking into account such factors as overall abundance of the population, abundance in the study area, likelihood of occurrence in the SAMP area, ESA-listing status, sensitivity to specific anthropogenic activities, and existence of other known threats to the population.

The following are brief summaries of our conclusions for each of the forty species, sorted by the conservation priority rankings. Priority 1 species are all common in the study area, listed as Endangered under the ESA, and likely to occur in the SAMP area at least seasonally. Priority 2 species fall into two categories—common and ESA-listed, but not likely to occur in abundance in the SAMP area; or common, very abundant, and likely to occur frequently in the SAMP area. Priority 3 includes one ESA-listed whale species that is very unlikely to occur in the SAMP area, two ESA-listed sea turtle species where data are lacking but where juveniles may occur in or pass through the SAMP area, and several other species that are common but mainly found outside of the SAMP area. In Priority 4 is one rare to accidental ESA-listed whale species. There are also several species that are regular to rare with far offshore distributions. And there are three seal species that are all common, but where mostly juveniles occur in the study area. Finally, Priority 5 includes species that are clearly accidental in the study area. For each species, we show the priority level (1–5), the occurrence classification relative to the study area (common, regular,

or rare), the ESA-listing status (Endangered, Threatened, or unlisted), and the page number in the report where the full species account can be found.

North Atlantic Right Whale (Priority 1A, Common, Endangered, p. 39): The North Atlantic right whale almost deserves to be in a category by itself. The species is one of the rarest mammals in the world, there is serious concern about long-term population viability, and there is known anthropogenic mortality from ship collisions, as well as from entanglement in commercial fishing gear. Right whales were hunted in southern New England until the early 20th Century. Shore-based whaling in Long Island took right whales year-round, but catches peaked in spring during the northbound migration from calving grounds off the southeastern U.S. to feeding grounds in the Gulf of Maine. In recent years, right whales have occurred in southern New England in all seasons, and in the SAMP area in spring and fall. There may be occasional years when they linger in the SAMP area for feeding for days or weeks rather than just transiting through on migration.

Humpback Whale (Priority 1B, Common, Endangered, p. 51): Humpbacks occur off southern New England in all four seasons, with peak abundance in spring and summer. They may be present in the SAMP area in spring and summer. Their presence in the region varies a great deal between years; they tend to most abundant in southern New England in years when stocks of sand lance, a principal prey species, are low in Cape Cod Bay and Massachusetts Bay.

Fin Whale (Priority 1B, Common, Endangered, p. 64): Fin whales are the most abundant large whale in southern New England, and are widespread in continental shelf waters. They can occur in the SAMP area and just offshore of the area in all seasons, and are most common in summer.

Leatherback Sea Turtle (Priority 1B, Common, Endangered, p. 263): Leatherbacks are the most likely sea turtle species to be encountered in the SAMP area. Their occurrence is during the warmest part of the year in summer and early fall. Although the areas where they can be abundant are beyond the SAMP area, they can occur in the SAMP area, and they are a global conservation priority with a Critically Endangered designation on the IUCN Red List.

Sperm Whale (Priority 2, Common, Endangered, p. 93): Sperm whales are primarily deep-water residents with a distribution at the shelf break and farther offshore. However, in southern

New England they frequently venture into nearshore areas. Sperm whales have been seen in the SAMP area, mainly in the summer.

Loggerhead Sea Turtle (Priority 2, Common, Threatened, p. 270): Although loggerheads are much more abundant off the Northeast than leatherbacks, they are less likely to be seen in cooler and nearshore waters. It is possible for loggerheads to occur occasionally in the SAMP area in summer or fall.

Harbor Porpoise (Priority 2, Common, Unlisted, p. 128): The harbor porpoise is one of three very abundant small cetaceans that are likely to occur frequently in the SAMP area. They can occur in the SAMP area in all seasons of the year, but are likely to be most abundant in spring when they are migrating toward Gulf of Maine feeding grounds from wintering areas in the mid-Atlantic and/or offshore.

Atlantic White-sided Dolphin (Priority 2, Common, Unlisted, p. 162): The Atlantic white-sided dolphin is one of three very abundant small cetaceans that are likely to occur frequently in the SAMP area. They can occur in the SAMP area in all seasons of the year, but are usually most abundant more offshore and beyond the SAMP area.

Short-beaked Common Dolphin (Priority 2, Common, Unlisted, p. 187): The short-beaked common dolphin, also known as the saddleback dolphin, is one of three very abundant small cetaceans that are likely to occur frequently in the SAMP area. They can occur in the SAMP area in all seasons of the year, with less variability between seasons than other species and peak occurrence in fall and winter. Common dolphins concentrate on the outer shelf offshore of the SAMP area, but may occur in the deeper parts of the SAMP area.

Harbor Seal (Priority 2, Common, Unlisted, p. 212): Seals are very difficult to spot during surveys, so their occurrence in the study area is known mainly from stranding records. Harbor seals are the only marine mammal that can be considered as resident in Rhode Island. They are common in fall, winter, and spring, and relatively rare in summer. They are known to occupy regular haul-out sites on the periphery of Block Island, where they could be subject to disturbance from development activities.

Sei Whale (Priority 3, Regular, Endangered, p. 76): Sei whales are absent from the study area in most years, but significant numbers may visit the area irregularly in an occasional year.

Their primary area of occurrence in the spring is to the east on Georges Bank. On the rare occasions when sei whales do occur in southern New England waters, it is not likely to be within the SAMP area.

Kemp's Ridley Sea Turtle (Priority 3, Regular, Endangered, p. 276): Kemp's ridley sea turtles have been sighted off southern New England only a few times, including within the SAMP area. Their main center of distribution is off the southeastern U.S. and in the Gulf of Mexico. However, small juveniles—too small to be detected during surveys—are known to utilize shallow developmental habitats around eastern Long Island and Cape Cod, and might transit through the SAMP area.

Green Sea Turtle (Priority 3, Rare, Threatened [species], Endangered [Florida nesting population], p. 280): There has been only one recent sighting of a green sea turtle off southern New England, outside of the SAMP area. They are primarily found in shallow, tropical waters. However, small juveniles—too small to be detected during surveys—are known to utilize shallow developmental habitats around eastern Long Island and Cape Cod, and might transit through the SAMP area.

Common Minke Whale (Priority 3, Common, Unlisted, p. 84): Common minke whales are relatively abundant and widespread across the shelf in southern New England in spring and summer, including within the SAMP area but mainly beyond it.

Long-finned Pilot Whale (Priority 3, Common, Unlisted, p. 138): Long-finned pilot whales are relatively abundant off southern New England. They occur widespread across the shelf, but mainly on the outer shelf. They occur year-round, with a peak abundance in spring. They may occur on occasion within the SAMP area.

Risso's Dolphin (Priority 3, Common, Unlisted, p. 155): Risso's dolphins are relatively abundant off southern New England. They may occur year-round, but are primarily concentrated during the warmer parts of the year. Their distribution is primarily offshore, and they are not likely to be seen in the SAMP area.

Common Bottlenose Dolphin (Priority 3, Common, Unlisted, p. 175): Bottlenose dolphins are relatively abundant off southern New England, but the issue is complicated by the presence of separate coastal and offshore populations, which may actually be two separate species.

Bottlenose dolphins occur in the region year-round with highest abundance in summer and a mainly offshore distribution. Only in summer are they likely to be seen in the outer part of the SAMP area.

Blue Whale (Priority 4, Rare, Endangered, p. 62): Blue whales appear to occur only accidentally within the study area. There were three sightings in 1990, which could all have been the same whale, and one killed by a ship collision in 1998. They are mainly found more to the north, with the nearest known population center in the Gulf of St. Lawrence. However, their winter range is believed to be in deep water beyond the shelf, including mid-Atlantic latitudes, so occasional migratory transits are possible.

Pygmy Sperm Whale (Priority 4, Regular, Unlisted, p. 104): Pygmy sperm whales are known to inhabit deep, offshore waters in tropical, subtropical, and warm-temperate regions. They are known mainly from strandings, and knowledge of their occurrence is complicated by detectability and species identification issues. They are not likely to occur within the SAMP area.

Dwarf Sperm Whale (Priority 4, Rare, Unlisted, p. 104): Dwarf sperm whales are known to inhabit deep, offshore waters in tropical, subtropical, and warm-temperate regions. They are known mainly from strandings, and knowledge of their occurrence is complicated by detectability and species identification issues. They are probably more common than is apparent from the existing data, but still rarer than pygmy sperm whales. They are not likely to occur within the SAMP area.

Cuvier's Beaked Whale (Priority 4, Rare, Unlisted, p. 110): All six of the North Atlantic beaked whales have distributions that are concentrated in very deep water beyond the shelf break, and are unlikely to occur within the SAMP area. However, they all have an additional level of management concern because they appear to be especially sensitive to acoustic disturbance. Cuvier's beaked whales are one of the three species that are probably most common off southern New England.

Blainville's Beaked Whale (Priority 4, Rare, Unlisted, p. 110): All six of the North Atlantic beaked whales have distributions that are concentrated in very deep water beyond the shelf break, and are unlikely to occur within the SAMP area. However, they all have an additional level of management concern because they appear to be especially sensitive to

acoustic disturbance. Blainville's beaked whales are one of the three species that are probably most common off southern New England.

Gervais' Beaked Whale (Priority 4, Rare, Unlisted, p. 110): All six of the North Atlantic beaked whales have distributions that are concentrated in very deep water beyond the shelf break, and are unlikely to occur within the SAMP area. However, they all have an additional level of management concern because they appear to be especially sensitive to acoustic disturbance. Gervais' beaked whales have mainly a warm-water distribution, and southern New England waters are probably near the northern edge of their range.

Sowerby's Beaked Whale (Priority 4, Rare, Unlisted, p. 110): All six of the North Atlantic beaked whales have distributions that are concentrated in very deep water beyond the shelf break, and are unlikely to occur within the SAMP area. However, they all have an additional level of management concern because they appear to be especially sensitive to acoustic disturbance. Sowerby's beaked whales have a mainly cold-water distribution, and southern New England waters are probably near the southern edge of their range.

True's Beaked Whale (Priority 4, Rare, Unlisted, p. 110): All six of the North Atlantic beaked whales have distributions that are concentrated in very deep water beyond the shelf break, and are unlikely to occur within the SAMP area. However, they all have an additional level of management concern because they appear to be especially sensitive to acoustic disturbance. True's beaked whales are one of the three species that are probably most common off southern New England.

Striped Dolphin (Priority 4, Regular, Unlisted, p. 197): Striped dolphins are probably the second most abundant cetacean species off the Atlantic coast of the U.S. after common dolphins. However, their distribution is mainly offshore in very deep water over the continental slope, and it is very unlikely that striped dolphins would occur within the SAMP area.

Gray Seal (Priority 4, Common, Unlisted, p. 231): Gray seals are very common in the stranding records from Rhode Island and the rest of southern New England. However, the majority of individuals in the study area appear to be juveniles dispersing from the main population centers of adult occurrence and breeding around Nantucket and Cape Cod, Massachusetts, on the coast of Maine, and at Sable Island, Nova Scotia. The relatively frequent strandings appear to be simply a component of natural juvenile mortality.

Harp Seal (Priority 4, Common, Unlisted, p. 240): Harp seals have been very common since the early 1990s in the stranding records from Rhode Island and the rest of southern New England. However, the majority of individuals in the study area appear to be juveniles dispersing from the main population centers of adult occurrence and breeding around Newfoundland and Greenland. The relatively frequent strandings appear to be simply a component of natural juvenile mortality.

Hooded Seal (Priority 4, Common, Unlisted, p. 249): Hooded seals have been relatively common since the early to mid-1990s in the stranding records from Rhode Island and the rest of southern New England. However, the majority of individuals in the study area appear to be juveniles dispersing from the main population centers of adult occurrence and breeding around Newfoundland and Greenland. The relatively frequent strandings appear to be simply a component of natural juvenile mortality.

West Indian Manatee (Priority 5, Rare, Endangered, p. 259): Manatees clearly occur accidentally in southern New England, with only four individuals known to have visited the region since 1996. They are tropical and subtropical animals that rarely travel north of the Carolinas.

Bryde's Whale (Priority 5, Rare, Unlisted, p. 82): Bryde's whales are tropical baleen whales that occur accidentally off southern New England. Only two records are known—one sighting of a live whale in 1982 and some baleen collected in a bottom dredge sample in 1952.

Northern Bottlenose Whale (Priority 5, Rare, Unlisted, p. 110): All six of the North Atlantic beaked whales have distributions that are concentrated in very deep water beyond the shelf break, and are unlikely to occur within the SAMP area. However, they all have an additional level of management concern because they appear to be especially sensitive to acoustic disturbance. Northern bottlenose whales are accidental in southern New England, with only two known occurrences in 1867. The closest known population is off Nova Scotia.

Beluga Whale (Priority 5, Rare, Unlisted, p. 122): Belugas are primarily Arctic residents, with a relict population in the Gulf of St. Lawrence in eastern Canada. Occasional wanderers from that population visit the northeastern and mid-Atlantic U.S., with three known individuals in the southern New England study area.

Short-finned Pilot Whale (Priority 5, Rare, Unlisted, p. 138): Short-finned pilot whales are the more tropical of the two pilot whale species found in the North Atlantic. A stranding on Block Island is the only confirmed record for north of New Jersey. Because at-sea sightings can rarely be identified to species, short-finned pilot whales may be somewhat more common than is apparent from the existing data, but are still not likely to occur in the SAMP area.

Killer Whale (Priority 5, Rare, Unlisted, p. 150): Despite occurring in the North Atlantic from the tropics to the sub-Arctic, killer whales have been seen in southern New England on only very rare occasions.

False Killer Whale (Priority 5, Rare, Unlisted, p. 153): False killer whales are primarily tropical and subtropical inhabitants. A few animals were seen in a localized area for short periods in three out of four summers in 1990–1993, possibly the same group each time.

White-beaked Dolphin (Priority 5, Regular, Unlisted, p. 171): White-beaked dolphins have mainly a cold-water distribution across the North Atlantic. The nearest consistent center of occurrence is in Nova Scotia.

Atlantic Spotted Dolphin (Priority 5, Rare, Unlisted, p. 205): Both species of spotted dolphins are primarily tropical and subtropical. Off the U.S. mid-Atlantic, they primarily occur in very deep slope water and farther offshore.

Pantropical Spotted Dolphin (Priority 5, Rare, Unlisted, p. 205): Both species of spotted dolphins are primarily tropical and subtropical. Off the U.S. mid-Atlantic, they primarily occur in very deep slope water and farther offshore.

Ringed Seal (Priority 5, Rare, Unlisted, p. 257): Ringed seals are very abundant residents of the high Arctic, which occur only accidentally in New England.

Table of Contents

List of Figures

List Of Tables

Abstract

We reviewed all available information to assess the distribution and relative abundance of marine mammals and sea turtles in Block Island Sound, Rhode Island Sound, and nearby coastal and continental shelf areas. Forty species—30 cetaceans, 5 seals, 1 manatee, and 4 sea turtles—are known to occur in the area. Those species were ranked into five levels of conservation priority relative to the Ocean Special Area Management Plan, taking into account such factors as overall abundance of the population, abundance in the study area, likelihood of occurrence in the SAMP area, endangered status, sensitivity to specific anthropogenic activities, and existence of other known threats to the population. Priority 1 species are all common in the study area, listed as Endangered, and likely to occur in the SAMP area at least seasonally. They include North Atlantic right whale, humpback whale, fin whale, and leatherback sea turtle. Priority 2 species fall into two categories—common in occurrence and listed as Endangered or Threatened), but not likely to occur in abundance in the SAMP area (sperm whale and loggerhead sea turtle); or common, very abundant, and likely to occur frequently in the SAMP area (harbor porpoise, Atlantic white-sided dolphin, short-beaked common dolphin, and harbor seal). Priority 3 includes one Endangered whale species that is very unlikely to occur in the SAMP area (sei whale), two Endangered sea turtle species where data are lacking but where juveniles may occur in or pass through the SAMP area (Kemp's ridley and green sea turtles), and several other species that are common but mainly found outside of the SAMP area (common minke whale, long-finned pilot whale, Risso's dolphin, and common bottlenose dolphin). In Priority 4 is one rare to accidental Endangered whale species, the blue whale. There are also several species that are regular to rare with far offshore distributions—pygmy and dwarf sperm whales, five species of beaked whales, and striped dolphin. And there are three seal species that are all common, but where mostly juveniles occur in the study area—gray, harp, and hooded seals. Finally, Priority 5 includes species that are clearly accidental in the study area—manatee (Endangered); Bryde's, northern bottlenose, beluga, short-finned pilot, killer, and false killer whales; white-beaked, Atlantic spotted, and pantropical spotted dolphins; and ringed seal.

1 Introduction

The Rhode Island State Office of Energy Resources (OER), at the request of Governor Carcieri, has set a goal of obtaining 15% (150 MW out of 1000 MW) of the state's energy needs from renewable sources, particular wind and wave-energy resources. To meet this demand requires approximately 450 MW of new energy-generating capacity, given the intermittent nature of wind and waves. The focus has been on obtaining this energy from offshore wind farms located in state and adjacent federal coastal waters. OER retained Applied Technology & Management (ATM) to identify the most viable areas for wind energy development and assess the potential energy generation for each of these sites. ATM identified the viable sites by establishing selection criteria and then performing a screening analysis using Geographic Information Systems (GIS) methods and data sources (ATM, 2007). Their report concluded that it was possible to reach the 15% target from winds, almost all from offshore areas.

One of the areas of concern that was not adequately addressed by the ATM site-selection review was the presence of protected marine species. They used the RIGIS rare-species data layer to assess all sites, however that dataset explicitly includes only terrestrial species, not aquatic or marine species. At least 25–30 species of marine mammals and 4 species of sea turtles were known or suspected to occur in the marine waters of Narragansett Bay, Block Island Sound, Rhode Island Sound, and nearby Atlantic continental shelf waters off southern New England (CETAP, 1982; Shoop & Kenney, 1992; Kenney & Nawojchik, 1996; Nawojchik, 2002; Waring et al., 2008; Whitaker et al., in prep). All marine mammals are protected under the federal Marine Mammal Protection Act (16 U.S.C. 1361–1421h), which prohibits all "takes[1]" including disturbance. In addition, 11 of the species (six whales, the manatee, and all four turtles) are listed as Endangered or Threatened under the federal Endangered Species Act (16 U.S.C. 1531–1544). Any potential impacts on federally protected species during the construction or operation of alternative energy projects, either in federal or state waters, must be assessed under these statutes before the project can proceed.

OER has agreed to fund the development of an Ocean Special Area Management Plan (SAMP) for siting of renewable energy facilities in state and nearby federal waters. The URI

[1] By regulation, a take under the MMPA means "to harass, hunt, capture, collect, or kill, or attempt to harass, hunt, capture, collect, or kill" any marine mammal. Under the ESA, a take means "to harass, harm, pursue, hunt, shoot, wound, kill, trap, capture, or collect," or attempt to do any of the preceding.

Center of Excellence for Offshore Renewable Energy is working cooperatively with the RI Coastal Resources Management Council (CRMC) in developing the SAMP. The SAMP project is being spearheaded by the URI Coastal Resources Center and RI Sea Grant.

As a component of the Ocean SAMP project, we proposed to collate and analyze existing data on the marine mammals and sea turtles that occur in the region. Our objective was to conduct detailed analyses and mapping of the spatial and temporal distributions and relative abundances of all marine mammals and sea turtles in the marine waters of the State of Rhode Island and adjacent areas, and to make recommendations for any future research that might be necessary. This report is the result of that analysis.

The most recent reviews of marine mammals specific to Rhode Island were a summary by Cronan and Brooks (1968) and a checklist by August et al. (2000). Lazell (1976, 1980) reviewed New England occurrences of sea turtles. A major survey program took place between late 1978 and early 1982 (CETAP, 1982). It was funded by the U.S. Dept. of the Interior, Bureau of Land Management (through the Outer Continental Shelf studies program that later moved from BLM to the Minerals Management Service). The objective of CETAP was to develop information on species diversity, distributions in space and time, and abundance for environmental impact assessments related to oil and gas exploration on Georges Bank and in the mid-Atlantic. Surveys were conducted year-round of the continental shelf from North Carolina to Maine. There have been other survey efforts since then, but none have matched CETAP in geographic scope or year-round coverage. (See section 2.2.5 for an amplified discussion of historical data sources.)

The marine mammal taxonomy and nomenclature followed here is based on Rice (1998) as modified by more recent information. This follows the standards established in the editorial policies of both *Marine Mammal Science* and *Journal of Cetacean Research and Management*. To maintain consistency, all measurements have been converted to metric units regardless of how they were originally reported, with the exception of material directly quoted from original sources.

2 Methods

2.1 Study Area

The area defined for the Rhode Island Ocean SAMP study includes Rhode Island Sound, Block Island Sound, and adjacent continental shelf waters out to about the 50-m isobath (Fig 1). Existing survey effort for marine mammals and sea turtles within the SAMP study area is relatively sparse, detectability of marine animals can be quite low during surveys, and large marine vertebrates are capable of long-distance movements over short time scales. Developing a good understanding of marine mammal and turtle occurrence with the SAMP study area therefore requires looking at data over a significantly larger area. In addition, the process of developing the relative abundance models (see 2.3.2) requires including spatial data from well beyond the actual study area for effective interpolation and to avoid artifacts from edge-effects within the study area. Initially, data were extracted for a very large area—between 68°W and 74°W and north of 39°N. Data from that area were used to derive the relative abundance models. A smaller area was used to extract the data for quantifying overall levels of occurrence and creating simple maps (see 2.3.1). That area was between 70°W and 73°W and north of 39°30'N, roughly encompassing the coastal and shelf waters south of New England between Cape Cod, Massachusetts and the middle of Long Island, New York (Fig. 1). We shall refer to this area as the "Rhode Island study area" in this report for convenience and clarity.

2.2 Data Sources

There were four primary types of data records included in this review, from a variety of original sources—survey data, opportunistic sighting records, stranding records, and fishery bycatch records.

2.2.1. Survey Data

There have been aerial and shipboard surveys for marine mammals and turtles in southern New England waters since the late 1970s. Most of the existing survey data for the region have been obtained and archived by the North Atlantic Right Whale Consortium (NARWC, http://www.rightwhaleweb.org). The NARWC database is managed and continually updated at the University of Rhode Island Graduate School of Oceanography (Kenney, 2001), with funding support from the National Marine Fisheries Service. By definition, in addition to records of all

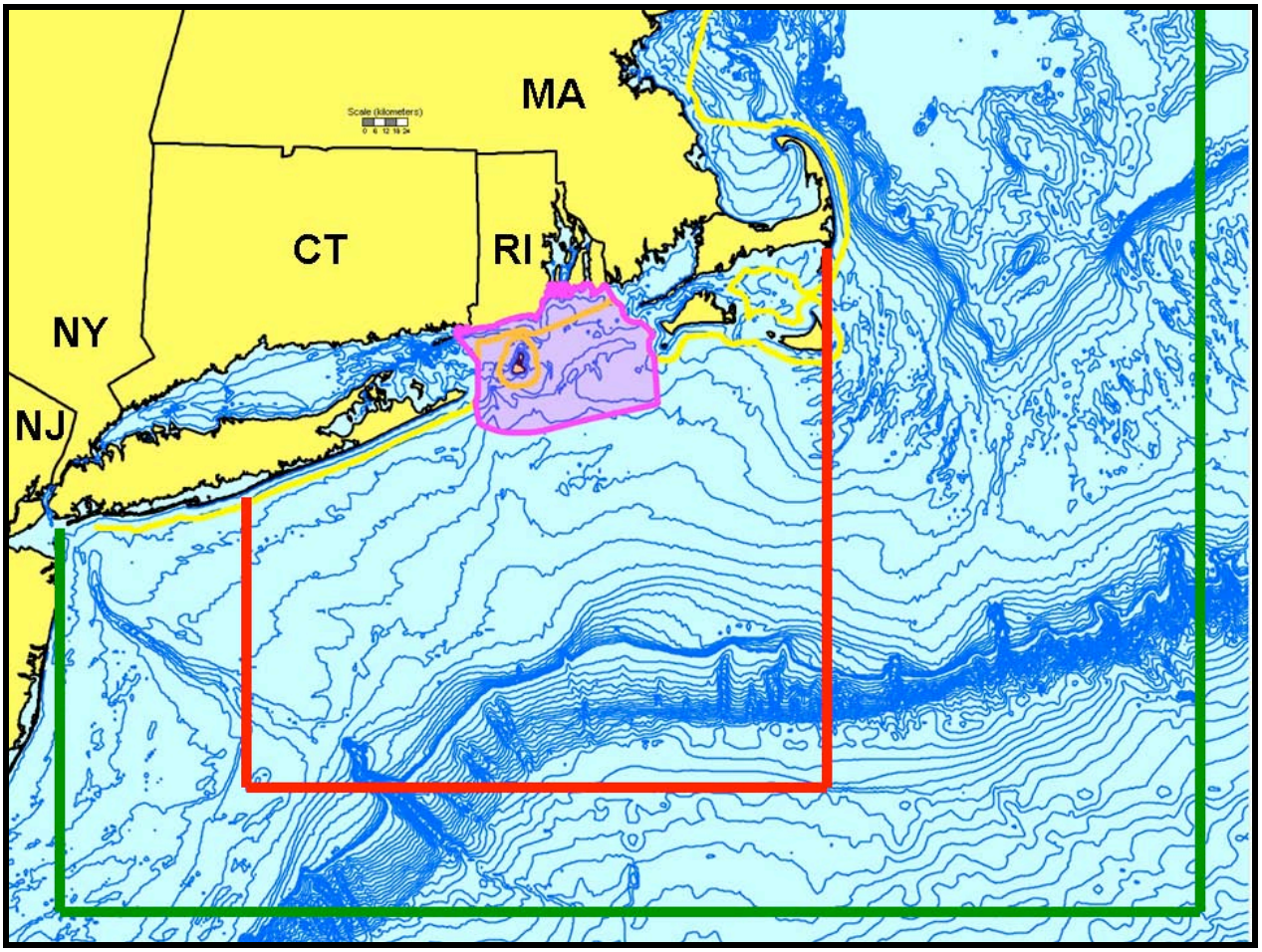

Figure 1. The study areas used in analyzing marine mammal and sea turtle occurrence for the Rhode Island Ocean SAMP. The broadest area outlined in green is the area used for extracting data for the relative abundance modeling procedure. The smaller area enclosed in the red line is the Rhode Island study area defined for this report. The smallest area outlined and shaded in pink is the formally defined SAMP study area. The yellow line shows the state waters boundary (3 nautical miles). The bathymetry shown is at 10-m contour intervals to 200 m, then at 100-m intervals.

target species (and sometimes non-target species) sighted, survey data include detailed information on the track of the survey platform (e.g., ship or aircraft) and associated environmental conditions, allowing for subsequent reconstruction of the survey and quantification of effort. The principal sources of survey data in the NARWC database from the southern New England are surveys in 1978–1982 by the Cetacean and Turtle Assessment Program (CETAP, 1982), surveys specifically focused on right whales and multi-species stock

assessment surveys conducted since the 1990s by the National Marine Fisheries Service's Northeast Fisheries Science Center (NMFS-NEFSC, Woods Hole, MA), and aerial surveys for right whales conducted in 2005 and 2006 by the Riverhead Foundation for Marine Research and Preservation (Riverhead, NY).

2.2.2 Sighting Records

The NARWC database also includes substantial numbers of opportunistic sighting records that have no associated survey data. Many of these represent records collected during CETAP or historical data that were aggregated and archived as part of CETAP. Other sightings have been contributed by a variety of individuals, including Navy, Coast Guard, other federal agencies, mariners, commercial fishermen, and recreational boaters. An additional collection of opportunistic sighting records was obtained from Dr. Arthur Kopelman of the Coastal Research and Education Society of Long Island, Inc. (CRESLI). The sightings came originally from the Okeanos Ocean Research Foundation (Samuel S. Sadove, executive director; Okeanos is no longer in existence), and were recorded from commercial whale-watching vessels out of Montauk in late spring and summer of 1981–1994 (primarily the *Finback*). These sightings are heavily concentrated in the area between eastern Long Island and Block Island and during the whale-watching season, and therefore somewhat biased, but provide valuable information on several less-common species. An attempt was also made to acquire sighting records collected by naturalists working aboard whale-watching boats operating from Galilee, Rhode Island. George O. Klein provided humpback whale sighting records collected aboard the *Super Squirrel* and *Super Squirrel II* in 1986–1988. Charles Avenengo provided his logbooks from the Frances Fleet whale-watch boats (*Lady Frances* and *Gail Frances*) for 1992–1996. We have been unsuccessful thus far in getting more recent records from the Frances Fleet.

2.2.3 Stranding Records

Dead or debilitated marine mammals and sea turtles occasionally wash up on shore, or strand (Geraci et al., 1999). Sometimes apparently healthy animals (on occasion in groups) strand, which, without human intervention, often results in mortality (seals are more likely to be successfully "rescued" than cetaceans). Because of federal protection in the U.S. since the early 1970s, all stranding response in the region is conducted by organizations that have been issued federal permits and that are part of the Northeast Regional Stranding (NERS) network (marine

mammals) or the Sea Turtle Stranding and Salvage Network (sea turtles). Network participants within the region are: New York plus Block Island, Rhode Island—Riverhead Foundation (who took over from Okeanos in the mid-1990s); Connecticut and the rest of Rhode Island—Mystic Aquarium and Institute for Exploration (Mystic, CT); and Massachusetts—several different organizations, with the mix changing over the years.

Both stranding networks are coordinated from the NMFS Northeast Regional Office (NERO, Gloucester, MA). The complete marine mammal stranding database for Rhode Island to New Jersey (but not including Massachusetts) for 1993–2005 was obtained from Mendy Garron, NERS Network Coordinator, NMFS-NERO. A database of pre-1993 records for the same region (plus additional records from a broader region for baleen whales only) was obtained from Dr. James G. Mead at the Smithsonian Institution, National Museum of Natural History. That dataset included strandings, museum specimen records (including a number of cross-references to specimens in the collections of other museums), sightings collected during a former program known as the Scientific Events Alert Network, records of intentional captures, and a variety of records that had been extracted from published reports. A few relevant museum specimen records were also obtained from the American Museum of Natural History and the Harvard University Museum of Comparative Zoology. Combining datasets required careful removal of duplicate records that were included in more than one source. Many of the older records in these datasets had only approximate descriptions of localities that would not have been precise enough to enable mapping them. We used Google Earth and a variety of other on-line search engines and mapping utilities to locate as many as possible and to generate latitude/longitude coordinates. The same process was used to derive corrected latitude/longitude coordinates for records where mapping uncovered obvious location errors (e.g., stranding and sighting records that mapped far inland or stranding records that mapped offshore). The Smithsonian dataset included only cetacean records, so we did not have a complete record of seal strandings prior to 1993. We were able to get pre-1993 seal stranding records for Rhode Island only from the stranding program at Mystic Aquarium, courtesy of Heather Medic, the stranding coordinator at that time. We were not able to obtain the data from the sea turtle stranding network; the only turtle stranding records we had were a few in the CETAP database, a few from the Rhode Island Sea Turtle Disentanglement Network, and 20 records from Block Island tabulated in Nawojchik (2002).

2.2.4 Bycatch Records

Marine mammals are often captured accidentally in the course of normal operations by commercial fisheries (Beddington et al., 1985; Woodley and Lavigne, 1991; Perrin et al., 1994b; Northridge and Hofman, 1999; Northridge, 2002; Waring et al., 2008). This incidental take, or bycatch, includes both animals that are killed and animals that are released alive from the gear. The NMFS Fisheries Sampling Branch (FSB, Woods Hole, MA) collects bycatch data from fishery observers placed aboard commercial fishing vessels in the northeastern U.S. to quantify fishery-related marine mammal mortality, in addition to collecting standard fisheries data. NMFS-FSB (David Potter and Sara Quinn) provided an extensive dataset of marine mammal bycatch records for the northeastern U.S. Because of confidentiality issues with the individual bycatch records, they have been fully integrated with the sighting and stranding records so they can not be identified separately, no specific information or details will be presented, and the bycatch locations will not be differentiated on the maps.

2.2.5 Notes on Historical Data Sources

In *The Mammals of Rhode Island* (first published in 1962, revised in 1968), John M. Cronan and Albert Brooks say that they have written "the first comprehensive study of the mammals of Rhode Island." They cited two previously published checklists of the state's mammalian fauna. One, "The Native Mammals of Rhode Island," was published in 1900 as Circular 1 of the Newport Natural History Society by Edgar A. Mearns (1856–1916), an Army surgeon and naturalist who was stationed at Fort Adams in 1899 and 1900. That publication was essentially a request for information toward the goal of developing a detailed catalog of the state's mammals, and included simple listings of 50 "wild mammals known to have inhabited the State of Rhode Island during the historic period" and another 32 species "whose occurrence … may be looked for with some degree of probability." The second was by Roland C. Clement, Audubon Society of Rhode Island, in 1952. It was simply a checklist, and included only terrestrial species. Two checklists were published following Cronan and Brooks. The state Water Resources Board (WRB) published a checklist of all fish and wildlife species in 1976, but again included only terrestrial mammals. August et al. (2001) published a checklist of the state's mammals, including an up-to-date list of marine species, as a chapter in the vertebrate volume of the Rhode Island Natural History Survey's "Biota of Rhode Island" series.

Because of their high economic value, the baleen whales historically have been the focus of substantially more scientific effort than other cetaceans. A particularly valuable source is Glover M. Allen's[2] 1916 monograph—*The Whalebone Whales of New England*[3]. Allen exhaustively reviewed seemingly everything that had been written before him about whales in New England, back to the earliest accounts from the colonial era. The specific records he published were then painstakingly extracted and computerized in the Smithsonian Institution's database, through the efforts of marine mammal curator James G. Mead. In 1908, Joel A. Allen published a paper reviewing information on North Atlantic right whales, which was a primary source for Allen (1916) for that species. Frederick W. True's (1904) baleen whale monograph was also an important source for Allen (1916); True also published a monograph on the Delphinidae (also including Phocoenidae and Monodontidae) in 1889. Another major source for Allen (1916) was Clark (1887), which was a review of American whaling as part of a massive review of the fisheries industry for the federal government.

Joseph H. Waters and C. Jean-Jacques Rivard published a review of the mammals of Massachusetts in 1962. Their volume was intended for a non-professional audience. The marine mammal accounts were relatively sparse and seemed to be based heavily on anecdotal information. They did include a table of sightings and strandings (for cetaceans, but not for the seals; also extending to Rhode Island) since 1940. Their primary sources besides those recent occurrences were two checklists published very recently before their summary (Grayce, 1957; Carpenter and Siegler, 1958), Allen (1916) for the baleen whales, and a very small number of recent papers in the primary literature.

James Ellsworth De Kay (1842) published the first comprehensive review of the mammal fauna of New York, although his treatment of the marine mammals was relatively incomplete

[2] There were two Harvard-educated American naturalists of the Victorian era named "Allen" who both published major works on mammals, and specifically on marine mammals. Joel Asaph Allen (1838–1921) was probably best known for his work on birds. He was the first curator of birds and mammals at the American Museum of Natural History. His major work on marine mammals was a monograph on North American pinnipeds in 1880. Glover Morrill Allen (1879–1942) was the curator of mammals at Harvard's Museum of Comparative Zoology (where J.A. Allen had gotten his professional start in 1872 as assistant in ornithology). To confuse things even more, J.A. Allen reviewed G.M. Allen's 1916 baleen whale monograph in *Science*, so there are two "Allen (1916)" publications with the same title (though we have cited only the monograph, not the review).

[3] Interestingly, many of the Rhode Island records included by Allen in this volume came to him from Major Edgar A. Mearns, who was apparently the same person who published "The Native Mammals of Rhode Island" in 1900. Since many of the observations occurred well before Major Mearns was posted to Fort Adams in 1899, it seems that he collected all available reports of Rhode Island baleen whales for his summary and also sent them on to Allen.

and relied heavily on second-hand anecdotal sources, and consequently has a number of errors. Paul F. Connor published a comprehensive review of the mammals of Long Island in 1971, as one piece of a never-completed region-by-region review of the New York mammal fauna. Connor's review summarized what was published in all of the historical sources mentioned herein and others, evidence from contemporary strandings and other specimens, and reliable reports from fishermen and others. J. G. Mead considered Connor's reports of sufficient reliability to extract them as occurrence records in the Smithsonian database. One of us (RDK) has written the marine mammal chapters for an updated *Mammals of New York* book (Whitaker et al., in preparation); much of the basic text of the species accounts included in this report has been abridged from that manuscript.

J.H. Linsley (1842) published an early review of the mammals of Connecticut, including marine species. Some of his information drew on De Kay's as-yet-unpublished treatise. A century later, Goodwin (1935) relied heavily on Linsley and De Kay for his review of Connecticut mammals.

Harold Lester Babcock, M.D. published a monograph on New England turtles in 1919, including four sea turtle species. He included listings of 19th and early 20th Century records from New England and New York, attempting to eliminate questionable reports from fishermen and others. James D. Lazell, Jr. published *This Broken Archipelago* in 1976. It was an extensive review of historical and recent data on the reptiles and amphibians of Cape Cod and the nearby islands of Massachusetts. In 1980, he published the information for only the sea turtles in a paper in *Copeia*, where he argued that New England waters comprised important habitats for as many as four of the five Atlantic sea turtle species. Lazell's work comprised the most complete source for New England sea turtles prior to results from the extensive CETAP surveys (CETAP, 1982; Shoop and Kenney, 1992).

2.3 Analytical Methods

2.3.1 General Occurrence and Distribution

All data records from the Rhode Island study area (Fig. 1) were extracted to assess the general levels of occurrence of all species in the region. Data were processed, analyzed, and archived in SAS 9.1.3 (SAS Institute, Inc., Cary, NC), using our own purpose-designed programs. Descriptive, order-of-magnitude occurrence levels were defined as:

- "common to abundant" is more than 100 records,
- "regular" is 10–100 records, and
- "rare or accidental" is fewer than 10 records.

Seasonal distribution maps of all available data, including sightings, strandings, intentional captures, and bycatch, were created for each species using MyWorld GIS 4.0.5 (Northwestern University, Evanston, IL). Seasons were defined as:

- Winter—December, January, February;
- Spring—March, April, May;
- Summer—June, July, August;
- Fall—September, October, November;

which matches very closely with the annual cycle of monthly mean air temperatures at Block Island (Shonting and Cook, 1970).

All histograms of frequency distributions were created using the GCHART procedure in SAS/GRAPH.

2.3.2 Modeling Relative Abundance Patterns

A major issue with the interpretation of distribution and habitat-use patterns based on raw sighting and stranding data is that the patterns are usually biased by the distribution of survey coverage ("effort"). We already were aware going into this project that the data were seriously biased by the intensive whale-watching concentrated in a relatively small geographic area during a few months of the year. One method to overcome this potential bias is to quantify survey effort, and then to correct sighting frequencies for differences in effort, producing an index termed sightings-per-unit-effort (SPUE). The units are numbers of animals sighted per unit length of survey track. To standardize the SPUE data even further, the data can be limited to only a subset of the survey tracklines which meet pre-defined criteria for "acceptability." The effort criteria can vary between studies; ours included having at least one observer formally on watch, visibility of at least 2 nautical miles (3.7 km), sea state of Beaufort class 3 or below, and altitudes below 1,200 feet (366 m, applicable only to aerial surveys). SPUE values are computed for consistent spatial units and can therefore be mapped or be statistically compared across areas,

seasons, years, etc. Development of this method was begun during CETAP (1982), and it has been used in a variety of analyses (Kenney and Winn, 1986; Winn et al., 1986; Kenney, 1990; Hain et al., 1992; Shoop & Kenney, 1992; Kraus et al., 1993; DoN, 2005; Pittman et al., 2006). Because the method requires regular location and environmental data to reconstruct the survey tracks and quantify effort, only a subset of the sighting data can be included, and stranding data are entirely excluded.

The SPUE method involves partitioning the study area into a regular grid based on latitude and longitude. The grid size selected is a compromise between resolution (smaller cells) and sample sizes (larger cells), and cannot be determined without preliminary examination of the available survey data. Previous studies based on the NAWRC data have used cells ranging from 1 min X 1 min (1.9 X 1.4 km) to 10 min X 10 min (18.5 X 13.9 km). For this project we used a 5 min X 5 min grid (9.3 X 7.0 km). All acceptable aerial and shipboard survey tracks were parsed into grid cells and their lengths computed and summed by season. Sightings were similarly assigned to cells and the numbers of animals sighted were summed by cell and season. Finally, the number of animals in each cell/season was divided by the corresponding effort value, then multiplied by 1,000 to avoid small decimal values, generating a SPUE index in units of animals sighted per 1,000 km of survey track. All of this analysis was done using our own custom programs in SAS 9.1.3 (SAS Institute, Inc., Cary, NC).

Species can differ substantially in their detectability from different survey platforms, especially between aircraft and ships. For example, sea turtles are very difficult to spot from shipboard surveys (Shoop & Kenney, 1992), while harbor porpoises and minke whales are more readily sighted from a shipboard survey (Kraus et al., 1983; Kenney et al., 1997). Given a large number of cells sampled with sufficient numbers of sightings from both platform types within the same cells and seasons, it is possible to derive and incorporate a correction factor into the SPUE calculation for a single species to account for inter-platform differences, as was done for a SPUE analysis of basking sharks from Florida to Nova Scotia (Campana et al., 2008). The level of analysis required to conduct the same type of scaling separately for each of the species in the Rhode Island study was beyond the scope of the SAMP project.

It is possible to map the gridded SPUE data directly (e.g., Shoop & Kenney, 1992; Kraus et al., 1993), however the effort data and resulting SPUE data are often sparse (see Fig. 2) and can

be difficult to interpret. Interpolation can smooth out the relative density contours and fill in predicted values in some un-sampled areas. Pittman et al. (2006) used inverse-distance weighting to create interpolated relative density maps. For a Navy Marine Resources Assessment (DoN, 2005), the kriging function in Spatial Analyst within the ArcGIS environment was used for that purpose (Watterson et al., in review). We used the same kriging process in ArcGIS 9.2 (ESRI, Inc, Redlands, CA) to produce interpolated GIS maps of seasonal relative densities, contoured in ten levels, for all of the species with sufficient sightings during surveys. One difference from the Watterson et al. work was that we used the elliptical search option instead of circular. Marine animal distributions are expected to be related to habitat variables, and bathymetry (water depth, bottom slope) consistently has been shown to be an important habitat parameter in defining or predicting distributions (e.g., Hui, 1979; CETAP, 1982; Kenney and Winn, 1986; Baumgartner, 1997; Hamazaki, 2002; Ferguson et al., 2006). In our restricted study area the bathymetric contours are consistently east-west, although in practicality we saw very little difference between the two search options when experimenting with them during preliminary mapping trials.

3 Results

3.1 Overview

In all, 41 species of marine mammals and sea turtles have been recorded at some time within the Rhode Island study area, including 31 cetaceans, 5 seals, 1 manatee, and 4 sea turtles (Table 1). For the mammals, this represents a substantial increase over the 15 species listed by Mearns (1900)—including 11 known to occur (9 cetaceans and 2 seals) and 4 others that might be expected (3 cetaceans and 1 seal) (Table 1). There were just over 8,000 records in total for the study area (N = 8,010). Sixteen species are classified as common, six as regular, and eighteen as rare; and one species was known to have occurred historically but is now extinct. Five other cetaceans, all delphinids—pygmy killer whale (*Feresa attenuata*), melon-headed whale (*Peponocephala electra*), rough-toothed dolphin (*Steno attenuata*), spinner dolphin (*Stenella longirostris*), and Clymene dolphin (*Stenella clymene*); two pinnipeds—bearded seal (*Erignathus barbatus*) and walrus (*Odobenus rosmarus*); and one hard-shelled sea turtle—hawksbill sea turtle (*Eretmochelys imbricata*) might be considered as hypothetical species with the remote potential to occur in the region at some time, based on known occurrences off the U.S. East

Table 1. Marine mammals and sea turtles of the Rhode Island region, showing the total numbers of records, occurrence classification, and whether included as known to occur in the state (X) or possible to occur (?) by Mearns (1900).

Species	N	Occurrence	Mearns
Class Mammalia			
Order Cetacea – whales, dolphins, and porpoises			
Suborder Mysticeti – baleen whales			
Family Balaenidae – right whales			
North Atlantic right whale	156	common	X
Family Eschrichtiidae – gray whales			
Gray whale	1	extinct	
Family Balaenopteridae – rorquals			
Humpback whale	611	common	
Blue whale	5	rare	
Fin whale	1,762	common	X
Sei whale	35	regular	
Bryde's whale	2	rare	
Common minke whale	504	common	
Suborder Odontoceti – toothed whales			
Family Physeteridae – sperm whales			
Sperm whale	103	common	X
Family Kogiidae – pygmy and dwarf sperm whales			
Pygmy sperm whale	26	regular	
Dwarf sperm whale	2	rare?*	
Family Ziphiidae – beaked whales			
Northern bottlenose whale	2	rare	X
Cuvier's beaked whale	4	rare	
Blainville's beaked whale	3	rare	
Gervais' beaked whale	1	rare	
Sowerby's beaked whale	2	rare	
True's beaked whale	2	rare	
Family Monodontidae – beluga and narwhal			
Beluga whale	4	rare	X
Family Phocoenidae – porpoises			
Harbor porpoise	374	common	X
Family Delphinidae – dolphins			
Long-finned pilot whale	43	common*	X
Short-finned pilot whale	1	rare*	
Killer whale	7	rare	?
False killer whale	9	rare	
Pygmy killer whale	0	hypothetical	
Melon-headed whale	0	hypothetical	
Risso's dolphin	208	common	?
Rough-toothed dolphin	0	hypothetical	
Atlantic white-sided dolphin	210	common	?
White-beaked dolphin	11	regular	
Common bottlenose dolphin	182	common	X

Table 1. (continued)

Species	N	Occurrence	Mearns
Short-beaked common dolphin	435	common	X
Striped dolphin	41	regular	
Atlantic spotted dolphin	3	rare	
Pan-tropical spotted dolphin	3	rare	
Spinner dolphin	0	hypothetical	
Clymene dolphin	0	hypothetical	
Order Carnivora – carnivores			
Suborder Caniformia – doglike carnivores			
Superfamily Pinnipedia – seals, sea lions, fur seals, and walrus			
Family Phocidae – seals			
Harbor seal	507	common	X
Gray seal	193	common	
Harp seal	703	common	X
Hooded seal	97	regular	?
Ringed seal	1	rare	
Bearded seal	0	hypothetical	
Family Odobenidae – walrus			
Walrus	0	hypothetical	
Order Sirenia – sea cows			
Family Trichechidae – manatees			
West Indian manatee	4	rare	
Class Reptilia			
Order Testudines – turtles			
Family Dermochelyidae – leatherback sea turtle			
Leatherback sea turtle	142	common	
Family Cheloniidae – hard-shelled sea turtles			
Loggerhead sea turtle	233	common	
Kemp's ridley sea turtle	14	regular	
Green sea turtle	1	rare	
Hawksbill sea turtle	0	hypothetical	

*Some species, particularly those that are difficult to identify, are known or suspected to be more abundant than is shown by the number of records alone; see the individual species accounts for details.

Coast. The hypothetical species are included in Table 1 for the sake of completeness, but are not addressed in the remainder of this report.

Out of the total sighting, stranding, and bycatch records, 1,141 or 14% were unidentified. The unidentified categories covered a wide range of observer certainty. Some were as narrow as "fin or sei whale," "Atlantic spotted or bottlenose dolphin," or "*Stenella* sp." On the other end of the scale, some were as broad as "unidentified whale," "unidentified dolphin/porpoise," "unidentified seal," or "unidentified turtle." These unidentified records have not been included in

our analyses, with two exceptions. (1) Sightings identified as "unidentified fin or sei whale" were counted in the SPUE analysis, assuming a 97.8% likelihood of being a fin whale and 2.2% likelihood of being a sei whale—based on the proportions of identified sightings. This worked for fin whales, but not for sei whales. (2) Unidentified seal sightings were combined with harbor seal and gray seal sightings in one SPUE model because they represented a substantial majority of the seal sightings during surveys.

Survey coverage varied between seasons (Fig. 2). Non-zero effort values were classified into ten categories from lowest to highest, and mapped by the 5x5-minute grids without interpolation. Coverage was essentially complete in spring, and relatively complete in the other four seasons—with the fewest holes in fall, followed by summer and winter. Except for winter, the most intense survey coverage was consistently in the region east of Cape Cod and Nantucket, a known right whale habitat that has been surveyed every year since 1979 except for several years in the1990s. Cape Cod Bay, another right whale habitat, had high effort in all seasons. Survey intensity south of New England has been consistently lower. Only in spring was there high survey effort within the Ocean SAMP study area. Effort in the SAMP area was moderate during summer, and somewhat lower and about equivalent in both fall and winter.

Strandings, excluding intentional captures in the pre-1993 Smithsonian data as much as possible, are summarized in Table 2. The total number was 1,803, with 1,763 since 1970. In terms of stranding frequencies, the four species of seals are at the top of the list. Note that the comparisons between species are not entirely consistent, since seals were not included in the pre-1993 data obtained from the Smithsonian and we were unable to obtain a copy of the sea turtle stranding dataset. Additionally, we do not have the complete stranding dataset for Massachusetts, but that is consistent across all the marine mammals. Finally, identifying stranding records from electronic databases (other than the NMFS stranding network data) is not always simple, since live strandings might not be categorized the same as dead animals on the beach or floating in the water. Each dataset has its own unique formats and codes. The historical stranding data also may be complicated by capture records, and some strandings during the whaling era may actually have been animals harpooned by whalers but not recovered. Identifying strandings often required manual verification of the records, assuming that sufficient information was included. It is quite likely that a few records are mis-classified one way or the other.

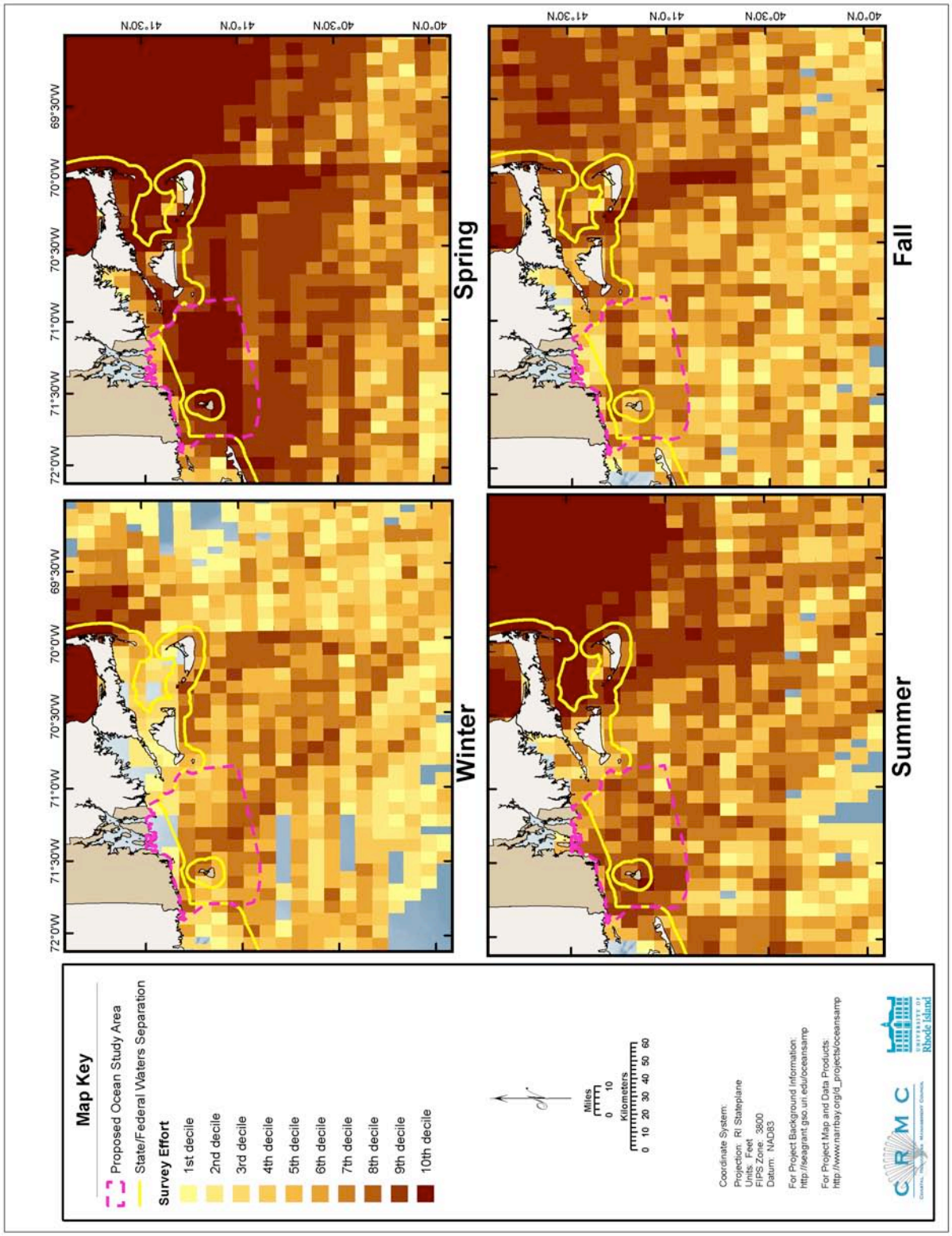

Figure 2. Seasonal summary maps of combined aerial and shipboard survey effort, in km of trackline per 5-minute grid cell.

Table 2. Stranding frequencies for marine mammals and sea turtles in the Rhode Island study area, for all years combined and for 1970–2005 only, in descending order of occurrence in the recent data.

Species	All Years	1970–2005
Harp seal	688	688
Harbor seal	446	446
Gray seal	155	155
Hooded seal	96	96
Harbor porpoise	87	83
Short-beaked common dolphin	71	68
Long-finned pilot whale	35	34
Common minke whale	31	29
Fin whale	39	28
Striped dolphin	27	25
Atlantic white-sided dolphin	21	21
Common bottlenose dolphin	23	18
Pygmy sperm whale	17	17
Humpback whale	17	16
Risso's dolphin	13	13
North Atlantic right whale	7	5
Globicephala sp.	4	4
Sperm whale	4	2
Blainville's beaked whale	3	2
Dwarf sperm whale	2	2
White-beaked dolphin	2	2
Blue whale	2	1
True's beaked whale	2	1
Pan-tropical spotted dolphin	2	1
Kogia sp.	1	1
Gervais' beaked whale	1	1
Beluga	1	1
Short-finned pilot whale	1	1
Atlantic spotted dolphin	1	1
Cuvier's beaked whale	2	0
Northern bottlenose whale	1	0
Killer whale	1	0

3.2 Species Accounts

The following section includes species accounts for the forty species classified as common, regular, or rare in Table 1, plus an abbreviated account for the extinct North Atlantic gray whale population. Rather than include separate sections for higher-level taxa (families, orders, etc.), very brief summaries are included within the accounts for the first species in that taxon. There

are four cases (i.e., pygmy and dwarf sperm whales, six species of beaked whales, long-finned and short-finned pilot whales, and Atlantic spotted and pan-tropical spotted dolphins) where the species are difficult or impossible to differentiate in the field, with the result that much of the available information is for all species combined. In those cases, one species account combining all of the species is presented, including species-specific information where available. Each species account includes the seven sections and primary sources outlined below. The extent of the information that is included for any particular species tends to be proportional to a combination of three factors—the species' regional abundance, management concerns or the significance of potential threats to the species, and the likelihood of it being present in or near the SAMP study area:

Description: a brief description of the species characteristics, mainly based on Wynne & Schwartz (1999) and Jefferson et al. (1993).

Status: Current status of a species or population under the U.S. Endangered Species Act[4] was obtained from USFWS (2009). Rhode Island state status[5] is as shown in *Rare Native Animals of Rhode Island* (RIDEM, 2006). International status[6] is as shown on *The IUCN Red List of Threatened Species* (IUCN, 2008). Current estimates of abundance of the population that occurs in the Rhode Island study area were based on the most recently published edition (2007) of the NMFS marine mammal stock assessment report (SAR: Waring et al., 2008) that was available at the time this report was first written. Note that: (1) The SAR abundance estimate may not cover the entire range of a population, so it may only be relevant to the portion of the range off the U.S. East Coast. If estimates are available for wider areas from the literature or other sources, they will also be included. (2) The SAR is updated annually and consequently the numbers are always subject to change. For example, the draft 2008 edition has been released for public review and comment, and should be published in final form soon (Note: it was officially released on 29 April 2009, however the estimates and citations in this report have not been updated; many did not change). (3) The current SAR, all previous editions, and the draft of the next edition, once released for comment, are all available on the NMFS Office of Protected Resources web page

[4] Categories, in decreasing order, are Endangered, Threatened, or Candidate (i.e., proposed for listing).
[5] Categories are Federally Endangered, Federally Threatened, State Endangered, State Threatened, Concern, and State Historical (i.e., extirpated).
[6] Categories are Extinct, Extinct in the Wild, Critically Endangered, Endangered, Vulnerable, Near Threatened, Least Concern, and Data Deficient.

(http://www.nmfs.noaa.gov/pr/sars/). (4) The SAR does not include sea turtles, as there is no statute equivalent to the MMPA that mandates annually updated reviews of abundance and mortality. The SAR is also the source for estimates of human-caused mortality to marine mammal populations, which are presented as 5-year averages (2001–2005 in the 2007 edition). Other conservation and management issues are summarized from the SAR and other sources.

Ecology and life history: a summary of information on biology, feeding, reproduction, etc., focusing on aspects relevant to habitat use and/or occurrence in the Rhode Island study area.

General distribution: a description of the species' distribution pattern, world-wide and in the North Atlantic.

Historical occurrence: details of known occurrences prior to the early or mid-1970s (i.e., before passage of the MMPA and ESA) in Rhode Island, in the Rhode Island study area, and in nearby areas of southern New England. These are based primarily on the records included in the data obtained from the Smithsonian, although many of those records were originally obtained from published literature.

Recent occurrence: This section will present the details of the analyses conducted specifically for this report. Each species (or species complex for those which were combined) account will include seasonal maps of the combined sighting, stranding, and bycatch records. For species with sufficient sightings in the survey data, there will also be seasonal maps of the effort-corrected relative abundance model outputs. Any analyses of recent trends within the study area will also be addressed here.

Conclusions: a summary of any information and details about species occurrence that are particularly relevant to the Rhode Island Ocean SAMP. See also Section 4, Recommendations, for a ranked list of species in the area prioritized by conservation concerns.

3.2.1 North Atlantic Right Whale *Eubalaena glacialis* (Müller 1776)

Cetacea includes 14 families and approximately 90 species world-wide, with 8 families and 30 species confirmed as occurring within the Rhode Island study area and 1 more extinct species in another family. Cetaceans are fully aquatic; their dramatic modifications for life in the water have obscured their evolutionary relationships to hoofed mammals (Barnes, 2002a). The body is

more or less fusiform and covered by smooth, hairless skin; they are insulated by a layer of blubber. The hind limbs have been lost, and the forelimbs have been simplified into paddle-like flippers. Swimming is powered by the tail, which is modified into a horizontal pair of "flukes" that are supported only by stiff connective tissue. The external nostrils have migrated to the top of the head.

Baleen whales (Mysticeti) are a suborder of Cetacea. They are readily distinguished from Odontoceti (toothed whales) by having baleen instead of teeth, two nostrils ("blowholes") rather than one, and a variety of skeletal features (Bannister, 2002; Hooker, 2002; Rommel and Reynolds, 2002; Rommel et al., 2002). Baleen consists of hundreds of keratin plates that grow down from the palate (Pivorunas, 1976, 1979; St. Aubin et al., 1984; Rice, 2002). The plates are oriented perpendicular to the body axis and set in two rows along the sides of the palate. They grow continuously, and the inner edges separate into fibers that are used for filtering prey from the water. The number, size, shape, and color of the plates and the color and diameter of the fibers are species-specific characteristics, and the plate spacing and fiber diameter are correlated with the size range of prey that can be filtered. Mysticetes and odontocetes also differ significantly in sociality and associated life history characteristics (Tyack, 1986). Mysticetes are largely asocial and do not form stable groups, while most odontocetes live in permanent herds (or "pods").

The family Balaenidae includes three species of right whales, in the North Atlantic, North Pacific, and Southern Ocean (Rosenbaum et al., 2000; Kenney, 2009), plus the bowhead whale, an Arctic species that does occur in the northernmost extremes of the North Atlantic (Reeves and Leatherwood, 1985; Rugh and Shelden, 2002). Balaenids are characterized by rotund bodies with thick blubber layers, relatively large heads with strongly bowed skulls, absence of a dorsal fin, and forelimbs that retain all five digits (Kenney, 2009; Rugh and Shelden, 2002; Reeves and Kenney, 2003). The baleen plates of balaenids are long, narrow, and flexible with very fine fringing hairs, and they feed on smaller prey organisms than other baleen whales (Nemoto 1970).

Description: North Atlantic right whale adults are 11–17 m long, with a maximum recorded length of 18 m (Cummings, 1985b; Jefferson et al., 1993; Wynne and Schwartz, 1999). Females are slightly larger than males. Calves are about 4.5 m in length and 800 kg in weight at birth. The body is very robust, with girth frequently exceeding half or even three-quarters of body length.

The back is very broad and smooth, with no dorsal fin. The color is usually black, and some animals have irregular white patches on the belly. The head is relatively large, comprising about a quarter or third of the body length. The top of the head in front of the blowholes (the rostrum) is narrow and arched, and the curve of the mouth opening is very strongly arched. There are irregular whitish patches called "callosities" on the rostrum, on the chin, along the lower jaw, and over the eye, usually behind the blowholes, and sometimes on the lower lips. The callosities are patches of thickened, keratinized skin inhabited by dense populations of light-colored whale lice (Payne and Dorsey, 1983). The callosity patterns are individually distinctive and used for photographic identification of individuals (Payne et al., 1983; Kraus et al., 1986). The flippers are large (up to 1.7 m long) and squarish. The flukes are broad (up to 6 m across), black on both surfaces, and tapered to points with a smooth trailing edge and deep central notch. Right whale baleen plates are mostly dark gray to black and are relatively long and narrow (Nemoto, 1970; Pivorunas, 1979). The maximum length is 2.7 m, with the longest plates in the middle of the row (see Figs 21.3 and 21.5 in Reeves and Kenney, 2003). There are 200–270 plates in each row (Jefferson et al., 1993; Wynne and Schwartz, 1999). The fringing hairs are very fine, about the same thickness as human hair (Mayo et al., 2001).

Status: North Atlantic right whales are listed as Endangered under the U.S. Endangered Species Act, as Federally Endangered on the Rhode Island state list, and as Endangered on the IUCN Red List. They are considered to be one of the most imperiled mammals in the world (Clapham et al., 1999). The most recent SAR gives the minimum number known to be alive in the population in 2002 as 313, but work in progress shows the number to have increased to at least 345 in 2005 (Kenney et al., in preparation), and the current population is probably around 400 animals (NARWC, 2007).

North Atlantic right whales were the first targets of commercial whaling, beginning along the Bay of Biscay in about the 11th century (Aguilar, 1986). By the 16th century, right whaling had expanded throughout the North Atlantic (Barkham, 1984). Along the south shore of Long Island, a shore-based fishery for right whales operated from 1650 to 1924 (reviewed by Reeves and Mitchell, 1986), although the last whale landed was in 1918. At least 550 whales were taken over that period, although records before 1820 are incomplete and certainly underestimate the actual catch. The highest estimated catch in one year was 111 whales in 1707, and the total take over the entire period likely exceeded 2,000 animals. Right whales have been protected from

commercial whaling since the first International Convention for the Regulation of Whaling was ratified in 1935 (Hain, 1975). Only six have been intentionally killed in the North Atlantic since that time (Moore, 1953; Brown, 1986; Mitchell et al., 1986).

Substantial anthropogenic mortality on North Atlantic right whales is continuing, and is suspected to be retarding recovery of the population (Kraus, 1990; Kenney and Kraus, 1993; IWC, 2001; Knowlton and Kraus, 2001; Laist et al., 2001; Kraus et al., 2005). The two most significant sources of mortality are collisions with ships and entanglement in commercial fishing gear. The average annual mortality in the western North Atlantic population during 2001–2005 was estimated as 1.4 killed by entanglement and 1.8 by ship strikes. A Take Reduction Plan is in effect to reduce fishery-related mortality, including closures and gear modification, with additional regulations due to take effect in April 2009 and others to be considered in the near future. A management regime to reduce mortalities from ship strikes, which includes limiting ship speed to 10 knots within 20 nautical miles of mid-Atlantic ports during right whale migration periods, took effect in December 2008. Other hypothesized anthropogenic impacts on right whales include toxic contaminants, habitat loss, and global climate change (Reeves et al., 2001a; Kenney, 2007).

Ecology and life history: Right whales in all oceans are strongly migratory, moving annually between high-latitude feeding grounds and low-latitude calving and breeding grounds (Cummings, 1985b; Kenney, 2009). The known feeding grounds in the North Atlantic are in the Gulf of Maine and adjacent waters, and the calving ground is in coastal waters off Florida and Georgia, but the location of breeding is unknown (Winn et al., 1986). Given the timing of births in winter and the 12–13 month gestation period, mating most likely occurs in November-January, when most adult males and non-calving adult females are absent from all known habitats (Winn et al. 1986, Brown et al. 2001).

Feeding by right whales is accomplished by "skimming" (Nemoto, 1970; Pivorunas, 1979), and the anatomy of the head, mouth, and baleen apparatus are all adapted to skim-feeding (Baumgartner et al., 2007). They feed by simply swimming forward with the mouth open. Water flows in through the opening at the front—below the rostrum, above and around the tongue, and between the two rows of baleen. Water then passes laterally through the baleen filter, straining prey organisms from the water and collecting them on the inside. The structure of the mouth

appears to develop a pattern of pressure gradients that maintains smooth water flow through the baleen. Feeding can occur at or just below the surface (Watkins and Schevill, 1976, 1979; Mayo and Marx, 1990), where it can be observed easily, or more often at depth and out sight (Murison and Gaskin, 1989, Kenney et al., 1995; Nowacek et al., 2001; Baumgartner and Mate, 2003; Baumgartner et al., 2003a, 2003b, 2007). Typical feeding dives last for 10–20 minutes (Winn et al.; 1995).

Right whales are obligate planktivores, with the principal prey in the North Atlantic being large, late-stage juveniles and adults of the copepod *Calanus finmarchicus* (crustaceans approximately the size of a grain of rice). At times they also feed on other zooplankton, including smaller copepods, euphausiids ("krill"), barnacle larvae, and pteropods (Collett, 1909; Nemoto, 1970; Watkins and Schevill, 1976; Mayo and Marx, 1990). They can probably be somewhat opportunistic, feeding on any prey of a size that can be filtered efficiently by the baleen, which does not swim strongly enough to escape, and which is concentrated into sufficiently dense patches to trigger feeding behavior. On the other hand, they can also be considered as extremely specialized predators occupying a very narrow niche. The sizes of predator and prey differ by a factor of 50 billion, consequently right whales can feed successfully only in areas where their prey are aggregated into extremely dense concentrations (Kenney et al. 1986, 1995; Wishner et al. 1988, 1995; Kenney and Wishner 1995; Baumgartner et al., 2007). Studies of right whale feeding grounds have shown that prey aggregations result from a combination of bottom topography, water column structure and stratification, currents, and prey behavior (Kenney et al. 1986, 1995; Wishner et al. 1988, 1995; Murison and Gaskin, 1989; Kenney and Wishner, 1995; Beardsley et al., 1996). The sensory mechanisms involved in prey detection and foraging probably include at least sight and touch, if not also sound and possibly taste (Kenney et al., 2001).

Female right whales give birth to single calves in winter; most births are in December–February in the western North Atlantic, peaking in early January (Kraus et al., 1993, 2001; Knowlton et al., 1994). The gestation period of southern right whales is approximately 12–13 months (Best, 1994); mostly likely the same holds for North Atlantic and North Pacific right whales. Most calves are probably weaned toward the end of their first year of life (Hamilton et al., 1995, Burnell, 2001). Following weaning, the female typically takes a year to "rest"—feeding and rebuilding blubber stores before mating the following winter. The result is a 3-year

interbirth interval under good conditions with adequate prey resources available. Calving intervals in southern right whales are generally 3–4 years (Best, 1990; R. Payne et al., 1990; Burnell, 2001, Cooke et al., 2001). The same was true of North Atlantic right whales until the early 1990s (Knowlton et al., 1994), but the average calving interval in the North Atlantic population increased to over 5 years by 2000 (Kraus et al., 2001), then returned to a predominance of 3-year intervals by 2004–2005 (Kraus et al., 2007). Environmentally driven interannual variability in prey resources appears to underlie the marked variability in calving success (Greene et al., 2003; Greene and Pershing, 2004; Kenney, 2007).

General distribution: North Atlantic right whales historically were widespread in continental shelf waters from subtropical to cold regions on both sides of the North Atlantic (Cummings, 1985b), but have been greatly reduced in number and range by centuries of whaling. Their original range extended from Florida and northwestern Africa north to the Gulf of Maine, Newfoundland, Labrador, Greenland, Iceland, the British Isles, and Norway (Kenney, 2009; Reeves and Kenney, 2003). The remnant population in the western North Atlantic occurs primarily between northeastern Florida and the Gulf of Maine region (Winn et al., 1986; Kenney et al., 2001). There is an annual migratory pattern from winter calving grounds in the nearshore waters off Florida and Georgia to feeding grounds in Cape Cod Bay (late winter-early spring), in the Great South Channel east of Cape Cod (late spring-early summer), and in the Bay of Fundy and Roseway Basin near Nova Scotia (late summer-fall). Other than the calving ground, habitat use during the winter is very poorly known. Migratory pathways between the calving/wintering and feeding areas are also poorly known. Other habitats in the Gulf of Maine also constitute feeding grounds in some years, and animals are occasionally observed in distant areas including deeper waters beyond the shelf edge, Gulf of Mexico, Gulf of St. Lawrence, Greenland, Iceland, Norway, and southwestern Europe (Reeves et al., 1978; Winn et al., 1986; Lien et al., 1989; Martin and Walker, 1997; Mate et al., 1997; Slay and Kraus, 1998; Knowlton et al., 1992; Jacobsen et al., 2004).

Historical occurrence: The Smithsonian data included four historical records from Rhode Island, three of which were extracted from Allen (1916). In February 1828, “a Right Whale forty-four feet long, and rated at about seventy barrels of oil, was killed in the waters off Providence, R.I., after having been seen for several days ‘sporting in our river’.” “1893.—Major E.A. Mearns furnishes me with a note of what was said to have been a Right Whale, about 50

feet in length, that was stranded on Ochre Point, Newport, R.I. The blubber had already been removed by one Mr. Church at Tiverton, where the whale had been killed. The carcass was finally sunk at sea by order of the City Council. The exact date is not available." Although this is an extreme example, it should be noted that there is some probability that any stranding during the whaling era was actually killed by whalers but not recovered ("struck and lost" in whaling statistics). "1894.—Major Mearns also sends me the record of a Right Whale that appeared off Beaver Tail, Conanicut Island, R.I., in this year. It finally was sighted off Fort Adams, where it was shot and killed (exact date unknown). He adds that Mr. Joshua P. Clark, formerly in charge of the Life Saving Station at Watch Hill, R.I., told him that Right Whales have been seen off Block Island in more recent years, although the most part of the whales seen in those waters are Finbacks." The single non-Allen record is a specimen record from the Academy of Natural Sciences of Philadelphia (ANSP3227)—right whale skull fragments from Rhode Island from November 1857. Cronan and Brooks (1968) reported the same three records as Allen, but knew of no others.

The records of the Long Island right whale fishery clearly reflect what is known about the migratory pattern of the population (Reeves and Mitchell, 1986). Both De Kay (1842) and Connor (1971) were very aware of the Long Island right whale fishery, and it was their principal source of information for the species. Most of the kills occurred in winter and early spring, from January through May with a peak in April, and included a high proportion of mothers and calves. The fishery was primarily targeting northbound animals during the spring migration. The Smithsonian dataset included more than 50 records from the whalers in eastern Long Island, dating back to 1707 (although no effort was expended to geolocate all of those old records for mapping). The AMNH has a mounted skeleton that was originally collected from Amagansett whalers on 22 February 1907 by Roy Chapman Andrews (Andrews, 1908, 1909, 1916). That individual, at 16.5 m, is the largest right whale known from the western North Atlantic and the second largest from the entire North Atlantic.

Allen (1916) also included large numbers of right whale records from Cape Cod, Nantucket, and Martha's Vineyard in Massachusetts, as well as Long Island, from 1620 to the early 20th Century. His summary of the annual cycle of right whale occurrence in Massachusetts waters closely mirrors the pattern seen in the last 40 years. Waters and Rivard (1962) tabulated sightings of "schools" of right whales in Cape Cod Bay in 1955, May 1958, May 1959, and May 1960,

three off Martha's Vineyard in April 1956, one in the Cape Cod Canal in June 1957, and one in Plymouth Harbor "chasing herring" in May 1958, as well as a stranding of a right whale in Nantucket in June 1961—killed by a ship collision. Their description is a good example of their mix of recent observations and unsupported conjecture—"a herd of forty to fifty may be seen each May in Cape Cod Bay. From June to October they are in the waters off Labrador and Greenland, and the return to warm, southern waters, by way of the Gulf Stream without stopping off in Cape Cod Bay, takes place in October and November."

Recent occurrence: North Atlantic right whales have occurred in the Rhode Island study area in all seasons of the year (Fig. 3[7]). They are most common in spring (58.3%), less common in winter (19.2%) and summer (16.0%), and relatively scarce in fall (4.5%). There were only 14 sightings from the various whale-watch boats, so there is not a substantial bias in the seasonal patterns; without those data the respective percentages are 62.0% spring, 21.1% winter, 10.6% summer, and 4.2% fall. Right whale occurrence in the region is consistent with both the historical record from the Long Island fishery (Reeves and Mitchell, 1986) and their known annual migratory cycle (Winn et al., 1986). Animals in this region are mainly migrating between winter calving grounds in the southeastern U.S. and feeding grounds in and around the Gulf of Maine. Winn et al. (1986) hypothesized that the southbound migration in fall was more diffuse and farther offshore than the spring migration. Additionally, traveling whales are believed to have a reduced probability of detection (Hain et al., 1999), therefore their presence in the region may be greater than apparent from the full sighting record.

Sightings in the Rhode Island study area tend to be concentrated relatively close to shore. Knowlton et al. (2002) reported that 94% of all right whale sightings between South Carolina and Nantucket were within 55.6 km (30 nautical miles) of the coastline and 64% were within 18.5 km (10 nautical miles). Some of that pattern is caused by the concentration of observers closer to shore. The proportion of sightings close to shore is significantly higher south of Cape Hatteras, North Carolina than to the north. One might hypothesize that northward migrating right

[7] Notes for all maps of this type: (1) the maps are Mercator projections with boundaries at: east = 70°00'W, west = 73°00'W, south = 39°30'N, north = 42°06'N; (2) records within Cape Cod Bay were excluded; (3) the pink outline shows the SAMP area and the yellow line shows the state waters boundary; (4) the same color code for seasons (winter = blue, spring = green, summer = red, fall = brown, unknown = black) is used whether the seasons are plotted on four separate maps or combined on one; (5) records with unknown season could not be classified because month was missing and are shown only for species with one combined map; (6) although the complete dataset may go back to the 17th or 18th Century for some species, the vast majority of records are from the 1970s and later.

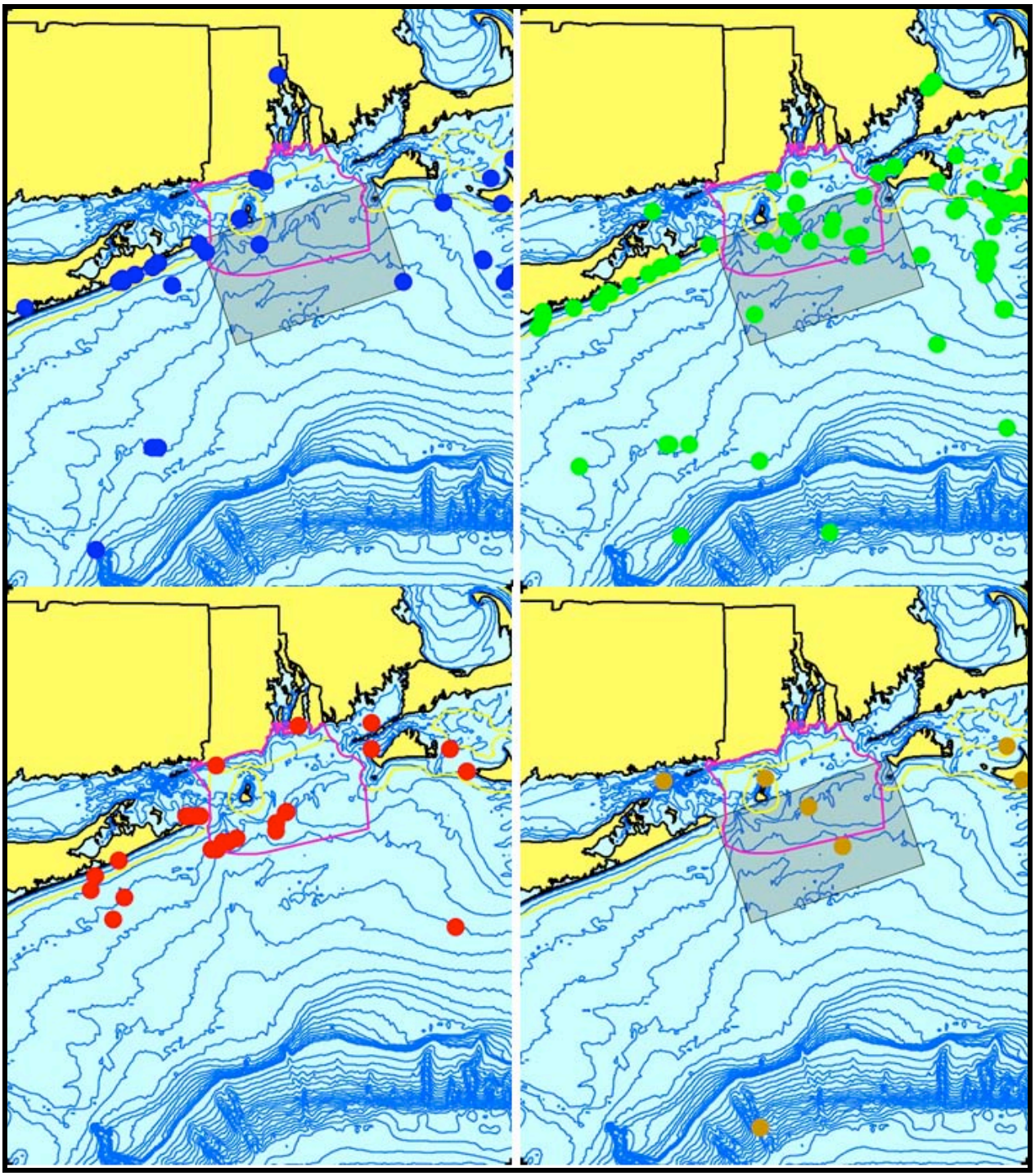

Figure 3. Aggregated sighting, stranding, and bycatch records of North Atlantic right whales in the Rhode Island study area, 1828–2007 (n = 156: winter = 30, spring = 91, summer = 25, fall = 7; unknown = 3). The gray-shaded box is the Block Island Sound Seasonal Management Area, in effect from November through April (see Conclusions).

whales in late winter and spring travel along shore until reaching Cape Hatteras, after which they spread out more, with some continuing to follow the coast while others take a more direct route towards Massachusetts. Right whales in the Rhode Island study area seem to show that pattern, with the majority of records in a band relatively close to shore, but others that are more offshore and may be on a migratory pathway between Cape Hatteras and the Great South Channel. Within the SAMP area, most right whales appear to remain in the offshore part of the area.

The relative abundance patterns resulting from kriging the 5-minute X 5-minute gridded SPUE data, corrected for survey effort, show right whales in or near the Rhode Island study area in all four seasons, but in the SAMP area only in spring and fall (Fig. 4). This is consistent with their known migratory cycle. Relative abundance in the SAMP area in both spring and fall is in the lowest class. The highest relative abundance of right whales in the area analyzed was in the Great South Channel east of Nantucket in spring and summer, which matches the known population distribution (Winn et al., 1986; Kenney et al., 1995, 2001). They were present at the lowest level of abundance south of Nantucket in winter and summer, and at the second-lowest level in spring.

Feeding by right whales is occasionally observed in the Rhode Island region, but is likely an opportunistic response to relatively rare occurrences of appropriate prey patches. An aggregation of feeding right whales that persisted for about two weeks was seen just east of Block Island in April 1998. The whales were first seen by fishermen, who reported their observations to the RI Division of Fish & Wildlife, who then passed on the reports to NMFS. NMFS directed their aerial surveys to investigate on 14, 19, and 21 April. On the 19th at least 16 whales were present and observed to be feeding at and just below the surface. To date 11 have been matched to the right whale catalog—mostly males (8) and ranging in age from 2-year-olds to adults. One other whale (an adult female) was identified from the photos (not dated) submitted by RIDFW. The NMFS crew photographed seven animals on the 14th and four have been identified—all different ones (3 adult males and 1 adult female). Five of the six whales they photographed on the 21st have been identified; three were resightings from the 19th and two were new—an adult male and a 2-year-old male. Eighteen different whales were identified in all, but the low rate of resightings suggests that substantially more than 18 whales were feeding in Rhode Island Sound in April 1998. (NOTE: This phenomenon occurred in the very first year of the NMFS aerial survey program, and they did not yet have complete and effective data collection protocols in

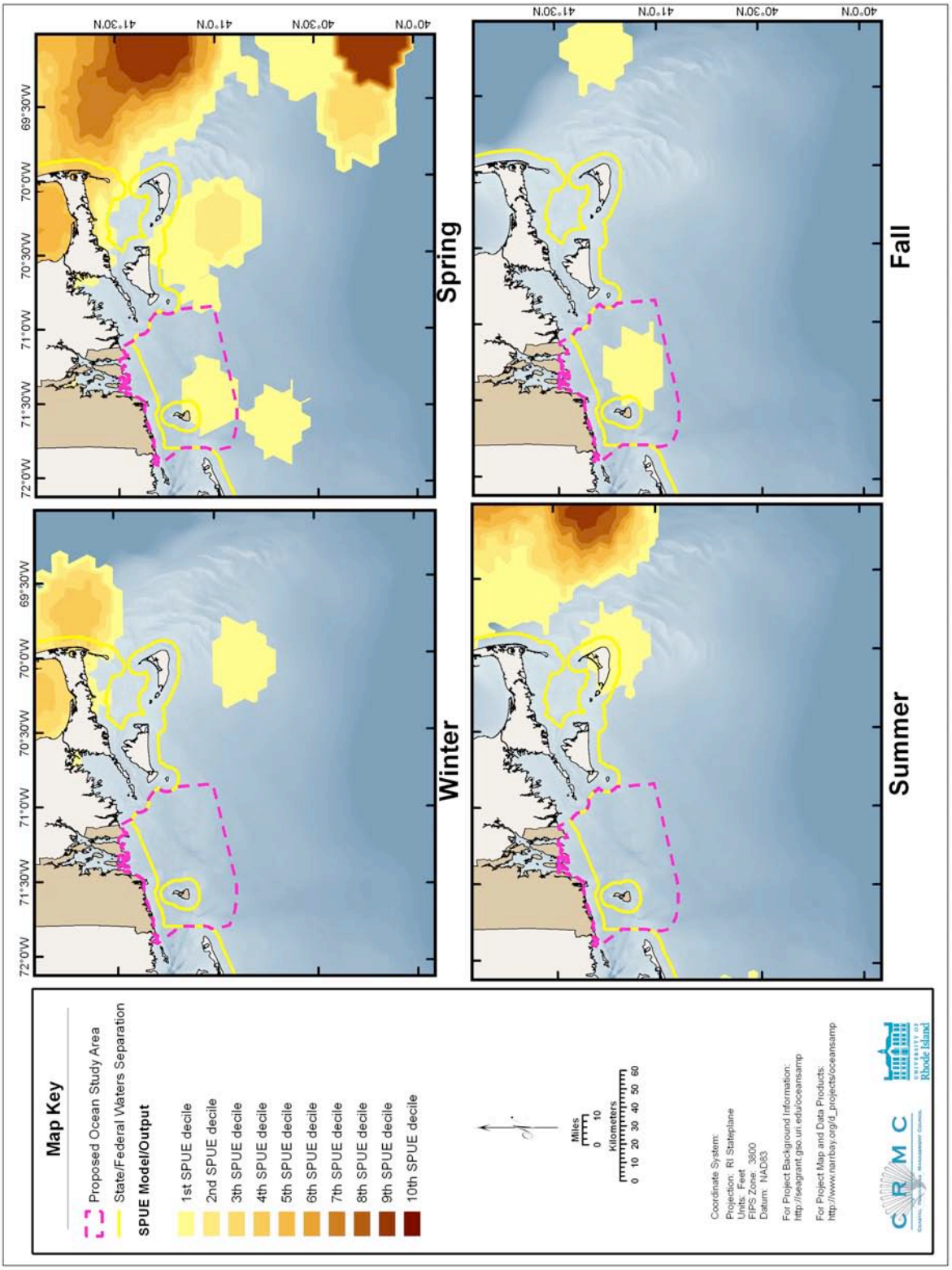

Figure 4. Modeled seasonal relative abundance patterns of North Atlantic right whales in the Rhode Island study area, corrected for uneven survey effort.

place. Therefore, the data are included in the sightings shown in Fig. 3, but could not be included in the analysis shown in Fig. 4.) (NOTE: On 20 April 2010, while this report was being finalized, 98 right whales, with many observed to be feeding at or near the surface, were reported in or near Rhode Island Sound by a NMFS aerial survey. These sightings have not been included in either Fig. 3 or Fig. 4).

There were five strandings in the Rhode Island study area in recent decades. A freshly dead animal washed ashore, with the tail severed by a ship collision, at Wainscott, New York on 5 March 1979; it was not identified as a known individual. A dead 10.0-m right whale stranded on Second Beach in Middletown on 17 July 1995 with multiple wraps of rope around one flipper, deeply embedded, even into the bone. It was eventually identified as a 2.5-year-old male (catalog #2366). It was first seen entangled as a 1-year-old off Georgia in December 1993. The entanglement appeared relatively benign, but as the whale grew the wraps became much tighter, eventually causing a massive systemic infection that led to the animal's death. A 3-year-old female (catalog #2701) was found floating dead 15–18 km southeast of Block Island on 19 January 2000. The carcass could not be retrieved and the cause of death was never determined, although there was fishing gear or rope on the animal. A 1-year-old female (#3107) washed ashore on Nantucket on 12 October 2002, but high surf prevented a necropsy until the 14th. It had first been seen entangled in what was probably inshore lobster gear near Brier Island, Nova Scotia, on 6 July. The gear was removed on a September in the Bay of Fundy, leaving severe lacerations on the tailstock. The whale likely succumbed to infection from the injuries. A NMFS aerial survey on 13 May 2005 sighted a dead right whale 39 km south of Martha's Vineyard, which was never recovered or identified. There was an additional record in 2006 that was not in the stranding data and has yet to be added to the NARWC database; a dead right whale was located on 21 May 2006 floating 56 km south of Block Island, after first having been reported by the Coast Guard three days previously. No cause of death could be determined; analysis of photos and genetic samples may eventually identify the individual.

Conclusions: Right whales are the marine mammal species of highest management concern in U.S. Atlantic waters because of their critically endangered status and known human impacts—most notably mortality from ship collisions but also entanglement in commercial fishing gear. They have the potential to occur in the SAMP area in any season, but would be most likely during the spring, when they are migrating northward, and secondarily in the fall during the

southbound migration. In most years, the whales would be expected to transit through the SAMP area or pass by just offshore of the area, however there may be some years when right whales encounter suitable prey resources and linger for some time, as occurred in April 1998. Note again that the April 1998 event was not captured in the relative abundance pattern (Fig. 4) because the appropriate survey data were not collected during the relevant flights.

Potential impacts on right whiles must be considered for all construction activities or on-going operations for any alternative energy development. In addition, a Right Whale Ship Strike Reduction Rule (50 CFR 224.105) went into effect on 9 December 2008. Among other provisions, it established a Block Island Seasonal Management Area (BI-SMA; Fig. 3). Under the Rule, all vessels 65 ft (19.8 m) or longer transiting through the BI-SMA are required to travel at speeds of 10 knots or less from 1 November through 30 April.

3.2.2 Humpback Whale *Megaptera novaeangliae* (Borowski, 1781)

Balaenopteridae is the most diverse family of baleen whales, with two genera and six species long recognized (Jonsgård, 1966; Nowak, 1999) and three species recognized more recently (Rice, 1998; Wada et al., 2003). They are collectively referred to as "rorquals," from the Norwegian meaning "furrow whale" in reference to the ventral grooves. Externally, the grooves look like long, parallel slits extending back from the tip of the lower jaw to as far as the umbilicus in some species, but are actually distensible pleats involved in feeding behavior. Rather than continuous, mouth-open skimming as in balaenids, rorquals are "gulpers" (Nemoto, 1970; Pivorunas, 1979; Lambertsen, 1983). The mouth is opened, engulfing a large volume of water and prey within the distended lower jaw and ventral pouch. Then the mouth is closed, the pouch contracted, and the water forced out through the baleen filter—retaining the prey on the inside. The baleen plates of rorquals are shorter and broader than in right whales, and the rostrum of the skull is flatter and broader. Rorquals have dorsal fins and retain only four digits in the forelimb (Bannister, 2002).

Description: Humpback whales are the easiest to identify of the rorquals and are clearly distinguished from *Balaenoptera* spp. based on morphology (Winn and Reichley, 1985; Jefferson et al., 1993; Wynne and Schwartz, 1999; Clapham, 2002), but genetic studies generally agree that they are not phylogenetically separate (Árnason and Best, 1991, Árnason et al., 1992,

1993; Árnason and Gullberg, 1994, 1996; Nikaido et al., 2001; Hatch et al., 2006; Sasaki et al., 2006). Adults typically range from 11 to 16 m in length. They have a more robust, stout body form than *Balaenoptera* spp., but are not as rotund as right whales. The body is black, often with some amount of white on the belly. The dorsal fin can be extremely variable in shape, from small and rounded to prominent to falcate or hooked. There is a prominent rounded hump in front of the dorsal, and a series of projections along the ridge from the dorsal fin to the tail. Their most distinctive features are their flippers, which are very long (about a third of the body length), with a relatively smooth trailing margin and a series of prominent bumps (the "knuckles") on the leading margin. The flippers usually white in North Atlantic humpbacks. The rostrum is broad and flat with a somewhat rounded tip. There are rows of rounded knobs down the center and along the edges of the rostrum and on the lower jaw. Each knob has a 1–3-cm stiff sensory hair in the center. There is also a prominent knob on the chin, which is covered by a clump of barnacles—actually by acorn barnacles attached to the whale and stalked barnacles attached to the acorn barnacles. There are also barnacles on the "knuckles" of the flippers, the margins of the flukes, the edges of the head, and scattered in other areas. The flukes have a deep central notch and a concave trailing edge with a ragged or serrated margin, and their underside is patterned in black and white (from all black to all white, most often black in the center and white toward the ends). The patterns are unique and can be used to identify individual whales (Katona et al., 1979). The ventral grooves extend all the way to the navel, and are more widely spaced than in any other rorquals, numbering only 12–36.

Status: Humpback whales are listed as Endangered under the U.S. Endangered Species Act, are classified as Federally Endangered on the Rhode Island state list, and are classified as Least Concern on the IUCN Red List. A review of the status of North Atlantic humpback stocks under the Endangered Species Act is being contemplated (Waring et al., 2008), and could potentially result in a proposal to down-list the North Atlantic humpback population to Threatened or even to de-list it completely. The number of humpback whales in the North Atlantic was estimated at 11,570 in 1992–93 by applying mark-recapture methods on the collection of photographs of known individuals (Stevick et al., 2003). That estimate is known to be negatively biased from spatial heterogeneity in sampling. In addition, the population appears to be increasing at 3% to as much as 6.5% per year (Barlow and Clapham, 1997; Stevick et al., 2001). North Pacific and Southern Ocean populations also appear to be growing (Clapham, 2002). Recent estimates of

abundance for only the Gulf of Maine feeding stock are 850–900 whales (Waring et al., 2008).

Humpback whaling in the North Atlantic began in the 1600s in Bermuda and continued into the 20th Century (reviews by Mitchell and Reeves, 1983; Reeves and Smith, 2002). Many thousands were killed by 19th and 20th Century whalers, seriously depleting populations. Most North Atlantic humpback whaling occurred in the 19th Century. Yankee whalers hunted humpbacks on the wintering grounds in the West Indies and Cape Verdes between sperm whaling seasons, leaving behind traditional whale fisheries in both locations. North Atlantic humpback whaling in the 20th century was mainly from shore stations in Canada, Greenland, Iceland, the Faroe Islands, the British Isles, and Norway. Humpback whaling ended world-wide in 1966 (Clapham, 2002). The only North Atlantic hunting since the International Whaling Commission (IWC) instituted a moratorium on commercial whaling in 1986 (see the fin whale account for more details) has been the occasional subsistence take in West Greenland (1 each in 1988 and 1990–1992, 2 in 1989) and 1 or 2 a year by a small, traditional fishery that has survived in Bequia, St. Vincent and the Grenadines, West Indies (see Table 21.3 in Reeves and Kenney, 2003 for a summary of all North Atlantic whaling in 1986–2000; for subsequent years see the annual reports of the IWC in the supplement to each volume of *Journal of Cetacean Research and Management*).

The 2001–2005 average annual human-related mortality from the Gulf of Maine humpback stock was estimated as 2.8 killed by fishery entanglements and 1.4 by ship collisions (Waring et al., 2008). Fisheries involved in humpback entanglements have included pelagic driftnets, sink gillnets, and lobster traps. Biotoxins have also been implicated in humpback whale mortalities. In 1987, 14 humpback whales died acutely near Cape Cod and Nantucket after eating mackerel containing saxitoxin produced by *Alexandrium tamarense*, the "red tide" organism that is responsible for paralytic shellfish poisoning in humans (Geraci et al. 1989). Domoic acid, produced by the diatom *Pseudo-nitzschia* sp., has been hypothesized as a cause of death of 12–15 humpbacks offshore on Georges Bank in 2003, but the data were sparse and results inconclusive (Waring et al. 2008).

Ecology and life history: Humpback whale habitat use patterns and distributions on their feeding grounds are not static, but change over time. Along with shifts in the relative abundance of herring and sand lance, the two principal forage fish species in the Gulf of Maine system, the

distribution of humpback whales has similarly changed (P. M. Payne et al. 1986, 1990; Kenney et al., 1996; Weinrich et al., 1997). Herring and mackerel stocks were severely depleted by commercial fisheries in the 1960s and early 1970s, and sand lance populations expanded greatly in response. Humpback whales shifted from feeding mostly in the northern Gulf of Maine to concentrating in Cape Cod Bay and east of Cape Cod. In the early 1980s, sand lance populations declined and herring began to recover. Humpback and fin whales declined around Cape Cod, and were nearly absent in 1986. Similar shifts in humpback distribution that coincided with changes in prey populations have been observed in Newfoundland (Lien et al., 1979; Whitehead and Lien, 1983) and southeastern Alaska (Bryant et al., 1981).

Humpbacks are gulp-feeders like the other rorquals (Nemoto 1970, Pivorunas 1979), but they display a much wider variety of feeding behaviors (Ingebrigtsen, 1929; Jurasz and Jurasz, 1979; Hain et al., 1982, 1995; Hays et al., 1985; Weinrich et al., 1992; Swingle et al., 1993). They may lunge violently with the mouth open, or surface open-mouthed very slowly and smoothly. They also routinely use bubbles in feeding—either columns of large bubbles in lines or partial or complete circles ("bubble-nets") or large clouds of tiny bubbles that are apparently released from the mouth rather than exhaled through the blowholes ("bubble clouds"). Some whales add tail-slaps or other vigorous splashing to the feeding behaviors. There is evidence that feeding behaviors are learned from the mother (Weinrich et al., 1992).

Humpbacks feed on a variety of small, schooling prey, including krill and fish (Watkins and Schevill, 1979; Kenney et al., 1985a; Winn and Reichley, 1985; Clapham, 1996, 2002). The principal prey species in the Gulf of Maine are herring and sand lance (Overholtz and Nicolas, 1979; CETAP, 1982; Kenney and Winn, 1986; P. M. Payne et al. 1986, 1990; Kenney et al., 1985a, 1996; Weinrich et al., 1997). In the northern Gulf of Maine, euphausiids may also be important prey (Sutcliffe and Brodie, 1977; Paquet et al., 1997).

Sexual maturity in both male and female humpback whales is reached at about 5 years of age on average, ranging from 4 to 9 years (Clapham and Mayo 1987, 1990; Clapham 1992, 1996, 2002; Craig and Herman, 2000). Calving is strongly seasonal, with calves in the Northern Hemisphere born from January to March after a gestation period of about 11 or 12 months (Rice, 1967; Johnson and Wolman, 1984; Clapham 1996, 2002). Calves are born at about 4–5 m in length and reach 8–9 m by the time they are weaned (Winn and Reichley, 1985). Calves are fully

weaned at about 1 year old, but begin to feed independently while still nursing at only 5 or 6 months old (Clapham, 1992). The intervals between calves are usually 2–3 years, although females occasionally give birth in successive years (Clapham and Mayo, 1990; Glockner-Ferrari and Ferrari, 1990; Clapham, 1996, Steiger and Calambokidis, 2000).

General distribution: Humpback whales occur in all of the world's oceans, making some of the longest migrations known for any mammal between high-latitude feeding grounds and low-latitude calving and breeding grounds (Kellogg, 1929; Jonsgård, 1966; Winn and Reichley, 1985; Rice, 1998; Clapham, 2002). North Atlantic humpbacks occur from the Caribbean Sea and Cape Verde Islands in the extreme south to as far north as Greenland, Iceland, Svalbard, and the Barents Sea (Jonsgård, 1966; Winn et al., 1975; Winn and Winn, 1978; Whitehead and Moore, 1982; Martin et al., 1984; Winn and Reichley, 1985; Katona and Beard, 1990; Clapham et al. 1992, 1993a, 1993b; Clapham, 1996; Palsbøll et al., 1997; Rice, 1998; Stevick et al., 1998; Smith et al., 1999). The vast majority of sightings in both the feeding and calving grounds are in nearshore and continental shelf waters, but the whales apparently migrate across deep oceanic regions. Reeves et al. (2004) mapped humpback whale sightings recorded in the logbooks of 18th and 19th Century sperm whalers. There were large numbers of sightings in the middle of the North Atlantic just west of the Mid-Atlantic Ridge, especially in April-July. The distribution confirmed migration routes far offshore, and also suggested that there might be offshore feeding grounds that are still unknown.

North Atlantic feeding grounds are occupied from spring through fall, and are located in continental shelf areas. The feeding range extends from southern New England and the British Isles north to Davis Strait, Greenland, Iceland, Svalbard, and Norway (Martin et al., 1984; Katona and Beard, 1990; Sigurjónsson and Gunnlaugsson, 1990; Clapham et al., 1992; Clapham, 1996; Palsbøll et al., 1997; Stevick et al., 1998). Humpbacks show strong matrilineal habitat fidelity (Baker et al. 1994). A calf learns the feeding grounds from its mother during its first year, and then tends to return to the same feeding areas each year (Clapham and Mayo, 1987). The result is genetically identifiable "feeding stocks," with very little interchange between stocks (Christensen et al., 1992; Palsbøll et al., 1995, 1997, 2001; Larsen et al., 1996). Separate feeding stocks have been recognized from the Gulf of Maine/Nova Scotia, Gulf of St. Lawrence, Newfoundland/Labrador, West Greenland, Iceland/Denmark Strait, and Norway. There is further subdivision on even finer scales. Clapham et al. (2003) showed that humpbacks in the Gulf of

Maine and on the Nova Scotian Shelf only partially overlap. Within feeding ranges, humpbacks tend to aggregate at specific locations where prey is most abundant.

During the winter, humpbacks from all North Atlantic feeding grounds migrate south to calving and breeding grounds on shallow banks in the West Indies/Caribbean region, where they mix together (Katona and Beard, 1990; Clapham et al., 1993b; Palsbøll et al., 1997; Stevick et al., 1998; Bérubé et al., 2004). The peak calving and breeding season is January–March, with some whales arriving as early as December and a few not leaving until June (Reeves et al., 2001b).

Historical occurrence: Historical occurrences of humpback whales in the southern New England region west of Massachusetts were very rare and were unknown to De Kay (1842), Linsley (1842), and Goodwin (1935). Allen (1916) reported only one from Rhode Island, in 1836—"A note in the Providence Courier makes mention of a whale that had been seen several times off Newport, R.I., during the last of June. It was finally captured in Newport Harbor, 'north of the asylum[8]; it measures fifty feet in length, and is of the Humpback species and is supposed to be the same which was seen off Pawtuxet on Wednesday morning last'." Cronan and Brooks (1968) reported that the only other humpback in Rhode Island was an 8.2-m calf stranded at Matunuck Beach in South Kingstown in June 1957, although the notes with the Smithsonian data record state that the photo showed an animal more likely 6 m long. Connor (1971) reported that the 1957 Rhode Island stranding was the only humpback known from southern New England, but he suspected that humpbacks had occasionally been taken by Long Island shore whalers hunting right whales.

There was one additional historical record of a humpback whale that was not included in the Smithsonian data. Both of us were graduate students of Professor Howard E. Winn (1926–1995) at GSO. It was common knowledge around the lab that a humpback had been seen in Mount Hope Bay at some time in the 1960s, but no record is in any database to our knowledge. However, in a box of photographs salvaged during the cleanout of Dr. Winn's files after his death was an envelope with ten black & white prints of a humpback whale, labeled "Humpback; Bristol, R.I., Nov. 4, 1968." One image clearly shows the Braga Bridge in Fall River in the

[8] The Newport Asylum for the Poor was built in 1822 on Coasters Harbor Island, which was turned over to the Navy in 1882. The original asylum building is now the Naval War College Museum.

background. We also found an old newspaper clipping about the event ("A tape recorder may save Howie: Scientists want to 'talk' to whale"), but the date and source had been cut off.

Allen (1916) reported many humpbacks, mostly animals killed by whalers, from Massachusetts to Maine, beginning with one that stranded in the inner harbor at Nantucket in 1608 and was killed by a group of Indians. Waters and Rivard (1962) said that humpbacks were "unusual but not rare in New England coastal waters," but described an erroneous migratory pattern similar to what they had for right whales. They reported only two specific records—a stranding of an 18-m humpback in Barnstable in August 1941 and a sighting of a "school" in Cape Cod Bay off the canal entrance on 3 May 1951.

Recent occurrence: Humpback whales occur throughout the region in all four seasons, with many sightings from whale-watching boats concentrated south and east of Montauk in summer and spring (Fig. 5). Including those data, 71.2% of records are in the summer, 15.7% in the spring, 10.3% in the fall, and 2.6% in the winter. Without the whale-watching sightings, the seasonal differences are less dramatic and the peak season switches to the spring (45.8%), followed by summer (33.6%), fall (10.3%), and winter (9.7%). Sightings are distributed across the shelf, especially in the spring. Except for the summer concentration from the whale-watchers' data, the sightings tend to be more common in the eastern half of the study area.

The effort-corrected relative abundance patterns show that humpbacks are most abundant east of the Rhode Island study area in the Great South Channel (Fig. 6). Humpbacks are strongly concentrated there in spring, summer, and fall, and present at lower abundances in winter. Areas of low predicted humpback abundance extend into the SAMP area in spring and summer. Areas of slightly higher abundance are south and/or southeast of the SAMP area in winter, spring, and summer. Only in fall are humpbacks absent from the Rhode Island study area in the relative abundance model output.

Humpback distributions in the Gulf of Maine have fluctuated markedly over the years, largely tracking patterns of abundance of their principal prey species—Atlantic herring, sand lance, and krill (P.M. Payne et al., 1986, 1990; Kenney et al., 1996). In the years during the 1980s when humpbacks were scarce off Cape Cod, there were numerous humpback sightings between Long Island and Martha's Vineyard by Montauk and Galilee whale-watch boats. The peak year for sightings from the Montauk boat was 1987, with 63 sightings (compared with 2 in 1986 and 9 in

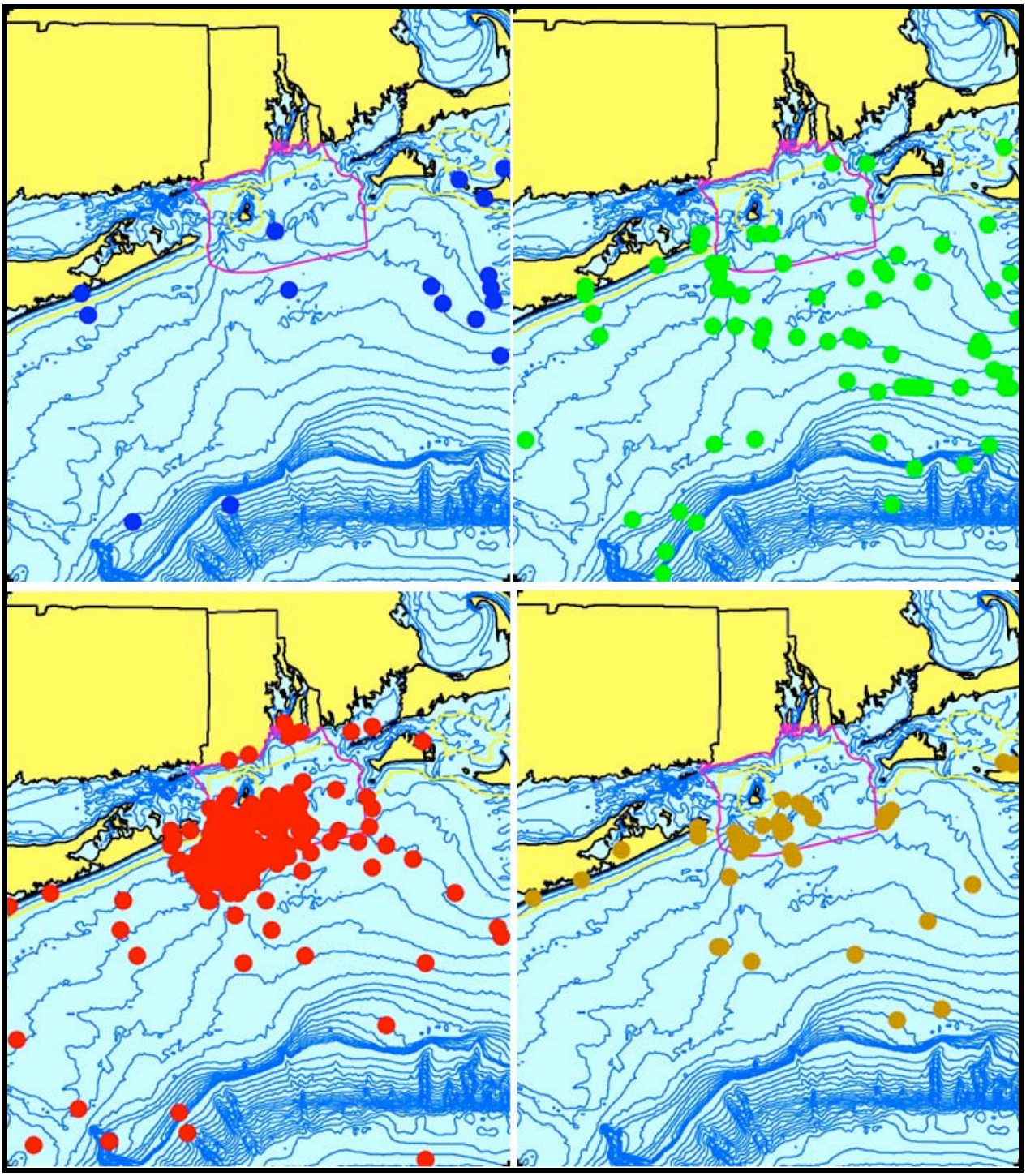

Figure 5. Aggregated sighting, stranding, and bycatch records of humpback whales in the Rhode Island study area, 1608–2007 (n = 611: winter = 16, spring = 96, summer = 435, fall = 63, unknown = 1).

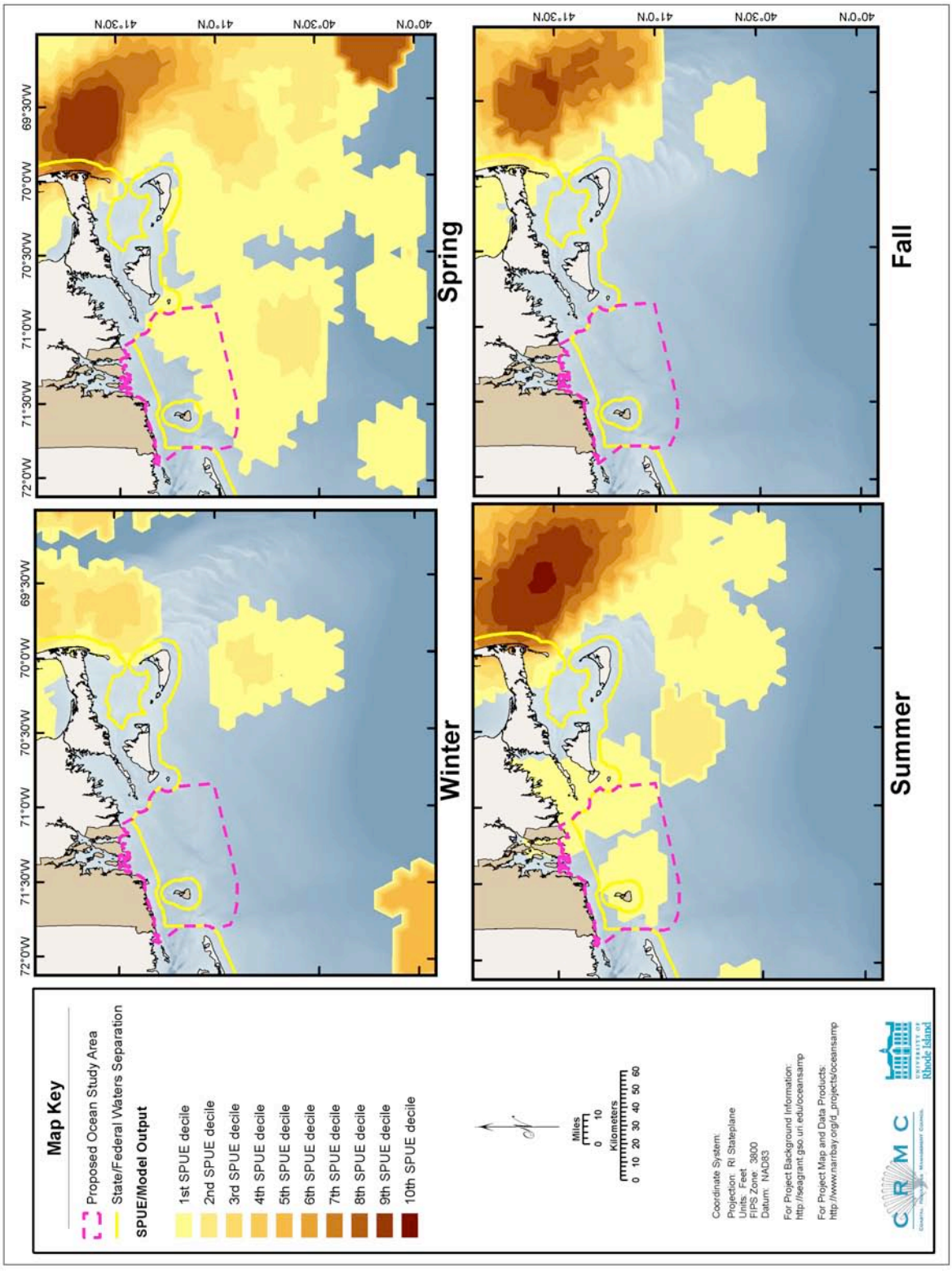

Figure 6. Modeled seasonal relative abundance patterns of humpback whales in the Rhode Island study area, corrected for uneven survey effort.

1988), and 1987 was also the best year for the Galilee boat. In 1987, the whales targeted by the whale-watching boats slowly shifted eastward over the course of the season—from the southwestern part of the SAMP area near Montauk and Block Island to the eastern part, near Noman's Land off the southwestern corner of Martha's Vineyard (G. O. Klein, pers. comm.). Sand lance populations in Cape Cod waters subsequently recovered, then went through another decline and recovery in the early 1990s, closely tracked again by whale sighting frequencies in the same area (Weinrich et al., 1997). There was similarly another increase in humpback sightings off Montauk in 1992 and 1993, and less dramatically in 1994 and 1991. The survey data, however, are far too sparse for an effective analysis of inter-annual trends in humpback abundances in the Rhode Island study area.

After an absence in the Rhode Island stranding record for more than 40 years, there were four humpback strandings in the state in 2001–2005: on 22 June 2001 behind "The Breakers" in Newport; on 10 August 2001 on the western side of Sachuest Point National Wildlife Refuge in Middletown; on 3 June 2004 on East Beach in the Ninigret Conservation Area in Charlestown; and on 6 July 2005 on Bailey's Beach in Newport. There were also four strandings around the Massachusetts Islands—in October 1987, November 1988, January 1991, and June 1992. There were also strandings on the south shore of eastern Long Island in February 1992, November 1992, October 1993, August 1997 (in Weesuck Creek off the northwestern part of Shinnecock Bay), and April 2004. Finally, there were two observations of a floating carcass on 20 May 2004—an opportunistic report to NMFS in western Vineyard Sound between Cuttyhunk and Nashawena and a sighting by the NMFS aerial survey team about 28 km west of there and 9 km southeast of Sakonnet Point. It is impossible to determine if both sightings were the same dead whale, or if that was the individual that washed up two weeks later in Charlestown. Although annual stranding frequencies of humpbacks in the Rhode Island study area are low, they do hint at a pattern of occasional peaks that may correspond to the years of peak occurrence in the area (Fig. 7). The first two peaks do match the peaks in sightings from the whale-watchers; unfortunately, we do not have sighting records from whale-watching boats in the region after 1996, so we are unable to check if sighting frequencies were also up in other years when strandings occurred.

Conclusions: Humpback whales have occurred in the Rhode Island study area and within the Ocean SAMP area in all four seasons of the year. Sightings are most frequent in spring, and the

whales show up in the relative abundance maps in the SAMP area in spring and summer. Because they are listed as Endangered under the ESA, they must be considered carefully in any development planning. Humpback occurrence in significant numbers in southern New England is relatively unpredictable and likely to be highly dependent on prey availability, both locally and in their primary feeding grounds in the Gulf of Maine. They are likely to be relatively rare in most years in the SAMP area, but may be locally abundant in certain years.

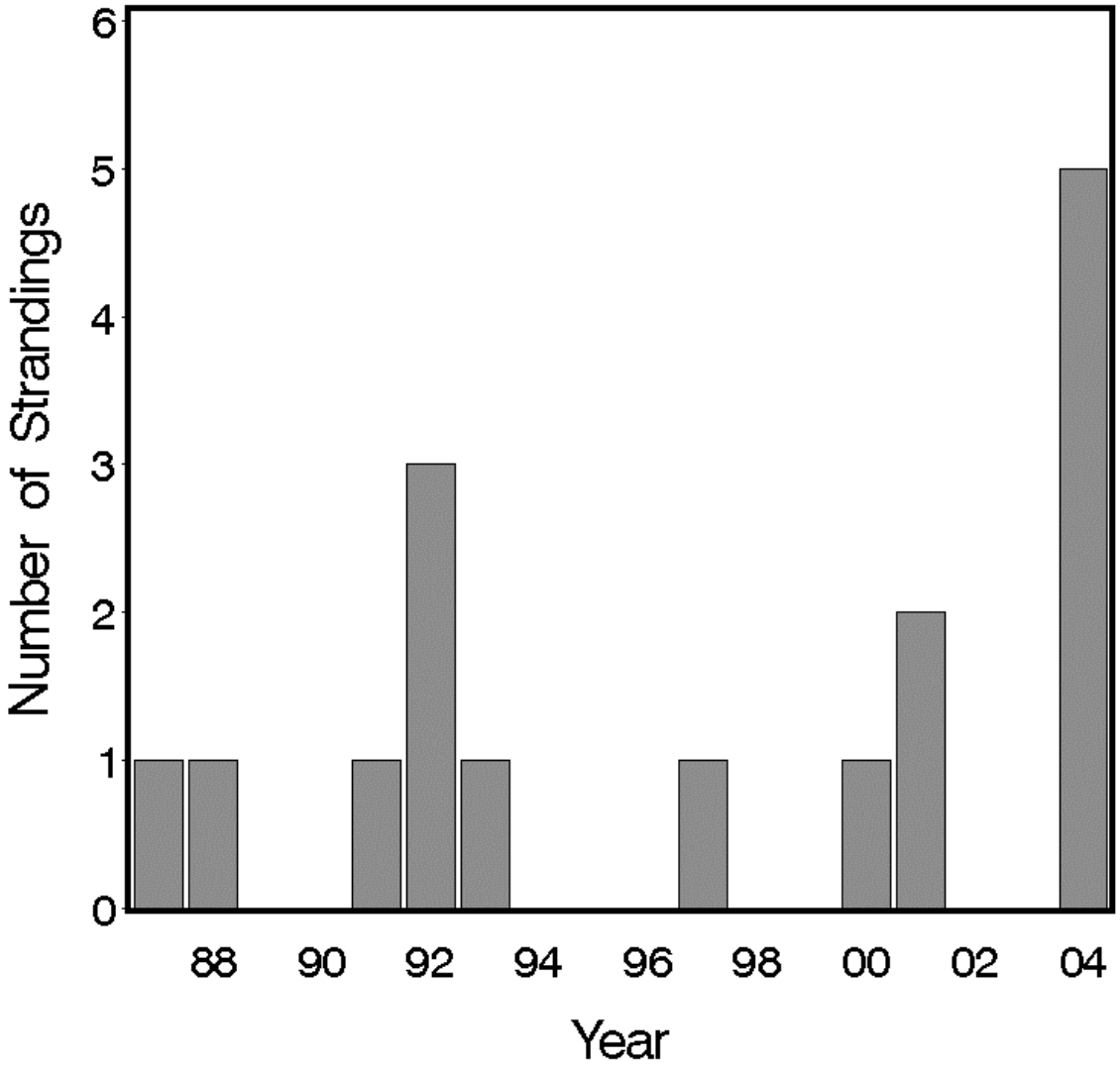

Figure 7. Annual stranding frequencies for humpback whales in the Rhode Island study area, 1987–2004.

3.2.3 Blue Whale *Balaenoptera musculus* (Linnaeus, 1758)

Description: Blue whales are the largest living animals, reaching lengths of 23–28 m and weights of 125,000 kg in the Northern Hemisphere, and over 30 m and 150,000 kg in the Southern Hemisphere (Yochem and Leatherwood 1985; Jefferson et al., 1993; Wynne and Schwartz, 1999; Sears, 2002). The rostrum is broad, U-shaped in dorsal view, and very flat. Coloration is blue-gray with distinctive light mottling. There are 55–88 ventral grooves that extend back to the umbilicus. There are 270–395 very broad baleen plates; they are black with coarse black fringes.

Status: Blue whales are classified as Endangered under the U.S. Endangered Species Act, but are not included on the Rhode Island state list. North Atlantic blue whales are classified as Vulnerable on the IUCN Red List, where the listing is noted as "needs updating." Stocks world-wide were seriously depleted by modern industrial whaling, with hundreds of thousands taken in the Antarctic and about 11,000 in the North Atlantic (Yochem and Leatherwood, 1985; Reeves et al., 1998; Sears, 2002; Reeves and Kenney, 2003). There are no precise estimates of original abundance in the North Atlantic. Yochem and Leatherwood (1985) proposed an original population of about 15,000 in the North Atlantic, but Reeves et al. (1998) suggested that might be too high. Over 320 different individuals have been identified though photographs in the Gulf of St. Lawrence (Reeves et al., 1998), and there may be 1,500 at the present time in the North Atlantic (IUCN, 2008). There is no current estimate of the number of blue whales in U.S. Atlantic waters (Waring et al., 2008).

Ecology and life history: Blue whales feed almost exclusively on euphausiid crustaceans ("krill"). Females mature at 5–15 years of age, and calves are born in the winter (Mizroch et al., 1984; Yochem and Leatherwood, 1985; Sears, 2002). Calves are 7 or 8 m long at birth and grow to about 16 m by the time they are weaned in as little as 6 or 7 months. The typical calving interval is 2 years.

General distribution: Blue whales are distributed in all the world's oceans; in the western North Atlantic, they are most commonly sighted from Nova Scotia north (Jonsgård, 1966; Yochem and Leatherwood, 1985; Sigurjónsson and Gunnlaugsson, 1990; Sears, 2002; Reeves and Kenney, 2003). There are occasional sightings and strandings along the U.S. east coast from the Gulf of Maine to the Gulf of Mexico (reviewed in Reeves et al., 1998). Acoustic detections

of blue whales (Clark, 1995) show that they occur broadly in winter in the deeper central Atlantic as far south as the subtropics, supporting the hypothesis of an inshore-offshore annual migration and a deep-water winter range (Kellogg, 1929).

Historical occurrence: Historical blue whale records in southern New England are very rare. Allen (1916) reported a stranding at Narragansett Pier in 1882 (another report from Major E.A. Mearns). While he reported it as a large female fin whale, in the Smithsonian database it is listed as a probable blue whale because of its reported size at over 30 m long (even allowing for exaggeration, it was larger than would be likely for a fin whale). There were also strandings at Ocean City, New Jersey in October 1891 and Barnegat Inlet, New Jersey in December 1927. Edwards and Rattray (1932) reported an earlier stranding (date unknown) at Sagaponack, Long Island. Waters and Rivard (1962) said that blue whales were rare in New England and had occurred in Massachusetts Bay, but reported no specific records.

Recent occurrence: There are only four recent occurrences of blue whales in the Rhode Island study area (Fig. 8). On 3 March 1998, a dead 20-m blue whale was carried into Rhode Island coastal waters on the bow of the *Botany Triumph*, a 148-m tanker carrying a load of caustic soda from Belgium, bound for Providence. After drifting for a few days, the whale was towed ashore for necropsy on the 7th at Second Beach in Middletown. The location where the whale was first struck by the ship is not known and is believed to have been outside of U.S. jurisdiction (Waring et al., 2008). That animal's skeleton has been mounted and is on display at the New Bedford Whaling Museum. Three blue whale sightings southeast of Montauk Point were recorded by whale-watchers over a one-week period—on 27 July, 31 July, and 3 August 1990. A single animal was seen each time, possibly the same one.

With no sightings from any surveys, a SPUE analysis for blue whales would result in zero values in all locations and all seasons.

Conclusions: Blue whale occurrence is very rare to accidental in southern New England. Consequently, blue whales pose no real concern for the Rhode Island Ocean SAMP.

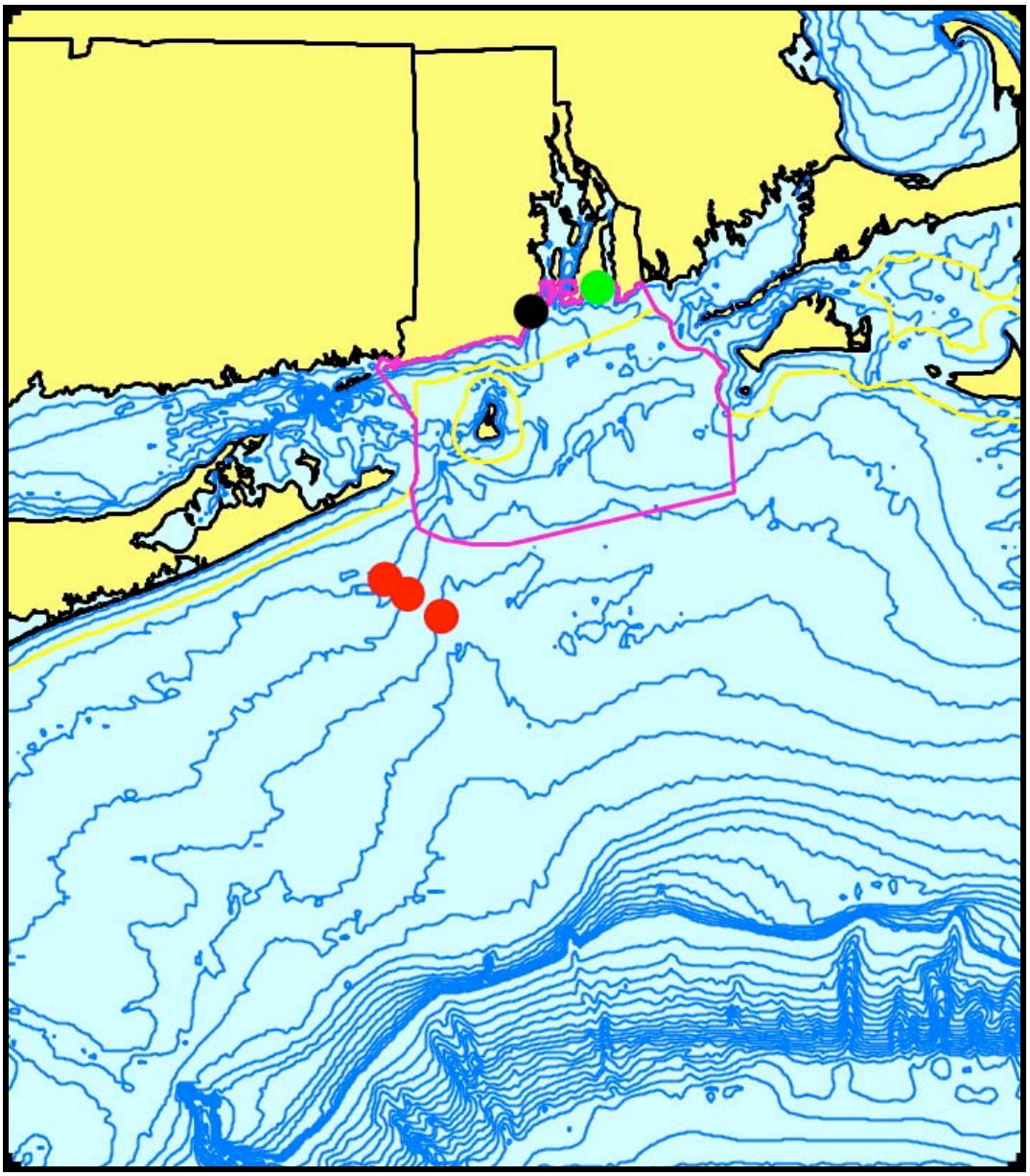

Figure 8. Aggregated sighting, stranding, and bycatch records of blue whales in the Rhode Island study area, 1882–1998 (n = 5: winter = 0, spring = 1, summer = 3, fall = 0, unknown = 1).

3.2.4 Fin Whale *Balaenoptera physalus* (Linnaeus, 1758)

Description: Fin whales are the second-largest species of living whale, with adults 17–24 m long (Gambell, 1985a; Jefferson et al., 1993; Wynne and Schwartz, 1999; Aguilar, 2002). Females are slightly larger than males, with Northern Hemisphere adults averaging about 22.5 m for females and 21 m for males (Aguilar, 2002). There is evidence that the fin whales off the

northeastern U.S. are smaller than animals from farther north (Hain et al., 1992). The mean adult length from animals measured from aerial photographs was 16.1 m, significantly smaller than fin whales taken in modern Icelandic whaling even after accounting for size selection by the whalers. Possible explanations suggested by Hain et al. (1992) included size differences between stocks or habitat segregation by age with the largest adults remaining farther offshore.

A fin whale has a very sleek, streamlined body with a flattened, tapered rostrum. The falcate dorsal fin is about 60 cm tall, set about two-thirds or even three-quarters of the way back on the body. There is a distinct ridge along the back from the dorsal fin to the tail. Fin whales are unique among mammals in being asymmetrically colored, with the lower jaw white on the right and dark on the left. The body color ranges from gray to brownish, with a much lighter belly. Above the flippers, there is a pale, forward-pointing V-shaped chevron on the back and swirls of lighter color on the sides, especially on the right side. There are 55–100 ventral grooves that extend back to the umbilicus.

Status: Fin whales are classified as Endangered under the U.S. Endangered Species Act, as Federally Endangered on the Rhode Island state list, and as Endangered on the IUCN Red List. There is no precise estimate of the total abundance of fin whales in the North Atlantic. Perry et al. (1999) estimated that there may be 50,000 to 60,000. Aguilar (2002) gave estimates of 3,500 in the western Mediterranean, 4,500 off northwestern Spain, 7,500 in the eastern temperate Atlantic, 700 around the Faeroe Islands, 1,850 off Norway, 15,600 in East Greenland and Iceland, 1,000 in West Greenland, and 10,800 off Nova Scotia, Newfoundland, and Labrador. Those estimates sum to 45,450. The most recent estimate for the U.S./Nova Scotia stock is 2,269, however that estimate did not include a correction factor for submerged animals that were missed during surveys. A more realistic estimate for the northeastern U.S. shelf in about 1979–1981, including a correction factor, would be on the order of 5,000–6,000 fin whales (CETAP, 1982; Hain et al., 1992; Kenney et al., 1997).

Fin whales began to be targeted after the depletion of blue whale stocks early in the modern whaling era, beginning off Norway in the 1870s (Tønnessen and Johnsen, 1982; Aguilar, 2002). The whaling stations in Norway closed by 1904 because nearby stocks were depleted, and the hunt expanded across the North Atlantic and into the Antarctic. Tens of thousands of Northern Hemisphere fin whales were taken during the 20th century. A total of 3,528 was taken from three

shore whaling stations in eastern Canada in 1965–1971, with 1,402 at Blandford, Nova Scotia (Mitchell, 1974, Sutcliffe and Brodie, 1977). Fin whaling in U.S. Atlantic waters ended around the turn of the 20th Century (Allen, 1916).

In July 1982, the International Whaling Commission approved a measure setting whaling catch limits to zero for all stocks beginning in 1986 (IWC, 1983; Gambell, 1999), establishing a moratorium on all commercial whaling. Legal whaling since 1986 has been conducted only under (1) the exception for "aboriginal subsistence" whaling (Reeves, 2002), (2) scientific research permits, or (3) objection (under the terms of the Convention, nations that formally object to specific IWC regulations are not bound by them). After 1986, Iceland took 292 fin whales from 1986 to 1989 under a research permit, and subsequently withdrew from IWC membership (Reeves and Kenney, 2003). The subsistence hunt in West Greenland takes 10–15 fin whales per year (Aguilar, 2002). Iceland rejoined the IWC in 2002, and in October 2006 announced the intention to resume small-scale commercial whaling and issued licenses to take 9 fin whales in 2007. Seven were taken. No fin whale quota was set for 2008.

The average annual human-related mortality of fin whales from the U.S./Nova Scotia stock in 2001–2005 was 0.8 from fisheries entanglement and 1.6 from ship collisions. Ship-struck fin whale carcasses are sometimes discovered in New York harbor or nearby in New Jersey. Other serious conservation concerns are rare (Aguilar, 2002). There are detectible contaminant levels in fin whales from waters near industrialized coasts such as the Mediterranean and North Atlantic, but they appear to be relatively low. Feeding relatively low on the food chain makes them less likely to accumulate harmful concentrations.

Ecology and life history: Fin whales appear to be similar to humpback whales in exhibiting maternally-directed habitat fidelity. Agler et al. (1993) use photoidentification of individual whales to demonstrate that adult females showed preferences for either northern or southern Gulf of Maine feeding areas. They suggested that age and sex segregation occurred on local scales, similar to what Hain et al. (1992) suggested for broader geographic scales. Even though individual fin whales are more difficult to identify than humpbacks, both Seipt et al. (1990) and Clapham and Seipt (1991) were able to show relatively high resighting rates, concluding that females tend to return to the same feeding grounds consistently.

Habitat use patterns by fin whales off the northeastern U.S. have shifted significantly in some years. P. M. Payne et al. (1990) showed a decline in fin whale and humpback occurrence in the southern Gulf of Maine in 1985 and 1986, coinciding with a minimum in sand lance abundance. Kenney et al. (1996) hypothesized that changes in relative abundance of herring and sand lance in different portions of the Gulf of Maine, driven by past commercial fishery practices, led to changes in whale distribution. Fin whale sightings south of the Gulf of Maine from summer surveys during the 1990s were more concentrated along the shelf edge than they had been previously (Waring et al., 2008), which might suggest an additional habitat shift, however at least some of the difference is likely due to differences in survey design and timing. Coakes et al. (2005) reported unusual numbers of fin whales off Halifax, Nova Scotia in 1997, also correlated with unusually high local abundance of whale prey.

Fin whales are fast swimmers and capable of moving substantial distances in relatively short times. They normally swim at 5–8 knots (9–15 km/hr), but are capable of short bursts of 15 (28 km/hr) or even 20 knots (37 km/hr) (Gambell, 1985a; Aguilar, 2002). Watkins (1981) tracked a radio-tagged fin whale between Iceland and Greenland that traveled 2,095 km in ten days and covered 292 km in a single day.

Like the other rorquals, fin whales are gulp feeders (Nemoto, 1970; Pivorunas, 1979). They often roll onto their right sides during feeding. Mitchell (1972) speculated that their asymmetric coloration was related to feeding, maintaining counter-shading when rolled to the right. Tershy and Wiley (1992) did show quantitatively that fin whales rolled most often to the right (97% of the time in the North Pacific, 81% in the North Atlantic), but that symmetrically colored blue and Bryde's whales also did. While Southern Hemisphere fin whales feed mainly on euphausiid crustaceans (krill), Northern Hemisphere whales prey upon a wide variety of small, schooling prey, including many small fishes (herring, sand lance, capelin, sardine, etc.), squids, and crustaceans such as krill and copepods (Gambell, 1985a; review in Kenney et al., 1985a; Hain et al., 1992; Kawamura, 1994; Aguilar, 2002).

Fin whale calves are born in the late fall and winter, probably offshore (Mitchell, 1974; Haug, 1981; Gambell, 1985a; Hain et al., 1992; Aguilar, 2002). Length at birth is about 6 m and weight is 1,000 kg or more, and the gestation period is about 11 months. Calves are weaned at 6–11 months old and about doubled in length to 11–13 m (Best, 1966; Haug, 1981; Gambell, 1985a;

Aguilar, 2002). Female fin whales mature at 7–8 years of age and males at 6–7, with the corresponding body lengths in the Northern Hemisphere around 17–18.5 m in females and somewhat smaller in males (Lockyer, 1972, 1984; Gambell, 1985a; Aguilar, 2002). Full physical maturity in both sexes might not be attained until around age 25. The inter-birth interval is usually 2 or 3 years (Christensen et al., 1992; Agler et al., 1993). The mean calving interval for identified individuals in the Gulf of Maine was 2.71 years, but may have been as low as 2.24 if potential missed calving years were taken into account.

General distribution: Fin whales are broadly distributed throughout the world's oceans, from the temperate regions poleward (Gambell, 1985a). Their range in the North Atlantic extends from the Gulf of Mexico, Caribbean Sea, and Mediterranean Sea in the south to Greenland, Iceland, and Norway in the north (Jonsgård, 1966; Gambell, 1985a). They are the most commonly sighted large whales in continental shelf waters from the Mid-Atlantic coast of the U.S. to Nova Scotia (Sergeant, 1977; Sutcliffe and Brodie, 1977; CETAP, 1982; Hain et al., 1992; Waring et al., 2008), which comprises the range of the U.S./Nova Scotia stock. Fin whales in other regions of the North Atlantic—Newfoundland/Labrador, West Greenland, East Greenland/Iceland, Norway, western Europe, and the Mediterranean—are believed to belong to different stocks (Donovan, 1991; Bérubé et al., 1998). Fin whales off the northeastern U.S. are most abundant from spring through fall, with smaller numbers of animals remaining through the winter (Hain et al., 1992). Most of the fin whales are believed to migrate offshore and south during the winter, which has been supported by passive acoustic tracking information developed in cooperation with the Navy (Clark, 1995).

Historical occurrence: Fin whales are the most common large whale in the Rhode Island region at the present time, and likely were common historically. Cronan and Brooks (1968) reported five 19th Century fin whale records from Rhode Island, all of which were included in Allen (1916), but stated that the last known occurrence was in 1884. The Smithsonian database included a larger number of records in or near Rhode Island from the late 19th Century, all also from Allen (1916), with the major difference probably being "definite" versus "probable" identifications. One whale was sighted off Point Judith on 28 October 1858. Allen quotes a newspaper account from 16 August 1873—"The skipper of the sloop *Annie*, of Saybrook, Conn., reports a large school of whales in close proximity to home. Monday, while midway between Southeast Point, Block Island, and Montauk, a school of whales, numbering probably thirty-five,

was seen from the *Annie's* deck, gamboling near the Block Island shore where they had been lured, it is supposed, by the prospect of a good feeding-ground. In the school very few Finbacks or Humpback Whales were to be seen. The majority were large whales, some of them being not less than 70 feet in length." It was far more likely that those whales were fin whales than blue whales. Large schools of whales were seen around Noman's Land, Cuttyhunk, Gay Head, and Vineyard Sound in October 1874, chasing "great shoals of herring." A stranding of a very large fin whale was reported near the life-saving station in "Wakefield"[9] on 18 April 1880. Several whales were sighted off Block Island in early summer 1882. There were two sightings off Block Island in July of 1884—several whales on the tenth and about 20 at mid-month. A fin whale was sighted off Newport in 1885—"In the summer of this year a Finback was seen in Easton's Bay, R.I., by a number of people, including Mr. Philip Peckham, Jr., on whose authority Major E.A. Mearns reports the fact to me." An 1887 incident was included by Allen as a possible minke whale, but recorded in the Smithsonian data as more likely a fin whale—"Major E.A. Mearns sends me the account of a capture of a small whale that was supposed to have been a 'young Finback,' but was perhaps a Little Piked Whale. The incident occurred in Narragansett Bay, R.I., but the exact date is not available. By some curious accident, the whale in rising to the surface caught its head between the stern and the propellor blades of the government steamer *Munroe* as it lay at the South Dock. In its struggles to free itself the whale nearly lifted the stern of the vessel out of the water. The Captain, seeing that the whale was caught fast, turned on full steam in order to dislodge it. This had the desired result, but the swiftly revolving blades inflicted such injuries on the whale's head that it rushed upon a shoal at the head of Brenton's Cove and became stranded. It was finally killed there by soldiers from Fort Adams. ... It was said to have been a female, about thirty feet long." There were sightings of single whales off Newport on 2 June 1897 and 11 March 1899. Finally, a 15.5-m fin whale stranded at Point Judith on 28 August 1900.

Fin whales were not mentioned by De Kay (1842) or by Linsley (1842). Fin whales were commonly observed by the shore-based right whalers in eastern Long Island, but were rarely pursued because they were too fast and yielded less oil than right whales (Edwards and Rattray, 1932; Connor, 1971). Fin whales were not targeted by whaling in New England until the development of modern technology in the second half of the 19th Century, although the first

[9] Narragansett was not established as a separate town from South Kingstown until 1901.

recorded attempt to kill fin whales, which was unsuccessful, was by Capt. John Smith in 1614, off Monhegan Island, Maine (Allen, 1916). Allen lists many sightings, strandings, and attempted captures (mostly unsuccessful) of fin whales off Massachusetts before the mid-19th Century. Waters and Rivard (1962) stated that fin whales were the most common whales in New England and very common in Cape Cod Bay. They tabulated 11 fin whale records between 1946 and 1958, including seven more or less typical strandings, one stranding with the tail severed by a ship propeller, two caught in fish weirs, and one entangled in the steel cable of a trawl net. Goodwin (1935) knew of only one record from the Connecticut coast, an 18-m whale killed in New Haven Harbor on 5 May 1834. Connor (1971) reported that fin whales were commonly sighted off Long Island, and he knew of strandings in 1916, 1936, and 1946.

Recent occurrence: Fin whales occur throughout continental shelf waters in the region in all four seasons (Fig. 9). Sightings are strongly concentrated in summer (80.9%) and spring (11.6%) and in the area between Block Island and Montauk Point, however both the spatial and temporal patterns are strongly biased by the whale-watching data, which generated 1,246 out of the 1,762 records (71%). Without those data, the seasonal differences are far less dramatic, with 52.7% of occurrences in summer, 29.8% in spring, 9.9% in fall, and 7.2% in winter, however the pattern of peak abundance is summer is still there. Strandings as a proportion of all records appear to be higher in the fall. It might be hypothesized that the observed seasonal increase in stranding frequency corresponds to the expected time of weaning.

After correcting for survey effort patterns (and including unidentified fin/sei sightings at 97.8% weighting), fin whales are present in the Rhode Island study area in all four seasons (Fig. 10). In spring, summer, and fall the main center of their distribution is in the Great South Channel area to the east of Cape Cod, which is a well-known feeding ground (Kenney and Winn, 1986). Winter is season of lowest overall abundance, but they do not depart the area entirely. In all four seasons, there are areas of higher fin whale occurrence both in inner shelf waters and near the shelf break. The highest occurrence within the SAMP area and nearby is in the outer half of the area from south of Montauk Point to south of Nantucket—in precisely the same area as the dense aggregations of sighting records from the whale-watching boats (Fig. 9). Therefore the pattern in the raw sighting data is not entirely due to bias in the data. That does make sense, since whale-watching would not be a viable operation if there were no whales, and they should be expected to focus their trips where they expect to find whales.

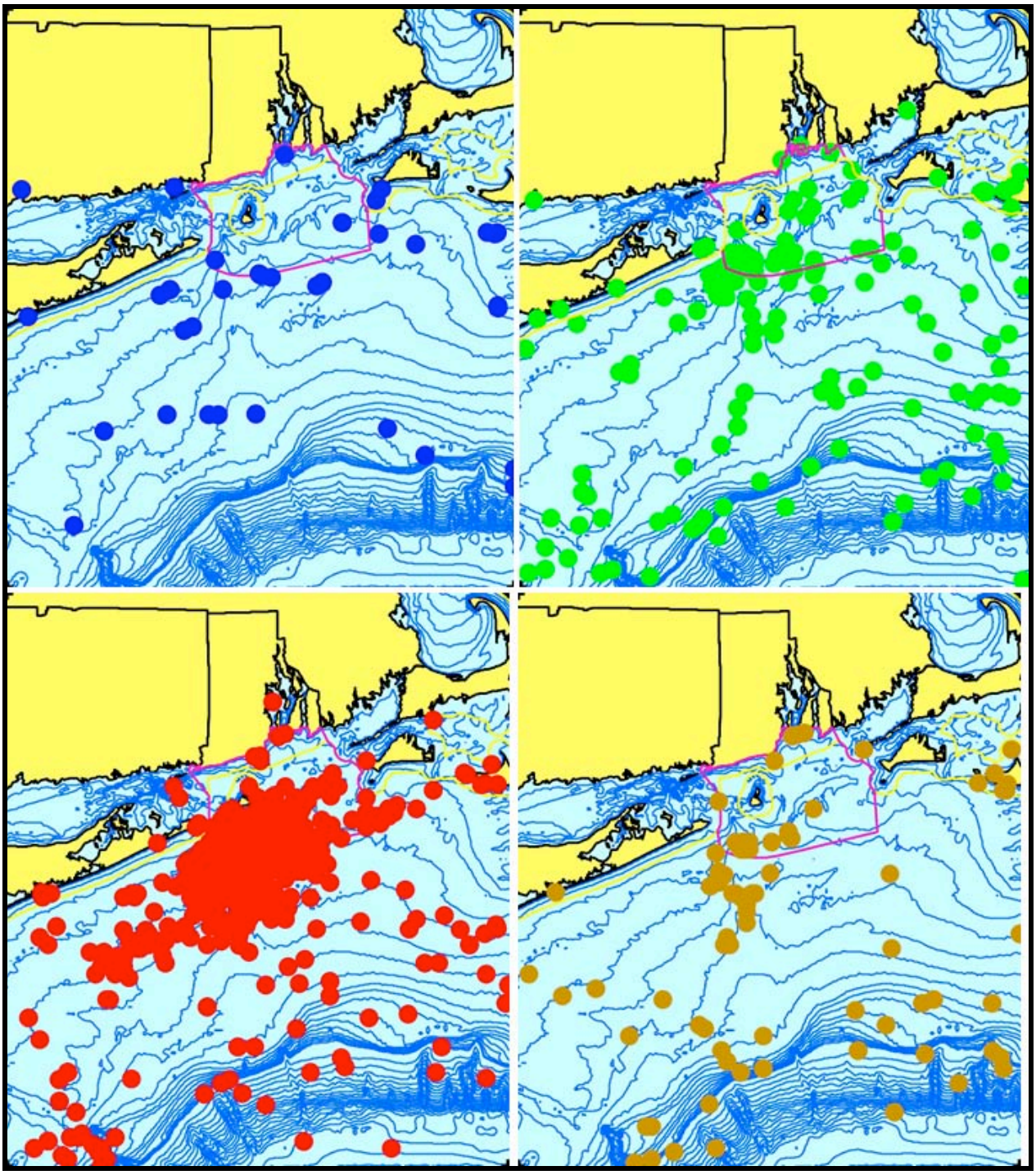

Figure 9. Aggregated sighting, stranding, and bycatch records of fin whales in the Rhode Island study area, 1834–2008 (n = 1,762: winter = 37, spring = 205, summer = 1,425, fall = 93, unknown = 2).

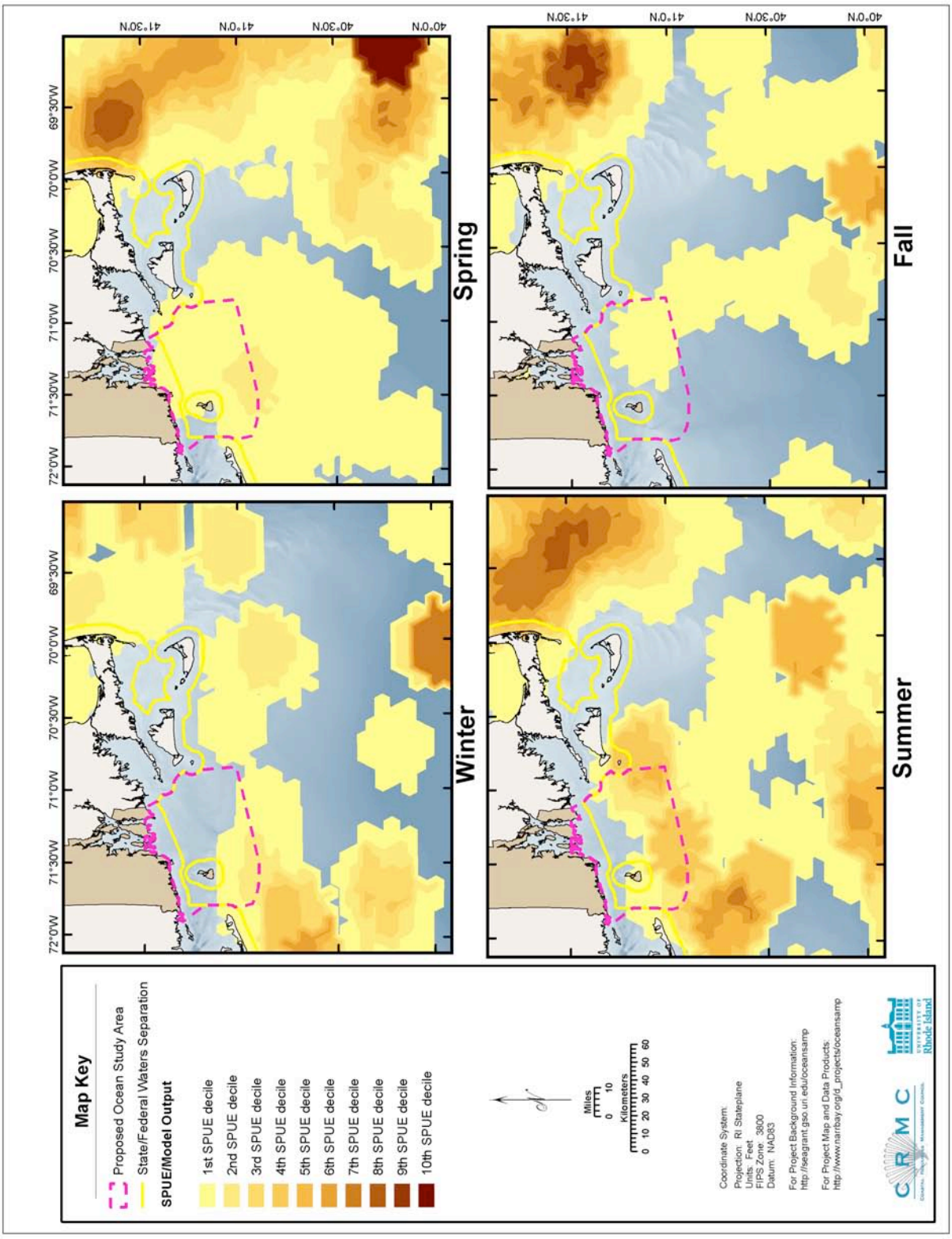

Figure 10. Modeled seasonal relative abundance patterns of fin whales in the Rhode Island study area, corrected for uneven survey effort.

Fin whales are the most commonly stranded large whale in the Rhode Island study area, with 28 records since 1970 (Table 2). One of the more interesting recent fin whale observations was in July 1983, when a headless carcass was seen drifting for several days. It was seen southwest of Block Island on the 27th and 5 km south of Point Judith on the 31st, with a number of great white sharks feeding on it. In August, as the dead whale continued drifting near Block Island, fishermen took the opportunity to target the feeding sharks (Casey and Pratt, 1985). Three very large male white sharks—480, 484, and 497 cm—were harpooned, two even larger animals (estimated at 518 and 610 cm) were tagged, and at least three others were seen. On 13 July 1989, a moderately decomposed immature female fin whale was found near Quonset Point; it was hauled up at Pier 2 in Davisville the following day. It had a fractured lower jaw and rope entangling the right flipper. On 27 July 1991, an 11-m whale was seen drifting near the south shore; it came ashore on East Matunuck State Beach on the 28th. On 30 April 1996, a 12.8-m fin whale stranded on Warren's Point in Little Compton. Three fin whales stranded this century in Newport—one in Castle Hill Cove on 25 November 2002, one at Fort Adams State Park on 13 June 2004, and one at Brenton Point State Park on 24 December 2004. There were also two strandings in Connecticut: on Long Point in Groton on 28 January 1976—a 13.5-m whale with injuries from a ship collision, and in New Haven harbor on 18 December 1983—a 12-m female that was stuck in an area of broken pilings for several hours before it died. Fin whale strandings are common in the Rhode Island study area both east and west of Rhode Island, as well as beyond the study area in New York, New Jersey, and Massachusetts. Shark scavenging on fin whale carcasses seems to be common from Rhode Island west. There are peaks in the stranding frequency in the study area in 1975–1985 and 2001–2005 (Fig. 11), which is a different pattern than what was shown for humpback whales (Fig. 7.) The underlying cause is not obvious. Plotting the annual stranding frequencies from 1987 to 2005 (Fig. 12) to match the humpback graph shows the fin whale stranding rate to be very consistent across years, with 0–2 strandings per year and no obvious clusters. However, plotting the previous 19-year period in the same format shows a very clear spike in 1983 at more than triple the maximum in any other year, which was also noted by Hain et al. (1992). The underlying reason is not known, but could potentially be fluctuations in prey resources, a disease event, a biotoxin event, other natural or anthropogenic impact, or simply random variability in mortality.

Conclusions: Fin whales are the most common large whale encountered in continental shelf

waters south of New England and into the Gulf of Maine. They are the whales most often encountered by local whale-watching operations in most years, and are quite likely to occur in SAMP area. Despite their relative abundance, they are listed as Endangered under the ESA. Fin whales must be considered in construction and operational planning for any developments in the SAMP area.

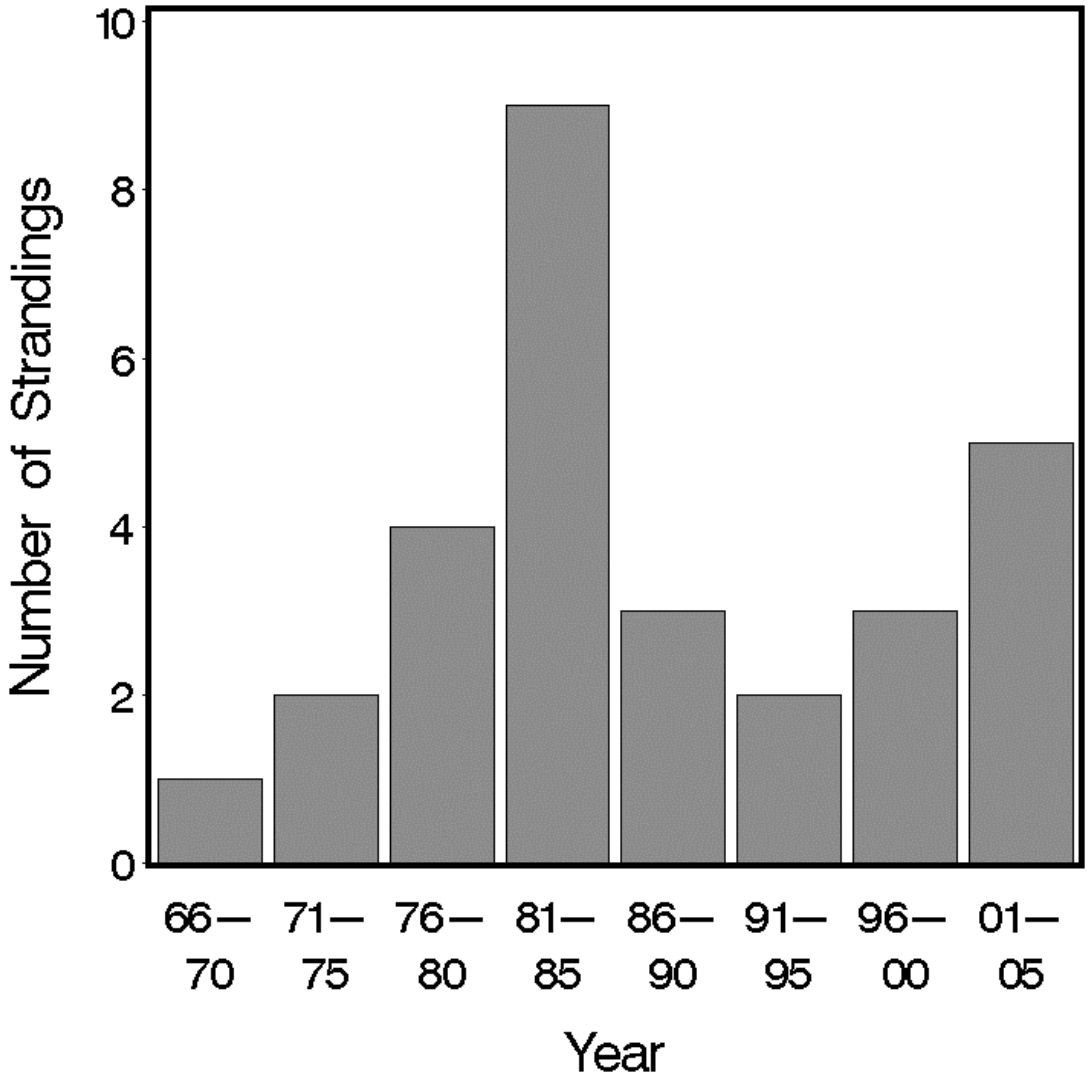

Figure 11. Five-year stranding frequencies for fin whales in the Rhode Island study area, 1966–2005.

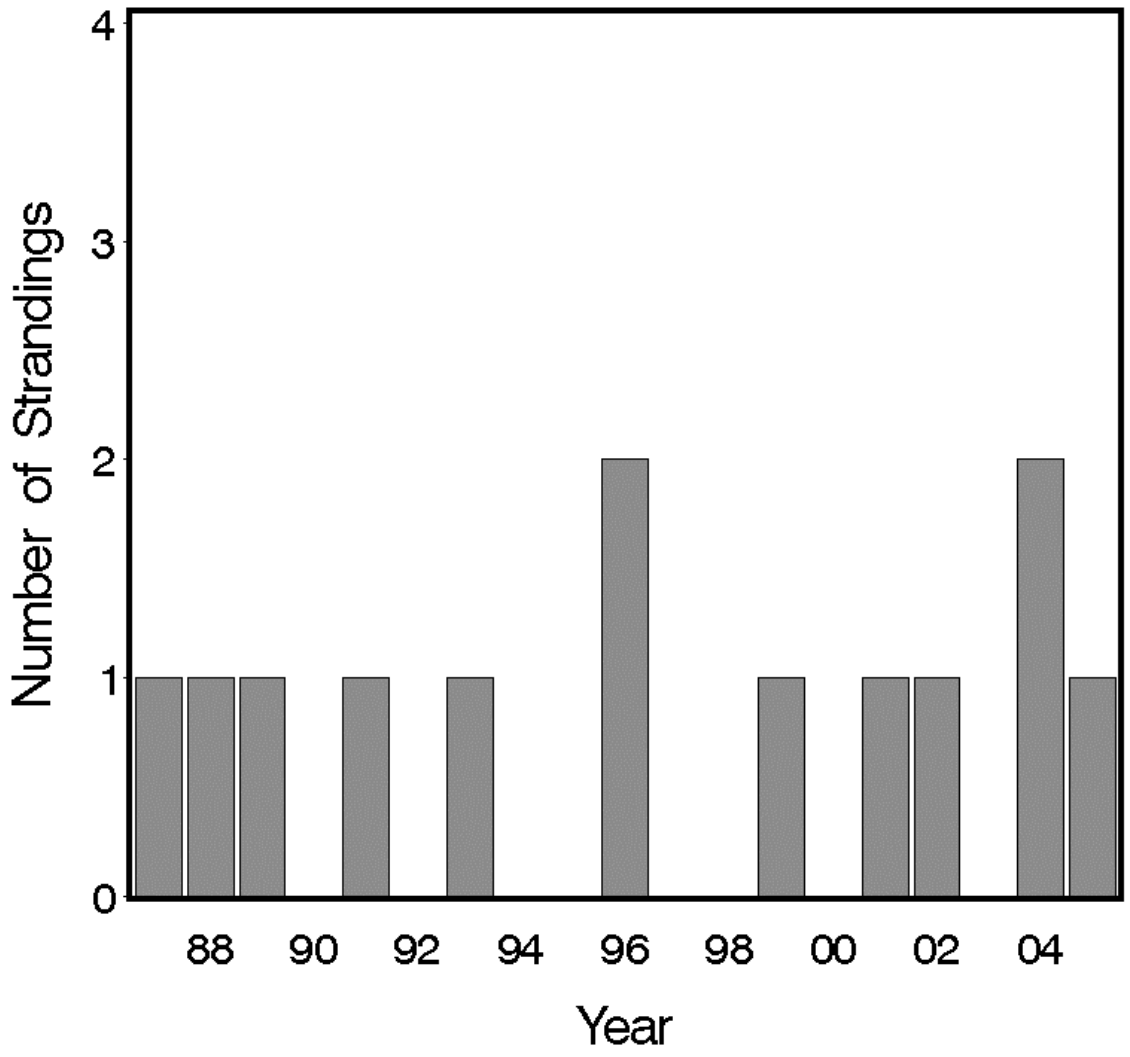

Figure 12. Annual stranding frequencies for fin whales in the Rhode Island study area, 1987–2005, for comparison with humpback whales (Fig. 7).

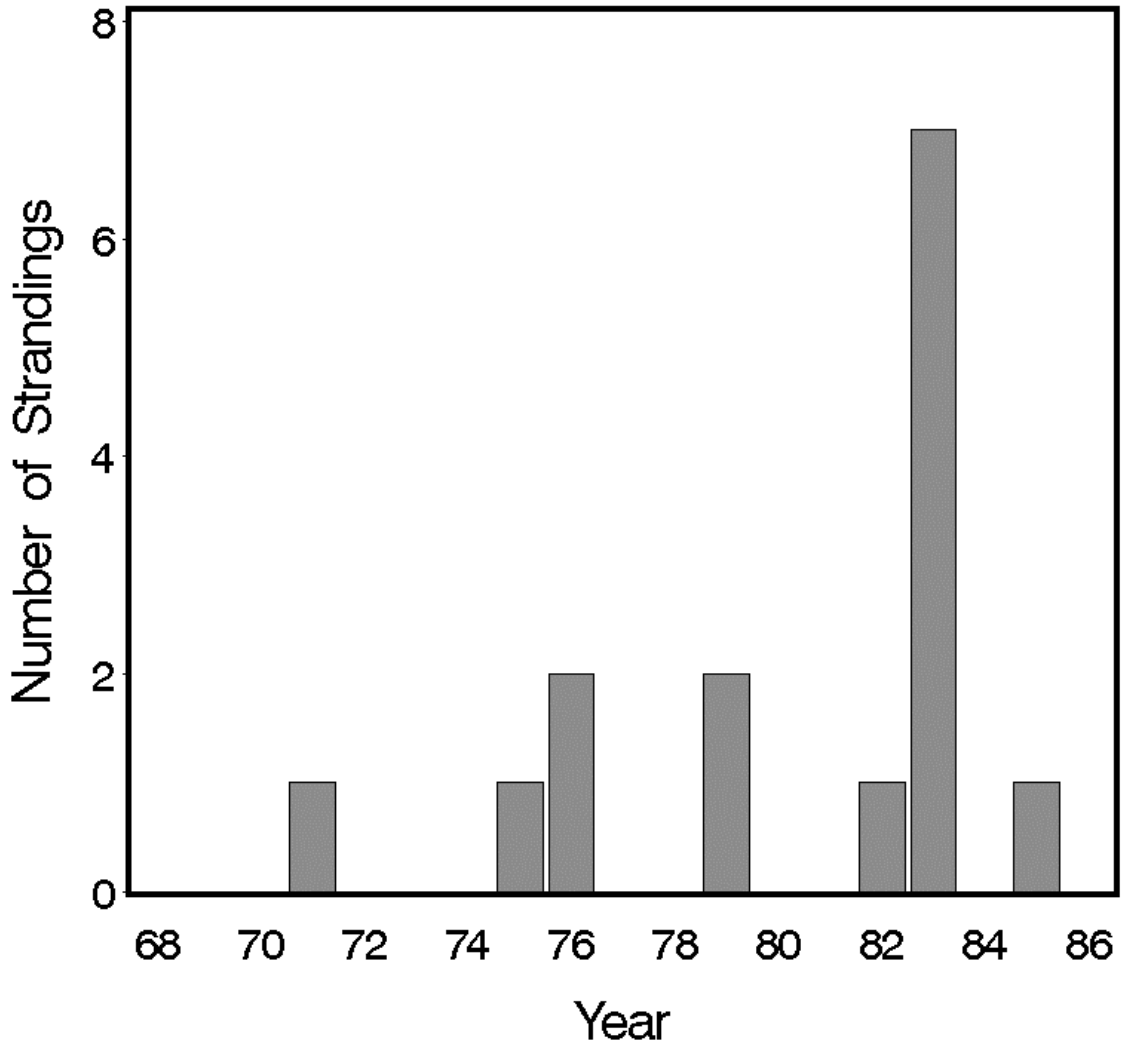

Figure 13. Annual stranding frequencies for fin whales in the Rhode Island study area, 1968–1986.

3.2.5 Sei Whale *Balaenoptera borealis* Lesson 1828

Description: Adult sei whales are 12–17 m in length, with a very sleek, slender, and streamlined appearance (Gambell, 1985b; Jefferson et al., 1993; Wynne and Schwartz, 1999). Typical maximum sizes in the whaling catches in Iceland were about 14 m in males and 15 m in females (Horwood, 1987). They are dark gray or brown to almost black in color, with a lighter belly, and frequently with pale mottling or scars. The rostrum is sharply pointed with a single longitudinal ridge, and curves noticeably downward towards the sides and tip. The dorsal fin is

erect and very falcate, and is located about 2/3 of the way back on the animal. There are 40–55 ventral grooves, which end about mid-way between the flippers and the navel.

Status: Sei whales are classified as Endangered under the U.S. Endangered Species Act, and are not included on the Rhode Island state list. They are currently classified as Endangered on the IUCN Red List, however the classification was based mainly on depletion of Southern Hemisphere stocks by 20th Century whaling. There is no reliable estimate of the total abundance of sei whales in the North Atlantic (Perry et al., 1999). The IWC recognizes three more or less arbitrarily-defined stocks in the North Atlantic: Nova Scotia (the one occurring off the U.S. Atlantic coast); Iceland-Denmark Strait; and Eastern (Donovan, 1991). Recent surveys suggest that there are about 10,000 in the Iceland-Denmark Strait stock (Horwood, 2002), but they seem to remain very rare off Europe (IUCN, 2008). Recent summer surveys in the Gulf of Maine in 2004 and 2006 yielded estimates of 386 and 207 sei whales, respectively (Waring et al., 2008), however the estimates are not corrected for diving and the surveys may have been later in the year than the spring peak occurrence of the whales around Georges Bank. Mitchell and Chapman (1977) estimated the Nova Scotia stock at 1,400–2,200 whales, which is similar to the estimate of about 2,200 for the U.S. Atlantic from the CETAP (1982) survey data if corrected for diving using the same correction factor derived for fin whales (Kenney et al., 1997).

Commercial whaling on sei whales did not begin until modern technology allowed the capture of fast-swimming rorquals, beginning in the second half of the 19th Century. In the North Atlantic, sei whales have been hunted in the waters off mainland Europe, Norway, the British Isles, Iceland, Greenland, and Canada, with total takes of more than 14,000 whales (Horwood, 1987), plus an unknown proportion of the 30,000 whales taken that were not identified to species (IUCN, 2008). About 1,200 sei whales were taken off eastern Canada in the 1960s and 1970s (IUCN, 2008), including 825 by whalers operating from a station in Blandford, Nova Scotia (Mitchell, 1975b). Since the IWC moratorium began in 1986, the only North Atlantic sei whales killed have been 70 taken in Iceland in 1986–1988 under a scientific research permit, and the possibility of an occasional accidental take in subsistence hunting for fin whales in Greenland (Reeves and Kenney, 2003).

Other human-related mortalities of sei whales appear to be rare (Waring et al., 2008). There have been no known fishery entanglement mortalities in U.S. Atlantic waters. There have been

three known ship-strike mortalities in the last two decades. A dead sei whale was found on the bow of a container ship in Boston on 17 November 1994, and a similar event happened on 2 May 2001 in New York Harbor. A dead sei whale with extensive injuries was found floating near the Navy base in Norfolk, Virginia on 19 February 2003.

Ecology and life history: Sei whales are normally observed alone or in groups of 2–5 animals. During the 1979–1981 surveys off the northeastern U.S., the most common sighting was a single whale, the average group size was the largest of all the baleen whales at 3.0, and the range was from 1 to 40 (CETAP, 1982). They are sometimes observed in feeding aggregations with other baleen whales, including fin, humpback, and right whales. Kenney and Winn (1987a) described a large whale feeding aggregation observed on 18 April 1980 in the vicinity of Hydrographer Canyon, which included 9 humpback whales, 10 right whales, at least 20 fin whales, and at least 40 sei whales, all feeding on probable euphausiid patches.

Sei whales are "switch-hitters" in their feeding behavior (Ingebrigtsen, 1929; Nemoto, 1970; Pivorunas, 1979; Watkins and Schevill, 1979; Gambell, 1985b). Sometimes they are gulp-feeders like blue, fin, or humpback whales—lunging forward with the mouth gaping widely, then closing the mouth and squeezing out the water. At other times sei whales skim-feed, opening the mouth only part-way, then swimming ahead with the mouth open for longer periods continuously filtering prey from the water. The feeding method is likely determined by prey type—skimming for smaller prey and gulping larger prey.

The principal prey species of sei whales are primarily copepods and secondarily euphausiids (Kawamura, 1974; Mitchell, 1975b; Jonsgård and Darling, 1977; Mitchell and Chapman, 1977; Christensen et al., 1992; Schilling et al., 1992). Their very fine baleen fringes allow them to filter out smaller prey than the other rorquals. It should be noted that the location of the sei whale sightings in the vicinity of the SAMP area, south of Montauk Point and Block Island (Fig. 14), is also a location where right whale sightings tend to be aggregated (Fig. 3), suggesting that dense copepod concentrations occasionally develop in that vicinity.

Sei whale calves are born in the winter at a length of 4.4–4.5 m and weight of about 650 kg (Mitchell and Chapman, 1977; Rice, 1977; Lockyer and Martin, 1983; Gambell, 1985b; Horwood, 1987, 2002; Boyd et al., 1999). The gestation period is believed to be 10.5–12 months, perhaps slightly longer in the Southern Ocean than in the North Atlantic and North Pacific,

therefore mating also occurs in the winter. Calves are weaned at 6 to 9 months old and about 9 m long, following the typical mysticete pattern of doubling in body length by the time of weaning. Both sexes typically reach sexual maturity at 5–15 years of age, with a peak at 8–10 years, and at about 13 m long. Females give birth every 2–3 years.

General distribution: Sei whales occur in all of the world's oceans, migrating between feeding grounds in temperate and sub-polar latitudes and wintering grounds at lower latitudes (Gambell, 1985b; Horwood, 1987, 2002; Reeves and Kenney, 2003). Most North Atlantic sightings are along the continental shelf edge and slope (Mitchell, 1975b; CETAP, 1982; Martin, 1983; Hain et al., 1985). Sei whales that occur off the northeast U.S. have been hypothesized to migrate from spring feeding grounds around the southern and eastern edges of Georges Bank, to the Nova Scotian shelf in June and July, further eastward perhaps as far as Newfoundland and the Grand Banks in late summer, back to the Scotian Shelf in the fall, and possibly offshore during the winter (Mitchell, 1975b; Mitchell and Chapman, 1977; CETAP, 1982). The winter range is poorly known, but there are scattered records from the southeastern U.S., Gulf of Mexico, and Caribbean (Mead, 1977; Schmidly, 1981; Gambell, 1985b). Sei whales also are known for their unpredictable sporadic occurrences in areas where they are not regularly seen (Gambell, 1985b; Horwood, 1987; P. M. Payne et al., 1990; Schilling et al., 1992; Clapham et al., 1997).

Historical occurrence: Historical sei whale records from southern New England are extremely rare. Cronan and Brooks (1968) knew of no occurrences in Rhode Island. Allen (1916) reported a stranding from Chatham, Massachusetts in August 1910, which he believed to be the first record from the U.S. Waters and Rivard (1962) said they were rare in New England, and reported only one Massachusetts occurrence, a stranding of an emaciated, 11.9-m male in the Jones River in Kingston on 21 October 1948. De Kay (1842) wrote that Dr. Mitchill[10] told him of an 11.6-m whale that was captured in 1804 near Reedy Island at the mouth of the Delaware River and then exhibited in New York. He assigned the whale to "*Rorqualus borealis,* the northern rorqual" (i.e., sei whale). No specimen from that whale survives. Allen (1916) believed that it was most likely a humpback whale, but it is recorded in the Smithsonian data as *Balaenoptera* sp. based on De Kay's account and subsequent literature reports. De Kay reported

[10] Presumably Samuel Latham Mitchill, 1764–1831, physician, naturalist, New York Assemblyman, U.S. Congressman and Senator, professor at Columbia, and co-founder of the Rutgers medical school.

no other sei whale occurrences, nor did Linsley (1842), Goodwin (1935), or Connor (1971).

Recent occurrence: Sei whales have occurred infrequently in the Rhode Island study area, with 35 records in total (Fig. 10) and a strong concentration in the spring (82.9%). The primary spring feeding area on Georges Bank shown by CETAP (1982) does not extend west of 70ºW longitude. Most of the sightings are more offshore—from the middle of the shelf to the shelf break and slope. The sightings do confirm the typical pattern of irregular occurrences by sei whales. The small cluster of five inshore sightings south of Montauk Point and Block Island included three on three different days in July 1981 (including the two inside the SAMP area—on 23 and 26 July), one in August 1982 (the only one from any whale-watching boat), and one in May 2003. All five were single individuals. The only other year with more than one sighting was 2001, when a NMFS aerial survey on 7 May recorded 23 sei whale sightings, totaling 112 individuals, within a relatively small area at mid-shelf south of Nantucket. There were single sightings in April 1983, May 1985, October 1987, April 2000, November 2004, April 2005, and April 2006.

For the sei whale SPUE estimates, we included 2.2% of the survey sightings identified as "unidentified fin/sei whale," based on the relative proportion of identified sightings of the two species. The resulting maps looked very similar to the fin whale model outputs. While it is quite probable that 2.2% of the fin/sei sightings in the study were sei whales (i.e., one or two of the 59 sightings), assuming that every sighting has the same probability of being a sei whale resulted in an obviously erroneous relative abundance model, which is not shown here. Since 60% of the identified sei whale sightings in the Rhode Island study area occurred on a single day in May 2001, and there were only six sightings in seasons other than spring, their occurrence in the region is too sparse to derive meaningful relative abundance patterns from the identified sightings alone.

There are no known strandings, either historical or recent, in the state or in the study area. The closest known stranding "as the crow flies" would be the 1948 incident in Kingston, Massachusetts mentioned above. The next two would be Allen's 1910 Chatham whale and one in September 2002 on the south shore of Long Island just west of Fire Island Inlet.

Conclusions: Although sei whales are sometimes known to occur unpredictably and irruptively, there have only been two sightings of single sei whales within the RI Ocean SAMP

area—three days apart in July 1981. They are not expected to occur within the SAMP area except as a very rare visitor. Although sei whales are listed as Endangered under the ESA, they pose very little concern for any development with the SAMP area.

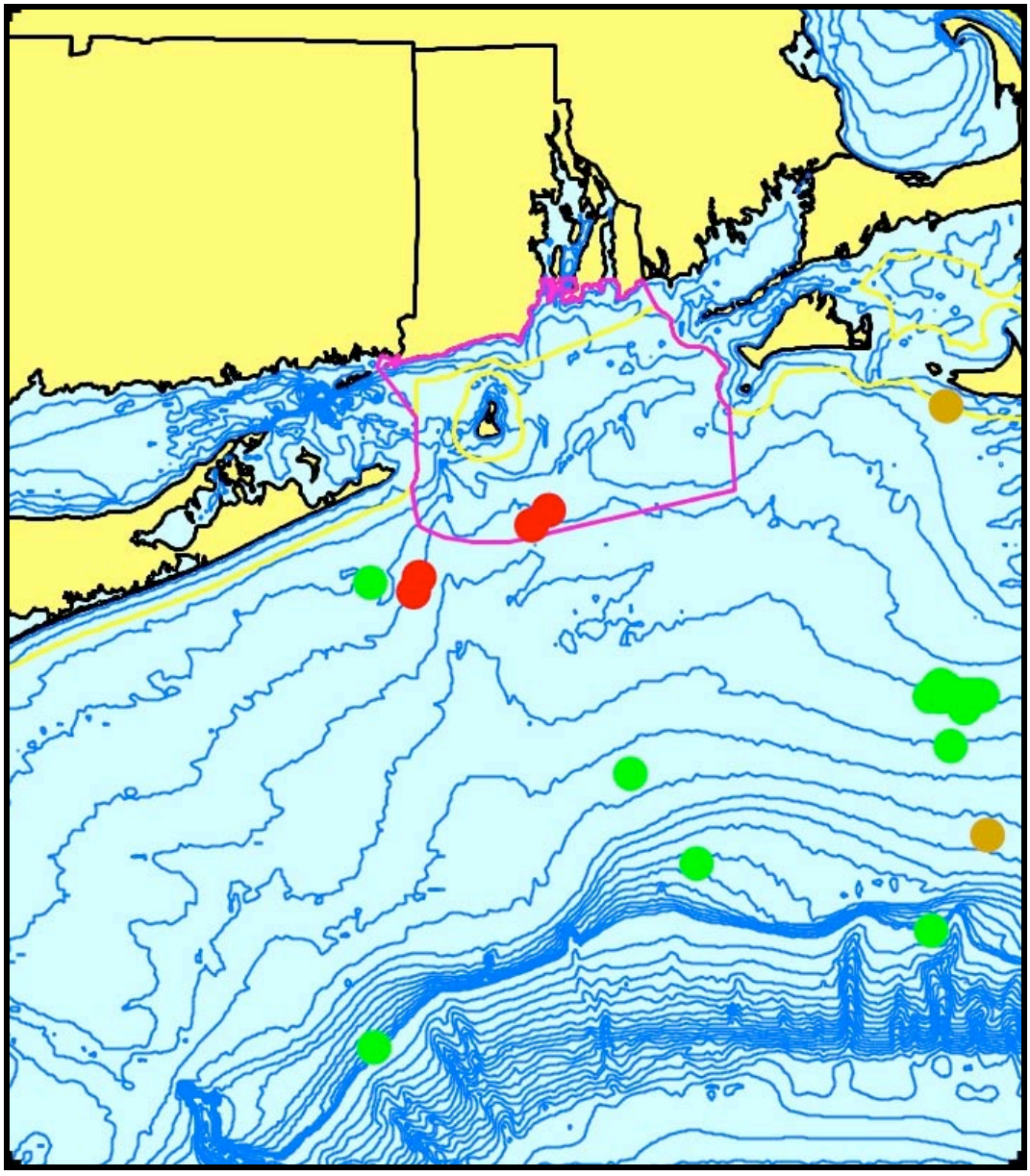

Figure 14. Aggregated sighting, stranding, and bycatch records of sei whales in the Rhode Island study area, 1981–2006 (n = 35: winter = 0, spring = 29, summer = 4, fall = 2).

3.2.6 Bryde's Whale *Balaenoptera brydei* Olsen, 1913

Description: Bryde's whales appear very similar to sei whales, but are slightly smaller, with adults up to 13–15.5 m in length (Cummings, 1985a; Jefferson et al., 1993; Wynne and Schwartz, 1999; Kato, 2002). They are dark colored, lighter ventrally, with a pointed, slightly rounded rostrum and a prominent, falcate dorsal fin. The definitive distinguishing characteristic of Bryde's whales is the presence of three longitudinal ridges on top of the rostrum—one down the middle and a parallel ridge on each side of it. There are 40–70 ventral grooves that extend to or past the navel. The baleen is dark gray with coarse, lighter gray fringes, and there are 250–350 plates on each side. The most anterior plates are sometimes lighter-colored or striped.

Status: Bryde's whales are not listed under the U.S. Endangered Species Act, are not included on the Rhode Island state list, and are classified as Data Deficient on the IUCN Red List. There are no abundance estimates for the North Atlantic except for a small stock in the Gulf of Mexico. The most recent abundance estimate there is 15 (Waring et al., 2008), but there are previous estimates of 35–40.

In the North Pacific, Japan began taking Bryde's whales under a scientific research permit in 2000, and currently takes 50 per year. North Atlantic Bryde's whales have never been targets of commercial whaling, although traditional whalers in the West Indies very occasionally take one (Reeves and Kenney, 2003), and some may have been included in catch totals for sei whales prior to 1972 (IUCN, 2008).

Ecology and life history: Prey of Bryde's whales include krill, other crustaceans, pelagic fish, and squid, with diets varying between regions (Best, 1977; Kawamura, 1980; Cummings, 1985a; Kato, 2002). Reproductive biology is not well known and is probably similar to other rorquals.

General distribution: Bryde's whales are the most tropical rorquals and are found in all oceans (Cummings, 1985a; Kato, 2002; Rice, 1998), although the existing taxonomic questions and the fact that they were probably confused with sei whales in commercial whaling records for many years limits historical information on distribution.

Historical occurrence: There are no published records of Bryde's whales in the region. There is a specimen of Bryde's whale baleen in the Harvard Museum of Comparative Zoology (MCZ48537) that was dredged from the bottom in about 150 meters of water south of Nantucket,

Massachusetts in 1952 (Fig. 15). The northernmost confirmed stranding record from the U.S. east coast is in Virginia (Mead, 1977).

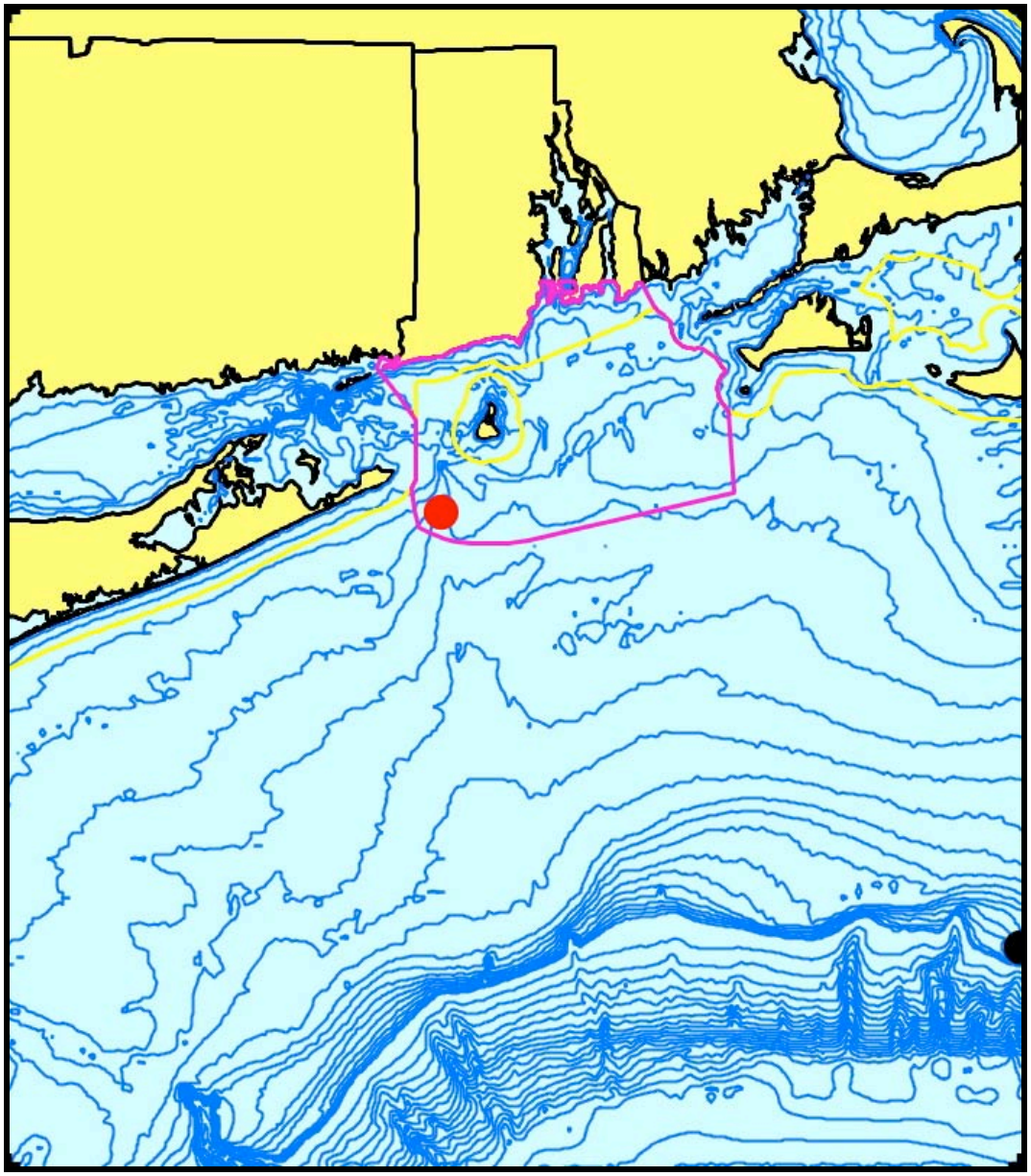

Figure 15. Aggregated sighting, stranding, and bycatch records of Bryde's whales in the Rhode Island study area, 1952 and 1982 (n = 2: winter = 0, spring = 0, summer = 1, fall = 0, unknown = 1).

Recent occurrence: There was one sighting of a single Bryde's whale southeast of Montauk from a whale-watch boat in August 1982 (Fig. 15).

Conclusions: Bryde's whales are clearly accidental off the northeastern U.S. and not a concern in the SAMP area.

3.2.7 Common Minke Whale *Balaenoptera acutorostrata* Lacépède 1804

Description: Common minke whales (There is a closely related species, the Antarctic minke whale *B. bonaerensis*, that has recently been accepted as a valid species, requiring the term "common" to designate this species.) are the smallest of the North Atlantic baleen whales, with adults generally 6–9 m long and reaching maximum lengths of 9–10 m (Stewart and Leatherwood, 1985; Jefferson et al., 1993; Wynne and Schwartz; 1999; Perrin and Brownell, 2002). The body is somewhat more robust than in the larger *Balaenoptera* species. The head is shorter relative to the body than in the other balaenopterids, and the rostrum is very sharply pointed with a prominent median ridge. The body is dark gray to black with a pale belly, and frequently shows pale areas on the sides that may extend up onto the back. The flippers are smooth and taper to a point, and the middle third of each flipper has a conspicuous bright white band. The dorsal fin is tall, prominent, and falcate, and is located about two-thirds of the way back along the body. The ventral grooves number 50–70, ending well forward of the navel. Minke whales were formerly known as little piked whales.

Status: Common minke whales are not listed under the U.S. Endangered Species Act or the Rhode Island state list, and are classified as Least Concern on the IUCN Red List. There are more than 180,000 minke whales in the North Atlantic (IUCN, 2008). The Northeast Atlantic stock is over 80,000 animals, the Central North Atlantic stock totals about 94,000, and the West Greenland stock is about 3,500. The Canadian East Coast stock includes the minke whales off the U.S. East Coast. The most recent estimate for a portion of the range from the Gulf of Maine to the Gulf of St. Lawrence is 3,312 (Waring et al., 2008), however that is likely to be a significant underestimate because minke whales tend to be under-sampled in most surveys. NMFS surveys in 1991 and 1992 designed specifically for harbor porpoises, also inconspicuous and difficult to detect, resulted in an estimate of 2,650 minke whales for just the northern Gulf of Maine and Bay of Fundy. Kenney et al. (1997) used those data in conjunction with CETAP

(1982) density estimates to suggest that a more likely range for minke whale abundance off the northeast U.S. was 10,000 to as many as 13,000 animals.

Minke whales are the smallest of the rorquals and did not have great commercial value until modern industrial whaling in the Southern Ocean decimated populations of the larger whales. Antarctic whalers started taking minke whales in the 1970s (Perrin and Brownell, 2002). In the North Atlantic, there is a long history of hunting for minke whales (reviews in Stewart and Leatherwood, 1985; Horwood, 1990; Reeves and Kenney, 2003). Small-scale minke whaling in Norway dates back to at least the Middle Ages, and modern whaling methods were first developed in Norway in the mid-19th Century. In the 20th Century, over 100,000 North Atlantic minke whales were killed by whalers, mostly Norwegians, on the high seas. Whalers from shore stations in Canada and West Greenland took about 1,000 and 8,000, respectively. Canada ceased whaling in 1972.

After the IWC moratorium began, Norway filed an objection and took 379 minke whales in 1986 and 375 in 1987 (Reeves and Kenney, 2003). In 1988–1992, catches ranged from 1 to 95 per year under a research permit. Norway resumed commercial minke whaling under objection in 1993, and presently takes several hundred each year. There is also an aboriginal subsistence hunt in Greenland that takes at least 150 minke whales per year. Iceland rejoined the IWC in 2002 and began taking small numbers of minke whales under a research permit beginning in 2003, with annual takes of 37, 25, 39, 60, and 39 through 2007. In October 2006, they announced the intention to resume small-scale commercial whaling and issued licenses to take 30 minke whales in 2007, but only 7 were taken. In 2008 they took 39 from a quota of 40.

Minke whales are occasionally entangled, with some killed and some released alive, in several east coast commercial fisheries, including the sink gillnet, pelagic driftnet, tuna purse seine, herring weir, and lobster trap fisheries, and there are occasional ship-strike mortalities. The average human-related mortality in 2001–2005 from the Canadian East Coast minke whale stock was estimated at 2.4 whales per year from entanglement and 0.4 per year from ship strikes (Waring et al., 2008).

Ecology and life history: Minke whales are typical baleen whales, most often seen as solitary individuals (Perrin and Brownell, 2002). The average group size sighted off the northeastern U.S. was 1.5 whales (CETAP, 1982). Large groups are occasionally observed, but those are

temporary aggregations in areas of rich food supplies, often associated with other species that feed on the same prey, including fin whales, humpback whales, Atlantic white-sided dolphins, and harbor porpoises (CETAP, 1982).

Minke whales feed on a wide variety of prey types, including copepods, krill, pteropods, squid, and many kinds of small and medium-sized fishes (reviewed in Horwood, 1990). In the northeastern North Atlantic, where stomach contents have been studied extensively, krill and herring are the principal prey, followed by several gadoids (including cod, haddock, and pollack), and capelin (Folkow et al., 2000). Off the northeastern U.S., primary prey species are most likely clupeids, gadoids, sand lance, and mackerel. Feeding is by the typical rorqual gulp-feeding mode (Nemoto, 1970; Pivorunas, 1979). Minke whales can probably be more flexible in their prey choices than the larger rorquals, since they require smaller prey schools to feed efficiently.

Minke whales mature at about 7 years of age and 7.2 m long in females and 6 years and 6.8 m for males (Stewart and Leatherwood, 1985; Horwood, 1990; Perrin and Brownell, 2002). Mating has not been observed, but the timing has been inferred from fetal development curves derived from whaling data. In the North Atlantic, mating occurs from October to March. The gestation period is 10–11 months, therefore births are concentrated in winter. Calves are born at about 2.4–2.7 m long, and are weaned in only 4–6 months. Pregnancy rates in adult females taking in commercial whaling range from about 85% up to nearly 100%, therefore most females in good condition give birth on an annual cycle.

General distribution: Common minke whales are broadly distributed in the Northern Hemisphere from the edge of the ice to the tropics (Stewart and Leatherwood, 1985; Horwood, 1990; Rice, 1998; Perrin and Brownell, 2002). The distribution of the dwarf minke (a sub-species) in the Southern Hemisphere is less well known, and is perhaps more coastal than Antarctic minkes (a separate species). In the western North Atlantic, minkes are common from Virginia north to the ice edge, and they occur as far south as the West Indies and Gulf of Mexico. In continental shelf waters off the northeast U.S. and eastern Canada, minke whales are abundant in spring and summer, less abundant but still common in fall, and largely absent in winter (CETAP, 1982). There are stranding records from the southeast U.S. Atlantic coast and Gulf of Mexico, as well as sightings and strandings from the West Indies and Caribbean, all of which are

concentrated mainly in the winter. This had led to the hypothesis that minke whales migrate offshore and south to wintering grounds in the West Indies and deep water south and east of Bermuda (Mitchell, 1991).

Historical occurrence: Cronan and Brooks (1968) reported five 19th Century minke whale records from Rhode Island, apparently from Allen (1916), but one is the whale injured by the ship propeller that was included above as a fin whale based on the species as recorded in the Smithsonian database. The others included: a 5.5–6.1-m whale killed near Point Judith on 15 May 1849, a 7.6-m whale killed (2 others were sighted) at the mouth of the Sakonnet River on 20 August 1867, a sighting off Newport in September 1887, and an 8.2-m whale killed near Fort Adams on 5 September 1889. Cronan and Brooks also reported a minke whale that drowned in a fish trap off Sakonnet Point on 11 June 1961 and a 4.6-m juvenile found in the Sakonnet River in July 1967.

The minke whale was included by De Kay (1842) as the "beaked rorqual (*Rorqualus rostratus*)", with "swimming paws white in the middle." He reported the capture of a 4.9–5.5-m animal in lower New York Bay in 1822 that was the basis for his description. Helmuth (1931) reported a specimen about 8 m long that was killed off Montauk Point and towed to shore on 16 August 1931. Connor (1971) knew of no additional New York records beyond those two, but said that minke whales were more frequent farther east in Rhode Island and Massachusetts. Allen (1916) said that, despite few previously published records, minke whales were common in New England, but Waters and Rivard (1962) erroneously concluded that they were rare. They knew only of a 6-m male that was caught in a fish trap off Barnstable and released alive, and the 1961 Rhode Island record.

Recent occurrence: Minke whales occur in the Rhode Island study area in all four seasons (Fig. 16). The largest proportion of records is in summer (74.6%) and spring (19.6%), however that is clearly biased by the large number of sightings from the whale-watching boats. Without the dense concentration of sightings between Block Island and Montauk Point in spring and summer, minke whales are still strongly seasonal—most widespread in the region during the spring (48.8%) and summer (41.7%), and relatively rare in the fall (7.1%) and winter (2.4%). Without the aggregation of records from the whale-watching boats, minke whales are distributed across the shelf from nearshore to the slope.

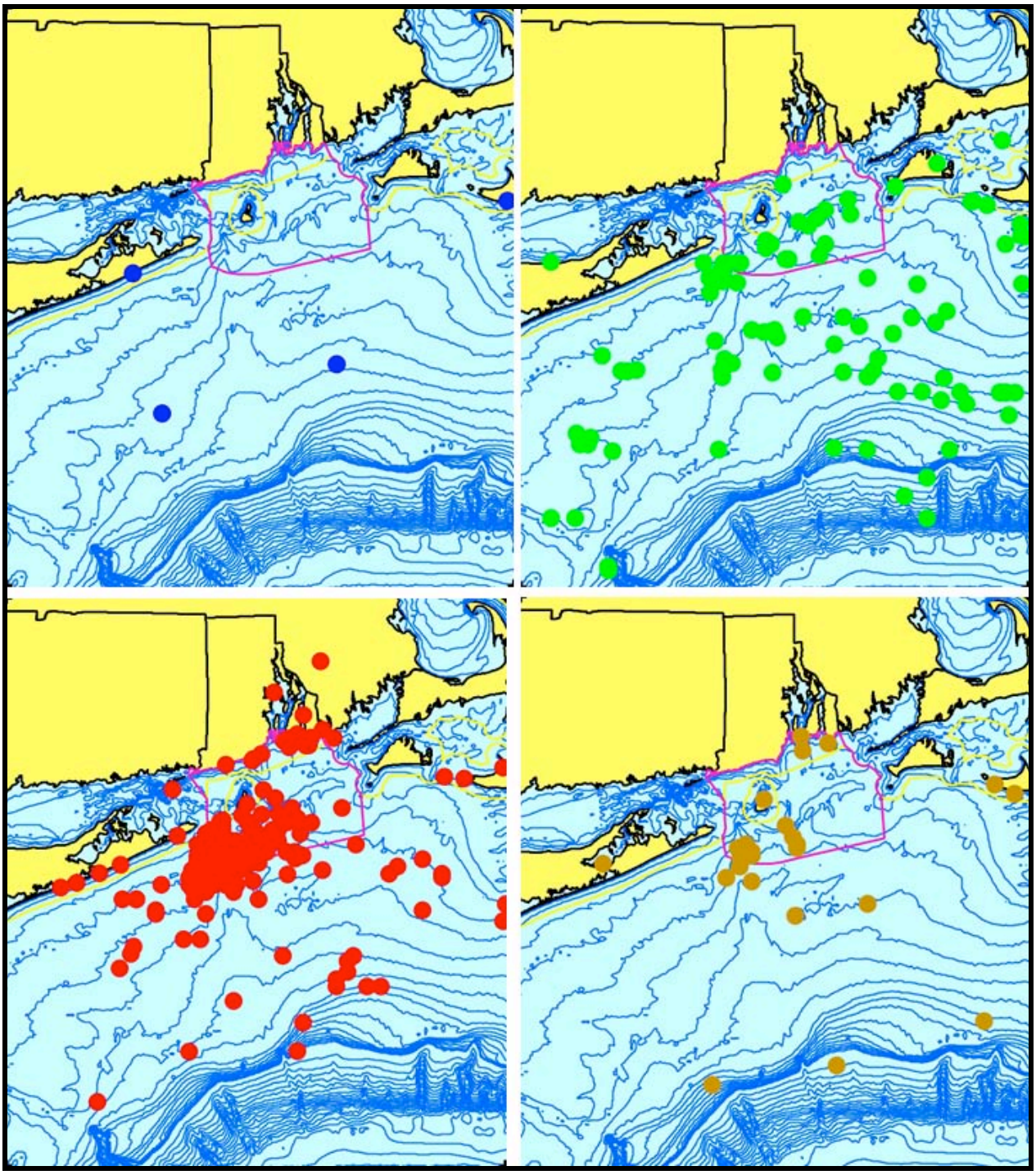

Figure 16. Aggregated sighting, stranding, and bycatch records of common minke whales in the Rhode Island study area, 1849–2008 (n = 504: winter = 4, spring = 99, summer = 376, fall = 25).

The effort-corrected relative abundance patterns of common minke whales (Fig. 17) show the same concentration in the Great South Channel east of Cape Cod and Nantucket as there was for humpback whales and fin whales (Figs. 6 & 10). Great South Channel minke whale abundance was highest in summer, followed in decreasing order by spring, fall, and winter. Kenney and Winn (1986) showed that the area in question was the most intensively utilized cetacean habitat off the northeastern U.S., primarily because of large stocks of sand lance. In the spring, there was also an area of high minke whale abundance on the outer shelf south of Nantucket, which extended west at lower levels as far as Montauk. Within the SAMP area, there is a widespread area of low minke abundance in spring, and another in summer that is only in the southwestern quadrant. There is also an area of moderate minke whale abundance on the outer shelf south of the SAMP area in summer.

Minke whales are the most commonly stranded baleen whale in the Rhode Island study area in recent decades, just nosing out fin whales with 29 strandings since 1970 (Table 2). There were 18 minke whale strandings in Rhode Island between 1976 and 2003: 31 July 1976—drowned in a fish trap off Sakonnet Point; 30 August 1981—stranded on First Beach, Newport, with possible rope marks; 26 November 1987—stranded on Mansion Beach, Block Island; 20 September 1988—stranded on Sakonnet Point; 5 July 1989—drowned in a fish trap off Point Judith; 18 August 1989—stranded in Newport; 19 July 1990—stranded in Newport, missing the tail but badly decomposed; 6 July 1991—stranded on Crescent Beach, Block Island, scavenged by sharks; 1 July 1992—stranded in Little Compton; 18 June 1995—stranded on Second Beach, Middletown; 10 July 1997—stranded in Little Compton; 3 July 1999—stranded in Tiverton; 2 August 1999—stranded in Jerusalem; 16 July 2000—stranded on East Beach, Charlestown; 30 July 2001—stranded at Black Point, Narragansett; 17 August 2001—stranded on Second Beach, Middletown; 12 August 2002—stranded near First Beach, Middletown; 22 June 2003—stranded near the Cliff Walk, Newport. There is a clearly obvious seasonality to the Rhode Island strandings, with two in June, nine in July, five in August, and one each in September and November. It is likely that many of the stranded minkes are recently weaned young of the year; their timing corresponds well with winter calving and a 4–6 month weaning time.

An interesting nearby minke whale occurrence was in Massachusetts in July 1994 (which at first glance looks like a mapping error in Fig. 16). A 405-cm female minke whale was seen in the

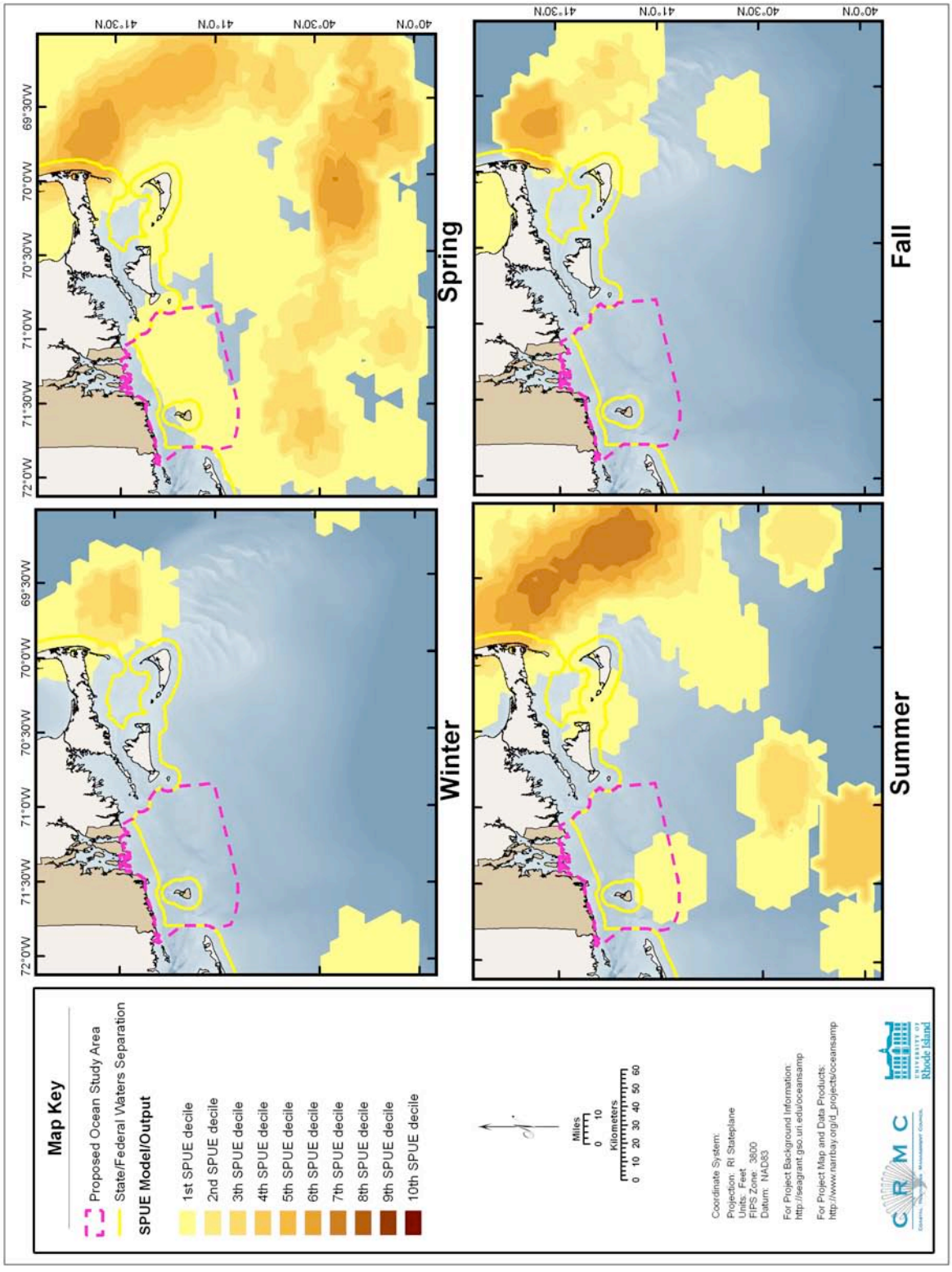

Figure 17. Modeled seasonal relative abundance patterns of common minke whales in the Rhode Island study area, corrected for uneven survey effort.

Taunton River in Dighton on the 23rd, about 13 km upstream from where the river empties into Mount Hope Bay at Fall River. The animal stranded in a marsh and was pushed off. It was found floating dead in the river two days later.

Five-year stranding frequencies in the Rhode Island study area (Fig. 18) show absence from 1966 to 1975, only one stranding in 1976–1980, then higher and relatively consistent strandings

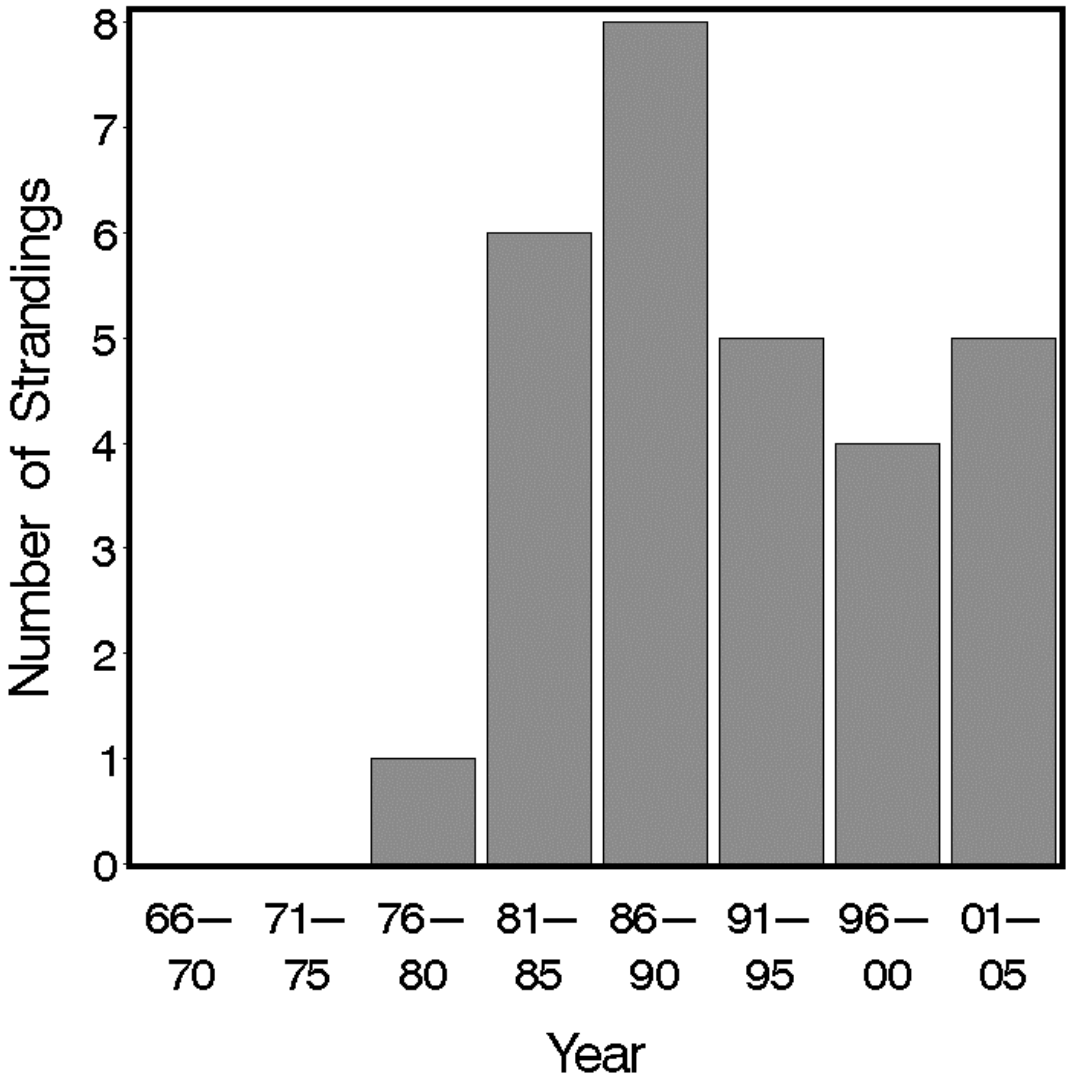

Figure 18. Five-year stranding frequencies for common minke whales in the Rhode Island study area, 1966–2005.

from 1981 to 2005. It is not known whether this pattern was caused by a lack of attention to minke whale strandings prior to the mid-1980s or a real increase in frequency afterwards.

Conclusions: The relative abundance models predict that common minke whales can be expected in the SAMP area in spring and summer, but not in fall or winter. There are some sighting records within the SAMP area in fall, but they were not during surveys, and the absence of minke whales in that season in the SPUE data is probably related to a combination of low abundance and low survey effort. Minke whales are not listed under the ESA, and should be considered a mid-level conservation priority relative to the SAMP.

3.2.8. Gray Whale *Eschrichtius robustus* (Lilljeborg, 1861)

Description: A gray whale is more robust in form than any of the *Balaenoptera* spp., but less so than a humpback (Wolman, 1985; Jefferson et al., 1993). Calves are born at 4.6–5 m, and adults reach 11–15 m. The head is relatively short, with a moderately curved and tapered rostrum. There is no dorsal fin; there is low hump followed by a series of "knuckles"—similar to the form in the sperm whale. There are 2–5 short, deep creases on the ventral surface in the throat region. The flippers are relatively broad and tapered to points, containing only four digits as in the rorquals. The color of the body is gray to brownish gray, lighter in adults and darker in calves, with extensive irregular mottling and patches of barnacles and whale lice. There are 130–180 short, yellowish baleen plates on each side of the mouth, with very coarse fringes.

Status: Gray whales were extirpated in the North Atlantic in early historical times, by the late 17th or 18th Century (Mead and Mitchell, 1984; Lindquist, 2000; Jones and Swartz, 2002), apparently persisting long enough to have been hunted by early whalers on both sides of the basin. The youngest specimen from the eastern North Atlantic dates to 1655 ± 260 years (Bryant, 1995). If, in fact, whaling were the cause of their disappearance, North Atlantic gray whales would be the only whale population hunted to extinction by commercial whaling.

Ecology and life history: Gray whales are primarily benthic feeders, specializing on ampeliscid amphipods, which live in mats of tubes in the sediment (Nemoto, 1970; Johnson and Nelson, 1984; Nerini, 1984; Kvitek and Oliver, 1986; Nelson and Johnson, 1987). A foraging gray whale swims to the bottom; rolls onto its side; sucks up a mouthful of sediment, water,

amphipods, and their tubes; then forces a cloud of muddy water back out through the baleen filter. Gray whales can also feed on prey up in the water column, including krill, small schooling fishes, and squid, with a total of over 80 prey species recorded (Jones and Swartz, 2002).

General distribution: Gray whales occurred only in the Northern Hemisphere, and today survive in two separate populations on the eastern (the "California" stock) and western (the "Korean" stock) sides of the North Pacific (Wolman, 1985; Swartz, 1986; Jones and Swartz, 2002; Reeves and Kenney, 2003). Extant gray whales have a primarily coastal distribution, so it seems reasonable to presume that North Atlantic gray whales were similarly coastal animals. Gray whales undertake some of the longest migrations known for any mammal. Very little is known of the distribution and migration of the former North Atlantic population. Subfossil remains have been found at scattered sites in northern Europe and along the east coast of the U.S. (Jones and Swartz, 2002). Mead and Mitchell (1984) speculated that early American colonial reports of whales using Delaware Bay as a calving ground, generally presumed to have been right whales, may have actually represented North Atlantic gray whales.

Historical occurrence: The Smithsonian dataset includes one record of a gray whale bone from the Rhode Island study area—a mandible carbon-dated to the very early 18th Century (± 35 years) found in Southampton, New York in 1977 (Mead and Mitchell, 1984). There is a second record from New Jersey—a mandible dated to the 16th Century found in Tom's River in 1855. Interestingly, Block Island Sound is known to have dense populations of ampeliscid amphipods (Steimle, 1982), and one might speculate that it was historically a gray whale feeding ground.

Conclusions: North Atlantic gray whales are extinct, therefore they pose no conservation issues relative to the Rhode Island Ocean SAMP.

3.2.9. *Physeter macrocephalus* Linnaeus 1758: Sperm Whale

Odontoceti includes a variety of species known as whales, dolphins, and porpoises. They are characterized by having teeth in one or both jaws (although in some species teeth only erupt in adult males) and a single blowhole (Hooker, 2002). They use echolocation for navigation and foraging, producing mid- to high-frequency sounds and listening to the echoes. Many of the unique characters of the skull, lower jaw, and facial region of odontocetes are related to

echolocation (Au, 2002). Odontocete species vary widely with respect to sexual dimorphism—some species are strongly dimorphic with males much larger than females, while others are slightly dimorphic, slightly reverse dimorphic (i.e., females larger), or monomorphic. Most odontocete species are highly social, living in more or less permanent groups of closely related individuals (Tyack, 1986). Twenty-four odontocete species in six families have been recorded from the waters or beaches of Rhode Island and adjacent areas, five other species are hypothetical (Table 1).

A number of authors consider the living sperm whale (*Physeter*) and two species of *Kogia* to be in the same family, but in separate subfamilies (e.g., Mead and Brownell, 2005). Fordyce and Barnes (1994) and Rice (1998) maintained Physeteridae and Kogiidae as two separate but closely related families. Characters shared by both families include (Nowak, 1999): a skull with a broad, flat rostrum and a large concavity in the facial region; a spermaceti organ in the forehead; and a narrow lower jaw that is significantly shorter than the rostrum. Sperm whales differ from pygmy and dwarf sperm whales in several characters (Caldwell and Caldwell, 1989; Rice, 1989; Nowak, 1999; McAlpine, 2002; Whitehead, 2002). Physeterids are much larger than kogiids (although there is a 5-m fossil physeterid: Mchedlidze, 2002). The head in *Physeter* is also much larger, comprising a quarter to a third of total body length, compared with only an eighth to a sixth in *Kogia*. Among other skull characters, *Kogia* has the shortest rostrum of any odontocete at less than half of the total skull length, while the rostrum of a sperm whale makes up two-thirds to three-quarters of the total length of the skull. Finally, the blowhole of a sperm whale is S-shaped and located on the left anterior corner of the head, while *Kogia* has a C-shaped blowhole on top of the head and slightly left of center.

Sperm whales are the only odontocetes large enough to be included with the baleen whales among the so-called "great whales." They were the basis of Yankee whaling in the 18th and 19th Centuries, as memorialized in Melville's classic *Moby Dick*.

Description: Sperm whales are the largest of the toothed whales and the most sexually dimorphic of all cetaceans (Rice, 1989; Jefferson et al., 1993; Wynne and Schwartz, 1999; Whitehead, 2002; Reeves and Read, 2003). Adult males may reach 18.3 m in length, and Tomilin (1967) reported males from the North Pacific of 19 or 20 m, while the maximum size for adult females is only 12.5 m. More typical adult sizes are 12–16 m in males and 8.5–11 m in

females. The head is large and squarish, comprising up to a third of the body length, with a very narrow, underslung lower jaw. The body color is from medium to dark gray-brown, often with light areas on the belly and around the mouth. The skin on the head is smooth, but forms longitudinal wrinkles or corrugations on the rest of the body. The flippers are relatively short, rounded, paddle-like, and set relatively high on the body so they do not project down below the belly when viewed from the side. The dorsal fin is low, blunt, and triangular—so low that some sources say that a dorsal fin is absent (e.g., Leatherwood et al., 1976; Nowak, 1999). There are distinct "knuckles" on the ridge between the dorsal fin and the tail. The trailing edge of the flukes is generally very straight across with a deep notch in the center, although they may become damaged and irregular in older animals.

Status: Sperm whales are listed as Endangered under the U.S. Endangered Species Act, are not included on the Rhode Island state list, and are classified as Vulnerable on the IUCN Red List, although the analysis concluded that a Near Threatened classification was almost as well-supported. There are statistically reliable estimates of abundance of sperm whales only for rather limited portions of their entire range, and a wide variety of extrapolations to global populations. Rice (1989) summarized the extrapolated estimates available at that time as 190,000 in the North Atlantic, 930,000 in the North Pacific, and 780,000 in the Southern Ocean. The worldwide total of 1.9 million represents a reduction from a pre-whaling population of 2.8–3 million. Whitehead's (2002) range of estimates for current stocks is substantially lower at 200,000 to 1.5 million, and stocks in some areas like the eastern South Pacific appear to be still severely impacted by past whaling. The most recent abundance estimate for sperm whales off the east coast of the U.S. from Florida to Maine is 4,804, with an additional 1,665 in the Gulf of Mexico (Waring et al., 2008). Those estimates are minimum values because they are not adjusted for whales missed due to diving.

Hundreds of thousands of sperm whales have been killed worldwide since the beginning of Yankee whaling in the early 18th Century. The total take in 1800–1910 was over 700,000, with an additional 600,000 or more killed since 1910 (Reeves and Read, 2003). Commercial hunting of sperm whales ended worldwide with the IWC moratorium in 1986. There is presently no hunting at all for any purpose in the North Atlantic, and a few are taken each year in the North Pacific under scientific research permits by the Japanese.

Sperm whales are occasionally entangled in fishing gear off the east coast of the U.S. or struck and killed by ships, but the level of mortality is not believed to be biologically significant (Waring et al., 2008). Sperm whales feed relatively high on the food chain and could potentially accumulate high levels of toxic contaminants, however they appear to have lower levels than odontocetes from more coastal waters (Whitehead, 2002). There is also concern that sperm whales could be subject to negative impacts from increasing levels of noise in the oceans, from sources including shipping, naval sonar, and seismic exploration for oil and gas (Reeves and Read, 2003).

Ecology and life history: Like most odontocetes, sperm whales are very social and live in permanent matrilineal groups (Caldwell et al., 1966; Best, 1979; Rice, 1989; Whitehead et al., 1991; Christal et al., 1998; Whitehead and Weilgart, 2000; Whitehead, 2002; Reeves and Read, 2003). Off the northeastern U.S., the average number of animals at a sighting was 3 (CETAP, 1982), and group sizes ranged as high as 100 whales. More than half of all sightings were solitary individuals, and typical group sizes were 2–10 whales. The basic unit of sperm whale social organization is the "mixed school" consisting of females of all ages and immature males (Best, 1979). Mixed schools are predominantly female, 70% or more. Adult females in the school are closely related, and the calves and immatures of both sexes are their offspring. Females in the mixed schools remain associated for their entire lives. Males leave the mixed schools as early as ages 4–5 and completely by age 15, forming bachelor schools. Whalers measured the size of a whale based on the oil yield. A New Bedford whaling captain quoted by Best (1979) indicated that the largest adult females or bulls in mixed schools yielded 35 barrels of oil. Bachelor bulls were caught in schools of same-sized animals, which decreased in number as the whales got larger. The largest bachelor schools were the 40-barrel bulls, and the next largest the 50-barrel bulls. Schools of 60-barrel bulls were generally 8–10 whales, 70-barrel bulls were in schools of 4–5 whales, and larger bulls were solitary or in pairs or trios. The whalers believed that mixed schools were "harems" controlled by a dominant bull, but mature males actually rove between mixed schools (Whitehead and Weilgart, 2000).

Sperm whales tend to remain relatively motionless at the surface or to swim ahead slowly during surface sequences, often tightly grouped. Surface sequences are generally much longer than in baleen whales, usually about 8–10 minutes but sometimes 15–60 minutes. Yankee whalers believed that a sperm whale needed to blow once for each minute spent submerged during the

previous dive. Sperm whales are positively buoyant, and raise the flukes above the surface on the final dive in a surfacing sequence (Kenney and Winn, 1987b). Sperm whales are known to breach on rare occasions.

Sperm whales are prodigious divers (Watkins et al., 1985, 1993, 1999, 2002; Papastavrou et al., 1989; Rice, 1989; Whitehead, 2002; Amano and Yoshioka, 2003; Reeves and Read, 2003; Watwood et al., 2006). Dives are typically 30–40 minutes, but dives lasting an hour or more are relatively common, and Watkins et al. (1985) recorded one dive of 2 hours and 18 minutes. Dive depths depend on the depth of the water, as they are capable of diving to the bottom. Average dives are to about 400 m, but dives deeper than 2000 m are known. Descents and ascents may be nearly vertical. Watkins et al. (1999) tracked three sperm whales in the Caribbean using radio tags. Whales made relatively short surfacings of 7–10.5 minutes, both day and night, for respiration between long dives and for extended periods of rest and socializing during the day. They spent about 27% of their time surfaced during daylight and 15–17% during the night. Watkins et al. (2002) tracked a tagged 12-m sperm whale in the Caribbean for 4.6 days in April–May 1995. During that time it traveled 295 km and made 158 dives longer than 3 minutes. There were 65 relatively shallow dives (< 200 m) and 93 deeper dives that averaged 990 m (range = 420–1330) and 44.4 min (18.2–65.3). The whale spent 23% of its time at or near the surface, 23% in shallow dives, and 54% in deep dives.

An important characteristic that separates mysticetes and odontocetes is the use of echolocation ("sonar") for foraging (Tyack, 1986, 1999; Au, 2002). Probably all cetaceans use sound for communication, but only odontocetes are known to echolocate. Echolocation involves the production of short-duration, high-amplitude, broadband pulses ("clicks") and listening for echoes returning from objects in the environment. Clicks are produced in the nasal complex of air sacs and associated structures in the facial region and focused into a relatively narrow beam by the melon or spermaceti organ, and the echoes are received at the posterior portion of the mandibles (Norris, 1968, Norris and Harvey, 1974; Cranford et al., 1996; Møhl et al., 1999; Cranford, 2000; Au, 2002; Frankel, 2002). Click duration, frequency range, bandwidth, repetition rate, and amplitude vary among species. Many odontocetes, but not all, also produce tonal sounds ("whistles," etc.) that are used for communication but have no role in echolocation. Sperm whales do not whistle, but use clicks for both echolocation and communication (Rice, 1989; Whitehead, 2002; Reeves and Read, 2003). Diving sperm whales click regularly once or

twice per second as they search for prey. The whales in the school can certainly hear each other as they spread out during foraging dives, and they may be using clicks at the same time as contact calls. There are occasionally accelerating series of clicks ("creaks" or "buzzes") as a whale homes in on a prey item (Miller et al., 2004; Watwood et al., 2006). Socially interacting whales also produced patterned sequences of 3 to about 20 clicks called "codas" (Watkins and Schevill, 1977). Codas vary by region and between schools and are probably passed on culturally within matrilineal groups. There are also very loud and slow (6–8 seconds apart) clicks called "clangs" that appear to be produced by large males; their function is not clear.

The primary prey of sperm whales is squid (Rice, 1989; Whitehead, 2002; Reeves and Read, 2003). Many species of mesopelagic and demersal squid are consumed, including very large ones up to the size of giant squid. The majority of the diet consists of medium-sized squids with mantle lengths of 20 cm to 1 m. Males feed on larger prey than do females and juveniles. Medium to large demersal fishes, including rays, sharks, and a variety of bony fishes, comprise small portions of the diet in most regions, but may be the predominant prey in certain areas, especially in high latitudes where only male sperm whales tend to occur. Other prey items include benthic octopus, crabs, and other crustaceans. Sperm whales consume a wider variety of squid than do northern bottlenose whales or Cuvier's beaked whales, which correlates with range of movements within each species (Whitehead et al., 2003).

Feeding occurs at depth, apparently all the way to the bottom at times, since stomach contents sometime include stones, sediment, shells, and other non-food items from the sea floor. Feeding behavior has not been observed and can only be inferred or hypothesized (reviewed in Rice, 1989). Suction feeding is probably used. There are paired, expansible throat grooves that would allow rapid expansion of the buccal cavity. The teeth are apparently not necessary for feeding—stomachs often contain completely intact and unmarked prey items, and juveniles with no erupted teeth and adults with badly injured and useless lower jaws are able to feed effectively. Sperm whales may simply scan for prey using echolocation. An alternative suggestion is that the whale hangs motionless at depth with the mouth wide open, waiting for prey to be attracted to the white lips or the luminescent squid mucus on the jaw and teeth. The so-called "big bang" hypothesis is that a sperm whale (or smaller odontocete) can produce clicks of high enough intensity to stun prey items. Fristrup and Harbison (2002) suggested that sperm whale simply may use vision in feeding, either by searching upward for prey silhouetted against the brighter

background or by searching for bioluminescence produced by prey species directly or indirectly by swimming through other bioluminescent organisms.

Sperm whales are at the extreme end of the mysticete-odontocete dichotomy in life histories (Caldwell et al., 1966; Best, 1974, 1979; Rice, 1989; Whitehead et al., 1991; Whitehead and Weilgart, 2000; Whitehead, 2002; Reeves and Read, 2003). Single calves are born at 4 m long following a 14–18-month gestation. In the Northern Hemisphere, mating occurs from December to August with a peak in March–May. Large mature bulls rove from one mixed school to the next. Adult females in a mixed school tend to come into estrus synchronously, and a bull's stay with a particular school might only be a few hours. Calves nurse for at least two years, but begin feeding on solid food at about a year old. Some calves may continue nursing much longer, past age 7 in females and 13 in males. Females reach sexual maturity at age 7–13 and at about 9 m long. Growth then slows until they reach maximum size at about age 30. Maturation in males is a prolonged process, beginning at about age 10 and lasting for 10 years. They continue to grow at a more rapid rate than females, and do not reach their full size and complete physical maturity until about age 50. Males generally do not begin breeding successfully until their late twenties. The interval between calves for prime-age females is about 5 years.

General distribution: Sperm whales are found from tropical to subpolar waters in all oceans of the world (Rice, 1989, 1998; Whitehead, 2002; Reeves and Read, 2003). In the western North Atlantic, they occur from the edge of the pack ice south to the Gulf of Mexico and Caribbean. Mature males penetrate farther into high-latitude waters than females or immatures (Best, 1974; 1979). The northern distributional limit of female/immature schools in the western North Atlantic is probably around Georges Bank and the Nova Scotian shelf (CETAP, 1982; Whitehead et al., 1992). Sperm whales are very wide-ranging and migratory, and it is likely that all sperm whales in the North Atlantic belong to a single population (Reeves and Whitehead, 1997; Dufault et al., 1999). A whale tagged off Nova Scotia in 1966 was captured off Spain in 1973 (Mitchell, 1975c). Even on a global scale, sperm whales show very low genetic variability (Lyrholm and Gyllensten, 1998; Lyrholm et al., 1999).

Most sperm whale sightings around the world are in waters deeper than 200 m, however significant numbers of sightings have occurred in shallow continental shelf waters south of New England and on the Nova Scotian shelf (CETAP, 1982; Whitehead et al., 1992; Scott and

Sadove, 1997). Most sightings have been along the shelf break and the edge of the Gulf Stream, but there has been little or no survey effort farther seaward, and sperm whales can probably occur almost anywhere in the deep ocean.

Sperm whales occur year-round off the northeastern U.S., but with some seasonal variability (CETAP, 1982). They occur in highest numbers in spring and summer all the way from Cape Hatteras to Nova Scotia. In fall there are fewer whales, and the distribution contracts south and west of Georges Bank. The smallest numbers of sperm whales are in winter, and the sightings tend to be aggregated east of Cape Hatteras. There are few sightings south of Cape Hatteras, but that is more likely a result of little survey effort except relatively near shore (Waring et al., 2008). There are scattered strandings from North Carolina to Florida, and a few recent sightings far offshore south of Cape Hatteras. However the area east of South Carolina was very well known to the Yankee whalers (the "Charleston Grounds"). Sperm whales were taken there year-round, a few nearshore but very large numbers offshore (Townsend, 1935).

Historical occurrence: Given that sperm whales are primarily offshore animals and rarely seen near shore, the historical record is dominated by whaling takes. Cronan and Brooks (1968) reported only one stranding in Rhode Island, a 4.4-m animal (i.e., a calf) in Charlestown on 20 February 1967 (which is rumored to be buried somewhere on the URI Bay Campus). They added that sperm whales had "also been found within a few miles of Rhode Island with records from Stonington, Connecticut, and New Bedford and Nantucket, Massachusetts." This seems to be a common issue in the literature—interpreting earlier reports of whaling captures as having been killed at the reported location rather than having been landed there—although it is not clear whether Cronan and Brooks did the misinterpreting or simply repeated it from someone else. For example, Linsley (1842) listed sperm whales for Stonington, by which he surely meant landed at Stonington but taken somewhere more offshore, however Goodwin (1935) seemed to interpret it otherwise: "The sperm whale was recorded by Linsley (1842) at Stonington, Conn." Goodwin seems to have been a primary source for Cronan and Brooks, as well as for Waters and Rivard (1962), who said that the sperm whales had occurred "from the Gulf of Maine to Long Island Sound." Note also that Stonington, New Bedford, and Nantucket were all major whaling ports.

Sperm whales were probably rarely, if ever, taken or even seen by the shore-based Long Island right whalers. The tale, likely apocryphal, is that Yankee sperm whaling began in about

1712, when Capt. Christopher Hussey, while hunting right whales from Nantucket, was blown offshore in a storm and took the first sperm whale. The sperm whale fishery expanded greatly, with voyages from a number of southern New England ports including Sag Harbor, Long Island; New London and Stonington, Connecticut; several localities in Rhode Island; and Nantucket, Woods Hole, and New Bedford, Massachusetts (Starbuck, 1878; Clark, 1887).

De Kay (1842) claimed that sperm whales were formerly abundant near Long Island, but provided very little specific information. Connor (1971) gave the oldest New York record as a 12-m whale captured in Fishers Island Sound in December 1894, and knew of a stranding on Fire Island in February 1918. There was one earlier stranding from Long Island, a 4.8-m animal at East Hampton on 19 March 1891, extracted for the Smithsonian dataset from an account published in the *East Hampton Star*. Waters and Rivard (1962) tabulated two strandings, one at West Yarmouth on 15 June 1954 and one at Nantucket in September 1961.

Recent occurrence: The distribution of sperm whales in the Rhode Island study area is concentrated along the edge of the shelf, with 57.3% of the records in the summer, 18.5% in fall, 16.5% in spring, and 7.8% in winter (Fig. 19). Southern New England is one of the rare locations in the world where sperm whales occur frequently well inshore of the shelf break (CETAP, 1982; Scott and Sadove, 1997). Sightings on the shelf in waters shallower than 200 m occurred in all four seasons, including seven sightings in summer, three in spring, and one in fall from the whale-watching boats. Many of them are aggregated in a relatively narrow band extending north-south along the shelf valley offshore of Montauk Point and Block Island. It is often speculated that sperm whale occurrence in shelf waters corresponds with inshore movements of spawning squid.

The effort-corrected relative abundance patterns show that sperm whales are generally not predicted to occur in the SAMP area (Fig. 20). Only in summer does one area of low abundance slightly intersect the SAMP area. Sperm whales are predicted to be present in all four seasons, but scattered and in low abundance. All of the high-abundance areas are offshore and beyond the boundaries mapped in Figure 20. The area of sperm whale occurrence in shallow water over the shelf valley between Block Island/Montauk and Block Canyon does not show up in the relative abundance outputs. This suggests that the phenomenon is sufficiently rare that it takes intensive searching, like repeated trips by whale-watching boats, to detect it.

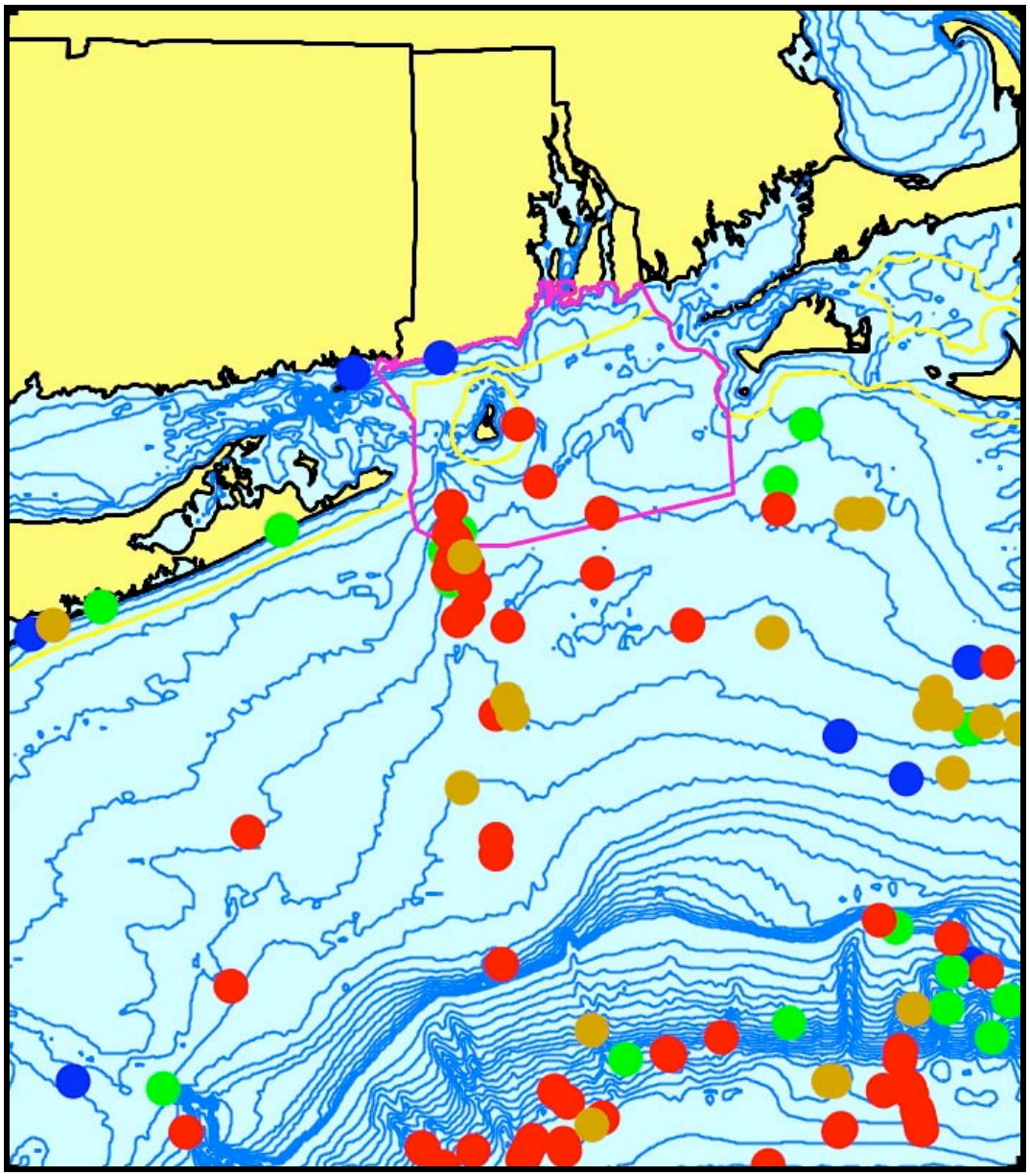

Figure 19. Aggregated sighting, stranding, and bycatch records of sperm whales in the Rhode Island study area, 1891–2004 (n = 103: winter = 8, spring = 17, summer = 59, fall = 19).

There have been no sperm whale strandings in Rhode Island since 1967. There have been occasional strandings in both Massachusetts and Long Island. The most publicized Long Island sperm whale stranding was in April 1981. On the 15th, a live, 732-cm, juvenile male sperm whale stranded at Coney Island and was pushed off the beach. The following day, it stranded again about 55 km east at Oak Beach near Fire Island Inlet. It was towed to a boat basin at a state

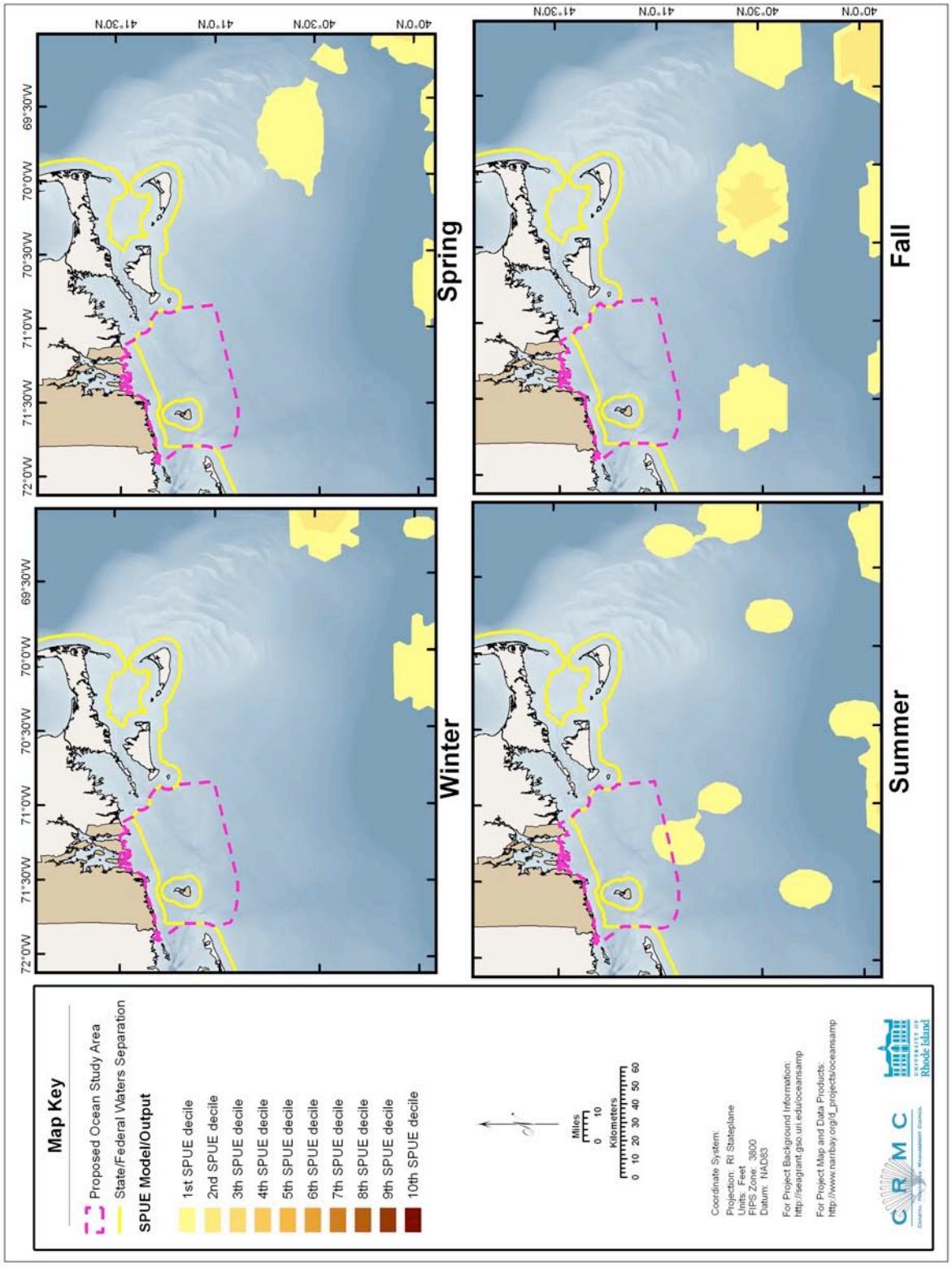

Figure 20. Modeled seasonal relative abundance patterns of sperm whales in the Rhode Island study area, corrected for uneven survey effort.

park 2–3 km away, where it was diagnosed with pneumonia and nick-named "Physty." Eventually, divers coaxed him into eating squid, so he could be treated for the pneumonia by being fed squid containing antibiotic tablets. On 25 April the whale was herded by small boats out of the boat basin and through the inlet back into the Atlantic.

Conclusions: Sperm whales are primarily offshore animals, and are not predicted to occur within the SAMP area. However, they are known to regularly enter shallower waters over the shelf south of New England. They may occur within the southwestern quadrant of the SAMP area, most likely during the summer. Sperm whales are listed as Endangered under the ESA. Because they are toothed whales, they are highly dependent on sound for navigation, foraging, and communication. Planning for any development activities in the SAMP area, particularly activities that produce loud sounds, must consider the possible presence of sperm whales.

3.2.10. Pygmy Sperm Whale *Kogia breviceps* (Blainville, 1838)
Dwarf Sperm Whale *Kogia sima* (Owen, 1866)

The two *Kogia* species are rarely seen except as strandings, and are difficult to distinguish at sea or even with intact specimens on the beach. Many mammalogists considered them to be conspecific as late as the mid-20th Century (see Rice, 1998 for a review); identifications of stranded specimens before that time (and even since then) may be questionable. The two species are often pooled in reporting and analyses. They are considered together here for those reasons.

Description: Pygmy and dwarf sperm whales are very similar in appearance and nearly identical in body form (Caldwell and Caldwell, 1989; Jefferson et al., 1993; Wynne and Schwartz, 1999; McAlpine, 2002). Pygmy sperm whales are larger at 3–3.7 m in adult length. They are dark gray in color with a lighter belly and a pale, crescent-shaped mark between the eye and flipper that resembles the gill opening of a fish. The head is square or conical, broad, and blunt, often appearing shark-like, with a tiny underslung lower jaw. The single C-shaped blowhole is located on top of the head, but offset slightly left of center. The flippers are short, rounded, and placed very close to the head. The dorsal fin is very small and falcate, placed well behind the midpoint of the body, and rises off the back at a relatively low angle. The head is slightly longer and more rounded than in the dwarf species.

Dwarf sperm whales are smaller at 2.1–2.7 m. The dorsal fin is relatively tall, pointed, dolphin-like, falcate, placed about in the middle of the animal, and rises off the back at a relatively steep angle. The head is slightly shorter and more pointed than in the pygmy sperm whale, and they have a pair of inconspicuous throat creases.

Status: The pygmy sperm whale is not listed under the U.S. Endangered Species Act, is not included on the Rhode Island state list, and is classified as Data Deficient on the IUCN Red List. Dwarf sperm whales are not listed under the U.S. Endangered Species Act, are not included on the Rhode Island state list, and are classified as Data Deficient on the IUCN Red List. There are no estimates of the populations worldwide of either *Kogia* species, but both may be relatively common. In the NMFS SAR (Waring et al., 2008) abundance is estimated for both species combined because of the identification difficulty. Off the east coast of the U.S. and Canada, the abundance of *Kogia* spp. was estimated as 695 in 1998 (Florida to the Gulf of St. Lawrence) and 395 in 2004 (Florida to the Bay of Fundy); the estimates of the Gulf of Mexico were 742 in 1996–2001 and 453 in 2003–2004 (the differences are not statistically significant).

There is no significant hunting of pygmy or dwarf sperm whales beyond very small numbers taken in traditional fisheries in the Caribbean, Sri Lanka, Japan, and Indonesia (Caldwell and Caldwell, 1989). Fisheries-related mortalities of both species have been documented in U.S. Atlantic waters. One *K. breviceps* was released alive but seriously injured in the pelagic longline (swordfish) fishery off Florida in 2000. Stranded animals are sometimes recorded with evidence of entanglement in fishing gear, propeller marks, or with plastic in their stomachs (though not necessarily determined as the cause of death). One *K. sima* was killed in the pelagic swordfish driftnet fishery in 1995 (Waring et al., 2008).

Ecology and life history: Pygmy and dwarf sperm whales are very poorly known, with most information coming from stranded animals (Nagorsen, 1985; Caldwell and Caldwell, 1989; McAlpine, 2002). Most strandings are single individuals, or occasionally mother-calf pairs. Sightings at sea may be small groups, up to about 6 animals. They seem to spend long periods relatively motionless at the surface. Diving animals tend to sink without rolling forward, and both are believed to be capable of deep and long dives. Both species exhibit a unique response to being startled—defecating a dark reddish-brown liquid into the water, producing a dense cloud in the water that might screen an animal from a predator or other danger as it dives away. Both

species have an expanded, balloon-like section of the lower intestine that is filled with up to 12 liters of liquid described by Caldwell and Caldwell (1989) as having the color and consistency of chocolate syrup.

Stomach contents of stranded pygmy and dwarf sperm whales are dominated by squid of a wide variety of species, sometimes with small amounts of fish or crustaceans (Nagorsen, 1985; Caldwell and Caldwell, 1989; McAlpine, 2002). Their anatomy (small jaw, reduced teeth, well-developed hyoid apparatus) also predicts a diet based on suction-feeding upon cephalopods. Most feeding appears to be at or near the bottom. Santos et al. (2006) analyzed stomach contents of 14 *K. breviceps* stranded in 1984–2002 in Europe (5 in Spain, 7 in France, and 2 in Scotland. Thirteen stomachs had almost entirely squid with some small amounts of crustaceans and fish, and one animal contained mainly crabs.

Little is known about reproduction, with nearly all information coming from strandings (Caldwell and Caldwell, 1989; McAlpine, 2002). Dwarf sperm whale calves appear to be born in spring at 1–1.2 m long. Gestation may be as short as 9 to as long as 11 months, and lactation lasts about a year. Females reach sexual maturity at about 2.7 m. Males probably attain maturity at similar sizes. Female pygmy sperm whales have been recorded that were simultaneously pregnant and lactating, indicating that a reproductive cycle with calving every year is possible. Female dwarf sperm whales reach sexual maturity at about 2.1 m, and newborn calves are under 1 m in length.

In addition to the usual range of diseases and parasites seen in stranded cetaceans, stranded adults in both species of *Kogia* frequently present with cardiomyopathy and other symptoms associated with heart failure (Bossart et al., 1985). The hearts in those animals are characterized grossly by pale, flabby ventricular muscle and by lesions that can be detected by detailed histopathology. The underlying cause is not known.

General distribution: Both pygmy and dwarf sperm whales are apparently broadly distributed in warm temperate, subtropical, and tropical waters around world (Caldwell and Caldwell, 1989; Rice, 1998; McAlpine, 2002). In the western North Atlantic, their distributions are entirely in deeper water offshore of the continental shelf edge. There was only one sighting of a single *Kogia* sp. off the northeastern U.S. during the CETAP surveys in 1979–1981, east of Delaware Bay in continental slope waters deeper than 2500 m in June 1981 (CETAP, 1982). The more

recent NMFS stock assessment surveys in the summers of 1998 and 2004 extended much farther offshore, resulting in at least 25 sightings between the shelf break and very deep pelagic waters from Georges Bank to Florida. Survey sightings are all in summer, and strandings are scattered throughout the year, so there is no information on seasonal patterns of distribution or migration. There are no data on stock separation, so it is unknown whether pygmy or dwarf sperm whales off the Atlantic coast of the U.S. belong to the same populations as those in the Gulf of Mexico and Caribbean. Barros et al. (1998) speculated from stable-isotope data that pygmy sperm whales may the more inshore of the two species, although prey data from stomach contents suggests the opposite (Caldwell and Caldwell, 1989; McAlpine, 2002).

Historical occurrence: Cronan and Brooks (1968) knew of no records of either species of *Kogia* in Rhode Island, but said that *K. breviceps* was likely to be present based on occurrences in Massachusetts and Long Island. They did not even mention *K. sima*. Strandings of both species are relatively common along the southeastern coast of the U.S. (Handley, 1966; Waring et al., 2008), outnumbered only by bottlenose dolphins. Connor (1971) reported at least eight records in New York between 1914 and 1968. The Smithsonian and American Museum datasets include more than 90 records from New York, New Jersey, and Rhode Island, dating back to 1883. All records prior to 1970 are identified as *Kogia breviceps*, or in a few cases as *Kogia* sp., however the prudent course at this time would be to consider all records without a thorough review of specimens, data, and photographic documentation to be *Kogia* sp.

Recent occurrence: Strandings strongly dominate the occurrence record for *Kogia* in the Rhode Island study area (Fig. 21), with only a few scattered sightings. This is likely due to a combination of factors including rarity, low sightability, occurrence far offshore where survey effort is lowest, and difficulty in identification at sea. There are strandings all along the shore of Long Island, and a few in Rhode Island, and no occurrences within Long Island Sound. There is some evidence of seasonality, with 25.8% of records in both winter and spring, 45.2% in summer, and only 3.2% in fall. Sightings were far too few to derive SPUE estimates or produce relative abundance maps.

There were four recent strandings of pygmy sperm whales in Rhode Island: at Lloyd's Beach, Sakonnet Point, on 19 January 1976; near Providence on 21 January 1976 (given the close proximity in time, one might speculate whether the two animals came in together, however they

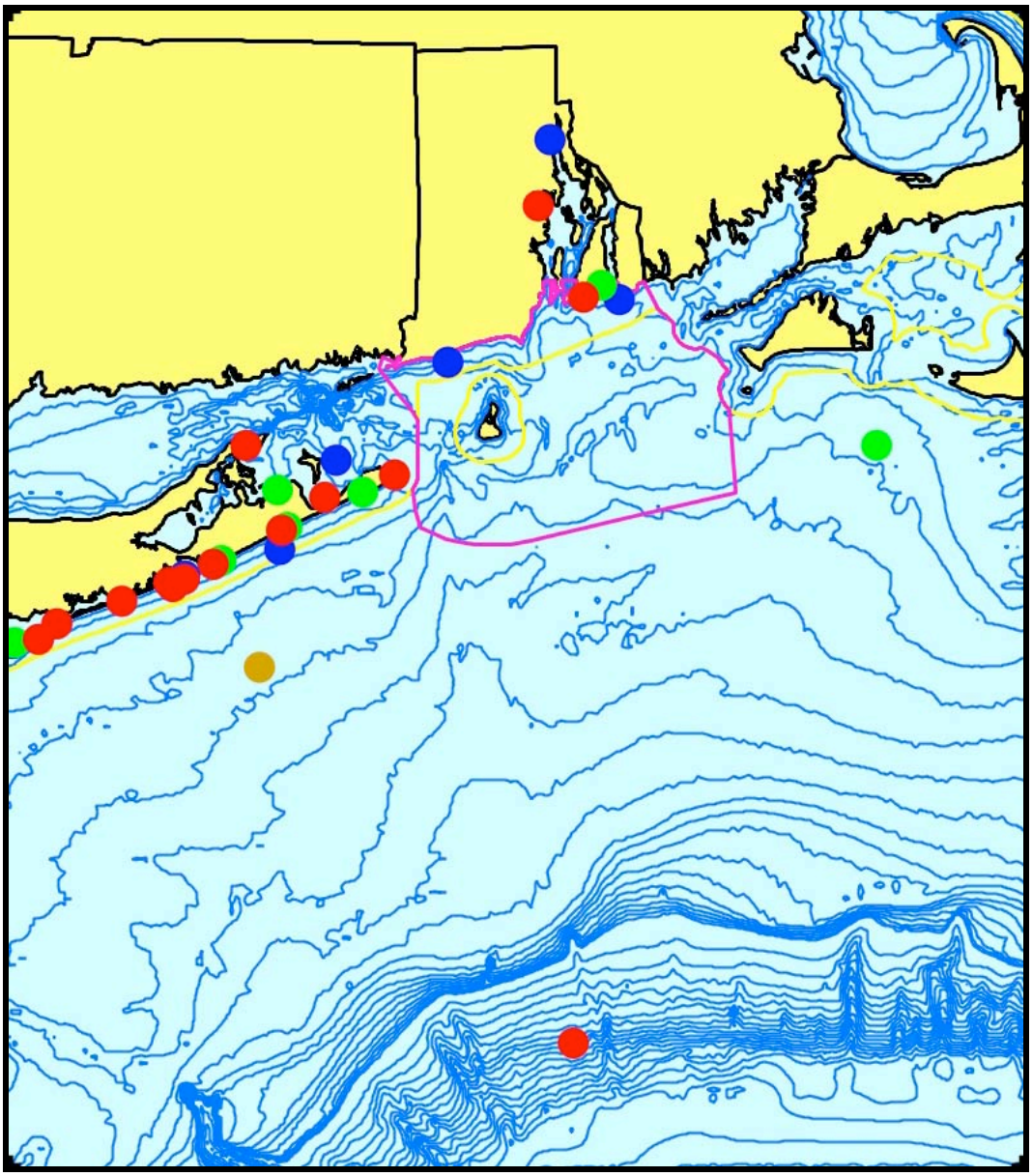

Figure 21. Aggregated sighting, stranding, and bycatch records of pygmy sperm whales, dwarf sperm whales, and unidentified *Kogia* sp. in the Rhode Island study area, 1941–2004 (n = 31: winter = 8, spring = 8, summer = 14, fall = 1).

were both adult-sized at 289 cm and 376 cm, respectively, therefore were not a mother-calf pair); on Third Beach, Middletown, on 22 March 2001; and near "Rosecliff" in Newport on 18 August 2003. There were also two strandings identified as dwarf sperm whales—one at the Quonochontaug Breachway in Charlestown on 29 December 1990 and one on the Goddard

Memorial State Park beach in Warwick on 10 June 1995. Based only on those records, the relative abundance of the two species in the region is 2:1. On the other hand, along the entire length of Long Island, there were 27 strandings between 1972 and 2005, but they were all recorded as *K. breviceps*.

It appears relatively clear from the post-1970 stranding record that *K. breviceps* is the more common species in the Rhode Island study area (Fig. 22). *K. breviceps* is known from strandings

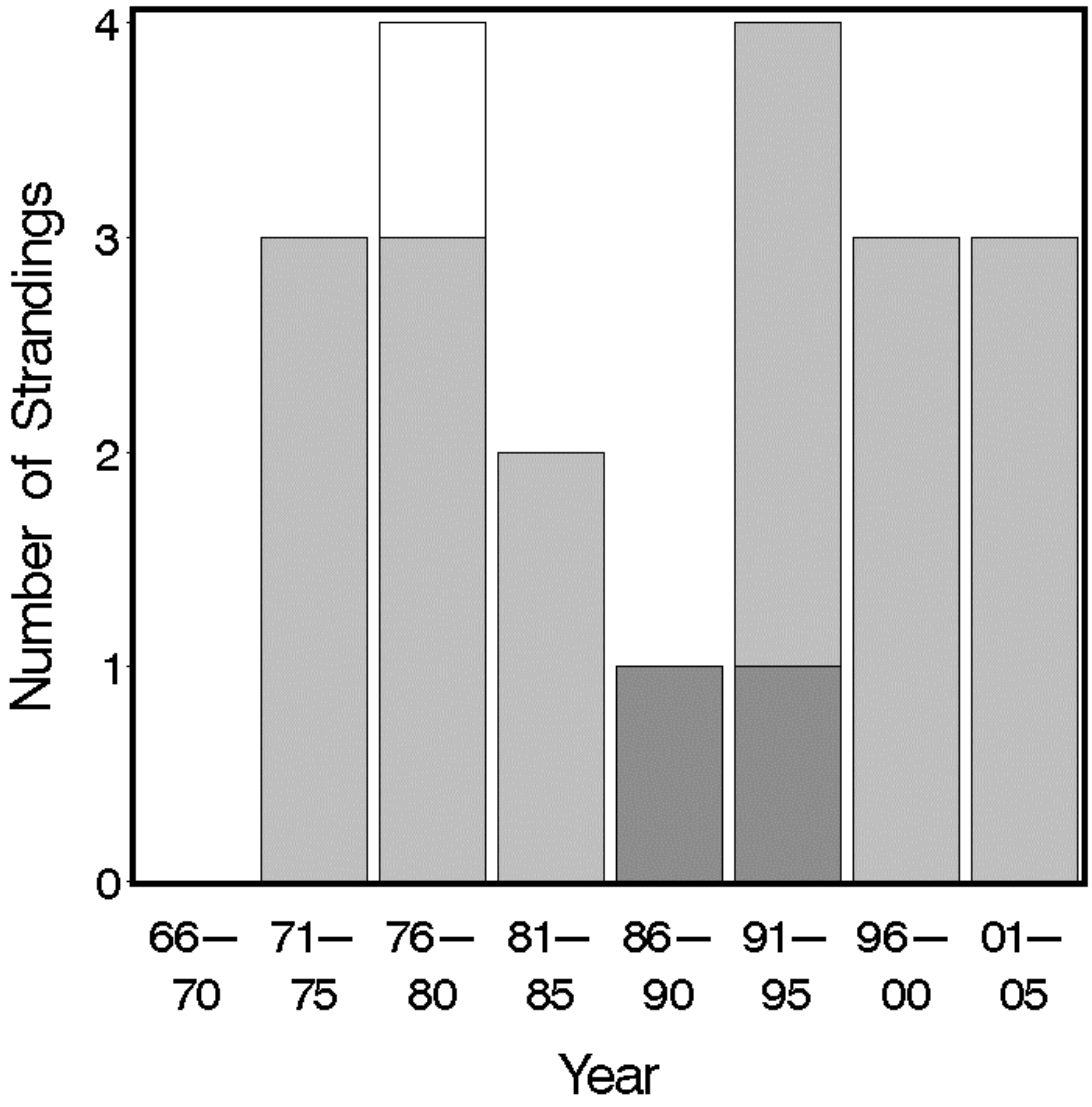

Figure 22. Five-year stranding frequencies for pygmy sperm whales (light gray bars), dwarf sperm whales (dark gray), and unidentified *Kogia* sp. (white) in the Rhode Island study area, 1966–2005.

in eastern Canada (Baird et al., 1996). The northernmost confirmed records of *K. sima* are the two strandings from Rhode Island, and *K. sima* has never been recorded from Canada (Willis and Baird, 1998). From 1999 through 2005, there were 260 *Kogia* strandings, identified to species, between Florida and Nova Scotia, including 200 *K. breviceps* and 60 *K. sima* (Waring et al., 2008). From Virginia north, 89.5% were *K. breviceps*; while from North Carolina south the strandings were 75.9% *K. breviceps*, indicating that pygmy sperm whales have a somewhat more northerly distribution. The level of expertise is not entirely consistent across all stranding groups, so it is impossible to conclude with certainty from the present data whether those differences represent true differences in species occurrence.

Conclusions: Both pygmy sperm whales and dwarf sperm whales are offshore species with main centers of distribution in relatively warm waters. There has never been a sighting of either in the SAMP area. Both species can safely be ignored for any development planning.

3.2.11. Beaked Whales: Northern Bottlenose Whale *Hyperoodon ampullatus* (Forster, 1770)
Cuvier's Beaked Whale *Ziphius cavirostris* G. Cuvier, 1823
Blainville's Beaked Whale *Mesoplodon densirostris* (Blainville, 1817)
Gervais' Beaked Whale *Mesoplodon europaeus* (Gervais, 1855)
Sowerby's Beaked Whale *Mesoplodon bidens* (Sowerby, 1804)
True's Beaked Whale *Mesoplodon mirus* True, 1913

Ziphiidae constitutes the second most speciose family of Cetacea, with 6 genera and 21 species (most in *Mesoplodon*) now recognized, second only to Delphinidae (Mead, 2002). Some species are still known only from stranded specimens and have never been seen alive (or even as a completely intact carcass). Ziphiids are collectively known as beaked whales. They all occur in deep water, far offshore. Six species are known from the North Atlantic, and all six have occurred in the Rhode Island study area. Many beaked whale species are difficult to differentiate with intact specimens at hand and nearly impossible to identify at sea, and sightings identified to species were extremely rare before the late 20th Century. All six species are considered together here.

Description: Except for a few larger species, including only *Hyperoodon ampullatus* in the North Atlantic, all of the beaked whales are medium-sized animals (adult lengths of 4–7 m) that

share a number of distinctive characters (Mead, 1989a, 1989b, 2002; Heyning, 1989, 2002; Gowans, 2002; Pitman, 2002). They have tail flukes that lack a central notch and small triangular dorsal fins located in the rear third of the body. The flippers are relatively small, with relatively long arm bones and short digits. On the ventral surface of the lower jaw there are two so-called throat grooves, which likely are involved in expansion of the oral cavity for suction feeding. The head has a pronounced, elongated rostrum that is continuous with the forehead without a distinct break or crease. In most species there is only one more or less tusk-like tooth in each mandible, which erupts only in adult males.

Northern bottlenose whales are the largest of the Atlantic beaked whales, with males reaching a maximum length of 9.8 m and females reaching 8.7 m (Mead, 1989b; Jefferson et al., 1993; Wynne and Schwartz, 1999; Gowans, 2002). The body is robust with a relatively wide back. The head is rounded and bulbous, which becomes increasingly pronounced in older, larger animals and nearly square with a flattened, vertical forehead in adult males. The blowhole is located in a shallow depression on top of the head, and the blow is short and bushy, and may be angled slightly forward. There is a pronounced, elongate, dolphin-like beak. They are tan to dark chocolate brown in color, with a lighter belly and often with lighter blotches, scratches, and scars. The head and neck are whitish on large adults. The dorsal fin is prominent, falcate, darker in color than the body, and located about two-thirds of the way back along the body.

Adult Cuvier's beaked whales reach 7–7.5 m long (Heyning, 1989, 2002; Jefferson et al., 1993; Wynne and Schwartz, 1999). They have relatively robust, cigar-shaped bodies with small conical heads and short, tapered flippers. There is often a visible concavity or depression at the top of the forehead. There is little or no distinct beak, and the line of the mouth is relatively short and curved upward toward the rear. The teeth of adult males may be visible at the tip of the lower jaw, and are sometimes covered by clumps of stalked barnacles. The body is tan to reddish brown to dark gray, often mottled and covered with circular white scars and parallel pairs of scratches. The head and neck are often white, especially in adults, with a dark patch around the eye. Much of the back may be whitish in older males.

Beaked whales in the genus *Mesoplodon* are much smaller than northern bottlenose whales and smaller than Cuvier's beaked whales. In addition, they have elongate, tapered beaks which differ from both the very short conical head of Cuvier's beaked whales and the bulbous head

with a dolphin-like beak of bottlenose whales. Identifying individuals to species becomes much more difficult. All species are about the same size and have the same general shape, show indistinct blows, have relatively small triangular to falcate dorsal fins located about 2/3 back on the body, and have flippers that fit into shallow depressions on the side of the body (Mead, 1989a).

Blainville's beaked whales may be the easiest of the four North Atlantic *Mesoplodon* species to differentiate, assuming a close look under optimum conditions (Mead, 1989a; Jefferson et al., 1993; Wynne and Schwartz, 1999; Pitman, 2002). They are up to 4.7 m long. The body is relative robust and spindle-shaped, with a relatively thick beak. The forehead appears flattened in front of the blowhole, and there is little or no obvious indentation at the blowhole. The rear half of the lower jaw has an obvious upward arch, which enlarges and extends higher than the top of the upper jaw in adult males. Adult males have two massive, flattened, triangular, forward-tilting teeth growing from the top of the arch in the lower jaw that are clearly visible when the mouth is closed. The color is dark gray to black on the back with lighter sides and a white belly. There may be a dark circular patch around the eye, and large oval scars and scratches are common.

Female Gervais' beaked whales are up to 5.2 m long, while males only reach 4.6 m (Mead, 1989a; Jefferson et al., 1993; Wynne and Schwartz, 1999; Norman and Mead, 2001; Pitman, 2002). The body is slender and laterally compressed, with an elongate, tapered beak and a prominent melon with a small indentation behind it at the blowhole. Gervais' and True's beaked whales are very similar, with the beak in the former having relatively flattened sides. The flippers are set very low on the body. The color is dark gray on the back and sides with irregular white patches and a lighter belly.

Sowerby's beaked whales are up to 5 m long (Mead, 1989a; Jefferson et al., 1993; Wynne and Schwartz, 1999; Pitman, 2002). The body is slender and spindle-shaped, with an elongate, tapered beak and a very prominent melon with a pronounced indentation behind it at the blowhole. The color is dark gray to brown on the back with somewhat lighter sides and an even lighter belly.

True's beaked whales are up to 5.2 m long (Mead, 1989a; Jefferson et al., 1993; Wynne and Schwartz, 1999; Pitman, 2002). The body is relatively robust and tapers noticeably toward the tail. There is an elongate, tapered, somewhat dolphin-like beak with rounded sides and a

prominent melon with a small indentation behind it at the blowhole. There is a sharp ridge from dorsal fin to the flukes. The color is gray to brown, gradually paling from a dark back to lighter sides to a whitish belly, with a darker band down the center of the back. The dorsal fin, lips, and a circular eye patch are black.

Status: None of the North Atlantic beaked whales are listed under the U.S. Endangered Species Act and none are included on the Rhode Island state list. Northern bottlenose whales and all four *Mesoplodon* species are classified as Data Deficient on the IUCN Red List, but Cuvier's beaked whale is classified as Least Concern. Under the Species at Risk Act in Canada, the Scotian Shelf population of *Hyperoodon* is classified as Endangered and Sowerby's beaked whale is classified as Special Concern (CWS, 2006).

The original population of northern bottlenose whales prior to whaling may have been as many as 90,000, and the current number may be 40–50,000 (Mead, 1989b; Gowans, 2002; IUCN, 2008). The most recent estimate of the northern bottlenose whale population in the Gully, based on photoidentification of individual whales, is 163 animals (Whitehead and Wimmer, 2005). Genetic studies show that the populations in the Gully, Davis Strait, and Iceland are distinct, suggesting little interchange between the areas (Dalebout et al., 2006). There is no abundance estimate for U.S. waters in the SAR because they occur so rarely. There are no North Atlantic ocean-wide estimates of abundance for any of the other beaked whales, although the global abundance of *Ziphius* is believed to be over 100,000 animals. They are pooled in abundance estimates in U.S. Atlantic waters because of species identification issues; the most recent pooled abundance estimate for all five species combined is 3,513 whales from Florida to Georges Bank in summer 2004 (Waring et al., 2008). For the Gulf of Mexico, there are separate abundance estimates for *Ziphius*—95 in 1996–2001 and 65 in 2003–2004, *Mesoplodon* spp.—106 in 1996–2001 and 57 in 2003–2004, and unidentified beaked whales—146 in 1996–2001 and 337 in 2003–2004. None of those estimates are corrected for diving and beaked whales tend to be long divers, therefore the actual numbers are likely to be substantially greater. It is possible that some beaked whales are rather abundant and that their apparent rarity is due more to their offshore distribution, low detectability, and tendency to avoid ships.

Commercial whaling for northern bottlenose whales began in the second half of the 19th Century and lasted until 1973 (Mead, 1989b; Gowans, 2002). At least 80,000 were killed over

that time, with peak catches in the 1890s. During 1962–1967, 87 were killed in the Gully by whalers from Nova Scotia (Mitchell, 1974). They are occasionally killed by small-scale whalers in the Faroe Islands, two in 2001 and six in 2002 (IWC, 2005, 2006). *Ziphius* was taken opportunistically in the Japanese fishery for North Pacific bottlenose whales, up to 35 in a single year (Heyning, 1989), and was occasionally taken by traditional whalers in the West Indies (Caldwell and Caldwell, 1971). There have been no directed hunts for *Mesoplodon* spp. (Mead, 1989a), although there have been occasional opportunistic takes in small cetacean fisheries, e.g. *M. bidens* in Newfoundland (Sergeant and Fisher, 1957).

Before it was shut down due to excessive marine mammal bycatch rates, the pelagic driftnet fishery for swordfish off the northeastern U.S. had a relatively high rate of beaked whale bycatch. Forty-six mortalities were recorded by NMFS fishery observers from 1989 to 1998, including 24 Sowerby's, 4 True's, and 1 Cuvier's, with 17 not identified to species (Waring et al., 2008). The extrapolated total annual average mortality from that fishery was 23 beaked whales killed per year. More recently, an average of 1.0 beaked whale per year strands along the U.S. Atlantic coast from human-caused mortality (ship collisions or entanglement in fishing gear), which is not thought to represent a serious impact on any of the species present.

There has been concern in recent years that very loud mid-frequency sounds, most notably naval active sonar and seismic exploration for oil and gas, could have serious impacts on beaked whales (Frantzis, 1998; Balcomb and Claridge, 2001; Evans and England, 2001). There have been several mass stranding events that have coincided with naval exercises—in the Bahamas, Canary Islands, and Mediterranean. Cuvier's beaked whales are most often affected, but some events have included Blainville's or Gervais' beaked whales. One hypothesis is that the loud sounds cause the whales to panic and surface very rapidly from depth, releasing nitrogen bubbles and causing the equivalent of the "bends" (Jepsen et al., 2003). The debilitated whales then strand, and eventually die from the physiological stresses associated with stranding (Cox et al., 2006). There may be other, more subtle impacts of anthropogenic sound. Aguilar Soto et al. (2006) suggested from their tagging study that intense ship noise might impact foraging behavior. On one of the dives by the tagged *Ziphius*, the animal made significantly fewer "buzzes" when the tag was receiving a high level of ship noise.

Ecology and life history: Northern bottlenose whales are usually encountered in small groups

of up to four whales (Mead, 1989b). Short-lived aggregations of up to 20 animals are observed (Gowans, 2002). Associations between adult females tend to be short-lived, but some male associations persist for years, suggesting a fission-fusion social structure with male coalitions, similar to that of bottlenose dolphins (Gowans et al., 2001; Gowans, 2002). They typically spend 10 minutes or more on the surface before dives that may last 1–2 hours. The median dive depth is 1000 m, and they are likely diving to the bottom for foraging (Hooker and Baird, 1999).

Northern bottlenose whales specialize mostly on one genus of deep-water squid, *Gonatus* sp., especially *G. fabricii* (Mead, 1989b; Hooker et al., 2001), although they feed on other species of squid and deep-water fishes. Whitehead et al. (2003) concluded that northern bottlenose whales have a much narrower feeding niche (measured as number of genera of squid eaten) than either sperm whales or *Ziphius*. Their dietary specialization is probably related to their restricted distribution and movement patterns, foraging primarily along the 1000-m isobath.

Reproduction in *Hyperoodon* is the best known of the North Atlantic ziphiids from data collected during 20th Century commercial whaling (Mead, 1989b). Sexual maturity in females occurs at a minimum length of 6.0 m and average length and age of 6.9 m and 11 years. In males the minimum length at maturity is 7.3 m, and the averages are 7.5 m and 7–11 years. Gestation lasts about 12 months, and lactation lasts at least 1 year and is possibly prolonged. Calves average 3.5 m at birth. The mean calving interval is 2 years, although some females have been observed accompanied by newborns and yearlings simultaneously.

Given that observations of living animals are rare and that most species are believed to actively avoid close approaches by vessels, the behavior of most beaked whale species is very poorly known (Heyning, 1989, Mead, 1989a). Adult male beaked whales often bear multiple scars that match the spacing of the tusks in that species, indicating that the scars are inflicted during aggressive encounters between males (Mead, 1989a). Heyning (1984) concluded from the scarring that the blows were struck with the mouth closed, and that the dense, fused bones of the rostrum in adult males were adapted for intraspecific aggression. Cuvier's beaked whales are typically observed in groups of 1–7 animals, with most groups of four or fewer (Heyning, 1989, 2002). *Mesoplodon* spp. tend to occur in small groups (1–6 whales, usually 2 or 3) of mixed large and small animals and probably have a social system like many other toothed whales (Mead, 1989a; Pitman, 2002). Groups at the surface tend to stay tightly clustered, no more than a

body length or two apart (Pitman, 2002).

All beaked whales are probably capable of long and deep dives. *Ziphius* dive durations are generally 20–40 minutes (Heyning, 1989). *Mesoplodon* spp. dives are typically 20 to over 45 minutes, with groups of animals generally surfacing and diving simultaneously (Pitman, 2002). Recent telemetry tagging studies on *Ziphius cavirostris* and *Mesoplodon densirostris* show their use of echolocation during foraging dives is similar to that in sperm whales, with regular clicks produced continuously at depth and short series of closely spaced clicks ("buzzes") when closing in on targeted prey items (Johnson et al., 2004; Madsen et al., 2005; Zimmer et al., 2005).

All species of beaked whales are squid specialists (Heyning, 1989, 2002; Mead, 1989a, 1989b; Gowans, 2002; Pitman, 2002). Data on stomach contents of *Mesoplodon* spp. are very sparse, but also show a predominance of deep-water squid and occasionally fish (Mead, 1989a), with some of the fish remains probably introduced secondarily in the stomach contents of squids consumed by the whale.

Data from Japanese whaling indicated mean lengths at maturity for *Ziphius* as 5.8 m in females and 5.5 m in males (Heyning, 1989). The data for females may have been biased, since a 5.1-m pregnant female stranded in Florida. Calves average 2.7 m at birth. Reproductive data for *Mesoplodon* spp. are extremely sparse (Mead, 1989a; Pitman, 2002). One stranded female *M. densirostris* was observed with 9 growth layers in the teeth and one corpus albicans in an ovary, indicating recent sexual maturity. *M. europaeus* is the only species with enough data to estimate mean size at maturity—4.5 m in females.

General distribution: Northern bottlenose whales occur only in the North Atlantic, from Nova Scotia and the British Isles in the south to Baffin Island, Greenland, Iceland, Jan Mayen, and Svalbard in the subarctic north (Mead, 1989b; Gowans, 2002). There are six known areas of aggregation—two near Norway, west of Svalbard, north of Iceland, in Davis Strait west of Greenland, and in the Gully, a large submarine canyon east of Sable Island off Nova Scotia. They occasionally occur south to the edge of Georges Bank, where sightings were recorded near the shelf break in 1980, 1993, and 1996, all in late spring or summer (CETAP, 1982; Waring et al., 2008). Seasonality is poorly known, however the known strandings in eastern Canada and New England are scattered throughout the year (Reeves et al., 1993). Bottlenose whales occur in the Gully year-round, and some individuals have been sighted in other canyons along the edge of

the Nova Scotian shelf (Gowans et al., 2000; Hooker et al., 2002; Wimmer and Whitehead, 2004).

Cuvier's beaked whale is the most cosmopolitan of all beaked whales, occurring in cold temperate to tropical waters world-wide (Heyning, 1989, 2002). There were six identified sightings in 1979 and 1980 off the northeastern U.S. (CETAP, 1982), and a number of additional sightings in more recent surveys off the Northeast and in the Gulf of Mexico (Waring et al., 2008). Sightings have been in spring and summer, and concentrated in deeper waters from the shelf break to further offshore. They are also known from strandings along the east coast from Nova Scotia to Florida to the West Indies.

Blainville's beaked whale has the widest distribution of any *Mesoplodon* species, occurring world-wide in warm temperate to tropical waters (Moore, 1966; Mead, 1989a). In the North Atlantic, they are more common in North America than in Europe. Strandings in the western North Atlantic are known from Nova Scotia south to Florida, the Gulf of Mexico, the Bahamas, and the Caribbean.

Gervais's beaked whales were once thought to occur only in the North Atlantic, but there were three strandings on Ascension Island in the tropical South Atlantic in 1980. They are the most common beaked whale in the stranding record from the east coast of the U.S. (Moore, 1966; Mead, 1989a; Norman and Mead, 2001). Fisher's Island, New York is the northernmost occurrence. Strandings occur south to Florida, the Gulf of Mexico, the West Indies, and the Caribbean. Occurrences on the eastern side of the North Atlantic are rare and scattered, occurring in France, Spain, the Canary Islands, Mauritania, and Guinea-Bissau.

Sowerby's beaked whales are known from cold temperate waters on both sides of the North Atlantic, but are much more common on the European side than on the North American side (Moore, 1966; Mead, 1989a). In the western North Atlantic, strandings are known from southern New England north to Newfoundland and Labrador. There is one stranding record from the Gulf of Mexico coast of Florida, however that is believed to be a stray far outside the normal range of the species.

As with Gervais' beaked whale, True's beaked whales were believed to occur only in temperate North Atlantic waters, but recently specimens have been identified from strandings on the Indian Ocean coasts of South Africa and Australia. Strandings are known from the northeast

Atlantic (Scotland, Ireland, and France) and in the western North Atlantic from Nova Scotia south to Florida and the Bahamas (Moore, 1966; Mead, 1989a).

Historical occurrence: The only documented historical records of northern bottlenose whale in southern New England were in Rhode Island in 1867—an 8.2-m animal was killed off Newport in February and a second was seen but escaped, and two 7.5-m animals stranded near the Stone Bridge in Tiverton on an unknown date. Mitchell and Kozicki (1975) concluded that there was only one occurrence that was inadvertently confused and repeated by various authors, however the specificity of the locality descriptions would seem to argue otherwise, and they are included in the Smithsonian database as separate records. There was also a stranding within Cape Cod Bay at North Dennis, Massachusetts in January 1869 (Mitchell and Kozicki, 1975). These were the southernmost known occurrences for the species in the western North Atlantic (Mead, 1989b) until a sighting of two animals near the shelf break east of Cape May, New Jersey in June 1981 (CETAP, 1982). Connor (1971) concluded that all earlier published reports for Long Island were in error. For example, Goodwin (1935) wrote "Linsley (1842) reported a whale of this species at Stonington, Conn." He clearly mistook Linsley's account of a minke whale ("*Rorqualus costatus* [sic] Dekay, Beaked Whale") for *Balaena rostrata*, a once-commonly used junior synonym for bottlenose whale. Waters and Rivard (1962) perpetuated the error, saying that bottlenose whales had been "recorded from the Gulf of Maine to Long Island Sound," but they included no specific occurrence records from Massachusetts.

There are two historical stranding records for Cuvier's beaked whale in Rhode Island, both described in Cronan and Brooks (1968). A 564-cm animal stranded in Newport in October 1901. A 580-cm, 2,535-kg animal stranded alive in Newport on 13 March 1961 and died the next day. The photo in Cronan and Brooks shows visible teeth, so it was an adult male. There were no stranding records in the study area in New York, although there were several farther west in Long Island and others in New Jersey. Waters and Rivard (1962) stated that there had been many strandings over the years in Massachusetts, mainly in spring, and reported three recent records—two in Falmouth in March 1958 and one on Nauset Beach in August 1961, killed by a ship collision.

There are no historical stranding records for any of the *Mesoplodon* species in Rhode Island, and few in the study area. There is one record of Blainville's beaked whale in eastern Long

Island, on 12 May 1925 in Southampton. There was one stranding of True's beaked whale on Mason's Island in Mystic, Connecticut on 19 November 1937, the only Connecticut occurrence for any beaked whale. There are multiple historical records of Blainville's, Gervais', and True's beaked whales in western Long Island and New Jersey. Goodwin (1935) suggested that a stranding at Southampton, New York was probably a Sowerby's but gave no evidence or even a date. Waters and Rivard (1962) reported that Blainville's, Sowerby's, and True's beaked whales were all known from strandings in Massachusetts.

Recent occurrence: The general pattern for beaked whales in the Rhode Island study area is strandings on the beaches and sightings at the shelf break and farther offshore, with a few scattered occurrences in between (Fig. 23). Most records that are identified to species are strandings; conversely, very few sightings are identified to species. There were two identified Cuvier's beaked whale sightings in the study area—one animal from a whale-watching boat in August 1986 in relatively shallow water near the 60-m isobath southeast of Montauk Point and a pair from a NOAA ship in deep water over the slope about 175 km offshore in August 1995. There were also two identified sightings of Sowerby's beaked whales in deep slope waters from a NOAA ship in 2004—three animals on 11 July and two animals on 2 August. Sowerby's was the most common beaked whale species taken incidentally by the swordfish driftnet fishery (see Status, above), which operated on the southern edge of Georges Bank just to the east. There are no identified sightings of Blainville's, Gervais', or True's beaked whales in the Rhode Island study area. There are few data for any species on migration or seasonality; sightings have tended to be mostly in the summer, but that may reflect more on patterns of survey effort and good weather than presence of whales (Table 3). Blainville's beaked whale is the only species that does not occur most often in summer, with two spring records and one in winter.

A stranding on Fishers Island (part of New York, but physically closer to Connecticut than to Long Island) on 17 July 1999 was originally identified as Sowerby's beaked whale and reported as such to the stranding network. It would have been the first documented occurrence of the species in the Rhode Island study area and the only record for New York. Subsequently, the skull was cleaned and photographs were sent to J. G. Mead at the Smithsonian, who identified it as Gervais' beaked whale (R. Nawojchik, Mystic Aquarium, pers. comm.), the sole record of that species in the Rhode Island study area. To balance the ledger, there was a stranding on Block

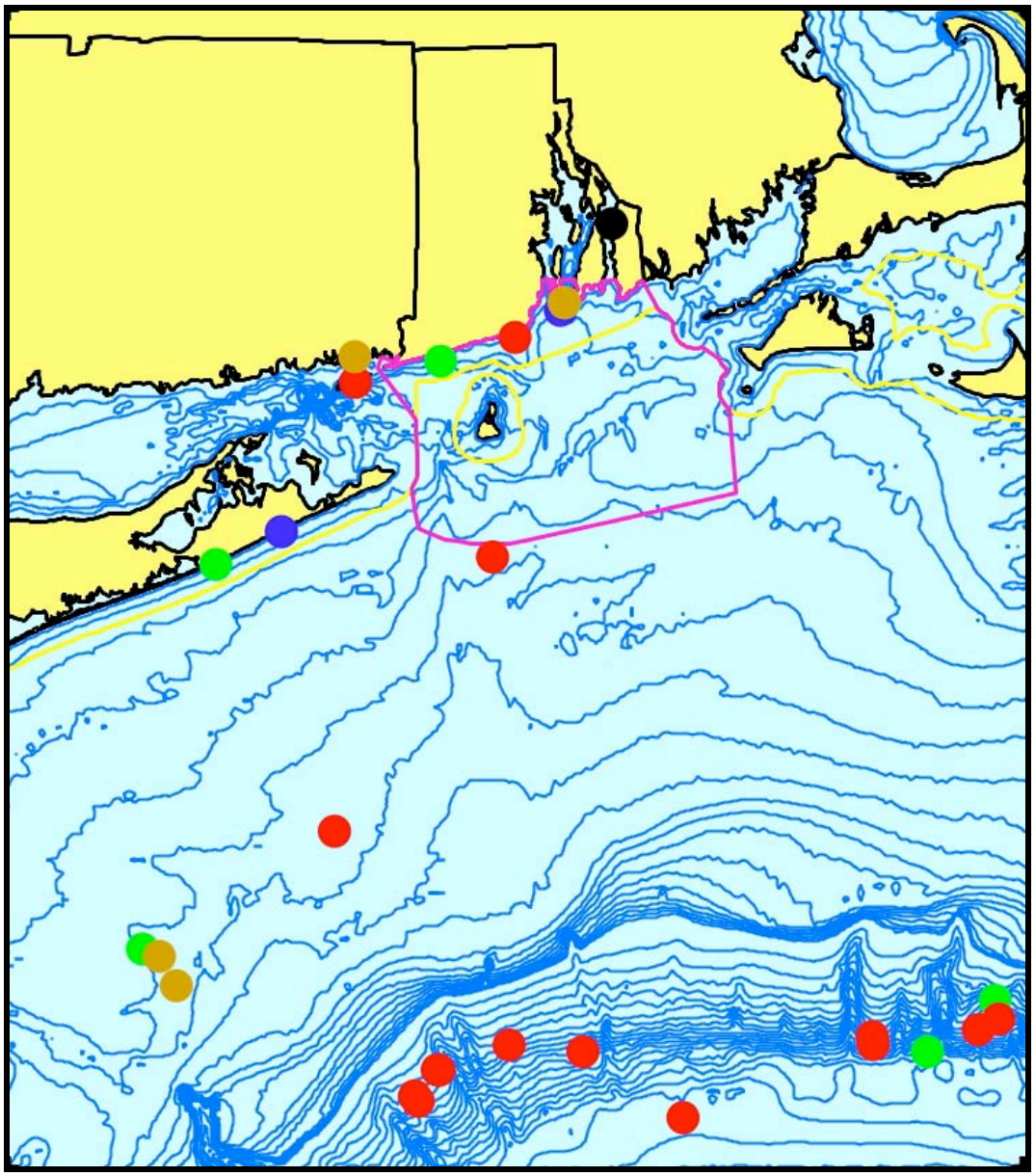

Figure 23. Aggregated sighting, stranding, and bycatch records of northern bottlenose whales, Cuvier's beaked whales, Blainville's beaked whales, Gervais' beaked whales, Sowerby's beaked whales, True's beaked whales, unidentified *Mesoplodon* sp., and unidentified beaked whales in the Rhode Island study area, 1867–2005 (n = 29: winter = 2, spring = 6, summer = 16, fall = 4, unknown = 1).

Table 3. Seasonal frequencies of all beaked whale records in the database (except for one 1857 northern bottlenose whale stranding where the date was not known).

Species	Winter	Spring	Summer	Fall
Northern bottlenose whale	1	0	0	0
Cuvier's beaked whale	0	1	2	1
Blainville's beaked whale	1	2	0	0
Gervais' beaked whale	0	0	1	0
Sowerby's beaked whale	0	0	2	0
True's beaked whale	0	0	1	1
Mesoplodon sp.	0	0	4	0
Unidentified beaked whale	0	3	6	2
Total	2	6	16	4

Island on 22 February 2007 (it occurred after obtaining the stranding database, so is not included on Fig. 23). It was identified at first by a local volunteer as a "dolphin," but photos were sent to Mystic Aquarium and then eventually forwarded to the Smithsonian. Dee Allen at the Smithsonian identified it as definitely a *Mesoplodon* and most likely Sowerby's beaked whale (*M. bidens*), but in the interim a storm washed the carcass back out to sea so no specimen could be collected to document the identification.

A 420-cm, 781-kg Blainville's live-stranded at East Hampton, New York on 14 February 1986. It died soon after stranding. On 21 March 1991, a 404-cm female Blainville's beaked whale stranded just west of the Quonochontaug Breachway in Charlestown, Rhode Island (Nawojchik, 1994). It was lactating, but there was no sign of the calf.

There was only one recent stranding of a True's beaked whale in the Rhode Island study area. A badly decomposed 463-cm carcass washed up on 2 August 1983 at Sand Hill Cove in Narragansett.

There have been no recent strandings of northern bottlenose whale, Cuvier's beaked whale, or

Sowerby's beaked whale (except for possibly the 2007 Block Island stranding discussed above) in the Rhode Island study area. Taking into account all of the historical and recent information, the general conclusion would be that the study area is situated well beyond the normal range of northern bottlenose whales, near the southwestern edge of the range of Sowerby's beaked whale, near the northeastern edge of the range of Gervais' beaked whale, and well within the range of the other three species.

Conclusions: At least three species of beaked whales probably occur regularly within the Rhode Island study area, and two others may occur. Beaked whales normally occur far offshore at the shelf break and beyond, and so would not be expected within the SAMP area.

3.2.12. Beluga Whale *Delphinapterus leucas* (Pallas, 1776)

Monodontidae includes two species of Arctic endemics, the narwhal (*Monodon monoceros*) and the beluga. The two living species are relicts of a family that was formerly more widespread in Northern Hemisphere temperate latitudes (Barnes, 2002b). Belugas are also known as white whales; the word "beluga" or "belukha" is the Russian word for "white."

Description: Beluga whales may be the easiest cetaceans to identify (Brodie, 1989; Jefferson et al., 1993; O'Corry-Crowe, 2002). Adult females are up to 4 m long. The maximum recorded size for a male was 6 m, but they usually do not reach more than about 4.5 m. Belugas have stocky bodies with no dorsal fin, instead there is a low dorsal ridge about 50 cm long but only 1–3 cm high along the mid-back. There may be thick folds of blubber, especially along the ventral surface. There is an obvious neck, which is much more flexible and mobile than in other cetaceans. The head is rounded and tapered in calves, with only the slightest indication of a beak. The melon expands with age, creating a bulbous forehead and a more obvious short, broad beak. The flippers are broad, blunt, and flat, but develop a distinct upward curve on the lateral edge in adult males that can be used to differentiate sexes in the field. The flukes have convex trailing edges. Belugas' most conspicuous character is their color—adults are completely snow-white. Calves are born dark slaty gray and gradually become lighter with age, becoming all white at the time of sexual maturity. Adults sometimes appear yellow, however that seems to be associated with molt.

Status: Belugas are not listed under the U.S. Endangered Species Act or on the Rhode Island state list, and are classified as Near Threatened on the IUCN Red List. The St. Lawrence Estuary stock is listed as Threatened under the Species At Risk Act in Canada (CWS, 2006). It had been classified as Endangered by COSEWIC (Committee on the Status of Endangered Wildlife in Canada), but their role is advisory only, with the SARA listing made by the federal government. The total abundance of beluga whales worldwide is estimated to be at least 150,000, spread across 29 separate identified regional populations (IUCN, 2008). The St. Lawrence Estuary stock was estimated at 1,221 whales in 1997, with the number of calves observed suggesting a slow recovery (CWS, 2006). There is no estimate of the number in U.S. Atlantic waters (Waring et al., 2008).

Belugas are taken by subsistence hunters in many parts of the species' range. Statistics collated by the International Whaling Commission's Scientific Committee summarize the 2000–2004 annual subsistence takes in Greenland (610, 398, 399, 430, 196), Russia (22, 7, 20, 66, unknown), and Alaska (240, 463, 394, 271, 262) (IWC, 2005, 2006). Canada reported a subsistence take of 375 in 2001, but takes in other years are not known (IWC, 2006; Canada is not an IWC member). In the St. Lawrence estuary, they were hunted for over 400 years until the hunt was prohibited in 1979 (CWS, 2006). The peaks years of the St. Lawrence beluga hunt were 1880–1950, when as many as 15,000 whales were killed. Béland (1996) estimated that the St. Lawrence beluga population was about 5,000–10,000 at the beginning of the 20th Century, declining to only about 350 individuals in the 1970s.

A serious concern with St. Lawrence estuary beluga whales is the issue of toxic contamination and associated health effects (Béland et al., 1993; Martineau et al., 1994, 1999; De Guise et al., 1994, 1998; Measures et al., 1995; Béland, 1996; Mathieu et al., 1997; Gauthier et al., 1999; Hickie et al., 2000). The St. Lawrence River is the outlet from the Great Lakes and a substantial watershed in the industrial center of North America. There are contaminants in the water and sediments, accumulating up the food chain to the belugas at the top. St. Lawrence belugas have much higher loads of contaminants than Arctic belugas, including lead, mercury, selenium, PCB's, DDT, dioxins, furans, Mirex, and PAH's. The effects of these contaminants include direct toxicity, suppression of the immune system, effects on the reproductive system, mutation, and cancer. There is evidence for higher rates of disease and parasitism in St. Lawrence beluga whales. One beluga with both testes and ovaries was recorded in 1994, and many females appear

to cease reproduction after reaching about age 21, which is not known from other beluga populations. Finally, over a third of all known tumors recorded from cetaceans have been in St. Lawrence River belugas.

Ecology and life history: Beluga whales are highly social and gregarious (Brodie, 1989; O'Corry-Crowe, 2002). They generally are seen in small groups of 2–10 animals, however they often occur in aggregations of over 1,000 animals in their summer habitats. Sightings off the northeastern U.S. are usually single individuals, although there was one group of six animals seen for two months in the vicinity of Portland, Maine in August–September 1927 (Reeves and Katona, 1980). Reeves and Katona reviewed hypotheses for why belugas have not expanded their range south of the St. Lawrence while at the same time there were so many extralimital records off the northeastern U.S. The possible explanations were temperature, avoidance of predators, competition, and prey abundance including the effects of commercial fishing, of which they considered competition the most likely. It is more likely that matrilineal habitat fidelity plays an important role, but that research was not available in 1980.

Belugas follow a distinct annual movement pattern (Brodie, 1989; O'Corry-Crowe, 2002). After the spring break-up of the sea ice, they move into summering areas in near-shore waters and in river mouths and estuaries. They frequently occur in extremely shallow water, sometimes barely deep enough to swim. They are apparently capable of swimming backwards, which may help them avoid being stranded by the out-going tide. At times they have been observed getting stuck on an out-going tide and simply waiting for the next high tide to re-float them. One hypothesis for using shallow waters in summer is that water temperatures may warm more quickly, providing a thermoregulatory benefit to young calves. In addition, belugas are the only cetacean known to undergo an annual molt in summer (St. Aubin et al., 1990). The entire outer layer of the skin turns yellow and is sloughed off. During the molt, belugas are known to rub themselves on gravel bottoms in shallow water to help scrape off the old skin (Smith et al., 1992). In winter, belugas are thought to mainly move offshore with the ice edge, however satellite tracked radio-tagging has shown them traveling long distances to as far as 1100 km offshore and as much as 700 km deep in the ice pack (Suydam et al., 2001).

Beluga whales are capable of diving to the sea floor in much of their habitat (Martin and Smith, 1992; Martin et al., 1998; Suydam et al., 2001). Satellite-linked time-depth-recorder tags

show that they routinely dive to 300–600 m and are capable of dives to more than 1000 m with durations up to 25 minutes.

The diet of beluga whales is extremely broad, although little is known for the winter season (Brodie, 1989; Stewart and Stewart, 1989; Measures et al., 1995; Béland, 1996; O'Corry-Crowe, 2002). Prey species include benthic and demersal fishes such as flounders, gadids, and sand lance; pelagic fish such as capelin, herring, and smelt; migratory fishes like salmonids and eels; squid; octopus; shrimp; and benthic worms, clams, and crabs. Evidence for bottom feeding includes occasional seaweed, sand, and gravel in stomach contents.

Calving takes place in a relatively short period in the summer, with the timing differing slightly between different stocks (Brodie, 1989; Stewart and Stewart, 1989; O'Corry-Crowe, 2002). Calving peaks in July in the St. Lawrence population. Calves average 1.6 m at birth. Mating takes place in the spring, and the gestation period is 14–14.5 months. Males attain sexual maturity at about age 8, and females around 5–6. Lactation lasts 20–24 months, with the calf beginning to feed on easily captured prey like crabs, worms, and mollusks during its second year. The inter-birth interval for most females is 3 years.

General distribution: The beluga is primarily an Arctic species, occurring in high latitudes around the Northern Hemisphere (Brodie, 1989; Stewart and Stewart, 1989; Nowak, 1999; O'Corry-Crowe, 2002). They are found along Alaska (south into the Bering Sea), Arctic Canada (south to Labrador and Hudson Bay), east and west Greenland, Svalbard, northern Norway, and Arctic Russia (south into the Sea of Okhotsk in the northwest Pacific). Stock divisions are maintained by very strong matrilineal fidelity to summering sites, even where there are few barriers between sites. Genetic studies have been used to elucidate stock structuring in belugas. Nuclear DNA markers show that North American belugas partition into two groups, eastern and western, suggestive that they occupied two separate refugia during the Pleistocene Ice Age (Brown Gladden et al., 1999b). Mitochondrial DNA shows the finer structure indicative of matrilineal habitat fidelity (Brennin et al., 1997; Brown Gladden et al., 1997). There are isolated relict populations in Cook Inlet in southern Alaska and in the Gulf of St. Lawrence and adjacent bays and rivers in eastern Canada. There have been occasional occurrences of belugas along the Atlantic coast from Nova Scotia to New Jersey (Reeves and Katona, 1980), which are believed to be individuals from the St. Lawrence population. Brown Gladden et al. (1999a) confirmed via

genetic sampling that a beluga stranded in Nova Scotia did come from the St. Lawrence population.

Historical occurrence: Cronan and Brooks (1968) knew of no occurrences of belugas in Rhode Island, but stated that "there are records from New Hampshire; Cape Cod, Massachusetts; and Atlantic City, New Jersey; it therefore seems likely that the white whale may someday be seen off Rhode Island." The occurrence of belugas at Atlantic City is one of those errors that get passed down through the literature based a previous misinterpretation and then a series of repeated citations. Reeves and Katona (1980) concluded that the error traced back to someone's mis-reading of True (1910), who reported behavioral observations of two captive belugas that were held in a tank in Atlantic City in 1908. Reeves examined the skull of one of those animals in the Smithsonian collection (USNM238104), and it did have a tag labeled "from Atlantic City," but the curatorial records show that it was captured in the St. Lawrence River. Connor (1971) knew of no confirmed records of belugas in or near Long Island. He said that Roy Latham had reported a 3–4-m white cetacean that he concluded was a beluga in Long Island Sound between Orient Point and Mattituck for four days in June 1942. Connor judged the report to be reliable, and there is a record in the Smithsonian database based on Connor's publication, the only mid-Atlantic beluga record in the Smithsonian database older than 1978. Reeves and Katona (1980) also accepted Latham's report as likely in their review of extralimital beluga occurrences off the northeastern U.S.

Recent occurrence: Belugas are rare in the Rhode Island study area, with only four records (Fig. 24; note that the numbers of sightings can be misleading, because an animal seen repeatedly for up to several months is typically represented in the data by only one or two records). Somewhat surprisingly, they occur more frequently in western Long Island and New Jersey (including one seen in Delaware Bay and the Delaware River in April 2005, as far upstream as Trenton). Individuals that do occur south of Cape Cod commonly stay for extended periods, usually very near the coast (Reeves and Katona, 1980). The study area records include the June 1942 sighting off Orient Point reported in Connor (1971). A single beluga was seen off Moriches Inlet on the south shore of Long Island on 22 June 1980. In February 1985, a beluga was seen in the harbor at New Haven, Connecticut. It was sighted repeatedly over the succeeding months. On 13 May 1986 it was found dead and entangled in fishing gear in Long Island Sound south of New Haven, however the cause of death was determined at necropsy to be from a

gunshot wound.

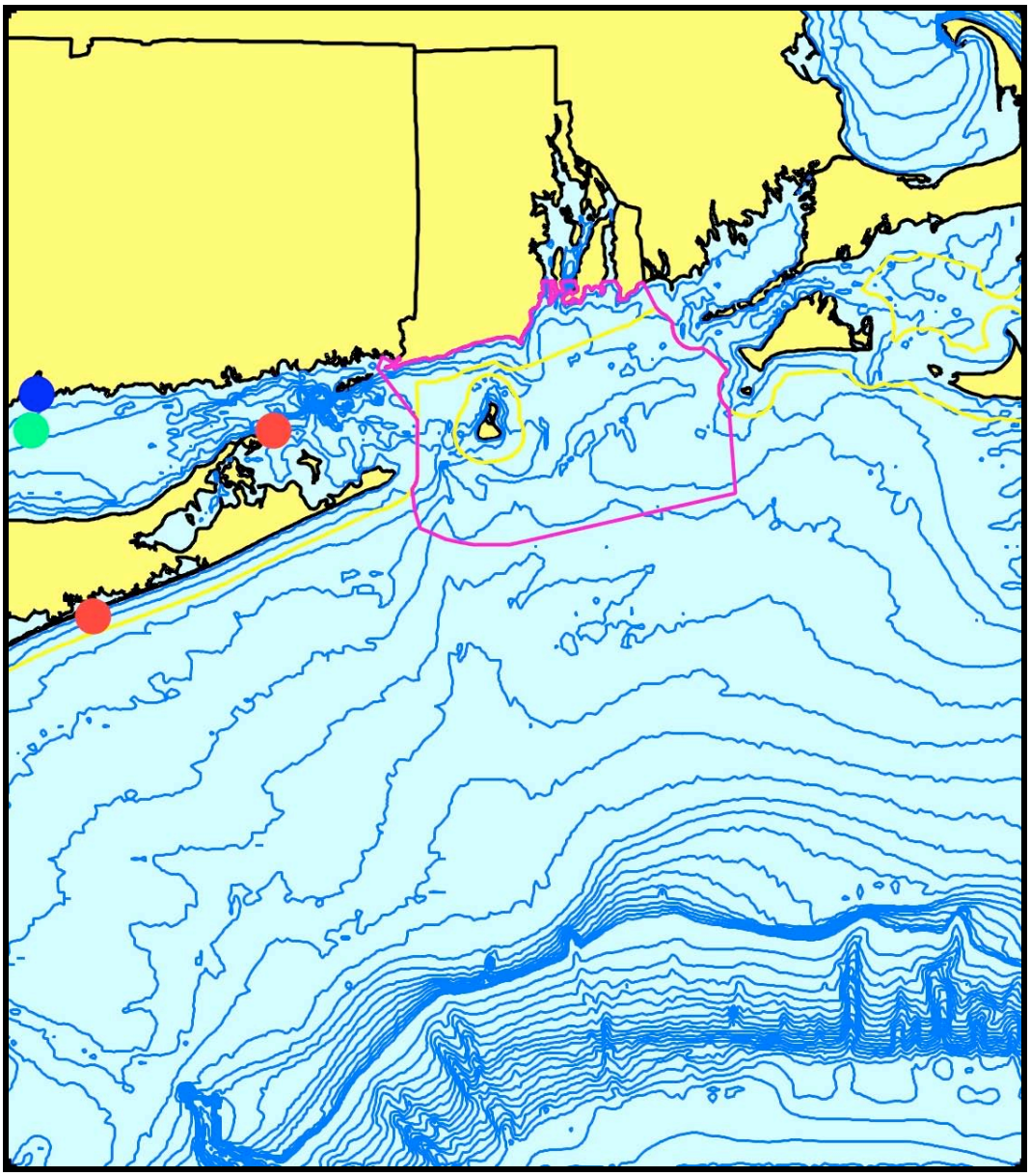

Figure 24. Aggregated sighting, stranding, and bycatch records of beluga whales in the Rhode Island study area, 1942–1986 (n = 4: winter = 1, spring = 1, summer = 2, fall = 0).

Conclusions: Belugas clearly occur only accidentally on rare occasions in the Rhode Island study area and are not expected in the SAMP area.

3.2.13. Harbor Porpoise *Phocoena phocoena* (Linnaeus 1758):

Phocoenidae includes three genera and six species of small toothed whales known as the porpoises, which are the smallest of the living cetaceans (Read, 2002). They are sometimes referred to as the "true" porpoises, most likely because the term "porpoise" has frequently been used in the U.S. as equivalent to "dolphin." Porpoises are closely related to the dolphins, and were long included in the Delphinidae. They are now recognized as a separate family, but are included with Delphinidae and Monodontidae in the superfamily Delphinoidea (Rice, 1998).

Porpoises are easily differentiated from dolphins by having spatulate rather than conical teeth (Read, 2002). The exposed portion of a porpoise tooth is flattened, somewhat wider than the base diameter, and slightly curved. A porpoise has a conical head without a beak. Their skulls resemble the skulls of very young dolphins, with delayed fusion of cranial sutures. The rostrum of the skull is much shorter than in small dolphins, and there are paired rounded protuberances on the premaxillae just in front of the braincase, which is relatively large and rounded. Porpoises have small but robust bodies, with relatively small flippers and dorsal fins (the dorsal fin is absent in the finless porpoise), which is likely related to conservation of heat for a relatively small animal living in cold water. Most species have epidermal tubercles on the leading edge of the dorsal fin. Porpoise life histories are more like those of mysticetes than like other odontocetes', with early maturation, rapid growth, short inter-birth intervals, and a low degree of sociality (Read and Hohn, 1995).

Description: Harbor porpoises are the smallest cetaceans occurring in the North Atlantic, reaching only 1.4–1.9 meters. They exhibit reverse sexual dimorphism; an average female is 160 cm and 60 kg, an average male is 145 cm and 50 kg, and the largest individual known was a 200-cm, 70-kg female (Bjørge and Tolley, 2002). The size ranges of mature porpoises from the Bay of Fundy were: females—131–168 cm (mean = 157, n = 32), 42–76 kg (mean = 62); males—129–157 cm (mean = 144, n = 62), 36–61 kg (mean = 49) (Read, 1999). The body is stocky, dark gray to black on the back and white on the belly with little or no distinctive patterning (Gaskin et al., 1974; Jefferson et al., 1993; Read, 1999; Wynne and Schwartz, 1999; Bjørge and Tolley, 2002). The sides may be mottled or simply transition gradually from dark to light. There are often one or more dark stripes from the corner of the mouth to the flipper. Individuals may show darker eye, chin, and lip patches. The head is bluntly conical with no distinct beak. The flippers

are small and pointed, and the dorsal fin is small, triangular (sometimes slightly falcate), and located slightly behind the middle of the back.

Status: Harbor porpoises are not listed under the U.S. Endangered Species Act. A proposal made in 1993 to list the Gulf of Maine/Bay of Fundy stock as Threatened because of excessive bycatch mortality in the sink gillnet fishery was withdrawn in 1999 after an extensive review (NMFS, 1999) and the species was removed from the Candidate list in 2001 (NMFS, 2001). Harbor porpoises are not included on the Rhode Island state list and are classified as Least Concern on the IUCN Red List. Northwest Atlantic harbor porpoises are listed as Special Concern under the Species at Risk Act in Canada (CWS, 2006). The total number of harbor porpoises in the North Atlantic is likely to be over 500,000 (IUCN, 2008). The current estimate for the Gulf of Maine/Bay of Fundy stock is 89,054 (Waring et al., 2008).

Harbor porpoises were the subject of an organized hunt in Denmark for oil and meat from at least the 14th Century until World War II, and had probably been hunted in that area since the Stone Age (Kinze, 1995). Average annual catches probably exceeded 1,000 animals. Inuit subsistence hunters in Greenland took 1,607 porpoises in 2000, 1,946 in 2001, 1,373 in 2002, 2,320 in 2003, and 2,238 in 2004 (IWC, 2005, 2006). Micmac and Passamaquoddy Indians in the Bay of Fundy and along the coast of Maine hunted porpoises for both meat and oil in the 19th and 20th Centuries (reviewed by Reeves and Read, 2003). They hunted from canoes using shotguns, but there is no archeological evidence that hunting occurred before the introduction of firearms. The blubber was rendered down to 2–3 gallons of oil that was used for lighting and lubrication. Much more valuable was the "jaw oil" from the mandibular fat, which was used for lubricating clocks, watches, and other precision instruments. Jaw oil was obtained by hanging the lower jaw over a can and allowing the oil to drip out, producing about a half-pint per animal. Total takes were likely several hundred per year.

Mortality of harbor porpoises and other phocoenids as bycatch in commercial fisheries is a global concern (Perrin et al., 1994b; D'Agrosa et al., 1995; Read and Wade, 2000). The most significant fishery bycatch occurs in sink gillnet fisheries. As pointedly noted by Reeves and Read (2003), the first U.S. government fisheries report in 1886 detailing the efficiency of gillnet fishing for cod also reported incidental captures of harbor porpoises. The stock assessment for Gulf of Maine/Bay of Fundy harbor porpoise stock (Waring et al., 2008) reported annual average

mortality of 725 porpoises in gillnet fisheries during 2001–2005—475 in the northeastern U.S., 177 in the mid-Atlantic, and 73 in Canada. There are also lower levels of mortality in other fisheries. A Take Reduction Plan is in effect in U.S. Atlantic waters, involving fishery closures in specific areas at times when the probability of porpoise bycatch is high, plus a requirement for the use of acoustic alarms ("pingers") to alert porpoises to the presence of gear. Bycatch mortality did decline for a time, however then began to increase, perhaps due to declining compliance with the Take Reduction Plan.

Harbor porpoises are the most common stranded cetacean in the Rhode Island study area (Table 2). Fishery-related mortality is likely to be a significant component of the stranding record. Of those strandings where a cause of death could be determined, over a quarter showed evidence of fishery interactions (Waring et al., 2006b). In another 18%, the animals were judged to be emaciated and most likely were newly weaned calves that were unsuccessful at feeding independently.

Given that harbor porpoises live in coastal waters adjacent to areas with high human population densities and industrial development, the potential effects of toxic pollution are of concern. In some areas harbor porpoises do have high levels of organochlorines and heavy metals in their body tissues, but no correlations have been shown with adverse health effects or body condition (Read, 1999).

Ecology and life history: The most common harbor porpoise sighting off the northeastern U.S. is a single individual, with pairs and trios common (CETAP, 1982). This is consistent with observations in other areas (Read, 1999; Bjørge and Tolley, 2002). Groups of 6–10 are often observed, or even larger groups on rare occasions, however these are not stable social groupings as in many other toothed whales. Harbor porpoise groupings are fluid, short-term associations in a "fission-fusion" social structure (Reeves and Read, 2003). The largest reported groups are most likely aggregations of un-associated animals in areas of abundant prey.

Harbor porpoises exhibit a clear seasonal pattern of distribution and movement, however there is little evidence for a coordinated annual migration (Reeves and Reed, 2003). Off the northeastern U.S., porpoise abundance declines in the Gulf of Maine in winter, coincident with the peak occurrence in the mid-Atlantic region. However, evidence from genetic sampling of stranded and bycaught individuals shows that some proportion of the animals in the mid-Atlantic

region do not come from the Gulf of Maine/Bay of Fundy stock (Rosel et al., 1999). In addition, the majority of stranded and bycaught porpoises in the mid-Atlantic are juveniles. Although juvenile mortality rates can be expected to be higher, there also may be age differences in seasonal movements, perhaps with younger animals wintering in more inshore areas than older animals.

Most dives by harbor porpoises are just about a minute or a little longer, but they are capable of diving for 5 minutes to depths exceeding 200 m (Westgate et al. 1995). Their surfacings are very brief. Read and Westgate (1997) studied movements of Gulf of Maine harbor porpoises using satellite-tracked radio tags. Average daily movements were 14–58 km. Tagged animals commonly remained resident in small, localized areas for extended periods, then made relatively rapid, directed movements lasting hours or days to different areas. Tagged porpoises ranged over the entire Bay of Fundy and Gulf of Maine area.

Harbor porpoises primarily feed on fish and secondarily on squid and crustaceans (Gaskin et al., 1974; Read, 1999; Bjørge and Tolley, 2002; Reeves and Read, 2003). They preferentially feed on non-spiny fishes with relatively high fat content that are less than 40 cm long (usually 10–30 cm). Clupeids and gadoids dominate. Their primary prey species in the Bay of Fundy are herring and silver hake. Other commonly eaten species include anchovies, sprat, sardines, and capelin, and calves apparently begin feeding on small crustaceans. Stomach contents of stranded porpoises in the Rhode Island study area frequently include herring and squid (Sadove and Cardinale, 1993). Harbor porpoises do not forage cooperatively, and often feed near the bottom (Read, 1999). Their daily ration ranges from 5% to 14% of body weight, and is highest in immatures and in pregnant and lactating females.

Harbor porpoise reproduction is strongly seasonal, with the timing varying between regions (Read, 1999; Reeves and Read, 2003). In the Gulf of Maine/Bay of Fundy population, ovulation occurs within a few weeks in late spring and early summer (Read, 1990a). Only the left ovary matures. There is also marked reproductive seasonality in the males, with testis mass and sperm production varying on an annual cycle and peaking at the same time as ovulation (Reeves and Read, 2003). At the peak of the breeding season, the testes in an adult male comprise about 4% of total body mass. The mating system is probably promiscuous with sperm competition occurring. Gestation is 10–11 months, with most calves born in May in the Gulf of Maine, and

June-July in Europe.

Calves are about 75 cm long and weigh about 6 kg at birth, and triple their weight in about 3 months (Read, 1999; Reeves and Read, 2003). Lactation lasts at least 8 months and possibly as long as a year, but weaning is gradual and calves begin feeding independently well before being completely weaned. Post-partum estrus and mating is common in harbor porpoise females, resulting in simultaneous pregnancy and lactation and 1-year intervals between calves. Most females give birth annually in the Gulf of Maine and European populations, but every other year in the California population (Read, 1990b; Read and Hohn, 1995).

Harbor porpoises typically reach sexual maturity in their third or fourth years, but are not physically mature until about age 5 in males and 7 in females (Read, 1999). The mean age at sexual maturity for Gulf of Maine/Bay of Fundy females is 3.44 years, at an average length of 143 cm (Read, 1990b).

Some harbor porpoises from the Bay of Fundy have tested positive for antibodies to morbillivirus (Duignan et al., 1995). A few porpoises died during the 1988 PDV epizootic in the North Sea harbor seals. Van Bressem et al. (2001) reported 16.7% morbillivirus seropositives in mature porpoises from the British Isles, but no positive tests in immatures from the British Isles or in either immatures or adults from the North Sea.

General distribution: Harbor porpoises are known from cool temperate to subpolar waters around both the North Atlantic and North Pacific (Gaskin et al., 1974; Read, 1999; Bjørge and Tolley, 2002; Reeves and Read, 2003). They occur most often in relatively shallow continental shelf and coastal waters. The sightings from the 1978–1981 CETAP surveys showed porpoises in spring most concentrated in the southwestern Gulf of Maine around Nantucket Shoals and western Georges Bank but also occurring throughout the Gulf of Maine and southern New England shelf, followed by a marked concentration into the northern Gulf of Maine and Bay of Fundy in the summer (CETAP, 1982). Sightings were much less frequent and extremely scattered in fall and winter, and it was hypothesized that many individuals migrated to the mid-Atlantic or offshore waters. Strandings are widespread from Maine to North Carolina. There are two stranding records for Florida in the 1980s and one in 2003 (Waring et al., 2008), however they are considered to be extralimital, since there are no other records south of North Carolina.

Historical occurrence: Cronan and Brooks (1968) knew of no records of harbor porpoises in

Rhode Island, but did mention occurrences nearby in Mount Hope Bay in July 1931 and September 1934 that "would have to go through Rhode Island waters to arrive in or leave Mount Hope Bay." In the Smithsonian database there is a record of a stranding at Brenton's Point in Newport on 5 July 1901, collected by E. A. Mearns, plus another undated specimen record from Newport, also collected by Major Mearns. There are also records of a 119-cm, 26-kg porpoise stranded at Narragansett Pier in February 1972, and 139-cm animal stranded on First Beach in Newport in March 1976.

There are historical stranding and capture records in the Smithsonian data for eastern Long Island, and quite a few more for western Long Island and New Jersey. The earliest harbor porpoise record in those data was a report of a porpoise taken more than 30 km up the Connecticut River in Middletown, Connecticut in 1850. One of the Smithsonian records is a sighting of 25 porpoises off Orient Point on 7 December 1921 extracted from Connor (1971), which might be suspect (see below). There is also a record of a live-stranding of a 120-cm, 20-kg porpoise in Niantic, Connecticut that was collected and survived for a short time at Mystic Aquarium. Waters and Rivard (1962) said that harbor porpoises occurred all along the coasts of New England, but were not very common in Cape Cod Bay. They presented only one recent record—a stranding up a river in Annisquam on Cape Ann in 1955.

Historical accounts of harbor porpoises in southern New England study area must be treated with some level of skepticism because of the common use of the word "porpoise" to also refer to dolphins, as pointed out by Connor (1971) with regard to sighting reports for Long Island during summers in the 1950s and 1960s. In addition, the recent data show harbor porpoises to be relatively rare in summer (see below). Also somewhat suspect are the accounts of porpoises in large schools, sometimes up to hundreds of animals (e.g., Miller, 1899; Rowley, 1902; Turrell, 1939: as cited by Conner, 1971; Cronan and Brooks, 1968). De Kay (1842) reported that porpoises were "formerly so abundant on the shores of Long Island as to have induced the inhabitants to form establishments for their capture." His account was derived from a 1792 report by E. L'Hommedieu in *Transactions of the Society in the State of New-York for the Promotion of Agriculture, Arts, and Manufactures*, which described a net fishery in eastern Long Island taking small cetaceans for oil and leather. Mead (1975) concluded that the fishery was not for harbor porpoises, but was most likely for bottlenose dolphins, in part because the average oil yield reported (6 gallons) was too high for *Phocoena* but matched that from the Cape Hatteras

Tursiops fishery. In addition, the capture method described matched what was used at Cape Hatteras. Linsley's (1842) report that "Numbers of the common porpoise are taken in this town for the sake of the oil, which is usually from three to seven gallons" suffers from the same weakness.

Recent occurrence: Harbor porpoise occurrence in the Rhode Island study area is strongly seasonal, with 69.5% of all records in spring, followed by winter (19.5%), summer (7.8%), and fall (2.7%) (Fig. 25). Sightings are widespread across the shelf. Strandings have occurred all along the south shore of Long Island and in parts of coastal Rhode Island. There were also strandings along both sides of Long Island Sound and occasional occurrences in bays, estuaries, and rivers. Seasonal stranding frequencies partly mirror the sighting frequencies—highest in winter and second-highest in spring. Harbor porpoises are relatively common in the winter in eastern Long Island Sound, Gardiner's Bay, and Peconic Bay (Sadove and Cardinale, 1993), however bays and sounds are excluded from survey areas so there are few documented sighting records. They probably also occur in winter in Narragansett Bay, although we have only second- and third-hand anecdotal reports for evidence.

The effort-corrected relative abundance patterns show that harbor porpoises occurred within the SAMP area in all four seasons of the year (Fig. 26). The data probably under-represent occurrence, because of their relatively low detectability during surveys. In winter, they were present at low to moderate abundances in the eastern part of the SAMP area, as well as south of Martha's Vineyard and Nantucket and offshore along the entire study area. In spring, porpoises occurred throughout the SAMP area, at relative high abundances in the offshore portion. They also occurred at relatively high abundance throughout much of the study area, and in highest abundance over Nantucket Shoals and eastward. Spring is when harbor porpoises are known to be migrating from wintering areas in the mid-Atlantic and offshore toward their spring and summer feeding grounds in the Gulf of Maine (CETAP, 1982; Read, 1999; Waring et al., 2008). In summer, porpoises were present in lower numbers in the eastern half of the SAMP area, and still in high abundance in the Nantucket Shoals area. Their abundance was lowest in fall—in the western half of the SAMP area around Block Island, plus relatively limited areas offshore, at Nantucket Shoals, and near Cape Cod and Nantucket.

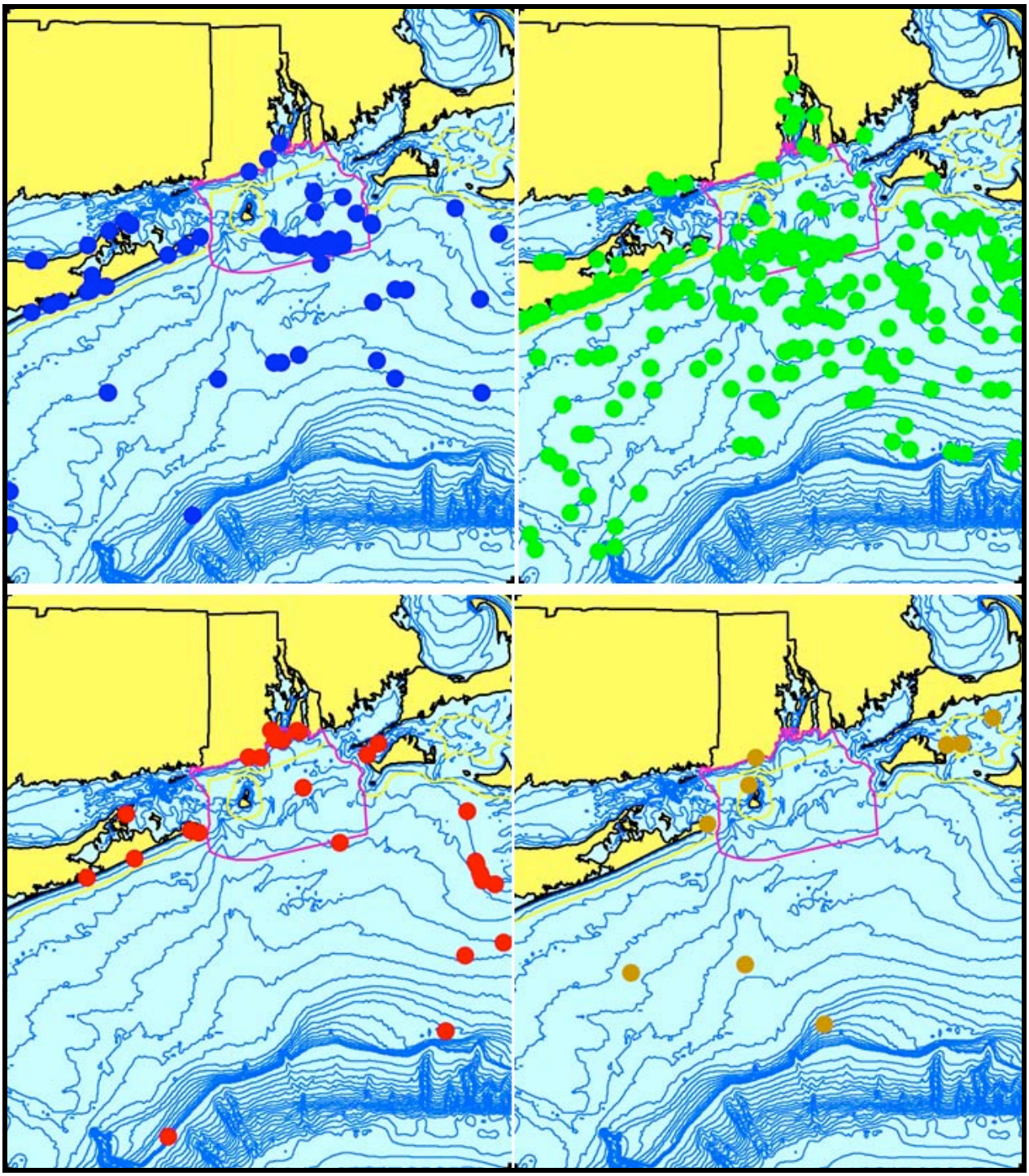

Figure 25. Aggregated sighting, stranding, and bycatch records of harbor porpoises in the Rhode Island study area, 1850–2007 (n = 376: winter = 73, spring = 262, summer = 29, fall = 10, unknown = 2).

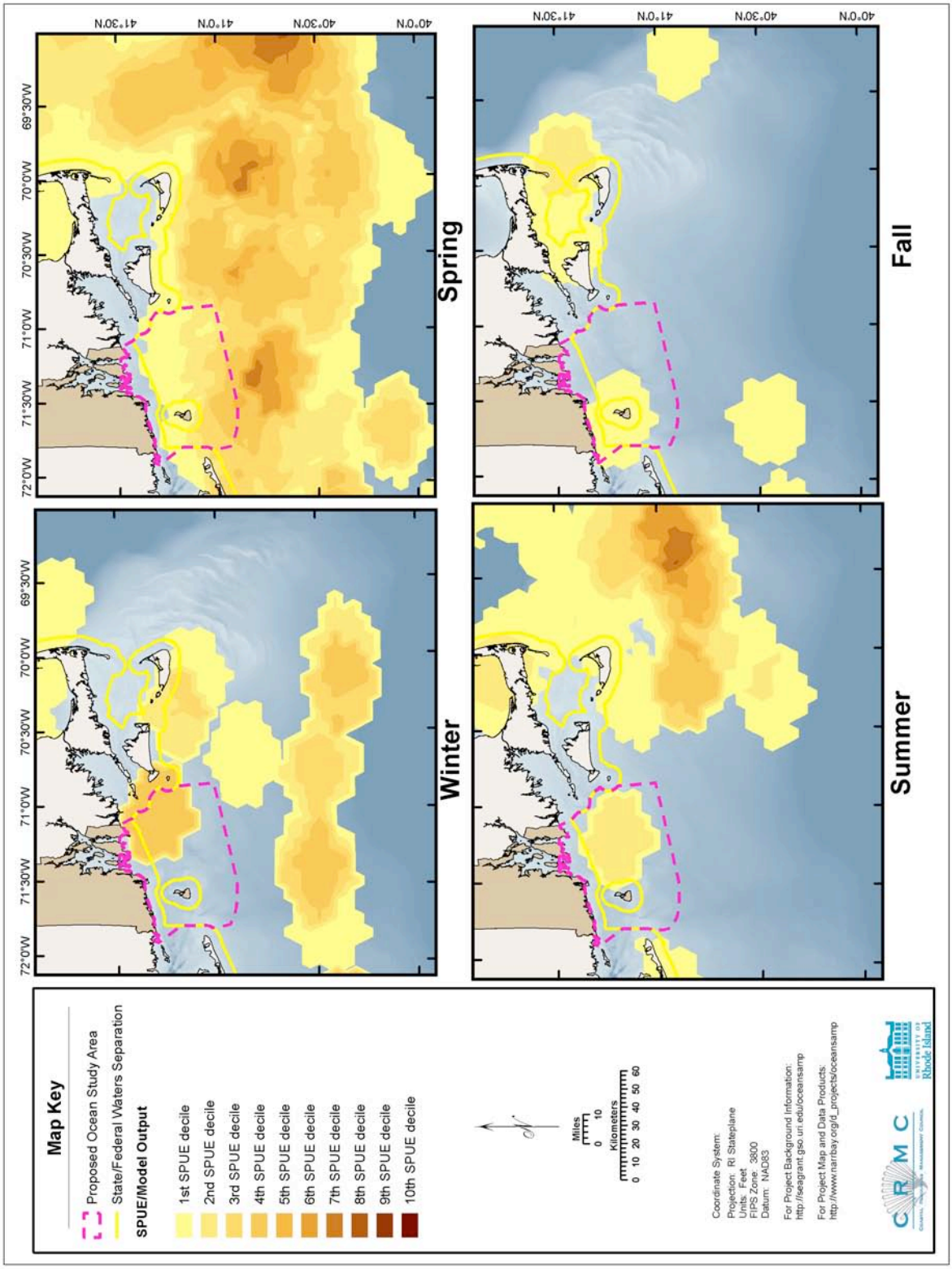

Figure 26. Modeled seasonal relative abundance patterns of harbor porpoises in the Rhode Island study area, corrected for uneven survey effort.

Stranding frequencies show a clear increasing trend beginning in the late 1980s (Fig. 27). One can only speculate about underlying causes. A high proportion of stranded porpoises have thin blubber, with starvation a contributing factor to their deaths (Nawojchik, 2002). Increased strandings could be related to increasing porpoise abundance in the region or to declines in prey availability. Some proportion of stranded porpoises also shows evidence of interaction with fisheries, primarily sink gillnets (Waring et al., 2008). Increasing strandings may reflect changes in fisheries—perhaps expansion of gillnet fishing for monkfish and dogfish. Landings of both increased sharply beginning about 1990.

The current Harbor Porpoise Take Reduction Plan (http://www.nero.noaa.gov/prot_res/porptrp) includes measures that recognize the high levels of mortality of harbor porpoises in gillnet fisheries off Rhode Island. The TRP established a Cape Cod South closure area to protect harbor porpoises. The closure area extends from 71°45' W (approximately the longitude of Weekapaug) east to 70°30' W (eastern Martha's Vineyard), and from the shoreline to 40°40' N. Gillnet fishing is prohibited completely in March. In December–February and April–May, gillnet fishing is allowed only using nets equipped with acoustic alarms ("pingers") that alert porpoises to the presence of the nets.

Conclusions: Harbor porpoises can occur in the SAMP area at any time of year, but are most abundant in spring, when they are moving inshore and northeastward. They are among the most abundant cetacean species in the SAMP area or the Rhode Island study area. Although they are not listed under the ESA, their abundance increases the likelihood of effects from development. In addition, seasonal restrictions on activities to mitigate potential impacts on right whales and other endangered species would mean that those activities would occur at times when harbor porpoises were likely to be abundant. This combination of factors suggests that harbor porpoise should be included in the second tier of conservation priorities for the SAMP (see Recommendations).

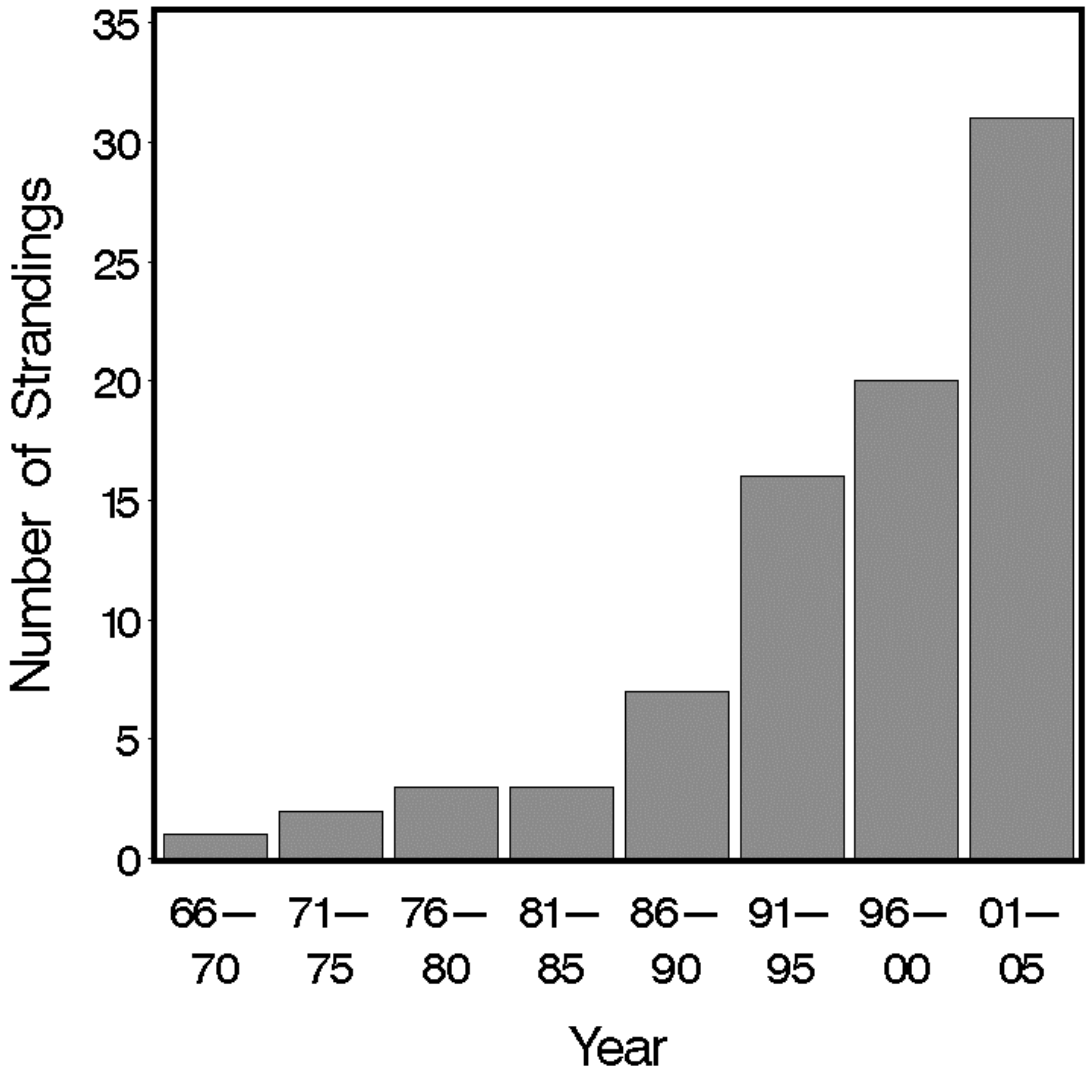

Figure 27. Five-year stranding frequencies for harbor porpoises in the Rhode Island study area, 1966–2005.

3.2.14. Long-finned Pilot Whale *Globicephala melas* (Traill, 1809)

Short-finned Pilot Whale *Globicephala macrorhynchus* Gray, 1846

Delphinidae is the most diverse and speciose family of cetaceans, with 17 currently accepted genera. Smaller delphinids are generally called "dolphins" and the larger ones "whales," perhaps

somewhat arbitrarily. In the recent past, the term "porpoise" was often used instead of "dolphin," especially in the U.S. The latter term could be confusing, because it also refers to tropical game and food fish in the genus *Coryphaena*. "Dolphin" is now used less often to refer to the fish in favor of the Hawaiian or Spanish name (mahi mahi or dorado, respectively).

All of the large, black, blunt-headed delphinids are sometimes collectively referred as blackfish, an old whalers' and fishermen's term. Pilot whales are sometimes also called potheads. The two species of pilot whales are well-defined and mostly parapatric, however, their ranges overlap in the waters off the mid-Atlantic coast of the U.S. They are also extremely difficult to differentiate in the field, so much of the information below refers to the two species combined.

Description: Pilot whales are easy to identify, but differentiating the long-finned and short-finned species in the field is exceedingly difficult (Jefferson et al., 1993; Bernard and Reilly, 1999; Wynne and Schwartz, 1999; Olson and Reilly, 2002). Both species are large, robust animals with a distinct "barrel-chested" appearance. Both are sexually dimorphic, with males larger than females. The head is rounded and bulbous with a very prominent melon, a slight beak, and an upturned mouth. The tailstock has prominent dorsal and ventral keels. The flippers are curved, tapered, and pointed. The dorsal fin is low, rounded to somewhat falcate, broad-based, and located well in front of the middle of the body. The color is black, dark gray, or brown overall, except for a whitish "anchor" mark on the chest, lighter gray "eyebrow" streaks from the eyes to the back, and a light gray "saddle" behind the dorsal fin.

Long-finned males may be as long as 7.6 m, while females reach a maximum of only 5.7 m. Their flippers are longer at about one-fifth of body length, with an obvious "elbow," but the length ranges overlap, making the difference in flipper length nearly useless as a field character for sightings of live animals. Short-finned pilot whales are somewhat smaller, and possibly slightly more thick-bodied, with males up to 6 m and females up to 5.5 m. The flippers in short-fins are shorter (about one-sixth of body length) and more curved, but the length ranges overlap, making the difference in flipper length nearly useless as a field character for sightings of live animals. In both species, dorsal fin shape changes in older adult males, with a tendency to become more broad-based in long-fins and more broad-based and hooked in short-fins. Additionally, in at least some short-fins, the saddle and lighter streaks on the head may be more

distinct, and the overall color more brown than black. Range may be helpful, but should not be relied upon for identification.

Status: Both long-finned and short-finned pilot whales are not listed under the U.S. Endangered Species Act and are classified as Data Deficient on the IUCN Red List. On the Rhode Island state list, long-finned pilot whales are classified as Unprotected, while short-finned pilots are not included.

The total abundance of either species of pilot whale in the North Atlantic is not well known, although the long-finned species is better known. Early estimates of the total size of the population impacted by directed harvests in eastern Canada concluded that there were 50,000–60,000 long-finned pilot whales in the western North Atlantic (Mitchell, 1974; Mercer, 1975). Hay (1982) estimated the abundance of long-finned pilot whales off Newfoundland and Labrador at 6,731–19,603; Kingsley and Reeves (1998) estimated 1,600 in the Gulf of St. Lawrence in late summer 1995; and Buckland et al. (1993) estimated 778,000 in the eastern and central North Atlantic. Because of the difficulty in identifying pilot whales at sea, off the eastern U.S. the two species currently must be combined for estimating abundance. Based on a 2004 summer survey, the combined stocks of both species between Florida and the Bay of Fundy were estimated at 31,139 animals (Waring et al., 2008). Efforts are underway to use a combination of genetic data from biopsy sampling, spatial modeling, color differences, and morphometrics to partition the estimates by species. In the Gulf of Mexico only short-finned pilot whales occur; recent abundance estimates for parts of the Gulf are 2,388 in 1996–2001 and 716 in 2003–2004.

Directed pilot whale fisheries on both species have occurred in many places around the world (reviewed in Bernard and Reilly, 1999). A drive fishery in Newfoundland took almost 10,000 pilot whales in 1956 but declined during the 1960s and eventually ended. Small-scale pilot whale fisheries formerly took place in Norway, Greenland, Iceland, Ireland, and Cape Cod, and Inuit subsistence hunters in Greenland took 5 in 2000, 45 in 2001, 24 in 2002, 195 in 2003, and 208 in 2004 (IWC, 2005, 2006). The drive fishery for long-finned pilot whales in the Faroe Islands is the only substantial hunt still continuing in the North Atlantic. It dates back to at least the 16th Century. Catches were about 1,500 per year in the 1970s and 2,500 per year in the 1980s, with little evidence for any negative impacts on overall pilot whale stocks in the northeastern Atlantic. Annual catches in 2000–2003 were 588, 918, 626, and 503 (IWC, 2005, 2006). Short-finned

pilot whales were hunted for centuries in Japan, and there are still catches of a few hundred per year (304 in 2000, 389 in 2001, 176 in 2002, 160 in 2003: IWC, 2005, 2006). In the North Atlantic, Yankee whalers left behind traditional fisheries in both the West Indies and the Azores that persisted into the 1980s.

Pilot whales are also impacted by bycatch in commercial fisheries. In U.S. Atlantic waters, average annual fishery-related mortality of both species combined in 2001–2005 was 163 animals. The predominant source of mortality is the pelagic long-line fishery for swordfish (86 per year), and pilot whales are also taken in bottom and mid-water trawl fisheries for squid, groundfish, and herring. Pilot whales were formerly taken in the pelagic swordfish driftnet and tuna pair-trawl fisheries, both now closed.

Ecology and life history: Pilot whales live in permanent social groups of about 10–50 animals, but at times pods join to form aggregations of hundreds of animals (Bernard and Reilly, 1999; Olson and Reilly, 2002). Off the northeastern U.S., group sizes observed ranged from 1 to 500, with a mode of 10 and mean of 20 (CETAP, 1982). In this region they commonly associate with other cetaceans. The most frequently observed mixed-species herds in the shelf-edge habitat off the northeastern U.S. were pilot whales and offshore bottlenose dolphins. They also have been observed associated with Risso's, common, and spotted dolphins and sperm whales, as well as in the same areas as fin and humpback whales in more inshore waters.

Short-finned pilot whales that were trained by the U.S. Navy routinely dived to 300 m and were capable of dives of 15 minutes and to at least 500 m and probably over 600 m (Bernard and Reilly, 1999).

In the North Pacific, there are differences in northern and southern stocks of short-finned pilot whales off Japan in size, markings, and life history (Kasuya and Tai, 1993; Bernard and Reilly, 1999). In the southern stock, mating is mostly in April–May and births are in July–August, but some births occur year round. In the northern stock calving is more strictly seasonal, with breeding in September and calving in December. Calves are about 1.7 m long at birth. The age at weaning is longer than in long-fins at 3.5–5.5 years. An older female might nurse her last calf for as long as 15 years (Marsh and Kasuya, 1991). Females reach sexual maturity at 9 years on average and males at about 16 years. A significant proportion of females become senescent, ceasing reproduction during or after their 30s.

Details of the social structure of long-finned pilot whale herds have been examined by genetic sampling from groups killed in a fishery in the Faroe Islands (located in the northeastern North Atlantic between Scotland and Iceland) (Amos et al., 1993). Entire herds are driven into a fjord or bay and killed, providing a complete picture of the inter-relationships among group members. All of the adults in a pod are related to one another. The calves and juveniles are offspring of the adult females in the pod, but the pod's adult males are not their fathers. Both males and females remain with their mothers for their entire lives, similar to the situation in killer whales. It is believed that mating occurs in large temporary aggregations, when the adult males are able to breed with females in other pods. Pilot whales also are one of the only non-human mammals with evidence of reproductive senescence, with post-reproductive individuals contributing to the survival of the young. In this system, the long-term benefits of group-living, social facilitation, and learning are maximized while still avoiding inbreeding.

Both species of pilot whales are known to strand commonly in large groups (Geraci and Lounsbury, 1993; Bernard and Reilly, 1999; Perrin, 2002f). Mass stranding is a phenomenon that occurs only in social odontocetes, including sperm whales, pilot whales, false killer whales, and some dolphin species. The causes of mass strandings are not well understood, and there are numerous hypotheses, including disease, parasites, geomagnetic anomalies interfering with navigation, social cohesiveness, and others. It is likely that there is no single cause, and that multiple causes interact. A common site for long-finned pilot whale mass strandings is on the inside of Cape Cod. In fact, a tidal creek in Wellfleet is called Blackfish Creek for the pilot whale strandings that have happened in that area at least since colonial times. Stranding events there tend to happen in winter, after storms when the water is murky and visibility limited. The bottom slope is nearly flat, so that echolocation provides no cue as to which direction is offshore, which also means that very wide mud flats are exposed at low tide. There is a known area of geomagnetic anomalies. It also may be possible that the usual direction to safety offshore for western North Atlantic pilot whales is south and east, which does not hold true inside Cape Cod Bay. In some strandings, rescue attempts are unsuccessful as animals seem to intentionally beach themselves again. Sometimes it appears that one or more individuals may be debilitated by disease or other cause, and the rest of the herd is trying to stay together. The adaptive value of social cohesion may be maladaptive under those circumstances.

On two occasions long-finned finned pilot whales that stranded in New England were rehabilitated and then released with satellite-tracked radio tags that provided information on movements and diving. Mate et al. (2005) tagged a 3-m, 2-year-old male in a group of three juveniles released after 7 months in captivity. They were released together on 29 June 1987 on the outer edge of Georges Bank about 160 km southeast of Cape Cod. The tagged whale was tracked for 94.5 days and a minimum distance traveled of 3144 km. It spent 10 days on Georges Bank, then moved offshore beyond the shelf edge for 9 days, then traveled 2 days north into the central Gulf of Maine, where it remained for the next 67 days. On day 20 it was observed in a group of pilot whales. The percent of time spent at the surface per day ranged from 5 to 47%. The average dive time was only about 40 seconds, but the average included short respiratory dives between breaths at the surface. The overall range of dive times was 6 seconds to almost 28 minutes, with a higher probability of short dives during the daytime and longer dives at night.

Nawojchik et al. (2003) released two juvenile males on 20 October 17 km south of Montauk Point (they had stranded on 28 June). They first headed west along the Long Island shore, then turned east and traveled to Nantucket. At that point they moved offshore to the outer part of Georges Bank and around the eastern end of the back into the basins to its north in November–December, then made a clockwise loop around the northern Gulf of Maine in January and ended up in the Great South Channel area east of Cape Cod in February. Most dives were less than 2 minutes and shallower than 15 m. Both whales made dives exceeding 26 minutes. Their deepest dives were 312 and 320 m, which is approximately the depth to the bottom in the area where they were at the time.

The preferred prey of both pilot whale species is squid, although at least long-finned pilot whales have been observed to feed on fish in the North Atlantic (Sergeant, 1962; Mercer, 1975; Kenney et al., 1985a; Desportes and Mauritsen, 1993; Bernard and Reilly, 1999; Olson and Reilly, 2002). Pilot whales were commonly taken in foreign fishing activities that were conducted in December–May 1977–1991 along the shelf edge off the northeastern U.S., with 391 taken in the mackerel fishery and 41 taken in the squid fishery (Waring et al., 1990; Fairfield et al., 1993). It is unclear whether mackerel is an important prey item in winter in our region, or whether the whales were simply feeding opportunistically on mackerel scavenged from the trawl nets.

Based on samples from fisheries in Newfoundland and the Faroe Islands, long-finned pilot whale calves in the North Atlantic are born in July–October (Bernard and Reilly, 1999). Calves are about 1.7 m long at birth (Wynne and Schwartz, 1999). Estimates of gestation period range from 12 months to as long as 15–16 months. Calves are weaned at about 22 months, and females that are simultaneously pregnant and lactating are rare. The average inter-birth interval is about 40 months. Females reach sexual maturity at 6–8 years (3.6–3.8 m) and males at about 12–17 years (4.8 m) (Desportes et al., 1993; Martin and Rothery, 1993). The occurrence of reproductive senescence seems to be less common than in short-finned pilot whales; a pregnant 55-year-old was observed in the Faroes, though ovulations appear to be spaced further apart in older females.

General distribution: Long-finned and short-finned pilot whales have mostly parapatric distributions, but they overlap in several areas of the world (Rice, 1998; Bernard and Reilly, 1999; Olson and Reilly, 2002). Long-finned pilot whales occur in the entire Southern Ocean south of 40ºS and in the North Atlantic north of about 30ºN, overlapping with short-fins (see below) from Australia to South America in the South Pacific, on the Atlantic coast of South America, and around South Africa. The broadest overlap is in the North Atlantic, from the east coast of the U.S. across to the eastern North Atlantic from France to northwestern Africa. Long-finned pilot whales range from North Carolina north to Newfoundland, Greenland, and Iceland, with possibly extralimital occurrences represented by strandings in South Carolina and Georgia. Fullard et al. (2000) proposed that there were two stocks of long-finned pilot whale in the North Atlantic—a cold-water population distributed north and west of the Gulf Stream, and a warm-water population associated with the Gulf Stream across the basin from North America to Europe.

Short-fins are found world-wide in warm-temperate to tropical waters on both sides of the equator, primarily in deeper offshore areas. Their southern limit is about 40ºS latitude around the entire Southern Ocean, to about 50ºN in the North Pacific and 42ºN in the North Atlantic. In the western North Atlantic, the range of short-finned pilot whales includes the southern U.S., Gulf of Mexico, Caribbean, West Indies, and the coast of South America. The northern limit of the range off the Atlantic coast is not well known, but believed to be between Virginia and New Jersey, probably varying seasonally.

Off the northeastern U.S., pilot whales (both species combined) are found primarily along the

shelf edge and around the edges of Georges Bank in all four seasons, most scattered in the winter (CETAP, 1982). Pilot whales occupied the most inshore depth zone of the shelf-edge cetaceans, along with common dolphins and offshore bottlenose dolphins (CETAP, 1982; Kenney, 1990). The patterns of seasonal distributions seen in the CETAP surveys and gaps in those patterns were suggestive of spatial partitioning between the species. In the winter, the densest concentration of sightings was offshore of New Jersey and southern New England, with scattered sightings along the edge of Georges Bank. South of New Jersey there were very few sightings except for a small cluster just off Cape Hatteras, North Carolina. In the spring, pilot whales were widespread from Maryland north to Georges Bank, and into shallower water on the shelf. There was a larger group of sightings off North Carolina than in winter, and still a hiatus in sightings east of Virginia. During the summer, there was a distinct concentration of pilot whales along the outer shelf from North Carolina to Delaware Bay, then a distinct gap south of Long Island and Cape Cod, and then sightings all around Georges Bank and into the central Gulf of Maine. Payne and Heinemann (1993) also noted the tendency for pilot whales to move into the deeper basins north of Georges Bank in late spring and summer. The pattern in fall was similar, except the gap in the middle was somewhat wider and extended farther south. More recent summer stock assessment surveys in 1998 and 2004 also showed a gap in pilot whale sightings approximately between the longitudes of eastern Long Island and Cape Cod (Waring et al., 2008). Those surveys also resulted in pilot whale sightings much farther offshore, mainly associated with the edge of the Gulf Stream.

Historical occurrence: The earliest pilot whale records for the Rhode Island study area were reported by De Kay (1842), who described a stranding at Fairfield Beach, Connecticut in October 1832 and two animals captured at the eastern end of Long Island in 1834. Cronan and Brooks (1968) reported three records from Rhode Island. One stranded in Middletown on 1 September 1959 and a 197-cm calf was caught in a fish trawl on 19 March 1961 about 50 km south of Narragansett Bay. The third was "the famous 'Willy the Whale' that cavorted about in the upper Providence River in July 1962. 'Willy,' who was actually a female, was over 18 feet in length." Connor (1971) mentioned several 20th Century stranding records from New York plus reports of frequent sightings. Waters and Rivard (1962) said that long-finned pilot whales were the most common whale in Cape Cod Bay, usually occurring in herds of up to 300, but that a large group of 1,975 had been seen off Blackfish Creek in Wellfleet in 1895. They also said that

pilot whales occurred year-round, but were most abundant in July and August. However, they did not list any recent records.

Recent occurrence: Pilot whales occur in the Rhode Island study area in all four seasons (Fig. 28), with a very strong peak in the spring (70.7%), and roughly equivalent proportions in the other seasons (winter – 8.1%, summer – 13.3%, fall – 7.4%). There are 43 records identified as long-finned pilot whales, only 1 as short-finned pilot whale, and 226 as only *Globicephala* sp. The seasonal proportions are nearly identical for long-finned pilot whales and *Globicephala* sp. There were only 12 sightings from the whale-watching data, 9 in summer and 3 in spring. Sightings were across the entire study area from the inner shelf to the slope, with more in shallow water in the spring, mirroring the pattern seen in CETAP (1982). In the Rhode Island to New Jersey stranding data, the ratio of long-finned to short-finned pilot whale is 9:1, but with the exception of the single Rhode Island record, short-finned pilot whale strandings have occurred only in New Jersey, and mainly in the southern part of that state. While there is a likelihood that some strandings might be misidentified, it is probably justifiable to conclude that pilot whales in the Rhode Island study area are usually the long-finned species, with short-fins occurring relatively rarely. A substantial proportion of the 226 unidentified pilot whale records in the combined data are more likely to have been long-finned pilot whales, consequently they were classified as "common" (Table 2) even though there were far fewer than 100 identified records.

The pattern in the effort-corrected relative abundance data (Fig. 29) is quite similar to that seen in the total occurrence data. Pilot whales occur in the Rhode Island study area year-round, but are most abundant in spring, most likely related to the inshore spawning of long-fin squid (*Loligo pealei*). Spring is also the only season when the relative abundance output predicts that pilot whales might occur in the SAMP area—in the southwestern corner of the area. In winter, there is an area of low abundance just offshore of the SAMP area and somewhat higher abundances farther offshore near the shelf edge. In summer, the abundances are maximum, but mainly east of the study area and offshore. The pattern in fall is similar to summer, however at lower abundance.

There was a mass stranding of 11 long-finned pilot whales in Cow Cove on Block Island, Rhode Island on 22 December 1983. The following day only five remained, all dead, but it is unclear from the Smithsonian data record whether the others were pushed off, left on their own,

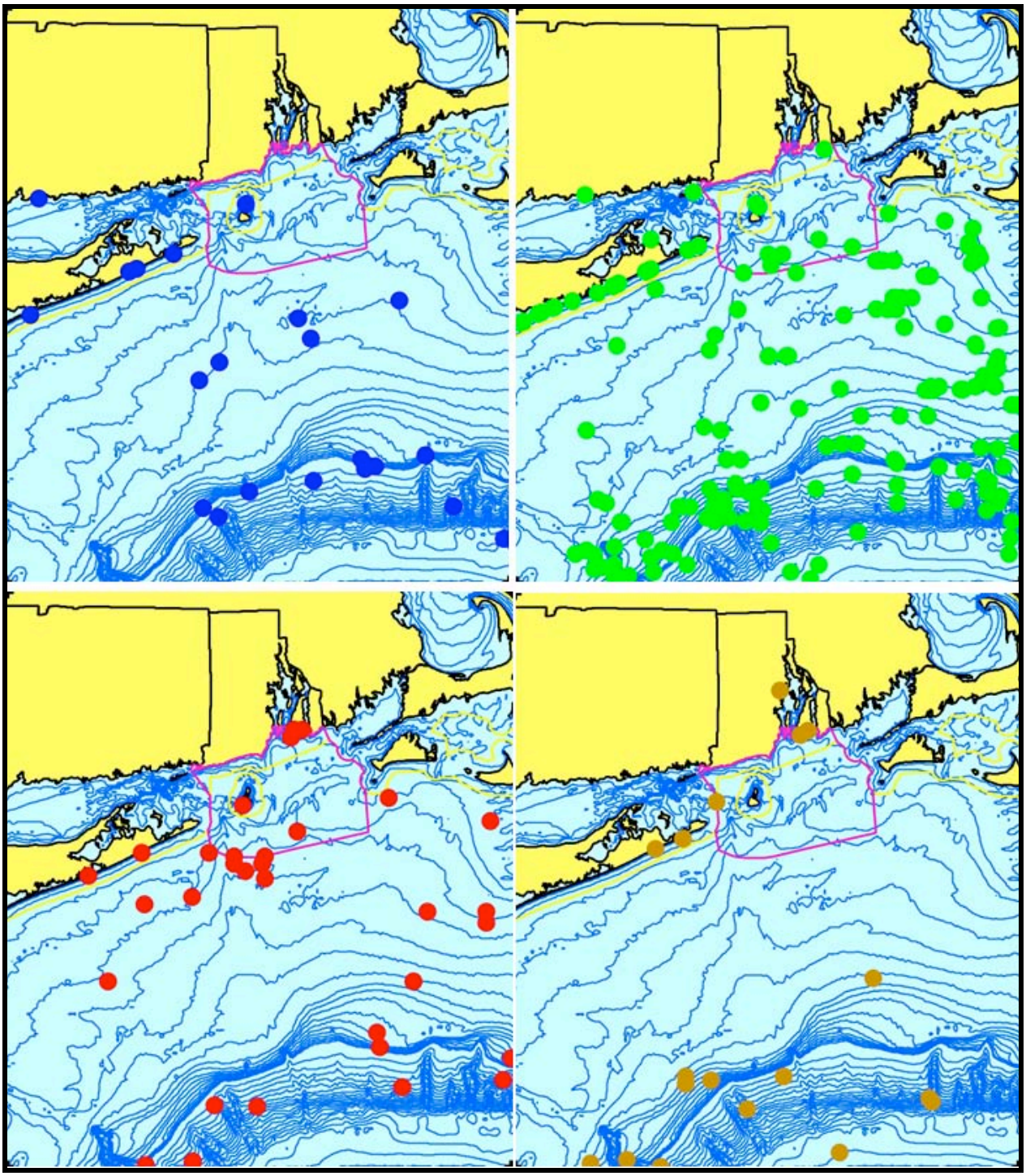

Figure 28. Aggregated sighting, stranding, and bycatch records of long-finned, short-finned, and unidentified pilot whales in the Rhode Island study area, 1834–2006 (n = 270: winter = 22, spring = 191, summer = 36, fall = 20, unknown = 1).

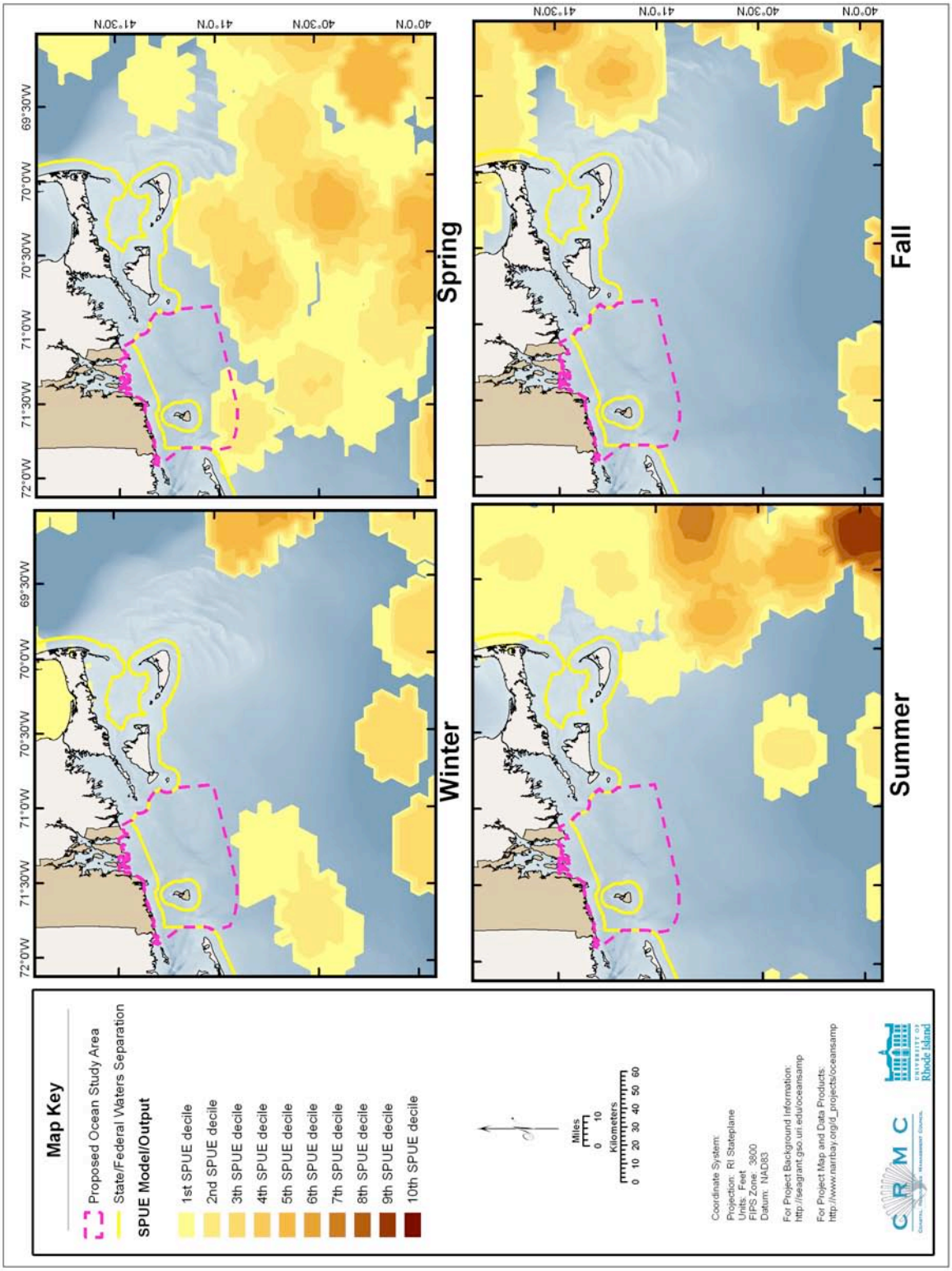

Figure 29. Modeled seasonal relative abundance patterns of pilot whales in the Rhode Island study area, corrected for uneven survey effort.

or died and washed out with the tide and waves. From necropsies of the five carcasses, the 1983 Block Island event was not a typical pilot whale mass stranding with a cross-section of ages and sexes (Nawojchik, 2002). All five were adult females of about the same size (442–457 cm) that all had some sort of medical problems (missing or broken teeth, thin blubber, kidney abnormality, abdominal fluid build-up).

Pilot whale stranding frequencies spiked in the late 1980s, and then declined but to a somewhat higher level than observed prior to 1985 (Fig. 30). The years 1987–1991 comprised a period of increased standings, with two in 1987, five in 1988, four in 1989, two in 1990, and three in 1991. Nearly all were in the spring, except for one in winter 1987, one in fall 1989, and one in winter 1991. Long-finned pilot whale strandings in Rhode Island occurred in Newport on 5 May 1974, in Newport on 28 November 1989 (a 192-cm calf), in Little Compton on 27 April 1990, at Clay Head on Block Island on 19 April 1994, near Goddard Park in Warwick on 8 October 1998, at Third Beach in Middletown on 2 June 2002, at Easton's Beach in Newport on 28 July 2003, and at Sandy Point on Block Island on 18 May 2004. There were also two strandings in Connecticut—in Madison on 5 April 1989 and in Branford on 9 February 1991. The latter animal had been reported alive along the Connecticut shore for five days before it washed up dead.

The only short-finned pilot whale record in the state or in the study area was a single animal stranded on 6 June 2001 at Snake Hole Beach on Block Island.

There were four strandings in the state of unidentified pilot whales: 18 December 1981 at Apponaug Cove in Warwick, 27 December 1985 at Brenton Cove in Newport, 18 February 1987 in Newport, and 17 March 1987 in Newport.

Conclusions: Although pilot whales (most likely long-finned pilot whales) are relatively abundant in the Rhode Island study area, they are not likely to occur within the SAMP area. The highest likelihood of occurrence would be in spring, and intensive whale-watching trips occasionally recorded pilot whale sightings southwest of Block Island. Pilot whales are not a significant concern for the SAMP.

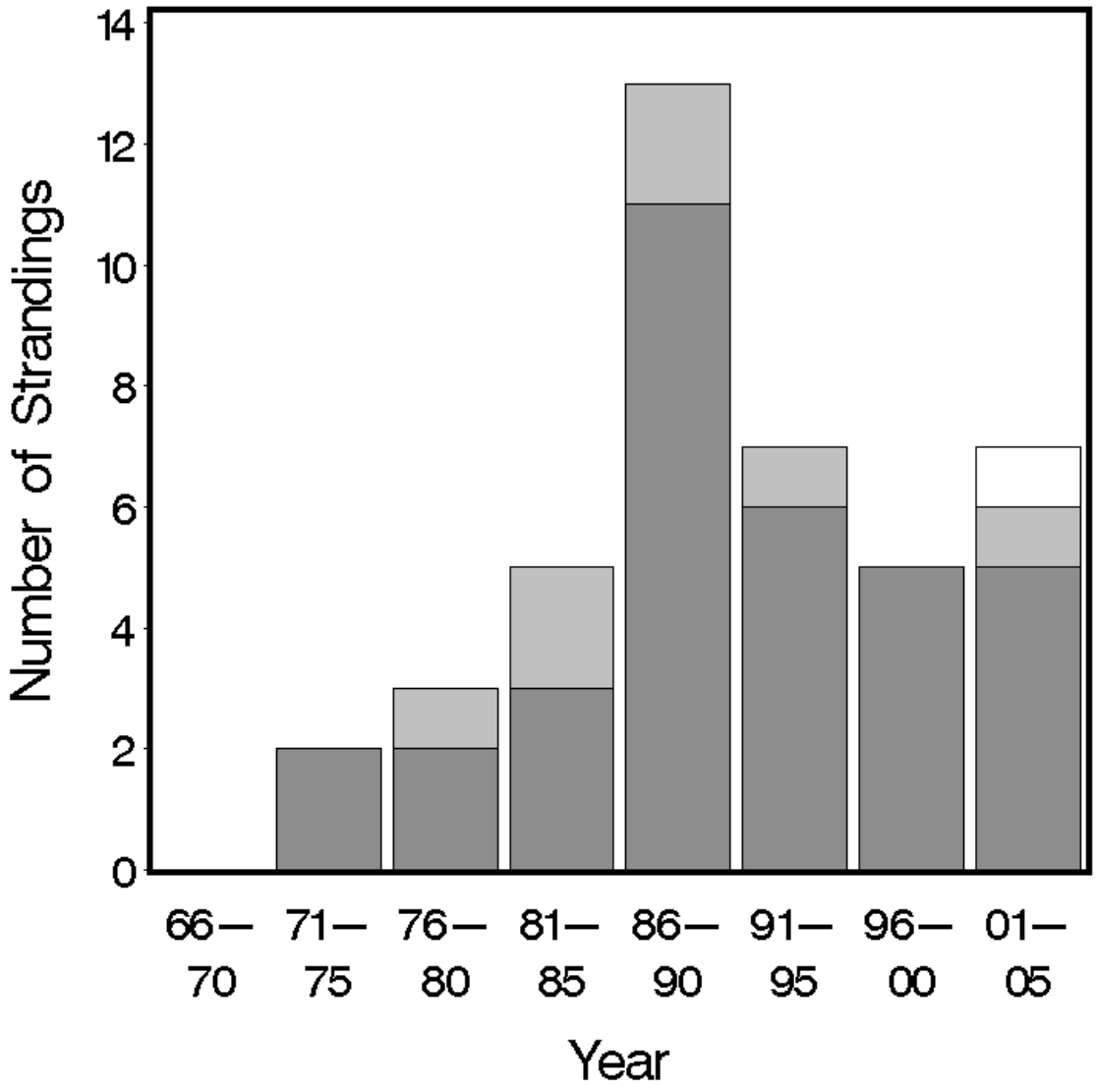

Figure 30. Five-year stranding frequencies for long-finned pilot whales (dark gray bars), short-finned pilot whales (white), and unidentified pilot whales (light gray) in the Rhode Island study area, 1965–2005.

3.2.15. Killer Whale *Orcinus orca* (Linnaeus, 1758)

Description: Killer whales, or orcas, are the largest of all delphinids. They are sexually dimorphic, with males up to 9.8 m and females up to 7–8.5 m (Jefferson et al., 1993; Wynne and Schwartz, 1999). They are very distinctive and easily recognized. The body is robust with a

rounded head and very large, rounded flippers. The dorsal fin is about 1 m tall and falcate in females and juveniles, and 2 m high and erect in adult males. The color pattern is strikingly distinct, with a black back, dorsal fin, flukes, and flippers clearly contrasting with white under the belly, chin, and flukes. The white belly extends in a narrow lobe up and back on both sides behind the dorsal fin, and there is an oval white patch behind and above each eye. There is also a gray saddle patch behind the dorsal fin. Killer whales have 10–12 large, slightly curved teeth on each side of both upper and lower jaws.

Status: Killer whales are not listed under the U.S. Endangered Species Act, although the Southern Resident stock in the eastern North Pacific has recently been listed as Endangered (NMFS, 2005). They are not included on the Rhode Island state list, and are classified as Data Deficient on the IUCN Red List. There are no abundance estimates for the entire North Atlantic, although there are estimates based on photoidentification or similar methods for limited areas (Dahlheim and Heyning, 1999), including 500–1500 off Norway and 143 off Iceland. There is also no estimate for U.S. Atlantic waters, and an estimate of 133 for the northern Gulf of Mexico (Waring et al., 2008). Killer whales were formerly taken by small-scale coastal whaling in a number of locations; 13 were killed by subsistence hunters in Greenland in 2002 (IWC, 2006).

Ecology and life history: Killer whales are extensively studied, and are known to live in permanent pods of up to 50 individuals (reviews in Dahlheim and Heyning, 1999 and Ford, 2002). Pods are matrilineal social groups that are formed of females, their sons and daughters, and the offspring of the daughters. Unlike most mammals, both females and males remain in their natal pods for life. The maximum life span of orcas may be 80 or 90 years, which results in pods containing as many as four generations together.

General distribution: Killer whales are cosmopolitan, and may be the most broadly distributed of all cetaceans (Heyning and Dahlheim, 1988; Dahlheim and Heyning, 1999; Ford, 2002). They occur in all oceans of the world from the tropics to the edge of the polar ice, and from estuaries and shallow coastal waters to deep, offshore waters. They appear to be most common in colder, nearshore waters. In the western North Atlantic, they are known from the Arctic to the tropics, but are not common anywhere. There were only 12 sightings off the northeastern U.S. during the CETAP study (CETAP, 1982) and none during the more recent NMFS assessment surveys (Waring et al., 2008), although over a longer term they appear to be

regular visitors to the Gulf of Maine (Gormley, 1990; M. Lutcavage, University of New Hampshire, pers. comm.).

Historical occurrence: Cronan and Brooks (1968) said they had one record of a killer whale stranding in Rhode Island, but provided no details, however Waters and Rivard (1962) included in their table a stranding of a 5.5-m animal in Narragansett in December of 1956. Waters and Rivard said that killer whales were fairly common in Massachusetts waters, and also cited records of one killed in Lewis Bay in Hyannis in March 1949, a pod seen off Provincetown in August 1949, and a stranding of a 5.2-m whale on Waquoit Beach in Falmouth in 1956. De Kay (1842) reported several sightings of killer whales off Long Island, and suggested without documentation that they were formerly more numerous. Connor (1971) described a live-stranded 730-cm orca at Orient, Long Island in January 1944 and a large male that followed a fishing boat for more than 30 km on its way back to Montauk in July 1958 (both records were in the Smithsonian data).

Recent occurrence: There are five additional killer whale records in the more recent data (Fig. 31). One or more orcas were reported by fishermen in Long Island Sound off Mattituck in August 1977. A group of 20 was sighted about 16 km southeast of Block Island on 22 September 1981. There were also three sightings in deep water south of Cape Cod—a group of 6 on 25 July 1979, a single animal on 5 October 1981, and a group of 19 on 13 September 1991.

Conclusions: Killer whales are sufficiently rare in the Rhode Island study area as to be ignored relative to development in the SAMP area.

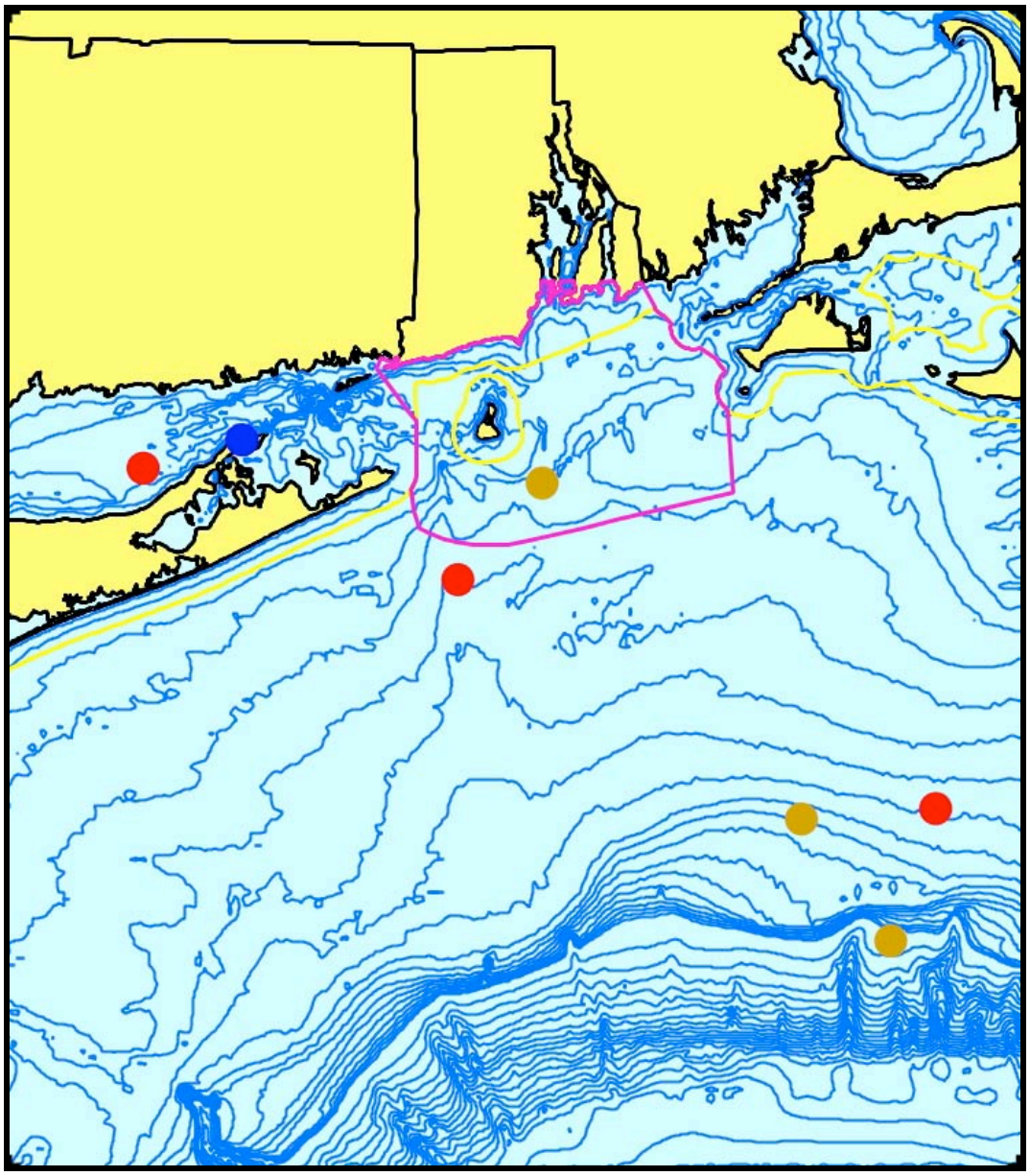

Figure 31. Aggregated sighting, stranding, and bycatch records of killer whales in the Rhode Island study area, 1944–1991 (n = 7: winter = 1, spring = 0, summer = 3, fall = 3).

3.2.16. False Killer Whale *Pseudorca crassidens* (Owen, 1846)

Description: False killer whales were so named because of the resemblance of the skull to that of a killer whale, not because of similar appearances (Odell and McClune, 1999). In fact, they look more like slimmed-down pilot whales, with which they are included as the larger "blackfish" (Jefferson et al., 1993; Wynne and Schwartz, 1999). They are long and slender,

uniformly black with a pale anchor mark on the chest, no cape, and no white markings visible anywhere on the head or back. Total length is up to 5.5 m in males and 4.8 m in females. The head is narrow and tapered, with no beak and a small, rounded melon that overhangs the lower jaw. The flippers have a distinctive hump on the leading edge, which makes them look permanently bent. The dorsal fin is dolphin-like, narrow-based, located at mid-back, falcate, and often rounded at the tip. There are 7–12 large (up to 1.8 cm in basal diameter) teeth in each side of both jaws.

Status: False killer whales are not listed under the U.S. Endangered Species Act, are not included on the Rhode Island state list, and are classified as Data Deficient on the IUCN Red List. There are no estimates of the total number of false killer whales in the North Atlantic, none have been sighted from any stock assessment surveys off the U.S. Atlantic, and the number in the northern Gulf of Mexico is estimated as 1,038 (Waring et al., 2008). False killer whales are taken in low numbers (5–26 in a year in 2000–2004) in coastal small-cetacean fisheries in Japan (IWC, 2005, 2006).

Ecology and life history: False killer whales are believed to feed primarily on deep-sea squid and fishes, but have been seen to attack smaller dolphins escaping from tuna nets (Odell and McClune, 1999; Baird, 2002a). There was one observation each of an attack on a humpback whale calf and on a group of sperm whales. They appear to be very gregarious, but their social organization and life history are very poorly known.

General distribution: False killer whales are found in pelagic tropical, subtropical, and warm temperate seas in all oceans of the world (Stacey et al., 1994; Odell and McClune, 1999; Baird, 2002a). In the western Atlantic, they occur from Maryland south to the Gulf of Mexico, Caribbean Sea, West Indies, and off mainland South America to the tip of Tierra del Fuego. Sightings are typically in deep water beyond the shelf break. Little is known of seasonality of occurrence.

Historical occurrence: There are no historical records of false killer whales in the Rhode Island study area, and they were not mentioned by Cronan and Brooks (1968) or any of the other regional sources consulted.

Recent occurrence: There have been no false killer whale strandings in the Rhode Island study area. There were nine sightings in the whale-watching data over a four-year period in

1990–1993, all in the same general vicinity south of Block Island and Montauk Point between the 50- and 70-m isobaths (Fig. 32). The sightings occurred during very short periods each year: 22–29 May 1990, 31 May–13 June 1992, and 3 May 1993. The largest group seen at any one time was five, and on the only day with two sightings (28 May 1990), there were groups of two and three whales seen. One could speculate that a small group of five false killer whales returned to the same vicinity at the same time of year for several years in a row. From other sighting records in the NARWC database, the pattern of occasional occurrences in unusual locations seems to be characteristic of false killer whales. Although most sightings have been off the southeastern U.S., there are records far to the east in the mid-ocean, a sighting in Cape Cod Bay in March 1978, and sightings on Georges Bank in 1980 and 1987.

Conclusions: Although false killer whales may occur on very rare occasions in the SAMP area, they may safely be ignored.

3.2.17. Risso's Dolphin *Grampus griseus* (G. Cuvier, 1812)

Description: Risso's dolphins are large, robust animals, 3–4 m in length, which are relatively easy to identify (Jefferson et al., 1993; Kruse et al., 1999; Wynne and Schwartz, 1999; Baird, 2002b). The body is thick and robust from the dorsal fin forward and relatively slender behind. The impression is that of a shorter, more barrel-chested pilot whale. The head is blunt with a squarish profile and a slight but distinctive vertical crease down the forehead. The mouth curves noticeably upward, and there is no beak. The flippers are very long and pointed but broader than in pilot whales, and the dorsal fin is very tall, slender, and falcate. The color pattern is distinctive and unique. Calves are uniformly light gray, and gradually darken to dark gray or brown with a white belly and white "anchor" mark on the chest as juveniles. Older animals get gradually whiter, mainly from scars and scratches, especially on the head. Old adults may be entirely white except for the dorsal fin, flippers, and flukes.

Status: Risso's dolphins are not listed under the U.S. Endangered Species Act or on the Rhode Island state list, and are classified as Least Concern on the IUCN Red List. There are no estimates of the total number of Risso's dolphins in the North Atlantic, and no information on stock separation. The most recent estimate of abundance of Risso's dolphins along the U.S.

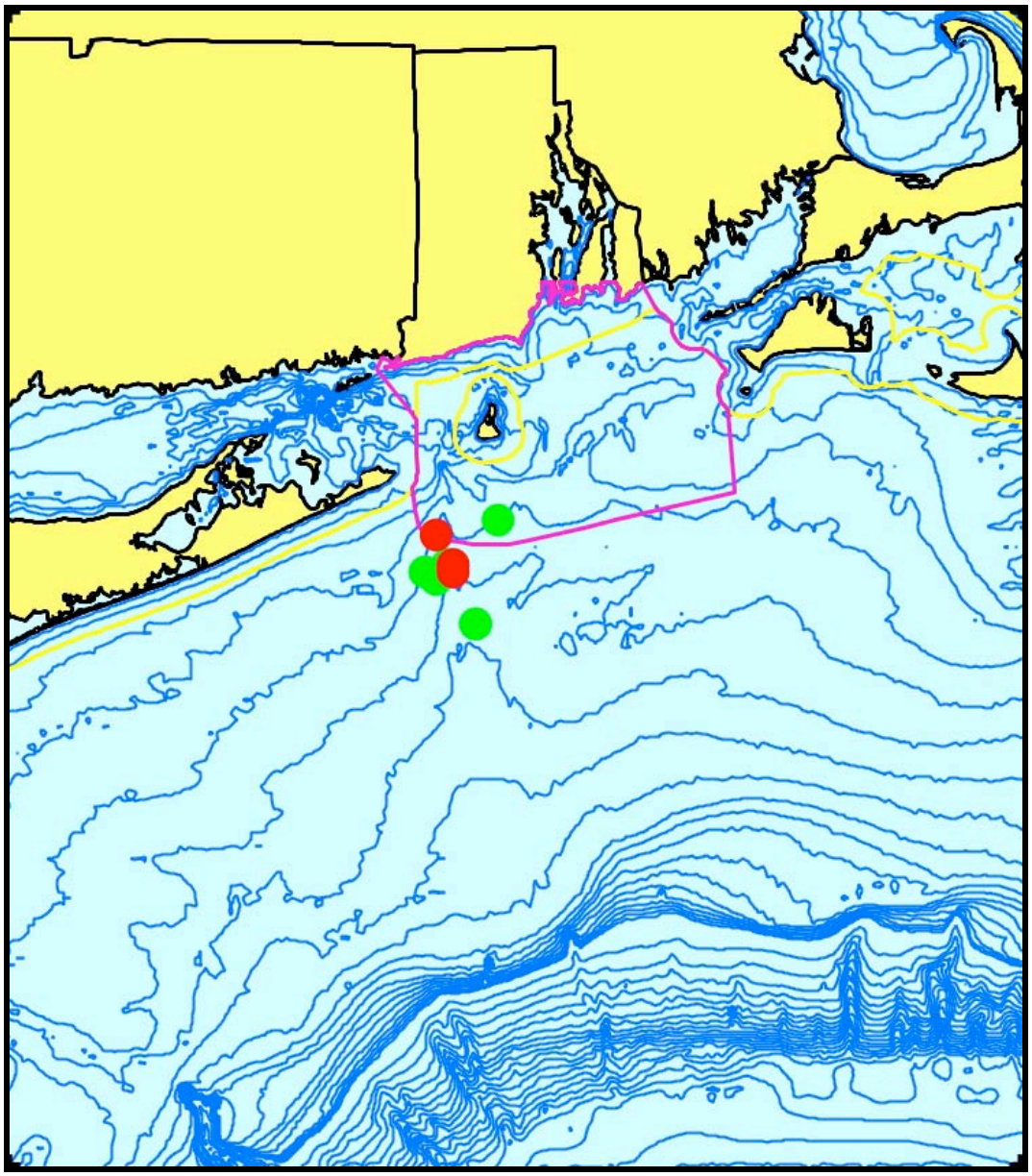

Figure 32. Aggregated sighting, stranding, and bycatch records of false killer whales in the Rhode Island study area, 1990–1993 (n = 9: winter = 0, spring = 6, summer = 3, fall = 0).

Atlantic coast was 20,479, with an additional 1,589 in the northern Gulf of Mexico (Waring et al., 2008). Surveys in 1998 estimated the Atlantic stock at 28,164.

Risso's dolphins have been taken in a number of small-cetacean fisheries around the world, but have never been the focus of a large-scale fishery (Kruse et al., 1999). They have been taken in Europe, Canada, the West Indies, the Azores, Peru, and Japan. Recent takes in Japanese small-

cetacean fisheries were 506 in 2000, 474 in 2001, 386 in 2002, 373 in 2003, and 6 in 2004 (IWC, 2005, 2006). They are also subject to incidental take in variety of commercial fisheries (Read, 1996). The average annual fishery-related mortality of Risso's dolphins in U.S. Atlantic fisheries in 2001–2005 was 40 (Waring et al., 2008). Most mortality (37 per year on average) was in the pelagic swordfish long-line fishery, with the remainder in the sink gillnet fishery. There was formerly mortality in the pelagic swordfish driftnet and tuna pair-trawl fisheries, both of which are now closed.

Ecology and life history: Risso's dolphins generally occur in small groups of 10–50 animals, but may be sighted as single individuals and in herds of several hundred or more (Kruse et al., 1999; Baird, 2002b). Off the northeastern U.S. the mean group size was 17, with a range from 1 to 400 (CETAP, 1982). They frequently perform aerial behaviors such as breaching, spy-hopping, and lob-tailing, but rarely bow-ride. They were sighted at times in association with pilot whales, offshore bottlenose dolphins, and other species (CETAP, 1982). In the North Pacific they associate with many other species in mixed groups (Kruse et al., 1999).

There are almost no data on diving capabilities. They appear to be capable of dives up to 30 minutes (Kruse et al., 1999).

Risso's dolphins are believed to feed exclusively or almost exclusively on squid (Kruse et al., 1999; Baird, 2002b). Reduction in the number of teeth is believed to be an adaptation to the squid-feeding habit (Clarke, 1986). Based on observations of activity patterns off Santa Catalina Island, California, Risso's dolphins are mainly nocturnal feeders (Shane, 1995).

Life history data for Risso's dolphins are sparse (Kruse et al., 1999; Baird, 2002b). Calves are born at 110–150 cm, and calving may peak in the winter. Size at sexual maturity is 2.6–2.8 m in females and 2.6–3.0 m in males. There is no information on gestation or lactation periods or inter-birth intervals.

Amano and Miyazaki (2004) reported on a school of 79 killed in a drive fishery in Japan. There were 49 females and 30 males, for a sex ratio of 1.63:1. Of the females, 2 were pregnant, 9 lactating, 2 both pregnant and lactating, 14 resting, 14 immature, and 8 unknown (66% mature). Their age at maturity was probably 8–10 years, and the oldest was 34.5. Of the males, 23 were immature, 4 were maturing, 1 was mature, and 2 were unknown (18% mature). The estimated age at maturity was 10–12, but the sample size was very small. The oldest male was 16.5. The

sex and age structure of the school suggests a life history pattern where males leave their natal groups when mature and remain segregated from schools of females and immatures.

General distribution: Risso's dolphins are found in tropical and temperate waters world-wide (Rice, 1998; Kruse et al., 1999; Baird, 2002b). In the Atlantic, they occur from Newfoundland and the British Isles south to the southern tips of Africa and South America, although the distribution is poorly known along the coasts of east-central South America and western Africa. Their distribution is primarily in deeper pelagic waters, and is poorly known in the central ocean regions. In the western North Atlantic they are found primarily along the shelf break, but are also sighted commonly in shallower waters to about mid-shelf, as well as much farther offshore. Off the northeastern U.S., Risso's dolphins occurred along the entire shelf in spring and summer, with dense concentrations from about Virginia to Cape Cod in spring and from Virginia to Georges Bank in summer (CETAP, 1982). In the fall, the number of sightings declined and the distribution contracted to Virginia–Long Island. There were many fewer sightings in winter, mostly east of Maryland and Virginia. Summer surveys in 1998, 1999, and 2004 extended farther offshore and resulted in numerous sightings, often associated with edges of the Gulf Stream and warm-core rings (Waring et al., 2008). The recent surveys also resulted in sightings offshore of the 100-m isobath off the southeastern U.S.

Historical occurrence: Cronan and Brooks (1968) were aware of no Risso's dolphin occurrences in Rhode Island. Neither De Kay (1842) nor Linsley (1842) mentioned the species. Schevill (1954) reported a sighting of more than 60 Risso's dolphins on 20 August 1952 about 140 km due south of Block Island near the shelf break. That record seemed to be the basis for conjectures about occurrence by Cronan and Brooks (1968), Waters and Rivard (1962), and Connor (1971). In their table of records from the 1940s and 1950s, Waters and Rivard included only Schevill's 1952 sighting (however giving the number of animals as one) and a sighting of three 350 km east of Cape Cod. Of course, none of those authors had the benefit of seeing the results of CETAP and subsequent surveys to know that Risso's dolphins are quite common in the area of Schevill's sighting. There are no historical strandings in the Rhode Island study area, although they are relatively common in New Jersey and less so in western Long Island. The only historical sighting in the study area was a group of 3 near Hudson Canyon on 29 May 1960 reported by Ulmer (1980) and included in the Smithsonian data.

Recent occurrence: Risso's dolphins are present year-round, but with strong seasonality (Fig. 33). They are most common in summer with 56.3% of the records, followed by 25.0% in fall, 15.9% in spring, and only 2.9% in winter. The sighting distribution is primarily along the shelf break and slope, with a few sightings in waters shallower than 100 m. There was only one spring sighting in the SAMP area, although there were strandings in or nearby in every season. Even with very intensive whale-watching over more than 15 years, they recorded only one sighting of Risso's dolphin—a group of 15 on 28 July 1992, which was on an offshore trip.

The patterns in the relative abundance data (Fig. 34) show the same thing as the total data. Abundance is lowest in winter and spring and highest in summer and fall. In addition, the species' distribution is centered far offshore in all seasons, with no areas of predicted occurrence in or near the SAMP area.

In the recent stranding record for the Rhode Island study area, Risso's dolphins have been relatively scarce. The first known stranding in the area was a 288-cm "old" adult on 17 July 1987 at Schooner Point on Block Island. A 192-cm immature male stranded at Newport on 28 November 1989. On 14 December 1991 a live Risso's dolphin was seen in a cove on the west side of Hog Island, but it was found dead the next day. A 250-cm adult stranded on Cooneymus Beach on Block Island on 3 March 1994. Risso's dolphins stranded in South Kingstown on 1 August 2004 and at Mackerel Cove in Jamestown on 25 August 2005. There were also strandings on the south shore of eastern Long Island in January 1995, March 2002, June and July 2004, and July, August, and September 2005. There is a very clear recent spike in the stranding record—of 13 total strandings during 1987–2005, 7 (53.8%) were in the last two years. To see whether that trend was more widespread and if it continued beyond the end of the stranding database we used, we reviewed the 2007 (Waring et al., 2008), 2008 (Waring et al., 2009), and draft 2009 stock assessments (NMFS, unpublished). The total numbers of Risso's dolphin strandings from Maine to Virginia were: 3 in 2001, 7 in 2002 (5 in Massachusetts), 13 in 2003 (10 in Mass.), 13 in 2004, 25 in 2005, 5 in 2006, and 7 in 2007. The 2004–05 spike seen in strandings in the study area was also present in the entire Northeast; it appeared to begin a year earlier in Massachusetts, and it did not continue beyond 2005.

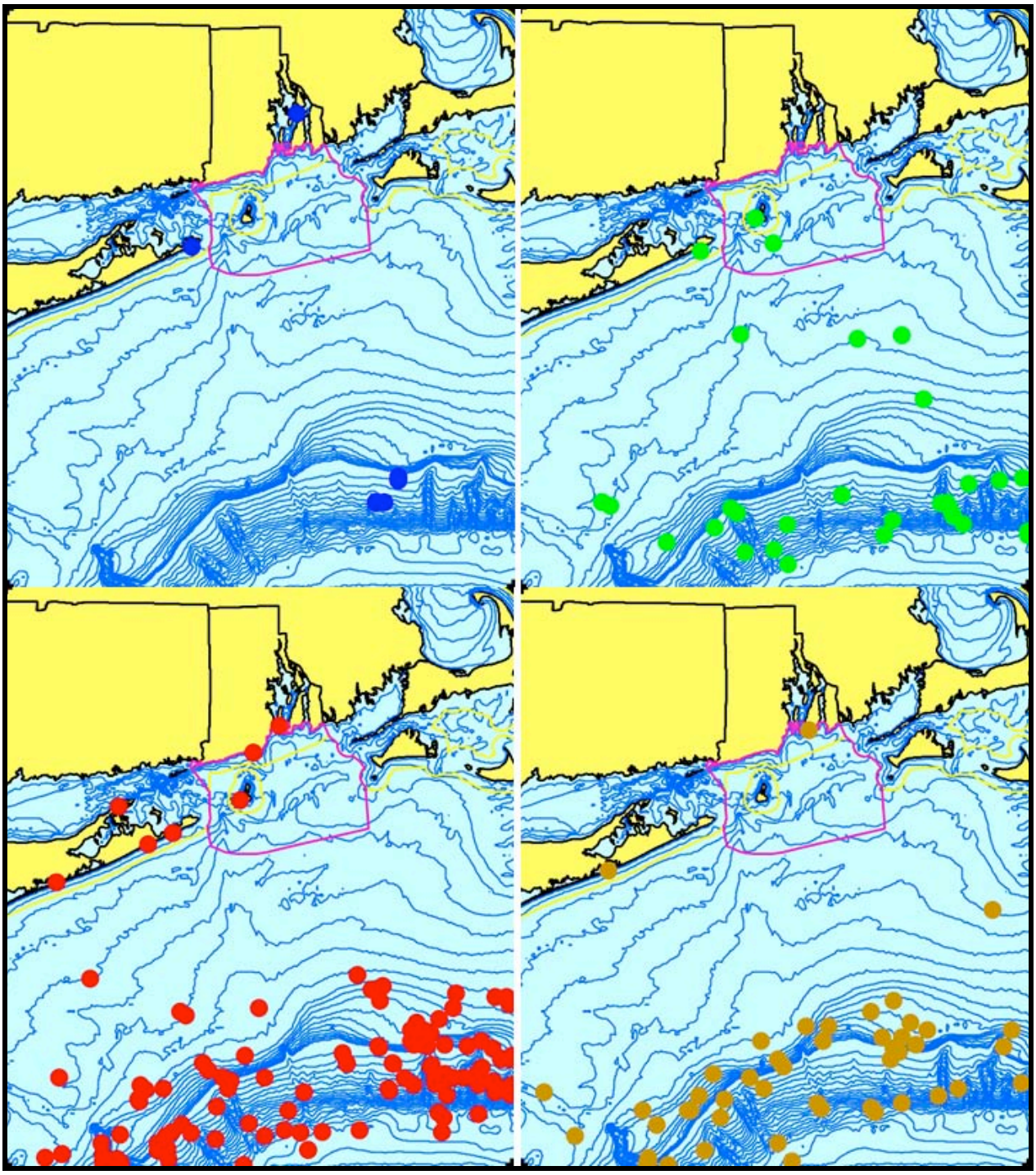

Figure 33. Aggregated sighting, stranding, and bycatch records of Risso's dolphins in the Rhode Island study area, 1960–2005 (n = 208: winter = 6, spring = 33, summer = 117, fall = 52).

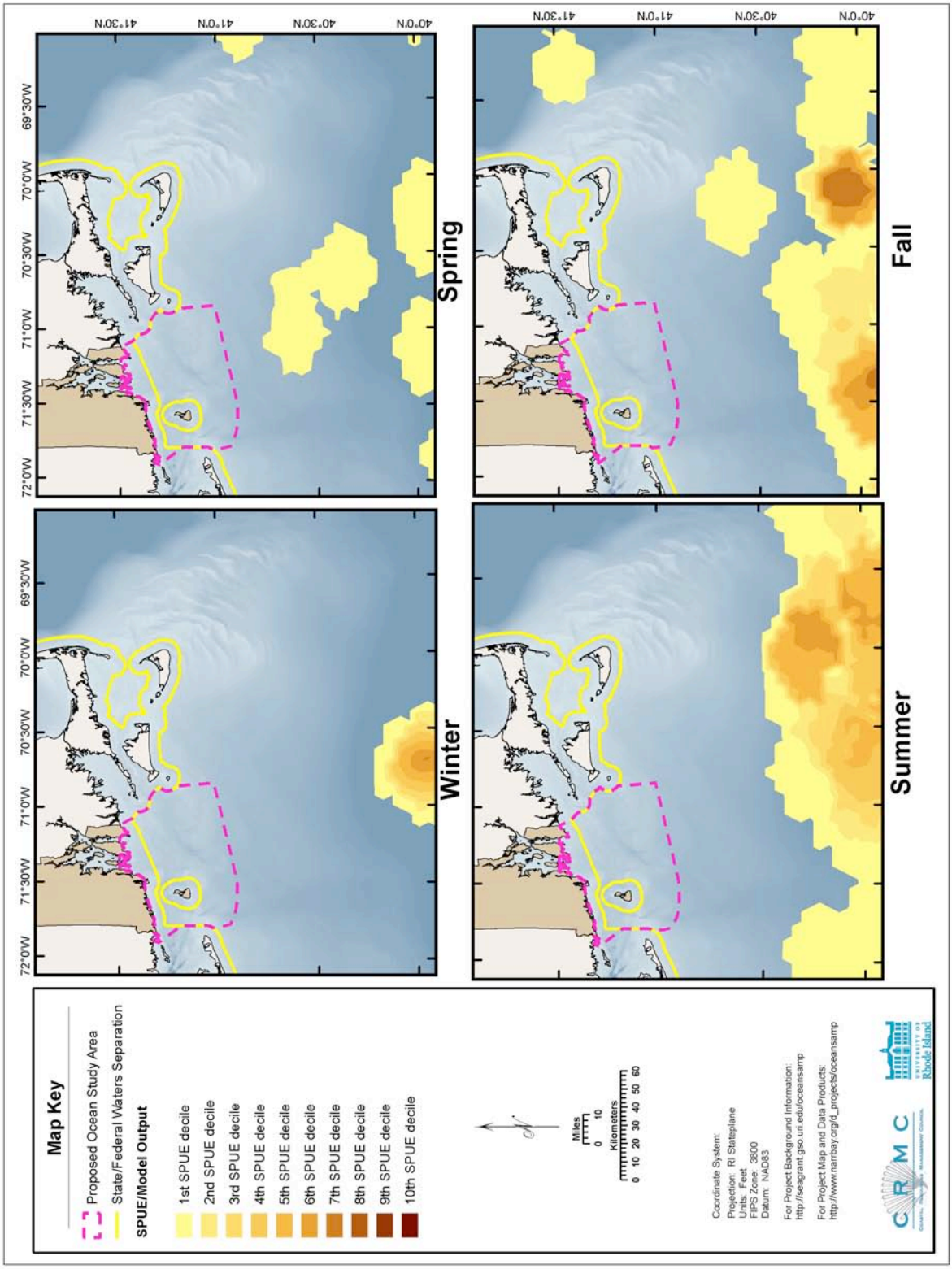

Figure 34. Modeled seasonal relative abundance patterns of Risso's dolphins in the Rhode Island study area, corrected for uneven survey effort.

Conclusions: Risso's dolphins are offshore animals and are not expected to occur in the SAMP area. They are clearly much more common in the study area than the previous species, false killer whale, and easier to identify, however the respective numbers of sightings of the two species from the whale-watching boats were one and nine. That confirms just how unlikely Risso's dolphins are to occur in the SAMP area.

3.2.18. Atlantic White-sided Dolphin *Lagenorhynchus (Leucopleurus) acutus* (Gray, 1828)

The six species of dolphins that have been included in the genus *Lagenorhynchus* appear very similar; all have robust bodies with tall falcate dorsal fins, very short beaks, and bold, distinctive color patterns (Jefferson et al., 1993; Folkens et al., 2002). LeDuc et al. (1999) and Cipriano (1997) both showed that the two North Atlantic species are genetically very divergent from the other four species and from each other. *L. albirostris* is the designated type species of the genus, and therefore should maintain the current name. The available generic name would *Leucopleurus* Gray, 1866 for the Atlantic white-sided dolphin. A detailed genetic analysis by May-Collado and Agnarsson (2006) supported the recognition of Atlantic white-sided dolphin as *Leucopleurus acutus*.

Description: Atlantic white-sided dolphins have robust bodies about 2.5–2.8 m in length; prominent sharp keels on the top and bottom of the tailstock; short, thick beaks; and very prominent, tall, falcate, pointed, broad-based dorsal fins (Jefferson et al., 1993; Reeves et al., 1999a; Wynne and Schwartz, 1999; Cipriano, 2002). Females are about 20 cm shorter than males. The basic color pattern is three-banded, with a black cape, a gray band along the side, and a white belly, all with clear, distinct, relatively horizontal margins. On the flank, below and slightly behind the dorsal fin, there is a brilliant white patch or band below the edge of the cape, which extends up and back into the cape as a yellowish-tan band. The cape extends all the way back from the dorsal fin to the tail, though from above and behind it may look like a narrow black stripe along the dorsal keel between the two yellow bands on the sides. On the beak, the upper jaw is black and the lower is white. The eye is surrounded by a round black patch, which is connected by a narrow black stripe to the upper jaw. There may also be a narrow, less distinct gray stripe from the eye to the black flipper, and there is a black patch around the genital slit.

Status: Atlantic white-sided dolphins are not listed under the U.S. Endangered Species Act or

on the Rhode Island state list, and are classified as Least Concern on the IUCN Red List. There are no precise estimates of the number of white-sided dolphins inhabiting the North Atlantic, though the number is roughly estimated as a few hundred thousand (Cipriano, 2002). They were one of the two most abundant dolphins observed during the CETAP studies (the other was the common dolphin), with seasonal abundances off the northeastern U.S. in spring through fall of 38,000 to 42,000 (CETAP, 1982; Kenney et al., 1997). The most recent estimates for the Gulf of Maine and surrounding area have been extremely variable—51,640 in 1999, 109,141 in 2002, 2,330 in 2004, and 17,594 in 2006 (Waring et al., 2008). Kingsley and Reeves (1998) estimated the number in the Gulf of St. Lawrence in 1995 at 11,740.

A directed fishery for Atlantic white-sided dolphins formerly occurred in Norway, and small numbers are taken by subsistence hunters in Greenland (Reeves et al., 1999a). Large numbers were taken in some years in the former pilot whale drive fishery in Newfoundland (Sergeant and Fisher, 1957). In the Faroe Islands, white-sided dolphins continue to be taken in their pilot whale drive fishery, with total takes of 255 in 2000, 546 in 2001, 714 in 2002, and 186 in 2003 (IWC, 2005, 2006).

White-sided dolphins are also taken as bycatch in commercial fisheries (Addink et al., 1997; Couperus, 1997; Palka et al., 1997; Reeves et al., 1999a). The 2001–2005 average annual mortality from incidental take in U.S. Atlantic commercial fisheries was 357, including 31 in sink gillnet fishery, 221 in bottom trawls, 103 in mid-water trawls, and 2 in herring trawls (Waring et al., 2008). There were earlier takes known in swordfish driftnets (fishery now closed), Canadian sink gillnets, and Spanish deepwater trawlers off the Grand Banks.

Ecology and life history: White-sided dolphins generally occur in groups of a few to 50 or 60 animals, with some differences between areas (Reeves et al., 1999a; Cipriano, 2002). In the Gulf of Maine, they appear to travel in tight groups of 6–10 animals that are sometimes loosely associated in larger herds. In the CETAP (1982) data, group sizes ranged from 1 to 800, with a mean of 54.3, but the most frequently observed group size was 8 dolphins. White-sided dolphins are very active, fast-swimming animals, and are known to breach and tail-slap, as well as to bow-ride in front of vessels and surf in their wakes. They have been observed swimming directly in front of large whales, which is thought to be the same bow-riding behavior seen in front of vessels.

White-sided dolphins have been observed in mixed-species aggregations with long-finned pilot whales in eastern Canadian waters, with white-beaked dolphins in the North Sea, and with white-beaked, bottlenose, and common dolphins off Ireland (Reeves et al., 1999a). In the Gulf of Maine, white-sided dolphins are frequently (i.e., at about a quarter of all sightings) sighted in association with other species known to feed on sand lance and other small fishes, including fin, humpback, and minke whales (CETAP, 1982). This was the most commonly observed multi-species association during the CETAP surveys. The association in this case is fundamentally different from the mixed schools of pilot whales, bottlenose dolphins, and other delphinids seen in offshore waters. In mixed schools of shelf-edge delphinids, they clearly are swimming together in a coordinated group, and the group sizes of each species were not significantly different between associated and non-associated sightings (i.e., a mixed school of, e.g., *Globicephala* and *Tursiops* is simply a typical school of each that have joined together). In the baleen whale/white-sided dolphin associations, group sizes for each species are significantly larger when associated with other species than when not associated, suggested that the multi-species sightings are adventitious groups of animals that occur when each species individually aggregates to feed on the same patchy prey resource, but there is no true interaction.

Mass strandings of white-sided dolphins are relatively common. Such strandings have been known since antiquity, and are probably a naturally occurring phenomenon (Gaskin, 1992). Such occurrences show a clear spatial pattern, with about 85–90% of all stranded white-sided dolphins between North Carolina and Nova Scotia occurring in Massachusetts.

White-sided dolphins do not appear to be deep divers. A satellite-tracked tagged animal made no dive longer than 4 minutes and most of its dives were less than 1 minute (Mate et al., 1994).

White-sided dolphins feed on a wide variety of small fishes and squid, with differences in the species consumed between areas and seasons (reviewed by Reeves et al., 1999a). Sand lance is an important prey in the spring in the Gulf of Maine. Other fish prey include herring, smelt, mackerel, silver hake, and a variety of other gadoids.

Sergeant et al. (1980) and Perrin and Reilly (1994) summarized the available information on life history in white-sided dolphins. Calves are born at around 110 cm long in May to early August, peaking in June–July, however the calving period may be more prolonged in the northeastern Atlantic. The gestation period is 10–12 months. Lactation lasts about 18 months,

and about a quarter of mature females are simultaneously pregnant and lactating. The resulting average inter-birth interval is 2–3 years. Sexual maturity in males is at 230–240 cm and 8–9 years of age; females mature at 201–222 cm and 6–8 years old.

General distribution: Atlantic white-sided dolphins and white-beaked dolphins are both found only in the North Atlantic, with broadly overlapping distributions (Rice, 1998; Reeves et al. 1999a, 1999b; Cipriano, 2002; Kinze, 2002). White-sided dolphins are found in temperate to subarctic waters on both sides of the basin, with the northern limits of the range not very clear, but probably very similar to the white-beaked dolphin's—to Newfoundland, Greenland, Iceland, Svalbard, and the North Cape of Norway. The southern distributional limit of white-sided dolphins is further south, at least on the western side of the North Atlantic, where they occur to the mid-Atlantic. Both species occur south to the Bay of Biscay on the eastern side of the basin. In the western North Atlantic, their range extends from the U.S. mid-Atlantic to Greenland. They are common in the Gulf of Maine and Gulf of St. Lawrence, but seem to be relatively rare along the Atlantic coast of Nova Scotia. Palka et al. (1997) suggested that there were separate stocks in the Gulf of Maine, Gulf of St. Lawrence, and Labrador Sea.

Off the northeastern U.S., white-sided dolphins occur regularly from Hudson Canyon east to Georges Bank and north to the Bay of Fundy (CETAP, 1982; Selzer and Payne, 1988; Waring et al., 2008). They are the most common and abundant dolphin in the Gulf of Maine. They occur throughout the Gulf, but are most concentrated in the western portions from the Great South Channel east of Cape Cod to the Maine coast. During the CETAP surveys in 1979–1981, the annual pattern showed strong aggregation between Cape Cod and Georges Bank in the spring, dispersal throughout the Gulf of Maine in summer, a weaker aggregation in the central Gulf in fall, and a near-absence in the winter. The distribution in those years may have been driven by the distribution of sand lance, which were extremely abundant at that time. Strandings in the mid-Atlantic were mainly in the winter, leading to an hypothesis for a winter migration offshore and to the south.

Prior to the 1970s, however, white-sided dolphins were very rarely seen within the Gulf of Maine. A sighting of a small group of about 12 east of Cape Cod was worthy of publication in the *Journal of Mammalogy* (Schevill, 1956), and their range was believed to be centered along the outer edge of the shelf, as is apparently the case off Newfoundland and Europe (Reeves et al.,

1999a; Northridge et al., 1997). During the 1970s, white-beaked dolphins were more commonly observed in the Gulf of Maine. Kenney et al. (1996) hypothesized that white-sided and white-beaked dolphins in the Gulf of Maine shifted distributions after drastic changes in the stocks of small pelagic forage fishes caused by commercial fisheries. Intense fishing by foreign fleets in the 1960s and early 1970s caused a major decline in herring stocks, which were replaced by an explosion of sand lance (Sherman et al., 1981). The hypothesis was that white-beaked dolphins preferred herring, and moved east on the Nova Scotian shelf, and white-beaked dolphins shifted from an offshore to inshore habitat to fill the vacated niche. White-sided dolphins appeared in the stranding record in the mid-Atlantic during the 1970s and gradually expanded to the south, which seems to fit that same pattern of an offshore-to-inshore habitat shift, perhaps accompanied by growth of the population.

Historical occurrence: Cronan and Brooks (1968) reported only one known occurrence of white-sided dolphin in Rhode Island—a stranding at Monahan's Dock in Narragansett Pier on 22 July 1967. Neither De Kay (1842) nor Linsley (1842) included white-sided dolphin as a species occurring in New York or Connecticut. Goodwin (1935) stated that the nearest record to Connecticut was from Cape Cod, Massachusetts. The nearest record Connor (1971) knew of was the stranding reported by Cronan and Brooks. Waters and Rivard (1962) reported that the species "may range south to Cape Cod, but it does so rarely. There are only a few recorded sightings in the area of Cape Cod." They reported strandings in Wellfleet in March 1949 and May 1960, and a mass stranding of 12 animals on Monomoy Island in September 1954. There were no other records in the Rhode Island study area prior to 1973.

Recent occurrence: The first recent record of Atlantic white-sided dolphin in the Rhode Island study area was a stranding at Bellport, Long Island in December 1973. The first Rhode Island stranding after the 1967 event was a 202-cm dolphin on First Beach in Newport on 1 May 1976. Later that same year, on 17 August, came the first live sighting record—a group of 200 dolphins seen in the southwestern end of Buzzard's Bay. Since then, the species has become common in the study area, and is the third most frequently recorded small cetacean (Table 1). There are occasional unconfirmed opportunistic reports of white-sided dolphins in Narragansett Bay, typically in fall and winter. Atlantic white-sided dolphins in the Rhode Island study area are inhabitants of the continental shelf, with a slight tendency to occur in shallower water in the spring (Fig. 35). They are most common in spring, with 61.4% of all records, evident in both

sightings and strandings, followed by summer (21.0%), winter (10.0%), and fall (7.6%). There is an obvious aggregation of sightings southeast of Montauk Point, in that area where deeper water comes closest to shore—in spring and secondarily in summer. In the data from the whale-watching boats, there were 16 spring sightings and 7 summer sightings; their removal has almost no effect on the pattern of seasonality and little effect on the spatial pattern. The spring-summer concentration southeast of Montauk is not caused by bias from the whale-watch sightings. It is likely that the same prey resources that draw fin whales to that area also attract white-sided dolphins. There was one stranding in the spring on the Connecticut shore of Long Island Sound; there was one more in Connecticut and one in Long Island west of the study area boundary.

The effort-corrected patterns of relative abundance show that Atlantic white-sided dolphins occur in the Ocean SAMP area in all four seasons (Fig. 36). In winter, they occur at low abundance in the offshore half of the SAMP area, but more abundantly in deeper water on the outer part of the shelf. In spring they occur throughout the SAMP area in low numbers. The area of highest abundance is offshore of the southeastern corner of the SAMP area, and the distribution is in somewhat shallower water than in winter. There is also an area of relatively high abundance in the Great South Channel region east of Cape Cod. In summer, there is an area of moderate abundance in the eastern half of the SAMP area, the zone of abundance south of the SAMP has moved a little farther offshore, and the highest abundance is in the Great South Channel. The pattern in fall is similar to spring, but at lower abundances.

Atlantic white-sided dolphin strandings in the Rhode Island study area have been relatively rare (Fig. 37). There was a spike in 2001–2005, but the annual average was still low at only 1.2 per year. Four of the six strandings in that 5-year period were in Rhode Island—two in 2002 and 2 in 2005 (Waring et al., 2008), but the stranding rate is minimal in comparison with Massachusetts. Of 285 white-sided dolphins stranded from North Carolina to Nova Scotia in 2001–2005, 222 (78%) were in Massachusetts, mostly in mass strandings. Strandings in the study area were less strongly seasonal than sightings, with six in winter (29%), ten in spring (48%), and five in summer (24%).

After the first two Rhode Island strandings in 1967 and 1976, the next was on 21 February 1997 at Snug Harbor, when a 140-cm, 50-kg juvenile that was disoriented in Point Judith Pond was live-captured, then released alive after blood samples tested normal. Two dolphins stranded

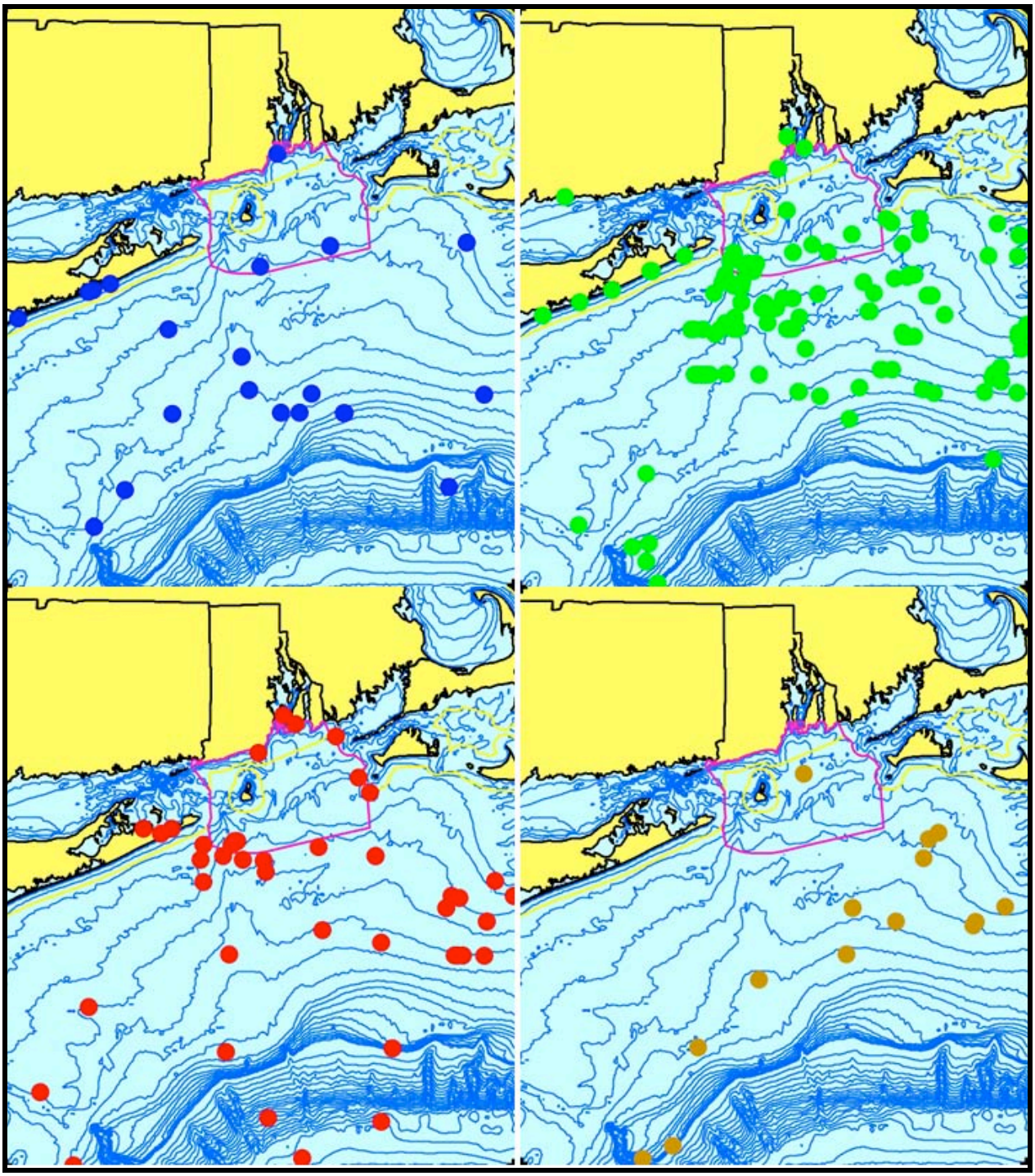

Figure 35. Aggregated sighting, stranding, and bycatch records of Atlantic white-sided dolphins in the Rhode Island study area, 1973–2006 (n = 210: winter = 21, spring = 129, summer = 44, fall = 16).

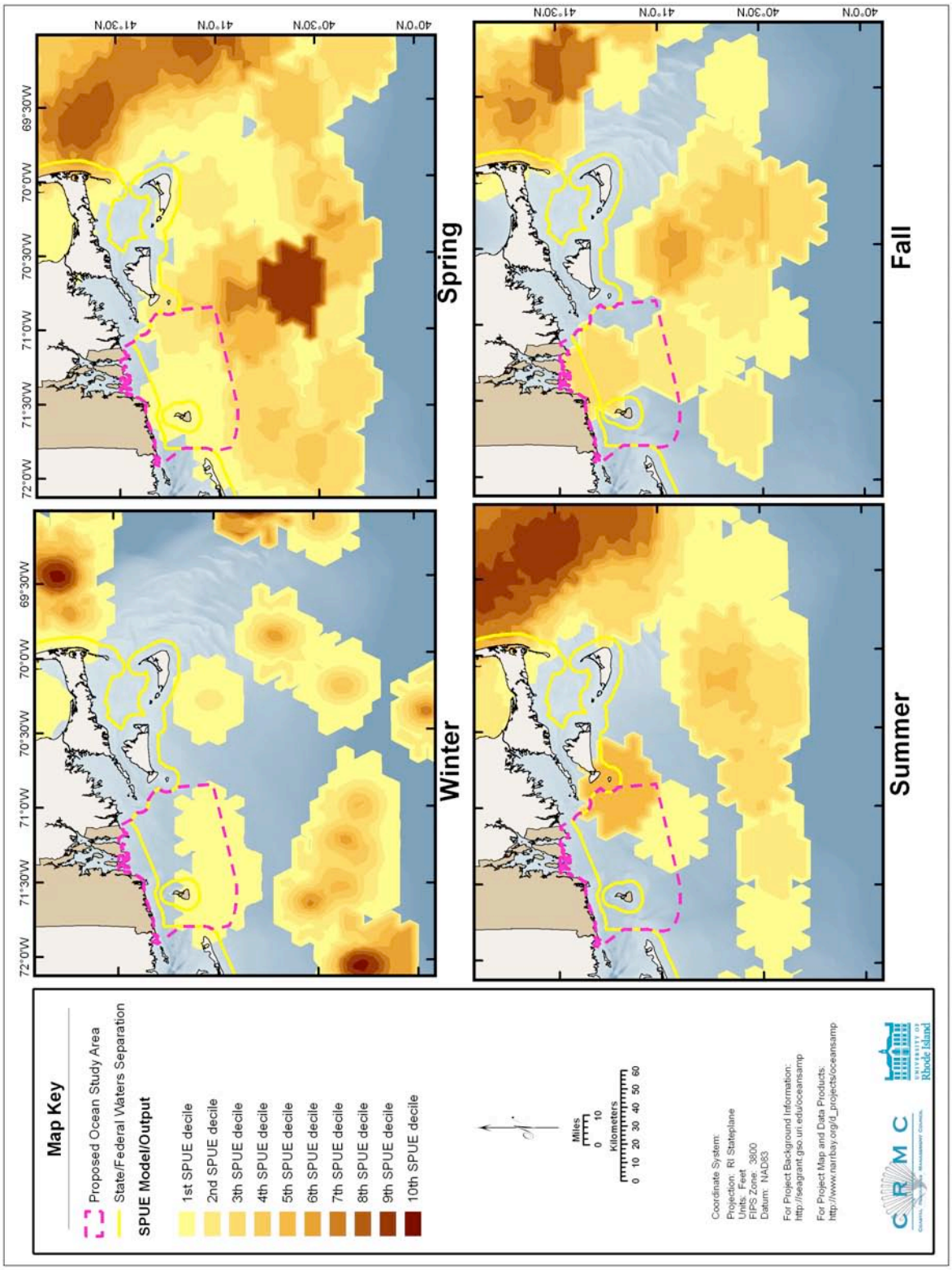

Figure 36. Modeled seasonal relative abundance patterns of Atlantic white-sided dolphins in the Rhode Island study area, corrected for uneven survey effort.

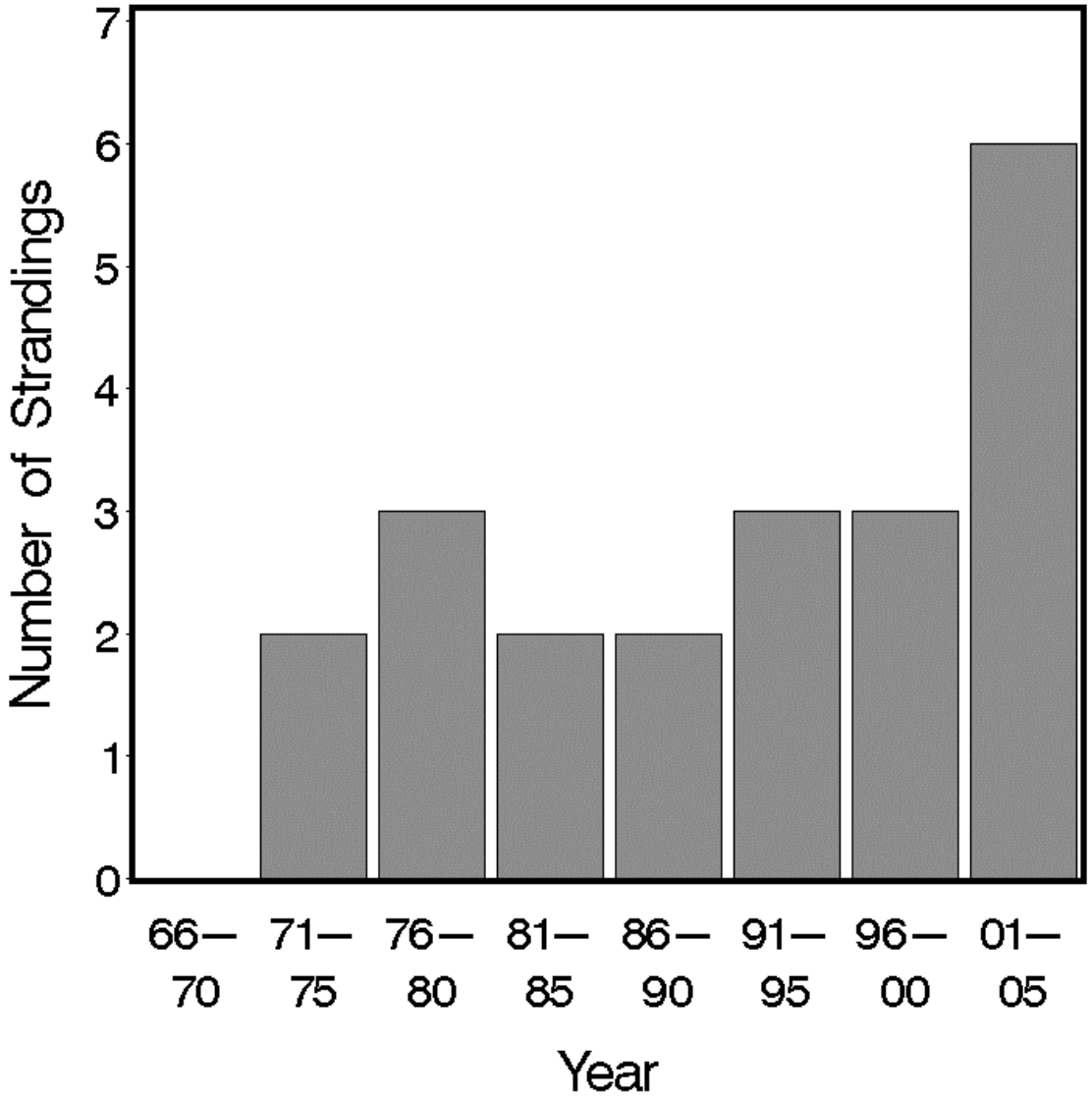

Figure 37. Five-year stranding frequencies for Atlantic white-sided dolphins in the Rhode Island study area, 1966–2005.

on Scarborough Beach in Narragansett on 31 March 2002, one stranded on First Beach in Newport on 8 June 2002, one stranded at Plum Point in North Kingstown on 6 March 2005, and one stranded on the eastern side of Jamestown on 7 July 2005. There was one stranding in Connecticut—at Branford in May 2003. The other 14 white-sided dolphin strandings in the study

area were all in eastern Long Island, in 1973 (mentioned above), 1974, 1978, 1979, 1981, 1985, 1987, 1988, 1991, 1995 (two), 1996, 1997, and 2004. The strandings are rare and localized: 1997, 2002, and 2005 were the only years with two strandings, and only in 1997 were there strandings in more than one state.

Conclusions: Atlantic white-sided dolphins are not ESA-listed, but they are probably the cetacean species that occurs seasonally in the highest numbers in the SAMP area. As such, they would be in the second tier of species that need to be considered carefully relative to the SAMP (see section 4, Recommendations).

3.2.19. White-beaked Dolphin *Lagenorhynchus albirostris* (Gray, 1846)

Description: White-beaked dolphins are very similar in overall body form to Atlantic white-sided dolphins, with robust bodies; prominent keels on the top and bottom of the tailstock; short, thick beaks; and very prominent, tall, falcate dorsal fins (Jefferson et al., 1993; Reeves et al., 1999b; Wynne and Schwartz, 1999; Kinze, 2002). White-beaked dolphins are slightly larger, reaching 3–3.2 m in length. Both species are counter-shaded with black backs and white bellies, but remaining details of their color patterns are distinctively different. In white-beaks, as their common name indicates, the white belly area includes both the upper and lower jaws and a little of the melon, though a close look is necessary to see this well in free-swimming animals. In front of the dorsal fin, there is a black cape, a white or pale gray patch below, and a dark gray to black patch below that. The cape and the darker patch on the side blend together at the head. Behind the dorsal fin, most of the animal is medium to very pale gray to nearly white, without distinct edges between different colors.

Status: White-beaked dolphins are not listed under the U.S. Endangered Species Act or on the Rhode Island state list, and are classified as Least Concern on the IUCN Red List. There are no synoptic estimates of the number of white-beaked dolphins across the Atlantic, though from estimates in separate smaller areas it is possible that the number is in the highs tens to low hundreds of thousands (Reeves et al., 1999b). Individual estimates from eastern Canadian waters range up to several thousand. None were sighted during the CETAP census surveys, although a single estimate of 573 was calculated from a special right whale survey east of Cape Cod in May 1980 (CETAP, 1982). An aerial survey in the Gulf of Maine in August 2006 resulted in the first

available estimate from any of the NMFS stock assessment surveys—2003 white-beaked dolphins (Waring et al., 2008).

White-beaked dolphins were at times the subject of small-scale opportunistic hunting in Norway, Iceland, Greenland, Newfoundland, and Nova Scotia. Some of the dolphins taken in the Faroe Islands pilot whale fishery may be white-beaked rather than white-sided dolphins. They were formerly hunted for food in Newfoundland and Labrador, with up to several hundred killed per year (Alling and Whitehead, 1987). Present takes in that region are apparently limited to only the most remote regions of Labrador (Lien et al., 2001). There are no records of human-related mortality in U.S. waters (Waring et al., 2008), although they are known to be killed by entanglement in fixed fishing gear in eastern Canadian waters (Alling and Whitehead, 1987; Read, 1994; Hai et al., 1996) and also in Europe (Kinze et al., 1997).

Ecology and life history: White-beaked dolphins typically are sighted in groups a few to 50 animals, most commonly in small groups of fewer than 10, but may at time aggregate in herds of hundreds (Reeves et al., 1999b; Kinze, 2002). There is a suggestion that juveniles segregate into separate groups from adults and calves, but the data are very sparse. They are very active, and are known to leap and breach, as well as bow-ride in front of vessels. They are very fast swimmers, and may create a rooster-tail of spray when surfacing.

White-beaked dolphins appear to feed primarily on fish and secondarily on squid, and also on octopus and benthic crustaceans (Reeves et al., 1999b; Kinze, 2002). The major types of fish eaten are herring and other clupeids, cod and other gadids, hake, capelin, mackerel, flounders, and sand lance.

There are very few available life-history data for white-beaked dolphins (Reeves et al., 1999b; Kinze, 2002). Calves are born at 110–120 cm over an extended period, probably from May to August or September. The gestation period is 10–11 months, but the length of lactation is not known. Information on maturity is based on very small samples. The smallest mature male known was 251 cm, and the largest immature male was 257 cm. In females the range is much wider—the smallest known mature individual was 174 cm and the largest immature was 246 cm. Physical maturity appears to be at an average length and age of 281 cm and 13 years in males and 261 cm and 16 years in females.

General distribution: Atlantic white-sided dolphins and white-beaked dolphins are both

found only in the North Atlantic, with broadly overlapping distributions (Rice, 1998; Reeves et al. 1999a, 1999b; Cipriano, 2002; Kinze, 2002). White-beaked dolphins are found in temperate to subarctic waters on both sides of the basin, with the northern limits around Newfoundland, Greenland, Iceland, Svalbard, the North Cape of Norway, and the White Sea. The southern distributional limit is about the same as white-sided dolphins on the European side of the ocean, to about the Bay of Biscay, but on the North American side they are common only to the Nova Scotian shelf currently, and formerly to the Gulf of Maine, with occasional occurrences as far south as North Carolina and Portugal. In the northeastern Atlantic, white-sided dolphins typically occur farther offshore than white-beaked dolphins. In the western North Atlantic, their range extends from southeastern New England and Nova Scotia to Greenland, although there was one sighting of 15 "probable" white-beaked dolphins on the outer shelf east of northern North Carolina border in May 1979 (CETAP, 1982). Prior to the 1970s, they were the most common species of dolphin occurring within the Gulf of Maine, with sightings concentrated around Massachusetts in April through June or July. Since then, however, they have been very rare in the Gulf of Maine (Waring et al., 2008), though still common off Nova Scotia and farther north (see discussion under white-sided dolphin).

Historical occurrence: There are no historical records of white-beaked dolphins in the Rhode Island study area. They were not mentioned at all by Cronan and Brooks (1968), nor by De Kay (1842), Linsley (1842), Goodwin (1935), or Connor (1971). Waters and Rivard (1962) wrote that the species "very rarely enters New England coastal waters. A sighting on 27 April 1961, thirty miles north of Cape Cod, is said to be the first specimen record from New England." They also reported a stranding on Nauset Beach on the outer Cape on 29 April 1961. The first known occurrence in the study area was the sighting in February 1975 (see below).

Recent occurrence: There were only 11 scattered occurrences of white-beaked dolphins in the Rhode Island study area (Fig. 38), all but one in spring or summer. The first was a sighting of six dolphins at the shelf break near Hudson Canyon on 15 February 1975. The sightings are concentrated in a few years. There were sightings in Vineyard Sound in August 1977 and March 1979, a sighting south of Martha's Vineyard in June 1979, one over the slope east of Hudson Canyon in August 1979, one animal seen from a whale-watching boat about 2 km off Montauk Point on 4 July 1981, and another sighting of one dolphin just south of Block Island on 5 August 1981. Then there were no sightings for 17 years. There were two strandings, quite possibly

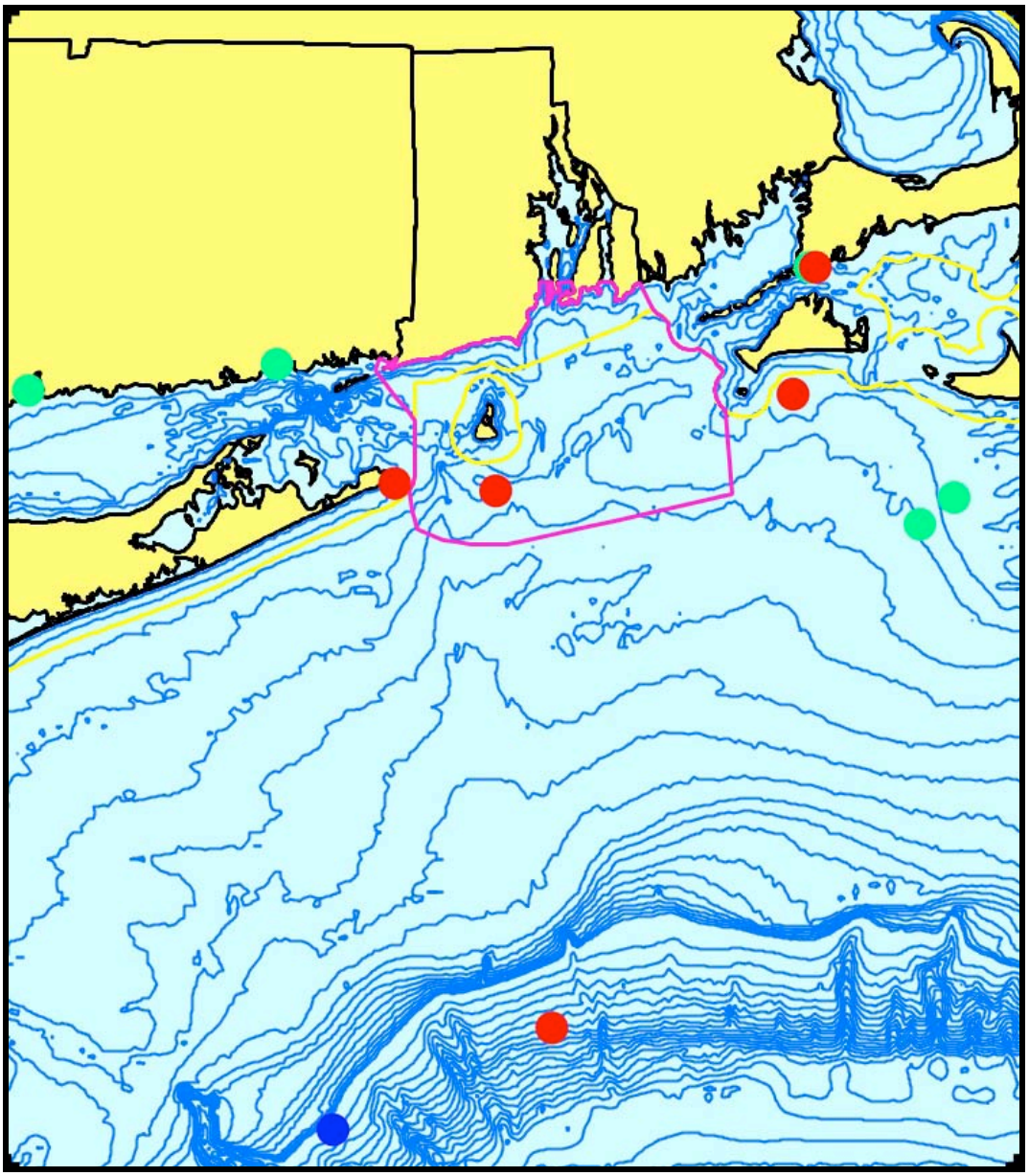

Figure 38. Aggregated sighting, stranding, and bycatch records of white-beaked dolphins in the Rhode Island study area, 1975–1998 (n = 11: winter = 1, spring = 5, summer = 5, fall = 0).

related, in Connecticut in May 1986—in West Haven (the westernmost) on the 22nd and in Niantic on the 25th. The last two sightings were from an aerial survey south of Nantucket on 22 May 1998—one group of 40 dolphins and another group of 2.

Conclusions: White-beaked dolphins occur in the study area only rarely, and are probably less likely now than they may have been 40 years ago. Despite the intensive whale-watching,

only one sighting was recorded in 1981. White-beaked dolphins can reliably be assigned to the lowest priority group of species relative to the SAMP.

3.2.20. Common Bottlenose Dolphin *Tursiops truncatus* (Montagu, 1821)

At least one other species of bottlenose dolphin is recognized—the Indian Ocean bottlenose dolphin, *Tursiops aduncus*, and other species are likely to be (Rice, 1998). In addition, in many areas of the world including the western North Atlantic, there are diagnosable inshore and offshore populations (Mead and Potter, 1990, 1995; Rice, 1998). Off the eastern U.S. the inshore and offshore populations are currently considered to be "ecotypes" or "morphotypes" of a single species for management purposes (Waring et al., 2008). Recent genetic results, however, show them to be sufficiently distinct to be considered separate species (Kingston and Rosel, 2004). The type specimen of *T. truncatus* matches the characteristics of the offshore population; available names for a separate inshore species include *T. erebennus* (Cope, 1865) and *T. subridens* (Flower, 1884) (Mead and Potter, 1995).

Description: Bottlenose dolphins are the "plainest" and least distinctively marked of all of the beaked dolphins in the North Atlantic (Jefferson et al., 1993; Wells and Scott, 1999, 2002; Wynne and Schwartz, 2002). Body size is extremely variable between populations; adults may be 2–3.8 m long. Offshore animals average about 15% larger than inshore animals along the U.S. Atlantic coast (Mead and Potter, 1995). The body is relatively thick and robust (especially in offshore animals), with a tall, falcate dorsal fin. The beak is well-defined and prominent, of moderate length (shorter than in *Stenella* and *Delphinus*, but significantly longer than in *Lagenorhynchus*), and stout. The body is basically gray to brownish, darkest on the back and lightest on the belly. There may be a clearly visible darker cape, or the color may simply fade gradually from the back to the belly. There may be indistinct stripes on the head or spots, and some animals may have a faint version of the spinal blaze that is seen prominently in striped and Atlantic spotted dolphins. In addition to consistent genetic and biochemical differences, inshore bottlenose dolphins in the western North Atlantic are significantly smaller than offshore animals, are usually lighter-colored, have flippers and beaks that are larger relative to body length, as well as narrower skulls and rostrums, feed on different types of prey, and carry different types of parasites (Hersh and Duffield, 1990; Mead and Potter, 1990, 1995; Hoelzel et al., 1998).

Status: Common bottlenose dolphins are not listed under the U.S. Endangered Species Act or on the Rhode Island state list, and are classified as Least Concern on the IUCN Red List. Coastal bottlenose dolphins along the U.S. Atlantic coast were designated as Depleted under the Marine Mammal Protection Act in 1993 (NMFS, 1993) because of high mortality in a 1987 epizootic (Scott et al., 1988). However, the impact of that event was seriously overestimated because the mortality occurred from Florida to New Jersey, but the only available estimate of abundance was for Cape Hatteras to New Jersey. In addition, no subsequent surveys have been able to detect a decrease in the abundance of coastal dolphins. A review of the depleted designation that is presently applied to all coastal stocks is needed (Waring et al., 2008). There are no reliable estimates of the total abundance of bottlenose dolphins in the North Atlantic. The existence of inshore and offshore populations (or species) and multiple stocks within populations makes it difficult to synoptically survey the entire region or to estimate the abundance of individual components. Mitchell (1975a) estimated the size of the stock subject to the North Carolina dolphin fishery in the 1880s at around 14,000. The CETAP data suggested that there were 11,000–13,000 bottlenose dolphins north of Cape Hatteras in spring and summer, with probably only 1,000 or fewer in the inshore stock (CETAP, 1982; Kenney, 1990). Subsequent surveys have been conducted in both inshore and offshore waters along the entire east coast (Waring et al., 2008). The Atlantic offshore population was estimated at 81,588 dolphins in 2002–2004 from Florida to Georges Bank. The total of all coastal stocks along the Atlantic coast was estimated at about 44,000 animals, including 17,466 in northern migratory stock—the only one that occurs in the mid-Atlantic. Additional bottlenose dolphin stocks occur in the Gulf of Mexico.

Bottlenose dolphins have been the targets of directed fisheries in several areas of the world (Wells and Scott, 1999, 2002; Reeves and Read, 2003). A fishery once existed in several countries around the Black Sea that took both bottlenose dolphins and harbor porpoises for oil, meat, and leather. Dolphin fisheries also exist in Peru, Sri Lanka, and Japan, taking dolphins for food, for bait in other fisheries, and to eliminate perceived competition for declining fish stocks. Recent takes of bottlenose dolphins in coastal small-cetacean fisheries in Japan have been 1,426 in 2000, 247 in 2001, 729 in 2002, 164 in 2003, and 16 in 2004 (IWC, 2005, 2006). There was a bottlenose dolphin fishery in operation at Cape Hatteras, North Carolina at least sporadically from 1797 to 1929 (Mead, 1975). A similar fishery was prosecuted at Cape May, New Jersey in 1884–1885, and one may have operated in the 18th Century or earlier in Long Island, depending

on what De Kay (1842) and earlier writers were referring to regarding "porpoise" fisheries. Reeves and Read (2003) provide a good review of the fishery methods. Catches at Cape Hatteras were mostly in spring and fall, with very few in summer; so they were apparently targeting migrating animals moving north or south and not residents.

Another directed effort has been the live-capture dolphin fishery for public display and other purposes (including research and military use) (Reeves and Leatherwood, 1984; Reeves and Mead, 1999; Wells and Scott, 1999, 2002). Over 1,500 were captured between the late 1930s and early 1980s, mostly in the southeastern U.S. A May 2000 inventory by NMFS showed 392 captive bottlenose dolphins in 35 facilities in the U.S. alone, with at least several hundred more in at least 16 other countries.

Bottlenose dolphins are taken incidentally as bycatch in a number of different commercial fisheries around the world (Northridge, 1991; Perrin et al., 1994b; Wells and Scott, 2002). The average annual mortalities in 2001–2005 in U.S. Atlantic waters are summarized in Waring et al. (2008). One observed take of an offshore dolphin in 1991 in the New England sink gillnet fishery extrapolated to an annual average of 26 individuals. Previous takes included an annual average in the swordfish driftnet fishery in 1989–1998 of 31.7 (that fishery is now closed), an average of 38.4 in the pelagic tuna pair-trawl fishery in 1991–1995 (also now closed), and one animal taken in a bottom trawl in 1991 (extrapolated to a total estimated take that year of 91). There was one take in the mid-Atlantic coastal gillnet fishery in 1998 that was probably an offshore animal, and one take in 2001 in the coastal-offshore overlap zone that was not included in the extrapolated estimate for the fishery due to uncertainty as to the stock identity. Annual average takes of coastal bottlenose in the mid-Atlantic coastal gillnet fishery were 233 per year in 1996–2000 and 61 per year in 2001–2005, with all takes in North Carolina and north and most in North Carolina in the winter. Bottlenose dolphins are probably also killed or injured by recreational fishing gear, but it is not well quantified (Gorzelany, 1998; Wells et al, 1998).

Bottlenose dolphins are the most frequently stranded cetacean on the U.S. Atlantic coast—292 in 2003, 359 in 2004, and 284 in 2005 (Waring et al., 2008), occasionally in mass strandings and primarily from New Jersey south. Some proportion of stranded animals bear marks of netting or ropes and were probably killed by entanglement in fishing gear.

Ecology and life history: Bottlenose dolphins are gregarious, usually occurring in small

groups of around 2–15 animals, but groups larger than 1000 have been reported (Wells et al., 1999; Wells and Scott, 1999, 2002). They generally are seen in smaller groups in bays and sounds than offshore, but group size is not a linear function of distance from shore. Off the northeastern U.S., the average group size was 14.8, with a mode of 2 and a range of 1–350 (CETAP, 1982), but that combined inshore and offshore sightings.

Group membership is dynamic, with sex, age, reproductive status, kinship, and affiliation history all involved (Wells et al., 1987; Scott et al., 1990; Wells and Scott, 1999, 2002; Connor et al., 2000; Reeves and Read, 2003). The social structure has been called a "fission-fusion" society. Some subgroups are stable for long terms, some may be repeated over periods of years, and others are more ephemeral. The basic social units are nursery schools of adult females and their calves, mixed-sex juvenile schools, and adult males, either solitary or in strongly bonded pairs and trios. Male-male bonds may last for decades, probably to enhance mating success and predator defense (Wells et al., 1987, 1990; Connor et al., 1992). There is no evidence for male coalitions in Moray Firth, Scotland, although those animals would be the same as the U.S. Atlantic offshore stock where there is very little information. Dominance hierarchies are observed in captivity—maintained by aggressive behaviors, including posturing, loud jaw claps, and physical contact.

Bottlenose dolphins commonly occur in mixed-species schools with other cetaceans. Scott and Chivers (1990) reported that bottlenose in the offshore eastern tropical Pacific were seen 16% of the time with one other species and 4% with two or more other species. They associated mostly with short-finned pilot whales, and pantropical spotted dolphins, and also with Risso's, rough-toothed, and spinner dolphins, sperm whales, and others. Norris and Prescott (1961) and Norris and Dohl (1980) similarly reported a common association of bottlenose dolphins and pilot whales in the North Pacific. Offshore bottlenose dolphins off the northeastern U.S. occur in mixed herds at 10% of all sightings, mostly with pilot whales, and also with Risso's, common, and striped dolphins (CETAP, 1982). Mixed delphinid schools often included calves and juveniles of one or both species.

There many reports on the prey of bottlenose dolphins, including observational studies and analyses of stomach contents, mostly dealing with inshore animals (Leatherwood, 1975; Leatherwood et al., 1978; Barros and Odell, 1990; Shane, 1990; Mead and Potter 1990, 1995;

Barros and Wells, 1998; Walker et al., 1999; Wells and Scott, 1999, 2002; Reeves and Read, 2003). The dominant prey are fishes, primarily from three families—sciaenids (weakfish, croaker, spot, etc.), scombrids (mackerels), and mugilids (mullets). Mead and Potter (1990) reported 40 different families of bony fishes, plus skates, rays, sharks, squid, shrimp, and isopods in the stomachs of *Tursiops* from the U.S. Atlantic coast. The four principal prey species were all sciaenids, including weakfish (also known as spotted sea trout), Atlantic croaker, spot, and silver perch. Stomachs of offshore animals were dominated by myctophids and squid.

Female bottlenose dolphins give birth after a 1-year gestation to a single calf that is 84–140 cm at birth, with substantial differences between populations (Wells and Scott, 1999, 2002; Reeves and Read, 2003). In Gulf of Mexico coastal dolphins, calves average 110 cm at birth (Fernandez and Hohn, 1998). Calving seasonality varies between populations (Scott et al., 1990; Urian et al., 1996; Fernandez and Hohn, 1998; Connor et al., 2000). In the long-term stranding data, Mead and Potter (1990) recorded neonates of 106–132 cm, and estimated a mean size at birth of 117 cm and 20.4 kg. They reported a mode in neonate strandings in March, and suggested a prolonged calving season with a peak in spring, with no evidence of a fall peak. During the CETAP (1982) study off the northeastern U.S., bottlenose calves were seen all year, recorded at 12% of sightings in spring, 12% in summer, 16% in fall, and 5% in winter. Thayer et al. (2003) reported that neonate strandings in North Carolina peaked in April–May and were lowest in fall and winter, but that births to known females were in May–June with one in fall. They speculated that the differences could be because of the presence of multiple stocks, or due to bias because out of season births may be more likely to lead to neonate mortality.

Mothers and calves rarely separate during the first few months (Mann and Smuts, 1998). A calf may nurse for several years, but begins foraging independently during its first or second year, maybe as young as four months (Wells et al., 1987; Wells and Scott, 2002). A calf is generally weaned completely at around the time the mother gives birth to the next calf, with overall duration a function of the age, nutritional condition, and social status of the mother (Wells et al., 1987; Mann et al., 2000; Whitehead and Mann, 2000; Wells and Scott, 2002). The typical inter-birth interval is 3–6 years (Scott et al., 1990; Wells and Scott, 2002).

The mating system in both species of bottlenose dolphins appears to be promiscuous with "roving" males (Wells et al., 1987, 1999; Scott et al., 1990; Connor et al., 1992; 2000; Wells and

Scott, 1999, 2002). Associations between males and females are extremely short-term. Coalitions of males travel more widely than any other groups, fighting for access to receptive females. Older males tend to be heavily scarred from fighting. In Australia, *T. aduncus* male coalitions aggressively separate receptive females from their bands and herd them away, which has not been observed in other populations.

In 1987–1988, there was a mass mortality of bottlenose dolphins along the U.S. Atlantic coast between New Jersey and Florida, which killed at least 740 animals (Scott et al., 1988). It was estimated at the time that the event killed 50% of the coastal migratory stock of *Tursiops*, however the only available abundance estimate (from CETAP, 1982) was for a much smaller area than that impacted by the epizootic. The dolphins died acutely from a wide variety of opportunistic viral and bacterial infections, but the underlying cause was first attributed to immune suppression caused by ingestion of prey containing a "red tide" toxin—brevitoxin produced by the dinoflagellate *Karenia* (formerly *Ptychodiscus*) *brevis* (Geraci, 1989). That finding was never widely accepted, particularly since there was no published literature showing a chronic immuno-suppressive effect of brevitoxin. In addition, bottlenose dolphins feed high on the food chain and could be subject to bioaccumulation of toxic contaminants. Animals in U.S. Atlantic waters have high concentrations of PCB's and PBB's (Kuehl et al., 1991; Lahvis et al., 1995). Organochlorines, even at relatively low levels, have the potential to affect immune response and may play a part in the apparent in increase in disease outbreaks (O'Shea et al., 1999; Wells and Scott, 2002). Males tend to accumulate higher loads than females, who reduce their own levels by transfer in milk lipids to their calves. In South African bottlenose dolphins, it was estimated that first-born calves received 80% of the mother's body burden of PCB's and dieldrin (Cockcroft et al., 1989). Subsequent reanalysis of archived tissue samples has suggested that morbillivirus may have played a role in the 1987–88 epizootic (Lipscomb et al., 1994). Morbillivirus has also been implicated in other bottlenose dolphin epizootics in the Gulf of Mexico (Duignan et al., 1996; Lipscomb et al., 1996).

General distribution: Bottlenose dolphins occur in temperate and tropical waters of all oceans of the world, as well as in the Mediterranean, Black, and Red Seas (Rice, 1998; Wells and Scott, 1999, 2002; Reeves and Read, 2003). The limit of the distribution in the Southern Hemisphere is around 40ºS. The distribution in the North Pacific extends north to the Sea of Okhotsk and Kuril Islands in the west and to central California in the east. Because of very extensive surveys

undertaken to assess the stocks of dolphins impacted by the tuna purse-seine fishery, there are substantial numbers of sightings of bottlenose dolphins across an immense area of the eastern tropical Pacific—as far as 3,000 km and more offshore (Scott and Chivers, 1990). In the North Atlantic their range extends north to southern Greenland, Iceland, and northern Norway. In the western North Atlantic, bottlenose dolphins occur from the equator north to at least Nova Scotia, with some records to Newfoundland.

Within that overall distribution, the picture is complicated by the existence of multiple species, populations, and/or stocks. Surveys in 1979–1981 showed clearly separated inshore and offshore bottlenose dolphins off the northeastern U.S. (CETAP, 1982; Kenney, 1990). There was one band of sightings very close to shore from Cape Hatteras to Delaware Bay and southern New Jersey, and a second band along the shelf break from Cape Hatteras to the Nova Scotian shelf, with scattered sightings far offshore in deep water. In the vicinity of Cape Hatteras, where the continental shelf becomes quite narrow, the two areas of sightings overlapped. South of Cape Hatteras the presence of coastal bottlenose dolphins was well known, but the continuous distribution of the offshore stock was not clear until NMFS conducted marine mammal stock assessment surveys beginning in the 1990s (Waring et al., 2008). The inshore and offshore dolphins are distinct, and possibly represent two different species (reviewed above). Kenney (1990) suggested that inshore and offshore dolphins could be split spatially by partitioning sightings into classes in waters deeper or shallower than 25 m, however no simple scheme has been successful. Torres et al. (2003) analyzed *Tursiops* skin biopsies collected both inshore and offshore from Florida to Georges Bank by incorporating the genetic results into a spatial model. Within 7.5 km from shore, only inshore animals were sampled. In areas more than 34 km offshore and in water deeper than 34 m, only offshore animals were sampled. In between was the "gray zone" where both types can occur, and there were three locations where both types were biopsied within the same school.

On top of the inshore-offshore pattern there is also a definite seasonal pattern to bottlenose distribution off the northeastern U.S. (CETAP, 1982; Kenney, 1990). Offshore dolphins occurred on the outer shelf along the entire study area from Hatteras to southern Nova Scotia in spring and summer. In the fall the distribution became sparser in the northern half of that range. In winter, sightings of offshore dolphins were very sparse, but still scattered along the entire shelf break. The seasonality was much more dramatic in the inshore distribution, which extended to

Delaware Bay in spring and summer, contracted to Virginia and south in fall, and contracted completely to south of Hatteras in winter.

Historical occurrence: Cronan and Brooks (1968) reported two bottlenose dolphin records from Rhode Island, a 315-cm male stranded at Sand Hill Cove in Narragansett on17 September 1967 and one previously at Newport on an unknown date. That is likely to refer to the specimen from Newport in the Smithsonian, collected by Major E. A. Mearns on 13 December 1899—the oldest bottlenose record in the Rhode Island study area. The species was not included by De Kay (1842) as part of New York's marine mammal fauna, unless it had been confused or inadvertently combined with the "common porpoise." Neither Linsley (1842) nor Goodwin (1935) knew of occurrences in Connecticut. Connor (1971) summarized a number of published and anecdotal records of bottlenose dolphins along the shores of Long Island and nearby, indicating that the species was rather common. The Smithsonian data include stranding and sighting records around eastern Long Island between 1921 and 1960, plus several non-dated sightings, all extracted from Connor's review. There were two other relevant records—a sighting in 1936 "off Block Island" but with no more specifics, reported by Remington Kellogg in a 1940 *National Geographic* article; and a specimen collected during the Atlantis Expedition in May 1939 "100 miles south of Montauk" (beyond the study area). Waters and Rivard (1962) said that bottlenose dolphins were uncommon migrants in Massachusetts waters, and cited only one specific record, a stranding in Plymouth in December 1947.

Recent occurrence: The spatial and temporal distribution of bottlenose dolphins in the Rhode Island study area essentially mirrors what was described above from the CETAP data (Fig. 39). Sightings of offshore dolphins occurred year-round in waters of the outer shelf, shelf break, and upper slope. Summer was the peak season (45.6%), followed by spring (31.3%), fall (18.1%), and winter (4.4%). There were a number of more inshore sightings in summer, but they were in waters deeper than 40–50 m, so there is no clear sighting or distributional evidence for the occurrence of coastal bottlenose dolphins in the study area. (Note, however, that detailed analyses of skull morphometrics, blood profiles, genetics, etc. of stranded specimens would be necessary to say anything about the population origins of individual stranded animals). Fourteen sightings came from the whale-watching boats, about equally in summer and fall, however the fall sightings were all on offshore trips. There were no sightings within the SAMP area, although there were several close by in summer.

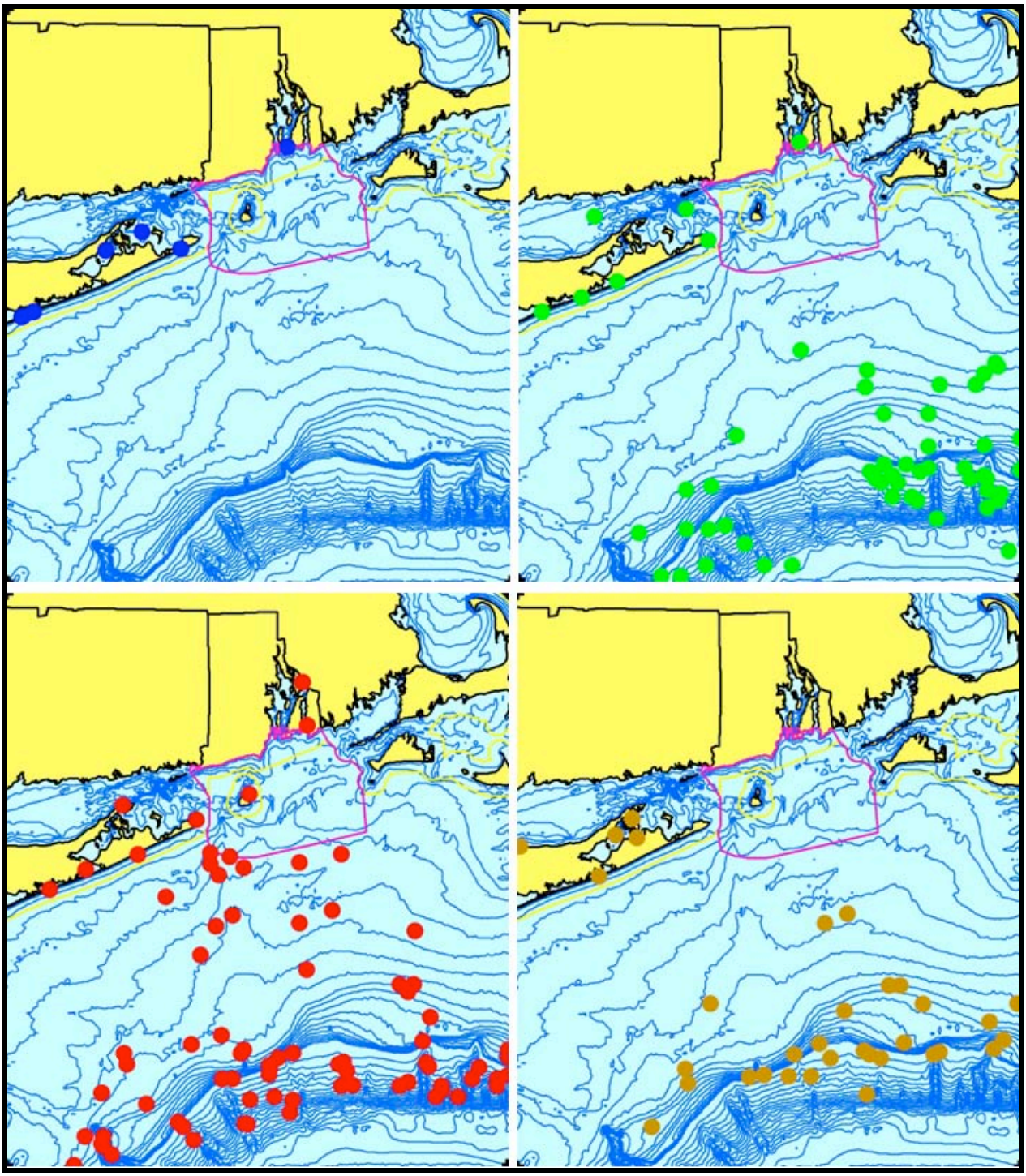

Figure 39. Aggregated sighting, stranding, and bycatch records of common bottlenose dolphins in the Rhode Island study area, 1899–2006 (n = 182: winter = 8, spring = 57, summer = 83, fall = 33, unknown = 1).

The first true offshore bottlenose dolphin sightings in the study area were in the 1970s. On 16 May 1974, a group of fifty dolphins was sighted from a U.S. Coast Guard cutter near the shelf break about 150 km south of Montauk Point. On 8 October 1978 a group of thirty was seen in the vicinity of Block Canyon. That sighting was extracted as an opportunistic sighting record in the early phase of CETAP from the Smithsonian's Scientific Event Alert Network bulletin, so it is also included in the Smithsonian data (among the many duplicates across datasets that needed to be identified and removed). The dolphins were originally seen by Paul Connor and the sighting published by Ulmer (1980).

The effort-corrected relative abundance patterns (Fig. 40) reinforce the suggestion that bottlenose dolphins in the Rhode Island study area are from the offshore population. There were no areas of predicted occurrence in the nearshore zone in the study area. There are areas of predicted bottlenose dolphin occurrence in all four seasons—always offshore. Overall relative abundance is lowest in the winter and highest in the summer, and the areas of highest abundance are outside the study area. Summer was the only season when the analysis showed that bottlenose might be expected within the SAMP area—in the most offshore portion and at the lowest level of abundance.

Bottlenose dolphins are the eighth most frequently stranded cetaceans in the Rhode Island study area (Table 2), which is much lower than the ranking in New York (third) or in New Jersey and states to the south (first). This is certainly due to the northern extent of the range of the inshore population. The seasonality in the strandings is different than seen in the total records, with about equal numbers in winter through summer (6, 6, and 7, respectively) and lower in the fall (3), which is more like the known temporal pattern of the offshore stock off southern New England than the inshore stock. There was a long gap in the stranding record for the study area between 1960 and 1983. Beginning in 1983, there have been four bottlenose strandings in Rhode Island, one on Fisher's Island, and thirteen in eastern Long Island (Fig. 41). There are two spikes in the time series. Of the five strandings in 1986–1990, four were in 1988, and may have been related to the epizootic. The second spike was six during 1996–2000, but those were more spread out, with three in 2000 and one each in 1996, 1998, and 1999.

On 16 August 1983, a 265-cm bottlenose dolphin live-stranded on the shore of Mount Hope Bay in Warren. It was taken to New England Aquarium in Boston, but its fate was not noted in

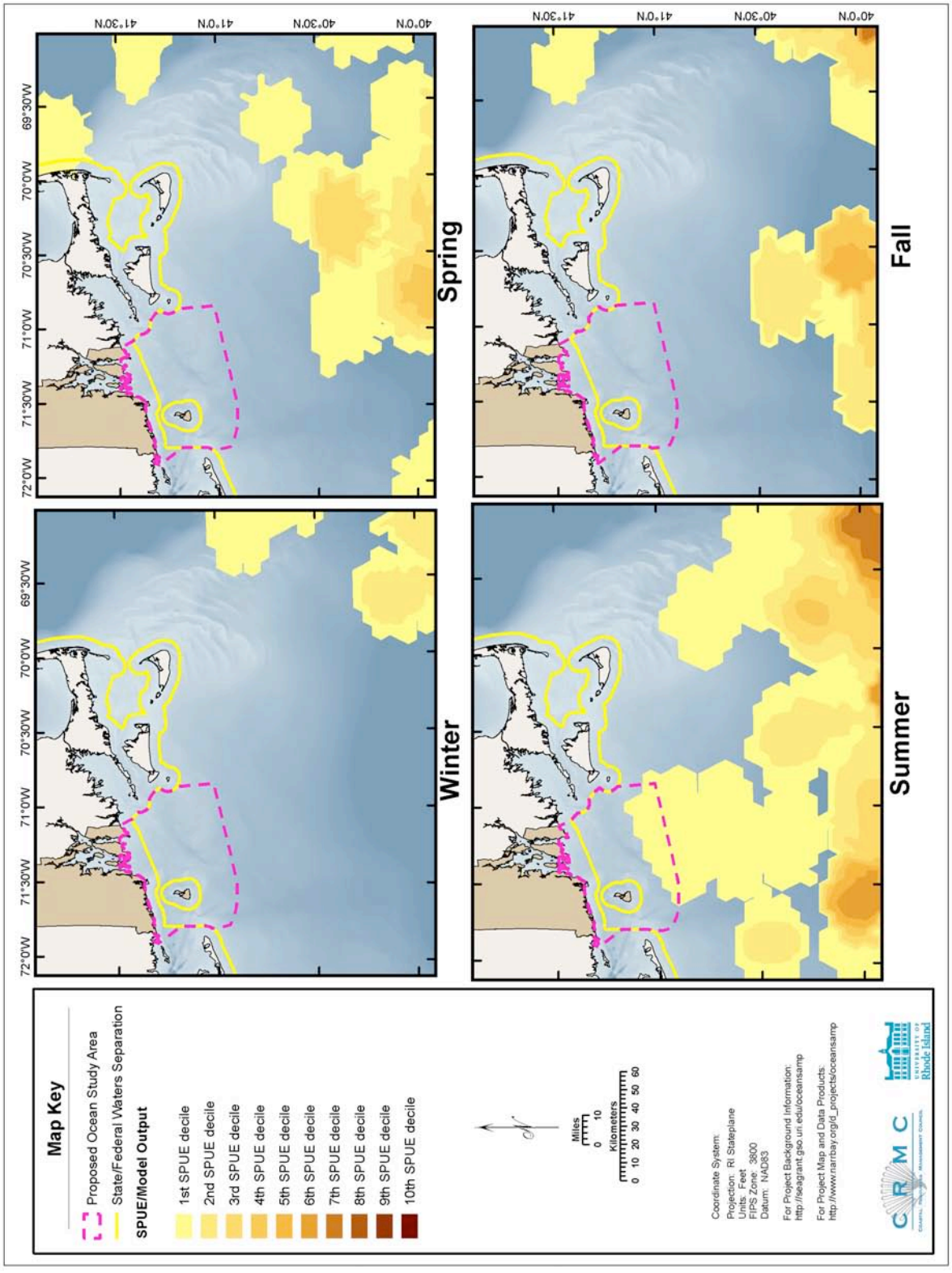

Figure 40. Modeled seasonal relative abundance patterns of common bottlenose dolphins in the Rhode Island study area, corrected for uneven survey effort.

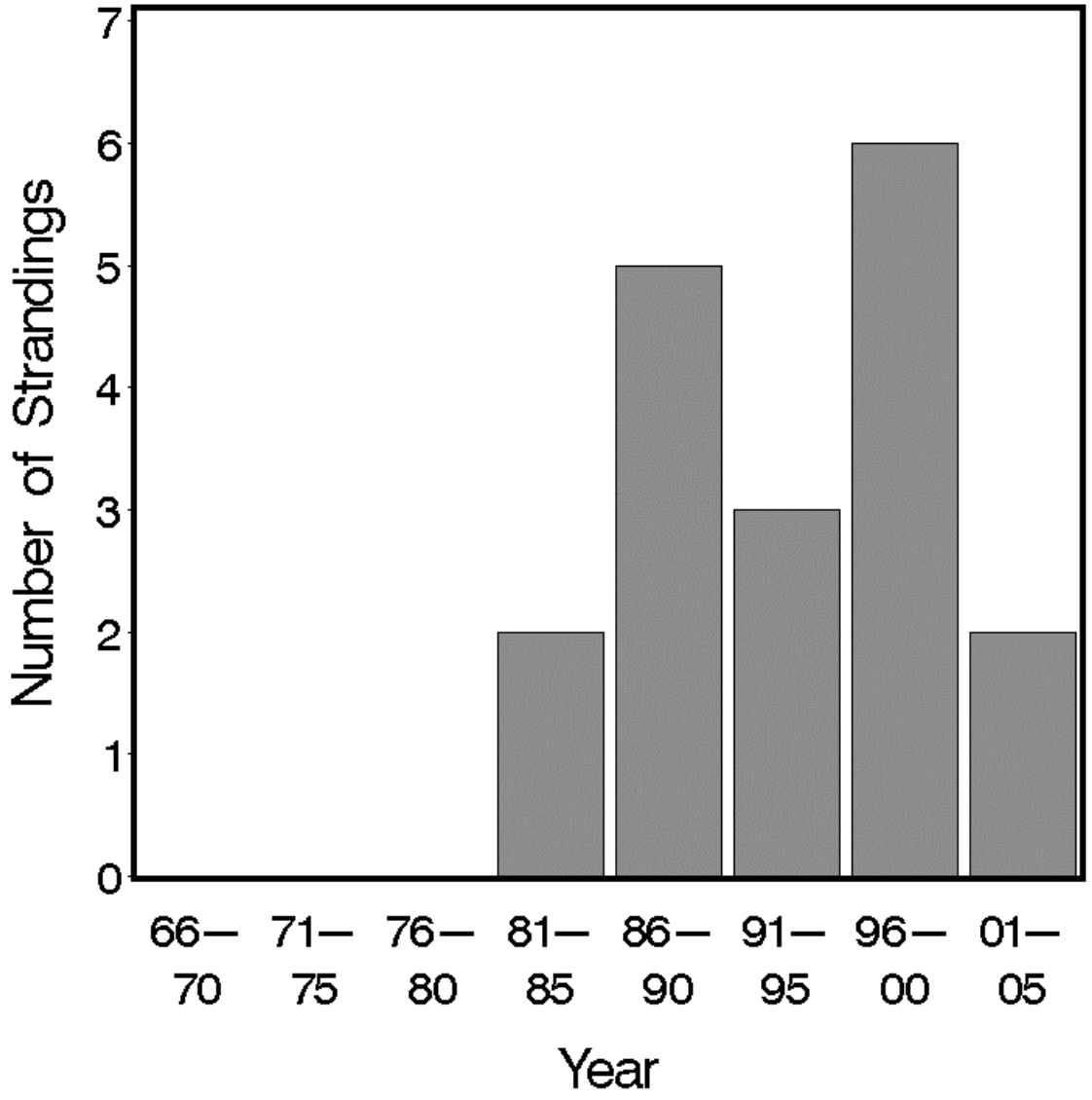

Figure 41. Five-year stranding frequencies for common bottlenose dolphins in the Rhode Island study area, 1966–2005.

the data record. On 31 August 1992, a 310-cm dolphin stranded on the east side of the Sakonnet River in Little Compton, which was noted as most likely from the offshore population. The last two Rhode Island strandings were both in 2004. One was on the Navy base in Newport on 7 March and the other was on Block Island on 12 July. The Fisher's Island stranding was in

August 1984. It was a very large male, 310 cm long and weighing 496 kg. A stranding on Montauk December 1988 was also a large animal at 311 cm; the record notes that analysis of a blood sample showed it to be an offshore bottlenose.

Conclusions: The sparse data suggest that bottlenose dolphins in the Rhode Island study area are more likely to come from the offshore population than from the coastal stock complex, which still is designated as "depleted" under the MMPA. Therefore the level of management concern is somewhat lower. Bottlenose dolphins are relatively abundant in the Rhode Island study area, but not in the SAMP area.

3.2.21. Short-beaked Common Dolphin *Delphinus delphis* Linnaeus 1758

Rice (1998) recognized three different species of *Delphinus*—the short-beaked common dolphin (*D. delphis*), the long-beaked common dolphin (*D. capensis*), and the Indian Ocean common dolphin (*D. tropicalis*), which may actually be a longer-beaked subspecies of *D. capensis* endemic to the Indian Ocean (Heyning and Perrin, 1994; Jefferson and Van Waerebeek, 2002). Only *D. delphis* is known from the North Atlantic (Heyning and Perrin 1994; Perrin 2002c).

Description: Common dolphins have the typical form of oceanic dolphins, with a streamlined fusiform body, a distinct beak that is separated from the melon by a crease, and a prominent dorsal fin (Jefferson et al., 1993; Evans, 1994; Wynne and Schwartz, 1999; Perrin, 2002c). Short-beaked common dolphins are slender, and range up to 2.3–2.6 m in length, with males slightly larger than females. Their color pattern is striking and distinctive. William Perrin developed a scheme for systematically classifying the pigmentation patterns of small cetaceans (summarized in Perrin, 2002b). There are two areas of dorsal pigmentation—the "cape," which is generally smaller and more anterior, and the "dorsal overlay," which is larger and extends farther posteriorly. The overlap of the two results in the typical pattern for a particular species. In common dolphins the cape is yellowish-tan, with a lower margin that runs back from the forehead crease, just below the eye, slightly downward to a lowest point between the flippers and the dorsal fin, then curves up to the back midway between the dorsal fin and the tail. The dorsal overlay is light gray; its lower margin starts on the forehead, curves upward over the eye to its highest point in front of the dorsal fin, then curves back downward to the belly in the area of the

genital slit. Where the two areas overlap, the color is dark gray to black, resulting in a dorsal field that is a rather narrow band from the head back that widens to a sharp point directly below the dorsal fin (the "saddle," where the margins of the cape and the dorsal overlay cross), then narrows to a point on the mid-back behind the dorsal fin. Anterior to the saddle the color on the side is yellowish tan (the cape alone), posterior to it and onto the back near the tail the color is gray (dorsal overlay alone). The belly is white. There is a prominent black blaze extending upward and forward from the genital slit to near the point of the saddle, which is thinner and paler in females. The complex pattern on the side of the animal gives rise to the alternative common names saddleback, hourglass, and criss-cross dolphin. The dorsal fin is tall, falcate, in the middle of the back, and black, often with a paler gray center. The lips, flippers, flukes, and a small circle around the eye are black. There are thin black stripes from the upper beak to the eye, and from chin to the flipper.

Status: Short-beaked common dolphins are not listed under the U.S. Endangered Species Act or on the Rhode Island state list, and are classified as Least Concern on the IUCN Red List. There is no estimate for the total abundance of short-beaked common dolphins in the North Atlantic. The CETAP (1982) survey results showed that common dolphins were one of the most abundant cetaceans off the northeastern U.S., with about 45,000 present in winter. More recent surveys (all in the summer) estimated a smaller population, until a summer shipboard survey from Florida to the Bay of Fundy in 2004 resulted in an estimate of 120,743 common dolphins (Waring et al., 2008).

There was a directed fishery (for human consumption) on common dolphins, bottlenose dolphins, and harbor porpoises in the Black Sea (Evans, 1994). The fishery began in the late 19th Century, and was conducted by Turkey, the Soviet Union, Romania, and Bulgaria. Tens of thousands of animals were taken annually, with peak kills perhaps as high as 200,000. The fishery ended in 1966, except in Turkey where it continued to 1983.

Common dolphins are taken incidentally in a number of commercial fisheries worldwide, in particular in gillnets (Perrin et al., 1994b) and in the eastern tropical Pacific tuna purse-seine fishery (Allen, 1985; NRC, 1992; Gosliner, 1999; Gerrodette, 2002). In the western North Atlantic, common dolphin bycatch mortalities occur in a number of different fisheries (Waring et al., 2008). The pelagic swordfish driftnet fishery killed an average of 303 annually in 1989–

1998, but has since been shut down. An experimental mid-water pair-trawl fishery for tuna killed 16 per year in 1991–1995, but it has also been closed. The most recent five-year average fishery-related mortality of common dolphins for U.S. Atlantic waters was 151 per year for 2001–2005, primarily in trawl fisheries, with a few in sink gillnets.

Ecology and life history: Common dolphins are known to aggregate into extremely large herds at times, however those schools are composed of smaller groups of 20–30 related individuals (Evans, 1994; Perrin, 2002c). Large herds chased during tuna fishing operations would break up into successively smaller groups, but the smallest groups of 20–30 animals remained tightly aggregated and never separated. Offshore fishermen tell of seeing herds of common dolphins on Georges Bank that take hours to pass by. Off the northeastern U.S. in 1979–1981, the average group size sighted was 54.8 dolphins, but the average was skewed by a few sightings of groups as large as 2000 individuals (CETAP, 1982). The modal group size was 8 animals. Off the northeastern U.S. they were sighted in mixed groups less often than a number of other species (CETAP, 1982). Other cetaceans with which they were associated on four or five occasions included fin whales, pilot whales, striped dolphins, and Risso's dolphins.

Common dolphins do not appear to be deep divers. Tagging studies show that most dives are to less than 50 m, with a few dives to as deep as 200 m.

Common dolphins feed on small fishes and squids, including species that school in near-surface waters and mesopelagic species that occur near the surface at night (Evans, 1994; Perrin, 2002c). Tagging studies in the North Pacific showed that foraging dives commenced at dusk and continued all night long. They were apparently feeding on deep-scattering layer fishes (dominated by myctophids or "lanternfishes") that migrate upwards at dusk and return to mid-depths at dawn, as well as on the squid that were also feeding on the small fishes. Hassani et al. (1997) looked at the stomach contents of common and striped dolphins taken as bycatch in a pelagic driftnet fishery in the northeastern Atlantic. Both species fed primarily on squid (50% or more of the prey items). Secondary prey in common dolphins, about equal in occurrence, were crustaceans (shrimp and krill) and fish (especially myctophids). Major (1986) reported a school of common dolphins on the southern edge of Georges Bank attacking and feeding on squid that had been lured near a research vessel at night by bright lights.

Most information about reproduction and life history comes from populations where large

numbers were taken in directed fisheries, as in the Black Sea, or as bycatch in commercial fisheries, as in the eastern tropical Pacific (Evans, 1994; Perrin, 2002c). Sexual maturity occurs at 6–7 years and 195–208 cm in females, and 7–12 years and about 200 cm in males. Ages at maturity appear to be significantly lower in the Black Sea, possibly a density-dependent response to high exploitation rates. Gestation is 10–11 months. Calves are born at about 80–90 cm in length, and wean in about 5 or 6 months, but begin feeding on solid food as young as 2–3 months. In the Pacific, there are two peaks in calving, in the spring and fall. At any one time, about 10% of adult females off California are "resting" (i.e., neither pregnant nor lactating); in the eastern tropical Pacific the proportion of resting females is about 17% in fall and winter and 30% in spring and summer.

General distribution: Common dolphins occur in tropical to temperate waters around the world, although understanding of distributional details is somewhat muddied by questions of species identity in the older data (Evans, 1994; Rice, 1998; Perrin, 2002c). Evans (1994) shows the Atlantic distribution as continuous from Norway to equatorial west Africa on the east and in Iceland, Greenland, Labrador, and Newfoundland, then continuous to Argentina in the west, but that includes both *D. delphis* and *D. capensis*. In the western North Atlantic, common dolphins occur from Iceland south, but the southern limit of the distribution is unclear and appears to vary between years. Older reports of common dolphins off Florida or in the Gulf of Mexico and Caribbean are likely to be misidentifications of Clymene dolphins (Jefferson et al., 1992; Jefferson, 1997; Jefferson and Curry, 2003). Off the northeast U.S., common dolphin sightings occur over the outer half of the continental shelf and continental slope from North Carolina to Nova Scotia, with occasional sightings in shallower waters in the Gulf of Maine (CETAP, 1982; Waring et al., 2008). Of all of the shelf-edge odontocetes of the region, common dolphins occurred in the zone closest to shore, a habitat they shared with pilot whales and offshore bottlenose dolphins (CETAP, 1982; Kenney, 1990). In the overall record for the broader mid-Atlantic, common dolphins are the most frequently stranded delphinid in Rhode Island and New York; while in New Jersey and south bottlenose dolphins are much more common.

Common dolphins have an atypical seasonal pattern off the northeastern U.S., with peak abundance in winter—very different from all other dolphin species (CETAP, 1982; Selzer and Payne, 1988). In spring during 1979–1981, intermediate densities of common dolphins occurred along the entire outer shelf from Virginia to Georges Bank. Sightings were widely scattered in

summer, with very low densities. The animals were thought to move north and east along the Nova Scotian shelf, however recent surveys did not observe substantial numbers of common dolphins there (Waring et al., 2008). Perhaps they move even farther north and east, or more offshore. In the fall, they were concentrated on Georges Bank in very high densities, extending west to about the longitude of Montauk Point. They reached their peak abundance in the winter, when they were again distributed all along the outer shelf from Virginia north.

Historical occurrence: Cronan and Brooks (1968) reported two historical records of common dolphins in Rhode Island—a specimen from Block Island with no date given and one captured alive in Point Judith Pond on 12 August 1966. The former most likely refers to the oldest known record in the study area in the Smithsonian dataset—a 203-cm dolphin captured "off Block Island" on 7 August 1882. Waters and Rivard (1962) said that common dolphins were relatively common in Cape Cod Bay, but made the counter-intuitive (and incorrect) conclusion that "even though most strandings take place in the winter, it is probably more abundant there in the warmer months." They reported two specific Massachusetts records—a mass stranding of eleven in Wellfleet in February 1949 and a stranding in Dennis in January 1950. De Kay (1842) listed common dolphins as part of the New York fauna, but said they rarely came into shallow water. Linsley (1842) reported that they occurred in Long Island Sound, which Goodwin (1935) extrapolated to "it is probably not an uncommon visitor to the shores of this state [i.e., Connecticut]." Connor (1971) summarized a number of sighting, stranding, and capture records for New York from a variety of sources. Of note was the occurrence of a herd of 30–40 common dolphins seen in the Hudson River in October 1936, almost as far upriver as Albany (Stoner, 1938). There are seven stranding records in the Smithsonian dataset from eastern Long Island between 1923 and 1951, all taken from Connor (1971), but none in Rhode Island.

Recent occurrence: Common dolphins occur in the Rhode Island study area year-round, across much of the shelf but most commonly in waters deeper than about 60 m (Fig. 42). Seasonality is not particularly strong, with 33.6% of records in spring, 26.2% in summer, 18.2% in fall, and 21.8% in winter. Sightings are somewhat more common in the spring. Strandings also occur year-round. A concentration of sightings in summer southeast of Montauk Point is evident, in the area where the 60-m isobath comes closer to shore. Without the sightings from the whale-watching boats (2 in spring, 39 in summer, and 5 in fall), the spring peak is slightly stronger, but

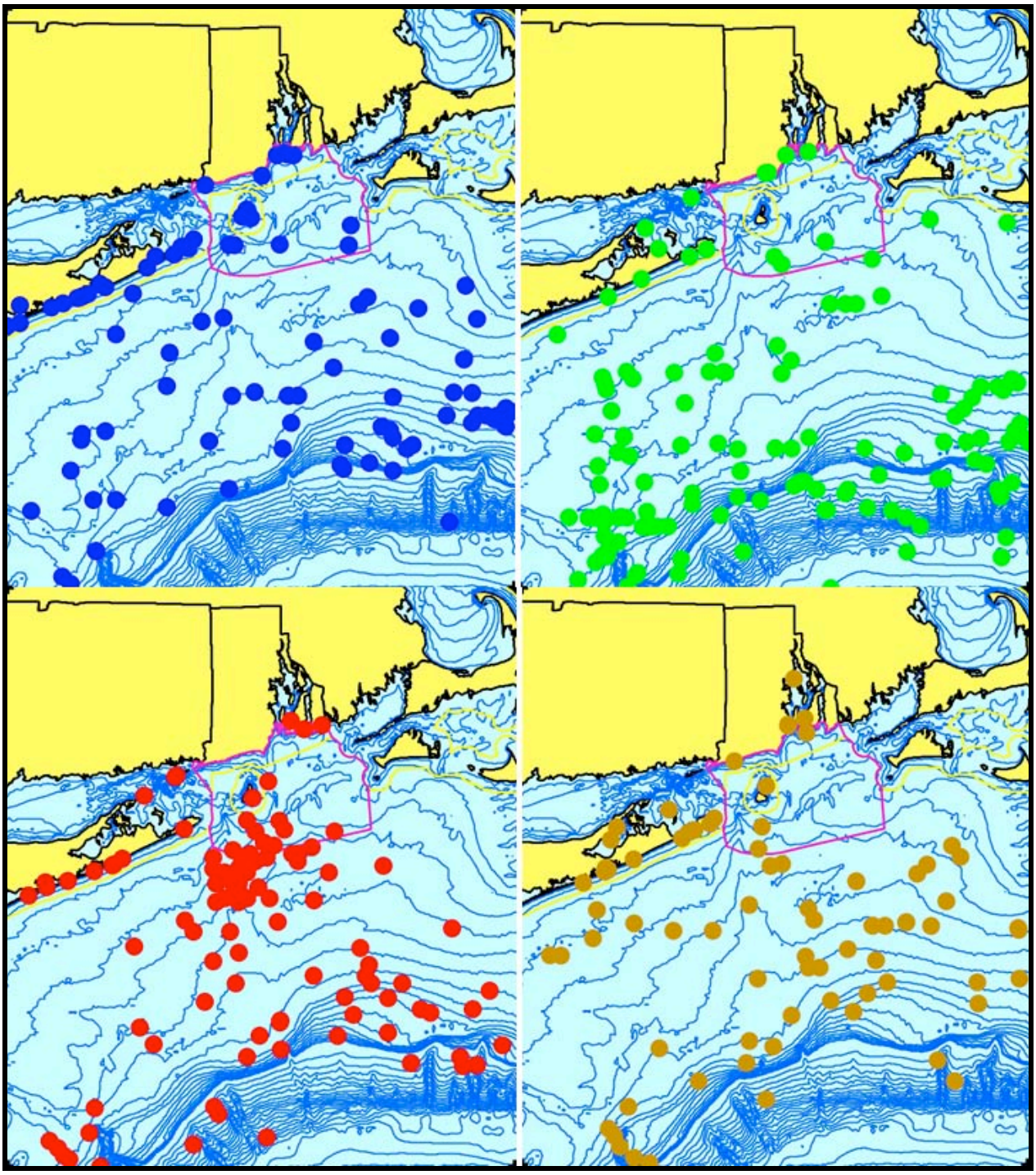

Figure 42. Aggregated sighting, stranding, and bycatch records of short-beaked common dolphins in the Rhode Island study area, 1882–2007 (n = 435: winter = 95, spring = 146, summer = 114, fall = 79, unknown = 1).

the seasonality during the rest of the year flattens out even more (24.4% winter, 37.0% spring, 19.3% summer, and 19.0% fall).

There are no recent records of common dolphins far up rivers, however such occurrences would only show up in the stranding database if the stranding network responded, and there is no centralized clearinghouse for opportunistic sightings of that type. In Rhode Island, there are occasional opportunistic reports of common dolphins in Narragansett Bay up as far as the Providence River, usually in winter.

The patterns of relative abundance show that short-beaked common dolphins are present in the Rhode Island study area in all four seasons (Fig. 43). They are consistently found on the outer half of the shelf, but do occur within the SAMP area in all seasons. Peak abundance in the study area is in the winter; peak abundance in the SAMP area is in the fall.

In the stranding record for the Rhode Island study area, common dolphins are the second most frequently stranded cetacean (exceeded only by harbor porpoises) and the most common delphinid (Table 2). There were 68 strandings in the study area between 1972 and 2005, including 23 in Rhode Island alone (Table 4). The rest were all in New York, including three on Fisher's Island—one in May 1981 and two in August 1995, six days apart. The first 1995 Fisher's Island animal was a 115-cm, 24-kg juvenile that was live-stranded, collected, and rehabilitated at Mystic Aquarium. The second was a dead 192-cm female, which may have been the juvenile's mother. There was one stranding in Connecticut during the period, but it was west of the study area in Fairfield. Strandings are even more frequent in Massachusetts, with 148 in 2001–2005 (Waring et al., 2008), but those are almost all on Cape Cod and include several mass strandings (e.g., 41 dolphins in four events in 2005). Stranding frequency spiked in 1996–2000, and was somewhat lower but still elevated in 2001–2005 (Fig. 44). The underlying reason for the increase is not known. There is also a clear seasonal pattern in the strandings, with a peak in the winter, a minimum in spring, and a smaller peak in summer (Fig. 45). Seasonal percentages were 40% in winter, 13% in spring, and 24% in both summer and fall.

Conclusions: Short-beaked common dolphins are very likely the most abundant marine mammal in the Rhode Island study area. They are also likely to occur in the SAMP area in all four seasons of the years. Although there are few serious management concerns about the

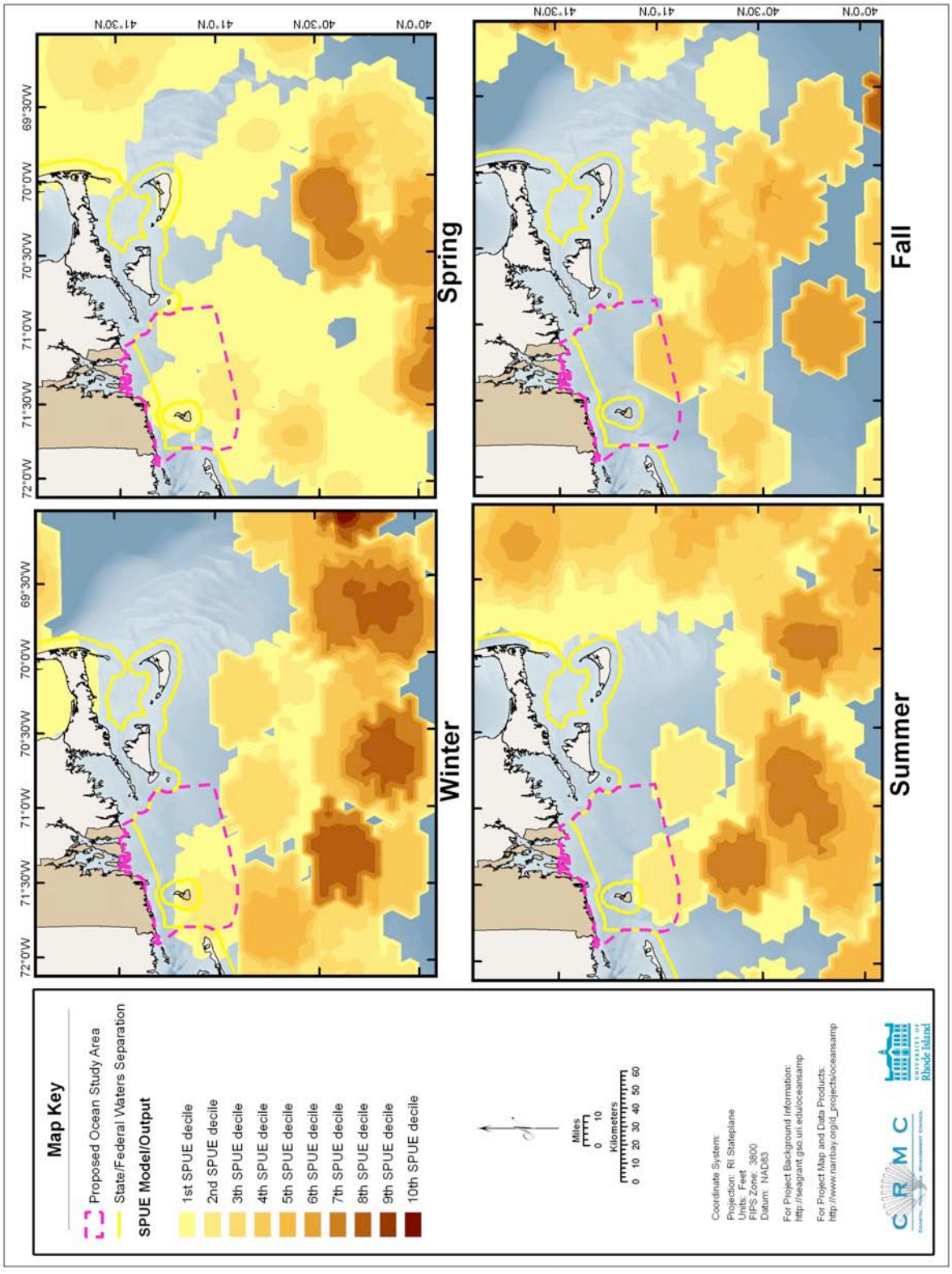

Figure 43. Modeled seasonal relative abundance patterns of short-beaked common dolphins in the Rhode Island study area, corrected for uneven survey effort.

Table 4. Rhode Island strandings of short-beaked common dolphins

Date	Locality	Notes
21 Nov 1983	Block Island, N of state beach	225-cm female
31 May 1986	Newport, near the mansions	live-stranded, was pushed off
25 Jun 1990	Newport, Coasters Harbor	205-cm female, alive, died 2 days later
02 Dec 1991	Newport, Bailey's Beach	181-cm male
26 Feb 1996	Point Judith, just inside east wall	206-cm, 78-kg male; both mandibles fractured, undigested food in stomach
14 Mar 1996	Narragansett, near Ft. Varnum	216-cm male
05 Dec 1996	Block Island, near Dories Cove	219-cm male
14 Feb 1997	Block Island, SW corner	176-cm male, propeller wounds
19 Jan 1998	Newport, Price's Cove	
15 Jul 1998	Middletown, Sachuest Point	
01 Jun 1999	Little Compton	
04 Nov 1999	Newport, Bailey's Beach	
05 Nov 1999	Westerly, Weekapaug Beach	
06 Dec 1999	Jamestown, Beavertail Point	
31 Dec 1999	Block Island	
30 Mar 2000	South Kingstown, Matunuck	
05 Apr 2000	South Kingstown, Town Beach	
09 Jun 2000	Block Island, Old Harbor	
14 Dec 2000	Westerly, Misquamicut Beach	
22 Dec 2002	Block Island, Old Harbor	
05 Jan 2003	Portsmouth, Island Park	
27 Oct 2003	Narragansett, Bonnet Shores	198-cm female, lactating, probably the mother of the calf seen earlier that day swimming alone off the Bay Campus; very worn teeth and thin blubber
05 Sep 2004	Warwick	

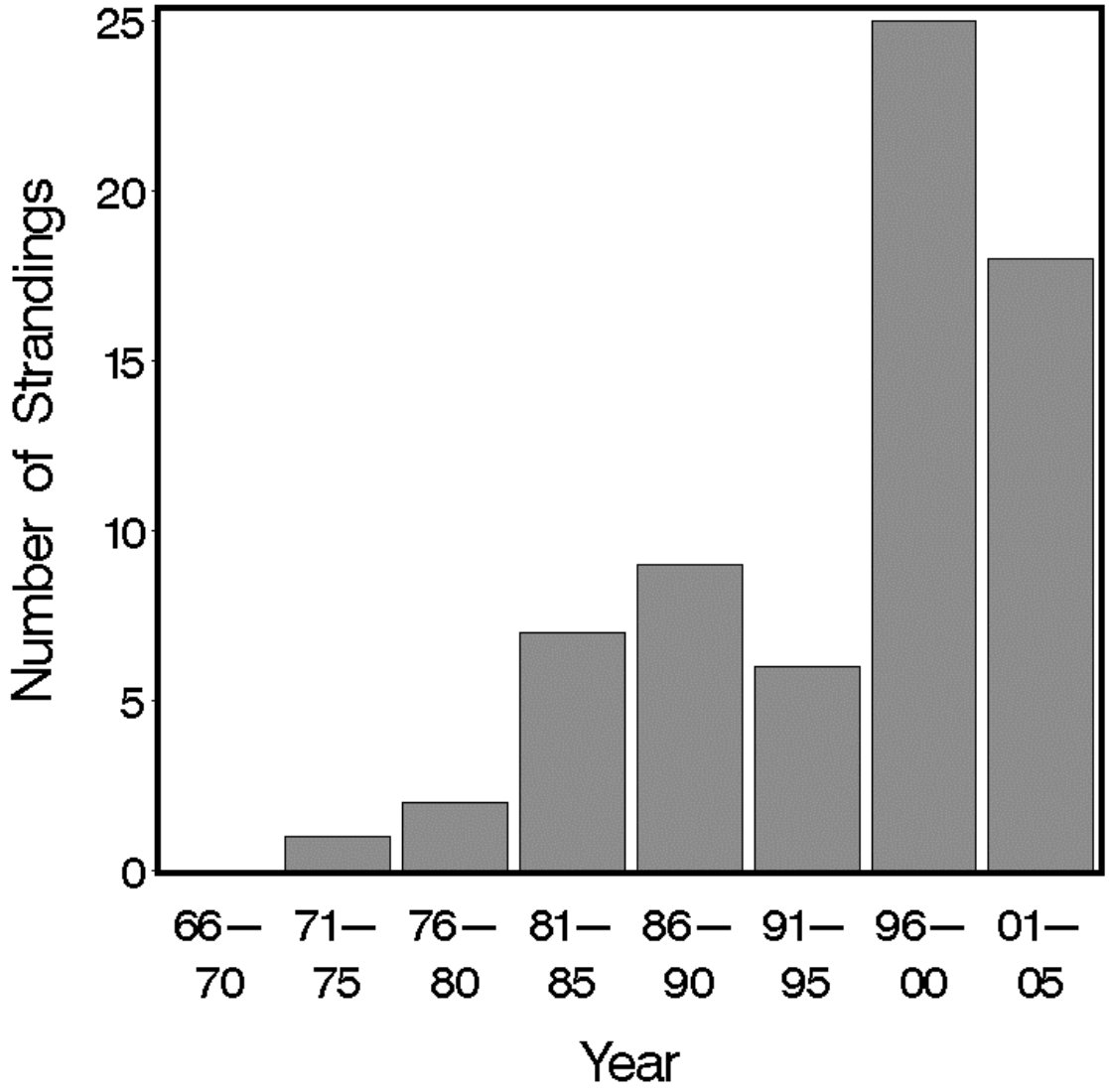

Figure 44. Five-year stranding frequencies for short-beaked common dolphins in the Rhode Island study area, 1966–2005.

population, their relative abundance would put them in the second tier of priority species relative to the SAMP.

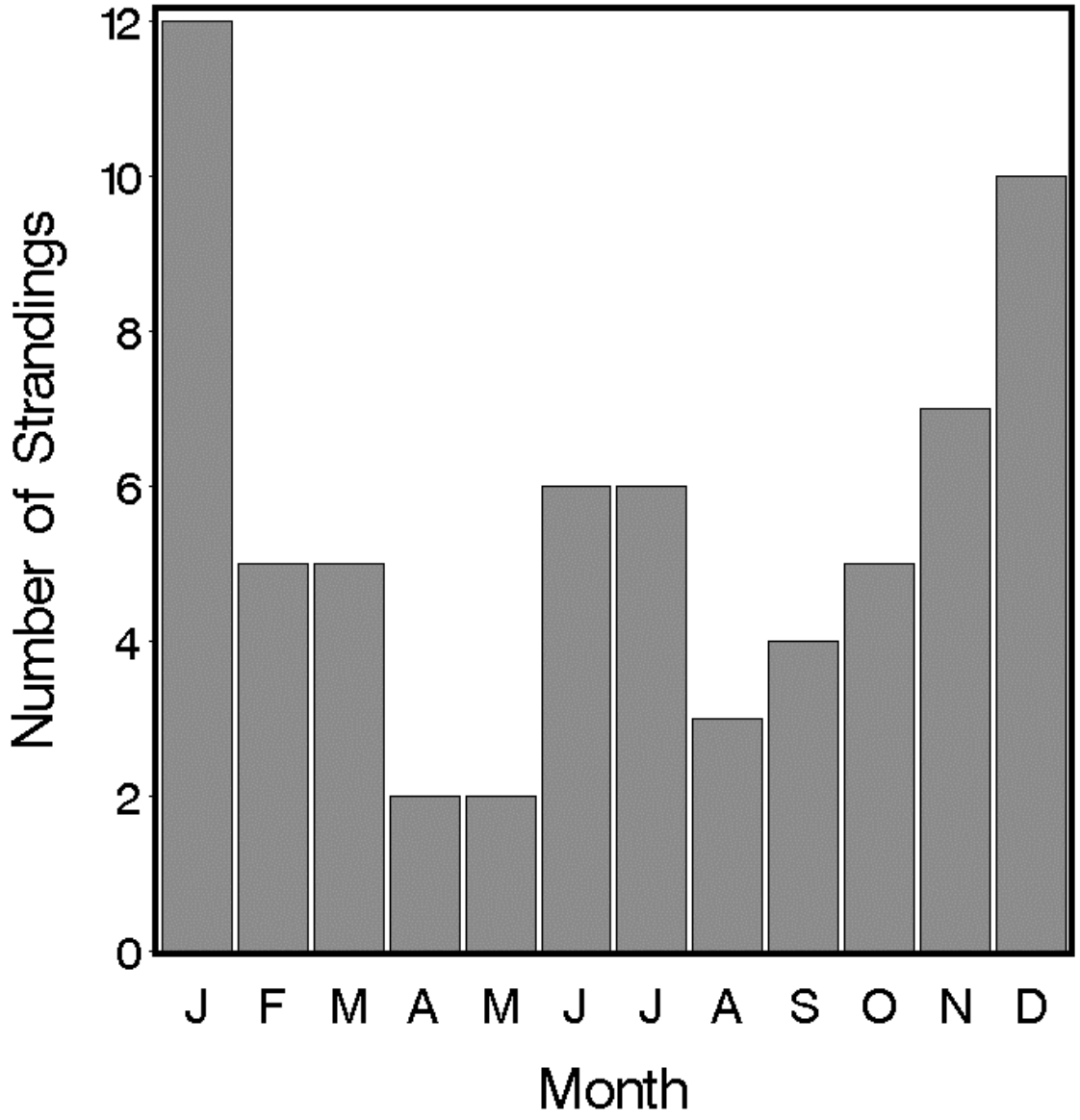

Figure 45. Monthly stranding frequencies of short-beaked common dolphins in the Rhode Island study area.

3.2.22. Striped Dolphin *Stenella coeruleoalba* (Meyen, 1833)

Description: Striped dolphins are typical of all the *Stenella* species in size and shape, and are very distinctively patterned (Jefferson et al., 1993; Perrin et al., 1994c; Archer and Perrin, 1999;

Wynne and Schwartz, 1999; Archer, 2002). They are slender and long-beaked, with tall falcate dorsal fins. Adults are up to 1.5–2.5 m long, with the largest animal known at 256 cm. Animals in the Mediterranean may be somewhat smaller than those in the North Atlantic. The cape is dark blue-gray, very narrow above the eye and widest in front of the dorsal fin (at about the midpoint of the flipper), and ends less than halfway back from the dorsal fin to the tail. There is a prominent pale band (the spinal blaze) extending from just above the flipper upward and backward into the cape toward the dorsal fin. Below and behind the cape, the sides and back are lighter gray, fading into a whitish (sometimes pink) belly. The upper beak is black, and the lower is gray to black. There is a bold black stripe from the upper jaw to the eye, where it divides into one stripe to the flipper, often a short thin stripe ending above the flipper, and a very bold stripe extending the length of the body back to the anus.

Status: Striped dolphins are not listed under the U.S. Endangered Species Act or on the Rhode Island state list and are classified as Least Concern the IUCN Red List. There are no reliable estimates of the total abundance of striped dolphins in the North Atlantic. The first abundance estimate off the U.S. Atlantic coast was from the CETAP (1982) surveys, which estimated that there were 4,300 striped dolphins in the spring. That number was negatively biased for two reasons. The CETAP study used only aerial surveys for estimating abundances, and many aerial sightings could only be identified to *Stenella* sp. Secondarily, the aerial surveys were almost entirely limited to continental shelf waters, and the majority of the striped dolphin sightings during the program were beyond the shelf (by shipboard observers). Kenney et al. (1997) attempted to address the first of those negative biases by partitioning the estimated abundances of unidentified *Stenella* sp. based on the proportions of identified sightings of striped, spotted, and spinner dolphins, which derived striped dolphin estimates of 6,491 in winter, 12,025 in spring, 16,320 in summer, and 13,482 in fall. More recent NMFS surveys for marine mammal stock assessments (Waring et al., 2008), using shipboard surveys that extended well beyond the edge of the shelf, produced estimates of striped dolphin abundance off the U.S. east coast of 49,945 in 1998 and 94,462 in 2004, with an additional 6,505 in the Gulf of Mexico.

There has been a directed small-cetacean fishery in a number of coastal villages in Japan, with records back to the mid-19th Century but probably dating back to at least the early 15th Century (Perrin et al., 1994c; Archer and Perrin, 1999). Takes averaged 8,000–9,000 annually along one section of the coast, and overall takes were about 14,000 per year, during the 1940s and 1950s,

with peak catches of over 21,000 in 1942 and 1959 (Kishiro and Kasuya, 1993). Recent takes of striped dolphins in coastal small-cetacean fisheries in Japan were 300 in 2000, 484 in 2001, 642 in 2002, and 450 in 2003 (IWC, 2005, 2006). There have also been directed harvests in the Lesser Antilles and in the Mediterranean (Archer, 2002).

Mortality of striped dolphins as bycatch in commercial fisheries has been observed in a number of locations around the world (Archer and Perrin, 1999; Archer, 2002), including the Pacific tuna purse-seine fishery. There was no known bycatch mortality of striped dolphins in U.S. Atlantic commercial fisheries in 2001–2005 (Waring et al., 2008). In previous years, there was bycatch estimated in two fisheries. Two striped dolphins were killed in the bottom trawl fishery in 1991, which extrapolated to an estimated mortality for the entire fishery of 181 animals. The average annual striped dolphin mortality in the pelagic swordfish driftnet fishery in 1989–1998 (now closed) was 17.

A dolphin morbillivirus epizootic in the western Mediterranean Sea killed over 1,100 striped dolphins in 1990–1992 (Aguilar and Raga, 1993; Perrin et al., 1994c). A later survey estimated the Mediterranean population of striped dolphins at 225,000, which would suggest that the mortality rate from the epizootic was relatively insignificant (less than 0.5%). Toxic contaminants, particularly organochlorines, were suspected to have played a role, acting as an immunosuppressant that then allowed a naturally occurring virus to cause disease (Aguilar and Raga, 1993; Aguilar and Borrell, 1994). Blubber PCB levels as high as 2,500 ppm were measured in the stranded striped dolphins during that event, which were among the highest levels ever recorded in a cetacean.

Ecology and life history: Striped dolphins are gregarious and may be observed in very large herds. In the eastern tropical Pacific average school size was 28–83 animals (Wade and Gerrodette, 1992). The mean school size in Japan is about 100, while in the eastern North Atlantic it is only 10–30 (Perrin et al., 1994c; Archer and Perrin, 1999). The average school size observed off the northeastern U.S. was 64.9 (CETAP, 1982), with a range 1 to 500. This was the largest average school size of all species observed, nevertheless the modal group size was still relatively small at 20.

Striped dolphins are known to segregate into juvenile, adult, and mixed schools, and adult and mixed schools can be either breeding or non-breeding (Miyazaki and Nishiwaki, 1978; Perrin et

al., 1994c; Archer and Perrin, 1999). Calves leave the mixed schools 1–2 years after weaning and join juvenile schools. Within breeding schools there are structured subgroups of only adult males or adult females.

Striped dolphins are very active and acrobatic, with frequent leaps, spins, and somersaults, and they may bow-ride (Perrin et al., 1994c; Archer and Perrin, 1999; Archer, 2002). They are known for an aerial behavior called "roto-tailing," which involves making a high jump while rapidly rotating the tail.

Striped dolphins sometimes associate with yellowfin tuna in the eastern tropical Pacific, but less than short-beaked common dolphins and much less than spinner or pan-tropical spotted dolphins (Archer and Perrin, 1999). They are known to occur commonly in mixed schools with short-beaked common dolphins off Japan and in the Mediterranean. Off the northeastern U.S. they were observed to be associated with other species only on a few occasions, usually with common dolphins (CETAP, 1982). Globally, striped and short-beaked common dolphins tend to occur in areas where spinner and pan-tropical spotted dolphins do not (Perrin et al., 1994c).

Mass strandings are rarely observed in striped dolphins (Archer, 2002). There was a stranding of a group of 12 striped dolphins in North Carolina in 2005 (Waring et al., 2008).

Striped dolphins overall feed on a very wide variety of fish and squid, including both pelagic and benthic species, with sharp differences among geographic regions (Perrin et al., 1994c; Archer and Perrin, 1999; Archer, 2002). The dominant prey items off Japan are mesopelagic myctophids ("lanternfishes"). In the northeastern Atlantic their main prey is cod, and in the Mediterranean they primarily eat squid. Extrapolating from prey species, they may commonly dive to 200–700 m for foraging. Stomachs of all stranded specimens examined in Long Island have contained squid beaks, suggesting a preference for squid in the Rhode Island study area (S. S. Sadove, pers. comm.).

Hassani et al. (1997) looked at the stomach contents of common and striped dolphins taken as bycatch in a pelagic driftnet fishery in the northeastern Atlantic. Both species fed primarily on squid, which comprised nearly 60% of the prey items in striped dolphins. Secondary prey in striped dolphins were crustaceans (shrimp and krill, about a third of diet), and fish were a relatively minor component.

The majority of the life-history data are derived from animals taken in the directed fishery in Japan, with additional data from animals caught in the tuna fishery (Perrin et al., 1994c; Archer and Perrin, 1999; Archer, 2002). Calves are born at 93–100 cm in length after a gestation period of 12–13 months. Calving may occur at almost any time of year with one or two diffuse peaks—winter and summer off Japan, spring or spring and fall in other areas. Lactation lasts for 1–1.5 years. Off Japan, calves grow to an average length of 166 cm at age 1, and to 180 cm at age 2. Between 2 and 3 years of age, males and females diverge in body size, with males growing larger and typically exceeding females by 10–15 cm as adults. Mean length at sexual maturity in females is 2.1–2.2 m. Maturity in females occurs at 5–13 years of age and in males at 7–15. Fecundity in females declines markedly at around age 30, but reproduction does not stop completely. In striped dolphins in Japan, the female age at maturity declined from 9.7 to 7.2 years, and the inter-birth interval dropped from 4 to 3 years, with both believed to be density-dependent responses to population declines caused by the small-cetacean fishery.

General distribution: Striped dolphins are distributed world-wide in temperate to tropical waters, although the distribution is poorly known in the South Atlantic where research has been sparse (Perrin et al., 1994c; Rice, 1998; Archer and Perrin, 1999; Archer, 2002). In the North Atlantic, they have the most temperate distribution of the five *Stenella* species, extending from northern South America to New England and Nova Scotia and from the Mediterranean to the British Isles. They are the most commonly sighted cetacean in the Mediterranean. There are a few sightings from Newfoundland, southern Greenland, Iceland, and the Faroe Islands, which may be extralimital. Striped dolphins are frequently sighted off the northeastern U.S. and Nova Scotia (CETAP, 1982; Gowans and Whitehead, 1995; Waring et al., 2008). Their distribution off the northeastern U.S. during the CETAP surveys was primarily along the outer shelf and into deeper waters, despite the very strong bias of the sampling to the shelf. Unlike all other cetaceans of the region, there was very little seasonal pattern to their distribution. In addition, their depth distribution in the CETAP data was significantly deeper than any other species, with an average sighting depth of 2,076 m and with 90% of the sightings between 101 and 3,749 m. There have been no sightings south of Cape Hatteras during any of the recent NMFS surveys, although there are strandings in Florida to North Carolina and striped dolphins do occur in the Gulf of Mexico (Waring et al. 2008). Nothing is known of stock structure, e.g., whether the animals seen in the Gulf of Mexico and off the northeastern U.S. come from the same or separate stocks.

Historical occurrence: Cronan and Brooks (1968) reported a stranding of an "old," 241-cm male on the town beach in Narragansett on 5 December 1966. They also indicated that there was a previous record for Woods Hole, Massachusetts. Waters and Rivard (1962) said that the species was very rare in New England and cited no recent Massachusetts records. Striped dolphins were not mentioned in De Kay (1842), Linsley (1842), or Goodwin (1935). Connor (1971) reported two historical stranding records for Long Island, but only one was within the Rhode Island study area—in May 1929 at Bellport. That is the oldest striped dolphin record in the study area. Other than the 1929 Bellport and 1966 Narragansett strandings, there is only one other pre-1970 striped dolphin record from the study area. The Harvard Museum of Comparative Zoology has a specimen from a 62-kg animal collected about 150 km south of Block Island on 27 July 1961 by M. R. Bartlett (MCZ51071).

Recent occurrence: Striped dolphins in the Rhode Island study area are observed either stranded on a beach or very far offshore, with few observations in between (Fig. 46). The records occur in approximately equivalent numbers in all four seasons, with 31.7% in the winter, 29.3% in summer, 18.5% in fall, and 19.5% in spring. That pattern may be misleading, however, since the sightings and strandings follow opposite trends. Striped dolphins are the sixth most common stranded cetacean in the region (Table 2). Strandings are primarily in fall (8, 29%) and winter (11, 39%), followed by spring (5, 18%) and summer (4, 14%). There are fewer than half as many sightings (13, including captures) as strandings (28), and they are mainly in the summer (8, 73%), with 3 (23%) in spring, 2 (15%) in fall, and none in winter. The seasonality in the sightings is surely due to sampling effort, especially from shipboard surveys beyond the shelf break. The survey data included too few sightings within our analysis area to develop SPUE estimates or produce relative abundance maps.

Stranding frequency has been relatively constant over time (Fig. 47). The small spike in the early 1990s may not be anything more than random interannual variability. Eleven of 26 strandings in the study area since 1966 have been in Rhode Island, which is a higher proportion than any for other cetacean. On 10 December 1978, a 174-cm striped dolphin stranded in Charlestown. A 147-cm juvenile stranded on First Beach in Middletown on 3 October 1980. A 121-cm calf stranded on the south shore of Little Compton on 26 June 1985. Later that year, on 7 September, a 241-cm adult live-stranded near the Stone Bridge in Portsmouth, but it died later that same day. A 235-cm adult male washed ashore on Matunuck Beach on 10 February with

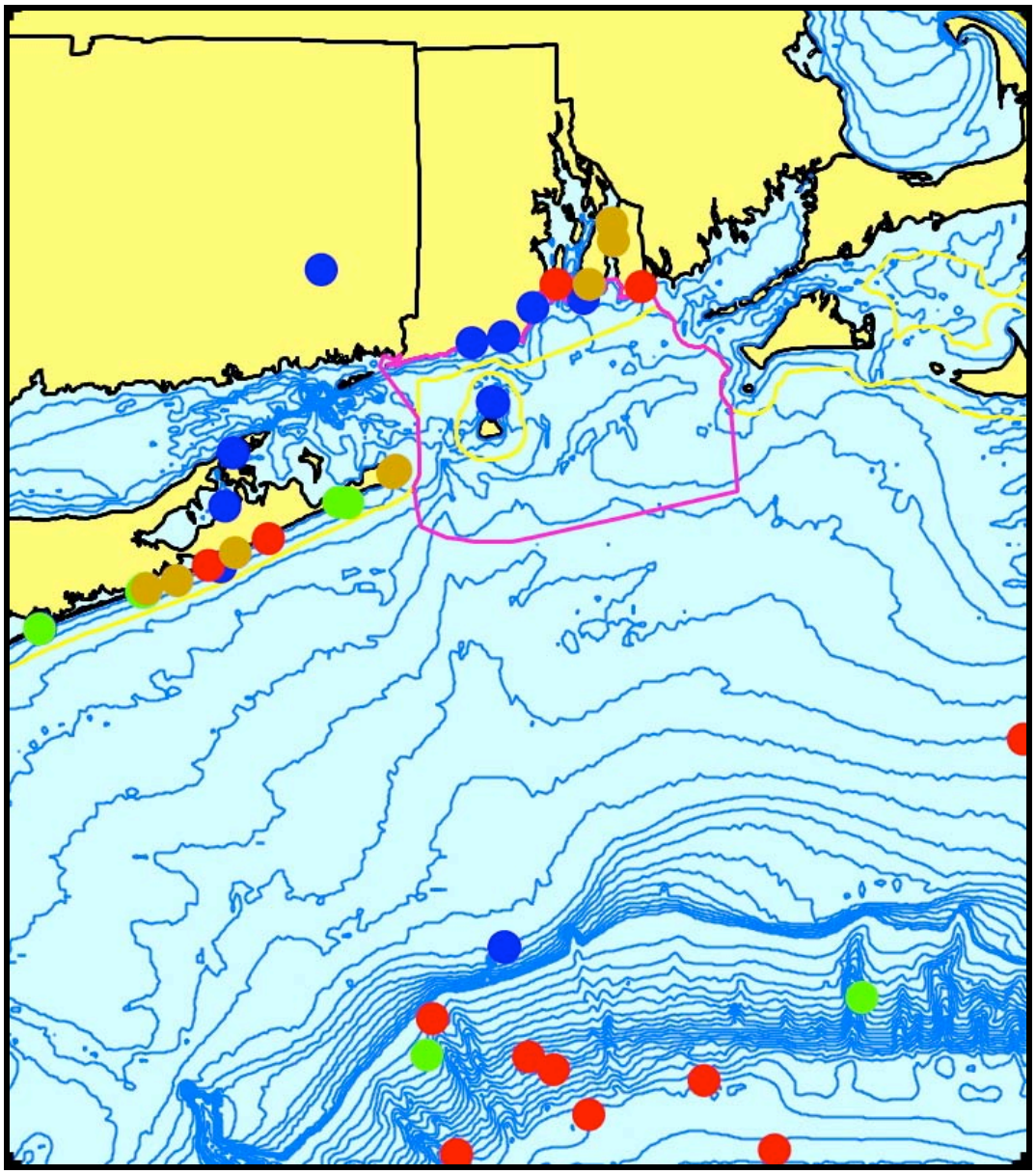

Figure 46. Aggregated sighting, stranding, and bycatch records of striped dolphins in the Rhode Island study area, 1929–2004 (n = 41: winter = 13, spring = 8, summer = 12, fall = 8).

both jaws severely fractured; the trauma was judged to be evidence of some sort of collision. A 136-cm, 27-kg juvenile female was seen swimming near Seapowet Beach in Tiverton on the morning of 20 November 1995; it died and stranded that afternoon. Striped dolphins stranded in Cow Cove at the northern end of Block Island on 10 January 1997 and 22 January 2000. On 4 June 2001 at 15:30, Jamestown police reported that a dolphin was seen swimming erratically and

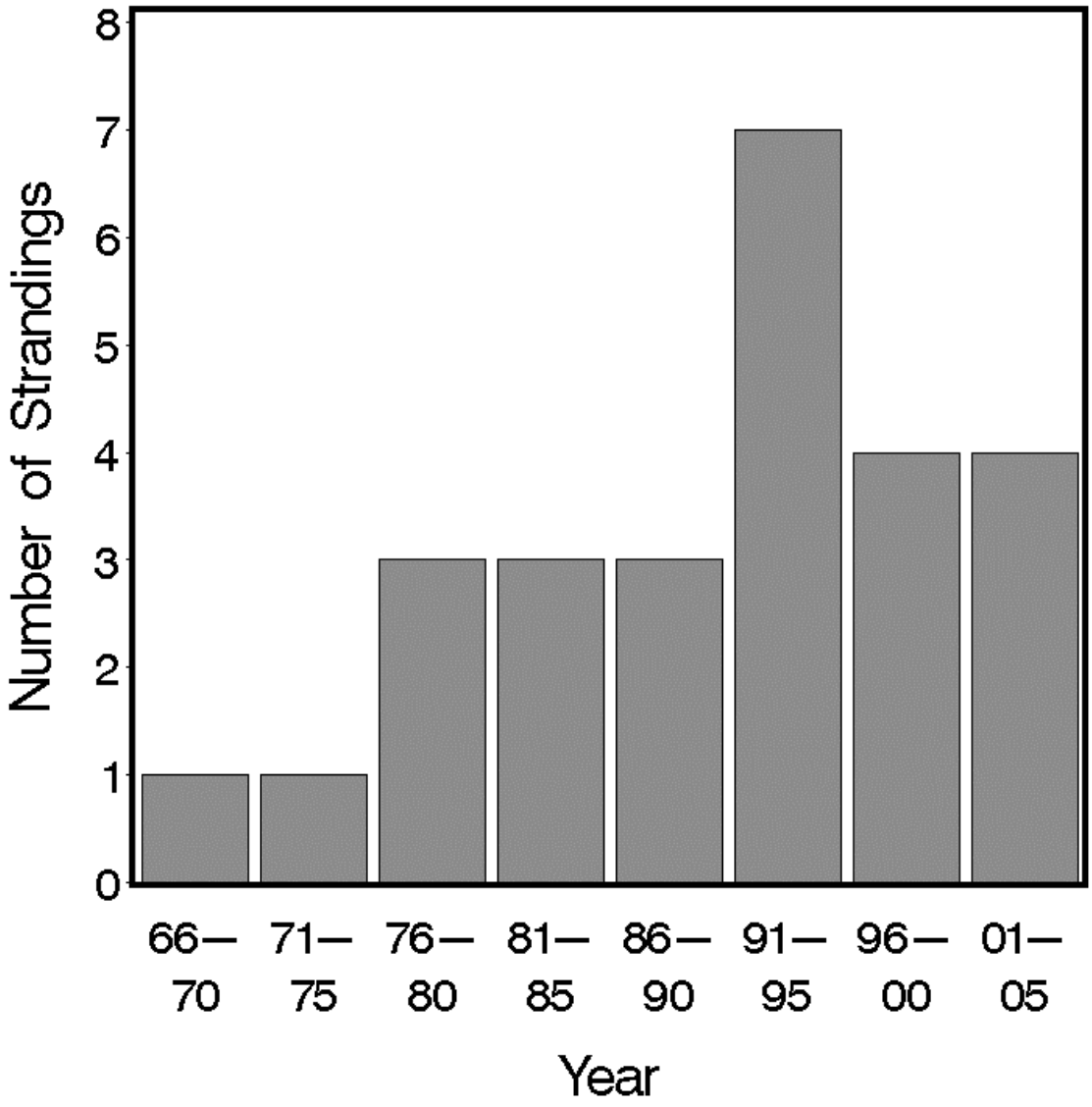

Figure 47. Five-year stranding frequencies for striped dolphins in the Rhode Island study area, 1966–2005.

seemingly in distress just off the beach at Mackerel Cove. It died and stranded by 17:15, when the carcass was recovered from the beach. It was a 201-cm adult or sub-adult male, and there was no discernible cause of death. Finally, a striped dolphin stranded near Sheep Point on the east side of Newport on 11 January 2002.

Conclusions: While striped dolphins are one of the most abundant cetaceans off the

northeastern U.S., their distribution is very far offshore. They have never been sighted in or near the SAMP area, and do not pose any concern relative to the SAMP.

3.2.23. Atlantic Spotted Dolphin *Stenella frontalis* (G. Cuvier, 1829)

Pan-tropical Spotted Dolphin *Stenella attenuata* (Gray, 1846)

The two species of spotted dolphins are broadly sympatric in the North Atlantic, are difficult to distinguish at sea, and have been frequently combined in survey and bycatch data, sometimes even in stranding data. It was not until the paper by Perrin et al. (1987) that the taxonomy of the spotted dolphins was sorted out. Prior to that, a variety of different common and scientific names were used, so it is not always clear which species may be referred to in particular instances. For example, Leatherwood et al. (1976) used the binomial *Stenella plagiodon* for the Atlantic spotted dolphin (*Stenella frontalis*), and used the common name bridled dolphin and binomial *Stenella frontalis* for the pan-tropical spotted dolphin (*Stenella attenuata*). Both are known from the Rhode Island study area, and they are combined here.

Description: Atlantic spotted dolphins are the most robust-bodied of the *Stenella* species, enough so that a young, unspotted animal may be mistaken for a young bottlenose dolphin. Adults are 1.7–2.3 m in length, with a tall, falcate dorsal fin, long but relatively thick beak, and moderately developed keels (Perrin et al., 1987, 1994a; Jefferson et al., 1993; Wynne and Schwartz, 1999; Perrin, 2002a, 2002e). They have a three-toned color pattern, with a dark gray cape that is widest below the dorsal fin, lighter gray sides, and a white belly. The tailstock is almost uniformly gray top and bottom. There is a pale gray "spinal blaze" that starts in the "shoulder" area above the flipper and extends upwards and backwards into the cape towards the dorsal fin, which may not be clearly visible on all individuals. The combination of spinal blaze and spots is diagnostic for *S. frontalis*. Calves are born without spots. Dark ventral spots begin to appear at about the time of weaning. Around puberty, the ventral spotting increases and pale dorsal spots begin to appear. The spotting intensifies, such that it can largely obscure the margins of the cape and lateral gray bands, but the ventral spots remain distinct in adults and do not fuse together. The tip of the beak is often distinctly white, there may be thin white borders along the lips, and there is a dark stripe from the corner of the mouth to the eye and then to the flipper. This latter character is variable, with some specimens having the mouth-to-flipper stripe passing

below the eye. Along the eastern U.S., there are relatively distinct inshore and offshore forms, with the offshore animals smaller, lighter, and less heavily spotted than the inshore animals, i.e., more similar in appearance to pan-tropical spotted dolphins. The larger, more spotted inshore animals represent the stock that may be a separate subspecies referable to *Stenella frontalis plagiodon*. Some offshore animals may be nearly unspotted, even as adults.

Pan-tropical spotted dolphins are very similar in body form to spinner dolphins, with a slender body, long thin beak, and prominent keels on the tailstock (Perrin et al., 1987; Jefferson et al., 1993; Perrin and Hohn, 1994; Wynne and Schwartz, 1999; Perrin, 2001, 2002d). The beak is shorter and the dorsal fin is more falcate than in spinners. Body size in adults is 1.6–2.6 m, with averages of 187 cm for females and 200 cm for males. They are more slender than Atlantic spotted dolphins, averaging 10–30 kg less at the same body length. The basic body pattern appears essentially two-toned. The dark gray cape is very narrow at the head, curving up well above the eye, and dips low on the side in front of the dorsal fin. There is no pale spinal blaze in the cape as in *S. frontalis* and *S. coeruleoalba*. Behind the dorsal fin the cape margin rises to the back and behind it the tailstock is clearly two-toned, lighter gray dorsally and white ventrally. The tip of the beak is often white, and there may be thin white borders along the lips. There is a black stripe from the upper jaw to the eye, and one from the corner of the mouth to the flipper. Overlaid on top of the basic pattern is the spotting. Calves are born without spots—dark gray above and ivory white below. The belly gradually turns light gray. Spotting begins with dark gray spots on the throat and abdomen, followed by pale dorsal spots. The ventral spots gradually increase in number and size, first touching each other and causing a mottled ventral appearance, then fusing and fading to a slightly mottled to uniform pale gray. The spotting does not obscure the margin of the cape. The flippers, flukes, and dorsal fins are smaller than in Atlantic spotted dolphins.

Status: Atlantic spotted dolphins are not listed under the U.S. Endangered Species Act or on the Rhode Island state list, and are classified as Data Deficient on the IUCN Red List. Pan-tropical spotted dolphins are not listed under the U.S. Endangered Species Act, are not included on the Rhode Island state list, and are classified as Least Concern on the IUCN Red List. There are no estimates of the total North Atlantic abundance number of either species of spotted dolphin. For continental shelf waters between Cape Hatteras and the Gulf of Maine, CETAP (1982) estimated only a few hundred undifferentiated spotted dolphins, however those estimates

were exclusively from aerial surveys, and a large proportion of aerial sighting could be identified only to *Stenella* sp. Kenney et al. (1997) partitioned the abundance estimates of "unidentified *Stenella*" into striped dolphin, spotted dolphin, and spinner dolphin based on the proportions of identified sightings—with estimates of spotted dolphins (both species combined) of 589 in winter, 1,689 in fall, 1,975 in spring, and 2,441 in summer. The estimated abundances from the more recent NMFS stock assessment surveys are substantially greater, since the surveys included the area from Florida to the Nova Scotian shelf and extended much farther offshore (Waring et al., 2008). Atlantic spotted dolphins were estimated at 46,481 in 1998 and 50,978 in 2004. There is also an estimate of 30,947 in the Gulf of Mexico. Pantropical spotted dolphins were estimated at 13,090 in 1998 and 4,439 in 2004, with 91,321 in the Gulf of Mexico.

Atlantic spotted dolphins are intentionally taken in small numbers by traditional fisheries in St. Vincent in the Lesser Antilles and maybe at some of the other islands (Perrin, 2002e). They are also taken as bycatch in tuna purse seines off West Africa. Offshore stocks of pan-tropical spotted dolphins and spinner dolphins were most seriously impacted by bycatch mortality in the Pacific tuna purse-seine fishery. There is also a directed fishery for small cetaceans in some coastal villages in Japan. Takes of pan-tropical spotted dolphins in Japan totaled 39 in 2000, 10 in 2001, 418 in 2002, and 132 in 2003 (IWC, 2005, 2006). There are also similar small-cetacean fisheries in the southwestern Pacific (Perrin, 2002d).

The average annual mortality of spotted dolphins in U.S. Atlantic commercial fisheries in 2001–2005 was 6, all in the swordfish longline fishery (Waring et al., 2008). From 1989 to 1998, the average annual mortality of spotted dolphins (not differentiated to species) in the pelagic swordfish driftnet fishery was 16 animals per year, ranging from 0 to 51. That fishery was shut down after the 1998 season for excessive marine mammal bycatch. Six spotted dolphins from the driftnet bycatch were sent to the Smithsonian for examination and identification, and all six were the pantropical species.

Ecology and life history: Atlantic spotted dolphins tend to occur in groups of fewer than 50, most often 1–15, although schools of 100 or more may occur offshore (Perrin et al., 1994a; Perrin, 2002a, 2002e). They are very active, acrobatic, and frequent bow-riders, and commonly break the surface with the tip of the beak when surfacing. Long-term studies in the Bahamas by Herzing (1997) show very fluid groupings of individuals, with some evidence of segregation by

age and sex. In the Bahamas, Atlantic spotted dolphins frequently associate with bottlenose dolphins (Herzing and Johnson, 1997). A tagged individual in the Gulf of Mexico made dives up to 40–60 m deep and 6 minutes in duration, but the majority of dives were shallower than 10 m (Davis et al., 1996).

Stenella frontalis feeds on small to large epipelagic and mesopelagic fishes and squid, and sometimes on benthic invertebrates (Perrin et al., 1994a; Perrin, 2002a, 2002e). It is probable that the diet differs between the inshore and offshore forms.

The available data for Atlantic spotted dolphins are more limited than for pan-tropical spotters, since there are not large samples of by-caught animals (Perrin et al., 1994a; Perrin, 2002a, 2002e). Calves are probably born at 90–100 cm. Females mature at about 190 cm along the U.S. Atlantic and 180 cm in St. Vincent in the West Indies. Males mature at 170–180 cm. The age at maturity in females in the Bahamas is estimated to be 9–15 years old (Herzing, 1997). The inter-birth interval is 1–5 years, averaging about 3.

Pan-tropical spotted dolphins may occur in schools from a few animals to several thousand (Perrin and Hohn, 1994; Perrin, 2001, 2002d). Within a large school there are distinct subgroups separated by age and sex—mother and calves, adult males, and juveniles—which tend to remain stable. There is evidence for an annual cycle of migration, inshore in spring and summer and offshore in fall and winter. They are very active, acrobatic, and frequent bow-riders. Dive data are limited, with dives known only up to 3.4 minutes in duration. In the Pacific, they commonly associate with spinner dolphins, short-beaked common dolphins, and yellowfin tuna.

Stenella attenuata in offshore Pacific waters feeds primarily on small epipelagic fishes, squid, and crustaceans, with some mesopelagic species (Perrin et al., 1973; Robertson and Chivers, 1997; Perrin and Hohn, 1994; Perrin, 2001, 2002d). Flying fish appear to be important prey, at least at times. The large inshore Pacific form may feed on larger benthic fishes. Archer and Robertson (2004) analyzed 203 stomachs from dolphins killed in the tuna fishery. Calves began to feed on myctophids at about 6 months of age while still nursing, then shifted their diet more to squid during weaning.

Pan-tropical spotted dolphins are born at 80–85 cm, and reach body lengths of 129–142 cm by 1 year of age (Perrin and Hohn, 1994; Perrin, 2001, 2002d). Calving is spread out over an extended period, with peaks in spring and fall, and maybe also in summer. Both males and

females begin to mature at about 160 cm, at which time males have a secondary growth spurt. Females mature at 9–11 years old, males at 12–15. The gestation period is 11.2–11.5 months. Lactation lasts is 1.4–2.1 years; the mean age and size at weaning in the Pacific bycatch sample analyzed by Archer and Robertson (2004) was 9 months and 122 cm. The inter-birth interval is 2–3 years. Both lactation period and inter-birth interval appear to vary in a density-dependent fashion with population status.

General distribution: Atlantic spotted dolphins are found only in subtropical and tropical waters of both the North and South Atlantic Oceans, between about 50ºN and 25ºS (Perrin et al., 1994a; Rice, 1998, Perrin, 2002a, 2002e). They appear to be more common on the western side of the basin—along the U.S. east coast to the Gulf of Mexico, Caribbean, and West Indies. There are scattered records from the South Atlantic near South America and Africa, and offshore, but there has been little research in those areas so they could be more common than the current data show. They are also known from the Azores, Canaries, and Cape Verdes, but not from Europe. There are numerous stranding records and older sighting records from the southeast U.S. for this species, and a few strandings along the northeast U.S. coast to Massachusetts.

Pan-tropical spotted dolphins are found in subtropical and tropical waters on both sides of the equator in all oceans between approximately 30–40ºN and 20–40ºS, a distribution nearly identical to that of the spinner dolphin (Perrin and Hohn, 1994; Rice, 1998; Perrin, 2001, 2002d). In the Atlantic the distribution seems to be mainly offshore and around oceanic islands. There are stranding records from Florida, and a scattering of strandings from North Carolina to Massachusetts.

In the western North Atlantic, distributional information about spotted dolphins has been confused by the occurrence of two similar species with overlapping ranges, confounded by the previous uncertainty regarding common and scientific names. Sightings of spotted dolphins were relatively numerous north of Cape Hatteras during the CETAP (1982) surveys, comprising about 40% of the identified *Stenella* sightings, but they were not differentiated to species, principally because the majority of the sightings came from aerial surveys. (Striped dolphin was the most frequently sighted *Stenella*, at 57% of the identified sightings, with a few spinner dolphin sightings and one Clymene sighting). The spotted dolphin sightings ranged from the middle of the shelf out into very deep water, were most common off North Carolina and Virginia, and were

rare north and east of Hudson Canyon. There were a few sightings identified to species, which were about three-quarters Atlantic and one-quarter pan-tropical spotters.

There have been additional sightings during the more recent NMFS assessment surveys, which have included a much larger shipboard component and have been able to identify a higher proportion of spotted dolphins to species (Waring et al, 2008). Spotted dolphins now make up 48% of the total *Stenella* sightings (with striped dolphins down to 49%), and pan-tropical spotters are less than 10% of the identified spotted dolphins. Sightings identified to pan-tropical spotters are almost all very far offshore, and mostly south of Cape Hatteras, but there were three sightings on the edge of Georges Bank. Pan-tropical spotted dolphins are the most commonly observed offshore cetacean species in the Gulf of Mexico, and are relatively common in the West Indies.

Historical occurrence: There are no historical records of either spotted dolphin from the Rhode Island study area. Cronan and Brooks (1968) did not mention either species for Rhode Island. The same is true for Waters and River (1962) for Massachusetts. Neither De Kay (1842) nor Linsley (1842) reported either species of spotted dolphins from New York or Long Island Sound, but both species were poorly known at that time, if at all. Goodwin (1935) mentioned Atlantic spotted dolphin (as *Prodelphinus plagiodon*) and said that the nearest known specimen was from New Jersey. Connor (1971) stated that *Stenella* "*plagiodon*" was a southern species reported from southern New Jersey.

Recent occurrence: There have been only nine scattered occurrences of spotted dolphins in the Rhode Island study area (Fig. 48). The first two confirmed spotted dolphin records for the Rhode Island study area were only two weeks apart in 1979. A shipboard observer sighted a pair of unidentified spotted dolphins offshore of the shelf break in the southeastern part of the Rhode Island study area on 16 August. On 1 September a CETAP aerial survey sighted a group of 100 unidentified spotters was sighted over the slope west of the August sighting. Another CETAP survey sighted a group of 40 on 22 August 1981 in the mid-shelf area south of Block Island. The other three sightings, all far offshore near or beyond the shelf break, came from an opportunistic sighting database originally created to map seabird distributions (PIROP, Programme Intégré des Recherches sur les Oiseaux Pélagiques)—two sightings of Atlantic spotters in July and October 1982 and one sighting of pan-tropical spotters in July 1984. All spotted dolphin sightings from

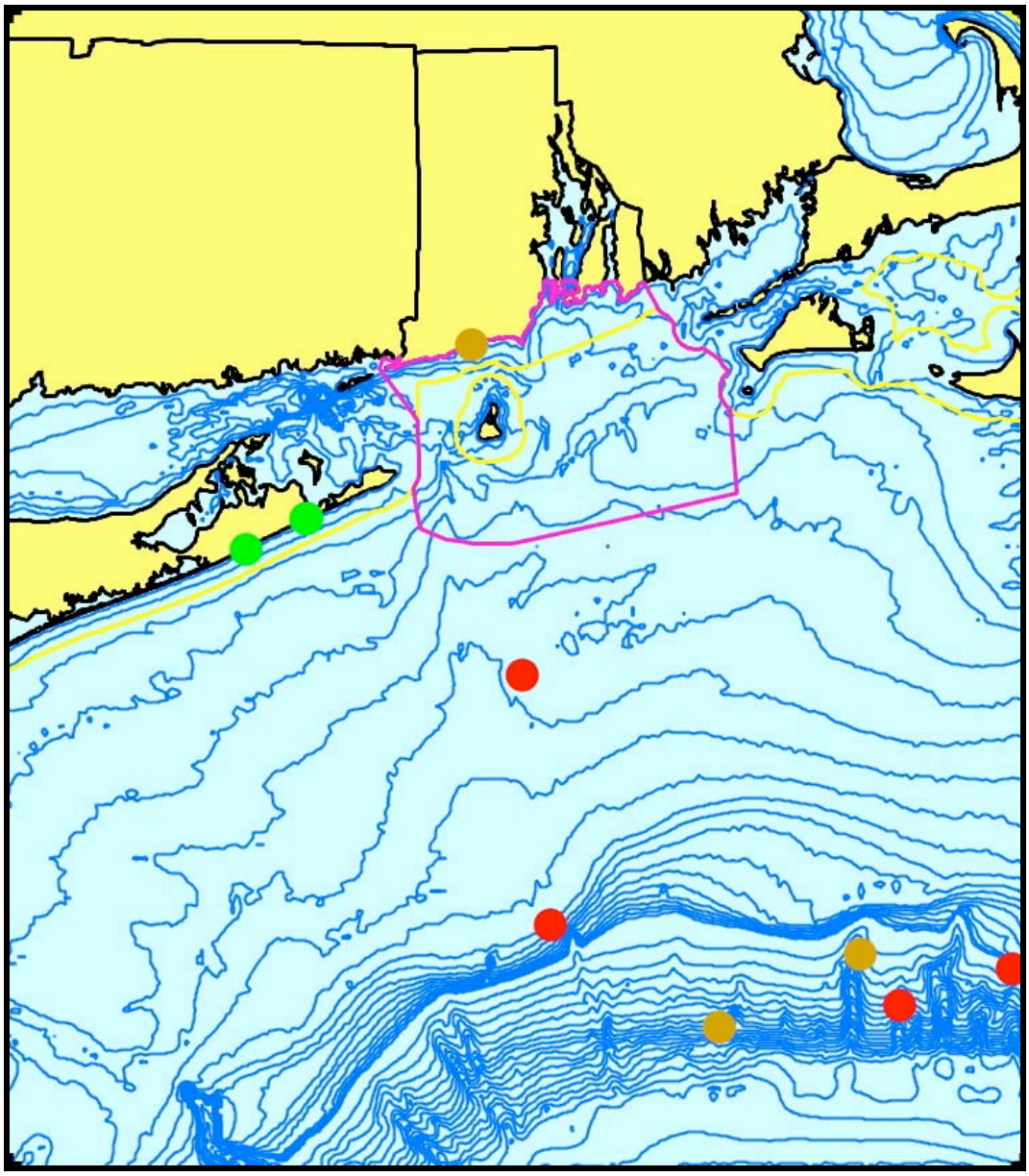

Figure 48. Aggregated sighting, stranding, and bycatch records of Atlantic, pan-tropical, and unidentified spotted dolphins in the Rhode Island study area, 1979–1988 (n = 9: winter = 0, spring = 3, summer = 3, fall = 3).

the NMFS cruises beginning in the 1990s have been farther offshore and beyond the study area. Based on the overall sighting record now available from those surveys (Waring et al., 2008), it is most likely that spotted dolphins encountered in the Rhode Island study area would be *Stenella frontalis*, but *Stenella attenuata* is possible.

In addition to the six sightings, there have been three spotted dolphin strandings in the Rhode Island study area. There was a live-stranding of a 216-cm, 47-kg pan-tropical spotted dolphin in Charlestown, Rhode Island on 11 October 1983. It died at Mystic Aquarium three days later. A 203-cm, 107-kg, pan-tropical spotter stranded in Amagansett, New York on 7 May 1983. The only confirmed Atlantic spotted dolphin stranding in the study area was a 209-cm animal stranded at Bridgehampton, Long Island on 23 May 1988.

Conclusions: Both spotted dolphin species have more subtropical and offshore distributions, and are not likely to occur in the SAMP area. Neither poses any conservation concern relative to the SAMP.

3.2.24. Harbor Seal *Phoca vitulina* Linnaeus, 1758

Pinnipedia includes three families of marine carnivores that are characterized by retention of all four limbs as flattened, simplified flippers—Phocidae (seals), Otariidae (sea lions and fur seals), and Odobenidae (walrus). Pinnipeds are not as completely adapted to the marine habitat as are cetaceans or sirenians, since all species must leave the water to give birth, either to a terrestrial habitat or onto sea ice. Recent morphological and molecular studies have concluded that Pinnipedia belongs within Order Carnivora, Suborder Caniformia (Rice 1998; Wozencraft 2005).

Phocids are sometimes referred to as “hair seals,” “earless seals,” or “true seals.” Phocids and otariids differ in a number of anatomical and life-history characteristics, with the walrus often intermediate (see Table 4 in Riedman, 1990 for a more detailed review). Otariids possess external ear pinnae, which are absent in seals and walrus. Seal flippers are completely furred with well-developed terminal claws. The hind-flippers are oriented directly backwards with opposed soles, and cannot be rotated underneath the body for locomotion on land, which is accomplished by caterpillar-like wriggling. In water, seals swim via alternating, lateral strokes of the hind-flippers, while using the fore-flippers mainly for maneuvering. Sea lions and fur seals have at least partially furless flippers with more rudimentary, subterminal claws. The pelvis and hind limbs can rotate underneath the body for walking on land. In water, they swim by simultaneous flapping of the long fore-flippers and use the hind limbs more as rudders. Seal coats have little underfur, and a seal is insulated by a thick layer of blubber. Fur seals have dense

underfur for thermal insulation and the least developed blubber layer, while sea lions have less dense underfur and moderately thick blubber. The walrus moves on land like a sea lion and in the water like a seal. It is essentially hairless with thick blubber. Seal pups grow extremely fast and wean quickly. The mother fasts completely during lactation in almost all species. In otariids and walrus, lactation can last two years or more, pup growth is slower, and the mother feeds during lactation.

There are no sea lions or fur seals in the North Atlantic. Pinnipeds of the North Atlantic and adjacent waters include the walrus and nine species of Phocidae. Only five seal species are confirmed as occurring in the Rhode Island study area. Three seal species have (or had) very restricted distributions—the Caspian seal (*Pusa caspica*), Mediterranean monk seal (*Monachus monachus*), and Caribbean monk seal (*Monachus tropicalis*, extinct since the mid-20th Century). The walrus (*Odobenus rosmarus*) and bearded seal (*Erignathus barbatus*) have Arctic distributions and occur rarely in U.S. waters but not south of Cape Cod. Although De Kay (1842) wrote that walrus "were formerly numerous on our coast, but are now scarcely ever found south of Cape Sable," there is no evidence to support his conjecture. There are no confirmed records in the Rhode Island study area. Historical walrus breeding populations in the Gulf of St. Lawrence and on Sable Island off Nova Scotia were extirpated in the early 18th Century (Lavigne and Kovacs, 1988). The nearest recorded walrus occurrences to New York were in Massachusetts in 1734 and 1937 (Cardoza et al., 2006). Similarly, there is a bearded seal stranding record in Massachusetts in 2002 (Sardi and Merigo, 2006), but none in the mid-Atlantic.

Description: Harbor seals are relatively small animals, with adults 1.7–1.9 m long (Jefferson et al., 1993; Wynne and Schwartz, 1999). Males are slightly larger than females. Harbor seals vary in color from very light gray or tan to brown to almost black, with extensive spotting. The basic spotting pattern is light with dark spots. In some individuals the spots coalesce, particularly on the back, giving the appearance of a dark color with sparse, light mottling. In general the belly is lighter than the back. Whether an individual is wet or dry will greatly change its appearance, with completely dry individuals often light-colored. Pups shed their white fetal coat (lanugo) in utero and are born with the same spotted coat pattern as adults. A harbor seal has a rounded head with a concave puppy-like face and only a short distance from eyes to nose. Nostrils are close together at the bottom and look like the letter "V" when seen from head-on.

Status: Harbor seals are not listed under the U. S. Endangered Species Act or on the Rhode Island state list, and are classified as Least Concern on the IUCN Red List.

A peak count of 271 harbor seals between the Massachusetts-Rhode Island border and eastern Long Island Sound was reported for March 1987 (Payne and Selzer, 1989). They suggested an upper bound of 374 based on their highest counts at each haul-out. Only Fishers Island, New York consistently had more than 50 animals, with a peak of 101 in March 1986. Schroeder (2000) estimated that the total number present in Narragansett Bay in 1999 was between 825 and 1,047. Ronald and Gots (2003) reported that the total seal count in southern New England in the spring of 1999 was nearly 6,100 animals.

The increase in harbor seals south of Cape Cod parallels that observed in the population's breeding range along the Maine coast. Gilbert et al. (2005) used aerial surveys to count seals hauled out on ledges along the entire Maine coast, and used radio-tagging data to correct for the proportion of seals hauled out at any given time. Between 1981 and 2001, seal counts increased from 10,543 to 38,014 (6.6% per year). Counts of pups increased at an even higher annual rate of 14.4%. The corrected estimate of the total abundance of harbor seals in Maine in late May and June of 2001 was 99,340 (95% CI = 83,118–121,397). The number of ledges used as haul-out sites also increased over that span of years, from 336 to 556, with the number used as pupping sites growing from 186 to 496.

Harbor seals were hunted by Native Americans for subsistence, then by early European settlers for oil, meat, and leather (Lavigne and Kovacs, 1988). In recent times, commercial hunting has never been of any great importance. Seals are commonly perceived as competitors for commercially valuable fish stocks. Bounties were paid on harbor (and gray) seals in both Maine and Massachusetts into the 1960s, resulting in depletion of the population overall and its extirpation from pupping sites in Massachusetts (Katona et al., 1993). Bounty payments in New Brunswick, Canada persisted until 1976 and were re-instituted in at least two years in the 1980s (Terhune, 1985). Harbor seals were also hunted for sport in the U.S. prior to passage of the Marine Mammal Protection Act in 1972, as reported for eastern Long Island by Connor (1971).

Harbor seals are taken as by-catch in a variety of U.S. and Canadian commercial fisheries, including gillnets, drift nets, long-lines, bottom trawls, midwater trawls, purse seines, trammel nets, fish traps, herring weirs, and even lobster traps (Woodley and Lavigne, 1991; Waring et al.,

2008). The 2001–2005 estimate of average numbers of harbor seals killed annually in the northeastern U.S. sink gillnet fishery was 882, plus an undetermined number in the bottom trawl fishery. It is as yet unclear how much of the U.S. fishery-related mortality represents seals from breeding sites in the U.S. versus Canada. Other known sources of human-related mortality in the northeastern U.S. and Canada include boat strikes, entrainment in power plant intakes, entanglement in aquaculture facilities, and intentional shooting.

More is known about disease as a population impact for harbor seals than for other marine mammals (Bigg, 1981). A relatively large number of diseases are known, and there have been several significant epizootics. Epizootics where the underlying cause was never determined were reported in Iceland in 1918 (Dietz et al., 1989b) and in the Shetland Islands in the 1920s (Bonner, 1972). There have also been several recent epizootics where the cause has been determined.

At least 500 harbor seals died in New England in 1979–80 (Geraci et al., 1982). The epizootic began in Cape Cod Bay in December 1979 and spread north along the Maine coast. The animals died from bacterial pneumonia caused by *Mycoplasma* spp. These bacteria are normally present in healthy seals, and can cause an infection known as "seal finger" in humans who have been bitten by a seal (Hartley and Pitcher, 2002; Mazet et al., 2004). At least three different species have been isolated from harbor seals or humans bitten by harbor seals (Geibel et al., 1991; Ruhnke and Madoff, 1992; Baker et al., 1998). The seals that contracted pneumonia were also infected with a strain of influenza A, and the hypothesized explanation was that the influenza lowered their immune response to the *Mycoplasma*.

There was a second, smaller epizootic in New England harbor seals in 1982 that killed only about 60 animals (Hinshaw et al., 1984). It was first recognized in Narragansett Bay. In that case, the underlying cause was a different strain of influenza A virus that normally is found in birds.

The most significant epizootic to date in harbor seals occurred in the North Sea in 1988, killing about 18,000 seals (Dietz et al., 1989b; Heide-Jørgensen et al. 1992). It began in April on Anholt Island in the Kattegat between Denmark and Sweden. It spread from there to the north along the coast of Norway and west to the Netherlands, Great Britain, and Ireland. Seal counts declined by 60% in the Kattegat and Skagerrak. Some areas experienced 90% mortality in 40–60 days, and in the Wadden Sea the number of carcasses recovered exceeded the highest previous

aerial survey count. The highest incidences occurred in areas where seals had congregated for pupping or molting, with less severe outbreaks where first introduced in the fall. The immediate cause of mortality was acute bacterial pneumonia, with *Bordetella bronchisepta* an important cause. There were secondary infections by herpes and picorna viruses, but the underlying cause appeared to be a morbillivirus. It was first identified as canine distemper virus (CDV) (Dickson, 1988; Osterhaus et al., 1988). Eventually the infectious agent was identified as a closely related morbillivirus now called phocine distemper virus (PDV) (Cosby et al., 1988; Osterhaus and Vedder, 1988). Dietz et al. (1989a) tested samples from 40 harp seals and 90 ringed seals collected in Greenland in 1985, prior to the 1988 epizootic, for the presence of antibodies to CDV, and found 30% positive in the harp seals and 4% in the ringed seals. It is now hypothesized that the virus was introduced to North Sea harbor seals from harp seals in a year when the harp seals dispersed unusually far southward (Heide-Jørgensen et al., 1992; Markussen and Have, 1992). A smaller PDV outbreak in the North Sea in 2002 killed hundreds of seals (Jensen et al., 2002).

Duignan et al. (1993) reported PDV in harbor seals from Long Island, New York. In an expanded study, Duignan et al. (1995) detected PDV antibodies in 37% of harbor seals and 73% of gray seals from New England, but not at all in Pacific harbor seals. There was usually little or no evidence of disease. In the winter of 1991–92, strandings increased in New England, and the PDV antibody detection rate increased to 83%. Morbillivirus lesions were observed in six animals, and a case of morbilliviral encephalitis was detected in archived tissue from an animal stranded in 1988. The authors hypothesized that high levels of PDV without disease outbreaks in gray seals are maintained by their large population size, high recruitment rate, and innate resistance, while infection is maintained in the smaller harbor seal population through contact with gray seals.

Dunn and Wolke (1976) reported seal heartworm infestation in harbor seals from New England. They found pulmonary, vascular, and hepatic lesions caused by both adult worms and microfilariae. The 1988 PDV epizootic in the North Sea provided very large sample sizes for parasite studies, and North Sea harbor seals carried a variety of nematodes, cestodes, trematodes, and acanthocephalans (Claussen et al., 1991a, 1991b). Five species of nematodes were very common. Seal heartworm was present in 32% of individuals. The lungworms *Otostrongylus* and *Parafilaroides* were present in 26% and 27%, respectively. The presence of heartworm and

lungworm was inverse to age, with *Parafilaroides* and heartworms absent in adults. The two common gut nematodes, *Contracecum* and *Pseudoterranova* (sealworm), present in 10% and 88% of animals, increased in occurrence with age.

Ecology and life history: Harbor seals are generally solitary when in the water, but gregarious when hauled out (Bigg, 1981; Burns, 2002; Ronald and Gots, 2003). Unlike many other pinnipeds that haul out only for reproduction and molting, harbor seals regularly haul out for resting. When hauled out, seals are observed sleeping for short periods with intervals of scratching, vocalization, yawning, jostling for position, or scanning for predators or other disturbance. Sometimes there are gray seals mixed in at harbor seal haul-outs, especially from Massachusetts north. In the Rhode Island study area, however, gray seals are most often juveniles and are difficult to identify except by experienced observers. Groups of seals on haul-outs show no evidence of sociality or structuring, but are simply aggregations of individuals that come together in order to utilize a limited resource. In addition, hauling out in groups is believed to be an anti-predator strategy. Terhune (1985) showed that as the number of seals in the group increased, the duration of time spent scanning decreased and the intervals between scans increased.

Hauling-out behavior is a function of tide stage, wind, temperature, precipitation, and time of day (Pauli and Terhune, 1987a, 1987b; Schneider and Payne, 1983; Burns, 2002; Ronald and Gots, 2003). The largest numbers of seals are likely to be hauled out at low tide in late afternoon on a calm, sunny day. Haul-out use also drops off when air temperatures get very cold. The seals are also extremely sensitive to disturbance when hauled out, and they may retreat to the water with only slight provocation—by humans, boats, aircraft, or potential predators.

What appears to be a relatively simple behavior pattern of hauling out at low tide each day and returning to the water between haul-out periods, presumably for foraging, can actually be quite complex. Individual harbor seals have been rehabilitated after stranding and released with satellite-linked radio tags. Single individuals have been recorded as using multiple haul-outs between Cape Cod, Massachusetts and Downeast Maine, interspersed with apparent foraging trips to one or more consistent locations tens of kilometers offshore in the Gulf of Maine. (see the WhaleNet satellite tagging program page at http://whale.wheelock.edu/whalenet-

stuff/stop_cover.html for both currently active tags on a variety of marine vertebrates and archived data and maps from previous tags.)

Harbor seals are relatively flexible in their selection of haul-outs, and can be found on rocky ledges and reefs, islets, mudflats, sand bars, gravel bars, sandy beaches, cobble beaches, glacial icebergs, sea ice, and man-made objects such as floating rafts and docks (Boulva and McLaren, 1979; Burns, 2002; Ronald and Gots, 2003). Important characteristics include protected locations that are relatively inaccessible from the land side and that have unobstructed access to water. Since harbor seals do not maintain breathing holes in the ice, when bays, inlets, and other nearshore waters freeze, the seals are pushed offshore where the ice edge provides water access (Ronald and Gots, 2003).

Annual molt occurs over two or three months from midsummer through early fall, after pupping (Bigg, 1981; Burns, 2002). Haul-out frequency increases somewhat during the molt. Yearlings molt first, followed by subadults, adult females, and then adult males. During molt there is an overlapping progression of age and sex classes.

Typical harbor seal dives last 3–4 minutes, but they are capable of diving for 30 minutes and to depths of 500 meters (Bigg, 1981; Burns, 2002). Frost et al. (2006) reported a study of Alaskan harbor seal pups using satellite-linked telemetry tags. Tagged pups increased their amount of time in the water and maximum dive depths during their first 3–6 months. Then time in the water and maximum dive depth both decreased, suggesting foraging seasonality. Percent time in the water was lowest in July (68%) and highest in November (89%). Tagged pups spent 50% of their swimming time diving in the upper third of the water column and only 5% in the deepest third, evidence that pups do not feed on or near the bottom during their first year.

Harbor seals are flexible in their prey selection (Bigg, 1981; Nowak, 1999; Burns, 2002; Ronald and Gots, 2003). Small to medium-sized fishes are the dominant prey, followed by squid and octopus, and then by crabs and shrimp. Types of fish eaten include a number of economically important commercial species. Among these are cods, hakes, mackerel, herring, sardines, anchovy, smelt, shad, capelin, sand lance, trout, salmon, rockfish, sculpins, and flounders. Shrimp may be particularly important prey for pups after weaning. Seals appear to feed on what is most abundant. Payne and Selzer (1989) collected scats from haul-outs in Maine and Massachusetts to look at prey preferences. They found clear geographic differences. Sand

lance was the dominant prey at all three Cape Cod, Massachusetts sites: 87% of the diet at Race Point (tip of Cape Cod), 85% at Monomoy Island (at the "elbow"), and 50% at Jeremy Point (on the west side in the middle of the "forearm"). Squid comprised the next most abundant food item (22%) and then gadids, herring, and flounders in decreasing importance. Mackerel and skate were also eaten. At the Isles of Shoals off southern Maine (about 100 km from Race Point), there was no dominant prey type. Gadids and rockfishes were about equal at 22% each, flounders and herring both were >10% of the diet, and cunner, sand lance, and skate were also eaten. The diet of harbor seals along Long Island, based on stomach contents of stranded animals and some observations of feeding, includes herring, mackerel, squid, flounder, green crabs, mussels, cod, and silver hake (S. S. Sadove, pers. comm.).

Harbor seal pupping in the Gulf of Maine takes place in late May and June (Katona et al. 1993). Pupping occurs from the Isles of Shoals at the Maine/New Hampshire boundary northward into Canada. Pupping formerly occurred south to Cape Cod (Katona et al., 1993), and recent evidence indicates that pupping has resumed at Manomet, Massachusetts on the west side of Cape Cod Bay. Single pups are born approximately 70 cm long and weighing about 10 kg (Wynne and Schwartz, 1999). The white lanugo is shed in utero, and the pup is born in a spotted juvenile coat, essentially the same as the adult pattern.

Harbor seals are unique among phocids. In most other seals, pups remain at the birth site until after weaning, and the mother tends to remain with or close by the pup for the entire lactation period, feeding little or not at all (Riedman, 1990). Harbor seal pups are precocial, swimming and following the mother within hours of birth (Bigg, 1981; Riedman, 1990; Burns, 2002; Ronald and Gots, 2003). At many pupping sites the pup has no other option, since the location is submerged at high tide. After the mother and pup leave the birth site, the pup follows the mother closely, sometimes riding on her back during the first week. They haul out at intervals, when nursing takes place. Adult females spend a larger proportion of their time hauled out during lactation (Thompson et al., 1989), but are able to feed throughout lactation (Burns, 2002). Pups are weaned at 3–6 weeks of age (Bigg, 1981; Burns, 2002). Harbor seal pups may continue to remain with and follow their mothers for 2–4 weeks after weaning.

Ovulation and mating occur very soon after weaning (Bigg, 1981; Thompson, 1988; Riedman, 1990; Burns, 2002). Mating takes place in the water. Males are largely unable to defend breeding

sites or females, resulting in a promiscuous or slightly polygynous mating system (Riedman, 1990). Implantation of the embryo is delayed for 1.5 to 3 months.

Female harbor seals become sexually mature at 2–5 years of age, most at age 3 or 4, and reach physical maturity at age 6 or 7 (Bigg, 1981; Burns, 2002). Males take about a year longer. Most (85–92%) mature females give birth each year. First-year mortality rate is 20–60%, after which it is 5–20% (Boulva and McLaren, 1979), and the mortality rate in males is higher than in females after sexual maturity. It is commonly assumed that a large proportion or even a majority of the harbor seals in southern New England are juveniles, and there is some published support for this (Payne and Schneider, 1984; Whitman and Payne, 1990; Katona et al., 1993). Waring et al. (2006a) captured and radio-tagged 21 harbor seals and estimated age for 17 near Cape Cod, Massachusetts in March 2001. Fourteen (82%) were adults, one (6%) was a subadult, and two (12%) were juveniles. It is still possible that the proportion of juveniles is higher in the Rhode Island study area. Alternatively, perhaps perceptions of the age structure in the region are somewhat biased by the reliance on strandings for data. Adults, sub-adults, and juveniles cannot be easily differentiated except by close examination, and mortality and stranding rates can be expected to be higher for younger animals. Gilbert and Wynne (1987) reported that all of the harbor seals taken in the gillnet fishery in the Gulf of Maine were young of the year.

In harbor seals, predation impacts pups to a larger extent than adults. Predators of pups include polar bears, red foxes, Arctic foxes, Steller's sea lions, eagles, ravens, and gulls (Burns, 2002; Ronald and Gots, 2003). In eastern Canada, the three major sources of mortality in the pups are stillbirth, abandonment after birth, and sharks (Boulva and McLaren, 1979). Stobo and Lucas (2000) reported that the rate of shark predation (with Greenland shark an important predator) on harbor seal pups at Sable Island increased markedly, from 20% of pups in 1980–1993 to about 25% in 1994 and 1995 to 45% in 1996. Shark attacks on adult seals seem to be directed preferentially towards females. In recent years white shark occurrence near Cape Cod seems to have increased, presumed to be related to the increased summer abundance of both harbor seals and gray seals (G. Skomal, Massachusetts Div. of Marine Fisheries, pers. comm.).

General distribution: Harbor seals occur in coastal waters of both the North Atlantic and North Pacific (Bigg, 1981; Riedman, 1990; Burns, 2002; Ronald and Gots, 2003). In the western North Atlantic, they are common from southern New England north to Labrador, Greenland, and

Iceland. They are mainly seen hauled out or relatively close to the shore. North of Cape Cod harbor seals can occur year-round. However, south of Cape Cod (Rhode Island to New Jersey) seals occur only during winter migration (October to early May) (Payne and Selzer, 1989). There are occasional records from as far south as Florida (Caldwell and Golley, 1965; Caldwell and Caldwell, 1969; Caldwell et al., 1971; Waring et al., 2008). As with pinnipeds in general, records of in-water observations are much less common than records of stranded animals or seals on haul-out sites. Harbor seal sighting and bycatch records away from shore are concentrated in relatively shallow water. Lens (1997) reported seven individuals taken in a Spanish deep-water trawl fishery on the southern edge of the Grand Banks, showing that harbor seals are capable of long-distance foraging movements and can occur far offshore.

The annual patterns of movement in the harbor seals of New England and Atlantic Canada are complex (Bigg, 1981; Riedman, 1990; Katona et al., 1993; Nowak, 1999; Burns, 2002; Ronald and Gots, 2003). Some sources call harbor seals migratory, while others say they are non-migratory, sometimes differentiating between migration and "seasonal movements." In Maine and Atlantic Canada, harbor seals can be observed year-round (Boulva and McLaren, 1979; Katona et al., 1993; Baird, 2001), while in southern New England they are very clearly seasonal, occurring from September to late April–early May (Payne and Schneider, 1984; Payne and Selzer, 1989; Sadove and Cardinale, 1993; Schroeder, 2000). Only a minority of the population winters in the Rhode Island study area, and does not remain for pupping. However, since the 1990s, small numbers have been reported to remain around Long Island year-round and pupping has been observed on Great Gull Island and Fishers Island (S. S. Sadove, pers. comm.). One hypothesis for why harbor seals depart from the Rhode Island study area just prior to the time of pupping is the presence of predators. Many large predatory sharks are more common south of Cape Cod than to the north in the Gulf of Maine (Kenney et al., 1985b; Collette and Klein-MacPhee, 2002).

Historical occurrence: Harbor seals have long been recognized as common residents in the northeastern U.S. (De Kay 1842; Allen 1880). (The Smithsonian dataset we obtained included only cetacean records, so we had no historical data from that source.) Cronan and Brooks (1968) reported seven 20th Century records from Rhode Island or nearby between 1933 and 1967. Seals were seen in Mount Hope Bay in 1933, 1938, and 1941. One was sighted off the URI Bay Campus on 10 December 1956, and another was seen in the Sakonnet River in November 1957.

A dead seal was found floating in the Bay in the fall of 1957 and collected as a specimen for the survey conducted by Cronan and Brooks for their study. One seal was captured in a fish net off Newport in August 1967. Waters and Rivard (1962) wrote that harbor seals were usually seen in southeastern Massachusetts in late winter and early spring and had formerly been much more abundant, but were rare south of Massachusetts. All historical sources concur that harbor seals were relatively common around Long Island and Connecticut (De Kay, 1842; Linsley, 1842; Merriam, 1884; Goodwin, 1935; Connor, 1971).

Recent occurrence: Harbor seals are regularly observed around all coastal areas throughout the Rhode Island study area, and occasionally well inland up bays, rivers, and streams (Fig. 49). It should be noted for all the seals that the available data are strongly dominated by stranding records, which comprised 446 out of 507 total records for harbor seals (88%). Seals are very difficult to detect during surveys, since they tend to be solitary and the usual sighting cue is only the seal's head above the surface. In addition, seals were specifically excluded from data collection efforts during CETAP, and there is no centralized repository for opportunistic seal sighting information outside of small localized collections. Although the harbor seal is generally referred to as a winter resident in the region, their period of occurrence is significantly broader. Of the available records, 52.5% are in spring, 31.2% in winter, 9.5% in summer, and 6.9% in fall. In the Rhode Island study area, there are no records offshore of the 90-m isobath (Fig. 49). From counts on haul-outs in Narragansett Bay, Schroeder (2000) showed that seals usually start arriving in September, steadily increase in numbers until April, then depart relatively abruptly in May.

Payne and Selzer (1989) identified six haul-outs in Narragansett Bay in the 1980s. Their peak counts were 43 at the Dumplings off Jamestown and 36 at Rome Point in North Kingstown, and only one animal was ever seen at Block Island. The numbers of harbor seals in the Rhode Island study area have increased dramatically since then. Schroeder (2000) reported 21 haul-outs around Narragansett Bay and 6 at Block Island during 1994–1999 (Fig. 50). The largest haul-out was a clump of rocks located 230–370 m off Rome Point in North Kingstown, with a maximum count of 170 animals. However, some haul-outs used in the 1960s–1980s had apparently been abandoned or nearly abandoned. The maximum count at the Dumplings was 2. The peak counts at the two largest haul-outs in Block Island were 54 and 16 (see below). Her results indicated that

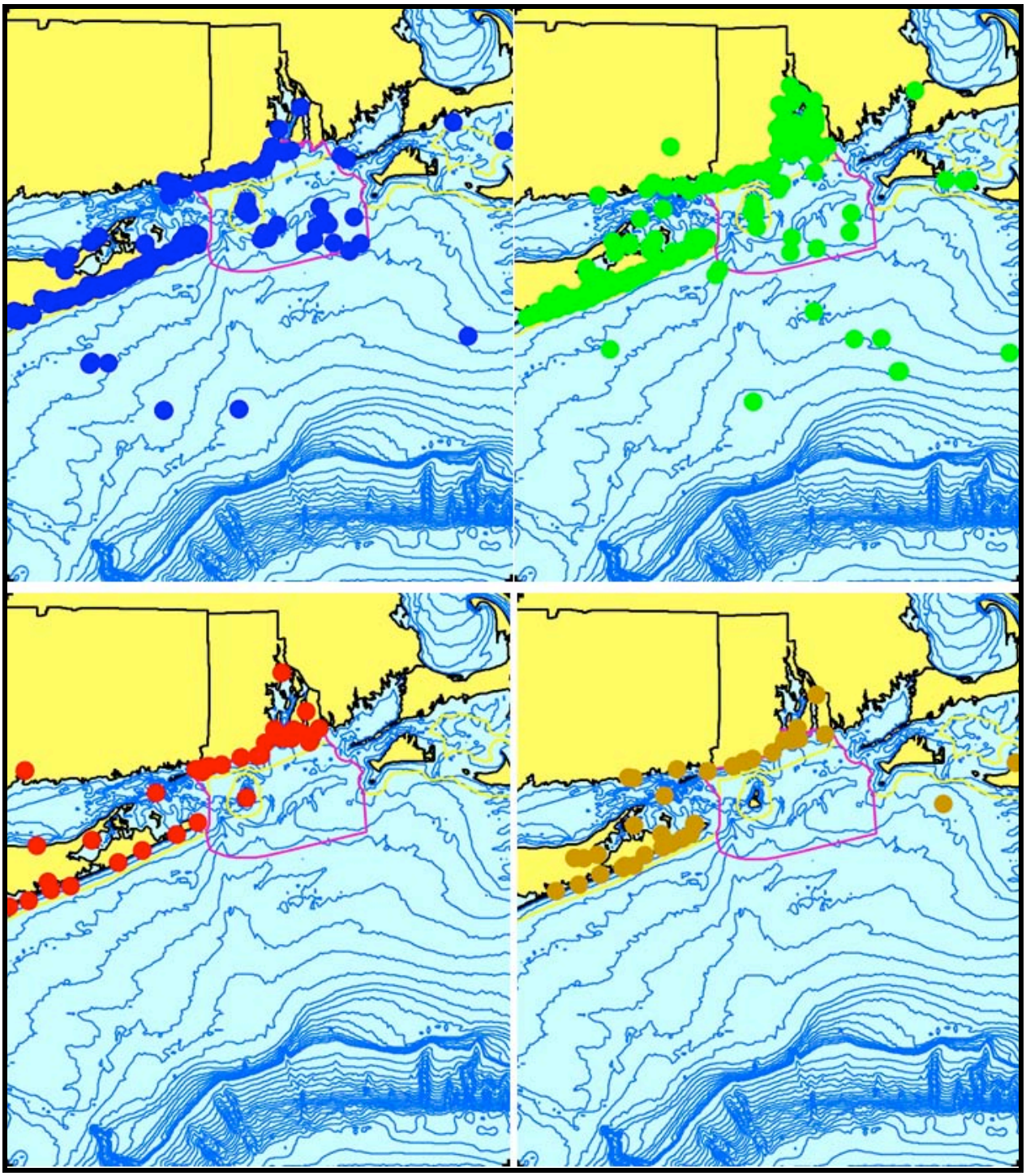

Figure 49. Aggregated sighting, stranding, and by-catch records of harbor seals in the Rhode Island study area, 1954–2005 (n = 507: winter = 158, spring = 266, summer = 48, fall = 35).

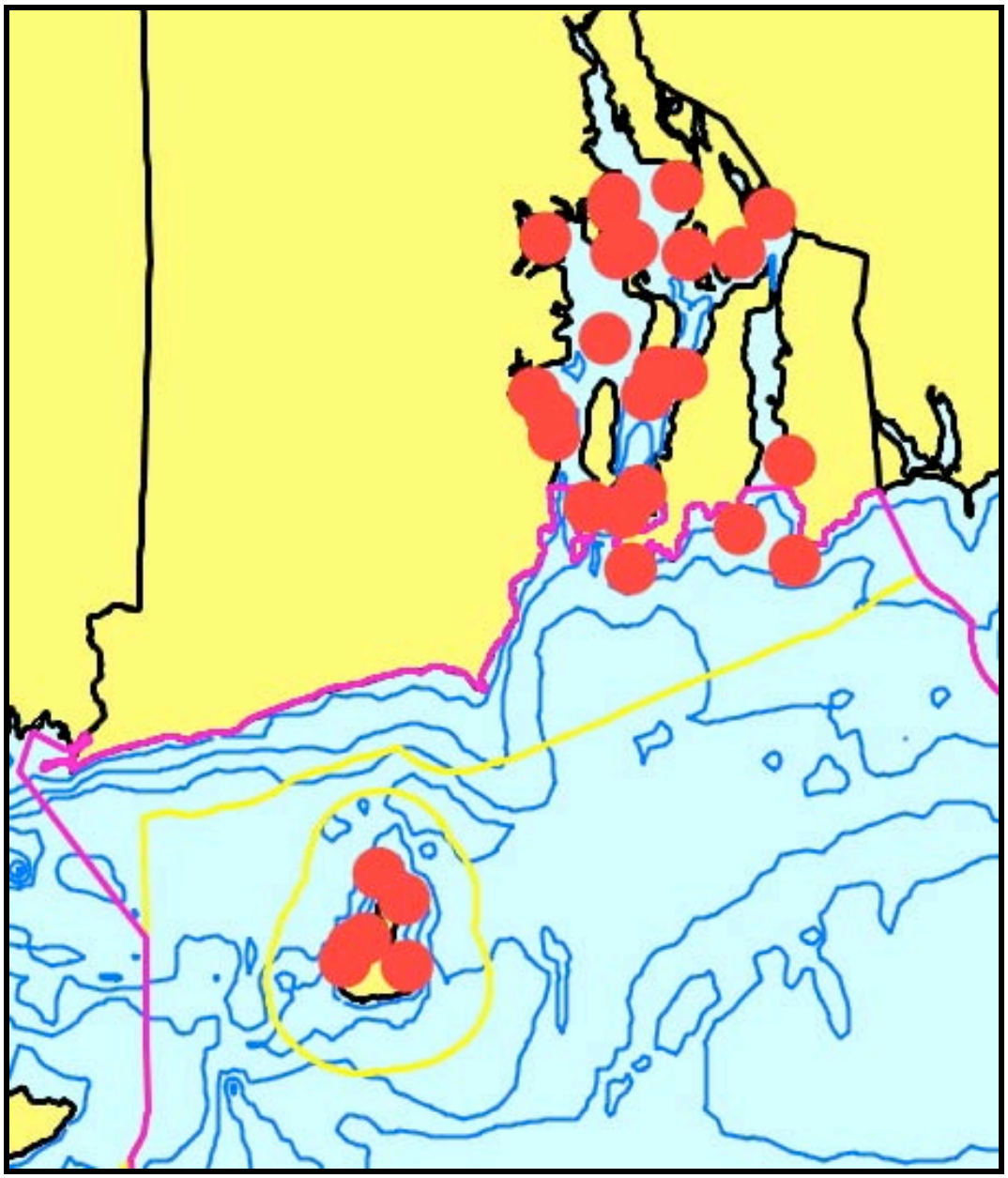

Figure 50. Harbor seal haul-outs in Rhode Island: 1966–1976, 1981, 1986–1987, and 1994–1999 (based on Schroeder, 2000).

the number of harbor seals in Rhode Island had increased by an order of magnitude from the 1960s to the late 1990s.

Schroeder (2000), collaborating with Scott Comings of The Nature Conservancy, identified six harbor seal haul-outs at Block Island (Table 5). The largest haul-out is at Cormorant Cove in

the southwestern corner of Great Salt Pond (see below). The other five are around the periphery of the island. Pebble Beach is on the southeastern part of the island, near Old Harbor. Two haul-outs are at the northern end of the island, at Clay Head and Sandy Point. Finally, there are two haul-outs on the southwestern side, first identified during the final season of Schroeder's research—Dorie's Cove and Grace's Cove.

Table 5. Maximum monthly counts of harbor seals at the six Block Island haul-outs during the 1997–98 and 1998–99 seasons (Schroeder, 2000).

	Month					
Haul-out (season)	**Dec**	**Jan**	**Feb**	**Mar**	**Apr**	**May**
Cormorant Cove (97–98)	–	–	47	52	22	0
Pebble Beach (97–98)	–	–	–	12	14	0
Clay Head (97–98)	–	–	–	8	0	0
Sandy Point (97–98)	–	–	–	0	2	0
Cormorant Cove (98–99)	52	52	54	53	43	0
Pebble Beach (98–99)	16	8	8	10	9	0
Clay Head (98–99)	3	5	4	6	10	0
Sandy Point (98–99)	2	3	0	6	0	0
Dorie's Cove (98–99)	0	1	2	3	3	0
Grace's Cove (98–99)	0	0	1	2	4	2

In Rhode Island, seals utilize different haul-out types around Narragansett Bay compared to those on Block Island (Schroeder, 2000). Nearly all of the haulouts around the Bay are rocky ledges and isolated rocks that are mostly submerged at high tide. The exception is Spar Island, which is a man-made dredge-spoil island in Mount Hope Bay. At Block Island, there are several haul-outs on cobble and sandy beaches around the island, but the haul-out used by the largest number of seals is a wooden raft moored in Cormorant Cove. Around the eastern end of Long Island, Payne and Selzer (1989) identified the most important haulouts in the 1980s, in order of

decreasing counts, as Fishers Island, Great Gull Island, Montauk Point, Gardiners Island, Sag Harbor, and Falkner Island (CT). These continue to have the largest aggregations, and constitute locations where access is restricted by physical characteristics or by extensive private or government property holdings. There are other haul-outs all around the eastern end of Long Island and along both the Atlantic and Long Island Sound shores (Sadove and Cardinale, 1993). The numbers of individuals at Long Island haul-outs range from about 20 to 500 (S. S. Sadove, pers. comm.). There are also known haul-outs in Connecticut (A. Ferland, Maritime Aquarium, pers. comm., R. Nawojchik and H. Medic, Mystic Aquarium, pers. comm.).

The vast majority of seal sightings during surveys come from aerial surveys flown by the National Marine Fisheries Service or the Provincetown Center for Coastal, focused primarily on right whales and mainly around Cape Cod. In the survey data for the broader area used in the relative abundance modeling (Fig. 1), there were 976 seal sightings—including 16 identified as gray seals, 151 identified as harbor seals, and 809 recorded simply as unidentified seals. In addition to the difficulty in identifying seals at sea from an airplane, the survey crews very often do not take the time from their primary mission to identify hauled-out seals. The number of animals at a sighting averaged 39.6, and ranged from 1 to 3,000. Over half of all sightings were single animals, but about 20% were groups of 4 or more, mainly on or near haul-outs.

All of the survey sightings of harbor, gray, and unidentified seals were combined in calculating the SPUE values and in creating the relative abundance maps (Fig. 51). The pattern shows concentration around the major haul-outs near Cape Cod and Nantucket in all four seasons. In winter, there is also an area of moderate abundance near the coast from eastern Long Island to Buzzards Bay and Vineyard Sound. There are areas of occurrence offshore in three seasons of the year, but at much lower levels of abundance than near the haul-outs. There was no survey effort in Narragansett Bay or the Sakonnet River except for a little at the mouth of the Bay in summer, therefore the occurrences in the Bay/River in all four seasons result from the GIS kriging and extrapolation procedure.

Annual stranding frequencies since 1993 (the start of the NE regional stranding network dataset available from NERO) are shown in Figure 52. Strandings were highest in the early 1990s. The numbers of strandings were lower on average in 1997–2002, with one-year spikes in 1998 and 2001, then generally higher again.

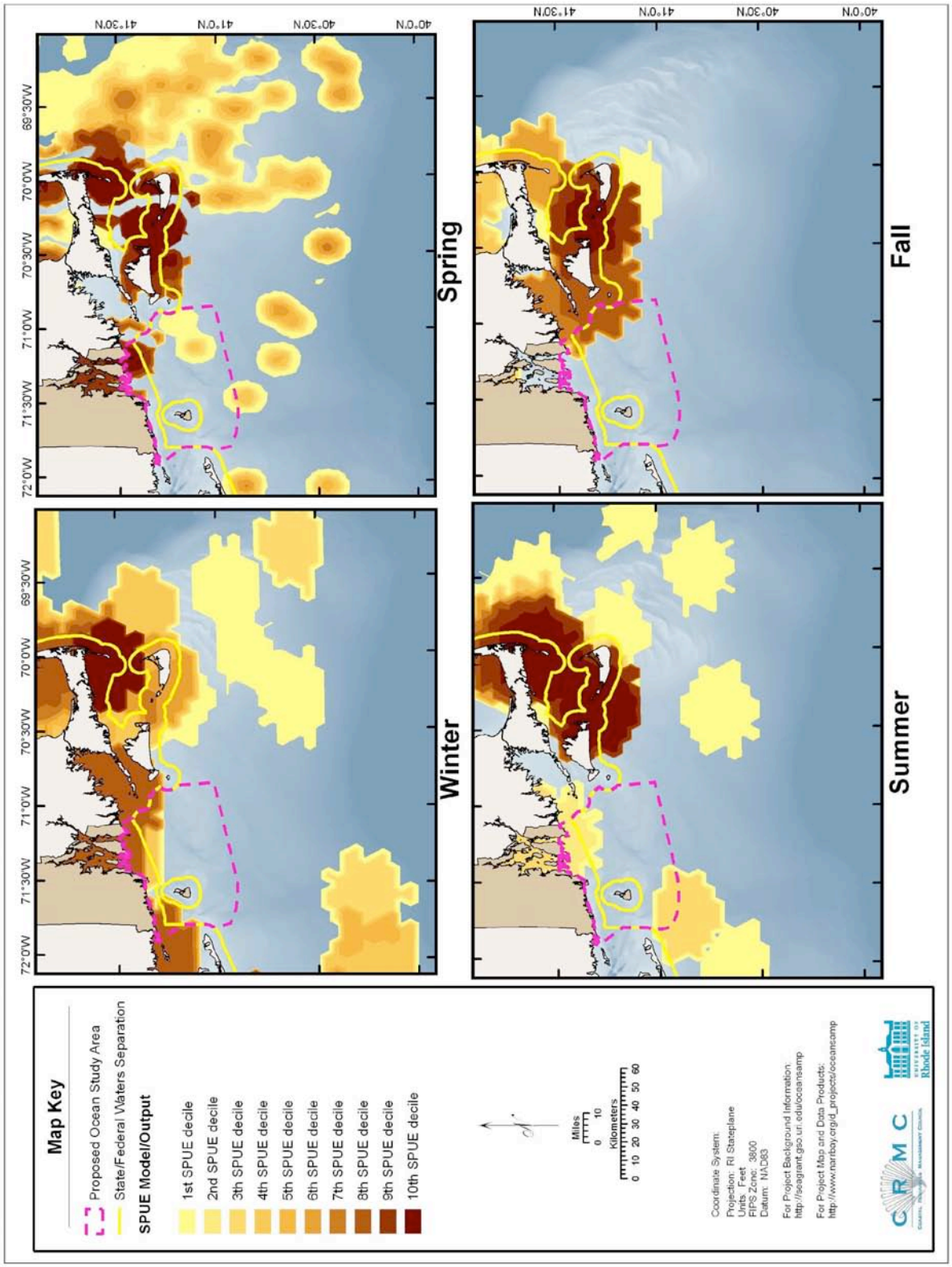

Figure 51. Modeled seasonal relative abundance patterns of seals (harbor seals, gray seals, and unidentified seals combined) in the Rhode Island study area, corrected for uneven survey effort.

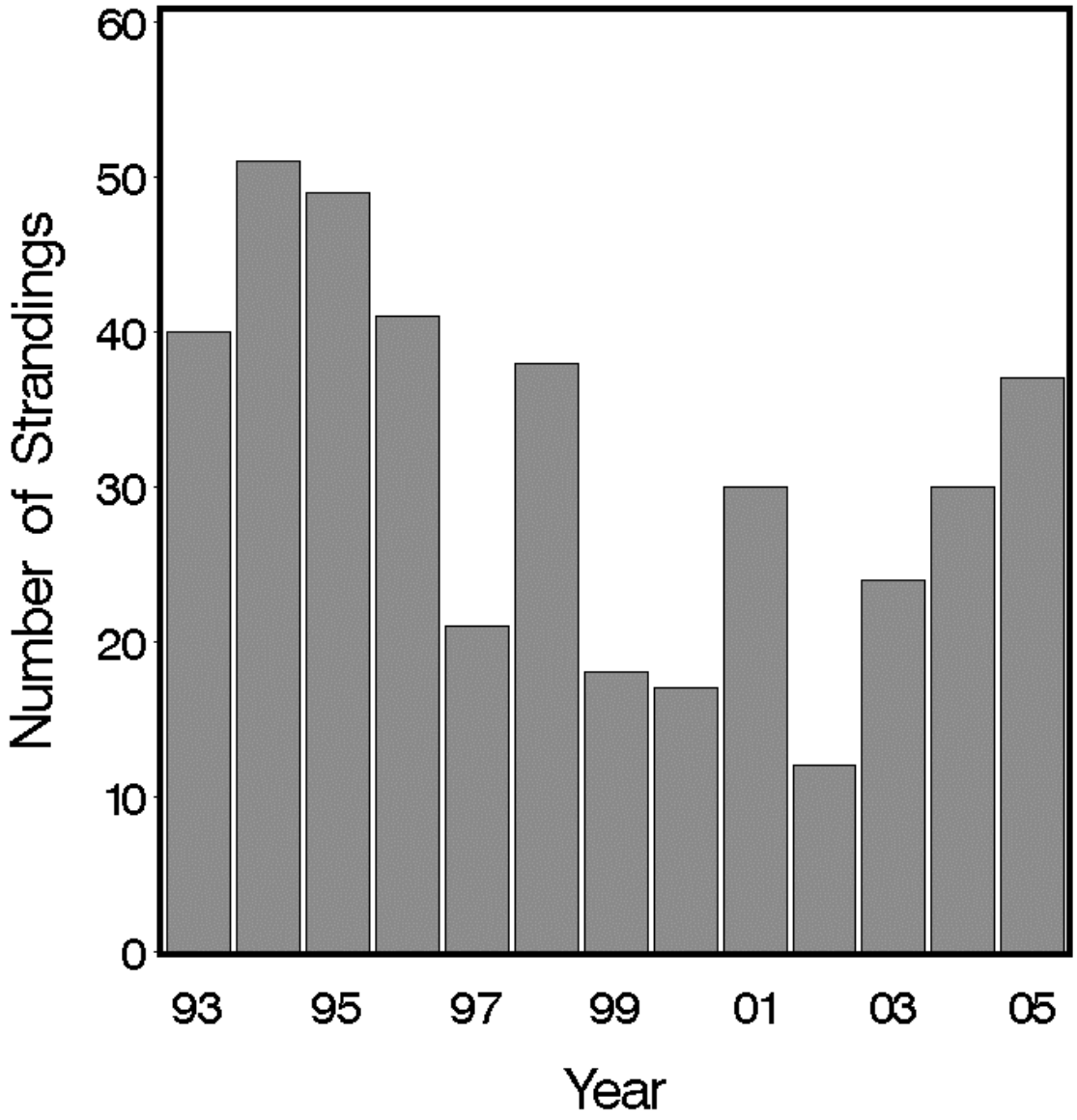

Figure 52. Annual stranding frequencies for harbor seals in the Rhode Island study area, 1993–2005.

Harbor seal strandings occur year-round in the study area, with a seasonal trend that closely mirrors the trends in counts on Rhode Island haul-outs shown by Schroeder (2000; Fig. 53). Strandings are least common in July and August and more frequent from November to June, with a peak in April and May. The stranding records from Mystic Aquarium included 44 harbor seal

strandings in Rhode Island in 1976–1992. Combined with the Rhode Island records from the NERS data, there were strandings in Rhode Island every year beginning in 1985, and in significant numbers beginning in 1987 (Fig. 54). There is no evidence for an increase in 1991-92, during the regional PDV epizootic. The pattern is similar to that seen in the regional data, with higher numbers in 1987–1998, a lower rate in 1999-2002, and then a return to similar levels.

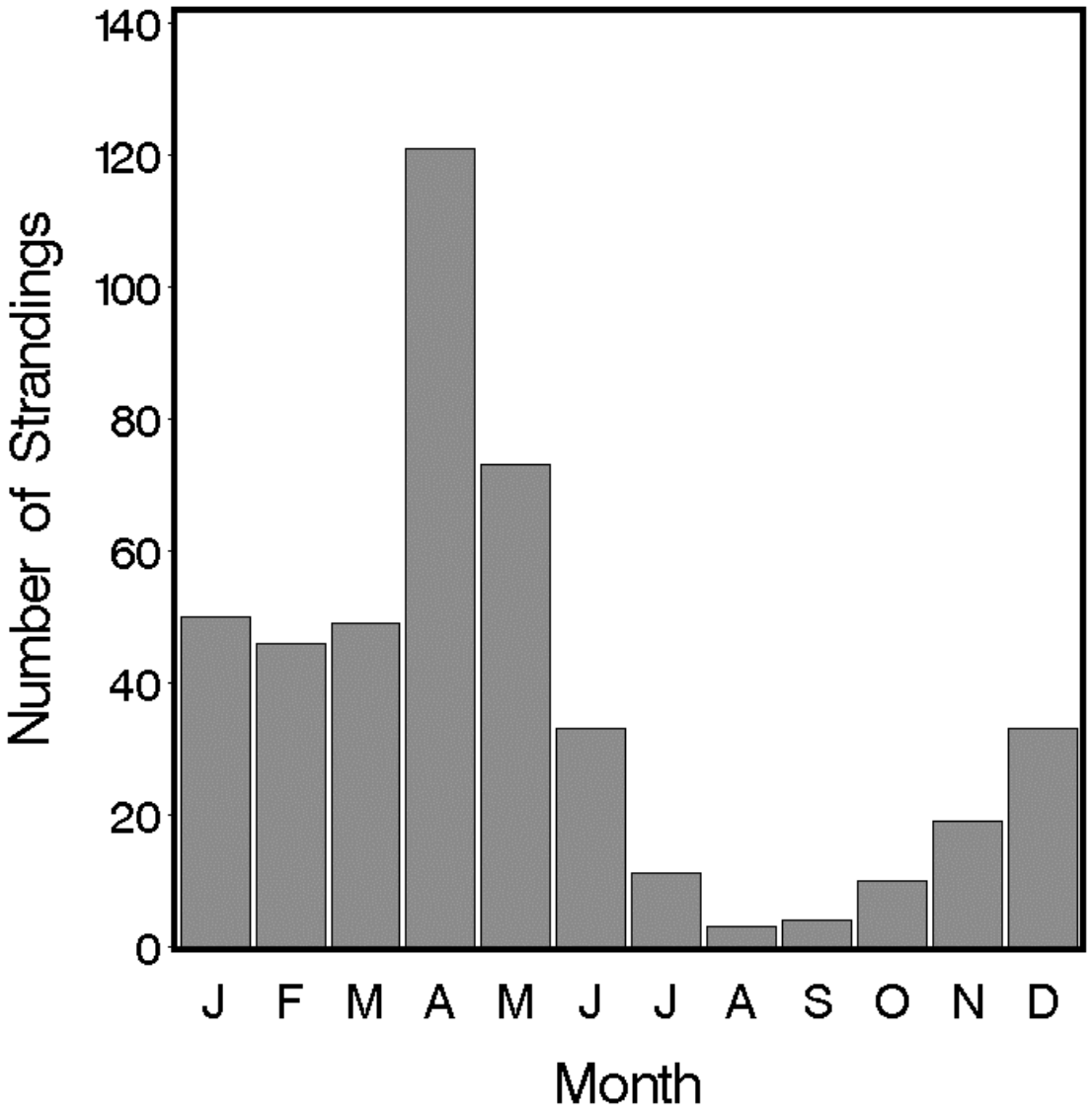

Figure 53. Monthly stranding frequencies of harbor seals in the Rhode Island study area.

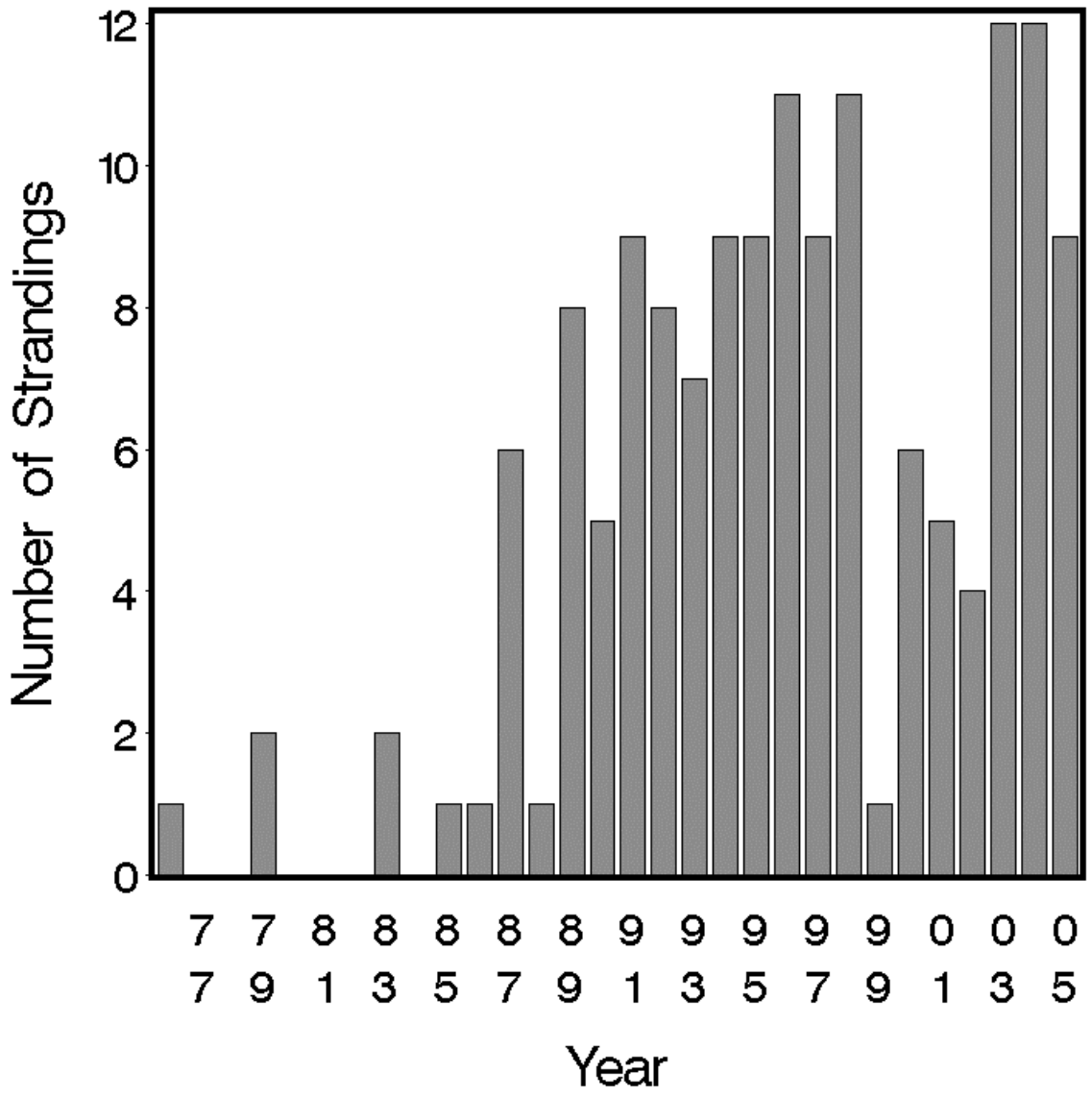

Figure 54. Annual stranding frequencies for harbor seals in Rhode Island alone, 1976–2005.

Conclusions: Harbor seals are really the only resident marine mammal within Rhode Island state waters, including Narragansett Bay and Block Island. If construction activities for a wind farm or other development project were to be restricted to winter in order to mitigate potential impacts on endangered whales and sea turtles, one effect would be to put those activities into a season of higher seal numbers. The proposed installation of wind turbines in state waters

southeast of Block Island would be closest to the seal haul-out at Pebble Beach near Old Harbor, where there might be 15 or more seals at any one time (Table 5). That construction might require both an Incidental Harassment Authorization or specific mitigation elements.

3.2.25. Gray Seal *Halichoerus grypus* (Fabricius, 1791)

Description: Gray seals are sexually dimorphic, with adult males up to 2.3 m long and females up to 2.0 m (Jefferson et al., 1993; Wynne and Schwartz, 1999). Sexes also differ in color—males mainly dark with irregular light patches and females light with dark spots. Pups are born with a solid white or yellowish coat, and molt to a spotted coat in 2–4 weeks. Gray seals (including pups) are distinguished from harbor and harp seals by the distinctive shape of the head. Gray seals have an elongate snout with a flat or slightly convex profile. The distance between the eyes and nose is about twice the distance between the eyes and the ear openings. The neck and chest of males may be wrinkled, scarred, and often devoid of fur. The latter is believed to result from male-male fights over access to females. Females are sleeker and lack scarring (Hall, 2002). The nostrils are widely separated and from the front look like the letter "M" or "W."

Status: Gray seals are not listed under the U.S. Endangered Species Act or on the Rhode Island state list, and are classified as Least Concern on the IUCN Red List. Gray seal populations in both the northeastern U.S. and eastern Canada have grown significantly since low points in the 1960s. Starting from a handful of animals and no pupping, the Massachusetts colony now has an annual pup production of over 1,000 and >5,600 seals total. There are >1,700 animals present in Maine (Waring et al., 2008). The eastern Canadian population was estimated at only 5,600 seals in the 1960s (Mansfield, 1966), but grew to 144,000 in 1993, 195,000 in 1997, and 209,000–223,000 in 2004 (Lesage and Hammill, 2001; Hammill, 2005).

Gray seals were hunted by Native Americans for subsistence. They were hunted by European settlers, for oil, meat, and leather, to the point where abundance was extremely low from the mid-19th to mid-20th centuries (Lavigne and Kovacs, 1988). In the modern era, commercial hunting has been relatively limited because of low abundance and relatively low pelt value. Most modern hunting has been primarily for population control to reduce sealworm infestation and minimize damage to commercial fishery gear and seal consumption of commercial fish stocks

(Bonner, 1981). Bounties paid by state authorities in both Maine and Massachusetts were one factor leading to the near extirpation in the 1960s of gray seals in the northeastern U.S. (Andrews and Mott, 1967; Rough, 1995). In Canada, gray seal stocks were also greatly reduced (Mansfield, 1966). There were culls at Sable Island averaging over 1,700 per year from the late 1960s to the early 1980s (Waring et al., 2008). At present there is a small commercial hunt in the Gulf of St Lawrence (few hundred per year), and hunting is not permitted at Sable Island (Waring et al., 2008). In addition, a personal hunting license in Canada allows killing up to six gray seals (Lesage and Hammill, 2001). The 2001–2005 annual average bycatch mortality of gray seals from entanglement in the northeastern and mid-Atlantic U.S. sink gillnet fisheries was 304 animals, with unknown levels of mortality in the bottom trawl fishery and some Canadian fisheries (Waring et al., 2008).

Ecology and life history: Like harbor seals, but unlike harp and hooded seals, gray seals haul out routinely for resting and not only for breeding or molting. They appear to be flexible in selection of haul-out substrates, utilizing rocky ledges, sandy beaches, and sea ice.

After the winter breeding season, there is a post-breeding pelagic feeding period in February–April. This is followed by a haul-out for molting in May or June, then another dispersed feeding period until the next winter's pupping season begins (Lesage and Hammill, 2001). Juveniles disperse more widely than adults during feeding phases of the annual cycle (Ronald and Gots, 2003). Three gray seals were taken in 1996 by Spanish trawlers on southern edge of the Grand Banks (Lens, 1997), suggesting they are capable of moving long distances and far offshore during pelagic feeding. Recent satellite-linked tagging studies have confirmed that Canadian gray seals commonly travel long distances far from their breeding sites (Beck et al., 2002; Austin et al., 2003).

Gray seals feed on a variety of fish species and cephalopods, with no evidence for significant dietary differences between first-year juveniles and adults (Bonner, 1981). Scat samples from Muskeget Island, Massachusetts, included flounder, silver hake, sand lance, skates, and gadids (Rough, 1995). Species identified from scats collected from Sable Island, Grand Manan Island, and eastern Nova Scotia include sand lance, herring, silver hake, cod, pollack, capelin, flounders, mackerel, and squid (W. D. Bowen et al., 1993; Bowen and Harrison, 1994). In New York waters, stomach contents of stranded gray seals show herring to be the predominant prey, as well

as mackerel, gadids, and flounders (S. S. Sadove, pers. comm.).

Gray seals give birth to single pups in January or February (Bonner, 1981; Riedman, 1990; Nowak, 1999; Hall, 2002). Adult females attend their pups continuously from birth to weaning and do not feed at all during that time. The breeding fast is even longer for adult males, since they arrive first to stake out and defend territories. Pups are weaned and abandoned in about 18 days, followed by a post-weaning fast of 10–28 days. Pups are born with a white lanugo coat that is molted around the time of weaning. Ovulation and mating take place late in lactation, and implantation is delayed for about 3.4 months.

Age at sexual maturity differs between sexes (Bonner, 1981; Hall, 2002). Most females mature at 4 or 5 years. Males mature at 6 years, but do not begin to breed until 8 years. Most breeding bulls are 12 to 18 years old.

Sharks prey on gray seals around Sable Island (Brodie and Beck, 1983; Stobo and Lucas, 2000). A variety of different shark species has been implicated, but Greenland sharks are suspected as a principal predator.

Bonner (1981) reviewed the occurrence of disease and parasites in gray seals. Most disease incidences are known from pups where the immune system has been compromised by starvation, rendering them subject to a variety of opportunistic infections. Common infections include pneumonia, conjunctivitis, and septicemia. External parasites include seal lice (*Echinophthirius horridus*) and nasal mites (*Halarachne halichoeri*). Internal parasites include a variety of nematodes, acanthocephalans, cestodes, and trematodes in the gut, lungs, liver, and kidneys. Of particular interest is the anisakine nematode *Pseudoterranova decipiens*, the sealworm or codworm (Templeman, 1990). The penultimate phase of the parasite's life cycle is as a large juvenile encysted in the muscle tissue of a fish like cod or haddock, greatly reducing the palatability and marketability of the fillets. Piscivorous seals are the final host in the life cycle of the worms, which mature and reproduce in the seal's gut. Sealworms infect other seal species, but are most commonly found in gray seals in most areas, which has led to seal reduction programs such as bounties or culls. Disease and parasites are better known in harbor seals, and it is likely that many of the same organisms affect gray seals.

General distribution: Gray seals are found only in the North Atlantic (Bonner 1981; Riedman 1990; Nowak 1999; Hall 2002; Ronald and Gots 2003). There are three separate populations: a

Canadian stock that occurs from Massachusetts to Labrador, a European stock that occurs from France north to Russia and west to Iceland, and a third stock in the Baltic Sea. There are two principal pupping concentrations of the Canadian stock: one in the Gulf of St. Lawrence and the other on Sable Island off the southern coast of Nova Scotia. The Massachusetts population has grown substantially, and at least two pupping colonies are now established in Maine (Waring et al. 2008).

Historical occurrence: Gray seals were largely absent from Rhode Island and nearby waters until recently. Cronan and Brooks (1968) reported that the species was unknown from Rhode Island, but said that there was one record to the south. That surely referred to Goodwin's (1933) report of a juvenile male taken in a net at Young's Million Dollar Pier in Atlantic City, New Jersey in 1931. Archaeological finds indicate that Native Americans utilized gray seals on Block Island and along the Connecticut coast (Waters, 1967), however, the number of individuals was apparently relatively small. It is quite possible that the Indians simply made opportunistic use of stranded animals at no greater frequency than current stranding rates. Neither De Kay (1842) nor Connor (1971) knew of any occurrences in New York. Similarly, Linsley (1842) did not mention gray seals for Connecticut, and Goodwin (1935) stated that the species had not been recorded in Connecticut.

Waters and Rivard (1962) said that gray seals might occur in low numbers in winter off Massachusetts to as far south as Block Island. There was a small breeding colony of gray seals in Massachusetts during the first half of the 20th Century (Andrews and Mott, 1967; Rough, 1995). They pupped on Muskeget Island, a low sandy island off the west end of Nantucket. They had been nearly extirpated by the 1960s due to hunting, primarily for bounties paid by state authorities in both Maine and Massachusetts. Annual pup production of the Massachusetts colony declined from 14–19 in the early 1950s to only 1 by the end of 1960s. No pups were observed and adults were scarce in 1971–1979, but the number of seals increased during the 1980s and pupping resumed by 1988 (Rough, 1995).

Recent occurrence: The recovery of the Massachusetts and Canadian populations led to an increased occurrence in southern New England and mid-Atlantic waters. There are gray seal specimens in the Smithsonian collection from strandings in New Jersey in 1973 and 1978. These were the first records west of Massachusetts after the 1931 Atlantic City animal. The three

earliest strandings in Rhode Island, all from Block Island, were in 1980, 1986, and 1988 (Nawojchik, 2002), although the 1980 specimen was misidentified and labeled as a harbor seal and then lost in a freezer for 24 years (Kenney, 2005). The first sighting of a gray seal in eastern Long Island was in about 1980 (S. S. Sadove, pers. comm.). Strandings and occasional sightings throughout the region have become common beginning in the 1990s.

Gray seal occurrences in the Rhode Island study area are mostly represented by stranding records—155 of 193 total records (80%). Gray seal records in the region are primarily from the spring (87.1%), with much smaller numbers in all other seasons—5.7% in winter, 5.2% in summer, and 2.1% in fall. Strandings were broadly distributed along ocean-facing beaches in Long Island and Rhode Island, with a few spring records in Connecticut (Fig. 55). There were no strandings on the north shore of Long Island.

As with other seals, habitat use by gray seals in the Rhode Island study area is poorly known. They are seen mainly when stranded or hauled out and infrequently at sea. No definitive conclusions about habitat preferences should be drawn from strandings. Gray seals are frequently observed mixed in with groups of harbor seals at haul-out sites in Massachusetts and northward. There are very few observations of gray seals in Rhode Island other than strandings. In New York, apparently healthy gray seals are similarly seen at harbor seal haul-outs, usually only one or two animals but in larger numbers on a few occasions (S. S. Sadove, pers. comm.). The most regular occurrences are at the haul-outs on Great Gull Island and Fisher's Island.

The annual numbers of gray seal strandings in the Rhode Island study area since 1993 have fluctuated markedly, from a low of 1 in 1999 to a high of 23 in 2004 (Fig. 56). There is some suggestion of a 3-4 year periodicity, but any underlying factors are not understood.

The very strong seasonality observed in gray seal occurrence in the study area is clearly related to the timing of pupping in January–February. The majority of individuals in the study area appear to be post-weaning juveniles, and starved or starving juveniles are the most common stranded individuals encountered (Nawojchik, 2002; Kenney, 2005). The expected period of feeding dispersal by newly weaned pups that have just completed their post-weaning fast and molt would be in March and April. A peak in gray seal stranding frequency in the study area occurs in April (n = 82, 43%), followed by March (61, 32%) and May (25, 13%) (Fig. 57).

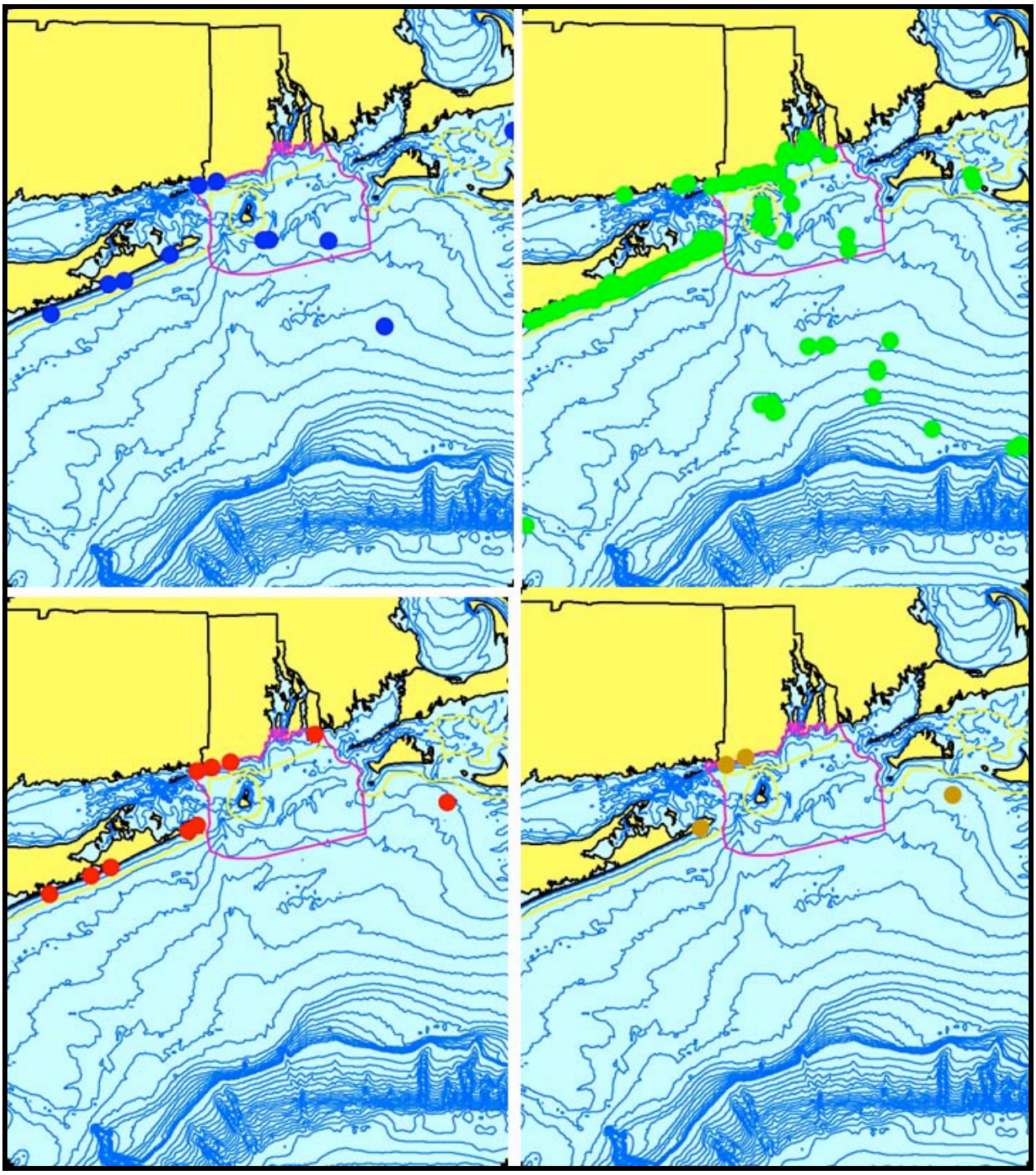

Figure 55. Aggregated sighting, stranding, and bycatch records of gray seals in the Rhode Island study area, 1986–2008 (n = 193: winter = 11, spring = 168, summer = 10, fall = 4).

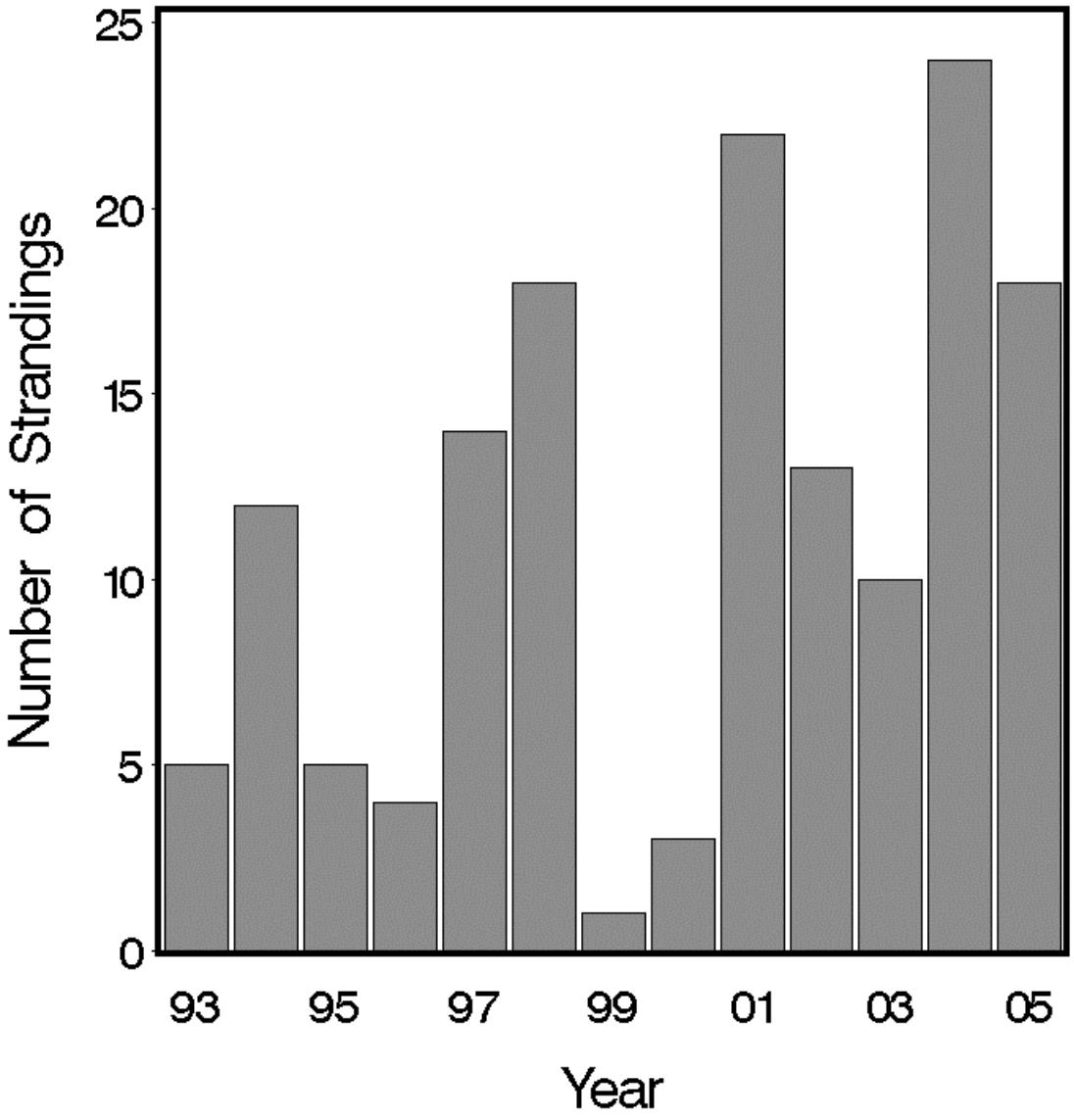

Figure 56. Annual stranding frequencies for gray seals in the Rhode Island study area, 1993–2005.

Including six pre-1993 stranding records provided by Mystic Aquarium, gray seal strandings in Rhode Island alone have been relatively uncommon (Fig. 58). Most years had 0–3 strandings, but there was a short-term spike with 7 in 2003 and 8 in 2004.

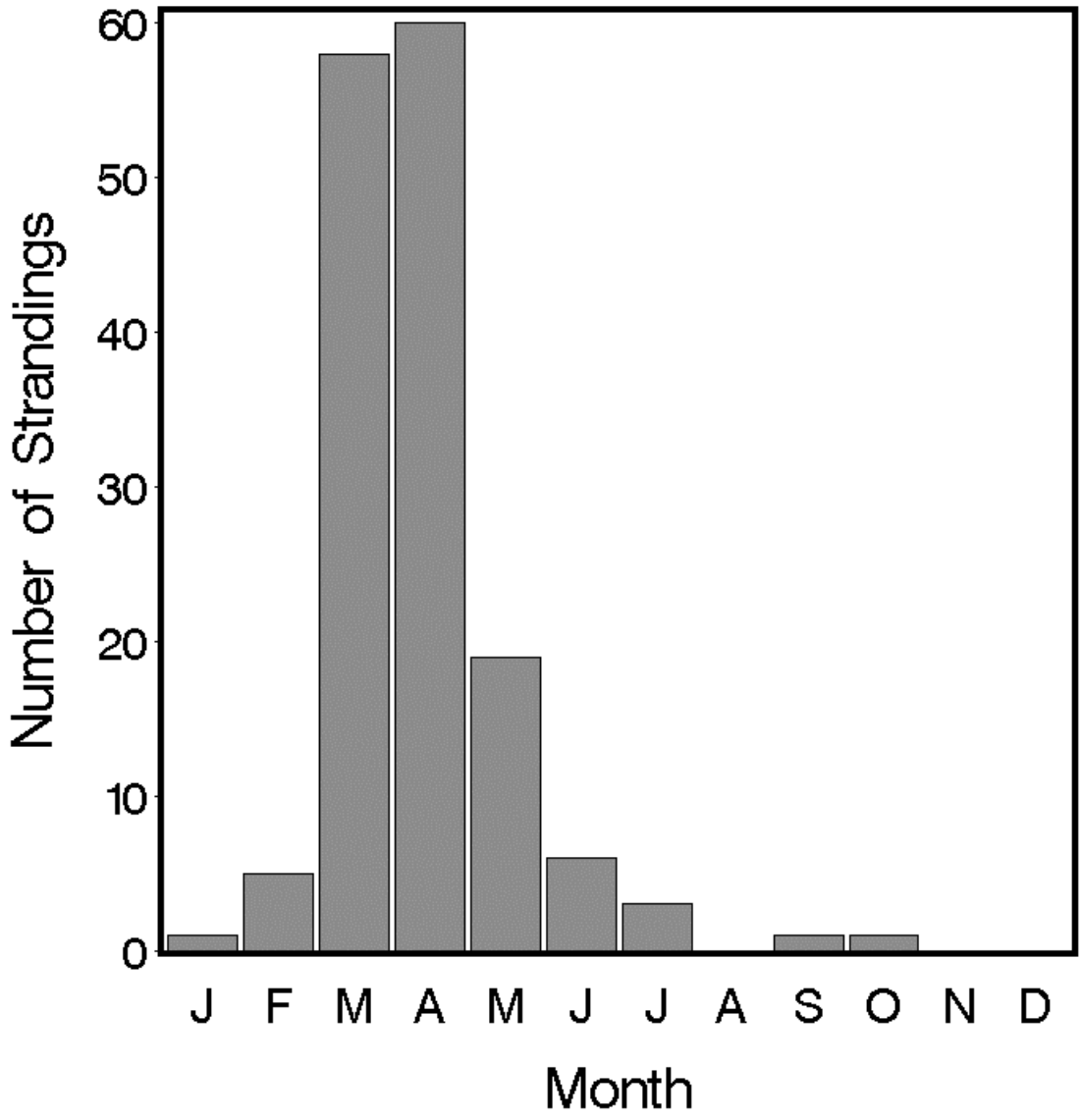

Figure 57. Monthly stranding frequencies for gray seals in the Rhode Island study area.

Conclusions: The occurrence of gray seals in the Rhode Island study area appears to be increasing over time, but the seals present are mostly dispersing juveniles in the spring. There are no consistent haul-out locations in the study area except for the sandy shoals around Nantucket and Monomoy in Massachusetts. Consequently, gray seals are not a significant concern relative to the SAMP. Over the longer term, one might speculate that continued expansion of the

breeding colony in Massachusetts could lead to establishment of pupping at Sandy Point at the northern end of Block Island, which might have the right combination of habitat and low disturbance.

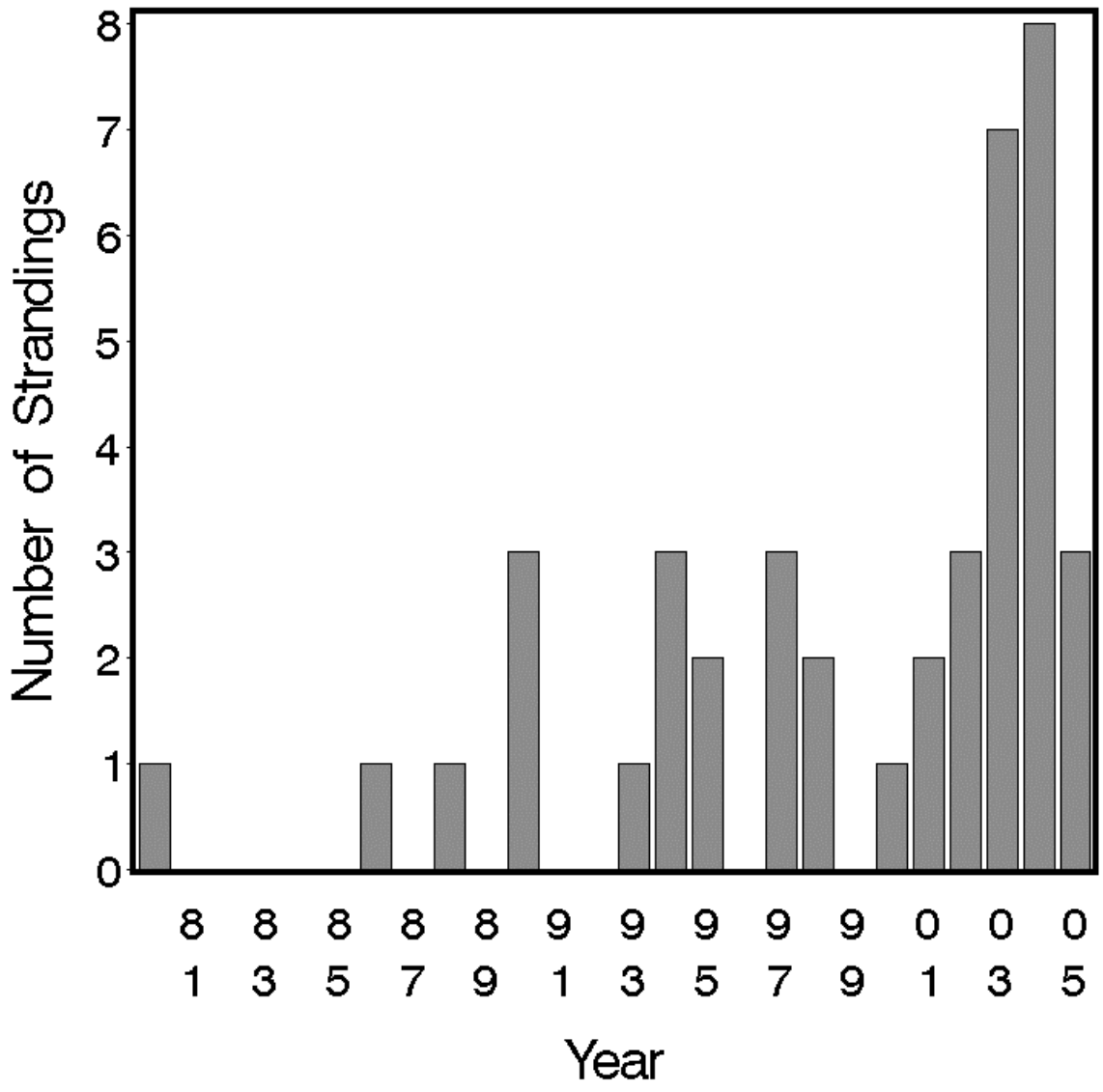

Figure 58. Annual stranding frequencies for gray seals in Rhode Island alone, 1980–2005.

3.2.26. Harp Seal *Pagophilus groenlandicus* (Erxleben, 1777)

Description: Adult harp seals are relatively distinctive and easily recognized. While they are roughly the same size (1.7–1.9 m) and shape as harbor seals, with heads that appear slightly smaller, their color pattern is distinctive (Jefferson et al., 1993; Wynne and Schwartz, 1999). An adult has a pale white to silvery-gray body with a black face and a black inverted V- or harp-shaped marking on the back. Juveniles are silvery gray with scattered large black blotches, and are much less spotted than similar-sized harbor seals. Harp seals go through a sequence of pelages from neonate to adult (Lavigne, 2002). Pups known as "thin white-coats" are born covered in a fine, white fetal fur or lanugo. They become "fat white-coats" as they gain weight during nursing. At weaning, the juvenile coat has filled in and is visible under the white lanugo. The pup is now known as a "gray-coat." The lanugo is shed after weaning, and the pup then has a silvery juvenile coat with scattered dark blotches. At this stage young seals are referred to as "beaters" because of their awkward, splashing manner of swimming on the surface. The second molt occurs at 13 to 14 months into a similar "bedlamer" pelage, with somewhat more dark patches. Juvenile and adult seals molt annually, hauling out in dense aggregations on the pack ice north of the breeding areas in April and May (Ronald and Gots, 2003). Adult pelage is attained at the time of sexual maturity. The transition tends to be much quicker in males than females, with some females never completely developing the harp pattern. Adults with the intermediate pattern of both a partially developed harp marking and typical juvenile dark blotches are known as "spotted harps."

Status: Harp seals are not listed under the U.S. Endangered Species Act or on the Rhode Island state list, and are classified as Least Concern on the IUCN Red List. Despite substantial annual harvests by commercial and subsistence hunters, the abundance of harp seals in the eastern Canadian populations appears to have increased steadily (Waring et al., 2008). Abundance is estimated using production models based on pup counts. The total Canadian population was estimated at 3.1 million in 1990, 4.8 million in 1994, 5.2 million in 1999, 5.5 million in 2000, and 5.9 million in 2004. The other two populations are substantially smaller—0.3 million near Jan Mayen and 1.5–2.0 million in the White Sea (Lavigne, 2002). There are no estimates for the numbers of harp seals off the northeastern U.S. or in the Rhode Island study area.

Harp seals have traditionally been hunted for subsistence use by the Inuit in Greenland and eastern Canada (MacLean et al., 2002). They still are hunted in Greenland; one of the first returns of a flipper tag from a live-stranded harp seal that had been rehabilitated and released by Mystic Aquarium came from an Inuit hunter in Greenland (R. Nawojchik, pers. comm.). Lavigne and Kovacs (1988) extensively reviewed the history of the eastern Canadian seal hunt. Early European settlers did not immediately exploit harp seals, since other species were more accessible. The walrus was the first species hunted for ivory, oil, and leather, but it was extirpated in the Gulf of St. Lawrence and off Nova Scotia by the early 18th century. Hunters also took gray seals and, to a lesser extent, harbor seals for oil, meat, and skins. Winter harp seal hunting began in the St. Lawrence River in the mid-17th century. Hunting methods quickly shifted from shooting seals on the ice from boats to the use of nets, adopting the Inuit methods. By the mid-18th century, harp sealing spread throughout the Gulf and along the northeastern coast of Newfoundland. Total annual takes ranged from 7,000 to 128,000 seals. It was also in the 18th century that the early spring hunt for white-coat pups began. During those years whelping patches, on the pack ice, were easily accessible from shore. In the 19th century, technological advances such as steam-powered ships enabled additional expansion of the hunt. Annual takes ranged from more than 500,000 to 740,000 seals. Hooded seals were also taken. Oil rendered from the blubber layer was the main product of the seal hunt, until tanning methods (developed in the 1940s and 1950s) made the pelts of white-coat harp seals and, especially, blue-back hooded seals extremely valuable. Beginning in the 1960s, opposition to the white-coat hunt became a major campaign of environmental organizations. Because of widespread opposition and a European ban on importation of white-coat pelts, commercial hunting of seal pups was banned in Canada in 1987. Hunting is now restricted to non-breeding adults, juveniles, and independent, post-weaning pups. The harp seal hunt is currently managed under quotas set by the Canadian Dept. of Fisheries and Oceans (Waring et al., 2008). Total annual take in Canada and Greenland, by commercial and subsistence hunters, including animals struck and lost, is about 440,000 harp seals. There is also substantial mortality caused by entanglement in gillnets in the Canadian lumpfish fishery, varying between 5,000 and 19,000 annually. Entanglement mortality in U.S. fisheries is lower, averaging 73 per year in 2001–2005 in the sink gillnet fishery plus an undetermined number in the bottom trawl fishery.

Starvation is by far the most frequent cause of mortality and morbidity for harp seals in the

Rhode Island study area. The most common harp seal encountered is a stranded, starved or starving juvenile in winter or early spring. The timing coincides with the feeding transition period, when 1-year-olds must switch from near-surface feeding on krill to diving deeper for fish, and some proportion of animals simply do not seem to make that transition successfully. Lucas et al. (2003) reported the same phenomenon at Sable Island, where three-quarters of the harp and hooded seals encountered were starved or emaciated juveniles. They also reported on the prevalence of gravel in the stomachs, and concluded that juveniles were often unable to feed successful. Disease and parasites are much better known in harbor seals, and it is likely that many of the same organisms affect harp seals.

Ecology and life history: Harp seals are gregarious in their northern range, hauling out for pupping and molting in large aggregations. In the Rhode Island study area, however, they are most often solitary. Nearly all individuals observed are juveniles. Three adults (one stranded dead, one photographed alive but extremely emaciated, and one apparently healthy) have been reported in Rhode Island, and Sadove and Cardinale (1993) reported one stranded adult in New York. An adult was captured in 1945 in Virginia (McAlpine and Walker, 1990), and adult markings were described for a harp seal in New Jersey by Allen (1880) (see Historical Occurrence below).The increase in juvenile harp seal occurrences in the Rhode Island study area in the 1990s coincided with growth of the seal population in Canada and declines in fish stocks. One might speculate that juveniles are forced to disperse more widely because of competition for prey (McAlpine et al., 1999a). However, complicating factors such as changes in climatic and oceanographic conditions (Frank, 2003) prevent taking the idea much beyond speculation.

Harp seals in their usual range are associated with sea ice, with an annual migration following the annual cycle of pack ice, moving north in summer and south in winter (Ronald and Healey, 1981; Lavigne, 2002; Ronald and Gots, 2003). Off the northeastern U.S., almost nothing is known of their habitat preferences except for stranded individuals. Like hooded seals, they are most likely to occur on relatively flat, sandy beaches.

Adult harp seals feed on a wide variety of small pelagic and demersal fishes, squid, and crustaceans, especially on capelin and Arctic cod (Wallace and Lawson, 1997). Pups undergo a transition in prey type and feeding depth during their first year (Ronald and Healey, 1981). After the post-weaning fast, pups first feed mainly on euphausiid crustaceans ("krill") in near-surface

waters. At about one year of age, they make a transition to diving to intermediate depths and feeding on pelagic fishes. Stomach contents of harp seals stranded in New York sometimes include herring or similar fishes (S. S. Sadove, pers. comm.). Often, stomachs are empty, or at times filled with stones and shells, leading to serious medical complications or death (Medic, 2005). No reason for the pathologic ingestion of stones has been determined, but it is speculated that it is a consequence of their habit of eating ice as a source of fresh water. Stranding response protocols for harp and hooded seals have been modified in an attempt to recover starving juveniles as soon as possible before they have a chance to start eating stones.

Female harp seals give birth to single pups on the dense pack ice (Ronald and Healey, 1981; Lavigne and Kovacs, 1988; Lavigne, 2002; Ronald and Gots, 2003). Females select areas of thick, hummocky ice that provides protection for pups. These locations are some distance from the ice margin but where open water is still accessible. Females gather in aggregations separated only by a couple of meters from one another. The timing differs slightly among breeding populations. Most pups in the Gulf herd are born between 20 February and 10 March, while births are slightly later in the Front herd.

Pups average a meter in length, weigh 11–12 kg at birth, and have little blubber. They nurse for 10–12 days on milk that is up to 43% fat and 10% protein, gaining 2.2 kg per day. Females fast entirely, or feed little, during lactation. They abandon the pups immediately after weaning. At weaning the pups have a 5-cm thick layer of blubber and weigh ca. 36 kg. Pups then remain on the ice for a post-weaning fasting period as long as 6 weeks, during which they can lose up to half of their body mass.

Mating occurs just after the pup is weaned. It usually takes place in the water, though there have been observations of mating on the ice. Implantation of the embryo is delayed about three months. Adult females breed annually, and both males and females can remain reproductively active into their twenties (Ronald and Healey, 1981). Both males and females reach sexual maturity at an average age of 5.5 years, but males generally are not reproductively active and successful until age 8 (Ronald and Healey, 1981).

General distribution: Harp seals are found only in the North Atlantic and Arctic, from eastern Canada east to northwestern Siberia (Ronald and Healey, 1981; Lavigne and Kovacs, 1988; Riedman, 1990; Nowak, 1999; Lavigne, 2002; Ronald and Gots, 2003). There are three breeding

populations—in the White Sea north of Russia, in the Greenland Sea near Jan Mayen, and in two locations near Newfoundland—the "Front herd" to the northeast and the "Gulf herd" to the west. Harp seal breeding patches are located somewhat inshore of those of hooded seals. Their distribution during the remainder of their annual cycle is poorly known.

Historical occurrence: Until recently harp seals were very rare in the Rhode Island study area and nearly as rare from Massachusetts to Maine (McAlpine and Walker, 1990). Cronan and Brooks (1968) cited one earlier report of a harp seal in Connecticut (but see the following), but knew of no records from Rhode Island. Waters and Rivard (1962) described harp seals as rare winter visitors to New England, but gave no specific records. Linsley (1842) reported a single occurrence in Connecticut: "The white seal, commonly called the harp seal, is very rare, and has been seen only at Stonington a few times on the rocks. During the past winter, attempts were made to take him, but unfortunately the hunters went to the windward side of him, and though they came so near as to shoot at him while sliding off, he escaped. I have information from J. H. Trumbull, Esq., of Stonington, who says 'his color was a dusky white throughout.' I conclude, therefore, it must be the *groenlandica*." Given that (1) the identification was based only on color from a second-hand report, (2) the report said nothing about markings, (3) harp seals in southern New England are more likely to haul out on flat sand than rocks, and (4) some harbor seals, especially when dry, appear very pale-colored, it seems that Linsley's seal was more likely a harbor seal. Goodwin (1935) and Connor (1971) repeated Linsley's account, and Connor added an unsubstantiated report from Kieran (1959) of harp seals offshore at Coney Island in winter. Allen (1880) reported a harp seal at Trenton, New Jersey and did include reasonable identifying details, but it was a third-hand report without documentation. Goodwin (1954) reported an adult male captured at Cape Henry, Virginia, in March 1945, documented by a newspaper photograph that was reprinted by McAlpine and Walker (1990), making it the only well-documented historical record south of Massachusetts.

Recent occurrence: Harp seals in the Rhode Island study area are known almost exclusively from strandings (688 of 703 records = 98%). Strandings are widespread on ocean-facing beaches throughout Long Island and Rhode Island (Fig. 58). The apparent absence in Massachusetts is due only to the geographic scope of the stranding dataset we had acquired. The records are almost entirely from spring (68.3%) and winter (30.4%). Harp seals are nearly absent in summer

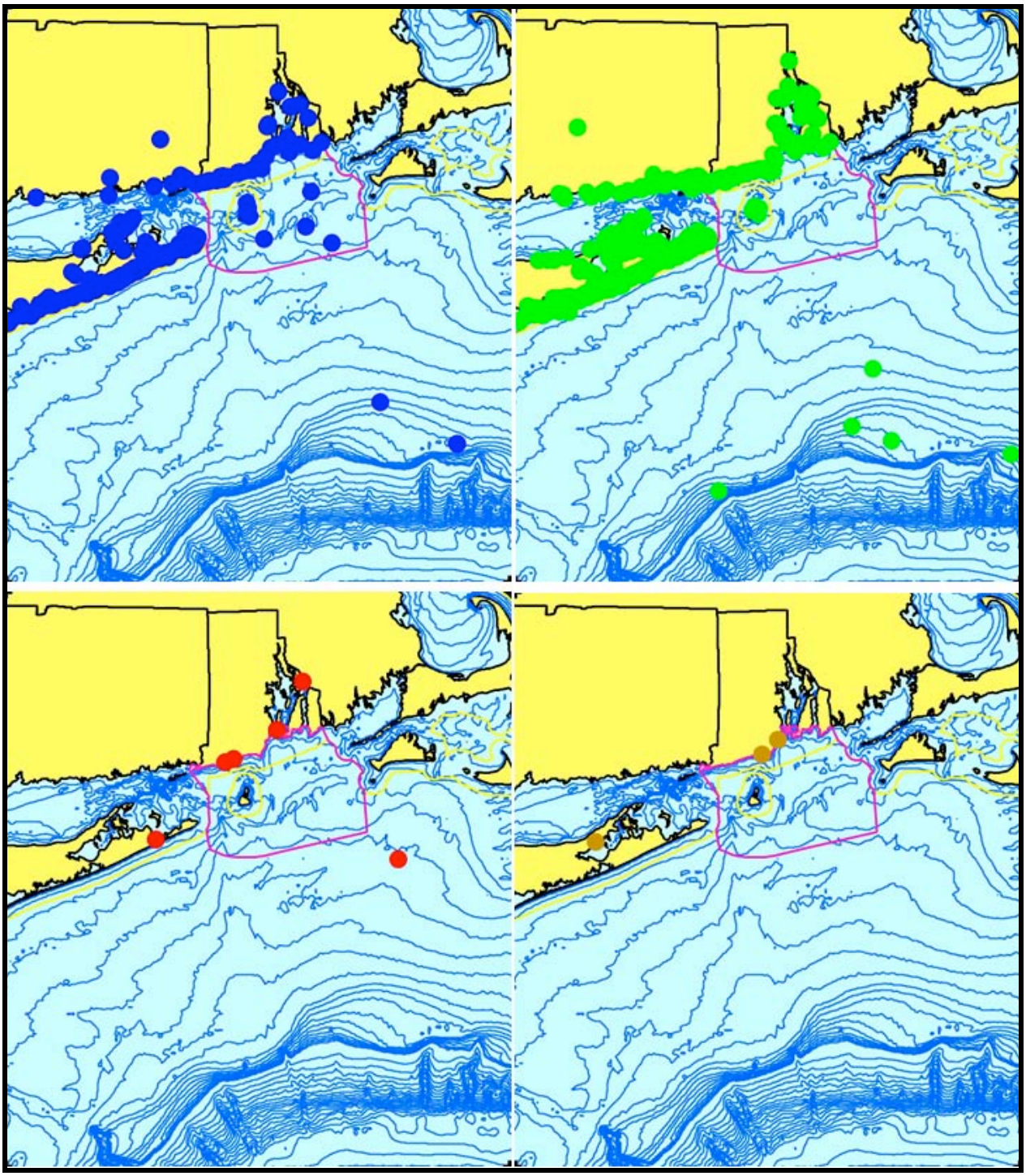

Figure 59. Aggregated stranding, sighting, and bycatch records of harp seals in the Rhode Island study area, 1989–2007 (n = 703: winter = 214, spring = 480, summer = 6, fall = 3).

and fall. Strandings are common on both sides of Long Island Sound, more than any other

species of seal. Harp seals also make occasional appearances well inland up rivers.

Beginning in the late 1980s harp seal occurrences began to increase in the Gulf of Maine (McAlpine and Walker, 1990; Stevick and Fernald, 1998; McAlpine et al., 1999a; Harris et al., 2002). The available regional stranding dataset for the Rhode Island study area begins in 1993, when there were 9 harp seal strandings (Fig. 60). Harp seal records in the region more than quadrupled to 38 in 1994, then increased to 55 in 1995 and to a peak of 67 in 1996. In 1995, for the first time harp seals exceeded the total for harbor seals. They have been the most common stranded seal in the region since, with the exception of 2003. Strandings spiked sharply in 2001 at 150% higher than the average annual rate in the other years from 1994 to 2005.

Monthly stranding frequencies provide a clearer view of the trend in harp seal strandings over the year (Fig. 61). Strandings peak in late winter-early spring, with very few outside of January–May. Peak strandings are in March (42%), with 22% in both February and April. The timing is too late for the strandings to be pups born in late February–early March in Newfoundland, confirming that strandings in the region are primarily yearlings.

It appears from the study area stranding trend that harp seal occurrence increased sharply in 1994 (Fig. 60), but that dataset doesn't quite capture the beginning of their presence in the region. There were three earlier strandings in Rhode Island—near the Quonochontaug Breachway in Charlestown in May 1989, on Napatree Point in Westerly in April 1990, and at Mackerel Cove in Jamestown in January 1992. There were also strandings before 1993 in New York (Sadove and Cardinale, 1993), but we don't have those records. Looking only at Rhode Island (Fig. 62), the stranding trend closely matches that for the entire study area, confirming that 1994 was the year when their presence really began to increase. The spike in 2001 is even higher in Rhode Island, at 284% above the 1994–2005 average background rate.

Conclusions: While harp seals may be relatively abundant in the Rhode Island study area, they are predominantly juveniles dispersed from a population center far to the north in eastern Canada. They are not of concern relative to the SAMP.

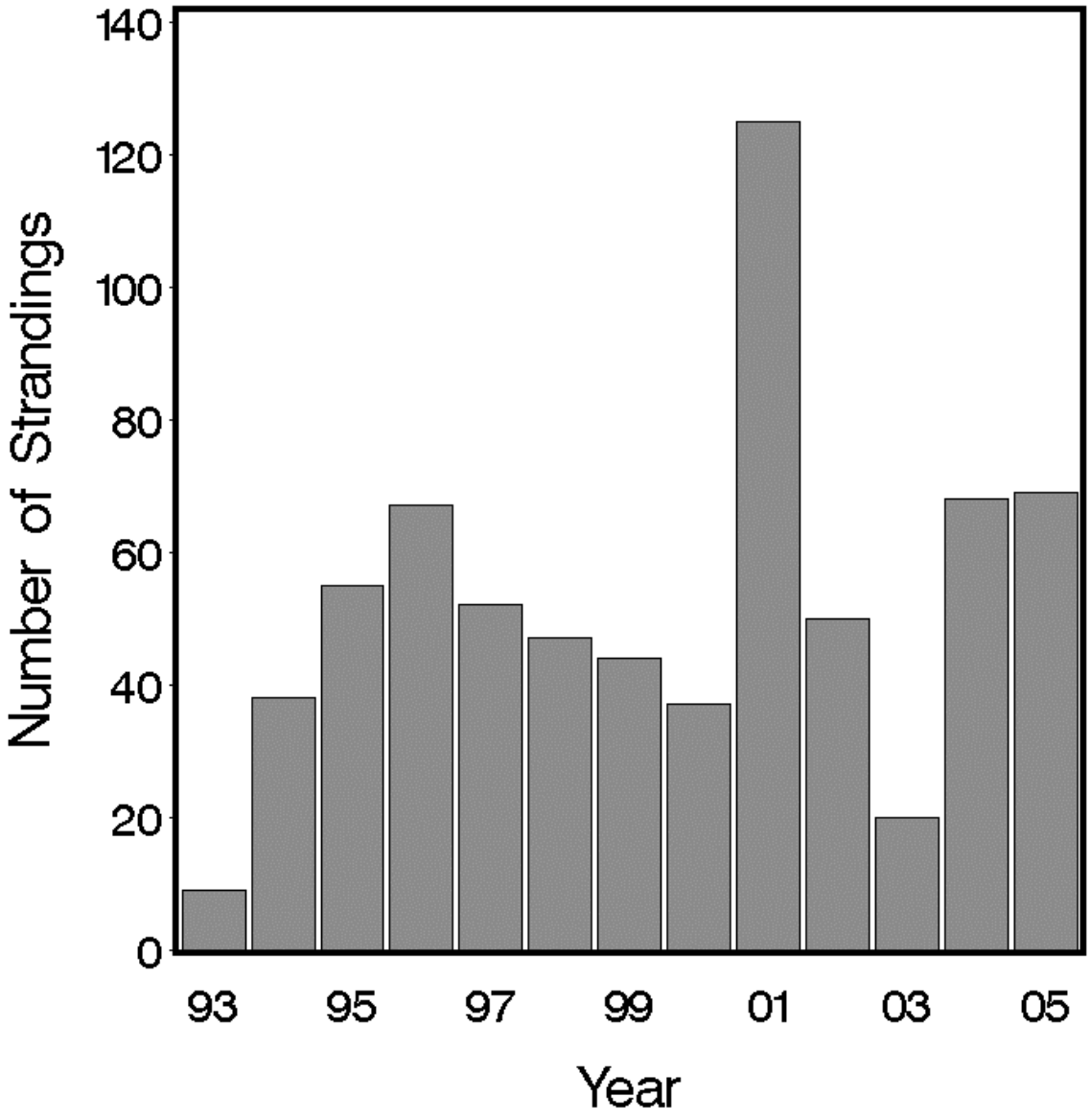

Figure 60. Annual stranding frequencies for harp seals in the Rhode Island study area, 1993–2005.

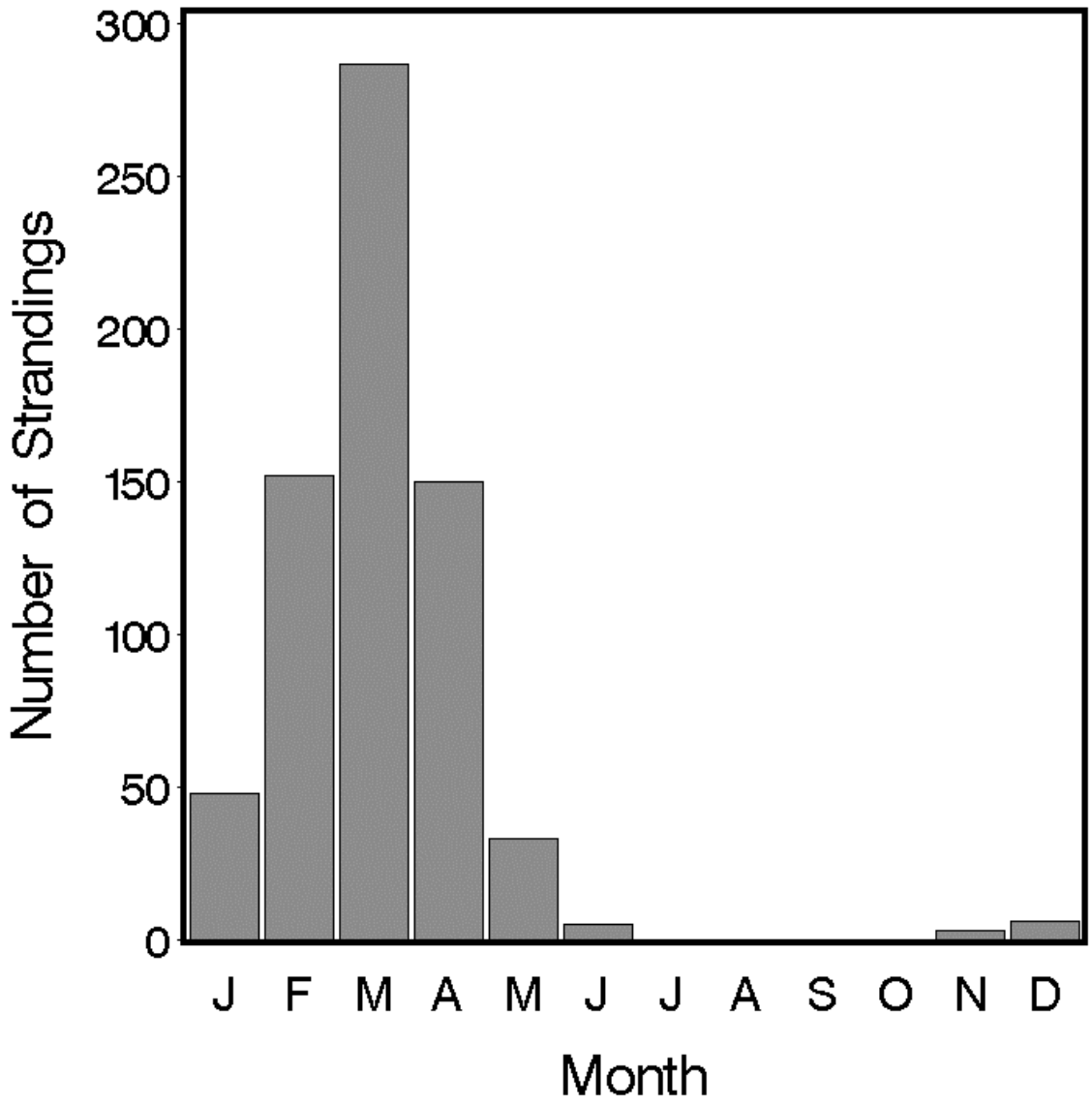

Figure 61. Monthly stranding frequencies of harp seals in the Rhode Island study area.

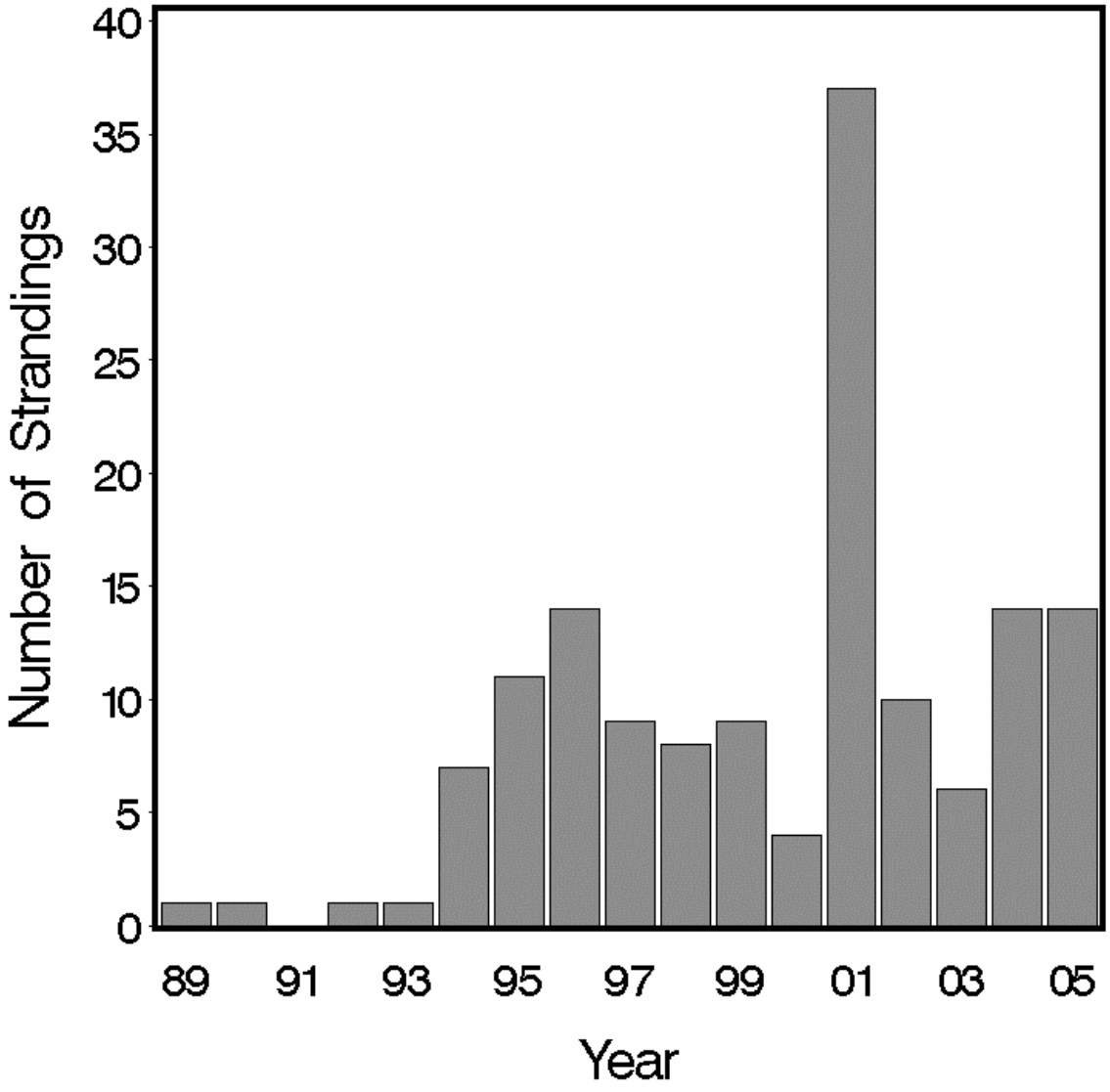

Figure 62. Annual stranding frequencies for harp seals in Rhode Island alone, 1989–2005.

3.2.27. Hooded Seal *Cystophora cristata* (Erxleben, 1777)

Description: Hooded seals are moderately sexually dimorphic, with males 2.3–2.7 m long and females 2.0–2.2 m (Jefferson et al. 1993; Wynne and Schwartz 1999). Adult males have a two-lobed, inflatable proboscis or hood on the top of the snout. They can also inflate the nasal septum out of one nostril like a red balloon. Adults are silvery blue-gray with a black face, irregular

black blotches, and a lighter belly. Pups, known as "blue-backs," are solid dark blue-gray above, with a creamy whitish belly clearly demarcated from the dark back. The head is broader, flatter, and rounder, with noticeably larger eyes, than other Atlantic seals.

Status: Hooded seals are not listed under the U.S. Endangered Species Act or on the Rhode Island state list, and are classified as Vulnerable on the IUCN Red List. There is no current, reliable estimate of abundance for the entire hooded seal population in the North Atlantic or for the animals within U.S. waters or in the Rhode Island study area (Waring et al., 2008). Breeding herd abundance estimates are extrapolated from pup counts assuming a ratio of 1:5 (pups:total population). The most recent estimates were from counts in 2005 (IUCN, 2008). The total abundance of the Northwest Atlantic stock (in eastern Canada and western Greenland) was estimated at 592,000, which represents a moderate increase since 1980. The West Ice stock (east of Greenland) was estimated at about 70,000, which is a decline of 85–90% in the last 60 years, and pup production declined from 24,000 in 1997 to 15,250 in 2005. The cause of the decline is not understood, but it is the reason for the Vulnerable classification on the Red List.

Hooded seals have long been hunted both by subsistence hunters (MacLean et al., 2002) and commercial sealers (Lavigne and Kovacs, 1988; Waring et al., 2008). There is no longer any hunting of blue-backs for their pelts. The annual commercial quota for the Front herd off eastern Newfoundland has been set at 10,000 since 1998, but recent catches have been low, and no commercial hunting is allowed in the Gulf of St. Lawrence or Davis Strait (Waring et al., 2008). The West Ice commercial hunt is jointly managed by Norway and Russia, with several thousand taken each year (NMFCA, 2006). An average of 16 hooded seals per year have been killed in recent years in U.S. waters by entanglement in the sink gillnet fishery, and others are taken as bycatch in Canadian fisheries (Waring et al., 2008). The total incidental take from all sources is believed to be low relative to the population's total abundance.

Ecology and life history: Hooded seals are solitary and aggressive (Kovacs, 2002). Most of the year they are widely dispersed and asocial. Even when aggregating during the breeding and molting season, they are aggressive with one another. Adult males fight for prime space near a mother and pup, but a female will keep a larger male at a distance from her pup. Even newly weaned pups have a reputation for aggressiveness.

Almost nothing is known of habitat use by healthy hooded seals in the Rhode Island study area. The species is known exclusively from strandings, which are nearly all recently weaned blue-back pups, many of which are under-nourished or even starving. A subadult male that live-stranded in Westerly in February 1999 was an exception. It was rehabilitated and released (see below). In their normal range, hooded seals are most often associated with sea ice. As with harp seals, the other ice seal that occurs in the Rhode Island study area, hooded seals are most often observed on relatively flat sandy beaches.

Outside of the breeding season, hooded seals are most likely highly pelagic. Scholander (1940) recorded a month-old hooded seal pup diving to a depth of 75 m on its first dive. Based on telemetry tagging, hooded seals are capable of dives deeper than 1000 m and lasting almost an hour (Folkow and Blix, 1995; Kovacs, 2002).

In their normal Arctic range, adult hooded seals feed on deepwater fish species such as Greenland halibut, redfish, and a variety of other fishes and squids (Reeves and Ling, 1981; Kovacs and Lavigne, 1986; Kovacs, 2002; Ronald and Gots, 2003), while pups feed more on crustaceans at shallower depths. Their prey preferences in the Rhode Island study area are poorly known. Stomachs of stranded animals contain a variety of prey items, probably reflecting local prey availability.

Hooded seal reproduction was reviewed by Reeves and Ling (1981), Kovacs and Lavigne (1986), Lavigne and Kovacs (1988), and Kovacs (2002). Single pups are born in late March, with pupping in all the stocks occurring synchronously. Pupping takes place on loose pack ice, with females at least 50 m apart. Hooded seals tend to pup farther offshore than harp seals in all areas except the Gulf of St. Lawrence. Pups are about 1 m in length and weigh 20–25 kg at birth. They shed the gray lanugo in utero and are born in a relatively advanced state in their juvenile blue-back coats. They are nursed on milk that averages 60% fat content, and weaned at 50–60 kg in only four days, the shortest known lactation period of any mammal (Bowen et al., 1985).

Each female-pup pair is usually guarded by a single male. Males compete vigorously for the opportunity via displays at first, but competition frequently escalates to violent, bloody fights. After weaning, the female abandons the pup and returns to the water, where mating takes place. At an earlier time, these mother-pup-male triads were anthropomorphically interpreted as families, and hooded seals were presumed to have a monogamous mating system. However, after

mating with one female the male is free to move to another, resulting in a polygynous mating system (Boness et al., 1988). The most successful males may mate with up to 8 females in one breeding season. Implantation of the embryo is delayed for about four months, extending gestation to match a tightly synchronized annual cycle. Adults then disperse until aggregating, along with juveniles, for molting in June and July.

Pups remain alone on the ice for a post-weaning fast period of at least several days. They then disperse widely. They skip the molt during their first year and undergo the first post-natal molt at 14 months of age.

Females mature at age 3. Males mature at 4–6 years, but probably need to be older in order to successfully compete for mating opportunities (Lavigne and Kovacs, 1988).

General distribution: Like most pinnipeds, the distribution of hooded seals is well-known only for the portion of their annual cycle when they haul out for pupping ("whelping"). Hooded seals occur only in two separate breeding stocks in the North Atlantic (Reeves and Ling, 1981; Kovacs, 2002). The Northwest Atlantic stock pups in three areas, two in eastern Canada—the Gulf herd in the Gulf of St. Lawrence west of Newfoundland and the Front herd northeast of Newfoundland and east of Labrador, and in the Davis Strait between eastern Canada and Greenland. The West Ice stock pups in the Greenland Sea, east of Greenland and near Jan Mayen. After the breeding season, adults and pups disperse, then seals from all areas, except pups, re-aggregate in the Denmark Strait between Greenland and Iceland to molt, with a second molting area farther north off the east coast of Greenland for some of the West Ice animals (Nowak, 1999). Their distribution at sea is poorly known, but they apparently disperse widely through much of the northwestern North Atlantic and into the Arctic Ocean (Lavigne and Kovacs, 1988). A few hooded seals, particularly pups and juveniles, have been known to disperse surprisingly far from their breeding areas, including the Caribbean and the North Pacific. Strandings have recently increased in frequency in New England, primarily between January and May coinciding with the breeding season (McAlpine et al., 1999b; Harris et al., 2001).

Historical occurrence: Historical literature confirms both the presence and extreme rarity of hooded seals in the Rhode Island study area or in southern New England more generally. Cronan and Brooks (1968) reported a single record in the Providence River, but the date was unknown to

them. Waters and Rivard (1962) also mentioned the Providence occurrence and one other at Newburyport on the Massachusetts north shore. De Kay (1824) reported that an adult male was killed in Westchester County, New York. Linsley (1842) and Goodwin (1935) stated that they were not known from Connecticut. Connor (1971) added a second New York record—an anecdotal report of a hooded seal in a New York Harbor tributary "within just the last few years."

Recent occurrence: Hooded seal occurrences in the Rhode Island study area are almost entirely strandings (96 of 97 records, 99%). The first confirmed strandings were recorded in 1993, though there were scattered anecdotal reports earlier than that (Sadove and Cardinale, 1993). They have been relatively common since. Hooded seal strandings are broadly distributed across ocean-facing beaches in the region, with only rare occurrences in Long Island Sound (Fig. 63). Strandings are most common in spring and winter (45% and 36% of all records, respectively), and rare in summer and fall. They occasionally occur well up rivers—for example, in southeastern Connecticut in spring, but less often than harp seals.

The time-series of strandings in the study area showed a marked spike in 1998 (Fig. 64). The same pattern is seen if only Rhode Island strandings are considered, where the 1993–2005 background level was 0–2 strandings per year with 3 in 1996, but there were 9 in 1998 (Fig. 65). There were no hooded seal strandings in Rhode Island before 1993. The reason for the sharp short-term increase is not known, but it may be related to hydrographic patterns in the region. In 1998 a cold mass of Labrador Subarctic Slope Water just offshore of the continental shelf extended much farther south than normal, reaching the latitude of southern New Jersey by February (Greene et al., 2003). The phenomenon was linked to a sharp decrease in the North Atlantic Oscillation Index in 1996.

Monthly stranding frequencies show maximum values in February (31%) and March (29%), but the occurrence is more spread out than in either gray seals or harbor seals (Fig. 66). As with harp seals, the peak in strandings is too early in the year to be pups. Most strandings are therefore yearlings, although summer and fall blueback strandings may be pups of the year. There was one interesting stranding event in 1999. On the 8th of February there was a report from Block Island of a live seal, possibly in distress, that sounded from the description like an adult hooded seal. The next day a subadult male hooded seal stranded on Misquamicut Beach in

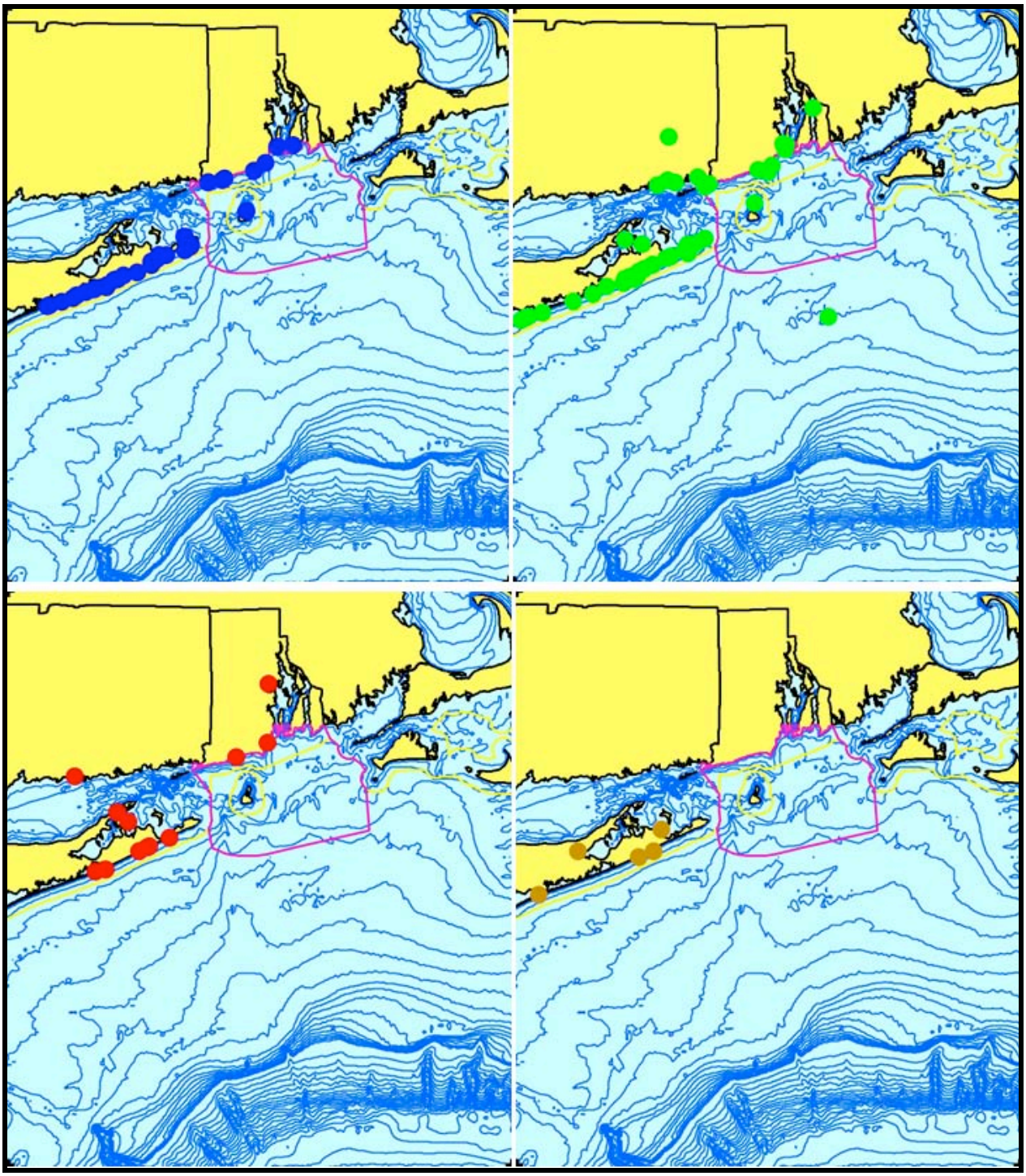

Figure 63. Aggregated sighting, stranding, and bycatch records of hooded seals in the Rhode Island study area, 1993–2005 (n = 97: winter = 36, spring = 43, summer = 13, fall = 5).

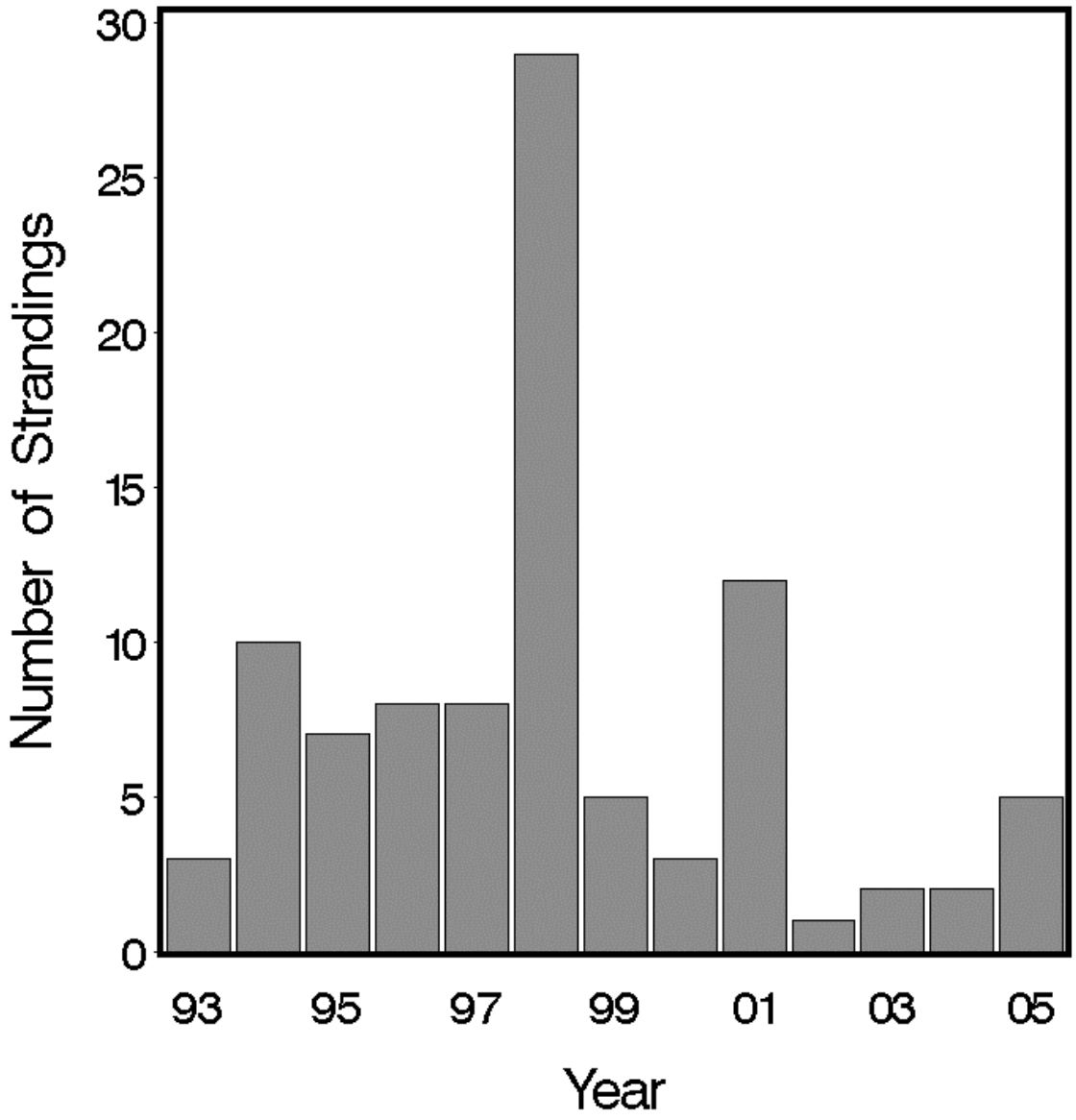

Figure 64. Annual stranding frequencies for hooded seals in the Rhode Island study area, 1993–2005.

Westerly. It was in very poor condition and was not expected to survive overnight (R. Nawojchik, pers. comm.). Contrary to expectations, it gained over 100 kg over the next month and was released at Monahan's Dock in Narragansett Pier.

Conclusions: As with harp seals, hooded seals in the Rhode Island study area are predominantly juveniles dispersed from a population center far to the north in eastern Canada. They are not of concern relative to the SAMP.

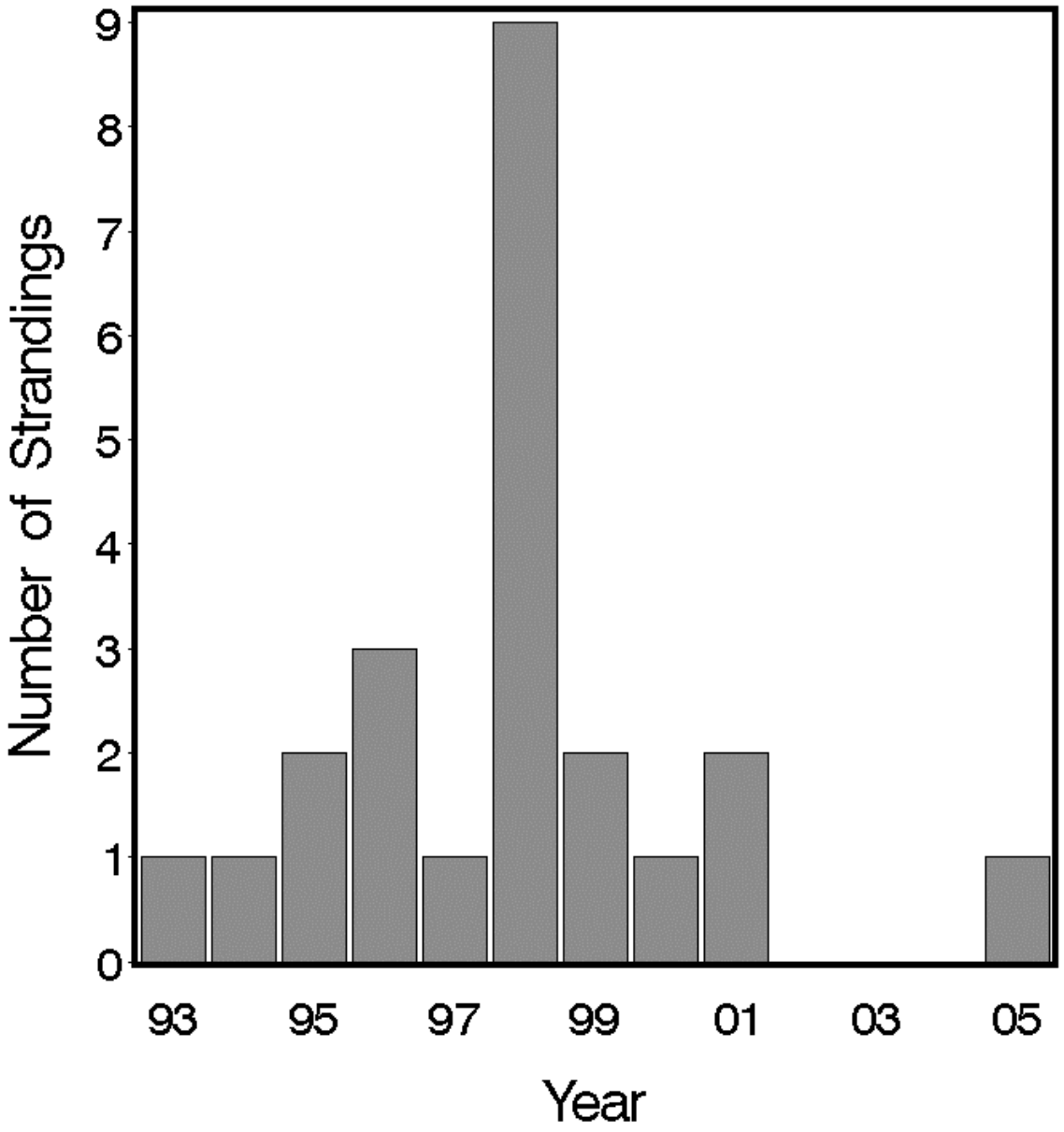

Figure 65. Annual stranding frequencies for hooded seals in Rhode Island alone, 1993–2005.

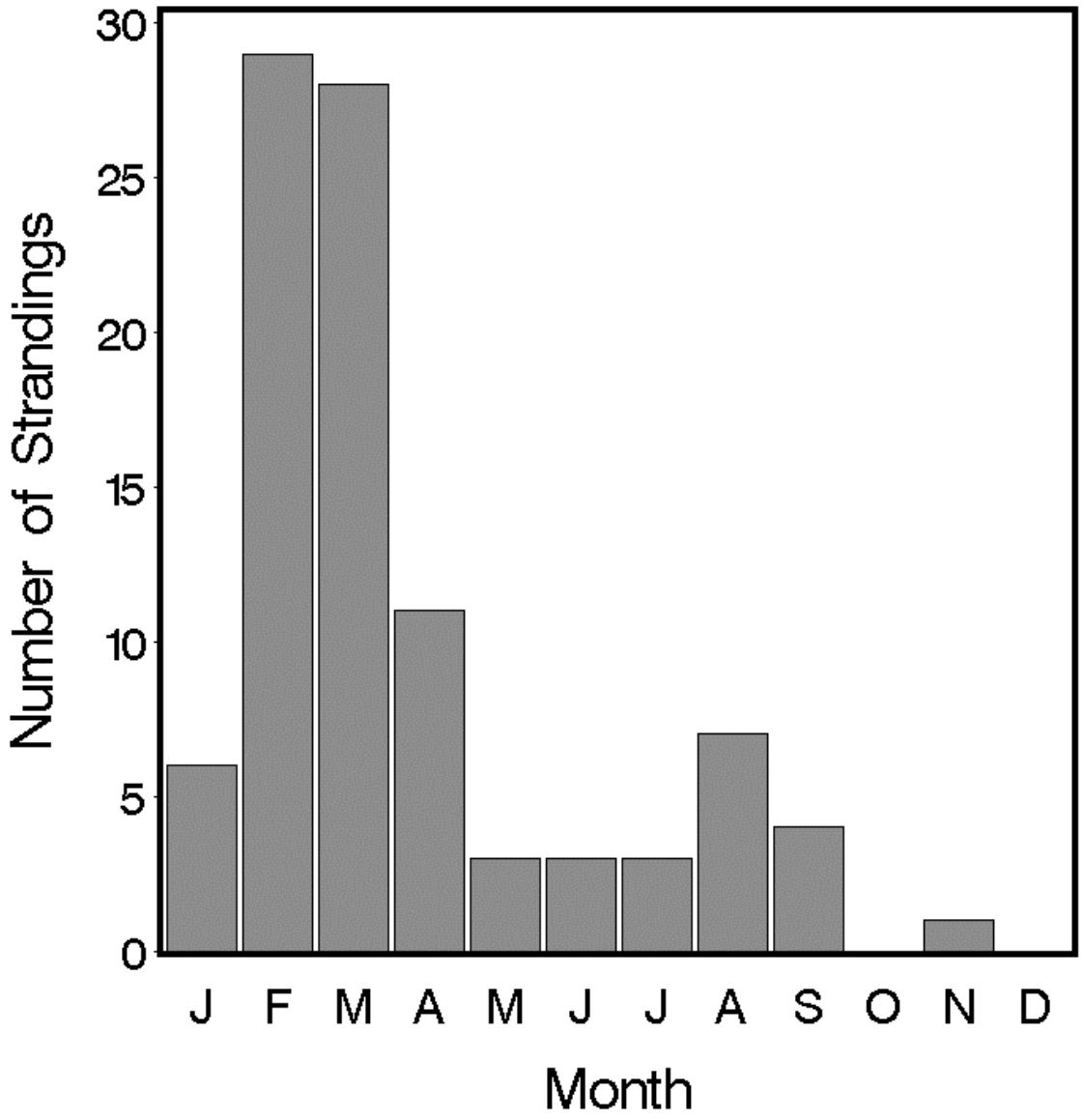

Figure 66. Monthly stranding frequencies of hooded seals in the Rhode Island study area.

3.2.28. Ringed Seal *Pusa hispida* (Schreber, 1775)

Description: Ringed seals are the smallest pinnipeds of the North Atlantic, with average adult lengths of 1.2–1.4 m (Frost and Lowry, 1981) and maximum length of about 1.6 m (Jefferson et al., 1993). They are plumper than harbor seals (maximum girth up to 80% of total length), with a shorter, almost cat-like snout. The ventral aspect of the adult coat is a solid light silver; dorsally

it is dark gray with oval spots that are about the same or slightly darker than the background and surrounded by pale rings. Pups are born covered in a fine white lanugo that is shed between 2 and 8 weeks after birth; juveniles are colored like adults but without the spots.

Status: Ringed seals are not listed under the U.S. Endangered Species Act or on the Rhode Island state list, and are classified as Least Concern on the IUCN Red List. There is no reliable estimate of ringed seal abundance in the North Atlantic. World-wide abundance has been estimated as high as 7 million (Kelly, 1988) and is at least 2.5 million (Miyazaki, 2002). Ringed seals are taken in subsistence hunts by natives around the Arctic (MacLean et al., 2002), but are not hunted commercially.

Ecology and life history: Ringed seals feed on a variety of small fishes and crustaceans (Frost and Lowry, 1981; Miyazaki, 2002), and they are known to dive to depths of at least 90 m (Lavigne and Kovacs, 1988).

Ringed seal pups are born in late March or early April in birth lairs constructed under the snow on stable, shore-fast ice (Frost and Lowry, 1981; Miyazaki, 2002). Pups are weaned in 5–7 weeks and then abandoned, at just around the time of ice break-up. As is typical of all phocids, mating takes place just around weaning (Riedman, 1990), therefore in late April–early May in ringed seals. Implantation of the embryo is then delayed for some time, synchronizing pupping to a tight annual cycle. That delay varies with the length of lactation, and is about three and a half months in ringed seals. Both sexes mature at 5–7 years of age, and record longevity is 43 years (Frost and Lowry, 1981; Miyazaki, 2002).

General distribution: Ringed seals are widely distributed around the Arctic (Miyazaki, 2002). In the North Atlantic they occur from Labrador, Iceland, and Norway to the North Pole, with isolated populations (recognized as three separate subspecies) in the Baltic Sea, Lake Ladoga, and Lake Saimaa (Frost and Lowry, 1981). They are associated with sea ice most of the year. Their distribution both during the pupping season and in the remainder of the year is extremely dispersed, likely driven by polar bear predation.

Historical and recent occurrence: There are no ringed seal records in Rhode Island. In New York waters, ringed seals are known only from very rare strandings and opportunistic sightings. There is one confirmed ringed seal stranding record in the Northeast regional dataset—in Easthampton in eastern Long Island in February 1998, and several other earlier anecdotal

observations (Sadove and Cardinale, 1993). There was also a live-stranded sub-adult male ringed seal on the north shore of Long Island in 2006, which was rehabilitated and released (RFMRP, 2006).

Conclusions: Ringed seals are clearly rare, accidental visitors to the Rhode Island study area and are not recorded from the SAMP area. They are not a concern relative to the SAMP.

3.2.29. West Indian manatee *Trichechus manatus* Linnaeus, 1758

Sirenia includes the marine and aquatic species known collectively as "sea cows" (Reynolds and Odell, 1991; Shoshani, 2005). There are four extant species in two families—three manatees of the tropical Atlantic (*Trichechus* spp.: Trichechidae) and the dugong (*Dugong dugon*: Dugongidae) of the tropical Indo-Pacific. A fifth species, Steller's sea cow (*Hydrodamalis gigas*), a sub-Arctic dugongid found only around the Commander Islands in the western Bering Sea, was both discovered and extirpated in the 18th Century.

Sirenians are fully aquatic, with many adaptations similar to those seen in the cetaceans, including a more or less fusiform body, absence of hair except for well-developed vibrissae on the muzzle, loss of the hind limbs, forelimbs modified into paddle-like flippers, and swimming powered by a horizontally flattened tail. They were long considered to be herbivorous cetaceans (e.g., Hamilton, 1839) and De Kay (1842) included the "Manatidae" as family I in the Cetacea, but sirenians are not closely related to the other marine mammals in the Cetacea and Carnivora. All sirenians are obligate herbivores, feeding primarily on seagrasses and also on submerged and floating aquatic vegetation.

Description: West Indian manatees are large, rotund, docile, and slow-moving, ranging in length from 2.5 to 4.5 m (Jefferson et al., 1993; Wynne and Schwartz, 1999). The body is tapered and somewhat streamlined, with a relatively small head and a large, rounded tail. The skin is relatively smooth, hairless, and uniformly gray or gray-brown, often with distinctive scars from boat collisions. The eyes are small and deep-set, and the fleshy muzzle is covered with stiff vibrissae. The only teeth present, except for vestigial incisors that are resorbed soon after birth, are 5–7 molars in each upper and lower jaw, which are replaced from the rear and drop out at the front of the row when worn (Husar, 1978; Caldwell and Caldwell, 1985). The skull and post-

cranial bones are very dense, perhaps adapted to serve as internal "dive weights." The forelimbs are relatively long and flexible, with blunt, rounded ends and elephant-like nails. The forelimbs are often used in feeding, in conjunction with the nearly prehensile upper lips, for manipulating vegetation into the mouth.

Status: West Indian manatees are classified as Endangered under the U.S. Endangered Species Act, are not included on the Rhode Island state list, and are classified as Vulnerable on the IUCN Red List, although both the Florida population and the population in the West Indies are classified as Endangered. Florida manatee numbers have been assessed since 1991 by aerial surveys following winter cold fronts, which concentrate the animals into the available warm-water refuges (FFWCC, 2006). The highest count was 3,807 in January 2009, more than 500 higher than the previous high of 3,300 in 2001 (FFWCC, 2009). Mortality is high, averaging 183 deaths annually since 1974 and more than 300 per year in the last decade or so. About 30% of the mortality can be attributed as human-related mortalities, primarily collisions with watercraft (24%) but also including crushing in floodgates and canal locks, poaching, ingestion of persistent debris, and drowning or entanglement in fishing gear. Categories of natural mortalities include perinatal, cold stress, and biotoxins from "red tides."

Ecology and life history: Manatees feed on a wide variety of marine, estuarine, and aquatic vegetation, including seagrasses, algae, mangrove leaves and seedlings, floating aquatic plants, overhanging and streamside terrestrial plants, and even acorns (Reynolds and Odell, 1991). Manatees typically spend 6–8 hours a day feeding. They are not deep divers, but are capable of remaining submerged for as long as 20 minutes.

Manatees become sexually mature at 6–10 years old and about 2.7 m in length (Reynolds and Odell, 1991). Gestation is believed to be about 12–13 months. Calves are born at about 1.2 m and 60 kg. In Florida, births can occur at any time of year, most are in spring and summer. Lactation lasts for about a year, although a calf may remain with its mother for another year. Intervals between births range from 2 to 5 years.

General distribution: West Indian manatees occur in warm subtropical and tropical waters of the western North Atlantic (Husar, 1978; Caldwell and Caldwell, 1985; Reynolds and Powell, 2002). They are primarily found in freshwater systems, estuaries, and shallow, nearshore, coastal waters. The species ranges from the southeastern U.S. to Central and northern South America,

the Caribbean, and the West Indies. Florida manatees disperse in summer to feeding grounds as far north as the Chesapeake (Reynolds and Odell, 1991; Reynolds and Powell, 2002).

Historical occurrence: There are no historical records of manatees in the Rhode Island study area.

Recent occurrence: One individual (an adult male known as "Chessie") was the first manatee confirmed to occur in Rhode Island waters. He was captured in a Chesapeake tributary as winter approached in 1994 (ORG, 2003). He was transported to Florida, equipped with a radio transmitter that could be tracked by satellite, and released. When the weather warmed the following spring, he departed from Florida and headed north along the coast. Chessie did not make the expected left turn into Chesapeake Bay, but continued north past New Jersey into New York Harbor and then into Long Island Sound. He traveled the entire length of the Sound before finally reaching Point Judith on the 16th of August. Then he turned around and went back. He eventually lost the tag near New Haven, Connecticut, but was sighted in Virginia on 23 September and recognized back in his normal winter habitat in Florida in November. Chessie was re-sighted in August 2001 in Virginia (USGS, 2006).

Three other manatees have since visited the study area (Fig. 67)[11]. A manatee was seen in Montauk Harbor for about a week in late July of 1998 (Kimberly Durham, Riverhead Foundation, pers. comm.). Another wayward manatee visited southern New England in the summer of 2006, leaving an extensive trail of sighting reports (Hamilton and Puckett, 2006). It was first reported in Ocean City, Maryland on 11 July. It was then seen in Delaware Bay on 14 July and at Barnegat Inlet, New Jersey on 22–23 July. Next it lingered for about a week in the Hudson River, from the 1st to the 8th of August, and was sighted off Manhattan and Harlem and more than 40 km upriver north of the Tappan Zee Bridge in Westchester County. The next sighting was far to the east, in Quissett Harbor near Woods Hole, Massachusetts, on 17 August, before it turned around and started on the return trip. It was seen on the 19th in Westport, Massachusetts, and then caused a brief media furor in Rhode Island—drinking from a storm drain for the Channel 10 television cameras in a marina in Greenwich Bay on 20 August, and making brief appearances in Wickford harbor on the 22nd and Bristol harbor on the 27th or 28th.

[11] Another manatee was sighted in 2009; it is not included on the figure.

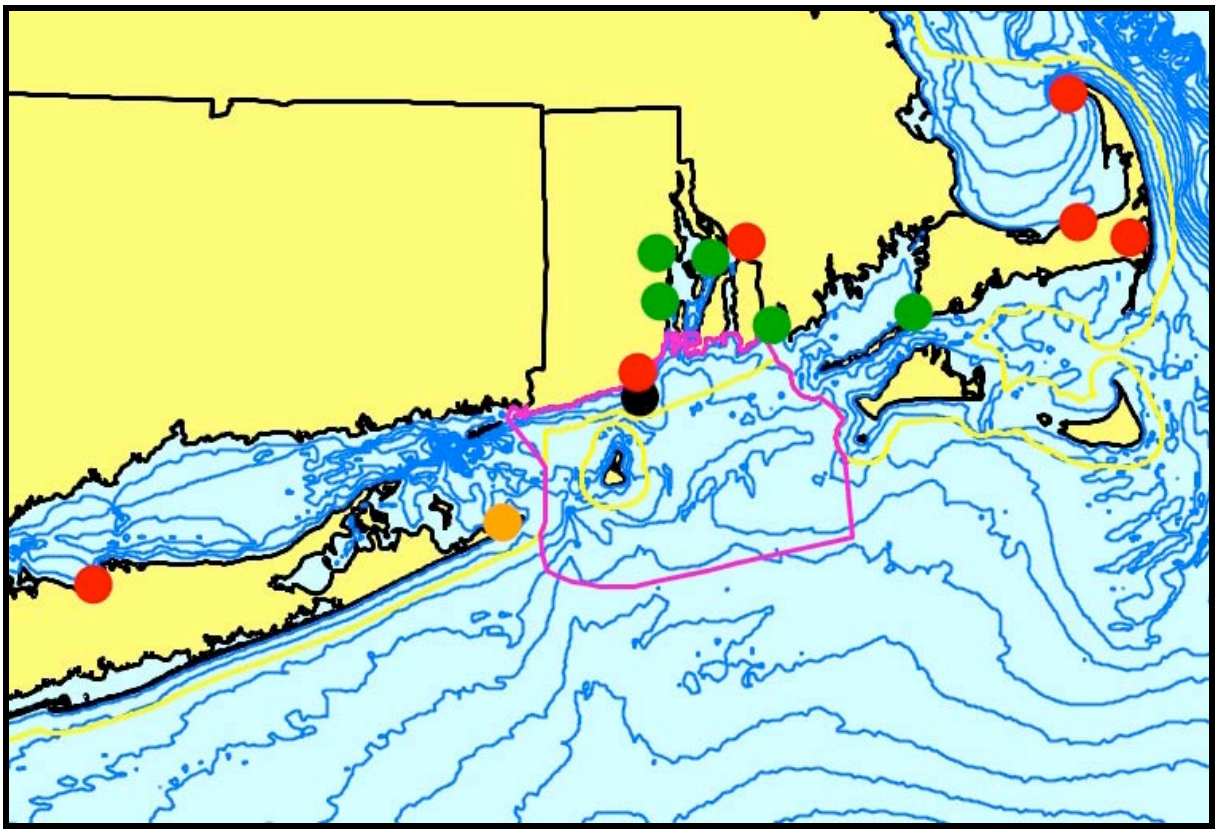

Figure 67. Sightings of four individual manatees in and near the Rhode Island study area, in 1995 (black), 1998 (orange), 2006 (green), and 2008 (red).

It has not been seen since (though there was an undocumented report of a manatee in Barnegat Bay, New Jersey in September), and is assumed to have returned home.

The last manatee to visit Rhode Island was in 2008; its locations and movements were extracted from a series of media reports. It first was seen on 11 August off Crown Point, on the South Kingstown side of Point Judith Pond and near Skip's Dock in Snug Harbor. The next report, on 21 August, came from a family fishing from a dock in Stony Brook Harbor on the north shore of Long Island. Then it laid low for almost a month, until the Massachusetts Division of Marine Fisheries reported on 19 September that a manatee had been seen for a couple of days under the Braga Bridge in Fall River. It showed up five days later on the 24th in a cove off Pleasant Bay in Harwich, Massachusetts—on the outside of Cape Cod. It apparently then went around the outer Cape, showing up on the 29th near the whale-watching boats in Provincetown harbor. The next day it was seen in Sesuit Harbor in Dennis, in the southeast corner of Cape Cod

Bay, where it remained until 11 October. On that day it was captured for relocation to Florida, however it died in transit from cold stress.

Conclusions: Florida manatees are clearly accidental visitors to the SAMP study area, and are most likely to occur on those occasions in shallow waters very close to shore, where there are sea grass beds. They can safely be ignored in planning for any developments in the SAMP area.

3.2.30. Leatherback sea turtle *Dermochelys coriacea* (Vandelli, 1761)

A turtle, encased within its shell (comprised of an upper carapace and a lower plastron), is something that is instantly recognizable to most people. The sea turtles include seven or eight species in two closely related families. Sea turtles spend their entire lives at sea except for nesting; adult females deposit their eggs in nests dug above the high-tide mark on sandy beaches in the tropics and sub-tropics. Their limbs are adapted for swimming—modified into simplified, flattened flippers. Sexes are generally indistinguishable, except that adult males usually can be identified by their very long tails. Only five species typically occur in the North Atlantic, although one other may occur accidentally in the West Indies (Ernst et al., 1994; Spotila, 2004). Four species are known from the Rhode Island study area—leatherback, loggerhead, Kemp's ridley, and green sea turtles (Table 1). The hawksbill sea turtle is known from single historical stranding records in Massachusetts in 1968 (Lazell, 1980; McAlpine et al. 2007) and New York in 1938 (Morreale et al., 1992), and is considered to be hypothetical for this analysis.

Description: The leatherback sea turtle is one of the largest living reptiles, and is the only living species in its family, Dermochelyidae (Ernst et al., 1994). Leatherbacks differ from all other sea turtles in lacking the outer layer of keratin plates or scutes on the shell. The bony shell, composed of a mosaic of thousands of tiny dermal bones, is covered by a layer of soft, leathery skin. Carapace lengths (the standard for measuring a turtle is to measure the length and width of the carapace without including the head, tail, or limbs) of adults are up to 1.8–2 m or more, and large leatherbacks can reach weights of 1,000 kg (Wynne and Schwartz, 1999). The carapace tapers from front to back, and there are seven longitudinal ridges. The overall color is black, and there are usually white or pinkish spots, especially underneath. The front flippers are very long and flexible; both front and rear flippers lack claws.

Status: Leatherback sea turtles are classified as Endangered under the U.S. Endangered Species Act, as Federally Endangered on the Rhode Island state list, and as Critically Endangered on the IUCN Red List. The status of populations in the North Atlantic does not seem to be as precarious as it is for those in the Pacific, where nesting populations have declined by more than 80%. Estimates of the total number of adult females in the world declined from 115,000 in 1982 to 20–30,000 in 1996 (IUCN, 2008).

Estimates of sea turtle population abundance for any region are rare or non-existent. Sea turtles are wide-ranging, difficult to detect at sea, and capable of long submergences; in addition, aerial surveys detect only individuals above a certain size threshold—about 75 cm carapace lengths (Shoop and Kenney, 1992). The northeastern U.S. is one of a few locations where there have been published estimates of abundance of pelagic sea turtle populations, based on line-transect aerial surveys (CETAP, 1982). Shoop and Kenney (1992) summarized the CETAP estimates, which showed that 100–900 leatherbacks occurred off the northeastern U.S. in the summer. Those numbers are minimum values, since they do not account for animals missed because they were below the surface and not visible when the survey aircraft passed.

Abundance is more typically indexed by counts of nesting adult females. There are seven known leatherback nesting populations in the Atlantic (reviewed in TEWG, 2007; NMFS & USFWS, 2007c), with the total number of adults estimated at 34,000–94,000. The Florida population grew from 98 nests in 1988 to 800–900 per year in the early 2000s, with a 17% increase rate on index beaches. The Northern Caribbean population nests on Puerto Rico and the Virgin Islands. Nests in Puerto Rico increased at 10% annually, from 9 in 1978 to 469–882 in 2000–2005. Nesting in the U.S. Virgin Islands increased at 10% from 1986 to 2004, and at 13% from 1994 to 2001. There were 143 nests in 1990 and 1008 in 2001. The number of nests in the British Virgin Islands increased from a few in the late 1980s to 35–65 in the 2000s, at a rate of 20% in 1994–2004. The Western Caribbean populations nests from Honduras to Colombia, especially in Costa Rica, Panama, and Colombia, and shows declining trends. At the major nesting beach in Tortuguero, Costa Rica, nesting declined by 68% between 1995 and 2006. The Southern Caribbean population nests in Guyana, Suriname, French Guiana, Trinidad, Dominica, and Venezuela, with perhaps 40% of the world's leatherback nesting in Suriname and French Guyana. The trend is generally stable to a slight increase. The other three populations are in the South Atlantic—Brazil, West Africa, and South Africa.

All sea turtle species share a nearly identical suite of survival threats (reviews in NRC, 1990; Lutcavage et al., 1997; Spotila, 2004; NMFS & USFWS, 2007a, 2007b, 2007c, 2007d). Harvesting of adults and eggs depleted populations in many areas of the world, and continues in some places. Predators, both natural and introduced, take significant numbers of eggs, hatchlings, and juveniles. There are two additional significant anthropogenic impacts on sea turtles—loss or degradation of nesting habitat and incidental capture in fisheries. While there are natural sources of habitat loss (e.g., beach erosion, hurricanes), development of beachfronts for residences or tourism, beach armoring, disorientation of hatchlings by artificial lighting, sand mining, beach replenishment, and spread of non-native vegetation are much more serious. Sea turtles are captured frequently in many fisheries, including pelagic longlines, high-sea driftnets, sink gillnets, pound nets, trap and pots, and trawls; turtles can also be entangled in other types of persistent debris. Other anthropogenic impacts include boat strikes and plastic ingestion.

Lewison et al. (2004) estimated that 50,000 leatherbacks were killed in pelagic longline fisheries worldwide in 2005, mainly in the Pacific. About 3,000 a year were killed in the U.S. Atlantic and Gulf of Mexico shrimp fishery; leading NMFS to require a larger escape opening in Turtle Excluder Devices (TEDs) beginning in 2003 (NMFS & USFWS, 2007c). Morreale and Standora (1998) reported eight leatherback turtles that were entangled in fishing gear near Long Island during 1987–1992 and released after tagging. In Rhode Island waters, a leatherback entangled in buoy lines for lobster traps is the most common sea turtle entanglement.

Ecology and Life History: The basic picture of sea turtle life history has long been known, is very similar across all species, and has been well-described in the works of Archie Carr and his colleagues (Carr, 1967, 1980, 1986, 1987, 1995; Carr and Meylan, 1980; Hamner, 1988; Musick and Limpus, 1997). An adult female crawls up onto a sandy beach, digs a nest hole, deposits a clutch of eggs, covers it over, and returns to the sea. About two months later a batch of hatchlings emerges from the nest and scrambles down the beach and into the ocean. The hatchlings swim straight out to sea and disappear until they next show up as small juveniles—long termed the "lost year." Carr theorized, which was later confirmed, that hatchlings get passively carried in ocean current systems and collect in sargassum patches and other surface convergences, where they feed on a wide variety of plant parts and invertebrates. Pelagic post-hatchlings grow into small juveniles, who move into developmental habitats, usually in coastal waters, although leatherbacks and olive ridley remain pelagic during this phase. Larger juveniles

move into the same foraging habitats as the adults.

Sea turtles are very difficult to age, so that the durations of the various life-stages were not known. For leatherbacks, growth seemed to be relatively fast, and the age at maturity had been estimated from as short as 2–3 years to as long as 13–14 years (Pritchard and Trebbau, 1984; Rhodin, 1985; Zug and Parham, 1996; Dutton et al., 2005). More recent work, however, suggests that the median age for first-time nesting females in the western North Atlantic is 24.5 to 29 years (Avens et al., 2009).

Adult leatherback sea turtles feed mainly on jellyfish and other gelatinous invertebrates, especially the lion's mane jelly *Cyanea capillata* (Bleakney, 1965; Lazell, 1980; Bjorndal, 1985; Mortimer, 1995).

General distribution: The leatherback sea turtle has the widest distribution of any species of sea turtle, extending worldwide from tropical and subtropical at least into cold-temperate waters and sometimes even more poleward (Ernst et al., 1994; Spotila, 2004; NMFS & USFWS, 2007c). In the North Atlantic, leatherbacks have been observed in waters of the U.S., Nova Scotia, Europe, the eastern Mediterranean, Newfoundland and Labrador, Greenland, the North Sea, and the Barents Sea (Bleakney, 1965; Brongersma, 1972, 1995; Threlfall, 1978; Goff and Lein, 1988; Marquez, 1990; Casale et al., 2003; Hays et al., 2004, 2006; James et al., 2005; McAlpine et al., 2007). They are capable of maintaining a body temperature well above ambient through a combination of anatomy, physiology, and behavior (Frair et al., 1972; Greer et al., 1973).

Off the northeastern U.S., leatherbacks were sighted commonly in summer in shelf waters from North Carolina to Maine, and in much lower numbers in spring and fall (Shoop and Kenney, 1992). The densest aggregation of sightings was in the nearshore waters south of central Long Island. Despite being present in much lower numbers than loggerheads (less than 5% of the number of sightings) leatherbacks were far more likely to occur within the Gulf of Maine north of Cape Cod—consistent with their known tolerance for colder water.

Historical occurrence: Lazell (1980) reported that the first recorded occurrence of a leatherback turtle in New England was in 1886 by the Monomoy lighthouse keeper. However, Babcock (1919) reported that the first New England occurrence was in Massachusetts Bay in 1824, and that the specimen was in the collection of the Boston Society of Natural History. He

reported two earlier records—in 1811 at an unknown locality and in 1816 at Sandy Hook, New Jersey. He listed a total of 31 known records between 1811 and 1917, ranging from New Jersey to Maine, including three from Rhode Island and seven others from the Rhode Island study area. The Rhode Island records included one in Narragansett Bay in 1878 and two off Southeast Point, Block Island around 30 July 1886. The plate illustrating leatherbacks in his monograph included two photos of one of the Block Island specimens. The other leatherback records in the study area included: 1826—Long Island Sound; 1875—one at Stonington, Connecticut, another between New London and Montauk; 1876—Stonington; 1879—Buzzards Bay at Marion, Massachusetts; 1891—caught in a fish trap in Buzzards Bay near Woods Hole; 1907—fouled in an anchor rope a few miles south of Noman's Land.

Lazell (1980) also mapped a number of leatherback sightings from Brongersma (1972) and Lazell (1976) along the New England coast from Rhode Island to Downeast Maine, concluding that "the greatest concentrations of non-nesting leatherback records in the Atlantic are around the Gulf of Maine."

Recent occurrence: Leatherback turtles occur relatively commonly in the Rhode Island study area (Fig. 68), and are almost entirely limited to summer (57.7%) and fall (41.6%). Leatherbacks occurred over much of the continental shelf in the study area. There is an aggregation of occurrences in the SAMP area, but 20 of those are strandings on Block Island extracted from Nawojchik (2002). There is also somewhat of an aggregation south of central Long Island, in the same area noted by Shoop and Kenney (1992) as a leatherback concentration area. There were 24 sightings in summer and 5 in fall from the whale-watching boats.

The relative abundance patterns (Fig. 69) show leatherbacks to be relatively dispersed and not particularly abundant. The areas of higher abundance are all beyond the boundary of the mapped area, and the model output does not predict occurrence within the SAMP area.

Leatherback strandings are relatively common in Rhode Island, however we did not have access to most of those records. Nawojchik and St. Aubin (2003) reported that, of the 146 sea turtle strandings responded to by Mystic Aquarium from 1987 to 2001, 124 (84.9%) were in Rhode Island, and 120 of the 146 were leatherbacks. All strandings occurred during June through November, with the biggest numbers in August and September. This is fully consistent with the sighting data. Leatherbacks were the only sea turtle species to strand on Block Island.

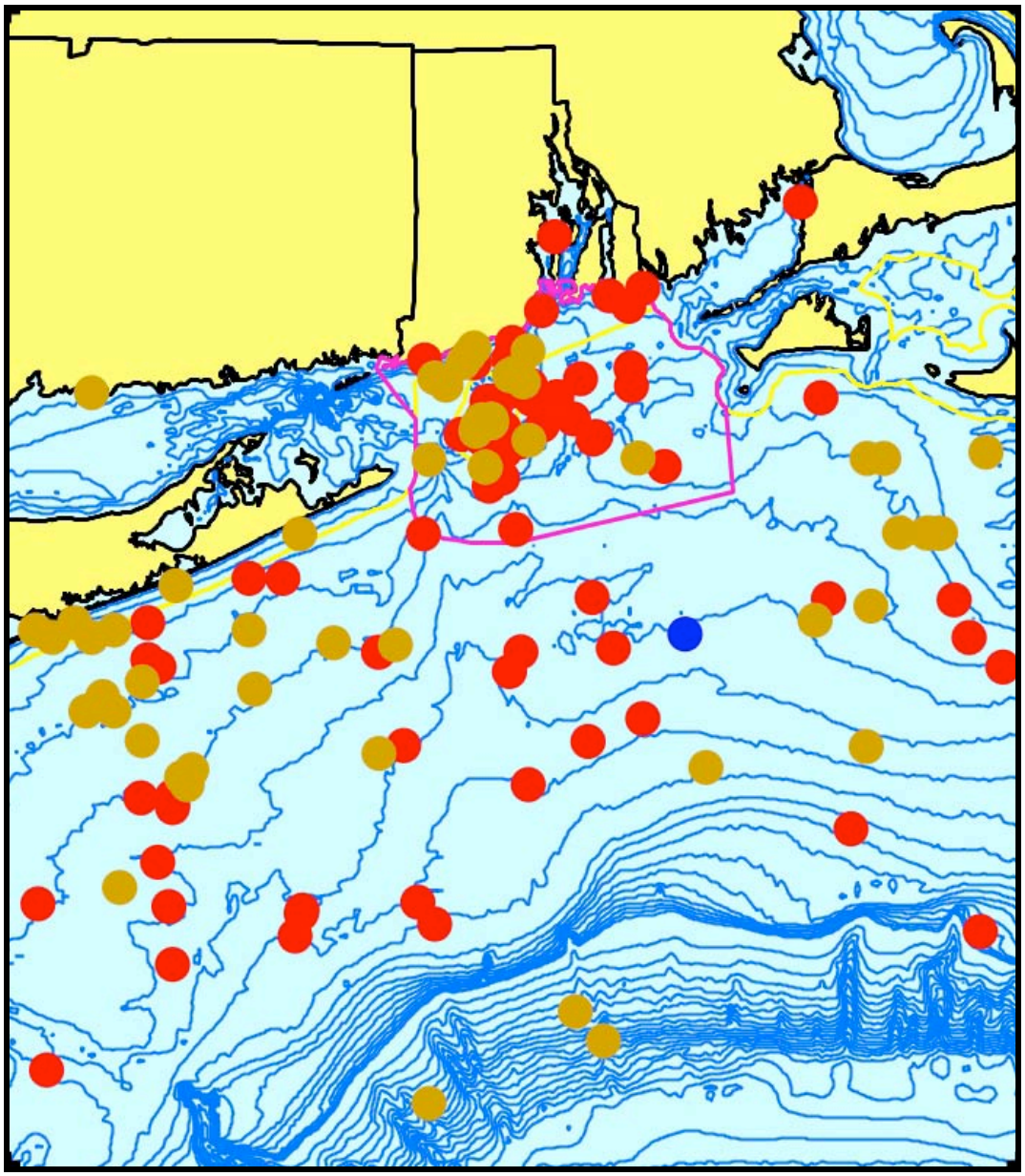

Figure 68. Aggregated sighting, stranding, and bycatch records of leatherback sea turtles in the Rhode Island study area, 1974–2008 (n = 142: winter = 1, spring = 0, summer = 82, fall = 59).

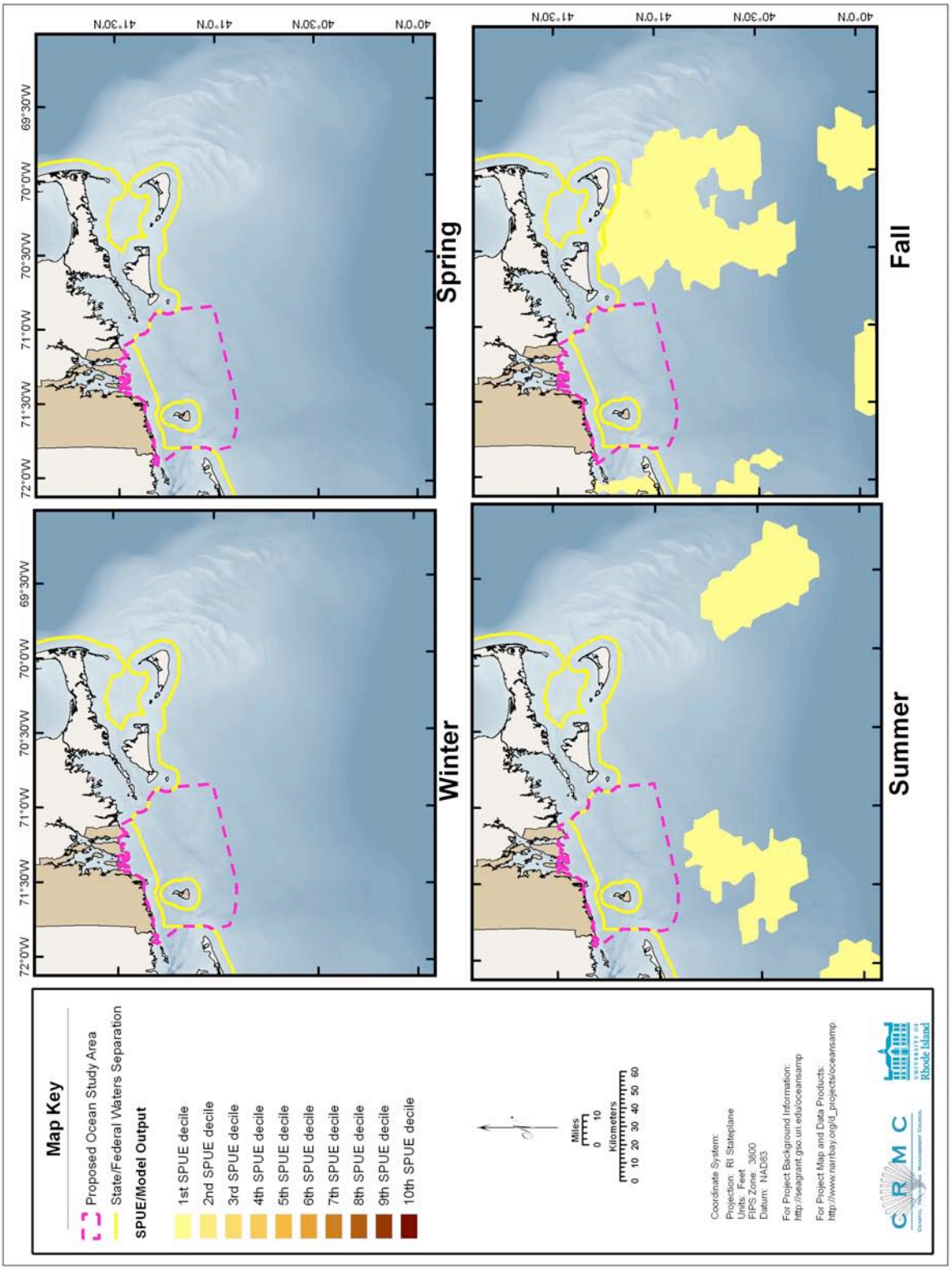

Figure 69. Modeled seasonal relative abundance patterns of leatherback sea turtles in the Rhode Island study area, corrected for uneven survey effort.

Conclusions: The relative abundance analysis does not predict that leatherback sea turtles will occur in the Ocean SAMP area (Fig. 69), however the more extensive data, including sightings from the whale-watching boats, show that leatherbacks do occur in the SAMP area. The lower survey effort in summer and fall may explain some of the difference. Given the leatherback's status as an Endangered species, they should be considered in any planning process.

3.2.31. Loggerhead sea turtle *Caretta caretta* (Linnaeus, 1758)

All of the sea turtles other than leatherbacks belong to a separate family—Cheloniidae, the so-called "shelled" sea turtles. The bony shell is much thicker and heavier than in leatherbacks, and it is covered by a layer of keratin plates or scutes. The arrangements and numbers of scutes are important characters used to identify species, especially small individuals or decomposed carcasses.

Description: The loggerhead sea turtle is one of the two species of larger shelled turtles found in the North Atlantic, with adult carapace lengths of 85-120 cm (Wynne and Schwartz, 1999), although the maximum known length was 213 cm (Ernst et al., 1994). The shell is shaped like a broad oval, tapering toward the rear. The head is much larger relative to body size than in the other sea turtle species, with broad crushing surfaces on both the upper and lower jaws. The color is a distinctive yellowish- to reddish-brown.

Status: Loggerhead sea turtles are classified as Threatened under the U.S. Endangered Species Act, as Federally Threatened on the Rhode Island state list, and as Endangered on the IUCN Red List. Shoop and Kenney (1992) estimated the summer pelagic population off the northeastern U.S. of large juveniles and adults detectable from aerial surveys at 2,200–11,000, not accounting for diving behavior, with less than half as many in spring and fall. There are no more recent comparable estimates.

TEWG (2000), Ehrhart et al. (2003), and NMFS & USFWS (2007d) reviewed the status of loggerhead nesting populations in the North Atlantic. The largest is in the southeastern U.S. and Gulf of Mexico, which is the second largest loggerhead nesting population in the world after the one in the eastern Indian state of Orissa. The total numbers of nests and nesting females per year are estimated at 53,000–92,000 and 32,000–56,000, respectively. The population is divided into

five sub-populations. The Northern sub-population nests in Georgia and the Carolinas. The average number of nests per year is 5,151, with a 1.9% declining trend over 1989–2005. The largest sub-population is South Florida, with an average of 65,460 nests and 15,966 females and a declining trend of 22.3% in 1989–2005. That decline may be accelerating. The Dry Tortugas sub-population shows no detectable trend and has annual averages of 246 nests and 60 females. The averages for the Florida Panhandle sub-population in 1995–2005 were 910 nests, 222 females, and a declining trend of 6.8%. The Yucatan sub-population increased from 903 nests in 1987 to 2,331 in 2001, but may currently be decreasing.

Other western North Atlantic populations include the eastern Bahamas, with 500–600 nests per year, and Cuba, with 250–300. Loggerheads formerly nested on Jamaica, Haiti, the Dominican Republic, and Puerto Rico, but no longer do so. The nesting population in northeastern Brazil has shown a long-term increase, with 4,837 nests in 2004. The only nesting population in the eastern North Atlantic is in the Cape Verde islands, with several thousand nests per year. Loggerheads also nest in the eastern Mediterranean, where nest counts can exceed 7,000 per year, although monitoring is incomplete.

Impacts on loggerheads are the same as for other sea turtles. Lewison et al. (2004) estimated that 60,000–80,000 loggerheads were killed annually by incidental capture in Atlantic pelagic longline fisheries, primarily in the western Mediterranean, and 200,000 globally. NRC (1990) estimated that, prior to regulations requiring TEDs, 5,000–50,000 loggerheads were killed each year in the southeastern U.S. and Gulf of Mexico shrimp trawl fishery.

In southern New England, juvenile sea turtles sometimes strand dead, comatose, or seemingly paralyzed. The event happens in the fall of the year, when water temperatures decline, and is referred to as “cold-stunning.” In 1985, 56 cold-stunned turtles stranded in eastern Long Island (Meylan, 1986), sparking the establishment of a monitoring, research, and rehabilitation program. A similar program exists in Cape Cod Bay.

Ecology and Life History: Loggerheads follow the typical sea turtle life history pattern. Post-hatchlings disperse and are entrained in ocean currents (Carr, 1986). Small juveniles are present in high abundance around the Azores (Bolten, 2003), where they remain resident for extended periods and feed on pelagic invertebrates such as siphonophores, jellies, salps, gastropods, barnacles, and isopods. Small juveniles may also congregate on the Grand Banks off

Newfoundland. In the Mediterranean, genetic profiling has shown that small and medium juvenile loggerheads come from both the eastern Mediterranean nesting population and from western North Atlantic populations (B. W. Bowen et al., 1993). Eventually juveniles reach the size where they return to coastal waters, first into shallower developmental habitats in bays and estuaries and then into adult foraging habitats. The diet of juveniles in developmental habitats is dominated by crabs (Burke et al., 1993). Adults feed on a wide variety of benthic prey, including bivalves, gastropods, crabs, sea pens, anemones, and seaweeds (reviewed by Bjorndal, 1997).

General distribution: Loggerhead sea turtles are distributed worldwide in subtropical and temperate waters (Ernst et al., 1994; Ehrhart et al., 2003). In the western North Atlantic, they are common off the southeastern U.S. and in the Gulf of Mexico. Off the northeastern U.S., there are few sightings north of the latitude of Long Island, and only one in the northern Gulf of Maine (CETAP, 1982; Shoop and Kenney, 1992), although there are inshore records from Nova Scotia and juveniles are commonly taken as bycatch in fisheries on the Newfoundland Grand Banks (Bleakney, 1965; Brongersma, 1972, 1995; Bolten, 2003; McAlpine et al., 2007).

From Long Island south to North Carolina, loggerhead occurrence is strongly seasonal (CETAP, 1982; Shoop and Kenney, 1992). They are nearly absent in winter. In spring they spread northward from south of Cape Hatteras. The distribution is most extensive in summer—from the shore to the mid-shelf area and also along the outer shelf. The distribution then contracts southward in the fall.

Historical occurrence: Babcock (1919) stated that loggerhead turtles "not uncommonly visit Long Island Sound and the Massachusetts coast." He reported that "a number of specimens usually about two feet in length [were] taken every year" in fish traps in Menemsha Bight of the northwestern side of Martha's Vineyard. He also included an interesting report that small loggerheads were "taken in Long Island Sound in a benumbed condition as late as December 4," possibly one of the first reports of cold-stunning from the region.

Lazell (1980) wrote that loggerhead turtles were "common in New England waters and the Canadian portions of the Gulf of Maine." However, McAlpine et al. (2007) suggested that Lazell was going beyond the limits of his available data in trying to make his point, and that loggerheads were rare north of Cape Cod.

Recent occurrence: The occurrence of loggerhead sea turtles in the Rhode Island study area (Fig. 70) is fully consistent with the reports of CETAP (1982) and Shoop and Kenney (1992). Sightings are strongly concentrated in the summer (73.4%), and then the fall (26.2%). The concentration of sightings is highest in the western half of the study area, and sightings in the eastern half are more on the outer part of the shelf. There is one cluster of sightings in the southwestern quarter of the SAMP area, which includes the majority of the 10 summer sightings and 1 fall sighting from the whale-watching boats.

As with leatherbacks, the areas of high relative abundance were to the west of the area mapped (Fig. 71). Within the study area, most areas of predicted loggerhead summer and fall occurrence were offshore of the SAMP area. One area of lowest abundance extended into the SAMP area's southwest corner in the fall, and there was an area of moderate occurrence on the outer shelf southeast of Nantucket in summer.

We did not have access to sea turtle stranding data for the study area. Nawojchik and St. Aubin (2003) reported that 23 of the 146 sea turtle strandings in Rhode Island and Connecticut (15.8%) were loggerheads—many fewer than leatherbacks even though the population in shelf waters is estimated to be an order of magnitude larger.

Many of the loggerheads that occur in coastal embayments such as Peconic Bay in eastern Long Island or Cape Cod Bay are juveniles that are too small to be detected during surveys. Morreale et al. (1992) reported that 28 juvenile loggerheads collected in eastern Long Island in 1986–1988 ranged from 36.6 to 59.6 cm, with a mean of 49.5. Over a longer period from 1984 to 1998, the mean size of 298 juvenile loggerheads in Long Island was smaller at 45.5 cm (SD = 18.0; Saari et al., 2000). Shoop et al. (1999) considered that 45 cm was the lower end of the 45-85 cm size range of large, benthic-feeding juveniles found off Georgia. Assuming a normal distribution, that would suggest that loggerheads around Long Island are about half and half small juveniles <45 cm and large juveniles >45 cm.

The species proportions differ between areas and between collection methods (Table 6). Collecting turtles for measurement, sampling, and tagging from those caught in fishing gear should sample more across the available size range than collecting individuals debilitated by declining temperatures in the fall ("cold-stunned"), which

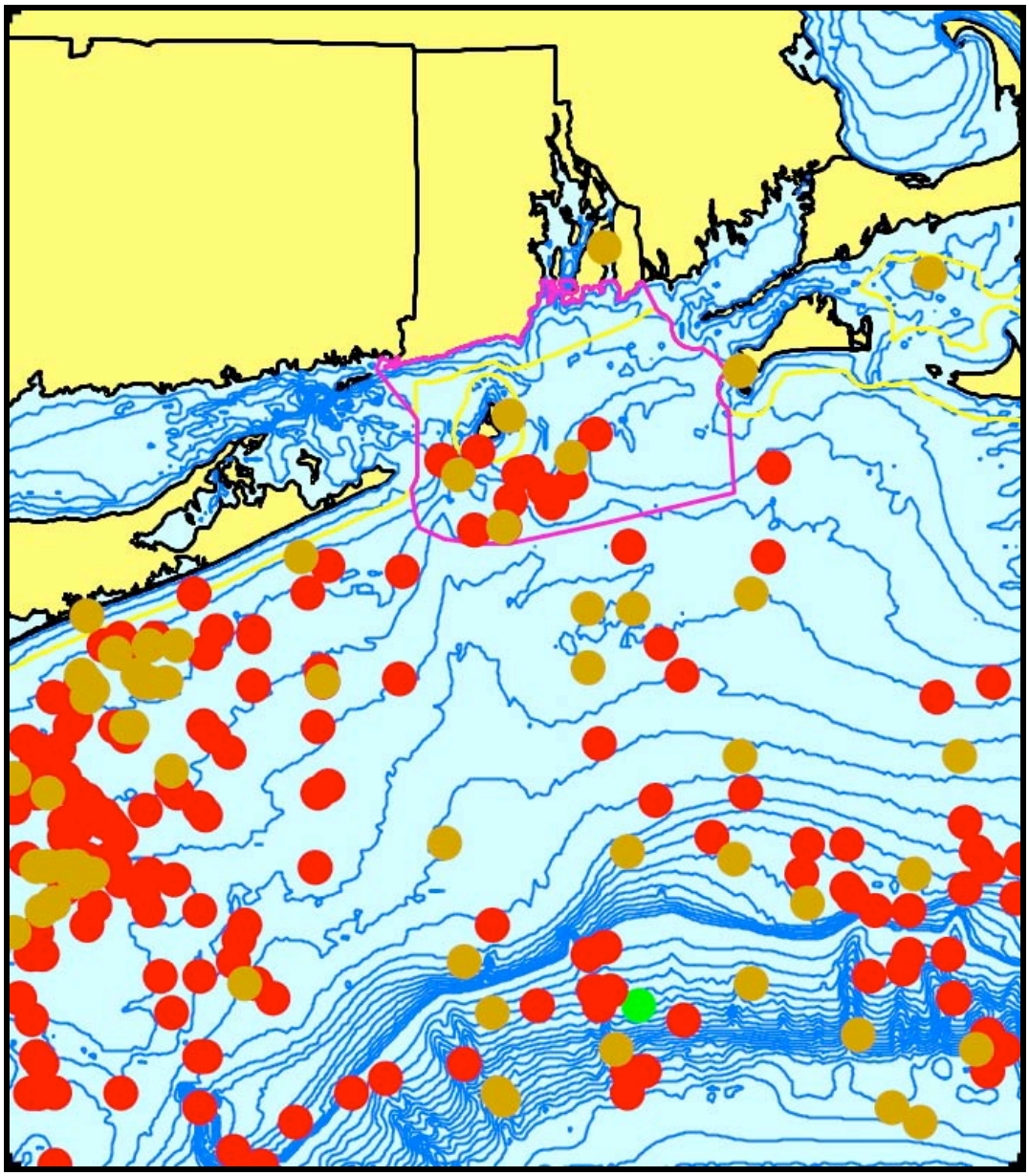

Figure 70. Aggregated sighting, stranding, and bycatch records of loggerhead sea turtles in the Rhode Island study area, 1963–2006 (n = 233: winter = 0, spring = 1, summer = 171, fall = 61).

affects juveniles more than adults. Of 519 turtles live-captured around eastern Long Island in 1984–1998, 298 (57.4%) were loggerheads (Saari et al., 2000). However, of 130 cold-stunned turtles in 1986–1988, only 28 (21.5%) were loggerheads (Morreale et al., 1992). In Rhode Island stranding records, loggerheads are far less frequent than leatherbacks (Nawojchik and St. Aubin, 2003).

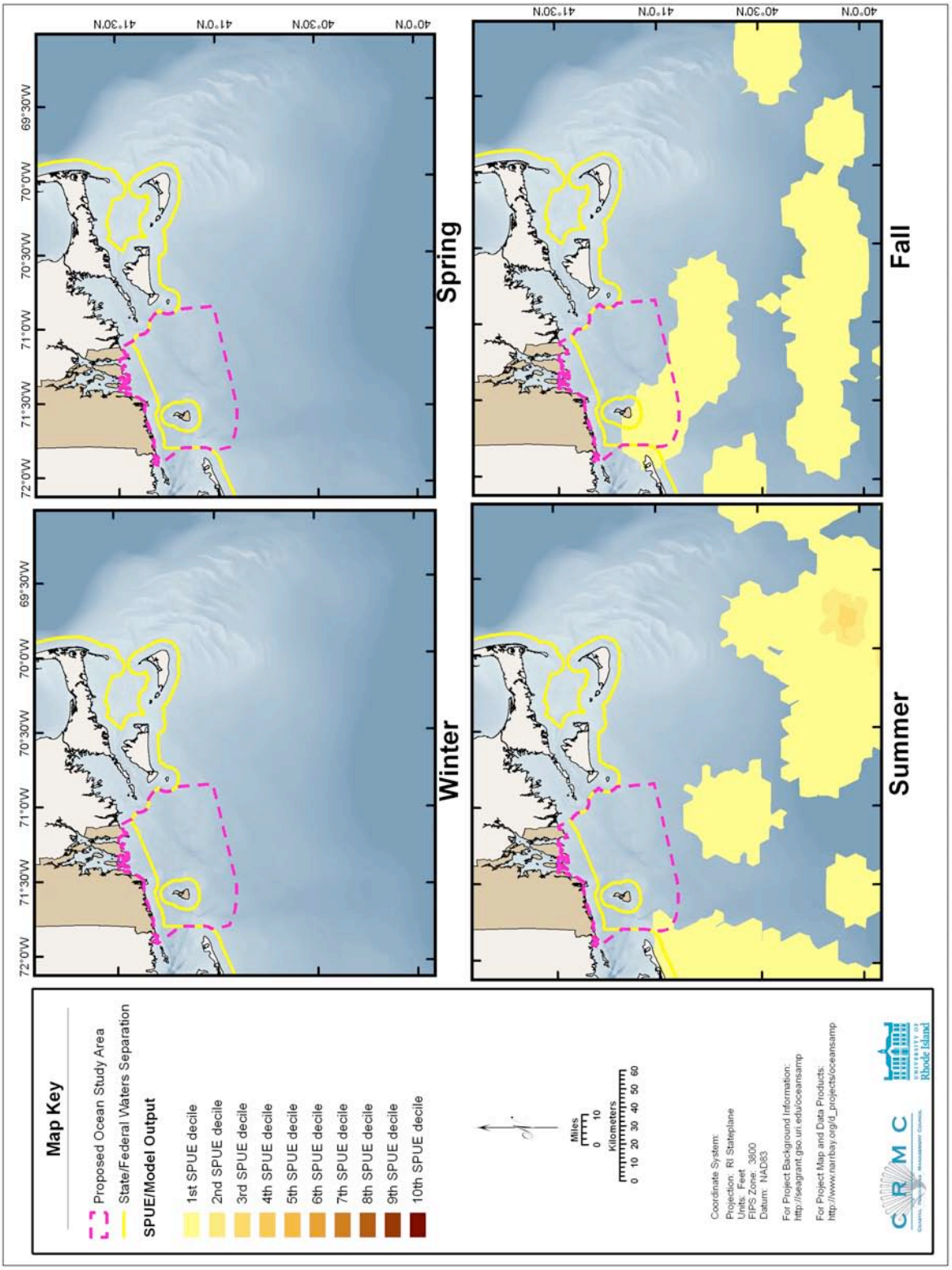

Figure 71. Modeled seasonal relative abundance patterns of loggerhead sea turtles in the Rhode Island study area, corrected for uneven survey effort.

Table 6. Comparisons of relative frequencies and percentages of leatherback (LeTu), loggerhead (LoTu), Kemps' ridley (KRTu) and green (GrTu) sea turtles in different collections from southern New England localities.

Collection and Source	LeTu	LoTu	KRTu	GrTu
RI (85%) & CT (15%) strandings, 1987–2001	120	23	1	2
(Nawojchik and St. Aubin, 2003)	82.2%	15.8%	0.7%	1.4%
Long Island live captures, 1984–1998	0	298	120	101
(Saari et al., 2000)	–	57.4%	23.1%	19.5%
Long Island cold-stunned, 1986–1988	0	28	97	5
(Morreale et al., 1992)	–	21.5%	74.6%	3.8%
Peconic Bay live captures, 2002–2003	0	2	11	16
(Aguirre et al., 2008)	–	6.9%	37.9%	55.2%
Cape Cod Bay cold-stunned, 1979–2003	0	272	983	30
(Dodge et al., 2008)	–	21.1%	76.3%	2.3%

Conclusions: Although loggerhead turtles are much more abundant off southern New England than leatherbacks (about 20:1 in numbers of sightings), they are less likely to occur in nearshore waters or in the SAMP area (1:6 in stranding frequency, also compare Figs. 69 and 71). Even though they are listed as a Threatened species, they can probably be discounted in planning for any development in the SAMP area, since mitigation taken for leatherbacks will also benefit loggerheads.

3.2.32. Kemp's ridley sea turtle *Lepidochelys kempii* (Garman, 1880)

Description: Kemp's ridleys are smaller shelled sea turtles, with adult carapace lengths of 60-80 cm (Ernst et al., 1994; Wynne and Schwartz, 1999). Individuals encountered off the northeastern U.S. are mostly juveniles. The shell is slightly heart-shaped to nearly circular, and is usually gray.

Status: Kemp's ridley sea turtles are classified as Endangered under the U.S. Endangered

Species Act, are not included on the Rhode Island state list, and are classified as Critically Endangered on the IUCN Red List.

At least 60% of all Kemp's ridley nesting takes place on one 40-km stretch of beach near Rancho Nuevo, Tamaulipas, Mexico (Ernst et al., 1994; TEWG, 2000; NMFS & USFWS, 2007b). As many as 40,000 females nested there on a single night in 1947 (Carr, 1963). By 1985, the total number of nests per year had declined to 740, and nesting females to about 250 (TEWG, 2000). Nesting increased through the 1990s. In 2002 there were over 4,000 nests at Rancho Nuevo and 6,000 in all of Mexico. In 2006 the respective counts were 7,866 and 12,143, with about 100 nests in the U.S., mainly at Padre Island, Texas. Given average estimates of nests per female per season and years between nesting years, the total number of adult females in the population is estimated at 7,000–8,000 (TEWG, 2000; NMFS & USFWS, 2007b).

There are no estimates of the number of Kemp's ridleys off the northeastern U.S. (Shoop and Kenney, 1992). Even most adults are too small to be sighted during aerial surveys, so the numbers of sightings are far too few to calculate densities.

Ecology and Life History: Kemp's ridley sea turtles follow the typical sea turtle life history pattern (reviewed in TEWG, 2000). Hatchlings are entrained in oceanic current patterns and passively drift about in the Gulf of Mexico and North Atlantic until they reach about 20 cm in carapace length (Collard and Ogren, 1990). At that point, which takes 1–4 years, they transition from a pelagic existence to a benthic-feeding juvenile stage and migrate into shallow developmental habitats. They reach sexual maturity at about 60 cm, by which time they have moved into typical adult foraging habitats and migratory patterns (Morreale et al., 2007). The total time from hatching to maturity is not well known, and is estimated to vary from 7 to 15 years (TEWG, 2000; Heppell et al., 2003, 2005). The typical re-migration interval for adult females (i.e., years between nesting years) is 2 years; 60% of females are on 2-year cycles, 20% on annual cycles, 15% on 3-year cycles, and 5% on 4-year cycles.

Pelagic post-hatchlings and small juveniles probably feed on the same types of prey as loggerheads of the same life-stage, but are poorly known (Bjorndal, 1997). Benthic juveniles and adults feed primarily on crabs (Shaver, 1991; Burke et al., 1994; Bjorndal, 1997; Morreale and Standora, 1998).

General distribution: Kemp's ridley sea turtles occur only in the North Atlantic (Ernst et al.,

1994; Spotila, 2004) and nearly all nesting is in the western Gulf of Mexico. Sighting and stranding records are concentrated heavily in the Gulf of Mexico and southeastern U.S. Atlantic (TEWG, 2000). Juveniles are dispersed about the Gulf of Mexico and North Atlantic. Brongersma (1972) pointed out the very interesting phenomenon that the smallest known Kemp's ridleys outside of hatchlings leaving the nesting beach were strandings in western Europe, and the second smallest were strandings in New England. Carr (1967) wrote that "The greatest concentration of positively identified Atlantic ridleys that I ever heard of (away from Tamaulipas) occurred in just about the most unlikely place that anybody could imagine. It was Martha's Vineyard, Massachusetts." Until relatively recently, it was often assumed that small ridleys in the temperate North Atlantic represented "waifs" that were lost to the population, however it now appears well established that they are a normal component of the species life history.

Historical occurrence: Babcock (1919) did not include Kemp's ridley sea turtles as occurring in New England, however Shoop et al. (1981) suggested that Babcock had incorrectly included many Kemp's ridley records as hawksbills. At that time, many did not accept that Kemp's ridleys were a valid species, and instead believed them to be hybrids of other species ("bastard turtles") (Carr, 1967). In addition, juvenile ridleys have a sharp, beak-like mouth similar to a hawksbill's. Babcock quoted several sources who said that small hawksbills were occasionally taken in fish traps in Massachusetts, and wrote that they were "reported to be more common in Buzzard's Bay than loggerheads." However only one or two specimens were ever collected.

Lazell (1980) summarized the substantial numbers of records of Kemp's ridley sea turtles in southern New England that had been collected to that time. He argued that New England waters constituted normal and important habitat for the species, and should be protected by designation as "Critical Habitat" under the ESA.

Recent occurrence: We had only 14 records of Kemp's ridley sea turtles in the Rhode Island study area—12 (85.7%) in summer and 2 (14.3%) in fall (Fig. 72). Four of the summer records came from whale-watching boats. Kemp's ridleys occurred either in the southwestern corner of the study area, or in or near the SAMP area. The sightings were far too few to generate relative abundances. There was one very recent stranding in Rhode Island—a live juvenile that was caught in a fisherman's net in Greenwich Bay in late October of 2004 (Wyman et al., 2004); its photo

graced the front page of the Fall/Winter 2004 issue of *Narragansett Bay Journal*. Only one other Kemp's ridley stranding from Rhode Island and Connecticut was recorded in 1987–2001 (Nawojchik and St. Aubin, 2003), although the exact year and location are not known to us.

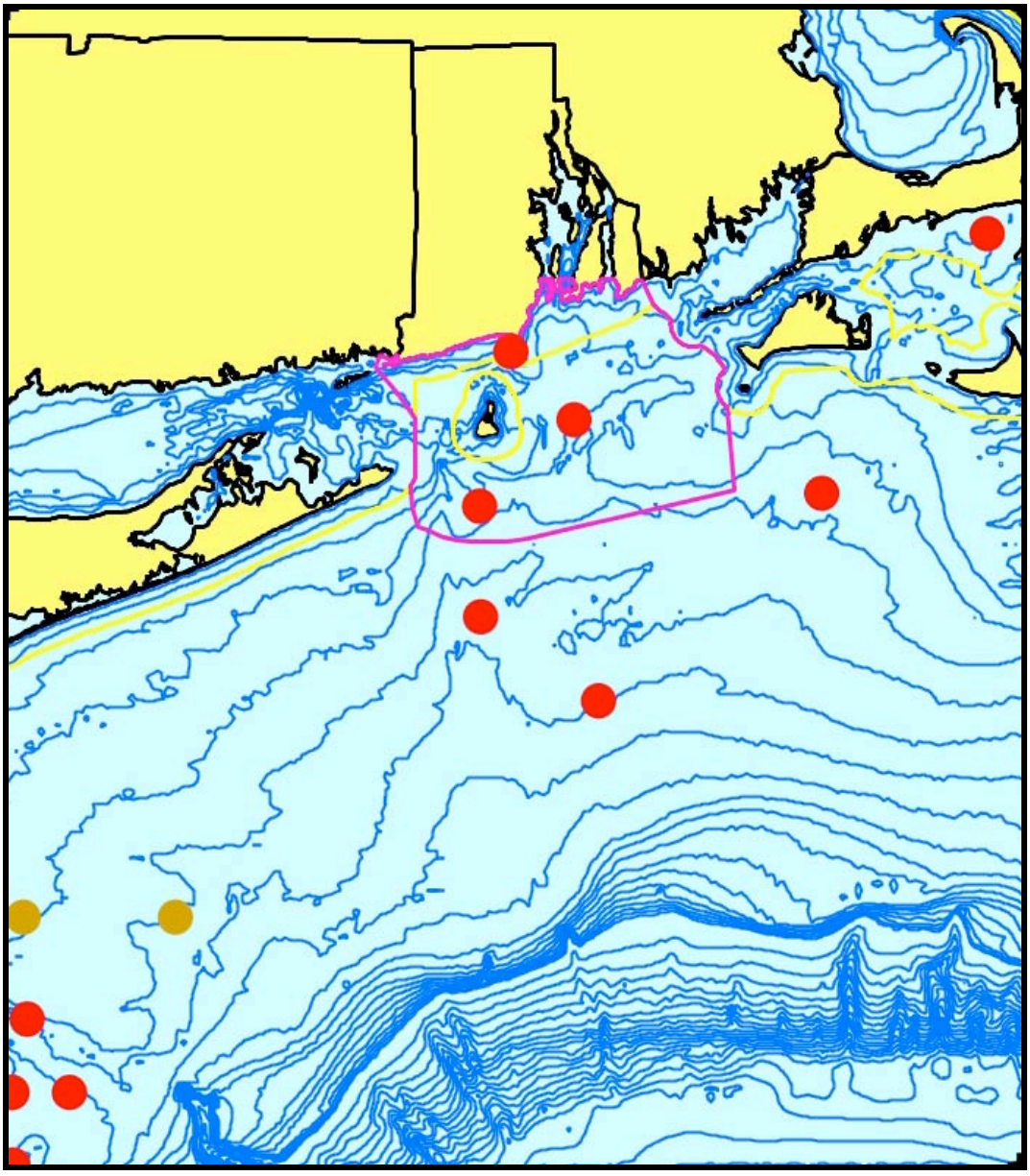

Figure 72. Aggregated sighting, stranding, and bycatch records of Kemp's ridley sea turtles in the Rhode Island study area, 1979–2002 (n = 14: winter = 0, spring = 0, summer [red] = 12, fall [brown] = 2).

The occurrence record for Kemp's ridleys in the study area is biased due to two factors. Most are simply too small to be detected from surveys. Morreale et al. (1992) reported that the carapace lengths of cold-stunned Kemp's ridleys in eastern Long Island in 1986–1988 ranged from 22.5 to 37.6 cm (N = 97, mean = 29.4). Dodge et al. (2008) reported that the typical cold-stunned Kemp's ridley in Cape Cod Bay was the size of a 2-year-old juvenile, based on sizes of some known-age individuals that had been tagged as hatchlings. The second factor is that the shallow bays and estuaries utilized by ridleys within the study area are usually excluded from survey designs. It is very clear that juvenile Kemp's ridleys are relatively common both around eastern Long Island and in Cape Cod Bay (Table 6). It is likely that Rhode Island simply does not have equivalent environments that would constitute good habitat for juvenile ridleys or other juvenile sea turtles. Given that they are common both east and west of Rhode Island, it is possible, however, that small ridleys regularly transit the Rhode Island and SAMP study areas.

Conclusions: Kemp's ridley sea turtles have occurred in the SAMP area, but they are much rarer in the study area than leatherbacks or loggerheads. There is some small concern that the small juvenile ridleys that are found around eastern Long Island or Cape Cod might transit through the SAMP area during their migrations. Any mitigation relative to the SAMP or development activities for leatherbacks would also benefit Kemp's ridleys, so it does not seem necessary to consider them separately.

3.2.33. Green sea turtle *Chelonia mydas* (Linnaeus, 1758)

Description: Green turtle adults are usually about the same size as or slightly larger than loggerheads, although the largest adults reach only about 150 cm (Ernst et al., 1994; Wynne and Schwartz, 1999). The shell is not as broad as in the loggerhead, and is more oval and less tapered. The color can be extremely variable, from pale olive to dark brown, with distinctive mottling or radiating patterns on the scutes. The head is much narrower than in loggerheads and lacks the broad crushing plates on the jaws.

Status: At the species level, green sea turtles are classified as Threatened under the U.S. Endangered Species Act, however the Florida nesting population is listed as Endangered. Since the population identity of any individual green turtle encountered off the northeastern U.S. is impossible to determine, the risk-averse strategy would be to consider them as Endangered.

Green turtles are not included on the Rhode Island state list, and are classified as Endangered on the IUCN Red List.

There are 46 identified nesting concentrations of green turtles in the world, including 13 in the Atlantic (reviewed in NMFS & USFWS, 2007a): five in the western North Atlantic, four in the eastern Mediterranean, one in Brazil, two in western Africa, and one on Ascension Island. The total number of nesting adult females worldwide is estimated between 110,000 and 150,000. The five western North Atlantic nesting populations include: Florida, with an average of 5,055 nests per year, mostly in Brevard and Palm Beach Counties, and with an increasing trend in 2001–2005; Yucatan, with 1,500 nests in the 2000s and an increasing trend; Costa Rica, with 17,402–37,290 nesting females in a year during 1999–2003, and with an increasing trend; Venezuela, with 335–443 nesting females and no detectable trend; and Suriname, with 1,803 nesting females in 1995 and an increasing trend.

There are no estimates of the number of green sea turtles off the northeastern U.S. (Shoop and Kenney, 1992). The numbers of sightings are far too few to calculate densities, and many individuals are too small to be sighted during aerial surveys.

Ecology and Life History: Green sea turtles follow the typical sea turtle life history pattern (reviewed in NMFS and USFWS, 2007a). Hatchlings are entrained in oceanic current patterns and passively drift about in association with sargassum patches (Carr, 1987). After 5–6 years of pelagic existence, they reach 20–25 cm in carapace length and move into developmental habitats in shallow coastal waters. They spend about 6 years in these habitats, then move into typical adult foraging habitats. The total time from hatching to maturity may be as long as 40 years (Limpus and Chaloupka, 1997). Adult females exhibit remigration intervals of 2–5 years, on average deposit three nests per breeding year, and have a reproductive lifetime of 17–23 years.

Green sea turtle adults and benthic feeding juveniles are herbivores, feeding on a variety of sea grasses and algae (Bjorndal, 1985, 1995, 1997; Mortimer, 1995). They also consume small amounts of animal material, including jellyfish, salps, and sponges (Bjorndal, 1997). Juvenile green turtles from Long Island were recorded as feeding on eel-grass, three species of green algae, and two species of brown algae (Burke et al., 1991). Pelagic post-hatchlings and small juveniles are not herbivorous, but are probably omnivores feeding more on animal food than on plant material (Bjorndal, 1985, 1997).

General distribution: Green sea turtles are globally distributed in tropical and sub-tropical regions, with some individuals occurring in cooler, temperate regions (Ernst et al., 1994; NMFS & USFWS, 2007a). In the western North Atlantic, they are most common in the Gulf of Mexico and Caribbean. Because of their herbivorous diet, green turtles are most likely to occur in shallow, nearshore habitats with extensive sea grass meadows.

Historical occurrence: Babcock (1919) wrote that green sea turtles were occasionally recorded in southern New England. He reported that one was captured in New Bedford harbor in September 1878, but that there were no other records from Buzzards Bay, where he expected they should occur. He also said that there were numerous records from Long Island Sound back to 1840, including two captured in the Housatonic River in Connecticut. Lazell (1980) recounted anecdotal evidence for a resident population of juvenile green turtles in Nantucket Sound, where they were regularly caught in pound nets and were often sold as exhibit specimens to commercial aquaria.

Recent occurrence: There has been only one confirmed green turtle sighting in the Rhode Island study area—on 25 March 2005 south of Long Island between the 40- and 50-m isobaths (Fig. 73). The sighting was made during an aerial survey for right whale monitoring, and was assigned an identification reliability of "probable." Nawojchik and St. Aubin (2003) reported only two strandings in Connecticut and Rhode Island during 1987–2001, but the dates and locations are not known to us. However, like Kemp's ridleys, juvenile green turtles are known to be present in shallow waters around eastern Long Island and Cape Cod (Table 6). Those data suggest that green turtles are relatively more common around Long Island than they are in Massachusetts.

Conclusions: Green sea turtles have never been recorded in the SAMP area, and they are much rarer in the study area than leatherbacks or loggerheads. There is some small concern that the juvenile green turtles that are found around eastern Long Island or Cape Cod might transit through the SAMP area during their migrations. Any mitigation relative to the SAMP or development activities for leatherbacks would also benefit green turtles, so it does not seem necessary to consider them separately.

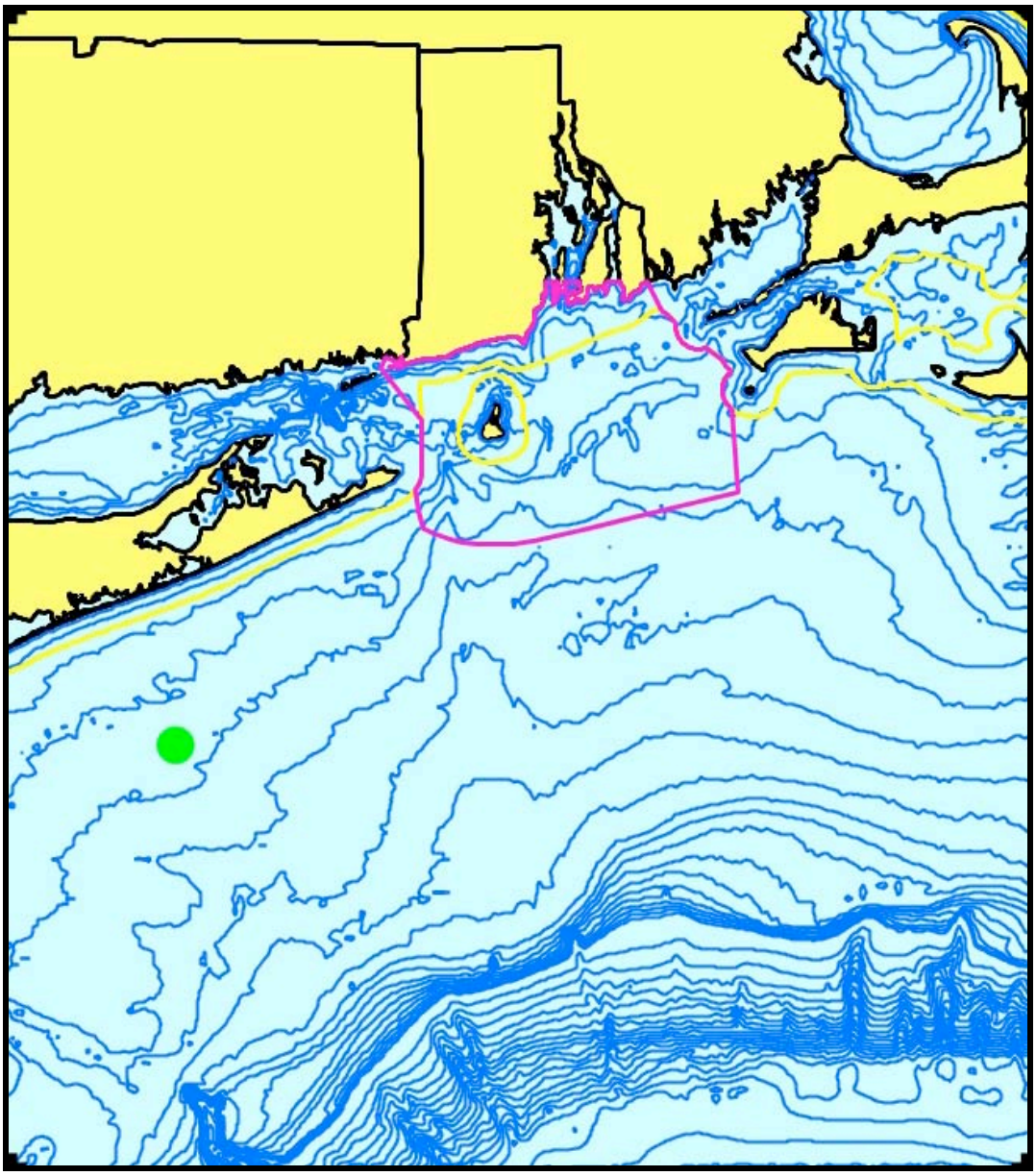

Figure 73. Aggregated sighting, stranding, and bycatch records of green sea turtles in the Rhode Island study area, 2005 (n = 1: winter = 0, spring [green] = 1, summer = 0, fall = 0).

4 Conclusions and Recommendations

Forty species of marine mammals and sea turtles are known to occur in the waters of the Rhode Island study area—encompassing Narragansett Bay, Block Island Sound, Rhode Island Sound, and nearby coastal and continental shelf areas. Sixteen are categorized as common to abundant, six as regular, and eighteen as rare to accidental. Eleven of those species—six whales,

the manatee, and four sea turtles—are listed as Endangered or Threatened under the U.S. Endangered Species Act. One other species was present historically but is now extinct in the North Atlantic. Eight other species, including one Endangered sea turtle, are considered to be hypothetical in the study area—with one or more records nearby.

Every species does not pose the same level of conservation concern relative to the Rhode Island Ocean SAMP or to the development of alternative energy projects or other industrial/ commercial projects in our coastal waters. Factors that influence the level of concern include overall abundance of the population, abundance in the study area, seasonal distribution patterns and likelihood of occurrence in or near any area of development, ESA-listing status, sensitivity to specific anthropogenic activities, and existence of other known threats to the population.

The 40 marine mammal and sea turtle species known to occur in the study area have been ranked into five levels of conservation priority relative to the SAMP. The ranking has been done using the factors outlined above. The general characteristics of each priority level are summarized in Table 7, and the species included in each priority class are summarized in Table 8.

4.1 Priority 1

The highest priority level includes species that are common in the Rhode Island study area, that are known to occur in the SAMP area at least seasonally, and that are listed as Endangered under the U.S. Endangered Species Act. The North Atlantic right whale almost deserves to be in a category by itself. The species is one of the rarest mammals in the world, there is serious concern about long-term population viability, and there is known anthropogenic mortality from ship collisions, as well as from entanglement in commercial fishing gear. The populations of humpback whales and fin whales are at least an order of magnitude larger than the right whale's, but they can be abundant in or near the SAMP area, and they are also subject to human-caused mortality from ship strikes and fishery entanglements. Leatherback sea turtles are a global conservation priority, and are the most likely sea turtle species to be encountered in the SAMP area. Leatherbacks are subject to anthropogenic mortality from fishery entanglements, vessel collisions, and debris ingestion. Other threats not relevant to the SAMP region are loss or degradation of nesting habitat and intentional harvest of eggs and/or adults.

Table 7. Summarized definitions of the five levels used to prioritize conservation rankings of marine mammals and sea turtles relative to the Rhode Island Ocean Special Area Management Plan.

Rank	Defining characteristics
1	Species common in the Rhode Island study area, known to occur in the SAMP area at least seasonally, and listed as Endangered under the ESA
2	(a) ESA-listed species that are common in the Rhode Island study area, but not likely to occur more than rarely to occasionally in the SAMP area; (b) very abundant species likely to occur in significant numbers within the SAMP area at least seasonally
3	(a) ESA-listed species that are not known to occur in the SAMP area, but might visit irregularly or pass through undetected as juveniles; (b) species common in the study area, but likely to occur in the SAMP area only infrequently
4	(a) ESA-listed species with accidental occurrences over an extended period; (b) rare species with offshore distributions at the shelf edge and beyond; (3) common pinniped species with main centers of the distribution elsewhere and present in the study area mainly as dispersing juveniles
5	Very rare or accidental species, including ESA-listed species only occurring very recently

4.2 Priority 2

The second level of priority includes species in two different classes. The first would include sperm whales and loggerhead sea turtles. Both are ESA-listed, sperm whales as Endangered and loggerheads as Threatened, and both are common in the Rhode Island study area. However, neither species is likely to occur more than rarely to occasionally in the SAMP area, with sperm whales more likely offshore and loggerheads more offshore and to the southwest on the shelf. The other group includes four very abundant marine mammals. Harbor porpoises, Atlantic white-sided dolphins, and short-beaked common dolphins are probably the most abundant marine mammals in the study area, and all are likely to occur in significant numbers within the SAMP area at least seasonally. Harbor seals are the most common seal species in the study area, and are the only marine mammal that can be considered as resident in Rhode Island. They are known to occupy haul-out sites on the periphery of Block Island, where they could be subject to disturbance from development activities.

Table 8. Prioritized conservation rankings of 49 species of marine mammals and sea turtles relative to the Rhode Island Ocean Special Area Management Plan. Species listed as Endangered or Threatened under the U.S. Endangered Species Act are identified by *E* or *T*, respectively.*

Rank	Species included
1a	North Atlantic right whale (*E*)
1b	humpback whale (*E*), fin whale (*E*), leatherback sea turtle (*E*)
2	sperm whale (*E*), harbor porpoise, white-sided dolphin, short-beaked common dolphin, harbor seal, loggerhead sea turtle (*T*)
3	sei whale (*E*), common minke whale, long-finned pilot whale, Risso's dolphin, bottlenose dolphin, Kemp's ridley sea turtle (*E*), green sea turtle (*T* & *E*)
4	blue whale (*E*), pygmy sperm whale, dwarf sperm whale, Cuvier's beaked whale, Blainville's beaked whale, Gervais' beaked whale, Sowerby's beaked whale, True's beaked whale, striped dolphin, gray seal, harp seal, hooded seal
5	Bryde's whale, northern bottlenose whale, beluga, short-finned pilot whale, killer whale, false killer whale, white-beaked dolphin, Atlantic spotted dolphin, pantropical spotted dolphin, ringed seal, West Indian manatee (*E*)
na	Atlantic gray whale, pygmy killer whale, melon-headed whale, rough-toothed dolphin, spinner dolphin, Clymene dolphin, bearded seal, walrus, hawksbill sea turtle (*E*) [1 extirpated and 8 hypothetical species]

* the order of species within any ranking category does not imply any priority within that category; it is simply the order in which the species appear in this report.

4.3 Priority 3

The third level of priority includes five cetacean species and two sea turtles. Sei whales are considered regular in the Rhode Island study area and are ESA-listed as Endangered, however they are not likely to occur in the SAMP area, typically occur beyond the study area, and are only likely to visit the study area irregularly in a small number of years. Kemp's ridley and green sea turtles are ESA-listed, but have mainly tropical and sub-tropical distributions and are not known to occur in the SAMP area. However juveniles of both species are known to utilize shallow developmental habitats around eastern Long Island and Cape Cod and may well occur within or transit through the SAMP area. Minke whales, long-finned pilot whales, Risso's

dolphins, and bottlenose dolphins are all common species in the study area, but likely to occur in the SAMP area only infrequently.

4.4 Priority 4

The fourth level of priority includes mostly rare species with known centers of occurrence outside of the SAMP area, or even beyond the Rhode Island study area. Blue whales are endangered, but occur accidentally in southern New England, and have a long historical record of doing so in the region. Pygmy sperm whales, dwarf sperm whales, Cuvier's beaked whales, Blainville's beaked whales, Gervais' beaked whales, Sowerby's beaked whales, True's beaked whales, and striped dolphins are all regular or rare species in the study area with distributions that are primarily offshore—at the shelf edge and beyond. Gray seals, harp seals, and hooded seals are all common species in the study area and very frequently stranded. However, for all three species the majority of individuals in the study area appear to be dispersing juveniles, the main centers of the adult populations are elsewhere in the western North Atlantic, and the strandings appear to be simply a component of natural juvenile mortality.

4.5 Priority 5

The lowest level of priority includes all rare species, with many occurring only accidentally in the study area—Bryde's whale, northern bottlenose whale, beluga whale, short-finned pilot whale, killer whale, false killer whale, white-beaked dolphin, Atlantic spotted dolphin, pantropical spotted dolphin, ringed seal, and West Indian manatee. The manatee is the only ESA-listed species here, and it has a record of occurrence in the Northeast going back only to 1996.

4.6 Recommendations

In the event that a full EIS is required at some point in the future for a wind farm, other alternative energy project, or other commercial/industrial development, there could well be a need to estimate the levels of "take" of protected species. Calculating take estimates will require estimating the densities (animals per km^2) of each species present. The relative abundances generated in this technical report will not be sufficient, nor can statistically defensible density

estimates be derived from the data that we used. Only line-transect or similar surveys can produce density estimates. There are old seasonal, stratified density estimates from CETAP based on aerial line-transect surveys in 1979–1981 (CETAP, 1982; Kenney et al., 1985a). The sampling design was year-round, and there were two survey strata that could approximate the SAMP area. However, the sampling coverage was relatively low and was reduced each year of the project. Later NMFS aerial and shipboard surveys were designed to estimate stock abundances for the annual stock assessment reports (e.g., Waring et al., 2008) that were required under the 1994 amendments to the MMPA. However, the surveys were almost all in summer, the coverage was low with one-off surveys spaced several years apart, many of the surveys concentrated on offshore waters coverage, the objective was to generate one abundance estimate and not densities by local sampling areas, and the actual densities are not published in the stock assessments. The most recent attempt to generate density estimates was for the Navy (DoN, 2007), done by Geo-Marine, Inc. with input from NMFS Science Center staff. That project tried to break down the estimates into smaller areas, however they were based on only a subset of the NMFS aerial surveys, and again were mainly from summer (exclusively so in the vicinity of the SAMP study area). In addition, it is possible that those estimates have never been externally reviewed outside of the agencies involved in generating them.

New appropriately designed line-transect surveys might be necessary to generate regionally specific seasonal density estimates of protected species. They could be either aerial or shipboard surveys, however a combination of both would be ideal to capture species that are best sampled by only one or the other. An ideal survey program would need to run year-round to adequately capture seasonal variability, for at least 2–3 years to capture interannual variability, and at sufficient intensity and sample sizes to generate reliable estimates with reasonably low CVs. A statistical review of the previous line-transect surveys in the region and a power analysis would be necessary to define the level of survey intensity and frequency needed to generate robust density estimates for the SAMP area, but the required survey program clearly would not be a simple or inexpensive undertaking.

Passive acoustic monitoring (PAM) would be a valuable addition to future studies for species that regularly produce underwater sounds (i.e., cetaceans). PAM studies have an advantage over visual boat- or aircraft-based surveys in not being restricted by reduced visibilities at night or during adverse weather conditions. For vocalizing animals, PAM can generate very good

presence-absence information over extended periods on a continuous basis. Currently, however, it is not possible from PAM data alone to generate estimates of density or abundance, however that capability is an objective of on-going research. Tagging studies might provide additional data on habitat use and movement patterns of animals of concern for specific projects, for example small sea turtles or resident seals.

Relatively low-cost, long-term monitoring during the summer could be accomplished by supporting student interns who would ride on the whale-watching boat from Galilee and collect sighting records and associated effort data in standardized form. Such an intern could also assist the company in computerizing their previous logbooks for additional trend analyses. An additional, although lower-priority, project for such an intern would be incorporating any still-outstanding stranding data, including seal strandings from the Smithsonian for prior to 1993, Massachusetts marine mammal strandings, marine mammal strandings for 2006 and beyond, and full sea turtle stranding data.

5 Acknowledgements

Thanks are due to a large number of individuals, too many to thank separately by name, whose efforts went into creating the CETAP and NARWC databases. Thanks to NMFS for access to the stranding and bycatch datasets; and to Jim Mead at the Smithsonian for access to their historical data. We are grateful to the individuals who collected and/or provided sighting records from the various whale-watching boats in Galilee, Rhode Island and Montauk, New York, including Sam Sadove, Artie Kopelman, George Klein (who passed away unexpectedly while this SAMP project was on-going), and Charles Avenengo. Allison Seifter, an undergraduate work-study student, completed the task of deciphering Charles' hand-written log entries and entering the data into a computer spreadsheet. Helpful reviews of the draft report were contributed by Malia Schwartz, URI Dept. of Fisheries, Animal, and Veterinary Sciences; Jaclyn Daly, NMFS Office of Protected Resources; Molly Lutcavage, University of New Hampshire, and Eugenia Marks, Audubon Society of Rhode Island.

References

Addink, M., M. García Hartmann, and B. Couperus. 1997. A note on life-history parameters of the Atlantic white-sided dolphin (*Lagenorhynchus acutus*) form animals bycaught in the northeastern Atlantic. *Report of the International Whaling Commission* 47: 637–639.

Agler, B. A., R. L. Schooley, S. E. Frohock, S. K. Katona, and I. E. Seipt. 1993. Reproduction of photographically identified fin whales, *Balaenoptera physalus*, from the Gulf of Maine. *Journal of Mammalogy* 74: 577–587.

Aguilar, A. 1986. A review of old Basque whaling and its effect on the right whales (*Eubalaena glacialis*) of the North Atlantic. *Report of the International Whaling Commission, Special Issue* 10: 191–199.

Aguilar, A. 2002. Fin whale *Balaenoptera physalus*. Pp. 435–438 in: W. F. Perrin, B. Würsig, and H. G. M. Thewissen, eds. *Encyclopedia of Marine Mammals*. Academic Press, San Diego, CA.

Aguilar, A., and A. Borrell. 1994. Abnormally high polychlorinated biphenyl levels in striped dolphins *Stenella coeruleoalba* affected by the 1990–1992 Mediterranean epizootic. *Science of the Total Environment* 154: 237–247.

Aguilar, A., and J. A. Raga. 1993. The striped dolphin epizootic in the Mediterranean Sea. *Ambio* 22: 524–528.

Aguilar Soto, N., M. Johnson, P. T. Madsen, P. L. Tyack, A. Bocconcelli, and J. F. Borsani. 2006. Does intense ship noise disrupt foraging in deep-diving Cuvier's beaked whales (*Ziphius cavirostris*)? *Marine Mammal Science* 22: 690–699.

Aguirre, A., M. Sims, K. Durham, M. K. McGonagle, R. DiGiovanni, and S. Morreale. 2008. Assessment of sea turtle health in Peconic Bay of eastern Long Island. P. 108 in: R. B. Mast, B. J. Hutchinson, and A. H. Hutchinson, eds. *Proceedings of the Twenty-Fourth Annual Symposium on Sea Turtle Biology and Conservation*. NOAA Technical Memorandum NMFS-SEFSC-567. National Marine Fisheries Service, Miami, FL.

Allen, G. M. 1916. The whalebone whales of New England. *Memoirs of the Boston Society of Natural History* 8(2): 107–322.

Allen, J. A. 1880. *History of North American Pinnipeds. A Monograph of the Walruses, Sea-lions, Sea-bears and Seals of North America*. Miscellaneous Publications, No. 12. U.S. Geological and Geographical Survey of the Territories, Washington, DC. 785 pp.

Allen, J. A. 1908. The North Atlantic right whale and its near allies. *Bulletin of the American Museum of Natural History* 24: 277–329.

Allen, R. L. 1985. Dolphins and the purse-seine fishery for yellowfin tuna. Pp. 236–252 in: J. R. Beddington, R. J. H. Beverton, and D. M. Lavigne, eds. *Marine Mammals and Fisheries*. Allen and Unwin, Boston, MA.

Alling, A. K., and H. P. Whitehead. 1987. A preliminary study of the status of white-beaked dolphins, *Lagenorhynchus albirostris*, and other small cetaceans off the coast of Labrador. *Canadian Field-Naturalist* 101: 131–135.

Amano, M., and N. Miyazaki. 2004. Composition of a school of Risso's dolphins, *Grampus griseus. Marine Mammal Science* 20: 152–160.

Amano M., and M. Yoshioka. 2003. Sperm whale diving behavior monitored using a suction-cup-attached TDR tag. *Marine Ecology Progress Series* 258: 291–295.

Amos, B., C. Schlotterer, and D. Tauz. 1993. Social structure of pilot whales revealed by analytical DNA profiling. *Science* 260: 670–672.

Andrews, J. C., and P. R. Mott. 1967. Gray seals at Nantucket, Massachusetts. *Journal of Mammalogy* 48: 657–658.

Andrews, R. C. 1908. Notes upon the external and internal anatomy of *Balaena glacialis* Bonn. *Bulletin of the American Museum of Natural History* 24: 171–182.

Andrews, R. C. 1909. Further notes on *Eubalaena glacialis* (Bonn.). *Bulletin of the American Museum of Natural History* 26: 273–275.

Andrews, R. C. 1916. *Whale Hunting With Gun and Camera*. D. Appleton and Co., New York, NY. 333 pp.

Archer, F. I. II. 2002. Striped dolphin *Stenella coeruleoalba*. Pp. 1201–1203 in: W. F. Perrin, B. Würsig, and H. G. M. Thewissen, eds. *Encyclopedia of Marine Mammals*. Academic Press, San Diego, CA.

Archer, F. I. II, and W. F. Perrin. 1999. *Stenella coeruleoalba. Mammalian Species* 603: 1–9.

Archer, F. I. II, and K. M. Robertson. 2004. Age and length at weaning and development of diet of pan-tropical spotted dolphins, *Stenella attenuata*, from the eastern tropical Pacific. *Marine Mammal Science* 20: 232–245.

Árnason, Ú., and P. B. Best. 1991. Phylogenetic relationships within the Mysticeti (whalebone whales) based upon studies of highly repetitive DNA in all extant species. *Hereditas* 114: 263–269.

Árnason, Ú., and A. Gullberg. 1994. Relationship of baleen whales established by cytochrome *b* gene sequence comparison. *Nature* 367: 726–728.

Árnason, Ú., and A. Gullberg. 1996. Cytochrome *b* nucleotide sequences and the identification of five primary lineages of extant cetaceans. *Molecular Biology and Evolution* 13: 407–417.

Árnason, Ú., S. Grétarsdóttir, and B. Widegren. 1992. Mysticete (baleen whale) relationships based upon the sequence of the common cetacean DNA satellite. *Molecular Biology and Evolution* 9: 1018–1028.

Árnason, Ú., S. Grétarsdóttir, and B. Widegren. 1993. Cetacean mitochondrial DNA control region: sequences of all extant baleen whales and two sperm whale species. *Molecular Biology and Evolution* 10: 960–970.

ATM (Applied Technology & Management). 2007. *Final Report, RIWINDS, Phase I: Wind Energy Siting Study.* Applied Technology & Management, Inc., Newport, RI. 131 pp.

Au, W. W. L. 2002. Echolocation. Pp. 358–367 in: W. F. Perrin, B. Würsig, and J. G. M. Thewissen, eds. *Encyclopedia of Marine Mammals*. Academic Press, San Diego, CA.

August, P. V., R. D. Kenney, and T. P. Husband. 2001. Mammals. Pp. 60–66 in: P. V. August, R. W. Enser, and L. L. Gould, eds. *Vertebrates of Rhode Island*. Biota of Rhode Island, volume 2. Rhode Island Natural History Survey, Kingston, RI.

Austin, D., J. I. McMillan, and W. D. Bowen. 2003. A three-stage algorithm for filtering erroneous Argos satellite locations. *Marine Mammal Science* 19: 371–383.

Avens, L., J. C. Taylor, L. R. Goshe, T. T. Jones, and M. Hastings. 2009. Use of skeletochrononological analysis to estimate the age of leatherback sea turtles *Dermochelys coriacea* in the western North Atlantic. *Endangered Species Research* 8: 165–177.

Babcock, H. L. 1919. The turtles of New England. *Memoirs of the Boston Society of Natural History* 8(3): 325–431 + plates 17–32.

Baird, R. W. 2001. Status of harbor seals, *Phoca vitulina*, in Canada. *Canadian Field-Naturalist* 115: 663–675.

Baird, R. W. 2002a. False killer whale *Pseudorca crassidens*. Pp. 411–412 in: W. F. Perrin, B. Würsig, and H. G. M. Thewissen, eds. *Encyclopedia of Marine Mammals*. Academic Press, San Diego, CA.

Baird, R. W. 2002b. Risso's' dolphin *Grampus griseus*. Pp. 1037–1039 in: W. F. Perrin, B. Würsig, and H. G. M. Thewissen, eds. *Encyclopedia of Marine Mammals*. Academic Press, San Diego, CA.

Baird, R. W., D. Nelson, J. Lien, and D. W. Nagorsen. 1996. The status of the pygmy sperm whale, *Kogia breviceps*, in Canada. *Canadian Field-Naturalist* 110: 525–532.

Baker, A. S., K. L. Ruoff, and S. Madoff. 1998. Isolation of *Mycoplasma* species from a patient with seal finger. *Clinical Infectious Disease* 27: 1168–1170.

Baker, C. S., R. W. Slade, J. L. Bannister, R. B. Abernethy, M. T. Weinrich, J. Lien, J. Urban, P. Corkeron, J. Calambokidis, O. Vazquez, and S. R. Palumbi. 1994. The hierarchical structure of mitochondrial DNA gene flow among humpback whales worldwide. *Molecular Ecology* 3: 313–327.

Balcomb, K. C., and D. Claridge. 2001. A mass stranding of cetaceans caused by naval sonar. *Bahamas Journal of Science* 5: 2–12.

Bannister, J. L. 2002. Baleen whales. Pp. 62–72 in: W. F. Perrin, B. Würsig, and H. G. M. Thewissen, eds. *Encyclopedia of Marine Mammals*. Academic Press, San Diego, CA.

Barkham, S. H. 1984. The Basque whaling establishments in Labrador 1536–1632—a summary. *Arctic* 37: 515–519.

Barlow, J., and P. J. Clapham. 1997. A new birth-interval approach to estimating demographic parameters of humpback whales. *Ecology* 78: 535–546.

Barnes, L. G. 2002a. Cetacea, overview. Pp. 204–208 in: W. F. Perrin, B. Würsig, and H. G. M. Thewissen, eds. *Encyclopedia of Marine Mammals*. Academic Press, San Diego, CA.

Barnes, L. G. 2002b. Delphinoids, evolution of the modern families. Pp. 314–316 in: W. F. Perrin, B. Würsig, and H. G. M. Thewissen, eds. *Encyclopedia of Marine Mammals*. Academic Press, San Diego, CA.

Barros, N. B., and D. K. Odell. 1990. Food habits of bottlenose dolphins in the southeastern United States. Pp. 309–328 in: S. Leatherwood and R. R. Reeves, eds. *The Bottlenose Dolphin.* Academic Press, San Diego, CA.

Barros, N. B., and R. W. Wells. 1998. Prey and feeding patterns of resident bottlenose dolphins (*Tursiops truncatus*) in Sarasota Bay, Florida. *Journal of Mammalogy* 79: 1045–1049.

Barros, N. B., D. A. Duffield, P. H. Ostrom, D. K. Odell, and V. R. Cornish. 1998. Nearshore vs. offshore ecotype differentiation of *Kogia breviceps* and *K. simus* based on hemoglobin, morphometric and dietary analyses. World Marine Mammal Science Conference Abstracts, Society for Marine Mammalogy, Lawrence, KS.

Baumgartner, M. F., and B. R. Mate. 2003. Summertime foraging ecology of North Atlantic right whales. *Marine Ecology Progress Series* 264: 123–135.

Baumgartner, M. F., T. V. N. Cole, P. J. Clapham and B. R. Mate. 2003a. North Atlantic right whale habitat in the lower Bay of Fundy and on the SW Scotian Shelf during 1999–2001. *Marine Ecology Progress Series* 264: 137–154.

Baumgartner, M. F., T. V. N. Cole, R. G. Campbell, G. J. Teegarden and E. G. Durbin. 2003b. Associations between North Atlantic right whales and their prey, *Calanus finmarchicus*, over diel and tidal time scales. *Marine Ecology Progress Series* 264: 155–166.

Baumgartner, M. F., C. A. Mayo, and R. D. Kenney. 2007. Enormous carnivores, microscopic food, and a restaurant that's hard to find. Pp. 138–171 in: S. D. Kraus and R. M. Rolland, eds. *The Urban Whale: North Atlantic Right Whales at the Crossroads*. Harvard University Press, Cambridge, MA.

Beardsley, R. C., A. W. Epstein, C. Chen, K. F. Wishner, M. C. Macaulay, and R. D. Kenney. 1996. Spatial variability in zooplankton abundance near feeding right whales in the Great South Channel. *Deep-Sea Research* 43: 1601–1625.

Beck, C. A., J. I. McMillan, and W. D. Bowen. 2002. An algorithm to improve geolocation positions using sea surface temperature and diving depth. *Marine Mammal Science* 18: 940–951.

Beddington, J. R., R. J. H. Beverton, and D. M. Lavigne. 1985. *Marine Mammals and Fisheries.* George Allen & Unwin, London. xxi + 354 pp.

Béland, P. 1996. The belugas of the St. Lawrence River. *Scientific American* 274(5): 74–81.

Béland, P., S. De Guise, C. Girard, A. Lagacé A., D. Martineau, R. Michaud, D. C. G. Muir, R. J. Norstrom, É. Pelletier, S. Ray, and L. R. Shugart. 1993. Toxic compounds and health and reproductive effects in St. Lawrence beluga whales. *Journal of Great Lakes Research* 19: 766–775

Bernard, H. J., and S. B. Reilly. 1999. Pilot whales *Globicephala* Lesson, 1828. Pp. 245–279 in: S. H. Ridgway and R. Harrison, eds. *Handbook of Marine Mammals. Volume 6: The Second Book of Dolphins and the Porpoises.* Academic Press, London.

Bérubé, M., A. Aguilar, D. Dendanto, F. Larsen, G. Notarbartolo di Sciara, R. Sears, J. Sigurjónsson, J. Urbán-R., and P. J. Palsbøll. 1998. Population genetic structure of North Atlantic, Mediterranean, and Sea of Cortez fin whales, *Balaenoptera physalus* (Linnaeus, 1758): analysis of mitochondrial and nuclear loci. *Molecular Ecology* 15: 585–599.

Bérubé, M., M. B. Rew, T. Cole, S. L. Swartz, E. Zolman, N. Øien, and P. J. Palsbøll. 2004. Genetic identification of an individual humpback whale between the eastern Caribbean and the Norwegian Sea. *Marine Mammal Science* 20: 657–663.

Best, P. B. 1966. A case for prolonged lactation in the fin whale. *Norsk Hvalfangst-tidende* 55: 118–122.

Best, P. B. 1974. The biology of the sperm whale as it relates to stock management. Pp. 257–293 in: W. E. Schevill, ed. The *Whale Problem: A Status Report*. Harvard University Press, Cambridge, MA.

Best, P. B. 1977. Two allopatric forms of Bryde's whale off South Africa. *Report of the International Whaling Commission, Special Issue* 1: 10–38.

Best, P. B. 1979. Social organization in sperm whales, *Physeter macrocephalus*. Pp. 227–289 in: H. E. Winn and B. L. Olla, eds. *Behavior of Marine Animals: Current Perspectives in Research. Volume 3: Cetaceans.* Plenum Press, New York, NY.

Best, P. B. 1990. Natural markings and their use in determining calving intervals in right whales off South Africa. *South African Journal of Zoology* 25: 114–123.

Best, P. B. 1994. Seasonality of reproduction and the length of gestation in southern right whales *Eubalaena australis*. *Journal of Zoology*, London 232: 175–189.

Best, P. B., A. Brandão, and D. S. Butterworth. 2001. Demographic parameters of southern right whales off South Africa. *Journal of Cetacean Research and Management, Special Issue* 2: 161–169.

Bigg, M. A. 1981. Harbour seal *Phoca vitulina* Linnaeus, 1758 and *Phoca largha* Pallas, 1811. Pp. 1–27 in: S. H. Ridgway and R. Harrison, eds. *Handbook of Marine Mammals. Volume 2: Seals.* Academic Press, London.

Bjørge, A., and K. A. Tolley. 2002. Harbor porpoise *Phocoena phocoena*. Pp. 549–551 in: W. F. Perrin, B. Würsig, and J. G. M. Thewissen, eds. *Encyclopedia of Marine Mammals*. Academic Press, San Diego, CA.

Bjorndal, K. A. 1985. Nutritional ecology of sea turtles. *Copeia* 1985: 736–751.

Bjorndal, K. A. 1995. The consequences of herbivory for the life history pattern of the Caribbean green turtle, *Chelonia mydas*. Pp. 111–116 in: K. A. Bjorndal, ed. *Biology and Conservation of Sea Turtles*, Revised Edition. Smithsonian Institution Press, Washington, DC.

Bjorndal, K. A. 1997. Foraging ecology and nutrition of sea turtles. Pp. 199–231 in: P. L. Lutz and J. A. Musick, eds. *The Biology of Sea Turtles.* CRC Press, Boca Raton, FL.

Bleakney, J. S. 1965. Reports of marine turtles from New England and eastern Canada. *Canadian Field-Naturalist* 79: 120–128.

Bolten, A. B. 2003. Active swimmers—passive drifters: the oceanic juvenile stage of loggerheads in the Atlantic system. Pp. 63–78 in: A. B. Bolten and B. E. Witherington, eds. *Loggerhead Sea Turtles.* Smithsonian Books, Washington, DC.

Bonness, D. J., W. D. Bowen, and O. T. Oftedal. 1988. Evidence of polygyny from spatial patterns of hooded seals (*Cystophora cristata*). *Canadian Journal of Zoology* 66: 703–

706.

Bonner, W. N. 1972. The grey seal and common seal in European waters. *Oceanography and Marine Biology Annual Review* 10: 461–507.

Bonner, W. N. 1981. Grey seal *Halichoerus grypus* Fabricius, 1791. Pp. 111–144 in: S. H. Ridgway and R. Harrison, eds. *Handbook of Marine Mammals. Volume 2: Seals.* Academic Press, London.

Bossart, G. D., D. K. Odell, and N. H. Altman. 1985. Cardiomyopathy in stranded pygmy and dwarf sperm whales. *Journal of the American Veterinary Medical Association* 187: 1137–1140.

Boulva, J., and I. A. McLaren. 1979. Biology of the harbour seal, *Phoca vitulina*, in eastern Canada. *Bulletin of the Fisheries Research Board of Canada* 200: 1–25.

Bowen, B. W., J. C. Avise, J. I. Richardson, A. B. Meylan, D. Margaritoulis, and S. R. Hopkins-Murphy. 1993. Population structure of loggerhead turtles (*Caretta caretta*) in the northwestern Atlantic Ocean and Mediterranean Sea. *Conservation Biology* 7: 834–844.

Bowen, W. D., and G. Harrison. 1994. Offshore diet of gray seals *Halichoerus grypus* near Sable Island, Canada. *Marine Ecology Progress Series* 112: 1–11.

Bowen, W. D., O. T. Oftedal, and D. J. Boness. 1985. Birth to weaning in 4 days: Remarkable growth in the hooded seal. *Canadian Journal of Zoology* 63: 2841–2846.

Bowen, W. D., J. W. Lawson, and B. Beck. 1993. Seasonal and geographic variation in the species composition and size of prey consumed by grey seals (*Halichoerus grypus*) on the Scotian Shelf. *Canadian Journal of Fisheries and Aquatic Sciences* 50: 1768–1778.

Boyd, I. L., C. Lockyer, and H. D. Marsh. 1999. Reproduction in marine mammals. Pp. 218–286 in: J. E. Reynolds III and S. A. Rommel, eds. *Biology of Marine Mammals*. Smithsonian Institution Press, Washington, DC.

Brennin, R., B. W. Murray, M. K. Friesen, L. D. Maiers, J. W. Clayton, and B. N. White. 1997. Population genetic structure of beluga whales (*Delphinapterus leucas*): mitochondrial DNA sequence variation within and among North American populations. *Canadian Journal of Zoology* 75:795–802.

Brodie, P. F. 1989. The white whale *Delphinapterus leucas* (Pallas, 1776). Pp. 119–144 in: S. H. Ridgway and R. Harrison, eds. *Handbook of Marine Mammals. Volume 4: River Dolphins and the Larger Toothed Whales.* Academic Press, London.

Brodie, P., and B. Beck. 1983. Predation by sharks on the grey seal (*Halichoerus grypus*) in eastern Canada. *Canadian Journal of Fisheries and Aquatic Sciences* 40: 267–271.

Brongersma, L. D. 1972. European Atlantic turtles. *Zoologische Verhandelinger* 121: 1–317

Brongersma, L. D. 1995. Marine turtles in the eastern Atlantic Ocean. Pp. 407-416 in: K. A. Bjorndal, ed. *Biology and Conservation of Sea Turtles*, Revised Edition. Smithsonian Institution Press, Washington, DC.

Brown, M. W., S. Brault, P. K. Hamilton, R. D. Kenney, A. R. Knowlton, M. K. Marx, C. A. Mayo, C. K. Slay, and S. D. Kraus. 2001. Sighting heterogeneity of right whales in the

western North Atlantic: 1980–1992. *Journal of Cetacean Research and Management, Special Issue* 2: 245–250.

Brown, S. G. 1986. Twentieth-century records of right whales (*Eubalaena glacialis*) in the northeast Atlantic Ocean. *Report of the International Whaling Commission, Special Issue* 10: 121–127.

Brown Gladden, J. G., M. M. Ferguson, and J. W. Clayton. 1997. Matriarchal genetic population structure of North American beluga whales *Delphinapterus leucas* (Cetacea: Monodontidae). *Molecular Ecology* 6: 1033–1046.

Brown Gladden, J. G., P. F. Brodie, and J. W. Clayton. 1999a. Mitochondrial DNA used to identify an extralimital beluga whale (*Delphinapterus leucas*) from Nova Scotia as originating from the St. Lawrence population. *Marine Mammal Science* 15: 556–558.

Brown Gladden, J. G., M. M. Ferguson, M. K. Friesen, and J. W. Clayton. 1999b. Population structure of North American beluga whales (*Delphinapterus leucas*) based on nuclear DNA microsatellite variation and contrasted with the population structure revealed by mitochondrial DNA variation. *Molecular Ecology* 8: 347–363.

Bryant, P. J. 1995. Dating remains of gray whales from the eastern North Atlantic. *Journal of Mammalogy* 76: 857–861.

Bryant, P. J., G. Nichols, T. B. Bryant, and K. Miller. 1981. Krill availability and the distribution of humpback whales in southeastern Alaska. *Journal of Mammalogy* 62: 427–430.

Buckland, S. T., D. Bloch, K. L. Cattanach, T. Gunnlaugsson, K. Hoydal, S. Lens, and S. Sigurjónsson. 1993. Distribution and abundance of long-finned pilot whales in the North Atlantic, estimated from NASS-87 and NASS-89 data. *Report of the International Whaling Commission, Special Issue* 14: 33–49.

Burke, V. J., E. A. Standora, and S. J. Morreale. 1991. Factors affecting strandings of cold-stunned juvenile Kemp's ridley and loggerhead sea turtles in Long Island, New York. *Copeia* 1991: 1136–1138.

Burke, V. J., E. A. Standora, and S. J. Morreale. 1993. Diet of juvenile Kemp's ridley and loggerhead sea turtles from Long Island, New York. *Copeia* 1993: 1176–1180.

Burke, V. J., S. J. Morreale, and E. A. Standora. 1994. Dietary composition of Kemp's ridley sea turtles in the waters of New York. *Fishery Bulletin* 92: 26–32.

Burnell, S. R. 2001. Aspects of the reproductive biology, movements and site fidelity of right whales off Australia. *Journal of Cetacean Research and Management, Special Issue* 2: 89–102.

Burns, J. J. 2002. Harbor seal and spotted seal *Phoca vitulina* and *P. largha*. Pp. 552–560 in: W. F. Perrin, B. Würsig, and H. G. M. Thewissen, eds. *Encyclopedia of Marine Mammals*. Academic Press, San Diego, CA.

Caldwell, D. K., and M. C. Caldwell. 1969. The harbor seal, *Phoca vitulina concolor*, in Florida. *Journal of Mammalogy* 50: 379–380.

Caldwell, D. K., and M. C. Caldwell. 1971. Beaked whales, *Ziphius cavirostris*, in the Bahamas. *Florida Academy of Science Quarterly Journal* 34: 157–160.

Caldwell, D. K., and M. C. Caldwell. 1985. Manatees *Trichechus manatus* Linnaeus, 1758; *Trichechus senegalensis* Link, 1795 and *Trichechus inunguis* (Natterer, 1883). Pp. 33–66 in: S. H. Ridgway and R. Harrison, eds. *Handbook of Marine Mammals. Volume 3: The Sirenians and Baleen Whales*. Academic Press, London.

Caldwell, D. K., and M. C. Caldwell. 1989. Pygmy sperm whale *Kogia breviceps* (de Blainville, 1838): dwarf sperm whale *Kogia simus* Owen, 1866. Pp. 235–260 in: S. H. Ridgway and R. Harrison, eds. *Handbook of Marine Mammals. Volume 4: River Dolphins and the Larger Toothed Whales.* Academic Press, London.

Caldwell, D. K., and F. B. Golley. 1965. Marine mammals from the coast of Georgia to Cape Hatteras. *Journal of the Elisha Mitchell Scientific Society* 81: 24–32.

Caldwell, D. K., M. C. Caldwell, and D. W. Rice. 1966. Behavior of the sperm whale *Physeter catodon* L. Pp. 677–717 in: K.S. Norris, ed. *Whales, Dolphins, and Porpoises.* University of California Press, Berkeley, CA.

Caldwell, D. K., H. Neuhauser, M. C. Caldwell, and H. W. Coolidge. 1971. Recent records of marine mammals from the coasts of Georgia and South Carolina. *Cetology* 5: 1–12.

Campana, S. E., J. Gibson, J. Brazner, L. Marks, W. Joyce, J.-F. Gosselin, R. D. Kenney, P. Shelton, M. Simpson, and J. Lawson. 2008. *Status of Basking Sharks in Atlantic Canada/État du Requin-Pèlerin de l'Atlantique Canadien.* CSAS Research Document 2008/004. Canadian Science Advisory Secretariat, Department of Fisheries and Oceans, Dartmouth, Nova Scotia, Canada. 67 pp.

Cardoza, J. E., G. S. Jones, and T. W. French. 2006. MassWildlife's State Mammal List. Massachusetts Division of Fish and Wildlife, Boston, MA. http://www.mass.gov/dfwele/dfw/dfwmam.htm

Carpenter, R. G., 2nd, and H. R. Sigler. 1958. *A List of New Hampshire Mammals and Their Distribution*. New Hampshire Fish and Game Dept., Concord, NH. 20 pp.

Carr, A. 1963. Panspecific reproductive convergence in *Lepidochelys kempi*. *Ergebnisse der Biologie 26: 298–303.*

Carr, A. 1967. *So Excellent a Fishe: A Natural History of Sea Turtles*. Natural History Press, New York, NY. x + 248 pp.

Carr, A. 1980. Some problems of sea turtle ecology. *American Zoologist* 20: 489–498.

Carr, A. 1986. Rips, FADs and little loggerheads. *Bioscience* 36: 92–100.

Carr, A. 1987. New perspectives on the pelagic stage of sea turtle development. *Conservation Biology* 1: 103–121.

Carr, A. 1995. Notes on the behavioral ecology of sea turtles. Pp. 19-26 in: K. A. Bjorndal, ed. *Biology and Conservation of Sea Turtles*, Revised Edition. Smithsonian Institution Press, Washington, DC.

Carr, A., and A. B. Meylan. 1980. Evidence of passive migration of green turtle hatchlings in sargassum. Copeia 1980: 366–368.

CETAP (Cetacean and Turtle Assessment Program, University of Rhode Island). 1982. *A Characterization of Marine Mammals and Turtles in the Mid- and North Atlantic Areas*

of the U. S. Outer Continental Shelf, Final Report. Contract AA551-CT8-48. Bureau of Land Management, Washington, DC. 586 pp

Christal, J., H. Whitehead, and E. Lettevall. 1998. Sperm whale social units: variation and change. *Canadian Journal of Zoology* 76: 1431–1440.

Christensen, I., T. Haug, and N. Øien. 1992. A review of feeding and reproduction in large baleen whales (Mysticeti) and sperm whales *Physeter macrocephalus* in Norwegian and adjacent waters. *Fauna Norvegica*, Series A 13: 39–48.

Cipriano, F. 1997. Antitropical distributions and speciation in dolphins of the genus *Lagenorhynchus*: a preliminary analysis. Pp. 305–316 in: A. E. Dizon, S. J. Chivers, and W. F. Perrin, eds. *Molecular Genetics of Marine Mammals*. Special Publication no. 3. Society for Marine Mammalogy, Lawrence, KS.

Cipriano, F. 2002. Atlantic white-sided dolphin *Lagenorhynchus acutus*. Pp. 49–51 in: W. F. Perrin, B. Würsig, and H. G. M. Thewissen, eds. *Encyclopedia of Marine Mammals*. Academic Press, San Diego, CA.

Clapham, P. J. 1992. Age at attainment of sexual maturity in humpback whales, *Megaptera novaeangliae*. *Canadian Journal of Zoology* 70: 1470–1472.

Clapham, P. J. 1996. The social and reproductive biology of humpback whales: an ecological perspective. *Mammal Review* 26: 27–49.

Clapham, P. J. 2002. Humpback whale *Megaptera novaeangliae*. Pp. 589–592 in: W. F. Perrin, B. Würsig, and H. G. M. Thewissen, eds. *Encyclopedia of Marine Mammals*. Academic Press, San Diego, CA.

Clapham, P. J., and C. A. Mayo. 1987. Reproduction and recruitment of individually identified humpback whales, *Megaptera novaeangliae*, observed in Massachusetts Bay, 1979–1985. *Canadian Journal of Zoology* 65: 2853–2863.

Clapham, P. J., and C. A. Mayo. 1990. Reproduction of humpback whales (*Megaptera novaeangliae*) in the Gulf of Maine. *Report of the International Whaling Commission, Special Issue* 12: 171–175.

Clapham, P. J., and I. E. Seipt. 1991. Resightings of independent fin whales, *Balaenoptera physalus*, on maternal summer ranges. *Journal of Mammalogy* 72: 788–790.

Clapham, P. J., P. J. Palsbøll, D. K. Mattila, and O. Vásquez. 1992. Composition and dynamics of humpback whale competitive groups in the West Indies. *Behaviour* 122: 182–194.

Clapham, P. J., L. S. Baraff, C. A. Carlson, M. A. Christian, D. K. Mattila, C. A. Mayo, M. A. Murphy, and S. Pittman. 1993a. Seasonal occurrence and annual return of humpback whales, *Megaptera novaeangliae*, in the southern Gulf of Maine. *Canadian Journal of Zoology* 71: 440–443.

Clapham, P. J., D. K. Mattila, and P. J. Palsbøll. 1993b. High-latitude-area composition of humpback whale competitive groups in Samana Bay: further evidence for panmixis in the North Atlantic population. *Canadian Journal of Zoology* 71: 440–443.

Clapham, P. J., S. Leatherwood, I. Szczepaniak, and R. L. Brownell, Jr. 1997. Catches of humpback and other whales from shore stations at Moss Landing and Trinidad, California, 1919–1926. *Marine Mammal Science* 13: 368–394.

Clapham, P. J., S. B. Young, and R. L. Brownell, Jr. 1999. Baleen whales: conservation issues and the status of the most endangered populations. *Mammal Review* 29: 35–60.

Clapham, P. J., J. Barlow, T. Cole, D. K. Mattila, R. Pace, D. Palka, J. Robbins, and R. Seton. 2003. Stock definition, abundance and demographic parameters of humpback whales from the Gulf of Maine. *Journal of Cetacean Research and Management* 4: 135–141.

Clark, A. H. 1887. History and present condition of the fishery. Pp. 3–218 in: G. B. Goode, ed. *The Fisheries and Fishery Industries of the United States. Section 5. History and Methods of the Fisheries. Volume 2, Part 15. The Whale Fishery*. Government Printing Office, Washington, DC.

Clark, C. W. 1995. Annex M. Matters arising out of the discussion of blue whales; Annex M1. Application of the US Navy underwater hydrophone arrays for scientific research on whales. *Report of the International Whaling Commission* 45: 210–212.

Clarke, M. R. 1986. Cephalopods in the diet of odontocetes. Pp. 282–321 in: M. M. Bryden and R. Harrison, eds. *Research on Dolphins*. Clarendon Press, Oxford, UK.

Claussen, D., V. Strauss, S. Ising, M. Jager, T. Schneider, and M. Stoye. 1991a. The helminth fauna from the common seal (*Phoca vitulina*, Linne, 1758) of the Wadden Sea in Lower Saxony. Part 1: Trematodes, cestodes, and acanthocephalans. *Zentralblatt für Veterinärmedizin* B 38: 641–648.

Claussen, D., V. Strauss, S. Ising, M. Jager, T. Schneider, and M. Stoye. 1991b. The helminth fauna from the common seal (*Phoca vitulina*, Linne, 1758) of the Wadden Sea in Lower Saxony. Part 2: Nematodes. *Zentralblatt für Veterinärmedizin* B 38: 649–656.

Clement, R. C. 1952. An Annotated Check-list of the Land Mammals of Rhode Island. Audubon Society of Rhode Island, Providence, RI. 8 pp.

Coakes, A., S. Gowans, P. Simard, J. Giard, C. Vashro, and R. Sears. 2005. Photographic identification of fin whales (*Balaenoptera physalus*) off the Atlantic coast of Nova Scotia, Canada. *Marine Mammal Science* 21: 323–326.

Cockcroft, V. G., A. C. De Kock, D. A. Lord, and G. J. B. Ross. 1989b. Organochlorines in bottlenose dolphins *Tursiops truncatus* from the east coast of South Africa. *South African Journal of Marine Science* 8: 207–217.

Collard, S. B., and L. H. Ogren. 1990. Dispersal scenarios for pelagic post-hatchling sea turtles. *Bulletin of Marine Science* 47: 233–243.

Collett, R. 1909. A few notes on the whale *Balaena glacialis* and its capture in recent years in the North Atlantic by Norwegian whalers. *Proceedings of the Zoological Society of London* 1909: 91–98.

Collette, B. B., and G. Klein-MacPhee, eds. 2002. *Bigelow and Schroeder's Fishes of the Gulf of Maine,* third edition. Smithsonian Press, Washington, DC. xxxiv + 748 pp.

Connor, P. F. 1971. *The Mammals of Long Island, New York*. Bulletin 146. New York State Museum & Science Service, Albany, NY. v + 78 pp.

Connor, R. C., R. A. Smolker, and A. F. Richards. 1992. Dolphin alliances and coalitions. Pp. 415–443 in: A. H. Harcourt and F. B. M. de Waal, eds. *Coalitions and Alliances in Humans and Other Animals*. Oxford University Press, Oxford, UK.

Connor, R. C., R. S. Wells, J. Mann, and A. J. Read. 2000. The bottlenose dolphin: social relationships in a fission-fusion society. Pp. 91–126 in: J. Mann, R. C. Connor, P. L. Tyack, and H. Whitehead, eds. *Cetacean Societies: Field Studies of Dolphins and Whales*. University of Chicago Press, Chicago, IL.

Cooke, J., V. J. Rowntree, and R. Payne. 2001. Estimates of demographic parameters for southern right whales (*Eubalaena australis*) observed off Peninsula Valdés, Argentina. *Journal of Cetacean Research and Management, Special Issue* 2: 125–132.

Cosby, S. L., S. McQuaid, N. Duffy, C. Lyons, B. K. Rima, G. M. Allen, S. J. McCullough, S. Kennedy, J. A. Smyth, F. McNeilly, and C. Orvell. 1988. Characterization of a seal morbillivirus. *Nature* 336: 115–116.

Couperus, B. 1997. Interactions between Dutch midwater trawl and Atlantic white-sided dolphins (*Lagenorhynchus acutus*) southwest of Ireland. *Journal of Northwest Atlantic Fisheries Science* 22: 209–218.

Cox, T. M., T. Ragen, A. J. Read, E. Vos, R. W. Baird, K. Balcomb, J. Barlow, J. Caldwell, T. Cranford, L. Crum, A. D'Amico, G. D'Spain, A. Fernandez, J. Finneran, R. Gentry, W. Gerth, F. Gulland, J. Hildebrand, D. Houser, T. Hullar, P. D. Jepson, D. Ketten, C. D. MacLeod, P. Miller, S. Moore, D. Mountain, D. Palka, P. Ponganis, S. Rommel, T. Rowles, B. Taylor, P. Tyack, D. Wartzok, R. Gisiner, J. Mead, and L. Benner. 2006. Understanding the impacts of anthropogenic sound on beaked whales. *Journal of Cetacean Research and Management* 7: 177–187.

Craig, A., and L. M. Herman. 2000. Habitat preferences of female humpback whales *Megaptera novaeangliae* in the Hawaiian Islands are associated with reproductive status. *Marine Ecology Progress Series* 193: 209–216.

Cranford, T. W. 2000. In search of impulse sound sources in odontocetes. Pp. 109–156 in: W. W. L. Au, A. N. Popper, and F. R. Fay, eds. *Hearing By Whales and Dolphins*. Springer-Verlag, New York, NY.

Cranford, T. W., M. Amundin, and K. S. Norris. 1996. Functional morphology and homology in the odontocete nasal complex—implications for sound generation. *Journal of Morphology* 228: 223–285.

Cronan, J. M., and A. Brooks. 1968. *The Mammals of Rhode Island*. Wildlife Pamphlet no. 6. Rhode Island Dept. of Agriculture and Conservation, Division of Fish and Game, Providence, RI. ix + 133 pp.

Cummings, W. C. 1985a. Bryde's whale *Balaenoptera edeni* Anderson, 1878. Pp. 137–154 in: S. H. Ridgway and R. Harrison, eds. *Handbook of Marine Mammals. Volume 3: The Sirenians and Baleen Whales.* Academic Press, London.

Cummings, W. C. 1985b. Right whales *Eubalaena glacialis* (Müller, 1776) and *Eubalaena*

australis (Desmoulins, 1822). Pp. 275–304 in: S. H. Ridgway and R. Harrison, eds. *Handbook of Marine Mammals. Volume 3: The Sirenians and Baleen Whales.* Academic Press, London.

CWS (Canadian Wildlife Service). 2006. Species at risk. Canadian Wildlife Service, Ottawa, Ontario. http://www.speciesatrisk.gc.ca/default_e.cfm

D'Agrosa, C., O. Vidal, and W. C. Graham. 1995. Mortality of the vaquita (*Phocoena sinus*) in gillnet fisheries during 1993–94. *Report of the International Whaling Commission, Special Issue* 16: 283–291.

Dahlheim, M. E., and J. E. Heyning. 1999. Killer whale *Orcinus orca* (Linnaeus, 1758). Pp. 281–322 in: S. H. Ridgway and R. Harrison, eds. *Handbook of Marine Mammals. Volume 6: The Second Book of Dolphins and the Porpoises.* Academic Press, London.

Dalebout, M. L., D. E. Ruzzante, H. Whitehead, and N. Øien. 2006. Nuclear and mitochondrial markers reveal distinctiveness of a small population of bottlenose whales, *Hyperoodon ampullatus*, in the western North Atlantic. *Molecular Ecology* 15: 3115–3129.

Davis, R. W., G. A. J. Worthy, B. Würsig, and S. K. Lynn. 1996. Diving behavior and at-sea movements of an Atlantic spotted dolphin in the Gulf of Mexico. *Marine Mammal Science* 12: 569–581.

De Guise S., A. Lagacé, and P. Béland. 1994. True hermaphroditism in a St. Lawrence beluga whale (*Delphinapterus leucas*). *Journal of Wildlife Diseases* 30: 287–290.

De Guise S., D. Martineau, P. Béland, and M. Fournier. 1998. Effects of in vitro exposure of beluga whale leukocytes to selected organochlorines. *Journal of Toxicology and Environmental Health* A 55: 479–493.

De Kay, J. E. 1824. An account of the *Phoca cristata*, recently taken in the vicinity of this city. *Annals of the Lyceum of Natural History of New York* 1: 94–99.

De Kay, J. E. 1842. *Zoology of New York; or, the New York Fauna; Comprising Detailed Descriptions of All the Animals Hitherto Observed Within the State of New York; With Brief Notices of Those Occasionally Found Near Its Borders, and Accompanied by Appropriate Illustrations. Part I. Mammalia*. W. & A. White and J. Visscher, Albany, NY. 188 pp.

Desportes, G., and R. Mouritsen. 1993. Preliminary results on the diet of long-finned pilot whales off the Faeroe Islands. *Report of the International Whaling Commission, Special Issue* 14: 305–324.

Desportes, G., M. Saboreay, and A. Lacroix. 1993. Reproductive maturity and seasonality of male long-finned pilot whales, off the Faroe Islands. *Report of the International Whaling Commission, Special Issue* 14: 233–262.

Dickson, D. 1988. Canine distemper may be killing North Sea seals. *Science* 241: 1284.

Dietz, R., C. T. Hanse, P. Have, and M.-P. Heide-Jørgensen. 1989a. Clue to seal epizootic. *Nature* 338: 627.

Dietz, R., M.-P. Heide-Jørgensen, and T. Härkönen. 1989b. Mass deaths of harbor seals (*Phoca vitulina*) in Europe. *Ambio* 18: 258–264.

Dodge, K. D., R. Prescott, D. Lewis, D. Murley, and C. Merigo. 2008. A review of cold stun strandings on Cape Cod, Massachusetts from 1979–2003. P. 123 in: R. B. Mast, B. J. Hutchinson, and A. H. Hutchinson, eds. *Proceedings of the Twenty-Fourth Annual Symposium on Sea Turtle Biology and Conservation*. NOAA Technical Memorandum NMFS-SEFSC-567. National Marine Fisheries Service, Miami, FL.

DoN (Department of the Navy). 2005. *Marine Resources Assessment for the Northeast Operating Areas: Atlantic City, Narragansett Bay, and Boston.* Technical report, contract number N62470-02-D-9997, task order number 0018. Naval Facilities Engineering Command, Norfolk, VA and Geo-Marine, Inc., Plano, TX. 554 pp.

DoN (Department of the Navy). 2007. *Navy OPAREA Density Estimates (NODE) for the Northeast OPAREAS: Boston, Narragansett Bay, and Atlantic City.* Technical report, contract number N62470-02-D-9997, task order number 0045. Naval Facilities Engineering Command, Norfolk, VA and Geo-Marine, Inc., Plano, TX. 216 pp.

Donovan, G. P. 1991. A review of IWC stock boundaries. *Report of the International Whaling Commission, Special Issue* 13: 39–68.

Dufault, S., H. Whitehead, and M. Dillon. 1999. An examination of the current knowledge on the stock structure of sperm whales (*Physeter macrocephalus*) worldwide. *Journal of Cetacean Research and Management* 1: 1–10.

Duignan, P. J., S. Sadove, J. T. Saliki, and J. R. Geraci. 1993. Phocine distemper in harbor seals (*Phoca vitulina*) from Long Island, New York. *Journal of Wildlife Diseases* 29: 465–469.

Duignan, P. J., J. T. Saliki, D. J. St. Aubin, G. Early, S. Sadove, J. A. House, K. Kovacs, and J. R. Geraci. 1995. Epizootiology of morbillivirus infection in North American harbor seals (*Phoca vitulina*) and gray seals (*Halichoerus grypus*). *Journal of Wildlife Diseases* 31: 491–501.

Duignan, P. J., C. House, D. K. Odell, R. S. Wells, L. J. Hansen, M. T. Walsh, D. J. St. Aubin, B. K. Rima, and J. R. Geraci. 1996. Morbillivirus infection in bottlenose dolphins: evidence for recurrent epizootics in the western Atlantic and Gulf of Mexico. *Marine Mammal Science* 12: 499–515.

Dunn, J. L., and R. E. Wolke. 1976. *Dipetalonema spirocauda* infection in the Atlantic harbor seal (*Phoca vitulina concolor*). *Journal of Wildlife Diseases* 12: 531–538.

Dutton, D. L., P. H. Dutton, M. Chaloupka, and R. H. Boulon. 2005. Increase of a Caribbean *Dermochelys coriacea* nesting population linked to long-term nest protection. *Biological Conservation* 126: 184–194.

Edwards, E. J., and J. E. Rattray. 1932. *Whale Off! The Story of American Shore Whaling*. Frederick A. Stokes Co., New York, NY. 285 pp. (reprinted 1956, Coward-McCann, New York, NY.)

Ehrhardt, L. M., D. A. Bagley, and W. E. Redfoot. 2003. Loggerhead turtles in the Atlantic Ocean: geographic distribution, abundance, and population status. Pp. 157–174 in: A. B. Bolten and B. E. Witherington, eds. *Loggerhead Sea Turtles.* Smithsonian Books, Washington, DC.

Ernst, C. H., R. W. Barbour, and J. E. Lovitch. 1994. *Turtles of the United States and Canada*.

Smithsonian Institution Press, Washington, DC. xxxviii + 578 pp.

Evans, D. L., and G. R. England. 2001. *Joint Interim Report, Bahamas Marine Mammal Stranding, Event of 15–16 March 2000*. U.S. Dept. of Commerce and Secretary of the Navy, Washington, DC. 59 pp.

Evans, W. E. 1994. Common dolphin, white-bellied porpoise *Delphinus delphis* Linnaeus, 1758. Pp. 191–224 in: S. H. Ridgway and R. Harrison, eds. *Handbook of Marine Mammals. Volume 5: The First Book of Dolphins.* Academic Press, London.

Fairfield, C. P., G. T. Waring, and M. H. Sano. 1993. Pilot whales incidentally taken during the distant water fleet Atlantic mackerel fishery in the Mid-Atlantic Bight, 1984–88. *Report of the International Whaling Commission, Special Issue* 14: 107–116.

Fernandez, S., and A. A. Hohn. 1998. Age, growth, and calving season of bottlenose dolphins, *Tursiops truncatus*, off coastal Texas. *Fishery Bulletin* 96: 357–365.

FFWCC (Florida Fish and Wildlife Conservation Commission). 2006. *Draft Manatee Management Plan,* Trichechus manatus latirostris. Florida Fish and Wildlife Conservation Commission, Tallahassee, FL. xiv + 231 pp.

FFWCC. 2009. Press release: FWC records high counts during statewide manatee survey. Florida Fish and Wildlife Conservation Commission, Fish and Wildlife Research Institute, St. Petersburg, FL. http://www.floridamarine.org/news/view_article.asp?id=31685

Folkens, P., R. R. Reeves, B. S. Stewart, P. J. Clapham, and J. A. Powell. 2002. *National Audubon Society Guide to Marine Mammals of the World.* A. A. Knopf, New York, NY. 528 pp.

Folkow, L. P., and A. S. Blix. 1995. Distribution and diving behavior of hooded seals. Pp. 193–200 in: A. S. Blix, L. Walløe, and Ø. Ulltang, eds. *Whales, Seals, Fish and Man.* Elsevier Science, Amsterdam, Netherlands.

Folkow, L. P., T. Haug, K. T. Nilssen, and E. S. Nordøy. 2000. Estimated food consumption of minke whales *Balaenoptera acutorostrata* in northeast Atlantic waters in 1992–1995. *North Atlantic Marine Mammal Commission Scientific Publications* 2: 65–80.

Ford, J. K. B. 2002. Killer whale *Orcinus orca*. Pp. 669–676 in: W. F. Perrin, B. Würsig, and H. G. M. Thewissen, eds. *Encyclopedia of Marine Mammals*. Academic Press, San Diego, CA.

Ford, J. K. B., G. M. Ellis, D. R. Matkin, K. C. Balcomb, D. Briggs, and A. B. Morton. 2005. Killer whale attacks on minke whales: prey capture and antipredator tactics. *Marine Mammal Science* 21: 603–618.

Fordyce, R. E., and L. G. Barnes. 1994. The evolutionary history of whales and dolphins. *Annual Review of Earth and Planetary Sciences* 22: 419–455.

Frair, W., R. G. Ackman, and N. Mrosovsky. 1972. Body temperature of *Dermochelys coriacea*: warm turtle from cold water. *Science* 177: 791–793.

Frank, K. 2003. *State of the Eastern Scotian Shelf Ecosystem*. Maritimes Region Ecosystem Studies Report 2003/04. Scientific Advisory Secretariat, Canada Dept. of Fisheries and

Oceans, Dartmouth, Nova Scotia. 25 pp.

Frankel, A. S. 2002. Sound production. Pp. 1126–1138 in: W. F. Perrin, B. Würsig, and J. G. M. Thewissen, eds. *Encyclopedia of Marine Mammals*. Academic Press, San Diego, CA.

Frantzis, A. 1998. Does acoustic testing strand whales? *Nature* 392: 29.

Fristrup, K. M., and G. R. Harbison. 2002. How do sperm whales catch squids? *Marine Mammal Science* 18: 42–54.

Frost, K. J., and L. F. Lowry. 1981. Ringed, Baikal and Caspian seals *Phoca hispida* Schreber, 1775, *Phoca sibirica* Gmelin, 1788 and *Phoca caspica* Gmelin, 1788. Pp. 29–53 in: S. H. Ridgway and R. Harrison, eds. *Handbook of Marine Mammals. Volume 2: Seals.* Academic Press, London.

Frost, K. J., M. A. Simpkins, R. J. Small, and L. F. Lowry. 2006. Development of diving by harbor seal pups in two regions of Alaska: Use of the water column. *Marine Mammal Science* 22: 617–643.

Fullard, K. J., G. Early, M. P. Heide-Jørgensen, D. Bloch, A. Rosing-Asvid, and W. Amos. 2000. Population structure of long-finned pilot whales in the North Atlantic: a correlation with sea surface temperature? *Molecular Ecology* 9: 949–958.

Gambell, R. 1985a. Fin whale *Balaenoptera physalus* (Linnaeus, 1758). Pp. 171–192 in: S. H. Ridgway and R. Harrison, eds. *Handbook of Marine Mammals. Volume 3: The Sirenians and Baleen Whales*. Academic Press, London.

Gambell, R. 1985b. Sei whale *Balaenoptera borealis* Lesson, 1828. Pp. 155–170 in: S. H. Ridgway and R. Harrison, eds. *Handbook of Marine Mammals. Volume 3: The Sirenians and Baleen Whales*. Academic Press, London.

Gambell, R. 1999. The International Whaling Commission and the contemporary whaling debate. Pp. 179–198 in: J. R. Twiss, Jr. and R. R. Reeves, eds. *Conservation and Management of Marine Mammals*. Smithsonian Institution Press, Washington, DC.

Gaskin, D. E. 1992. Status of Atlantic white-sided dolphin, *Lagenorhynchus acutus*, in Canada. *Canadian Field-Naturalist* 106: 64–72.

Gaskin, D. E., P. W., Arnold, and B. A. Blair. 1974. *Phocoena phocoena. Mammalian Species* 42: 1–8.

Gauthier J. M., H. Dubeau, É. Rassart, W. M. Jarman, and R. S. Wells. 1999. Biomarkers of DNA damage in marine mammals. *Mutation Research* 444: 427–439.

Geibel, J., J. Meier, A. Binder, J. Flossdorf, J. B. Poveda, R. Schmidt, and H. Kirchhoff. 1991. *Mycoplasma phocarhinus* sp. nov. and *Mycoplasma phocacerebrale* sp. nov., two new species from harbor seals (*Phoca vitulina* L.). *International Journal of Systematic Bacteriology* 41: 39–44.

Geraci, J. R. 1989. Investigation of the 1987–1988 mass mortality of the bottlenose dolphin. *Naval Research Reviews* 41(2): 2–10.

Geraci, J. R., and V. J. Lounsbury. 1993. *Marine Mammals Ashore: A Field Guide for Strandings*. Texas A&M University, Sea Grant College Program, College Station, TX. 305 pp.

Geraci, J. R., D. J. St. Aubin, I. K. Barker, R. G. Webster, V. S. Hinshaw, W. J. Bean, H. L. Ruhnke, J. H. Prescott, G. Early, A. S. Baker, S. Madoff, and R. T. Schooley. 1982. Mass mortality of harbor seals: pneumonia associated with influenza A virus. *Science* 215: 1129–1131.

Geraci, J. R., D. M. Anderson, R. J. Timperi, D. J. St. Aubin, G. Early, J. H. Prescott, and C. A. Mayo. 1989. Humpback whales (*Megaptera novaeangliae*) fatally poisoned by dinoflagellate toxins. *Canadian Journal of Fisheries and Aquatic Sciences* 46: 1895–1898.

Geraci, J. R., J. Harwood, and V. J. Lounsbury. 1999. Marine mammal die-offs; Causes, investigations, and issues. Pp. 367–395 in: J. R. Twiss, Jr. and R. R. Reeves, eds. *Conservation and Management of Marine Mammals.* Smithsonian Institution Press, Washington, DC.

Gerrodette, T. 2002. Tuna-dolphin issue. Pp. 1269–1273 in: W. F. Perrin, B. Würsig, and H. G. M. Thewissen, eds. *Encyclopedia of Marine Mammals*. Academic Press, San Diego, CA.

Gilbert, J. R., and K. Wynne. 1987. *Marine Mammal Interactions with New England Gillnet Fisheries.* Final report, contract no. NA-84-EAC-00070. National Marine Fisheries Service, Woods Hole, MA. 21 pp.

Gilbert, J. R., G. T. Waring, K. M. Wynne, and N. Guldager. 2005. Changes in abundance of harbor seals in Maine, 1981–2001. *Marine Mammal Science* 21: 519–535.

Glockner-Ferrari, D. A., and M. J. Ferrari. 1990. Reproduction in the humpback whale (*Megaptera novaeangliae*) in Hawaiian waters, 1975–1988: The life history, reproductive rates and behaviour of known individuals identified through surface and underwater photography. *Report of the International Whaling Commission, Special Issue* 12: 161–169.

Goff, G. P., and J. Lien. 1988. Atlantic leatherback turtles, *Dermochelys coriacea*, in cold water off Newfoundland and Labrador. *Canadian Field-Naturalist* 102: 1-5.

Goodwin, G. G. 1933. Occurrence of a gray seal at Atlantic City, New Jersey. *Journal of Mammalogy* 14: 73.

Goodwin, G. G. 1935. *The Mammals of Connecticut*. Bulletin no. 53. State of Connecticut, State Geological and Natural History Survey, Hartford, CT. 221 pp. + 33 pl.

Goodwin, G. G. 1954. Southern records for Arctic mammals and a northern record for Alfaro's rice rat. *Journal of Mammalogy* 35: 258.

Gormley, G. 1990. *Orcas of the Gulf: A Natural History.* Sierra Club Books, San Francisco, CA. xiv + 295 pp.

Gorzelany, J. F. 1998. Unusual deaths of two free-ranging Atlantic bottlenose dolphins (*Tursiops truncatus*) related to ingestion of recreational fishing gear. *Marine Mammal Science* 14: 614–617.

Gosliner, M. L. 1999. The tuna-dolphin controversy. Pp. 120–155 in: J. R. Twiss, Jr. and R. R. Reeves, eds. *Conservation and Management of Marine Mammals*. Smithsonian Institution Press, Washington, DC.

Gowans, S. 2002. Bottlenose whales *Hyperoodon ampullatus* and *H. planifrons*. Pp. 128–129 in: W. F. Perrin, B. Würsig, and J. G. M. Thewissen, eds. *Encyclopedia of Marine Mammals*. Academic Press, San Diego, CA.

Gowans, S., and H. Whitehead. 1995. Distribution and habitat partitioning by small odontocetes in the Gully, a submarine canyon on the Scotian Shelf. *Canadian Journal of Zoology* 73: 1599–1608.

Gowans, S., H. Whitehead, J. K. Arch, and S. K. Hooker. 2000. Population size and residency patterns of northern bottlenose whales (*Hyperoodon ampullatus*) using the Gully, Nova Scotia. *Journal of Cetacean Research and Management* 2: 2201–210.

Gowans, S., H. Whitehead, and S. K. Hooker. 2001. Social organization in northern bottlenose whales (*Hyperoodon ampullatus*): not driven by deep water foraging? *Animal Behaviour* 62: 369–377.

Grayce, R. L. 1957. Checklist of New England Mammals. *Bulletin of the Massachusetts Audubon Society* 41(1): 15-24, 26.

Greene, C. H., and A. J. Pershing. 2004. Climate and the conservation biology of North Atlantic right whales: the right whale at the wrong time? *Frontiers in Ecology and the Environment* 2: 29–34.

Greene, C. H., A. J. Pershing, R. D. Kenney, and J. W. Jossi. 2003. Impact of climate variability on the recovery of endangered North Atlantic right whales. *Oceanography* 16(4): 98–103.

Greer, A. E., J. D. Lazell, Jr., and R. M. Wright. 1973. Anatomical evidence for a counter-current heat exchanger in the leatherback turtle (*Dermochelys coriacea*). *Nature* 244: 181.

Hai, D. J., J. Lien, D. Nelson, and K. Curren. 1996. A contribution to the biology of the white-beaked dolphin, *Lagenorhynchus albirostris*, in waters off Newfoundland. *Canadian Field-Naturalist* 110: 278–287.

Hain, J. H. W. 1975. The international regulation of whaling. *Marine Affairs Journal* 3: 28–48.

Hain, J. H. W., G. R. Carter, S. D. Kraus, C. A. Mayo, and H. E. Winn. 1982. Feeding behavior of the humpback whale, *Megaptera novaeangliae*, in the western North Atlantic. *Fishery Bulletin* 80: 259–268.

Hain, J. H. W., M. A. M. Hyman, R. D. Kenney, and H. E. Winn. 1985. The role of cetaceans in the shelf-edge region of the northeastern United States. *Marine Fisheries Review* 47: 13–17.

Hain, J. H. W., M. J. Ratnaswamy, R. D. Kenney, and H. E. Winn. 1992. The fin whale, *Balaenoptera physalus*, in waters of the northeastern United States continental shelf. *Report of the International Whaling Commission* 42: 653–669.

Hain, J. H. W., S. L. Ellis, R. D. Kenney, P. J. Clapham, B. K. Gray, M. T. Weinrich, and I. G. Babb. 1995. Apparent bottom feeding by humpback whales on Stellwagen Bank. *Marine Mammal Science* 11: 464–479.

Hain, J. H. W, S. L. Ellis, R. D. Kenney, and C. K. Slay. 1999. Sightability of right whales in coastal waters of the southeastern United States with implications for the aerial monitoring program. Pp. 191–207 in: G. W. Garner, S. C. Amstrup, J. L. Laake, B. F. J. Manly, L. L. McDonald, and D. G. Robertson, eds. *Marine Mammal Survey and Assessment Methods*. A. A. Balkema, Rotterdam, Netherlands.

Hall, A. 2002. Gray seal *Halichoerus grypus*. Pp. 522–524 in: W. F. Perrin, B. Würsig, and H. G. M. Thewissen, eds. *Encyclopedia of Marine Mammals*. Academic Press, San Diego, CA.

Hamilton, H., and C. Puckett. 2006. Manatee traveler in northeastern waters not Chessie. *Sound Waves* FY2006(87): 6–7. http://soundwaves.usgs.gov/2006/09/research2.html

Hamilton, P. K., M. K. Marx, and S. D. Kraus. 1995. Weaning in North Atlantic right whales. *Marine Mammal Science* 11: 386–390.

Hamilton, R. 1839. *The Natural History of the Amphibious Carnivora, Including the Walrus and Seals, Also of the Herbivorous Cetacea, &c., Illustrated by Thirty-Three Plates, With Memoir and Portrait of Peron.* The Naturalist's Library XXIII, Mammalia Vol. VIII. W. H. Lizars, Edinburgh. 396 pp.

Hammill, M. O. 2005. *Abundance of Northwest Atlantic Grey Seals in the Gulf of St. Lawrence and Along the Nova Scotia Eastern Shore/Abondance des Phoques Gris du Nord-Ouest de l'Atlantique dans le Golfe du Saint-Lawrent et le Long de la Côte Est de la Novelle-Écosse.* CSAS Research Document 2005/036. Canadian Science Advisory Secretariat, Department of Fisheries and Oceans, Dartmouth, Nova Scotia, Canada. 15 pp.

Hamner, W. H. 1988. The 'lost year' of the sea turtle. *Trends in Ecology and Evolution* 3: 116-118.

Handley, C. O., Jr. 1966. A synopsis of the genus *Kogia* (pygmy sperm whales). Pp. 62–69 in: K. S. Norris, ed. *Whales, Dolphins, and Porpoises*. University of California Press, Berkeley, CA.

Harris, D. E., B. Lelli, G. Jakush, and G. Early. 2001. Hooded seal (*Cystophora cristata*) records from the southern Gulf of Maine. *Northeastern Naturalist* 8: 427–434.

Harris, D. E., B. Lelli, and G. Jakush. 2002. Harp seal records from the southern Gulf of Maine: 1997–2001. *Northeastern Naturalist* 9: 331–340.

Hartley, J. W., and D. Pitcher. 2002. Seal finger—tetracycline is first line. *Journal of Infection* 45: 71–75.

Hassani, S., L. Antoine, and V. Ridoux. 1997. Diets of albacore, *Thunnus albacares*, and dolphins, *Delphinus delphis* and *Stenella coeruleoalba*, caught in the northeast Atlantic albacore drift-net fishery: a progress report. *Journal of Northwest Atlantic Fisheries Science* 22: 119–123.

Hatch, L. T., E. B. Dopman, and R. G. Harrison. 2006. Phylogenetic relationships among the baleen whales based on maternally and paternally inherited characters. *Molecular Phylogenetics and Evolution* 41: 12–27.

Haug, T. 1981. On some reproduction parameters in fin whales *Balaenoptera physalus* (L.) caught off Norway. *Report of the International Whaling Commission* 31: 373–378.

Hay, K. 1982. Aerial line-transect estimates of abundance of humpback, fin, and long-finned pilot whales in the Newfoundland-Labrador area. *Report of the International Whaling Commission* 32: 475–480.

Hays, H. E., H. E. Winn, and R. Petricig. 1985. Anomalous feeding behavior of a humpback whale. *Journal of Mammalogy* 66: 819–821.

Hays, G. C., J. D. R. Houghton, and A. E. Myers. 2004. Pan-Atlantic leatherback turtle movements. Nature 429: 522.

Hays, G. C., V. J. Hobson, J. D. Metcalfe, D. Righton, and D. W. Sims. 2006. Flexible foraging movements of leatherback turtles across the North Atlantic Ocean. Ecology 87: 2647–2656.

Heide-Jørgensen, M.-P., T. Härkönen, R. Dietz, and P. M. Thompson. 1992. Retrospective of the 1988 European seal epizootic. *Diseases of Aquatic Organisms* 13: 37–62.

Helmuth, W. T. 1931. *Balaenoptera acutorostrata* off Montauk Point, New York. *Journal of Mammalogy* 12: 72–73.

Heppell, S. S., M. L. Snover, and L. B. Crowder. 2003. Sea turtle population ecology. Pp. 275–306 in: P. L. Lutz, J. A. Musick, and J. Wyneken, eds. *The Biology of Sea Turtles*, volume II. CRC Press, Boca Raton, FL.

Heppell, S. S., D. T. Crouse, L. B. Crowder, S. P. Epperly, W. Gabriel, T. Henwood, R. Márquez, and N. B. Thompson. 2005. A population model to estimate recovery time, population size, and management impacts on Kemp's ridley sea turtles. *Chelonian Conservation and Biology* 4: 767–773.

Hersh, S. L., and D. A. Duffield. 1990. Distinction between northwest Atlantic pelagic and coastal bottlenose dolphins based on hemoglobin profile and morphometry. Pp. 129–139 in: S. Leatherwood and R. R. Reeves, eds. *The Bottlenose Dolphin.* Academic Press, San Diego, CA.

Herzing, D. L. 1997. The life history of free-ranging Atlantic spotted dolphins (*Stenella frontalis*): Age classes, color phases, and female reproduction. *Marine Mammal Science* 13: 576–595.

Herzing, D. L., and C. M. Johnson. 1997. Interspecific interactions between Atlantic spotted dolphins (*Stenella frontalis*) and bottlenose dolphins (*Tursiops truncatus*) in the Bahamas, 1985–1995. *Aquatic Mammals* 23: 85–99.

Heyning, J. E. 1984. Functional morphology involved in the interspecific fighting of the beaked whale *Mesoplodon carlhubbsi. Canadian Journal of Zoology* 62: 145–1654.

Heyning, J. E. 1989. Cuvier's beaked whale *Ziphius cavirostris* G. Cuvier, 1823. Pp. 289–308 in: S. H. Ridgway and R. Harrison, eds. *Handbook of Marine Mammals. Volume 4: River Dolphins and the Larger Toothed Whales.* Academic Press, London.

Heyning, J. E. 2002. Cuvier's beaked whale *Ziphius cavirostris*. Pp. 305–307 in: W. F. Perrin, B. Würsig, and J. G. M. Thewissen, eds. *Encyclopedia of Marine Mammals*. Academic Press, San Diego, CA.

Heyning, J. E., and M. E. Dahlheim. 1988. *Orcinus orca. Mammalian Species* 304: 1–9.

Heyning, J. E., and W. F. Perrin. 1994. Evidence for two species of common dolphins (genus *Delphinus*) from the eastern North Pacific. *Natural History Museum of Los Angeles County Contributions in Science* 442: 1–35.

Hickie B. E., M. C. S. Kingsley, P. V. Hodson, D. C. G. Muir., P. Béland, and D. A. Mackay. 2000. Modelling-based perspective on the past, present and future polychlorinated biphenyl contamination of the St. Lawrence beluga whale (*Delphinapterus leucas*) population. *Canadian Journal of Fisheries and Aquatic Sciences* 57(Suppl. 1): 101–112.

Hinshaw, V. S., W. J. Bean, R. G. Webster, J. E. Rehg, P. Fiorelli, G. Early, J. R. Geraci, and D. J. St. Aubin. 1984. Are seals frequently infected with avian influenza viruses? *Journal of Virology* 51: 863–865.

Hoelzel, A. R., C. W. Potter, and P. B. Best. 1998. Genetic differentiation between parapatric "nearshore" and "offshore" populations of bottlenose dolphins. *Proceedings of the Royal Society of London* B 265: 1177–1183.

Hooker, S. K. 2002. Toothed whales, overview. Pp. 1252–1260 in: W. F. Perrin, B. Würsig, and H. G. M. Thewissen, eds. *Encyclopedia of Marine Mammals*. Academic Press, San Diego, CA.

Hooker, S. K., and R. W. Baird. 1999. Deep-diving behaviour of the northern bottlenose whale, *Hyperoodon ampullatus* (Cetacea: Ziphiidae). *Proceedings of the Royal Society of London* B 266: 671–676.

Hooker, S. K., S. J. Iverson, P. Ostrom, and S. C. Smith. 2001. Diet of northern bottlenose whales inferred from fatty-acid and stable-isotope analyses of biopsy samples. *Canadian Journal of Zoology* 79: 1442–1454.

Hooker, S. K., H. Whitehead, S. Gowans, and R. W. Baird. 2002. Fluctuations in distribution and patterns of individual range use of northern bottlenose whales. *Marine Ecology Progress Series* 225: 287–297.

Horwood, J. 1987. *The Sei Whale. Population Biology, Ecology and Management*. Croom Helm, New York, NY. 375 pp.

Horwood, J. 1990. *Biology and Exploitation of the Minke Whale*. CRC Press, Boca Raton, FL. 238 pp.

Horwood, J. 2002. Sei whale *Balaenoptera borealis*. Pp. 1069–1071 in: W. F. Perrin, B. Würsig, and H. G. M. Thewissen, eds. *Encyclopedia of Marine Mammals*. Academic Press, San Diego, CA.

Husar, S. L. 1978. *Trichechus manatus. Mammalian Species* 93: 1–5.

Ingebrigtsen, A. 1929. Whales caught in the North Atlantic and other seas. *Rapports et Procès-verbaux des Réunions, Conseil Permanent International pour L'exploration de la Mer* 56(2): 1–26.

IUCN (International Union for the Conservation of Nature and Natural Resources). 2008. *2008 IUCN Red List of Threatened Species.* International Union for the Conservation of Nature and Natural Resources, Species Survival Commission Red List Programme, Cambridge, UK. http://www.iucnredlist.org

IWC (International Whaling Commission). 1983. Chairman's report of the thirty-fourth annual meeting. *Report of the International Whaling Commission* 33: 20–42.

IWC(International Whaling Commission). 2001. Report of the workshop on the status and trends of western North Atlantic right whales. *Journal of Cetacean Research and Management, Special Issue* 2: 61–87.

IWC(International Whaling Commission). 2005. Annex L. Report of the subcommittee on small cetaceans. *Journal of Cetacean Research and Management* 7(Supplement): 307–326.

IWC (International Whaling Commission). 2006. Annex L. Report of the subcommittee on small cetaceans. *Journal of Cetacean Research and Management* 8(Supplement): 221–240.

Jacobsen, K.-O., M. Marx, and N. Øien. 2004. Two-way trans-Atlantic migration of a North Atlantic right whale (*Eubalaena glacialis*). *Marine Mammal Science* 20: 161–166.

James, M. C., C. A. Ottensmeyer, and R. A. Myers. 2005. Identification of high-use habitat and threats to leatherback sea turtles in northern waters: new directions for conservation. *Ecology Letters* 8: 195–201.

Jefferson, T. A. 1997. Distribution of cetaceans in the offshore Gulf of Mexico. *Mammal Review* 27: 27–50.

Jefferson, T. A., and B. E. Curry. 2003. *Stenella clymene. Mammalian Species* 726: 1–5.

Jefferson, T. A., and K. Van Waerebeek. 2002. The taxonomic status of the nominal dolphin species *Delphinus tropicalis* van Bree 1971. *Marine Mammal Science* 19: 787–818.

Jefferson, T. A., S. Leatherwood, L. K. M. Shoda, and R. L. Pitman. 1992. *Marine Mammals of the Gulf of Mexico: A Field Guide for Aerial and Shipboard Observers.* Texas A&M University Printing Center, College Station, TX. 92 pp.

Jefferson, T. A, S. Leatherwood, and M. A. Webber. 1993. *FAO Species Identification Guide; Marine Mammals of the World.* United Nations Environment Programme, Food and Agriculture Organization of the United Nations, Rome. viii + 320 pp.

Jensen, T., M. van de Bildt, H. H. Dietz, T. H. Andersen, A. S. Hammer, T. Kuiken, and A. Osterhaus. 2002. Another phocine distemper outbreak in Europe. *Science* 297: 209.

Jepsen, P. D., M. Arbelo, R. Deaville, I. A. P. Patterson, P. Castro, J. R. Baker, E. Degollada, H. M. Ross, P. Herráez, A. M. Pocknell, R. Rodríguez, F. E. Howie, A. Espinoza, R. J. Reid, J. R. Jaber, V. Martín, A. A. Cunningham, and A. Fernández. 2003. Gas-bubble lesions in stranded cetaceans. *Nature* 425: 575–576.

Johnson, J. H., and A. A. Wolman. 1984. The humpback whale (*Megaptera novaeangliae*). *Marine Fisheries Review* 46(4): 30–37.

Johnson, K. R., and C. H. Nelson. 1984. Side-scan sonar assessment of gray whale feeding in the Bering Sea. *Science* 225: 1150–1152.

Johnson, M., P. T. Madsen, W. M. X. Zimmer, N. Aguilar de Soto, and P. Tyack. 2004. Beaked whales echolocate on prey. *Proceedings of the Royal Society of London* B (Suppl.) 271: S383–S386.

Jones, M. L., and S. L. Swartz. 2002. Gray whale *Eschrichtius robustus*. Pp. 524–536 in: W. F. Perrin, B. Würsig, and H. G. M. Thewissen, eds. *Encyclopedia of Marine Mammals*. Academic Press, San Diego, CA.

Jonsgård, Å. 1966. The distribution of Balaenopteridae in the North Atlantic Ocean. Pp. 114–124 in: K. S. Norris, ed. *Whales, Dolphins, and Porpoises.* University of California Press, Berkeley, CA.

Jonsgård, Å., and K. Darling. 1977. On the biology of the eastern North Atlantic sei whale, *Balaenoptera borealis* Lesson. *Report of the International Whaling Commission, Special Issue* 1: 124–129.

Jurasz, C. M., and V. P. Jurasz. 1979. Feeding modes of the humpback whale, *Megaptera novaeangliae*, in southeast Alaska. *Scientific Reports of the Whales Research Institute*, Tokyo 31: 69–83.

Kasuya, T., and S. Tai. 1993. Life history of short-finned pilot whale stocks off Japan and a description of the fishery. *Report of the International Whaling Commission, Special Issue* 14: 439–473.

Kato, H. 2002. Bryde's whales *Balaenoptera edeni* and *B. brydei*. Pp. 171–177 in: W. F. Perrin, B. Würsig, and H. G. M. Thewissen, eds. *Encyclopedia of Marine Mammals*. Academic Press, San Diego, CA.

Katona, S. K., and J. A. Beard. 1990. Population size, migrations and feeding aggregations of the humpback whale (*Megaptera novaeangliae*) in the western North Atlantic Ocean. *Report of the International Whaling Commission, Special Issue* 12: 295–305.

Katona, S., B. Baxter, O. Brazier, S. Kraus, J. Perkins, and H. Whitehead. 1979. Identification of humpback whales by fluke photographs. Pp. 33–44 in: H. E. Winn and B. L. Olla, eds. *Behavior of Marine Animals: Current Perspectives in Research. Volume 3: Cetaceans.* Plenum Press, New York, NY.

Katona, S. K., V. Rough, and D. T. Richardson. 1993. *A Field Guide to Whales, Porpoises, and Seals From Cape Cod to Newfoundland*, fourth edition, revised. Smithsonian Institution Press, Washington, DC. xix + 316 pp.

Kawamura, A. 1974. Food and feeding ecology in the southern sei whale. *Scientific Reports of the Whales Research Institute*, Tokyo 26: 25–144.

Kawamura, A. 1980. Food habits of the Bryde's whales taken in the South Pacific and Indian oceans. *Scientific Reports of the Whales Research Institute,* Tokyo 32: 1–23.

Kawamura, A. 1994. A review of baleen whale feeding in the Southern Ocean. *Report of the International Whaling Commission* 44: 261–271.

Kellogg, R. 1929. What is known of the migration of some of the whalebone whales. *Annual Report of the Smithsonian Institution* 1928: 467–494.

Kelly, B. P. 1988. Ringed seal, *Phoca hispida*. Pp. 57–75 in: J. W. Lentfer, ed. *Selected Marine Mammals of Alaska: Species Accounts with Research and Management Recommendations.* Marine Mammal Commission, Washington, DC.

Kenney, R. D. 1990. Bottlenose dolphins off the northeastern United States. Pp. 369–396 in: S.

Leatherwood and R. R. Reeves, eds. *The Bottlenose Dolphin.* Academic Press, San Diego, CA.

Kenney, R. D. 2001. The North Atlantic Right Whale Consortium databases. *Maritimes* 43(2): 3–5.

Kenney, R.D. 2005. Paleostratigraphy in the campus freezer: re-discovery of an early gray seal stranding from Block Island, Rhode Island. *Rhode Island Naturalist* 12(2): 5–9.

Kenney, R. D. 2007. Right whales and climate change: Facing the prospect of a greenhouse future. Pp. 436–459 in: S.D. Kraus and R.M. Rolland, eds. *The Urban Whale: North Atlantic Right Whales at the Crossroads*. Harvard University Press, Cambridge, MA.

Kenney, R. D. 2009. Right whales *Eubalaena glacialis*, *E. japonica*, and *E. australis*. Pp. 962–972 in: W. F. Perrin, B. Würsig, and J. G. M. Thewissen, eds. *Encyclopedia of Marine Mammals*, second edition. Academic Press/Elsevier, San Diego, CA.

Kenney, R. D., and S. D. Kraus. 1993. Right whale mortality—A correction and an update. *Marine Mammal Science* 9: 445–446.

Kenney, R.D. and H.E. Winn. 1986. Cetacean high-use habitats of the northeast United States continental shelf. *Fishery Bulletin* 84: 345– 357.

Kenney, R. D., and H. E. Winn. 1987a. Cetacean biomass densities near submarine canyons compared to adjacent continental shelf/slope areas. *Continental Shelf Research* 7: 107–114.

Kenney, R. D., and H. E. Winn. 1987b. Why some whales fluke: suggesting a novel hypothesis. *Cetus* 7(2): 15–19.

Kenney, R. D., and K. F. Wishner. 1995. The South Channel Ocean Productivity Experiment. Continental Shelf Research 15: 373–384.

Kenney, R. D., M. A. M. Hyman, and H. E. Winn. 1985a. *Calculation of Standing Stocks and Energetic Requirements of the Cetaceans of the Northeast United States Outer Continental Shelf*. NOAA Technical Memorandum NMFS-F/NEC-41. National Marine Fisheries Service, Woods Hole, MA. iv + 99 pp.

Kenney, R. D., R. E. Owen, and H. E. Winn. 1985b. Shark distributions off the northeast United States from marine mammal surveys. *Copeia* 1985: 220–223.

Kenney, R. D., M. A. M. Hyman, R. E. Owen, G. P. Scott, and H. E. Winn. 1986. Estimation of prey densities required by western North Atlantic right whales. *Marine Mammal Science* 2: 1–13.

Kenney, R. D., H. E. Winn, and M. C. Macaulay. 1995. Cetaceans in the Great South Channel, 1979–1989: right whale (*Eubalaena glacialis*). *Continental Shelf Research* 15: 385–414.

Kenney, R. D., P. M. Payne, D. J. Heinemann, and H. E. Winn. 1996. Shifts in Northeast shelf cetacean distributions relative to trends in Gulf of Maine/Georges Bank finfish abundance. Pp. 169–196 in: K. Sherman, N. A. Jaworski, and T. J. Smayda, eds. *The Northeast Shelf Ecosystem: Assessment, Sustainability, and Management*. Blackwell Science, Boston, MA.

Kenney, R. D., G. P. Scott, T. J. Thompson, and H. E. Winn. 1997. Estimates of prey consumption and trophic impacts of cetaceans in the USA northeast continental shelf ecosystem. *Journal of Northwest Atlantic Fisheries Science* 22: 155–171.

Kenney, R. D., C. A. Mayo, and H. E. Winn. 2001. Migration and foraging strategies at varying spatial scales in western North Atlantic right whales: A review of hypotheses. *Journal of Cetacean Research and Management, Special Issue* 2: 251–260.

Kenney, R. D., R. M. Pace III, P. K. Hamilton, and T. R. Frasier. In preparation. Trends in Minimum Number Alive: Are Gulf of Maine right whales approaching carrying capacity?

Kieran, J. 1959. *A Natural History of New York City.* Houghton Mifflin, Boston, MA. 428 pp. (not seen, cited by Connor, 1971)

Kingsley, M. C. S., and R. R. Reeves. 1998. Aerial surveys of cetaceans in the Gulf of St. Lawrence in 1995 and 1996. *Canadian Journal of Zoology* 76: 1529–1550.

Kingston, S. E., and P. E. Rosel. 2004. Genetic differentiation among recently diverged delphinid taxa determined using AFLP markers. *Journal of Heredity* 95: 1–10.

Kinze, C. C. 1995. Exploitation of harbour porpoises (*Phocoena phocoena*) in Danish waters: a historical review. *Report of the International Whaling Commission, Special Issue* 16: 141–153.

Kinze, C. C. 2002. White-beaked dolphin *Lagenorhynchus albirostris*. Pp. 1332–1334 in: W. F. Perrin, B. Würsig, and H. G. M. Thewissen, eds. *Encyclopedia of Marine Mammals*. Academic Press, San Diego, CA.

Kinze, C. C., M. Addink, C. Smeenk, M. García Hartmann, H. W. Richards, R. P. Sonntag, and H. Benke. 1997. The white-beaked dolphin (*Lagenorhynchus albirostris*) and the white-sided dolphin (*Lagenorhynchus acutus*) in the North and Baltic seas: Review of available information. *Report of the International Whaling Commission* 47: 675–681.

Kishiro, T., and T. Kasuya. 1993. Review of the Japanese dolphin drive fisheries and their status. *Report of the International Whaling Commission* 43: 439–452.

Knowlton, A. R., and S. D. Kraus. 2001. Mortality and serious injury of northern right whales (*Eubalaena glacialis)* in the western North Atlantic Ocean. *Journal of Cetacean Research and Management, Special Issue* 2: 193–208.

Knowlton, A. R., J. Sigurjónsson, J. N. Ciano, and S. D. Kraus. 1992. Long-distance movements of North Atlantic right whales (*Eubalaena glacialis*). *Marine Mammal Science* 8: 397–405.

Knowlton, A. R., S. D. Kraus, and R. D. Kenney. 1994. Reproduction in North Atlantic right whales (*Eubalaena glacialis*). *Canadian Journal of Zoology* 72: 1297–1305.

Knowlton, A. R., J. Beaudin-Ring, and B. Russell. 2002. *Right Whale Sightings and Survey Effort in the Mid-Atlantic Region: Migratory Corridor, Time Frame, and Proximity to Port Entrances.* Unpublished report. Northeast Implementation Team Ship Strike Subcommittee, National Marine Fisheries Service, Gloucester, MA. 25 pp. http://www.nero.noaa.gov/shipstrike/ssr/midatanticreportrFINAL.pdf

Kovacs, K. M. 2002. Hooded seal *Cystophora cristata*. Pp. 580–582 in: W. F. Perrin, B. Würsig, and J. G. M. Thewissen, eds. *Encyclopedia of Marine Mammals*. Academic Press, San Diego, CA.

Kovacs, K. M., and D. M. Lavigne. 1986. *Cystophora cristata*. *Mammalian Species* 258: 1–9.

Kraus, S. D. 1990. Rates and potential causes of mortality in North Atlantic right whales (*Eubalaena glacialis*). *Marine Mammal Science* 6: 278–291.

Kraus, S. D., J. R. Gilbert, and J. H. Prescott. 1983. A comparison of aerial, shipboard, and land-based survey methodology for the harbor porpoise *Phocoena phocoena*. *Fishery Bulletin* 84: 910–913.

Kraus, S. D., K. E. Moore, C. A. Price, M. J. Crone, W. A. Watkins, H. E. Winn, and J. H. Prescott. 1986. The use of photographs to identify individual North Atlantic right whales (*Eubalaena glacialis*). *Report of the International Whaling Commission, Special Issue* 10: 145–151.

Kraus, S. D., R. D. Kenney, A. R. Knowlton, and J. N. Ciano. 1993. *Endangered Right Whales of the Southwestern North Atlantic*. Final Report, Contract No. 14-35-0001-30486. U. S. Department of the Interior, Minerals Management Service, Herndon, Virginia. 69 pp.

Kraus, S. D., P. K. Hamilton, R. D. Kenney, A. R. Knowlton, and C. K. Slay. 2001. Reproductive parameters of the North Atlantic right whale. *Journal of Cetacean Research and Management, Special Issue* 2: 231–236.

Kraus, S. D., M. W. Brown, H. Caswell, C. W. Clark, M. Fujiwara, P. K. Hamilton, R. D. Kenney, A. R. Knowlton, S. Landry, C. A. Mayo, W. A. McLellan, M. J. Moore, D. P. Nowacek, D. A. Pabst, A. J. Read, and R. M. Rolland. 2005. North Atlantic right whales in crisis. *Science* 309: 561–562.

Kraus, S. D., R. M. Pace III, and T. R. Frasier. 2007. High investment, low return: the strange case of reproduction in *Eubalaena glacialis.* Pp. 172-199 in*:* S. D. Kraus and R. M. Rolland, eds. *The Urban Whale: North Atlantic Right Whales at the Crossroads*. Harvard University Press, Cambridge, MA.

Kruse, S., D. K. Caldwell, and M. C. Caldwell. 1999. Risso's dolphin *Grampus griseus* (G. Cuvier, 1812). Pp. 183–212 in: S. H. Ridgway and R. Harrison, eds. *Handbook of Marine Mammals. Volume 6: The Second Book of Dolphins and the Porpoises.* Academic Press, London.

Kuehl, D. W., R. Haebler, and C. Potter. 1991. Chemical residues in dolphins from the U.S. Atlantic coast including Atlantic bottlenose obtained during the 1987/88 mass mortality. *Chemosphere* 22: 1071–1084.

Kvitek, R. G., and J. S. Oliver. 1986. Side-scan sonar estimates of the utilization of gray whale feeding grounds along Vancouver Island, Canada. *Continental Shelf Research* 6: 639–654.

Lahvis, G. P., R. S. Wells, D. W. Kuehl, J. L. Stewart, H. L. Rhinehart, and C. S. Via. 1995. Decreased lymphocyte responses in free-ranging bottlenose dolphins (*Tursiops truncatus*) are associated with increased concentrations of PCBs and DDT in peripheral blood. *Environmental Health Perspectives* 103(Supplement 4): 67–72.

Laist, D. W., A. R. Knowlton, J. G. Mead, A. S. Collett, and M. Podesta. 2001. Collisions between ships and whales. *Marine Mammal Science* 17: 35–75.

Lambertsen, R. H. 1983. The internal mechanism of rorqual feeding. *Journal of Mammalogy* 64: 76–88.

Larsen, A. H., I. Sigurjónsson, N. Øien, G. Vikingsson, and P. Palsbøll. 1996. Population genetic analysis of mitochondrial and nuclear genetic loci in skin biopsies collected from central and northeastern North Atlantic humpback whales (*Megaptera novaeangliae*): population identity and migratory destinations. *Proceeding of the Royal Society of London* B 263: 1611–1618.

Lavigne, D. J. 2002. Harp seal *Pagophilus groenlandicus*. Pp. 560–562 in: W. F. Perrin, B. Würsig, and J. G. M. Thewissen, eds. *Encyclopedia of Marine Mammals*. Academic Press, San Diego, CA.

Lavigne, D. J., and K. M. Kovacs. 1988. *Harps and Hoods: Ice Breeding Seals of the Northwest Atlantic.* University of Waterloo Press, Waterloo, Ontario. xviii + 174 pp.

Lazell, J. D., Jr. 1976. *This Broken Archipelago: Cape Cod and the Islands, Amphibians, and Reptiles.* Quadrangle Press, Harper and Row, New York, NY. xi + 260 pp.

Lazell, J. D., Jr. 1980. New England waters: Critical habitat for marine turtles. *Copeia* 1980(2): 290–295.

Leatherwood, S. 1975. Some observations of feeding behavior of bottle-nosed dolphins (*Tursiops truncatus*) in the northern Gulf of Mexico and (*Tursiops* cf *gilli*) off southern California, Baja California, and Nayarit, Mexico. *Marine Fisheries Review* 37(9): 10–16.

Leatherwood, S., D. K. Caldwell, and H. E. Winn. 1976. *Whales, Dolphins, and Porpoises of the Western North Atlantic: A Guide to Their Identification.* NOAA Technical Report NMFS CIRC-396. National Marine Fisheries Service, Seattle, WA. iv + 176 pp.

Leatherwood, S., M. W. Deerman, and C. W. Potter. 1978. Food and reproductive status of nine *Tursiops truncatus* from the northeastern United States coast. *Cetology* 28: 1–6.

LeDuc, R. G., W. F. Perrin, and A. E. Dizon. 1999. Phylogenetic relationships among the delphinoid cetaceans based on full cytochrome *b* sequences. *Marine Mammal Science* 15: 619–648.

Lens, S. 1997. Interactions between marine mammals and deep water trawlers in the NAFO regulatory area. Meeting document C.M. 8/Q. International Council for the Exploration of the Sea, Copenhagen. 10 pp.

Lesage, V. and M. O. Hammill. 2001. The status of the grey seal, *Halichoerus grypus*, in the Northwest Atlantic. *Canadian Field-Naturalist* 115: 653–662.

Lewison, R. L., S. A. Freeman, and L. B. Crowder. 2004. Quantifying the effects of fisheries on threatened species: the impact of pelagic longlines on loggerhead and leatherback sea turtles. Ecology Letters 7: 221–231.

Lien, J., S. Johnson, and B. Merdsoy. 1979. Whale distribution in Newfoundland during 1979. *Osprey* 11(2): 21–32.

Lien, J., R. Sears, G. B. Stenson, P. W. Jones, and I-H. Ni. 1989. Right whale, *Eubalaena glacialis*, sightings in waters off Newfoundland and Labrador and the Gulf of St. Lawrence, 1978–1987. *Canadian Field-Naturalist* 103: 91–93.

Lien, J., D. Nelson, and D. J. Hai. 2001. Status of the white-beaked dolphin, *Lagenorhynchus albirostris*, in Canada. *Canadian Field-Naturalist* 115: 118–126.

Limpus, C., and M. Chaloupka. 1997. Nonparametric regression modelling of green sea turtle growth rates (southern Great Barrier Reef). *Marine Ecology Progress Series* 149: 23–34.

Lindquist, O. 2000. *The North Atlantic Gray Whale (*Eschrichtius robustus*): An Historical Outline Based on Icelandic, Danish-Icelandic, English and Swedish Sources Dating From ca 1000 AD to 1792.* Occasional Papers, No. 1. The Centre for Environmental History and Policy, Universities of St. Andrews and Stirling, Scotland. 53 pp.

Linsley, J. H. 1842. A catalogue of the Mammalia of Connecticut. *American Journal of Science* 43(7): 345–354.

Lipscomb, T. P., F. Y. Schulman, D. Moffett, and S. Kennedy. 1994. Morbilliviral disease in Atlantic bottlenose dolphins (*Tursiops truncatus*) from the 1987–1988 epizootic. *Journal of Wildlife Diseases* 30: 567–571.

Lipscomb, T. P., S. Kennedy, D. Moffett, A. Krafft, B. A. Klaunberg, J. H. Lichy, G. T. Regan, G. A. J. Worthy, and J. K. Taubenberger. 1996. Morbilliviral epizootic in bottlenose dolphins of the Gulf of Mexico. *Journal of Veterinary Diagnostic Investigations* 8: 283–290.

Lockyer, C. 1972. The age at sexual maturity of the southern fin whale (*Balaenoptera physalus*) using the annual layer counts in the ear plug. *Journal du Conseil International pour L'exploration de la Mer* 34: 276–294.

Lockyer, C. 1984. Review of baleen whale (Mysticeti) reproduction and implications for management. *Report of the International Whaling Commission, Special Issue* 6: 27–50.

Lockyer, C., and A. R. Martin. 1983. The sei whale off western Iceland: II Age, growth and reproduction. *Report of the International Whaling Commission* 33: 465–476.

Lucas, Z., P.-Y. Daoust, G. Conboy, and M. Brimacombe. 2003. Health status of harp seals (*Phoca groenlandica*) and hooded seals (*Cystophora cristata*) on Sable Island, Nova Scotia, Canada, concurrent with their expanding range. *Journal of Wildlife Diseases* 39: 16–28.

Lutcavage, M. E., P. Plotkin, B. Witherington, and P. L. Lutz. 1997. Human impacts on sea turtle survival. Pp. 387–409 in: P. L. Lutz and J. A. Musick, eds. *The Biology of Sea Turtles.* CRC Press, Boca Raton, FL.

Lyrholm, T., and U. Gyllensten. 1998. Global matrilineal population structure in sperm whales as indicated by mitochondrial DNA sequences. *Proceedings of the Royal Society of London* B 265: 1679–1684.

Lyrholm, T., O. Leimar, B. Johanneson, and U. Gyllensten. 1999. Sex-biased dispersal in sperm whales: contrasting mitochondrial and nuclear genetic structure of global populations. *Proceedings of the Royal Society of London* B 266: 347–354.

MacLean, S. A., G. W. Sheehan, and A. M. Jensen. 2002. Inuit and marine mammals. Pp. 641–652 in: W. F. Perrin, B. Würsig, and J. G. M. Thewissen, eds. *Encyclopedia of Marine Mammals*. Academic Press, San Diego, CA.

Madsen, P.T., M. Johnson, N. Aguilar de Soto, W. M. X. Zimmer, and P. Tyack. 2005. Biosonar performance of foraging beaked whales (*Mesoplodon densirostris*). *Journal of Experimental Biology* 208: 181–191.

Major, P. F. 1986. Notes on a predator-prey interaction between common dolphins (*Delphinus delphis*) and short-finned squid (*Illex illecebrosus*) in Lydonia Submarine Canyon, western North Atlantic Ocean. *Journal of Mammalogy* 67: 769–770.

Mann, J., and B. B. Smuts. 1998. Natal attraction: Allomaternal care and mother-infant separations in wild bottlenose dolphins. *Animal Behaviour* 55: 1097–1113.

Mann, J., R. C. Connor, L. M. Barre, and M. R. Heithaus. 2000. Female reproductive success in wild bottlenose dolphins (*Tursiops* sp.): Life history, habitat, provisioning, and group size effects. *Behavioral Ecology* 11: 210–219.

Mansfield, A. W. 1966. The grey seal in eastern Canadian waters. *Canadian Audubon Magazine* 28(Nov–Dec): 161–166.

Markussen, N. H., and P. Have. 1992. Phocine distemper virus infection in harp seals (*Phoca groenlandica*). *Marine Mammal Science* 8: 19–26.

Marquez M., R. 1990. *Sea Turtles of the World: An Annotated and Illustrated Catalogue of Sea Turtle Species Known to Date.* FAO Fisheries Synopsis No. 125, Volume 11. Food and Agriculture Organization of the United Nations, Rome, Italy. iv + 81 pp.

Marsh, H., and T. Kasuya. 1991. An overview of the changes in the role of a female pilot whale with age. Pp. 281–285 in: K. Pryor and K. S. Norris, eds. *Dolphin Societies—Discoveries and Puzzles.* University of California Press, Berkeley, CA.

Martin, A. R. 1983. The sei whale off western Iceland. I. Size, distribution and abundance. *Report of the International Whaling Commission* 33: 457–463.

Martin, A. R., and P. Rothery. 1993. Reproductive parameters of female long-finned pilot whales (*Globicephala melas*) around the Faroe Islands. *Report of the International Whaling Commission, Special Issue* 14: 263–304.

Martin, A. R. and T. G. Smith. 1992. Deep diving in wild, free-ranging beluga whales, *Delphinapterus leucas*. *Canadian Journal of Fisheries and Aquatic Sciences* 49: 462–466.

Martin, A. R., and F. J. Walker. 1997. Sighting of a right whale (*Eubalaena glacialis*) with calf off S. W. Portugal. *Marine Mammal Science* 13: 139–140.

Martin, A. R., S. K. Katona, D. Mattila, D. Hembree, and T. D. Waters. 1984. Migration of humpback whales between the Caribbean and Iceland. *Journal of Mammalogy* 65: 330–333.

Martin, A. R., T. G. Smith, and O. P. Cox. 1998. Dive form and function in belugas *Delphinapterus leucas* of the eastern Canadian High Arctic. *Polar Biology* 20: 218–228.

Martineau, D., S. De Guise, M. Fournier, L. Shugart, C. Girard, A. Lagacé, and P. Béland. 1994. Pathology and toxicology of beluga whales from the St. Lawrence Estuary, Quebec, Canada. Past, present, and future. *Science of the Total Environment* 154: 201–215.

Martineau D., S. Lair, S. De Guise, T. Lipscomb, P. Béland. 1999. Cancer in beluga whales from the St. Lawrence Estuary, Quebec, Canada: A potential biomarker of environmental contamination. *Journal of Cetacean Research and Management, Special Issue* 1: 249–265.

Mate, B. R., K. M. Stafford, R. Nawojchik, and J. L. Dunn. 1994. Movements and dive behavior of a satellite-monitored Atlantic white-sided dolphin (*Lagenorhynchus acutus*) in the Gulf of Maine. *Marine Mammal Science* 10: 116–121.

Mate, B. R., S. L. Nieukirk, and S. D. Kraus. 1997. Satellite-monitored movements of the northern right whale. *Journal of Wildlife Management* 61: 1393–1405.

Mate, B. R., B. A. Lagerquist, M. Winsor, J. Geraci, and J. H. Prescott. 2005. Movements and dive habits of a satellite-monitored longfinned pilot whale (*Globicephala melas*) in the Northwest Atlantic. *Marine Mammal Science* 21: 136–144.

Mathieu, A., J. F. Payne, L. L. Fancey, R. M. Santella, and T. L. Young. 1997. Polycyclic aromatic hydrocarbon-DNA adducts in beluga whales from the Arctic. *Journal of Toxicology and Environmental Health* 51: 1–4.

May-Collado, L., and I. Agnarsson. 2006. Cytochrome *b* and Bayesian inference of whale phylogeny. *Molecular Phylogenetics and Evolution* 38: 344–354.

Mayo, C. A., and M. K. Marx. 1990. Surface foraging behaviour of the North Atlantic right whale, *Eubalaena glacialis*, and associated zooplankton characteristics. *Canadian Journal of Zoology* 68: 2214–2220.

Mayo, C. A., B. H. Letcher, and S. Scott. 2001. Zooplankton filtering efficiency of the baleen of a North Atlantic right whale, *Eubalaena glacialis*. *Journal of Cetacean Research and Management, Special Issue* 2: 225–229.

Mazet, J. A. K., T. D. Hunt, and M. H. Ziccardi. 2004. *Assessment of the Risk of Zoonotic Disease Transmission to Marine Mammal Workers and the Public: Survey of Occupational Risks.* Final Report no. K0005486-01 to the U.S. Marine Mammal Commission. Wildlife Health Center, School of Veterinary Medicine, University of California, Davis, CA. 55 pp.

McAlpine, D. F. 2002. Pygmy and dwarf sperm whales *Kogia breviceps* and *K. sima*. Pp. 1007–1009 in: W. F. Perrin, B. Würsig, and H. G. M. Thewissen, eds. *Encyclopedia of Marine Mammals*. Academic Press, San Diego, CA.

McAlpine, D. F., and R. H. Walker. 1990. Extralimital records of the harp seal, *Phoca groenlandica*, from the western North Atlantic: a review. *Marine Mammal Science* 6: 243–247.

McAlpine, D. F., P. T. Stevick, and L. D. Murison. 1999a. Increase in extralimital occurrences of ice-breeding seals in the northern Gulf of Maine region: More seals or fewer fish? *Marine Mammal Science* 15: 906–911.

McAlpine, D. F., P. T. Stevick, L. D. Murison, and S. D. Turnbull. 1999b. Extralimital records of

hooded seals (*Cystophora cristata*) in the Bay of Fundy and northern Gulf of Maine. *Northeastern Naturalist* 6: 225–230.

McAlpine, D. F., M. C. James, J. Lien, and S. A. Orchard. 2007. Status and conservation of sea turtles in Canadian waters. Pp. 85–112 in: C. N. L. Seburn and C. A. Bishop, eds. *Ecology, Conservation, and Status of Reptiles in Canada.* Herpetological Conservation Number 2. Society for the Study of Amphibians and Reptiles, Salt Lake City, UT.

Mchedlidze, G. A. 2002. Sperm whales, evolution. Pp. 1172–1174 in: W. F. Perrin, B. Würsig, and J. G. M. Thewissen, eds. *Encyclopedia of Marine Mammals*. Academic Press, San Diego, CA.

Mead, J. G. 1975. Preliminary report on the former net fisheries for *Tursiops truncatus* in the western North Atlantic. *Journal of the Fisheries Research Board of Canada* 32: 1155–1162.

Mead, J. G. 1977. Records of sei and Bryde's whales from the Atlantic coast of the United States, Gulf of Mexico and the Caribbean. *Report of the International Whaling Commission, Special Issue* 1: 113–116.

Mead, J. G. 1989a. Beaked whales of the genus *Mesoplodon*. Pp. 349–430 in: S. H. Ridgway and R. Harrison, eds. *Handbook of Marine Mammals. Volume 4: River Dolphins and the Larger Toothed Whales.* Academic Press, London.

Mead, J. G. 1989b. Bottlenose whales *Hyperoodon ampullatus* (Forster, 1770) and *Hyperoodon planifrons* Flower, 1882. Pp. 321–348 in: S. H. Ridgway and R. Harrison, eds. *Handbook of Marine Mammals. Volume 4: River Dolphins and the Larger Toothed Whales.* Academic Press, London.

Mead, J. G. 2002. Beaked whales, overview, Ziphiidae. Pp. 81–84 in: W. F. Perrin, B. Würsig, and J. G. M. Thewissen, eds. *Encyclopedia of Marine Mammals*. Academic Press, San Diego, CA.

Mead, J. G., and R. L. Brownell, Jr. 2005. Order Cetacea. Pp. 723–743 in: D. E. Wilson and D. M. Reeder, eds. *Mammal Species of the World, A Taxonomic and Geographic Reference*, 3rd edition, volume 1. Johns Hopkins University Press, Baltimore, MD.

Mead, J. G., and E. D. Mitchell. 1984. Atlantic gray whales. Pp. 33–53 in: M. L. Jones, S. L. Swartz, and S. Leatherwood, eds. *The Gray Whale* Eschrichtius robustus. Academic Press, Orlando, FL.

Mead, J. G., and C. W. Potter. 1990. Natural history of bottlenose dolphins along the central Atlantic coast of the United States. Pp. 165–195 in: S. Leatherwood and R. R. Reeves, eds. *The Bottlenose Dolphin.* Academic Press, San Diego, CA.

Mead, J. G., and C. W. Potter. 1995. Recognizing two populations of the bottlenose dolphin (*Tursiops truncatus*) off the Atlantic coast of North America: morphological and ecological considerations. *IBI Reports* 5: 31–39.

Mearns, E. A. 1900. The native mammals of Rhode Island. *Circular of the Newport Natural History Society* 1: 1–4.

Measures, L. N., P. Béland, D. Martineau, and S. De Guise. 1995. Helminths of an endangered population of belugas, *Delphinapterus leucas*, in the St Lawrence Estuary, Canada. *Canadian Journal of Zoology* 73: 1402–1409.

Medic, H. 2005. Wandering hooded seals. *Rhode Island Naturalist* 12(2): 9–10.

Mercer, M. C. 1975. Modified Leslie-DeLury population models of the long-finned pilot whale (*Globicephala melaena*) and annual production of the short-finned squid (*Illex illecebrosus*) based upon their interactions at Newfoundland. *Journal of the Fisheries Research Board of Canada* 32: 1145–1154.

Merriam, C. H. 1884. *The Mammals of the Adirondack Region, Northeastern New York, With an Introductory Chapter Treating of the Location and Boundaries of the Region, Its Geological History, Topography, Climate, General Features, Botany, and Faunal Position.* L. S. Foster, New York, NY. 316 pp. (reprinted 1974, Arno Press, New York, NY)

Meylan, A. 1986. The riddle of the ridley. *Natural History* 95: 90–96.

Miller, G. S., Jr. 1899. Preliminary list of the mammals of New York. *Bulletin of the New York State Museum* 6: 271–390. (not seen; cited by Connor, 1971)

Miller, P., M. Johnson, and P. Tyack. 2004. Sperm whale behavior indicates the use of rapid echolocation click buzzes "creaks" in prey capture. *Proceedings of the Royal Society of London* B 271: 2239–2247.

Mitchell, E. 1972. Whale pigmentation and feeding behavior. *American Zoologist* 12: 655.

Mitchell, E. 1974. Present status of northwest Atlantic fin and other whale stocks. Pp. 108–169 in: W. E. Schevill, ed. *The Whale Problem, A Status Report*. Harvard University Press, Cambridge, MA.

Mitchell, E. 1975a. *Porpoise, Dolphin and Small Whale Fisheries of the World: Status and Problems.* IUCN Monograph 3. International Union for the Conservation of Nature and Natural Resources, Morges, Switzerland. 129 pp.

Mitchell, E. 1975b. Preliminary report on Nova Scotia fishery for sei whales (*Balaenoptera borealis*). *Report of the International Whaling Commission* 25: 218–225.

Mitchell, E. 1975c. Preliminary report on Nova Scotian fishery for sperm whales (*Physeter catodon*). *Report of the International Whaling Commission* 25: 226–235.

Mitchell, E. D., Jr. 1991. Winter records of the minke whale (*Balaenoptera acutorostrata acutorostrata* Lacépède 1804) in the southern North Atlantic. *Report of the International Whaling Commission* 41: 455–457.

Mitchell, E., and D. G. Chapman. 1977. Preliminary assessment of stocks of northwest Atlantic sei whales (*Balaenoptera borealis*). *Report of the International Whaling Commission, Special Issue* 1: 117–120.

Mitchell, E., and V. M. Kozicki. 1975. Autumn stranding of a northern bottlenose whale (*Hyperoodon ampullatus*) in the Bay of Fundy, Nova Scotia. *Journal of the Fisheries Research Board of Canada* 32: 1019-1040.

Mitchell, E., and R. R. Reeves. 1983. Catch history, abundance, and present status of northwest Atlantic humpback whales. *Report of the International Whaling Commission, Special Issue* 5: 153–212.

Mitchell, E., V. M. Kozicki, and R. R. Reeves. 1986. Sightings of right whales, *Eubalaena glacialis*, on the Scotian Shelf, 1966–72. *Report of the International Whaling Commission, Special Issue* 10: 83–107.

Miyazaki, N. 2002. Ringed, Caspian, and Baikal seals, *Pusa hispida*, *P. caspica*, and *P. sibirica*. Pp. 1033–1037 in: W. F. Perrin, B. Würsig, and J. G. M. Thewissen, eds. *Encyclopedia of Marine Mammals*. Academic Press, San Diego, CA.

Miyazaki, N. and M. Nishiwaki. 1978. School structure of the striped dolphin off the Pacific coast of Japan. *Scientific Reports of the Whales Research Institute*, Tokyo 30: 65–115.

Mizroch, S. A., D. W. Rice, and J. M. Breiwick. 1984. The fin whale *Balaenoptera physalus*. *Marine Fisheries Review* 46(4): 20–24.

Møhl, B., W. W. L. Au, J. L. Pawloski, and P. E. Nachtigall. 1999. Dolphin hearing: Relative sensitivity as a function of point of application of a contact sound source in the jaw and head region. *Journal of the Acoustical Society of America* 105: 3421–3424.

Moore, J. C. 1953. Distribution of marine mammals to Florida waters. *American Midland Naturalist* 49: 117–158.

Moore, J. C. 1966. Diagnoses and distribution of beaked whales of the genus *Mesoplodon* known from North American waters. Pp. 32–61 in: K. S. Norris, ed. *Whales, Dolphins and Porpoises*. University of California Press, Berkeley, CA.

Morreale, S. J., and E. A. Standora. 1998. *Early Life Stage Ecology of Sea Turtles in Northeastern U.S. Waters.* NOAA Technical Memorandum NMFS-SEFSC-413. National Marine Fisheries Service, Miami, FL. iii + 49 pp.

Morreale, S. J., A. Meylan, S. S. Sadove, and E. A. Standora. 1992. Annual occurrence and winter mortality of marine turtles in New York waters. *Journal of Herpetology* 26: 301–308.

Morreale, S. J., P. T. Plotkin, D. J. Shaver, and H. J. Kalb. 2007. Adult migration and habitat utilization. Pp. 213–219 in: P. T. Plotkin, ed. *Biology and Conservation of Ridley Sea Turtles.* Johns Hopkins University Press, Baltimore, MD.

Mortimer, J. A. 1995. Feeding ecology of sea turtles. Pp. 103–109 in: K. A. Bjorndal, ed. *Biology and Conservation of Sea Turtles*, Revised Edition. Smithsonian Institution Press, Washington, DC.

Murison, L. D., and D. E. Gaskin. 1989. The distribution of right whales and zooplankton in the Bay of Fundy, Canada. *Canadian Journal of Zoology* 67: 1411–1420.

Nagorsen, D. 1985. *Kogia simus. Mammalian Species* 239: 1–6.

NARWC (North Atlantic Right Whale Consortium). 2006. North Atlantic right whale report card: November 2005–October 2006. North Atlantic Right Whale Consortium, Boston, MA. 5 pp. http://www.rightwhaleweb.org/papers/pdf/NARWC_Report_Card2006.pdf

Nawojchik, R. 1994. First record of *Mesoplodon densirostris* (Cetacea: Ziphiidae) from Rhode Island. *Marine Mammal Science* 10: 477–480.

Nawojchik, R. 2002. Marine mammals and sea turtles of Block Island, Rhode Island. Pp. 169–181 in: P. W. Paton, L. L. Gould, P. V. August, and A. O. Frost, eds. *The Ecology of Block Island*. Rhode Island Natural History Survey, Kingston, RI.

Nawojchik, R., and D. J. St Aubin. 2003. Sea turtles in Connecticut and Rhode Island: information from strandings (1997–2001). Pp. 270–271 in: J. A. Seminoff, ed. *Proceedings of the Twenty-Second Annual Symposium on Sea Turtle Biology and Conservation*. NOAA Technical Memorandum NMFS-SEFSC-503. National Marine Fisheries Service, Miami, FL.

Nawojchik, R., D. J. St. Aubin, and A. Johnson. 2003. Movements and dive behavior of two stranded, rehabilitated long-finned pilot whales (*Globicephala melas*) in the Northwest Atlantic. *Marine Mammal Science* 19: 232–239.

Nelson, C. H., and K. R. Johnson. 1987. Whales and walruses as tillers of the sea floor. *Scientific American* 255: 112–117.

Nemoto, T. 1970. Feeding patterns of baleen whales in the ocean. Pp. 241–252 in: J. H. Steele, ed. *Marine Food Chains*. University of California Press, Berkeley, CA.

Nerini, M. 1984. A review of gray whale feeding ecology. Pp. 423–450 in: M. L. Jones, S. L. Swartz, and S. Leatherwood, eds. *The Gray Whale* Eschrichtius robustus. Academic Press, Orlando, FL.

Nikaido, M., F. Matsumo, H. Hamilton, R. L. Brownell, Jr., Y. Cao, W. Ding, Z. Zuoyan, A. M. Shedlock, R. E. Fordyce, M. Hasegawa, and N. Okada. 2001. Retroposon analysis of major cetacean lineages: The monophyly of toothed whales and paraphyly of river dolphins. *Proceedings of the National Academy of Sciences of the USA* 98: 7384–7389.

NMFCA (Norwegian Ministry of Fisheries and Coastal Affairs). 2006. Marine stocks: hooded seals. NMFCA, Oslo, Norway. http://www.fisheries.no/marine_stocks/mammals/seals/marine_stocks_marine_mammals_hooded_seals.htm

NMFS (National Marine Fisheries Service). 1993. Taking and importing of marine mammals; depletion of the coastal migratory stock of bottlenose dolphins along the U.S. Mid-Atlantic coast—final rule. *Federal Register* 58: 17789–17791.

NMFS (National Marine Fisheries Service). 1999. Threatened fish and wildlife: Listing of the Gulf of Maine/Bay of Fundy population of harbor porpoise as threatened under the Endangered Species Act (ESA). *Federal Register* 64: 465–471.

NMFS (National Marine Fisheries Service). 2001. Status review of the Gulf of Maine/Bay of Fundy population of harbor porpoise under the Endangered Species Act (ESA). *Federal Register* 66: 53195–53197.

NMFS (National Marine Fisheries Service). 2005. Endangered and threatened wildlife and plants: Endangered status for southern resident killer whales. *Federal Register* 70: 69903–69912.

NMFS (National Marine Fisheries Service) and USFWS (U.S. Fish and Wildlife Service). 2007a. *Green Turtle (*Chelonia mydas*) 5-Year Review: Summary and Evaluation*. National

Marine Fisheries Service, Office of Protected Resources, Silver Spring, MD and U.S. Fish and Wildlife Service, Southeast Region, Jacksonville Ecological Service Field Office, Jacksonville, FL. 105 pp.

NMFS (National Marine Fisheries Service) and USFWS (U.S. Fish and Wildlife Service). 2007b. *Kemp's Ridley Sea Turtle (*Lepidochelys kempii*) 5-Year Review: Summary and Evaluation*. National Marine Fisheries Service, Office of Protected Resources, Silver Spring, MD and U.S. Fish and Wildlife Service, Southeast Region, Jacksonville Ecological Service Field Office, Jacksonville, FL. 50 pp.

NMFS (National Marine Fisheries Service) and USFWS (U.S. Fish and Wildlife Service). 2007c. *Leatherback Sea Turtle (*Dermochelys coriacea*) 5-Year Review: Summary and Evaluation*. National Marine Fisheries Service, Office of Protected Resources, Silver Spring, MD and U.S. Fish and Wildlife Service, Southeast Region, Jacksonville Ecological Service Field Office, Jacksonville, FL. 81 pp.

NMFS (National Marine Fisheries Service) and USFWS (U.S. Fish and Wildlife Service). 2007d. *Loggerhead Sea Turtle (*Caretta caretta*) 5-Year Review: Summary and Evaluation*. National Marine Fisheries Service, Office of Protected Resources, Silver Spring, MD and U.S. Fish and Wildlife Service, Southeast Region, Jacksonville Ecological Service Field Office, Jacksonville, FL. 67 pp.

Norman, S. A., and J. G. Mead. 2001. *Mesoplodon europaeus. Mammalian Species* 688: 1–5.

Norris, K. S. 1968. The echolocation of marine mammals. Pp. 391–423 in: H. T. Andersen, ed. *The Biology of Marine Mammals*. Academic Press, New York, NY.

Norris, K. S., and T. P. Dohl. 1980. The structure and function of cetacean schools. Pp. 211–261 in: L. M. Herman, ed. *Cetacean Behavior: Mechanisms and Functions*. John Wiley, New York, NY.

Norris, K. S., and G. W. Harvey. 1974. Sound transmission in the porpoise head. *Journal of the Acoustical Society of America* 56: 659–664.

Norris, K. S., and J. H. Prescott. 1961. Observations on Pacific cetaceans of California and Mexican waters. *University of California Publications in Zoology* 63: 291–402.

Northridge, S. P. 1991. An updated world review of interactions between marine mammals and fisheries. *FAO Technical Paper* 251(Supplement 1): 1–58.

Northridge, S. 2002. Fishing industry, effects of. Pp. 442–446 in: W. F. Perrin, B. Würsig, and J. G. M. Thewissen, eds. *Encyclopedia of Marine Mammals*. Academic Press, San Diego, CA.

Northridge, S. P., and R. J. Hofman. 1999. Marine mammal interactions with fisheries. Pp. 99–119 in: J. R. Twiss, Jr. and R. R. Reeves, eds. *Conservation and Management of Marine Mammals.* Smithsonian Institution Press, Washington, DC.

Northridge, S., M. Tasker, A. Webb, K. Camphuysen, and M. Leopold. 1997. White beaked *Lagenorhynchus albirostris* and Atlantic white-sided dolphin *L. acutus* distributions in northwest European and U.S. Atlantic waters. *Report of the International Whaling Commission* 47: 797–805.

Nowacek, D. P., M. P. Johnson, P. L. Tyack, K. A. Shorter, W. A. McLellan, and D. A. Pabst. 2001. Buoyant balaenids: the ups and downs of buoyancy in right whales. *Proceedings of the Royal Society of London* B 268: 1811–1816.

Nowak, R. M. 1999. *Walker's Mammals of the World*, sixth edition, volume II. Johns Hopkins University Press, Baltimore, MD. x + 1100 pp.

NRC (National Research Council). 1990. *The Decline of the Sea Turtle: Causes and Prevention*. National Academy Press, Washington, DC. xv + 260 pp.

NRC (National Research Council). 1992. *Dolphins and the Tuna Industry*. National Academy Press, Washington, DC. 176 pp.

O'Corry-Crowe, G. M. 2002. Beluga whale *Delphinapterus leucas*. Pp. 94–99 in: W. F. Perrin, B. Würsig, and J. G. M. Thewissen, eds. *Encyclopedia of Marine Mammals*. Academic Press, San Diego, CA.

Odell, D. K., and K. M. McClune. 1999. False killer whale *Pseudorca crassidens* (Owen, 1846). Pp. 213–243 in: S. H. Ridgway and R. Harrison, eds. *Handbook of Marine Mammals. Volume 6: The Second Book of Dolphins and the Porpoises.* Academic Press, London.

Olson, P. A., and S. B. Reilly. 2002. Pilot whales *Globicephala melas* and *G. macrorhynchus*. Pp. 898–903 in: W. F. Perrin, B. Würsig, and J. G. M. Thewissen, eds. *Encyclopedia of Marine Mammals*. Academic Press, San Diego, CA.

ORG (Oceanic Research Group). 2003. The Chessie watch page. Oceanic Research Group, North Reading, MA. http://www.oceanicresearch.org/chessie.html

O'Shea, T. J., R. R. Reeves, and A. K. Long, eds. 1999. *Marine Mammals and Persistent Ocean Contaminants: Proceedings of the Marine Mammal Commission Workshop, Keystone, Colorado, 12–15 October 1998*. Marine Mammal Commission, Bethesda, MD. vii + 150 pp.

Osterhaus, A. D. M. E., and E. J. Vedder. 1988. Identification of virus causing recent seal deaths. *Nature* 335: 20.

Osterhaus, A. D. M. E., J. Groen, P. DeVries, F. G. C. M. Uytde Haag, B. Klingenborn, and R. Zarnke. 1988. Canine distemper virus in seals. *Nature* 335: 403–404.

Overholtz, W. J., and J. R. Nicolas. 1979. Apparent feeding by the fin whale, *Balaenoptera physalus*, and humpback whale, *Megaptera novaeangliae*, on the American sand lance, *Ammodytes americanus*, in the western North Atlantic. *Fishery Bulletin* 77: 285–287.

Palka, D., A. Read, and C. Potter. 1997. Summary of knowledge of white-sided dolphins (*Lagenorhynchus acutus*) from the U.S. and Canadian North Atlantic waters. *Report of the International Whaling Commission* 47: 729–734.

Palsbøll, P. J., , P. J. Clapham, D. K. Mattila, F. Larsen, R. Sears, H. R. Seigismund, J. Sigurjónsson, O. Vasquez, and P. Actander. 1995. Distribution of mtDNA haplotypes in North Atlantic humpback whales: the influence of behavior on population structure. *Marine Ecology Progress Series* 116: 1–10.

Palsbøll, P. J., J. Allen, M. Bérubé, P. J. Clapham, T. P. Feddersen, P. Hammond, H. Jørgensen, S. Katona, A. H. Larsen, F. Larsen, J. Lien, D. K. Mattila, J. Sigurjónsson, R. Sears, T.

Smith, R. Sponer, P. Stevick, and N. Øien. 1997. Genetic tagging of humpback whales. *Nature* 388: 767–769.

Palsbøll, P. J., J. Allen, T. H. Anderson, M. Bérubé, P. J. Clapham, T. P. Feddersen, N. Friday, P. Hammond, H. Jørgensen, S. K. Katona, A. H. Larsen, F. Larsen, J. Lien, D. K. Mattila, F. B. Nygaard, J. Robbins, R. Sponer, R. Sears, J. Sigurjónsson, T. D. Smith, P. T. Stevick, G. Vikingsson, and N. Øien. 2001. Stock structure and composition of the North Atlantic humpback whale, *Megaptera novaeangliae*. Unpublished document SC/53/NAH11. International Whaling Commission, Cambridge, United Kingdom.

Papastavrou, V., S. C. Smith, and H. Whitehead. 1989. Diving behaviour of the sperm whale, *Physeter macrocephalus*, off the Galapagos Islands. *Canadian Journal of Zoology* 67: 839–846.

Paquet, D., C. Haycock, and H. Whitehead. 1997. Numbers and seasonal occurrence of humpback whales (*Megaptera novaeangliae*) off Brier Island, Nova Scotia. *Canadian Field-Naturalist* 111: 548–552.

Pauli, B. D., and J. M. Terhune. 1987a. Meteorological influences on harbour seal haul-out. *Aquatic Mammals* 13: 114–118.

Pauli, B. D., and J. M. Terhune. 1987b. Tidal and temporal interaction on harbour seal haul-out patterns. *Aquatic Mammals* 13: 93–95.

Payne, P. M., and D. W. Heinemann. 1993. The distribution of pilot whales (*Globicephala* spp.) in shelf/shelf edge and slope waters of the north-eastern United States. *Report of the International Whaling Commission, Special Issue* 14: 51–68.

Payne, P. M., and D. C. Schneider. 1984. Yearly changes in the abundance of harbor seals, *Phoca vitulina* at a winter haul-out site in Massachusetts. *Fishery Bulletin* 82: 440–442.

Payne, P. M., and L. A. Selzer. 1989. The distribution, abundance and selected prey of the harbor seal, *Phoca vitulina concolor*, in southern New England. *Marine Mammal Science* 5: 173–192.

Payne, P. M., J. R. Nicolas, L. O'Brien, and K. D. Powers. 1986. The distribution of the humpback whale, *Megaptera novaeangliae*, on Georges Bank and in the Gulf of Maine in relation to densities of the sand eel, *Ammodytes americanus*. *Fishery Bulletin* 84: 271–277.

Payne, P. M., D. N. Wiley, S. B. Young, S. Pittman, P. J. Clapham, and J. W. Jossi. 1990. Recent fluctuations in the abundance of baleen whales in the southern Gulf of Maine in relation to changes in selected prey. *Fishery Bulletin* 88: 687–696.

Payne, R., and E. M. Dorsey. 1983. Sexual dimorphism and aggressive use of callosities in right whales (*Eubalaena australis*). Pp. 295–329 in: R. Payne, ed. *Communication and Behavior of Whales.* AAAS Selected Symposium 76. Westview Press, Boulder, CO.

Payne, R., O. Brazier, E. M. Dorsey, J. S. Perkins, V. J. Rowntree, and A. Titus. 1983. External features in southern right whales (*Eubalaena australis*) and their use in identifying individuals. Pp. 371–445 in: R. Payne, ed. *Communication and Behavior of Whales*. AAAS Selected Symposium 76. Westview Press, Boulder, CO.

Payne, R., V. Rowntree, J. S. Perkins, J. G. Cooke, and K. Lankester. 1990. Population size, trends and reproductive parameters of right whales (*Eubalaena australis*) off Peninsula Valdes, Argentina. *Report of the International Whaling Commission, Special Issue* 12: 271–278.

Perrin, W. F. 2001. *Stenella attenuata. Mammalian Species* 683: 1–8.

Perrin, W. F. 2002a. Atlantic spotted dolphin *Stenella frontalis*. Pp. 47–49 in: W. F. Perrin, B. Würsig, and H. G. M. Thewissen, eds. *Encyclopedia of Marine Mammals*. Academic Press, San Diego, CA.

Perrin, W. F. 2002b. Coloration. Pp. 236–245 in: W. F. Perrin, B. Würsig, and H. G. M. Thewissen, eds. *Encyclopedia of Marine Mammals*. Academic Press, San Diego, CA.

Perrin, W. F. 2002c. Common dolphins *Delphinus delphis, D. capensis*, and *D. tropicalis*. Pp. 245–248 in: W. F. Perrin, B. Würsig, and H. G. M. Thewissen, eds. *Encyclopedia of Marine Mammals*. Academic Press, San Diego, CA.

Perrin, W. F. 2002d. Pantropical spotted dolphin *Stenella attenuata*. Pp. 865–867 in: W. F. Perrin, B. Würsig, and H. G. M. Thewissen, eds. *Encyclopedia of Marine Mammals*. Academic Press, San Diego, CA.

Perrin, W. F. 2002e. *Stenella frontalis. Mammalian Species* 702: 1–6.

Perrin, W. F. 2002f. Stranding. Pp. 1192–1197 in: W. F. Perrin, B. Würsig, and J. G. M. Thewissen, eds. *Encyclopedia of Marine Mammals*. Academic Press, San Diego, CA.

Perrin, W. F., and R. L. Brownell, Jr. 2002. Minke whales *Balaenoptera acutorostrata* and *B. bonaerensis*. Pp. 750–754 in: W. F. Perrin, B. Würsig, and J. G. M. Thewissen, eds. *Encyclopedia of Marine Mammals*. Academic Press, San Diego, CA.

Perrin, W. F., and A. A. Hohn. 1994. Pantropical spotted dolphin *Stenella attenuata* (Gray, 1846). Pp. 71–98 in: S. H. Ridgway and R. Harrison, eds. *Handbook of Marine Mammals. Volume 5: The First Book of Dolphins.* Academic Press, London.

Perrin, W. F., and S. B. Reilly. 1994. Reproductive parameters of dolphins and small whales of the family Delphinidae. *Report of the International Whaling Commission, Special Issue* 6: 97–133.

Perrin, W. F., R. R. Warner, C. H. Fiscus, and D. B. Holts. 1973. Stomach contents of porpoise, *Stenella* spp., and yellowfin tuna, *Thunnus albacares*, in mixed-species aggregations. *Fishery Bulletin* 71: 1077–1092.

Perrin, W. F., E. D. Mitchell, J. G. Mead, D. K. Caldwell, P. J. H. van Bree, and W. H. Dawbin. 1987. Revision of the spotted dolphins, *Stenella* spp. *Marine Mammal Science* 3: 99–170.

Perrin, W. F., D. K. Caldwell, and M. C. Caldwell. 1994a. Atlantic spotted dolphin *Stenella frontalis* (G. Cuvier, 1829). Pp. 173–190 in: S. H. Ridgway and R. Harrison, eds. *Handbook of Marine Mammals. Volume 5: The First Book of Dolphins.* Academic Press, London.

Perrin, W. F., G. P. Donovan, and J. Barlow, eds. 1994b. *Gillnets and Cetaceans, Incorporating the Proceedings of the Symposium and Workshop on the Mortality of Cetaceans in Passive Fishing Nets and Traps. Report of the International Whaling Commission,*

Special Issue 15. International Whaling Commission, Cambridge, UK. ix + 629 pp.

Perrin, W. F., C. E. Wilson, and F. I. Archer II. 1994c. Striped dolphin *Stenella coeruleoalba* (Meyen, 1833). Pp. 129–159 in: S. H. Ridgway and R. Harrison, eds. *Handbook of Marine Mammals. Volume 5: The First Book of Dolphins.* Academic Press, London.

Perry, S. L., D. P. DeMaster, and G. K. Silber. 1999. The great whales: history and status of six species listed as endangered under the U. S. Endangered Species Act of 1973. *Marine Fisheries Review* 61: 1–74.

Pitman, R. L. 2002. Mesoplodont whales *Mesoplodon* spp. Pp. 738–742 in: W. F. Perrin, B. Würsig, and J. G. M. Thewissen, eds. *Encyclopedia of Marine Mammals*. Academic Press, San Diego, CA.

Pitman, R. L., and P. Ensor. 2003. Three forms of killer whales (*Orcinus orca*) in Antarctic waters. *Journal of Cetacean Research and Management* 5: 131–139.

Pittman, S., B. Costa, C. Moy, D. Wiley, and R. D. Kenney. 2006. Cetacean distribution and diversity. Pp. 265-326 in: T. Battista, R. Clark, and S. Pittman, eds. *An Ecological Characterization of the Stellwagen Bank National Marine Sanctuary Region: Oceanographic, Biogeographic, and Contaminants Assessment*. NOAA Technical Memorandum NCCOS 45. Center for Coastal Monitoring and Assessment, NOAA National Centers for Coastal Ocean Science, Silver Spring, MD.

Pivorunas, A. 1976. A mathematical consideration on the function of baleen plates and their fringes. *Scientific Reports of the Whales Research Institute*, Tokyo 28: 37–55.

Pivorunas, A. 1979. The feeding mechanisms of baleen whales. *American Scientist* 67: 432–440.

Pritchard, P. C. H., and P. Trebbau. 1984. The Turtles of Venezuela. Contribution to Herpetology, No. 2. Society for the Study of Amphibians and Reptiles, Salt Lake City, UT. 403 pp.

Read, A. J. 1990a. Reproductive seasonality in harbour porpoises, *Phocoena phocoena*, from the Bay of Fundy. *Canadian Journal of Zoology* 68: 284–288.

Read, A. J. 1990b. Age as sexual maturity and pregnancy rates of harbour porpoises *Phocoena phocoena* from the Bay of Fundy. *Canadian Journal of Fisheries and Aquatic Sciences* 47: 561–565.

Read, A. J. 1994. Interactions between cetaceans and gillnet and trap fisheries in the northwest Atlantic. *Report of the International Whaling Commission, Special Issue* 15: 133–147.

Read, A. J. 1996. Incidental catches of small cetaceans. Pp. 109–128 in: M. P. Simmonds and J. D. Hutchinson, eds. *The Conservation of Whales and Dolphins: Science and Practice.* John Wiley & Sons, Chichester, UK.

Read, A. J. 1999. Harbour porpoise *Phocoena phocoena* (Linnaeus, 1758). Pp. 323–355 in: S. H. Ridgway and R. Harrison, eds. *Handbook of Marine Mammals. Volume 6: The Second Book of Dolphins and the Porpoises.* Academic Press, London.

Read, A. J. 2002. Porpoises, overview. Pp. 982–985 in: W. F. Perrin, B. Würsig, and J. G. M. Thewissen, eds. *Encyclopedia of Marine Mammals*. Academic Press, San Diego, CA.

Read, A. J., and A. A. Hohn. 1995. Life in the fast lane: The life history of harbor porpoises from

the Gulf of Maine. *Marine Mammal Science* 11: 423–440.

Read, A. J., and P. R. Wade. 2000. Status of marine mammals in the United States. *Conservation Biology* 14: 929–940.

Read, A. J., and A. J. Westgate. 1997. Monitoring the movements of harbour porpoises (*Phocoena phocoena*) with satellite telemetry. *Marine Biology* 130: 315–322.

Reeves, R. R. 2002. The origins and character of 'aboriginal subsistence' whaling: a global review. *Mammal Review* 32: 71–106.

Reeves, R. R., and S. K. Katona. 1980. Extralimital records of white whales (*Delphinapterus leucas*) in eastern North American waters. *Canadian Field-Naturalist* 94: 239–247.

Reeves, R. R., and R. D. Kenney. 2003. Baleen whales, *Eubalaena* spp. and allies. Pp. 425–453 in: G. A. Feldhamer, B. C. Thompson, and J. A. Chapman, ed. *Wild Mammals of North America: Biology, Management, and Economics*, second edition. Johns Hopkins University Press, Baltimore, MD.

Reeves, R. R., and S. Leatherwood. 1984. Live-capture fisheries for cetaceans in USA and Canadian waters, 1973–1982. *Report of the International Whaling Commission* 34: 497–507.

Reeves, R. R., and S. Leatherwood. 1985. Bowhead whale *Balaena mysticetus* Linnaeus, 1758. Pp. 305–344 in: S. H. Ridgway and R. Harrison, eds. *Handbook of Marine Mammals. Volume 3: The Sirenians and Baleen Whales.* Academic Press, London.

Reeves, R. R., and J. K. Ling. 1981. Hooded seal *Cystophora cristata* Erxleben, 1777. Pp. 171–194 in: S. H. Ridgway and R. Harrison, eds. *Handbook of Marine Mammals. Volume 2: Seals.* Academic Press, London.

Reeves, R. R., and J. G. Mead. 1999. Marine mammals in captivity. Pp. 412–436 in: J. R. Twiss, Jr. and R. R. Reeves, eds. *Conservation and Management of Marine Mammals*. Smithsonian Institution Press, Washington, DC.

Reeves, R. R., and E. Mitchell. 1986. The Long Island, New York, right whale fishery: 1650–1924. *Report of the International Whaling Commission, Special Issue* 10: 201–220.

Reeves, R. R., and A. J. Read. 2003. Bottlenose dolphin, harbor porpoise, sperm whale, and other toothed cetaceans. Pp. 397–424 in: G. A. Feldhamer, B. C. Thompson, and J. A. Chapman, ed. *Wild Mammals of North America: Biology, Management, and Economics*, second edition. Johns Hopkins University Press, Baltimore, MD.

Reeves, R. R., and T. D. Smith. 2002. Historical catches of humpback whales in the North Atlantic Ocean: an overview of sources. *Journal of Cetacean Research and Management* 4: 219–234..

Reeves, R. R., and H. Whitehead. 1997. Status of the sperm whale (*Physeter macrocephalus*) in Canada. *Canadian Field-Naturalist* 111: 293–307.

Reeves, R. R., J. G. Mead, and S. Katona. 1978. The right whale, *Eubalaena glacialis*, in the western North Atlantic. *Report of the International Whaling Commission* 28: 303–312.

Reeves, R.R., E. Mitchell, and H. Whitehead. 1993. Current status of the northern bottlenose whale, *Hyperoodon ampullatus*. *Canadian Field-Naturalist* 107: 490–508.

Reeves, R. R., P. J. Clapham, R. L. Brownell, Jr., and G. K. Silber. 1998. *Recovery Plan for the Blue Whale (*Balaenoptera musculus*)*. U. S. Department of Commerce, National Oceanic and Atmospheric Administration, National Marine Fisheries Service, Office of Protected Resources, Silver Spring, Maryland, USA. iv + 39 pp.

Reeves, R. R., C. Smeenk, R. L. Brownell, Jr., and C. C. Kinze. 1999a. Atlantic white-sided dolphin *Lagenorhynchus acutus* (Gray, 1828). Pp. 31–56 in: S. H. Ridgway and R. Harrison, eds. *Handbook of Marine Mammals. Volume 6: The Second Book of Dolphins and the Porpoises.* Academic Press, London.

Reeves, R. R., C. Smeenk, C. C. Kinze, R. L. Brownell, Jr., and J. Lien. 1999b. White-beaked dolphin *Lagenorhynchus albirostris* Gray, 1846. Pp. 1–30 in: S. H. Ridgway and R. Harrison, eds. *Handbook of Marine Mammals. Volume 6: The Second Book of Dolphins and the Porpoises.* Academic Press, London.

Reeves, R. R., R. Rolland, and P. J. Clapham, eds. 2001a. Report of the workshop on the causes of reproductive failure in North Atlantic right whales: New avenues of research. Northeast Fisheries Science Center Reference Document 01-16. National Marine Fisheries Service, Woods Hole, MA. 54 pp.

Reeves, R. R., S. L. Swartz, S. E. Wetmore, and P. J. Clapham. 2001b. Historical occurrence and distribution of humpback whales in the eastern and southern Caribbean Sea, based on data from American whaling logbooks. *Journal of Cetacean Research and Management* 3: 117–129.

Reeves, R. R., T. D. Smith, E. A. Josephson, P. J. Clapham, and G. Woolmer. 2004. Historical observations of humpback and blue whales in the North Atlantic Ocean: Clues to migratory routes and possibly additional feeding grounds. *Marine Mammal Science* 20: 774–786.

Reidman, M. 1990. *The Pinnipeds: Seals, Sea Lions, and Walruses.* University of California Press, Berkeley, CA. xxxiii + 439 pp.

Reynolds, J. E. III, and D. K. Odell. 1991. *Manatees and Dugongs.* Facts on File, New York, NY. xiv + 192 pp.

Reynolds, J. E. III, and J. A. Powell. 2002. Manatees *Trichechus manatus*, *T. senegalensis*, and *T. inunguis*. Pp. 709–720 in: W. F. Perrin, B. Würsig, and J. G. M. Thewissen, eds. *Encyclopedia of Marine Mammals*. Academic Press, San Diego, CA.

RFMRP (Riverhead Foundation for Marine Research and Preservation). 2006. "Ringy," ringed seal Phoca hispida). RFMRP, Riverhead, NY. http://www.riverheadfoundation.org/ research/content. asp?code=Ringed%20seal

Rhodin, A. G. J. 1985. Comparative chondro-osseus development and growth of marine turtles. *Copeia* 1985: 752–771.

Rice, D. W. 1967. Cetaceans. Pp. 291–324 in: S. Anderson and J. K. Jones, eds. *Recent Mammals of the World: A Synopsis of Families*. Ronald Press, New York, NY.

Rice, D. W. 1977. Synopsis of biological data on the sei whale and Bryde's whale in the eastern North Pacific. *Report of the International Whaling Commission, Special Issue* 1: 92–97.

Rice, D. W. 1989. Sperm whale *Physeter macrocephalus* Linnaeus 1758. Pp. 177–233 in: S. H.

Ridgway and R. Harrison, eds. *Handbook of Marine Mammals. Volume 4: River Dolphins and the Larger Toothed Whales.* Academic Press, London.

Rice, D. W. 1998. *Marine Mammals of the World: Systematics and Distribution*. Special Publication No. 4. Society for Marine Mammalogy, Lawrence, Kansas.

Rice, D. W. 2002. Baleen. Pp. 61–62 in: W. F. Perrin, B. Würsig, and J. G. M. Thewissen, eds. *Encyclopedia of Marine Mammals*. Academic Press, San Diego, CA.

Robertson, K. M., and S. Chivers. 1997. Prey occurrence in pantropical, *Stenella attenuata*, spotted dolphins from the eastern tropical Pacific. *Fishery Bulletin* 95: 334–348.

Rommel, S. A., and J. E. Reynolds III. 2002. Skeletal anatomy. Pp.1089–1103 in: W. F. Perrin, B. Würsig, and J. G. M. Thewissen, eds. *Encyclopedia of Marine Mammals*. Academic Press, San Diego, CA.

Rommel, S. A., D. A. Pabst, and W. A. McLellan. 2002. Skull anatomy. Pp. 1103–1117 in: W. F. Perrin, B. Würsig, and J. G. M. Thewissen, eds. *Encyclopedia of Marine Mammals*. Academic Press, San Diego, CA.

Ronald, K., and B. L. Gots. 2003. Seals: Phocidae, Otariidae, and Odobenidae. Pp. 789–854 in: G. A. Feldhamer, B. C. Thompson, and J. A. Chapman, eds. *Wild Mammals of North America: Biology, Management, and Economics*, second edition. Johns Hopkins University Press, Baltimore, MD.

Ronald, K., and P. J. Healey. 1981. Harp seal *Phoca groenlandica* Erxleben, 1777. Pp. 55–81 in: S. H. Ridgway and R. Harrison, eds. *Handbook of Marine Mammals. Volume 2: Seals.* Academic Press, London.

Rosel, P. E., S. C. France, J. Y. Wang, and T. D. Kocher. 1999. Genetic structure of harbour porpoise *Phocoena phocoena* populations in the northwest Atlantic based on mitochondrial and nuclear markers. *Molecular Ecology* 8: S41–S54.

Rosenbaum, H. C., R. L. Brownell, Jr., M. W. Brown, C. Schaeff, V. Portway, B. N. White, S. Malik, L. A. Pastene, N. J. Patenaude, C. S. Baker, M. Goto, P. B. Best, P. J. Clapham, P. Hamilton, M. Moore, R. Payne, V. Rowntree, C. T. Tynan, J. L. Bannister, and R. DeSalle. 2000. World-wide genetic differentiation of *Eubalaena*: questioning the number of right whale species. *Molecular Ecology* 9: 1793–1802.

Rough, V. 1995. *Gray Seals in Nantucket Sound, Massachusetts, Winter and Spring, 1994*. Contract report no. T10155615. Marine Mammal Commission, Washington, DC. 31 pp.

Rowley, J. 1902. The mammals of Westchester County, New York. *Proceedings of the Linnaean Society of New York* 13,14: 31–60. (not seen; cited by Connor, 1971)

Rugh, D. J., and K. E. W. Sheldon. 2002. Bowhead whale *Balaena mysticetus*. Pp. 129–131 in: W. F. Perrin, B. Würsig, and J. G. M. Thewissen, eds. *Encyclopedia of Marine Mammals*. Academic Press, San Diego, CA.

Ruhnke, H. L., and S. Madoff. 1992. *Mycoplasma phocidae* sp. nov., isolated from harbor seals (*Phoca vitulina* L.). *International Journal of Systematic Bacteriology* 42: 211–214.

Saari, V., B. Purinton, S. S. Sadove, and S. E. Shumway. 2000. Seasonality and capture location relationships for sea turtles in New York State. Pp. 172–174 in: H. Kalb and T. Wibbels,

eds. *Proceedings of the Nineteenth Annual Symposium on Sea Turtle Biology and Conservation*. NOAA Technical Memorandum NMFS-SEFSC-443. National Marine Fisheries Service, Miami, FL.

Saayman, G. S., and C. K. Tayler. 1973. Some behaviour patterns of the southern right whale Eubalaena australis. *Zeitschrift für Säugetierkunde* 38: 172–183.

Sadove, S. S., and P. Cardinale. 1993. *Species Composition and Distribution of Marine Mammals and Sea Turtles in the New York Bight*. Final report to U. S. Fish and Wildlife Service, Southern New England–New York Bight Coastal Estuaries Project. Okeanos Ocean Research Foundation, Hampton Bays, NY. 48 pp.

Santos, M. B., G. J. Pierce, A. López, R. J. Reid, V. Ridoux, and E. Mente. 2006. Pygmy sperm whales *Kogia breviceps* in the northeast Atlantic: New information on stomach contents and strandings. *Marine Mammal Science* 22: 600–616.

Sardi, K. A., and C. Merigo. 2006. *Erignathus barbatus* (bearded seal) vagrant in Massachusetts. *Northeastern Naturalist* 13: 39–42.

Sasaki, T., M. Nikaido, S. Wada, T. K. Yamada, Y. Cao, M. Hasegawa, and N. Okada. 2006. *Balaenoptera omurai* is a newly discovered baleen whale that represents an ancient evolutionary lineage. *Molecular Phylogenetics and Evolution* 41: 40–52.

Schevill, W. E. 1954. Sight records of the gray grampus, *Grampus griseus* (Cuvier). *Journal of Mammalogy* 35: 123–124.

Schevill, W. E. 1956. *Lagenorhynchus acutus* off Cape Cod. *Journal of Mammalogy* 37: 128–129.

Schilling, M. R., I. Seipt, M. T. Weinrich, S. E. Frohock, A. E. Kuhlberg, and P. J. Clapham. 1992. Behavior of individually-identified sei whales *Balaenoptera borealis* during an episodic influx into the southern Gulf of Maine in 1986. *Fishery Bulletin* 90: 749–755.

Schmidly, D. J. 1981. *Marine Mammals of the Southeastern United States Coast and the Gulf of Mexico*. USFWS Biological Services Program Report FWS/OBS-80/41. U. S. Fish and Wildlife Service, Washington, DC. 163 pp.

Schneider, D. C., and P. M. Payne. 1983. Factors affecting haul-out of harbor seals at a site in southern Massachusetts. *Journal of Mammalogy* 64: 518–520.

Scholander, P. F. 1940. Experimental investigations on the respiratory function in diving mammals and birds. *Hvålradets Skrifter* 22: 1–131.

Schroeder, C. L. 2000. *Population Status and Distribution of the Harbor Seal in Rhode Island Waters*. M.S. thesis. University of Rhode Island, Graduate School of Oceanography, Narragansett, RI. xiii + 197 pp.

Scott, G. P, D. M. Burn, and L. J. Hansen. 1988. The dolphin die-off: long-term effects and recovery of the population. Pp. 819–823 in: *Proceedings of the Oceans '88 Conference, Baltimore, MD, October 31 – November 2, 1988.* Marine Technology Society and IEEE, Piscataway, NJ.

Scott, M. D., and S. J. Chivers. 1990. Distribution and herd structure of bottlenose dolphins in the eastern tropical Pacific Ocean. Pp. 387–402 in: S. Leatherwood and R. R. Reeves, eds.

The Bottlenose Dolphin. Academic Press, San Diego, CA.

Scott, M. D., R. S. Wells, and A. B. Irvine. 1990. A long-term study of bottlenose dolphins on the west coast of Florida. Pp. 387–402 in: S. Leatherwood and R. R. Reeves, eds. *The Bottlenose Dolphin.* Academic Press, San Diego, CA.

Scott, T. M., and S. S. Sadove. 1997. Sperm whale, *Physeter macrocephalus*, sightings in shallow shelf waters off Long Island, New York. *Marine Mammal Science* 13: 317–321.

Sears, R. 2002. Blue whale *Balaenoptera musculus*. Pp. 112–116 in: W. F. Perrin, B. Würsig, and J. G. M. Thewissen, eds. *Encyclopedia of Marine Mammals*. Academic Press, San Diego, CA.

Seipt, I. E., P. J. Clapham, C. A. Mayo, and M. P. Hawvermale. 1990. Population characteristics of individually identified fin whales, *Balaenoptera physalus*, in Massachusetts Bay. *Fishery Bulletin* 88: 271–278.

Selzer, L. A., and P. M. Payne. 1988. The distribution of white-sided (*Lagenorhynchus acutus*) and common dolphins (*Delphinus delphis*) vs. environmental features of the continental shelf of the northeastern United States. *Marine Mammal Science* 4: 141–153.

Sergeant, D. E. 1962. The biology of the pilot or pothead whale *Globicephala melaena* (Traill) in Newfoundland waters. *Bulletin of the Fisheries Research Board of Canada* 132: 1–84.

Sergeant, D. E. 1977. Stocks of fin whales *Balaenoptera physalus* L. in the North Atlantic Ocean. *Report of the International Whaling Commission* 27: 460–473.

Sergeant, D. E., and H. D. Fisher. 1957. The smaller Cetacea of eastern Canadian waters. *Journal of the Fisheries Research Board of Canada* 14: 83–115.

Sergeant, D. E., D. J. St. Aubin, and J. R. Geraci. 1980. Life history and northwest Atlantic status of the Atlantic white-sided dolphin, *Lagenorhynchus acutus. Cetology* 17: 1–12.

Shane, S. H. 1990. Behavior and ecology of the bottlenose dolphin at Sanibel Island, Florida. Pp. 245–265 in: S. Leatherwood and R. R. Reeves, eds. *The Bottlenose Dolphin.* Academic Press, San Diego, CA.

Shane, S. H. 1995. Behavior patterns of pilot whales and Risso's dolphins off Santa Catalina Island, California. *Aquatic Mammals* 21: 195–197.

Shaver, D. J. 1991. Feeding ecology of wild and head-started Kemp's ridley sea turtles in south Texas waters. Journal of Herpetology 25: 327–334.

Sherman, K., C. Jones, L. Sullivan, W. Smith, P. Berrien, and L. Ejsymont. 1981. Congruent shifts in sand eel abundance in western and eastern North Atlantic ecosystems. *Nature* 291: 486–489.

Shonting, D. H., and G. S. Cook. 1970. On the seasonal distribution of temperature and salinity in Rhode Island Sound. *Limnology and Oceanography* 15: 100–112.

Shoop, C. R., and R. D. Kenney. 1992. Distributions and abundances of loggerhead and leatherback sea turtles in northeastern United States waters. *Herpetological Monographs* 6: 43–67.

Shoop, C. R., T. L. Doty, and N. E. Bray. 1981. Sea turtles in the region between Cape Hatteras and Nova Scotia in 1979. Pp. IX.2–IX.85 in: CETAP (Cetacean and Turtle Assessment

Program, University of Rhode Island). *A Characterization of Marine Mammals and Turtles in the Mid- and North Atlantic Areas of the U. S. Outer Continental Shelf, Annual Report for 1979.* Contract AA551-CT8-48. Bureau of Land Management, Washington, DC.

Shoop, C. R., C. A. Ruckdeschel, and R. D. Kenney. 1999. Long-term trends in size of stranded juvenile loggerhead sea turtles (*Caretta caretta*). *Chelonian Conservation and Biology* 3: 501–504.

Shoshani, J. 2005. Order Sirenia. Pp. 92–93 in: D. E. Wilson and D. M. Reeder, eds. *Mammal Species of the World, A Taxonomic and Geographic Reference*, 3rd edition, volume 1. Johns Hopkins University Press, Baltimore, MD.

Sigurjónsson, J., and T. Gunnlaugsson. 1990. Recent trends in abundance of blue (*Balaenoptera musculus*) and humpback whales (*Megaptera novaeangliae*) off west and southwest Iceland, with a note on occurrence of other cetacean species. *Report of the International Whaling Commission* 40: 537–551.

Slay, C. K., and S. D. Kraus. 1998. Right whale tagging in the North Atlantic. *Marine Technology Society Journal* 32: 102–103.

Smith, T. D., J. Allen, P. J. Clapham, P. S. Hammond, S. Katona, F. Larsen, J. Lien, J., D. Mattila, P. J. Palsbøll, J. Sigurjónsson, P. T. Stevick, and N. Øien. 1999. An ocean-basin-wide mark-recapture study of the North Atlantic humpback whale (*Megaptera novaeangliae*). *Marine Mammal Science* 15: 1–32.

Smith, T. G., D. J. St. Aubin, and M. O. Hammill. 1992. Rubbing behaviour of belugas, *Delphinapterus leucas*, in a High Arctic estuary. *Canadian Journal of Zoology* 70: 2405–2409.

Spotila, J. R. 2004. *Sea Turtles: A Complete Guide to Their Biology, Behavior, and Conservation.* Johns Hopkins University Press, Baltimore, MD. 240 pp.

Stacey, P. J., S. Leatherwood, and R. W. Baird. 1994. *Pseudorca crassidens. Mammalian Species* 456: 1–6.

Starbuck, A. 1878. *History of the American Whale Fishery; From Its Earliest Inception to the Year 1876. Report of the U.S. Commission on Fish and Fisheries, Part IV*. U.S. Commission on Fish and Fisheries, Washington, DC. 779 pp.

St. Aubin, D. J., R. H. Stinson, and J. R. Geraci. 1984. Aspects of the structure and composition of baleen, and some effects of exposure to petroleum hydrocarbons. *Canadian Journal of Zoology* 62: 193–198.

St. Aubin, D. J., T. G. Smith, and J. R. Geraci. 1990. Seasonal epidermal molt in beluga whales, *Delphinapterus leucas*. *Canadian Journal of Zoology* 68: 339–367.

Steiger, G. H., and J. Calambokidis. 2000. Reproductive rates of humpback whales off California. *Marine Mammal Science* 16: 220–239.

Steimle, F.W., Jr. 1982. The benthic invertebrates of Block Island Sound. *Estuarine, Coastal, and Shelf Science* 15: 1–16.

Stevick, P. T., and T. W. Fernald. 1998. Increase in extralimital records of harp seals in Maine. *Northeastern Naturalist* 5: 75–82.

Stevick, P. T., N. Øien, and D. Mattilla. 1998. Migration of a humpback whale (*Megaptera novaeangliae*) between Norway and the West Indies. *Marine Mammal Science* 14: 162–166.

Stevick, P. T., J. Allen, P. J. Clapham, N. Friday, S. K. Katona, F. Larsen, J. Lien, D. K. Mattila, P. J. Palsbøll, R. Sears, J. Sigurjónsson, T. D. Smith, G. Vikingsson, N. Øien, and P. S. Hammond. 2001. Trends in abundance of North Atlantic humpback whales, 1979–1993. Unpublished document SC/53/NAH2. International Whaling Commission, Cambridge, United Kingdom.

Stevick, P. T., J. Allen, P. J. Clapham, N. Friday, S. K. Katona, F. Larsen, J. Lien, D. K. Mattila, P. J. Palsbøll, J. Sigurjónsson, T. D. Smith, N. Øien, and P. S. Hammond. 2003. North Atlantic humpback whale abundance and rate of increase four decades after protection from whaling. *Marine Ecology Progress Series* 258: 263–273.

Stewart, B. E., and R. E. A. Stewart. 1989. *Delphinapterus leucas*. *Mammalian Species* 336: 1–8.

Stewart, B. S., and S. Leatherwood. 1985. Minke whale *Balaenoptera acutorostrata* Lacépède, 1804. Pp. 91–136 in: S. H. Ridgway and R. Harrison, eds. *Handbook of Marine Mammals. Volume 3: The Sirenians and Baleen Whales.* Academic Press, London.

Stobo, W. T., and Z. Lucas. 2000. Shark-inflicted mortality on a population of harbour seals (*Phoca vitulina*) at Sable Island, Nova Scotia. *Journal of Zoology*, London 252: 405–414.

Stoner, D. 1938. New York State records for the common dolphin, *Delphinus delphis*. *New York State Museum Circular* 21: 1–16.

Sutcliffe, W. H., and P. F. Brodie. 1977. *Whale Distributions in Nova Scotia Waters*. Canadian Fisheries and Marine Service Technical Report 722. Marine Ecology Laboratory, Bedford Institute of Oceanography, Dartmouth, Nova Scotia. vi + 83 pp.

Suydam, R. S., L. F. Lowry, K. J., Frost, G. M. O'Corry-Crowe, and D. Pikok, Jr. 2001. Satellite tracking of eastern Chukchi Sea beluga whales in the Arctic Ocean. *Arctic* 54: 237–243.

Swartz, S. L. 1986. Gray whale migratory, social and breeding behavior. *Report of the International Whaling Commission, Special Issue* 8: 207–229.

Swingle, W. M., S. G. Barco, T. D. Pitchford, W. A. McLellan, and D. A. Pabst. 1993. Appearance of juvenile humpback whales feeding in the nearshore waters of Virginia. *Marine Mammal Science* 9: 309–315.

Templeman, W. 1990. Historical background to the sealworm problem in eastern Canadian waters. Pp. 1–16 in: W. D. Bowen, ed. *Population Biology of Sealworm (*Pseudoterranova decipiens*) in Relation to its Intermediate and Seal Hosts*. Canadian Bulletin of Fisheries and Aquatic Sciences No. 222. Dept. of Fisheries and Oceans, Ottawa, Ontario.

Terhune, J. M. 1985. Scanning behavior of harbor seals on haul-out sites. *Journal of Mammalogy* 66: 392–395.

Tershy, B. R., and D. N. Wiley. 1992. Asymmetric pigmentation in the fin whale: a test of two feeding related hypotheses. *Marine Mammal Science* 8: 315–318.

TEWG (Turtle Expert Working Group). 2000. *Assessment Update for the Kemp's Ridley and Loggerhead Sea Turtle Populations in the Western North Atlantic*. NOAA Technical Memorandum NMFS-SEFSC-444. National Marine Fisheries Service, Miami, FL. 155 pp.

TEWG (Turtle Expert Working Group). 2007. *An Assessment of the Leatherback Turtle Population in the Atlantic Ocean.* NOAA Technical Memorandum NMFS-SEFSC-555. National Marine Fisheries Service, Miami, FL. 116 pp.

Thayer, V. G., A. J. Read, A. S. Friedlander, D. R. Colby, A. A. Hohn, W. A. McLellan, D. A. Pabst, J. L. Dearolf, N. I. Bowles, J. R. Russell, and K. A. Rittmaster. 2003. Reproductive seasonality of western North Atlantic bottlenose dolphins off North Carolina, U.S.A. *Marine Mammal Science* 19: 617–629.

Thompson, P. 1988. Timing of mating in the common seal (*Phoca vitulina*). *Mammal Review* 18: 105–112.

Thompson, P. M., M. A. Fedak, B. J. McConnell, and K. Nicholas. 1989. Seasonal and sex-related variation in the activity patterns of common seals (*Phoca vitulina*). *Journal of Applied Ecology* 26: 521–535.

Tomilin, A. G. 1967. *Mammals of the U. S. S. R. and Adjacent Countries. Vol. 9, Cetacea.* Translated from Russian, Israel Program for Scientific Translations. 717 pp. (First published in Russian, 1957.)

Tønnessen, J. N., and A. O. Johnsen. 1982. *The History of Modern Whaling*. University of California Press, Berkeley. xx + 798 pp.

Torres, L. G., P. E. Rosel, C. D'Agrosa, and A. J. Read. 2003. Improving management of overlapping bottlenose dolphin ecotypes through spatial analysis and genetics. *Marine Mammal Science* 19: 502–514.

Townsend, C. H. 1935. The distribution of certain whales as shown by logbook records of American whaleships. *Zoologica* 19: 1–50.

True, F. W. 1889. *Contributions to the Natural History of the Cetaceans; A Review of the Family Delphinidae*. Bulletin no. 36. U. S. National Museum, Washington, DC. 192 pp.

True, F. W. 1904. The whalebone whales of the western North Atlantic. *Smithsonian Contributions to Knowledge* 33: 1–332.

True, F. W. 1910. Observations on living white whales (*Delphinapterus leucas*); with a note on the dentition of *Delphinapterus* and *Stenodelphis*. *Smithsonian Miscellaneous Collections* 5: 325–330.

Turrell, L. W. 1939. *The Natural History of Smithtown*. Arts-Craft Press, St. James, New York. 89 pp. (not seen; cited by Connor, 1971)

Tyack, P. 1986. Population biology, social behavior and communication in whales and dolphins. *Trends in Ecology and Evolution* 1: 144–150.

Tyack, P. L. 1999. Communication and cognition. Pp. 287–323 in: J. E. Reynolds III and S. A. Rommel, eds. *Biology of Marine Mammals.* Smithsonian Institution Press, Washington, DC.

Ulmer, F. A., Jr. 1980. New Jersey's dolphins and porpoises. *New Jersey Audubon Society Occasional Paper* 137: 1–11.

Urian, K. W., D. A. Duffield, A. J. Read, R. S. Wells, and E. D. Shell. 1996. Seasonality of reproduction in bottlenose dolphins, *Tursiops truncatus. Journal of Mammalogy* 77: 394–403.

USFWS (U.S. Fish and Wildlife Service). 2006. USFWS Threatened and Endangered Species System (TESS). U.S. Fish and Wildlife Service, Dept. of the Interior, Washington, DC. http://ecos.fws.gov/tess_public/SpeciesReport.do?groups=A&listingType=L

USGS (U.S. Geological Survey). 2006. Chessie the manatee is seen again! U.S. Geological Survey, Florida Integrated Science Center, Gainesville, FL. http://cars.er.usgs.gov/Manatees/Manatee_Sirenia_Project/Manatee_Chessie_Surfaces/manatee_chessie_surfaces.html

Van Bressem, M.-F., K. Van Waerebeek, P. D. Jepsen, J. A. Raga, P. J. Duignan, O. Neilsen, A. P. Di Beneditto, S. Siciliano, R. Ramos, W. Kant, V. Peddemors, R. Kinoshita, P. S. Ross, A. López-Fernandez, K. Evans, E. Crespo, and T. Barrett. 2001. An insight into the epidemiology of dolphin morbillivirus worldwide. *Veterinary Microbiology* 81: 287–304.

Wada, S., M. Oishi, and T. K. Yamada. 2003. A newly discovered species of living baleen whale. *Nature* 426: 278–281.

Wade, P., and T. Gerrodette. 1992. Estimates of dolphin abundance in the eastern tropical Pacific. Preliminary analysis of five years of data. *Report of the International Whaling Commission* 42: 532–539.

Walker, J. L., C. W. Potter, and S. A. Macko. 1999. The diets of modern and historic bottlenose dolphin populations reflected through stable isotopes. *Marine Mammal Science* 15: 335–350.

Wallace, S. D., and J. W. Lawson. 1997. *A Review of Stomach Contents of Harp Seals (*Phoca groenlandica*) from the Northwest Atlantic: An Update*. Technical Report 97-01. International Marine Mammal Association, Guelph, Ontario. 99 pp.

Waring, G. T., P. Gerrior, P. M. Payne, B. L. Parry, and J. R. Nicolas. 1990. Incidental take of marine mammals in foreign fishery activities off the northeast United States. *Fishery Bulletin* 88: 347–360.

Waring, G. T., J. R. Gilbert, J. Loftin, and N. Cabana. 2006a. Short term movements of radio tagged harbor seals in New England. *Northeastern Naturalist* 13: 1–24.

Waring, G. T., E. Josephson, C. P. Fairfield, and K. Maze-Foley, eds. 2006b. *U.S. Atlantic and Gulf of Mexico Marine Mammal Stock Assessments—2005.* NOAA Technical Memorandum NMFS-NE-194. National Marine Fisheries Service, Woods Hole, MA. vi + 346 pp.

Waring, G. T., E. Josephson, C. P. Fairfield, and K. Maze-Foley, eds. 2008. *U.S. Atlantic and Gulf of Mexico Marine Mammal Stock Assessments—2007.* NOAA Technical Memorandum NMFS-NE-205. National Marine Fisheries Service, Woods Hole, MA. vii + 415 pp. (updated annually, available at http://www.nmfs.noaa.gov/pr/sars/)

Waring, G. T., E. Josephson, C. P. Fairfield, and K. Maze-Foley, eds. 2009. *U.S. Atlantic and Gulf of Mexico Marine Mammal Stock Assessments—2008.* NOAA Technical Memorandum NMFS-NE-210. National Marine Fisheries Service, Woods Hole, MA. vii + 429 pp.

Waters, J. H. 1967. Gray seal remains from southern New England archaeological sites. *Journal of Mammalogy* 48: 139–141.

Waters, J. H., and C. J.-J. Rivard. 1962 *Terrestrial and Marine Mammals of Massachusetts and Other New England States.* Standard-Modern Printing Co., Brockton, MA. vi + 151 pp.

Watkins, W. A. 1981. Activities and underwater sounds of fin whales. *Scientific Reports of the Whales Research Institute*, Tokyo 33: 83–117.

Watkins, W. A., and W. E. Schevill. 1976. Right whale feeding and baleen rattle. *Journal of Mammalogy* 57: 58–66.

Watkins, W. A., and W. E. Schevill. 1977. Sperm whale codas. *Journal of the Acoustical Society of America* 62: 1485–1490.

Watkins, W. A., and W. E. Schevill. 1979. Aerial observations of feeding behavior in four baleen whales: *Eubalaena glacialis*, *Balaenoptera borealis*, *Megaptera novaeangliae*, and *Balaenoptera physalus*. *Journal of Mammalogy* 60 155–163.

Watkins, W. A., K. E. Moore, and P. Tyack. 1985. Sperm whale acoustic behavior in the southeast Caribbean. *Cetology* 49: 1–15.

Watkins, W. A., M. A. Daher, K. M. Fristrup, T. J. Howard, and G. Notarbartolo di Sciara. 1993. Sperm whales tagged with transponders and tracked underwater by sonar. *Marine Mammal Science* 9: 55–67.

Watkins, W. A., M. A. Daher, N. A. DiMarzio, A. Samuels, D. Wartzok, K. M. Fristrup, D. P. Gannon, P. W. Howey, R. R. Maiefski, and T. R. Spradlin. 1999. Sperm whale surface activity from tracking by radio and satellite tags. *Marine Mammal Science* 15: 1158–1180.

Watkins, W. A., M. A. Daher, N. A. DiMarzio, A. Samuels, D. Wartzok, K. M. Fristrup, P. W. Howey, and R. R. Maiefski. 2002. Sperm whale dives tracked by radio tag telemetry. *Marine Mammal Science* 18: 55–68.

Watterson, J. C., R. D. Kenney, A. Richardson, A. Kumar, C. L. Schroeder, R. Crossland, J. T. Bell, and D. R. Rees. In review. Method for predicting seasonal distributions of protected species through geostatistical modeling. *Journal of Wildlife Management.*

Watwood, S. L., P. J. O. Miller, M. Johnson, P. T. Madsen, and P. L. Tyack. 2006. Deep–diving foraging behaviour of sperm whales (*Physeter macrocephalus*). *Journal of Animal Ecology* 75: 814–825.

Weinrich, M. T., M. R. Schilling, and C. R. Belt. 1992. Evidence for acquisition of a novel feeding behavior: lobtail feeding in humpback whales, *Megaptera novaeangliae*. *Animal Behavior* 44: 1059–1072.

Weinrich, M. T., M. Martin, R. Griffiths, J. Bove, and M. Schilling. 1997. A shift in distribution of humpback whales, *Megaptera novaeangliae*, in response to prey in the southern Gulf of Maine. *Fishery Bulletin* 95: 826–836.

Wells, R. S., and M. D. Scott. 1999. Bottlenose dolphin *Tursiops truncatus* (Montagu, 1821). Pp. 137–182 in: S. H. Ridgway and R. Harrison, eds. *Handbook of Marine Mammals. Volume 6: The Second Book of Dolphins and the Porpoises.* Academic Press, London.

Wells, R. S., and M. D. Scott. 2002. Bottlenose dolphins *Tursiops truncatus* and *T. aduncus*. Pp. 122–128 in: W. F. Perrin, B. Würsig, and H. G. M. Thewissen, eds. *Encyclopedia of Marine Mammals*. Academic Press, San Diego, CA.

Wells, R. S., M. D. Scott, and A. B. Irvine. 1987. The social structure of free-ranging bottlenose dolphins. Pp. 247–205 in: H. H. Genoways, ed. *Current Mammalogy 1*. Plenum Press, New York, NY.

Wells, R. S., L. J. Hansen, A. Baldridge, T. P. Dohl, D. L. Kelly, and R.H. Defran. 1990. Northward extension of the range of bottlenose dolphins along the California coast. Pp. 421–431 in: S. Leatherwood and R. R. Reeves, eds. *The Bottlenose Dolphin.* Academic Press, San Diego, CA.

Wells, R. S., S. Hofmann, and T. L. Moors. 1998. Entanglement and mortality of bottlenose dolphins, *Tursiops truncatus*, in recreational fishing gear in Florida. *Fishery Bulletin* 96: 647–650.

Wells, R. S., D. J. Boness, and G. B. Rathbun. 1999. Behavior. Pp. 324–422 in: J. E. Reynolds III and S. A. Rommel, eds. *Biology of Marine Mammals*. Smithsonian Institution Press, Washington, DC.

Westgate, A. J., A. J. Read, P. Berggren, H. N. Koopman, and D. E. Gaskin. 1995. Diving behaviour of harbour porpoises, *Phocoena phocoena. Canadian Journal of Fisheries and Aquatic Sciences* 52: 1064–1073.

Whitaker, J. O., Jr., A. Hicks, H. H. Thomas, J. Bopp, and R. D. Kenney. In preparation. *The Mammals of New York.*

Whitehead, H. 2002. Sperm whale *Physeter macrocephalus*. Pp. 1165–1172 in: W. F. Perrin, B. Würsig, and H. G. M. Thewissen, eds. *Encyclopedia of Marine Mammals*. Academic Press, San Diego, CA.

Whitehead, H., and J. Lien. 1983. Changes in the abundance of whales, and whale damage, along the Newfoundland coast 1973–1981. *Report of the International Whaling Commission* 33: 775.

Whitehead, H., and J. Mann. 2000. Female reproductive strategies of cetaceans: Life histories and calf care. Pp. 219–246 in: J. Mann, R. C. Connor, P. L. Tyack, and H. Whitehead, eds. *Cetacean Societies: Field Studies of Dolphins and Whales*. University of Chicago Press, Chicago, IL.

Whitehead, H., and M. J. Moore. 1982. Distribution and movements of West Indian humpback whales in winter. *Canadian Journal of Zoology* 60: 2203–2211.

Whitehead, H., and L. Weilgart. 2000. The sperm whale: social females and roving males. Pp. 154–172 in: J. Mann, R. C. Connor, P. Tyack, and H. Whitehead, eds. *Cetacean*

Societies. University of Chicago Press, Chicago, IL.

Whitehead, H. and T. Wimmer. 2005. Heterogeneity and the mark-recapture assessment of the Scotian Shelf population of northern bottlenose whales (*Hyperoodon ampullatus*). *Canadian Journal of Fisheries and Aquatic Sciences* 62: 2573–2585.

Whitehead, H., S. Waters, and T. Lyrholm. 1991. Social organization in female sperm whales and their offspring: constant companions and casual acquaintances. *Behavioral Ecology and Sociobiology* 29: 395–389.

Whitehead, H., S. Brennan, and D. Grover. 1992. Distribution and behaviour of male sperm whales on the Scotian Shelf, Canada. *Canadian Journal of Zoology* 70: 912–918.

Whitehead, H., C. D. MacLeod, and P. Rodhouse. 2003. Differences in niche breadth among some teuthivorous mesopelagic marine mammals. *Marine Mammal Science* 19: 400–405.

Whitman, A. A., and P. M. Payne. 1990. Age of harbour seals, *Phoca vitulina concolor*, wintering in southern New England. *Canadian Field-Naturalist* 104: 579–582.

Willis, P. M., and R. W. Baird. 1998. Status of the dwarf sperm whale, *Kogia simus*, with special reference to Canada. *Canadian Field-Naturalist* 112: 114–115.

Wimmer, T., and H. Whitehead. 2004. Movements and distribution of northern bottlenose whales, *Hyperoodon ampullatus*, on the Scotian Slope and in adjacent waters. *Canadian Journal of Zoology* 82: 1782–1794.

Winn, H. E., and N. E. Reichley. 1985. Humpback whale *Megaptera novaeangliae* (Borowski, 1781). Pp. 241–273 in: S. H. Ridgway and R. Harrison, eds. *Handbook of Marine Mammals. Volume 3: The Sirenians and Baleen Whales.* Academic Press, London.

Winn, H. E., and L. K. Winn. 1978. The song of the humpback whale (*Megaptera novaeangliae*) in the West Indies. *Marine Biology* 47: 97–114.

Winn, H. E., R. K. Edel, and A. G. Taruski. 1975. Population estimate of the humpback whale (*Megaptera novaeangliae*) in the West Indies by visual and acoustic techniques. *Journal of the Fisheries Research Board of Canada* 32: 499–506.

Winn, H. E., C. A. Price, and P. W. Sorensen. 1986. The distributional ecology of the right whale *Eubalaena glacialis* in the western North Atlantic. *Reports of the International Whaling Commission, Special Issue* 10: 129–138.

Winn, H. E., J. D. Goodyear, R. D. Kenney, and R. O. Petricig. 1995. Dive patterns of tagged right whales in the Great South Channel. *Continental Shelf Research* 15: 593–611.

Wishner, K., E. Durbin, A. Durbin, M. Macaulay, H. Winn, and R. Kenney. 1988. Copepod patches and right whales in the Great South Channel off New England. *Bulletin of Marine Science* 43: 825–844.

Wishner, K., J. R. Schoenherr, R. Beardsley, and C. Chen. 1995. Abundance, distribution and population structure of the copepod *Calanus finmarchicus* in a springtime right whale feeding area in the southwestern Gulf of Maine. *Continental Shelf Research* 15: 475–507.

Wolman, A. A. 1985. Gray whale *Eschrichtius robustus* (Lilljeborg, 1861). Pp. 67–90 in: S. H. Ridgway and R. Harrison, eds. *Handbook of Marine Mammals. Volume 3: The Sirenians and Baleen Whales.* Academic Press, London.

Woodley, T. H., and D. M. Lavigne. 1991. *Incidental Capture of Pinnipeds in Commercial Fishing Gear.* Technical Report 91-01. International Marine Mammal Association, Guelph, Ontario, Canada. 35 pp.

Wozencraft, W. C. 2005. Order Carnivora. Pp. 532–628 in: D. E. Wilson and D. M. Reeder, eds. *Mammal Species of the World, A Taxonomic and Geographic Reference*, 3rd edition, volume 1. Johns Hopkins University Press, Baltimore, MD.

WRB (Water Resources Board). 1976. *Fish & Wildlife: Inventory of Rhode Island's Fish and Wildlife.* Water and Related Land Resources Planning, task no. 10. State of Rhode Island, Water Resources Board, Providence, RI. 100 pp.

Wyman, J., K. Almeida, and T. Ardito. 2004. Fisherman rescues rare turtle. Narragansett Bay Journal 9: 6.

Wynne, K., and M. Schwartz. 1999. *Guide to Marine Mammals & Turtles of the U. S. Atlantic & Gulf of Mexico*. Rhode Island Sea Grant, Narragansett, RI. vi + 114 pp.

Yochem, P. K., and S. Leatherwood. 1985. Blue whale *Balaenoptera musculus* (Linnaeus, 1758). Pp. 193–240 in: S. H. Ridgway and R. Harrison, eds. *Handbook of Marine Mammals. Volume 3: The Sirenians and Baleen Whales*. Academic Press, London.

Zimmer, W. M. X., M. Johnson, P. T. Madsen, and P. Tyack. 2005. Echolocation clicks of free-ranging Cuvier's beaked whales (*Ziphius cavirostris*). *Journal of the Acoustical Society of America* 117: 3919–3927.

Zug, G. R., and J. F. Parham. 1996. Age and growth in leatherback turtles, *Dermochelys coriacea* (Testudines: Dermochelyidae): a skeletochronological analysis. *Chelonian Conservation and Biology* 2: 244–249.

11.

Spatial Distribution, Abundance, and Flight Ecology of Birds in Nearshore and Offshore Waters of Rhode Island

Interim Technical Report for the Rhode Island Ocean Special Area Management Plan 2010

by

Peter Paton, Kristopher Winiarski, Carol Trocki, and Scott McWilliams

Department of Natural Resources Science
University of Rhode Island

University of Rhode Island, June 17, 2010

Executive Summary

This interim report for the Rhode Island Special Area Management Plan (SAMP) summarizes our research conducted from January 2009 through mid-February 2010. This research is the first attempt to quantify the spatial distribution and abundance of birds using the nearshore and offshore waters of Rhode Island. Avian research is still ongoing, with ship-based line transect surveys and land-based seawatches continuing from Feb through July 2010. In addition, aerial surveys are planned to continue from Feb 2010 through May 2011. Results from this ongoing research will be presented in another technical report in 2011.

Our objectives for avian research as part of the Ocean Special Area Management Plan (SAMP) were to: (1) Summarize historical studies of avian use of nearshore and offshore waters within Ocean SAMP study area boundaries, (2) Assess seasonal variation in the spatial distribution and abundance of birds in RI nearshore and coastal waters, (3) Assess diel patterns of avian use of RI nearshore and offshore waters, (4) Quantify flight ecology for birds in RI nearshore and offshore waters, and (5) Investigate Roseate Tern use of the Ocean SAMP study area.

The Ocean SAMP study area encompasses 3,800 km^2 (about 1,500 $miles^2$) that includes Block Island Sound, Rhode Island Sound, and the Inner Continental Shelf. One of the primary factors determining the spatial distribution and abundance of birds using nearshore and offshore areas is bathymetry. Water depths in the Ocean SAMP study area are relatively deep compared to adjacent areas and average 35 m ± 10 m deep, with 8% of the SAMP area <20 m deep and 86% of the area between 20-50 m deep.

Prior to the current Ocean SAMP avian study, only two systematic surveys of offshore avian communities had been conducted within the Ocean SAMP area. First, avian observers stationed on National Marine Fisheries Service (NMFS) and Coast Guard vessels in 1978-79 detected 4,532 birds in 665 different flocks and 21 bird species. Gulls [38% of detections], shearwaters [26%], and storm-petrels [13%] dominated NMFS surveys. Second, the largest historical offshore survey was the Cetacean and Seabird Assessment Program (CSAP) conducted from 1980 to 1988. CSAP surveyed 101 15-min transects throughout the year using Manomet Bird Observatory observers stationed on vessels conducting plankton, groundfish, and shellfish surveys. CSAP surveys detected 34 species of birds from a total of 14,045 detections, with gulls (69% of detections), shearwaters (16% of detections), and storm-petrels (6% of detections) dominating counts. However, data were too sparse to map the historical spatial distribution and density of birds in the Ocean SAMP study area.

Much more historical information about avian use of nearshore habitats of Narragansett Bay, coastal promontories and peninsulas, and coastal ponds is available from surveys conducted by DEM biologists, volunteers coordinated by EPA, and biologists from US Fish and Wildlife

Service's Rhode Island National Wildlife Refuge complex. Narragansett Bay is home to thousands of wintering waterfowl, with an average of 21,256 ± 12,051 (SD) individuals counted annually, with a maximum of 58,706 individuals in 2001. The most abundant species in the Narragansett Bay based on DEM aerial surveys over the past 27 years included scaup (mean = 6,600 individuals ± 5100 (SD) annually), Canada Geese, (6,300 ± 5400), American Black Duck (2,200 ± 1200), and Common Eider (1250 ± 3000).

Exposed promontories along the coast, such as Sachuest Point NWR, were surveyed by USFWS biologists in the winters from 1992-2003. These areas were dominated by seaducks including Common Eider (560 ± 880 annually), Surf Scoter (110 ± 130), Harlequin Ducks (80 ± 16), and Common Goldeneye (90 ± 30). Surveys conducted throughout the year by DEM biologist C. Raithel at Napatree from 1982 to the present provide valuable information on migration phenology and relative abundance of birds in the northwest corner of the Ocean SAMP area.

Coastal ponds, such as Trustom and Ninigret NWR, have been surveyed during winter by USFWS biologists since 1992. The abundance of dabbling ducks (e.g., American Black Duck, Mallard, American Wigeon, Green-winged Teal and Gadwall) and diving ducks (Greater and Lesser Scaup, Canvasback, Ring-necked Duck and Ruddy Duck) in these coastal ponds demonstrate the value of these habitats for wintering waterfowl.

We used five primary survey methods to assess avian use of the Ocean SAMP area: (1) six 1-2 hr land-based seawatches (≤ 3 km from shore) per month at 11 stations along coastal mainland Rhode Island from 23 Jan 2009 to mid-Feb 2010; (2) systematic ship-based line-transect surveys approximately once a month from February to May 2009 on two 4 by 5 nm grids and then approximately four times per month from June 2009 until March 2010 on eight 4 by 5 nm grids; (3) aerial strip-transect surveys (24 transects, 3 km apart) flown from November 2009 to March 2010 at a fixed altitude of 152 m and at a constant speed of 160 km/hr; (4) boat-based line transect surveys in nearshore waters in the NW corner of the Ocean SAMP area conducted during July and August 2009 to assess the distribution and abundance of Roseate Terns; and (5) a study by ornithologists from New Jersey Audubon Society using both a dual horizontial and vertical radar unit on Block Island to monitor the movement ecology of birds from March to mid-December 2009, 24 hrs per day, 7 days per week (see Appendix K).

We conducted 796 1-2 hr land-based seawatches during this 13-month period. We had 465,039 detections of 121 species during land-based seawatches. The most commonly detected species were scoters, eiders, Herring Gulls, and Great Black-backed Gulls (all scientific names are given in Appendix A). From these data, we were able to assess spatial variation the relative abundance of birds and to model the phenology of common waterbirds using the Ocean SAMP study area.

We conducted 54 ship-based line transect surveys of 8 grids on 27 days between 10 June 2009 and 13 February 2010. We detected 56 species during these surveys, of which 11 species were relatively common: Herring Gull, Wilson's Storm-Petrel, Northern Gannet, Great Black-backed Gull, Cory's Shearwater, Common Loon, Greater Shearwater, Black-legged Kittiwake, Razorbill, Common Murre, and Dovekie. Using program DISTANCE, we estimated the seasonal change in the spatial distribution and density of these common species.

We conducted 10 aerial surveys between 18 November 2009 and 22 February 2010. During aerial surveys, we had 9,414 detections of 17 species or guilds, of which the following were most common: Common Eider, unidentified gulls, Northern Gannet, Herring Gulls, unidentified scoters, Common Loon, and unidentified alcids. We compared these data to the spatial distribution and density estimates for common species from the ship-based line transect surveys and developed bathymetry profiles for select species.

We had 125 Roseate Tern detections during land-based point counts, with most detections at the NW corner of the Ocean SAMP study area. We had 8 Roseate Tern detections on 3 ship-based line transect grids in Block Island Sound, but we did not detected Roseate Terns in Rhode Island Sound or the Inner Continental Shelf during ship-based surveys.

Highlights for avian guilds include:

Loons: Both Common and Red-throated Loon are abundant species during winter months in the Ocean SAMP area. Estimates of the number of Common Loons wintering in the Ocean SAMP area (2,901 individuals (95% CI = 2535-3321), suggest this area provides critical wintering habitat for a significant number of loons. In 2009, an estimated 5,400 adult loons were nesting in New York, Vermont, New Hampshire, Massachusetts, and Maine (NE Loon Study Group, pers. comm.). Therefore the Ocean SAMP area supports the equivalent of 54% of the Northeast loon breeding population during the winter. We primarily detected loons in nearshore waters that are <35 m deep, but some loons were documented in deeper offshore waters of Rhode Island Sound.

Grebes: Two species were observed, Horned and Red-necked Grebe, wintering in the Ocean SAMP area. Both species generally occurred only in nearshore areas.

Shearwaters: Four migratory species were detected in offshore waters from May through August, with two species seasonally abundant (Cory's and Greater Shearwaters). Cory's Shearwater was more likely to venture into nearshore areas, but peak densities for both species occurred in southern, central sections of Rhode Island Sound. On average 3,350 (95% CI = 3005-3712) Greater Shearwaters and 2,643 (1979-3530) Cory's Shearwaters occur in the Ocean SAMP study area from May through August. Since we could not estimate the passage rate of shearwaters through the area, we could not calculate the total number of birds using the Ocean

SAMP area during the summer of 2009. However, tens of thousands of shearwaters likely migrate through and forage in the SAMP study area.

Storm-Petrels: We detected two species, Wilson's and Leach's Storm-petrel, of which only Wilson's Storm-Petrel was abundant. These migratory, pelagic species are found in deep, offshore sections of the Ocean SAMP study area throughout the summer, with peak numbers in July. We estimated 16,335 Wilson's Storm-Petrel (95% CI = 10,879-24,527) were within the Ocean SAMP study area on an average day in summer. We do not know passage rates of this species in the Ocean SAMP study area, thus were unable to estimate the total number of Wilson's Storm-Petrels that used the area during summer 2009. However, this species is one of the most abundant birds in the world and it is conceivable that tens of thousands of Wilson's Storm-Petrels pass through the Ocean SAMP study area every summer.

Gannet: Northern Gannets are a common spring and fall migrant through the Ocean SAMP study area. This piscivorous specialist tends to occur in areas where water depths were >30 m deep. In addition, gannets tended to be concentrated around active fishing vessels in the western half of the study area. Gannet densities peaked in a zone approximately 3 miles offshore from Block Island and mainland Rhode Island in both fall and winter. We estimated an average density of 4,474 individuals during days in winter (95% CI = 3688-5187), however we do not know passage rates of gannets, so were unable to estimate the total number of gannets using the area.

Cormorants: We detected two species of cormorant that were both restricted to nearshore habitats. Double-crested Cormorants are an abundant local breeding species (>2,000 nesting pairs in Narragansett Bay), with thousands of individuals migrating along the coast in fall. Great Cormorants are much less abundant during the winter months.

Waterfowl: We detected two species of swans (Mute and Tundra), two species of geese (Canada Goose and Brant), seven species of dabbling ducks (Wood Duck, Mallard, American Black Duck, Gadwall, Northern Pintail, American Wigeon, and Green-winged Teal), and one species of bay duck (Greater Scaup) during fieldwork, all of which were associated with nearshore habitats along coastal mainland Rhode Island.

Seaducks: Eiders, scoters, and related species were among the most abundant birds we observed using nearshore habitats during the winter months. The most common species we observed included Common Eider, Surf, and Black Scoter. We documented substantial interannual variation in scoter and eider abundance during land-based seawatches, with fewer birds in the area in 2009-10 when ship-based line transect surveys and aerial surveys were conducted. . We primarily detected seaducks in nearshore areas in the NE corner of Rhode Island Sound, the northern edge of Block Island Sound, and south and southwest of Block Island.

Previous research suggested that the primary foraging depths for seaducks was <20 m. We found seaducks were consistently foraging in waters up to 25 m deep in the SAMP study area. It is important to note that night time roosting locations of seaducks in the Ocean SAMP area are still unknown. We found that seaducks traveled offshore daily just before or after dusk to roost in deeper waters (1 to 5 km offshore), likely to avoid nearshore predators. A Surf Scoter satellite telemetry project being conducted by URI biologists in the winter of 2010-2011 will hopefully provide us with more insight regarding important roosting areas for seaducks.

Shorebirds: We documented four species of plover and 13 species of sandpipers, primarilyduring land-based seawatches. We had a few detections of six species of shorebirds during ship-based line transects. No shorebird species was detected frequently using any survey method because shorebirds mainly use nearshore and intertidal areas. We were unable to model their spatial distribution and density within the Ocean SAMP study area due to low detection rates.

Jaegers: We detected three species, but all species were rare (< 20 detections). We were only able to model their migration phenology. We were unable to model their spatial distribution and density within the Ocean SAMP study area due to low detection rates.

Gulls: We detected six gull species, of which two were local breeding species and the other species were migrants into the Ocean SAMP study area. Herring Gulls and Great Black-backed Gulls are two of the most abundant waterbirds utilizing the Ocean SAMP study area. During the summer, their movements appear to be restricted to nearshore habitats by nesting colonies. In summer, we estimated 1,454 individual Herring Gulls in the Ocean SAMP study area (95% CI = 1,246 – 1,697). For Great Black-backed Gulls, we estimated 1,869 individuals in summer (95% CI = 1,255 -2,786). During the fall, both species dispersed to offshore habitats and their numbers in the Ocean SAMP study area increased dramatically (7,332 individual Herring Gulls (6,000-8,961) and 2,680 individual Great Black-backed Gulls (2366-3036). By winter, their numbers declined dramatically to 1,082 individual Herring Gulls (1,042-1,124) and 682 Great Black-backed Gulls (627-743) estimated throughout the Ocean SAMP area.

Kittiwakes: Black-legged Kittiwakes are an offshore specialist that winter in the Ocean SAMP study area. They are primarily found far offshore in deeper water (>50 m deep). During winter, we estimated that a daily average of 291 (95% CI = 548-707) kittiwakes winter in the Ocean SAMP study area. We do not know the passage rate of kittiwakes through the area, so cannot estimate the total number of kittiwakes using the Ocean SAMP area.

Terns and skimmer: We detected seven species of terns and Black Skimmer during fieldwork, of which only Common, Least, and Roseate Terns were moderately common in nearshore areas. All terns were detected in the Ocean SAMP area only during summer months, with more birds in

the area during the post-breeding season. Few terns were detected during ship-based line transect surveys, so we were unable to model their spatial distribution or density. We did detect small number of Roseate Terns, primarily in NW corner of Ocean SAMP, with a few detections around Block Island. One observer on Block Island detected moderate numbers of Roseate Terns on the Island during post-breeding staging.

Alcids: We detected six species of alcids during fieldwork including Razorbills, Common and Thick-billed Murres, Atlantic Puffin, Black Guillemot, and Dovekie. All alcids are migrants that winter in the Ocean SAMP study area. Three of the species were rarely observed (Thick-billed Murre, Atlantic Puffin, and Black Guillemot), while the other three species were relatively common. We were able to model the spatial distribution and density of Razorbills, Common Murre, and Dovekie. These species exhibited spatial segregation in the Ocean SAMP study area, with Razorbills specializing in the northern sections that were shallower and closer to land, Common Murre tending to use the central latitudes of the area, while Dovekies were the offshore specialist that reached peak densities in the southern sections of Rhode Island Sound and the Continental Shelf. We were able to estimate average daily abundance for three alcids in winter: Razorbill averaged 1,390 individuals (95% CI = 996-1,940), Dovekie had an estimated 5,771 individuals (4,222-7,888), and Common Murre was the least abundant with 623 individuals (548 – 707). As with other migrants, we do not know passage rates of any of these species through the study area, so we were unable to estimate the total number of individuals using the Ocean SAMP study area during the winter of 2009-2010.

Landbirds and Passerines: During land-based seawatches, we detected 7 species of raptors and 27 other species of landbirds including Mourning Dove, Short-eared Owl, Chimney swift, Ruby-throated Hummingbird, Belted Kingfisher, Northern Flicker, a flycatcher, three species of jays and crows, Horned Lark, six species of swallows, a thrush, a pipit, a waxwing, three species of warblers, a bunting, three species in the blackbird family, and a goldfinch. However, with the exception of Tree Swallows, which are diurnal migrants along the coast, we detected very few songbirds or other types of landbirds during our land-based seawatches. During ship-based line transect surveys, we detected Mourning Dove and 7 species of songbirds (Bank and Tree Swallow; Blackpoll and Yellow-rumped Warbler; Dark-eyed Junco, Savannah Sparrow, and Snow Bunting). This is not surprising as most landbirds, particularly songbirds, are nocturnal migrants, and can therefore only be monitored by radar. We did have a radar unit on Block Island throughout 2009 and results from that research are included in an appendix to this interim report (see Appendix K).

Table of Contents

List of Figures

List of Tables

List of Attachments and Appendices

Abstract

This interim report for the Rhode Island Special Area Management Plan (SAMP) summarizes research conducted from January 2009 through mid-February 2010. This research is the first attempt to quantify the spatial distribution and abundance of birds using the offshore waters of Rhode Island. Avian research is still ongoing and will continue through at least May 2011. Our objectives were to: (1) Summarize historical studies of avian use of nearshore and offshore waters, (2) Assess seasonal variation in the spatial distribution and abundance of birds in RI nearshore and coastal waters, (3) Assess diel patterns of avian use of RI nearshore and offshore waters, (4) Quantify flight ecology for birds in RI nearshore and offshore waters, and (5) Investigate Roseate Tern use of the study area.

There are no similar avian studies within the Ocean SAMP boundaries, although avian offshore research has been conducted in continental shelf waters of the NE Atlantic Ocean. In addition, ongoing research along the coast, in coastal ponds, and in Narragansett Bay that we summarized provides valuable long-term baseline information for avian species that use nearshore habitats. We used five survey methods to assess avian use of the study area: (1) land-based seawatches at 11 stations along coastal mainland Rhode Island from 23 Jan 2009 to mid-Feb 2010 to survey birds out to 3 km offshore; (2) systematic ship-based line-transect surveys on up to 8 grids from February 2009 - March 2010; (3) aerial strip-transect surveys spaced at 3 km intervals perpendicular to the coast from November 2009 to March 2010; (4) boat-based nearshore line transect surveys for Roseate Terns from August 2009 to early September 2009; and (5) observations monitoring the movement ecology of birds 24 hrs per week, 7 days a week from March to mid-December 2009 using horizontal and vertical radars on Block Island.

We conducted 796 1-2 hr land-based seawatches and had 465,039 detections of 121 species. We used these surveys to model the phenology of common species and spatial variation to assess relative abundance. We conducted 54 ship-based surveys on 8 grids over 27 days and detected 56 species. We used these results in program DISTANCE to model the distribution and abundance of 11 common species that included loons, shearwaters, storm-petrels, gannets, gulls, and alcids in summer, fall and winter. During summer, we estimated 16,335 Wilson's Storm-Petrels (95% CI = 10,879-24,527) were using deeper sections of Rhode Island Sound and the Inner Continental Shelf. In winter, the average daily abundance of Common Loons (average = 2,901, 95% CI = 2535-3321) suggests the Ocean SAMP study area provides critical wintering habitat for loons. We also detected large number of alcids in winter (Razorbill =1,390 individuals [95% CI = 996-1,940], Dovekie = 5,771 individuals [4,222-7,888]), with strong evidence of spatial segregation among species in bathymetry preferences. During 10 aerial surveys, we had a total of 9,414 detections from 17 species or guilds. We used aerial survey results to verify spatial distribution patterns and to assess bathymetry preferences for various species. We occasionally detected Roseate Tern during land-based point counts in the NW corner of the Ocean SAMP study area, while we rarely observed Roseate Terns offshore. Once surveys are complete, we will use this quantitative information to aid the Ocean SAMP process in determining where various types of development can take place that would minimize impacts to avian populations.

1 Introduction

1.1 Ocean SAMP background and the scope this report.

This interim report summarizes avian research conducted for the Rhode Island Special Area Management Plan (SAMP) from January 2009 through March 2010. We will continue to collect original data from March 2010 to at least May 2011. Our goal for this preliminary summary of results is to present the results and identify patterns in the spatial distribution and abundance of birds in the Ocean SAMP study area that are evident from data collected for over one year (up to March 2010). We will provide a final analysis of land-based and boat-based surveys in an updated report in December 2010, and a full report of all surveys in a final report in mid 2011. What is lacking from this preliminary report is longer-term information on interannual variation in avian distribution patterns or movement ecology in the Ocean SAMP study area. Avian studies in Nantucket Sound associated with the Cape Wind offshore wind farm documented considerable interannual variation in the distribution of large flocks of various species of seaducks (Perkins et al. 2004, 2005). This is why it is important that we continue to conduct surveys over time so that an accurate baseline assessment of the distribution and abundance of birds is available for comparison with data collected before, during, and after proposed development projects.

The focus of this report is avian use of Rhode Island's offshore waters. Based on previous research primarily in Europe, birds are likely to be one of the taxonomic groups most affected by energy development (e.g., offshore wind farm development) through: (1) increased mortality from collisions, (2) displacement from used habitats, or (3) enhancement of existing habitats (JNCC 2004; Maclean 2006). Therefore, understanding avian abundance, spatial distribution, phenology and movement ecology in the Ocean SAMP study area is crucial. The scientific information summarized in this report provides essential biological data that will inform development of Ocean SAMP policy. Federal agencies such as the U.S. Fish and Wildlife Service and the U.S. Army Corps of Engineers, and state agencies including the R.I. Department of Environmental Management, will review this and other SAMP documents because these agencies are responsible for assessing potential impacts of offshore development on all wildlife, including birds. In addition, the public will have opportunities throughout the SAMP process to have input into SAMP documents and to shape policies.

Special Area Management Plans, or SAMPs, are federally recognized management and regulatory documents that promote ecosystem-based management, as well as coastal-dependent economic activity. Rhode Island's coastal management agency, the Coastal Resource Management Council (CRMC), is the state agency in charge of the SAMP process. CRMC has regulatory functions and is responsible for preserving, protecting, developing, and where possible, restoring the state's coastal resources.

CRMC has already worked with scientists, planners, and public stakeholders to create six Rhode Island SAMPs in nearshore waters. These SAMPs encompass a variety of uses from industrial ports to conservation areas. As with other SAMPs, the Ocean SAMP will define use zones for offshore waters using a research and planning process, with input from the public. Using the best available science from a variety of disciplines and open public input and involvement, the SAMP is an adaptive planning tool that promotes comprehensive ecosystem-based management. It is the intent of the SAMP to facilitate coordination between state and federal agencies and the people of Rhode Island.

The Ocean SAMP will make Rhode Island the first state in the nation to zone its offshore waters for diverse activities including renewable energy development. This process will also protect current uses and habitats through zones for commercial fishing; critical habitats for fish, marine animals, and birds; marine transport; and other important uses of offshore waters. This planning process involves data collection by scientists from a variety of disciplines, including biologists.

1.2 Description of the study area.

The Ocean SAMP study area encompasses about 3,800 km^2 that includes Rhode Island Sound, Block Island Sound, and the Inner Continental Shelf. The Inner Continental Shelf is defined as the area south of Rhode Island and Block Island Sounds that extends to the Continental Shelf Slope (Armsby 2010; Fig. 1). In the Ocean SAMP Ecology Chapter, Armsby (2010) effectively described the geological, physical, chemical, and biological oceanogeography of the Ocean SAMP region, thus we urge readers interested in an in-depth overview of any of these characteristics of the region to read the Ecology chapter. However, we describe below some of the key geological and physical features that likely affect the spatial distribution of avian populations within the Ocean SAMP.

Bathymetry is one of the primary physical features determining where many species of waterbirds roost and forage. The Ocean SAMP study area is characterized by shallow, nearshore continental shelf waters, with water depths averaging 34.9 m ± 9.9 (SD); about 8% of the area is <20 m deep and 86% is between 20-50 m deep (Fig. 2). The area is interconnected to Narragansett Bay, Buzzards Bay, Long Island Sound, and the Atlantic Ocean via the Inner Continental Shelf. Outflow from large freshwater rivers (e.g., Connecticut River) enter Block Island Sound via Long Island Sound, which affects the physical, chemical, and biological characteristics of the Ocean SAMP study area (Armsby 2010). A 15-25 m deep glacial end moraine extends from Montauk Point to Block Island, which partially buffers Block Island Sound from large wave impacts from the Continental Shelf. The deepest water of the Ocean SAMP study area is Block Channel (maximum depth of about 60 m), which is an undersea canyon between Block Island and Martha's Vineyard formed by outflow from a glacial lake

about 20,000 years ago (Uchupi et al. 2001) that now forms an underwater connection between Block Island Sound and the Inner Continental Shelf .

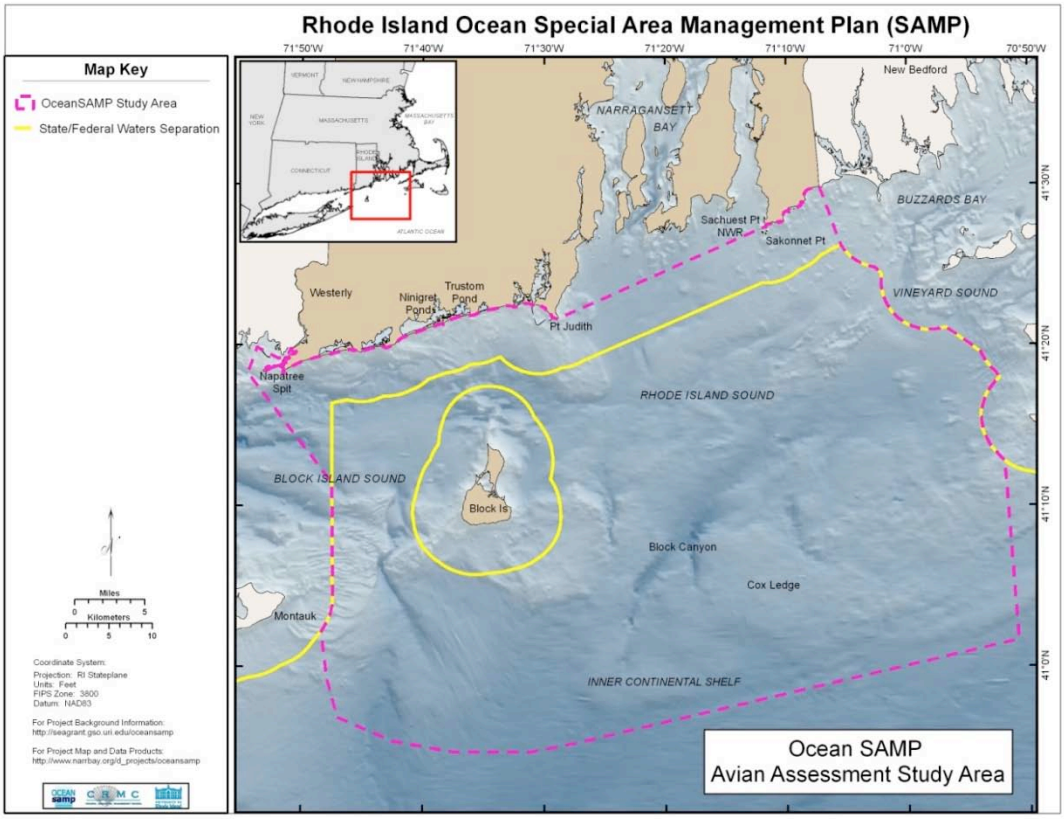

Fig. 1. Study boundaries for the Rhode Island Ocean Special Area Management Plan. Yellow line represents a boundary 3 miles offshore and in state waters, pink line is 16 miles offshore at its nearest point, hence in federal waters.

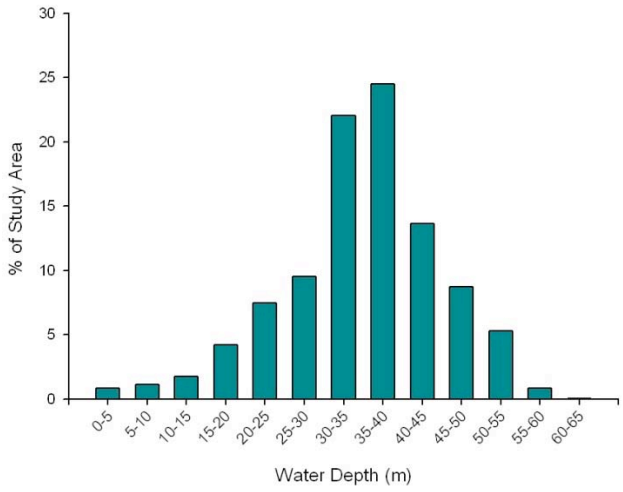

Fig. 2. Bathymetry of the Ocean SAMP study area based on 6500 uniformly distributed points placed within study area boundaries. Approximately 8% of the area is <20 m deep and 86% is 20-50 m deep.

Water temperatures in winter ranges from 3-6°C, with water on the bottom several degrees warmer than surface temperatures. In summer, water temperature ranges from 10-21°C, with surface temperatures 10°C warmer than bottom water. Thus, the water column tends to be stratified in the summer, while there is less stratification in the winter. During the summer, this stratification can reduce dissolved oxygen to levels that are detrimental to benthic marine fauna and the animals that eat them. During winter, the warmest waters occur offshore in the area around Cox Ledge, while the lowest temperatures occur next to mainland Rhode Island. In the summer, the warmest waters occur in northern and central Rhode Island Sound, while cool water from Long Island Sound makes western portions of the area cooler (Codiga and Ullman 2010).

The benthic community in the Ocean SAMP study area is dominated by tube-dwelling amphipod species, with bivalves, marine polychaete worms, and small crustaceans also common in the region. Some of these benthic species are important prey for a number of avian species including seaducks and other diving ducks during winter, as well as demersal fish. Unfortunately, there currently are no large-scale studies that have mapped the spatial distribution of the benthic community in the Ocean SAMP study area, nor are the habitat associations of various species of benthic fauna clearly understood. Thus, we know little about the spatial distribution patterns of the benthic community within the Ocean SAMP boundaries. We know even less about variation between years in abundance and distribution of benthic prey, which could be one of the main factors determining where seaducks forage annually.

The topography and composition of the seafloor within the Ocean SAMP study area is primarily the result of glacial processes. The seafloor has been subdivided into four depositional environments, which vary as a function of particle grain size: (1) depositional platform sand sheet [medium-grained sand], (2) cross-shore swaths [medium to coarse sand], (3) depositional gravel pavement [cobble gravel], and (4) glacial moraine [gravels to boulders]) (Boothroyd in prep). The glacial moraines are relatively static, while other depositional environments can be dynamic and move during storm events. In addition, upwelling, downwelling, and ocean currents, among other forces, can affect their characteristics and location.

Winds in the Ocean SAMP region tend to be diurnal during summer months. Dominant wind direction varies seasonally, with southwest winds in the summer and northwest winds in winter. Average wind speeds tend to be at least two times greater in winter. Northwest winds in winter can generate up to 7 m waves in Block Island Sound, which probably affects the local distribution of birds in the Ocean SAMP study area. Mean wave height in the area is 1.2 m, with most waves coming from a southerly direction. Tides in the Ocean SAMP study area are semi-diurnal (about twice per day) and have a range of about 1 m.

Water circulation patterns in the Ocean SAMP study area vary between Rhode Island Sound, Block Island Sound, and the Inner Continental Shelf. In general, water circulates from the SW to

SE in Rhode Island Sound. In contrast, outflow of fresher water from Long Island Sound causes shallow water to flow from west to east or south in Block Island Sound, while deeper water tends to flow from east to west (Codiga and Ullman 2010; Armsby 2010: Fig 2.13).

1.3 Research objectives

Most baseline investigations of seabird use of an area prior to construction of some major development occur for two or three years before construction in the seasons in which birds are most likely to be present in significant numbers (JNCC 2004; Maclean et al. 2006), although this obviously varies between projects. Several years of baseline information is needed because avian populations can fluctuate dramatically among years, as can the spatial distribution of preferred foraging habitat. Thus, multiple years of data are often needed to obtain a clear understanding of avian abundance, spatial distribution, phenology and movement ecology (Maclean 2006).

In New England, the largest concentrations of offshore birds occur in winter, although large numbers of some migratory birds (shearwaters, storm-petrels) use offshore habitats in the summer. There are no major seabird colonies located in the Ocean SAMP area (although there are wading bird, gull, cormorant, and tern colonies in adjacent nearshore waters in Narragansett Bay and in coastal Rhode Island; there is also a small wading bird colony on Block Island and some gulls also nest on Block Island). Thus, our avian monitoring efforts were primarily designed to assess the abundance and distribution of migrants and birds wintering in Rhode Island's offshore waters.

As Maclean et al. (2006) pointed out, baseline surveys conducted for at least two full seasons are needed to assess the seasonal abundance of birds and its annual variability (JNCC 2004; Kahlert et al. 2002, 2004). The principal methods used to assess habitat use by seabirds in relation to offshore wind farms are ship and aerial surveys (Innogy 2003), with land-based seawatches also used to assess the phenology of migration and abundance trends (e.g., Wynn and Yesou 2007).

Our objectives for assessing avian distribution and abundance for this Ocean SAMP include:

1) *Assess historical avian use of nearshore and offshore waters*. We conducted a thorough review of peer-reviewed literature that was pertinent to avian use of any part of the Ocean SAMP study area. We also summarized unpublished data obtained from local state and federal biologists that included surveys of birds in nearshore and offshore waters of Rhode Island.

2) *Assess seasonal variation in the spatial distribution and abundance of birds in RI nearshore and offshore waters*. We conducted a coordinated series of systematic land-based sea watches, ship-based line transect surveys on randomly placed grids, and aerial strip transect surveys that

enabled us to estimate bird distribution and abundance across the entire study area. All surveys were conducted monthly so that we could assess seasonal variation in the spatial distribution and movement ecology of birds throughout the study area.

3) *Assess diel patterns of avian use of RI nearshore and offshore waters*. We conducted land-based seawatches from dawn to dusk to determine how avian distribution and movements changed throughout the day in nearshore habitats. In addition, we stationed a radar unit on Block Island that monitored avian abundance throughout the day and night (24 hrs per day/7 days per week).

4) *Quantify flight ecology for birds in RI nearshore and offshore waters*. We gathered flight ecology information as part of all surveys and radar monitoring. During land-based seawatches, we recorded altitude and flight direction for all flying birds. During ship-based line-transect surveys, we also recorded altitude and flight direction for all flying birds. Radar data from Block Island included flight altitude, flight direction, and number of targets passing by the radar unit throughout each day and night from March to December 2009.

5) *Determine foraging and roosting sites for Roseate Terns*. The Roseate Tern is the only bird species regularly detected flying over the Ocean SAMP study area that is listed by the federal government as endangered. Piping Plovers occur within the Ocean SAMP study area, but are generally restricted to coastal beaches, with the exception of migratory periods. Thus, in addition to recording Roseate Terns during the standard monthly land-based and boat-based surveys, we also conducted additional land-based seawatches during late-summer that focused on the movement phenology of Roseate Terns in nearshore habitats. We also conducted additional boat-based line transect surveys during late-summer in nearshore waters from Point Judith to Napatree to investigate the spatial distribution, abundance, and foraging ecology of post-breeding Roseate Terns.

NOTE: Scientific names of all bird species mentioned in this report are given in Appendix A.

1.4 Review of Historical Data

1.4.1 Offshore surveys

We could not find any publications or reports that focused solely on avian use of offshore waters within either Block Island Sound or Rhode Island Sound. Most previously conducted systematic surveys that focused on Rhode Island birds have concentrated effort on nearshore habitats along mainland coastal Rhode Island, coastal ponds along the south shore, or within Narragansett Bay (see sections below). Two systematic ship-based bird surveys were conducted along the entire

northeastern United States that recorded bird species and numbers within the RI Ocean SAMP study area. These ship-based surveys were conducted by US Fish and Wildlife Service observers on National Marine Fisheries Service (NMFS) and U.S. Coast Guard vessels during 1978 and 1979 (hereafter NMFS surveys). NMFS survey transects were recorded in 10-min periods from January 1978 through February 1980, with a total of 42 days of survey effort in the RI Ocean SAMP study area during 1978 (19 days of survey effort) and 1979 (23 days) (Table 1). NMFS surveys in the RI Ocean SAMP study area occurred throughout the year, with more surveys conducted in March, July, and November (Table 2).

Table 1. Number of days per year when ship-based surveys were conducted within the Ocean SAMP study area from 1978 to 1988 during NMFS and CSAP avian surveys (MBO 1988).

Year	Number of Surveys
NMFS	
1978	19
1979	23
Subtotal	42
CSAP	
1980	9
1981	10
1982	5
1983	12
1984	19
1985	12
1986	11
1987	15
1988	8
Subtotal	101

The other systematic offshore survey effort in Rhode Island was the Cetacean and Seabird Assessment Program (CSAP) conducted by observers from Manomet Bird Observatory (now the Manomet Center for Conservation Sciences). This unprecedented program was conducted for the Northeast Fisheries Science Center (NEFSC) of the National Marine Fisheries Service from 1980 to 1988. CSAP was designed to provide a quantitative assessment of the abundance and distribution of cetaceans, seabirds and marine turtles in the shelf waters of the northeastern United States. These data represent the largest, highest quality historical dataset for the northwest Atlantic U.S. waters (USGS 2010). There is no other dataset for the northeastern United States that includes observations of birds at this large spatial and temporal scale. A total of 101 survey days during 1980-1988 were conducted within Rhode Island waters, with 5 to 19 survey days in a given year (Table 1). These 101 surveys within the RI Ocean SAMP study area

were distributed across months such that on average 8.4 surveys were conducted each month (Table 2).

During 42 days of NMFS surveys in the RI Ocean SAMP study area, observers detected 4,532 birds in 665 different flocks and documented 21 bird species (Table 3; Fig. 3). About 17.5% of all detections were not identified to species, but most observations were identified to at least a guild (e.g., unidentified loon). Although we were unable to standardize survey effort to develop quantitative abundance estimates of birds based on NMFS surveys, it appears that species that tend to be most common during summer months dominated their survey results because gulls (37.9% of detections), shearwaters (25.8%) and storm-petrels (13%) were the most common taxa detected. One of the most interesting species detected during these surveys was an unidentified albatross, which was probably a Yellow-nosed Albatross, as this is the only species of albatross to have been detected in Rhode Island waters (D. Ferren, unpubl. manuscript).

Table 2. Seasonal variation (number of days per month when surveys were conducted) in survey effort during NMFS and CSAP offshore ship-based surveys conducted from 1978-1988 within RI Ocean SAMP study area boundaries.

Month	CSAP Number of surveys	NMFS Number of Surveys
January	9	1
February	2	0
March	12	6
April	2	4
May	11	4
June	5	4
July	15	7
August	8	1
September	14	1
October	9	7
November	10	6
December	4	1
Total	**101**	**42**

Few alcids (i.e., puffins, Razorbills, murres, etc) were detected during NMFS surveys (43 detections, <1% of total detections), with only Razorbills identified to species. The paucity of alcid detections during NMFS surveys is not unexpected, as only 2 surveys were conducted from December through Feb, when alcids tend to be most common (see Alcid section below). Apparently the few offshore NMFS surveys that took place were in nearshore areas, as no deep water species (e.g., Common Murre or Dovekies) were detected.

During the nine years of CSAP surveys, observers recorded 34 species from a total of 14,045 detections of 1447 flocks (Table 3; Fig. 3). During CSAP surveys, gulls accounted for the

majority of detections (6 species; 69.1% of all detections), while shearwaters (4 species; 15.7%), and storm-petrels (2 species; 6%) were the other most common taxa detected.

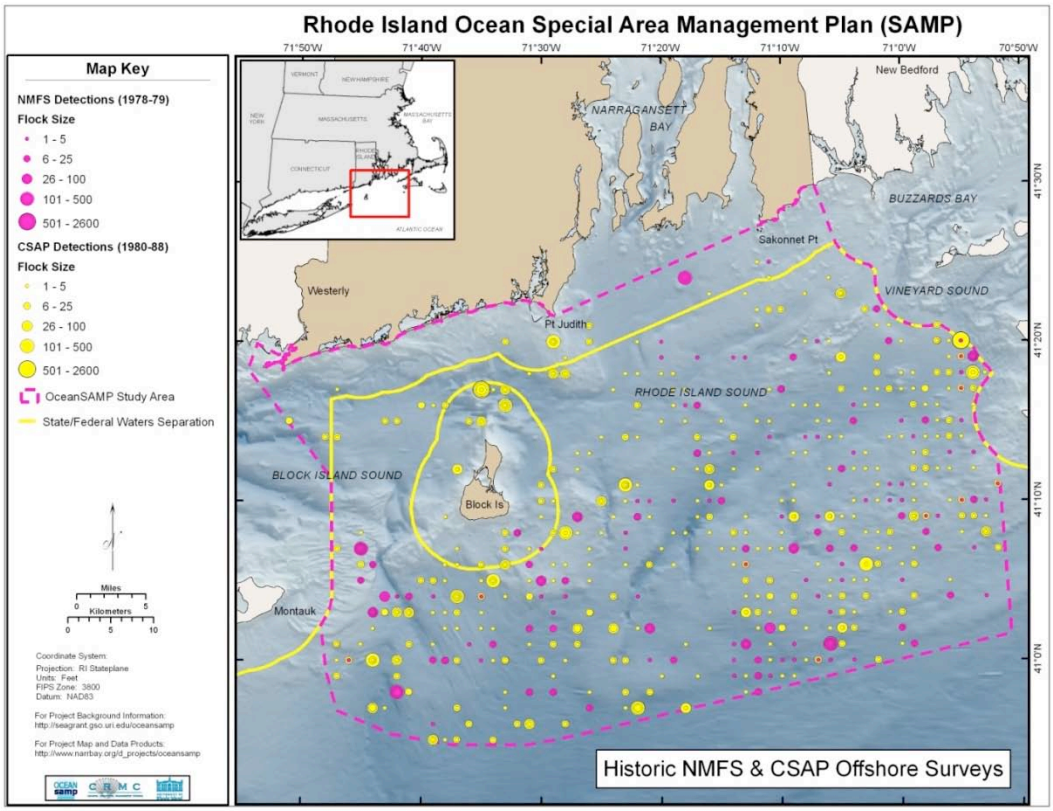

Fig. 3. Distribution of avian flocks detected during NMFS (1978-1979) and CSAP (1980-1987) offshore surveys within the RI Ocean SAMP study area. Both surveys encompassed offshore waters throughout the Northeast, thus these detections in the RI Ocean SAMP study area represent only a small fraction of the total number of birds detected during the all surveys. See Table 3 for a summary of species detected during these surveys.

Similar to NMFS surveys, alcids were rarely observed during CSAP surveys (4 species including Dovekie and Atlantic Puffin; 0.3% of all detections; Table 3). Although 15 survey days were conducted from December through February during CSAP, the paucity of alcid sightings (81 total detections in NMFS and CSAP datasets combined) in these historical datasets is somewhat puzzling because much of the sampling took place in offshore waters where alcids occur (Fig. 3). Because we could not determine survey effort within RI Ocean SAMP boundaries during NMFS and CSAP surveys, we cannot directly compare these historical datasets to our own ship-based results.

Table 3. Total number of detections and flocks recorded for 32 species of birds detected during CSAP and NMFS offshore ship-based surveys within the RI Ocean SAMP study area boundaries from 1978 to 1987 (MBO 1988). See Fig. 3 for locations of birds detected during these historical offshore surveys.

	CSAP 1980-1987			NMFS 1978-1979		
Species	**Birds**	**%detections**	**Flocks**	**Birds**	**%detections**	**Flocks**
Unidentified bird	0	0	0	208	4.59	2
Unidentified Loon	7	0.05	4	2	0.04	2
Common Loon	41	0.29	30	11	0.24	5
Red-throated Loon	14	0.10	8	0	0	0
Unidentified Albatross	0	0	0	1	0.02	1
Northern Fulmar	28	0.20	12	0	0	0
Unidentified Shearwater	150	1.07	12	23	0.46	5
Manx Shearwater	8	0.06	6	1	0.02	1
Greater Shearwater	1198	8.52	74	432	9.53	45
Sooty Shearwater	48	0.34	17	89	1.96	22
Cory's Shearwater	799	5.68	61	625	13.78	43
Unidentified storm-petrel	8	0.06	6	4	0.09	3
Wilson's Storm-petrel	796	5.66	66	587	12.95	35
Leach's Storm-petrel	32	0.23	10	1	0.02	1
Northern Gannet	781	5.56	160	135	2.98	51
Unidentified Cormorant	14	0.10	3	5	0.11	2
Double-crested Cormorant	204	1.45	6	70	1.54	2
Great Cormorant	9	0.06	3	2	0.04	1
Common Eider	56	0.40	2	0	0	0
Long-tailed Duck	5	0.04	2	0	0	0
Unidentified Scoter	0	0	0	120	2.65	3
White-winged Scoter	50	0.36	12	72	1.59	0
Surf Scoter	1	0.01	1	18	0.40	1
Unidentified Phalarope	1	0.02	1	18	0.40	1
Red-breasted Merganser	1	0.01	1	0	0	0
Unidentified Jaeger	3	0.02	3	3	0.07	3
Pomarine Jaeger	5	0.04	4	1	0.02	1
Parasitic Jaeger	4	0.03	4	0	0	0
Long-tailed Jaeger	0	0	0	1	0.02	1
Unidentified Gull	4,824	34.31	43	405	8.93	27
Black-legged Kittiwake	818	5.82	161	131	2.89	36
Bonaparte's Gull	163	1.16	11	94	2.07	3
Ring-billed Gull	65	0.46	15	2	0.04	2
Laughing Gull	125	0.89	48	2	0.04	2
Herring Gull	2,033	14.46	385	1,084	23.91	244
Great Black-backed Gull	1,687	12.00	247	339	7.48	108
Arctic Tern	8	0.06	2	0	0	0
Common Tern	22	0.16	7	25	0.55	2
Roseate Tern	3	0.02	2	0	0	0
Unidentified Alcid	10	0.08	1	22	0.49	3
Razorbill	7	0.05	3	21	0.46	4
Common Murre	12	0.09	5	0	0	0
Dovekie	4	0.03	2	0	0	0
Atlantic Puffin	5	0.04	4	0	0	0

Total	**14,045**	**1447**	**4,532**	**665**

NEARSHORE SURVEYS

Most of the historical information available regarding phenology, abundance and spatial distribution of different avian groups in Rhode Island are from surveys of nearshore waters, coastal ponds, and the Narragansett Bay estuary that were conducted by several state and federal biologists over the past 30 years. These data were provided by biologists from the Rhode Island Department of Environmental Management Division of Fish and Wildlife (RIDFW, Jay Osenkowski, Waterfowl Biologist, Chris Raithel, Non-game Biologist), the U.S. Fish and Wildlife Service's Rhode Island National Wildlife Refuge Complex (USFWS, Suzanne Paton, Senior Refuge Biologist), and the Environmental Protection Agency (EPA, Dr. Rick McKinney). We also present long-term data on landbird abundance and phenology from the bird banding program at Kingston Wildlife Research Station, operated by the University of Rhode Island in conjunction with the Audubon Society of Rhode Island. Most data were land-based surveys (with the exception of aerial surveys conducted by RI Division of Fish and Wildlife Biologists) that were conducted in areas along the northern boundary or inland of the RI Ocean SAMP study area. These data provide useful baseline information on avian abundance and phenology in parts of the Ocean SAMP study area that were helpful for designing avian surveys for the RI Ocean SAMP.

Below we describe these various surveys:

RIDFW Mid-Winter Aerial Survey of Narragansett Bay and coastal wetlands

The Rhode Island Division of Fish and Wildlife (RIDFW) conducted a mid-winter waterfowl survey every January since 1955. We had access to data collected over 27 years from 1979 to 2008 that were collected in three zones, with Zones 1 and 2 adjacent to the RI Ocean SAMP study area (Fig. 4). These aerial surveys were conducted from a helicopter by Charlie Allin from 1979-2003, and Jason Osenkowski from 2004-2008. This survey takes place one day per year in January, with efforts focused on assessing the abundance of each species of waterfowl present in Narragansett Bay and coastal ponds. This survey does not follow a strict sampling protocol (e.g., flight elevation was not consistent throughout the survey, there were not predetermined transects to follow, the time when various sites are surveyed varies among years, and these surveys did not use either a strip transect or line transect methodology), so density of birds cannot be estimated from these surveys. However, these data can be used to assess interannual changes in relative abundance. Using total counts for Zones 1-3 for each survey, we calculated mean annual abundance, two estimates of variance (SD and Coefficient of Variation [CV]; SD/Mean X 100), the maximum number of individuals during any survey over the 27 winters, and the percent of years when the species was detected. Similar aerial surveys were conducted during mid-winter in every state in the eastern U.S. during the same time period, so that annual and spatial variation in waterfowl abundance can be assessed on a larger scale as well.

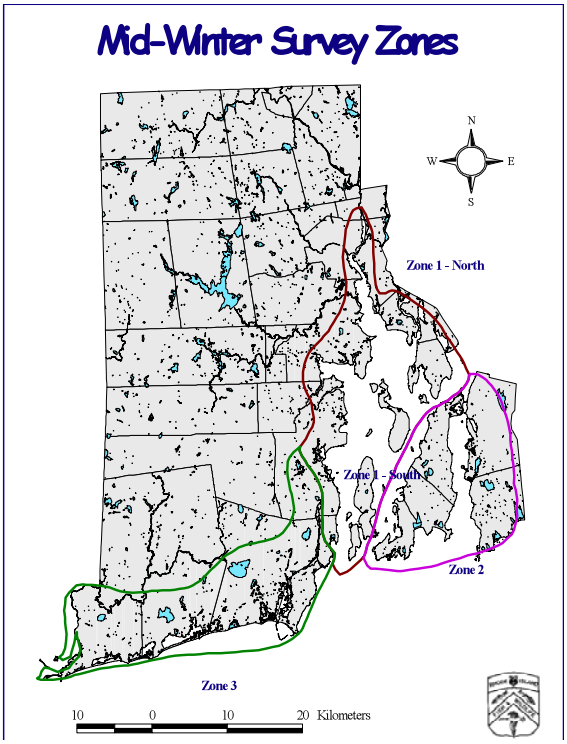

Fig. 4. Flight zones of aerial surveys conducted every January by the Rhode Island Fish and Wildlife Service (1979-present) to monitor waterfowl population trends (J. Osenkowski, unpubl. data).

Napatree Avian Surveys

Chris Raithel of the Rhode Island Division of Fish and Wildlife (RIDFW) conducted land-based transect surveys at Napatree Point in Watch Hill, RI from 1982 to the present. For this report, we analyzed surveys conducted by Raithel approximately every 1-2 weeks from 1982 to mid-2005 (1,418 total surveys; an average of 59.1 ± 15.5 (SD) surveys per year). In fact, this dataset is unique in that Raithel was the only observer and the duration of the surveys was extensive (in terms of being conducted for all months of the year over such a long time period). Most surveys took ca. 2-3 hours to complete. Weather data were also recorded at the beginning and end of each survey and included: weather condition, temperature, wind direction and speed, moon phase, tide and recent weather. Although these data are from one location, the strength of this dataset is that it was collected by the same experienced observer using the same methodology every year since 1982 and it includes counts of all bird species observed. Thus, these data provide strong quantitative insights into the migration phenology of birds in the region. They also provide useful information about annual variation in avian abundance at one study site. To assess annual variation, we calculated the maximum number of individuals detected per year for each species. We then used these maximum counts to quantify mean abundance per year, two estimates of variance (Standard Deviation [SD] and Coefficient of Variation [CV]), the maximum count over all surveys, and the percent of years when the species was detected.

US EPA Land-based Mid-winter Narragansett Bay Waterfowl Survey

Dr. Rick McKinney (US Environmental Protection Agency; EPA) has been coordinating a winter (mid-January) waterfowl survey in Narragansett Bay since 2004 with biologists from the EPA, URI, and RIDFW, as well as local birders (EPA 2010). This land-based survey provides a one-day assessment of waterfowl abundance throughout Narragansett Bay every January. Surveys were conducted at a standardized set of survey locations on one day using six teams of at least two biologists each. At each survey site, observers used spotting scopes and binoculars to record the abundance of each species, along with weather conditions. Surveys began at dawn and took most of the day to be completed. Surveys conducted close to the mouth of Narragansett Bay were adjacent to the RI Ocean SAMP study area. Since this survey was conducted one day a year (similar to the RIDFW aerial mid-winter survey), it only provides a snapshot view of waterfowl abundance in Narragansett Bay. However, it captures the interannual variation in the number of waterfowl overwintering in the bay at a given time during winter, as many individual waterfowl exhibit site fidelity to the same wintering location between years. For the EPA data, we calculated mean annual abundance, two estimates of variance (SD and Coefficient of Variation [CV]; CV = SD/mean X 100), the maximum number of individuals during any survey over the 6 winters, and the percent of years when the species was detected.

Sachuest Point NWR

Land-based waterbird surveys have been conducted from 1992 to the present at Sachuest Point National Wildlife Refuge by volunteers working with USFWS refuge staff. We had access to data collected from 1992 to 2003. We summarized 94 surveys that occurred from November through the end of April when waterfowl and waterbirds were most abundant. Over the 11 years, there was an average of 8.6 ± 3.8 surveys per year during this winter period. Most surveys were conducted in the morning hours from 10 observation points on both the east and west sides of Sachuest Point. At each survey point, observers used a spotting scope to identify species and numbers of all birds detected. Weather data were also recorded including temperature, wind direction and speed, percent clouds and precipitation. Surveys were conducted by numerous observers so that there is the potential for observer variation to bias these survey results. However, these data provide useful information about annual variation in avian abundance at a site used by relatively large numbers of waterbirds, particularly seaducks. For each winter (1 Nov to 30 April), we first calculated the maximum number of individuals detected for each species. We then used these estimates of maximum abundance within a winter to calculate mean annual abundance, two estimates of variance (SD and Coefficient of Variation [CV]; CV = SD/mean X 100), the maximum number of individuals during any survey over the 10 winters, and the percent of years when each species was detected. To assess annual variation in the total number of birds using Sachuest, we summed the maximum counts for each species within a winter season. We then calculated the mean, SD, CV, and maximum for these summed winter counts to determine total abundance.

Pt. Judith Waterbird Surveys

The movement ecology of waterbirds was investigated from the fall of 1997 to the fall of 1998 at Pt. Judith by researchers from the University of Rhode Island as part of an assessment for wind farm development at this coastal site. Observers recorded species abundance, flock size (total number of individuals), time the flock was detected, flight direction (compass bearing), and estimated height above the water (in meters) for birds in flight. Also recorded was the behavior of the birds(s) including flying, loafing on water, roosting on the breakwater, hovering, or circling. Weather variables were recorded including: wind speed, direction, temperature, cloud cover, ceiling height, vertical visibility, precipitation, and sea swell height. Vertical visibility was recorded if the clouds were <300 m high. These surveys were conducted by the same observers through time.

Coastal Ponds

Ninigret Pond: We summarized waterbird surveys conducted annually by USFWS biologists at 11 sites at Ninigret Pond from 1992-2008 (16 winters), with surveys conducted approximately 2-4 weeks apart. On average, 7.4 ± 2.1 (SD) surveys were conducted each winter between 1 November to 30 March (a total of 119 surveys), which coincided with peak waterfowl use of this coastal pond. We calculated mean abundance, two estimates of variance (SD and Coefficient of Variation [CV]; CV = SD/Mean X 100), the maximum number of individuals during any survey over the 10 winters, and the percent of years when the species was detected. To assess annual variation in the total number of birds using Ninigret, we summed the maximum counts for each species within a winter season. We then calculated the mean, SD, CV, and maximum for these summed winter counts to determine total abundance.

Trustom Pond: Waterbird surveys have been conducted by biologists with the US Fish and Wildlife Service at Trustom Pond NWR, Mud Pond, and Card's Pond intermittently from 1992 to the present. We report here data for 10 winters from 1992 to 2006 (1992-93 to 1993-94, 1998-99 to 2005-2006). The timing of surveys varied annually, but typically occurred at two-week intervals from October through April, which represents the peak of waterfowl use of coastal ponds in southern New England. We analyzed 88 total surveys, with an average of 8.8 ± 2.4 (SD) surveys per winter. Most surveys were conducted in the morning hours from 10 fixed observation points. At each survey point, all individuals were recorded to species. Weather data were also recorded including temperature, wind direction and speed, percent clouds and precipitation. Surveys were conducted by numerous observers. To characterize interannual variation in waterbird abundance, we calculated the maximum number of individuals detected each winter for each species. We then calculated mean abundance, two estimates of variance (SD and Coefficient of Variation [CV];CV = SD/mean X 100), the maximum number of individuals during any survey over the 10 winters, and the percent of years when the species was detected. To assess annual variation in the total number of birds using Trustom, we summed the

maximum counts for each species within a winter season. We then calculated the mean, SD, CV, and maximum for these summed winter counts to determine total abundance.

Trustom Pond offers some of the best waterfowl habitat for diving and dabbling ducks in the region during the winter months. These data provide quantitative information on the phenology of waterfowl and relative abundance of waterbirds using this important wintering and stopover habitat along the south coast of Rhode Island.

SUMMARY OF THE PHENOLOGY, DISTRIBUTION, ABUNDANCE AND BEHAVIOR OF AVIAN GROUPS INHABITING THE OCEAN SAMP STUDY AREA BASED ON HISTORICAL DATASETS

Waterfowl

Waterfowl occur in Rhode Island throughout the year, but are most abundant during winter months (November to April) in Rhode Island. Mid-winter aerial surveys conducted by Rhode Island Division of Fish and Wildlife every January since 1979 have detected an average of 21,256 ± 12,051 (SD) waterfowl annually, with a maximum of 58,706 individuals in 2001 (RIDFW; Table 4). On average 12.7 ± 2.6 species were detected during these RIDFW surveys, with a cumulative total of 24 species detected over the years (Table 4). The most abundant species (>1,000 individuals annually) during these mid-winter surveys include scaup (which were primarily Greater Scaup, with some Lesser Scaup based on EPA land-based survey results of Narragansett Bay – Table 5), Canada Goose, American Black Duck, and Common Eider (Table 4). There was considerable interannual variation in RIDFW survey results, with coefficients of variation (CV) averaging 240.1 ± 167.7 (SD). However, the most abundant species tend to have CV's <100, although Common Eider exhibit considerable interannual variation (CV = 237.9).

The other large-scale investigation of annual variation in waterbird abundance in Rhode Island was the EPA's mid-winter survey of Narragansett Bay (EPA). This land-based, one day survey counted an average of 22,725.0 ± 3,557.4 (SD) waterbirds annually (Table 5). Dominant species during these surveys were Greater Scaup, Canada Goose, Brant, Common Eider, Lesser Scaup, and American Black Duck. Coefficients of variation (CV) for these land-based point counts of Narragansett Bay averaged 83.4 ± 60.2 which were considerably lower than that of the RIDFW surveys. Given that the same areas were sampled from land-based stations in a similar manner during the EPA mid-winter counts, the EPA surveys were probably more accurate and precise than RIDFW aerial surveys. Therefore, the CVs detected during the EPA land-based surveys (Table 5) are probably more reflective of annual variation in waterbird counts for birds in Rhode Island.

At a smaller spatial scale, surveys of waterbirds at Sachuest Point NWR from 1992-2003 provided another estimate of annual variation in bird abundance in nearshore habitats (Table 6). During these surveys at Sachuest Point NWR, a cumulative total of 31 species were detected with an average of 1,300.6 ± 1,056.0 individuals counted annually (Table 6). Dominant waterfowl species were Common Eider, Surf Scoter, Harlequin Duck, Common Goldeneye, Bufflehead, Black Scoter, and American Black Duck (Table 6). There was considerable annual variation in these land-based surveys, with Coefficients of Variation (CV) averaging 174.1 ± 89.9 (SD) and 26 of 31 species having CVs greater than 100 (Table 6).

Surveys at Napatree by Raithel provided the best long-term dataset for a wide variety of waterbirds in the region. We summarized annual variation in waterbirds that are typically associated with nearshore and offshore waters (i.e., loons, grebes, cormorants, tubenoses, waterfowl, gulls and alcids; Table 7). There were 14 species whose maximum count on a survey within a year averaged over 100 individuals per year, with 12 of 14 of these common species having CVs <100 (mean CV for these 14 species = 89.9 ± 65.1). However, Northern Gannet abundance was more variable between years (CV = 313.3).

Terns often forage and roost at Napatree, plus many terns migrate past this sandy promontory. Raithel detected 10 species of terns over the years, with three species consistently detected (Least, Common, and Roseate). Mean maximum annual counts for these three species (56, 262, and 161 individuals, respectively; Table 7) were relatively consistent over the years, as CVs for these three species (mean = 70.0 ± 18.1 [SD]) were relatively low.

Table 4. Mean abundance per year, interannual variation, maximum number observed in a given year, and frequency of occurrence (% of years detected) for 21 species of waterfowl detected over 27 years during RIDFW mid-winter waterfowl surveys of Narragansett Bay and nearshore habitats along coastal mainland from 1979-2008 from Zones 1-3 combined (J. Osenkowski, RIDFW, unpubl. data; see Fig. 4 for zones). These helicopter-based aerial surveys were conducted on one day during January each year.

Species	Mean	SD	CV	Maximum	% of years
Mute Swan	845.1	438.4	51.9	1,788	100
Canada Goose	6,262.3	5,401.1	86.2	28,096	100
Brant	761.9	954.6	125.3	3,165	74
Mallard	860.8	692.0	80.4	3,220	100
American Black Duck	2,174.2	1,205.4	55.4	6,697	100
Gadwall	33.7	70.2	208.0	290	37
American Wigeon	148.0	206.7	139.6	835	70
Green-winged Teal	0.1	0.8	519.6	4	4
Canvasback	359.6	425.3	118.3	1,693	96
Redhead	0.3	1.3	519.6	7	4
Ring-necked Duck	0.7	3.8	519.6	20	4
Scaup unidentified	6,558.0	5,090.9	77.6	23,095	100
Common Eider	1,249.8	2,973.0	237.9	14,100	56
Harlequin Duck	11.3	25.2	222.4	100	30

Long-tailed Duck	2.6	7.9	299.6	30	11
Scoter unidentified	260.4	692.3	265.9	3,600	56
White-winged Scoter	9.3	39.3	424.6	200	7
Common Goldeneye	331.9	437.8	131.9	1,590	82
Bufflehead	608.7	409.3	67.2	1,387	93
Hooded Merganser	11.7	43.9	375.9	225	15
Merganser unidentified	590.2	538.4	91.2	2,396	93
Common Merganser	2.2	9.7	438.3	50	7
Red-breasted Merganser	170.2	352.9	207.4	1,187	30
Ruddy Duck	2.9	14.4	499.3	75	7
Overall abundance	21,256.0	12,050.6	56.7	58,706	
Species richness	12.7	2.6			

Table 5. Mean abundance per year, interannual variation, maximum number observed in a given year, and frequency of occurrence (% of years detected) for 23 species of waterbirds detected during EPA mid-winter surveys within the Narragansett Bay estuary from 2004-2009 (see EPA 2010). Birds were counted from land-based routes one day during January each year.

Species	Mean	SD	CV	Max	% of surveys
Common Loon	63.2	36.6	57.9	119	100.0
Horned Grebe	145.7	230.2	158.0	609	100.0
Cormorants unidentified	33.3	33.9	101.6	90	100.0
Mute Swan	572.5	147.7	25.8	775	100.0
Canada Goose	2,655.5	1,467.0	55.2	4,882	100.0
Brant	2,402.2	853.2	35.5	3,808	100.0
Mallard	1,012.5	449.3	44.4	1,478	100.0
American Black Duck	1,267.7	183.2	14.5	1,474	100.0
Gadwall	133.5	129.6	97.1	395	100.0
American Wigeon	481.3	369.3	76.7	1,060	100.0
Greater Scaup	4,638.2	2,978.3	64.2	7,889	100.0
Lesser Scaup	1,214.2	2,578.6	212.4	6,462	66.7
Common Eider	1,423.0	669.2	47.0	2,465	100.0
Harlequin Duck	71.7	25.6	35.7	105	100.0
Long-tailed Duck	1.5	2.1	138.2	5	50.0
White-winged Scoter	97.5	160.7	164.8	411	83.3
Surf Scoter	74.0	66.9	90.5	165	100.0
Black Scoter	125.0	67.2	53.8	204	100.0
Common Goldeneye	1,485.3	629.9	42.4	2,323	100.0
Barrow's Goldeneye	0.2	0.4	244.9	1	16.7
Bufflehead	901.5	424.3	47.1	1,530	100.0
Hooded Merganser	106.3	66.0	62.1	187	100.0
Red-breasted Merganser	710.8	209.6	29.5	1,022	100.0
Common Merganser	12.7	12.9	101.9	27	66.7
Gulls unidentified	3,095.8	854.0	27.6	4,015	100.0
Overall abundance	**22,725.0**	**3,557.4**	**15.7**	**26,950**	**100.0**
Species richness[1]	**21.8**	**1.2**			

[1]unidentified cormorants or gulls were not included in this calculation

Table 6. Mean abundance per year, interannual variation, maximum number observed in a given year, and frequency of occurrence (% of years detected) for 32 species of waterbirds detected in nearshore waters at Sachuest Point National Wildlife Refuge from 1992-2003 (USFWS, unpubl. data). Birds were counted from land-based routes every 2-4 weeks during November-April each year.

Species	Mean	SD	CV	Maximum	% of surveys
Common Loon	33.9	51.2	150.9	182	91
Red-throated Loon	1.8	2.2	122.5	6	55
Horned Grebe	16.2	20.3	125.6	72	91
Red-necked Grebe	2.2	3.9	177.3	11	36
Double-crested Cormorant	3.1	9.0	291.3	30	18
Great Cormorant	0.6	1.4	225.2	4	18
Mute Swan	2.6	3.4	130.6	10	64
Snow Goose	0.5	1.8	331.7	6	9
Canada Goose	5.1	11.6	227.6	37	46
Brant	12.4	14.3	115.4	38	73
Mallard	0.7	1.0	138.7	2	36
American Black Duck	55.3	46.3	83.7	160	100
American Wigeon	0.4	0.8	222.5	2	18
Gadwall	1.9	4.9	257.1	16	18
Redhead	0.1	0.3	331.7	1	9
Lesser Scaup	2.4	6.6	277.6	22	27
Greater Scaup	49.3	41.6	84.5	155	100
Common Eider	559.0	880.1	157.4	3011	100
King Eider	2.6	6.1	229.6	19	27
Harlequin Duck	80.5	16.0	19.9	107	100
Common Merganser	2.5	8.1	331.7	27	9
Long-tailed Duck	1.9	2.5	131.4	8	55
White-winged Scoter	31.4	40.4	128.9	115	100
Surf Scoter	109.1	128.3	117.6	368	91
Black Scoter	57.3	90.8	158.6	300	82
Common Goldeneye	87.7	31.8	36.2	143	100
Barrow's Goldeneye	0.2	0.4	222.5	1	18
Bufflehead	57.7	46.2	80.1	165	100
Hooded Merganser	0.3	0.9	331.7	3	9
Red-breasted Merganser	48.6	20.4	42.0	77	100
Ruddy Duck	8.3	12.0	144.7	30	46
Purple Sandpiper	65.2	94.1	144.4	250	46
Overall abundance	**1,300.6**	**1,056.0**	**81.2**	**4,053**	**100**

COASTAL PONDS

In coastal ponds, more species of dabbling ducks and diving ducks were detected at Trustom Pond NWR and Ninigret Pond NWR than within Narragansett Bay. For example, 41 species of waterbirds were detected at Trustom Pond, with 34 species of waterfowl detected and an average of 26.4 species of waterbirds detected annually during systematic surveys (Table 8). Nine species of dabbling ducks (genus *Anas*) were detected during Trustom Pond surveys, with Mallards and American Black Ducks the most abundant species. For the five most common species of dabbling ducks (American Black Duck, Mallard, American Wigeon, Green-winged Teal, and Gadwall), the overall mean CV was 94.7 ± 34.1 (SD), which was similar to land-based point counts of waterfowl during EPA mid-winter Narragansett Bay surveys (83.4 ± 60.2; Table 5). Large numbers of diving ducks (genus *Aythya*) were also prevalent at Trustom, with six species detected; Greater Scaup was the most abundant diving duck at Trustom with maximum counts of over 600 detected annually (Table 8). Ruddy Ducks were also prevalent at Trustom (over 300 annually), which is one of the few places where this species is common in Rhode Island. For the four common diving ducks (Greater and Lesser Scaup, Canvasback, and Ring-necked Duck) and Ruddy Duck, the overall mean CV was 128.5 ± 58.9, which was slightly higher than the estimate for dabbling ducks at Trustom (94.7 ± 34.1).

At Ninigret Pond, USFWS biologists detected 30 species of waterfowl over the years, with an average of 13.5 ± 2.9 (SD) species detected each winter (Table 9). Thus species richness was lower at Ninigret compared to Trustom. The number of dabbling ducks tends to be much lower at Ninigret than at Trustom, although American Black Ducks (over 200 individuals annually) were common at Ninigret. Certain species of ducks tended to be more abundant at Ninigret compared to Trustom, specifically Buffleheads, Common Goldeneye, and Red-breasted Mergansers. CVs for common diving ducks and seaducks (Greater and Lesser Scaup, Common Goldeneye, Bufflehead, Hooded and Red-breasted Merganser) averaged 115.9 ± 79.4, which was similar to that for diving ducks at Trustom (above).

Table 7. Mean abundance per year, interannual variation, maximum number observed in a given year, and frequency of occurrence (% of years detected) for 72 species of birds detected from Napatree Spit, Rhode Island during land-based surveys conducted over 24 years from 1982 to 2005 at Napatree Spit (C. Raithel, RI Div of Fish and Wildlife, unpubl. data). Birds were counted from land-based routes every 2 weeks throughout each year (1,418 total surveys). .

Species	Mean	SD	CV	Maximum	% of years
Common Loon	26.9	17.7	65.7	80	100
Red-throated Loon	15.0	10.3	68.9	35	100
Horned Grebe	27.9	8.9	32.0	47	100
Red-necked Grebe	1.1	1.0	89.9	4	75
Pied-billed Grebe	0.0	0.2	489.9	1	4
Eared Grebe	0.1	0.3	270.3	1	13
Sooty Shearwater	0.0	0.2	489.9	1	4
Wilson's Storm-Petrel	0.5	1.7	363.8	8	13
Leach's Storm-Petrel	0.0	0.2	489.9	1	4
Double-crested Cormorant	1528.7	1678.6	109.8	7640	100
Great Cormorant	26.6	12.6	47.3	50	100
Northern Gannet	193.1	605.0	313.3	3000	92
American White Pelican	0.0	0.2	489.9	1	4
Brown Pelican	0.0	0.2	489.9	1	4
G. White-fronted Goose	0.1	0.4	489.9	2	4
Snow Goose	37.3	112.9	303.0	495	42
Brant	424.6	130.7	30.8	580	100
Canada Goose	216.5	178.6	82.5	735	100
Mute Swan	116.2	67.3	57.9	250	100
Tundra Swan	0.1	0.6	489.9	3	4
Wood Duck	1.5	1.9	131.0	6	50
Gadwall	10.0	7.9	79.8	29	96
Eurasian Wigeon	0.0	0.2	489.9	1	4
American Wigeon	7.5	8.8	117.4	35	79
American Black Duck	222.6	181.3	81.4	750	100
Mallard	39.5	82.6	209.4	400	100
Blue-winged Teal	1.7	4.2	247.4	20	42
Northern Shoveler	0.2	0.6	282.4	2	13
Northern Pintail	2.0	2.7	132.0	10	54
Green-winged Teal	4.4	5.4	123.3	21	71
Canvasback	0.8	2.8	373.5	13	8
Redhead	0.1	0.4	358.7	2	8
Ring-necked Duck	0.0	0.2	489.9	1	4
Greater Scaup	44.9	88.9	197.9	400	96
Lesser Scaup	0.6	1.1	188.6	4	29
King Eider	0.4	0.9	222.9	4	25
Surf Scoter	35.2	44.2	125.6	171	100
Black Scoter	35.5	39.8	112.2	140	100
Harlequin Duck	0.4	0.7	156.9	2	33
White-winged Scoter	21.9	16.2	74.2	66	100
Common Eider	76.7	152.5	198.7	620	96
Bufflehead	42.5	42.1	99.1	220	100

Common Goldeneye	101.3	57.1	56.4	199	100

Table 7 continued. Birds observed at Napatree by Raithel (RIDEM).

Species	Mean	SD	CV	Maximum	% of years
Barrow's Goldeneye	0.7	2.2	315.6	11	29
Hooded Merganser	0.7	1.3	201.1	6	33
Common Merganser	1.1	2.5	221.4	11	33
Red-breasted Merganser	247.7	103.6	41.8	500	100
Ruddy Duck	0.1	0.4	489.9	2	4
Laughing Gull	283.3	255.6	90.2	1000	96
Little Gull	0.1	0.3	338.8	1	8
Black-headed Gull	0.1	0.3	270.3	1	13
Bonaparte's Gull	53.3	57.0	107.0	250	100
Ring-billed Gull	121.5	118.2	97.3	400	100
Herring Gull	496.8	313.6	63.1	1500	100
Lesser Black-backed Gull	0.3	0.4	176.9	1	25
Glaucous Gull	0.1	0.3	338.8	1	8
Great Black-backed Gull	167.5	143.7	85.8	500	100
Black-legged Kittiwake	0.8	1.4	181.2	6	38
Iceland Gull	0.3	0.5	159.2	1	29
Least Tern	55.8	34.3	61.5	140	96
Gull-billed Tern	0.1	0.3	270.3	1	13
Caspian Tern	1.3	1.4	105.8	5	63
Black Tern	1.3	1.8	132.1	7	63
Roseate Tern	160.9	146.1	90.8	500	96
Common Tern	261.9	151.2	57.7	700	96
Royal Tern	0.8	1.7	217.1	7	33
Sandwich Tern	0.3	0.9	275.0	4	17
Forster's Tern	2.4	2.1	89.4	7	83
Parasitic Jaeger	0.0	0.2	489.9	1	4
Dovekie	0.0	0.2	489.9	1	4
Razorbill	0.1	0.3	270.3	1	13
Black Guillemot	0.1	0.3	338.8	1	8
Osprey	20.3	15.9	78.2	53	100
Bald Eagle	0.5	0.9	172.0	4	38
Northern Harrier	5.8	3.1	53.4	15	100
Sharp-shinned Hawk	118.3	149.1	126.1	532	96
Cooper's Hawk	4.0	4.3	106.6	16	88
Northern Goshawk	0.5	0.8	143.8	3	42
Red-shouldered Hawk	0.3	0.5	159.2	1	29
Red-tailed Hawk	1.4	1.3	95.5	5	75
Broad-winged Hawk	1.9	5.1	266.4	25	42
Rough-legged Hawk	0.1	0.3	338.8	1	8
American Kestrel	51.9	58.6	113.0	195	96
Merlin	8.0	5.9	73.3	22	96
Gyrfalcon	0.1	0.3	338.8	1	8
Peregrine Falcon	1.6	1.6	100.2	8	88

Table 8. Mean abundance per year, interannual variation, maximum number observed in a given year, and frequency of occurrence (% of years detected) for 41 species of waterbirds detected using the coastal pond at Trustom Pond National Wildlife Refuge over 11 winters from fall 1992 thru spring 2006 (data were not available from Dec 1995 through spring 1998). Birds were counted from land-based routes every 2-4 weeks during November-April each year.

Species	Mean	SD	CV	Maximum	% of years
Common Loon	14.8	19.9	134.2	45	45
Red-throated Loon	3.4	5.4	158.8	14	45
Red-necked Grebe	0.9	1.3	143.0	3	36
Horned Grebe	11.2	21.4	191.1	59	45
Eared Grebe	0.3	0.7	225.0	2	18
Pied-billed Grebe	4.9	4.7	96.4	17	82
Great Cormorant	2.6	8.2	316.2	26	9
Mute Swan	21.5	23.9	111.3	78	91
Canada Goose	684.8	359.1	52.4	1260	91
Brant	0.9	2.2	248.2	7	18
Greater White-fronted Goose	0.3	0.9	316.2	3	9
Snow Goose	30.2	59.2	196.1	185	73
Wood Duck	6.1	13.6	222.3	44	55
Mallard	119.4	97.8	81.9	338	91
Mallard/Black Duck Hybrid	0.2	0.6	316.2	2	9
American Black Duck	167.0	78.0	46.7	309	91
Gadwall	15.9	20.4	128.6	72	91
Northern Pintail	8.4	6.0	71.7	18	91
American Wigeon	38.0	48.0	126.3	129	82
Northern Shoveler	1.2	1.8	151.1	5	36
Blue-winged Teal	2.5	6.2	249.6	20	27
Green-winged Teal	28.8	25.9	89.9	96	91
Eurasian Wigeon	0.5	0.8	170.0	2	27
Canvasback	75.1	78.1	104.0	210	91
Redhead	2.3	2.8	119.6	7	55
Tufted Duck	0.1	0.3	316.2	1	9
Ring-necked Duck	15.3	23.5	153.8	75	73
Greater Scaup	622.3	300.3	48.3	1260	91
Lesser Scaup	88.5	182.8	206.6	598	64
Common Eider	10.2	23.3	228.0	75	36
King Eider	0.1	0.3	316.2	1	9
Unidentified seaduck	1.0	3.2	316.2	10	9
Unidentified scoter	5.0	15.8	316.2	50	9
Long-tailed Duck	0.1	0.3	316.2	1	9
Surf Scoter	18.5	56.8	306.8	180	36
Black Scoter	4.2	8.3	198.2	25	45

White-winged Scoter	15.2	43.9	288.7	140	45

Table 8. continued. Birds observed at Trustom Pond NWR.

Species	Mean	SD	CV	Maximum	% of years
Common Goldeneye	110.9	57.5	51.8	196	91
Bufflehead	21.6	17.5	80.8	57	91
Hooded Merganser	69.6	39.4	56.6	138	91
Common Merganser	12.2	30.4	249.0	98	64
Red-breasted Merganser	97.7	49.1	50.2	179	91
Ruddy Duck	342.5	393.5	114.9	1,244	91
American Coot	81.2	99.1	122.1	304	82
Overall abundance	2,757.4	1,004.2	36.4	4,324	
Species richness	**26.4**	**4.9**			

Table 9. Mean abundance per year, interannual variation, maximum number observed in a given year, and frequency of occurrence (% of years detected) for 32 species of waterfowl detected at Ninigret Pond from 1992-2008 (S. Paton, USFWS, unpubl. data).

Species	**Mean**	**SD**	**CV**	**Maximum**	**% of years**
Mute Swan	10.4	7.2	69.3	26	100
Canada Goose	55.8	52.0	93.3	150	88
Brant	4.3	7.2	169.3	25	44
Snow Goose	0.1	0.3	273.3	1	13
Wood Duck	0.4	0.8	215.0	2	19
Mallard	15.4	14.4	93.7	46	100
American Black Duck	202.4	155.9	77.0	642	100
Gadwall	2.9	5.8	198.7	22	31
Northern Pintail	1.1	2.5	231.7	8	19
American Wigeon	7.2	24.9	346.1	100	31
Blue-winged Teal	0.1	0.3	400.0	1	6
Green-winged Teal	0.8	1.5	197.8	5	25
Canvasback	5.6	11.2	198.9	35	38
Redhead	0.3	0.7	225.3	2	19
Ring-necked Duck	0.6	1.8	317.8	7	13
Greater Scaup	196.2	200.5	102.2	534	69
Lesser Scaup	34.4	93.9	272.7	306	25
Common Eider	0.1	0.3	400.0	1	6
King Eider	0.1	0.3	400.0	1	6
Long-tailed Duck	0.4	1.0	235.6	3	19
Surf Scoter	0.8	1.1	150.1	3	38
Black Scoter	0.3	0.8	309.8	3	13
White-winged Scoter	2.0	6.2	309.8	24	13
Common Goldeneye	215.4	186.3	86.5	768	100
Barrow's Goldeneye	0.1	0.3	400.0	1	6
Bufflehead	550.6	453.4	82.3	1745	100
Hooded Merganser	45.9	47.7	103.7	147	100
Common Merganser	7.7	8.0	103.8	22	81
Red-breasted Merganser	280.1	134.9	48.2	418	100
Ruddy Duck	2.6	5.9	223.4	21	31
Overall abundance	1,643.8	891.5	54.2	3,055	100

Species richness	13.5	2.9

SEADUCKS

Seaducks are among the most common waterbirds inhabiting the Ocean SAMP study area in winter. Common seaducks in the Ocean SAMP study area include: Common Eider, Black Scoter, White-winged Scoter, Surf Scoter, and Long-tailed Duck. With the exception of Sachuest Point (Table 6) and Napatree (Table 7), there is little historical information available on seaduck abundance in the nearshore and offshore waters of Rhode Island. The RIDFW mid-winter survey primarily focuses on Narragansett Bay and the coastal ponds, and thus does not adequately sample Rhode Island nearshore and offshore waters (J. Osenkowski, RIDFW, pers. comm.; Table 4). We know that large numbers of seaducks (>10,000 scoters) have been observed in some years on the southwest ledge of Block Island (C. Raithel, RIDFW, pers. comm.), but this area southwest of Block Island has not been systematically surveyed by boat or plane prior to our Ocean SAMP surveys.

Based on our analyses of Raithel's surveys at Napatree (Fig. 5) and USFWS surveys at Sachuest (Fig. 6), we know that seaduck numbers tend to peak in Rhode Island from November to March. A few first-year nonbreeding seaducks (e.g., Common Eiders) spend the summer in Rhode Island rather than migrating to their northern breeding grounds. Groups of 30 Common Eiders at the Harbor of Refuge just west of Pt. Judith in July are not uncommon.

Fig. 5. Seasonal changes in number of seaducks detected during surveys at Napatree Point from 1982-2008 (C. Raithel, RIDFW, unpubl. data). For survey date, first number represents month, second number is 10-day period (1 = 1-10, 2 = 11-20, 3 = 21-31).

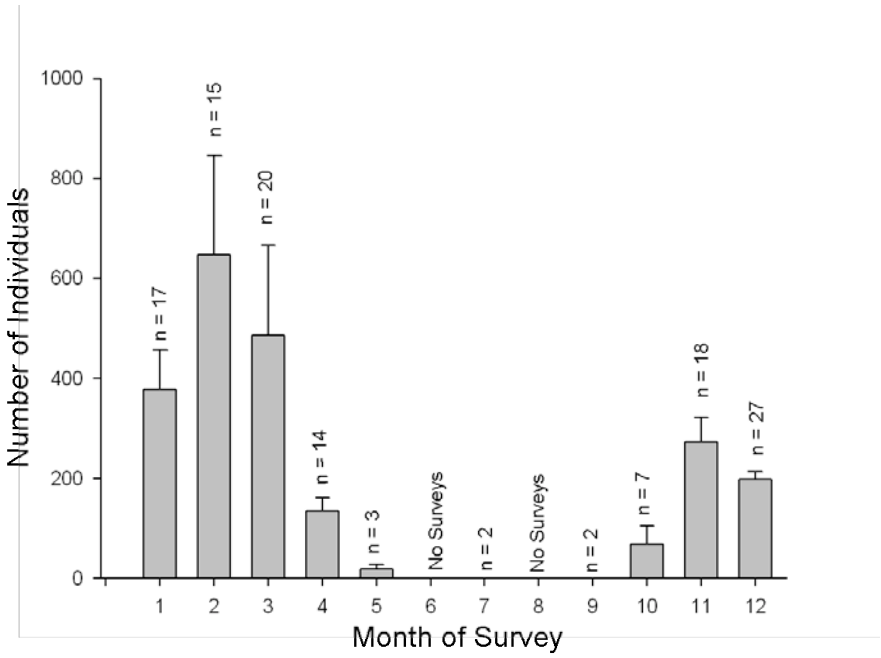

Fig. 6. Seasonal change (mean ± SD) in the number of seaducks detected each month at Sachuest Point NWR from 1993-2002 (USFWS, unpubl. data). January is Month 1. Sample sizes (n) above bar refer to number of surveys per month.

Harlequin Ducks winter along the south coast of Rhode Island and are currently a state-listed species of special concern. They are also currently listed as endangered in Canada and threatened in the state of Maine. Harlequin Ducks are common in RI from November to May (USFWS; Fig. 7). In Rhode Island, Harlequin Ducks are typically found close to shore in areas with rocky shorelines, with most birds detected at either Sachuest or Beavertail (Caron and Paton 2007). At Sachuest, an average of 80 Harlequin Ducks was detected (Table 6), although their numbers have declined recently at Sachuest, and birds have apparently shifted to Beavertail (Caron and Paton 2007). Harlequins have been found foraging to 20 m depths, but commonly dive in much shallower nearshore waters (<10 m) and usually stay within 15 m of the shoreline (Robertson and Goudie 1999). Their diet on their wintering grounds mainly consists of crabs, amphipods and gastropods (Fischer 1998; Gaines and Fitzner 1987; Goudie and Ankney 1986; Vermeer 1983; Palmer 1949).

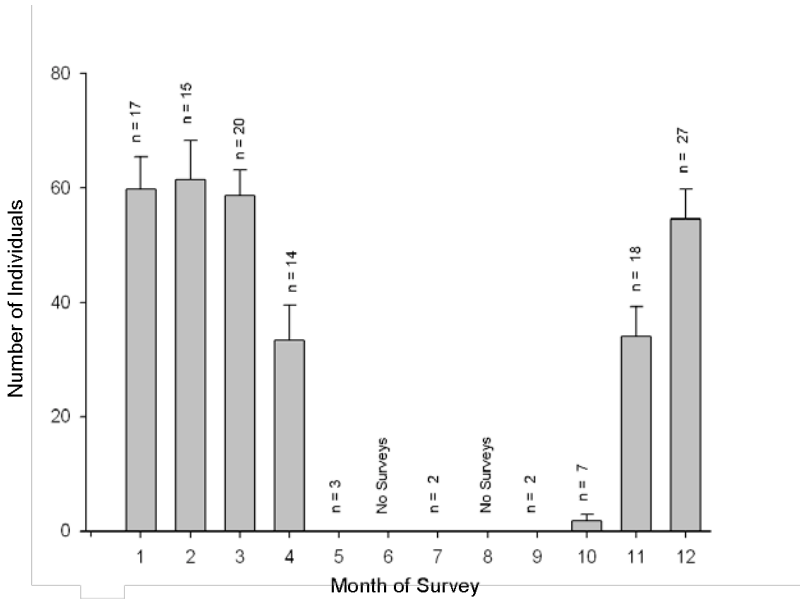

Fig. 7. Seasonal change (mean ± SD) in the mean number of Harlequin Ducks (*Histronicus histronicus*) detected per survey at Sachuest Point NWR from 1993-2002 (USFWS, unpubl. data). January is Month 1. Sample sizes (n) above bar refer to number of surveys per month.

Preferred sea duck foraging areas are strongly correlated with environmental variables such as water depth, bottom substrate, bivalve community, and bivalve density and size (Vaitkus and Bubinas 2001). Currently, bathymetric data (water depth, bottom substrate) for the Ocean SAMP study area is well known, but relatively little is known about bivalve communities and densities, especially further offshore. Foraging depths of seaducks differ among species and are a function of preferred diet, but average depths tend to be less than 20 m for most species (Table 10). Common Eiders typically forage in water <10 m during the winter when diving over rocky substrate and kelp beds (Goudie et al. 2000; Guillemette et al. 1993). The preferred diet of Common Eiders changes with season and foraging location, but mainly consists of mollusks and crustaceans (Goudie et al. 2000; Palmer 1976; Cottam 1939).

Table 10. Foraging depths of seaducks based on the literature.

Species	Dive depth	Reference
Common Eider	0-15 m	Ydenberg and Guillemetter 1991.
Common Eider	<16 m deep	NERI Report 2006.
Surf Scoter	90% of dives <20 m depth during diurnal period – used deeper waters at night – but rarely dived at night	Lewis et al. 2005.
Black Scoter	>95% of observations were in waters <20m deep	Kaiser et al. 2006.
Black Scoter	<20 m deep	NERI Report 2006.
White-winged Scoter	~90% of diver <20 m depth – might use deeper waters at night	Lewis et al. 2005.

Maximum diving depths of scoters are about 25 m, although most birds probably forage in water less than 20 m deep, particularly during the winter months (Vaitkus and Bubinas 2001; Bordage and Savard 1995). Scoter diet in marine environments predominantly consists of mollusks (Bordage and Savard 1995; Durinck et al. 1993; Madsen 1954; Cottam 1939). Long-tailed Ducks forage deeper (>60 m) and forage father offshore than other sea duck species (Robertson and Savard 2002; Ellarson 1956; Schorger 1947, 1951). Their diet on the wintering grounds consists mainly of epibenthic crustaceans including: amphipods, isopods, and mysids (Robertson and Savard 2002; Jamieson et al. 2001; Goudie and Ankney 1986, Johnson 1984; Cottam 1939). Much of the study area is relatively deep (> 25 m), thus much of the SAMP area is probably not preferred foraging habitat for seaducks, although seaducks can roost in deeper waters (Fig. 8).

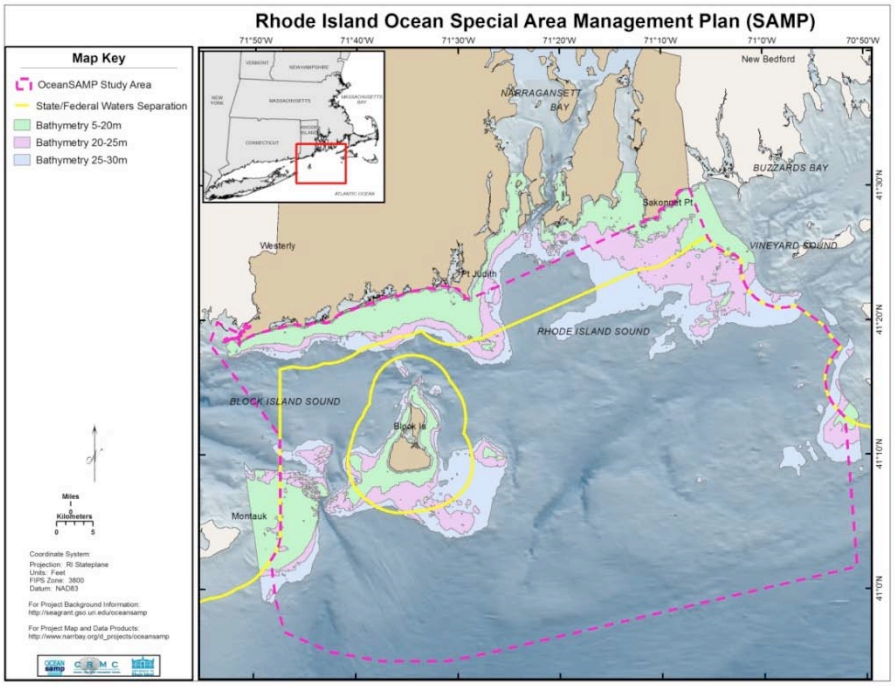

Fig. 8. Areas of the Ocean SAMP potentially suitable for seaduck foraging based on water depths ranging from 5 – 20 m deep (light green), which literature suggests are primary foraging depths.

Seaducks tend to forage and roost in different locations. Movements to feeding locations from roosting locations usually takes place just after sunrise and movements back to roosting locations usually occur just before or after sunset. Distances between foraging areas and roosting locations can be >10 km, although little is known about sea duck roosting locations in Rhode Island. Long-tail Ducks that forage around the area of Nantucket Shoals roost farther offshore in Nantucket Sound (Kerlinger and Hatch 2001). Sea ducks also tend to move short distances during daytime hours. Rafts of resting sea ducks are often moved off of forage areas by strong tides and wind and these ducks frequently fly short distances to return to areas with high prey densities. Seaducks generally fly low over the water surface (<15 m), but are known to fly at higher when flying over land, to roosting locations, or during migration (Fig. 9).

DIVING DUCKS

Diving ducks are another common winter resident in Rhode Island and the Ocean SAMP study area. The most abundant species include Common Goldeneye, Bufflehead, Greater Scaup, Lesser Scaup, Ruddy Duck, Canvasback and Redhead. Diving duck species are most common from November to March (USFWS; Fig. 10), with abundance greatest in Narragansett Bay where thousands of Greater and Lesser Scaup were detected during both RIDFW (max >23,000 scaup in one year, Table 4) and EPA (max = 7,889

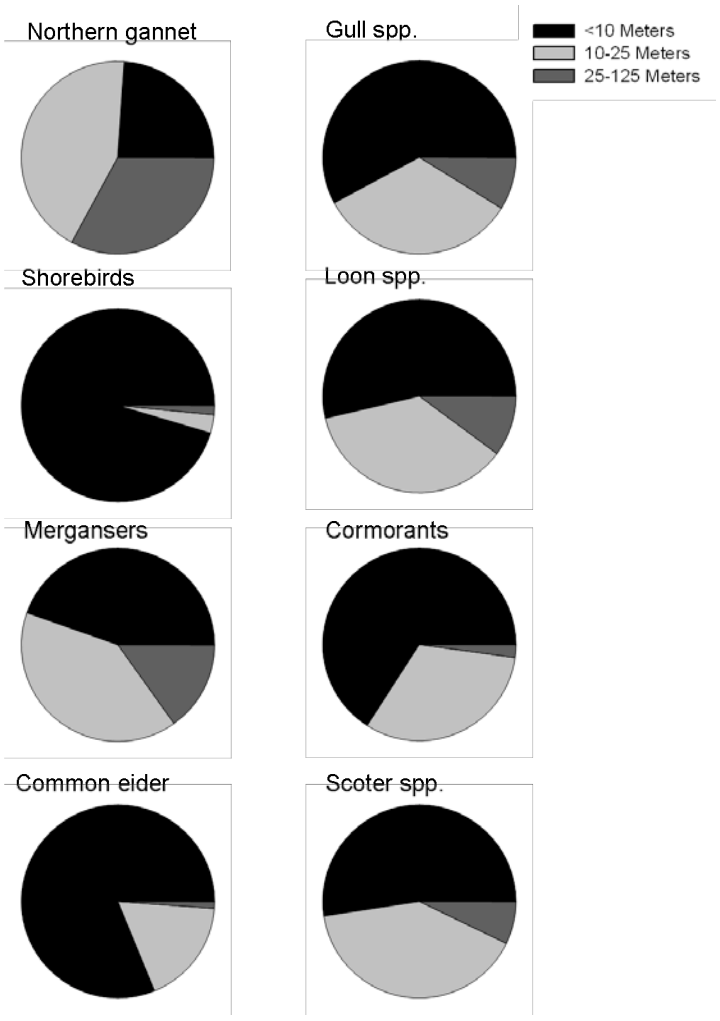

Fig. 9. Estimated flight altitude above ocean surface for various avian guilds based on ocular estimates during land-based surveys at Pt. Judith in 1998 (URI, unpubl. data).

Greater Scaup and 6,452 Lesser Scaup; Table 5) mid-winter surveys. Scaup are also relatively common in the southern coastal ponds (Tables 8 and 9) along the northern border of the SAMP area, but not as abundant in nearshore waters along the Rhode Island coastline (e.g., Napatree [Table 7] or Sachuest Point NWR [Table 6]). Dietary preferences differ among species and vary between seasons, but many species forage on bivalves, snails and other benthic invertebrates

(Kessel et al. 2002; Gauthier 1993). Diving duck species migrate through the Ocean SAMP study area during fall and spring migration, although abundance and migration corridors are poorly known. Available evidence suggests that diving ducks typically fly low over the ocean surface (typically <25 m above the water surface), but can also be found flying relatively high (>50 m), especially during migration (Kerlinger and Hatch 2001).

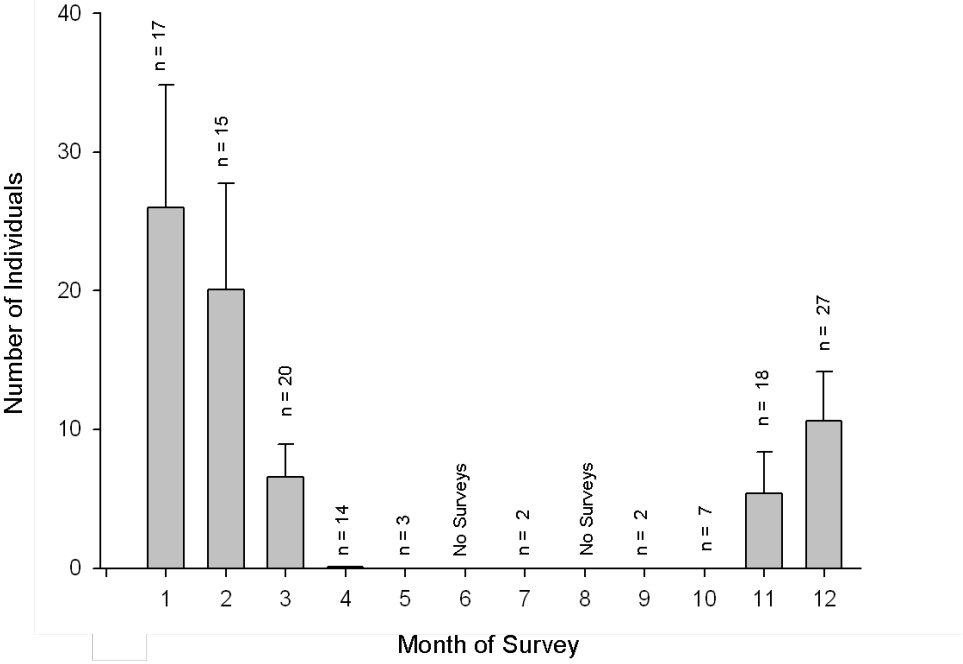

Fig. 10. Seasonal change (mean ± SD) in mean number of diving ducks detected per survey at Sachuest Point NWR from 1993-2002 (USFWS, unpubl. data). January is month 1. Sample sizes (n) above bar refer to number of surveys per month.

DABBLING DUCKS

Dabbling ducks commonly winter in nearshore and inland coastal ponds in southern Rhode Island. They are more abundant in freshwater, coastal ponds and salt marsh habitats (e.g., Trustom Pond NWR [Table 8] and Ninigret Pond [Table 9]), but can also be found along protected rocky and sandy beaches bordering Narragansett Bay and Block Island Sound. Common dabbling duck species include American Black Duck, Mallard, Gadwall, American Wigeon, Green-winged Teal and Northern Pintail. Dabbling ducks occur in Rhode Island year round, but are much more abundant from November to April (USFWS; Fig 11). Dabbling ducks likely migrate through much of the Ocean SAMP study area. Dabblers tend to fly high when migrating, sometimes reaching elevations > 125 m.

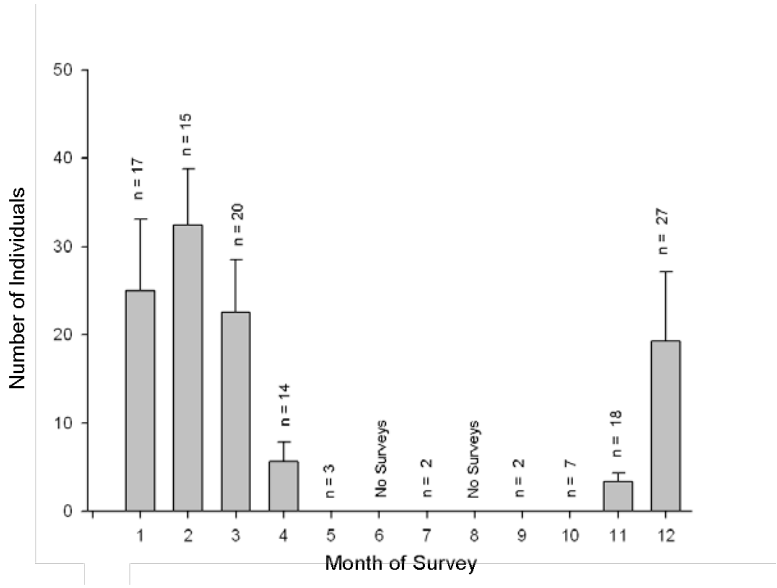

Fig. 11. Seasonal change (mean ± SD) in the mean number of dabbling ducks detected per survey at Sachuest Point NWR from 1992-2005 (USFWS, unpubl. data). January is month 1. Sample sizes (n) above bar refer to number of surveys per month.

MERGANSERS

Red-breasted Mergansers are abundant Rhode Island residents during the winter months, while Common Mergansers are uncommon migrants (see survey results for Napatree and Ninigret, Tables 7 and 9). Common Mergansers prefer freshwater bodies of water for foraging, while red-breasted mergansers tend to forage in harbors, estuaries, and tidal rivers (Mallory and Metz 1999). Common Mergansers become more common along the coast when freshwater lakes and rivers freeze during prolonged cold spells.

Red-breasted Mergansers are common in RI from November to April (USFWS; Fig. 12). Their wintering numbers apparently fluctuate less than many species of waterfowl in the region because CVs were relatively low (e.g., CV = 29.5, 41.8, and 48.2, for EPA [Table 5], Napatree [Table 7], and Ninigret [Table 9], respectively). Red-breasted Mergansers are an abundant species in nearshore waters, especially in Narragansett Bay. Red-breasted Merganser diets in the winter along the New England coast consist primarily of small fish including; mummichog (*Fundulus heteroclitus*), silversides (*Menidia menidia*) and blueback herring (*Alosa aestevalis*) (Titman 1999; Stott and Olson 1973). Red-breasted Mergansers generally fly low over the water (<15 m), but can be seen flying at heights up to <50 m during migration (Fig. 9).

GEESE

Brant and Canada Geese are common winter residents in Rhode Island and common migrants in coastal Rhode Island and Narragansett Bay (e.g., almost 800 Brant and over 6,000 Canada Geese

are counted annually during RIDFW mid-winter survey; Table 4). Canada Geese are also common breeding birds throughout the state. Snow Geese are uncommon migrants that pass through Rhode Island during spring and fall migration on their way to and from mid-Atlantic wintering grounds (see Napatree survey results; Table 7). Brant arrive from the breeding grounds in October and are common residents until April. Brant densities in the winter are highest in the upper portions of Narragansett Bay

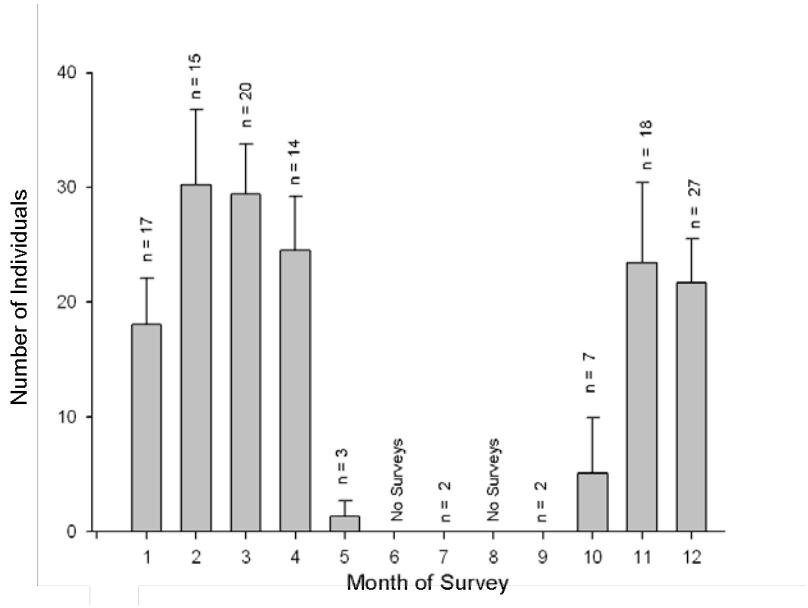

Fig. 12. Seasonal change (mean ± SD) in the mean number of Red-breasted Mergansers recorded per survey at Sachuest Point NWR from 1993-2002 (USFWS, unpubl. data). January is month 1. Sample sizes (n) above bar refer to number of surveys per month.

(e.g., an average of approx. 2,400 are counted during EPA mid-winter survey; Table 5), but are also common along the mouth of Narragansett Bay and the south shore (e.g., over 400 annually at Napatree, Table 7). Brant spend much of their time foraging close to shore on eel grass, macro algae, and salt marsh cord grass (Reed et al. 1998). In some areas, Brant are found foraging frequently in terrestrial habitats on lawn grass and agricultural fields (Ward et al. 2005). Canada Geese spend a majority of their time foraging in terrestrial environments including agricultural fields and turf grass farms (Mowbray et al. 2002). They often roost in coastal ponds and on Narragansett Bay. Like other waterfowl, wintering populations of geese tend to fluctuate annually depending on weather and available forage , although CVs for Canada Geese (CV = 55) and Brant (CV = 36) during EPA mid-winter surveys (Table 5) suggest that geese populations tend to fluctuate less annually than other waterfowl in the region. Brant fly relatively low (<30 m) when moving from roost locations to foraging locations. Canada Geese generally fly higher (>50 m) when moving from roost to foraging locations.

Waterbirds

TERNS

Terns are a common inhabitant of the study area from May through September (Fig. 13). Common species of terns in the SAMP area include Common Tern, Least Tern, Forster's Tern, and Roseate Tern (see survey results from Napatree spit; Table 7). Common Terns nest in Rhode Island and breed in a number of locations on the northern border of the Ocean SAMP study area (Ferren and Myers 1997).

Roseate Terns are federally-listed as an endangered species. The total number of breeding pairs averages 3,500 – 4,000 in the northeastern United States. The population is concentrated in two colonies near Rhode Island: Great Gull Island, NY is within 20 km of Rhode Island waters, and both Bird and Ram Island, MA which are just over 40 km away. Great Gull and Bird Island colonies contain over 80% of the Northeastern United States population (Nisbet 1989). Their numbers peaked at 4,310 breeding pairs in 2000, but have declined to just over 3,200 in 2008, coupled with a long term drop in the total number of breeding sites (Mostello 2007). Adult Roseate Terns disperse up to 30 km on foraging flights for their young, particularly in years with low fish productivity (Nisbet 1981, Duffy 1986; Heinemann 1992), thus Rhode Island may be within foraging range of some breeding birds (see Grist 2010 for a more detailed description of Roseate Terns in Rhode Island). We know of no recent nesting records of Roseate Terns in Rhode Island. However, Roseate Terns were commonly detected in Rhode Island from late July to early September at Napatree Point (Fig. 14; RIDFW).

In addition, adults and young can disperse large distances during the post-breeding season, but dispersal studies have only recently been initiated. In particular, observations of large congregations of Roseate and Common Terns occur at Cape Cod, Massachusetts, with over 20 staging sites documented which had 1,000 to 20,000 birds per site. Post-breeding terns from as far away as Great Gull Island, NY and Nova Scotia were documented at staging sites on Cape Cod (MAS 2010)

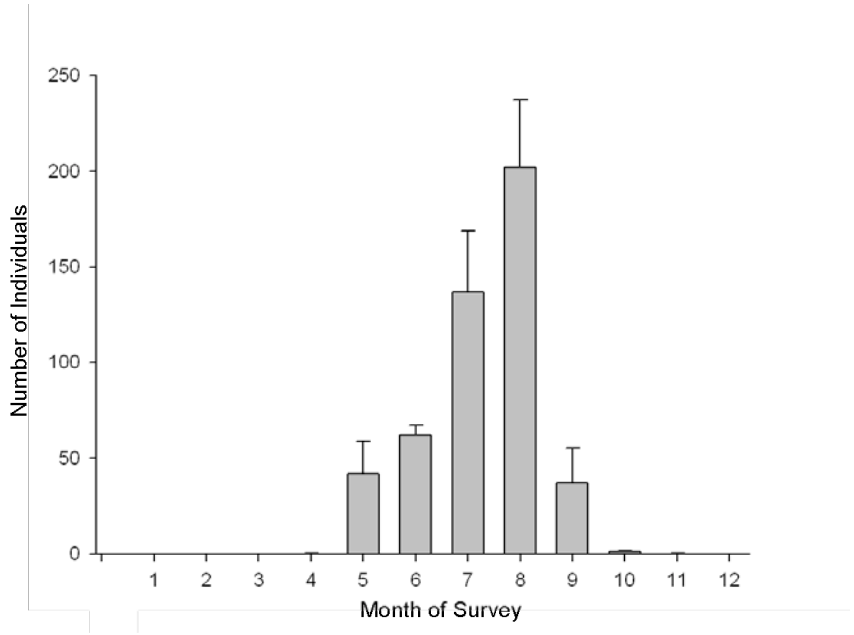

Fig. 13. Seasonal change (mean ± SD) in the number of terns recorded during surveys at Napatree Point. Surveys were conducted 1982-2008 (C. Raithel, RIDFW). All tern species were pooled for this analysis.

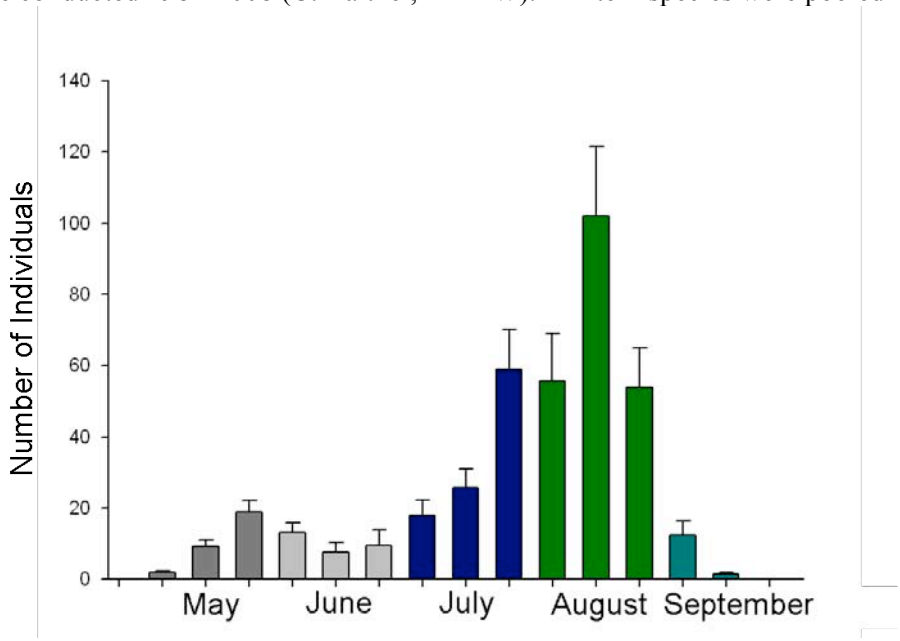

Fig. 14. Seasonal change (mean ± SD) in the mean number of Roseate Terns recorded during surveys at Napatree Point from 1982 to 2008 (C. Raithel, RIDFW). (Each similarly-colored bar represents a 10-day period within the same month. (Each similarly-colored bar represents a 10-day period. Bar 1 = 1-10, Bar 2 = 11-20, Bar 3 = 21-31).

Least Terns are listed as State Threatened by the state of Rhode Island (RINHP 2006). In 2008, 193 pairs of Least Terns nested along the south shore beaches and coastal ponds that border the northern edge of the Ocean SAMP study area (USFWS, unpubl. data). Most tern species generally stay close to shore (<5 km) during the breeding season, but are occasionally found in

low densities offshore along the continental shelf during spring and fall migration (Nisbet 2002; Powers et al. 1980; Haney and Stone 1988). Terns forage primarily on small fish including Atlantic silversides (*Menidia menidia*), American sand lance (*Ammodytes dubius*), and Atlantic herring (*Clupea harengus*). Terns observed during surveys for the Cape Wind project generally flew low, at elevations less than 18 m above the water surface (Kerlinger and Hatch 2001).

LOONS

Common Loons and Red-throated Loons are more abundant during migration and the winter months, but they have been recorded year round in Narragansett Bay and the Ocean SAMP study area (C. Raithel at Napatree; Fig. 15). Common Loons tend to be more abundant than Red-throated Loon; for example, at Sachuest NWR peak counts for Common Loons were 34 birds compared to only two Red-throated Loons (Table 6). Less than 70 Common Loons are typically counted in Narragansett Bay during the mid-winter aerial survey (Table 4), whereas survey data at Napatree suggest that peak counts of Red-throated Loons (mean = 15 individuals) are 50% lower than peak counts of Common Loons (mean = 27 individuals; Table 7). Loon abundance also changed between years (CV = ca. 65, Table 7). Red-throated Loons and Common Loons are most concentrated within nearshore areas (<10 km from shore) and prefer water <20 m deep for foraging, although they can be found much farther offshore depending on weather conditions and the locations of forage fish (Daub 1989). The diet of Red-throated and Common Loons consists mainly of live fish, but also includes other aquatic vertebrates and invertebrates (McIntyre and Barr 1997). Loons generally fly low over the water (<15 m), but can be detected flying over 50 m high when migrating (McIntyre and Barr 1997; Sibley 1993).

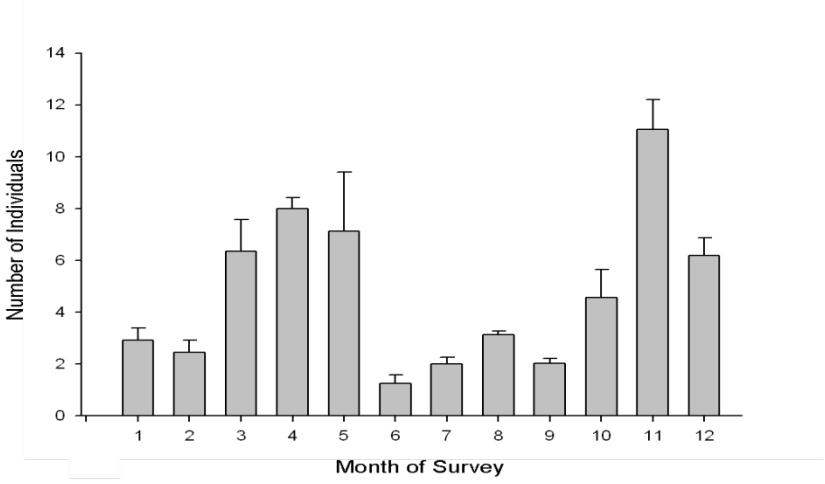

Fig. 15. Seasonal change (mean ±SD) in the mean number of loons detected during surveys at Napatree Point. Surveys were conducted from 1982-2008 (C. Raithel, RIDFW). January is month 1.

GREBES

In nearshore coastal waters, the most common grebe species occurring in Rhode Island is Horned Grebe mean annual peak count of 27.9 ± 8.9, with a maximum of 47 during Napatree surveys,

Table 7), while Pied-billed Grebe is more common in coastal ponds such as Trustom (mean annual peak count of 4.9 ± 4.7, maximum = 17; Table 8). In addition, small numbers of Red-necked Grebes winter in nearshore waters (see Tables 6 and 7). Horned Grebe and Red-necked Grebes are migratory winter residents in the Ocean SAMP study area, whereas Pied-billed Grebes breed in coastal ponds in Rhode Island. Grebes forage in nearshore and inshore areas within relatively shallow water (<6 m) on small schooling fish (Stedman 2000; Dewar 1924). Grebes generally fly low over the water when moving to and from foraging areas (<5 m).

CORMORANTS

Double-crested Cormorants and Great Cormorants are common in Rhode Island and the SAMP area. Mean annual peak counts of Double-crested Cormorants averaged 1,529 ± 1,679 individuals, with a maximum daily count of 7,640 at Napatree (Table 7). In contrast, Great Cormorants, were much less abundant with mean peak counts of 26.6 ± 12.6 individuals and a maximum daily count of 50 at Napatree (Table 7). CVs were higher for Double-crested Cormorants compared to Great Cormorants, 110 vs. 47, respectively during Napatree surveys (Table 7). Double-crested Cormorants reed in Rhode Island and often forage in large flocks on Narragansett Bay and the Ocean SAMP area during summer and during migration (RIDFW; Fig. 16). Great Cormorants are common winter residents in coastal Rhode Island . Double-crested and Great Cormorants are generally found close to shore (<5 km) and tend to forage in shallow (<8 m) open water (Hatch and Weseloh 1999). Great Cormorants tend to forage in water that is less than 20 m deep (Hatch et al. 2000). Their diets consist primarily of schooling species of fish (Hatch and Weseloh 1999). Cormorants generally fly low over the water (<15 m) when moving from foraging areas to roosting areas or wing-drying perches, but are found flying much higher (>100 m) when flying over land or during migratory flights when they are often seen flying in formation (Fig. 9).

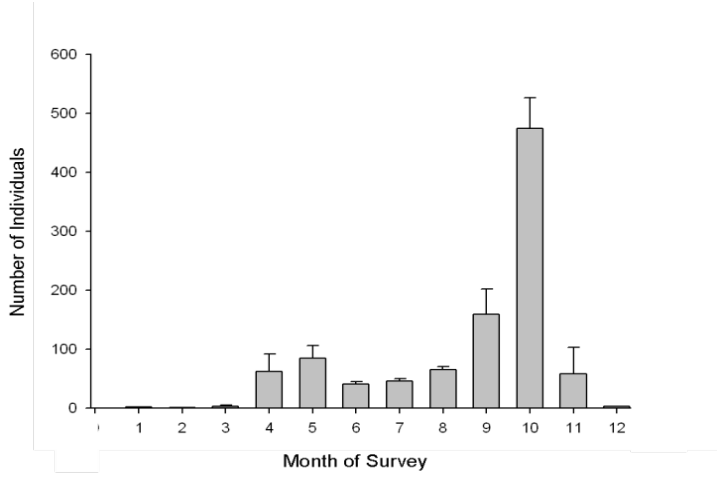

Fig. 16. Seasonal change (mean ± SD) in the mean number of Double-crested Cormorants detected during surveys at Napatree Point. Surveys were conducted from 1982-2008 (C. Raithel, RIDFW). January is month 1.

GULLS

There are at least 15 species of gulls that could occur in the Ocean SAMP study area, and gulls are among the most abundant avian groups using the Ocean SAMP study area. Common gull species using Rhode Island's nearshore and offshore waters include Great Black-backed Gull, Herring Gull, Bonaparte's Gull, Laughing Gull, Ring-billed Gull and Black-legged Kittiwake. Herring and Great Black-backed Gulls breed in Rhode Island and are abundant in the study area throughout the year (Ferren and Myers 1998). Black-legged Kittiwakes and Bonaparte's Gulls are only found in the area during the winter months. Laughing Gulls breed north of Rhode Island and winter in the southern US, and thus are found migrating through the Ocean SAMP study area prior to the nesting season and during early fall. Gulls are generally found in nearshore habitats, with the exception of Black-legged Kittiwakes which are almost always found offshore. Most species of gulls also venture offshore, except Ring-billed Gull, which are rarely found offshore. Dietary preferences differ among gull species but they are generally opportunistic and prey on intertidal marine invertebrates, fish, insects, and human waste (Good 1998; Pierotti and Good 1994). Gulls are usually found flying low to the water when actively foraging (<15 m) but are also commonly seen flying high, especially when they are soaring to search food over a large area (Fig. 9).

NORTHERN GANNETS

Northern Gannets are abundant in the Ocean SAMP study area during migration and are winter residents in offshore waters. Northern Gannets generally forage far offshore on larger surface-schooling pelagic fish (i.e., herring, mackerel) and squid (Mowbray 2002). However, they can be detected from land-based survey stations. Raithel regularly detected gannets flying off of Napatree, with mean annual peak counts of 193 ± 605 (SD), and a peak daily count of 3,000 birds. Gannet numbers are highly variable (e.g., CV at Napatree = 313), probably because they actively follow concentrations of small bait fish which tend to vary in space and time. They can be seen foraging in small groups, but are often in large flocks foraging on large concentrations of surface schooling fish (Mowbray 2002). They are often seen in mixed flocks with Herring and Great Black-backed Gulls foraging behind commercial trawlers (K. Winiarski, pers. obs.). Common flight elevations are 5-50 m when not foraging (Fig. 9).

ALCIDS

Common alcid species (Alcidae) in Rhode Island include Razorbills, Common Murre, and Thick-billed Murre. They are common offshore winter residents, although little is known about their abundance and distribution in the Ocean SAMP study area. These species were rarely detected during NMFS or CSAP surveys from 1978-1988 (Table 3). They are generally found in small groups (<40 individuals). Dovekie, Black Guillemot, and Atlantic Puffin are uncommon

off the coast of Rhode Island because they usually winter farther north. Alcids mainly forage on fish, but will also forage on crustaceans and other invertebrates (Hipfner and Chapdelaine 2002; Ainley et al. 2002). In the Atlantic, alcids are typically found foraging on the continental shelf or slope, regularly in relatively shallow water 20 to 40 m deep (Hipfner and Chapdelaine 2002; Gaston and Hipfner 2000). They generally fly lower than 10 m above the water.

STORM-PETRELS

Wilson's Storm-Petrel are one of the most abundant seabird species in the world (IUCN 2006) and are common in Rhode Island's offshore waters. They are rarely detected during land-based surveys, with <1 seen most years at Napatree (Table 7). They are most common off of the New England coast from May to September (they breed in southern hemisphere during October-April) (Quillfeldt 2001). Leach's Storm-Petrels are uncommon and only found in small numbers off of the New England coast during the late fall. Storm-petrels are generally found in offshore areas where upwellings or floating debris concentrate forage on the surface (Huntington *et al.* 1996). Petrels are generally omnivorous and forage primarily on plankton, nekton, fishes, squids, crustaceans and jelly fishes (Huntington et al. 1996) Wilson's Storm-Petrels observed during surveys for the Cape Wind project were found flying below 3 m (Kerlinger and Hatch 2001).

SHEARWATERS

Greater Shearwater and Sooty Shearwater are common migrants in the offshore areas of the Ocean SAMP area, but are rarely seen from land-based survey locations (Table 7). Manx Shearwater and Cory's Shearwater are found in small numbers off of the coast of New England in late summer and during fall when they migrate through the area. In northern New England, shearwaters are commonly found in shallower areas of the continental shelf foraging in areas where water depth is between 20 to 200 m (Lee and Haney 1996). Shearwaters feed mainly on small fish and squid (Brown et al. 1981) and tend to fly just above the ocean surface.

JAEGERS

Pomarine Jaeger and Parasitic Jaeger are common offshore migrants in New England from July to October, but are rarely seen from land (e.g., Napatree survey results, Table 7). Parasitic Jaegers are generally found closer to shore than Pomarine Jaegers because of their kleptoparasitic foraging strategy which commonly targets tern species (Haven and Lee 1999). Pomarine Jaegers are not commonly found foraging in nearshore coastal waters and tend to be found foraging along the continental shelf (Lee 1995). Jaegers forage primarily on fish and squid and generally fly at low elevations (5-10 m), while foraging and migrating (Haven and Lee 2000).

Wading Birds

HERONS AND EGRETS

Herons and egrets are common colonial breeders and migrants in Rhode Island (Myers and Ferren 1998). Narragansett Bay and the coastal ponds offer acres of shallow water habitat that these birds prefer for hunting nekton (small fish and crustaceans). Common species include Great Blue Heron, Little Blue Heron, Black-crowned Night Heron, Great Egret and Snowy Egret. Herons and egrets breed on many of the islands in Narragansett Bay, just north of the SAMP area (Myers and Ferren 1998). Herons and egrets likely migrate in small numbers in nearshore habitats north of the Ocean SAMP study area during fall and spring migration, with much of the study area too deep for foraging. Herons and egrets are known to fly relatively high (>150 m) during migration.

Shorebirds

Shorebirds are common in Rhode Island from May to September (RIDFW; Fig. 17). Large numbers of shorebirds probably migrate over the Ocean SAMP study area and forage in intertidal areas at the edges of the SAMP area. Piping Plovers breed in Rhode Island and are federally listed as a threatened species. They breed on both the south shore beaches of Rhode Island, and rarely on Block Island (USFWS, unpubl. data).

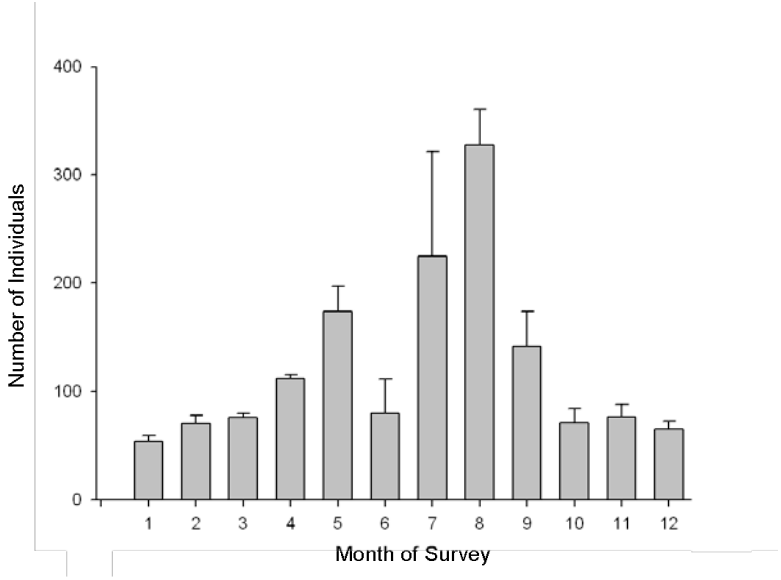

Fig. 17. Seasonal change (mean ± SD) in the mean number of shorebirds recorded during surveys at Napatree Point. Surveys were conducted from 1982-2008 (C. Raithel, RIDFW). January is month 1.

PLOVERS AND SANDPIPERS

The most common plover and sandpiper species in Rhode Island include Piping Plover, Semipalmated Plover, Black-bellied Plover, Semipalmated Sandpiper, Dunlin, Purple Sandpiper, Least Sandpiper and Sanderling. Piping Plovers breed on coastal beaches in mainland Rhode Island and Block Island and are likely common migrants through the Ocean SAMP study area (Ferren and Myers 1998). Since Piping Plovers are federally listed as a threatened species, they are closely monitored by the USFWS and local conservation organizations. In 2008, a total of 63 pairs were found breeding along the south coast of Rhode Island (USFWS, unpubl. data). All nests were along the south shore of RI and within the northern border of the SAMP area. Piping Plover forage primarily on marine invertebrates in the intertidal zone and are believed to stay close to their nest location while breeding (Elliot-Smith and Haig 2004).

Semipalmated Plover, Black-bellied Plover, Semipalmated Sandpiper, and Least Sandpiper are common spring and fall migrants through the area. Sanderlings, Dunlin, and Purple Sandpipers are winter residents in Rhode Island. Shorebirds mainly forage on marine invertebrates in tidal flats, beaches and coastal ponds. It is likely that tens of thousands of shorebirds migrate over the study area, but since they are known to migrate at high elevations (>400 m) they are difficult to detect. However, they are often found flying at lower elevations (<10 m) when foraging or after initial takeoff or when descending after a migratory flight (Fig. 9).

PHALAROPES

Red-necked Phalarope and Red Phalarope are common offshore migrants during late summer and early fall. Distribution and abundance of phalaropes in the Ocean SAMP area is not well known (see Table 3). Phalaropes are members of the shorebird family, but unlike many shorebird species they spend up to 11 months annually offshore (Tracy et al. 2002; Rubega et al. 2000). Phalaropes forage primarily on plankton and are usually found in areas where there is significant upwelling and mixing, areas which support high plankton concentrations (Rubega et al. 2000). In the southeastern United States, they are generally found 40 to 80 km from shore, in water that is 20 to 40 m deep (Rubega et al. 2000). Phalaropes generally fly low to the water when foraging, but likely fly at much higher elevations when migrating long distances.

Landbirds

PASSERINES

Songbirds spend most of their time on land, but during migration, large numbers of passerine species migrate over large water bodies and concentrate along the southern coast of Rhode Island and Block Island. Block Island has been designated by The Nature Conservancy as an important

bird area because of a high abundance of songbirds during migration (Parrish 2000). Due to the consistency of cold fronts and associated northwest winds during the fall, larger numbers of songbird migrants pass through the area during fall migration than during the spring migration when southwest winds that provide optimal conditions for bird movement through the area are less consistent (Reinert et al. 2002; Drury and Keith 1962). Fall migration peaks in October and the most common migrants captured in Rhode Island and Block Island include: Yellow-rumped Warbler, Gray Catbird, Golden-crowned Kinglet and Red-eyed Vireo (KWRS; Fig. 18 and 19). In the fall, nearly 97% of individuals captured are hatch year birds that fledged 1-4 months prior to being captured (Reinert et al 2002). Spring migration peaks in May and the most common migrants captured in the area include: Gray Catbird, Common Yellowthroat, Yellow-rumped Warbler and White-throated Sparrow.

Large numbers of songbirds likely migrate through the Ocean SAMP study area at high elevations (>500 m), but likely fly at much lower elevations when beginning or ending migratory flights. Occasionally songbirds have been observed flying low over the offshore water surface (<5 m) during ship-based avian surveys off of the coast of Block Island (Winiarski, unpubl. data). It is unclear if these individuals were attracted to the ship at the end of a migratory flight or if they commonly move across the study area at low elevations.

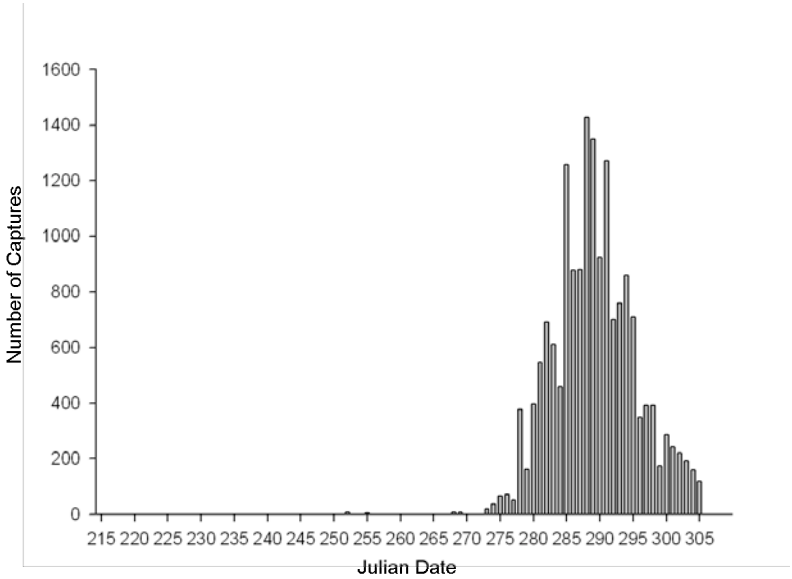

Fig. 18. Seasonal change in the total number of Yellow-rumped Warblers captured at the Kingston Wildlife Research Station from 1960-2007. Day 275 is 2 October in most years.

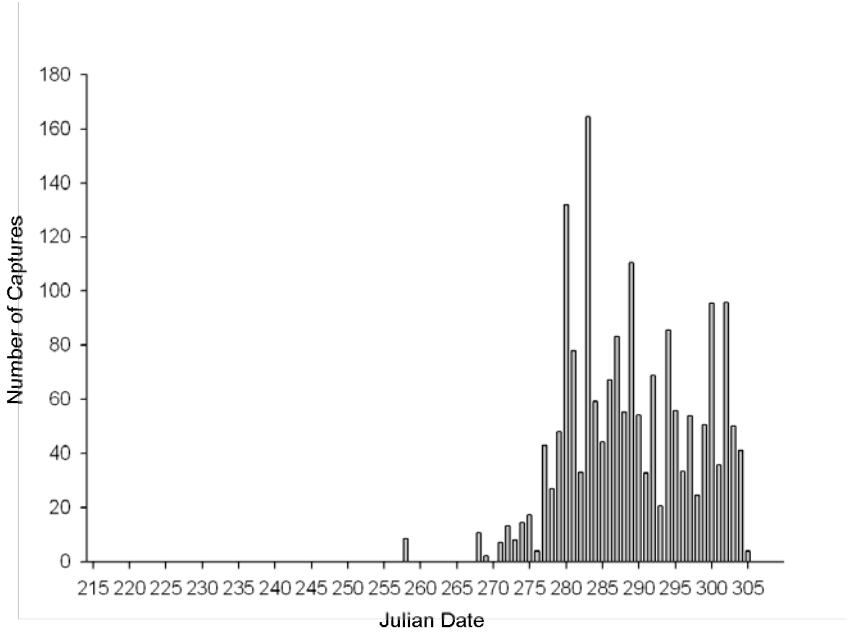

Fig. 19. Seasonal change in the total number of Golden-crowned Kinglets captured at the Kingston Wildlife Research Station from 1960-2007. Day 275 is 2 October in most years.

DIURNAL RAPTORS

Common diurnal raptor species in Rhode Island include: Red-tailed Hawk, Sharp-shinned Hawk, Cooper's Hawk, Northern Harrier, Broad-winged Hawk, Peregrine Falcon, Merlin and Osprey (e.g., see Napatree surveys by Raithel, Table 7). Raptors spend the majority of their time on land, but like songbirds are found in large numbers during migration in southern Rhode Island especially in September and October (RIDFW; Fig. 20). Most raptor species will only migrate over narrow water bodies, in particular buteos (e.g., Red-tailed Hawk) are rarely seen along the coast during migration (mean daily peak counts of 1.4 ± 1.3 (SD) individuals per year at Napatree; Table 7) and rarely venture out to Block Island. Accipters, particularly Sharp-shinned Hawk (Napatree mean daily peak counts = 118.3 ± 149.1) and Cooper's Hawk (4.0 ± 4.3) often migrate along the coast during fall migration on days with strong NW winds (Table 7), but are much less common on Block Island. In contrast, falcons (Merlin and Peregrine Falcon), ospreys and harriers will fly over large expanses of open water and are commonly observed on Block Island.

In addition, Napatree is an area well known for raptor concentration during fall migration. Peregrine Falcons observed during a ship-based survey off of the coast of Block Island were seen flying at altitudes up to 50 m, while Merlins were observed flying less than 5 m above the ocean surface (Winiarski unpublished data).

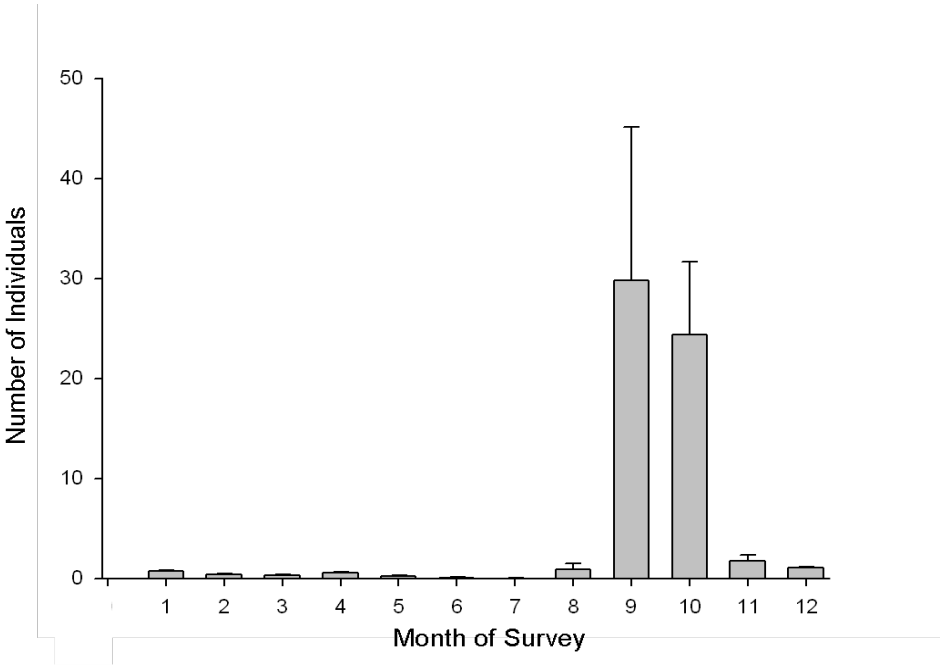

Fig. 20. Seasonal change (mean ± SD) in the number of raptors recorded during surveys at Napatree Point. Surveys were conducted from 1982-2008 (C. Raithel, RIDFW). January is month 1.

SUMMARY OF PREVIOUS AVIAN RESEARCH IN OCEAN SAMP STUDY AREA

Data sets available from prior avian surveys conducted within the Ocean SAMP study area document the phenology, abundance, spatial distribution in nearshore habitats, and movement ecology of many avian groups, but also highlight the lack of information regarding a number of avian groups, particularly those groups common to offshore waters. Surveys conducted in a manner that allow for a quantitative analysis of avian density and spatial distribution (especially in offshore waters) will be crucial to assess potential and actual impacts of future development. Additional research effort must target threatened and endangered species and those species considered of conservation concern.

1.5 Rationale for selected survey and analysis techniques.

Ship-based surveys that involve observers recording all birds observed on the water have been used extensively for surveying seabirds (Camphuysen et al. 2004; JNCC 2004). The advantages of ship-based surveys are that they can provide accurate information on the density and behavior of species present in the area of interest. Ship-based transects surveys have been used by ornithologists for almost 100 years (Jespersen 1924) and have been the primary means to estimate seabird abundance for almost 50 years (Brown et al. 1974). Standardized survey protocols have been in place for over 25 years (Tasker 1984). Recent advances in density

estimation based on line transect methods have increased the accuracy and precision of model estimates of seabird distribution and abundance (Ronconi and Burger 2009).

Most current ship-based surveys use line transect distance-sampling methods (Buckland et al. 2001), with observers recording the number of each species present, their behavior, and flight direction (Innogy 2003; Camphuysen et al. 2004). Importantly, if observers also accurately record the distance of each observed bird from the boat, then a detection function for each species can be determined and then used to more accurately estimate density for each bird species within the survey area (Buckland et al. 2001).

Aerial surveys are used extensively in western Europe to investigate the spatial distribution and abundance of offshore birds, particularly when assessing the potential impacts of wind farms. In fact, standardized aerial survey protocols have been developed by COWRIE (Camphuysen et al. 2004) and are now widely adopted as standard protocols. COWRIE recommends a twin-engine (for safety) high-wing aircraft be used, that allows good visibility for observers. Helicopters are not recommended because they have a tendency to disturb seabirds on the water (Camphuysen et al. 2004). Standardized protocols in the UK and Denmark recommend a line-transect methodology with the aircraft flying at 185 km/hr at 80 m altitude, with transects spaced 2 km apart to minimize the probability of double-counting birds. They also record birds in three-band distances from the line of flight (44-163 m; 164-432 m and 433-1000 m), so that detection functions can be calculated. Finally, Camphuysen et al. (2004) recommend that two trained observers be used for each aerial survey, one conducting observations on each side of the aircraft, with all observations recorded continuously on a Dictaphone. The time of each bird sighting is recorded, ideally to the nearest second. Locations are later determined by cross-referencing these with a GPS track that is obtained throughout the flight with locations and times recorded at least every 5 seconds.

Effective study designs for conducting aerial surveys place line transects perpendicular to major environmental axes (Buckland et al. 2001, Maclean et al. 2006). For example, seabirds are often distributed according to food availability and water depth. Thus, transects should be established perpendicular to the coast to gather information on the entire range of densities for each individual transect, as the sampling unit is each transect. For investigators using Distance sampling, Laursen et al. (1997) recommended 20 transects within an area of interest. Maclean et al. (2006) also recommended that at least four flights of the whole area be undertaken during the winter (mid-October to mid-March), with counts carried out across the whole period if possible.

2 Methods

2.1 Nearshore Avian Assessment: Land-based Point Counts (Jan 2009 to 12 Mar 2010)

2.1.1 Survey Techniques

We initiated systematic land-based avian point counts on 23 January 2009 and they will be continued until the end of July 2010. These land-based sea watches occurred at 11 fixed point count stations ("stations") located along four survey routes ("routes") from Watch Hill to Sakonnet Point (Fig. 21). Three routes had three stations each, while the eastern route (Sakonnet area) had two stations. We surveyed each station at least six times per month, with three morning surveys and three afternoon surveys.

During morning surveys, we surveyed the first station on the route for 120 min starting at dawn, whereas the next two stations were surveyed for 60 min each. For afternoon surveys, the first two stations were surveyed for 60 min each, whereas the last station of the day was surveyed for 120 min. Afternoon surveys were scheduled so that they were completed just prior to dusk when low light levels made it difficult to see and identify individuals to species or guild. We varied the order that stations were surveyed using a stratified random selection sampling scheme. We ensured that each station was surveyed once per month during the 120-min early morning and late afternoon sampling blocks.

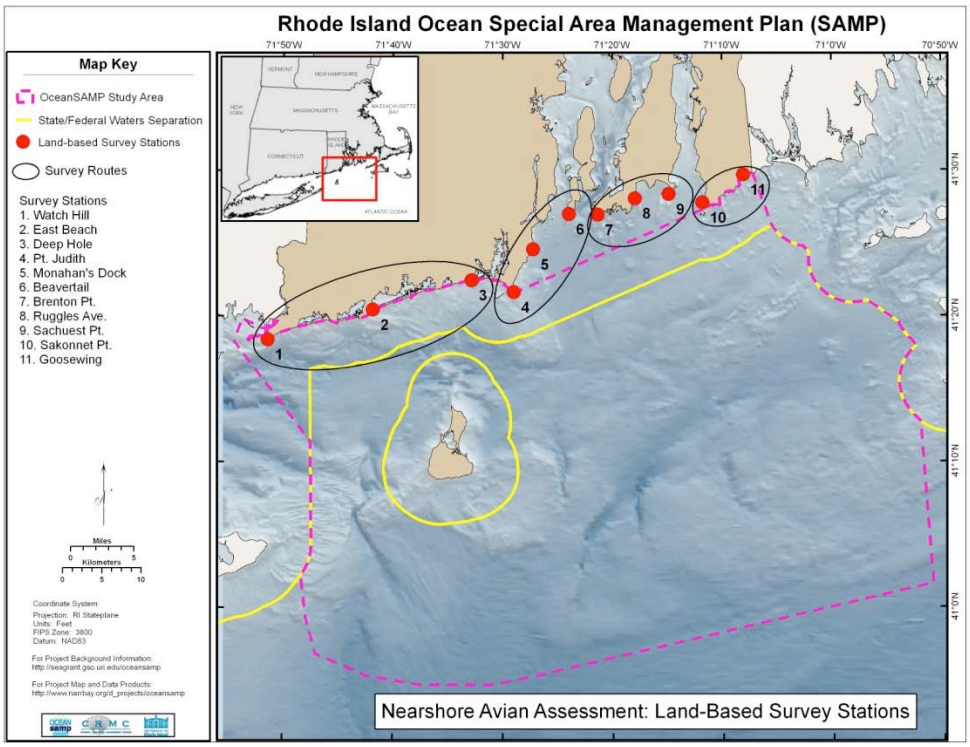

Fig. 21. Distribution of 11 land-based seawatch stations (red circles) along 4 survey routes (black ovals) where 1-2 hr morning and evening seawatches were conducted from January 2009 through July 2010. Stations include: 1) Watch Hill Lighthouse, 2 = East Beach, 3 = Deep Hole, 4 = Point Judith, 5 = Monahan's Dock, 6 = Beavertail Lighthouse, 7 = Brenton Point, 8 = Ruggles Ave., 9 = Sachuest Point NWR, 10 = Sakonnet Point, and 11 = Goosewing Beach.

During land-based surveys, one observer recorded all birds on or flying over the water that were within 3 km of the station (Fig. 22). Observers used a combination of a 20-60 power spotting scope (Swarovski HD-ATS 80) and a pair of 10 x 42 binoculars (Swarovski EL) to effectively scan the point count area. Observers scanned the ocean surface out to 3 km and equally scanned the airspace above the water surface (>200m) and recorded the number and species for all flying individuals or flocks for the specified survey period 60 or 120 minutes). For birds on the water, we separately recorded abundance of birds at four distance increments: 0-0.5 km, 0.5 – 1 km, 1 – 2 km and 2 – 3 km from the observer (Fig. 22). If individuals were observed in flight, we categorized flight elevation into five altitude categories: <10 m above the ocean, 10-25 m, 26-125 m, 126-200 m, >200 m. In addition, we also estimated true flight direction (N, NE, E, SE, S, SW, W, NW, variable). We also recorded environmental parameters and observation conditions at the beginning of each survey or when conditions changed including: wind speed (km/hr), wind direction, visibility distance, cloud cover (0-100%), and weather (e.g., precipitation). We did not conduct land-based surveys when the Beaufort sea state was 5 or higher (Table 11). We recorded observations in the field using a handheld PDA (Juno Trimble) equipped with Cybertracker data collection software (Cybertracker: www.cybertracker.co.za).

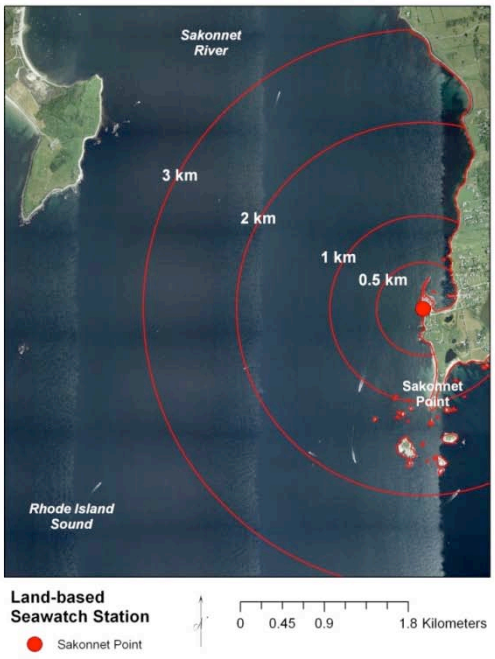

Fig. 22. During land-based point counts, birds were counted out to 3 km offshore in 4 distance bands. Here is an example of distance bands at Sakonnet Point.

Table 11. Beaufort scale used to describe sea state. We only list up to Beaufort 6, as no surveys were conducted in sea states above a 5.

Beaufort number	Description	Wind speed	Wave height	Sea conditions
0	Calm	<1 km/hr (< 1 mph)	0 m	Flat
1	Light air	1.1-5.5 km/hr (1-3 mph)	0-0.2 m	Ripples without crests
2	Light breeze	5.6 – 11 km/hr (4-7 mph)	0.2-0.5 m	Small wavelets, Crests of glassy appearance, not breaking
3	Gentle breeze	12-19 km/hr 8-12 mph	0.5 – 1 m	Large wavelets, crests begin to break, scattered whitecaps
4	Moderate breeze	20-28 km/hr (13-17 mph)	1-2 m	Small waves with breaking crests. Fairly frequent white caps
5	Fresh breeze	29-38 km/hr (18-24 mph)	2-3 m	Moderate waves of some length, many white caps, small amounts of spray
6	Strong breeze	39-49 km/hr (25-30 mph)	3-4 m	Long waves begin to form, white foam crests are frequent, some airborne spray present.

2.2 Offshore Avian Assessment: Ship-based Surveys (Feb 2009 to Feb 2010)

2.2.1 Survey Techniques

We conducted systematic ship-based surveys approximately once a month from February to May 2009 and then approximately once a week from June 2009 until Feb 2010 to quantify the abundance of all species of waterbirds within the Ocean SAMP study area. We conducted all surveys on a 27.5 m (90ft) ship operated by the Frances Fleet (Galilee, RI). From February 2009 to May 2009 surveys were conducted on two sampling grids, one grid (A) located south of Block Island and one grid (B) located to the east of Block Island (Fig. 23). The ship traversed each sampling grid along four 9.3 km (5 nautical miles [nm]) long parallel transects (i.e., 37 km [20 nm] surveyed) that were oriented north to south. Starting June 2009, we added 6 more grids, and change the survey pattern within grids to be a sawtooth pattern using program DISTANCE to generate the transects (Fig. 24).

All ship-based surveys used the following line-transect sampling method (modified from Camphuysen et al. 2004) so that we could later estimate density of each bird species or guild in the study area given their likelihood of detection. Two sampling grids were sampled per survey day and the order of surveying of these grids was randomized from month to month. We began surveys at sunrise when there was enough light to allow observers to identify individuals to species. During surveys, the ship traveled at a constant speed of 10 knots (11.5 mph), which was slow enough to allow for detection of all individuals along the ships trackline. We conducted all observations from the upper level of the vessel at the bow of the ship and from either the port or starboard side of the ship (depending on which side offered optimal viewing conditions). Observers used their unaided eye or a pair of 10 x 42 binoculars to detect birds. We conducted all surveys using an observer and an observer/recorder. We recorded observations in the field using a handheld PDA (Juno Trimble) equipped with Cybertracker data collection software (Cybertracker: www.cybertracker.co.za).

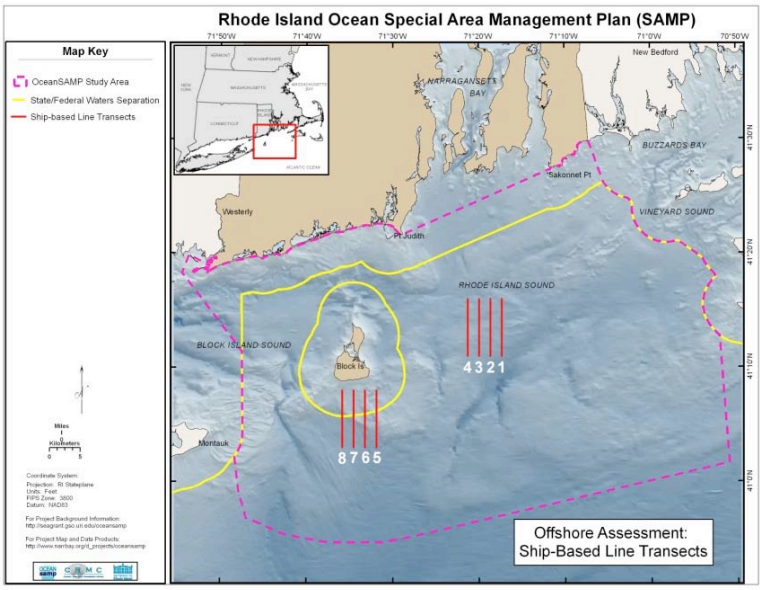

Fig. 23. Location of two ship-based line-transect grids S and E of Block Island that were monitored from Feb to May 2009.

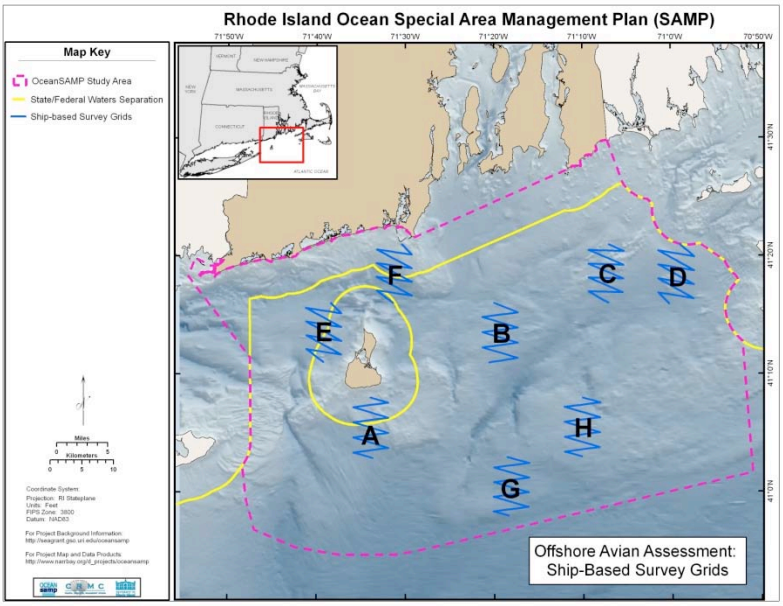

Fig. 24. Distribution of eight survey grids used for ship-based line transect surveys from June 2009 through mid-Feb 2010. Each grid was 4 by 5 nm and had 25 nm of line transects.

Occasionally, when viewing conditions were difficult (e.g., birds were backlit) or birds quickly dove underwater upon detection, we identified individuals to a guild (e.g., large shearwater, Surf or Black scoter (either Surf or Black Scoter, alcid). We visually estimated perpendicular distance from the trackline to each bird on the water and in flight. From February 2009 to

September 2009, we only measured distance to birds on the water and we estimated this distance from the ships trackline as <50m, 50-100m, 101-200m, 201-300m. From September 2009 to July 2010, we estimated the actual distance (m) and the bearing to each detection (an individual bird or a flock of birds) regardless of whether the bird was on the water or in flight. We estimated the bearing by using a large protractor mounted at the bow of the ship. This allowed us to calculate a perpendicular distance to the transect line for all individuals using the formula x = r * sin (bearing angle), where x is the distance to the transect line from the bird or flock, r is the estimated distance from bird or flock to observer, and bearing angle was estimated by the observer using the large protractor (Fig. 25).

Fig. 25. Ship-based line transect surveys were conducted on a large vessel (>27.5 m), with one primary observer and one observer/recorder. Angle to birds was measured using a large protractor mounted to bridge railing. Note recorder (K. Winiarski) taking observations on a PDA, while primary observer (B. Harris) is actively searching for birds with both naked eye and binoculars.

We also recorded the behavior of all observed individuals or flocks as feeding, loafing, resting, or millingfor bird(s) on the water. For birds in flight, we recorded birds as feeding if so observed. For individuals or flocks in flight, vertical flight elevation was estimated into discrete elevation bins (<10m, 10-25m, 26-125m, 126-200, >200m) along with the individual or flocks flight direction (N, NE, E, SE, S, SW, W, NW, variable). Birds following the ship ("ship followers") were ignored and not recorded. Information on anthropogenic influences during the survey that may have been attracting birds to the sampling area was also recorded (e.g., fishing boats or floating debris).

We recorded environmental data at the beginning of each line transect including: wind speed, wind direction, sea state, visibility and weather (% cloud cover, precipitation). Surveys did not take place when the Beaufort sea state was 4 or higher (Table 11). Data were recorded with a handheld GPS-enabled PDA (Trimble Juno) loaded with Cybertracker data collection software

(www.cybertracker.org). A handheld Garmin unit (Garmin Marine GPS 76) recorded a trackline when the ship was on survey (unit recorded a GPS location every 15 seconds).

2.2.2 Analytic Methods: Detection Functions and Density Surface Modeling (DSM)

We utilized the 'count method' of Hedley and Buckland (2004) and used sighting data collected on ship-based surveys to model the surface density and to visually depict the foraging area of those species common to the Ocean SAMP study area. Species were modeled by season: Summer (surveys conducted from 10 June 2009 to 25 August 009), Fall (surveys conducted from 8 Sept 2009 to 17 Nov 2009) and Winter (surveys conducted from 19 Nov 2009 to 13 Feb 2010). Creating a surface density model is a multiple step process (Fig. 26) that first includes modeling a detection function based on the observed distance data collected from line transect sampling. These detection functions are then included in the creation of models that relate observation data with spatial covariates to predict densities across both areas sampled and those not sampled (Fig 26; Katsanevakis 2007).

It is important to note that the standard line transect sampling methods that we used (e.g. surveying within a set 300m distance) violated key assumptions of Distance sampling when recording birds in flight, so we opted not to fit a detection function to data on birds in flight. Instead, we assumed 100% detection of flying individuals in the 300m sampling "box" (e.g., strip transect). For all surface density models we used either data for birds in flight or for birds on the water, and we used the frequency of observations to determine which data to use for a given species. For example, Greater Shearwater, Cory's Shearwater and Wilson's Storm-Petrel were rarely sighted on the water, and so we used only data on birds in flight to model their surface density. Most other species were predominately observed on the water and so we used these data to model surface density. For the few species (e.g., gulls and gannets) that were frequently observed both flying and on the water, we selected the data set with the greatest number observations to construct the predictive models.

The detection function, g(y), was estimated using Distance 6.0 software (Thomas et al. 2006) following the method outlined by Buckland et al. (2001). A single parameter half-normal function or a two parameter hazard rate formula were considered as possible detection functions. Akaike Information Criteria was used to select the "best" model and Q-Q plots were used to assess model fit. The highest ranking detection functions were chosen for each avian species and each season that was modeled.

We used two physical spatial covariates, depth and distance to land, to model the foraging distribution of species common to the Ocean SAMP study area. Each line transect was divided into 830 m long segments using ArcMap 9.3 (total of 465 segments). Depth was measured at the midpoint of the segment from the NOAA Coastal Relief Model data set. Distance to land was

also calculated from the midpoint of the segment, and measured to the nearest point of land using ArcMap 9.3. The total number of birds within each segment, independent of spatial covariates, was calculated using the Horvitz-Thompson-like estimator (Hedley et al. 2004). Expected values of abundance in each segment were calculated using Generalized Additive Models (GAMs; Hastie and Tibshirani 1990). Four different GAMs were fitted for each density surface model: two univariate models for depth and distance to land, a model including both depth and distance to land, and a model with a depth and distance to land interaction. Model selection was based on the lowest Generalized Cross Validation score (GCV; Wood 2006). For this analysis we used the mgcv package (Wood 2000, 2006) written in R v.2.9.1 (R Development Core Team 2009) within Distance 6.0 (Thomas et al. 2006). The steps we took to develop a DSM are shown in Fig. 26.

Using ArcMap 9.3 software (ESRI), a prediction grid was created overlaying the map of the study area with 920 square cells, each 4 km^2 in area (Fig. 26). Abundance in the study area for each species and season was estimated as the sum of prediction cells, where abundance predictions for each cell were calculated with the selected GAM model. The abundance estimation was conducted using the DSM analysis engine of the Distance 6 software (Thomas et al. 2006). Based on the predictions for each of the 920 grid cells, we produced a distribution map of individual species for the Ocean SAMP study area using ArcMap 9.3.

A variance component was calculated for each model following Seber (1982) that included both the variance associated with fitting the detection function and that associated with the density surface model (e.g. the two steps in creating a density surface model). To calculate the variability associated with the density surface model estimates, we ran a parameteric bootstrap with 499 reiterations for each model (Efron and Tibshirani 1993). The bootstrap used a moving block of three segments to reduce the effects of spatial autocorrelation.

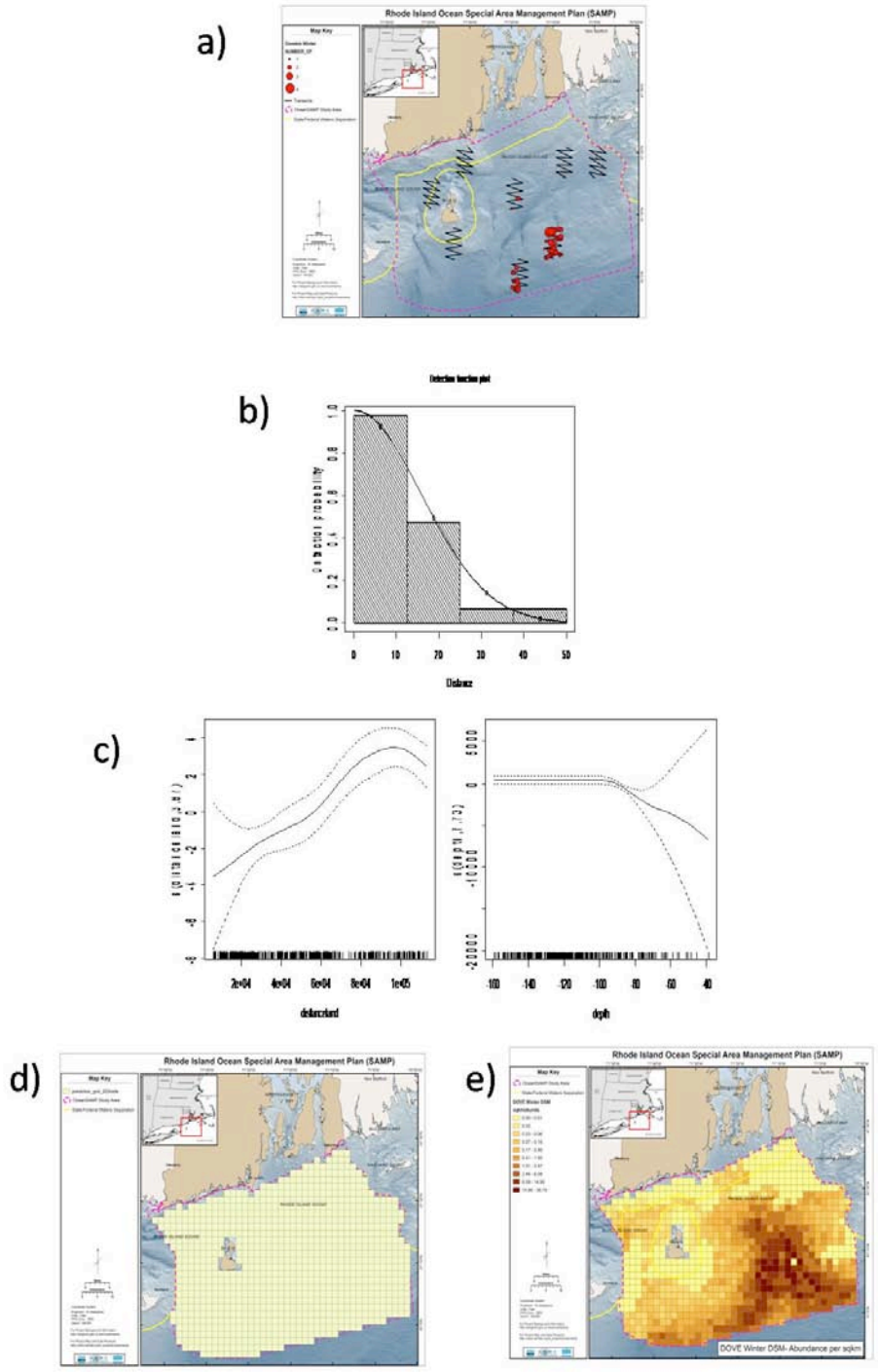

Fig. 26. Example of the steps involved in creating a surface density model (DSM) for Dovekie in winter: (a) Raw data collected from ship-based line-transects (b) Detection function (Half-normal) fitted to distance data. (c) Generalized additive models (GAMs) modeled with two physical variables, depth and distance from shore. (d) Grids (each cell is 4 km^2) created to predict avian densities across study area. (e) Predicted density in cells based on GAM model output with water depth and distance to shore (calculated at the midpoint of each cell).

2.3 Offshore Avian Assessment: Aerial Surveys (Nov 2009 to Feb 2010)

2.3.1 Survey Techniques

We performed aerial surveys approximately once a week starting in November 2009. Aerial surveys will continue monthly through May 2011. Based on our observations of the movement phenology of waterbirds during land-based point counts of nearshore habitats from January to Feb 2009, we conducted the aerial surveys during mid-day (usually 1000-1500 hrs) to coincide with when birds had completed their post-dawn or pre-sunset movements from roosting to feeding areas. We conducted surveys along 24 transect lines that were spaced 3 km apart, with average transect length of 46.26 km ± 12.34 km (SD) (min = 7.77 km, max = 57.97 km) (Fig. 27). Transects were oriented perpendicular to the coast and equally covered all of the SAMP study area. We conducted all aerial surveys from a twin engine Cessna Skymaster aircraft that flew at an altitude of 152 m (500ft) above mean sea level at a constant speed of 160 km/hr (100 miles/hr).

We realize that many previous aerial surveys for seabirds were conducted at a lower altitude (76-80 m or 250 feet) and at a speed of 185 km/hr (Camphuysen et al. 2004; Maclean et al. 2006). However, we flew at an altitude of 152 m for three reasons: (1) if these data were used for pre-construction surveys for wind power, we wanted to maintain constant detection probabilities post-construction. Since offshore wind turbines can be over 120 m tall, we needed to fly above the height of wind turbine blades, (2) aerial surveys for the adjacent Cape Wind project were conducted at an altitude of 152 m to minimize disturbance to seaducks (Perkins et al. 2004), thus we hoped our survey results could be compared to abundance estimates from Cape Wind avian surveys directly, and (3) current Federal Aviation Administration regulations for these types of surveys restricted our Part 135 certified pilot to elevations greater than 152 m.

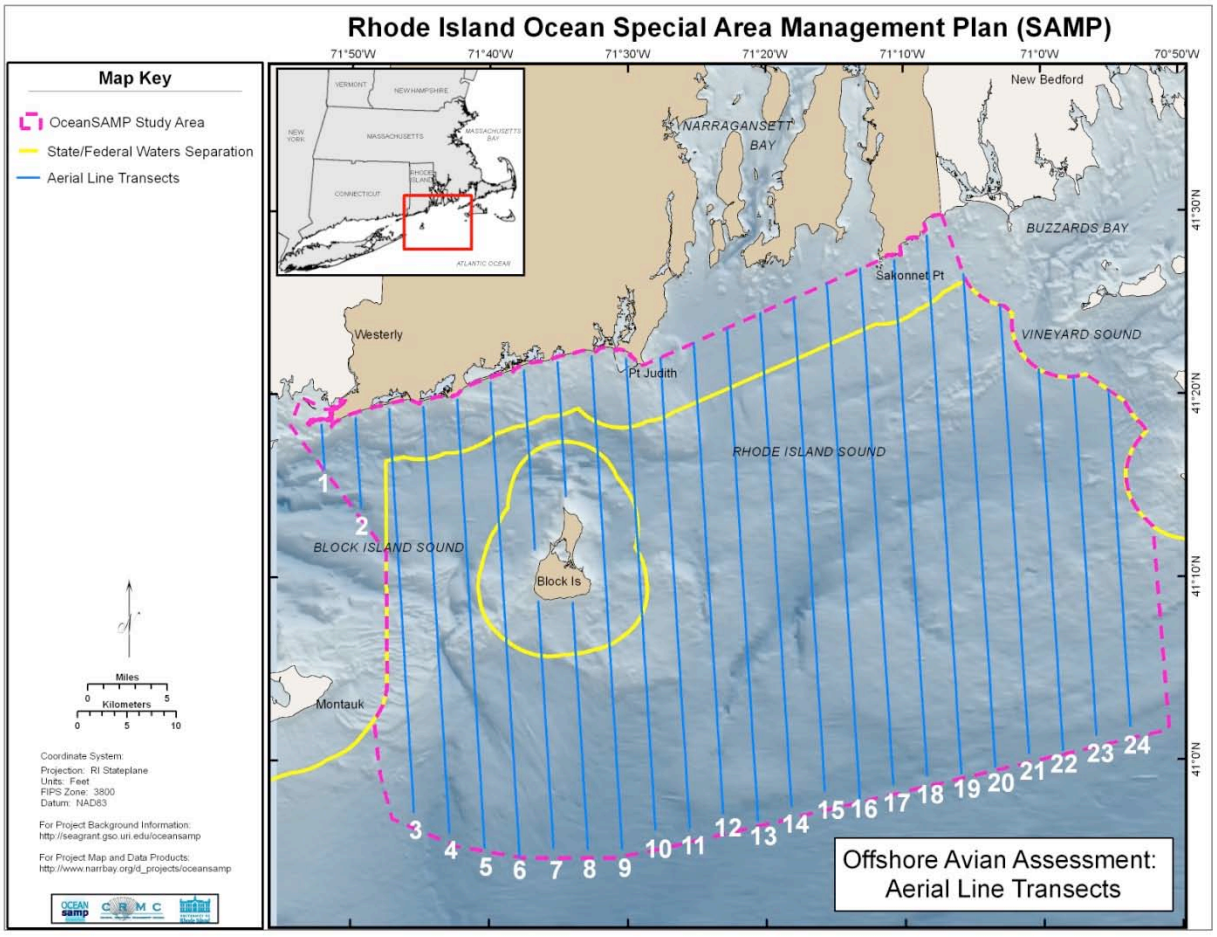

Fig. 27. Location of 24 aerial transects sampled from 18 Nov 2009 to 22 Feb 2010 for this report. Surveys continued after Feb 2010 and current plans are to continue sampling through May 2011.

We had two observers on each survey flight who were located behind the pilot and co-pilot seats (one on each side of the plane). Observers scanned a fixed-width strip transect (107 m [350ft]) on their side of the plane. To ensure that observers only recorded birds within this fixed distance, we used a clinometer to mark set angles (38 to 58 degrees) with black electrical tape on the aircraft's wing struts to aid observers in determining which individuals were in or out of the strip transect. Observers recorded all individuals and flocks to species when possible or to an avian guild (e.g., alcid spp., loon spp.) when necessary. Individuals or flocks were recorded as either on the water or in flight.

We also recorded whether any anthropogenic influences during the survey were apparently attracting birds to the area (e.g., fishing boats, whales or floating debris). We recorded the following environmental data at the beginning of each transect line or when conditions changed: wind direction, wind speed, wave height, glare (none, minimal, moderate, and heavy) and whitecaps (none, minimal, moderate, and heavy).

Observers recorded individual sightings with a time stamp (to the nearest second) into a digital voice recorder. Each observer had a digital stopwatch that was time stamped to a handheld Garmin (Garmin handheld Marine 76) that recorded the aircraft's position every 5 seconds. Surveys were not performed when wind speed was greater than 20 knots (23 mph) and waves were > 1.2 m (4 ft) tall. Unfortunately, due to the orientation of the transect lines and the orientation of the sun; glare was an issue on sunny days when surveying transect lines from north to south. If glare compromised detection of birds on one side of the plane, these data were not included in the final analyses.

Analytic Methods

For this report, we provide descriptive statistics on the number of detections for aerial surveys. We also used GIS to calculate depth at each observed flock to compare the depth profile of the Ocean SAMP study area to locations were each species (or guild) was detected.

2.4 Roseate Tern specific surveys (July 2010 to September 2010)

We designed some surveys specifically to focus on Roseate Tern use of coastal and nearshore waters along mainland Rhode Island. We conducted surveys of potential roosting sites for Roseate Terns, particularly tidal sandflats. We identified three main areas as previous or potential Roseate Tern roosting habitat (Raithel, pers comm.): Ninigret Pond, Quonochotaug Pond and Napatree Point, which were surveyed once a week during mornings or evenings from mid July to the end of August with 10 x 42 power binoculars and a 20-60 power spotting scope. Each survey was conducted for one hour, with the order determined by random generation. All tern species present were counted and identified, and where possible, identified down to individual level by field-readable leg bands. Flying terns were also recorded and additional data was collected for these individuals including flight elevation (<10m, 10-25m, 26-125m, 126-200m, >200m), distance offshore, flight direction and behavior (e.g.. feeding, commuting). During this same time period, each beach in southern Rhode Island was also walked during different time periods and in a random order to determine any further sites of interest. Three more sites were identified at the beginning as being possible roosting sites and included in surveys: Sandy Point, Moonstone Beach and East Beach. Behavioral observations were conducted during roosting surveys. Focal observations were conducted for 100-sec periods on randomly selected birds to determine foraging rate and food type.

To assess spatial distribution and abundance of foraging aggregations of Roseate Terns, we conducted nearshore boat surveys along a 104 km long sawtooth transect line (Fig. 28) on 8 days from 10 August to 3 September 2009. These surveys were designed to focus on terns using nearshore water within the Ocean SAMP study area. Surveys were conducted during August when Roseate Terns are known to be most abundant (Fig. 14) and dispersing from nesting

colonies in Long Island and Connecticut through the study area to staging areas in Cape Cod prior to migration to wintering grounds (Harris 2008). We conducted surveys in the morning hours (06:25 to 12:45), using a 6.4 m (21ft) center-console boat, with a 250 hp outboard.

Each survey sampled the sawtooth grid that covered nearshore waters extending out to 7.4 km from shore from Watch Hill to Pt. Judith (Fig. 28). During each survey, we had two observers and a boat operator. Observers used 10 x 42 power binoculars to scan a 300-m wide strip transect on the port and starboard side of the boat, moving at a constant speed of 10 knots (11.5 mph). For each observed tern, the species, age, behavior, flight elevation (<10m, 10-25m, 26-125m, 126-200m, >200m) and flight direction was recorded, as well as location (with a GPS). We also recorded wind direction and speed, cloud cover, visibility and sea state (Table 11). When approaching a large flock of feeding terns, we often stopped the boat to get an accurate estimate of species composition and age composition of the flock. Stopping the boat also allowed observers to listen for Roseate Tern calls, which often enabled observers to pick out Roseate Terns in large tern flocks when they often only made up less than 5% of the flock. Surveys were conducted when the Beaufort sea state was below state three to ensure identification of terns to the species level (Table 11). We recorded all observations using a handheld GPS enabled PDA (Trimble Juno), which used Cybertracker data collection software that we had programmed for ease of date entry (www.cybertracker.org).

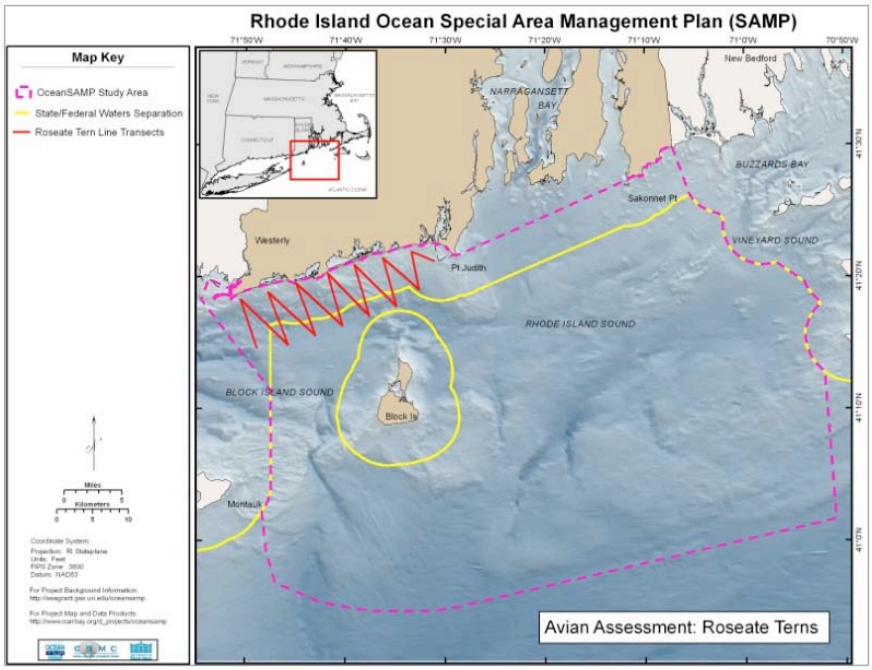

Fig. 28. Location of boat-based sawtooth line-transects used to survey Roseate Terns on 8 days from 10 August to 3 September 2009.

2.5 Radar studies – See Appendix K.

3 Results

3.1 Summary Statistics

3.1.1 Land-based Point Counts

We conducted a total of 796 surveys from 23 January 2009 to 21 February March 2010, with a total of 66,517 minutes (1,108 hours) of survey effort conducted at the 11 point count stations (Table 12). We conducted an average of 72.3 ± 11.7 (SD) surveys per station (1-hr and 2-hr surveys combined). We conducted an average of 42.6 ± 10.9 1-hr long surveys per station and 26.8 ± 4.2 2-hr long surveys per station. Although the survey protocol called for 3 morning and 3 evening surveys per site per month, we ended up averaging slightly more morning surveys (average = 39.9 ± 8.1 surveys per site) than evening surveys (mean = 32.5 ± 4.5 surveys per site) because weather conditions tended to be poorer in the afternoon. Overall, we averaged about 100 hours of observation time (mean = 100.8 ± 13.5 hr per site) at each land-based survey site (Table 12).

Table 12. Summary of survey effort during 796 land-based seawatches from 11 stations along coastal Rhode Island (see Fig. 21) from 23 January 2009 to 21 February 2010.

	Total number of surveys					Mean number of surveys		
Location	All	1-hr long*	2-hr long *	AM	PM	1-hr per month**	2 hr per month**	Hours of Observation
Watch Hill	77	48	27	44	33	6.9	3.8	104
East Beach	78	47	28	47	31	6.7	3.9	108
Deep Hole	80	50	28	48	32	7.1	3.9	109
Pt. Judith	85	47	35	47	38	6.7	4.9	122
M. Dock	90	63	23	51	39	9.0	3.2	115
Beavertail	81	48	32	43	38	6.9	4.4	114
Brenton Point	65	40	23	31	34	6.2	3.5	89
Ruggles	65	37	22	34	31	5.3	3.4	90
Sachuest	62	37	22	34	28	5.3	3.1	86
Sakonnet Point	56	24	27	30	26	3.7	4.1	86
Goosewing	57	28	28	30	27	4.3	3.9	86
Grand Total	796	469	295	439	357	67.0	41.4	1109

*Note: Total number of 1- and 2-hr surveys will not equal 796 because some surveys in Jan 2009 were intermediate in length.
**Note: In January 2009 we did not survey for a complete month, did not conduct 1-hr surveys, and did not yet conduct 2-hr surveys at all sites; therefore, January 2009 surveys were not included in the calculation of monthly mean.

During land-based seawatches throughout the year conducted from 23 Jan 2009 to 21 Feb 2010, we had a total of 465,039 detections from 121 species (Table 13). We detected three species of loons (Gaviidae), two species of grebes (Podicipedidae), four species of shearwaters (Procellariidae), two species of storm-petrels (Hydrobatidae), two species of cormorants (Phalacrocoracidae), one species of gannet (Sulidae), six species of herons/egrets (Ardeidae), one ibis (Threskiornithidae), 26 species of waterfowl (Anatidae), 7 species of diurnal raptors (Acciptridae and Falconidae), 18 species of shorebirds [four plovers (Charadriidae), one oystercatcher (Haematopodidae), 13 sandpipers and allies (Scolopacidae)], two species of jaegers (Stercorariidae), 15 larids [7 species of gulls (Laridae), 7 species of terns (Sternidae) and a skimmer (Rynchopidae)], four alcids (Alcidae), and 28 species of landbirds (Columbidae, Strigidae, Apodidae, Trochilidae, Alcedinidae, Picidae, and various Passeriformes).

As expected, seaducks and gulls were the most frequently observed birds in these nearshore habitats during land-based seawatches. The 15 most abundant species (or species groups), in terms of overall detections, were unidentified scoter (105,656 detections; these were primarily either Surf or Black Scoters),Common Eider (80,445), Herring Gull (59,614), Surf Scoter (42,704), Black Scoter (32,274), Double-crested Cormorant (25,626), unidentified gull (23,860), Tree Swallow (14,025), Great Black-backed Gull (12,583), Laughing Gull (12,097), Northern Gannet (8,718), Red-breasted Merganser (7,926), Common Loon (6,770), White-winged Scoter (6,750), unidentified seaducks (5,303, mainly eider and scoters far offshore), and Ring-billed Gull (3,723) (Table 13).

Since Herring Gulls and Great Black-backed Gulls are widespread, year-round residents that breed in coastal Rhode Island, is it not surprising that those two species were detected on more land-based seawatches than all other species, 96.7% and 89.9% of all surveys, respectively (Table 13). Other species seen on over 50% of land-based seawatches included Common Loon (75.8%), Common Eider (66.5%), Double-crested Cormorants (59.8%), Red-breasted Merganser (55.8%), and Ring-billed Gull (Table 13).

There were considerable differences in detection rates among months during land-based seawatches (Fig. 29; Appendix D). Because there were more seaducks using nearshore habitats in 2009 compared to 2010, detection rates were much higher in 2009. However, seasonal trends were still evident with greater detection rates during the winter and early spring (Nov through March). There was a pulse of birds coming through in October, which was due in part to the influx of Tree Swallows in coastal areas.

Species richness per individual survey during land-based seawatches tended to be lowest in the summer months (June through September; Fig. 30, Appendix D). However, the cumulative number of species detected over all surveys within a month was actually greatest from May to

Sept (50, 51, 58, 39, and 57 total species detected per month, respectively). In contrast, fewer species were detected from Dec through Feb (40, 40, 36 total species per month, respectively).

Table 13. Relative abundance of 121 species of birds detected during 796 land-based seawatches from 23 January 2009 to 21 February 2010 at 11 stations along the Rhode Island coast (Fig. 21). We summarized for each species the mean (SD) number of detections per survey, total number of detections, the frequency of detections (% of surveys with a detection), and percent of surveys where detections were of birds on the water or in flight.

Species	Mean Number of Detections per Survey	SD Number of Detections per Survey	Total Number of Detections Over All Surveys	% of Surveys with a Detection	% of Surveys with a Detection, On the Water	% Surveys with a Detection, In Flight
Red-throated Loon	3.11	8.78	2473	40.1	28.0	26.3
Pacific Loon	0.00	0.06	3	0.4	0.1	0.3
Common Loon	8.51	18.20	6770	75.8	66.0	40.8
Loon spp.	0.83	4.53	661	13.9	1.5	13.2
Red-necked Grebe	0.10	0.57	82	6.5	4.4	2.3
Horned Grebe	1.90	13.11	1515	30.7	29.5	4.8
Cory's Shearwater	3.02	26.06	2401	5.7	0.9	5.7
Greater Shearwater	0.02	0.30	14	0.8	n/a	0.8
Manx Shearwater	0.01	0.11	7	0.8	n/a	0.8
Sooty Shearwater	0.01	0.09	5	0.5	n/a	0.5
Shearwater spp.	1.92	33.19	1526	2.9	0.1	2.9
Wilson's Storm-Petrel	1.56	14.55	1241	6.3	0.1	6.3
Leach's Storm-Petrel	0.00	0.04	1	0.1	n/a	0.1
Storm-petrel spp.	0.00	0.04	1	0.1	n/a	0.1
Great Cormorant	2.82	7.89	2243	41.6	13.2	39.3
Double-crested Cormorant	32.19	79.88	25626	59.8	45.9	57.8
Northern Gannet	10.95	45.80	8718	42.0	4.4	41.6
Great Blue Heron	0.05	0.56	38	1.8	n/a	1.8
Great Egret	0.06	0.39	45	3.3	0.4	3.0
Snowy Egret	0.02	0.18	12	0.9	0.1	0.8
Cattle Egret	0.00	0.05	2	0.3	n/a	0.3
Green Heron	0.01	0.13	5	0.3	n/a	0.3
Black-crowned Night-Heron	0.01	0.07	4	0.5	n/a	0.5
Glossy Ibis	0.04	0.91	34	0.5	n/a	0.5
Mute Swan	0.14	0.76	111	5.5	1.6	3.9
Tundra Swan	0.00	0.07	2	0.1	n/a	0.1
Canada Goose	3.16	16.13	2513	14.1	2.3	12.9
Atlantic Brant	1.84	8.06	1464	13.6	2.4	11.9
Wood Duck	0.01	0.21	10	0.4	n/a	0.4
Mallard	0.09	0.58	74	4.1	0.9	3.4
American Black Duck	0.88	5.53	700	13.2	6.9	9.0
Gadwall	0.03	0.28	22	1.1	0.4	0.8
Northern Pintail	0.01	0.18	7	0.4	n/a	0.4
American Wigeon	0.02	0.25	14	0.8	0.6	0.3

Green-winged Teal	0.05	0.73	38	0.6	0.1	0.5
Teal spp.	0.00	0.04	1	0.1	n/a	0.1
Anas spp.	0.08	0.92	65	1.9	n/a	1.9
Greater Scaup	1.26	12.10	1000	4.3	2.8	1.8

Table 13 continued. Relative abundance of birds during land-based seawatches.

Species	Mean Number of Detections per Survey	SD Number of Detections per Survey	Total Number of Detections Over All Surveys	% of Surveys with a Detection	% of Surveys with a Detection, On the Water	% Surveys with a Detection, In Flight
Scaup spp.	0.57	9.58	454	1.9	0.4	1.6
Aythya Spp.	0.06	0.80	49	0.9	n/a	0.9
Common Eider	101.06	296.80	80445	65.6	55.8	50.8
King Eider	0.03	0.29	26	1.8	1.6	0.1
Harlequin Duck	1.64	5.60	1305	14.1	11.6	7.3
Long-tailed Duck	0.59	3.01	470	13.3	4.3	10.1
Surf Scoter	53.65	385.48	42704	34.5	17.2	24.1
Black Scoter	40.55	193.38	32274	41.1	22.1	28.6
Surf or Black Scoter	4.21	22.23	3350	18.2	1.3	18.0
White-winged Scoter	8.48	39.81	6750	40.6	19.5	29.4
Scoter spp.	100.54	517.05	80030	35.4	9.0	32.0
Common Goldeneye	2.47	7.64	1966	24.4	21.5	9.5
Barrow's Goldeneye	0.00	0.05	2	0.3	0.3	n/a
Bufflehead	0.84	3.61	668	10.1	8.0	3.6
Hooded Merganser	0.02	0.34	12	0.3	n/a	0.3
Red-breasted Merganser	9.96	23.51	7926	55.8	43.8	42.5
Common Merganser	0.00	0.05	2	0.3	n/a	0.3
Seaduck spp.	6.66	89.65	5303	2.5	0.4	2.1
Ruddy Duck	0.02	0.40	16	0.3	0.3	n/a
Northern Harrier	0.01	0.09	7	0.9	n/a	0.9
Sharp-shinned Hawk	0.00	0.08	3	0.3	n/a	0.3
Cooper's Hawk	0.00	0.04	1	0.1	n/a	0.1
Osprey	0.06	0.29	48	5.0	n/a	5.0
Merlin	0.01	0.09	6	0.8	n/a	0.8
American Kestrel	0.01	0.09	6	0.8	n/a	0.8
Peregrine Falcon	0.01	0.10	8	1.0	0.1	0.9
Falcon spp.	0.00	0.05	2	0.3	n/a	0.3
Black-bellied Plover	0.02	0.28	19	1.1	n/a	1.1
Piping Plover	0.01	0.15	9	0.8	0.3	0.5
Semipalmated Plover	0.20	1.63	158	4.8	0.4	4.5
Killdeer	0.01	0.07	4	0.5	n/a	0.5
American Oystercatcher	0.02	0.17	14	1.3	n/a	1.3
Greater Yellowlegs	0.03	0.68	22	0.5	n/a	0.5
Lesser Yellowlegs	0.02	0.27	13	0.6	n/a	0.6
Yellowlegs spp.	0.00	0.04	1	0.1	n/a	0.1
Willet	0.03	0.42	22	0.9	n/a	0.9
Spotted Sandpiper	0.01	0.14	8	0.6	0.3	0.5
Whimbrel	0.03	0.40	26	0.9	n/a	0.9
Ruddy Turnstone	0.17	1.56	138	3.8	n/a	3.8
Purple Sandpiper	2.55	11.62	2029	11.8	1.4	11.1

Sanderling	3.21	20.34	2558	11.1	0.5	10.9
Dunlin	0.11	1.08	87	1.4	0.1	1.4
White-rumped Sandpiper	0.00	0.04	1	0.1	n/a	0.1
Semipalmated Sandpiper	1.66	24.94	1318	5.7	0.3	5.4

Table 13 continued. Relative abundance of birds during land-based seawatches.

Species	Mean Number of Detections per Survey	SD Number of Detections per Survey	Total Number of Detections Over All Surveys	% of Surveys with a Detection	% of Surveys with a Detection, On the Water	% Surveys with a Detection, In Flight
Sandpiper spp.	1.00	6.28	799	5.3	n/a	5.3
Least Sandpiper	0.06	0.50	50	2.1	n/a	2.1
Short-billed Dowitcher	0.29	2.80	231	2.0	n/a	2.0
Shorebird spp.	1.26	6.74	1000	10.7	n/a	10.7
Pomarine Jaeger	0.00	0.07	2	0.1	n/a	0.1
Parasitic Jaeger	0.02	0.37	19	0.8	n/a	0.8
Jaeger spp.	0.00	0.06	3	0.4	n/a	0.4
Bonaparte's Gull	0.55	2.76	436	9.7	2.3	9.0
Laughing Gull	15.20	53.86	12097	36.7	8.2	36.4
Ring-billed Gull	4.68	15.22	3723	52.6	9.7	50.0
Herring Gull	74.89	368.88	59614	96.7	51.3	94.5
Iceland Gull	0.00	0.04	1	0.1	0.1	n/a
Great Black-backed Gull	15.81	79.01	12583	89.9	46.1	82.9
Black-legged Kittiwake	0.07	0.67	58	2.8	0.3	2.5
Gull spp.	29.97	134.37	23860	26.8	1.9	25.9
Caspian Tern	0.00	0.07	2	0.1	n/a	0.1
Royal Tern	0.01	0.10	6	0.6	n/a	0.6
Common Tern	4.58	19.41	3647	18.8	0.3	18.6
Forster's Tern	0.01	0.17	11	0.8	n/a	0.8
Roseate Tern	0.16	1.08	125	3.9	n/a	3.9
Least Tern	0.61	3.17	485	9.9	n/a	9.9
Black Tern	0.02	0.20	15	1.1	n/a	1.1
Sterna spp.	1.65	15.70	1317	9.0	0.1	9.0
Black Skimmer	0.00	0.11	3	0.1	n/a	0.1
Thick-billed Murre	0.00	0.05	2	0.3	0.3	n/a
Murre spp.	0.00	0.04	1	0.1	n/a	0.1
Razorbill	0.36	2.15	290	6.7	3.0	4.5
Dovekie	0.001	0.04	1	0.1	0.1	n/a
Black Guillemot	0.00	0.05	2	0.3	0.1	0.1
Alcid spp.	0.14	1.16	110	3.3	0.3	3.0
Mourning Dove	0.01	0.09	5	0.5	n/a	0.5
Short-eared Owl	0.00	0.04	1	0.1	n/a	0.1
Chimney Swift	0.00	0.06	3	0.4	n/a	0.4
Ruby-throated Hummingbird	0.00	0.05	2	0.3	n/a	0.3
Belted Kingfisher	0.00	0.05	2	0.3	n/a	0.3
Northern Flicker	0.00	0.04	1	0.1	n/a	0.1
Eastern Kingbird	0.00	0.04	1	0.1	n/a	0.1
Blue Jay	0.03	0.85	24	0.1	n/a	0.1
American Crow	0.03	0.42	26	1.0	n/a	1.0
Fish Crow	0.01	0.25	11	0.4	n/a	0.4

Corvid spp.	0.03	0.51	21	0.9	n/a	0.9
Horned Lark	0.00	0.05	2	0.3	n/a	0.3
Purple Martin	0.01	0.11	7	0.8	n/a	0.8
Northern Rough-wd Swallow	0.13	1.16	102	2.5	n/a	2.5

Table 13 continued. Relative abundance of birds during land-based seawatches.

Species	Mean Number of Detections per Survey	SD Number of Detections per Survey	Total Number of Detections Over All Surveys	% of Surveys with a Detection	% of Surveys with a Detection, On the Water	% Surveys with a Detection, In Flight
Bank Swallow	0.02	0.32	18	1.0	n/a	1.0
Tree Swallow	17.62	359.01	14025	6.3	0.1	6.3
Cliff Swallow	0.00	0.04	1	0.1	n/a	0.1
Barn Swallow	0.29	1.37	230	8.7	n/a	8.7
Swallow spp.	0.25	2.07	196	5.2	n/a	5.2
American Robin	0.01	0.26	9	0.3	n/a	0.3
American Pipit	0.01	0.09	5	0.5	n/a	0.5
Cedar Waxwing	0.00	0.05	2	0.3	n/a	0.3
Yellow Warbler	0.02	0.19	13	0.9	n/a	0.9
Yellow-rumped Warbler	0.05	1.21	36	0.4	n/a	0.4
Palm Warbler	0.00	0.04	1	0.1	n/a	0.1
Warbler spp.	0.01	0.18	9	0.5	n/a	0.5
Snow Bunting	0.04	0.80	30	0.5	n/a	0.5
Bobolink	0.00	0.04	1	0.1	n/a	0.1
Brown-headed Cowbird	0.01	0.20	9	0.4	n/a	0.4
Common Grackle	0.01	0.19	10	0.5	0.1	0.4
American Goldfinch	0.02	0.47	16	0.4	n/a	0.4
Passerine spp.	0.02	0.29	19	1.1	n/a	1.1

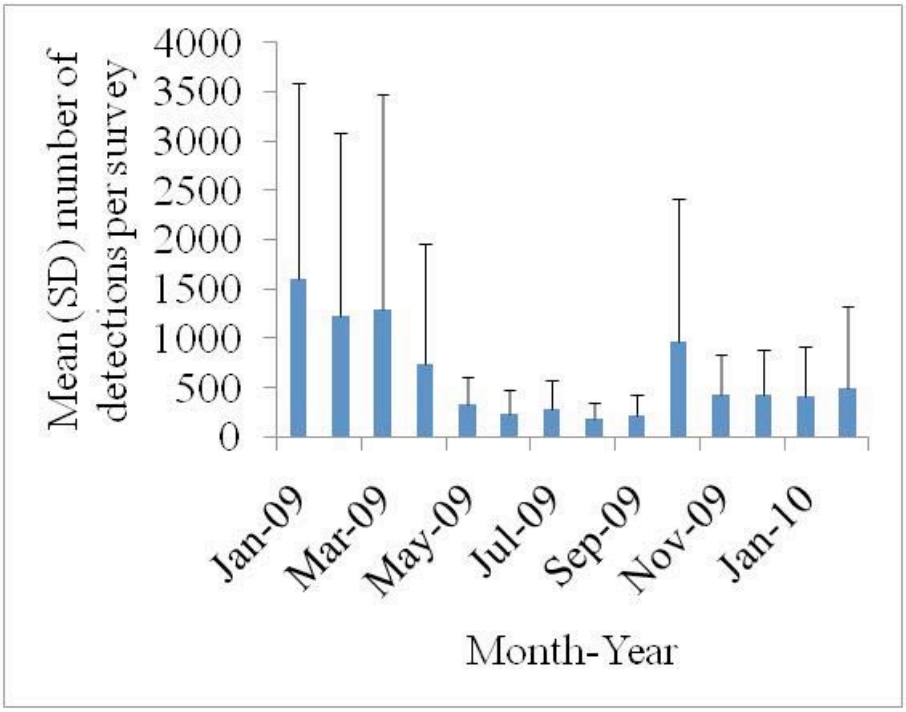

Fig. 29. Seasonal change in overall detection rate (mean ± SD detection per survey) during land-based seawatches (N = 796) from 23 January 2009 to 21 February 2010 at 11 stations (Fig. 21).

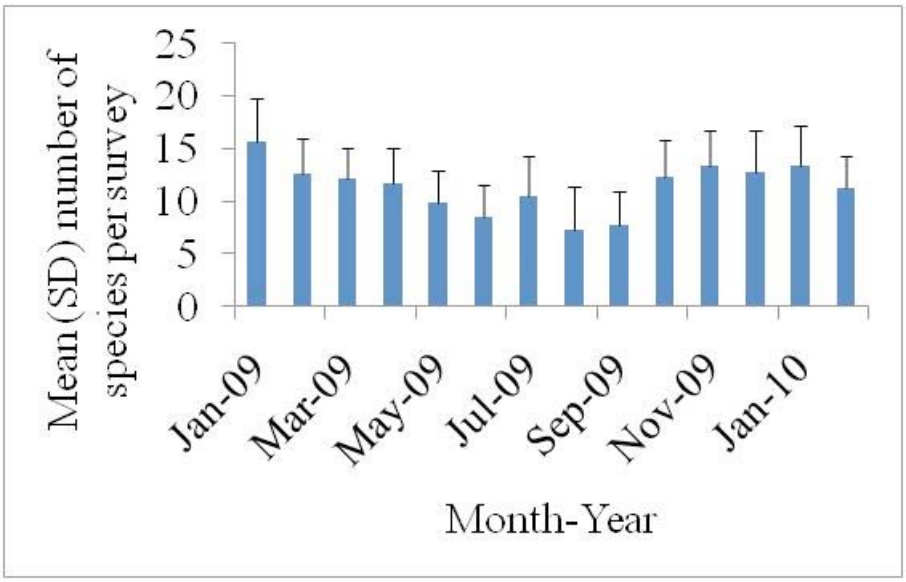

Fig. 30. Seasonal change in species richness (mean ± SD number of species detected per survey) during land-based seawatches (N = 796) from 23 January 2009 to 21 February 2010 at 11 stations (Fig. 21).

Overall detection rates varied considerably among land-based seawatch stations (Tables 1, Fig. 31). Detection rates were greatest at Brenton Point on the SW corner of Aquidneck Island, with an average of 1,379 ± 2,279 (SD) detections per surveys. This was primarily due to the large numbers of seaducks (scoters and eiders) that used this site throughout the winter. Ruggles Ave, on Aquidneck Island, had the second highest detection rates (889 ± 1563), likely also due to large rafts of wintering seaducks. Goosewing (771 ± 1280) and Watch Hill (692 ± 1481) had relatively high detection rates as well. In contrast, detection rates were lowest at Monahan's Dock (239 ± 224), which was located in the SW corner of Narragansett Bay, south of Narragansett Town Beach.

Table 14. Differences among 11 land-based stations in number of detections per survey, and species richness per survey based on pooled 1-hr and 2-hr seawatches from Jan 2009 through Feb 2010.

	Number of detections per survey				Species detected per survey			
Station	Mean	SD	CV	Total	Mean	SD	Total	N
Watch Hill	692.5	1481.4	214	53,321	10.5	3.6	69	77
East Beach	607.4	955.7	157	47,377	10.6	3.8	72	78
Deep Hole	397.2	539.3	136	31,778	10.3	3.5	67	80
Pt. Judith	362.6	502.5	139	30,823	12.2	4.8	78	85
M. Dock	239.1	223.8	94	21,518	10.5	3.6	68	90
Beavertail	409.7	641.8	157	33,182	11.0	4.3	60	81

Brenton Pt.	1379.7	2279.2	165	89,683	11.7	3.9	62	65
Ruggles Ave.	890.0	1563.1	176	57,849	11.8	4.2	52	65
Sachuest Pt.	430.0	501.2	117	26,663	11.8	4.3	61	62
Sakonnet Pt.	516.0	485.2	94	28,894	11.5	4.3	66	56
Goosewing	771.1	1280.9	166	43,951	11.2	3.1	59	57

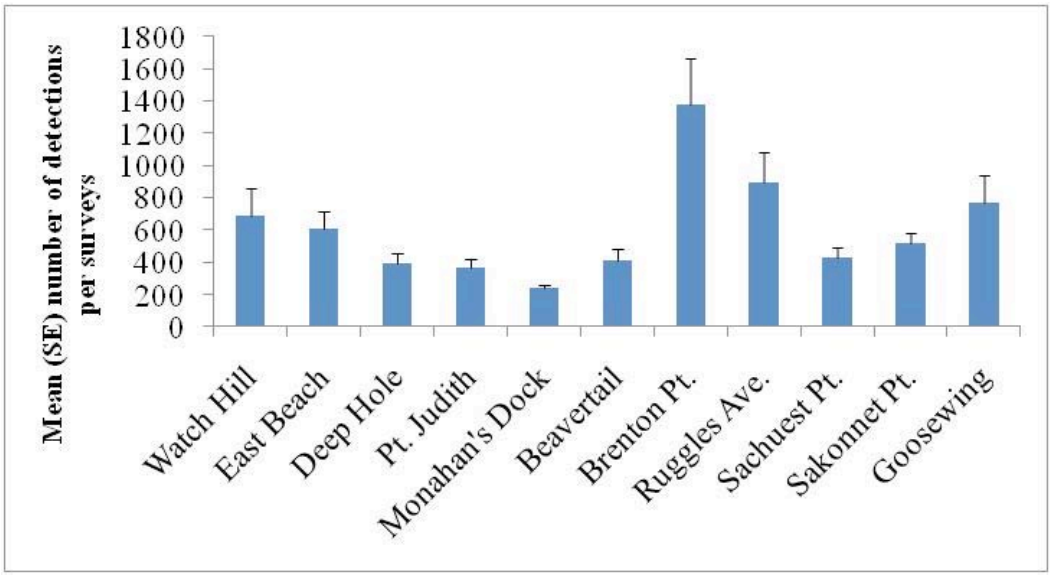

Fig. 31. Mean (SE) number of detections per survey at 11 land-based seawatch stations from January 2009 through February 2010 (see Fig. 21 for locations).

The 11 land-based seawatch stations averaged between 10.3 (Deep Hole) to 12.2 (Point Judith) species per survey from January 2009 through February 2010 (Fig. 32), with the cumulative number of species detected at each station ranging from 52 (Ruggles) to 78 (Point Judith; Table 1). There was a tendency for stations located at the north end of Rhode Island Sound to have greater species richness than stations located at the north end of Block Island Sound.

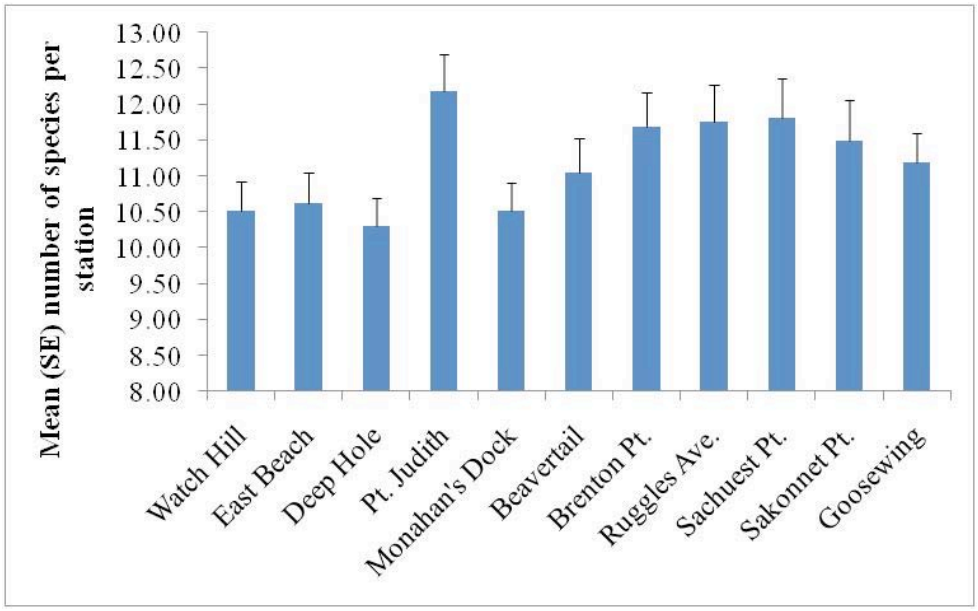

Fig. 32. Mean (SE) number of species detected per survey at 11 land-based point count stations during seawatches from Jan 2009 through Feb 2010.

We estimated flight altitude (m above sea level) for 250,992 detections of birds in flight during land-based seawatches into four height categories (Table 15). Most detections (69%) were of birds flying < 10 m altitude. Certain guilds of birds almost always flew <10 m altitude including shearwaters, storm-petrels, seaducks (although many flew between 10-25 m altitude), and alcids. About 24% of detections were of birds flying between 10-25 m. About 7.7% of detections were of birds flying over 25 m, with only 0.4% of detections >125 m altitude. There was considerable variation among species in altitudes, and altitudes tended to vary throughout the year for some species. For example, loons were generally observed on the water, but during migration periods large numbers of Common Loons were observed flying >25 m high (24% of all detections; Table 15).

Table 15. Altitude (m) above sea level for birds detected in flight during land-based seawatches.

	Percent Detections by Elevation (m)				
	<10	10-25	25-125	>125	Total
Red-throated Loon	80.5	12.4	6.0	1.1	1,226
Pacific Loon	50.0	50.0	0.0	0.0	2
Common Loon	58.0	19.2	20.1	2.7	2,762
Loon spp.	58.9	23.4	14.8	2.9	615
Red-necked Grebe	91.7	8.3	0.0	0.0	24
Horned Grebe	76.5	0.0	23.5	0.0	85
Cory's Shearwater	99.6	0.4	0.0	0.0	2,229
Greater Shearwater	100.0	0.0	0.0	0.0	14
Manx Shearwater	100.0	0.0	0.0	0.0	7
Sooty Shearwater	100.0	0.0	0.0	0.0	5
Shearwater spp.	100.0	0.0	0.0	0.0	1,525
Wilson's Storm-Petrel	100.0	0.0	0.0	0.0	1,240
Leach's Storm-Petrel	100.0	0.0	0.0	0.0	1

Storm-petrel spp.	100.0	0.0	0.0	0.0	1
Great Cormorant	79.8	12.9	5.8	1.5	2,014
Double-crested Cormorant	81.3	9.4	7.9	1.4	22,328
Northern Gannet	54.6	35.4	9.9	0.1	8,560
Great Blue Heron	18.4	5.3	73.7	2.6	38
Great Egret	60.0	32.5	7.5	0.0	40
Snowy Egret	54.5	27.3	18.2	0.0	11
Cattle Egret	0.0	0.0	100.0	0.0	2
Green Heron	0.0	40.0	60.0	0.0	5
Black-crowned Night-Heron	25.0	50.0	25.0	0.0	4
Glossy Ibis	5.9	82.4	11.8	0.0	34
Mute Swan	60.2	32.5	7.2	0.0	83
Tundra Swan	100.0	0.0	0.0	0.0	2
Canada Goose	31.7	35.9	30.2	2.2	2,021
Atlantic Brant	53.1	22.2	22.5	2.2	1,152
Wood Duck	70.0	0.0	30.0	0.0	10
Mallard	9.4	29.7	53.1	7.8	64
American Black Duck	24.1	39.2	35.5	1.2	324
Gadwall	25.0	41.7	16.7	16.7	12
Northern Pintail	0.0	100.0	0.0	0.0	7
Species	<10	10-25	25-125	>125	Total
American Wigeon	33.3	66.7	0.0	0.0	6
Green-winged Teal	100.0	0.0	0.0	0.0	37
Teal spp.	0.0	0.0	100.0	0.0	1
Anas spp.	6.2	52.3	38.5	3.1	65
Greater Scaup	65.7	31.5	2.8	0.0	143
Scaup spp.	85.3	14.7	0.0	0.0	224
Aythya Spp.	20.4	8.2	57.1	14.3	49
Common Eider	92.9	6.9	0.2	0.0	24,195
King Eider	100.0	0.0	0.0	0.0	1
Harlequin Duck	99.3	0.7	0.0	0.0	291
Long-tailed Duck	90.3	9.7	0.0	0.0	259
Surf Scoter	94.1	5.2	0.7	0.0	3,498
Black Scoter	94.1	5.7	0.2	0.0	4,756
Black or Surf Scoter	77.5	21.2	1.4	0.0	2,764
White-winged Scoter	78.0	15.0	4.1	2.9	2,973
Scoter spp.	92.2	7.0	0.7	0.0	34,373
Common Goldeneye	50.6	38.1	11.3	0.0	336
Bufflehead	80.3	19.7	0.0	0.0	142
Hooded Merganser	75.0	0.0	25.0	0.0	12
Red-breasted Merganser	78.2	16.4	5.4	0.0	2,245
Common Merganser	0.0	0.0	100.0	0.0	2
Seaduck spp.	94.0	4.8	0.7	0.5	2,228
Northern Harrier	28.6	57.1	14.3	0.0	7
Sharp-shinned Hawk	33.3	66.7	0.0	0.0	3
Cooper's Hawk	0.0	100.0	0.0	0.0	1
Osprey	2.1	31.3	60.4	6.3	48
Merlin	16.7	66.7	16.7	0.0	6
American Kestrel	16.7	66.7	16.7	0.0	6
Peregrine Falcon	28.6	28.6	28.6	14.3	7

Falcon spp.	0.0	50.0	50.0	0.0	2
Black-bellied Plover	57.9	5.3	36.8	0.0	19
Piping Plover	100.0	0.0	0.0	0.0	6
Semipalmated Plover	87.5	8.3	4.2	0.0	144
Killdeer	0.0	25.0	75.0	0.0	4
American Oystercatcher	64.3	35.7	0.0	0.0	14
Greater Yellowlegs	90.9	0.0	9.1	0.0	22
Lesser Yellowlegs	38.5	53.8	7.7	0.0	13
Yellowlegs spp.	0.0	0.0	100.0	0.0	1
Willet	54.5	31.8	13.6	0.0	22
Spotted Sandpiper	100.0	0.0	0.0	0.0	5
Whimbrel	26.9	15.4	57.7	0.0	26
Ruddy Turnstone	71.7	25.4	2.9	0.0	138
Purple Sandpiper	99.9	0.1	0.0	0.0	1,594
Sanderling	90.8	6.6	2.6	0.0	2,262
Dunlin	100.0	0.0	0.0	0.0	75
White-rumped Sandpiper	100.0	0.0	0.0	0.0	1
Semipalmated Sandpiper	73.6	19.4	7.1	0.0	1,316
Peep spp.	82.6	10.9	6.5	0.0	799
Least Sandpiper	68.0	26.0	6.0	0.0	50
	<10	10-25	25-125	>125	Total
Short-billed Dowitcher	66.2	25.1	8.7	0.0	231
Shorebird Spp.	81.6	12.0	6.4	0.0	1,000
Pomarine Jaeger	100.0	0.0	0.0	0.0	2
Parasitic Jaeger	63.2	15.8	21.1	0.0	19
Jaeger spp.	100.0	0.0	0.0	0.0	3
Bonaparte's Gull	70.3	28.9	0.8	0.0	357
Laughing Gull	58.7	36.2	4.9	0.1	11,350
Ring-billed Gull	50.8	39.5	9.5	0.1	3,227
Herring Gull	51.9	33.2	14.7	0.3	51,036
Great Black-backed Gull	65.8	25.8	8.0	0.5	8,610
Black-legged Kittiwake	76.8	23.2	0.0	0.0	56
Gull spp.	66.6	22.5	10.3	0.7	22,808
Caspian Tern	0.0	100.0	0.0	0.0	2
Royal Tern	33.3	66.7	0.0	0.0	6
Common Tern	53.5	42.7	3.8	0.0	3,644
Forster's Tern	36.4	63.6	0.0	0.0	11
Roseate Tern	40.0	60.0	0.0	0.0	125
Least Tern	56.1	39.0	4.9	0.0	485
Black Tern	73.3	26.7	0.0	0.0	15
Sterna spp.	29.9	58.6	11.4	0.0	1,293
Black Skimmer	100.0	0.0	0.0	0.0	3
Murre spp.	100.0	0.0	0.0	0.0	1
Razorbill	100.0	0.0	0.0	0.0	135
Black Guillemot	100.0	0.0	0.0	0.0	1
Alcid spp.	100.0	0.0	0.0	0.0	106
Mourning Dove	20.0	80.0	0.0	0.0	5
Short-eared Owl	100.0	0.0	0.0	0.0	1
Chimney Swift	0.0	100.0	0.0	0.0	3
Ruby-throated Hummingbird	0.0	50.0	50.0	0.0	2

Belted Kingfisher	0.0	100.0	0.0	0.0	2
Northern Flicker	0.0	100.0	0.0	0.0	1
Eastern Kingbird	0.0	100.0	0.0	0.0	1
Blue Jay	0.0	0.0	100.0	0.0	24
American Crow	0.0	69.2	3.8	26.9	26
Fish Crow	0.0	100.0	0.0	0.0	11
Corvid spp.	4.8	19.0	76.2	0.0	21
Horned Lark	0.0	0.0	100.0	0.0	2
Purple Martin	28.6	28.6	28.6	14.3	7
Northern Rough-wd. Swallow	62.7	32.4	4.9	0.0	102
Bank Swallow	27.8	72.2	0.0	0.0	18
Tree Swallow	11.2	83.3	5.4	0.0	14,017
Cliff Swallow	100.0	0.0	0.0	0.0	1
Barn Swallow	65.2	29.1	5.7	0.0	230
Swallow spp.	53.6	41.8	4.6	0.0	196
American Robin	0.0	0.0	100.0	0.0	9
American Pipit	0.0	0.0	100.0	0.0	5
Cedar Waxwing	0.0	0.0	100.0	0.0	2
Yellow Warbler	0.0	7.7	92.3	0.0	13
Yellow-rumped Warbler	0.0	38.9	61.1	0.0	36
	<10	10-25	25-125	>125	Total
Warbler spp.	22.2	0.0	77.8	0.0	9
Snow Bunting	73.3	0.0	26.7	0.0	30
Bobolink	0.0	0.0	100.0	0.0	1
Brown-headed Cowbird	0.0	55.6	44.4	0.0	9
Common Grackle	0.0	25.0	75.0	0.0	8
American Goldfinch	0.0	18.8	81.3	0.0	16
Passerine spp.	42.1	47.4	5.3	5.3	19
Overall	68.9	23.5	7.3	0.4	250,992

3.1.2 Ship-based Surveys

We conducted a total of 54 surveys of 8 grids on 27 days between 10 June 2009 and 13 February 2010 (Table 16). We had planned on surveying each of the 8 grids one time per month during this eight month period. However, because we only conducted ship-based surveys when the sea state was ≤3 (Table 11), we had a difficult time some months surveying all eight grids

Table 16. Days when we conducted ship-based surveys on 8 grids from 10 June 2009 to 13 Feb 2010. We conducted at total of 54 grid survey days. See Fig. 24 for survey grid locations.

Date	A	B	C	D	E	F	G	H
6/10/2009	X	X						
6/30/2009	X	X						
7/10/2009			X	X				
7/15/2009					X	X		
7/22/2009							X	X
8/5/2009	X				X			
8/10/2009			X	X				
8/25/2009		X				X		

9/8/2009							X	X
9/15/2009	X				X			
10/6/2009			X	X				
10/9/2009		X				X		
10/22/2009							X	X
10/27/2009			X	X				
11/5/2009		X				X		
11/17/2009	X				X			
11/19/2009							X	X
12/2/2009			X	X				
12/8/2009		X				X		
12/18/2009	X				X			
12/31/2009							X	X
1/5/2010		X				X		
1/11/2010			X	X				
1/21/2010	X				X			
2/3/2010							X	X
2/5/2010		X				X		
2/13/2010			X	X				
Total	**7**	**8**	**7**	**7**	**6**	**7**	**6**	**6**

During ship-based surveys, we detected a total of 56 species, which included 6 species of Procelliformes (tubenoses), 9 Anseriformes (waterfowl), 5 species of gulls, two species of terns, three species of jaegers, and five species of alcids (Table 17). The five most abundant species, in terms of mean number of detections per survey were Herring Gull (30.6 detections per survey), Wilson's Storm-Petrel (28.0), Northern Gannet (23.7), Great Black-backed Gull (18.5), and Cory's Shearwater (9.6). Herring (94.4% of surveys) and Great-Black-backed Gulls (94.4% of surveys) were detected more frequently than other species; Northern Gannets (68.5%) and Common Loon (59.3%) were also frequently seen.

We have summarized variation in the average number of detections per grid for all birds detected during ship-based surveys from 10 June 2009 through mid-Feb 2010 (Table 18). Species richness was greatest on grid A (33 species detected; south of Block Island) and grid F (32 species detected; SW of Harbor of Refuge/Pt. Judith), which were also the two grids closest to shore. The average abundance of birds was greatest on grids A (343 detections per survey) and E (338 detections per survey; Table 18). We used these data to model the spatial distribution and abundance of the most commonly detected species of waterbirds (see species accounts below).

We have also summarized the average number of detections across all grids for 24 species during the summer (10 June to 25 August 2009; Appendix E), when tubenoses (shearwaters and storm-petrels) were common, and jaegers were observed. In the fall, 29 species were detected (8 Sept thru 19 Nov 2009; Appendix F), with seaducks, gannets, gulls (both Herring and Great Black-backed Gulls) becoming common in offshore areas of the Ocean SAMP study area. Finally in winter 21 species we detected (18 Dec 2009 to 13 Feb 2010; Appendix G), and overall detections declined, although detection rates for Common Loons and Northern Gannets increased. We have

presented these summary statistics in appendices for those readers interested in the total number of detections for individual grids for a particular species at a specific time of year (see Appendices E, F, and G).

Table 17. Mean (SD) number of detections per grid, CV of detection rate, total number of detections, and % of surveys (n = 54) with a detection within a grid) during ship-based line transect surveys on all 8 grids (see Fig. 24) conducted from 10 June 2009 through 13 Feb 2010.

Species	Mean	SD	CV	Total	% of surveys
Common Loon	5.41	7.69	142.19	292	59.3
Red-throated Loon	1.96	4.68	238.53	106	29.6
Loon unid.	0.09	0.45	481.55	5	5.6
Red-necked Grebe	0.02	0.14	734.85	1	1.9
Great Cormorant	0.28	0.94	338.41	15	11.1
Double-crested Cormorant	0.19	0.52	279.00	10	13.0
Northern Gannet	23.67	78.19	330.36	1278	68.5
Wilson's Storm-Petrel	27.98	72.24	258.16	1511	31.5
Manx's Shearwater	0.04	0.19	514.69	2	3.7
Sooty Shearwater	0.30	1.18	396.80	16	7.4
Greater Shearwater	4.43	13.04	294.68	239	31.5
Cory's Shearwater	9.63	24.02	249.41	520	33.3
Shearwater small unid.	0.04	0.27	734.85	2	1.9
Shearwater unid.	0.50	1.97	393.82	27	13.0
Northern Fulmar	0.09	0.40	433.45	5	5.6
Great Blue Heron	0.02	0.14	734.85	1	1.9
Brant	0.31	2.31	734.85	17	1.9
Mallard	0.02	0.14	734.85	1	1.9
Dabbling duck unid.	0.20	1.50	734.85	11	1.9
Green-winged Teal	0.19	1.36	734.85	10	1.9
Bay duck unid.	0.15	1.09	734.85	8	1.9
Scaup unid.	1.02	5.26	516.89	55	3.7
Common Eider	5.44	21.00	385.73	294	25.9
Black Scoter	5.13	18.86	367.75	277	20.4
Surf Scoter	3.87	23.80	614.98	209	16.7
White-winged Scoter	2.98	5.68	190.46	161	40.7
Surf or Black Scoter	4.41	14.75	334.55	238	16.7
Scoter unid.	0.07	0.54	734.85	4	1.9
Long-tailed Duck	0.39	1.16	297.27	21	16.7
Red-breasted Merganser	0.04	0.19	514.69	2	3.7
Semipalmated Plover	0.04	0.27	734.85	2	1.9
Least Sandpiper	0.04	0.27	734.85	2	1.9
Purple Sandpiper	0.07	0.54	734.85	4	1.9
Lesser Yellowlegs	0.07	0.54	734.85	4	1.9
Short-billed Dowitcher	0.09	0.68	734.85	5	1.9
Whimbrel	0.09	0.56	603.27	5	3.7
Red-necked Phalarope	0.44	3.27	734.85	24	1.9
Phalarope unid	0.04	0.19	514.69	1	3.7
Shorebird unid.	0.06	0.30	543.57	2	3.7
Bonaparte's Gull	0.33	1.08	324.47	18	13.0
Laughing Gull	3.15	13.59	431.78	170	27.8
Ring-billed Gull	0.59	1.70	286.75	32	20.4
Herring Gull	30.59	109.43	357.71	1652	94.4

Great Black-backed Gull	18.54	71.35	384.89	1001	94.4

Table 17 continued. Abundance of birds during ship-based line transect surveys.

Species	Mean	SD	CV	Total	% of surveys
Gull spp.	1.07	5.03	468.09	58	9.3
Black-lg. Kittiwake	1.02	1.90	186.38	55	27.8
Common Tern	1.13	5.15	455.97	61	11.1
Roseate Tern	0.15	0.68	461.87	8	5.6
Tern unid	0.22	0.63	285.50	11	13.0
Parasitic Jaeger	0.02	0.14	734.85	1	1.9
Pomarine Jaeger	0.02	0.14	734.85	1	1.9
Long-tailed Jaeger	0.02	0.14	734.85	1	1.9
Razorbill	1.72	4.41	255.83	93	29.6
Common Murre	2.43	8.54	352.02	131	20.4
Thick-billed Murre	0.06	0.30	543.57	3	3.7
Murre unid.	0.11	0.60	543.57	6	3.7
Dovekie	2.31	10.87	469.78	125	11.1
Atlantic Puffin	0.09	0.68	734.85	5	1.9
Alcid unid	1.54	6.49	422.15	83	20.4
Merlin	0.02	0.14	734.85	1	1.9
Mourning Dove	0.02	0.14	734.85	1	1.9
Bank Swallow	0.04	0.27	734.85	2	1.9
Tree Swallow	0.15	0.86	577.65	8	3.7
Swallow unid.	0.04	0.19	514.69	2	3.7
Blackpoll Warbler	0.04	0.19	514.69	2	3.7
Yellow-rumped Warbler	0.02	0.14	734.85	1	1.9
Warbler unid.	0.06	0.30	543.57	3	3.7
Dark-eyed Junco	0.04	0.27	734.85	2	1.9
Savannah Sparrow	0.02	0.14	734.85	1	1.9
Snow Bunting	0.02	0.14	734.85	1	1.9

Table 18. Mean (SD) number of detections per survey for 56 bird species recorded on eight grids (A-H; see Fig.24) over all ship-based line transects conducted from 10 June 2009 to 15 Feb 2010. Total represents the cumulative number of detections over all surveys. Unid = Unidentified to species.

Species	A	B	C	D	E	F	G	H	Total
Loon Unid	0.4 ± 1.0	0 ± 0	0 ± 0	0 ± 0	0 ± 0	0.1 ± 0.3	0 ± 0	0 ± 0	5
Common Loon	13.8 ± 19.1	6.0 ± 8.5	11.2 ± 14.1	5.7± 4.9	18.9 ± 20.3	12.3 ± 10.6	1.0 ± 2.1	1.5 ± 2.3	611
Red-throated Loon	5.4 ± 7.0	2.3 ± 4.7	0.6± 1.0	1.7± 2.9	4.3 ± 7.3	5.2 ± 7.1	1.1 ± 2.11	0.9 ± 1.8	190
Pacific Loon	0.1 ± 0.3	0.1 ± 0.3	0 ± 0	0 ± 0	0 ± 0	0 ± 0	0 ± 0	0 ± 0	2
Red-necked Grebe	0 ± 0	0 ± 0	0 ± 0	0 ± 0	0.1 ± 0.4	0.1 ± 0.3	0 ± 0	0 ± 0	2
Shearwater Unid	0.1± 0.3	0.3 ± 0.7	1.4 ± 4.0	0.2 ± 0.7	0 ± 0	0 ± 0	1.0 ± 2.8	0.3 ± 0.7	29
Cory's Shearwater	7.2 ± 14.1	2.0 ± 4.2	14.7± 35.0	14.7± 36.3	3.1 ± 8.3	1.9 ± 6.0	10.8 ± 29.2	5.5 ± 12.2	520
Greater Shearwater	1.4 ± 4.0	1.3 ± 3.5	4.4 ± 9.9	1.1 ± 2.3	0.14 ± 0.4	0 ± 0	8 ± 19.5	12.3 ± 25.1	239
Manx Shearwater	0.1 ± 0.3	0.1 ± 0.3	0 ± 0	0 ± 0	0 ± 0	0 ± 0	0.1 ± 0.4	0.1 ± 0.4	4
Sooty Shearwater	0.1 ± 0.3	0.1 ± 0.3	0.7 ± 2	0.6± 1.7	0 ± 0	0 ± 0	0.1 ± 0.4	0.6 ± 1.4	19
Wilson's Storm-Petrel	44.4 ± 69.8	9.6 ± 16.5	10.1 ± 24.9	6.7± 14.1	11 ± 29.1	5.2 ± 10.9	21.5 ± 40.9	70.4 ± 164.1	1511
Leach's Storm-Petrel	0 ± 0	0.2 ± 0.6	0 ± 0	0 ± 0	0 ± 0	0 ± 0	0 ± 0	0 ± 0	2
Northern Fulmar	0 ± 0	0 ± 0	0 ± 0	0 ± 0	0 ± 0	0 ± 0	0.4 ± 0.7	0.3 ± 0.7	5
Northern Gannet	16.6 ± 23.5	12.5 ± 20.3	9 ± 13.4	4.8± 5.1	70.1 ± 168.9	43.8 ± 113.8	4.5 ± 7.7	9.3 ± 9.3	1437
Double-crd Cormorant	0.1 ± 0.3	0 ± 0	0 ± 0	0.2 ± 0.4	1.3 ± 2.9	4.7 ± 12.4	0 ± 0	0 ± 0	59
Great Cormorant	0.9 ± 1.5	0.5 ± 1.3	0 ± 0	0.1 ± 0.3	0 ± 0	0.5 ± 1.6	0 ± 0	0 ± 0	19
Great Blue Heron	0 ± 0	0 ± 0	0 ± 0	0 ± 0	0.14 ± 0.4	0 ± 0	0 ± 0	0 ± 0	1
Brant	0 ± 0	0 ± 0	0 ± 0	0 ± 0	0 ± 0	1.7 ± 5.4	0 ± 0	0 ± 0	17
Canada Goose	0 ± 0	0 ± 0	0 ± 0	0 ± 0	0 ± 0	0 ± 0	0 ± 0	0.3 ± 0.7	2
Dabbling duck Unid	1.2± 3.7	0 ± 0	0 ± 0	0 ± 0	0 ± 0	0 ± 0	0 ± 0	0 ± 0	11
Mallard	0 ± 0	0.1 ± 0.3	0 ± 0	0 ± 0	0 ± 0	0 ± 0	0 ± 0	0 ± 0	1
Green-winged Teal	0 ± 0	0 ± 0	0 ± 0	0 ± 0	0 ± 0	0.1 ± 0.3	0 ± 0	0 ± 0	10
Bay Duck Unid	0 ± 0	0 ± 0	0 ± 0	0 ± 0	0 ± 0	0.8 ± 2.5	0 ± 0	0 ± 0	8
Scaup Unid	0 ± 0	0 ± 0	3.3 ± 10	0 ± 0	0 ± 0	2.5 ± 7.9	0 ± 0	0 ± 0	55
Red-bd. Merganser	0.1 ± 0.3	0 ± 0	0 ± 0	0 ± 0	0.3 ± 0.8	0.2 ± 0.4	0 ± 0	0 ± 0	5
Common Eider	8.4 ± 21.7	1.5 ± 4.7	3.7± 10.6	4.3 ± 6.1	3.4 ± 5.7	33.1 ± 55.6	0 ± 0	0 ± 0	518
Scoter Unid.	88.8 ± 266.6	0 ± 0	0 ± 0	0 ± 0	0 ± 0	0 ± 0	0 ± 0	0.5 ± 1.4	804

Table 18 continued. Abundance of birds detected during ship-based grid surveys on individual grids.

Species	A	B	C	D	E	F	G	H	Total
Black Scoter	1.7 ± 2.6	17.5 ± 38.9	3.8± 9.9	0.2 ± 0.7	0.1 ± 0.4	8.6 ± 16.6	0 ± 0	0 ± 0	313
Surf Scoter	6.3 ± 15.7	39.2 ± 82.9	2.6 ± 5.8	0 ± 0	3.3 ± 7.4	2.3 ± 3.4	0 ± 0	5.6 ± 15.9	563
White-winged Scoter	54.9 ± 148.7	3.7 ± 6.8	2.1 ± 2.6	6.1 ± 8.7	2.9 ± 2.9	4.0 ± 6.5	0.6 ± 1.8	1.5 ± 2.1	682
Black or Surf Scoter	14.4 ± 21.9	38.9 ± 100.9	0 ± 0	6 ± 11.7	0.4 ± 1.2	10.4 ± 23.5	0 ± 0	7.3 ± 20.5	738
Long-tailed Duck	0.6 ± 1.1	0.1 ± 0.3	0 ± 0	0.3 ± 0.7	0.6 ± 1.1	1.0 ± 2.2	0 ± 0	0.1 ± 0.4	24
Merlin	0 ± 0	0 ± 0	0.1 ± 0.3	0 ± 0	0 ± 0	0 ± 0	0 ± 0	0 ± 0	1
Shorebird Unid	0 ± 0	0 ± 0	0 ± 0	0 ± 0	0.3 ± 0.8	0 ± 0	0 ± 0	0.1 ± 0.4	3
Short-billed Dowitcher	0 ± 0	0 ± 0	0 ± 0	0.6± 1.7	0 ± 0	0 ± 0	0 ± 0	0 ± 0	5
Semipalmated Plover	0 ± 0	0 ± 0	0 ± 0	0 ± 0	0.3 ± 0.8	0 ± 0	0 ± 0	0 ± 0	2
Purple Sandpiper	0.4 ± 1.3	0 ± 0	0 ± 0	0 ± 0	0 ± 0	0 ± 0	0 ± 0	0 ± 0	4
Lesser Yellowlegs	0 ± 0	0 ± 0	0 ± 0	0 ± 0	0 ± 0	0 ± 0	0 ± 0	0.5 ± 1.4	4
Whimbrel	0.1 ± 0.3	0 ± 0	0 ± 0	0 ± 0	0 ± 0	0.4 ± 1.3	0 ± 0	0 ± 0	5
Phalarope Unid	0 ± 0	0.1 ± 0.3	0 ± 0	0 ± 0	0 ± 0	0 ± 0	0.1 ± 0.4	0 ± 0	2
Red-necked Phalarope	0 ± 0	0 ± 0	0 ± 0	0 ± 0	0 ± 0	0 ± 0	0 ± 0	3.0 ± 8.5	24
Gull Unid	0 ± 0	0.1 ± 0.3	0.1 ± 0.3	0 ± 0	0 ± 0	5.6 ± 10.9	0.8 ± 2.1	0 ± 0	64
Herring Gull	25.7± 20.6	28.1 ± 44.8	9.9 ± 7.3	5.8± 5.9	129.4 ±	36.8 ± 64.2	12.8 ± 13.1	11.1 ± 8.8	2118
Great Black-bd. Gull	19.3± 17.9	13.7 ± 21.2	5 ± 5.5	3.1 ± 2.8	80.9 ± 196.3	27.7 ± 56.5	10 ± 12.4	4.1 ± 3.6	1340
Ring-billed Gull	0.2 ± 0.7	0.8 ± 2.2	0.1 ± 0.3	0 ± 0	0.9 ± 1.5	5.6 ± 12.8	0 ± 0	0 ± 0	73
Laughing Gull	0.3 ± 0.7	0.8 ± 1.5	1 ± 2.3	1.3 ± 2.6	2.1 ± 4.8	12.4 ± 30.7	0 ± 0	0 ± 0	171
Bonaparte's Gull	0.44 ± 1.0	0.2 ± 0.6	0.44 ± 1.3	0 ± 0	0.14 ± 0.4	0.3 ± 0.9	0.8 ± 2.1	0.1 ± 0.4	21
Black-ld Kittiwake	0.9 ± 1.5	0.9 ± 2.0	0.6± 1.3	0.6± 1.7	0.14 ± 0.4	0.3 ± 0.7	2.0 ± 2.8	1.1 ± 2.1	56
Long-tailed Jaeger	0 ± 0	0 ± 0	0 ± 0	0 ± 0	0 ± 0	0 ± 0	0 ± 0	0.1 ± 0.4	1
Parasitic Jaeger	0 ± 0	0 ± 0	0 ± 0	0 ± 0	0 ± 0	0.1 ± 0.3	0 ± 0	0 ± 0	1
Pomarine Jaeger	0.1 ± 0.3	0 ± 0	0 ± 0	0 ± 0	0 ± 0	0 ± 0	0 ± 0	0 ± 0	1
Razorbill	13.8 ± 24.5	4.3 ± 8.8	4.8 ± 8.1	6.22 ± 15.1	2.1 ± 2.7	3.3 ± 7.5	1.8 ± 4.6	4.4 ± 7.5	363
Dovekie	0.2 ± 0.4	2.1 ± 6.6	0.1 ± 0.3	0.1 ± 0.3	0 ± 0	0 ± 0	4.6 ± 9.9	9.6 ± 25.6	139
Murre Unid	0.1 ± 0.3	0.2 ± 0.6	0 ± 0	0 ± 0	0 ± 0	0 ± 0	0.5 ± 1.4	0 ± 0	7
Common Murre	5.7± 16.3	4.2 ± 11.3	1.1 ± 2.9	2.1 ± 5.9	0.3 ± 0.8	0.8 ± 2.2	0.8 ± 1.4	0.6 ± 1.2	143
Thick-billed Murre	0 ± 0	0.2 ± 0.6	0 ± 0	0 ± 0	0 ± 0	0 ± 0	0 ± 0	0.1 ± 0.4	3
Atlantic Puffin	0 ± 0	0 ± 0	0 ± 0	0.2 ± 0.7	0 ± 0	0 ± 0	0.8 ± 1.7	0.1 ± 0.4	9

Table 18 continued. Abundance of birds detected during ship-based grid surveys on individual grids.

Species	A	B	C	D	E	F	G	H	Total
Alcid Unid	5.1 ± 14.9	0.9 ± 2.0	0.7 ± 1.4	2 ± 5.3	0.4 ± 1.1	0.1 ± 0.3	1.1 ± 2.1	0.6 ± 1.2	97
Common Tern	2.3 ± 6.3	0.4 ± 1.3	0 ± 0	0 ± 0	0 ± 0	3.4 ± 10.4	0 ± 0	0.3 ± 0.7	61
Roseate Tern	0.1 ± 0.3	0 ± 0	0 ± 0	0 ± 0	0.4 ± 1.1	0.4 ± 1.3	0 ± 0	0 ± 0	8
Tern Unid	0.44 ± 0.9	0.2 ± 0.6	0 ± 0	0.1 ± 0.3	0.4 ± 1.1	0.1 ± 0.3	0 ± 0	0.1 ± 0.4	12
Mourning Dove	0 ± 0	0 ± 0	0 ± 0	0.1 ± 0.3	0 ± 0	0 ± 0	0 ± 0	0 ± 0	1
Swallow Unid	0 ± 0	0 ± 0	0 ± 0	0.1 ± 0.3	0 ± 0	0.1 ± 0.3	0 ± 0	0 ± 0	2
Tree Swallow	0 ± 0	0 ± 0	0 ± 0	0.9 ± 2.0	0 ± 0	0.2 ± 0.6	0 ± 0	0 ± 0	10
Barn Swallow	0 ± 0	0 ± 0	0 ± 0	0.1 ± 0.3	0 ± 0	0.2 ± 0.6	0 ± 0	0 ± 0	3
Warbler Unid	0 ± 0	0 ± 0	0.1 ± 0.3	0.2 ± 0.7	0 ± 0	0 ± 0	0 ± 0	0 ± 0	3
Blackpoll Warbler	0 ± 0	0.1 ± 0.3	0 ± 0	0.1 ± 0.3	0 ± 0	0 ± 0	0 ± 0	0 ± 0	2
Yellow-rp. Warbler	0 ± 0	0 ± 0	0 ± 0	0.1 ± 0.3	0 ± 0	0 ± 0	0 ± 0	0 ± 0	1
Dark-eyed Junco	0.2 ± 0.7	0 ± 0	0 ± 0	0 ± 0	0 ± 0	0 ± 0	0 ± 0	0 ± 0	2
Savannah Sparrow	0 ± 0	0 ± 0	0 ± 0	0 ± 0	0 ± 0	0 ± 0	0.1 ± 0.4	0 ± 0	1
Snow Bunting	0 ± 0	0 ± 0	0 ± 0	0 ± 0	0.1 ± 0.4	0 ± 0	0 ± 0	0 ± 0	1
Summary total	342.9±459.9	193.3±257.9	91.6±52.5	76.4±36.4	338.1±645.5	237.2±207.5	85.1±63.9	152.4±186.4	13170
Species richness	33	30	23	28	27	32	20	26	56

During ship-based surveys, we recorded flight altitudes of birds into 5 categories (< 10 m, 10-25 m, 25-125 m, 125-200 m, >200 m) altitude above the ocean surface; Table 19). Of 8,927 detections during ship-based surveys from June 2009 through mid-Feb 2010, most birds were in flight at <10 m altitude (58%), while substantial percentages were either on the water (22%) or flying at intermediate altitudes of 10-25 m (15 %). Few birds were observed between 25-125 m elevation (6%), and <1% were >125 m high (Table 19).

Table 19. Summary of flight altitude (m above sea level) for 54 species of birds detected during ship-based line-transect surveys from June 2009 through mid-February 2010. Altitude for each detection was based on ocular estimates, with observers stationed at 6 m elevation on the flying bridge of a ship.

	% of birds detected in altitude category (m)					
Species	**0**	**<10**	**10-25**	**25-125**	**>125**	**N**
Common Loon	81.8	7.9	4.5	5.1	0.7	292
Red-thd. Loon	5.7	30.2	35.8	21.7	6.6	106
Loon spp.	100.0	0.0	0.0	0.0	0.0	5
Red-nd. Grebe	100.0	0.0	0.0	0.0	0.0	1
Northern Fulmar	20.0	80.0	0.0	0.0	0.0	5
Cory's Shearwater	21.7	78.3	0.0	0.0	0.0	520
Greater Shearwater	9.6	90.4	0.0	0.0	0.0	239
Manx Shearwater	50.0	50.0	0.0	0.0	0.0	2
Sooty Shearwater	0.0	100.0	0.0	0.0	0.0	16
Small shearwater unid	0.0	100.0	0.0	0.0	0.0	2
Shearwater unid	48.1	51.9	0.0	0.0	0.0	27
Wilson's Storm-Petrel	49.8	50.2	0.0	0.0	0.0	1511
Double-ct. Cormorant	30.0	70.0	0.0	0.0	0.0	10
Great Cormorant	13.3	80.0	6.7	0.0	0.0	15
Northern Gannet	9.0	46.1	38.1	6.7	0.2	1278
Great Blue Heron	0.0	100.0	0.0	0.0	0.0	1
Brant	0.0	100.0	0.0	0.0	0.0	17
Mallard	0.0	0.0	100.0	0.0	0.0	1
Green-winged Teal	0.0	100.0	0.0	0.0	0.0	10
Dabbling duck unid.	0.0	36.4	63.6	0.0	0.0	11
Bay duck unid.	0.0	100.0	0.0	0.0	0.0	8
Scaup unid.	0.0	0.0	45.5	54.5	0.0	55
Common Eider	8.8	90.8	0.3	0.0	0.0	294
Long-tailed Duck	9.5	76.2	14.3	0.0	0.0	21
Surf Scoter	0.0	9.6	90.4	0.0	0.0	209
Black Scoter	0.0	92.4	7.6	0.0	0.0	277
White-winged Scoter	2.5	70.2	27.3	0.0	0.0	161
Surf or Black Scoter	3.4	81.1	15.5	0.0	0.0	238
Scoter unid.	0.0	0.0	100.0	0.0	0.0	4
Red-brd. Merganser	0.0	0.0	100.0	0.0	0.0	2
Merlin	0.0	0.0	100.0	0.0	0.0	1
Semipalmated Plover	0.0	100.0	0.0	0.0	0.0	2
Least Sandpiper	0.0	100.0	0.0	0.0	0.0	2
Purple Sandpiper	0.0	100.0	0.0	0.0	0.0	4
Lesser Yellowlegs	0.0	100.0	0.0	0.0	0.0	4
Whimbrel	0.0	100.0	0.0	0.0	0.0	5

Table 19 cont. Flight altitude of birds detected during ship-based surveys.

	% of birds detected					
Species	**0**	**<10**	**10-25**	**25-125**	**>125**	**N**
Short-bd Dowitcher	0.0	100.0	0.0	0.0	0.0	5
Red-nd. Phalarope	95.8	4.2	0.0	0.0	0.0	24
Phalarope unid.	0.0	100.0	0.0	0.0	0.0	2
Shorebird unid.	0.0	100.0	0.0	0.0	0.0	3
Long-td. Jaeger	0.0	0.0	100.0	0.0	0.0	1
Parasitic Jaeger	0.0	100.0	0.0	0.0	0.0	1
Pomarine Jaeger	0.0	100.0	0.0	0.0	0.0	1
Bonaparte's Gull	27.8	50.0	22.2	0.0	0.0	18
Laughing Gull	31.2	48.2	17.6	2.9	0.0	170
Ring-billed Gull	3.1	37.5	37.5	18.8	3.1	32
Herring Gull	7.6	64.7	13.9	12.8	1.0	1652
Great-Black-bd Gull	15.8	67.3	8.1	8.0	0.8	1001
Black-lg. Kittiwake	9.1	32.7	47.3	10.9	0.0	55
Gull spp.	0.0	0.0	1.7	39.7	58.6	58
Common Tern	4.9	36.1	47.5	11.5	0.0	61
Roseate Tern	0.0	37.5	50.0	12.5	0.0	8
Tern unid.	0.0	33.3	66.7	0.0	0.0	12
Common Murre	55.0	45.0	0.0	0.0	0.0	131
Thick-billed Murre	33.3	66.7	0.0	0.0	0.0	3
Murre unid	33.3	66.7	0.0	0.0	0.0	6
Razorbill	41.9	58.1	0.0	0.0	0.0	93
Dovekie	77.6	22.4	0.0	0.0	0.0	125
Alcid unid.	13.3	86.7	0.0	0.0	0.0	83
Atlantic Puffin	100.0	0.0	0.0	0.0	0.0	5
Mourning Dove	0.0	100.0	0.0	0.0	0.0	1
Bank Swallow	0.0	100.0	0.0	0.0	0.0	2
Tree Swallow	0.0	50.0	37.5	12.5	0.0	8
Swallow unid.	0.0	0.0	100.0	0.0	0.0	2
Blackpoll Warbler	0.0	100.0	0.0	0.0	0.0	2
Yellow-rd Warbler	0.0	100.0	0.0	0.0	0.0	1
Warbler unid	0.0	100.0	0.0	0.0	0.0	3
Dark-eyed Junco	0.0	0.0	100.0	0.0	0.0	2
Savannah Sparrow	0.0	100.0	0.0	0.0	0.0	1
Snow Bunting	0.0	100.0	0.0	0.0	0.0	1
Grand Total	**21.5**	**57.6**	**14.6**	**5.5**	**0.8**	**8,927**

3.1.2 Aerial Surveys

Survey Effort

We conducted 10 flights between 18 Nov 2009 and 22 Feb 2010 (Table 20). During Round 1 in 2009, we surveyed 6 transects during each flight which took approximately 2.5 hours to complete, thus it took 4 flights to completely sample all 24 transects. During Rounds 2 and 3, we surveyed 8 transects per day, which took approximately 3 hours of flight time on transects, thus we could survey all 24 transects in 3.35 flights.

Table 20. Summary of dates and transects sampled during aerial surveys of Ocean SAMP study area from 18 Nov 2009 to 22 Feb 2010 (see Fig. 27 for locations of transects).

	Round 1 (2009)				**Round 2 (2010)**			**Round 3 (2010)**		
Transect	**18 Nov**	**2 Dec**	**7 Dec**	**8 Dec**	**11 Jan**	**14 Jan**	**27 Jan**	**5 Feb**	**13 Feb**	**22 Feb**
1	X						X			X
2			X			X				
3				X	X			X		
4		X					X			X
5	X					X			X	
6			*		X			X		
7				X			X			X
8		X				X			X	
9	X				X			X		
10			X				X			X
11				X		X			X	
12		X			X			X		
13	X						X			X
14			X			X			X	
15				X	X			X		
16		X					X			X
17	X					X			X	
18			X		X			X		
19				X			X			X
20		X				X			X	
21	X				X			X		
22			X				X			X
23				X		*			X	
24		X			X			X		

*data discarded due to navigational error

During aerial surveys, we had a total of 9,414 detections from 17species or guilds (i.e., cormorants, scoters, shorebirds, gulls, alcid; Table 21). The most common species, in terms of total detections, were Common Eider (3,571 detections), unidentified gulls (1,293 detections),

Northern Gannet (885 detections), Herring Gulls (856), unidentified scoters (716 detections), Common Loon (632 detections), and unidentified alcids (589 detections).

There was considerable variation among survey flights in detection rates between days. During Round 1, when 6 transects were sampled per fight, there were an average of 878 ± 561 total detections per day (CV = 63.8). During Rounds 2 and 3, there was less variation among days (CV = 39.0) based on an average of 983 ± 383 total detections per day

Table 21. Total number of detections for 17 avian species or guilds during 10 aerial surveys of the Ocean SAMP study area from 18 Nov 2009 to 22 Feb 2010.

Species	18 Nov	2 Dec	7 Dec	8 Dec	11 Jan	14 Jan	27 Jan	5 Feb	13 Feb	22 Feb	Total
Loons	20	79	19	45	13	94	126	34	60	170	660
Cormorants	1	0	4	1	0	0	0	0	0	0	6
N. Gannet	225	200	17	285	21	94	35	1	6	1	885
Common Eider	345	44	22	781	406	137	604	303	275	654	3571
Scoter spp.	2	2	3	35	130	128	604	2	20	20	946
Long-tailed Duck	0	0	0	0	0	0	0	0	0	15	15
R-b. Merganser	0	0	0	0	3	0	0	0	0	2	5
Shorebird spp.	0	0	0	0	0	0	3	0	0	14	17
Bonaparte's Gull	0	0	0	0	0	0	1	0	0	0	1
Herring Gull	59	207	37	215	97	67	19	8	72	75	856
Great B-b. Gull	8	70	21	85	10	13	18	2	25	17	269
B-l Kittiwake	3	2	7	11	117	20	12	18	2	0	192
Gull spp.	347	265	6	31	11	286	36	310	0	1	1293
Razorbill	0	0	0	0	4	0	13	7	1	21	46
Murre spp.	0	0	0	0	0	0	1	0	0	0	1
Dovekie	0	0	0	0	0	59	1	2	0	0	62
Alcid spp.	0	1	3	5	63	426	97	47	24	32	698
Total	**1010**	**870**	**139**	**1494**	**871**	**1265**	**1555**	**725**	**484**	**1001**	**9414**

During aerial surveys, 68% of all detections were birds observed on the water, although this varied among species (Table 22). Cormorants, shorebirds, and gulls were more likely to be detected while in flight, whereas seaducks and alcids were more likely to be observed on the water. Since observers only estimated the number of detections in one distance band, we were unable to calculate detection functions for birds detected during aerial surveys. We were unable to estimate avian density based on aerial survey due to time limitations in preparing this report, however raw plotted data has been provided within the sections covering individual species and groups below. We will present DSM modeled estimates of avian densities within the Ocean SAMP study area based on aerial strip-transect surveys.

Table 22. Percent of flocks in flight or on the water for 14 avian guilds during aerial surveys in 2009 and 2010 in the Ocean SAMP study area.

Species	% fly	% water	N
Loons	6	94	454
Cormorants	100	0	3
Northern Gannet	49	51	209
Common Eider	11	89	118
Scoters	37	63	38
Long-tailed Duck	0	100	2
R-b. Merganser	100	0	4
Shorebirds	100	0	2
Bonaparte's Gull	100	0	1
Herring Gull	81	19	296
Great B-b. Gull	58	42	146
B-l Kittiwake	98	2	62
Gulls	29	71	28
Alcids	4	96	435
Total	32	68	1803

3.2 Endangered Species Assessment

Roseate Terns:

We detected small numbers of Roseate Terns during systematic ship- and land-based surveys. During ship-based surveys, Roseate Terns were relatively uncommon and we only had 8 Roseate Tern detections on 3 grids (Table 23). Roseate Terns were detected on ship-based line transect surveys in Block Island Sound from mid-July to late August 2009; SW of the Harbor of Refuge, NW of Block Island and S of Block Island (Fig. 33). No Roseate Terns were detected on grids in Rhode Island Sound or within Inner Continental Shelf during ship-based surveys.

Table 23. Spatial distribution of tern detections on survey grids (see Fig. 33 for locations) during ship-based offshore line transect surveys in the summer and fall of 2009.

	Grid Cell						
Species	**A**	**B**	**D**	**E**	**F**	**H**	**Total**
Common Tern	21	4	0	0	34	2	61
Roseate Tern	1	0	0	3	4	0	8
Sterna spp.	4	2	1	3	1	1	12
Total	**26**	**6**	**1**	**6**	**39**	**3**	**81**

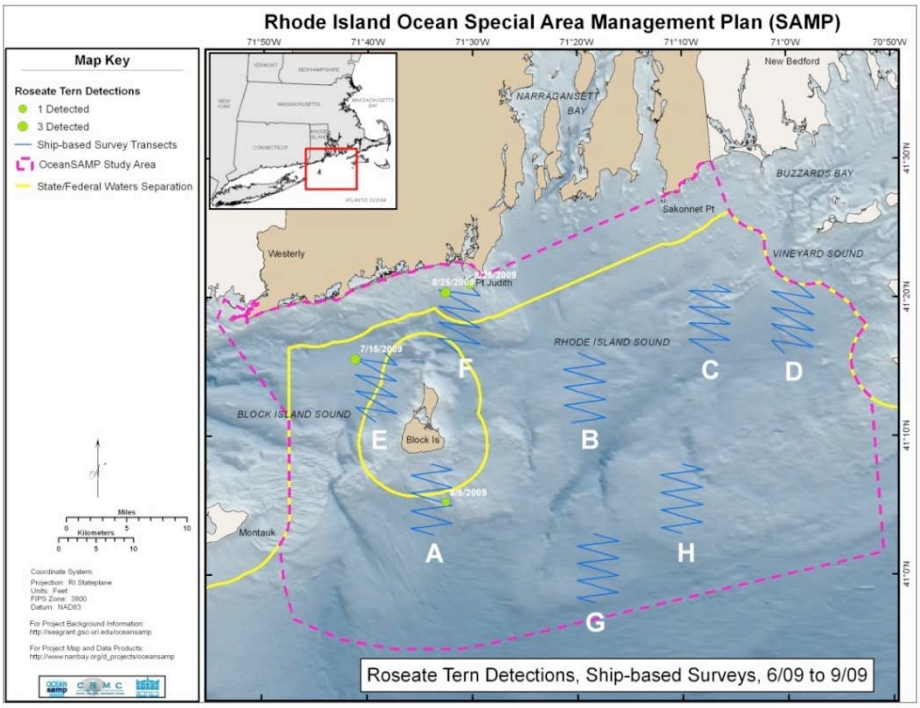

Fig. 33. Spatial distribution of Roseate Tern detections (green circles) during ship-based surveys on 8 grids from June through September 2009.

We had 125 Roseate Tern detections during land-based seawatches, with most detections at the NW corner of the Ocean SAMP study area (Table 24). Detections were concentrated at Watch Hill Lighthouse (34% of 125 detections) and Point Judith (25%). In contrast, Common Tern detections during land-based surveys tended to be more uniformly dispersed throughout the 11 survey stations. Finally, there were large numbers of unidentified terns, particularly at Watch Hill Lighthouse and at Ruggles Ave. survey stations. It is likely that a low percentage of these birds were in fact Roseate Terns, as Common and Roseate Terns often forage together on aggregations of sand lance (Grist 2009).

Table 24. Distribution and abundance (total number of detections) of Common (COTE), Roseate (ROST), and unidentified terns (UNID) at 11 seawatch stations (Fig. 21) from May to Sep 2009.

	Station*											
Species	**1**	**2**	**3**	**4**	**5**	**6**	**7**	**8**	**9**	**10**	**11**	**Total**
COTE	682	170	237	637	289	555	448	129	150	203	147	3647
ROST	42	11	18	31	5	5	1		4	8		125
UNID	104	195	55	126	23	47	18	414	119	159	57	1317
Total	828	376	310	794	317	607	467	543	273	370	204	5089

*1 = Watch Hill, 2 = East Beach, 3 = Deep Hole, 4 = Pt. Judith, 5 = Monahan's Dock, 6= Beavertail, 7 = Brenton Point, 8 = Ruggles Ave., 9 = Sachuest Pt., 10 = Sakonnet Pt, 11 = Goosewing.

During onshore roosting surveys, Grist (2009) observed 5 banded Roseate Terns at Charlestown Breachway, all of which came from the Great Gull Island, NY colony (Table 25).

Table 25. Observations of banded Roseate Terns at Charlestown Breachway from June to Aug 2009 by Grist (2009). All birds were originally banded at Great Gull Island, New York.

Age	Left leg	Right leg	Age banded	Date banded
Adult	1182-07600	00/B6	Chick	23/06/1996
Adult	9822-43697	A6/97	Chick	28/06/2003
Adult	1182-078?1	?1/B8	Chick	XX/06/03
Adult	1182-04883	83/H8	Adult	23/06/2002
Adult	6B/88	1182-03688	Chick	23/06/2000

We had 935 detections of terns during boat-based surveys of nearshore habitats between Point Judith and Napatree on 8 survey days between 10 Aug and 3 Sept 2009 (Table 26). Roseate Terns were detected on 4 of 8 survey days, with a total of 29 detections (15 adults, 4 juveniles, and age was not known for 4 detections). Common Terns were much more abundant than other tern species during these boat surveys (87% of 935 detections). We also detected three other species (Black, Forster's, and Least). Terns tended to be more abundant on the western half of the sawtooth grid (Fig. 34). The few Roseate Terns that were detected also were on the western half of the grid, with most detections occurring near the western edge of Quonochotaug Pond (Fig. 35)

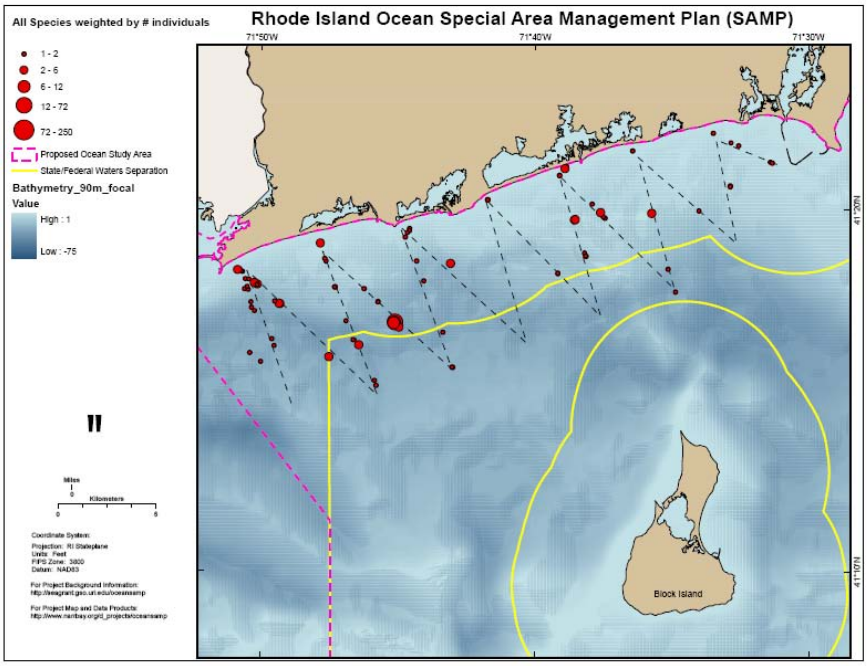

Fig. 34. Distribution of terns (all species: Common, Roseate, Least, Forster's, and Black) detected during boat-based strip surveys in nearshore habitats during summer 2009.

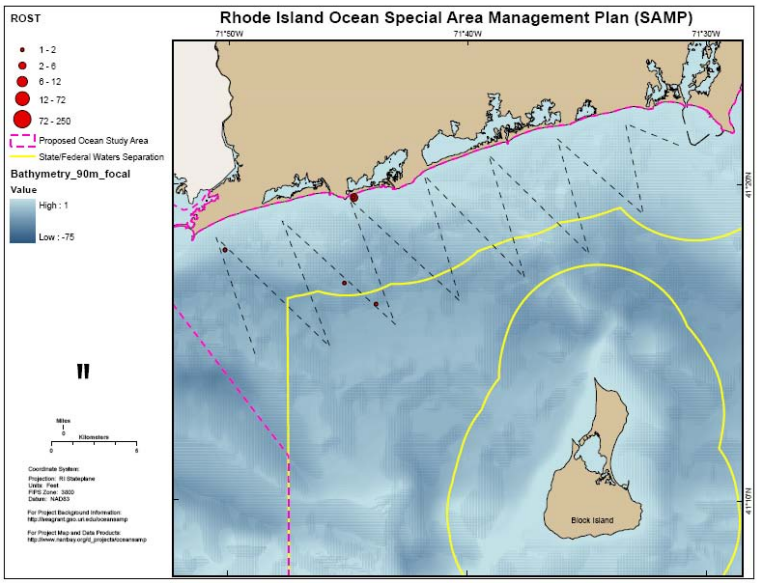

Fig. 35. Distribution of Roseate Terns detected during boat-based strip-transect surveys in nearshore habitats from Napatree to Point Judith during July and August 2009.

Table 26. Total number of terns detected during boat-based surveys in nearshore habitats between Pt. Judith and Napatree from 10 Aug to 3 Sept 2009 (see Fig. 34 for location of transects).

Species	Age	10 Aug	14 Aug	18 Aug	19 Aug	25 Aug	27 Aug	1 Sept	3 Sept	Total
Roseate Tern	Adult		7		1		4	3		15
Roseate Tern	Juv		3				1			4
Roseate Tern	Unk		10							10
Common Tern	Adult	4	50	1	86	12	3	2		158
Common Tern	Juv	1	50	1	15	11	1	17	1	97
Common Tern	unk		255	1	3	6	254	40		559
Black Tern	Adult							1		1
Black Tern	Juv						1	3		4
Black Tern	Unk							38		38
Forster's Tern	Adult		1					1		2
Least Tern	Adult	5	5		5					15
Sterna spp.	Unk		3					24	5	32
Total		10	384	3	110	29	264	129	6	935

During 2009, an ornithologist working for New Jersey Audubon Society maintaining the radar unit on Block Island consistently observed Roseate Terns at a number of sites (Table 27). Magarian (pers. comm.) detected Roseate Terns on the island from 21 July through 30 August, where he observed up to 100 Roseate Terns observed on the island on any given day.

Table 27. Observations of adult and immature Roseate Terns on Block Island during July and August 2009 (Tom Magarian, New Jersey Audubon Society, pers. comm.)

		Age		
Date	**Location**	**Adult**	**Immature**	**Unknown**
21-Jul	Andy's Way	2		
22-Jul	Westside Beach/Beane Pt			3
24-Jul	Andy's Way	75	20	
25-Jul	North end	1		
25-Jul	Cormorant Cove	25	5	
26-Jul	Andy's Way	5	3	
27-Jul	Andy's Way	30	10	
28-Jul	Andy's Way	3	5	
29-Jul	Andy's Way	3	2	
30-Jul	North end	1		
31-Jul	Andy's Way	4		
1-Aug	Cormorant Cove	5	3	
2-Aug	North end	1		
2-Aug	Andy's Way			1
7-Aug	Andy's Way	15	3	
9-Aug	North end	2		
9-Aug	Andy's Way	2		
11-Aug	Andy's Way			1
12-Aug	Andy's Way	3		
15-Aug	Andy's Way	2		
16-Aug	Andy's Way			1
17-Aug	Andy's Way	2		
20-Aug	Andy's Way	1		
22-Aug	Andy's Way	50	20	
23-Aug	North radar site			2
23-Aug	Sandy Point			100
24-Aug	Cormorant Cove	2		
25-Aug	Trimms Pond	45	5	
29-Aug	Andy's Way	3	1	
29-Aug	Trimms Pond	7	1	
30-Aug	Spring Street	4		

3.3 Loons

We detected three species of loons (Gaviidae) in the Ocean SAMP study area: Common Loon, Red-throated Loon, and Pacific Loon. Common Loons were the most abundant species of loon in the Ocean SAMP area, and this species had detection rates 2 to 4 times greater than Red-throated Loons during land-based seawatches. We detected one species of loon rare to the east coast, Pacific Loon, twice during land-based seawatches.

Seasonal changes in abundance - Loons are primarily winter residents and migrants in the Ocean SAMP area (Sibley 2000). Common and Red-throated Loons that winter farther south migrate through Rhode Island waters during their fall migration mostly in October and November, and then pass through again in April and May during spring migration to their northern breeding lakes (Figs. 36 and 37).

Large numbers of loons, both Common and Red-throated Loons, also are winter residents in the Ocean SAMP area from October through May. Loon abundance in nearshore waters peaked in December (birds on water, Figs. 36 and 37), and then gradually declined through May. There is some indication that loons disperse farther offshore starting in January, when they are in flightless molt. Thus, this decline in nearshore areas could be a redistribution of birds offshore and not an actual reduction in overall abundance in the study area. A few Common Loons were detected during land-based seawatches during the summer, when no Red-throated Loons were detected.

Flight altitude of birds - Most loons that we observed during land-based and ship-based surveys were flying at elevations of <10 m (49% of observations), although 9% of birds flew at altitudes greater than 25 m (1% flew over 125 m high; Fig. 38).

Spatial patterns in abundance in nearshore waters - In nearshore areas, Common Loons tend to be more abundant off of sandy beaches in Block Island Sound than rocky headlands of Rhode Island Sound, although loons were common at Brenton Point and Ruggles Ave. on the southern end of Aquidneck Island (Fig. 39). See Appendices B and C for data on loon abundance at each of the land-based seawatch stations for each month surveyed.

During fall ship-based line transect surveys, we primarily detected Common and Red-throated Loons in southerly-directed flight at the northern end of the Ocean SAMP study area (Figs. 40 and 41). However, in late winter, both species of loons were more widely dispersed in the Ocean SAMP area as birds in flight were detected throughout the Ocean SAMP area (Figs. 40 and 41).

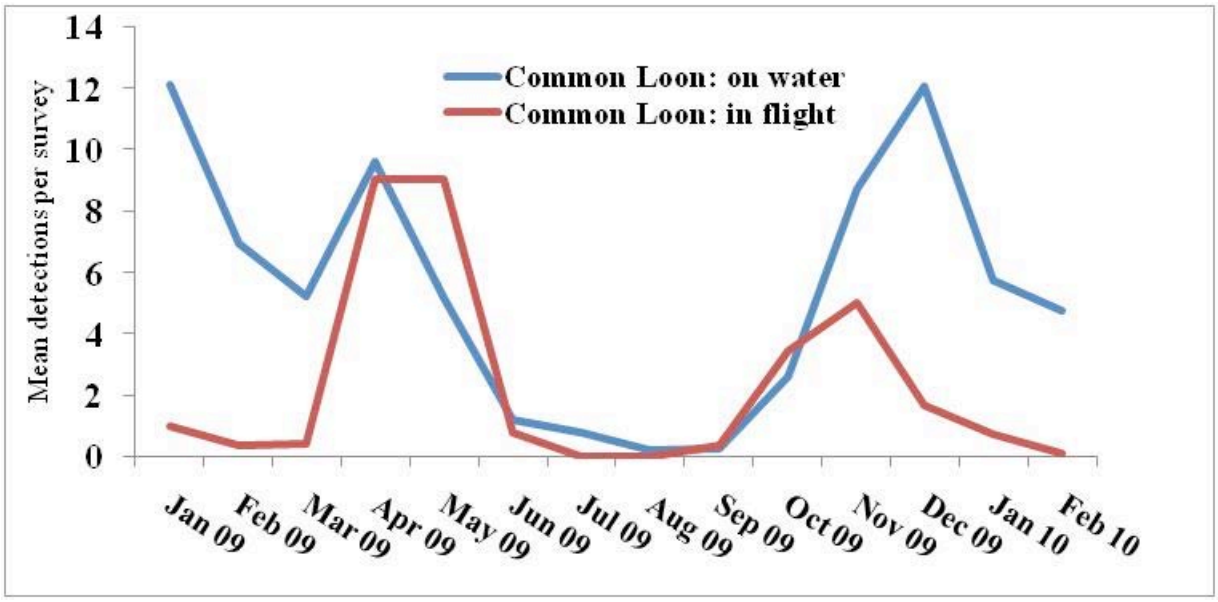

Fig. 36. Monthly differences in the mean number of Common Loons detected on the water and in flight (birds per hr) during surveys at 11 land-based seawatch stations along the Rhode Island coastline

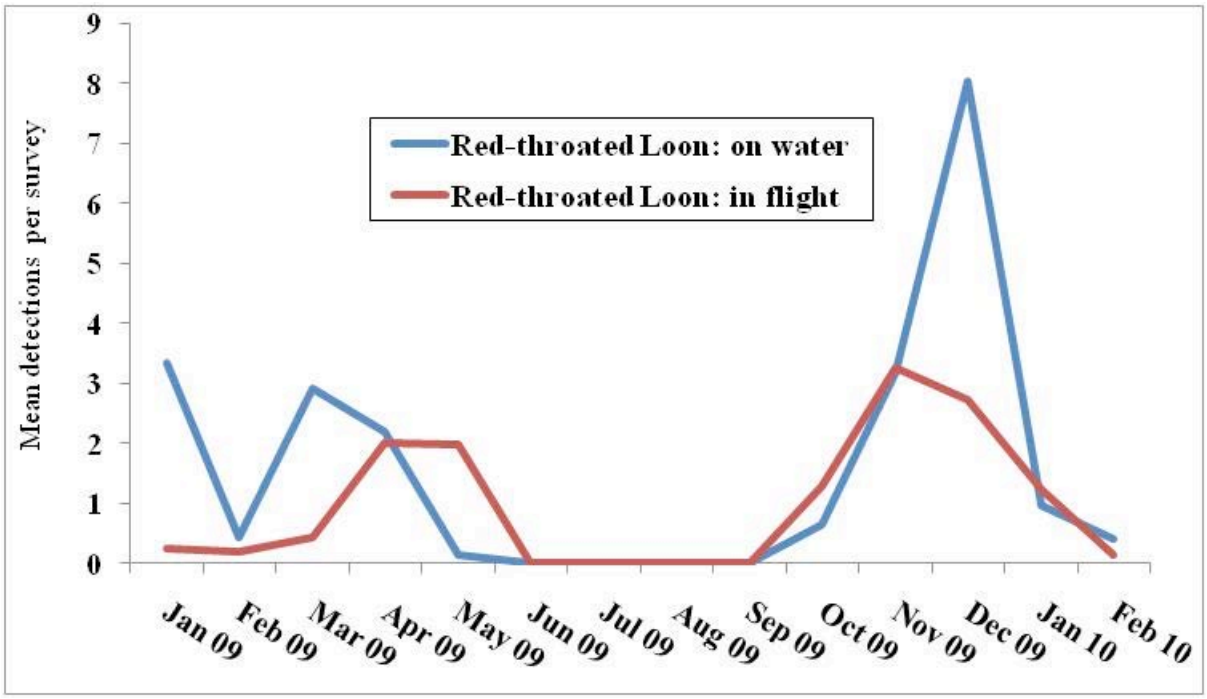

Fig. 37. Mean number of Red-throated Loons detected on the water and in flight (birds per hr) per survey per month at 11 land-based seawatch stations along the Rhode Island coastline

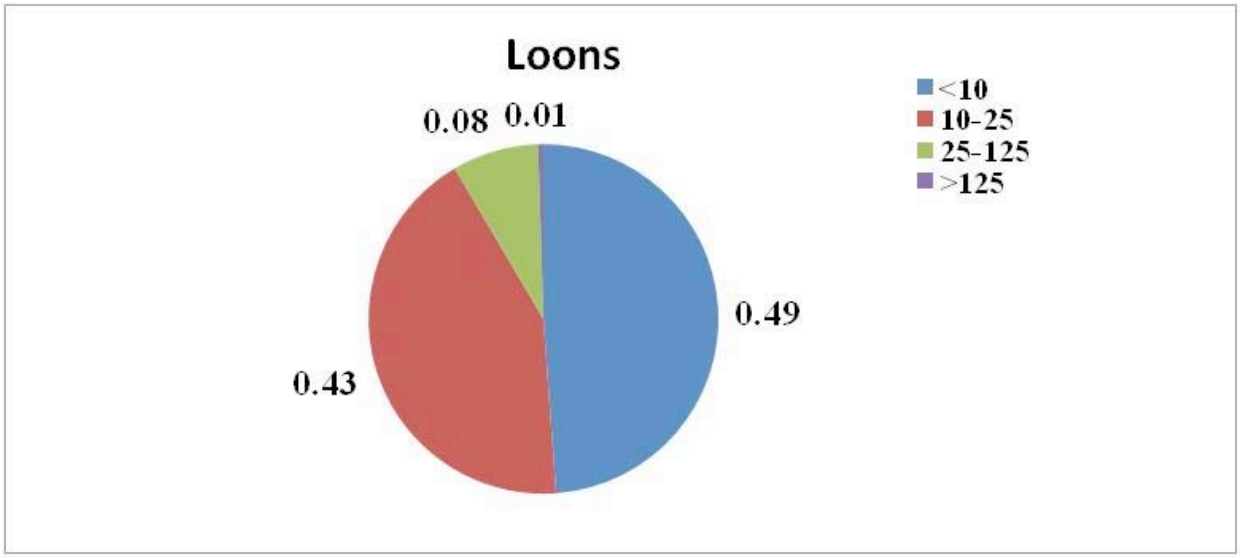

Fig. 38. Flight altitude of loons (m above sea level; N = 1,806 detections) based on visual estimates during land-based seawatches and ship-based line transects. Proportion of birds in four altitude categories is shown.

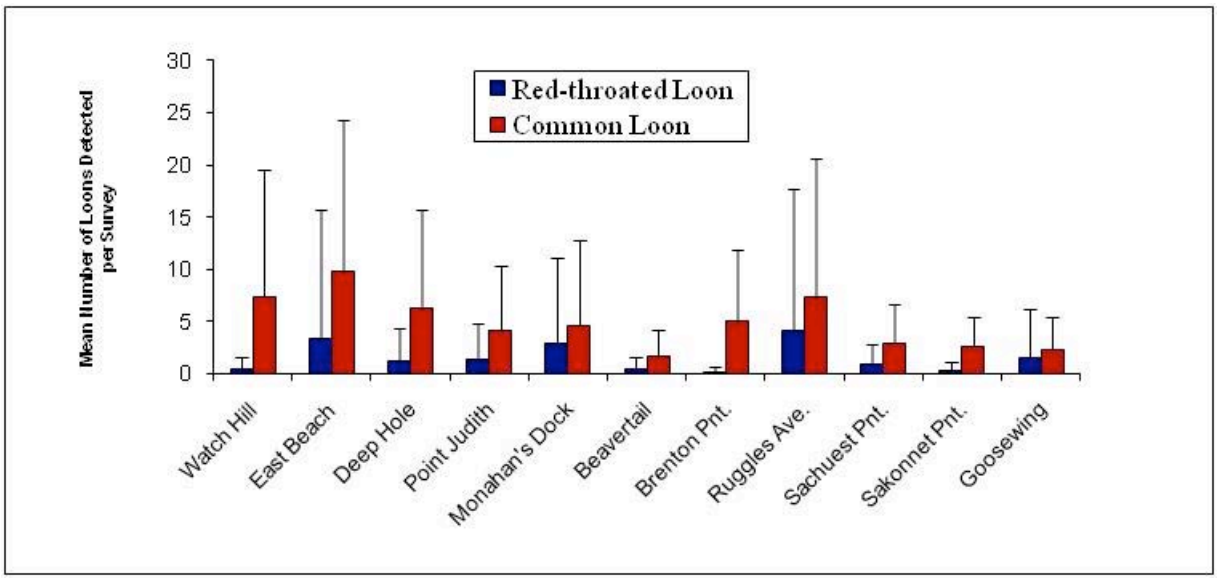

Fig. 39. Mean (SD) number of Common and Red-throated Loons detected per survey at 11 land-based seawatch stations (see Fig. 21 for locations of stations).

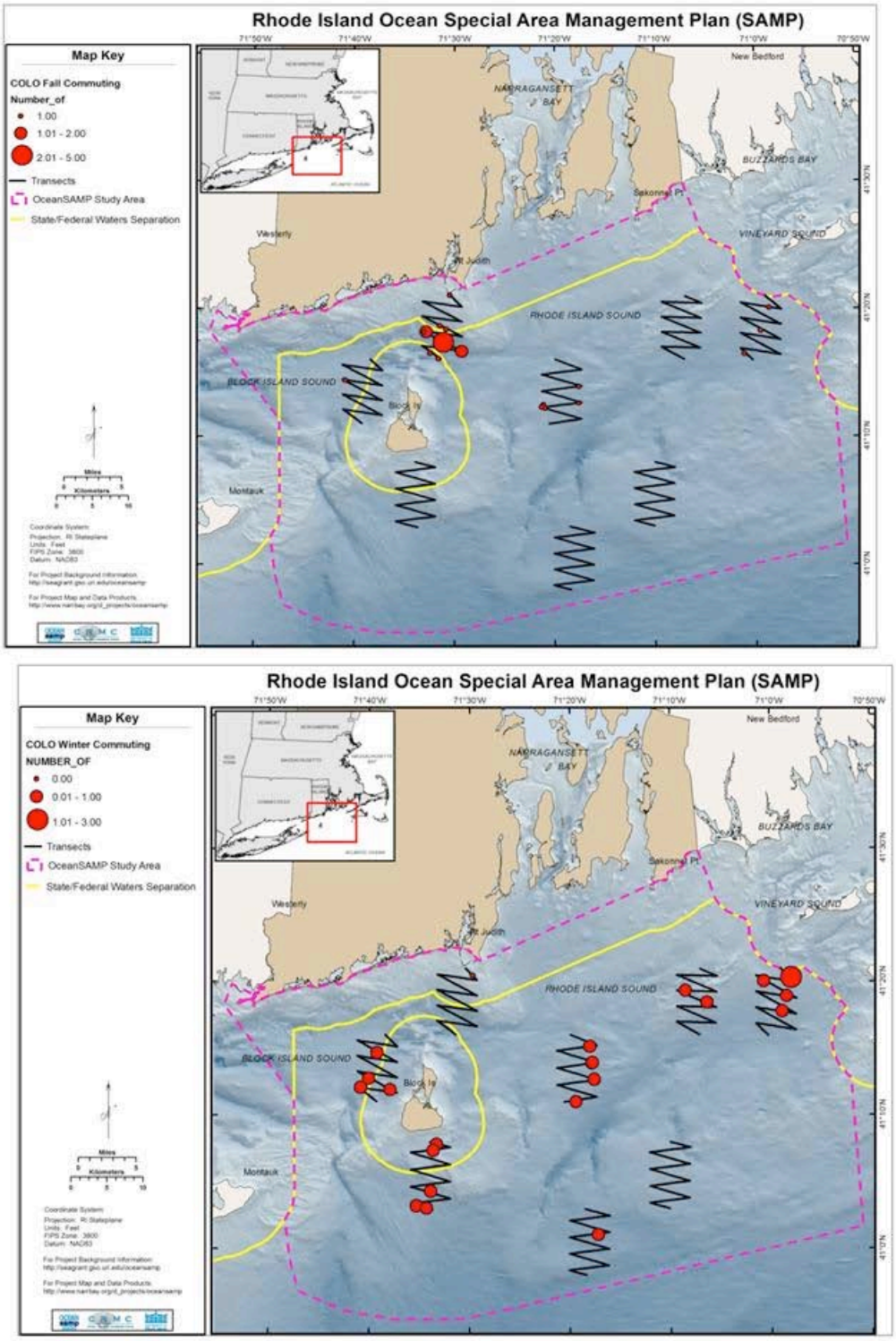

Fig. 40. Locations of Common Loons in flight in fall (upper) and winter (lower) in the Ocean SAMP study area during on ship-line transect surveys.

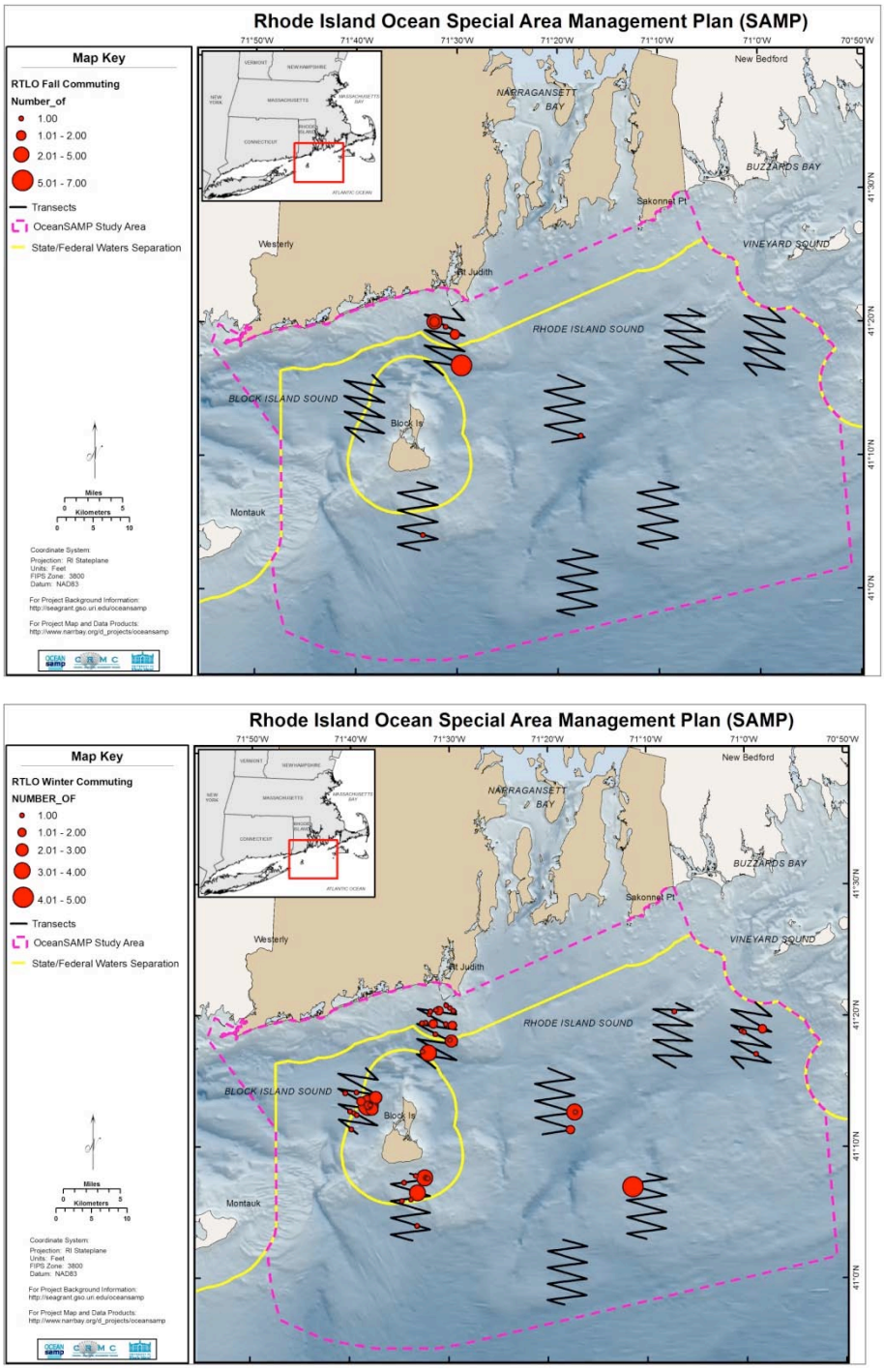

Fig. 41. Locations of Red-throated Loons in flight in fall (upper) and winter (lower) in the Ocean SAMP study area during on ship-line transect surveys.

Spatial patterns in abundance in nearshore and offshore waters – We present the detection function plot that was derived from the observed abundance of Common Loons on the water from ship-based surveys, and the associated GAM plot in Appendix J. The best-fit Density Surface Model (DSM) explained 21.5% of the spatial variation in observed abundance of Common Loons (see Appendix H for full model results). Common Loon densities during winter were highest closer to shore (densities of up to 5 loons per km^2), particularly along the northern edge of the Ocean SAMP study area, and in waters surrounding Block Island (Fig. 42). In addition, estimated densities during winter were relatively high in Block Island Sound between Block Island and Long Island. In contrast, estimated loon densities during winter were lower in the southern, central sections of Rhode Island Sound and all of the Inner Continental Shelf, where waters tend to be much deeper. However, there is less certainty about the density estimates in these southern sections of Rhode Island Sound during winter, where CVs for model density estimates were relatively high (Fig. 43). We were unable to model Common Loon densities in offshore areas during summer and fall due to low detection rates during ship-based line transects. We had too few detections of Red-throated Loons during ship-based line transects to model their density or spatial distribution. The literature, and our low detection rate for Red-throated Loons, suggests that Red-throated Loons are particularly sensitive to disturbance and appear to disperse from the ship's path before they can be detected.

Population size in the Ocean SAMP area - Based on the Common Loon DSM (Appendix H), we estimated that during the winter of 2009-2010, there were 2,901 Common Loons (95% CI = 2,525 to 3,321) in the Ocean SAMP study area (Appendix I). We provide no population estimate for Red-throated Loons because we detected too few during ship-based surveys for reliable DSM modeling. However, Red-throated loons were abundant at times in nearshore habitats, with an average of 3.1 individuals detected during land-based seawatches (Table 13). It is unknown what proportion of loons detected in offshore waters and recorded as "loon species" during aerial surveys were Red-throated Loons.

Spatial patterns in abundance in relation to bathymetry – The distribution and abundance of loons detected during aerial surveys were consistent with the estimated densities from the Common Loon DSM (Fig.44). Most observations of loons during aerial surveys were in nearshore habitats in Block Island Sound, at the northeast corner of the Ocean SAMP study area, south of Sakonnet Pt., and in nearshore waters south and southwest of Block Island. Based on locations where loons were detected during aerial surveys, loons were primarily found in areas where the water depth was < 35 m deep (Fig. 45).

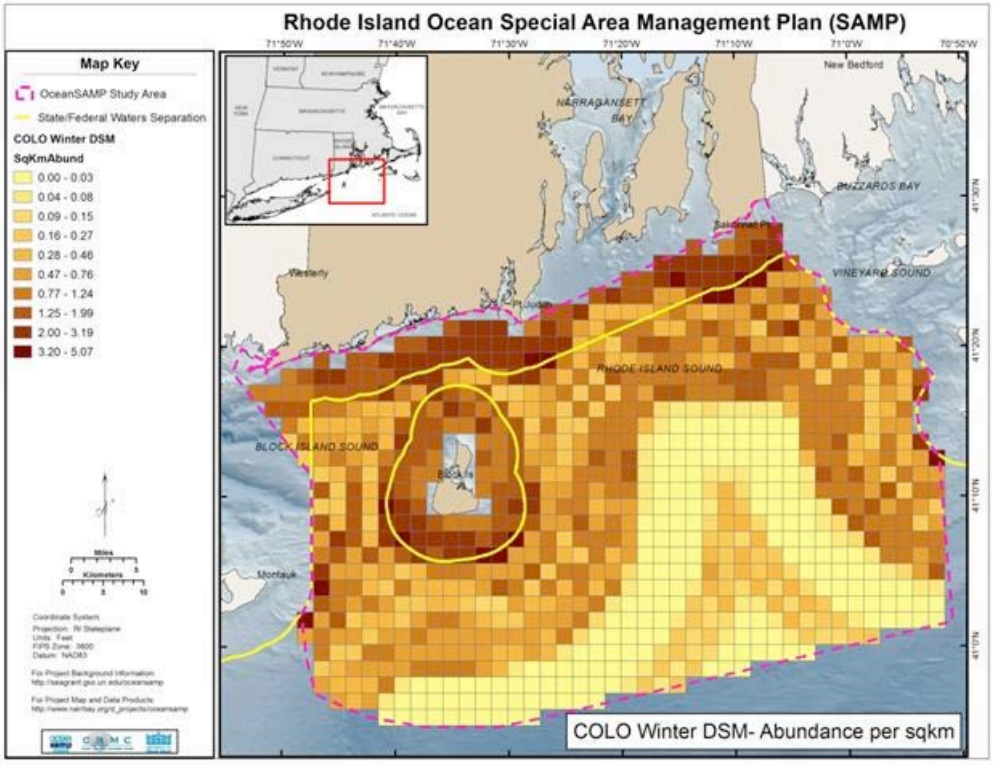

Fig. 42. DSM estimates of the spatial distribution and density of Common Loons in winter in the Ocean SAMP study area based on ship line-transect surveys. Densities were as great as 5 birds per km^2.

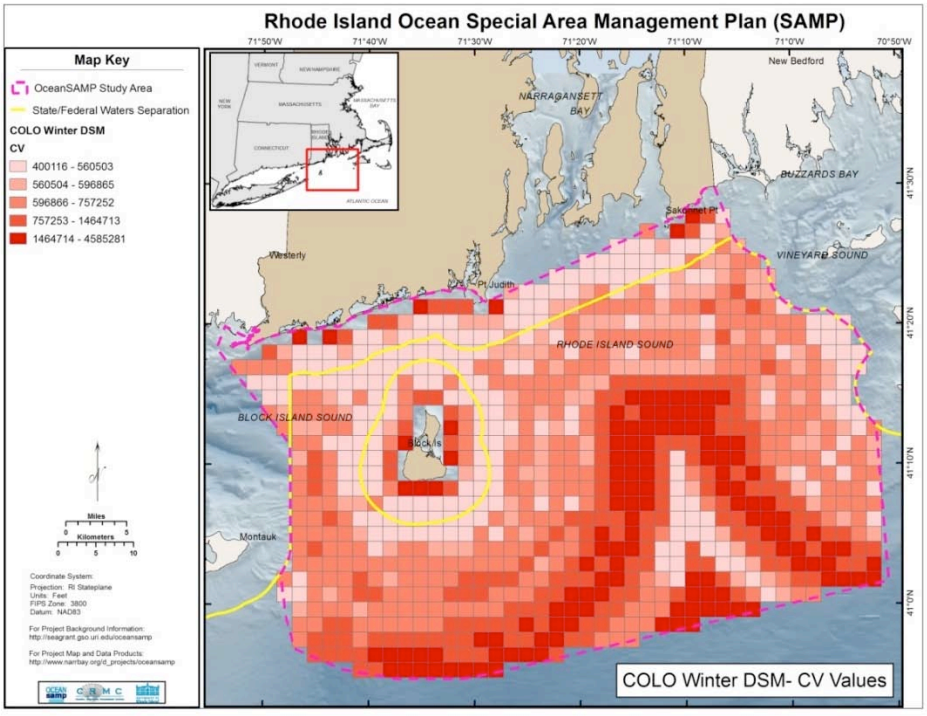

Fig. 43. Coefficient of Variation for DSM modeled loon density estimates based on ship line transect surveys shown in Fig. 43. Areas that are deeper red have less certainty in density estimates

.

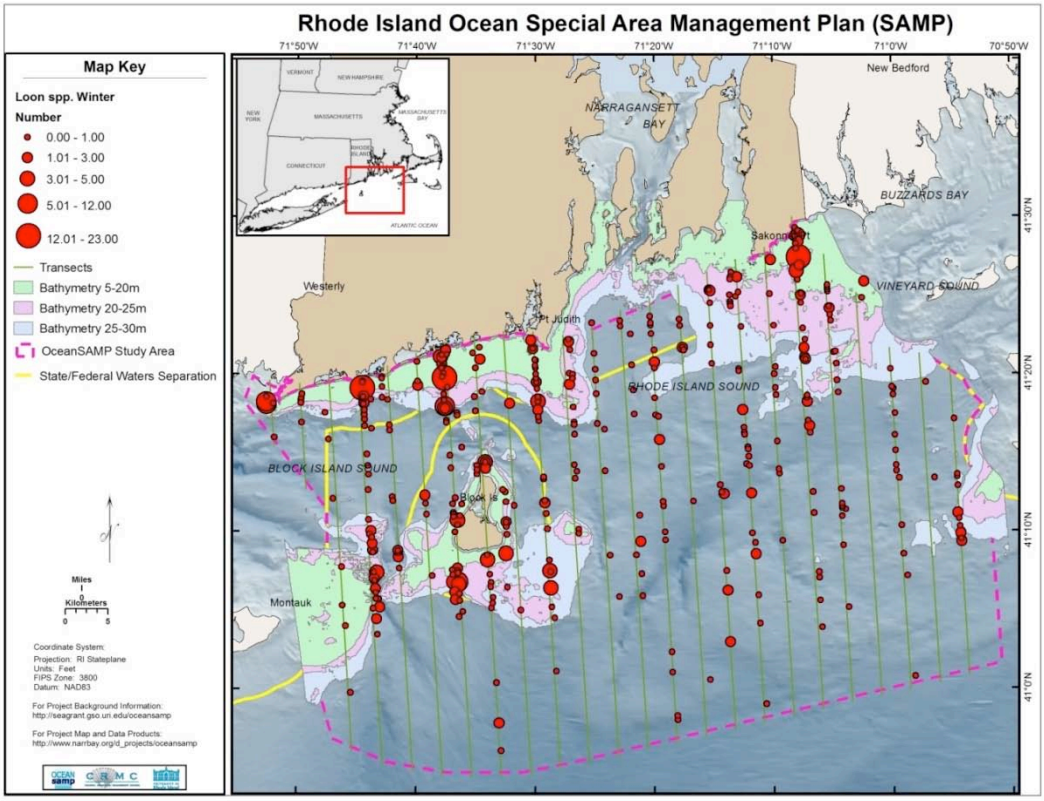

Fig. 44. Distribution of loons during aerial surveys in the winter of 2009-2010 in the Ocean SAMP study area.

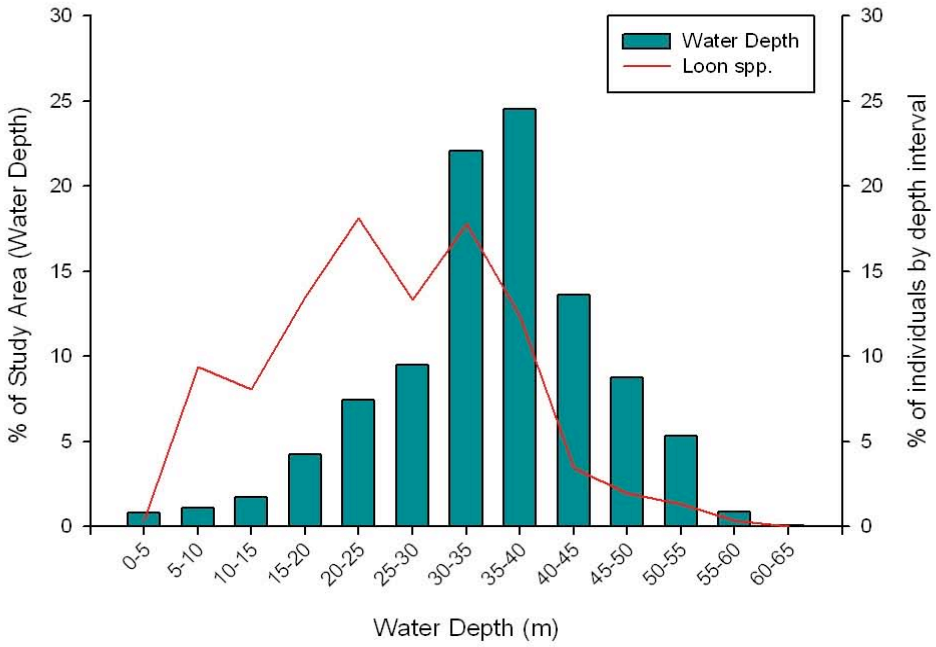

Fig. 45. Bathymetry of Ocean SAMP study area (green histogram) compared to depths where loons were detected during aerial surveys (red line)(Fig 44).

3.4 Grebes

We detected two species of grebes (Podicipedidae) in the Ocean SAMP study area: Horned Grebe and Red-necked Grebe. Horned Grebes are relatively common in small numbers in nearshore habitats, while Red-necked Grebes are also found in nearshore habitats but are relatively uncommon.

Seasonal changes in abundance - Both species of grebe occur in Rhode Island only during winter (Fig. 46) and then spend the breeding season north of Rhode Island. Peak abundance of Horned Grebes occurred in March indicating that birds wintering farther south migrate through Rhode Island waters during their spring migration to more northerly breeding lakes (Fig. 46, Appendices B and C).

Flight altitude of birds - Neither species of grebe were detected often in flight (Tables 15 and 19); however, those detected flying during daytime surveys were at altitudes <10 m (Fig. 47).

Spatial patterns in abundance in nearshore waters - Horned Grebes were relatively common at East Beach, Brenton Point, and Ruggles Ave., while Red-necked Grebes were seen more often at Pt. Judith and Sachuest Pt. (Fig. 48). See Appendices B and C for data on grebe abundance at each of the land-based seawatch stations for each month surveyed.

Spatial patterns in abundance in nearshore and offshore waters – We had too few detections of Horned and Red-necked Grebe during ship-based line transects to model their density or spatial distribution. However, a comparison of grebe detections during land-based versus ship-based surveys clearly shows that they almost exclusively were found in nearshore habitats. For example, Horned Grebes were never observed during offshore ship-based surveys (Table 17), and we detected only two Red-necked Grebes during offshore surveys (Table 17).

Population size in the Ocean SAMP area - We had too few detections of grebes during ship-based line transects in all seasons to estimate their population size in the study area.

Spatial patterns in abundance in relation to bathymetry – We did not detect grebes during winter aerial surveys, thus we did not explore grebe abundance in relation to water depth in the Ocean SAMP study area. During land-based seawatches, grebes were detected in waters <20 m deep.

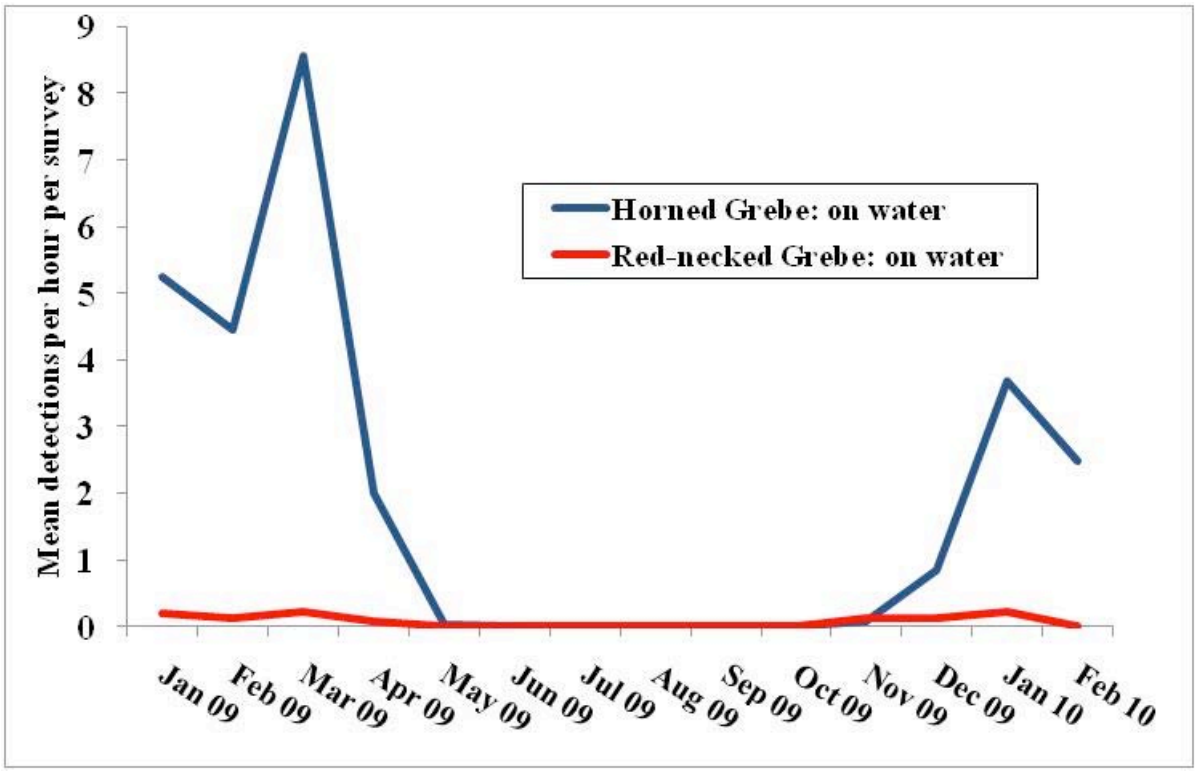

Fig. 46. Mean number of Horned and Red-necked Grebes detected on the water per survey per month at 11 land-based seawatch stations along the Rhode Island coastline.

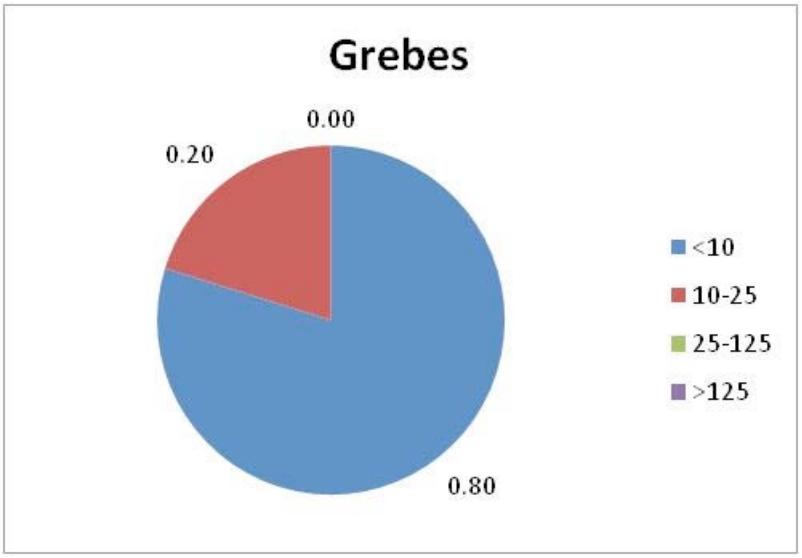

Fig. 47. Flight altitude of grebes (m above sea level; N = 109 detections) based estimates during land-based seawatches and ship-based line transects. Shown are proportion of birds in four altitude categories.

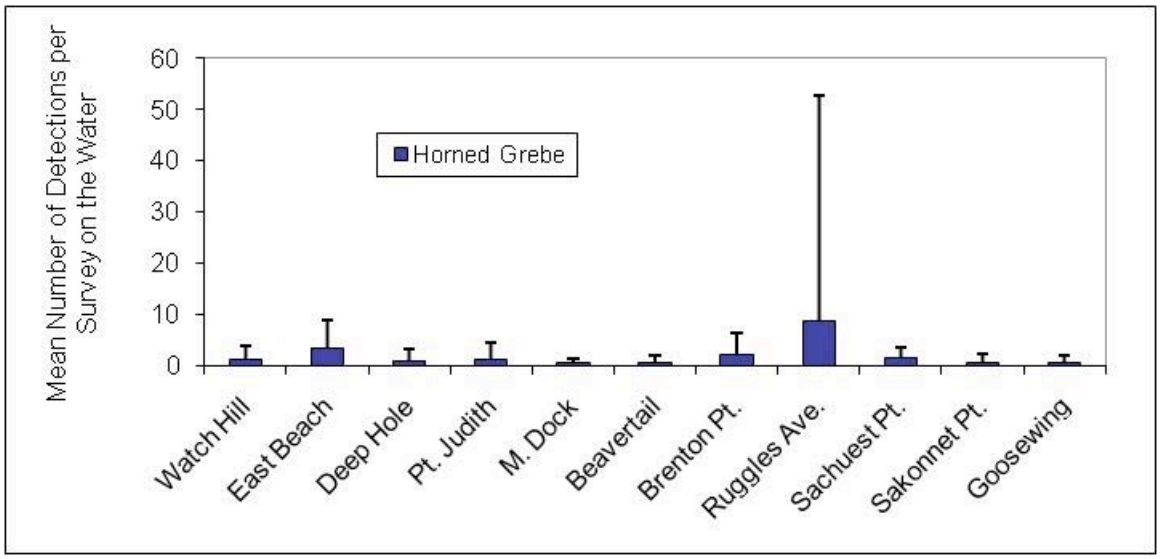

Fig. 48. Mean (SD) number of Horned Grebes detected per survey at 11 land-based seawatch stations (see Fig. 21 for locations of stations).

3.5 Shearwaters

We detected four species of shearwaters (Procellariidae) in the Ocean SAMP study area: Manx, Cory's, Greater, and Sooty Shearwater. Cory's Shearwater and Greater Shearwater are seasonally abundant and the most common species of shearwater in the SAMP study area, with Manx and Sooty Shearwaters relatively common but found in relatively low numbers.

Seasonal changes in abundance – Shearwaters are pelagic species that are found in the Ocean SAMP area during the summer months (Appendices B and C). During land-based surveys, Cory's Shearwater, was detected only during mid-summer during land-based surveys (July; Fig. 49). Greater, Cory's, and Sooty Shearwaters breed in the southern hemisphere and so reside in Rhode Island waters during the nonbreeding "winter" period of their annual cycle.

Flight altitude of birds - Shearwaters are almost always observed flying low over the water as they take advantage of small wind currents near the ocean surface to efficiently search for food near the ocean surface. All shearwaters that we observed flew at altitudes of <10 m (N = 665 detections).

Spatial patterns in abundance in nearshore waters – Cory's Shearwater the only species of shearwater that were detected regularly during land-based seawatches (>2400 detections; Table 13), where they were most common at East Beach, Deep Hole, Brenton Pt. and Ruggles Ave (Fig. 50). Greater (14 detections), Sooty (7 detections), and Manx Shearwaters (five detections) were rarely detected during land-based seawatches (Table 13). See Appendices B and C for

data on shearwater abundance at each of the land-based seawatch stations for each month surveyed.

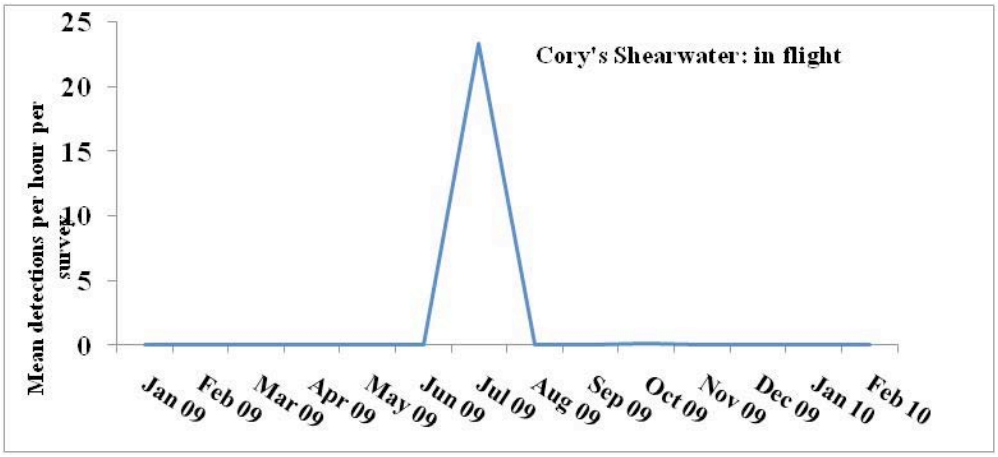

Fig. 49. Mean number of Cory's Shearwaters detected in flight per survey per month at 11 land-based seawatch stations along the Rhode Island coastline

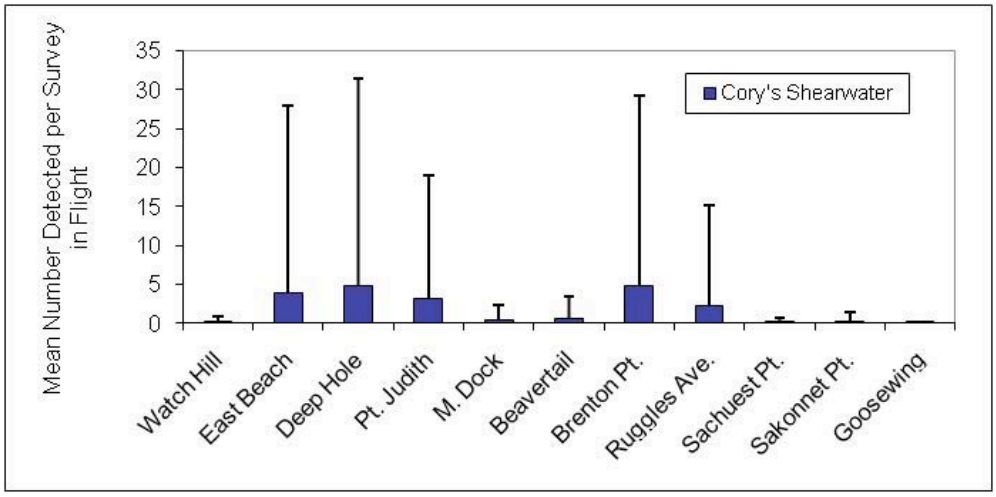

Fig. 50. Mean (SD) number of Cory's Shearwaters detected per survey at 11 land-based seawatch stations (see Fig. 21 for locations of stations).

Spatial patterns in abundance in nearshore and offshore waters –The best-fit Density Surface Model (DSM) for Cory's and Greater Shearwaters in summer explained 26.3% and 50.8% of the spatial variation in observed abundance, respectively (Appendix H for full model results). Cory's Shearwater density during summer was lowest in nearshore areas at the north end of the Ocean SAMP area and highest in south, central Rhode Island Sound and the Inner Continental Shelf (Fig. 51). In general, the spatial distribution of Greater Shearwater during summer was similar to that for Cory's Shearwater, although Greater Shearwater was less common closer to the coast than Cory's Shearwater (Fig. 51). Cory's Shearwater densities (over 5 detections per

km^2) were on average higher than Greater Shearwater peak densities (2.5 detections per km^2; Fig. 51). The greatest uncertainty in shearwater density estimates occurred in the southern, central sections of Rhode Island Sound and the Inner Continental Shelf (Fig. 52).

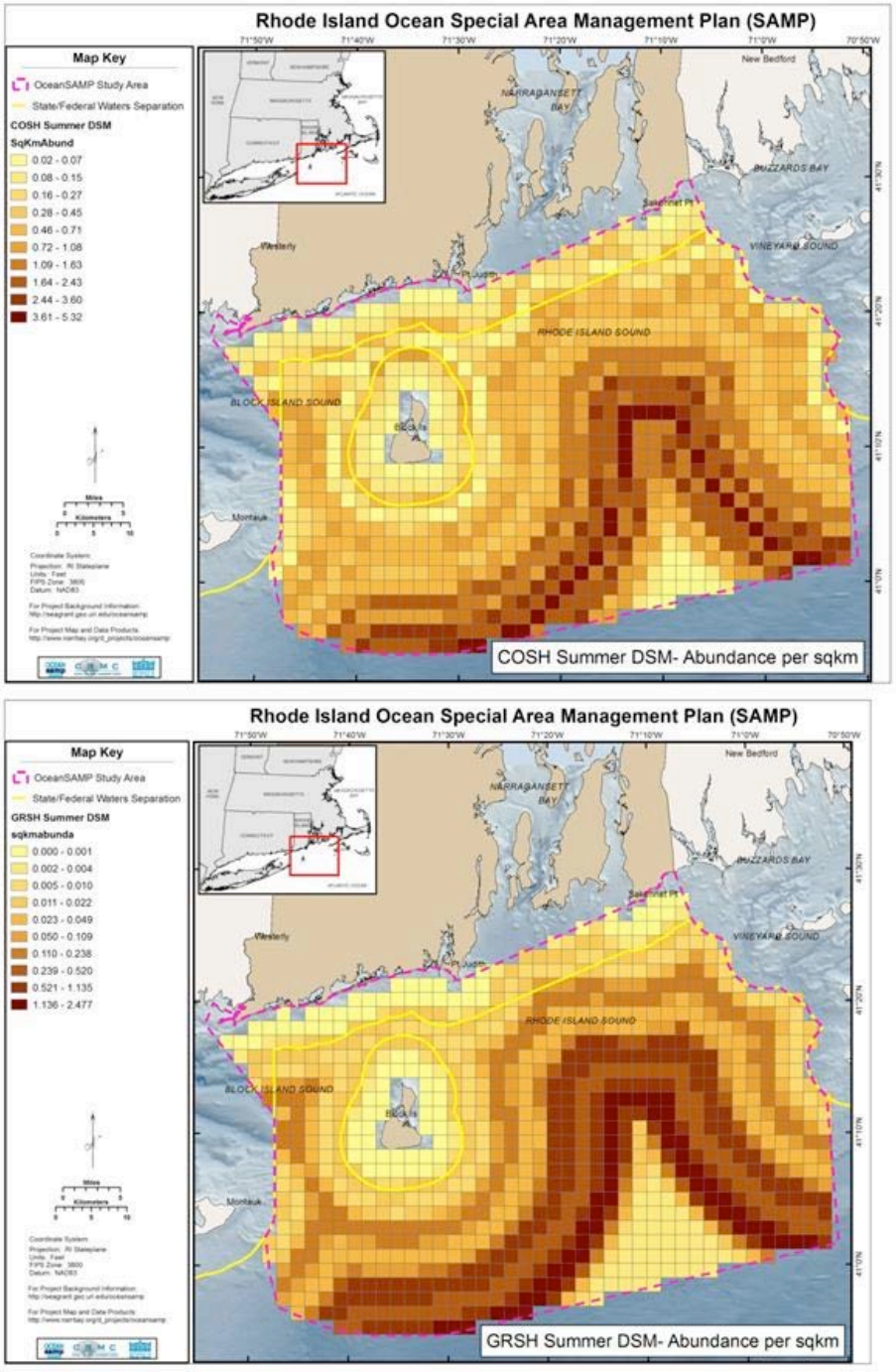

Fig. 51. DSM estimates of the spatial distribution and density of Cory's Shearwaters (upper) and Greater Shearwater (lower) in summer in the Ocean SAMP study area based on ship line-transect surveys.

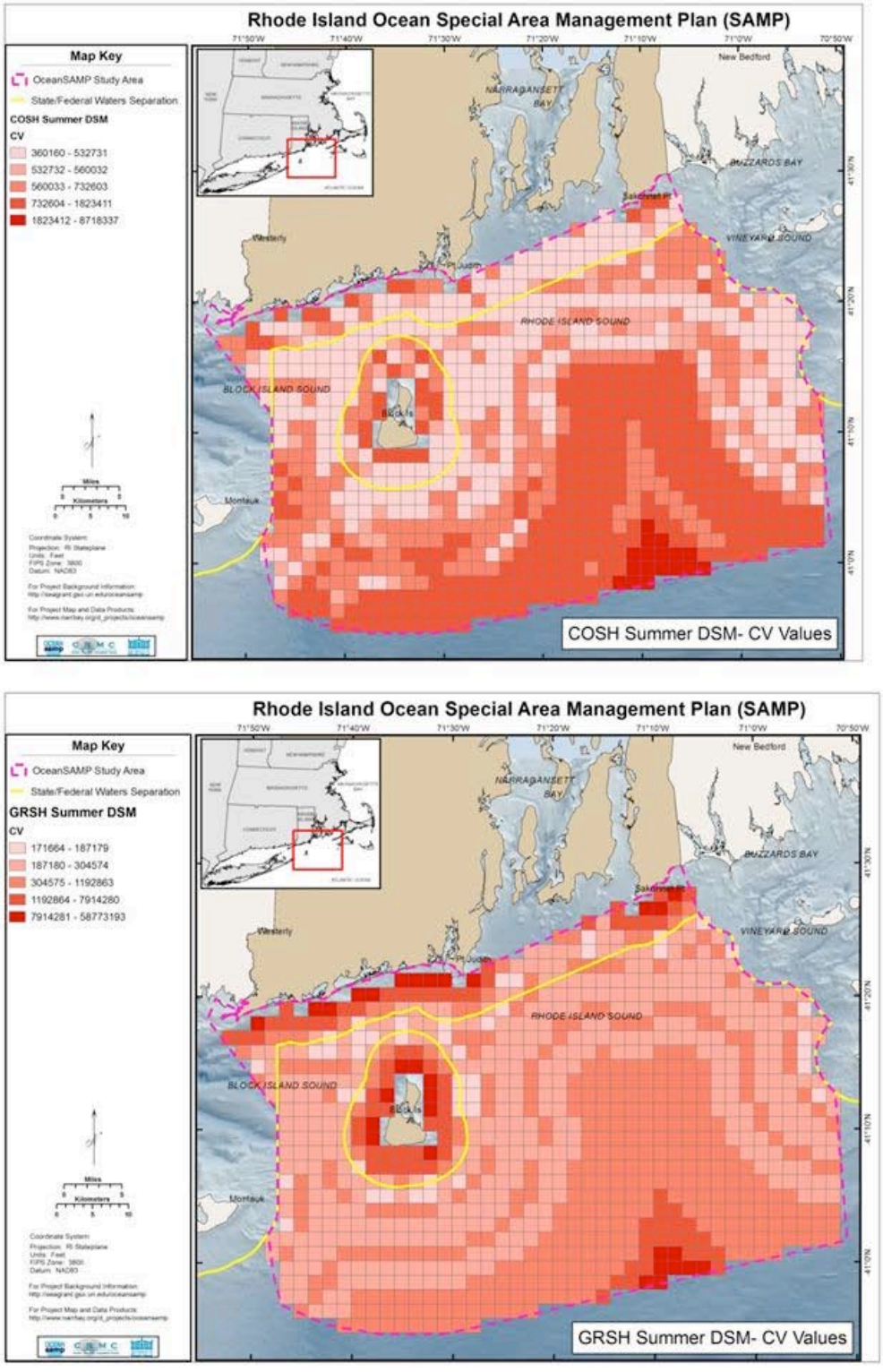

Fig. 52. Coefficient of Variation for DSM modeled density estimates for Cory's Shearwater (upper) and Greater Shearwater (lower) based on ship line transect surveys shown in Fig. 51.

Population size in the Ocean SAMP area – Based on the DSM models (Appendix H), we estimated that during summer 2009 there were 2,643 (95% CI: 1,979 to 3,530) Cory's Shearwaters and 3,350 (95% CI: 3,005 to 3,712) Greater Shearwaters in the Ocean SAMP study area (Appendix I). This is a conservative estimate of shearwater population for both species because it assumes no turnover of individuals. However, shearwaters travel great distances as they move from their southern hemisphere breeding areas to northern hemisphere nonbreeding areas including the Rhode Island Ocean SAMP study area. Thus, these population estimates likely greatly underestimate the actual number of shearwaters that inhabit the study area from June to August.

3.6 Storm-petrels

We detected two species of storm-petrels (Hydrobatidae) in the Ocean SAMP area, Wilson's Storm-Petrel and Leach's Storm-Petrel. Wilson's Storm-Petrels are common and seasonally abundant in the SAMP study area, while Leach's Storm-Petrels are uncommon. Wilson's Storm-Petrels breed in the southern hemisphere and so reside in Rhode Island waters during the nonbreeding "winter" period of their annual cycle.

Seasonal changes in abundance – Storm-petrels are pelagic species that are most common in the Ocean SAMP area during the summer months (Fig. 53).

Flight altitude of birds - Storm-Petrels are like shearwaters in that they are almost always observed flying low over the water as they take advantage of small wind currents near the ocean surface to efficiently search for food near the ocean surface. All storm-petrels were detected in flight and always at altitudes <10 m during land-based seawatches and ship-based surveys (N = 2,001 detections; Tables 15 and 19).

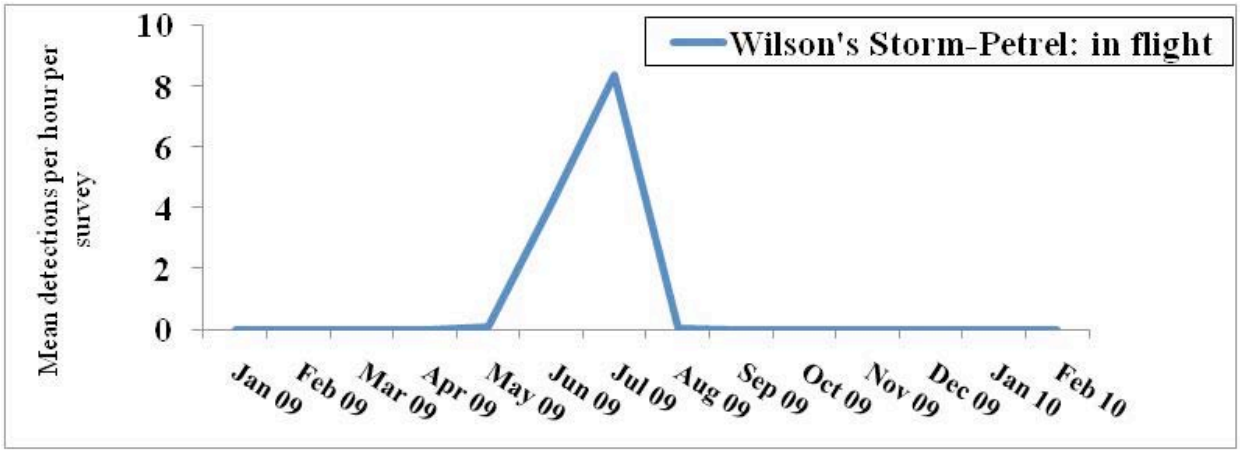

Fig. 53. Mean number of Wilson's Storm-Petrels detected in flight per survey per month at 11 land-based seawatch stations along the Rhode Island coastline

Spatial patterns in abundance in nearshore waters – We detected Wilson's Storm-Petrels from seawatch stations on both Block Island and Rhode Island Sound, with concentrations at East Beach, Deep Hole, and Pt. Judith (Fig. 54). In contrast, Leach's Storm-Petrels were only detected once during land-based seawatches, at Deep Hole (Table 13). See Appendices B and C for data on storm-petrel abundance at each of the land-based seawatch stations for each month surveyed.

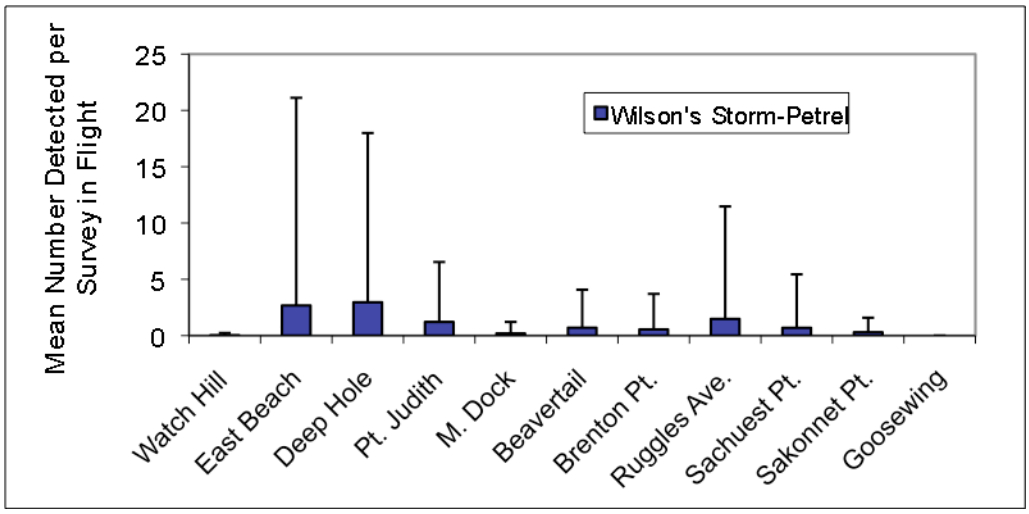

Fig. 54. Mean (SD) number of Wilson's Storm-Petrels detected per survey at 11 land-based seawatch stations (see Fig. 21 for locations of stations).

Spatial patterns in abundance in nearshore and offshore waters – We present the GAM plot that was derived from the observed abundance of Wilson's Storm -Petrels in flight from ship-based surveys during summer in Appendix J. The best-fit Density Surface Model (DSM) explained 33.5% of the spatial variation in observed abundance of Wilson's Storm Petrels in summer (see Appendix H for full model results). Wilson's Storm-Petrel density during summer was unique compared to other species (e.g., shearwater spp.) in that they were relatively abundant in a band about 3 miles offshore in Block Island Sound and Rhode Island Sound and were most densely concentrated over the Inner Continental Shelf (22 individuals per km^2; Fig. 55). The greatest uncertainty in Wilson's Storm Petrel density estimates occurred along the southern boundary of Rhode Island Sound and along the moderately deep sections of the Inner Continental Shelf (Fig. 56).

Population size in the Ocean SAMP area – Based on the DSM models (Appendix H), we estimated that during summer 2009 there were 16,335 (95% CI: 10,879 to 24,527) Wilson's Storm-Petrels in the Ocean SAMP study area (Appendix I), which made this species among the most abundant in offshore waters of the Ocean SAMP study area. This is a conservative estimate of Wilson's Storm-Petrel population because it assumes minimal turnover of

individuals. However, Wilson's Storm-Petrel travel great distances as they move from their southern hemisphere breeding areas to northern hemisphere nonbreeding areas including the Rhode Island Ocean SAMP study area. Thus, this population estimate likely greatly underestimates the actual number of Wilson's Storm-Petrel that inhabit the study area from June to August.

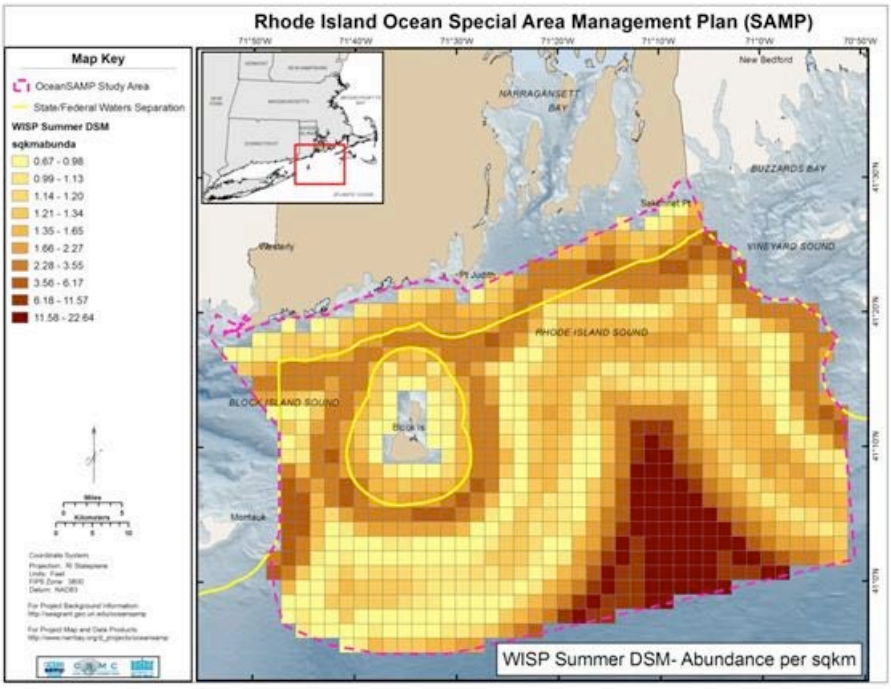

Fig. 55. DSM estimates of the spatial distribution and density of Wilson's Storm-Petrels in summer in the Ocean SAMP study area based on ship line-transect surveys.

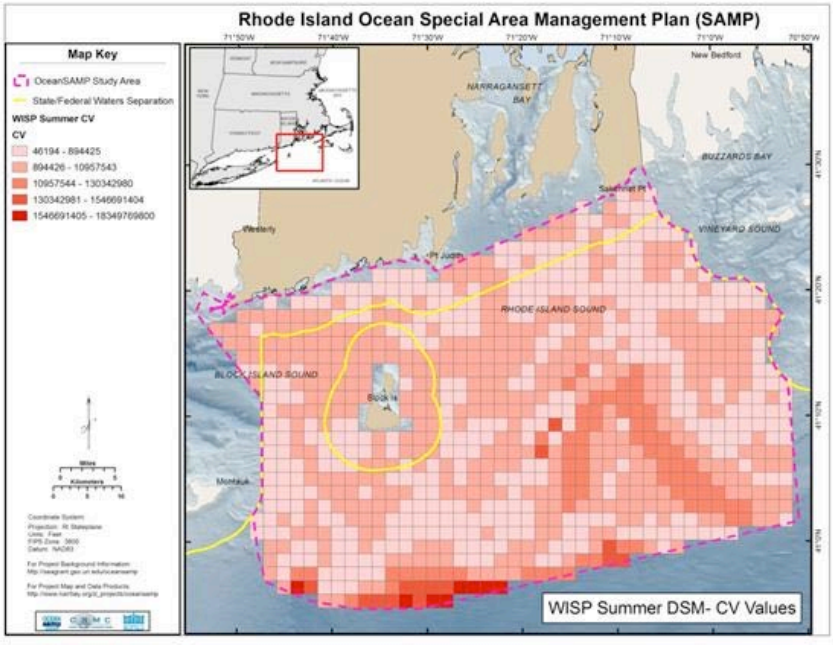

Fig. 56. Coefficient of Variation for Wilson's Storm-Petrel density estimates based on ship line transect surveys shown in Fig. 55.

Spatial patterns in abundance in relation to bathymetry – We did not detect storm-petrels during aerial surveys because flights were conducted too late in the season for storm-petrels. Thus, in our final report produced during 2011, we will estimate a bathymetric profile for storm-petrels as we did for other taxa.

3.7 Gannets

Northern Gannets are the only member of the family Sulidae that are found in the SAMP area. Northern Gannets are common and seasonally abundant during migration from their breeding grounds in Canada to wintering areas along the southern Atlantic Coast and into the Gulf of Mexico (Sibley 2000).

Seasonal changes in abundance – Northern Gannets are a common migrant and winter resident in nearshore and offshore waters of the Ocean SAMP area. Peak passage rates in the spring occur during April and May, whereas gannets during fall migration are most abundant in November and December (Fig. 57).

Flight altitude of birds – Gannets observed during land-based and ship-based surveys flew at a broad range of altitudes in part because they plunge-dive from an altitude of 10-40 m for fish that can be up to 20 m below the ocean surface . Most flying birds (54%) were at altitudes <10 m, with 36% flying between 10-25 m altitude, and 10% between 25-125 m (Fig. 58).

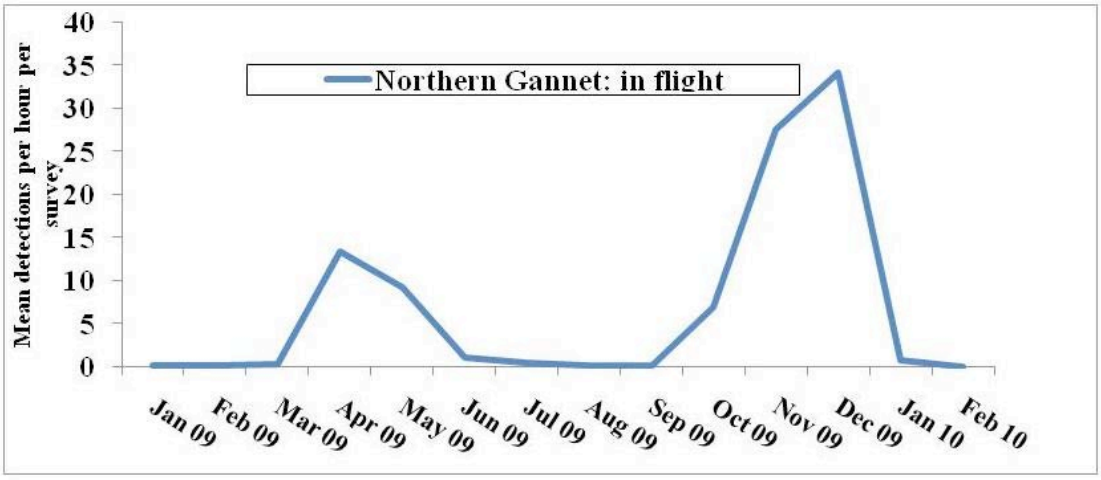

Fig. 57. Mean number of Northern Gannets detected in flight per survey per month at 11 land-based seawatch stations along the Rhode Island coastline.

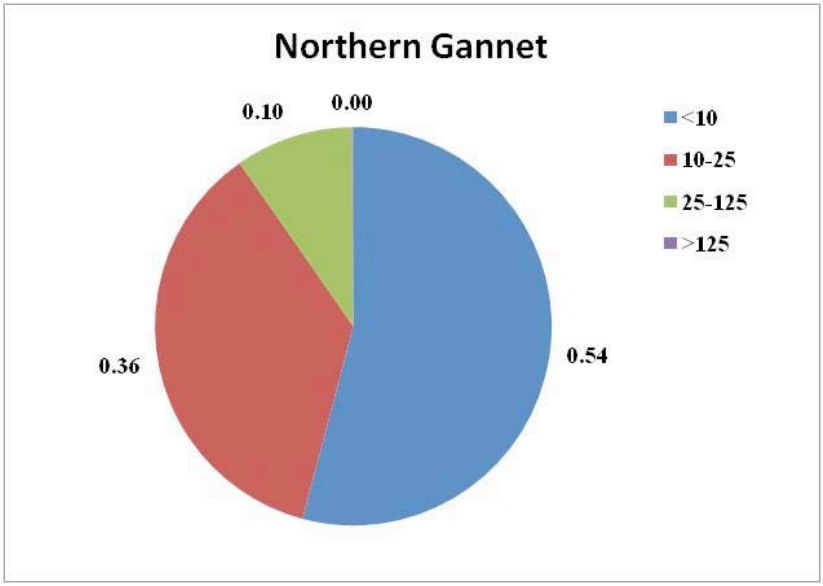

Fig. 58. Flight altitude of Northern Gannets (m above sea level: N = 9724) based estimates during land-based seawatches and ship-based line transects. Shown are proportion of birds in four altitude categories.

Spatial patterns in abundance in nearshore waters - In nearshore areas, gannets were common in Block Island Sound and Rhode Island Sound, with the greatest detection rates at Pt. Judith (Fig. 59). See Appendices B and C for data on Northern Gannet abundance at each of the land-based seawatch stations for each month surveyed.

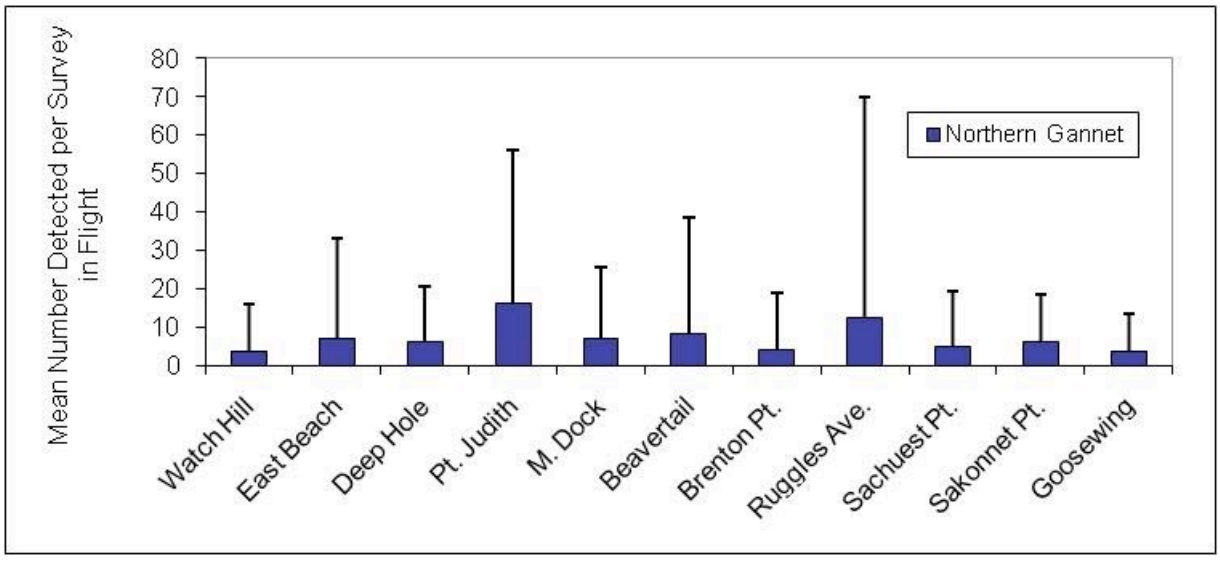

Fig. 59. Mean (SD) number of Northern Gannets detected per survey at 11 land-based seawatch stations (see Fig. 21 for locations of stations).

Spatial patterns in abundance in nearshore and offshore waters – We present the GAM plot that was derived from the observed abundance of Northern Gannets in flight from ship-based surveys during fall and winter in Appendix J. The best-fit Density Surface Models (DSM) for fall and winter explained 34.8% and 36.6% of the spatial variation, respectively (see Appendix H for full model results). Northern Gannet densities during fall were highest about 4 km off the south shore of mainland Rhode Island and around Block Island, as well as from the edge of Block Canyon extending SW to the Inner Continental Shelf (Fig. 60). Spatial patterns of gannet densities during the winter were generally similar to that during fall, although gannets were on average higher in density during winter (up to 51 birds per km^2 in winter and 33 birds per km^2 in fall; Fig. 60). The greatest uncertainty in gannet density estimates occurred along coast and in deeper sections of Rhode Island Sound in the fall and in a band of center of Rhode Island Sound in the winter (Fig. 61).

Population size in the Ocean SAMP area – Based on the Northern Gannett DSM (Appendix H), we estimated that during the fall there were 3,987 (95% CI = 3,336 to 4,764) Northern Gannets and during winter there were 4,373 (3,688 to 5,187) Northern Gannets within the Ocean SAMP area (Appendix I). In North America, gannets breed in only six colonies, three in the Gulf of St. Lawrence and three off of Newfoundland, with birds wintering as far south as Florida and into the Gulf of Mexico. Thus, these population estimates are likely conservative because it assumes minimal turnover of individuals and we know gannets migrate through Rhode Island waters during both spring and fall.

Spatial patterns in abundance in relation to bathymetry – The distribution and abundance of gannets detected during aerial surveys were generally consistent with the estimated densities from the Northern Gannet DSM (Fig. 62). During aerial surveys it was obvious that Northern Gannet distribution was often associated with commercial fishing boats, and we often observed Gannets plunge-diving for fish bycatch by trawlers (K. Winiarski, pers. obs.). The depth profile of gannets was similar to the depth profile of the study area, with peak abundance in ocean waters that were 30-45 m deep (Fig. 63).

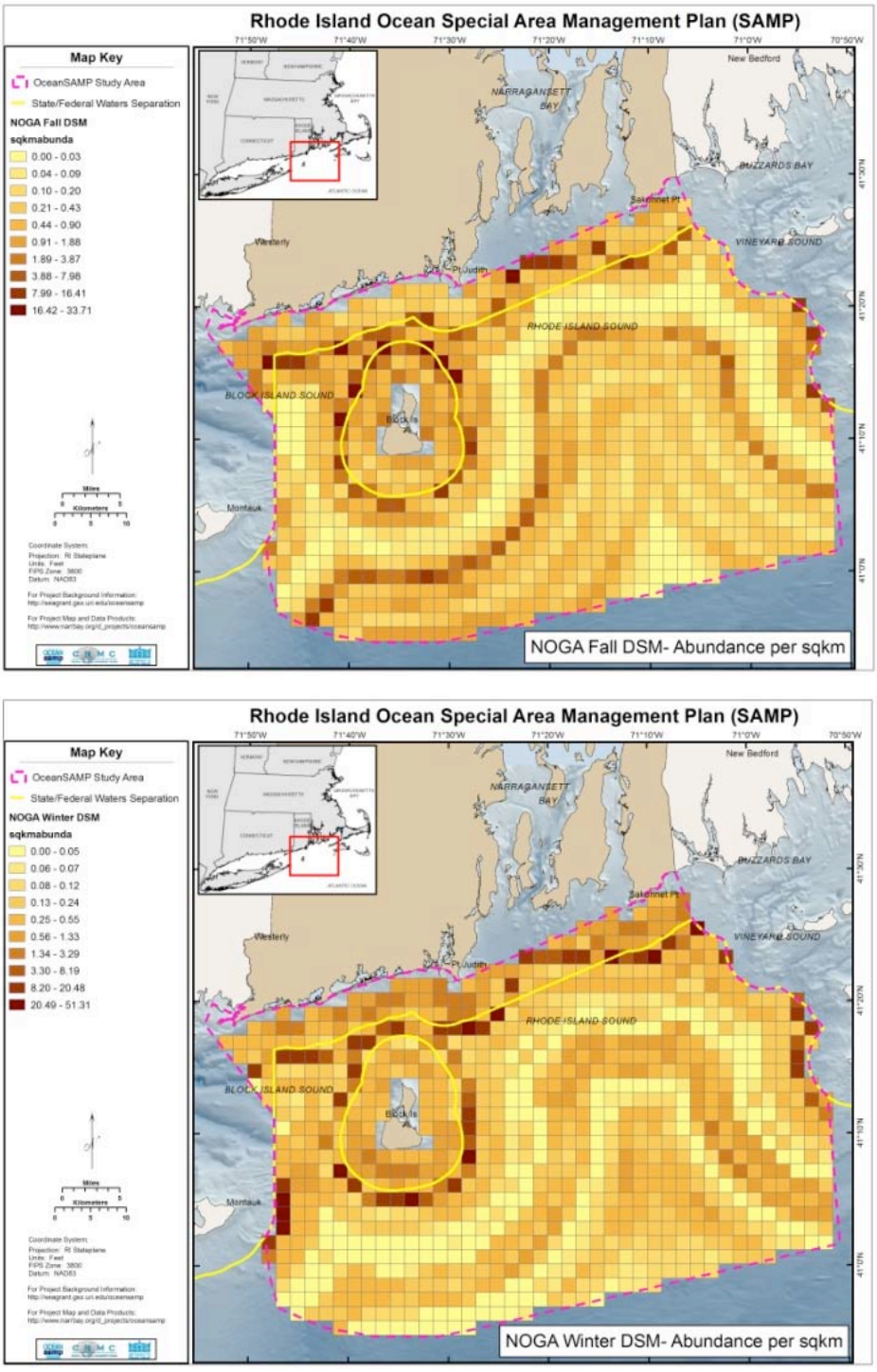

Fig. 60. DSM estimates of the spatial distribution and density of Northern Gannets in fall (upper) and winter (lower) in the Ocean SAMP study area based on ship line-transect surveys.

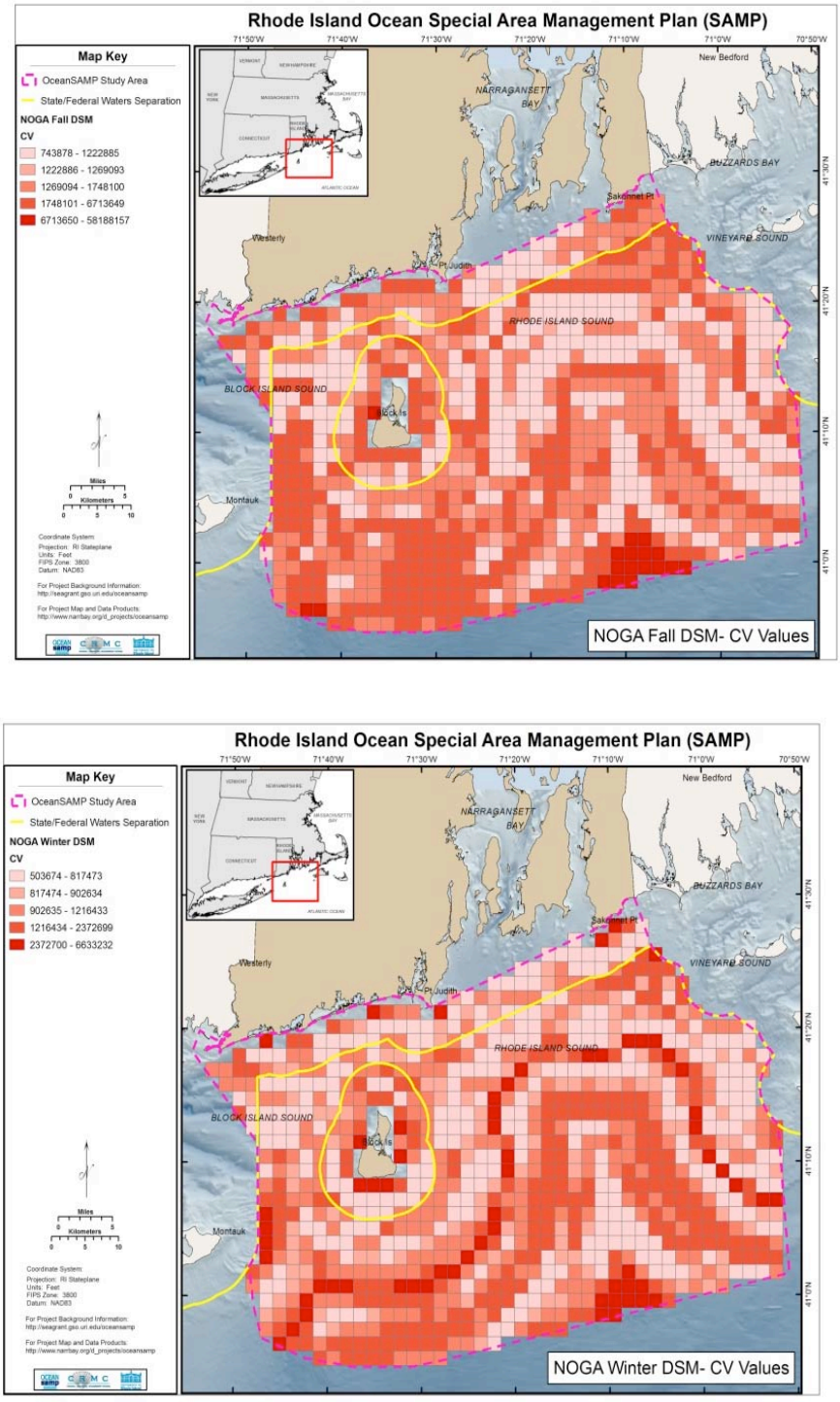

Fig. 61. Coefficient of Variation for DSM modeled gannet density estimates based on ship line transect surveys in fall (upper) and winter (lower) shown in Fig. 60.

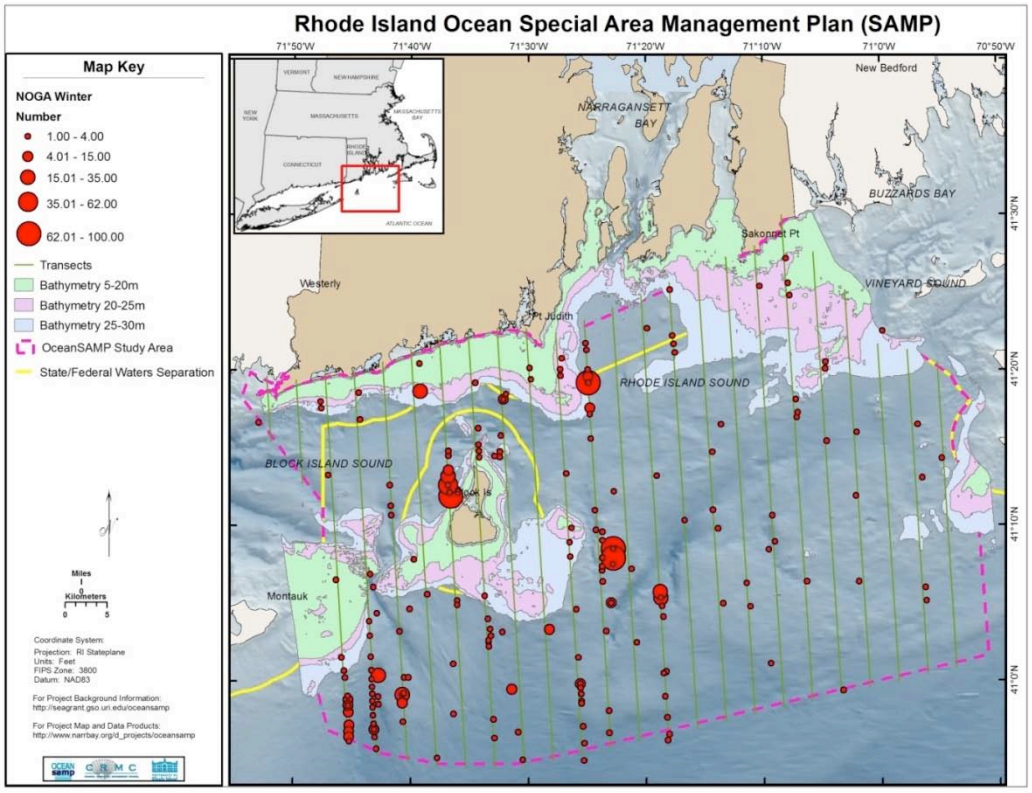

Fig. 62. Distribution of Northern Gannet flocks during aerial surveys in winter 2009-10. Large flocks were often trailing commercial fishing vessels.

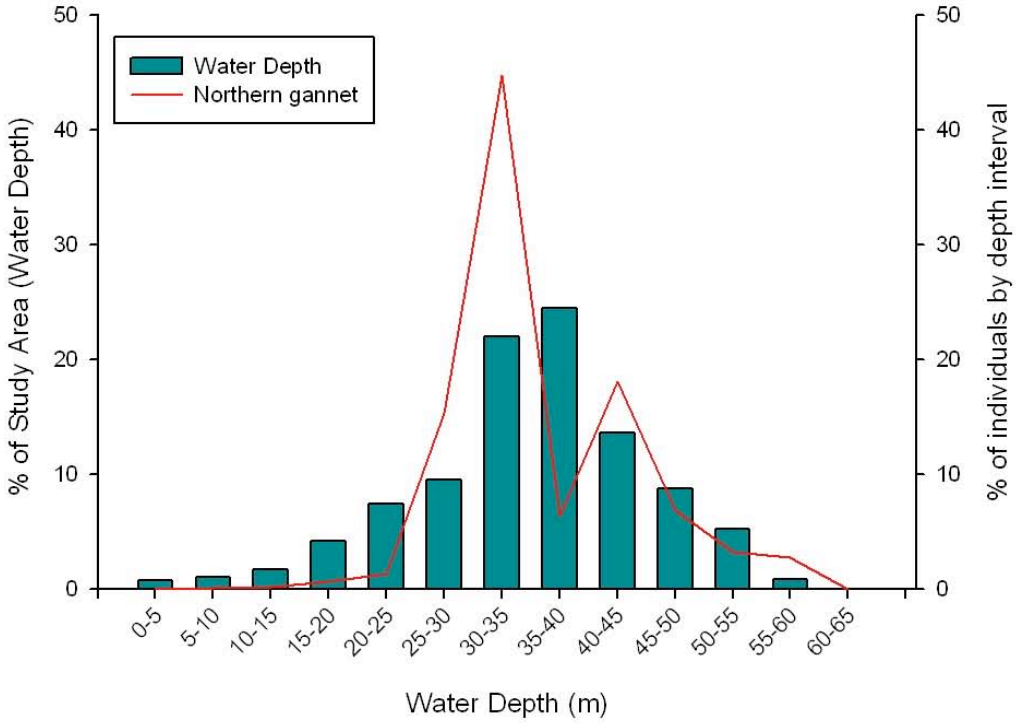

Fig. 63. Bathymetry of Ocean SAMP study area (green histogram) compared to depths where gannets were detected during aerial surveys (red line) (Fig. 62)

3.8 Cormorants

We detected two species of cormorants (Phalacrocoracidae) in the Ocean SAMP study area: Double-crested Cormorant and Great Cormorant. Double-crested Cormorants were the most abundant species of cormorant in the Ocean SAMP area, and this species had 10 times more detections than Great Cormorants during land-based seawatches; >25,000 detections vs. >2,200 detections, respectively (Table 13).

Seasonal changes in abundance - Cormorants are breeders, winter residents and migrants in the Ocean SAMP area. Around 2,000 pairs of Double-crested Cormorants nest on islands in Narragansett Bay (C. Raithel, unpublished data 2009; Ferren and Myers 1998). Hence, they occur in large numbers in the Ocean SAMP area from April through October (Fig. 64). Double-crested Cormorants migrate through Rhode Island waters during their fall migration mostly in September and October, and then peak again in May and June during spring migration (Fig. 64). Great Cormorants breed in a few colonies from Maine to Greenland, and only spend the winter months (Nov through March) in the Ocean SAMP study area (Fig. 64). Great Cormorants migrate winter in Rhode Island from November through March, with a possible peak influx of birds into the region in December (Fig. 64).

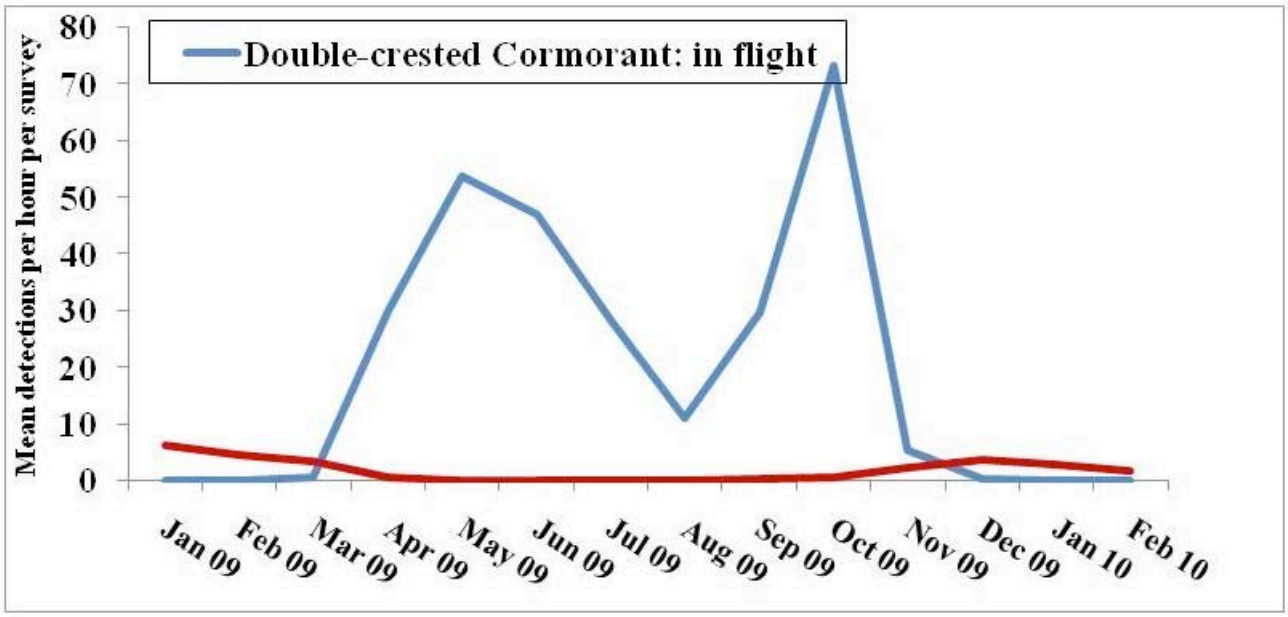

Fig. 64. Mean number of Double-crested and Great Cormorants detected in flight per survey per month at 11 land-based seawatch stations along the Rhode Island coastline

Flight altitude of birds - Flight altitudes of cormorants were variable. In the majority of our observations, cormorants were flying at <10 m altitude (81% of observations; Fig. 65). Of the birds flying higher than 10 m, approximately equal percentages were flying between 10-25 m (10%), and 25-125 m (8%) elevation, while about 1% were flying over 125 m in altitude. Birds flying this high were generally migratory flocks of Double-crested Cormorants flying near the mainland coast.

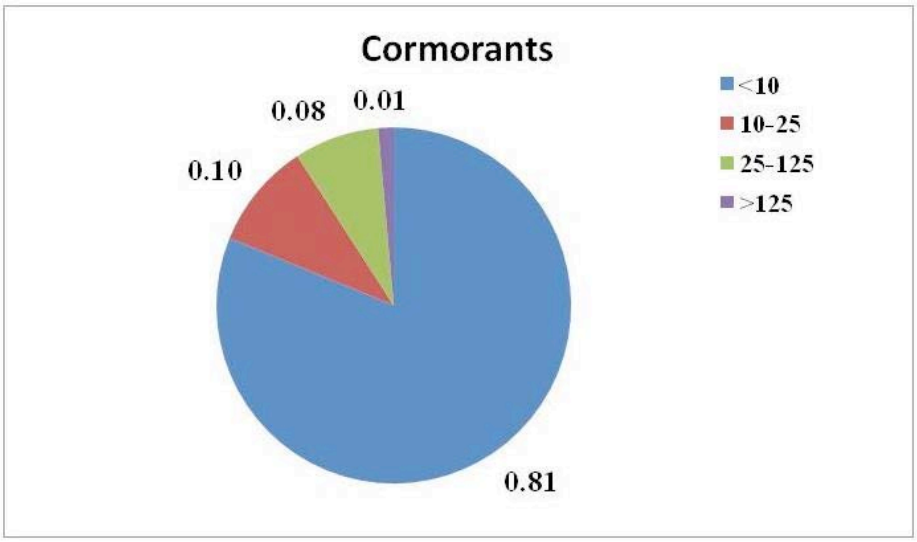

Fig. 65. Flight altitude of cormorants (m above sea level; N = 24,362 detections) based estimates during land-based seawatches and ship-based line transects. Proportion of birds in four altitude categories are shown.

Spatial patterns in abundance in nearshore waters - In nearshore areas, Double-crested Cormorants tend to be more abundant off of Deep Hole, Brenton Pt, Sachuest NWR, and Sakonnet Pt, in part due to the location of nearby breeding sites (Fig. 66). Great Cormorants are uniformly distributed across the study area (Fig. 66). See Appendices B and C for data on cormorant abundance at each of the land-based seawatch stations for each month surveyed.

Spatial patterns in abundance in nearshore and offshore waters – We had too few detections of Double-crested and Great Cormorants during ship-based line transects to model their density or spatial distribution (Table 17). However, a comparison of cormorant detections during land-based versus ship-based surveys clearly shows that they are almost exclusively found in nearshore habitats. For example, Double-crested Cormorants were only detected five times and Great Cormorants were only detected once during offshore ship-based surveys (Table 17), while we had over 25,000 detections of Double-created Cormorants and over 2,000 detections of Great Cormorants during land-based seawatches (Table 13).

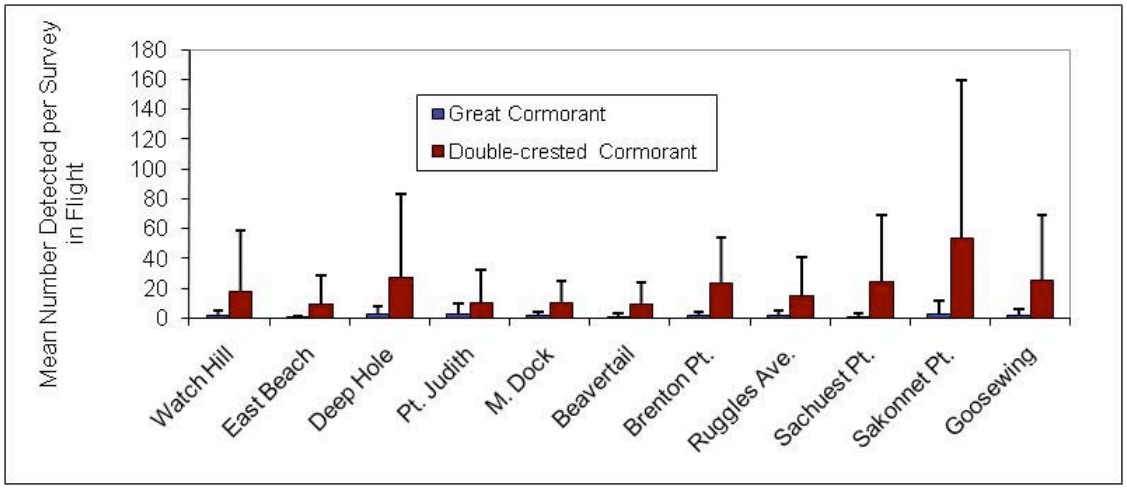

Fig. 66. Mean (SD) number of Double-crested and Great Cormorants detected per survey at 11 land-based seawatch stations (see Fig. 21 for locations of stations).

Population size in the Ocean SAMP area - We had too few detections of Double-crested and Great Cormorants during ship-based line transects to estimate their population size in the study area.

Spatial patterns in abundance in relation to bathymetry – We did not have any detections of cormorants sitting on the water during winter aerial surveys (Table 21), thus we did not explore cormorant abundance in relation to water depth in the SAMP study area. 3.9 Wading Birds

We detected seven species of wading birds (Herons and egrets; Ardeidae, Ibises; Threskiornithidae) in the Ocean SAMP area: Great Blue Heron, Great Egret, Snowy Egret, Cattle Egret, Green Heron, Black-crowned Night-Heron, and Glossy Ibis.

Seasonal changes in abundance - Wading birds breed in Rhode Island on islands throughout Narragansett Bay and small numbers of three species (Great Egret, Snowy Egret, and Black-crowned Night-Heron) nest on Block Island (C. Raithel, unpublished data 2009; Ferren and Myers 1998). Hence, they are most common in the Ocean SAMP are from May through September (Appendices B and C). All wading birds that nest in Rhode Island are migrants, with the exception of Great Blue Heron. Thus there is probably some migration by wading birds along the coast during migratory events, but the primary migratory routes are probably restricted to nearshore areas or over the land.

Flight altitude of birds - Flight altitudes of wading birds were variable. In the majority of our observations, 30% of wading birds were flying at <10 m altitude, 37% were at 10-25 m altitude, 32% at 25-125 m, and <1% >125 m (N = 134 detections;Table 15).

Spatial patterns in abundance in nearshore waters - In nearshore areas, wading birds tended to be sparse everywhere during land-based seawatches, since most species of wading birds appear to avoid flying out over the ocean. See Appendices B and C for data on wading bird abundance at each of the land-based seawatch stations for each month surveyed.

Spatial patterns in abundance in nearshore and offshore waters – We had too few detections of wading birds during ship-based line transects to model their density or spatial distribution.

Population size in the Ocean SAMP area - We had too few detections of wading birds during ship-based line transects to estimate their population size in the study area.

3.9 Waterfowl

We detected 18 species of waterfowl (Anatidae) in the Ocean SAMP study area: two species of swans (Mute and Tundra Swan), two species of geese (Canada and Brant Geese), seven species of dabbling ducks (Mallard, Black Duck,Wood Duck, Gadwall, Northern Pintail, American Widgeon and Green-winged Teal), one species of bay duck (Greater Scaup) and six species of seaducks (Common Eider, King Eider, Black Scoter, Surf Scoter, White-winged Scoter and Long-tailed Duck). Swans are common year round residents in Rhode Island, but found in relatively small numbers in the Ocean SAMP area. Geese and dabbling ducks are seasonally abundant and common migrants, but found in relatively small numbers in the Ocean SAMP area. Seaducks are common migrants and winter residents and abundant in the Ocean SAMP area.

Swans: We detected two species, Mute Swan (111 detections during land-based seawatches; Table 13) and Tundra Swan (2 detections during land-based seawatches; Table 13). No swans were detected offshore during ship-based line transects (Table 17) or during aerial surveys (Table 21). Both species primarily use coastal ponds in Rhode Island [e.g., Trustom (Table 8) and Ninigret Pond (Table 9)], although they are occasionally detected flying over nearshore areas along the mainland coast of Rhode Island. Due to low detection rates, we could not model the movement ecology or spatial distribution of swans.

Geese: We detected two species during fieldwork: Brant and Canada Goose. We often detected Brant during land-based seawatches (mean = 1.8 detections per survey), as well as Canada Geese (mean = 3.2 detections per survey; Table 13). We detected Brant offshore on Grid F (NW of Harbor of Refuge; Table 18) during ship-based line transects and during aerial surveys (Table 21). Both species are restricted to nearshore habitats or inland areas. Brant are common

in Narragansett Bay (Tables 4 and 5) and along the coast at Napatree Point (Table 7). Due to low detection rates, we could not model the movement ecology or spatial distribution of geese.

Dabbling ducks (Genus *Anas*): We detected seven species of dabbling ducks during land-based seawatches of birds flying over the ocean or birds resting/foraging on the surface. Species we recorded included Wood Duck (10 detections), Mallard (74 detections), American Black Duck (700 detections), Gadwall (22 detections), Northern Pintail (7 detections), American Wigeon (14 detections) and Green-winged Teal (38 detections). American Black Ducks were the only species that was relatively common along the coastline (mean = 0.9 detections per survey; Table 13) because they regularly foraging in the intertidal zone on algae that is exposed at low tide (pers. obs.) Gadwalls and Mallards also will occasionally forage in the intertidal zone, however dabbling ducks are more common found in coastal ponds (Tables 8 and 9) or freshwater lakes inland. We rarely detected dabbling ducks during ship-based surveys (Table 17). Due to low detection rates, we could not model the movement ecology or spatial distribution of dabbling ducks.

Diving Ducks: We detected one species of bay duck during land-based seawatches, Greater Scaup, with an average of 1.3 detections per survey (Table 13). We also detected large numbers of Red-breasted Mergansers, Common Goldeneye, and Buffhead.

Seasonal changes in abundance- Diving ducks were most abundant during the winter months (Nov through May; Fig. 67).

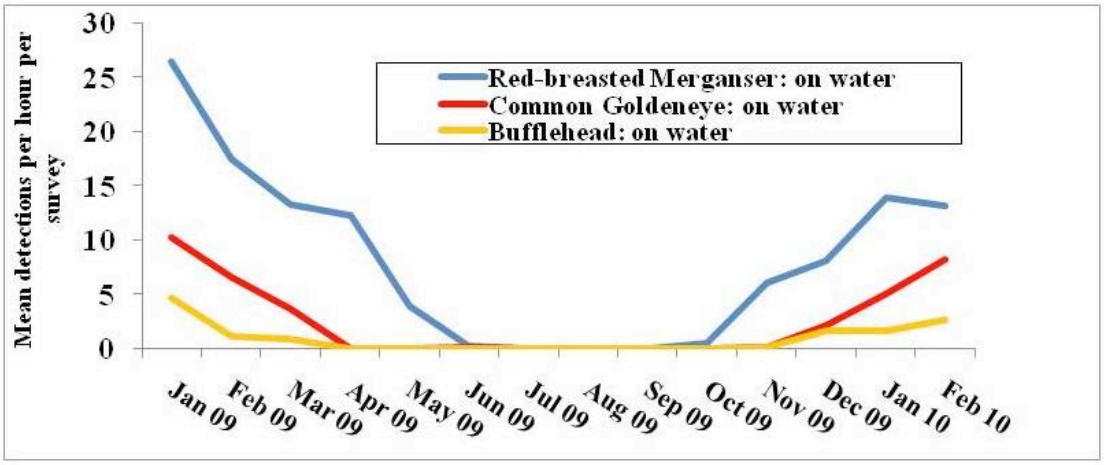

Fig. 67. Mean number of diving ducks detected per survey per month during land-based seawatches.

Flight altitude of birds.- Diving ducks were usually detected flying <10 m altitude (Table 15).

Spatial patterns in abundance in nearshore waters. – Diving ducks, in particular Red-breasted Mergansers, were most abundant at Deep Hole, Pt. Judith, and Brenton Pt, while Common Goldeneye were most abundant at Brenton Pt. (Fig. 68, see also Appendices B and C).

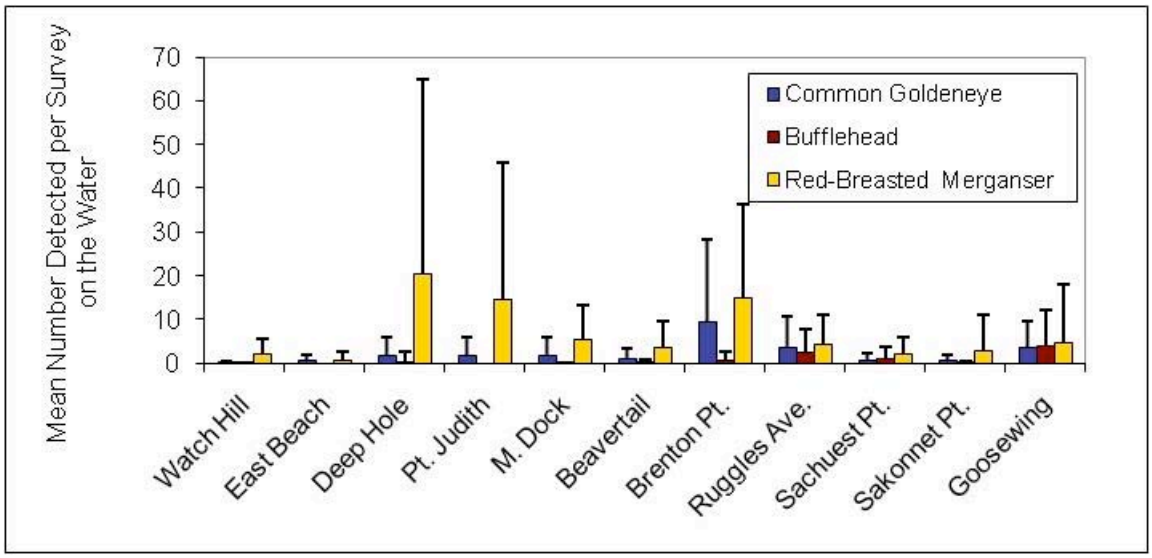

Fig. 68. Mean (SD) number of diving ducks detected per survey at 11 land-based seawatch stations (see Fig. 21 for locations of stations).

Spatial patterns in abundance in nearshore and offshore waters. – Diving ducks were rarely detected during ship-based line transects, or aerial surveys so we could not model their movement ecology or spatial distribution patterns. During ship-based line transects, scaup were detected in flight, once each on Grid C and Grid F (Table 18). Bay ducks are more abundant in Narragansett Bay (Tables 4 and 5) and in coastal ponds (Tables 8 and 9) than in the Ocean SAMP study area.

Population size in the Ocean SAMP area. – We had too few detections during ship-based line transect to estimate the population size of diving ducks in the Ocean SAMP study area.

Seaducks: Seaducks include eiders, scoters, and related species and are the most abundant species we detected in nearshore habitats in winter. We detected two species of eider, Common Eider, a very common species in nearshore areas with an average of 101 detections per survey (> 80,000 detections overall) during land-based seawatches and King Eider (26 total detections; Table 13). Long-tailed Ducks are uncommon in the Ocean SAMP study area, with 470 detections during land-based seawatches (0.6 detections per survey; Table 13). We detected all three species of scoters, Surf, Black, and White-winged Scoter, which were among the most abundant species in nearshore habitats in the Ocean SAMP study area.

Seasonal changes in abundance. – Seaducks primarily winter in Rhode Island, although large numbers also migrate through the region to winter farther south (Sibley 2000). During fall migration, birds start to move into the Ocean SAMP area from October through November. During spring migration, there appears to be a influx of birds starting February and peaking in March (Fig. 69). We noticed considerable interannual variation in numbers of birds in the study area between 2009 and 2010.

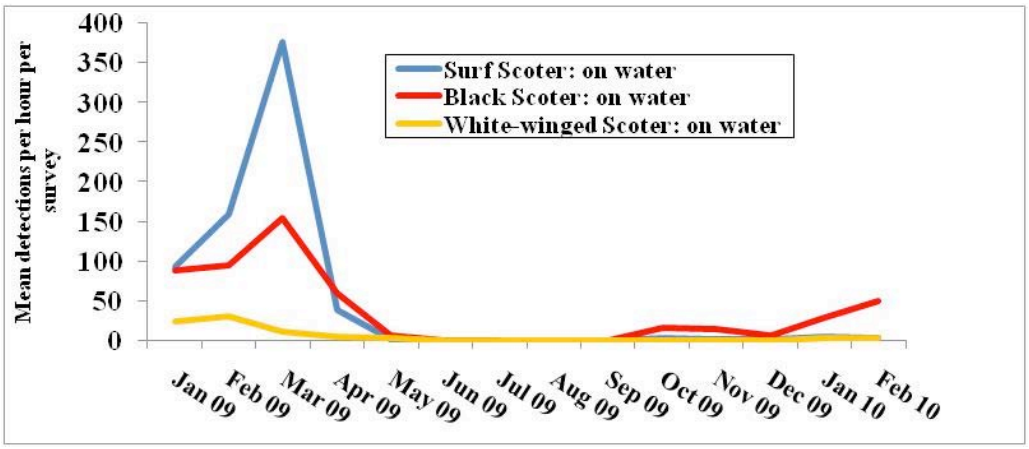

Fig. 69. Mean number of scoter detections per survey per month at 11 land-based seawatch stations.

Flight altitude of birds. –Most (91%) seaducks flew <10 m high, although 8% flew beween 10-25 m (Fig. 70)

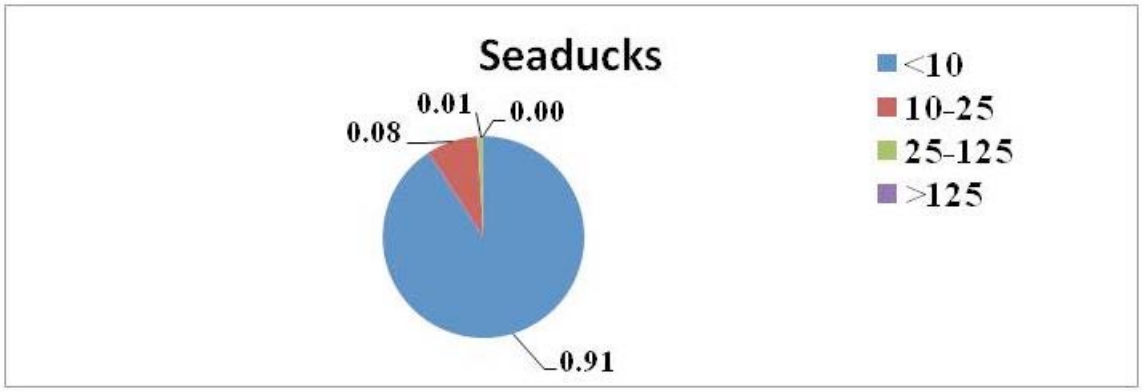

Fig. 70. Flight altitude of seaducks (m above sea level; N = 79,209 detections; eiders, scoters, and mergansers) based estimates during land-based seawatches and ship-based line transects. Shown are proportion of birds in four altitude categories.

Spatial patterns in abundance in nearshore waters. – The largest concentrations of scoters and eider were observed at Brenton Point, although we had relatively high numbers of scoter at Watch Hill, East Beach, Ruggles Ave, and Sakonnet Point (Figs. 71 and 72).

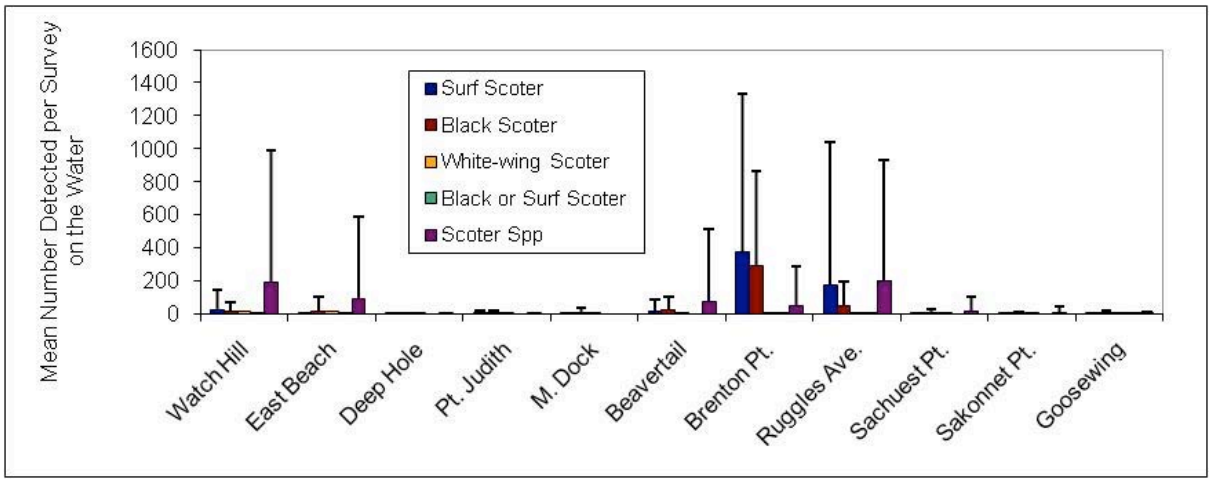

Fig. 71. Mean (SD) number of scoters detected per survey at 11 land-based seawatch stations (see Fig. 21 for locations of stations).

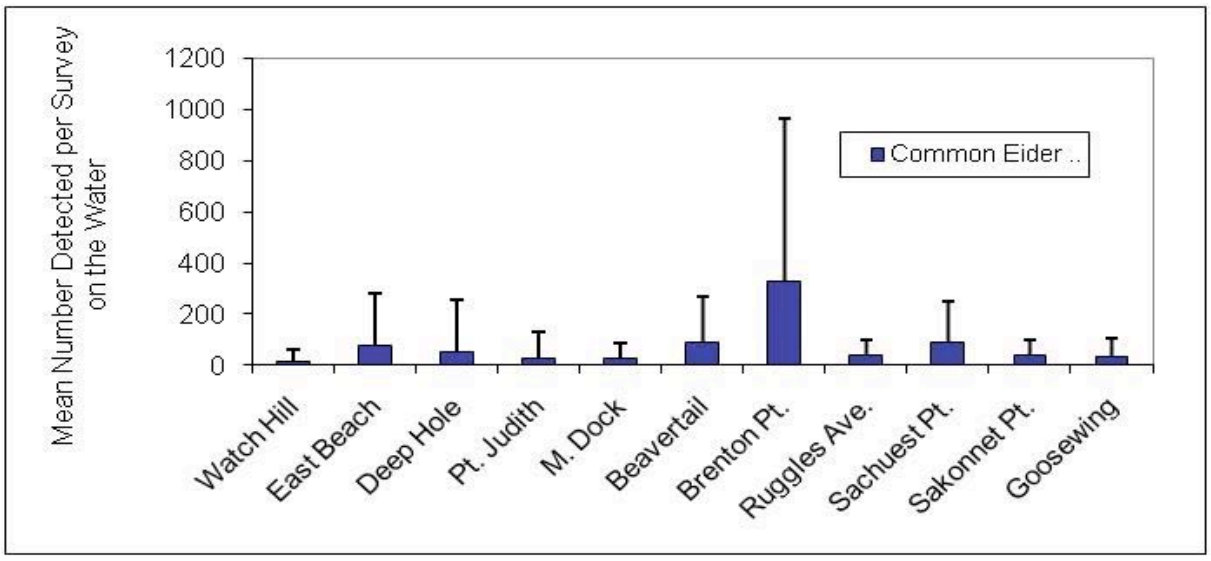

Fig. 72. Mean (SD) number of Common Eider detected per survey at 11 land-based seawatch stations (see Fig. 21 for locations of stations).

Spatial patterns in abundance in nearshore and offshore waters.- We had too few detections of seaducks during ship-based line transects in all seasons to model their density or spatial distribution. We believe limited detections of seaducks which are abundant in the Ocean SAMP area are a result of both (a) limited ship-based survey effort in waters shallow enough for seaduck foraging (waters <25 m), and (b) seaducks are more sensitive to the presence of the survey ship compared to other avian species. Seaducks routinely flush 700 m to 1000 m ahead of the ship making on-the-water detections difficult (K. Winiarski, pers. obs.). We plan on developing Density Surfact Models of their distribution and density based on aerial survey data

(collected both in the winter of 2009-10 and winter of 2010-11) for a future Ocean SAMP report.

Athough we did not detected Surf or Black Scoters away from nearshore areas, we occasionally observed White-winged Scoters commuting throughout offshore sections of Rhode Island and Block Island Sounds and even as far out as the Inner Continental Shelf (Fig. 73). This suggests that land-based seawatches may underestimate the number of White-winged Scoters in the Ocean SAMP area.

Population size in the Ocean SAMP area - We had too few detections of seaducks during ship-based line transects in all seasons to estimate their population size in the study area.

Spatial patterns in abundance in relation to bathymetry – We often detected seaducks (eider and scoter) during our winter aerial surveys, however the number of seaducks in the area was relatively low during the winter of 2009-2010 compared to the previous year (Fig. 69). During aerial surveys, seaducks tended to be found in nearshore areas in the NW and NE corners of the Ocean SAMP study area, as well as S of Block Island and between Block Island and Montauk, Long Island (Fig. 74). Based on the bathymetry at locations where seaducks were detected during aerial surveys, scoter and eider seem to select shallow waters < 25 m deep (Fig. 75). There was some indication that scoter selected areas in the transition zone at about 20 m depth, but more detailed research is needed to determine the exact bathymetry requirements of scoters or eiders in the Ocean SAMP area.

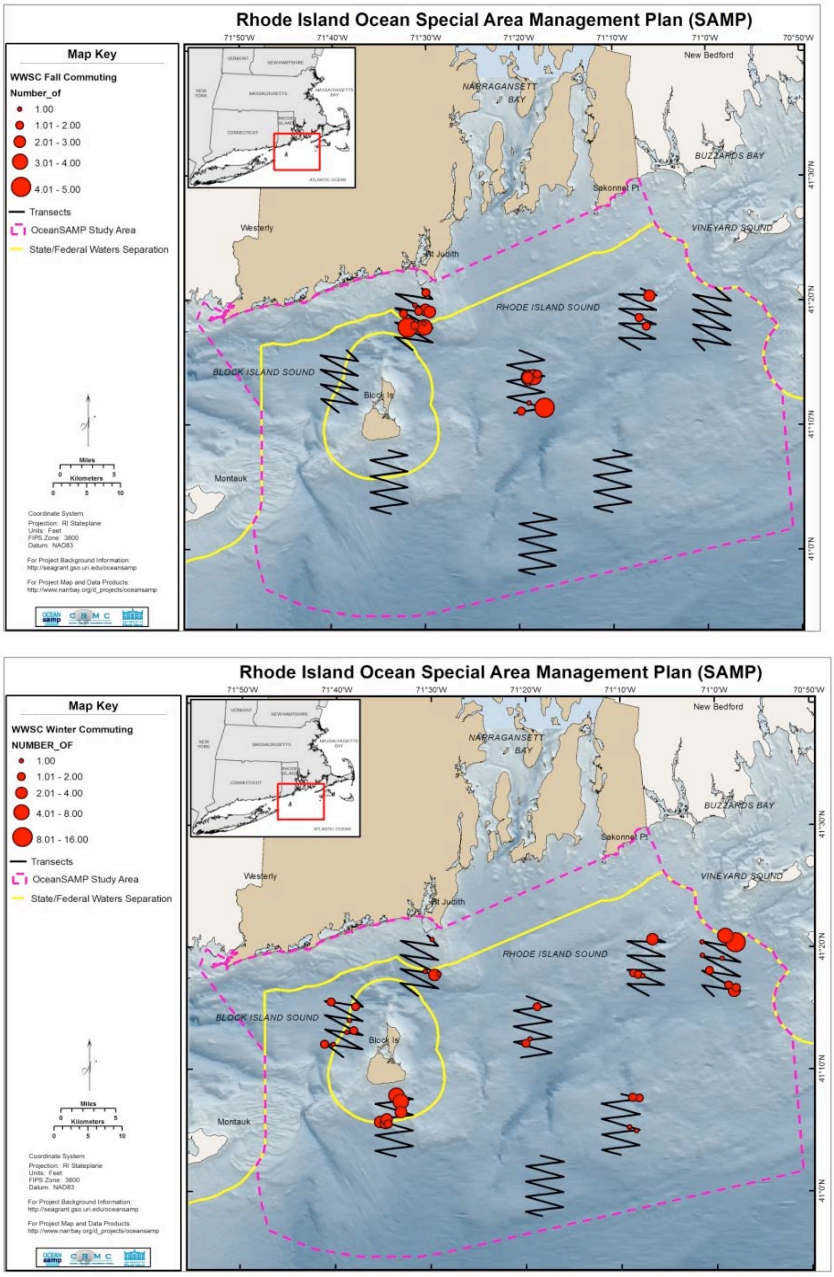

Fig. 73. Distribution of White-winged Scoter flocks in flight in fall (upper) and winter (lower) in the Ocean SAMP study area based on ship line-transect surveys.

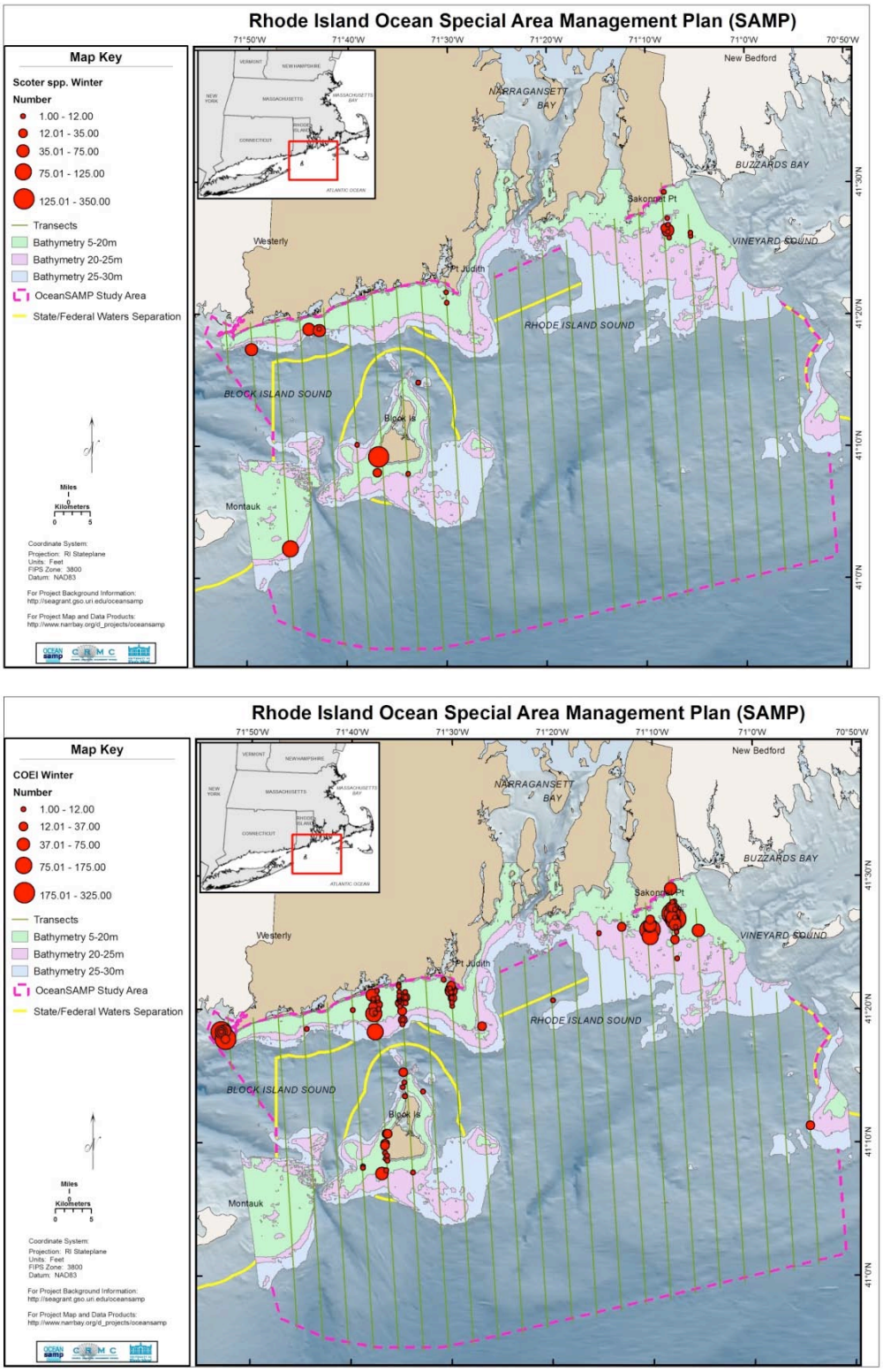

Fig. 74. Distribution of seaducks, scoter (upper) and Common Eider (lower) flocks during aerial surveys in winter 2009-10 in the Ocean SAMP study area.

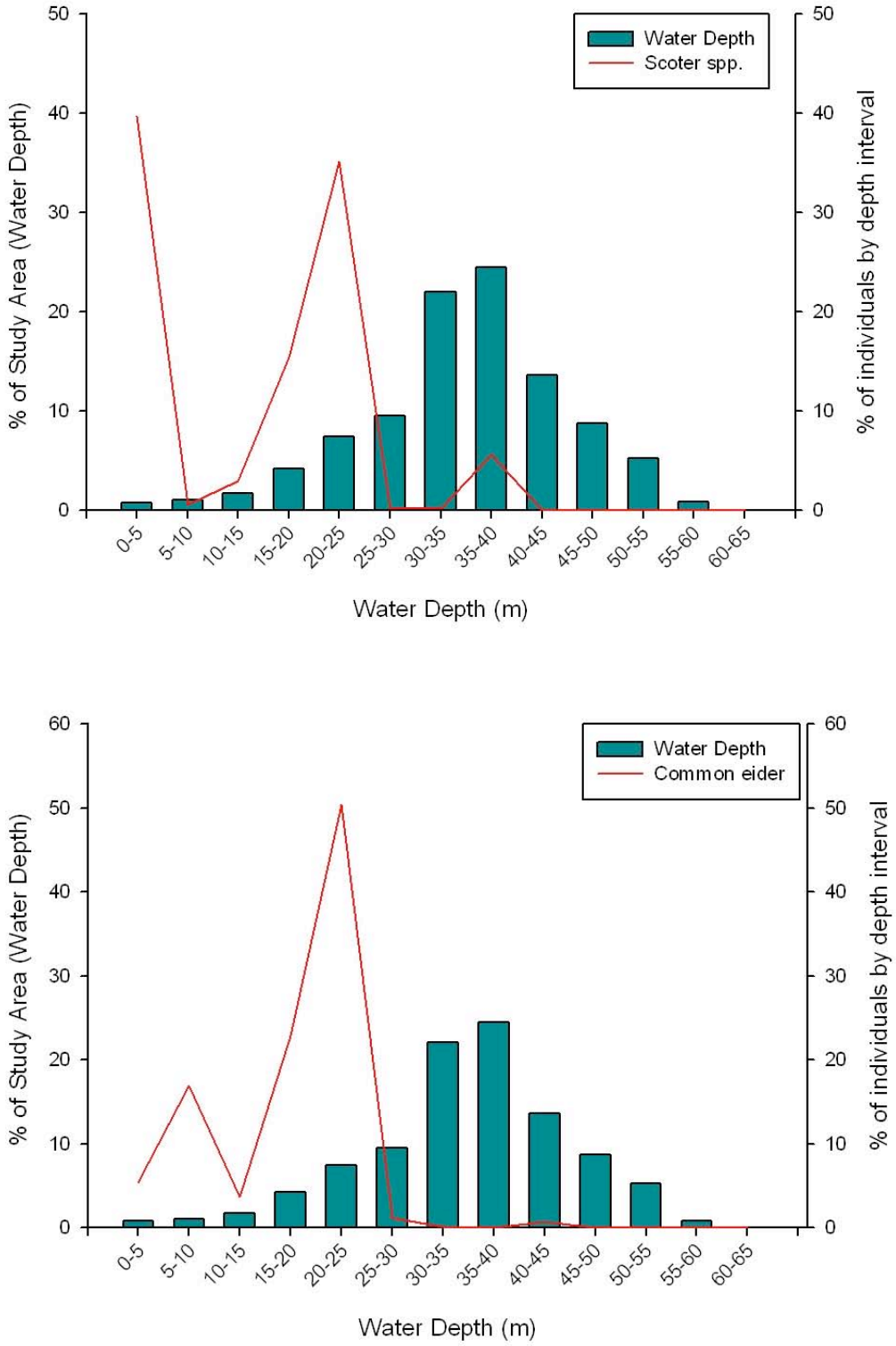

Fig. 75. Bathymetry of Ocean SAMP study area (green histogram) compared to depths where scoters (upper) and eiders (lower) were detected during aerial surveys (red line) (Fig. 74)

3.10 Shorebirds

We detected 19 species of shorebirds (Scolopacidae) in the Ocean SAMP area: four species of plovers (Black-bellied Plover, Piping Plover, Semipalmated Plover and Killdeer), one oystercatcher (American Oystercatcher), 13 species of sandpipers (Greater and Lesser Yellowlegs, Spotted Sandpiper, Whimbrel, Ruddy Turnstone, Purple Sandpiper, Sanderling, Dunlin, White-rumped Sandpiper, Semipalmated Sandpiper, Least Sandpiper, and Short-billed Dowitcher) and one species of phalarope (Red-necked phalarope). Shorebirds are common to the study area but found in relatively low numbers in the Ocean SAMP area, although Semipalmated Plovers, Ruddy Turnstone, Purple Sandpipers, Sanderlings, Dunlin, Semipalmated Sandpipesr and Short-billed Dowitcher were detected fairly often during land-based seawatches (Table 13).

Seasonal changes in abundance - Shorebirds are breeders, winter residents and migrants in the Ocean SAMP area. Most shorebirds migrate through Rhode Island waters during their fall migration mostly in August through September, and then peak again in May and June during spring migration. Around 80 pairs of Piping Plovers nest on the beaches of southern Rhode Island and Block Island (W. Edwards, USFWS, pers. comm.). Some shorebirds winter in Rhode Island (Purple Sandpiper, Sanderling, and Dunlin) which is why they had relatively high detection rates.

Spatial patterns in abundance in nearshore waters - In nearshore areas, shorebirds tend to be occasionally detected throughout the study area during land-based seawatches. See Appendices B and C for data on shorebird abundance at each of the land-based seawatch stations for each month surveyed.

Flight altitude of birds - Flight altitudes of shorbirds were variable. In the majority of our observations, 87% of shorebirds were flying at <10 m altitude, with 9% flying 10-25 m, and 4% flying 25-125 m (N = 6512 detections; Table 15).

Spatial patterns in abundance in nearshore and offshore waters – We had too few detections of shorebirds during ship-based line transects in all seasons to model their density or spatial distribution. We had few detections of shorebirds away from nearshore areas. During ship-based line transects we detected 6 species (Short-billed Dowitcher, Semipalmated Plover, Purple Sandpiper, Lesser Yellowlegs, Whimbrel, and Red-necked Phalarope on a variety of grids; Table 18). Red-necked Phalarope, a pelagic specialist, was only detected on Grid H over the Inner continental Shelf.

Population size in the Ocean SAMP area - We had too few detections of shorebirds during ship-based line transects to estimate their population size in the study area.

Spatial patterns in abundance in relation to bathymetry – With the exception of phalaropes, shorebirds generally only use water <10 cm deep. We only had a small number of detections of shorebirds during winter aerial surveys, thus we did not explore shorebird abundance in relation to water depth in the Ocean SAMP study area. All detections were of birds in flight likely migrating through the Ocean SAMP area.

3.11 Jaegers

We detected three species of jaegers (Stercorariidae) in the Ocean SAMP study area: Long-tailed, Parasitic and Pomarine Jaeger. All three species are relatively uncommon in the SAMP area; Parasitic Jaeger was the most regularly detected jaeger species during land-based seawatches.

Seasonal changes in abundance - Jaegers breed in the Arctic tundra and migrate through the Ocean SAMP area during spring and fall migration from May through October (Fig. 76; Appendix B and C).

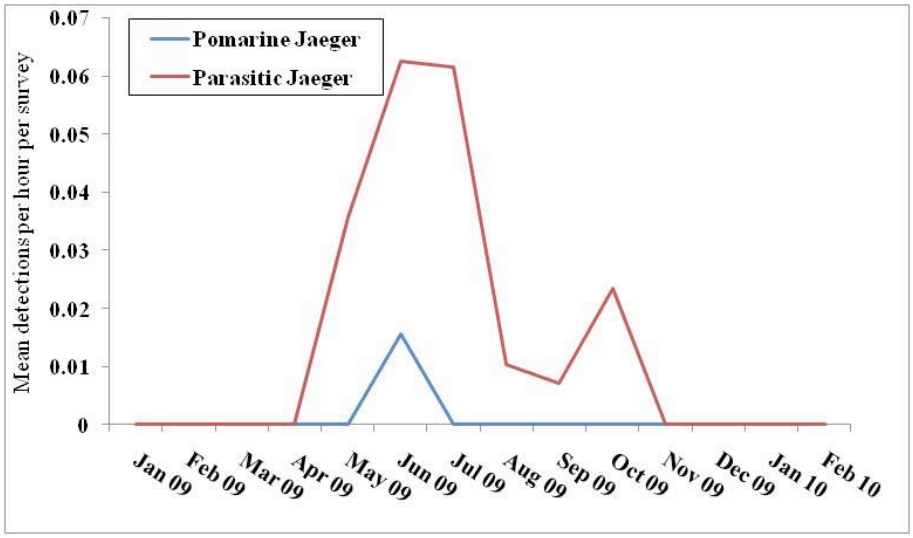

Fig. 76. Monthly differences in average number of Pomarine and Parasitic Jaegers detected in flight per survey at 11 land-based seawatch stations along the Rhode Island coastline

Flight altitude of birds - Flight altitudes of jaegers were similar to gulls. In the majority of our observations, 70% of jaegers were flying at <10 m altitude, 13% at 10-25 m, and 17% at 25-125 m (N = 24 detections; Table 15).

Spatial patterns in abundance in nearshore waters - In nearshore areas, jaegers tend to be more abundant off of Deep Hole, Pt. Judith, and Goosewing; Fig. 77). Parasitic Jaeger was the most common jaeger detected during land-based seawatches with 19 detections, while Pomarine Jaeger was detected only twice (Table 13). This is probably because Parasitic Jaegers specialize in kleptoparasitism of terns, which tend to be concentrated in nearshore areas during the post-breeding season. See Appendices B and C for data on jaeger abundance at each of the land-based seawatch stations for each month surveyed.

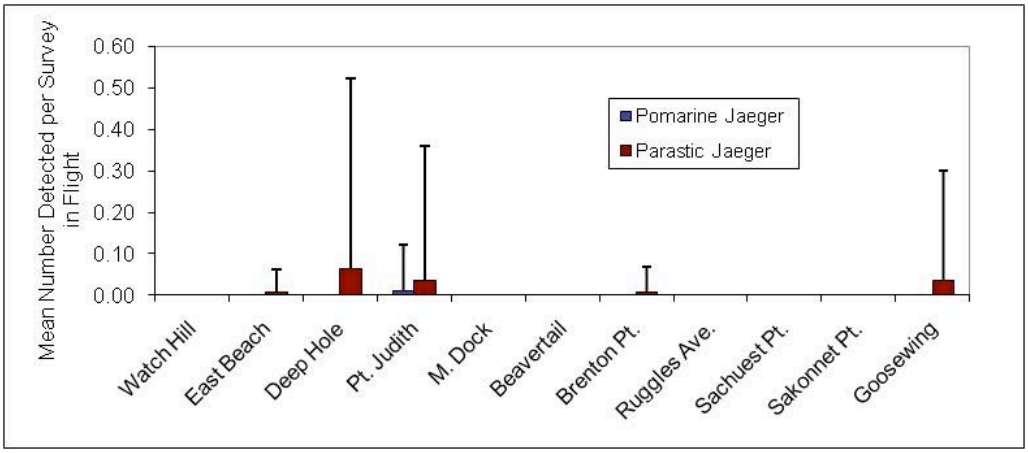

Fig. 77. Mean (SD) number of Pomarine and Parasitic Jaegers detected per survey at 11 land-based seawatch stations (see Fig. 21 for locations of stations).

Spatial patterns in abundance in nearshore and offshore waters – We had too few detections of jaegers during ship-based line transects in all seasons to model their density or spatial distribution. Jaegers were rarely detected during ship-based line transect surveys, with only one detection of Long-tailed Jaeger on Grid H (at the edge between Rhode Island Sound and Block Island Sound), one detection of Parasitic Jaeger on Grid F (SW of Harbor of Refuge in a nearshore area) and one detection of Pomarine Jaeger on Grid A (S of Block Island; Table 18).

Population size in the Ocean SAMP area - We had too few detections of jaegers during ship-based line transects in all seasons to estimate their population size in the study area.

Spatial patterns in abundance in relation to bathymetry – We had no detections of jaegers during winter aerial surveys, thus we did not explore jaeger abundance in relation to water depth in the Ocean SAMP study area.

3.12 Gulls

We detected six species of gulls (Laridae) in the Ocean SAMP study area: Bonaparte's, Laughing, Ring-billed, Herring, Iceland, and Great Black-backed Gull. Ring-billed Gull, Laughing Gull, Herring Gull, and Great Black-backed Gull were among the most abundant species detected in the Ocean SAMP area (Table 13). Bonaparte's Gulls are common during the winter months but found in relatively low numbers in the Ocean SAMP area. Iceland Gulls are rare in the study area, and we had just one detection during our surveys.

Seasonal changes in abundance - Herring Gulls and Great Black-backed Gulls nest in Rhode Island and are year-round residents, thus were detected throughout the year during our surveys. Herring Gull and Great Black-backed Gull numbers in flight peak in March when they are moving to their breeding colonies along the coast (Fig. 78). Bonaparte's, Ring-billed, and Laughing Gulls are common migrants and winter residents in the SAMP area that breed outside of Rhode Island, with their detection rates peaking in October (Fig. 79; see also Appendix D).

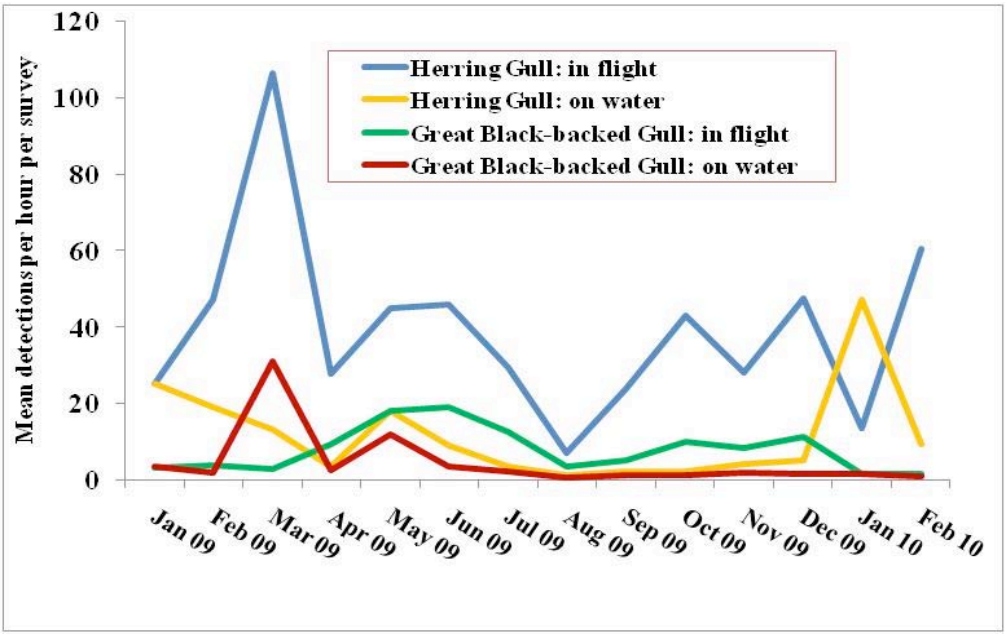

Fig. 78. Mean number of Herring and Great Black-backed Gulls detected on the water and in flight per survey per month at 11 land-based seawatch stations along the Rhode Island coastline.

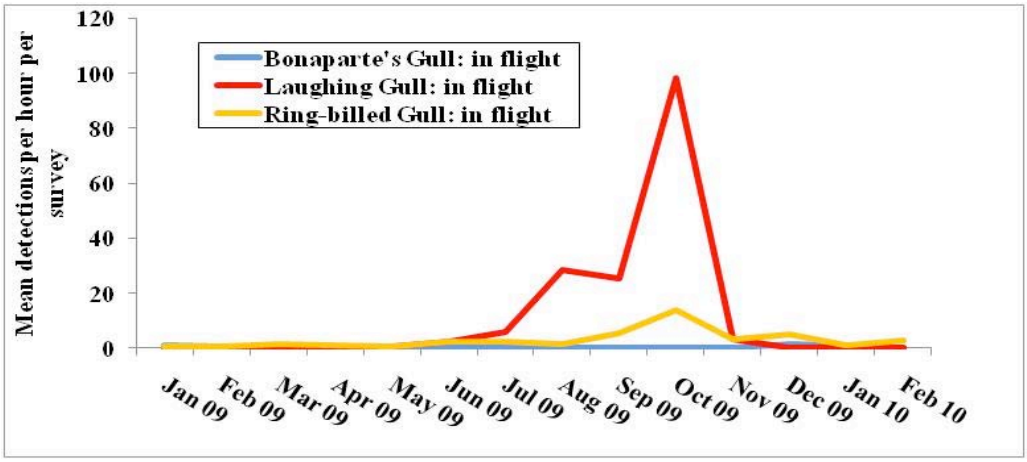

Fig. 79. Mean number of Bonaparte's, Laughing, and Ring-billed Gulls detected in flight per survey per month at 11 land-based seawatch stations along the Rhode Island coastline

Spatial patterns in abundance in nearshore waters - In nearshore areas, large gulls (Herring and Great Black-backed Gulls) tend to be widely dispersed in the study area. However, Herring Gulls detection rates peak near Goosewing, which is near both a nesting colony and a winter roost (Fig. 80). All three of the common small gulls (Bonaparte's, Laughing, and Ring-billed Gull) tend to be uniformly distributed throughout the study area (Fig. 81). See Appendices B and C for data on gull abundance at each of the land-based seawatch stations for each month surveyed.

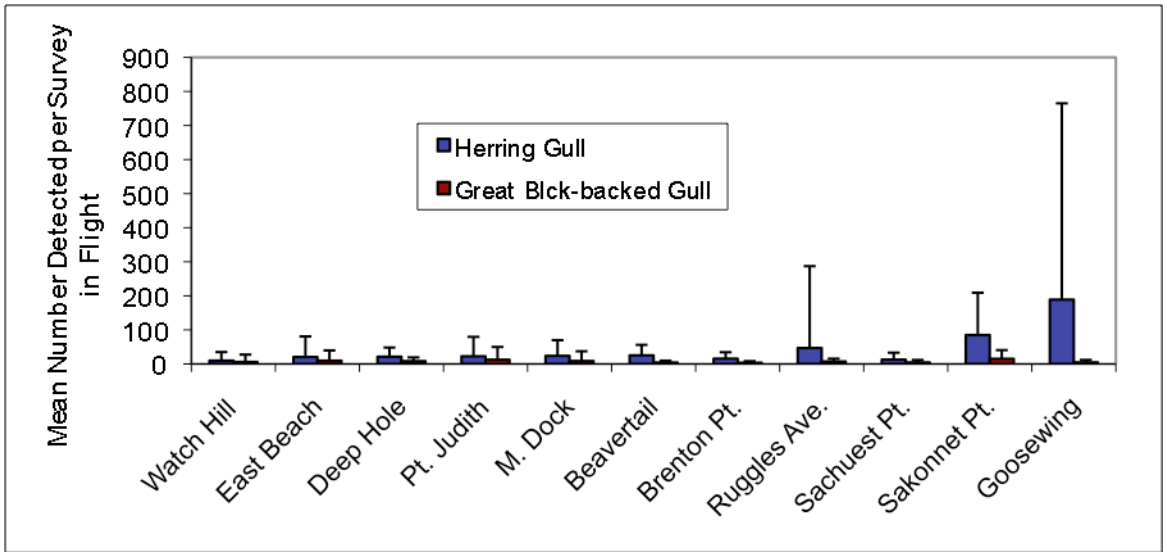

Fig. 80. Mean (SD) number of Herring and Great Black-backed Gulls detected per survey at 11 land-based seawatch stations (see Fig. 21 for locations of stations).

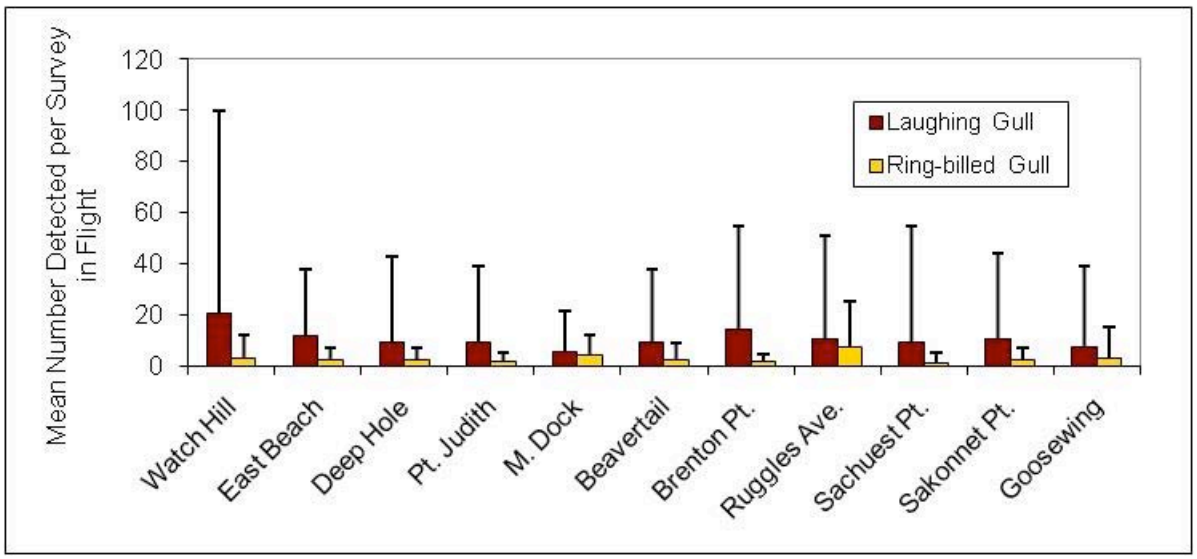

Fig. 81. Mean (SD) number of Laughing and Ring-billed Gulls detected per survey at 11 land-based seawatch stations (see Fig. 21 for locations of stations).

Flight altitude of birds - Gulls exhibit a broad range of flight altitudes (Fig. 82). During our surveys, most (58%) gulls were flying <10 m altitude, with substantial numbers flying between 10-25 m (30%), moderate numbers (12%) flying between 25-125 m, and <1% flying >125 m high.

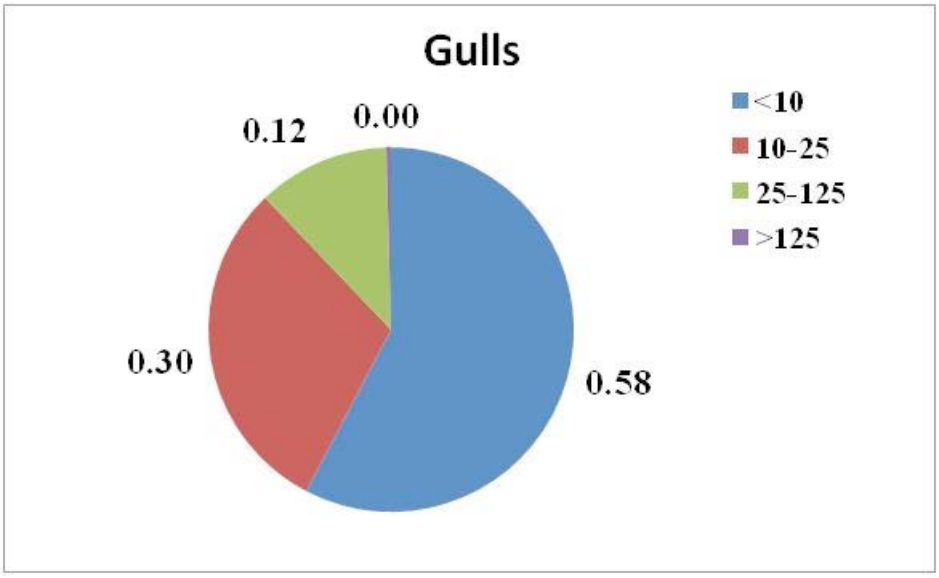

Fig. 82. Flight altitude of gulls (m above sea level; N = 100,031 detections) based estimates during land-based seawatches and ship-based line transects. Shown are the proportion of birds in four altitude categories.

Spatial patterns in abundance in nearshore and offshore waters –The best-fit Density Surface Model (DSM) for Herring Gulls explained 27.1%, 32.3% and 8.6% of the spatial variation in observed abundance during summer, fall and winter, respectively (see Appendix H for full model results). The best-fit DSM for Great Black-backed Gulls explained 19.1%, 43.9% and 7.5% of the spatial variation in observed abundance of Great Black-backed Gulls during summer, fall and winter, respectively (see Appendix H for full model results).

Herring Gulls were concentrated in nearshore areas adjacent to breeding colonies in the summer. During fall, densities increased to up to 40 birds per km^2 and gulls moved to offshore areas in Rhode Island Sound and the Inner Continental Shelf. During winter, Herring Gull densities declined (peak densities of 1.7 birds per km^2), and birds appeared to be more restricted to nearshore habitats, although some birds were using offshore areas (Fig. 83). In all three seasons, most of the variation in density estimates of Herring Gulls occurred in offshore areas (Fig. 84).

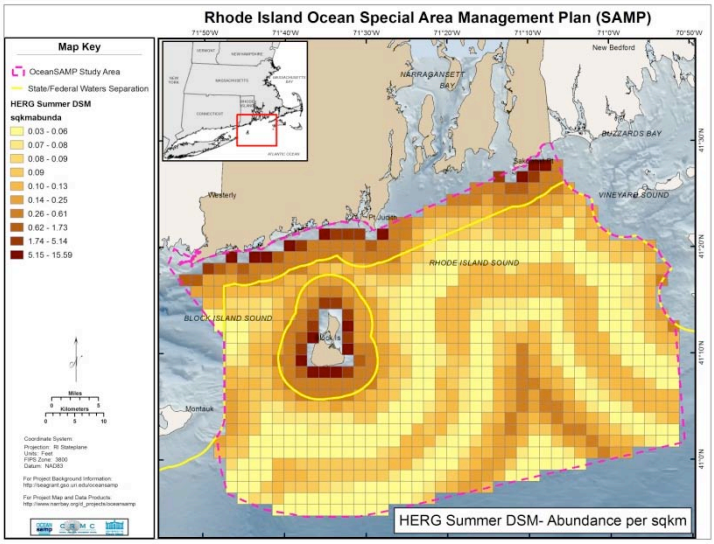
Rhode Island Ocean Special Area Management Plan (SAMP)
Map Key
OceanSAMP Study Area
State/Federal Waters Separation
HERG Summer DSM
sqkmabunda
0.03 - 0.06
0.07 - 0.08
0.08 - 0.09
0.09
0.10 - 0.13
0.14 - 0.25
0.26 - 0.61
0.62 - 1.73
1.74 - 5.14
5.15 - 15.59
NARRAGANSETT BAY
BUZZARDS BAY
VINEYARD SOUND
RHODE ISLAND SOUND
BLOCK ISLAND SOUND
Montauk
New Bedford
Westerly
Pt Judith
HERG Summer DSM- Abundance per sqkm

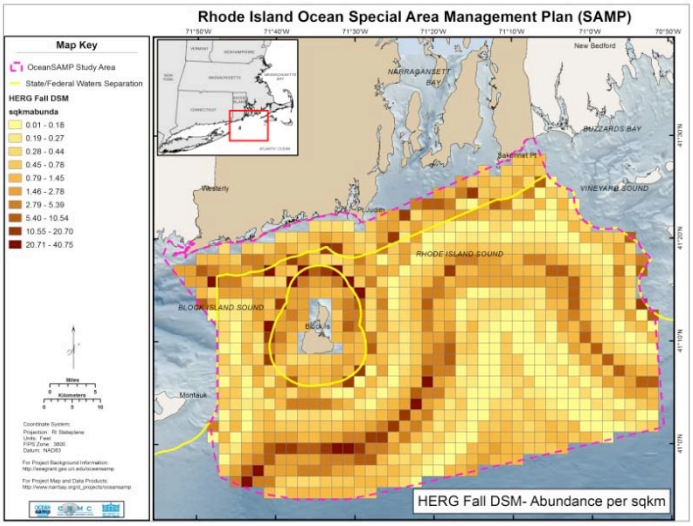
Rhode Island Ocean Special Area Management Plan (SAMP)
Map Key
OceanSAMP Study Area
State/Federal Waters Separation
HERG Fall DSM
sqkmabunda
0.01 - 0.18
0.19 - 0.27
0.28 - 0.44
0.45 - 0.78
0.79 - 1.45
1.46 - 2.78
2.79 - 5.39
5.40 - 10.54
10.55 - 20.70
20.71 - 40.75
NARRAGANSETT BAY
BUZZARDS BAY
VINEYARD SOUND
RHODE ISLAND SOUND
BLOCK ISLAND SOUND
Montauk
New Bedford
Westerly
Pt Judith
HERG Fall DSM- Abundance per sqkm

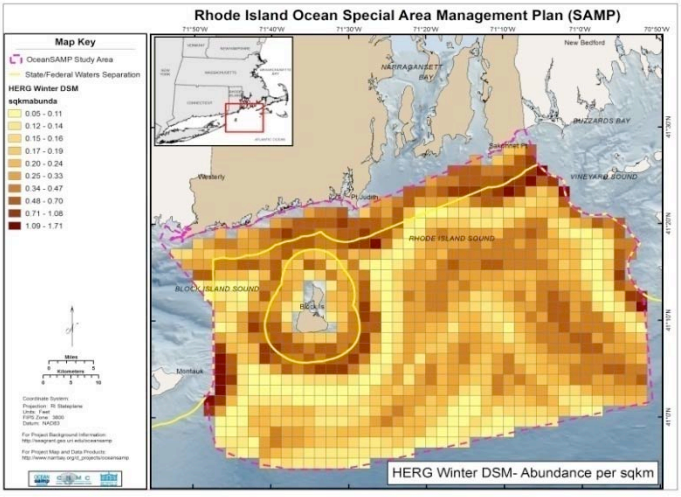
Rhode Island Ocean Special Area Management Plan (SAMP)
Map Key
OceanSAMP Study Area
State/Federal Waters Separation
HERG Winter DSM
sqkmabunda
0.05 - 0.11
0.12 - 0.14
0.15 - 0.16
0.17 - 0.19
0.20 - 0.24
0.25 - 0.33
0.34 - 0.47
0.48 - 0.70
0.71 - 1.08
1.09 - 1.71
NARRAGANSETT BAY
BUZZARDS BAY
VINEYARD SOUND
RHODE ISLAND SOUND
BLOCK ISLAND SOUND
Montauk
New Bedford
Westerly
Pt Judith
HERG Winter DSM- Abundance per sqkm

Fig. 83. DSM estimates of the spatial distribution and density of Herring Gulls in summer (upper), fall (middle), and winter (lower) in the Ocean SAMP study area based on ship line-transect surveys.

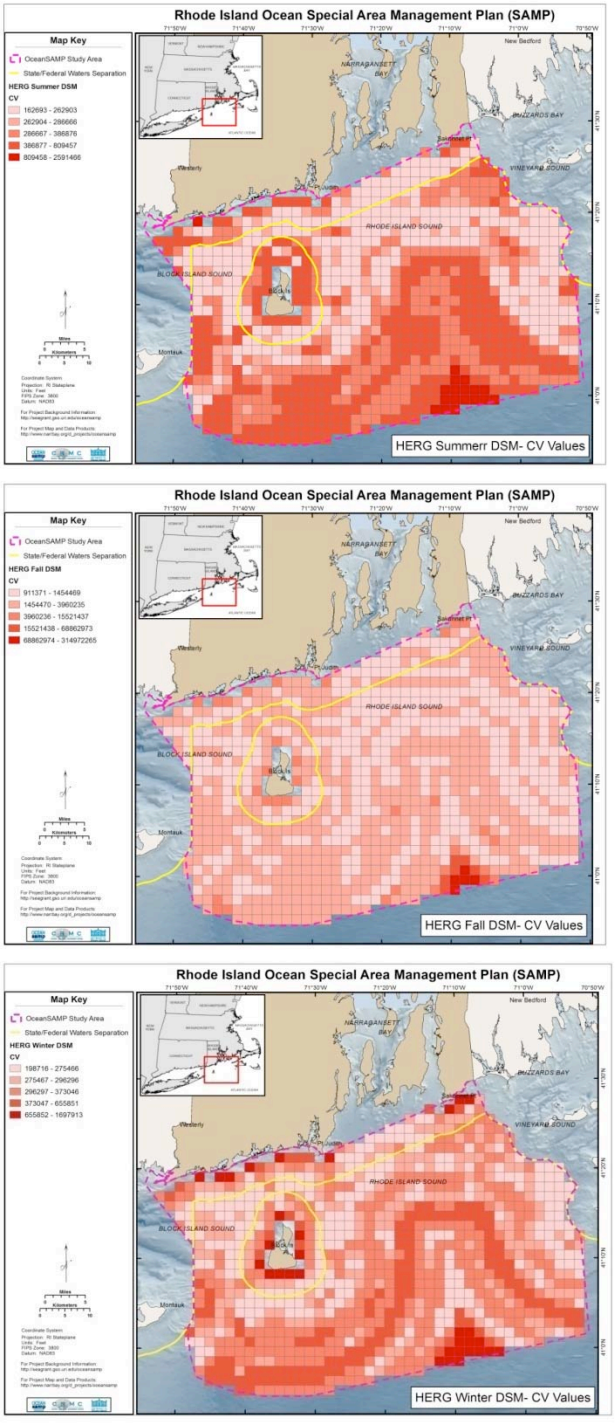

Fig. 84. Coefficient of Variation for DSM modeled Herring Gull density estimates in summer (upper), fall (middle), and winter (lower) density estimates based on ship line transect surveys shown in Fig. 83.

Great Black-backed gulls were concentrated, similar to Herring Gulls in nearshore areas, adjacent to breeding colonies in the summer (Fig. 85). In the fall, Great Black-backed Gulls dispersed to offshore areas in Block Island and Rhode Island Sounds, although estimated densities were very low in deeper, central, offshore sections of Rhode Island Sound and the Inner Continental Shelf (Fig. 85). During the fall, densities peaked at 36 individuals per km^2. During the winter, numbers of Great Black-backed Gulls in the Ocean SAMP area apparently declined substantially to only 3.6 individuals per km^2. In all three seasons, most of the variation in density estimates of Great Black-backed Gulls occurred in offshore areas (Fig. 86).

Population size in the Ocean SAMP area – Based on the DSM models (Appendix H), we estimated that during summer 2009 there were 1,454 Herring Gulls in the Ocean SAMP area (95% CI = 1,246 to 1,697), an increase to 7,332 individuals (6,000 to 8,961) in fall, and a dramatic decline to 1,082 individuals (1,042 to 1,124) during the winter season (Appendix I). In summer, we estimated 1,869 Great Black-backed Gulls in the Ocean SAMP area (95% CI = 1,255 to 2,786), an increase to 2,680 individuals (2,366 to 3,036) in fall, and a dramatic decline to 682 individuals (627 to 743) during the winter season (Appendix I).

Spatial patterns in abundance in relation to bathymetry – The distribution and abundance of gulls detected during aerial surveys were generally consistent with the estimated densities from the Herring Gull and Great Black-backed Gull winter DSM (Fig. 87). During aerial surveys it was obvious that Herring and Great Black-backed Gull distribution was often associated with commercial fishing boats, and we often observed gulls feeding behind boats (K. Winiarski, pers. obs.). The depth profile of Gulls was similar to the depth profile of the study area, with peak abundance in ocean waters that were 30-45 m deep (Fig. 88).

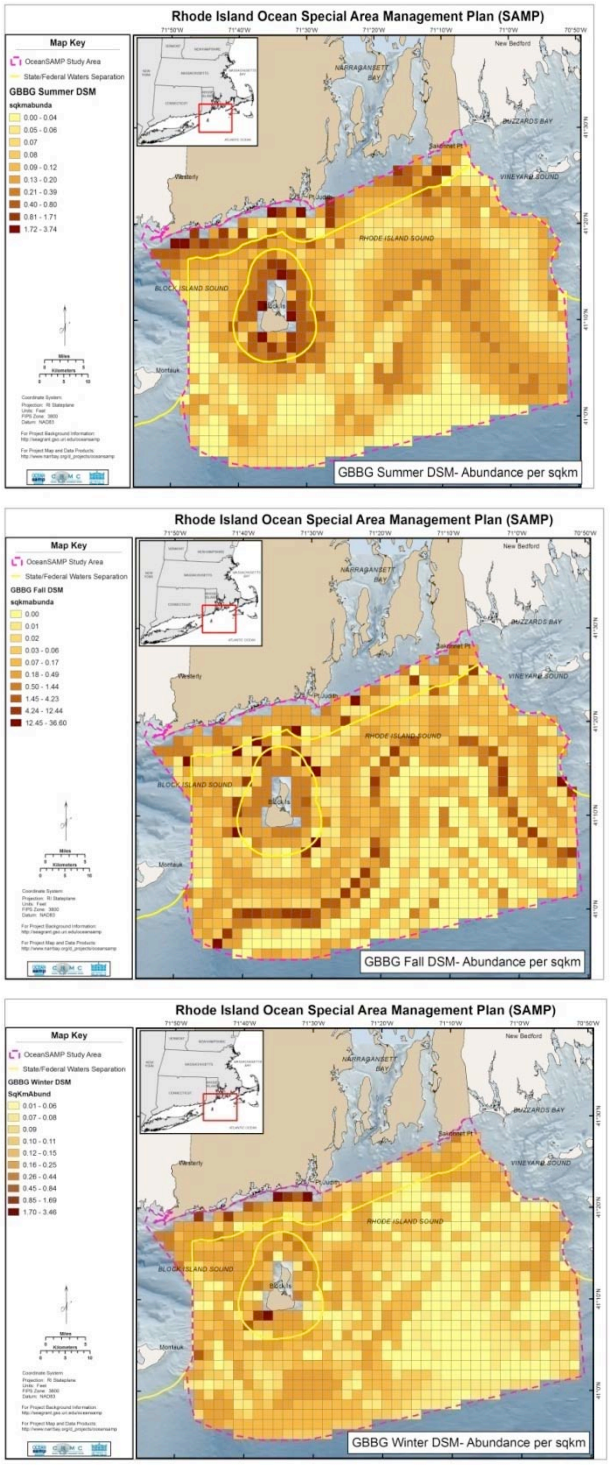

Fig. 85. DSM estimates of the spatial distribution and density of Great Black-backed Gulls in summer (upper), fall (middle) and winter (lower) in the Ocean SAMP study area based on ship line-transects.

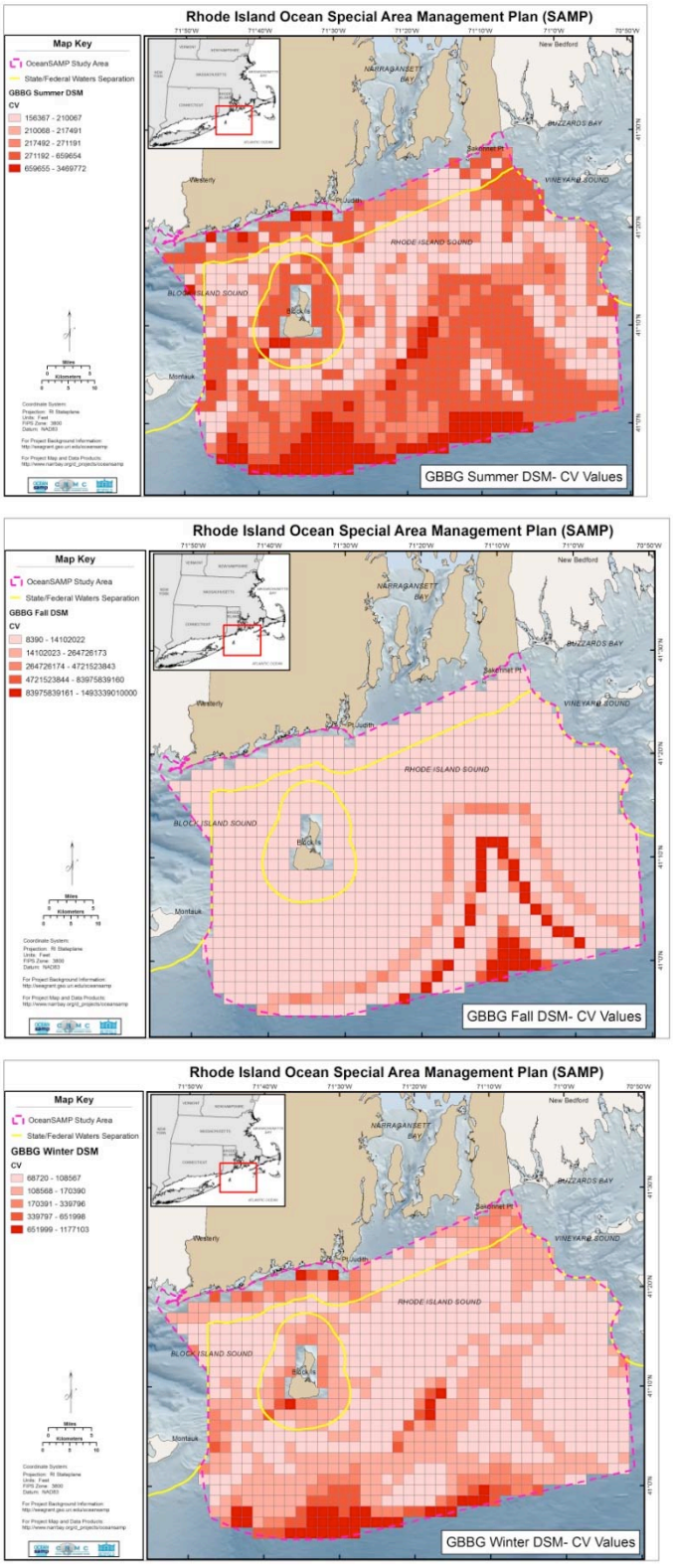

Fig. 86. Coefficient of Variation for DSM modeled Great Black-backed Gulls density estimates in summer (upper), fall (middle) and winter (lower) based on ship line transect surveys shown in Fig. 85. Density estimates exhibit more variation in areas in bright red.

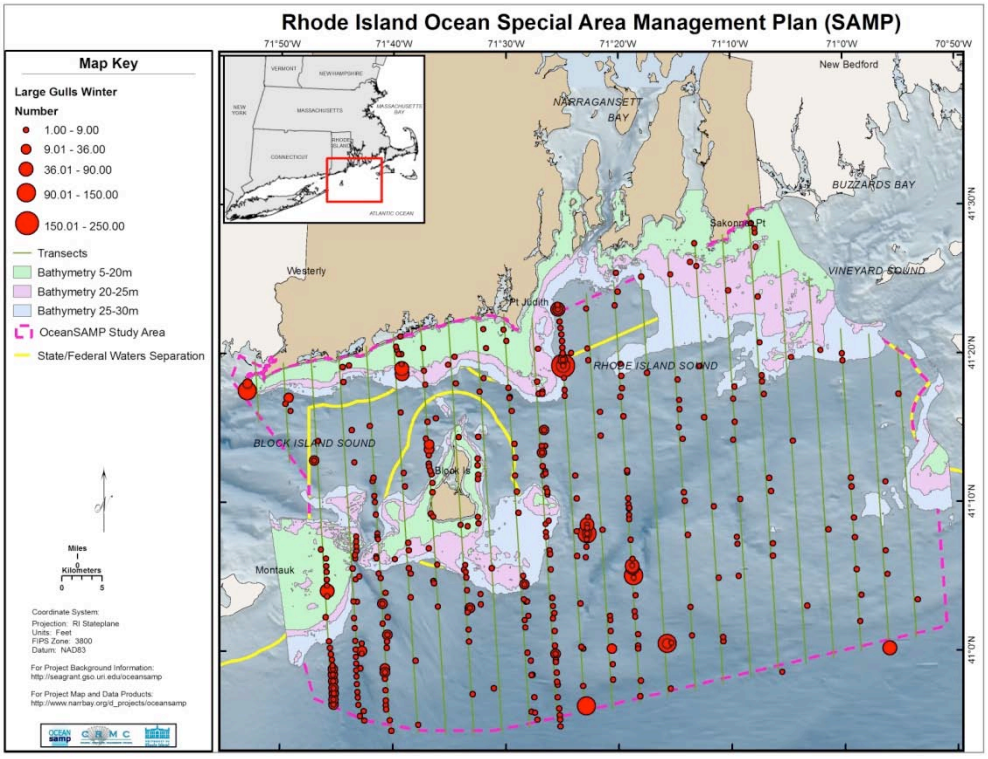

Fig. 87. Distribution of gulls detected during aerial surveys in the winter of 2009-2010. Large flocks tended to be associated with fishing vessels.

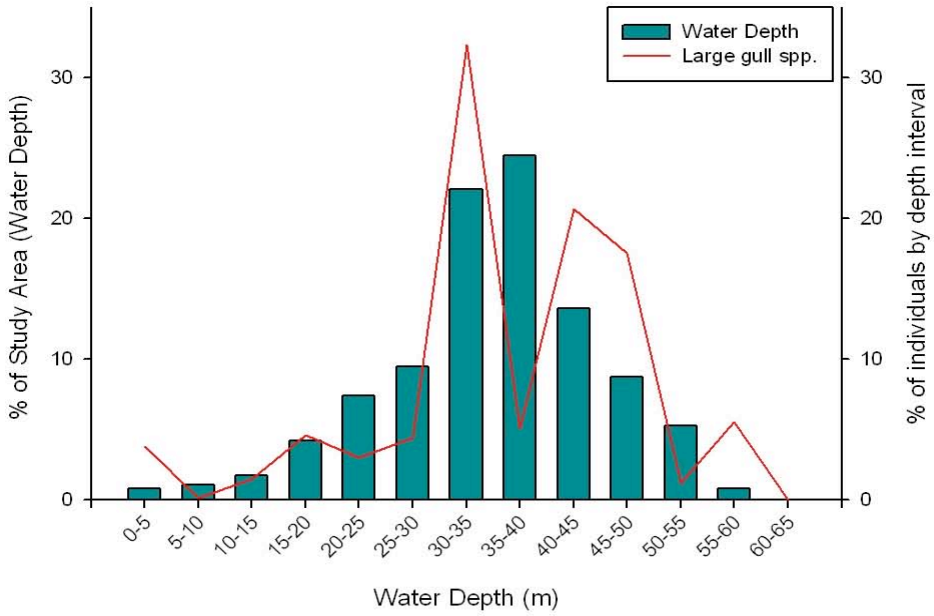

Fig. 88. Bathymetry of Ocean SAMP study area (green histogram) compared to depths where Herring and Great Black-backed Gulls were detected during aerial surveys (red line) (Fig. 87).

3.13 Kittiwakes

We detected one species of kittiwake (Laridae) in the Ocean SAMP study area, the Black-legged Kittiwake. The Black-legged Kittiwake is an offshore specialist that is not commonly found close to shore.

Seasonal changes in abundance – Black-legged Kittiwakes are winter residents and migrants in the Ocean SAMP area most commonly found from November through March (Fig. 89).

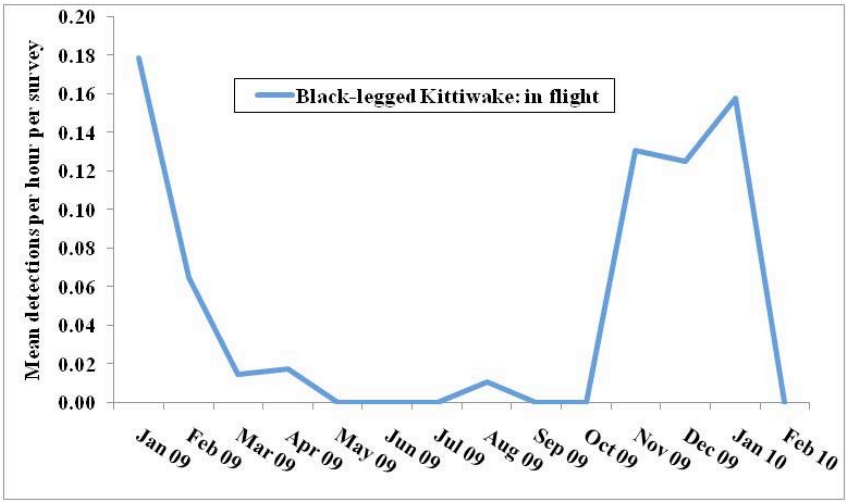

Fig. 89. Mean number of Black-legged Kittiwakes detected in flight per survey per month at 11 land-based seawatch stations along the Rhode Island coastline

Flight altitude of birds - Kittiwakes fly at similar altitudes as other gulls, with 58% of detections flying at altitudes <10 m high, 37% between 10-25 m, and about 6% flying over 25 m high (Fig. 90).

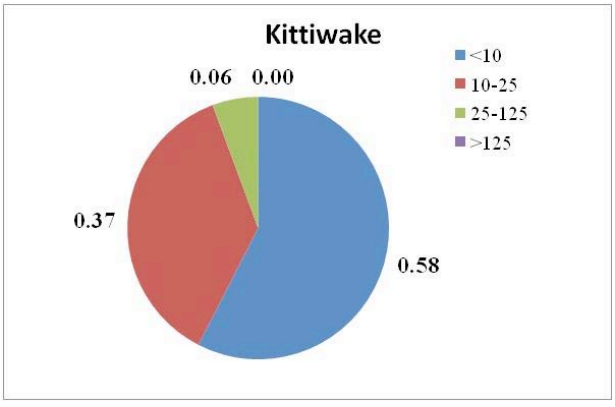

Fig. 90. Flight altitude of kittiwakes (m above sea level; N = 106 detections) based estimates during land-based seawatches and ship-based line transects. Shown are proportion of birds in four altitude categories.

Spatial patterns in abundance in nearshore waters - The only nearshore locations where kittiwakes were seen fairly regularly were Point Judith, Beavertail, Brenton Pt., and Ruggles Ave. (Fig. 91). See Appendices B and C for data on kittiwake abundance at each of the land-based seawatch stations for each month surveyed.

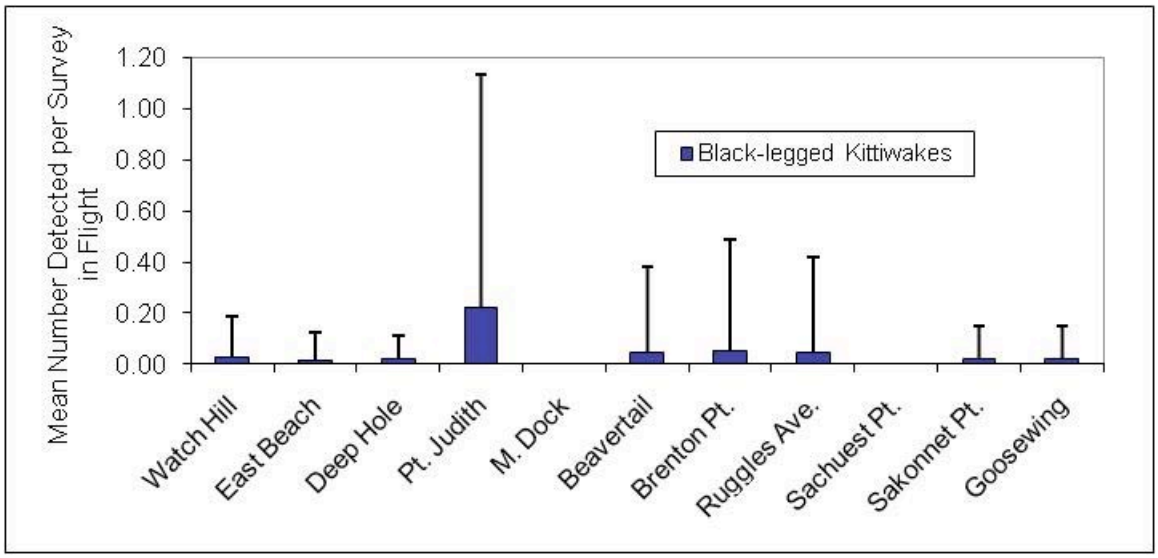

Fig. 91. Mean (SD) number of Black-legged Kittiwakes detected per survey at 11 land-based seawatch stations (see Fig. 21 for locations of stations).

Spatial patterns in abundance in nearshore and offshore waters –The best-fit Density Surface Model (DSM) explained 9.7% of the spatial variation in observed abundance of Black-legged Kittiwakes (see Appendix H for full model results). Black-legged Kittiwake densities during winter were greatest in the deeper waters of central Rhode Island Sound and the Inner Continental Shelf (Fig. 92). Densities were also high in a band about 3 miles south of the mainland coast and off of Block Island. However, there was considerable uncertainty about kittiwake use of nearshore habitats off of mainland Rhode Island and Block Island. The scarcity of kittiwake observations at land-based seawatch stations suggests the DSM model is fairly accurate concerning the paucity of kittiwakes using nearshore habitats. CVs for these density estimates are shown in Fig. 92.

Population size in the Ocean SAMP area - Based on the Black-legged Kittiwake DSM (Appendix H), we estimated that during the winter of 2009-2010, there were 291Black-legged Kittiwake (95% CI = 283 to 299) in the Ocean SAMP study area (Appendix I). This is a daily estimate during winter. Since kittiwakes are actively migrating through the area, we have no

accurate estimates concerning their turnover rates in the study area, and so cannot determine how many kittiwakes use the area overall.

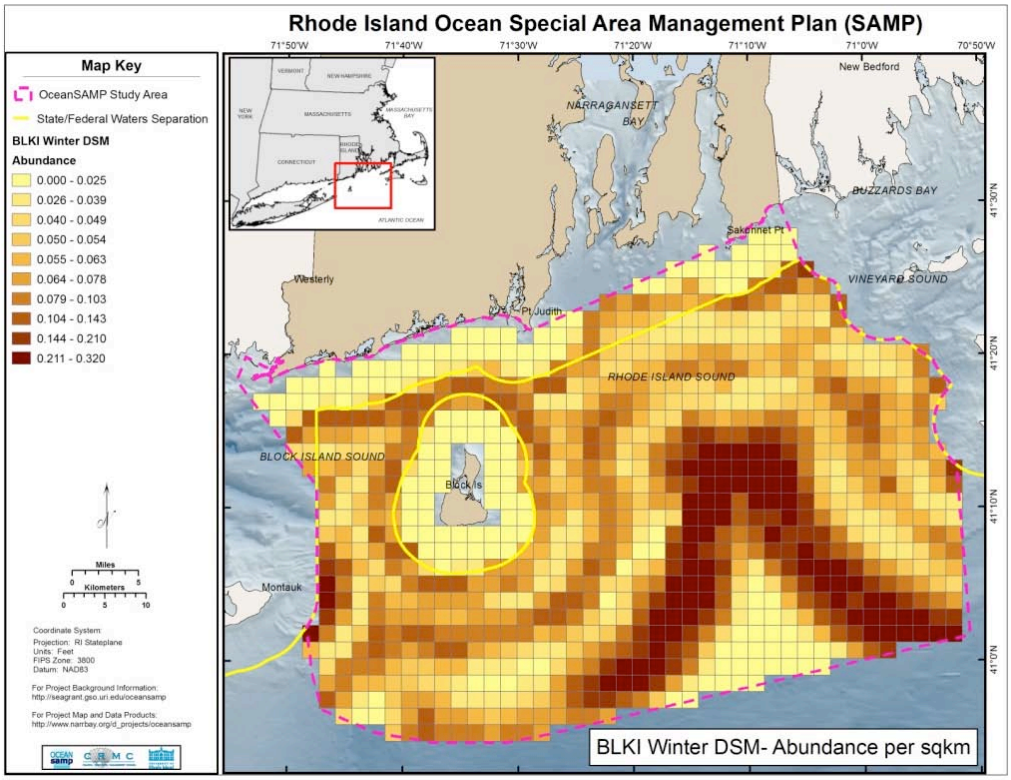

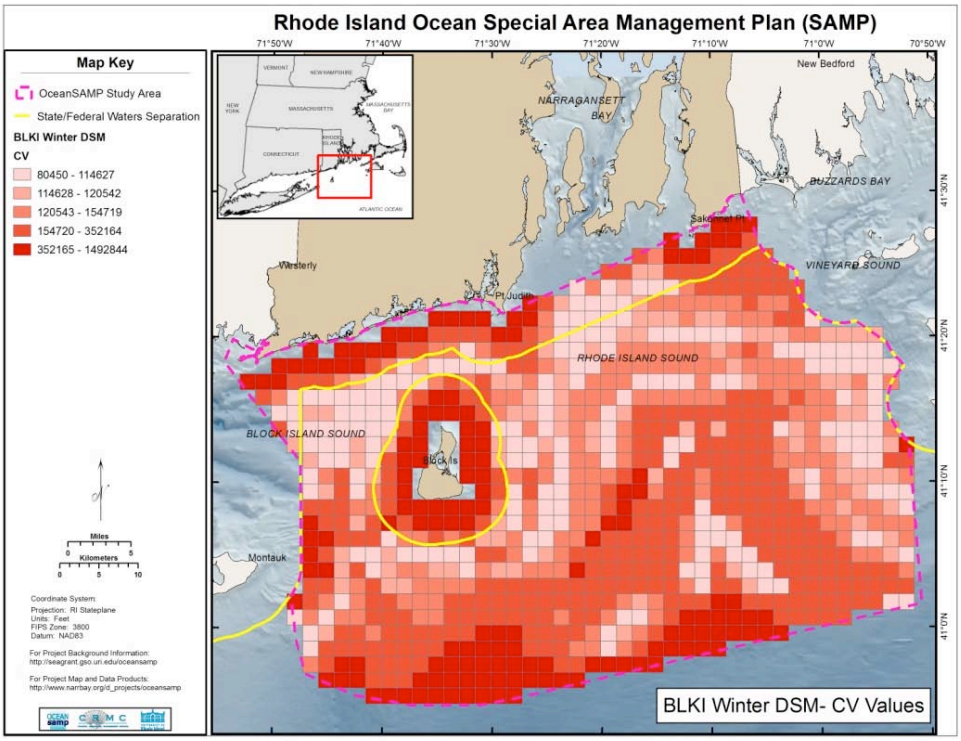

Fig. 92. DSM estimates of the spatial distribution and density of Black-legged Kittiwakes (upper) and CV estimates (lower) in winter in the Ocean SAMP study area based on ship line-transect surveys.

Spatial patterns in abundance in relation to bathymetry – The distribution and abundance of Black-legged Kittiwakes detected during aerial surveys were consistent with the estimated densities from the Black-legged Kittiwake DSM (Fig. 93). Most observations of kittiwakes during aerial surveys were on the Inner Continental Shelf and in southern sections of Rhode Island Sound (Fig. 93). Kittiwakes were primarily found in deeper waters of the Ocean SAMP area, with peak detections in waters that were 50-55 m deep (Fig. 94).

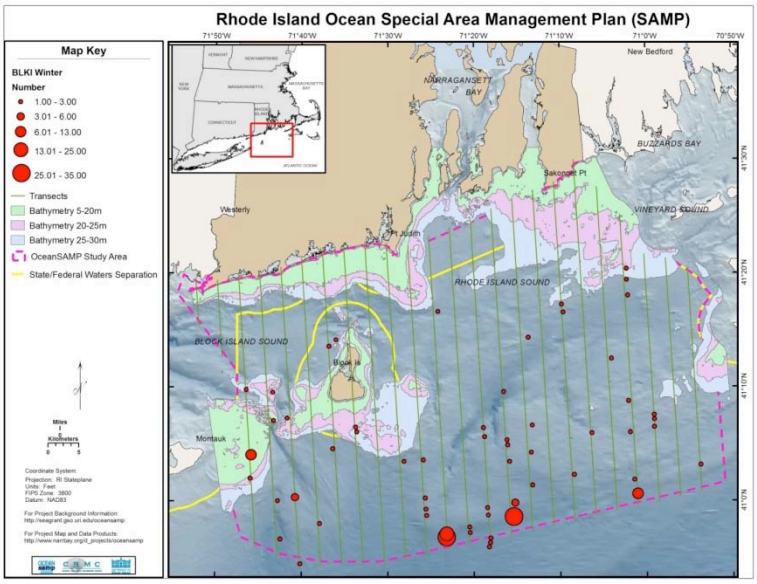

Fig. 93. Distribution of Black-legged Kittiwakes detected during aerial surveys in winter in the Ocean SAMP study area

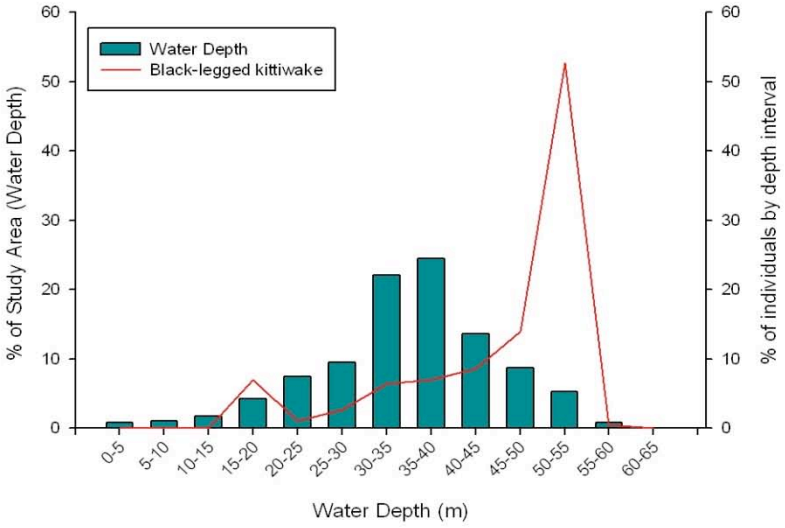

Fig. 94. Depth profile of Ocean SAMP study area (green histogram) compared to depths where Black-legged Kittiwakes were detected during aerial surveys (red line) (Fig. 93).

3.14 Terns and skimmers

We detected seven species of terns (Sternidae) and one species of skimmer (Rynchopidae) in the Ocean SAMP study area: Caspian, Royal, Common, Forster's, Roseate, Least, Black Tern and Black Skimmer. Common, Least and Roseate are the most abundant tern species detected in the Ocean SAMP area. Caspian Tern, Royal Tern, Forster's Tern, Black Tern and Black Skimmer are relatively uncommon in the SAMP area.

Seasonal changes in abundance - Terns are breeders and migrants in the Ocean SAMP area. Common and Least Terns are both species that breed locally in Rhode Island (C. Raithel unpublished data 2009; Ferren and Meyers 1998), which explains in part their high detection rates from May to September (Fig. 95). Roseate Terns breed in colonies near Rhode Island, and are primarily post-breeding migrants into the area from mid-July to early September (a detailed summary of Roseate Terns using the Ocean SAMP area is provided in section 3.2 above). All species of terns and skimmer spend only a maximum of six months in Rhode Island waters. For example, Common Terns are in the region from May through October (Fig 95), which is slightly longer than other migratory terns that only pass through the area to and from their breeding grounds (Royal, Caspian, Forster's, and Black Terns).

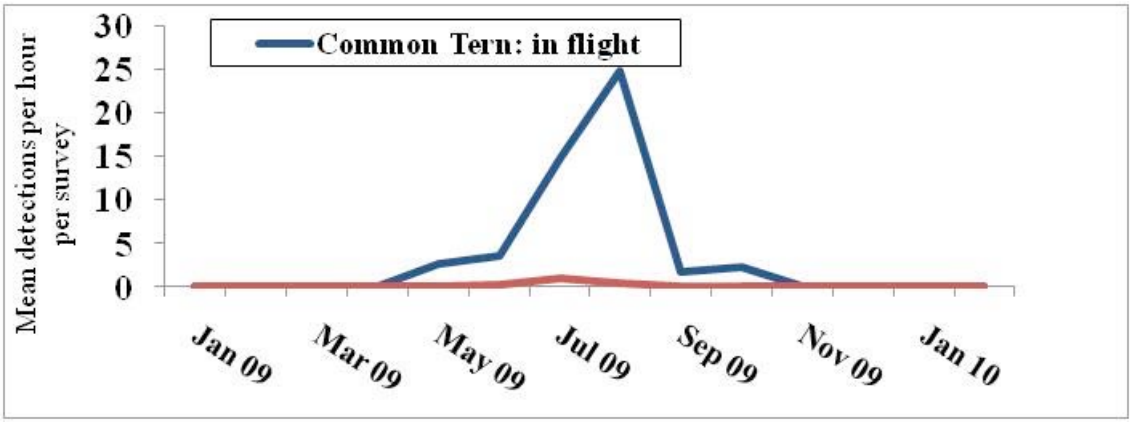

Fig. 95. Mean number of Common (blue line) and Roseate Terns (red line) detected in flight per survey per month at 11 land-based seawatch stations along the Rhode Island coastline.

Flight altitude of birds - Most terns (94%) were flying at altitudes of <25 m when we observed them during land-based seawatches and ship-based line-transect surveys (Fig. 96).

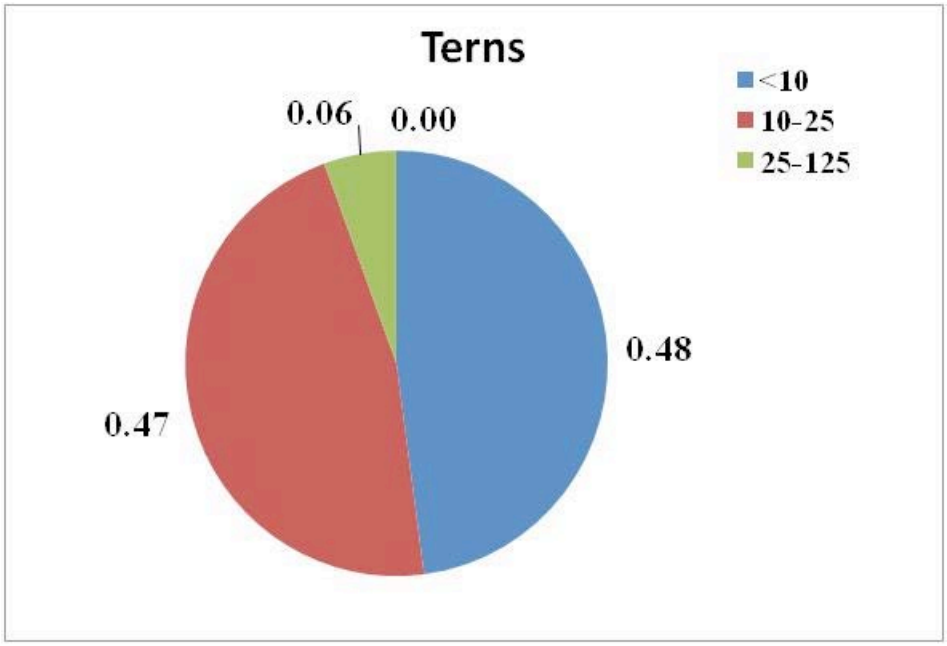

Fig. 96. Flight altitude of terns (m above sea level; N = 5,592 detections) based estimates during land-based seawatches and ship-based line transects. Shown are proportion of birds in four altitude categories.

Spatial patterns in abundance in nearshore waters – Common Terns tend to be detected throughout nearshore waters in the Ocean SAMP study area, while Least Terns tend to be more abundant in Block Island Sound and near Goosewing (Fig. 97). The distribution of Roseate Terns is discussed in detail in section 3.2 above. See Appendices B and C for data on tern and skinner abundance at each of the land-based seawatch stations for each month surveyed.

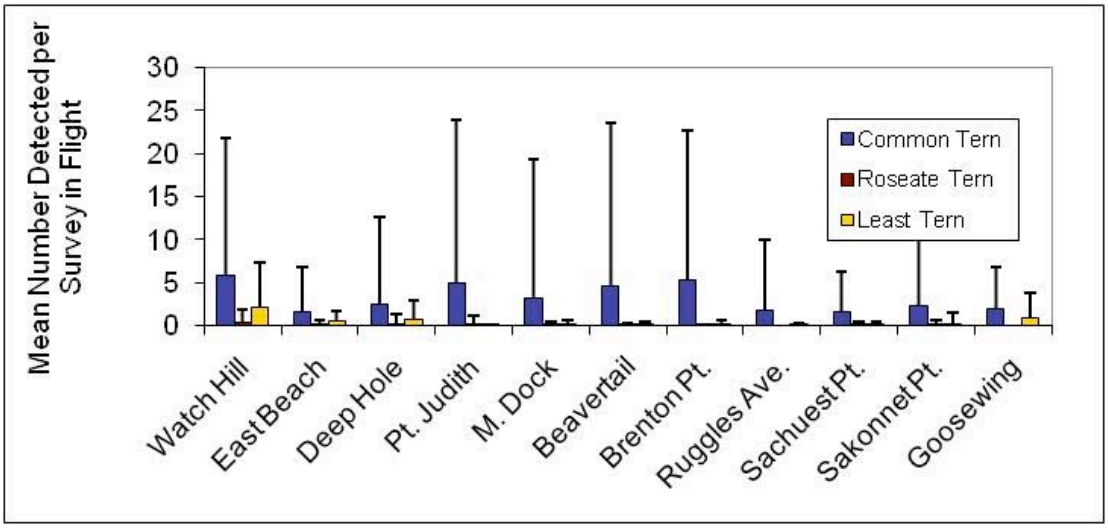

Fig. 97. Mean (SD) number of Common, Roseate, and Least Terns detected per survey at 11 land-based seawatch stations (see Fig. 21 for locations of stations).

Spatial patterns in abundance in nearshore and offshore waters –We detected a small number of commuting terns in offshore areas during ship-based surveys but not enough to confidently model the distribution and density of terns in the SAMP area (Fig. 98).

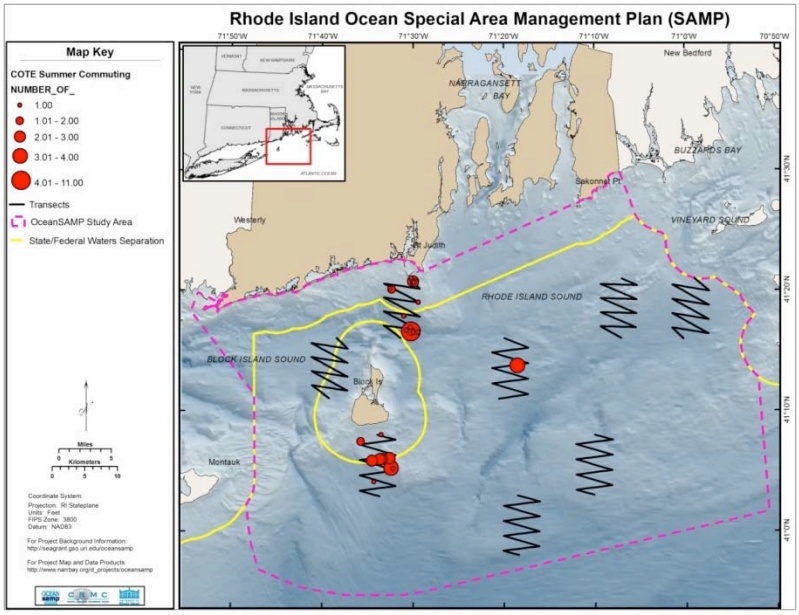

Fig. 98. Distribution of Common Tern flocks detected during ship line-transects in the summer in the Ocean SAMP study area

Population size in the Ocean SAMP area - We had too few detections of terns and skimmers during ship-based line transects in to estimate their population size in the study area.

Spatial patterns in abundance in relation to bathymetry – We had no detections of terns or skimmers during winter aerial surveys, thus we did not explore tern abundance in relation to water depth in the Ocean SAMP study area.

3.15 Alcids

We detected six species of alcids (Alcidae) in the Ocean SAMP study area: Razorbill, Common Murre, Thick-billed Murre, Dovekie, Black Guillemot, and Atlantic Puffin. Razorbills, Common Murre and Dovekies are common and abundant in the SAMP area. Thick-billed Murre, Black Guillemot and Atlantic Puffin are common but found in relatively low numbers in the Ocean SAMP study area.

Seasonal changes in abundance - Alcids are winter residents and migrants in the Ocean SAMP area. Based on land-based seawatch data of Razorbills, alcids start to appear Rhode Island in

December, their numbers peak in January, and most have departed by mid-March (Fig. 99; see also Appendix D).

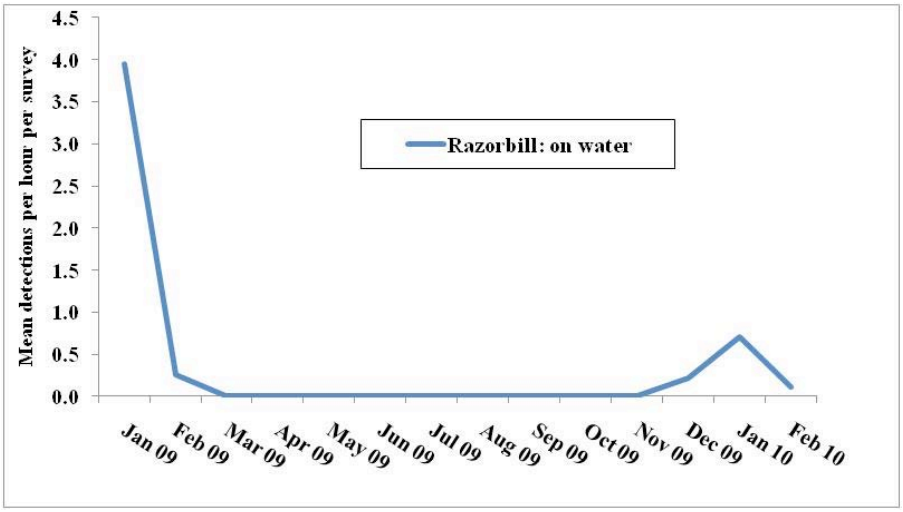

Fig. 99. Mean number of Razorbills detected on the water per survey per month at 11 land-based seawatch stations along the Rhode Island coastline

Flight altitude of birds - As with most pelagic species, alcids remain near the ocean surface when in flight; all birds observed were flying at altitudes <10 m (N = 401 detections; see also Tables 15 and 19).

Spatial patterns in abundance in nearshore waters - Razorbills were detected most often at rocky promontories (Pt. Judith, Beavertail; Fig. 100.). See Appendices B and C for data on alcid abundance at each of the land-based seawatch stations for each month surveyed.

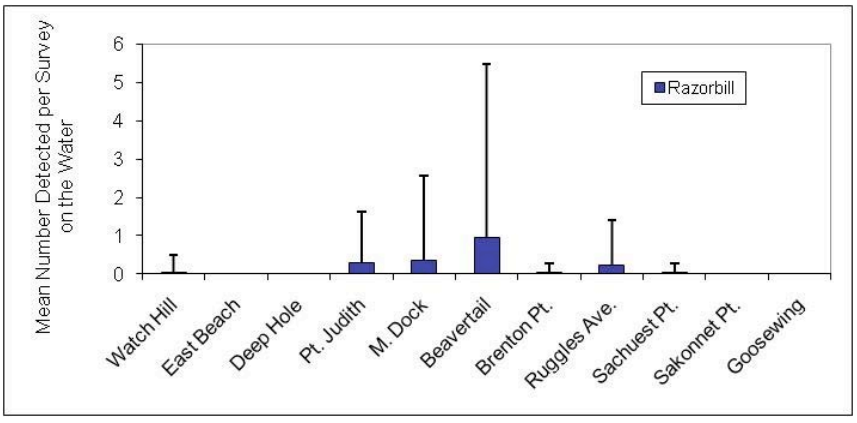

Fig. 100. Mean (SD) number Razorbills detected per survey at 11 land-based seawatch stations (see Fig. 21 for locations of stations).

Spatial patterns in abundance in nearshore and offshore waters – We present the detection function plots that were derived from the observed abundance of alcids on the water from ship-based surveys, and the associated GAM plot (Appendix J). The best-fit Density Surface Model (DSM) for Razorbills, Common Murres and Dovekies explained 11.3%, 23.5% and 34.6% of the spatial variation in observed abundance, respectively (see Appendix H for full model results). DSM models revealed a clear pattern of spatial segregation among these three species within the Ocean SAMP area. Razorbills tend to have their greatest density estimates (up to 1.5 birds per km^2) in the northern edge of the study area and south of Block Island in shallower waters (Fig. 101). Common Murres tend to be concentrated in the middle of the Ocean SAMP study area, in areas with slightly deeper water (Fig 101). High densities of Common Murres (up to 2.2 birds per km^2) occur north of Block Island and across the middle sections of Rhode Island Sound. Finally, Dovekies tended to occur in the deeper water sections of Rhode Island Sound and the Inner Continental Shelf, where densities can be much higher (up to 36.8 individuals per km^2) than any of the other alcids in the region (Fig. 101). We were unable to model the densities or distribution of the other three alcids due to their low detection rates. For all three alcids we modeled, we had the greatest uncertainty about density estimates in southern sections of Rhode Island Sound (Fig. 102).

Population size in the Ocean SAMP area - Based on the alcid DSMs (Appendix H), we estimated that during the winter of 2009-2010, Dovekies were the most abundant species, with 5,771 individuals (95% CI = 4,222 to 7,888), Razorbills the second most common, with 1,390 individuals (95% CI: 996 to1,940) and Common Murres the least abundant, with 623 individuals (95% CI: 548 to 707: Appendix I).

Spatial patterns in abundance in relation to bathymetry – The distribution and abundance of alcids detected during aerial surveys were consistent with the estimated densities from the alcid DSMs (Figure 103). When you compare the depth at alcid detections during aerial surveys compared to the depth profile of the Ocean SAMP area, it is apparent that alcids prefer deeper water (>30 m deep; Fig. 104).

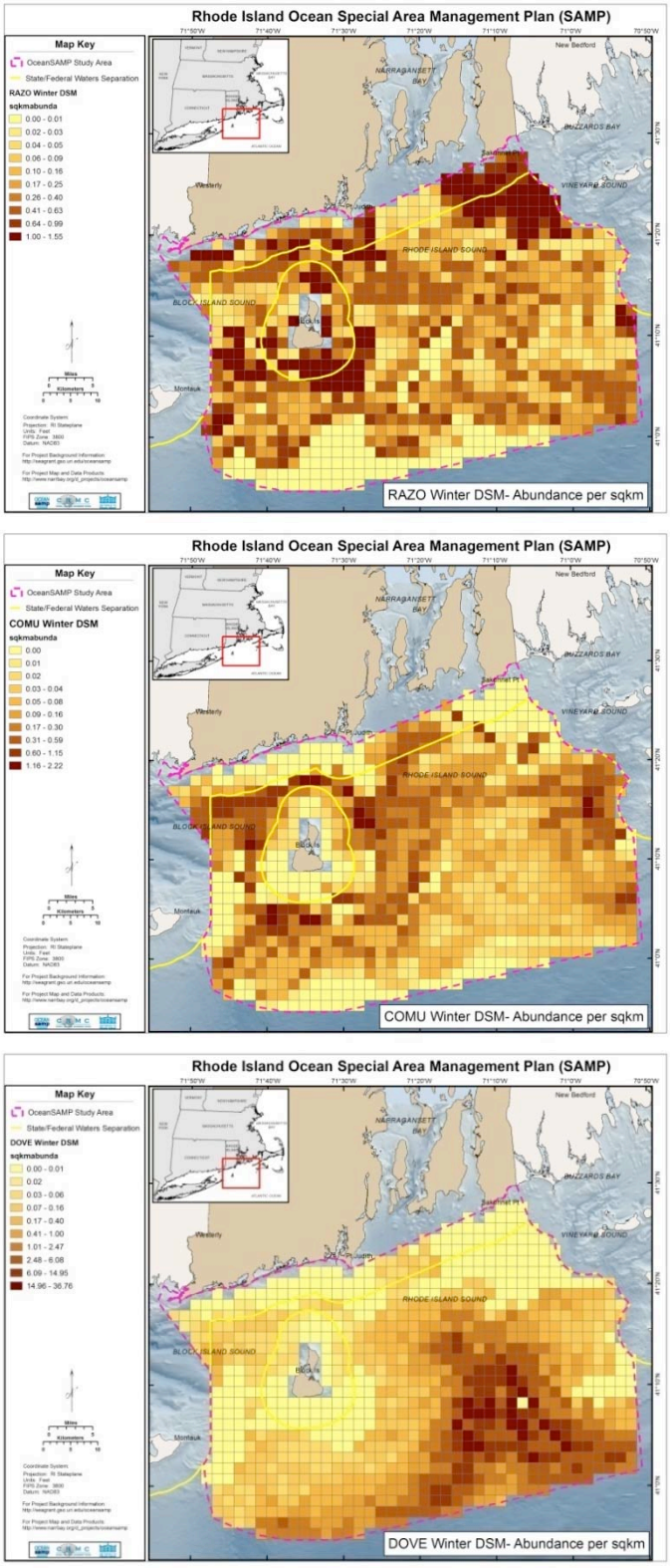

Fig. 101. DSM estimates of the spatial distribution and density of Razorbills (upper), Common Murre (middle) and Dovekie (lower) in winter in the Ocean SAMP study area based on ship line-transect surveys.

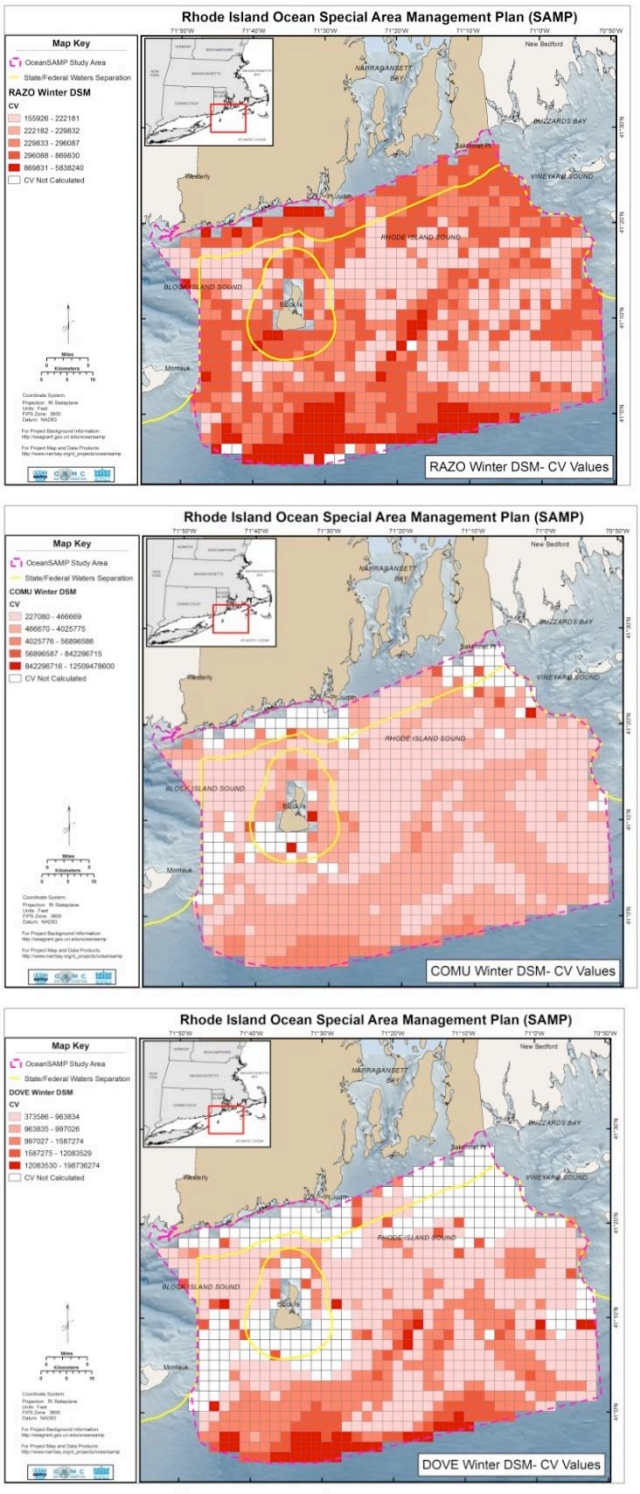

Fig. 102. Coefficient of Variation for DSM density estimates for Razorbills (upper), Common Murre (middle) and Dovekie (lower) based on ship line transect surveys shown in Fig. 101.

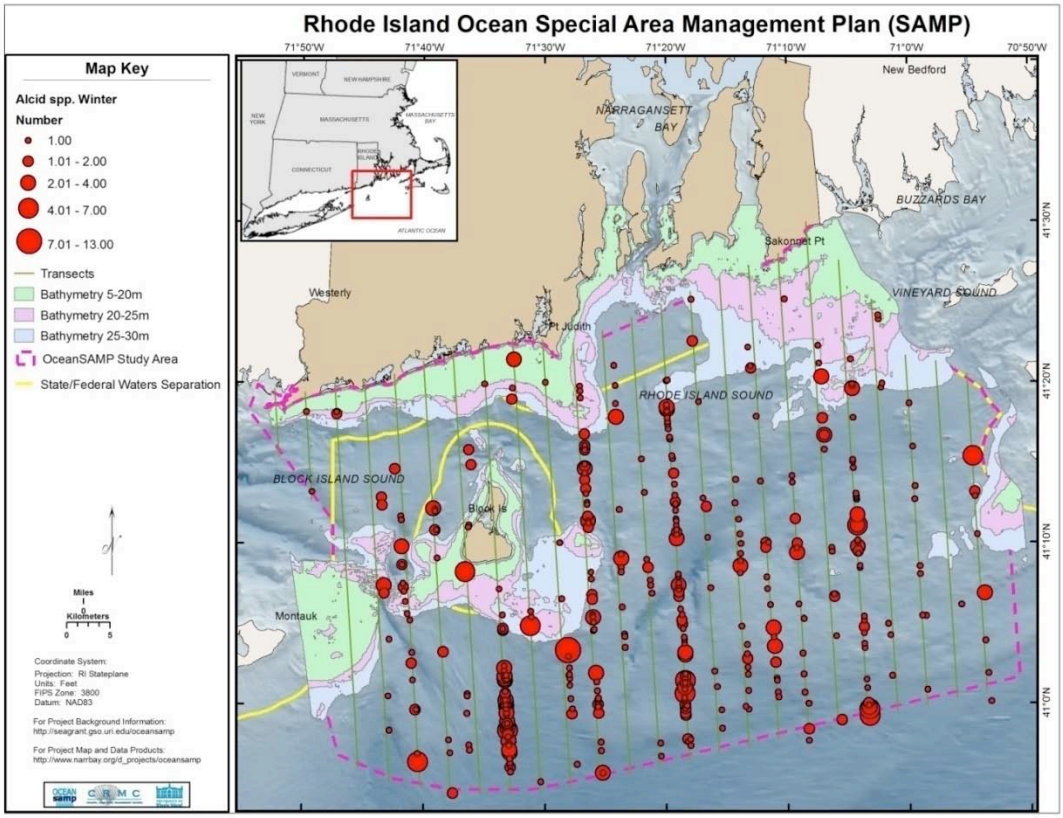

Fig. 103. Distribution of alcid flocks (e.g., Razorbills Common Murre, and Dovekie) based on aerial surveys in winter in the Ocean SAMP study area. We could not identify species during flights.

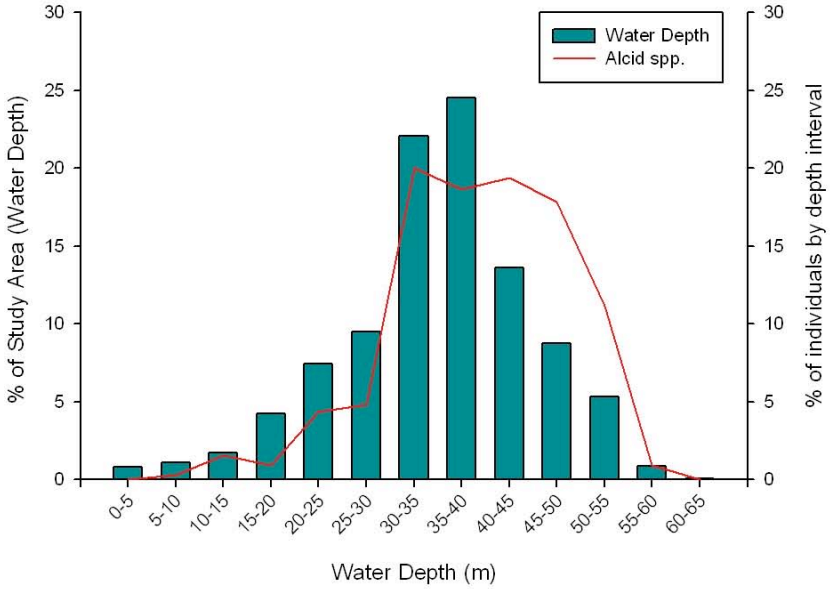

Fig. 104. Depth profile of Ocean SAMP study area (green histogram) compared to depths where alcids were detected during aerial surveys (red line) (Fig. 103).

3.16 Landbirds

We detected seven species of raptors (Accipitidae, Pandonidae and Falconidae), a dove species (Columbidae), an owl species (Strigidae), a swift (Apodidae), a hummingbird (Trochilidae), a kingfisher (Cerylidae), a flycatcher (Muscicapidae), three species of corvids (Corvidae), a lark (Alauidae), six species of swallows (Hirundinidae), a thrush (Turdidae), a pipit (Motacillidiae), a waxing (Bombycillidae), three warblers (Parulidae), a bunting (Emberizidae), a finch (Fringillidiae) , a junco (Emberizidae), three icterids (Icteridae) and a sparrow (Passeridae). Landbirds are relatively uncommon in the Ocean SAMP area (excluding Block Island) since they are generally associated with terrestrial habitats. The only raptor we detected regularly was Osprey, which is not surprising given that they often forage in nearshore habitats and regularly migrate along the coast. All other raptors were detected <10 times. Most raptors, with the exception of falcons, avoid crossing large water bodies, thus are rarely observed on Block Island.

Seasonal changes in abundance – Landbirds were recorded during land-based seawatches year round. Tree Swallows were among the most abundant landbirds and found in large numbers in the fall during migration (Appendices B-D).

Flight altitude of birds - Of the passerines we observed, 99% were flying at altitudes <25 m (Fig. 105). However, this is likely a biased estimate of flight altitudes and is not representative of flight altitudes of passerines because birds flying at higher elevations are unlikely to have been detected with our survey methods. A more quantitative unbiased sample of passerine flight altitudes is obtained from data collected by radar, which are available in Appendix K.

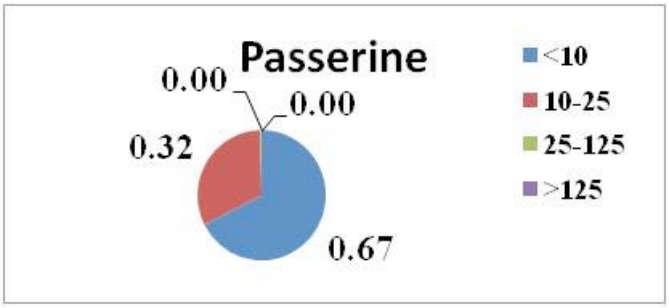

Fig. 105. Flight altitude of songbirds (m above sea level; N = 2,881) based on ocular estimates during land-based seawatches and ship-based line transects. Proportion of birds in four altitude categories is shown.

Spatial patterns in abundance in nearshore waters –Landbirds were distributed throughout seawatch stations (Appendices B and C).

Spatial patterns in abundance in nearshore and offshore waters – We had too few detections of landbirds during ship-based line transects in all seasons to model their density or spatial distribution. During ship-based line transects, we did detect a Mourning Dove and 7 species of songbirds (Bank and Tree Swallow; Blackpoll and Yellow-rumped Warbler; Dark-eyed Junco, Savannah Sparrow, and Snow Bunting; Table 18). The farthest offshore we detected a passerine was a Savannah Sparrow on Grid G.

Population size in the Ocean SAMP area - As expected, we had too few detections of landbirds during ship-based surveys to estimate their population size in the study area. This study was not designed to estimate the population size of landbirds migrating over Ocean SAMP study area.
Spatial patterns in abundance in relation to bathymetry – We had no detections of landbirds during aerial surveys, thus we did not explore Landbird abundance in relation to water depth in the SAMP study area.

4 Discussion

This interim report for the Rhode Island Special Area Management Plan (SAMP) summarizes our research conducted from January 2009 through mid-February 2010. This study represents the first attempt to quantify the spatial distribution and abundance of birds using the offshore waters of Rhode Island. However, our research is ongoing with ship-based and land-based surveys continuing through at least July 2010 and aerial surveys continuing until at least May 2011. Results from this ongoing research will be presented in another technical report published in 2011, along with a more comprehensive discussion of those final results. We provide here some discussion of the results presented in this interim report.

Previous Studies of Birds That Inhabit Rhode Island Waters
We compiled and summarized in this report the results from systematic surveys conducted in the Ocean SAMP study area in the late 1970s and throughout the 1980s. The largest historical offshore survey in the region was the Cetacean and Seabird Assessment Program surveys conducted from 1980-1988. This was a large-scale research program focused on investigating cetacean and seabird distribution and abundance from Cape Hatteras, North Carolina to Nova Scotia, Canada (MBO 1988). They surveyed within all shelf and shelf-edge waters < 183m (100 fathoms) deep in the Gulf of Maine, Georges Bank, southern New England waters, and the mid-Atlantic Bight (MBO 1988). They conducted a total of 1690 15-min long transects in the Inner Continental Shelf of the southern New England region from 1980 -1987, but only 101 transects were conducted within the Ocean SAMP study area boundaries over this 8-year study. Therefore, these surveys were too sparse over space and time to quantify baseline density or spatial distribution for birds within the Ocean SAMP boundaries. However, at larger spatial scales, these surveys summarize valuable information on avian distribution and abundance in this large-scale Atlantic offshore region (Power et al. 1980, Powers 1983).

We also summarized in this report the considerable historical information on avian abundance and distribution in Narragansett Bay, nearshore habitats along the southern Rhode Island coast (e.g., Sachuest Point NWR and Napatree Spit), and some coastal ponds. This summary makes it clear that a different suite of bird species uses Narragansett Bay and the coastal ponds than most of the Ocean SAMP study area that we surveyed. For example, although a diversity of dabbling ducks, geese, swans, and bay ducks are found in Narragansett Bay and the coastal ponds, those guilds occur only in low densities or are absent from the Ocean SAMP study area. Given this lack of historical baseline surveys, the results we present in this report provide the first quantitative estimates of the spatial distribution and abundance of birds inhabiting the offshore waters of Rhode Island.

Species Richness and Abundance of Birds in the Ocean SAMP Area

Importance of Nearshore Habitats

Our avian surveys along with historical avian surveys in Rhode Island nearshore waters, as well as bird surveys conducted in Nantucket Sound by Massachusetts Audubon as part of the Cape Wind research project, show the importance of nearshore, shallow waters for a wide range of avian species including seaducks, loons, grebes, cormorants, geese, gulls, gannets and one species of alcid (Razorbill). Of the 796 1-2 hr land-based surveys that we conducted, we detected 465,039 individuals of 121 different avian species. During the summer, nearshore waters were important for terns (including the federally endangered Roseate Tern), gulls, and shorebirds. During winter, seaducks and loons (both Common and Red-throated Loons) were also abundant throughout the Ocean SAMP study area. In Nantucket Sound, large numbers of loons (2,200 and 4,600 were detected in the winters of 2003-04 and 2004-05, respectively) and Razorbills (2,600 and 2,800, respectively) inhabited nearshore, shallow waters (Perkins et al. 2005). Thus, these nearshore, shallow water habitats in southern New England provide vital habitat for many avian species and possibly millions of migratory birds inhabit these nearshore waters in the Ocean SAMP study area during some portion of their annual life cycle.

Common Loons deserve mention because a significant portion of the population that nests in New England freshwater lakes spends the winter in Rhode Island waters. Common Loons primarily utilize nearshore areas in the SAMP area during December and January, though there is some indication that they move farther offshore as the winter progresses, potentially during their flightless molt period. Kenow et al. (2009), in a satellite telemetry study of 17 Common Loons, found that 95% of locations were within 10.5 km of a coastal land mass, with a maximum distance from shore of 26.6 km. Mean water depth at loon telemetry locations was <20 m for loons monitored by Kenow et al. (2009), and averaged 13 m. Kenow et al. (2009) documented winter home ranges of adult Common Loons from 43 to 1,159 km^2, indicating

loons ranged widely during winter. This telemetry study documented movement of loons between Rhode Island Sound and Buzzards Bay, Massachusetts. Another adult spent 3 months in Cape Cod Bay and then moved 87 km to Narragansett Bay in early February. However, the local movement patterns of resident wintering loons in the Ocean SAMP study area are still poorly understood and need further investigation. We estimated a surprisingly large population of Common Loons (2,901 individuals (95% CI = 2535-3321) during winter within the Ocean SAMP study area. Given that New York, Vermont, New Hampshire, Massachusetts, and Maine had 5,400 adults nesting during 2009 (NE Loon Study Group, pers. comm.), the Ocean SAMP area supports the equivalent of 54% of the Northeast loon breeding population during the winter. Thus, the nearshore waters within the Ocean SAMP area provide critical wintering habitat for significant numbers of loons that inhabit New England.

Importance of Offshore Habitats

Offshore areas in Rhode Island Sound and the Inner Continental Shelf provide important habitat for a different suite of birds than nearshore areas. On the 54 ship-based line transects (conducted from Jun 2009 to Feb 2010) we detected 13,170 individuals of 56 species. In contrast to avian species that use the ocean for part of their annual cycle (e.g., Loons [Gaviiformes], Grebes [Podicipiformes], and waterfowl [Anseriformes]), three orders of seabirds (Charadriiformes, Procellariiformes, and Pelecaniiformes) have specific adaptations that make them dependent throughout the year on the ocean for their food resources (Durant et al. 2004) and many of these seabirds primarily inhabit offshore waters. In the summer, thousands of shearwaters and storm-petrels use the southern sections of Rhode Island Sound and the Inner Continental Shelf during their large-scale movements throughout the Atlantic Ocean (Powers et al. 1983). In the fall and spring, Northern Gannets migrate through the SAMP area, taking advantage of abundant schools of sandlance (*Ammodytes* spp.) and mackerel (*Scomber scombrus*) (MBO 1988). Recent investigations of gannet migration from their breeding grounds in NE Canada to wintering sites off of SE North America document large-scale movements of gannets from nearer shore areas to pelagic waters hundreds of kilometers offshore (Montevecchi 2010).

During the winter, large numbers of alcids (Common and Thick-billed Murre, Dovekie) move into southern New England to feed on krill (e.g., euphausiids), decapods, fish and squid (Brown 1988, Huettmann et al. 2005) and they inhabit the deeper, offshore waters of the Ocean SAMP study area. These movements of alcids can be quite episodic. For example, Huettmann et al. (2005) conducted systematic boat-based surveys for alcids off Grand Manan Island, New Brunswick, and detected an average of 3,327 ± 4,058 (CV = 123; min = 160) large alcids between 3 Jan to 3 April 1998. However, on one survey in the middle of this survey period they detected 45,278 large alcids. In Jan 2010, we observed a similar influx of alcids during aerial surveys (average number of alcids from 18 Nov to 22 Feb = 70 ± 129; CV = 184; Table 26). In sum, these offshore, deeper water habitats in the Ocean SAMP study area provide vital habitat

for many avian species and it is likely that millions of migratory birds inhabit these offshore waters during some portion of their annual life cycle.

Endangered Species (Roseate Terns)

Roseate Terns are the only federally-listed endangered species of bird found in the Ocean SAMP study area. Our land-based and ship-based surveys that specifically focused on Roseate Terns (e.g., small boat tern surveys) revealed that Roseate Terns reside in the SAMP area only during mid-July to late-August (post-breeding) and this species is relatively uncommon. We observed most Roseate Terns in nearshore waters during seawatches, although we detected eight Roseate Terns during ship-based surveys in August. An ornithologist working for New Jersey Audubon Society on Block Island consistently observed up to 100 Roseate Terns on the island on any given day during August. This suggests that Roseate Terns are commuting through offshore waters during this post-breeding period before they eventually reach Cape Cod prior to fall migration.

Bathymetry as an Important Driver of Avian Species Composition: A Comparison with Nantucket Sound

We found water depth to be an important physical variable driving spatial distribution and abundance of avian species within the SAMP study area, and this is a relatively unique aspect of the Ocean SAMP study area. For example, the bathymetry of Nantucket Sound is much shallower (primarily <20 m deep) than the Ocean SAMP study area (<8% of the Ocean SAMP study area is <20 m deep) and avian community composition between Nantucket Sound and the RI Ocean SAMP study area was strikingly dissimilar. We found that seaducks in the Ocean SAMP area were mostly restricted to waters <25 m deep (Fig. 75), which is a relatively small portion of the study area, and we detected far fewer seaducks in the Ocean SAMP study area during the winter of 2009-2010 than in Nantucket Sound in the mid-2000s.

Perkins et al. (2005) estimated 280,000 and 204,000 Common Eider; 83,000 and 277,000 scoter in the winters of 2004-04 and 2004-05, respectively, in Nantucket Sound. Seaduck abundance within Nantucket Sound reflects the availability of benthic prey for scoters and eiders that typically utilize shallow habitats <20 m deep for feeding (Ydenberg and Guillemetter 1991, Lewis 2005, Kaiser 2006, NERI 2006). In contrast, thousands of shearwaters and storm-petrels use the deeper southern sections of the SAMP area during summer and large numbers of alcids (Razorbill, Common and Thick-billed Murre, Dovekie) move into the SAMP area to feed on krill (e.g., euphausiids), decapods, fish and squid (Brown 1988, Huettmann et al. 2005) during the winter. These species are much less common in Nantucket Sound because deepwater foraging habitat is not available. The bathymetry of Rhode Island Sound and Block Island Sound provides seaducks and seabirds with a much broader spectrum of water depth choices,

including much deeper areas, than in Nantucket Sound. Consequently, water depth is an important determinant of the distribution, abundance, and species composition of birds in the Ocean SAMP study area.

Review of Survey Methodology

The survey methods that we used provide an accurate assessment of the distribution and abundance of birds in the Ocean SAMP study area on mostly fair-weather days during the diurnal portion of the study period. The 800 land-based seawatch surveys that were conducted throughout the year for this report allowed us to quantify migration phenology and spatial variation in use of nearshore habitats. In addition, compared to ship-based and aerial surveys, land-based seawatches were relatively inexpensive to conduct. However, land-based seawatches only provide information about bird distribution and abundance relatively close to the coast (<3 km from shore). In addition, it is extremely difficult to standardize protocols among stations (e.g., elevation of the observer above the ocean surface, area sampled at each station, habitat characteristics vary among stations); thus, these point count data are too complex to analyze in a DISTANCE framework (Buckland et al. 2001) to estimate density patterns among stations.

One of the primary methods we used to accurately assess the spatial distribution, abundance, and behavior of birds in the Ocean SAMP study area was ship-based surveys, which have been used by ornithologists for almost 100 years (Jespersen 1924), with standardized protocols in place for 25 years (Tasker 1984, Camphuysen et al. 2004). However, because standardized survey protocols recommend the vessels moves at 10 km/hr, many hours (multiple days) of survey effort are needed to adequately cover a study area as large as the Ocean SAMP area. Yet, recent advances in line transect methods allowed us to model the spatial distribution and abundance of bird density across the entire study area from these restricted surveys (Ronconi and Burger 2009).

We also used aerial strip transect surveys along with the land-based and ship-based surveys to document distribution and abundance of birds in the Ocean SAMP study area. Aerial surveys allowed observers to cover portions of the entire Ocean SAMP study area in one day (approximately 3 hrs to survey every third transect; Fig. 26). Disadvantages of aerial surveys include identification of all birds to species is not possible (e.g., diving loons, small alcids, dark scoters) and flight altitude and flight direction of flying birds cannot be recorded. Despite these limitations, aerial transect surveys remain the primary method of choice for large-scale studies of nearshore and offshore birds especially in relation to offshore development projects (e.g., Camphuysen et al. 2004). After we complete at least one year of aerial surveys, we will use the DISTANCE framework (Buckland et al. 2001) and the data from both the aerial and ship-based surveys to estimate density of birds throughout the Ocean SAMP study area.

Importance of Long Term Avian Research: Inter-annual Variation in Avian Abundance

We documented considerable inter-annual variation in spatial distribution and abundance of birds during our surveys from Jan 2009 to Feb 2010, which is consistent with other longer-term studies of seabirds and seaducks. Seaducks were relatively more abundant during land-based seawatches in the winter of 2008-2009 compared to the winter of 2009-2010. For example, at Brenton Point (a primary foraging spot for seaducks) from 27 Jan to 25 March 2009, we counted on average 5,730 ± 4,250 (SD) scoters and eiders during each survey on the water (max = 16,055 on 6 March 2009). In contrast, from 2 Nov 2009 to 18 Feb 2010, we only detected on average 412 ± 192 (max = 1,107) scoters and eiders on the water. Thus, although we detected relatively few seaducks during aerial and ship based surveys during 2009-2010, it was likely a reflection of the relatively low numbers of seaducks in Rhode Island that winter. Locally, Perkins et al. (2004, 2005) documented substantial annual variation in the spatial distribution and abundance of seaduck flocks in Nantucket Sound. This inter-annual variation in abundance of birds makes it necessary to conduct avian surveys over an extended time period so that an accurate baseline assessment of the distribution and abundance of birds is available for comparison with data collected before, during, and after proposed development projects.

Daily Movement Patterns of Birds

Our surveys were designed to reliably estimate bird distribution and abundance throughout the year, but such surveys do not provide direct information about local daily movement patterns of seaducks in the Ocean SAMP study area. Near Nantucket Island, Long-tailed Ducks commute daily from nocturnal roosting sites in Nantucket Sound to Nantucket Shoals, up to 70 km offshore where they forage for pelagic amphipods in waters <20 m deep (White et al. 2009). We detected very few Long-tailed Ducks during our fieldwork. However, we did observe large numbers of scoters (primarily Surf and Black Scoter) emigrating south of the Sakonnet River into Rhode Island Sound every evening and then large numbers of birds immigrating north back up the Sakonnet River in the evening from January through March 2010. Documenting such regular daily movements of large numbers of birds within the Ocean SAMP study area would help delineate commuting corridors and help determine nocturnal roosting sites of seaducks, important information to consider when determining the location of offshore development projects. During 2011-2012, we will monitor the local movements of Surf Scoters implanted with satellite transmitters so that commuting corridors and frequently used nocturnal roosting sites can be delineated.

Summary

This report provides the first quantitative estimates of the spatial distribution and abundance of birds in the nearshore and offshore waters of Rhode Island. We have documented substantial avian use of nearshore habitats throughout the year. During winter, these nearshore waters are especially vital to a variety of species including seaducks, loons, grebes, gannets and cormorants. During summer, these nearshore waters become important for terns, gulls, and shorebirds. In contrast, offshore areas in Rhode Island Sound and the Inner Continental Shelf provide important wintering habitat for alcids, kittiwakes, gannets, gulls, and other species. During summer, these offshore areas provide critical habitat for a variety of seabirds that migrate long distances to reach Rhode Island waters. Storm-Petrels, from breeding colonies in Antarctica, and shearwaters, from breeding colonies in the southern central Atlantic Ocean, pass through Rhode Island during their annual migration around the perimeter of the Atlantic Ocean. These long-distance migrants are among the most numerous birds in the Ocean SAMP study area during this time. The distribution, abundance, and species composition of birds that we have documented in the Ocean SAMP study area are in part the product of the broad spectrum of water depths in Rhode Island Sound and Block Island Sound, its associated effects on many aspects of the ecosystem (e.g., water temperature, circulation, productivity), and the geographic location of Rhode Island waters with respect to one of the major bird migration corridors in North America.

Acknowledgements

A research project this broad in scope is impossible without the coordinated efforts of many excellent biologists, land managers, statisticians, computer geeks, boat captains, pilots, and others. We wish to thank the following people for their assistance with various aspects of this project. For help collecting data for this project, we thank Alex Patterson, John Veale, Hannah Grist and Everett Swanson. In particular, we thank Brian Harris for collecting excellent data while enduring often miserable working conditions in the middle of winter during freezing land-based seawatches and ship-based surveys – Brian is a skilled biologist who maximized the number of species we detected during surveys.

For access to historical data, we thank Chris Raithel (RI DEM – Napatree Point surveys), Jay Osenkowski and Charlie Allin (RI DEM – waterfowl surveys), Suzanne Paton (USFWS-Trustom Pond, Ninigret Point, and Sachuest Point NWRs), Rick McKinney (US EPA waterfowl surveys), and Allan O'Connell and Andrew Gilbert (USGS – access to NMFS and CSAP survey data). It is because of their foresight and dedication that some important baseline information about bird distribution and availability has been collected – thanks for letting us summarize this information here. We also thank the many unnamed volunteers who helped collect these data over the years.

We thank Sharon Marino and Tom Halavik (USFWS, Southern New England – NY Bight Coastal Program) for logistical support so that we could conduct boat-based Roseate Tern surveys in coastal Rhode Island waters. We thank the Francis Fleet (Galilee, RI) for assistance with conducting ship-based transects throughout the year in often inclement weather, and for their patience as we figured out schedules. Special thanks to Captains Don and Pauly for their excellent captain skills, their help collecting accurate data by staying on transect lines under adverse conditions, and for safely bringing us back to port every time. We thank EagleCap Aviation (LaGrande, Oregon) for providing excellent planes for aerial surveys. We especially want to thank Captain George Breen for unerringly piloting the Skymaster, for good company, and for getting our feet safely back on the ground after every survey.

We thank Chris Damon and Aimee Mandeville (URI EDC) for assistance with GIS analysis. We thank Dr. Eric Rexstad and Louise Burt (CREEM, Univ of St. Andrews) for assistance analyzing survey data in Program DISTANCE. We thank Dr. Tony Fox for advice about study design and many other things. We thank Rob Lancellotti of Swarovski Optiks for providing the survey crew with excellent optics at a discounted price.

Finally, we thank the entire Ocean SAMP research team for making this an exciting scientific as well as management and planning process. Special thanks to Jen McCann, Sam DeBow, and Kate Manning for their coordination skills, for keeping us on track (most of the time), and for answering our (many) questions. Extra special thanks to Grover Fugate who made this all possible and for being the ultimate captain.

References

Ainley, D. G., Nettleship, D.N., Carter, H.R., and Storey, A.E. 2002. Common Murre (*Uria aalge*). In: *The Birds of North America*. Poole, A. and Gill, F. (eds.). The Birds of North America, Inc., Philadelphia, PA.

Akaike, H. 1973. Information theory and an extension of the maximum likelihood principle. In: *Second international symposium on information theory. Akademiai Kiado*, pp. 267-281. Petrov, B.N., Csaaki, F., (eds). Budapest.

Boothroyd, J.C. in prep. Coarse-Grained Sediment Transport in Sounds, Bays, Estuaries, and Lagoons. In: *Sound Connections: The Science of Rhode Island & Block Island Sounds.* Proceedings of the 7th Annual Ronald C. Baird Sea Grant Science Symposium. Rhode Island Sea Grant, Narragansett, RI. October 2008.

Bordage, D. and Savard, J.L. 1995. Black Scoter (*Melanitta nigra*). In: *The Birds of North America*. Poole, A. and Gill, F. (eds.). The Birds of North America, Inc., Philadelphia, PA.

Brown, R.G. B., Barker, S. P., Gaskin, D.E. and Sandeman, M.R. 1981. The foods of Greater and Sooty shearwaters *Puffinus gravis* and *P. griseus* in eastern Canadian waters. *Ibis* 123:19–30.

Brown, R.G.B. 1988. Oceanographic factors as determinants of the winter range of the Dovekie (*Alle alle*) off Atlantic Canada. *Colonial Waterbirds* 11:176-180.

Buckland, S.T., Anderson, D.R, Burnham, K.P., Laake, J.L., Borchers, D.L., and Thomas, L. 2001. Introduction to distance sampling: estimating abundance of biological populations. Oxford University Press, London.

Burnham, K.P., and Anderson, D.R. 2002. Model selection and multimodel inference: a practical information-theoretic approach, 2nd ed. Springer, Berlin.

Burnham, K.P., Buckland, S.T., Laake, J.L., Borchers, D.L., Marques, T.A., Bishop, J.R.B., and Thomas, L. 2004. Further topics in distance sampling. In: Buckland, S.T., Anderson, D.R., Burnham, K.P., Laake, J.L., Borchers, D.L. and Thomas, L. (eds) Advanced distance sampling: estimating abundance of biological populations. Oxford University Press, New York, pp. 307-392.

Caron, C. M. and P.W.C. Paton. 2008. Population trends and habitat use of Harlequin Ducks in Rhode Island. *Journal of Field Ornithology* 78:254-262.

Certain, G., Bellier, E., Planque, B., and Bretagnolle, V. 2007. Characterising the temporal variability of the spatial distribution of animals: an application to seabirds at sea. *Ecography* 30: 695-708.

Conway, R.A. 1979. Field checklist of Rhode Island birds. Bulletin No. 1, Rhode Island Ornithological Club, Audubon Society of Rhode Island, Smithfield, RI.

Codiga, D.L., and Ullman, D.S. 2010 (*draft).* Characterizing the physical oceanography of coastal waters off Rhode Island: Literature review, available observation, and a representative model simulation. Final Report Part 1 for Rhode Island Ocean Special Area Management Plan.

Cottam, C. 1939. Food habits of North American diving ducks. U.S. Department of Agriculture Technical Bulletin No. 643., Washington, D.C.

Daub, B.C. 1989. Behavior of Common Loons in winter. *Journal of Field Ornithology* 60:305-311.

Desholm, M. and Kahlert, J. 2005. Avian collision risk at an offshore wind farm. *Biology Letters* 1: 296-298.

Dewar, J. M. 1924. The bird as a diver. Witherby, London.

Drewitt, A.L. and Langston, R.H.W. 2006. Assessing the impacts of wind farms on birds. *Ibis* 148:29-42.

Drury, W. H., and Keith, J.A .1962. Radar studies of songbird migration in coastal New England. *Ibis* 104:449–489.

Duffy, D.C. 1977. Breeding populations of terns and skimmers on Long Island Sound and eastern Long Island. *Proceedings of Linnean Society* 73: 1-48.

Durant, J.M.,Stenseth, N.C., Anker-Nilssen, T., Harris, M.P., Thompson, P.M., and Wanless. S. 2004. Marine birds and climate fluctuation in the North Atlantic. In: *Marine Ecosystems and Climate Variation*. Pp. 95-108. Oxford University Press,

Durinck, J., Christensen, K.D., Skov, H., and Danielsen, F.1993. Diet of the Common Scoter *Melanitta nigra* and Velvet Scoter *Melanitta fusc*a wintering in the North Sea. *Ornis Fennica* 70:215–218.

Efron, B. and Tibshirani, R.J. 1993. An introduction to the bootstrap. Chapman and Hall, New-York.

Ellarson, R. S. 1956. A study of the Old-squaw Duck on Lake Michigan. Ph.D. thesis, University of Wisconsin, Madison.

Elliott-Smith, E., and Haig, S.M. 2004. Piping Plover (*Charadrius melodus*). In: *The Birds of North America*. Poole, A. and Gill, F. (eds.). The Birds of North America, Inc., Philadelphia, PA.

Fischer, J. B. 1998. Feeding behavior, body condition, and oil contamination of wintering Harlequin Ducks (*Histrionicus histrionicus*) at Shemya Island, Alaska. M.S. thesis, University of Massachusetts, Amherst.

Gaines, W. L. and Fitzner, R.E. 1987. Winter diet of the Harlequin Duck at Sequim Bay, Puget Sound, Washington. *Northwest Science* 61:213–215.

Gauthier, G. 1993. Bufflehead (*Bucephala albeola*). In: *The Birds of North America*. Poole, A. and Gill, F. (eds.). The Birds of North America, Inc., Philadelphia, PA.

Gaston, A. J. and Hipfner, J.M. 2000. Thick-billed Murre (*Uria lomvia*). In: *The Birds of North America*. Poole, A. and Gill, F. (eds.). The Birds of North America, Inc., Philadelphia, PA.

Good, T. P. 1998. Great Black-backed Gull (*Larus marinus*). In: *The Birds of North America*. Poole, A. and Gill, F. (eds.). The Birds of North America, Inc., Philadelphia, PA.

Goudie, R. I. and Ankney, C.D. 1986. Body size, activity budgets, and diets of sea ducks wintering in Newfoundland. *Ecology* 67: 1475–1482.

Goudie, R. I., Robertson, G.J. and Reed, A. 2000. Common Eider (*Somateria mollissima*). In: *The Birds of North America*. Poole, A. and Gill, F. (eds.). The Birds of North America, Inc., Philadelphia, PA.

Grist, H. 2009. Rhode Island Ocean Special Area Management Plan: Post-breeding ecology of Roseate Terns (*Sterna dougalii*). M.S. thesis, Oxford Univ, England.

Guillemette, M., Himmelman, J.H., Barette, C. and Reed, A. 1993. Habitat selection by common eiders in winter and its interaction with flock size. *Canadian Journal of Zoology* 71: 1259-1266.

Guillemette, M., Woakes, A.J., Henaux, V., Grandbois, J. and Butler, P. 2005. The effect of depth on the diving behavior of common eiders. *Canadian Journal of Zoology* 82: 1818-1826.

Hastie, T.J. and Tibshirani, R.J. 1993. An introduction to the bootstrap. Chapman and Hall, New-York.

Hatch, J. J. and Weseloh, D.V. 1999. Double-crested Cormorant (*Phalacrocorax auritus*). In: *The Birds of North America*. Poole, A. and Gill, F. (eds.). The Birds of North America, Inc., Philadelphia, PA.

Hatch, J.J., Brown, K.V., Geoffrey, G.H. and Morris, R.D. 2000. Great Cormorant (*Phalacrocorax carbo*). In: *The Birds of North America*. Poole, A. and Gill, F. (eds.). The Birds of North America, Inc., Philadelphia, PA.

Haney, J. C. and Stone, A.E. 1988. Seabird foraging tactics and water clarity: are plunge-divers really in the clear? *Marine Ecology Progress Series* 49: 1–9.

Haven, R.W. and Lee, D.S. 1999. Parasitic Jaeger (*Stercorarius parasiticus*). In: *The Birds of North America*. Poole, A. and Gill, F. (eds.). The Birds of North America, Inc., Philadelphia, PA.

Haven, R.W. and Lee, D.S. 2000. Pomarine Jaeger (*Stercorarius pomarinus*). In: *The Birds of North America*. Poole, A. and Gill, F. (eds.). The Birds of North America, Inc., Philadelphia, PA.

Hedley, S.L. and Buckland, S.T. 2004. Spatial models for line transect sampling. Journal of Agricultural Biology Environmental Statistics 9:181-199.

Hedley, S.L., Buckland, S.T., and Borchers, D.L. 2004. Spatial distance sampling models. In: *Advanced distance sampling: estimating abundance of biological populations.* pp 48-70, Buckland, S.T., Anderson, D.R., Burnham, K.P., Laake, J.L., Borchers, D.L. and Thomas, L. (eds). Oxford University Press, New York,

Heinemann, D. 1992. Foraging ecology of Roseate Terns in Bird Island, Massachusetts. US Fish and Wildlife Service Report, MA

Hipfner, J.M. and Chapdelaine, G. 2002. Razorbill (*Alca torda*). In: *The Birds of North America*. Poole, A. and Gill, F. (eds.). The Birds of North America, Inc., Philadelphia, PA.

Huntington, C. E., Butler, R.G. and Mauck, R.A. 1996. Leach's Storm-Petrel (*Oceanodroma leucorhoa*). In: *The Birds of North America*. Poole, A. and Gill, F. (eds.). The Birds of North America, Inc., Philadelphia, PA.

Hurvich, C.M., & Tsai, C.L. 1989. Regression and time series model selection in small samples. *Biometrika* 76: 297-307.

Innogy 2003. North Hoyle offshore wind farm baseline monitoring report. NH/MonR/Rev 1.

IUCN. 2006. *Oceanites oceanicus*. IUCN Red List of Threatened Species. www.iucnredlist.org.

Jamieson, S. E., Robertson, G.J. and Gilchrist, H.G. 2001. Autumn and winter diet of Long-tailed Ducks wintering in the Belcher Islands, Nunavut, Canada. *Waterbirds* 23:129–132.

Jaspersen, P. 1924. The frequency of birds over the high Atlantic Ocean. Nature 114:281-283.

JNCC. 2004. Guidance on offshore windfarm development – extract on draft guidance on bird survey techniques. JNCC, Peterborough.

Johnson, S. R. 1984. Prey selection by Oldsquaws in a Beaufort Sea lagoon, Alaska. In:*Marine birds: their feeding ecology and commercial fisheries relationships*. G. A. Sanger, G.A.

and Springer,P.F. (eds.). pp. 12-19.Canadian Wildlife Service Special Publication, Ottawa, ON.

Kahlert, J., Desholm, M., Clausager, I., and Petersen, I.K. 2000. Environmental impact assessment of an offshore wind park at Rodsand: technical report on birds. National Environmental Research Institute, Ministry of the Environment, Denmark.

Kahlert, J., Petersen, I.K, Desholm, and Therkildsen, O. 2004. Investigations of birds during operation of Nysted offshore wind farm at Rodsand: Results and conclusions, 2004. National Environmental Research Institute, Ministry of the Environment, Denmark.

Kaiser, M.J., Galanidi, M., Showler, D.A and Elliott, A.J. 2006. Distribution and behavior of Common Scoter *Melanitta nigra* relative to prey resources and environmental parameters. *Ibis* 148:110-128.

Katsanevakis, S. 2007. Density surface modeling with line transect sampling as a tool for abundance estimation of marine benthic species: the *Pinna nobilis* example in a marine lake. *Marine Biology* 152:77-85.

Kenow, K. P., Adams, D., Schoch, N., Evers, D. C., Hanson, W., Yates, D., Savoy, L., Fox, T. J., Major, A., Kratt, R. and Ozard. J. 2009. Migration patterns and wintering range of Common Loons breeding in the Northeastern United States. *Waterbirds* 32:234-247.

Kerlinger, P. 1985. Water-crossing behavior of raptors during migration. *Wilson Bulletin* 97: 109-113.

Kerlinger, P., and Hatch, J.J. 2001. Preliminary avian risk assessment for the Cape Wind Energy Project. November 2001. Report prepared for Cape Wind Associates, LLC and Environmental Services, Inc. (Appendix 5.7-A).

Kessel, B., Rocque, D.A. and Barclay, J.S. 2002. Greater Scaup (*Aythya marila*). In: *The Birds of North America*. Poole, A. and Gill, F. (eds.). The Birds of North America, Inc., Philadelphia, PA.

Koch, S.L., and Paton, P.W.C. 2009. Shorebird migration chronology at a stopover site in Massachusetts. *Wader Study Group Bulletin* 116:145-152.

Lee, D. S. 1995. Marine birds off the coast of North Carolina. Chat 59: 113–171.

Lee, D. S. and Haney, J.S. 1996. Manx Shearwater (*Puffinus puffinus*). In: *The Birds of North America*. Poole, A. and Gill, F. (eds.). The Birds of North America, Inc., Philadelphia, PA.

Lewis, T.L., Esler, D. and Boyd, W.S. 2005. Nocturnal foraging behavior of wintering Surf and White-winged Scoters. *Condor* 107:637-647

Maclean, I.M.D., Skov, H., Rehfisch, M.M. and Piper, W.. 2006. Use of aerial surveys to detect bird displacement by offshore windfarms. BTO Research Report No. 446 to COWRIE, BTO, Thetford, England.

Madsen, F. J. 1954. On the food habits of diving ducks in Denmark. *Danish Review of Game Biology* 2:157–266.

Mallory, M. and Metz, K. 1999. Common Merganser (*Mergus merganser*). In: *The Birds of North America*. Poole, A. and Gill, F. (eds.). The Birds of North America, Inc., Philadelphia, PA.

Massachusetts Audubon Society (MAS). 2010. http://www.massaudubon.org/cwp/.

Mcintyre, J. W. and Barr, J.F. 1997. Common Loon (*Gavia immer*). In: *The Birds of North America*. Poole, A. and Gill, F. (eds.). The Birds of North America, Inc., Philadelphia, PA.

Montevecchi, W.A. 2010. Seabird migration. Accessed 10 June 2010. http://play.psych.mun.ca/~mont/discoverymigration.html.

Mostello, C. S. 2007. Roseate Tern. Massachusetts Natural Heritage Endangered Species Program, West Borough, MA. http://www.mass.gov/dfwele/dfw/nhesp/species_info/nhfacts/roseate_tern.pdf

Mowbray, T. B., Ely, C.R., Sedinger, J.S. and Trost, R.E. 2002. Canada Goose (*Branta canadensis*). In: *The Birds of North America*. Poole, A. and Gill, F. (eds.). The Birds of North America, Inc., Philadelphia, PA.

Mowbray, T. B. 2002. Northern Gannet (*Morus bassanus*). In: *The Birds of North America*. Poole, A. and Gill, F. (eds.). The Birds of North America, Inc., Philadelphia, PA.

NERI Report 2006. Final results of birds studies at the offshore wind farms at Nysted and Horns Rev, Denmark

Nisbet, I. C. T., and Spendelow, J.A. 1999. Contribution of research to management and recovery of the Roseate Tern: Review of a twelve-year project. *Waterbirds* 22:239-252.

Nisbet, I.C.T. 1981. Biological characteristics of the Roseate Tern (*Sterna dougallii*). US Fish and Wildlife Service Report, MA.

Nisbet, I.C.T. 1989. Status and biology of the northeastern population of the Roseate Tern (*Sterna dougallii*): a literature survey and update. US Fish and Wildlife Service Report, MA.

Nisbet, I.C. 2002. Common Tern (*Sterna hirundo*). In: *The Birds of North America*. Poole, A. and Gill, F. (eds.). The Birds of North America, Inc., Philadelphia, PA.

Palmer, R. S. 1949. Maine birds. Harvard Mus. Comp. Bull. 102, Cambridge, MA.

Palmer, R. S. 1976. Handbook of North American birds. Vol. 3. Yale Univ. Press, New Haven, CT.

Parrish, J. D. 2000. Behavioral, energetic, and conservation implications of foraging plasticity during migration. *Studies in Avian Biology* 20:53–70.

Perkins, S., G. Sadoti, T. Allison, and A. Jones. Relative waterfowl abundance within Nantucket Sound, Massachusetts during the 2003-2004 winter season. Massachusetts Audubon Society, Lincoln, Massachusetts.

Perkins, S., G. Sadoti, T. Allison, E. Jedrey, and A. Jones. Relative waterfowl abundance within Nantucket Sound, Massachusetts during the 2004-2005 winter season. Massachusetts Audubon Society, Lincoln, Massachusetts.

Pierotti, R. J. and Good, T.P. 1994. Herring Gull (*Larus argentatus*). In: *The Birds of North America*. Poole, A. and Gill, F. (eds.). The Birds of North America, Inc., Philadelphia, PA.

Powers, K. D., Pittman, G.L. and Fitch, S.J. 1980. Distribution of marine birds on the mid- and North Atlantic U.S. outer continental shelf. U.S. Dept. Energy, Washington, D.C.

Powers, K.D. 1983. Pelagic distribution of marine birds off the northeastern United States. Technical Report. NMFS-F/NEC-27, Woods Hole, Massachusetts.

Quillfeldt, P. 2001. Variation of breeding success in Wilson's Storm-Petrels: influence of environmental factors. *Antarctic Science* 13: 400-409.

R Development Core Team 2006. R: A language and environment for statistical computing. R foundation for Statistical Computing. Vienna. Austria ISBN 3-900051-07-0. http://www.r-project.org

Reed, A., Ward, D.H., Derksen, D.V., and Sedinger, J.S. 1998. Brant (*Branta bernicla*). In: *The Birds of North America*. Poole, A. and Gill, F. (eds.). The Birds of North America, Inc., Philadelphia, PA.

Reinert, S. E., Lapham, E. and Gaffet, K.. 2002. Landbird migration on Block Island: community composition and conservation implications for an island stopover habitat. In: *The ecology of Block Island: proceedings of the Rhode Island Natural History Survey Conference*. Paton, P.W.C., Gould, L.L., August, P.V., and Frost, A.O.(eds). pp. 1510163.. Rhode Island Natural History Survey, Kingston, USA.

Rhode Island Natural Heritage Program. 2006. Rare native animals of Rhode Island. http://www.rinhs.org/wp-content/uploads/ri_animals_2006.pdf.

Robertson, G. J. and Goudie, R.I. 1999. Harlequin Duck (*Histrionicus histrionicus*). In: *The Birds of North America*. Poole, A. and Gill, F. (eds.). The Birds of North America, Inc., Philadelphia, PA.

Robertson, G. J. and Savard, J.P.L. 2002. Long-tailed Duck (*Clangula hyemalis*). In: *The Birds of North America*. Poole, A. and Gill, F. (eds.). The Birds of North America, Inc., Philadelphia, PA.

Ronconi, R. A., and Burger, A.E. 2009. Estimating seabird densities from vessel transects: distance sampling and implications for strip transects. *Aquatic Biology* 4:297-309.

Rubega, M.A., Schamel, D. and Tracy, D.M. 2000. Red-necked Phalarope (*Phalaropus lobatus*). In: *The Birds of North America*. Poole, A. and Gill, F. (eds.). The Birds of North America, Inc., Philadelphia, PA.

Schorger, A. W. 1947. The deep diving of the Loon and the Old-squaw and its mechanism. *Wilson Bulletin* 59:151–159.

Schorger, A. W. 1951. Deep diving of the Oldsquaw. *Wilson Bulletin* 63: 112.

Seber, G.A.F. 1982. The estimation of animal abundance and related parameters, 2nd edn. Griffin, London.

Sibley, D. 1993. Birds of Cape May. New Jersey Audubon Society, Cape May Point, NJ.

Sibley, D. 2000. The Sibley guide to birds. National Audubon Society, A. Knopf, New York.

Stedman, S. J. 2000. Horned Grebe (*Podiceps auritus*). In: *The Birds of North America*. Poole, A. and Gill, F. (eds.). The Birds of North America, Inc., Philadelphia, PA.

Stewart, G.G., Coles, C.F. and Pullin, A.S. 2004. Effects of Wind Turbines on Bird Abundance. Systematic Review no. 4. Birmingham, UK: Centre for Evidence-based Conservation.

Stott, R. S. and Olson, D.P. 1973. Food-habitat relationship of sea ducks on the New Hampshire coastline. *Ecology* 54: 996–1007.

Tasker, M.L., Jones, P.H., Dixon, T., and Blake, B.F. 1984. Counting seabirds at sea from ships: a review of methods employed and a suggestion for a standardized approach. Auk 101:567-577.

Terres, J. K. 1980. The Audubon encyclopedia of North American birds. Alfred A. Knopf, New York.

Thomas, L., Laake, J.L., Rexstad, E., Strindberg, S., Marques, F.F.C., Buckland, S.T., Borchers, D.L., Anderson, D.R., Burnham,K.P., Burt, M.L., Hedley, S.L., Pollard, J.H., Bishop, J.R.B., & Marques, T.A. 2006. Distance 6.0 Release Beta 1. Research Unit for Wildlife Population Assessment, University of St. Andrews, UK. http://www.ruwpa.st-and.ac.uk/distance/

Titman, R. D. 1999. Red-breasted Merganser (*Mergus serrator*). In: *The Birds of North America*. Poole, A. and Gill, F. (eds.). The Birds of North America, Inc., Philadelphia, PA.

Tracy, D. M., Schamel, D. and Dale, J. 2002. Red Phalarope (*Phalaropus fulicarius*). In: *The Birds of North America*. Poole, A. and Gill, F. (eds.). The Birds of North America, Inc., Philadelphia, PA.

Uchupi, E., Driscoll, N., Ballard, R.D., and Bolmer, S.T. 2001. Drainage of late Wisconsin lakes and the morphology of later Quaternary stratigraphy of the New Jersey-southern New England continental shelf and slope. *Marine Geology* 172:117–145.

Vaitkus, G., and A. Bubinas. 2001. Modeling of sea duck spatial distribution in relation to food resources in Lithuanian offshore waters under the gradient of winter climatic conditions. *Acta Zoologica Lituanica* 11: 1392-1657.

Vermeer, K. 1983. Diet of the Harlequin Duck in the Strait of Georgia, British Columbia. *Murrelet* 64: 54–57.

Ward, D.H., Reed, A., Sedinger, J.S., Black, J.M., Derksen, D.V.and Castelli, P.M. 2005. North American Brant: effects of changes in habitat and climate on population dynamics. *Global Change Biology* 11: 869-880.

White, T.P., Veit, R.R. and Perry, M.C. 2009. Feeding ecology of Long-tailed Ducks *Clangula hyemalis* wintering on the Nantucket Shoals. *Waterbirds* 293: 293-299.

Wood, S.N. 2000. Modelling and smoothing parameter estimation with multiple quadratic penalties. *Journal of the Royal Statistical Society Series B*, 62:413-428.

Wood, S.N. 2006. Generalized additive models: an introduction with R. Chapman and Hall/CRC, Florida.

Wynn, R.B., and P. Yesou. 2007. Changing status of the Balearic Shearwater (*Puffinus mauretanicus*) in northwest European waters. *British Birds* 100:392-406.

Ydenberg, R. and M. Guillemetter. 1991. Diving and foraging in the Common Eider. *Ornis Scandinavica* 22:349-352.

APPENDICES

Appendix A. List of birds that could occur in Ocean SAMP study area. Given are common name, scientific name, Status (A= abundant, C = Common, U = uncommon, O = occasional, V = vagrant; based on Conway 1979), and whether the species was detected during any Ocean SAMP survey from Jan 2009 through mid-Feb 2010 (either land-based seawatch, ship-based grid, or aerial survey).

Common Name	Scientific Name	Status	On SAMP Surveys?
Red-throated Loon	*Gavia stellata*	A	Yes
Pacific Loon	*Gavia pacifica*	V	Yes
Common Loon	*Gavia immer*	A	Yes
Pied-billed Grebe	*Podilymbus podiceps*	U	
Horned Grebe	*Podiceps auritus*	C	Yes
Red-necked Grebe	*Podiceps grisegena*	U	Yes
Yellow-nosed Albatross	*Thalassarche chlororhynchos*	V	
Northern Fulmar	*Fulmarus glacialis*	U	Yes
Cory's Shearwater	*Calonectris diomedea*	A	Yes
Greater Shearwater	*Puffinus gravis*	A	Yes
Sooty Shearwater	*Puffinus griseus*	C	Yes
Manx Shearwater	*Puffinus puffinus*	C	Yes
Audubon's Shearwater	*Puffinus lherminieri*	V	
Wilson's Storm-Petrel	*Oceanites oceanicus*	A	Yes
Leach's Storm-Petrel	*Oceanodroma leucorhoa*	U	Yes
Red-billed Tropicbird	*Phaethon aethereus*	V	
Northern Gannet	*Morus bassanus*	A	Yes
American White Pelican	*Pelecanus erythrorhynchos*	V	
Brown Pelican	*Pelecanus occidentalis*	V	
Double-crested Cormorant	*Phalacrocorax auritus*	A	Yes
Great Cormorant	*Phalacrocorax carbo*	C	Yes
Magnificent Frigatebird	*Fregata magnificens*	V	
American Bittern	*Botaurus lentiginosus*	U	
Least Bittern	*Ixobrychus exilis*	O	
Great Blue Heron	*Ardea herodias*	C	Yes
Great Egret	*Ardea alba*	C	Yes
Snowy Egret	*Egretta thula*	C	Yes
Little Blue Heron	*Egretta caerulea*	U	
Tricolored Heron	*Egretta tricolor*	U	
Cattle Egret	*Bubulcus ibis*	U	Yes

Green Heron	*Butorides virescens*	C	Yes
Black-crowned Night-Heron	*Nycticorax nycticorax*	C	Yes
Yellow-crowned Night-Heron	*Nyctanassa violacea*	U	
White Ibis	*Eudocimus albus*	V	
Glossy Ibis	*Plegadis falcinellus*	C	Yes
Mute Swan	*Cygnus olor*	C	Yes
Tundra Swan	*Cygnus columbianus*	V	Yes
Greater White-fronted Goose	*Anser albifrons*	V	
Snow Goose	*Chen caerulescens*	U	
Brant	*Branta bernicla*	C	Yes
Cackling Goose	*Branta hutchinsii*	O	
Canada Goose	*Branta canadensis*	A	Yes
Wood Duck	*Aix sponsa*	C	Yes
Gadwall	*Anas strepera*	C	Yes
Eurasian Wigeon	*Anas penelope*	V	
American Wigeon	*Anas americana*	A	Yes
American Black Duck	*Anas rubripes*	A	Yes
Mallard	*Anas platyrhynchos*	A	Yes
Blue-winged Teal	*Anas discors*	C	
Northern Shoveler	*Anas clypeata*	O	
Northern Pintail	*Anas acuta*	C	
Green-winged Teal	*Anas crecca*	C	Yes
Canvasback	*Aythya valisineria*	U	
Redhead	*Aythya americana*	C	Yes
Ring-necked Duck	*Aythya collaris*	C	Yes
Tufted Duck	*Aythya fuligula*	V	
Greater Scaup	*Aythya marila*	A	Yes
Lesser Scaup	*Aythya affinis*	C	Yes
King Eider	*Somateria spectabilis*	V	Yes
Common Eider	*Somateria mollissima*	A	Yes
Harlequin Duck	*Histrionicus histrionicus*	C	Yes
Surf Scoter	*Melanitta perspicillata*	A	Yes
White-winged Scoter	*Melanitta fusca*	A	Yes
Black Scoter	*Melanitta nigra*	A	Yes
Long-tailed Duck	*Clangula hyemalis*	U	Yes
Bufflehead	*Bucephala albeola*	C	Yes
Common Goldeneye	*Bucephala clangula*	C	Yes
Barrow's Goldeneye	*Bucephala islandica*	V	
Smew	*Mergellus albellus*	V	
Hooded Merganser	*Lophodytes cucullatus*	C	Yes
Common Merganser	*Mergus merganser*	U	Yes

Red-breasted Merganser	*Mergus serrator*	A	Yes
Ruddy Duck	*Oxyura jamaicensis*	A	Yes
Black Vulture	*Coragyps atratus*	U	
Turkey Vulture	*Cathartes aura*	C	
Osprey	*Pandion haliaetus*	C	Yes
Swallow-tailed Kite	*Elanoides forficatus*	V	
Bald Eagle	*Haliaeetus leucocephalus*	U	
Northern Harrier	*Circus cyaneus*	C	Yes
Sharp-shinned Hawk	*Accipiter striatus*	C	Yes
Cooper's Hawk	*Accipiter cooperii*	C	Yes
Northern Goshawk	*Accipiter gentilis*	U	
Red-shouldered Hawk	*Buteo lineatus*	U	
Broad-winged Hawk	*Buteo platypterus*	C	Yes
Red-tailed Hawk	*Buteo jamaicensis*	C	
Rough-legged Hawk	*Buteo lagopus*	U	
American Kestrel	*Falco sparverius*	U	Yes
Merlin	*Falco columbarius*	C	Yes
Peregrine Falcon	*Falco peregrinus*	C	Yes
Clapper Rail	*Rallus longirostris*	U	
King Rail	*Rallus elegans*	U	
Virginia Rail	*Rallus limicola*	C	
Sora	*Porzana carolina*	C	
Common Moorhen	*Gallinula chloropus*	U	
American Coot	*Fulica americana*	C	
Sandhill Crane	*Grus canadensis*	O	
Black-bellied Plover	*Pluvialis squatarola*	C	Yes
American Golden-Plover	*Pluvialis dominica*	O	
Semipalmated Plover	*Charadrius semipalmatus*	C	Yes
Piping Plover	*Charadrius melodus*	U	Yes
Killdeer	*Charadrius vociferus*	C	Yes
American Oystercatcher	*Haematopus palliatus*	U	Yes
Black-necked Stilt	*Himantopus mexicanus*	V	
American Avocet	*Recurvirostra americana*	V	
Spotted Sandpiper	*Actitis macularius*	O	Yes
Solitary Sandpiper	*Tringa solitaria*	U	
Greater Yellowlegs	*Tringa melanoleuca*	C	Yes
Willet	*Tringa semipalmata*	C	Yes
Lesser Yellowlegs	*Tringa flavipes*	U	Yes
Upland Sandpiper	*Bartramia longicauda*	O	
Whimbrel	*Numenius phaeopus*	O	Yes
Hudsonian Godwit	*Limosa haemastica*	O	

Ruddy Turnstone	*Arenaria interpres*	A	Yes
Red Knot	*Calidris canutus*	U	
Sanderling	*Calidris alba*	C	
Semipalmated Sandpiper	*Calidris pusilla*	C	Yes
Western Sandpiper	*Calidris mauri*	O	
Least Sandpiper	*Calidris minutilla*	C	Yes
White-rumped Sandpiper	*Calidris fuscicollis*	O	Yes
Baird's Sandpiper	*Calidris bairdii*	O	
Pectoral Sandpiper	*Calidris melanotos*	O	
Purple Sandpiper	*Calidris maritima*	C	Yes
Dunlin	*Calidris alpina*	A	Yes
Ruff	*Philomachus pugnax*	V	
Short-billed Dowitcher	*Limnodromus griseus*	C	Yes
Long-billed Dowitcher	*Limnodromus scolopaceus*	O	
Wilson's Snipe	*Gallinago delicata*	U	
American Woodcock	*Scolopax minor*	C	
Wilson's Phalarope	*Phalaropus tricolor*	O	
Red-necked Phalarope	*Phalaropus lobatus*	O	Yes
Red Phalarope	*Phalaropus fulicarius*	O	
Black-legged Kittiwake	*Rissa tridactyla*	C	Yes
Sabine's Gull	*Xema sabini*	V	
Bonaparte's Gull	*Chroicocephalus philadelphia*	U	Yes
Little Gull	*Hydrocoloeus minutus*	V	Yes
Laughing Gull	*Leucophaeus atricilla*	A	Yes
Franklin's Gull	*Leucophaeus pipixcan*	V	
Black-tailed Gull	*Larus crassirostris*	V	
Ring-billed Gull	*Larus delawarensis*	C	Yes
Herring Gull	*Larus argentatus*	A	Yes
Iceland Gull	*Larus glaucoides*	O	Yes
Lesser Black-backed Gull	*Larus fuscus*	O	
Glaucous Gull	*Larus hyperboreus*	O	
Great Black-backed Gull	*Larus marinus*	A	Yes
Sooty Tern	*Onychoprion fuscatus*	V	
Least Tern	*Sternula antillarum*	C	Yes
Gull-billed Tern	*Gelochelidon nilotica*	V	
Caspian Tern	*Hydroprogne caspia*	O	Yes
Black Tern	*Chlidonias niger*	U	Yes
Roseate Tern	*Sterna dougallii*	C	Yes
Common Tern	*Sterna hirundo*	A	Yes
Arctic Tern	*Sterna paradisaea*	O	
Forster's Tern	*Sterna forsteri*	U	

Royal Tern	*Thalasseus maximus*	O	Yes
Sandwich Tern	*Thalasseus sandvicensis*	V	
Black Skimmer	*Rynchops niger*	O	Yes
Pomarine Jaeger	*Stercorarius pomarinus*	C	Yes
Parasitic Jaeger	*Stercorarius parasiticus*	U	Yes
Long-tailed Jaeger	*Stercorarius longicaudus*	O	Yes
Dovekie	*Alle alle*	A	Yes
Common Murre	*Uria aalge*	C	Yes
Thick-billed Murre	*Uria lomvia*	U	Yes
Razorbill	*Alca torda*	A	Yes
Black Guillemot	*Cepphus grylle*	U	Yes
Long-billed Murrelet	*Brachyramphus perdix*	V	
Atlantic Puffin	*Fratercula arctica*	O	Yes
Rock Pigeon	*Columba livia*	A	Yes
Mourning Dove	*Zenaida macroura*	A	Yes
Yellow-billed Cuckoo	*Coccyzus americanus*	O	
Black-billed Cuckoo	*Coccyzus erythropthalmus*	O	
Barn Owl	*Tyto alba*	O	
Eastern Screech-Owl	*Megascops asio*	U	
Great Horned Owl	*Bubo virginianus*	C	
Snowy Owl	*Bubo scandiacus*	O	
Barred Owl	*Strix varia*	O	
Great Gray Owl	*Strix nebulosa*	V	
Long-eared Owl	*Asio otus*	O	
Short-eared Owl	*Asio flammeus*	O	Yes
Northern Saw-whet Owl	*Aegolius acadicus*	C	
Common Nighthawk	*Chordeiles minor*	U	
Whip-poor-will	*Caprimulgus vociferus*	C	
Chimney Swift	*Chaetura pelagica*	C	Yes
Ruby-throated Hummingbird	*Archilochus colubris*	C	Yes
Belted Kingfisher	*Megaceryle alcyon*	C	Yes
Yellow-bellied Sapsucker	*Sphyrapicus varius*	U	
Downy Woodpecker	*Picoides pubescens*	A	
Hairy Woodpecker	*Picoides villosus*	U	
Northern Flicker	*Colaptes auratus*	A	Yes
Pileated Woodpecker	*Dryocopus pileatus*	O	
Eastern Wood-Pewee	*Contopus virens*	C	
Acadian Flycatcher	*Empidonax virescens*	O	
Alder Flycatcher	*Empidonax alnorum*	O	
Willow Flycatcher	*Empidonax traillii*	O	
Least Flycatcher	*Empidonax minimus*	O	

Eastern Phoebe	*Sayornis phoebe*	C	
Say's Phoebe	*Sayornis saya*	V	
Great Crested Flycatcher	*Myiarchus crinitus*	C	
Eastern Kingbird	*Tyrannus tyrannus*	C	Yes
Scissor-tailed Flycatcher	*Tyrannus forficatus*	V	
Northern Shrike	*Lanius excubitor*	U	
White-eyed Vireo	*Vireo griseus*	O	
Yellow-throated Vireo	*Vireo flavifrons*	O	
Blue-headed Vireo	*Vireo solitarius*	O	
Philadelphia Vireo	*Vireo philadelphicus*	O	
Red-eyed Vireo	*Vireo olivaceus*	C	
Blue Jay	*Cyanocitta cristata*	A	Yes
American Crow	*Corvus brachyrhynchos*	C	Yes
Fish Crow	*Corvus ossifragus*	C	Yes
Common Raven	*Corvus corax*	O	
Horned Lark	*Eremophila alpestris*	U	Yes
Purple Martin	*Progne subis*	U	Yes
Tree Swallow	*Tachycineta bicolor*	A	Yes
N. Rough-winged Swallow	*Stelgidopteryx serripennis*	O	Yes
Bank Swallow	*Riparia riparia*	U	Yes
Cliff Swallow	*Petrochelidon pyrrhonota*	O	Yes
Cave Swallow	*Petrochelidon fulva*	V	
Barn Swallow	*Hirundo rustica*	C	Yes
Black-capped Chickadee	*Poecile atricapillus*	A	
Tufted Titmouse	*Baeolophus bicolor*	A	
Red-breasted Nuthatch	*Sitta canadensis*	C	
Brown Creeper	*Certhia americana*	C	
Carolina Wren	*Thryothorus ludovicianus*	C	
House Wren	*Troglodytes aedon*	C	
Winter Wren	*Troglodytes troglodytes*	O	
Sedge Wren	*Cistothorus platensis*	O	
Marsh Wren	*Cistothorus palustris*	O	
Golden-crowned Kinglet	*Regulus satrapa*	C	
Ruby-crowned Kinglet	*Regulus calendula*	C	
Blue-gray Gnatcatcher	*Polioptila caerulea*	O	
Northern Wheatear	*Oenanthe oenanthe*	V	
Eastern Bluebird	*Sialia sialis*	U	
Veery	*Catharus fuscescens*	C	
Gray-cheeked Thrush	*Catharus minimus*	O	
Bicknell's Thrush	*Catharus bicknelli*	O	
Swainson's Thrush	*Catharus ustulatus*	O	

Hermit Thrush	*Catharus guttatus*	O	
Wood Thrush	*Hylocichla mustelina*	C	
American Robin	*Turdus migratorius*	A	Yes
Varied Thrush	*Ixoreus naevius*	V	
Gray Catbird	*Dumetella carolinensis*	A	
Northern Mockingbird	*Mimus polyglottos*	C	
Brown Thrasher	*Toxostoma rufum*	U	
European Starling	*Sturnus vulgaris*	A	
American Pipit	*Anthus rubescens*	U	
Bohemian Waxwing	*Bombycilla garrulus*	U	
Cedar Waxwing	*Bombycilla cedrorum*	A	Yes
Blue-winged Warbler	*Vermivora pinus*	C	
Golden-winged Warbler	*Vermivora chrysoptera*	O	
Tennessee Warbler	*Vermivora peregrina*	O	
Orange-crowned Warbler	*Vermivora celata*	O	
Nashville Warbler	*Vermivora ruficapilla*	O	
Northern Parula	*Parula americana*	U	
Cape May Warbler	*Dendroica tigrina*	O	
Black-throated Blue Warbler	*Dendroica caerulescens*	U	
Yellow-rumped Warbler	*Dendroica coronata*	A	Yes
Black-throated Green Warbler	*Dendroica virens*	C	
Blackburnian Warbler	*Dendroica fusca*	U	
Yellow Warbler	*Dendroica petechia*	C	Yes
Chestnut-sided Warbler	*Dendroica pensylvanica*	C	
Magnolia Warbler	*Dendroica magnolia*	U	
Yellow-throated Warbler	*Dendroica dominica*	O	
Pine Warbler	*Dendroica pinus*	C	
Prairie Warbler	*Dendroica discolor*	C	
Palm Warbler	*Dendroica palmarum*	U	Yes
Bay-breasted Warbler	*Dendroica castanea*	O	
Blackpoll Warbler	*Dendroica striata*	C	Yes
Cerulean Warbler	*Dendroica cerulea*	O	
Black-and-white Warbler	*Mniotilta varia*	C	
American Redstart	*Setophaga ruticilla*	C	
Prothonotary Warbler	*Protonotaria citrea*	O	
Worm-eating Warbler	*Helmitheros vermivorum*	O	
Ovenbird	*Seiurus aurocapilla*	C	
Northern Waterthrush	*Seiurus noveboracensis*	O	
Louisiana Waterthrush	*Seiurus motacilla*	O	
Kentucky Warbler	*Oporornis formosus*	O	
Connecticut Warbler	*Oporornis agilis*	O	

Mourning Warbler	*Oporornis philadelphia*	O	
Common Yellowthroat	*Geothlypis trichas*	C	
Hooded Warbler	*Wilsonia citrina*	U	
Wilson's Warbler	*Wilsonia pusilla*	O	
Canada Warbler	*Wilsonia canadensis*	U	
Yellow-breasted Chat	*Icteria virens*	O	
Green-tailed Towhee	*Pipilo chlorurus*	V	
Eastern Towhee	*Pipilo erythrophthalmus*	C	
American Tree Sparrow	*Spizella arborea*	C	
Chipping Sparrow	*Spizella passerina*	C	
Clay-colored Sparrow	*Spizella pallida*	O	
Field Sparrow	*Spizella pusilla*	C	
Vesper Sparrow	*Pooecetes gramineus*	O	
Lark Sparrow	*Chondestes grammacus*	O	
Savannah Sparrow	*Passerculus sandwichensis*	U	Yes
Grasshopper Sparrow	*Ammodramus savannarum*	O	
Nelson's Sparrow	*Ammodramus nelsoni*	U	
Saltmarsh Sparrow	*Ammodramus caudacutus*	C	
Seaside Sparrow	*Ammodramus maritimus*	U	
Fox Sparrow	*Passerella iliaca*	U	
Song Sparrow	*Melospiza melodia*	A	
Lincoln's Sparrow	*Melospiza lincolnii*	U	
Swamp Sparrow	*Melospiza georgiana*	U	
White-throated Sparrow	*Zonotrichia albicollis*	A	
White-crowned Sparrow	*Zonotrichia leucophrys*	U	
Dark-eyed Junco	*Junco hyemalis*	A	Yes
Lapland Longspur	*Calcarius lapponicus*	U	
Snow Bunting	*Plectrophenax nivalis*	U	Yes
Summer Tanager	*Piranga rubra*	O	
Scarlet Tanager	*Piranga olivacea*	U	
Rose-breasted Grosbeak	*Pheucticus ludovicianus*	U	
Blue Grosbeak	*Passerina caerulea*	O	
Indigo Bunting	*Passerina cyanea*	U	
Dickcissel	*Spiza americana*	O	
Bobolink	*Dolichonyx oryzivorus*	U	Yes
Red-winged Blackbird	*Agelaius phoeniceus*	C	
Eastern Meadowlark	*Sturnella magna*	O	
Yellow-headed Blackbird	*X. xanthocephalus*	O	
Rusty Blackbird	*Euphagus carolinus*	O	
Common Grackle	*Quiscalus quiscula*	C	Yes
Brown-headed Cowbird	*Molothrus ater*	A	Yes

Orchard Oriole	*Icterus spurius*	O	
Baltimore Oriole	*Icterus galbula*	U	
Purple Finch	*Carpodacus purpureus*	U	
House Finch	*Carpodacus mexicanus*	C	
Red Crossbill	*Loxia curvirostra*	U	
White-winged Crossbill	*Loxia leucoptera*	O	
Common Redpoll	*Acanthis flammea*	O	
Pine Siskin	*Spinus pinus*	U	
American Goldfinch	*Spinus tristis*	C	Yes
House Sparrow	*Passer domesticus*	A	

Appendix B. Mean (SD) number of detections of birds **on the water** at 11 land-based seawatch stations along coastal Rhode Island at northern edge of Ocean SAMP study area from Jan 2009 through mid-Feb 2010. N = total number of detections at that station (Watch Hill to Pt. Judith).

	Watch Hill			East Beach			Deep Hole			Pt Judith		
	Mean	SD	N	Mean	SD	N	Mean	SD	N	Mean	SD	N
Red-throated Loon	0.43	1.15	33	3.38	12.30	264	1.18	3.18	94	1.36	3.47	116
Pacific Loon	0.01	0.11	1	0.00	0.00	0	0.00	0.00	0	0.00	0.00	0
Common Loon	7.40	12.22	570	9.81	14.53	765	6.29	9.47	503	4.21	6.09	358
Loon spp.	0.21	1.23	16	0.26	2.26	20	0.03	0.22	2	0.01	0.11	1
Red-necked Grebe	0.00	0.00	0	0.03	0.16	2	0.01	0.11	1	0.13	0.43	11
Horned Grebe	1.16	2.66	89	3.22	5.59	251	0.93	2.12	74	1.14	3.14	97
Cory's Shearwater	0.00	0.00	0	0.10	0.91	8	0.00	0.00	0	0.79	7.27	67
Wilson's Storm-Petrel	0.00	0.00	0	0.00	0.00	0	0.00	0.00	0	0.01	0.11	1
Great Cormorant	0.27	1.10	21	0.03	0.16	2	0.01	0.11	1	0.55	1.28	47
Double-c. Cormorant	7.10	15.71	547	1.19	2.93	93	2.19	10.73	175	2.98	6.76	253
Northern Gannet	0.04	0.25	3	0.37	2.74	29	0.20	1.58	16	0.44	2.85	37
Snowy Egret	0.00	0.00	0	0.01	0.11	1	0.00	0.00	0	0.00	0.00	0
Mute Swan	0.04	0.34	3	0.01	0.11	1	0.05	0.35	4	0.04	0.24	3
Canada Goose	0.00	0.00	0	0.64	5.66	50	0.00	0.00	0	0.00	0.00	0
Atlantic Brant	1.45	10.53	112	0.00	0.00	0	0.00	0.00	0	0.00	0.00	0
Am. Black Duck	0.05	0.32	4	0.05	0.32	4	0.08	0.38	6	0.02	0.22	2
Greater Scaup	0.00	0.00	0	0.00	0.00	0	4.33	22.75	346	0.00	0.00	0
Common Eider	16.47	44.56	1268	73.83	209.27	5759	54.11	198.47	4329	27.59	100.51	2345
Long-tailed Duck	0.16	0.67	12	0.24	1.06	19	0.16	1.14	13	0.48	2.06	41
Surf Scoter	23.62	123.13	1819	0.73	3.98	57	0.04	0.19	3	2.72	13.11	231
Black Scoter	12.73	55.11	980	13.90	91.01	1084	0.88	5.35	70	2.99	13.79	254
Surf or Black Scoter	1.23	10.83	95	0.38	3.40	30	0.00	0.00	0	0.00	0.00	0
White-winged Scoter	16.29	73.09	1254	13.13	60.84	1024	0.03	0.16	2	0.01	0.11	1
Scoter spp.	192.3	799.87	14808	91.54	492.64	7140	0.14	1.23	11	0.15	0.87	13
Common Goldeneye	0.08	0.31	6	0.49	1.47	38	1.58	4.32	126	1.65	4.33	140

Appendix B. continued.

	Watch Hill			East Beach			Deep Hole			Pt Judith		
	Mean	SD	N	Mean	SD	N	Mean	SD	N	Mean	SD	N
Bufflehead	0.03	0.16	2	0.00	0.00	0	0.41	2.30	33	0.00	0.00	0
Red-brd Merganser	1.96	3.44	151	0.77	2.00	60	20.46	44.28	1637	14.61	31.14	1242
Seaduck spp.	0.00	0.00	0	38.46	251.87	3000	0.00	0.00	0	0.00	0.00	0
Ruddy Duck	0.00	0.00	0	0.21	1.27	16	0.00	0.00	0	0.00	0.00	0
Purple Sandpiper	0.00	0.00	0	0.00	0.00	0	0.00	0.00	0	0.11	0.98	9
Sanderling	0.00	0.00	0	3.14	20.40	245	0.00	0.00	0	0.00	0.00	0
Semipal. Sandpiper	0.00	0.00	0	0.01	0.11	1	0.00	0.00	0	0.00	0.00	0
Bonaparte's Gull	0.01	0.11	1	0.00	0.00	0	0.01	0.11	1	0.02	0.15	2
Laughing Gull	1.12	4.14	86	0.91	3.75	71	0.19	0.75	15	0.39	2.87	33
Ring-billed Gull	0.05	0.22	4	0.55	2.43	43	0.61	2.76	49	0.04	0.19	3
Herring Gull	3.16	7.12	243	9.68	32.09	755	5.51	14.16	441	3.15	6.84	268
Great Black-bd. Gull	1.01	1.93	78	5.26	20.66	410	2.16	5.05	173	3.05	5.64	259
Black-ld. Kittiwake	0.00	0.00	0	0.00	0.00	0	0.00	0.00	0	0.01	0.11	1
Gull spp.	0.58	3.80	45	2.69	18.21	210	0.10	0.89	8	0.12	1.08	10
Common Tern	0.00	0.00	0	0.00	0.00	0	0.00	0.00	0	0.01	0.11	1
Thick-billed Murre	0.00	0.00	0	0.00	0.00	0	0.00	0.00	0	0.01	0.11	1
Razorbill	0.05	0.46	4	0.00	0.00	0	0.00	0.00	0	0.28	1.35	24
Dovekie	0.00	0.00	0	0.00	0.00	0	0.00	0.00	0	0.01	0.11	1
Black Guillemot	0.00	0.00	0	0.00	0.00	0	0.00	0.00	0	0.01	0.11	1
Alcid spp.	0.00	0.00	0	0.00	0.00	0	0.00	0.00	0	0.04	0.33	3
Common Grackle	0.00	0.00	0	0.00	0.00	0	0.03	0.22	2	0.00	0.00	0
Overall	289.0	839.84	22255	275.03	681.75	21452	101.69	212.50	8135	69.13	132.14	5876

Appendix B continued. Birds detected on the water during land-based seawatches (Monahan's Dock to Ruggles Ave)

	M. Dock			Beavertail			Brenton Point			Ruggles		
	Mean	SD	N	Mean	SD	N	Mean	SD	N	Mean	SD	N
Red-throated Loon	2.93	8.14	264	0.42	1.22	34	0.17	0.45	11	4.15	13.55	270
Common Loon	4.61	8.23	415	1.63	2.65	132	5.06	6.90	329	7.29	13.30	474
Loon spp.	0.04	0.30	4	0.00	0.00	0	0.00	0.00	0	0.00	0.00	0
Red-necked Grebe	0.07	0.25	6	0.07	0.31	6	0.06	0.35	4	0.32	1.54	21
Horned Grebe	0.36	0.83	32	0.49	1.34	40	2.15	4.10	140	8.65	44.18	562
Cory's Shearwater	0.14	1.37	13	0.00	0.00	0	0.85	6.82	55	0.43	3.12	28
Shearwater spp.	0.00	0.00	0	0.00	0.00	0	0.02	0.12	1	0.00	0.00	0
Great Cormorant	0.22	0.99	20	0.67	1.57	54	0.28	1.53	18	0.71	1.85	46
Double-c. Cormorant	3.74	12.97	337	2.17	3.48	176	6.63	11.79	431	2.66	4.62	173
Northern Gannet	0.34	2.10	31	0.00	0.00	0	0.18	0.85	12	0.20	0.83	13
Great Egret	0.01	0.11	1	0.00	0.00	0	0.00	0.00	0	0.00	0.00	0
Mute Swan	0.06	0.27	5	0.00	0.00	0	0.00	0.00	0	0.02	0.12	1
Canada Goose	0.47	3.11	42	0.01	0.11	1	0.00	0.00	0	5.08	19.60	330
Atlantic Brant	0.08	0.46	7	1.05	8.79	85	0.80	2.77	52	0.00	0.00	0
Mallard	0.03	0.32	3	0.02	0.22	2	0.03	0.17	2	0.00	0.00	0
Am. Black Duck	0.14	0.63	13	0.11	0.50	9	0.18	0.85	12	0.18	0.63	12
Gadwall	0.00	0.00	0	0.02	0.22	2	0.06	0.50	4	0.00	0.00	0
American Wigeon	0.00	0.00	0	0.02	0.22	2	0.03	0.25	2	0.00	0.00	0
Green-winged Teal	0.00	0.00	0	0.00	0.00	0	0.02	0.12	1	0.00	0.00	0
Greater Scaup	0.02	0.21	2	0.04	0.33	3	0.05	0.28	3	0.03	0.25	2
Common Eider	24.08	63.48	2167	87.48	182.16	7086	327.09	638.37	21261	37.88	62.75	2462
King Eider	0.00	0.00	0	0.02	0.16	2	0.35	0.96	23	0.00	0.00	0
Harlequin Duck	0.00	0.00	0	6.78	9.99	549	0.02	0.12	1	0.46	1.43	30
Long-tailed Duck	0.00	0.00	0	0.05	0.22	4	1.86	7.27	121	0.00	0.00	0
Surf Scoter	0.08	0.40	7	16.10	65.77	1304	376.00	959.43	24440	172.55	864.2	11216
Black Scoter	6.99	27.50	629	22.25	78.61	1802	291.71	572.49	18961	45.29	150.7	2944
Surf or Black Scoter	0.00	0.00	0	0.00	0.00	0	5.40	28.37	351	1.62	10.35	105

Appendix B. Continued.

	M. Dock			Beavertail			Brenton Point			Ruggles		
	Mean	SD	N	Mean	SD	N	Mean	SD	N	Mean	SD	N
White-winged Scoter	0.01	0.11	1	0.52	1.18	42	5.51	18.87	358	6.68	20.61	434
Scoter spp.	0.00	0.00	0	74.69	434.46	6050	51.18	232.78	3327	196.52	730.6	12774
Common Goldeneye	1.57	4.53	141	0.98	2.31	79	9.32	19.01	606	3.43	7.20	223
Barrow's Goldeneye	0.00	0.00	0	0.00	0.00	0	0.02	0.12	1	0.00	0.00	0
Bufflehead	0.01	0.11	1	0.12	0.75	10	0.51	2.05	33	2.58	5.32	168
Red-brd Merganser	5.53	7.69	498	3.69	5.81	299	14.94	21.39	971	4.20	7.04	273
Semipalmated Plover	0.00	0.00	0	0.00	0.00	0	0.06	0.39	4	0.00	0.00	0
Spotted Sandpiper	0.00	0.00	0	0.00	0.00	0	0.02	0.12	1	0.00	0.00	0
Purple Sandpiper	0.40	3.22	36	0.00	0.00	0	4.77	24.11	310	0.95	6.36	62
Sanderling	0.00	0.00	0	0.00	0.00	0	0.02	0.12	1	0.00	0.00	0
Bonaparte's Gull	0.60	2.49	54	0.23	1.19	19	0.03	0.17	2	0.00	0.00	0
Laughing Gull	1.17	9.01	105	0.53	2.33	43	1.42	9.11	92	2.48	11.77	161
Ring-billed Gull	1.76	9.28	158	0.47	2.10	38	0.29	1.54	19	0.22	0.78	14
Herring Gull	8.26	23.09	743	7.80	17.66	632	11.83	21.67	769	3.43	7.25	223
Great Black-bd. Gull	1.66	5.03	149	1.57	4.34	127	33.46	248.79	2175	1.63	3.11	106
Black-ld Kittiwake	0.01	0.11	1	0.00	0.00	0	0.00	0.00	0	0.00	0.00	0
Gull spp.	1.33	12.65	120	0.62	3.98	50	0.03	0.25	2	1.55	8.95	101
Sterna spp.	0.00	0.00	0	0.00	0.00	0	0.00	0.00	0	0.37	2.98	24
Thick-billed Murre	0.01	0.11	1	0.00	0.00	0	0.00	0.00	0	0.00	0.00	0
Razorbill	0.36	2.21	32	0.95	4.54	77	0.03	0.25	2	0.22	1.18	14
Alcid spp.	0.00	0.00	0	0.00	0.00	0	0.00	0.00	0	0.02	0.12	1
Tree Swallow	0.09	0.84	8	0.00	0.00	0	0.00	0.00	0	0.00	0.00	0
Overall	67.18	90.09	6046	231.59	611.50	18759	1152.43	2244.00	74908	511.80	1236.4	33267

Appendix B continued. Birds detected on the water during land-based seawatches (Sachuest to Goosewing).

	Sachuest			Sakonnet			Goosewing		
Species	Mean	SD	N	Mean	SD	N	Mean	SD	N
Red-throated Loon	0.89	2.01	55	0.29	0.85	16	1.58	4.62	90
Common Loon	2.94	3.80	182	2.64	2.77	148	2.32	3.17	132
Loon spp.	0.03	0.18	2	0.00	0.00	0	0.02	0.13	1
Red-necked Grebe	0.11	0.55	7	0.00	0.00	0	0.00	0.00	0
Horned Grebe	1.26	2.19	78	0.61	1.51	34	0.58	1.28	33
Cory's Shearwater	0.02	0.13	1	0.00	0.00	0	0.00	0.00	0
Great Cormorant	0.11	0.41	7	0.05	0.30	3	0.18	0.63	10
Double-crested Cormorant	2.71	6.10	168	7.75	18.61	434	8.84	45.97	504
Northern Gannet	0.16	0.85	10	0.02	0.13	1	0.05	0.40	3
Great Egret	0.00	0.00	0	0.07	0.37	4	0.00	0.00	0
Mute Swan	0.00	0.00	0	0.00	0.00	0	0.19	1.33	11
Canada Goose	0.00	0.00	0	0.63	4.54	35	0.60	3.99	34
Atlantic Brant	0.50	2.55	31	0.30	1.91	17	0.14	1.06	8
Mallard	0.00	0.00	0	0.00	0.00	0	0.05	0.23	3
American Black Duck	0.89	3.62	55	0.27	0.88	15	4.28	14.16	244
Gadwall	0.00	0.00	0	0.00	0.00	0	0.07	0.53	4
American Wigeon	0.02	0.13	1	0.00	0.00	0	0.05	0.29	3
Greater Scaup	0.66	2.62	41	0.00	0.00	0	8.07	34.19	460
Scaup spp.	0.00	0.00	0	0.07	0.53	4	3.96	20.98	226
Common Eider	86.79	162.01	5381	39.91	61.13	2235	34.26	72.45	1953
Harlequin Duck	5.84	8.36	362	1.27	3.01	71	0.00	0.00	0
Long-tailed Duck	0.00	0.00	0	0.00	0.00	0	0.02	0.13	1
Surf Scoter	0.82	3.37	51	0.70	2.26	39	0.68	2.38	39
Black Scoter	5.55	21.28	344	2.14	11.09	120	5.79	11.57	330
Surf or Black Scoter	0.00	0.00	0	0.00	0.00	0	0.09	0.66	5
White-winged Scoter	3.27	8.63	203	2.89	9.13	162	5.19	10.09	296
Scoter spp.	15.69	83.81	973	7.20	34.41	403	2.77	11.27	158

Appendix B. Continued.

	Sachuest			Sakonnet			Goosewing		
Species	Mean	SD	N	Mean	SD	N	Mean	SD	N
Common Goldeneye	0.60	1.77	37	0.55	1.55	31	3.56	6.14	203
Barrow's Goldeneye	0.00	0.00	0	0.00	0.00	0	0.02	0.13	1
Bufflehead	0.98	2.61	61	0.05	0.30	3	3.77	8.26	215
Red-breasted Merganser	1.98	3.89	123	2.82	8.35	158	4.70	13.27	268
Seaduck spp.	0.00	0.00	0	0.00	0.00	0	1.32	9.93	75
Peregrine Falcon	0.00	0.00	0	0.02	0.13	1	0.00	0.00	0
Piping Plover	0.00	0.00	0	0.00	0.00	0	0.05	0.29	3
Semipalmated Plover	0.00	0.00	0	0.00	0.00	0	0.18	1.32	10
Spotted Sandpiper	0.03	0.25	2	0.00	0.00	0	0.00	0.00	0
Purple Sandpiper	0.24	1.91	15	0.05	0.40	3	0.00	0.00	0
Sanderling	0.00	0.00	0	0.00	0.00	0	0.88	6.62	50
Dunlin	0.19	1.52	12	0.00	0.00	0	0.00	0.00	0
Semipalmated Sandpiper	0.00	0.00	0	0.00	0.00	0	0.02	0.13	1
Laughing Gull	0.47	1.91	29	0.61	2.81	34	0.89	5.01	51
Ring-billed Gull	0.18	1.05	11	0.41	2.15	23	2.25	10.32	128
Herring Gull	1.65	4.25	102	12.93	40.43	724	63.58	331.64	3624
Iceland Gull	0.00	0.00	0	0.00	0.00	0	0.02	0.13	1
Great Black-backed Gull	0.48	0.94	30	5.46	15.22	306	2.77	5.50	158
Gull spp.	0.00	0.00	0	0.00	0.00	0	8.88	47.35	506
Common Tern	0.00	0.00	0	0.02	0.13	1	0.00	0.00	0
Razorbill	0.03	0.25	2	0.00	0.00	0	0.00	0.00	0
Overall	135.10	205.44	8376	89.73	91.16	5025	172.67	365.05	9842

Appendix C. Mean (SD) number of birds detected per hour **in flight** at 11 land-based seawatch stations along coastal Rhode Island from Jan 2009 to mid-Feb 2010. N = total number detections at that station (Watch Hill to Pt. Judith).

	Watch Hill			East Beach			Deep Hole			Point Judith		
Species	Mean	SD	N	Mean	SD	N	Mean	SD	N	Mean	SD	N
Red-throated Loon	0.9	2.6	66	0.57	2.33	45	0.98	3.57	79	2.80	5.98	238
Pacific Loon	0.0	0.0	0	0.00	0.00	0	0.01	0.11	1	0.01	0.05	1
Common Loon	1.8	4.7	137	2.39	6.26	187	3.91	12.32	313	3.99	13.61	339
Loon spp.	0.3	1.5	25	0.95	6.20	74	0.61	1.96	49	0.29	1.30	25
Red-necked Grebe	0.0	0.1	1	0.01	0.11	1	0.04	0.25	3	0.06	0.21	5
Horned Grebe	0.2	1.1	14	0.01	0.11	1	0.03	0.16	3	0.07	0.29	6
Cory's Shearwater	0.1	0.8	9	3.81	24.21	297	4.79	26.61	383	3.12	15.92	266
Greater Shearwater	0.0	0.0	0	0.02	0.13	2	0.00	0.00	0	0.01	0.05	1
Manx Shearwater	0.0	0.0	0	0.00	0.00	0	0.00	0.00	0	0.01	0.11	1
Sooty Shearwater	0.0	0.0	0	0.00	0.00	0	0.01	0.11	1	0.00	0.00	0
Shearwater spp.	0.0	0.0	0	1.04	8.51	82	3.79	33.54	304	0.25	1.20	22
Wilson's St.-Petrel	0.0	0.2	3	2.68	18.44	209	2.96	15.03	237	1.22	5.32	104
Leach's Storm-Petrel	0.0	0.0	0	0.00	0.00	0	0.01	0.06	1	0.00	0.00	0
Storm-Petrel spp.	0.0	0.0	0	0.00	0.00	0	0.01	0.11	1	0.00	0.00	0
Great Cormorant	1.9	3.3	143	0.47	0.95	37	2.23	5.26	179	3.00	6.34	255
Double-c Cormorant	17.8	40.9	1370	9.04	19.37	706	26.84	56.64	2148	10.42	21.40	886
Northern Gannet	3.8	12.3	290	6.90	26.27	538	5.89	14.69	472	16.04	40.17	1363
Great Blue Heron	0.0	0.0	0	0.03	0.16	2	0.09	0.73	8	0.02	0.12	2
Great Egret	0.0	0.2	2	0.02	0.13	2	0.01	0.06	1	0.01	0.05	1
Snowy Egret	0.0	0.1	1	0.03	0.16	2	0.04	0.24	3	0.00	0.00	0
Cattle Egret	0.0	0.0	0	0.00	0.00	0	0.00	0.00	0	0.01	0.05	1
Green Heron	0.0	0.0	0	0.00	0.00	0	0.04	0.34	3	0.00	0.00	0
Blk-c N-Heron	0.0	0.0	0	0.00	0.00	0	0.01	0.06	1	0.00	0.00	0
Glossy Ibis	0.0	0.0	0	0.18	1.42	14	0.00	0.00	0	0.00	0.00	0
Mute Swan	0.0	0.1	1	0.08	0.36	6	0.04	0.19	3	0.04	0.25	4
Canada Goose	0.9	3.8	71	0.35	1.46	27	0.63	2.84	50	1.14	4.26	97

Appendix C Continued.

	Watch Hill			East Beach			Deep Hole			Point Judith		
Species	Mean	SD	N	Mean	SD	N	Mean	SD	N	Mean	SD	N
Atlantic Brant	0.4	1.6	31	0.37	1.42	29	0.37	1.40	30	1.38	4.39	117
Wood Duck	0.1	0.5	4	0.00	0.00	0	0.04	0.34	3	0.00	0.00	0
Mallard	0.0	0.1	1	0.06	0.30	5	0.21	1.28	17	0.05	0.35	5
Am Black Duck	0.1	0.4	7	0.12	0.66	9	0.16	0.50	13	0.05	0.49	5
Gadwall	0.0	0.2	2	0.00	0.00	0	0.00	0.00	0	0.00	0.00	0
Northern Pintail	0.0	0.0	0	0.00	0.00	0	0.00	0.00	0	0.01	0.05	1
American Wigeon	0.0	0.2	2	0.00	0.00	0	0.00	0.00	0	0.00	0.00	0
Green-winged Teal	0.0	0.0	0	0.03	0.23	2	0.06	0.50	5	0.16	1.52	14
Teal spp.	0.0	0.0	0	0.00	0.00	0	0.01	0.06	1	0.00	0.00	0
Anas spp.	0.0	0.0	0	0.13	1.13	10	0.04	0.24	3	0.01	0.11	1
Greater Scaup	0.0	0.0	0	0.02	0.17	2	0.18	1.36	14	0.19	1.79	17
Scaup spp.	0.0	0.0	0	0.05	0.45	4	0.01	0.11	1	0.04	0.27	4
Aythya Spp.	0.0	0.0	0	0.03	0.23	2	0.21	1.11	17	0.00	0.00	0
Common Eider	38.7	191.4	2983	9.71	42.93	757	14.37	46.21	1150	23.94	85.50	2035
Long-tailed Duck	0.5	1.5	35	0.41	2.34	32	0.11	0.36	9	0.40	1.29	34
Surf Scoter	6.3	45.5	484	0.88	2.23	69	1.24	5.60	100	7.92	34.91	674
Black Scoter	7.4	36.8	571	1.63	5.43	128	1.26	6.34	101	15.11	73.64	1284
Surf or Black Scoter	0.6	2.3	44	1.44	4.72	112	1.99	7.16	160	3.39	11.96	288
White-winged Scoter	6.3	21.9	489	4.87	16.03	380	0.74	1.97	60	2.51	5.96	213
Scoter spp.	10.3	28.3	795	65.06	315.6	5075	4.98	8.85	398	18.79	78.74	1597
Common Goldeneye	0.0	0.2	3	0.05	0.27	4	0.16	0.67	13	0.30	1.28	26
Bufflehead	0.0	0.3	3	0.00	0.00	0	0.12	0.67	10	0.00	0.00	0
Hooded Merganser	0.0	0.0	0	0.00	0.00	0	0.02	0.17	2	0.00	0.00	0
Red-bd Merganser	1.3	2.5	100	0.85	2.08	67	1.62	2.87	130	4.45	9.88	379
Common Merganser	0.0	0.0	0	0.00	0.00	0	0.01	0.06	1	0.00	0.00	0
Seaduck spp.	0.0	0.0	0	8.65	58.92	675	0.83	3.79	66	0.11	0.98	9
Northern Harrier	0.0	0.1	1	0.01	0.11	1	0.00	0.00	0	0.00	0.00	0

Appendix C continued.

	Watch Hill			East Beach			Deep Hole			Point Judith		
Species	Mean	SD	N	Mean	SD	N	Mean	SD	N	Mean	SD	N
Osprey	0.1	0.2	5	0.05	0.21	4	0.09	0.33	8	0.01	0.11	1
Merlin	0.0	0.2	2	0.01	0.06	1	0.00	0.00	0	0.01	0.08	1
American Kestrel	0.0	0.2	3	0.00	0.00	0	0.00	0.00	0	0.00	0.00	0
Peregrine Falcon	0.0	0.0	0	0.00	0.00	0	0.00	0.00	0	0.02	0.12	2
Black-bellied Plover	0.0	0.1	1	0.02	0.13	2	0.01	0.11	1	0.00	0.00	0
Piping Plover	0.0	0.0	0	0.04	0.34	3	0.01	0.06	1	0.00	0.00	0
Semipal. Plover	0.1	0.4	5	0.40	2.47	32	0.19	0.73	16	0.01	0.11	1
Killdeer	0.0	0.0	0	0.00	0.00	0	0.00	0.00	0	0.02	0.12	2
Am. Oystercatcher	0.0	0.1	1	0.00	0.00	0	0.00	0.00	0	0.02	0.12	2
Greater Yellowlegs	0.0	0.0	0	0.01	0.11	1	0.01	0.06	1	0.00	0.00	0
Lesser Yellowlegs	0.0	0.0	0	0.04	0.26	4	0.01	0.11	1	0.08	0.76	7
Willet	0.1	0.6	5	0.06	0.37	5	0.00	0.00	0	0.01	0.05	1
Spotted Sandpiper	0.0	0.1	1	0.00	0.00	0	0.00	0.00	0	0.00	0.00	0
Whimbrel	0.0	0.2	4	0.12	0.91	9	0.00	0.00	0	0.08	0.58	7
Ruddy Turnstone	0.2	1.3	14	0.11	0.70	9	0.05	0.35	4	0.09	0.58	8
Purple Sandpiper	0.3	1.4	24	0.11	0.68	9	0.26	2.24	21	0.98	4.91	84
Sanderling	3.1	18.6	236	7.63	26.85	595	0.74	3.02	60	1.41	8.28	120
Dunlin	0.0	0.0	0	0.10	0.71	8	0.18	1.14	15	0.00	0.00	0
Semipal. Sandpiper	3.4	26.8	260	0.51	2.76	40	0.76	3.49	61	3.47	28.19	295
Peep spp.	0.7	3.4	53	1.72	8.31	134	0.53	3.19	43	1.22	5.43	104
Least Sandpiper	0.1	0.8	10	0.00	0.00	0	0.00	0.00	0	0.03	0.19	3
Short-bd Dowitcher	0.5	3.0	40	0.26	1.95	20	0.29	2.52	24	0.42	2.18	36
Shorebird Spp.	1.2	5.6	91	1.40	6.96	109	0.45	1.90	36	1.42	6.24	121
Pomarine Jaeger	0.0	0.0	0	0.00	0.00	0	0.00	0.00	0	0.01	0.11	1
Parasitic Jaeger	0.0	0.0	0	0.01	0.06	1	0.06	0.46	5	0.04	0.33	3
Jaeger spp.	0.0	0.0	0	0.00	0.00	0	0.01	0.06	1	0.00	0.00	0
Bonaparte's Gull	0.1	0.3	5	0.38	1.80	30	0.24	0.94	19	0.58	2.01	49

Appendix C Continued.

	Watch Hill			East Beach			Deep Hole			Point Judith		
Species	Mean	SD	N	Mean	SD	N	Mean	SD	N	Mean	SD	N
Laughing Gull	20.6	78.9	1587	11.31	26.60	882	9.24	33.43	739	8.85	30.27	752
Ring-billed Gull	3.0	8.8	232	1.99	4.63	155	1.97	4.68	157	1.63	3.56	138
Herring Gull	9.8	25.2	751	20.41	60.20	1592	21.28	26.87	1702	22.58	56.93	1919
Great Black-bd Gull	5.9	21.5	454	9.59	30.18	748	8.37	10.84	670	12.48	37.45	1061
Black-l. Kittiwake	0.0	0.2	2	0.01	0.11	1	0.02	0.10	2	0.22	0.91	19
Gull spp.	16.1	60.5	1236	32.66	141.19	2548	66.76	160.67	5341	6.13	31.69	521
Caspian Tern	0.0	0.0	0	0.01	0.11	1	0.00	0.00	0	0.00	0.00	0
Royal Tern	0.0	0.0	0	0.03	0.23	2	0.00	0.00	0	0.01	0.05	1
Common Tern	5.9	15.9	455	1.65	5.11	129	2.51	10.19	201	4.98	19.00	424
Forster's Tern	0.1	0.3	5	0.01	0.11	1	0.00	0.00	0	0.01	0.11	1
Roseate Tern	0.3	1.5	26	0.11	0.57	9	0.20	1.06	16	0.25	0.91	21
Least Tern	2.2	5.2	168	0.45	1.20	35	0.65	2.22	52	0.02	0.12	2
Black Tern	0.0	0.2	2	0.04	0.34	3	0.01	0.06	1	0.01	0.05	1
Sterna spp.	1.3	10.5	98	2.42	12.62	189	0.51	1.94	41	1.35	10.86	115
Black Skimmer	0.0	0.0	0	0.02	0.17	2	0.00	0.00	0	0.00	0.00	0
Murre spp.	0.0	0.0	0	0.00	0.00	0	0.00	0.00	0	0.01	0.05	1
Razorbill	0.1	0.5	5	0.01	0.11	1	0.03	0.22	2	0.64	2.08	54
Black Guillemot	0.0	0.0	0	0.00	0.00	0	0.00	0.00	0	0.01	0.05	1
Alcid spp.	0.0	0.1	1	0.06	0.46	5	0.01	0.08	1	0.47	2.10	40
Mourning Dove	0.0	0.1	1	0.00	0.00	0	0.00	0.00	0	0.01	0.11	1
Chimney Swift	0.0	0.1	1	0.00	0.00	0	0.00	0.00	0	0.00	0.00	0
Ruby-t Hummbird	0.0	0.0	0	0.01	0.11	1	0.00	0.00	0	0.01	0.11	1
Belted Kingfisher	0.0	0.1	1	0.00	0.00	0	0.00	0.00	0	0.00	0.00	0
Northern Flicker	0.0	0.0	0	0.00	0.00	0	0.00	0.00	0	0.01	0.05	1
Eastern Kingbird	0.0	0.0	0	0.01	0.06	1	0.00	0.00	0	0.00	0.00	0
Blue Jay	0.2	1.4	12	0.00	0.00	0	0.00	0.00	0	0.00	0.00	0
Fish Crow	0.1	0.6	5	0.06	0.57	5	0.00	0.00	0	0.00	0.00	0

	Watch Hill			East Beach			Deep Hole			Point Judith		
Species	Mean	SD	N	Mean	SD	N	Mean	SD	N	Mean	SD	N
Horned Lark	0.0	0.1	1	0.00	0.00	0	0.00	0.00	0	0.00	0.00	0
Purple Martin	0.0	0.0	0	0.02	0.13	2	0.02	0.12	2	0.01	0.05	1
N Rough-w Swallow	0.0	0.2	2	0.05	0.45	4	0.00	0.00	0	0.15	0.75	13
Bank Swallow	0.0	0.0	0	0.00	0.00	0	0.00	0.00	0	0.08	0.45	7
Tree Swallow	130.6	1144.6	10058	1.67	11.41	130	1.13	8.91	91	0.36	2.79	31
Cliff Swallow	0.0	0.0	0	0.01	0.11	1	0.00	0.00	0	0.00	0.00	0
Barn Swallow	0.4	2.0	34	0.21	0.97	17	0.11	0.45	9	0.08	0.41	7
American Pipit	0.0	0.0	0	0.00	0.00	0	0.01	0.06	1	0.00	0.00	0
Cedar Waxwing	0.0	0.0	0	0.00	0.00	0	0.00	0.00	0	0.01	0.11	1
Yellow Warbler	0.0	0.2	3	0.00	0.00	0	0.01	0.11	1	0.02	0.12	2
Palm Warbler	0.0	0.0	0	0.00	0.00	0	0.00	0.00	0	0.01	0.05	1
Snow Bunting	0.1	0.6	6	0.01	0.11	1	0.00	0.00	0	0.00	0.00	0
Brown-hd Cowbird	0.0	0.0	0	0.00	0.00	0	0.00	0.00	0	0.08	0.48	7
Common Grackle	0.0	0.0	0	0.00	0.00	0	0.00	0.00	0	0.04	0.24	3
Total	306.3	1184.5	23586	218.84	373.75	17069	199.22	245.34	15938	191.94	252.55	16315

Appendix C continued. Birds detected **in flight** during land-based seawatches (Monahan's Dock to Ruggles Ave).

	Monahan's Dock			Beavertail			Brenton Point			Ruggles		
Species	Mean	SD	N	Mean	SD	N	Mean	SD	N	Mean	SD	N
Red-throated Loon	0.9	2.1	82	0.6	1.5	50	0.8	3.7	53	0.8	2.1	49
Common Loon	2.1	6.1	191	1.4	4.2	110	1.3	2.8	87	3.6	16.4	233
Loon spp.	0.8	4.3	74	0.3	1.0	26	0.2	1.1	12	0.5	2.8	32
Red-necked Grebe	0.0	0.1	1	0.0	0.1	1	0.0	0.1	1	0.0	0.1	2
Horned Grebe	0.0	0.1	1	0.0	0.2	4	0.3	2.5	22	0.1	0.6	8
Cory's Shearwater	0.4	2.0	33	0.6	2.8	51	4.8	24.5	312	2.3	12.8	151
Greater Shearwater	0.0	0.0	0	0.0	0.1	1	0.1	0.5	4	0.0	0.1	1
Manx Shearwater	0.0	0.2	3	0.0	0.1	1	0.0	0.0	0	0.0	0.0	0
Sooty Shearwater	0.0	0.1	1	0.0	0.0	0	0.0	0.1	1	0.0	0.1	1

Appendix C. Continued.

	Monahan's Dock			Beavertail			Brenton Point			Ruggles		
Species	Mean	SD	N	Mean	SD	N	Mean	SD	N	Mean	SD	N
Shearwater spp.	0.2	0.9	17	0.4	2.7	29	5.6	44.3	361	0.3	2.4	22
Wilson's Storm-Petrel	0.2	1.0	18	0.7	3.4	57	0.6	3.2	36	1.5	10.0	97
Great Cormorant	1.4	2.9	125	0.9	1.7	76	1.3	2.5	87	1.5	3.4	100
Double-cd Cormorant	9.9	15.3	888	9.5	13.8	770	23.0	31.1	1492	14.9	25.7	968
Northern Gannet	7.1	18.3	636	8.0	30.4	645	4.2	14.7	271	12.2	57.6	796
Great Blue Heron	0.0	0.1	1	0.1	0.4	5	0.0	0.1	1	0.0	0.2	2
Great Egret	0.2	0.7	17	0.0	0.0	0	0.0	0.0	0	0.0	0.2	3
Snowy Egret	0.0	0.1	1	0.0	0.0	0	0.0	0.0	0	0.0	0.0	0
Cattle Egret	0.0	0.0	0	0.0	0.0	0	0.0	0.1	1	0.0	0.0	0
Black-crd Night-Heron	0.0	0.1	1	0.0	0.0	0	0.0	0.0	0	0.0	0.0	0
Glossy Ibis	0.0	0.2	2	0.0	0.0	0	0.0	0.0	0	0.0	0.0	0
Mute Swan	0.1	0.5	10	0.0	0.1	1	0.0	0.1	1	0.0	0.2	2
Canada Goose	5.1	12.8	456	1.4	10.1	114	0.7	3.5	43	7.0	24.1	456
Atlantic Brant	1.6	5.7	143	2.2	7.3	180	0.9	3.9	59	1.8	9.7	116
Mallard	0.1	0.4	6	0.0	0.1	2	0.1	0.4	6	0.0	0.1	1
American Black Duck	0.1	0.5	12	0.0	0.2	3	0.3	1.7	20	0.3	1.1	17
Gadwall	0.0	0.1	1	0.0	0.0	0	0.1	0.3	5	0.0	0.0	0
American Wigeon	0.0	0.0	0	0.0	0.2	2	0.0	0.0	0	0.0	0.0	0
Green-winged Teal	0.0	0.0	0	0.1	1.3	12	0.0	0.0	0	0.0	0.0	0
Anas spp.	0.1	0.7	7	0.0	0.3	4	0.0	0.1	1	0.0	0.2	3
Greater Scaup	0.0	0.3	4	0.0	0.2	2	0.0	0.0	0	0.0	0.2	2
Scaup spp.	0.0	0.2	3	0.3	2.3	28	0.0	0.0	0	0.0	0.0	0
Aythya Spp.	0.1	0.5	5	0.0	0.2	2	0.0	0.0	0	0.0	0.0	0
Common Eider	11.7	39.4	1054	18.2	43.1	1475	40.8	122.4	2650	15.8	32.8	1029
King Eider	0.0	0.0	0	0.0	0.0	0	0.0	0.1	1	0.0	0.0	0
Harlequin Duck	0.0	0.1	1	0.7	2.6	58	0.5	1.7	30	0.1	0.6	9
Long-tailed Duck	0.1	0.3	7	0.2	0.5	14	0.2	1.1	16	0.1	0.5	5

Appendix C. Continued.

	Monahan's Dock			Beavertail			Brenton Point			Ruggles		
Species	Mean	SD	N	Mean	SD	N	Mean	SD	N	Mean	SD	N
Surf Scoter	0.7	4.0	59	0.9	2.0	70	0.9	3.4	58	3.3	10.7	213
Black Scoter	2.0	13.6	178	3.2	10.2	256	4.4	15.1	283	1.9	4.8	120
Surf or Black Scoter	2.2	15.9	196	1.8	9.1	148	0.7	3.0	46	3.2	8.6	208
White-winged Scoter	0.9	5.3	84	0.6	1.7	48	4.7	35.3	304	1.4	4.9	93
Scoter spp.	8.5	56.3	763	5.9	32.6	477	14.3	70.4	931	64.6	301.8	4197
Common Goldeneye	0.3	1.5	27	0.1	0.3	6	0.3	1.1	18	0.8	4.0	54
Bufflehead	0.0	0.4	4	0.0	0.0	0	0.0	0.1	1	0.1	0.3	5
Red-breasted Merganser	1.6	3.4	147	1.1	2.7	90	1.9	4.5	122	2.9	6.7	188
Common Merganser	0.0	0.0	0	0.0	0.0	0	0.0	0.1	1	0.0	0.0	0
Seaduck spp.	0.0	0.0	0	0.0	0.1	1	0.0	0.0	0	0.7	4.0	47
Northern Harrier	0.0	0.1	1	0.0	0.0	0	0.0	0.0	0	0.0	0.2	3
Osprey	0.1	0.2	5	0.0	0.1	1	0.0	0.3	3	0.0	0.2	3
American Kestrel	0.0	0.0	0	0.0	0.0	0	0.0	0.1	1	0.0	0.0	0
Peregrine Falcon	0.0	0.0	0	0.0	0.2	2	0.0	0.0	0	0.0	0.0	0
Falcon spp.	0.0	0.0	0	0.0	0.1	1	0.0	0.0	0	0.0	0.0	0
Black-bellied Plover	0.0	0.0	0	0.0	0.0	0	0.0	0.2	3	0.0	0.0	0
Semipalmated Plover	0.0	0.2	3	0.1	0.6	9	0.3	1.0	18	0.0	0.1	1
American Oystercatcher	0.0	0.1	1	0.0	0.1	2	0.0	0.0	0	0.0	0.0	0
Willet	0.0	0.1	1	0.0	0.0	0	0.0	0.0	0	0.0	0.0	0
Spotted Sandpiper	0.0	0.0	0	0.0	0.0	0	0.0	0.0	0	0.0	0.1	1
Ruddy Turnstone	0.0	0.3	3	0.0	0.0	0	0.5	2.2	31	0.1	0.6	7
Purple Sandpiper	2.0	9.0	178	1.0	5.3	81	3.1	9.5	201	2.0	5.8	132
Sanderling	2.5	7.2	227	0.6	2.9	45	0.2	1.5	12	0.5	3.0	34
Dunlin	0.2	1.3	17	0.0	0.1	1	0.0	0.0	0	0.0	0.0	0
Semipalmated Sandpiper	0.3	1.9	24	0.1	0.6	7	0.3	1.1	17	0.2	1.5	12
Peep spp.	1.1	6.5	103	0.4	2.7	35	0.1	0.4	6	0.3	2.1	17
Least Sandpiper	0.1	0.4	5	0.0	0.1	1	0.2	0.7	12	0.0	0.0	0

Appendix C. Continued.

	Monahan's Dock			Beavertail			Brenton Point			Ruggles		
Species	Mean	SD	N	Mean	SD	N	Mean	SD	N	Mean	SD	N
Short-billed Dowitcher	0.0	0.1	1	0.1	0.8	9	0.0	0.4	3	0.0	0.0	0
Shorebird Spp.	1.3	5.8	119	0.7	4.1	55	0.6	2.1	39	0.0	0.1	1
Parasitic Jaeger	0.0	0.0	0	0.0	0.0	0	0.0	0.1	1	0.0	0.0	0
Jaeger spp.	0.0	0.0	0	0.0	0.1	1	0.0	0.0	0	0.0	0.0	0
Bonaparte's Gull	0.6	2.0	54	0.7	2.0	60	0.1	0.5	5	0.1	0.3	5
Laughing Gull	5.4	15.9	483	9.2	28.3	743	13.9	40.6	904	10.1	40.5	659
Ring-billed Gull	4.2	7.8	378	2.2	6.9	178	1.4	3.0	93	7.1	18.0	465
Herring Gull	23.7	46.1	2135	25.3	30.8	2049	15.7	18.8	1020	46.7	240.3	3039
Great Black-backed Gull	8.6	28.6	777	4.3	5.0	348	3.7	4.5	242	7.4	8.1	480
Black-legged Kittiwake	0.0	0.0	0	0.0	0.3	4	0.1	0.4	4	0.0	0.4	3
Gull spp.	20.9	83.1	1883	9.4	34.1	759	1.1	5.3	75	4.7	14.6	305
Royal Tern	0.0	0.1	1	0.0	0.1	1	0.0	0.0	0	0.0	0.0	0
Common Tern	3.1	16.2	281	4.6	19.1	370	5.3	17.3	347	1.7	8.2	110
Forster's Tern	0.0	0.0	0	0.0	0.1	1	0.0	0.0	0	0.0	0.0	0
Roseate Tern	0.1	0.3	5	0.0	0.2	3	0.0	0.1	1	0.0	0.0	0
Least Tern	0.1	0.5	13	0.1	0.4	6	0.1	0.5	6	0.1	0.2	4
Black Tern	0.0	0.1	1	0.0	0.1	2	0.0	0.0	0	0.0	0.0	0
Sterna spp.	0.2	0.8	17	0.3	1.4	26	0.3	1.6	17	3.1	22.8	204
Razorbill	0.1	0.3	6	0.2	0.6	13	0.0	0.1	1	0.0	0.1	2
Alcid spp.	0.1	0.2	5	0.1	0.5	9	0.0	0.2	2	0.0	0.2	2
Chimney Swift	0.0	0.1	1	0.0	0.0	0	0.0	0.0	0	0.0	0.0	0
Belted Kingfisher	0.0	0.1	1	0.0	0.0	0	0.0	0.0	0	0.0	0.0	0
American Crow	0.0	0.0	0	0.0	0.0	0	0.0	0.0	0	0.4	1.4	23
Fish Crow	0.0	0.1	1	0.0	0.0	0	0.0	0.0	0	0.0	0.0	0
Corvid spp.	0.0	0.0	0	0.0	0.0	0	0.0	0.0	0	0.2	0.9	11
Horned Lark	0.0	0.1	1	0.0	0.0	0	0.0	0.0	0	0.0	0.0	0
N Rough-wd Swallow	0.1	0.7	12	0.0	0.2	2	0.0	0.0	0	0.4	1.7	25

Appendix C. Continued

	Monahan's Dock			Beavertail			Brenton Point			Ruggles		
Species	Mean	SD	N	Mean	SD	N	Mean	SD	N	Mean	SD	N
Bank Swallow	0.0	0.0	0	0.0	0.3	3	0.0	0.0	0	0.0	0.0	0
Tree Swallow	2.3	12.1	205	0.0	0.3	4	0.0	0.3	3	0.2	1.6	13
Barn Swallow	0.4	1.2	40	0.1	0.7	12	0.5	1.9	34	0.2	0.6	11
Swallow spp.	0.2	0.8	18	0.0	0.2	3	0.0	0.2	3	0.0	0.3	3
American Robin	0.0	0.0	0	0.0	0.0	0	0.0	0.2	2	0.0	0.0	0
American Pipit	0.0	0.0	0	0.0	0.0	0	0.0	0.1	1	0.0	0.1	1
Yellow Warbler	0.0	0.3	3	0.0	0.0	0	0.0	0.0	0	0.0	0.0	0
Common Grackle	0.0	0.1	1	0.0	0.0	0	0.0	0.0	0	0.0	0.0	0
Passerine spp.	0.0	0.1	1	0.0	0.0	0	0.0	0.0	0	0.0	0.0	0
Total	136.2	150.6	12255	119.2	106.2	9655	160.5	199.8	10433	227.6	420.8	14795

Appendix C. Continued. Birds detected **in flight** during land-based seawatches (Sachuest and Goosewing).

	Sachuest			Sakonnet			Goosewing		
Species	Mean	SD	N	Mean	SD	N	Mean	SD	N
Red-throated Loon	1.63	3.51	101	0.70	2.11	39	0.46	1.85	26
Common Loon	1.42	3.10	88	1.13	2.10	64	1.75	7.87	100
Loon spp.	0.19	1.08	12	0.57	1.98	32	1.43	5.27	82
Red-necked Grebe	0.01	0.10	1	0.02	0.13	1	0.00	0.00	0
Horned Grebe	0.06	0.31	4	0.04	0.16	2	0.01	0.07	1
Cory's Shearwater	0.10	0.56	6	0.20	1.13	11	0.01	0.07	1
Manx Shearwater	0.00	0.00	0	0.00	0.00	0	0.01	0.07	1
Shearwater spp.	0.00	0.00	0	0.01	0.07	1	0.00	0.00	0
Wilson's Storm-Petrel	0.69	4.75	43	0.30	1.29	17	0.00	0.00	0
Great Cormorant	1.05	1.88	65	2.93	8.59	164	1.43	4.22	82
Double-crested Cormorant	24.60	44.26	1525	53.01	106.24	2969	24.97	44.34	1424
Northern Gannet	4.71	14.62	292	6.26	12.35	351	3.71	9.71	212
Appendix C. Continued									

	Sachuest			Sakonnet			Goosewing		
Species	Mean	SD	N	Mean	SD	N	Mean	SD	N
Great Blue Heron	0.05	0.28	3	0.02	0.13	1	0.00	0.00	0
Great Egret	0.01	0.06	1	0.04	0.27	3	0.02	0.13	1
Green Heron	0.00	0.00	0	0.04	0.27	2	0.00	0.00	0
Black-crowned Night-Heron	0.00	0.00	0	0.03	0.15	2	0.00	0.00	0
Glossy Ibis	0.00	0.00	0	0.00	0.00	0	0.07	0.53	4
Mute Swan	0.02	0.13	1	0.05	0.23	3	0.35	1.01	20
Tundra Swan	0.00	0.00	0	0.00	0.00	0	0.04	0.26	2
Canada Goose	0.43	2.60	27	0.55	2.67	31	1.34	5.02	77
Atlantic Brant	0.79	3.62	49	0.53	1.97	30	0.15	1.06	9
Wood Duck	0.00	0.00	0	0.00	0.00	0	0.03	0.20	2
Mallard	0.00	0.00	0	0.06	0.23	4	0.07	0.42	4
American Black Duck	0.24	0.67	15	0.40	0.81	23	1.65	7.52	94
Gadwall	0.00	0.00	0	0.04	0.27	2	0.00	0.00	0
Northern Pintail	0.00	0.00	0	0.05	0.34	3	0.00	0.00	0
Anas spp.	0.00	0.00	0	0.10	0.67	6	0.05	0.29	3
Greater Scaup	0.08	0.64	5	0.01	0.07	1	0.75	4.52	43
Scaup spp.	0.00	0.00	0	0.19	1.40	11	1.76	12.91	101
Common Eider	18.02	56.76	1117	14.00	32.68	784	5.93	10.99	338
Harlequin Duck	1.04	2.75	65	0.22	0.65	13	0.04	0.19	2
Long-tailed Duck	0.14	0.39	9	0.24	1.00	14	0.00	0.00	0
Surf Scoter	6.46	17.28	401	2.96	11.30	166	0.11	0.79	6
Black Scoter	4.21	9.60	261	3.74	10.97	210	0.32	0.95	18
Surf or Black Scoter	5.11	23.10	317	2.60	8.46	146	1.93	11.93	110
White-winged Scoter	2.56	4.35	159	4.34	9.35	243	0.59	1.89	34
Scoter spp.	53.35	205.24	3308	32.17	143.00	1802	4.87	11.39	278
Common Goldeneye	0.76	3.27	47	0.23	0.61	13	0.38	1.13	22
Bufflehead	0.88	3.04	55	0.04	0.24	3	0.18	0.86	11

Appendix C. Continued.

	Sachuest			Sakonnet			Goosewing		
Species	Mean	SD	N	Mean	SD	N	Mean	SD	N
Hooded Merganser	0.07	0.57	5	0.00	0.00	0	0.00	0.00	0
Red-breasted Merganser	1.71	3.61	106	1.40	2.41	78	1.01	2.15	58
Seaduck spp.	7.07	53.17	439	0.98	7.35	55	1.22	8.94	70
Northern Harrier	0.00	0.00	0	0.01	0.07	1	0.00	0.00	0
Sharp-shinned Hawk	0.01	0.06	1	0.02	0.13	1	0.00	0.00	0
Cooper's Hawk	0.00	0.00	0	0.01	0.07	1	0.00	0.00	0
Osprey	0.02	0.13	1	0.03	0.15	2	0.06	0.27	4
Merlin	0.02	0.13	1	0.00	0.00	0	0.00	0.00	0
American Kestrel	0.01	0.06	1	0.01	0.07	1	0.00	0.00	0
Peregrine Falcon	0.02	0.13	1	0.00	0.00	0	0.03	0.15	2
Falcon spp.	0.00	0.00	0	0.00	0.00	0	0.01	0.07	1
Black-bellied Plover	0.00	0.00	0	0.05	0.40	3	0.07	0.53	4
Piping Plover	0.00	0.00	0	0.01	0.07	1	0.02	0.13	1
Semipalmated Plover	0.00	0.00	0	0.12	0.60	7	0.17	0.61	10
Killdeer	0.00	0.00	0	0.00	0.00	0	0.03	0.15	2
American Oystercatcher	0.00	0.00	0	0.08	0.33	5	0.00	0.00	0
Greater Yellowlegs	0.00	0.00	0	0.36	2.54	20	0.00	0.00	0
Yellowlegs spp.	0.00	0.00	0	0.02	0.13	1	0.00	0.00	0
Willet	0.00	0.00	0	0.00	0.00	0	0.01	0.07	1
Spotted Sandpiper	0.02	0.14	2	0.00	0.00	0	0.00	0.00	0
Ruddy Turnstone	0.06	0.29	4	0.09	0.36	5	0.02	0.13	1
Purple Sandpiper	3.60	11.93	223	2.43	6.34	136	0.00	0.00	0
Sanderling	0.87	3.74	54	0.00	0.00	0	2.73	9.20	156
Dunlin	0.03	0.25	2	0.00	0.00	0	0.32	1.90	19
White-rumped Sandpiper	0.02	0.13	1	0.00	0.00	0	0.00	0.00	0
Semipalmated Sandpiper	0.01	0.06	1	0.04	0.16	2	0.10	0.55	6
Peep spp.	0.06	0.29	4	0.94	6.43	53	0.32	2.38	18

Appendix C. Continued.

	Sachuest			Sakonnet			Goosewing		
Species	Mean	SD	N	Mean	SD	N	Mean	SD	N
Least Sandpiper	0.04	0.32	3	0.04	0.16	2	0.00	0.00	0
Short-billed Dowitcher	0.04	0.32	3	0.00	0.00	0	0.00	0.00	0
Shorebird Spp.	0.69	3.84	43	0.46	1.84	26	1.03	6.64	59
Parasitic Jaeger	0.00	0.00	0	0.00	0.00	0	0.04	0.26	2
Jaeger spp.	0.01	0.06	1	0.00	0.00	0	0.00	0.00	0
Bonaparte's Gull	0.00	0.00	0	0.32	1.68	18	0.02	0.13	1
Laughing Gull	9.26	45.13	574	10.18	33.50	570	7.42	31.21	423
Ring-billed Gull	1.02	3.98	64	2.26	4.47	127	2.96	12.04	169
Herring Gull	12.64	20.41	784	84.89	124.19	4754	188.98	576.08	10772
Great Black-backed Gull	4.64	7.08	288	15.22	25.36	853	4.78	7.09	272
Black-legged Kittiwake	0.00	0.00	0	0.02	0.13	1	0.02	0.13	1
Gull spp.	4.35	11.79	270	10.55	44.19	591	40.27	133.35	2296
Royal Tern	0.00	0.00	0	0.02	0.13	1	0.00	0.00	0
Common Tern	1.55	4.63	96	2.30	9.42	129	1.91	4.96	109
Roseate Tern	0.06	0.40	4	0.07	0.53	4	0.00	0.00	0
Least Tern	0.06	0.40	4	0.22	1.30	13	0.91	2.88	52
Black Tern	0.00	0.00	0	0.04	0.27	2	0.00	0.00	0
Sterna spp.	1.10	5.79	69	2.70	19.11	151	0.73	2.77	42
Razorbill	0.07	0.40	5	0.02	0.13	1	0.00	0.00	0
Alcid spp.	0.05	0.38	3	0.00	0.00	0	0.00	0.00	0
Mourning Dove	0.00	0.00	0	0.00	0.00	0	0.03	0.15	2
Short-eared Owl	0.00	0.00	0	0.01	0.07	1	0.00	0.00	0
American Crow	0.02	0.13	1	0.01	0.10	1	0.00	0.00	0
Crows	0.00	0.00	0	0.01	0.07	1	0.00	0.00	0
Purple Martin	0.00	0.00	0	0.00	0.00	0	0.02	0.13	1
N. Rough-winged Swallow	0.00	0.00	0	0.45	3.34	25	0.02	0.09	1
Bank Swallow	0.03	0.25	2	0.00	0.00	0	0.01	0.07	1

Appendix C. Continued.

	Sachuest			Sakonnet			Goosewing		
Species	Mean	SD	N	Mean	SD	N	Mean	SD	N
Tree Swallow	11.67	61.86	724	4.50	22.22	252	18.56	77.52	1058
Barn Swallow	0.08	0.34	5	0.21	1.34	12	0.07	0.36	4
Swallow spp.	0.09	0.54	6	0.34	2.04	19	0.39	1.83	22
American Robin	0.06	0.44	4	0.00	0.00	0	0.00	0.00	0
American Pipit	0.00	0.00	0	0.01	0.07	1	0.00	0.00	0
Cedar Waxwing	0.01	0.06	1	0.00	0.00	0	0.00	0.00	0
Yellow Warbler	0.01	0.06	1	0.00	0.00	0	0.00	0.00	0
Yellow-rumped Warbler	0.29	2.16	18	0.00	0.00	0	0.02	0.13	1
Warbler spp.	0.01	0.06	1	0.04	0.27	2	0.00	0.00	0
Snow Bunting	0.00	0.00	0	0.39	2.94	22	0.00	0.00	0
Bobolink	0.01	0.06	1	0.00	0.00	0	0.00	0.00	0
American Goldfinch	0.26	1.67	16	0.00	0.00	0	0.00	0.00	0
Passerine spp.	0.06	0.51	4	0.00	0.00	0	0.05	0.40	3
Total	190.38	252.71	11804	269.68	301.32	15102	328.70	593.97	18736

Appendix D. Mean number of detections (±1 SD) per survey for each month from 23 January 2009 to 21 February 2010 for 121 species of birds detected during 796 land-based seawatches at 11 stations along the Rhode Island coast. Note: One and two hour surveys, birds in flight and birds on the water have been pooled.

	Jan 2009		Feb 2009		Mar 2009		Apr 2009	
Species	Mean	SD	Mean	SD	Mean	SD	Mean	SD
Red-throated Loon	3.76	6.25	0.72	1.09	3.47	8.06	5.43	11.42
Pacific Loon	0.00	0.00	0.00	0.00	0.00	0.00	0.00	0.00
Common Loon	13.62	11.12	7.48	5.92	5.93	4.59	24.16	43.14
Loon spp.	0.14	0.36	0.09	0.29	0.07	0.31	0.72	2.74
Red-necked Grebe	0.19	0.51	0.13	0.39	0.25	1.48	0.12	0.42
Horned Grebe	5.71	4.56	4.56	4.78	9.21	42.93	2.00	5.08
Cory's Shearwater	0.00	0.00	0.00	0.00	0.00	0.00	0.00	0.00
Greater Shearwater	0.00	0.00	0.00	0.00	0.00	0.00	0.00	0.00
Manx Shearwater	0.00	0.00	0.00	0.00	0.00	0.00	0.00	0.00
Sooty Shearwater	0.00	0.00	0.00	0.00	0.00	0.00	0.00	0.00
Shearwater spp.	0.00	0.00	0.00	0.00	0.00	0.00	0.00	0.00
Wilson's Storm-Petrel	0.00	0.00	0.00	0.00	0.00	0.00	0.00	0.00
Leach's Storm-Petrel	0.00	0.00	0.00	0.00	0.00	0.00	0.00	0.00
Storm-petrel spp.	0.00	0.00	0.00	0.00	0.00	0.00	0.00	0.00
Great Cormorant	12.86	21.11	7.52	11.68	5.50	8.96	0.79	2.67
Double-cd Cormorant	0.00	0.00	0.00	0.00	2.24	13.37	51.24	155.05
Northern Gannet	0.33	0.97	0.11	0.50	0.50	1.67	24.31	107.42
Great Blue Heron	0.00	0.00	0.00	0.00	0.00	0.00	0.02	0.13
Great Egret	0.00	0.00	0.00	0.00	0.00	0.00	0.07	0.32
Snowy Egret	0.00	0.00	0.00	0.00	0.00	0.00	0.05	0.22
Cattle Egret	0.00	0.00	0.00	0.00	0.00	0.00	0.00	0.00
Green Heron	0.00	0.00	0.00	0.00	0.00	0.00	0.00	0.00
Blk-crd Night-Heron	0.00	0.00	0.00	0.00	0.00	0.00	0.00	0.00
Glossy Ibis	0.00	0.00	0.00	0.00	0.00	0.00	0.00	0.00
Mute Swan	0.33	1.53	0.35	0.87	0.13	1.09	0.00	0.00
Tundra Swan	0.00	0.00	0.00	0.00	0.00	0.00	0.00	0.00
Canada Goose	10.24	24.39	5.76	17.31	4.12	11.94	0.88	2.06
Atlantic Brant	5.05	9.98	6.52	15.80	6.25	16.81	1.21	5.06
Wood Duck	0.00	0.00	0.00	0.00	0.04	0.36	0.00	0.00
Mallard	0.05	0.22	0.00	0.00	0.06	0.34	0.09	0.39
Am Black Duck	8.29	18.73	2.74	10.51	1.10	2.29	0.05	0.29
Gadwall	0.43	1.03	0.04	0.27	0.03	0.24	0.00	0.00
Northern Pintail	0.00	0.00	0.00	0.00	0.00	0.00	0.00	0.00
American Wigeon	0.33	1.32	0.04	0.27	0.01	0.12	0.00	0.00
Green-winged Teal	0.00	0.00	0.00	0.00	0.01	0.12	0.00	0.00
Teal spp.	0.00	0.00	0.00	0.00	0.00	0.00	0.00	0.00
Anas spp.	0.00	0.00	0.00	0.00	0.06	0.49	0.00	0.00
Greater Scaup	11.43	51.46	2.59	10.82	1.31	10.31	0.12	0.70
Scaup spp.	14.57	52.48	0.09	0.49	0.00	0.00	0.07	0.53
Athya Spp.	0.00	0.00	0.00	0.00	0.00	0.00	0.09	0.66
Common Eider	273.05	674.14	214.00	564.17	165.72	395.14	38.26	91.30
King Eider	0.00	0.00	0.07	0.54	0.12	0.68	0.10	0.45

Appendix D continued.

	Jan 2009		Feb 2009		Mar 2009		Apr 2009	
Species	Mean	SD	Mean	SD	Mean	SD	Mean	SD
Harlequin Duck	1.67	3.64	4.63	11.66	3.63	7.70	1.52	3.50
Long-tailed Duck	2.05	2.69	2.93	9.42	1.01	3.11	0.62	2.59
Surf Scoter	99.00	305.62	167.94	670.81	379.49	1103.53	66.64	148.08
Black Scoter	94.19	221.56	101.15	340.12	160.07	501.31	75.22	186.36
Black or Surf Scoter	0.00	0.00	0.00	0.00	0.00	0.00	0.14	1.05
White-winged Scoter	28.52	59.30	36.28	122.88	17.65	28.93	12.57	22.47
Scoter spp.	814.62	1646.0	408.89	892.60	183.03	574.49	337.0	1037.5
Common Goldeneye	14.43	14.10	8.44	10.49	4.78	7.00	0.33	1.57
Barrow's Goldeneye	0.00	0.00	0.00	0.00	0.00	0.00	0.00	0.00
Bufflehead	6.29	10.99	1.35	3.51	0.88	2.58	0.00	0.00
Hooded Merganser	0.00	0.00	0.06	0.41	0.00	0.00	0.00	0.00
Red-brd Merganser	31.14	60.40	23.30	39.62	16.90	22.40	18.05	19.56
Common Merganser	0.00	0.00	0.04	0.19	0.00	0.00	0.00	0.00
Seaduck spp.	9.90	22.54	66.72	309.35	21.10	126.17	0.00	0.00
Ruddy Duck	0.00	0.00	0.00	0.00	0.00	0.00	0.00	0.00
Northern Harrier	0.00	0.00	0.00	0.00	0.01	0.12	0.02	0.13
Sharp-shinned Hawk	0.00	0.00	0.00	0.00	0.00	0.00	0.00	0.00
Cooper's Hawk	0.00	0.00	0.00	0.00	0.00	0.00	0.00	0.00
Osprey	0.00	0.00	0.00	0.00	0.00	0.00	0.02	0.13
Merlin	0.00	0.00	0.00	0.00	0.00	0.00	0.03	0.18
American Kestrel	0.05	0.22	0.00	0.00	0.01	0.12	0.03	0.18
Peregrine Falcon	0.00	0.00	0.00	0.00	0.00	0.00	0.00	0.00
Falcon spp.	0.00	0.00	0.00	0.00	0.00	0.00	0.00	0.00
Black-bellied Plover	0.00	0.00	0.00	0.00	0.00	0.00	0.00	0.00
Piping Plover	0.00	0.00	0.00	0.00	0.00	0.00	0.00	0.00
Semipalmated Plover	0.00	0.00	0.00	0.00	0.00	0.00	0.00	0.00
Killdeer	0.00	0.00	0.00	0.00	0.00	0.00	0.00	0.00
Am Oystercatcher	0.00	0.00	0.00	0.00	0.03	0.17	0.02	0.13
Greater Yellowlegs	0.00	0.00	0.00	0.00	0.00	0.00	0.34	2.50
Lesser Yellowlegs	0.00	0.00	0.00	0.00	0.00	0.00	0.00	0.00
Yellowlegs spp.	0.00	0.00	0.00	0.00	0.00	0.00	0.00	0.00
Willet	0.00	0.00	0.00	0.00	0.00	0.00	0.00	0.00
Spotted Sandpiper	0.00	0.00	0.00	0.00	0.00	0.00	0.00	0.00
Whimbrel	0.00	0.00	0.00	0.00	0.00	0.00	0.00	0.00
Ruddy Turnstone	0.00	0.00	0.00	0.00	0.00	0.00	0.00	0.00
Purple Sandpiper	10.05	22.55	9.80	28.84	4.12	13.67	5.62	15.12
Sanderling	0.71	2.85	0.37	2.34	1.41	6.25	0.00	0.00
Dunlin	0.00	0.00	0.50	2.59	0.21	1.70	0.00	0.00
White-rpd Sandpiper	0.00	0.00	0.00	0.00	0.00	0.00	0.00	0.00
Semipalm.Sandpiper	0.00	0.00	0.00	0.00	0.00	0.00	0.00	0.00
Peep spp.	0.00	0.00	0.00	0.00	0.00	0.00	0.00	0.00
Least Sandpiper	0.00	0.00	0.00	0.00	0.00	0.00	0.00	0.00
Short-bd Dowitcher	0.00	0.00	0.00	0.00	0.00	0.00	0.00	0.00
Shorebird Spp.	0.05	0.22	0.52	3.41	1.40	7.11	2.07	7.85

Appendix D continued.

	Jan 2009		Feb 2009		Mar 2009		Apr 2009	
Species	Mean	SD	Mean	SD	Mean	SD	Mean	SD
Pomarine Jaeger	0.00	0.00	0.00	0.00	0.00	0.00	0.00	0.00
Parasitic Jaeger	0.00	0.00	0.00	0.00	0.00	0.00	0.00	0.00
Jaeger spp.	0.00	0.00	0.00	0.00	0.00	0.00	0.00	0.00
Bonaparte's Gull	2.33	4.89	0.76	2.77	0.03	0.17	0.00	0.00
Laughing Gull	0.00	0.00	0.00	0.00	0.00	0.00	0.09	0.43
Ring-billed Gull	0.71	1.01	1.17	3.66	2.62	9.48	1.71	4.56
Herring Gull	69.10	61.17	97.65	259.84	216.85	1052.51	45.34	78.42
Iceland Gull	0.00	0.00	0.00	0.00	0.00	0.00	0.00	0.00
Great Bk-backed Gull	8.29	9.27	7.56	15.43	34.94	243.08	14.86	25.21
Black-ld Kittiwake	0.43	1.33	0.07	0.33	0.01	0.12	0.02	0.13
Gull spp.	48.33	125.94	34.07	73.08	38.71	188.16	3.19	18.66
Caspian Tern	0.00	0.00	0.00	0.00	0.00	0.00	0.00	0.00
Royal Tern	0.00	0.00	0.00	0.00	0.00	0.00	0.00	0.00
Common Tern	0.00	0.00	0.00	0.00	0.00	0.00	0.00	0.00
Forster's Tern	0.00	0.00	0.00	0.00	0.00	0.00	0.00	0.00
Roseate Tern	0.00	0.00	0.00	0.00	0.00	0.00	0.00	0.00
Least Tern	0.00	0.00	0.00	0.00	0.00	0.00	0.00	0.00
Black Tern	0.00	0.00	0.00	0.00	0.00	0.00	0.00	0.00
Sterna spp.	0.00	0.00	0.00	0.00	0.00	0.00	0.00	0.00
Black Skimmer	0.00	0.00	0.00	0.00	0.00	0.00	0.00	0.00
Thick-billed Murre	0.05	0.22	0.02	0.14	0.00	0.00	0.00	0.00
Murre spp.	0.00	0.00	0.00	0.00	0.00	0.00	0.00	0.00
Razorbill	5.19	8.46	0.89	2.51	0.21	0.94	0.12	0.70
Dovekie	0.05	0.22	0.00	0.00	0.00	0.00	0.00	0.00
Black Guillemot	0.05	0.22	0.00	0.00	0.00	0.00	0.02	0.13
Alcid spp.	1.00	3.92	0.26	0.85	0.26	1.25	0.09	0.66
Mourning Dove	0.00	0.00	0.00	0.00	0.00	0.00	0.00	0.00
Short-eared Owl	0.00	0.00	0.00	0.00	0.00	0.00	0.00	0.00
Chimney Swift	0.00	0.00	0.00	0.00	0.00	0.00	0.00	0.00
Ruby-t Hummingbird	0.00	0.00	0.00	0.00	0.00	0.00	0.00	0.00
Belted Kingfisher	0.00	0.00	0.00	0.00	0.00	0.00	0.02	0.13
Northern Flicker	0.00	0.00	0.00	0.00	0.00	0.00	0.02	0.13
Eastern Kingbird	0.00	0.00	0.00	0.00	0.00	0.00	0.00	0.00
Blue Jay	0.00	0.00	0.00	0.00	0.00	0.00	0.00	0.00
American Crow	0.05	0.22	0.17	1.09	0.00	0.00	0.00	0.00
Fish Crow	0.00	0.00	0.00	0.00	0.00	0.00	0.19	0.93
Corvid spp.	0.00	0.00	0.00	0.00	0.00	0.00	0.05	0.22
Horned Lark	0.00	0.00	0.00	0.00	0.00	0.00	0.00	0.00
Purple Martin	0.00	0.00	0.00	0.00	0.00	0.00	0.00	0.00
N Rough-w. Swallow	0.00	0.00	0.00	0.00	0.00	0.00	0.43	1.49
Bank Swallow	0.00	0.00	0.00	0.00	0.00	0.00	0.00	0.00
Tree Swallow	0.00	0.00	0.00	0.00	0.01	0.12	0.00	0.00
Cliff Swallow	0.00	0.00	0.00	0.00	0.00	0.00	0.00	0.00
Barn Swallow	0.00	0.00	0.00	0.00	0.00	0.00	0.10	0.55

Appendix D continued.

	Jan 2009		Feb 2009		Mar 2009		Apr 2009	
Species	Mean	SD	Mean	SD	Mean	SD	Mean	SD
Swallow spp.	0.00	0.00	0.00	0.00	0.00	0.00	0.03	0.26
American Robin	0.00	0.00	0.00	0.00	0.00	0.00	0.00	0.00
American Pipit	0.00	0.00	0.00	0.00	0.00	0.00	0.00	0.00
Cedar Waxwing	0.00	0.00	0.00	0.00	0.00	0.00	0.00	0.00
Yellow Warbler	0.00	0.00	0.00	0.00	0.00	0.00	0.00	0.00
Yellow-rd Warbler	0.00	0.00	0.00	0.00	0.00	0.00	0.00	0.00
Palm Warbler	0.00	0.00	0.00	0.00	0.00	0.00	0.00	0.00
Warbler spp.	0.00	0.00	0.00	0.00	0.00	0.00	0.00	0.00
Snow Bunting	0.00	0.00	0.00	0.00	0.00	0.00	0.00	0.00
Bobolink	0.00	0.00	0.00	0.00	0.00	0.00	0.00	0.00
Brown-hd Cowbird	0.00	0.00	0.00	0.00	0.00	0.00	0.16	0.74
Common Grackle	0.00	0.00	0.00	0.00	0.00	0.00	0.07	0.37
American Goldfinch	0.00	0.00	0.00	0.00	0.00	0.00	0.00	0.00
Passerine spp.	0.00	0.00	0.00	0.00	0.00	0.00	0.00	0.00
Grand Total	1608.6	1973.2	1228.3	1860.3	1295.5	2182.4	736.6	1215.8

Appendix D continued (May-June)

	May		Jun		Jul		Aug	
Species	Mean	SD	Mean	SD	Mean	SD	Mean	SD
Red-throated Loon	2.66	5.83	0.03	0.18	0.02	0.12	0.00	0.00
Pacific Loon	0.02	0.13	0.00	0.00	0.00	0.00	0.00	0.00
Common Loon	17.95	31.52	2.28	3.96	0.78	1.87	0.23	0.83
Loon spp.	3.41	11.65	0.00	0.00	0.00	0.00	0.00	0.00
Red-necked Grebe	0.02	0.13	0.02	0.13	0.00	0.00	0.00	0.00
Horned Grebe	0.02	0.13	0.00	0.00	0.00	0.00	0.00	0.00
Cory's Shearwater	0.00	0.00	0.00	0.00	36.88	84.65	0.00	0.00
Greater Shearwater	0.00	0.00	0.00	0.00	0.20	1.03	0.00	0.00
Manx Shearwater	0.13	0.38	0.00	0.00	0.00	0.00	0.00	0.00
Sooty Shearwater	0.02	0.13	0.03	0.25	0.03	0.17	0.00	0.00
Shearwater spp.	0.02	0.13	0.05	0.38	23.38	114.77	0.00	0.00
Wilson's Storm-Petrel	0.09	0.67	6.47	23.88	12.62	43.51	0.04	0.29
Leach's Storm-Petrel	0.00	0.00	0.00	0.00	0.02	0.12	0.00	0.00
Storm-petrel spp.	0.00	0.00	0.02	0.13	0.00	0.00	0.00	0.00
Great Cormorant	0.02	0.13	0.00	0.00	0.00	0.00	0.00	0.00
Double-cd Cormorant	78.05	96.60	72.50	101.31	46.60	53.47	17.06	21.49
Northern Gannet	11.00	16.76	1.33	2.05	0.51	1.37	0.08	0.35
Great Blue Heron	0.00	0.00	0.00	0.00	0.20	0.94	0.00	0.00
Great Egret	0.25	1.05	0.28	0.70	0.08	0.41	0.00	0.00
Snowy Egret	0.00	0.00	0.05	0.28	0.05	0.37	0.06	0.43
Cattle Egret	0.00	0.00	0.00	0.00	0.02	0.12	0.00	0.00
Green Heron	0.00	0.00	0.03	0.25	0.05	0.37	0.00	0.00
Black-c Night-Heron	0.00	0.00	0.06	0.24	0.00	0.00	0.00	0.00
Glossy Ibis	0.07	0.53	0.08	0.45	0.38	3.10	0.00	0.00
Mute Swan	0.07	0.37	0.38	1.56	0.12	0.67	0.00	0.00
Tundra Swan	0.00	0.00	0.00	0.00	0.00	0.00	0.00	0.00

Canada Goose	0.61	2.22	0.69	4.26	0.00	0.00	0.00	0.00
Atlantic Brant	0.00	0.00	0.02	0.13	0.00	0.00	0.00	0.00
Wood Duck	0.00	0.00	0.00	0.00	0.00	0.00	0.00	0.00
Mallard	0.23	0.76	0.14	0.47	0.17	0.67	0.00	0.00
Am. Black Duck	0.04	0.27	0.00	0.00	0.00	0.00	0.00	0.00
Gadwall	0.00	0.00	0.00	0.00	0.00	0.00	0.00	0.00
Northern Pintail	0.00	0.00	0.00	0.00	0.00	0.00	0.00	0.00
American Wigeon	0.00	0.00	0.00	0.00	0.00	0.00	0.00	0.00
Green-winged Teal	0.00	0.00	0.00	0.00	0.00	0.00	0.00	0.00
Teal spp.	0.00	0.00	0.00	0.00	0.00	0.00	0.00	0.00
Anas spp.	0.36	2.67	0.00	0.00	0.02	0.12	0.00	0.00
Greater Scaup	0.00	0.00	0.00	0.00	0.00	0.00	0.00	0.00
Scaup spp.	0.00	0.00	0.00	0.00	0.00	0.00	0.00	0.00
Athya Spp.	0.00	0.00	0.00	0.00	0.00	0.00	0.00	0.00
Common Eider	6.52	15.63	1.80	4.43	1.15	3.56	2.98	8.73
King Eider	0.00	0.00	0.00	0.00	0.00	0.00	0.00	0.00
Harlequin Duck	0.02	0.13	0.00	0.00	0.00	0.00	0.00	0.00
Long-tailed Duck	0.05	0.23	0.00	0.00	0.00	0.00	0.00	0.00
Surf Scoter	5.93	14.40	0.08	0.32	0.00	0.00	0.00	0.00
Black Scoter	8.02	22.17	0.03	0.18	0.05	0.28	0.33	1.89
Black or Surf Scoter	0.00	0.00	0.00	0.00	0.00	0.00	0.04	0.29
White-winged Scoter	21.05	59.65	0.16	0.54	0.15	0.89	0.02	0.14
Scoter spp.	31.20	113.43	0.11	0.76	0.03	0.25	0.00	0.00
Common Goldeneye	0.00	0.00	0.05	0.38	0.00	0.00	0.00	0.00
Barrow's Goldeneye	0.00	0.00	0.00	0.00	0.00	0.00	0.00	0.00
Bufflehead	0.00	0.00	0.00	0.00	0.00	0.00	0.00	0.00
Hooded Merganser	0.00	0.00	0.00	0.00	0.00	0.00	0.00	0.00
Red-bd Merganser	5.89	16.36	0.23	0.79	0.02	0.12	0.00	0.00
Common Merganser	0.00	0.00	0.00	0.00	0.00	0.00	0.00	0.00
Seaduck spp.	0.00	0.00	0.00	0.00	0.00	0.00	0.00	0.00
Ruddy Duck	0.00	0.00	0.00	0.00	0.00	0.00	0.00	0.00
Northern Harrier	0.00	0.00	0.00	0.00	0.00	0.00	0.00	0.00
Sharp-shinned Hawk	0.00	0.00	0.00	0.00	0.00	0.00	0.00	0.00
Cooper's Hawk	0.00	0.00	0.00	0.00	0.00	0.00	0.00	0.00
Osprey	0.13	0.47	0.23	0.50	0.20	0.54	0.04	0.20
Merlin	0.00	0.00	0.00	0.00	0.00	0.00	0.00	0.00
American Kestrel	0.00	0.00	0.00	0.00	0.00	0.00	0.00	0.00
Peregrine Falcon	0.00	0.00	0.00	0.00	0.00	0.00	0.00	0.00
Falcon spp.	0.00	0.00	0.00	0.00	0.00	0.00	0.00	0.00
Black-bellied Plover	0.00	0.00	0.03	0.25	0.02	0.12	0.19	0.67
Piping Plover	0.11	0.49	0.03	0.18	0.02	0.12	0.00	0.00
Semipalmated Plover	0.00	0.00	0.00	0.00	0.42	1.45	1.63	5.77
Killdeer	0.02	0.13	0.00	0.00	0.02	0.12	0.00	0.00
Am. Oystercatcher	0.05	0.30	0.05	0.28	0.08	0.37	0.00	0.00
Greater Yellowlegs	0.02	0.13	0.00	0.00	0.00	0.00	0.00	0.00
Lesser Yellowlegs	0.00	0.00	0.00	0.00	0.12	0.88	0.02	0.14
Yellowlegs spp.	0.00	0.00	0.00	0.00	0.00	0.00	0.02	0.14
Willet	0.11	0.80	0.06	0.30	0.18	1.25	0.00	0.00
Spotted Sandpiper	0.00	0.00	0.00	0.00	0.06	0.39	0.08	0.35

	May		Jun		Jul		Aug	
Species	Mean	SD	Mean	SD	Mean	SD	Mean	SD
Whimbrel	0.00	0.00	0.00	0.00	0.38	1.35	0.02	0.14
Ruddy Turnstone	0.07	0.53	0.00	0.00	0.74	3.05	1.71	4.99
Purple Sandpiper	1.48	7.24	0.02	0.13	0.00	0.00	0.00	0.00
Sanderling	0.00	0.00	0.03	0.25	14.54	48.50	1.25	5.86
Dunlin	0.00	0.00	0.00	0.00	0.00	0.00	0.00	0.00
White-rd Sandpiper	0.00	0.00	0.00	0.00	0.00	0.00	0.00	0.00
Semipalm. Sandpiper	0.02	0.13	0.09	0.75	17.25	85.98	3.58	8.45
Peep spp.	0.00	0.00	0.00	0.00	7.49	15.42	5.31	14.14
Least Sandpiper	0.00	0.00	0.00	0.00	0.26	0.91	0.40	1.27
Short-bd. Dowitcher	0.00	0.00	0.00	0.00	2.77	7.65	1.06	6.53
Shorebird Spp.	0.41	1.57	0.06	0.35	7.68	18.78	1.75	3.82
Pomarine Jaeger	0.00	0.00	0.03	0.25	0.00	0.00	0.00	0.00
Parasitic Jaeger	0.04	0.27	0.13	1.00	0.11	0.75	0.02	0.14
Jaeger spp.	0.00	0.00	0.00	0.00	0.00	0.00	0.00	0.00
Bonaparte's Gull	0.25	1.61	0.09	0.64	0.02	0.12	0.00	0.00
Laughing Gull	0.80	1.80	2.92	4.29	9.69	15.85	41.25	78.32
Ring-billed Gull	1.14	2.60	4.22	16.81	4.52	10.82	3.46	10.94
Herring Gull	82.68	124.95	69.89	102.78	42.38	71.58	12.90	27.82
Iceland Gull	0.00	0.00	0.00	0.00	0.00	0.00	0.00	0.00
Great Bk-backed Gull	36.21	43.61	29.08	50.99	17.11	31.71	5.98	8.38
Black-ld Kittiwake	0.00	0.00	0.00	0.00	0.00	0.00	0.02	0.14
Gull spp.	6.89	25.53	24.91	75.17	9.06	25.91	9.83	58.03
Caspian Tern	0.00	0.00	0.00	0.00	0.00	0.00	0.00	0.00
Royal Tern	0.00	0.00	0.02	0.13	0.06	0.30	0.02	0.14
Common Tern	3.34	7.59	4.80	9.62	20.45	33.61	35.10	54.57
Forster's Tern	0.00	0.00	0.00	0.00	0.02	0.12	0.17	0.60
Roseate Tern	0.00	0.00	0.20	0.96	1.40	3.24	0.44	1.27
Least Tern	1.91	5.03	3.45	8.22	1.94	4.29	0.65	2.29
Black Tern	0.00	0.00	0.00	0.00	0.06	0.30	0.23	0.69
Sterna spp.	0.84	3.68	0.33	1.14	3.03	9.07	18.83	59.27
Black Skimmer	0.00	0.00	0.00	0.00	0.00	0.00	0.00	0.00
Thick-billed Murre	0.00	0.00	0.00	0.00	0.00	0.00	0.00	0.00
Murre spp.	0.00	0.00	0.00	0.00	0.00	0.00	0.00	0.00
Razorbill	0.00	0.00	0.00	0.00	0.00	0.00	0.00	0.00
Dovekie	0.00	0.00	0.00	0.00	0.00	0.00	0.00	0.00
Black Guillemot	0.00	0.00	0.00	0.00	0.00	0.00	0.00	0.00
Alcid spp.	0.00	0.00	0.00	0.00	0.00	0.00	0.00	0.00
Mourning Dove	0.00	0.00	0.00	0.00	0.02	0.12	0.04	0.29
Short-eared Owl	0.00	0.00	0.00	0.00	0.00	0.00	0.00	0.00
Chimney Swift	0.02	0.13	0.02	0.13	0.02	0.12	0.00	0.00
Ruby-t Hummingbird	0.02	0.13	0.00	0.00	0.00	0.00	0.02	0.14
Belted Kingfisher	0.00	0.00	0.00	0.00	0.02	0.12	0.00	0.00
Northern Flicker	0.00	0.00	0.00	0.00	0.00	0.00	0.00	0.00
Eastern Kingbird	0.00	0.00	0.02	0.13	0.00	0.00	0.00	0.00
Blue Jay	0.43	3.21	0.00	0.00	0.00	0.00	0.00	0.00
American Crow	0.00	0.00	0.02	0.13	0.00	0.00	0.00	0.00
Fish Crow	0.00	0.00	0.00	0.00	0.00	0.00	0.00	0.00

	May		Jun		Jul		Aug	
Species	Mean	SD	Mean	SD	Mean	SD	Mean	SD
Corvid spp.	0.00	0.00	0.00	0.00	0.00	0.00	0.00	0.00
Horned Lark	0.00	0.00	0.00	0.00	0.00	0.00	0.00	0.00
Purple Martin	0.00	0.00	0.05	0.21	0.03	0.25	0.02	0.14
N Rough-w Swallow	0.75	3.70	0.19	0.83	0.35	1.32	0.00	0.00
Bank Swallow	0.04	0.19	0.02	0.13	0.17	1.05	0.08	0.35
Tree Swallow	0.00	0.00	0.02	0.13	0.49	1.34	5.75	28.26
Cliff Swallow	0.00	0.00	0.00	0.00	0.02	0.12	0.00	0.00
Barn Swallow	1.02	2.35	0.48	1.28	0.78	1.87	1.38	3.56
Swallow spp.	0.70	3.25	0.02	0.13	0.40	1.04	2.44	7.25
American Robin	0.04	0.27	0.00	0.00	0.00	0.00	0.00	0.00
American Pipit	0.00	0.00	0.00	0.00	0.00	0.00	0.00	0.00
Cedar Waxwing	0.00	0.00	0.02	0.13	0.00	0.00	0.00	0.00
Yellow Warbler	0.13	0.00	0.00	0.12	0.57	0.06	0.32	0.13
Yellow-rd. Warbler	0.00	0.00	0.00	0.00	0.00	0.00	0.00	0.00
Palm Warbler	0.00	0.00	0.00	0.00	0.00	0.00	0.00	0.00
Warbler spp.	0.00	0.00	0.00	0.00	0.00	0.00	0.00	0.00
Snow Bunting	0.00	0.00	0.00	0.00	0.00	0.00	0.00	0.00
Bobolink	0.00	0.00	0.00	0.00	0.00	0.00	0.00	0.00
Brown-hd Cowbird	0.00	0.00	0.00	0.00	0.00	0.00	0.00	0.00
Common Grackle	0.53	0.03	0.25	0.00	0.00	0.00	0.00	0.53
American Goldfinch	0.00	0.00	0.00	0.00	0.00	0.00	0.00	0.00
Passerine spp.	0.00	0.00	0.00	0.00	0.00	0.00	0.00	0.00
Grand Total	272.0	228.4	252.4	288.0	287.7	176.6	171.2	272.0

Appendix D continued. (Sept – Dec 2009)

	Sep		Oct		Nov		Dec	
Species	Mean	SD	Mean	SD	Mean	SD	Mean	SD
Red-throated Loon	0.03	0.17	3.00	9.23	7.99	10.61	12.10	19.93
Pacific Loon	0.00	0.00	0.00	0.00	0.01	0.12	0.00	0.00
Common Loon	0.79	2.03	6.67	8.72	16.22	19.51	14.72	18.25
Loon spp.	0.00	0.00	0.43	1.72	4.00	9.50	1.40	3.09
Red-necked Grebe	0.00	0.00	0.09	0.34	0.26	0.80	0.12	0.32
Horned Grebe	0.00	0.00	0.02	0.13	0.10	0.35	0.85	1.84
Cory's Shearwater	0.04	0.20	0.02	0.13	0.00	0.00	0.00	0.00
Greater Shearwater	0.01	0.12	0.00	0.00	0.00	0.00	0.00	0.00
Manx Shearwater	0.00	0.00	0.00	0.00	0.00	0.00	0.00	0.00
Sooty Shearwater	0.00	0.00	0.00	0.00	0.00	0.00	0.00	0.00
Shearwater spp.	0.03	0.17	0.00	0.00	0.00	0.00	0.00	0.00
Wilson's Storm-Petrel	0.00	0.00	0.00	0.00	0.00	0.00	0.00	0.00
Leach's Storm-Petrel	0.00	0.00	0.00	0.00	0.00	0.00	0.00	0.00
Storm-petrel spp.	0.00	0.00	0.00	0.00	0.00	0.00	0.00	0.00
Great Cormorant	0.34	1.37	0.60	1.76	3.71	4.97	7.13	16.20
Double-cd Cormorant	53.39	91.37	88.36	124.47	9.93	22.89	0.67	1.49
Northern Gannet	0.15	0.79	11.78	30.68	40.07	58.26	49.73	91.63
Great Blue Heron	0.08	0.37	0.24	1.71	0.00	0.00	0.07	0.41
Great Egret	0.01	0.12	0.05	0.29	0.00	0.00	0.00	0.00
Snowy Egret	0.00	0.00	0.00	0.00	0.00	0.00	0.00	0.00

Cattle Egret	0.00	0.00	0.02	0.13	0.00	0.00	0.00	0.00
Green Heron	0.00	0.00	0.00	0.00	0.00	0.00	0.00	0.00
Black-cd N-Heron	0.00	0.00	0.00	0.00	0.00	0.00	0.00	0.00
Glossy Ibis	0.00	0.00	0.00	0.00	0.00	0.00	0.00	0.00
Mute Swan	0.01	0.12	0.26	0.83	0.10	0.39	0.08	0.38
Tundra Swan	0.00	0.00	0.00	0.00	0.00	0.00	0.03	0.26
Canada Goose	0.65	5.46	0.02	0.13	1.25	6.75	13.93	32.16
Atlantic Brant	0.00	0.00	4.24	11.49	1.65	5.98	0.15	1.04
Wood Duck	0.04	0.36	0.00	0.00	0.06	0.48	0.00	0.00
Mallard	0.03	0.24	0.10	0.48	0.09	0.61	0.27	1.47
Am Black Duck	0.07	0.49	0.12	0.59	0.20	0.80	3.45	12.13
Gadwall	0.00	0.00	0.00	0.00	0.00	0.00	0.00	0.00
Northern Pintail	0.00	0.00	0.00	0.00	0.00	0.00	0.03	0.18
American Wigeon	0.00	0.00	0.00	0.00	0.03	0.24	0.00	0.00
Green-winged Teal	0.00	0.00	0.60	2.65	0.03	0.24	0.00	0.00
Teal spp.	0.00	0.00	0.02	0.13	0.00	0.00	0.00	0.00
Anas spp.	0.01	0.12	0.17	0.60	0.00	0.00	0.47	1.92
Greater Scaup	0.00	0.00	0.00	0.00	0.29	1.55	1.43	8.76
Scaup spp.	0.00	0.00	2.10	15.23	0.12	0.74	0.15	1.04
Athya Spp.	0.00	0.00	0.00	0.00	0.36	2.24	0.32	1.47
Common Eider	5.69	12.77	282.40	403.57	172.49	230.11	77.63	90.06
King Eider	0.00	0.00	0.02	0.13	0.00	0.00	0.00	0.00
Harlequin Duck	0.00	0.00	0.16	0.72	2.09	5.87	2.20	5.36
Long-tailed Duck	0.00	0.00	0.43	1.51	0.67	1.36	0.58	2.73
Surf Scoter	0.14	0.64	8.84	22.13	2.78	11.19	2.38	5.66
Black Scoter	0.37	2.02	40.38	123.76	19.09	57.70	10.50	25.84
Black or Surf Scoter	0.55	1.87	18.22	46.06	8.54	29.39	6.20	14.86
White-winged Scoter	0.54	1.76	4.00	8.39	2.45	2.94	1.43	3.35
Scoter spp.	0.38	1.86	4.59	11.18	6.81	17.46	2.40	6.18
Common Goldeneye	0.00	0.00	0.00	0.00	0.16	0.74	2.42	6.35
Barrow's Goldeneye	0.00	0.00	0.00	0.00	0.00	0.00	0.02	0.13
Bufflehead	0.00	0.00	0.00	0.00	0.88	4.33	1.70	5.06
Hooded Merganser	0.00	0.00	0.00	0.00	0.00	0.00	0.00	0.00
Red-bd Merganser	0.03	0.24	2.19	4.06	12.74	22.86	12.97	15.38
Common Merganser	0.00	0.00	0.00	0.00	0.00	0.00	0.00	0.00
Seaduck spp.	0.00	0.00	0.95	7.22	0.00	0.00	0.03	0.26
Ruddy Duck	0.00	0.00	0.28	1.47	0.00	0.00	0.00	0.00
Northern Harrier	0.01	0.12	0.00	0.00	0.03	0.17	0.02	0.13
Sharp-shinned Hawk	0.04	0.26	0.00	0.00	0.00	0.00	0.00	0.00
Cooper's Hawk	0.01	0.12	0.00	0.00	0.00	0.00	0.00	0.00
Osprey	0.11	0.36	0.03	0.18	0.00	0.00	0.00	0.00
Merlin	0.04	0.20	0.02	0.13	0.00	0.00	0.00	0.00
American Kestrel	0.00	0.00	0.03	0.18	0.00	0.00	0.00	0.00
Peregrine Falcon	0.10	0.30	0.02	0.13	0.00	0.00	0.00	0.00
Falcon spp.	0.03	0.17	0.00	0.00	0.00	0.00	0.00	0.00
Black-bellied Plover	0.01	0.12	0.00	0.00	0.09	0.72	0.00	0.00
Piping Plover	0.00	0.00	0.00	0.00	0.00	0.00	0.00	0.00
Semipalmated Plover	0.49	1.80	0.31	0.88	0.00	0.00	0.00	0.00
Killdeer	0.01	0.12	0.00	0.00	0.01	0.12	0.00	0.00

	Sep		Oct		Nov		Dec	
Species	Mean	SD	Mean	SD	Mean	SD	Mean	SD
Am. Oystercatcher	0.00	0.00	0.00	0.00	0.00	0.00	0.00	0.00
Greater Yellowlegs	0.01	0.12	0.00	0.00	0.00	0.00	0.00	0.00
Lesser Yellowlegs	0.06	0.33	0.00	0.00	0.00	0.00	0.00	0.00
Yellowlegs spp.	0.00	0.00	0.00	0.00	0.00	0.00	0.00	0.00
Willet	0.00	0.00	0.00	0.00	0.00	0.00	0.00	0.00
Spotted Sandpiper	0.00	0.00	0.00	0.00	0.00	0.00	0.00	0.00
Whimbrel	0.00	0.00	0.00	0.00	0.00	0.00	0.00	0.00
Ruddy Turnstone	0.01	0.12	0.03	0.26	0.00	0.00	0.00	0.00
Purple Sandpiper	0.00	0.00	0.10	0.79	2.20	7.58	4.65	13.46
Sanderling	9.51	38.18	9.17	29.58	1.51	4.20	0.72	3.70
Dunlin	0.13	0.79	0.26	1.22	0.22	1.69	0.12	0.90
White-rd Sandpiper	0.00	0.00	0.02	0.13	0.00	0.00	0.00	0.00
Semipalm. Sandpiper	0.24	0.90	0.02	0.13	0.00	0.00	0.00	0.00
Peep spp.	0.80	5.94	0.00	0.00	0.00	0.00	0.00	0.00
Least Sandpiper	0.20	0.90	0.00	0.00	0.00	0.00	0.00	0.00
Short-bd Dowitcher	0.00	0.00	0.00	0.00	0.00	0.00	0.00	0.00
Shorebird Spp.	1.32	4.38	0.71	2.93	0.12	0.85	0.00	0.00
Pomarine Jaeger	0.00	0.00	0.00	0.00	0.00	0.00	0.00	0.00
Parasitic Jaeger	0.01	0.12	0.00	0.00	0.00	0.00	0.00	0.00
Jaeger spp.	0.01	0.12	0.03	0.18	0.00	0.00	0.00	0.00
Bonaparte's Gull	0.00	0.00	0.22	0.82	0.38	1.59	3.15	7.34
Laughing Gull	37.69	41.13	108.52	144.32	4.04	8.60	0.02	0.13
Ring-billed Gull	7.86	13.90	13.83	28.95	4.26	5.55	8.12	18.51
Herring Gull	40.69	93.16	24.86	45.68	48.29	140.61	89.08	194.58
Iceland Gull	0.00	0.00	0.00	0.00	0.00	0.00	0.00	0.00
Great Bl-backed Gull	8.34	8.99	5.93	5.94	11.74	26.42	22.57	88.35
Black-ld Kittiwake	0.00	0.00	0.00	0.00	0.19	0.93	0.25	1.81
Gull spp.	18.49	43.46	116.21	293.59	44.71	174.31	64.42	221.58
Caspian Tern	0.03	0.24	0.00	0.00	0.00	0.00	0.00	0.00
Royal Tern	0.00	0.00	0.00	0.00	0.00	0.00	0.00	0.00
Common Tern	1.96	9.38	0.00	0.00	0.00	0.00	0.00	0.00
Forster's Tern	0.00	0.00	0.03	0.26	0.00	0.00	0.00	0.00
Roseate Tern	0.00	0.00	0.00	0.00	0.00	0.00	0.00	0.00
Least Tern	0.00	0.00	0.00	0.00	0.00	0.00	0.00	0.00
Black Tern	0.00	0.00	0.00	0.00	0.00	0.00	0.00	0.00
Sterna spp.	2.06	11.37	0.03	0.26	0.00	0.00	0.00	0.00
Black Skimmer	0.04	0.36	0.00	0.00	0.00	0.00	0.00	0.00
Thick-billed Murre	0.00	0.00	0.00	0.00	0.00	0.00	0.00	0.00
Murre spp.	0.00	0.00	0.00	0.00	0.00	0.00	0.02	0.13
Razorbill	0.00	0.00	0.00	0.00	0.00	0.00	0.53	1.64
Dovekie	0.00	0.00	0.00	0.00	0.00	0.00	0.00	0.00
Black Guillemot	0.00	0.00	0.00	0.00	0.00	0.00	0.00	0.00
Alcid spp.	0.00	0.00	0.02	0.13	0.04	0.27	0.33	1.63
Mourning Dove	0.01	0.12	0.02	0.13	0.00	0.00	0.00	0.00
Short-eared Owl	0.00	0.00	0.00	0.00	0.00	0.00	0.00	0.00
Chimney Swift	0.00	0.00	0.00	0.00	0.00	0.00	0.00	0.00
Ruby-t Hummingbird	0.00	0.00	0.00	0.00	0.00	0.00	0.00	0.00

	Sep		Oct		Nov		Dec	
Species	Mean	SD	Mean	SD	Mean	SD	Mean	SD
Belted Kingfisher	0.00	0.00	0.00	0.00	0.00	0.00	0.00	0.00
Northern Flicker	0.00	0.00	0.00	0.00	0.00	0.00	0.00	0.00
Eastern Kingbird	0.00	0.00	0.00	0.00	0.00	0.00	0.00	0.00
Blue Jay	0.00	0.00	0.00	0.00	0.00	0.00	0.00	0.00
American Crow	0.03	0.24	0.00	0.00	0.00	0.00	0.03	0.26
Fish Crow	0.00	0.00	0.00	0.00	0.00	0.00	0.00	0.00
Corvid spp.	0.00	0.00	0.26	1.84	0.01	0.12	0.03	0.26
Horned Lark	0.00	0.00	0.00	0.00	0.00	0.00	0.02	0.13
Purple Martin	0.01	0.12	0.00	0.00	0.00	0.00	0.00	0.00
N. Rough-w Swallow	0.00	0.00	0.00	0.00	0.00	0.00	0.00	0.00
Bank Swallow	0.00	0.00	0.00	0.00	0.00	0.00	0.00	0.00
Tree Swallow	25.94	78.75	204.71	1322.9	0.00	0.00	0.00	0.00
Cliff Swallow	0.00	0.00	0.00	0.00	0.00	0.00	0.00	0.00
Barn Swallow	0.24	1.15	0.03	0.26	0.00	0.00	0.00	0.00
Swallow spp.	0.13	0.53	0.03	0.18	0.00	0.00	0.00	0.00
American Robin	0.10	0.83	0.00	0.00	0.00	0.00	0.00	0.00
American Pipit	0.01	0.12	0.03	0.18	0.03	0.24	0.00	0.00
Cedar Waxwing	0.01	0.12	0.00	0.00	0.00	0.00	0.00	0.00
Yellow Warbler	0.01	0.12	0.00	0.00	0.00	0.00	0.00	0.00
Yellow-rd Warbler	0.01	0.12	0.02	0.13	0.00	0.00	0.00	0.00
Palm Warbler	0.01	0.12	0.00	0.00	0.00	0.00	0.00	0.00
Warbler spp.	0.10	0.54	0.03	0.26	0.00	0.00	0.00	0.00
Snow Bunting	0.00	0.00	0.03	0.26	0.41	2.71	0.00	0.00
Bobolink	0.01	0.12	0.00	0.00	0.00	0.00	0.00	0.00
Brown-hd Cowbird	0.00	0.00	0.00	0.00	0.00	0.00	0.00	0.00
Common Grackle	0.00	0.00	0.00	0.00	0.00	0.00	0.00	0.00
American Goldfinch	0.03	0.24	0.24	1.71	0.00	0.00	0.00	0.00
Passerine spp.	0.06	0.37	0.10	0.55	0.13	0.75	0.00	0.00
Grand Total	220.5	214.6	967.3	1440.3	433.6	405.2	421.6	469.6

Appendix D continued.

	Jan 2010		Feb 2010	
Species	Mean	SD	Mean	SD
Red-throated Loon	2.95	4.19	0.66	1.26
Pacific Loon	0.02	0.13	0.00	0.00
Common Loon	6.75	6.37	4.96	6.12
Loon spp.	0.51	1.57	0.02	0.15
Red-necked Grebe	0.26	0.58	0.00	0.00
Horned Grebe	3.98	7.75	2.55	2.54
Cory's Shearwater	0.00	0.00	0.00	0.00
Greater Shearwater	0.00	0.00	0.00	0.00
Manx Shearwater	0.00	0.00	0.00	0.00
Sooty Shearwater	0.00	0.00	0.00	0.00
Shearwater spp.	0.00	0.00	0.00	0.00
Wilson's Storm-Petrel	0.00	0.00	0.00	0.00
Leach's Storm-Petrel	0.00	0.00	0.00	0.00
Storm-petrel spp.	0.00	0.00	0.00	0.00
Great Cormorant	4.96	5.40	2.55	3.18
Double-cd Cormorant	0.02	0.13	0.02	0.15
Northern Gannet	1.37	3.98	0.04	0.29
Great Blue Heron	0.00	0.00	0.00	0.00
Great Egret	0.00	0.00	0.00	0.00
Snowy Egret	0.00	0.00	0.00	0.00
Cattle Egret	0.00	0.00	0.00	0.00
Green Heron	0.00	0.00	0.00	0.00
Black-cd N-Heron	0.00	0.00	0.00	0.00
Glossy Ibis	0.00	0.00	0.00	0.00
Mute Swan	0.07	0.42	0.17	0.64
Tundra Swan	0.00	0.00	0.00	0.00
Canada Goose	9.95	39.34	0.89	2.55
Atlantic Brant	1.65	4.97	1.00	2.71
Wood Duck	0.00	0.00	0.00	0.00
Mallard	0.02	0.13	0.00	0.00
Am Black Duck	0.63	1.76	0.62	1.29
Gadwall	0.05	0.40	0.13	0.65
Northern Pintail	0.00	0.00	0.11	0.73
American Wigeon	0.00	0.00	0.04	0.29
Green-winged Teal	0.00	0.00	0.00	0.00
Teal spp.	0.00	0.00	0.00	0.00
Anas spp.	0.00	0.00	0.02	0.15
Greater Scaup	3.04	14.87	5.21	25.14
Scaup spp.	0.00	0.00	0.00	0.00
Athya Spp.	0.00	0.00	0.00	0.00
Common Eider	103.23	142.71	207.28	490.58
King Eider	0.09	0.34	0.04	0.20
Harlequin Duck	4.02	7.73	3.62	8.28
Long-tailed Duck	0.63	1.62	0.40	0.92
Surf Scoter	7.00	16.50	6.21	15.39
Black Scoter	36.77	64.72	57.55	107.83

Appendix D continued.

	Jan 2010		Feb 2010	
Species	Mean	SD	Mean	SD
Black or Surf Scoter	13.81	29.73	10.55	51.47
White-winged Scoter	5.58	12.43	4.68	9.57
Scoter spp.	92.04	360.64	19.98	78.31
Common Goldeneye	5.28	7.31	8.57	19.47
Barrow's Goldeneye	0.02	0.13	0.00	0.00
Bufflehead	2.04	5.20	2.64	5.41
Hooded Merganser	0.16	1.19	0.00	0.00
Red-bd Merganser	17.19	25.06	15.02	38.34
Common Merganser	0.00	0.00	0.00	0.00
Seaduck spp.	0.00	0.00	0.00	0.00
Ruddy Duck	0.00	0.00	0.00	0.00
Northern Harrier	0.00	0.00	0.02	0.15
Sharp-shinned Hawk	0.00	0.00	0.00	0.00
Cooper's Hawk	0.00	0.00	0.00	0.00
Osprey	0.00	0.00	0.00	0.00
Merlin	0.00	0.00	0.00	0.00
American Kestrel	0.00	0.00	0.00	0.00
Peregrine Falcon	0.00	0.00	0.00	0.00
Falcon spp.	0.00	0.00	0.00	0.00
Black-bellied Plover	0.00	0.00	0.00	0.00
Piping Plover	0.00	0.00	0.00	0.00
Semipalmated Plover	0.00	0.00	0.00	0.00
Killdeer	0.00	0.00	0.00	0.00
Am Oystercatcher	0.00	0.00	0.00	0.00
Greater Yellowlegs	0.00	0.00	0.00	0.00
Lesser Yellowlegs	0.00	0.00	0.00	0.00
Yellowlegs spp.	0.00	0.00	0.00	0.00
Willet	0.00	0.00	0.00	0.00
Spotted Sandpiper	0.00	0.00	0.00	0.00
Whimbrel	0.00	0.00	0.00	0.00
Ruddy Turnstone	0.02	0.13	0.00	0.00
Purple Sandpiper	2.77	6.86	0.09	0.58
Sanderling	0.28	1.62	1.06	7.29
Dunlin	0.00	0.00	0.00	0.00
White-rd Sandpiper	0.00	0.00	0.00	0.00
Semipalm Sandpiper	0.00	0.00	0.00	0.00
Peep spp.	0.00	0.00	0.00	0.00
Least Sandpiper	0.00	0.00	0.00	0.00
Short-bd Dowitcher	0.00	0.00	0.00	0.00
Shorebird Spp.	0.05	0.40	0.00	0.00
Pomarine Jaeger	0.00	0.00	0.00	0.00
Parasitic Jaeger	0.00	0.00	0.00	0.00
Jaeger spp.	0.00	0.00	0.00	0.00
Bonaparte's Gull	1.58	4.08	0.11	0.73

Appendix D continued.

	Jan 2010		Feb 2010	
Species	Mean	SD	Mean	SD
Laughing Gull	0.00	0.00	0.00	0.00
Ring-billed Gull	1.51	3.86	7.38	33.21
Herring Gull	70.58	334.85	127.79	577.65
Iceland Gull	0.02	0.13	0.00	0.00
Great Black-bd Gull	3.72	4.79	3.47	6.35
Black-ld Kittiwake	0.25	0.93	0.00	0.00
Gull spp.	2.53	15.94	0.00	0.00
Caspian Tern	0.00	0.00	0.00	0.00
Royal Tern	0.00	0.00	0.00	0.00
Common Tern	0.00	0.00	0.00	0.00
Forster's Tern	0.00	0.00	0.00	0.00
Roseate Tern	0.00	0.00	0.00	0.00
Least Tern	0.00	0.00	0.00	0.00
Black Tern	0.00	0.00	0.00	0.00
Sterna spp.	0.00	0.00	0.00	0.00
Black Skimmer	0.00	0.00	0.00	0.00
Thick-billed Murre	0.00	0.00	0.00	0.00
Murre spp.	0.00	0.00	0.00	0.00
Razorbill	1.28	4.30	0.15	0.66
Dovekie	0.00	0.00	0.00	0.00
Black Guillemot	0.00	0.00	0.00	0.00
Alcid spp.	0.46	2.67	0.04	0.29
Mourning Dove	0.00	0.00	0.00	0.00
Short-eared Owl	0.00	0.00	0.02	0.15
Chimney Swift	0.00	0.00	0.00	0.00
Ruby-t Hummingbird	0.00	0.00	0.00	0.00
Belted Kingfisher	0.00	0.00	0.00	0.00
Northern Flicker	0.00	0.00	0.00	0.00
Eastern Kingbird	0.00	0.00	0.00	0.00
Blue Jay	0.00	0.00	0.00	0.00
American Crow	0.07	0.53	0.15	1.02
Fish Crow	0.00	0.00	0.00	0.00
Corvid spp.	0.00	0.00	0.00	0.00
Horned Lark	0.00	0.00	0.02	0.15
Purple Martin	0.00	0.00	0.00	0.00
N Rough-w Swallow	0.00	0.00	0.00	0.00
Bank Swallow	0.00	0.00	0.00	0.00
Tree Swallow	0.00	0.00	0.00	0.00
Cliff Swallow	0.00	0.00	0.00	0.00
Barn Swallow	0.00	0.00	0.00	0.00
Swallow spp.	0.00	0.00	0.00	0.00
American Robin	0.00	0.00	0.00	0.00
American Pipit	0.00	0.00	0.00	0.00
Cedar Waxwing	0.00	0.00	0.00	0.00

Appendix D continued.

	Jan 2010		Feb 2010	
Species	Mean	SD	Mean	SD
Yellow Warbler	0.00	0.00	0.00	0.00
Yellow-rd Warbler	0.60	4.50	0.00	0.00
Palm Warbler	0.00	0.00	0.00	0.00
Warbler spp.	0.00	0.00	0.00	0.00
Snow Bunting	0.00	0.00	0.00	0.00
Bobolink	0.00	0.00	0.00	0.00
Brown-headed Cowbird	0.00	0.00	0.00	0.00
Common Grackle	0.00	0.00	0.00	0.00
American Goldfinch	0.00	0.00	0.00	0.00
Passerine spp.	0.00	0.00	0.00	0.00
Grand Total	409.8	515.1	495.9	823.1

Appendix E. Mean (SD) number of detections per grid, CV of detection rate, total number of detections, and % of surveys (n = 16) with a detection within a grid) during ship-based line transect surveys for data pooled across all 8 grids (see Fig. 24) conducted in the summer of 2009 (10 June thru 25 Aug 2009).

Species	Mean	SD	CV	Total detections	% of surveys
Common Loon	0.38	0.72	191.7	6	25.00
Red-throated Loon	0.06	0.25	400.0	1	6.25
Shearwater unidentified	1.69	3.40	201.5	27	43.75
Small shearwater	0.13	0.50	400.0	2	6.25
Manx Shearwater	0.13	0.34	273.3	2	12.50
Greater Shearwater	12.06	21.84	181.1	193	62.50
Cory's Shearwater	30.94	36.59	118.3	495	75.00
Sooty Shearwater	1.00	2.03	203.3	16	25.00
Wilson's Storm-Petrel	82.00	112.96	137.8	1,312	93.75
Leach's Storm-Petrel	0.13	0.50	400.0	2	6.25
Northern Gannet	2.13	3.24	152.6	34	56.25
Double-crd. Cormorant	0.31	0.70	225.3	5	18.75
Great Cormorant	0.06	0.25	400.0	1	6.25
Great Blue Heron	0.06	0.25	400.0	1	6.25
Mallard	0.06	0.25	400.0	1	6.25
Shorebird unidentified	0.13	0.50	400.0	2	6.25
Semipalmated Plover	0.13	0.50	400.0	2	6.25
Whimbrel	0.25	1.00	400.0	4	6.25
Short-billed Dowitcher	0.31	1.25	400.0	5	6.25
Phalarope unidentified	0.06	0.25	400.0	1	6.25
Pomarine Jaeger	0.06	0.25	400.0	1	6.25
Long-tailed Jaeger	0.06	0.25	400.0	1	6.25
Parasitic Jaeger	0.06	0.25	400.0	1	6.25
Gull spp.	0.06	0.25	400.0	1	6.25
Laughing Gull	6.81	24.62	361.4	109	31.25
Herring Gull	8.94	13.80	154.4	143	93.75
Great Black-bd. Gull	11.38	13.23	116.3	182	100.00
Tern unidentified	0.69	1.01	147.6	11	37.50
Common Tern	3.69	9.14	247.9	59	31.25
Roseate Tern	0.50	1.21	242.2	8	18.75
Grand Total	**165.06**	**132.36**	**80.2**	**2,628**	

Appendix F. Mean (SD) number of detections per grid, CV of detection rate, total number of detections, and % of surveys (n = 18) with a detection within a grid) during ship-based line transect surveys for data pooled across all 8 grids (see Fig. 24) conducted during fall (8 Sept thru 19 Nov 2009).

Species	Mean	SD	CV	Total	% of surveys
Common Loon	2.94	6.82	231.7	53	50.0
Red-throated Loon	1.33	4.09	306.5	24	22.2
Loon spp.	0.17	0.71	424.3	3	5.6
Red-necked Grebe	0.06	0.24	424.3	1	5.6
Northern Fulmar	0.28	0.67	240.9	5	16.7
Greater Shearwater	2.56	5.26	205.8	46	38.9
Cory's Shearwater	1.39	2.91	209.8	25	33.3
Wilson's Storm-Petrel	11.06	32.21	291.4	199	11.1
Northern Gannet	36.44	104.90	287.8	656	72.2
Double-crd Cormorant	0.22	0.55	246.7	4	16.7
Bay duck unidentified	0.44	1.89	424.3	8	5.6
Green-winged Teal	0.56	2.36	424.3	10	5.6
Scaup unidentified	3.06	8.93	292.4	55	11.1
Common Eider	12.00	35.46	295.5	216	27.8
Scoter unidentified	0.22	0.94	424.3	4	5.6
Surf or Black Scoter	9.44	22.94	242.9	170	16.7
Surf Scoter	11.22	40.98	365.2	202	27.8
Black Scoter	14.17	31.22	220.4	255	27.8
White-winged Scoter	3.17	6.82	215.3	57	27.8
Long-tailed Duck	0.67	1.75	262.3	12	22.2
Merlin	0.06	0.24	424.3	1	5.6
Lesser Yellowlegs	0.22	0.94	424.3	4	5.6
Red-necked Phalarope	1.33	5.66	424.3	24	5.6
Purple Sandpiper	0.22	0.94	424.3	4	5.6
Whimbrel	0.06	0.24	424.3	1	5.6
Phalarope unidentified	0.06	0.24	424.3	1	5.6
Shorebird unidentified	0.06	0.24	424.3	1	5.6
Ring-billed Gull	0.89	2.11	237.5	16	38.9
Bonaparte's Gull	0.33	1.41	424.3	6	5.6
Laughing Gull	3.39	4.10	121.1	61	55.6
Herring Gull	72.50	185.23	255.5	1305	94.4
Great Black-backed Gull	39.33	122.38	311.1	708	83.3
Black-legged Kittiwake	0.56	1.65	297.5	10	11.1
Gull unidentified	1.67	7.07	424.3	30	5.6
Tern unidentified	0.06	0.24	424.3	1	5.6
Common Tern	0.11	0.47	424.3	2	5.6
Razorbill	0.22	0.43	192.5	4	22.2
Atlantic Puffin	0.28	1.18	424.3	5	5.6
Grand Total	**233.28**	**426.47**	**182.8**	**4199**	**100.0**

Appendix G. Mean (SD)) number of detections per grid, CV of detection rate, total number of detections, and % of surveys (n = 20) with a detection within a grid during ship-based line transect surveys for data pooled across all 8 grids (see Fig. 24) conducted during winter 2009-2010 (18 Dec 2009 through 13 Feb 2010).

Species	Mean	SD	CV	Total	% of surveys
Common Loon	11.65	7.40	63.5	233	95
Red-throated Loon	4.05	6.18	152.5	81	55
Loon spp.	0.10	0.31	307.8	2	10
Northern Gannet	29.40	81.35	276.7	588	75
Double-crd cormorant	0.05	0.22	447.2	1	5
Great Cormorant	0.70	1.45	207.8	14	25
Brant	0.85	3.80	447.2	17	5
Dabbling duck unidentified	0.55	2.46	447.2	11	5
Common Eider	3.90	6.11	156.7	78	45
Long-tailed Duck	0.45	0.89	197.1	9	25
White-winged Scoter	5.20	5.97	114.8	104	85
Surf or Black Scoter	3.40	9.70	285.2	68	30
Surf Scoter	0.35	0.75	212.9	7	20
Black Scoter	1.10	2.02	184.0	22	30
Red-breasted Merganser	0.10	0.31	307.8	2	10
Bonaparte's Gull	0.60	1.14	190.4	12	30
Ring-billed Gull	0.80	1.91	238.6	16	20
Herring Gull	10.20	7.74	75.9	204	95
Great Black-bd Gull	5.55	5.60	100.8	111	100
Black-legged Kittiwake	2.25	2.22	98.7	45	65
Gull unidentified	1.35	4.94	366.3	27	15
Razorbill	4.45	6.44	144.8	89	60
Murre unidentified	0.30	0.98	326.2	6	10
Common Murre	6.55	13.23	202.0	131	55
Thick-billed Murre	0.15	0.49	326.2	3	10
Dovekie	6.25	17.44	279.0	125	30
Alcid unidentified	4.15	10.30	248.1	83	55
Grand Total	**104.45**	**104.81**	**100.3**	**2089**	**100**

Appendix H. Model selection results for Density Surface Models (DSM) for various species of birds in the Ocean SAMP area.

Species	Season	Model	Deviance explained (%)	edf	CV (%)
Common Loon	Winter	s(depth ⊤ dis to land)	21.5	22.74	0.069
Northern Gannet	Fall	s(depth ⊤ dis to land)	34.8	18.82	0.091
Northern Gannet	Winter	s(depth ⊤ dis to land)	36.6	23.44	0.087
Cory's Shearwater	Summer	s(depth ⊤ dis to land)	26.3	22.07	0.054
Greater Shearwater	Summer	s(depth) + s(dis to land)	50.8	8.37	0.149
Wilson's Storm-Petrel	Summer	s(depth) + s(dis to land)	33.5	13.89	0.210
Herring Gull	Summer	s(depth ⊤ dis to land)	27.1	12.35	0.079
Herring Gull	Fall	s(depth ⊤ dis to land)	32.3	20.78	0.102
Herring Gull	Winter	s(depth ⊤ dis to land)	8.6	14.9	0.019
Great Black-backed Gull	Summer	s(depth) + s(dis to land)	19.1	11.12	0.206
Great Black-backed Gull	Fall	s(depth ⊤ dis to land)	43.9	27.61	0.064
Great Black-backed Gull	Winter	s(depth) + s(dis to land)	7.45	9.08	0.044
Black-legged Kittiwake	Winter	s(depth) + s(dis to land)	9.74	12.112	0.014
Razorbill	Winter	s(depth)	11.3	8.774	0.171
Common Murre	Winter	s(depth) + s(dis to land)	23.5	15.133	0.065
Dovekie	Winter	s(depth) + s(dis to land)	34.6	11.72	0.160

Appendix I. Estimated number of individuals (N) and 95% Confidence intervals for 11 species of birds in Ocean SAMP area during three seasons based on DSM models (Appendix H).

Species	Season	N	95% CI
Common Loon	Winter	2,901	2535-3321
Northern Gannet	Fall	3,987	3336-4764
Northern Gannet	Winter	4,373	3688-5187
Cory's Shearwater	Summer	3,340	3005-3712
Greater Shearwater	Summer	2,643	1979-3530
Wilson's Storm-Petrel	Summer	16,335	10879-24527
Herring Gull	Summer	1454	1246-1697
Herring Gull	Fall	7332	6000-8961
Herring Gull	Winter	1082	1042-1124
Great Black-bd. Gull	Summer	1869	1255-2786
Great Black-bd. Gull	Fall	2680	2366-3036
Great Black-bd. Gull	Winter	682	627-743
Black-legged Kittiwake	Winter	291	283-299
Razorbill	Winter	1390	996-1940
Common Murre	Winter	623	548-707
Dovekie	Winter	5771	4222-7888

Appendix J. Detection functions and Generalized Additive Model output used to develop Density Surface Models for 11 species of birds in the Ocean SAMP study area.

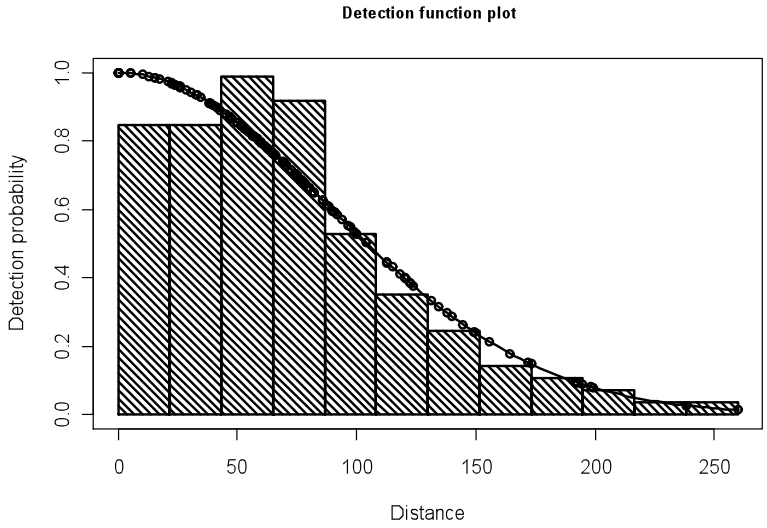

Figure J-1. Histogram of the distance data and the 'best' detection model (half-normal) for Common Loons in the study area during the winter season.

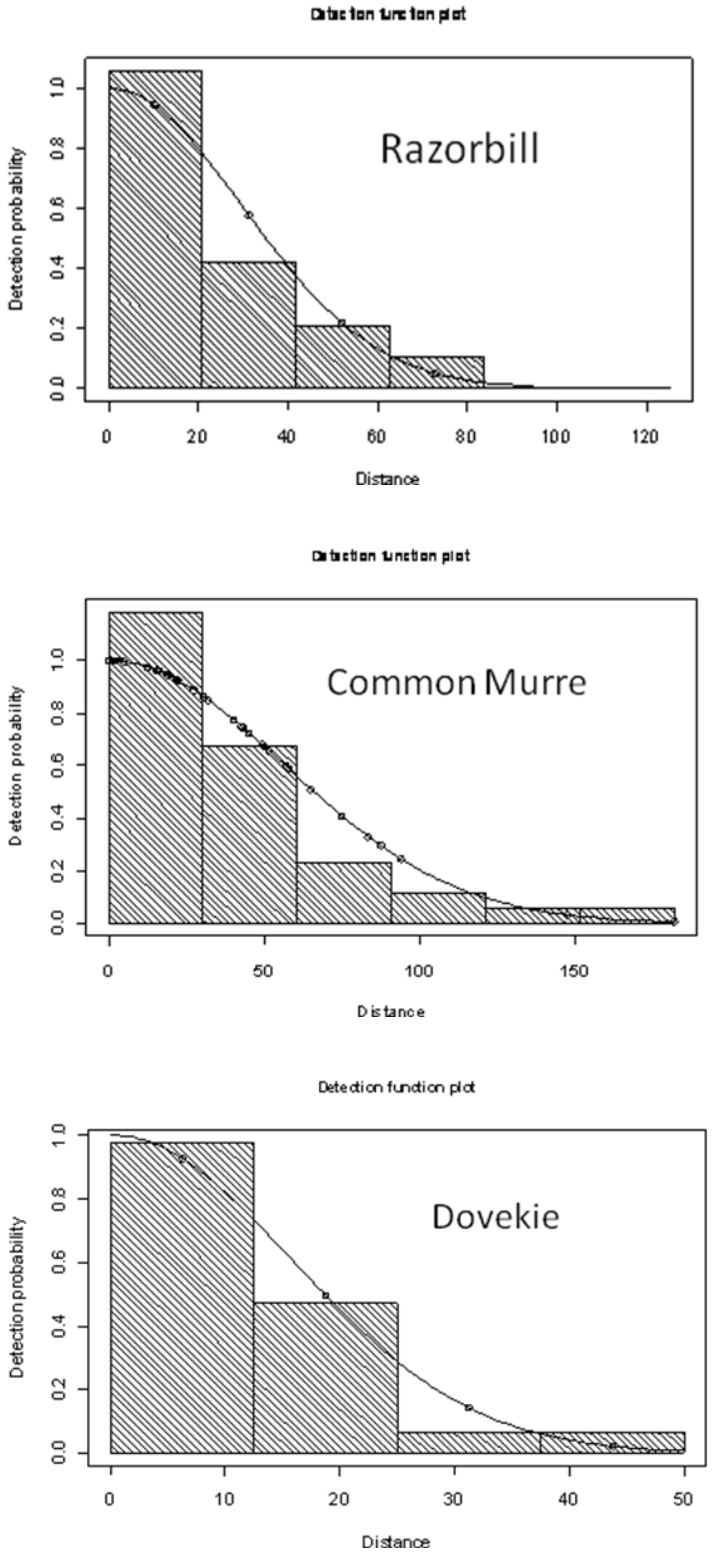

Fig. J-2.. Histogram of the distance data and the 'best' detection model (half-normal) for Razorbill, Common Murre and Dovekie in the study area during the winter season.

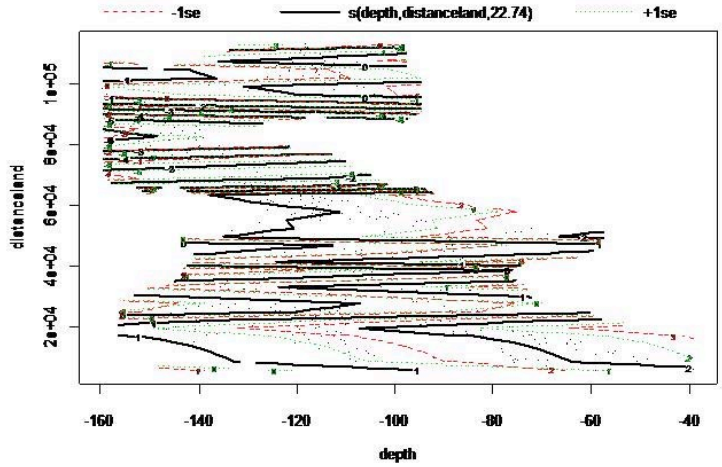

Fig. J-3. The output of the GAM model that best predicted Common Loon abundance in the study area during winter. The solid lines show the nature of the relationship as a contour plot (dotted lines are related to confidence intervals above and below the contour surface).

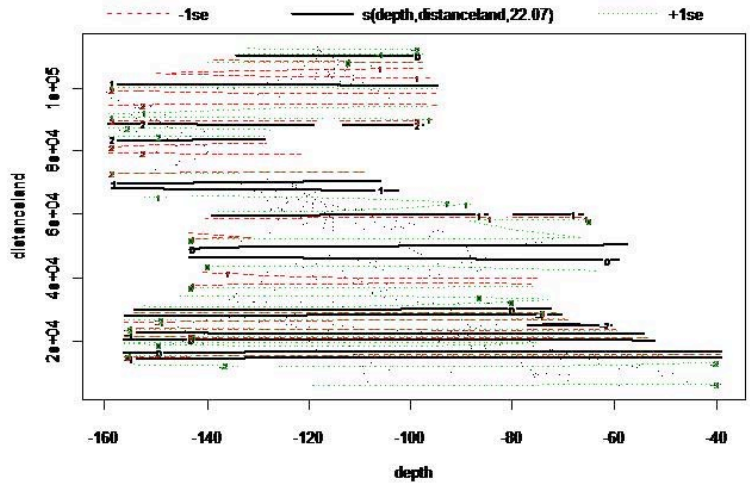

Fig. J-4. The output from the GAM model that best predicted Cory's Shearwater abundance in the study area during summer. The solid lines show the nature of the relationship as a contour plot (dotted lines are related to confidence intervals above and below the contour surface).

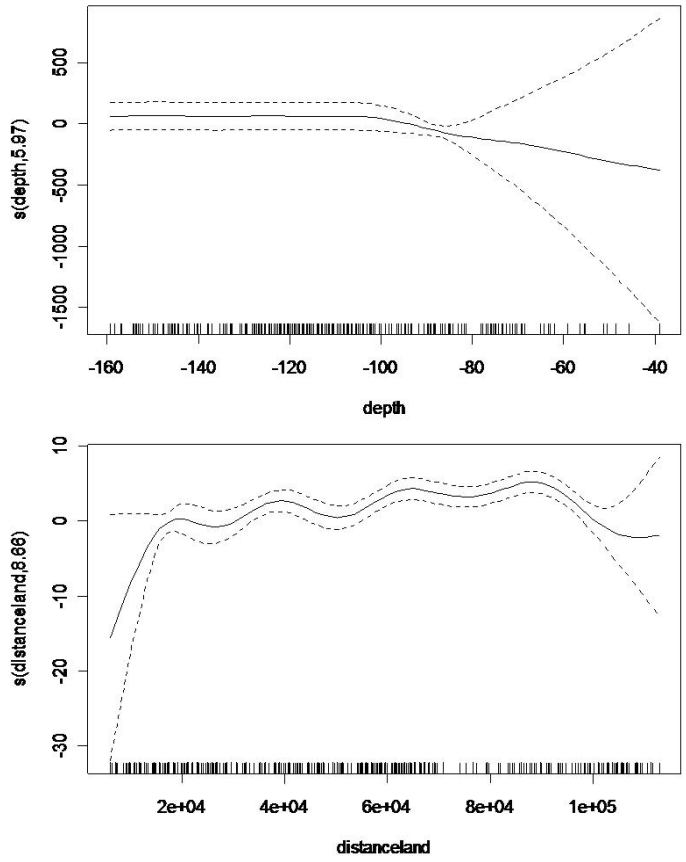

Figure J-5. The output from the GAM model that best predicted Greater Shearwater abundance in the study area during summer. The 95% confidence interval is represented with the dotted line and the distribution of data available to model (e.g. distribution of segments) is represented with the parallel lines on the x-axis.

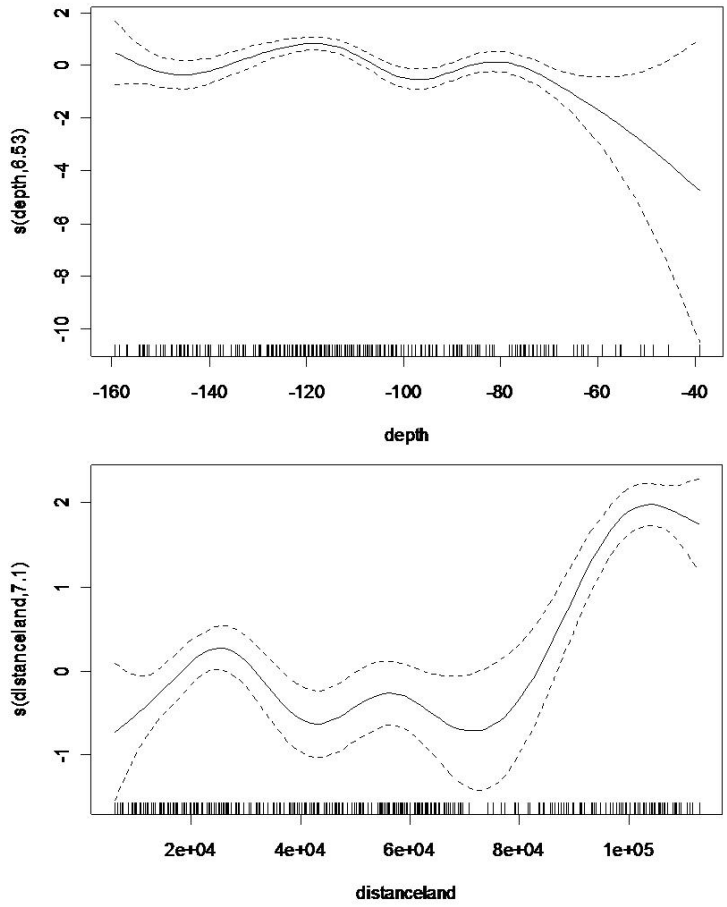

Fig. J-6. The output from the GAM model that best predicted Wilson Storm-Petrel abundance in the study area during summer. The 95% confidence interval is represented with the dotted line and the distribution of data available to model (e.g. distribution of segments) is represented with the parallel lines on the x-axis.

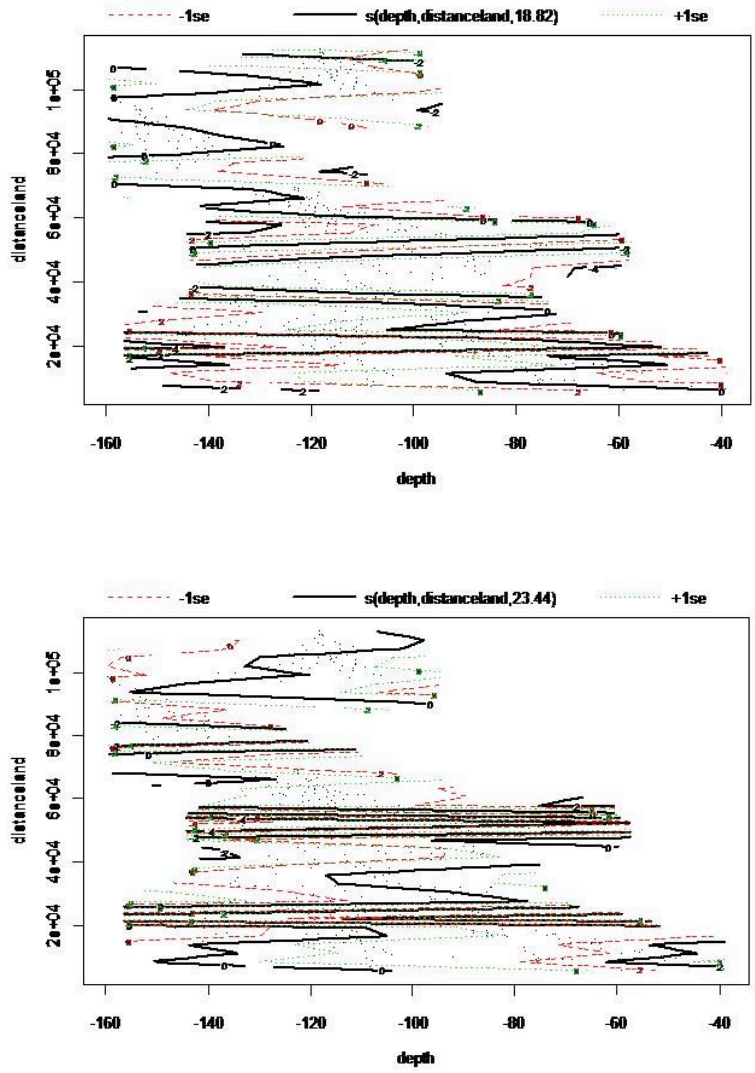

Fig. J-7. The output from the GAM model that best predicted Northern Gannet abundance in the study area during fall (top panel) and winter (bottom panel). The solid lines show the nature of the relationship as a contour plot (dotted lines are related to confidence intervals above and below the contour surface).

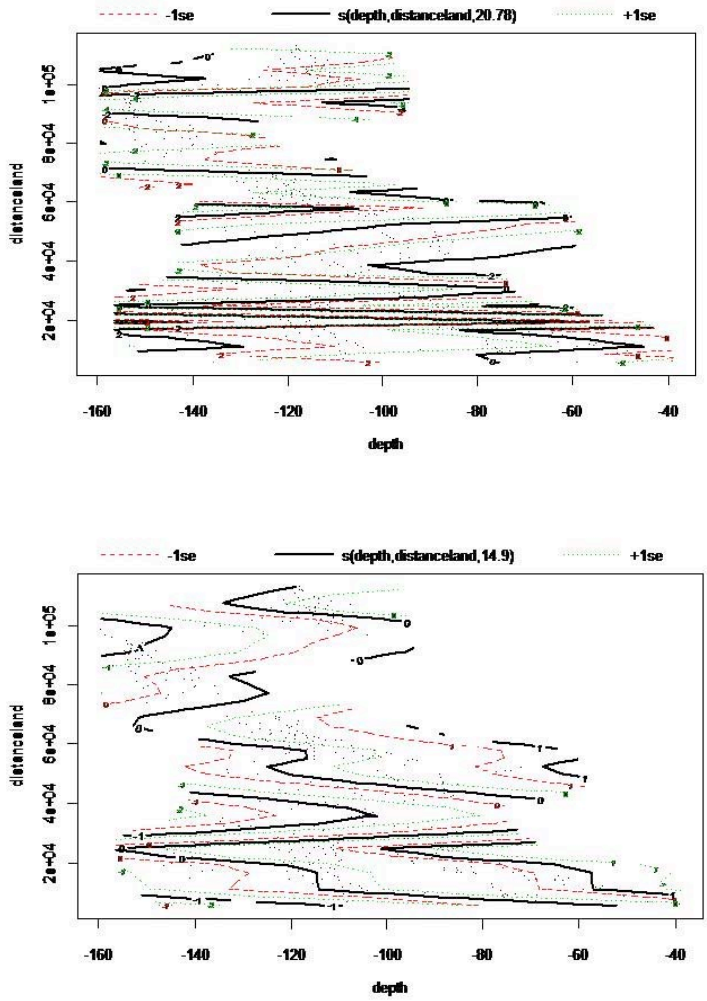

Fig. J-8. The output from the GAM model that best predicted Herring Gull abundance in the study area during summer (top panel), fall (middle panel) and winter (bottom panel). The solid lines show the nature of the relationship as a contour plot (dotted lines are related to confidence intervals above and below the contour surface).

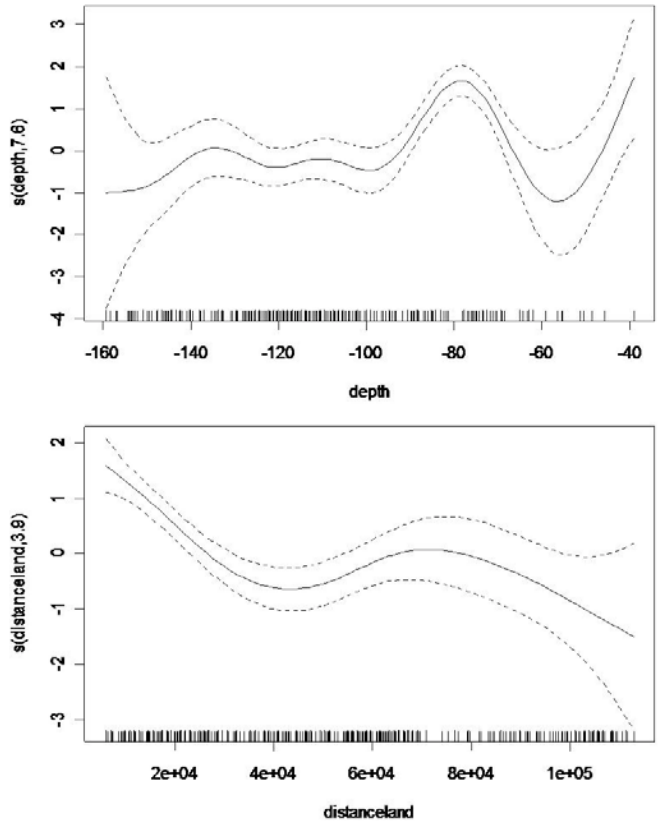

Fig. J-9. The output from the GAM model that best predicted Great Black-backed Gull in the study area during summer The 95% confidence interval is represented with the dotted line and the distribution of data available to model (e.g. distribution of segments) is represented with the parallel lines on the x-axis.

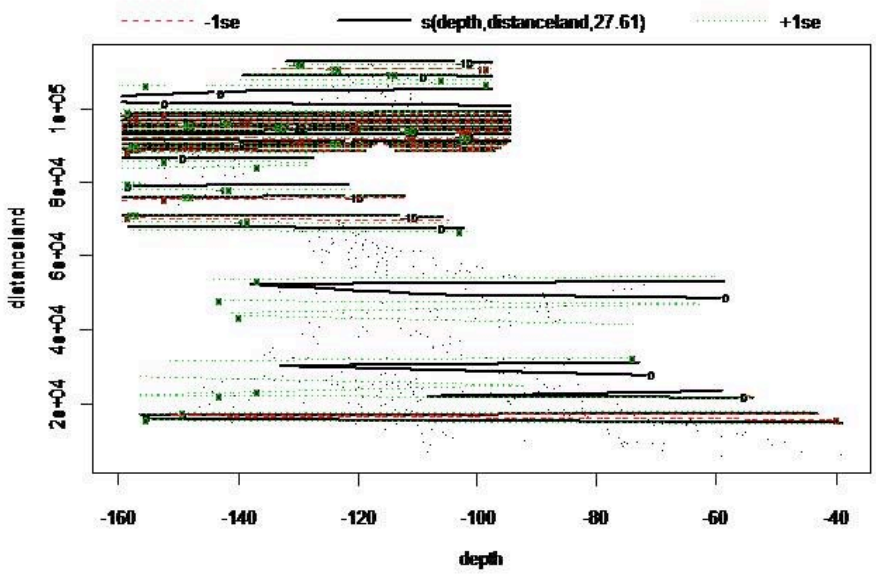

Fig. J-10. The output from the GAM model that best predicted Great Black-backed Gull abundance in the study area during fall. The solid lines show the nature of the relationship as a contour plot (dotted lines are related to confidence intervals above and below the contour surface).

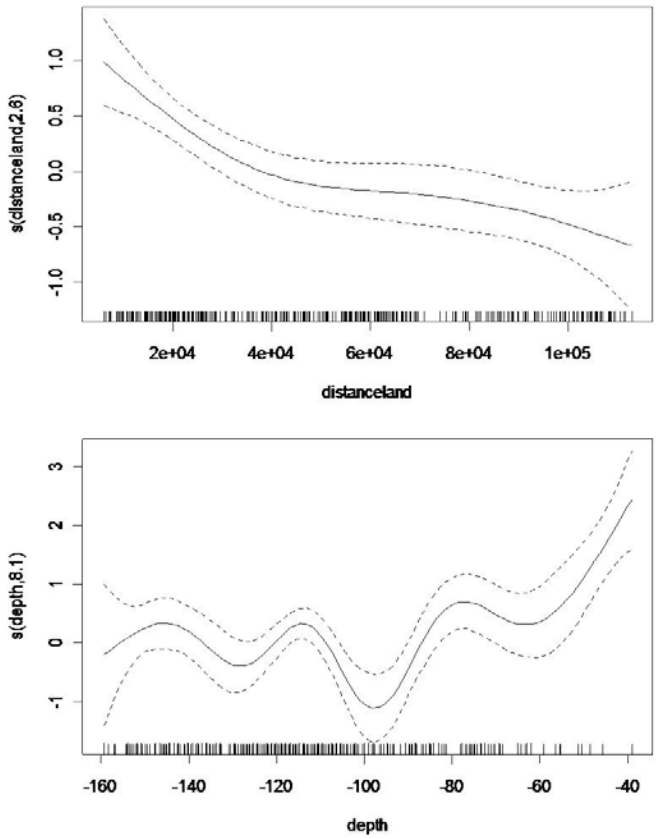

Fig. J-11. The output from the GAM model that best predicted Great Black-backed abundance in the study area during winter. The 95% confidence interval is represented with the dotted line and the distribution of data available to model (e.g. distribution of segments) is represented with the parallel lines on the x-axis.

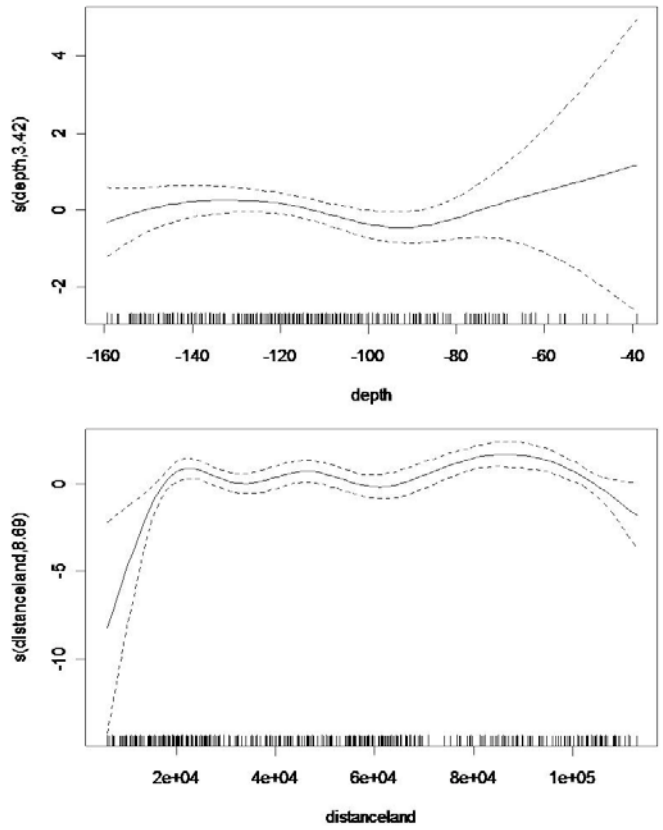

Fig. J-12. The output from the GAM model that best predicted Black-legged Kittiwake abundance in the study area during winter. The 95% confidence interval is represented with the dotted line and the distribution of data available to model (e.g. distribution of segments) is represented with the parallel lines on the x-axis.

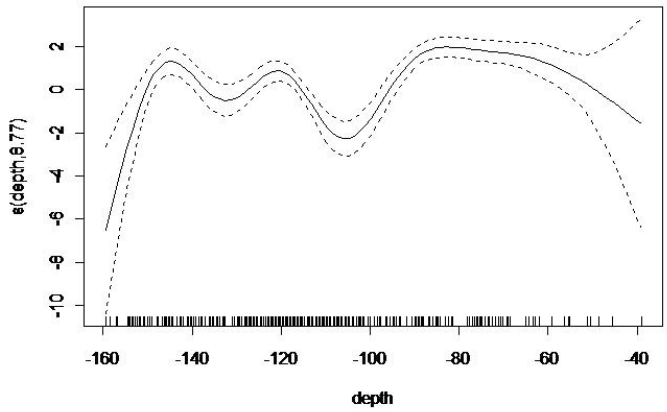

Fig. J-13. The output from the GAM model that best predicted Razorbill abundance in the study area during winter. The 95% confidence interval is represented with the dotted line and the distribution of data available to model (e.g. distribution of segments) is represented with the parallel lines on the x-axis.

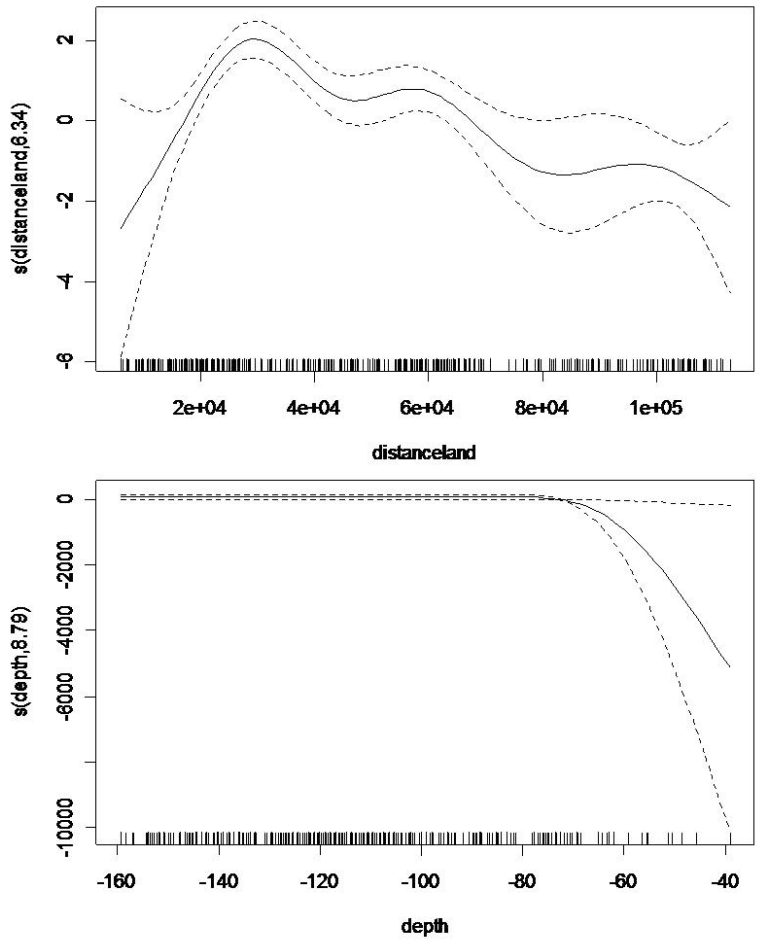

Fig. J-14. The output from the GAM model that best predicted Common Murre abundance in the study area during winter. The 95% confidence interval is represented with the dotted line and the distribution of data available to model (e.g. distribution of segments) is represented with the parallel lines on the x-axis.

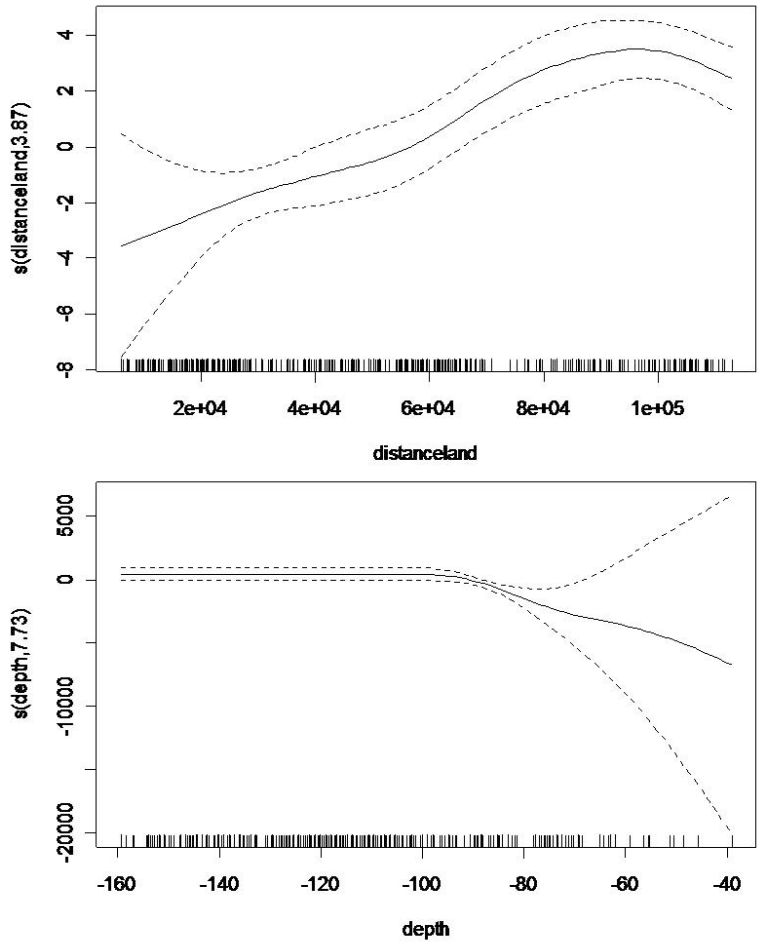

Fig. J-15. The output from the GAM model that best predicted Dovekie abundance in the study area during winter. The 95% confidence interval is represented with the dotted line and the distribution of data available to model (e.g. distribution of segments) is represented with the parallel lines on the x-axis.

Appendix K.

RADAR MONITORING OF BIRD AND BAT MOVEMENT PATTERNS ON BLOCK ISLAND AND ITS COASTAL WATERS

DRAFT INTERIM REPORT

Submitted to
University of Rhode Island
Department of Natural Resources Science

State of Rhode Island
Ocean Strategic Area Management Plan

Prepared by
Dr. David Mizrahi
Robert Fogg
Thomas Magarian
Vincent Elia
David La Puma

New Jersey Audubon Society
Department of Research and Monitoring

20 June 2010

GOALS AND OBJECTIVES

The goal of this task was to provide an improved understanding of bird and possibly bat movement patterns on Block Island, Rhode Island and in the local waters around the island. Specifically, our objectives were to (1) estimate nightly and seasonal passage patterns of aerial vertebrates (i.e., birds, bats) traversing Block Island and its coastal waters, (2) estimate altitudinal distributions of bird/bat movements and determine what proportion occurs at altitudes deemed a "risk" for collisions with wind turbines (3) determine flight directions and pathways of bird/bat "targets" in the study area and (4) investigate how meteorological conditions affect flight dynamics and behavior. This interim report will address Objectives 1-3. Results for Objective 4 and a discussion of all results relative to what is currently known about bird and bat movement patterns in other regions will be provided in a future report.

METHODS

Radar equipment and configuration

We used a dual mobile marine radar system to collect data on bird and bat flight dynamics and behavior. This system consists of two 25 kW Furuno X-band marine radars (frequency = 9410 GHz, wavelength = 3 cm, model # FAR2127BB, Furuno Electric Company, Nishinomiya, Japan) mounted to a trailer (12' long x 6' wide x 8' high, Fig. 1). The radars and all computer equipment connected to them were powered with a single Honda EU6500i fitted with a 15 gallon external gas tank to extend uninterrupted operating time.

The radars typically are fitted with standard 6.5' open array antennas (Fig. 1), which produce a fan-shaped electromagnetic beam 1.23° x 20°. The antennas rotate simultaneously to monitor various bird/bat flight dynamics and behavior patterns. In our system, one radar unit operates with the antenna rotating rotate in the vertical plane (i.e., "vertical radar"). This is accomplished by mounting the antenna turning unit perpendicular to the ground (Fig. 1). The antenna sweeps from horizon to horizon, describing a 180° arc above radar level (arl), 20° wide (Fig. 2). Data collected with the radar in this orientation were used to generate target (i.e., birds, bats) passage estimates and to quantify altitudinal distributions of targets (see Fig. 3 for data image example). During data collection at the southern end of the island (i.e., 19 March – 30 April), the vertical radar was positioned so that the antenna swept an arc from South to North. This was done to maximize the number of targets detected as waterbirds moved east to west along the southern coast of the island.

The second radar unit operates with the antenna rotating rotate in the horizontal plane (i.e., "horizontal radar"), describing a 360° arc every 2.5 seconds (Fig. 4). Data collected in this mode provided information on flight direction and in some cases, passage rates (see Fig. 5 for data image example). During the study we experienced persistent and often extensive backscatter of electromagnetic energy from wave action experienced at the southern site which dramatically affected the quality of data collected with the horizontal radar (Fig. 6 upper). On some days, this backscatter was extreme and it occluded the horizontal radar's entire view of the ocean sample area (Fig. 6 lower). Although, this is common problem when using radar in marine application, the southern site's elevation above sea level (i.e., ~45 m) exacerbated the problem. In an attempt to address this we experimented with a parabolic dish antenna (Fig. 7). This antenna produces a 4° conical-shaped electromagnetic beam and our mounting allowed it to be elevated in 2.5° above the scanning horizon. With the antenna elevated at 5° above the scanning horizon, we

were able to eliminate detection of most wave-generated backscattered energy. Raising the antenna this far above the scanning horizon reduced our ability to sample low to the ocean surface, so we opted not to use the parabolic dish antenna at the southern site. We did, however, use this antenna at the northern radar site for the last 9 weeks of the study (8 October – 15 December) to reduce backscatter problems. We were able to do this by elevating the antenna only 2.5° above the scanning horizon, thereby maintaining the radar's view of areas close to the ocean's surface.

The radar's pulse length (i.e., rate that electromagnetic energy is transmitted) can be set from 0.07 - 1.2 μsec and detection ranges from 0.125 - 96 nautical miles (nm). For both radars, we used a 0.15 μsec pulse length. For monitoring the sunrise – sunset period (i.e., diurnal period) we set the horizontal radars' range to 2 nm as we expected to monitor the movements of larger waterbirds (e.g., loons, sea ducks, gulls) during the day. During the sunset – sunrise period (i.e., nocturnal period) we set the radars' range to 1 nm to increase the detection of small passerines and shorebirds that typically migrate at night. The range for the vertical radar was always set to 1.0 nm detection range regardless of the time of day.

Short pulse lengths provide better target resolution and more accurate location and distance estimates. Similarly, short detection ranges result in improved resolution of small passerine or bat-sized targets. The radars we use feature color-coded target representation that indicates return signal strength. This allows for discrimination and removal of weak reflectors that could be insects. The radar units also are equipped with an integrated global positioning system (GPS) and target tracking feature that allowed us to determine each target's coordinates and quantify target flight directions.

Each radar's processor unit is connected directly to a computer equipped with a PCI frame grabber circuit board. Using proprietary scheduling software developed by New Jersey Audubon Society (NJAS), we automatically captured five consecutive radar sweep images as bitmap files for any interval and for any period. Typically we collect images for five consecutive radar sweeps, every 10 minutes, from sunrise to sunset (~360 images/night/radar). We chose 10 minute intervals because we believe this insures total turnover of targets between samples.

Study sites and data collection time frame
From 19 March – April 30 2009, our radar system collected data on Audubon Society of Rhode Island property near the Lewis Farm, at the southern end of Block Island (i.e., "southern" site, 41°08.98' N, 71° 36.18' W, Fig. 8). The site is approximately 50 m above sea level and was selected because of its wide field of view to the south that would allow monitoring of migration of waterbirds (e.g., scoters, loons) that typically winter along the SE coast of Block Island. This location provided a view of the ocean from approximately 170-300° (i.e., S – NW or 130° of arc, Fig. 9) for the horizontal radar. The radar's view of the ocean between 90-170° (i.e., E – S, or 80° of arc) was occluded by a rise along the edge of the landform. Areas from approximately 300-90° (NW – E, or 150° of arc) were over land.

From 1 May – 15 October 2009, the NJAS radar system was located on Town of New Shoreham property, at the north end of the island, along the SW shore of Sachem Pond (i.e., "northern" site, 41°13.11' N, 71° 34.30' W, Fig. 8). The site was selected primarily to monitor northward and

southward migration movements of passerines and other landbirds as well as waterbird (e.g., herons, egrets, terns) movements during the summer breeding season. The radar's view of the ocean was clear to the north, east and west. However backscatter of electromagnetic energy from trees and low-rising dunes occluded some of the radar's view of the surrounding landscape (Fig. 10). Unlike the southeastern study site, we experienced only minor problems in a limited area with backscatter of electromagnetic energy from wave action (i.e., from 15-40° or 25° of arc).

Although we anticipated moving the radar system back to the southern site on 1 Nov, (i.e., New Jersey Audubon Society, University of Rhode Island bird/bat monitoring principals) decided to leave the radar at the northern location through the end of the study period (i.e., 15 December). This was primarily because of issues related to extreme backscatter of radar energy from wave action experienced at the southern site (see above for description of problem).

To the extent possible, data were collected 24 hours/day, during the entire 272 day study period . The radar system was shut down approximately 30 min every two days to fill the generator's gas tank. From 9 – 14 July, the radar was offline for service.

Data Processing and Analysis

We collected approximately 1764 hours of data/radar during spring 2009 (74 days, mean = 23.83 hr/day) and reviewed approximately 52, 900 images/radar. For the summer period, we collected 934 hours of data per radar (39 days, mean = 23.97 hrs/day) and reviewed 28,900 images for each radar. From 9 – 14 July, the radar was offline for service. During the fall data collection period, we collected 3523 hours of data for each radar (147 days, mean = 23.97 hr/day) and reviewed approximately 105,600 images per radar. We experienced intermittent problems with the computer attached to the vertical radar on 6 – 8 December.

Image review was conducted to determine occurrences of bird/bat movement episodes and identify precipitation events, insect contamination or any other unwanted propagation. Precipitation and insects typically have distinct characteristics that allow trained observers to distinguish them from bird and bat targets. Data images with precipitation, insect contamination or any other unwanted propagation were removed from subsequent data analyses either using data processing software developed by NJAS or by manually removing images from data set before analyses. In extreme cases (e.g., continuous rain), we removed entire days or nights of data from analysis.

Vertical radar

Using image processing software developed by NJAS, we extracted target information from all data images collected with the vertical radar. The integrated image processing software:

1. Identifies the sample area and creates a template (Fig. 11) to remove stationary radar reflectors (i.e., ground clutter, sea clutter, main bang).
2. Removes targets with low signal strength likely to be insects (i.e., based on color value).
3. Smooths the data and locates and marks the centroid of each discrete target that remains
4. Exports a text file that includes information on every target's signal strength and its position (i.e., the distance of its centroid) in the *X*- and *Y*-planes relative to the radar's position

5. Outputs a bitmap image showing the transformed data with marked targets (Fig.12). This last feature allows us to review the data processing output to identify possible spurious targets and remove them from the data analysis step.

Using an analysis software program developed by NJAS staff, we summarized target counts, passage rates and altitudinal distribution (i.e., target position in the *Y*-plane relative to radar's position) for 10 min and hourly intervals. The software's output includes the total number of targets detected in each image and the mean number of targets detected in each five-image sample.

Our analysis software also quantifies the number of targets detected in discrete altitudinal bins (e.g., 100 m). Nineteen 100 m (approximately 1 nm) altitudinal bins were created from the data collected with the vertical radar. It also has a threshold feature that allows us to filter out data with unusually high target counts, typically indicating precipitation or insect contamination.

The results of analyses in this report are based on the average for each five-image sampling bout. These values are summed for the entire night's data collection (sum of the sample averages) to generate hourly, daily and nightly passage estimates. We believe using the sum of the sample averages is a more accurate assessment for the number of targets crossing through the study area because it minimizes the effect of enumerating the same targets multiple times during a single sampling bout. Analyses to quantify variation in target counts in successive images in a sampling bout indicated that coefficients of variation (CV) were very low (< 2%).

Horizontal radar

We used NJAS-developed software to calculate target directions from images collected with the horizontally radar. The program requires that the end of a target's trail and the target (in that order) be marked using the computer's mouse and cursor (Fig. 13). The program outputs the position of the trail's tail and the target and from these calculates the target's direction of movement. For day and night period, we analyzed one image for each hour of data collected on each sample day. Targets for each hour were compiled and we used Oriana© 3.0 circular statistical software (Kovach Computing 2006) to generate mean vectors (directional tendency), vector lengths (*r*, strength of directional tendency) and test statistical significance (i.e., Rayleigh's *Z* test, Zar 2003). We calculated second-order mean vectors (i.e., mean of mean vectors) for each season (i.e., day and night separately) and tested for statistical significance using Hotelling T^2 test (Mardia and Rupp 2000).

Statistical Analysis

We used General Linear Model procedures (GLM, Zar 1998) the effect of SEASON (i.e., SPRING migration: 19 Mar – 31 May, SUMMER: 1 June – 15 July, FALL migration: 16 July – 15 December) PERIOD (DAY: sunrise to sunset the same day, NIGHT: sunset to sunrise the following morning) and the interaction between the two variables on target passage and passage rates (i.e., targets/hr). We used the same statistical approach to investigate these factors on the proportion and number of targets detected in the two lowest altitudinal strata (i.e., $\leq$ 100 m, 100 $< x \leq$ 200 m). We used Bonferonni procedures to make *post hoc* pairwise comparisons when GLM procedures suggested significant affects of predictor variables (i.e., SEASON, PERIOD, SEASON*PERIOD interaction) on response variables.

We used Kolmogorov-Smirnoff two-sample tests (Corder and Foreman 2009) to compare altitudinal distributions among seasons and between periods and used GLM procedures to investigate relationships between targets detected and the proportion of targets detected in the two lowest altitudinal strata.

To estimate directional patterns of movement, we compiled hourly target azimuths generated by our software for each season and by period. We used circular statistical analysis procedures (Mardia and Rupp 2000) to generate mean vectors (directional tendency), vector lengths (*r*, strength of directional tendency) and test statistical significance (i.e., Rayleigh's *Z* test, Zar 2003) for each SEASON/PERIOD combination (e.g., spring/day, spring/night). Using means and circular variance output from Oriana, we calculated second-order mean vectors (i.e., mean of mean vectors) for each SEASON/PERIOD combination and tested for statistical significance using Hotelling T^2 test (Mardia and Rupp 2000).

Prior to statistical analyses, response and predictor variables were evaluated to determine if they met assumptions of parametric tests being employed. If assumptions were not met, data were transformed or non parametric tests were used. Based on these assessments we used arcsine transformations to normalize variables represented as proportions (e.g., proportion of targets detected in various altitudinal strata). We used the log transformation to normalize the response variable representing nightly number of targets detected, hourly rates of targets detected and targets detected within altitudinal strata. Although we present results of statistical analyses that used transformed variables, we present summary statistics (e.g., means, standard errors) for response variables in their untransformed state in textual, tabular and graphical accounts, unless otherwise indicated. All standard statistical analyses were performed using SAS® 9.2 (SAS Institute, Inc. 2004) and SYSTAT® 11.0 (SYSTAT Software, Inc. 2004). Statistical tests involving directional data (i.e., flight direction) were performed using Orianna 3.0© (Kovach Computing Services 2007). Results of statistical tests were considered significant at $\alpha \leq 0.05$.

RESULTS

Target passage and passage rates

Numbers of birds and bats detected during the study varied widely within and among seasons and between day and night periods (Tables 1 – 6, Figs. 14, 15, 16). Generally, sums of the 10-minute sample averages and hourly rates of targets detected raged 2-3 orders of magnitude within a single season or period and coefficients of variation were > 95%. These results indicate that seasonal bird/bat movements, especially during migration periods (i.e., both diurnal and nocturnal), were temporally episodic. The seasonal pattern in targets detection varied between day and night. Kolmogorov Smirnov two-sample tests suggested that day and night cumulative frequency distributions that characterized daily changes in target movements, were significantly different in spring (maximum difference = 0.402, $P < 0.001$, Fig. 17 upper) and summer (maximum difference = 0.605, $P < 0.001$, Fig. 17 center), but not in fall (maximum difference = 0.099, $P < 0.48$, Fig. 17 lower).

Despite large variability in indices of movement, we found statistically significant SEASON ($F_{2, 513} = 9.23$, $P = 0.0001$) and PERIOD (i.e., day, night, $F_{1, 514} = 10.38$, $P = 0.0014$) effects on the number of targets detected (i.e., sum of the sample averages). Targets detected during the

fall (mean = 141.24 ± SE 1.08) were significantly greater ($P = 0.003$) than in spring (mean = 89.90 ± SE 1.19) and summer ($P = 0.001$, mean = 76.54 ± SE 1.17), while spring and summer were not significantly different from each other. Targets detected at night (mean = 123.70 ± SE 1.10) were significantly greater ($P < 0.001$) than those detected during the day (mean = 79.32 ± SE 1.10). We also found a significant SEASON*PERIOD interaction ($F_{2, 513} = 14.47$, $P < 0.0001$). *Post hoc* comparisons suggested that targets detected during fall/night were significantly greater than all other SEASON/PERIOD combinations (all Ps < 0.0001, Fig. 18 upper) while none of the other combinations were statistically different from each other (Fig. 18 upper).

We found similar significant SEASON ($F_{2, 513} = 6.98$, $P = 0.001$) and PERIOD ($F_{1, 514} = 27.40$, $P < 0.0001$) effects on target detection rate (i.e., targets detected/hour). Again, fall target detection rate (mean = 14.95 ± SE 1.07) was significantly greater ($P = 0.01$) than spring (mean = 10.43 ± SE 1.11) and summer ($P = 0.008$, mean = 9.28 ± SE 1.15), while spring and summer were not significantly different from each other. Targets detection rates at night (mean = 15.68 ± SE 1.09) were also significantly greater ($P < 0.0001$) than those during the day (mean = 8.16 ± SE 1.09). We found a significant SEASON*PERIOD interaction ($F_{2, 513} = 14.47$, $P < 0.0001$). *Post hoc* comparisons indicated that target detection rate during fall/night was significantly greater than all other SEASON/PERIOD combinations (all Ps < 0.0001, Fig. 18 lower) while none of the other combinations were statistically different from each other (Fig. 18 lower).

Bird/bat movements also varied with time relative to sunrise and sunset. The diurnal period (i.e., sunrise – sunset) appeared to be characterized by distinct peaks in movement 6-8 hours after sunrise (Fig. 19). Peak movement during the nocturnal period (i.e., sunset – sunrise the following morning) appeared to occur 1-3 hours after sunset (Fig. 20). However, Kolmogorov Smirnov two-sample tests suggested that day and night cumulative frequency distributions, which characterized hourly changes in target detections, were not significantly different among seasons for day (Fig. 21 upper, all Ps > 0.60) or night (Fig. 21 lower, all Ps > 0.80) data collection periods. Additionally, comparisons of season-specific cumulative frequency distributions for day and night data collections periods were not significantly different (all Ps > 0.3, *cf* Fig. 21).

Target altitude

Results from Kolmogorov-Smirvov two-sample tests suggest that proportional distributions of targets detected in each 100 m strata (i.e., up to one nautical mile or approximately 1900 m) were not significantly different (all Ps > 0.10) among seasons for the diurnal (Fig. 22, upper) or nocturnal periods (Fig. 22, lower). Regardless of season or period, altitudinal distributions of detected targets generally increased with altitude to peak between 200 and 400 m (Figs. 23, 24), except during the spring/diurnal period when the greatest proportion of detected targets occurred in the 0-100 m stratum. At altitudes greater than 500 m the proportion of detected targets decreased asymptotically.

<u>0-100 meter stratum</u>

Our data also suggest extensive within-season variation in the proportion of and number of targets detected in the lowest altitudinal strata we considered (i.e., targets ≤ 100 m, Tables 1 – 6, Figs. 25, 26, 27). Kolmogorov Smirnov two-sample tests suggested that cumulative frequency

distributions that characterized daily changes in the proportion of target detected in the 0-100 m stratum, were significantly different between day and night data collection periods in spring (maximum difference = 0.402, $P < 0.001$, Fig. 28 upper), summer (maximum difference = 0.632, $P < 0.001$, Fig. 28, center) and fall (maximum difference = 0.160, $P < 0.05$, Fig. 28, lower). Additionally, Kolmogorov Smirnov two-sample tests suggested a significant difference in the cumulative frequency distributions among seasons for the day (*cf* Fig. 28, all *P*s < 0.005,) and night (*cf* Fig. 28, all *P*s < 0.0009,) data collection periods.

Although the proportional distributions of target altitudes were high day-to-day and night-to-night variability, we found significant SEASON ($F_{2, 513} = 4.49$, $P = 0.01$) and PERIOD ($F_{1, 514} = 36.19$, $P < 0.0001$) effects on the proportion of targets detected in the 0-100 m stratum. The proportion of targets detected in the 0-100 m stratum was significantly greater in summer ($P = 0.04$) during the (mean = 0.116 ± SE 0.000) compared to fall (0.086 ± SE 0.00) and nearly so compared to spring ($P = 0.08$, mean = 0.106 ± SE 0.000). Additionally, the proportion of targets detected in the 0-100 m stratum was significantly greater ($P < 0.0001$) during the day (mean = 0.132 ± SE 0.000) than at night (mean = 0.076 ± SE 0.00).

We found a significant SEASON*PERIOD interaction effect on the proportion of targets detected in the 0-100 m stratum ($F_{2, 513} = 3.98$, $P < 0.02$). *Post hoc* comparisons indicated that fall/night had a significantly smaller proportion (mean = 0.065 ± SE 0.005) than any other SEASON/PERIOD combination (all *P*s < 0.02) except summer/night (Fig. 29, upper). Summer/day had the greatest proportion of targets detected in the 0-100 m stratum (mean = 0.176 ± SE 0.018) and this was significantly greater than all SEASON/night combinations (all Ps < 0.02) but not greater than other SEASON/day combinations (Fig. 29, upper).

We found a significant SEASON effect on targets detected (i.e., sums of the 10-minute sample averages) in the 0-100 stratum ($F_{2, 513} = 3.49$, $P = 0.03$), but no significant PERIOD effect ($F_{1, 514} = 0.16$, $P = 0.69$). Targets detected in fall (mean = 10.43 ± SE 1.08) were significantly greater ($P = 0.05$) than in spring (mean = 7.70 ± SE 1.11) but not summer (mean = 7.66 ± SE 1.16). Targets we detected in spring and summer were not statistically different.

However, the SEASON*PERIOD interaction was significant. *Post hoc* comparisons indicated that targets detected in the 0-100 stratum for the fall/night combination (mean = 31.43 ± SE 3.86) were significantly greater (all *P*s < 0.004, Fig. 29, lower) than fall/day (mean = 16.68 ± SE 2.09), spring/night (mean = 11.68 ± SE 1.63) and summer night (mean = 14.40 ± SE 4.13). Other SEASON/PERIOD combinations were not statistically different from each other (Fig.29, lower).

The proportion and mean number of bird/bat targets detected in the 0-100 m altitudinal stratum showed extensive hour-to-hour variation during day and night data collection periods, regardless of season (spring: Figs. 30, summer: Fig. 31, fall: Fig. 32). Variation in the proportion and numbers of targets in the 0-100 m stratum appeared to follow patterns similar to those observed in the hourly proportion and total count of targets and patterns discussed in the previous section (*cf* Figs. 19, 20). That is, during the diurnal period (i.e., sunrise – sunset) distinct peaks in the mean proportion and number of targets detected in the lowest altitudinal strata occurred 6-8 hours after sunrise. During spring and summer nocturnal periods (i.e., sunset to sunrise the following morning), peak mean proportions and number of targets detected below 100 m

appeared to occur 1-3 hours after sunset (Figs. 30, 31). In fall, however, the mean proportion of targets detected at or below 100 m was smallest at sunrise and gradually increased to the greatest values as sunrise approached (Fig. 32, upper right). Conversely, the mean number of targets detected in this stratum was greatest at sunset and decreased gradually to reach the smallest values of the night at sunrise (Fig. 32 lower right).

However, Kolmogorov Smirnov two-sample tests suggested that cumulative frequency distributions that characterized hourly changes in the proportion of target detected in the 0-100 m stratum were not significantly different between day and night data collection periods in spring, summer or fall (all Ps > 0.20, Fig. 33). Additionally, Kolmogorov Smirnov two-sample tests suggested that there was no statistical difference in the cumulative frequency distributions that characterize hourly variation among seasons for the day (all Ps > 0.80, *cf* Fig. 33) and night (all Ps > 0.60, *cf* Fig. 33) data collection periods.

101-200 meter stratum

Similar to our findings for the 0-100 m stratum, our data also suggest extensive within-season variation in the proportion of and number of targets detected in the 101-200 m stratum, Tables 1 – 6, Figs. 24, 25, 26). Kolmogorov Smirnov two-sample tests suggested that cumulative frequency distributions that characterized daily changes in the proportion of target detected in the 101-200 m stratum, were significantly different between day and night data collection periods in spring (maximum difference = 0.240, P = 0.03, Fig. 34 upper) and summer (maximum difference = 0.526, P < 0.0001, Fig. 34, center), but not in fall (maximum difference = 0.126, P < 0.19, Fig. 28, lower). Additionally, Kolmogorov Smirnov two-sample tests suggested the fall cumulative frequency distribution for the day data collection period was significantly different than spring and summer (all Ps ≤ 0.003 *cf* Fig. 34), for spring and fall were statistically different (P = 0.69).

We found a significant SEASON ($F_{2, 513}$ = 5.29, P = 0.005) and PERIOD ($F_{1, 514}$ = 32.63, P < 0.0001) effects on the proportion of targets detected in the 101-200 m stratum. The proportion of targets detected in the 101-200 m stratum was significantly greater in summer (mean = 0.175 ± SE 0.000) compared with fall (P = 0.01, mean = 0.138 ± SE 0.000) and spring (P = 0.006, mean = 0.133 ± SE 0.000), but fall and spring were statistically different from each other (Fig. 35, upper). "Day" had significantly greater proportion (P < 0.0001, mean = 0.177 ± SE 0.000) of targets in the 101-200 m stratum than "night" (mean = 0.122 ± SE 0.000). A SEASON*PEROID effect on the proportion of targets detected in the 101-200 m stratum was not evident from our analyses ($F_{2, 513}$ = 1.65, P = 0.19, Fig. 35, upper).

Similar to results from the 0-100 m stratum, we found a significant SEASON effect on targets detected in the 101-200 stratum ($F_{2, 513}$ = 8.61, P = 0.0002) and no significant PERIOD effect ($F_{1, 514}$ = 0.60, P = 0.44). We detected significantly greater numbers of targets in fall (mean = 18.41 ± SE 1.08) compared with spring (P = 0.0002, mean = 10.56 ± SE 1.12). However, targets detected in fall and summer (mean = 13.00 ± SE 1.17) were not statistically different, nor were they for spring and summer. We also found a significant SEASON*PERIOD effect ($F_{2, 513}$ = 12.46, P < 0.0001) on targets detected in the 101-200 m stratum. Significant more targets were detected during fall/night (mean = 65.66 ± SE 7.08, (Fig. 35, lower) than all other SEASON/PERIOD combinations (all Ps ≤ 0.0004) except for summer/day (P = 0.09, mean =

30.82 ± SE 5.55, Fig. 35, lower). None of the other SEASON/PERIOD combinations were significantly different from each other (Fig. 35, lower).

As was the case for the 0-100 m altitudinal stratum, the proportion and mean number of bird/bat targets detected in the 101-200 m altitudinal stratum showed extensive hour-to-hour variation during day and night data collection periods, regardless of season (spring: Figs. 30, summer: Fig. 31, fall: Fig. 32). Variation in the proportion and numbers of targets in the 101-200 m stratum appeared to follow patterns observed in the hourly proportion and total count of targets discussed in the previous section (*cf* Figs. 19, 20) and for the 0-100 m stratum (Figs. 30, 31, 32). Generally, peaks in the mean proportion and number of targets detected in the lowest altitudinal strata occurred approximately 6-8 hours after sunrise during the diurnal period (i.e., sunrise – sunset). During spring and summer nocturnal periods (i.e., sunset to sunrise the following morning) these peaks occurred approximately 1-3 hours after sunset (Figs. 30, 31). In contrast, the mean proportion of targets detected in the 101-200 m stratum was smallest at sunrise and gradually increased to the greatest values as sunrise approached during the fall nocturnal period (Fig. 32, upper right), while the mean number of targets detected in this stratum was greatest at sunset and decreased gradually to reach the smallest values of the night at sunrise (Fig. 32 lower right).

However, Kolmogorov Smirnov two-sample tests suggested that cumulative frequency distributions that characterized hourly changes in the proportion of target detected in the 101-200 m stratum were not significantly different between day and night data collection periods in spring, summer or fall (all *P*s > 0.15, Fig. 36). Additionally, Kolmogorov Smirnov two-sample tests suggested that there was no statistical difference in the cumulative frequency distributions that characterize hourly variation among seasons for the day (all *P*s > 0.60, *cf* Fig. 36) and night (all *P*s > 0.80, *cf* Fig. 36) data collection periods.

Relationships between target altitude and movement magnitude

0-100 meter stratum

Generally, we found a negative relationship between the proportion of targets detected (i.e., arsine transformed, see Methods section, Statistical Analysis) in the 0-100 m stratum and total targets detected (i.e., log transformed, see Methods section, Statistical Analysis) across all strata. That is, as total targets detected increased, the proportion of targets in the lowest altitudinal stratum decreased regardless of season or period (Figs. 37, 38, 39). However, these relationships were only statistically significant for the night periods and the fall/day period (all *P*s < 0.02, Table 7).

101-200 meter stratum

For the 101-200 m stratum, only spring/day, fall/day and fall night exhibited a negative relationship between the proportion of targets detected and total targets detected across all strata (Figs. 37, 39). All of these relationships were statistically significant (all, *P*s < 0.01, Table 7). For spring/night, summer/day and summer/night periods, relationships between the proportion of targets detected and total targets detected across all strata were positive (Figs. 37, 38). However, only the relationship for summer/night was significant (*P* = 0.02).

Target flight direction

We conducted second-order analyses (i.e., means of means) on mean vectors and vector lengths calculated for each season/period combination (e.g., spring/day, summer/night, fall/night). We found that second-order mean vectors were significantly different from random for each period in spring and summer (Fig. 40). However, neither fall/day nor fall/night second-order mean vectors were statistically different from random (fall/day: mean vector = 328°, $r = 0.14$, $F_{1,145} = 2.82$, $P = 0.06$, fall/night: mean vector = 265°, $r = 0.09$, $F_{1,145} = 1.16$, $P = 0.31$). After visual inspection of the data, we noticed that many of the first-order mean vectors during July and August were oriented toward the north, while many from September – December were oriented to the south. Given this, we split the fall data into four groups: July – August, day and night, September – December, day and night. Of these, all second-order mean vectors were statistically significant (all Ps < 0.003, Fig. 41) except for September – December/day ($P = 0.22$, Fig. 41). We found not statistical difference when we compared season-specific day and night second-order mean vectors for each season (all Ps > 0.20). A comparison between September – December/day and September – December/night was not possible because the second-order mean vector of the former was no statistically significant.

Table 1. Results of marine radar image analyses for data collected on 73 days (i.e., sunrise to sunset the same day) during the spring 2009 migration period (19 March - 31 May on Block Island, New Shoreham, Rhode Island. "Total targets detected" are the number of birds/bats detected in all images collected. "Sum of the sample averages" refers to the target count averaged over the five successive images that constitute a sample (i.e., every 10 minutes). These values are summed for the entire night's data collection to generate a passage estimate. "Target detection rate" represents the number of targets detected per nautical mile of passage front per hour. We also present the proportion and number of targets detected within the three lowest altitudinal strata (i.e., 100, 200, 300 m).

Date	Julian day	Total targets detected	Sum of the sample averages	Target detection rate	Proportion of targets <=100 m	Number of targets <=100 m	Proportion of targets 101-200 m	Number of targets 101-200 m	Proportion of targets 201-300 m	Number of targets 201-300 m
03/20/09	79	3836	760	87.69	0.0201	15.26	0.0250	19.02	0.0344	26.15
03/21/09	80	200	37	3.31	0.1500	5.55	0.1450	5.37	0.2050	7.59
03/22/09	81	515	102	11.55	0.0388	3.96	0.0641	6.54	0.0583	5.94
03/23/09	82	337	65	6.39	0.0267	1.74	0.1454	9.45	0.2136	13.89
03/24/09	83	643	126	11.63	0.2504	31.55	0.2084	26.26	0.1882	23.71
03/25/09	84	438	87	7.68	0.1667	14.50	0.1895	16.49	0.2169	18.87
03/26/09	85	740	145	16.42	0.0595	8.62	0.0297	4.31	0.0419	6.07
03/27/09	86	265	52	4.73	0.3623	18.84	0.1623	8.44	0.1019	5.30
03/28/09	87	100	20	2.40	0.2100	4.20	0.1600	3.20	0.0100	0.20
03/29/09	88	32	7	2.80	0.0000	0.00	0.0000	0.00	0.0000	0.00
03/30/09	89	909	181	22.16	0.4070	73.67	0.0792	14.34	0.1045	18.92
03/31/09	90	193	37	3.47	0.1917	7.09	0.2021	7.48	0.0466	1.73
04/01/09	91	658	112	13.18	0.0106	1.19	0.0198	2.21	0.0198	2.21
04/02/09	92	290	56	13.44	0.0759	4.25	0.3414	19.12	0.2414	13.52
04/03/09	93	1171	232	32.37	0.0598	13.87	0.0102	2.38	0.0248	5.75
04/04/09	94	1837	363	31.11	0.0332	12.05	0.0430	15.61	0.0697	25.29
04/05/09	95	1876	374	31.61	0.2377	88.91	0.0608	22.73	0.0810	30.30
04/06/09	96	1066	212	48.92	0.0722	15.31	0.0394	8.35	0.0366	7.76
04/07/09	97	7191	1422	118.50	0.2356	334.98	0.0419	59.52	0.0334	47.46
04/08/09	98	6911	1359	151.00	0.1399	190.15	0.0865	117.59	0.0291	39.53
04/09/09	99	700	136	11.33	0.1043	14.18	0.0786	10.69	0.0829	11.27
04/10/09	100	697	142	13.27	0.1707	24.24	0.1306	18.54	0.0631	8.96
04/11/09	101	146	31	14.31	0.5822	18.05	0.2055	6.37	0.1096	3.40
04/12/09	102	278	52	6.50	0.2014	10.47	0.2734	14.22	0.0971	5.05
04/13/09	103	383	72	6.00	0.0783	5.64	0.1619	11.66	0.0836	6.02
04/14/09	104	566	114	12.67	0.0230	2.62	0.1131	12.89	0.0442	5.04
04/15/09	105	1225	245	19.86	0.0237	5.80	0.0914	22.40	0.0278	6.80
04/16/09	106	515	100	8.00	0.1087	10.87	0.1417	14.17	0.2039	20.39
04/17/09	107	319	62	4.89	0.0627	3.89	0.2414	14.97	0.0878	5.44
04/18/09	108	1426	282	23.50	0.0196	5.54	0.0743	20.96	0.0912	25.71
04/19/09	109	648	130	10.68	0.1204	15.65	0.2207	28.69	0.1651	21.47
04/20/09	110	351	56	7.81	0.1054	5.90	0.1966	11.01	0.0484	2.71
04/21/09	111	637	124	14.88	0.0471	5.84	0.0534	6.62	0.0518	6.42
04/22/09	112	632	124	15.18	0.0617	7.65	0.1535	19.03	0.1962	24.33
04/23/09	113	703	141	13.22	0.0327	4.61	0.1465	20.66	0.0484	6.82
04/24/09	114	332	63	4.91	0.0512	3.23	0.2078	13.09	0.1325	8.35

Table 1. Continued

04/25/09	115	3125	624	47.39	0.0109	6.79	0.0522	32.55	0.0915	57.11
04/26/09	116	745	157	11.92	0.0255	4.00	0.1812	28.45	0.0966	15.17
04/27/09	117	823	161	12.23	0.0413	6.65	0.1397	22.50	0.1701	27.39
04/28/09	118	1041	204	15.90	0.0384	7.84	0.0768	15.68	0.0384	7.84
04/29/09	119	473	92	7.26	0.1078	9.92	0.2452	22.56	0.1776	16.34
04/30/09	120	499	102	7.75	0.0301	3.07	0.2285	23.30	0.0541	5.52
05/01/09	121	490	97	18.19	0.1694	16.43	0.1735	16.83	0.0592	5.74
05/02/09	122	275	51	5.56	0.0618	3.15	0.1127	5.75	0.1055	5.38
05/03/09	123	354	69	27.60	0.6017	41.52	0.2797	19.30	0.0311	2.14
05/04/09	124	291	55	9.71	0.1271	6.99	0.3162	17.39	0.2543	13.99
05/05/09	125	157	32	5.33	0.4459	14.27	0.0892	2.85	0.0000	0.00
05/06/09	126	752	146	12.17	0.2061	30.09	0.2566	37.47	0.1702	24.85
05/07/09	127	807	163	16.58	0.0310	5.05	0.0756	12.32	0.0496	8.08
05/08/09	128	423	81	6.23	0.1348	10.91	0.1820	14.74	0.1560	12.64
05/09/09	129	205	37	4.04	0.0585	2.17	0.1366	5.05	0.1073	3.97
05/10/09	130	203	34	2.49	0.0985	3.35	0.4384	14.91	0.0640	2.18
05/11/09	131	178	34	2.68	0.2303	7.83	0.3652	12.42	0.0562	1.91
05/12/09	132	880	175	13.29	0.1534	26.85	0.2318	40.57	0.2966	51.90
05/13/09	133	660	128	9.85	0.0818	10.47	0.3152	40.34	0.2364	30.25
05/14/09	134	1134	227	25.22	0.5273	119.71	0.0820	18.62	0.0097	2.20
05/15/09	135	391	82	8.04	0.2992	24.54	0.1841	15.10	0.0946	7.76
05/16/09	136	213	40	3.16	0.2723	10.89	0.1737	6.95	0.1268	5.07
05/17/09	137	142	27	3.12	0.0282	0.76	0.1197	3.23	0.1056	2.85
05/18/09	138	127	23	2.38	0.2441	5.61	0.1969	4.53	0.1654	3.80
05/19/09	139	667	130	9.40	0.3418	44.44	0.2204	28.65	0.1934	25.14
05/20/09	140	233	40	3.00	0.0773	3.09	0.2146	8.58	0.0858	3.43
05/21/09	141	184	34	2.52	0.0815	2.77	0.3641	12.38	0.1304	4.43
05/22/09	142	277	50	3.80	0.0830	4.15	0.1769	8.84	0.1227	6.14
05/23/09	143	404	83	6.47	0.1089	9.04	0.1559	12.94	0.1535	12.74
05/24/09	144	384	75	5.77	0.0391	2.93	0.1589	11.91	0.0964	7.23
05/25/09	145	937	181	13.24	0.1889	34.19	0.1366	24.73	0.2038	36.90
05/26/09	146	580	110	7.95	0.3603	39.64	0.1931	21.24	0.1534	16.88
05/27/09	147	79	11	1.18	0.0759	0.84	0.1646	1.81	0.0759	0.84
05/28/09	148	103	20	2.93	0.1553	3.11	0.3786	7.57	0.0388	0.78
05/29/09	149	246	44	3.89	0.0203	0.89	0.2114	9.30	0.1138	5.01
05/30/09	150	440	81	5.86	0.0455	3.68	0.3341	27.06	0.2068	16.75
05/31/09	151	691	139	11.58	0.0434	6.03	0.1679	23.33	0.1042	14.48
Totals	73 days	58379	11462			1524		1246.11		933.17
Means		800	157	16	0.14	21	0.17	17	0.11	13

Table 2. Results of marine radar image analyses for data collected on 74 nights (i.e., sunset to sunrise the following morning) during the spring 2009 migration period (19 March - 31 May on Block Island, New Shoreham, Rhode Island. "Total targets detected" are the number of birds/bats detected in all images collected. "Sum of the sample averages" refers to the target count averaged over the five successive images that constitute a sample (i.e., every 10 minutes). These values are summed for the entire night's data collection to generate a passage estimate. "Target detection rate" represents the number of targets detected per nautical mile of passage front per hour. We also present the proportion and number of targets detected within the three lowest altitudinal strata (i.e., 100, 200, 300 m).

Date	Julian day	Total targets detected	Sum of the sample averages	Target detection rate	Proportion of targets <=100 m	Number of targets <=100 m	Proportion of targets 101-200 m	Number of targets 101-200 m	Proportion of targets 201-300 m	Number of targets 201-300 m
03/19/09	78	221.00	43	3.91	0.13	5.45	0.19	7.98	0.29	12.26
03/20/09	79	363.00	71	6.00	0.08	5.87	0.04	2.93	0.06	4.50
03/21/09	80	325.00	61	5.15	0.03	1.88	0.06	3.57	0.08	4.88
03/22/09	81	70.00	12	1.01	0.19	2.23	0.14	1.71	0.04	0.51
03/23/09	82	60.00	9	0.77	0.07	0.60	0.05	0.45	0.00	0.00
03/24/09	83	34.00	6	0.51	0.32	1.94	0.09	0.53	0.18	1.06
03/25/09	84	306.00	59	5.06	0.09	5.21	0.08	4.82	0.07	4.05
03/26/09	85	71.00	14	3.23	0.37	5.13	0.00	0.00	0.11	1.58
03/27/09	86	107.00	19	2.15	0.01	0.18	0.06	1.07	0.00	0.00
03/28/09	87	331.00	65	16.96	0.08	5.11	0.02	1.37	0.02	1.18
03/29/09	88	141.00	27	5.06	0.46	12.45	0.00	0.00	0.00	0.00
03/30/09	89	99.00	16	1.41	0.11	1.78	0.18	2.91	0.08	1.29
03/31/09	90	259.00	48	4.24	0.12	5.56	0.10	4.82	0.04	1.85
04/01/09	91	95.00	17	3.64	0.49	8.41	0.01	0.18	0.00	0.00
04/02/09	92	443.00	86	7.59	0.02	1.36	0.01	0.58	0.00	0.19
04/03/09	93	843.00	169	15.13	0.05	9.02	0.10	17.24	0.13	22.25
04/04/09	94	391.00	74	6.63	0.04	2.65	0.03	2.27	0.05	3.79
04/05/09	95	1017.00	204	18.27	0.16	32.50	0.08	16.05	0.08	16.05
04/06/09	96	930.00	180	18.62	0.11	19.94	0.06	10.65	0.06	11.03
04/07/09	97	4125.00	824	100.90	0.11	93.89	0.08	63.12	0.05	37.75
04/08/09	98	967.00	191	17.91	0.04	6.72	0.08	14.81	0.05	8.69
04/09/09	99	1027.00	203	18.74	0.05	10.67	0.09	19.17	0.09	17.59
04/10/09	100	347.00	70	12.35	0.18	12.91	0.01	1.01	0.03	1.82
04/11/09	101	237.00	47	4.78	0.21	9.72	0.08	3.77	0.02	0.99
04/12/09	102	123.00	24	2.22	0.20	4.68	0.18	4.29	0.26	6.24
04/13/09	103	421.00	83	7.66	0.12	9.66	0.26	21.69	0.23	19.12
04/14/09	104	249.00	53	8.37	0.06	3.41	0.17	8.94	0.17	8.94
04/15/09	105	1743.00	348	32.63	0.02	8.59	0.08	29.55	0.09	30.95
04/16/09	106	396.00	78	7.43	0.15	11.42	0.30	23.64	0.12	9.06
04/17/09	107	532.00	106	10.10	0.14	14.94	0.18	19.33	0.17	18.13
04/18/09	108	476.00	89	9.37	0.08	7.48	0.16	14.58	0.08	6.92
04/19/09	109	181.00	36	3.43	0.09	3.18	0.35	12.53	0.22	7.76
04/20/09	110	282.00	57	68.40	0.06	3.23	0.06	3.64	0.09	5.26
04/21/09	111	395.00	77	85.77	0.06	4.87	0.06	4.48	0.06	4.68
04/22/09	112	133.00	26	5.57	0.08	1.95	0.16	4.11	0.07	1.76
04/23/09	113	167.00	31	3.05	0.08	2.41	0.38	11.69	0.28	8.54

Table 2. Continued

04/24/09	114	856.00	172	16.65	0.09	14.67	0.17	29.34	0.19	32.75
04/25/09	115	1829.00	369	36.90	0.03	10.89	0.18	66.58	0.19	68.39
04/26/09	116	975.00	192	28.76	0.05	10.44	0.19	36.82	0.15	28.95
04/27/09	117	1582.00	310	31.00	0.04	11.17	0.11	34.10	0.18	55.46
04/28/09	118	738.00	147	18.77	0.06	8.17	0.13	19.52	0.09	13.35
04/29/09	119	308.00	60	6.00	0.04	2.14	0.28	16.75	0.11	6.43
04/30/09	120	1912.00	385	39.83	0.01	3.83	0.04	14.70	0.07	28.59
05/01/09	121	2654.00	531	75.21	0.02	10.60	0.06	33.01	0.17	91.63
05/02/09	122	1152.00	233	23.30	0.09	20.02	0.18	41.46	0.22	50.56
05/03/09	123	103.00	21	18.00	0.18	3.87	0.16	3.26	0.17	3.47
05/04/09	124	143.00	27	9.00	0.03	0.94	0.03	0.94	0.09	2.45
05/05/09	125	47.00	6	3.16	0.30	1.79	0.23	1.40	0.09	0.51
05/06/09	126	596.00	120	16.94	0.07	7.85	0.10	12.28	0.18	21.54
05/07/09	127	2446.00	489	56.42	0.09	44.98	0.15	72.77	0.15	75.77
05/08/09	128	2148.00	429	57.20	0.11	48.53	0.16	67.11	0.18	75.49
05/09/09	129	1232.00	250	25.86	0.07	17.05	0.15	37.95	0.14	35.31
05/10/09	130	114.00	17	1.79	0.24	4.03	0.33	5.67	0.10	1.64
05/11/09	131	976.00	193	19.97	0.14	27.29	0.22	42.91	0.22	42.12
05/12/09	132	570.00	109	11.47	0.11	12.05	0.22	23.52	0.24	26.58
05/13/09	133	284.00	56	6.11	0.07	3.75	0.13	7.10	0.16	8.87
05/14/09	134	46.00	8	16.00	0.41	3.30	0.04	0.35	0.02	0.17
05/15/09	135	1585.00	318	34.69	0.06	19.66	0.15	49.15	0.19	58.99
05/16/09	136	351.00	67	8.74	0.04	2.48	0.11	7.64	0.12	8.21
05/17/09	137	199.00	35	5.12	0.14	4.75	0.13	4.40	0.10	3.34
05/18/09	138	653.00	131	14.56	0.13	17.05	0.28	37.11	0.13	17.25
05/19/09	139	991.00	194	21.56	0.06	11.55	0.12	22.51	0.23	45.42
05/20/09	140	884.00	178	19.07	0.06	10.07	0.10	17.32	0.16	27.79
05/21/09	141	4167.00	832	34.47	0.03	28.95	0.07	57.10	0.09	75.27
05/22/09	142	1666.00	336	36.65	0.04	12.71	0.08	26.42	0.15	48.81
05/23/09	143	2876.00	573	76.40	0.03	15.14	0.07	40.25	0.08	48.41
05/24/09	144	2963.00	590	68.08	0.06	35.24	0.08	46.59	0.09	54.16
05/25/09	145	668.00	132	14.67	0.13	16.99	0.20	25.89	0.12	15.41
05/26/09	146	268.00	53	21.20	0.10	5.14	0.08	4.35	0.05	2.77
05/27/09	147	1548.00	309	33.71	0.11	35.53	0.22	66.87	0.26	79.65
05/28/09	148	144.00	27	3.24	0.08	2.25	0.06	1.69	0.17	4.50
05/29/09	149	1595.00	319	37.53	0.05	15.60	0.07	23.20	0.09	30.00
05/30/09	150	2546.00	510	57.74	0.04	19.83	0.11	55.29	0.13	68.71
05/31/09	151	302.00	60	3.33	0.12	7.35	0.41	24.64	0.04	2.58
Totals	74 nights	62024	12311			864.64		1417.43		1541.98
Means		838	166	20.72	0.11	11.68	0.13	19.15	0.12	20.84

Table 3. Results of marine radar image analyses for data collected on 39 days (i.e., sunrise to sunset the same day) during the 2009 non migration period (i.e., summer, 1 June - 15 July) on Block Island, New Shoreham, Rhode Island. Meteorological conditions resulted in data not being analyzed for one of the 39 nights during the study period. "Total targets detected" are the number of birds/bats detected in all images collected. "Sum of the sample averages" refers to the target count averaged over the five successive images that constitute a sample (i.e., every 10 minutes). These values are summed for the entire night's data collection to generate a passage estimate. "Target detection rate" represents the number of targets detected per nautical mile of passage front per hour. We also present the proportion and number of targets detected within the three lowest altitudinal strata (i.e., 100, 200, 300 m).

Date	Julian day	Total targets detected	Sum of the sample averages	Target detection rate	Proportion of targets <=100 m	Number of targets <=100 m	Proportion of targets 101-200 m	Number of targets 101-200 m	Proportion of targets 201-300 m	Number of targets 201-300 m
06/01/09	152	285	49	3.72	0.0877	4.30	0.3930	19.26	0.0807	3.95
06/02/09	153	736	145	11.15	0.0747	10.84	0.1807	26.20	0.1861	26.99
06/03/09	154	815	164	17.26	0.2025	33.20	0.1129	18.51	0.1215	19.92
06/04/09	155	547	107	11.26	0.2687	28.76	0.2066	22.10	0.2011	21.52
06/06/09	157	724	139	9.93	0.0829	11.52	0.3867	53.76	0.2500	34.75
06/07/09	158	1333	266	22.67	0.0480	12.77	0.1275	33.92	0.1605	42.70
06/08/09	159	648	130	9.51	0.0926	12.04	0.2685	34.91	0.1898	24.68
06/09/09	160	145	26	3.32	0.1448	3.77	0.2345	6.10	0.0552	1.43
06/10/09	161	187	31	2.24	0.0160	0.50	0.1016	3.15	0.0802	2.49
06/11/09	162	229	38	3.12	0.1528	5.81	0.4891	18.59	0.1135	4.31
06/12/09	163	311	60	6.10	0.0611	3.67	0.2186	13.12	0.0868	5.21
06/13/09	164	1206	244	18.30	0.1144	27.92	0.2405	58.67	0.1658	40.46
06/14/09	165	2404	481	39.53	0.0283	13.61	0.3760	180.88	0.5740	276.11
06/15/09	166	662	129	9.33	0.0695	8.96	0.5891	76.00	0.2085	26.89
06/16/09	167	477	93	6.72	0.2914	27.10	0.3836	35.68	0.1342	12.48
06/17/09	168	2004	398	29.12	0.0399	15.89	0.1407	56.01	0.1712	68.12
06/18/09	169	130	27	4.76	0.4462	12.05	0.1154	3.12	0.2077	5.61
06/19/09	170	163	31	2.30	0.1350	4.18	0.1963	6.09	0.1104	3.42
06/20/09	171	592	118	10.73	0.3564	42.06	0.2922	34.48	0.0895	10.56
06/21/09	172	206	41	4.10	0.4029	16.52	0.0437	1.79	0.0728	2.99
06/22/09	173	87	14	1.50	0.1839	2.57	0.2989	4.18	0.0460	0.64
06/23/09	174	103	19	1.94	0.3107	5.90	0.0388	0.74	0.1359	2.58
06/24/09	175	149	19	2.07	0.3423	6.50	0.1477	2.81	0.1946	3.70
06/25/09	176	462	89	6.51	0.2208	19.65	0.2100	18.69	0.1234	10.98
06/26/09	177	703	142	12.17	0.1323	18.79	0.1565	22.22	0.0811	11.51
06/27/09	178	1264	254	18.14	0.2983	75.76	0.1638	41.60	0.2468	62.70
06/28/09	179	248	47	3.32	0.2661	12.51	0.2419	11.37	0.1653	7.77
06/29/09	180	610	123	8.68	0.1639	20.16	0.3754	46.18	0.0967	11.90
06/30/09	181	1197	239	16.30	0.1170	27.95	0.1571	37.54	0.2272	54.31
07/01/09	182	177	36	4.24	0.2655	9.56	0.0678	2.44	0.1186	4.27
07/02/09	183	781	148	10.83	0.0755	11.18	0.3137	46.43	0.2113	31.27
07/03/09	184	1137	225	15.88	0.2841	63.92	0.2348	52.84	0.1073	24.14
07/04/09	185	256	43	3.00	0.1133	4.87	0.3516	15.12	0.0664	2.86
07/05/09	186	279	50	3.61	0.1541	7.71	0.2688	13.44	0.1649	8.24
07/06/09	187	2179	438	31.66	0.2446	107.14	0.2194	96.08	0.1703	74.57
Tabe 3. Continued										
07/08/09	189	928	184	13.46	0.1649	30.34	0.3071	56.51	0.2069	38.07
07/09/09	190	30	6	7.20	0.1667	1.00	0.0667	0.40	0.0333	0.20
07/15/09	196	16	1	0.38	0.0625	0.06	0.1875	0.19	0.2500	0.25
Totals	38 days	24410	4794			721		1171		985
Means		642.37	126.16	10.16	0.18	18.97	0.23	30.82	0.16	25.91

Table 4. Results of marine radar image analyses for data collected on 38 nights (i.e., sunset to sunrise the following morning) during the 2009 non migration period (1 June - 15 July) on Block Island, New Shoreham, Rhode Island. "Total targets detected" are the number of birds/bats detected in all images collected. "Sum of the sample averages" refers to the target count averaged over the five successive images that constitute a sample (i.e., every 10 minutes). These values are summed for the entire night's data collection to generate a passage estimate. "Target detection rate" represents the number of targets detected per nautical mile of passage front per hour. We also present the proportion and number of targets detected within the three lowest altitudinal strata (i.e., 100, 200, 300 m).

Date	Julian day	Total targets detected	Sum of the sample averages	Target detection rate	Proportion of targets <=100 m	Number of targets <=100 m	Proportion of targets 101-200 m	Number of targets 101-200 m	Proportion of targets 201-300 m	Number of targets 201-300 m
06/01/09	152	7172	1432	159.11	0.05	71.08	0.09	125.59	0.12	171.71
06/02/09	153	4776	959	106.56	0.12	115.46	0.28	267.46	0.20	188.35
06/03/09	154	4305	862	517.20	0.08	72.88	0.14	120.34	0.21	177.21
06/04/09	155	4145	830	93.96	0.08	68.48	0.17	142.97	0.23	190.83
06/05/09	156	13	3	3.60	0.46	1.38	0.00	0.00	0.00	0.00
06/06/09	157	265	53	31.80	0.15	8.00	0.20	10.80	0.21	11.20
06/07/09	158	2991	599	76.47	0.06	34.05	0.10	58.28	0.11	67.89
06/08/09	159	3850	772	107.72	0.05	36.29	0.11	88.03	0.16	124.72
06/09/09	160	2020	399	45.17	0.02	9.48	0.08	32.00	0.13	52.94
06/10/09	161	690	138	16.56	0.04	5.00	0.11	15.00	0.10	14.40
06/11/09	162	538	107	15.66	0.06	6.56	0.14	14.52	0.21	22.28
06/12/09	163	1244	246	28.94	0.07	18.19	0.19	47.66	0.19	46.67
06/13/09	164	155	30	12.00	0.10	2.90	0.12	3.48	0.17	5.23
06/14/09	165	370	74	8.71	0.09	6.40	0.16	11.80	0.15	10.80
06/15/09	166	187	35	4.38	0.22	7.86	0.18	6.18	0.17	5.99
06/16/09	167	285	57	6.71	0.03	1.80	0.22	12.40	0.23	13.00
06/17/09	168	183	33	4.13	0.08	2.70	0.09	3.07	0.17	5.59
06/18/09	169	35	6	3.60	0.23	1.37	0.00	0.00	0.00	0.00
06/19/09	170	829	166	19.53	0.03	4.41	0.13	20.83	0.12	20.42
06/20/09	171	105	21	15.75	0.16	3.40	0.30	6.20	0.19	4.00
06/21/09	172	63	9	1.13	0.00	0.00	0.08	0.71	0.06	0.57
06/22/09	173	120	21	2.52	0.03	0.53	0.08	1.75	0.28	5.95
06/23/09	174	218	41	4.92	0.06	2.63	0.19	7.90	0.20	8.09
06/24/09	175	140	27	3.68	0.14	3.86	0.14	3.66	0.28	7.52
06/25/09	176	492	97	10.98	0.07	6.31	0.07	6.90	0.11	10.45
06/26/09	177	211	42	5.60	0.08	3.38	0.12	4.98	0.16	6.57
06/27/09	178	389	75	8.82	0.04	2.70	0.11	8.48	0.26	19.86
06/28/09	179	347	67	8.20	0.06	4.25	0.16	11.01	0.18	11.97
06/29/09	180	513	105	12.60	0.07	7.57	0.16	16.78	0.21	22.31
06/30/09	181	589	115	14.38	0.06	6.64	0.19	22.26	0.18	20.70
07/01/09	182	165	34	4.00	0.08	2.88	0.16	5.56	0.15	4.95
07/02/09	183	319	62	7.29	0.05	2.92	0.12	7.58	0.08	5.05
07/03/09	184	256	47	5.32	0.05	2.20	0.21	9.91	0.18	8.63
07/04/09	185	174	31	3.96	0.07	2.32	0.14	4.45	0.12	3.74
07/05/09	186	355	71	8.04	0.07	5.20	0.22	15.40	0.12	8.60
Table 4. Continued										
07/06/09	187	485	96	11.08	0.06	5.34	0.14	13.86	0.17	16.03
07/08/09	189	297	57	6.45	0.06	3.45	0.09	5.18	0.05	2.69
07/15/09	196	524	106	11.56	0.07	7.48	0.22	23.26	0.22	22.86
Totals	38 nights	39815	7925			547.38		1156.24		1319.75
Means		1048	208.55	37.05	0.09	14.40	0.14	30.43	0.16	34.73

Table 5. Results of marine radar image analyses for data collected on 153 days (i.e., sunrise to sunset the same day) during the 2009 fall migration period (16 July -15 Dec) on Block Island, New Shoreham, Rhode Island. Radar malfunction, power loss and meteorological conditions resulted in data not being analyzed for 7 of the 153 days during the study period. "Total targets detected" are the number of birds/bats detected in all images collected. "Sum of the sample averages" refers to the target count averaged over the five successive images that constitute a sample (i.e., every 10 minutes). These values are summed for the entire night's data collection to generate a passage estimate. "Target detection rate" represents the number of targets detected per nautical mile of passage front per hour. We also present the proportion and number of targets detected within the three lowest altitudinal strata (i.e., 100, 200, 300 m).

Date	Julian day	Total targets detected	Sum of the sample averages	Target detection rate	Proportion of targets <=100 m	Number of targets <=100 m	Proportion of targets 101-200 m	Number of targets 101-200 m	Proportion of targets 201-300 m	Number of targets 201-300 m
07/16/09	197	279	49	3.27	0.1254	6.15	0.2545	12.47	0.1039	5.09
07/17/09	198	1404	284	34.08	0.3739	106.20	0.3063	86.98	0.1339	38.03
07/18/09	199	114	21	2.57	0.1140	2.39	0.1316	2.76	0.0877	1.84
07/19/09	200	515	97	6.61	0.1709	16.57	0.1320	12.81	0.0971	9.42
07/20/09	201	527	100	6.82	0.1575	15.75	0.1992	19.92	0.1252	12.52
07/21/09	202	139	28	15.27	0.1942	5.44	0.0288	0.81	0.1655	4.63
07/22/09	203	284	57	3.94	0.1056	6.02	0.2113	12.04	0.1585	9.03
07/23/09	204	300	59	8.43	0.2633	15.54	0.1567	9.24	0.1100	6.49
07/24/09	205	262	47	3.76	0.0802	3.77	0.1603	7.53	0.0992	4.66
07/25/09	206	530	101	6.97	0.2208	22.30	0.3377	34.11	0.1434	14.48
07/26/09	207	512	99	7.52	0.0586	5.80	0.2598	25.72	0.1621	16.05
07/27/09	208	226	40	2.76	0.0575	2.30	0.1770	7.08	0.1106	4.42
07/28/09	209	1223	242	16.88	0.0989	23.94	0.1872	45.31	0.1251	30.27
07/29/09	210	592	118	8.63	0.1385	16.34	0.1402	16.54	0.1470	17.34
07/30/09	211	362	67	4.90	0.0552	3.70	0.1188	7.96	0.1243	8.33
08/01/09	213	2468	496	34.60	0.1309	64.91	0.1625	80.59	0.1657	82.20
08/02/09	214	1175	239	19.38	0.0783	18.71	0.1438	34.38	0.1387	33.15
08/03/09	215	4771	958	66.84	0.0799	76.50	0.1140	109.23	0.1694	162.24
08/04/09	216	1818	360	25.12	0.2107	75.84	0.1634	58.81	0.1535	55.25
08/05/09	217	351	68	4.74	0.0969	6.59	0.2365	16.08	0.1624	11.04
08/06/09	218	950	190	17.01	0.1042	19.80	0.1768	33.60	0.1284	24.40
08/07/09	219	1415	278	19.62	0.0495	13.75	0.1647	45.78	0.1597	44.40
08/08/09	220	2525	508	36.29	0.0598	30.38	0.1750	88.93	0.1921	97.58
08/09/09	221	1406	277	20.52	0.1181	32.70	0.1600	44.33	0.1472	40.78
08/10/09	222	344	70	4.94	0.0610	4.27	0.1831	12.82	0.2413	16.89
08/11/09	223	3100	618	44.14	0.0432	26.71	0.1003	62.00	0.0987	61.00
08/12/09	224	4056	811	58.63	0.0372	30.19	0.0690	55.99	0.0587	47.59
08/13/09	225	184	37	11.10	0.1902	7.04	0.1250	4.63	0.0380	1.41
08/14/09	226	1102	218	15.57	0.2024	44.11	0.2414	52.62	0.1443	31.45
08/15/09	227	549	108	8.64	0.1457	15.74	0.1730	18.69	0.1548	16.72
08/16/09	228	716	144	10.41	0.0978	14.08	0.1872	26.95	0.1341	19.31
08/17/09	229	1136	227	16.41	0.1408	31.97	0.1461	33.17	0.1303	29.57
08/18/09	230	777	153	11.06	0.0656	10.04	0.1519	23.24	0.1158	17.72
08/19/09	231	502	99	7.24	0.1056	10.45	0.1653	16.37	0.1434	14.20

Table 5. Continued

08/20/09	232	1890	373	27.29	0.1910	71.24	0.1429	53.29	0.1418	52.89
08/21/09	233	1144	230	17.04	0.0367	8.44	0.1101	25.33	0.1075	24.73
08/22/09	234	516	100	7.50	0.0543	5.43	0.2384	23.84	0.2054	20.54
08/23/09	235	1660	333	24.67	0.0620	20.66	0.0873	29.09	0.0934	31.09
08/24/09	236	2162	432	31.61	0.0934	40.36	0.1610	69.54	0.1785	77.13
08/25/09	237	7344	1469	110.18	0.0556	81.61	0.1661	244.03	0.2394	351.65
08/26/09	238	1277	254	19.29	0.0360	9.15	0.0744	18.90	0.0681	17.30
08/27/09	239	3711	739	55.43	0.0318	23.50	0.0787	58.15	0.1692	125.06
08/28/09	240	733	148	24.67	0.1473	21.81	0.2374	35.13	0.2101	31.09
08/29/09	241	82	16	4.57	0.6098	9.76	0.0244	0.39	0.0000	0.00
08/30/09	242	634	125	13.16	0.0820	10.25	0.0852	10.65	0.1088	13.60
08/31/09	243	1047	208	18.91	0.0220	4.57	0.0879	18.28	0.0802	16.69
09/01/09	244	777	155	11.77	0.0579	8.98	0.1789	27.73	0.2625	40.69
09/02/09	245	488	99	7.62	0.2049	20.29	0.1844	18.26	0.1537	15.22
09/03/09	246	294	57	4.38	0.0816	4.65	0.2959	16.87	0.2177	12.41
09/04/09	247	3623	728	56.00	0.0171	12.46	0.1366	99.46	0.2236	162.76
09/05/09	248	7197	1437	110.54	0.1280	183.89	0.1620	232.81	0.1502	215.84
09/06/09	249	3320	662	51.58	0.0428	28.31	0.0720	47.66	0.0807	53.44
09/07/09	250	1191	236	18.39	0.1898	44.78	0.2057	48.55	0.2435	57.46
09/08/09	251	815	163	12.70	0.1448	23.60	0.2098	34.20	0.2650	43.20
09/09/09	252	725	140	10.91	0.2359	33.02	0.0814	11.39	0.1062	14.87
09/10/09	253	218	40	3.16	0.1881	7.52	0.1560	6.24	0.1009	4.04
09/11/09	254	47	9	4.91	0.4894	4.40	0.0000	0.00	0.0000	0.00
09/12/09	255	126	22	2.81	0.0397	0.87	0.1508	3.32	0.0714	1.57
09/13/09	256	690	138	11.66	0.1014	14.00	0.1942	26.80	0.1565	21.60
09/14/09	257	9543	1904	152.32	0.0725	138.07	0.0906	172.58	0.1293	246.21
09/15/09	258	4278	862	68.96	0.0622	53.60	0.0856	73.75	0.1206	103.97
09/16/09	259	2231	445	41.08	0.1443	64.23	0.1268	56.45	0.1954	86.97
09/17/09	260	275	53	4.30	0.1745	9.25	0.2182	11.56	0.0909	4.82
09/18/09	261	300	56	5.09	0.0800	4.48	0.1933	10.83	0.1600	8.96
09/19/09	262	756	152	12.49	0.0450	6.84	0.1164	17.69	0.1521	23.12
09/20/09	263	2061	414	33.57	0.0529	21.90	0.0932	38.57	0.1334	55.24
09/21/09	264	2052	407	33.00	0.0785	31.93	0.1096	44.63	0.1423	57.92
09/22/09	265	486	93	7.64	0.0802	7.46	0.1420	13.20	0.1379	12.82
09/23/09	266	315	61	5.23	0.0889	5.42	0.1079	6.58	0.1397	8.52
09/24/09	267	4636	929	76.36	0.0218	20.24	0.0567	52.70	0.1342	124.64
09/25/09	268	8312	1666	136.93	0.0381	63.54	0.0691	115.05	0.1207	201.03
09/26/09	269	767	152	12.67	0.0782	11.89	0.2008	30.52	0.1760	26.75
09/27/09	270	24	5	5.00	0.6667	3.33	0.0000	0.00	0.0833	0.42
09/28/09	271	662	134	11.32	0.0498	6.68	0.1042	13.97	0.1088	14.57
09/29/09	272	303	56	4.73	0.0363	2.03	0.1155	6.47	0.1089	6.10
09/30/09	273	383	73	6.35	0.0679	4.96	0.1645	12.01	0.1149	8.39
10/01/09	274	246	48	5.24	0.1098	5.27	0.1504	7.22	0.2561	12.29
10/02/09	275	330	62	5.47	0.2061	12.78	0.1000	6.20	0.1545	9.58
10/03/09	276	35	7	3.82	0.4571	3.20	0.0000	0.00	0.2000	1.40

Table 5. Continued

10/04/09	277	1220	226	33.90	0.0172	3.89	0.0910	20.56	0.0566	12.78
10/05/09	278	2487	498	42.69	0.0201	10.01	0.0133	6.61	0.0692	34.44
10/06/09	279	1148	231	20.09	0.0209	4.83	0.0235	5.43	0.0671	15.49
10/07/09	280	186	37	17.08	0.0430	1.59	0.3548	13.13	0.0753	2.78
10/08/09	281	142	4	2.67	0.0282	0.11	0.0704	0.28	0.0352	0.14
10/09/09	282	431	86	24.57	0.1508	12.97	0.1462	12.57	0.2065	17.76
10/10/09	283	618	121	11.71	0.0178	2.15	0.0437	5.29	0.1472	17.82
10/11/09	284	719	142	12.72	0.1001	14.22	0.1001	14.22	0.2017	28.64
10/12/09	285	619	121	10.84	0.1309	15.83	0.2132	25.80	0.2601	31.47
10/13/09	286	165	32	3.05	0.2000	6.40	0.2485	7.95	0.1455	4.65
10/14/09	287	543	109	9.76	0.1289	14.05	0.1805	19.67	0.2284	24.89
10/15/09	288	112	22	5.74	0.1786	3.93	0.1786	3.93	0.2500	5.50
10/16/09	289	152	28	3.50	0.1250	3.50	0.1513	4.24	0.1250	3.50
10/17/09	290	230	45	4.09	0.1261	5.67	0.2783	12.52	0.1696	7.63
10/19/09	292	514	102	9.42	0.1226	12.50	0.2257	23.02	0.1907	19.45
10/20/09	293	445	84	9.69	0.0719	6.04	0.1169	9.82	0.1708	14.35
10/21/09	294	4748	950	87.69	0.0278	26.41	0.0482	45.82	0.1666	158.27
10/22/09	295	441	82	7.57	0.1202	9.85	0.1270	10.41	0.1587	13.02
10/23/09	296	10	2	6.00	0.0000	0.00	0.0000	0.00	0.0000	0.00
10/24/09	297	91	15	1.80	0.1648	2.47	0.1209	1.81	0.3187	4.78
10/25/09	298	413	81	7.59	0.2155	17.46	0.1356	10.98	0.2155	17.46
10/26/09	299	613	127	12.10	0.1485	18.85	0.2382	30.25	0.2382	30.25
10/27/09	300	116	21	3.60	0.3276	6.88	0.1810	3.80	0.2241	4.71
10/28/09	301	19	2	0.71	0.6842	1.37	0.0000	0.00	0.0000	0.00
10/29/09	302	280	53	5.13	0.1964	10.41	0.1893	10.03	0.3536	18.74
10/30/09	303	452	89	8.61	0.1350	12.01	0.2412	21.46	0.2942	26.19
10/31/09	304	116	22	2.16	0.0603	1.33	0.3276	7.21	0.3534	7.78
11/01/09	305	169	29	3.22	0.1893	5.49	0.2840	8.24	0.0888	2.57
11/02/09	306	248	49	13.36	0.0968	4.74	0.1169	5.73	0.0766	3.75
11/03/09	307	251	47	4.62	0.0757	3.56	0.1633	7.68	0.1633	7.68
11/04/09	308	247	47	6.00	0.1903	8.94	0.1903	8.94	0.2389	11.23
11/05/09	309	430	89	11.87	0.1488	13.25	0.1628	14.49	0.0791	7.04
11/06/09	310	994	196	19.28	0.0644	12.62	0.1700	33.32	0.3099	60.73
11/07/09	311	565	108	10.62	0.2673	28.86	0.1416	15.29	0.2018	21.79
11/08/09	312	206	38	3.74	0.0631	2.40	0.1650	6.27	0.1117	4.24
11/09/09	313	251	47	4.70	0.1315	6.18	0.1992	9.36	0.1633	7.68
11/10/09	314	258	49	4.90	0.0930	4.56	0.1085	5.32	0.1008	4.94
11/11/09	315	659	129	12.90	0.4325	55.79	0.1912	24.66	0.0819	10.57
11/12/09	316	240	46	4.68	0.3292	15.14	0.1208	5.56	0.0833	3.83
11/13/09	317	57	11	6.00	0.0351	0.39	0.0877	0.96	0.0877	0.96
11/14/09	318	46	9	3.38	0.0000	0.00	0.2391	2.15	0.2391	2.15
11/15/09	319	86	13	1.39	0.0698	0.91	0.2558	3.33	0.0000	0.00
11/16/09	320	199	38	3.93	0.0653	2.48	0.1558	5.92	0.0754	2.86
11/17/09	321	357	70	7.24	0.1793	12.55	0.2101	14.71	0.2381	16.67
11/18/09	322	392	75	7.76	0.2398	17.98	0.2398	17.98	0.1327	9.95

Table 5. Continued

11/19/09	323	122	20	2.45	0.2869	5.74	0.2377	4.75	0.0738	1.48
11/20/09	324	73	12	1.50	0.0959	1.15	0.2877	3.45	0.0822	0.99
11/21/09	325	99	20	2.07	0.0606	1.21	0.2626	5.25	0.1414	2.83
11/22/09	326	181	37	3.83	0.2928	10.83	0.2818	10.43	0.1713	6.34
11/23/09	327	80	15	6.43	0.4750	7.13	0.1750	2.63	0.1750	2.63
11/24/09	328	86	14	1.47	0.2093	2.93	0.3605	5.05	0.0698	0.98
11/25/09	329	63	12	1.80	0.1270	1.52	0.0952	1.14	0.1905	2.29
11/26/09	330	145	24	2.53	0.1931	4.63	0.4828	11.59	0.1379	3.31
11/27/09	331	16	3	6.00	0.6875	2.06	0.3125	0.94	0.0000	0.00
11/28/09	332	60	7	0.74	0.0333	0.23	0.5333	3.73	0.1167	0.82
11/29/09	333	72	10	1.07	0.0000	0.00	0.4028	4.03	0.1111	1.11
11/30/09	334	19	4	0.71	0.2632	1.05	0.1579	0.63	0.0000	0.00
12/01/09	335	750	146	19.91	0.0187	2.73	0.2147	31.34	0.3067	44.77
12/02/09	336	120	20	2.40	0.1417	2.83	0.2667	5.33	0.0417	0.83
12/04/09	338	51	11	1.94	0.1569	1.73	0.3922	4.31	0.2157	2.37
12/09/09	343	40	8	2.67	0.5000	4.00	0.1000	0.80	0.0000	0.00
12/10/09	344	79	13	1.42	0.0000	0.00	0.3671	4.77	0.1392	1.81
12/11/09	345	87	11	1.20	0.0000	0.00	0.2414	2.66	0.2989	3.29
12/12/09	346	334	66	7.20	0.0329	2.17	0.3772	24.90	0.2335	15.41
12/13/09	347	47	9	1.59	0.1277	1.15	0.2979	2.68	0.1277	1.15
12/14/09	348	195	37	4.04	0.1077	3.98	0.3846	14.23	0.2000	7.40
12/15/09	349	38	3	0.33	0.1316	0.39	0.2632	0.79	0.0263	0.08
Totals	146 days	141762	28084			2435		3632		4209
Means		970.97	192.36	16.60	0.14	16.68	0.17	24.87	0.14	28.83

Table 6. Results of marine radar image analyses for data collected on 153 nights (i.e., sunset to sunrise the following morning) during the 2009 fall migration period (16 July -15 Dec) on Block Island, New Shoreham, Rhode Island. Radar malfunction, power loss and meteorological conditions resulted in data not being analyzed for 6 of the 153 nights during the study period. "Total targets detected" are the number of birds/bats detected in all images collected. "Sum of the sample averages" refers to the target count averaged over the five successive images that constitute a sample (i.e., every 10 minutes). These values are summed for the entire night's data collection to generate a passage estimate. "Target detection rate" represents the number of targets detected per nautical mile of passage front per hour. We also present the proportion and number of targets detected within the three lowest altitudinal strata (i.e., 100, 200, 300 m).

Date	Julian day	Total targets detected	Sum of the sample averages	Target detection rate	Proportion of targets <=100 m	Number of targets <=100 m	Proportion of targets 101-200 m	Number of targets 101-200 m	Proportion of targets 201-300 m	Number of targets 201-300 m
07/16/09	197	1198	242	29.04	0.13	30.70	0.24	59.19	0.16	38.38
07/17/09	198	1187	253	34.34	0.07	17.05	0.11	27.50	0.14	36.23
07/18/09	199	1526	305	33.27	0.02	7.20	0.14	43.37	0.21	62.56
07/19/09	200	2433	484	52.80	0.03	15.52	0.12	57.69	0.15	71.42
07/20/09	201	955	191	38.20	0.05	9.00	0.11	21.80	0.12	23.40
07/21/09	202	133	26	3.92	0.07	1.76	0.14	3.52	0.16	4.11
07/22/09	203	1808	364	39.71	0.05	17.31	0.15	56.17	0.13	47.11
07/23/09	204	256	51	25.50	0.51	25.90	0.02	0.80	0.43	21.91
07/24/09	205	588	122	14.94	0.07	8.51	0.10	11.62	0.12	14.32
07/25/09	206	650	130	13.93	0.06	7.40	0.25	32.00	0.17	22.40
07/26/09	207	466	95	10.18	0.04	3.47	0.16	15.29	0.11	9.99
07/27/09	208	728	145	15.26	0.04	5.98	0.14	19.92	0.16	23.10
07/28/09	209	858	175	18.75	0.11	19.58	0.14	24.88	0.13	22.64
07/29/09	210	541	108	12.96	0.04	4.19	0.11	11.58	0.13	14.17
07/30/09	211	1156	231	24.32	0.05	12.59	0.11	25.58	0.14	33.37
07/31/09	212	1635	327	57.71	0.01	3.60	0.03	11.40	0.11	34.60
08/01/09	213	3612	721	75.89	0.03	18.56	0.09	67.47	0.12	87.23
08/02/09	214	964	191	19.76	0.03	5.35	0.10	18.82	0.09	17.83
08/03/09	215	2225	446	46.14	0.05	20.25	0.12	52.92	0.17	74.37
08/04/09	216	722	144	14.90	0.05	7.38	0.17	24.33	0.19	26.93
08/05/09	217	17721	3542	360.20	0.02	55.17	0.03	110.13	0.08	279.03
08/06/09	218	6730	1343	134.30	0.04	47.69	0.07	97.58	0.11	143.28
08/07/09	219	14499	2897	294.61	0.02	52.95	0.04	122.48	0.11	314.90
08/08/09	220	6868	1373	137.30	0.04	48.98	0.10	137.54	0.12	158.33
08/09/09	221	2553	507	56.33	0.11	55.01	0.20	101.48	0.17	88.17
08/10/09	222	2421	486	48.60	0.02	11.64	0.12	57.41	0.19	90.13
08/11/09	223	16953	3391	339.10	0.05	172.42	0.12	415.45	0.17	592.67
08/12/09	224	990	197	168.86	0.06	12.54	0.04	7.16	0.08	14.92
08/13/09	225	3887	782	93.84	0.02	15.69	0.06	43.05	0.07	53.92
08/14/09	226	2439	489	48.90	0.04	19.25	0.09	44.91	0.11	53.13
08/15/09	227	2378	476	46.82	0.02	11.61	0.12	56.25	0.13	60.65
08/16/09	228	3616	723	71.11	0.02	16.80	0.10	70.18	0.14	99.97
08/17/09	229	4820	965	94.92	0.04	40.44	0.14	134.94	0.19	185.19
08/18/09	230	2968	594	57.48	0.05	30.82	0.16	93.66	0.16	95.66
08/19/09	231	7854	1568	151.74	0.05	73.07	0.11	176.88	0.13	199.24

Table 6. Continued

08/20/09	232	5347	1069	103.45	0.05	56.58	0.10	106.36	0.11	119.56
08/21/09	233	1198	244	23.61	0.06	14.46	0.16	39.72	0.24	58.66
08/22/09	234	7993	1600	195.92	0.02	28.42	0.04	59.45	0.05	87.88
08/23/09	235	10112	2024	192.76	0.03	54.04	0.08	158.53	0.11	230.58
08/24/09	236	26147	5232	490.50	0.03	163.48	0.07	369.18	0.10	537.87
08/25/09	237	11874	2376	222.75	0.03	67.83	0.10	246.32	0.12	294.75
08/26/09	238	13605	2720	286.32	0.06	165.54	0.13	351.47	0.13	355.67
08/27/09	239	23463	4691	439.78	0.04	175.34	0.08	395.47	0.11	499.43
08/28/09	240	701	129	154.80	0.24	30.92	0.21	27.05	0.13	16.93
08/29/09	241	3417	680	72.86	0.06	40.00	0.13	87.56	0.08	56.52
08/30/09	242	3266	656	60.55	0.06	36.76	0.14	92.60	0.16	102.84
08/31/09	243	6856	1378	127.20	0.04	54.47	0.09	121.60	0.10	137.48
09/01/09	244	2602	522	48.18	0.09	46.14	0.20	102.71	0.17	88.87
09/02/09	245	1706	340	30.91	0.08	25.51	0.17	58.59	0.14	48.63
09/03/09	246	1500	302	27.45	0.06	19.13	0.14	40.87	0.10	31.41
09/04/09	247	4291	858	78.00	0.05	42.59	0.10	89.58	0.12	102.98
09/05/09	248	7426	1493	135.73	0.03	49.86	0.06	85.65	0.09	134.10
09/06/09	249	2204	440	39.40	0.08	33.14	0.17	74.07	0.16	70.07
09/07/09	250	2358	471	42.18	0.08	38.35	0.21	96.68	0.15	72.71
09/08/09	251	2285	458	46.58	0.14	63.54	0.21	96.01	0.18	82.38
09/09/09	252	1632	327	28.85	0.05	15.03	0.08	24.65	0.12	40.07
09/10/09	253	466	93	9.00	0.04	3.59	0.14	12.57	0.11	10.38
09/11/09	254	142	25	2.73	0.03	0.70	0.10	2.46	0.07	1.76
09/12/09	255	3007	601	68.04	0.02	13.99	0.04	23.18	0.05	31.58
09/13/09	256	4697	936	81.39	0.06	54.40	0.09	83.90	0.10	90.47
09/14/09	257	3466	694	60.35	0.10	71.28	0.19	135.16	0.18	124.74
09/15/09	258	2867	571	77.86	0.09	53.57	0.18	99.98	0.16	92.41
09/16/09	259	2567	515	44.14	0.03	16.85	0.06	31.10	0.10	49.75
09/17/09	260	2091	419	35.91	0.06	26.05	0.12	50.10	0.16	65.53
09/18/09	261	2034	409	35.06	0.04	17.29	0.09	34.79	0.12	49.26
09/19/09	262	3322	662	56.74	0.07	49.22	0.16	104.82	0.16	107.61
09/20/09	263	1644	328	28.11	0.07	21.55	0.11	37.11	0.14	46.29
09/21/09	264	2188	438	37.54	0.04	16.82	0.16	69.86	0.18	78.27
09/22/09	265	2025	402	33.97	0.07	28.98	0.12	46.25	0.16	63.13
09/23/09	266	3395	677	60.63	0.04	24.73	0.08	53.44	0.08	57.43
09/24/09	267	23323	4668	394.48	0.05	249.58	0.11	518.98	0.13	610.04
09/25/09	268	7956	1591	132.58	0.04	61.99	0.08	123.58	0.10	160.98
09/26/09	269	3621	723	71.11	0.02	16.97	0.08	60.50	0.13	90.65
09/27/09	270	1505	306	25.15	0.04	12.00	0.09	26.03	0.06	17.89
09/28/09	271	1926	383	62.11	0.04	15.71	0.09	35.99	0.19	71.19
09/29/09	272	1155	231	18.99	0.04	10.20	0.13	30.80	0.10	22.80
09/30/09	273	6120	1222	99.08	0.03	36.94	0.09	116.01	0.13	156.14
10/01/09	274	1432	287	30.21	0.09	25.45	0.18	51.91	0.15	42.49
10/02/09	275	715	144	15.71	0.06	9.06	0.32	45.92	0.27	39.27
10/03/09	276	1880	376	31.77	0.11	41.80	0.15	56.80	0.12	46.60

Table 6. Continued

10/04/09	277	5091	1022	82.86	0.05	48.18	0.11	113.82	0.16	159.79
10/05/09	278	2997	599	48.57	0.05	29.98	0.11	64.76	0.11	68.75
10/06/09	279	1676	335	37.92	0.09	29.78	0.18	60.16	0.15	48.77
10/07/09	280	1401	280	22.11	0.06	17.39	0.11	30.78	0.13	36.57
10/08/09	281	20107	4016	330.08	0.09	345.54	0.16	629.75	0.18	739.01
10/09/09	282	4852	970	66.14	0.12	118.15	0.18	177.13	0.24	236.30
10/10/09	283	10820	2165	168.70	0.07	148.67	0.13	277.13	0.15	324.95
10/11/09	284	2175	436	33.97	0.04	17.44	0.09	40.49	0.16	67.76
10/12/09	285	2351	470	40.29	0.08	39.78	0.13	60.17	0.17	82.17
10/13/09	286	4274	860	67.89	0.02	16.50	0.05	39.84	0.08	65.19
10/14/09	287	5584	1112	86.65	0.06	70.69	0.12	136.41	0.14	154.53
10/16/09	289	2911	584	44.92	0.03	15.05	0.05	27.48	0.11	66.20
10/17/09	290	3031	606	84.56	0.03	15.79	0.06	33.79	0.13	77.37
10/18/09	291	172	36	4.41	0.09	3.14	0.21	7.53	0.08	2.72
10/19/09	292	7864	1571	119.32	0.09	136.24	0.10	161.42	0.09	147.63
10/20/09	293	2174	434	32.96	0.11	47.91	0.13	55.50	0.14	59.69
10/21/09	294	2271	455	34.56	0.07	33.46	0.12	53.29	0.16	73.93
10/22/09	295	1504	301	32.84	0.06	17.81	0.08	24.82	0.18	52.84
10/23/09	296	1033	202	22.44	0.10	19.75	0.27	54.75	0.26	53.19
10/24/09	297	512	105	12.60	0.10	10.25	0.05	5.33	0.13	14.15
10/25/09	298	5939	1187	89.03	0.06	75.15	0.08	94.54	0.11	127.31
10/26/09	299	2845	567	42.00	0.04	24.91	0.10	59.19	0.13	73.94
10/27/09	300	177	35	8.40	0.10	3.56	0.01	0.40	0.27	9.49
10/28/09	301	339	68	7.03	0.07	4.61	0.08	5.62	0.14	9.63
10/29/09	302	4943	986	74.89	0.03	30.12	0.04	35.31	0.06	59.04
10/30/09	303	303	58	4.64	0.07	3.83	0.09	4.98	0.21	12.06
10/31/09	304	148	28	3.91	0.16	4.54	0.05	1.51	0.13	3.59
11/01/09	305	3823	762	57.87	0.04	33.69	0.09	72.15	0.12	92.68
11/02/09	306	1094	220	16.10	0.08	18.10	0.12	26.34	0.17	38.41
11/03/09	307	242	44	3.26	0.14	6.18	0.14	6.18	0.16	6.91
11/04/09	308	866	173	18.54	0.17	28.97	0.17	29.57	0.17	29.77
11/05/09	309	486	96	13.09	0.12	11.46	0.13	12.64	0.20	19.36
11/06/09	310	2364	471	34.05	0.06	28.69	0.11	52.40	0.11	52.20
11/07/09	311	247	46	3.33	0.11	4.84	0.17	7.82	0.12	5.59
11/08/09	312	1806	359	25.64	0.03	11.73	0.07	26.84	0.13	45.32
11/09/09	313	399	76	5.43	0.05	3.62	0.07	4.95	0.18	13.52
11/10/09	314	1821	363	26.56	0.05	17.54	0.07	26.31	0.17	62.00
11/11/09	315	815	166	11.86	0.04	5.91	0.10	15.89	0.22	36.87
11/12/09	316	332	58	4.09	0.04	2.45	0.10	5.94	0.17	9.61
11/14/09	318	131	23	1.97	0.14	3.16	0.07	1.58	0.05	1.05
11/15/09	319	1656	329	23.22	0.07	22.85	0.08	25.63	0.11	35.16
11/16/09	320	1321	262	18.28	0.02	6.35	0.08	20.63	0.12	31.54
11/17/09	321	503	97	6.77	0.05	4.82	0.17	16.20	0.22	21.02
11/18/09	322	272	49	3.42	0.07	3.60	0.12	5.76	0.15	7.21
11/19/09	323	2057	408	36.00	0.03	13.29	0.08	33.52	0.14	58.51

Table 6. Continued

11/20/09	324	188	35	2.44	0.03	1.12	0.18	6.14	0.13	4.47
11/21/09	325	310	55	3.84	0.03	1.77	0.14	7.63	0.14	7.63
11/22/09	326	180	33	2.36	0.03	0.92	0.01	0.37	0.13	4.22
11/23/09	327	21	3	1.29	0.05	0.14	0.00	0.00	0.00	0.00
11/24/09	328	101	18	1.26	0.08	1.43	0.08	1.43	0.10	1.78
11/25/09	329	221	41	3.97	0.20	8.35	0.37	15.03	0.12	5.01
11/26/09	330	215	35	2.26	0.17	5.86	0.36	12.70	0.12	4.23
11/27/09	331	378	75	8.04	0.13	9.72	0.74	55.36	0.04	3.37
11/28/09	332	180	28	1.91	0.13	3.58	0.28	7.78	0.13	3.73
11/29/09	333	106	18	1.23	0.06	1.02	0.16	2.89	0.07	1.19
11/30/09	334	251	47	4.78	0.06	2.81	0.13	5.99	0.12	5.80
12/01/09	335	190	34	2.96	0.21	7.16	0.17	5.73	0.19	6.44
12/02/09	336	41	7	2.80	0.02	0.17	0.20	1.37	0.22	1.54
12/04/09	338	210	39	3.21	0.13	5.20	0.22	8.54	0.14	5.39
12/08/09	342	237	45	4.66	0.04	1.71	0.13	5.70	0.17	7.59
12/09/09	343	278	54	3.86	0.03	1.55	0.12	6.22	0.03	1.36
12/10/09	344	157	25	1.69	0.04	0.96	0.27	6.85	0.27	6.85
12/11/09	345	123	19	1.28	0.02	0.31	0.42	8.03	0.28	5.41
12/12/09	346	126	20	1.35	0.06	1.27	0.20	3.97	0.25	5.08
12/13/09	347	85	13	1.37	0.09	1.22	0.09	1.22	0.02	0.31
12/14/09	348	3200	638	45.57	0.00	0.00	0.00	0.00	0.00	0.00
12/15/09	349	1625	319	22.52	0.01	3.53	0.04	12.17	0.05	16.10
Totals	147 nights	470017	93886			4620.50		9651.66		11902.14
Means		3197.39	638.68	61.79	0.07	31.43	0.13	65.66	0.14	80.97

Table 7. Results from General Linear Model procedures investigating relationships between the proportion of targets detected in the two lowest altitudinal strata (i.e., 0-100, 101-200 m arcsine transformed) and total targets detected in all strata (i.e., sum of the 10-minute sample averages, log transformed).

Season		0-100			101-200		
	Period	Coefficient	*F*	*P*	Coefficient	*F*	*P*
Spring							
	Day	-0.036	0.48	0.49	-0.137	14.4	<0.0001
	Night	-0.183	45.95	<0.0001	0.006	0.04	0.85
Summer							
	Day	-0.037	0.67	0.42	0.067	2.21	0.15
	Night	-0.073	5.65	0.02	0.07	5.67	0.02
Fall							
	Day	-0.0001	8.92	0.003	-0.0001	8.42	0.004
	Night	-0.045	15.56	<0.0001	-0.04	6.71	0.01

Figure 1. Dual radar system with horizontally and vertically oriented antennas that operate simultaneously. This system allows for data collection on passage (horizontal and vertical), altitude (vertical) and flight direction (horizontal).

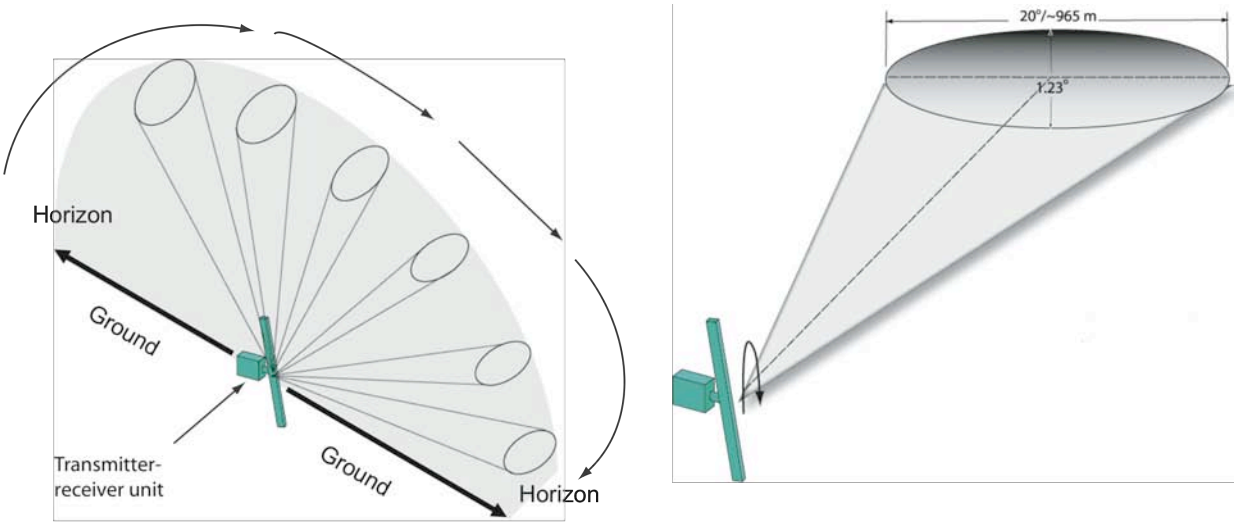

Figure 2. Graphical depiction of scanning operation of vertically-oriented radar. In this orientation, the transmitter-receiver unit is mounted perpendicular to the ground so that the radar antenna's rotation results in a 180^{o}, horizon-to-horizon scan (radar does not transmit when antenna is oriented groundward). When the radar's range is set to 0.75 nm (1.4 km, 4557 ft) it samples ~0.98 km3 of air space. Data collected in "vertical" scanning mode can be used to estimate (1) target altitude and (2) target passage magnitude.

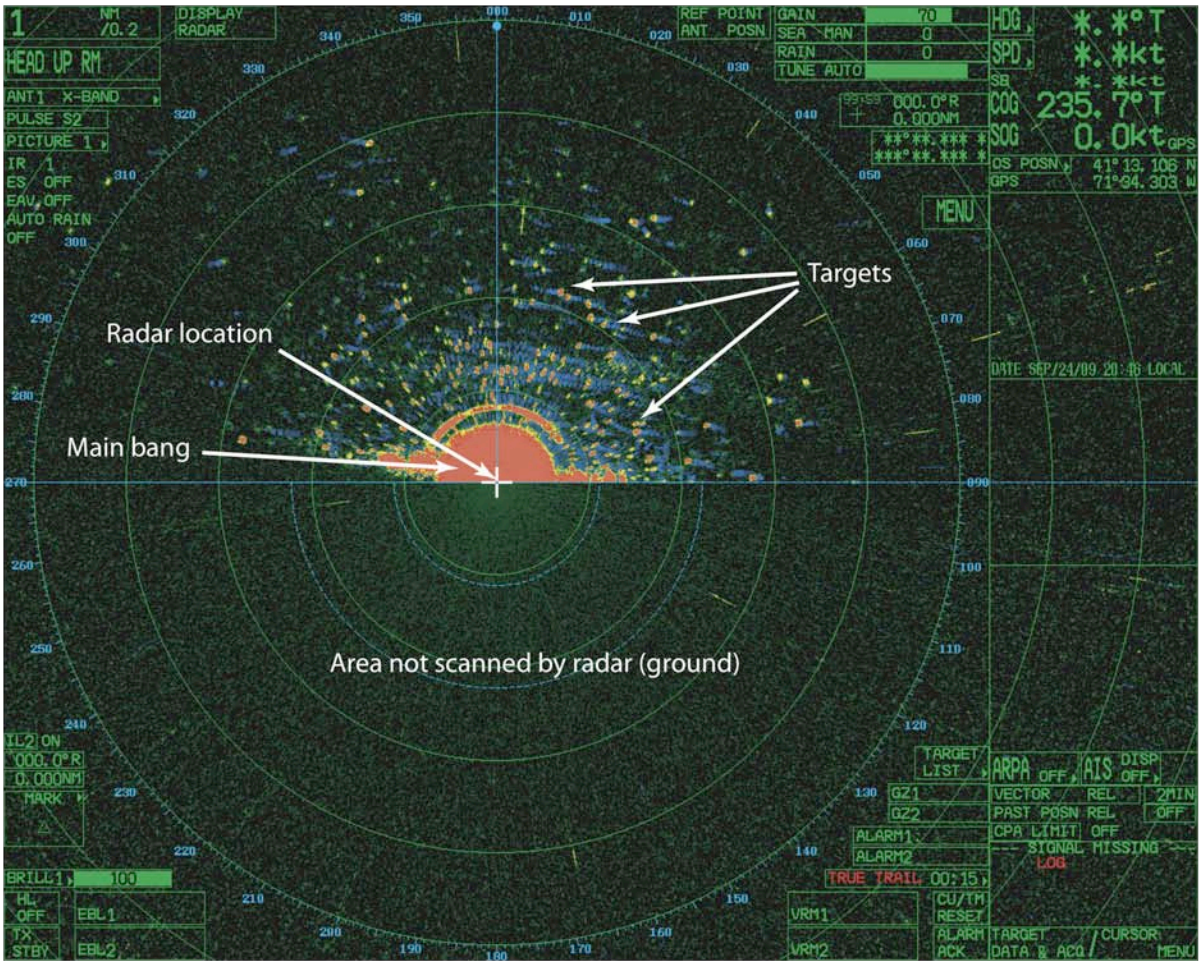

Figure. 3. Data image from the "vertical" radar collected on 8 October 2009 at 2133 EDT (9:33 PM). The small red ellipses with the blue tails are bird or bats flying through the radar's sample space. The height above the blue dotted line splitting the image indicates each target's altitude. The large, circular red area in the center of the image is the "main bang" an area of interference generated by an inherent to marine radars. Note that the radar in the vertical orientation does not transmit or receive electromagnetic energy when the antenna scans toward the ground so no targets are shown below the blue dotted line.

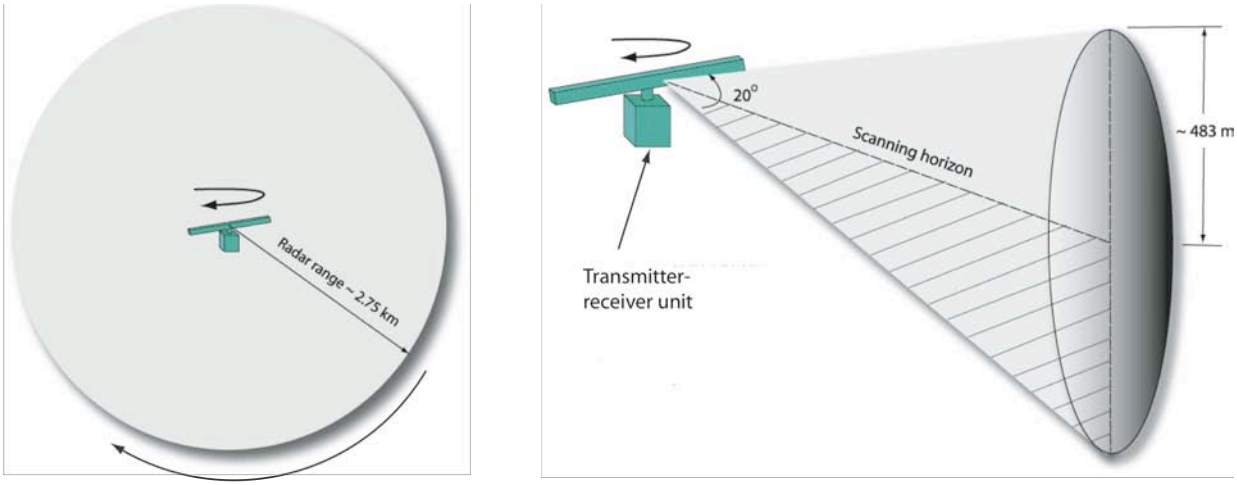

Figure 4. Graphic representation of scanning operation of horizontally-oriented radar. In this orientation, the antenna rotates in a plane parallel to the ground resulting in a 360^{o} scan with a that samples 10^{o} above and below the scanning horizon. With the radar's range set to 1 nautical mile (1.85 km, 6076 ft) which is the effective detection range for small passerines with 25 kW radar) it samples up to 483 m arl (above radar level) and ~4.0 km3 of air space. Data collected in "horizontal" scanning mode can be used to estimate (1) target flight direction and speed and (2) target passage magnitude.

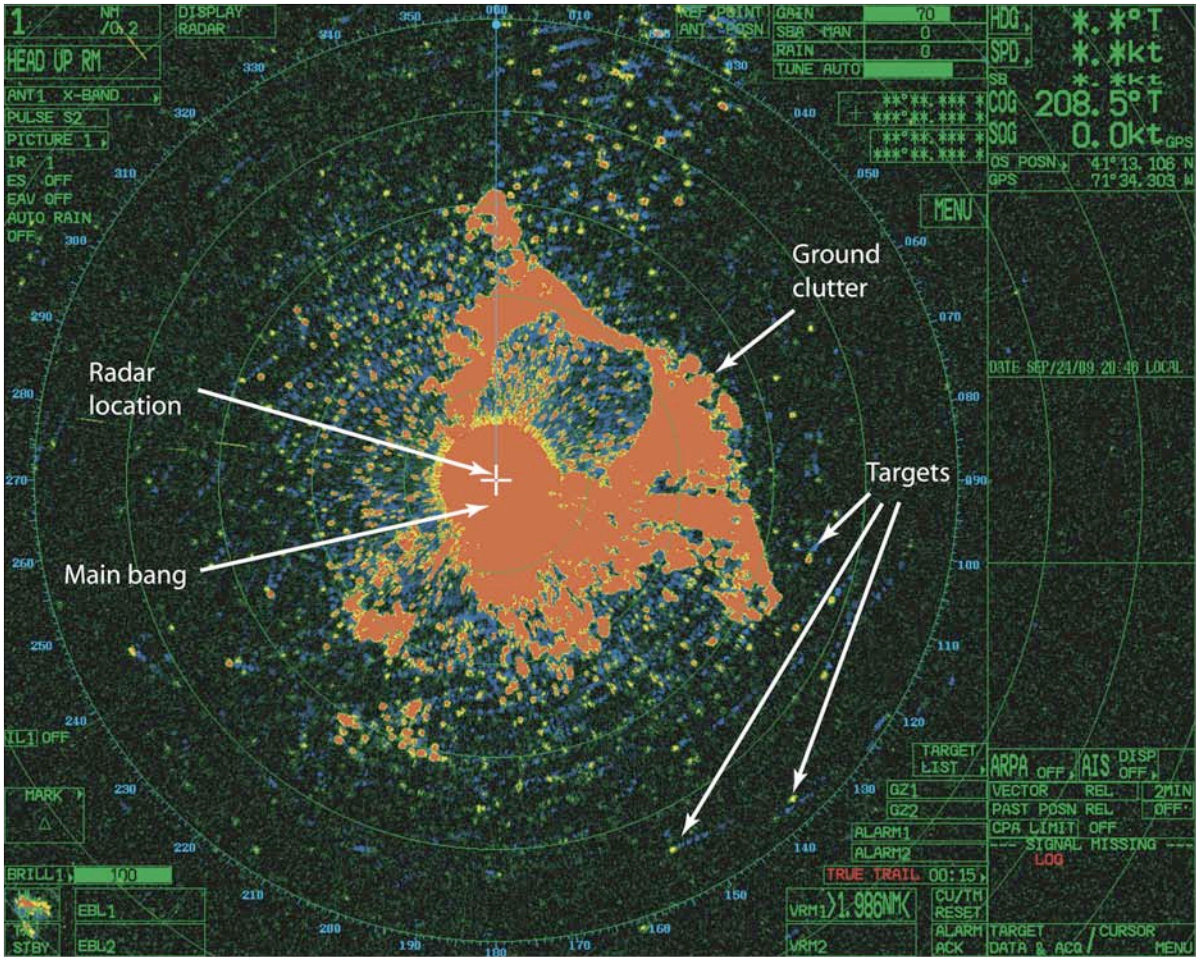

Figure 5. Data image from the "horizontal" radar collected on 8 October 2009 at 2133 EDT (9:33 PM). The small red ellipses with the blue trails are bird or bats flying through the radar's sample space. A blue trail shows the 15 second track history of its associated target, so represents its general flight direction. The large, cirucular red area in the center of the image is the "main bang" an area of interference or "ground clutter" generated by an inherent to marine radars. The large, irregularly-shaped areas primarily to the east of radar's location is electromagnetic energy being reflected from the surrounding landform.

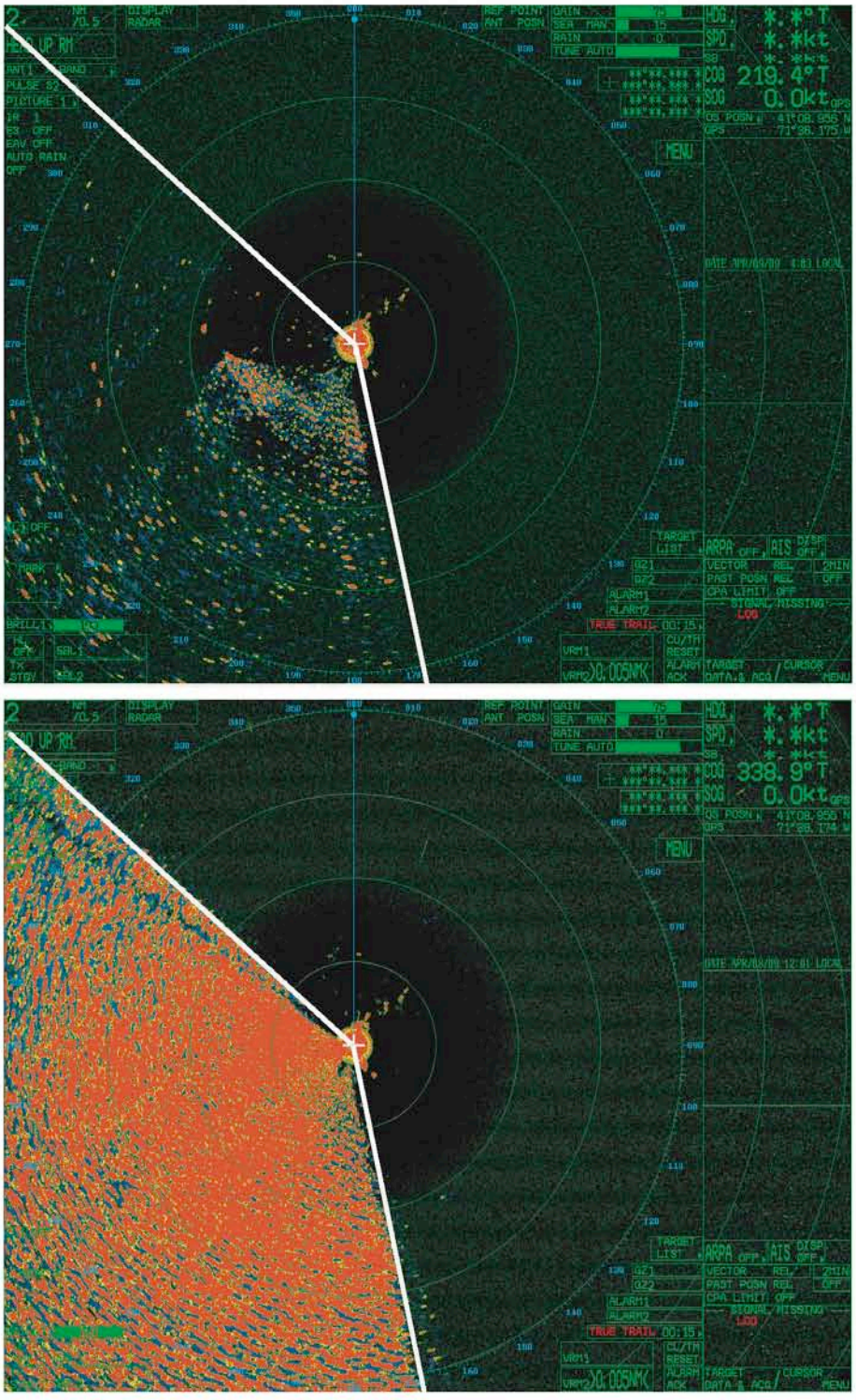

Figure 6. Images from horizontal radar showing backscatter of radar energy from wave action along the southeastern coast of Block Island. Upper panel show normal extent of backscatter. Lower panel shows extreme incidence of backscatter. White lines describe the radar's view of the ocean. View of the ocean from approximately 90-170° (i.e., E - S) was occluded by a rise along the edge of the landform. Areas from approximately 305-90° (NW-E) were over land so did not experience backscatter.

Figure 7. Radar unit with parabollic dish antenna. Custom mounting allow the antenna to be raised or lowered in 2.5° increments above the scanning horizon.

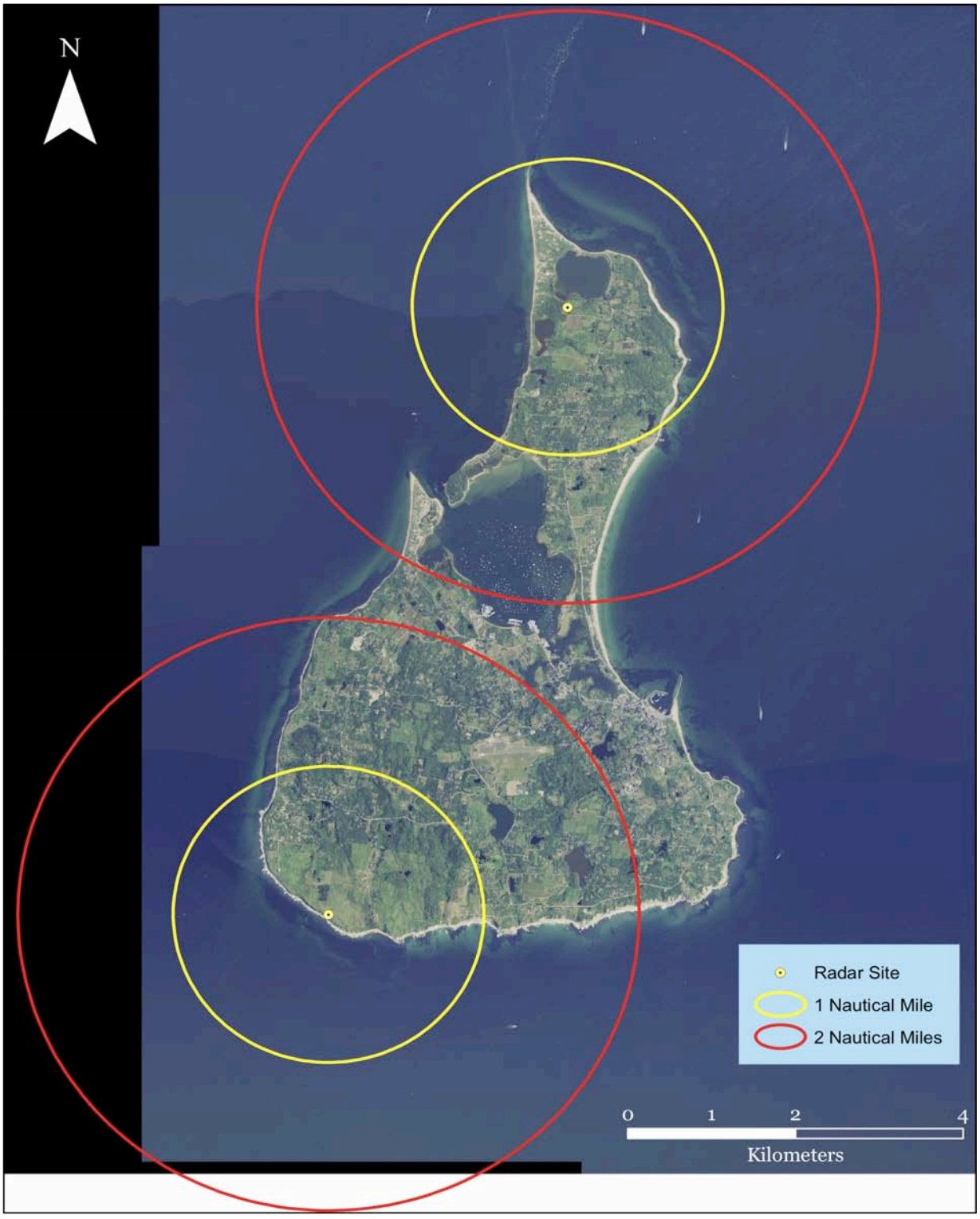

Figure 8. Radar study sites on Block Island, 2009. Study site along southeastern coast of the island was used from 19 March - 30 April. The radar system was located at the northern site 1 May - 15 December. Vertical radar

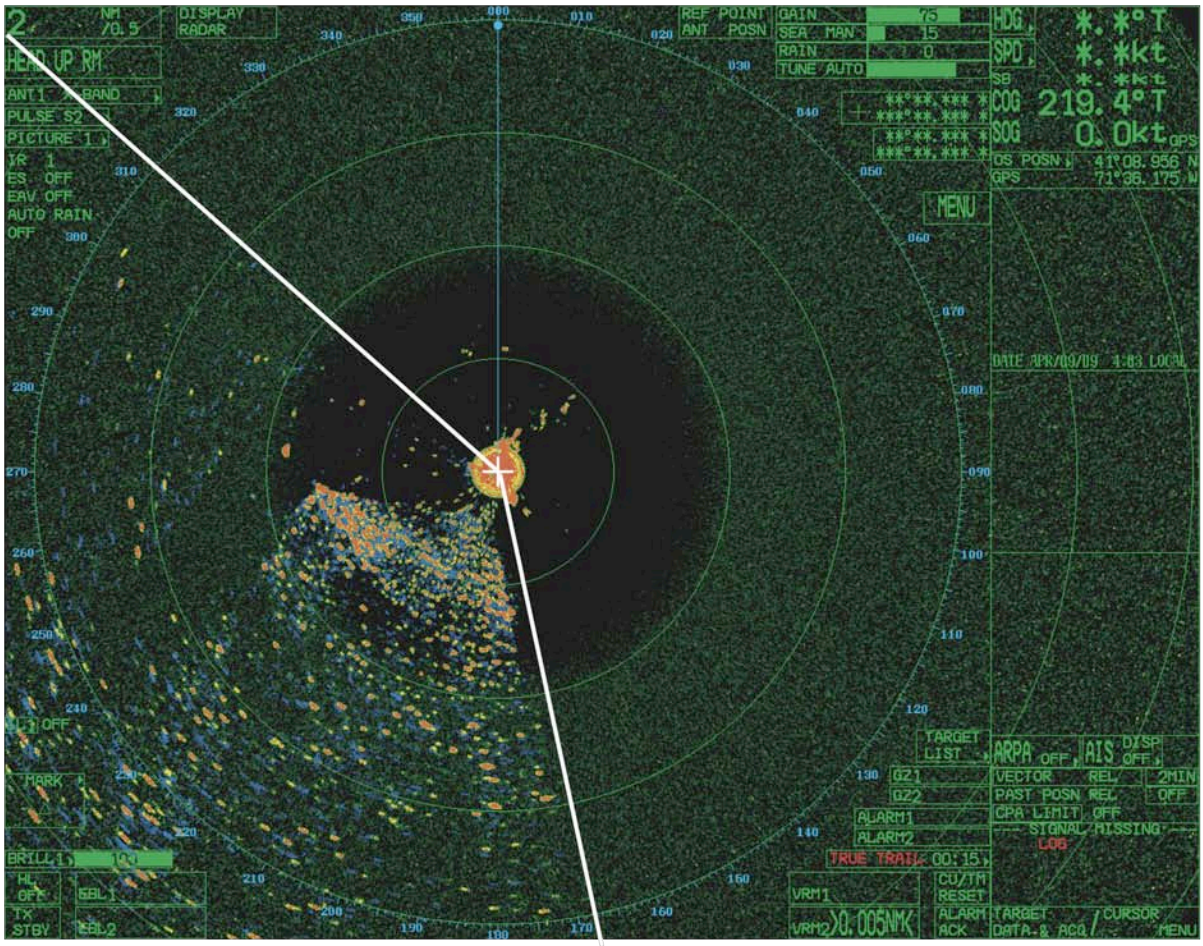

Figure 9. Horizontal radar's view from the southeastern study site. The view of the ocean occurred from approximately 170-300° (i.e., S-NW, ~130°area between white lines, rotating clockwise). The radar's view of the ocean between 90-170° (i.e., E - S) was occluded by a rise along the edge of the landform although the airspace above the landfrom was visible. Areas from approximately 305-90° (NW-E) were over land. This image shows mild backscatter from wave action along the coast out to at least 2 miles. Areas over land did not experience backscatter.

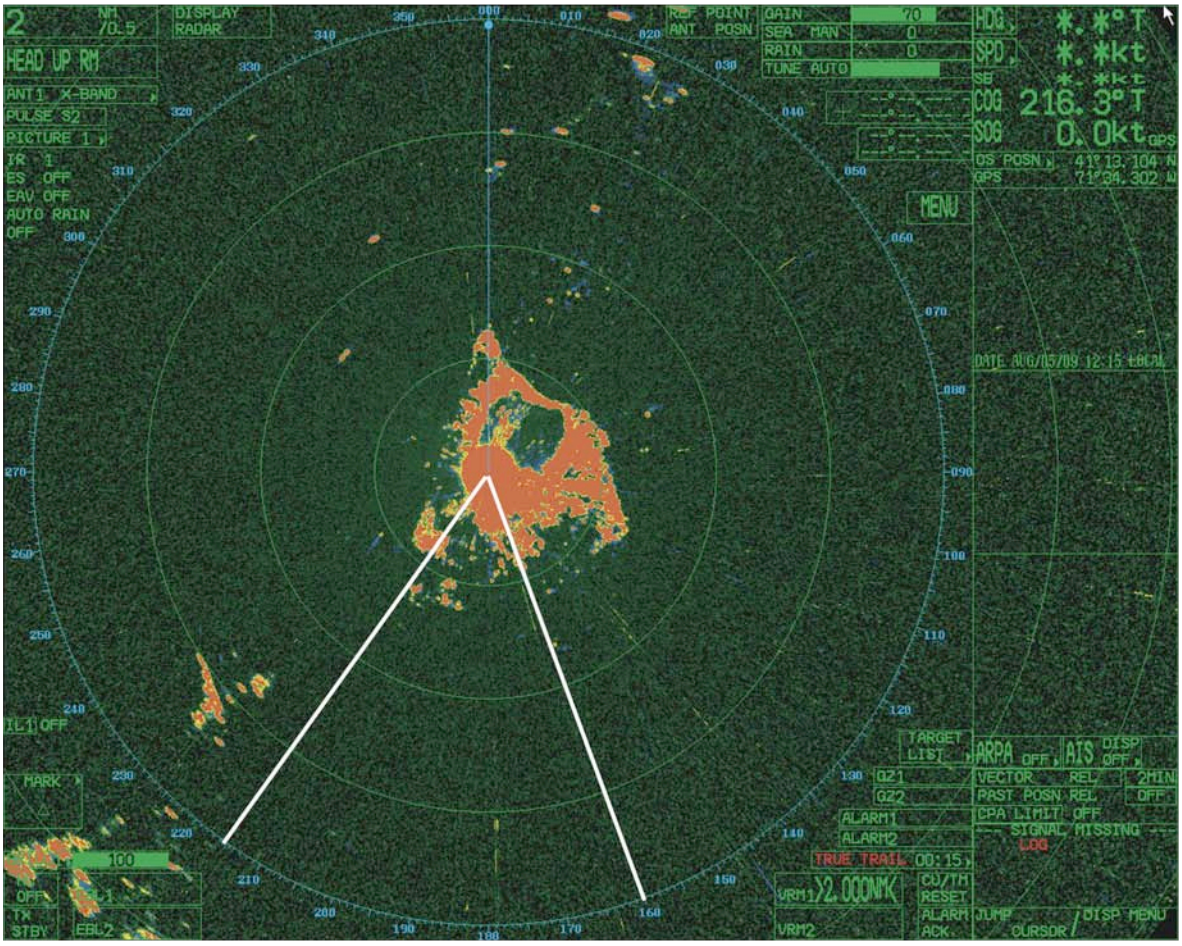

Figure 10. Horizontal radar's view from the northern study site. The view of the ocean occurred from approximately 215-160° (i.e., SW-SE, ~305°area between white lines, rotating clockwise). The large red areas near the center of the radar image is backscatter of eclectromagnetic energy from the surrounding landscape, which occluded target detection in this area.

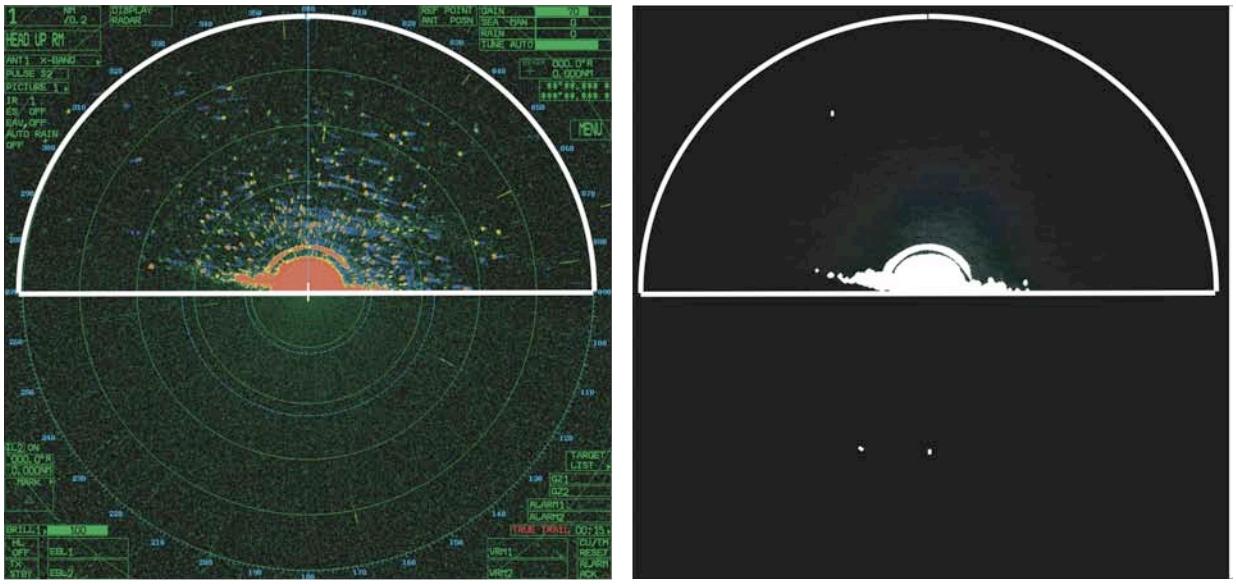

Figure 11. (Left) Data image from vertically oriented radar collected on 24 September 2009, 2046 EDT 08:46 PM). The thick white line graphically represents how NJAS's integrated image processing software defines the sample area. (Right) Template generated by NJAS's integrated image processing software for data collected on the same date as data image on the left. The template is used as a mask to remove stationary reflectors (i.e., main bang, ground clutter, see Figs. 3, 5 for reference) from data images.

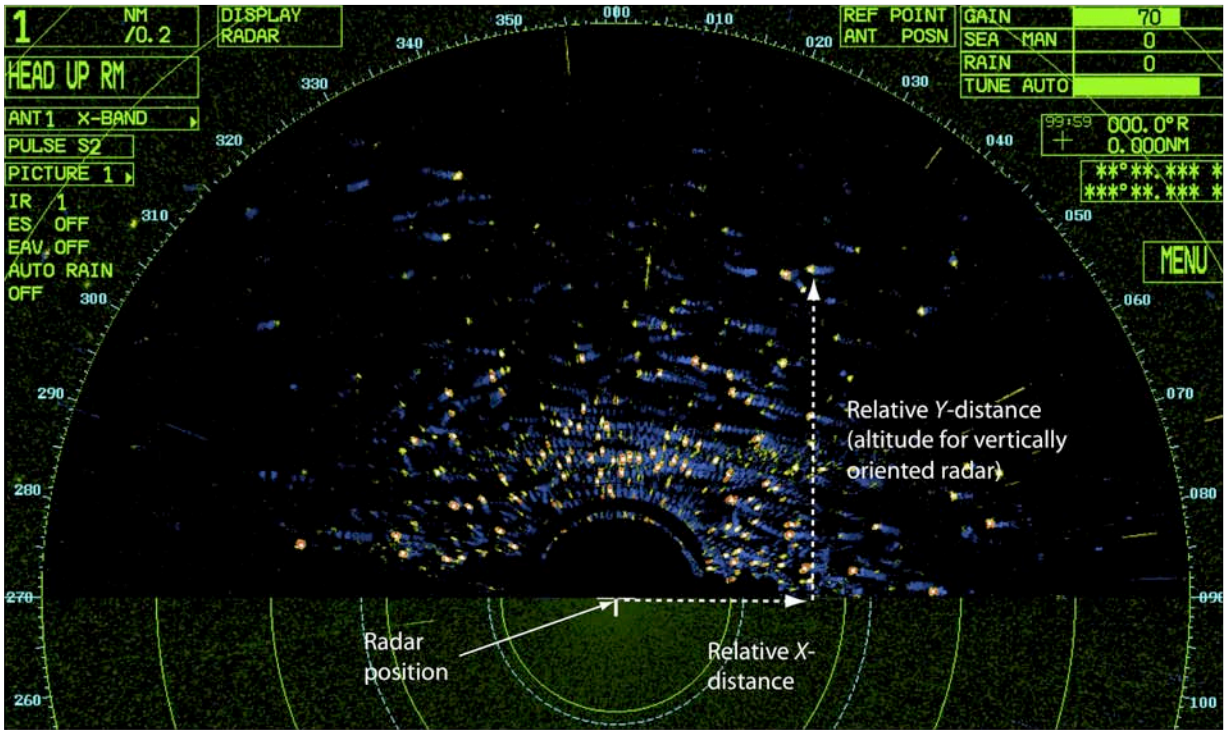

Figure 12. Data image collected on 24 September 2009 at 2046 EDT (8:46 PM), with the vertically-oriented radar. NJAS integrated image processing software removes targets with low reflectivity, smooths the data and locates and marks the centroid of each discrete target that remains. In this representation target centroids are marked with white dots. Because coordinates of the scan center (i.e., radar position, GPS) and the image's pixel dimensions are known, we can calculate a target's distance from the radar in the *X-, Y*-planes. This allows us to calculate any target's altitude (vertical radar) or *X-, Y*-coordinates (horizontal radar).

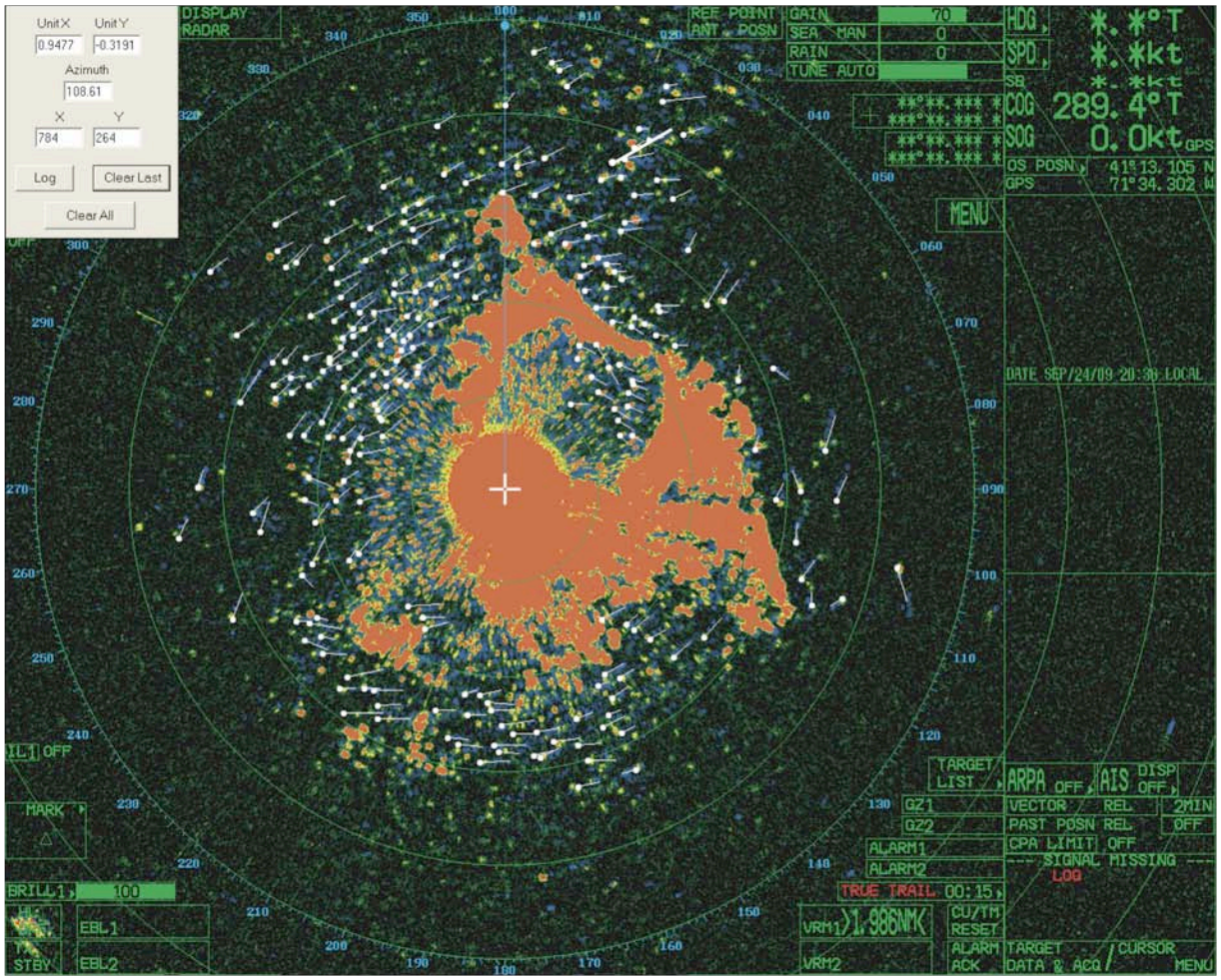

Figure 13. Data image collected on 24 September 2009 at 2036 EDT (8:36 PM) with the horizontal radar. The image shows target tracks (white circles with white tails) created using NJAS proprietary software to calculate target directions. The end of a target's trail (blue dotted line, see Figs. 3 and 5 for reference) and the target (green, yellow or red ellipses) is marked (in that order) using the computer's mouse and cursor. The program outputs the position of the trail's tail and the target and from these calculates the target's direction of movement.

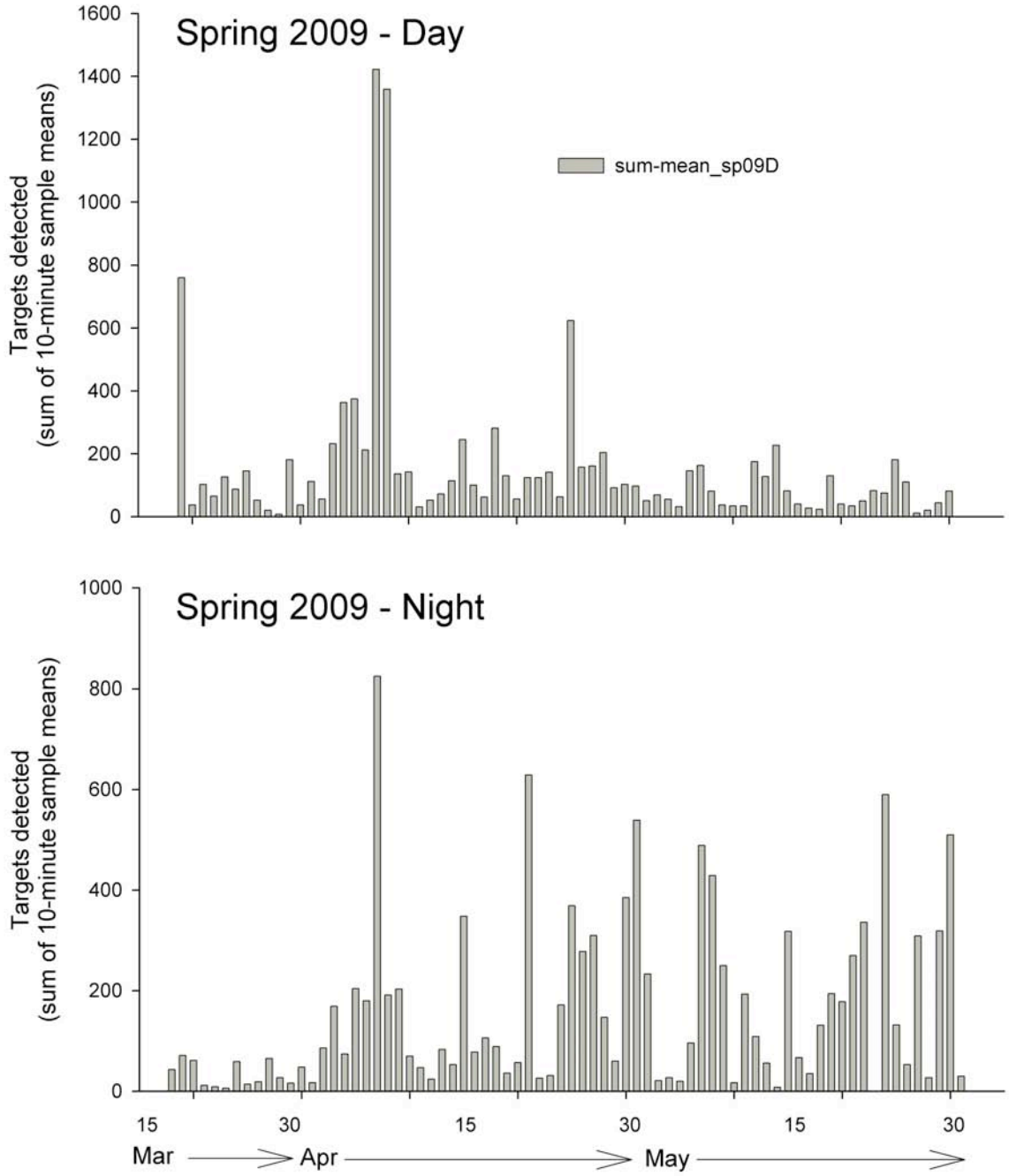

Figure 14. Seasonal temporal pattern in targets detected (sum of 10-minute sample means) during day (i.e. sunrise to sunset, upper panel) and night (sunset to sunrise the following morning, lower panel) data collection periods, spring (19 Mar-31 May) 2009.

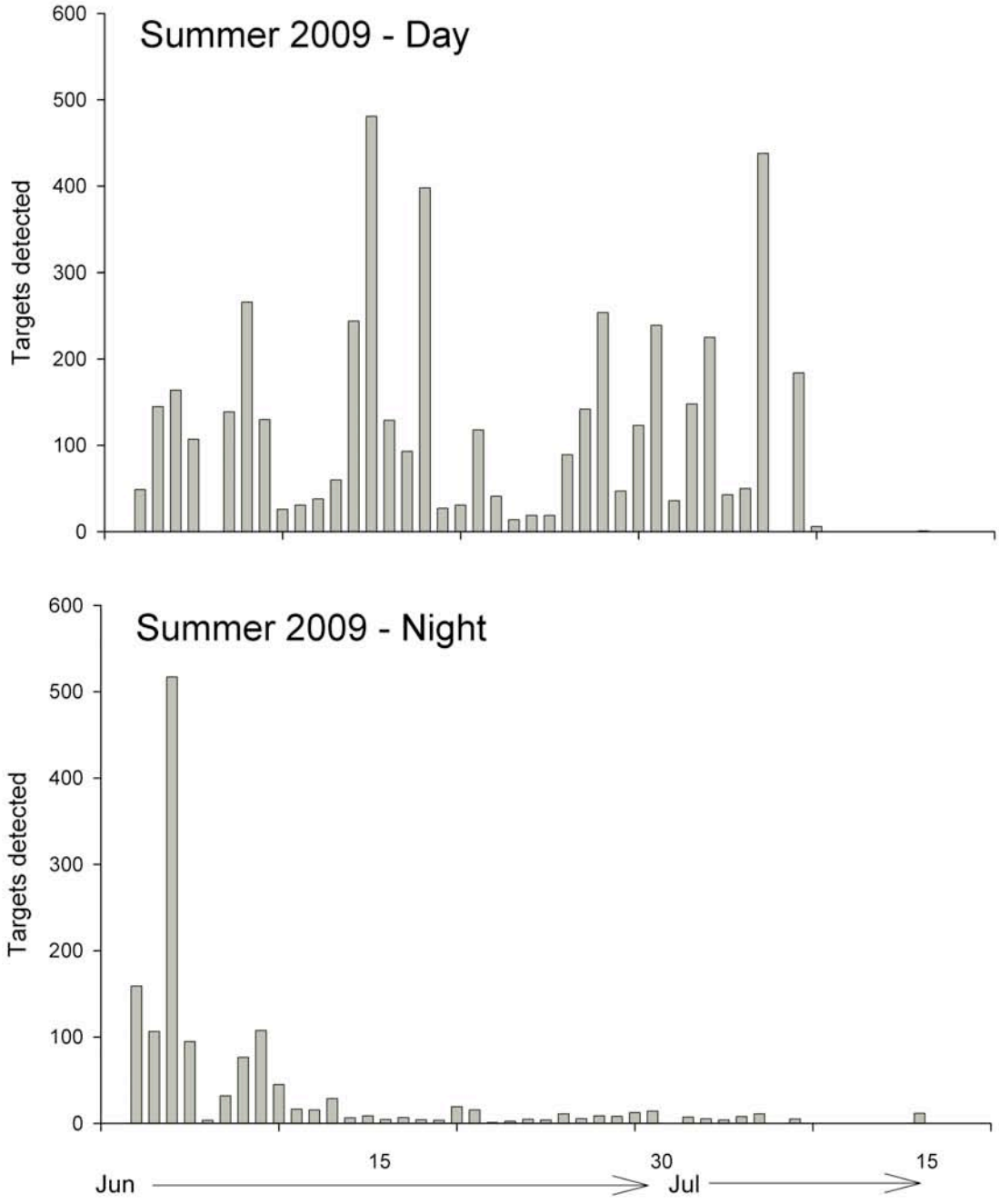

Figure 15. Seasonal temporal pattern in targets detected (sum of 10-minute sample means) during day (i.e. sunrise to sunset, upper panel) and night (sunset to sunrise the following morning, lower panel) data collection periods, summer (1 June - 31 July) 2009.

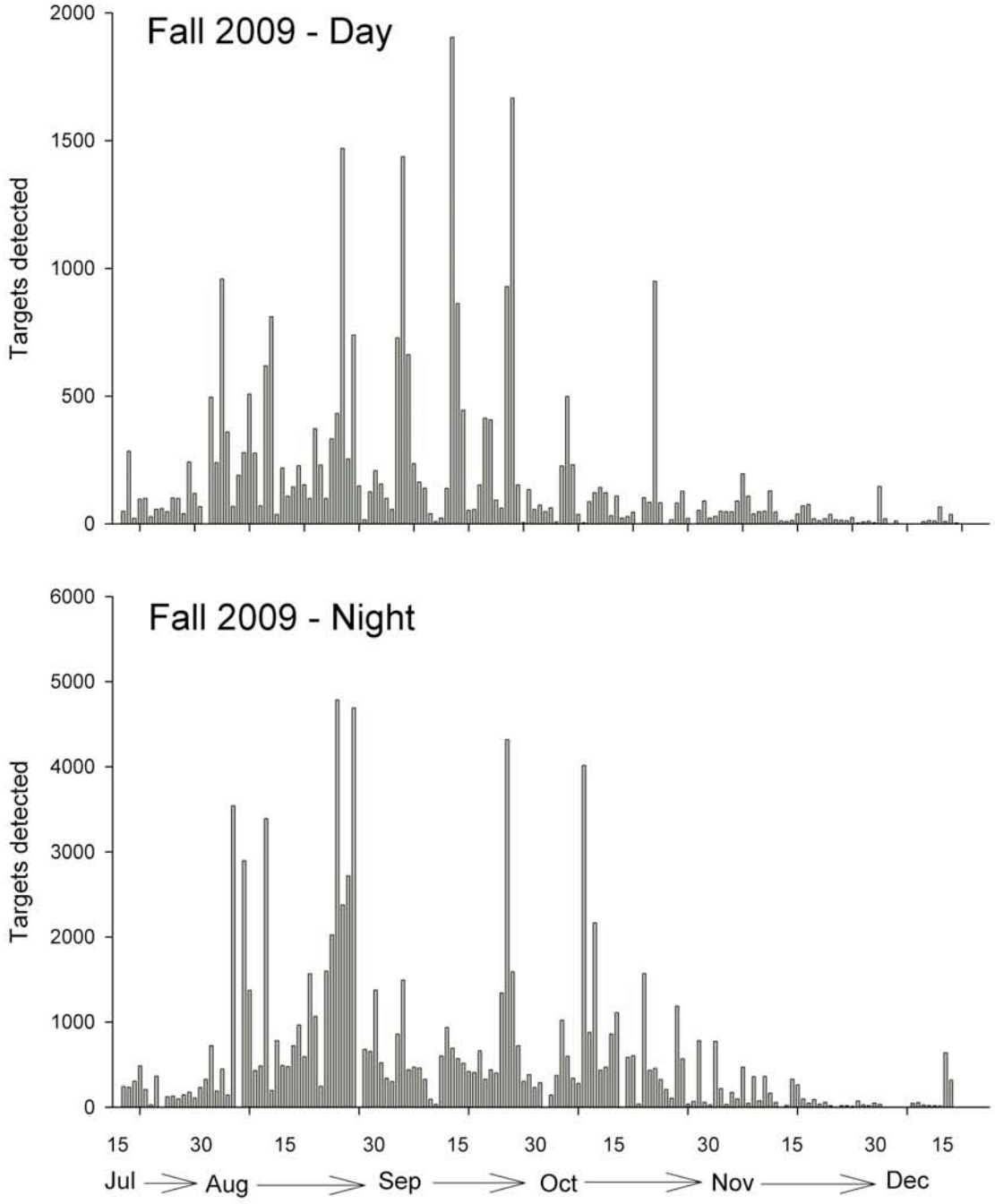

Figure 16. Seasonal temporal pattern in targets detected (sum of 10-minute sample means) during day (i.e. sunrise to sunset, upper panel) and night (sunset to sunrise the following morning, lower panel) data collection periods, fall (16 July - 15 December) 2009.

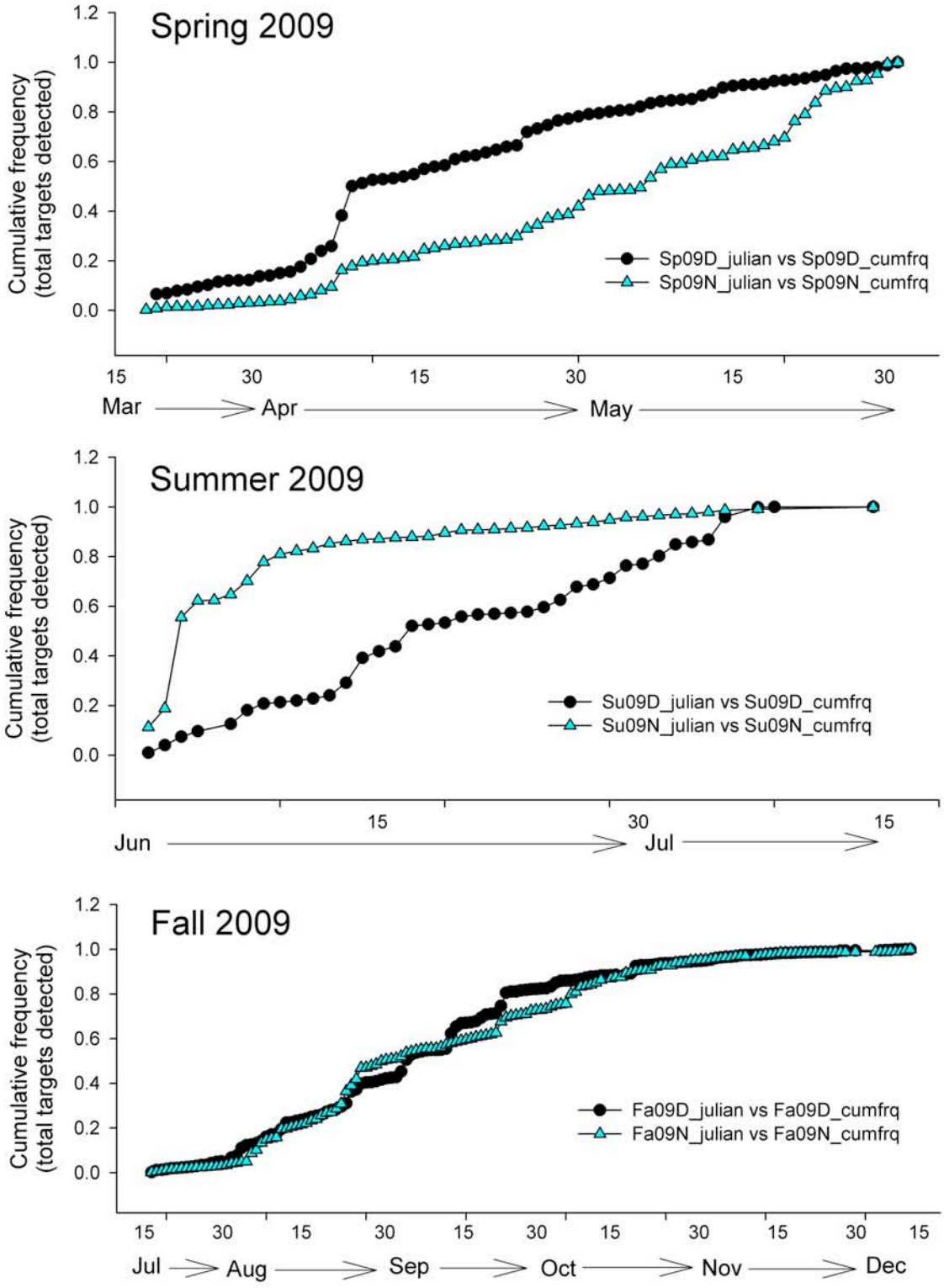

Figure 17. Cumulative frequency distributions for total targets detected (sum of 10-minute sample means) during day (i.e. sunrise to sunset, upper panel) and night (sunset to sunrise the following morning, lower panel) data collection periods, spring (upper), summer (center) and fall (lower) 2009.

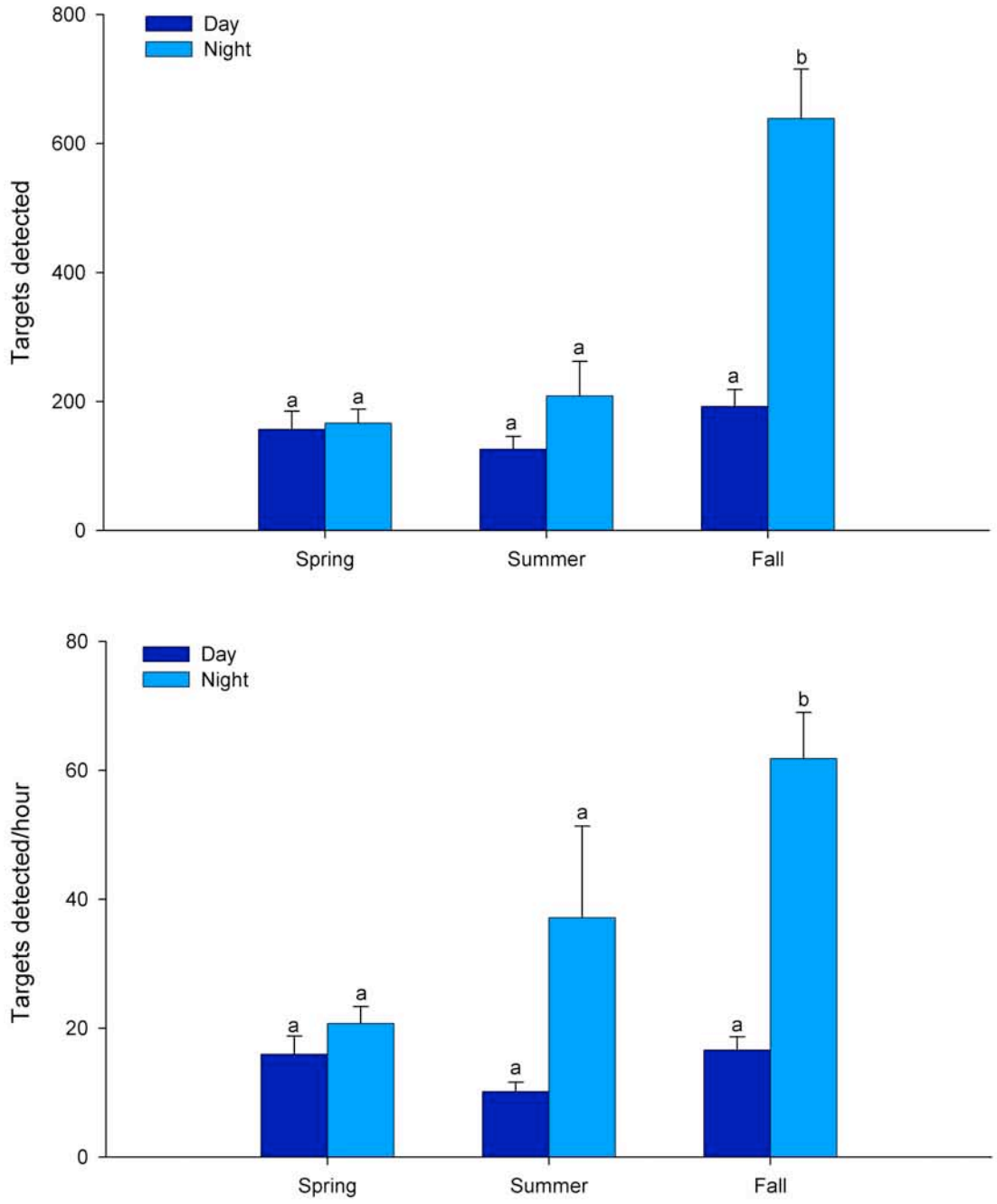

Figure 18. Targets detected (upper panel) and target detection rate (i.e., targets/hour, lower panel) for each season and period (i.e., day, night) during 2009 study of bird/bat movement patterns on Block Island, Rhode Island and in its near-coastal waters (within 2 nautical miles) . In each graph, bars with the same letter are not statistically different from each other.

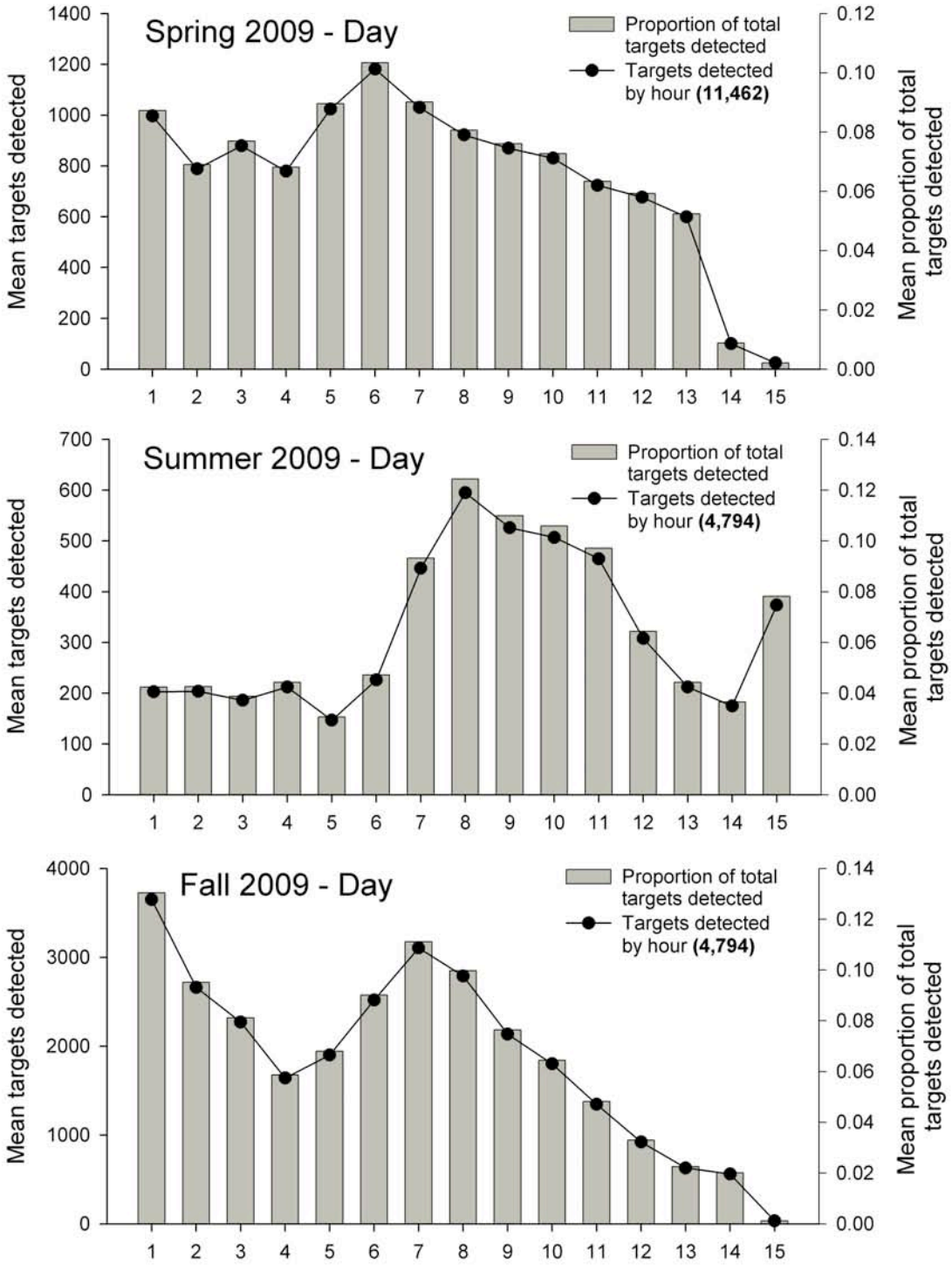

Figure 19. Mean targets detected and proportion of total targets detected by hour during the "day" (sunrise to sunset the same day) for spring migration (19 Mar - 31 May), summer (1 June - 15 July) and fall migration (16 July - 15 December) data collection periods.

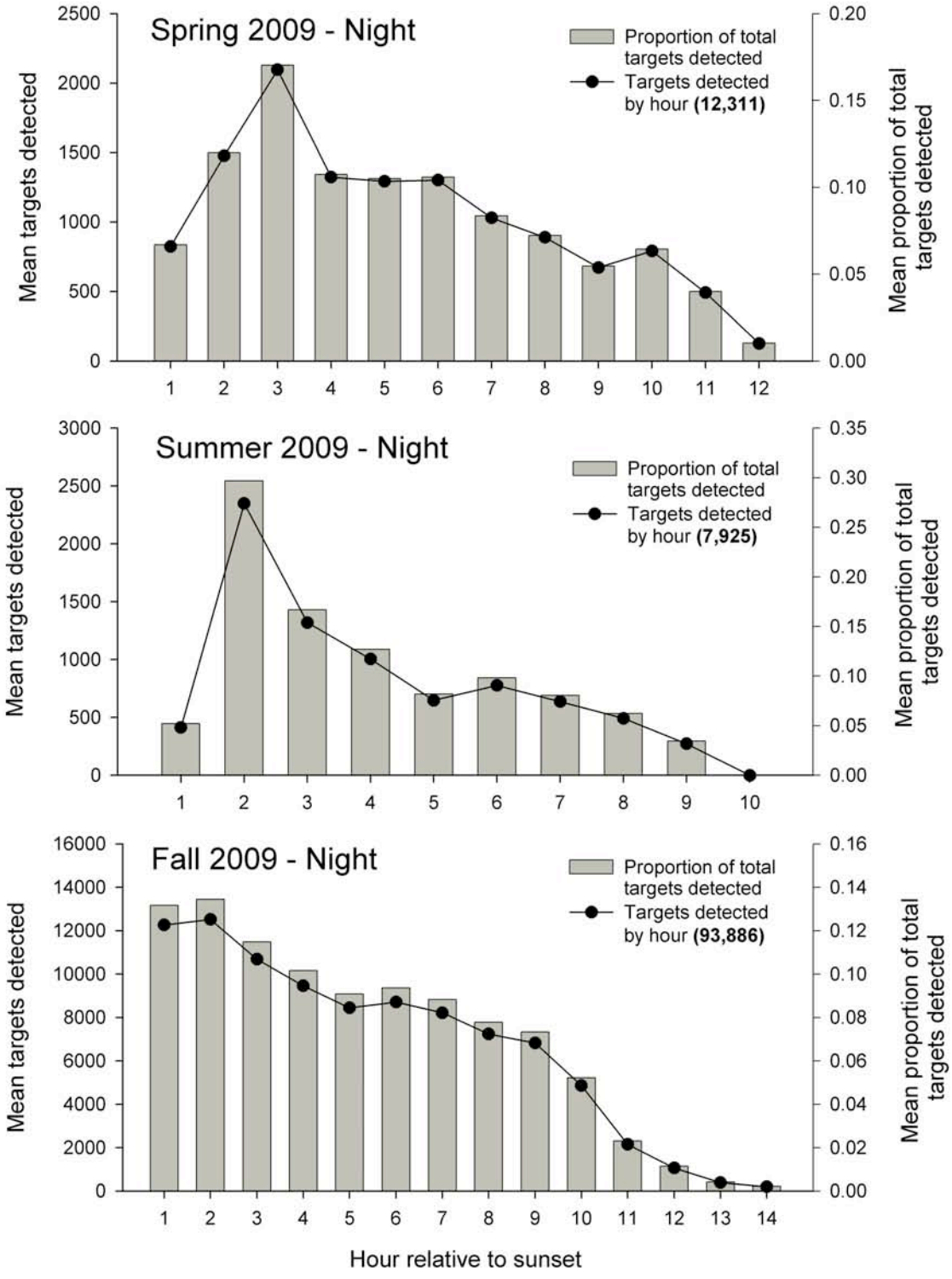

Figure 20. Mean targets detected and proportion of total targets detected by hour during the "night" (sunset to sunrise the following morning) for spring migration (19 Mar - 31 May), summer (1 June - 15 July) and fall migration (16 July - 15 December) data collection periods.

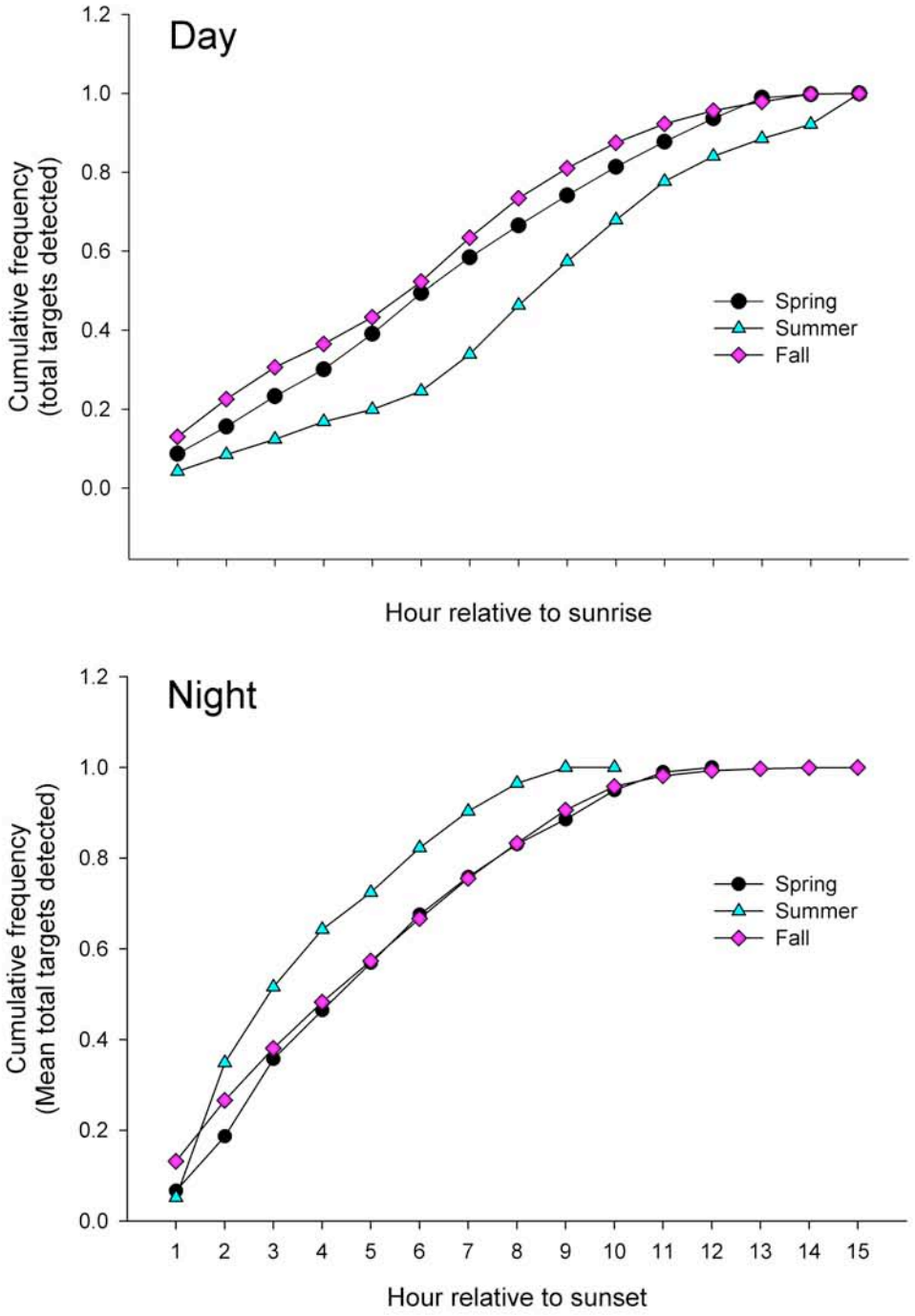

Figure 21. Hourly cumulative frequency distributions relative to sunrise (i.e., day data collection period, upper panel) and relative to sunset (i.e., night data collection, lower panel) for mean total targets detected (i.e., sum of 10-minute sample means for each hour averaged over entire season) during spring (19 Mar-31 May), summer (1 June - 15 July) and fall (16 July - 15 December) 2009.

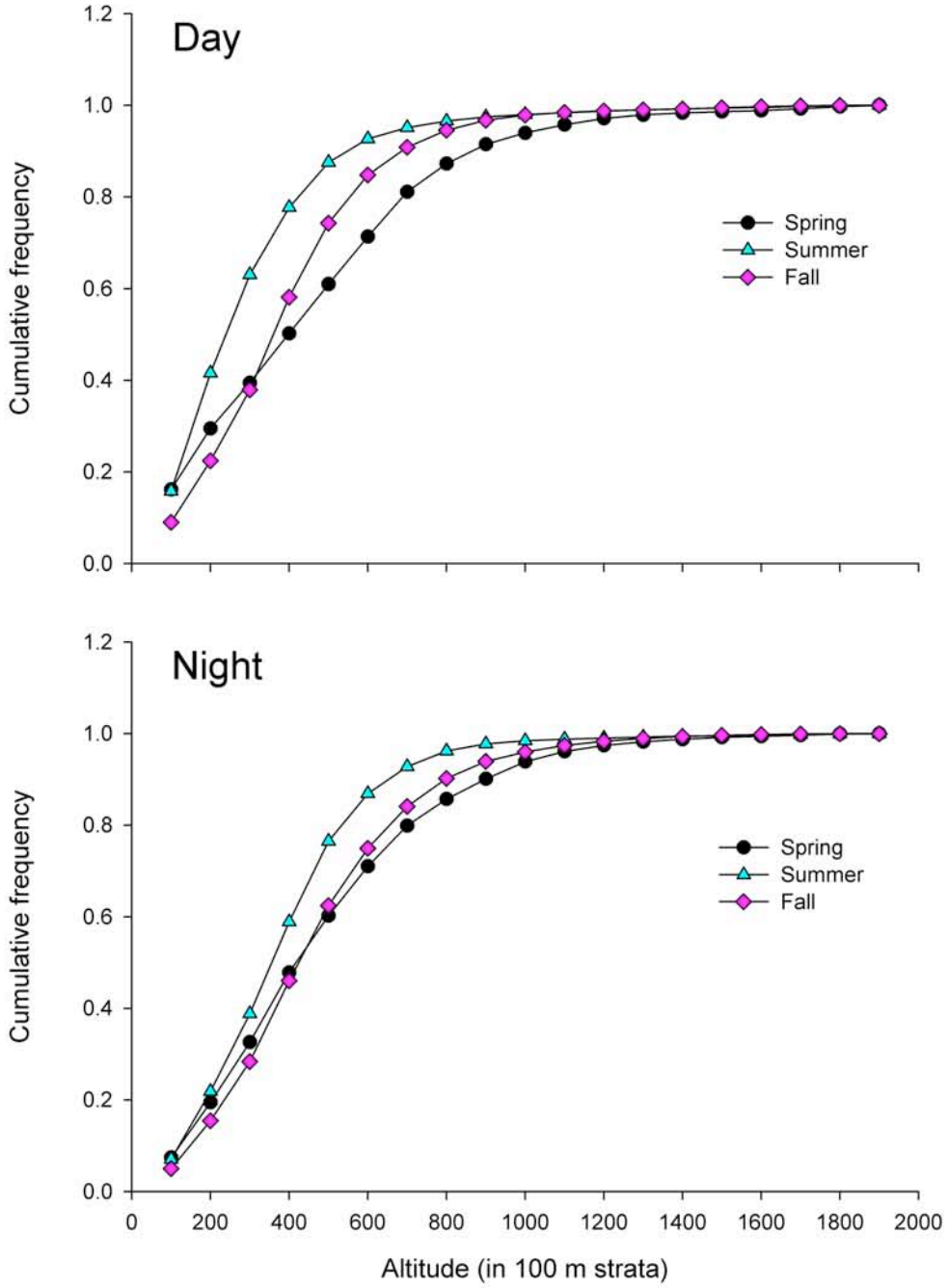

Figure 22. Cumulative frequency distributions for targets detected in each of 19, 100 m altitudinal strata (i.e., 1900 meters = ~1 nautical mile, the range setting for the vertical radar). during day (i.e. sunrise to sunset, upper panel) and night (sunset to sunrise the following morning, lower panel) data collection periods, spring (upper), summer (center) and fall (lower) 2009.

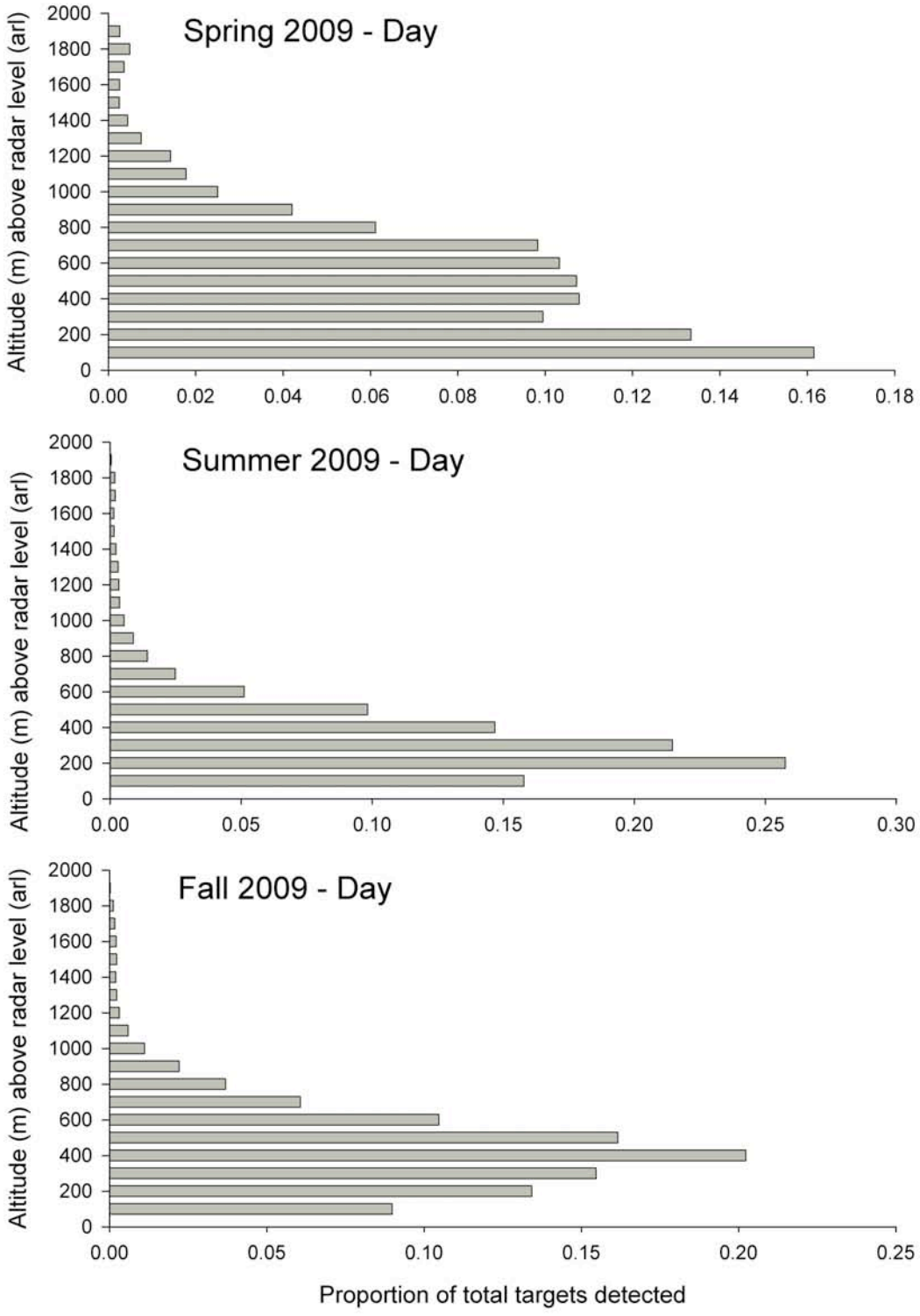

Fig. 23. Altitudinal distribution of targets detected in the day (sunrise-sunset the same day) during spring migration (19 Mar-31 May), summer (1 Jun-15 July) and fall migration (16 July-15 December) periods.

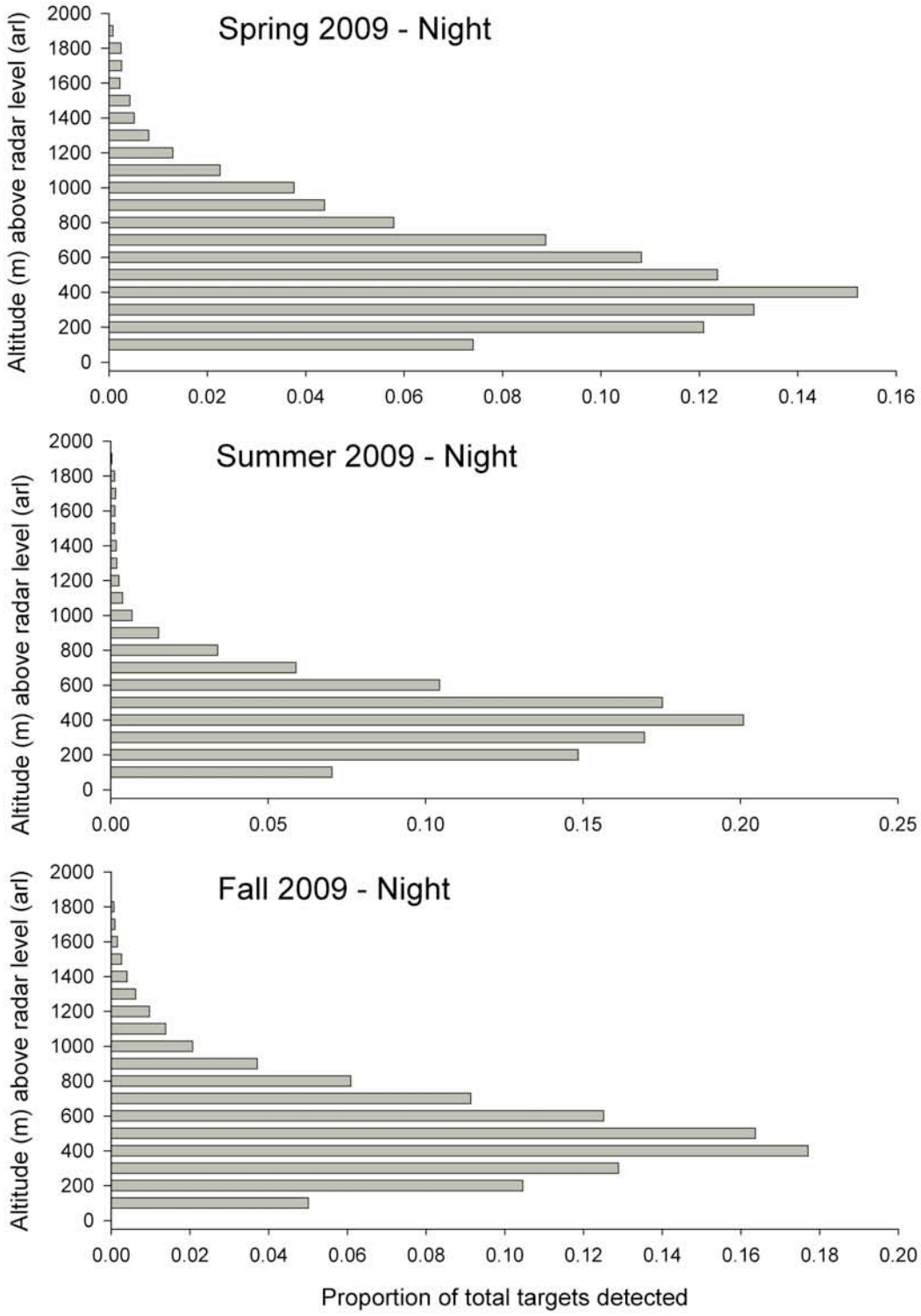

Fig. 24. Altitudinal distribution of targets detected at night (sunset-sunrise) the following morning) during spring migration (19 Mar-31 May), summer (1 Jun-15 July) and fall migration (16 July-15 December) periods.

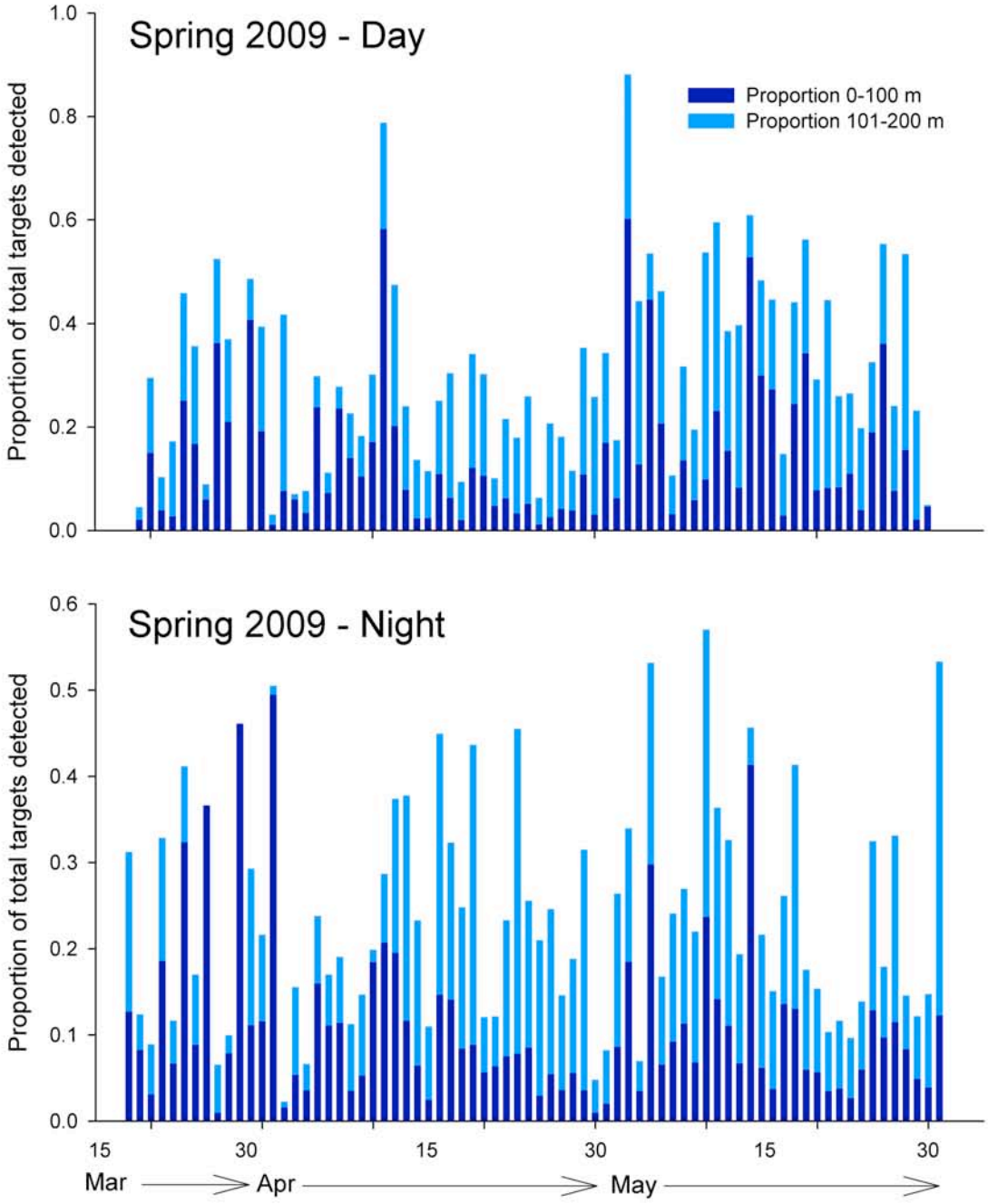

Figure 25. Seasonal temporal pattern in the proportion of targets detected <= 100 m and between 101 m and 200 m during day (upper panel) and night (lower panel) data collection periods, spring (19 Mar-31 May) 2009.

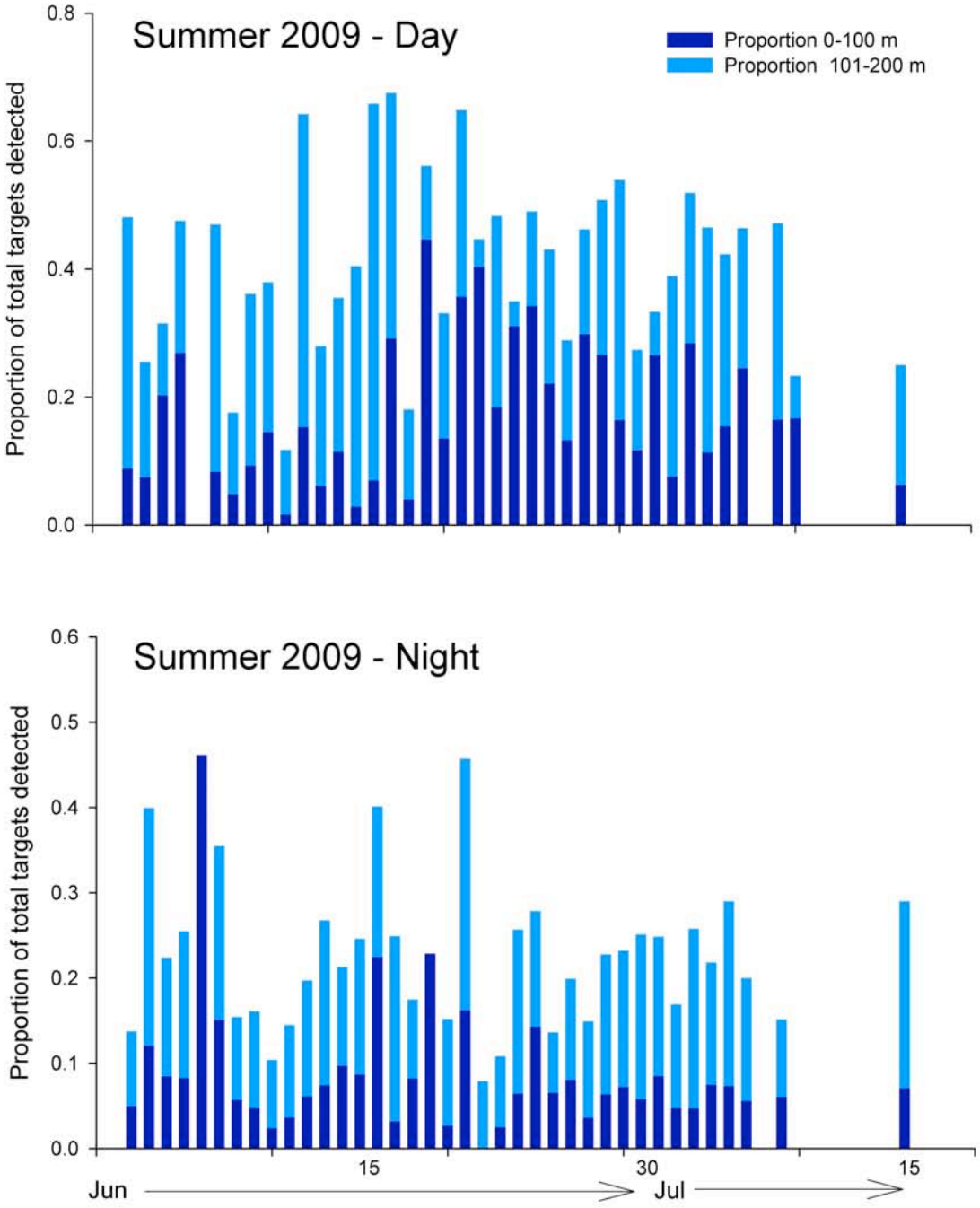

Figure 26. Seasonal temporal pattern in the proportion of targets detected <= 100 m and between 101 m and 200 m during day (upper panel) and night (lower panel) data collection periods, summer (1June - 15 July) 2009.

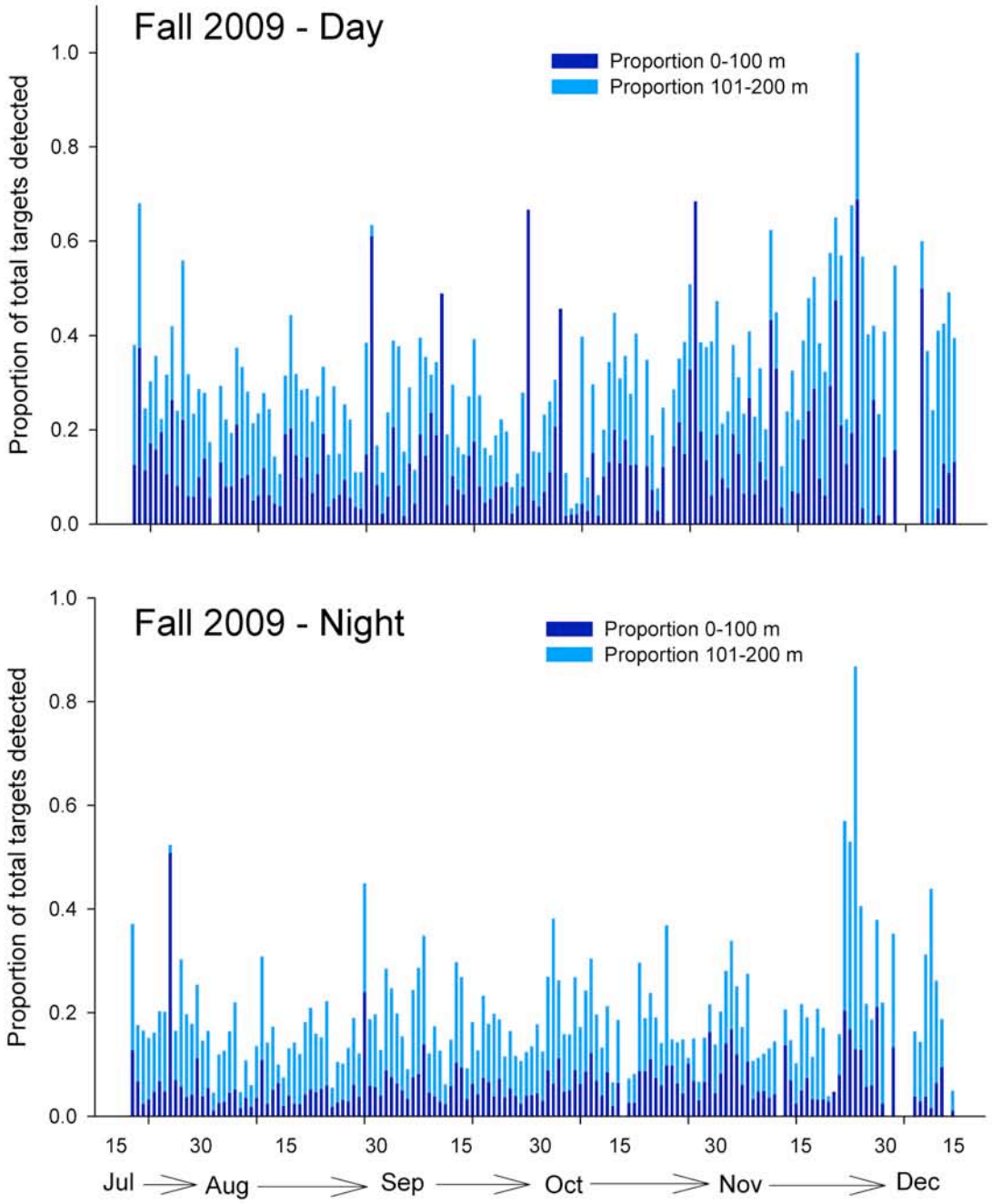

Figure 27. Seasonal temporal pattern in the proportion of targets detected <= 100 m and between 101 m and 200 m during day (upper panel) and night (lower panel) data collection periods, fall (16 July - 15 December) 2009.

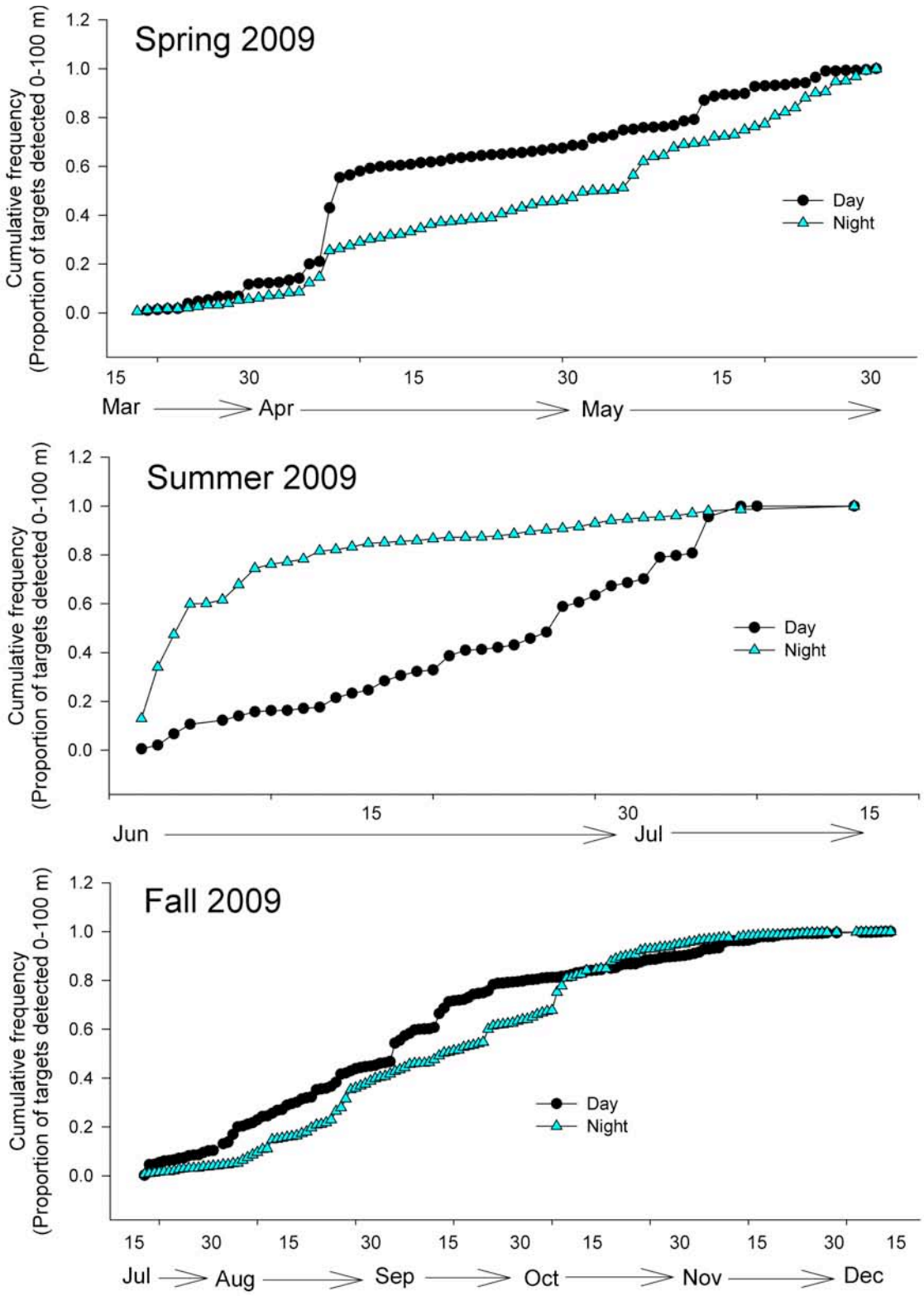

Figure 28. Cumulative frequency distributions for the proportion of targets detected in the 0-100 m strata) during day (i.e. sunrise to sunset) and night (sunset to sunrise the following morning) data collection periods, spring (upper), summer (center) and fall (lower) 2009.

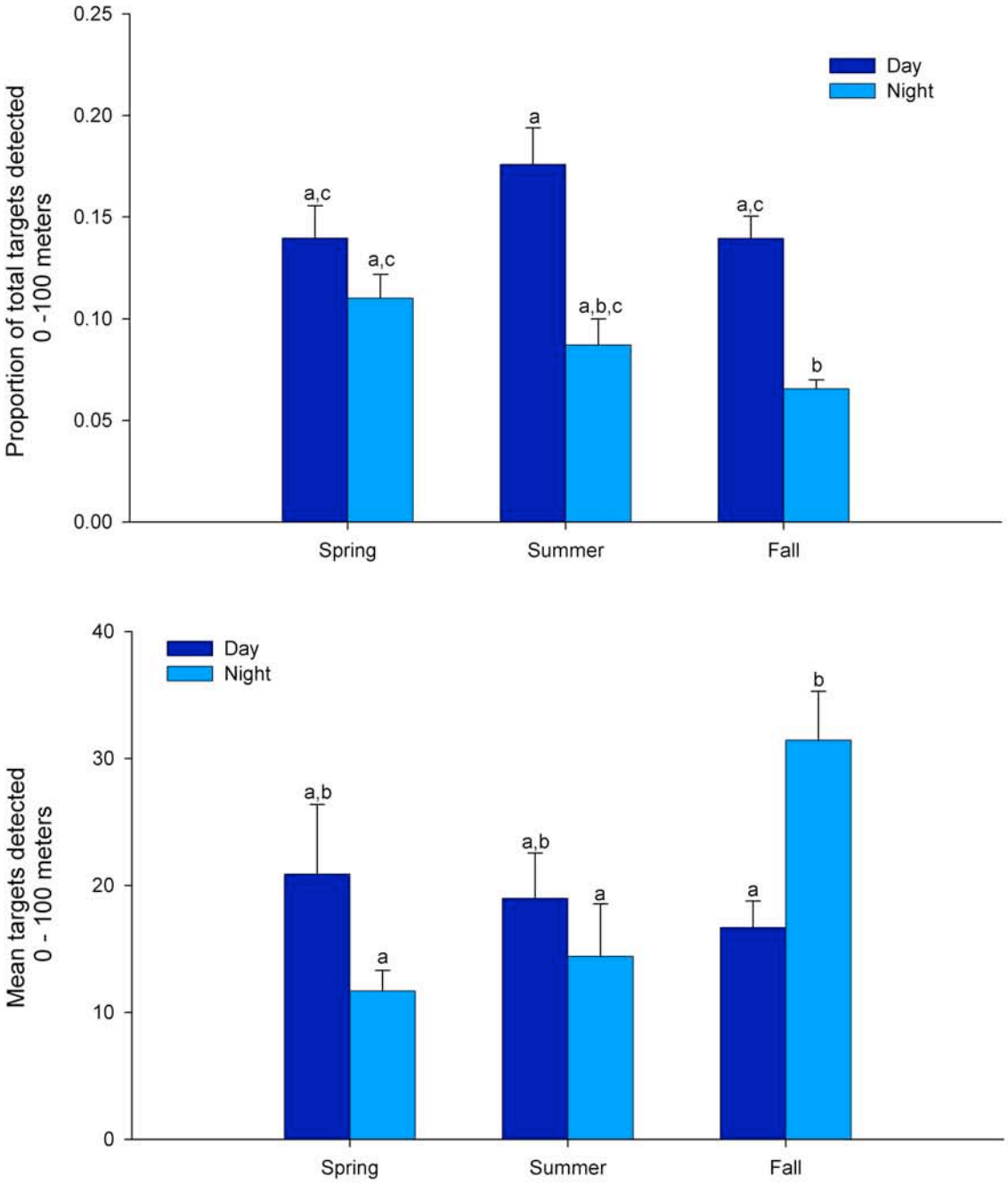

Figure 29. Proportion of targets detected (upper panel) and mean target detected (i.e., sums of 10-minutes sample averages, lower panel) in the 0-100 m for each season and period (i.e., day, night) during 2009 study of bird/bat movement patterns on Block Island, Rhode Island and in its near-coastal waters (within 2 nautical miles). In each graph, bars with the same letter are not statistically different from each other.

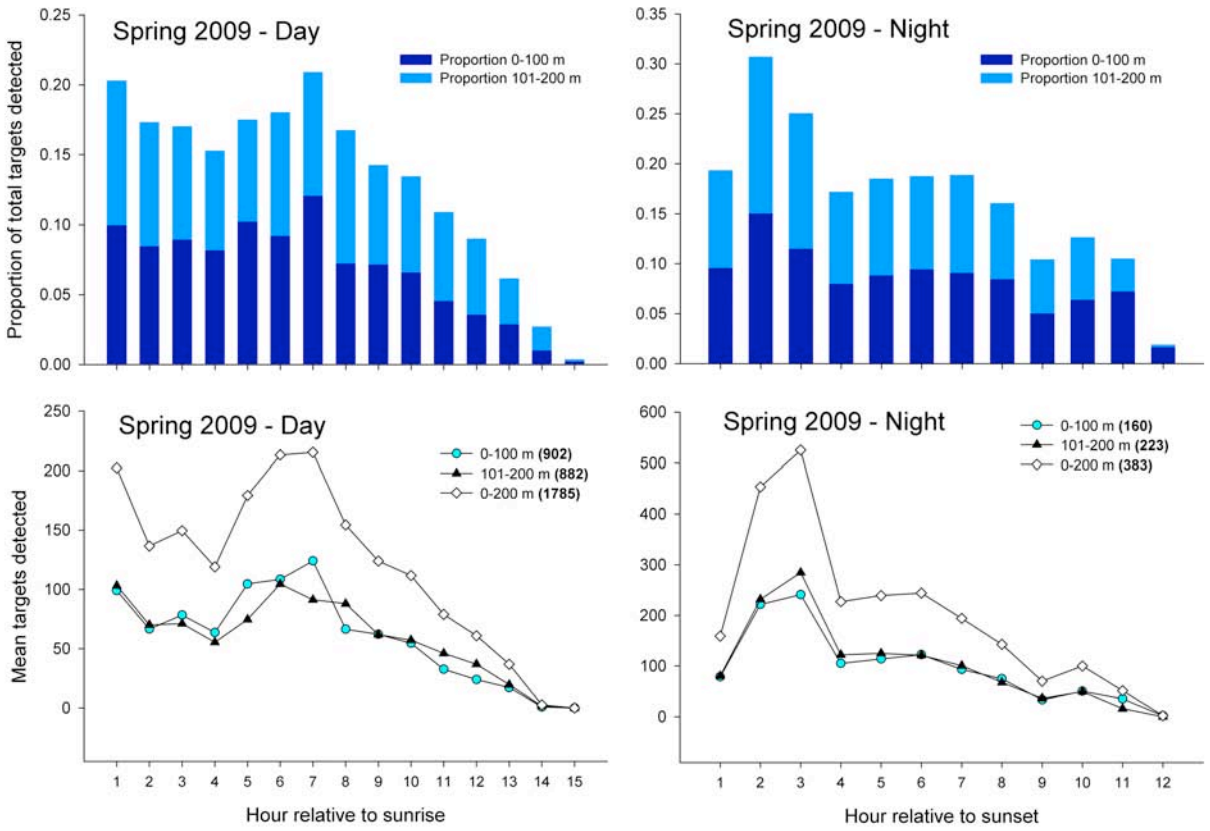

Figure 30. (Upper panels) Mean proportion of targets by hour detected <=100 m and between 101 m and 200 m above radar level (arl) in spring (19 Mar - 31 May 2009 during day and night sampling period. (Lower panels) Mean number of targets by hour detected at <=100 m and between 101 m and 200 m arl.

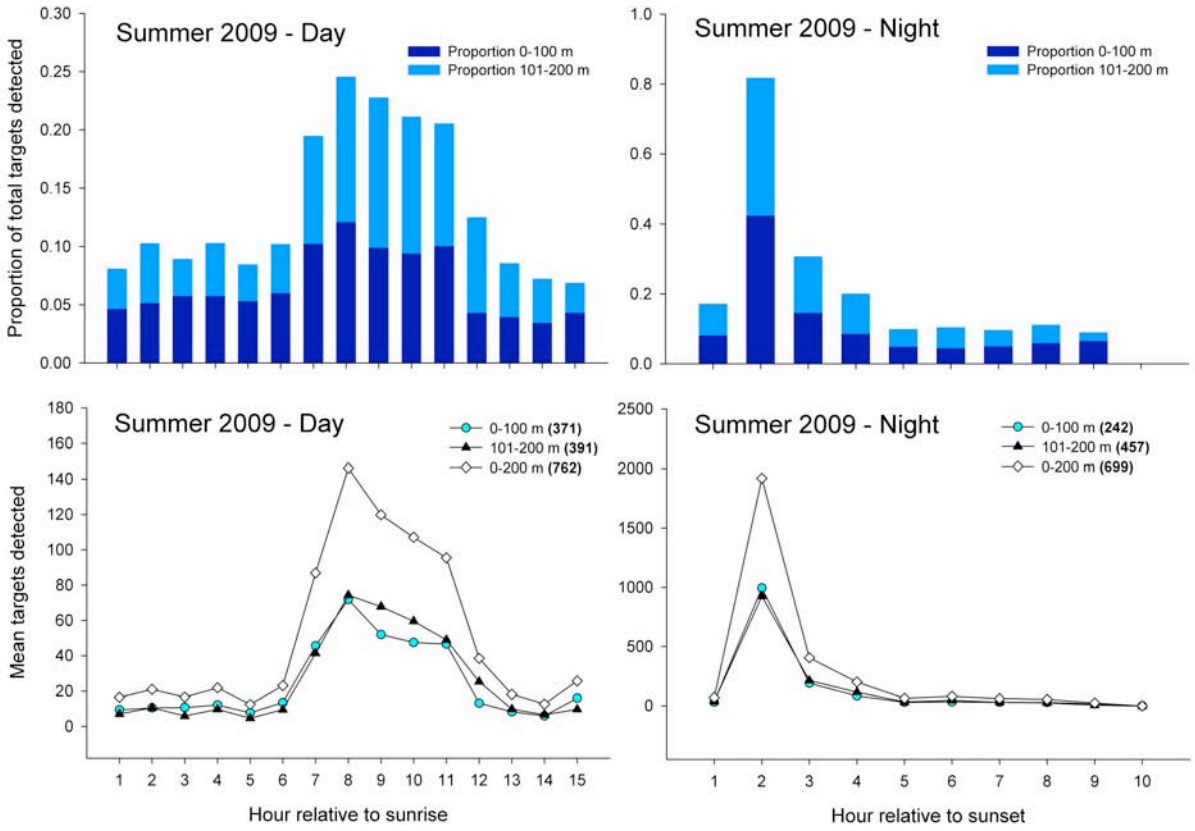

Figure 31. (Upper panels) Mean proportion of targets by hour detected <=100 m and between 101 m and 200 m above radar level (arl) in summer (1 Jun - 15 July 2009 during day and night sampling period. (Lower panels) Mean number of targets by hour detected at <=100 m and between 101 m and 200 m arl.

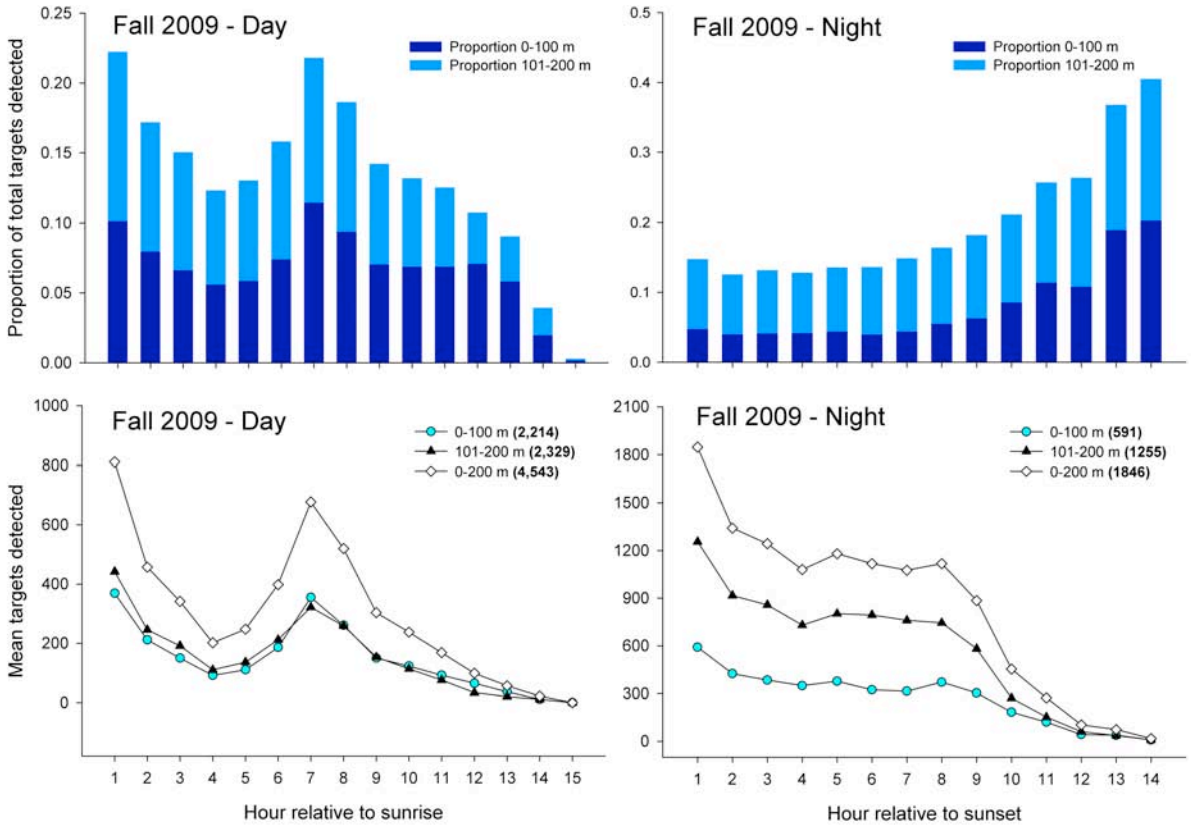

Figure 32. (Upper panels) Mean proportion of targets by hour detected <=100 m and between 101 m and 200 m above radar level (arl) in fall (16 July - 15 december 2009 during day and night sampling period. (Lower panels) Mean number of targets by hour detected at <=100 m and between 101 m and 200 m arl.

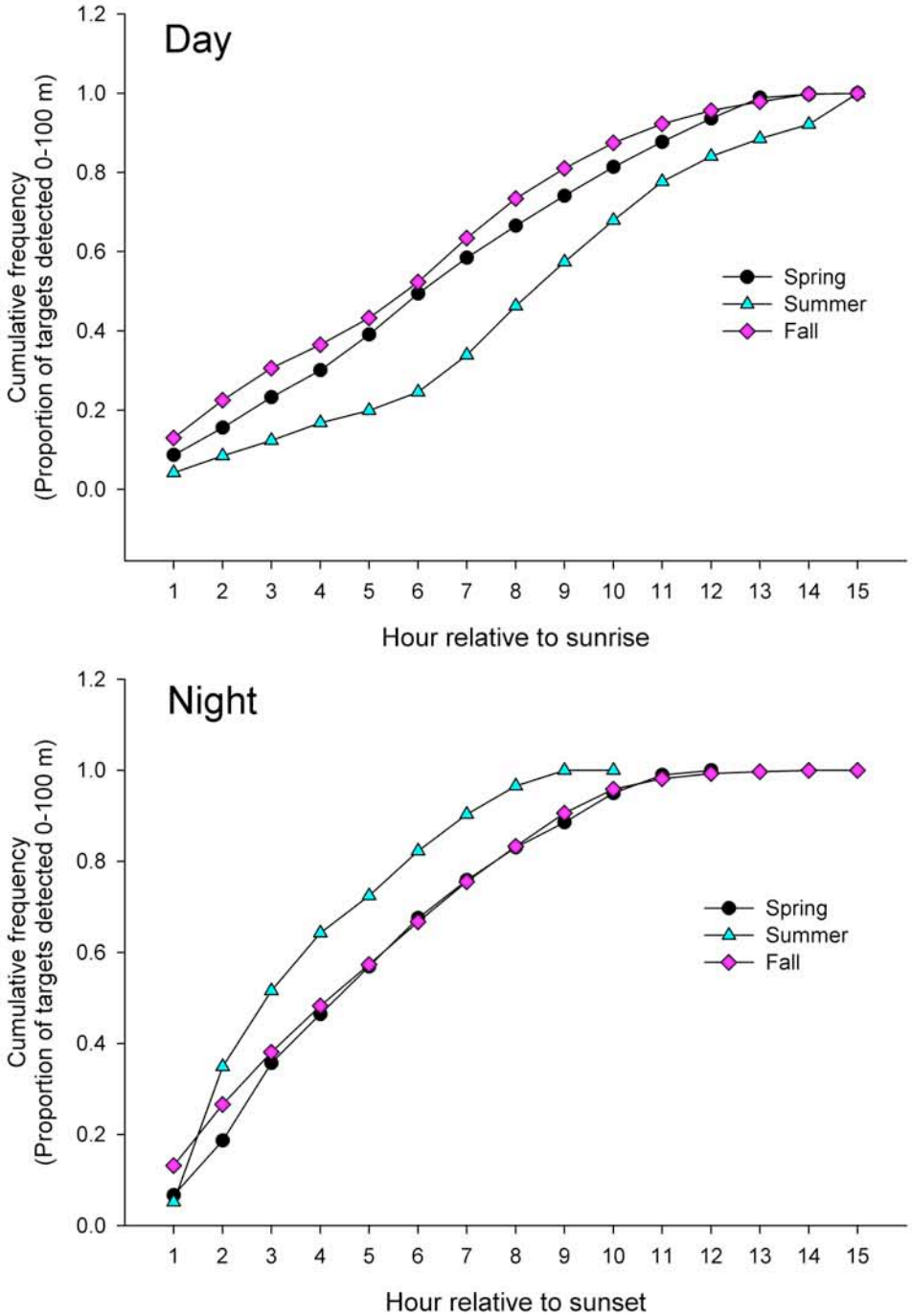

Figure 33. Hourly cumulative frequency distributions relative to sunrise (i.e., day data collection period, upper panel) and relative to sunset (i.e., night data collection, lower panel) for the proportion of targets detected at or below 100 m during spring (19 Mar-31 May), summer (1 June - 15 July) and fall (16 July - 15 December) 2009.

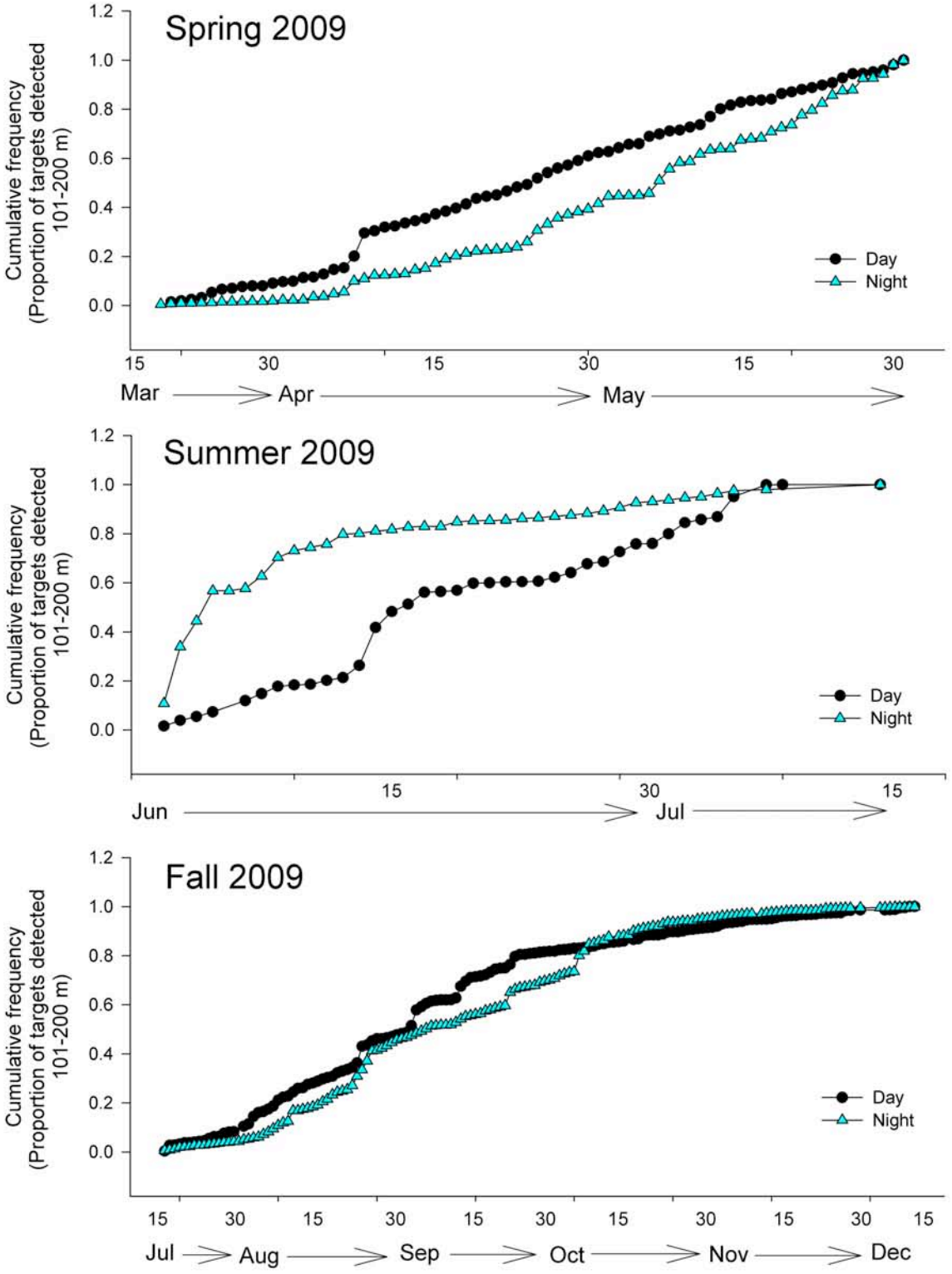

Figure 34. Cumulative frequency distributions for the proportion of targets detected in the 101-200 m strata during day (i.e. sunrise to sunset) and night (sunset to sunrise the following morning) data collection periods, spring (upper), summer (center) and fall (lower) 2009.

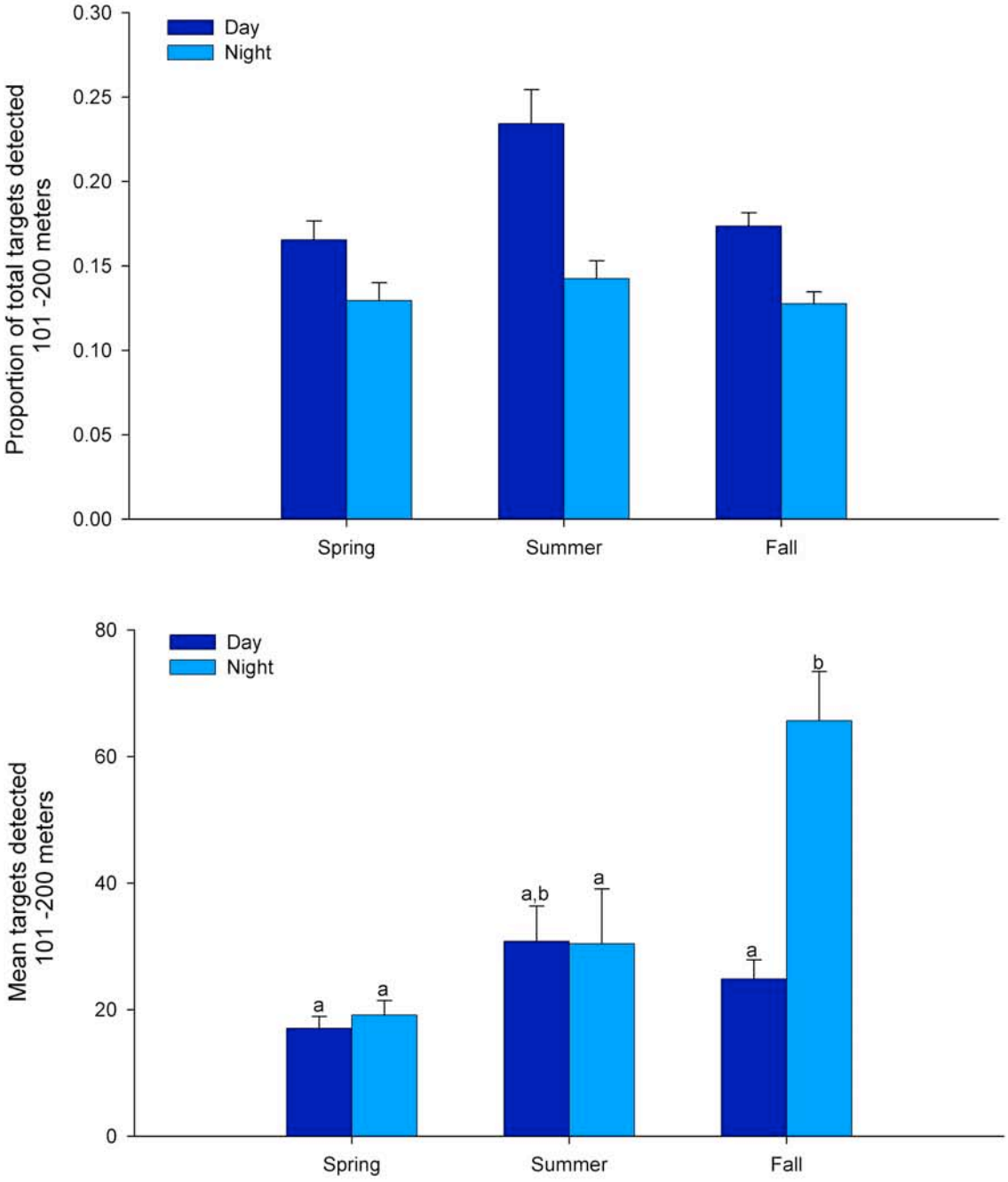

Figure 35. Proportion of targets detected (upper panel) and mean target detected (i.e., sums of 10-minutes sample averages, lower panel) in the 101-200 m stratum for each season and period (i.e., day, night) during 2009 study of bird/bat movement patterns on Block Island, Rhode Island and in its near-coastal waters (within 2 nautical miles). In each graph, bars with the same letter are not statistically different from each other.

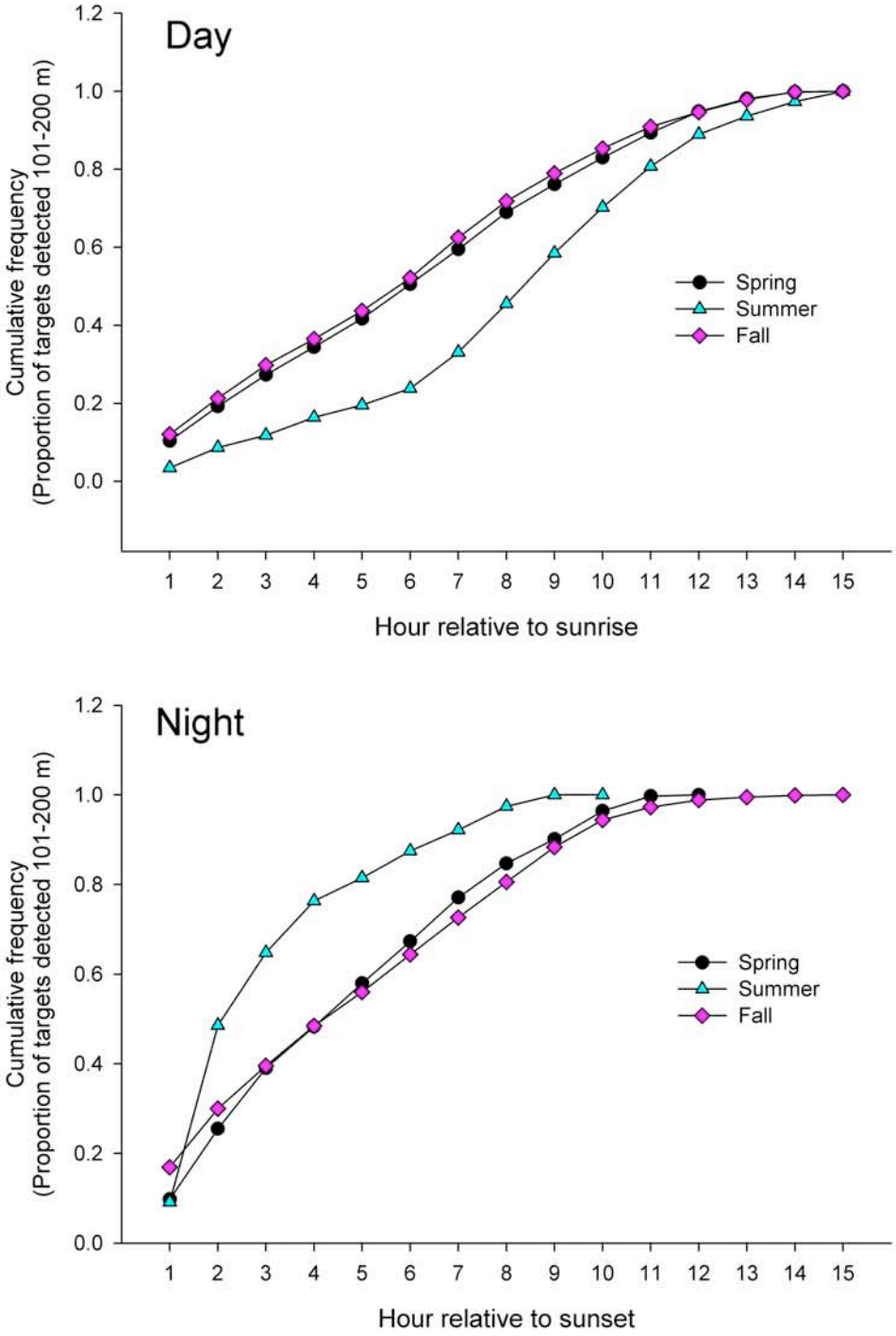

Figure 36. Hourly cumulative frequency distributions relative to sunrise (i.e., day data collection period, upper panel) and relative to sunset (i.e., night data collection, lower panel) for the proportion of targets detected in the 101-200 m stratum during spring (19 Mar-31 May), summer (1 June - 15 July) and fall (16 July - 15 December) 2009.

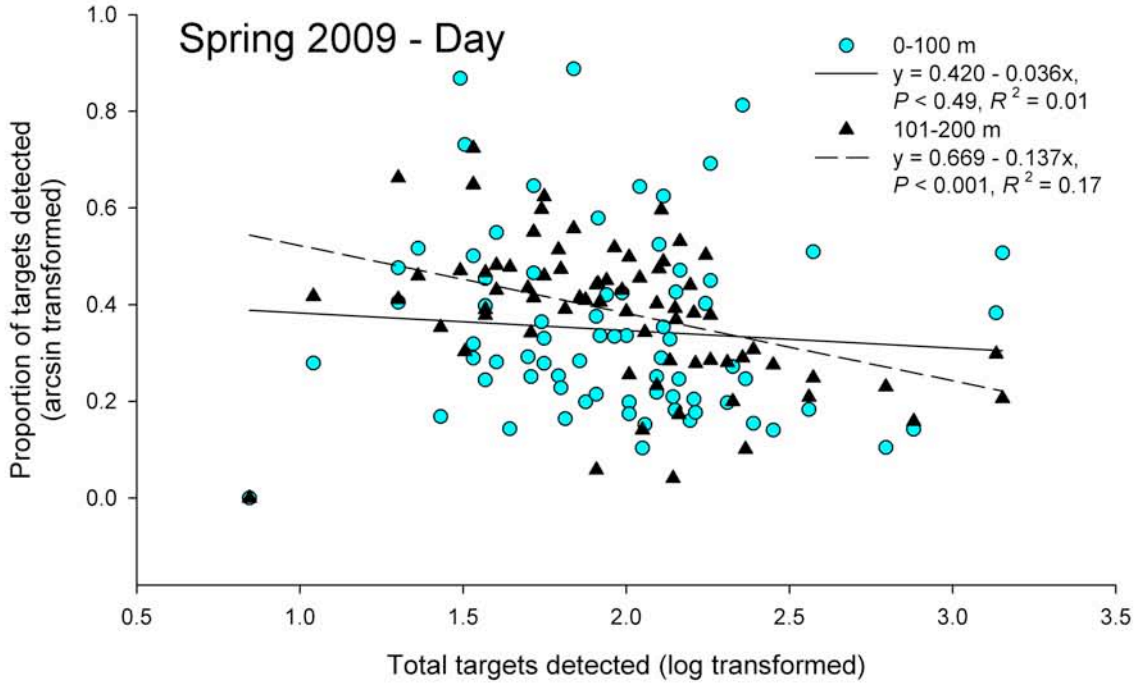

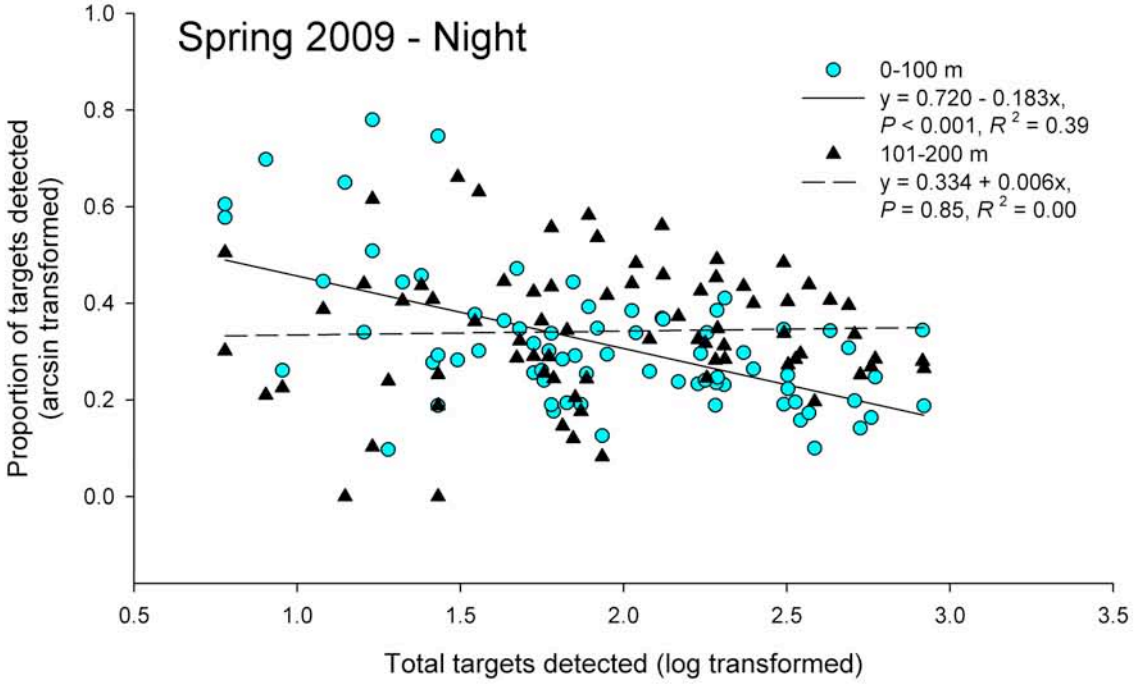

Figure 37. Relationship between the proportion of targets detected in the two lowest altitudinal strata (i.e., <= 100 m, between 100 and 200 m) and total targets detected (i.e., sum of the 10-minute sample averages) during day and night data collection periods, spring 2009.

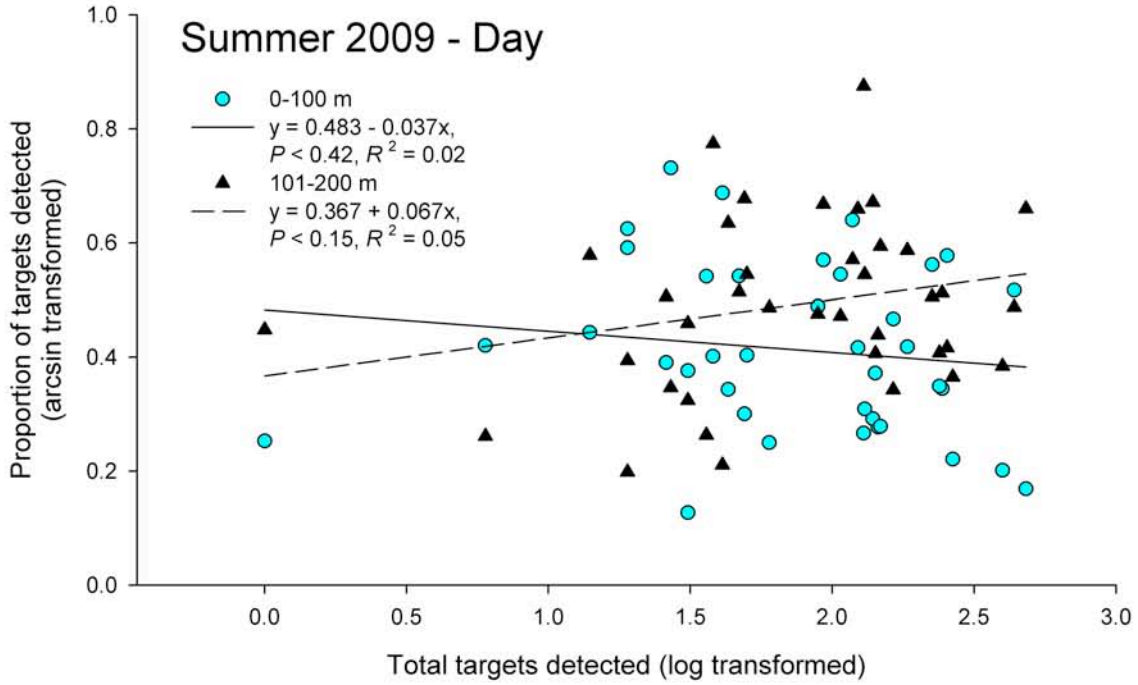

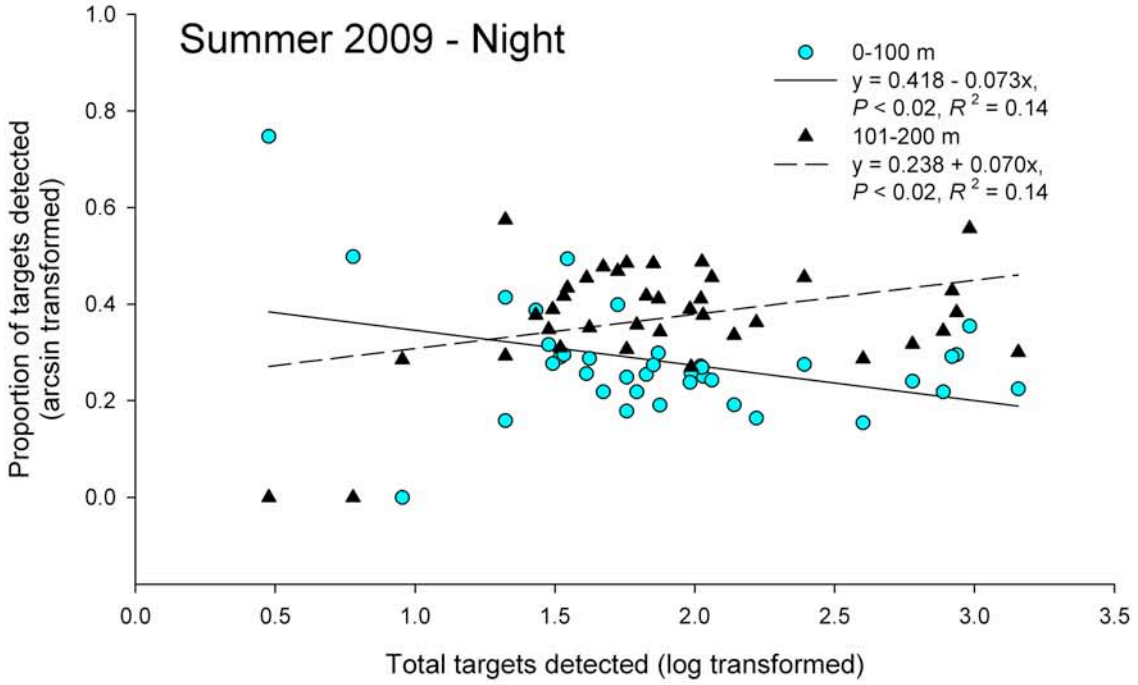

Figure 38. Relationship between the proportion of targets detected in the two lowest altitudinal strata (i.e., <= 100 m, between 100 and 200 m) and total targets detected (i.e., sum of the 10-minute sample averages) during day and night data collection periods, summer 2009.

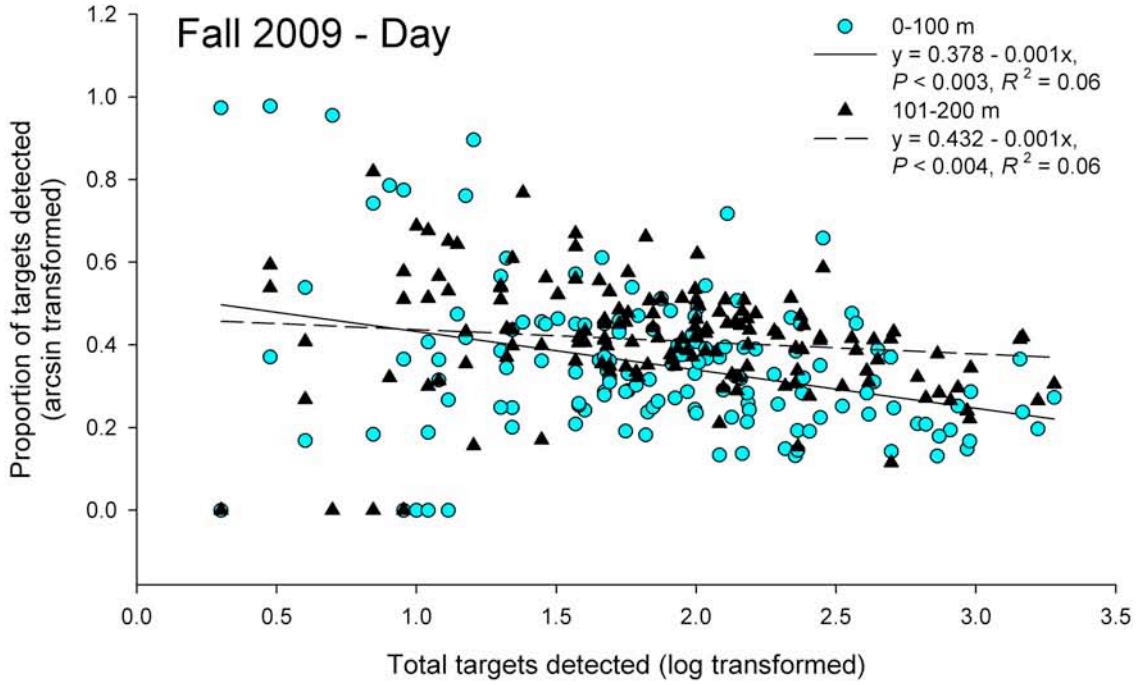

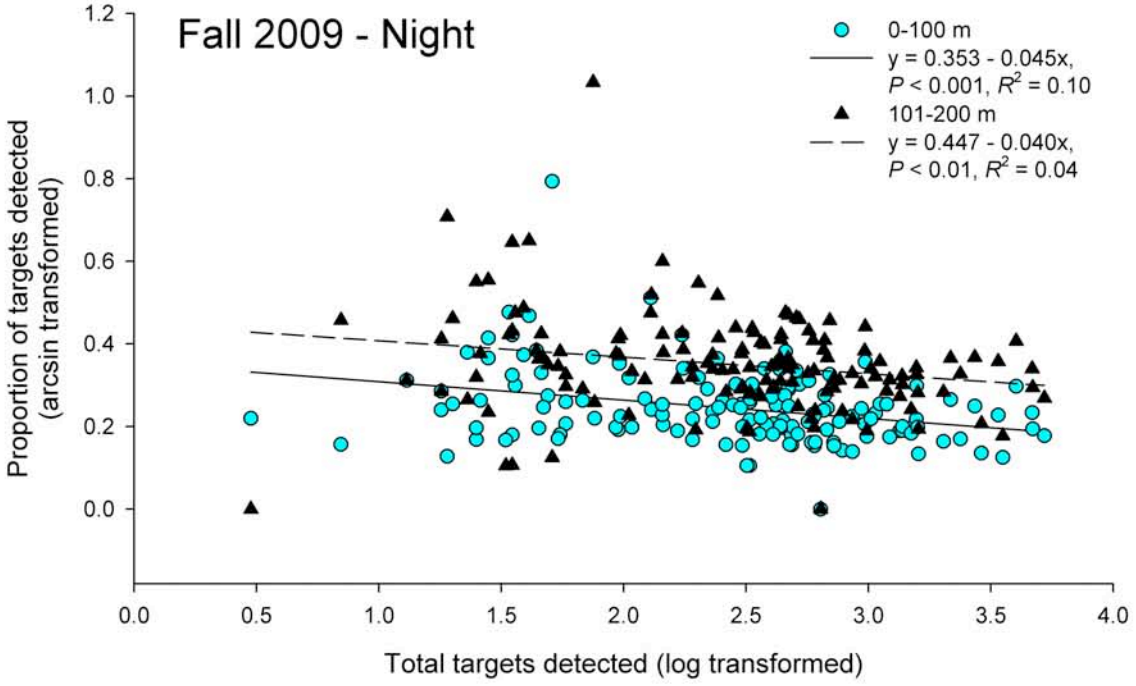

Figure 39. Relationship between the proportion of targets detected in the two lowest altitudinal strata (i.e., <= 100 m, between 100 and 200 m) and total targets detected (i.e., sum of the 10-minute sample averages) during day and night data collection periods, fall 2009.

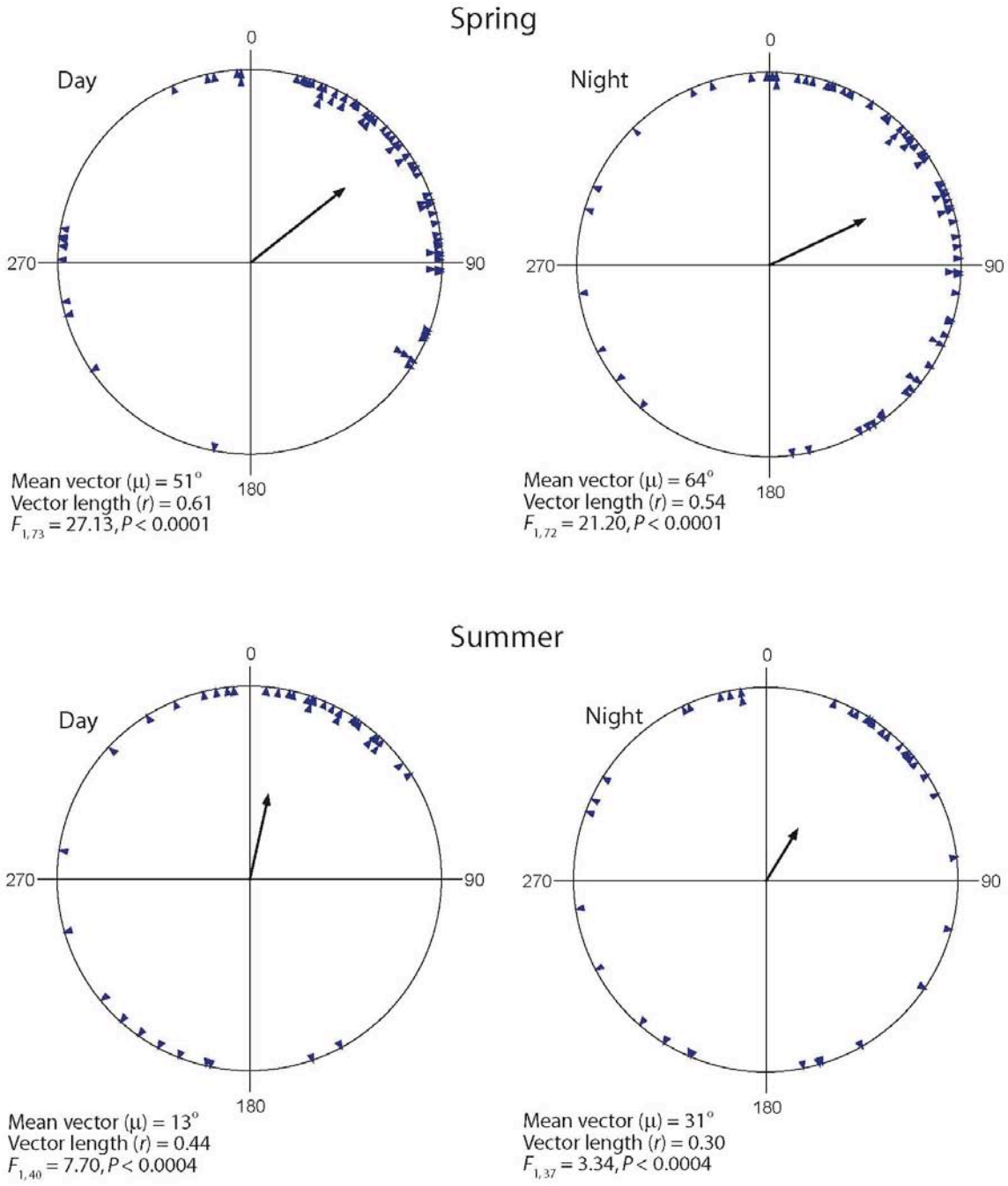

Fig. 40. Second-order mean vectors (i.e., mean of meanns) in spring and summer 2009 for day and night data collection periods. Blue triangles around the perimeter of each circle represent first-order mean vectors. Arrows point in the direction of the second-order mean vector and their length represents the vector length Vector lenght is an index or circular variance with values ranging between 0 and 1. The higher the value, the lower the variance in the mean vector.

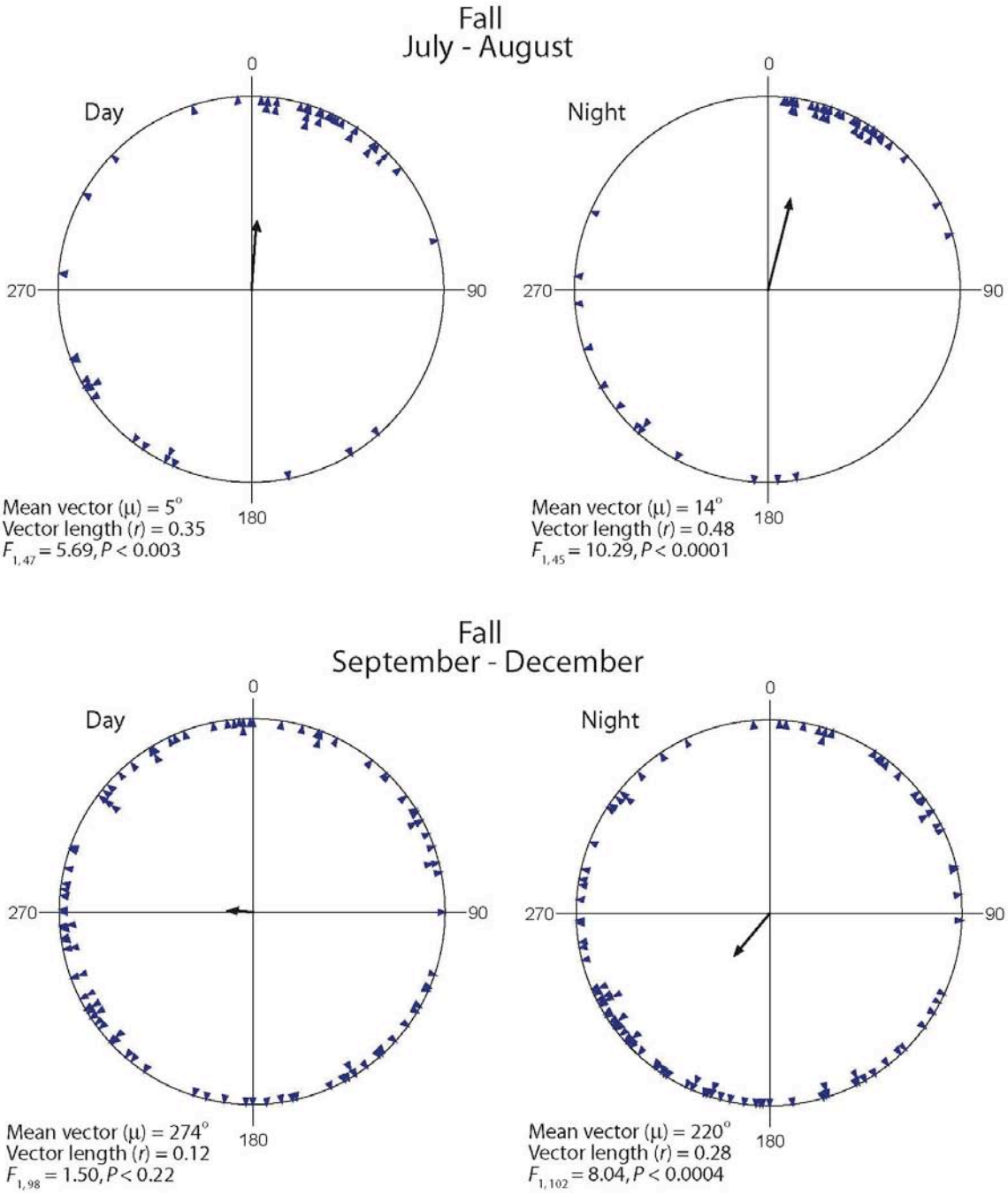

Fig. 41. Second-order mean vectors (i.e., mean of meanns) in fall, July - August and September - December 2009 for day and night data collection periods. Blue triangles around the perimeter of each circle represent first-order mean vectors. Arrows point in the direction of the second-order mean vector and their length represents the vector length Vector lenght is an index or circular variance with values ranging between 0 and 1. The higher the value, the lower the variance in the mean vector.

12.

Acoustic Noise and Electromagnetic Study in Support of the Rhode Island Ocean Special Area Management Plan 2010

by

James H. Miller, Gopu R. Potty, Kathleen Vigness-Raposa, David Casagrande, Lisa A. Miller, Jeffrey Nystuen, and Peter M. Scheifele

University of Rhode Island, June 30, 2010

Executive Summary

The goal of our study was to assess the environmental impact of an offshore wind farm consisting of 8 turbines in an area south of Block Island, Rhode Island. In this study, we considered the underwater acoustic noise generated by the various phases of the life cycle of a wind farm from site surveys, construction, operation, and decommissioning. In particular, the equipment can cause slightly elevated levels of noise in the area adjacent to the turbines both in the atmosphere and in the ocean. To understand the acoustic impact of the offshore wind farm on the surrounding area, a measurement program for the existing ambient noise field was undertaken. The major sources of underwater noise have been found to be shipping, wind-generated waves and bubbles, rain and marine animals. The modeling suggests that the operation of the 8 turbine wind farm would have little impact on marine life. The construction of the wind farm involves driving piles and noise from this operation would have a significant effect on any nearby animals. We recommend that the construction be done after the spring migration of right whales past Block Island. A larger farm being planned for an area east of Block Island was shown to increase the underwater noise levels inside the larger farm. One of recommendations from this study was to encourage the developer to design the support structures that would lower the underwater noise levels. Airborne noise was measured and we conclude that no turbine noise will be detectable on Block Island. In addition to the acoustic measurements, electric and magnetic ambient fields were measured at the candidate sites and at other sites associated with electric power transmission underwater. The fields have the potential to affect animals such as turtles, marine mammals, birds and fish within 30 feet of the underwater power transmission cables.

Table of Contents

List of Figures

List of Tables

Abstract

The goal of our study was to assess the environmental impact of an offshore wind farm consisting of 8 turbines in an area south of Block Island, Rhode Island. In this study, we considered the underwater acoustic noise generated by the various phases of the life cycle of a wind farm from site surveys, construction, operation, and decommissioning. In particular, the equipment can cause increased levels of noise both in the atmosphere and in the ocean. To understand the acoustic impact of the offshore wind farm on the ecosystem, a measurement program for the existing ambient noise field was undertaken. An ambient noise budget for the area was computed and showed that the major sources of underwater noise in this area was found to be shipping, wind-generated waves and bubbles, rain and marine animals. The underwater noise generated by the wind turbines was modeled using European data. The modeling suggests that the 8 turbine wind farm would have little impact on marine life. The construction of the wind farm involves driving piles and noise from this operation would have a significant effect on any nearby animals. We recommend that the construction be done after the spring migration of right whales past Block Island. A larger farm being planned for an area east of Block Island was shown to increase the underwater noise levels inside the larger farm. One of recommendations from this study was to encourage the developer to design the support structures that would lower the underwater noise levels as compared to the European wind farms. Airborne noise was measured and we conclude that no turbine noise will be detectable on Block Island. In addition to the acoustic measurements, electric and magnetic ambient fields were measured at the candidate sites and at other sites associated with electric power transmission underwater. The fields have the potential to affect animals such as turtles, marine mammals, birds and fish within 10 meters of the power transmission cables.

1 Introduction

The goal of this report is to assess the environmental impact of a planned offshore wind farm consisting of 8 turbines being considered in an area south of Block Island, Rhode Island. In this report, we consider the underwater acoustic noise generated by the various phases of the life cycle of a wind farm from site surveys, construction, operation, and decommissioning. We also document the potential effects of the electromagnetic fields generated by the production and transmission of the electrical power from the wind farm to shore. The equipment and facilities associated with generating offshore wind power have the potential to affect the surrounding environment. In particular, the equipment can cause increased levels of noise both in the atmosphere and in the ocean. Also, increased electric and magnetic fields can be generated in the process of creating the electrical power and in transmitting the power to shore. The fields have the potential to affect animals such as turtles, marine mammals, birds and fish.

Our approach for assessing the impact of underwater noise uses the concept of zones of influence to categorize the effects on marine life. These zones of influence vary from a small zone of injury just adjacent to the source of the noise to a large zone of audibility where the noise may be detectable by the marine animals. Beyond that, a zone of no effect is described where the wind farm noise cannot be detected against the ambient noise from shipping, wind, rain, and biological sources.

One of the fundamental activities in any environmental assessment is the measurement of the existing conditions at the proposed candidate site. The National Research Council's 2003 report, "Ocean Noise and Marine Mammals" (Frisk, et al., 2003) stated that ambient noise is "the noise associated with the background din emanating from a myriad of unidentified sources. Its distinguishing features are that it is due to multiple sources, individual sources are not identified (although the type of noise source—e.g., shipping, wind—may be known), and no one source dominates the received field."

The candidate site for an offshore wind farm south of Block Island has an ambient noise field that varies with season, wind speed, boat traffic, rainfall rate, etc. To understand the acoustic impact of the offshore wind farm on the ecosystem, a measurement program for the existing ambient noise field was undertaken. In addition to underwater noise, airborne noise was measured at the site and at Block Island. In addition to the acoustic measurements, electric and

magnetic ambient fields were measured at the candidate sites and at other sites associated with electric power transmission underwater.

European researchers have quantified the noise and other effects from offshore wind farms in Denmark. (DONG Energy, 2006) Recently, new injury and behavior criteria for marine mammals including cetaceans and pinnipeds have been published (Southall, et al., 2007). Our analysis of the effects of the additional noise caused by the offshore wind farm has utilized both new criteria and the existing criteria from the National Marine Fisheries Service (NMFS).

Pile driving and other activities associated with construction and removal of the wind turbine structures will have the most intense acoustic signals. (Richardson, Greene, Malme, & Thomson, 1998) In this report, we model the acoustic signature of pile driving using standard pile driving source functions, the geological and oceanographic properties of the potential sites, and the Monterey-Miami Parabolic Equation (MMPE) acoustic transmission loss model (Smith, 2006).

2. Wind Turbine Noise

2.1 Air Noise

In general, there are four different types of sounds produced by wind turbines: tonal, broadband, low frequency, and impulsive. Tonal sounds occur at discrete frequencies and can be caused by components within the turbine. Broadband sounds occur when the turbine blades spin through the air and interact with the atmospheric turbulence. Low frequency sounds are associated with downwind rotors. Finally, impulsive sounds are "short acoustic impulses…that vary in amplitude with time." (Rogers, Manwell, & Wright, 2002)

The sources of the noise produced by the operation of wind turbines can be divided into two categories: mechanical and aerodynamic. The mechanical sound is produced from both the gearbox and the control mechanism, such as cooling fans, the generator, and yaw drives. The emitted sounds are often tonal, as they are linked with the rotation of equipment (Rogers, Manwell, & Wright, 2002). Besides gear tone, it is primarily the aerodynamic generation mechanism that is the dominant source of noise from wind turbines. The broadband noise produced by the turbine often originates from airflow around the turbine blades and typically increases with rotor speed (Colby W. D., Dobie, Leventhall, Lipscomb, McCunney, & Seilo, 2009).

Environmental factors can also affect the noise produced by wind turbines. Often if the ground is very warm, the air will cause the produced noise to refract upwards, which results in reduced sound levels. Conversely, when the ground is very cool, the sound levels of the turbine noise increase. In addition to temperature, barriers, trees, shrubbery, etc can cause attenuation of the sound (Colby W. D., Dobie, Leventhall, Lipscomb, McCunney, & Seilo, 2009).

2.2 Underwater Noise

Underwater noise from the operation of offshore wind turbines is created by many of the same sources as air noise. However, the most efficient path for the noise from the turbine into the water is through the support structure. The noise transmitted through the air is of much lower level due to the impedance mismatch between air and water. To convert air intensity levels to water intensity level, we use the following expression SPL_{water} (dB re 1 μPa)= SPL_{air}(dB re 20 μPa) + 62. But the impedance contrast results in a transmission coefficient of -36 dB. Therefore, underwater noise generated directly by aerodynamic sources can be neglected. The underwater noise transmitted through the structure from the turbine is analogous to shipping noise, in that it is continuous, low frequency (<1000 Hz), and low level. Because there are no installed wind turbines in the waters off the US, we have relied on data measured at European wind farms. (Betke, Glahn, & Matuschek, 2004) Simultaneous measurements of vibration on the monopile showed that the noise was dominated by gear noise.

3. Zones of Influence

Our approach for assessing the impact of underwater noise uses the concept of zones of influence to categorize the effects on marine life. Figure 1 shows the zones of influence for the effects of noise on marine animals. (Richardson, Greene, Malme, & Thomson, 1998) At some range from the source of noise, there is a Zone of No Effect in which the sound levels are so low that they are not detectable in the ambient noise. Inside the Zone of No Effect, there is the Zone of Audibility where while the sound is detectable but is not intense enough to cause any observable response. Inside the Zone of Audibility, there is the Zone of Responsiveness where the sound is loud enough to cause a behavioral reaction such as a startle response, movement to or away from the source, etc. Closer to the source, there is the Zone of Masking where the sound from the source is loud enough to mask important acoustic signals including conspecific calls. Finally, very near the source, there is a Zone of Injury where the acoustic signals are intense enough to cause physical harm. It is important to note that Temporary Threshold Shift (TTS), a

short term degradation of the hearing capability of an animal is not considered injury per se because there is no tissue damage. (Southall, et al., 2007) Rather, TTS can be thought of as hearing fatigue, a phenomenon often observed in humans after concerts, auto races or operating loud machinery for a short time. Permanent Threshold Shift (PTS) is an injury to the ear which is permanent and not recoverable. The Zone of Injury is a region where PTS or more severe injury may occur.

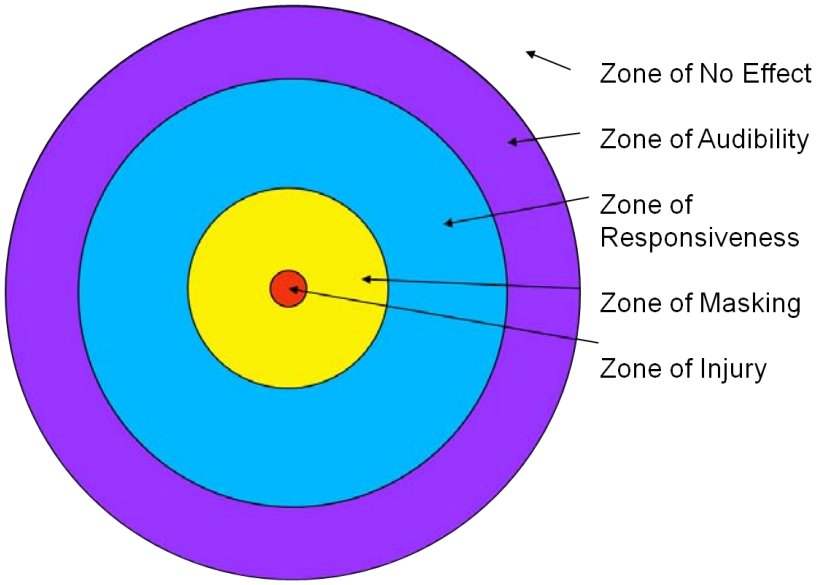

Figure 1: Zones of influence for the effects of noise on marine animals. Adapted from Richardson, et al, 1998.

Criteria for estimating the effects of noise on marine mammals are shown in Table 1. Another recent development of criteria is given by Southall (Southall, et al., 2007). The criteria suggested by Southall and his colleagues are higher than those listed in Table 1 for injury. Audibility is typically assumed to be 120 dB re 1 μPa rms (root mean square) or greater in water and we assume this level in this report. We assume that the existing NMFS criteria will apply to this development. Root mean square or rms is a property of signals can be thought of as the square root of the average power of a signal as is defined formally as

$$p_{rms} = \sqrt{\frac{1}{T}\int_0^T |p(t)|^2 \, dt}$$

Table 1: Criteria for estimating the effects of noise on marine animals. NMFS criteria taken from (Department of Commerce, 2008).

Criteria	NMFS Criteria
Level A Injury (Pinnipeds)	190 dB re 1 μPa rms (impulse)
Level A Injury (Cetaceans)	180 dB re 1 μPa rms (impulse)
Level B Harassment/Behavior	160 dB re 1 μPa rms (impulse)

4. Noise Budget

One way to quantify the potential effects of anthropogenic, underwater sound on marine animals is with an ambient noise budget (Miller, Bradley, & Nystuen, 2008). An ambient noise budget is a listing of the various sources of noise at a receiver and their associated ranking by some measure. A number of different types of budgets can be conceived using acoustic measures such as intensity, energy, or duration. These budgets are usually parameterized by frequency and are typically computed over bands such as 1/3 octave.

Noise budgets may be useful for marine mammal masking studies, habitat characterization, environmental studies, and for studies of the evolution of animal hearing. The use of a sound budget allows for the estimation of the acoustic environment prior to man's introduction of sound into the oceans and a computation of anthropogenic contributions to the noise environment. In addition, an understanding of how anthropogenic activities might be affecting animals can be produced. For example, noise from shipping may be interfering with the communication and behavior of marine mammals. (Tyack & Clark, 2000) The Wenz curves (Wenz, 1962), a common way to display the contributions of the myriad of oceanic sound sources, have been used as a basis for averaged noise budgets. The Wenz curves are shown in Figure 2. Note that the units of the Wenz curves are dB re 1 μPa2/Hz, i.e. the average intensity in a 1 Hz band. With the assumption that the curves correctly represent the acoustic environment of marine life, noise budgets will provide marine mammal hearing evolution studies with the baseline data for establishing mammal hearing response. More importantly, if that budget is changing with time, it provides details of the change and can be used to predict impact and adjustments that might be necessary to mitigate the change.

In 2003, a panel convened by the National Research Council of the US to study the effect of sound on marine animals wrote a report recommending the use of noise budgets. (Frisk, et al.,

2003) A conceptual framework was developed by the committee members using average intensity (AI) budget in 1/3-octave bands rather than the 1-Hz bands used by the Wenz curves. While 1-Hz bands are used for convenience, the 1/3-octave bands are very similar to the bandwidth of animal hearing. The intensity of sound in 1/3-octave bands has been considered to be appropriate for marine mammal hearing and masking studies (Ketten, 2000).

In an ocean with constant sound speed and density, the instantaneous intensity of a wave far from a small source labeled n is given by:

$$I_n(f,t) = \mathrm{Re}\left[p_n(f,t)u_n^*(f,t)\right] = \frac{|p_n(f,t)|^2}{\rho\, c}$$

where $p_n(f,t)$ is the acoustic pressure in a band of frequencies centered at frequency f and time t and $u_n(f,t)$ is the radial component of acoustic particle velocity. The average intensity in the frequency band is:

$$\langle I_n(f)\rangle = \frac{1}{T\rho\, c}\int_0^T |p_n(f,t)|^2\, dt$$

where T is the averaging time. If one is able to classify the source n of sound for all times between 0 and T, a noise budget can be calculated using the average intensity in the frequency band for each source.

Since the publication of the NRC report, a large of amount of noise data in various ocean sites using PAL (Passive Aquatic Listener) systems. (Ma, Nystuen, & Lien, 2005) (Nystuen, Moore, & Stabeno, 2010) Sound budgets based on temporal detections and classifications have been reported (Nystuen and Howe, 2005). These temporal detection (TD) noise budgets are closely related to the AI budget model but use the duration of maximum received level in frequency bands. Unique spectral characteristics of different sound sources are used to identify the sound source. Typical sources include breaking waves from wind (to measure wind speed), raindrop splashes (to measure rain), drizzle, shipping (both distant and local), and marine mammals (especially whales).

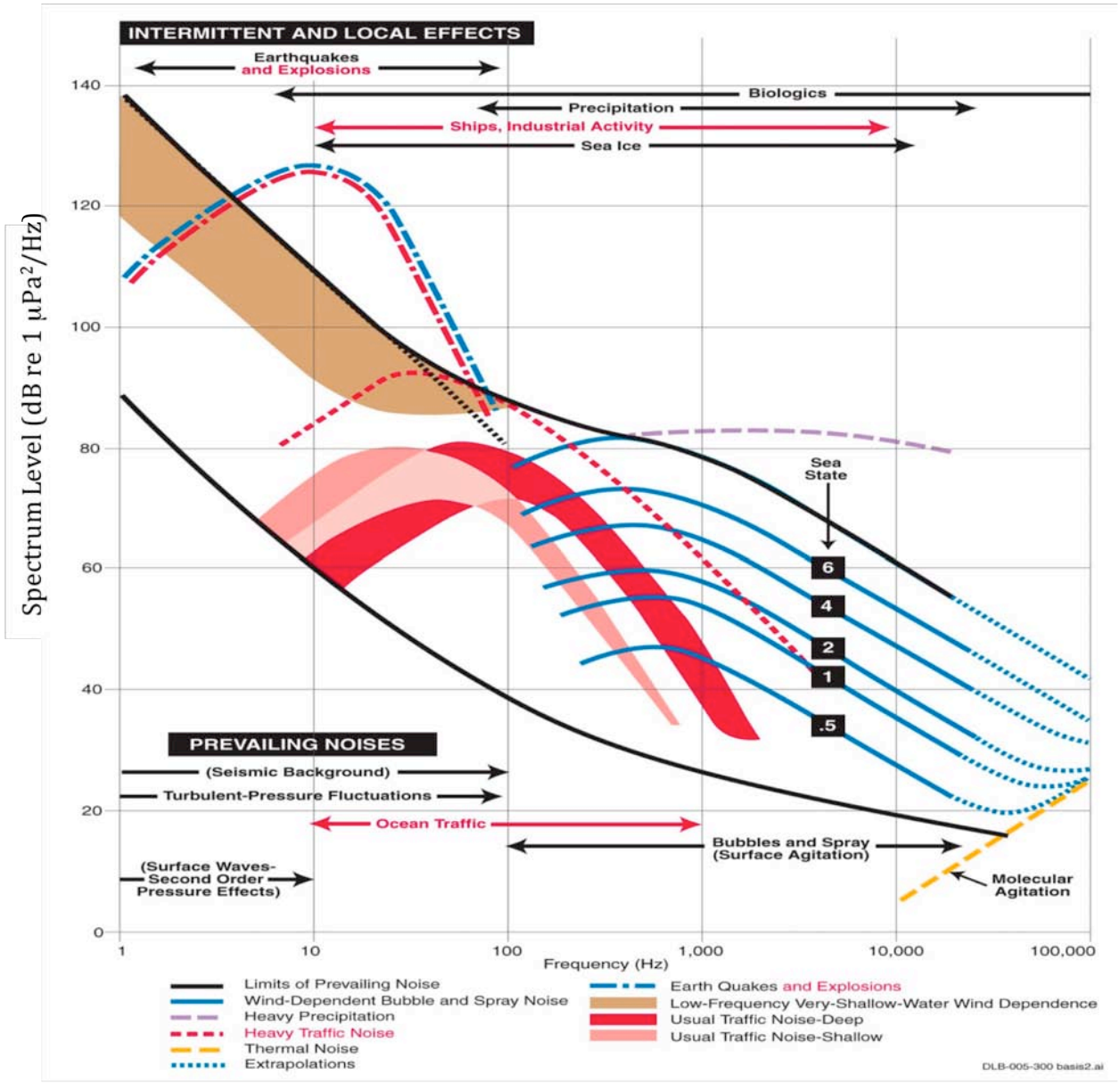

Figure 2: The Wenz curves depicting average ambient noise levels as a function of frequency for various sources. Note that the units are dB re 1 mPa2/Hz. (courtesy of David L. Bradley)

5. Air Noise

The human ear is capable of hearing a wide range of sounds based on their sound pressure level or frequency content. The average human ear is able to perceive sounds that range from 20 Hz to 20,000 Hz. Humans are affected by noise based on the intensity as follows (Rogers, Manwell, & Wright, 2002):

- <90 dBA: No adverse effects
- 115 dBA: Fatigue, Stomach Pains, Hypertension, etc.

- 120 dBA: Threshold of pain at 10 Hz
- >120 dBA: Exposure for 24 hours or longer can cause permanent physiology damage.

It is the low frequency sound, typically ranging from 10 to 200 Hz, that is the subject of concern of some physicians and scientists when it comes to the development of wind turbines near human habitats. Some believe that these sounds can cause adverse health effects such as "wind turbine syndrome". In a testimony before the New York State legislature Energy Committee (Pierpont, 2006), Dr. Nina Pierpont, a proponent of "wind turbine syndrome", defines it as a set of symptoms that include:

- Sleep Problems
- Headaches
- Dizziness
- Anxiety
- Concentration & Learning Problems
- Tinnitus

Low frequency sounds typically need to be at a high sound pressure level to be heard by an average human. As stated in the expert panel review conducted for both the American Wind Energy Association (AWEA) and Canadian Wind Energy Association (CanWEA), "As the annoyance of a given sound increases as loudness increases, there is also a more rapid growth of annoyance at low frequencies. However, there is no evidence for direct physiological effects from either infrasound or low frequency sound at the levels generated from wind turbines, indoors or outside. Effects may result from the sounds being audible, but these are similar to the effects from other audible sounds." (Colby W. D., Dobie, Leventhall, Lipscomb, McCunney, & Seilo, 2009)

Powerful and intense, but very short-duration sounds above 130 dBA (i.e. explosions) are capable of causing cochlear damage, as well as permanent hearing loss; but the majority of occupational hearing loss is due to prolonged exposure to high noise levels between 90 and 105 dBA. In 1983 in the US, the Occupational Safety and Health Administration authorities (OSHA, 1983), as well as in 1998 by the National Institute for Occupational Health and Safety (NIOSH, 1998), warned that the risk of occupational hearing loss begins at 85 dBA, over an eight hour day and a forty year career. Sound pressure levels that are below 75 dBA do not pose a danger of noise induced hearing loss and therefore the sound levels that are produced by wind turbines will

not cause noise induced hearing loss because they are simply not high enough. Through studies performed (Suter, 1991),it has been shown that simple tasks may be unaffected at noise levels as high as 115 dBA, but complex tasks may be affected at noise levels as low as 75 dBA. Noise levels that are below 70 dBA do not result in task interference. Therefore, the noise produced by the operation of wind turbines interferes with neither simple nor complex tasks. (Colby W. D., Dobie, Leventhall, Lipscomb, McCunney, & Seilo, 2009)

Annoyance is "a subjective response that varies among people to many types of sounds". Although annoyance can be a frustrating effect of certain sounds, it is not considered an adverse health effect. The belief that chronic noise exposure might lead to chronic health problems has been the subject of many debated and hundreds of contradictory studies. There is no definitive evidence that supports claims of "wind turbine syndrome" (The Health Impact of Wind Turbines: A Review of the Current White, Grey, and Published Literature , 2008).

6. Results of the Study

6.1 Acoustic data collection using calibrated systems in air

Air noise data were collected at the following three sites: 1) near the Portsmouth High School Wind Turbine (1.5 MW), 2) on Mohegan Bluffs on Block Island and 3) near sediment coring at sea near the Lift/Barge (L/B) Kayd. All air noise data were collected in 2009 using a Bruel and Kjaer Hand-Held Analyzer Type 2250L. A typical air noise spectrogram measured near the site south of Block Island is shown in Figure 3. The more intense epochs in Figure 3 are shown in red and are associated with gusts of wind. These gusts of wind contain low frequency noise typically below 500 Hz.

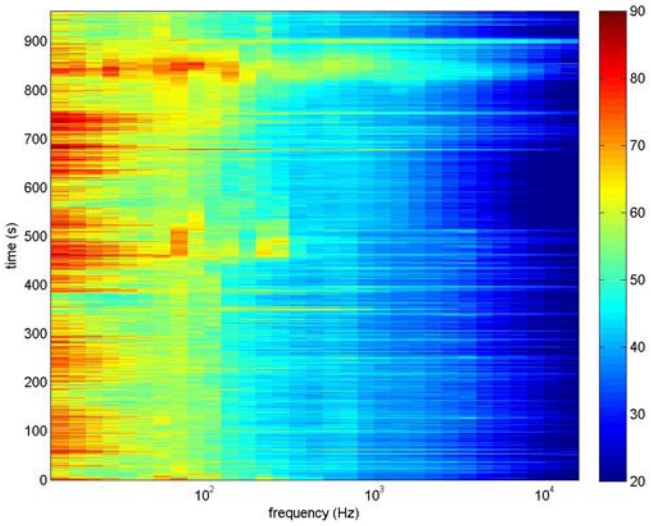

Figure 3: Air noise spectrogram as a function of frequency and time taken at sea just south of Block Island. The units are dB re 20 mPa^2 in a 1/3 octave band.

There have been reported instances of wind turbine syndrome from land-based systems in the US and Canada. (Pierpont, 2010) In the Canadian Province of Ontario, the Ministry of the Environment created noise guidelines to limit wind turbine noise levels 30 meters away from a dwelling or campsite to 40 dB(A). These regulations also set a minimum distance of 550 meters (1,804 feet) for a group of up to five relatively quiet [102 dB(A)] turbines within a 3-kilometer (1.86-mile) radius, rising to 1,500 meters (4,921 feet) for a group of 11 to 25 noisier (106-107 db(A)) turbines (Ontario Ministry of Environment, 2009).

The noise spectrogram for the Portsmouth High School Wind Turbine measured at a distance of 65 meters is shown in Figure 4. Units are dB re 20 μPa^2 in a 1/3-octave band. The color scale is the same as used in Figure 3. Based on these very typical air noise measurements described above and published reports on wind turbine noise in air, the noise from the 5-8 wind turbines planned for state waters south of Block Island (approximately 3 nm from the island) will not be detectable by residents on the island. It is possible that blade noise would be detectable by humans very near (<200 meters) from the wind turbines. Air noise from the impact pile driving may be detectable on Block Island especially at night when propagation conditions allow for downward refraction.

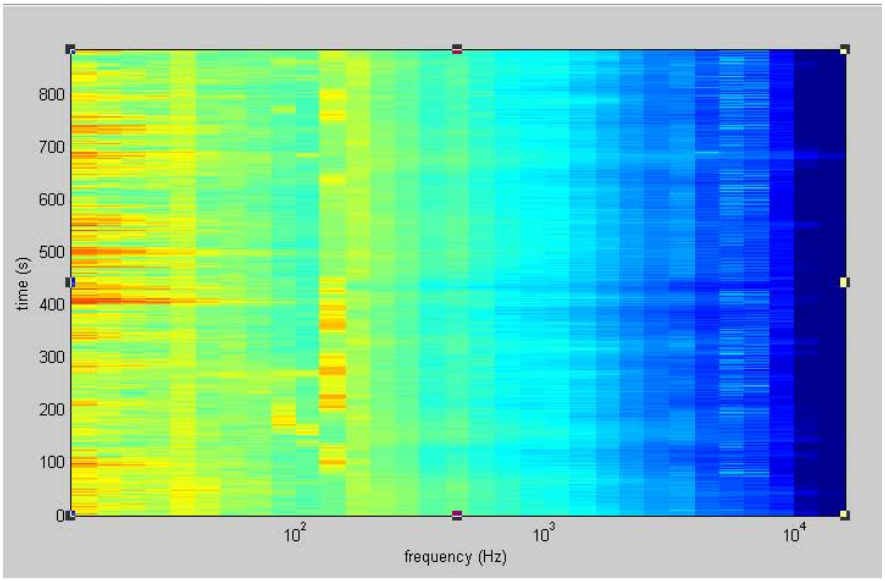

Figure 4: Noise spectrogram for the Portsmouth High School Wind Turbine measured at a distance of 65 meters. Units are dB re 20 mPa^2 in a 1/3-octave band. The color scale is the same as used in Figure 3.

6.2 Acoustic data collection using calibrated systems underwater

The ambient noise levels were measured underwater at the candidate locations. Underwater noise measurements were made with Passive Aquatic Listeners (PALs). This system was deployed for five weeks in October and November of 2008. Figure 5 shows the locations of the PALs and the Automated Identification System (AIS)-derived shipping for the period of October 6 through November 14, 2008. Two PAL systems were deployed off Block Island in the fall of 2009 and are due to be recovered in summer of 2010 providing data for the estimation of noise budgets for all four seasons.

The PALs were programmed to make a short recordings of 4.5 seconds every nine minutes, perform a Fourier Transform on the time series, and then do a spectral analysis to identify the sound source. If the sound is uniform during the sample, the source is deemed "background" and unique spectral characteristics for known background sources such as wind, rain and shipping are used to identify the sound source. The spectral components of the sample are saved, and the original temporal sample is discarded. However, transient sound within the 4.5 second sample are also detected. If the detection threshold of 13 dB signal-to-noise within a user chosen frequency band is met (user set), then an audio sample is saved in addition to the spectral data, um, and the delay before the next recording is decreased to two minutes. This allows repeated

adaptive sampling of relatively rare events (more frequent samples when something interesting is happening), but introduces a bias in that these events detections are overrepresented (higher temporal density of samples).

To remove this bias, each saved spectrum is weighted by the time between itself and the samples before and after it. For example, spectra are known at 0, 2, and 11 minutes. The spectrum at 2 minutes is representative of the time from 1 minute to 6.5 minutes. An unbiased time series of sound level is produced for each frequency of interest, allowing the creation of a histogram of sound level over the entirety of the data.

In summary, for each sound sample, the spectral characteristics of the sample are saved and used to identify the sound source. For most samples, this is a measure of background sound sources, and these sources are identified uniquely by their spectral characteristics. However, some sound samples contain transient signals. For these samples the PALs save the original audio sample as well as the spectral components. The source of the transient signal (anthropogenic, animal vocalization, etc. can often be identified by listening to it and comparing to known recording of these types of sounds. This allows a probable sound source to be identified for the majority of the PAL deployment. The mean sound intensity for each source is used to construct a noise budget.

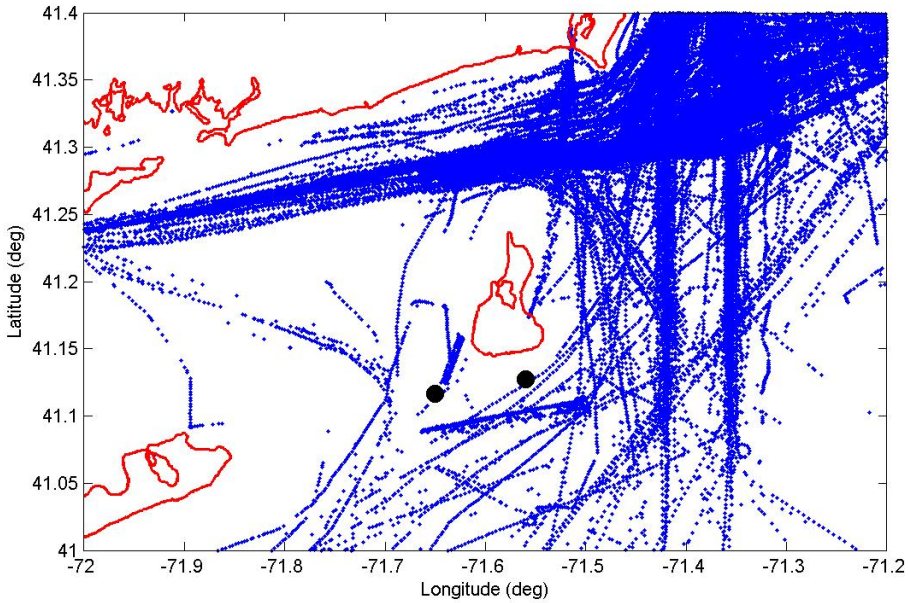

Figure 5: The solid black dots depict the locations of the two Passive Aquatic Listener systems labeled Eider on the western PAL and Puffin on the eastern PAL. The small blue dots indicate Automated Identification System (AIS)-derived ship positions. These data were collected October 6 – November 14, 2008.

A histogram for the 1/3-octave band centered at 500 Hz for PAL Eider is shown in Figure 6. A Gaussian probability density function was fitted to the data in a least square sense and the resulting pdf is also shown in Figure 6. The mean of the data was approximately 98 dB and the standard deviation was about 5 dB. The ambient noise budget for the Eider PAL in the 1/3-octave band centered at 500 Hz is shown in Figure 7. The main contributors to the noise budget at this location were shipping with 3244 pW/m^2 or 97 dB re 1 μPa^2 and wind related noise was with 3361 pW/m^2 or 97 dB re 1 μPa. Rain was next with 1167 pW/m^2 or 92 dB re 1 μPa^2 and lastly, biological noise with 341 pW/m^2 or 87 dB re 1 μPa^2.

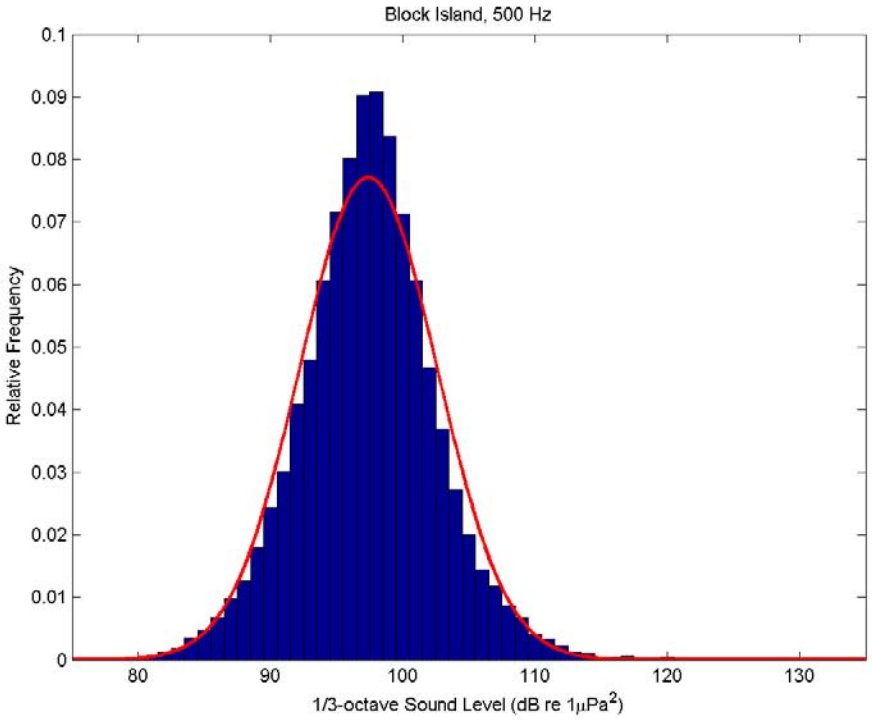

Figure 6: Histogram of ambient noise sound level in a 1/3-octave band centered at 500 Hz as measured on the Eider PAL.

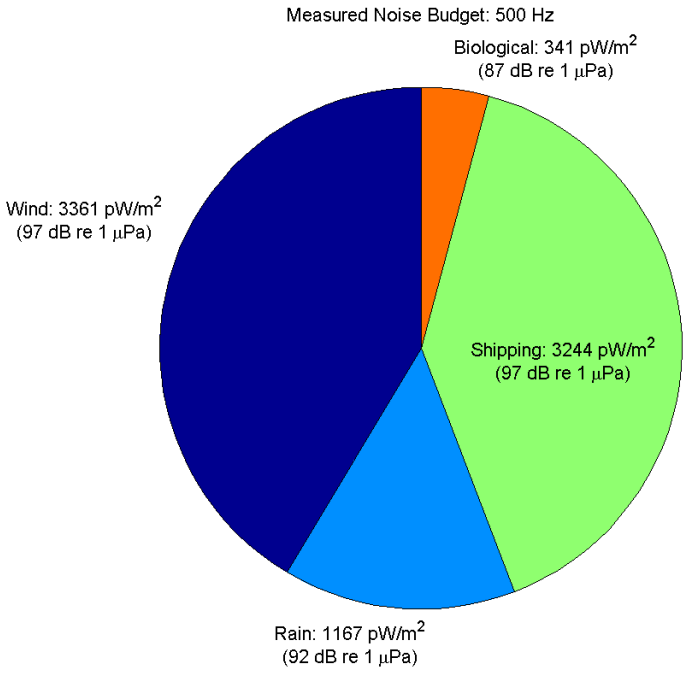

Figure 7: Noise budget as measured by PAL Eider south of Block Island in the 1/3 octave band centered at 500 Hz.

6.3 Transmission loss modeling

Transmission Loss (TL) is a measure of the rate at which sound energy is lost as a function of range, and is defined as:

$$TL = 10 \log_{10} (I_0/I_R) = 20 \log_{10} (P_0 / P_R)$$

where:

I_0 = acoustic intensity at a point one m away from the source

I_R = acoustic intensity at range R m from the source

P_0 = pressure at a point one m away from the source

P_R = pressure at range R m from the source

Transmission Loss results from geometric losses due to one of two types of spreading, spherical or cylindrical and attenuation due to absorption, scattering, viscosity, and thermal losses. The usual method of modeling the Transmission Loss due to spreading is using the expression:

$$TL = N \log_{10}(r)$$

where:

r = range from the source

N = coefficient of geometric spreading

The value of N is equal to 20 for spherical spreading and 10 for cylindrical spreading. In shallow water the value of N will lie between 10 and 20. Accurate modeling of transmission loss (TL) is usually done using standard acoustic propagation models such as Miami-Monterey Parabolic Equation (MMPE) propagation code. In the early 90's, a numerical code known as the University of Miami Parabolic Equation (UMPE) Model was documented and made available to the general research community. This model was based on the split-step Fourier (SSF) technique, and had been adapted from previous versions developed by Fred Tappert at the University of Miami. A subsequent version, known as the Monterey-Miami Parabolic Equation (MMPE) Model, was developed in the mid-90's that was more streamlined and user friendly. This code was thoroughly tested against several existing benchmark scenarios and was found to perform reasonably well during the Shallow Water Acoustic Modeling Workshop held in Monterey, CA in 1999.

Inputs to this propagation model include the environmental description i.e., sound speed in the water column as a function of depth, geoacoustic parameters of the sediment layer and basement i.e., compressional wave speed and attenuation, shear speed and attenuation and density. During the transmission loss field test in October, 2009, we deployed a CTD to measure the temperature and salinity which was then used to calculate the sound speed. The bottom was assumed to consist of a sediment layer and a basement. The sediment parameters and the thickness of the sediment layer were estimated using a simple iterative inversion by matching the modeled and measured TL. Water depth at the location was 35 m. Range independent conditions were assumed for the acoustic modeling.

Measurements of transmission loss at 200 Hz were made near Block Island in summer 2009 to support the modeling effort at the location shown in Figure 8. During the field test, an acoustic array of receive hydrophones and vector sensors were deployed from a small boat which remained stationary throughout the experiment. A J-15 sound source was deployed from another boat which moved away from the receiver ship. This provided us with a measurement of TL as a function of range assuming that the environmental conditions remained stationary. The depth of the source was 14 m and the receivers were at 9m and 21 m. These TL values correspond to the frequency of 200 Hz. Figure 9 shows the results of TL modeling using MMPE. The variation of

TL as a function of range and depth is shown in this figure. The two white straight lines in these figures represent the water-sediment interface and sediment-basement interface.

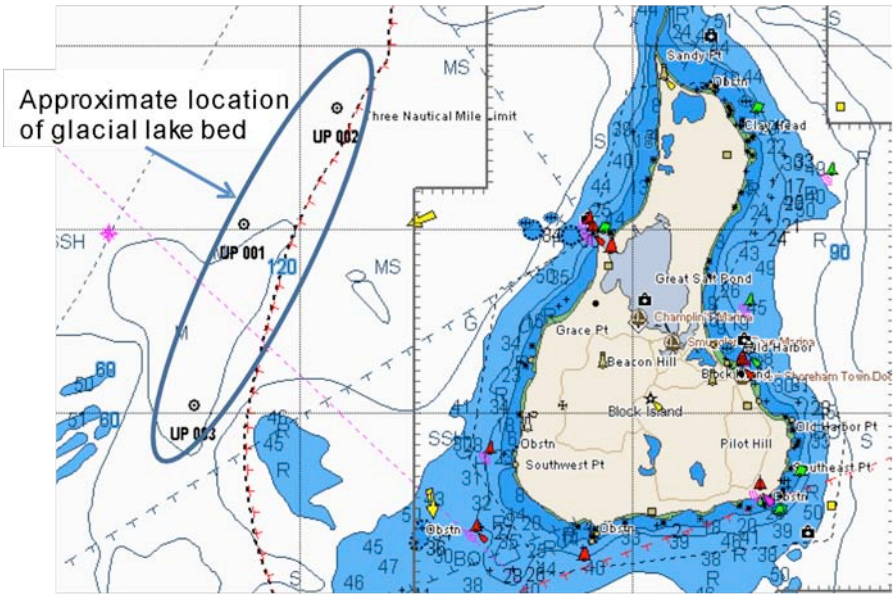

Figure 8: Location of measurements of transmission loss.

Figure 10 shows the measured transmission loss (red), modeled transmission loss using MMPE (blue). The green line represents the TL corresponding to N log(r). We tried different values for N to get a good fit and a value of N=17 provides a good fit as seen in the figure. In Figure 10 the green line represents TL calculated using 17log(r). Upper plot is TL at 9 meter depth and lower plot is at 21 meter depth. Frequency is 200 Hz. A simple TL model as 17 log(r) allows us to quickly compute TL for any acoustic propagation path without using a sophisticated propagation model.

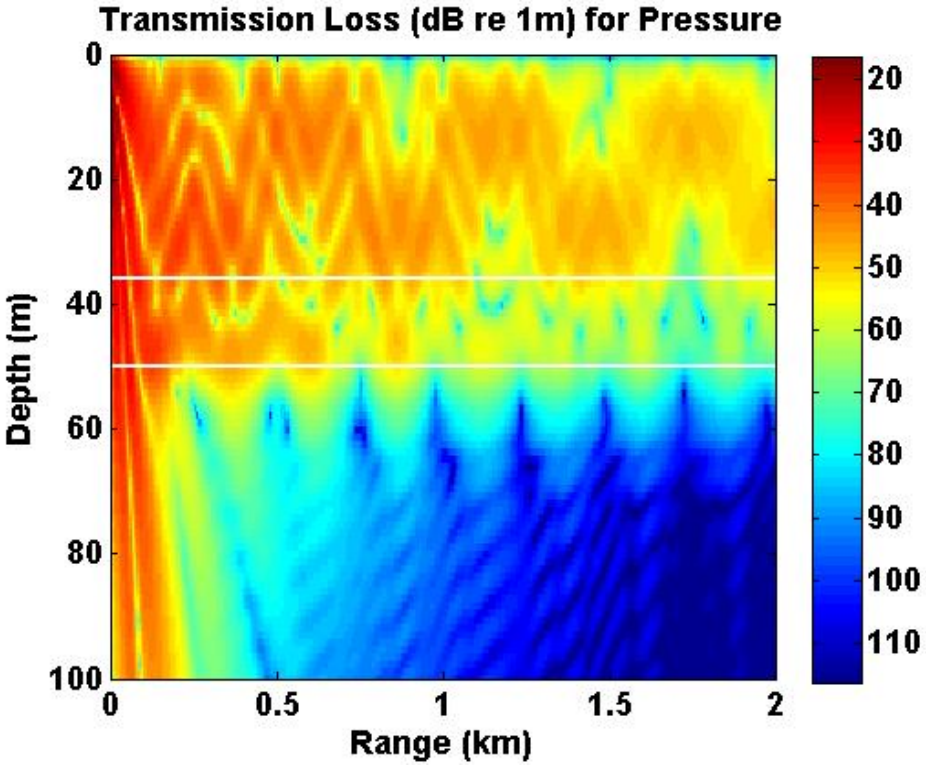

Figure 9: Modeled transmission loss at 200 Hz for a region near Block Island. Sediment parameters were adjusted to fir the measured TL.

6.4 Predicted levels of wind turbine operational noise underwater

Noise from the operation of offshore wind turbines is much lower in level than that of construction noise. This noise is more analogous to shipping noise, in that it is continuous, low frequency (<1000 Hz), and low level. Because there are no installed wind turbines in the waters off the US, we have relied on data measured at European wind farms. Measurements were taken at a range of 110 meters from a monopile-mounted 1.5 MW GE turbine in Utgruden, Sweden. (Betke, Glahn, & Matuschek, 2004) The measurement set-up is shown in Figure 11 where the water depth was about 10 meters. The underwater noise levels in 1/3 octave bands are shown in Figure 12 for four cases: a) 1500 kW, 17 m/s in September, 2003, b) 1500 kW, 12 m/s in September, 2003, c) 80 kW, 3.5 m/s in October, 2002 and d) 80 kW, 3.5 m/s in October, 2003. Betke concluded that the sound levels measured would not cause damage to the hearing organs of marine mammals, but might affect their behavior in the vicinity of the turbine.

With the information in Figure 12, we can estimate the average noise budget for various wind farm configurations near Block Island. The wind speed probability density function for the

waters south of Block Island was derived from US Army Corps of Engineering WIS Station 76 and shown in Figure 13 (Spaulding, 2010).

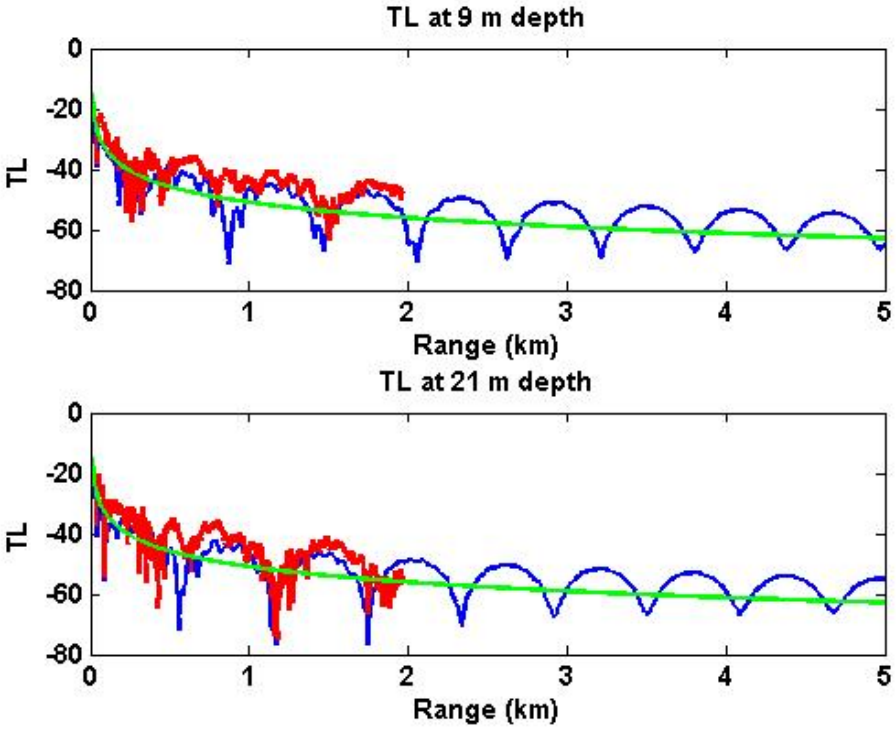

Figure 10: Measured transmission loss (red), modeled transmission loss using MMPE (blue) and 17log(r) (green). Upper plot is TL at 9 meter depth and lower plot is at 21 meter depth. The frequency is 200 Hz and the depth of the water is 35 meters. Sediments parameters were adjusted to match the measured and predicted TL.

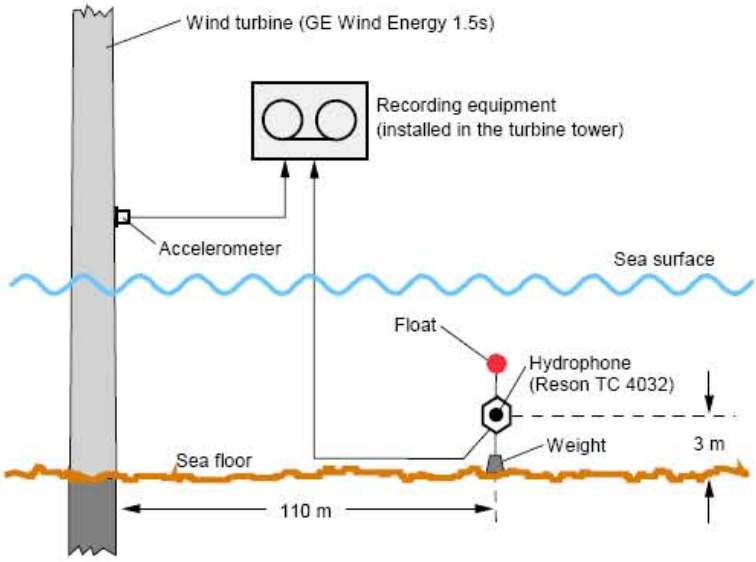

Figure 11: Measurement setup for monitoring underwater noise induced by an offshore wind turbine. Water depth was about 10 m (Betke, 2004).

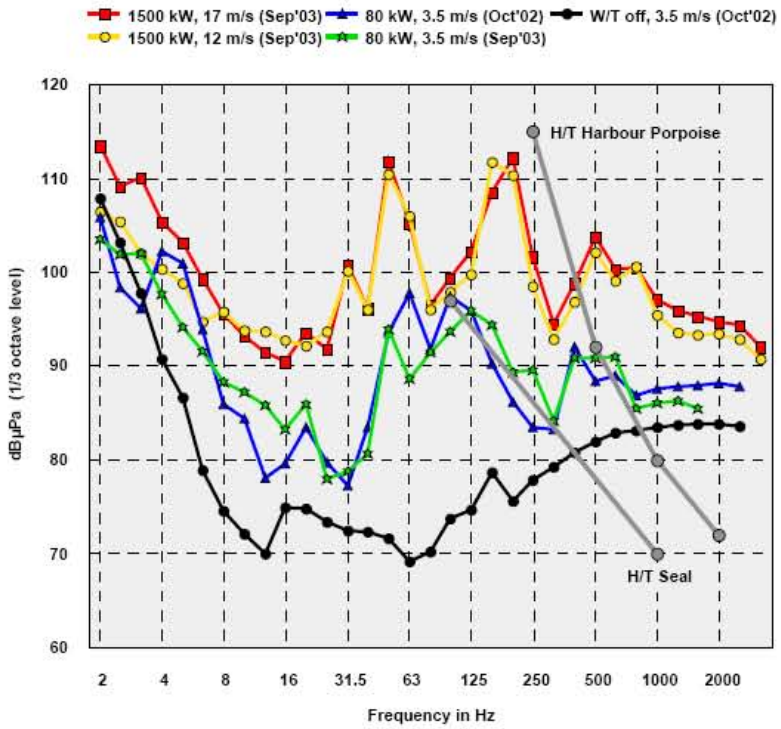

Figure 12: Measured underwater noise spectra in a 1/3-octave band for various wind speeds and power production. Also shown are the hearing thresholds for harbor porpoise and harbor seal (Betke, 2004).

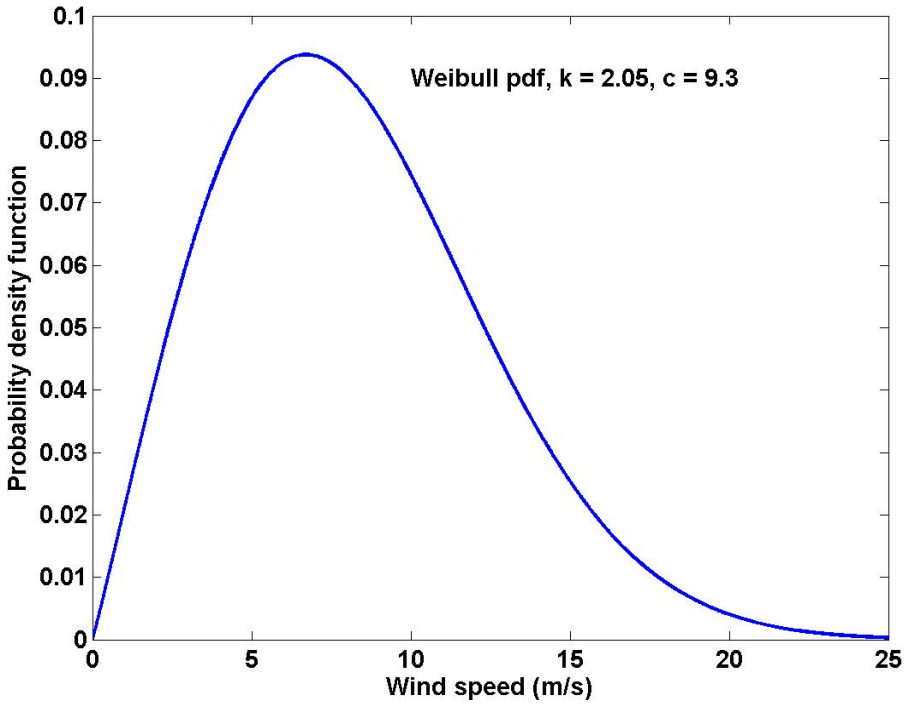

Figure 13: Probability density function for wind speed in the waters just south of Block Island. The Weibull pdf has a k-value of 2.05 and mean wind speed of 9.3 m/s.

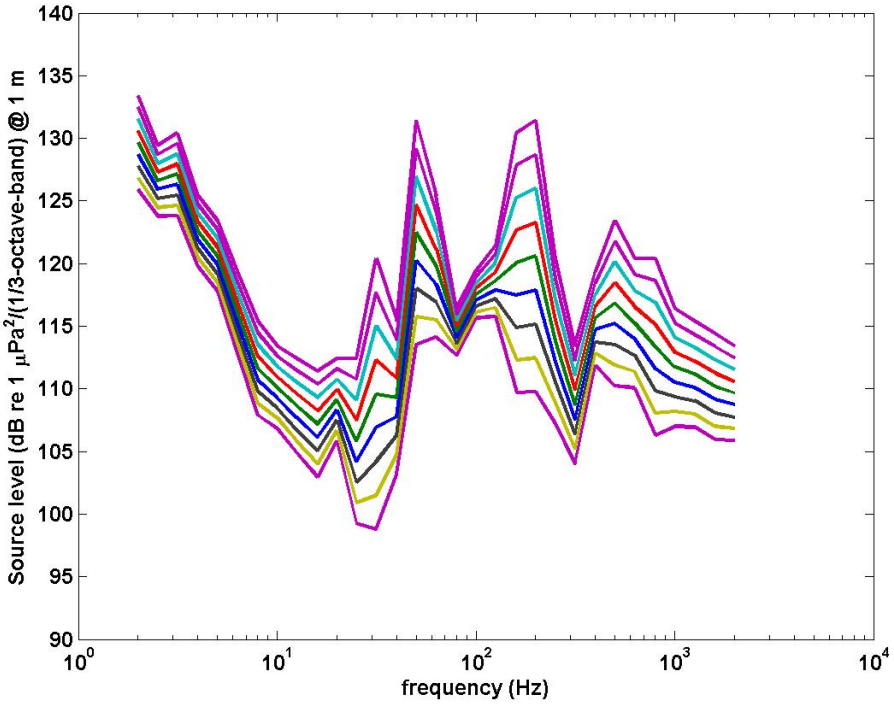

Figure 14: Calculated source level for a single wind turbine for various wind speeds from 3.5 to 12 m/s.

Figure 14 shows the interpolated source levels from a single 1.5 MW wind turbine for various wind speeds from 3.5 to 12 m/s. Using the levels in Figure 14, we are now able to calculate the additional noise from wind turbines in the noise budget originally presented in Figure 7. Figure 15 was developed by Robert Kenney and Kathleen Vigness Raposa for the Ocean SAMP study and shows the relative abundance of the northern right whale in the region south of New England. Within the Ocean SAMP region, the principal areas of northern right whale habitat are south of Block Island. We therefore computed the noise budget for a location 10 km south of the proposed experimental wind turbines near Block Island, in the area of high relative abundance of the northern right whale. The effect of the additional noise from the 8 wind turbines located near Block Island is shown in Figure 16 where the wind turbine noise is predicted to contribute 424 pW/m^2 or 88 dB re 1 μPa. The additional noise from the wind turbines is significantly less than noise from shipping, wind and rain. Also, the wind turbine noise is, on average, approximately the same as the biological noise in the budget.

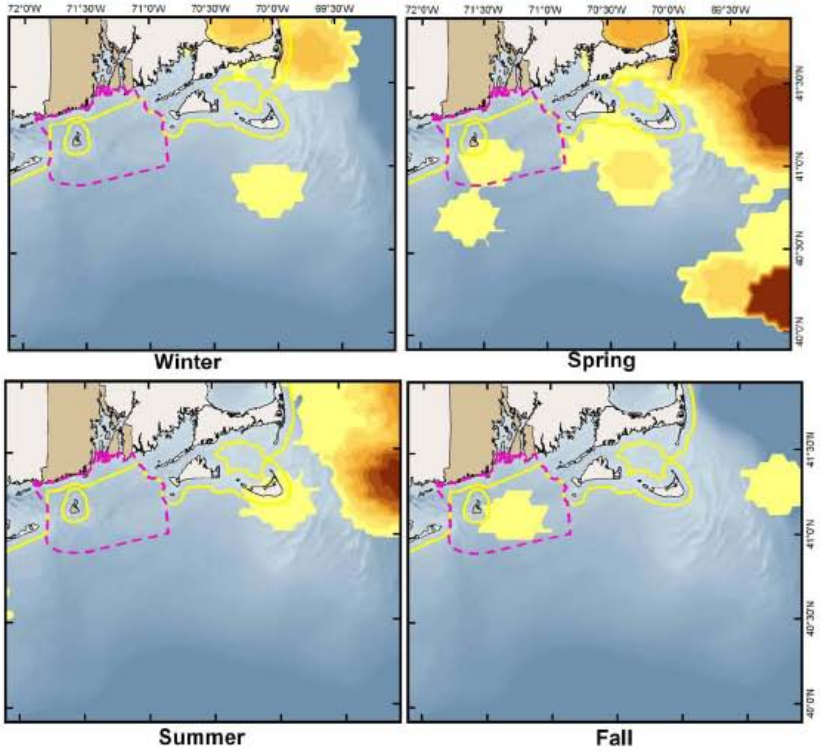

Figure 15: Relative northern right whale abundances are indicated by the yellow and brown in the region south of New England.

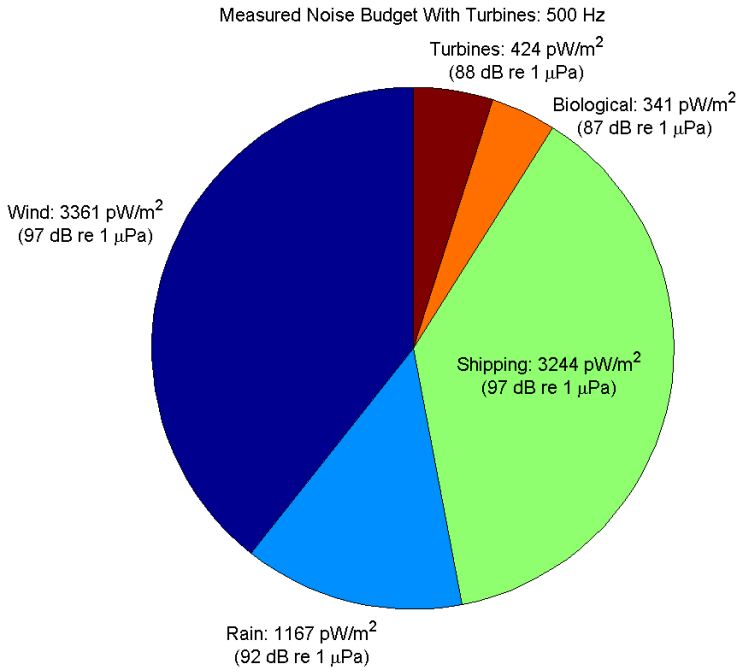

Figure 16: Noise budget as measured by the Eider PAL south of Block Island in the 1/3-octave band centered at 500 Hz with modeled turbine noise added.

For Phase 2 farm being considered (e.g. 70 turbines), the operational noise from all the turbines would add incoherently. Figure 17 shows three panels that illustrate the effect of two radiated noise levels at 100 meters. The left panel shows the noise in a 1/3 octave band at 200 Hz for a 70 turbine wind with 1 km spacing and a source level of 112 dB re 1 μPa^2 in a 1/3 octave band at 100 m. The middle panel is the radiated noise for a source level of 100 dB. The right panel is the measured ambient noise histogram from the Eider PAL deployed south of Block Island. The lowered radiated noise from the wind turbines brings the levels within the wind farm below the average ambient noise already present in the area.

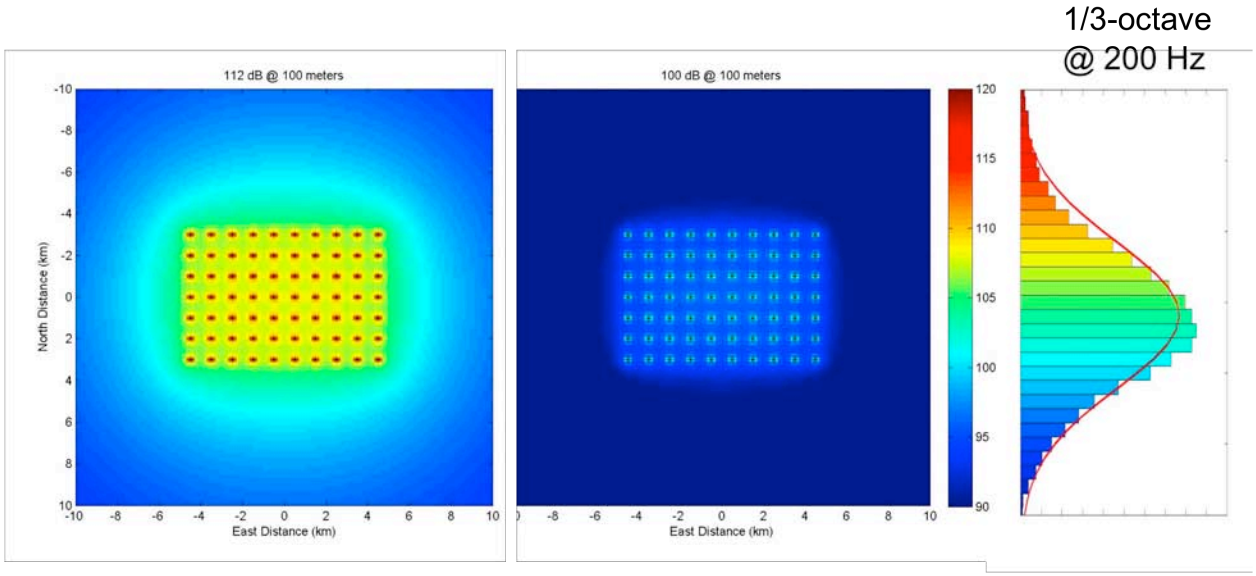

Figure 17: The left panel shows the noise in a 1/3 octave band at 200 Hz for a 70 turbine wind with 1 km spacing and a source level of 112 dB re 1 mPa^2 in a 1/3 octave band at 100 m. The middle panel is the radiated noise for a source level of 100 dB. The right panel is the measured ambient noise histogram from the Eider PAL deployed south of Block Island.

6.5 Prediction of pile driving noise

Using the propagation modeling approach discussed in the previous section, TL was modeled along tracks in all directions from the center of the proposed location of the wind farm. The approximate location is 41.1167 (N latitude); 71.5250 (W longitude) or 4554781 m (northing); 288009 m (easting). The tracks were spaced at 10 degrees apart. The ranges at which the received level exceeds 180 dB, 160 dB and 120 dB were picked based on the predicted received levels along each of these directions. The receive level at any range is calculated as the source level (@ 1m) minus the predicted TL at the range. Since no measurements of pile driving source levels were available at the location, we used published data from piles with comparable size in

similar water depths. Data (Andrews, 2009) show measured sound pressure levels at 10 m for a similar size pile as 210 dB. We back calculated the sound pressure levels at 1 m to estimate the source level and used that to calculate the receive levels. Contours of received levels corresponding to 180 dB, 160 dB and 120 dB were then constructed and mapped into a GIS layer as shown in Figure 18.

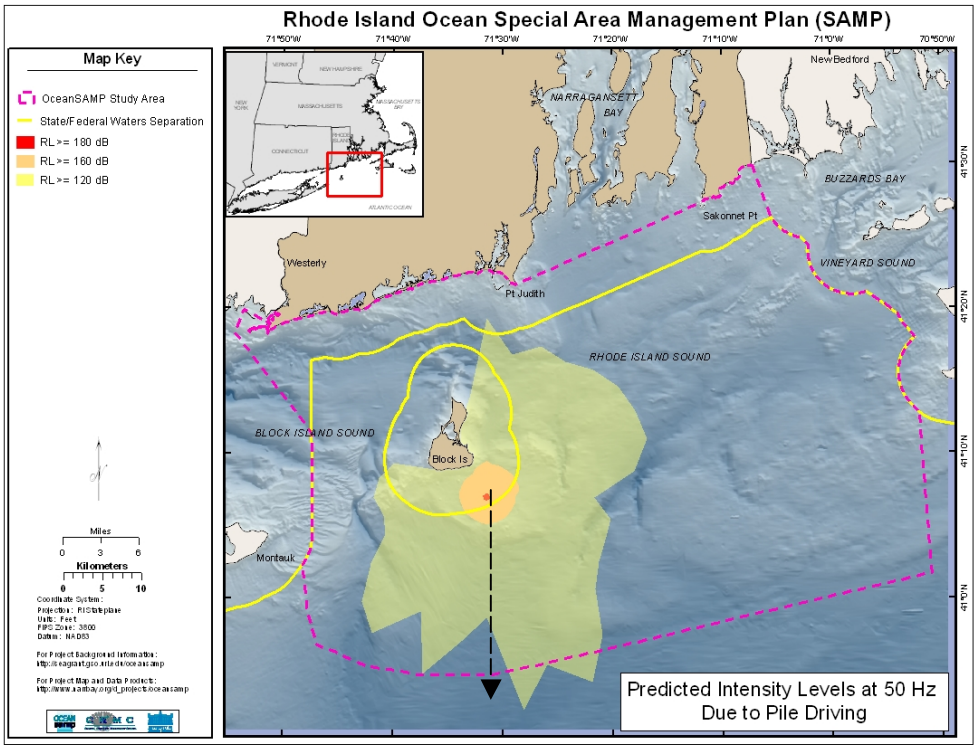

Figure 18: Estimate of the affected area in the vicinity of pile driving. Receive levels greater than 180 dB are indicated in red, 160 dB in orange, and 120 dB in yellow. The dashed arrow indicates the transect selected for modeling the broadband transmission loss.

Broadband acoustic modeling was carried out using the PE code MMPE. Calculations were made for a track as shown in Figure 18 out to a range of 30 km. Transmission Loss was calculated for frequencies from 5 Hz to 1000 Hz. Figure 19 shows the Transmission loss in dB as a function of depth (y-axis) and arrival time (x-axis) at 30 km. The ETOPO1 Global Relief Model provided the bathymetry along the propagation path. Measured temperature and salinity data were used to calculate the sound speed profile at the location. The sound speed and sediment geoacoustic properties were assumed range independent in these calculations.

Figure 19 provides the results of the calculation of broadband transmission loss on a transect directly to the south of the candidate turbine location southeast of Block Island. The minimum TL 85 dB is associated with peak intensity of the pile driving noise waveform. The peak SPL can then be calculated as SPL = SL – TL. Measured data (Andrews, 2009) show sound pressure levels at 10 m for a similar size pile as 210 dB re 1 μPa^2. If we assume cylindrical spreading near the pile, this corresponds to a source level of 220 dB re 1 μPa^2 at 1 meter. Therefore the peak SPL at 30 km is 135 dB re 1 μPa^2. This predicts that the pile driving noise would be detectable by animals at these ranges. This level is less than the Level A Injury Criterion or the Level B Behavioral Criterion presently being used by NMFS.

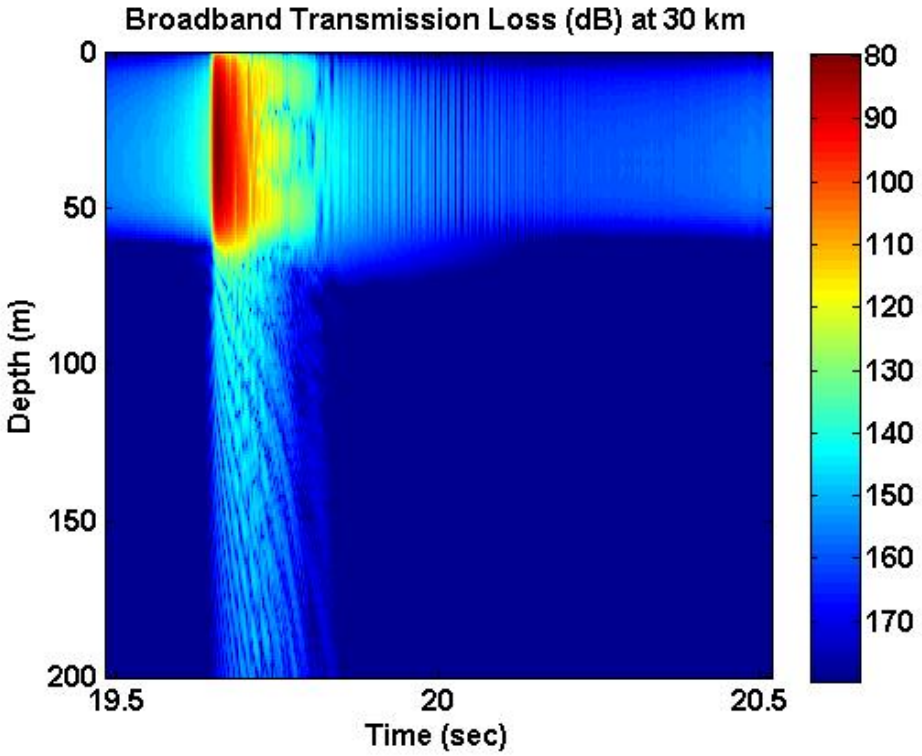

Figure 19. Broadband transmission loss on the transect to the south from candidate site out to a range of 30 km. The bandwidth of the transmission loss calculation using MMPE was 1 Hz to 10000 Hz.

6.6 Collected EM field data using calibrated systems in air in the fall of 2009

The electromagnetic field was measured at the underwater/underground cables from Newport to Jamestown and the data are shown in Figure 19. While this work is in progress, it is clear that these levels of magnetic field will also be present underwater near the power cable. This power cable is rated for 26 kVA and is similar to the cable to be installed for the 8 turbine farm near

Block Island. Elasmobranches (sharks, rays and skates) respond to magnetic fields in the range of 25 to 100 μTesla (.25 to 1 milliGauss). (Gill & Kimber, 2005) Reactions to EMF can be attraction or avoidance depending on species, levels, distance from transmission cable and other factors. However, it is clear that these effects will be confined to within 10's meters from the power transmission cables envisioned for the Block Island wind farm.

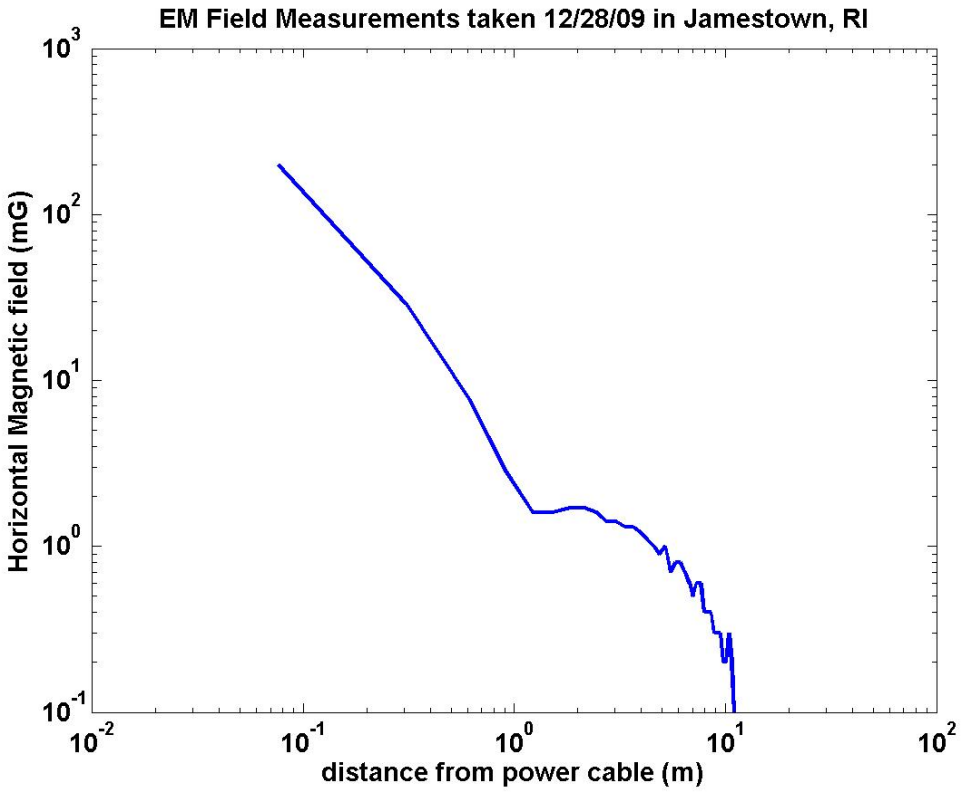

Figure 20: Horizontal magnetic field strength measurements taken on 12/28/2009 in Jamestown, RI near the underwater/underground power cable connecting Jamestown to Newport.

7 Conclusions and Recommendations

1) Pile driving impulses during construction may have significant physiological effects on marine life including whales and dolphins within 500 meters of the pile and pinnipeds within 150 meters of the pile.

> Mitigation Recommended: Pile driving should start slowly with at least a 2 minute ramp-up before maximum pile driving. The piles should be driven with pile caps made of wood or synthetic material to reduce the pressure pulse and increase the pulse rise time. Observers should be utilized to assure that no whales or dolphins are in an area of radius 500 meters from the pile driving (150 meters for pinnipeds). A monitoring system should be in operation during the pile driving to assure ramp up and measure the impulse time

series on appropriate hydrophones and geophones. We recommend that construction be delayed until after the spring migration of North Atlantic right whales past Block Island.

2) Pile driving impulses during construction may have observable behavioral effects on marine life including marine mammals, fish, turtles, and lobsters within 4000 meters of the pile.

Mitigation Recommended: The piles should be driven with pile cushions made of wood or synthetic material to reduce the pressure pulse and increase the pulse rise time. A monitoring system should be in operation during the pile driving to assure ramp up and measure the impulse time series on appropriate hydrophones and geophones.

3) Underwater noise from offshore wind turbines has been measured in Europe at 118 dB re 1 μPa^2 in any 1/3 octave band at a range of 100 meters at full power production. The noise is due to gear noise and transmitted in to the ocean through the monopile support structure. This noise would be greater than the ambient noise present within 1 km of the wind turbines. It is likely that the operational wind turbine noise at ranges of 10 km would be below the ambient noise in the region.

Mitigation Recommended: Reducing the levels of noise from the wind turbines to below the ambient noise level in the area nearest to the wind farm may able to be achieved using the lattice jacket structure (which should reduce the noise level as compared to a monopile structure), appropriate isolation technology in the design of the structure, and lower noise drive systems. A monitoring system deployed to measure the operational noise time series on appropriate hydrophones and geophones. In addition, accelerometers should be installed on at least one of the turbines to monitor structural vibration. A goal for the wind farm developer and operator is to have operational noise from wind turbines average less than or equal to 100 dB re 1 μPa^2 in any 1/3 octave band at a range of 100 meters at full power production.

4) Airborne noise from the offshore wind turbines for the Block Island site (~3 nm south of the island) will not be detectable by humans or animals on Block Island. Airborne noise from the turbines will be detectable by humans and animals within 200 meters of the turbines.

Mitigation Recommended: The developer and manufacturer should endeavor to minimize the radiated airborne noise from the wind turbines.

5) Noise from decommissioning of the wind turbine structures using explosives could have serious impact on marine life within 500 meters of the structure.

Mitigation Recommended: The minimum possible amount of explosives should be used for the structure removal and all charges should be set to detonate at least 3 meters below

the seafloor. A monitoring system should be in operation during the explosive removal to measure the operational noise time series on appropriate hydrophones and geophones.

6) Electromagnetic fields from transmission lines may have behavioral effects on marine life within 20 meters of the 26 kVA power lines likely to be used in the Block Island wind farm. The effects could include both attraction and repulsion.

Mitigation Recommended: A monitoring system including acoustical, optical and other sensors should be established near these facilities to quantify the effects

References

Andrews, J. (2009). *Technical Guidance for Assessment and Mitigation of the Hydroacoustic Effects of Pile Driving on Fish* . Sacramento, CA: ICF Jones & Stokes.

Betke, K., Glahn, M.-v., & Matuschek, R. (2004). Underwater noise emissions from offshore wind turbines. *Proceedings of the CFA/DAGA 2004* .

Department of Commerce. (2008, July 3). Taking of Marine Mammals Incidental to Specified Activities; Construction of the East Span of the San Francisco-Oakland Bay Bridge. *Federal Register* , pp. 38180-38183.

DONG Energy. (2006, November). *Danish Offshore Wind - Key Environmental Issues*. Retrieved from http://www.ens.dk/graphics/Publikationer/Havvindmoeller/havvindmoellebog_nov_2006_skrm.pdf

Frisk, G., Bradley, D. L., Caldwell, J., D'Spain, G., Gordon, J., Hastings, M., et al. (2003). *Ocean Noise and Marine Mammals*. Washington, DC: National Academy Press.

Gill, A. B., & Kimber, J. A. (2005). Elasmobranchs and offshore renewable energy. *J. Mar. Biol. UK* , 85, 1075-1081.

Ketten, D. (2000). Cetacean Ears. In W. W. Au, A. N. Popper, & R. R. Fay, *Hearing by Whales and Dolphins* (pp. 43-108). New York: Springer-Verlag.

Ma, B. B., Nystuen, J. A., & Lien, R.-C. (2005). Prediction of underwater sound levels from rain and wind. *J. Acoust. Soc. Am.* , 3555-3565.

Miller, J. H., Bradley, D. L., & Nystuen, J. L. (2008). Ocean Noise Budgets. *Bioacoustics* , 17(1-3), 133-136.

Nystuen, J. A., & Howe, B. (2005). Ambient Sound Budgets. *Proceedings of the Underwater Acoustics Measurements Conference*. Heraklion, Crete, Greece.

Nystuen, J. A., Moore, S., & Stabeno, P. (2010). An acoustic report from the Bering Sea: Wind speed, rainfall, shipping and other sources of underwater sound. *J. Acoust. Soc. Am.* , in press.

Ontario Ministry of Environment. (2009, June 9). *Wind Turbines – Proposed Requirements and Setbacks*. Retrieved May 13, 2010, from http://www.ene.gov.on.ca/en/news/2009/060901mb2.php

Pierpont, N. (2010). *Wind Turbine Syndrome*. Malone, NY: KSelected Books.

Richardson, W. J., Greene, C. R., Malme, C. I., & Thomson, D. H. (1998). *Marine Mammals and Noise*. New York: Academic Press.

Smith, K. B. (2006). Adjoint modeling with a split-step Fourier parabolic equation model. J. *Acoust. Soc. Am.* , 1190.

Southall, B. L., Bowles, A. E., Ellison, W. T., Finneran, J. J., Gentry, R. L., Greene, C. R., et al. (2007). Marine Mammal Noise Exposure Criteria: Initial Scientific Recommendations. *Aquatic Mammals* , 1-122.

Spaulding, M. (2010). Personal Communication.

Tyack, P., & Clark, C. W. (2000). Communication and acoustic behavior of dolphins and whales. In W. W. Au, A. N. Popper, & R. R. Fay, *Hearing by Whales and Dolphons* (pp. 156-272). New York: Springer-verlag.

Wenz, G. M. (1962). Acoustic Ambient Noise in the Ocean: Spectra and Sources. Journal of the *Acoustical Society of America* , 1936-1956.

13.
Chapter 5: Commercial and Recreational Fisheries

APPENDIX A

BASELINE CHARACTERIZATION: DATA SOURCES, METHODS, AND RESULTS

Erin Bohaboy, Anna Malek, and Jeremy Collie, URI Graduate School of Oceanography

1. Overview

The purpose of the baseline characterization was to provide baseline information on the current state of fisheries resources in the Ocean SAMP area based on existing survey data. It is not an assessment of individual fish stocks, nor is it an analysis of longer-term trends in Rhode Island's offshore fisheries resources. Data were obtained from multiple bottom trawl surveys occurring in and around the Ocean SAMP area. Ten years of data were used in this analysis as this provides enough data to smooth out interannual variability while retaining a focus on the current state of resources in the study area. Data included in this analysis were collected at survey stations within a polygon delineated by the following coordinates:

41° 30' N, 071° 50.5'W
40°50' N, 071° 50.5'W
41° 30' N, 070° 50'W
40°50' N, 070° 50'W

Survey stations that occur adjacent to but just outside the SAMP area were included in this analysis in order to allow for a comprehensive analysis of fisheries resources in and around the planning area. See Figure 1 for a map showing the location of each of the survey stations included in this analysis.

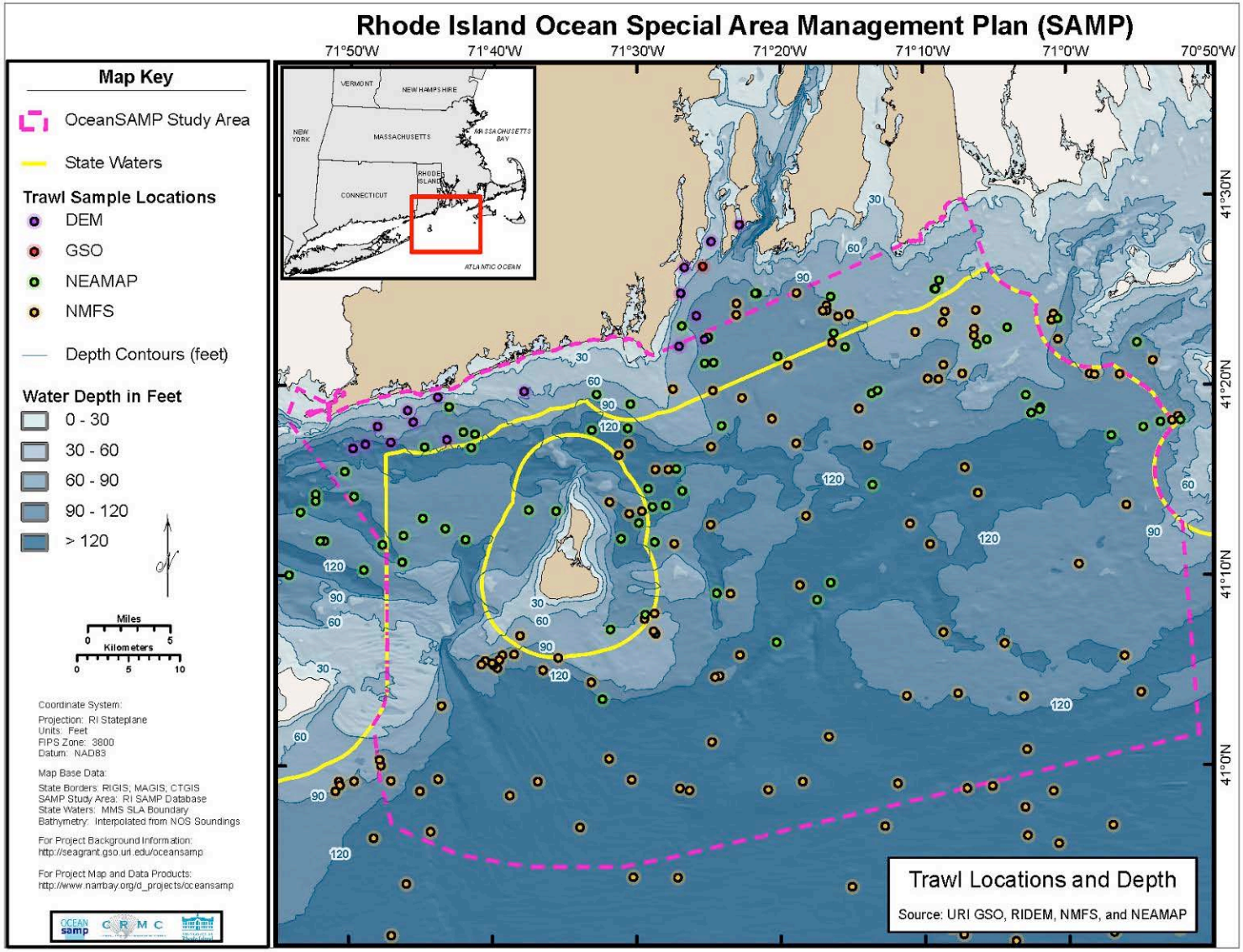

Figure 1. Locations of Survey Stations Included in Baseline Characterization Analysis

The following datasets are included in the data analyses:

- Rhode Island Department of Environmental Management (DEM): DEM data includes seasonal and monthly fixed stations along the southern Rhode Island coast (Block Island Sound) and the mouth of Narragansett Bay, 1999-2008. Biomass at monthly stations was converted to seasonal data each year by averaging April, May, and June tows to obtain a spring biomass and September, October, and November tows to obtain a fall biomass.
- University of Rhode Island Graduate School of Oceanography (GSO): GSO data includes one weekly fixed station in the mouth of Narragansett Bay, 1999-2008. Weekly biomass was converted to seasonal data each year by averaging April, May, and June tows to obtain a spring biomass and September, October, and November tows to obtain a fall biomass.
- Northeast Area Monitoring and Assessment Program (NEAMAP): NEAMAP data includes random stations throughout the nearshore waters off Rhode Island. The NEAMAP survey data analyzed include sampling in fall 2007, spring 2008, and fall 2008.
- National Marine Fisheries Service (NMFS): NMFS data includes random stations throughout the waters off Rhode Island, generally not inside Block Island Sound. Sampling occurred during spring and fall from 1999 through 2008.

The survey catch weight (biomass) was calculated for each survey by dividing the catch per tow (weight) by the area of each tow. Survey biomass units are milligrams per square meter (mg / m2). Tow area is the calculated area swept using the length of the tow and the distance between the net's wings, or wingspread:

Length of tow (m) x width of net (m) = area towed (m^2).

For the NMFS and NEAMAP surveys, the length of the tow and the wingspread were recorded by GPS and net sensors and used to calculate area swept. For the DEM and GSO surveys, area swept was estimated using the length of the tow, which is consistent, and gear specialists' estimates of wingspread based on net configuration. The purpose of these calculations was to allow for comparison between the surveys. However, these calculations do not account for all differences between the surveys, and results show that relative biomass estimates nonetheless vary significantly between the individual surveys. For this reason, all figures and map based on this analysis show the results for each individual survey.

2. Analysis of Total Catch

A. Methods

For analyses of total catch data, biomass was summed over all species listed in Table 1. Species in Table 1 were selected by the Ocean SAMP team and include commercially and recreationally targeted species as well as "Species of Concern", except for those (i.e. large pelagics) which cannot be adequately sampled through bottom trawl surveys. When noted, biomass values were transformed for some analyses by taking the natural logarithm (Ln) to reduce violation of the assumption of normally distributed residuals.

Common Name	Scientific Name
Alewife	*Alosa pseudoharengus*
American lobster	*Homarus americanus*
American shad	*Alosa sapidissima*
Atlantic cod	*Gadus morhua*
Atlantic herring	*Clupea harengus*
Atlantic mackerel	*Scomber scombrus*
Atlantic sea scallop	*Placopectin magellanicus*
Barndoor skate	*Dipturus laevis*
Black sea bass	*Centropristis striata*
Blueback herring	*Alosa aestivalis*
Bluefish	*Pomatomus saltatrix*
Butterfish	*Peprilus triacanthus*
Cusk	*Brosme brosme*
Dusky shark	*Carcharhinus obscurus*
Goosefish	*Lophius americanus*
Little skate	*Leucoraja erinacea*
Longfin squid	*Loligo peali*
Rainbow smelt	*Osmerus mordax*
Scup	*Stenotomus chrysops*
Silver hake	*Merluccius bilinearis*
Smooth dogfish	*Mustelus canis*
Spiny dogfish	*Squalus acanthias*
Striped bass	*Morone saxatilis*
Summer flounder	*Paralichthys dentatus*
Tautog	*Tautoga onitis*
Thorny skate	*Amblyraja radiate*
Winter flounder	*Pseudopleuronectes americanus*
Winter skate	*Leucoraja ocellata*
Yellowtail flounder	*Limanda ferruginea*

Table 1. Species considered in total biomass analyses

B. Results

Multi-way analysis of variance (ANOVA) based on Ln transformed biomass data indicate that the primary factors accounting for variation in total biomass are season, survey, and depth. Season was the most important factor effecting total biomass (Figure 2). Catch biomass is higher in fall and lower in spring. Survey is the second most important factor (Figure 3); the NMFS survey biomass is lowest and the NEAMAP survey biomass is highest. Even when accounting for differences in biomass caused by season and survey, there is a statistically significant trend in depth where survey sites at deeper depth are characterized by the highest biomass. Tukey's pair-wise means difference test based on Ln transformed biomass shows that the deep depth strata (60 to 90 ft and 90+ ft) have higher total biomass than either of the shallow depth strata (20 to 40 ft and 40 to 60 ft). Other factors that were investigated and found not to have a significant effect on biomass include region (Figure 5), year, and combined depth/region.

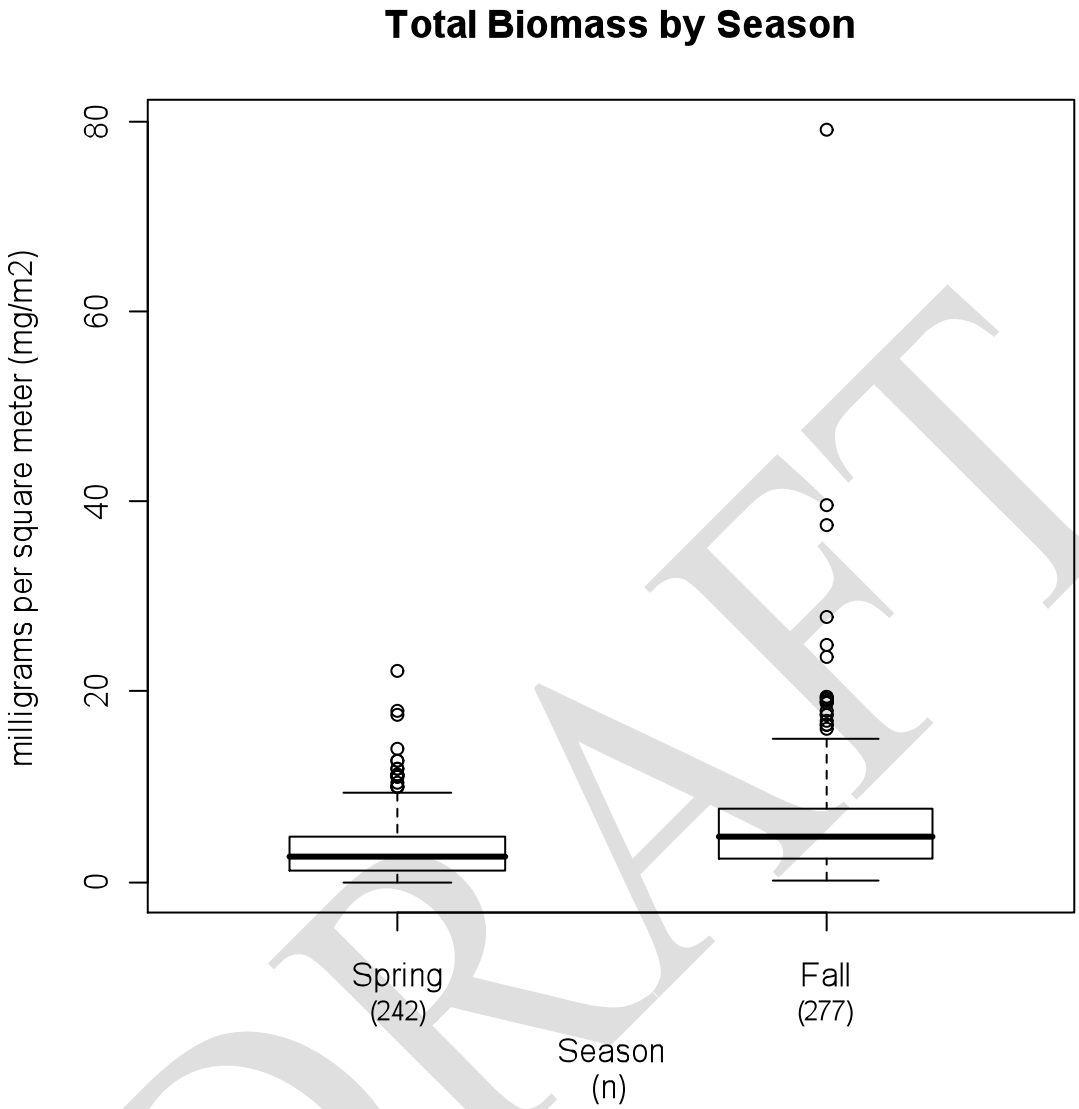

Figure 2. The mean, interquartile, range, and outliers of the biomass (mg/m2) summed by species. Multiple ANOVA based on Ln transformed biomass indicates that season differences are statistically significant at the 95% confidence level (actual p-value < 0.001). N = sample size for this analysis.

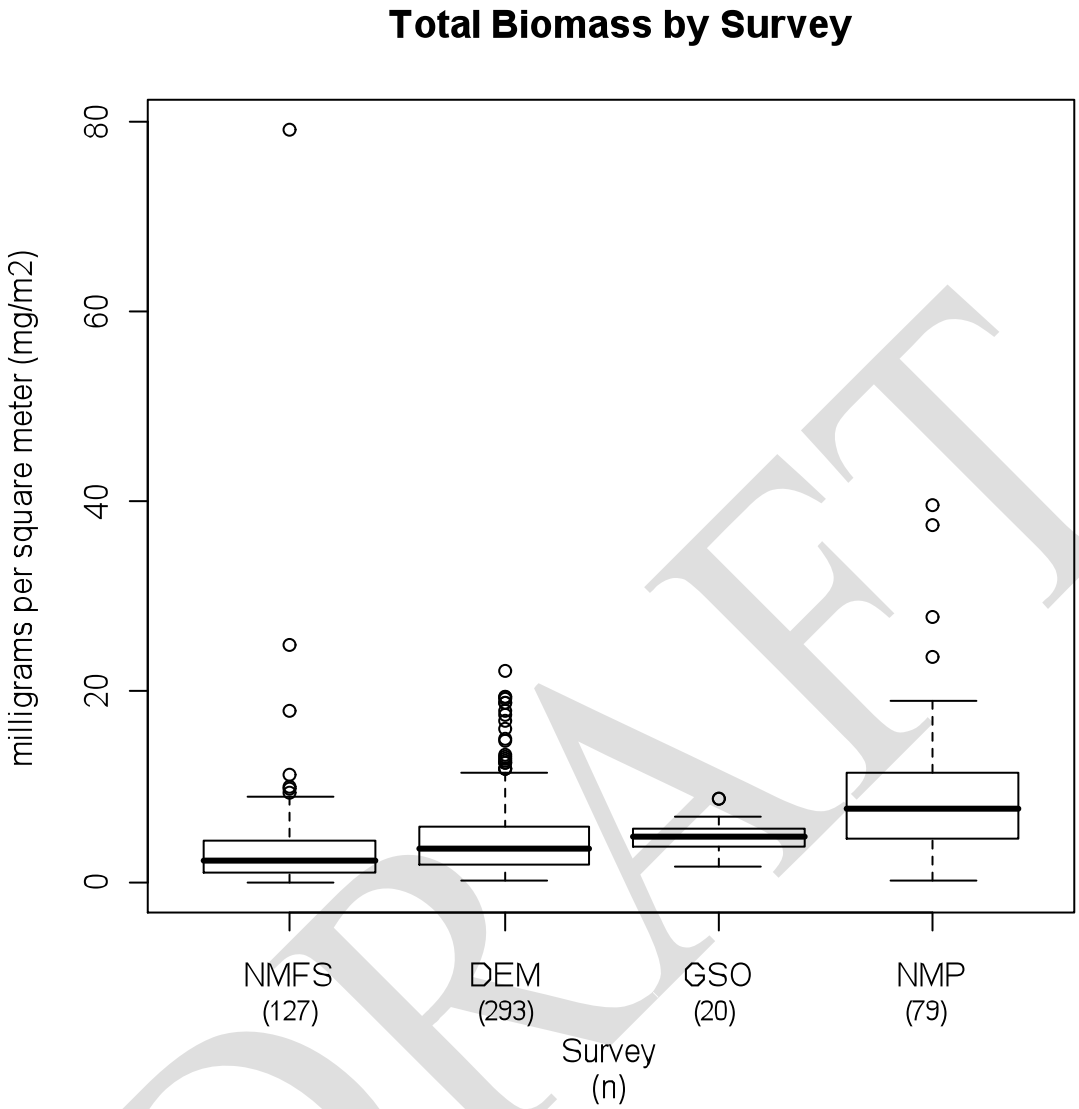

Figure 3. The mean, interquartile, range, and outliers of the biomass (mg per m2) summed by species. Multiple ANOVA based on Ln transformed biomass indicates that survey differences are statistically significant at the 95% confidence level (actual p-value < 0.001). N = sample size used in this analysis.

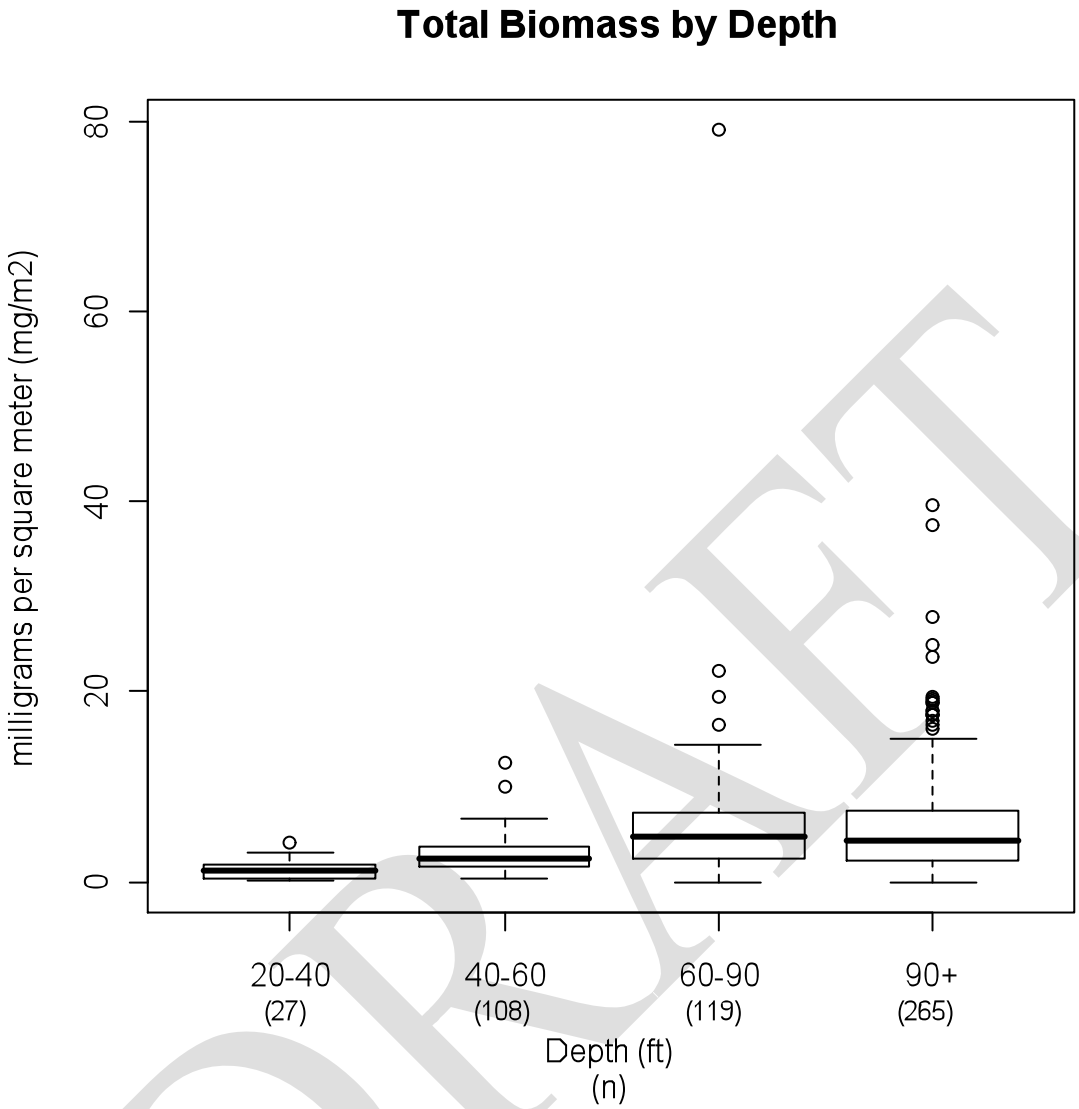

Figure 4. The mean, interquartile, range, and outliers of the biomass (mg per m2) summed by species. Multiple ANOVA based on Ln transformed biomass indicates that depth stratum is statistically significant at the 95% confidence level (actual p-value < 0.001). Tukey's pair-wise means difference test based on Ln transformed biomass shows that the deep depth strata (60 to 90 ft and 90+ ft) have higher total biomass than either of the shallow depth strata (20 to 40 ft and 40 to 60 ft). N = sample size used in this analysis.

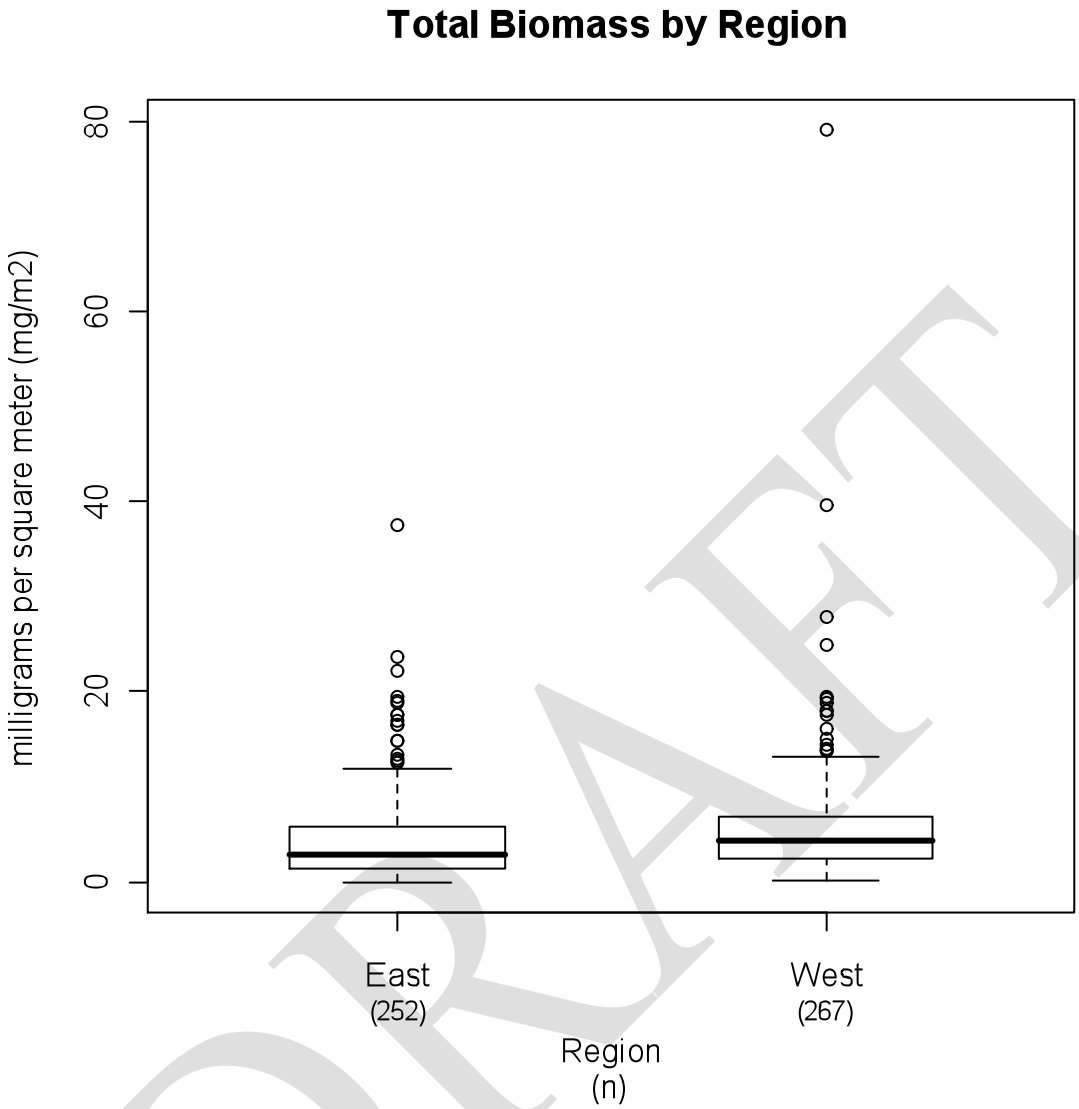

Figure 5. The mean, interquartile, range, and outliers of the biomass (mg per m2) summed by species. Multiple ANOVA based on Ln transformed biomass indicates that region (as defined by survey stations east or west of -71.38° (west) longitude) is not statistically significant (actual p-value = 0.29). N = sample size used in this analysis.

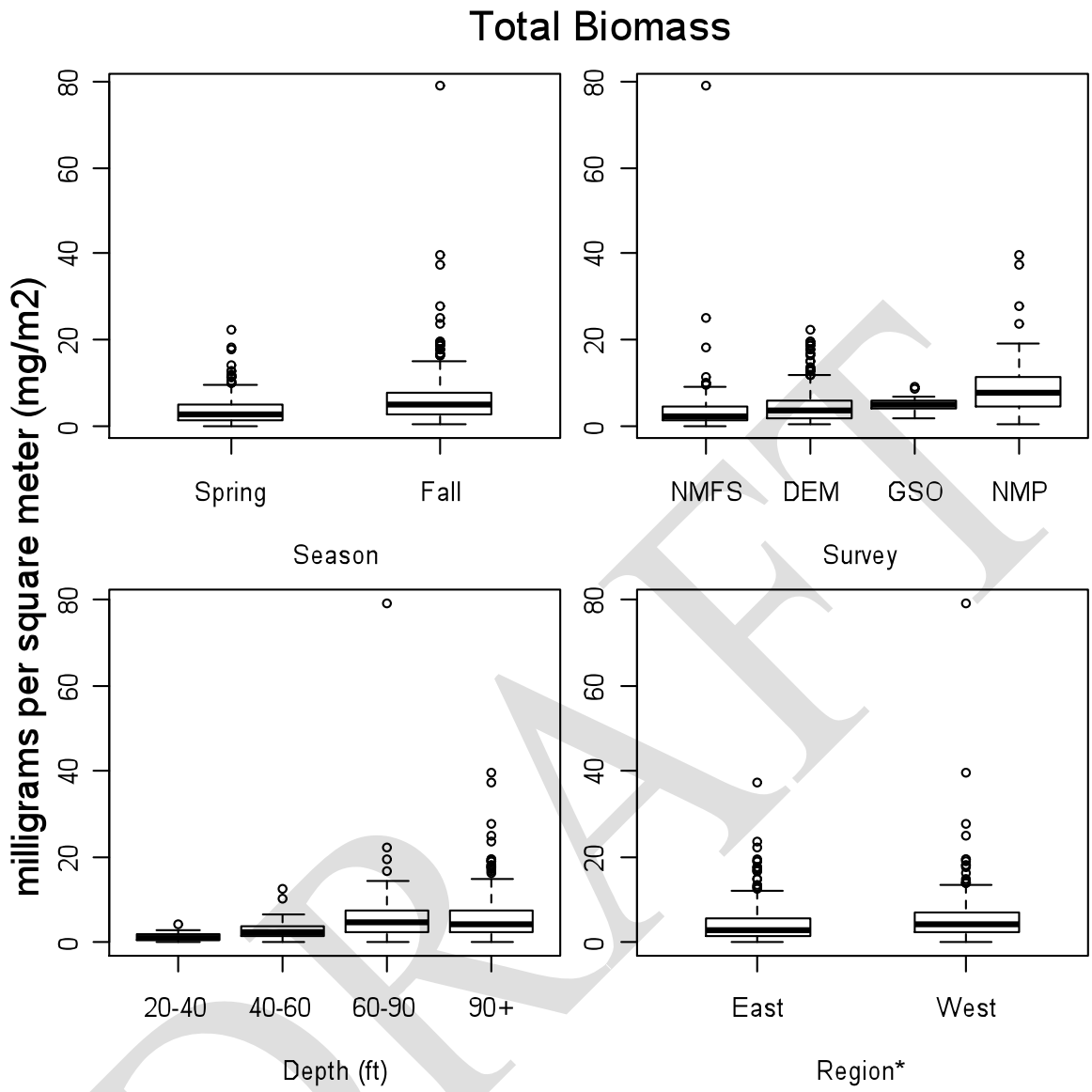

Figure 6. Summary results of multivariate analysis of total biomass. Region is defined as survey stations east or west of -71.38° (west) longitude. Sample size for each analysis is indicated in the individual figures (2-5).

3. Analysis of Catch by Species

A. Summary Data

Catch biomass data from the four trawl surveys were also used to assess individual species catch biomass for key species for which data were available. Figure 4 below shows a simple sum of individual species biomass within the study area based on RIDEM, GSO, and NMFS survey data from 1999-2008. NEAMAP data were not included in this figure as only two years of data are available. Figure 4 below illustrates that in the fall surveys, little skate, scup, and longfin squid were among the species with the highest relative biomass in the study area, whereas in the spring surveys, little skate, scup, and winter flounder were among the species with the highest relative biomass in the study area. Figures 5-8 below show the individual species biomass reflected in each individual survey. Note that all figures represent the total biomass on a logarithmic scale to allow for comparison between the figures.

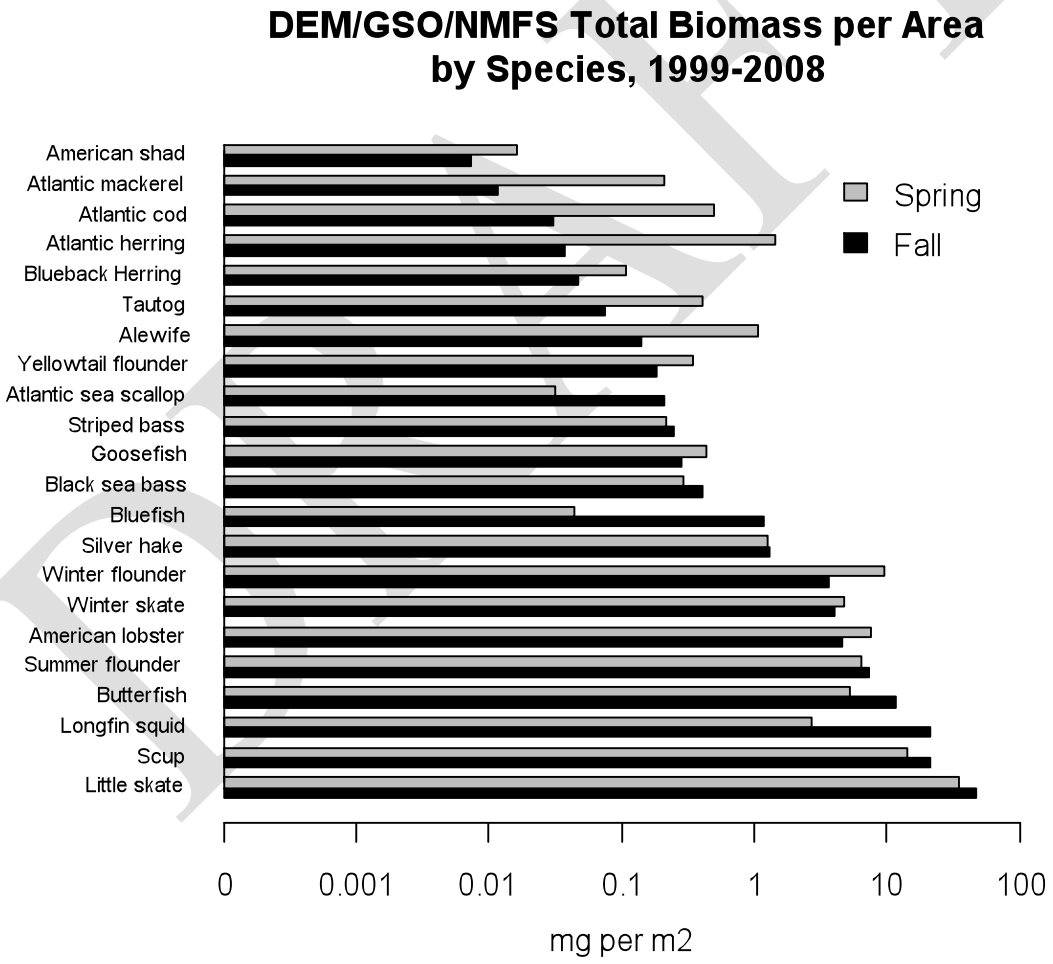

Figure 7. Total biomass per area by species, 1999-2008. Based on RIDEM, URI GSO, and NMFS trawl surveys. Includes all commercially and recreationally targeted species as well as those identified as drivers of demersal fish and invertebrate community composition (see BVStep analysis below).

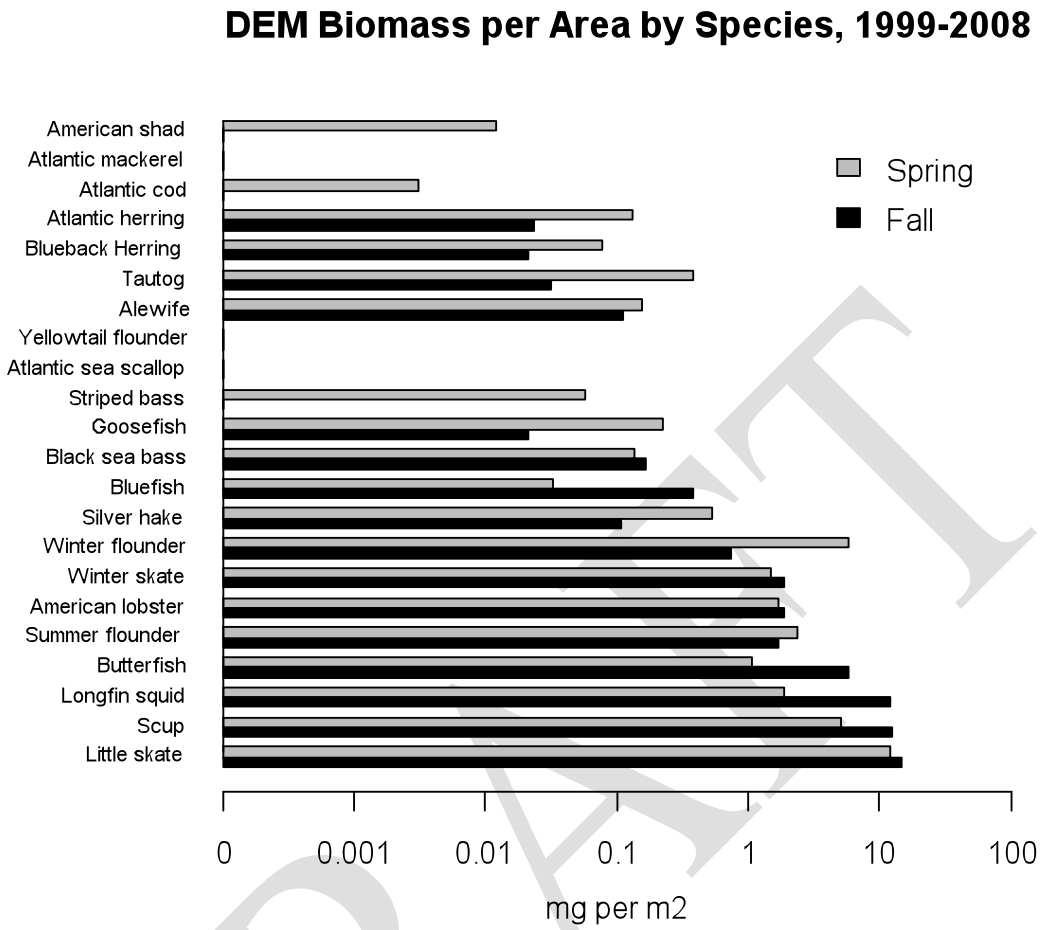

Figure 8. DEM trawl survey biomass per area by species. Includes all commercially and recreationally targeted species as well as those identified as drivers of demersal fish and invertebrate community composition (see BVStep analysis below).

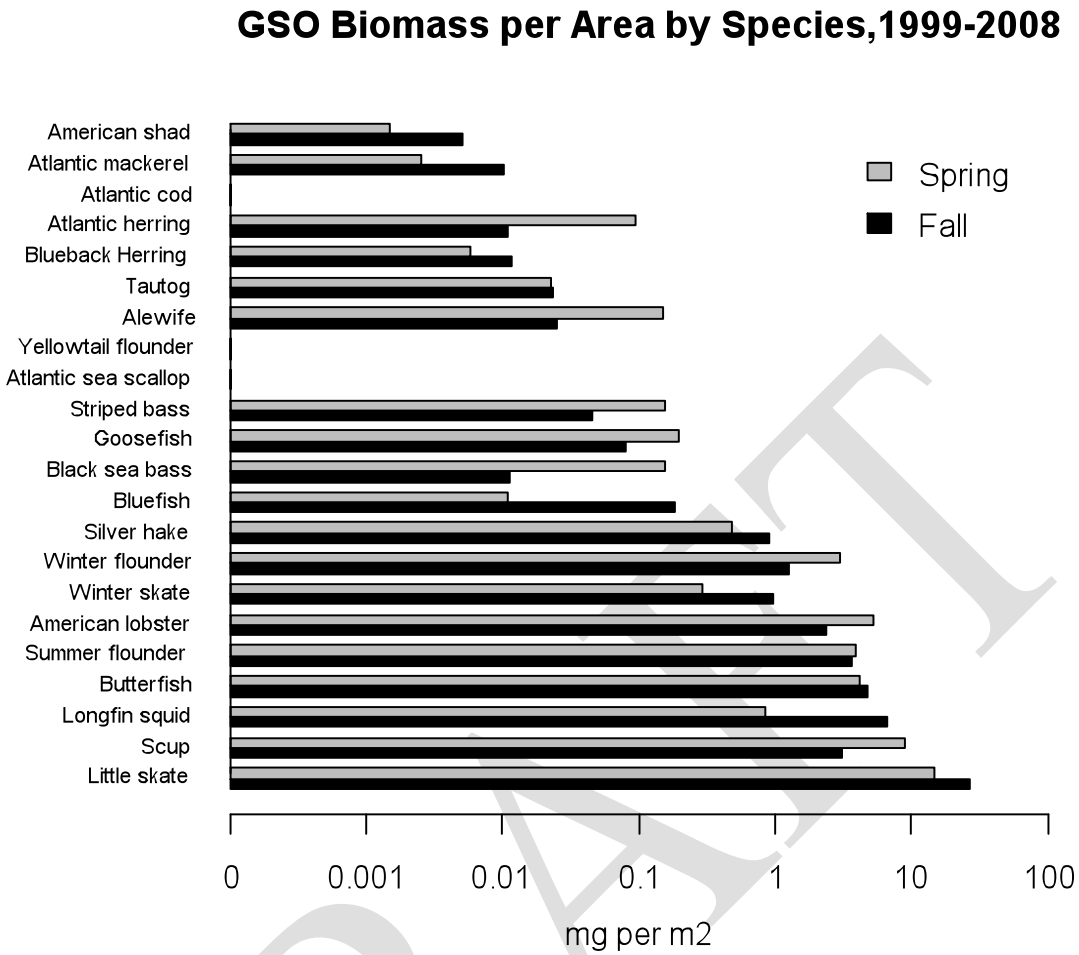

Figure 9. GSO trawl survey biomass per area by species. Includes all commercially and recreationally targeted species as well as those identified as drivers of demersal fish and invertebrate community composition (see BVStep analysis below).

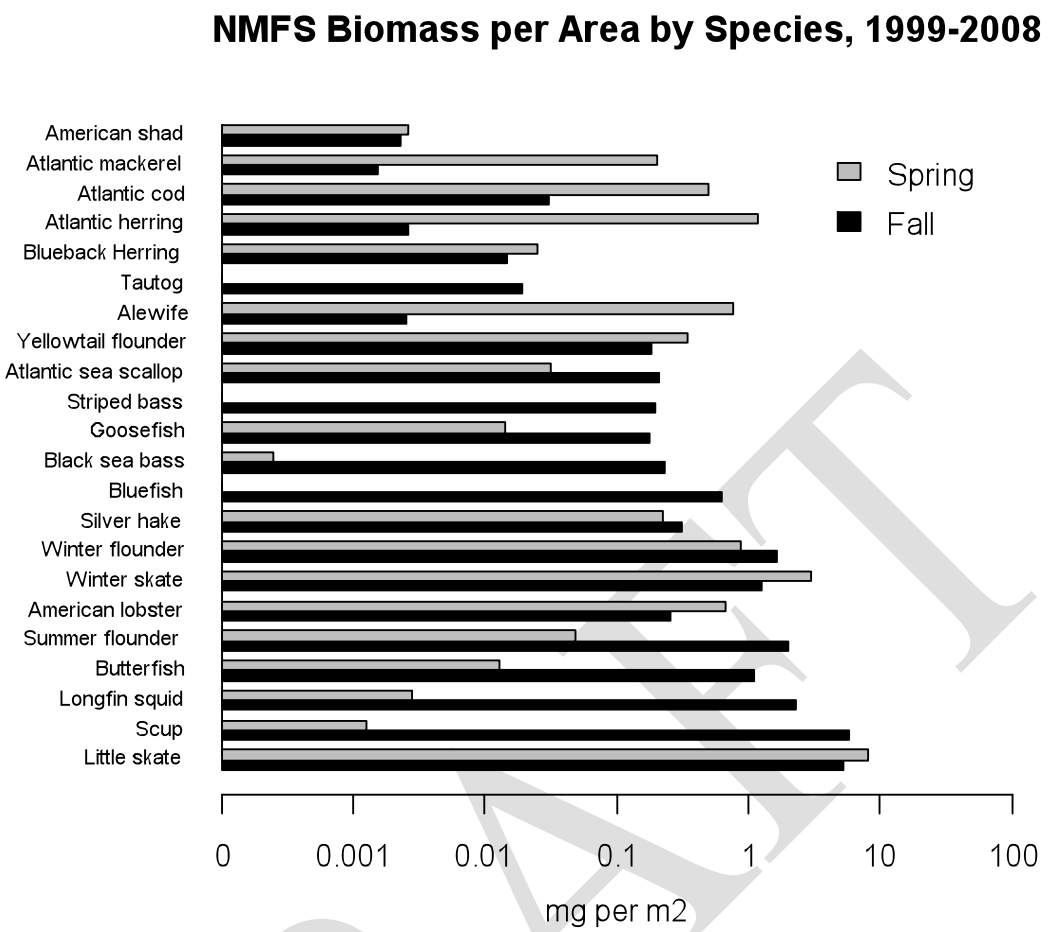

Figure 10. NMFS trawl survey biomass per area by species. Includes all commercially and recreationally targeted species as well as those identified as drivers of demersal fish and invertebrate community composition (see BVStep analysis below).

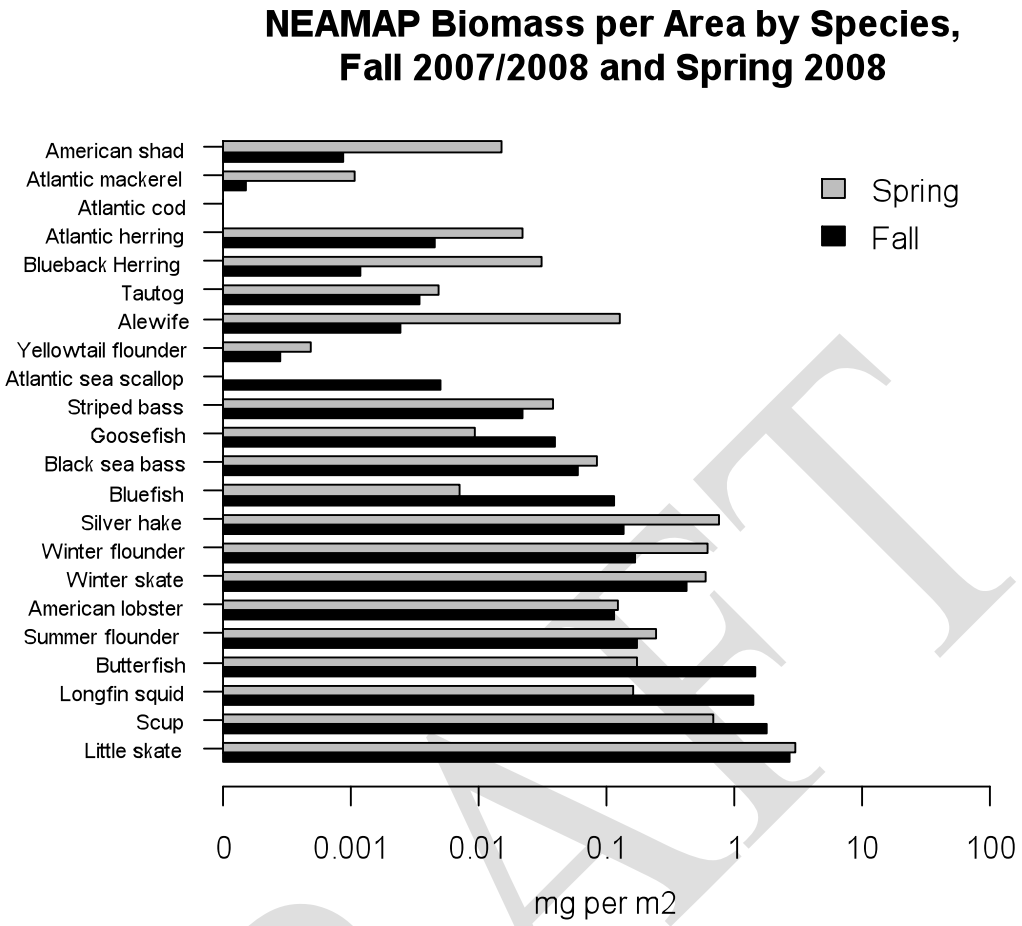

Figure 11. NEAMAP trawl survey biomass per area by species. Includes all commercially and recreationally targeted species as well as those identified as drivers of demersal fish and invertebrate community composition (see BVStep analysis below).

B. Multivariate Analysis Methods

All multivariate analysis was performed in Primer 6.0. Fisheries survey data from National Marine Fisheries Service (NMFS), Northeast Monitoring and Assessment Program (NEAMAP), Rhode Island Department of Environmental Management (DEM) and the Graduate School of Oceanography (GSO) were combined to identify patterns in fish an invertebrate species composition throughout Block Island Sound and Rhode Island Sound. All data was standardized to units of biomass (mg) per meter squared prior to multivariate analysis to account for differences in gear and sampling methods. Due to the omission of cancer crabs during DEM sampling, cancer crabs were excluded from these analyses.

Multidimentional scaling plots (MDS) were created as a visual representation of the unique species compositions within Block Island Sound and Rhode Island Sound as identified by the aforementioned surveys. Each point on the MDS plot represents one tow. Points that are closer together have more similar species composition than distant points. ANOSIM analyses were used to identify factors that affect species composition in the SAMP area as depicted in the MDS

plot. The following five factors were tested: Survey agency, Year, Season, Depth strata and SAMP region. A BVStep analysis was performed to identify the individual species that are most responsible for the pattern in demersal fish and invertebrate community composition within Block Island Sound and Rhode Island Sound.

C. Results

Of the five factors tested in the ANOSIM analysis (Survey agency, Year, Season, Depth strata and SAMP region), season and survey agency were shown to significantly affect fish and invertebrate species composition in the SAMP area (R=0.236 and R=0.266,respectively) . These results suggest that seasonal movement of demersal fish species influences the structure of local marine communities (Figure 5). Such seasonal variations in species composition should be considered when predicting the impacts of offshore development and resource exploitation. The ANOSIM results further indicate that a distinct composition of species is caught by each survey agency (Figure 6). This finding may be an artifact of slight differences in sampling methods and gear that were not fully corrected for during initial data processing. Such inconsistencies must be considered in further studies that combine data from various survey agencies. The ANOSIM results indicate that neither SAMP region or depth strata affect demersal fish and invertebrate species composition within Block Island Sound and Rhode Island Sound (R=0.043 and R=0.032, respectively). Despite differences in chemical and physical properties within the SAMP area, the species composition of the demersal community is not significantly different in the East and West sectors. More precise delineation of SAMP Area and depth strata, however, many reveal fine-scale patterns in species composition that were not detected in this analysis.

The BVStep analysis identified 17 species that most affect the demersal fish and invertebrate community composition within the SAMP area (Table 2, Figure 7). Although these species may not be the most abundant within the SAMP area, they are of immense ecological importance to the stability and resiliency of the local marine community. When attempting to predict the effects of development and exploitation on the demersal fish assemblage of the SAMP area, it is essential to consider these community-shaping species. Many of these species vary in abundance from fall to spring (Figure 7). Such seasonal community dynamics should also be considered when planning offshore construction and directed exploitation.

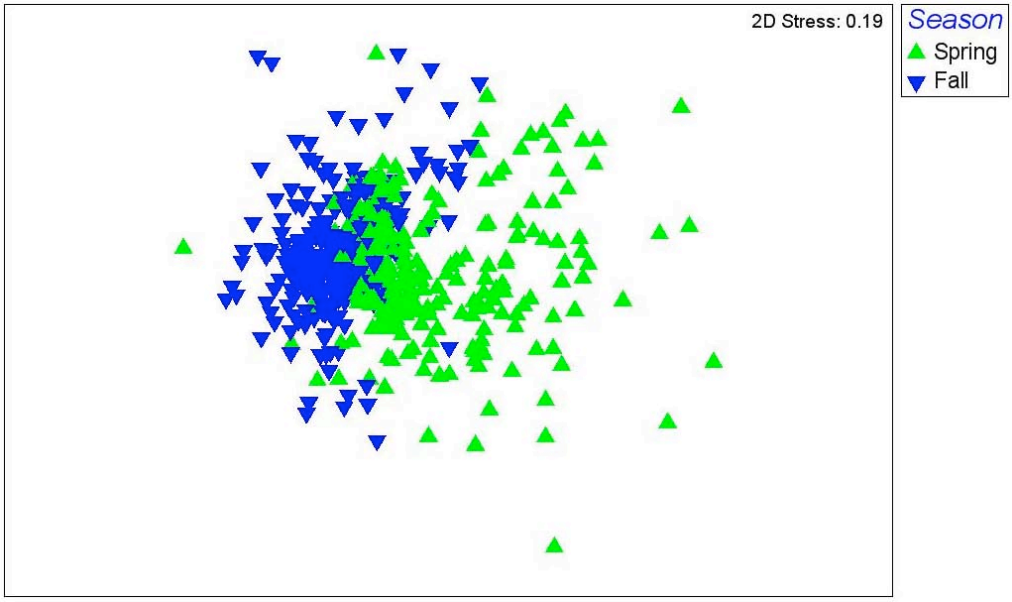

Figure 12. Ordination of the biomasses of SAMP species within Block Island Sound and Rhode Island Sound. This nonmetric multidimensional scaling plot (MDS) depicts the pattern in demersal fish and invertebrate species composition, with similar species compositions close together. Each point represents one tow. The green triangles represent spring tows and the blue inverted triangles represent fall tows. This shows that species composition within Rhode Island Sound and Block Island Sound is seasonally distinct (R=0.236).

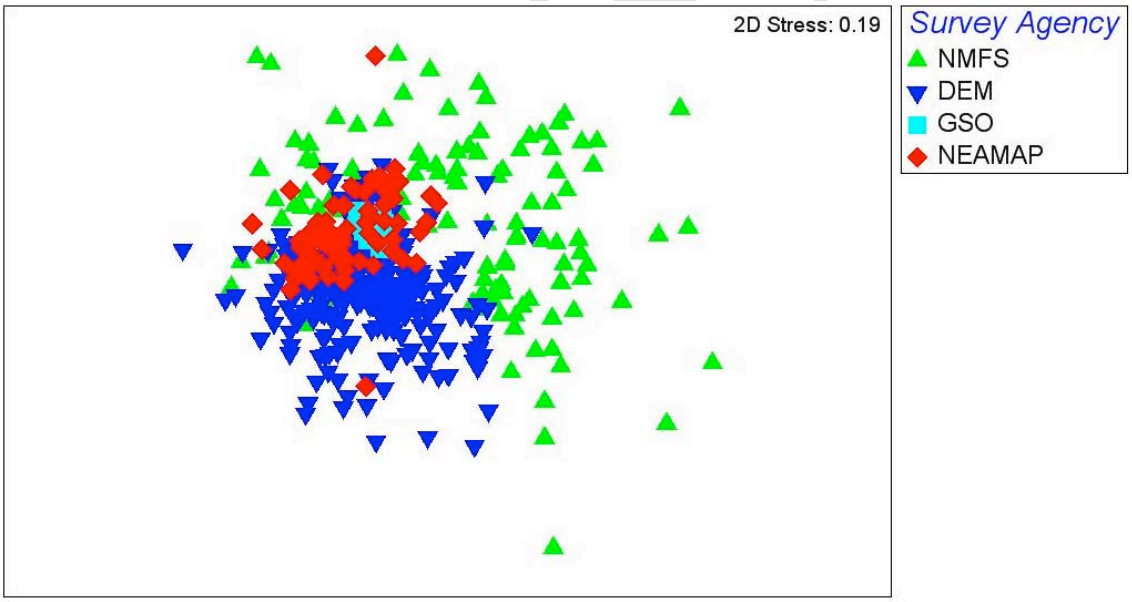

Figure 13. Ordination of the biomasses of SAMP species within Block Island Sound and Rhode Island Sound. This nonmetric multidimensional scaling plot (MDS) depicts the pattern in demersal fish and invertebrate species composition, with similar species compositions close together. Each point represents one tow. The green triangles represent NMFS tows and the blue inverted triangles represent DEM tows, the light blue squares represent GSO tows and the red diamonds represent NEAMAP tows. This plot shows that each survey agency catches a distinct composition of demersal fish species, which may be a source of bias (R=0.266).

	Biomass (mg m^{-2})	
Species	**Spring**	**Fall**
Alewife	0.109	0.059
American Lobster	0.315	0.309
American Shad	0.019	0.004
Atlantic Cod	0.042	0.014
Atlantic Herring	0.143	0.021
Atlantic Sea Scallop	0.008	0.046
Black Sea Bass	0.076	0.053
Blueback Herring	0.031	0.034
Bluefish	0.074	0.141
Butterfish	0.405	0.825
Longfin Squid	0.242	1.091
Scup	0.888	1.316
Silver Hake	0.243	0.118
Summer Flounder	0.360	0.243
Winter Flounder	0.508	0.190
Winter Skate	0.304	0.260
Yellowtail Flounder	0.071	0.052

Table 2. BVStep Results. The spring and fall biomass of each species identified as a driver of the pattern in demersal fish and invertebrate community composition within Block Island Sound and Rhode Island Sound. R=0.940.

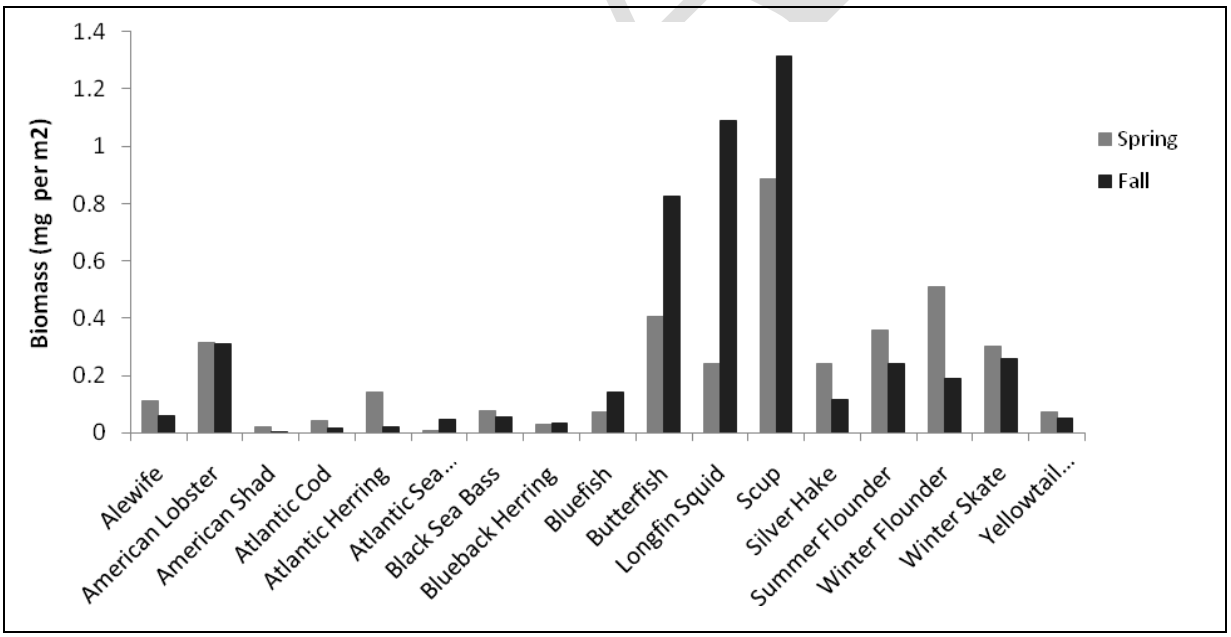

Figure 14. Spring and fall biomass of each species identified as a driver of the pattern in demersal fish and invertebrate community composition within Block Island Sound and Rhode Island Sound (Primer 6.0, BVStep, R=0.940).

D. Individual Species Trends

Individual species data were also used to plot recent trends in biomass caught sampled through these trawl surveys. Trends figures include only DEM, GSO, and NMFS trawl survey data as only two years of data are available through the NEAMAP program.

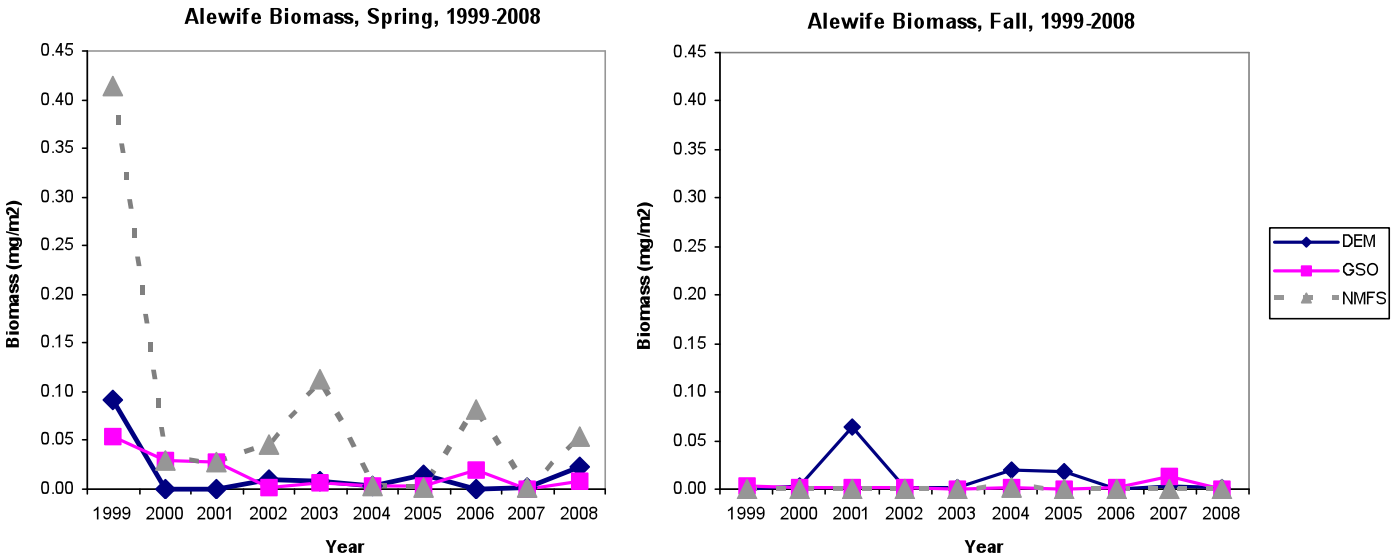

Figure 15. Alewife biomass 1999-2008 based on DEM, GSO, and NMFS survey data.

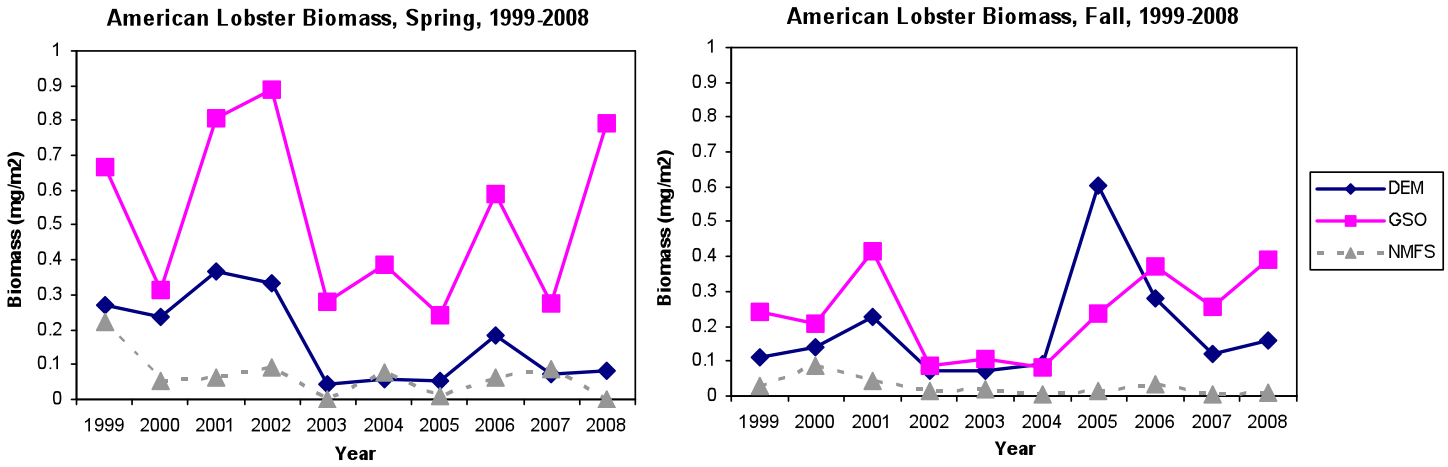

Figure 16. American lobster biomass 1999-2008 based on DEM, GSO, and NMFS survey data.

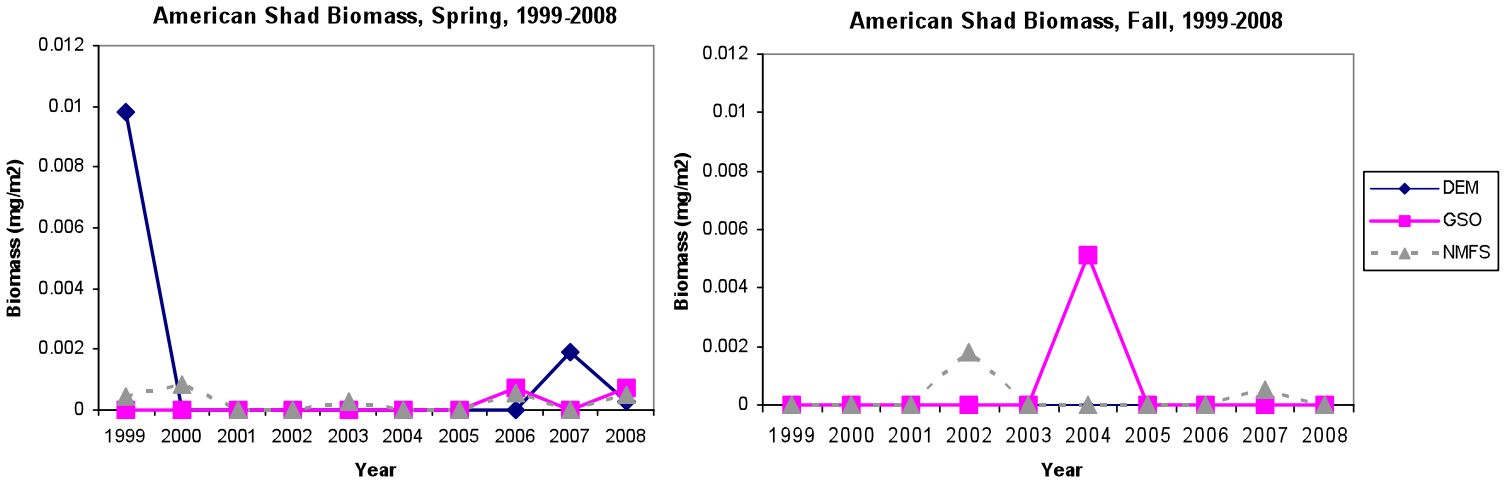

Figure 17. American shad biomass 1999-2008 based on DEM, GSO, and NMFS survey data.

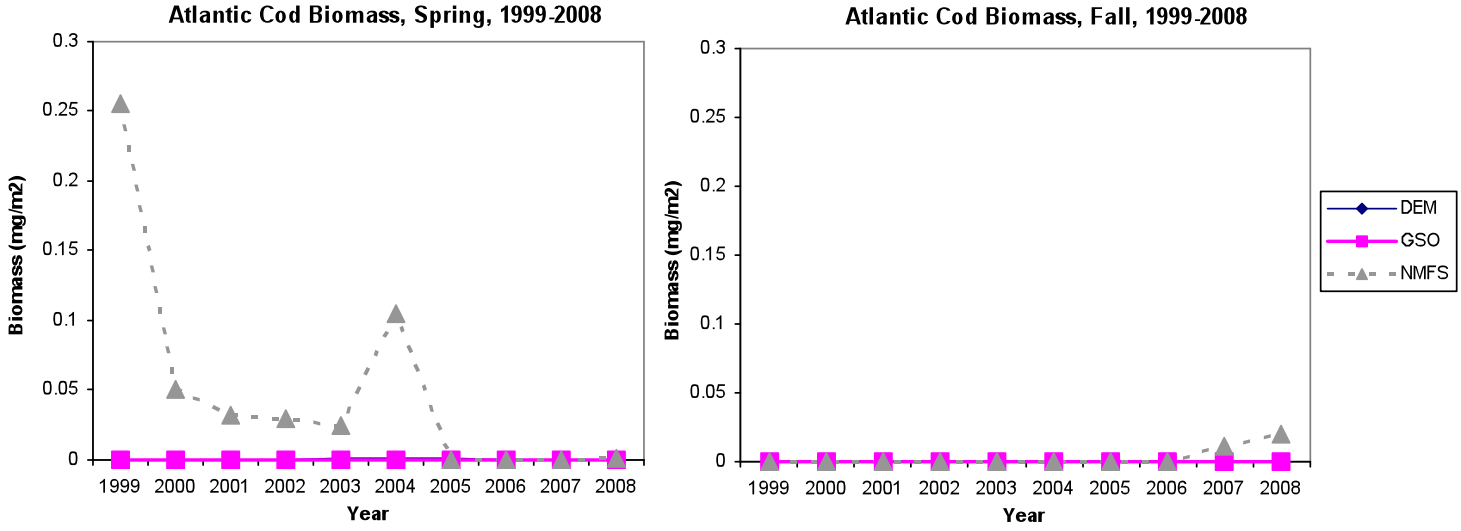

Figure 18. Atlantic cod biomass 1999-2008 based on DEM, GSO, and NMFS survey data.

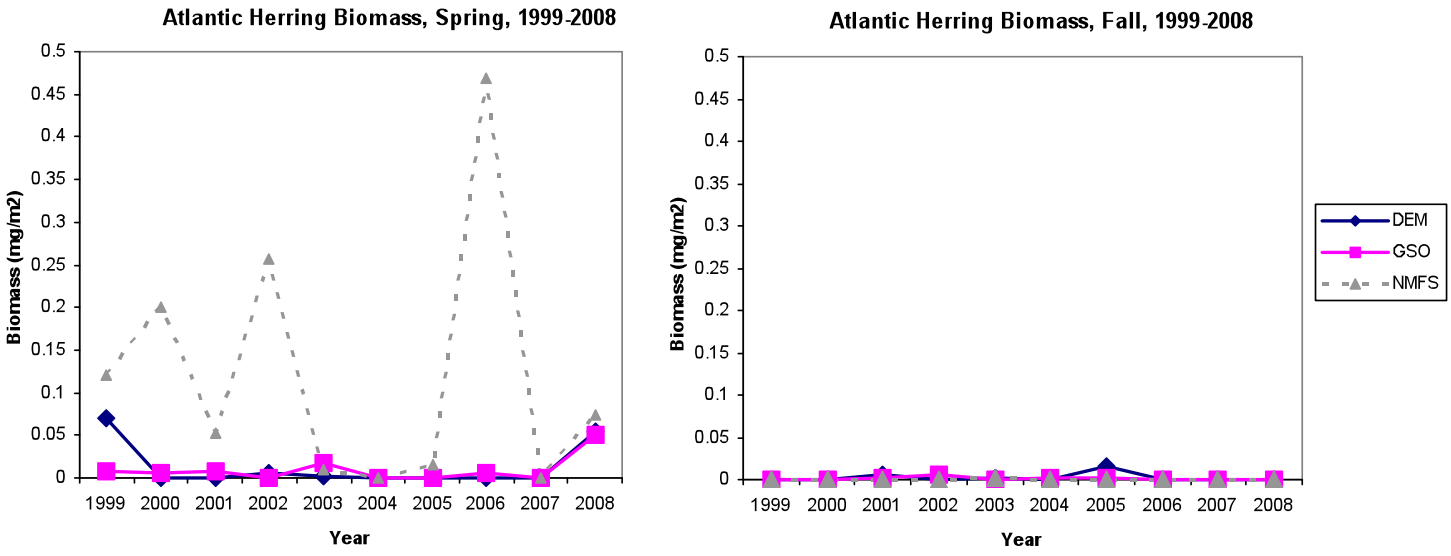

Figure 19. Atlantic herring biomass 1999-2008 based on DEM, GSO, and NMFS survey data.

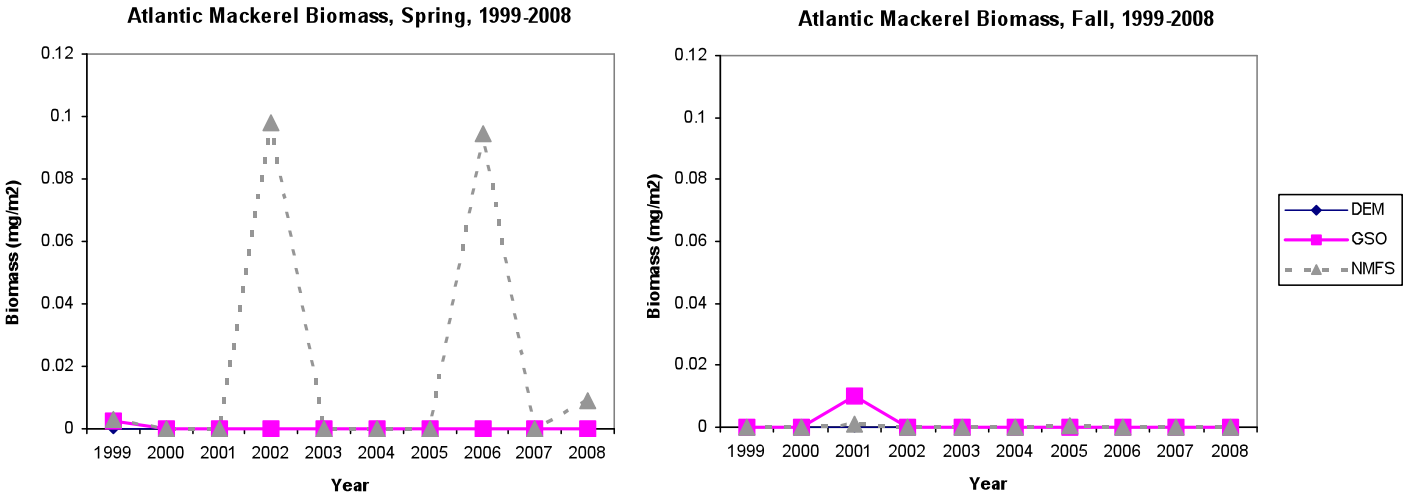

Figure 20. Atlantic mackerel biomass 1999-2008 based on DEM, GSO, and NMFS survey data.

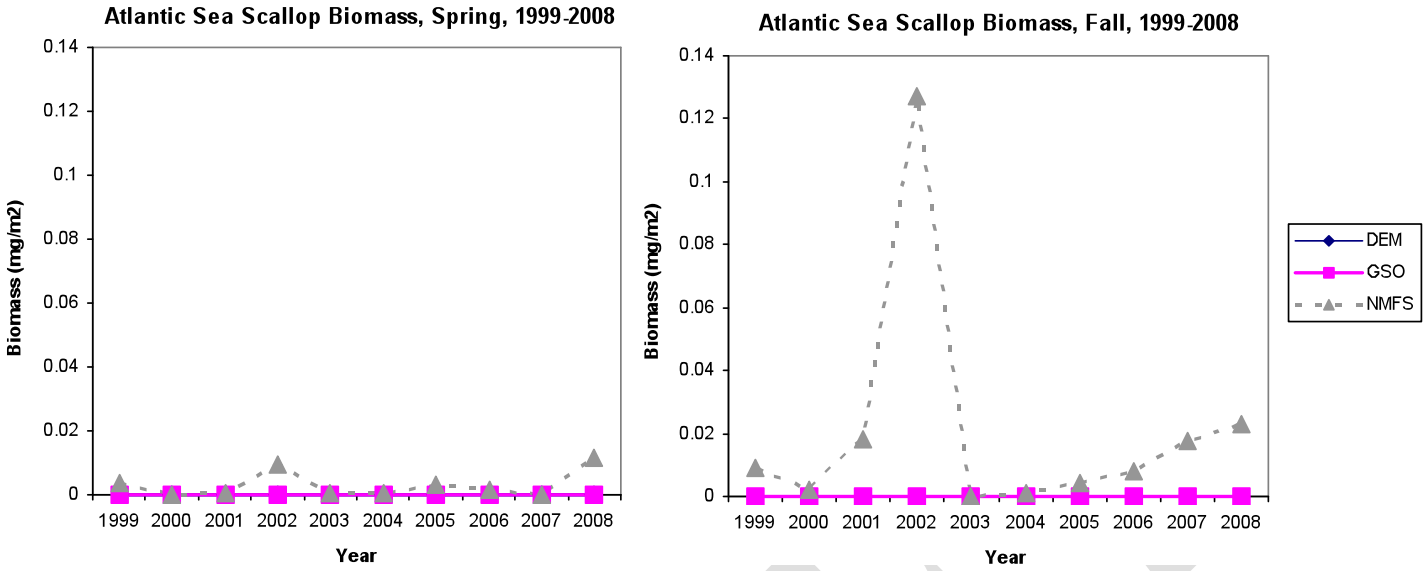

Figure 21. Atlantic sea scallop biomass 1999-2008 based on DEM, GSO, and NMFS survey data.

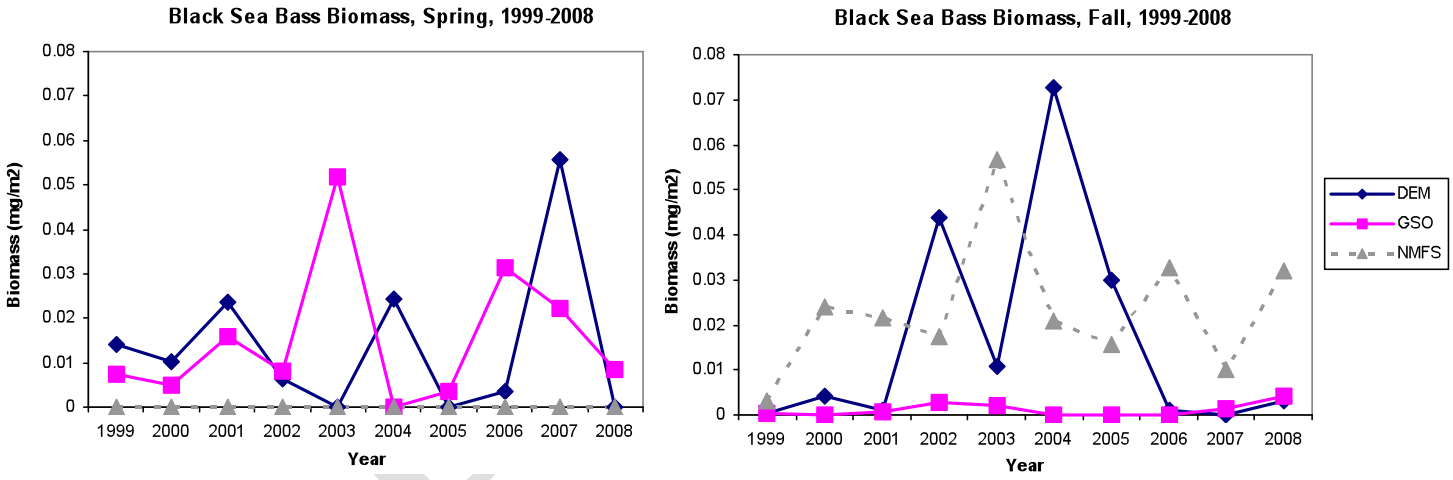

Figure 22. Black sea bass biomass 1999-2008 based on DEM, GSO, and NMFS survey data.

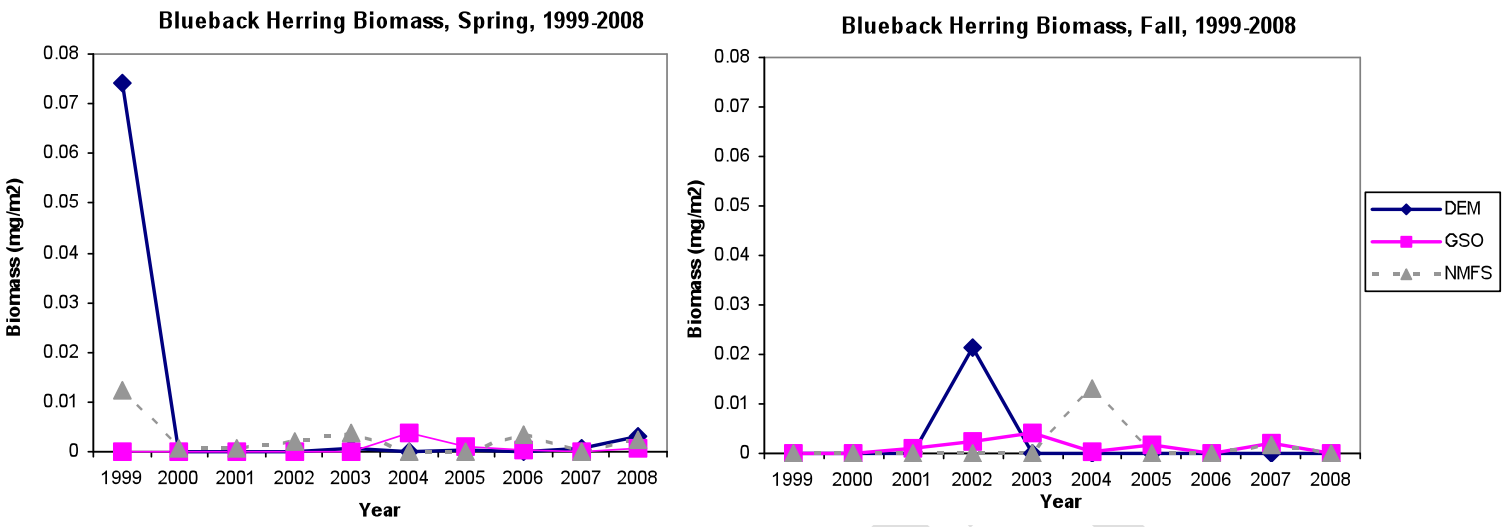

Figure 23. Blueback herring biomass 1999-2008 based on DEM, GSO, and NMFS survey data.

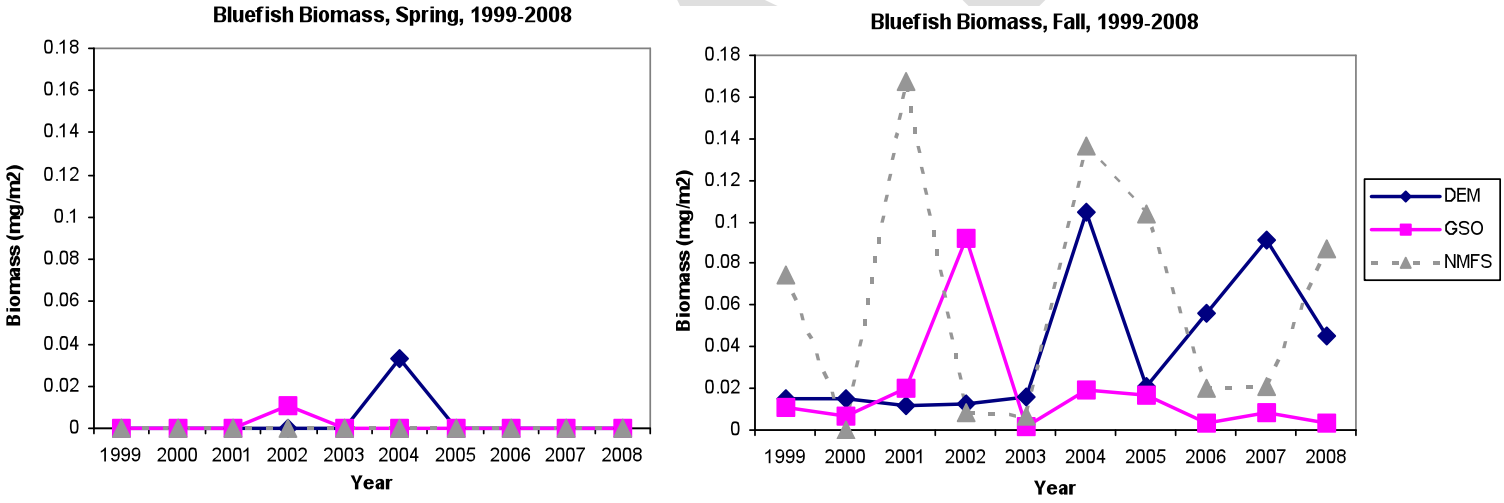

Figure 24. Bluefish biomass 1999-2008 based on DEM, GSO, and NMFS survey data.

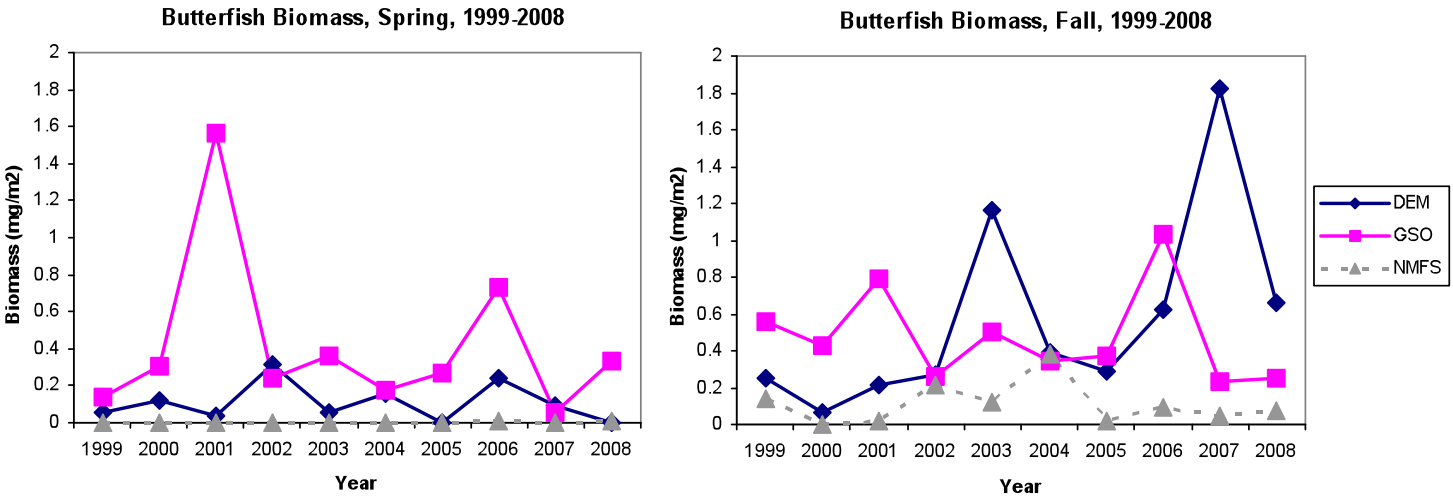

Figure 25. Butterfish biomass 1999-2008 based on DEM, GSO, and NMFS survey data.

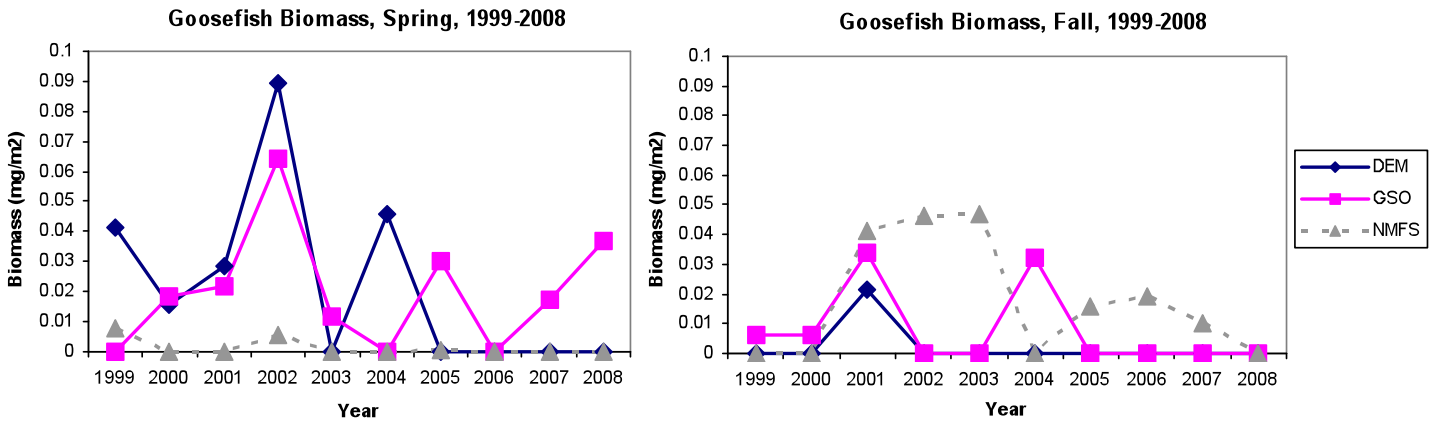

Figure 26. Goosefish (monkfish) biomass 1999-2008 based on DEM, GSO, and NMFS survey data.

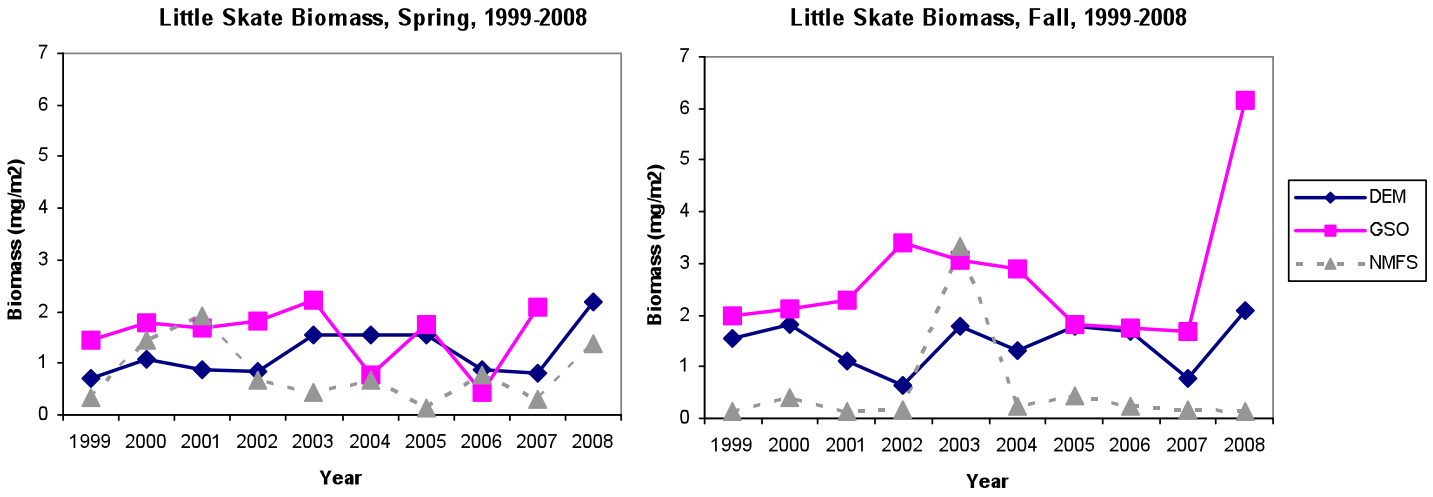

Figure 27. Little skate biomass 1999-2008 based on DEM, GSO, and NMFS survey data.

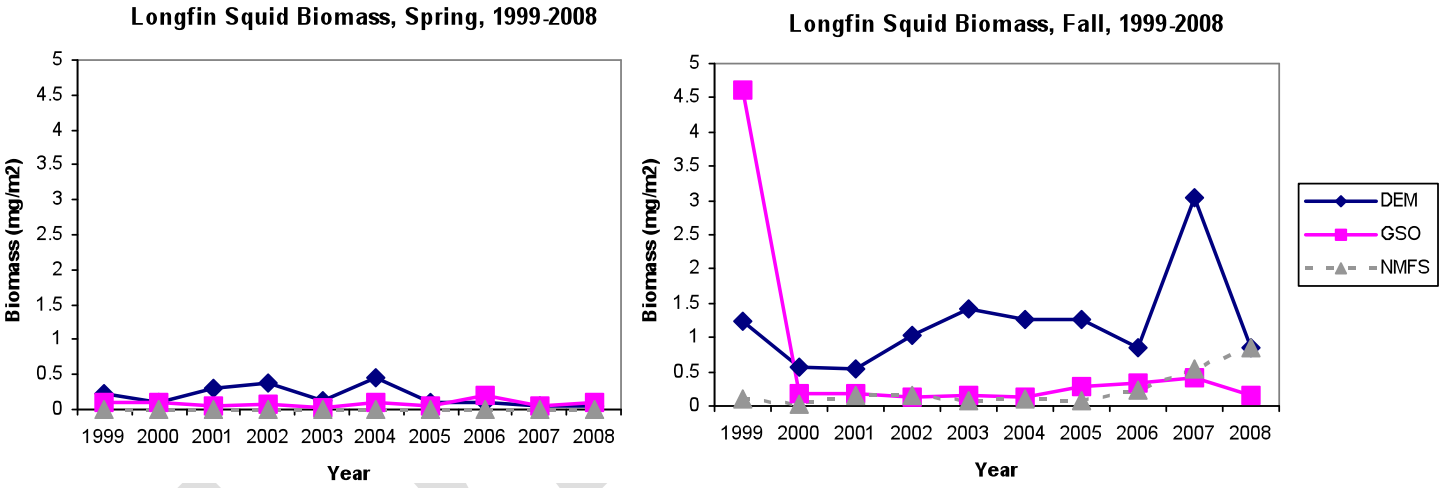

Figure 28. Longfin squid biomass 1999-2008 based on DEM, GSO, and NMFS survey data.

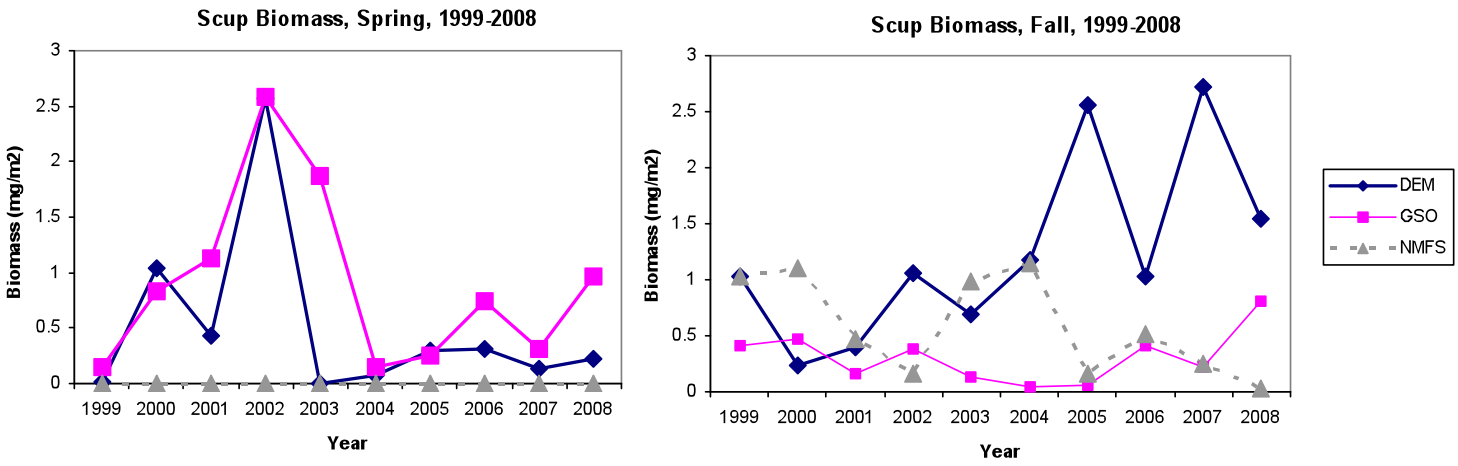

Figure 29. Scup biomass 1999-2008 based on DEM, GSO, and NMFS survey data.

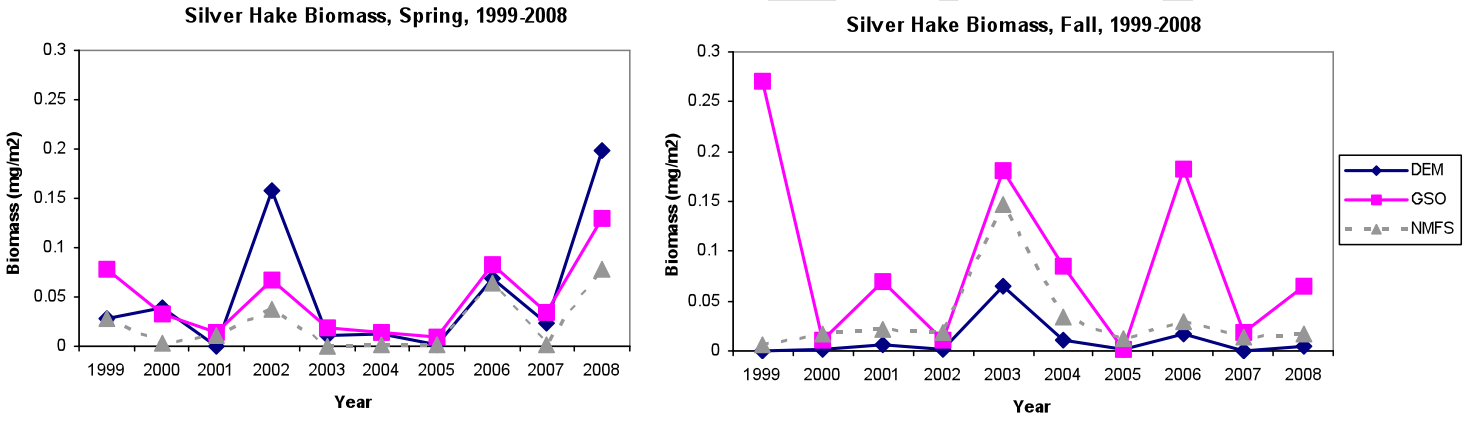

Figure 30. Silver hake biomass 1999-2008 based on DEM, GSO, and NMFS survey data.

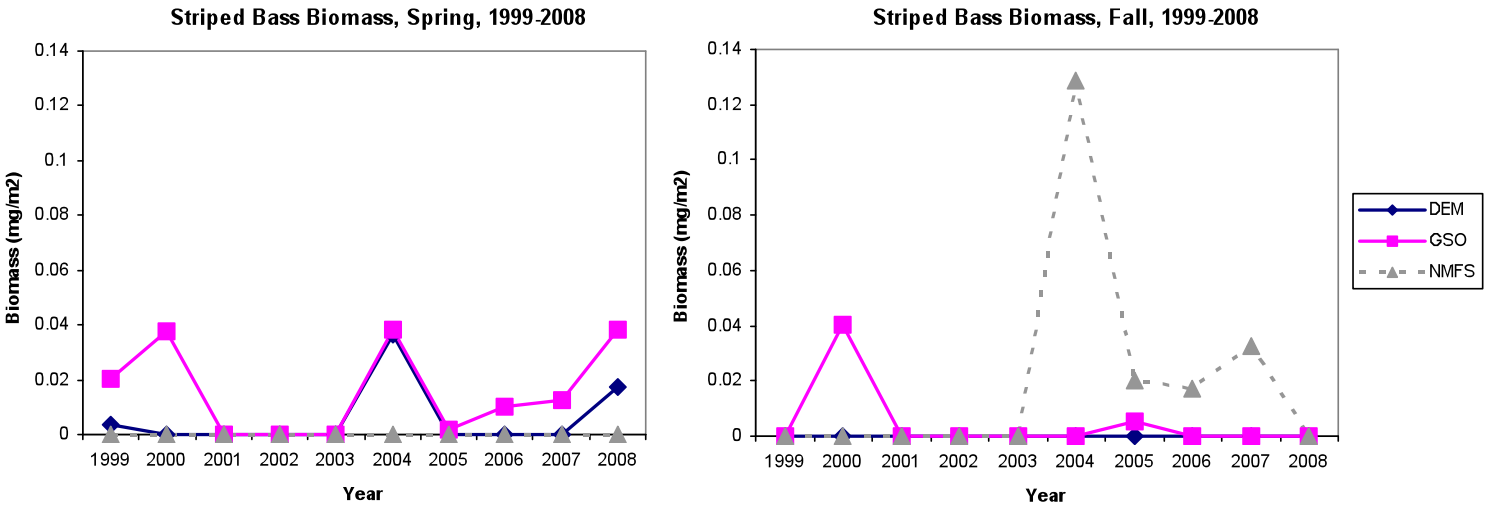

Figure 31. Striped bass biomass 1999-2008 based on DEM, GSO, and NMFS survey data.

Figure C-25. Summer Flounder Biomass

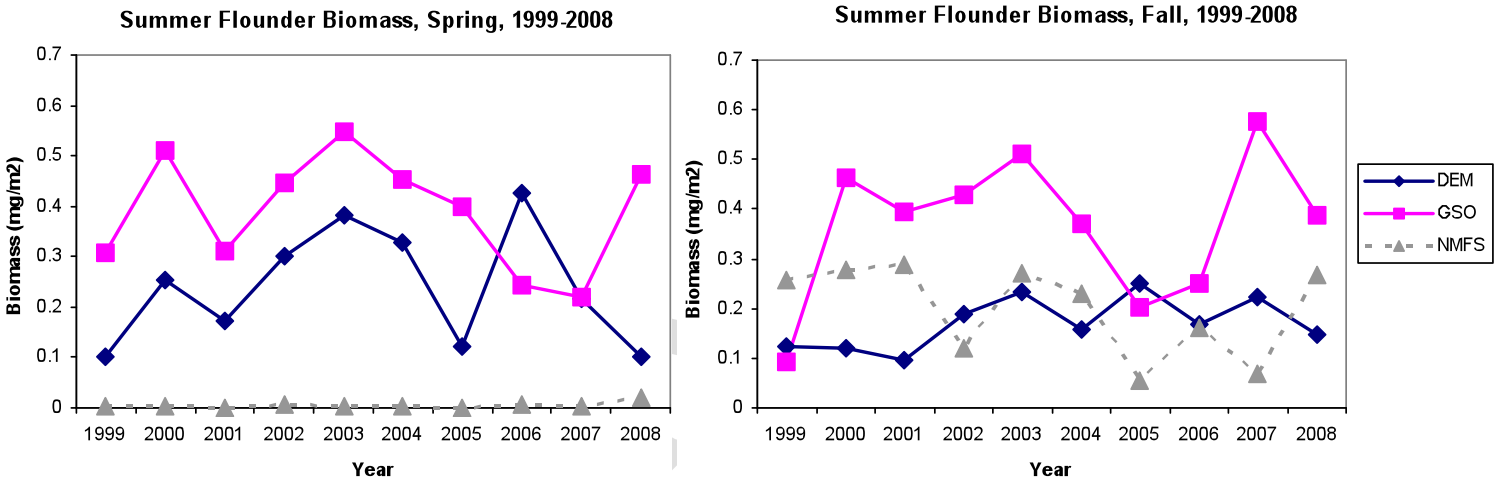

Figure 32. Summer flounder biomass 1999-2008 based on DEM, GSO, and NMFS survey data.

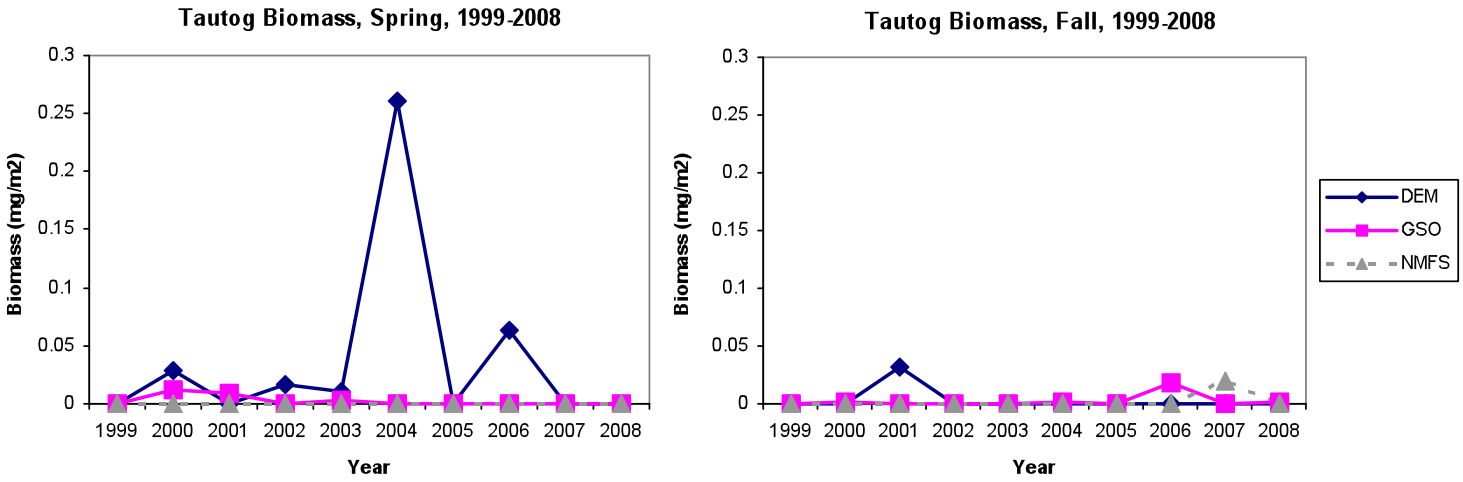

Figure 33. Tautog biomass 1999-2008 based on DEM, GSO, and NMFS survey data.

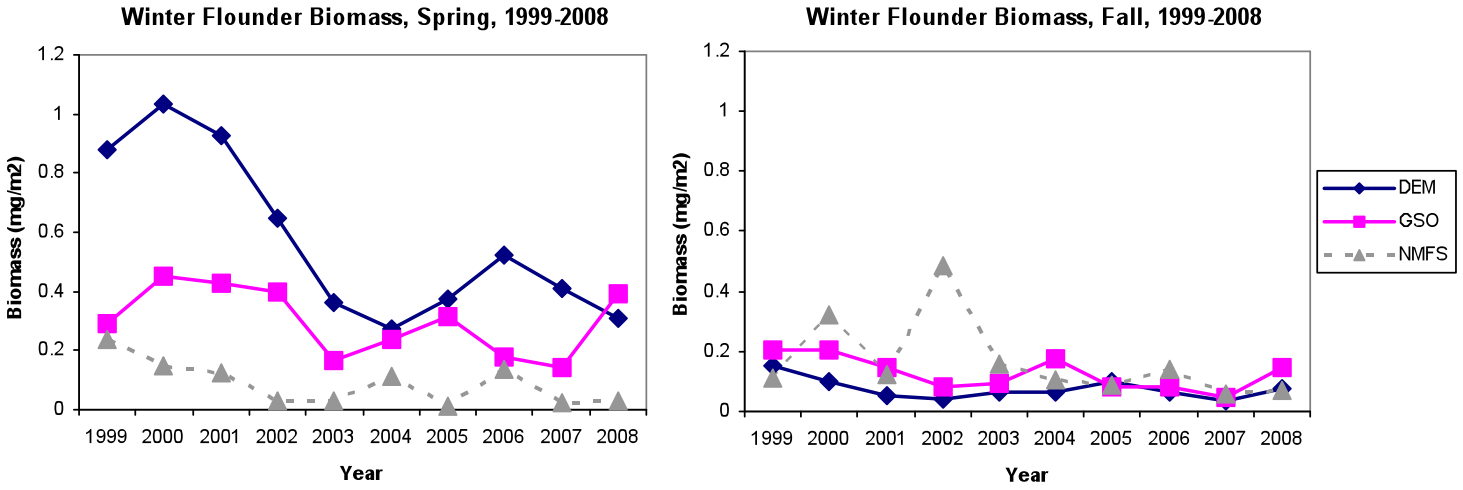

Figure 34. Winter flounder biomass 1999-2008 based on DEM, GSO, and NMFS survey data.

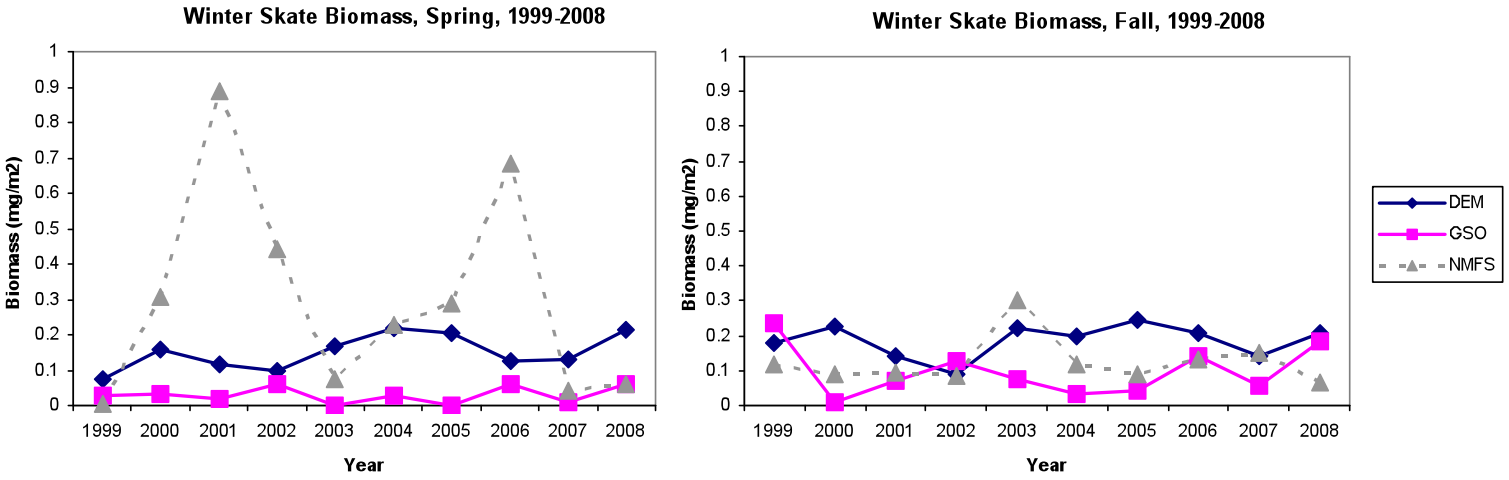

Figure 35. Winter skate biomass 1999-2008 based on DEM, GSO, and NMFS survey data.

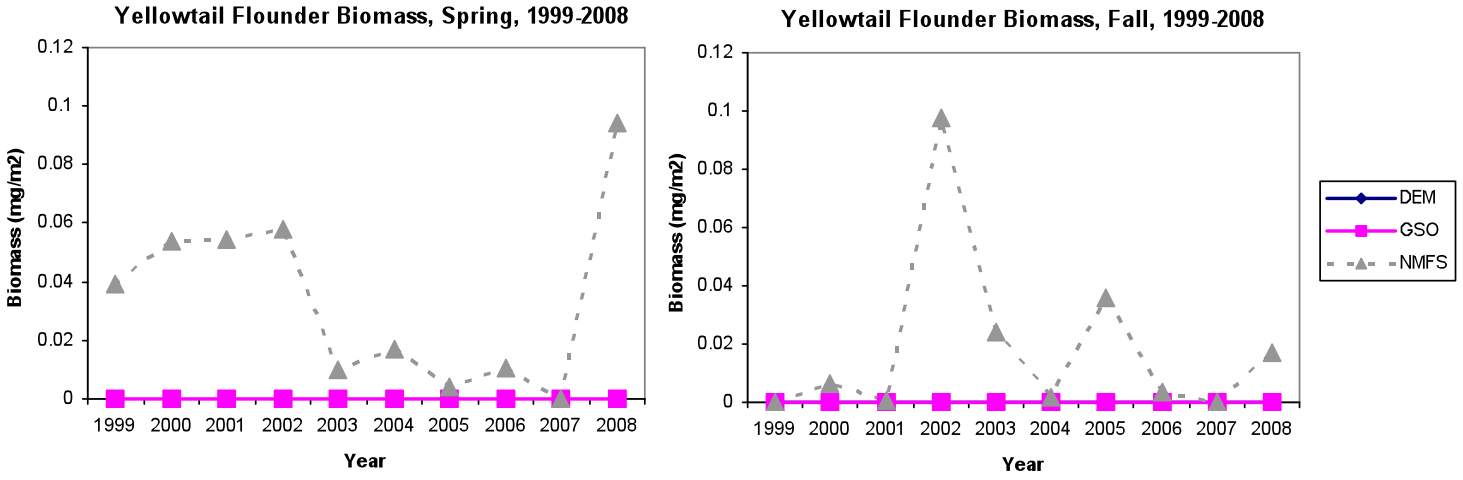

Figure 36. Yellowtail flounder biomass 1999-2008 based on DEM, GSO, and NMFS survey data.

5. Maps of Individual Species Biomass, Spring and Fall

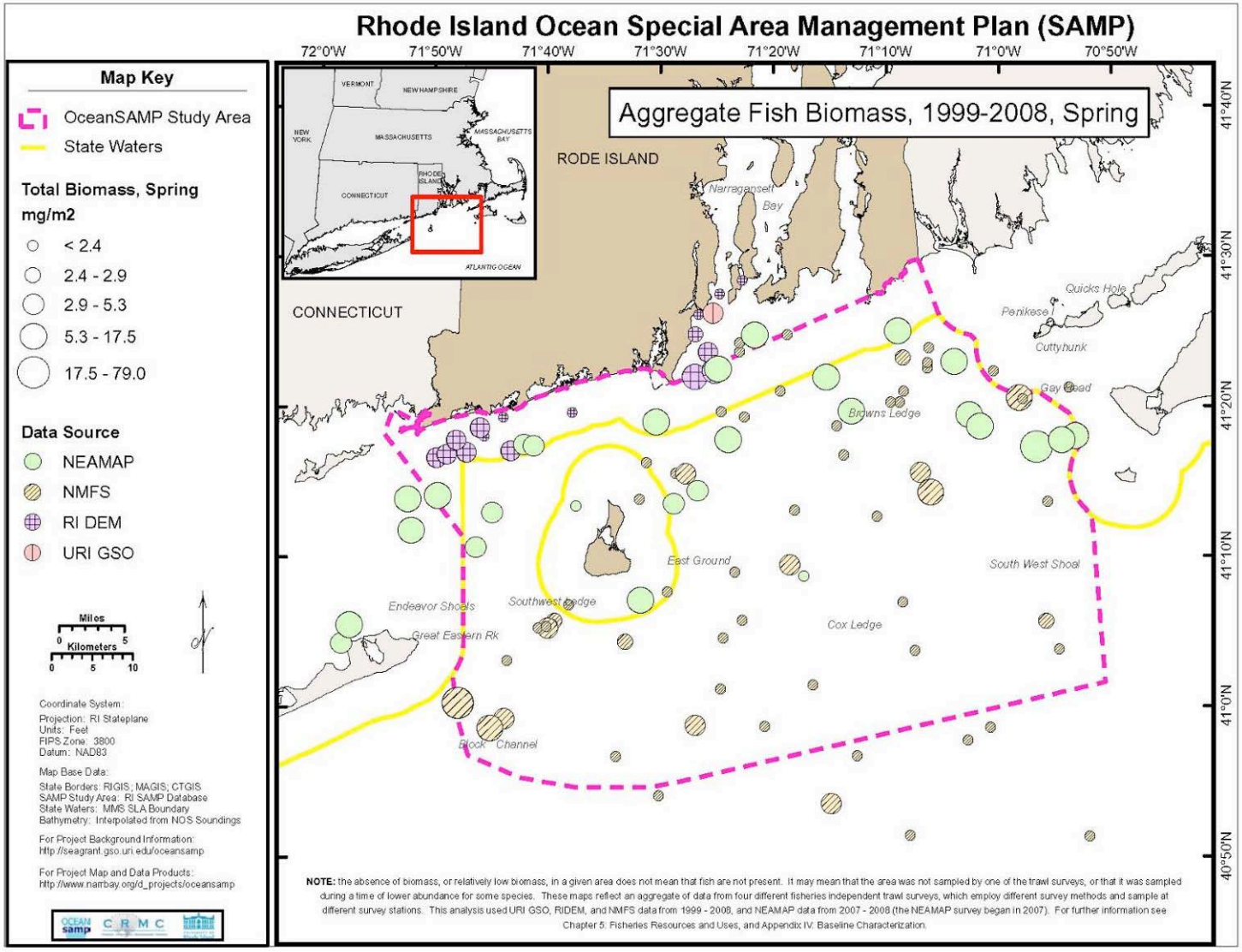

Figure 37. Aggregate Fish Biomass, 1999-2008, Spring

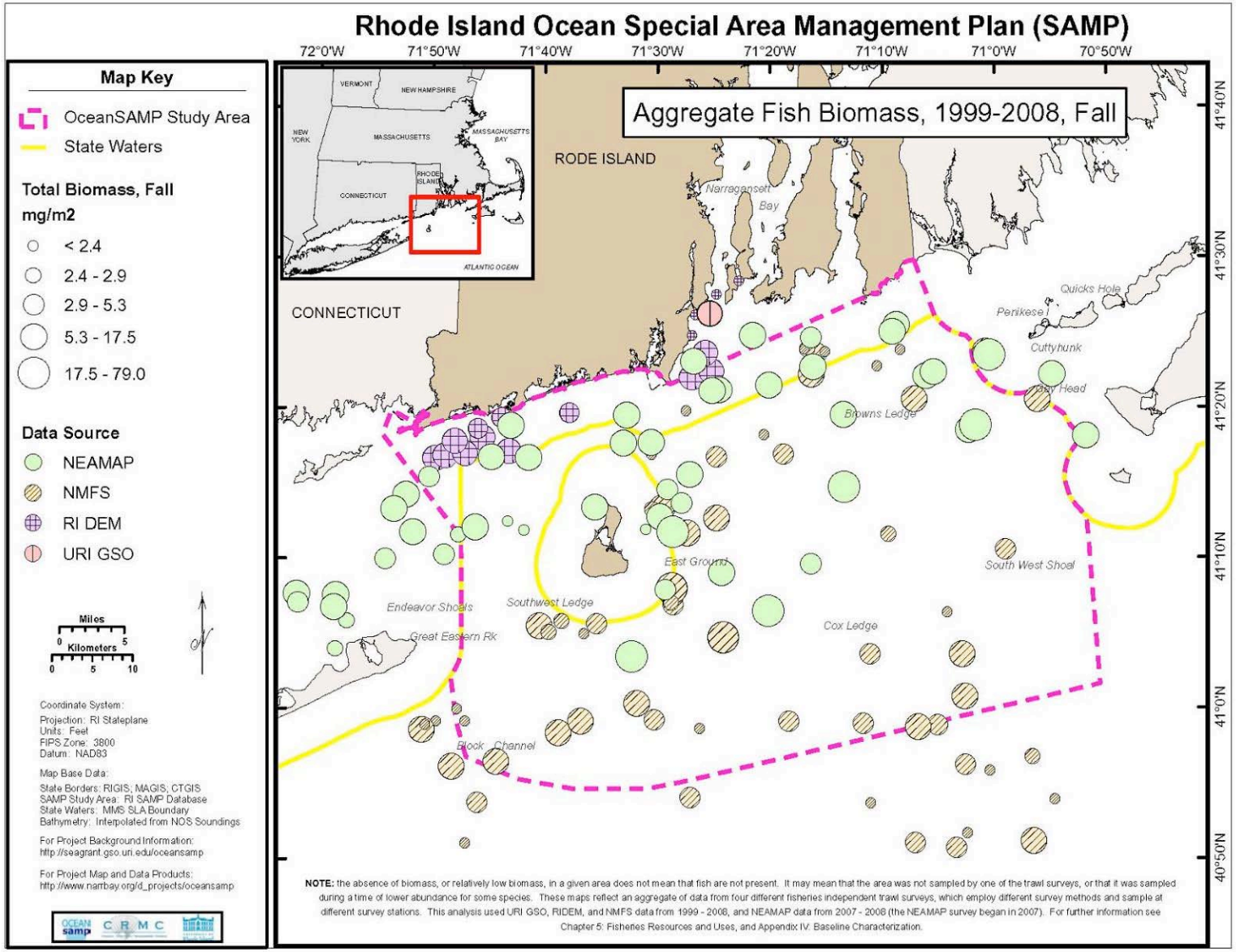

Figure 38. Aggregate Fish Biomass, 1999-2008, Fall

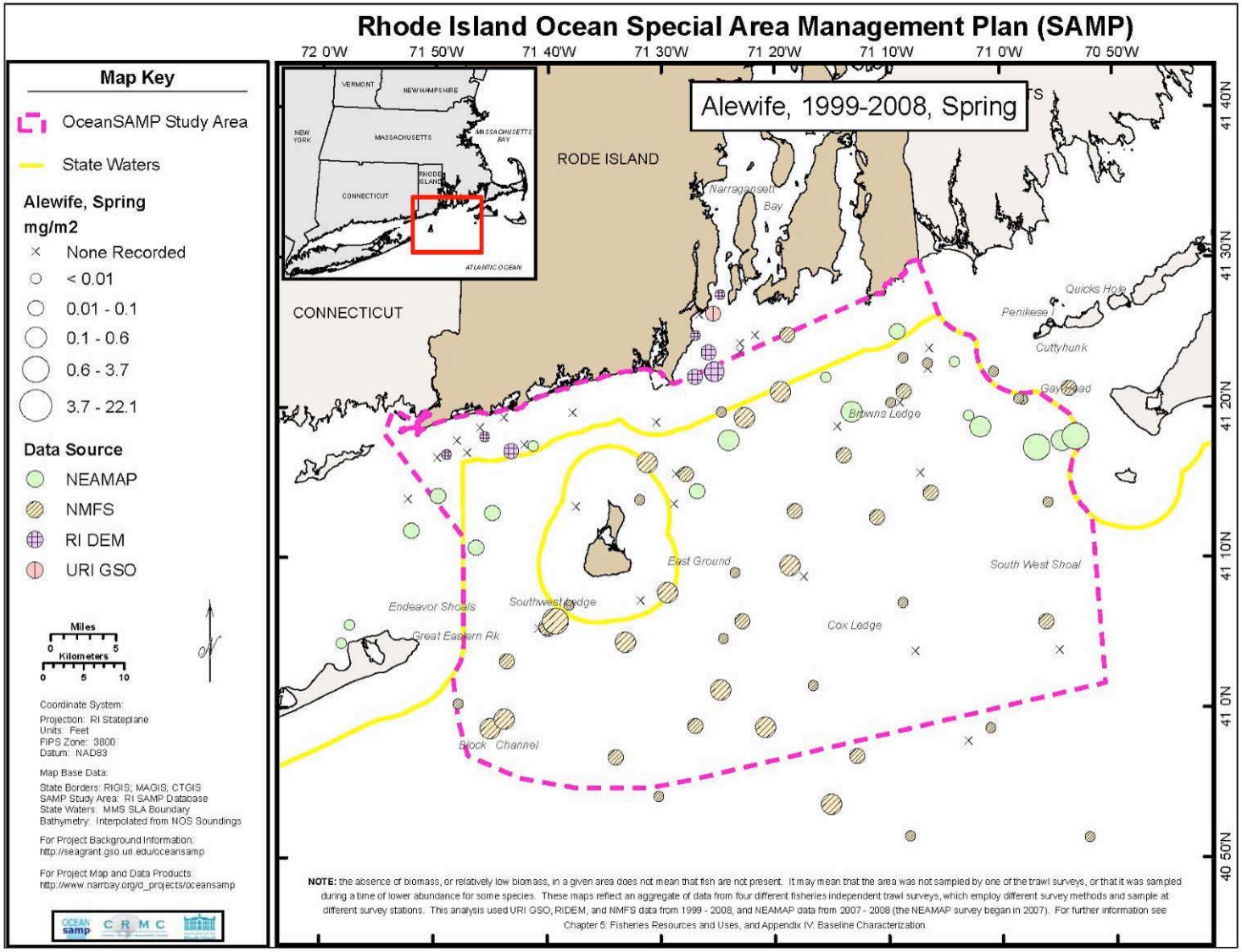

Figure 39. Alewife Biomass, Spring

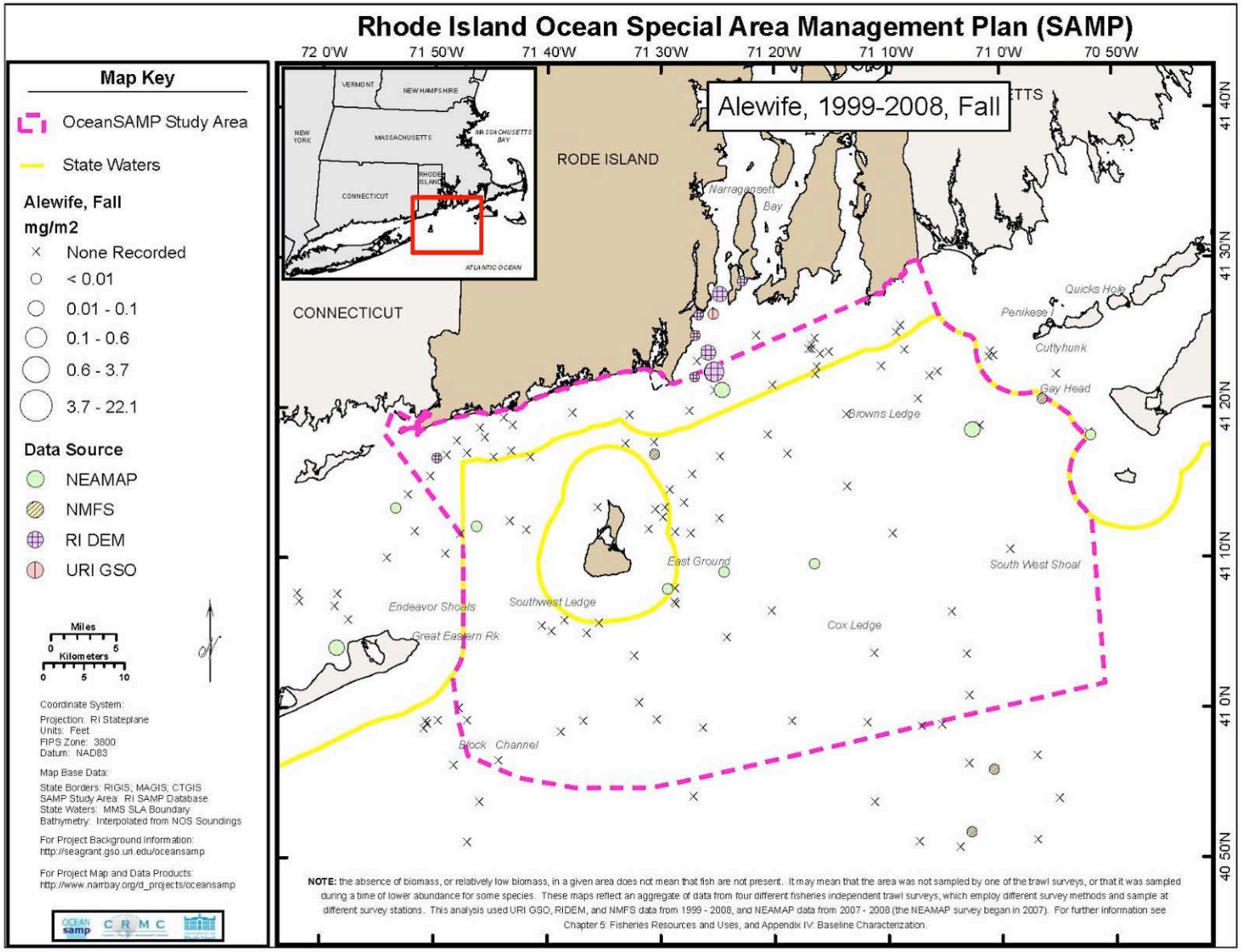

Figure 40. Alewife Biomass, Fall

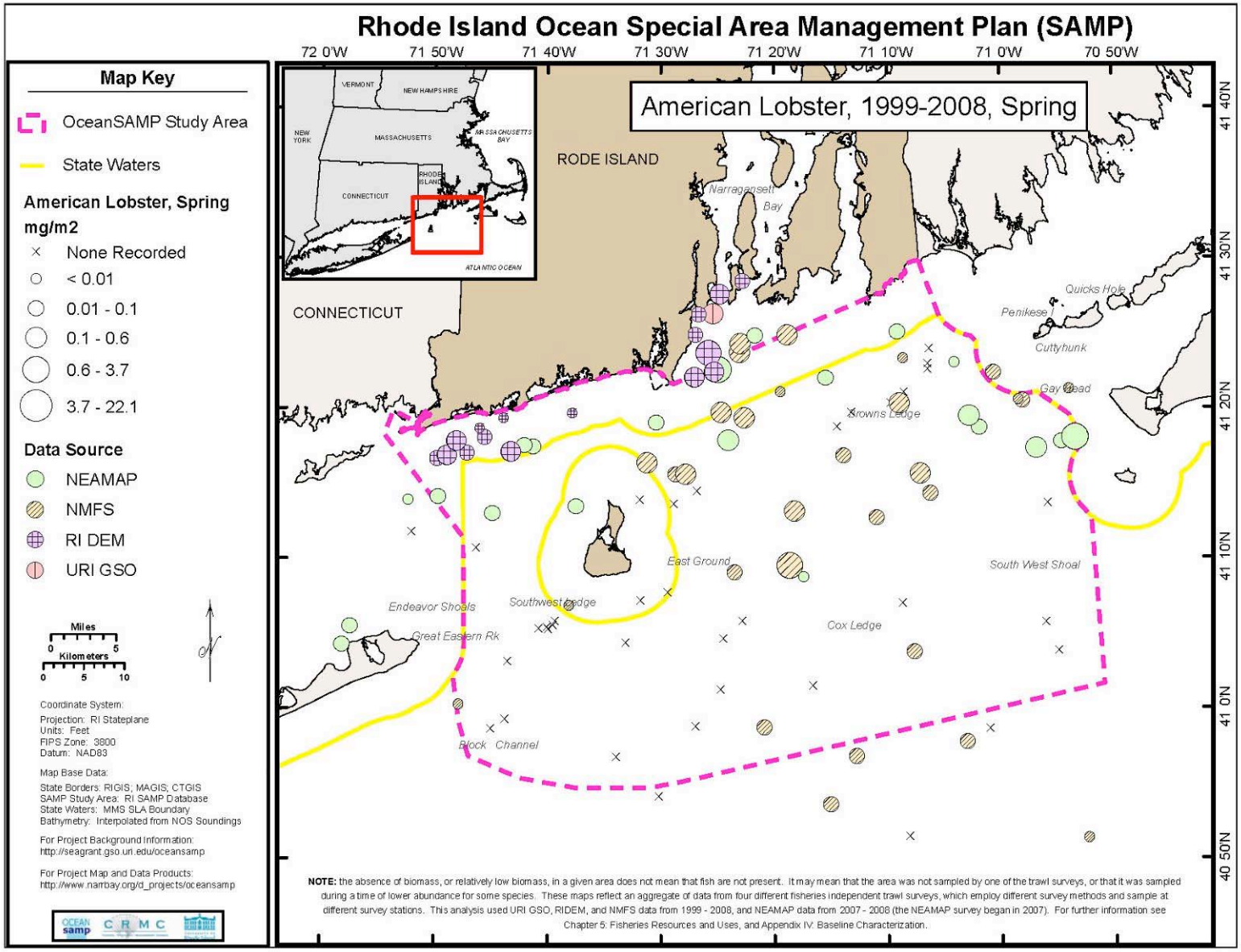

Figure 41. American Lobster Biomass, Spring

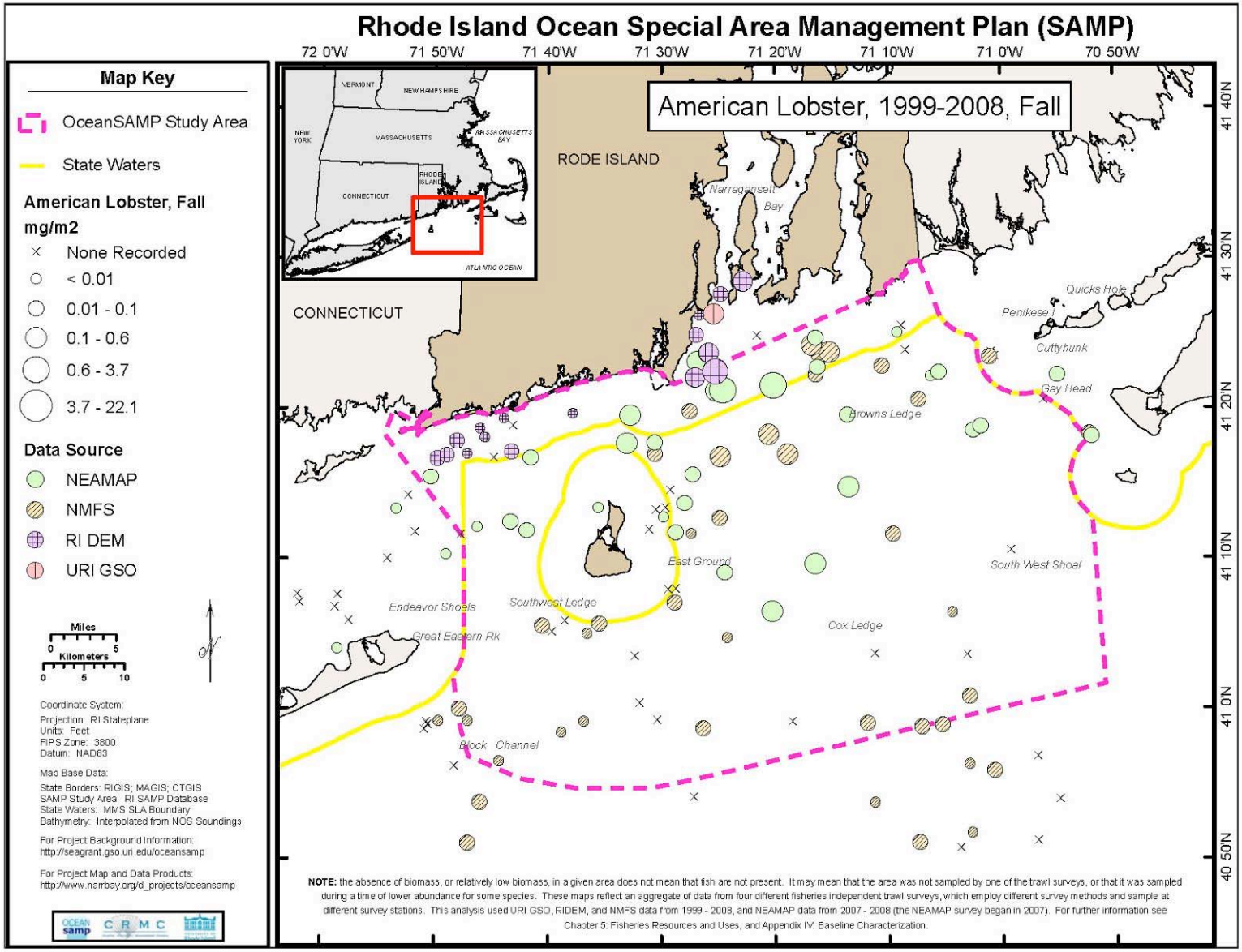

Figure 42. American Lobster Biomass, Fall

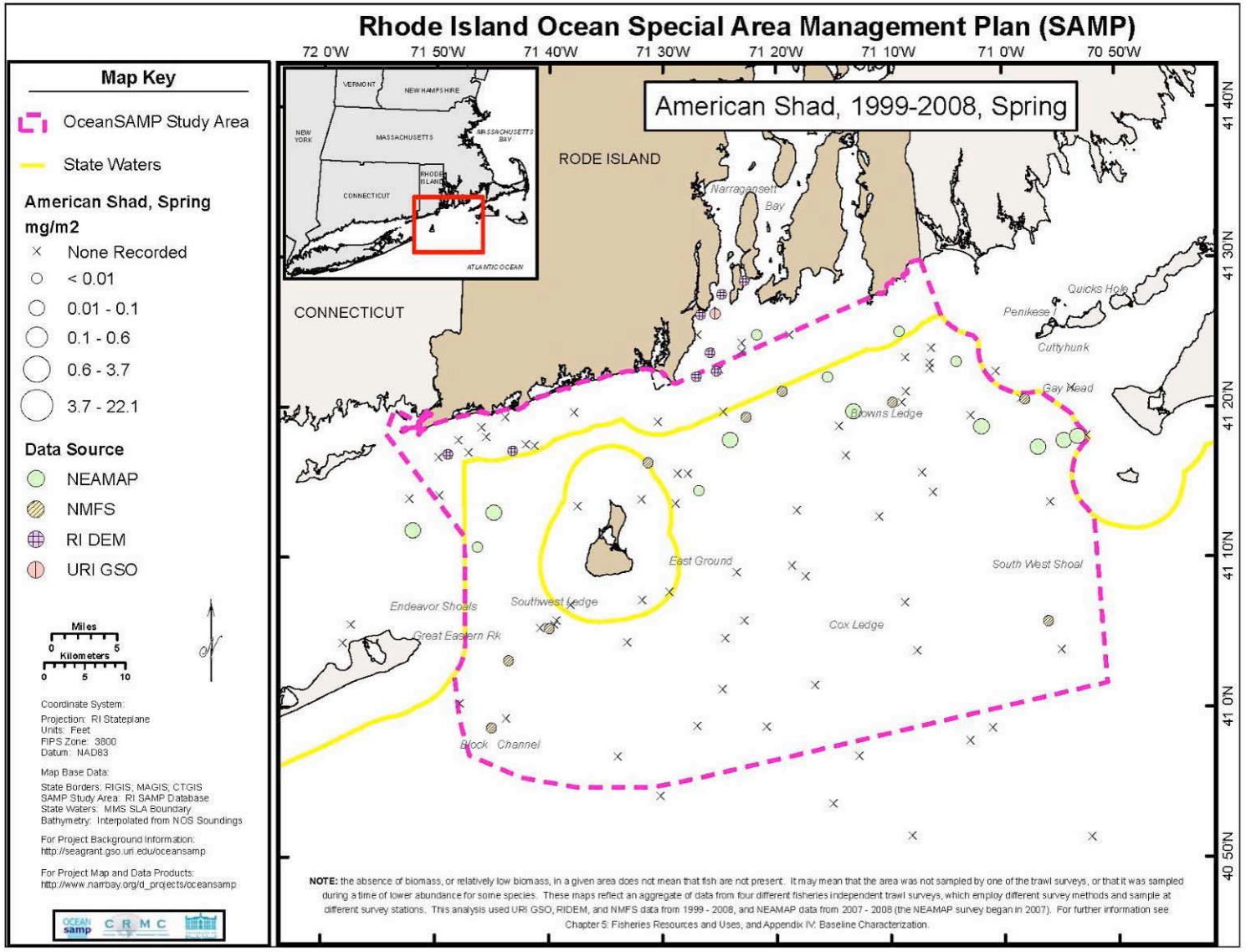

Figure 43. American Shad Biomass, Spring

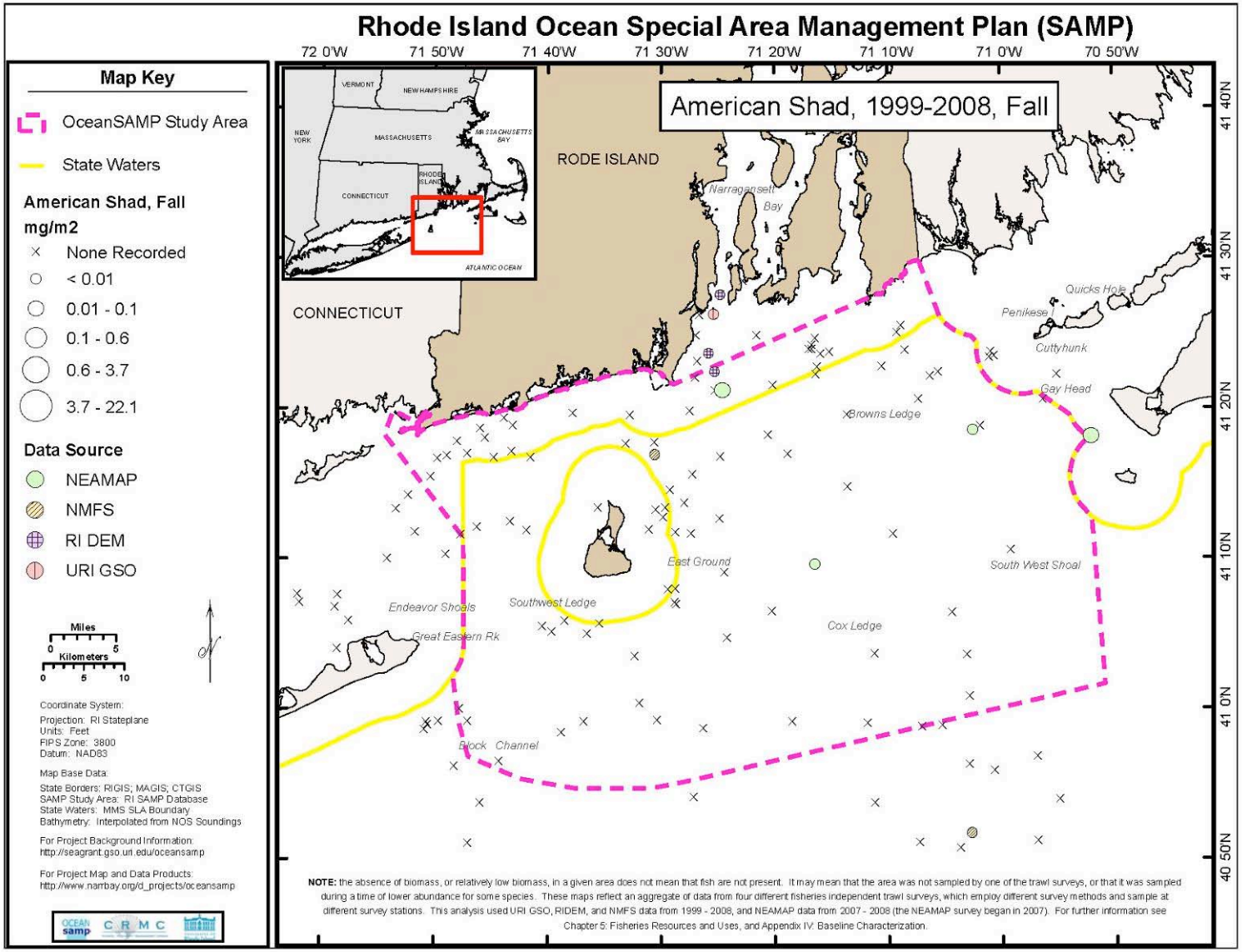

Figure 44. American Shad Biomass, Fall

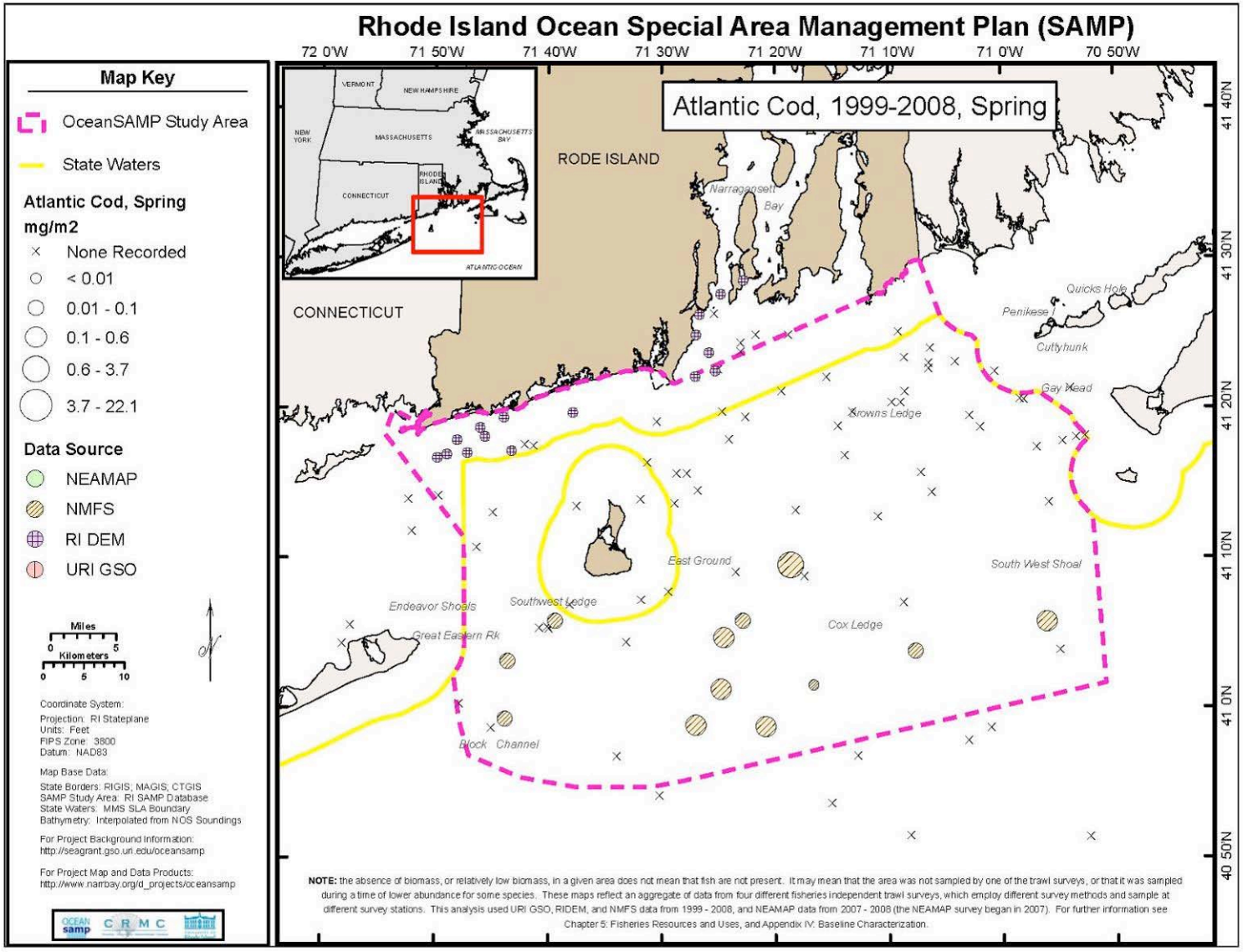

Figure 45. Atlantic Cod Biomass, Spring

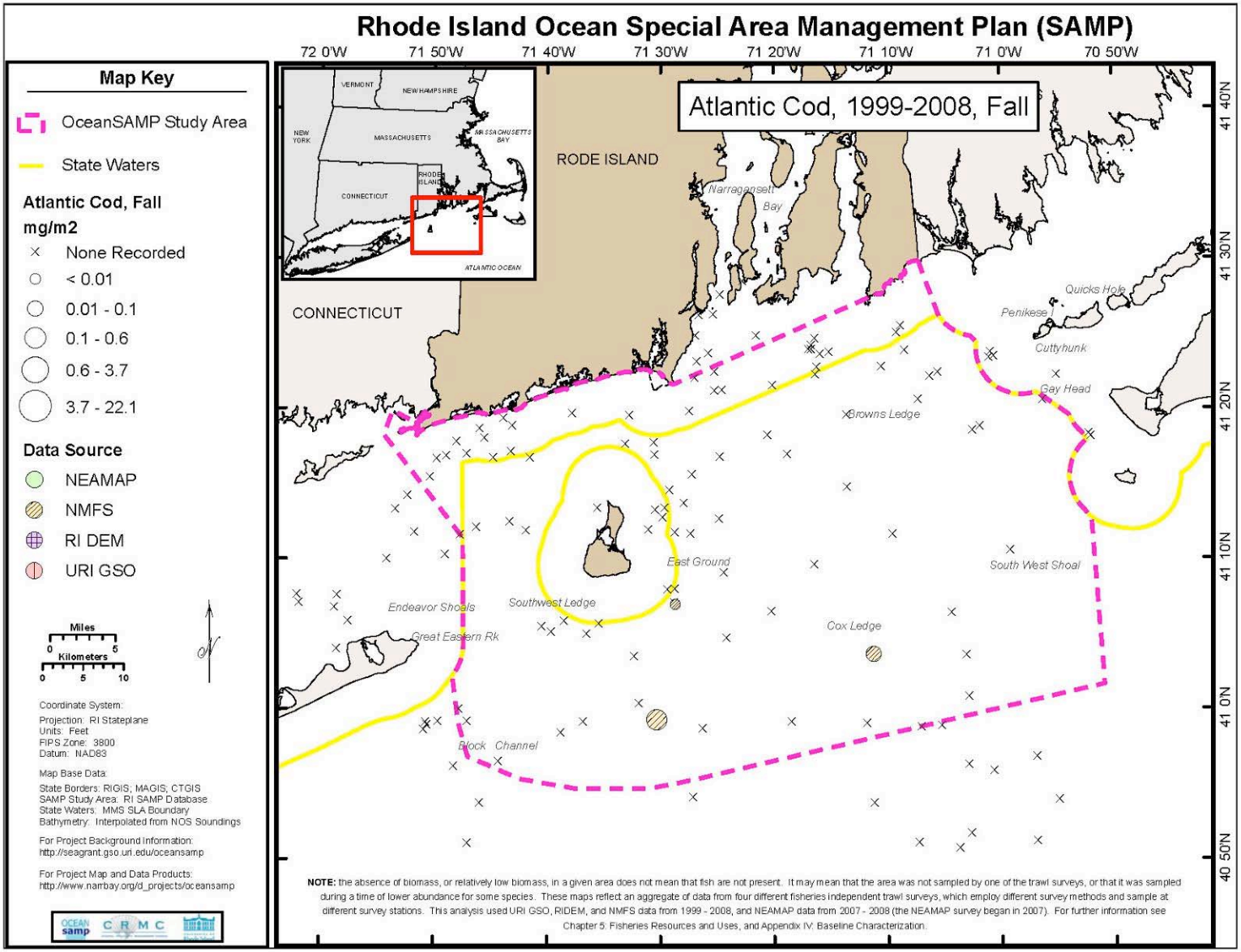

Figure 46. Atlantic Cod Biomass, Fall

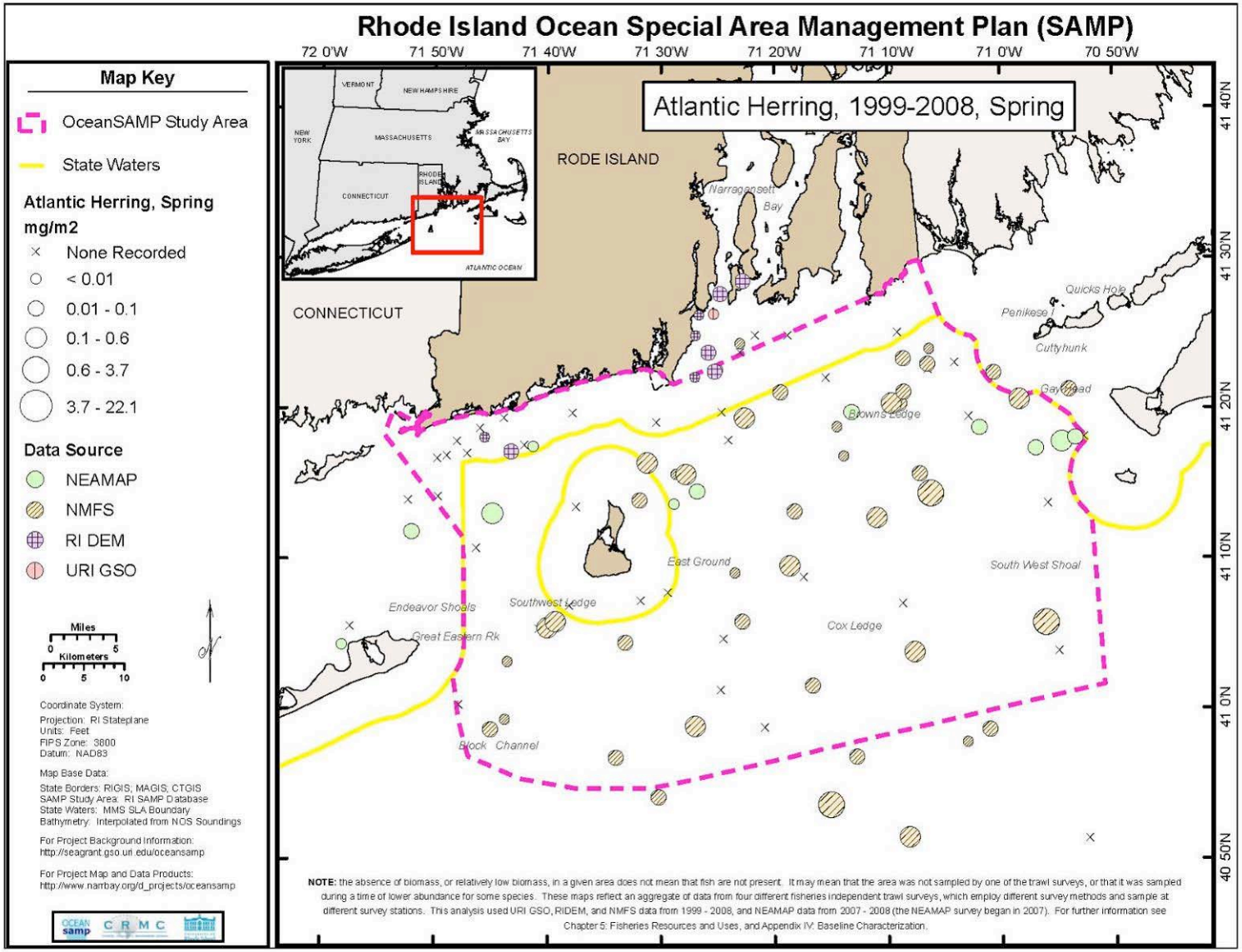

Figure 47. Atlantic Herring Biomass, Spring

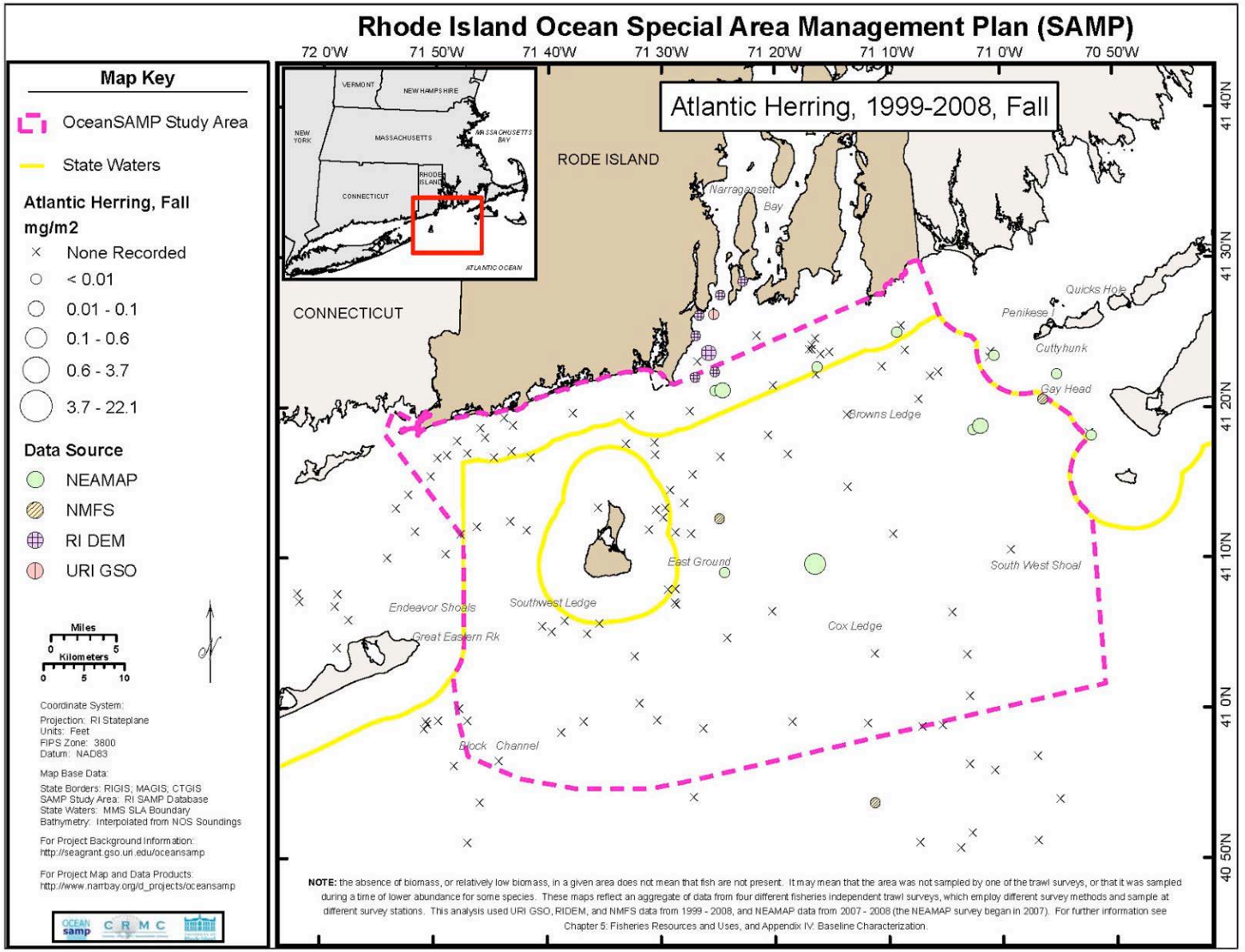

Figure 48. Atlantic Herring Biomass, Fall

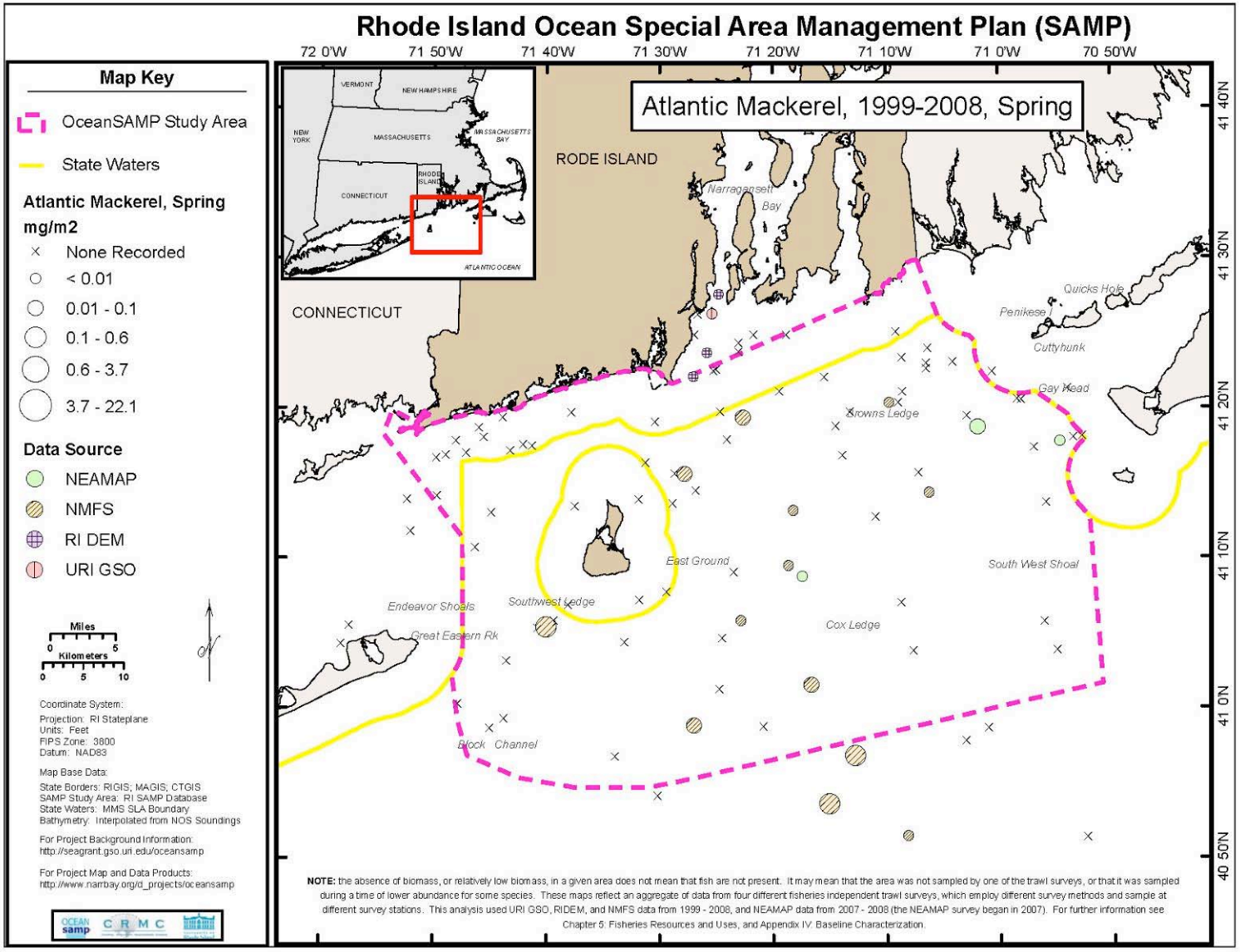

Figure 49. Atlantic Mackerel Biomass, Spring

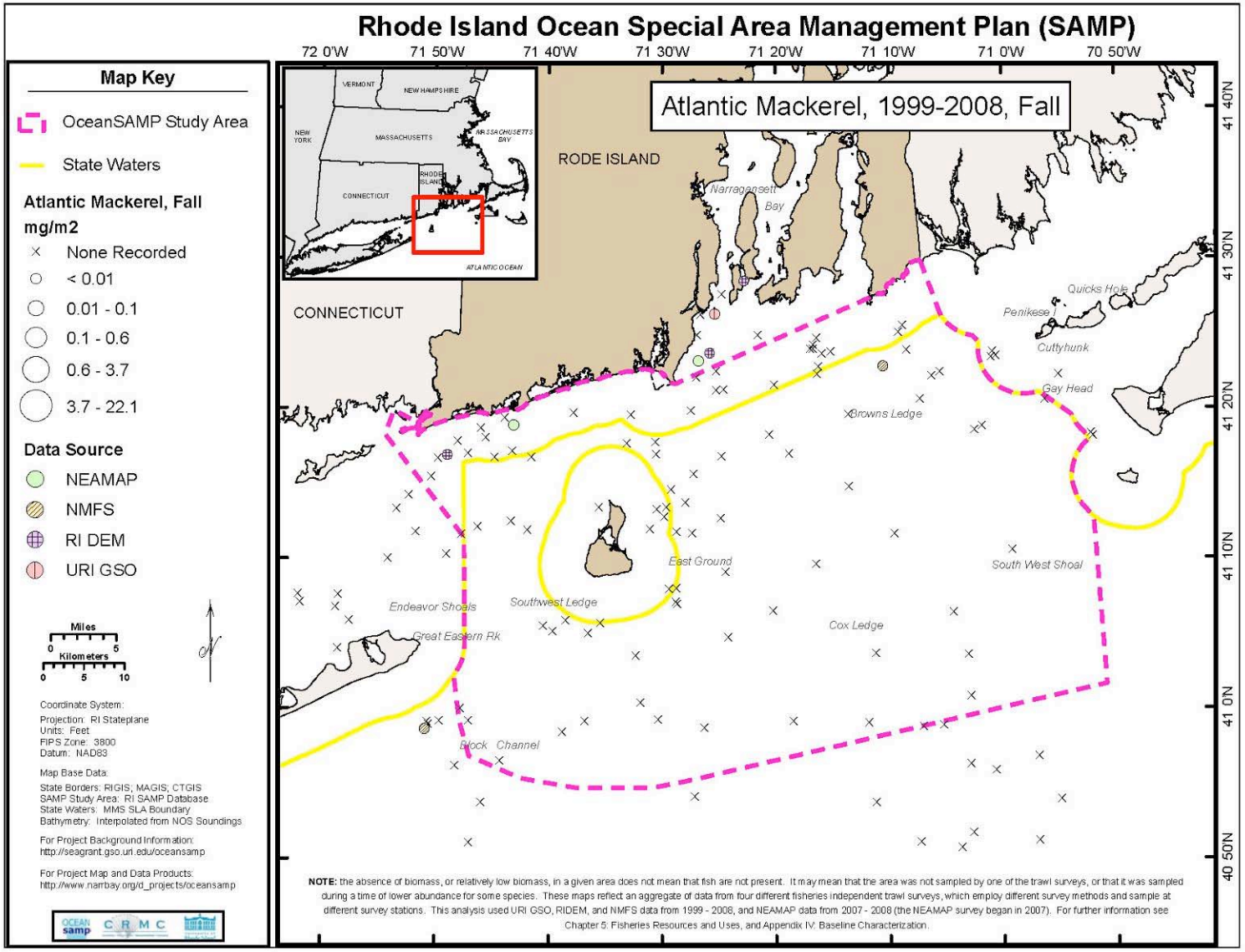

Figure 50. Atlantic Mackerel Biomass, Fall

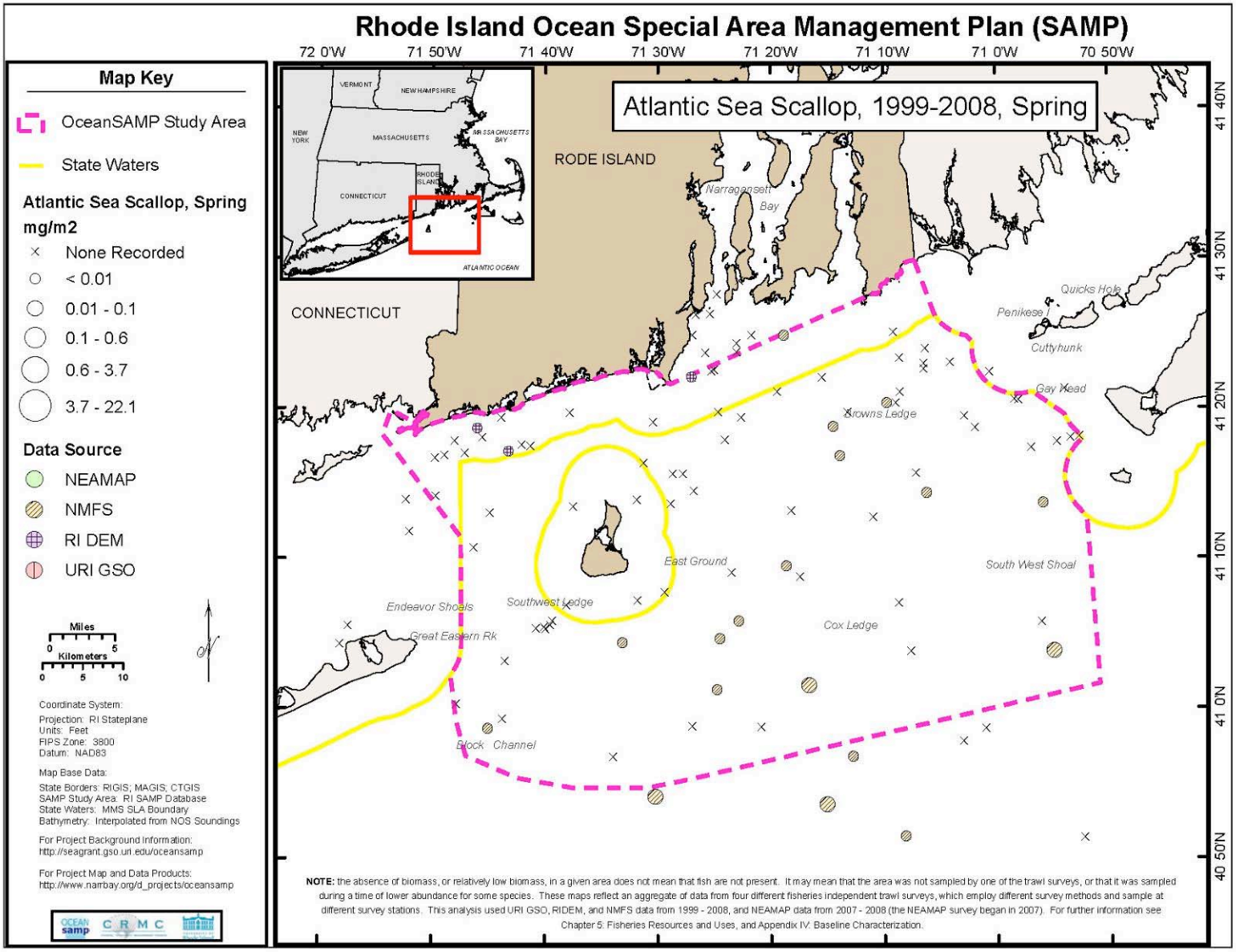

Figure 51. Atlantic Sea Scallop Biomass, Spring

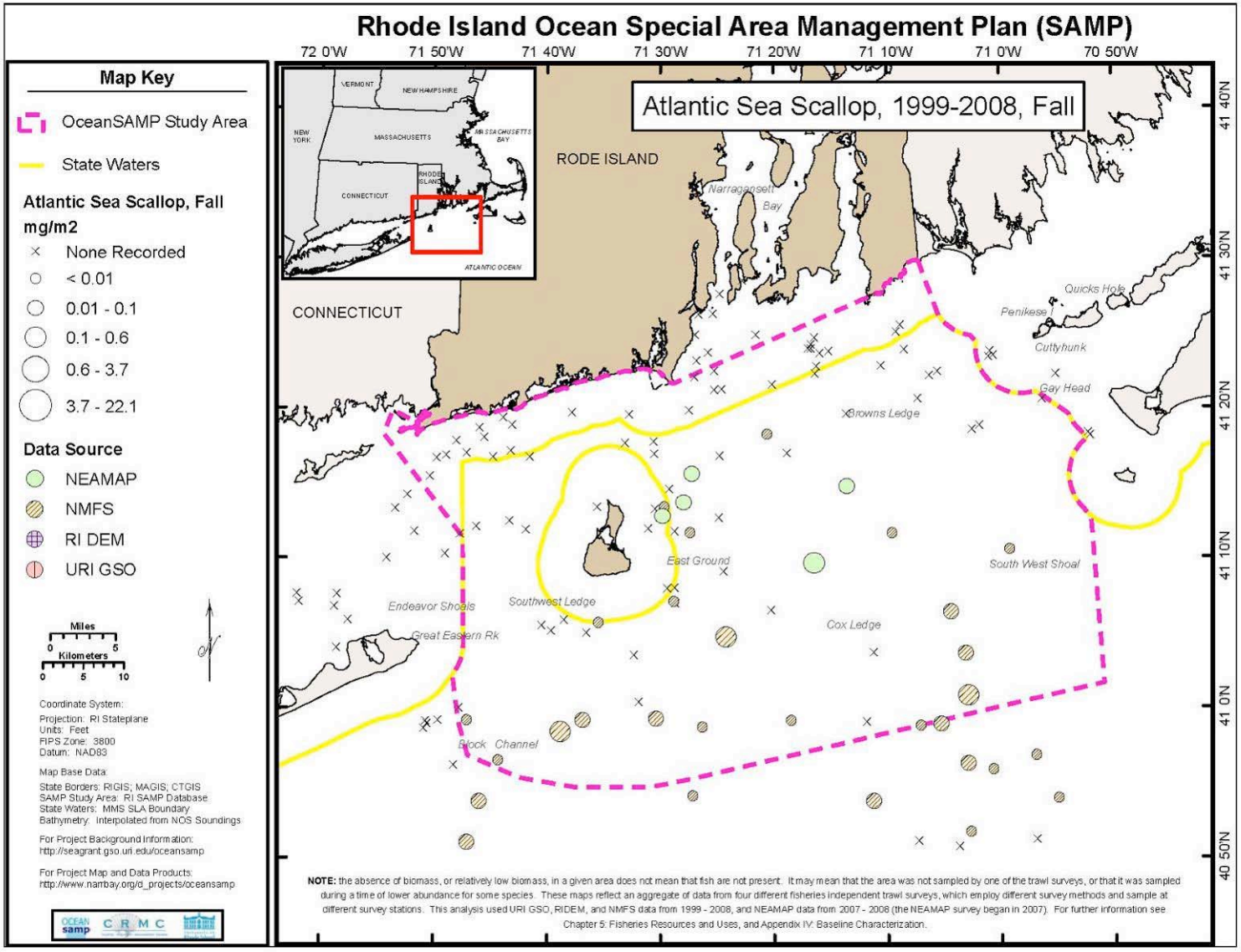

Figure 52. Atlantic Sea Scallop Biomass, Fall

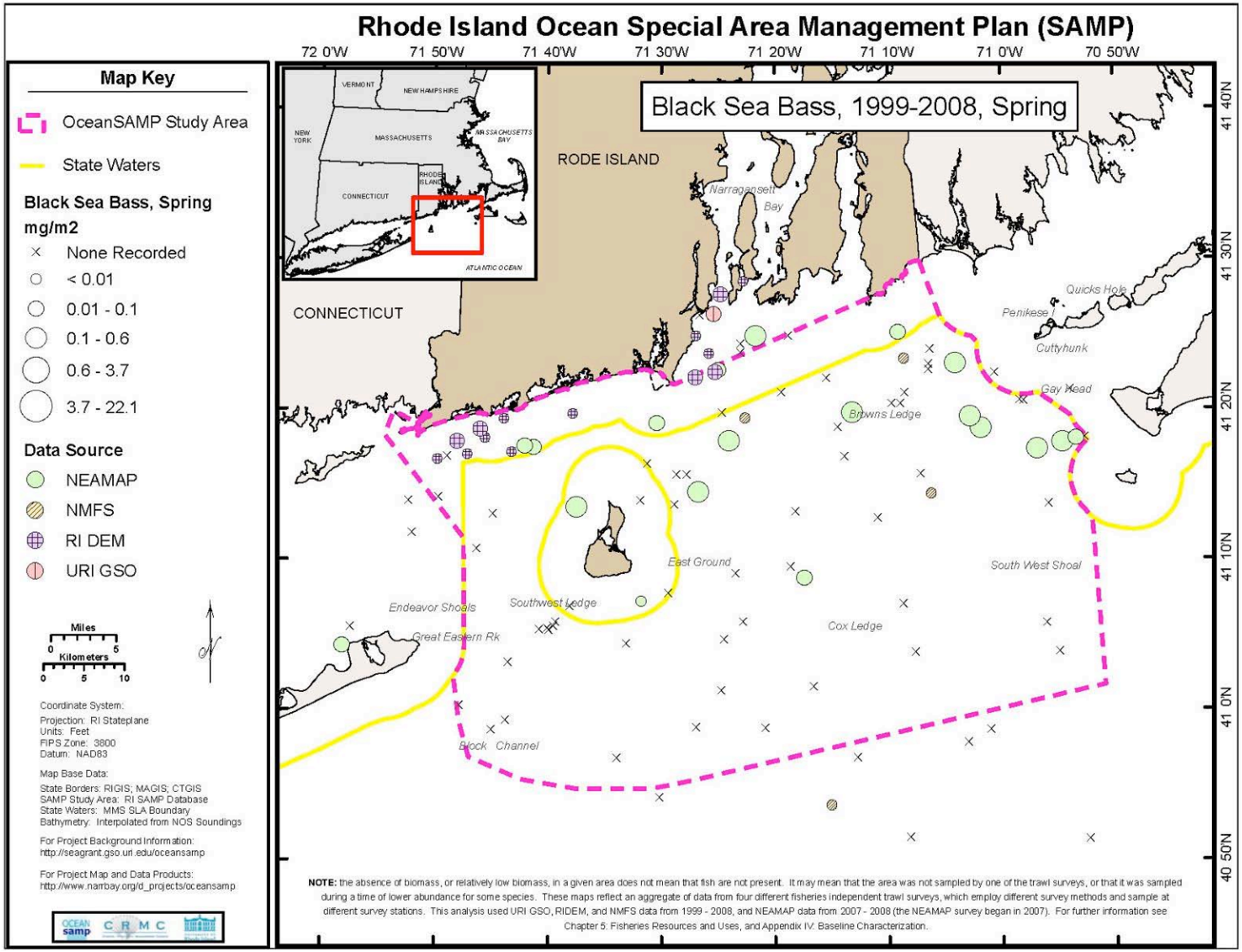

Figure 53. Black Sea Bass Biomass, Spring

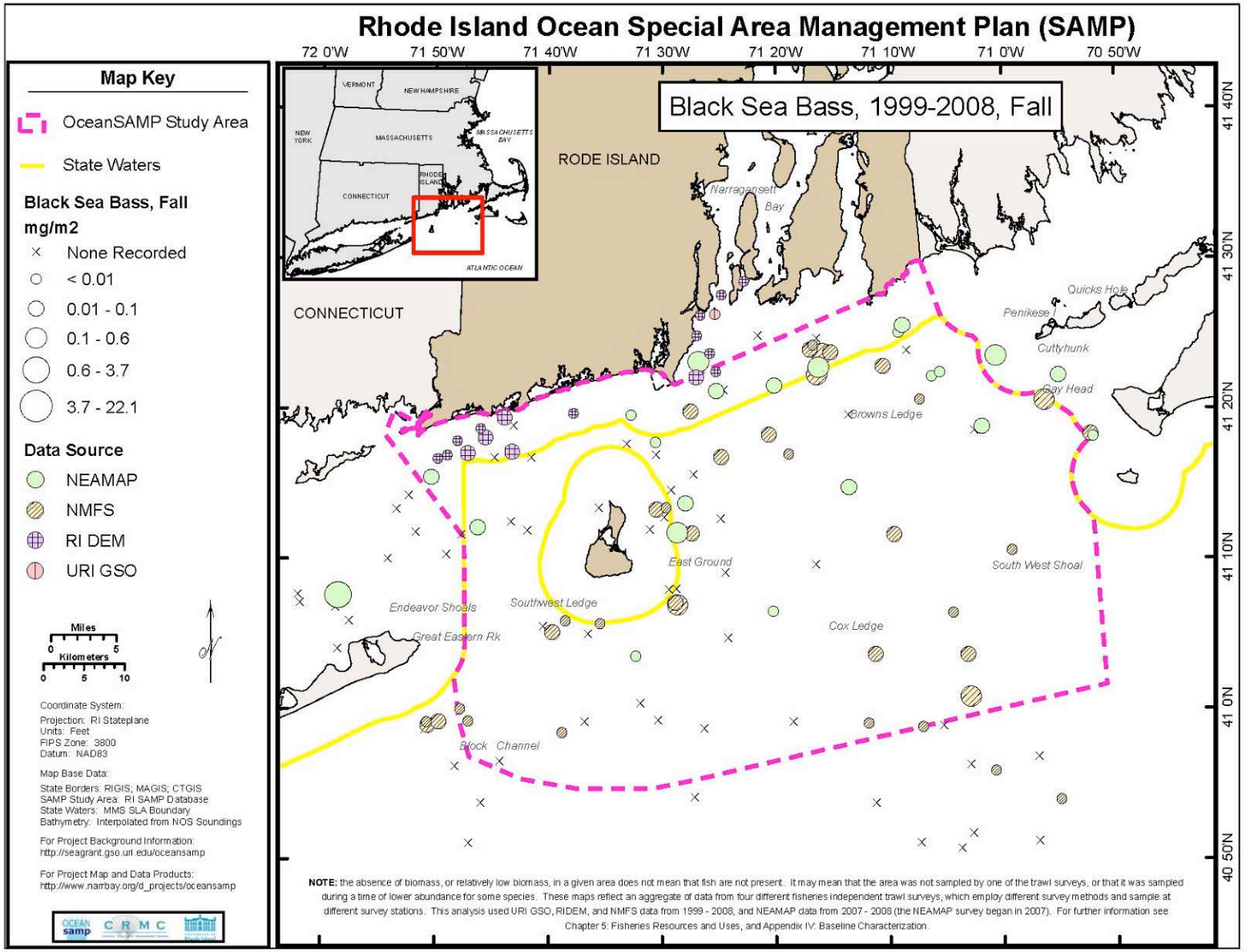

Figure 54. Black Sea Bass Biomass, Fall

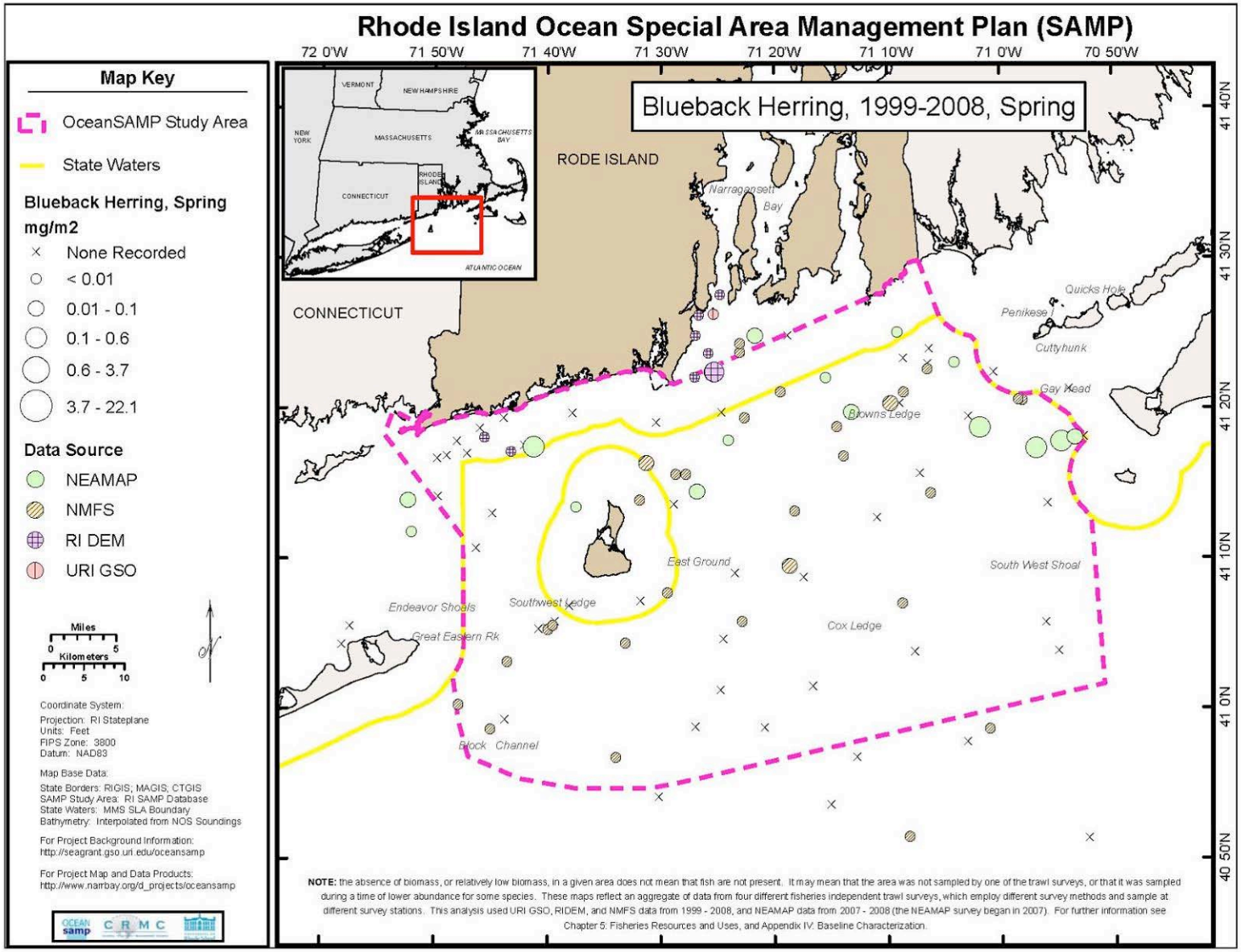

Figure 55. Blueback Herring Biomass, Spring

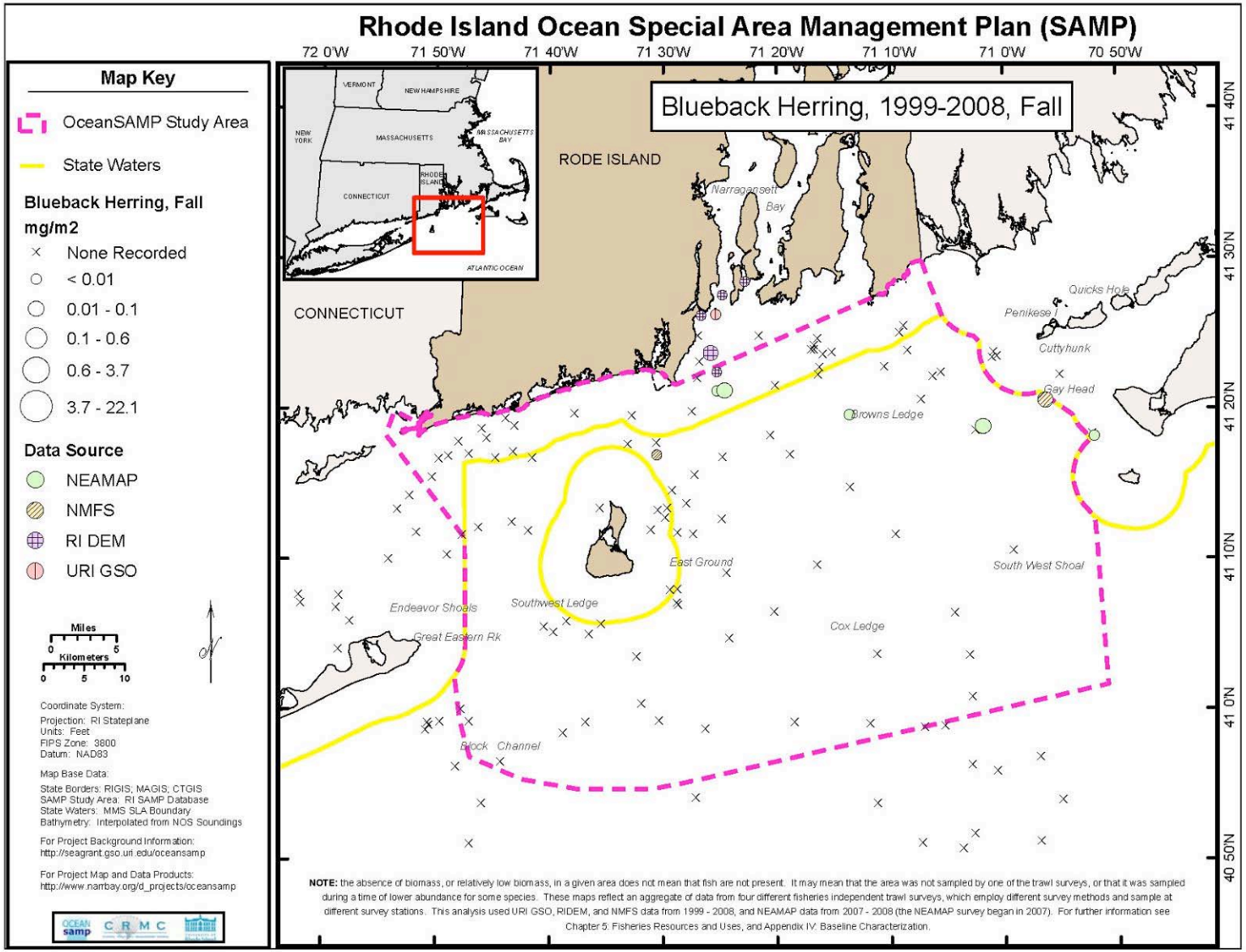

Figure 56. Blueback Herring Biomass, Fall

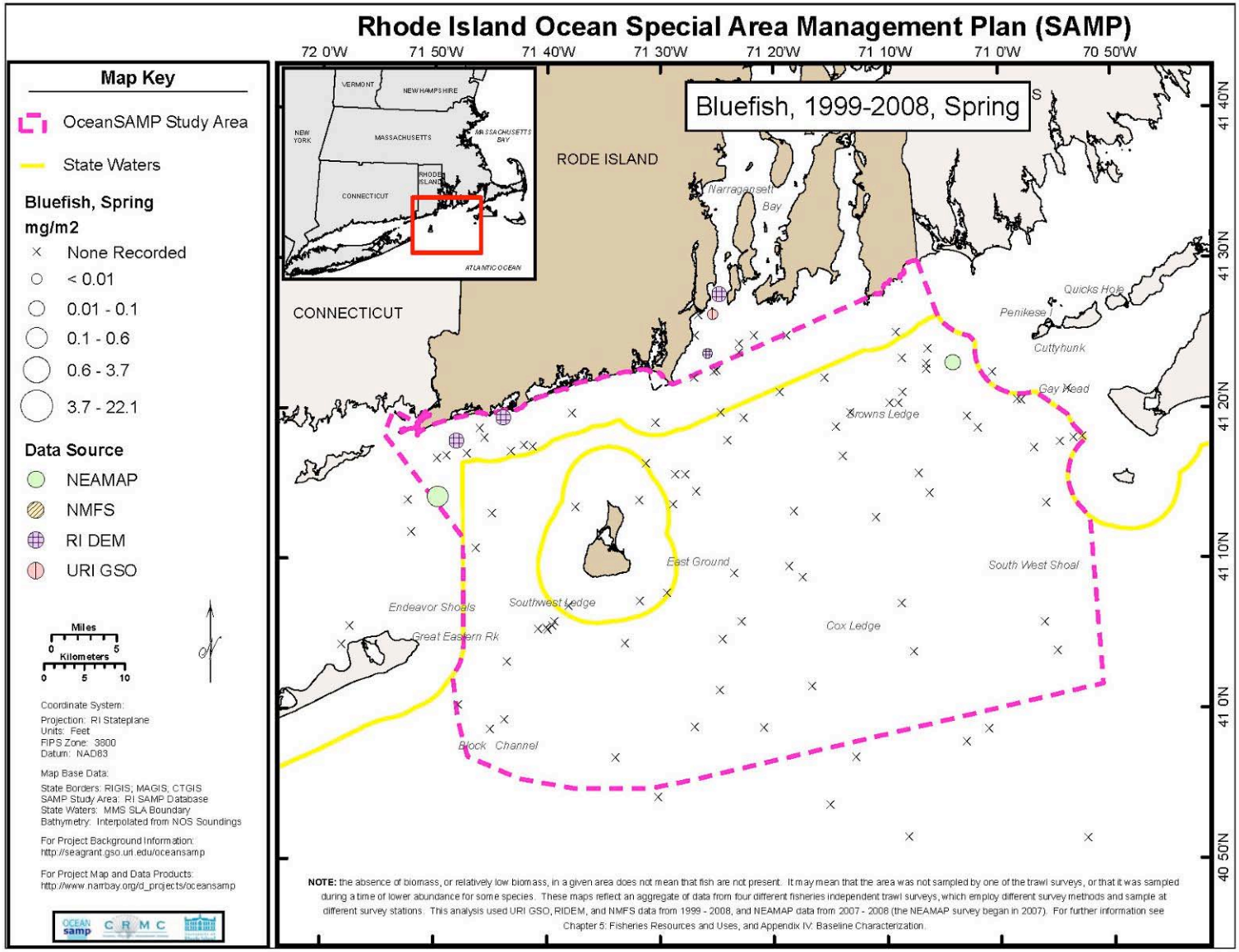

Figure 57. Bluefish Biomass, Spring

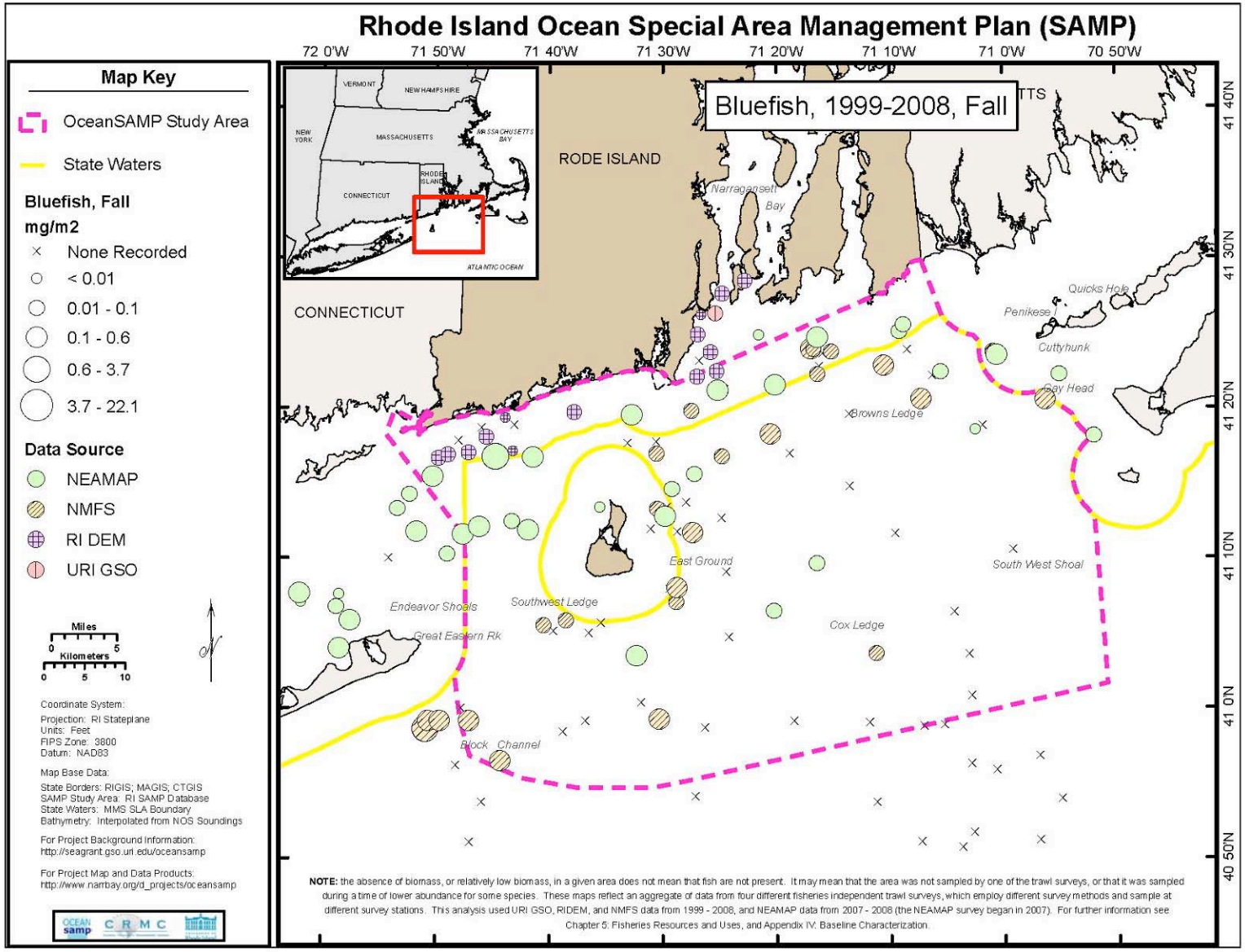

Figure 58. Bluefish Biomass, Fall

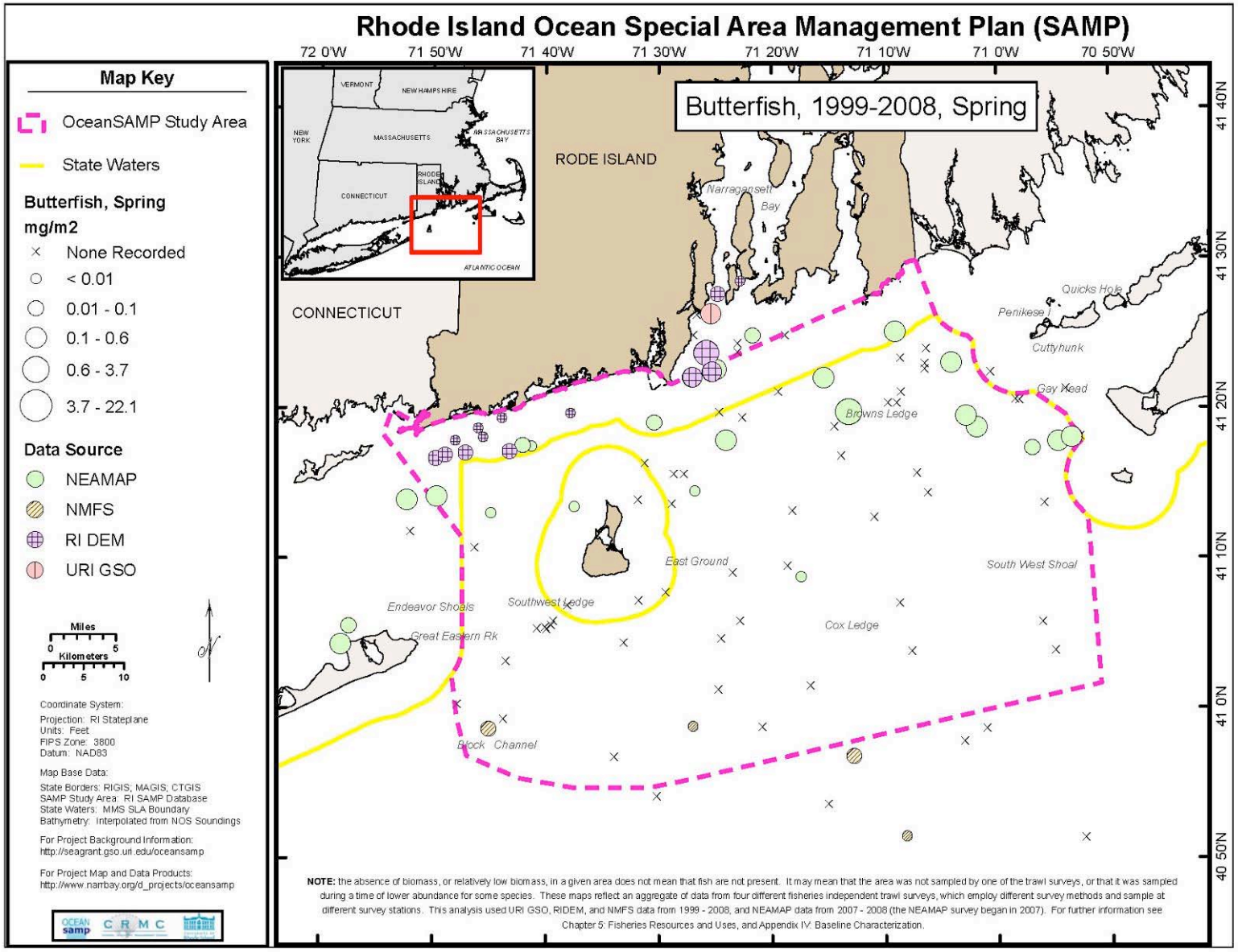

Figure 59. Butterfish Biomass, Spring

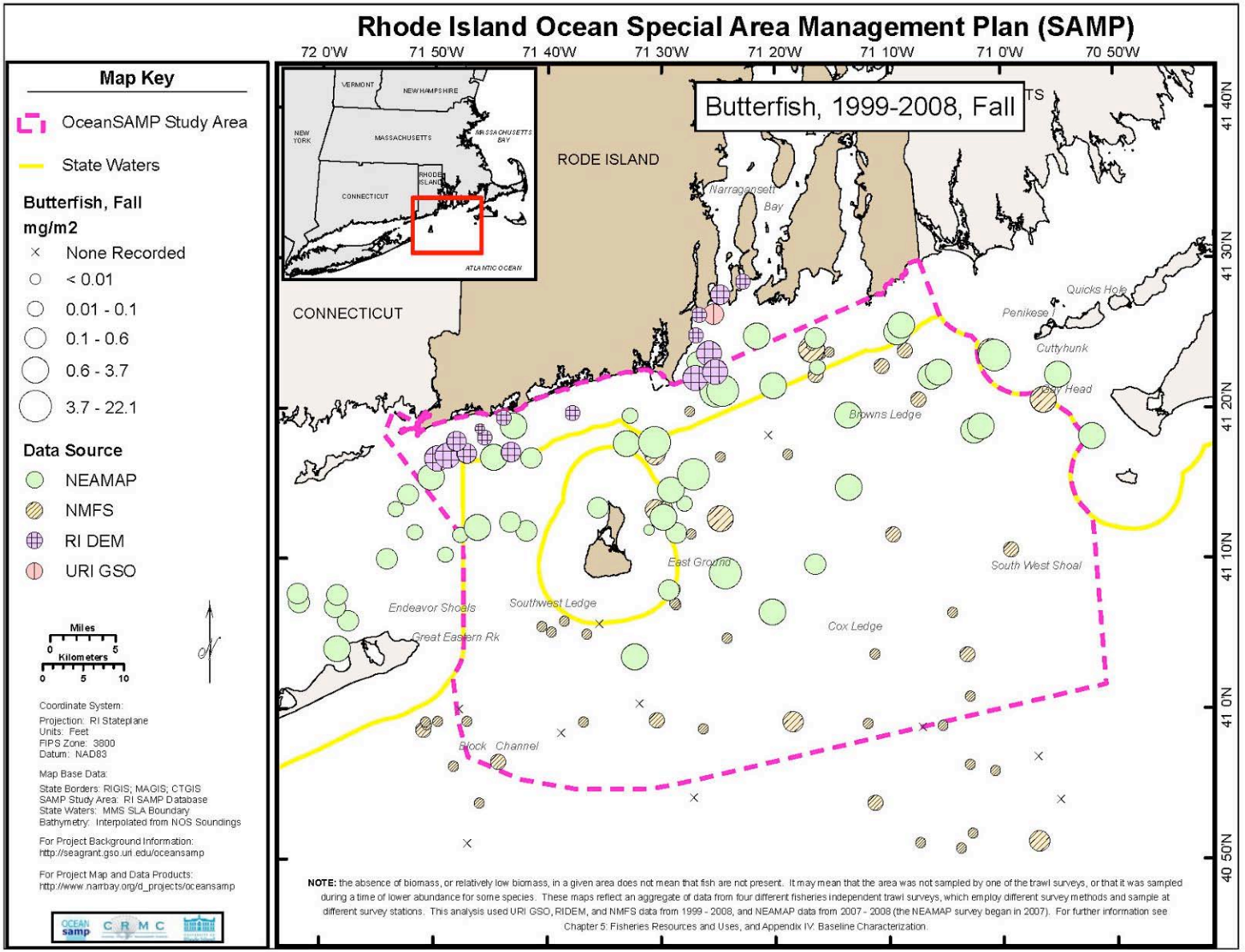

Figure 60. Butterfish Biomass, Fall

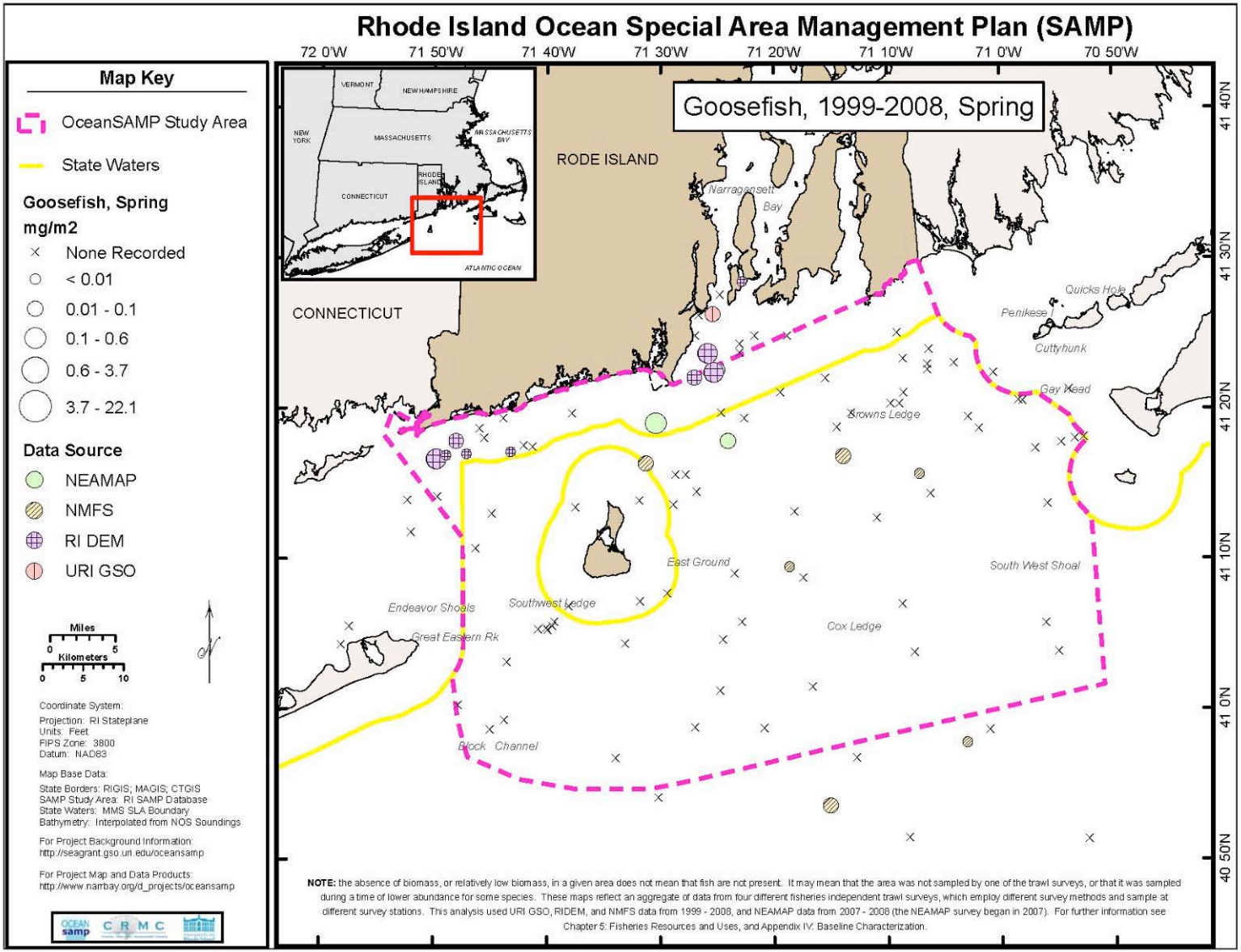

Figure 61. Goosefish Biomass, Spring

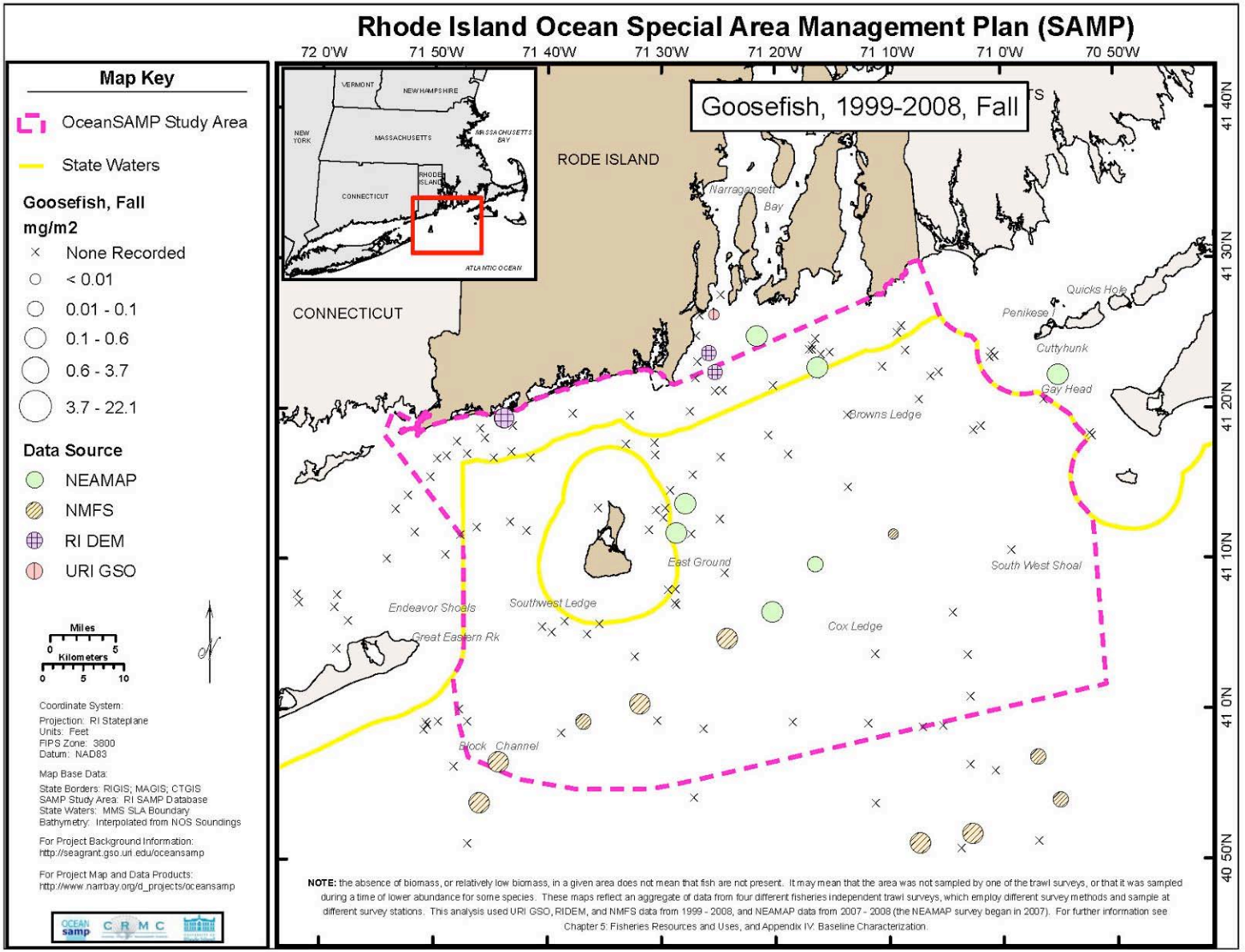

Figure 62. Goosefish Biomass, Fall

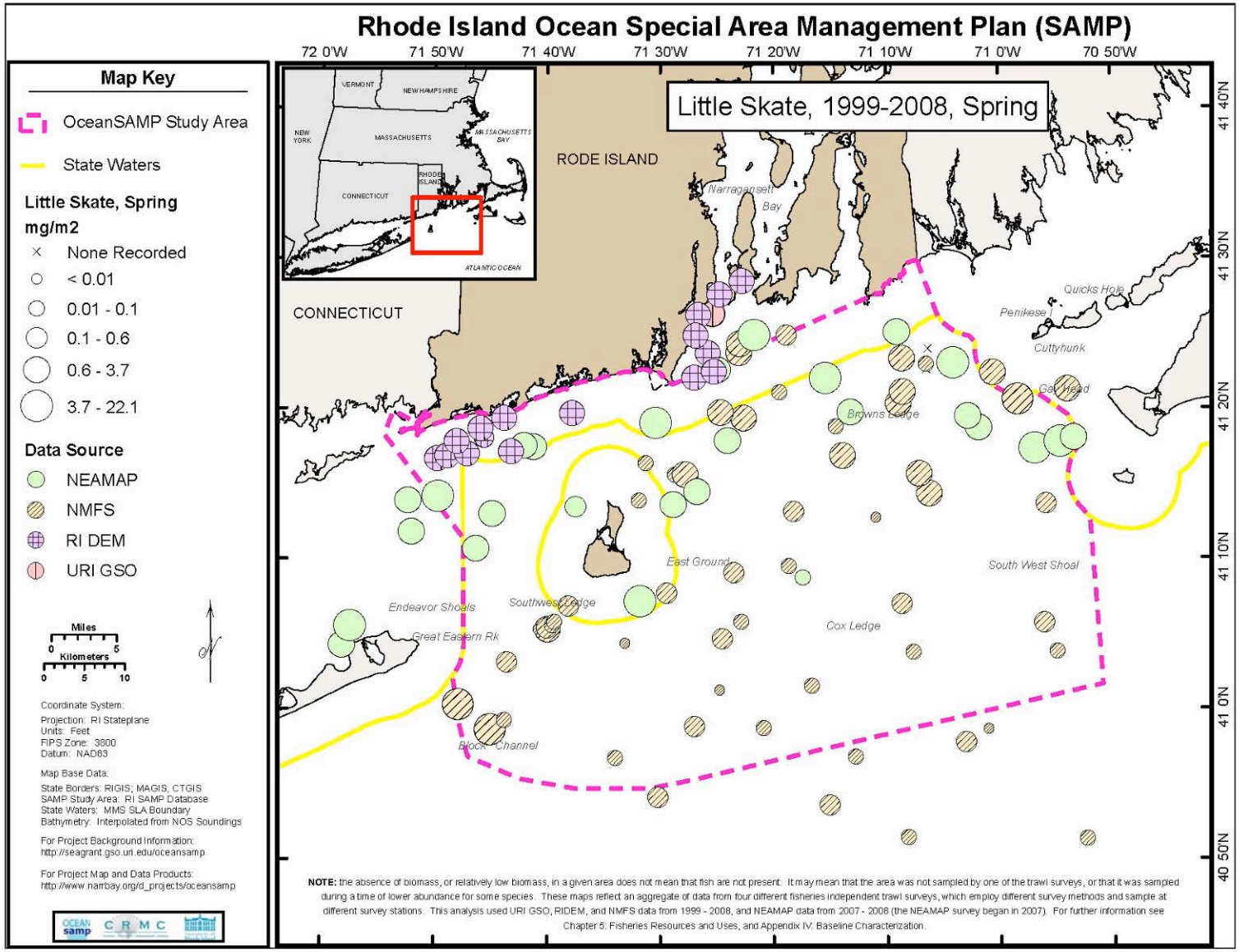

Figure 63. Little Skate Biomass, Spring

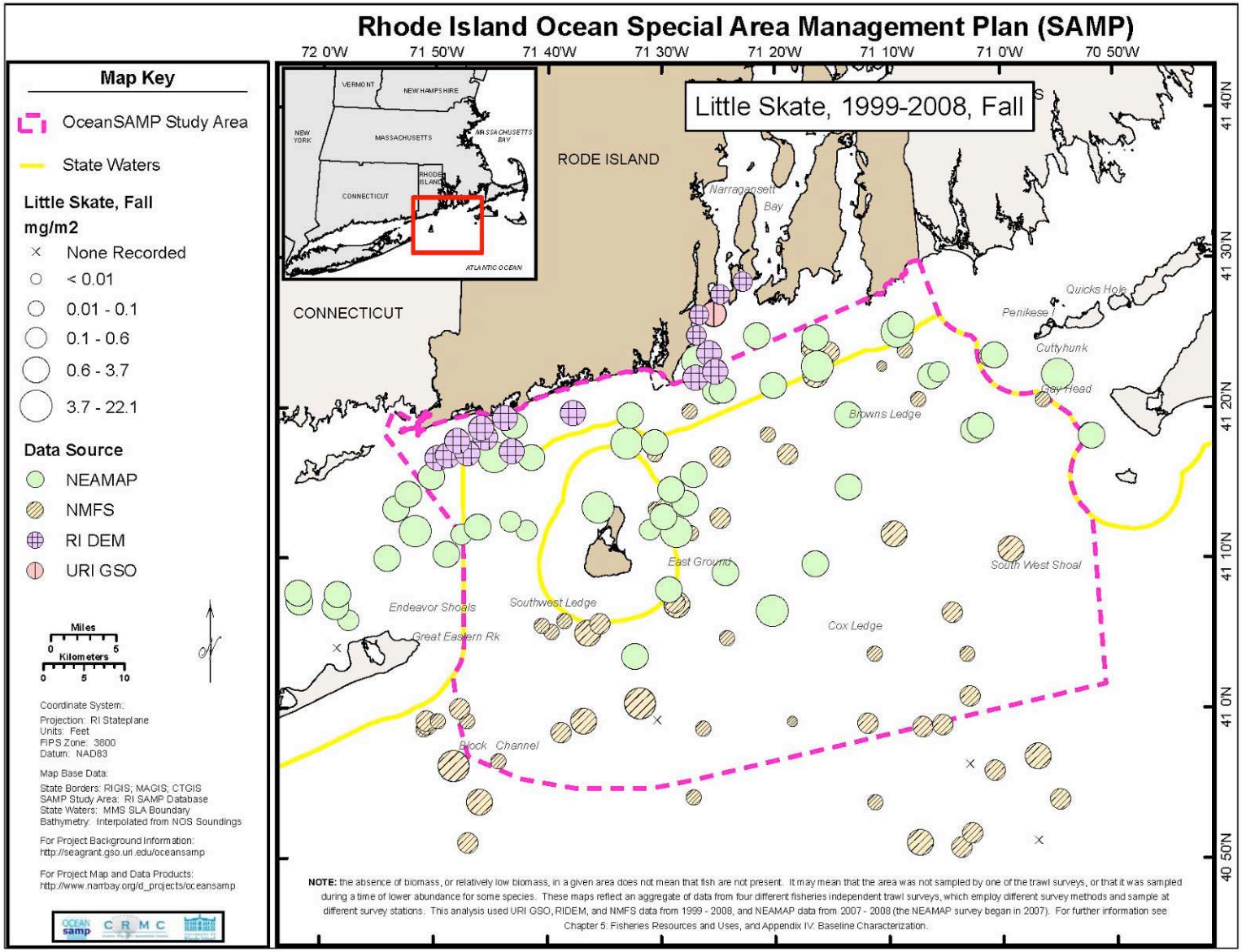

Figure 64. Little Skate Biomass, Fall

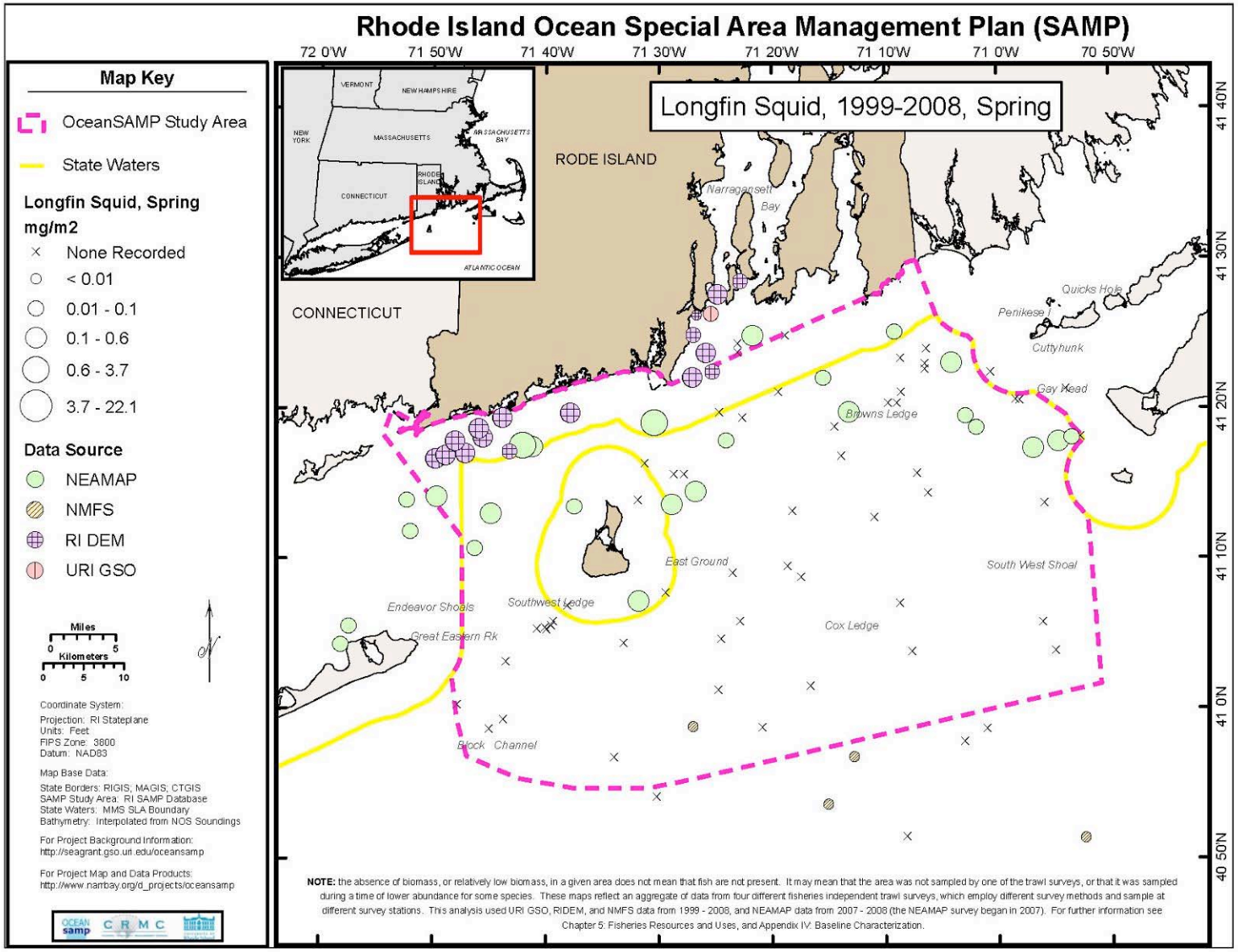

Figure 65. Longfin Squid Biomass, Spring

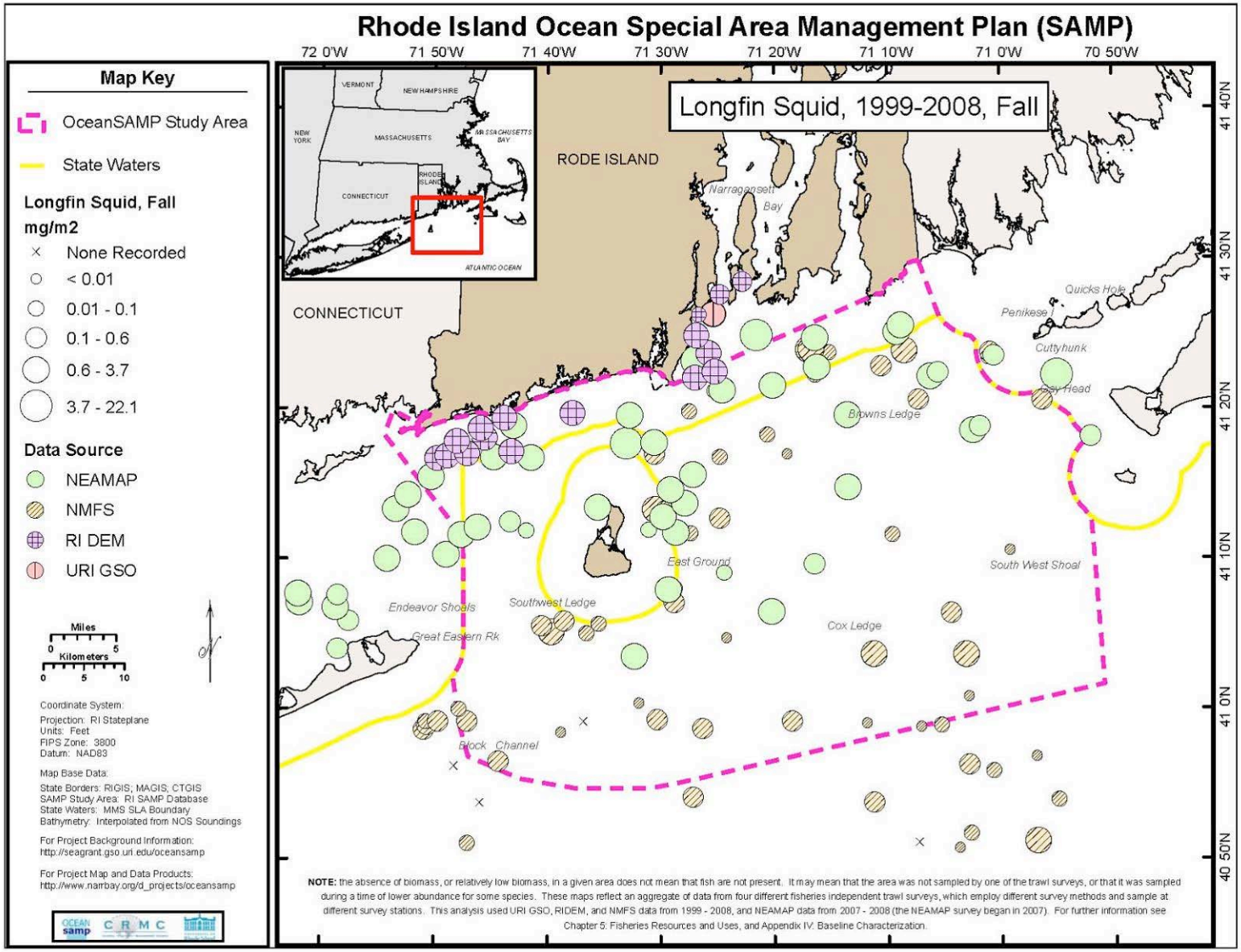

Figure 66. Longfin Squid Biomass, Fall

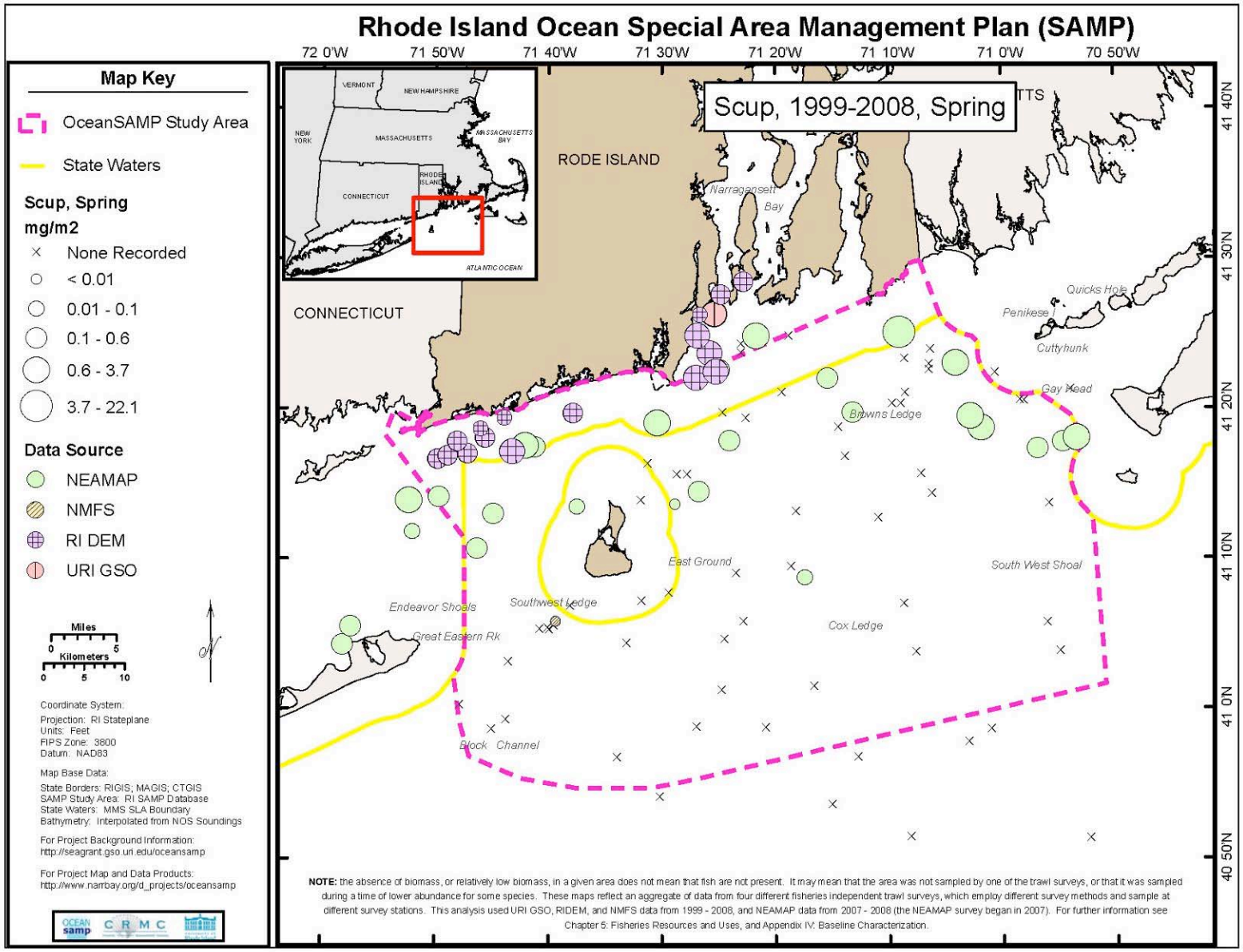

Figure 67. Scup Biomass, Spring

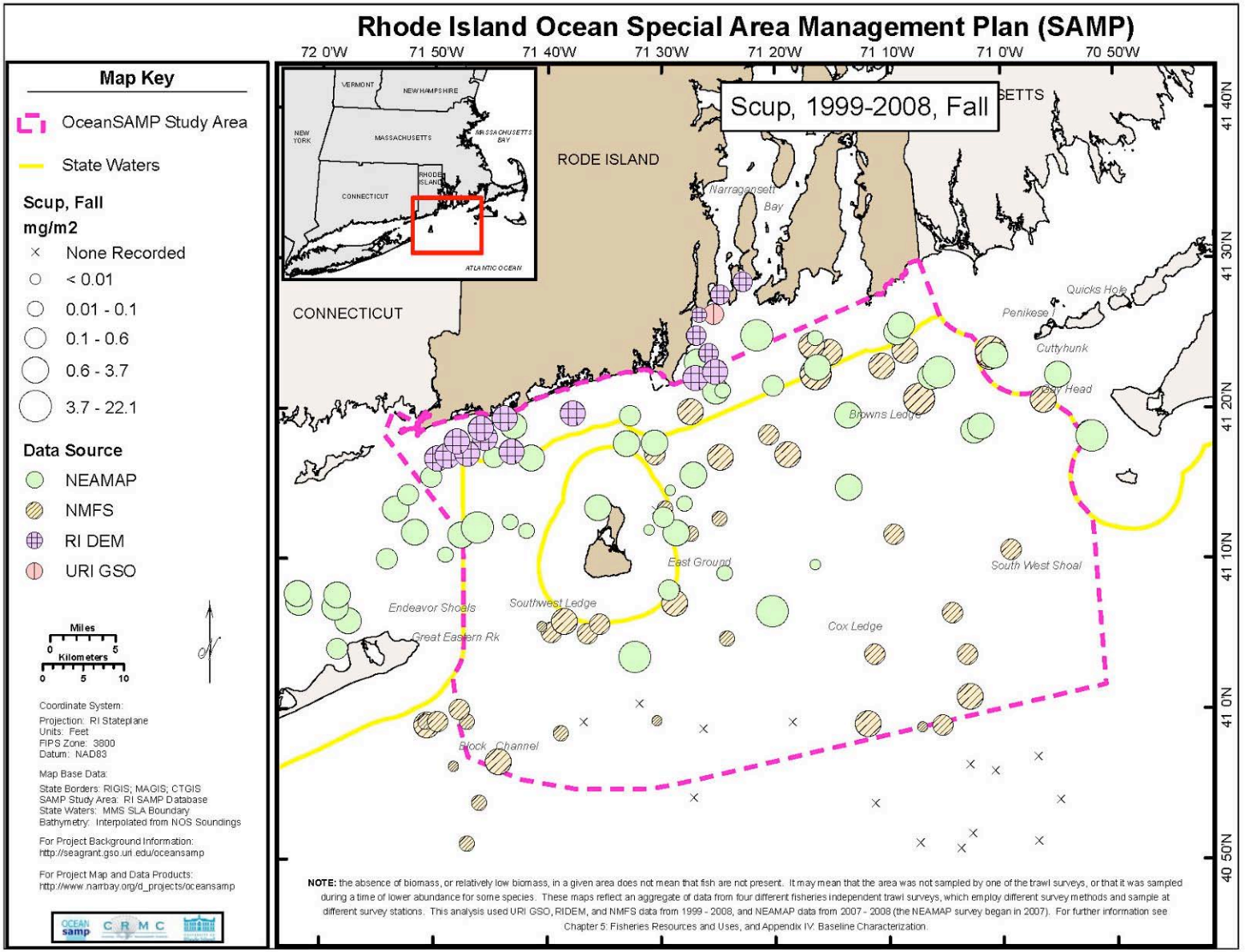

Figure 68. Scup Biomass, Fall

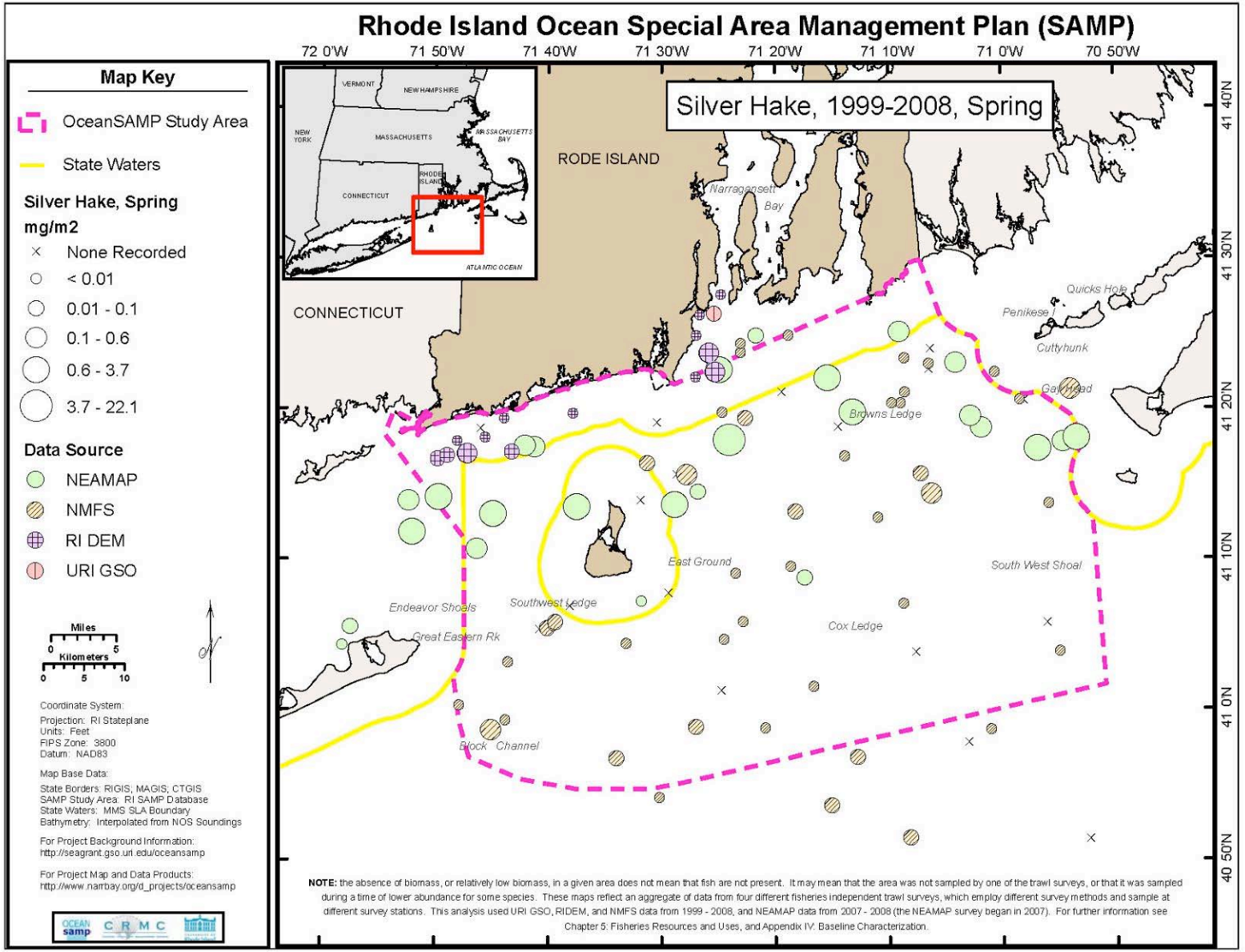

Figure 69. Silver Hake Biomass, Spring

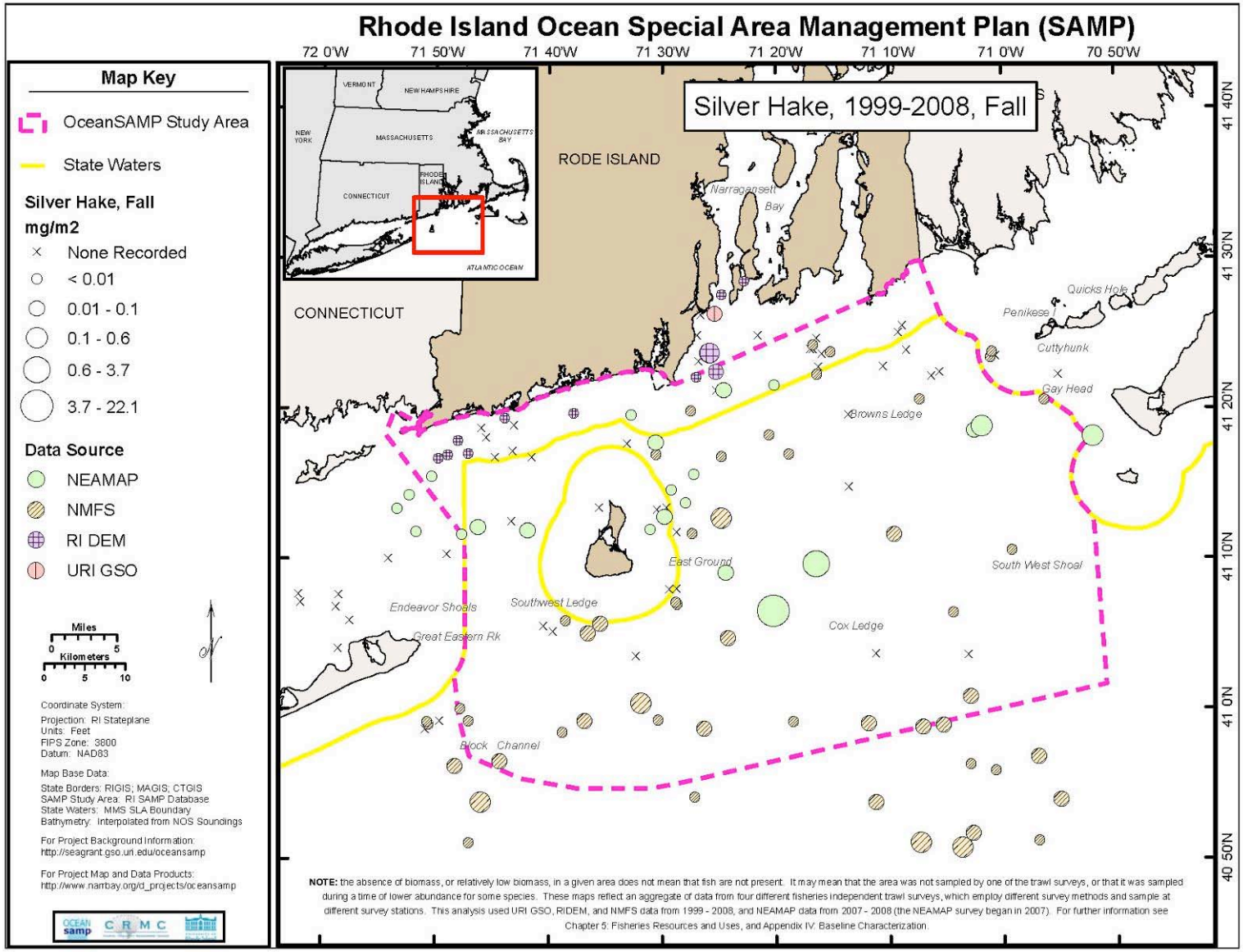

Figure 70. Silver Hake Biomass, Fall

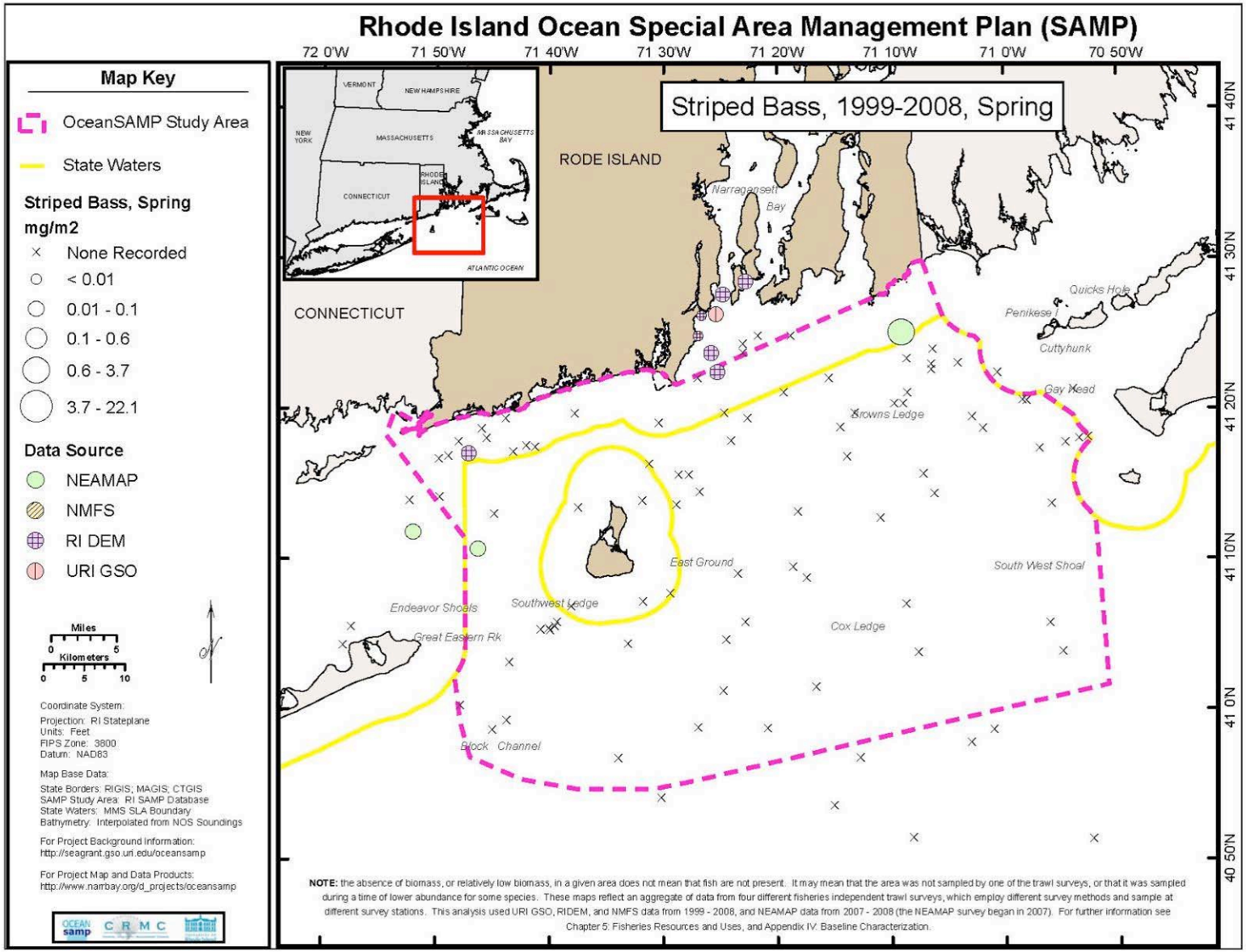

Figure 71. Striped Bass Biomass, Spring

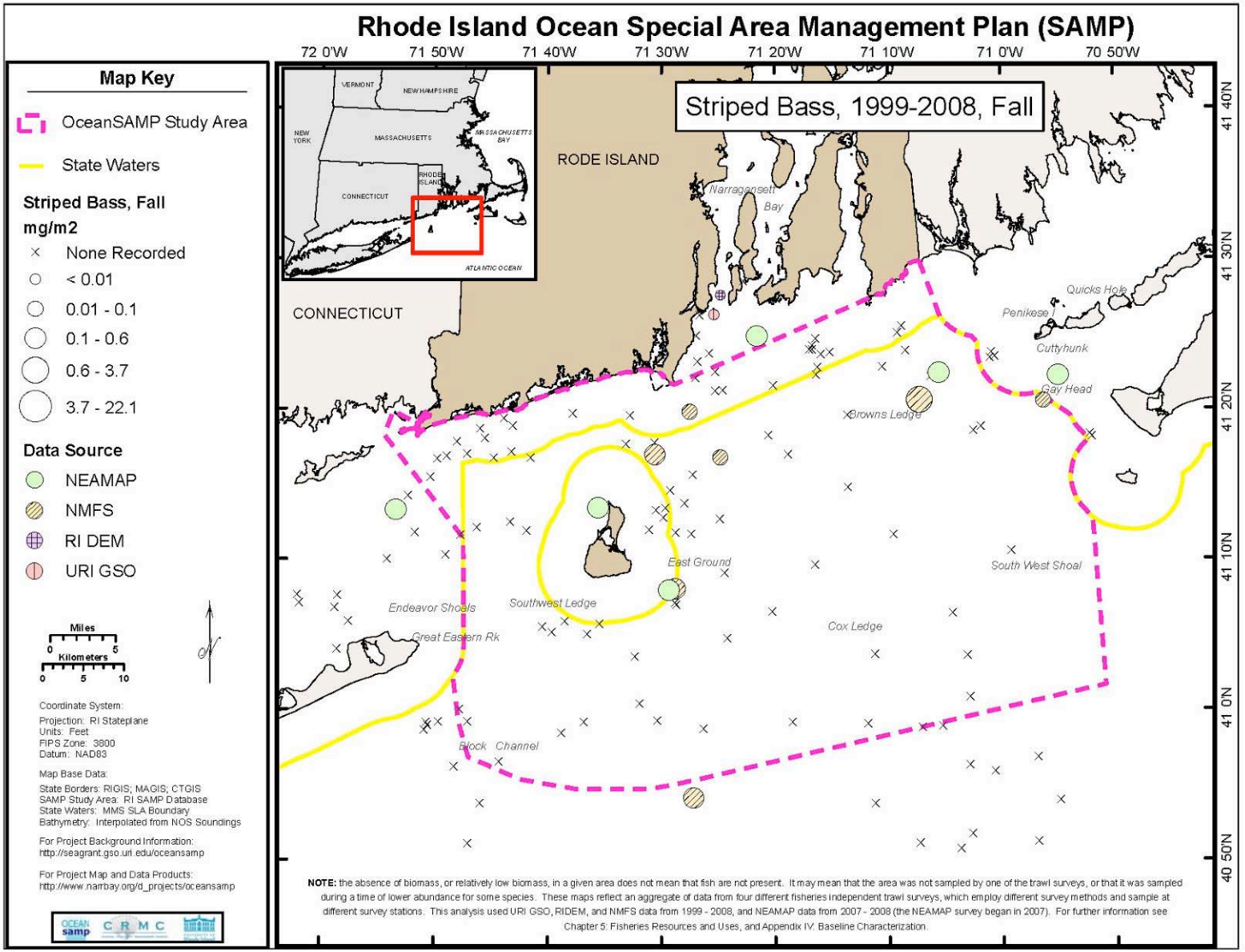

Figure 72. Striped Bass Biomass, Fall

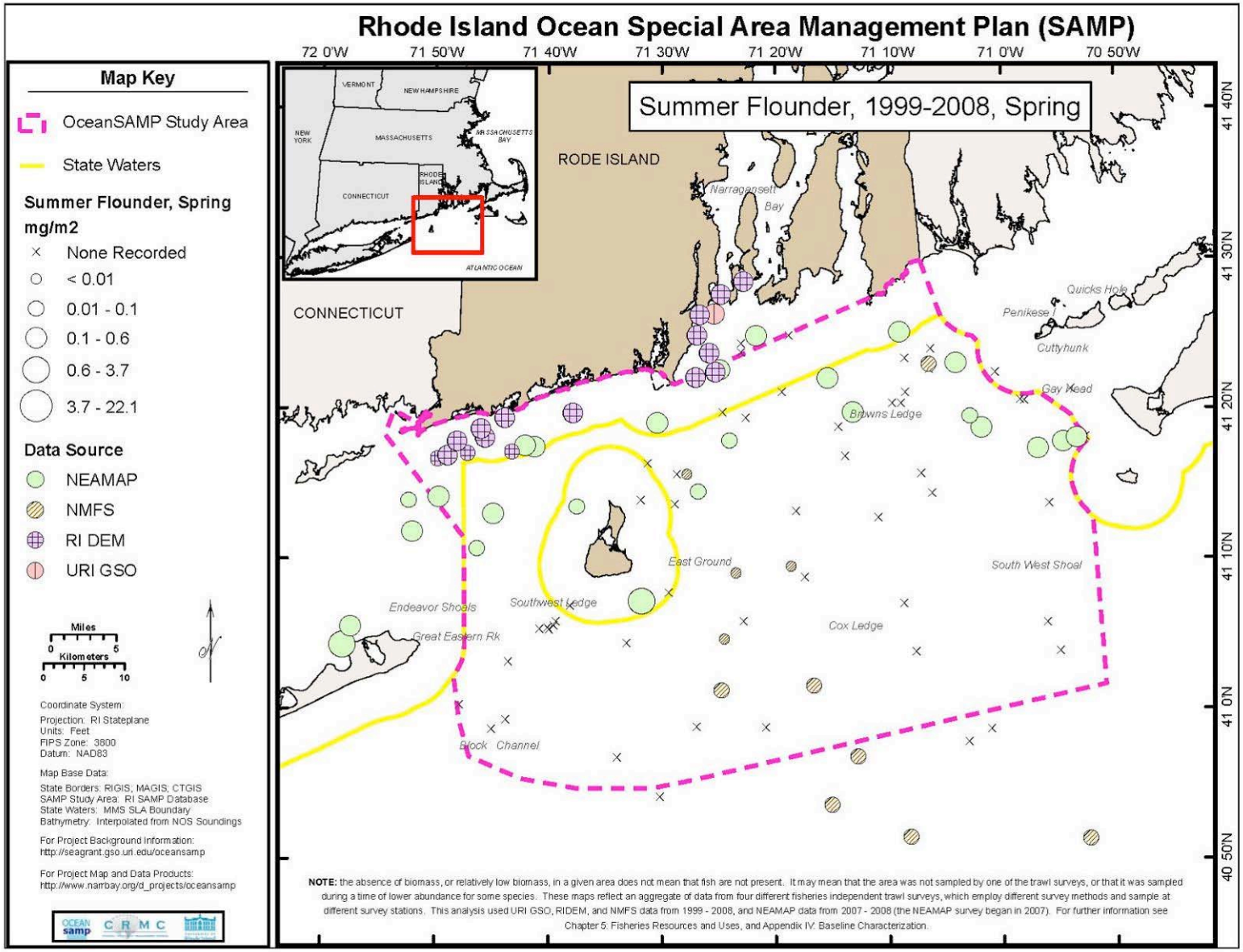

Figure 73. Summer Flounder Biomass, Spring

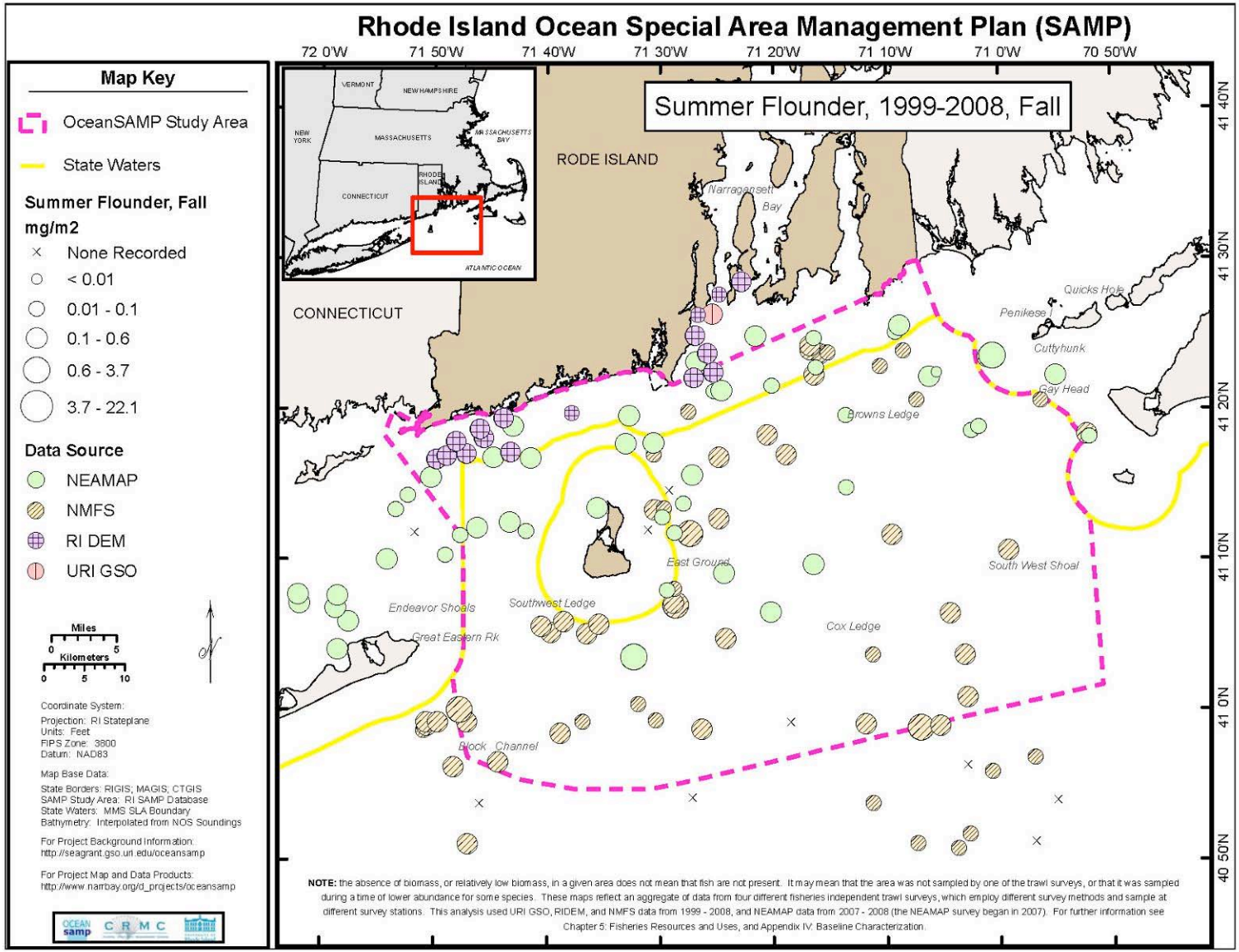

Figure 74. Summer Flounder Biomass, Fall

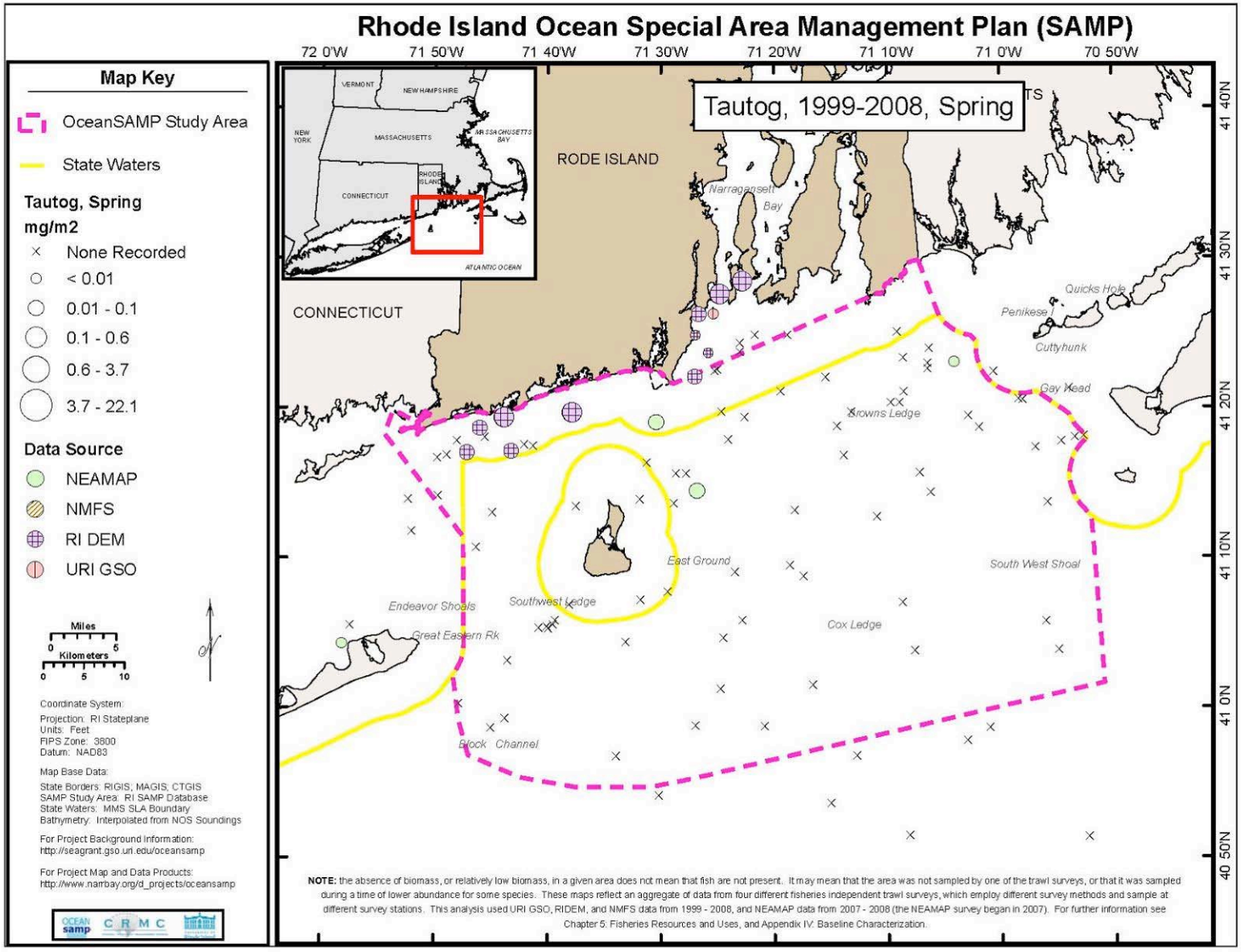

Figure 75. Tautog Biomass, Spring

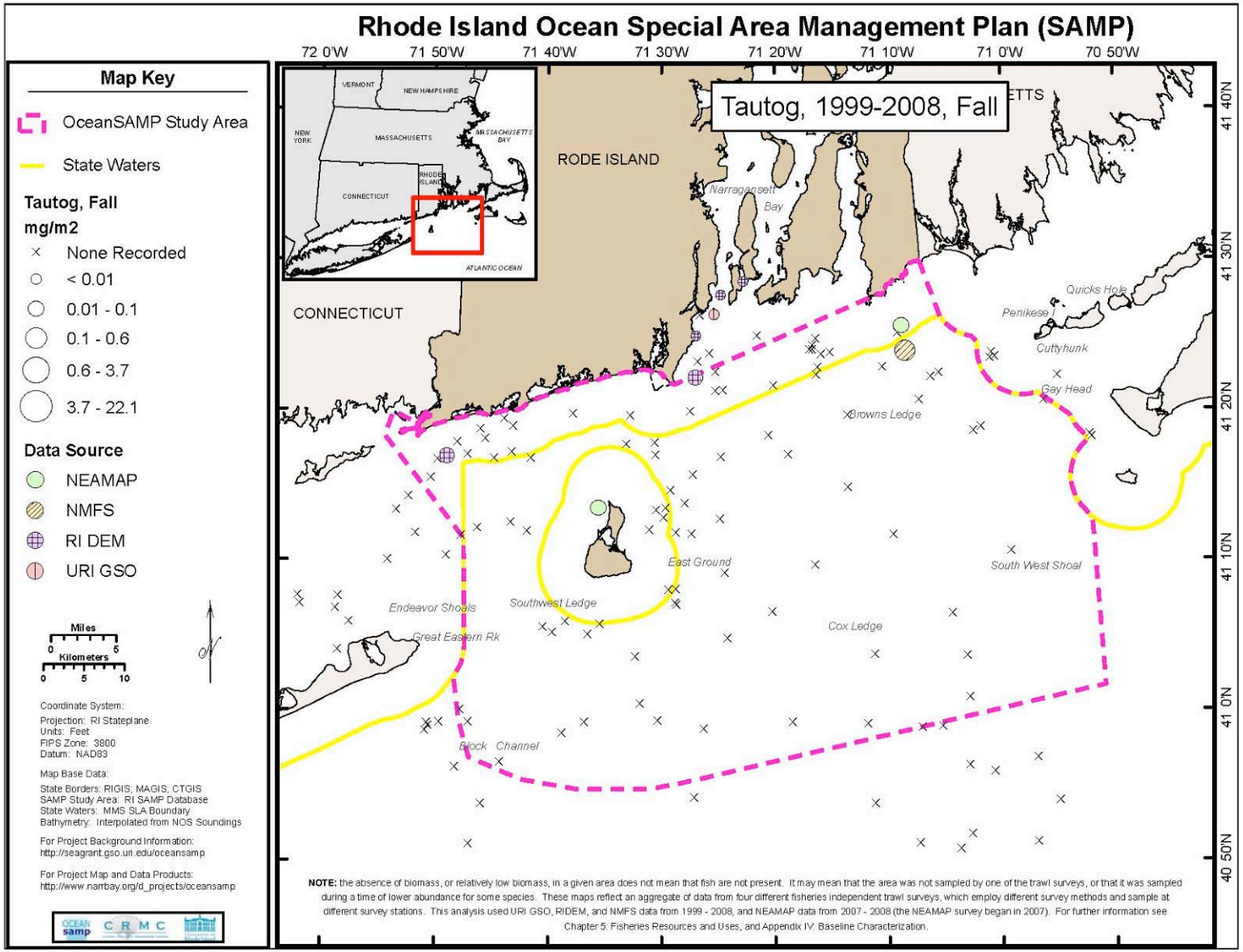

Figure 76. Tautog Biomass, Fall

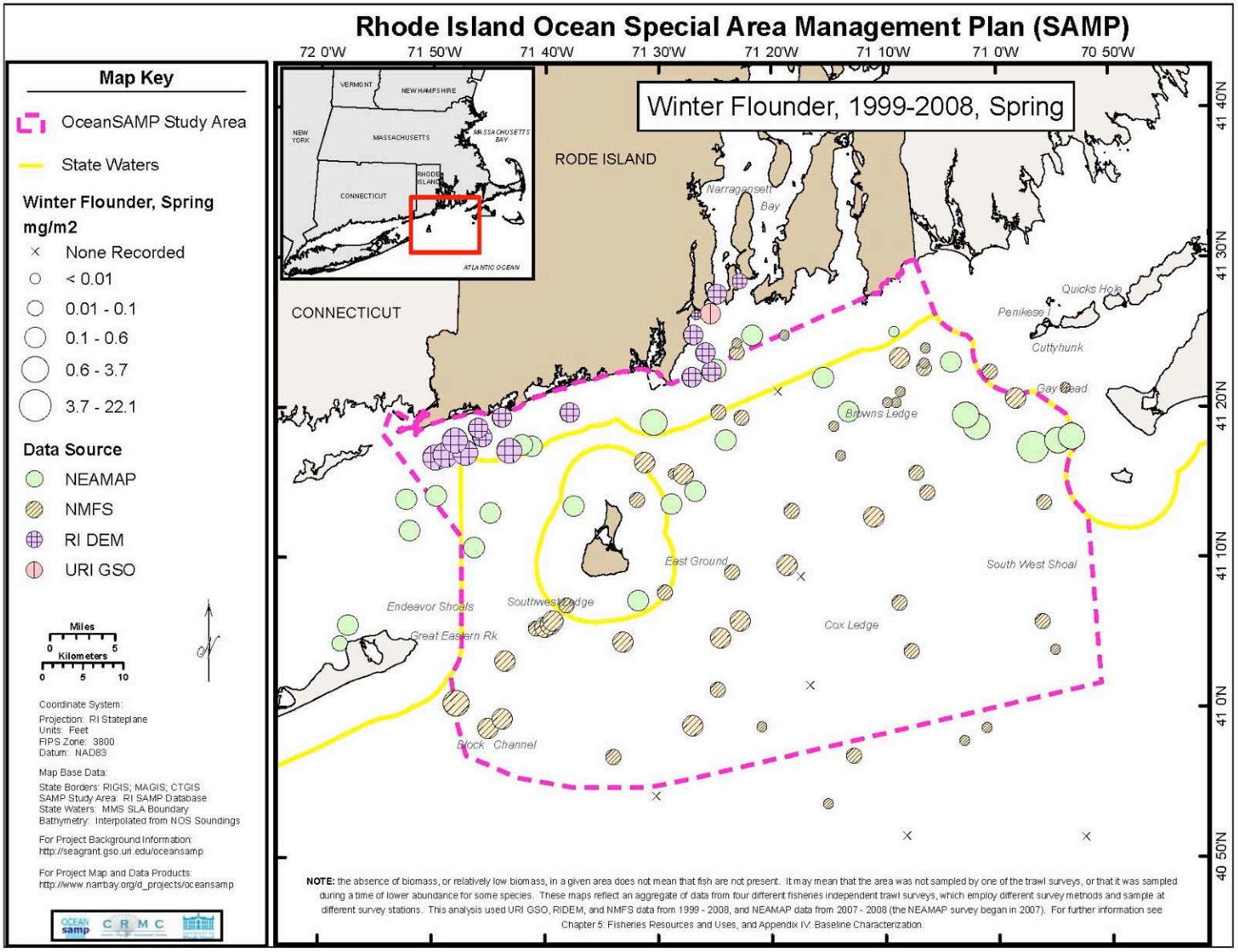

Figure 77. Winter Flounder Biomass, Spring

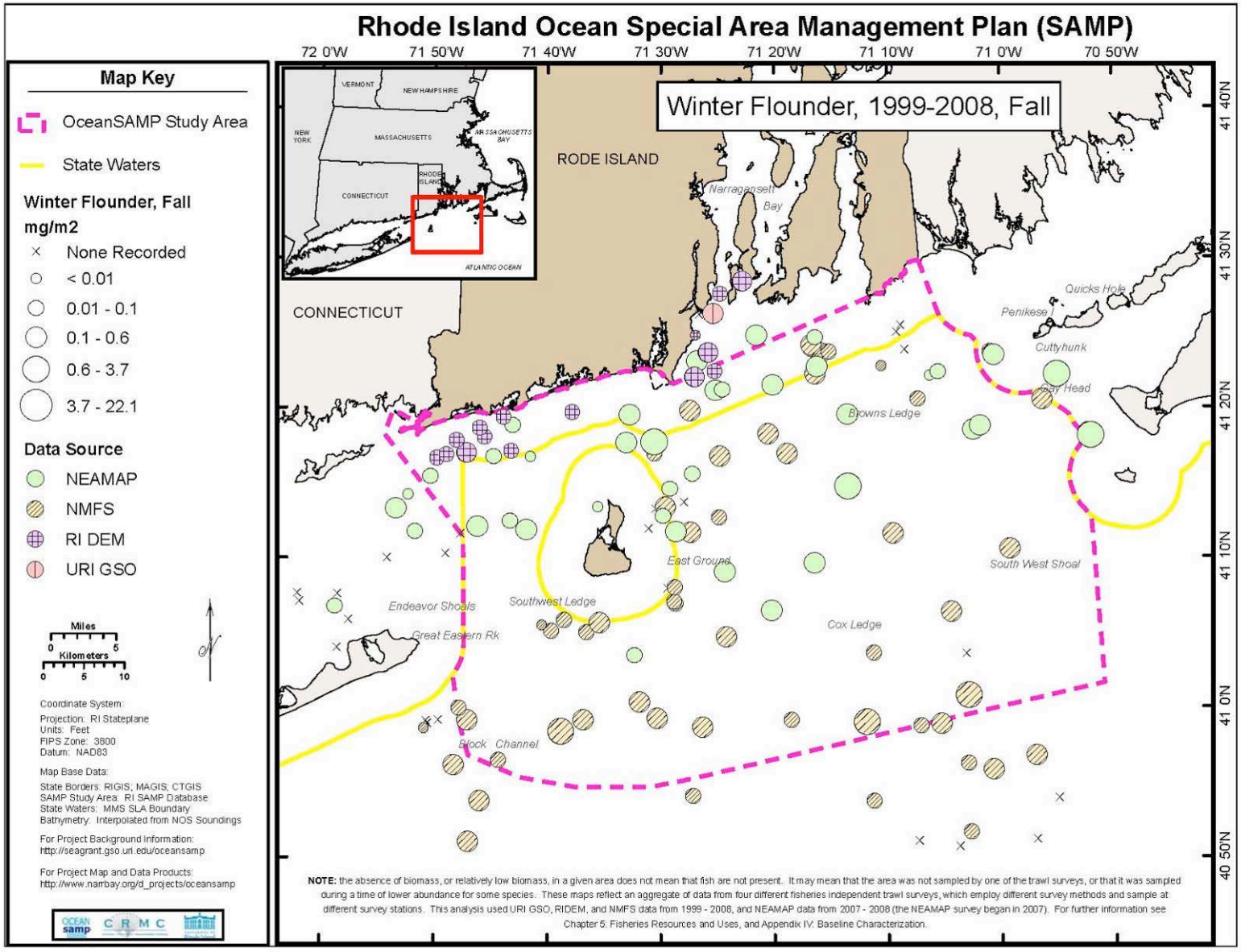

Figure 78. Winter Flounder Biomass, Fall

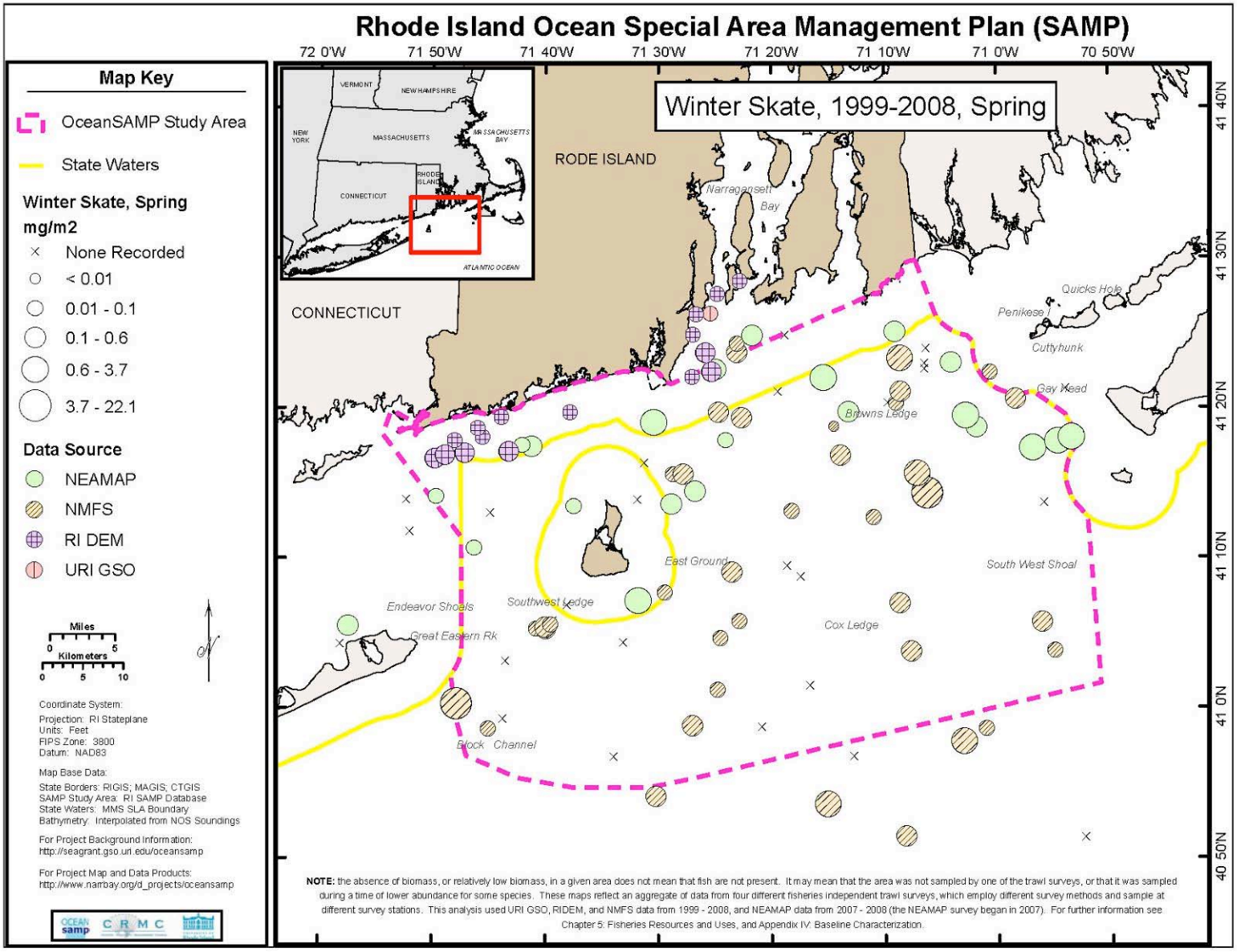

Figure 79. Winter Skate Biomass, Spring

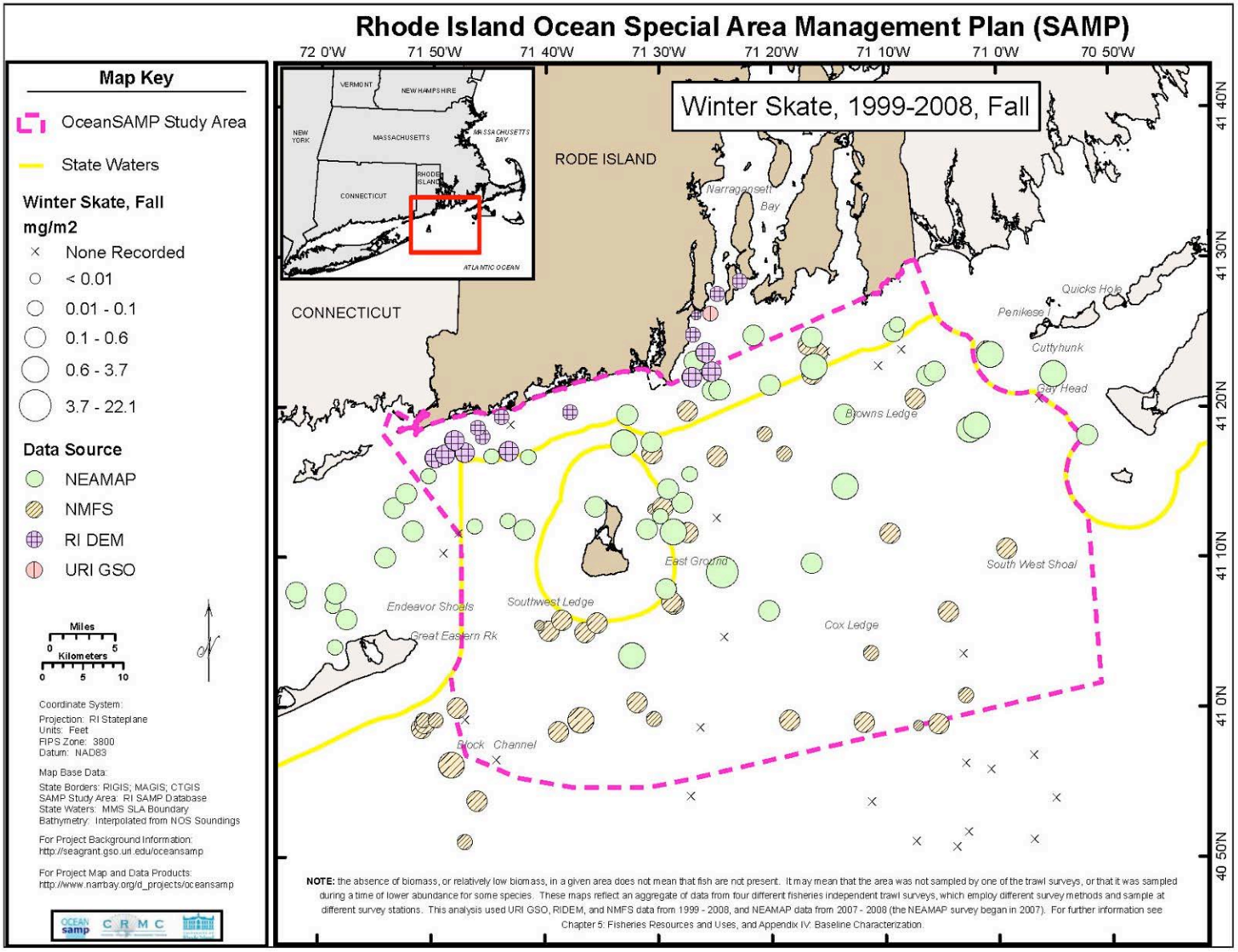

Figure 80. Winter Skate Biomass, Fall

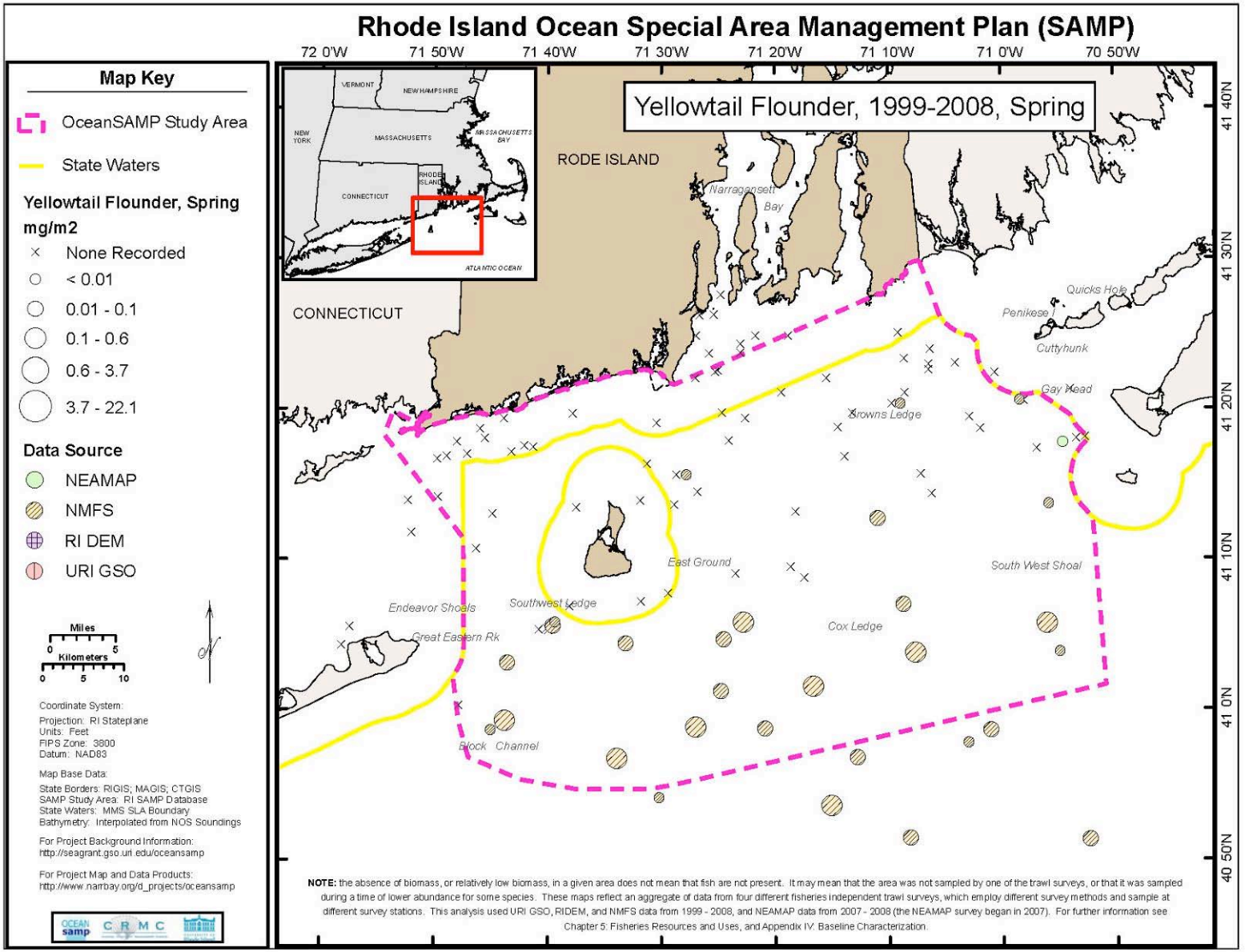

Figure 81. Yellowtail Flounder Biomass, Spring

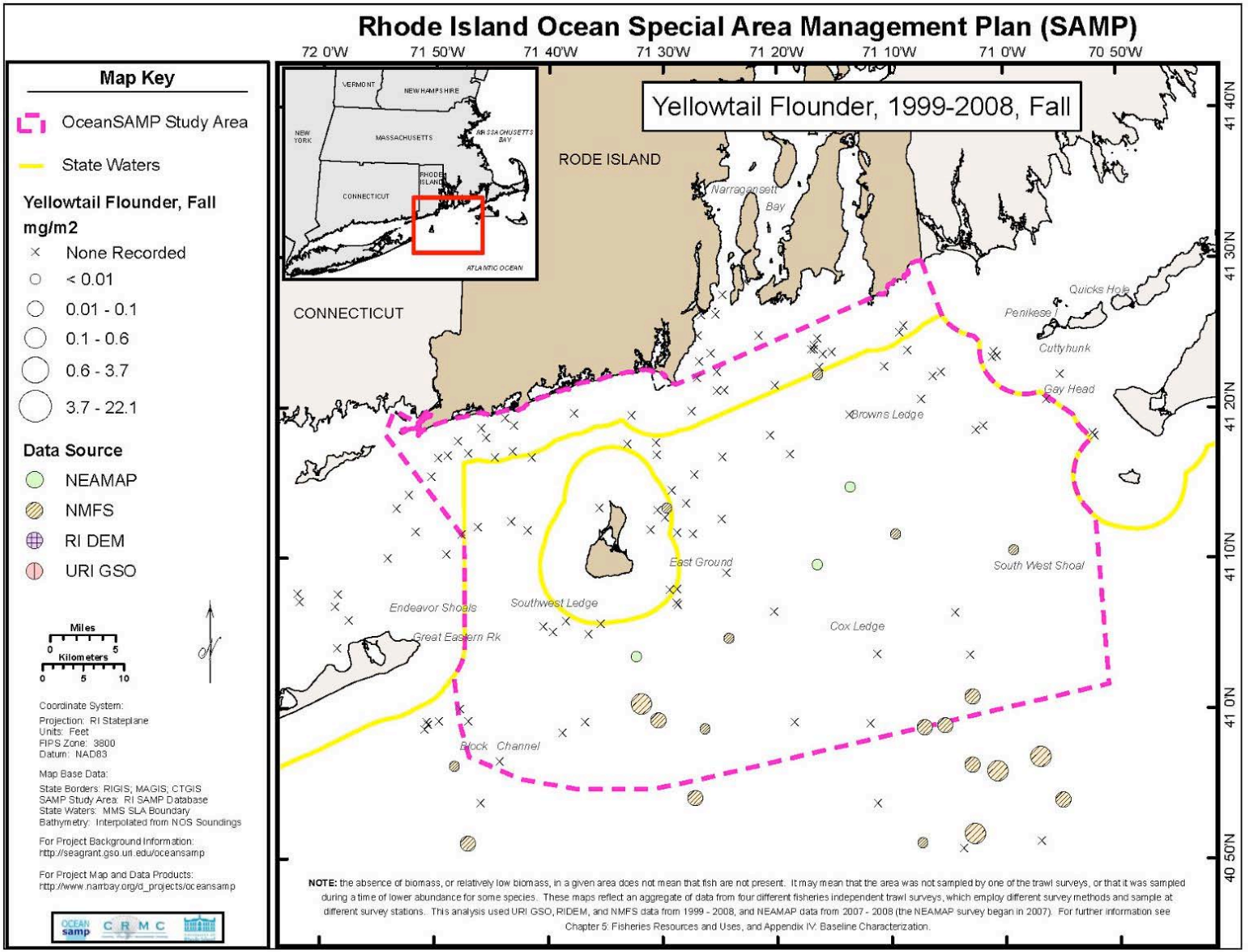

Figure 82. Yellowtail Biomass, Fall

14.

Fisheries Ecology and Benthic Habitat in Rhode Island and Block Island Sounds

for the Rhode Island Ocean Special Area Management Plan 2010

by

Anna Malek, Jeremy Collie, Monique LaFrance and John King

University of Rhode Island, June 25, 2010

Executive Summary

This study aimed to classify and map fisheries habitats and to improve understanding of the relationship between temperate demersal fish communities and benthic habitat. Fifteen sites within the RI Ocean SAMP study area were chosen for coupled acoustic surveys and bottom trawls. Full side-scan and bathymetric processing was carried out for five sites within the RI Ocean SAMP study area. Benthic surface roughness was calculated for all fifteen sites. Analysis of acoustically-derived benthic habitat variables revealed a trend toward greater habitat complexity in Block Island Sound. The demersal fish community was sampled at all fifteen sites in conjunction with the NEAMAP survey on September 30th and October 2nd, 2009. A number of spatial trends in fish community metrics were evident, such as greater fish abundance and biomass in Rhode Island Sound and greater fish community diversity in Block Island Sound. Further analyses revealed a relationship between fish community and depth, with larger, more evenly distributed fish communities in deep water habitats and smaller, more diverse communities in shallow water habitats. Coupling of benthic habitat and species-specific fish community data revealed a strong relationship between benthic habitat complexity and demersal fish community diversity, with more diverse fish communities occupying more complex habitats. Multivariate analysis identified two acoustically-derived benthic habitat variables that effect the species composition of the demersal fish assemblage, standard deviation of backscatter and number of bottom types. A larger sample size, however, is needed to determine if this relationship applies to the offshore ecosystem of Rhode Island Sound and Block Island Sound as a whole. This study provides the scientific community with a basic understanding of fish-habitat relationships in a temperate marine ecosystem and begins to elucidate the importance of benthic-pelagic coupling in supporting fish production. By understanding the role that benthic habitat plays in fish community dynamics in the transitional seas of Rhode Island Sound and Block Island Sound, we hope to guide the placement of offshore structures so as to preserve the ecological and economic value of the area.

Table of Contents

List of Figures

shipping lane). Inverted blue triangles represent site in Blocked Island Sound (west of the shipping lane). ANOSIM analysis indicates that location (RIS v. BIS) has an effect on the composition of the demersal fish assemblage (R = 0.113, p=0.10).

Figure 14. Comparison of benthic surface roughness between Block Island Sound and Rhode Island Sound. Mean benthic surface roughness data was calculated for each site in ArcMap (Figure 5).

List of Tables

List of Attachments and Appendices

Appendix I. Acoustically-determined abiotic benthic habitat variables for sites I, J, P, Q and U.

Abstract

This study aimed to classify and map fisheries habitats and to improve understanding of the relationship between temperate demersal fish communities and benthic habitat. Fifteen sites within the RI Ocean SAMP study area were chosen for coupled acoustic surveys and bottom trawls. Full side-scan and bathymetric processing was carried out for five sites within the RI Ocean SAMP study area. Benthic surface roughness was calculated for all fifteen sites. Analysis of acoustically-derived benthic habitat variables revealed a trend toward greater habitat complexity in Block Island Sound. The demersal fish community was sampled at all fifteen sites in conjunction with the NEAMAP survey on September 30th and October 2nd, 2009. A number of spatial trends in fish community metrics were evident, such as greater fish abundance and biomass in Rhode Island Sound and greater fish community diversity in Block Island Sound. Further analyses revealed a relationship between fish community and depth, with larger, more evenly distributed fish communities in deep water habitats and smaller, more diverse communities in shallow water habitats. Coupling of benthic habitat and species-specific fish community data revealed a strong relationship between benthic habitat complexity and demersal fish community diversity, with more diverse fish communities occupying more complex habitats. Multivariate analysis identified two acoustically-derived benthic habitat variables that effect the species composition of the demersal fish assemblage, standard deviation of backscatter and number of bottom types. A larger sample size, however, is needed to determine if this relationship applies to the offshore ecosystem of Rhode Island Sound and Block Island Sound as a whole. This study provides the scientific community with a basic understanding of fish-habitat relationships in a temperate marine ecosystem and begins to elucidate the importance of benthic-pelagic coupling in supporting fish production. By understanding the role that benthic habitat plays in fish community dynamics in the transitional seas of Rhode Island Sound and Block Island Sound, we hope to guide the placement of offshore structures so as to preserve the ecological and economic value of the area.

1 Introduction

Rhode Island Sound (RIS) and Block Island Sound (BIS) support a variety of commercial and recreational fishing activities, such as scallop dredging, otter trawling, long-lining and gill-netting. Many of these activities target specific areas with the benthic habitat characteristics thought to yield the best harvest (RI Ocean SAMP, Chapter 5). Due to the secrecy of such fishing spots, little is known about the distribution of fisheries resources and benthic habitat in RIS and BIS. Furthermore, research survey tows that are made in this area are sparse, and by the nature of the random sampling design, they are not habitat specific. Until recently, this area has been too far offshore for state surveys and too close to shore for federal surveys. While this data gap has been recognized for some time, filling it has now become a priority because of the desire to zone the area for multiple uses, including recent interest in offshore energy development, and the ongoing need to assess the status of overfished groundfish species that may be subject to cumulative impacts in this area.

The physical characteristics of marine benthic habitat have been shown to affect biological community structure in a variety of ecosystems (Luckhurst & Luckhurst 1978, Gratewick & Spite 2005). For example, Friedlander and Parrish (1998) found a distinct relationship between the rugosity and depth of benthic habitat and fish species assemblage on Hawaiian coral reefs. Unfortunately, very little is known about fish habitat use and feeding relationships in temperate, transitional waters, such as Rhode Island Sound and Block Island Sound. With the reality of offshore development rapidly approaching, it is essential to understand the basis of fish-habitat relationships, the functional role of different habitat types and the importance of benthic-pelagic coupling in supporting fish production. With global climate change shifting the range and species composition of many ecosystems, the relationship between habitat and fish community becomes even more significant. Accordingly, this study aimed to develop a baseline for measuring the cumulative effects of offshore development projects and global climate change as well as contributing a basic understanding of the fisheries ecosystem dynamics in Rhode Island's transitional waters.

This study focuses on the transitional seas, Rhode Island Sound (RIS), Block Island Sound (BIS) and the adjacent inner shelf, which separate the estuaries of Narragansett Bay and Long Island Sound from the outer continental shelf (Figure 1). Providing the link between near-shore

and offshore processes as well as state and federal waters, these transitional seas are both ecologically and economically important. To appropriately zone for offshore development in these transitional seas, a sound understanding of the fisheries ecosystem dynamics is essential. By investigating the distribution and relationship of benthic habitat complexity and demersal fish community within RIS and BIS, we hope to contribute information to assist in creating scientifically sound, ecosystem-based management decisions for Rhode Island's coastal waters.

2 Background

This study builds upon the baseline characterization, presented in RI Ocean SAMP Chapter 5, Section 510.7. The baseline characterization used data from bottom trawl surveys conducted between 1999 and 2008 in and around the RI Ocean SAMP area. Analyses revealed a strong seasonal effect, with higher biomass in the fall and lower biomass in the spring, as well as a trend in depth, whereby survey sites at deeper depth were characterized by the highest biomass (RI Ocean SAMP Chapter 5, Appendix A). Differences in survey methodology as well as natural interannual variability in fish stocks, however, confounded spatial analyses. This study aimed to develop a more comprehensive characterization of the benthic habitats and fish communities within Rhode Island Sound and Block Island Sound and their relationship with each other.

3 Methods

Acoustic mapping and bottom trawling were used to classify fisheries habitats, based on benthic habitat characteristics and site-specific fisheries data. Fifteen sites were chosen for habitat mapping and bottom trawling based on existing maps of bottom sediment composition (McMaster, 1960), side-scan sonar data (King, unpublished; Knebel et al., 1982; Driscoll, 1992), interpretation of NOAA hydrographic surveys (McMullen et al., 2007, 2008) and fishing location maps prepared by David Beutel in consultation with the mobile gear, fixed gear and recreational fishing sectors.

3.1 Habitat Mapping

Habitat mapping was conducted aboard the OSV Bold from August 24-29, 2009. All mapping was conducted with GSO's Teledyne/Benthos C3D/CHIRP III bathymetry/side-scan sonar instrument. Combining high-resolution imagery and wide-swath bathymetry, this system is ideal

for fisheries habitat mapping. The swath width was 240m at 30m water depth. At this depth, roughly 4 square miles can be mapped in 8 hours.

3.1.1 Side-scan and Bathymetry

Bathymetry data were processed to produce a mosaic with CARIS software, whereas the side-scan data were processed with QuesterTangent(QT) Sideview software to obtain a bottom classification based on the acoustic characteristics. A combination of visual discrimination and the QT Sideview classification was used to identify initial polygons of similar bottom type. ArcInfo was used to create a bottom type classification map for each site. Bottom type classifications were based on acoustic and geological characteristics (e.g. soft return with smooth texture; boulder field; hard return with sand waves).

Due to time constraints, a subset of five sites was selected for full side-scan and bathymetric analysis. The selected sites provide an accurate representation of the acoustic and biological features of Rhode Island and Block Island Sound as a whole. The sites selected for full side-scan and bathymetric analysis were I, J, P, Q and U (Figure 1).

Bathymetry and side-scan data were analyzed in ArcGIS to obtain depth and backscatter profiles of each site. The minimum, maximum, mean and standard deviation of backscatter and depth were calculated for each site at 2 meter, 25 meter and 50 meter resolutions (Table 1). Rugosity was calculated from bathymetry data with the Benthic Terrain Modeler Toolbox in ArcMap. The mean and standard deviation of backscatter and depth were independent of all other factors and were, therefore, included in analysis. In order to account for small-scale variability in benthic habitat, two-meter resolution was used in all analyses.

The number of bottom types and number of habitat interfaces within each site were also included as factors in statistical analysis (Table 1). The number of distinct bottom types, as indicated by side-scan imagery, was determined from the bottom type classification map created in ArcInfo (Figure 2). Bottom type classification was based on backscatter intensity, ranging from white to black. Light backscatter patterns represent harder surfaces, such as boulders, shell, and sand, whereas dark backscatter represents softer bottom types, including mud, silt, and clay. The number of bottom types was determined by counting the patches of unique backscatter intensity occurring within each site. A habitat interface was defined as a boundary between two bottom types. The number of habitat interfaces at each site was determined by overlaying bottom

trawl tracklines on the bottom type classification map and counting the number of habitat interfaces crossed by each sites's trackline.

3.1.2. Benthic Surface Roughness

Measurements of benthic surface roughness, as derived in the surface roughness map in the RI Ocean SAMP Ecology Chapter (Chapter 2, Figure 2.26), were used to measure the habitat complexity for each site (Figure 4). In this case, benthic surface roughness is measured as the standard deviation of the slope within a 1000 meter radius. The minimum, maximum, range, mean and standard deviation of benthic surface roughness were calculated for each site with ArcMap (Table 1).

3.2 Fish Community Dynamics

3.2.1. Bottom Trawling

The demersal fish community was sampled in conjunction with the ongoing NEAMAP survey, which is conducted by scientists at the Virginia Institute of Marine Science (VIMS) aboard the 90' FV *Darana R*, captained by James Ruhle (http://www.neamap.net/). Sampling was conducted in Block Island Sound on September 30th and in Rhode Island Sound on October 2nd, 2009.

Bottom trawls were used to obtain habitat-specific fish and invertebrate species composition at fifteen sites in Block Island and Rhode Island Sounds (Figure 1). Each tow was conducted with a 400 x 12 cm, three-bridle, four-seam bottom trawl, paired with a set of Thyboron, Type IV 66" trawl doors. All tows were 20 minutes in duration with a target tow speed of 3.1 knots.

The catch was processed at sea by a team of scientists from VIMS and URI. Once on board, the catch from each station was sorted by species and size class. Aggregate weights, counts and individual length measurements were recorded from all species collected.

3.2.2. Univariate Analysis

For analyses of total catch data, abundance and biomass were summed over all species caught during bottom trawling (Table 2). Hill's N1 and N2 were used as indexes of diversity and evenness, respectively (Hill 1973). For spatial analyses, the shipping lane to the east of Block Island acted as the delineation between Block Island Sound and Rhode Island sound. The shipping lane runs in a nearly straight line between 41°25'35''N, 71°23'22''W and 41°06'06''N, 71°23'22''W (RI Ocean SAMP, Chapter 7, Section 720.2). Trawls sites located to the west of

the shipping lane were considered to be in Block Island Sound, while trawl sites located to the east of the shipping lane were considered to be in Rhode Island Sound (Table 3).

NEAMAP depth strata and tow depth were used to investigate the relationship between depth and fish community dynamics (Table 3). NEAMAP depth stratum was determined for each trawl site based on pre-existing bathymetric maps, while NEAMAP tow depth was measured at the start of each trawl. Depth strata were defined as follows: Stratum 1: 20-40ft, Stratum 2: 40-60ft, Stratum 3: 60- 90ft, Stratum 4: 90-120ft, Stratum 5: >120ft. Comparisons of fish community metrics (i.e. abundance, biomass, diversity and evenness) were conducted among depth strata. Univariate regressions of tow depth against abundance, biomass, diversity and evenness were also conducted to investigate the relationship between the demersal fish community and depth.

3.2.3. Multivariate Analysis

Primer 6.0 was used to calculate a Bray-Curtis similarity index from fourth-root transformed fish abundance data from each site. This index measures similarities in species assemblage composition between sites. A multi-dimensional scaling plot (MDS plot) was derived from the similarity matrix to ordinate the sites in two dimensions. Individual ANOSIMs were used to test for the affect of location (Block Island Sound v. Rhode Island Sound) and depth strata on the fish assemblage.

3.3. Benthic Habitat and Fish Community Integration

Benthic habitat variables of the selected stations (i.e. backscatter, depth, rugosity, bottom type heterogeneity) were integrated with species-specific demersal fish community data in Primer 6.0. Table 1 lists all abiotic variables included in these analyses. A Draftsman plot, consisting of pairwise scatterplots, was used to select uncorrelated benthic habitat variables. Variables marked with an asterisk in Table 1 did not exhibit strong relationships with other variables and were, therefore, included in further analyses. All benthic habitat factors were normalized prior to analysis.

A multivariate algorithm, BIOENV, was used to identify the combination of abiotic benthic habitat variables that best explains the biotic structure of the selected stations. The Linktree function was used to split the stations into groups based on abiotic habitat features. These

Linktree-defined groups were further analyzed with SIMPER to investigate the contribution of individual species to the within-group similarity and between-group disparity.

Univariate regressions were conducted to investigate the relationship between acoustically-derived benthic habitat features and fish community characteristics (i.e. abundance, biomass, diversity and evenness).

Benthic surface roughness was also integrated with species-specific demersal fish community data in Primer 6.0. A Draftsman plot was used to select non-correlating benthic surface roughness variables, as previously described. Table 1 lists all roughness variables included in these analyses. The BIOENV function was used to match benthic surface roughness features to fish assemblage patterns throughout the SAMP area. The Link-tree function was used to identify groups of trawl sites with similar benthic surface roughness, providing a categorical ordination of roughness for each site. An ANOSIM was used to test for the affect of categorically defined benthic surface roughness on fish assemblage.

Univariate regressions were used to investigate the relationship between benthic surface roughness and fish community characteristics (abundance, biomass, diversity and evenness).

4 Results

4.1 Habitat Mapping

4.1.1. Side-scan and Bathymetry

Benthic habitat maps of the selected stations in Rhode Island Sound and Block Island Sound were constructed from side-scan backscatter and bathymetry data (Figure 2 and Figure 3). The minimum, maximum, mean, and standard deviation of backscatter and bathymetry for sites I, J, P, Q and U are given in Appendix I. Maps of bottom rugosity within sites I, J, P, Q and U are shown in Figure 4. There was a strong correlation ($r>0.9$) between low-resolution and high-resolution factors within these sites, indicating that benthic habitat is dominated by large-scale features, such as sand waves.

4.1.2. Benthic Surface Roughness

A map of the benthic surface roughness within Block Island Sound and Rhode Island Sound is given in Figure 5. The minimum and maximum of benthic surface roughness were highly correlated with both the mean and standard deviation of benthic surface roughness and were, therefore, excluded from further analysis. The range, mean and standard deviation of benthic

surface roughness were applied as environmental variables in the multivariate integration with fish community data (Table 1).

4.2 Fish Community Dynamics

Abundance, biomass, diversity and evenness of the fish community at all 15 sites are given in Table 4. Figure 6 and figure 7 show the relative abundance and biomass of the demersal fish community in the spatial context of Rhode Island Sound and Block Island Sound.

4.2.1. Univariate Analyses

Univariate analysis of fish community data revealed apparent trends towards higher abundance and biomass in Rhode Island Sound as compared to Block Island Sound (Figure 8). Overall species diversity, as defined by Hill's N1, was higher in Block Island Sound, while species evenness, as defined by Hill's N2, was higher in Rhode Island Sound (Figure 8). As a community becomes more diverse, the distribution of species abundance is expected to become less even, and, therefore, an inverse relationship between diversity and evenness is expected (Hill 1973). The trends toward greater evenness and higher abundance in Rhode Island Sound indicate that larger fish communities tend to have a more even species distribution.

Analysis of fish community data by depth revealed an apparent increase in fish abundance and biomass with depth (Figure 9, Figure 10). Inverse trends in diversity and evenness were also evident, with decreasing diversity and increasing evenness with depth (Figure 9, Figure 10). These results indicate that fish communities residing in deeper water are larger and less diverse than fish communities residing in shallower water.

4.2.2. Multivariate Analysis

A multidimentional scaling plot (MDS) was created as a visual representation of the unique species compositions at each of the sites within Block Island Sound and Rhode Island Sound (Figure 11). Each point on the MDS plot represents the species composition of one trawl site. Points that are closer together have more similar species composition than distant points.

ANOSIM analyses indicate that Block Island Sound and Rhode Island Sound support different communities of demersal fish (Figure 12, $R = 0.113$, $p = 0.1$). ANOSIM analyses also indicate that depth strata influences the species composition of demersal fish communities within Rhode Island Sound and Block Island Sound (Figure 13, $R=0.332$, $p=0.011$).

The BVStep analysis identified 11 species that account for most of the pattern in demersal fish and invertebrate community composition within the SAMP area (Table 2, p=0.953, p=0.01). These species are alewife, atlantic herring, black seabass, bluefish, butterfish, goosefish, quahog, round scad, silver hake and spiny dogfish. Although these species may not be the most abundant within the SAMP area, they are of ecological importance in defining the local marine community structure. When attempting to predict the effects of development and exploitation on the demersal fish assemblage of the SAMP area, it is essential to consider these community-shaping species.

4.3. Benthic Habitat and Fish Community Integration

Together, standard deviation of depth and number of bottom types, resulted in the highest rank correlation between biotic and abiotic variables (BIOENV: rho=0.709). A permutation test, however, indicated that, within the five selected sites, the aforementioned rank correlation between biotic and abiotic variables has a high probability of occurring due to chance alone (BIOENV: p=0.496). A number of benthic habitat variables most likely affect the fish community in Rhode Island's offshore waters, but the small number of sites included in these analyses prevents identification of such variables.

Based on the similarity of their abiotic features, the selected stations were divided into three groups. Group 1 included sites J and U. Group 2 included sites I and P. Group 3 included site Q only. Analysis of biological similarity within these groups, revealed a 62.4% similarity between stations J and U and a 75.4% similarity between stations I and P (SIMPER). Two pelagic species, butterfish and squid, accounted for most of the biological similarity.

Univariate regression analyses revealed a positive relationship between the number of bottom types and diversity as well as an inverse relationship between the number of bottom types and total abundance (R^2=0.691, p=0.081; R^2= 0.836, p=0.029, Table 5). There was no apparent relationship between the standard deviation of depth and total abundance or diversity (Table 5).

A relationship between large-scale benthic surface roughness and species distribution was also identified. Together, the mean and standard deviation of benthic surface roughness resulted in a rank correlation of 0.392 (BIOENV: rho=0.392). A permutation test indicated that the correlation between benthic surface roughness and the species composition of the demersal fish assemblage was not due to chance alone (BIOENV: p=0.02). When defined categorically,

however, benthic surface roughness was not significantly related to the demersal fish assemblage (ANOSIM: R=0.163, p=0.117).

Univariate regression revealed a weak inverse relationship between roughness and total abundance and a positive relationship between roughness and total biomass (Roughness v. Abundance: R^2=0.057, p=0.391; Roughness v. Biomass: R^2=0.300, p=0.034). These results suggest that a larger number of small fish (i.e. bait fish and juveniles), inhabit less complex benthic habitats, while a smaller number of large fish (i.e. top predators) inhabit more complex benthic habitats. Univariate regression also indicated that there is no apparent relationship between roughness and species diversity (R^2=0.014, p=0.679). There was, however, an evident trend towards higher benthic surface roughness in Block Island Sound (Figure 14).

5 Discussion

The fisheries ecosystem of Rhode Island and Block Island Sounds is influenced by a number of factors, such as location, depth, bathymetric complexity, habitat heterogeneity and benthic surface roughness. Understanding the relationship between these factors and the fish populations of Rhode Island's transitional seas will help to guide ecologically-sound spatial management decisions.

Spatial variability of the demersal fish community within Rhode Island and Block Island Sounds is apparent in the results from this study (Figure 6, Figure 7, Figure 8). As seen in figure 8, there is a pattern towards higher abundance and biomass of the fish community in Rhode Island Sound. This pattern may be related to the spatial variability in primary production. It has recently been suggested that primary production is higher in Rhode Island Sound than in Block Island Sound (Nixon et al. In press). If the typical bottom-up ecological model is followed, increased production in Rhode Island Sound would lead to increased fish abundance. The results of this study indicate that this is, indeed, the case (Figure 8).

While the size of the fish community appears to be larger in Rhode Island Sound, the species diversity appears to be higher in Block Island Sound (Figure 8). A general paradigm about marine benthic communities is that, as bottom complexity increases from smooth sand and mud to rock and cobble, ecological complexity and diversity increase. Areas with high bottom roughness correspond with prime fishing areas for several species targeted by commercial and recreational fisheries. Analysis of benthic surface roughness data indicates that Block Island

Sound contains more complex bottom terrain, making it more diverse than Rhode Island Sound (Figure 14). The high benthic habitat complexity of Block Island Sound supports a unique and more diverse demersal fish community (Figure 8, Figure 13). Identifying highly complex habitats from acoustic parameters and protecting them from anthropogenic influence will be a key tool in promoting ecosystem stability and resiliency in Rhode Island's transitional seas.

The preference of demersal fish for specific depth ranges has been observed in a variety of ecosystems (Persohn et al. 2009; Sonntag et al. 2009). The fish of Rhode Island and Block Island Sounds are no exception to this phenomenon. In this study, survey sites at deeper depth were characterized by the highest biomass, while survey sites at shallower depths were characterized by higher species diversity (Figure 9, Figure 10). This pattern suggests that deeper habitats support many of the most abundant demersal fish species within Rhode Island and Block Island Sounds, while shallower habitats support a more diverse and less abundant community of fish. When aiming to protect specific fish species, determining the location of the preferred depth range within the management area is essential. Creating small closed areas around the preferred habitat of a threatened species may provide the key to stock recovery.

The relationship between benthic habitat features and fish abundance and assemblage has been well documented in coral reefs and seagrass beds, but there has been little research in temperate, deep water environments, such as Block Island Sound and Rhode Island Sound (Aut & Johnson 1998; Christensen et al. 2003; Eriksson et al. 2006). The presumed relationship is that the more heterogeneous the habitat, the more species it can support (Eriksson et al. 2006). Through paired geological and biological sampling this study identified two biologically influential benthic habitat features: standard deviation of depth and the number of bottom types. The standard deviation of the depth is a measure of bathymetric complexity that is related to rugosity, while the number of bottom types is a measure of habitat heterogeneity. Our analyses indicate that habitat complexity and heterogeneity may have an effect on the species distribution within the demersal fish community, but our small sample size prevents definite conclusions (BIOENV: rho=0.709, p=0.496). The strong positive relationship between the number of bottom types and diversity within the selected stations, however, clearly indicates that the habitat-biology relationship so often seen in coral reefs and seagrass beds also applies to the temperate, deep-water environment of Rhode Island and Block Island Sounds. Understanding the functional importance of benthic habitat features, such as bathymetric complexity, to the demersal fish community is essential in developing strategies for rebuilding fish stocks important to Southern New England.

Differences in fish assemblage are most pronounced between areas with vastly different bottom types (i.e. sandy v. rocky bottom) (Gomelyuk 2009; Kendall et al. 2004). However, the acoustic surveys and fish trawls employed in this study mainly survey sandy bottom areas in order to avoid gear damage. To develop a full understanding of the functional importance of benthic habitat to the demersal fish community in Block Island and Rhode Island sound, a greater variety of bottom types must be mapped and sampled. We plan to use modified acoustic surveys, underwater videography and beam trawls to sample rocky benthic habitats in the near future. Utilizing data from a diverse range of bottom types would increase the accuracy of this analysis and provide a more reliable conclusion concerning the effect of bottom complexity on fish assemblage composition in Rhode Island and Block Island Sounds.

6 Conclusions

Based on 15 bottom trawls and 5 coupled acoustic surveys, the following conclusions can be made about the fisheries ecology and benthic habitats of Rhode Island and Block Island Sounds:

- Total abundance and biomass of the demersal fish community is higher in Rhode Island Sound than Block Island Sound.
- Diversity of the demersal fish community, as represented by Hill's N1, is higher in Block Island Sound than Rhode Island Sound.
- Benthic habitats in deep water support a larger, more evenly distributed community of small fish, while benthic habitats in shallow water support a smaller, more diverse community of larger fish.
- The benthic habitat complexity in Block Island Sound is greater than the benthic habitat complexity in Rhode Island Sound.
- Bathymetric complexity and habitat heterogeneity influence the species composition of the demersal fish community within Block Island and Rhode Island Sound, but additional sites must be analyzed to make a confident conclusion about this abiotic-biotic relationship.
- Our understanding of the role that benthic habitat plays in fish community dynamics in Rhode Island Sound and Block Island Sound will help to guide the placement of offshore structures so as to preserve the ecological and economic value of the area.

References

Ault, T.R. and Johnson, C.R. (1998) Spatially and temporally predictable fish communities on coral reefs. Ecological Monographs 68: 25-50.

Christensen, JD, Jeffrey, C.F.G. and Caldow, C. (2003) Cross-shelf habitat utilization patterns of reef fishes in south western Puerto Rico. Gulf and Caribbean Research 14: 9-27.

Driscoll, N.W. 1992. Side-scan sonar investigation of shallow-water depositional processes in and around Block Island Sound: before and after the Nor'easter of 1992. Storming Media Pentagon Reports, retrieved online from http://www.stormingmedia.us/48/4888/A488813.html.

Eriksson, B.K. , Ruback, A. , Hillebrand, H. 2006. Biotic habitat complexity controls species diversity and nutrient effects on net biomass production. Ecology 87(1):246-254.

Friedlander, A.M. and Parrish, J.D. 1998. Habitat characteristics affecting fish assemblages on a Hawaiian coral reef. Journal of Experimental Marine Biology and Ecology 224(1): 1-30.

Gratewick, B. and Speight, M.R. 2005. The relationship between fish species richness, abundance and habitat complexity in a range of shallow tropical marine habitats. Journal of Fish Biology 66: 650-667.

Gomelyuk, V.E. 2009. Fish assemblages composition and structure in three shallow habitats in north Australian tropical bay, Garig Ganuk Barlu National Park, Northern Territory, Australia. Journal of Marine Biological Association of the United Kingdom 89(3): 449-460.

Hill, M.O. 1973. Diversity and evenness: A unifying notation and its consequences. Ecology 54 (2): 327-432.

Kendall, M.S., Christensen, J.D., Caldow, C., Coyne, M., Jeffrey, C., Monaco, M.E., Morrison, W. and Hillis-Starr, Z. 2004. The influence of bottom type and shelf position on biodiversity of tropical fish inside a recently enlarged marine reserve. Aquatic Conservation: Marine and Freshwater Ecosystems 14(2): 113-132.

Knebel, H.J., Needell, S.W. and O'Hara, C.J. 1982. Modern sedimentary environments on the Rhode Island Inner Shelf, off the eastern United States. Marine Geology 49: 241-256.

Luckhurst B.E. & Luckhurst K. (1978) Analysis of the influence of substrate variables on coral reef fish communities. Marine Biology 49: 317-323.

McMaster, R.L. 1960. Sediments of Narragansett Bay system and Rhode Island Sound, Rhode Island. Journal of Sedimentary Petrology 30: 249-274.

McMullen, K.Y., Poppe, L.J., Twomey, E.R., Danforth, W.W., Haupt, T.A. and Crocker, J.M. 2007. Sidescan-sonar imagery, multibeam bathymetry, and surficial geologic interpretations of the sea floor in Rhode Island Sound, off Sakonnet Point, Rhode Island. U.S. Geological Survey Open-File Report 2007-1150, DVD-ROM. Also available online at http://pubs.usgs.gov/of/2007/1150.

McMullen, K.Y., Poppe, L.J., Denny, J.F., Haupt, T.A. and Crocker, J.M. 2008. Sidescan-sonar imagery and surficial geologic interpretations of the sea floor in central Rhode Island Sound: U.S. Geological Survey Open-File Report 2007-1366, DVD-ROM. Also available online at http://pubs.usgs.gov/of/2007/1366.

Nixon, S., Granger, S., Oviatt, C., Fields, L. and Mercer, J. In Press. Spatial and temporal variability of surface chlorophyll, primary production and benthic metabolism in Rhode Island and Block Island Sounds. Rhode Island Ocean Special Area Management Plan.

Persohn, C., Lorance, P. and Trenkel, V.M. 2009. Habitat preferences of selected demersal fish species in the Bay of Biscay and Celtic Sea, North-East Atlantic. Fisheries Oceanography 18 (4): 268-285.

Sonntag, N., Garthe, S. and Adler, S. 2009. A freshwater species wintering in a brackish environment: Habitat selection and diet of Slavonian grebes in the southern Baltic Sea. Estuarine, Coastal and Shelf Science 84 (2) :186-194.

Figure 1. RI Ocean SAMP study area and location of acoustic survey and bottom trawls sites. The red dashed line represents the boundaries of the SAMP area. The solid orange lines represent the boundaries of acoustically surveyed sites. Thick yellow lines represent bottom trawl track-lines. Each site with coupled geological-biological data is labeled with a letter. Sites selected for full acoustic analysis are highlighted in red.

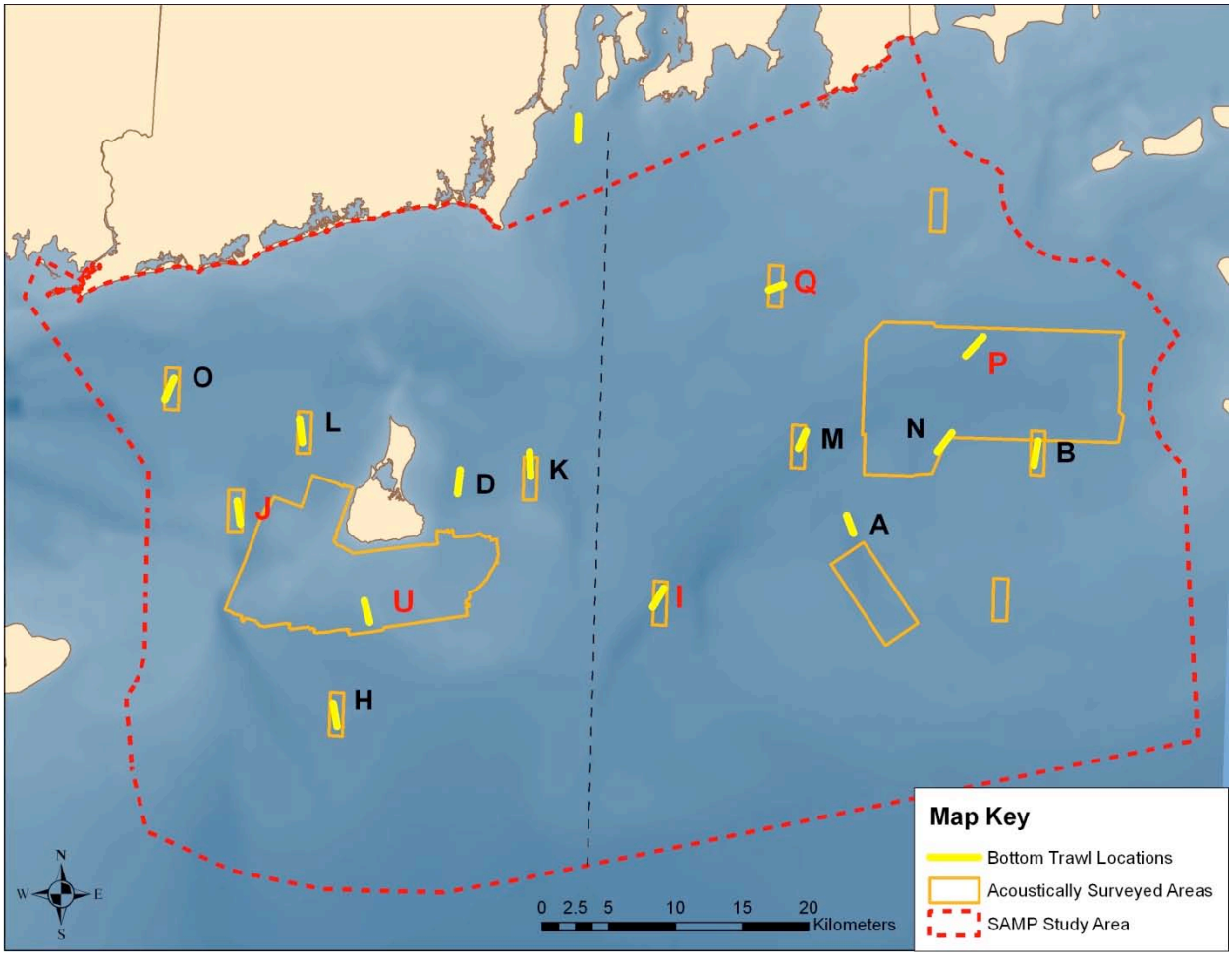

Figure 2. Side-scan backscatter of sites selected for full acoustic analysis (I,J,P,Q,U). Bottom trawl tracklines are represented by solid yellow lines. Light backscatter patterns represent highly reflective (harder) surfaces, such as boulders, shell, and sand, whereas dark backscatter represents less reflective (softer) bottom types, including mud, silt, and clay.

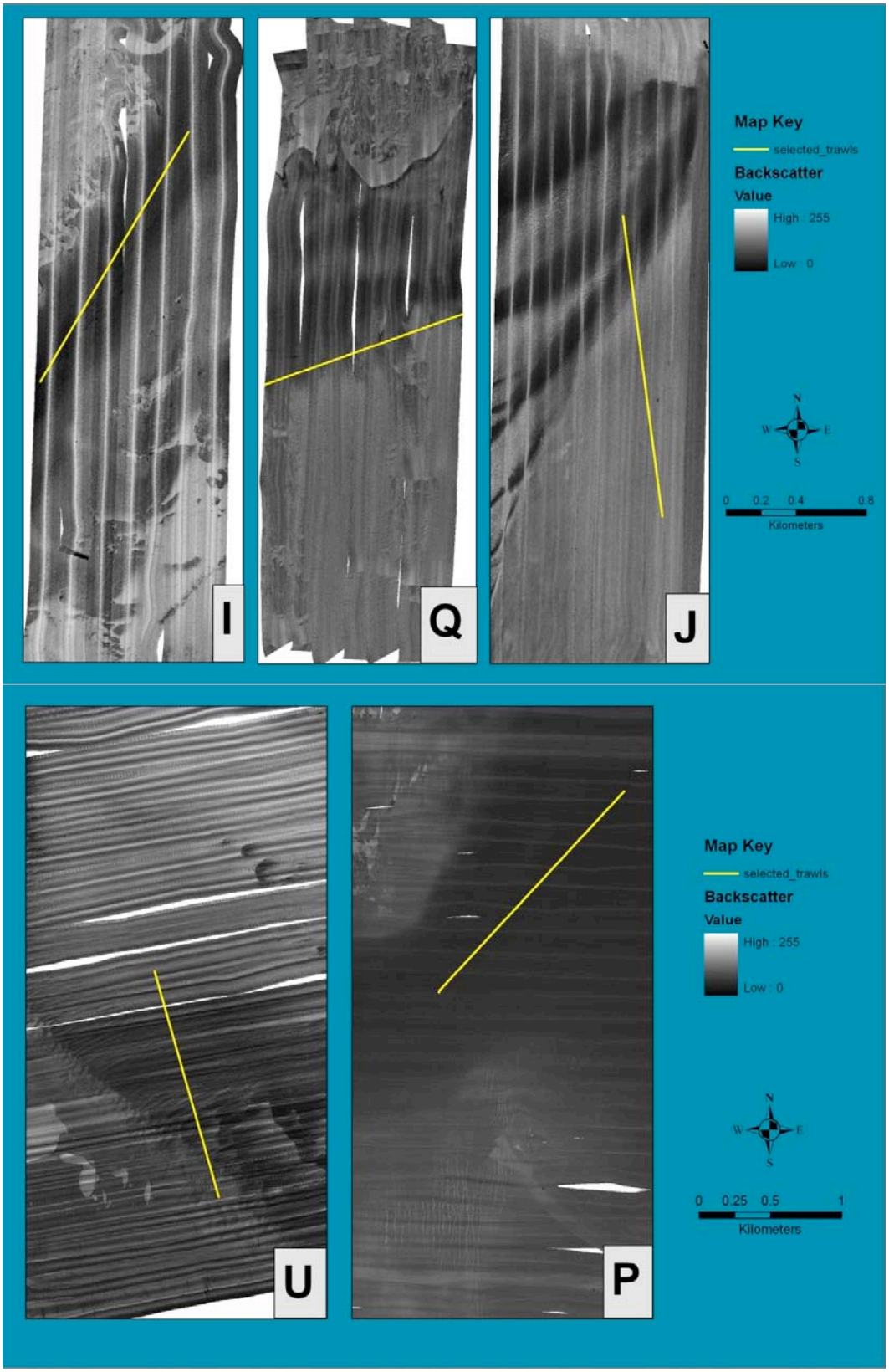

Figure 3. Bathymetry of sites selected for full acoustic analysis (I,J,P,Q,U). Light blue represents shallower water and dark pink represents deeper water. Bottom trawl tracklines are represented by solid yellow lines.

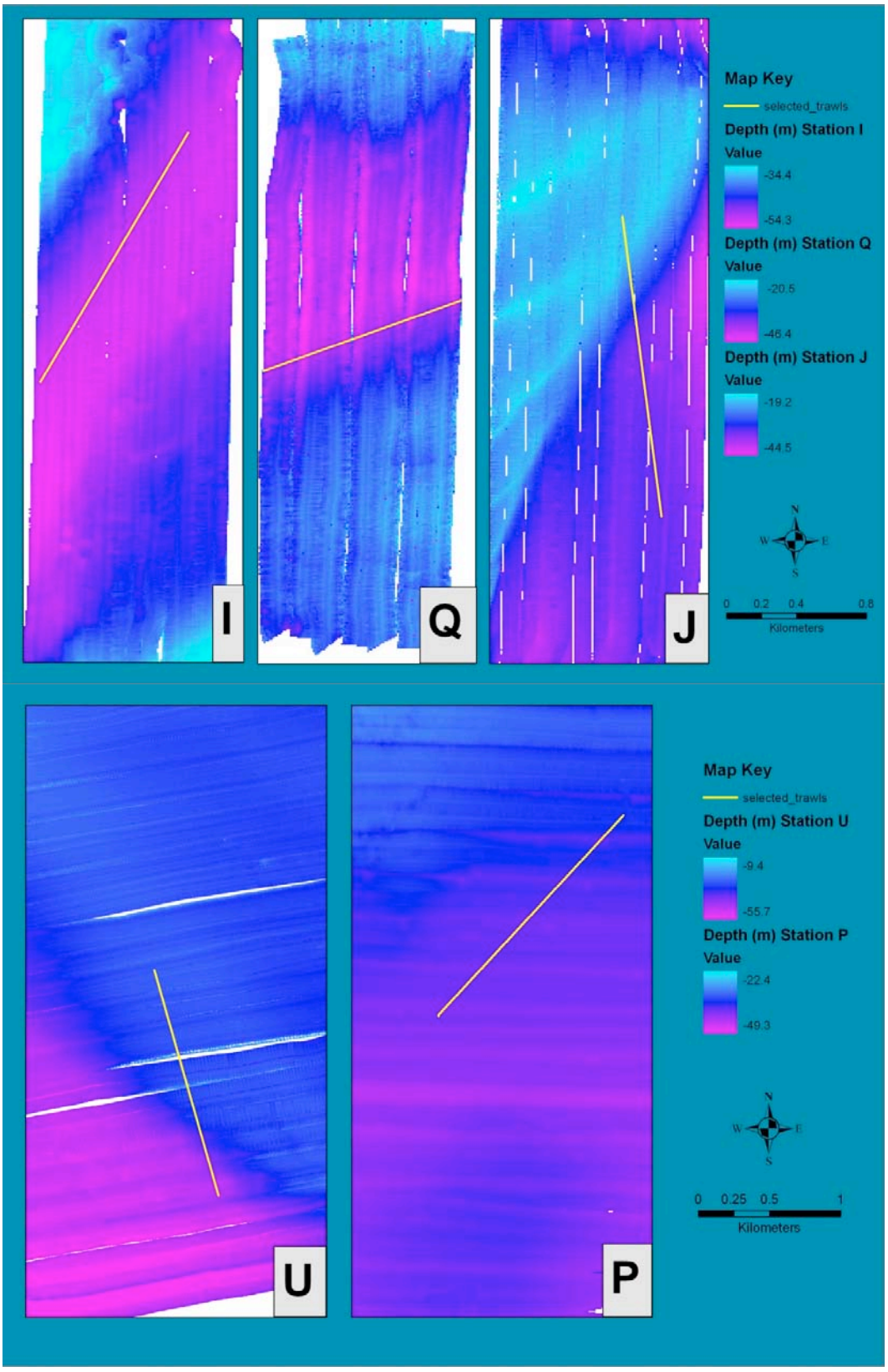

Figure 4. Rugostity of sites selected for full acoustic analysis. Rugosity was calculated from bathymetry data with the Benthic Terrain Modeler Toolbox in ArcMap. Bright yellow represents high rugosity and dark blue represents low rugosity. Bottom trawl tracklines are represented by solid yellow lines.

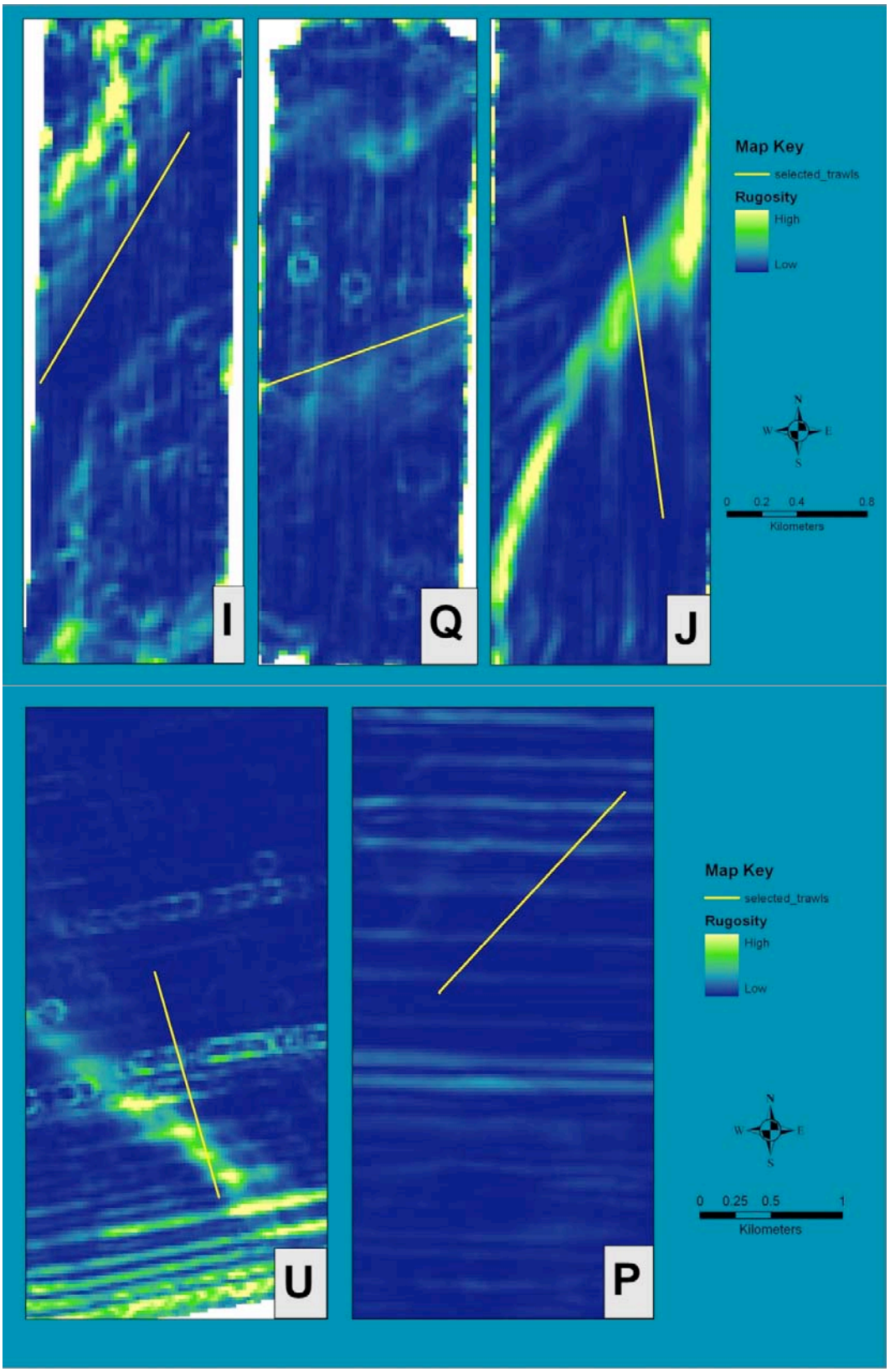

Figure 5. Map of benthic surface roughness in Rhode Island Sound and Block Island Sound. Light colors indicate low roughness and dark colors indicate high roughness. The RI Ocean SAMP area is outlined by a dashed red line. The solid orange lines represent the boundaries of acoustically surveyed sites. Thick yellow lines represent bottom trawl track-lines.

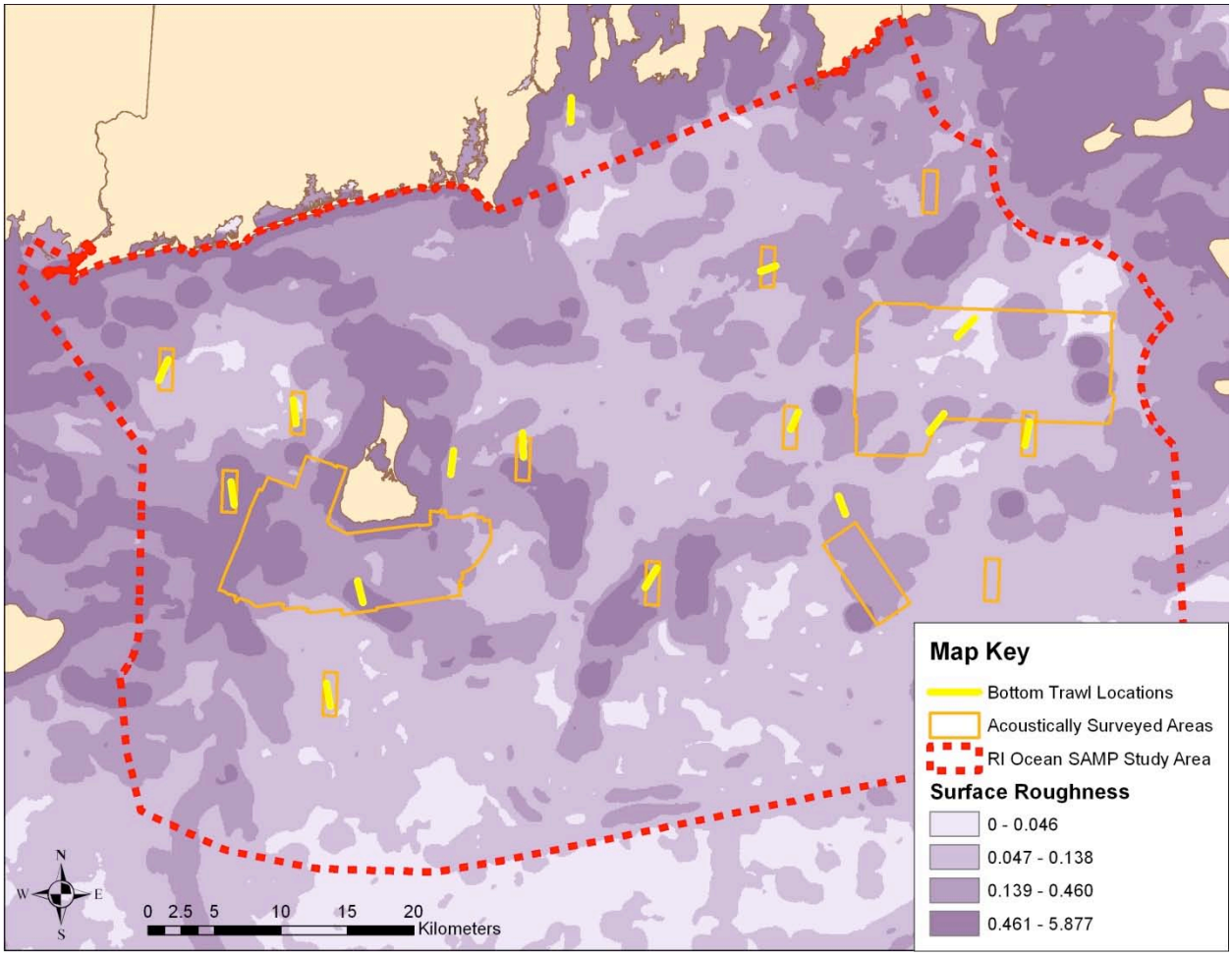

Figure 6. Aggregate fish abundance in Rhode Island Sound and Block Island Sound as measured by fifteen bottom trawls conducted in conjunction with the NEAMAP survey on September 30th and October 2nd, 2009 (http://www.neamap.net/). Green circles represent the total fish abundance at each site.

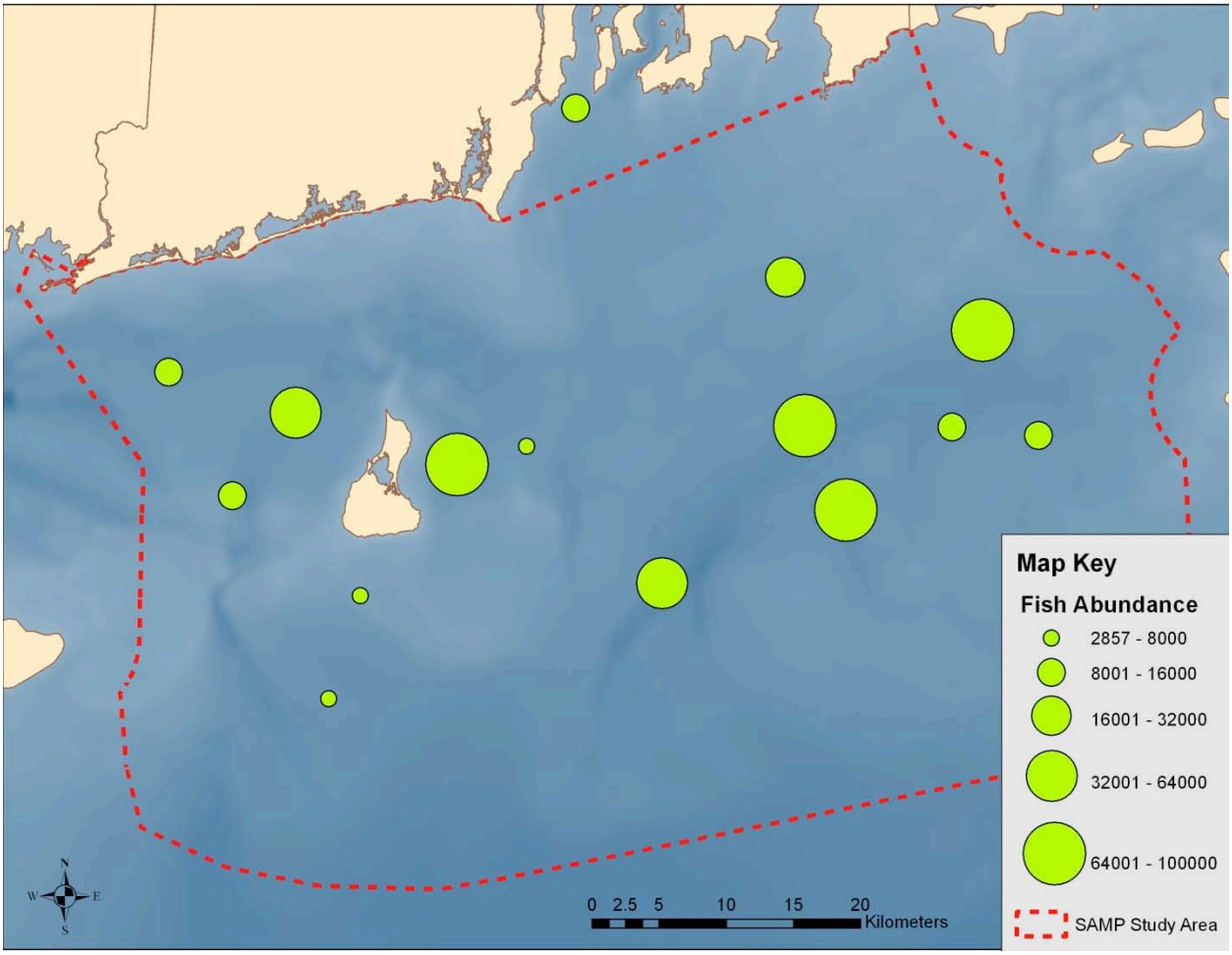

Figure 7. Aggregate fish biomass in Rhode Island Sound and Block Island Sound as measured by fifteen bottom trawls conducted in conjunction with the NEAMAP survey on September 30th and October 2nd, 2009 (http://www.neamap.net/). Blue circles represent the total fish biomass at each site.

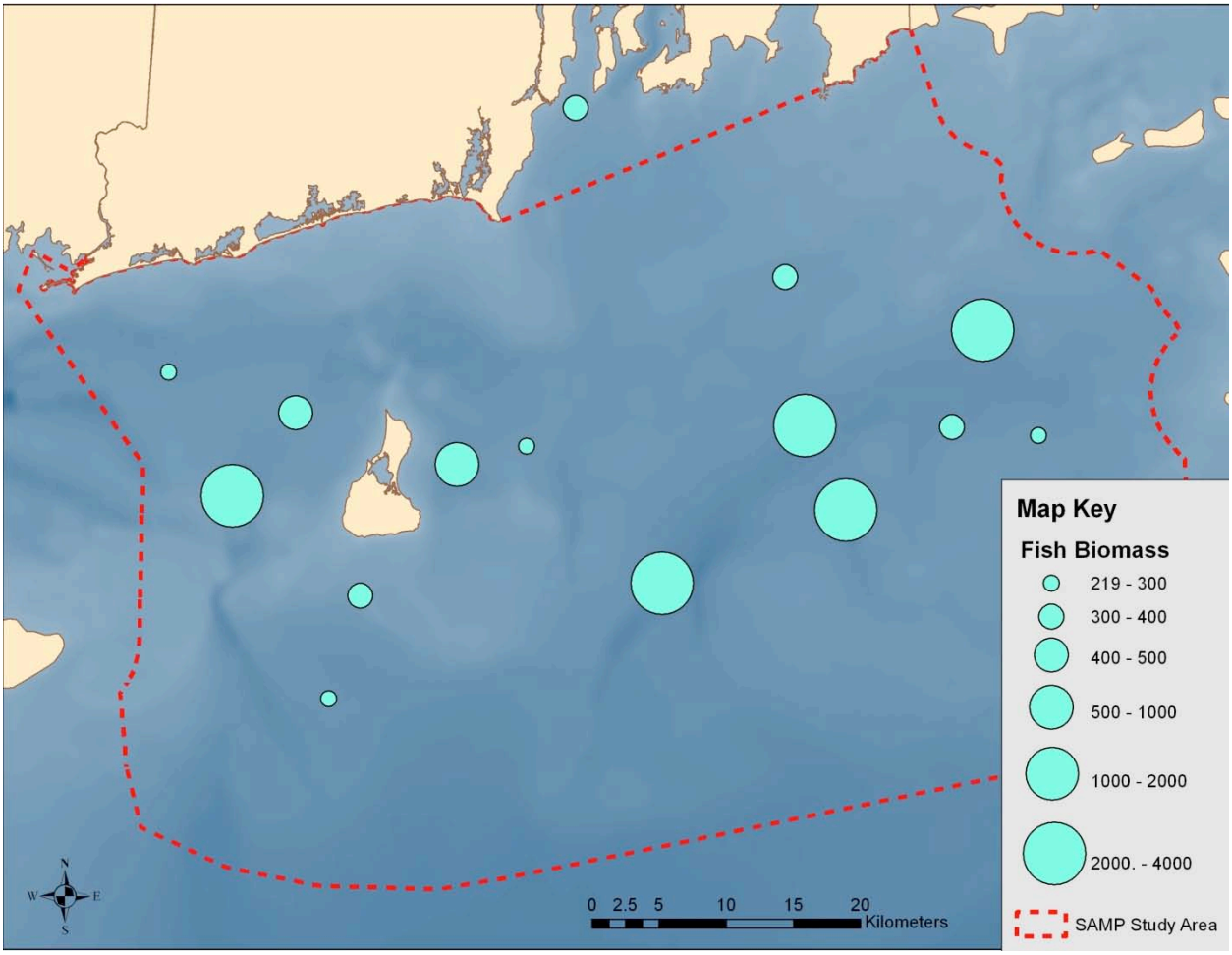

Figure 8. Comparison of total fish abundance, biomass, diversity and evenness between Rhode Island Sound and Block Island Sound. Hill's N1 and N2 were used as indices of diversity and evenness, respectively.

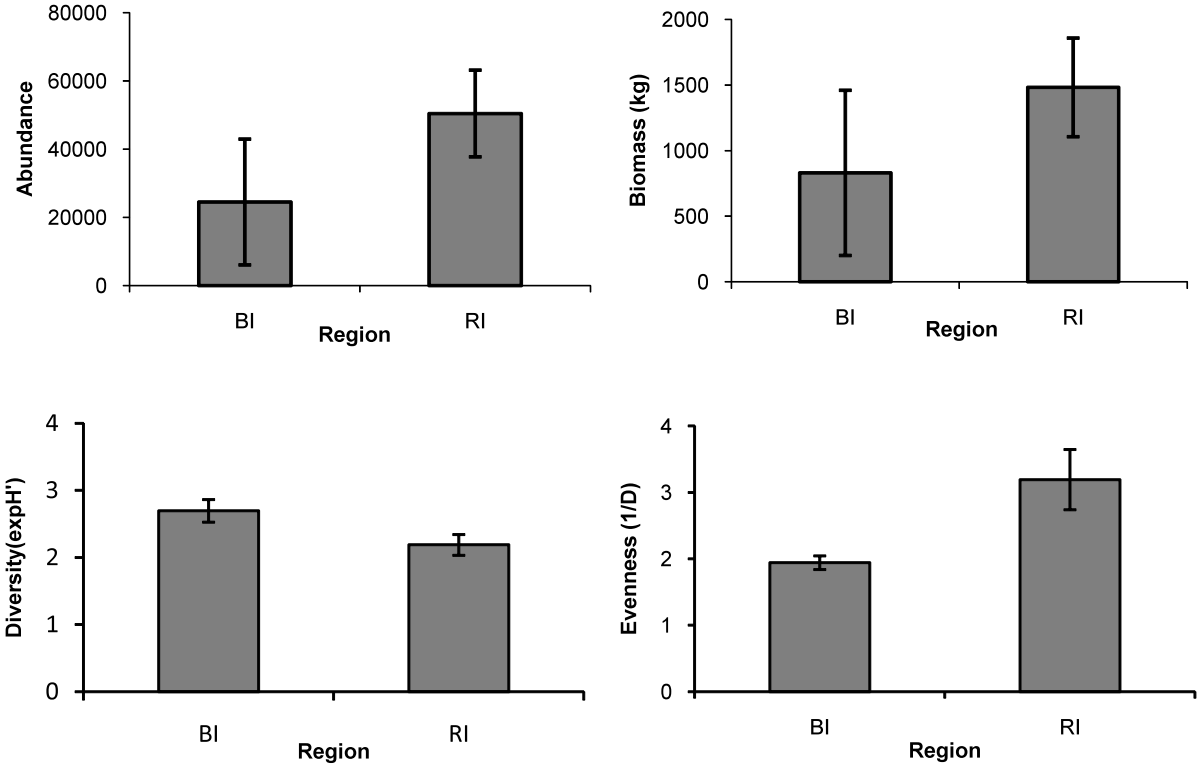

Figure 9. Comparison of total fish abundance, biomass, diversity and evenness between NEAMAP depth strata. The depth strata were defined as follows: Stratum 1: 20-40ft, Stratum 2 : 40- 60ft, Stratum 3: 60-90ft, Stratum 4 : 90-120ft, Stratum 5: >120ft.

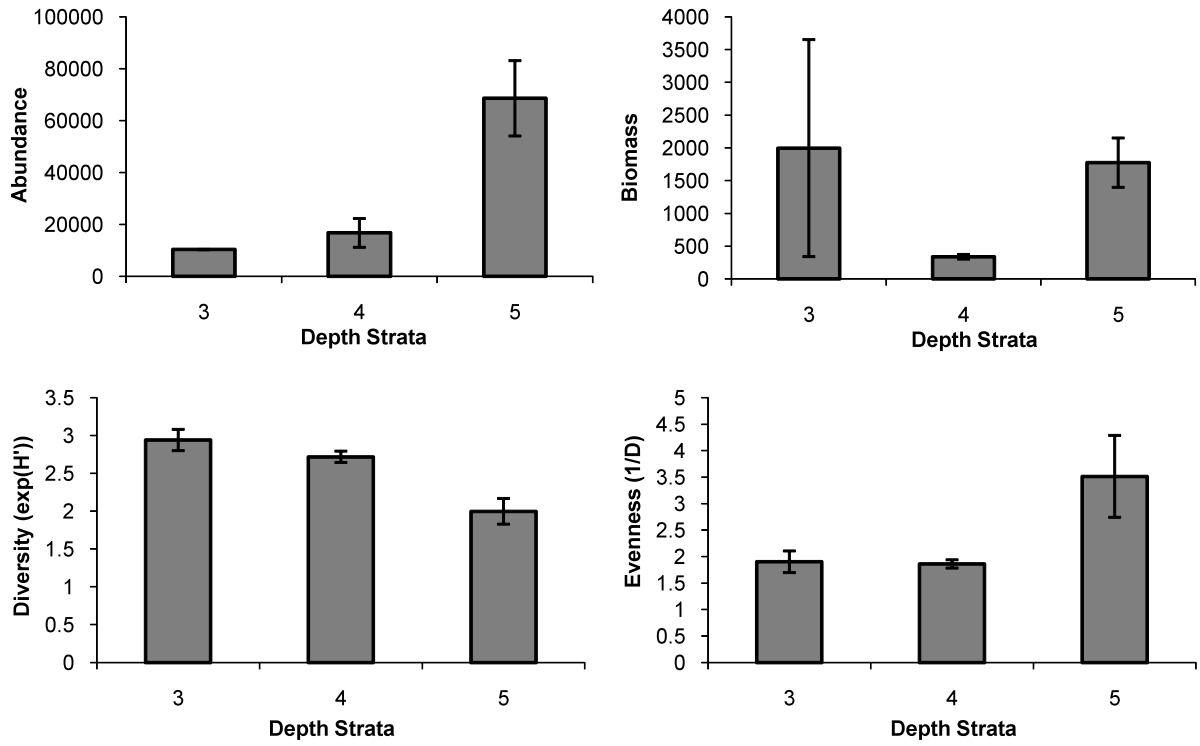

Figure 10. Univariate regressions between tow depth and fish abundance, biomass, diversity and evenness. Regression statistics are given in the upper right corner of each graph.

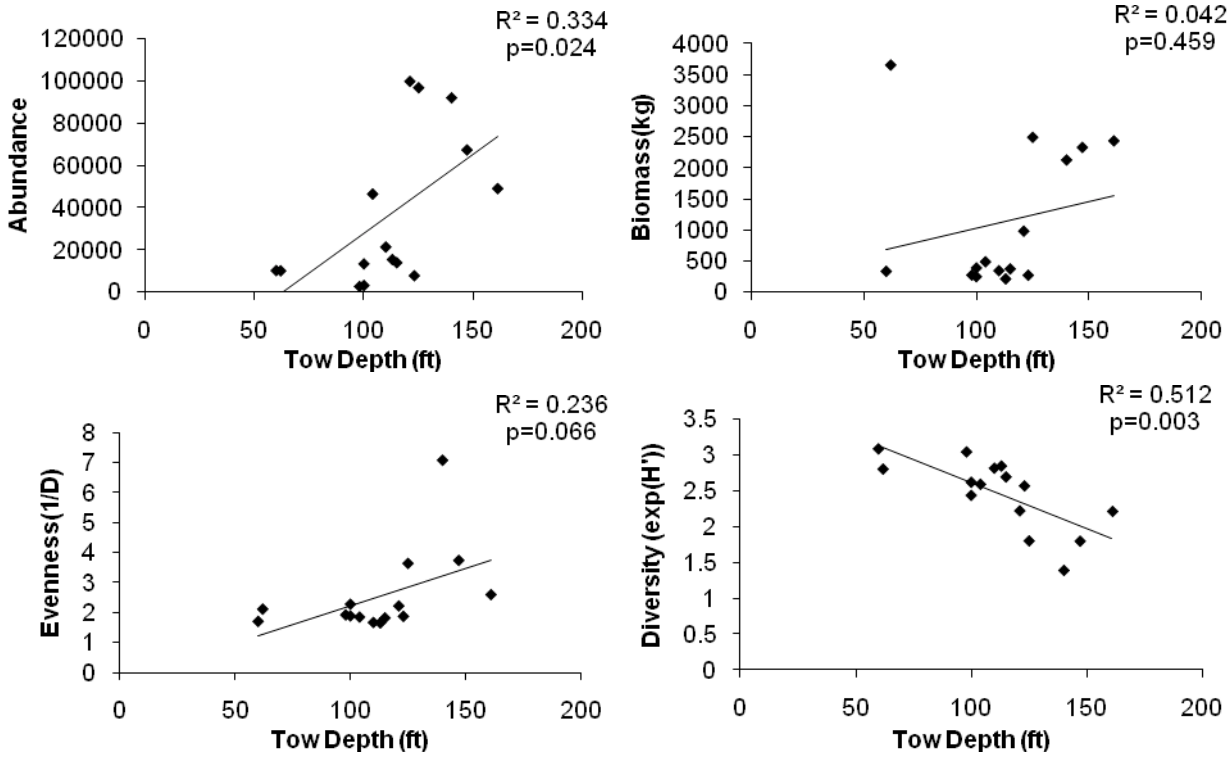

Figure 11. Ordination of the abundances of fish and invertebrate species sampled with demersal bottom trawls within Block Island and Rhode Island Sound. This nonmetric multidimensional scaling plot (MDS) depicts the pattern in demersal fish and invertebrate species composition, with similar species compositions close together. Each point represents one site.

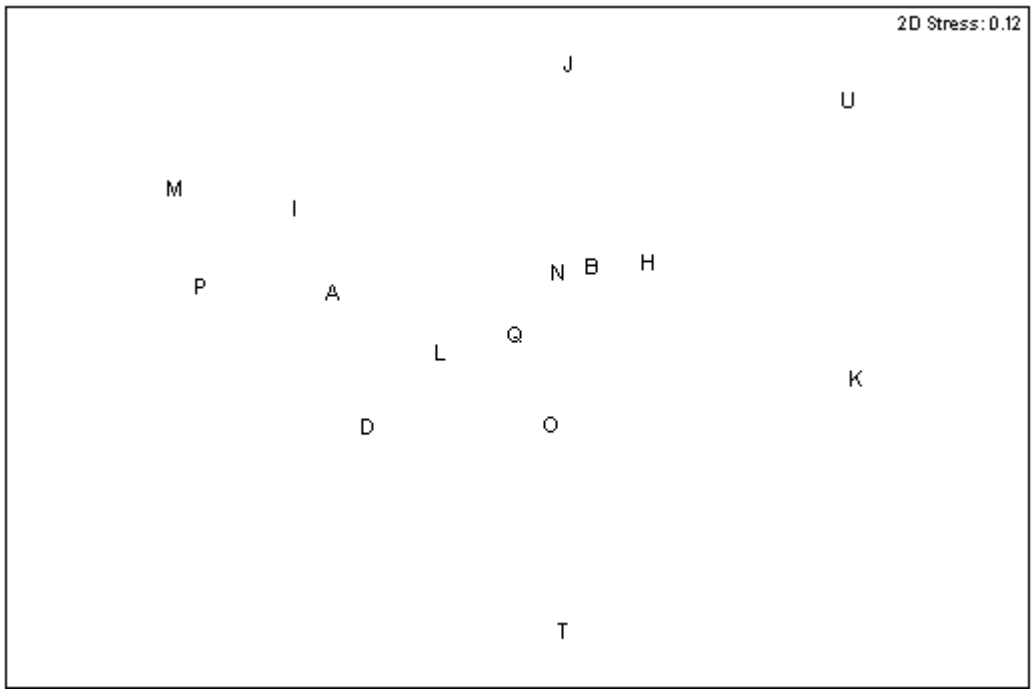

Figure 12. Multidimensional scaling plot (MDS) depicting the pattern in demersal fish and invertebrate species composition in Rhode Island Sound and Block Island Sound. Each point represents one site. Green triangles represent sites in depth stratum 5 (>120 ft), inverted blue triangles represent sites in depth stratum 4 (90-120ft) and light blue squares represent sites in depth stratum 3 (60-90ft). ANOSIM analysis indicates that depth strata has a significant effect on the composition of the demersal fish assemblage (R=0.337, p=0.011).

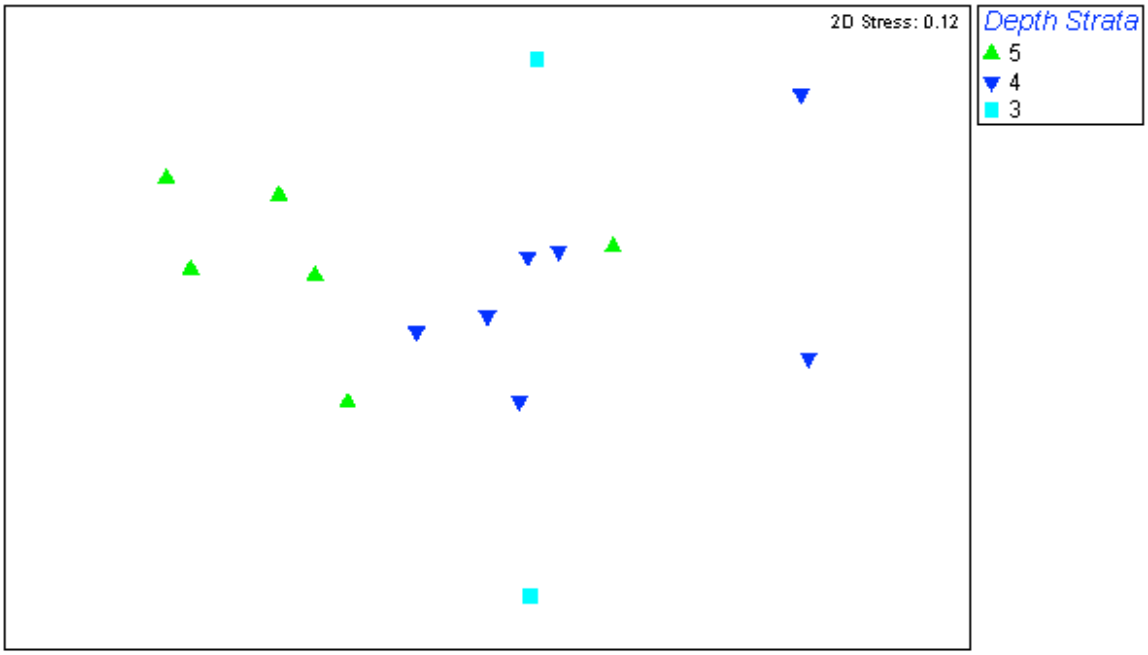

Figure 13. Multidimensional scaling plot (MDS) depicting the pattern in demersal fish and invertebrate species composition in Rhode Island Sound and Block Island Sound. Each point represents one sampling site. Green triangles represent sites in Rhode Island Sound (east of the shipping lane). Inverted blue triangles represent site in Blocked Island Sound (west of the shipping lane). ANOSIM analysis indicates that location (RIS v. BIS) has an effect on the composition of the demersal fish assemblage (R = 0.113, p= 0.10).

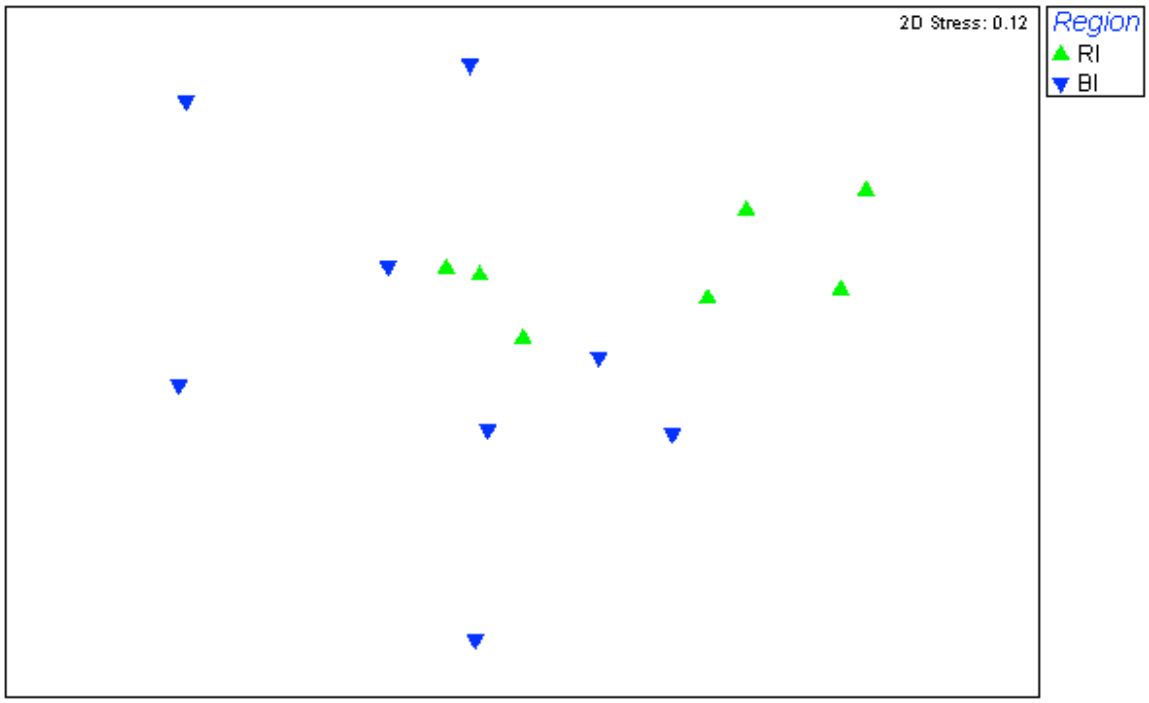

Figure 14. Comparison of benthic surface roughness between Block Island Sound and Rhode Island Sound. Mean benthic surface roughness data was calculated for each site in ArcMap. See Appendix I for more information.

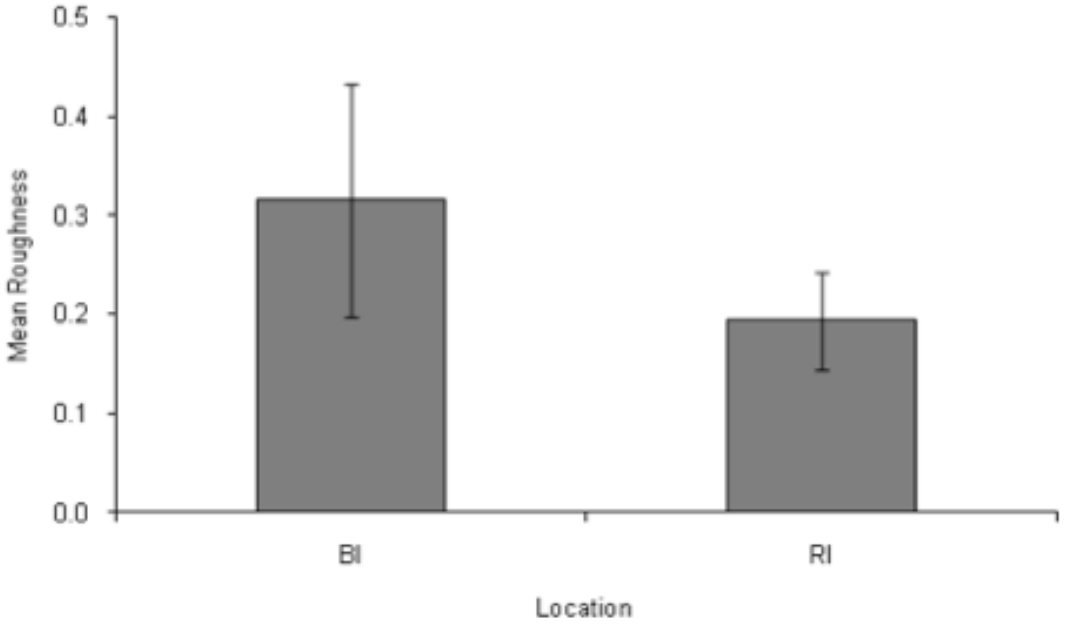

Table 1. Abiotic variables calculated from side-scan, bathymetry and roughness data. Rugosity was calculated from bathymetry data with the Benthic Terrain Modeler Toolbox in ArcMap. A Drafstman plot was used to identify highly correlated variables which were subsequently removed from analysis. Variables marked with an asterisk were uncorrelated and were used in final analyses.

Source	Resolution	Variable
Side-scan (Backscatter)	2m	Min*
		Max
		Mean*
		Standard Deviation*
	25m	Min
		Max
		Mean
		Standard Deviation
	50m	Min
		Max
		Mean
		Standard Deviation
	N/A	Number of Bottom Types*
		Number of Benthic Interfaces*
Bathymetry (Depth)	2m	Min
		Max
		Mean*
		Standard Deviation*
	25m	Min
		Max
		Mean
		Standard Deviation
	50m	Min
		Max
		Mean
		Standard Deviation
	25m	Rugosity*
Roughness (Damon, 2010)	100m	Min
		Max
		Range
		Mean*
		Standard Deviation*

Table 2. Mean abundance and biomass of the fish and invertebrate species caught during bottom trawl sampling in Rhode Island and Block Island Sounds on September 30th and October 2nd, 2009. All species listed below were included in calculations of total abundance, biomass, diversity and evenness as well as multivariate ordination of fish community composition. Species marked with an asterisk account for most of the pattern in the demersal fish assemblage within Block Island Sound and Rhode Island Sound (BVSTEP: rho=0.953).

Common Name	Scientific Name	Abundance	Biomass
Alewife*	*Alosa pseudoharengus*	183.7	11.4
American eel	*Anguilla rostrata*	1.2	0.2
American lobster	*Homarus americanus*	6.8	2.0
American shad	*Alosa sapidissima*	27.5	2.2
Atlantic herring*	*Clupea harengus*	188.0	2.9
Atlantic moonfish	*Selene setapinnis*	3.5	0.0
Atlantic torpedo	*Torpedo nobiliana*	1.0	20.9
Barndoor skate	*Dipturus laevis*	1.0	1.8
Black seabass*	*Centropristis striata*	2.0	2.2
Blueback herring	*Alosa aestivalis*	18.0	0.8
Bluefish*	*Pomatomus saltatrix*	4.8	3.3
Bluespotted cornetfish	*Fistularia tabacaria*	1.5	0.0
Butterfish*	*Peprilus triacanthus*	26104.3	371.5
Clearnose skate	*Raja eglanteria*	1.0	2.7
Crevalle jack	*Caranx hippos*	2.0	0.1
Cunner	*Tautogolabrus adspersus*	1.0	1.2
Fourspot flounder	*Paralichthys oblongus*	7.6	1.7
Goosefish*	*Lophius americanus*	2.5	6.8
Gulf Stream flounder	*Citharichthys arctif rons*	13.7	0.3
Horseshoe crab	*Limulus polyphemus*	1.0	2.5
Jonah crab	*Cancer borealis*	3.6	0.8
Little skate	*Leucoraja erinacea*	123.7	75.1
Longfin squid	*Loligo peali*	6258.9	86.3
Longhorn sculpin	*Myoxocephalus octodecemspinosus*	1.0	0.2
Northern searobin	*Prionotus carolinus*	1.0	0.1
Quahog*	*Mercenaria mercenaria*	3.0	0.7
Red hake	*Urophycis chuss*	12.5	1.6
Rock crab	*Cancer irroratus*	2.0	0.4
Rough scad	*Trachurus lathami*	5.9	0.2
Round herring	*Etrumeus sadina*	4.8	0.1
Round scad*	*Decapterus punctatus*	40.7	1.2
Scup	*Stenotomus chrysops*	3674.4	136.2
Sea raven	*Hemitripterus americanus*	10.0	5.4
Sea scallop*	*Placopecten magellanicus*	23.0	2.1
Silver hake*	*Merluccius bilinearis*	57.1	3.5
Smooth dogfish	*Mustelus canis*	1.7	5.4
Spider crab	*Libinia emarginata*	5.0	0.1
Spiny dogfish*	*Squalus acanthias*	161.6	442.1
Spot	*Leiostomus xanthurus*	1.0	0.1
Spotted hake	*Urophycis regius*	1.5	0.2
Striped bass	*Morone saxatilis*	2.0	8.6
Striped searobin	*Prionotus evolans*	2.3	1.1
Summer flounder	*Paralichthys dentatus*	8.1	14.6
Weakfish	*Cynoscion regalis*	7.5	0.6
Windowpane	*Scophthalmus aquosus*	3.5	0.8
Winter flounder	*Pseudopleuronectes americanus*	52.8	15.3
Winter skate	*Leucoraja ocellata*	13.2	25.6

Table 3. Depth strata, tow depth and region of all 15 sampling sites in Rhode Island and Block Island Sounds. Depth stratum was determined for each trawl site based on pre-existing bathymetric maps, while tow depth was measured at the start of each trawl. Depth strata were defined as follows: Stratum 1: 20-40ft, Stratum 2 : 40- 60ft, Stratum 3: 60- 90ft, Stratum 4 : 90-120ft, Stratum 5: >120ft. Region was classified as follows: Rhode Island Sound (RIS): East of the shipping lane, Block Island Sound: West of the shipping lane (Figure 1).

Site	Depth Strata	Tow Depth (ft)	Region
A	5	140	RIS
B	4	100	RIS
D	5	121	BIS
H	5	123	BIS
I	5	161	RIS
J	3	62	BIS
K	4	98	BIS
L	4	104	BIS
M	5	147	RIS
N	4	115	RIS
O	4	113	BIS
P	5	125	RIS
Q	4	110	RIS
T	3	60	BIS
U	4	100	BIS

Table 4. Total abundance, biomass, diversity and evenness of the fish community at 15 sites within Rhode Island Sound and Block Island Sound as measured by bottom trawls conducted in conjunction with the NEAMAP survey on September 30th and October 2nd, 2009. Hill's N1 (exp(H')) and Hill's N2 (1/D) were used as indices for diversity and evenness, respectively.

Site	Abundance	Biomass (kg)	Diversity	Evenness
A	91676	2127.971	1.390	7.062
B	13485	254.334	2.616	1.877
D	99417	985.733	2.219	2.210
H	7953	277.689	2.565	1.862
I	48949	2435.333	2.210	2.586
J	10232	3652.395	2.798	2.104
K	2857	280.103	3.038	1.912
L	46383	494.456	2.588	1.840
M	67133	2330.536	1.795	3.726
N	14078	379.556	2.689	1.810
O	15536	218.995	2.841	1.645
P	96436	2492.355	1.800	3.627
Q	21450	351.260	2.811	1.658
T	10359	341.235	3.079	1.695
U	3315	394.357	2.433	2.267

Table 5. Results of univariate regressions between acoustically-derived abiotic variables and fish community metrics. Significant relationships are marked with an asterisk.

X variable	Y variable	R^2	p	Relationship
# BT	Diversity	0.691	0.081*	+
# BT	Abundance	0.836	0.030*	-
# BT	Biomass	0.406	0.247	-
# BT	Evenness	0.809	0.038*	-
STDev Depth	Abundance	0.433	0.228	-
STDev Depth	Biomass	0.033	0.770	+
STDev Depth	Diversity	0.184	0.471	+
STDev Depth	Evenness	0.081	0.642	-

Appendix I. Acoustically-determined abiotic benthic habitat variables for sites I, J, P Q and U. All analyses were carried out in ArcMap.

			Station				
Source	**Resolution**	**Variable**	**I**	**J**	**P**	**Q**	**U**
Side-scan (Backscatter)	2m	Min	38	36	32	73	17
		Max	255	191	87	184	166
		Mean*	111.848	115.569	49.234	123.405	71.017
		Standard Deviation*	37.669	27.703	6.415	17.552	22.685
	25m	Min	62.091	31.098	41.882	73.346	26.663
		Max	255	255	121.905	255	136.266
		Mean	121.038	114.436	50.789	126.477	74.117
		Standard Deviation	30.932	24.545	5.675	21.477	20.651
	50m	Min	66.529	34.732	43.534	78.16	33.987
		Max	255	255	84.626	255	113.643
		Mean	121.249	114.546	50.785	127.668	73.965
		Standard Deviation	24.503	22.795	4.725	22.148	17.57
	N/A	Number of Bottom Types*	2	3	1	4	4
		Number of Benthic Interfaces*	1	2	0	9	3
Bathymetry (Depth)	2m	Min	51.248	20.345	37.678	32.042	17.584
		Max	53.617	34.951	40.492	36.584	36.863
		Mean*	52.424	28.943	39.34	34.734	26.269
		Standard Deviation*	0.396	3.841	0.686	0.46	3.415
	25m	Min	47.064	20.589	37.256	28.513	19.982
		Max	53.744	34.686	40.893	36.446	36.771
		Mean	52.052	28.673	39.299	34.515	26.627
		Standard Deviation	1.088	4.42	0.781	0.887	3.919
	50m	Min	47.901	20.68	37.574	27.946	21.587
		Max	53.615	34.676	40.814	36.246	36.02
		Mean	52.046	28.673	39.299	34.509	26.618
		Standard Deviation	1.079	4.413	0.777	0.88	3.906
	N/A	Rugosity	1.00002	1.00011	1	1.00002	1.00008
Roughness (Damon, 2010)	100m	Min	0.363	0.547	0.024	0.176	0.387
		Max	0.460	1.367	0.082	0.258	0.612
		Range	0.098	0.820	0.059	0.082	0.225
		Mean*	0.419	1.043	0.047	0.221	0.569
		Standard Deviation*	0.023	0.194	0.020	0.027	0.040

15.
Chapter 5: Commercial and Recreational Fisheries

APPENDIX B

FISHERIES ACTIVITY MAPS: METHODS AND DATA SOURCES

1. Fisheries Activity Maps Based on Qualitative Input

1. Commercial and recreational fisheries usage Geographic Information Systems (GIS) data layers and maps for Rhode Island's offshore waters were developed from September 2008 – August 2009 and finalized in October 2009. Three data layers and maps were created: recreational fishing usage areas; commercial fishing usage areas – mobile gear; and commercial fishing usage areas – fixed gear.

2. The main purpose of this data collection effort was to document the fishing grounds used by RI commercial and recreational fishermen. This effort took place as part of the Ocean SAMP planning process, and so data collection focused on the SAMP area, which encompassed RI's coastal and ocean waters, encompassing both state and federal jurisdictions, out to 20 miles offshore. These data layers were created for use in the Ocean SAMP planning process, but were also intended as an update and refinement to a similar set of maps created in 2004 by New England regional Sea Grant.

3. Fisheries usage data layers are based on qualitative data and were developed using standard qualitative research methods. Data were collected through interviews and mapping exercises conducted in person, both one-on-one and in small groups, with RI commercial and recreational fishermen. Interviews took place between September 2008 and January 2009. Approximately 30 fishermen, including representatives of commercial and recreational fishing groups and numerous unaffiliated fishermen, were interviewed. Interview subjects were identified by RI fisheries experts, and representatives from all RI fishing industry groups were invited to participate. Effort was made to schedule in-person meetings in places and at times that were convenient to fishermen. Groups that participated included the RI Fishermen's Alliance (RIFA), the RI Lobstermen's Association, the Eastern New England Scallop Association (ENESA), the RI Saltwater Anglers Association (RISAA), and the RI Party and Charter Boat Association (RIPCBA).

4. In each interview, fishermen were first given a brief introduction to the RI Ocean SAMP planning process and shown NOAA nautical charts of the SAMP area. Fishermen were also told that their individual input would be kept confidential, and that only aggregate data, in the form of GIS data layers, maps, and metadata, would be shared with the public. This was important in order to preserve individual fishermen's information about their most important fishing areas, which is essential to the success of their businesses. Researchers then asked the fishermen to describe where they fish, and to draw polygons encompassing these areas on the nautical charts. Fishermen were then asked follow-up questions about these areas, including (1) During which seasons do you fish in each

area?; (2) With what gear?; and in some cases (3) What are your target species in each area? This information was notated directly on NOAA nautical charts and additional notes were taken where appropriate. Fishermen were also asked if they had questions or concerns about the Ocean SAMP planning process. This input was recorded and used to shape the SAMP stakeholder process as well as the framework for developing the SAMP fisheries chapter.

5. Following these meetings, data were aggregated onto three sets of NOAA nautical charts to represent the three different data layers described above. The raw data, which exists in the form of the original nautical charts with fishermen's confidential information, are archived by David Beutel, Aquaculture Coordinator at the RI Coastal Resources Management Council. These aggregate charts were first compared with the 2004 maps for corroboration, and then combined with the 2004 data to complete the current information. Charts were then scanned and georeferenced and polygons were digitized in order to create Geographic Information Systems (GIS) shapefiles. Attribute fields were created for the data layers to record available information about either seasonality or gear type. See Chapter 5 for final maps based on these data layers.

6. This dataset has some limitations. In many cases, fixed gear areas are not always differentiated by gear type because this information was not available; for example, gillnet gear is not thoroughly differentiated from lobster gear, which is not further differentiated from fish pots. In addition, these data do not include out-of-state fisheries which may be conducted within the SAMP area, such as the herring mid-water trawling fishery based out of other New England ports.

7. While the data represented in these data layers is anecdotal, comparison with past usage maps shows that it is consistent. Moreover, there are few other data sources that indicate where fishermen fish, and none which is universally deemed reliable. See below for further discussion of other fisheries activity data sources.

2. Fisheries Activity Maps Based on Quantitative Data

1. Additional commercial fisheries usage GIS data layers and maps were created for the Ocean SAMP through the use of quantitative fisheries-dependent monitoring data obtained from NMFS. There is no one dataset, nor a combination of datasets, available that accurately represent the exact locations of all commercial fisheries activity. The best available data that provide insight into the spatial and temporal characteristics of commercial fishing activity are two NMFS monitoring datasets: Vessel Trip Report (VTR) data; and Vessel Monitoring Systems (VMS) data. VTR data are based on the individual fisherman reporting his or her activity, whereas VMS data are based on an independent electronic satellite tracking system, and reflect both vessel transits as well as fishing activity. Both of these datasets are subject to strict confidentiality provisions designed to protect fishermen's privacy. Because of numerous limitations associated with the use of VMS data in mapping, only VTR data were used to create maps for the Ocean SAMP.

2. As a means of monitoring fisheries activity, NMFS requires commercial fishermen with federally-permitted groundfish, scallop, and monkfish vessels operating in the SAMP

area to submit one VTR for each fishing trip. On each report, the fisherman reports the location of that trip as one set of coordinates (latitude/longitude or Loran). VTR location information is only an approximation of fishing activity because the fisherman self-reports only one set of coordinates for the trip, despite the fact that one trip may include multiple tows that take place in many different locations across a much wider area.

3. VTR data for Rhode Island-based vessels for 1998 – 2008 were obtained from NMFS, subject to data access agreements that are designed to ensure fishermen's privacy. Fishing activity maps were created by aggregating all VTRs as one set of point data, and then aggregating the data by gear type to reflect bottom trawling; scallop dredging; gillnetting; and mid-water trawling activity. A density plot was then created, using a 1-minute by 1-minute grid overlay, to determine the relative density of fishing trips by gear type and in aggregate. Darker-shaded areas represent the areas with a higher density of fishing activity; see Chapter 5 for the final maps based on these data. In addition, because VTR data include the dates of each fishing trip, data were aggregated by gear type and season (Winter: Jan 1 – March 31; Spring: April 1 – June 31; Summer: July 1 – September 30; Fall: October 1 – December 31) in order to highlight the seasonal variation in fishing activity; see Figures 1-12 below.

4. It is important to emphasize that VTR data have some limitations. As noted above, VTR location information is only an approximation of fishing activity because the fisherman self-reports only one set of coordinates for the trip, despite the fact that one trip may include multiple tows or sets that take place in many different locations across a much wider area. In addition, VTR data do not reflect lobstering, which is one of the main commercial fishing activities that takes place in the SAMP area. No equivalent dataset is available from any state or federal regulatory agency that can be used to map lobstering activity at this level of resolution. Whereas RIDEM collects logbook data (similar to VTRs) from lobstermen, these data include location information reported by statistical area only and are therefore insufficient for mapping fishing activity in the SAMP area.

Figure 1. Gillnet and Mobile Gear Fishing, Winter, Based on NMFS Vessel Trip Reports, 1998 - 2008

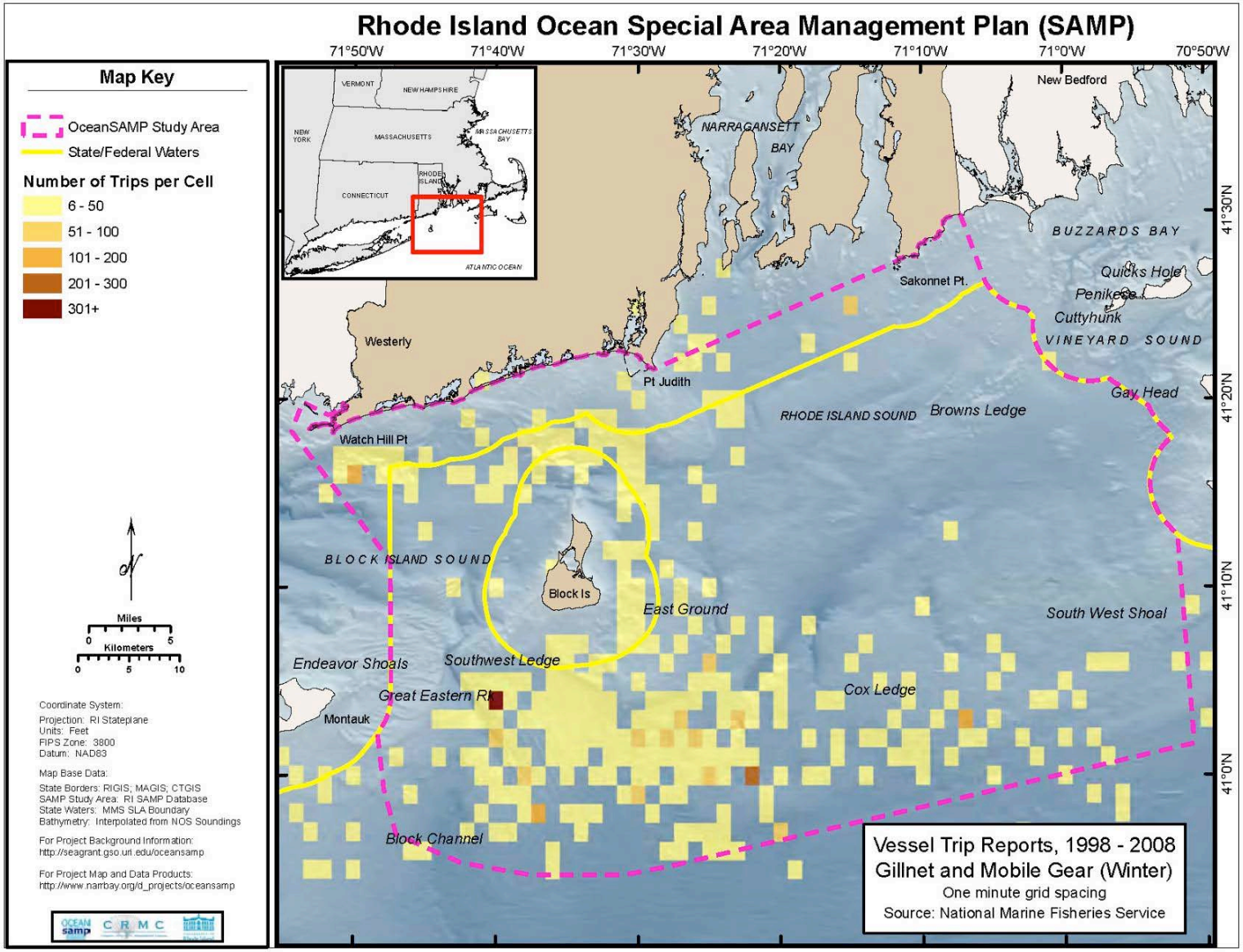

Figure 2. Gillnet and Mobile Gear Fishing, Spring, Based on NMFS Vessel Trip Reports, 1998 - 2008

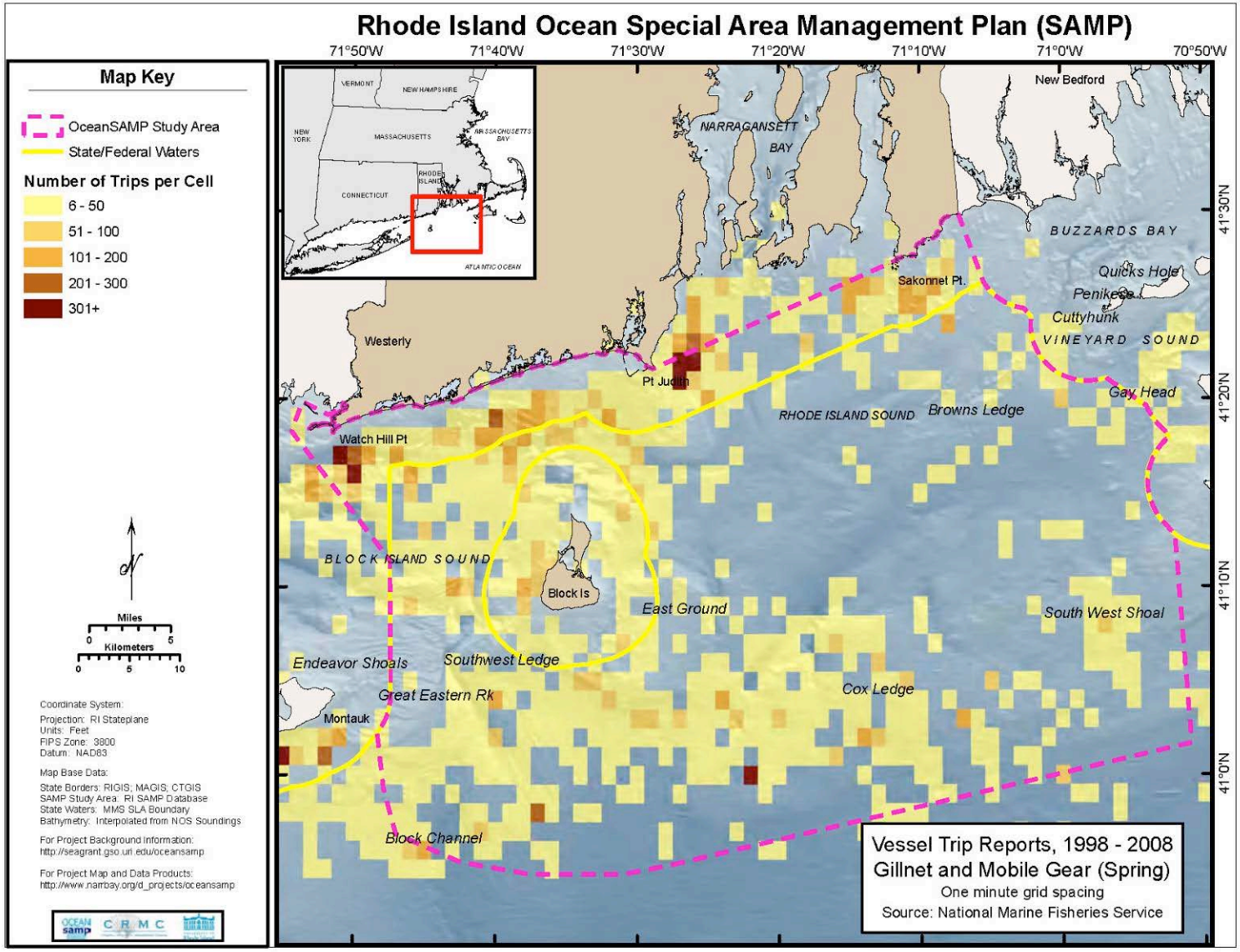

Figure 3. Gillnet and Mobile Gear Fishing, Summer, Based on NMFS Vessel Trip Reports, 1998 - 2008

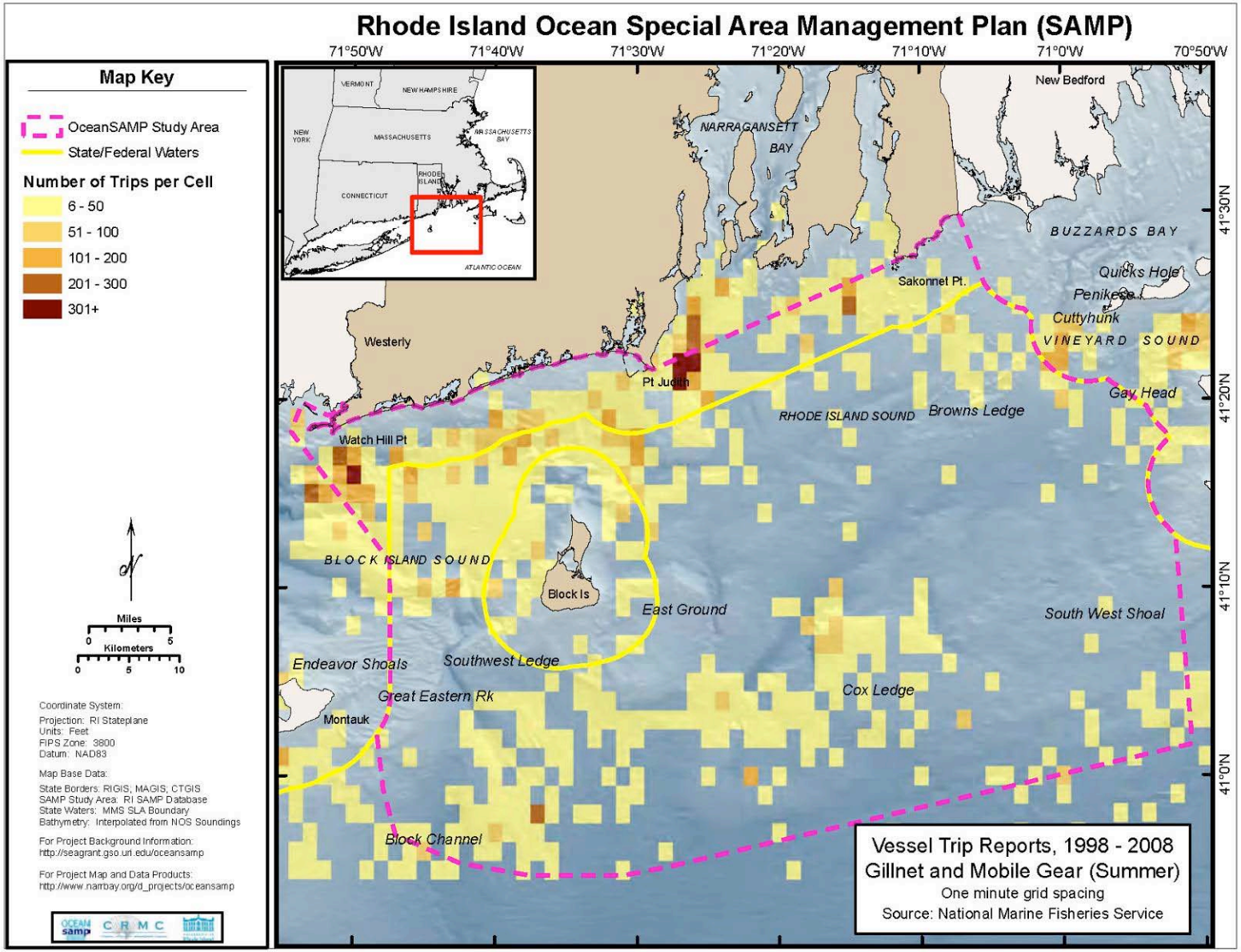

Figure 4. Gillnet and Mobile Gear Fishing, Fall, Based on NMFS Vessel Trip Reports, 1998 - 2008

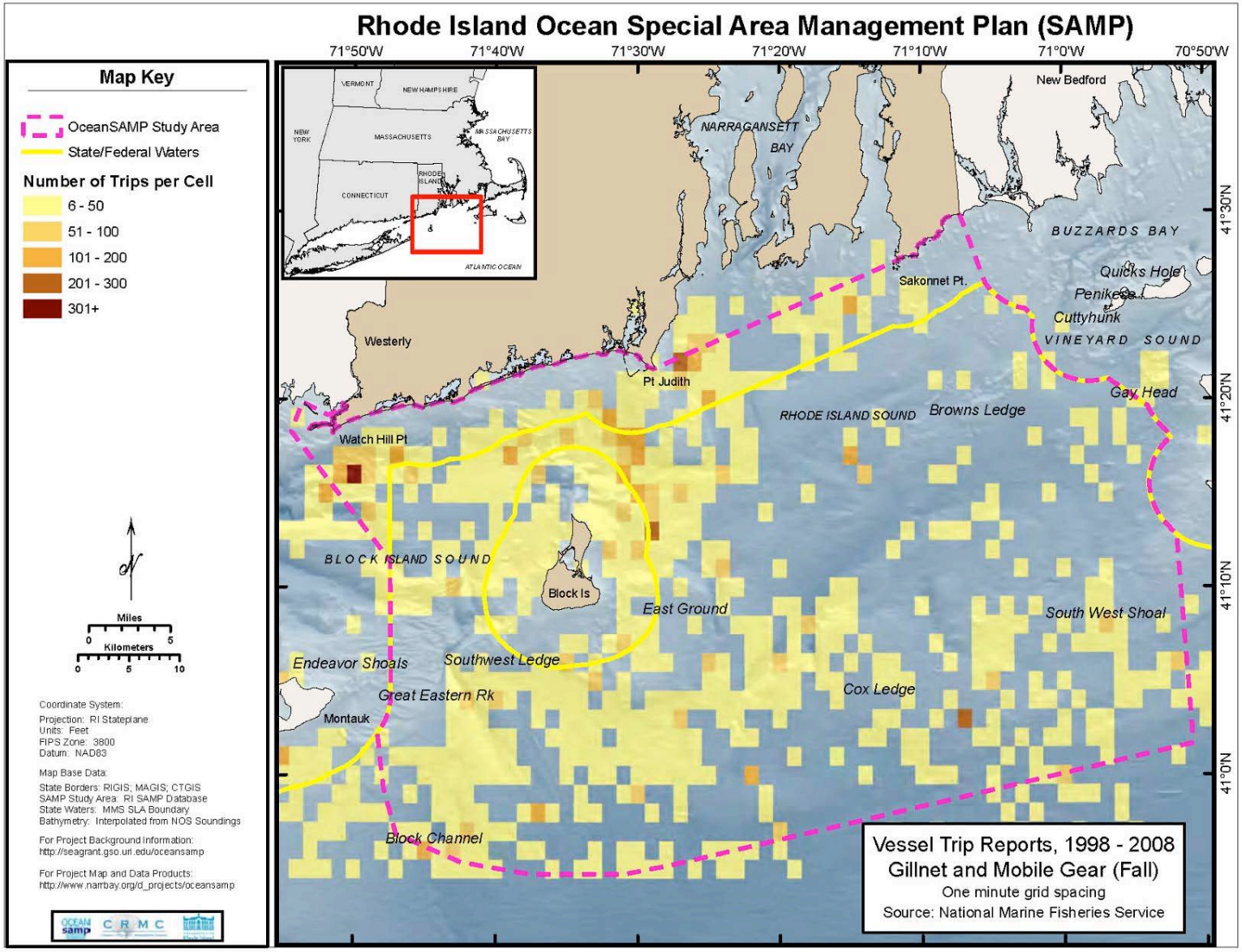

Figure 5. Bottom Trawling, Winter, Based on NMFS Vessel Trip Reports, 1998 - 2008

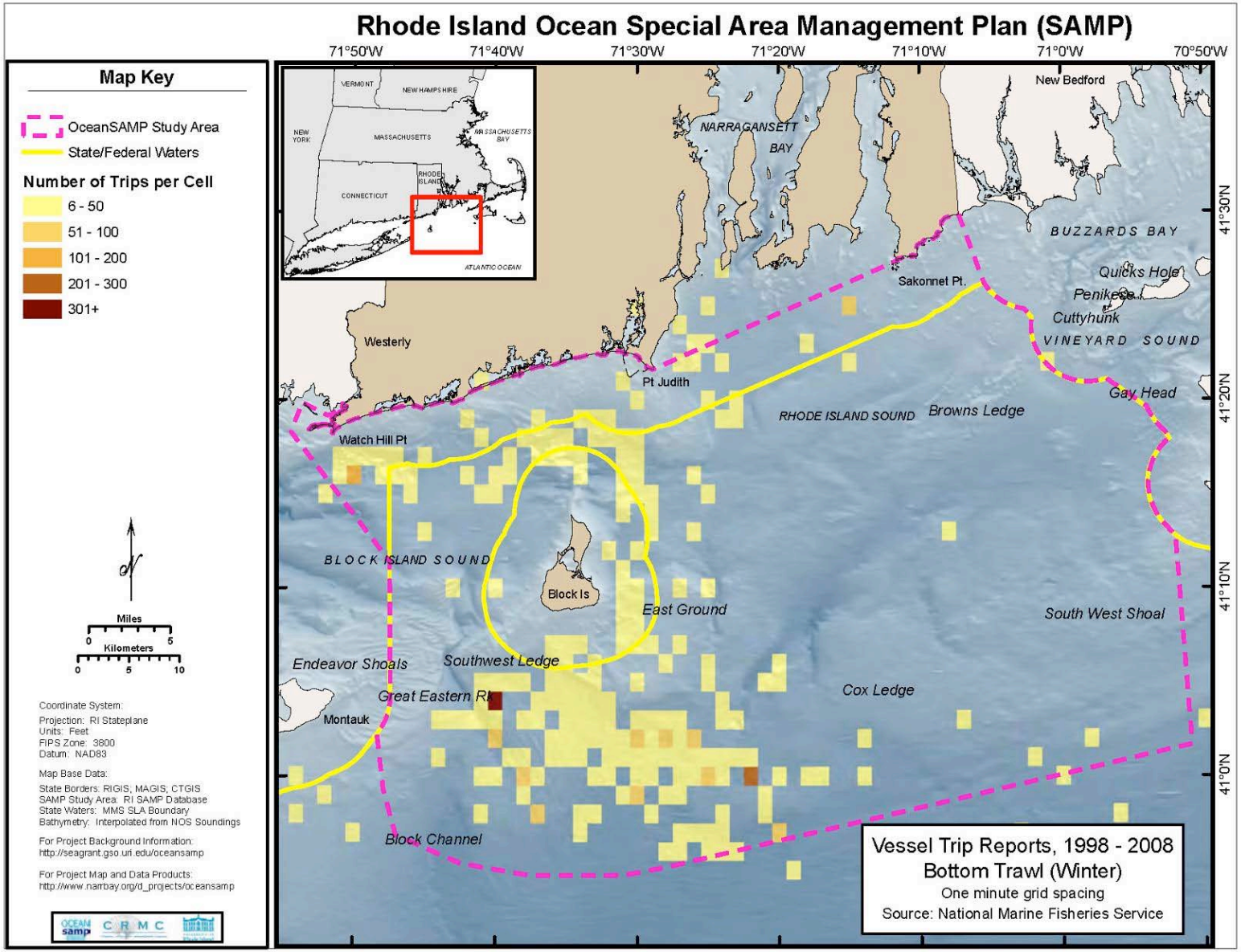

Figure 6. Bottom Trawling, Spring, Based on NMFS Vessel Trip Reports, 1998 - 2008

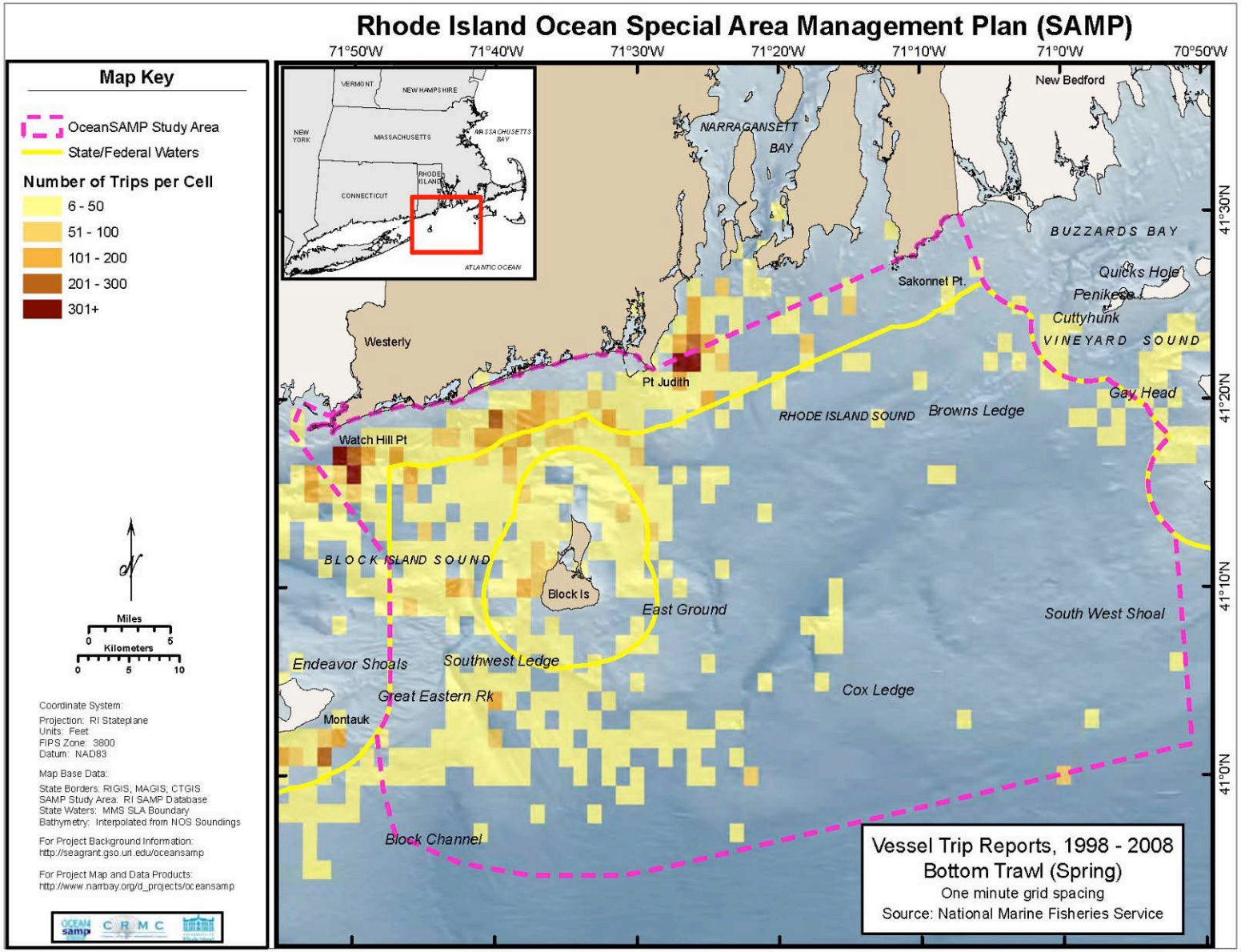

Figure 7. Bottom Trawling, Summer, Based on NMFS Vessel Trip Reports, 1998 - 2008

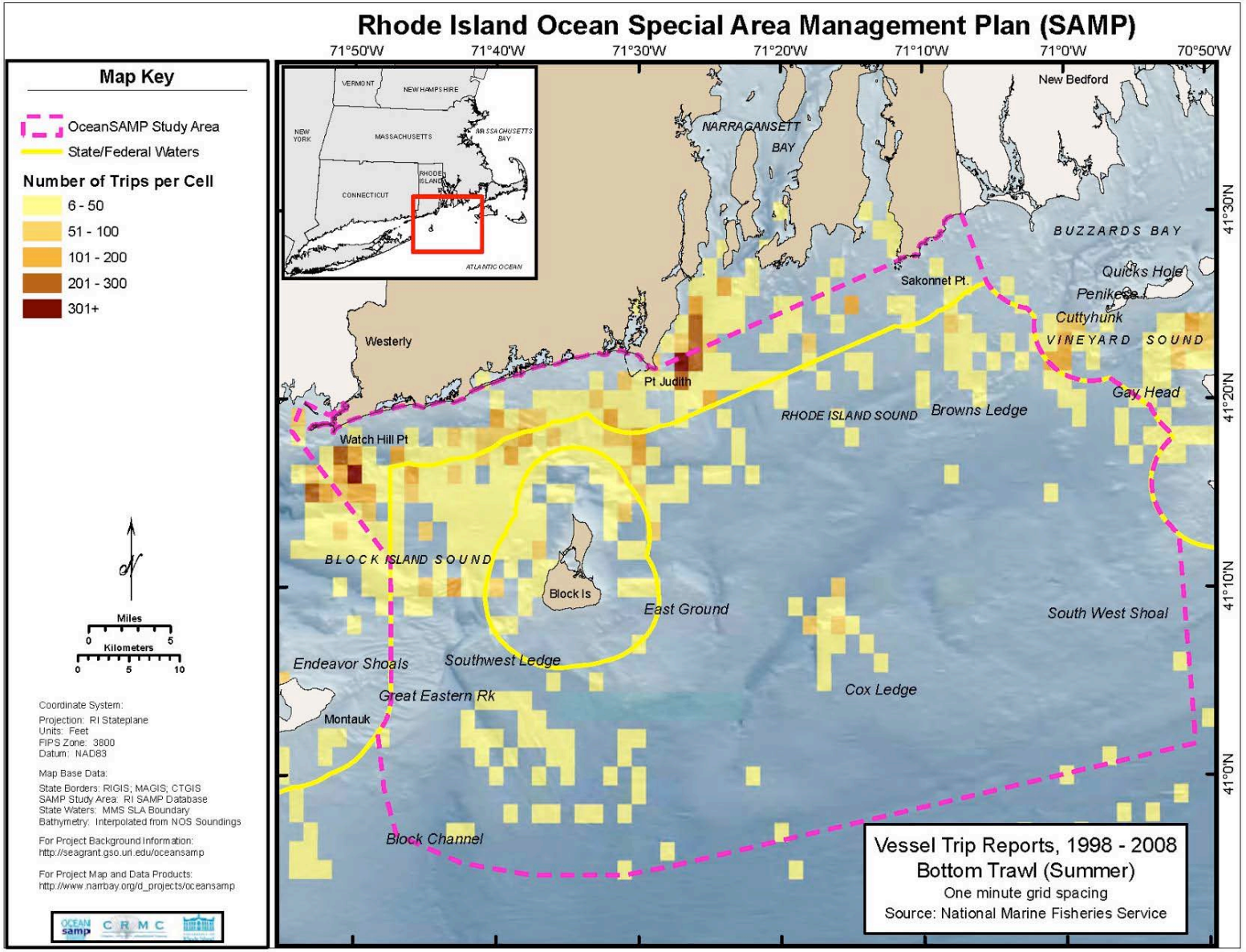

Figure 8. Bottom Trawling, Fall, Based on NMFS Vessel Trip Reports, 1998 - 2008

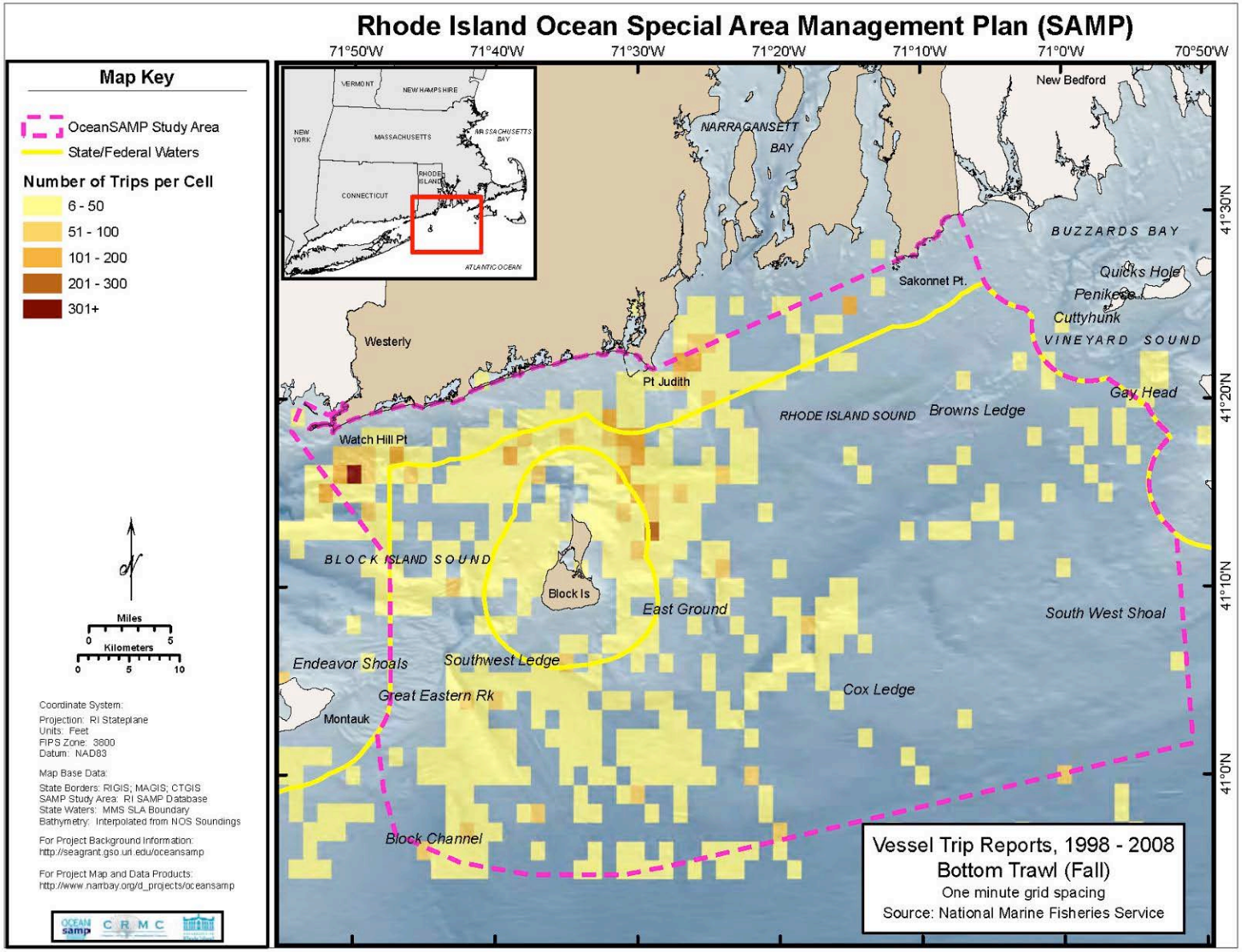

Figure 9. Gillnetting, Winter, Based on NMFS Vessel Trip Reports, 1998 - 2008

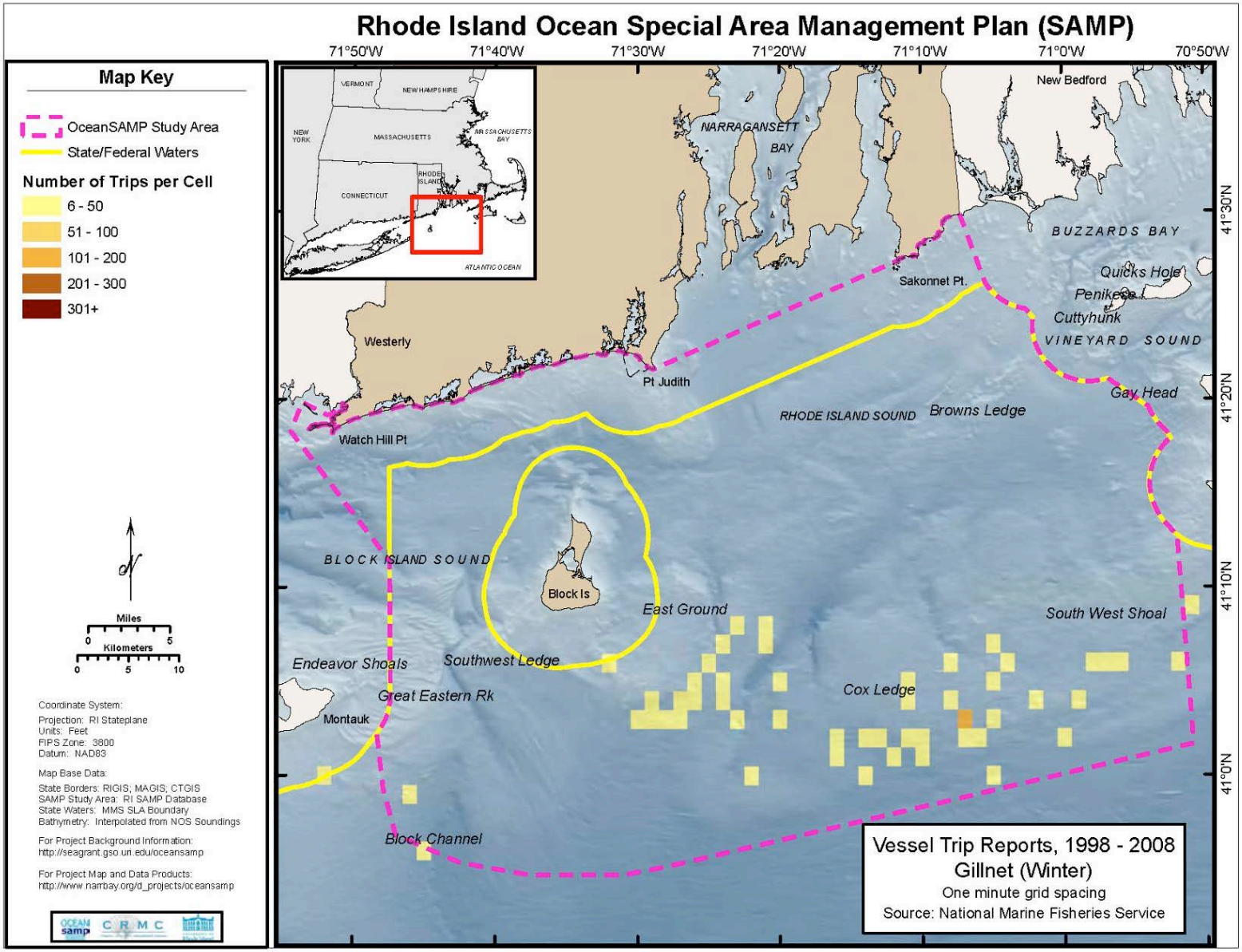

Figure 10. Gillnetting, Spring, Based on NMFS Vessel Trip Reports, 1998 - 2008

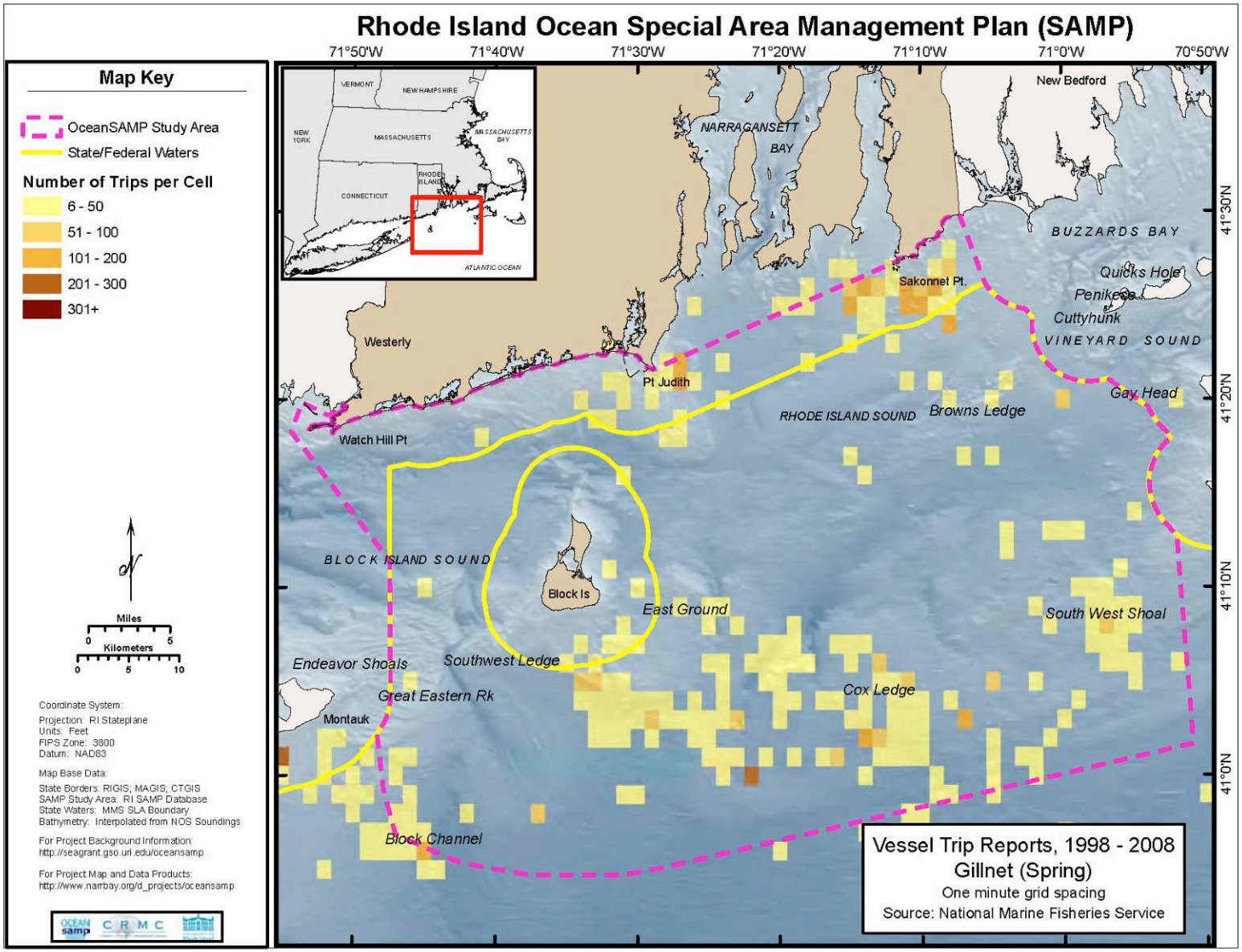

Figure 11. Gillnetting, Summer, Based on NMFS Vessel Trip Reports, 1998 - 2008

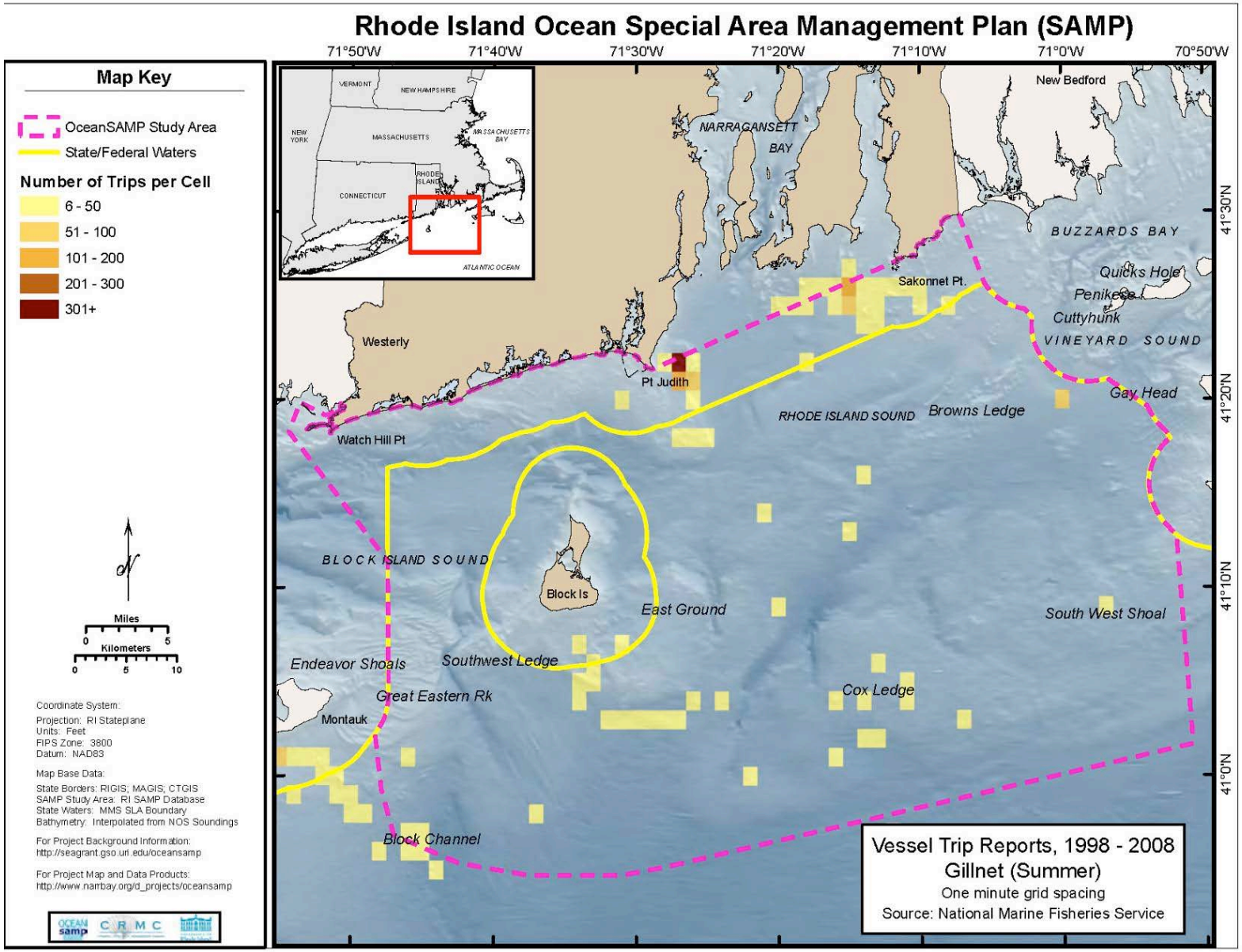

Figure 12. Gillnetting, Fall, Based on NMFS Vessel Trip Reports, 1998 - 2008

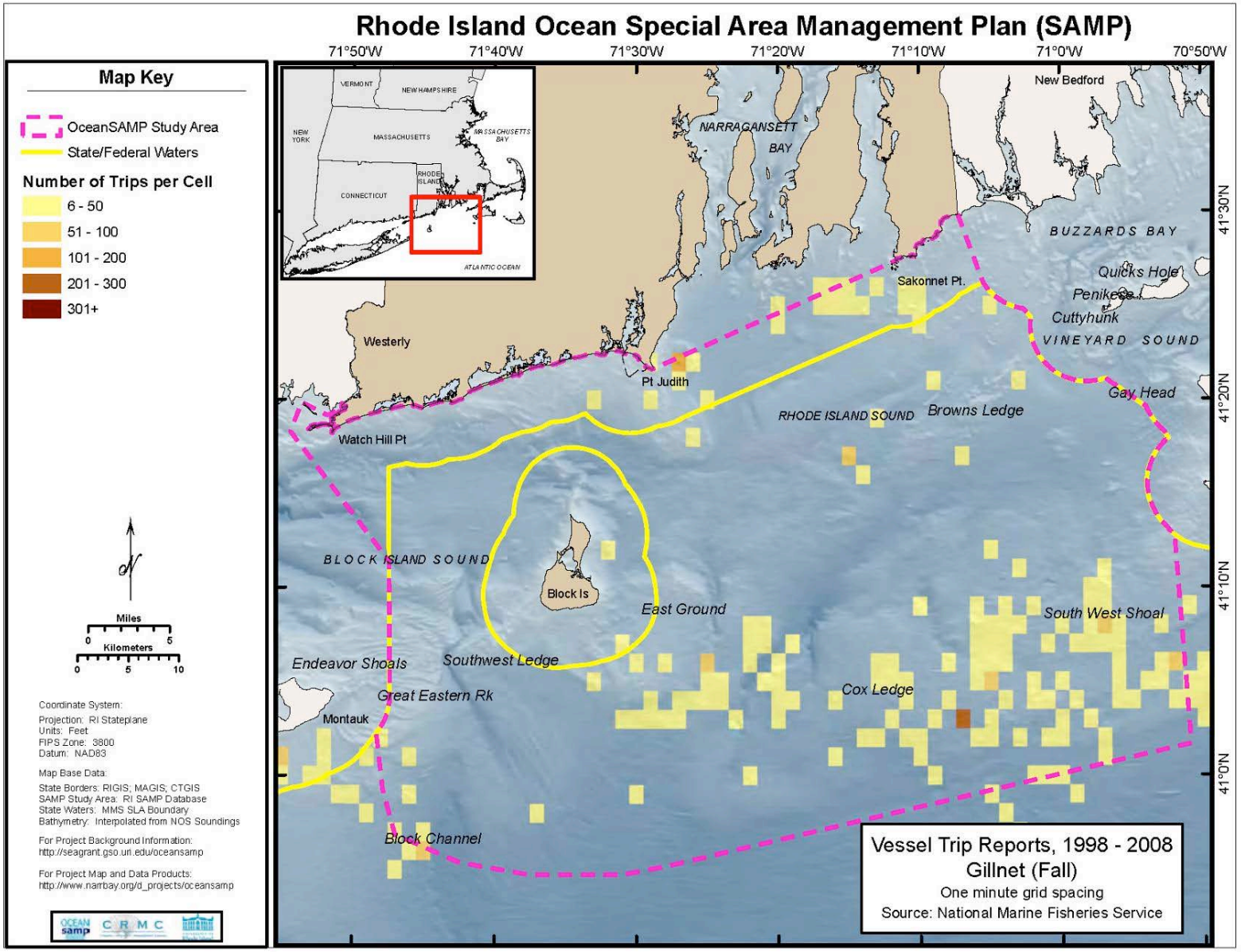

16.

Application of Technology Development Index and Principal Component Analysis and Cluster Methods to Ocean Renewable Energy Facility Siting for the Rhode Island Ocean Special Area Management Plan 2010

by

M. L. Spaulding[1], A. Grilli[1], C. Damon[2], and G. Fugate[3]

[1]Ocean Engineering, and [2]Environmental Data Center,

University of Rhode Island,

Narragansett, RI 02882

[3] RI Coastal Resources Management Council

Wakefield, RI 02879

February 2, 2010

Executive Summary

To assist in siting of offshore renewable energy facilities (wind, wave, and in-stream tidal and ocean current) a marine spatial planning based approach is proposed. The first level (Tier #1) screening determines the potential energy resource to be exploited and then identifies areas that are prohibited from siting because there is a direct, irreconcilable conflict, as determined by a stakeholder process and vetted by regulators. Areas that remain after these exclusions are implementeded are candidates for facility siting. The next step involves considering technical (engineering and economic) attributes of the proposed energy development that further restricts the area under consideration. Finally Tier #2 screening (not addressed here) evaluates other use conflicts such as recreational and commercial fishing areas, marine mammal feeding and breeding grounds and transit paths, bird migratory paths, feeding, and nesting areas, and similar that must be considered in facility siting.

To facilitate the application of technology constraints on siting, two methods are proposed, a Technology Development Index (TDI) and a Principal Components - Cluster Analysis (PCCA). The TDI method, developed by the authors and presented in this paper, is ratio of the Technical Challenge Index (TCI) to the Power Production Potential (PPP) of the energy extraction device. TCI is a measure of how difficult it is to site the device at a given location plus a measure of the distance to the closest electrical grid connection point. The PPP is an estimate of the annual power production of one of the devices. The site with the lowest TDI represents the optimum location. In practice, the study area is gridded and the TDI (TCI and PPP) is calculated for each grid. The method explicitly accounts for the spatial variability of all input data. Simulations can be performed either deterministically or stochastically, using a Monte Carlo method, so that uncertainties in the underlying input data are reflected in the estimated values of the TDI. The later approach allows detailed assessment of the sensitivity of the estimates to the input data and formulations of the TCI and PPP. The results are presented in the form of contours of TDI. The method can be applied to any offshore renewable energy type or extraction system once the technical attributes are specified.

The PCCA approach uses several spatially varying variables that describe the key attributes of the siting decision (e.g. water depth, power production potential, distance to shore, and seabed conditions). The principal components are first determined from the gridded data and then

clusters are identified. Finally the clusters are mapped to the study area. The attributes and spatial distribution of clusters provide insight into the optimum locations for development.

The two methods were employed in identifying potential areas for siting of a wind farm in coastal waters of Rhode Island, assuming lattice jacket support structures for the wind turbines. Both methods give consistent results and show locations where the ratio of technical challenge to power production is minimized.

Table of Contents

List of Figures

List of Tables

Abstract

To assist in siting of offshore renewable energy facilities (wind, wave, and in-stream tidal and ocean current) a marine spatial planning based approach is proposed. The first level (Tier #1) screening determines the potential energy resource to be exploited and then identifies areas that are prohibited from siting because there is a direct, irreconcilable conflict, as determined by a stakeholder process and vetted by regulators. Areas that remain after these exclusions are implementeded are candidates for facility siting. The next step involves considering technical (engineering and economic) attributes of the proposed energy development that further restricts the area under consideration. Finally Tier #2 screening (not addressed here) evaluates other use conflicts such as recreational and commercial fishing areas, marine mammal feeding and breeding grounds and transit paths, bird migratory paths, feeding, and nesting areas, and similar that must be considered in facility siting.

To facilitate the application of technology constraints on siting, two methods are proposed, a Technology Development Index (TDI) and a Principal Components - Cluster Analysis (PCCA). The TDI method, developed by the authors and presented in this paper, is ratio of the Technical Challenge Index (TCI) to the Power Production Potential (PPP) of the energy extraction device. TCI is a measure of how difficult it is to site the device at a given location plus a measure of the distance to the closest electrical grid connection point. The PPP is an estimate of the annual power production of one of the devices. The site with the lowest TDI represents the optimum location. In practice, the study area is gridded and the TDI (TCI and PPP) is calculated for each grid. The method explicitly accounts for the spatial variability of all input data. Simulations can be performed either deterministically or stochastically, using a Monte Carlo method, so that uncertainties in the underlying input data are reflected in the estimated values of the TDI. The later approach allows detailed assessment of the sensitivity of the estimates to the input data and formulations of the TCI and PPP. The results are presented in the form of contours of TDI. The method can be applied to any offshore renewable energy type or extraction system once the technical attributes are specified.

The PCCA approach uses several spatially varying variables that describe the key attributes of the siting decision (e.g. water depth, power production potential, distance to shore, and seabed conditions). The principal components are first determined from the gridded data and then

clusters are identified. Finally the clusters are mapped to the study area. The attributes and spatial distribution of clusters provide insight into the optimum locations for development.

The two methods were employed in identifying potential areas for siting of a wind farm in coastal waters of Rhode Island, assuming lattice jacket support structures for the wind turbines. Both methods give consistent results and show locations where the ratio of technical challenge to power production is minimized.

1 Background

Rhode Island's(RI) Coastal Resources Management Council (CRMC) is currently leading an Ocean Special Area Management Plan (SAMP) (http://seagrant.gso.uri.edu/oceansamp/) that will result in zoning of the state's coastal water to accommodate a wide variety of uses, including renewable energy development. In this effort, identification of sites for offshore renewable energy facilities (wind, wave, and in-stream tidal and ocean current) is being performed using a marine spatial planning based approach (geographic information system (GIS) analysis). The planning process is proceeding on an accelerated schedule and requires selection of those areas in the SAMP region where limited funds for site assessment should be focused. Basic level (Tier #1) analysis is therefore being used to identify those areas where detailed analysis on siting constraints and conflicts with other uses or ecosystem attributes is anticipated as being most valuable.

Methods for siting of offshore renewable energy facilities (wind, wave, and in-stream tidal and ocean current) have been under development for the past two decades in Europe but are just beginning in the US. The most well developed approaches (see Marine Resource Assessment System, MarS, used by the UK Crowne Estates as an example, http://www.thecrownestate.co.uk/mars) employ a multi-step, marine spatial planning protocol that develops geographic information system (GIS) maps of the energy resource and any constraints on siting of extraction facilities. This mapping and constraint analysis exercise identifies areas with conflicts in use and ultimately those with development potential. This is followed by a detailed sustainability and financial analysis for each development effort. The weighting methods used in performing these analyses are often treated as proprietary by the authority exercising control of the seabed and not available for review or evaluation.

In the US, offshore renewable energy siting studies (e.g. Cape Wind development in Nantucket Sound, MA, http://www.capewind.org/) have typically been led by the developer with evaluations of prime and alternative sites for the proposed facility. An assessment of the site selection process is performed as part of the environmental permitting process by either the US Army Corp of Engineers (for developments in state waters) or the Minerals Management Service (for federal waters). Since most state and federal waters are not explicitly zoned for renewable energy development the proposer has wide latitude in proposing prime and alternate sites. This

approach does not lend itself particularly well to marine spatial planning and its promise to help protect and restore ocean ecosystems while minimizing negative impacts and conflicts from human activities.

The present paper outlines the basic first level (Tier#1) marine spatial screening approach used in the RI Ocean SAMP study, including the use of one new method (Technology Development Index (TDI)) and the application of a well known technique (Principal Component – Cluster Analysis (PCCA)) for assessing the technical aspects of the development. The overall strategy is outlined first and the TDI and PCCA described in detail. As a demonstration, the Tier #1 approach is applied to siting of an offshore wind farm in RI coastal waters, with particular emphasis on the results of the application of the TDI and PCCA. Extension to Tier #2 screening, using the same conceptual strategy is currently in progress and will be reported in subsequent publications.

2 Approach

To provide a framework to assist in siting of offshore renewable energy facilities (wind, waves, in-stream tidal currents, and mean currents) a marine geospatial screening analysis is proposed. The analysis is divided into two separate tiers. Tier #1 screening begins with an assessment of the energy resource to be exploited. This information is normally given in terms of the speed of the flow or the energy density. As an example, for wind and water currents the resource could be specified in terms of mean speed (m/sec) or mean flow energy density (kW/m^2), while for waves one might use the mean wave energy density (kW/m). The values are typically displayed as gridded data on the area of interest. For wind and water currents the values are normally presented at hub height of the extraction device. If the speed or energy density is below a specified limit then exploitation of the resource is not economically viable and hence no further analysis is required. These thresholds are dependent on the local cost of energy (with or without subsidies) and the state of technology development. Some commonly used, but not definitive thresholds are: wind speeds greater than 7 m/sec at hub height, water current speeds greater than 1.5 m/sec, and wave energy densities greater than10 kW/m. It is important to note that since the energy densities are generally low, a large number of devices (10s to 100s) are typically required to generate grid scale power. These devices are typically distributed over a large area given the need to minimize the interaction between extraction devices. As an example, the spacing for offshore wind turbines is on the order of 10 blade diameters in the principal flow direction and 6 blade diameters in the cross flow direction.

If the energy density is sufficient to warrant development then an analysis is performed to determine any constraints imposed by existing uses within the study area. As example, existing uses or restrictions might include regulated marine transportation areas (shipping lanes, precautionary areas, preferred routes, ferry routes), regulated uses (disposal sites, unexploded ordnance, marine protected areas and conservations zones, military areas), areas permitted /licensed for existing developments (oil and gas, offshore renewable, aggregate extraction, aquaculture), set backs from airports, and a coastal buffer zone. These might be viewed as strong or hard constraints since the two uses are incompatible. Note that other uses (occasional vessel traffic, impacts on view shed) might be viewed as weak or soft constraints that can be evaluated as part of a tradeoff study). Whether a constraint is considered hard or soft is normally vetted through a stakeholder process and ultimately subject to review by regulators. This analysis is performed by overlaying GIS layers for each of the uses, with each layer further reducing the area available for energy facility siting.

In the next step, two fully independent methods are proposed to help further narrow the viable areas: the Technology Development Index (TDI) and application of the widely known Principal Component - Cluster Analysis (PCCA) approach. The motivation for this step is to determine from a technical point of view which areas are most appropriate for development. Each method is explained separately below. As an alternative to the strategy above, it is possible to perform the TDI and PCCA analyses first and then the constraint analysis.

2.1 Technology Development Index (TDI)

The Technology Development Index (TDI) is defined as the ratio of the Technical Challenge Index (TCI) to the Power Production Potential (PPP). In brief, it gives an estimate of how difficult it is to site the energy extraction device relative to the power production potential if the device is sited at that location. The method is normally applied on a square grid that represents the study area.The grid resolution is dependent on the availability of input data.

$$TDI = TCI/PPP \quad (1)$$

The minimum value of the TDI is the optimum siting location since it is the site with the lowest ratio of TCI to PPP.

$$PPP = W \times CF \quad (2)$$

where

W- annual mean power density at the extraction site (kW/m or kW/m^2)

CF- capacity factor is the ratio (normally expressed in percent, %) of a power plant's actual production over a given period of time with the amount of power the plant would have produced if it had run at full capacity for the same amount of time (Justus et al, 1976; Hennessey, 1976). CF principally depends on the temporal characteristics of the energy resource and the power production curve for the extraction device. It inherently accounts for the intermittency of the energy source. Note that the CF adjustment in Equation 2 is not necessary, if CF is assumed constant over the study area.

In the case of offshore winds, W is the mean annual power density (kW/m2) at hub height and CF is approximately 35% (RERL, 2008). For waves, W is the mean annual power density in kW/m of wave front and CF is comparable to the value for wind. Additional factors could be considered in the formulation of PPP, such as power production during peak usage periods, if desired by the user.

TCI represents the technical challenge associated with the placement of a extraction device at a given offshore location and delivery of power to the electric grid. It has two major components; the first represents the support and foundation structure for the device and the second the distance from the site to the closest electrical grid connection point. The TCI for the support and foundation system is based on the technology type. The value may be adjusted to address the impacts of water depth, extreme wind and wave loading conditions, mooring constraints, the difficulty in installing the foundation (driving piles, drilling and grouting) and others. It is noted that the cost or technical challenge of the extraction device itself (wind turbine, in stream tidal current turbine, or wave energy conversion device) is not included in the analysis since it is assumed to be the same at all sites and hence does not contribute toassessing the differences between various sites.

The proposed formulation is:

TCI = TT +CD (2)

where

TT- Technology Type. The values here depend on the energy extraction system and its associated support structure and foundation system.

CD – Prorated Cable Distance (distance to the electrical grid x SF/number of energy extraction devices in the field) where SF is a scaling factor. This formulation prorates the technical challenge of installing the main power cable to shore over all extraction devices in the

field. Cabling within the extraction device field is not included since it would be the same for any field of similar devices. The scaling factor weights the technical challenge of cable installation relative to the TT values used in the analysis. As an example, if the metric used in defining TT is monetary then SF is the cost of the cable per unit distance (Green et al, 2007) If the field contains a large number of devices (100s) CD is generally small compared to TT.

TCI can be estimated by numerical values assigned to each of the categories ranked in level of difficulty based on professional judgment (say 1 to 5, with 5 being the most difficult). Ideally TCI could be estimated from the structure design and installation and associated cost for a given location.

As an example of the later, Table 1 provides Roark's(2008) assessment of the relative costs with each technology type for mono-pile and lattice jacket based wind turbine support structures for varying water depths.

Table 1 TT values (cost) for mono-pile and lattice jacket wind turbine support structures as a function of water depth (Roark, 2008).

Mono-piles -	$ 2.9 M, water depths - 5 to 25 m, not viable in deeper water depths
Lattice Jacket –	$ 3.36 M water depths - 5 to 25 m
	$ 4.48 M water depths 25 to 45 m
	$ 5.76 M water depths 45 to 65 m

Comparable estimates for lattice jacket structures for the German North Sea AlphaVentus (30 m water depth) (Seidel, 2007) and Beatrice, Moray Firth, Scotland (42 m water depth) (Talisman Energy, 2004) projects are $3 M and $4.5 M, respectively and in reasonable agreement with the trends given in Table 1. Estimates in Table 1 might be adjusted to account for the effort required to install pilings to support the wind turbine. As an example, if the depth to bedrock is quite shallow, compared to the water depth, the TT values would be multiplied by a degree of difficulty to account for the increased technical challenges (drilling and grouting or alternatively vessel days on site) of installing the pilings. This multiplier could also be determined by cost.

In application, the TDI is calculated for a grid covering the study area. The resolution of the grid is typically dependent on the availability of input data. To minimize the computational effort, TDIs only need to be estimated where the energy resource is above the minimum threshold for power production and can exclude areas based on constraints imposed by the TT.

As an example, for a mono-pile based wind power device the mean wind speed at hub height must exceed 7 m/sec and the water depth be less than 25 m. Prediction of TDI can be made using discrete values at each site or performed as a Monte Carlo simulation where uncertainties in the input data can be approximated with an appropriate distribution function. The distribution functions may be different for different variables in the problem.

Model predictions are displayed in terms of the mean (and standard deviations if Monte Carlo simulations are employed) of the TDI for a given technology type. The TDIs can also be converted to non-dimensional form by dividing by the lowest possible TDI in the study area (the grid with the highest PPP, zero cable distance, and the lowest TT). (TDI in italics denotes the non dimensional form of TDI). The location of this site is really hypothetical since the highest PPP is not likely to be at the same position as the lowest TT. The non dimensional TDI values start at 1 and go higher, where values close to 1 represent optimum sites.

2.2 Principal Component – Cluster Analysis (PCCA)

Principal Component Analysis (PCA) is a mathematical procedure (Jolliffe, 2002; Zuur et al, 2007) that transforms a number of potentially correlated variables into a smaller number of uncorrelated variables called principal components. The first principal component accounts for as much of the variability of the data as possible and each succeeding component for as much of the remaining variability as possible. In practice the first several principal components account for most of the variability of the data. PCAs are often used in exploratory analysis of data and for developing predictive, data based models. They are typically used to reveal the internal structure of the data in a way that most simply explains the data variance.

The principal component data are then grouped into homogeneous clusters using the k-means clustering method (Lloyd, 1982 and Ding C. and X. He, 2004). In this approach, each cluster in the partition is defined by its member objects and centroid. The centroid for each cluster is the point from which the sum of distances from all objects in the cluster is minimized. The method uses Lloyd's iterative algorithm that minimizes the sum of distances from each object to its cluster centroid and over all clusters. Objects are relocated between clusters until the sum cannot be further decreased. The result is a set of clusters that are as compact and well-separated as possible and representative of the data. The clusters can then be mapped back to the grid from

which the original data were obtained to develop a picture of the spatial distribution of the clusters.

3 Application

To demonstrate the approach, an application of the screening methodology, through the Tier #1 level, to siting of an offshore wind farm in RI coastal waters is presented. An earlier screening study for offshore wind development has been performed by RI Office of Energy Resources (ATM, 2007a, b). The present work is part of an Ocean Special Area Management Plan (SAMP) being developed for these coastal waters and an extension of the earlier ATM investigation. The study area is shown in Figure 1 and is bounded by the RI coast on the north, Connecticut and New York state borders (Long Island Sound) to the west, Massachusetts state border to the east (Buzzards Bay), and the outer boundary, 50 km offshore. The area includes Block Island Sound (western side) and RI Sound (eastern side) in their entirety. The state waters boundaries (3 mi, 5.6 km) are provided. The figure also shows contours of the water depth based on the NOAA bathymetric data (NGDC Coastal Relief Model. http://www.ngdc.noaa.gov/mgg/coastal/coastal.html).

Figure 2 shows an overlay on Figure 1 of the regulated areas that are considered to be hard constraints for siting of a wind farm. These hard constraints were vetted through a stakeholder process, with concurrence of the state and federal regulators. These include designated shipping lanes, precautionary areas, preferred navigation routes, ferry routes, dredged material disposal and unexploded ordnance sites, military areas, set backs from airports, and a coastal buffer zone. There are no marine protected areas and conservations zones, or areas permitted /licensed for existing developments (oil and gas, offshore renewable, aggregate extraction, aquaculture) in the study area. The data for each of these regulated areas was acquired from the NOAA Electronic Navigation Chart data base (http://www.nauticalcharts.noaa.gov/mcd/enc/index.htm). While cable routes and areas are provided on the NOAA ENC's they are not included here since the cable locations are well mapped and not considered a conflict with siting of wind turbine support structures.

3.1 TDI Method

The TDI was estimated on a 100 m square grid covering the study area. PPP was determined at a proposed hub height of 80 m using AWS True Winds wind speed data (Brower, 2007) by interpolating wind speed data from model predictions made at heights of 70 and 100 m. The friction coefficient (Hsu et al, 1994) is estimated at each grid cell from AWS data at those two levels. The value is approximately constant at 0.134. Figure 3 shows the contours of wind speed for the study area. The wind speed data was then converted to wind power per unit area of the wind turbine. While the mean wind speed increases gradually with distance offshore, from 7 to 9.6 m/sec, 37%; the wind power increases by a factor of 2.6. Grilli and Spaulding (2009) have performed a detailed comparison of model predictions to observations in the study area. The difference between predictions and measurements is normally distributed with an average value of about 0.17 m/sec and a standard deviation of 0.13 m/sec.

The TT for each location was estimated using the data in Table 1, assuming use of lattice jacket support structures for the wind turbines. The data in the table were fit with a linear regression with water depth. The water depths (Figure 1) were obtained for the NOAA gridded bathymetric data. In this case, the cable length was assumed to be the closest straight line distance to shore and the field to contain 70 wind turbines. The scaling factor was set at 0.8 (Green et al, 2007).

Figure 4 provides a contour map of the non-dimensional TDI for the study area. The TDI varies from 1 to 2.1. The large scale pattern shows that the TDI decreases with distance from the coast, displays a broadly distributed minimum and then increases with further distance offshore. Near the coast the TDI is high because the wind energy available is low, this in spite of the fact that the water depths are generally low. TDI decreases with continuing distance off shore because the wind energy is growing substantially, even though water depth continues to increase. Near the outer boundary of the study domain the wind energy has reached its maximum and begins to level off (seaward of coastal boundary layer), while the water depth continues to increase, and hence results in increasing TDIs. Variations from this large scale pattern are principally a result of the bathymetric variations near the RI coast, south and west of Block Island, and the shallower area in the vicinity of Cox's Ledge and Southwest Shoals (Figure 1).

Sensitivity studies were performed varying the number of turbines in the wind farm and to alternate paths for the cable. These simulations showed that the TDI only became sensitive to variations in CD if the number of turbines in the farm was small.

The effort (and cost) of installing lattice jacket structures is known to be sensitive to composition of the seabed sediments within the upper 30 to 50 m of the sediment column, since piles used to provide the foundation for these four legged structures are typically driven into the seabed at depths comparable to the water depth. The piles are typically either driven or drilled into the sediments/bed rock depending on the geotechnical properties of these materials.

The seabed geology in the study area is dominated by glacial end moraine and lake floor sediments deposited in several incidents of glacial advancements and retreats. A broad summary of the deposits within the upper 50 m of the sediment column is provided in Figure 5. This map is based on the analysis of Stone and Borns (1966), Schafer and Hartshoren (1965), Stone and Sirkin (1996) and Sirkin (1982, 1996). Using this map and sub-bottom survey data collected by Needell and Lewis (1984) in Block Island Sound and Lewis and Needell (1987) in eastern Long Island Sound and smaller scale sub bottom mapping efforts in RI Sound by McMullen et al (2008), a construction effort (geology challenge) map (Figure 6) was developed by glacial geological experts familiar with southern RI waters (J. King and J. Boothroyd, personal communication). The effort was ranked on a scale of 1 to 5. A low ranking indicates deposits amenable to pile driving operations, while the highest values reflect areas with shallow depth to bed rock requiring drilling and grouting techniques to install the piles. Intermediate values (level 3) are indicative of complex end moraine sediment deposits, consisting of a mix of lake-floor sediments, and sand, gravel, and boulders of varying size. Lacking any detailed site specific data the TTs were multiplied by a factor varying from 1 (for Construction Effort Level 1) to 2.3 for Construction Level 5. Variations at intermediate construction efforts were by determined by linear interpolation with construction effort. The construction effort maps are initial estimates and will be refined as additional sub-bottom mapping and geotechnical studies are completed.

Figure 7 shows the TDI when the construction effort effects on the TCI are included. As expected the broad scale pattern remains the same as for the case with no consideration for geology (Figure 5). The range of TDI has however increased from 1 to 2.1 to 1 to 3.5. The largest values are found in the areas of highest construction effort (see area south of Sakonnet Pt in particular). In the end moraine sediments, the values are higher than for the no glacial geology case because of the intermediate values for construction effort. The optimum (lowest TDI) site in state waters is the shallow areas south and southwest of Block Island (Figure 1). For federal waters the optimum site, if distance to shore is considered, is the deep water tongue located

between two end moraine deposit sequences (Figure 5) just landward of Cox's Ledge-Southwest Shoals (Figure 1) in the center of RI Sound.

To understand the impact of uncertainties on the analysis, Monte Carlo simulations were performed to estimate the TDI. The uncertainty in the wind data was assumed to be normally distributed with an average value of about 0.17 m/sec and a standard deviation of 0.15 m/sec (Grilli and Spaulding, 2009). The uncertainty in TT was assumed as a top hat distribution, 15% higher and lower than the values reported in Table 1. The depth data was assumed to be accurate as provided. One hundred simulations were performed to assure an accurate estimate of the mean and distribution of the output. Figure 8 provides the predicted mean, and upper and lower 95% confidence limit TDI. These results can be directly compared to the deterministic case (Figure 7).

The TDI ranges are observed to be largest for the upper 95% confidence limit (1 to 10), smallest for the lower 95% confidence limit (1 to 6.4) and intermediate for the mean case (1 to 6.9). This compares to a range of 1 to 3.5 for the deterministic case (Figure 7). Independent of which analysis is evaluated the differential in TDI across the study area are preserved and identify the most appropriate sites.

In summary, the TCI increases with distance offshore since water depth generally increases with distance and hence the height (size) of the structure and length of support piles driven/drilled into the seabed increases and the distance to the closest grid connection increases. On the other hand, the wind energy (PPP) increases rapidly with distance offshore (Figure 3) as land based roughness effects on the atmospheric boundary layer decrease. This leads to a TDI saddle point (TDI minimum) at an intermediate distance offshore. Topographic variability alters this basic balance as does the effort of driving piles in end moraine and glacial lake deposits characteristically present in the area. The TDI method provides estimates that are robust to variability in the input data and is an objective and quantifiable method to facilitate this intermediate stage of site identification.

3.2 PCCA Method

The PCA analysis method was applied to the study area using the same grid as for the TDI method. The principal component analysis determines the new orthogonal/independent axes (u_i) with each being a linear combination of the original variables (y_i). For the present application four variables (y_i) were used for each grid: h- water depth, W- wind power, CD- distance to

shore, and E - construction effort. Table 2 provides the coefficients for the first two principal components.

Table 2 Dependence for the first two principal components (ui) on the initial four variables (yi) (W- wind power, CD-distance to grid, h- water depth and E- construction effort). A linear fit is assumed.

	u_1	u_2
y_1 (W)	0.5	-0.43
y_2 (CD)	0.52	0.38
y_3 (h)	0.48	-0.57
y_4 (E)	-0.49	-0.58

Application of the method showed that 70, 90, and 98% of the cumulative variance of the original data could be explained by the first, second, and third principal components, respectively.

The data were mapped to the first two principal components domain and from visual examination five clusters were a-priori assumed as a desirable partitioning. Given the five clusters, the k-means clustering method was used to extract the most appropriate clusters to minimize the variance within a cluster and maximizing the variance between cluster centroids. Figure 9 shows the clusters mapped to the first two principal component domain.

Table 3 shows the major attributes of each of the five clusters in terms of the four input variables. The dependence on each is noted in qualitative terms. None of the clusters explicitly represent the optimum for siting of a wind farm. Clusters 1 and 2 however are best, 3 and 5 worst, and 4 is intermediate.

Table 3 Qualitative summary of the major attributes of each cluster in terms of the four input variables.

	Wind Power	***Depth***	***Distance***	***Construction Challenge***
• Cluster 1	Highest	Deep	Far	Low
• Cluster 2	High	Mid	Mid	Low
• Cluster 3	Lowest	Shallow	Close	Mid
• Cluster 4	Mid-High	Mid	Mid	Mid-High
• Cluster 5	Mid-Low	Shallow	Close	High

Figure 10 shows the clusters mapped to the study area. The cluster distributions are primarily oriented in the long shore direction and banded from near shore to offshore. The most desirable sites are located at intermediate to far distances offshore and the least desirable sites close to the coast (see area off Sakonnet Pt). The impact of water depth and construction effort is clearly seen. Visually the basic pattern in the cluster distribution and identification of the most appropriate sites for wind farm development are fully consistent with the prior TDI analysis; the TDI minimum and Cluster 1 and 2 are in the same general locations. To quantify this visual comparison , mean and standard deviations of TDI values were estimated for each cluster (Table 4). The analysis shows that Clusters 1 and 2 have the lowest TDI (1.7 to 1.8), with the smallest standard deviations (0.18 – 0.19). TDIs for Clusters 3 and 5 are highest (2.7 to 2.8) and have the highest standard deviations (0.41 to 0.6). Cluster 4 has an intermediate TDI mean (2.4) and standard deviation (0.26). This quantitative analysis shows that the cluster analysis maps are statistically consistent with the TDI analysis.

Table 4 Mean and standard deviation of TDI for each cluster (see Table 3 for definitions of clusters).

TDI	C1	C2	C3	C4	C5
Mean	1.8	1.7	2.7	2.4	2.8
Std Dev	0.18	0.19	0.41	0.26	0.6

3.3 Other Considerations

To develop a sense of the impact of view shed considerations on siting, an analysis was performed where the size of the coastal buffer zone was progressively increased to 8, 10, 12, 15, and 20 km from all land masses (Figure 11). This progression explores decreasing visualize impact of wind turbines in the field, with the 20 km offset approaching the limit of visibility.

To further consider the impact of marine transportation (in and outside of regulated areas) on siting, Automated Information System (AIS) data was obtained for the study area for Sept 2007 to July 2008. The US Coast Guard mandated AIS provides vessel track data on all commercial traffic in the study area, for vessels with lengths greater than 20 m, with the exception of fishing vessels. Figure 12 shows a plot of vessel traffic density (1 km resolution grid) over the observation period in terms of number of vessel counts. Areas that have fewer than 24 counts are not shown. The high count areas are observed in the in- and out-bound shipping lanes to Narragansett Bay, the precautionary area at the mouth of Narragansett Bay, the preferred east-

west coastal transport route from Buzzards Bay, through RI and Block Island Sound, to Long Island Sound, and a route from the eastern end of Long Island Sound, through the Southwest Ledge channel, and then southwest parallel to the coast of Long Island.

Constraints can be imposed on marine traffic (AIS data), TDI levels, and coastal buffer distances to progressively refine site selection and to optimize for specified siting criteria. As an example, Figure 13 shows the impact of marine traffic restrictions. The upper panel shows the TDI map with no restrictions as a reference, the center panel, restrictions for exclusionary areas, and the lower panel, restrictions for exclusionary areas and areas with AIS counts greater than 24. Figure 14 shows the impact of restrictions on the TDI. The upper panel is once again the TDI map with no restrictions, the center panel, removal of areas with TDIs greater 3.0 (as well as exclusionary areas and AIS counts greater than 24) and the lower panel, the same as the center panel but with TDIs greater than 2.5 excluded. Finally, Figure 15 shows the impact of visual buffers. The upper panel is the TDI with no restrictions, the center panel, a visual buffer of 10 km (as well as exclusionary areas and AIS counts greater than 24), and the lower panel, the same as the center panel but with a visual buffer of 15 km. It is clear that this systematic process can identify sites that minimize TDI, impacts on marine transportation, and visualization. The map overlays also provide a methodology for assessing tradeoffs given varying constraints.

4 Conclusions

A marine spatial planning based screening method to facilitate siting of offshore renewable energy facilities has been presented. This basic strategy has been used for siting of other activities in the Ocean SAMP study area (dredged material, Battelle, 2003) and is an obvious candidate for the present application. Development and application of the TDI and PCCA methods have provided new quantitative tools to assist in the site selection process and in helping to identify and rank locations where facilities can be placed to minimize the technical challenge and maximize the power production potential.

Tier #1, of the two tier screening method, incorporating both the TDI and PCCA analysis methods, has been applied to siting a wind farm in coastal RI waters, as a demonstration case. The approach provides a logical step by step procedure to identify sites and to assess the impact of each input parameter on site selection. It is encouraging that both the TDI and PCCA methods provide consistent results on site selection even though the methods are dramatically different.

The first relies on a fundamental understanding of the development process while the later is based exclusively on the data. The very good agreement, as shown by a statistical comparison between the two, is, in part, due to the selection of parameters used as input to the PCCA. These are consistent with those used in the TDI. The TDI is preferred when TT is well known. The PCCA is very useful when the basic attributes of the energy device are not known. Its performance however is strongly dependent on the assumed input variables. The results of the TDI method are only as good as the input data and the formulation of the basic model. In the demonstration case, bathymetry and distance to the electric grid are judged to quite good. Wind power distribution data for this application is reasonable based on detailed comparisons to wind observations (Grilli and Spaulding, 2009). The seabed sediment maps are broadly consistent with the glacial geology of the study area. Interpretation of the seabed stratigraphy and associated construction effort map is supported by extensive sub-bottom profiles in Block Island Sound (Needell and Lewis, 1984), with penetration to 30 to 50 m or bed rock. There is however, very limited sub-bottom profile data for RI Sound.

The formulation for TT is based on data from a study reported by Roark (2008). The basic dependence of TT on water depth appears reasonable and consistent with data from AphaVentus (Siedel, 2007) and Beatrice developments (Talisman Energy, 2004). Additional validation needs to be performed. Work is progress in the European Mangrove Project (van der Tempel et al, 2008) to evaluate the cost for alternative structures for deep water applications. ODE (2007) and Papalexandrou (2008) have also evaluated costs of offshore wind farm development for varying turbine sizes, water depths, and foundation types. The formulation should also explicitly accounts for environmental loading from both extreme winds and waves. Hensel (2009) has recently developed a formula for TT as a function of structure and foundation weight for various soil conditions, based on sophisticated models for both the structure and foundation. The agreement with Roark (2008) is very good for the sandy soil case. Hensel's (2009) analysis considers sand, soft and stiff clays soils. In assessing the impact of pile driving or drilling operations in various sediment types a simple scaling protocol has been used. This estimate can be substantially improved if additional knowledge of the sea beds sediments (including cores) in the study area were available.

Extension of the basic strategy presented above is currently in progress for Tier #2 screening. An Ecosystem Services Value Index (ESVI) methodology is being developed that quantitatively measures the ecological services for natural resources located in the study area. Initial work on

the ESVI approach has clearly demonstrated that it will be difficult to develop a robust, numerical based planning tool given the lack of consensus on evaluation metrics and the absence and uncertainty of the input data required for the evaluation.

The TDI, PCAA, and ESVI should be viewed as new tools that will assist in an integrated, multi-disciplinary MSP process to assist in siting of renewable energy facilities.

5 Acknowledgements

Jon Boothroyd, Geosciences and John King, Graduate School of Oceanography, University of Rhode Island provided the background information on glacial geology and generated the construction effort map. The project was supported by the RI Ocean SAMP project, led by Grover Fugate, Director Coastal Resources Management Council. The RI Ocean SAMP was funded by the RI Renewable Energy Fund.

References

ATM, 2007a. RI WINDS Phase I, Wind Energy Siting Study, prepared for RI Office of Energy Resources, Providence, RI, April 2007.

ATM, 2007b. RI WINDS Summary Report, prepared for RI Office of Energy Resources, Providence, RI, September 2007

Battelle, 2003. Alternative site screening report, RI Region, Long term dredged material disposal site evaluation project, Contract Number DACW33-01-D-004, June 2003, US Army Corp of Engineers, New England Division, Concord, MA.

Brower, M., 2007. Wind resource maps of Southern New England, prepared by True Wind Solutions, LLC, 10 p.

Dhanju, A., P. Whitaker, and W. Kempton, 2007. Assessing offshore wind resources: an accessible methodology, Rewna Energy (2007), doi:10.1016/j.renene.2007.03.2006.

Ding C. and X. He, 2004. K-means clustering via Principal Component Analysis. Proc. of Int'l Conf. Machine Learning (ICML 2004), pp 225-232, July 2004.

Green, J. et al, 2007. Electrical collection and transmission systems for offshore wind power, Ocean Technology Conference, Houston, TX.

Grilli, A. and M. L. Spaulding, 2009. Evaluation of wind energy resources in southern RI coastal waters for wind energy development, RI Ocean SAMP study report.

Hensel, J.V., 2009. Jacket Structures for offshore wind turbines in RI, MS Thesis, Ocean Engineering, University of Rhode Island, Narragansett, RI, 159p.

Hennessey J.,1977: Some aspects of wind power statistics. Journal of Applied Climatology, Vol. 16,2, 119-128

Hsu, S. A., Eric A. Meindl, and David B. Gilhousen, 1994. Determining the power-law wind-profile exponent under near-neutral stability conditions at sea, Applied Meteorology, Vol. 33, No. 6, June 1994

Jolliffe I.T., 2002. *Principal Component Analysis*, Series: Springer Series in Statistics, 2nd ed., Springer, NY, 2002, XXIX, 487 p. 28 illus. ISBN 978-0-387-95442-4.

Justus C.G. et al., 1976. Nationwide assessment of potential output from wind –powered generators. Journal of Applied Meteorology, Vol. 15, 7, 673-678.

Lewis, R. S. and S. W. Needell, 1987. Maps showing the stratigraphic framework and quaternary geologic history of eastern Long Island Sound, U.S. Geological Survey Miscellaneous Field Studies Map MF-1939-A.

Lloyd, S. P, 1982. Least squares quantization in PCM. Special issue on quantization, IEEE Trans. Inform. Theory, 28, pp. 129–137.

McMullen, K. Y., L. J. Pope, J. F. Denny, T. A. Haupt, and J. M. Crocker,2008. Side-scan sonar imagery and surficial geologic interpretations of the sea floor in central Rhode Island Sound, US Geological Survey, Open File Report 2007-1366, DVD ROM. Also available online at http://pubs.usgs.gov/of/2007/1366/, US Department of Interior.

Needell, S.W., and R. S. Lewis, 1984, Geology of Block Island Sound, Rhode Island, and New York, U.S. Geological Survey Miscellaneous Field Studies Map MF-1621, Scale 1:125,000, 4 sheets.

Offshore Design Engineering (ODE), Ltd, 2007. Study of the costs of offshore wind generation, Report to the Renewables Advisory Board (RAB) and DTI, UK, p114.

Papalexandrou, M. ,2008. Economic analysis of offshore wind farms, Master of Science Thesis, KTH School of Energy and Environmental Technology, Stockholm, Sweden.

RERL, 2008. Wind Power: Capacity Factor, Intermittency, and what happens when the wind doesn't blow?"Renewable Energy Research Laboratory(RERL), University of Massachusetts at Amherst, Amherst, MA. http://www.ceere.org/rerl/about_wind/RERL_Fact_Sheet_2a_Capacity_Factor.pdf. Retrieved on 2008-10-16.

Roark, T., 2008. Offshore wind energy: An international perspective, Roger Williams University, Marine Law Symposium, October 23, 2008.

Schafer, J. P. and J. H. Hartshorn, 1965. The quaternary of New England, in Wright, H.E. Jr., and D. G. Frey (eds.), The Quaternary of the United States, pp 113-128. Princeton University Press, Princeton, New Jersey.

Seidel, M, 2007. Jacket substructures for the Repower 5 M turbine, Conference Proceedings European Offshore Wind 2007. Berlin, Germany, 8p.

Sirkin, L. A., 1982. Wisconsin glaciations of Long Island Sound, New York to Block Island, Rhode Island, in Larson, G. J., and Stone, B.D. (eds.) *Late Wisconsinian Glaciation of New England,* pp 35-39. Kendall/Hunt, Dubuque, Iowa.

Stone, B. D., and L. A. Sirkin., 1996, Geology. Pages 9-23 in A. I. Veeger, and H. E. Johnston, Hydrogeology and water resources of Block Island, Rhode Island: U. S. Geological Survey Water-Resources Investigations Report 94-4096, Providence, Rhode Island.

Sirkin, L., 1996, Block Island geology: History, processes and field excursions: Watch Hill, RI, Book and Tackle Shop, 203 p.

Stone, B.D. and H. Borns, Jr., 1986. Pleistocene glacial and interglacial stratigraphy of New England, Long Island and adjacent Georges Bank and Gulf of Maine, in Quaternary Glaciations in the Northern Hemisphere, Report of the International Geology Correlation Programme, Project 24, V. Sibrava, D. S. Bowen, and G. M. Richmond, (eds.), Pergamon Press, Oxford.

Talisman Energy, 2004. Deepwater offshore wind farm design fabrication and installation study, Final Report Number W/61/000635/00REP, RUN 04/1041, Talisman Energy UK Ltd.

Van der Tempel, J., W. de Vries, V. Krolis, D.C. Salzmann, T. Haverkort, R. Narold, R. Van Glist, H. J. Koopmand, and J. Peeringa, 2008. Mangrove Findings: Offshore wind energy in deeper waters, Delft University of Technology, The Netherlands

Zuur A.F. , E. N. Ieno , and G. M. Smith, 2007. Analyzing ecological data, Springer, New York, 672p.

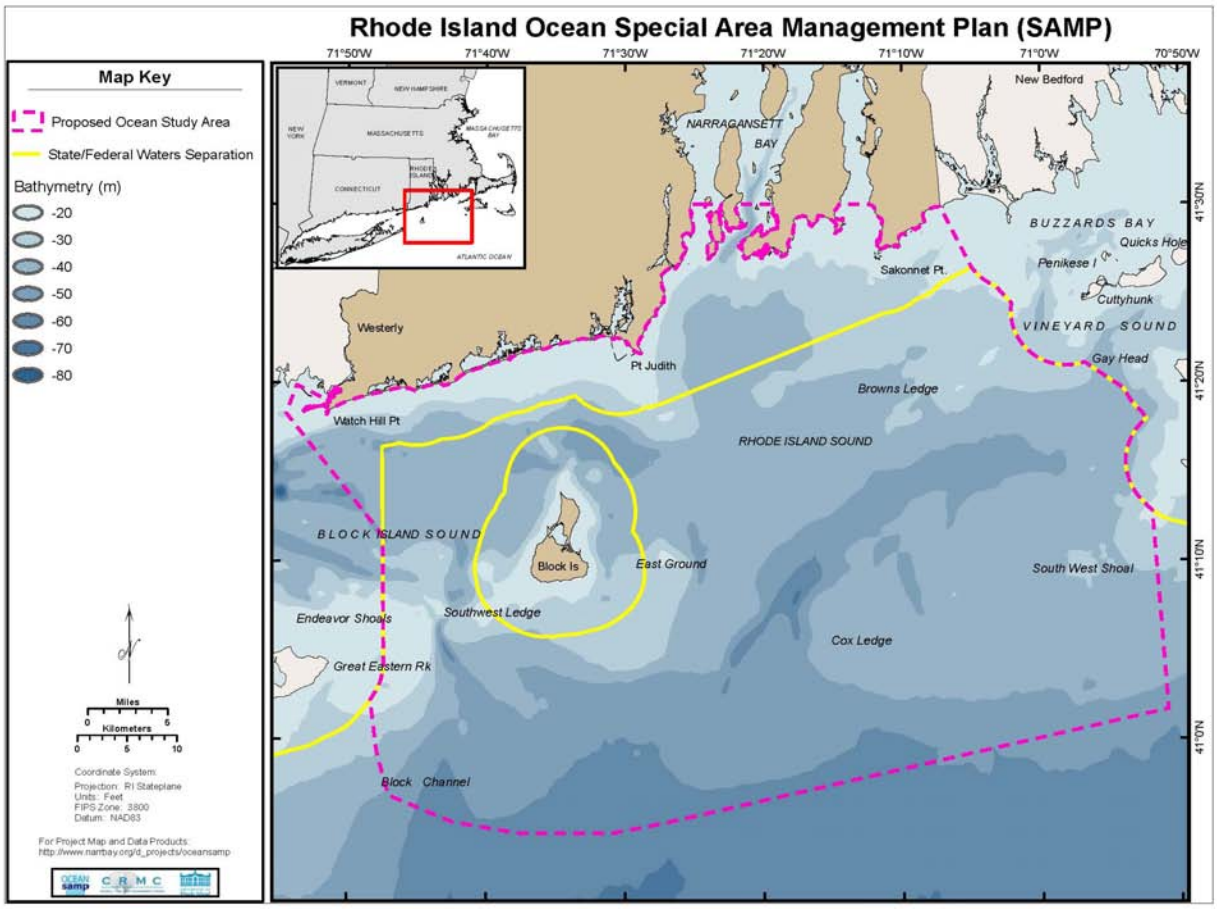

Figure 1 RI Ocean SAMP coastal study area. The dashed line is the study area boundary and the solid yellow line is the boundary of state waters. Key location names are provided as well.

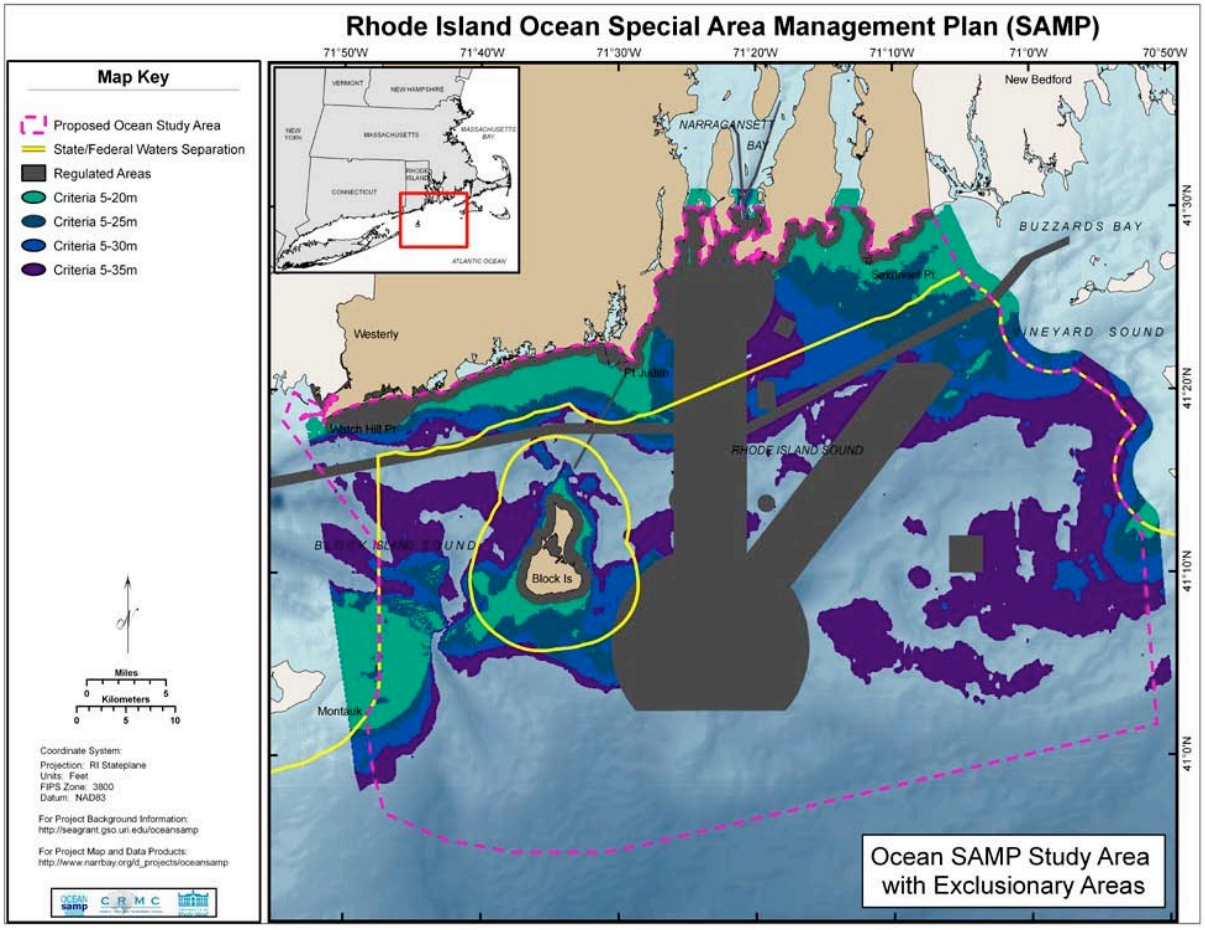

Figure 2 Study area with exclusionary areas (designated shipping lanes, precautionary areas, preferred navigation routes, ferry routes, dredged material disposal and unexploded ordnance sites, military areas, set backs from airports, and a coastal buffer zone) overlaid.

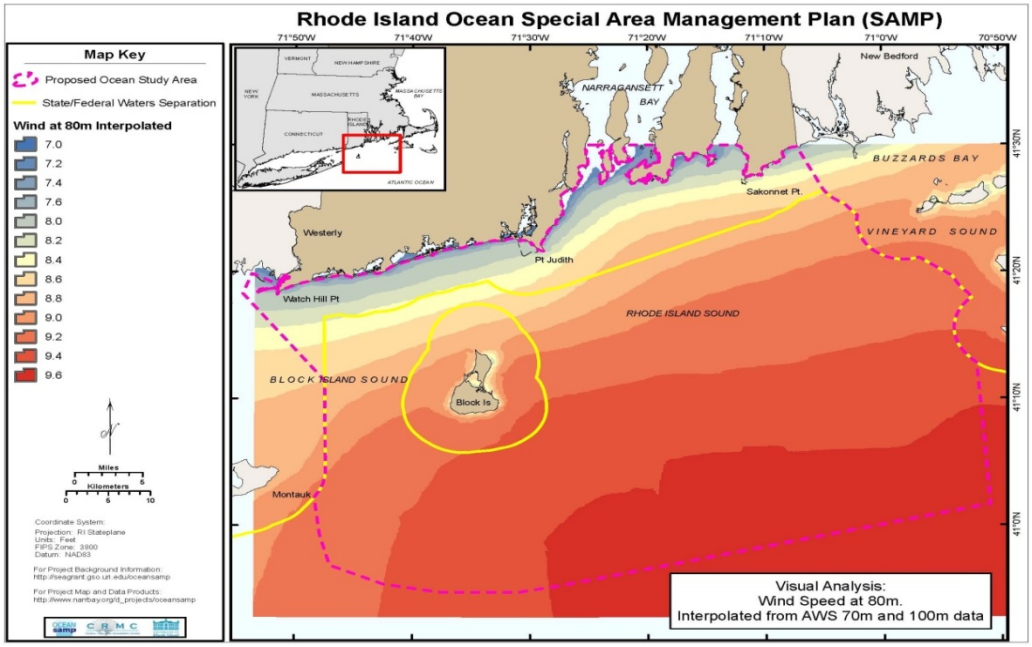

Figure 3 Wind speed contours at 80 m elevation interpolated from data at 70 and 100m from AWS True Solutions (Brower, 2007).

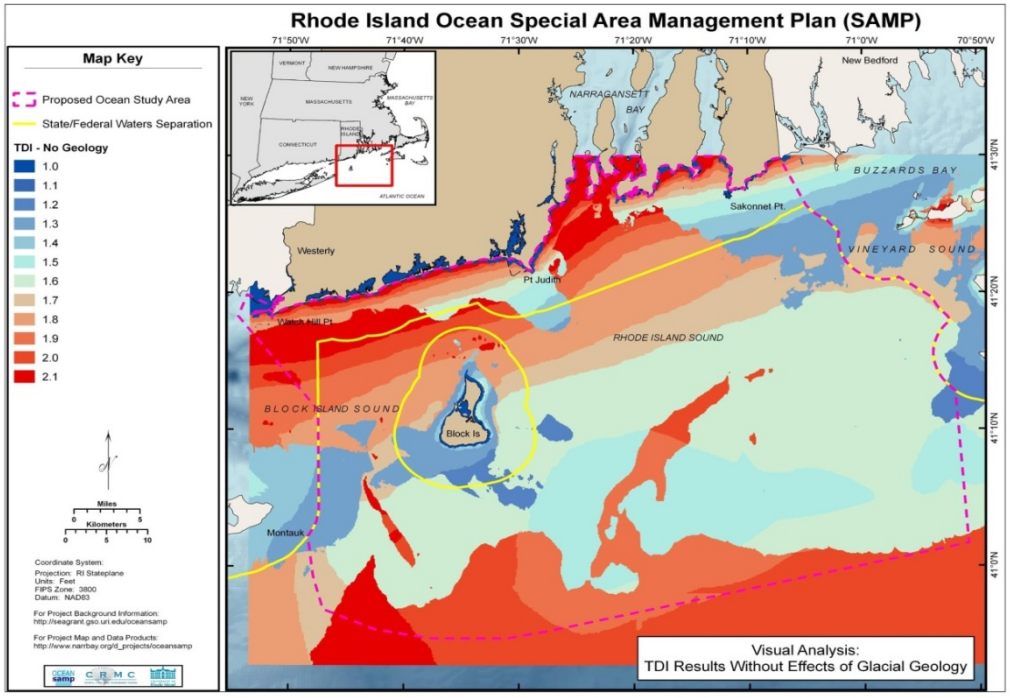

Figure 4 Contours of non-dimensional *TDI* for the study area, without glacial geology.

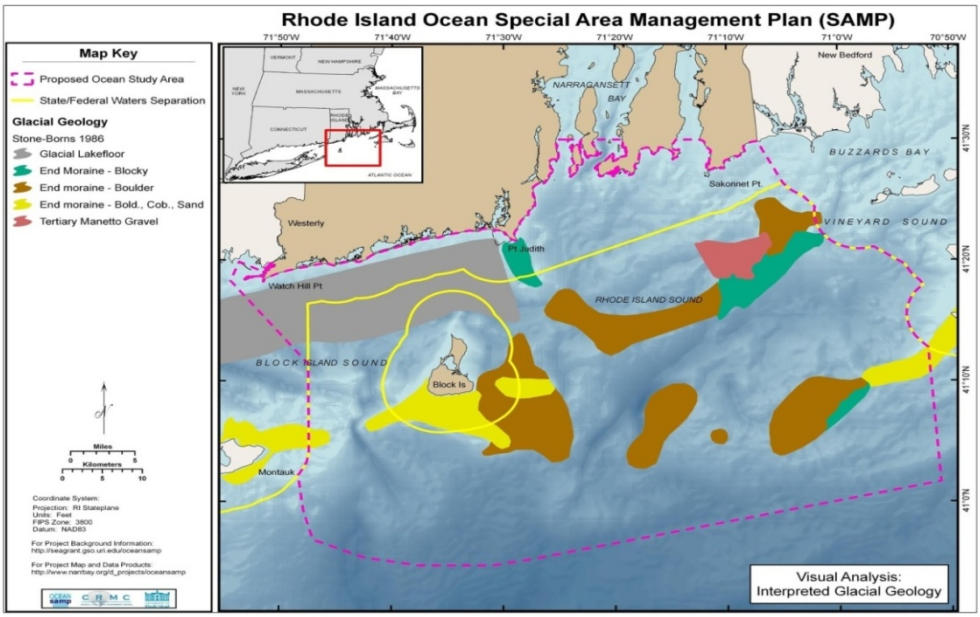

Figure 5 Glacial geology of the study area based on Schafer and Hartshorn (1965), Stone and Borns (1986), Stone and Sirkin (1996), and Sirkin (1982, 1996). Glacial lake floor, end moraine (blocky, boulder, cobble, and sand), and tertiary mannetto gravel deposits are shown.

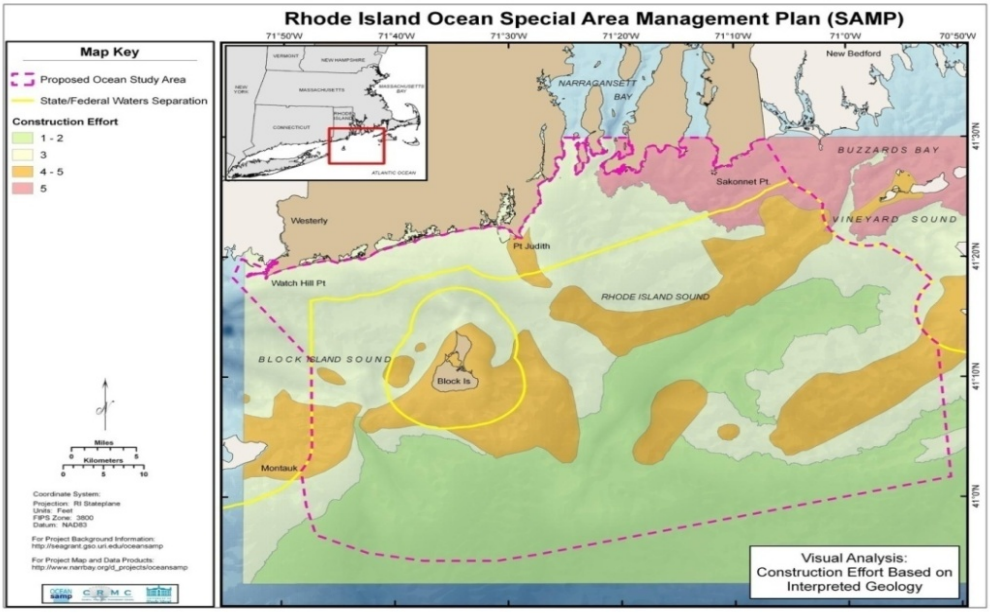

Figure 6 Estimates of the level of construction effort based on the glacial geology (Figure 5) and US Geological Survey (USGS) sub-bottom profile data (Needell and Lewis, 1984). Scale is 1 to 5, where 1 is lowest and 5 is the highest. Prepared by J. Boothroyd, Geosciences, and J. King, Graduate School of Oceanography, University of Rhode Island.

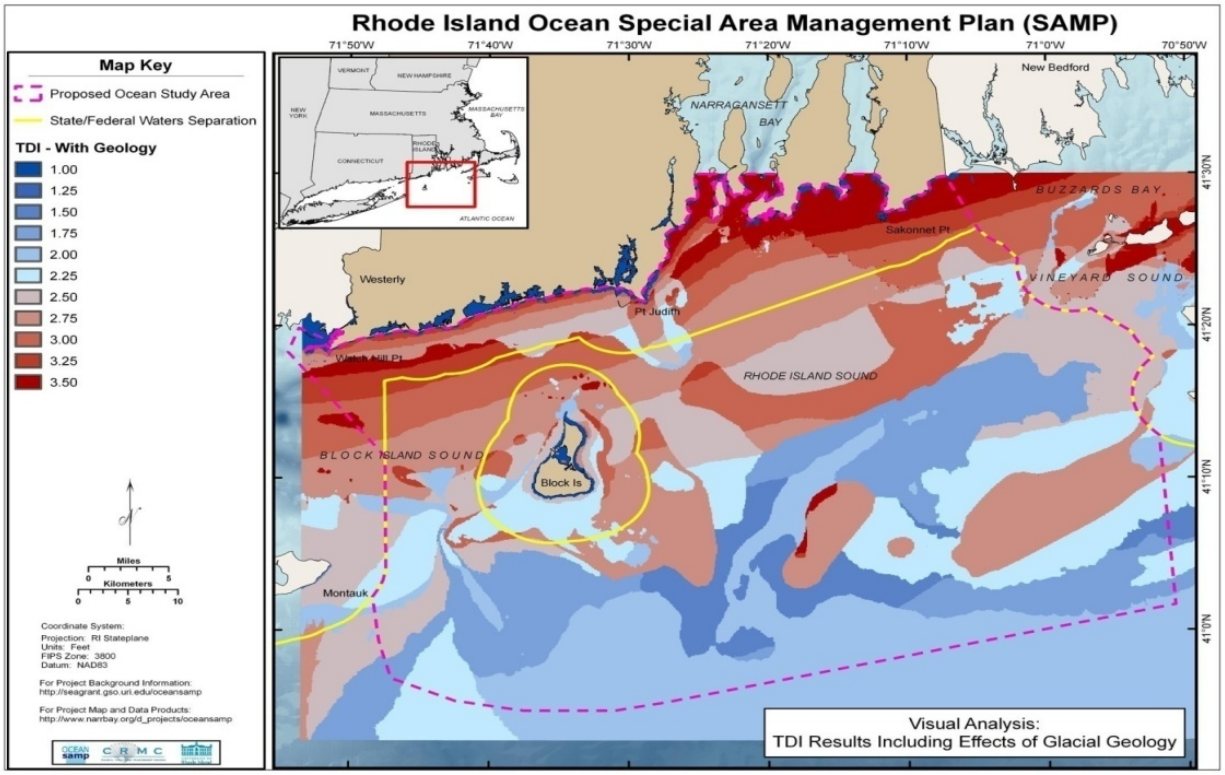

Figure 7 Contours of non-dimensional *TDI* for the study area, with glacial geology.

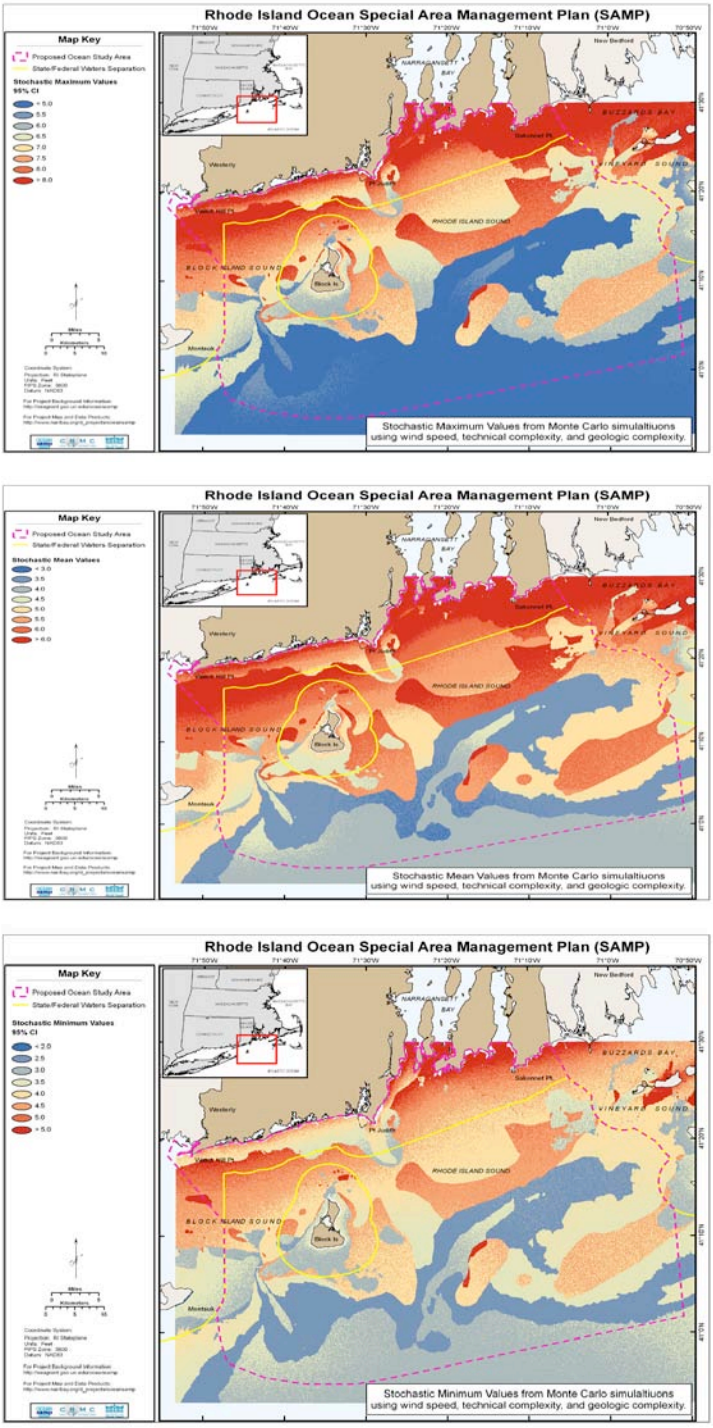

Figure 8 Contours of the non dimensional *TDI* with glacial geology based on Monte Carlo simulation, upper 95% confidence interval (top panel), mean (center panel) and lower 95% confidence interval (lower panel).

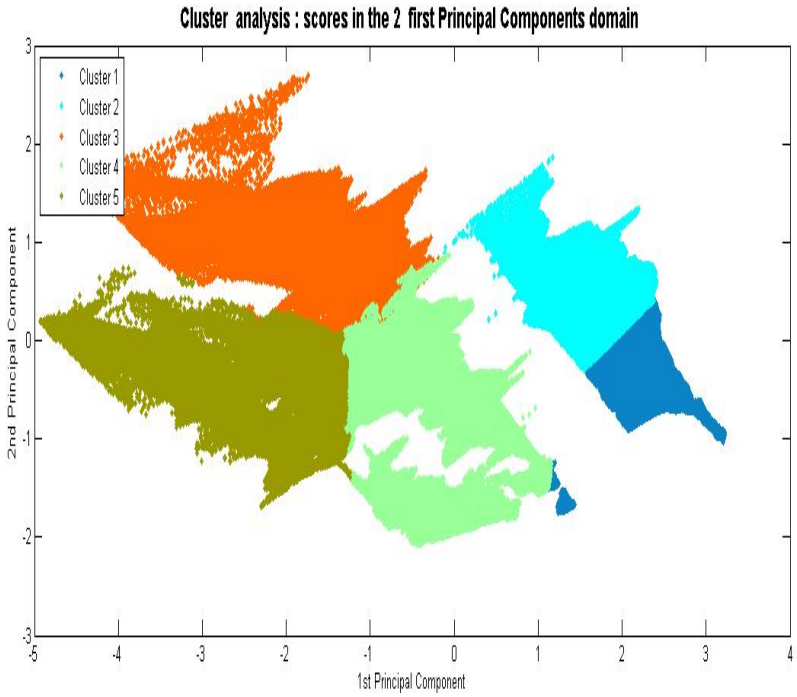

Figure 9 Identification of clusters using the first two principal components for the RI SAMP study area. Cluster definitions, in terms of the input variables, are given in Table 3.

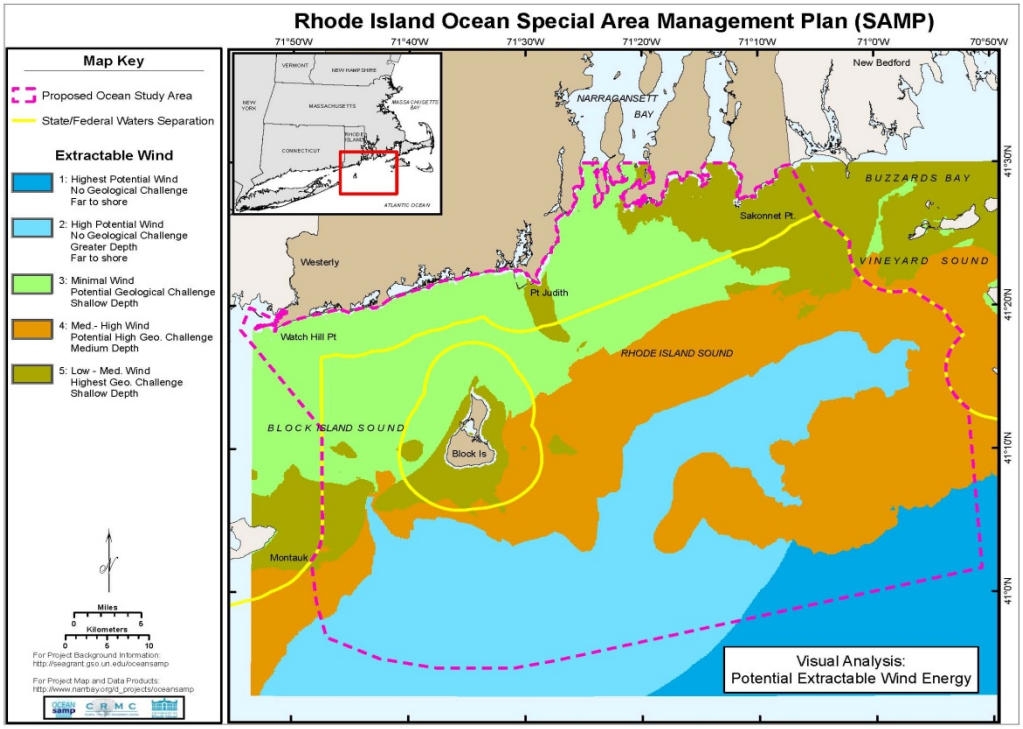

Figure 10 Spatial distribution of the five clusters for the study area. The principal attributes for each cluster are provided in the legend and Table 3.

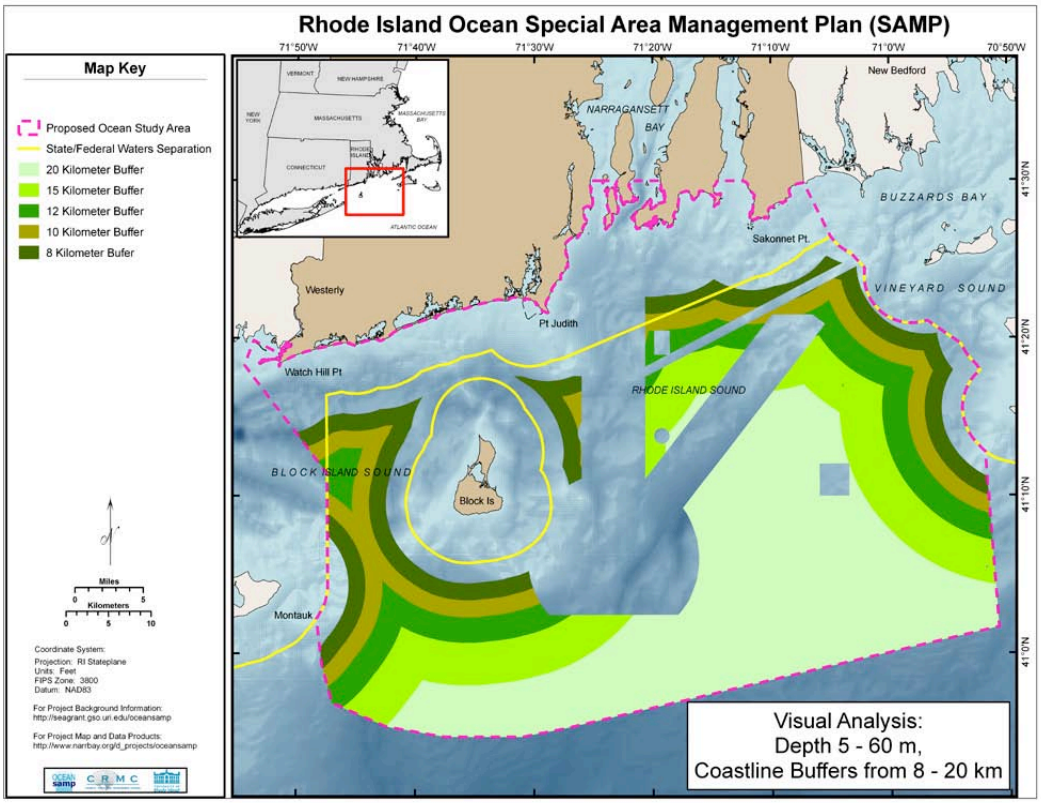

Figure 11 Coastal buffer offsets at 8, 10, 12, 15, and 20 km for the closest land mass.

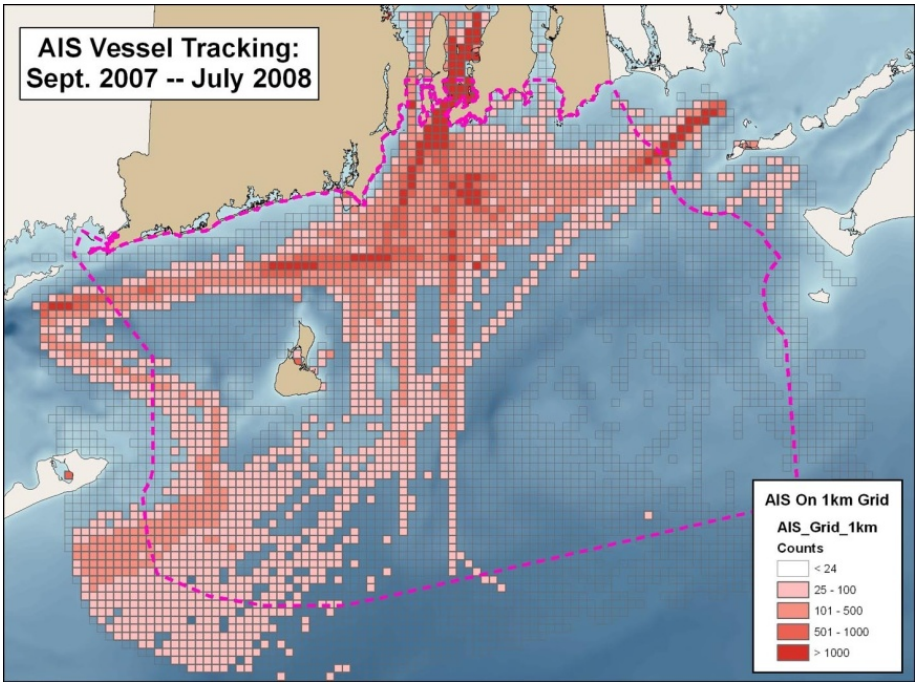

Figure 12 AIS vessel track density data from September 2007 to July 2008 for vessel counts greater than 24.

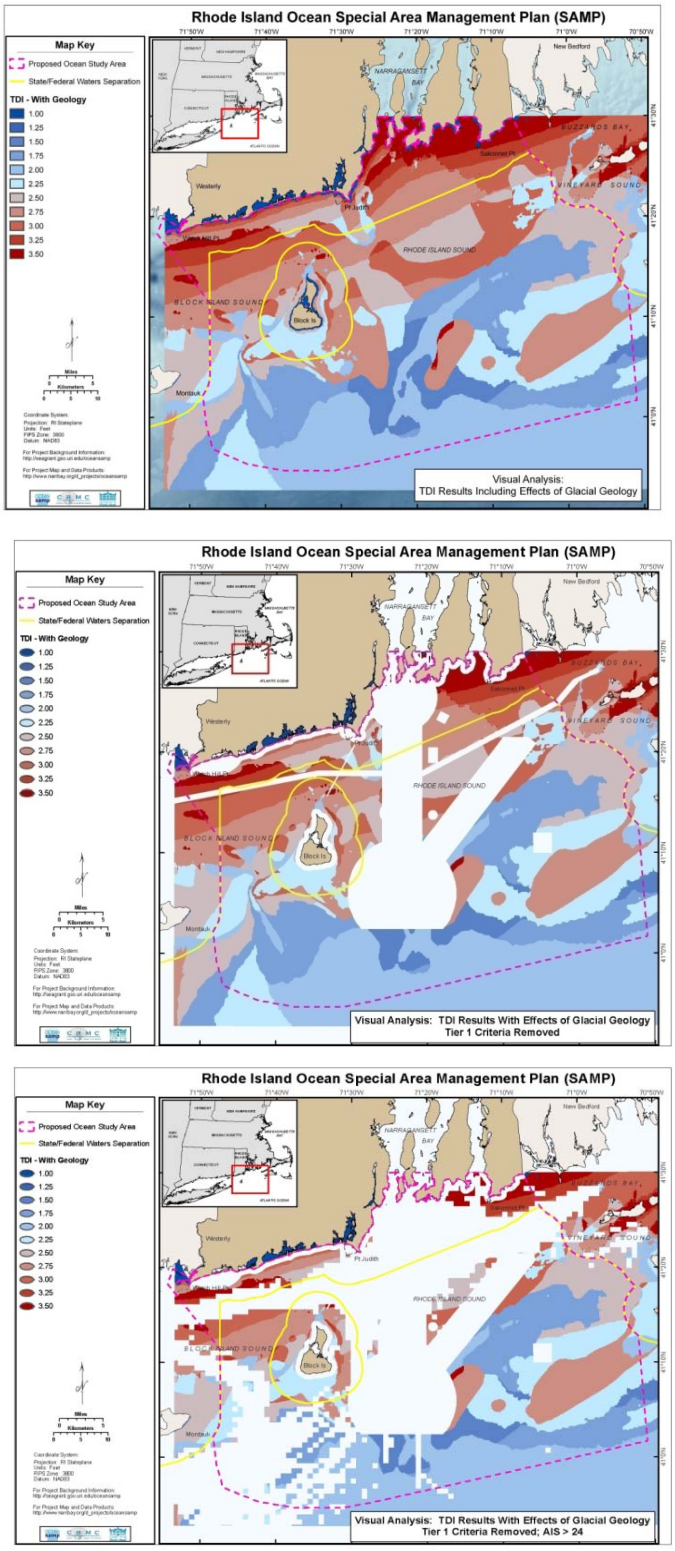

Figure 13 ***TDI*** **(upper panel),** ***TDI*** **with exclusionary areas removed (center panel) and** ***TDI*** **with exclusionary areas and AIS (above 24 counts) removed (lower panel).**

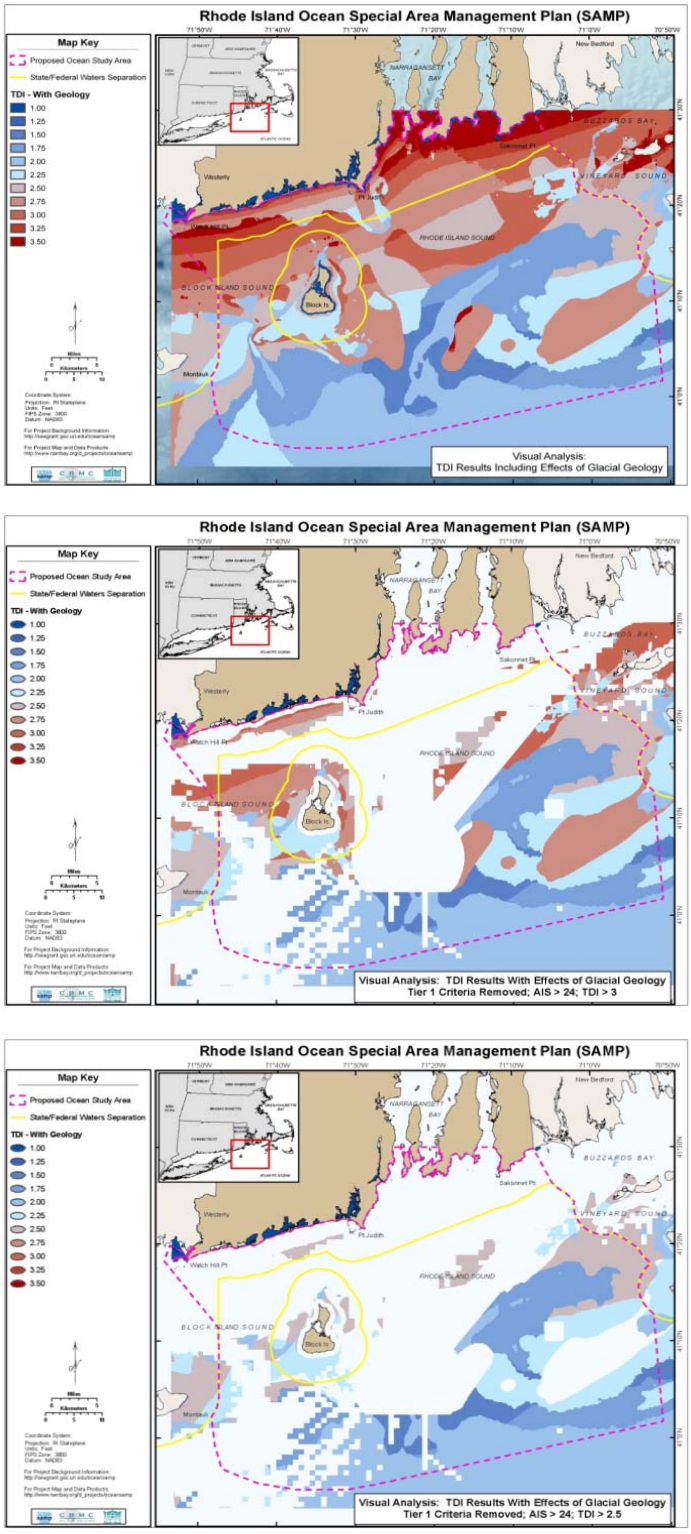

Figure 14 *TDI* (upper panel), *TDI* greater than 3, AIS greater than 24, and exclusionary areas removed (center panel), *TDI* greater than 2.5, AIS greater than 24, and exclusionary areas removed (lower panel).

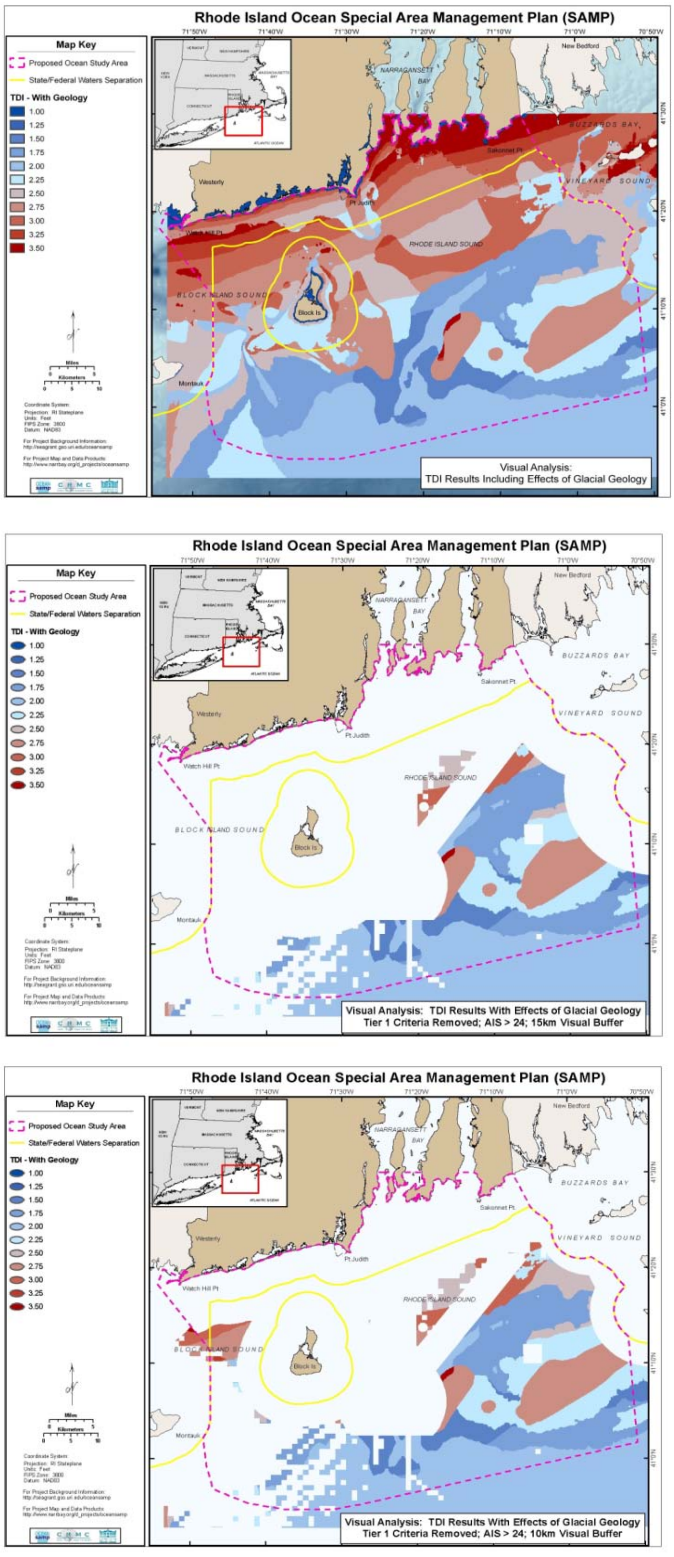

Figure 15 ***TDI*** **(upper panel),** ***TDI*** **with visual buffer 10 km, AIS greater than 24, and exclusionary areas removed (center panel), and** ***TDI*** **with visual buffer 15 km, AIS greater than 24, and exclusionary areas removed (lower panel).**

17.

High Resolution Application of the Technology Development Index (TDI) in State Waters South of Block Island

for the Rhode Island Ocean Special Area Management Plan 2010

by

Annette Grilli[1], Malcolm L. Spaulding[1], Chris Damon[2], and Ravi Sharma[1]

[1]Ocean Engineering

[2]Environmental Data Center, College of Environmental and Life Sciences

University of Rhode Island

Narragansett, RI 02882

April 15, 2010

Executive Summary

A technology development index (TDI) was developed by Spaulding et al. (2010) for the Rhode Island Ocean Special Area Management Plan (RI OSAMP). The TDI is an estimate of the technical challenge for siting wind farms in any state or federal waters and includes technology type, seabed geology, cable distance, and wind power in its calculation. TDI values of one are optimum, while higher values indicate increasing siting challenge and decreasing return. The relatively low-resolution study of Spaulding et al. (2010) show the values of the TDI in state waters south of Block Island are about 2.25 to 2.5 compared to values of 2.75 in state waters adjacent to the southern Rhode Island coastline. This mostly reflects the much higher wind power available at the Block Island site.

In this work we extend the TDI to higher resolution in the Block Island area employing meterological simulations for discrete directions, a wind frequency rose based on wind hindcast data from a station located immediately south of Block Island, and a newly determined construction effort map (sub-bottom geology). A high-resolution map of the TDI was constructed and shows values of TDI of 2.1 adjacent to the south coast of Block Island, with increasing values going south (2.0 to 2.3) and then decreasing to 1.6 to 1.8 in a band several kilometers wide SE and SW of the island near the state waters boundary with federal waters. The lowest TDI values are found S to SSW or S to E of the island depending on which wind speed data set is used (meterological model or AWS TrueWinds data, respectively), due to the lee effects of Block Island from NW winds.

Table of Contents

List of Figures

Abstract

A technology development index (TDI) was developed by Spaulding et al. (2010) for the Rhode Island Ocean Special Area Management Plan (RI OSAMP). The TDI is an estimate of the technical challenge for siting wind farms in any state or federal waters and includes technology type, seabed geology, cable distance, and wind power in its calculation. TDI values of one are optimum, while higher values indicate increasing siting challenge and decreasing return. The relatively low-resolution study of Spaulding et al. (2010) show the values of the TDI in state waters south of Block Island are about 2.25 to 2.5 compared to values of 2.75 in state waters adjacent to the southern Rhode Island coastline. This mostly reflects the much higher wind power available at the Block Island site.

In this work we extend the TDI to higher resolution in the Block Island area employing meterological simulations for discrete directions, a wind frequency rose based on wind hindcast data from a station located immediately south of Block Island, and a newly determined construction effort map (sub-bottom geology). A high-resolution map of the TDI was constructed and shows values of TDI of 2.1 adjacent to the south coast of Block Island, with increasing values going south (2.0 to 2.3) and then decreasing to 1.6 to 1.8 in a band several kilometers wide SE and SW of the island near the state waters boundary with federal waters. The lowest TDI values are found S to SSW or S to E of the island depending on which wind speed data set is used (meterological model or AWS TrueWinds data, respectively), due to the lee effects of Block Island from NW winds.

1 Introduction

Spaulding et al (2010) applied a technology development index (TDI) to the RI Ocean SAMP study area to assist in siting of wind farms in state and federal waters. The TDI estimates the technical challenge (technology type plus cable distance) in extracting offshore wind energy to the amount of wind energy (wind power) available at a given location. To facilitate comparisons and eliminate dependence on the units used in the analysis, the TDI is divided by the optimum TDI in the region to generate a non-dimensional TDI. Figure 1 shows the non dimensional TDI for the RI Ocean SAMP study area, including consideration for the seabed geology. Optimum sites have a TDI of one and those less desirable have values increasingly larger than one. The analysis was performed on a 100 m grid system. Bathymetric data was obtained from the NOAA

Electronic Navigation Charts (ENC) data set. Mean annual wind speed (power) data was obtained at hub height (80 m) from AWS True Winds data set for the Ocean SAMP study area (Brower, 2007). A lattice jacket support structure, with piles driven into the seabed, was assumed to support the tower and wind turbine. The cost of the lattice jacket structure, as a function of water depth, was provided by Roarke (2008) and confirmed by Hensel (2009). The impact of the glacially dominated subsea bed geology on construction effort (pile driving operations) was estimated using a construction effort (CE) map. The CE ranged from 1 (lowest effort) to 5 (highest effort). The map was generated by University of Rhode Island geology experts: Jon Boothroyd, GeoSciences and John King, Graduate School of Oceanography based on their analysis of existing data sets and literature resources. Chris Baxter, Ocean Engineering, a geotechnical engineer, recommended a scaling parameter to relate the construction effort to the challenge of pile driving or drilling operations. These scaling factors (SF) were applied directly to the technology type costs. (CE- 1 scale factor of 1 to CE-5 with a scale factor of 2.2).

A review of the results of the TDI analysis, with a focus on potential sites for offshore wind development in state waters (within 3 miles of the RI coast line or around island, yellow line in Figure 1), shows that the best location is south of Block Island. The value of the TDI in this area is about 2.25 to 2.5. This compares to values of 2.75 or higher in state waters adjacent to the southern RI coastline. In this region, while water depths are generally low, and hence the technology challenge is low, the wind power is low given the proximity to land and its enhanced roughness. South of Block Island the water depths are deeper but the wind power is considerably higher and hence is the preferred site in state waters, based on the TDI analysis.

2 High Resolution Application of TDI

In the interest of assessing the area south of Block Island for siting of a small wind farm (5 to 8 wind turbines) and taking advantage of new data generated by studies of wind resources and seabed geology in the Ocean SAMP, a high resolution TDI was performed. Figure 2 shows the study area for the high resolution analysis and the associated bathymetry. The bathymetric data set was once again obtained from the NOAA Electronic Navigation Charts (ENC) charts. The location of the state water boundary is shown. A 65 m grid was selected for this application.

Two wind data sources were considered for this study. The first (Figure 3) uses the same data employed in the SAMP wide study area at 80 m elevation obtained from AWS True Winds (Brower, 2007). The second (Figure 4) is based on a four level, nested, high resolution

meteorological simulations for discrete directions (eight points of the compass) and dates (performed by Titlow and Morris, 2010) and then scaled using a wind frequency rose based on wind hindcast data from the US Army Corp of Engineers Wave Information Study (WIS) (http://chl.erdc.usace.army.mil/wis), station 101, located immediately south of Block Island.

The construction effort map (Figure 5) was generated by John King and Rob Pockalny, Graduate School of Oceanography and Jon Boothroyd and Brian Oakley, Geosciences. The map is based on high resolution (250 m track line spacing) side scan and sub-bottom profiling data collected by King, with interpretation of seabed surface geology by Boothroyd and Oakley and sub seabed geology by King and. Pockalny. The construction effort ranged from 1 to 5, to be consistent with the prior effort (Spaulding et al , 2010). There is no data for several areas south of the state water boundary and hence construction effort has been estimated for these locations based on the large scale glacial geology. Chris Baxter, Ocean Engineering reviewed data from boring logs (typically 65 m in depth) that DeepWater Wind (DWW) collected at eight sites in the study area, SE of Block Island. Based on this data and his review of the construction effort maps he has developed a scaling factor of 1 for CE 1-2, 1.5 for CE-3, 1.8 for CE 4-5, and 2.2 for CE 5.

High resolution TDI maps (non dimensional) for the study area were prepared, once again assuming lattice jacket support structure, and are shown in Figures 6 and 7 for the two wind cases (Figures 3 and 4), respectively. Both maps show the same basic characteristics. High TDI (2.1 or greater) areas are located adjacent to the southern coast of Block Island with tongues protruding offshore. These are directly related to the construction effort (Figure 5) (areas with CE of 4-5). As one moves further south, the TDI progressively increases (2.0 to 2.3) due to increasing water depths. There is a band of low TDI values (1.6 to 1.8) several kilometers wide from approximately SE to SW of Block Island following the state line boundary. If AWS True Winds data is used (Figure 3), the lowest TDI (Figure 6) spans, in an arc, from the E to S. If the meteorological model scaled winds (Figure 4) are used, the areas (Figure 7) from the S to SSW of Block Island have the lowest TDIs. This difference is a direct result of the difference in wind speed contours to the SE of Block Island. AWS TrueWinds analyses show the wind speed contours wrapping around the southeastern side of the island, while those based on the meteorological model results show lower wind speeds in the area due to lee effects of Block Island from NW winds. Buoy based wind observations are currently being collected due south of Block Island at the state water boundary (Latitude - 41.1 and longitude - 71.56; October 2009 to

present). This data will help partially resolve the difference between the two approximations of the wind fields in the area.

References

Brower, M., 2007. Wind resource maps of Southern New England, prepared by True Wind Solutions, LLC, 10 p.

Hensel, J.V., 2009. Jacket Structures for offshore wind turbines in RI, MS Thesis, Ocean Engineering, University of Rhode Island, Narragansett, RI, 159p.

Roark, T., 2008. Offshore wind energy: An international perspective, Roger Williams University, Marine Law Symposium, October 23, 2008.

Titlow, J. and D. Morris, 2010. Block Island modeling analysis, WeatherFlow Inc. Poquoson, VA,, Model simulations by MetLogics, Boulder, CO.

Spaulding, M. L., A. Grilli, C. Damon, and G. Fugate, 2010, Application of Technology Development Index and Principal Component Analysis and Cluster Methods to Ocean Renewable Energy Facility Siting, Journal of Marine Technology, Special Edition on Offshore Wind, January February 2010

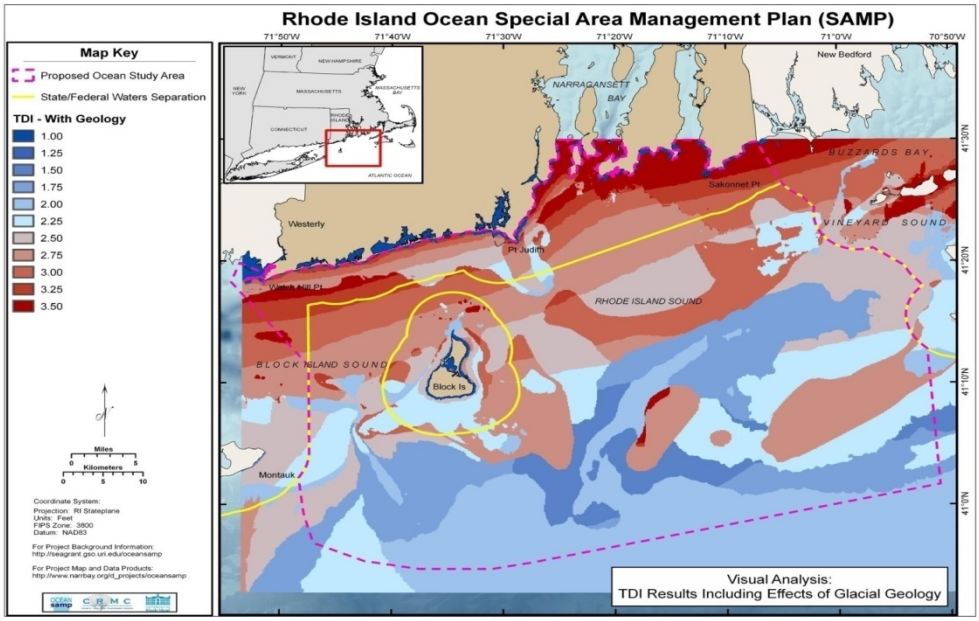

Figure 1 Contours of non-dimensional *TDI* for the Ocean SAMP study area, with glacial geology (Spaulding et al, 2010).

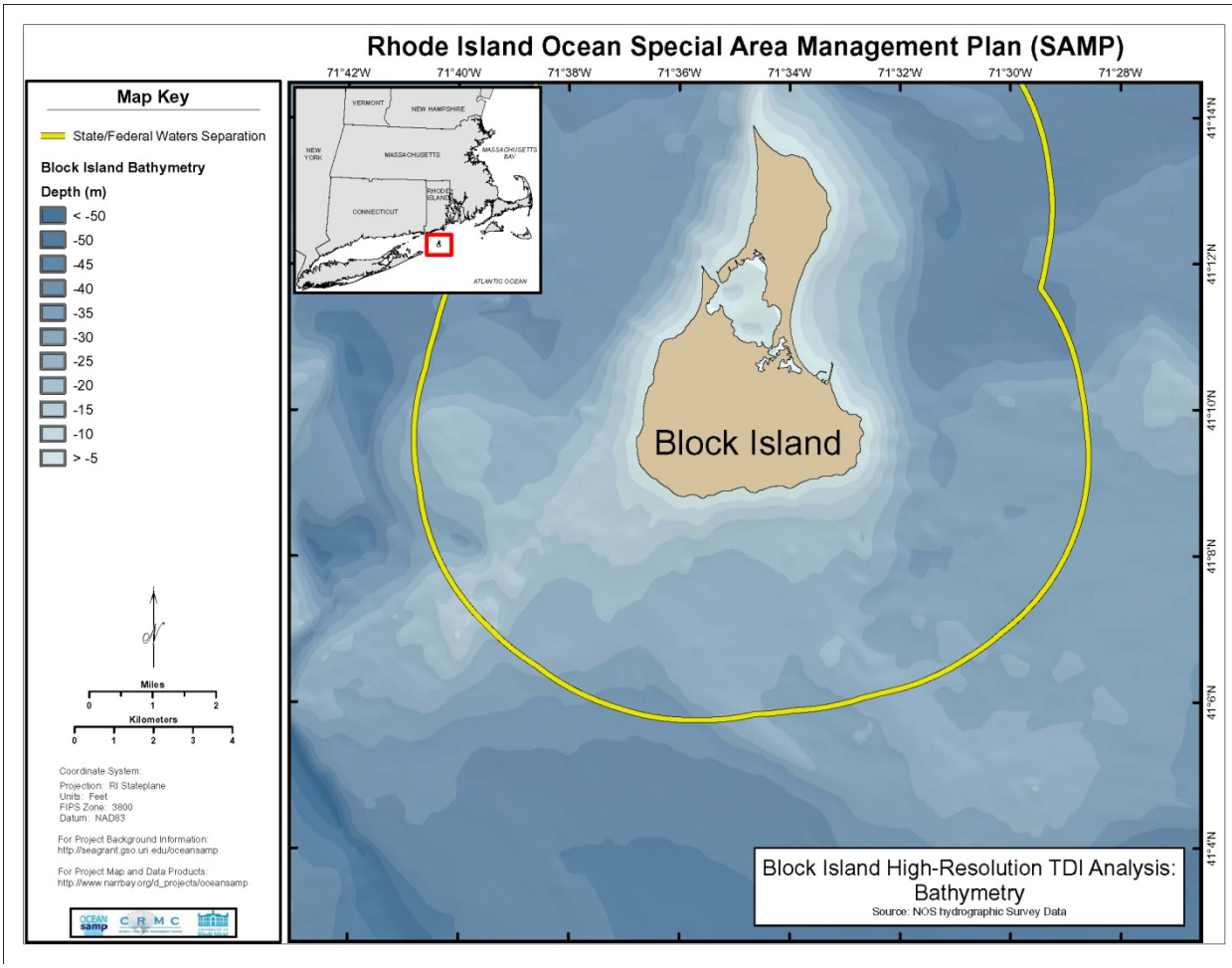

Figure 2 Block Island study area with NOAA ENC bathymetry.

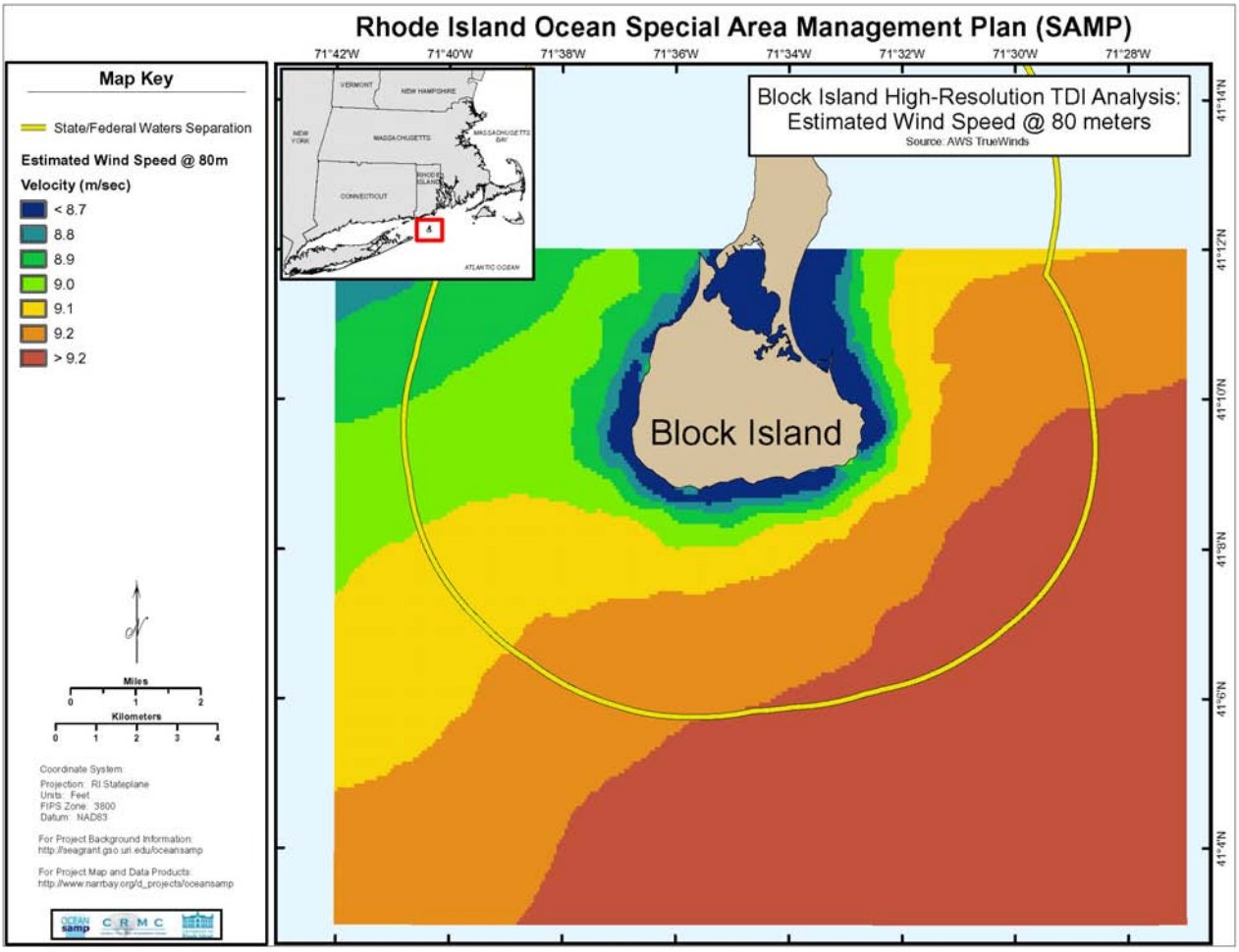

Figure 3 Estimated mean annual wind speed at 80 m from AWS TrueWinds data (Brower, 2007) for Block Island study area.

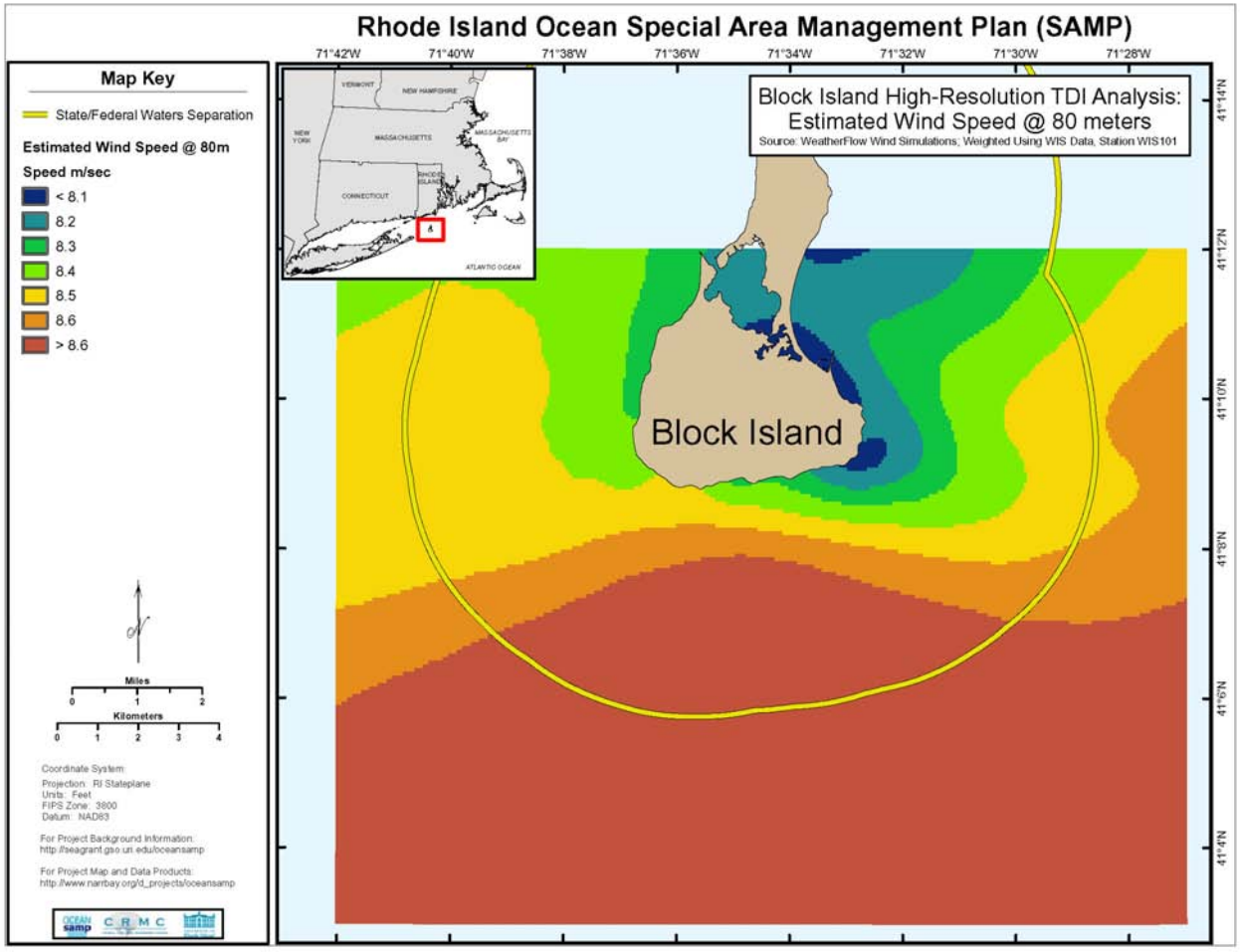

Figure 4 Estimated mean annual wind speed at 80 m with using meteorological modeling based strategy and US Army Corp of Engineers, Wave Information Study, WIS 101 wind rose for Block Island study area.

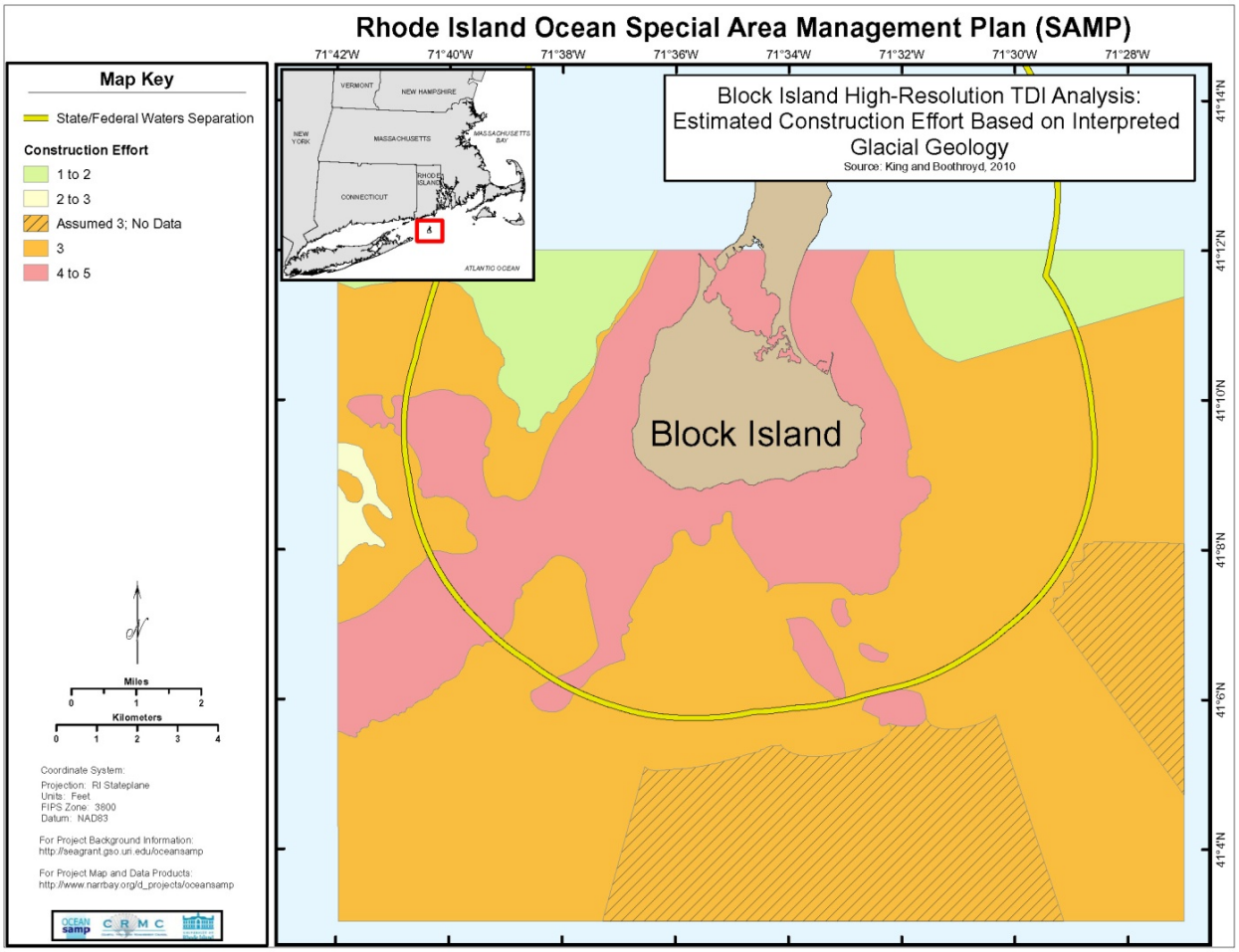

Figure 5 Construction effort map for Block Island study area (generated by John King, Rob Pockalny, Graduate School of Oceanography,and Jon Boothroyd and Brian Oakley, Geosciences.)

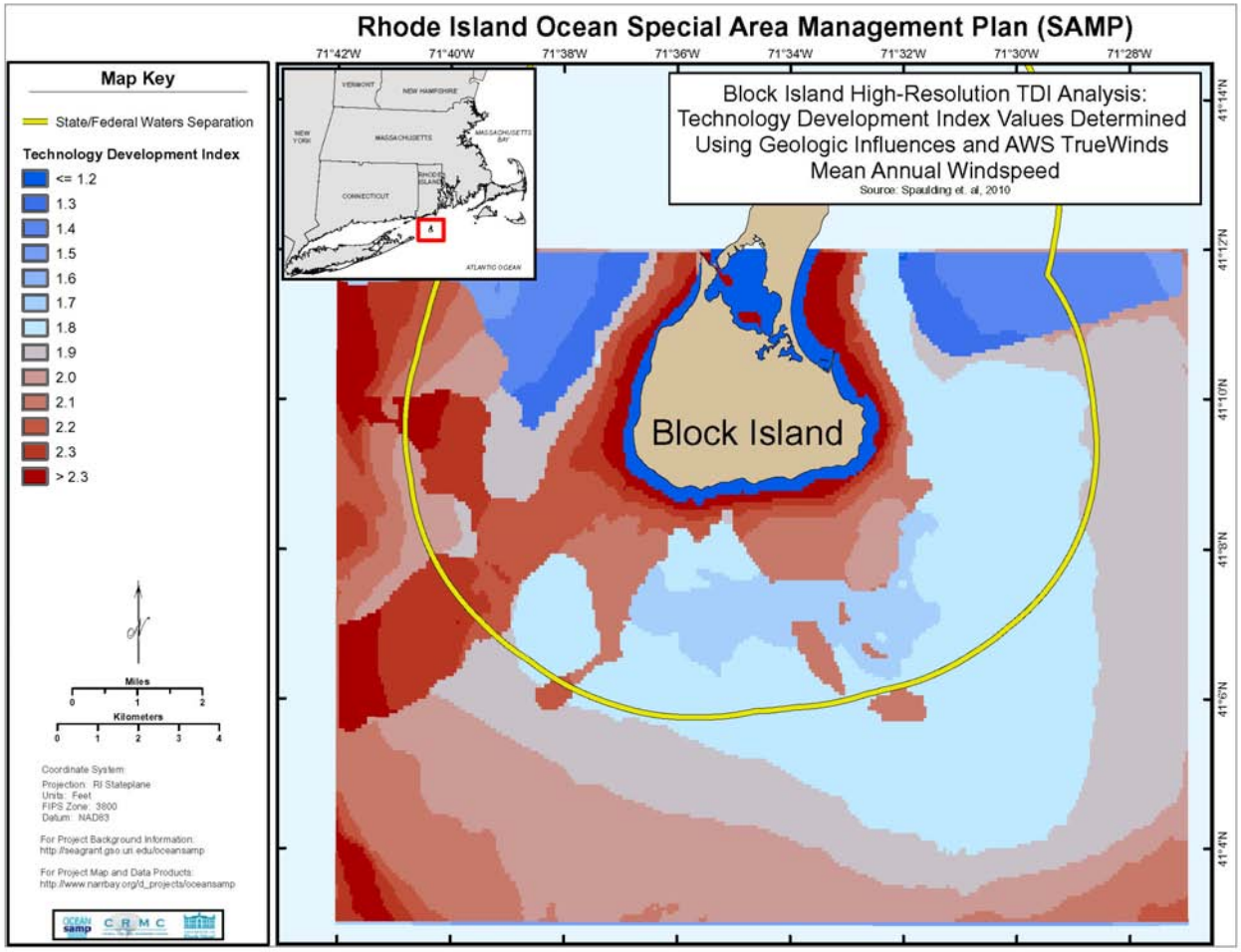

Figure 6 TDI for Block Island Study area with geology using AWS TrueWinds mean annual winds (Brower, 2007).

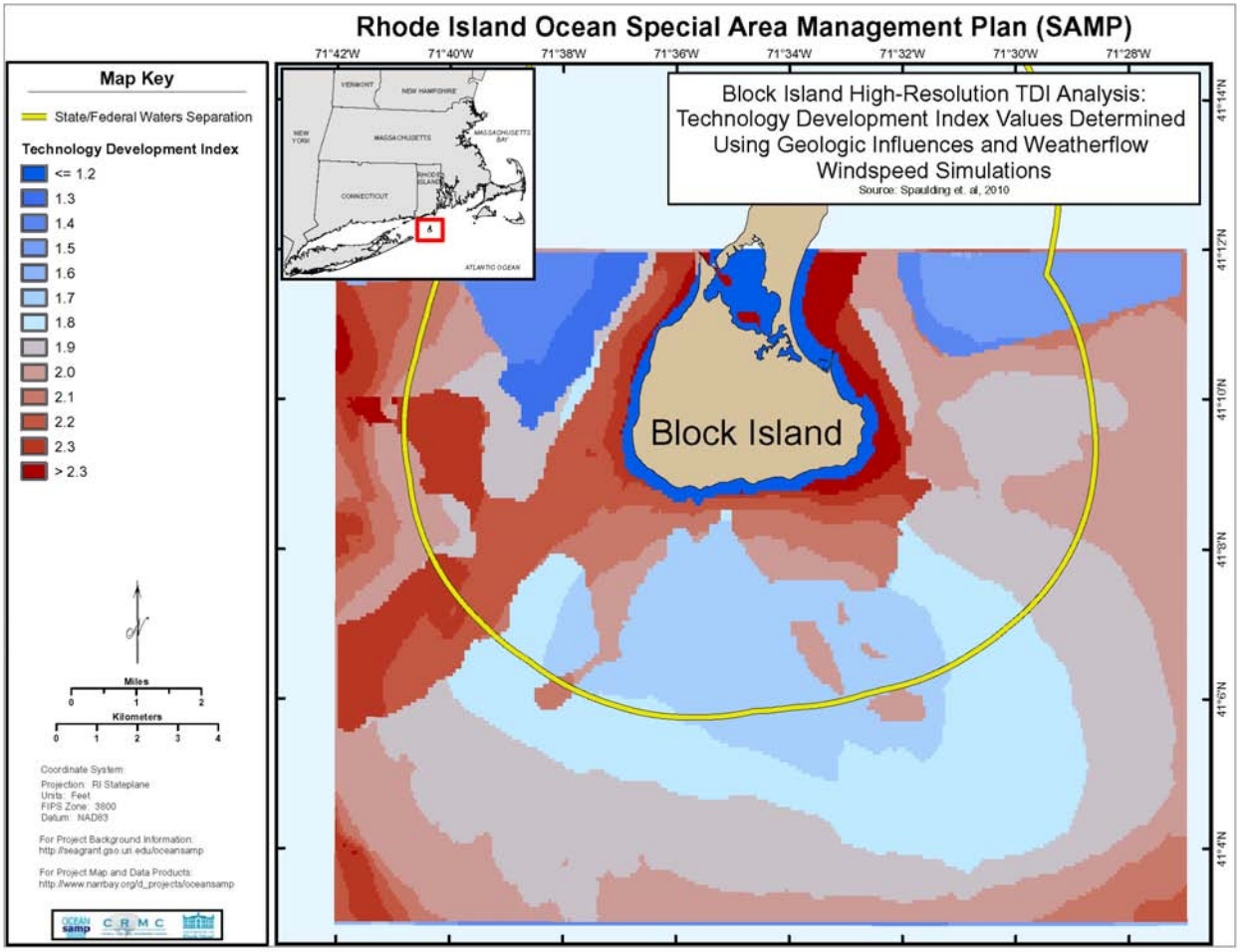

Figure 7 TDI for Block Island Study area with geology with model scaled winds based on WIS 101 wind rose.

18.

Development of a Technology Type Factor for Jacket Structures for Offshore Wind Turbines in Rhode Island

by

M.S. Ravi Sharma, Jonas Hensel, Christopher D.P. Baxter, and Sau-Lon James Hu

University of Rhode Island, June, 17, 2010

Executive Summary

A marine spatial planning approach is being used to locate possible sites for offshore wind development in Rhode Island. A Technology Development Index (TDI) was developed by Spaulding et al. (2010) to quantify the technical challenges of a particular site relative to its potential power production. A component of this index is the Technology Type (TT) factor, which quantifies the relative expensive of a structure/foundation system as a function of environmental loading, water depth, and soil conditions.

This report documents the development of TT factors for jacket structures supporting offshore wind turbines in Rhode Island Sound (Hensel 2009). TT factors were calculated by the total weight of the jacket and piles for a given water depth and soil conditions normalized by the weight of a reference structure. Jacket structure weights were determined by a frequency driven finite element analysis using the program ANSYS. The structure was subjected to hydrodynamic and quasi-static turbine loads from 50-year extreme wind and the 100-year extreme wave loading in Rhode Island Sound to determine the ultimate stresses in the structural members. Pile foundation weights were determined from an analysis of the axial capacity and the lateral capacity using commercially available pile design software. Jacket and foundation weights were calculated for water depths ranging from 30m to 60m and for three representative soil types.

These analyses resulted in a Technology Type factor that varies with water depth according to a 2nd order polynomial, and also with soil type. The results were compared to the weights of two existing jacket structures in Europe as well as existing Technology Type factors from the United Kingdom, and there was good agreement between the results.

Table of Contents

List of Figures

List of Tables

Abstract

A marine spatial planning approach is being used to locate possible sites for offshore wind development in Rhode Island. A Technology Development Index (TDI) was developed by Spaulding et al. (2010) to quantify the technical challenges of a particular site relative to its potential power production. A component of this index is the Technology Type (TT) factor, which quantifies the relative expensive of a structure/foundation system as a function of environmental loading, water depth, and soil conditions.

This report documents the development of TT factors for jacket structures supporting offshore wind turbines in Rhode Island Sound (Hensel 2009). TT factors were calculated by the total weight of the jacket and piles for a given water depth and soil conditions normalized by the weight of a reference structure. Jacket structure weights were determined by a frequency driven finite element analysis using the program ANSYS. The structure was subjected to hydrodynamic and quasi-static turbine loads from 50-year extreme wind and the 100-year extreme wave loading in Rhode Island Sound to determine the ultimate stresses in the structural members. Pile foundation weights were determined from an analysis of the axial capacity and the lateral capacity using commercially available pile design software. Jacket and foundation weights were calculated for water depths ranging from 30m to 60m and for three representative soil types.

These analyses resulted in a Technology Type factor that varies with water depth according to a 2nd order polynomial, and also with soil type. The results were compared to the weights of two existing jacket structures in Europe as well as existing Technology Type factors from the United Kingdom, and there was good agreement between the results.

1 Introduction

Offshore wind resources have been identified as an attractive source of renewable energy along the U.S. east coast, and there are several offshore wind energy projects under various stages of development. Most of these projects are planned for deeper water depths (e.g. 30-45 m in Rhode Island) than most of the existing European wind farms, which are typically in water depths less than 30 m (Musial and Butterfield, 2004; Westgate and DeJong, 2006). Usually, a detailed technological-economical analysis (siting analysis) is performed to find an optimum location within a given area for development of the wind farm. Since the technical and economical aspects of the offshore wind turbine system are influenced by spatial variation within a given site (e.g. water depth, environmental loading, wind potential, etc.), a marine spatial planning approach is often followed to determine an optimum location.

The siting analysis developed for the Ocean SAMP utilizes the Technology Development Index (*TDI*), which quantifies the relative difficulty in siting the offshore wind turbine compared to it power production potential (Spaulding et al., 2010). The *TDI* is expressed as

$$TDI = TCI/PPP \quad (1)$$

where *TCI* is the Technology Challenge Index and *PPP* is the Power Production Potential. *TCI* quantifies the costs associated with construction of offshore wind turbines and is influenced by environmental conditions (waves, wind, water depth, and soil type). *PPP* is influenced primarily by the mean annual wind power at the hub height of the turbines, which increases with distance from shore. Low *TDI* values indicate high power production and relatively low cost of installation. *PPP* and *TCI* can be rewritten as

$$PPP = W \, x \, CF \quad (2)$$

and

$$TCI = (TT \, x \, FF) + CD \quad (3)$$

where *W* is the hub height, *CF* is a capacity factor for the turbine, *TT* is a Technology Type Factor, *FF* is a Foundation Factor and *CD* is the distance to the grid connection. The Technology Type factor represents the supply costs of the support structure and depends on many parameters, including type of turbine used (e.g. 3.6 MW, 5 MW, etc.), substructure type (e.g. monopile, jacket structure, gravity, floating), foundation technology (e.g. gravity base, piles, suction buckets, anchors), water depth, and geotechnical conditions. To incorporate the relative difficulty of installation in different soil types, the Technology Type Factor can be multiplied by a Foundation Factor, FF.

At the outset of the Ocean SAMP siting exercise, *TT* values were obtained from a study in the United Kingdom that described the factors as the total supply costs of a jacket support structure in a given water depth in $millions/structure (Roark, 2008). The *TT* values were grouped based on the following water depths: 5m to 25m, *TT* = 3.36; 25m to 45m, *TT* = 4.48; and from 45m to 65m, *TT* = 5.76.

The objective of this study is to develop independent values of Technology Type factors specific to jacket structures and to the environmental conditions relevant to the Ocean SAMP study area. This is accomplished by relating the *TT* factor (or cost/structure) to the weight of the steel required for the jacket and pile foundations, an approach that has been used successfully to model the costs of monopile foundations for offshore wind turbines (Papalexandrou, 2008). Based on Ocean SAMP project requirements, a 5 MW turbine mounted on a jacket structure in water depths ranging from 25m to 65m on a foundation consisting of four piles is considered in this analysis. The weight of the transition piece weight and the rest of the structure is considered to be constant for the varying water depths and soil conditions, and is not included in the determination of the *TT* factors. Environmental loads and representative soil conditions are specific to the Ocean SAMP study area.

To obtain the weights of the jacket structure for different water depths, a frequency driven, Ultimate Limit State design was performed using finite element analyses. A “soft-stiff” design approach was utilized to avoid resonance between the natural frequencies of the structure, environmental loads, and the turbine. Structural members and dimensions of the jacket were varied in the order to meet the soft-stiff design criterion, and the weight of the optimal design was used to develop the *TT* factors. The finite element analyses were performed using the commercial software ANSYS. As a check on the calculated structural dimensions of the jacket, a yielding stress analysis was performed with loads from wind and waves based on the Ultimate Limit State.

The weight of the foundation was determined by determining the diameter and length of four, steel pipe piles that transfer the loads from the wind, waves, turbine, and jacket structure safety into the ground. As with the design of the jacket, the foundations were designed based on the Ultimate Limit State. To evaluate pile diameter and length, the "p-y method" (Reese, 1984) was employed using the commercial software L-Pile Plus. This software allows for simulation of the lateral load bearing behavior of piles under time varying loading. Soil properties were estimated from published geophysical data.

Loads on the jacket and foundation were estimated based on recommended design standards for offshore wind turbines, specifically from 50-year extreme wind and the 100-year extreme wave loading (DNV, 2007). The wave climate for extreme storm events were derived from hind cast data according to the Ultimate Limit State and the study area. Load effects on the structure were estimated using a hydrodynamic force effect calculation implemented in ANSYS. Turbine loads were estimated for the design storm from quasi-static loads determined for a Dutch research study on a comparable turbine under comparable environmental conditions (van der Tempel, 2006).

2 Design Considerations for Jacket Structures and Foundations

Offshore structures must be designed to withstand a variety of loads, including wind, wave, current, ice and other environmental forces (e.g. earthquakes). The design principle for these structures and foundations is aimed at satisfying the safety requirements during the design life of the structures. There are three codes currently available for the design of offshore wind turbine structures: Germanischer Lloyd (2005), International Electrotechnical Commission IEC 61400-3 (2006), and Det Norske Veritas DNV-OS-J101 (2007). These guidelines are developed based on the rich experience gained from the design guidelines recommended for oil and gas

platform structures (e.g American Petroleum Institute, 2000). The choice of a particular guideline is based on the local regulations and certification requirements dictated by the regulating government agency.

In DNV-OS-J101, the safety requirements are specified based on limit states of structural members at different load cases: ultimate limit state (ULS), the fatigue limit state (FLS), serviceability limit state (SLS), and accidental limit state (ALS). Ultimate limit state governs the safety requirements against the forces caused by extreme environmental conditions (e.g. 50-year return period wave) whereas fatigue limit state ensures the safety against damage accumulation caused by cyclic loading conditions. Serviceability and accidental limit states ensure safety during normal operating condition and accidental impact loads respectively. In most cases, depending on the environmental conditions in a given site, fatigue limit state governs the design of support structures of offshore wind turbine, followed by the ultimate limit state (Schaumann and Wilke, 2006).

In addition to the limit states criteria, the dynamic behavior of the coupled wind turbine structure (i.e. the Rotor-Nacelle Assembly, tower, and support structure including foundation piles) should also be considered in the design. To avoid dynamic magnification of load effects, the offshore wind turbine structures are designed as "soft-stiff" structures, meaning that the first eigen frequency of the structure is kept between the excitation frequency bands of turbine rotation and blade passing frequency (termed "1P and 3P"). The frequency band for typical ocean waves is 0.05-0.30Hz. 1P and 3P frequency bands depend on the operating speed of the turbine and are typically in the range of 0.14 - 0.20 Hz and 0.43 - 0.60 Hz (Seidel, 2007).

The support structure, which includes the jacket and four foundation piles, was modeled in a finite element analysis as steel tubular members (details are explained later) subjected to dynamic environmental loadings from waves and quasi-dynamic loads from turbine and wind, in addition to the self weight of the entire structure. The influence of soil stiffness in the dynamic response of the structure is considered by extending the foundation to a depth of six times the diameter of the piles (van der Tempel, 2006; Zaaijer, 2002). A fixity constraint was applied at this depth, and this condition has been shown to reasonably capture the nonlinear response of the foundation. The first natural frequency of the jacket structure was used as a design driver for determining the structure weight. The first mode of the natural frequency of the jacket structure was kept between 0.33-0.36Hz and the second mode was kept greater than 0.70Hz. The structures are designed in the ULS for a load combination of the 50-year extreme wind and the 100-year extreme wave loading. Ice and current loadings are not considered. Fatigue limit state was not considered in the design due to lack of time and insufficient load data. Moreover, the focus of this study was on estimating the relative change in weight of the support structure with water depth and soil conditions for a given turbine, it is assumed that fatigue consideration would not affect the relative change.

The foundation piles are designed for ultimate axial compression, axial tension and lateral loads obtained from the coupled structural analysis. The penetration depth of the piles for the jacket structure is determined based on the no-toe-kick-out criterion.

3 Estimation of Wind and Wave Loading

The water depth in the Ocean SAMP study area varies from approximately 5m to over 60m, and jacket support structures are designed for water depths ranging from 30m to 60m. Met-ocean data analysis for the study area resulted in an extreme wave height for a 100-year return period ($H_{max,100\text{-}year}$) of 16.2 m, and wave period (T) of 15s (Spaulding et al., 2010). Based on the range of water depth and wave parameters in the study area, Stokes 5th order wave theory was used to simulate wave kinematics time series (Det Norske Veritas, 2007). Wave forces on the slender tubular structures were calculated using Morison's equation within the ANSYS program. The influence of the attacking angle on the structure was investigated and the frontal attack was found to be the worst case scenario, resulting in the highest loads at the mudline.

Wind loads and moments on the turbine are dependent on the support structure stiffness, site specific wind conditions and the turbine itself. In this study, we used wind loads and moments reported by van der Tempel (2006) for a 5.5 MW turbine which is comparable to the turbine used in this study. Table 1 shows the forces and moments in the horizontal (x and y) and vertical (z) directions. These loads and moments were applied quasi-statically at the top of the tower. Additional wind loads and moments on the tower (with a cylindrical cross section) were estimated based on the extreme 50-year return period wind speed of 37m/s and then applied statically at the base of the tower.

Table 1. Estimated loads at the top of the tower from a 5.5MW GE Energy turbine. Design load case: ULS; turbine parked; extreme wind speed model (van der Tempel, 2006).

F_x (N)	F_y (N)	F_z (N)	M_x (Nm)	M_y (Nm)	M_z (Nm)
1.28E+5	2.10E+5	3.48E+5	4.25E+6	8.20E+6	1.24E+6

Due to the lack of detailed information about geotechnical data in the study area, three basic soil profiles (dense sand, soft clay and stiff clay) were considered in this study. These types are idealized soils and represent three major types of soils in the study zone: sand, till, and soft rock. This simplification of real soil conditions allows for distinguishing between weak, average, and strong soil conditions and helps to quantify the influence of the soil conditions on the foundation weight.

4 Methods

4.1 Jacket Weight Estimation

As the design of the jacket structure was optimized for various water depths, certain assumptions were made throughout the design process. Many of these assumptions were made to be consistent with both the Beatrice and Alpha Ventus projects. The geometry of the modeled jacket structure was arbitrarily fixed to have an area of 10m by 10m above the water line at the beginning of the transition piece. In addition, the four legs of the jacket structure were assumed to be inclined at an angle of 3.5^{o} degrees outward, thereby increasing the foot print with increasing water depth. A typical jacket structure geometry modeled using ANSYS is shown in Figure 1.

The structural model of the wind turbine system was analyzed at water depths of 30m, 38m, 45m, 53m, and 60m. At each water depth, only the jacket height and the corresponding self weight of the jacket were changed, while the rest of the components of wind turbine system, such as the Rotor-Nacelle Assemble (RNA), tower, transition piece and foundation piles, were kept constant in the analysis. The RNA was represented as a lumped mass of 435t on top of the tower. The tower was modeled as a tubular beam of 5.5m diameter and height of 75m. The transition piece was idealized as a rigid beam having a lumped mass of 160t connecting the tower and jacket. An additional four concentrated mass points (60t each) were included to idealize the pipe sleeve connecting the jacket and the foundation piles (Seidel, 2007). The foundation piles were modeled as tubular elements of 1.8m diameter and 0.05m wall thickness. The length of the piles below seabed was extended up to six times the diameter in the finite element analysis to ensure some incorporation of soil-structure interaction in the design. The structural members including tower, jacket legs and bracings and foundation piles were assumed to be tubular steel.

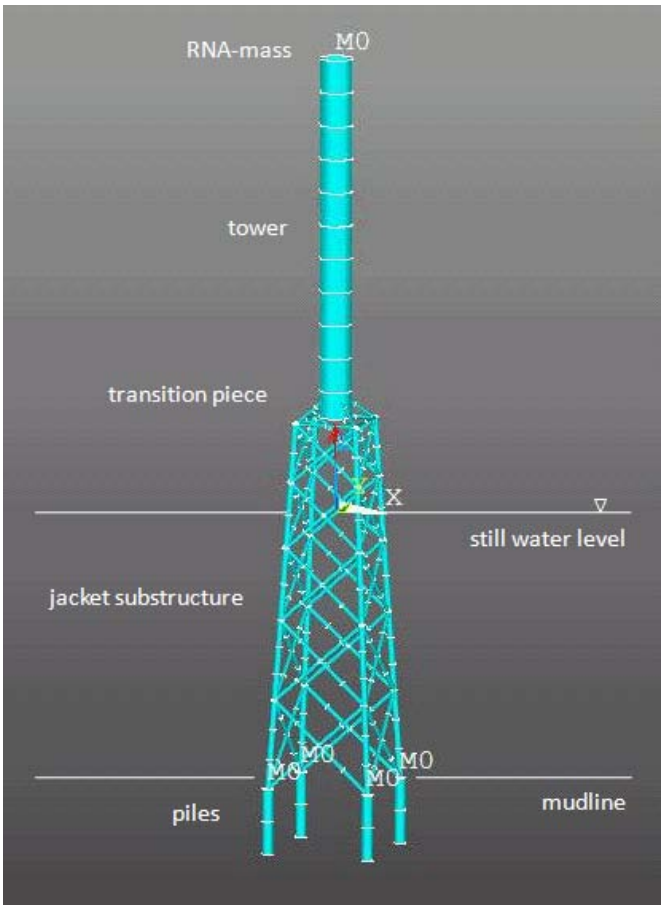

Figure 1. Typical geometry of the finite element model used to model the jacket support structure modeled using the program ANSYS.

For a given water depth, the total mass of the jacket structure was varied and the natural frequency of the entire system was estimated. During the modal analysis, for a given total mass of the jacket, the ratio of mass of the legs to mass of bracings was also varied and the appropriate jacket structure masses were estimated based on the first natural frequency that was within 0.33-0.36Hz and the second mode of the natural frequency that was greater than 0.7Hz. This

frequency criterion resulted in a set of possible jacket structure weights which were further analyzed based on the ULS criterion.

Following the modal analysis, a transient analysis in the time domain was performed to check the ULS requirements and also to determine the loads and moments at the mudline for foundation pile design. In this transient analysis, the structure was subjected to time varying loads from the waves and quasi-static loads from wind as explained above. An analysis time of 120s was chosen with time increments of 1s. A series of eight waves with a wave period of 15s were simulated. This duration was found to be sufficient to model the dynamic behavior of the structure. A relatively low damping is expected for the parked turbine and therefore 2% Rayleigh damping was used to model structural and material damping in the analysis (van der Tempel, 2006; Det Norske Veritas, 2007).

The structural integrity of the jacket in response to the transient loads was evaluated by comparing the maximum von-Mises stress within each structural member to the allowable yield stress of the steel member. This is consistent with U.S. guidelines for the design of offshore structures (American Petroleum Institute, 2000).

This analysis resulted in many combinations of leg and bracing sizes that satisfied both the frequency criterion and the structural integrity (i.e. ULS) criterion. Both the lower and upper bound of admissible jacket weights were obtained from the mean values of the lowest and highest jacket masses estimated for each first natural frequency varying from 0.33Hz to 0.36Hz. The lower bound mass represents the most economical structure with the smallest material consumption. The upper bound mass represents a less economic solution with higher material consumption.

This procedure was then repeated for different water depths and the variation of lower and upper bound weights for each water depth is shown in Figure 2. Figure 2 shows that jacket structure weight followed a quadratic relationship with water depth in contrast to the monopile structure for which a cubic polynomial relationship was proposed (Papalexandrou, 2008). Figure 2 also includes weight and water depth data for the Alpha Ventus (Seidel, 2007a) and Beatrice jacket structures (Talisman Energy, 2007). There is reasonable agreement between the weight of the actual structures and the estimated trends from the finite element analyses.

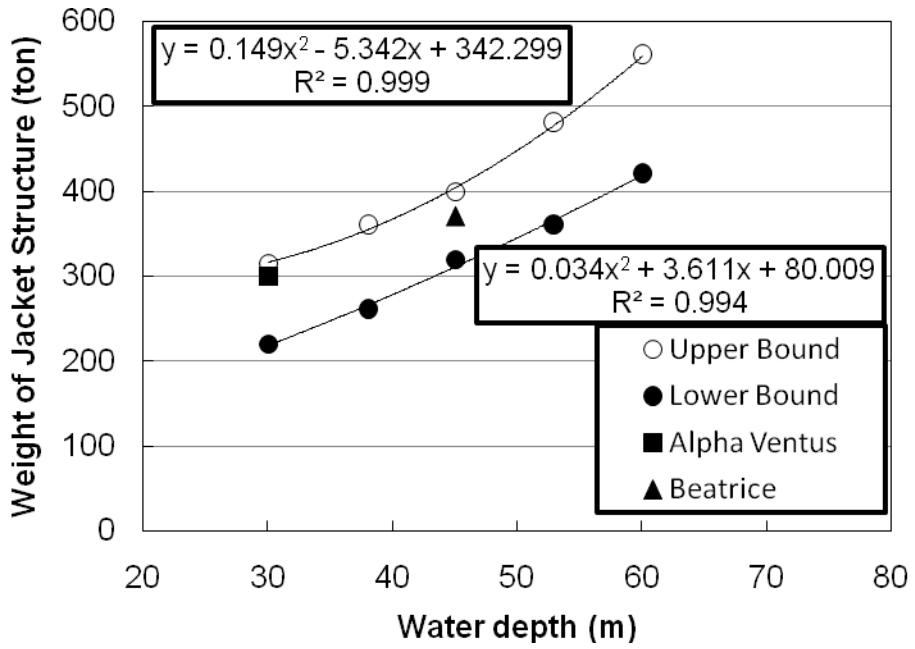

Figure 2. Variation of estimated jacket weight with water depth. Installed weights of two jackets from the Alphus Ventus and Beatrice projects are included for comparison.

The transient analysis was also performed to estimate the time history of forces and moments at mudline that would be applied to the head of the four foundation piles. A typical time history of axial load, horizontal load and moments at mudline is shown in Figure 3. The absolute maximum of loads and moments on the pile heads at the mudline were estimated for lower and upper bound cases of jacket weight at each water depth. These maximum loads and moments were then used for foundation pile design as explained below.

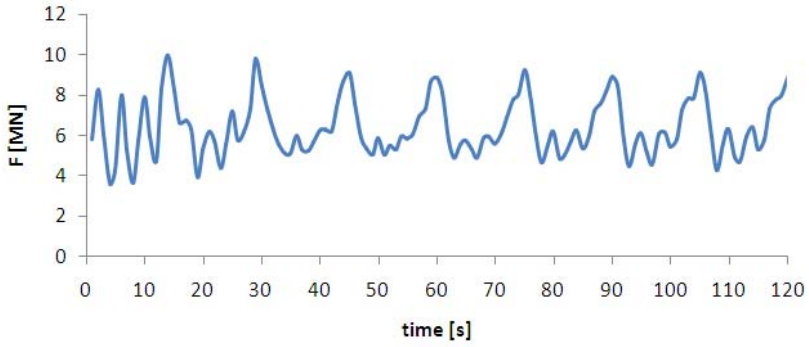

(a.)

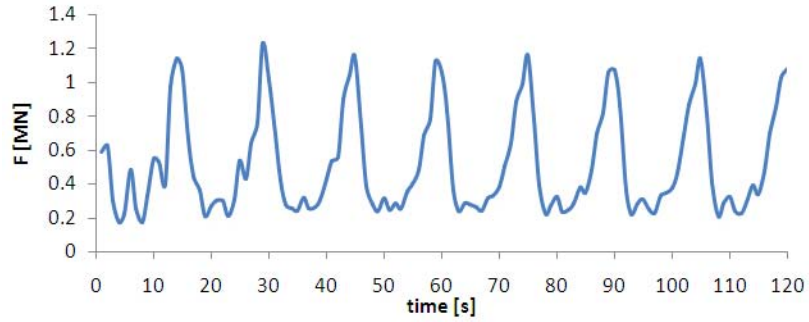

(b.)

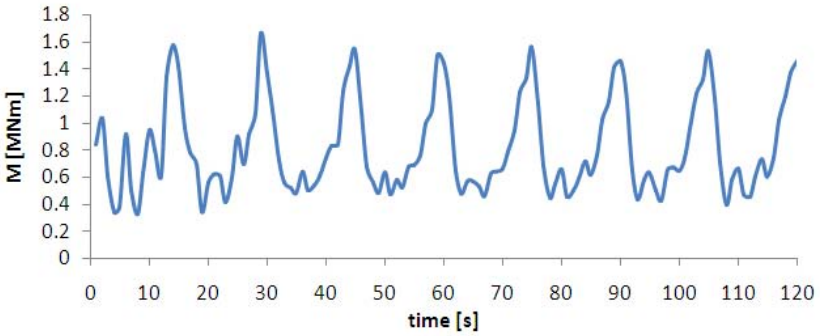

(c.)

Figure 3. Transient loads generated at the mudline for use in the geotechnical pile design, including a.) vertical force, b.) horizontal force, and c.) moments (45m water depth, f = 0.33Hz).

4.2 Foundation Pile Weight Estimation

The foundation piles consisted of four, vertically driven tubular steel piles. These piles were designed to carry the ultimate axial and lateral forces and moments at the pile head. The axial and lateral pile capacity was estimated according to the standard practice recommended in API (2000). The lateral capacity was estimated using a nonlinear soil stiffness model (p-y model) available within the software program L-Pile Plus. Based on the applied static ultimate loads, the pile penetration length was estimated using the zero deflection at pile toe (no toe-kick out) criterion. From the length and diameter of the pile the weight of the foundation piles were calculated for each water depths.

There is a lack of geotechnical data with depth throughout the study area, so three different uniform soil profiles that represent the range of soils that can be expected were considered in the pile design: sand, stiff clay, and soft clay. Assumed values of buoyant unit weight, undrained shear strength ratio, and effective stress strength parameters are shown in Table 2. The stiff clay is assumed to have an over consolidation ratio (OCR) of 5. The soft clay is assumed to be normally consolidated (OCR = 1). Pile capacity was estimated for all the three soil types and for the lower and upper bound loads and moments at different water depths. Based on these factors, the penetration length and hence the weight of the foundation piles for different soil conditions and water depths was determined, and the weights are shown in Figure 4.

Figure 4 shows that the influence of water depth on the foundation pile weight is negligible. This is due to the increasing size of the jacket footprint at the mudline with increasing water depth, which changes the distribution of axial loads, lateral loads, and moments at the pile head. Figure 4 also illustrates that the influence of soil type is significant on the weight of the foundations. The weight of the piles in the sand deposit is 50% less than the weight of the piles in soft clay. It is also noted that in the sand deposit the lateral capacity governs the pile design and there is no difference in foundation pile weight for lower and upper bound loads. In the soft and stiff clay deposits, the lower bound loads resulted in marginally lower penetration depths in the range of 2m to 5m when compared to upper bound loads.

The weight of the foundation piles at the Beatrice site is also shown in Figure 4. Soil conditions at the Beatrice site are dominated by clay of various densities and medium dense sands (Talisman Energy, 2007). There is good agreement between the weight of the Beatrice foundation and the weight estimated in this study for stiff clay at the same water depth.

Table 2. Soil types and geotechnical parameters assumed for estimation of pile lengths and weights.

Soil type	γ' (kN/m^3)	S_u/σ'_v	φ' (deg)	D_r (%)
Sand	11	-	34	65
Stiff clay	8	0.5	-	-
Soft clay	7	0.3	-	-

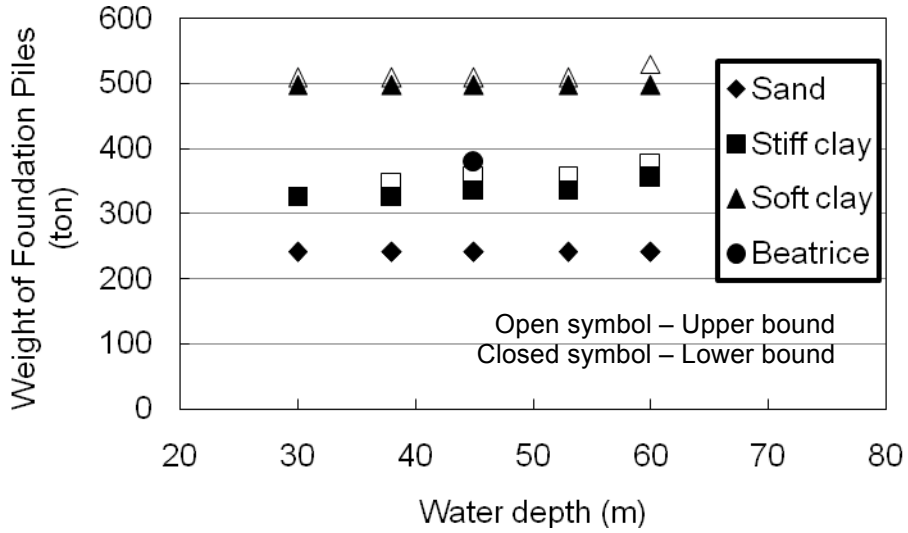

Figure 4. Estimated weight of foundation piles for different soil types and water depths. The weight of the Beatrice foundation piles are included for comparison.

5 Development of Technology Type Factors and Relative Cost Model

The total cost of development of a wind farm includes many factors, including the turbine, tower, support structures (e.g. transition piece, jacket, foundation piles, scour protection, etc.), electrical infrastructure, operation and maintenance (Papalexandrou, 2008). The cost of all the above components are influenced by the supply costs (e.g. materials used, manufacturing process, transportation and installation costs). However, in this study only the variation of supply costs for the jacket type support structure are considered. It is assumed that the unit cost for transportation and installation would remain the same for a given wind farm and therefore the relative cost model (and the related Technology Type factors) developed based on weight of the structural members is a reasonable approximation for support structure cost.

5.1 Technology Type Factors for the Ocean SAMP Study Area

The combined jacket and foundation weights for the upper and lower bound solutions and different soil types are shown in Figure 5a. Although the magnitude of the values differs between the upper and lower bound, the trends are almost identical. The Technology Type factors (*TT*) were obtained by normalizing the support structure weights by the weight at 30m water depth (Fig. 5b). Figure 5b shows that the *TT* factor increases with both water depth and soil type. For a

given soil type the increase in the *TT* factor (and thus the supply costs) of a structure from 30m to 60m is approximately 30%. As the *TT* factors between upper bound solution and lower bound solution did not vary significantly, only the upper bound solution was used in the further analysis.

Roark (2008) provided relative costs for lattice jacket type wind turbine support structures for varying water depths (Table 3). These costs were not very sensitive to moderate changes in water depth and did not distinguish between variations in soil conditions. These costs were also normalized by the cost at 30m water depth (i.e. $ 4.48M), and Figure 6 shows that there is reasonable agreement with the *TT* factors established independently in this study. Since Roark's costs are typical for North Sea conditions where soil types often consist of sands and stiff clays, the agreement of his *TT* values with the values for sand and stiff clays from this study is encouraging.

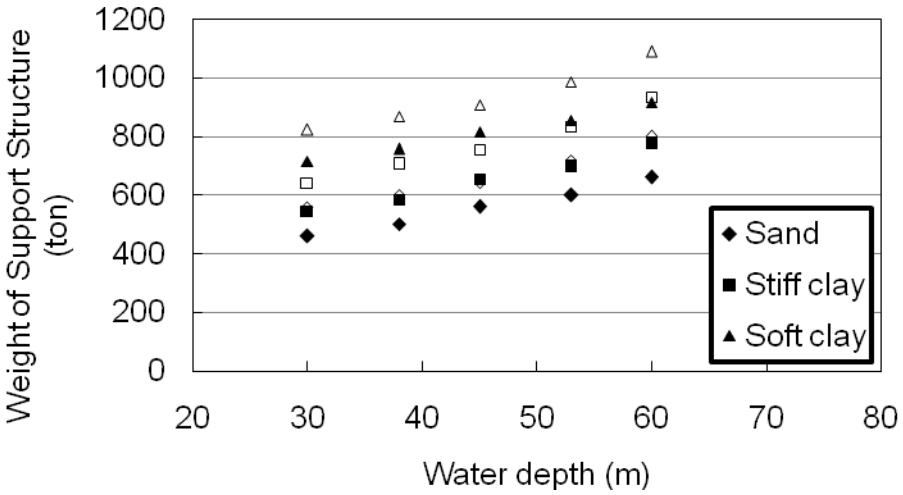

(a.)

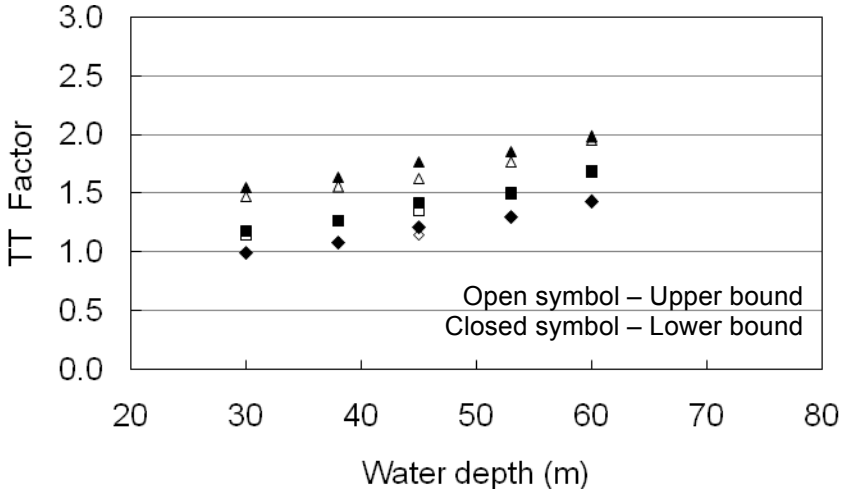

(b.)

Figure 5. Variation of a.) support structure weight and b.) Technology Type (*TT*) factor with soil type and water depth. The *TT* factors are the support structure weights at a given water depth divided by the support structure weight at 30m water depth.

Table 3. Published relative costs of jacket support structures of offshore wind turbines used as *TT* factors (Roark, 2008).

Water Depth (m)	Costs (Million USD)	*TT* Factor
5-25	3.36	1.75
25-45	4.48	1.0
45-65	5.76	1.28

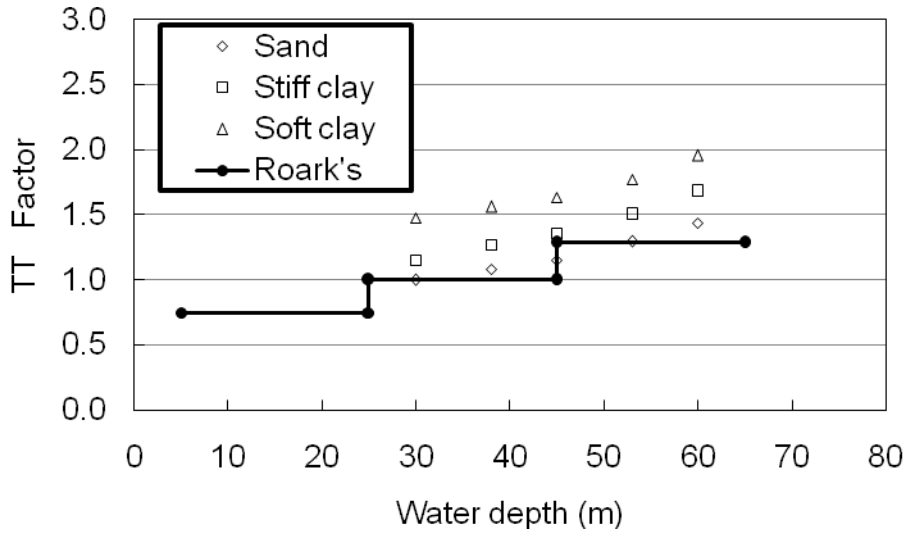

Figure 6. Comparison of Technology Type factor developed in this study with relative costs proposed by Roark (2008).

5.2 Relative Cost Model for Jacket Structures

The concept of using support structure weights to develop Technology Type factors can be expanded to a relative cost model for jacket structures. The simplest form of a cost model involves factoring the weight of the support structure by a supply and fabrication cost multiplier. To do this, it must first be recognized that the supply costs of a jacket are more than the supply costs of the foundation piles due to the additional effort required for fabrication. The relative cost of a jacket support structure (C_{ss}) can thus be expressed as:

$$C_{ss} = aW_j + bW_f \quad (4)$$

where W_j is the weight of jacket for a given water depth and soil type; W_f is the weight of piles; a is the material and manufacturing cost multiplier for jacket structure (e.g. $/ton); and b is the material and manufacturing cost multiplier for the piles.

Using the upper bound estimates of weight, W_j and W_f can be written as a function of water depth and soil type as shown in Table 4. With these relationships and accurate estimates of multipliers a and b, the variation of the cost of the support structure within the Ocean SAMP study area can be evaluated.

Table 4. List of weight functions

Support Structure Component	Soil Type	Weight (W) as a Function of Water Depth (d) (W in tons, d in m)	R^2
Jacket	all	$W_j=0.149d^2 - 5.342d + 342.299$	0.99
Foundation	Sand	$W_f = 241.6$	-
Foundation	stiff clay	$W_f = 0.005d^3 - 0.777d^2 +35.77d - 200.5$	0.98
Foundation	soft clay	$W_f = 0.004d^3 - 0.559d^2 + 22.380d + 217.5$	0.98

6 Conclusions

This study supports the Ocean SAMP *TDI* screening analysis by developing an independent measure of Technology Type (*TT*) factors for jacket structures supporting offshore wind turbines. *TT* factors are used to quantify the relative expense of a jacket structure and pile foundation system as the water depth increases and the soil conditions change, and is expressed as a non-dimensionless number. The factor is calculated from the total weight of the jacket and piles for a given water depth and soil conditions normalized by the weight of a reference structure. It takes into account environmental conditions from wind and waves specific to the Ocean SAMP study area.

Support structures were designed to safely carry a 5MW turbine. The structures were composed of a jacket substructure and a four pile foundation. The design of the jacket was based on two criteria. The first natural frequency of the structure had to be between the excitation frequencies of the rotating turbine and the passing blades. This is typically called a soft-stiff design and is important to avoid resonance during environmental loading. In addition, the allowable stresses in the structure and piles were kept below the yield strength of the material. This criterion is called the Ultimate Limit state.

Jacket weights were determined using the finite element program ANSYS. Thousands of combinations of different sized jacket legs and bracing were evaluated, and the designs that satisfied the two loading criteria were binned. Both upper and lower bound weights were determined for different water depths, and there was a consistent trend of increasing jacket weight with water depth. The foundation piles were designed using the API code (2000) for axial loads and the program L-Pile Plus for lateral loads. Designs were made for water depths ranging from 30m to 60m and for three different soil types: sand, stiff clay, and soft clay.

The combined weights of the jacket and piles were then compared to published values of weights from the Alpha Ventus jacket in Germany and the Beatrice jacket in Scotland. There was good agreement between the calculated and published values, which supports the validity of the design approach used in this study.

The combined weights of the jacket and piles were then used to directly calculate *TT* factors. The three weight functions (one for each soil type) were normalized by the weight of the

support structure in the shallowest water depth (30m) and for sandy soil, and the resulting *TT* factors range from approximately 1 to 1.44 for sandy soil condition , from 1.15 to 1.68 for stiff clay, and from 1.48 to 1.96 for soft clay. The results were compared to the weights of two existing jacket structures in Europe as well as existing Technology Type factors from the United Kingdom, and there was good agreement between the results.

References

American Petroleum Institute. (2000). Recommended Practice for Planning, Designing, and Constructing Fixed Offshore platforms - Working Stress Design, *API RP-2A-WSD*, 21st edition.

Det Norske Veritas. (2007). Design of Offshore Wind Turbine Structures, *DNV-OS-J101*.

Germanischer Lloyd. (2004). Guideline for the Certification of Offshore Wind Turbines.

Hensel, Jonas (2009). Jacket Structures for Offshore Wind Turbines in Rhode Island, M.S. Thesis, Department of Ocean Engineering, 145 pp.

International Electrotechnical Commission. (2006). Design Requirements for Offshore Wind Turbines, *IEC 61400-3*.

Musial, W. and Butterfield, S. (2004). Future for Offshore Wind Energy in the United States, *National Renewable Energy Laboratory,* Online: www.nrel.gov/docs/fy04osti/36313.pdf.

Papalexandrou, M. (2008). Economic analysis of offshore wind farms. Technical report, M.S. thesis. *KTH School of Energy and Environmental Technology,* Stockholm.

Reese, L.C. (1984). Handbook on Design of Piles and Drilled Shafts Under Lateral Load. *Report No. FHWA-IP-84-11*, U.S. Department of Transportation, Federal Highway Administration, Office of Implementation, Washington, D.C., 386 pp.

Roark, T. (2008). Offshore wind energy: An international perspective. *Marine Law Symposium*, October 23, Roger Williams University.

Schaumann, P. and Wilke, F. (2006). Enhanced Structural Design for Offshore Wind Turbines, *XICAT 2006, Xi'an International Conference of Architecture and Technology*, Xi'an, China.

Seidel, M. (2007). Jacket Substructures for the Repower 5M Wind Turbine, *Proceedings of European Offshore Wind Conf.,* Berlin.

Seidel, M. (2007a). Tragstruktur und Installation der Offshore-Windenergieanlage Repower 5M, *Stahlbau*, *76, 4*, 650-656 (in German).

Spaulding, M.L., Grilli, A. and Damon, C. (2010). Application of Technology Development Index and Principal Component Analysis and Cluster Methods to Ocean Renewable Energy Facility Siting. J. *Marine Technology Society* (in press).

Talisman Energy (2007). Beatrice Wind Farm Demonstrator Project Scoping Report, Final Report number W/61/000635/00REP, Online: http://www.beatricewind.co.uk/Uploads/Downloads/Scoping_doc.pdf.

van der Tempel, J. (2006). Design of Support Structures for Offshore Wind Turbines, *Ph.D. Dissertation*, TU Delft.

Westgate, Z.J. and DeJong, J.T. (2006) Geotechnical Considerations for Offshore Wind Farm Development, *WINDPOWER 2006*, June 4-7, Pittsburg, PA.

Zaaijer, M.B. (2002). Desing Methods for Offshore Wind Turbines at Exposed Sites, *TU Delft*, Online: Accessed on June 10th, 2009.

19.

Wind Resource Assessment in the Vicinity of a Small, Low Relief Coastal Island for the Rhode Island Ocean Special Area Management Plan 2010

by

Malcolm L. Spaulding[1], Marty Bell[2], Jay Titlow[3], Ravi Sharma[1], Annette Grilli[1], Alexander Crosby[1], Lauren Decker[4] and Daniel Mendelsohn[4]

[1] Ocean Engineering, University of Rhode Island, Narragansett, RI

[2]Metlogic, 212 West Mountain Avenue, Fort Collins, CO 80521

[3]WeatherFlow, 790 Poquoson Ave, Poquoson, VA 23662

[4]Applied Science Associates, 55 Village Square, South County Commons, South Kingstown, RI 02879

June 9, 2010

Executive Summary

The focus of the paper is to assess the wind resources for the area in state waters (4.5 km from land) immediately south of Block Island, a small, 9 km by 6 km, low relief (35 m elevation) pear shaped island located 15 km off the coast of RI, for the siting of a small (5 to 8 turbine) wind farm. The area is being considered for designation as the potential site for offshore wind development. A review of existing wind observations was performed and showed that the wind speed and power density roses were dominated by westerly winds with NW dominant in the winter and SW in the summer. Wind shear measurements from meteorological tower observations on the island showed low shears in the winter during unstable atmospheric conditions and higher values during the stable summer winds. The shears were also strongly impacted by the Block Island land cover and the positioning of the observation tower relative to these features.

A template based scaling method was used to estimate the annual mean wind speed and power density distribution in the vicinity of the southern end of the island. Hindcast simulations were performed using a four level nested version of RAMS for eight points of the compass for selected time periods over the last two years. These model predictions were compared to observations at two locations on the island and showed good agreement for direction and temporal trends of the speed but consistently under predicted the speed. The results of the simulations were used in conjunction with a wind speed frequency rose in the study area and, assuming linear speed scaling, estimates were made for the annual mean values. The large scale patterns showed wind speeds and power increasing with distance offshore. This pattern was modified in the vicinity of the island by lee effects from the predominant and strong NW winds. The impacted area extended at least 8 km to the SE of the island. Areas to the W-WSW of the island were impacted by lee effects from NE winds and roughness effects from Long Island, immediately to the west. Predictions showed the highest annual mean wind speeds and power densities to the S of the island with sites to the SW and SE having lower values. Power production potential was estimated for three sites: SE, S and SW of island. Wind power at the S site was 4.9 % and 6.9 % greater than the SW and SE sites, respectively.

Three separate wake models were applied to the SE and S sites to assess the impact of turbine layout. The SW site was not viable for a farm because of seabed geology making installation of pile foundations challenging. The turbines were nominally spaced 1 km apart. Simulations were

performed for each wind direction and showed wake losses as high as 14 %, when the wind was in alignment with the field. When weighted by data from a nearby wind rose, the annual losses were shown to be several percent at the SE site and about half of that at the S site. The difference is due to the fact that SW winds are dominant in the summer while W winds are less frequent.

Considering both lee effects from the island and wake effects, the S site is the preferred location for a small wind farm.

Table of Contents

List of Figures

Figure 25 Wind direction as a function of time for the eight directional cases at Block Island, Jetty, upper panel includes all data and the lower panel only data that were within 15 degrees of the desired direction.

List of Tables

List of Attachments and Appendices

Appendix A: Wind frequency and power density roses (seasonal and annual) and Weibull fits to all observations or hindcasts in the study area.

Appendix B: Titlow, J. and D. Morris, 2010. Block Island modeling analysis, WeatherFlow Inc., Poquoson, VA, with model simulations by MetLogics, Fort Collins, CO.

Appendix C: Step by step protocol for the template based prediction method, prepared by L. Decker and D. Mendelsohn, Applied Science Associates, South Kingstown, RI.

Appendix D: Evaluation of the linear scaling analysis used in the template based method.

Abstract

The focus of the paper is to assess the wind resources for the area in state waters (4.5 km from land) immediately south of Block Island, a small, 9 km by 6 km, low relief (35 m elevation) pear shaped island located 15 km off the coast of RI, for the siting of a small (5 to 8 turbine) wind farm. The area is being considered for designation as the potential site for offshore wind development. A review of existing wind observations was performed and showed that the wind speed and power density roses were dominated by westerly winds with NW dominant in the winter and SW in the summer. Wind shear measurements from meteorological tower observations on the island showed low shears in the winter during unstable atmospheric conditions and higher values during the stable summer winds. The shears were also strongly impacted by the Block Island land cover and the positioning of the observation tower relative to these features.

A template based scaling method was used to estimate the annual mean wind speed and power density distribution in the vicinity of the southern end of the island. Hindcast simulations were performed using a four level nested version of RAMS for eight points of the compass for selected time periods over the last two years. These model predictions were compared to observations at two locations on the island and showed good agreement for direction and temporal trends of the speed but consistently under predicted the speed. The results of the simulations were used in conjunction with a wind speed frequency rose in the study area and, assuming linear speed scaling, estimates were made for the annual mean values. The large scale patterns showed wind speeds and power increasing with distance offshore. This pattern was modified in the vicinity of the island by lee effects from the predominant and strong NW winds. The impacted area extended at least 8 km to the SE of the island. Areas to the W-WSW of the island were impacted by lee effects from NE winds and roughness effects from Long Island, immediately to the west. Predictions showed the highest annual mean wind speeds and power densities to the S of the island with sites to the SW and SE having lower values. Power production potential was estimated for three sites: SE, S and SW of island. Wind power at the S site was 4.9 % and 6.9 % greater than the SW and SE sites, respectively.

Three separate wake models were applied to the SE and S sites to assess the impact of turbine layout. The SW site was not viable for a farm because of seabed geology making installation of pile foundations challenging. The turbines were nominally spaced 1 km apart. Simulations were performed for each wind direction and showed wake losses as high as 14 %, when the wind was

in alignment with the field. When weighted by data from a nearby wind rose, the annual losses were shown to be several percent at the SE site and about half of that at the S site. The difference is due to the fact that SW winds are dominant in the summer while W winds are less frequent.

Considering both lee effects from the island and wake effects, the S site is the preferred location for a small wind farm.

1 Introduction

Spaulding et al (2010a) have recently performed an application of a Technology Development Index to the RI coastal waters to assist in siting of wind farms in the Ocean Special Area Management Plan (SAMP) study area (Figure 1). The TDI estimates the technical challenge (technology type plus cable distance) in extracting offshore wind energy to the wind energy (power) available at a given location. The analysis was performed on a grid of approximately 200 m. Optimum sites have low TDI (low technical challenge and high power production potential). To remove the dependence on units, the TDI is non-dimensionalized by the optimum value in the study area. Optimum sites have a TDI of one and less desirable sites have values increasingly larger than one. This analysis, assuming a lattice jacket support structure (Hensel, 2009; Roarke, 2008) as the technology type, turbine hub height at 80 m, and considering the difficulty of installing foundation piles in glacial, end moraine sediments showed that the optimum site in state waters (3 miles (4.8 km) from land) was immediately south of Block Island. Even though the water depths in the area range from 20 to 40 m, the wind resources are significantly higher than near the mainland shoreline, shallow water areas. Grilli et al (2010) subsequently performed a high resolution TDI (Figure 2) for this area and identified a band from east to the southwest approximately 2 km wide, bounded on the outer edge by the state water boundary as optimum for wind farm siting. This analysis used NOAA ENC bathymetry, results of high resolution side scan and sub-bottom imagery, supplemented by boring logs to determine the effort to install the pile foundation, and an estimate of the annual mean wind speed at 80 m provided by Brower (2007)(Figure 3).

Brower (2007) uses results from simulations performed with MASS (Mesoscale Atmospheric Simulation System). The model includes the fundamental physics of the atmosphere including conservation of mass, momentum, and energy, as well as the moisture phases. It also includes a turbulent kinetic energy module that accounts for the effects of viscosity and thermal stability on wind shear. The system creates a wind resource map by simulating weather conditions over 366 days selected from a 15-year period. The days are chosen through a stratified random sampling scheme so that each month and season is represented equally in the sample. Each simulation generates wind and other weather variables (including temperature, pressure, moisture, turbulent kinetic energy, and heat flux) throughout the model domain, and the information is stored at

hourly intervals. The analysis has been performed on a 2. 5 km grid, for the Ocean SAMP study area, and the data provided on a 200 m grid.

A review of the Brower (2007) estimates raises concern that this mean climatology does not adequately represent the wind fields in close proximity to Block Island (within state water boundary) given its topography (mean elevation of 35 m on the southern half of the island) (Figure 4) and surface roughness (Figure 5) and the potential for lee effects from winds from from the W to NE sector. The focus of this paper is to review the available observations to describe the wind fields in the vicinity of the island with a focus on mean annual conditions (Section 2), to apply a high resolution meteorological model (RAMS) (Section 3) to understand the basic flow patterns for eight points of the compass wind directions, and then to use the model predictions, in conjunction with observations, to estimate mean annual wind conditions to the south of the island. The sensitivity of these estimates to the wind rose used to represent the wind distribution and a comparison to Brower (2007) are provided. Finally comparisons are made if an 8 turbine wind farm is located to the SE and S of Block Island on the power generation. In addition, wake models (Section 6) are applied to determine the losses from each wind direction for the two sites and the total loss over the year. Conclusions are provided in Section 7.

2. Wind Observations

There are five sources of wind observations/hindcasts in the vicinity of Block Island. Each is briefly summarized below. These represent the principal observations for winds in the study area.

Army Corp of Engineers Wave Information Studies (WIS)-WIS101 (41 Lat, 71.58 Lon)(WIS101)

The US Army Corp performed a 20 yr hindcast (1980-1999) of the wind and wave conditions for a number of sites located along the southern boundary of the SAMP study area as part of the Wave Information Study (WIS)(http://www.frf.usace.army.mil/cgi-bin/wis/atl/atl_main.html). The locations of the southern New England hindcast sites are provided at the WIS web site. The site of primary interest in this investigation is WIS101, located immediately south of Block Island. Wind time series data are available at 10 m via the internet over the 20 yr hindcast period. Validation of the hindcasts was performed primarily using the NOAA NDBC offshore observations (Stations 44004, 44008, 440017, 440018, and 44025).

WeatherFlow Block Island Jetty (41.199 Lat, 71.593 Long)(BI Jetty)

WeatherFlow (http://www.weatherflow.com/) is a private firm that operates a network of meteorological observation towers in the SAMP study area. Data from their Block Island Jetty (western entrance to Great Salt Pond) station was obtained from WeatherFlow. Data was nominally at an elevation of 11 m. This data is available from December 2005 to 2009.

Department of Energy (DOE) Block Island Meteorological Tower (41.183 Lat, 71.57 Long)(DOE)

DOE made wind measurements at a site just south of Great Salt Pond as part of a feasibility study to investigate the siting of a wind turbine on the island (Renne et al, 1982). Measurements were made at two locations in the vertical (9.1 and 45.7 m). Wind data were available from 1979 through 1982, but with substantial periods of the record missing. The site is located on a hill top in rolling grass land on the southern edge of and overlooking Great Salt Pond.

Block Island Airport AWOS(41.168 Lat, 71.577 Long)(KBID)

An automated weather observation system (AWOS) is located on the northern side of the E-W oriented Block Island Airport runway (Figure 5). The runway is located on the southern end of the island with a mean elevation of approximately 35 m (Figure 4). Data is available from 1997 to present with observations at a 10 m height. The AWOS was located approximately 50 m eastward of the terminal building (peak height of 8.3 m) until the building was demolished and a new terminal constructed further to the west in 2009. The AWOS data collected prior to 2009 is considered suspect for westerly and northwesterly winds because it is in the immediate lee of the terminal building. In addition, there is strong topographic relief and tree cover to the west and northwest of the AWOS site (Figure 5) complicating accurate measurements of the wind.

Ocean SAMP Buoy MDS02 (41.1 Lat, 41.56 Long)(MDS)

The University of Maine, on behalf of the Ocean SAMP study, deployed an offshore buoy with meteorological and oceanographic sensors immediately south of Block Island at the state water boundary line. The buoy collects wind speed and direction and air and sea surface temperature data every 15 minutes. The data is distributed through the Northeast Regional Association of Coastal Ocean Observing Systems web site (www.neracoos.org) and has been in operation from October 1, 2009 to present.

AWS True Winds Block Island Meteorological Tower (41°11'49.96"N Lat, 71°35'30.34"W,Long.) (AWS Met)

AWS True Winds erected a meteorological tower at the western entrance to Great Salt Pond, in close proximity to WeatherFlow's Block Island Jetty Station. Wind speed and direction data are being collected at elevations of 9.9, 32, 47.6, and 57.4 m. Data is available from Aug 2009 to present.

Appendix A provides wind frequency and power density roses, average power rose, and a Weibull fit to the data for all sites in the study area. The reader is cautioned to note the duration of the observation or hindcast product and its elevation.

Figure 6 and 7 show the wind frequency and power density roses, respectively for all stations and the dates noted above. The reader should note that the data have been collected over different time periods and is of varying duration and at different elevations; so care should be taken in interpreting the data sets. The WIS data is a hindcast product and not actual observations. In all cases the data is presented at the lowest elevation of the measurements (typically in the range of 4 to 10 m).

Comparing the longer term data sets (DOE and WIS) it is observed that the wind frequency and power density roses are similar and dominated by winds from the west; NW and SW in particular. The wind data from KBID is substantially different from these two sets, likely due to the impact of the terminal building and the significant roughness elements NW of the measurement site. This data set is clearly not representative of oceanic conditions.

AWS Met and MDS data sets are from the winter of 2009-2010 and collected over the same period of time. Both data sets show that the dominant winds and power density are from the NW, with the next most frequent winds from the NE. A comparison of the both stations was made to the winter average from WIS 101 and showed good agreement (not shown here), with the exception that the NE winds were more frequent in 2009-2010. This is consistent with recent observations throughout the area showing enhanced NE winds during the 2009 to 2010 winter.

Figure 8 shows the average power density rose for each location. These plots are generated by frequency weighting the power density roses shown in Figure 7. The dominant wind power comes from the NW or W, except for KBID, which is SW dominated. The power density for KBID is more lower than any other station because of vegetative roughness effects. It is noted that wind power is particularly strong from the NE in both the AWS Met and MDS locations. This is consistent with strong NE winds occurring during the winter of 2009-2010.

An analysis was performed of the shear, using both the DOE and AWS Met data sets. Figure 9 shows the observed wind speed data at 9 m vs 45 m from the DOE site. The data have been fitted using a least squares regression line, which gives a shear coefficient of 0.228. This compares to a mean value over the record period of 0.245. A line representing the neutral boundary layer assumption is shown for reference. Figure 10 shows the shear coefficient by season and direction. The shear is lowest in the winter for NW winds and highest in both the summer and winter for SW winds. NW winds dominate in the winter and SW in the summer. The picture that emerges is that winter winds are typically unstable and hence the shear is primarily due to topographic relief and roughness of the island. In summer, the winds are stable and island topographic relief and roughness are significant over the steep southern face of Block Island and hence the shear is quite high.

Shear estimates were made from data collected at the AWS Met site from August 2009 to February 2010. The mean values decreased from 0.18 in August to 0.08 in November and remained in the range of 0.06 to 0.07 through February 2010. The shear was approximately the same, no matter which vertical levels were used to perform the analysis. The shear for the winter season at AWS Met is consistent with ocean conditions and stable transitioning to unstable atmosphere from late summer to winter. The impact of topographic relief and roughness is minimal as might be expected based on the station's location.

Grilli and Spaulding (2010) provide a comprehensive analysis of the data using Weibull distribution methodology. They demonstrate the transition from oceanic to land based roughness impacts on the wind field.

3. High Resolution Meteorological Modeling in Study Area

RAMS, the Regional Atmospheric Modeling System (Piekle et al, 1992; Tremback and Walko, 2010; RAMS, 2010), is a highly versatile numerical code developed by several groups over the years, including the scientists at Colorado State University, the *ASTER division of Mission Research Corporation, and ATMET. RAMS is used for simulating and forecasting meteorological phenomena, and for depicting the results.

RAMS is primarily a limited area model, and many of its parameterizations have been designed for mesoscale or higher resolution scale grids. There is no lower limit to the domain size or to the mesh cell size of the model's finite difference grid; microscale phenomena such as tornadoes and boundary layer eddies, as well as sub-microscale turbulent flow over buildings and

in a wind tunnel, have been simulated with this code. Two-way interactive grid nesting in RAMS allows local fine mesh grids to resolve small-scale atmospheric systems such as thunderstorms, while simultaneously modeling the large-scale environment of the systems on a coarser grid.

The atmospheric model is constructed around the full set of non-hydrostatic, compressible equations that include atmospheric dynamics and thermodynamics, plus conservation equations for scalar quantities such as water vapor and liquid and ice hydrometeor mixing ratios. These equations are supplemented with a large selection of parameterizations for turbulent diffusion, solar and terrestrial radiation, moist processes including the formation and interaction of clouds and precipitating liquid and ice hydrometeors, kinematic effects of terrain, cumulus convection, and sensible and latent heat exchange between the atmosphere and the surface, which consists of multiple soil layers, vegetation, snow cover, canopy air, and surface water.

For the present study daily simulations starting at 0Z were performed with RAMS version 6.1. The model employed a 500m horizontal grid spacing on the high resolution grid telescopically nested from 12 km, 6 km and 2 km grids (Figures 11 and 12). A range of horizontal grid resolutions from 4 km to 250 m were tested. In most cases, the convergence of results at the proposed turbine locations occurred at 1-2km. In some cases, where stable conditions existed and the proposed wind farm sites were downwind of the island, differences were apparent down to 500 m. 20 m vertical grid spacing, expanding upward with a geometric ratio of 1.15 was employed. Vertical grid resolutions from 40 m to 5 m were evaluated. Testing showed a loss in wind speed of up to 5 % when the vertical resolution was lowered from 5 to 20 m. 20 m was used in this study in order to complete the hindcasts in a timely fashion.

RAMS was initialized 6 hours prior to the 0Z start time (tau 0), firstly with a 2 grid run (outer grids only) from tau -6 to tau -3 (stage 1), then with all 4 grids from tau -3 to tau 0 (stage 2). Simulations were initialized from the 12 km North American Mesoscale Model (NAM) analysis, with grid 1 bounded by subsequent 6 hourly 12 km NAM analyses. In stage 1, the wind speed and direction, pressure, and air temperature model fields in the interior domain were strongly nudged to the interpolated NAM analysis values. In stage 2, the same variables were nudged, but far less strongly. The atmospheric moisture data was excluded from the nudging. This forces a balance to develop for the mechanical quantities between the model and the NAM analysis, while allowing moisture quantities (clouds and precipitation) to evolve.

The 3D (spatial and depth) soil moisture field was extracted from the 12km NAM analysis files and interpolated to the RAMS grids and soil levels. The 2D (spatial) snow cover field was

also extracted from the 12km NAM analysis files and interpolated to the RAMS grids. Sea surface temperature data was obtained from Operational Sea Surface Temperature and Sea Ice Analysis (OSTIA) which uses satellite data provided by the GHRSST project, together with in-situ observations to determine the sea surface temperature. The analysis is performed using a variant of optimal interpolation (OI) technique. The analysis is produced daily at a resolution of 1/20 degree, (approx. 5km).

Digital elevation data for Block Island was data was provided from ASTER GDEM, which has a 30 m grid resolution and is referenced to the WGS84/EGM96 geoid. Surface roughness, which is a significant factor in the results of this study, is formulated as a function of wind speed over water. Over land, contributions to the surface roughness come from the water bodies, soil, vegetative cover and topographical drag within the grid cell. RAMS partitions the land use effects into contributing patches, whose weighting on the grid scale is proportional the relative dominance of the water and vegetation cover from the MRLC land use dataset.

RAMs was applied to perform high resolution simulations for discrete events that characterized conditions typical of each direction of wind forcing experienced in the area. The dates and directions which they characterize are provided in Table 1. It is noted that from several of the directions (NE, S, and NW) more than one simulation was performed. While an attempt was made to ensure that the wind directions did not change significantly over the simulation period this was not always possible since the simulations represent real events. A detailed description of each simulation and a comparison of model predictions to wind observations at WeatherFlow's Block Island Jetty wind observation station and at the Block Island Airport (KBID) are provided in Titlow and Morris (2010) (Appendix B).

4. Model Application

Case examples

In the interest of space, only three examples are presented here: NW (Oct 30, 2008), SW (July 8, 2008), and NE (September 22, 2008). They have been selected because they are the predominant wind directions in the winter (NW), summer (SW), and during extra-tropical storms (NE), respectively.

For each case a brief description of the event is provided. This is followed by plan view plots of the wind speed and direction at 80 m for grids 3 and 4. Finally a plan view plot of the shear coefficient estimated from the model at 80 m for the highest resolution grid is provided. A

supporting figure is also given showing the wind shear coefficient as a function of elevation for Block Island Jetty, KBID, and sites to the SE and SW. Finally model predictions are compared to observations at Block Island Jetty and KBID. These are the only two stations collecting observations in the immediate vicinity of Block Island during the simulation periods.

October 30, 2008 – NW

Description

High pressure, 1030mb, building into the East Coast from the southwest, following the departure of a low pressure center tracking northeastward across Newfoundland. This is a relatively common synoptic setup. Since the passage of the cold front late on the 28th, wind directions veered into the west then NW through the 29th, becoming a well established northwesterly through Oct 30th. These post cold frontal northwesterly winds exhibit a characteristically gusty signature, with average morning wind speeds around 10 m/sec, with gusts to the upper teens. Through the afternoon, wind speeds ease slightly, in response to weakening pressure gradients. The gust to lull spread appears to remain relatively large irrespective of diurnal solar insolation and air temperatures over the land. Boundary layer mixing is largely occurring as a result of relatively warm sea surface temperatures warming the lower layers of post cold frontal air advecting into the region.

Wind Speed Contours

Wind speed contours for Grids 3 and 4 are shown in Figure 13, upper and lower panels, respectively, at 80 m. The large scale pattern (Grid 3) shows wind speeds progressively increasing with distance offshore. The contour lines are shore parallel. The rate of increase decreases with distance offshore. Immediately south of Block Island the winds reach their maximum speeds. The wind speeds in addition are impacted by the presence of Long Island immediately to the west. This pattern is a direct result of the decreasing surface roughness from land to the coastal ocean. The basic pattern is interrupted by the presence of Block Island. There are two areas to the SE of the island, at the northern and southern ends of the island that show lee effects from the island's topography and surface roughness. The wind speed deficient zones extend approximately 10 km from the island. The southern lee area is more pronounced than its northern counterpart due to the higher surface roughness and topography (Figure 3 and 4).

Shear

Figure 14 shows the wind shear coefficient at 80 m for Grid 4 at stations to the SE, SW, KBID and Block Island Jetty. Figure 15 shows the vertical structure of the shear coefficients at the same stations. Given the late fall conditions, the atmosphere is unstable (air temperatures colder than water temperatures) during this period and the shear coefficient is very low (0.05) for most of the field. The values over Block Island are considerably larger and reach 0.45 at KBID. The shear coefficient is observed to be strongly correlated with the topographic relief and land cover of the island. Block Island Jetty wind station is on the margins of the impacted area. In the lee of Block Island, SE, shear coefficient is predicted to be impacted by the presence of the island extending to the state water boundary.

Comparison with observations

A comparison of model predicted wind speeds and directions with observations as Block Island Jetty (upper left) and KBID (upper right) are shown in Figure 15. The large scale wind field for the US and Northeast are provided in the lower panels. Model predicted directions are in good agreement with observations. The temporal trend in wind speeds is correctly predicted but the model consistently under predicts the speed.

July 8, 2008- SW

Description

For this case a Bermuda high pressure, 1022 mb, established to the southeast with a weak, expansive low pressure system, 1002 mb, centered over Lake Superior, with associated cold front extending southwestward to Nebraska. A warm front extends from the low pressure center to Canadian Maritimes. This is a relatively common summer synoptic set up.

Southwesterly winds are established through the early morning hours with average wind speeds hovering around 5 to 6 m/sec, but unsteady with several periods of < 2.5 m/sec, and a couple of gusts to 7 to 9 m/sec. During the light period, wind directions veered more WSW to W briefly. Wind speeds began to increase after 0900, reaching a plateau between 1300 and 1600 (local time) with averages around 10 m/sec and gusts into the lower to mid teens.

Wind Speed Contours

The model predicted wind speed contours at 80 m for Grids 3 (upper) and 4 (lower) are provided in Figure 17. Compared to the NW case the coastal boundary layer is substantially compressed with speeds increasing to oceanic levels close to the RI shoreline. Areas on the western side of Block Island Sound are in the lee of Long Island. Wind fields NE of Block Island

show a large lee effect, extending at least 15 km. This effect covers the entire shadow zone of the island and is a result of the enhanced roughness and topographic relief at the southern end of the island (Figure 3).

Shear

Figure 18 shows the wind shear coefficient at 80 m for Grid 3. Figure 19 shows the vertical structure at the selected stations noted earlier. Given summer conditions, the atmosphere is very stable during this period and the shear coefficient is relatively high (0.25) for most of the oceanic field. The values over Block Island are considerably larger and reach 0.43 at KBID. The shear coefficient is again observed to be strongly correlated with the topographic relief and land cover of the island. The Block Island Jetty wind station is on the margins of the impact area. In the lee of Block Island, NE, the impact of the island on the shear coefficient is observed to extend a considerable distance from the island and exhibit lower shears (0.20) than in adjacent waters. The vertical structure of the shear is consistent among all locations with values highest at KBID, next highest at Block Island Jetty, and lowest and about the same at SE and SW sites.

Comparison with observations

A comparison of model predicted wind speeds and directions with observations as Block Island Jetty (upper left) and KBID (upper right) are shown in Figure 20. The large scale wind field for the US and Northeast are provided in the lower panels. Model predicted directions are in good agreement with observations. The temporal trend in wind speeds is correctly predicted but the model under predicts the speed at Block Island Jetty and substantially under predicts them at KBID.

September 22 -24, 2008 - NE

Description

Anti-cyclonic NE winds are observed across New England thanks to high pressure becoming established over Quebec following the passage of a cold front from NNW to SSE the previous day. A stationary frontal boundary and trough axis to the east of Cape Hatteras helps to enhance northeasterly pressure gradients across the region.

Northeast winds increase through the morning hours, from 0200: 5.5 to7 m/sec., to 0700: 8.5 to 9.8 m/sec. For the rest of the period northeast winds generally hold around 9 m/sec. mark. The lull-to-gust spread remains relatively small possibly indicating neutral or stable lower layers, and therefore more stratification rather than well mixed lower layers.

Wind Speed Contours

The wind speed contours (Figure 21) for this simulation are similar to those for SW case presented earlier, shore parallel with increasing wind speed with distance offshore. Reduced wind speeds are clearly observed on the western side of Block Island Sound. (The contours in Figure 21 are shown for February 24 not the 22 nd since the basic NE pattern is better depicted on this date.). Once again there is a low speed area in the lee of Block Island (SW). It extends about 10 km.

Shear

Figure 22 shows the wind shear coefficient at 80 m for the high resolution grid. Figure 23 shows the vertical structure at selected stations. Given fall storm conditions, the atmosphere is unstable during this period and the shear coefficient is relatively low (less than 0.10) for most of the field. The values over Block Island are considerably larger and once again reach 0.43 at KBID. The shear coefficient is again observed to be strongly correlated with the topographic relief and land cover of the island. Block Island Jetty wind station is on the margins of the impacted area. In the lee of Block Island, SW, the impact of the island on the shear coefficient is observed to extend a considerable distance from the island and exhibit lower shears (0.10) than in adjacent waters.

Comparison with observations

A comparison of model predicted wind speeds and directions with observations as Block Island Jetty (upper left) and KBID (upper right) are shown in Figure 24. The large scale wind field for the US and Northeast are provided in the lower panels. Model predicted directions are in reasonable agreement with observations and correctly capture the rapidly changing direction. The temporal trend in wind speeds is correctly predicted but the model substantially under predicts the speed at Block Island Jetty and at KBID.

5. Estimated Wind Resources South of Block Island

To estimate the mean annual wind speed (or power) a spatial template based weighting scheme was employed. (Appendix C provides a step by step protocol for the template based method.) This approach requires an estimate of the wind frequency or power rose at one location in the study area (ideally at hub height but more often at 10 m) and meteorological model predictions for each wind direction as function of elevation and location. Assuming that the wind spatial patterns are relatively constant over the 30 hr simulation period (Table 1) and that the

wind patterns scale linearly with speed, the wind speed map can be determined for each speed and direction bin. The dates given in italics were used as the base case in the analysis. Nominally eight (or some even multiple) direction and 10 or more wind speed bins are employed. The individual speed/direction bins are weighted by their occurrence from the wind frequency rose. If the wind rose is at a different elevation than the desired model predictions, the rose can be extrapolated to the appropriate height using the model predicted shear coefficient. This method assumes that the stratification (wind shear) from a given direction is represented in the model simulation. Note that model under or over prediction is not an issue, since we are only using the model spatial structure in the method.

To test the linearity assumption, hindcasts presented in Spaulding et al (2010b) using RAMS for the period from October 1, 2009 to February 28, 2010 were reviewed and 34 instances of NW winds identified. NW winds were selected since they generated the most power south of the island. The spatial patterns of all simulations were averaged to determine a mean wind speed map for all events. The wind speed maps for each individual event were divided by the mean spatial map to develop a scale map for each event. Appendix D provides the maps for each event. The scaling factors vary from a low of about 0.5 to a high of 2.0. For any given map the largest variation (lower to upper value) in scaling factor is on the order of 0.1 or 10% of the mean value. For all events the scale factor variation is +/- 3.3% of the mean value. This analysis confirms that linear scaling is a reasonable assumption.

Figure 25 shows the observed wind speed direction time series for each of the directional cases at the Block Island Jetty station (upper panel, all directions case). For cases with winds from the NW, E, SW, and W the wind direction does not vary significantly over the simulation period. The variations are much larger for the N, S, and SE cases and particularly large for the NE case. For the present analysis the directions of the cases were assumed to be constant as specified in Table 1.

Simulations were performed using the template weighting method described above and the WIS 101 (10 m) (Figure 26) rose to describe the wind speed directional distribution. WIS was selected as most representative of long term winds in the study area. Predictions of the mean annual wind speed and power, left and right panels, respectively are provided in Figure 27. The dots indicate locations E, ESE, SE, SSE, S, SSW, SW, WSW, and W of the island along the state water boundary line (Figure 5). The basic pattern is that the wind speed and power contours are approximately parallel to the RI shoreline with increasing values moving seaward. The presence

of Block Island and the prevalence of winds from the NW and W have resulted in a substantial area in the lee of the island (SE) with lower wind speeds and power levels. This clearly extends to the state water boundary. This area of reduced wind speed and power is a direct result of lee effects from the topographic relief and roughness of the island. Note a similar low power area is seen SE of the northern tip of Block Island.

An inspection of Figure 26 (upper panel) shows the directional variations of the winds was quite large for several of the cases (NE in particular). This will lead to smearing the directionality of the wind resource assessment. To assess the sensitivity of predictions to this issue, simulations were performed using only wind data that was within 15 degrees of the desired direction (Figure 26, lower panel). This is referred to as the "reduced direction" case.

Figure 28 show the wind speed and power contours, respectively at 80 m for the reduced direction case. The wind speeds and power levels are generally higher for this case but the underlying pattern is the same, extended lee effect E and SE of Block Island. The results from both cases are very similar showing the same large scale pattern. The wind resource to the SE is almost identical. SW of the island the all direction case predicts slightly lower wind power density than the reduced direction case (about 20 kW/m^2).

Template based model predictions were also performed using the AWS Met 57 m wind rose (Figure 26). It must be remembered that this rose is based on data from October 1, 2009 to February 28, 2010. Predictions of mean wind speed and power contours are shown in Figure 29. The basic pattern is again similar to the WIS101 case but with enhanced wind speeds and power since the time is restricted to the winter and spring seasons.

Model simulations, in addition, were performed using wind roses from WIS 100 and KBID. The power density contours are shown for each in Figure 30. Results for the WIS101 and AWS Met cases are also provided again to make facilitate comparisons. Model predictions for the WIS 101 and 100 are almost identical. The pattern for AWS Met is very similar to the WIS 101 cases although with stronger winds due to the winter time period. While the wind rose from KBID is not representative of the study area, as noted above (see Figure 26), predicted power contours are very similar to the other cases. All show strong lee effects to the SE of the island from NW and W winds. The lee effects are least pronounced in the KBID simulations and most prominent in the AWS Met case.

Additional simulations were performed to assess model predictions to which NW data case was used (Table 1). Each case was used separately and the average of all cases was used. There was very little difference among them.

Template based model predicted mean wind speeds and power density at selected sites E through W and at KBID, Block Island Jetty, AWS Met, and MDS are shown in Figure 31, using the WIS101 wind rose. The data show increasing speeds and power densities with distance offshore and lower values to the west compared to the east. The mean values for three potential locations for a small wind farm have been determined for sites SE (E, ESE, SE), S (SSE, S, SSW) and SW (SW,WSW,W) of the island. Mean powers are SE- 973 W/m^2, S- 1045 W/m^2, and SW- 994 W/m^2. The power production potentials at the S site are 6.9% and 4.9% greater than the SE and SW sites, respectively.

It is impossible to assess the uncertainty in the above estimates since there are no long term observations at any of the locations south of Block Island. To provide some sense of uncertainties a Weibull distribution was fit to the wind data at AWS Met, 57.4 m. This site was selected since it has the best quality data, at the highest elevation in the study area. Estimates were made of the mean and the upper and lower 95% confidence limits for the Weibull shape and amplitude parameters. The Weibull distribution was then used to estimate the mean and upper and lower 95% confidence limits for power and showed a +/- 2.5% variation around the mean.

Spaulding et al (2010b) applied the template method to predict the mean wind speeds and power density for a hindcast period for which RAMS hindcasts were performed (October 1, 2009 to February 28, 2010). The template method used directional simulations as noted in Table 1. These periods are hence completely independent of the hindcast period. The mean power density was determined directly from the model hindcasts and from the template based method using the wind rose at the AWS Met tower location as input. The template based model predictions were within +/- 5.3% of the hindcast estimates to the south of Block Island.

6. Wake Loss Modeling

Based on the TDI analysis there are two potential sites for a small, five to eight, turbine wind farm south of Block Island: SE and SSW (Figure 32). The spacing between the turbines is nominally 1 km, or about 10 blade diameters (100 m diameter blade). A site to the SW was not considered as it is not likely given the geological impacts on installation of the pile foundation

(Grilli et al, 2010). To assess the impact of wake losses at each site, simulations were performed with the three wake models incorporated in WinSim (www.winsim.com).

Model 1 (Jensen, 1983) is based on momentum deficit theory and expresses the radius of the area spread of momentum deficit behind the turbine as a linear function of the distance to the rotor, modulated by a decay factor. The decay factor increases with increasing levels of turbulence, which is directly related to the surface roughness (order of 10-2-10-4 for sea surface). Model 2 (Larsen, 1988) is based on turbulent boundary layer equations with the turbulence term expressed in terms of Prandtl's mixing length. Model 3 (Ishihara et al, 2004) introduces a semi-empirical term, the turbulent dependent recovery rate, that modulates the wake expansion. Since there is no model that is clearly superior to the others for the present applications simulations were performed with all three and the results averaged.

Figure 33 shows the average of all three models predictions as a function of wind direction. Simulations were performed for a constant wind speed of 9 m/sec at 80 m, with 12, equally spaced 30 degree direction bins. Three separate location cases are shown. Site 1 represents the SE location while Site 2 and 3 represent the SSW location, with Site 3 representing alignment of wind turbines in the E-W direction and Site 2, the same orientation but with staggering of every other turbine. The predicted losses are as large as 13 to 16 % when the wind farm layout is the same as the wind direction (E-W for Site 3 and NE-SW for site 1). Staggering the turbines substantially reduces the losses (compare Site 2 and 3). Slight curvature in the farm layout, as in Site 1, reduces the maximum loss but spreads it directionally.

To estimate the total loss at a site, a wind rose was used to characterize the frequency distribution of wind speed by direction, the wind losses for each direction and speed bin are determined, and the total determined by applying the frequency weighting to each case. The total wake loss was estimated using wind roses from WIS 101, Buzzard Bay CMAN station, and data collected by meteorological observations on Block Island, with 12 direction (30 degree) and 1 m/sec speed bins. The WIS101 represents the closest long term (20 yr) hindcast, the Buzzard Bay station represents the closest long term observation at elevation (23 m), and the data from the Block Island meteorological tower represents the closest observation but is of limited duration (5 months). The results are provided in Table 2, in terms of the minimum, mean, maximum and standard deviation of the three methods. The results are approximately independent of which wind rose is used. The losses are about twice as high at Site 1 (1.7 to 1.8%) than at Sites 2 and 3 (0.8 to 1%). Staggering at the SSW site reduces the losses slightly,

about 0.2% (Compare Sites 2 and 3). In the larger context, wake losses are predicted to be small and are below the uncertainty of the wind resource estimates in the vicinity of the island.

7. Conclusions

Annual wind speed and power roses in the vicinity of Block Island (WIS 101, DOE) are typically dominated by westerly winds: NW in the winter, SW in the summer, and W in the spring and fall. Winds at AWS Met and MDS are dominated by NW followed by NE winds, characteristic of the winter observation period (Oct to Feb). KBID winds are predominantly from the SW and are strongly impacted by land cover (trees) and resulting high roughness for winds from the W and NW. The speeds at KBID are substantially lower than those at DOE or AWS Met again because of roughness effects.

Wind shear at the DOE site showed seasonal and directional dependence. Wind shear was lowest in the winter months (0.15) (NW), highest during the summer (0.28) (SW), and intermediate in other seasons. The shear at this island based site is impacted both by the seasonal stability of the atmosphere and the land cover and topography upwind from the site: stable in the summer and unstable in the winter. Wind shear coefficient at the AWS Met site was consistent with the transition from late summer (0.15) to fall and winter conditions (0.06 to 0.09). These values are lower than at the DOE site for the comparable time of the year since the AWS Met is located much closer to the shoreline.

Simulations from the individual compass directions showed consistent large scale patterns. When the wind blew offshore (NW, N, NE) the wind speed increased with distance offshore reaching maximum values just seaward of Block Island. If the winds were from the west (W, SW) the wind speed contours were once again shore parallel but more closely spaced. Areas on the western side of Block Island were in the lee of Long Island, with lower wind speeds close to the island. Winds from the S and SE were rare. In the immediate vicinity of Block Island, wind speeds demonstrated a lee effect for all wind directions. The impacted area typically extended 8 km or more from the island. Details of the shape of the impacted area were dependent on the wind direction and its orientation relative to high roughness land cover and elevation of the southern and northern end of the island. For winds from the NW, two lee areas are predicted, consistent with higher elevations and greater roughness at the northern and southern end of the island. For winds from the NE and N and from the S and SW only one impacted area is predicted.

The template scaling method was applied using the model predicted wind pattern for discrete compass directions and the WIS 101 wind rose to determine the annual mean wind speed and power density for the study area. The predictions showed a basic pattern of increasing speeds and power with distance offshore. This pattern is altered with lower speed and power to the southeast of the island. This is due to the fact that NW winds dominate the wind power rose. Sites to the S of the island show the highest power production potential, followed by sites to the SW and SE.

Simulations were performed constraining the model predicted wind time series used to define the directional templates to be within 15 deg of the selected direction. The annual mean estimates showed the same general pattern as the prior case with same small alternations in magnitude.

Sensitivity studies were performed using wind rose data from WIS100, AWS Met, and KBID. All gave similar patterns with prominent lee effects to the SE of the island. The smallest lee effects were predicted KBID because of its enhanced SW winds and largest for AWS Met because the wind rose was from the winter spring season when NW winds dominate.

Power production potential was estimated for three sites: SE, S and SW of island. Wind power at the S site was highest and 4.7% and 6.9% lower, respectively, than the S site. This result is consistent with Spaulding et al (2010c) analysis based on a model hindcast of the period from October 1, 2009 to February 28, 2010.

Simulations were performed using three separate wake models to assess the impact of wake losses on siting of a small wind farm. Turbine spacing was nominally 1 km. The losses are highest (14%) when the winds are in alignment with the turbine layout and disappear in the cross wind directions. The results of the individual directional cases and the WIS 101 wind rose were used to estimate total losses. The losses are about twice as high at Site 1 (SE) (1.7 to 1.8%) than at Sites 2 (staggered) and 3 (0.8 to 1%)(SSW). Staggering at the SSW site reduces the losses slightly, about 0.2%. In the larger context wake losses are predicted to be very small and are well below the uncertainty of the wind resource estimates in the vicinity of the island (Spaulding et al, 2010c).

Considering both lee effects from the island and wake effects, the S site is the preferred location for a small wind farm.

References

Brower, M., 2007. Wind resource maps of Southern New England, prepared by True Wind Solutions, LLC, 10 p.

Grilli, A., M. L. Spaulding, C. Damon, and R. Sharma, 2010. High resolution application of the Technology Development Index (TDI) in state waters south of Block Island, Ocean SAMP project report, Ocean Engineering, University of Rhode Island, Narragansett, RI.

Grilli, A. and M. L. Spaulding, 2010. Estimation of offshore wind power resources based on Weibull distribution in Rhode Island coastal and offshore waters, Ocean Engineering, University of Rhode Island, Narragansett, RI.

Ishihara T., Yamaguchi A., Fujino Y., 2004. Development of a new wake model based on wind tunnel experiment, Poster in Global Wind Power, 2004,Tokyo, Japan.

Jensen, N.O., 1983. A note on wind generator interaction. RIS0-M-2411. RIS0 National Laboratory, Roskilde, Denmark, 16pp.

Larsen, G.C., 1988. A simple wake calculation procedure. RIS0-M-2760. RIS0 National Laboratory, Roskilde, Denmark, 58pp.

Hensel, J.V., 2009. Jacket Structures for offshore wind turbines in RI, MS Thesis, Ocean Engineering, University of Rhode Island, Narragansett, RI, 159p.

Pielke, R.A., W.R. Cotton, R.L. Walko, C.J. Tremback, W.A. Lyons, L.D. Grasso, M.E. Nicholls, M.D. Moran, D.A. Wesley, T.J. Lee, and J.H. Copeland, 1992: A comprehensive meteorological modeling system -- RAMS. Meteor. Atmos. Phys., 49, 69-91.

RAMS, 2010, Regional Atmospheric Modeling System Technical Manual, Weather Flow,

Renne, D. S., W. F. Sandusky, and D. L. Hadley, 1982. Meteorological field measurements at potential and actual wind turbine sites, US Department of Energy, Pacific Northwest Laboratory, Richland, WA, PNL -4431, UC-60, September 1982

Roark, T., 2008. Offshore wind energy: An international perspective, Roger Williams University, Marine Law Symposium, October 23, 2008.

Spaulding, M. L., A. Grilli, C. Damon, and G. Fugate, 2010a. Application of Technology Development Index and Principal Component Analysis and Cluster Methods to Ocean Renewable Energy Facility Siting, Marine Technology Society, Special Issue on Marine Technology for Offshore Wind, Vol. 44, No 1, January/ February 2010, pg 8-23.

Spaulding, M. L., M. Bell, J. Titlow, A. Grilli, R. Sharma, L. Decker, and D. Mendelsohn, 2010b. Meteorological model based wind resource assessment in the vicinity of Block Island, Ocean Engineering, University of Rhode Island, Narragansett, RI

Spaulding, M. L., A. Grilli, A. Crosby, and R. Sharma, 2010c, Evaluation of wind statistics and energy resources in southern RI coastal waters, Ocean Engineering, University of Rhode Island, Narragansett, RI

Titlow, J. and D. Morris, 2010. Block Island modeling analysis, WeatherFlow Inc., Poquoson, VA with model simulations by MetLogics, Fort Collins, CO.

Tremback, C. J. and R. L. Walko, 2010. Regional Atmospheric Modeling System, Users Guide-Introduction, Version 6.0, ATMET, Boulder, CO.

Table 1 List of WeatherFlow simulation dates and their associated directions.

1. ***North: January 4th 2008***
2. ***Northeast: September 22nd 2008***
3. ***Northeast 2: April 17th 2008***
4. ***East: September 24th 2008***
5. ***Southeast: October 25th 2008***
6. South: September 6th 2008
7. ***South 2: November 8th 2008***
8. ***Southwest: July 8th 2008***
9. ***West: December 22nd 2008***
10. Northwest 1: October 30, 2008
11. Northwest 2: November 22 2008
12. ***Northwest 3: February 23 2009***

*Sites in **bold italics** were used in the analysis as the base case.*

Table 2 Sensitivity to climatology

Wake effect: Sensitivity to climatology				
	Power loss (%)			
Climatology 1: WIS101	***min***	***max***	***mean***	***std***
Site1 (SE)	1.1	2.3	1.7	0.43
Site2 (SSW, Stag.)	0.6	1.0	0.8	0.14
Site3 (SSW, SE-W)	0.7	1.6	1.1	0.29
Climatology 2: Block Island Tower	***min***	***max***	***mean***	***std***
Site1 (SE)	1.4	2.3	1.8	0.35
Site2 (SSW, Stag)	0.7	1.1	0.9	0.16
Site3 (SSW, E-W)	0.6	1.3	0.9	0.25
Climatology 3: Buzzard Bay	***min***	***max***	***mean***	***std***
Site1 (SE)	1.1	2.4	1.8	0.46
Site2 (SSW,Stag.)	0.6	0.9	0.8	0.13
Site3 (SSW, E-W)	0.7	1.5	1.0	0.26

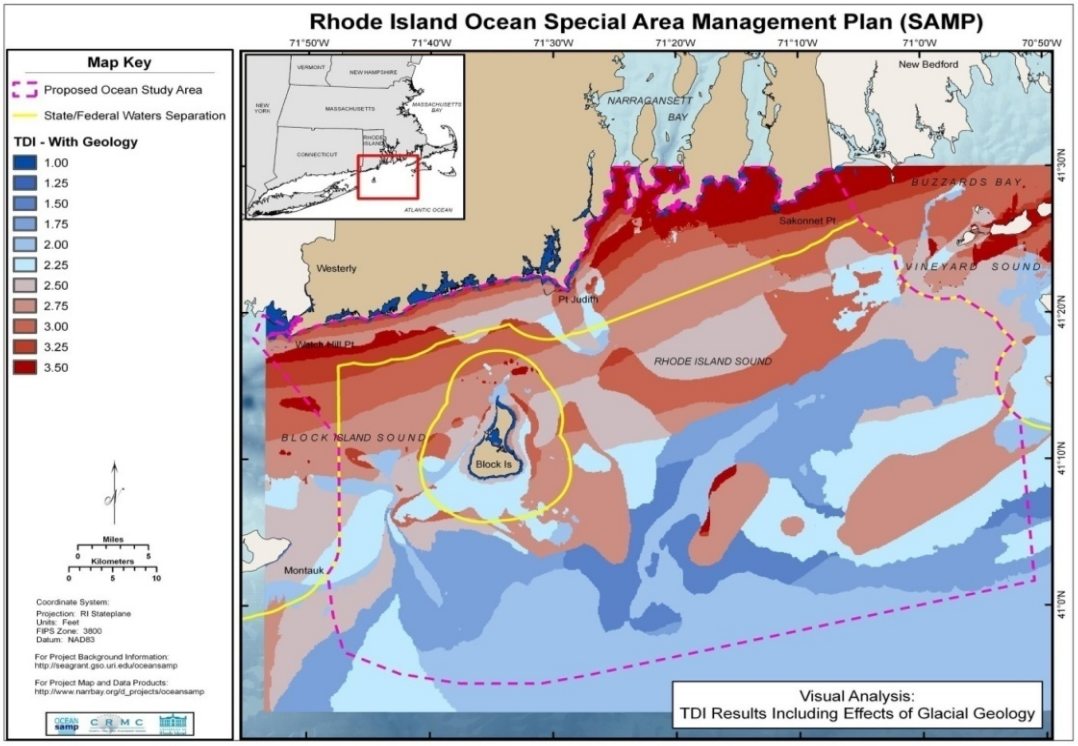

Figure 1 Contours of non-dimensional *TDI* for the Ocean SAMP study area, with glacial geology (Spaulding et al, 2010a).

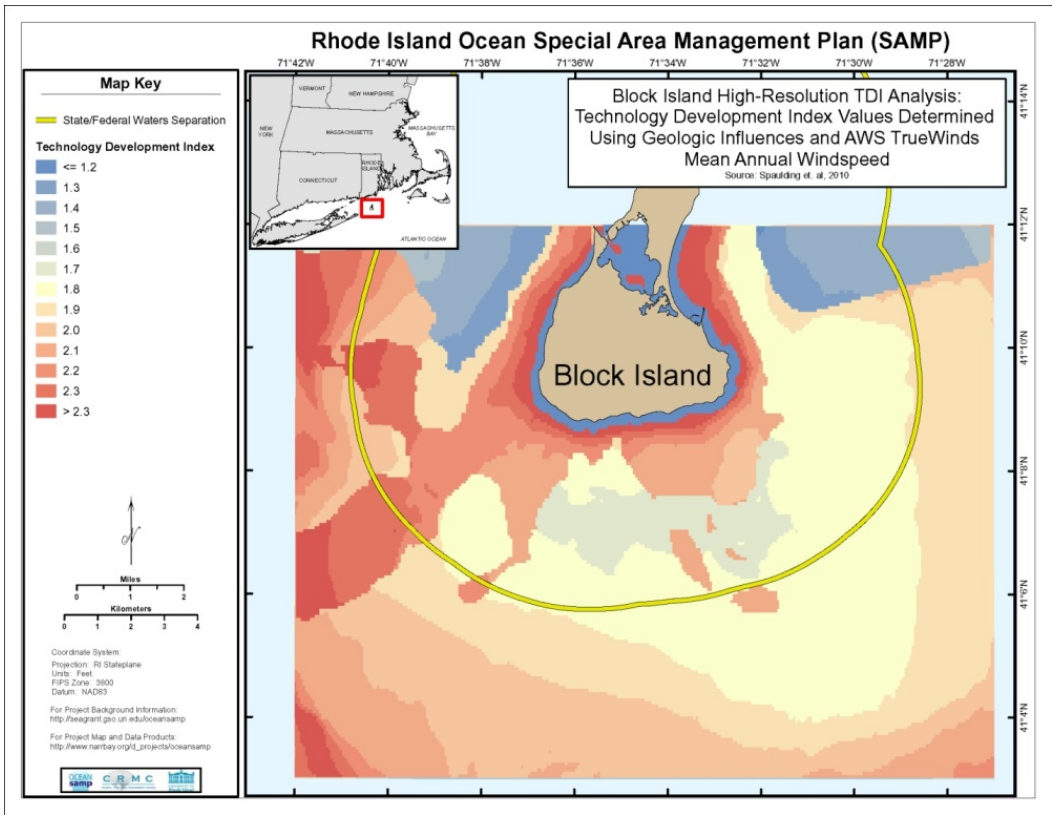

Figure 2 Technology Development Index (TDI) for Block Island Study area with geology (Grilli et al, 2010a) using AWS TrueWinds mean annual winds (Brower, 2007).

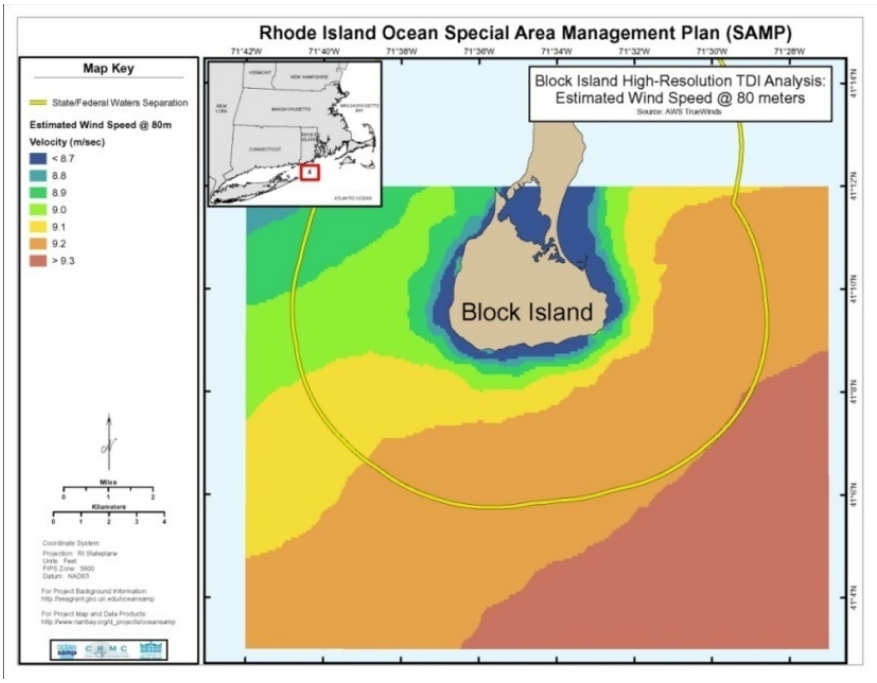

Figure 3 Estimated mean annual wind speed at 80 m from AWS TrueWinds data (Brower, 2007) for Block Island study area.

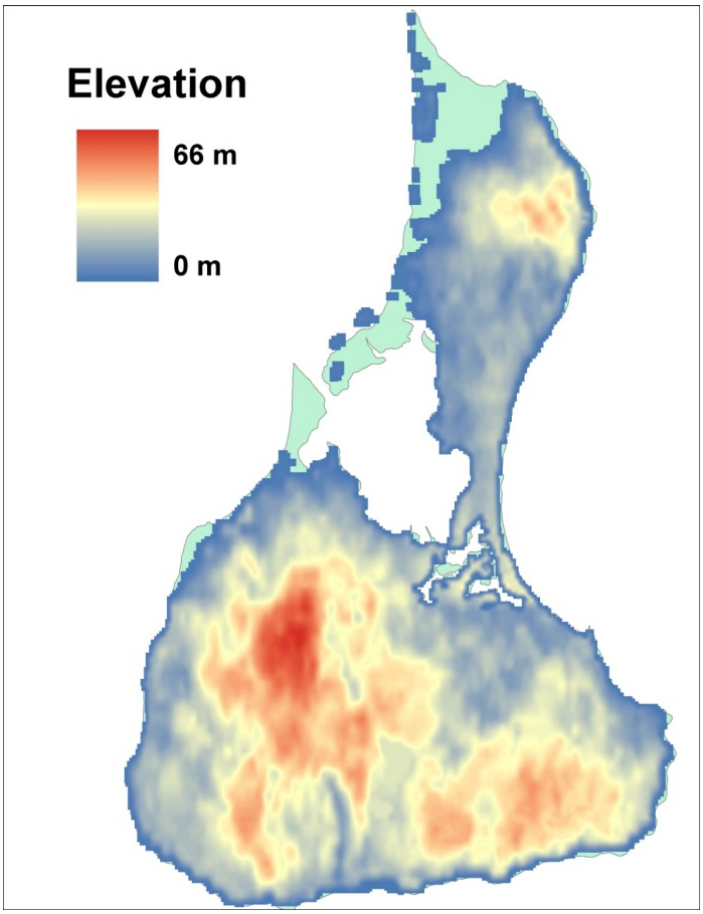

Figure 4 Block Island topography (RI GIS)

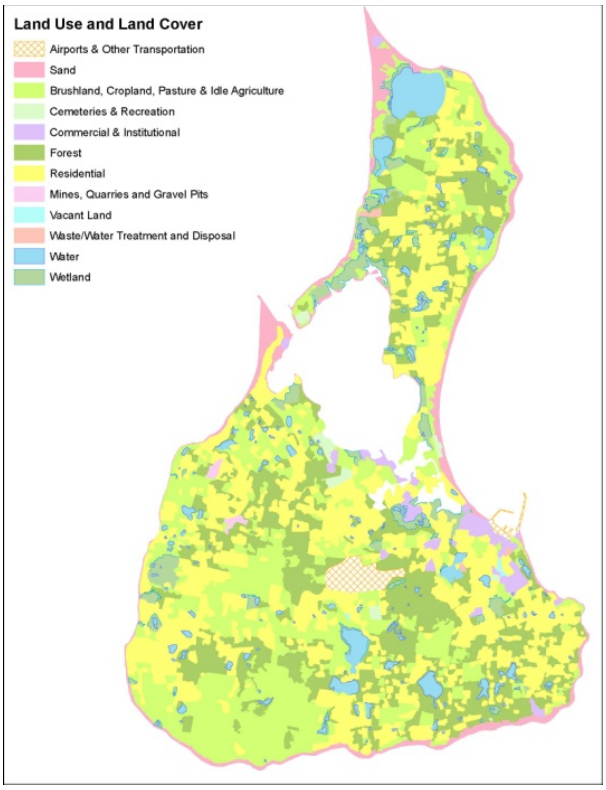

Figure 5 Block Island Land Cover (RI GIS).

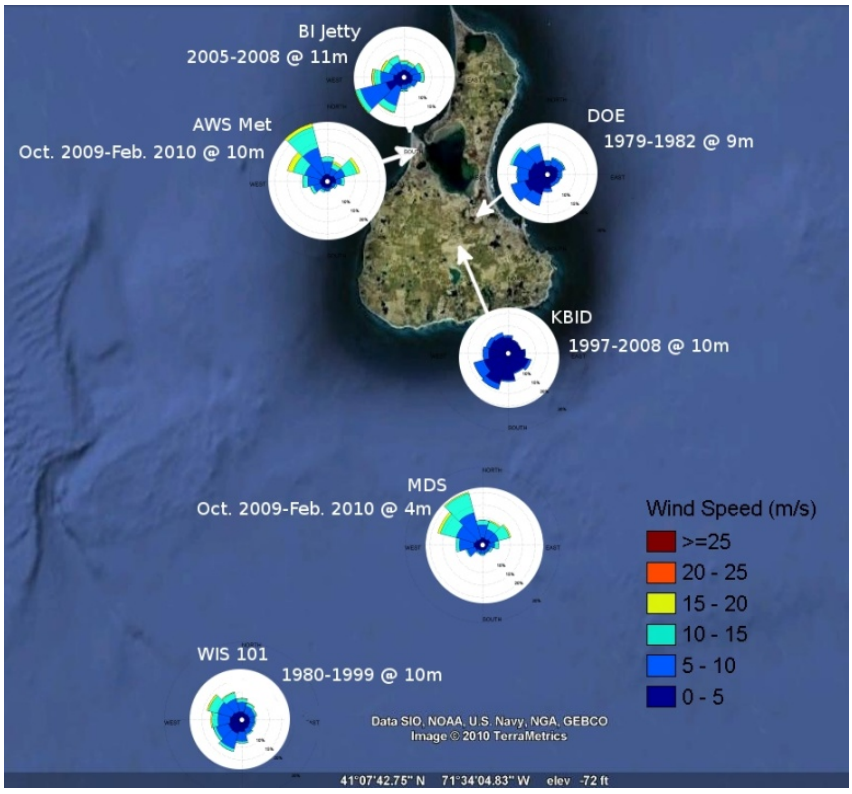

Figure 6 Wind speed frequency roses in the vicinity of Block Island.

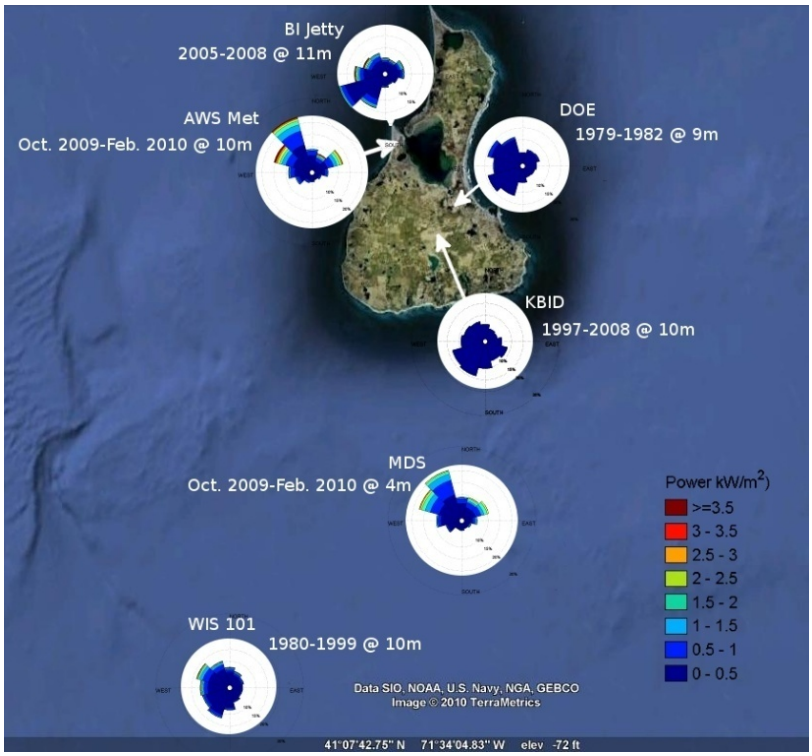

Figure 7 Wind power density roses in the vicinity of Block Island

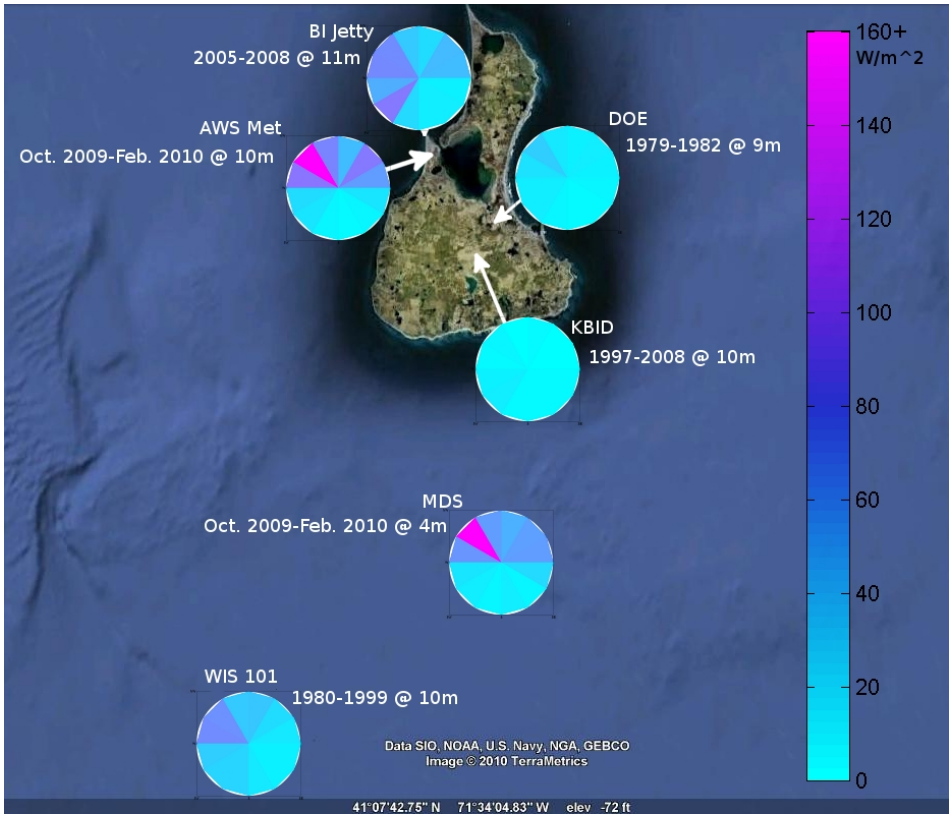

Figure 8 Average wind power density versus direction in the vicinity of Block Island.

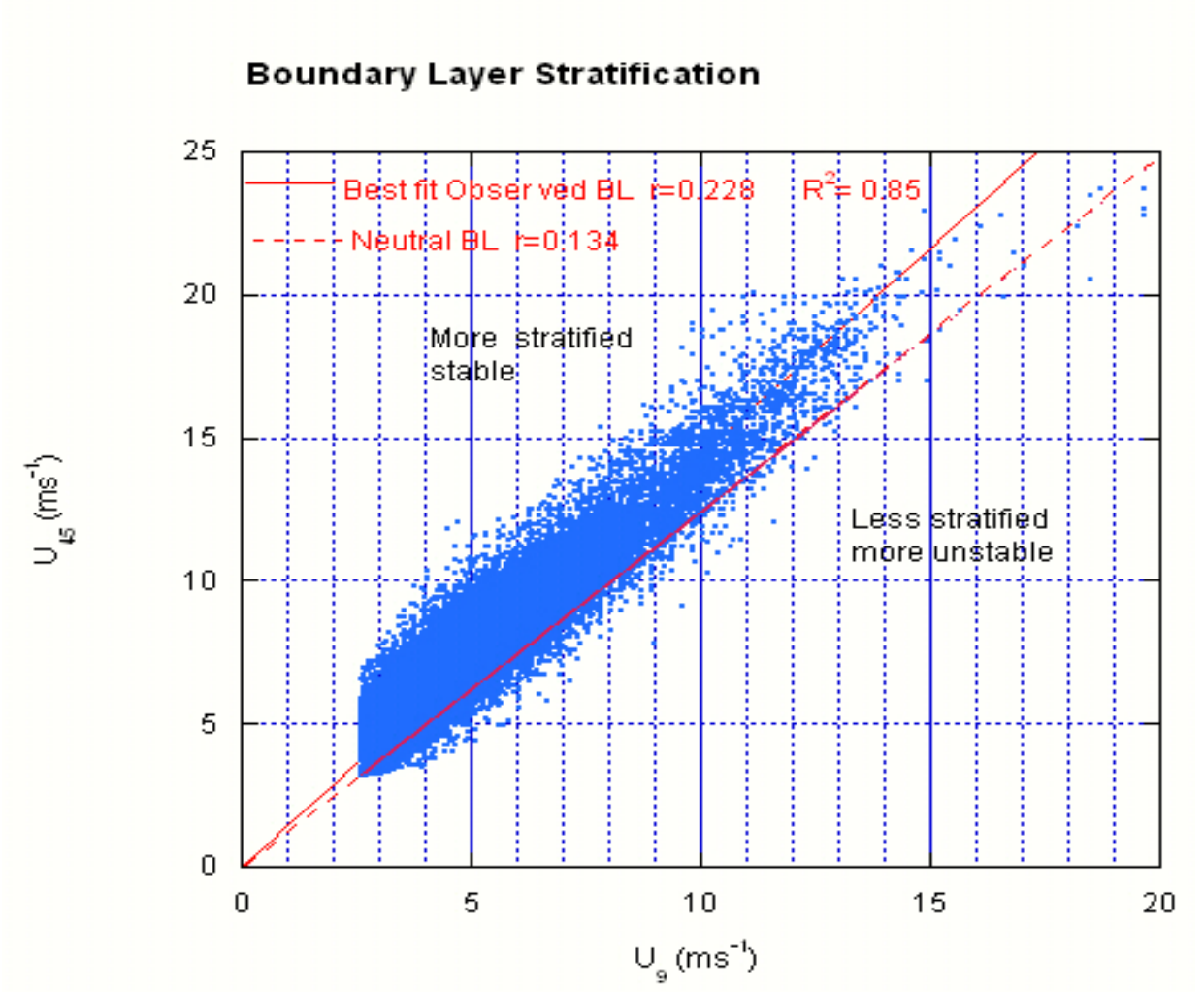

Figure 9 Observed wind speeds at 9 m vs those at 45 m from the DOE observations, 1979 to 1982. A neutral boundary layer is provided for reference and a linear least squares regression line for the shear coefficient is shown.

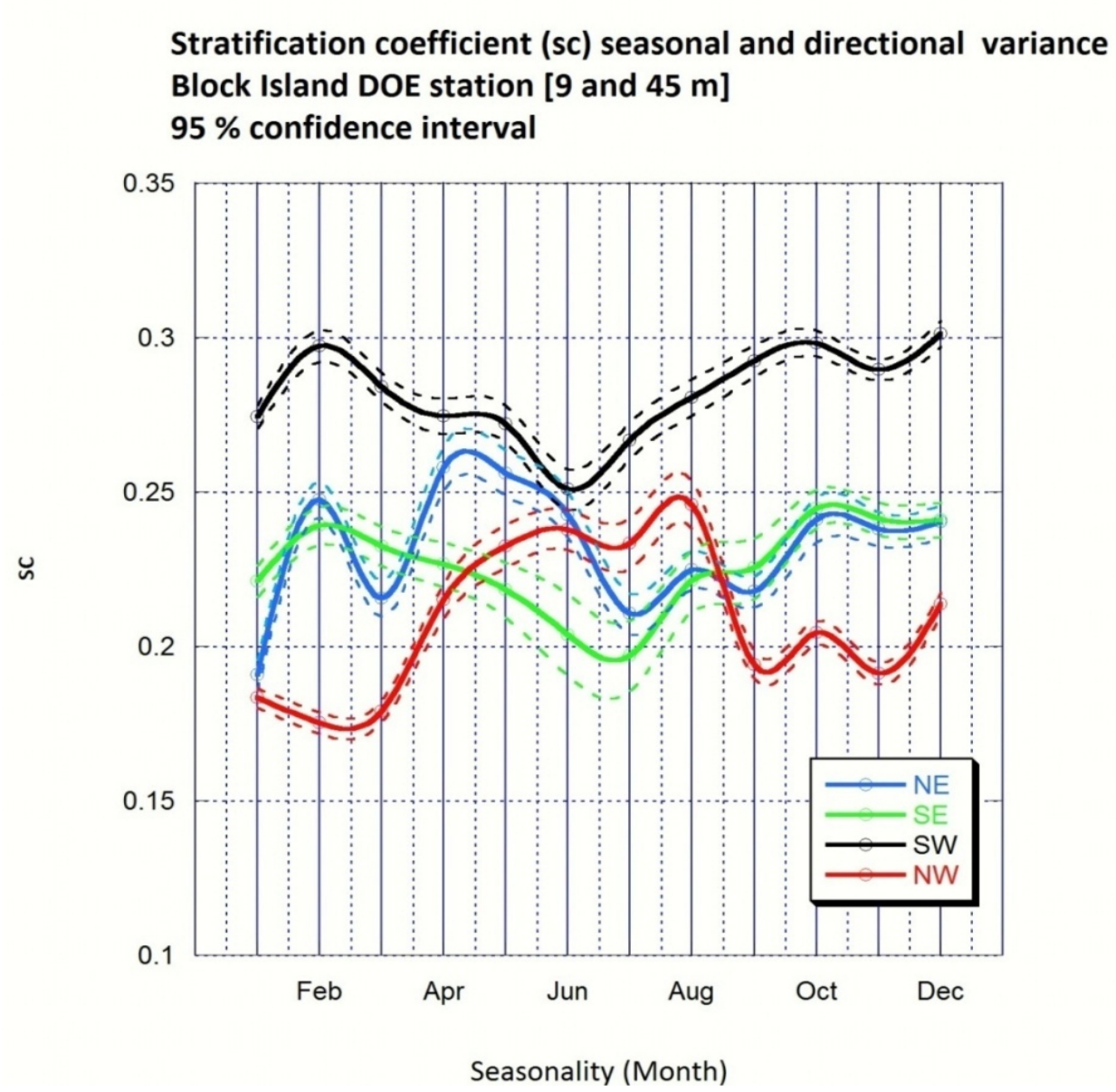

Figure 10 Shear coefficient for the DOE site vs month and direction. The upper and lower 95% confidence limits are shown.

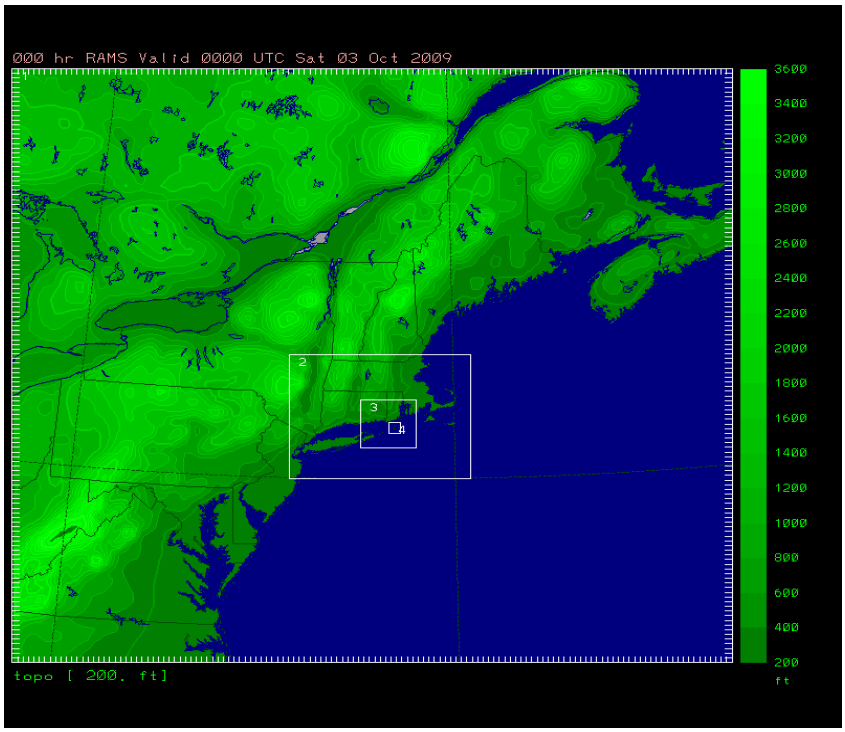

Figure 11 Nested grid system showing 6 km (Grid 2), 2 km (Grid 3) and 0.5 km (Grid 4) grid boundaries.

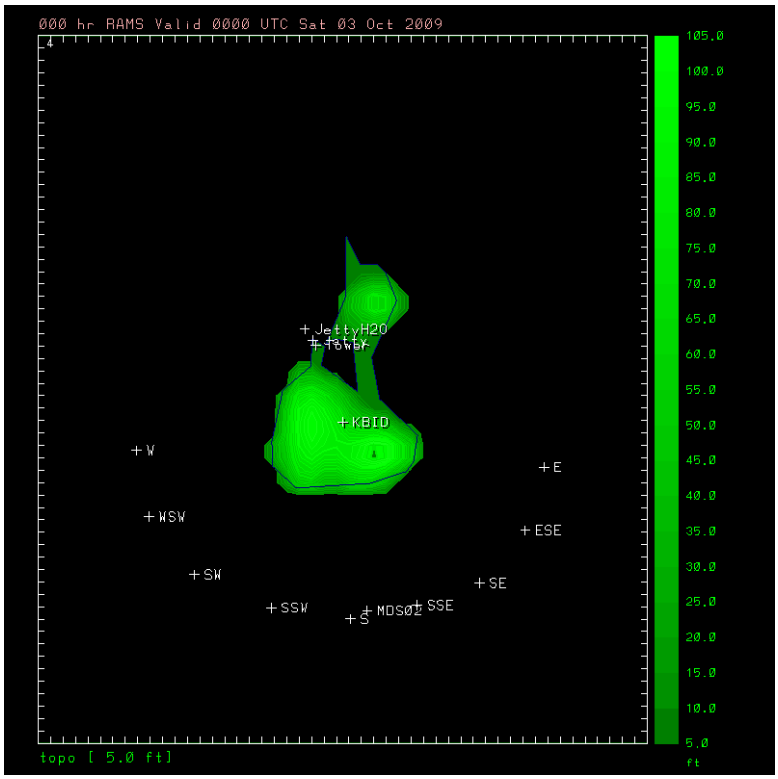

Figure 12 Grid 4 showing topographic relief of Block Island. The locations at which model time series were generated are shown, including E, ESE, SE, SSE, S, SSW, SW, WSW, and W along state water boundary line, and at observation locations KBID, BI Jetty, AWS Met, and MSD.

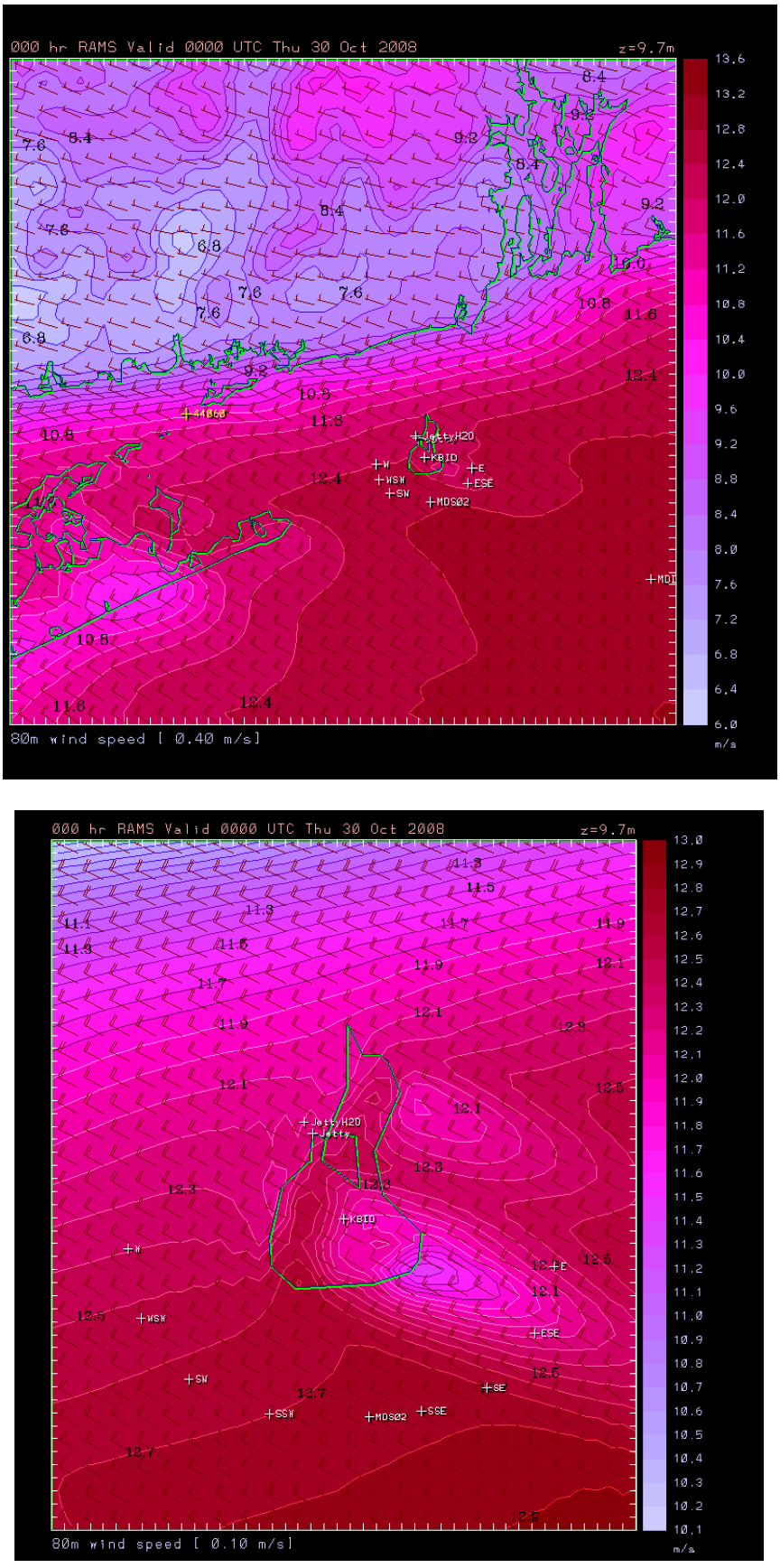

Figure 13 Model predicted wind speeds at 80 m at 0000 UTC on October 30, 2008 (NW). Upper panel Grid 3 and lower panel Grid 4.

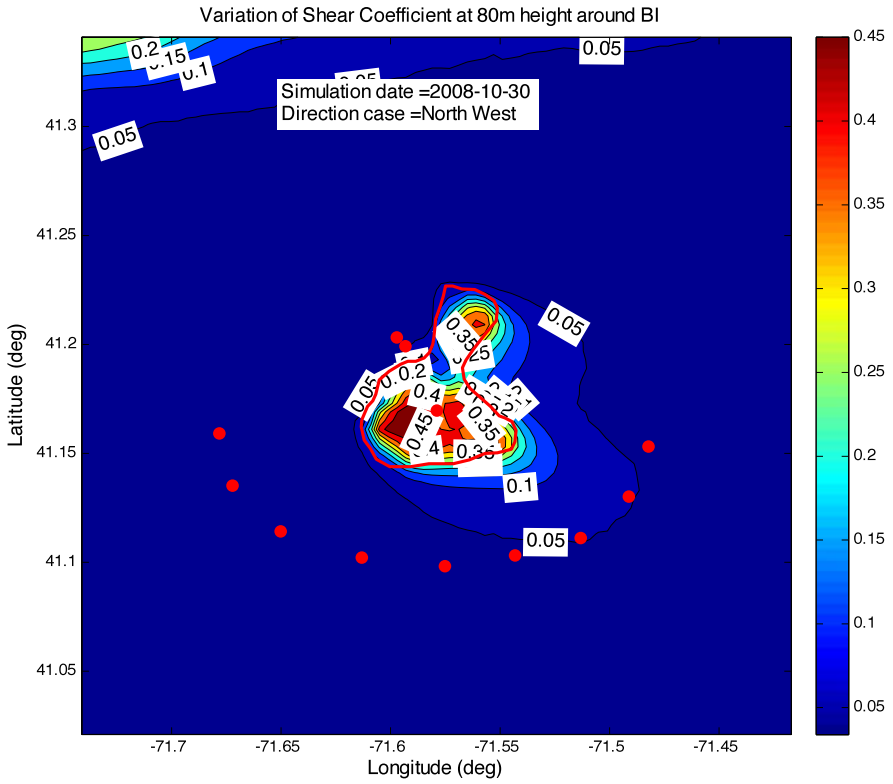

Figure 14 Model predicted shear coefficient for October 30, 2008 simulation.

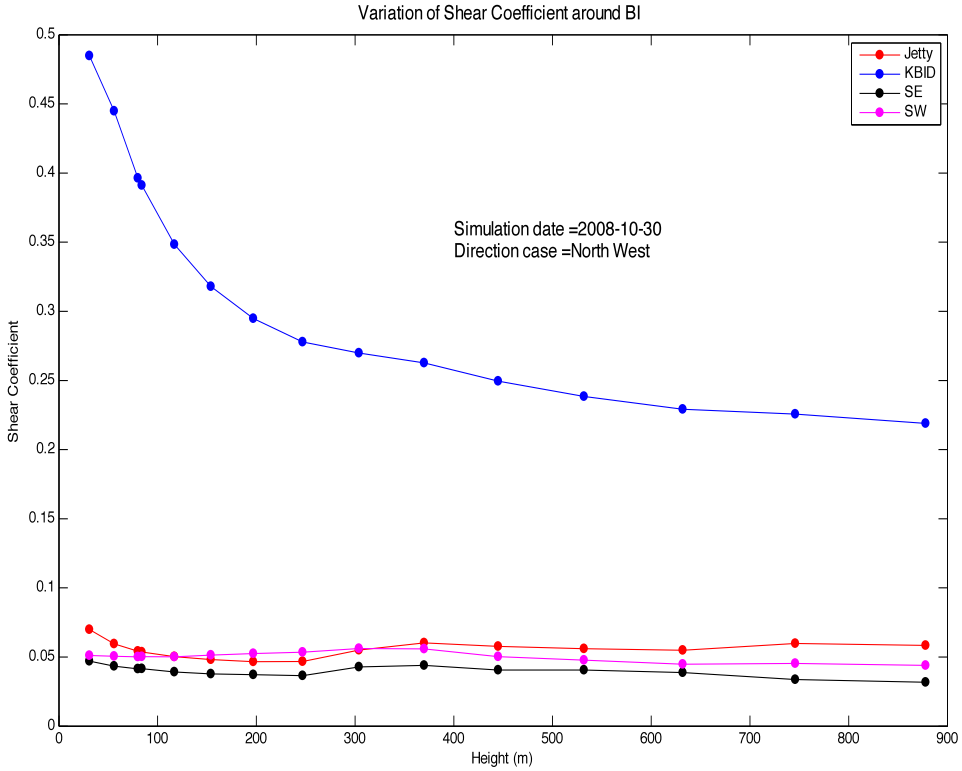

Figure 15 Model predicted shear coefficient at SE, SW, KBID, and Block Island Jetty locations for the October 30, 2008 simulation.

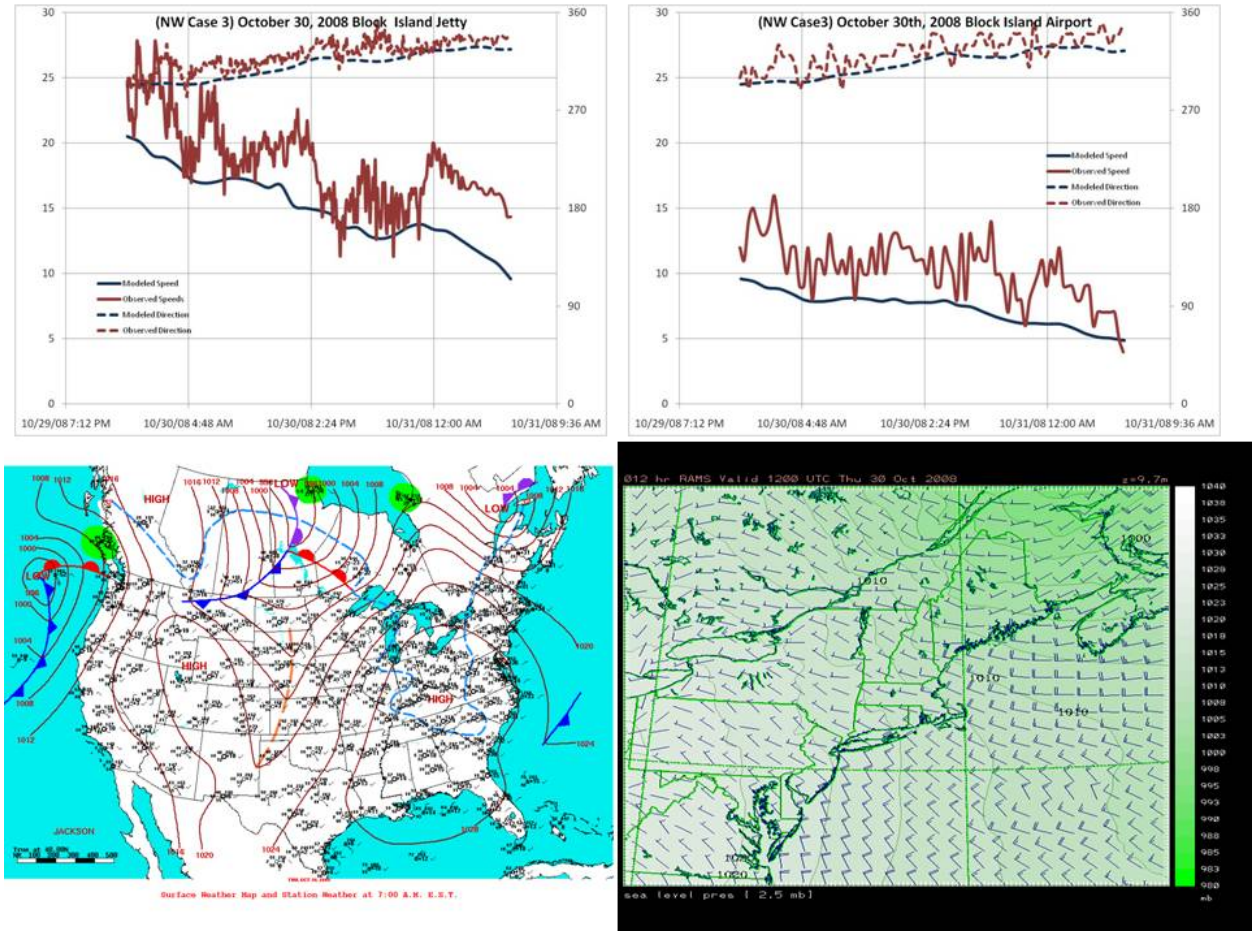

Figure 16 Comparison of model predictions to observations at Block Island Jetty (upper left) and KBID (upper right) on October 30, 2008. Large scale atmospheric forcing field (lower left) and NAM model predictions for Northeastern US (lower right).

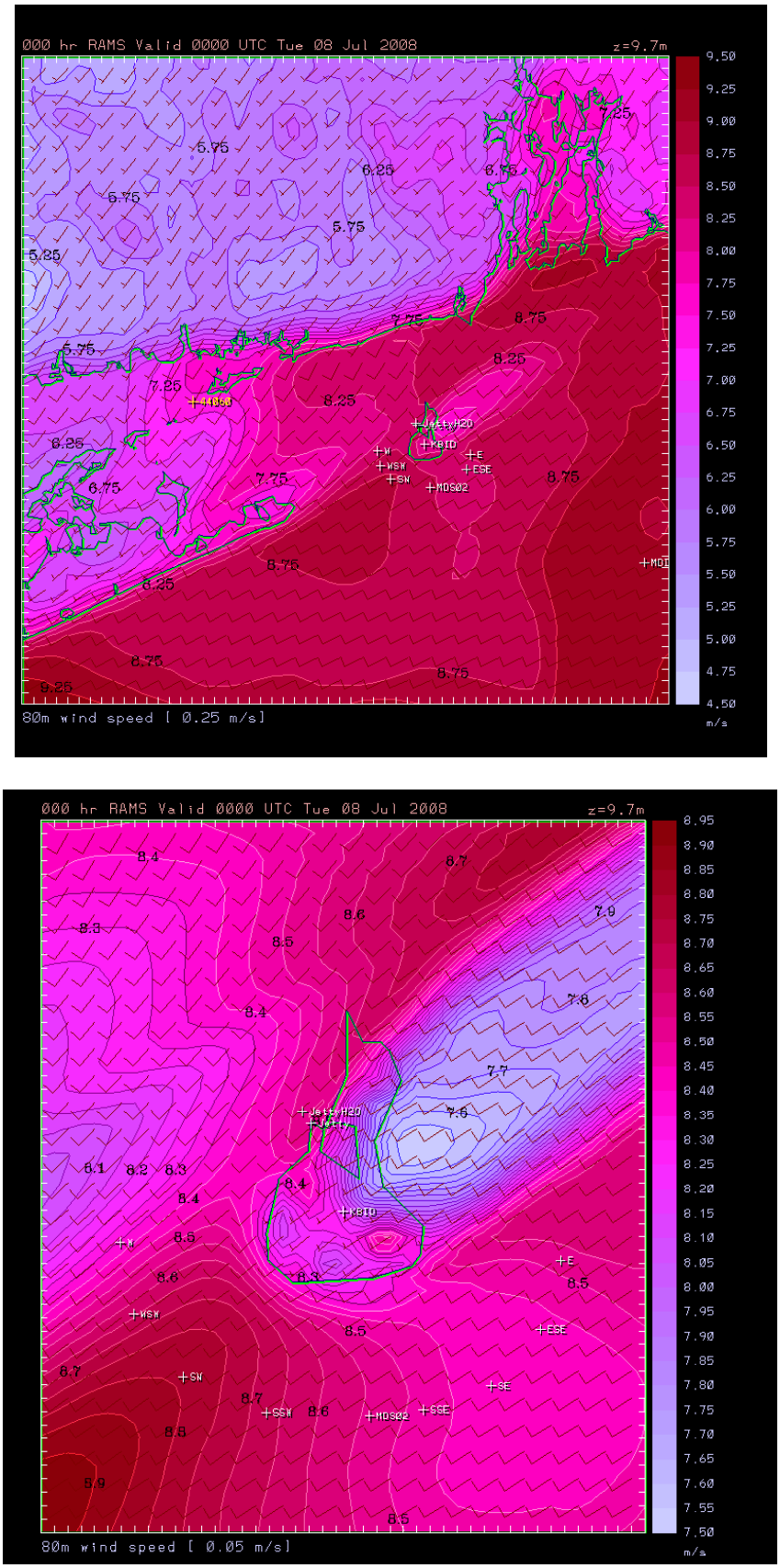

Figure 17 Model predicted wind speeds at 80 m at 0000 UTC on July 8, 2008 (SW). Upper panel- Grid 3 and lower panel - Grid 4.

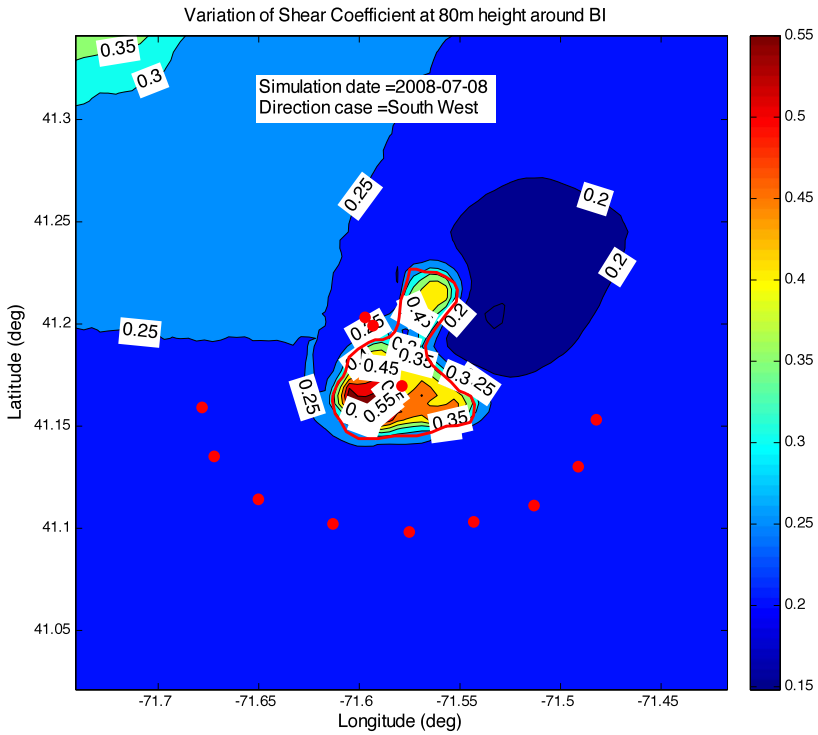

Figure 18 Model predicted shear coefficient for July 8, 2008 simulation.

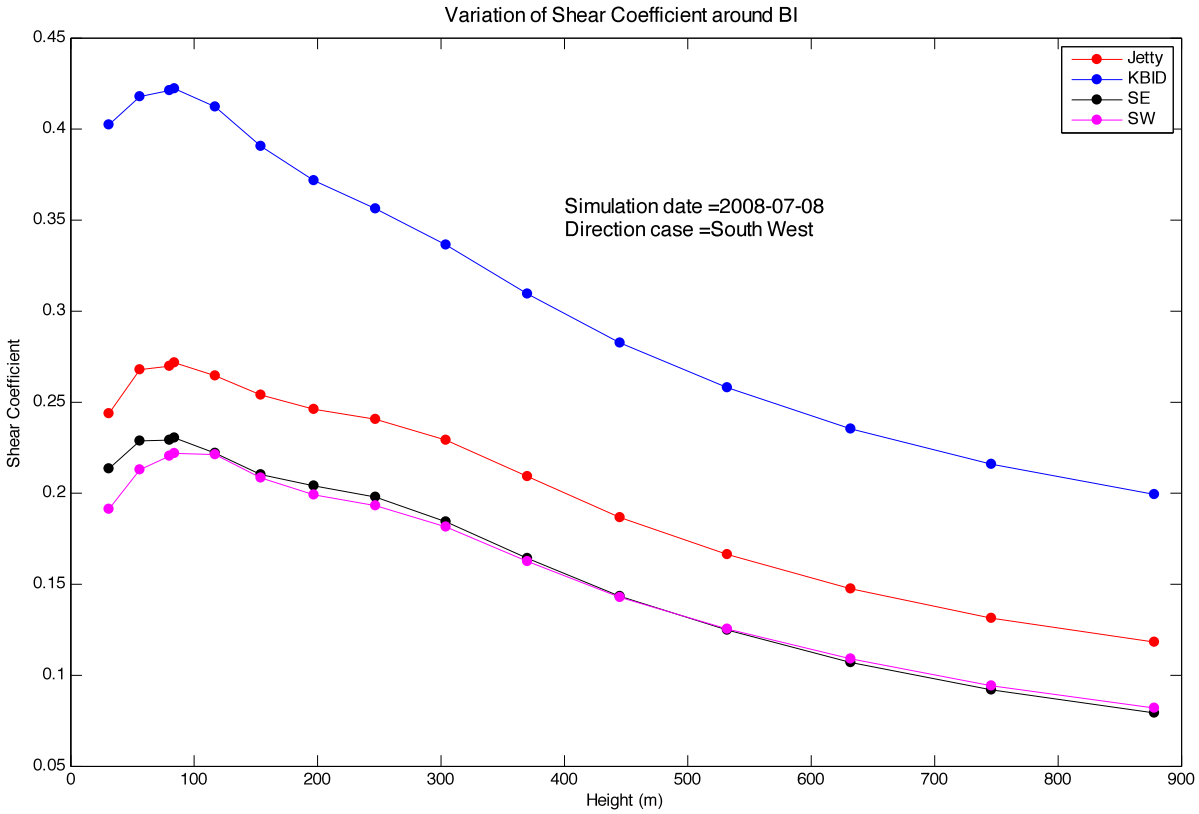

Figure 19 Model predicted shear coefficient at SE, SW, KBID, and Block Island Jetty locations for the July 8, 2008 simulation.

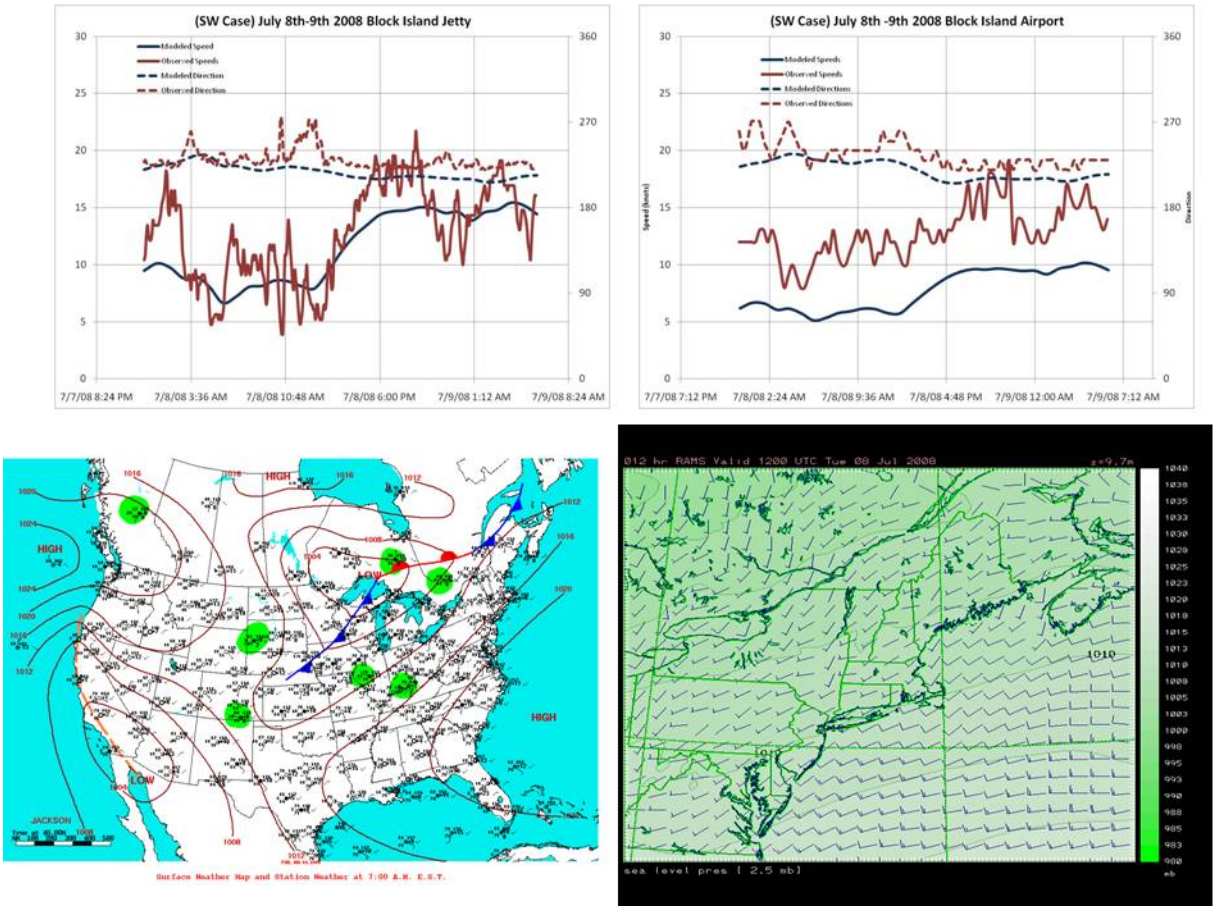

Figure 20 Comparison of model predictions to observations at Block Island Jetty (upper left) and KBID (upper right) on July 8, 2008. Large scale atmospheric forcing field (lower left) and NAM model predictions for Northeastern US (lower right).

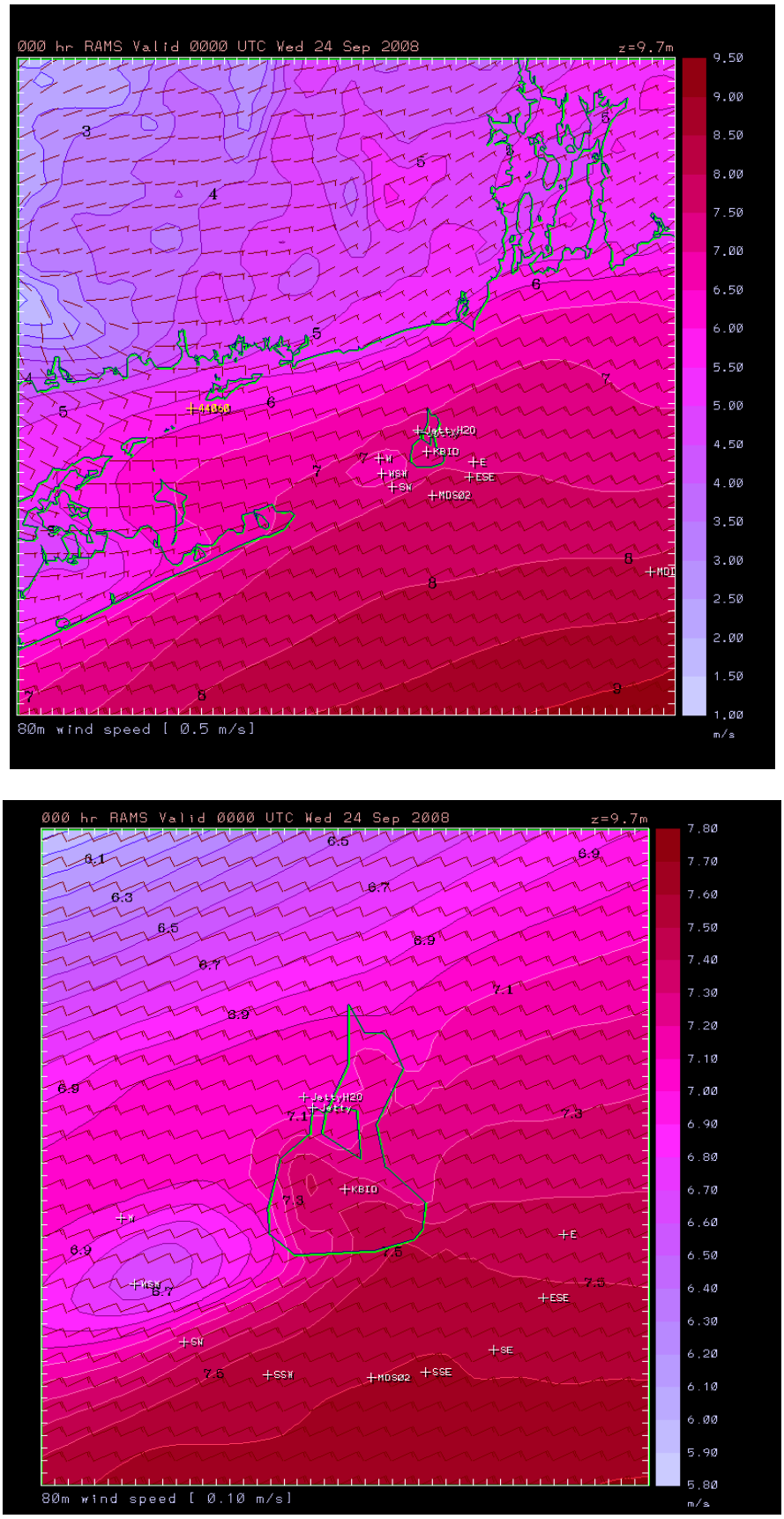

Figure 21 Model predicted wind speeds at 80 m at 0000 UTC on September 24, 2009 (NE). Upper panel - Grid 3 and lower panel - Grid 4.

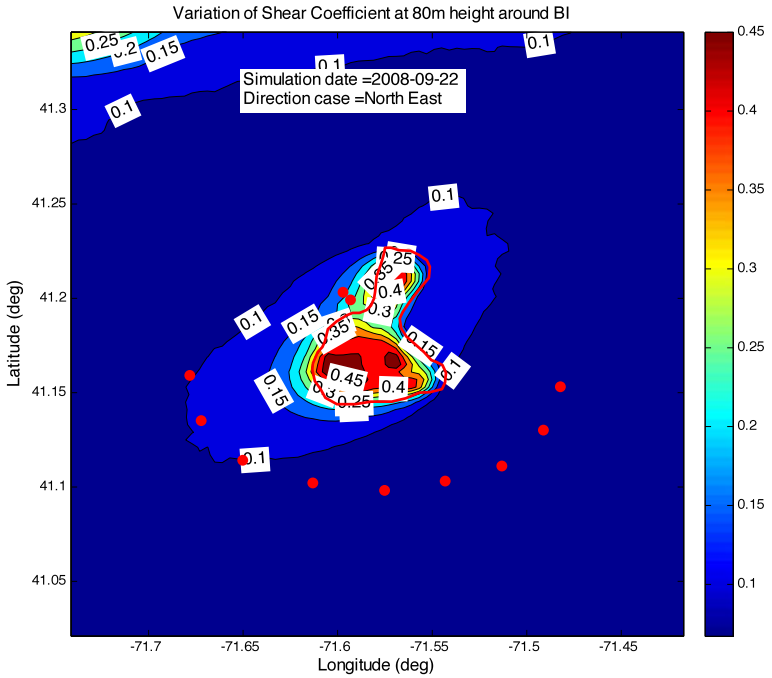

Figure 22 Model predicted shear coefficient for September 22, 2008 simulation.

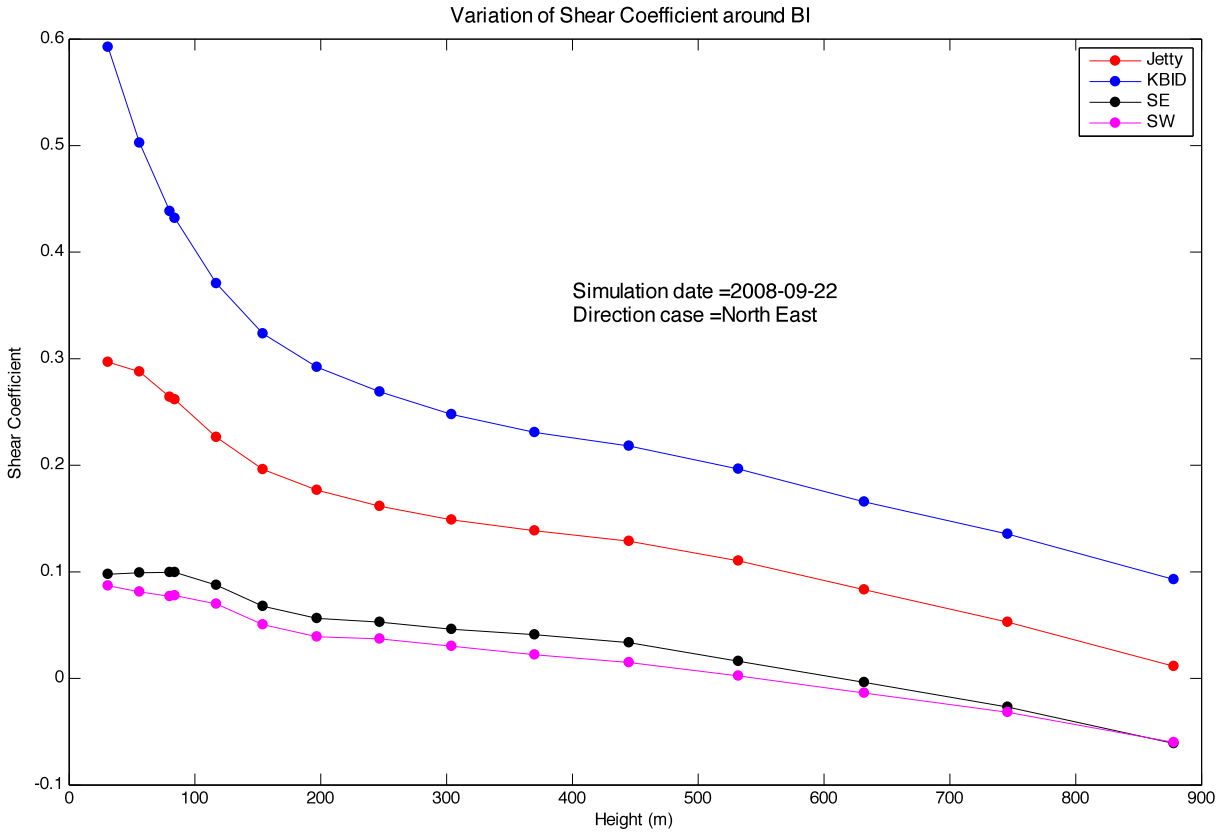

Figure 23 Model predicted shear coefficient at SE, SW, KBID, and Block Island Jetty locations for the September 22, 2008 simulation.

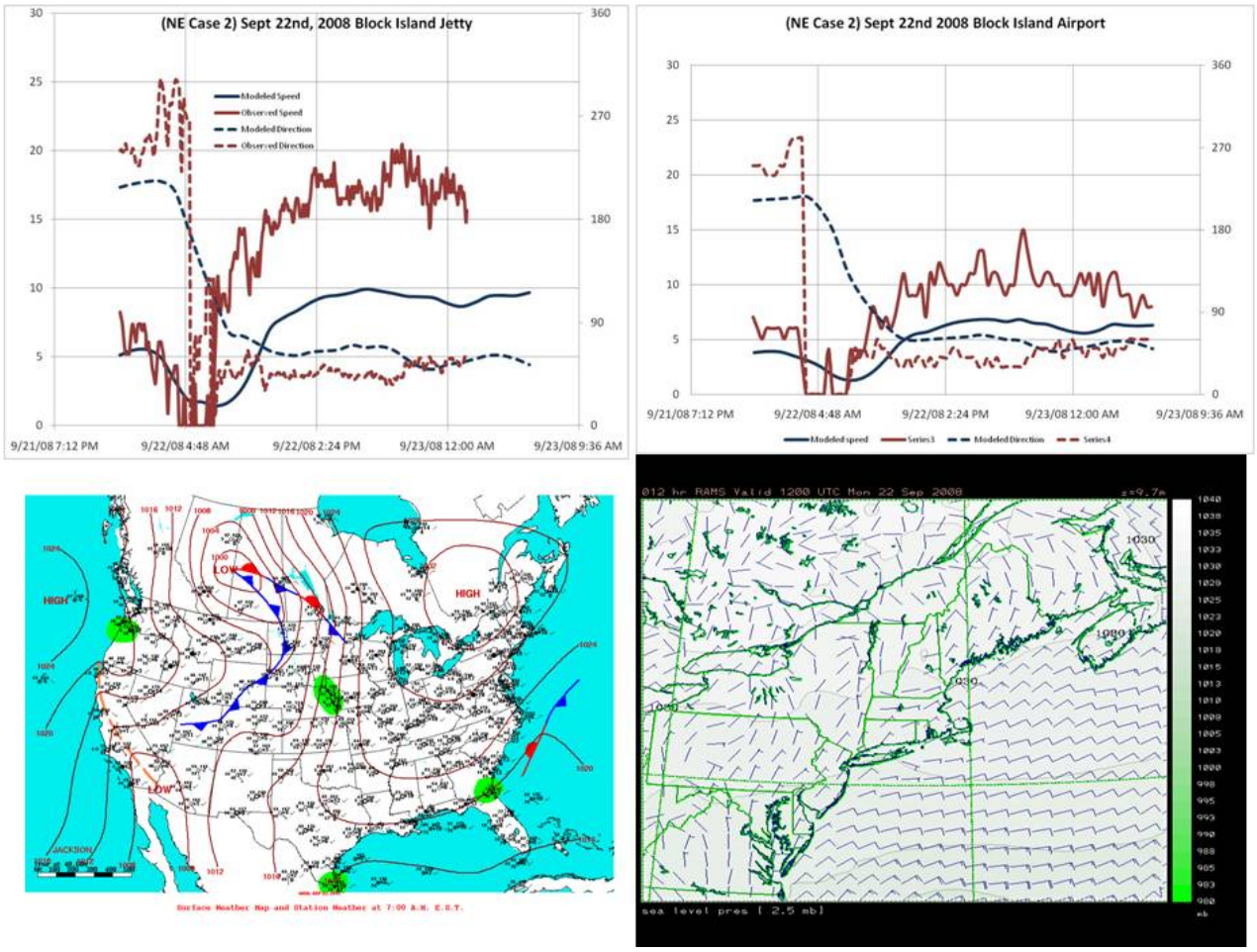

Figure 24 Comparison of model predictions to observations at Block Island Jetty (upper left) and KBID (upper right) on September 22, 2008. Large scale atmospheric forcing field (lower left) and NAM model predictions for Northeastern US (lower right).

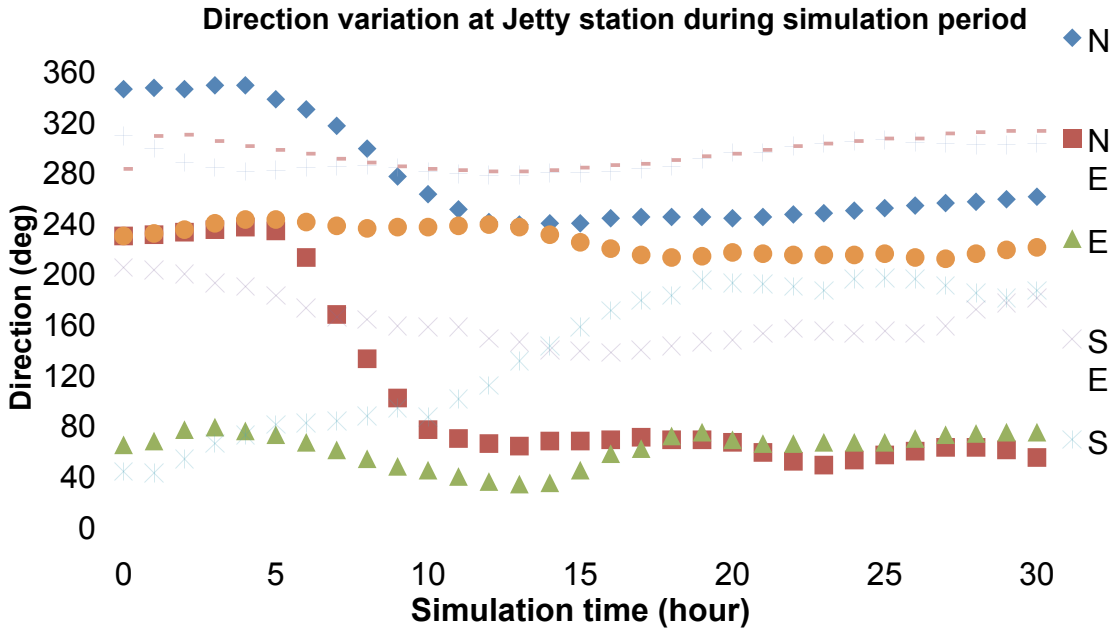

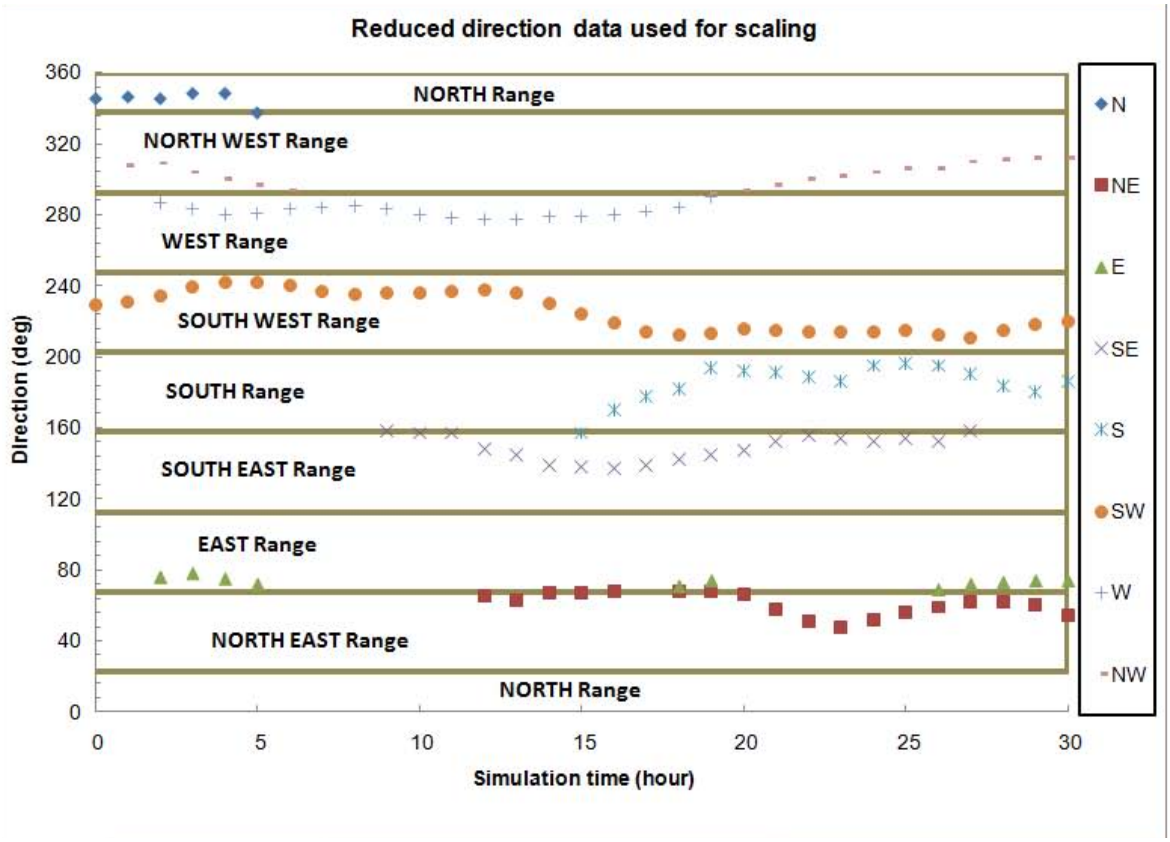

Figure 25 Wind direction as a function of time for the eight directional cases at Block Island, Jetty, upper panel includes all data and the lower panel only data that were within 15 degrees of the desired direction.

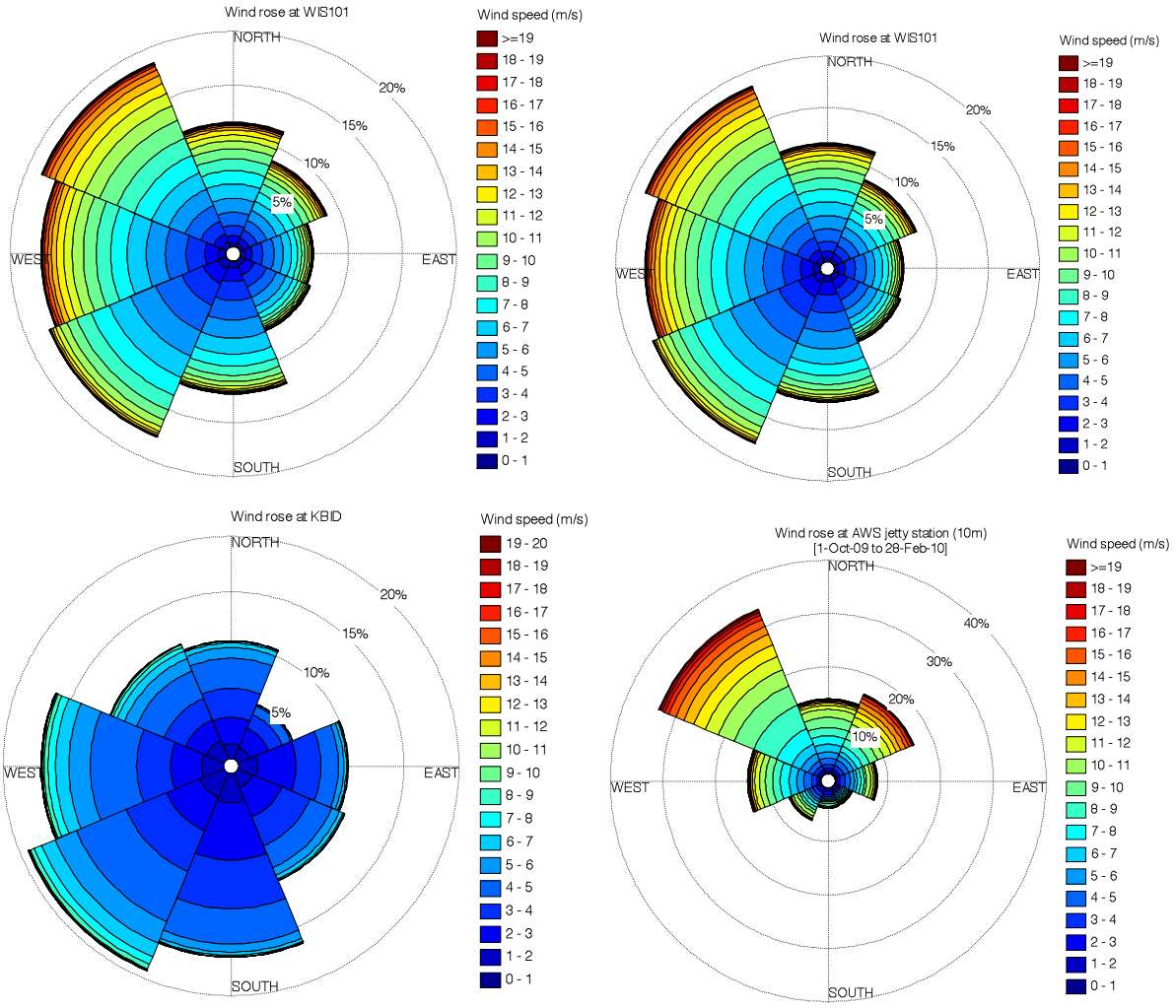

Figure 26 Wind roses at WIS100 and 101, KBID, and AWS Met all at 10 m.

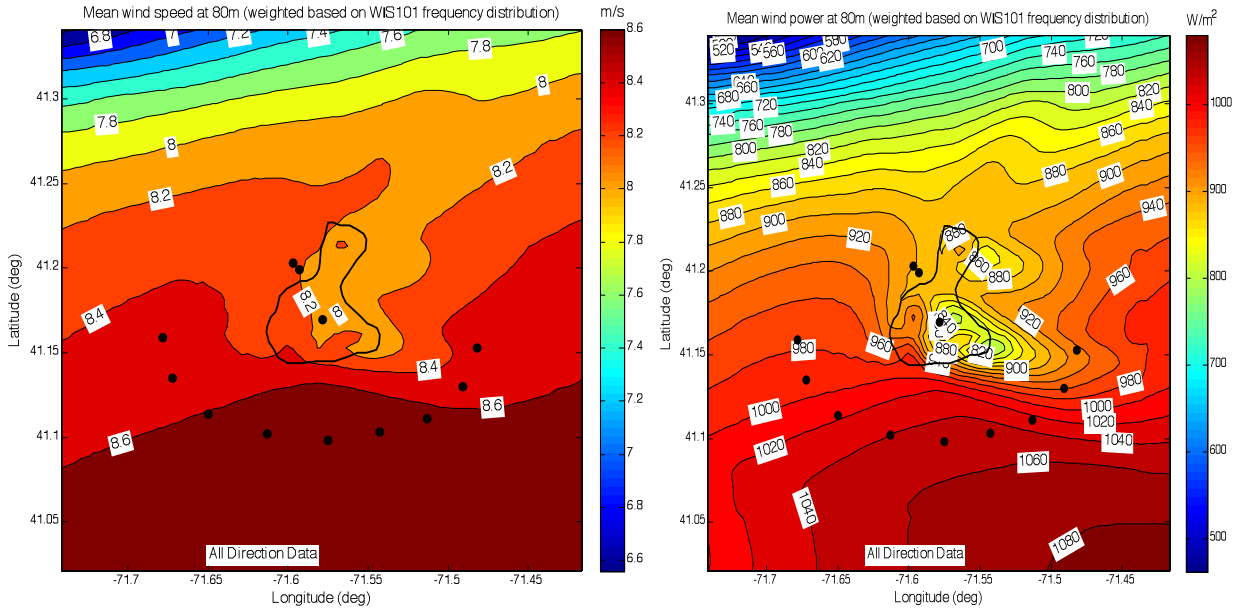

Figure 27 Template based model predictions of the mean annual wind speed (left) and wind power density (right) at 80 m, using the WIS101 wind rose. All direction data.

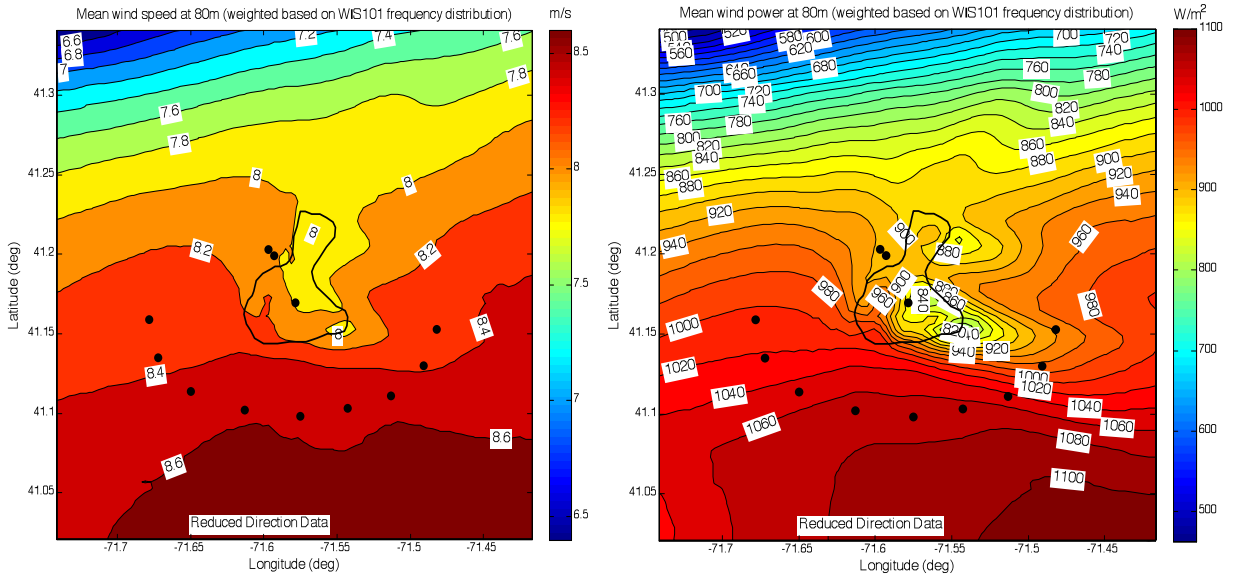

Figure 28 Template based model predictions of the mean annual wind speed (left) and wind power density (right) at 80 m, using the WIS101 wind rose. Reduced direction data.

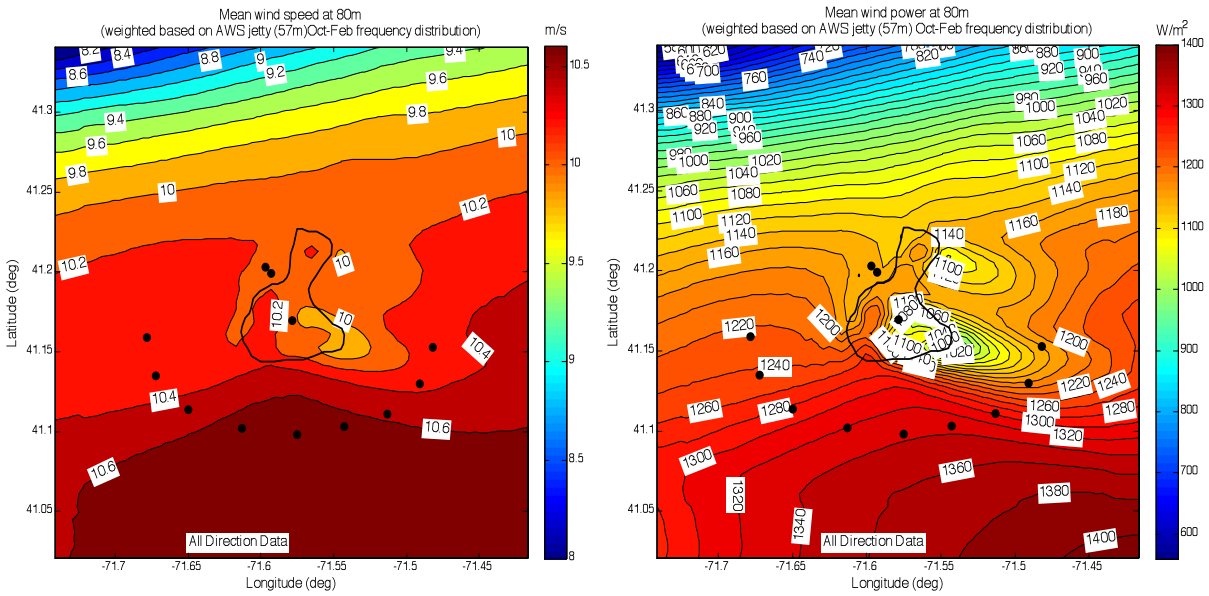

Figure 29 Template based model predictions of the mean annual wind speed (left) and wind power density (right) at 80 m, using the AWS Met 57m wind rose. All direction data.

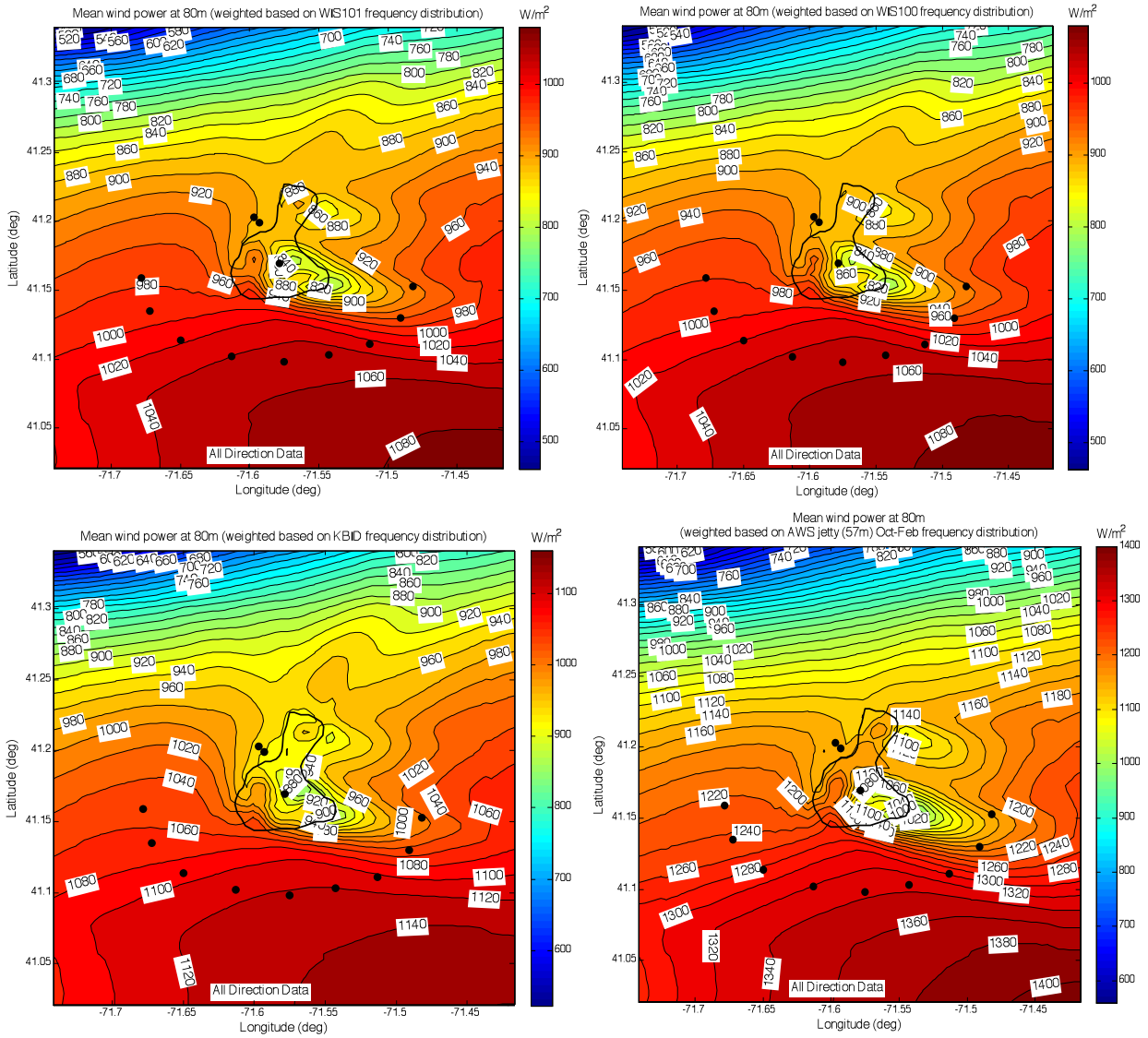

Figure 30 Template based method predictions of wind power density at 80 m using wind roses from WIS 101 (upper left), WIS 101 (upper right), KBID (lower left) and AWS Met (lower right).

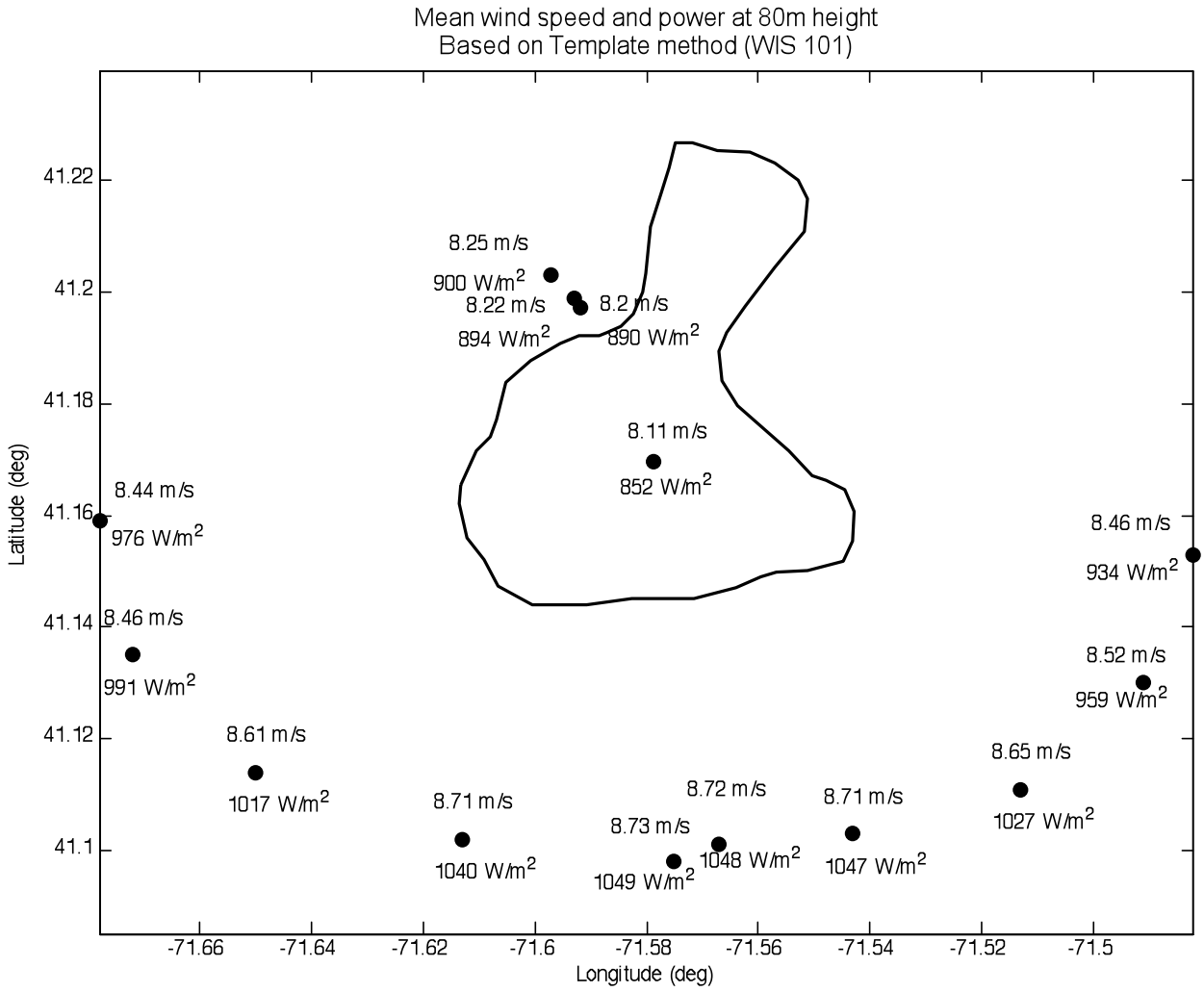

Figure 31 Template model predicted mean wind speed and power at selected locations along the state water boundary line as well as at KBID, Block Island Jetty, MDS, and AWS Met stations using WIS 101 wind rose.

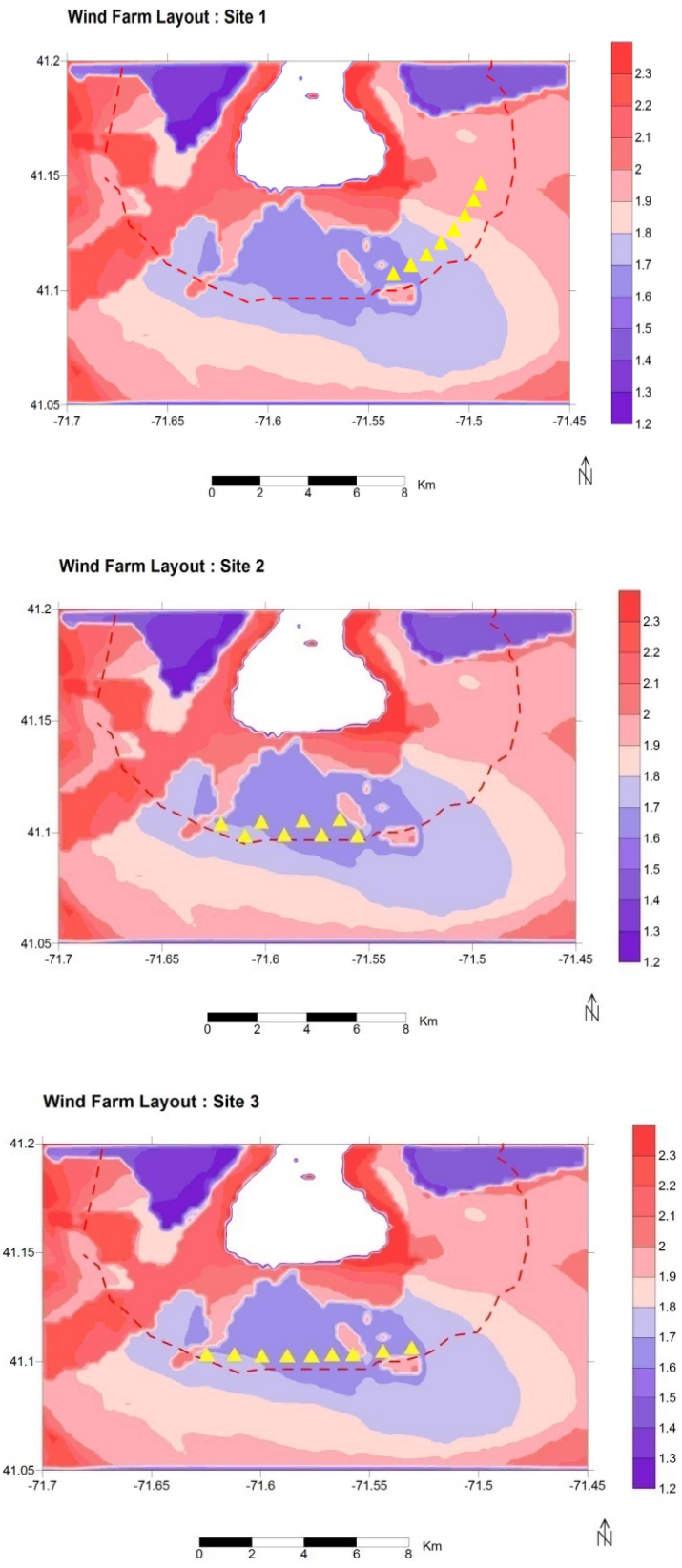

Figure 32 Location of proposed wind farm for wake loss study, SE - Site 1; S- Staggered, Site 2; and S – Un-staggered, Site 3.

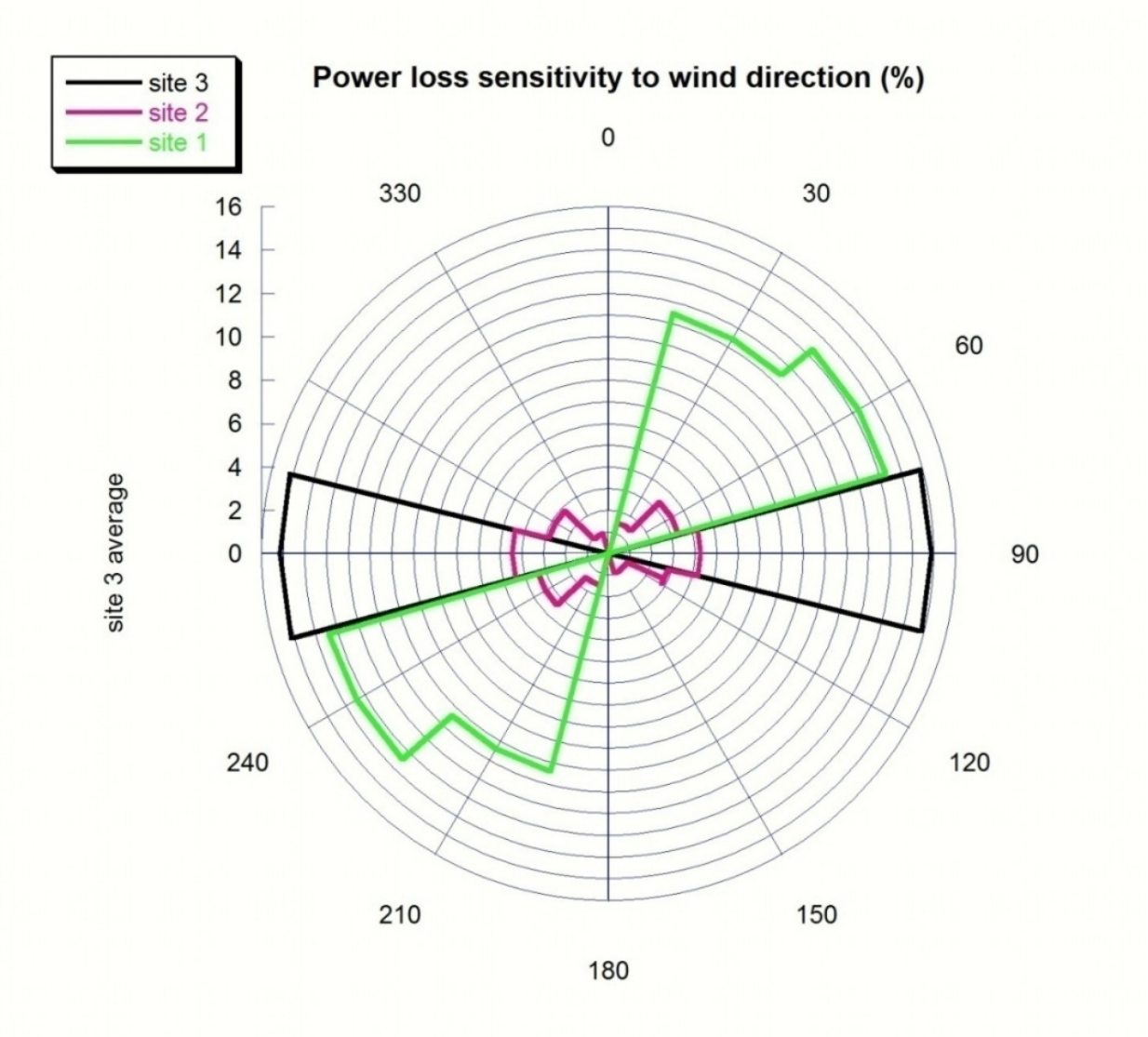

Figure 33 Power loss wind rose due to wake effects (%) for SE - Site 1; S- Staggered, Site 2; and S – Un-staggered, Site 3.

Appendix A

Wind frequency and power density (seasonal and annual) roses and Weibull distribution fits for selected stations in the SAMP study area.

Presented below are wind frequency and power density roses for selected stations in the SAMP study area. Locations are shown in Figures 1 (southern NE) and 2 (In vicinity of Block Island) for seasonal and annual average cases. Also provided are Weibull distribution fits to the data. In each case the data is reported at the elevation at which it was measured or hindcast. The period of observations is noted. In some cases the record lengths are shorter than one year and hence data for all seasons is not available.

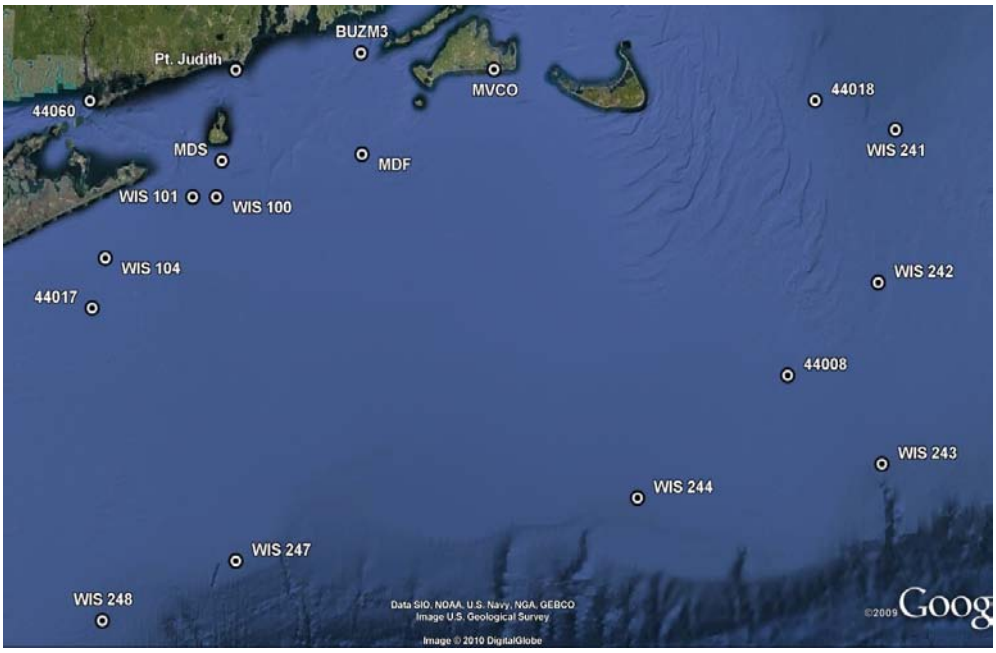

Figure 1 Location of wind observation and hindcast stations in the SAMP study area. US Army Corp of Engineers, WIS; NDBC (44018, 44017, 44060; BUZM3); Ocean SAMP: MDS, MDF; WeatherFlow's Pt Judith; and Martha's Vineyard Coastal Observatory (MVCO).

Figure 2 Location of wind observation stations in the vicinity of Block Island: WeatherFlow's Block Island Jetty, AWS Meteorological Tower, Block Island Airport (KBID), and DOE site.

Weibull distribution fit to the observed data. The start and end dates of the observation are provided as is the elevation of the observation. The Weibull amplitude, c, and shape, k, parameter and their upper and lower 95% confidence interval values are provided.

Wind speed and power density roses are provided. The start and end dates of the observation are provided as is the elevation of the observation. The four corners of the plot show the seasonal results and the center the annual values. The mean wind speed and power density for seasonal and annual results are given.

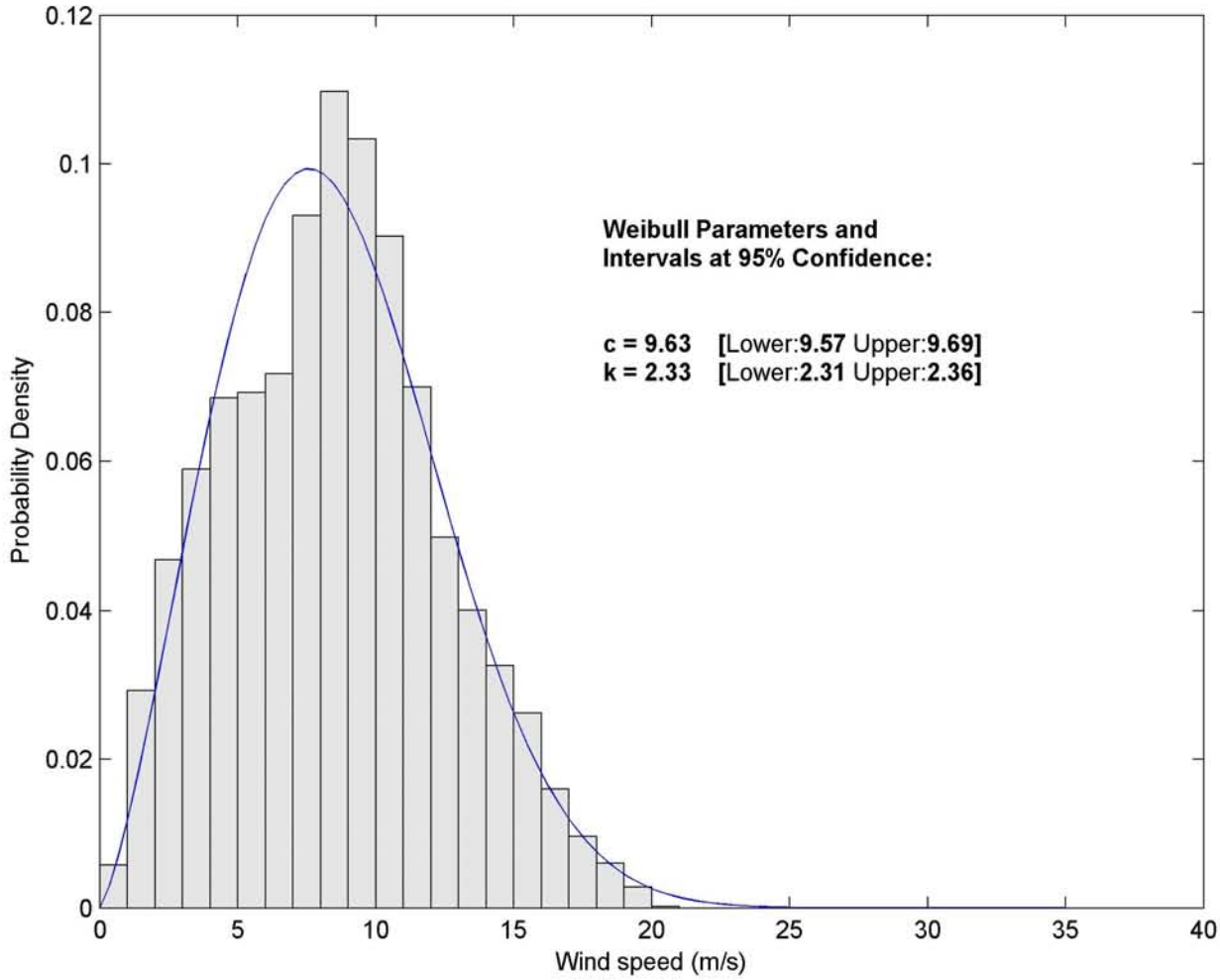
AWS Met Tower Probability Distribution
Dates: October 2009-February 2010
Elevation: 9.9m
Weibull Parameters and
Intervals at 95% Confidence:
c = 9.63 [Lower:9.57 Upper:9.69]
k = 2.33 [Lower:2.31 Upper:2.36]
Probability Density
Wind speed (m/s)
0
0.02
0.04
0.06
0.08
0.1
0.12
0
5
10
15
20
25
30
35
40

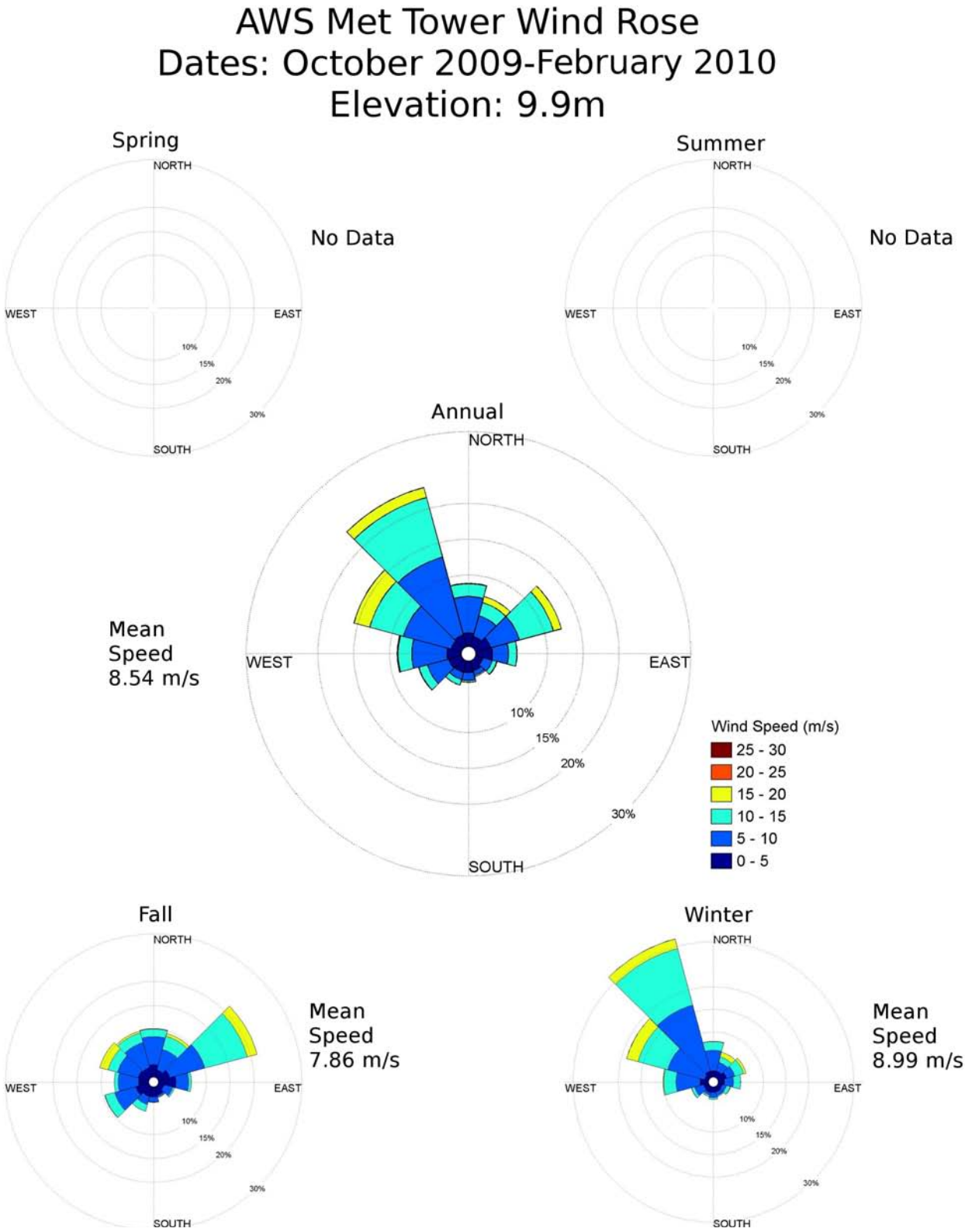
AWS Met Tower Wind Rose
Dates: October 2009-February 2010
Elevation: 9.9m
Spring
No Data
Summer
No Data
Annual
Mean
Speed
8.54 m/s
Fall
Mean
Speed
7.86 m/s
Winter
Mean
Speed
8.99 m/s
NORTH
SOUTH
EAST
WEST
10%
15%
20%
30%
Wind Speed (m/s)
25 - 30
20 - 25
15 - 20
10 - 15
5 - 10
0 - 5

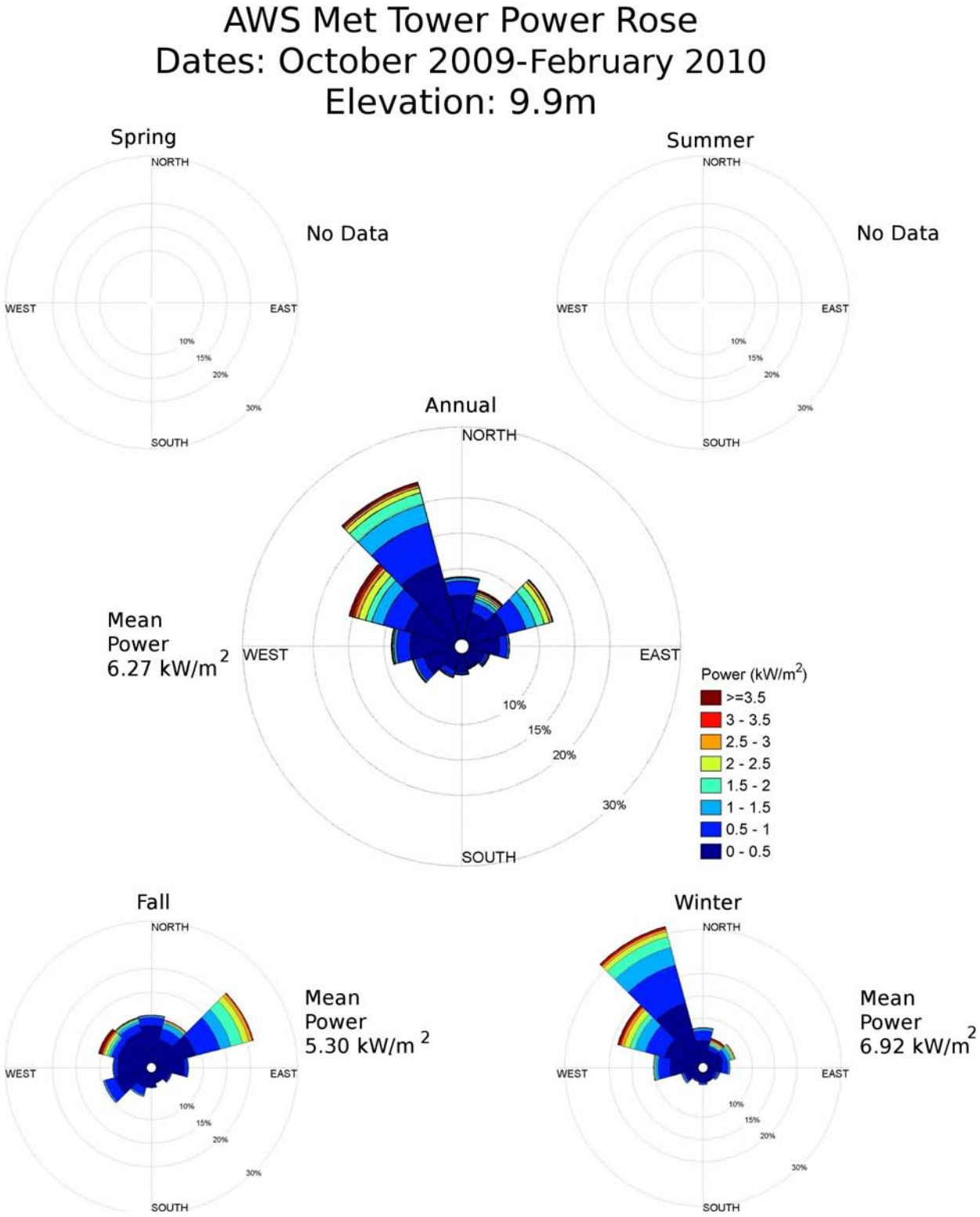
AWS Met Tower Power Rose
Dates: October 2009-February 2010
Elevation: 9.9m
Spring
No Data
Summer
No Data
Annual
Mean
Power
6.27 kW/m 2
Power (kW/m2)
>=3.5
3 - 3.5
2.5 - 3
2 - 2.5
1.5 - 2
1 - 1.5
0.5 - 1
0 - 0.5
Fall
Mean
Power
5.30 kW/m 2
Winter
Mean
Power
6.92 kW/m2
NORTH
SOUTH
EAST
WEST
10%
15%
20%
30%

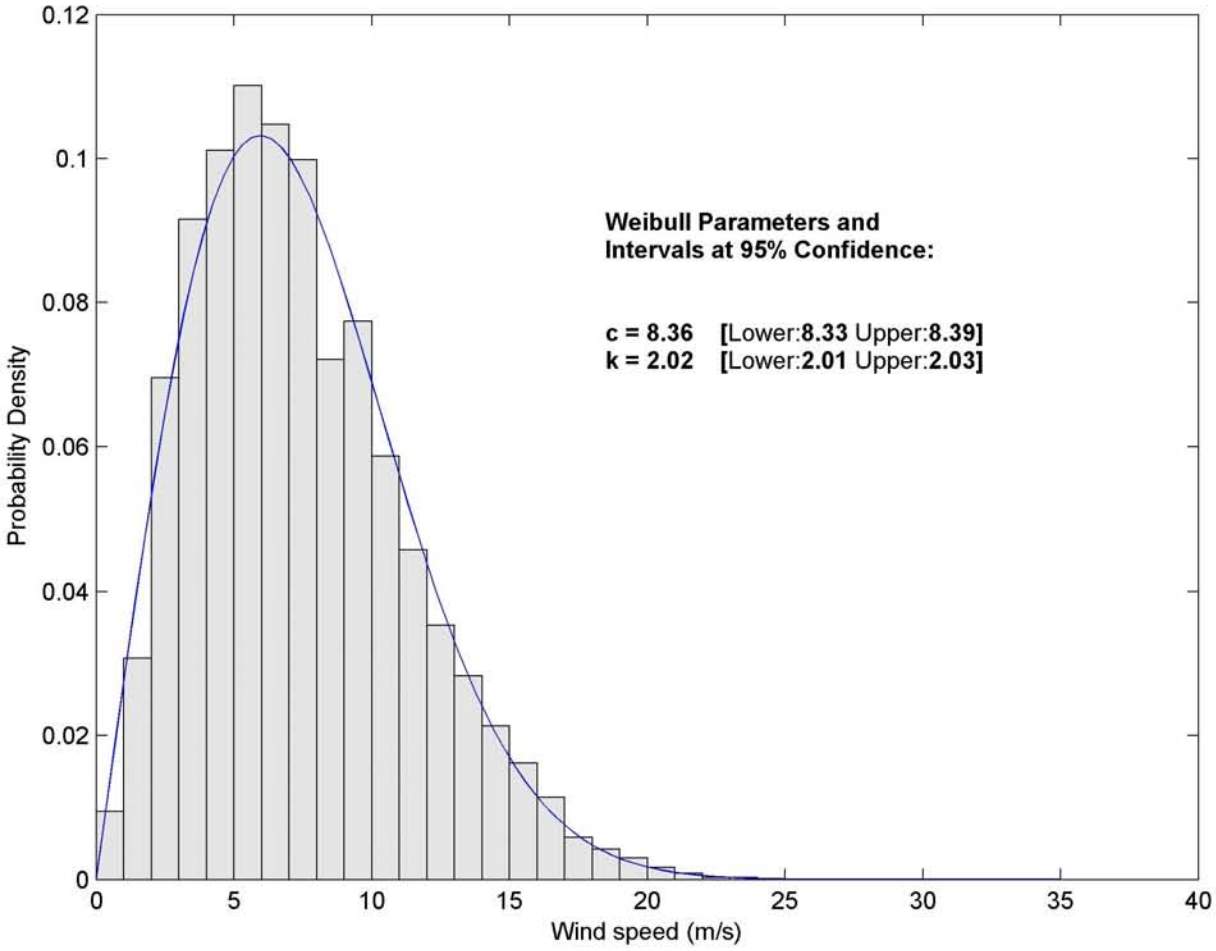
Block Island Jetty Probability Distribution
Dates: October 2005-September 2008
Elevation: 11m
Weibull Parameters and
Intervals at 95% Confidence:
c = 8.36 [Lower:8.33 Upper:8.39]
k = 2.02 [Lower:2.01 Upper:2.03]
Probability Density
Wind speed (m/s)
0
0.02
0.04
0.06
0.08
0.1
0.12
0
5
10
15
20
25
30
35
40

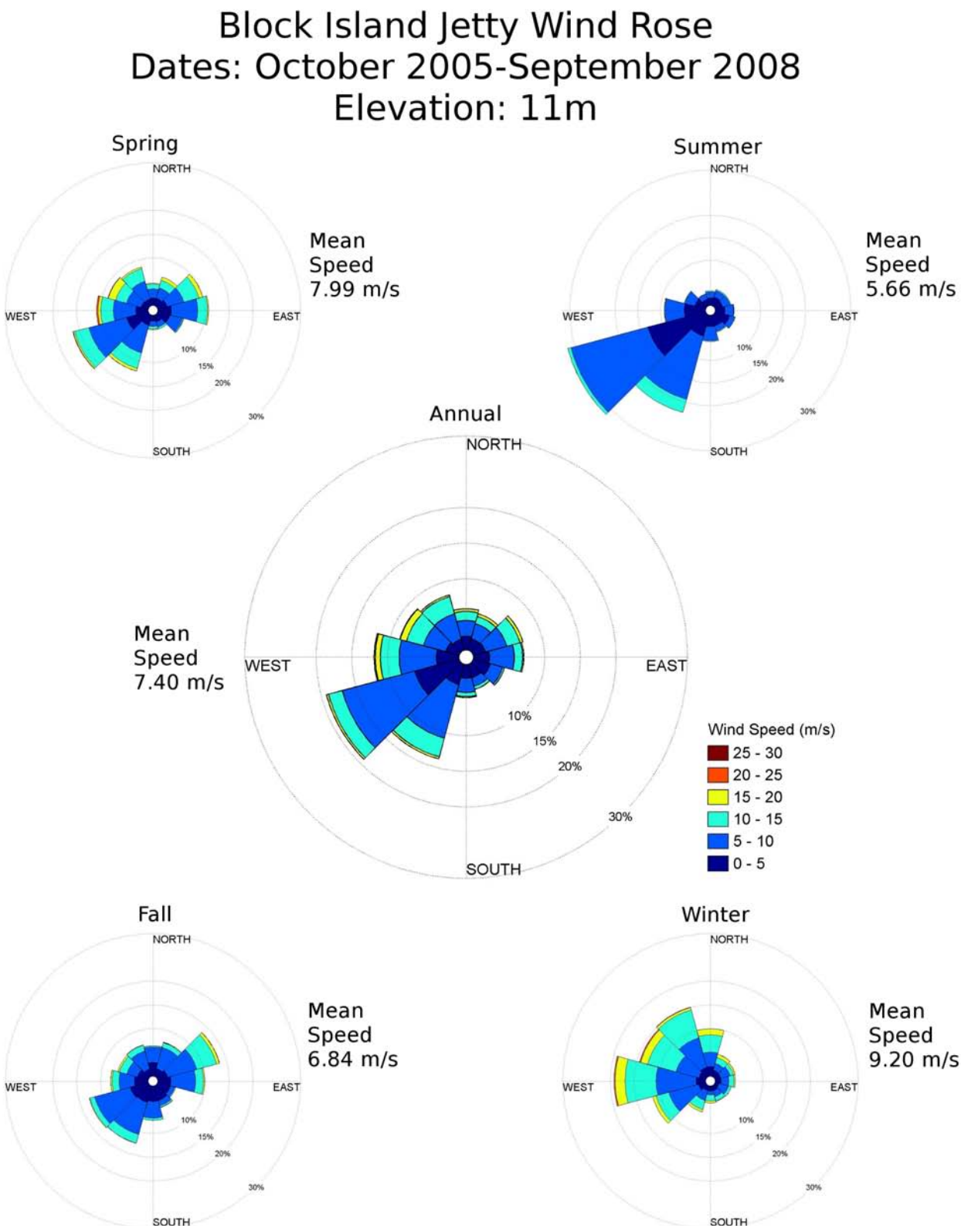
Block Island Jetty Wind Rose
Dates: October 2005-September 2008
Elevation: 11m
Spring
Mean Speed 7.99 m/s
Summer
Mean Speed 5.66 m/s
Annual
Mean Speed 7.40 m/s
Fall
Mean Speed 6.84 m/s
Winter
Mean Speed 9.20 m/s
NORTH
SOUTH
EAST
WEST
10%
15%
20%
30%
Wind Speed (m/s)
25 - 30
20 - 25
15 - 20
10 - 15
5 - 10
0 - 5

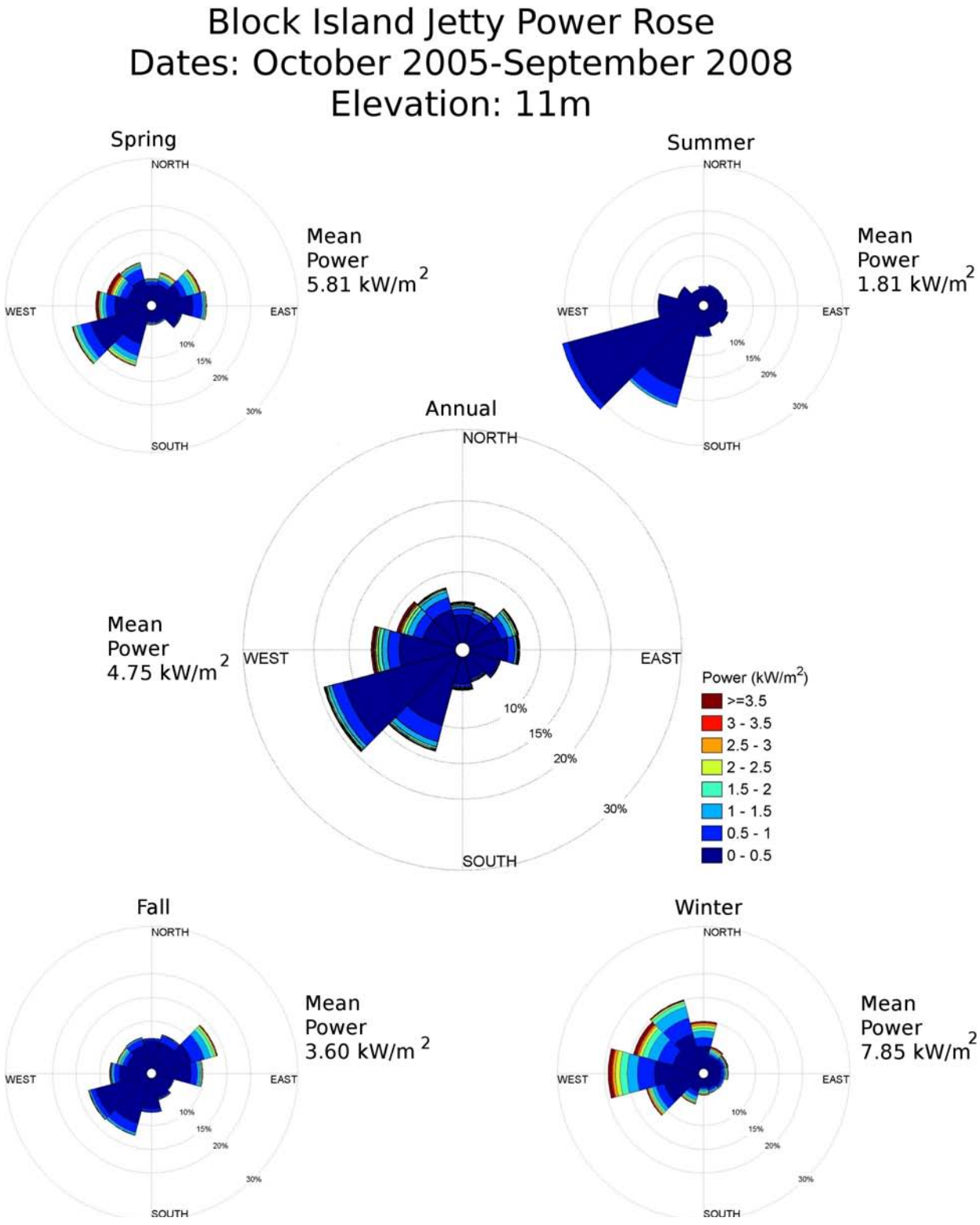
Block Island Jetty Power Rose
Dates: October 2005-September 2008
Elevation: 11m
Spring
Mean Power 5.81 kW/m2
Summer
Mean Power 1.81 kW/m2
Annual
Mean Power 4.75 kW/m2
Fall
Mean Power 3.60 kW/m2
Winter
Mean Power 7.85 kW/m2
NORTH
SOUTH
EAST
WEST
10%
15%
20%
30%
Power (kW/m2)
>=3.5
3 - 3.5
2.5 - 3
2 - 2.5
1.5 - 2
1 - 1.5
0.5 - 1
0 - 0.5

DOE Site Probability Distribution
Dates: 1977-1982
Elevation: 9m

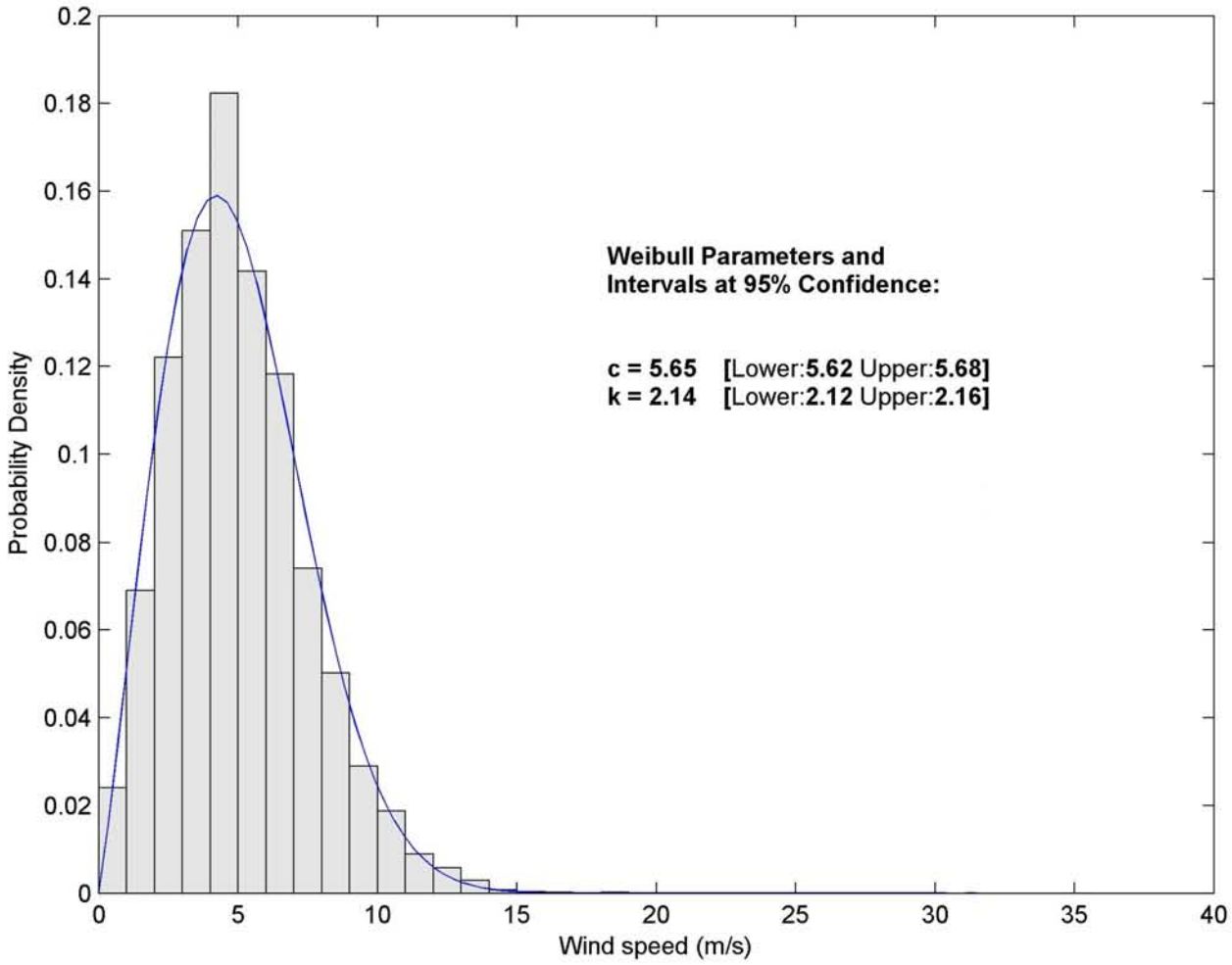

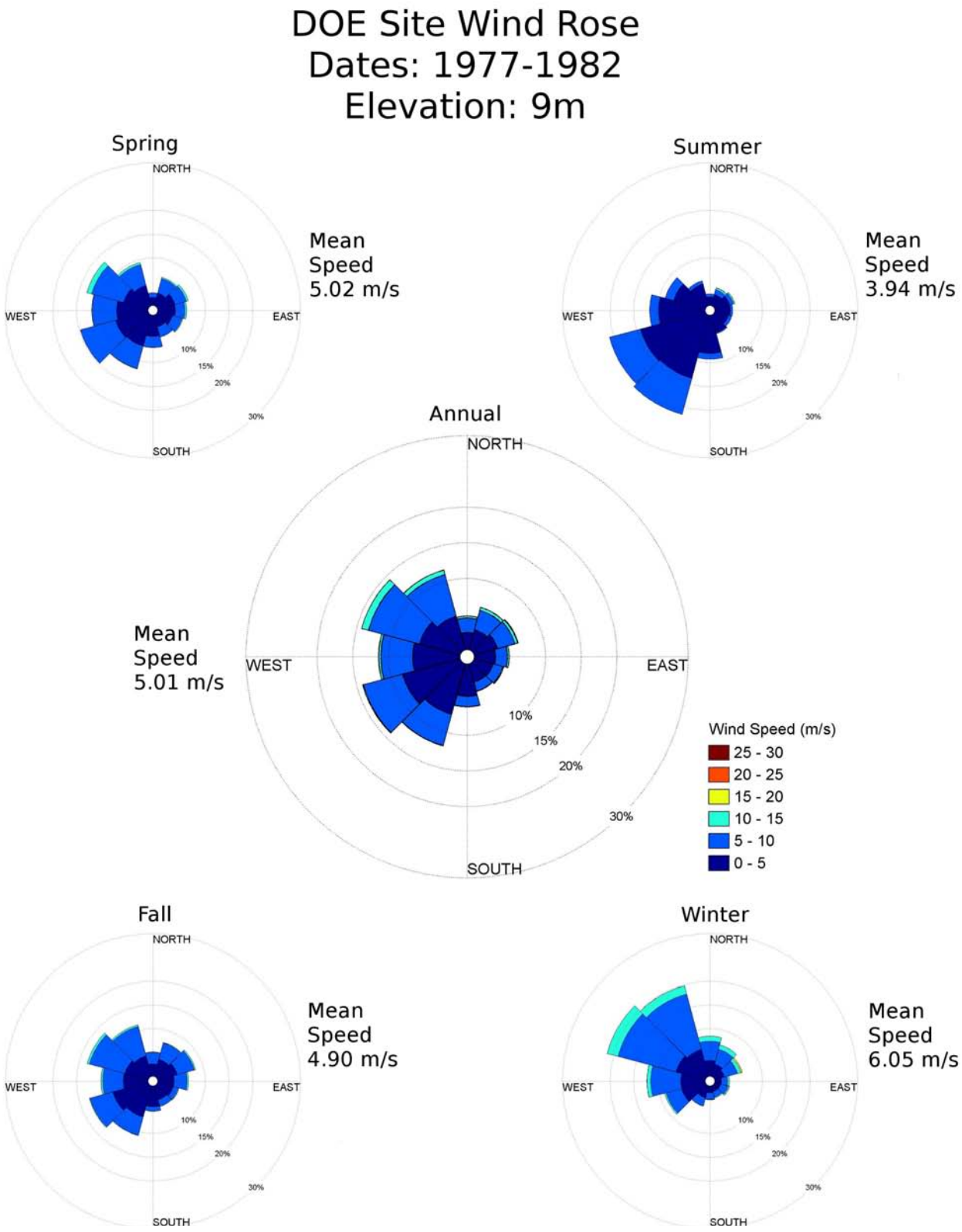
DOE Site Wind Rose
Dates: 1977-1982
Elevation: 9m
Spring
Mean Speed 5.02 m/s
Summer
Mean Speed 3.94 m/s
Annual
Mean Speed 5.01 m/s
Fall
Mean Speed 4.90 m/s
Winter
Mean Speed 6.05 m/s
NORTH
SOUTH
EAST
WEST
10%
15%
20%
30%
Wind Speed (m/s)
25 - 30
20 - 25
15 - 20
10 - 15
5 - 10
0 - 5

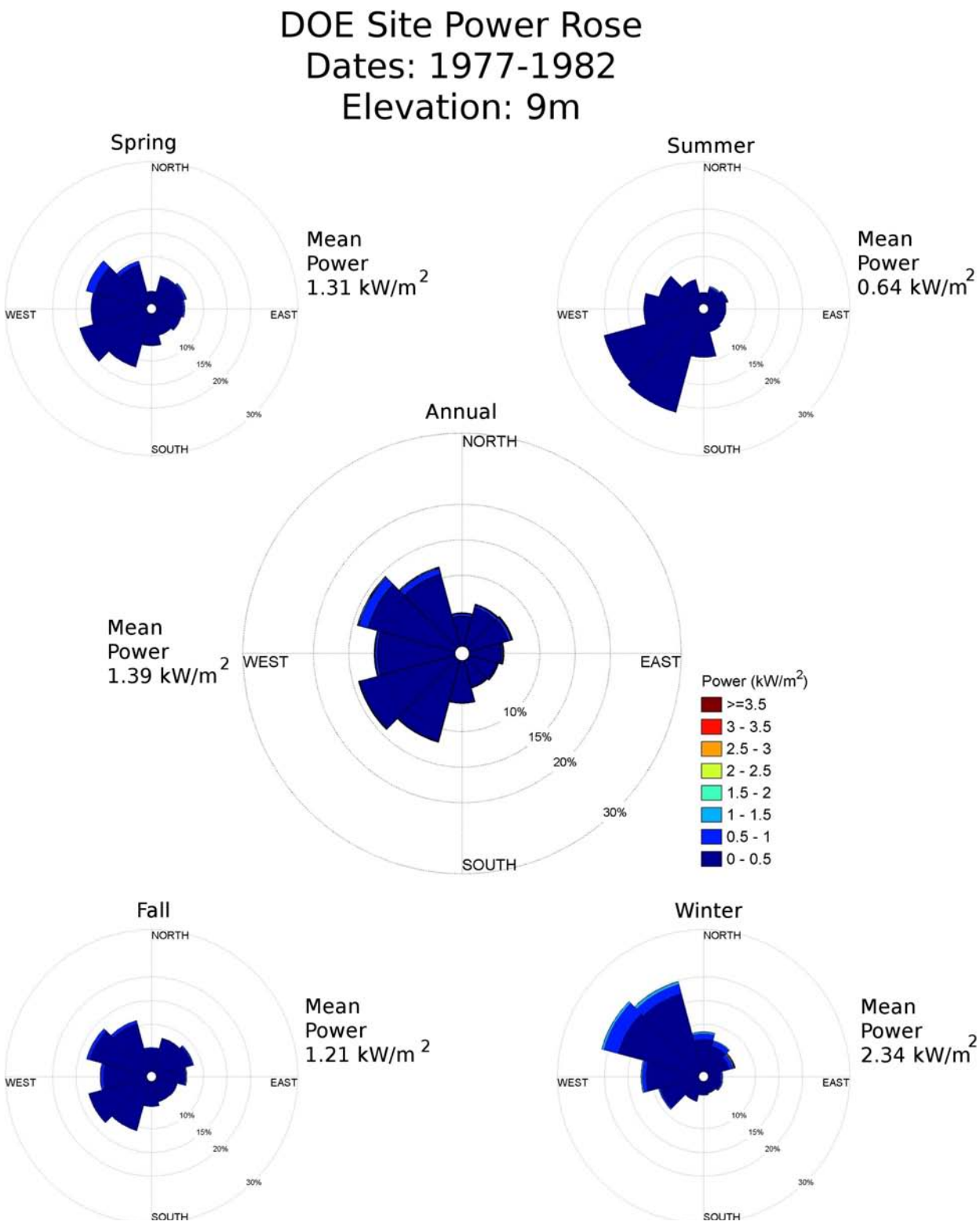
DOE Site Power Rose
Dates: 1977-1982
Elevation: 9m
Spring
Mean Power 1.31 kW/m2
Summer
Mean Power 0.64 kW/m2
Annual
Mean Power 1.39 kW/m2
Fall
Mean Power 1.21 kW/m2
Winter
Mean Power 2.34 kW/m2
NORTH
SOUTH
EAST
WEST
10%
15%
20%
30%
Power (kW/m2)
>=3.5
3 - 3.5
2.5 - 3
2 - 2.5
1.5 - 2
1 - 1.5
0.5 - 1
0 - 0.5

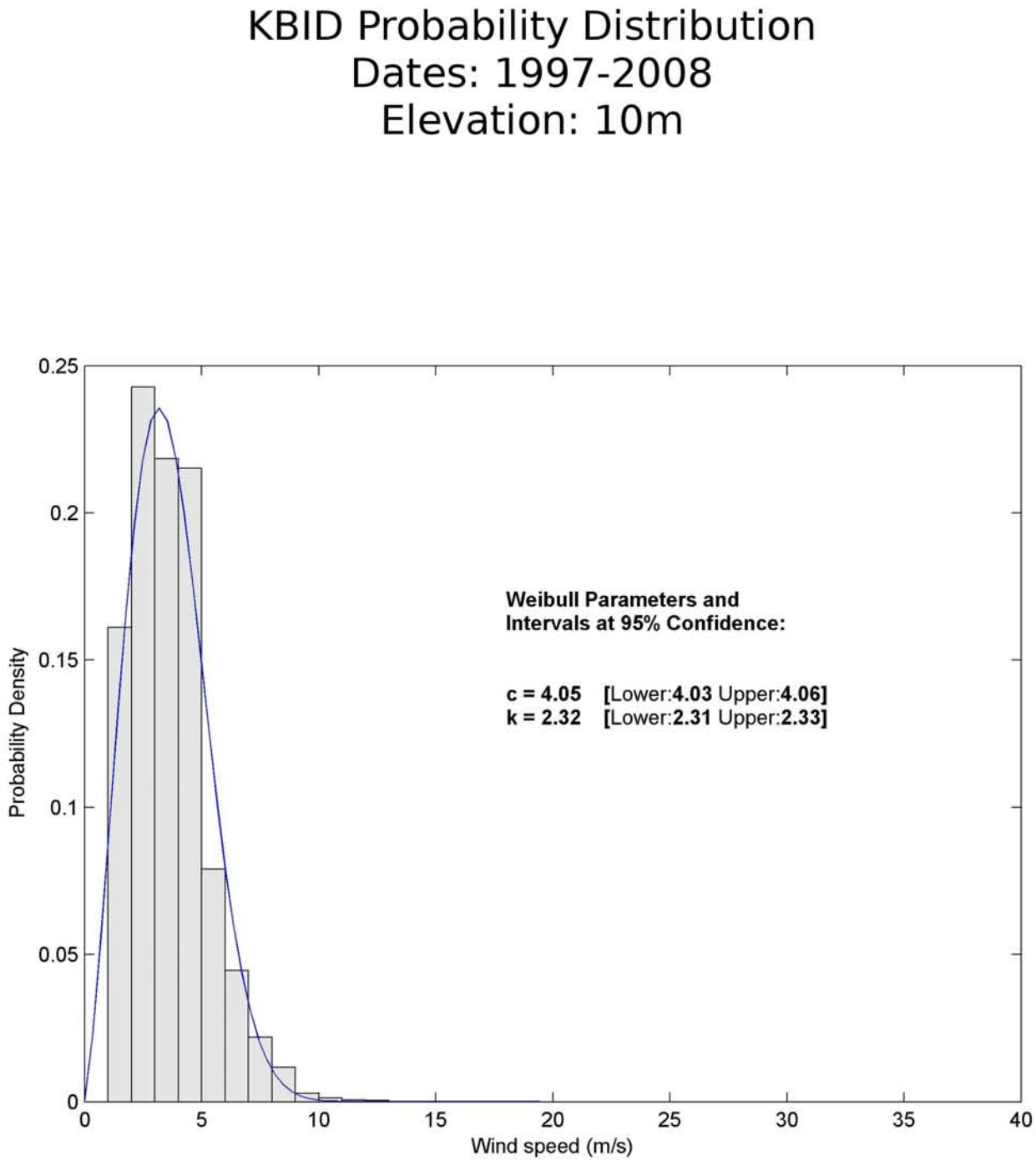
KBID Probability Distribution
Dates: 1997-2008
Elevation: 10m
Weibull Parameters and
Intervals at 95% Confidence:
c = 4.05 [Lower:4.03 Upper:4.06]
k = 2.32 [Lower:2.31 Upper:2.33]
Probability Density
Wind speed (m/s)
0
0.05
0.1
0.15
0.2
0.25
0
5
10
15
20
25
30
35
40

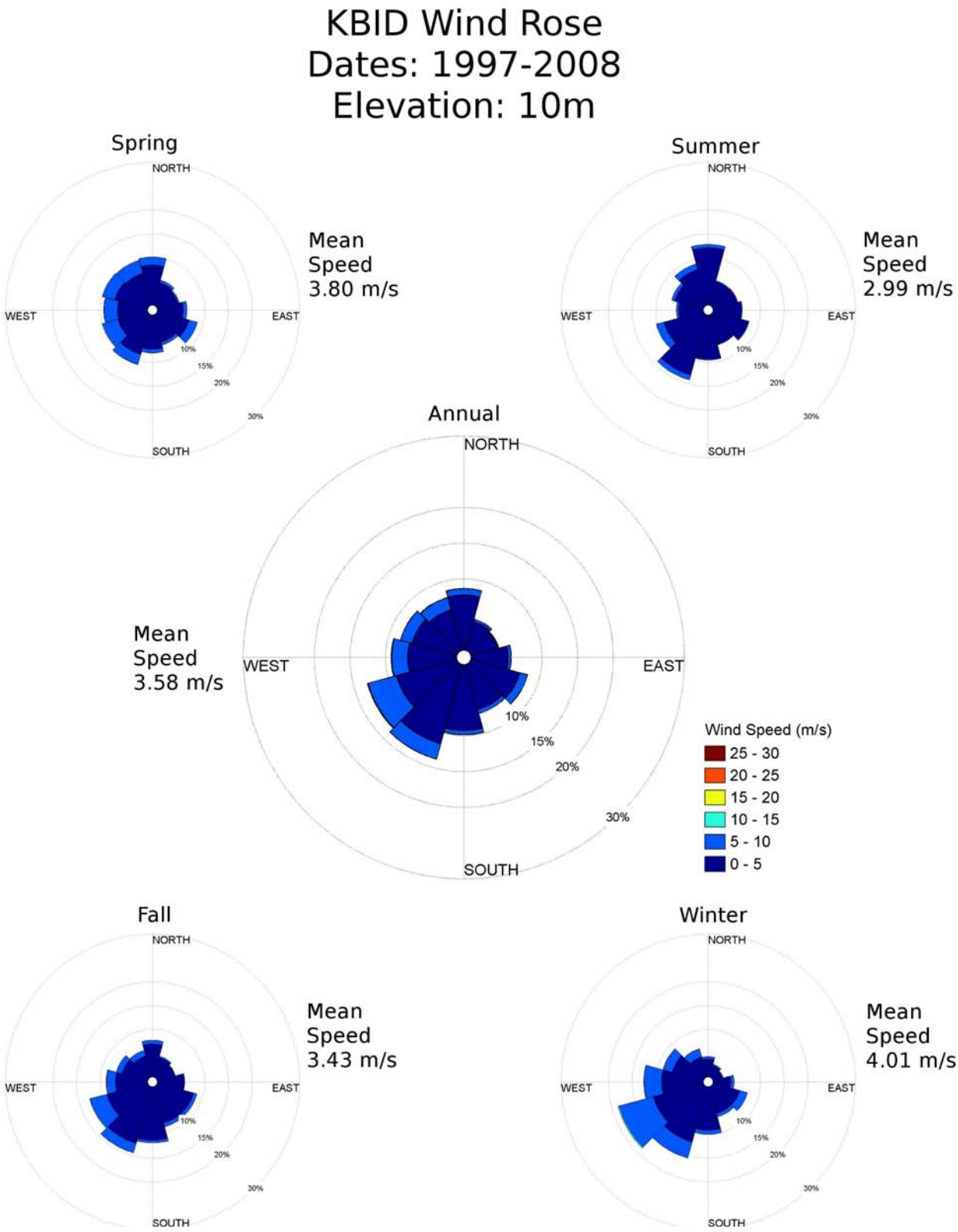
KBID Wind Rose
Dates: 1997-2008
Elevation: 10m
Spring
Mean Speed 3.80 m/s
Summer
Mean Speed 2.99 m/s
Annual
Mean Speed 3.58 m/s
Fall
Mean Speed 3.43 m/s
Winter
Mean Speed 4.01 m/s
NORTH
SOUTH
EAST
WEST
10%
15%
20%
30%
Wind Speed (m/s)
25 - 30
20 - 25
15 - 20
10 - 15
5 - 10
0 - 5

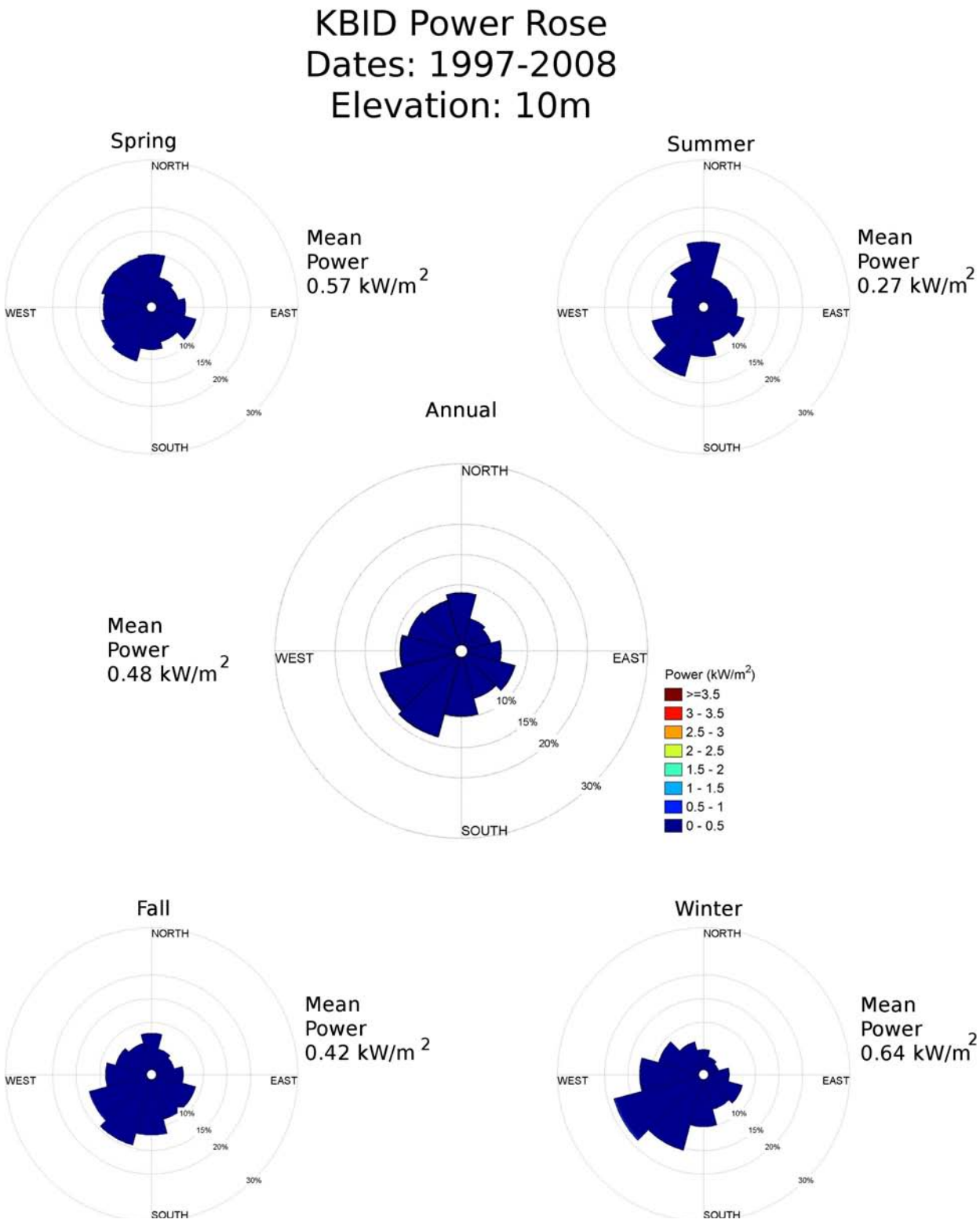
KBID Power Rose
Dates: 1997-2008
Elevation: 10m
Spring
Mean Power 0.57 kW/m2
Summer
Mean Power 0.27 kW/m2
Annual
Mean Power 0.48 kW/m2
Fall
Mean Power 0.42 kW/m2
Winter
Mean Power 0.64 kW/m2
NORTH
SOUTH
EAST
WEST
10%
15%
20%
30%
Power (kW/m2)
>=3.5
3 - 3.5
2.5 - 3
2 - 2.5
1.5 - 2
1 - 1.5
0.5 - 1
0 - 0.5

Martha's Vinyard Coastal Observatory Probability Distribution
Dates: June 2001-May 2010
Elevation: 12.5m

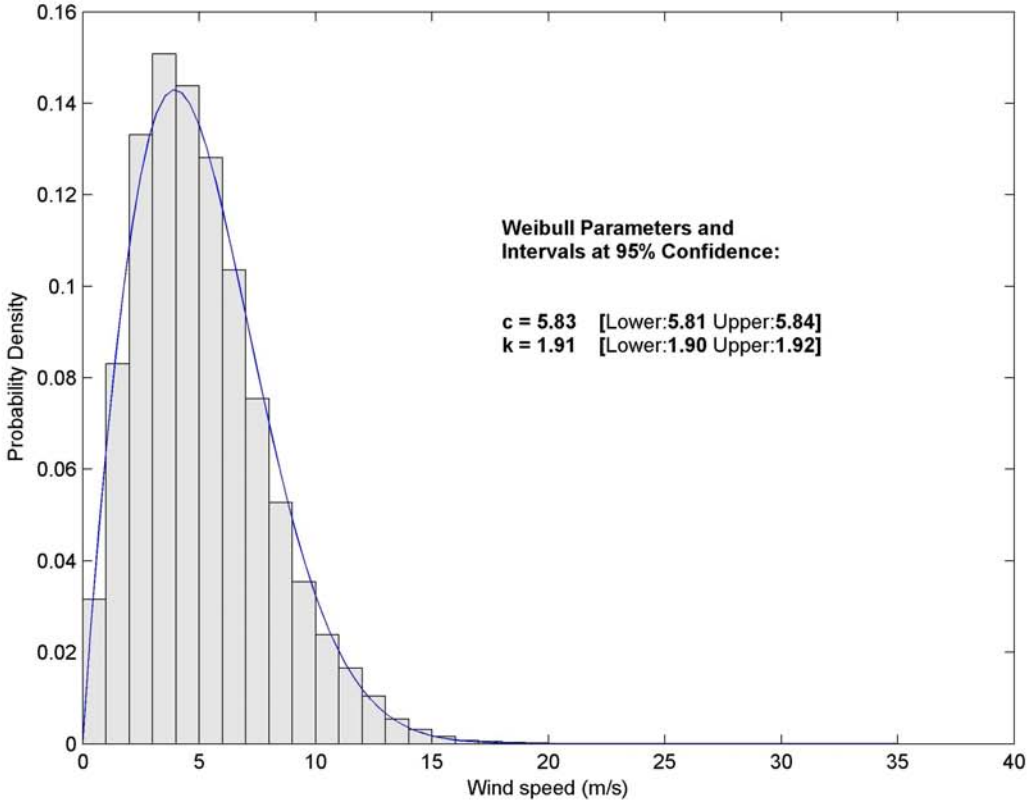

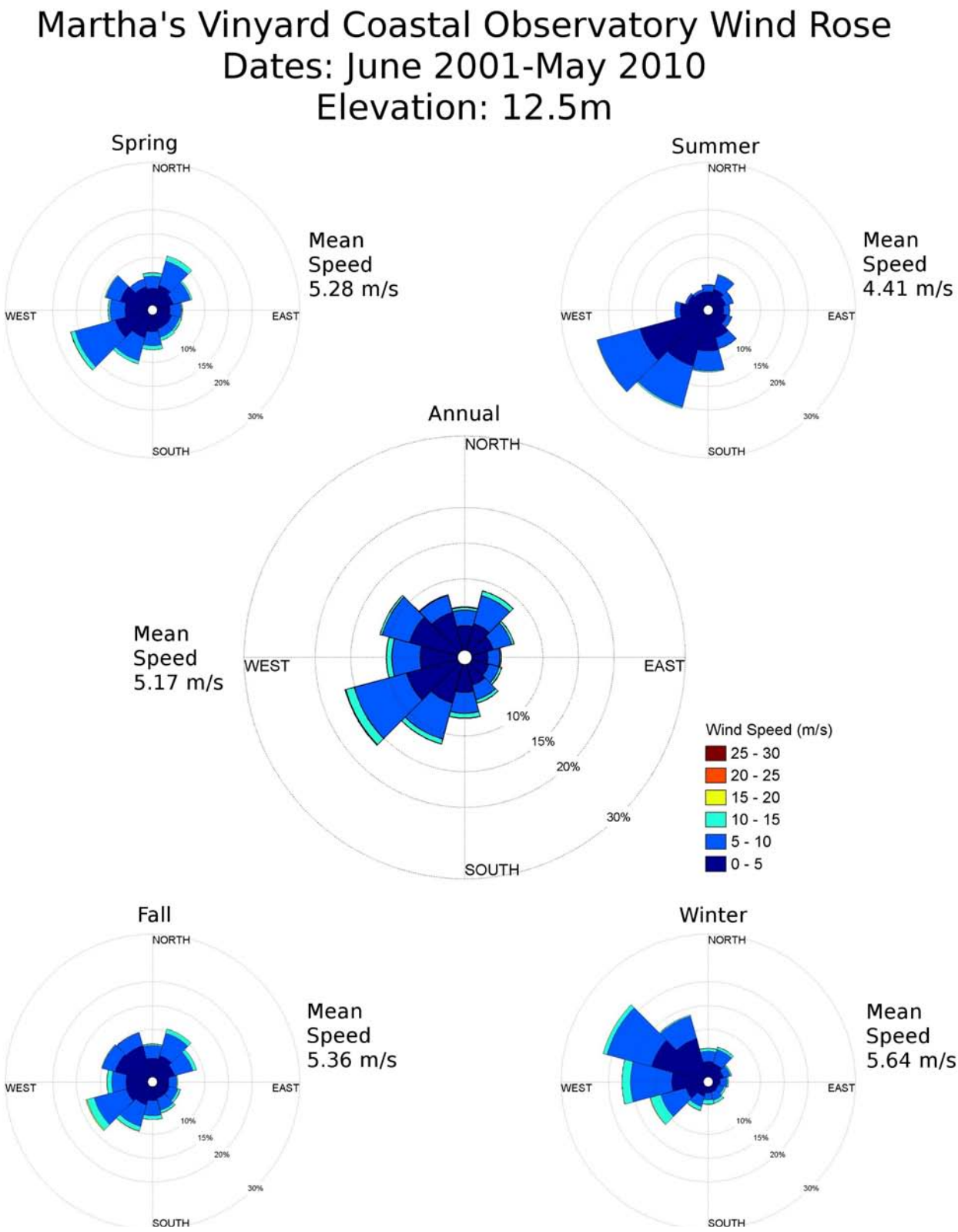
Martha's Vinyard Coastal Observatory Wind Rose
Dates: June 2001-May 2010
Elevation: 12.5m
Spring
Mean Speed 5.28 m/s
Summer
Mean Speed 4.41 m/s
Annual
Mean Speed 5.17 m/s
Fall
Mean Speed 5.36 m/s
Winter
Mean Speed 5.64 m/s
NORTH
SOUTH
EAST
WEST
10%
15%
20%
30%
Wind Speed (m/s)
25 - 30
20 - 25
15 - 20
10 - 15
5 - 10
0 - 5

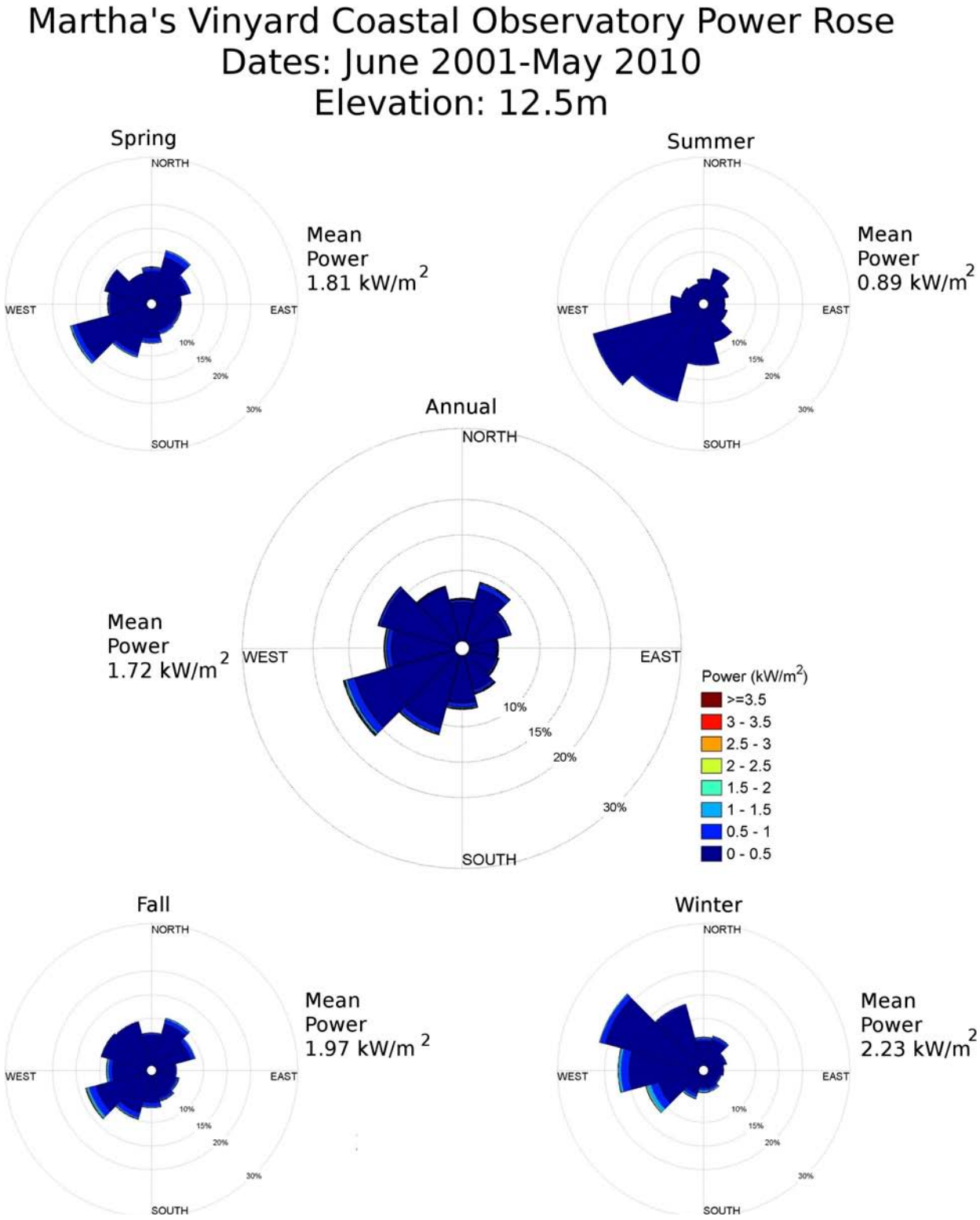
Martha's Vinyard Coastal Observatory Power Rose
Dates: June 2001-May 2010
Elevation: 12.5m
Spring
Mean Power 1.81 kW/m2
Summer
Mean Power 0.89 kW/m2
Annual
Mean Power 1.72 kW/m2
Fall
Mean Power 1.97 kW/m2
Winter
Mean Power 2.23 kW/m2
NORTH
SOUTH
EAST
WEST
10%
15%
20%
30%
Power (kW/m2)
>=3.5
3 - 3.5
2.5 - 3
2 - 2.5
1.5 - 2
1 - 1.5
0.5 - 1
0 - 0.5

NOAA NDBC 44008 Probability Distribution
Dates: 1988-2009
Elevation: 5m

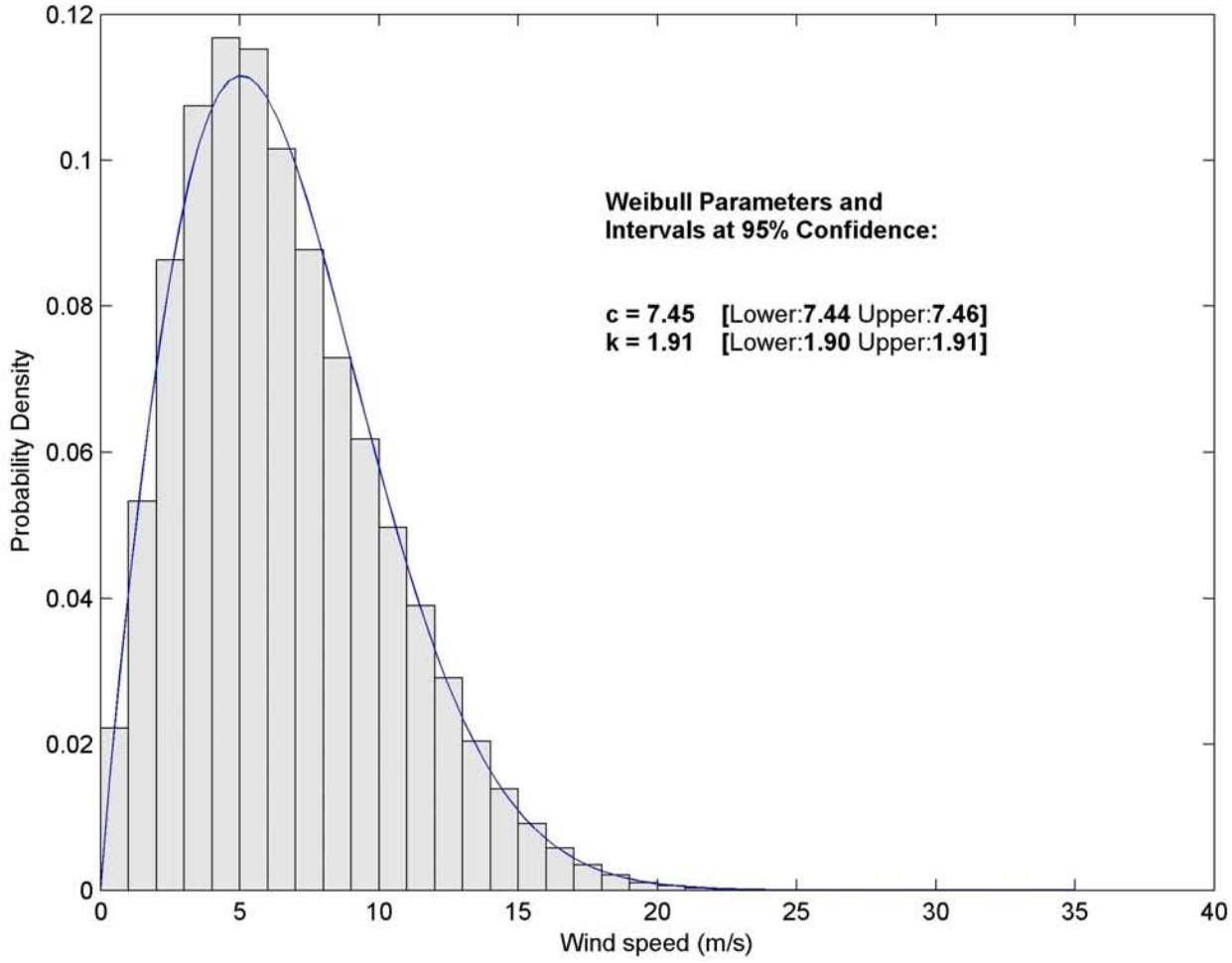

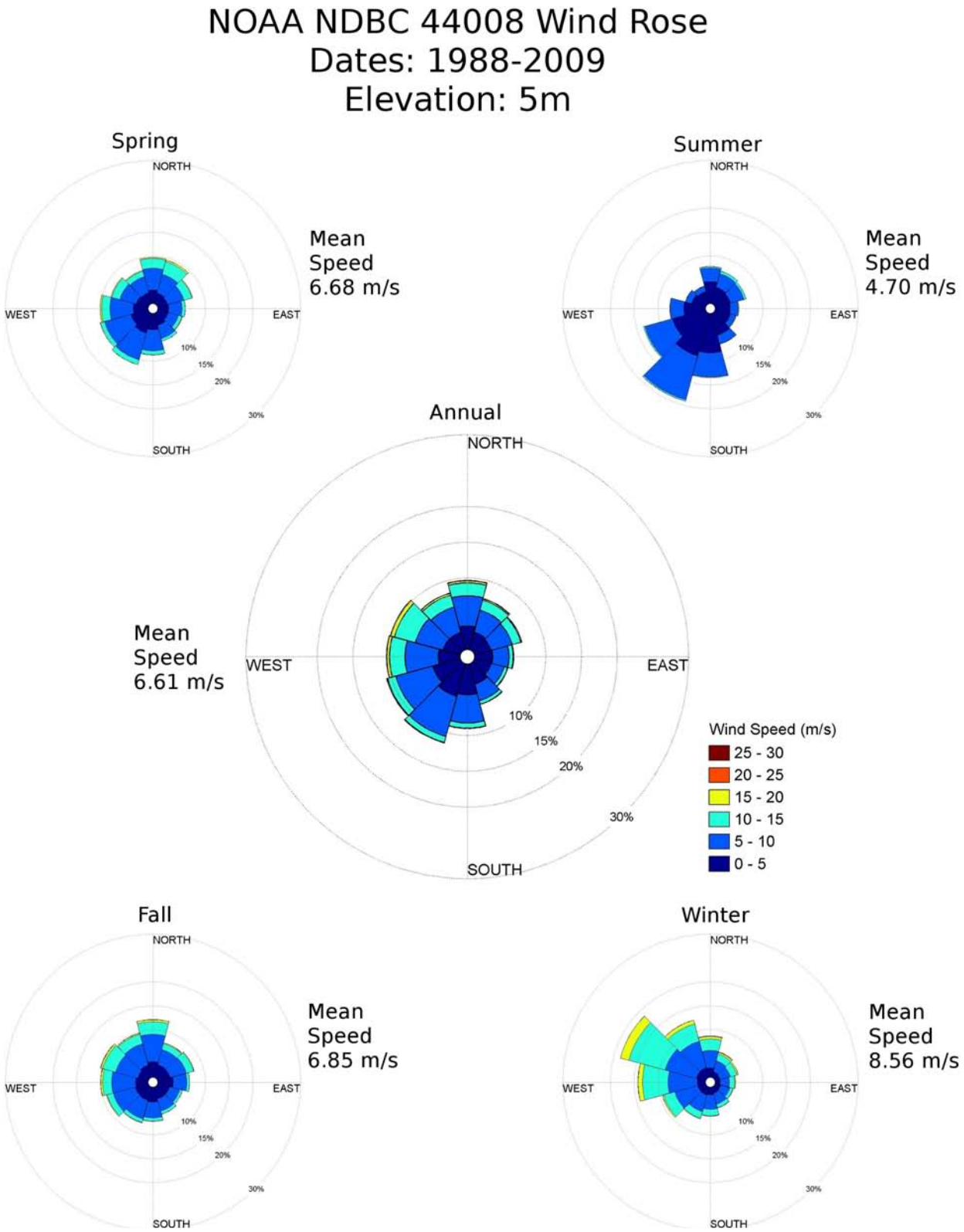
NOAA NDBC 44008 Wind Rose
Dates: 1988-2009
Elevation: 5m
Spring
Mean Speed 6.68 m/s
Summer
Mean Speed 4.70 m/s
Annual
Mean Speed 6.61 m/s
Fall
Mean Speed 6.85 m/s
Winter
Mean Speed 8.56 m/s
NORTH
SOUTH
EAST
WEST
10%
15%
20%
30%
Wind Speed (m/s)
25 - 30
20 - 25
15 - 20
10 - 15
5 - 10
0 - 5

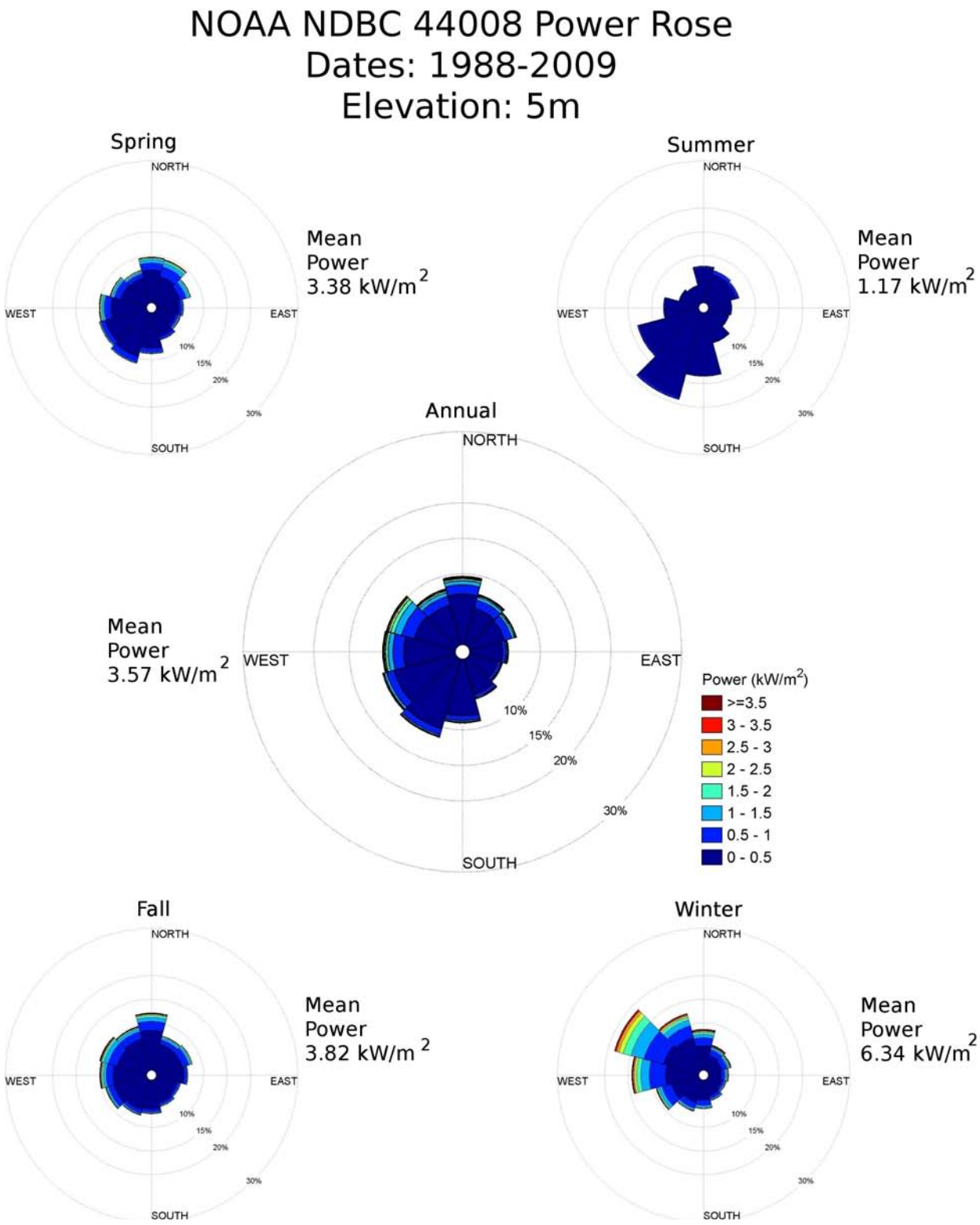
NOAA NDBC 44008 Power Rose
Dates: 1988-2009
Elevation: 5m
Spring
Mean Power 3.38 kW/m2
Summer
Mean Power 1.17 kW/m2
Annual
Mean Power 3.57 kW/m2
Fall
Mean Power 3.82 kW/m2
Winter
Mean Power 6.34 kW/m2
NORTH
SOUTH
EAST
WEST
10%
15%
20%
30%
Power (kW/m2)
>=3.5
3 - 3.5
2.5 - 3
2 - 2.5
1.5 - 2
1 - 1.5
0.5 - 1
0 - 0.5

NOAA NDBC 44017 Probability Distribution
Dates: 2002-2009
Elevation: 5m

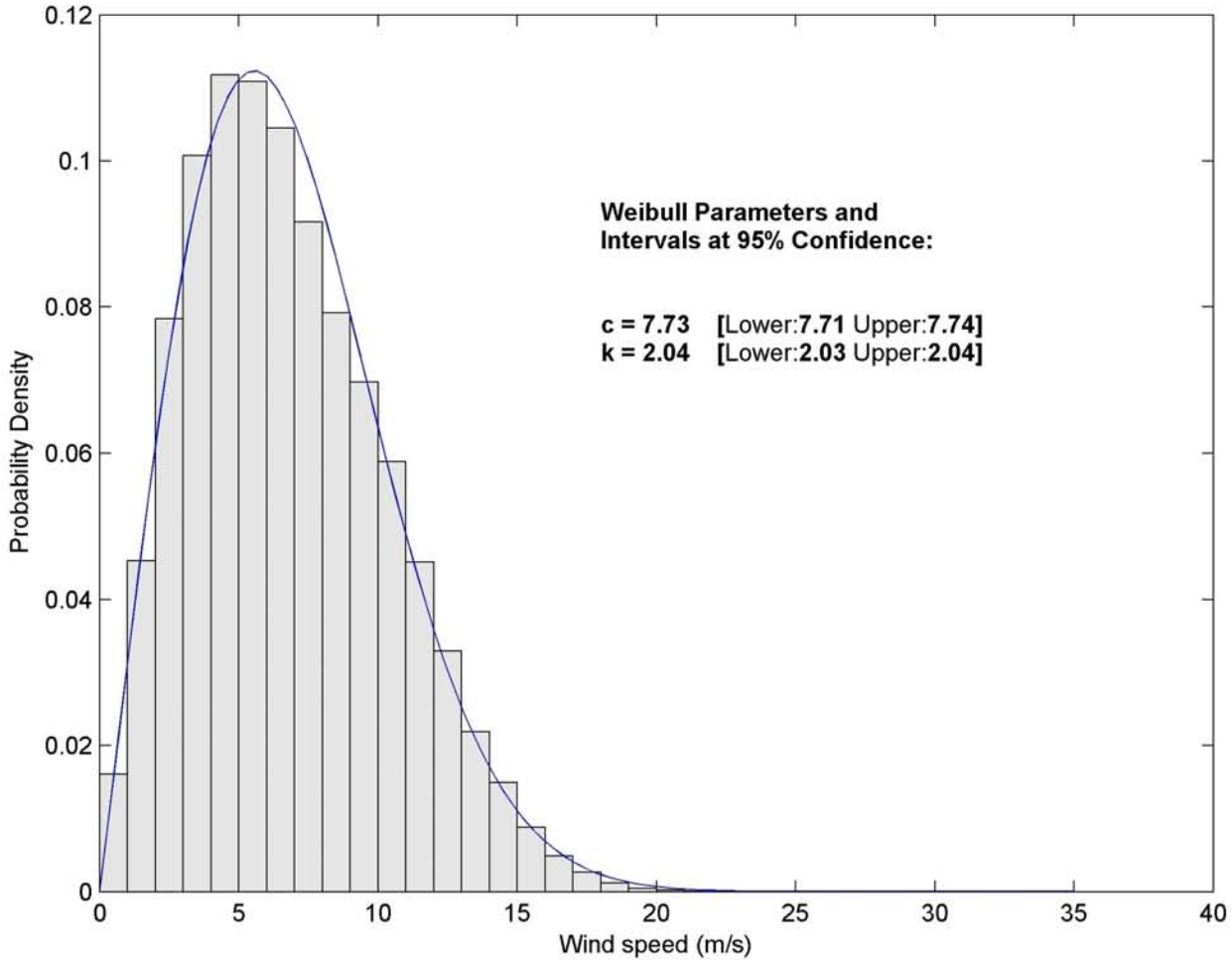

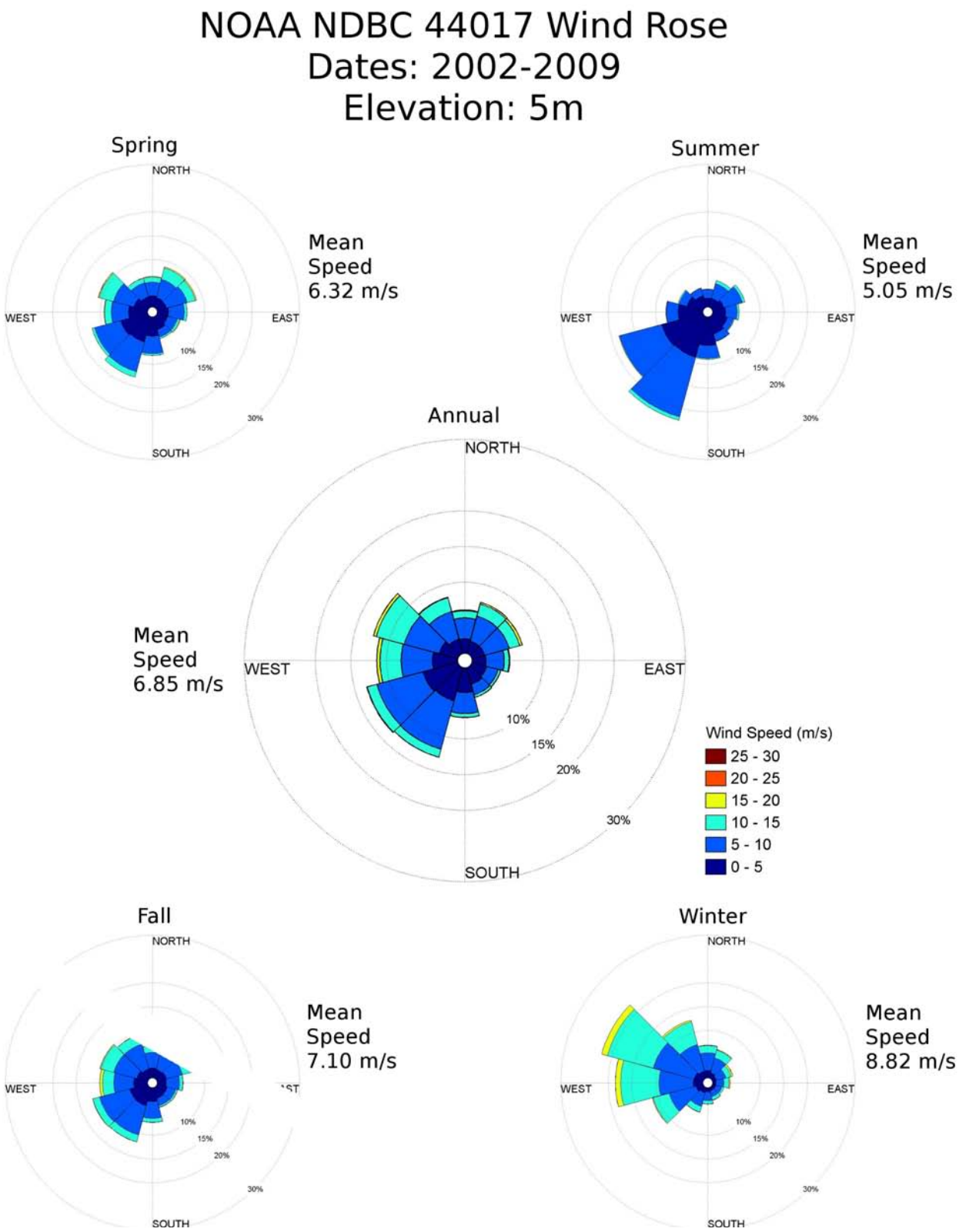
NOAA NDBC 44017 Wind Rose
Dates: 2002-2009
Elevation: 5m
Spring
Mean Speed 6.32 m/s
Summer
Mean Speed 5.05 m/s
Annual
Mean Speed 6.85 m/s
Fall
Mean Speed 7.10 m/s
Winter
Mean Speed 8.82 m/s
NORTH
SOUTH
EAST
WEST
10%
15%
20%
30%
Wind Speed (m/s)
25 - 30
20 - 25
15 - 20
10 - 15
5 - 10
0 - 5

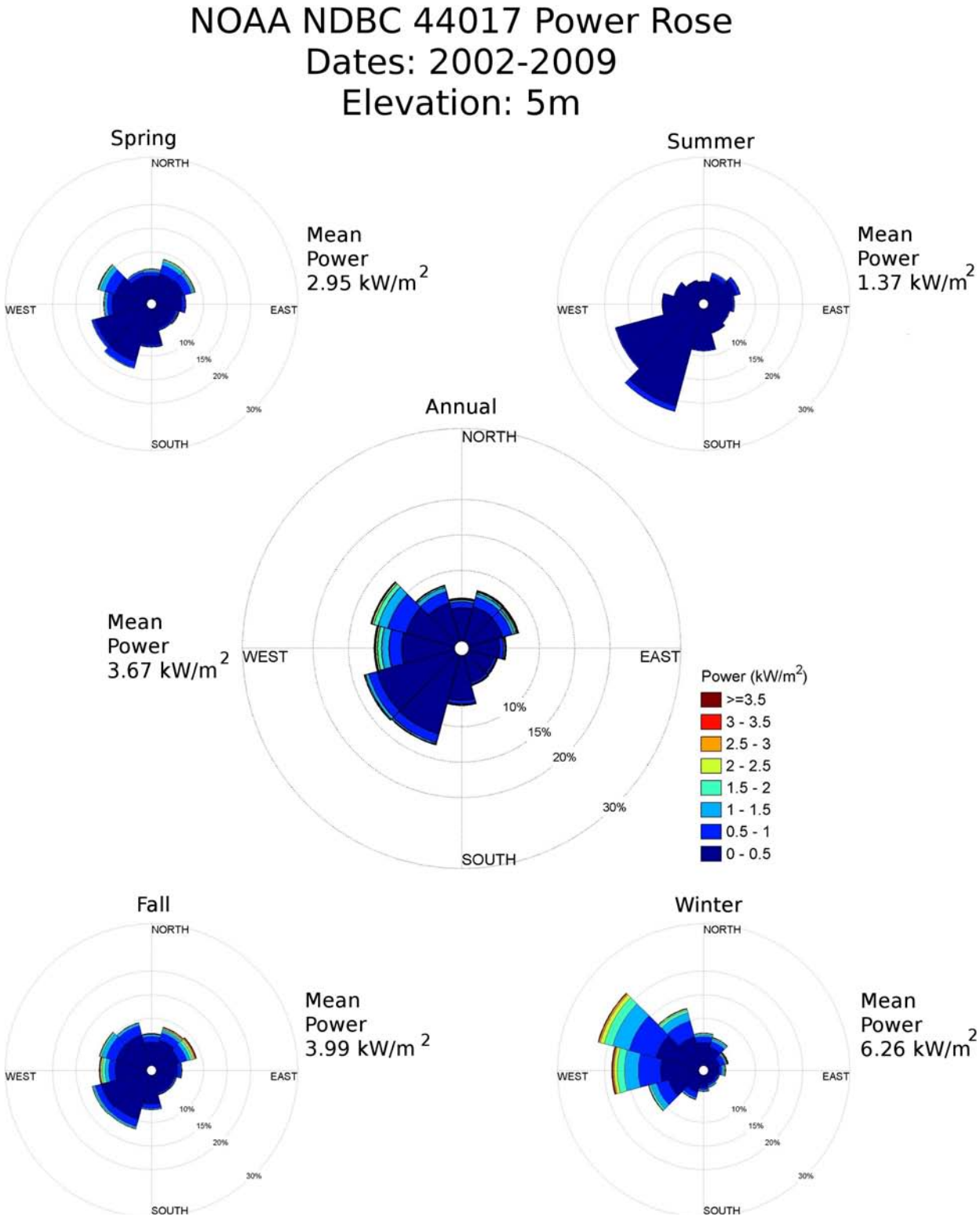
NOAA NDBC 44017 Power Rose
Dates: 2002-2009
Elevation: 5m
Spring
Mean Power 2.95 kW/m2
Summer
Mean Power 1.37 kW/m2
Annual
Mean Power 3.67 kW/m2
Fall
Mean Power 3.99 kW/m2
Winter
Mean Power 6.26 kW/m2
NORTH
SOUTH
EAST
WEST
10%
15%
20%
30%
Power (kW/m2)
>=3.5
3 - 3.5
2.5 - 3
2 - 2.5
1.5 - 2
1 - 1.5
0.5 - 1
0 - 0.5

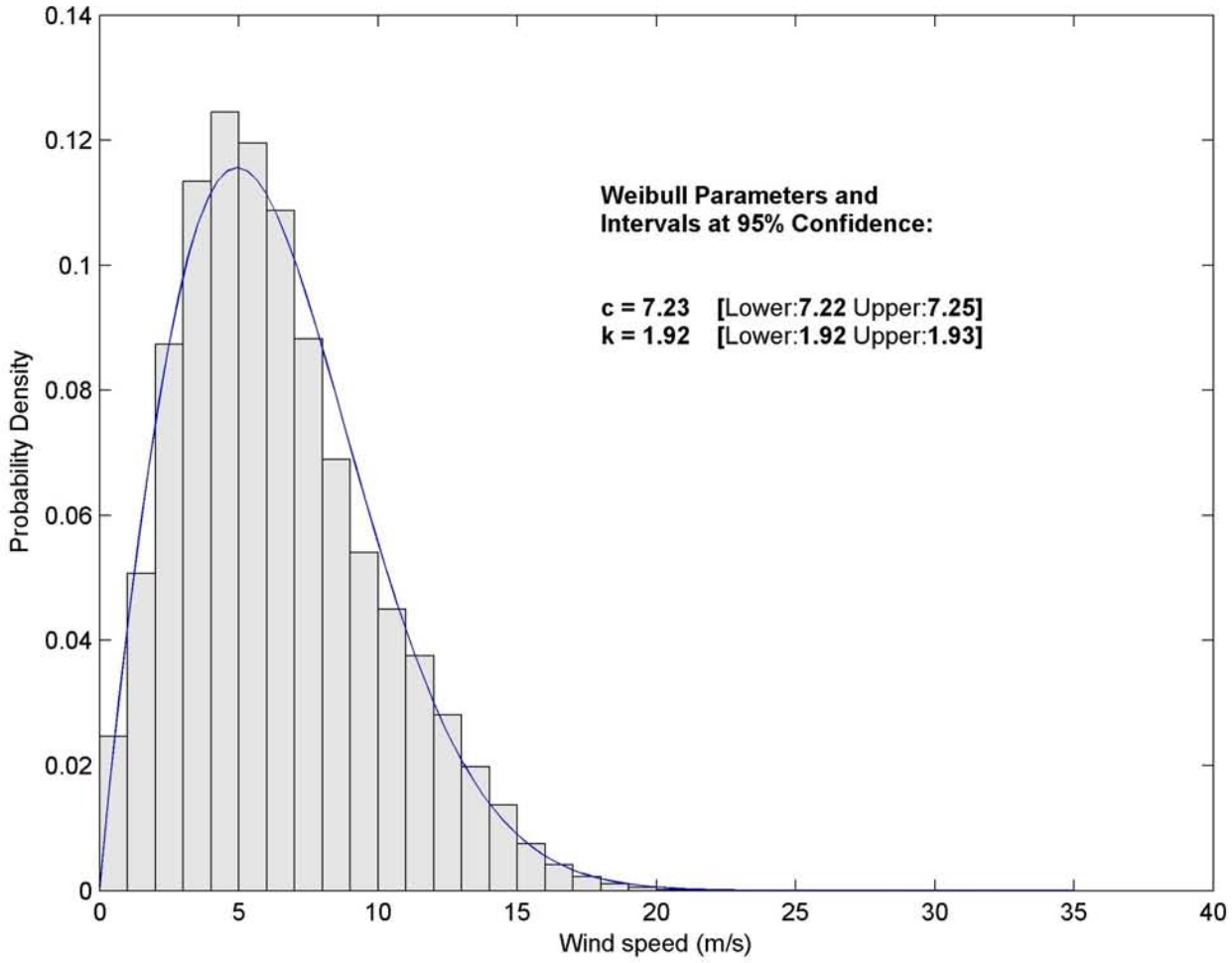
NOA NDBC 44018 Probability Distribution
Dates: 2002-2009
Elevation: 5m
Weibull Parameters and
Intervals at 95% Confidence:
c = 7.23 [Lower:7.22 Upper:7.25]
k = 1.92 [Lower:1.92 Upper:1.93]
Probability Density
Wind speed (m/s)
0.14
0.12
0.1
0.08
0.06
0.04
0.02
0
0
5
10
15
20
25
30
35
40

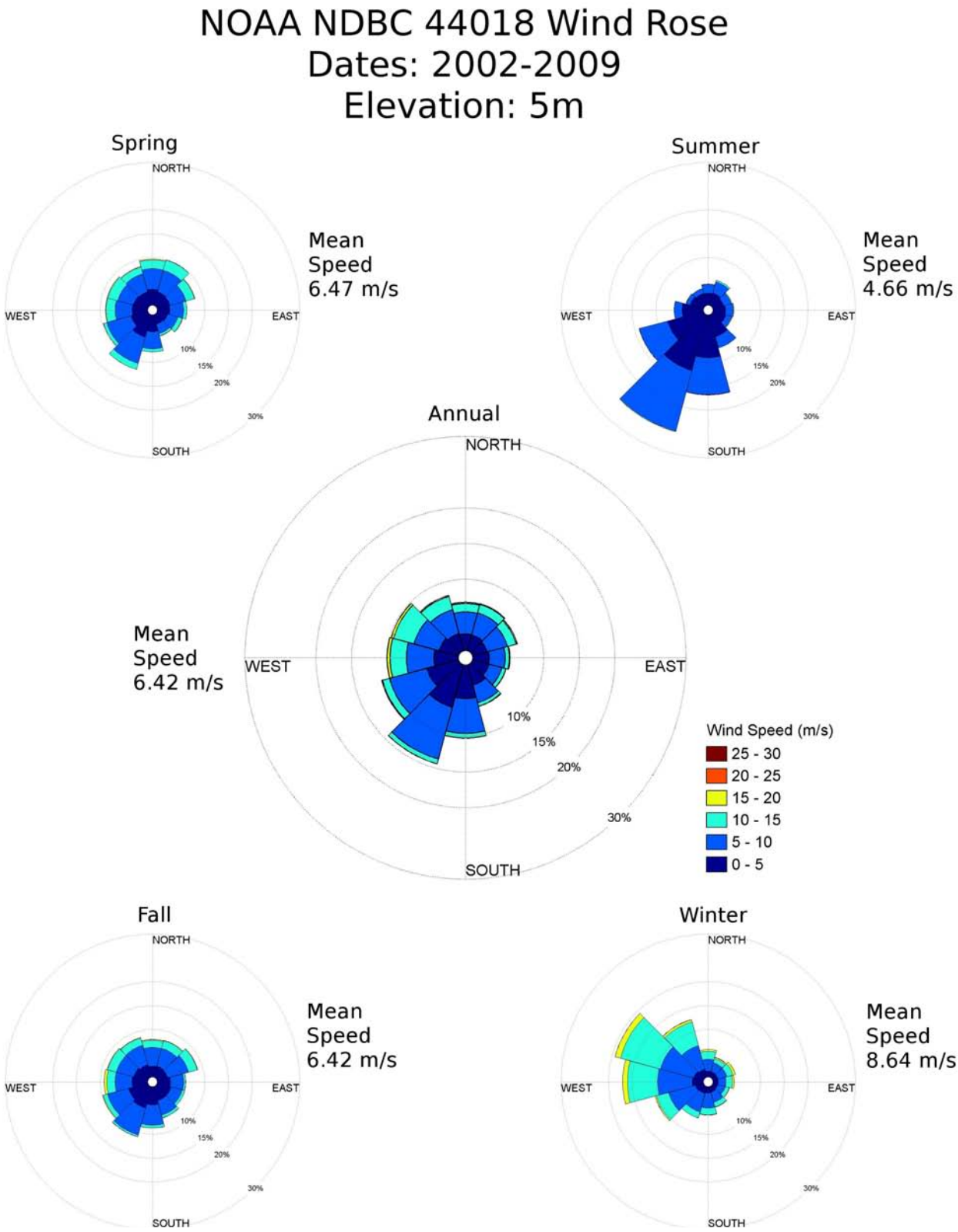
NOAA NDBC 44018 Wind Rose
Dates: 2002-2009
Elevation: 5m
Spring
Mean Speed 6.47 m/s
Summer
Mean Speed 4.66 m/s
Annual
Mean Speed 6.42 m/s
Fall
Mean Speed 6.42 m/s
Winter
Mean Speed 8.64 m/s
NORTH
SOUTH
EAST
WEST
10%
15%
20%
30%
Wind Speed (m/s)
25 - 30
20 - 25
15 - 20
10 - 15
5 - 10
0 - 5

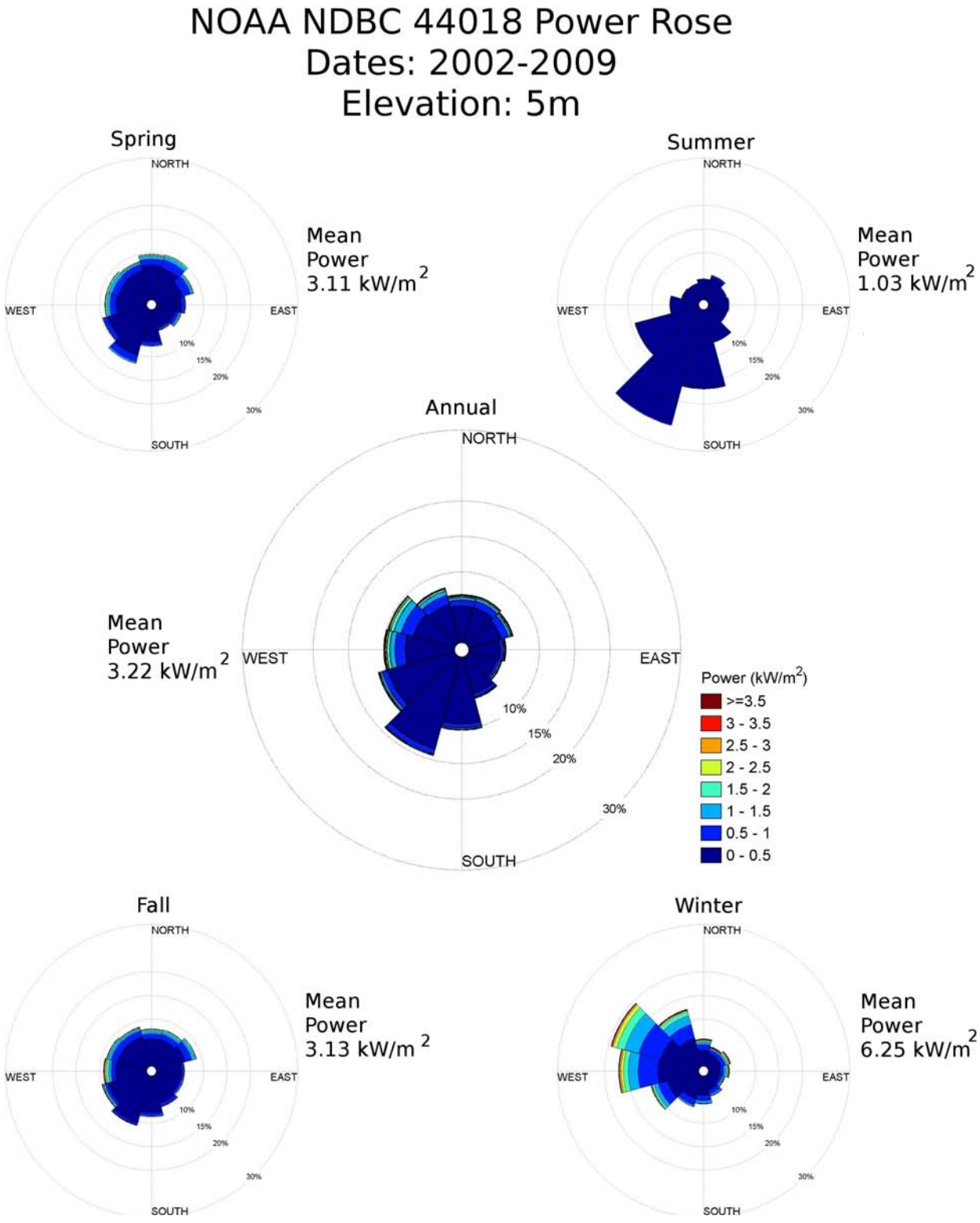
NOAA NDBC 44018 Power Rose
Dates: 2002-2009
Elevation: 5m
Spring
Mean
Power
3.11 kW/m 2
Summer
Mean
Power
1.03 kW/m 2
Annual
Mean
Power
3.22 kW/m 2
Fall
Mean
Power
3.13 kW/m 2
Winter
Mean
Power
6.25 kW/m 2
NORTH
SOUTH
EAST
WEST
10%
15%
20%
30%
Power (kW/m2)
>=3.5
3 - 3.5
2.5 - 3
2 - 2.5
1.5 - 2
1 - 1.5
0.5 - 1
0 - 0.5

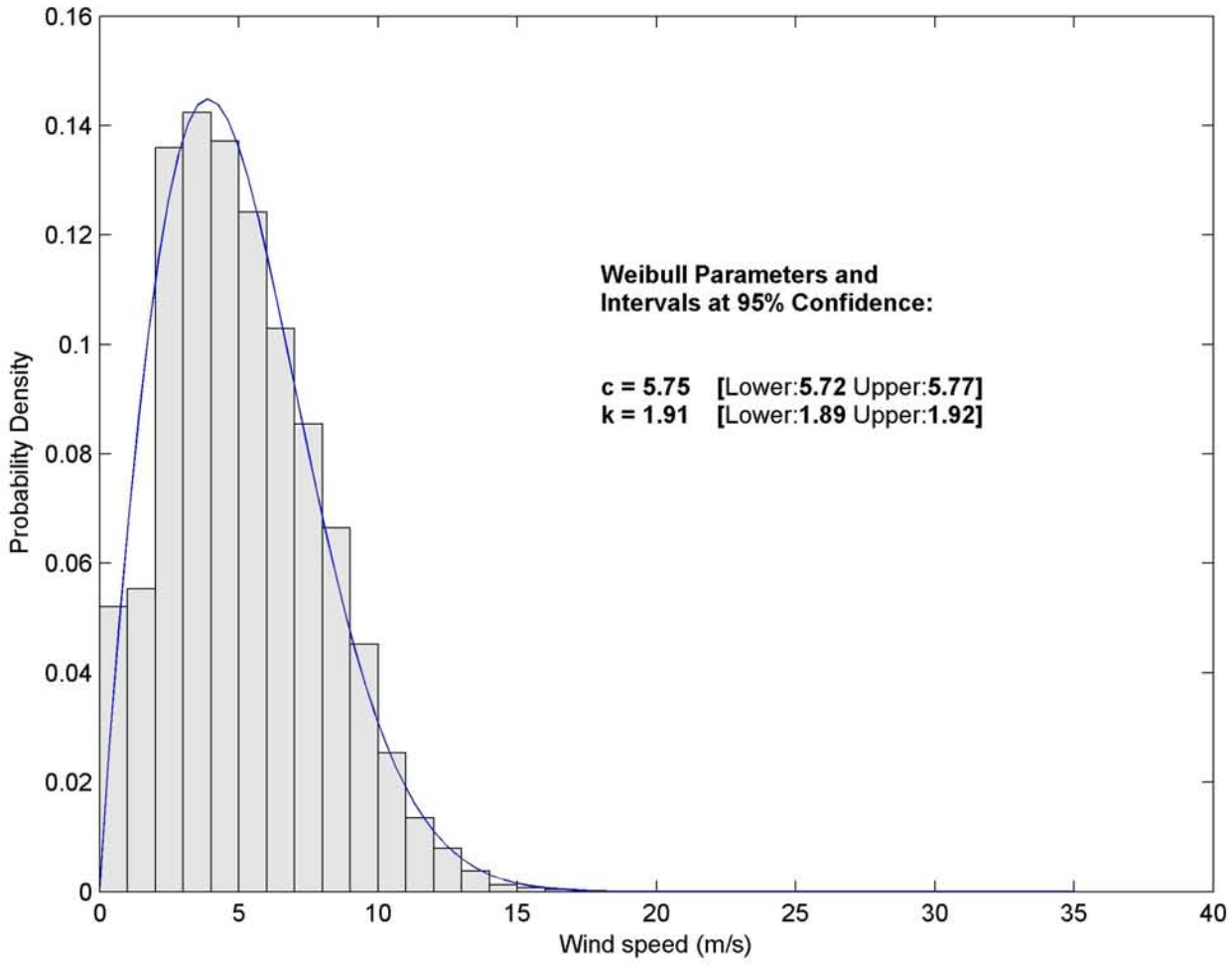
NOAA NDBC 44060 Probability Distribution
Dates: July 2007-June 2009
Elevation: 3.5m
Weibull Parameters and
Intervals at 95% Confidence:
c = 5.75 [Lower:5.72 Upper:5.77]
k = 1.91 [Lower:1.89 Upper:1.92]
Probability Density
Wind speed (m/s)
0.16
0.14
0.12
0.1
0.08
0.06
0.04
0.02
0
0
5
10
15
20
25
30
35
40

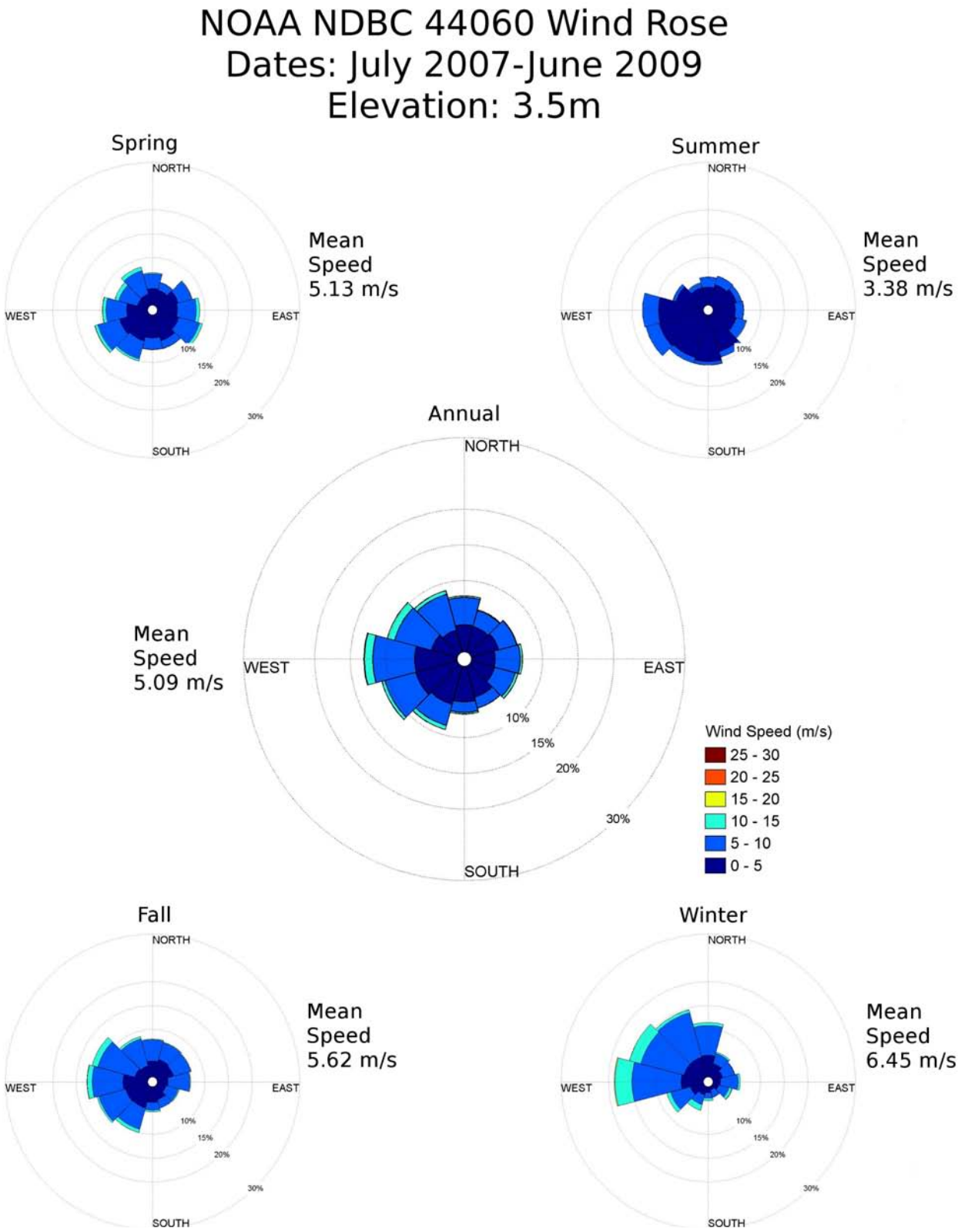
NOAA NDBC 44060 Wind Rose
Dates: July 2007-June 2009
Elevation: 3.5m
Spring
Mean Speed 5.13 m/s
Summer
Mean Speed 3.38 m/s
Annual
Mean Speed 5.09 m/s
Fall
Mean Speed 5.62 m/s
Winter
Mean Speed 6.45 m/s
NORTH
SOUTH
EAST
WEST
10%
15%
20%
30%
Wind Speed (m/s)
25 - 30
20 - 25
15 - 20
10 - 15
5 - 10
0 - 5

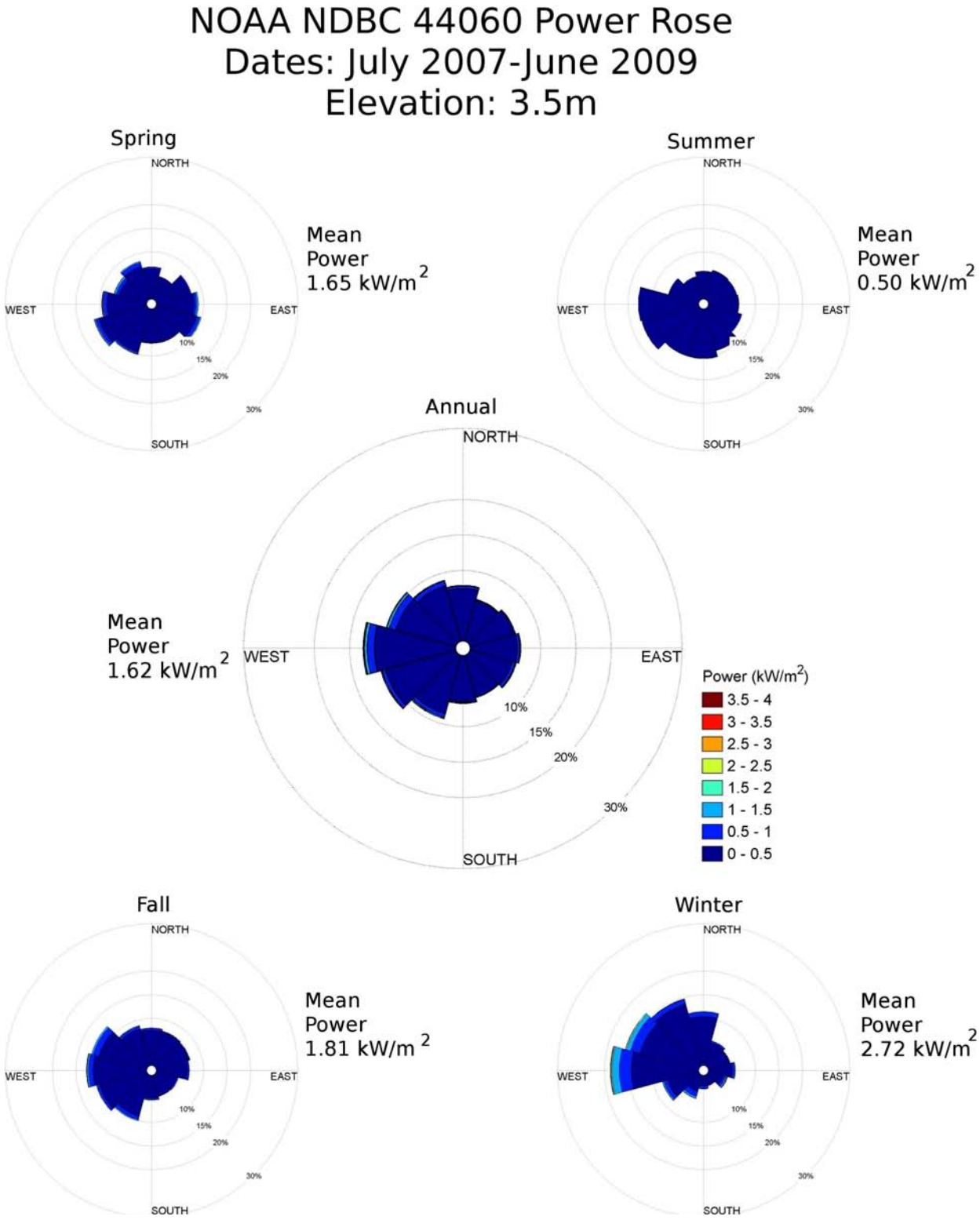
NOAA NDBC 44060 Power Rose
Dates: July 2007-June 2009
Elevation: 3.5m
Spring
Mean Power 1.65 kW/m2
Summer
Mean Power 0.50 kW/m2
Annual
Mean Power 1.62 kW/m2
Fall
Mean Power 1.81 kW/m2
Winter
Mean Power 2.72 kW/m2
NORTH
SOUTH
EAST
WEST
10%
15%
20%
30%
Power (kW/m2)
3.5 - 4
3 - 3.5
2.5 - 3
2 - 2.5
1.5 - 2
1 - 1.5
0.5 - 1
0 - 0.5

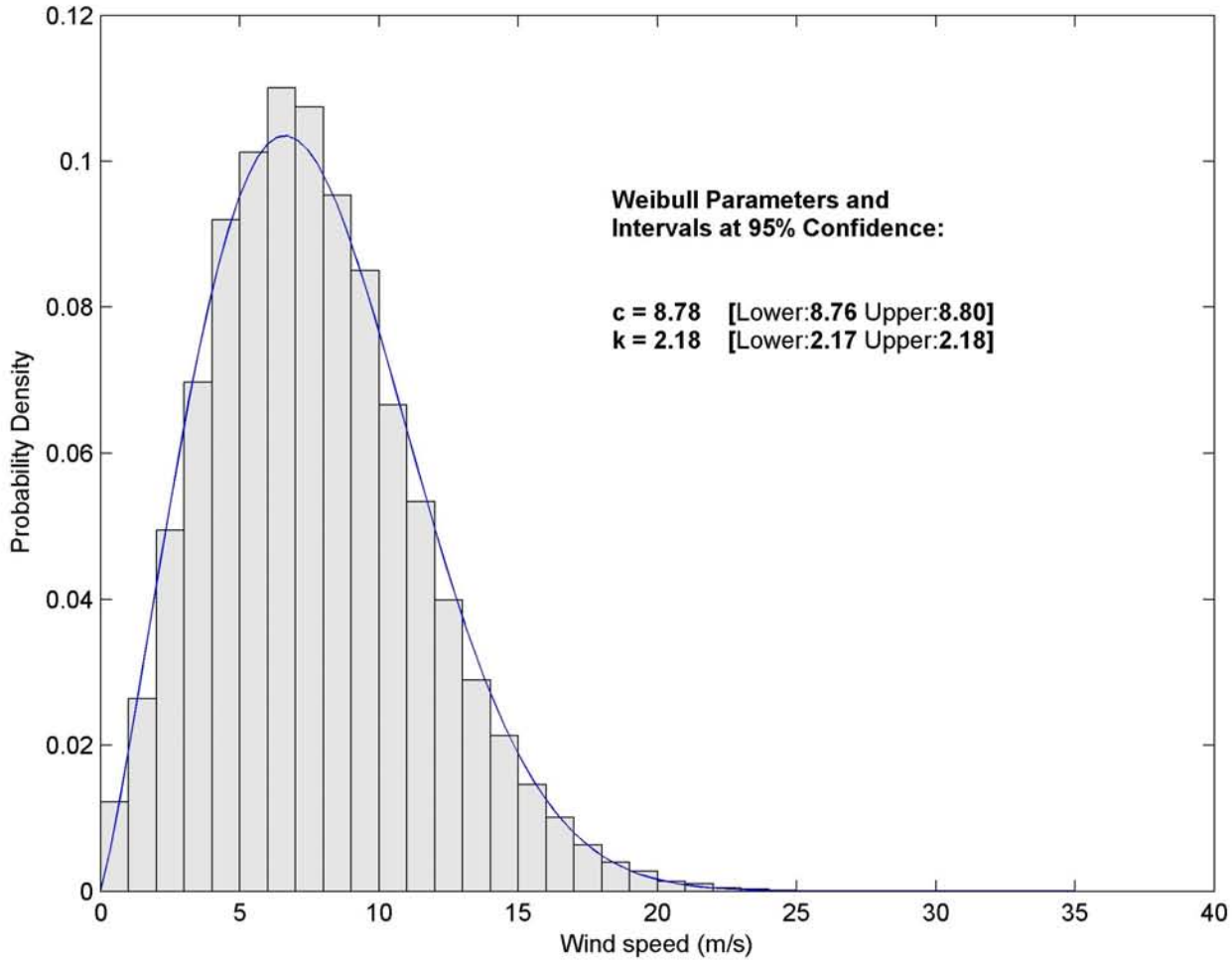
NOAA NDBC BUZM3 Probability Distribution
Dates: 1986-1993, 1998-2009
Elevation: 24.8m
Weibull Parameters and
Intervals at 95% Confidence:
c = 8.78 [Lower:8.76 Upper:8.80]
k = 2.18 [Lower:2.17 Upper:2.18]
Probability Density
Wind speed (m/s)
0
0.02
0.04
0.06
0.08
0.1
0.12
0
5
10
15
20
25
30
35
40

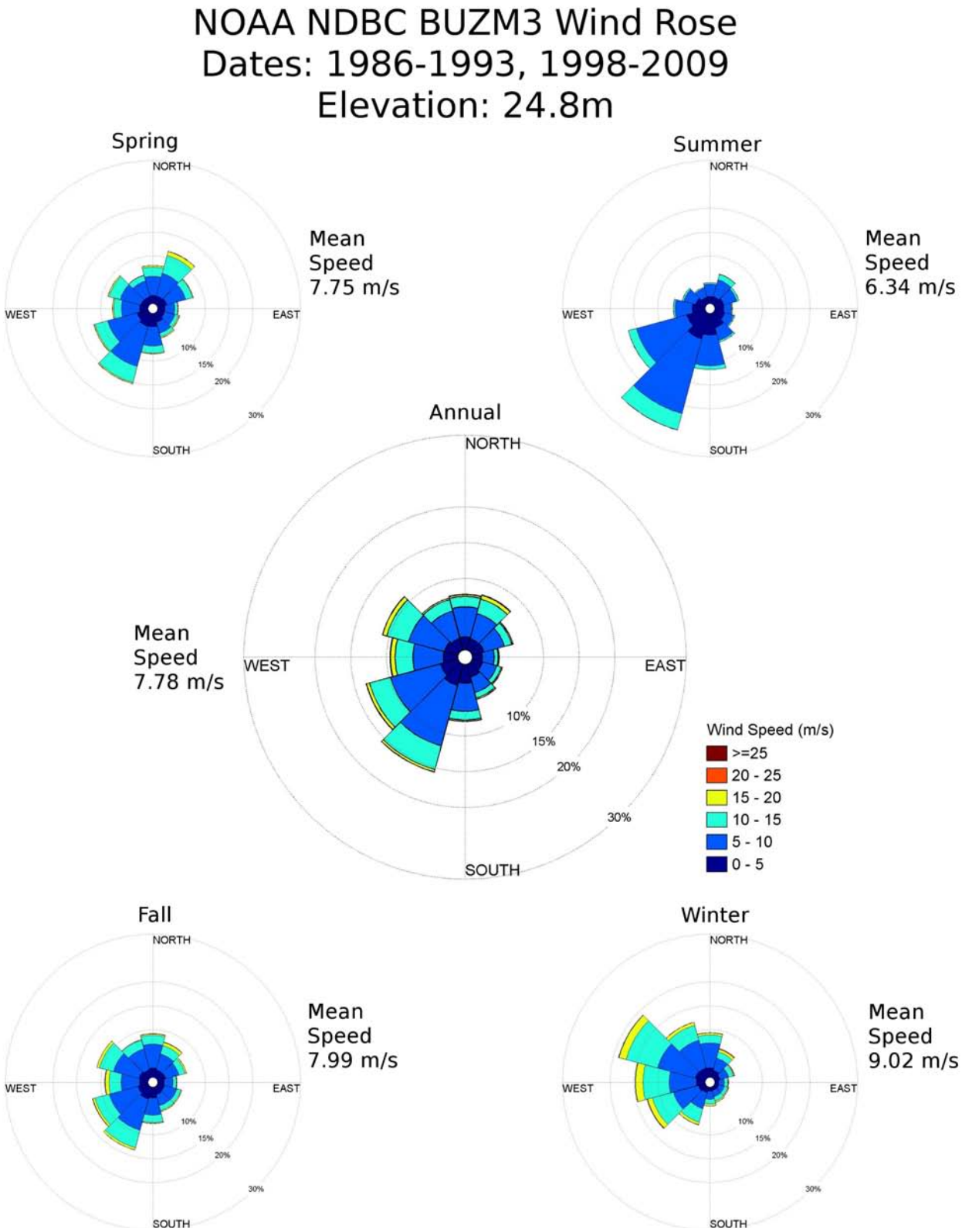
NOAA NDBC BUZM3 Wind Rose
Dates: 1986-1993, 1998-2009
Elevation: 24.8m
Spring
Mean Speed 7.75 m/s
Summer
Mean Speed 6.34 m/s
Annual
Mean Speed 7.78 m/s
Fall
Mean Speed 7.99 m/s
Winter
Mean Speed 9.02 m/s
NORTH
SOUTH
EAST
WEST
10%
15%
20%
30%
Wind Speed (m/s)
>=25
20 - 25
15 - 20
10 - 15
5 - 10
0 - 5

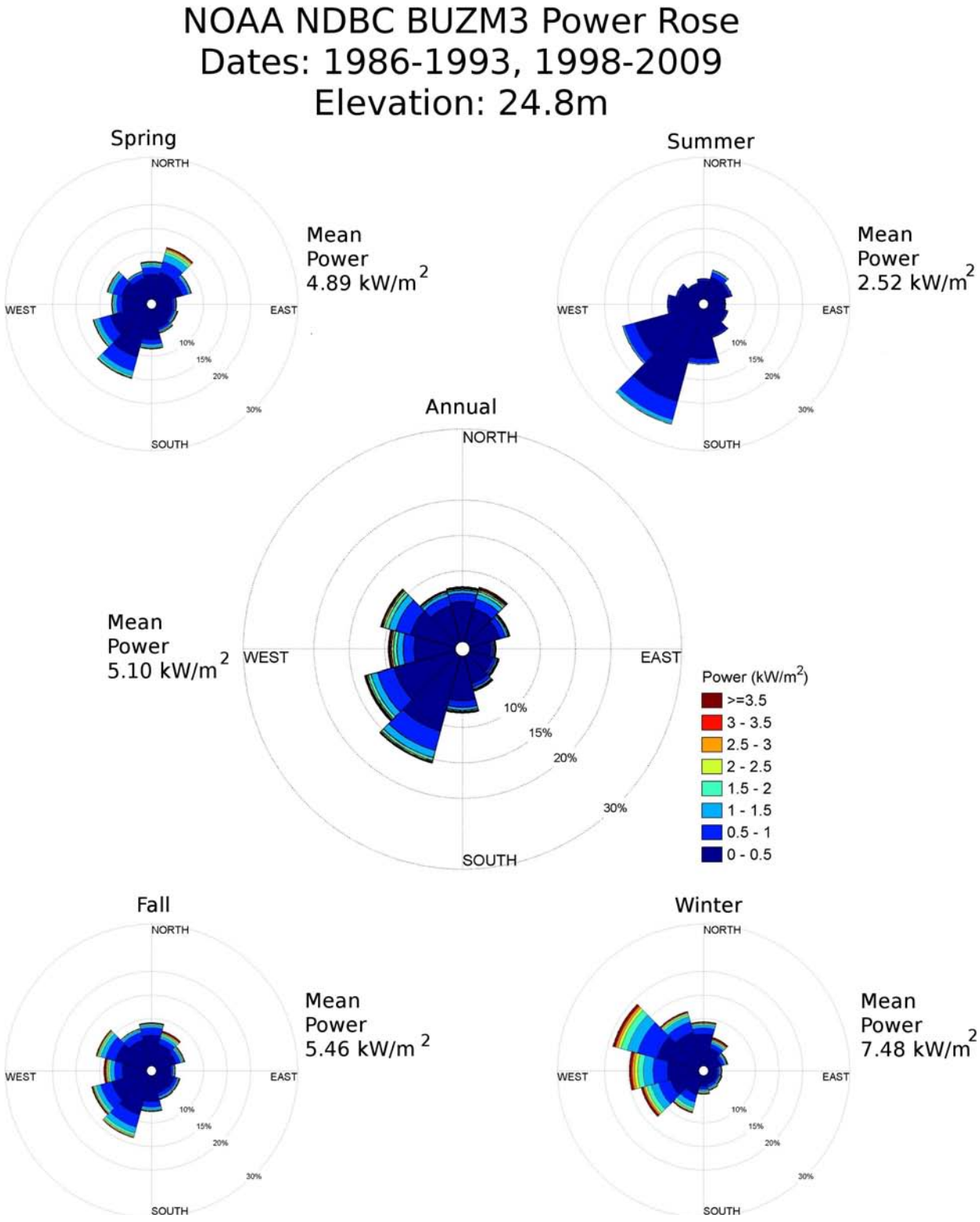
NOAA NDBC BUZM3 Power Rose
Dates: 1986-1993, 1998-2009
Elevation: 24.8m
Spring
Mean Power 4.89 kW/m2
Summer
Mean Power 2.52 kW/m2
Annual
Mean Power 5.10 kW/m2
Fall
Mean Power 5.46 kW/m2
Winter
Mean Power 7.48 kW/m2
NORTH
SOUTH
EAST
WEST
10%
15%
20%
30%
Power (kW/m2)
>=3.5
3 - 3.5
2.5 - 3
2 - 2.5
1.5 - 2
1 - 1.5
0.5 - 1
0 - 0.5

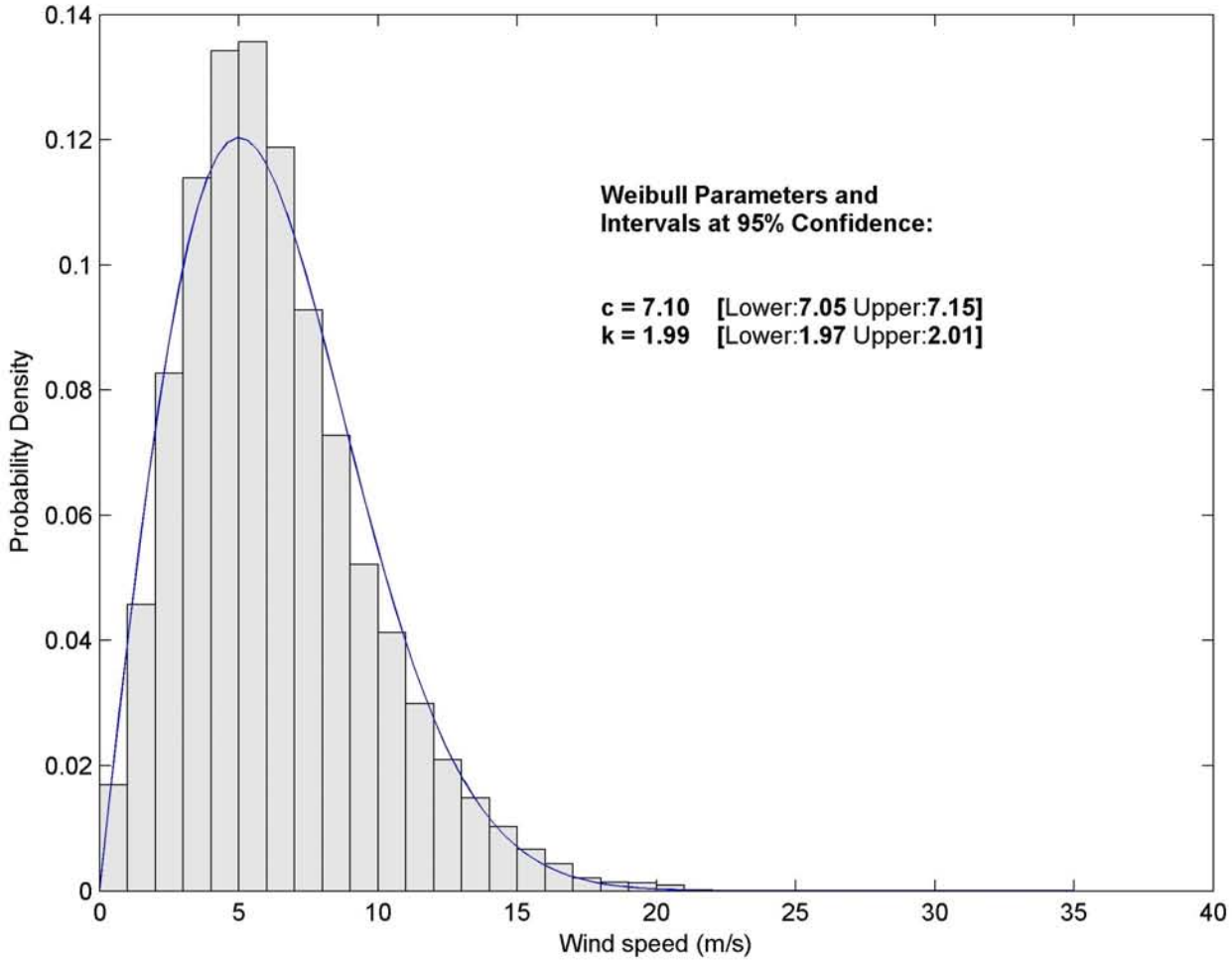
Pt. Judith Probability Distribution
Dates: 2005-2007
Elevation: 22.3m
Weibull Parameters and
Intervals at 95% Confidence:
c = 7.10 [Lower:7.05 Upper:7.15]
k = 1.99 [Lower:1.97 Upper:2.01]
Probability Density
Wind speed (m/s)
0.14
0.12
0.1
0.08
0.06
0.04
0.02
0
0
5
10
15
20
25
30
35
40

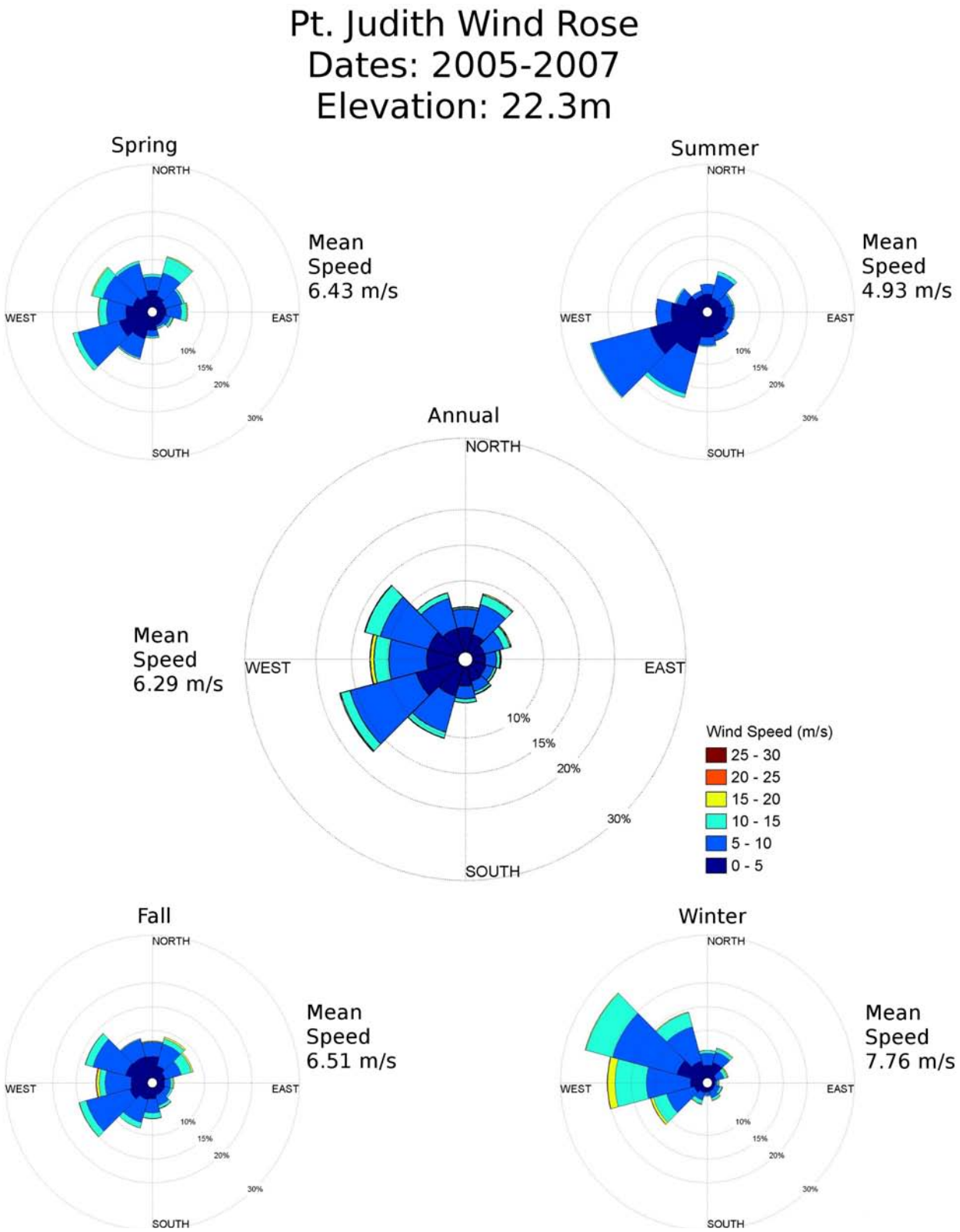
Pt. Judith Wind Rose
Dates: 2005-2007
Elevation: 22.3m
Spring
Mean
Speed
6.43 m/s
Summer
Mean
Speed
4.93 m/s
Annual
Mean
Speed
6.29 m/s
Fall
Mean
Speed
6.51 m/s
Winter
Mean
Speed
7.76 m/s
NORTH
SOUTH
EAST
WEST
10%
15%
20%
30%
Wind Speed (m/s)
25 - 30
20 - 25
15 - 20
10 - 15
5 - 10
0 - 5

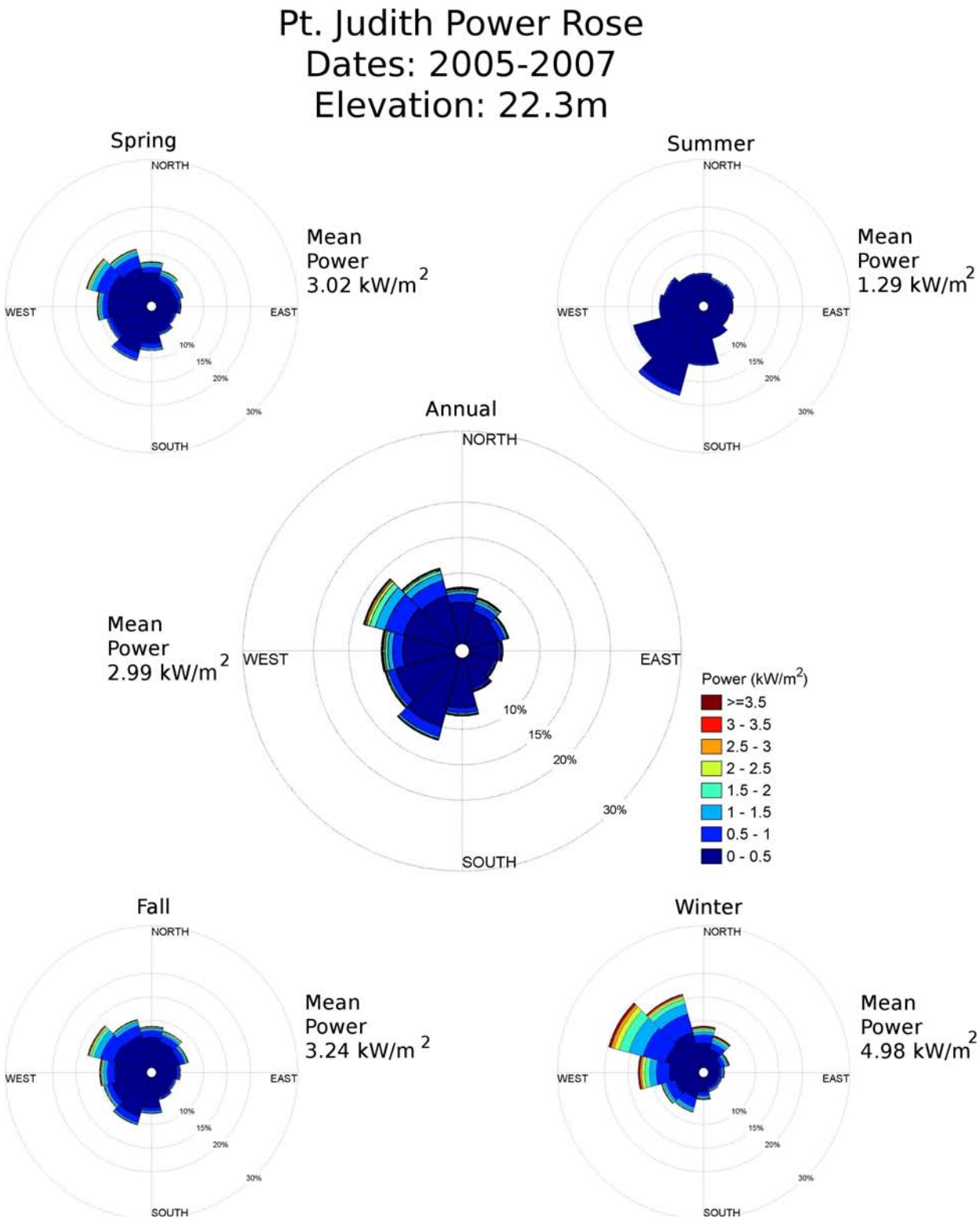
Pt. Judith Power Rose
Dates: 2005-2007
Elevation: 22.3m
Spring
Mean Power 3.02 kW/m2
Summer
Mean Power 1.29 kW/m2
Annual
Mean Power 2.99 kW/m2
Fall
Mean Power 3.24 kW/m2
Winter
Mean Power 4.98 kW/m2
NORTH
SOUTH
EAST
WEST
10%
15%
20%
30%
Power (kW/m2)
>=3.5
3 - 3.5
2.5 - 3
2 - 2.5
1.5 - 2
1 - 1.5
0.5 - 1
0 - 0.5

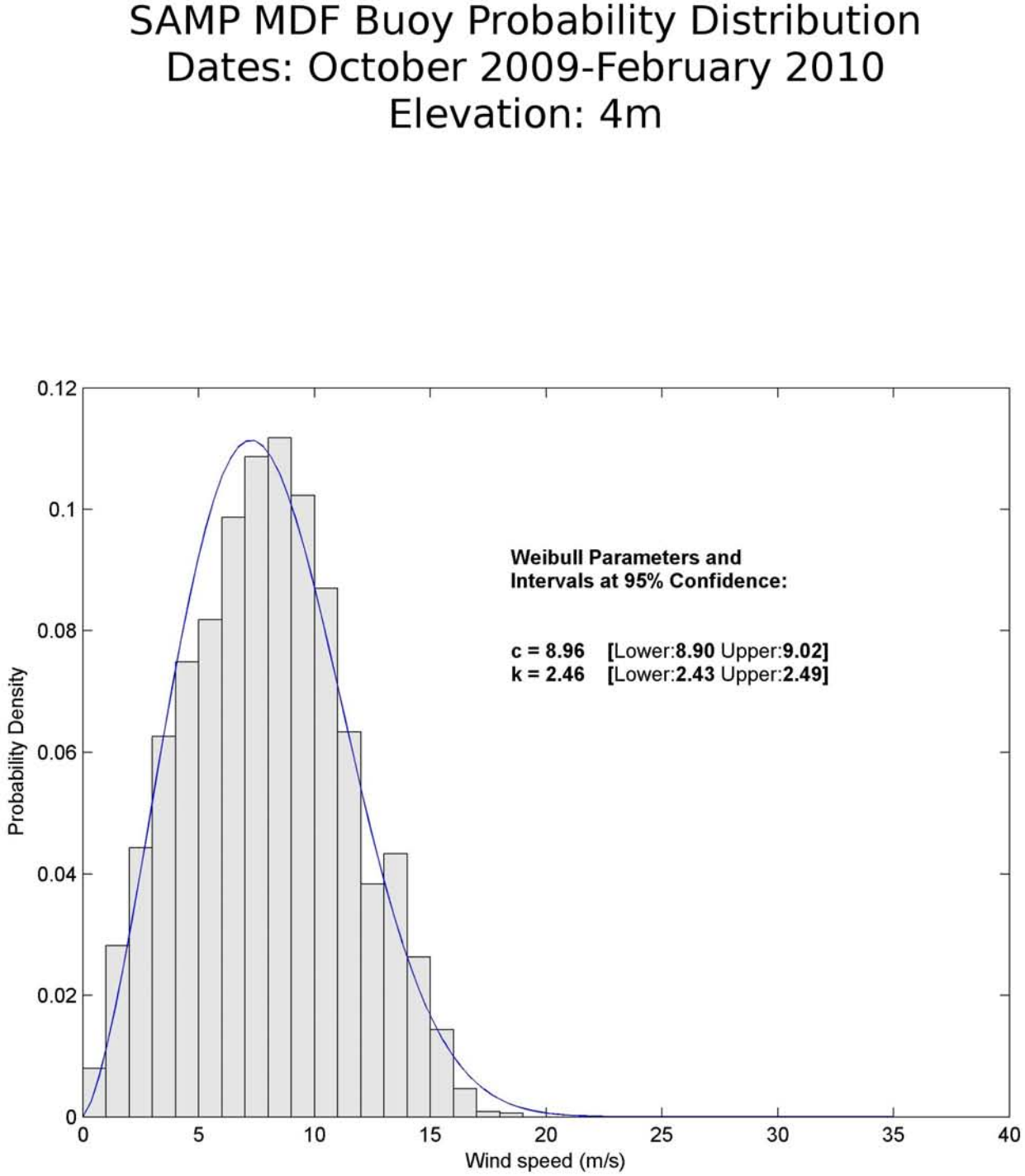
SAMP MDF Buoy Probability Distribution
Dates: October 2009-February 2010
Elevation: 4m
Weibull Parameters and
Intervals at 95% Confidence:
c = 8.96 [Lower:8.90 Upper:9.02]
k = 2.46 [Lower:2.43 Upper:2.49]
Probability Density
Wind speed (m/s)
0
0.02
0.04
0.06
0.08
0.1
0.12
0
5
10
15
20
25
30
35
40

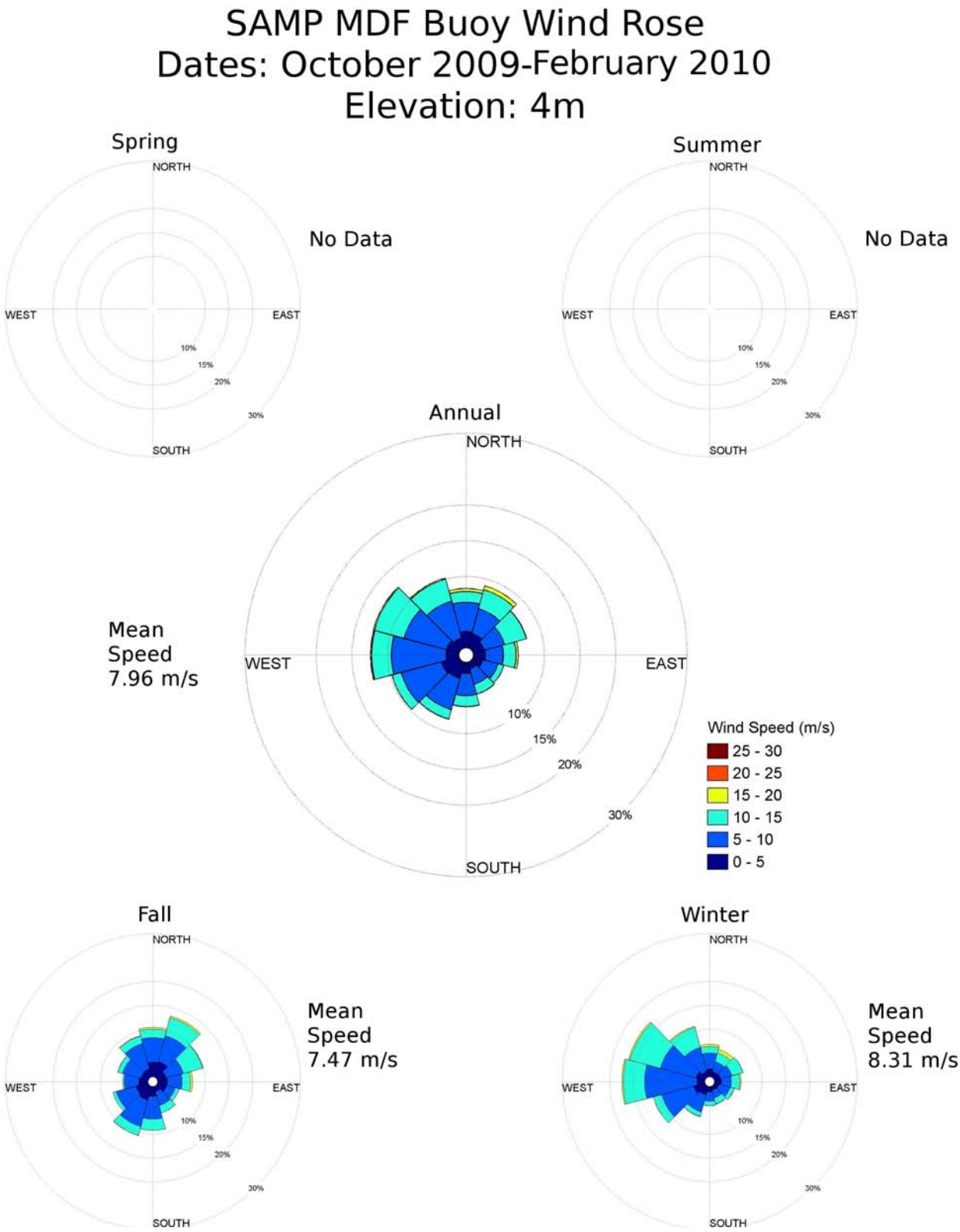
SAMP MDF Buoy Wind Rose
Dates: October 2009-February 2010
Elevation: 4m
Spring
No Data
Summer
No Data
Annual
Mean
Speed
7.96 m/s
Wind Speed (m/s)
25 - 30
20 - 25
15 - 20
10 - 15
5 - 10
0 - 5
Fall
Mean
Speed
7.47 m/s
Winter
Mean
Speed
8.31 m/s
NORTH
SOUTH
EAST
WEST
10%
15%
20%
30%

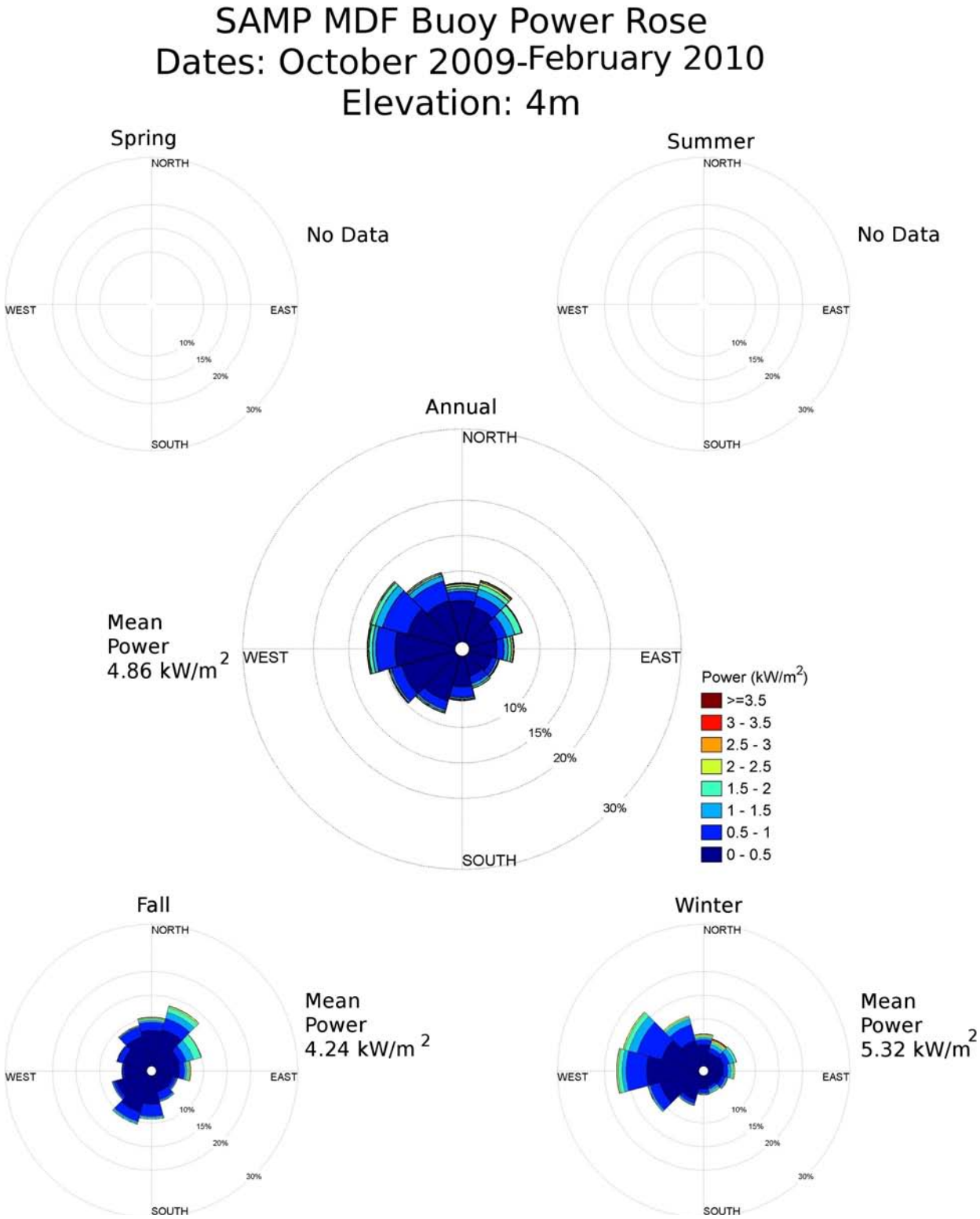
SAMP MDF Buoy Power Rose
Dates: October 2009-February 2010
Elevation: 4m
Spring
No Data
Summer
No Data
Annual
Mean
Power
4.86 kW/m 2
Fall
Mean
Power
4.24 kW/m 2
Winter
Mean
Power
5.32 kW/m 2
NORTH
SOUTH
EAST
WEST
10%
15%
20%
30%
Power (kW/m2)
>=3.5
3 - 3.5
2.5 - 3
2 - 2.5
1.5 - 2
1 - 1.5
0.5 - 1
0 - 0.5

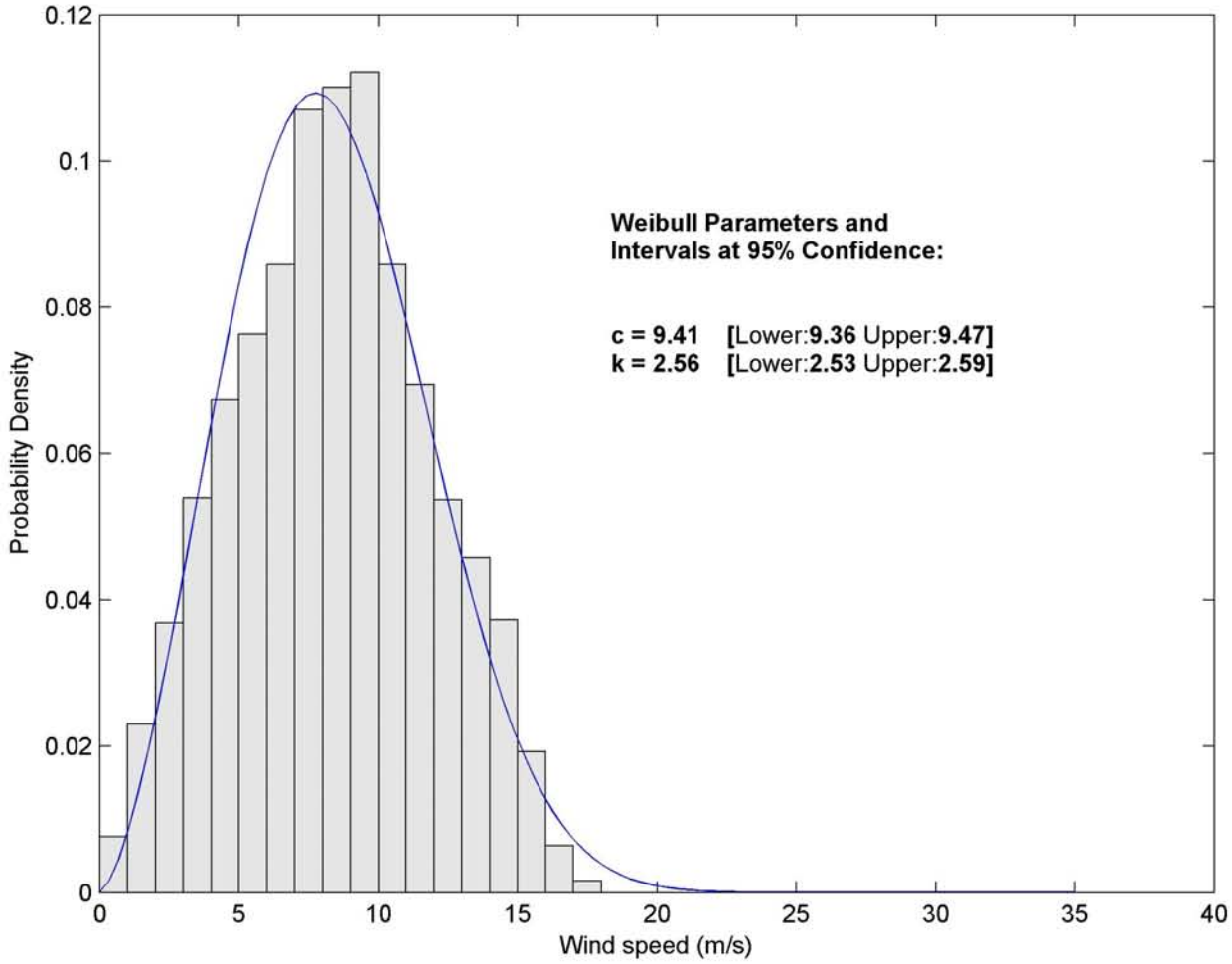
SAMP MDS Buoy Probability Distribution
Dates: October 2009-February 2010
Elevation: 4m
Weibull Parameters and
Intervals at 95% Confidence:
c = 9.41 [Lower:9.36 Upper:9.47]
k = 2.56 [Lower:2.53 Upper:2.59]
Probability Density
Wind speed (m/s)
0
0.02
0.04
0.06
0.08
0.1
0.12
0
5
10
15
20
25
30
35
40

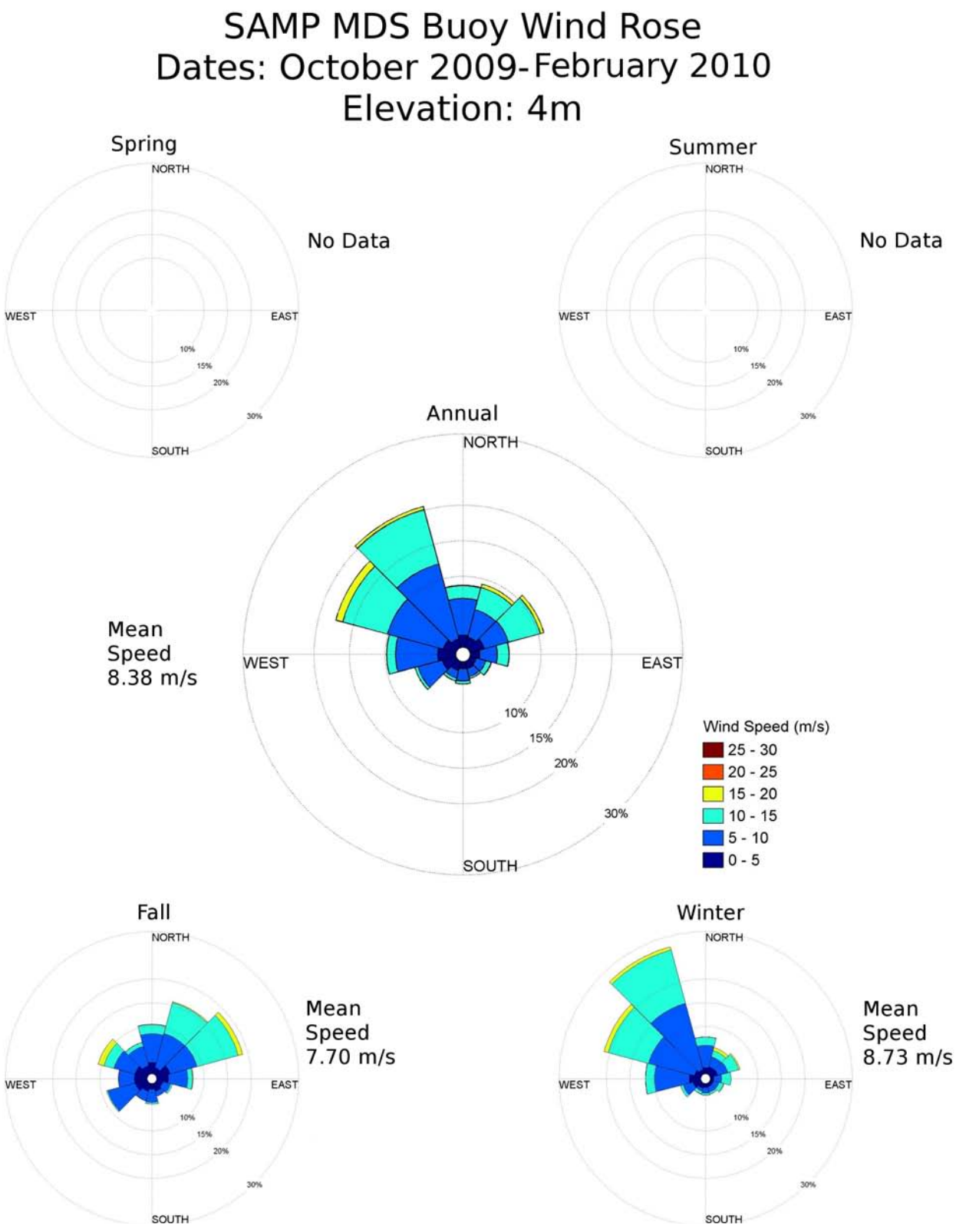
SAMP MDS Buoy Wind Rose
Dates: October 2009-February 2010
Elevation: 4m
Spring
No Data
Summer
No Data
Annual
Mean
Speed
8.38 m/s
Fall
Mean
Speed
7.70 m/s
Winter
Mean
Speed
8.73 m/s
NORTH
SOUTH
EAST
WEST
10%
15%
20%
30%
Wind Speed (m/s)
25 - 30
20 - 25
15 - 20
10 - 15
5 - 10
0 - 5

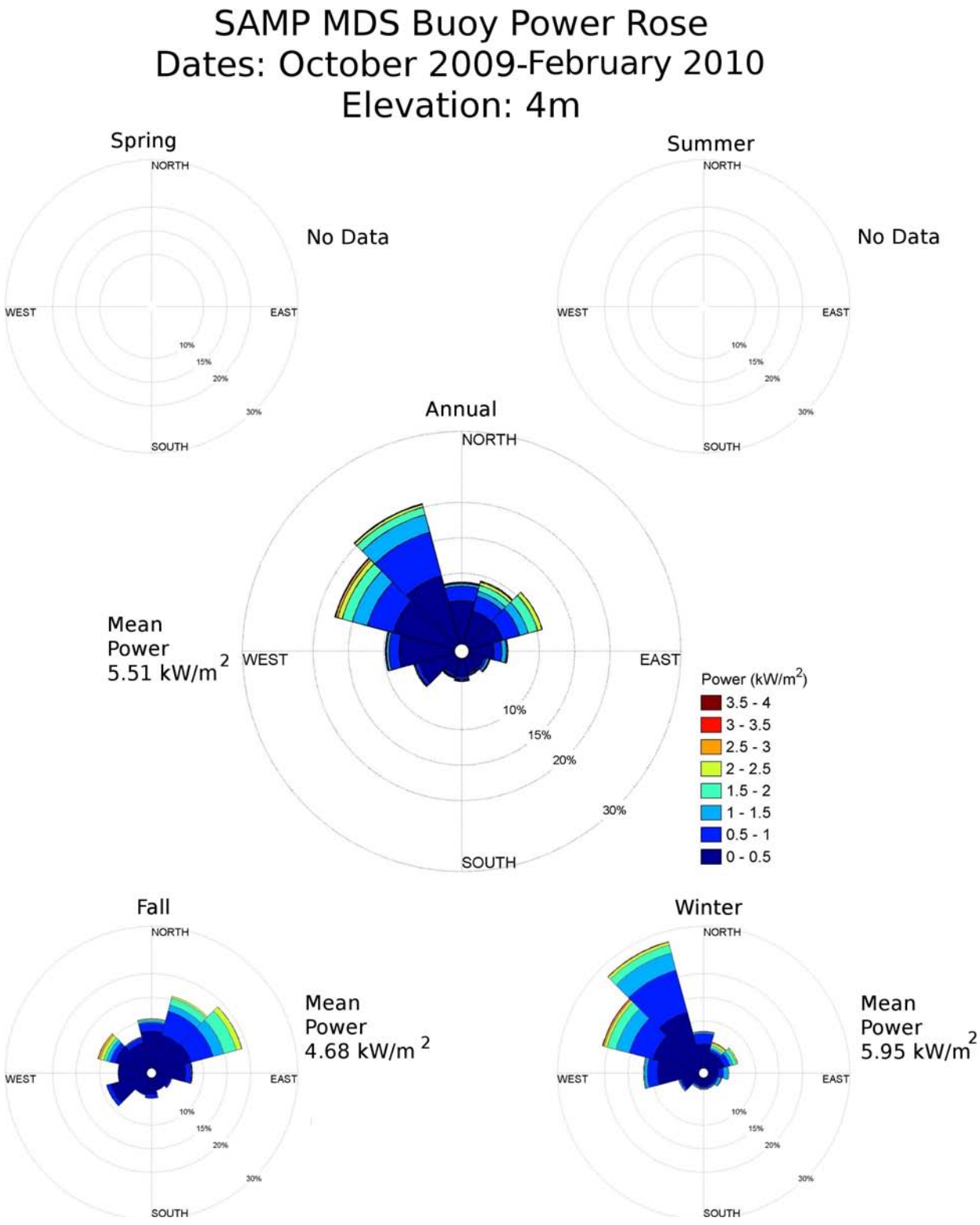
SAMP MDS Buoy Power Rose
Dates: October 2009-February 2010
Elevation: 4m
Spring
No Data
Summer
No Data
Annual
Mean
Power
5.51 kW/m 2
Power (kW/m2)
3.5 - 4
3 - 3.5
2.5 - 3
2 - 2.5
1.5 - 2
1 - 1.5
0.5 - 1
0 - 0.5
Fall
Mean
Power
4.68 kW/m 2
Winter
Mean
Power
5.95 kW/m 2
NORTH
SOUTH
EAST
WEST
10%
15%
20%
30%

WIS 100 Probability Distribution
Dates: 1980-1999
Elevation: 10m

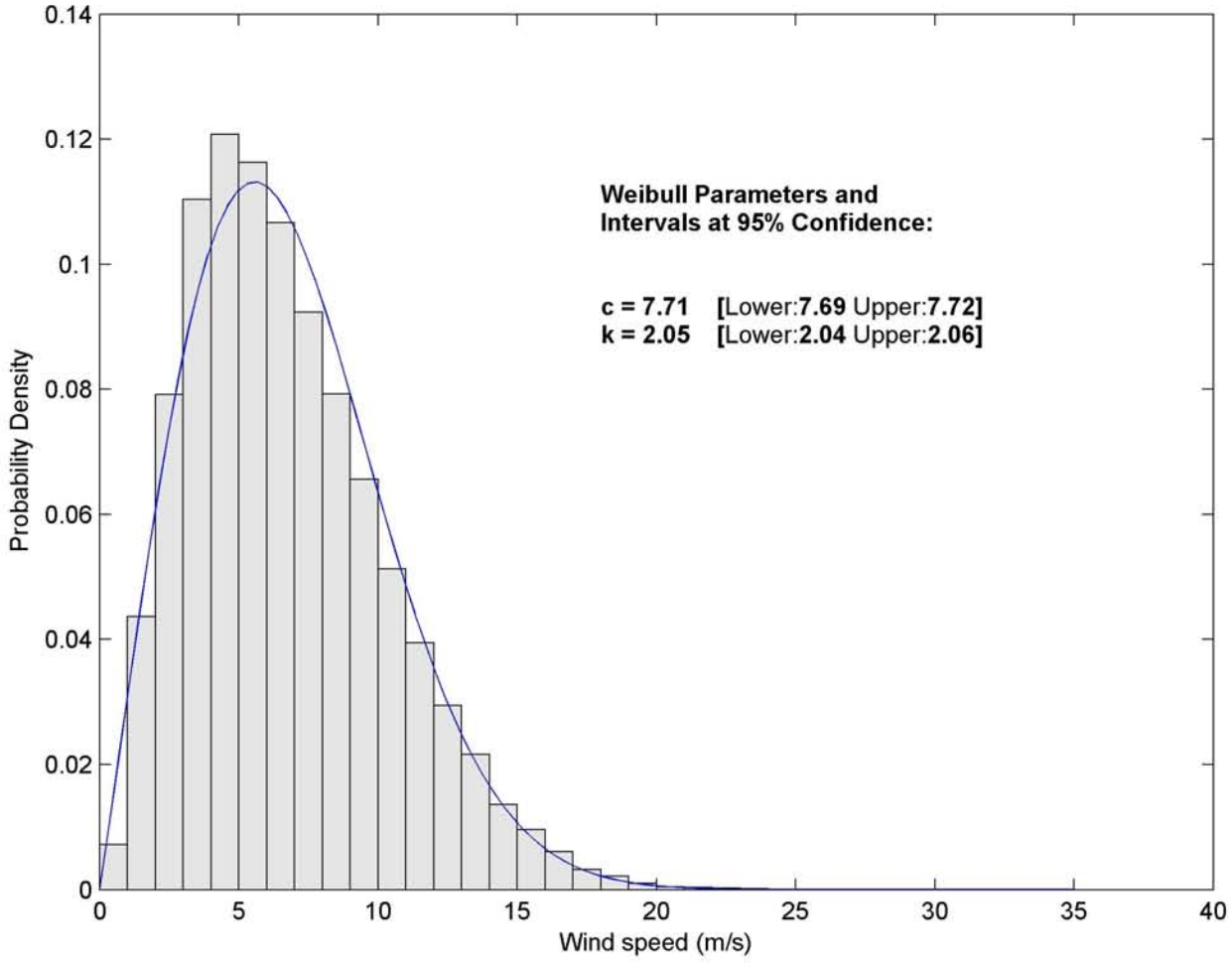

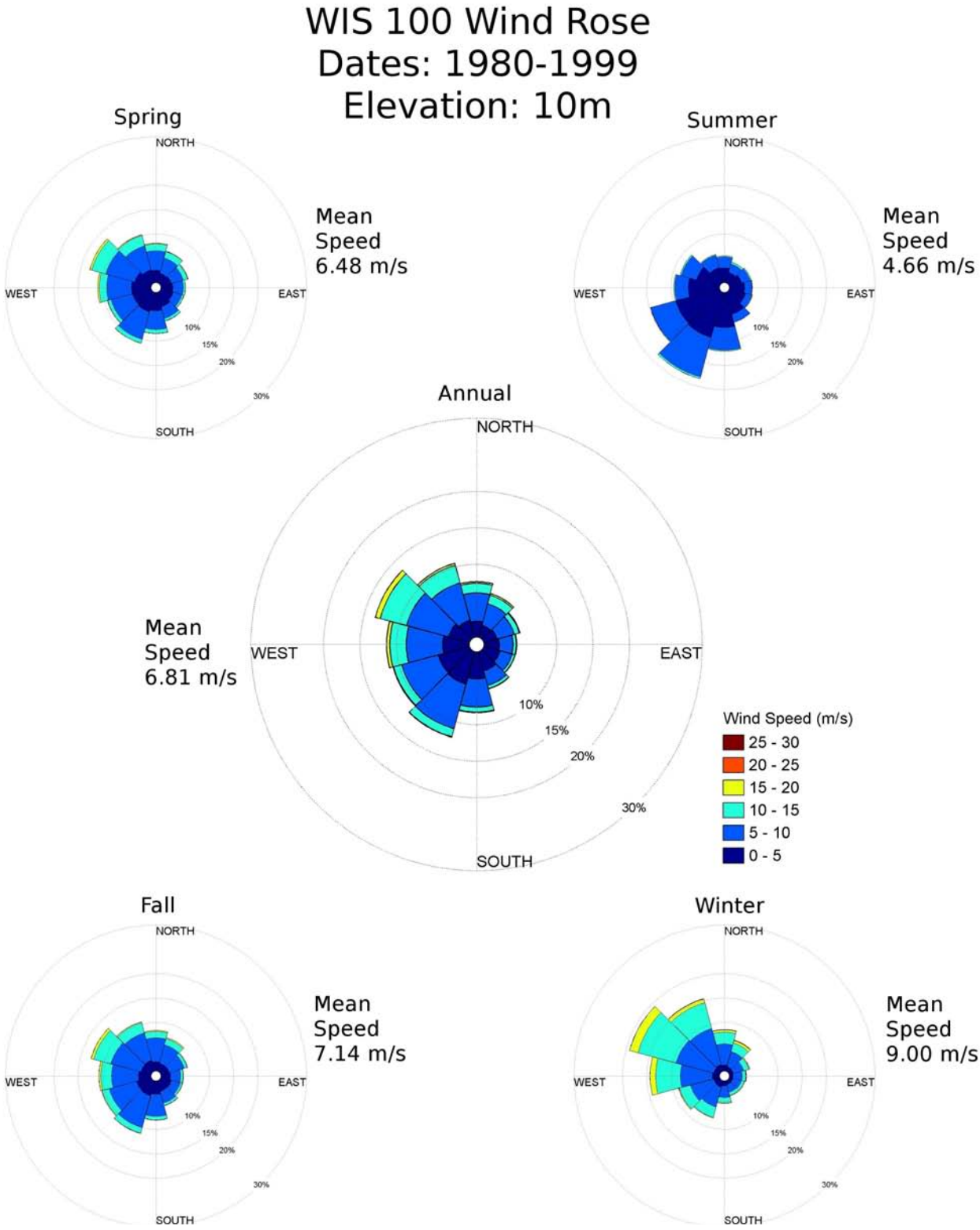
WIS 100 Wind Rose
Dates: 1980-1999
Elevation: 10m
Spring
Mean Speed 6.48 m/s
Summer
Mean Speed 4.66 m/s
Annual
Mean Speed 6.81 m/s
Fall
Mean Speed 7.14 m/s
Winter
Mean Speed 9.00 m/s
NORTH
SOUTH
EAST
WEST
10%
15%
20%
30%
Wind Speed (m/s)
25 - 30
20 - 25
15 - 20
10 - 15
5 - 10
0 - 5

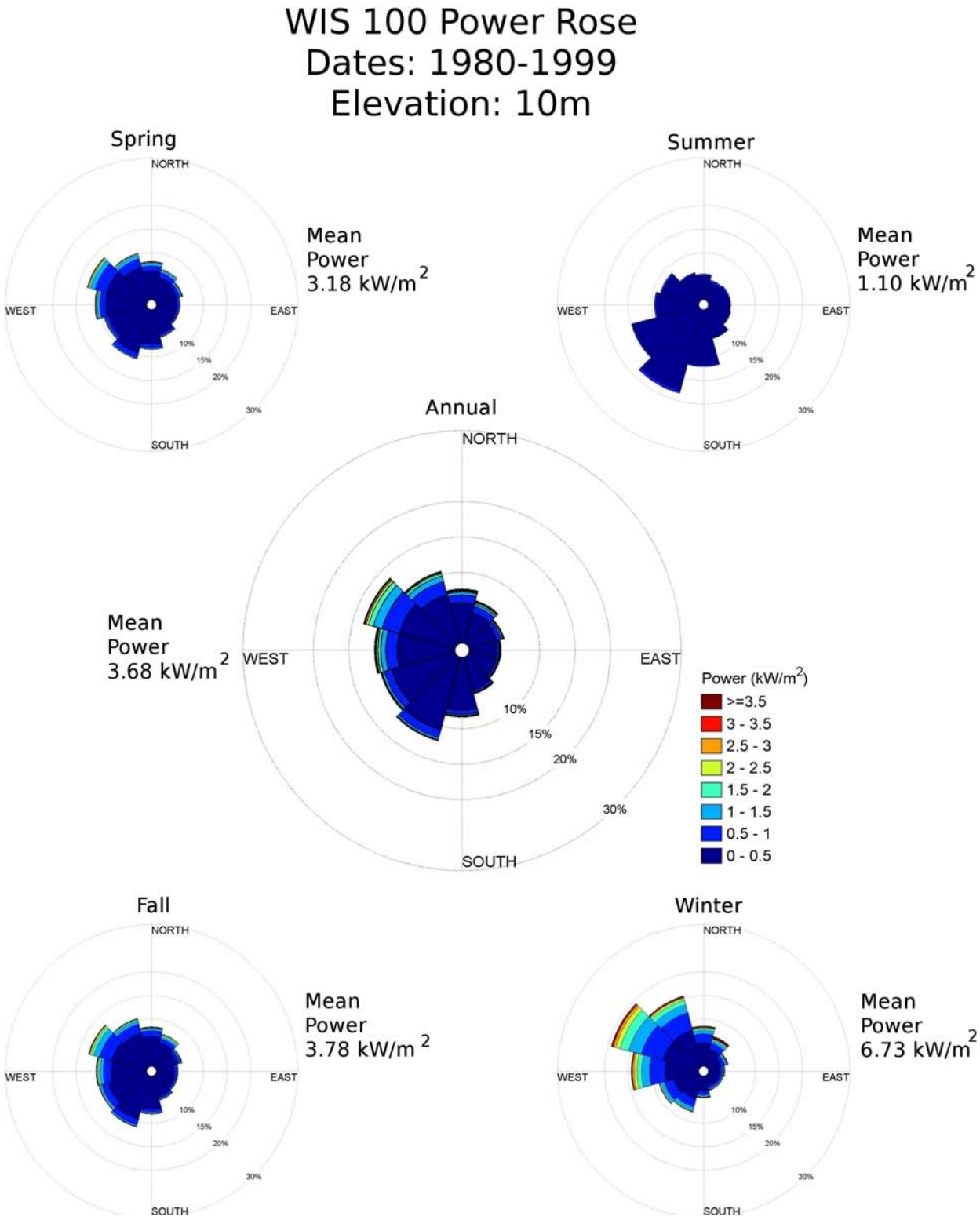
WIS 100 Power Rose
Dates: 1980-1999
Elevation: 10m
Spring
Mean Power 3.18 kW/m2
Summer
Mean Power 1.10 kW/m2
Annual
Mean Power 3.68 kW/m2
Fall
Mean Power 3.78 kW/m2
Winter
Mean Power 6.73 kW/m2
NORTH
SOUTH
EAST
WEST
10%
15%
20%
30%
Power (kW/m2)
>=3.5
3 - 3.5
2.5 - 3
2 - 2.5
1.5 - 2
1 - 1.5
0.5 - 1
0 - 0.5

WIS 101 Probability Distribution
Dates: 1980-1999
Elevation: 10m

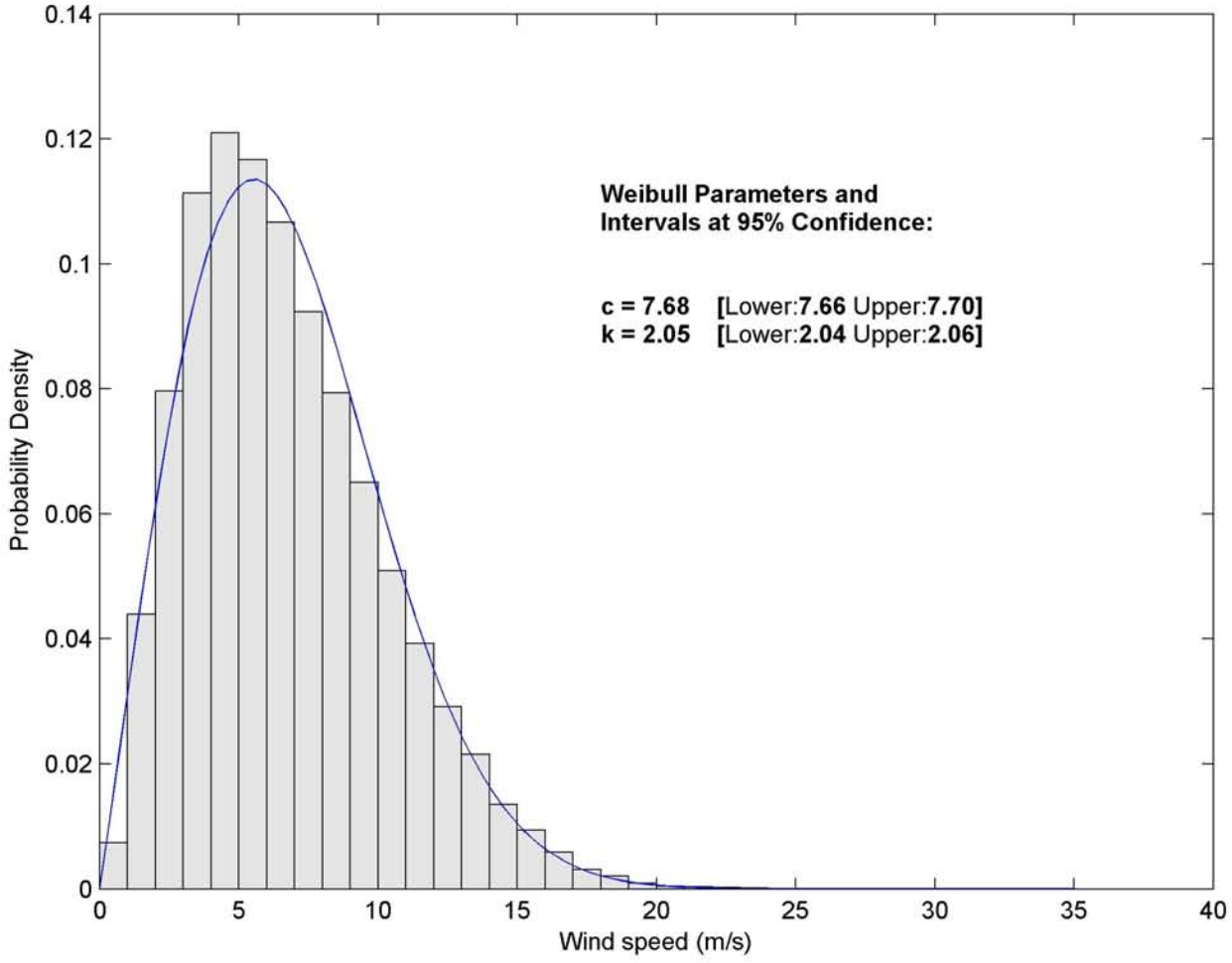

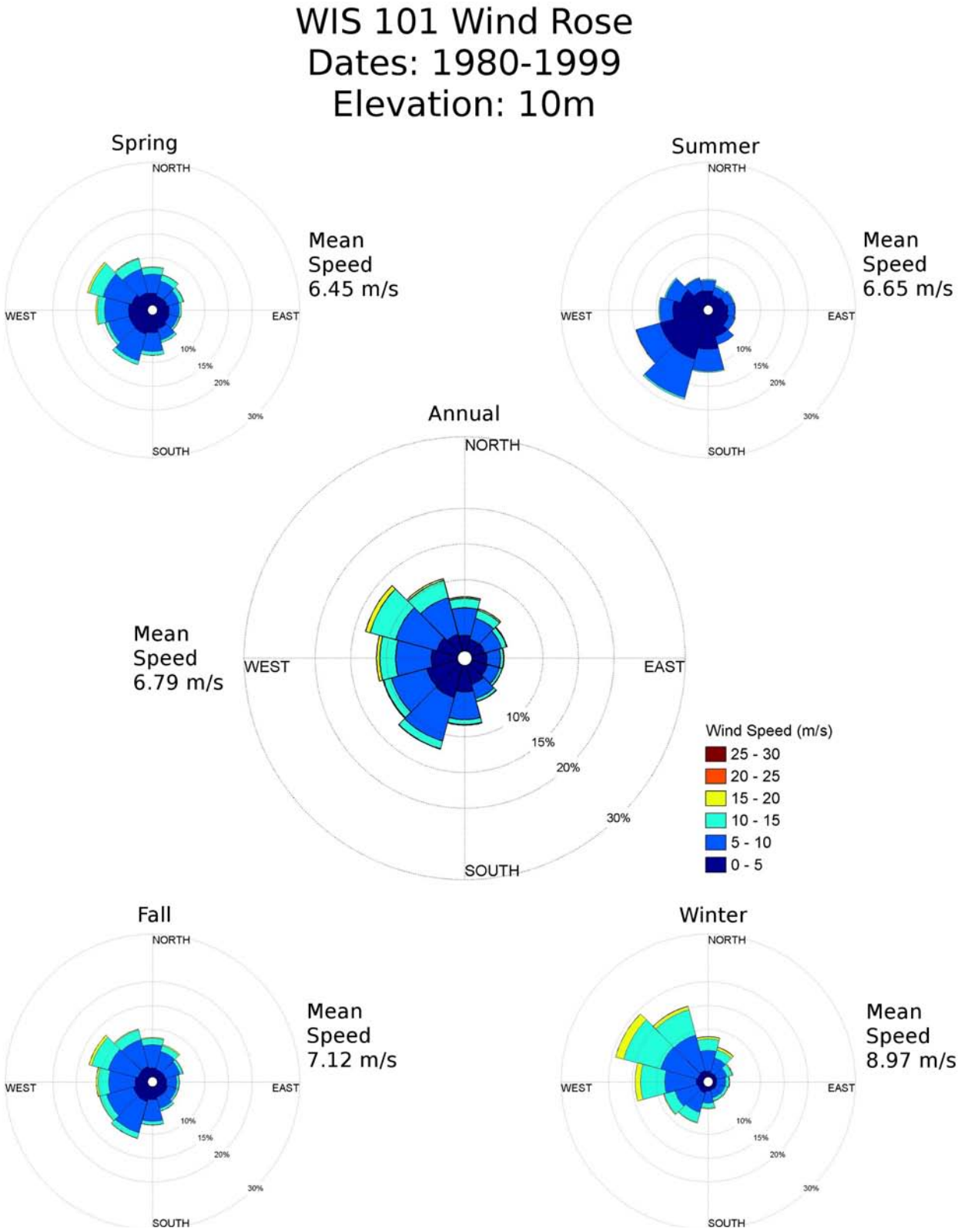
WIS 101 Wind Rose
Dates: 1980-1999
Elevation: 10m
Spring
Mean Speed 6.45 m/s
Summer
Mean Speed 6.65 m/s
Annual
Mean Speed 6.79 m/s
Fall
Mean Speed 7.12 m/s
Winter
Mean Speed 8.97 m/s
NORTH
SOUTH
EAST
WEST
10%
15%
20%
30%
Wind Speed (m/s)
25 - 30
20 - 25
15 - 20
10 - 15
5 - 10
0 - 5

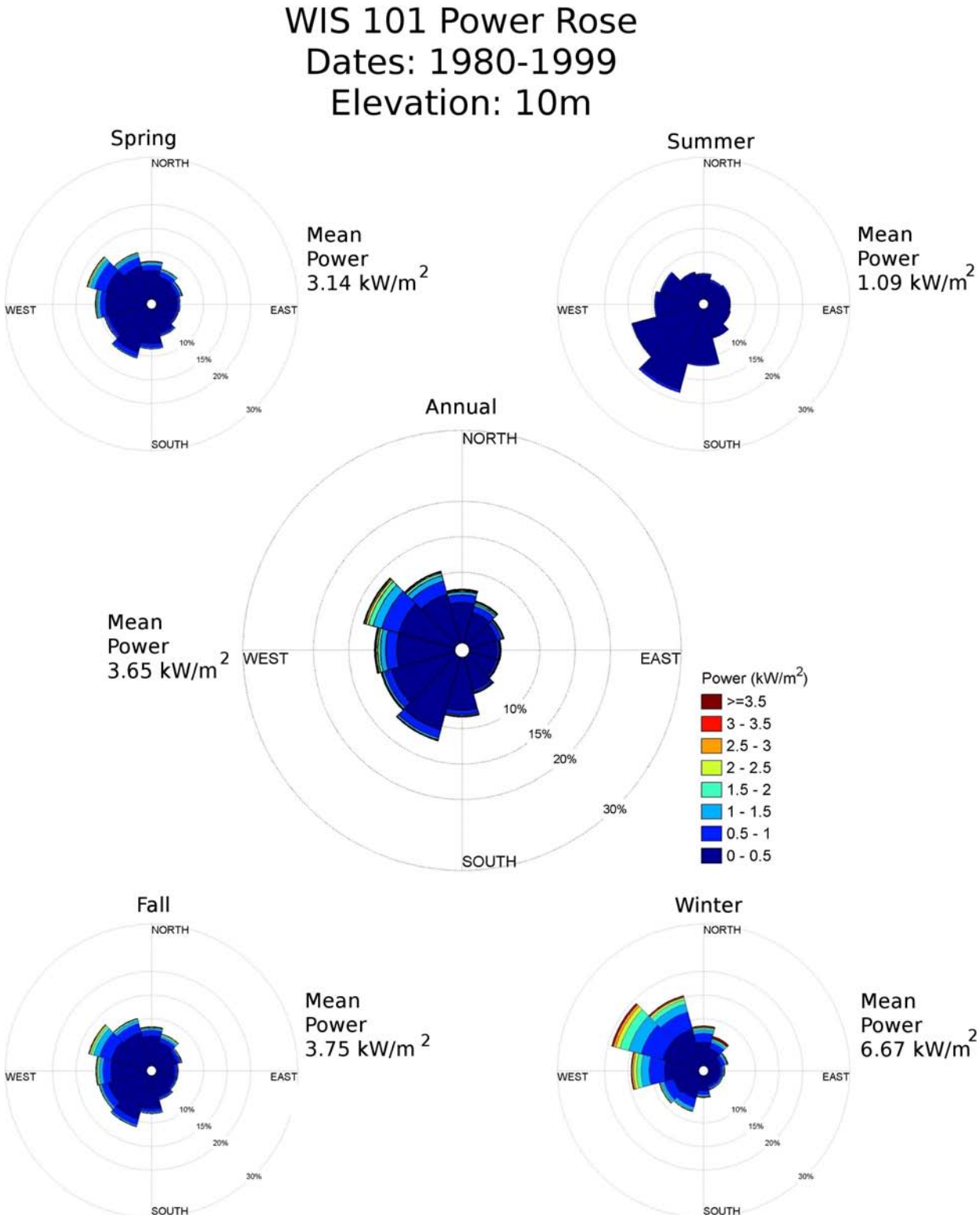
WIS 101 Power Rose
Dates: 1980-1999
Elevation: 10m
Spring
Mean Power 3.14 kW/m2
Summer
Mean Power 1.09 kW/m2
Annual
Mean Power 3.65 kW/m2
Fall
Mean Power 3.75 kW/m2
Winter
Mean Power 6.67 kW/m2
NORTH
SOUTH
EAST
WEST
10%
15%
20%
30%
Power (kW/m2)
>=3.5
3 - 3.5
2.5 - 3
2 - 2.5
1.5 - 2
1 - 1.5
0.5 - 1
0 - 0.5

WIS 104 Probability Distribution
Dates: 1980-1999
Elevation: 10m

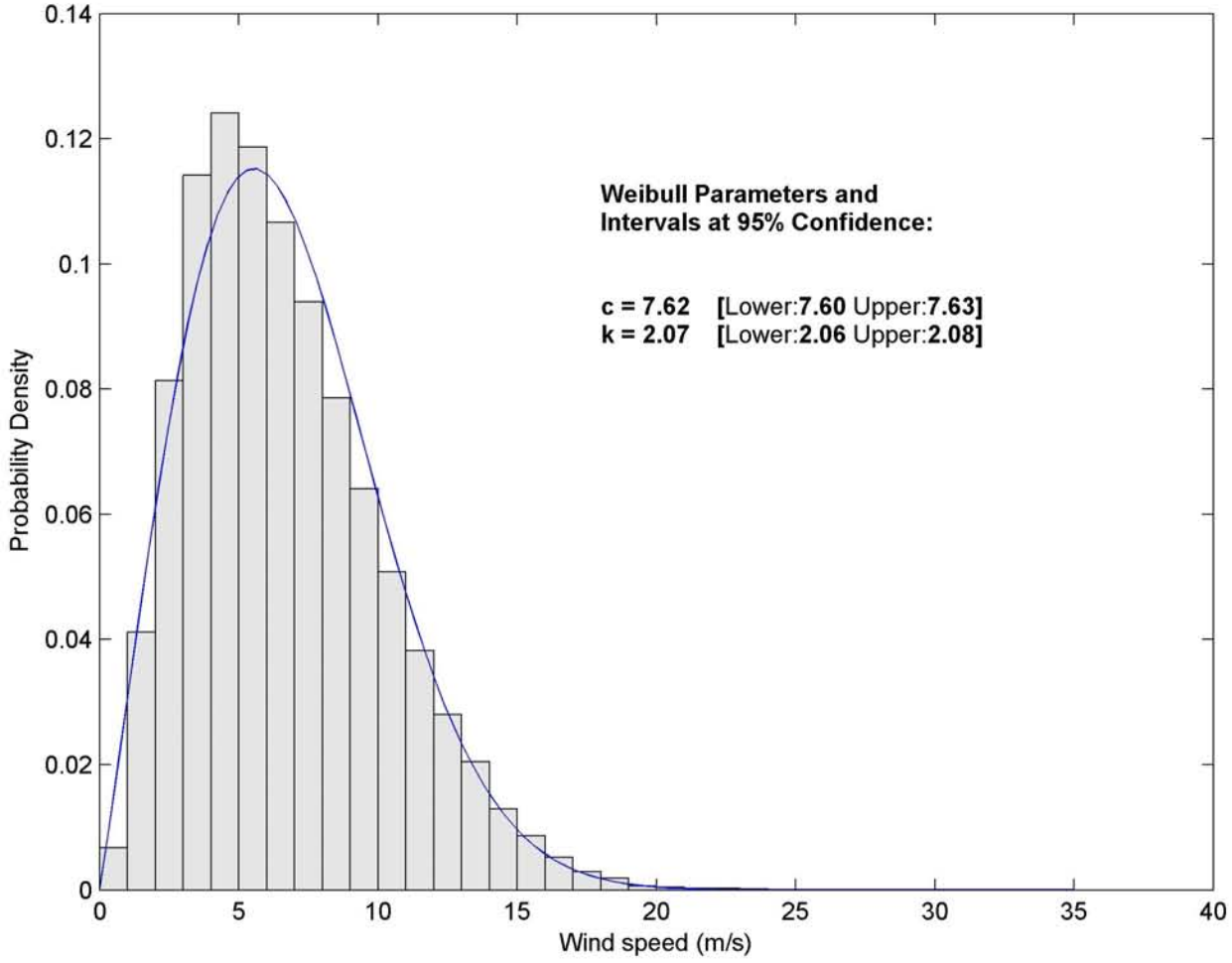

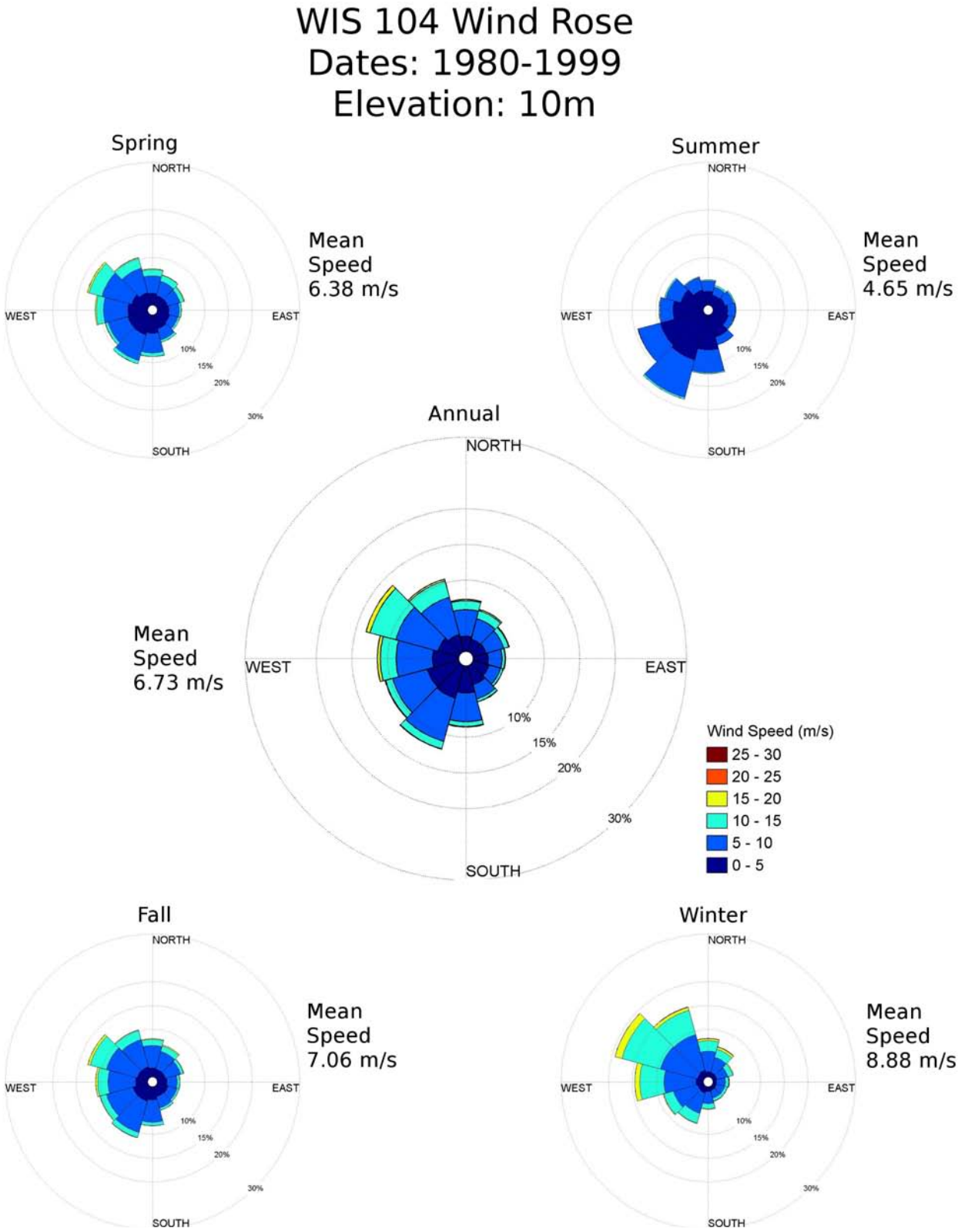
WIS 104 Wind Rose
Dates: 1980-1999
Elevation: 10m
Spring
Mean Speed 6.38 m/s
Summer
Mean Speed 4.65 m/s
Annual
Mean Speed 6.73 m/s
Fall
Mean Speed 7.06 m/s
Winter
Mean Speed 8.88 m/s
NORTH
SOUTH
EAST
WEST
10%
15%
20%
30%
Wind Speed (m/s)
25 - 30
20 - 25
15 - 20
10 - 15
5 - 10
0 - 5

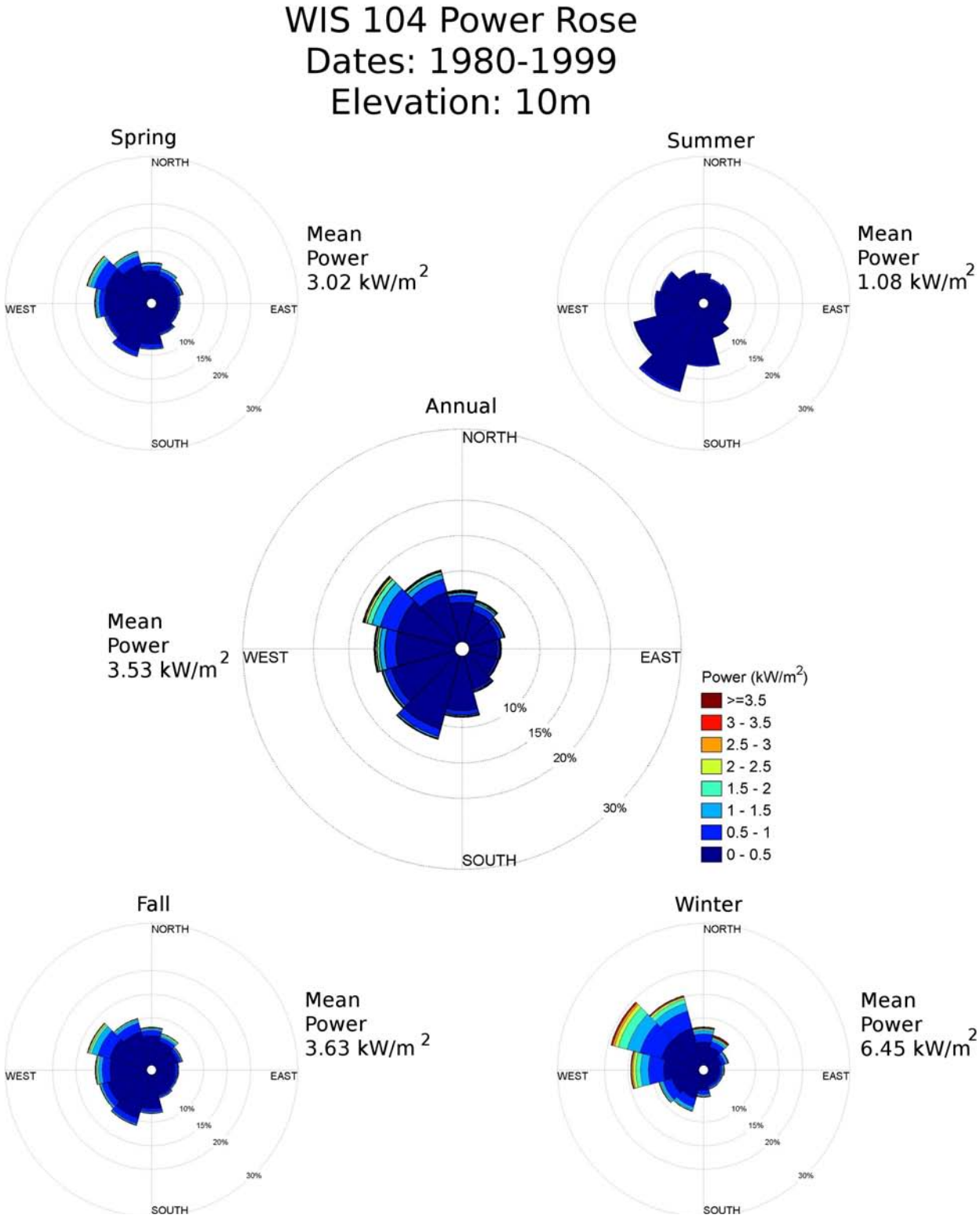
WIS 104 Power Rose
Dates: 1980-1999
Elevation: 10m
Spring
Mean Power 3.02 kW/m2
Summer
Mean Power 1.08 kW/m2
Annual
Mean Power 3.53 kW/m2
Fall
Mean Power 3.63 kW/m2
Winter
Mean Power 6.45 kW/m2
NORTH
SOUTH
EAST
WEST
10%
15%
20%
30%
Power (kW/m2)
>=3.5
3 - 3.5
2.5 - 3
2 - 2.5
1.5 - 2
1 - 1.5
0.5 - 1
0 - 0.5

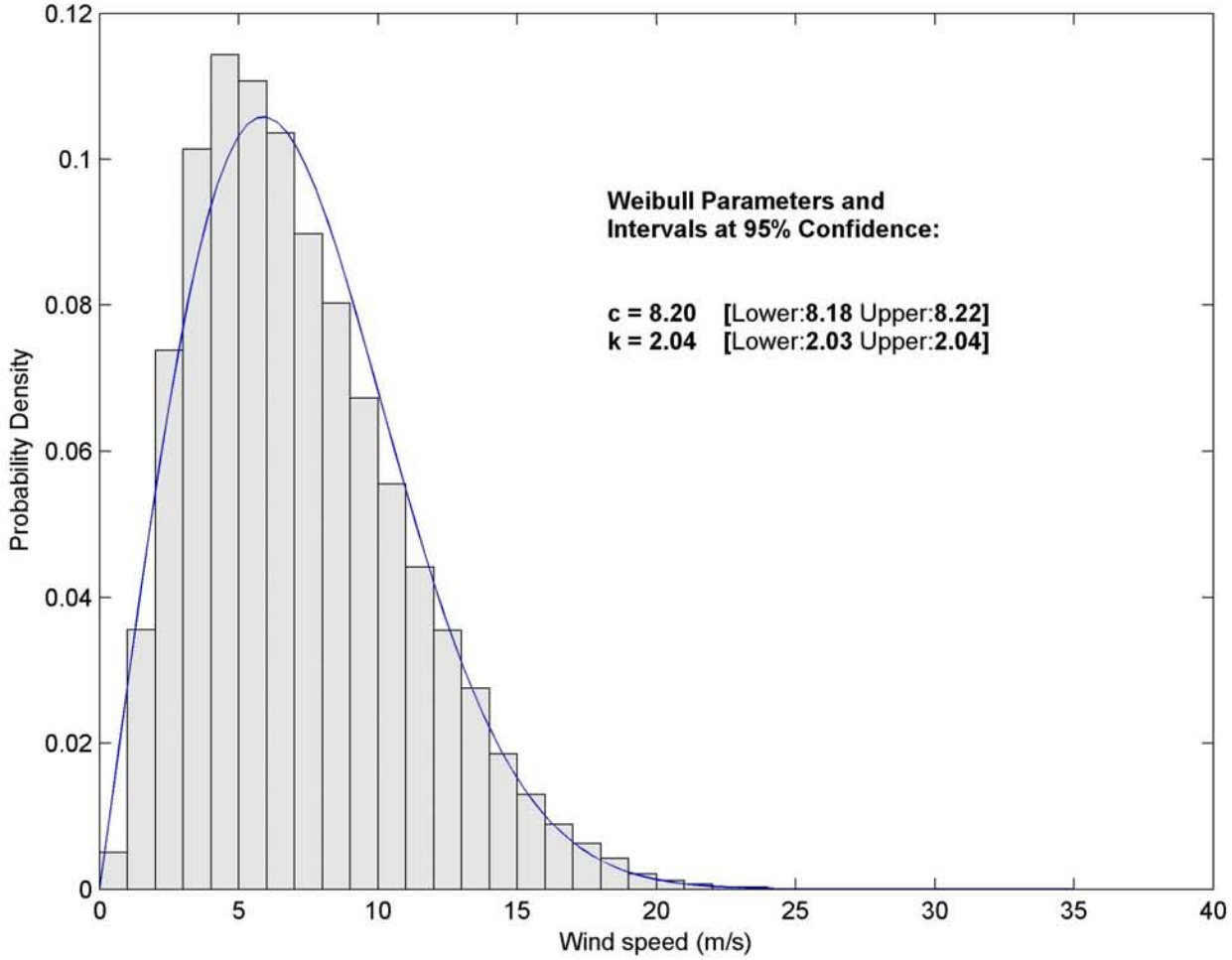
WIS 241 Probability Distribution
Dates: 1980-1999
Elevation: 10m
Weibull Parameters and
Intervals at 95% Confidence:
c = 8.20 [Lower:8.18 Upper:8.22]
k = 2.04 [Lower:2.03 Upper:2.04]
Probability Density
Wind speed (m/s)
0
0.02
0.04
0.06
0.08
0.1
0.12
0
5
10
15
20
25
30
35
40

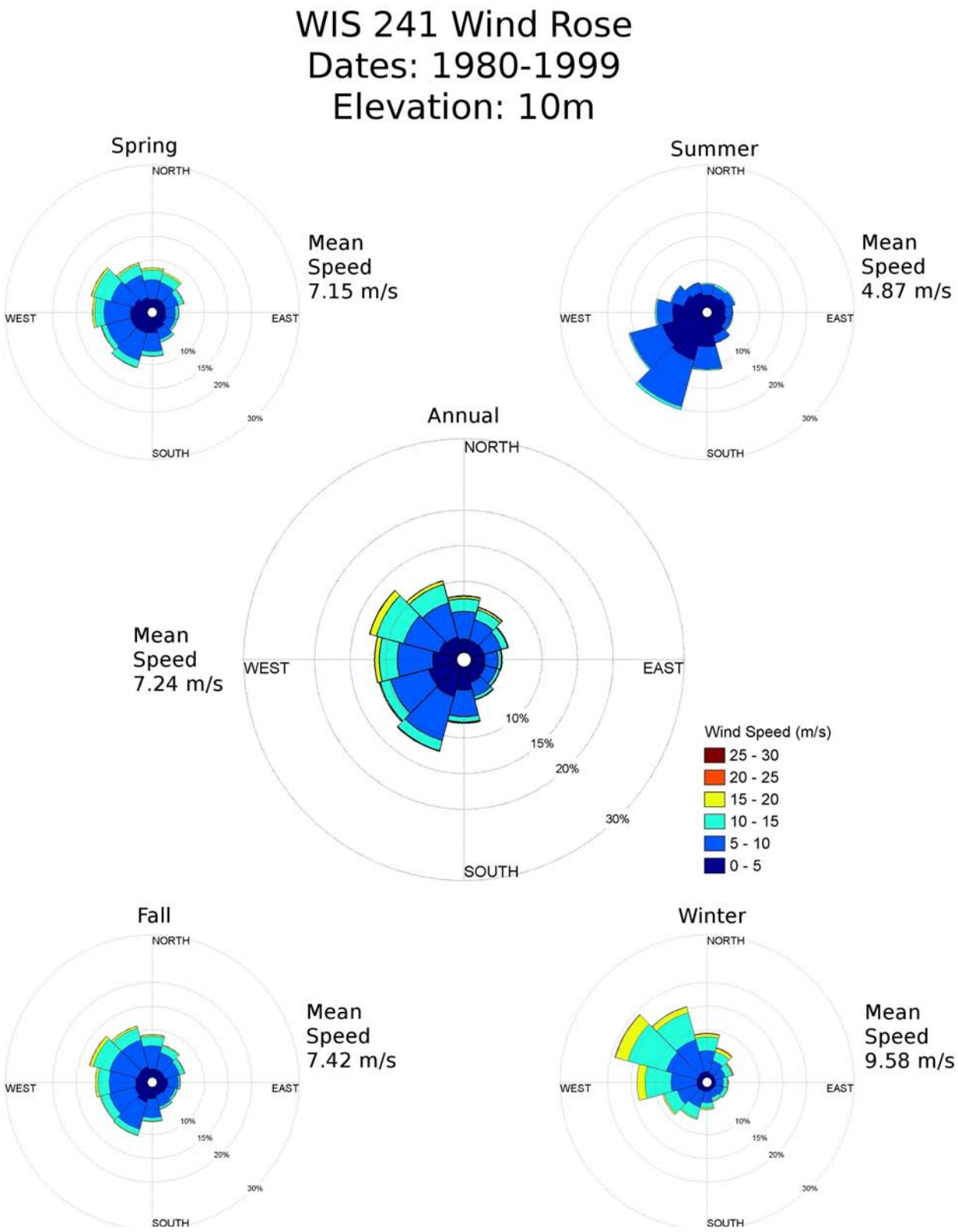
WIS 241 Wind Rose
Dates: 1980-1999
Elevation: 10m
Spring
Mean Speed 7.15 m/s
Summer
Mean Speed 4.87 m/s
Annual
Mean Speed 7.24 m/s
Fall
Mean Speed 7.42 m/s
Winter
Mean Speed 9.58 m/s
NORTH
SOUTH
EAST
WEST
10%
15%
20%
30%
Wind Speed (m/s)
25 - 30
20 - 25
15 - 20
10 - 15
5 - 10
0 - 5

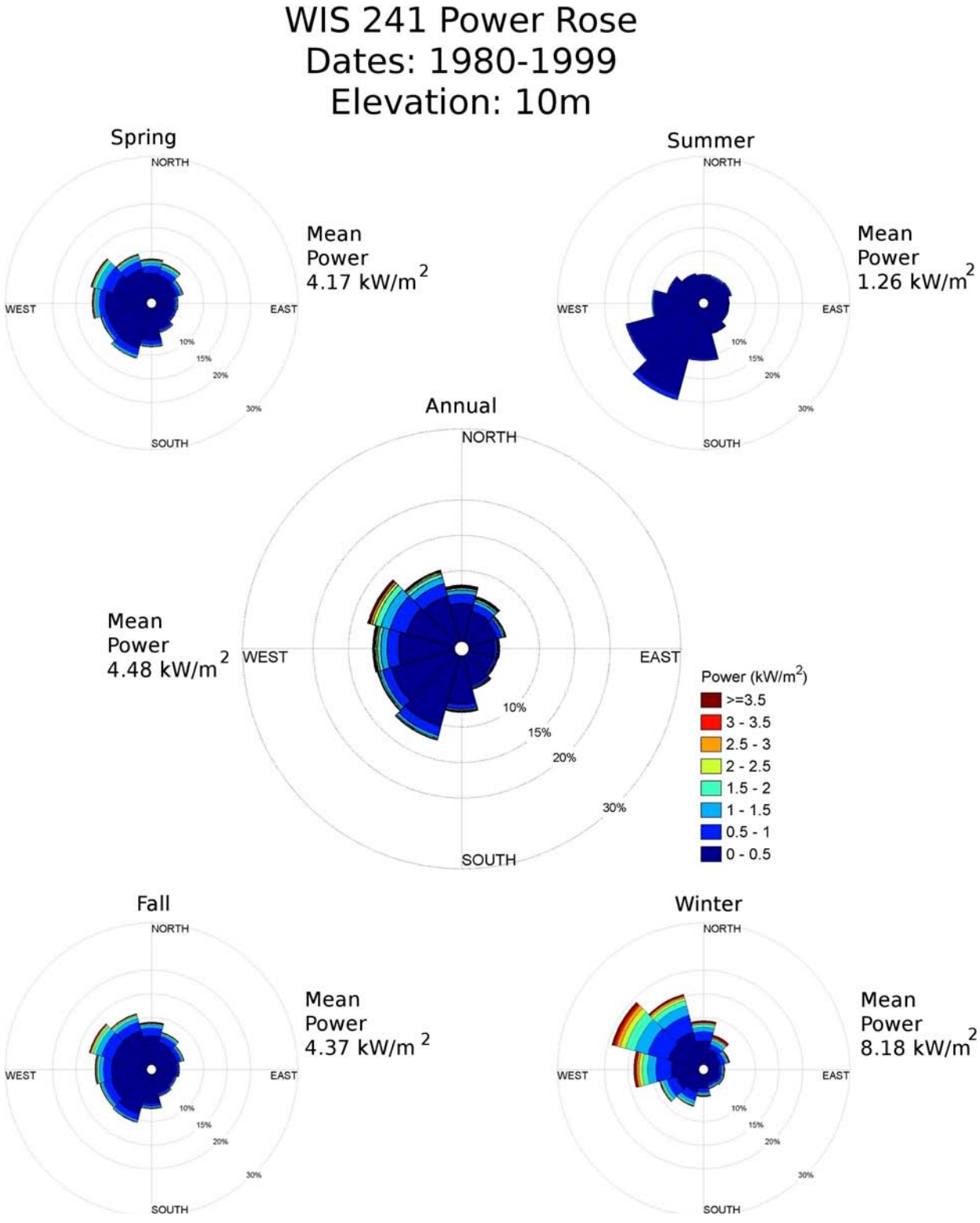
WIS 241 Power Rose
Dates: 1980-1999
Elevation: 10m
Spring
Mean Power 4.17 kW/m2
Summer
Mean Power 1.26 kW/m2
Annual
Mean Power 4.48 kW/m2
Fall
Mean Power 4.37 kW/m2
Winter
Mean Power 8.18 kW/m2
NORTH
SOUTH
EAST
WEST
10%
15%
20%
30%
Power (kW/m2)
>=3.5
3 - 3.5
2.5 - 3
2 - 2.5
1.5 - 2
1 - 1.5
0.5 - 1
0 - 0.5

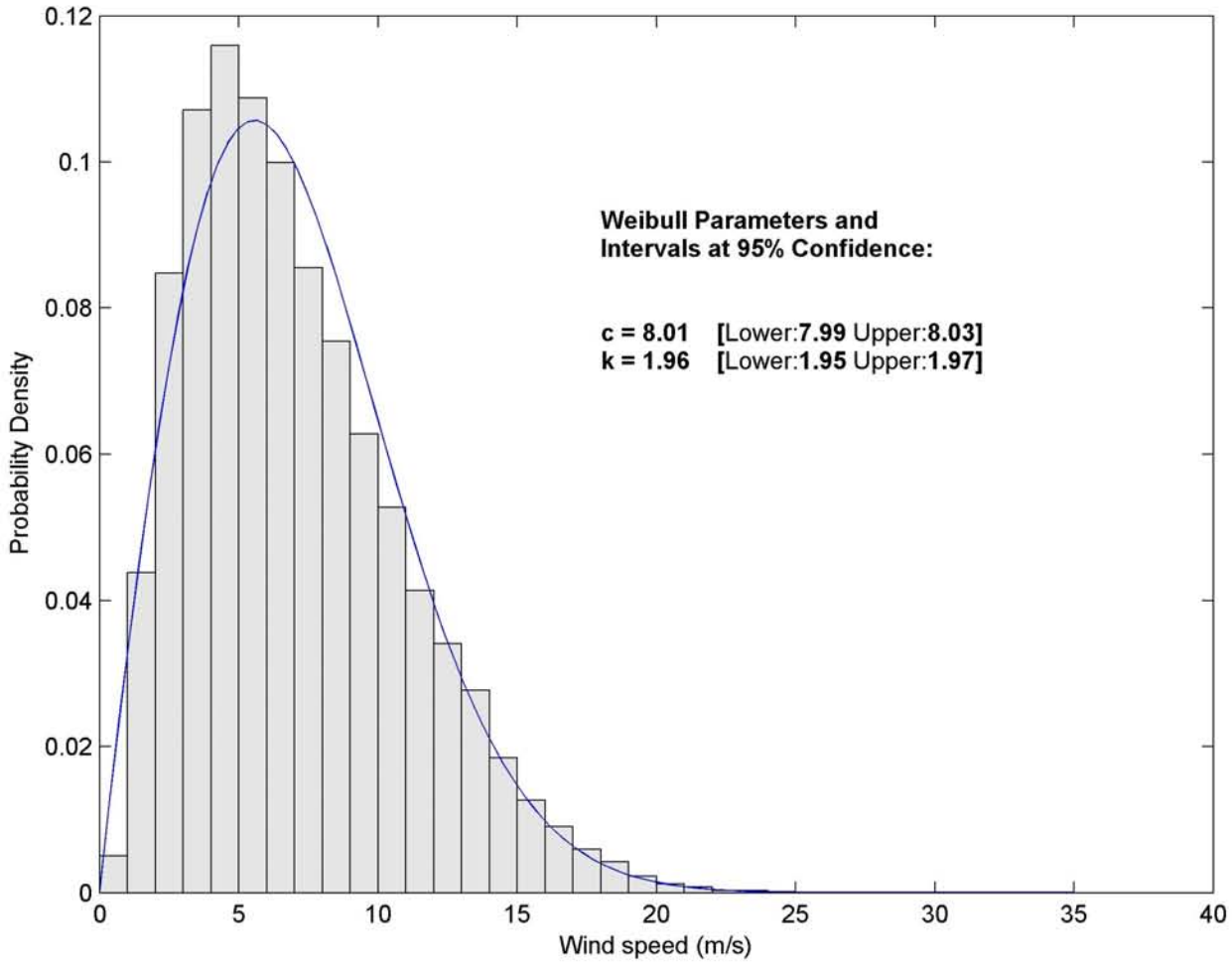
WIS 242 Probability Distribution
Dates: 1980-1999
Elevation: 10m
Weibull Parameters and
Intervals at 95% Confidence:
c = 8.01 [Lower:7.99 Upper:8.03]
k = 1.96 [Lower:1.95 Upper:1.97]
Probability Density
Wind speed (m/s)
0
0.02
0.04
0.06
0.08
0.1
0.12
0
5
10
15
20
25
30
35
40

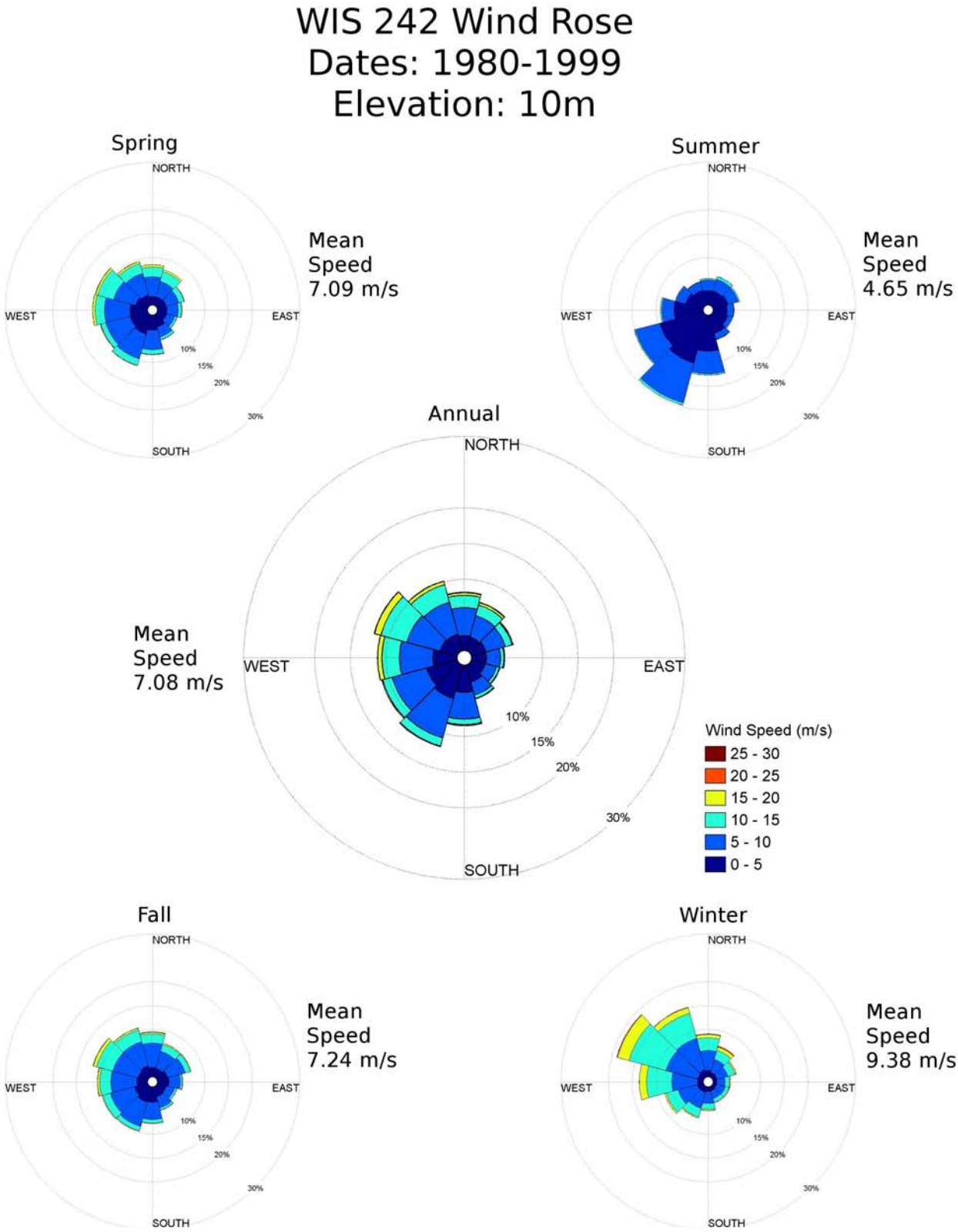
WIS 242 Wind Rose
Dates: 1980-1999
Elevation: 10m
Spring
Mean Speed 7.09 m/s
Summer
Mean Speed 4.65 m/s
Annual
Mean Speed 7.08 m/s
Fall
Mean Speed 7.24 m/s
Winter
Mean Speed 9.38 m/s
NORTH
SOUTH
EAST
WEST
10%
15%
20%
30%
Wind Speed (m/s)
25 - 30
20 - 25
15 - 20
10 - 15
5 - 10
0 - 5

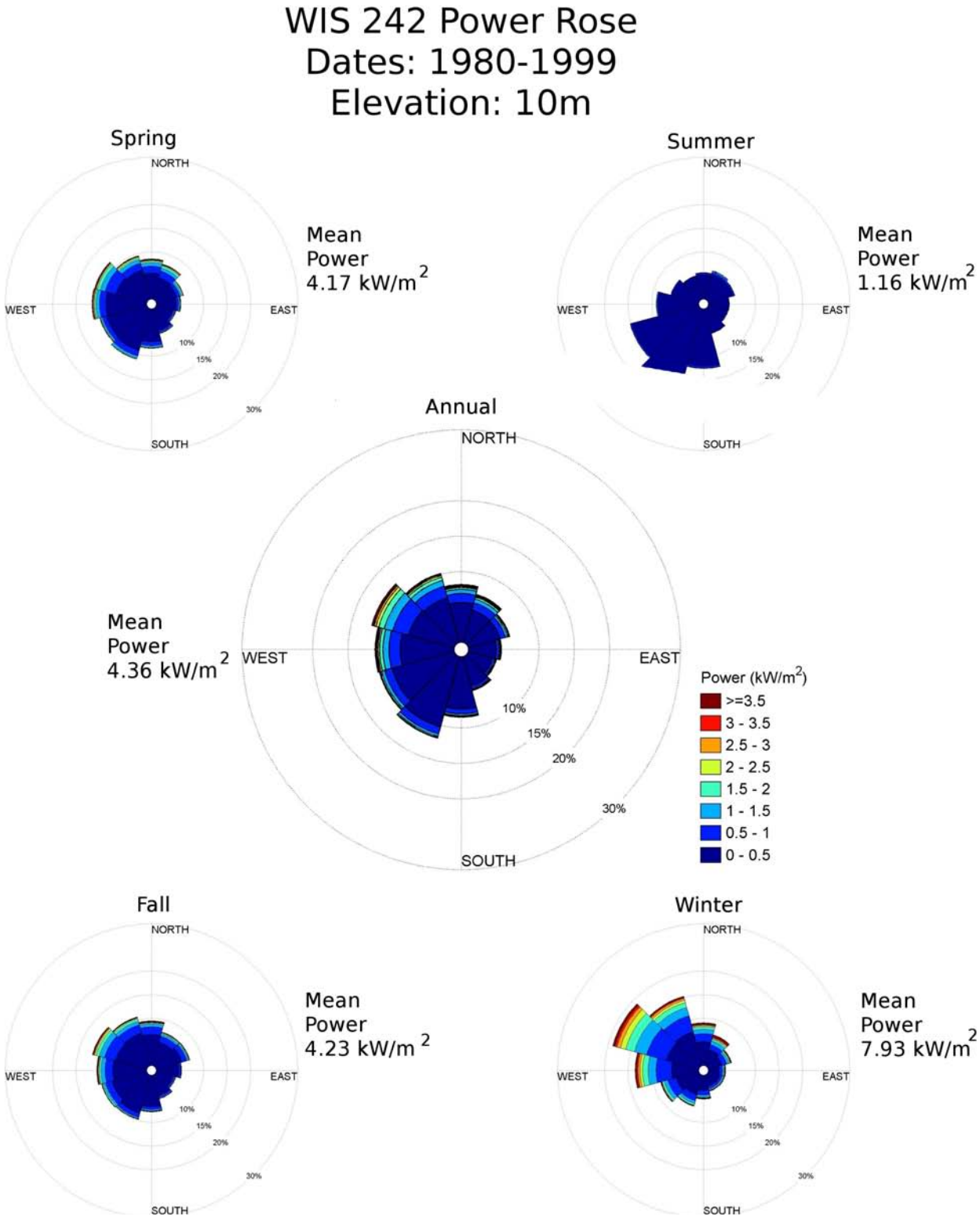
WIS 242 Power Rose
Dates: 1980-1999
Elevation: 10m
Spring
Mean Power 4.17 kW/m2
Summer
Mean Power 1.16 kW/m2
Annual
Mean Power 4.36 kW/m2
Fall
Mean Power 4.23 kW/m2
Winter
Mean Power 7.93 kW/m2
NORTH
SOUTH
EAST
WEST
10%
15%
20%
30%
Power (kW/m2)
>=3.5
3 - 3.5
2.5 - 3
2 - 2.5
1.5 - 2
1 - 1.5
0.5 - 1
0 - 0.5

WIS 243 Probability Distribution
Dates: 1980-1999
Elevation: 10m

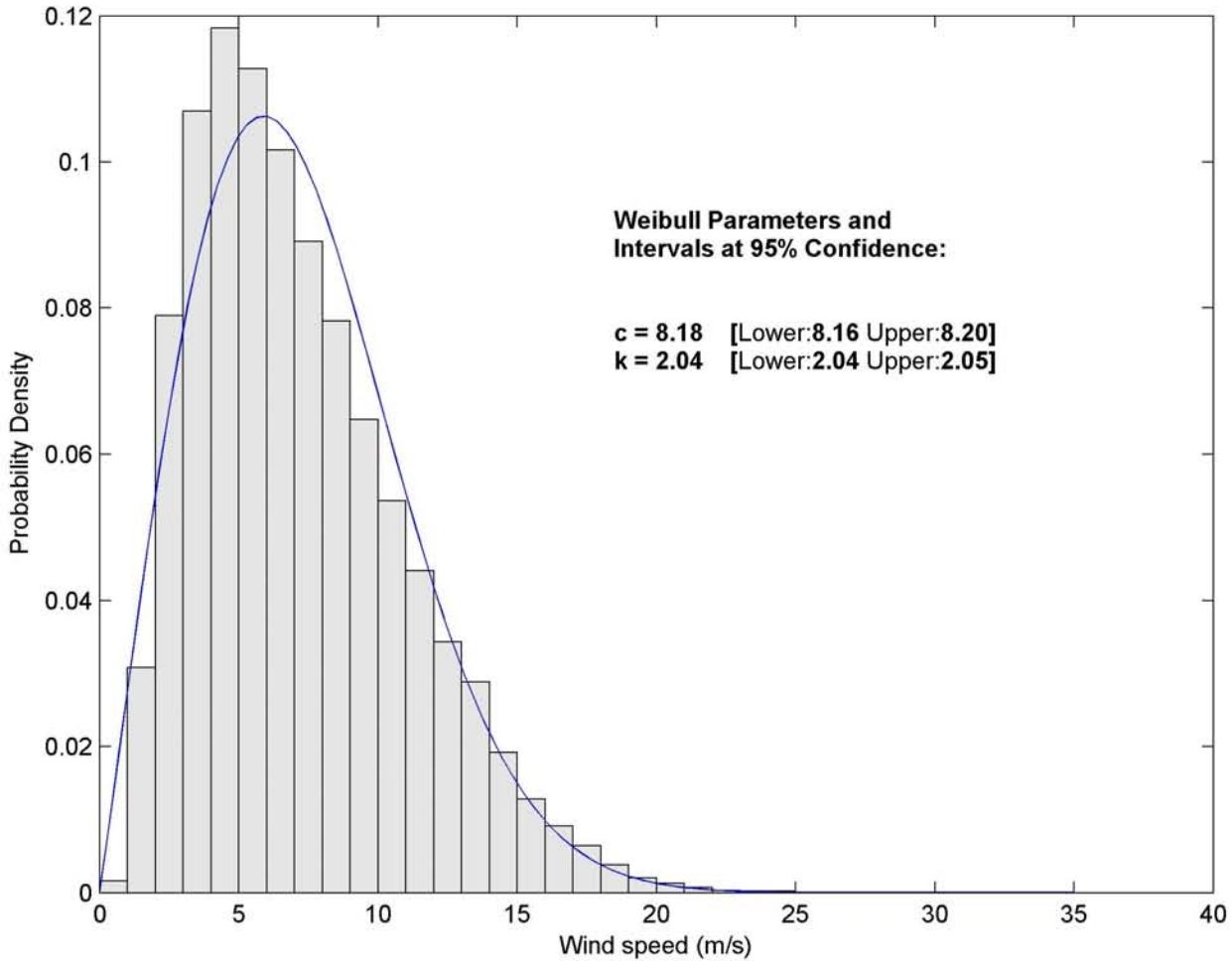

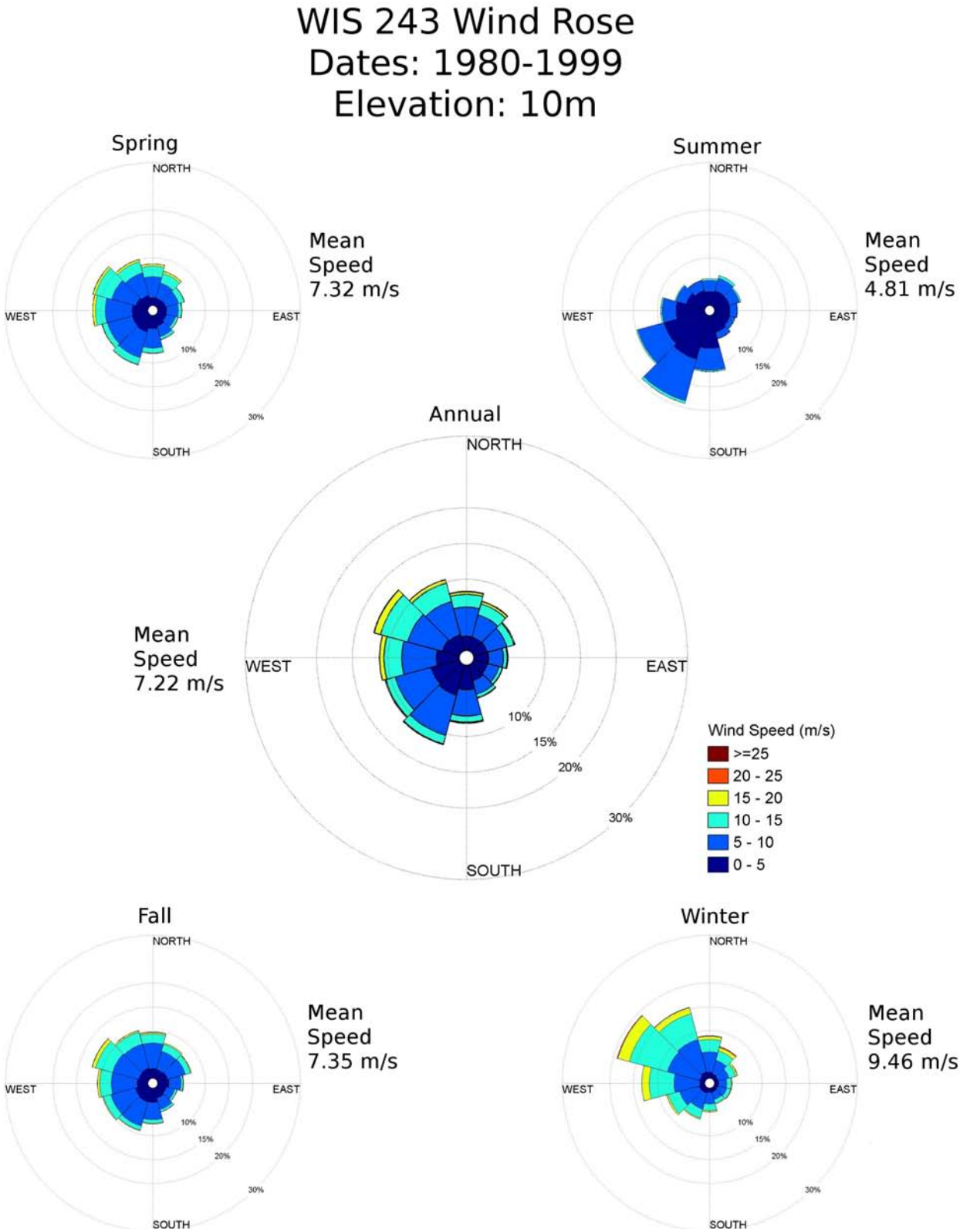
WIS 243 Wind Rose
Dates: 1980-1999
Elevation: 10m
Spring
Mean Speed 7.32 m/s
Summer
Mean Speed 4.81 m/s
Annual
Mean Speed 7.22 m/s
Fall
Mean Speed 7.35 m/s
Winter
Mean Speed 9.46 m/s
NORTH
SOUTH
EAST
WEST
10%
15%
20%
30%
Wind Speed (m/s)
>=25
20 - 25
15 - 20
10 - 15
5 - 10
0 - 5

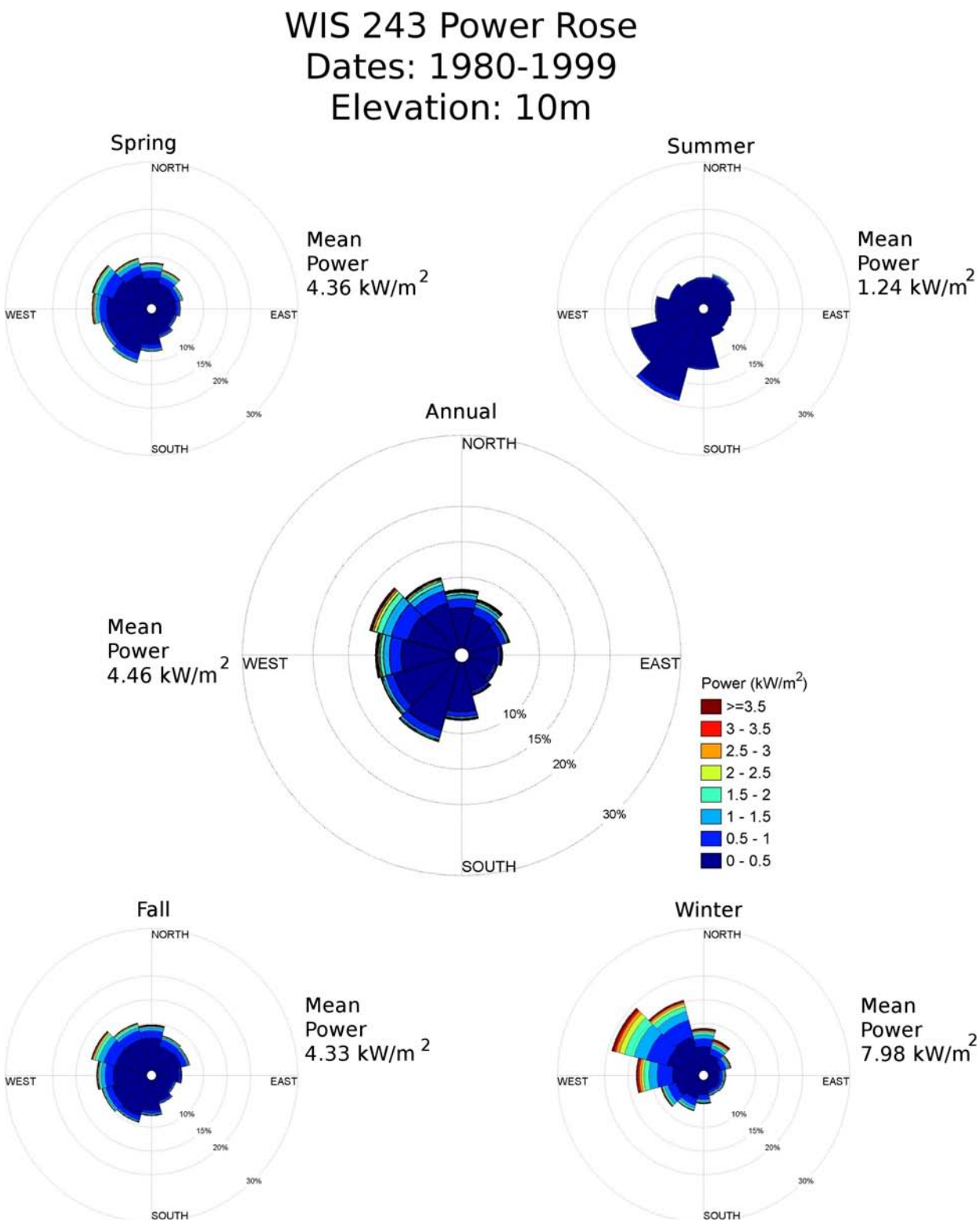
WIS 243 Power Rose
Dates: 1980-1999
Elevation: 10m
Spring
Mean Power 4.36 kW/m2
Summer
Mean Power 1.24 kW/m2
Annual
Mean Power 4.46 kW/m2
Fall
Mean Power 4.33 kW/m2
Winter
Mean Power 7.98 kW/m2
NORTH
SOUTH
EAST
WEST
10%
15%
20%
30%
Power (kW/m2)
>=3.5
3 - 3.5
2.5 - 3
2 - 2.5
1.5 - 2
1 - 1.5
0.5 - 1
0 - 0.5

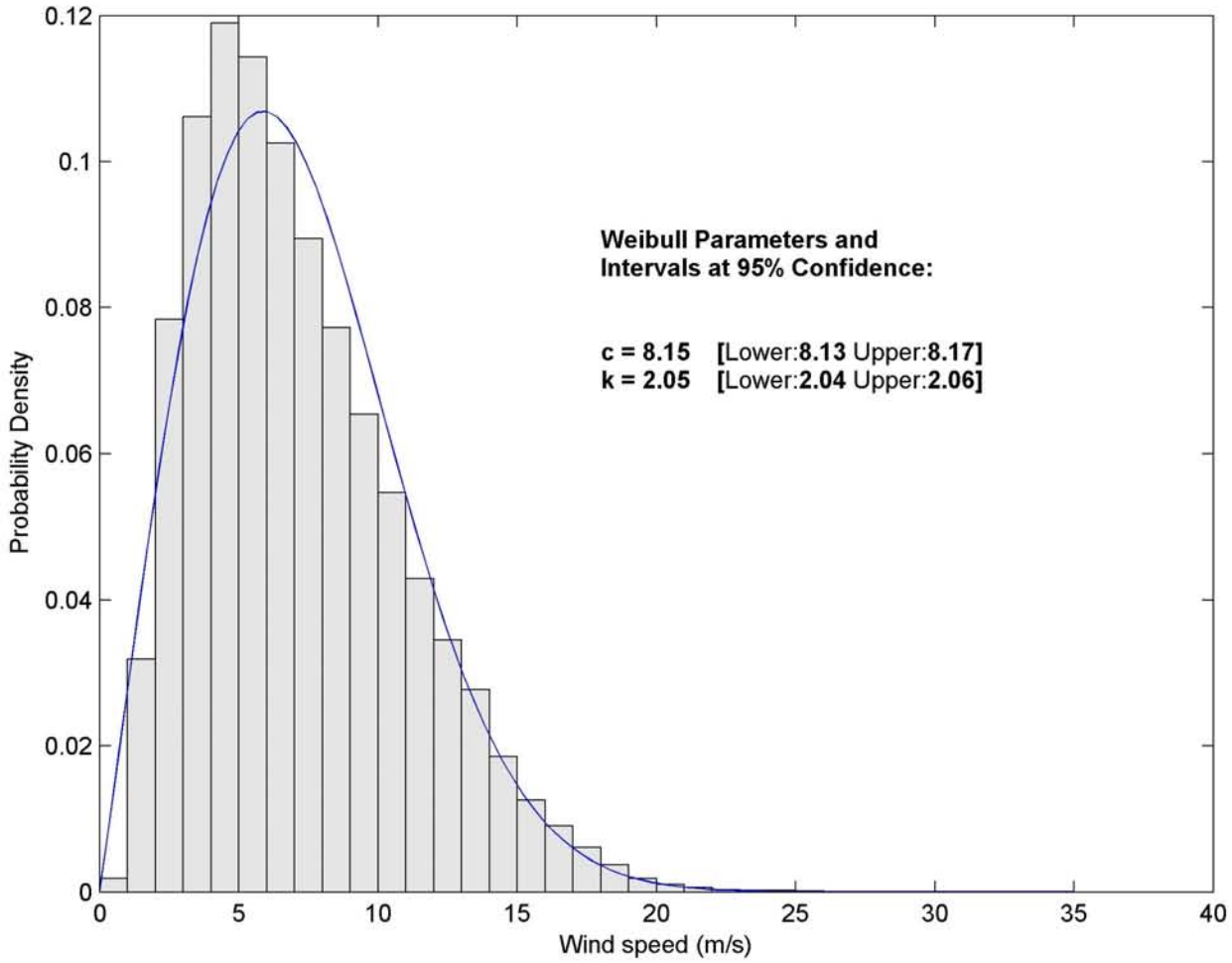
WIS 244 Probability Distribution
Dates: 1980-1999
Elevation: 10m
Weibull Parameters and
Intervals at 95% Confidence:
c = 8.15 [Lower:8.13 Upper:8.17]
k = 2.05 [Lower:2.04 Upper:2.06]
Probability Density
Wind speed (m/s)
0
0.02
0.04
0.06
0.08
0.1
0.12
0
5
10
15
20
25
30
35
40

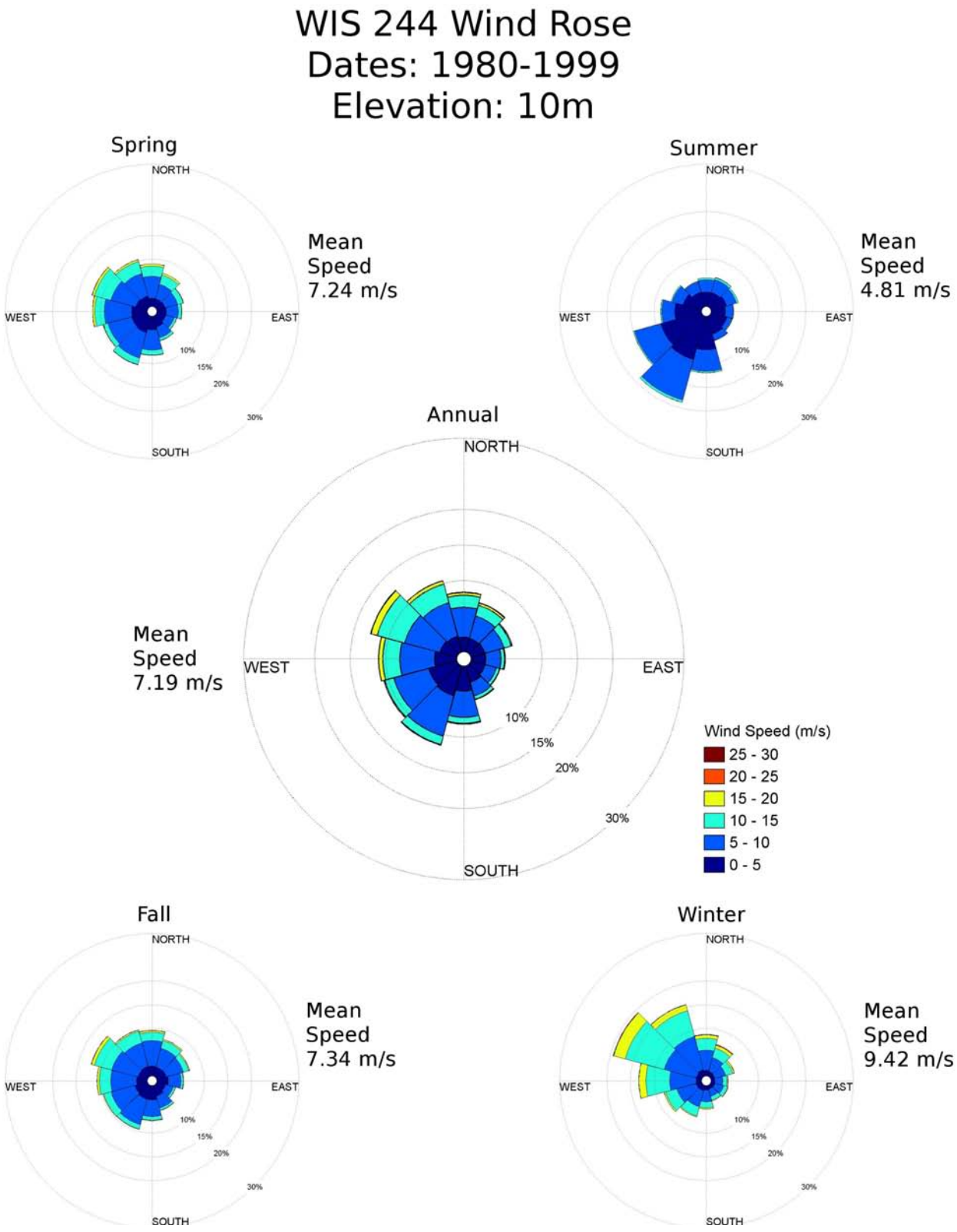
WIS 244 Wind Rose
Dates: 1980-1999
Elevation: 10m
Spring
Mean Speed 7.24 m/s
Summer
Mean Speed 4.81 m/s
Annual
Mean Speed 7.19 m/s
Fall
Mean Speed 7.34 m/s
Winter
Mean Speed 9.42 m/s
NORTH
SOUTH
EAST
WEST
10%
15%
20%
30%
Wind Speed (m/s)
25 - 30
20 - 25
15 - 20
10 - 15
5 - 10
0 - 5

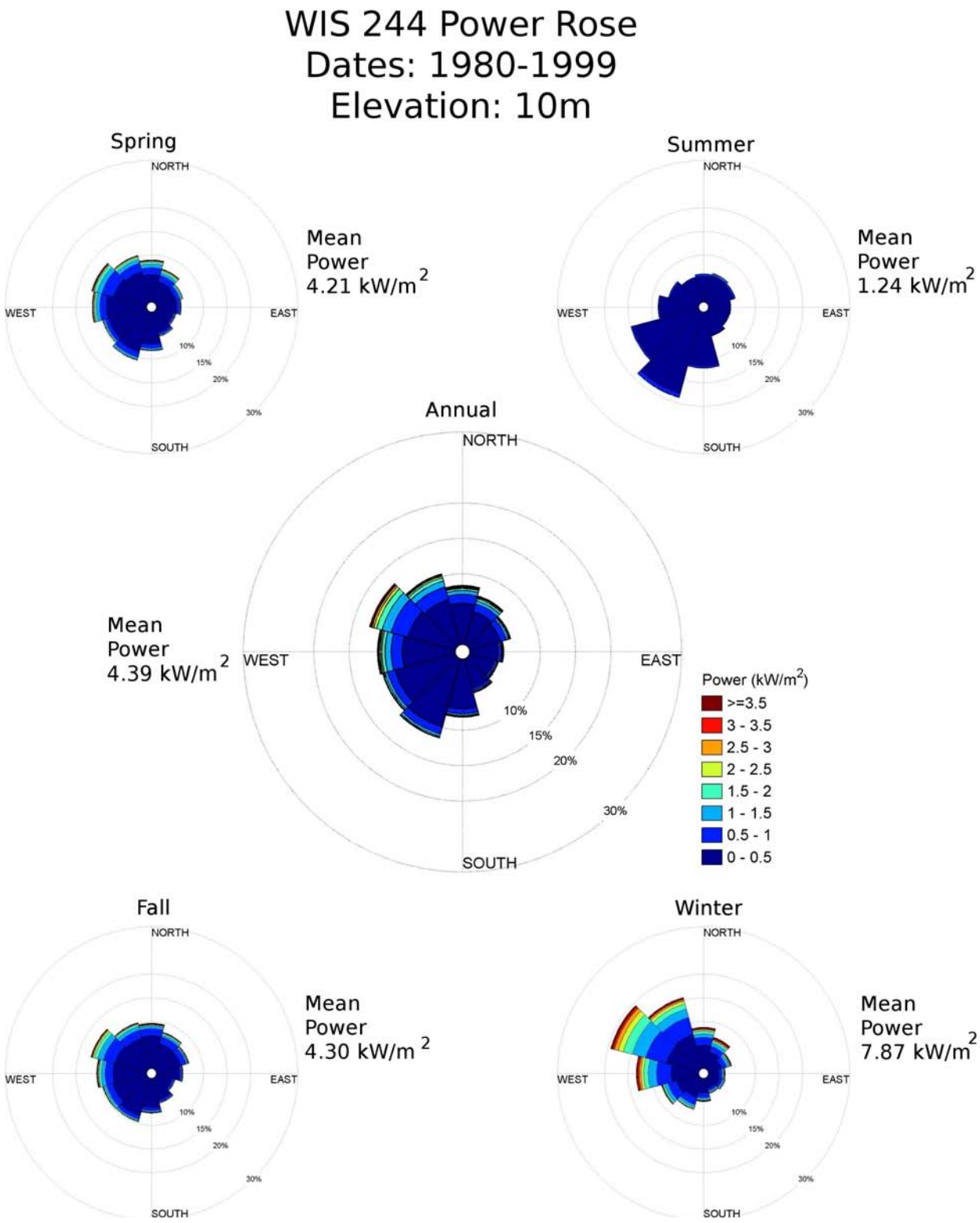
WIS 244 Power Rose
Dates: 1980-1999
Elevation: 10m
Spring
Mean Power 4.21 kW/m2
Summer
Mean Power 1.24 kW/m2
Annual
Mean Power 4.39 kW/m2
Fall
Mean Power 4.30 kW/m2
Winter
Mean Power 7.87 kW/m2
NORTH
SOUTH
EAST
WEST
10%
15%
20%
30%
Power (kW/m2)
>=3.5
3 - 3.5
2.5 - 3
2 - 2.5
1.5 - 2
1 - 1.5
0.5 - 1
0 - 0.5

WIS 247 Probability Distribution
Dates: 1980-1999
Elevation: 10m

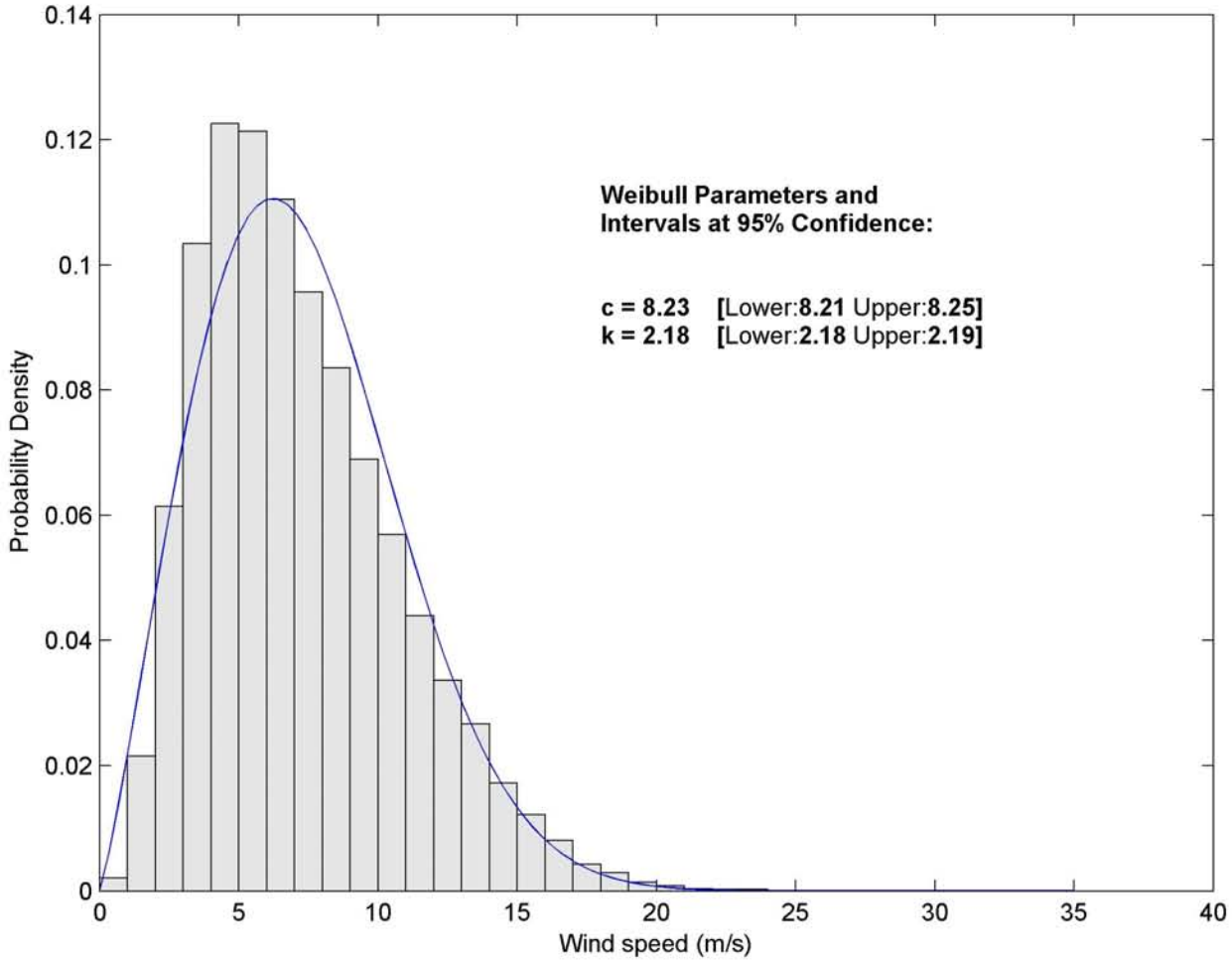

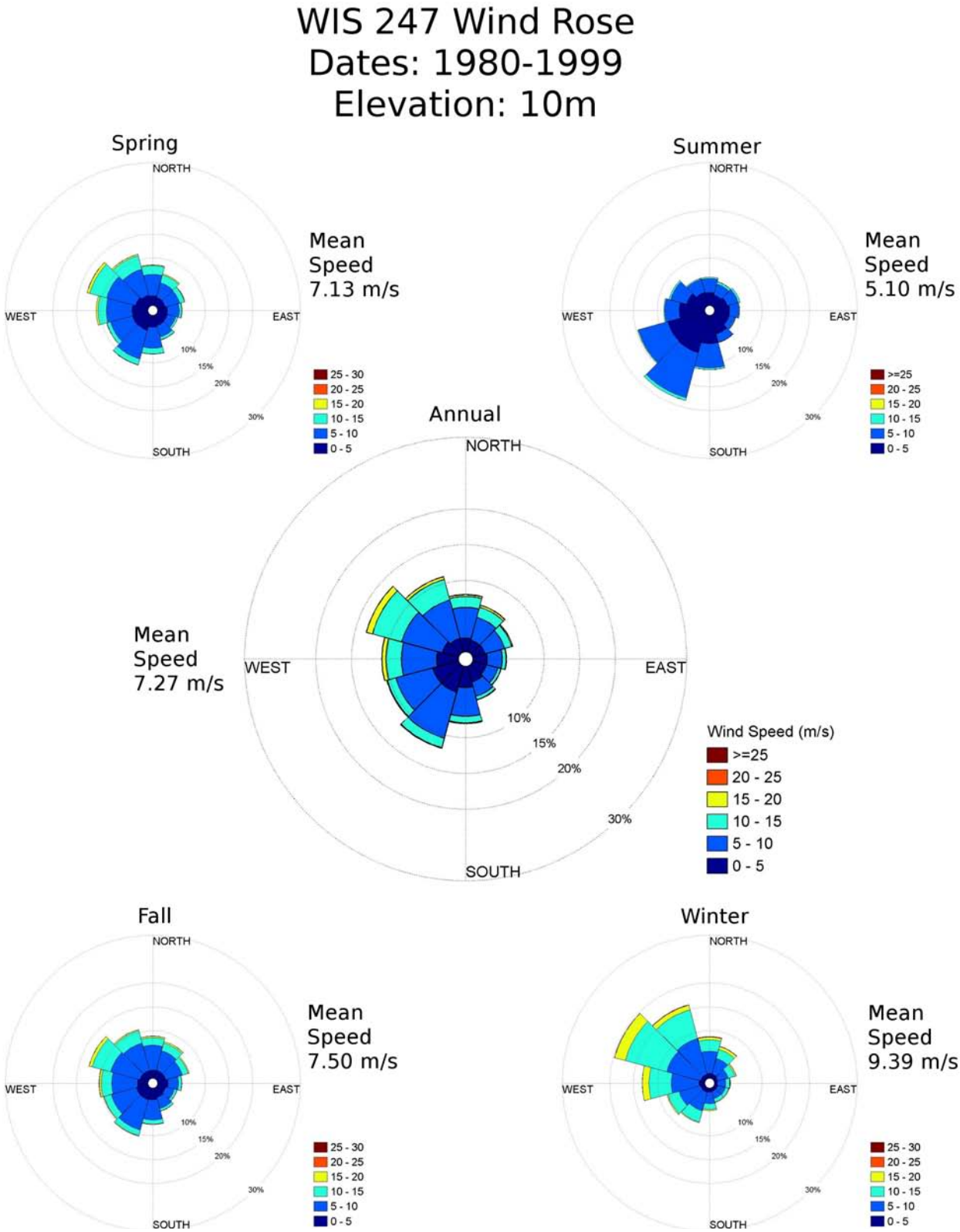
WIS 247 Wind Rose
Dates: 1980-1999
Elevation: 10m
Spring
Mean Speed 7.13 m/s
Summer
Mean Speed 5.10 m/s
Annual
Mean Speed 7.27 m/s
Fall
Mean Speed 7.50 m/s
Winter
Mean Speed 9.39 m/s
NORTH
SOUTH
EAST
WEST
10%
15%
20%
30%
Wind Speed (m/s)
>=25
20 - 25
15 - 20
10 - 15
5 - 10
0 - 5

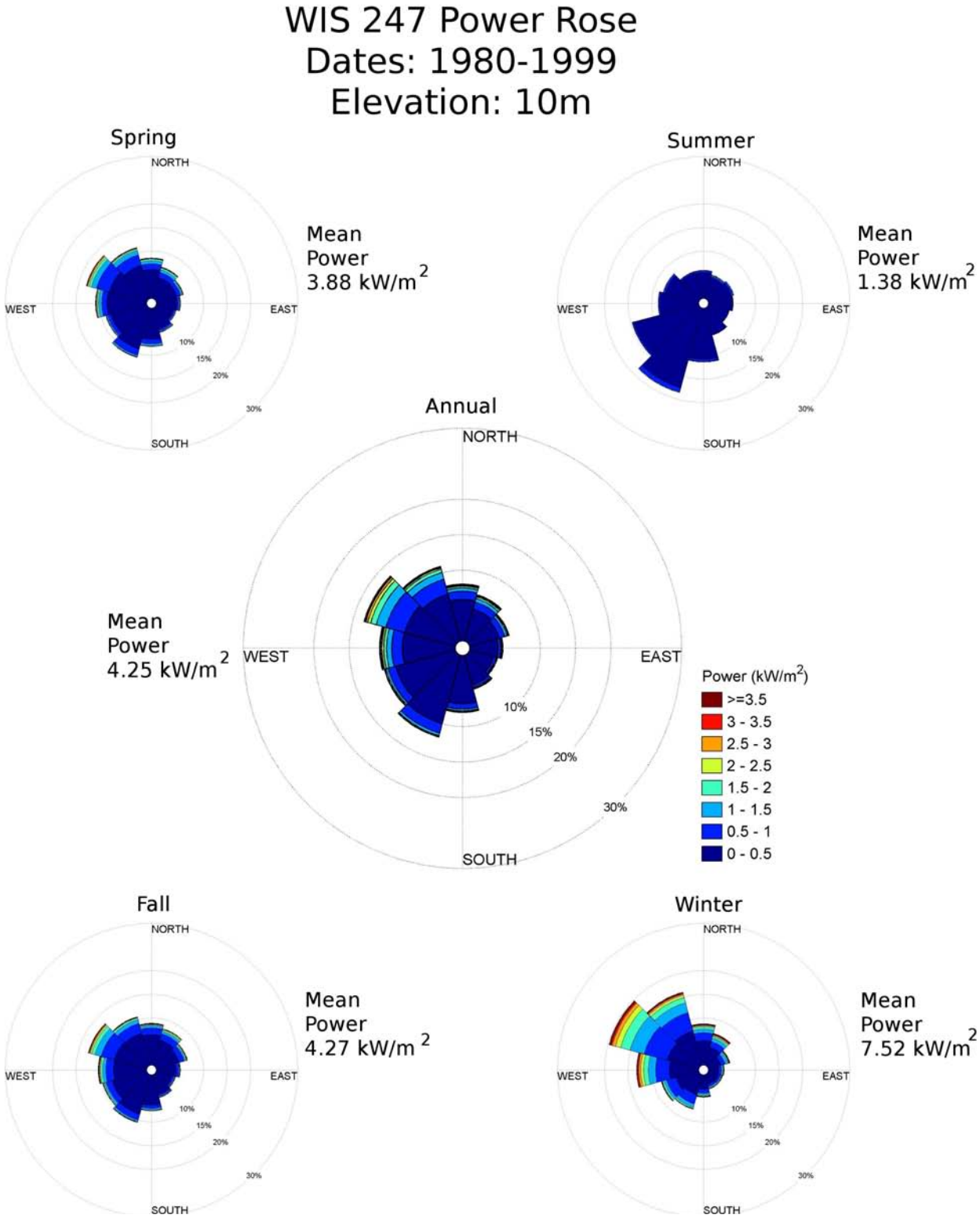
WIS 247 Power Rose
Dates: 1980-1999
Elevation: 10m
Spring
Mean Power 3.88 kW/m2
Summer
Mean Power 1.38 kW/m2
Annual
Mean Power 4.25 kW/m2
Fall
Mean Power 4.27 kW/m2
Winter
Mean Power 7.52 kW/m2
NORTH
SOUTH
EAST
WEST
10%
15%
20%
30%
Power (kW/m2)
>=3.5
3 - 3.5
2.5 - 3
2 - 2.5
1.5 - 2
1 - 1.5
0.5 - 1
0 - 0.5

WIS 248 Probability Distribution
Dates: 1980-1999
Elevation: 10m

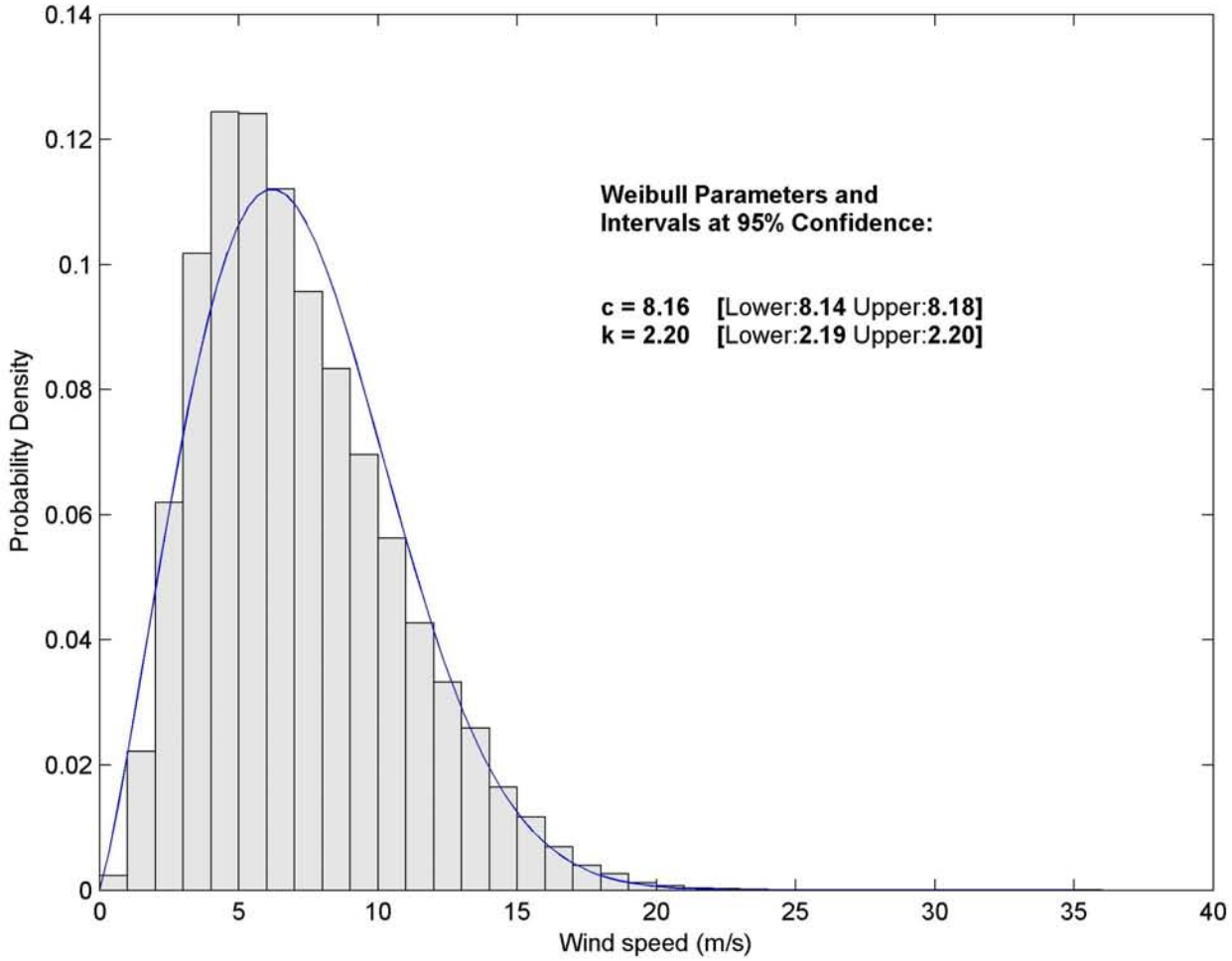

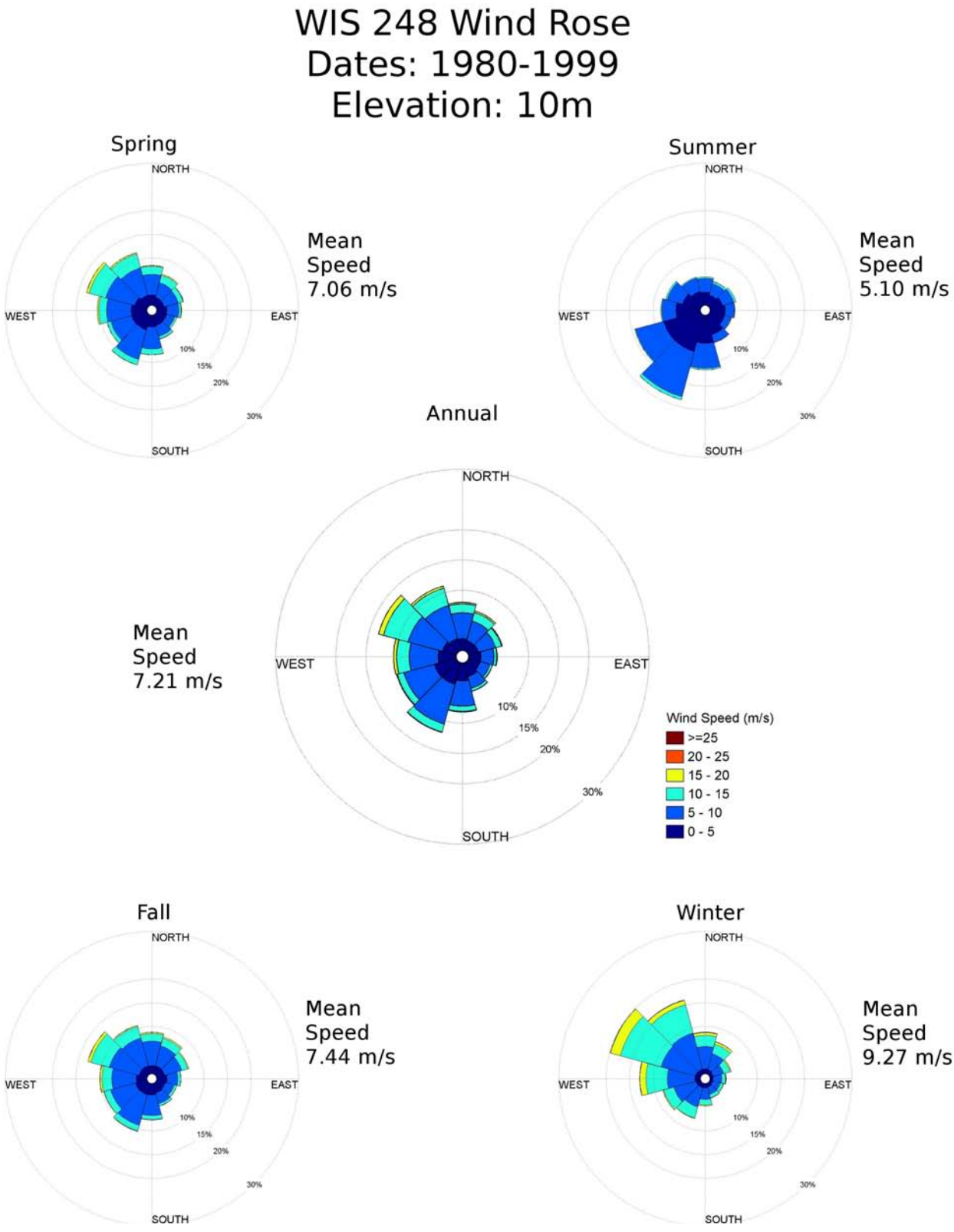
WIS 248 Wind Rose
Dates: 1980-1999
Elevation: 10m
Spring
Mean Speed 7.06 m/s
Summer
Mean Speed 5.10 m/s
Annual
Mean Speed 7.21 m/s
Fall
Mean Speed 7.44 m/s
Winter
Mean Speed 9.27 m/s
NORTH
SOUTH
EAST
WEST
10%
15%
20%
30%
Wind Speed (m/s)
>=25
20 - 25
15 - 20
10 - 15
5 - 10
0 - 5

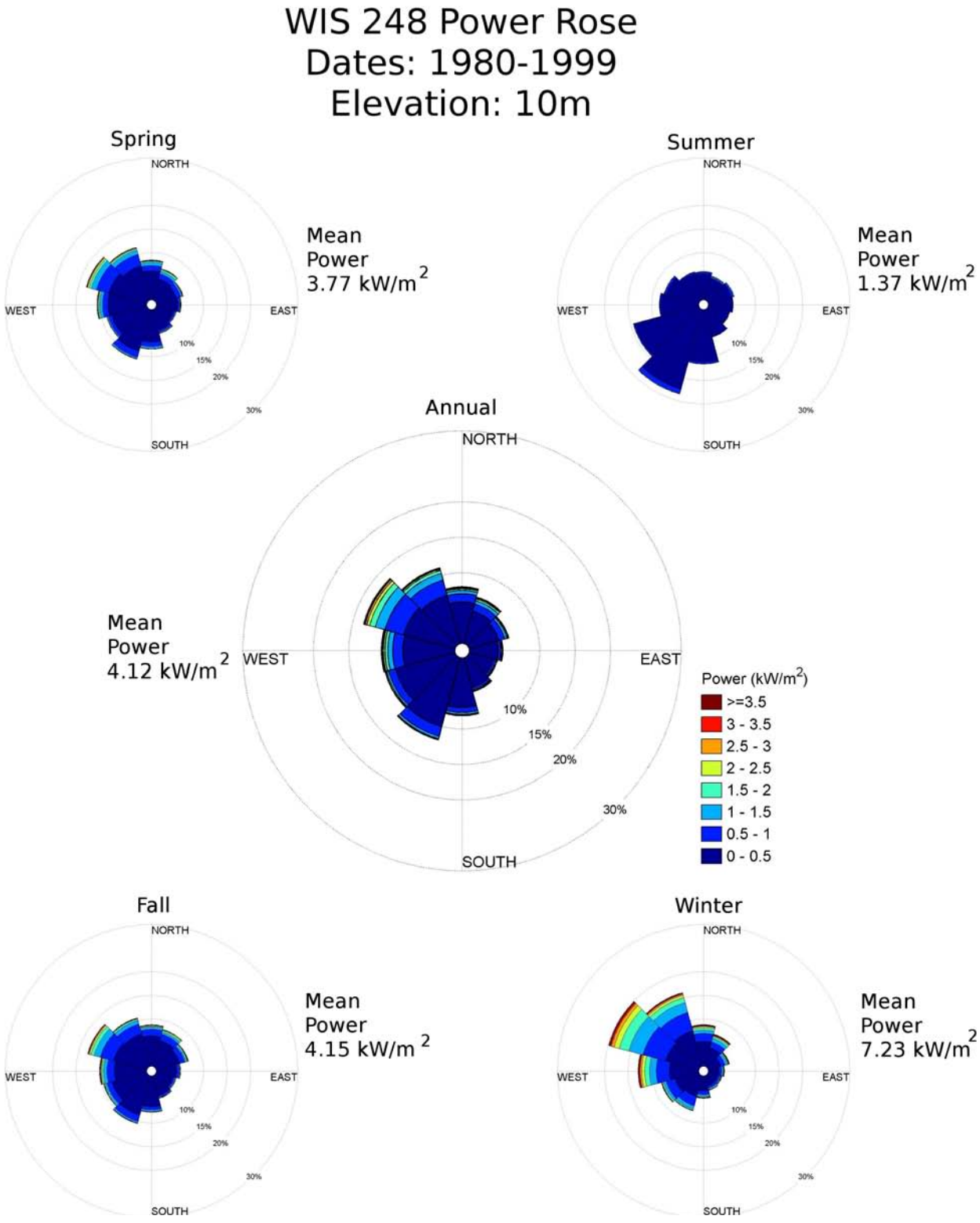
WIS 248 Power Rose
Dates: 1980-1999
Elevation: 10m
Spring
Mean Power 3.77 kW/m2
Summer
Mean Power 1.37 kW/m2
Annual
Mean Power 4.12 kW/m2
Fall
Mean Power 4.15 kW/m2
Winter
Mean Power 7.23 kW/m2
NORTH
SOUTH
EAST
WEST
10%
15%
20%
30%
Power (kW/m2)
>=3.5
3 - 3.5
2.5 - 3
2 - 2.5
1.5 - 2
1 - 1.5
0.5 - 1
0 - 0.5

Appendix B

Block Island Modeling Analysis

Report completed by Jay Titlow and David Morris of WeatherFlow, Inc.

Modeling results produced by MetLogic, Inc.

Project scope:

To complete a set of atmospheric model simulations to reveal flow patterns around Block Island with emphasis on the effect of the Island itself.

Product:

A set of 12 model runs, one for each octant compass direction from North clockwise through Northwest plus 4 additional runs to highlight seasonal variations of the more frequent flow regimes.

Table of Contents

Introduction

The modeling analysis was performed to increase the understanding of wind regimes in the coastal waters surrounding Block Island, Rhode Island. Special emphasis was placed on the influence of the island on surface to hub height flows both upwind and downwind in each particular compass direction.

An overview of the model runs can be found at:

http://rock.metlogic.com/overview.shtml

Results of this analysis can be viewed at the following web site:

http://rock.metlogic.com/index.shtml

Model, Configuration and Input Data

Simulation Details

- Simulations performed with RAMS version 6.1, the latest (unreleased) version from technology partner, ATMET.
- 500m horizontal grid spacing on the high resolution grid telescopically nested from 12km, 6km and 2km grids. A range of horizontal grid resolutions from 4km to 250m were tested. In most cases, the convergence of results at the proposed turbine locations occurred at 1-2km. In some cases, where stable conditions existed and the proposed wind farm sites were downwind of the island, differences with apparent down to 500m.
- 20m vertical grid spacing, expanding upward with a geometric ratio of 1.15. Vertical grid resolutions from 40m to 5m were tested. Most of the energy in the wind is captured at 20m vertical resolution, however, the wind speeds at 80m (hub height) at the wind farm sites are underestimated by up to 20%. It was not feasible within the time frame of the project to run the simulations at the time steps required for 5-10m vertical resolution.
- 0Z start times, simulating for 30 hours, with 6 hours of dynamic initialization prior to the 0Z start.
- Initialized from the 12km NAM analysis, with grid 1 bounded by subsequent 6 hourly 12km NAM analyses.

A complete configuration description can be found at: http://rock.metlogic.com/forecasts/bi/details.bi.shtml.

- *Dynamic Initialization:* RAMS was initialized 6 hours prior to the 0Z start time (tau 0), firstly with a 2 grid run (outer grids only) from tau -6 to tau -3 (stage 1), then with all 4 grids from tau -3 to tau 0 (stage 2). In stage 1, the dynamic model fields (U, V, P and T) in the interior domain were strongly nudged to the interpolated NAM analysis values. In stage 2, the same variables were nudged, but far less strongly. The atmospheric moisture data was excluded from the nudging. This forces a numerical balance to develop for the dynamic quantities (U,V,P and T) between the model and the NAM analysis, while allowing moisture quantities (clouds and precipitation) to evolve independently.

- *3D Soil Moisture Initialization*: The 3D (spatial and depth) soil moisture field was extracted from the 12km NAM analysis files and interpolated to the RAMS grids and soil levels.
- *2D Snow Cover Initialization*: The 2D (spatial) snow cover field was extracted from the 12km NAM analysis files and interpolated to the RAMS grids.

High Resolution Input Data

- *Operational Sea Surface Temperature and Sea Ice Analysis (OSTIA)*

OSTIA uses satellite data provided by the GHRSST project, together with in-situ observations to determine the sea surface temperature. The analysis is performed using a variant of optimal interpolation (OI) technique. The analysis is produced daily at a resolution of 1/200 (approx. 5km). OSTIA data is provided in GHRSST netCDF format every day.

http://ghrsst-pp.metoffice.com/pages/latest_analysis/ostia.html

- *ASTER Global Digital Elevation Model (ASTER GDEM)*

The ASTER GDEM covers land surfaces between 83°N and 83°S and is composed of 22,600 1°-by-1° tiles. Tiles that contain at least 0.01% land area are included. The ASTER GDEM is in GeoTIFF format with geographic lat/long coordinates and a 1 arc-second (30 m) grid of elevation postings. It is referenced to the WGS84/EGM96 geoid. Pre-production estimated accuracies for this global product were 20 meters at 95% confidence for vertical data and 30 meters at 95 % confidence for horizontal data.

http://www.ersdac.or.jp/GDEM/E/index.html

- *National Land Cover Database (NLCD 2001) Multi-zone Download Site*

The Multi-Resolution Land Characteristics Consortium (MRLC) has completed the National Land Cover Database (NLCD) 2001 products for the conterminous United States, Hawaii, Alaska and Puerto Rico at 30 m cell resolution. The NLCD 2001 products (land cover, impervious surface and canopy density) were generated from a standardized set of data layers mosaicked by mapping zone. Typical zonal layers included multi-season Landsat 5 and Landsat 7 imagery centered on a nominal collection year of 2001, and Digital Elevation Model based derivatives at 30 meters spatial resolution. NLCD 2001 used an improved classification algorithm from NLCD 1992, resulting in a more precise rendering of spatial boundaries between 16 classes of land cover (additional classes are available in coastal areas and Alaska only). A

shapefile with the standard NLCD zones as well as a mutlizone attribute is available for download here.

http://www.mrlc.gov/nlcd_multizone_map.php

List of model runs completed:

1. **North: January 4th 2008**
2. **Northeast: September 22nd 2008**
3. **Northeast 2: April 17th 2008**
4. **East: September 24th 2008**
5. **Southeast: October 25th 2008**
6. **South: September 6th 2008**
7. **South 2: November 8th 2008**
8. **Southwest: July 7th 2008**
9. **West: December 22nd 2008**
10. **Northwest 1: October 30, 2008**
11. **Northwest 2: November 22 2008**
12. **Northwest 3: February 23 2009**

Basic Wind Regimes of Block Island and Climatology

Wind behavior over southeastern New England, and in particular, coastal Rhode Island can be best described as progressive west to east flow with embedded mid-latitude synoptic waves, which are more frequent during the spring, fall, and winter. During the summer months basic flow remains westerly, but the jet stream and associated weather lifts northward allowing for periods of lighter flow. During these occasions, mesoscale processes such as sea breezes have a more pronounced effect on the region's weather.

Typical synoptic setups across Southern New England are as follows:

Persistent Bermuda high pressure to the southeast

Very common feature often occurring up to 5 to 7 days a week during the summer months, 3 to5 days a week during the spring and fall and 2 to 4 days a week during the winter.

Consistent SSW to SW synoptic flow is found across the region when this semi-permanent oceanic feature becomes established. From late spring, through summer to early autumn, Southern New England sea breezes enhance prevailing SSW, SW or WSW surface winds. The complex geography of the region from Long Island through to Buzzards Bay and Martha's Vineyard generates multiple convergence zones and varying effects. Examples of this synoptic set-up with mesoscale enhancement include accelerating SW flow into Buzzard Bay and channeled southerly flow into the East and West passages of Narragansett Bay.

High pressure to the west and northwest

The next most common feature, often occurring 1 to 2 days a week during the summer months, 2 to 4 days a week during the spring and fall and 3 to 5 days a week during the winter.

This is often the setup that results following the passage of a low pressure system tracking away to the east. Northwest wind strength depends upon the pressure gradients between the incoming anticyclone to the west and the departing low pressure system. Blocking high pressure can become well established across New England, or slowly migrate eastward and offshore. (In the summer, it is often more common to experience brief surges of NW flow that then die and back to the SW as high pressure weakens and the semi-permanent Bermuda High re-intensifies. Alternately, during the winter and late spring and fall, high pressure often tracks by to the north, veering the flow more NE.

High pressure to the northeast

Right behind B, this pattern is the third most common feature occurring, on average 1 day a week during the summer months, 2 to 3 days a week during the spring and fall and 3 to 4 days a week during the winter.

As previously mentioned, high pressure often becomes well established over the Canadian Maritimes, resulting in NE or ENE winds across Southern New England. This pattern can last a few days and may generate a backdoor cold front. Pressure gradients are sometimes

significantly tightened if an area of low pressure or a trough axis exists to the southeast or south. (Again, this is more frequent during the winter and early spring).

Mid-latitude low pressure systems

Finally, these systems, almost absent from July through mid August, can occur once or twice a month from late August through early October, become much more frequent from mid October all the way to early May, then wind down to one or two a month from mid May through June.

Mid latitude low pressure centers can track toward New England from varying directions. The most common arrive from anywhere between WNW through WSW to SSW. Alberta Clippers, originating in the North Pacific, reform in the lee of the Rocky Mountains and move rapidly across New England. Cyclogenesis also occurs further south, over the Great Plains, and these systems can track directly across Western New England, or push offshore from the Mid-Atlantic states and take a coastal route into Southern New England. Other systems can develop over the Gulf of Mexico or offshore of the Carolinas and approach Southern New England as a potent system. Occasionally, given favorable upper air conditions, a coastal low pressure system may loop back into Eastern New England. (During "normal" progressive patterns, these synoptic events are most responsible for the sporadic ramp-ups and ramp-downs experienced over a several day span).

Mesoscale features

A variety of smaller mesoscale features can also have a significant effect on the wind regimes in the region.

Sea breezes

The geography of Eastern Long Island, Block Island Sound, Buzzards Bay, and Vineyard Sound provides a complex region of sea breeze generation to interact with the overall synoptic flow. The South Coast of Long Island and the Connecticut Coast typically experience independent sea breeze onsets. Given favorable synoptic conditions, these two sea breeze regimes often merge into a larger scale enhanced flow through the course of the day. Typically, as the diurnal flow matures, surface wind directions usually veer from SW through WSW.

Under weak synoptic gradients, a weak thermal trough sometimes develops over Northern Rhode Island and Southeast Massachusetts. This often increases the strength and longevity of sea breeze enhanced SW surface flow into Southern Narragansett Bay, Buzzards Bay and Vineyard Sound. Sea breeze enhancement often begins on a relatively small scale through midday or early

afternoon, but by late afternoon and sometimes well into summer evenings a broad swath of increased SW flow exists across the entire coastline from Western Long Island through Block Island to Nantucket Sound.

The Rhode Island coast usually experiences more of a south or SSW sea breeze onset through East and West Passages and the entrance to the Sakonnet River. Some strengthening, due to channeling through these topographical gaps, is also common. The sea breeze front often shows up well as a distinctive line of Cu on visible satellite imagery. This may be well defined just inland of the Connecticut coast, but becomes less well defined along the Rhode Island coast. The sea breeze front usually propagates inland to the north of Providence and Fall River, a little more rapidly than further east.

The presence of afternoon cloud cover can significantly weaken SW potential on otherwise synoptically favorable days. Conditions in Buzzards Bay are occasionally influenced by the sea breeze from Cape Cod Bay, propagating toward the southwest. The resultant convergence is usually pushed back to the northeast as the dominant SW sea breeze strengthens. The convergence between these two opposing sea breeze onsets, which can extend along the spine of Cape Cod as far as Chatham, is often marked by a distinctive band of Cu.

Mid-latitude low pressure system low level jet

With a low pressure system positioned to the west or northwest, a well defined warm front often slides from south to north across Southern New England. With the associated cold front propagating eastward across Long Island Sound and Southern New England firmly established in the warm sector, a low level jet, associated with warm air advection, can exist for a time. This can commonly generate wind speeds at the 850mb level in the 40 to 70 knot range. This wind mechanism is problematic with respect to wind energy potential as this strong "ribbon of wind" is present aloft but the degree to which it propagates downward towards typical hub heights and to the surface is often related to near surface thermodynamics (if air temperatures are too cool at the surface, the atmosphere becomes too stable for the jet to reach the lower levels) or momentum transfer (in which moderate to heavy precipitation will pull the stronger wind down). Indeed, during a period of "spiked" higher speeds on October 25th, (case 6, SE flow) rain was observed in the area.

Nocturnal low level jet

The nocturnal low level jet is caused by changes in the vertical temperature structure, due to heat exchanges near the surface. This is thought to generate a nocturnal wind maximum a few hundred feet above the ground, at its strongest between 0000 and 0300 local time. When the inversion layer decays upward from the surface due to warming at the surface, the entire layer between the surface and the low level jet becomes more turbulent, increasing wind strengths at the surface and hub height as well as decreasing the strength of the low level jet itself. This effect is thought to be more prevalent during the summer months, however it is difficult to isolate an increase in wind at a station and say that it has been solely generated by a true nocturnal low level jet event, rather than the interaction of other meteorological processes. The nocturnal low level jet can be better visualized as a sheet or ribbon of wind maxima a few hundred feet above the surface.

a. Tropical systems

The winds associated with tropical storms and hurricanes obviously exceed the operational limits for wind turbines, and this region is impacted by these systems, most frequently at tropical storm strength. Consequently, winds of this magnitude must be factored in to project designs. While winds in a nor'easter are rather uniform in the vertical, this is not the case for tropical systems, in which speeds can be much stronger just aloft, introducing shear stresses and other operational issues.

Weather "Wildcard": The effects of Seasonal SST differences

The differing SST regimes found in the different seasons can also have a significant effect on the weather and winds found in the region. For example, in the late spring/early summer, with SSTs around Block Island hovering around the mid 40s F to low 50s F and a warm SW flow, the warmer air aloft usually struggles to mix to the surface resulting in stratification and shear between the lighter winds at the surface and the stronger winds aloft. (To the northeast of Block Island, given a period of solar insolation, there will be less stratification in the immediate lee of the island, and SW winds generally have more success in mixing to the surface). This stratification, or de-coupling effect, becomes much less noticeable with less thermal gradient (i.e. cooler air temps or warmer sea surface temperatures as found in late summer/early autumn).

During post cold frontal northwest winds in late summer and early fall, stronger winds will mix to the surface more readily. Sea surface temperatures at this time will usually be hovering around the upper 60'sF. Unstable conditions over the water generate convection, and result in Cu

or Sc development offshore. The well mixed convective boundary layer maintains strong and gusty conditions (dependent on pressure gradient) irrespective of solar insolation, throughout the night or under a blanket of cloud cover. This is in contrast to the generation of the convective boundary layer over the land, which requires solar insolation to generate diurnal thermal activity. Thus, during an early morning, post cold frontal day, the nocturnal inversion may be keeping surface winds light at Watch Hill and Westerly, whereas stronger NW winds are present on the NW facing shoreline of Block Island. Note that Block Island's nocturnal inversion may keep NW winds off the surface to the southeast of the island.

In addition, autumn NE winds can often have an extra "kick" as cooler air is flowing over relatively warmer waters. For example, case number 3 (NE, on September 22nd) depicts an excellent example of the markedly higher speeds recorded at the jetty location, whereas the airport does not experience the significantly higher speeds. Notice that the model unfortunately does not capture the enhanced speeds at the surface very well. In fact, the model will often perform better at speed forecasts at heights only 10s of meters above the surface, so this inadequacy may be less troublesome for wind energy assessment than for surface operations like Search and Rescue.

Qualitative Analysis of Results

General modeling results:

1. Wind directions verified well. This result is important as the primary focus of this study is to investigate the wind behavior in the Block Island region as a function of wind direction.

2. The model estimates the wind strength trends well, both on land and over water.

3. The model underestimates surface wind speeds on land with what appears to be a rather constant bias of about 5 knots once speeds rise to 5 knots or greater. Surface roughness differences between the model representation of the observation site, and the observation site itself are the primary cause for these differences. The surface roughness differences originate from two sources; deficiencies in the satellite derived land cover dataset used, and the spatial area in the model the observational site data is extracted from (a weighted interpolation from the 4 neighboring grid cells). These effects are minimized as you move vertically up towards elevated hub heights

4. The model also underestimates surface wind speeds over water, but the differences can range from near zero to double digit biases during the course of any particular run. We believe these biases are caused by poorly captured near surface thermal effects. Initial surges of colder air over warmer water associated with frontal passages, nocturnal instability, and interaction with low level jets are examples of events that could cause these thermally driven biases, which are more pronounced at the surface but still may be a factor at hub heights.

5. Finally, precipitation-altered speeds, which in fact, depending on the synoptic conditions, are known to both enhance and diminish speeds. These effects are generally not captured by models.

Event Descriptions and Verifications

1. North Case January 4th 2008

On 3 Jan an intense anticyclone, 1045mb, is established over Tennessee, with a ridge extending across the Great Lakes into Northern Quebec, resulting in cold northerly winds across New England. By Jan 4th, a fast moving low pressure center, propagates eastward across Hudson Bay and into Northern Quebec as the high pressure center to the south shows a weakening tendency and slips eastward across the Carolinas. This results in a steady backing of surface wind directions from northerly to westerly through the period. The high pressure center continues to slide offshore to the east through Jan 5th, resulting in a further backing to SW.

High pressure established inland can be a relatively common occurrence through the winter months, giving several days of N, NW or W winds for New England. During the summer months, high pressure generally becomes better established offshore, giving more days of southwesterly conditions.

Through 3 Jan, N and NNW winds eased slightly from around 30mph during the early hours to 20mph through the afternoon and evening dictated by pressure gradients. For the 4th, westerly winds built back up into the low thirties by 1000 (local time). Westerly winds then hovered around mid to upper twenties (mph) through much of the afternoon, diminishing into the evening.

Well modeled at both the Jetty and Airport.

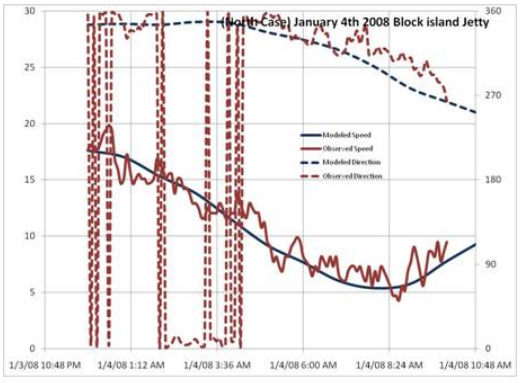

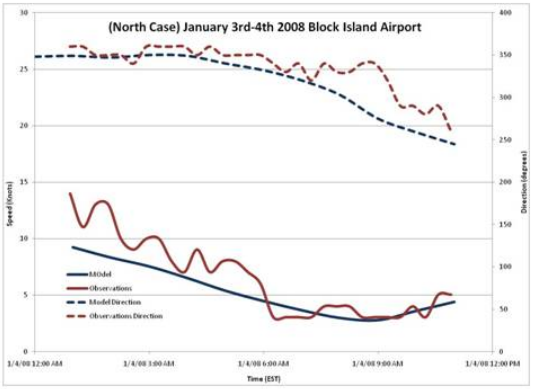

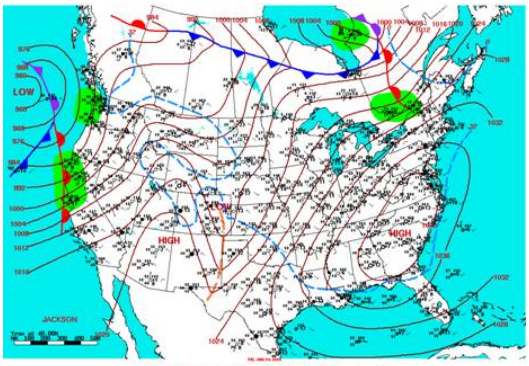

2. Northeast Case September 22nd 2008

Anticyclonic NE winds across New England thanks to high pressure becoming established over Quebec following the passage of a cold front from NNW to SSE the previous day. A stationary frontal boundary and trough axis to the east of Cape Hatteras helps to enhance northeasterly pressure gradients across the region.

Northeast winds increase through the morning hours, from 0200: 11g14mph, to 0700: 19 g22mph. For the rest of the period northeast winds generally hold around the 20mph mark. The lull-to-gust spread remains relatively small possibly indicating neutral or stable lower layers, and therefore more stratification rather than well mixed lower layers.

Directional trends captured well at both the jetty and airport. Speed trends captured well but magnitudes under-predicted at both locations. It is interesting to note that the speed magnitudes captured well with the dying SW flow at the beginning of the simulation, but once the cooler air arrives, the model totally misses the strong initial surge that occurs only over water, but then both locations settles into more of a systematic bias.

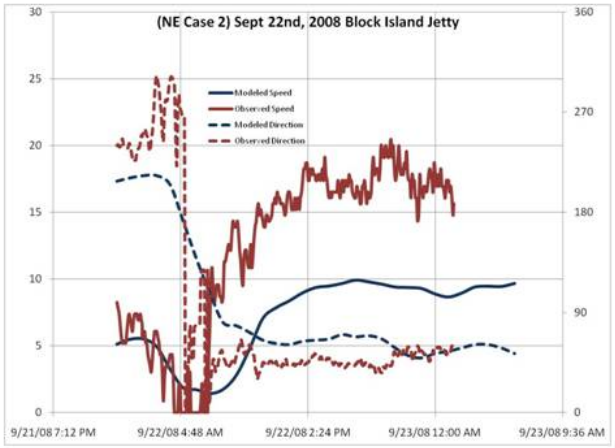

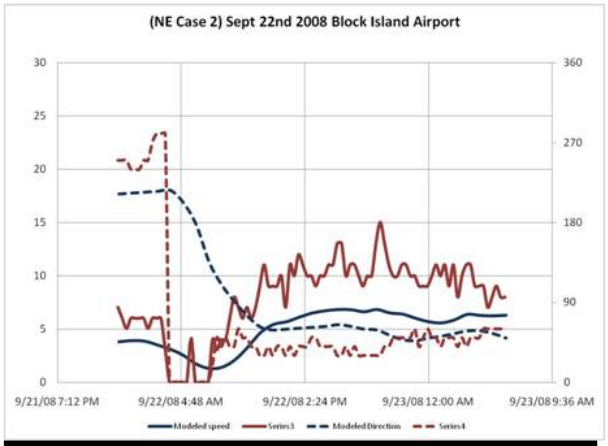

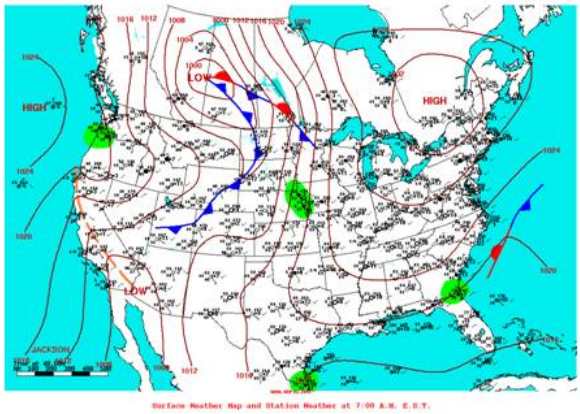

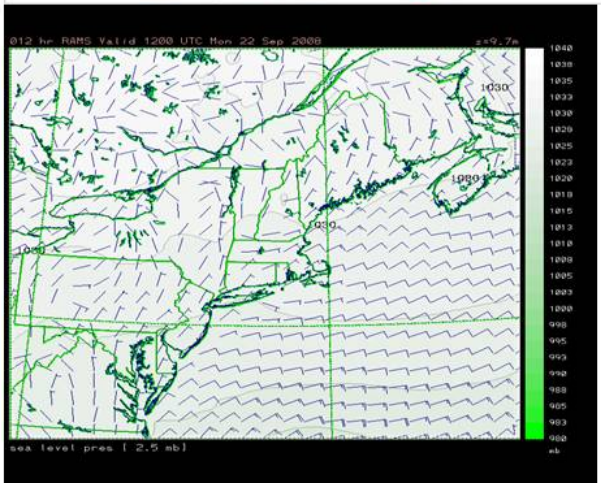

3. Northeast Case 2 April 17th 2008

Ridge of high pressure, 1024mb, extends from Nova Scotia to Florida Panhandle. Low pressure offshore Atlantic, maintaining northeast winds across Cape Cod, Block Island and Eastern Long Island. NE winds increase through the period, builds to 12mph through late morning and to 23mph through the afternoon. This is in response to tightening pressure gradients as low pressure edges westward across coastal New England.

Directional trends again are generally good, although the directional shift pattern at the beginning of the run occurred a couple of hours later than the model predicted, but the model recovered for awhile, only to lag again on a late backing trend. The onset of the speed increases was modeled well at both locations but eventually the prevalent under-prediction in speed occurred at both locations. Notice that the time series for both locations are quite similar with the magnitudes being higher over water.

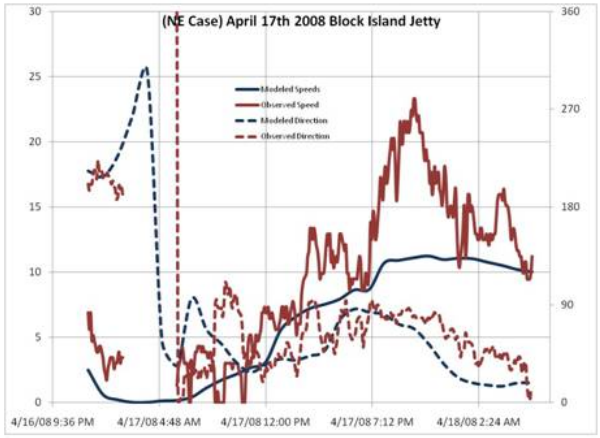

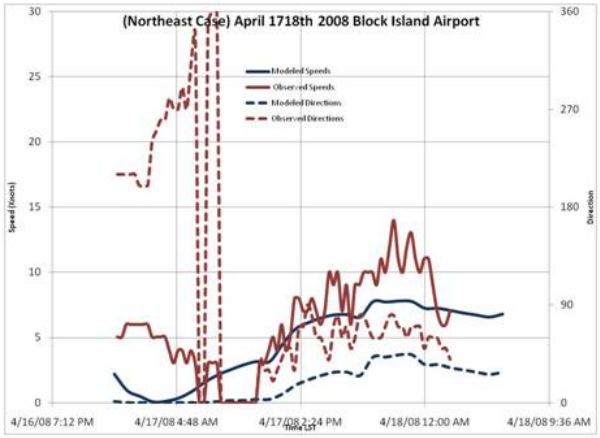

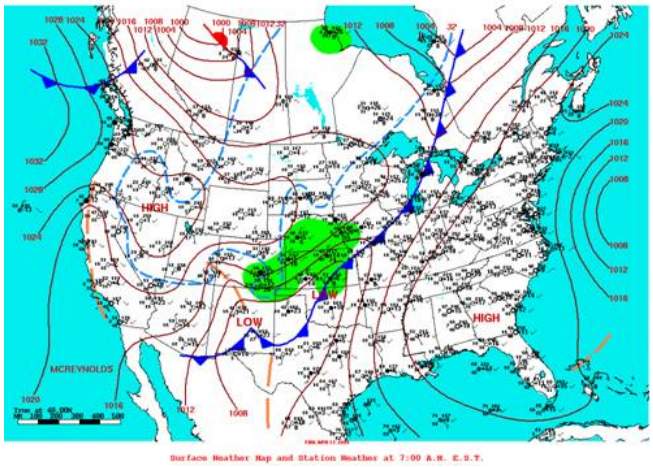

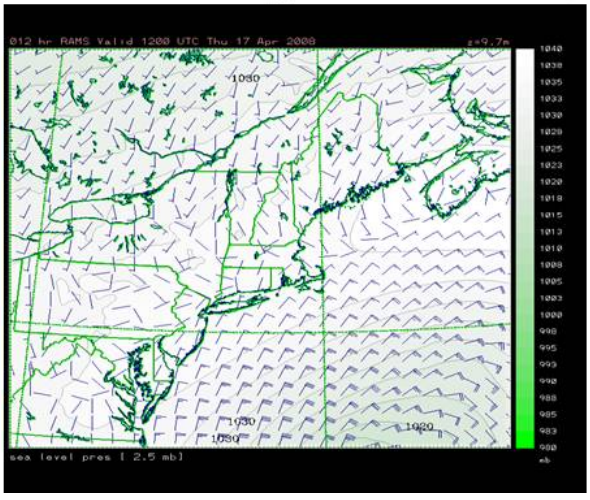

4. East Case September 24th 2008

High pressure, 1032mb, established over Northern New England. Trough axis and cyclogenesis east of Cape Hatteras. NE and ENE pressure gradients across coastal New England, becoming more easterly through the afternoon with some strengthening. Wind strengths through the beginning of the period were in the low teens (mph), building to mid teens by 0900 (local time), followed by a brief diminish through midday to low teens, and then building to mid and upper teens (with gusts to low twenties) by 1400 (local time). Afternoon wind directions become a better established easterly direction, holding into the evening.

This synoptic set up occurs occasionally, but when established (with high pressure and developing coastal low pressure to the south) can last for two to three days.

Directional trends look good, but again, observed speeds are higher at both the jetty and the airport. The differences were significantly higher at the jetty with little overall agreement, whereas the airport observed speed trends generally resemble the model.

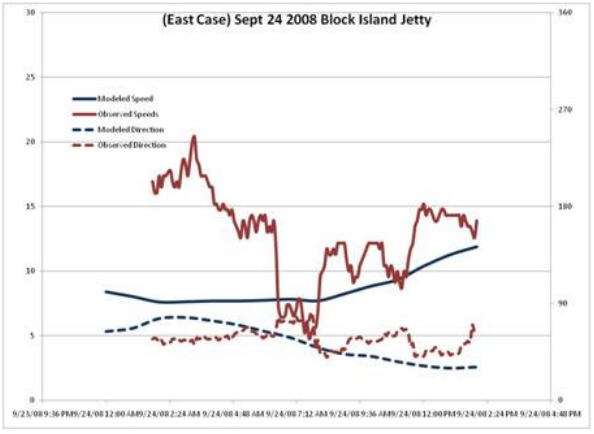

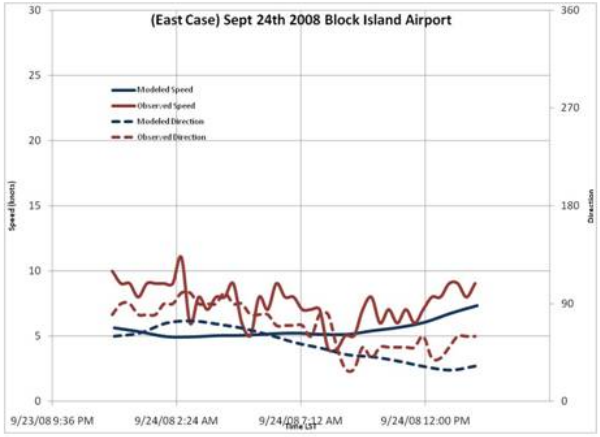

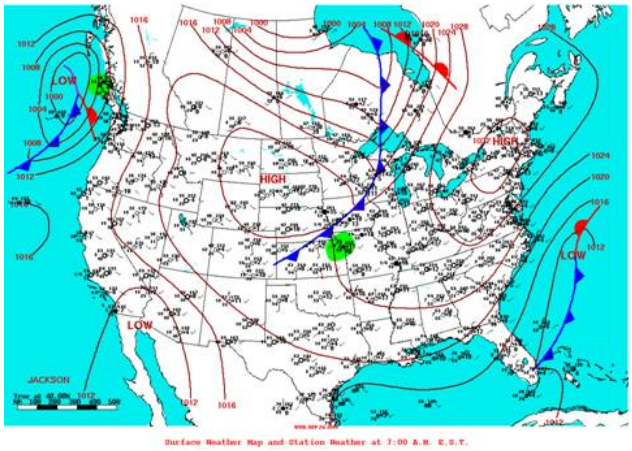

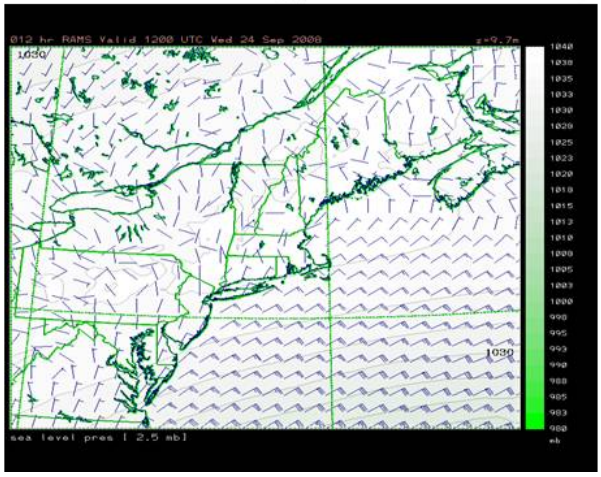

5. Southeast Case October 25th 2008

Quite a rare and short-lived synoptic set up. SE winds established for the day as New England high pressure slips northeastward over Nova Scotia. During the period a trough axis to the west deepens, eventually becoming a vigorous cold front that slides quickly offshore the following day. Through Oct 25th however, SE and SSE winds steadily increase from 14 g18mph at 0600 to 28 g 36 mph by 2300 (local).

Direction verification is quite good at both the jetty and the airport. In addition, observed speed trends also are well modeled. The under-prediction of speed is seen again, with a systematic approximate 5 knot under-prediction throughout most of the model run at the airport. At the jetty, speeds generally agree at both the beginning and end of the run, but during the period where winds backed to the ESE, observed values are significantly higher.

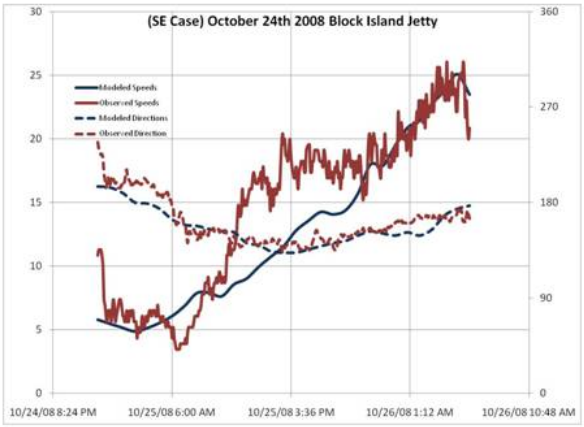

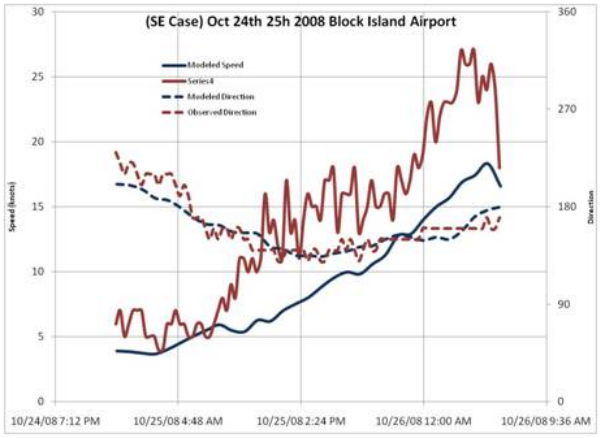

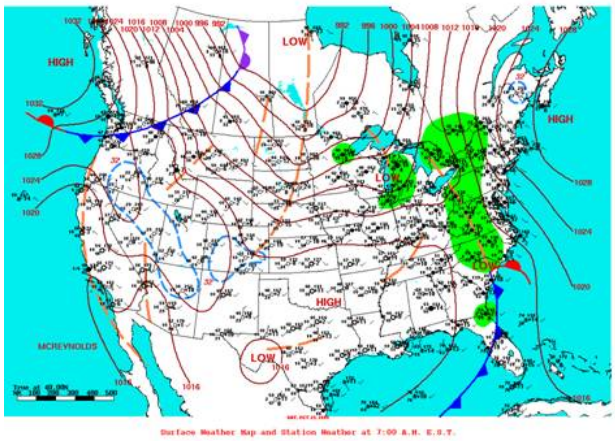

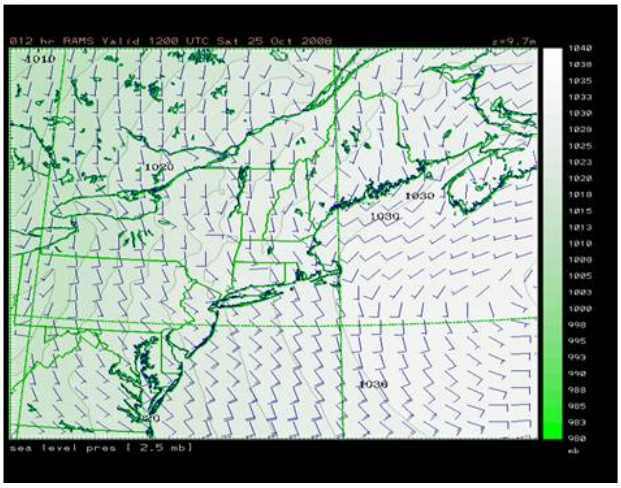

6. South Case September 6th 2008

Tropical Storm Hanna continues on her recurving path to the north, across NC and into VA. High pressure to the southeast of Nova Scotia, with a southerly becoming SE pressure gradient across Block Island. Pressure gradients tighten from 1600 onward (12 g 22mph) as wind directions become a better established SSE to SE. Wind strength maxima are reached between 2030 and 2215 (local time) with averages to 29mph and gusts to mid forties. Once again, southeasterly flow remains a relatively rare occurrence for Block Island, especially in combination with a tropical storm.

Verification for this case is harder to describe simply. This may be due to the complex dynamics associated with a decaying tropical system interacting with a frontal passage. There is general directional agreement during both the beginning and end of the model runs at both locations, but some significant veering and backing is missed mid run at both locales. Speeds are quite different with the most obvious glitch being the model missing the spike in speeds at both locales late in the run.

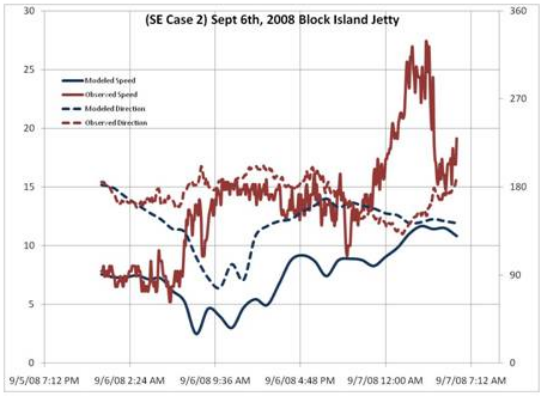

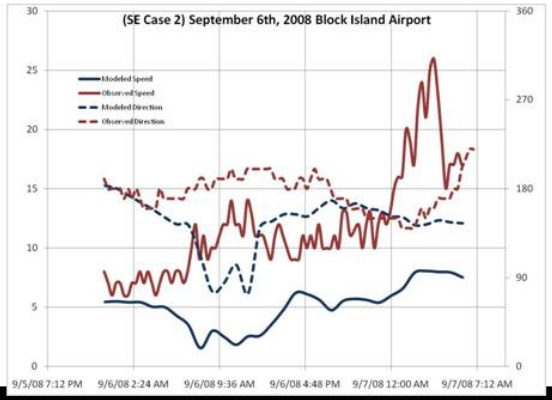

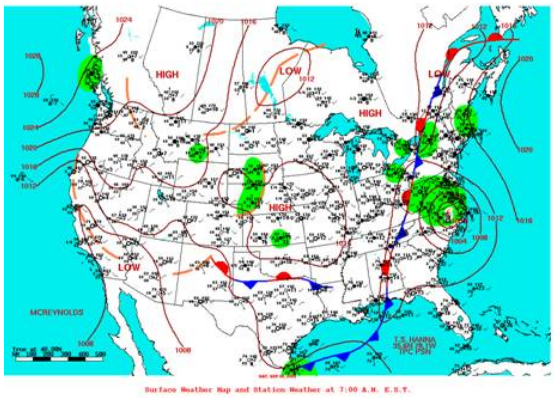

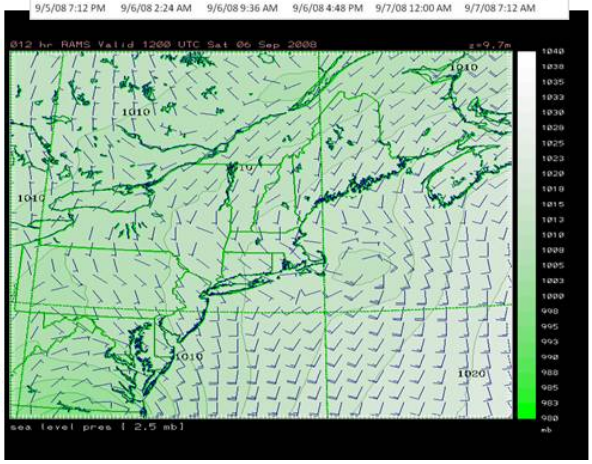

7. South Case 2 November 8th 2008

Low pressure complex, 999mb, over the Great Lakes. Warm front extending from Toronto, eastward across Maine to Nova Scotia. Cold front extending southward from Lake Ontario to Georgia. Warm air advection across New England through the day with tightening SSW to southerly pressure gradients associated with low level jet ahead of approaching cold front to the west. Light winds at Block Island through the early morning, then ramp up begins at 0800 (local time). SW wind maxima at 1415, with average to 18mph and gusts to 20. Wind directions becoming more southerly into the evening. Drops off to around 8mph by 1620, before increasing into the night with 21mph gusting to 27 by 2300. Also veering to SSW and SW by 2300 once again in response to approaching cold front. Cold frontal passage at Block Island eventually occurs around 0400 Nov 9th.

At the airport, some uncaptured directional oscillations. With speeds, an increasing trend is noted, but an under-prediction of speed is also evident, generally about 3 to 5 knots.

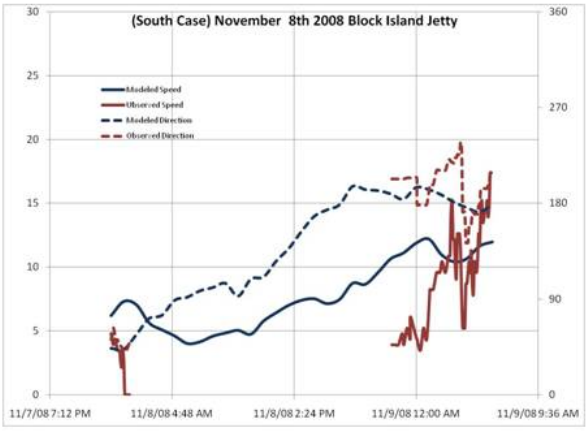

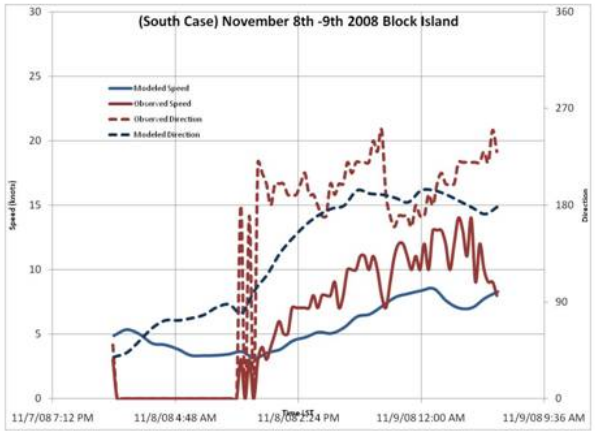

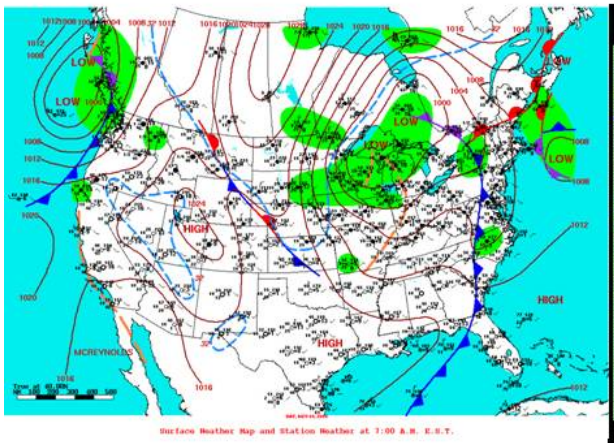

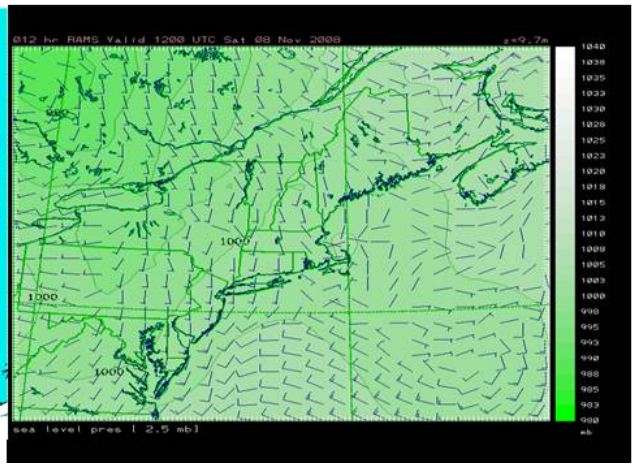

8. Southwest Case July 8th 2008

Bermuda high pressure, 1022mb, established to the southeast. Weak, expansive low pressure system, 1002mb, centered over Lake Superior with associated cold front extending southwestward to Nebraska. Warm front extending from low pressure center to Canadian Maritimes. This is a relatively common summer synoptic set up.

Southwesterly winds are established through the early morning hours with average wind speeds hovering around 10 to 12 mph, but unsteady with several periods of < 5mph, and a couple of gusts to 15 to 18mph. During the light period, wind directions veered more WSW to W briefly. Wind speeds began to ramp up after 0900, reaching a plateau between 1300 and 1600 (local time) with averages around 20mph and gusts into the mid to upper twenties.

Verification trends again very similar with directions in close agreement for both locations. For speeds, the airport exhibits the usual general agreement with trends, but a systematic approximate 5 knot under-prediction bias. Speed verification at the jetty is, at times, quite good with oscillations about near zero difference, but at others times 5 to 10 knots too low. Two such periods are observed during the overnight hours. Although the model does indicate enhanced flow, the model may struggle to capture the full effect of the nocturnal low-level jet.

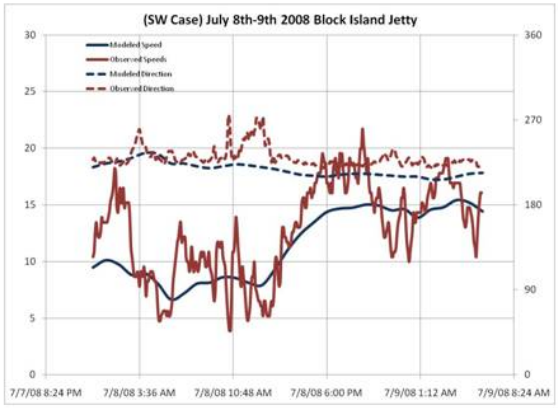

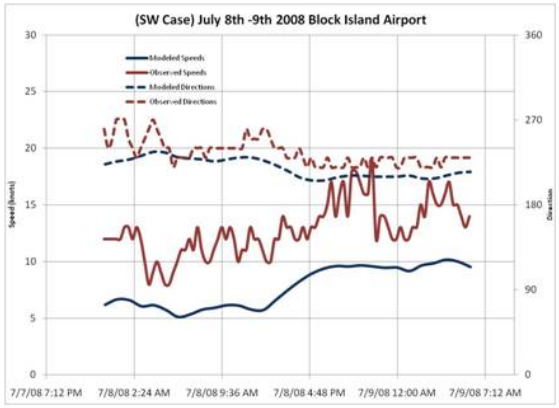

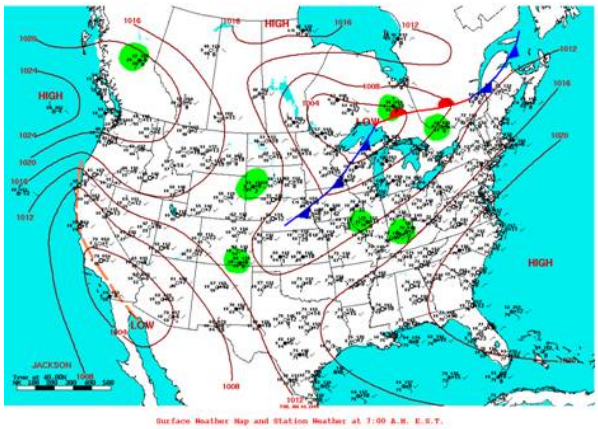

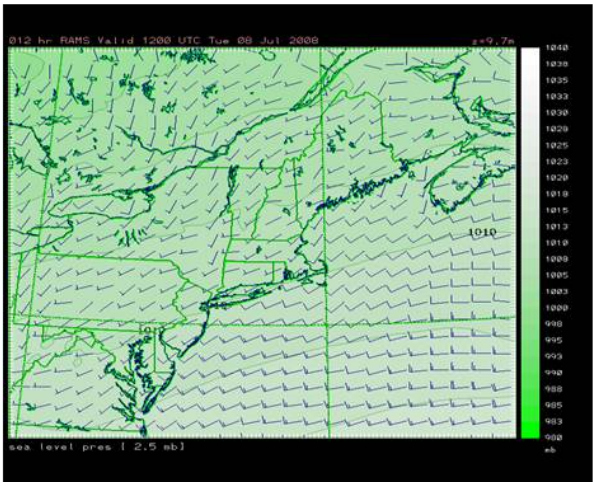

9. West Case December 22nd 2008

Developing low pressure tracks across New England through Dec 21st, deepening over Nova Scotia by Dec 22nd. High pressure, 1038mb, remains established over Missouri, generating northwest pressure gradients across New England and much of the East Coast. WNW winds, becoming NW through the early morning hours with average wind speeds easing from upper forties (mph) to 30mph. Once again, characteristic NW gustiness with a distinctive lull to gust spread throughout the day.

For this case, we were unable to retrieve observations from the airport, and so conducted verification using only the jetty, which reveals directional agreement with exception to a veer and back feature coinciding with lower speeds. This may simply be an embedded wave rotating around a departing deep low pressure system that the model failed to capture. Speed verification looks good although observed stronger flow continues into evening at the end of the model run at similar speeds to afternoon values. This discrepancy is typically problematic for models in near-coastal inland areas as decoupling (stabilization over land due to radiational cooling) may or may not occur based on highly local thermal effects (marsh or urban area may stay relatively unstable whereas an adjacent field may become stable). The vertical depth of the stable area is also difficult to model correctly in these regions.

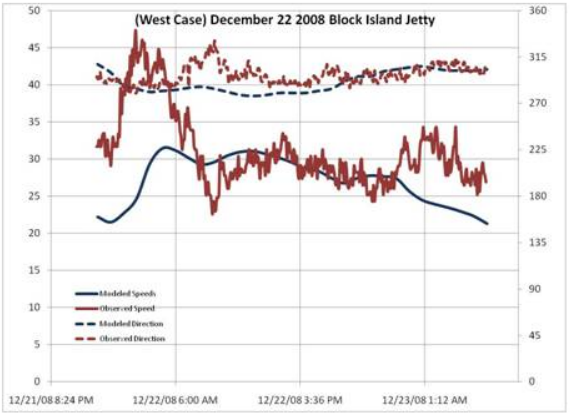

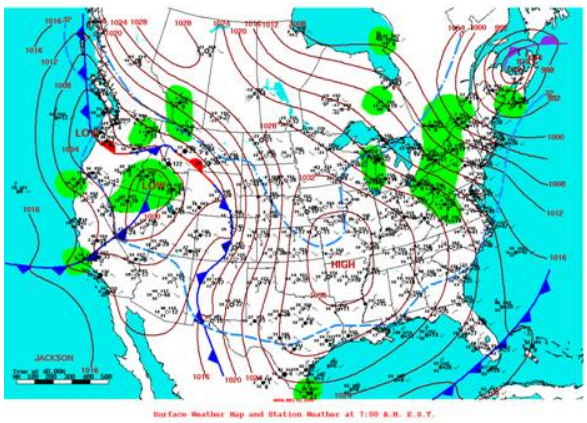

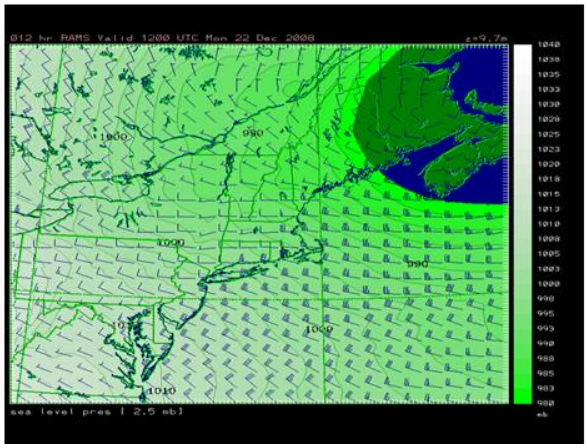

10. Northwest Case October 30th 2008

High pressure, 1030mb, building into the East Coast from the southwest, following the departure of a low pressure center now tracking northeastward across Newfoundland. This is a relatively common synoptic setup. Since the passage of the cold front late on the 28th, wind directions veered into the west then NW through the 29th, becoming a well established northwesterly through Oct 30th. These post cold frontal northwesterly winds exhibit a characteristically gusty signature, with average morning wind speeds around low 20s (mph), with gusts to upper twenties and low thirties. Through the afternoon, wind speeds ease slightly in response to weakening pressure gradients. The gust to lull spread appears to remain relatively large irrespective of diurnal solar insolation and air temps over the land. Boundary layer mixing is largely occurring as a result of relatively warm sea surface temperatures warming the lower layers of post cold frontal air advecting into the region.

Verification behavior is very similar to the other cases. Directional trends and magnitudes are well correlated. Modeled speeds at both locations are too low with the airport exhibiting more of a uniform bias throughout the run, whereas, once again, the jetty trends look good but the bias varies in a generally diurnal fashion, typical for cold air intrusions where both local differences between near-coastal air and water temperatures and nocturnal decoupling are quite sensitive to the resolution of the input fields.

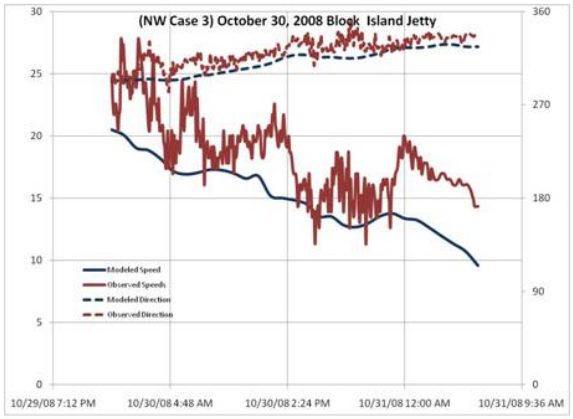

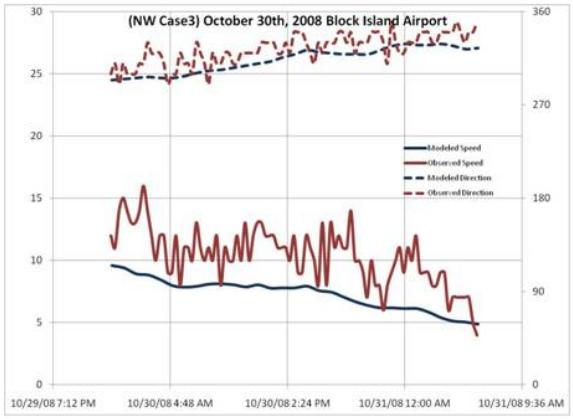

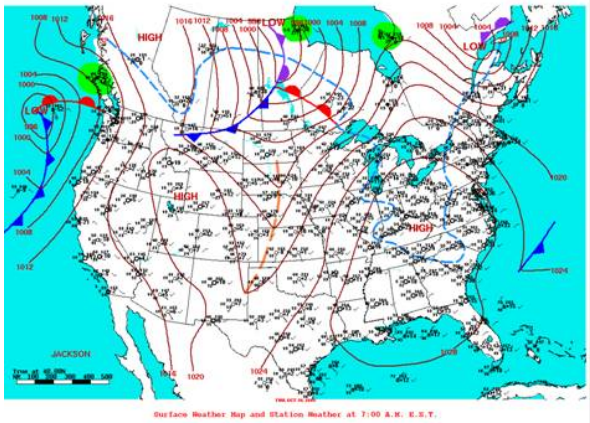

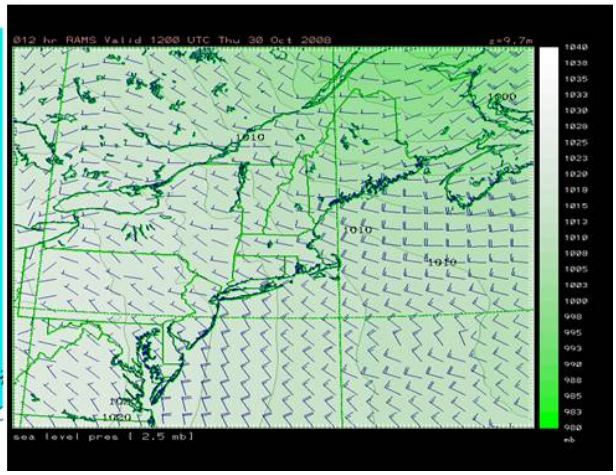

11. Northwest Case 2 November 22nd 2008

Tight NW pressure gradients generated by a low pressure center situated over the Canadian Maritimes and a high pressure system over the Carolinas. Strong and characteristically gusty NW conditions exist through Nov 22nd. Average wind speeds generally between mid twenties and low thirties through the morning hours, with gusts to mid and upper thirties (mph). Through the afternoon generally stronger conditions exist with averages in the low to upper thirties and gusts into the forties. Stronger winds are likely mixing to the surface from aloft as a result of cold air advection over relatively warm sea surface temperatures, as well as a component of mechanical turbulence generated over surface roughness.

Pressure gradients eased dramatically through the morning of Nov 23rd as high pressure built into New England from the southwest and low pressure pushed away to the northeast of the Canadian Maritimes.

Verification trends are similar to the previous northwest case with the only difference being that speeds are actually over predicted at the jetty for a short period and that same stronger speed feature is seen at the airport, yielding the only period during the run where the usual under-prediction bias is reduced to zero. Similar to the west wind case, the model does really "get it right" but more likely is unable to resolve an embedded wave from a departing strong low pressure system.

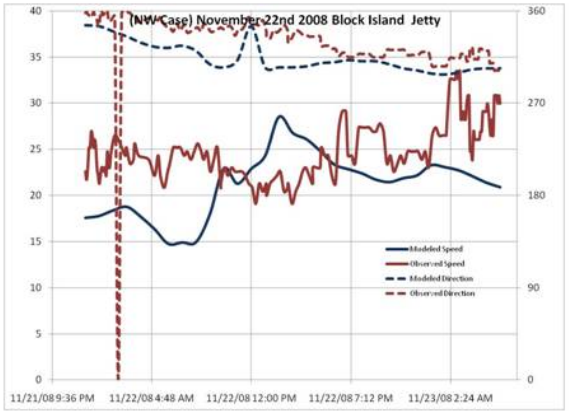

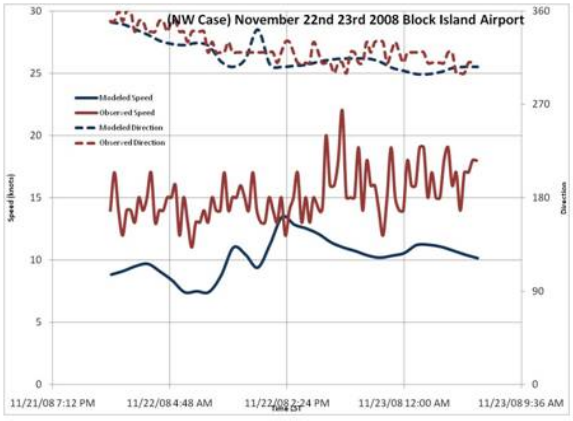

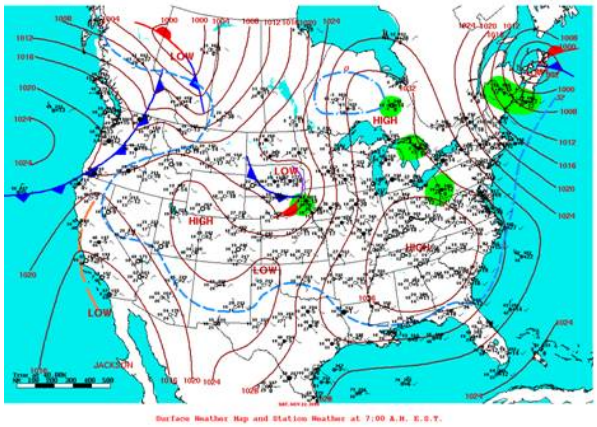

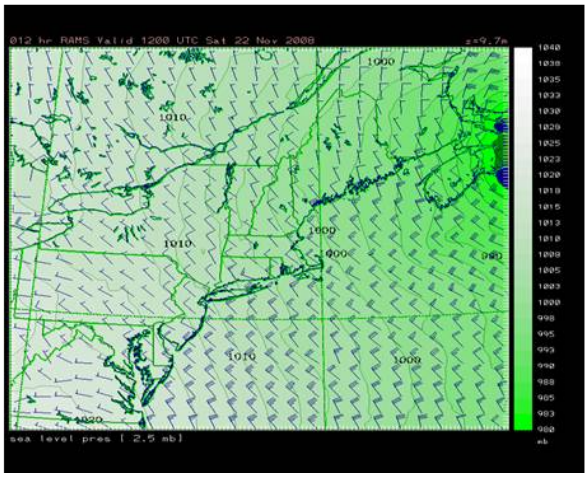

12. NW Case 3 February 23 2009

Low pressure, 992mb, centered over Nova Scotia, maintaining cyclonic flow across New England. Ridge of high pressure established to the west of the Great Lakes and moving gradually eastward. Strong WNW to NW winds throughout the day, starting out with averages to around 40mph and gusts to 50mph. As pressure gradients gradually relax through the day, wind speeds gradually ease into the mid to low thirties. Eventually wind strengths drop into the upper twenties by 2300 (local time).

Finally, for this third northwest case, with only jetty observations available from the archive, the results are roughly the same as with the previous cases - good agreement with observed and modeled direction and an under-prediction of speeds, highest during the initial surge of colder air over a relatively warm, unmixed water column. Of note, as stronger flow persists over time, the water column will mix and cool, thus reducing the difference between air and sea temperatures. The result is less efficient momentum transfer of stronger flow from aloft propagating down to the surface.

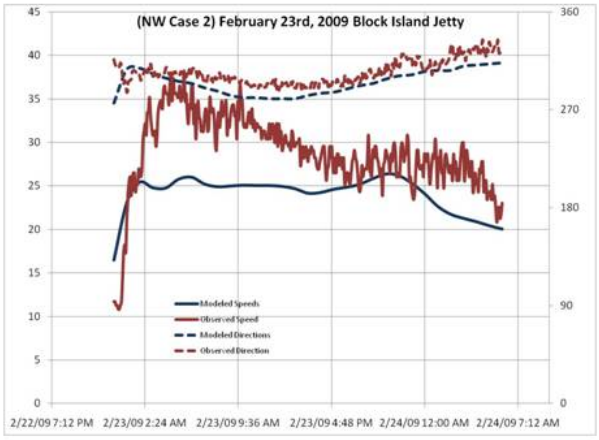

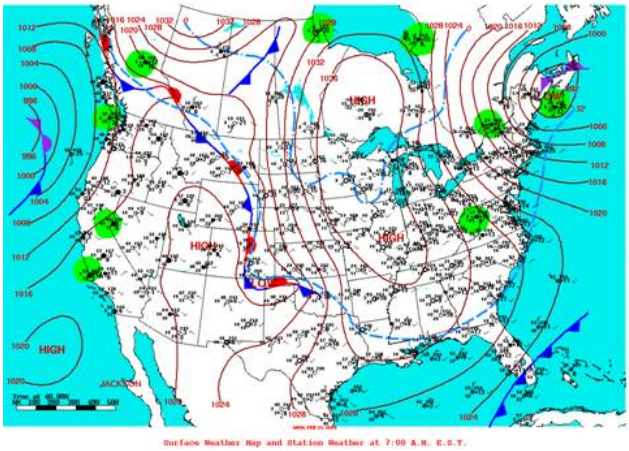

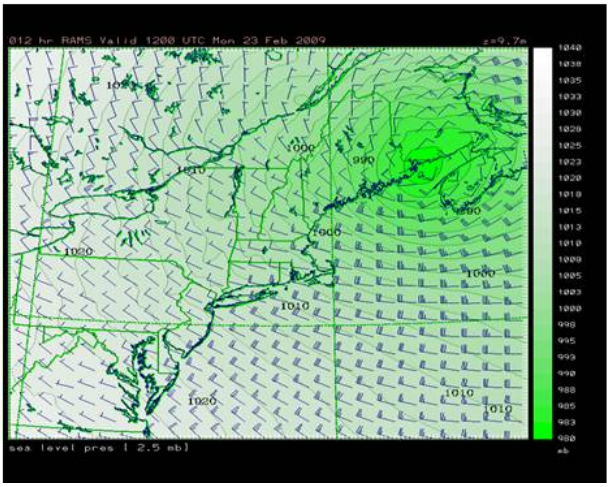

Appendix C

Template Method for Finding Average Annual Wind Speed

The template method for estimating the average annual winds at any point around the area of interest used wind patterns associated with wind fields emanating from the 8 points of the compass. The wind data used for the patterns was developed as hindcasts of 8 different wind regimes using a 3D, fine grid meteorological model of the area. In addition, the template method also used a long term wind speed directional distributions (rose) for determination of the frequency distribution of speeds and directions in the area.

The method for estimating the annual average wind speed is to use the long term wind rose (8 directions and 1 to 20m/s speed bins) from the WIS station and perform a weighted average of the 8 modeled wind regimes using the distributions. From that weighted average, an annual average wind speed is developed for every grid cell of the modeled domain. Using the 3D modeled templates, the estimates can be determined for any height, but the focus here was on the 80m hub height of proposed offshore wind turbines.

The methodology may be summarized as follows:

$$\sum_{w_{dir}=1}^{8} \sum_{w_I=1}^{20} \frac{Winds_{80}(w_{dir})}{SC_{80}(w_{dir})} * wndBin(w_I) * F(WIS_{10} * (80/10)^{\alpha w_{dir}} | (w_I, w_{dir}))$$

w_{dir} is the wind direction (N, NE, E, SE, S, SW, W, NW)

w_I is the wind speed (winds from 1 to 20 m/s)

$Winds_{80}(w_{dir})$ is the average wind speed for a given direction (wdir) at 80 meters based on the meteorological model

$wndBin(w_I)$ is the wind speed used: winds from 1 to 20 m/s

$SC_{80}(w_{dir})$ is the winds near the wind rose at 80 meters in the average meteorological model for a wind direction

WIS_{10}- wind frequency distribution at 10 meters at the wind rose location

$F(WIS_{10} * (80/10)^{alpha\text{-}wdir} | (w_{dir}, w_I))$ is the frequency distribution of rose data extrapolated to 80 meters with a directional alpha, and is dependent on the wind direction and wind speed.

Implementation of the methodology was performed using the following steps:

Build Template:

1) Gather meteorological model results for the 8 different wind directions. Each directional template consisted of a 30 hour hindcast of an actual time period with prevailing winds from the selected direction.

2) Using the location closest to the wind rose, at 80 meters, find the average wind direction for each individual hour of the hindcast. Using the expected wind direction, remove extraneous winds (time steps) that are not in the desired direction.

3) Average all remaining winds from a specific template at 10 and 80 meters.

4) Divide the wind speed values by the velocity in the region of the wind rose.

Determine Shear Coefficient Alpha:

Using the average winds from the template at 10 and 80 meters and the wind shear power law, solve for the wind shear coefficient (alpha):

alpha = (log(Velocity at 80 meters) - log(Velocity at 10 meters)) / (log(80) - log(10));

Find Wind Distribution:

1) Import the wind data to generate the wind rose (if not already available)

2) Using the wind shear equation, project 10m rose winds to 80m hub height. Scale the wind speed from rose location using the power law and the alpha determined in the previous step, to estimate winds at 80 meters:

V80 = V10 (80/10)alpha

Use alpha values as close to the wind rose station as possible.

3) Bin the values into direction and speed sets (8 wind directions and 0 to 20 m/s, 1 meter wind velocities.) Then divide by the number of wind measurements. Summing all values in the table will equal 100% of the data.

Final Annual Average Winds:

The final annual average wind speed estimate is a weighted average of the templates based on the wind distributions at the different speeds. For every wind speed and direction use the appropriate template, multiplied by the current wind speed bin and the distribution value. Then sum all weighted templates. The result is an average wind speed for each cell in the model domain based on the long term speed and direction frequency distribution. A similar strategy can be applied to estimate wind power.

Appendix D

Evaluation of the linear scaling analysis used in the template based method.

In the template based method, it is assumed that for a given wind direction the spatial pattern is similar and that wind speeds scale linearly relative to a reference location. To test this assumption, hindcast simulations for the period from October 1, 2009 to February 28, 2010 (Spaulding et al, 2010b) were reviewed to identify all the time periods for which winds were from the NW. NW winds have been selected since these dominant the hindcast period. These are also winds that dominate the wind power density roses in the vicinity of the renewable energy zone. These events are highlighted in blue in Figure 1. All wind speeds for each NW hindcast period were averaged over the study period to generate an average wind speed and power density map for NW winds (Figure 2). The mean wind speeds over a given event were divided by the average value over all events. The resulting map represents the scaling required to convert the mean wind speed map for all events to the wind speed map for a given event. The scaling maps for each NW event period are provided below. Table 1 (below) summarizes the upper and lower limits for each case. The differences in the scaling values for a given map are the focus here. Ideally the values are all the same, which represents linearly scaling. The scaling values for the various events range from 0.5 to 2, with most of values in the range of 0.8 to 1.2. The variation in the value of scaling parameters for a given time event is typically quite small and never larger than 10%. The average for all cases ranges from 0.979 to 1.05, or 6.6%. Linear scaling hence is a reasonable approximation.

Table 1 Scaling factors by time period for inner scaling of NW wind cases

Start Date	Start Time	End Date	End Time	Scale Factor Lower	Scale Factor Upper	Difference	% Difference
21-Feb	20	22-Feb	16	0.95	1	0.05	5.13
21-Feb	6	21-Feb	11	1.1	1.25	0.15	12.77
20-Feb	22	21-Feb	2	0.85	1.15	0.3	30.00
19-Feb	19	20-Feb	16	1.05	1.15	0.1	0.09
17-Feb	2	17-Feb	9	1.2	1.3	0.1	8.00
18-Feb	10	19-Feb	0	1.05	1.1	0.05	4.65
13-Feb	0	13-Feb	17	0.76	0.8	0.04	5.13
14-Feb	1	14-Feb	8	1.1	1.2	0.1	8.70
11-Feb	21	12-Feb	19	.95	1.05	0.1	10.00
8-Feb	16	9-Feb	16	1.1	1.2	0.1	8.70
7-Feb	14	8-Feb	10	1.09	1.1	0.01	0.91
4-Feb	2	5-Feb	16	0.85	0.9	0.05	5.71
2-Feb	4	2-Feb	16	0.505	0.55	0.045	8.53
29-Jan	4	29-Jan	14	1.55	1.7	0.15	9.23
30-Jan	2	30-Jan	18	1.17	1.2	0.03	2.53
13-Jan	9	14-Jan	7	0.63	0.65	0.02	3.13
12-Jan	4	13-Jan	1	0.68	0.7	0.02	2.90
10-Jan	20	11-Jan	2	0.68	0.71	0.03	4.32
9-Jan	2	9-Jan	22	0.92	1.1	0.18	17.82
8-Jan	3	8-Jan	15	0.45	0.5	0.05	10.53
6-Jan	2	7-Jan	17	0.95	0.95	0	0.00
5-Jan	2	7-Jan	17	0.95	0.95	0	0.00
3-Jan	13	5-Jan	14	1.23	1.3	0.07	5.53
3-Jan	0	3-Jan	9	1.9	2.05	0.15	7.53
29-Dec	14	30-Dec	16	1.35	1.4	0.05	3.54
23-Dec	20	24-Dec	11	1.1	1.15	0.05	4.44
20-Dec	17	23-Dec	9	1.25	1.35	0.1	7.69
17-Dec	2	18-Dec	3	1.25	1.25	0	0.00
16-Dec	2	16-Dec	19	1.06	1.1	0.04	3.70
8-Dec	8	8-Dec	23	0.6	0.6	0	0.00
6-Dec	11	7-Dec	12	0.77	0.8	0.03	3.82
4-Nov	3	4-Nov	17	0.9	0.95	0.05	5.41
19-Oct	19	20-Oct	10	0.45	0.5	0.05	10.53
8-Oct	6	9-Oct	5	1	1	0	0.00
1-Oct	0	1-Oct	11	0.95	0.9	0.05	5.71
			Avg.	0.98	1.04	0.066	6.19

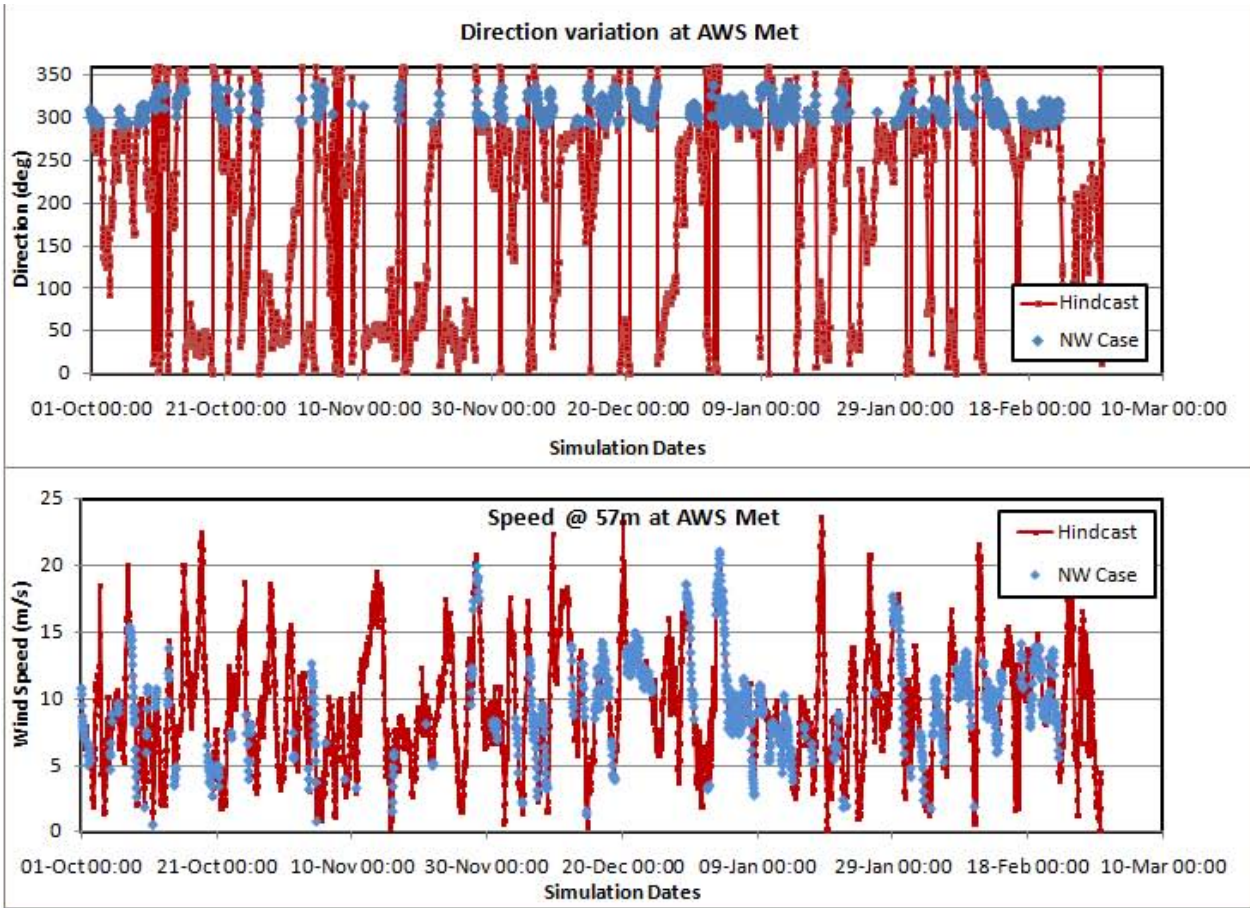

Figure 1 RAMS model predicted winds direction (upper panel) and speed (lower panel) at AWS Met, at 57 m elevation from October 1, 2009 through February 28, 2010.

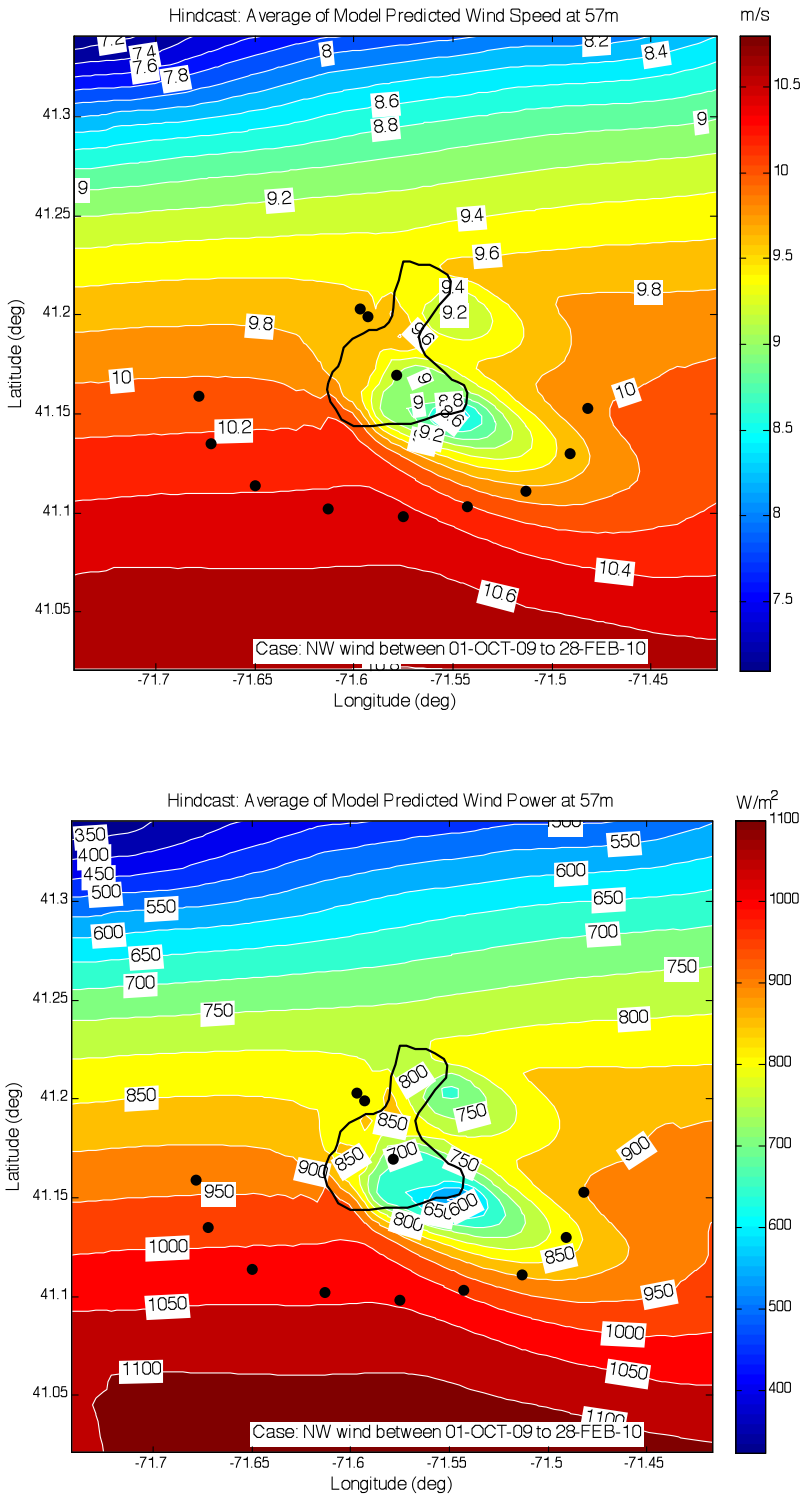

Figure 2 Model predicted average wind speed (upper panel) and wind power density (lower panel) at 57 m for all NW wind cases.

Figures that follow show model predicted scaling parameter, relative to the mean value over each individual event.

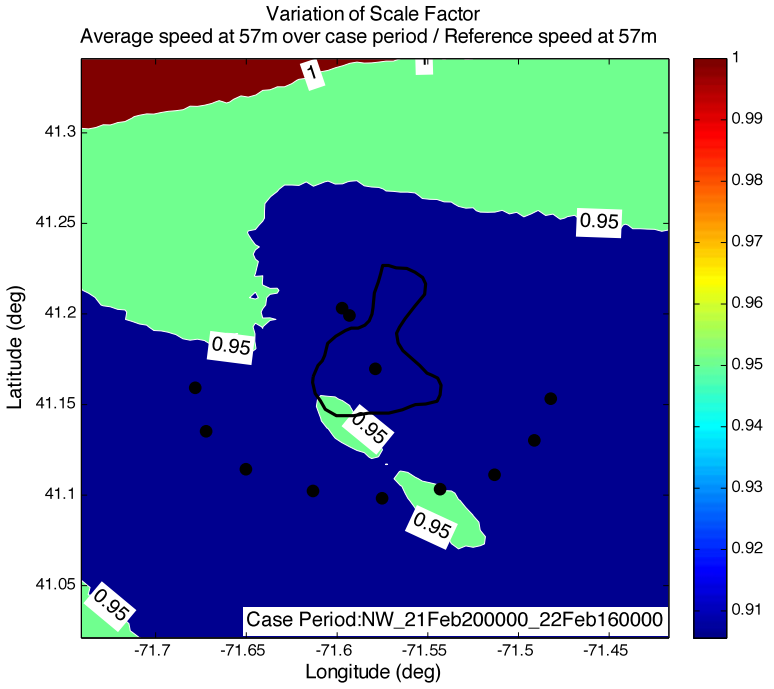
Variation of Scale Factor
Average speed at 57m over case period / Reference speed at 57m
1
0.95
0.95
0.95
0.95
Case Period:NW_21Feb200000_22Feb160000
Latitude (deg)
Longitude (deg)
41.3
41.25
41.2
41.15
41.1
41.05
-71.7
-71.65
-71.6
-71.55
-71.5
-71.45
1
0.99
0.98
0.97
0.96
0.95
0.94
0.93
0.92
0.91

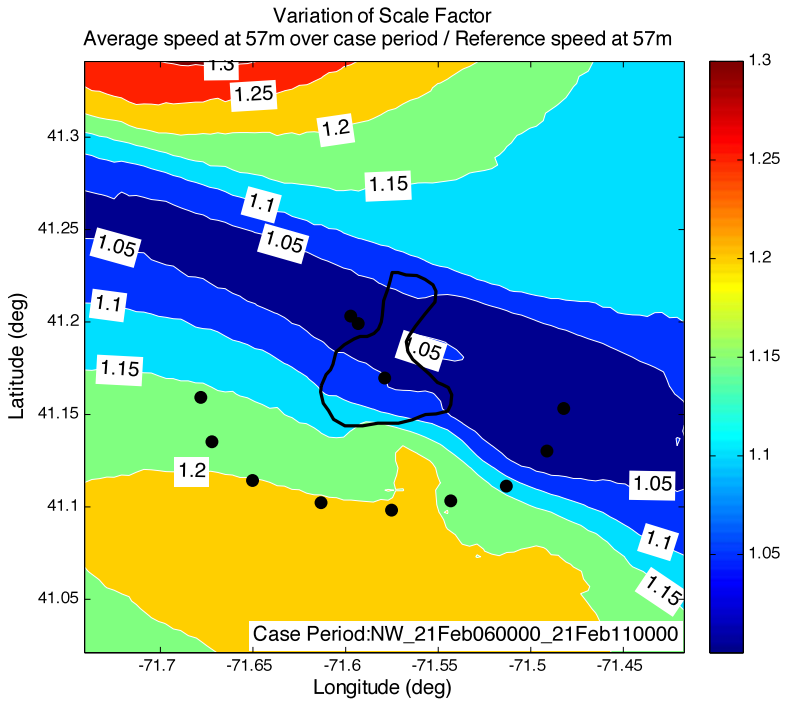
Variation of Scale Factor
Average speed at 57m over case period / Reference speed at 57m
1.25
1.2
1.15
1.1
1.05
1.05
1.1
1.15
1.2
1.05
1.05
1.1
1.15
Case Period:NW_21Feb060000_21Feb110000
Latitude (deg)
Longitude (deg)
41.3
41.25
41.2
41.15
41.1
41.05
-71.7
-71.65
-71.6
-71.55
-71.5
-71.45
1.3
1.25
1.2
1.15
1.1
1.05

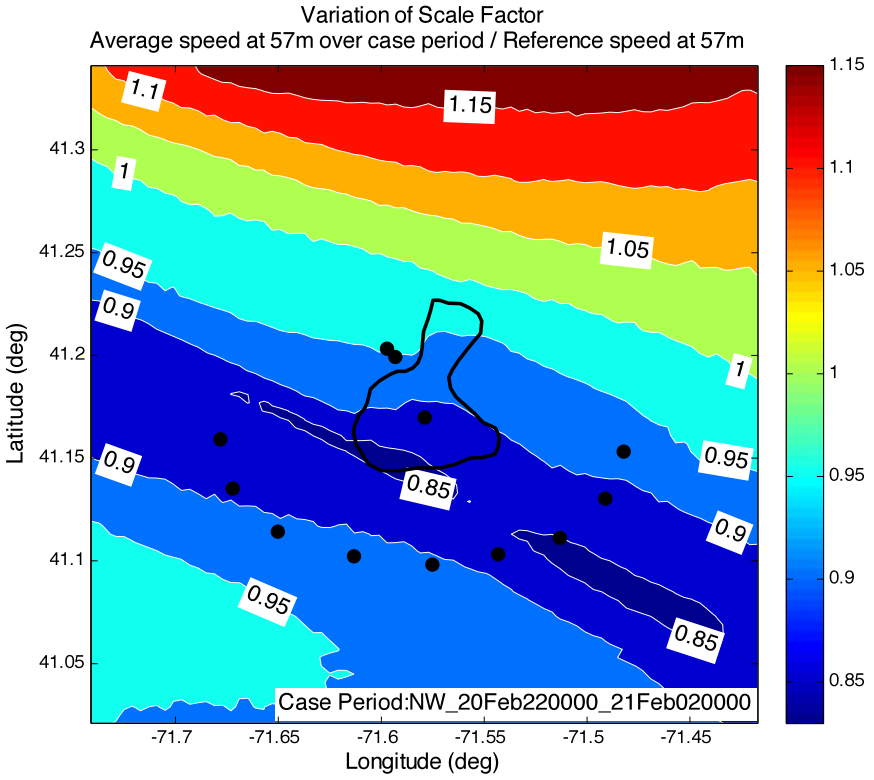
Variation of Scale Factor
Average speed at 57m over case period / Reference speed at 57m
1.1
1.15
1
1.05
0.95
0.9
0.85
Case Period:NW_20Feb220000_21Feb020000
Latitude (deg)
Longitude (deg)
41.3
41.25
41.2
41.15
41.1
41.05
-71.7
-71.65
-71.6
-71.55
-71.5
-71.45
1.15
1.1
1.05
1
0.95
0.9
0.85

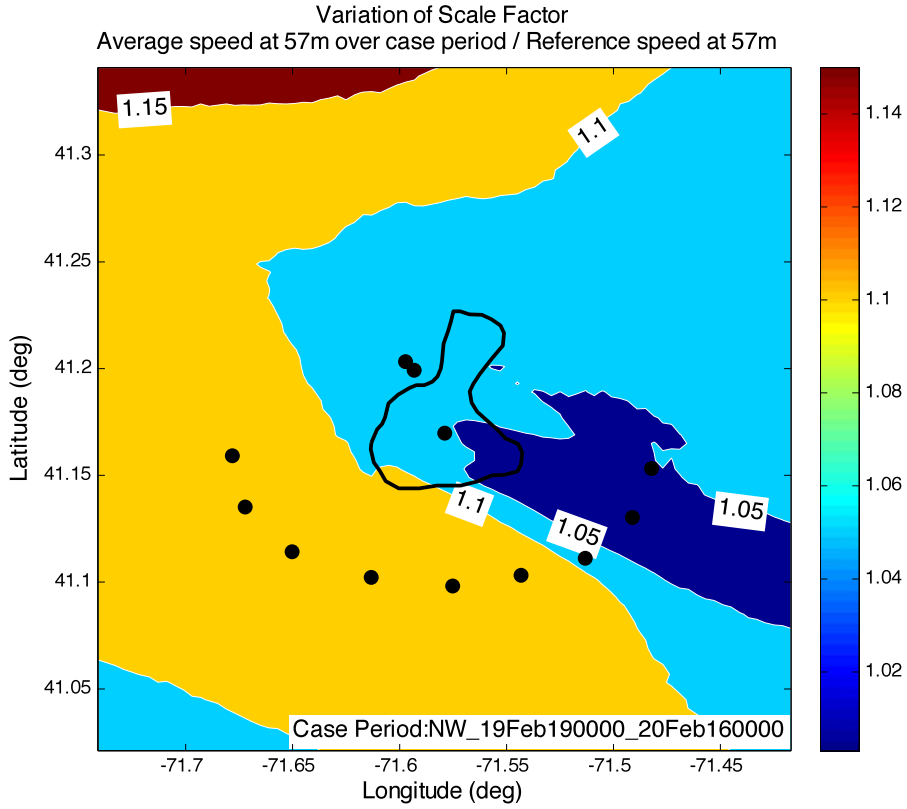
Variation of Scale Factor
Average speed at 57m over case period / Reference speed at 57m
1.15
1.1
1.05
Case Period:NW_19Feb190000_20Feb160000
Latitude (deg)
Longitude (deg)
41.3
41.25
41.2
41.15
41.1
41.05
-71.7
-71.65
-71.6
-71.55
-71.5
-71.45
1.14
1.12
1.1
1.08
1.06
1.04
1.02

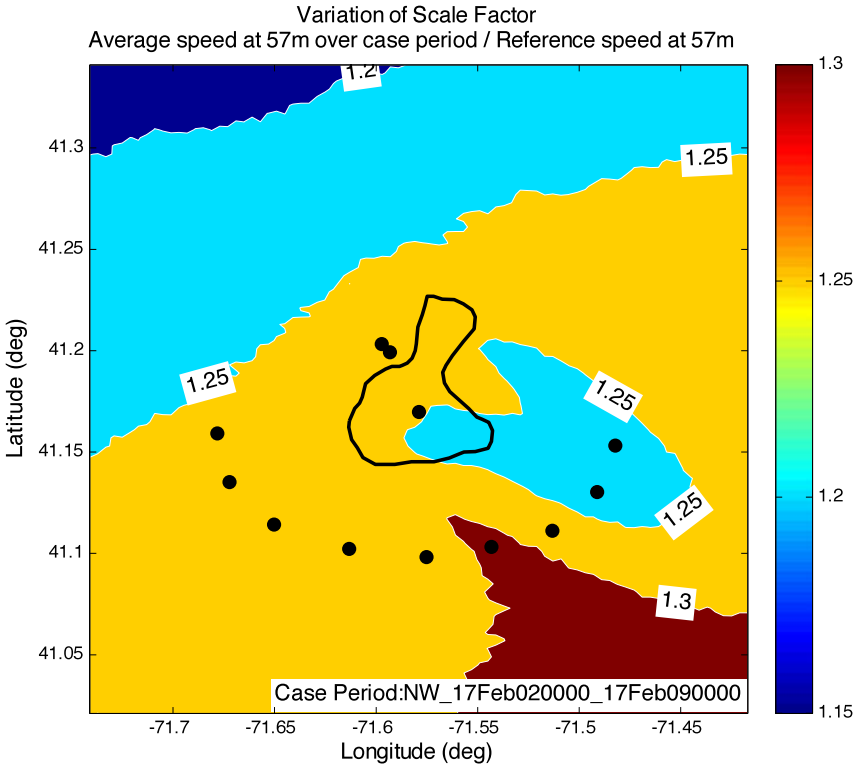
Variation of Scale Factor
Average speed at 57m over case period / Reference speed at 57m
1.25
1.25
1.25
1.25
1.3
Case Period:NW_17Feb020000_17Feb090000
Latitude (deg)
Longitude (deg)
41.3
41.25
41.2
41.15
41.1
41.05
-71.7
-71.65
-71.6
-71.55
-71.5
-71.45
1.3
1.25
1.2
1.15

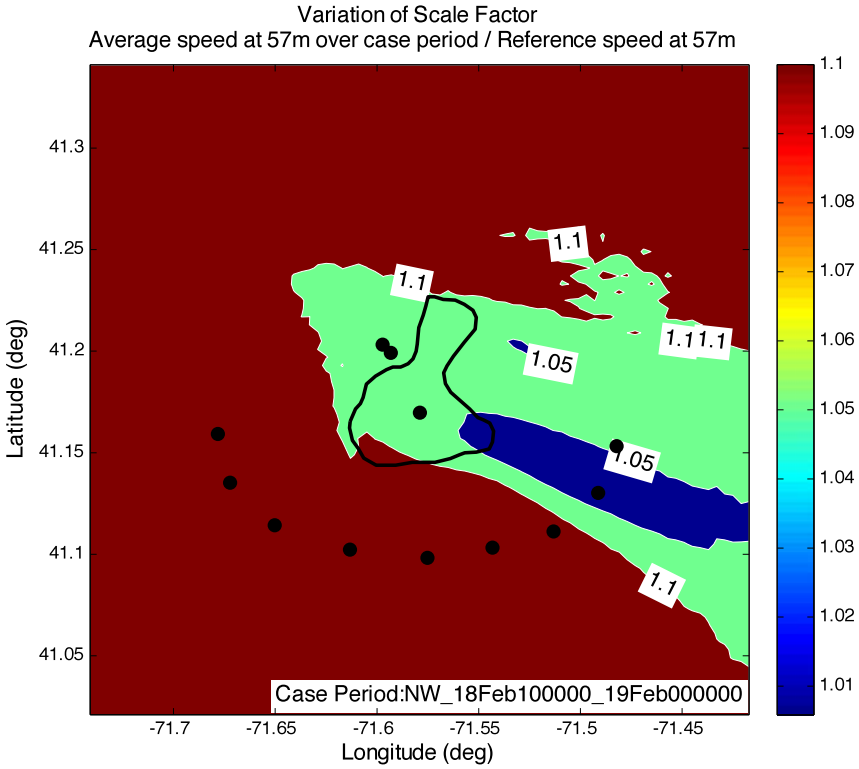
Variation of Scale Factor
Average speed at 57m over case period / Reference speed at 57m
1.1
1.1
1.1
1.1
1.05
1.05
Case Period:NW_18Feb100000_19Feb000000
Latitude (deg)
Longitude (deg)
41.3
41.25
41.2
41.15
41.1
41.05
-71.7
-71.65
-71.6
-71.55
-71.5
-71.45
1.1
1.09
1.08
1.07
1.06
1.05
1.04
1.03
1.02
1.01

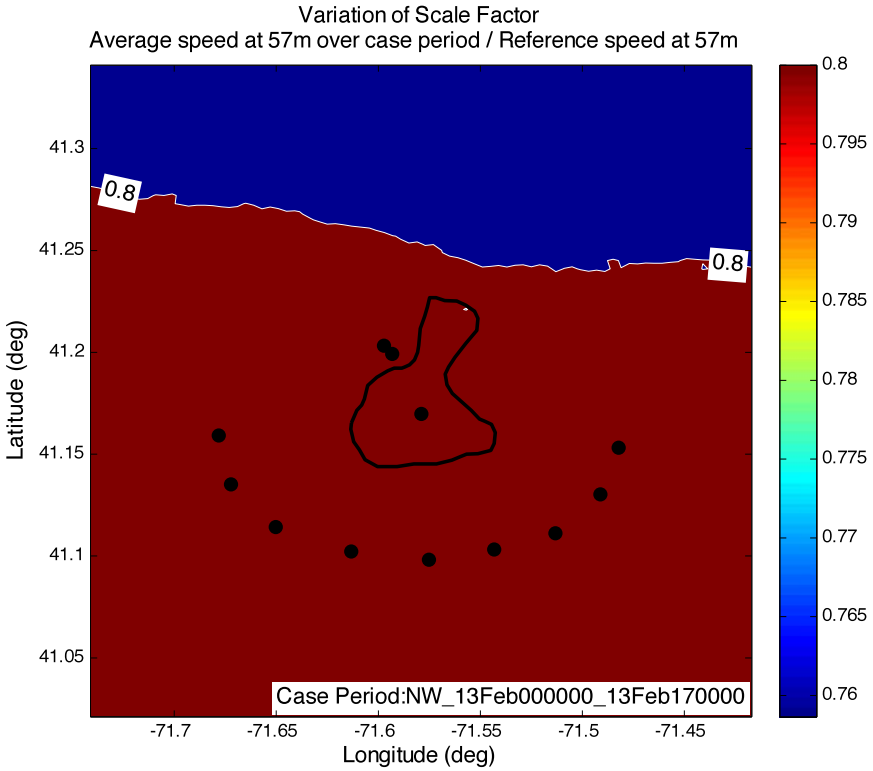
Variation of Scale Factor
Average speed at 57m over case period / Reference speed at 57m
0.8
0.8
Case Period:NW_13Feb000000_13Feb170000
Latitude (deg)
Longitude (deg)
41.3
41.25
41.2
41.15
41.1
41.05
-71.7
-71.65
-71.6
-71.55
-71.5
-71.45
0.8
0.795
0.79
0.785
0.78
0.775
0.77
0.765
0.76

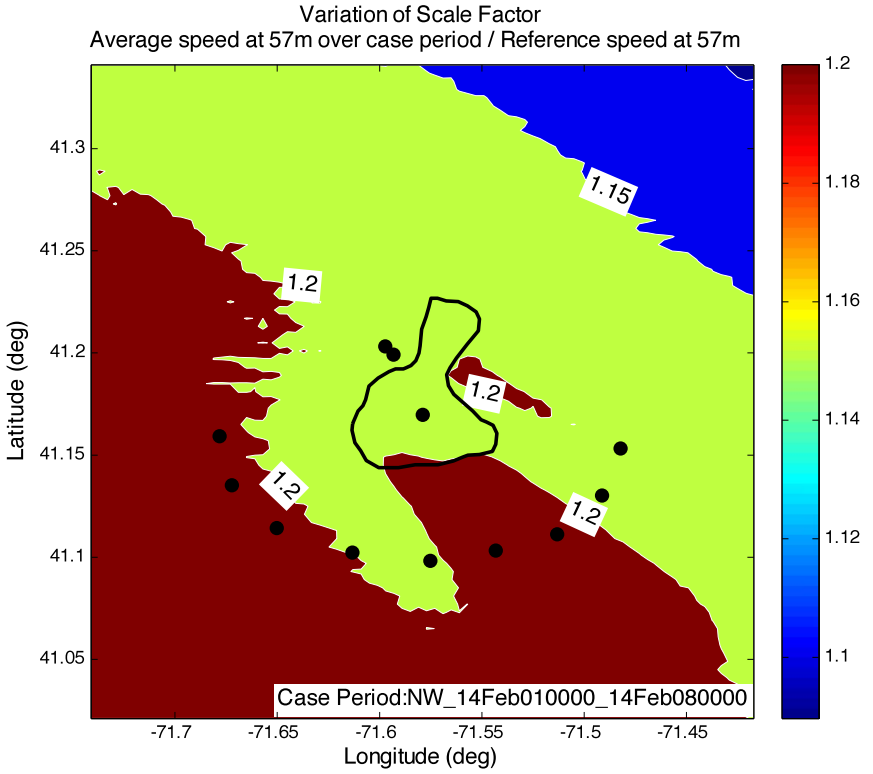
Variation of Scale Factor
Average speed at 57m over case period / Reference speed at 57m
1.15
1.2
1.2
1.2
1.2
Case Period:NW_14Feb010000_14Feb080000
Latitude (deg)
Longitude (deg)
41.3
41.25
41.2
41.15
41.1
41.05
-71.7
-71.65
-71.6
-71.55
-71.5
-71.45
1.2
1.18
1.16
1.14
1.12
1.1

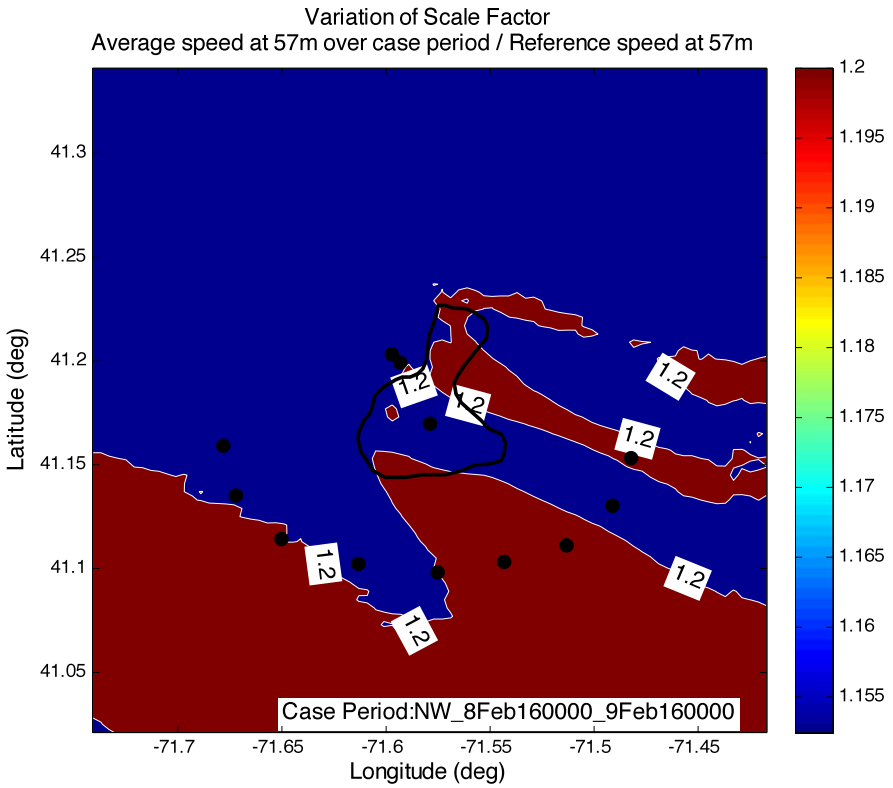
Variation of Scale Factor
Average speed at 57m over case period / Reference speed at 57m
Latitude (deg)
Longitude (deg)
41.3
41.25
41.2
41.15
41.1
41.05
-71.7
-71.65
-71.6
-71.55
-71.5
-71.45
1.2
1.195
1.19
1.185
1.18
1.175
1.17
1.165
1.16
1.155
Case Period:NW_8Feb160000_9Feb160000

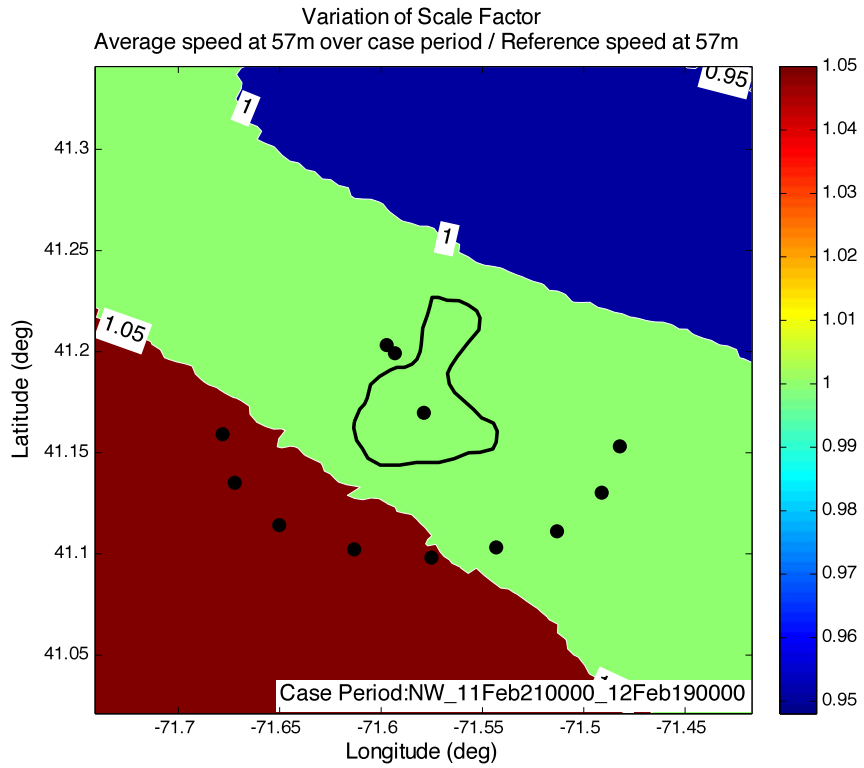
Variation of Scale Factor
Average speed at 57m over case period / Reference speed at 57m
Latitude (deg)
Longitude (deg)
41.3
41.25
41.2
41.15
41.1
41.05
-71.7
-71.65
-71.6
-71.55
-71.5
-71.45
1.05
1.04
1.03
1.02
1.01
1
0.99
0.98
0.97
0.96
0.95
Case Period:NW_11Feb210000_12Feb190000

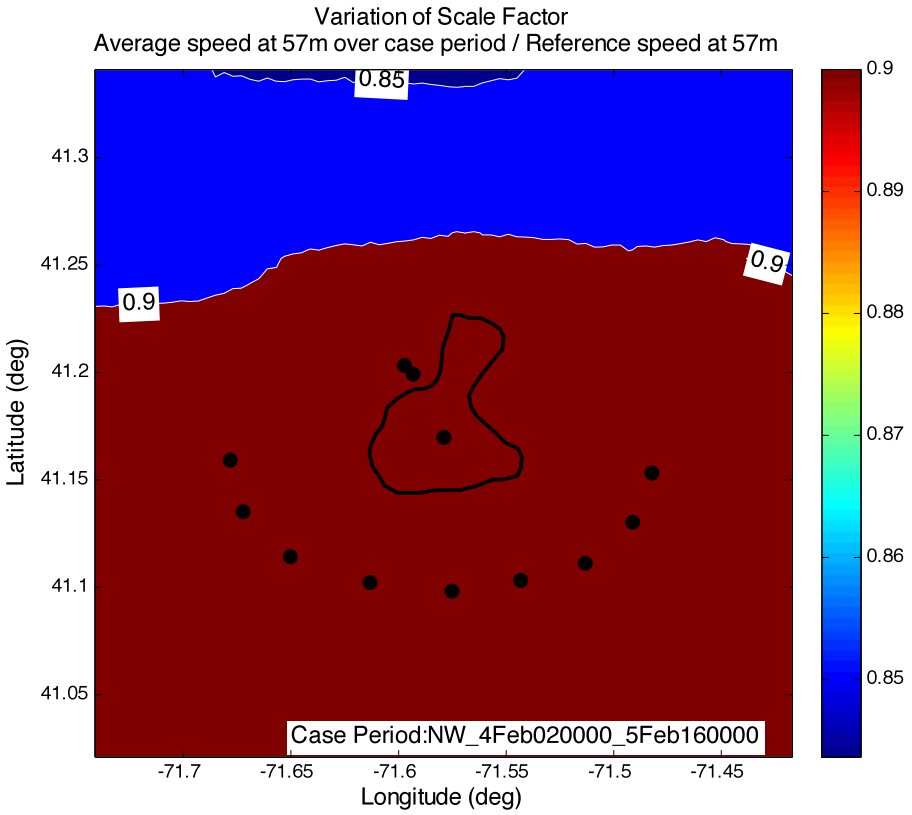
Variation of Scale Factor
Average speed at 57m over case period / Reference speed at 57m
0.85
0.9
0.9
Case Period:NW_4Feb020000_5Feb160000
Latitude (deg)
41.3
41.25
41.2
41.15
41.1
41.05
-71.7
-71.65
-71.6
-71.55
-71.5
-71.45
Longitude (deg)
0.9
0.89
0.88
0.87
0.86
0.85

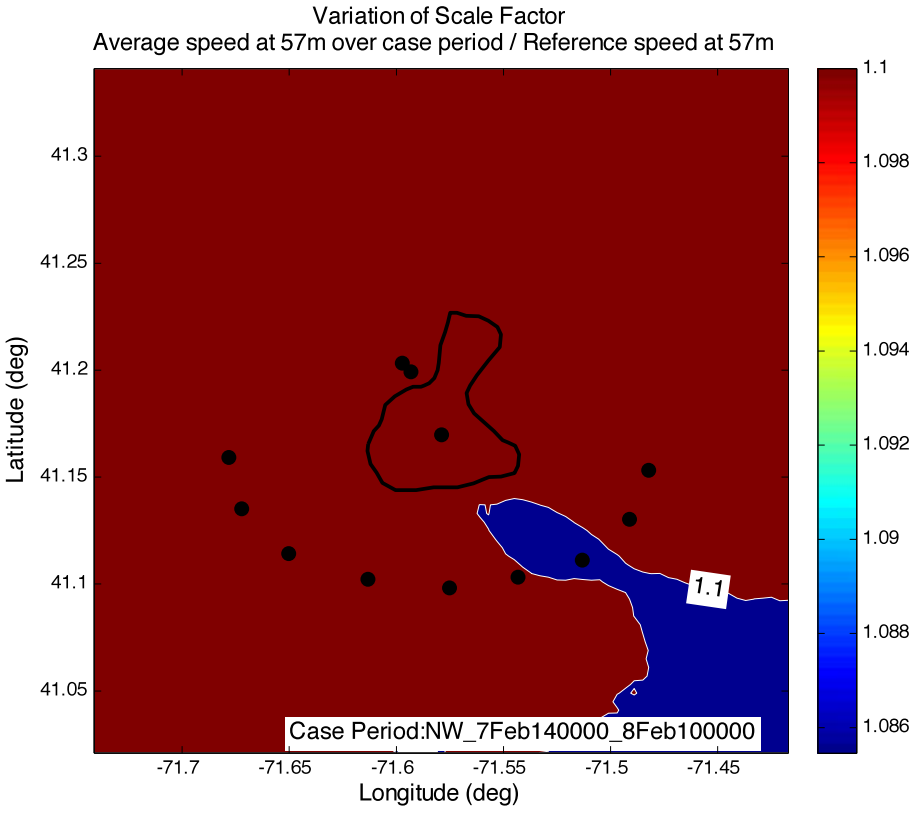
Variation of Scale Factor
Average speed at 57m over case period / Reference speed at 57m
1.1
Case Period:NW_7Feb140000_8Feb100000
Latitude (deg)
41.3
41.25
41.2
41.15
41.1
41.05
-71.7
-71.65
-71.6
-71.55
-71.5
-71.45
Longitude (deg)
1.1
1.098
1.096
1.094
1.092
1.09
1.088
1.086

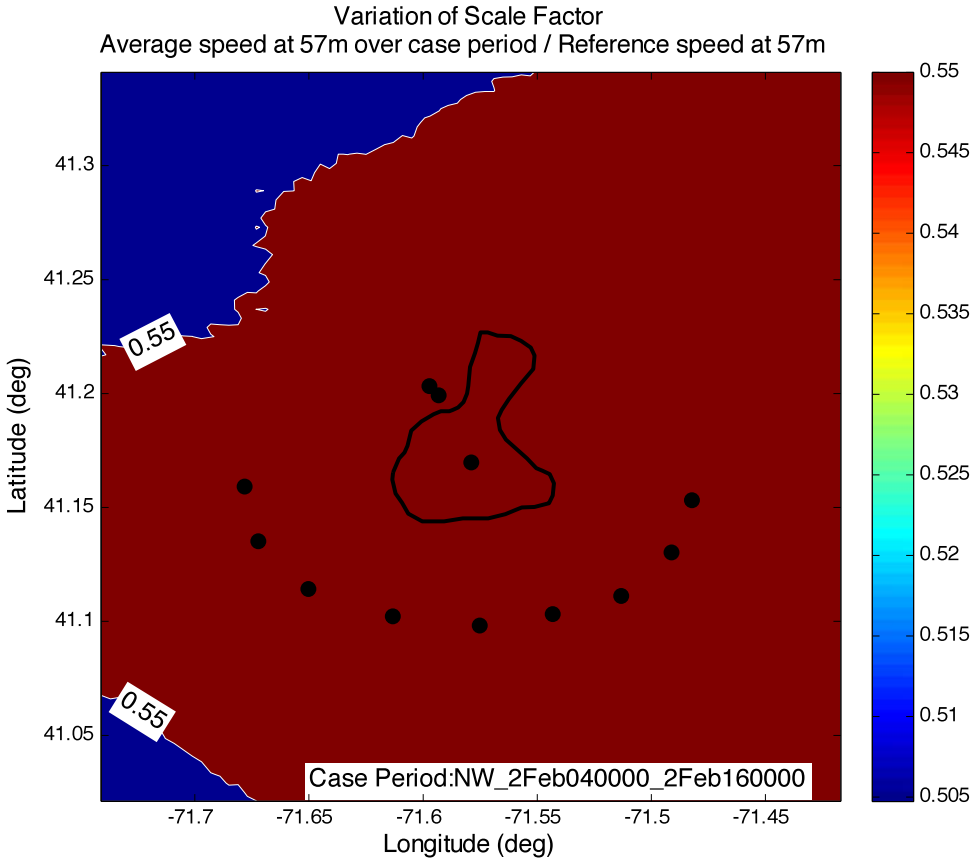
Variation of Scale Factor
Average speed at 57m over case period / Reference speed at 57m
0.55
0.55
Case Period:NW_2Feb040000_2Feb160000
Latitude (deg)
Longitude (deg)
41.3
41.25
41.2
41.15
41.1
41.05
-71.7
-71.65
-71.6
-71.55
-71.5
-71.45
0.55
0.545
0.54
0.535
0.53
0.525
0.52
0.515
0.51
0.505

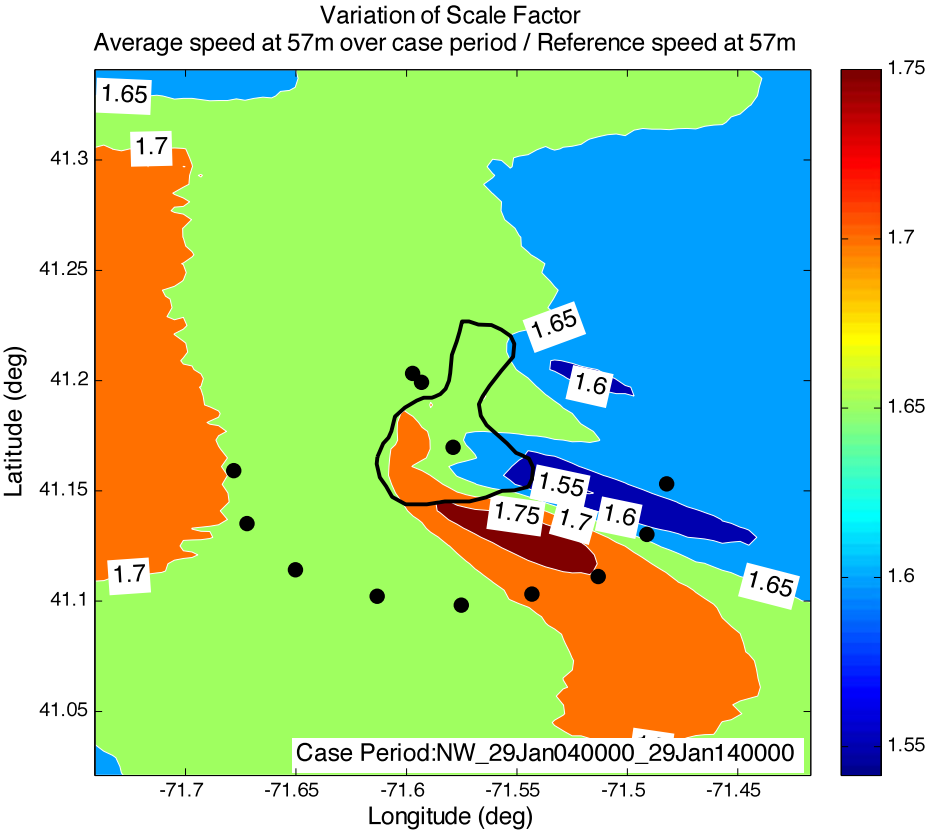
Variation of Scale Factor
Average speed at 57m over case period / Reference speed at 57m
1.65
1.7
1.65
1.6
1.55
1.75
1.7
1.6
1.7
1.65
Case Period:NW_29Jan040000_29Jan140000
Latitude (deg)
Longitude (deg)
41.3
41.25
41.2
41.15
41.1
41.05
-71.7
-71.65
-71.6
-71.55
-71.5
-71.45
1.75
1.7
1.65
1.6
1.55

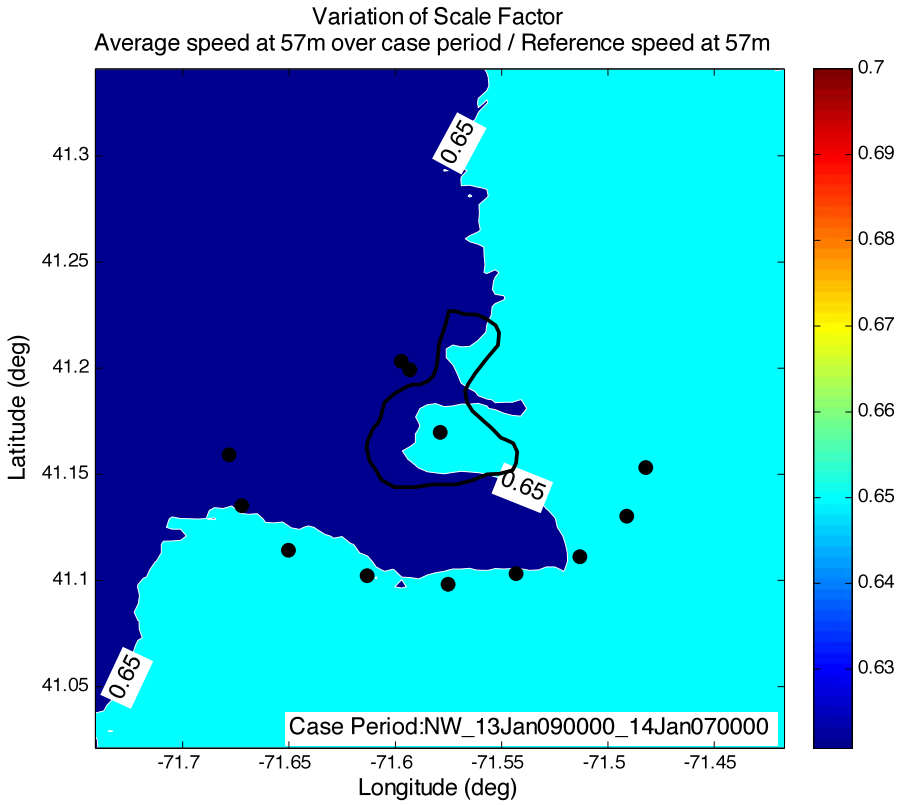
Variation of Scale Factor
Average speed at 57m over case period / Reference speed at 57m
0.65
0.65
0.65
Case Period:NW_13Jan090000_14Jan070000
Latitude (deg)
Longitude (deg)
41.3
41.25
41.2
41.15
41.1
41.05
-71.7
-71.65
-71.6
-71.55
-71.5
-71.45
0.7
0.69
0.68
0.67
0.66
0.65
0.64
0.63

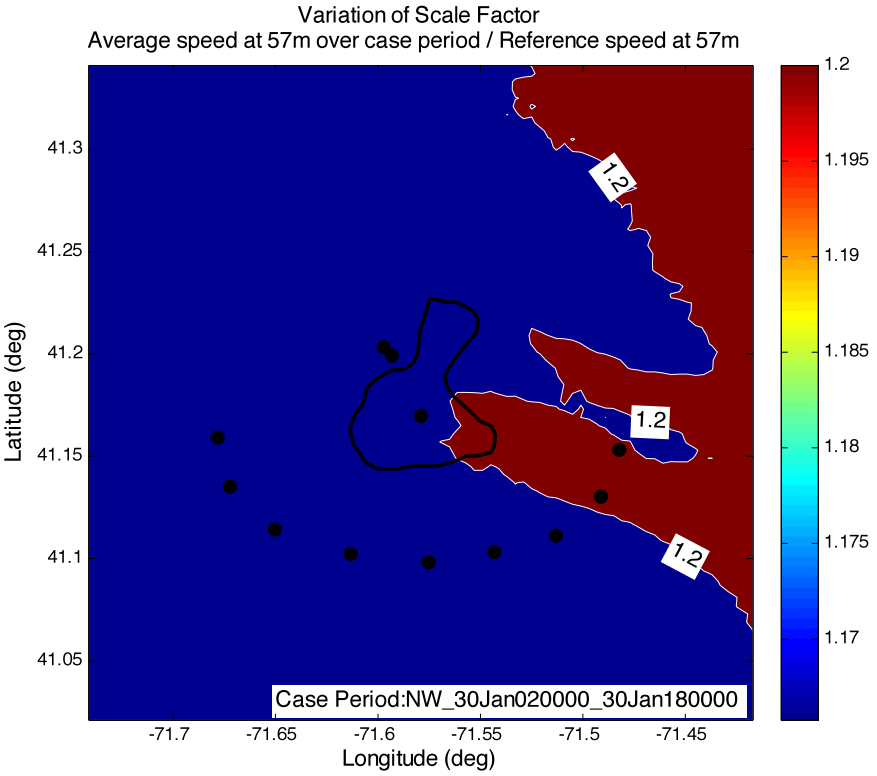
Variation of Scale Factor
Average speed at 57m over case period / Reference speed at 57m
1.2
1.2
1.2
Case Period:NW_30Jan020000_30Jan180000
Latitude (deg)
Longitude (deg)
41.3
41.25
41.2
41.15
41.1
41.05
-71.7
-71.65
-71.6
-71.55
-71.5
-71.45
1.2
1.195
1.19
1.185
1.18
1.175
1.17

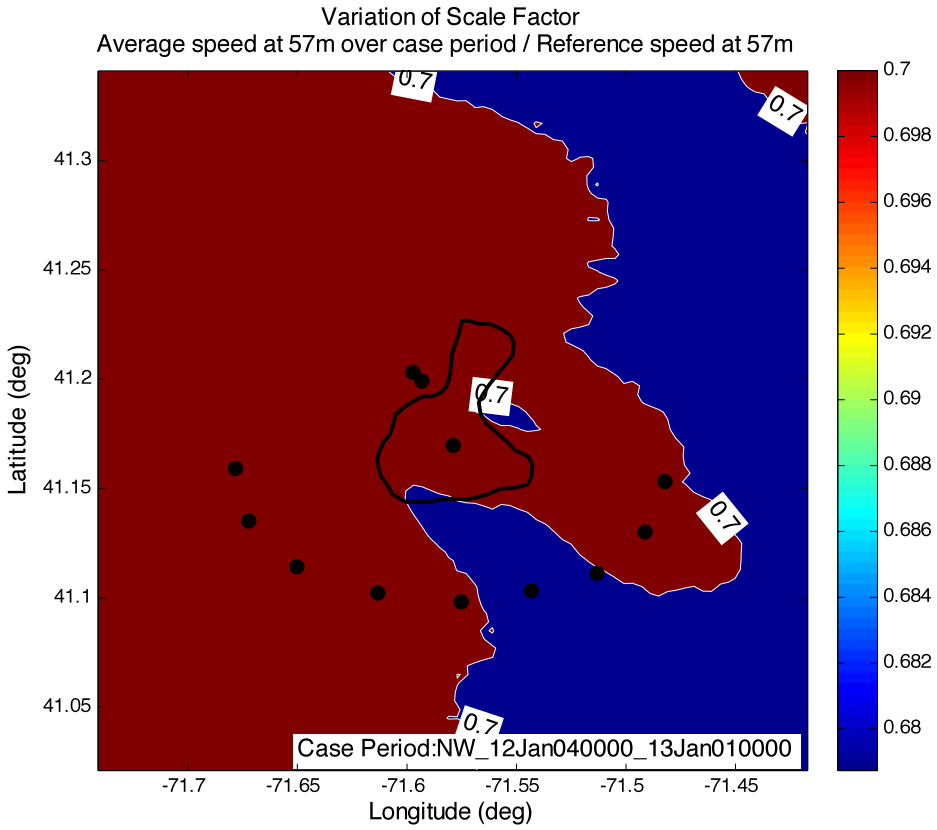
Variation of Scale Factor
Average speed at 57m over case period / Reference speed at 57m
0.7
0.7
0.7
0.7
0.7
Case Period:NW_12Jan040000_13Jan010000
41.3
41.25
41.2
41.15
41.1
41.05
Latitude (deg)
-71.7
-71.65
-71.6
-71.55
-71.5
-71.45
Longitude (deg)
0.7
0.698
0.696
0.694
0.692
0.69
0.688
0.686
0.684
0.682
0.68

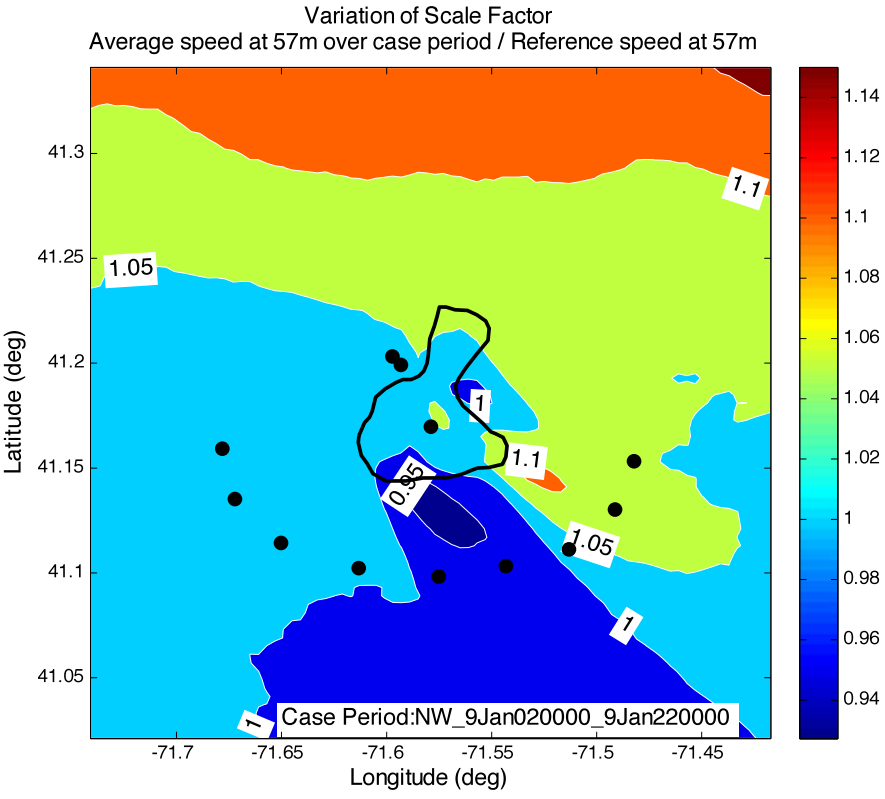
Variation of Scale Factor
Average speed at 57m over case period / Reference speed at 57m
1.1
1.05
1
1.1
0.95
1.05
1
1
Case Period:NW_9Jan020000_9Jan220000
41.3
41.25
41.2
41.15
41.1
41.05
Latitude (deg)
-71.7
-71.65
-71.6
-71.55
-71.5
-71.45
Longitude (deg)
1.14
1.12
1.1
1.08
1.06
1.04
1.02
1
0.98
0.96
0.94

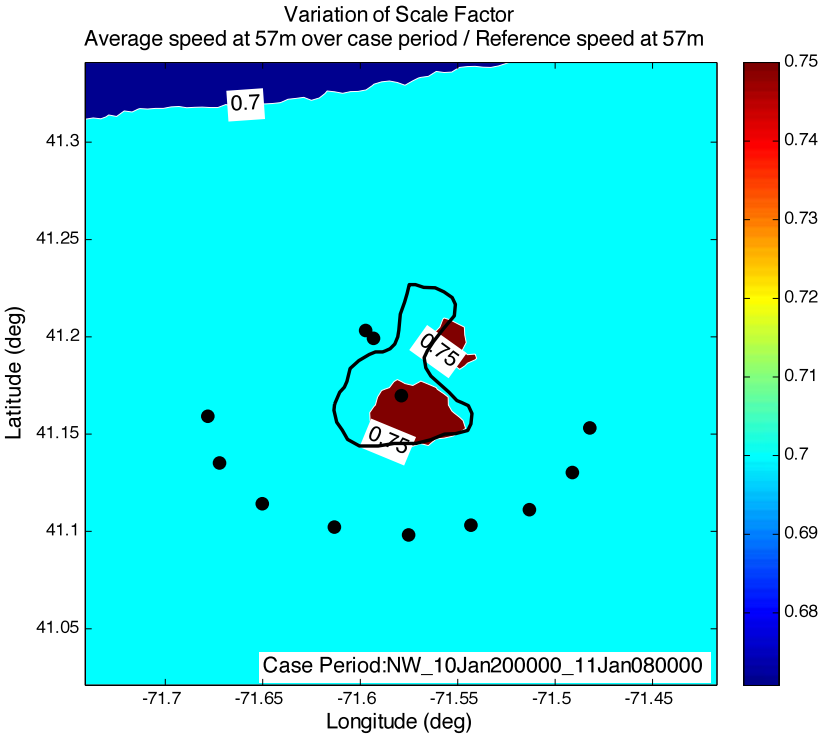
Variation of Scale Factor
Average speed at 57m over case period / Reference speed at 57m
0.7
0.75
0.75
Case Period:NW_10Jan200000_11Jan080000
Latitude (deg)
Longitude (deg)
41.3
41.25
41.2
41.15
41.1
41.05
-71.7
-71.65
-71.6
-71.55
-71.5
-71.45
0.75
0.74
0.73
0.72
0.71
0.7
0.69
0.68

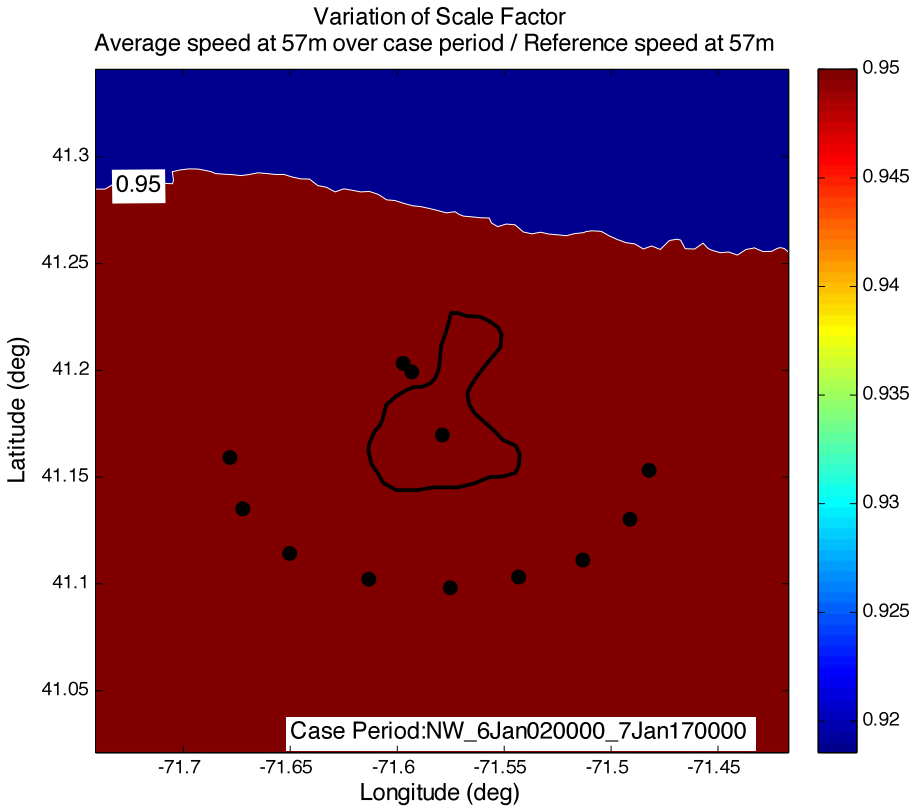
Variation of Scale Factor
Average speed at 57m over case period / Reference speed at 57m
0.95
Case Period:NW_6Jan020000_7Jan170000
Latitude (deg)
Longitude (deg)
41.3
41.25
41.2
41.15
41.1
41.05
-71.7
-71.65
-71.6
-71.55
-71.5
-71.45
0.95
0.945
0.94
0.935
0.93
0.925
0.92

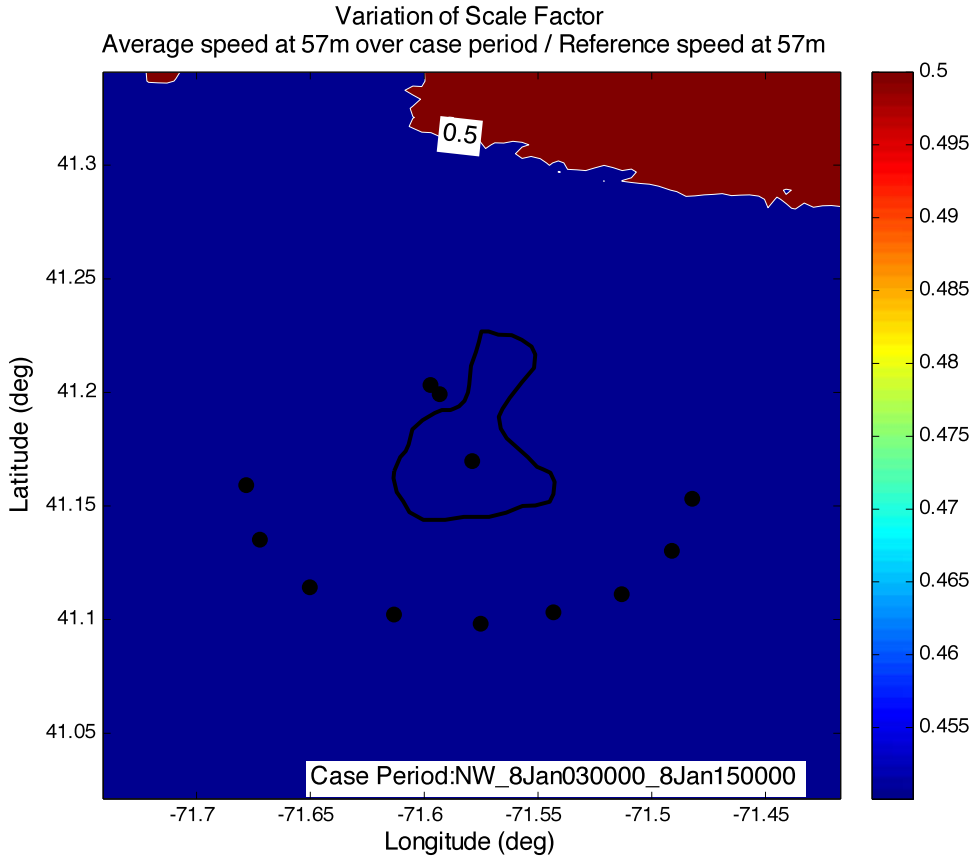
Variation of Scale Factor
Average speed at 57m over case period / Reference speed at 57m
0.5
Case Period:NW_8Jan030000_8Jan150000
Latitude (deg)
Longitude (deg)
41.3
41.25
41.2
41.15
41.1
41.05
-71.7
-71.65
-71.6
-71.55
-71.5
-71.45
0.5
0.495
0.49
0.485
0.48
0.475
0.47
0.465
0.46
0.455

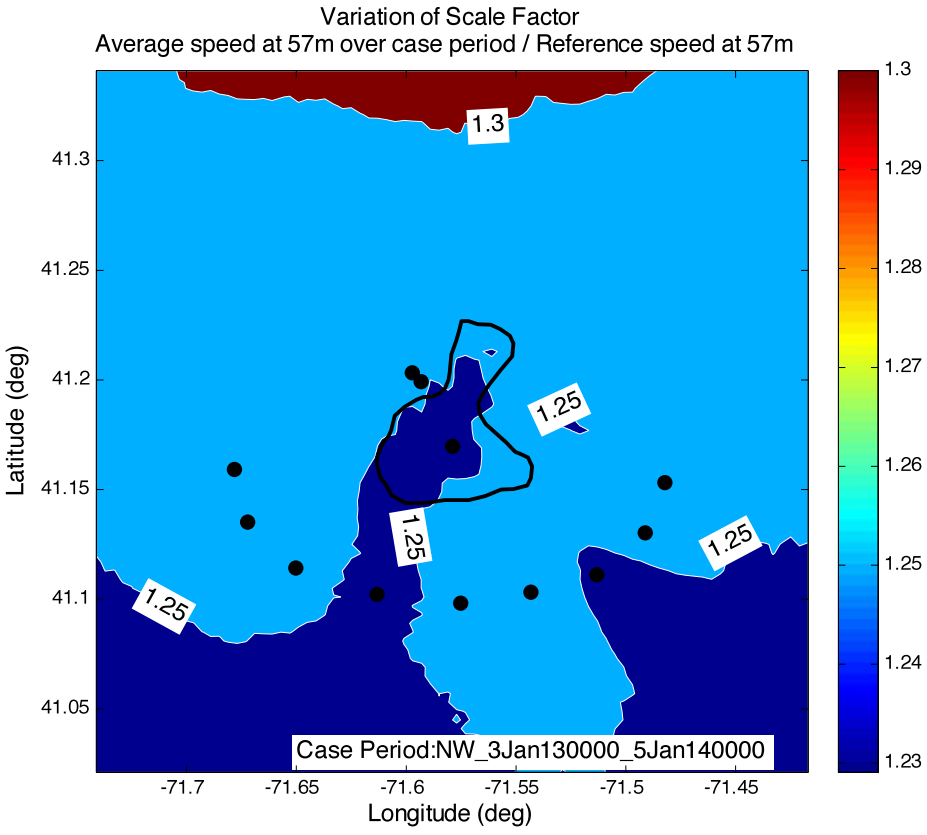
Variation of Scale Factor
Average speed at 57m over case period / Reference speed at 57m
1.3
1.25
1.25
1.25
Case Period:NW_3Jan130000_5Jan140000
Latitude (deg)
Longitude (deg)
41.3
41.25
41.2
41.15
41.1
41.05
-71.7
-71.65
-71.6
-71.55
-71.5
-71.45
1.3
1.29
1.28
1.27
1.26
1.25
1.24
1.23

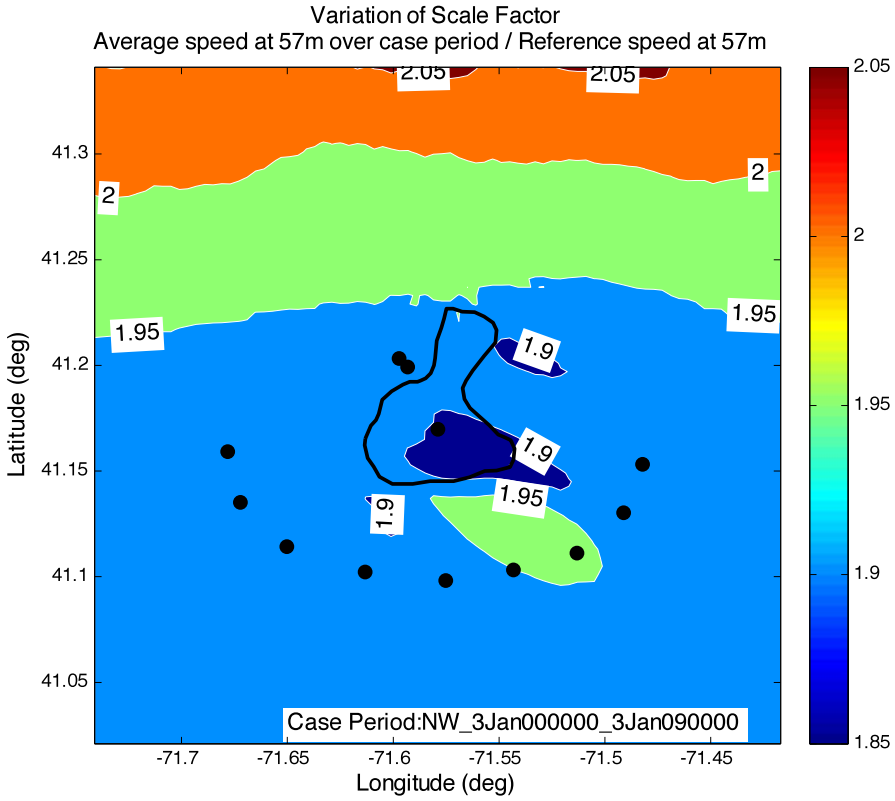
Variation of Scale Factor
Average speed at 57m over case period / Reference speed at 57m
2.05
2
1.95
1.9
1.85
41.3
41.25
41.2
41.15
41.1
41.05
Latitude (deg)
-71.7
-71.65
-71.6
-71.55
-71.5
-71.45
Longitude (deg)
Case Period:NW_3Jan000000_3Jan090000

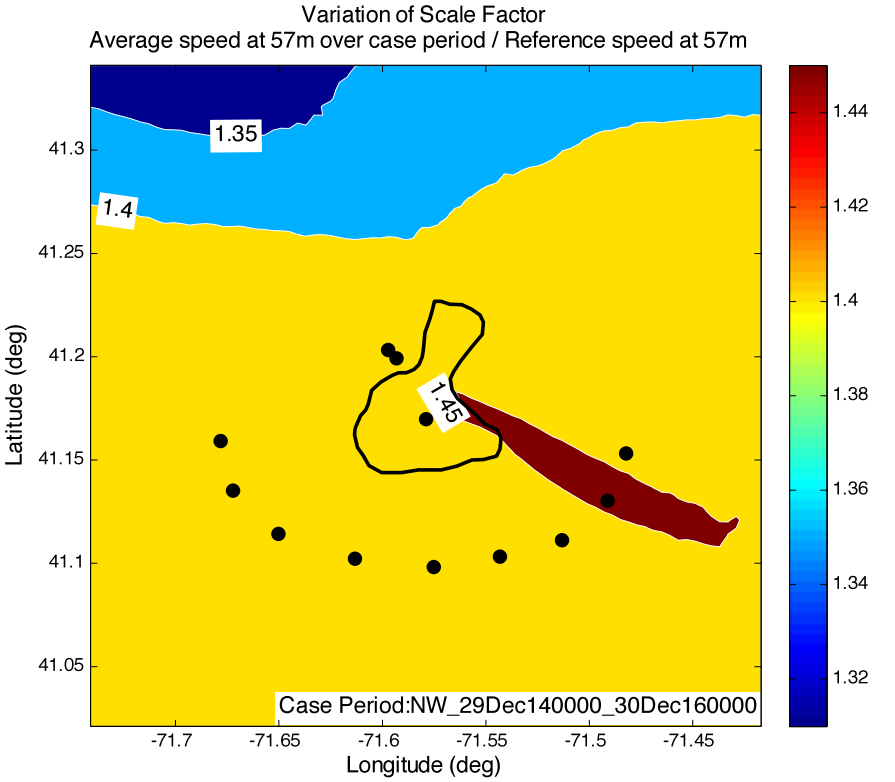
Variation of Scale Factor
Average speed at 57m over case period / Reference speed at 57m
1.44
1.42
1.4
1.38
1.36
1.34
1.32
1.35
1.4
1.45
41.3
41.25
41.2
41.15
41.1
41.05
Latitude (deg)
-71.7
-71.65
-71.6
-71.55
-71.5
-71.45
Longitude (deg)
Case Period:NW_29Dec140000_30Dec160000

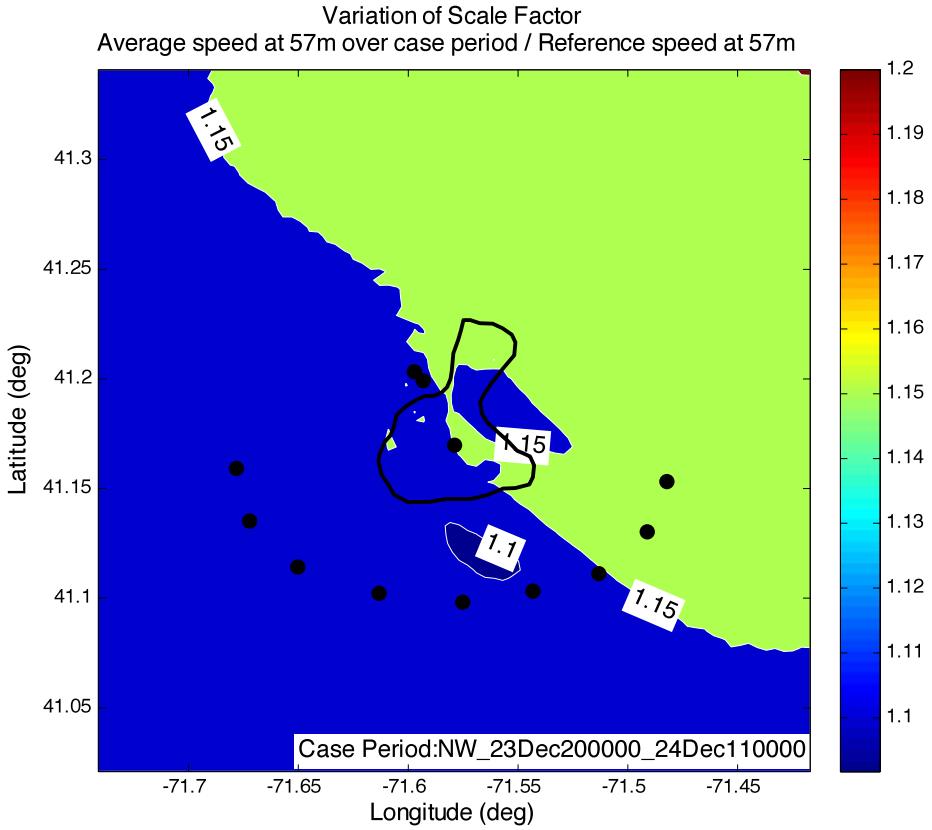
Variation of Scale Factor
Average speed at 57m over case period / Reference speed at 57m
1.15
1.15
1.1
1.15
Case Period:NW_23Dec200000_24Dec110000
Latitude (deg)
Longitude (deg)
41.3
41.25
41.2
41.15
41.1
41.05
-71.7
-71.65
-71.6
-71.55
-71.5
-71.45
1.2
1.19
1.18
1.17
1.16
1.15
1.14
1.13
1.12
1.11
1.1

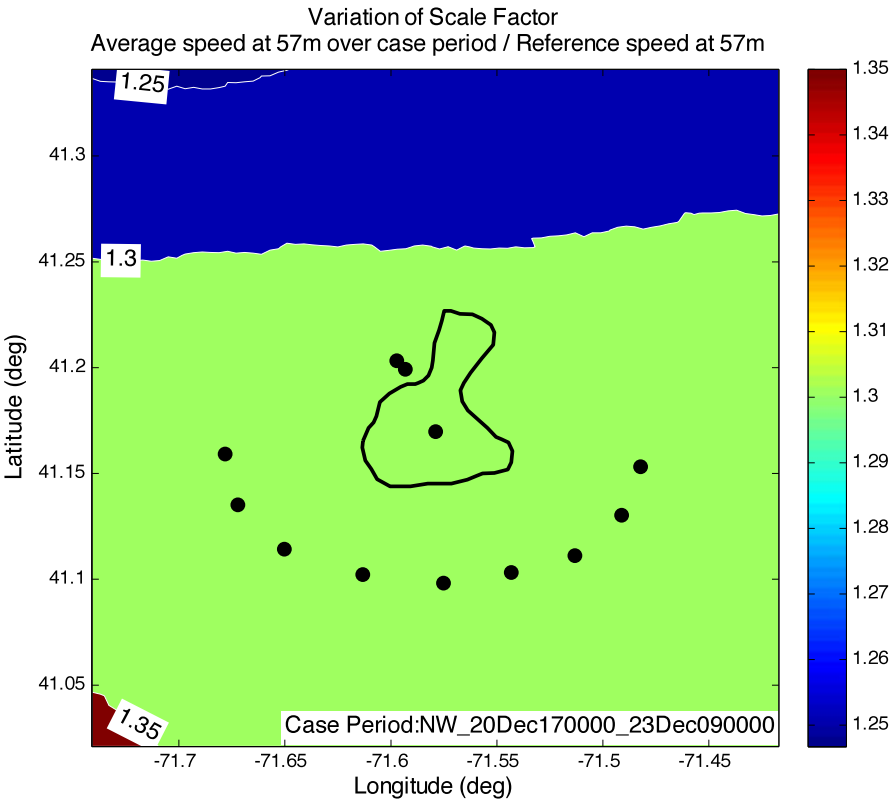
Variation of Scale Factor
Average speed at 57m over case period / Reference speed at 57m
1.25
1.3
1.35
Case Period:NW_20Dec170000_23Dec090000
Latitude (deg)
Longitude (deg)
41.3
41.25
41.2
41.15
41.1
41.05
-71.7
-71.65
-71.6
-71.55
-71.5
-71.45
1.35
1.34
1.33
1.32
1.31
1.3
1.29
1.28
1.27
1.26
1.25

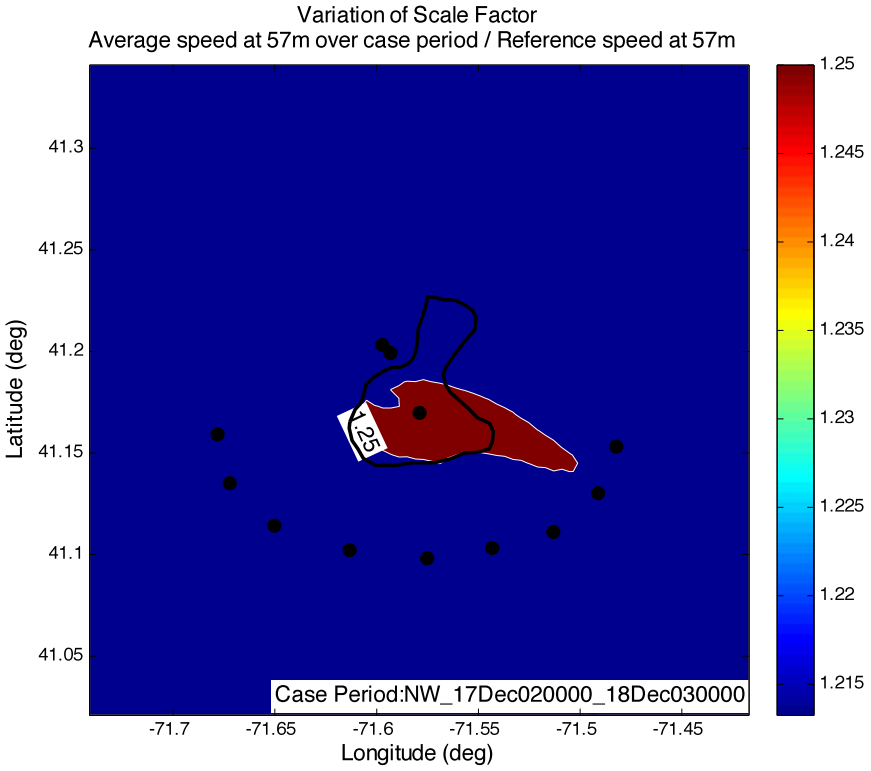
Variation of Scale Factor
Average speed at 57m over case period / Reference speed at 57m
1.25
Case Period:NW_17Dec020000_18Dec030000
Latitude (deg)
Longitude (deg)
41.3
41.25
41.2
41.15
41.1
41.05
-71.7
-71.65
-71.6
-71.55
-71.5
-71.45
1.25
1.245
1.24
1.235
1.23
1.225
1.22
1.215

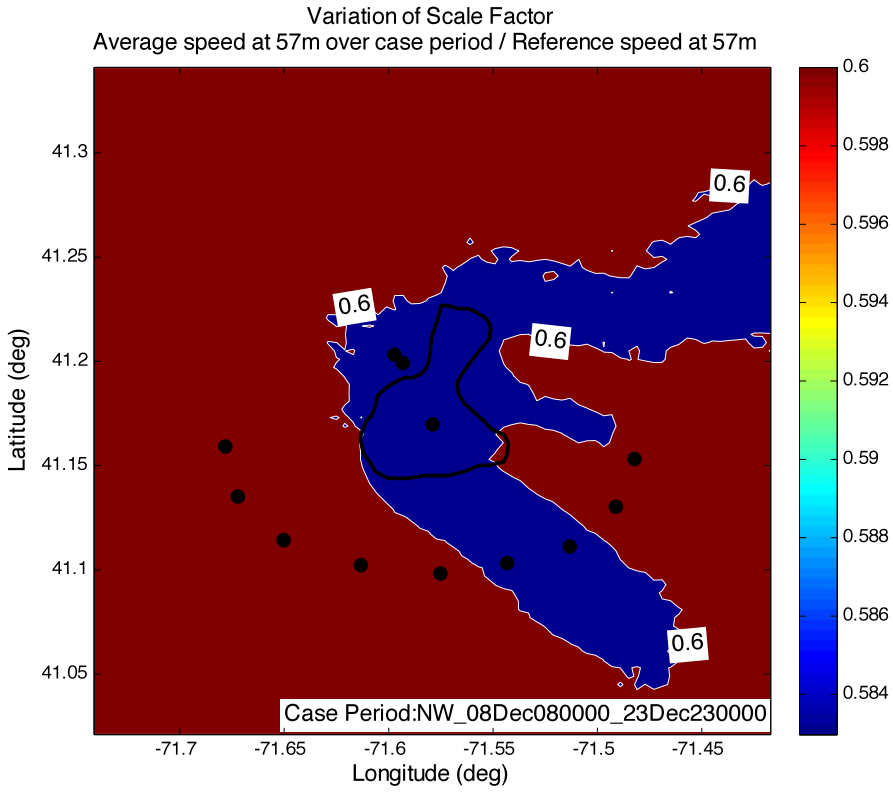
Variation of Scale Factor
Average speed at 57m over case period / Reference speed at 57m
0.6
Case Period:NW_08Dec080000_23Dec230000
Latitude (deg)
Longitude (deg)
41.3
41.25
41.2
41.15
41.1
41.05
-71.7
-71.65
-71.6
-71.55
-71.5
-71.45
0.6
0.598
0.596
0.594
0.592
0.59
0.588
0.586
0.584

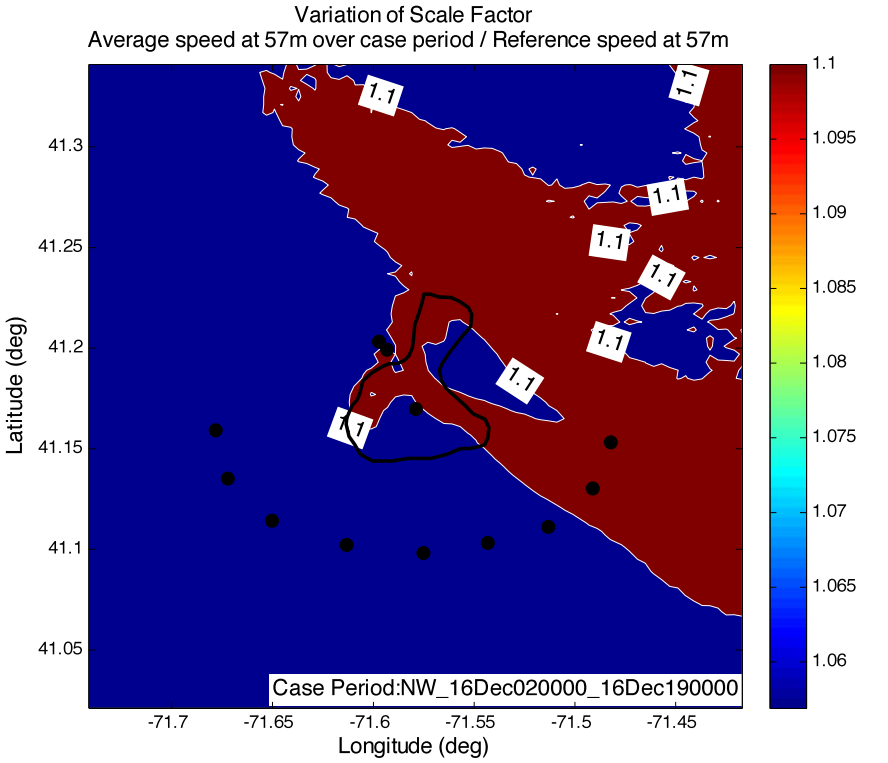
Variation of Scale Factor
Average speed at 57m over case period / Reference speed at 57m
Latitude (deg)
Longitude (deg)
Case Period:NW_16Dec020000_16Dec190000
1.1
1.095
1.09
1.085
1.08
1.075
1.07
1.065
1.06
41.3
41.25
41.2
41.15
41.1
41.05
-71.7
-71.65
-71.6
-71.55
-71.5
-71.45

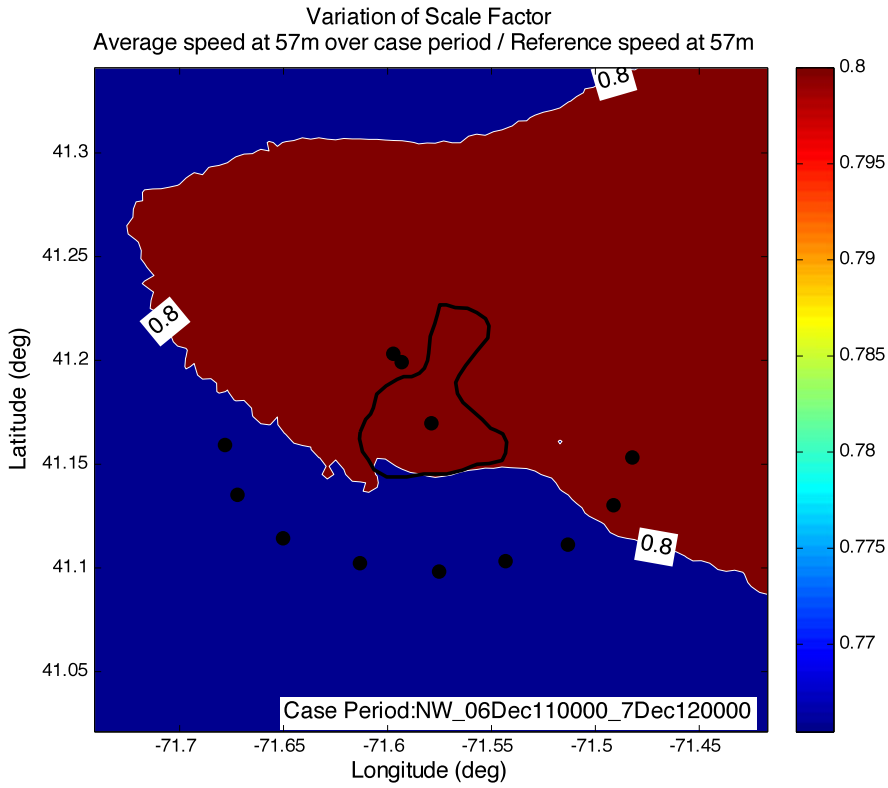
Variation of Scale Factor
Average speed at 57m over case period / Reference speed at 57m
Latitude (deg)
Longitude (deg)
Case Period:NW_06Dec110000_7Dec120000
0.8
0.795
0.79
0.785
0.78
0.775
0.77
41.3
41.25
41.2
41.15
41.1
41.05
-71.7
-71.65
-71.6
-71.55
-71.5
-71.45

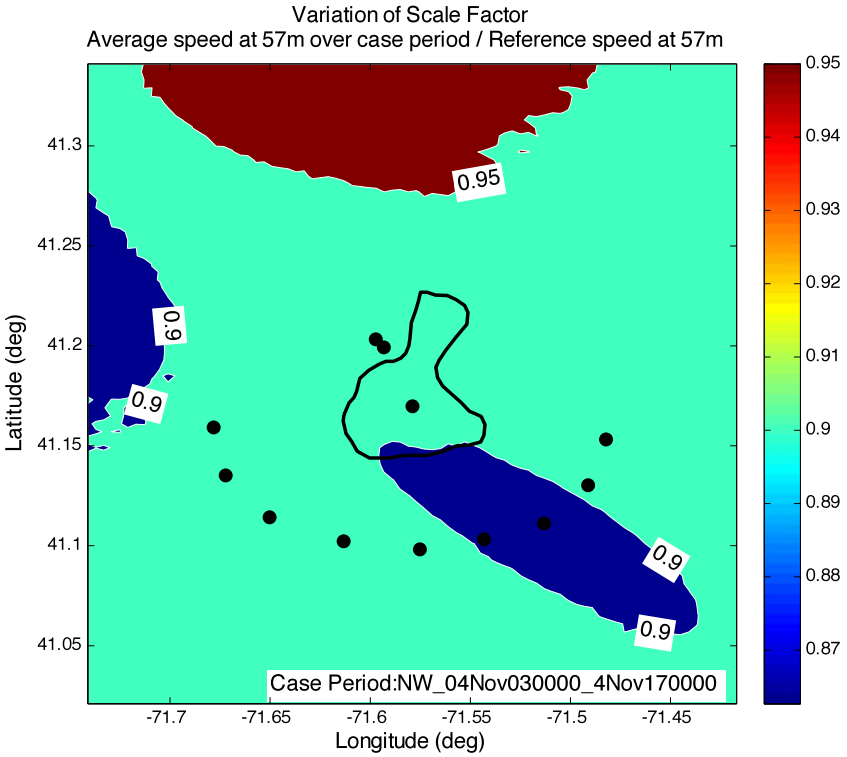
Variation of Scale Factor
Average speed at 57m over case period / Reference speed at 57m
0.95
0.9
0.9
0.9
Case Period:NW_04Nov030000_4Nov170000
Latitude (deg)
Longitude (deg)
41.3
41.25
41.2
41.15
41.1
41.05
-71.7
-71.65
-71.6
-71.55
-71.5
-71.45
0.95
0.94
0.93
0.92
0.91
0.9
0.89
0.88
0.87

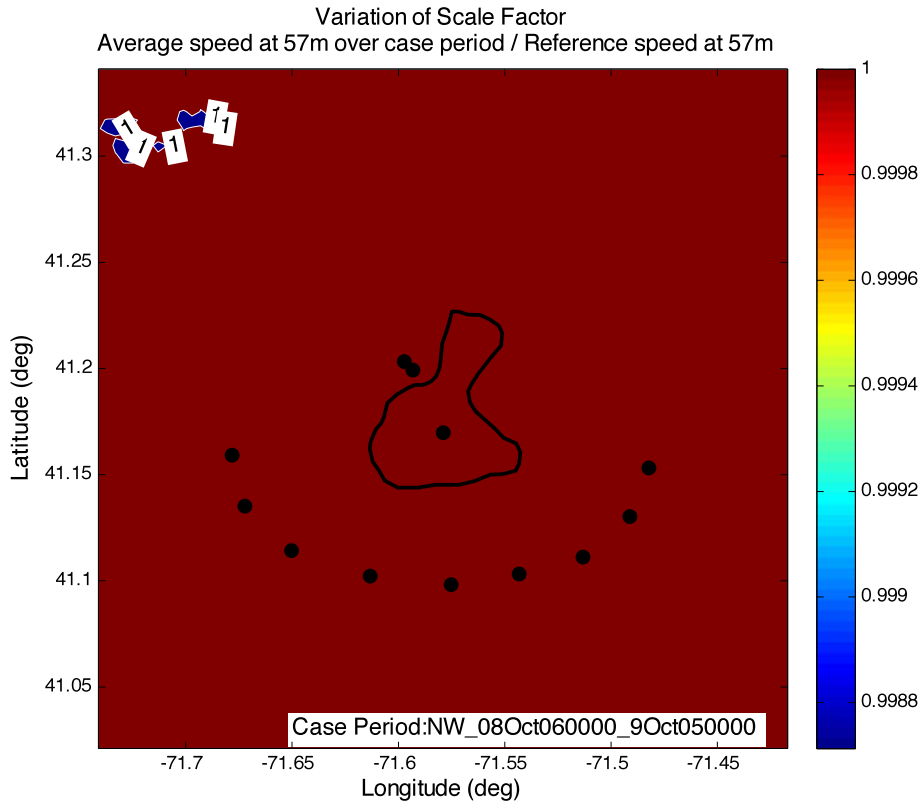
Variation of Scale Factor
Average speed at 57m over case period / Reference speed at 57m
1
1
1
1
Case Period:NW_08Oct060000_9Oct050000
Latitude (deg)
Longitude (deg)
41.3
41.25
41.2
41.15
41.1
41.05
-71.7
-71.65
-71.6
-71.55
-71.5
-71.45
1
0.9998
0.9996
0.9994
0.9992
0.999
0.9988

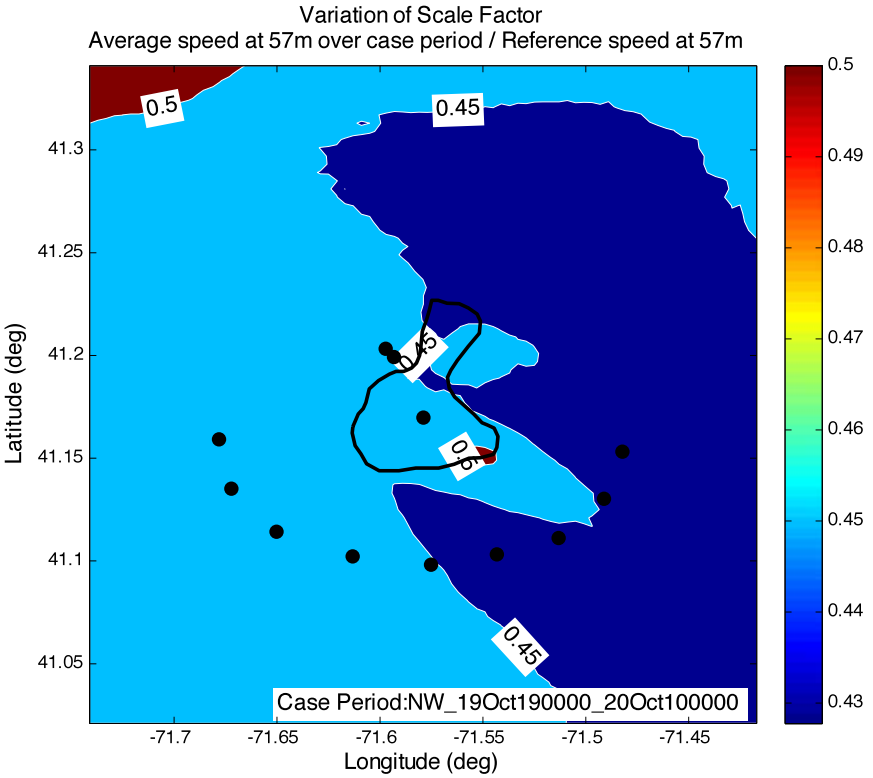
Variation of Scale Factor
Average speed at 57m over case period / Reference speed at 57m
0.5
0.45
0.45
0.45
0.45
Case Period:NW_19Oct190000_20Oct100000
41.3
41.25
41.2
41.15
41.1
41.05
-71.7
-71.65
-71.6
-71.55
-71.5
-71.45
Latitude (deg)
Longitude (deg)
0.5
0.49
0.48
0.47
0.46
0.45
0.44
0.43

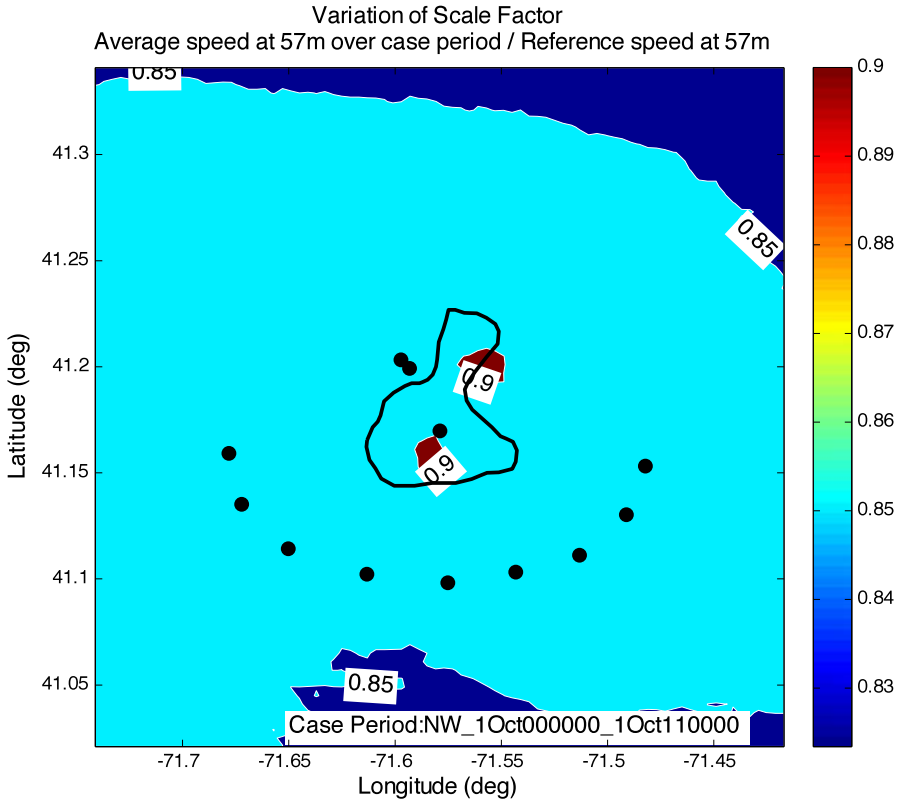
Variation of Scale Factor
Average speed at 57m over case period / Reference speed at 57m
0.85
0.85
0.9
0.9
0.85
Case Period:NW_1Oct000000_1Oct110000
41.3
41.25
41.2
41.15
41.1
41.05
-71.7
-71.65
-71.6
-71.55
-71.5
-71.45
Latitude (deg)
Longitude (deg)
0.9
0.89
0.88
0.87
0.86
0.85
0.84
0.83

20.

Evaluation of Wind Statistics and Energy Resources in Southern RI Coastal Waters for the Rhode Island Ocean Special Area Management Plan 2010

by

A. Grilli, M. L. Spaulding, A. Crosby, and R. Sharma

Ocean Engineering
University of Rhode Island
Narragansett, RI 02882

June 1, 2010

Executive Summary

The focus of the present study is to characterize the wind resources in southern RI coastal waters based on model simulations performed by AWS TrueWinds and historical observations and hindcasts in the study area. Both model predictions and observations show wind speeds increasing with distance offshore, with wind power approximately doubling between the RI shoreline and Block Island. Westerly winds are dominant in the study area with NW dominant west of Block Island and W and SW winds dominant to the east and near shore. Block Island Sound is in the lee for winds from the WSW to W from Long Island while Buzzards Bay and Nantucket Sound are in the lee of the main land for winds from the NW. Winds in the vicinity of Block Island are impacted by the topography and land cover on the island. Offshore buoy observations in coastal waters show a dominant NW to NE pattern off Block Island and a W dominance for observations in RI Sound for the observation period from Oct 2009 to May 2010. The northwesterly to westerly dominance is consistent with equivalent winter observation periods.

Table of Contents

List of Figures

List of Tables

List of Attachments and Appendices

Appendix A Wind frequency and power density(seasonal and annual) roses and Weibull distribution fits for selected stations in the SAMP study area.

Abstract

The focus of the present study is to characterize the wind resources in southern RI coastal waters based on model simulations performed by AWS TrueWinds and historical observations and hindcasts in the study area. Both model predictions and observations show wind speeds increasing with distance offshore, with wind power approximately doubling between the RI shoreline and Block Island. Westerly winds are dominant in the study area with NW dominant west of Block Island and W and SW winds dominant to the east and near shore. Block Island Sound is in the lee for winds from the WSW to W from Long Island while Buzzards Bay and Nantucket Sound are in the lee of the main land for winds from the NW. Winds in the vicinity of Block Island are impacted by the topography and land cover on the island. Offshore buoy observations in coastal waters show a dominant NW to NE pattern off Block Island and a W dominance for observations in RI Sound for the observation period from Oct 2009 to May 2010. The northwesterly to westerly dominance is consistent with equivalent winter observation periods.

1 Background

In 2006, the RI Office of Energy Resources contracted with ATM to assess to whether wind energy could meet the State's renewable energy goals of 15% of 1000 MW or 150 MW by 2016. Given a typical wind capacity factor, this would require an installed capacity of 450 MW. ATM (2007a,b) concluded that the goal could be met but would require development of offshore wind resources. Restricting their attention to water depths less than 23 m (75 ft), where mono-pile structures are feasible, they estimated that 95% of the available wind energy resource in RI was from offshore waters. The study also identified sites for potential offshore wind development that could either individually or collectively meet the state's renewable energy goal.In performing their assessment, ATM used data provided by AWS True Winds (Brower, 2007) to estimate wind energy resources. AWS True Winds provided annual mean wind speeds at 30, 50, 70, and 100 m and mean wind power at 50 m. The data were generated by AWS TrueWind's MesoMap meteorological modeling system and included the southern New England states (Rhode Island, Massachusetts, and Connecticut) and adjacent coastal waters. The data were provided on a 200 m by 200 m resolution grid. AWS validated the model predictions by comparison to 33 stations located in southern New England. The model root mean square error was reported to be 4% based on comparisons of annual mean wind speeds at an elevation of 65 m. Observed data at individual comparison sites were extrapolated from the observation height to the 65 m reference level using frictional scaling. The vast majority of sites used for validation were on land. There were only three validation sites in RI (Providence, Pt Judith and Block Island) and none in RI coastal waters. Buzzards Bay was the only validation site in southern New England coastal waters. National Renewable Energy Laboratory (NREL) reviewed the maps and found that they under predicted the winds in the area around Boston Harbor, based on a comparison to observations at Logan Airport, Boston Harbor, and other nearby stations. AWS True Winds adjusted the maps (5% increase in wind speed) to address this problem.

Anticipating the use of this data to define the wind energy resource as part of the marine spatial planning undertaken by the RI Ocean Special Area Management Plan (SAMP) and given the lack of validation of the estimates for SAMP study area (Figure 1) an independent analysis was performed and is the focus of the present report. This effort consisted of (1) obtaining AWS TrueWinds data from ATM, (2) identifying and collecting historical wind observations for all sites in the SAMP study area or immediately adjacent to it, and (4) then comparing mean annual

estimates from these observation stations to the model data product. Additional statistical analyses were performed on the observed data to support other SAMP study elements.

In related work, Spaulding et al (2010b and c) summarize observations in the immediate vicinity of Block Island. Spaulding et al 2010b use a template scaling method based on high resolution meteorological model (RAMS) predictions for discrete wind directions and a wind frequency rose to estimate mean annual wind speed and power fields south of the island. Spaulding et al (2010c) use the same meteorological model to predict wind speeds and power in the same study area to hindcast the winds from October 2009 to February 2010. Predictions are compared to observations from an offshore buoy and a meteorological tower located on Block Island.

2 The Data

Presented below is a summary of the data available to perform the analysis. An overview of the AWS True Winds model predicted data is presented first followed by the available observations. Details on each data set are provided in Table 1.

AWS True Winds Data

The modeling methodology used to generate the wind maps and their validation is presented in Brower (2007). Figure 2a to d show contour plots of the AWS TrueWinds mean annual wind speed maps at 30, 50, 70, and 100 m, respectively. The data at all vertical levels show a clear increase in wind speed as a function of distance offshore. The wind speeds are also observed to increase with height above the sea surface.

Assuming a neutrally stable atmosphere, on average, the wind speeds at 30 and 100 m were used to estimate the friction or shear coefficient, where wind speeds are U1 at height h1 and U2 at height h2, and r is the friction or shear coefficient (Hsu et al, 1994).

$$U_2 = U_1 \left[\frac{h_2}{h_1} \right]^r \qquad (1)$$

Based on this analysis the friction coefficient for the offshore study area was approximately constant at 0.134. For near shore sites the friction coefficient increased to 0.16 and higher reflecting the proximity of the coast and the greater roughness on the main land. The standard reference value used for a neutrally stable atmosphere is 1/7 or 0.143.

Observations

An in-depth review was performed to identify any data sets that might be used to compare to model predictions. The criterion were that the data had to be from a recognized source with suitable quality control and the wind observation period should be at least 1 yr, and preferably much longerideally 6 years . A summary of the data sets identified in this process are given below. The locations of the observation stations are provided in Figure 3a for the WIS stations and 3b for the rest.

Five data sources and associated data sets were identified: US Army Corp of Engineers, Wave Information Study (WIS), Martha's Vineyard Coastal Observatory, WeatherFlow, NOAA National Data Buoy Center (NBDC), and Department of Energy (DOE). The data sets including the station number/location, period, recording height, frequency of observation, and type (measured or hindcast) are provided in Table 1. Links to the sites from which the data were obtained are provided at the bottom of the table, if the data was available on line. Additional wind observations are currently being collected from two offshore buoys, one immediately south of Block Island, and one NNE of Cox's Ledge (October 1, 2009 to present). Measurements are also being made at four vertical levels from a meteorological tower on the coast of Block Island, nearby the western entrance to Great Salt Pond (August 1, 2009 to present). None of these measurements are discussed here because of their short record lengths. Selected analyses of the data are provided in Appendix A.

Army Corp of Engineers Wave Information Studies (WIS)

The US Army Corp performed a 20 yr hindcast (1980-1999) of the wind and wave conditions for a number of sites located along the southern boundary of the study area as part of the Wave Information Study (WIS). The locations of the southern New England hindcast sites are shown in Figure 3a. The sites of primary interest in this investigation are 74 to 79, 95, 100, and 101, located in a coast parallel configuration. Time series data are available via the internet at each location over the 20 yr hindcast period. Winds are estimated at 10 m elevation. The hindcast were made primarily validated with data from NOAA NDBC offshore observations (Stations 44004, 44008, 440017, 440018, and 44025).

Martha's Vineyard Coastal Observatory (MVCO)

Woods Hole Oceanographic Institution (WHOI) installed the MVCO to perform fundamental research in coastal meteorology. The meteorological tower from which the observations were made is in close proximity to the southern coast of Martha's Vineyard.

WeatherFlow

WeatherFlow is a private firm that operates a network of meteorological observation towers in very near to the coastal throughout the study area. The data is distributed through their IWindSurf web site. Historical data (not normally available) for the Pt Judith, Rose Island, Half Way Rock and Block Island Jetty (western entrance to Great Salt Pond) stations , were provided by WeatherFlow Inc. (J. Titlow, personal communication).

NOAA/ NDBC

NOAA/NBDC operates two meteorological observation close to the SAMP site, one at the entrance to Buzzards Bay (BUZM3) and the second a 3 m discus buoy (44017) located off the southern coast of Long Island (40.691 N 72.046 W). This is the closest NOAA/NDBC buoy to the study area. While data from BUZM3 are available from the mid 1980s to present, the data prior to 1999 had substantial discontinuities and therefore was not used.

Department of Energy (DOE)

DOE made wind measurements at a site just south of Great Salt Pond as part of a feasibility study to investigate the siting of a wind turbine on the island (Renne et al, 1982). This measurement program was unusual in that measurements were made at two locations in the vertical (9.1 and 45.7 m). The site is located on a hill top in rolling grass land.

Other

Wind observations were obtained under an educational institution license agreement from the meteorological tower established for the Cape Wind project on Horseshoe Shoals in Nantucket Sound, MA (http://capewind.whgrp.com/). This data set is not publically available. An analysis of the data was performed found to be consistent with the analyses that follow but Cape Wind would not allow its release at the time of this report.

Wind data is available from the Automated Weather Observation Stations (AWOS) at Block Island Airport (KBID) from 1997 to present. An analysis was performed of the data and showed a strong SW dominance. A decision was made not to use this data in the present analysis for the following reasons: (1) the site is on land with significant tree cover and topographic relief

immediately to the W and NW of the observation site. (Model simulations by Spaulding et al (2010 b, c) show very large shear, 0.45, year round in the vicinity of the airport), (2) the AWOS was located within 50 m of the airport terminal (height 12 m)(terminal to west of AWOS) until a new terminal was constructed in 2009. The short distance between the AWOS and the terminal building was in violation of FAA siting standards for AWOSs.

3 Data Analysis

Wind statistics

The data provided by AWS TrueWinds are annual mean values. Access to the underlying time series data or frequency distributions either by speed or direction was not available. Given this situation the first step in the analysis was to determine the mean wind speeds for each observation record at the observation height. These values were then adjusted to a standard reference height of 65 m using Equation 1. The vertical reference is the same as used by Brower (2007) in his validation of the AWS TrueWinds predictions. A friction coefficient of 0.1 was used to be consistent with the value employed by ATM (2007a). Table 2 summarizes the minimum, maximum, mean, median, skewness, and kurtosis for the observations at each station. Focusing on the means, it is noted that values for the various WIS sites are remarkably similar, with mean values of 8.15 m/sec. For locations closer to land (Pt Judith, MVCO) the means are lower at 6.4 to 7 m/sec, while at the BUZM3 site they are 8.5 m/sec., comparable to the WIS sites. Inside Narragansett Bay (Rose Island and Half Way Rock) the mean values decrease to 6.4 to 6.6 m/sec.

To assess the sensitivity of the mean values to the friction coefficient estimates were made at 24.5, 65, and 80 m elevations. The 24.5 m elevation was selected because it is the height of observations at the BUZM3 station (the most central, longest duration, and highest elevation observation in the study area), 65 m because it was used by Brower for validation, and 80 m since this is the projected hub height of the proposed wind power development in RI waters. Two values of friction coefficient were employed, 0.1 as in ATM (2007a) and 1/7 = 0.143, as this is a typical value (Hsu et al, 1994) and consistent with the AWS True Winds data for offshore areas (Figure 4). Table 2 presents the results of this analysis. The larger the value of the friction coefficient the higher the wind speed at a given elevation. At 65 m the mean wind speed

at the offshore sites increases about 0.4 to 0.5 m/sec as the friction coefficient increased from 0.1 to 0.143.

Figure 5 shows a comparison of the AWS True Wind estimates at each of the stations provided in Table 1 that are within the SAMP area or adjacent to it (BUZM3, MVCO). Values are provided at the 30 m elevation since this was the closest elevation of the AWS TrueWinds data to the vertical location of the observations. The data clearly show the gradient in wind speed with distance from shore; low values near the coast (Pt Judith (PJ)and MVCO) and higher values offshore (BB, WIS).

The probability distribution of the differences between the observations and predictions was estimated and found to be normally distributed (Figure 6) with a mean value of 0.17 m/s and a standard deviation of 0.14 m/s. The predicted AWS wind speed, at maximum, overestimates the observations by 0.44 m/s and, at minimum, underestimates measurements by 0.10 m/s (at the 95 % confidence interval). The AWS estimates are slightly higher than the observed values. Brower (2007) estimated the root mean square error between predicted and observed/extrapolated winds as 0.5 m/sec or 6.6% for the 32 stations where comparisons were made. He estimated a 0.1 m/sec bias with the predictions lower than the observations. The present results are generally consistent with his analysis.

One area of concern in analyzing the data is the impact of wind observation record length on estimates of the mean values. The observation record lengths vary substantially from 2 to 20 yrs (Table 1). The sensitivity of the mean wind speed value to the record length was performed for all WIS stations and BUZM3. These were selected since they have the longest hindcast and observed records (20 and 7 yrs, respectively) in the study area. Results were similar for all WIS stations therefore only the values from Station 101 are presented. The data were analyzed at a 10 m elevation for WIS 101 and 23.5 m for BUZM3. These are the original elevations at which the data were reported.

Annual and cumulative annual (from the beginning of the record) mean wind speed were estimated from the time series and are shown in Figure 7 and 8 for WIS101 and BUZM3, respectively. A review of the data shows that the annual variability is on the order of 0.4 m/sec. at both sites. The year to year variability can be as large as 0.8 m/sec at WIS101 and 1 m/sec at BUZM3. The averaging inherent in a cumulative analysis significantly reduces the variability with time. At WIS 101, approximately 6 yrs of data are required for the cumulative value to reach its long term mean. The data actually show a slight downward trend with time, but an

analysis shows the trend is not statistically significant. Cumulating the values reduces the variability for BUZM3 but the time to reach the long term mean is not clear.

An identical cumulative analysis, except backward in time, was performed for WIS 101. The results of both the forward and backward in time cumulative analyses are shown in Figure 9. Once again the 6 yr averaging time to achieve steady state conditions is shown.

Wind speed probability distributions

To provide additional insight into the winds in the study area, Weibull distributions were fit to the observation data. These distribution functions allow estimates of the wind power generation to be made and highlight the differences between the median and mean values observed in the analysis. Weibull distributions have two fit parameters, c (magnitude) and k (shape) that are varied to fit the data. These values were determined by a least squares fit for all observation stations. The results are reported in Table 2 (last two columns). Figure 10 shows a sample of the curve fit at 65 m elevation to WIS 74(upper panel) and BUZM3(lower panel), respectively. The values for c are very similar (c = 9.3) and k is close to 2 for the WIS and BUZM3 stations. The k values for the near shore stations, MVCO and Pt Judith, are comparable to the offshore stations. The c values (7 to 8) are substantially lower; consistent with the lower wind speeds at these locations (Table 2). For comparison ATM(2007a) estimated k = 2 and c = 7.22 (6.5 m/sec winds) and 7.78 (7 m/sec winds) for on shore sites. Grilli and Spaulding (2010) present a more comprehensive analysis using Weibull based distribution analysis. This paper shows how the shape and amplitude parameter vary with proximity to land. The paper also estimates the power production potential in the area using a Weibull based analysis.

Extreme wind speed analysis

An analysis was performed to estimate the mean and upper 95% percentile, once in 20, 50, 75, and 100 yr return period wind speeds as a function of wind direction at WIS 101. The estimates were determined by a Gumbel distribution fit to the maximum monthly mean wind speed data. Thirty (30) degree bins were used, centered on 90, 120, 150, 180, 210, and 240 degrees. The meteorological convention for wind direction was used. The results are reported in Table 4 for both mean and upper 95% confidence limit values. The wind speed increases with return period and the greatest exposure is from the north. The mean and upper 95% confidence limit maximum winds for 100 yr return period are 31 and 34 m/sec, respectively.

Wind and wind power directional distribution

Wind speed and power roses were prepared for all stations located in the SAMP study area and are shown in Figure 11 and 12, respectively. The figures show the directional values by speed or power for each direction. Figure 13 shows the average wind power by directions. This value is calculated by frequency weighting the value of power from each direction. (Appendix A provides wind speed, power density and average power roses for all sites.) The large scale trends show that the wind speeds and power roses are dominated by westerly winds. West of Block Island and offshore NW winds dominate, while east of the island and closer to show the winds are more westerly and southwesterly.

To assist in interpreting the wind roses Figures 14 (October 30, 2008- NW), 15 (July 8, 2008-SW), and 16 (September 24, 2008 – NE) show hindcast wind speed contours from a nested high resolution meteorological model applied to the SAMP study area. Spaulding et al (2010c) describe the model application and validation with observations in detail. These simulations represent typical winter (NW), summer (SW) and NE (storm conditions). All the simulations show that the wind speed increases with distance offshore reaching maximum values south of Block Island. The rate of increase is greatest for shore parallel winds (SW) and lowest for offshore winds (NW). The lee effect of Long Island is clearly evident in western Block Island Sound. At locations close to the shoreline the wind speeds from the NW are substantially reduced due to flow over land while those from the SW are unimpeded since the wind flow is over water; the closer to land the greater the effect.

Wind and wind power directional distribution

Wind data were analyzed at WIS 101 at 80m to determine the directional distribution for all observed winds and for winds that are appropriate for extraction of energy using current wind turbine technology. This site was selected as it representative of offshore waters. "Extractable" is defined as wind speeds above 3.5 m/sec (cut-in speed of the wind turbine) but below 27 m/sec (cut out speed of the turbine). These values depend on the characteristics of the specific wind turbine but the limits given above are reasonable for the current generation of technology. Figure 17 shows a wind rose giving the number of observations (hourly intervals over 20 yrs) by direction for all winds (left panel) and extractable winds (right panel). Note the two figures have difference scales. Figure 18 shows the probability of occurrence for both cases. Both figures show that winds are primarily from the west northwest and secondarily from the west and south west. Winds from the east are substantially less frequent. The extractable winds show the same pattern as the all winds case but at 90%.

Estimates of mean wind power by direction, for all and extractable wind cases, are shown in Figure 19. This value is calculated by taking the average of wind power for each 30 degree direction segment. Figure 20 shows seasonal plots of the all wind case. Figure 21 provides a histogram of the data show in Figure 19, top panel all winds and bottom panel extractable winds. The power is largest (1.3 kW/m^2) when the winds are from the west northwest and still substantial for winds from the north (1 kW/m^2). Mean wind power is much lower (0.6 kW/m^2) for winds from the southwest to the east. The all and extractable wind cases show similar directional distributions, but the extractable power is slightly lower. The mean, averaged over all directions, is 841 kW/m^2 for the all case and 825 kW/m^2 for the extractable case. Figure 20 clearly shows that winter winds have the highest energy levels (1.9 kW/m^2), fall and spring intermediate levels (1.2 kW/m^2), and summer the lowest levels (3.8 kW/m^2). The power levels are largest from the northwest for fall, winter and spring winds and from the north to northeast for summer winds. Wind power in the winter from all directions exceeds those from every other season

Figure 21 and 22 show corresponding plots for the directional average all and extractable wind cases. Average here is defined as the weighting of the mean power resource by frequency of occurrence (Figure 12). Given the dominance of the stronger westerly winds the average wind power is highest from the west to northwest (160 kW/m^2) and lowest from the east and southeast (2o kW/m2). Summing the average wind power over all directions gives 841 kW/m^2 for the all wind case and 825 kW/m^2 for the extractable case; the same values as the mean for the mean wind power results.

Estimates of the spatial distribution of the mean wind power were next made on a 100 m by 100 m grid covering the SAMP study area (Figure 1). To make this estimate a Weibull distribution was assumed at each of the grid locations in the study area. Based on the analyses presented in Table 2, the k value for the distribution was observed to be close to 2. For this special case, the Weibull distribution reduces to a Rayleigh distribution. For Rayleigh distributed winds c = U/0.886, where U is the mean wind speed at a given location. More details are given on the spatial distribution of the shape parameter in Grilli and Spaulding (2010), but in this approach, the shape coefficient is assumed to be equal to 2 and the distribution is therefore a simple function of the mean wind speed. At each grid cell, the Weibull parameters (c=f(U),k=2) are used to generate a wind speed distribution; 10,0000 wind speed vectors are randomly drawn from each distribution and converted into power. The mean power value is then calculated at

each grid cell . Power was alternatively calculated analytically from the Weibull parameters and results are comparable. The choice of the Monte Carlo method is driven by its flexibility to introduce the concepts of cut-in, cut –out, rated speed, although not use in this particular analysis. A detail analysis of the expected power spatial distribution is presented in a more comprehensive approach by Grilli and Spaulding (2010).The results of the analysis are presented in the form of contour plots of mean wind power. Figure 23 and 24 show the mean wind power contours for the study area for the all and extractable wind cases, respectively. These assume that the mean wind speed estimates from AWS are accurate. Both figures show the mean wind power increasing with distance offshore, consistent with the wind speed contours. The power levels just south of Block Island are 900 W/m2, twice their value along the southern RI coast line (450 W/m2) for the all wind case. The values for the extractable winds are about 10% lower than the all winds case. The spatial structure is exactly the same.

It has been shown earlier in the report that the winds from AWS are biased high (0.17 m/sec) from the observed winds. The spatial analysis was repeated using the AWS adjusted for the bias. These results are provided in Figures 20 and 21 for the all and extractable case, respectively. Not surprisingly the patterns are comparable to all winds case however the magnitudes are reduced by approximately 20 W/m2.

Recent observations

As part of the SAMP investigation three new sets or data have become available. The SAMP project deployed two buoys that are collecting data on wind speed and direction. The data is being collected at an elevation of 4 m. The stations are located (Figure 27) immediately south of Block Island (MDS) and NNE of Cox's ledge at MDF. In addition data is being collected at AWS meteorological tower located at the western entrance to Great Salt Pond on Block Island. Measurements are being made at 9.9, 32, 47.6, and 57.4 m. Data from the MDS and MDF are available from October 1, 2010 to present while data from AWS Met site from August 2009 to present.

Figure 28 shows the observed wind speed time series from the beginning of the recording period through mid February. The mean speeds are 8.01 m/sec at AWS Met, 8.35 m/sec at MDS and 7.95 m/sec at MDF. Wind speed frequency roses are shown in Figure 29 and power roses in Figure 30. The roses are strongly dominated by winds from the NW and secondarily from the NE at AWS Met and MDS. Winds from the westerly direction are dominant at MDF. This basic

pattern is consistent for winter winds and the transition for NW to W-SW dominance noted earlier.

Shear estimates were made from the AWS Met site using data at each of the various levels. The results showed that the values decreased from 0.18 in August to 0.08 in November and remained in the range of 0.06 to 0.07 through February 2010. The shear was approximately the same no matter which vertical levels were used to perform the analysis. The shear for the winter season at AWS Met is consistent with oceanic conditions and stable transitioning to an unstable atmosphere from late summer to winter. The impact of topographic relief and roughness is minimal, as might be expected based on the station's location near the shoreline at the entrance to Great Salt Pond.

4 Conclusions

A comparison was performed between the AWS True Wind predictions of annual mean wind speeds (200 m by 200 m grid) to all wind data publically available in the SAMP study area and those from nearby stations. The principal data sources, with record lengths ranging in duration from 2 to 20 yrs, were US Army Corp WIS, WeatherFlow, Martha's Vineyard Coastal Observatory, and NOAA/NBDC stations. Comparisons were made at an elevation of 65 m. Data sets were adjusted to this elevation using standard frictional scaling. The analysis showed that the wind speeds from the model and observations were in good agreement with the observations (mean difference of 0.17 m/sec and standard deviation of 0.14 m/sec). The mean annual wind speeds were 6.8 m/sec at coastal stations and 8.1 m/sec at offshore stations. Viewed in terms of an onshore-offshore transect, observations were only available very close to the shore and at a distance of about 40 km offshore, hence only two locations. Additional observations at intermediate and greater distances will be required to characterize the width of the coastal boundary layer.

Estimates of the frictional coefficient, based on the AWS True Winds data, were made at the observation sites and show that the value is constant for offshore waters (0.128) but increased substantially at near coastal stations (0.16 to 0.19). It was impossible to verify these estimates since wind observations were only available at one height at each station. The increased frictional resistance at very near coastal stations is consistent with increased roughness over land.

The annual variability of the mean wind speed was investigated at WIS 101 (20 yrs) and BUZM3 (7 yrs) and showed typical year to year variations of 0.4 m/sec, with maximum

differences on the order of 0.8 to 1 m/sec. A sensitivity study was performed on estimates of the annual mean value based on length of record used in the averaging. The analysis showed that 6 years of data were required at WIS101. No conclusion could be drawn at BUZM3 however since the record was only 7 years in length.

Wind observations at all stations were fit with a Weibull probability distribution function. The shape parameter, c, was approximately 2 for all stations. The amplitude parameter, k, was 9.3 at offshore sites but decreased to about 7 at near shore locations. This result is consistent with the gradient of wind speeds with distance offshore.

An extreme analysis of the once in 20, 50, 75, and 100 year return period wind speeds by direction was performed. Mean and upper 95% percentile values were estimated by 30 degree direction bins. The maximum mean and upper 95% values for the once in 100 year event were 31 and 34 m/sec from the north.

A directional analysis of the wind speed and power was performed for WIS site 101 at 80 m. The analysis shows that the winds from the northwest to southwest have the highest frequency of occurrence, with the power being from westerly to northwesterly winds. Wind power is substantially larger in the winter months, intermediate in spring and fall and smallest during the summary. The analysis was performed for all and extractable. The patterns are exactly the same but the magnitude of the later is about 90% of the former.

Using a Weibull distribution and the mean AWS wind speeds contour maps of wind power were generated for the study area. The wind power contours are shoreline parallel and increase with distance offshore from 450 kW/m2 to 900 kW/m2. The analysis was performed again correcting the mean AWS wind speeds for a positive bias. The power levels generally decreased about 20 kW/m2 when compared to AWS based estimates.

Recent measurements from AWS Met, MDS and MDF show a NW followed by NE dominant pattern for the first two and W dominance for MDF for the October 2009 to present measurement period. The pattern is consistent with historical data in the study and the transition for NW to W dominance as one moves eastward. The shear coefficient at AWS Met was low (0.08) typical of unstable winter winds.

References

ATM, 2007a. RI WINDS Phase I, Wind Energy Siting Study, prepared for RI Office of Energy Resources, Providence, RI, April 2007.

ATM, 2007b. RI WINDS Summary Report, prepared for RI Office of Energy Resources, Providence, RI, September 2007.

Brower, M., 2007. Wind resource maps of Southern New England, prepared by True Wind Solutions, LLC, 10 p.

Grilli, A and M. L. Spaulding, 2010. Estimation of offshore wind power resources based on Weibull distribution in Rhode Island coastal and offshore waters, Ocean Engineering, University of Rhode Island, Narragansett, RI.

Grilli, A., M. L. Spaulding, C. Damon, and R. Sharma, 2010. High Resolution Application of the Technology Development Index (TDI) in State Waters South of Block Island, Ocean Engineering, University of Rhode Island, Narragansett, RI.

Hsu, S. A., Eric A. Meindl, and David B. Gilhousen, 1994. Determining the power-law wind-profile exponent under near-neutral stability conditions at sea, Applied Meteorology, Vol. 33, No. 6, June 1994

Renne, D. S., W. F. Sandusky, and D. L. Hadley, 1982. Meteorological field measurements at potential and actual wind turbine sites, US Department of Energy, Pacific Northwest Laboratory, Richland, WA, PNL -4431, UC-60, September 1982.

Spaulding, M. L., A. Grilli, C. Damon, and G. Fugate, 2010a. Application of technology development index and principal component analysis and cluster methods to ocean renewable energy facility siting, Marine Technology Society, Special Issue on Marine Technology for Offshore Wind, Vol. 44, No 1, January/ February 2010, pg 8-23. *Format: Paper, Status: Published*

Spaulding, M. L, R. Sharma, A. Grilli, M. Bell, A. Crosby and Lauren Decker, 2010b. Wind resource assessment in the vicinity of a small, low relief coastal island, Ocean Engineering, University of Rhode Island, Narragansett, RI.

Spaulding, M. L. ,M. Bell, J. Titlow, A. Grilli, R. Sharma, L. Decker and D. Mendelsohn, 2010c. Meteorological model based wind resource assessment in the vicinity of Block Island, Ocean Engineering, University of Rhode Island, Narragansett, RI

Table 1 Wind observations used in analysis

Data Name		Period	Recording Height(m)	Frequency (hrs)	Type
US Army Corp of Engineers					
WIS Stations	74-79,89,95,100,101	1980-1999	10	1	Hindcast
Marthas Vineyard Coastal Observatory(MVCO)		2001-2008 (data missing 2005-2008)	12.5	0.33	Measured
WeatherFlow					
	Pt Judith	2005-2007	22.3	1	Measured
	Rose Island	2005-2007	10.7	1	Measured
	Half Way Rock	2005-2007	8.23	1	Measured
NOAA /NDBC					
	BUZM3	1999-2007	24.8	0.17	Measured
	Buoy 44017	2002-2007	5	0.17	Measured

Data Sources

WIS	http://www.frf.usace.army.mil/cgi-bin/wis/atl/atl_main.html
MVCO	http://mvcodata.whoi.edu/cgi-bin/mvco/mvco.cgi
WeatherFlow	http://www.weatherflow.com/
NOAA/NBDC	http://www.ndbc.noaa.gov/

Table 2 Wind speed statistics for WIS, Martha's Vineyard Coastal Observatory, WeatherFlow and NOAA/NDBC data

Descriptive statistics wind (m/s) at 65 m; wind@65m= wind@h0 * [65/h0]^alpha

Friction coefficient, alpha = 0.1

Station WIS	Period	Min m/s	Max m/s	Mean m/s	Median m/s	Skewness	Kurtosis	Weibull c Magnitude parameter	Weibull k Shape parameter
#74	1980-1999	0.24	42.57	8.23	7.60	0.77	0.46	9.31	2.02
#75		0.24	38.35	8.20	7.48	0.77	0.46	9.19	2.03
#76		0.24	39.19	8.16	7.48	0.77	0.45	9.27	2.03
#77		0.24	41.12	8.13	7.48	0.78	0.46	9.23	2.03
#78		0.24	40.28	8.12	7.48	0.77	0.44	9.23	2.03
#79		0.36	39.43	8.12	7.48	0.76	0.42	9.27	2.04
#89		0.24	32.20	8.15	7.48	0.76	0.41	9.19	2.03
#95		0.24	32.68	8.20	7.48	0.76	0.40	9.29	2.05
#100		0.24	33.64	8.21	7.60	0.76	0.40	9.19	2.03
#101		0.36	36.06	8.18	7.48	0.76	0.41	9.26	2.05
MARTHA'S VINEYARD									
Martha Son3D	2001-2008	0.12	24.65	6.53	6.13	0.70	0.46	6.89	2.15
	(missing data 2005-2008)								
WEATHER FLOW									
Point Judith	2005-2007	0.04	24.96	7.06	6.51	0.82	0.79	7.98	2.02
Rose Island	2005-2007	0.025	25.04	6.39	6.03	0.69	0.58	7.17	1.82
Halfway Rock	2005-2007	0.03	25.69	6.56	6.15	0.69	0.60	5.98	1.82
Buzzard Bay									
BUZM3	1999	0.01	26.60	8.30	7.94	0.52	0.14	9.36	2.14
	1999-2007	0.01	32.81	8.50	8.15	0.59	0.36	9.58	2.19

Table 3 Sensitivity of mean value at 65 m to assumption of friction coefficient

Roughness coefficient alpha = 0.1 or alpha=1/7
Criteria Choice of roughness coefficient : identical to ATM to compare with Buzzard Bay data

Station WIS	Period	Simulation height	Mean @ m/s r=1/7	Mean @ m/s r=1	Mean @ m/s r=0.1	Mean @ m/s r=1/7	Mean @ m/s r=1	Mean @ m/s r=0.1	Mean @80 m m/s r=1/7
#74	1980-19	10 m	6.83	7.77	7.48	8.23	8.92	8.41	9.19
#75		simulated	6.80	7.74	7.44	8.20	8.88	8.37	9.15
#76		data				8.16		8.33	
#77						8.13		8.30	
#78						8.12		8.29	
#79						8.12		8.29	
#89						8.15		8.32	
#95						8.20		8.37	
#100						8.21		8.38	
#101						8.18		8.35	

Station	Period	Anemo height (	U (m/s at Hre	Mean @ r=1/7	Mean @ m/s r=1	Mean @ m/s r=0.1	Mean @ m/s r=1/7	Mean @ m/s r=1	Mean @ r=0.1	Mean @80 m m/s r=1/7
MARTHA VINEYARD										
Martha	2001-20(	12.5 m	5.54	5.37	6.11	5.93	6.53	7.01	6.67	7.22
WEATHER FLOW										
Point Ju	2005-20(	22.25 m	6.34	5.65	6.44	6.41	7.06	7.39	7.20	7.61
Rose Is	2005-20(	10.66 m	5.34	5.29	6.02	5.81	6.39	6.91	6.53	7.12
Halfway	2005-20(	8.23 m	5.33	5.48	6.24	5.95	6.56	7.16	6.69	7.38
NOAA station										
Buzzarc	1999	24.8 m	7.53		7.53		8.30	8.66		
	1999-20(	24.8 M	7.72	6.80	7.72		8.50	8.86	8.68	9.10

Table 4 Extreme wind analysis for 20, 50, 75 and 100 yr return periods at WIS 101

Calculations based on Gumbel distribution fit through monthly maximum data
Directions assume meteorological convention
2 sets of extreme events: average value and upper limit of the 95 % confidence interval

		U(m/s)	U 95 % (m/s)			U(m/s)	U 95 % (m/s)
Direction		**90**		**Direction**		**180.0**	
	100	31.0	34.0		100	28.0	30.4
	75	30.1	33.0		75	27.3	29.6
	50	28.9	31.6		50	26.3	28.5
	20	26.1	28.4		20	24.0	25.9
Direction		**120.0**		**Direction**		**210.0**	
	100	29.7	32.5		100	29.2	31.7
	75	28.8	31.5		75	28.5	30.9
	50	27.6	30.2		50	27.5	29.7
	20	25.0	27.1		20	25.1	27.0
Direction		**150.0**		**Direction**		**240.0**	
	100	27.8	30.3		100	31.3	34.0
	75	27.0	29.4		75	30.5	33.1
	50	26.0	28.2		50	29.3	31.8
	20	23.6	25.6		20	26.7	28.9

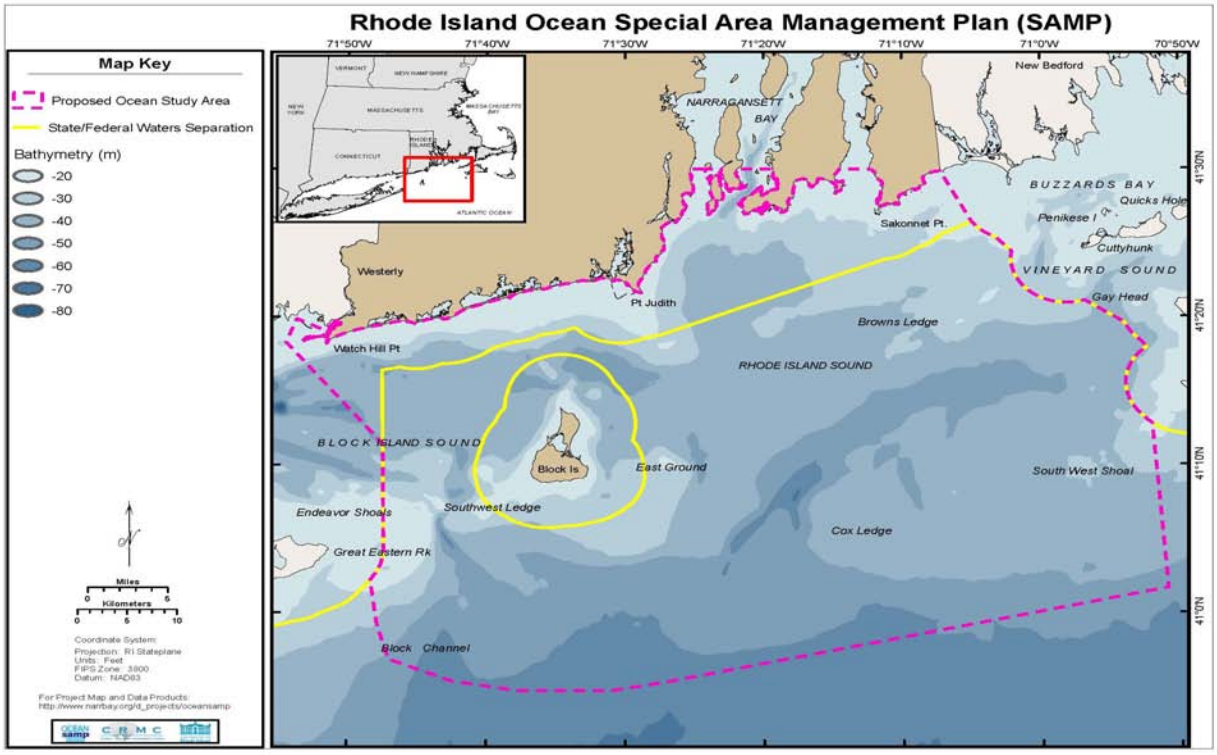

Figure 1 RI Ocean SAMP coastal study area. The dashed line is the study area boundary and the solid yellow line is the boundary of state waters. Key location names are provided as well.

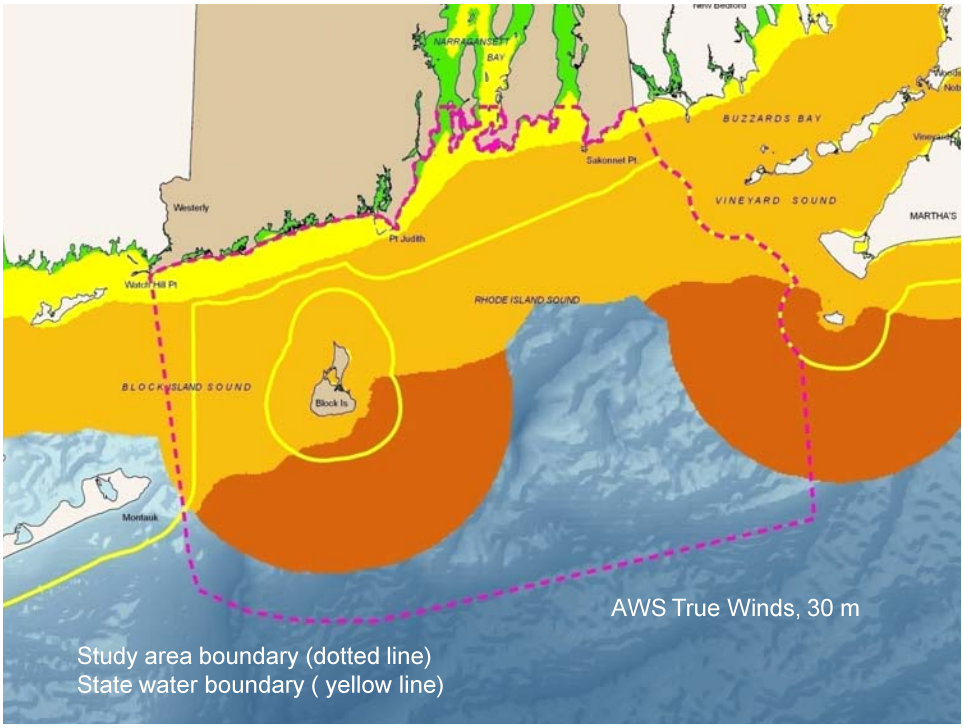

Figure 2a AWS TrueWinds mean annual wind speed at 30 m above sea level

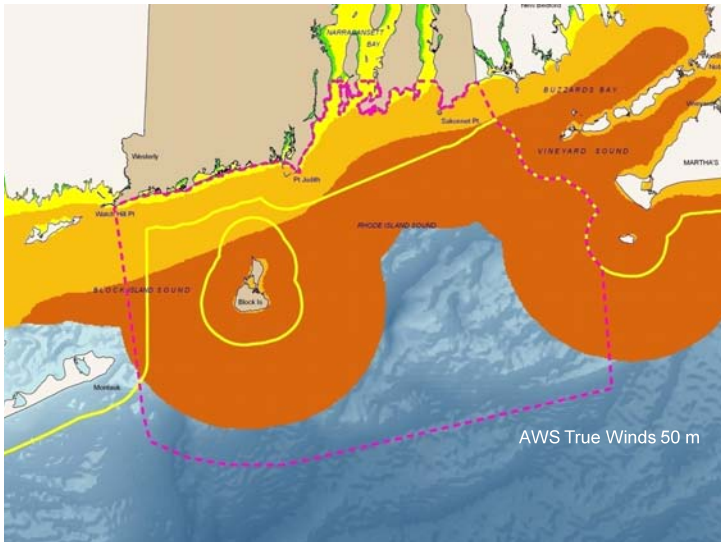

Figure 2b AWS TrueWinds mean annual wind speed at 50 m above sea level.

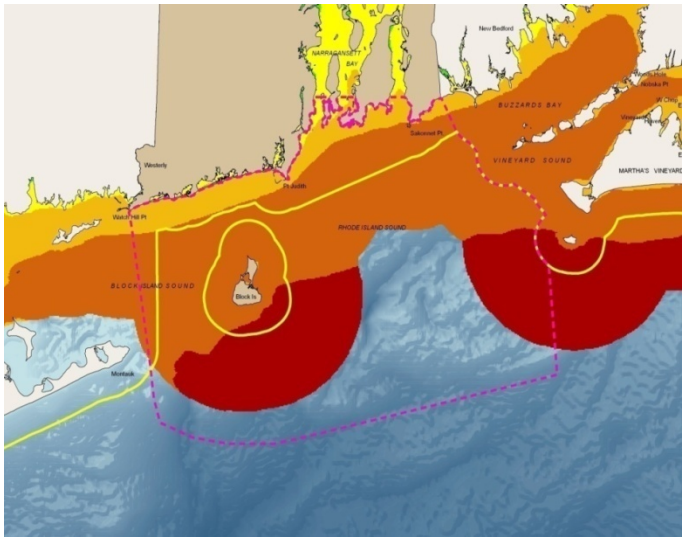

Figure 2c AWS TrueWinds mean annual wind speed at 70 m above sea level.

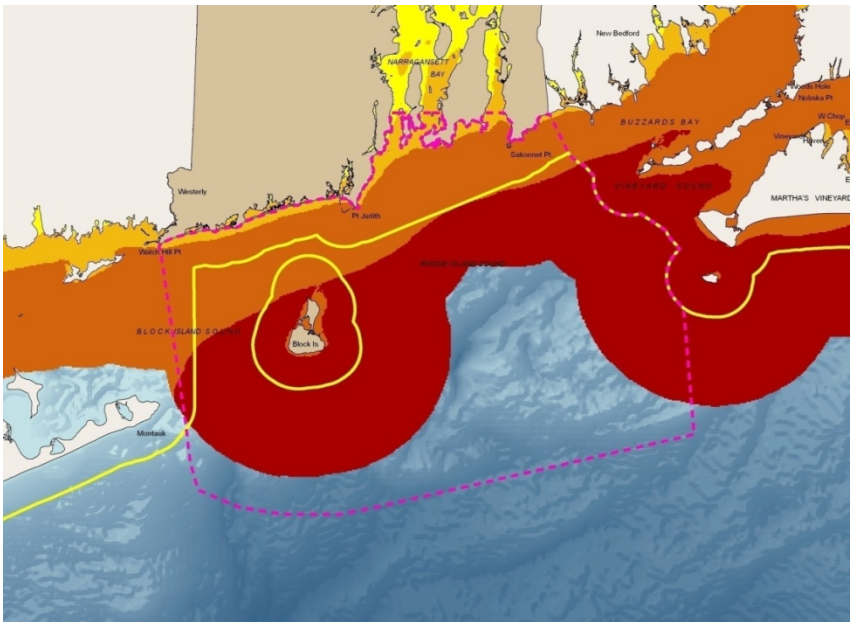

Figure 2d AWS TrueWinds mean annual wind speed at 100 m above sea level.

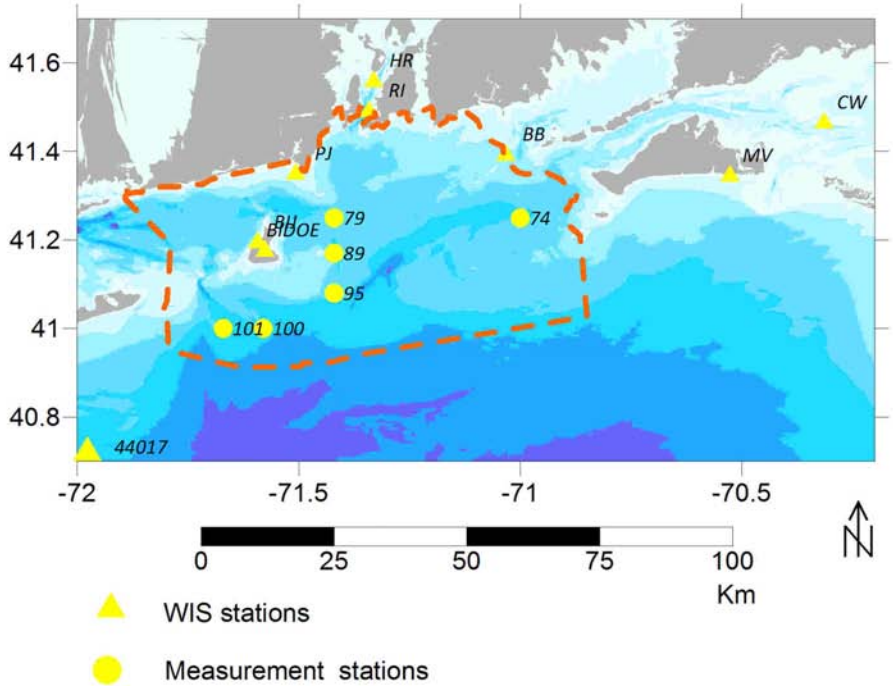

Figure 3 Location of U.S. Army corps of Engineer WIS stations and all measurement stations , Point Judith(PJ), Half Way Rock(HR), Buzzard Bay (BB), Martha's Vineyard (MV), Cape Wind(CW),Block Island Jetty(BIJ), Block Island DOE (DOE), NOAA 44017 (44017) (Cape Wind is not used in the analysis for reasons of confidentiality).

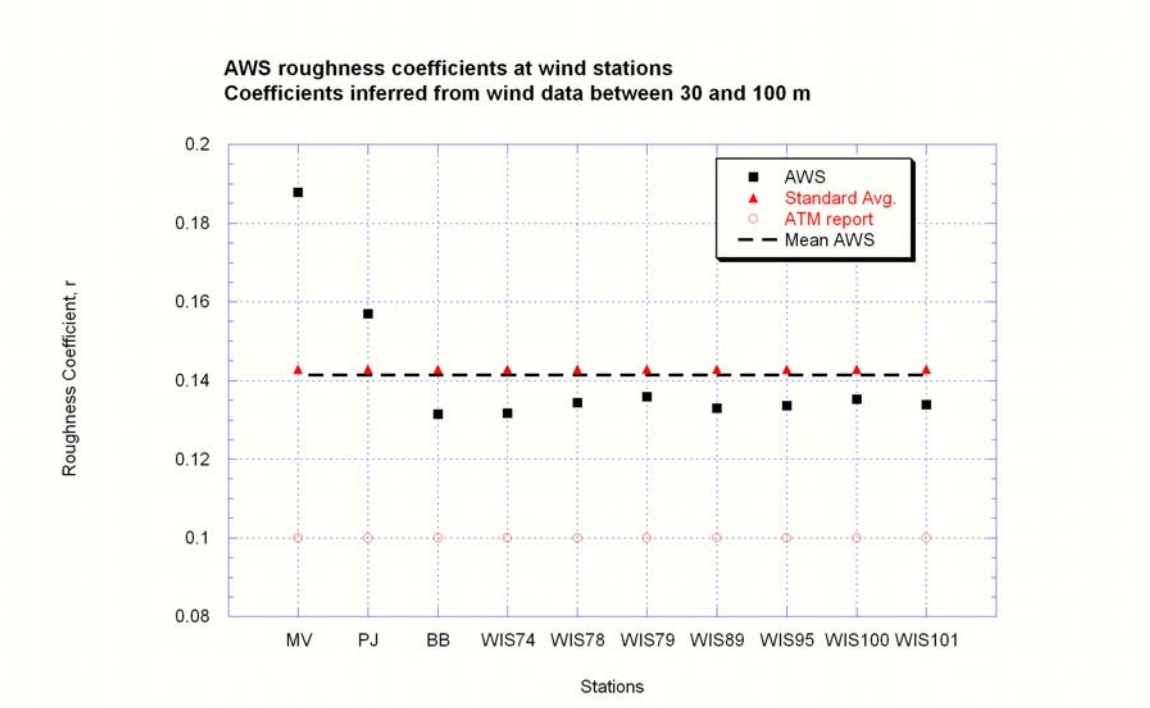

Figure 4 Friction coefficient for each observation station based on the AWS data, standard average value and the value assumed by ATM (2007a). The mean AWS value is also presented.

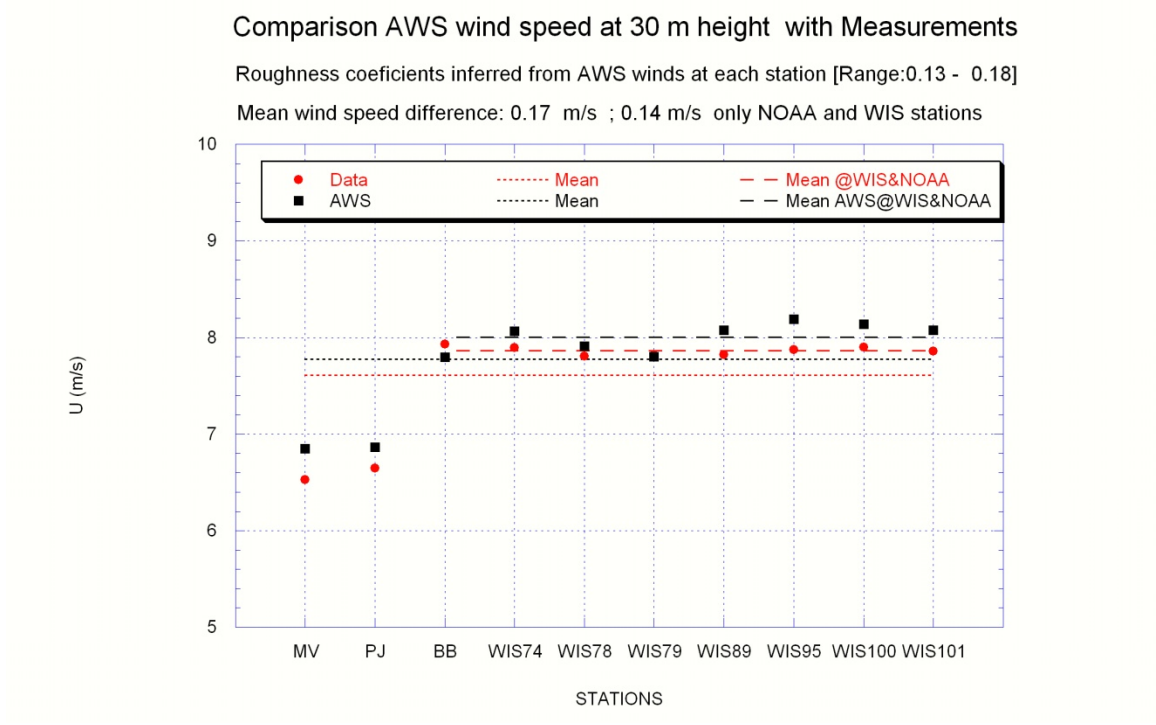

Figure 5 Comparison of the mean wind speed at each observation station with AWS True Winds data at an elevation of 30 m. The mean values for WIS and NOAA sites are also shown.

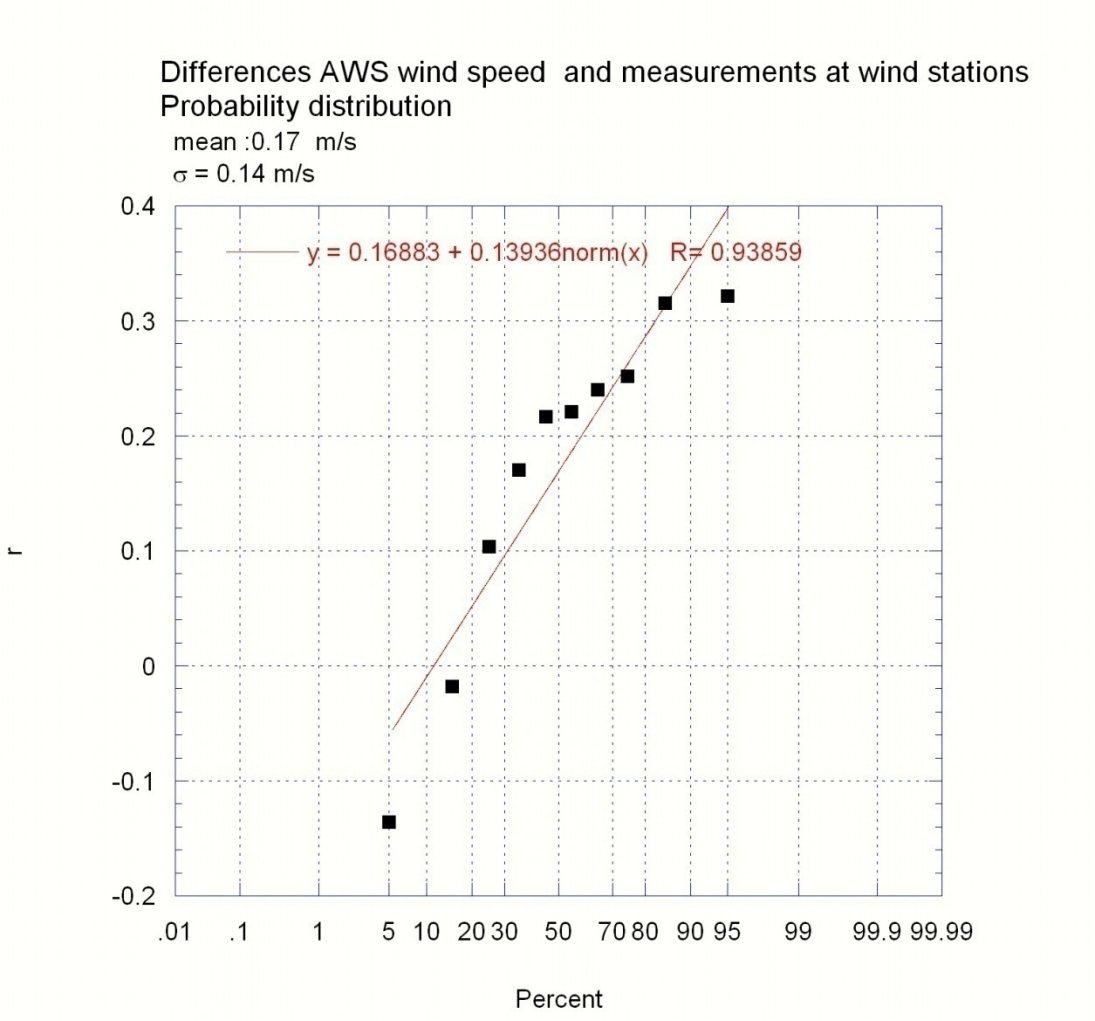

Figure 6 Probability distribution of the difference between observed and computed wind speeds at the selection observation locations at 30 m. A normal distribution curve fit to the difference data is shown.

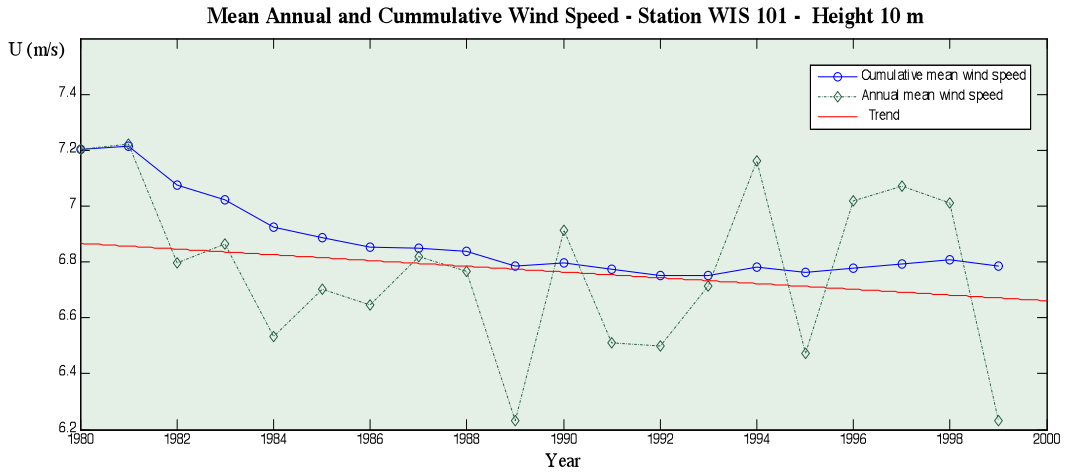

Figure 7 Mean annual and cumulative wind speed at WIS 101 versus time (1980-1999) at 10 m elevation. The trend line is also shown.

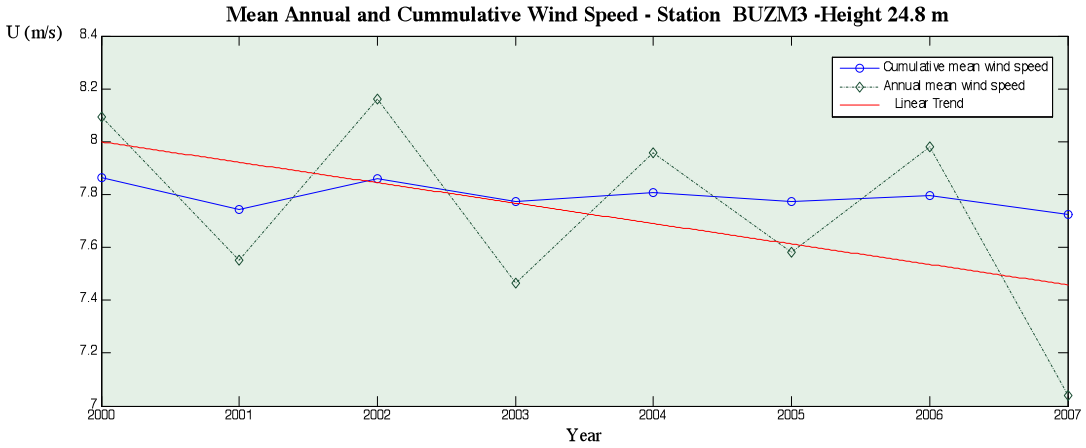

Figure 8 Mean annual and cumulative wind speed at BUZM3 versus time (2000- 2007) at 24.8 m elevation. The trend line is also shown.

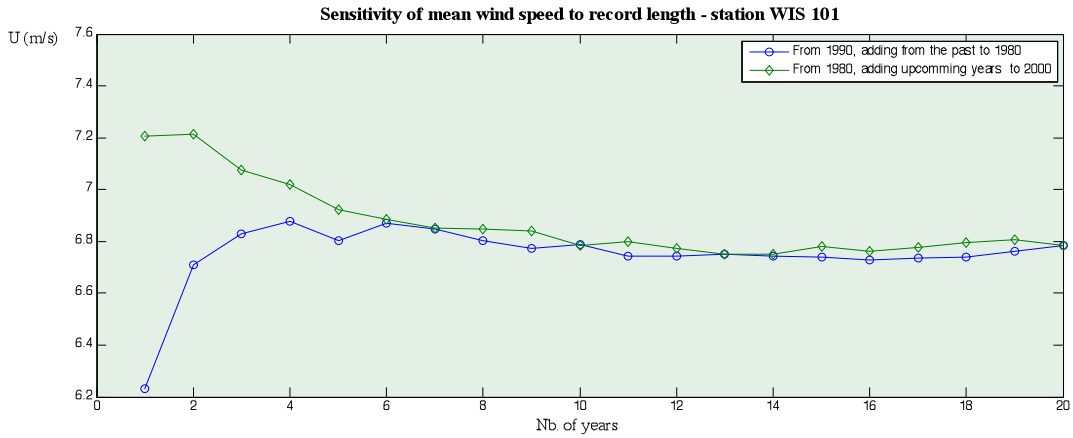

Figure 9 Cumulative mean wind speed versus number of years for both forward and backward averaging at WIS 101, 10 m elevation.

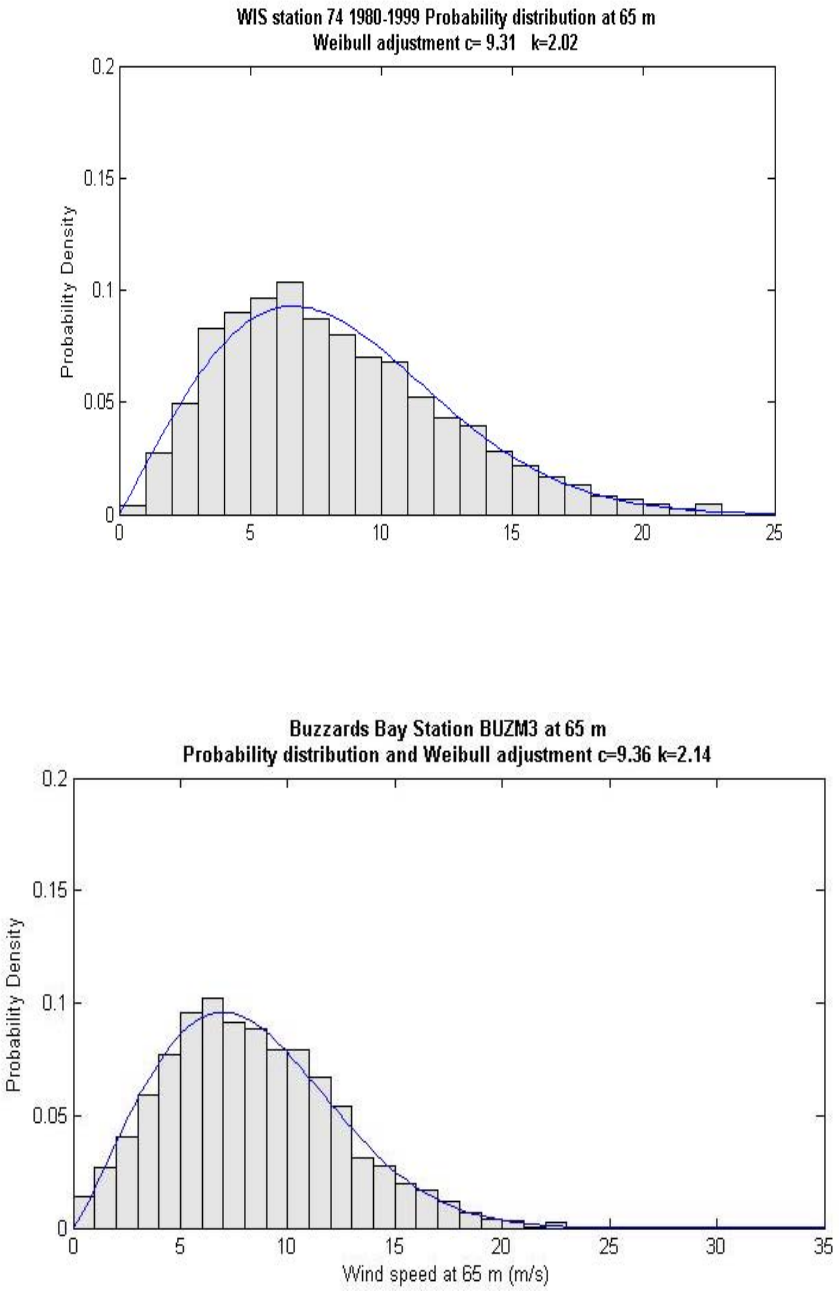

Figure 10 Probability distribution of wind speed at 65 m for WIS 74(upper panel) and BUZM3 (lower panel) stations. The solid line represents a least squares, Weibull distribution fit to the data, with the c and k values given in the header.

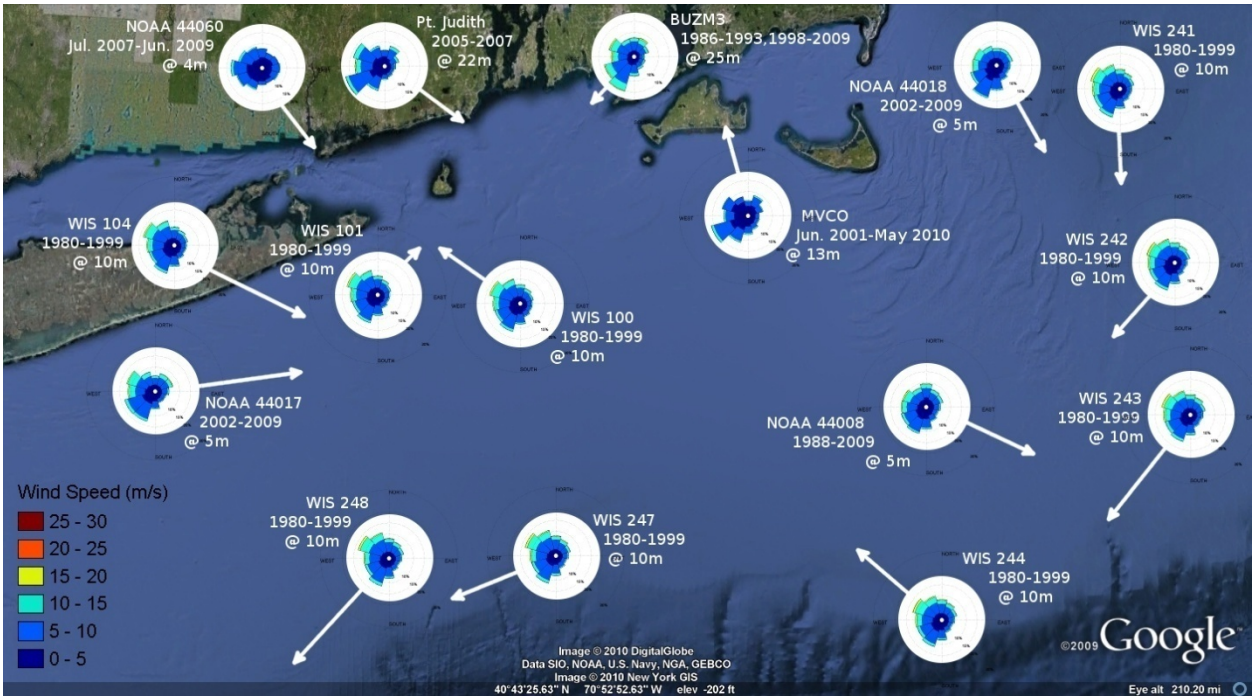

Figure 11 Wind speed frequency roses for SAMP study area.

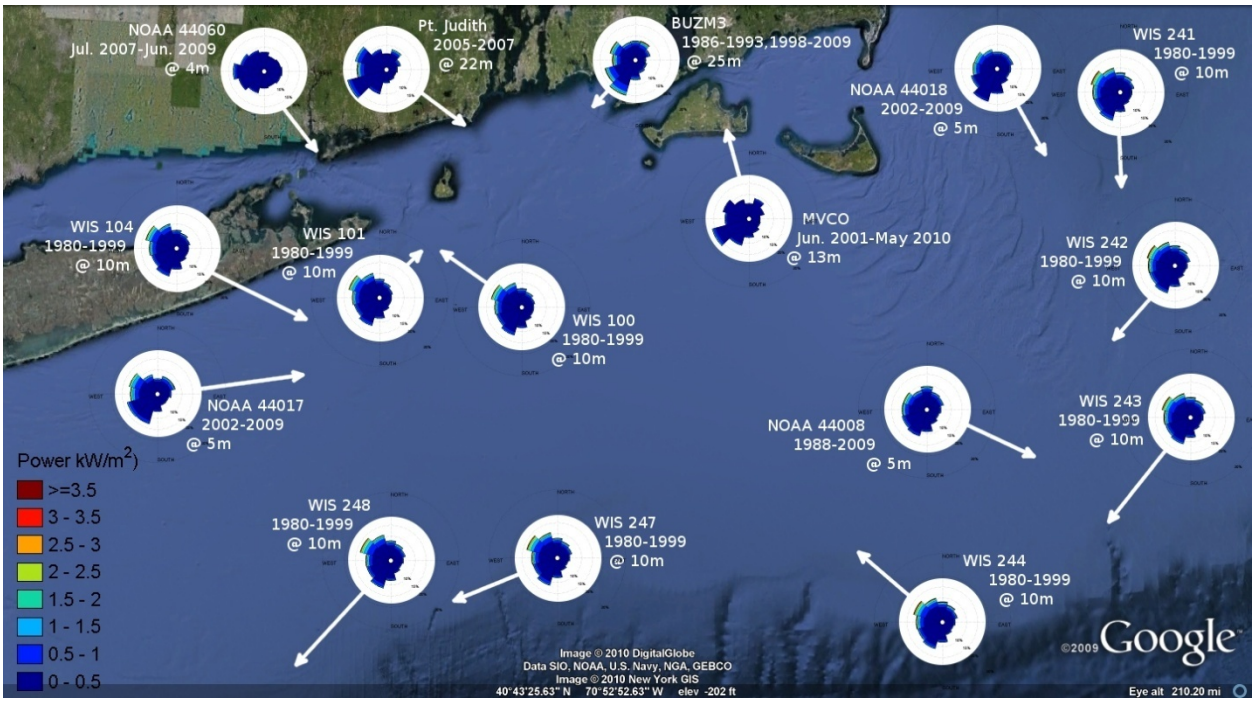

Figure 12 Wind power roses for SAMP study area.

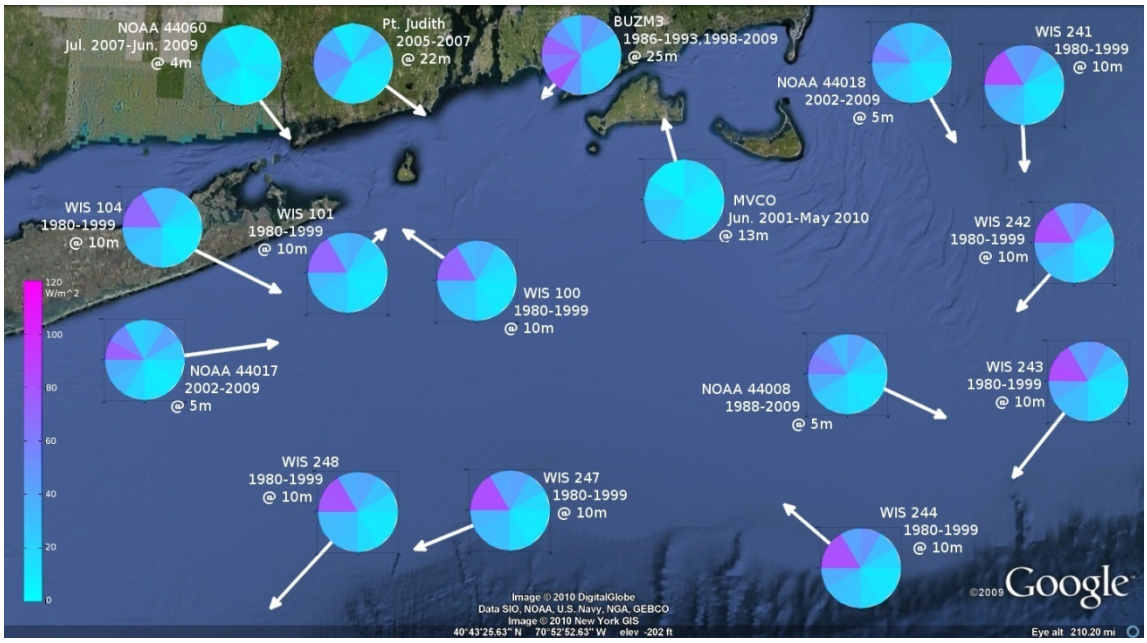

Figure 13 Mean wind power rose for SAMP study area.

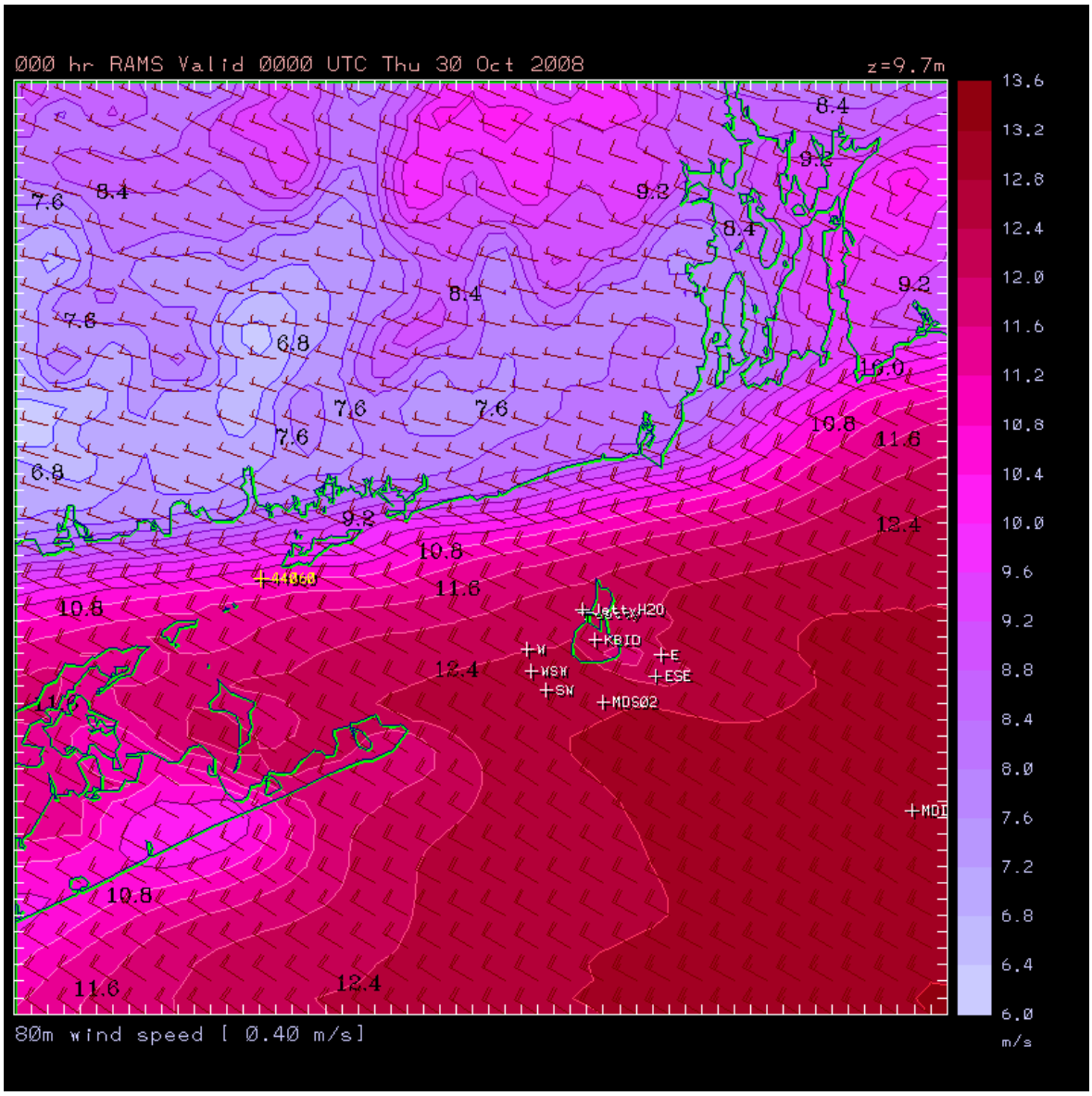

Figure 14 RAMS meteorological model predicted wind field in SAMP study area on October 30, 2008 (NW case).

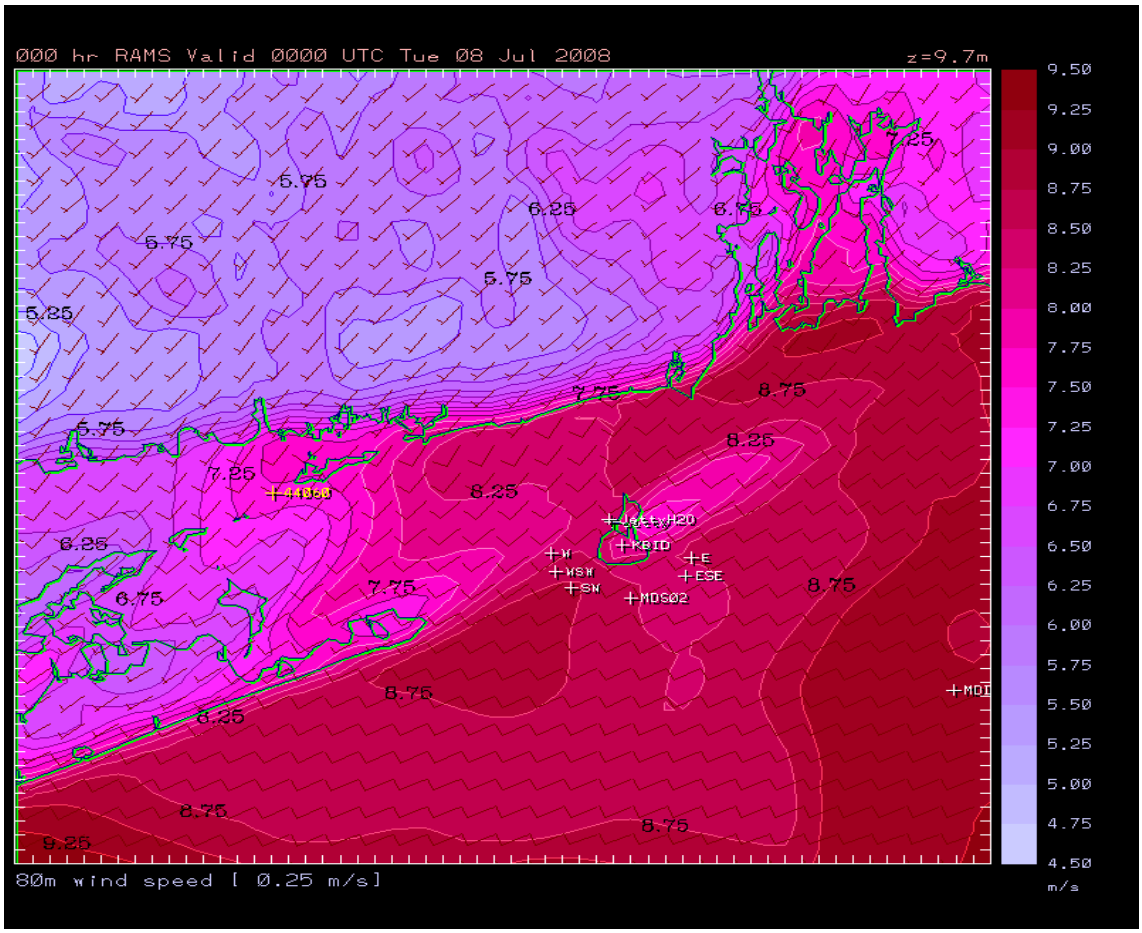

Figure 15 RAMS meteorological model predicted wind field in SAMP study area on July 8, 2008 (SW case).

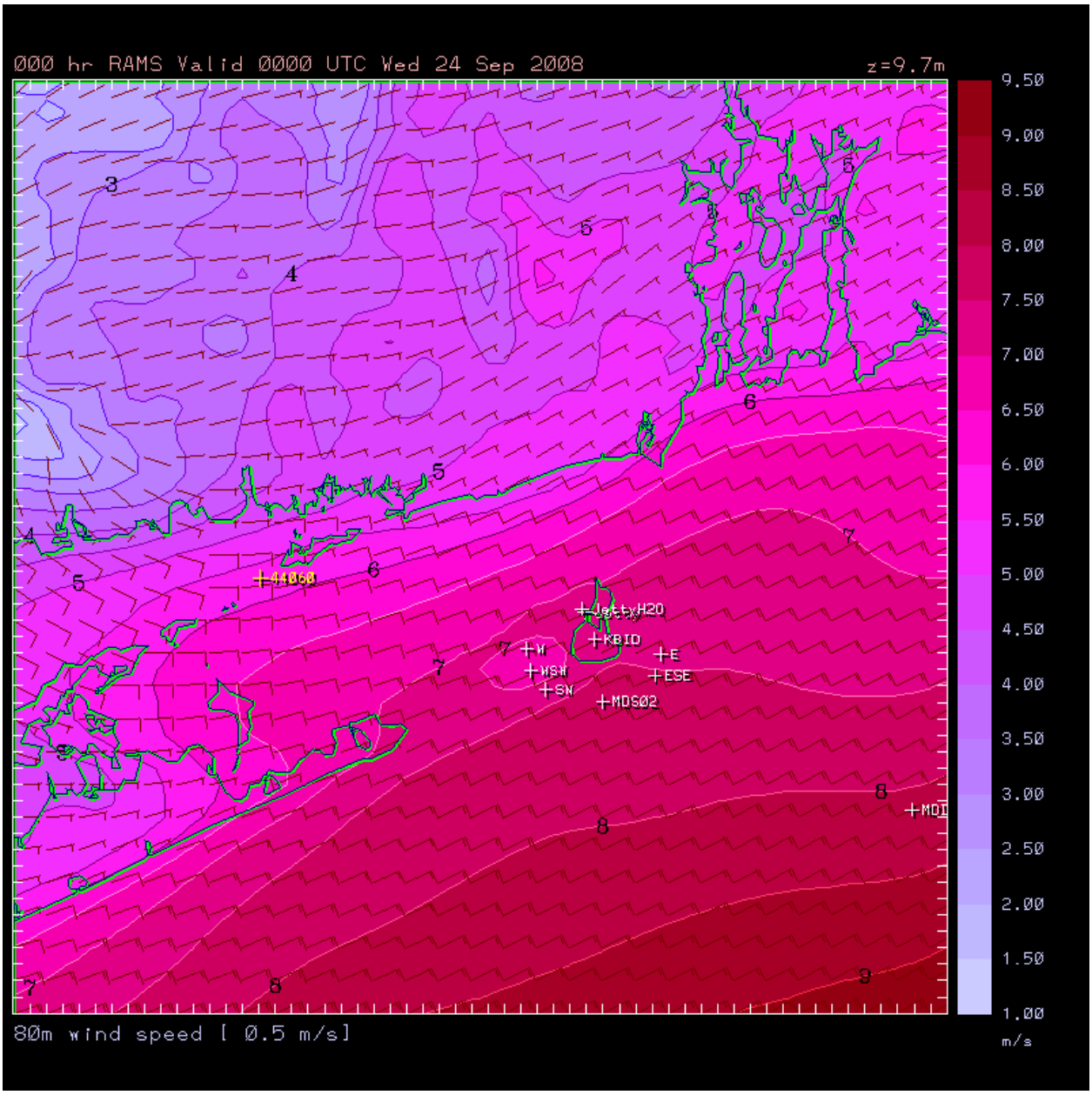

Figure 16 RAMS meteorological model predicted wind field in SAMP study area on September 24, 2008.

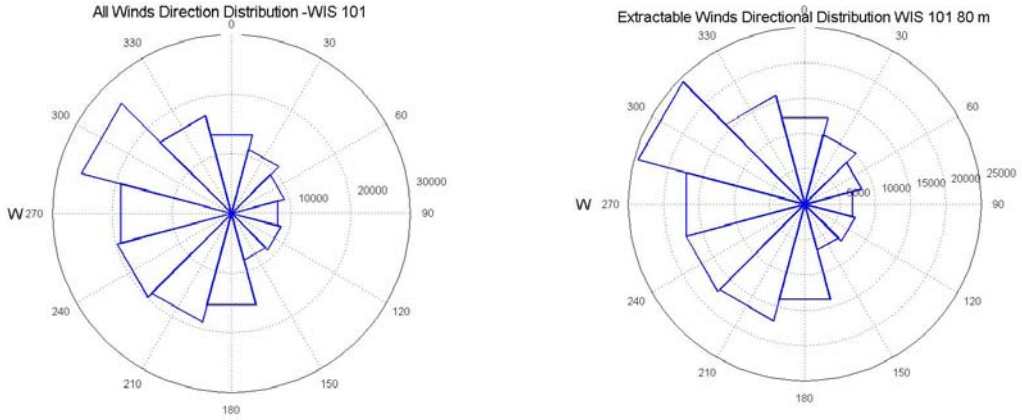

Figure 17 Wind directional distribution by count at 80 m elevation for WIS 101 (1980-1999, hourly data). Left panel includes all wind data and right panel extractable winds (3.5 to 27 m/sec). (Note difference in scale.)

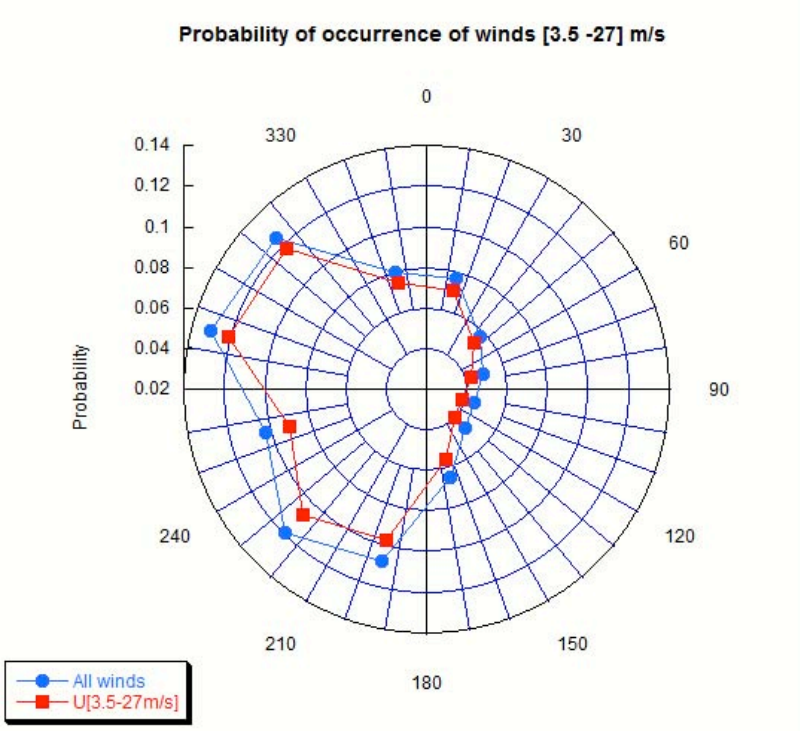

Figure 18 Probability of occurrence by direction for all and extractable winds at WIS101, 80 m elevation.

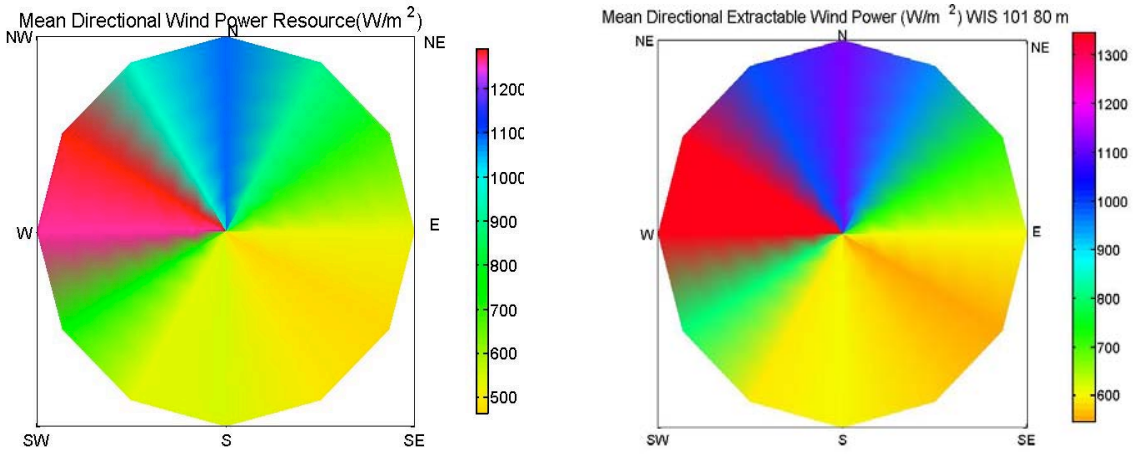

Figure 19 Mean directional wind power resource, all (left panel) and extractable (right panel).

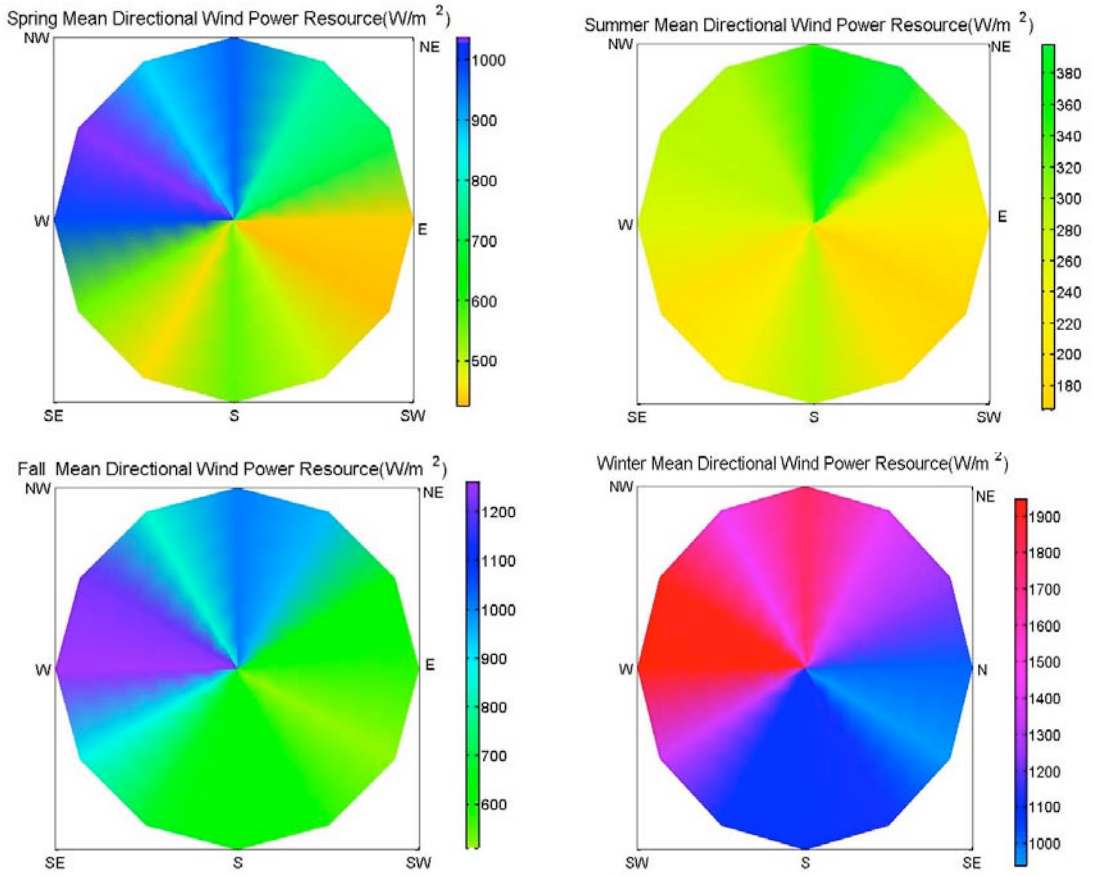

Figure 20 Mean wind power resource by direction for each season of the year, spring, summer (upper panel, left and right) and fall, winter (lower panel, left and right).

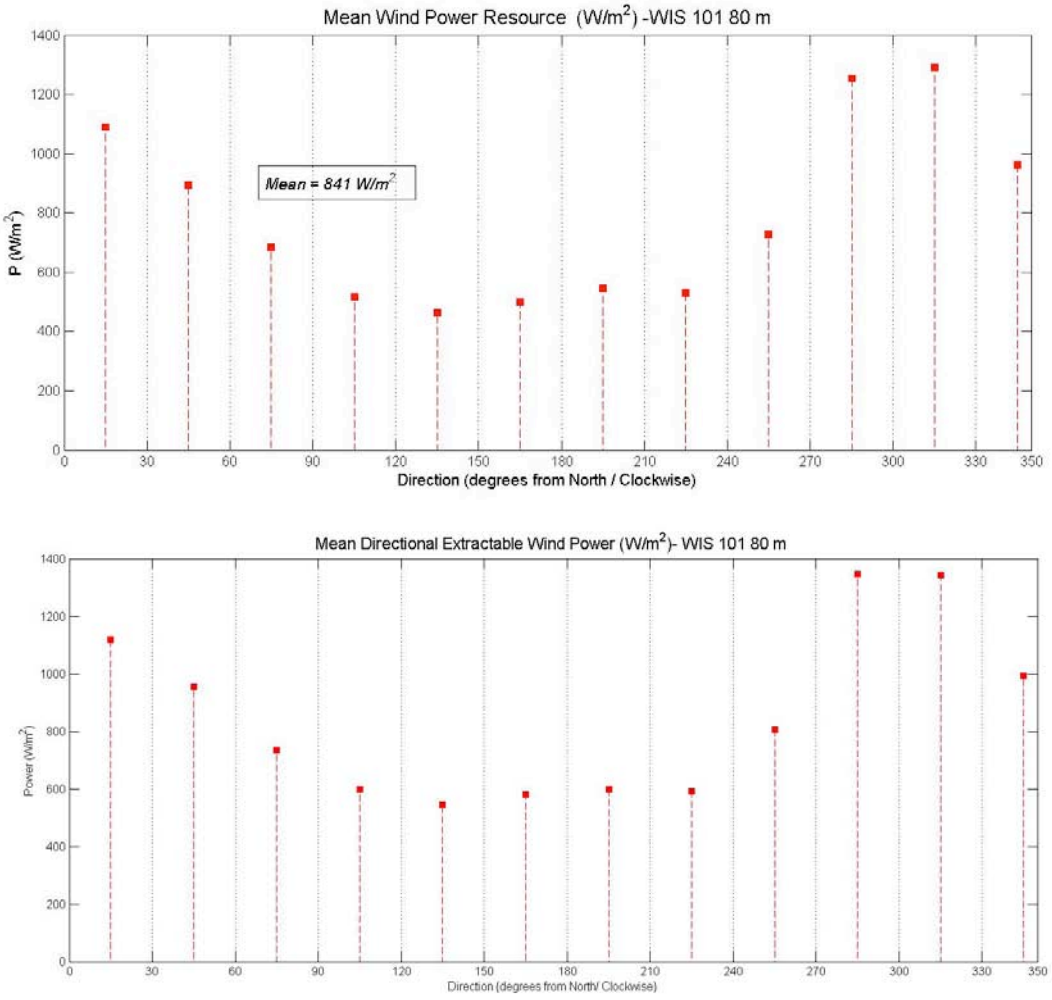

Figure 21a Mean wind power all (upper panel) and extractable (lower panel) by direction, WIS 101, 80 m.

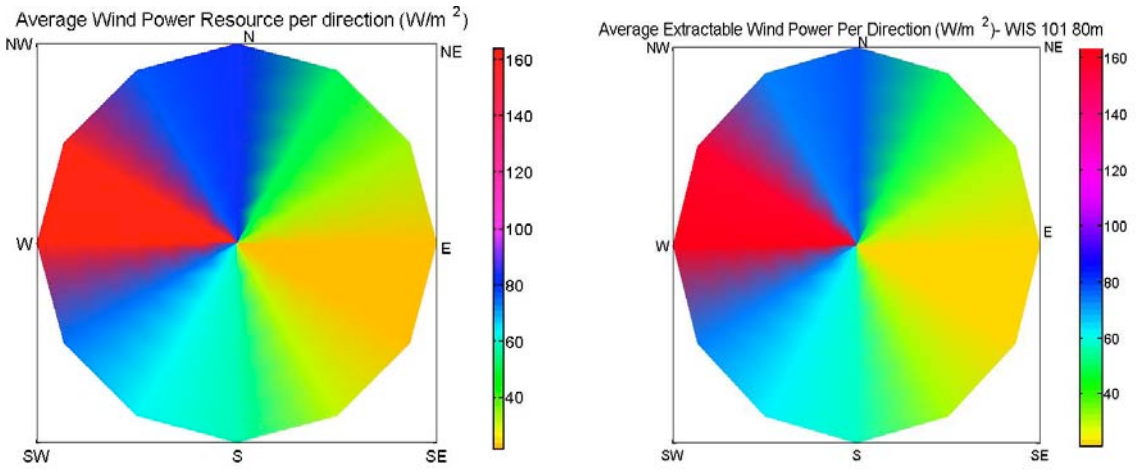

Figure 21b Average wind power resource by direction, total (left panel) and extractable (right panel), WIS 101, 80 m.

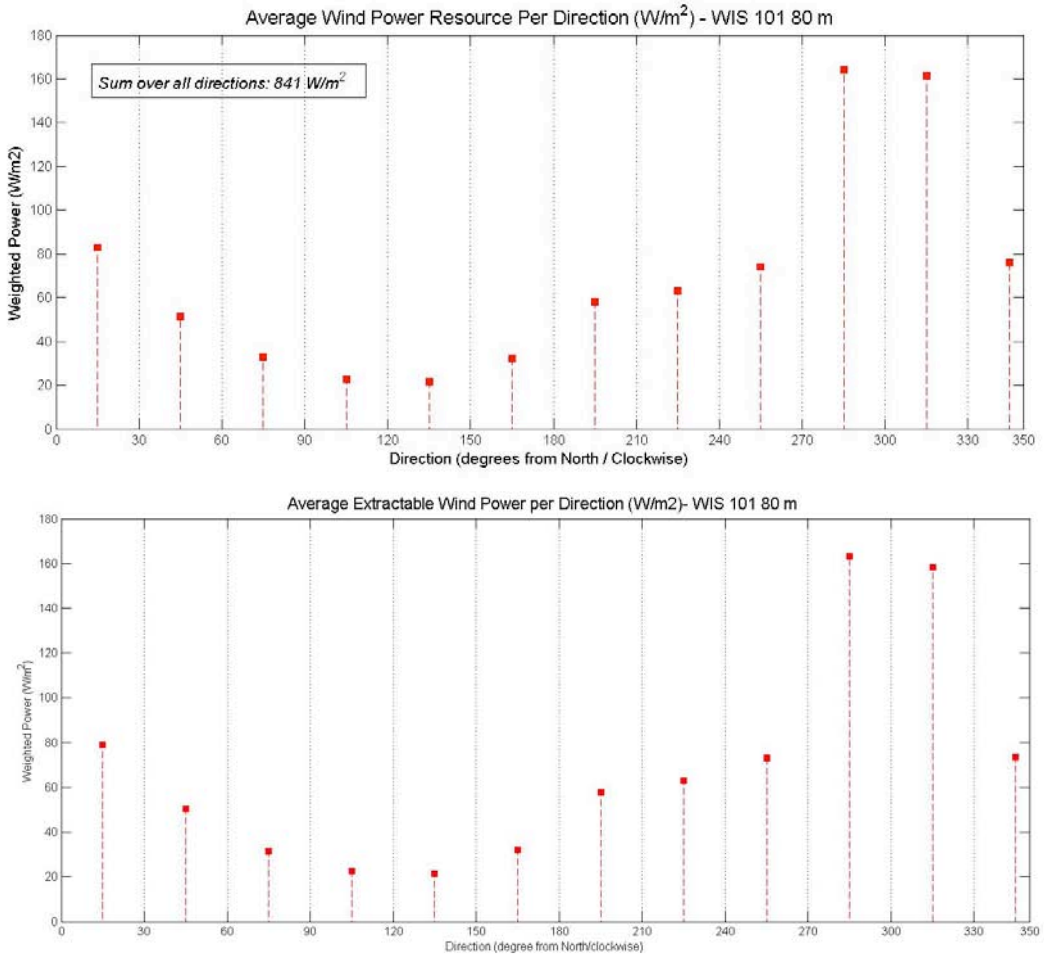

Figure 22 Average wind power by direction, all winds (upper panel) and extractable winds (lower panel), WIS 101, 80 m.

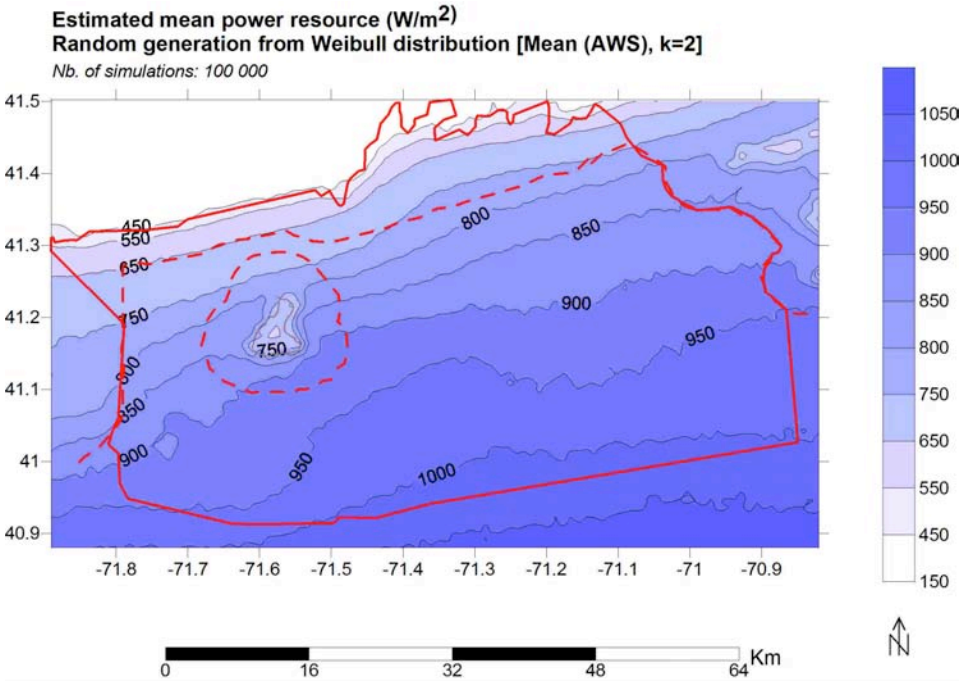

Figure 23 Contours of mean wind power in the study area based on AWS all winds.

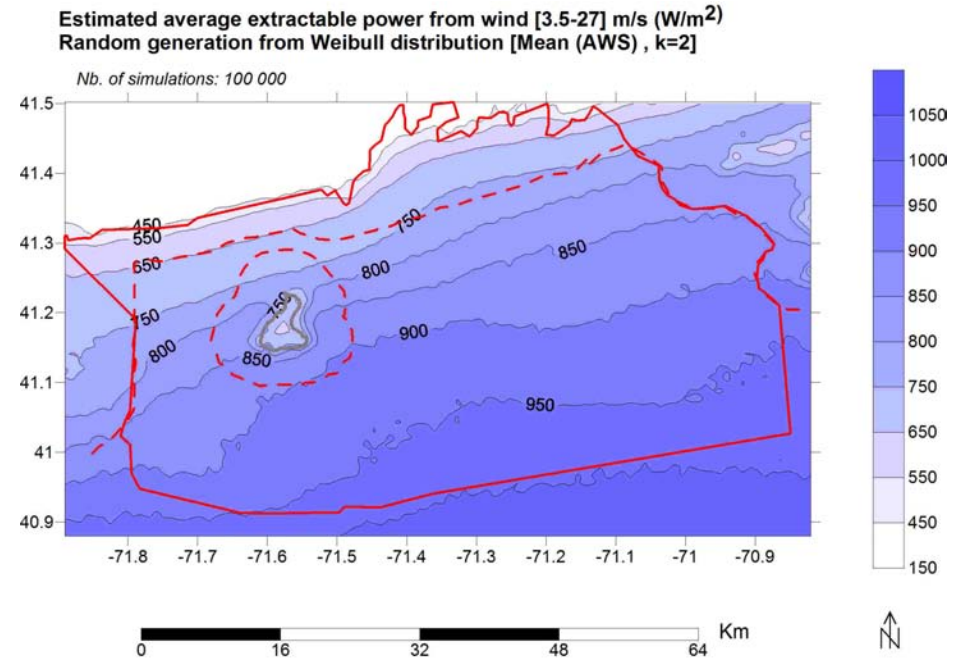

Figure 24 Contours of mean wind power in the study area based on AWS extractable winds.

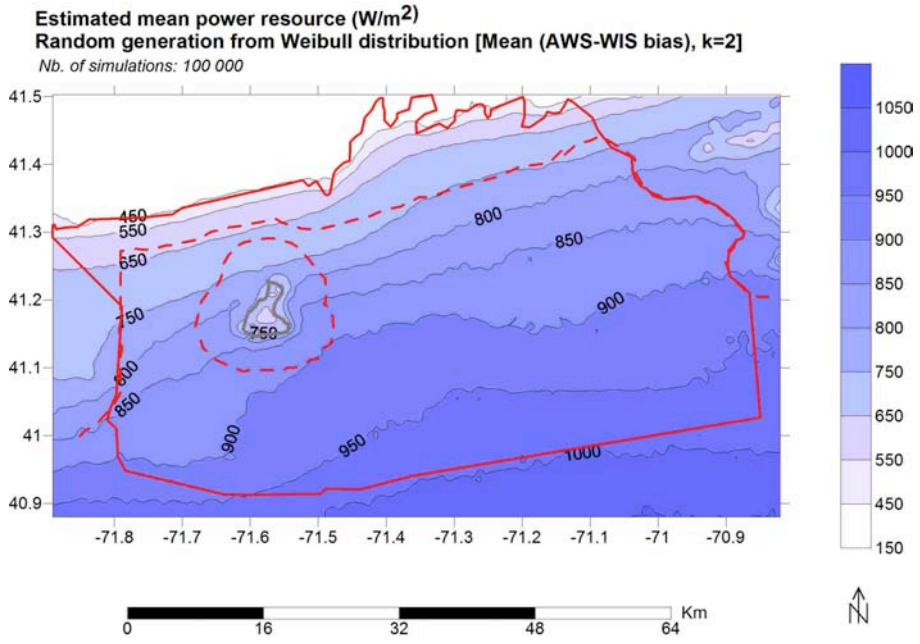

Figure 25 Contours of mean wind power in the study area based on AWS minus bias, all winds.

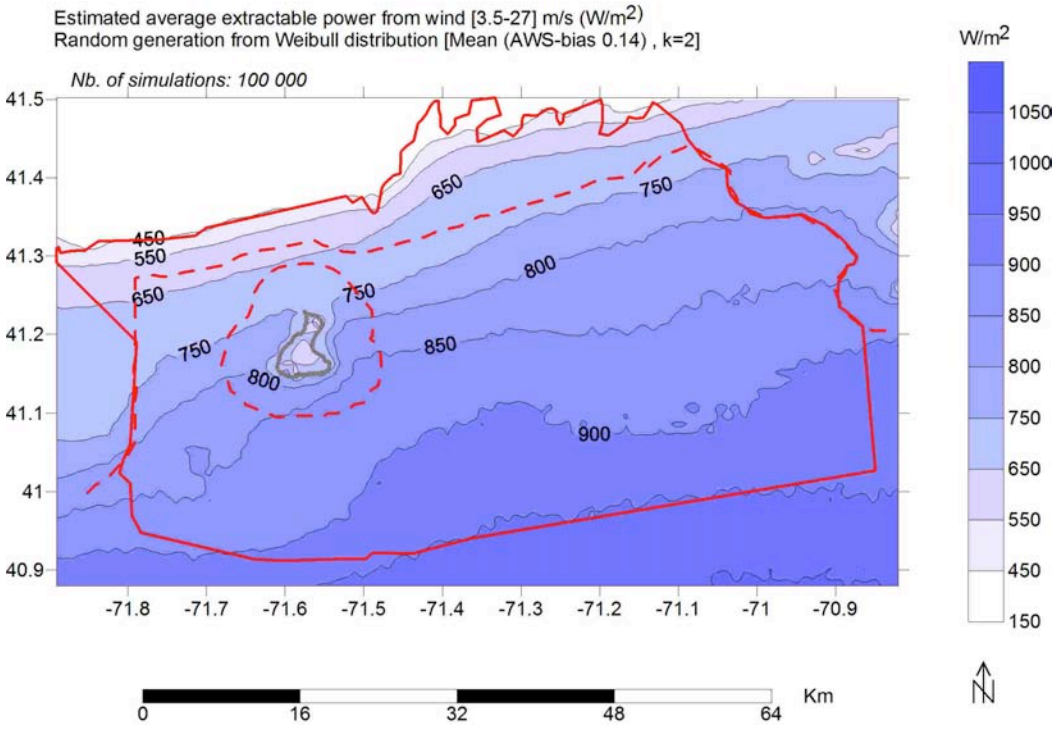

Figure 26 Contours of mean wind power in the study area based on AWS minus bias, extractable winds.

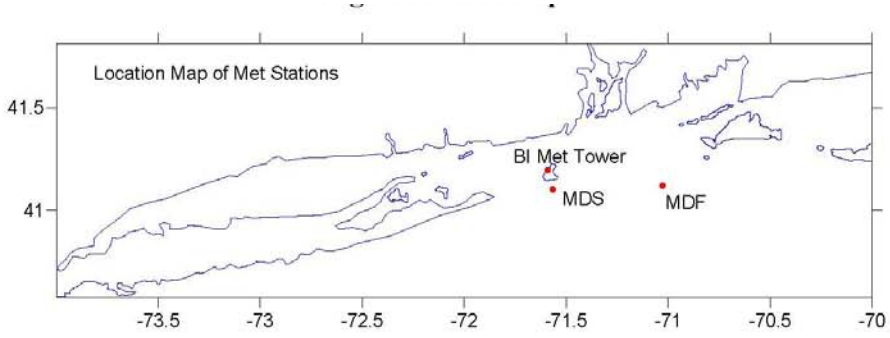

Figure 27 Location map for MDS, MDF and AWS Met tower.

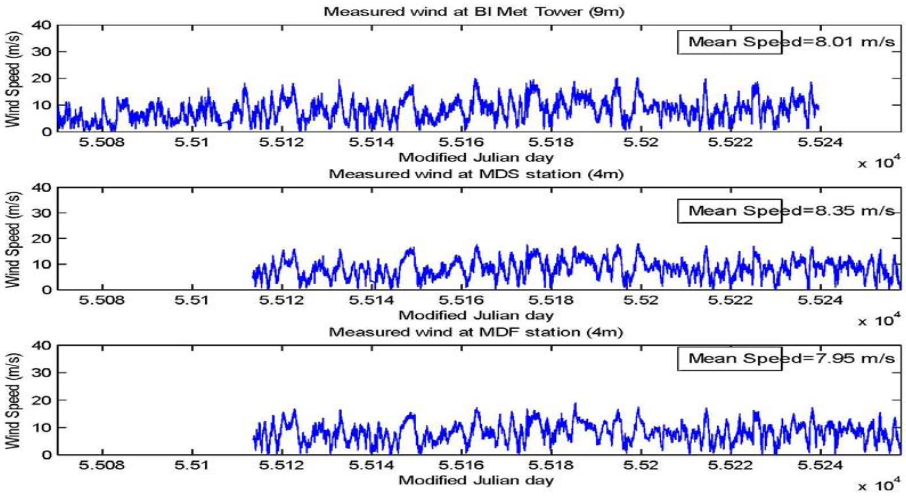

Figure 28 Wind time series at AWS Met, MDS, and MDF, from beginning of record to February 1, 2010.

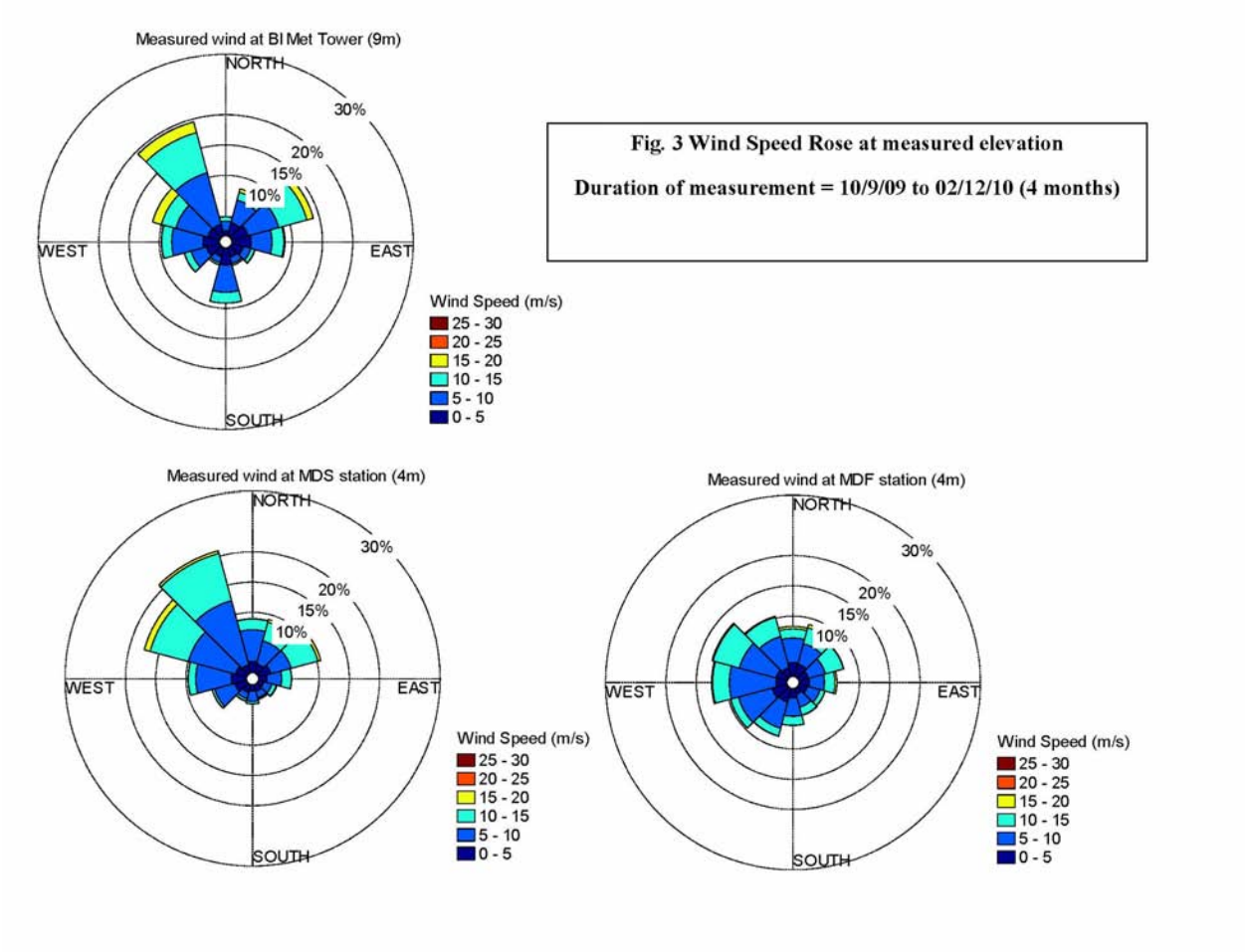

Figure 29 Wind speed rose for AWS Met, MDS, and MDF from October 9, 2009 to February 12, 2010.

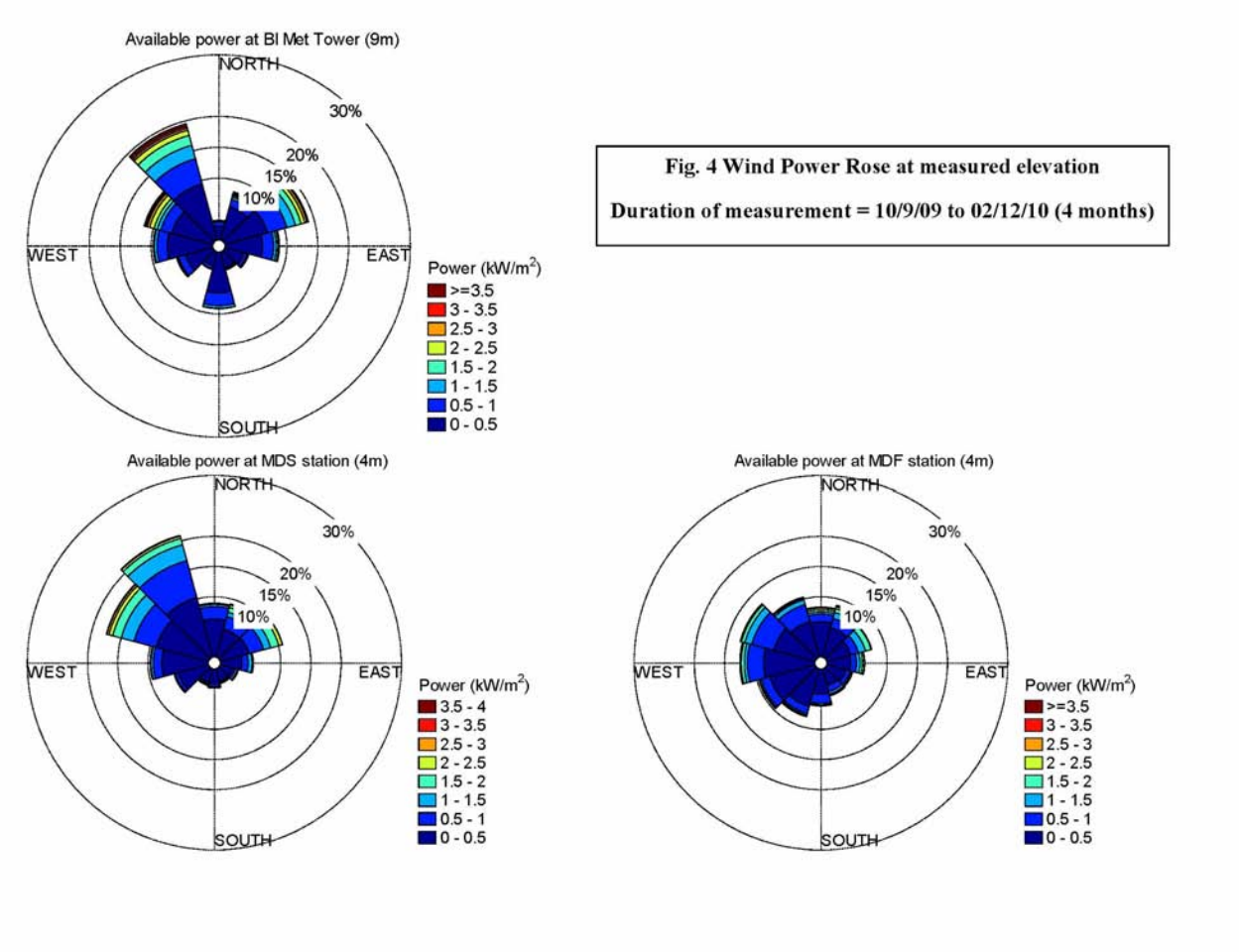

Figure 30 Wind power rose for AWS Met, MDS, and MDF from October 9, 2009 to February 12, 2010.

Appendix A

Wind frequency and power density (seasonal and annual) roses and Weibull distribution fits for selected stations in the SAMP study area.

For this appendix material, see Appendix A of Spaulding, et al., 2010, "Wind Resource Assesment in the Vicinity of a Small, Low Relief Coastal Island" – this report.

21.

Meteorological Model Based Wind Resource Assessment in the Vicinity of Block Island for the Rhode Island Ocean Special Area Management Plan 2010

by

Malcolm L. Spaulding[1], Marty Bell[2], Jay Titlow[3], Lauren Decker[4], Annette Grilli[1], Ravi Sharma[1], Alexander Crosby[1], and Daniel Mendelsohn[4]

[1] Ocean Engineering
University of Rhode Island
Narragansett, RI

[2]Metlogic
212 West Mountain Avenue
Fort Collins, CO 80521

[3]WeatherFlow
790 Poquoson Ave
Poquoson, VA 23662

[4]Applied Science Associates
55 Village Square
South County Commons
South Kingstown, RI 02879

June 7, 2010

Executive Summary

Hindcast simulations of the winds in the vicinity of Block Island were performed using the Regional Atmospheric Modeling System, RAMS, V6., from October 1, 2009 to February 28, 2010 to assist in evaluating various sites south of Block Island for a small wind farm. This period was selected since wind and air temperature observations were available from an offshore buoy (4 m elevation) immediately south (4.5 km) of the island and from a meteorological tower (9.9, 32, 47.6 and 57.4 m elevations) near the center, west coast of the island. The model was implemented in a four level nested system with grid resolutions of 12, 6, 2, and 0.5 km. The model was driven by NAM 12 km analyses. The model employed a 20 m vertical grid resolution at the surface, that geometrically increased with elevation. Island land cover and topography and sea surface temperature were provided by national digital data bases.

The winds during this period were predominantly from the NW, with the next most frequent direction from the NE. The wind distribution is typical of winter winds in the area, but with enhanced winds from the NE. The meteorological tower observations showed very low shear coefficients, 0.7 to 0.9, during the simulation period, typical of neutral to unstable, winter winds.

Model simulations were compared to meteorological tower observations at 57 m on shore of Block Island and showed good agreement with the data, with similar trends for passing weather events. The observed mean speed was 9.73 m/sec and the RAMS predicted was 9.3 m/sec (5.1% difference). The wind power followed a similar trend, 1000 kW/m^2 observed and 838 kW/m^2 RAMS (16.2% difference). The model predicted shear was higher than meteorological tower observations. The predicted shear coefficients increased dramatically over the island, reaching values as high as 0.45 over the southern end of the island where vegetative cover is dense. Model predictions also show lee effects from the topography/land cover at the southern end of the island (mean elevation of 35 m) for the two predominant wind directions. Lee effects were clearly noted 8 km from the island. Model predictions were also compared to winds (10 m elevation) from an offshore buoy and again showed good agreement (observed - 8.54 m/sec vs RAMS- 8.32 m/sec).

Simulations were performed for the dominant NW wind case to assess the sensitivity of the model to how the island was represented: by both its topography and land cover, or by each

separately. The model predictions showed that either topography or land cover contributed substantially to lee effects.

Model predictions were integrated over the simulation period to estimate mean wind speeds and average power at 80 m. The mean wind speed and power contour lines are parallel to the RI shoreline. Wind speeds decrease from 10.2 m/sec south of Block Island to 9.7 m/sec at the northern end of the island. Power decreases from 1150 kW/m^2 to 965 kW/m^2 over the same distance. Power estimates were made at three potential locations for a small wind farm (5 to 8 turbines), SE, S and SW of the island following the state water boundary line (5 km) from the island. Mean powers were predicted to be SE- 1097 kW/m^2, S - 1139 kW/m^2, and SW -1076 kW/m^2. The S site has the highest power production potential; 3.6 to 5.4% higher than the other two sites. The difference between the sites is due to lee effects from the island for NW winds at the SE site and for NE winds at the SW site. The SW site, in addition, is the lee of eastern end of Long Island (Montauk Point) for westerly winds. Lee effects at the S site are minimal since winds from the N are rare. Simulations have not been performed for spring and summer months where SW winds dominant. Winds from this direction are likely to be comparable at all three sites, since there is no lee effect and the locations are quite close. There is some degradation of winds from the W due however to lee effects from Long Island and an increase to the SW of the island due to channel enhancements for southerly winds.

Simulations, using a template based method, were performed using the observed wind rose at the AWS Met site and model predicted wind fields for eight compass directions. Predicted mean wind speeds and power densities were in generally good agreement with the hindcasts. The differences could be explained in part by the model predicting lower frequency for the NW winds and higher frequency for W winds than observed. When the model predicted wind rose at the AWS Met was used the predictive performance improved measurably.

Table of Contents

List of Figures

List of Attachments and Appendices

Appendix A: Hindcast Verification Project Oct 2009 Feb 2010

Appendix B: Comparison of WeatherFlow predictions and observations

Abstract

Hindcast simulations of the winds in the vicinity of Block Island were performed using the Regional Atmospheric Modeling System, RAMS, V6., from October 1, 2009 to February 28, 2010 to assist in evaluating various sites south of Block Island for a small wind farm. This period was selected since wind and air temperature observations were available from an offshore buoy (4 m elevation) immediately south (4.5 km) of the island and from a meteorological tower (9.9, 32, 47.6 and 57.4 m elevations) near the center, west coast of the island. The model was implemented in a four level nested system with grid resolutions of 12, 6, 2, and 0.5 km. The model was driven by NAM 12 km analyses. The model employed a 20 m vertical grid resolution at the surface, that geometrically increased with elevation. Island land cover and topography and sea surface temperature were provided by national digital data bases.

The winds during this period were predominantly from the NW, with the next most frequent direction from the NE. The wind distribution is typical of winter winds in the area, but with enhanced winds from the NE. The meteorological tower observations showed very low shear coefficients, 0.7 to 0.9, during the simulation period, typical of neutral to unstable, winter winds.

Model simulations were compared to meteorological tower observations at 57 m on shore of Block Island and showed good agreement with the data, with similar trends for passing weather events. The observed mean speed was 9.73 m/sec and the RAMS predicted was 9.3 m/sec (5.1% difference). The wind power followed a similar trend, 1000 kW/m^2 observed and 838 kW/m^2 RAMS (16.2% difference). The model predicted shear was higher than meteorological tower observations. The predicted shear coefficients increased dramatically over the island, reaching values as high as 0.45 over the southern end of the island where vegetative cover is dense. Model predictions also show lee effects from the topography/land cover at the southern end of the island (mean elevation of 35 m) for the two predominant wind directions. Lee effects were clearly noted 8 km from the island. Model predictions were also compared to winds (10 m elevation) from an offshore buoy and again showed good agreement (observed - 8.54 m/sec vs RAMS- 8.32 m/sec).

Simulations were performed for the dominant NW wind case to assess the sensitivity of the model to how the island was represented: by both its topography and land cover, or by each separately. The model predictions showed that either topography or land cover contributed substantially to lee effects.

Model predictions were integrated over the simulation period to estimate mean wind speeds and average power at 80 m. The mean wind speed and power contour lines are parallel to the RI shoreline. Wind speeds decrease from 10.2 m/sec south of Block Island to 9.7 m/sec at the northern end of the island. Power decreases from 1150 kW/m^2 to 965 kW/m^2 over the same distance. Power estimates were made at three potential locations for a small wind farm (5 to 8 turbines), SE, S and SW of the island following the state water boundary line (5 km) from the island. Mean powers were predicted to be SE- 1097 kW/m^2, S - 1139 kW/m^2, and SW -1076 kW/m^2. The S site has the highest power production potential; 3.6 to 5.4% higher than the other two sites. The difference between the sites is due to lee effects from the island for NW winds at the SE site and for NE winds at the SW site. The SW site, in addition, is the lee of eastern end of Long Island (Montauk Point) for westerly winds. Lee effects at the S site are minimal since winds from the N are rare. Simulations have not been performed for spring and summer months where SW winds dominant. Winds from this direction are likely to be comparable at all three sites, since there is no lee effect and the locations are quite close. There is some degradation of winds from the W due however to lee effects from Long Island and an increase to the SW of the island due to channel enhancements for southerly winds.

Simulations, using a template based method, were performed using the observed wind rose at the AWS Met site and model predicted wind fields for eight compass directions. Predicted mean wind speeds and power densities were in generally good agreement with the hindcasts. The differences could be explained in part by the model predicting lower frequency for the NW winds and higher frequency for W winds than observed. When the model predicted wind rose at the AWS Met was used the predictive performance improved measurably.

1 Introduction

The RI Ocean Special Area Management Plan (SAMP) has identified a potential renewable energy zone in state waters south of Block Island (Figure 1 and 2). Pear shaped, Block Island is approximately 9 km (N-S) by 6 km (widest at southern end, E-W) and was formed as an end moraine deposit from the most recent glacial ice sheet advance. The southern end of the island has a mean elevation of about 35 m (Figure 3) and is characterized by rolling hills, scrub and brush cover, and pockets of deciduous trees (Figure 4). The island is located about 15 km south of the southern RI coastal line and 23 km east northeast of Montauk Point, NY. This site was selected based on a comprehensive screening analysis and the application of a Technology Development Index (TDI) that evaluates the technical challenge to siting of lattice jacket supported wind turbines to the available power at the site (Spaulding et al, 2010a; Grilli et al, 2010). It was also identified in ATM's (2007a, b) initial screening study for offshore wind development. The analysis was performed on a 50 m spatial grid and included consideration of water depth, wind resources, cost of lattice jacket structures, and the construction effort for a pile foundation system. After consideration for marine traffic, and the impacts on marine fisheries, birds and marine mammals, a 2 km wide arc extending from SSW to E of the southern end of Block Island was selected (Figure 2). The seaward edge of the zone is bounded either by the state water boundary or the designated navigation precautionary area to the east.

One concern in the siting was the impact of topography and associated land cover on the wind resources in the immediate vicinity of the island, particularly for winds from the NW and NE, which are predominant in the winter. The concern was that the turbines would be adversely impacted by the lee effects of the island. Grilli et al's (2010) study addressed this issue by evaluating the sensitivity of predictions to two different wind resource estimates; one based on a coarse (2.5 km) grid meteorological model simulation product provided by Brower (2007) and the second based on a template scaling method using meteorological model predictions for eight compass directions and then scaling these estimates using an annual wind rose (Spaulding et al, 2010b). The two methods give substantially different results, with the later method showing more pronounced lee effects to the SE of the island.

The goal of the present study is to determine how the power production potential varies within the proposed renewable energy zone, during a winter period, when NW and NE winds dominate and the lee effects to the south of the island are expected to be important. To accomplish this goal, a four level nested version of the RAMs meteorological system is applied to predict the three dimensional wind, temperature, and pressure field in the vicinity of the island from October 1, 2009 to February 28, 2010. Wind data is available from an offshore buoy 5 km south of Block Island and from a meteorological tower located on the western coast, about mid island during this period. Model predictions are next validated with the observations. Finally wind power estimates are made for the renewable energy zone shown in Figure 2. Section 2 presents an overview of the observation data available and Section 3 a summary of the RAMS meteorological modeling system and its application to the study area. Selected model predictions for typical NW and NE winds are provided in Section 4. Section 5 presents a comparison of model predictions to observation and 6 summarizes the power estimates for the renewable energy zones. Conclusions are presented in Section 7.

2 Observations

Two data sets are available for model validation for the simulation period from October 1, 2009 through February 28, 2010. They are summarized below:

Ocean SAMP Buoy MDS02 (Lat: 41.1, Long: 41.56)(MDS)

The University of Maine, on behalf of the Ocean SAMP study, deployed an offshore buoy with meteorological and oceanographic sensors immediately south of Block Island at the state water boundary line. The buoy collects wind speed and direction and air and sea surface temperature data every 15 minutes. The data is distributed through the Northeast Regional Association of Coastal Ocean Observing Systems web site (www.neracoos.org). The buoy has been in operation from Oct 1, 2009 to present.

AWS True Winds Block Island Meteorological Tower (AWS Met) (Lat: 41°11'49.96"N, Long: 71°35'30.34"W)

AWS True Winds erected a meteorological tower at the western entrance to Great Salt Pond. Wind speed and direction data are being collected at elevations of 9.9, 32, 47.6, and 57.4 m. Data is available from Aug 2009 to present.

Additional data sets are available in the area from Army Corp WIS study (WIS101, hindcast, 1980-1999), Department of Energy Site (DOE, 1977-1981), Block Island Airport (KBID, 1997 to 2009), and WeatherFlow's site at Block Island Jetty (2005 to 2009). They are of secondary interest for the present study. Spaulding et al (2010b) discuss these data sets in detail.

Figure 5 and 6 show the wind frequency and power roses, respectively for MDS and AWS Met stations. Data for the other stations are shown for reference but are not discussed in depth since they represent annual estimates and were collected outside the simulation period. The observations at MDS are at a 4 m elevation and those at AWS Met are at 9.9 m. During the winter observation period, both wind frequency and power roses are dominated by NW winds, followed by NE winds. Figure 7 shows the average wind power density by direction, consistent with Figure 6, the power is dominated by NW winds. Wind and power roses were analyzed for additional elevations at AWS Met and showed a similar structure. Values are shown at 32 and 57 m in Figures 7 and 8, respectively. The figures also show Weibull distribution fits to the data. The shape parameter, k, is typically in the range of 2.15 to 2.21. The amplitude parameter, c, increases with elevation from 4.62 at 10 m, to 9.66 at 32 m, to 10.12 at 57 m. Over the period of interest the wind shear coefficients at this site were typically in the range of 0.06 to 0.09, indicating a neutral to unstable boundary layer and well mixed conditions. Buoy observations show that the air temperature was colder than the water temperature during most of this period, consistent with an unstable atmosphere.

3 High Resolution Meteorological Modeling in Study Area

RAMS, the Regional Atmospheric Modeling System (Piekle et al, 1992; Tremback and Walko, 2010), is a highly versatile numerical code developed by several groups over the years, including the scientists at Colorado State University, the *ASTER division of Mission Research Corporation, and ATMET. RAMS is used for simulating and forecasting meteorological phenomena, and for depicting the results.

RAMS is primarily a limited area model, and many of its parameterizations have been designed for mesoscale or higher resolution scale grids. There is no lower limit to the domain

size or to the mesh cell size of the model's finite difference grid; microscale phenomena such as tornadoes and boundary layer eddies, as well as sub-microscale turbulent flow over buildings and in a wind tunnel, have been simulated with this code. Two-way interactive grid nesting in RAMS allows local fine mesh grids to resolve small-scale atmospheric systems such as thunderstorms, while simultaneously modeling the large-scale environment of the systems on a coarser grid.

The atmospheric model is constructed around the full set of non-hydrostatic, compressible equations that atmospheric dynamics and thermodynamics, plus conservation equations for scalar quantities such as water vapor and liquid and ice hydrometeor mixing ratios. These equations are supplemented with a large selection of parameterizations for turbulent diffusion, solar and terrestrial radiation, moist processes including the formation and interaction of clouds and precipitating liquid and ice hydrometeors, kinematic effects of terrain, cumulus convection, and sensible and latent heat exchange between the atmosphere and the surface, which consists of multiple soil layers, vegetation, snow cover, canopy air, and surface water.

For the present study daily simulations starting at 0Z were performed with RAMS version 6.1. The model employed a 500 m horizontal grid spacing on the high resolution grid telescopically nested from 12 km, 6 km and 2 km grids (Figure 10 and 11). A range of horizontal grid resolutions from 4 km to 250 m were tested. In most cases, the convergence of results at the proposed turbine locations occurred at 1-2 km. In some cases, where stable conditions existed and the proposed wind farm sites were downwind of the island, differences were apparent down to 500 m. 20 m vertical grid spacing, expanding upward with a geometric ratio of 1.15 was employed. Vertical grid resolutions from 40 m to 5 m were evaluated. Testing showed a loss in wind speed of up to 5% when the vertical resolution was lowered from 5 to 20 m. 20 m was used in this study in order to complete the 5 months of hindcasting in a timely fashion.

RAMS was initialized 6 hours prior to the 0Z start time (tau 0), firstly with a 2 grid run (outer grids only) from tau -6 to tau -3 (stage 1), then with all 4 grids from tau -3 to tau 0 (stage 2). Simulations were initialized from the 12km NAM analysis, with grid 1 bounded by subsequent 6 hourly 12 km National Center for Environmental Prediction (NCEP) North America Meteorology Model (NAM) analyses. In stage 1, the wind speed and direction, pressure, and air temperature model fields in the interior domain were strongly nudged to the interpolated NAM analysis values. In stage 2, the same variables were nudged, but far less strongly. The atmospheric moisture data was excluded from the nudging. This forces a balance to develop for

the mechanical quantities between the model and the NAM analysis, while allowing moisture quantities (clouds and precipitation) to evolve.

The 3D (spatial and depth) soil moisture field was extracted from the 12 km NAM analysis files and interpolated to the RAMS grids and soil levels. The 2D (spatial) snow cover field was also extracted from the 12km NAM analysis files and interpolated to the RAMS grids. Sea surface temperature data was obtained from Operational Sea Surface Temperature and Sea Ice Analysis (OSTIA) which uses satellite data provided by the GHRSST project, together with in-situ observations to determine the sea surface temperature. The analysis is performed using a variant of optimal interpolation (OI) technique. The analysis is produced daily at a resolution of 1/20 degree, (approx. 5km).

Digital elevation data for the study area, including Block Island, was provided from ASTER GDEM which has a 30 m grid resolution and is referenced to the WGS84/EGM96 geoid. Surface roughness, which is a significant factor in this study, is formulated as a function of wind speed over water. Over land, contributions to the surface roughness come from the water bodies, soil, vegetative cover and topographical drag within the grid cell. RAMS partitions the land use effects into contributing patches, whose weighting on the grid scale is proportional the relative dominance of the water and vegetation cover from the MRLC land use dataset.

4 Selected Simulation Results

RAMS was used to perform high resolution simulations for the study period from October 1, 2009 through February 28, 2010. This period was selected since wind data from both the meteorological tower on Block Island (AWS Met) and the MDS buoy were available. To provide a sense of the results, model predicted winds for cases of the two predominant directions observed during the study period are provided. Figure 12a and b show wind fields for NE winds, October 29, 2009, for grids 3 and 4 (Figure 9), respectively. Figures 13a and b show similar model predictions for NW winds, January 4, 2010. Predictions are at 80 m consistent with the hub height of 3.5 MW turbines. Each case is discussed separately below.

NE, October 29, 2009

The basic pattern shows that the wind speeds increase with distance offshore from the RI coastline, with the speed contours parallel to the shoreline. There is clear evidence of lower

speed winds to the SW of the Block Island as a result of lee effects from the southern end of the island. These effects extend at least 8 km from the island.

NW, January 4, 2010

This basic pattern for the NW case is very similar to the NE example, wind speeds increasing with distance from the coast and lee effects to the SE of Block Island. The spatial extent is similar to that for the NE case. For this case, lee effects are also noted from the topography on the northern end of the island. The impact from the northern end of the island is much reduced compared to the southern end because of the more limited area and lower elevation (Figure 3).

Simulations were performed to assess the sensitivity of the model predictions to the representation of Block Island used as input to RAMS. Model predictions were performed for December 6, 2010, a NW wind case, where the impact of both topography and land cover were considered, and where land cover and topography were modeled separately. Figure 14 shows model predictions of the wind at 80 m for the three cases: topography and roughness (upper panel), roughness only (center panel), and topography only (lower panel). The patterns for the three cases are very similar. There are differences, but these are a matter of detail. An interesting observation is that either roughness or topography can result in significant lee effects. This has important implications in that westerly winds flowing over Long Island, which has a relatively low topographic relief, can result in a significant impacted area in its lee.

5 Comparison of Model Predictions to Observations

Model predictions were compared to wind observations at the 57 m elevation at the AWS Met for the simulation period. Figure 15, 16, and 17 show observed and model values vs time (upper panel) and differences between the two (lower panel) for wind speed, power density, and shear coefficient, respectively. Additional details are provided in Appendix A.

The model does well in representing the passage of weather events and the associated temporal variations in wind speeds (Figure 15). The mean speeds predicted by the model are 9.23 m/sec and for the observations 9.73 m/sec; a 5.1% under prediction. The model predicted wind power density (Figure 16) is very similar in temporal structure to the observed values. Over the simulation period the model under predicts the observed value (Observed: 1000 kW/m^2 versus RAMS: 838 kW/m^2 or a difference of 16.2%). This difference is consistent with the speed under prediction.

Cross correlations (Appendix B) were performed using observed and hindcast data at 32 and 57 m and showed high values – 0.90 or greater. Power spectral densities and coherence analysis were performed and showed high coherences (0.9) for periods of 3 days or longer. The one day coherence values decreased to 0.6. A wind power density directional analysis was performed and showed the winds from the model are slightly more westerly than those observed.

The observed and predicted shear (57.4 m vs 32.1 m) (upper panel)(differences between wind speeds at the two elevations) and differences (lower panel) vs time are provided in Figure 17. The model shows similar temporal trends to the data but the mean model predicted value (0.026) is considerably higher than the observed (0.014). The comparative mean shear coefficients are 0.08 for the observations and 0.16 for the model.

A comparison of model predicted and observed wind speed versus time at MDS, 10 m elevation, is provided in Figure 18. The model does a very good job of predicting the temporal pattern and mean winds: model mean of 8.23 m/sec compared to 8.54 m/sec for the observed or an average difference of 0.49 m/sec (5.7%). The model predictive performance is comparable to that at AWS Met.

6 Mean Wind Speed and Power Estimates

Model predicted wind speeds were averaged at 10 and 80 m elevations over the simulation period and are shown in Figure 19. The patterns are very similar at both elevations, shore parallel contours with speeds increasing with distance offshore. Winds at 80 m are approximately 25% stronger than at 10 m. The wind speed contours are distorted (bulge) immediately south of Block Island, predominantly to the SE and SW. The former due to lee effects from NW winds and the later from similar effects from NE winds.

Model predicted average wind power and cumulative wind power are shown at 10 and 80 m elevations in Figure 20 and 21, respectively. The patterns are of course identical to those in Figure 19. The magnitudes however scale as the cube of the wind speed.

Model predicted average shear coefficients are shown in Figure 22. These are determined based on model predictions from the surface to 80 m. Shear coefficients are typically 0.105 in the area around Block Island but increase dramatically over island. They reach values of 0.4 to 0.45 on the southern end of the island. It is noted that the area to the west of the Block Island Airport

has the highest shear coefficients on the island. These high shear values are consistent with the land cover distribution (Figure 4).

Model predicted time series of wind power density are provided in Figure 23 for the sites noted in Figure 10. These include a ring of sites from E to S to W, following the state water boundary line and at key observation stations (AWS Met, MDS, KBID, and WeatherFlow's BIock Island Jetty). The wind power varies dramatically over time scales of hours as a result of changing weather patterns. There are about 25 events where the wind power exceeds 4 kW/m^2. NW wind events are typically strong and sustained for several days

The values in Figure 23 were averaged over the simulation period and are shown in Figure 24. The state water boundary sites represent potential locations for a small wind farm. The values range from 1060 to 1146 kW/m^2. Power density was highest to the south of the island and lower toward the E and W. Power estimates were made at three potential locations for a small wind farm (5 to 8 turbines), SE (incorporates E, ESE, SE), S (SSE, S, SSW) and SW (SW,WSW,W) of the island following the state water boundary line (5 km) from the island. Mean powers were predicted to be SE- 1097 kW/m^2, S - 1138 kW/m^2, and SW -1076 kW/m^2. The S site has the highest power production potential; 3.6 to 5.4% higher than the other two sites. The difference between the sites is due to lee effects from the island for NW winds at the SE site and for NE winds at the SW site. The SW site, in addition, is in the lee of the eastern end of Long Island (Montauk Point) for westerly winds. Lee effects at the S site are minimal since winds from the N are rare. Winds are also enhanced at the S site by the channeling effect of Long Island for winds from the W to SW.

The SW location has been partially eliminated based on the TDI analysis (Grilli et al, 2010) due to substantially higher construct effort to install a pile foundation in the glacial end moraine sediments. Of the two remaining sites, the S site has a marginally higher power production potential. It should be noted that this analysis has not considered winds from other times of the year. During the remainder of the year winds are observed to be predominantly from the SW. With SW winds all three locations are anticipated to experience about the same winds and hence power production potential. The simulation period under investigation covers only 5 months (October through February) and does not incorporate the spring and fall season when SW winds are dominant. An evaluation of the data at WIS 101 shows that this represents 77% of the total energy for the year.

Spaulding et al (2010b), in a companion paper, have estimated the average wind speeds and power density for the study area using a template based scaling method. In this approach model simulations are performed for representative wind events from each point of the compass and the results weighted by a wind rose used to estimate the mean conditions. The template method was applied to the present hindcast period using the wind rose at AWS Met. The individual simulation cases were taken from 2008 and 2009 and hence are completely independent of the present hindcast period.

Figure 25 shows the template (upper panel), hindcast (center panel), and difference between the two (lower panel) for the mean wind speeds (left) and power (right) at 80 m. The template based method is in good agreement with the model hindcast. The spatial patterns are quite similar, both showing lee effects to the SE of the island. The largest differences, south of Block Island are an over prediction of the wind speed of about 0.4 m/sec or about 3.5% of the 10.2 m/sec winds. For power the template method predicts more pronounced lee effects from NW winds compared to the hindcast. The largest difference is on the order 100 kW/m^2 south of Block Island or 12% higher than of mean value.

Figure 26 shows the observed and hindcast wind roses at AWS Met 57 m. The model hindcast under predicts the winds from the NW and over predicts those from the W. This is particularly the case at higher wind speeds. This explains why the template derived results show a more pronounced lee effect to the SE than the hindcast.

To investigate this issue further, the template method was applied again but using the hindcast wind at the AWS Met site, rather than the observed values at this location. This estimate hence removes the difference in wind roses between the hindcast and observations and focuses on the just difference between the hindcast and template methods. Figure 27 shows the template (upper panel), hindcast (center panel), and difference between the two (lower panel) for the mean wind speeds (left) and power (right) at 80 m. Comparing to Figure 26, the template method predictive performance is measurably improved. The differences in mean wind speed have been reduced from 0.2 to 0.4 m/sec to 0.1 to 0.2 m/sec. Similar reductions in the differences are also observed for wind power; from 100 kW/m^2 to 60 kW/m^2.

7 Conclusions

The major conclusions from this study are:

NW and NE dominate the observed winds at MDS and AWS Met for this fall - winter study period. This pattern is consistent with wind hindcasts for the winter from the nearby WIS 101 site. The wind speeds increase with height and have low shear coefficients, consistent with unstable atmospheric conditions. The Weibull distribution shape parameter is approximately 2.12 and the amplitude parameter increases with observation height.

Model predicted wind speeds are in good agreement with observations for temporal trends. The model under predicts the observed wind speed at 57 m elevation at the AWS Met station by an average difference of 5.1% (Obs. - 9.73 m/sec vs RAMS -9.23 m/sec.). The model similarly under predicts the observed power at this location by 16.1 % (Obs. - 1000 kW/m^2 vs RAMS - 838 kW/m^2). RAMS predicted values at MDS (10 m elevation) are in good agreement with observations (Obs – 8.54 m/sec versus RAMS – 8.23 m/sec), under predicting the wind speed by 5.7%.

Model predicted wind speeds and power density distributions show the same basic pattern: shore parallel contours with speed or power density increasing with distance offshore. Regions to the S and SE of Block Island represent oceanic wind conditions, while those to the N and NW are strongly influenced by the adjacent land masses. The simulations show substantial lee effects that are predicted to extend at least 8 km from the island at 80 m. The location of the impacted area is dependent on the wind direction, lee effects SE of the island result from NW winds and SW for NE winds. The lee effects are most pronounced from the southern end of the island, which has the highest elevation and the highest roughness land cover. Model predicted shear coefficients are higher (0.18) than the observed values (0.08) at AWS Met. Shear coefficients are very large over the island reaching values as high as 0.45 on the southern end.

A sensitivity study was performed to assess the impact on winds in the lee of Block Island for NW winds assuming the island both topography and land cover, or each independently were used as input to the model. The simulations showed that either topography or land cover alone explained much of the observed lee effects.

Mean powers densities were predicted for a small wind farm located at the state water boundary line. The site locations and their power densities are: SE- 1097 kW/m^2, S - 1139 kW/m^2, and SW -1076 kW/m^2. The S site has the highest power production potential; 3.6 to 5.4% higher than the other two sites. The SW has been eliminated from consideration based on high construction effort due to end moraine sediments. Of the two remaining sites, the S site has a marginally higher power production potential than the SE site. It should be noted that this

analysis has not considered winds from other times of the year. During the remainder of the year, winds are observed to be predominantly from the SW. With SW winds all three locations are anticipated to experience about the same winds and hence power production potential.

Simulations for the hindcast period were compared to application of an independent template based method for the study period. The results showed the template based predictions were in generally good agreement with the hindcast mean winds, and correctly predicted the lee effects from both NW and NE winds. The template based method showed a more pronounced lee area to the SE. The predictive quality for wind power was comparable. A comparison of the observed and hindcast wind rose show the model under predicts the winds from the NW and over predicts those from the W, hence explaining in part the difference between the two estimates.

References

ATM, 2007a. RI WINDS Phase I, Wind Energy Siting Study, prepared for RI Office of Energy Resources, Providence, RI, April 2007.

ATM, 2007b. RI WINDS Summary Report, prepared for RI Office of Energy Resources, Providence, RI, September 2007.

Brower, M., 2007. Wind resource maps of Southern New England, prepared by True Wind Solutions, LLC, 10 p.

Grilli, A. M. L. Spaulding, C. Damon, and R. Sharma, 2010. High resolution application of the Technology Development Index (TDI) in state waters south of Block Island, Ocean SAMP project Report, Narragansett, RI.

Pielke, R.A., W.R. Cotton, R.L. Walko, C.J. Tremback, W.A. Lyons, L.D. Grasso, M.E. Nicholls, M.D. Moran, D.A. Wesley, T.J. Lee, and J.H. Copeland, 1992: A comprehensive meteorological modeling system -- RAMS. Meteor. Atmos. Phys., 49, 69-91.

RAMS, 2010, Regional Atmospheric Modeling System Technical Manual, Weather Flow,

Spaulding, M. L., A. Grilli, C. Damon, and G. Fugate, 2010a, Application of Technology Development Index and Principal Component Analysis and Cluster Methods to Ocean Renewable Energy Facility Siting, Journal of Marine Technology, Special Edition on Offshore Wind, January February 2010.

Spaulding, M.L., M. Bell, J. Titlow, R. Sharma , A. Grilli, A. Crosby, L. Decker and D. Mendelsohn, 2010b. Wind Resource Assessment in the Vicinity of a Small, Low Relief Coastal Island, University of Rhode Island, Narragansett, RI 02882.

Titlow, J. and D. Morris, 2010. Block Island modeling analysis, WeatherFlow Inc. Model simulations by MetLogics, Boulder, CO.

Tremback, C. J. and R. L. Walko, 2010. Regional Atmospheric Modeling System, Users Guide-Introduction, Version 6.0, ATMET, Boulder, CO.

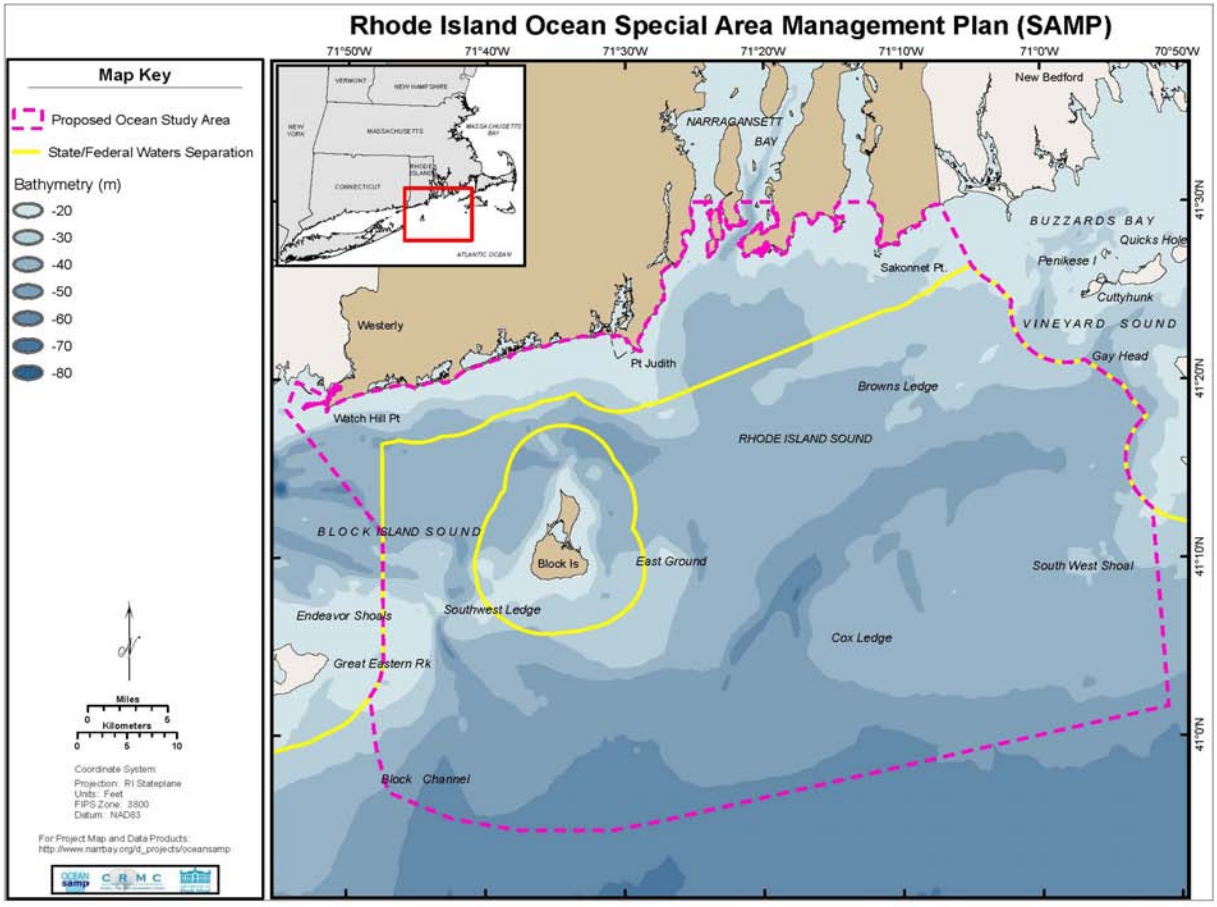

Figure 1 Ocean SAMP study area with bathymetry as background. Yellow lines are state water boundaries and dotted lines are study area boundaries.

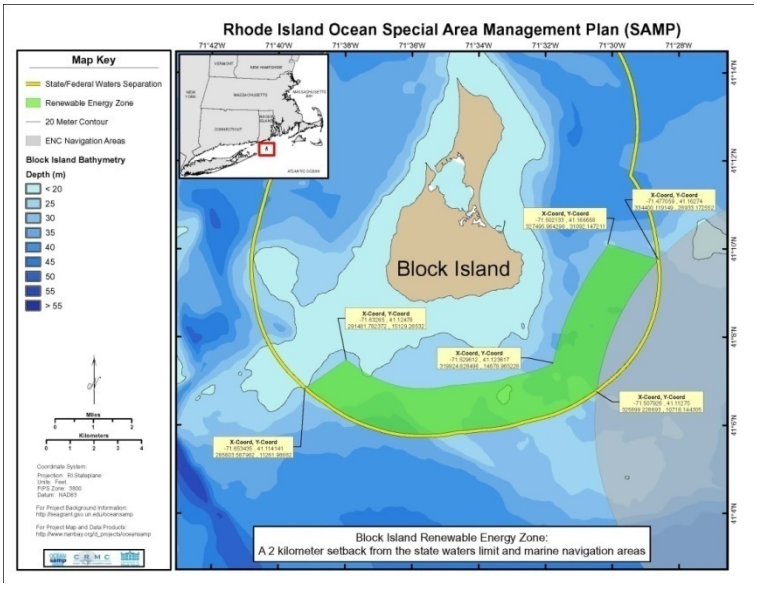

Figure 2 Proposed renewable energy zone south of Block Island. Latitude and longitude (state plane) coordinates are provided at key points.

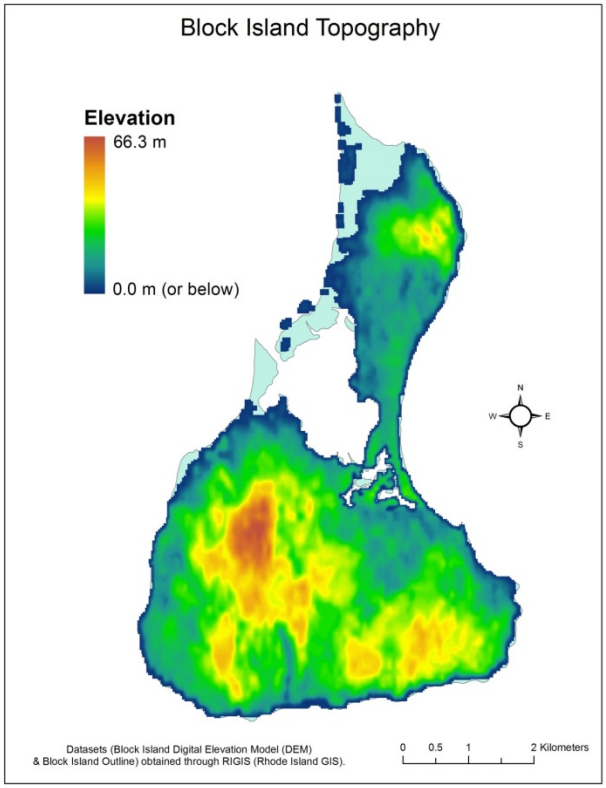

Figure 3 Block Island topography based on RI GIS digital elevation maps.

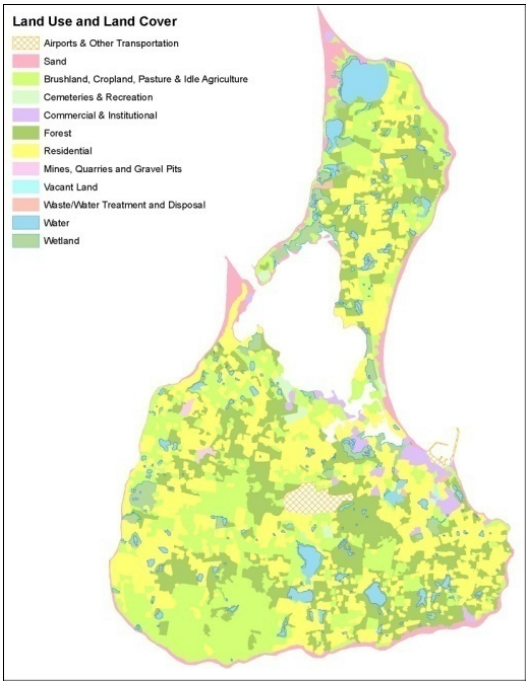

Figure 4 Block Island land cover (RI Geographic Information System).

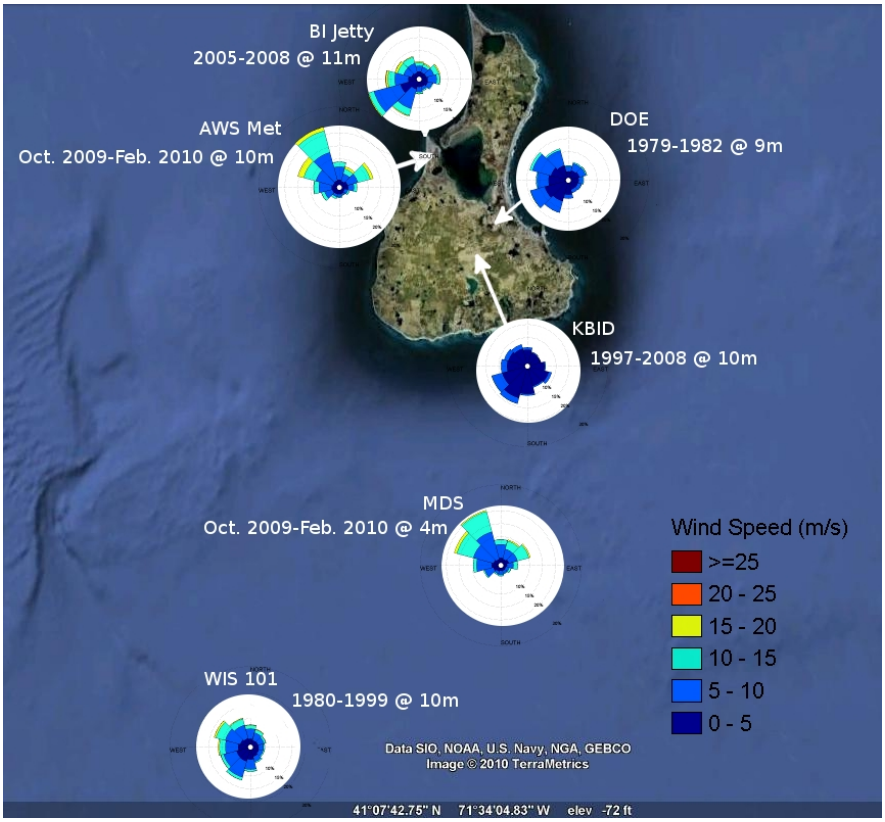

Figure 5 Wind speed frequency rose at AWS Met and MDS stations. Data is also shown for WIS101, Block Island Airport (KBID), DOE and WeatherFlow's Block Island Jetty.

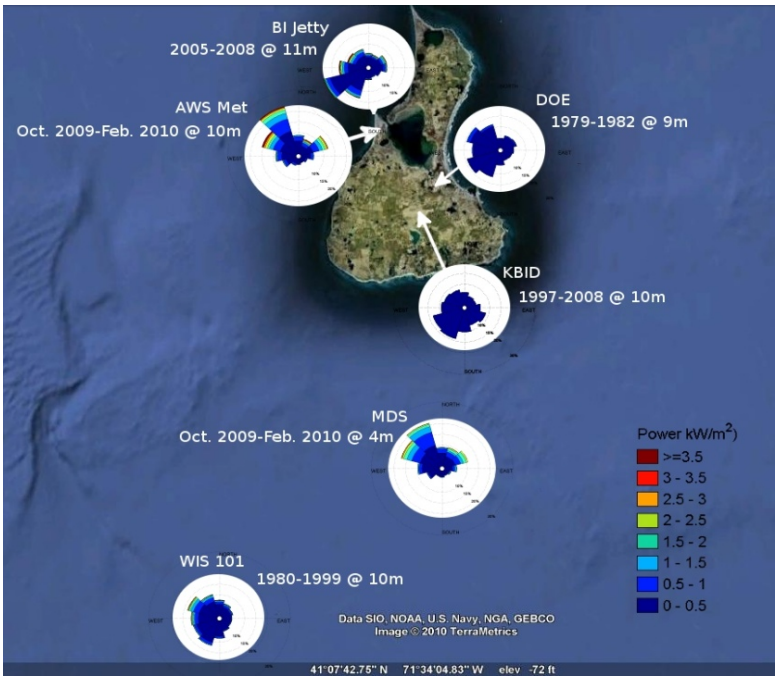

Figure 6 Wind power roses at AWS Met and MDS stations. Data is also shown for WIS101, Block Island Airport (KBID), DOE and WeatherFlow's Block Island Jetty.

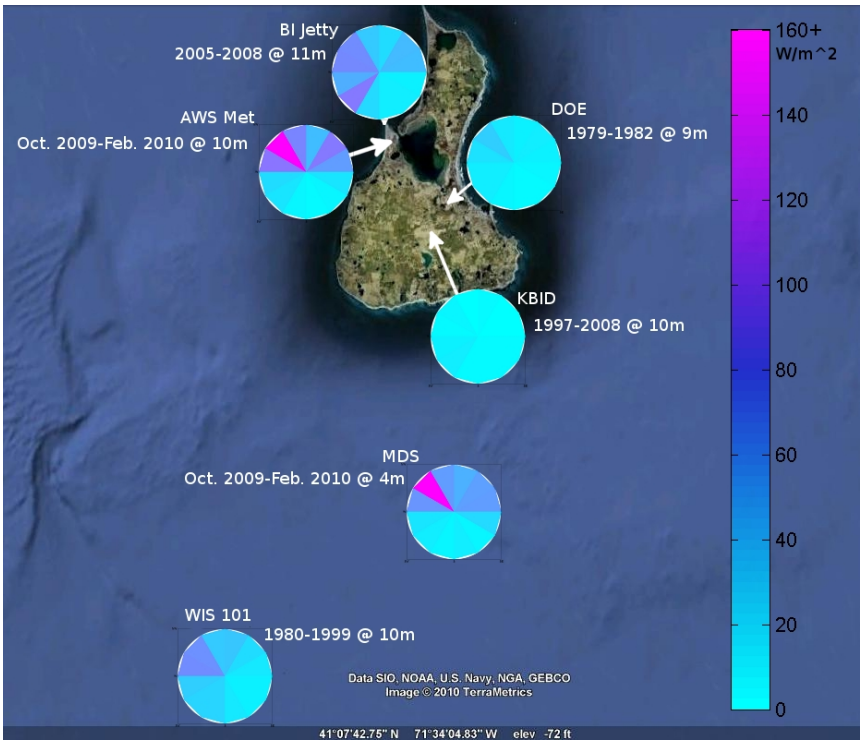

Figure 7 Average wind power by direction. Data is also shown for WIS101, Block Island Airport (KBID), DOE and WeatherFlow's Block Island Jetty.

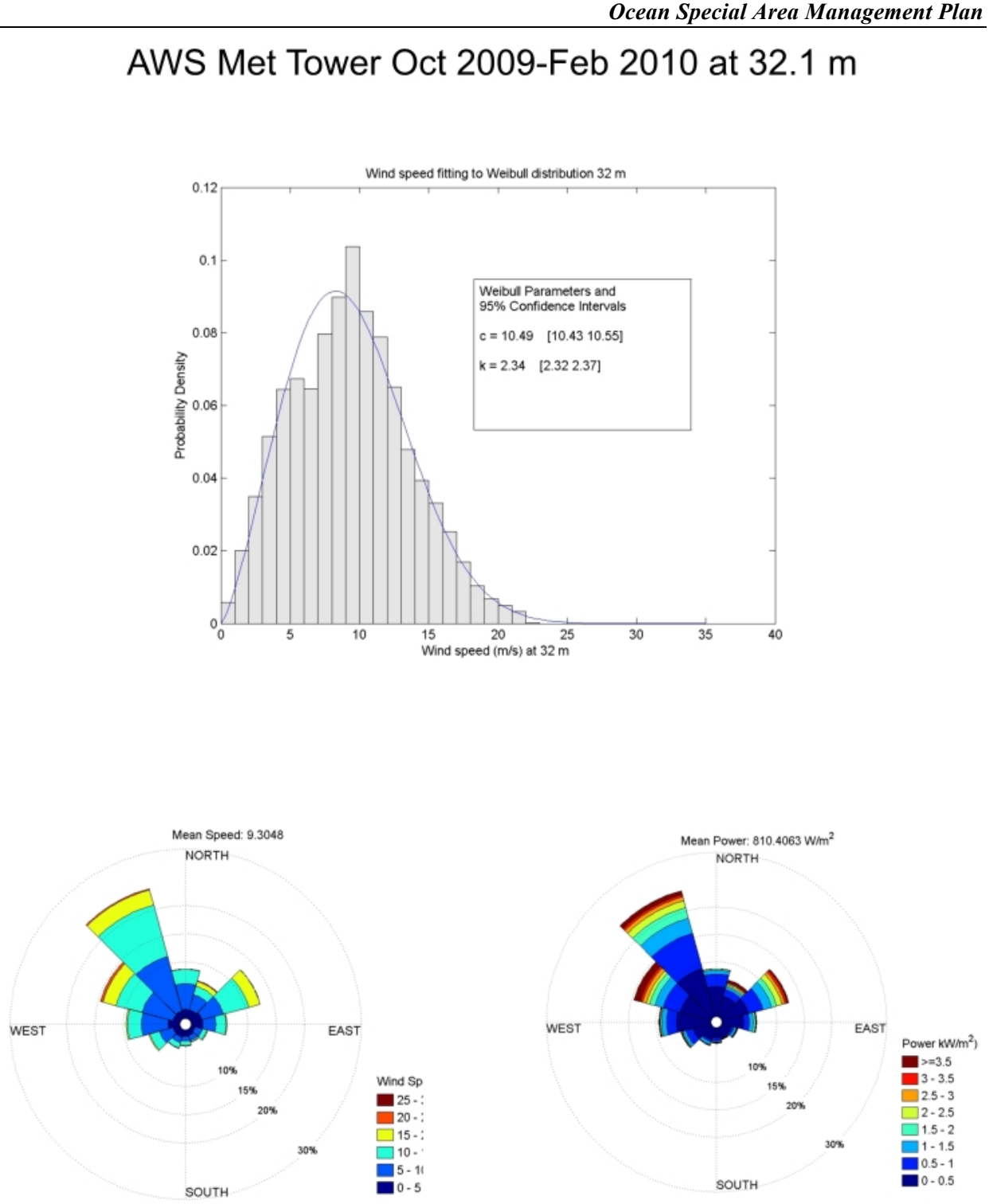

Figure 8 Weibull distribution, wind frequency and power roses for AWS Met, 32 m elevation.

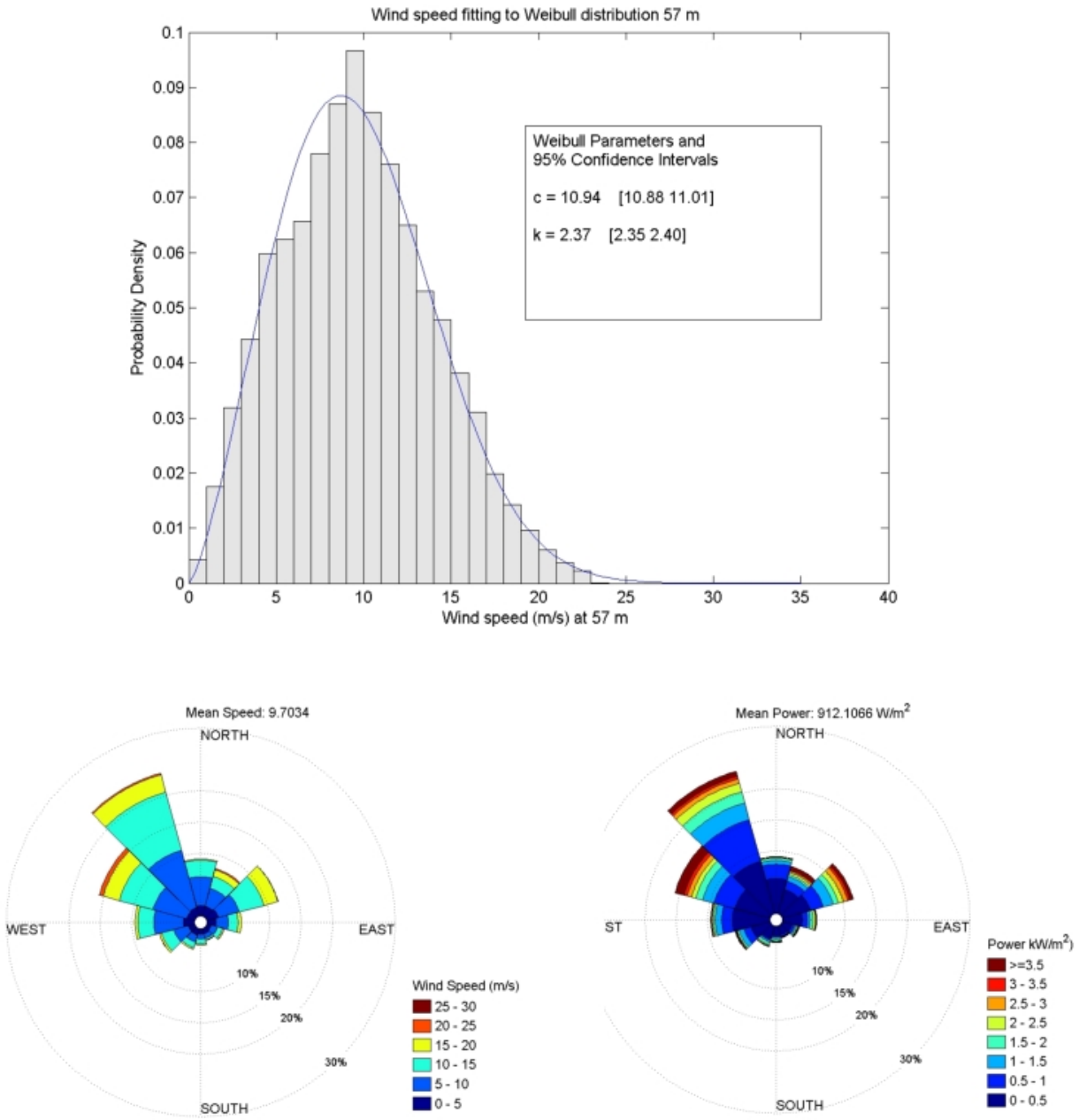

Figure 9 Weibull distribution, wind frequency and power roses for AWS Met, 57 m elevation.

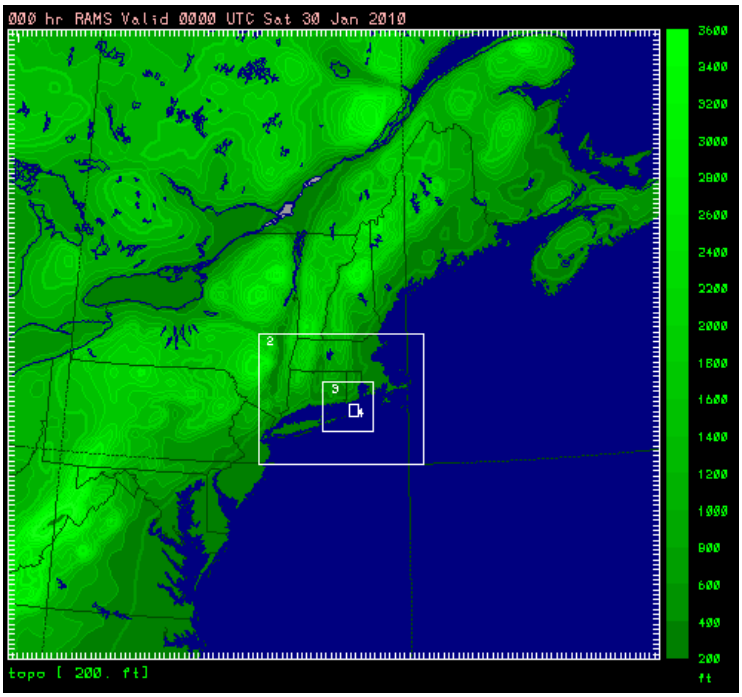

Figure 10 RAMS nested grid system showing 6 km (Grid 2), 2 km (Grid 3) and 0.5 km (Grid 4) grid boundaries. The outer NCEP NAM grid is 12 km.

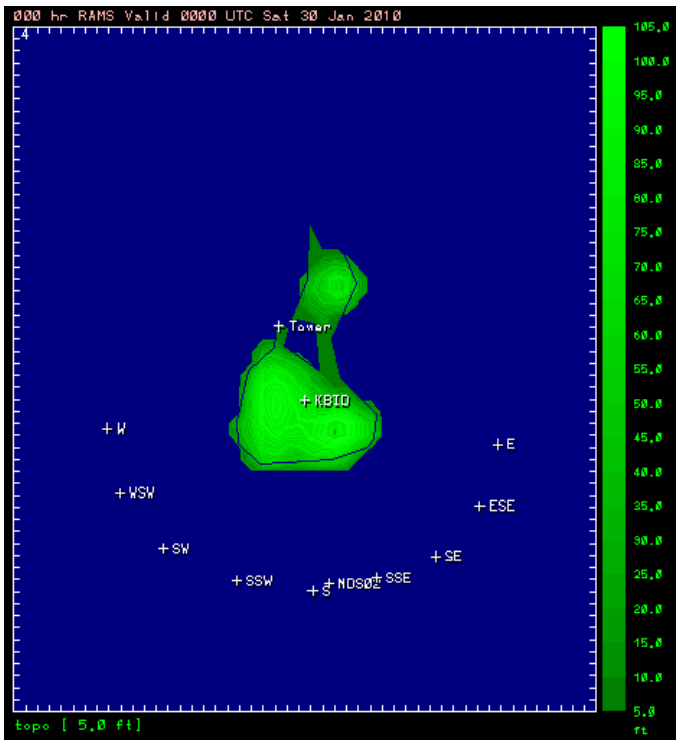

Figure 11 Grid 4 showing topographic relief of Block Island. The locations at which model time series were generated are shown, including E, ESE, SE, SSE, S, SSW, SW, WSW, and W along state water boundary line, and at observation locations KBID, BI Jetty, AWS Met, and MSD.

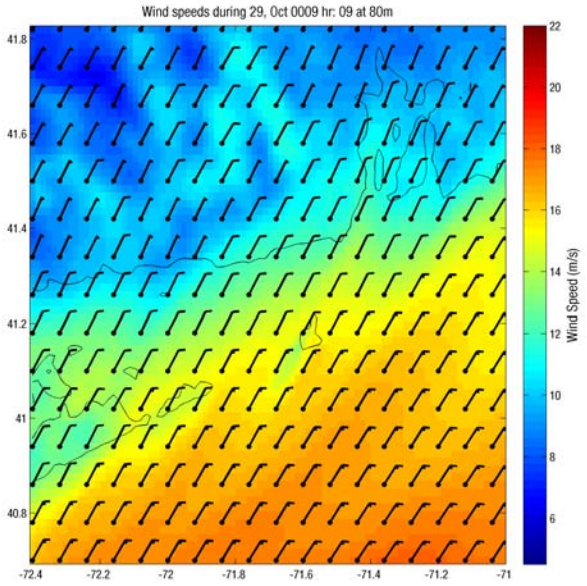

Figure 12a Model predicted wind speed contours (Grid 3) on October 29, 2009 at 80 m elevation on Grid 3. Wind barbs are provided to show wind direction.

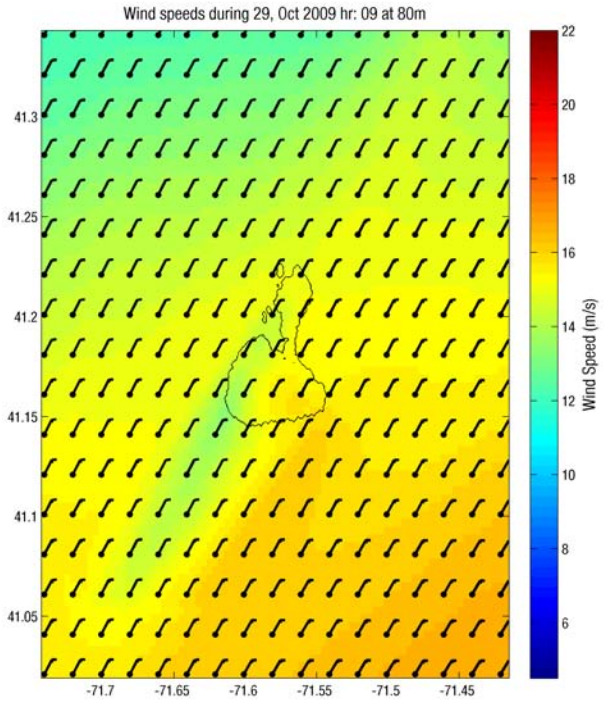

Figure 12b Model predicted wind speed contours (Grid 4) on October 29, 2009 at 80 m elevation on Grid 4. Wind barbs are provided to show wind direction.

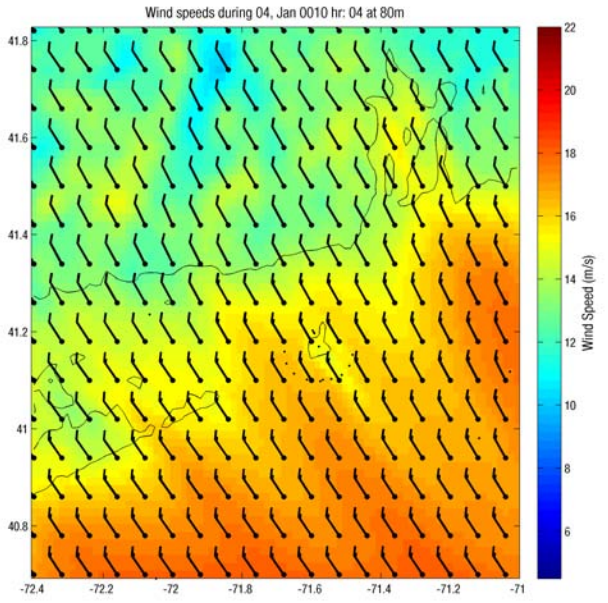

Figure 13a Model predicted wind speed contours (Grid 3) on January 4, 2010 at 80 m elevation. Wind barbs are provided to show wind direction.

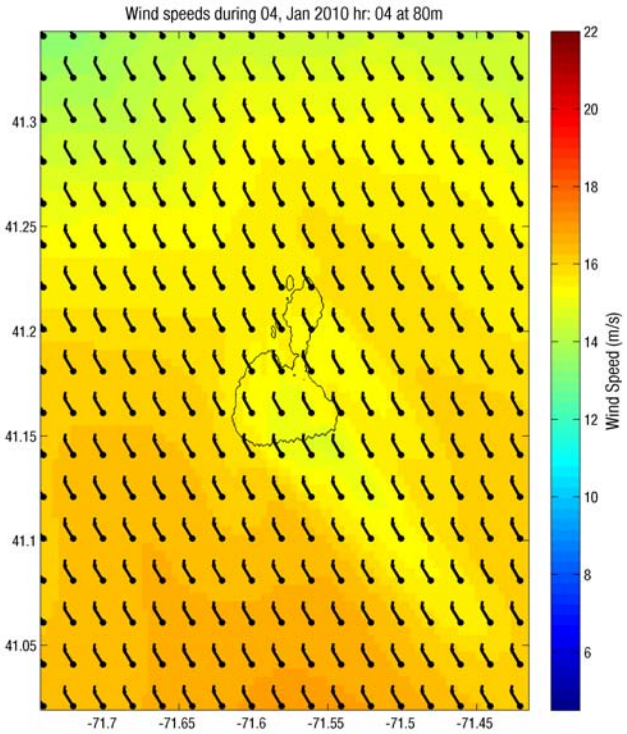

Figure 13b Model predicted wind speed contours (Grid 4) on January 4, 2010 at 80 m elevation. Wind barbs are provided to show wind direction.

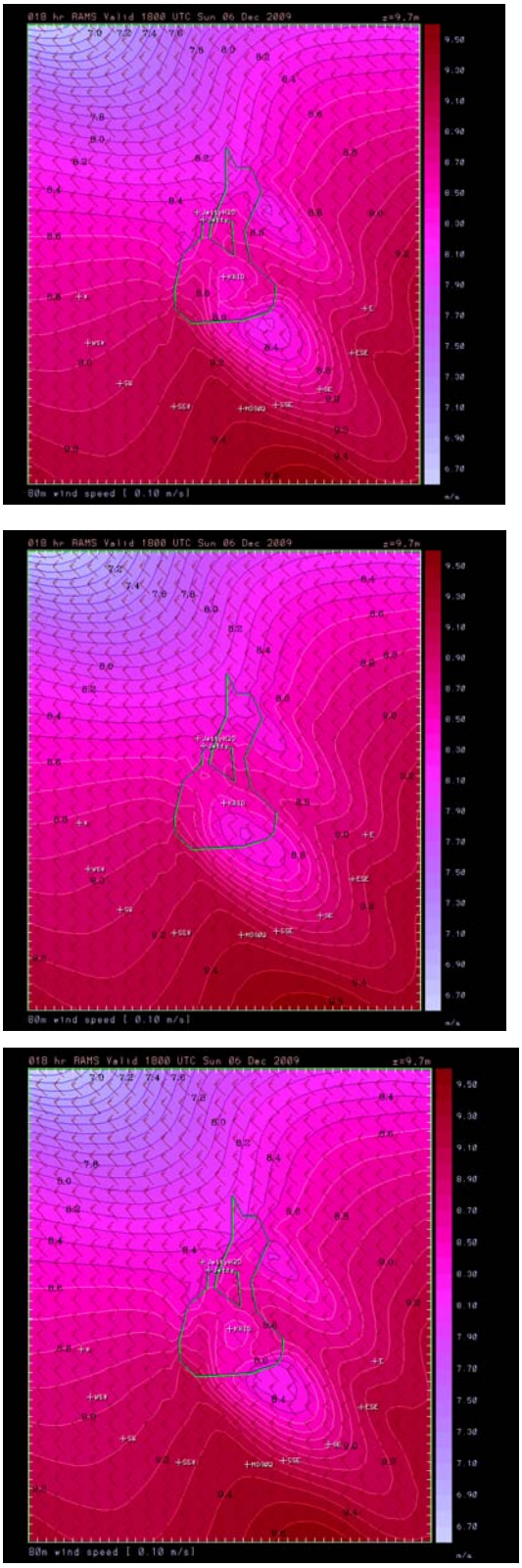

Figure 14 Model predicted wind field on December 6, 2009, 80 m elevation with topography and roughness (upper panel), with roughness only (center panel) and with topography only (lower panel).

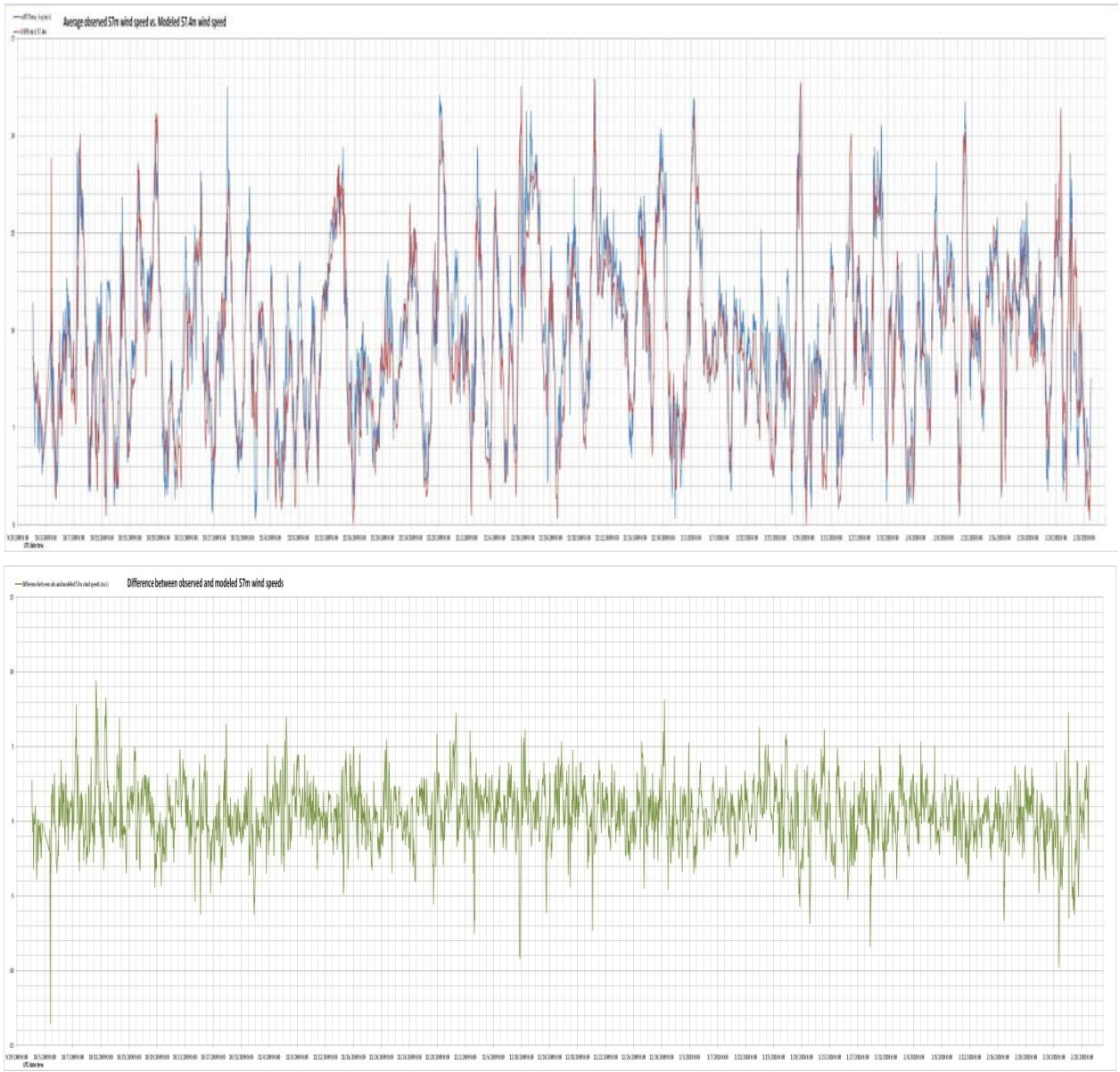

Figure 15 Model predicted and observed wind speed vs time (upper panel) and difference between the two (lower panel)(blue - observed, red - model) for the simulation period at AWS Met at 57 m elevation.

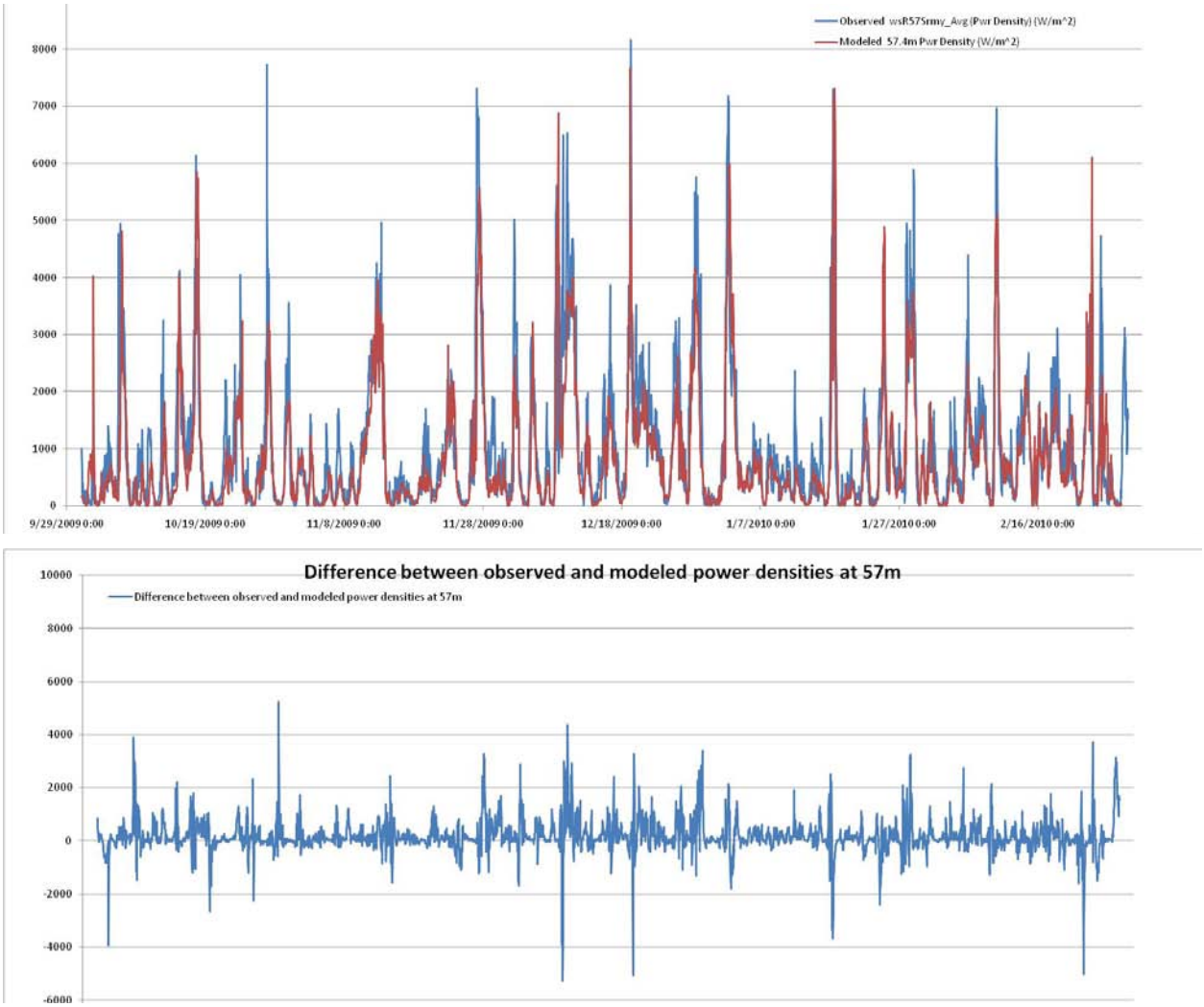

Figure 16 Model predicted and observed power density vs time (upper panel)(blue - observed, red-model) and difference between the two (lower panel) at the AWS Met 57 m elevation.

Figure 17 Model predicted and observed shear vs time (upper panel)(blue –observed, red- model) and difference between the two (lower panel) at the AWS Met 57 m elevation.

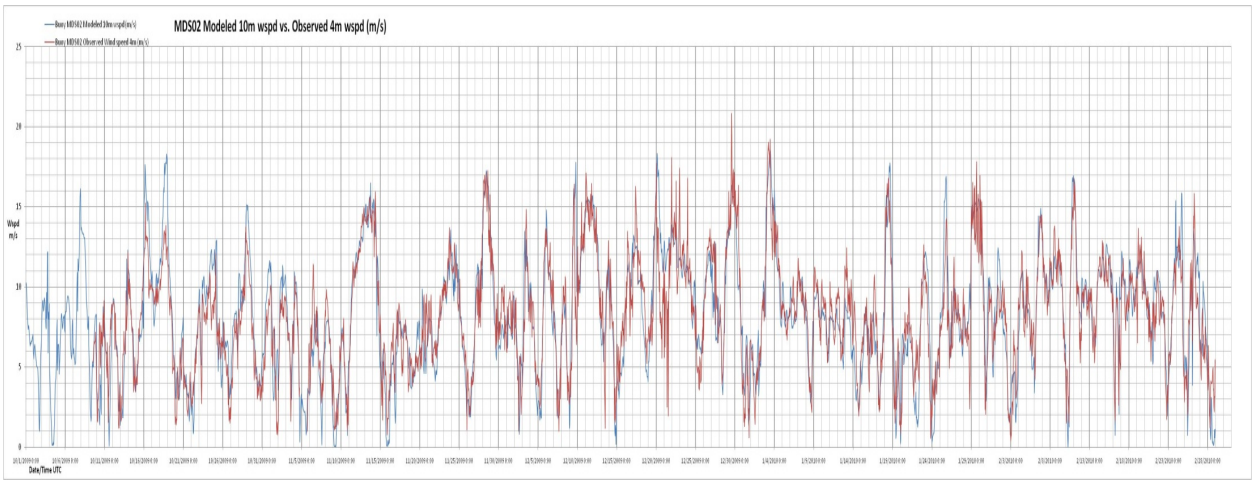

Figure 18 Model (red) predicted and observed (blue) winds at MDS at 10 m elevation.

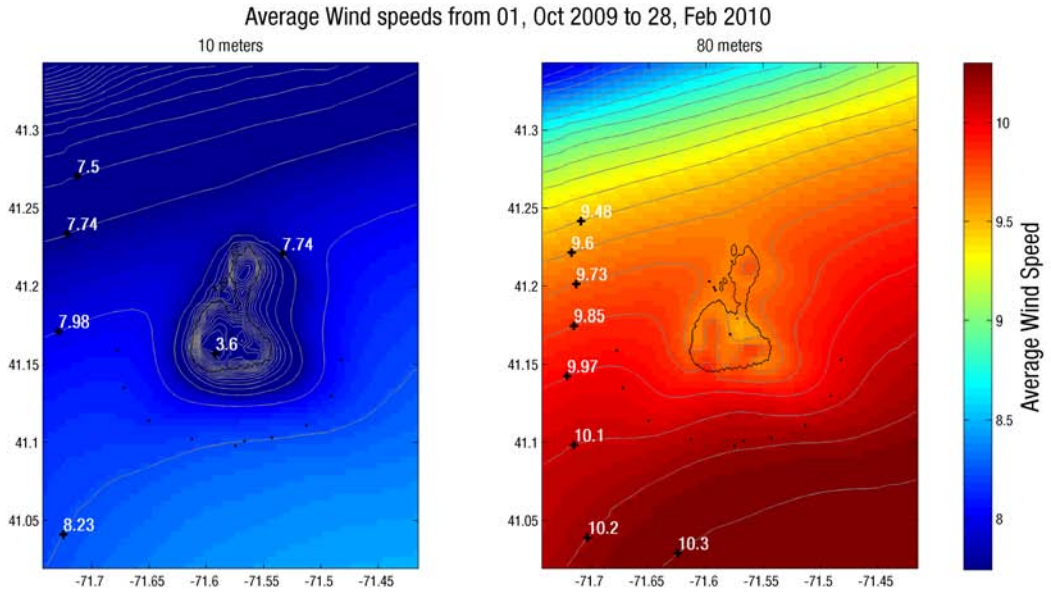

Figure 19 Average model predicted wind speed contours at 10 m (left) and 80 m (right) elevations over the simulation period.

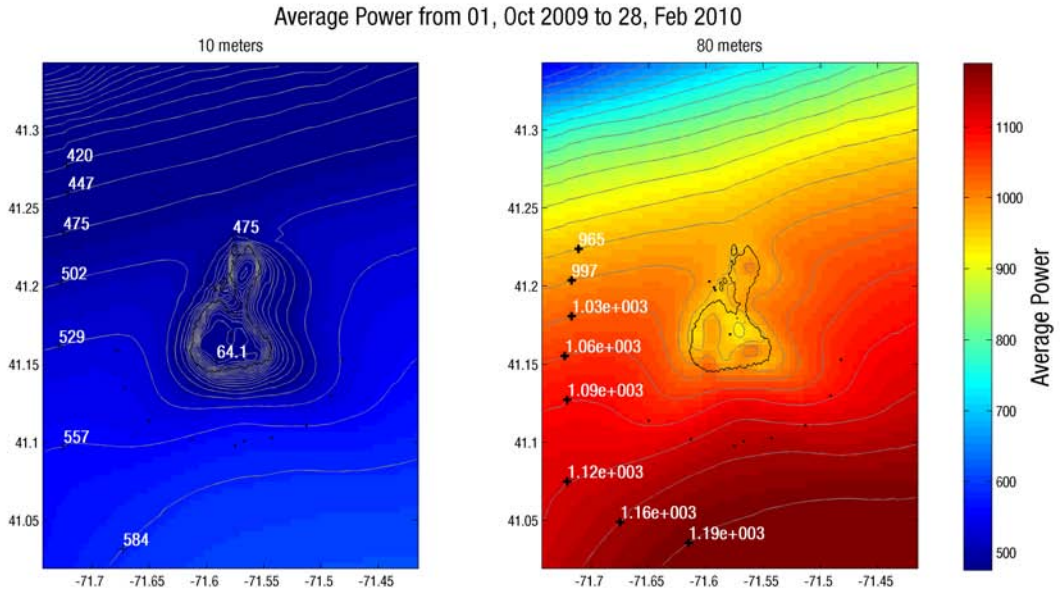

Figure 20 Average model predicted wind power (kW/m^2)contours at 10 m (left) and 80 m (right) elevations over the simulation period.

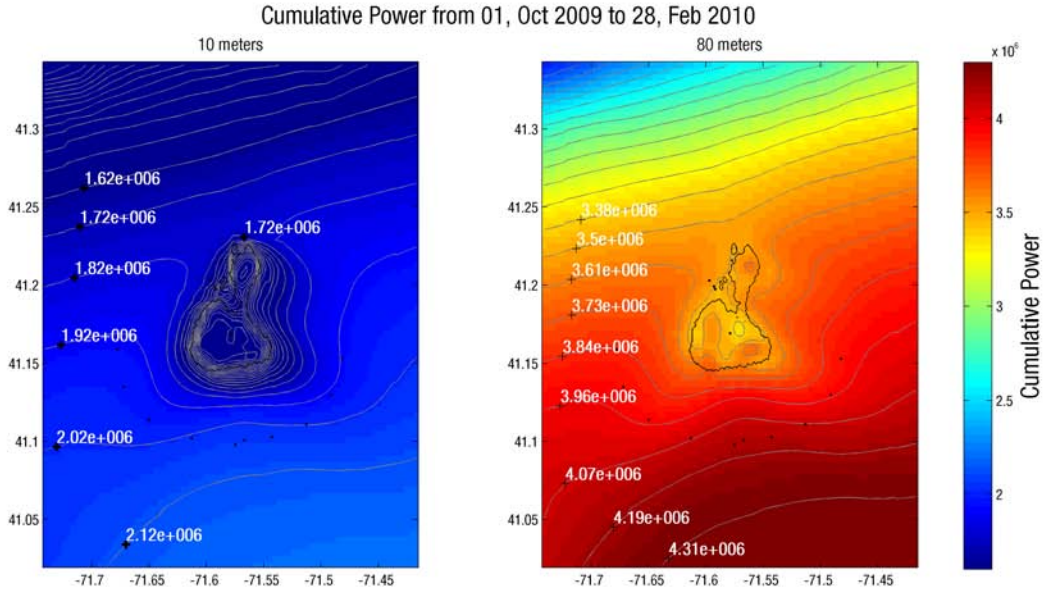

Figure 21 Average model predicted cumulative wind power (kW hrs/m2) contours at 10 m (left) and 80 m (right) elevations.

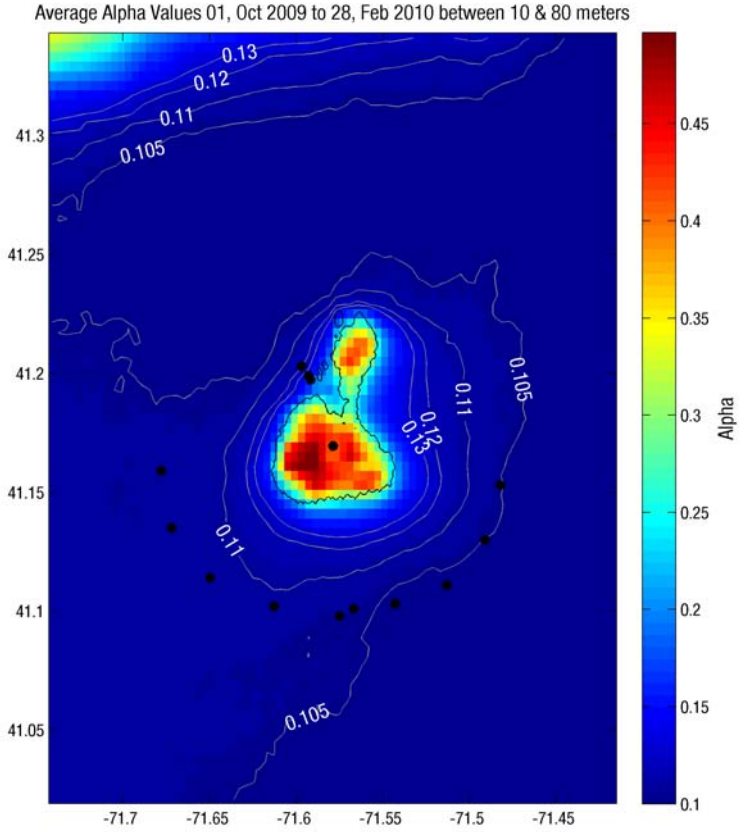

Figure 22 Model predicted average shear coefficient over the simulation period.

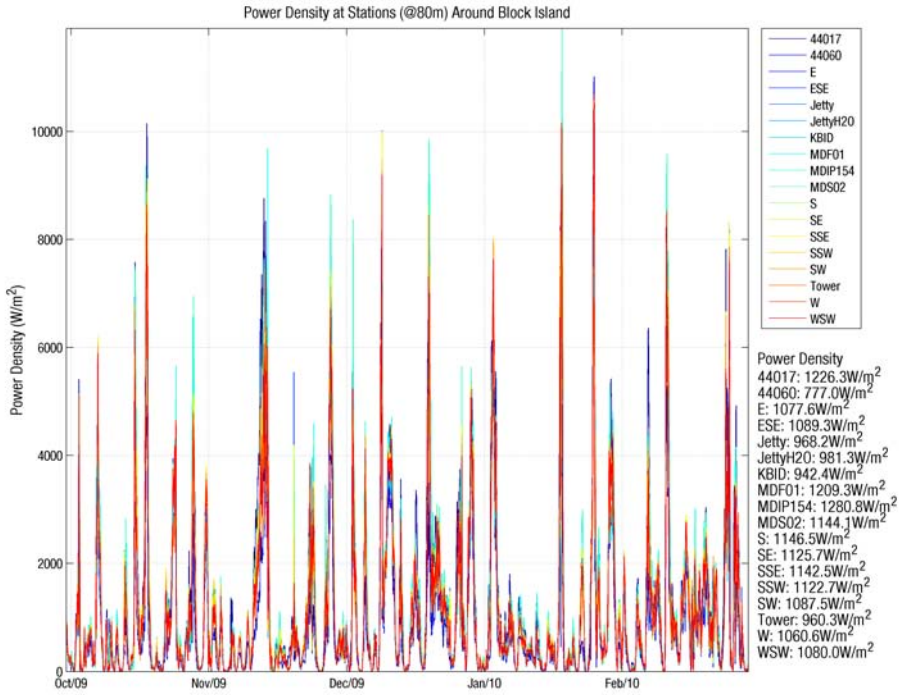

Figure 23 Model predicted time series of wind power density at selected sites (see Figure 11).

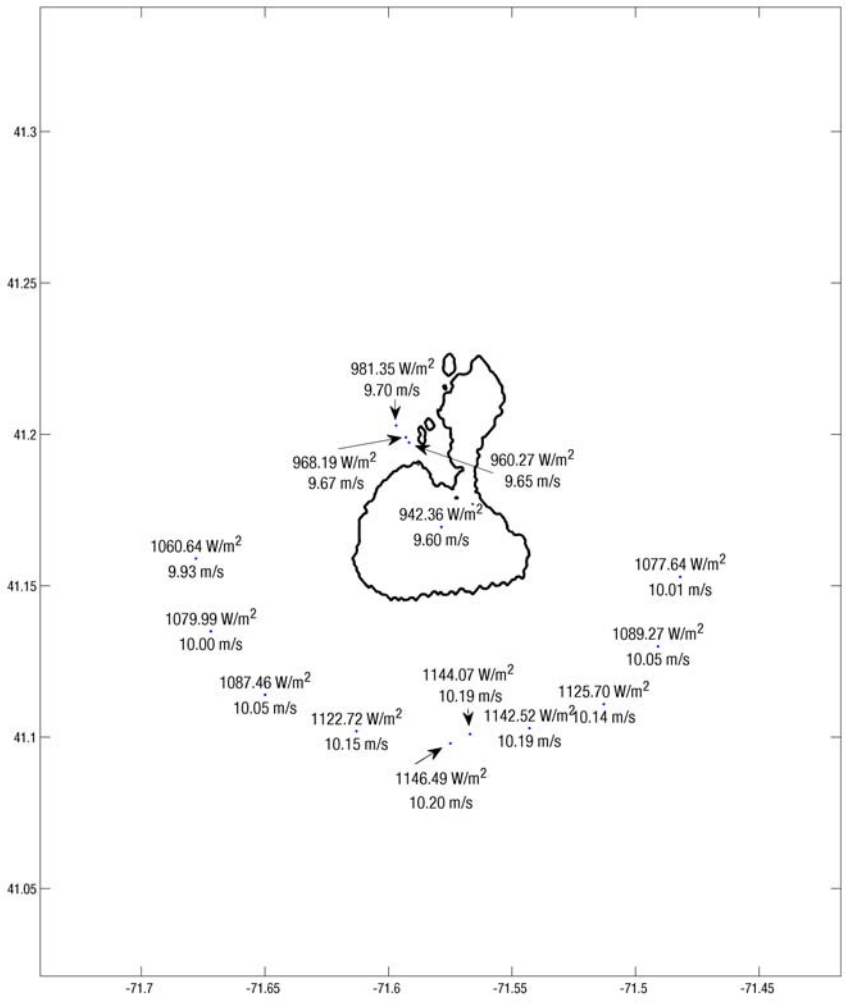

Figure 24 Model predicted mean wind power density at selected sites (see Figure 11).

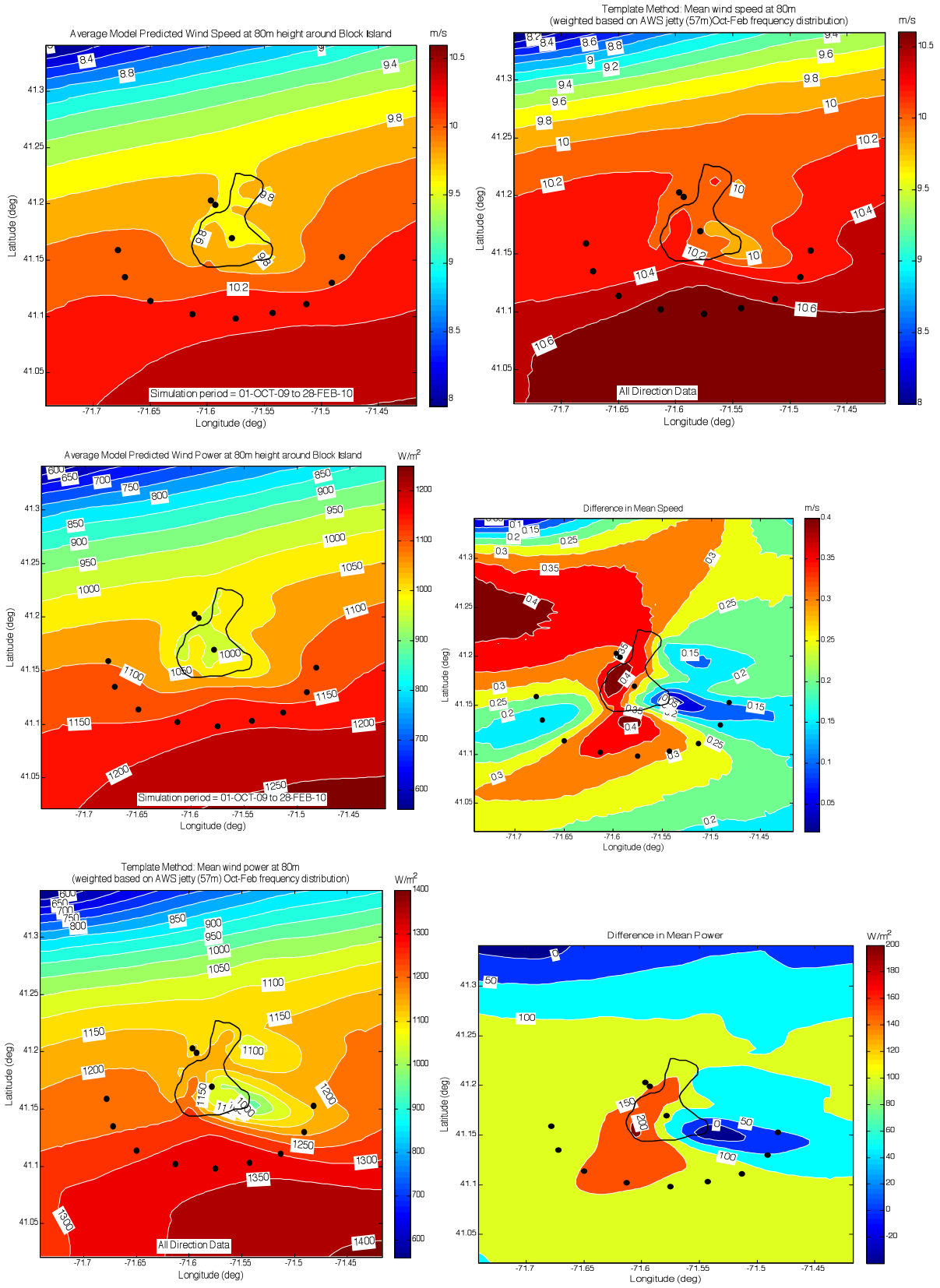

Figure 25 Mean wind speed (left) and power (right) at 80 m based on the template method (using AWS Met wind rose at 57m) (Spaulding et al, 2010b) (upper panel), present hindcast (center panel), and difference between the two methods (lower panel).

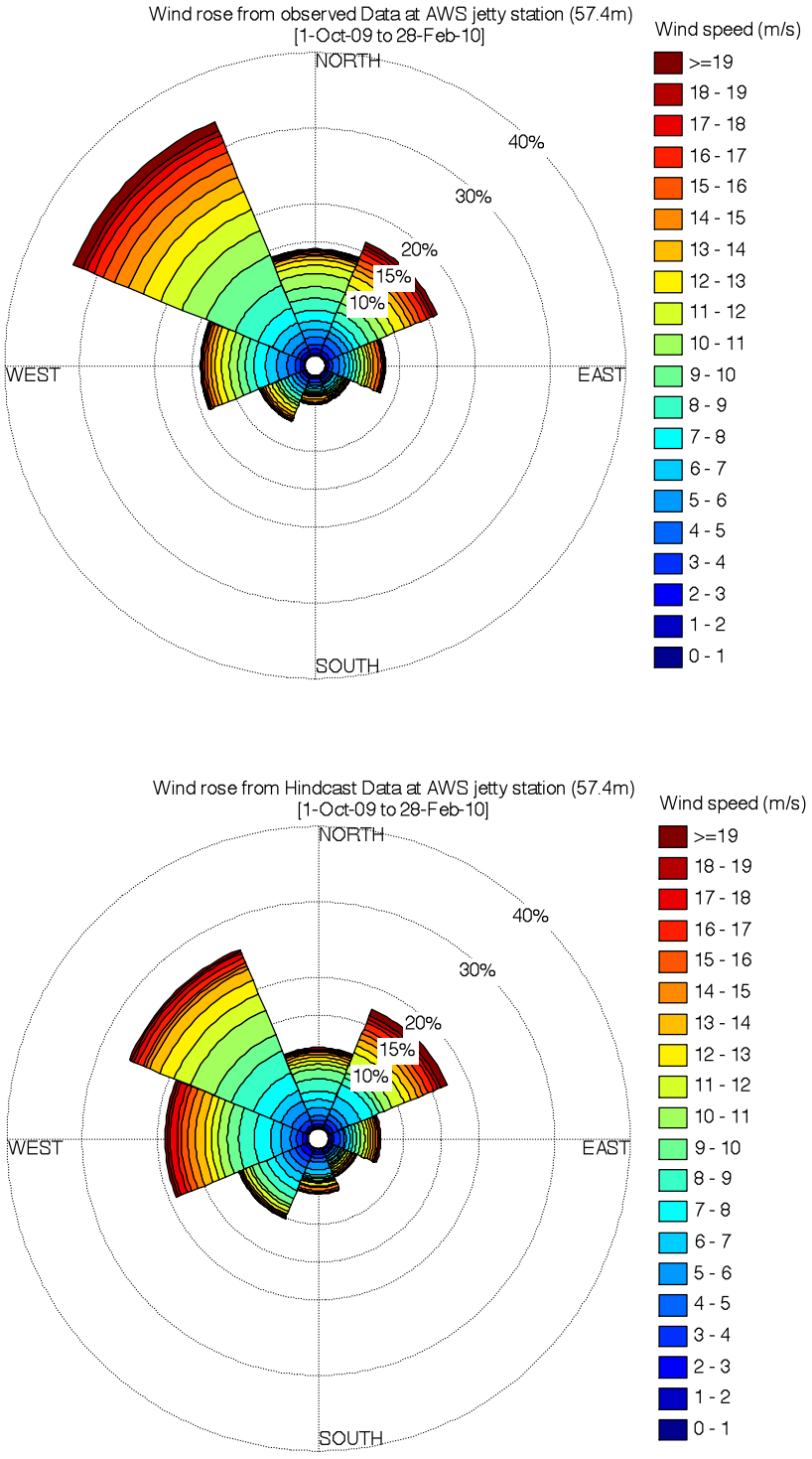

Figure 26 Observed (upper panel) and hindcast (lower panel) wind speed rose at AWS Met 57 m elevation.

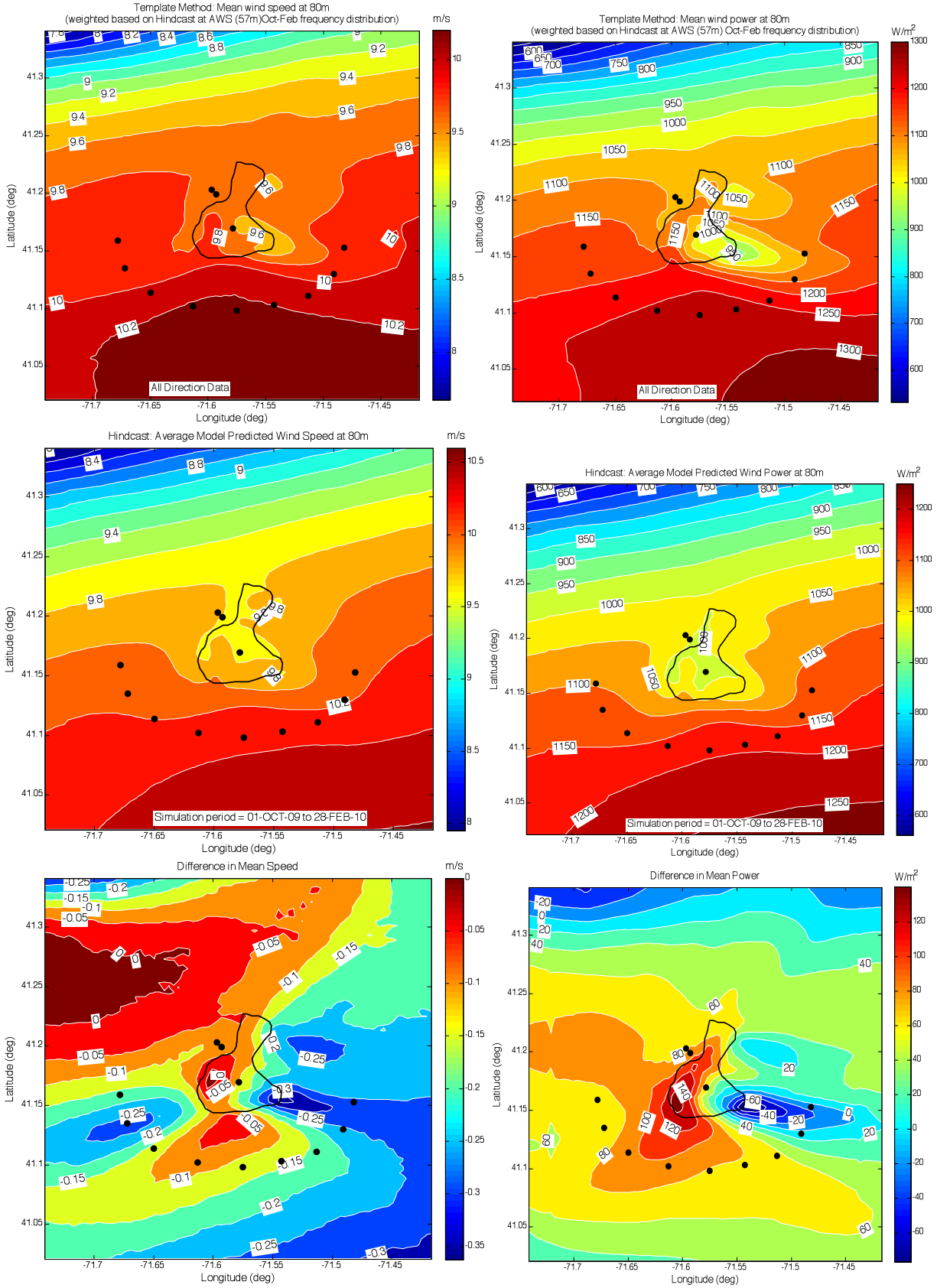

Figure 27 Mean wind speed (left) and power (right) at 80 m based on the template method (using hindcast wind rose at AWS Met location) (Spaulding et al, 2010b) (upper panel), present hindcast (center panel), and difference between the two methods (lower panel).

Appendix A

Titlow, J, 2010. Comparison of RAMS Model Predictions with Observations for the October 2009 to February 2010 Hindcast Period, WeatherFlow Inc., Poquoson, VA.

Appendix A is a twenty-seven slide Power Point presentation avialable on request from the frist author.

Appendix B

Comparison Weather Flow Simulations and Observations at AWS Met tower

Data

Observations

Period of record: 10/01/2009 to 28/02/2010

Sampling interval : 10 minutes

Data: wind speed at 32.1 m and 57.4 m

Observations at each level are used to infer the "observed" shear coefficient which is used to derive the "observed" wind speed and power at 80 m.

Modeled data

Period of simulation: 10/01/2009 to 28/02/2010

Time step: 1 hour

Data: wind speed at 32.1 m , 57.4 m, 80 m, shear coefficient, power at 80 m

Data analysis

1. Time series preparation

Observed data are smoothed and rei-interpolated on 1 hour time step to be synchronized with Weather Flow modeled data at each measurement level (Figure 1 and Figure 2). Visual comparison show a slight time lag between observation and simulations (about 5h). This lag is due to the fact the model predictions are provided in UTC and the observations in EST, a 5 hr time difference.

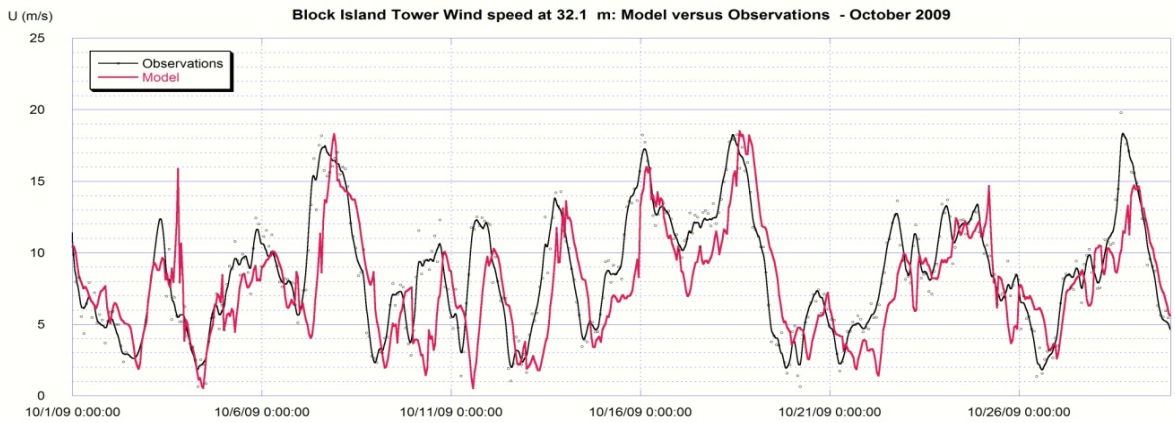

Figure 1: Time series of observed and modeled wind speed at 32.1 m at Block Island AWS Met Tower- Example for October 2009.

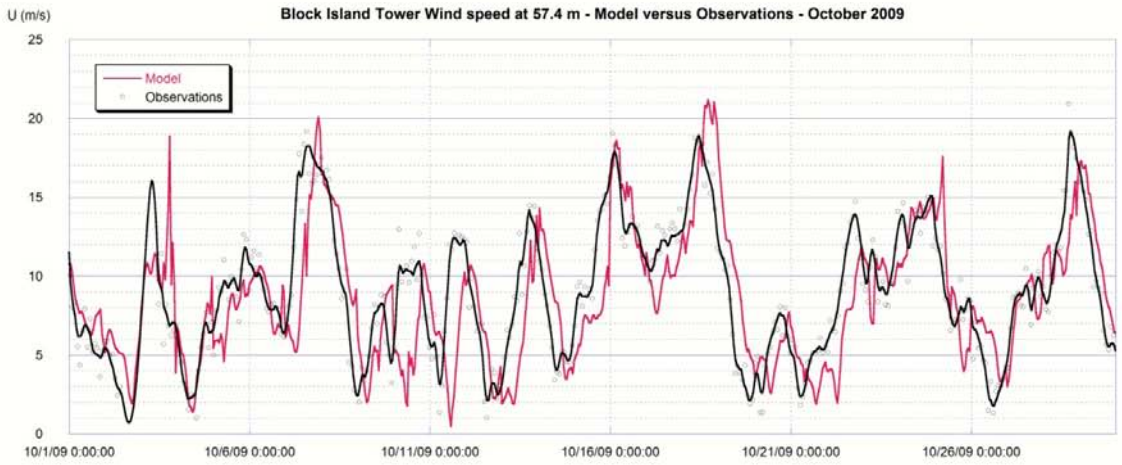

Figure 2: Time series of observed and modeled wind speeds at 57.4 m at Block Island Met Tower - Example for October 2009

2. Cross-correlation analysis

The Cross correlation coefficient function is calculated for each pair, observations-simulations : wind speed at at 32.1 m, 57.4 m , and 80 m, shear coefficient , wind power at 80 m. The function measures the degree of linear dependence between the 2 time series for any relative displacement τ , between them . Results are plotted for each pair for a range of τ between 0 and +- 20 (hours). The peak shows the optimal value of the correlation for the corresponding time lag. A consistent time lag of 5 hours is found between the 2 time series which is consistent with Figure 1 and Figure 2. The correlation coefficient is above 90% for wind speeds observations versus simulations, and 86% for simulated versus "observed" wind power at 80 m. The shear coefficient however is in poor agreement with a correlation coefficient of 0. 47.

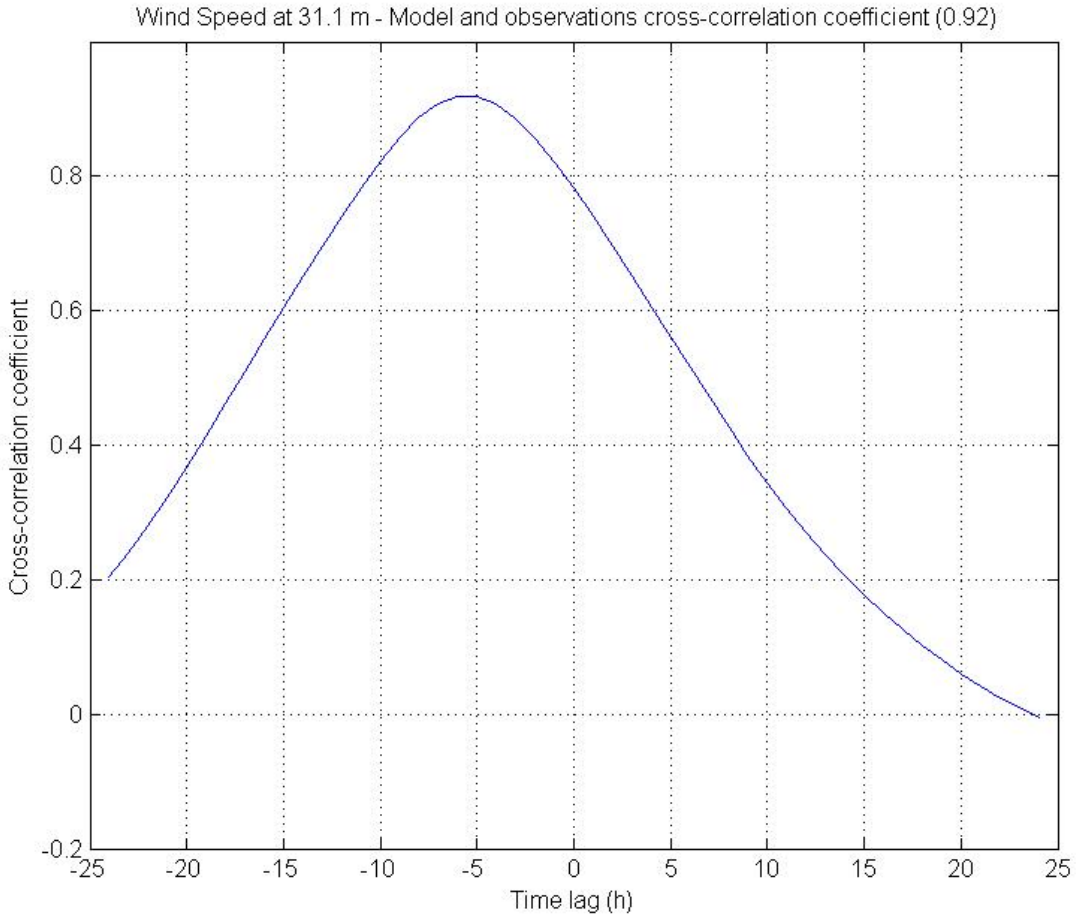

Figure 3: Cross-correlation coefficient for modeled and observed wind speeds at 32.1 m at Block Island AWS Met Tower.

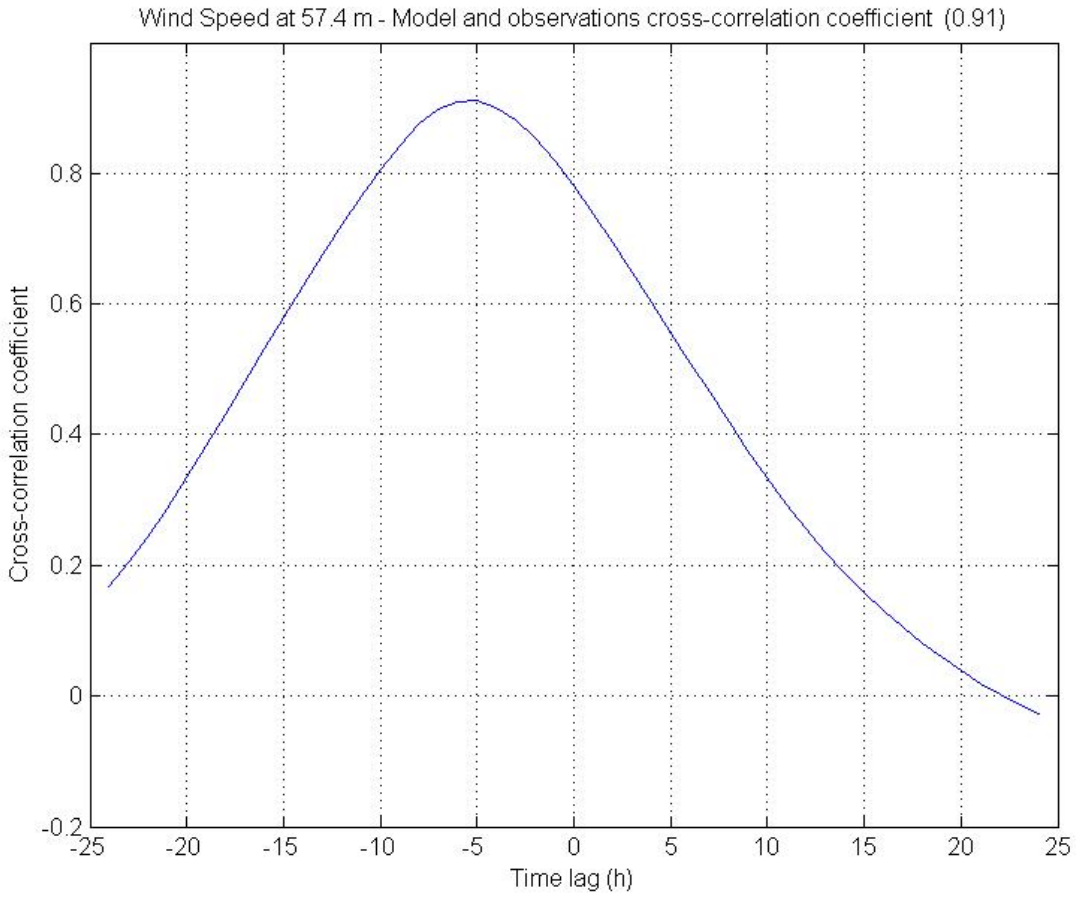

Figure 4: Cross-correlation coefficient for modeled and observed wind speeds at 57.4 m at Block Island AWS Met Tower.

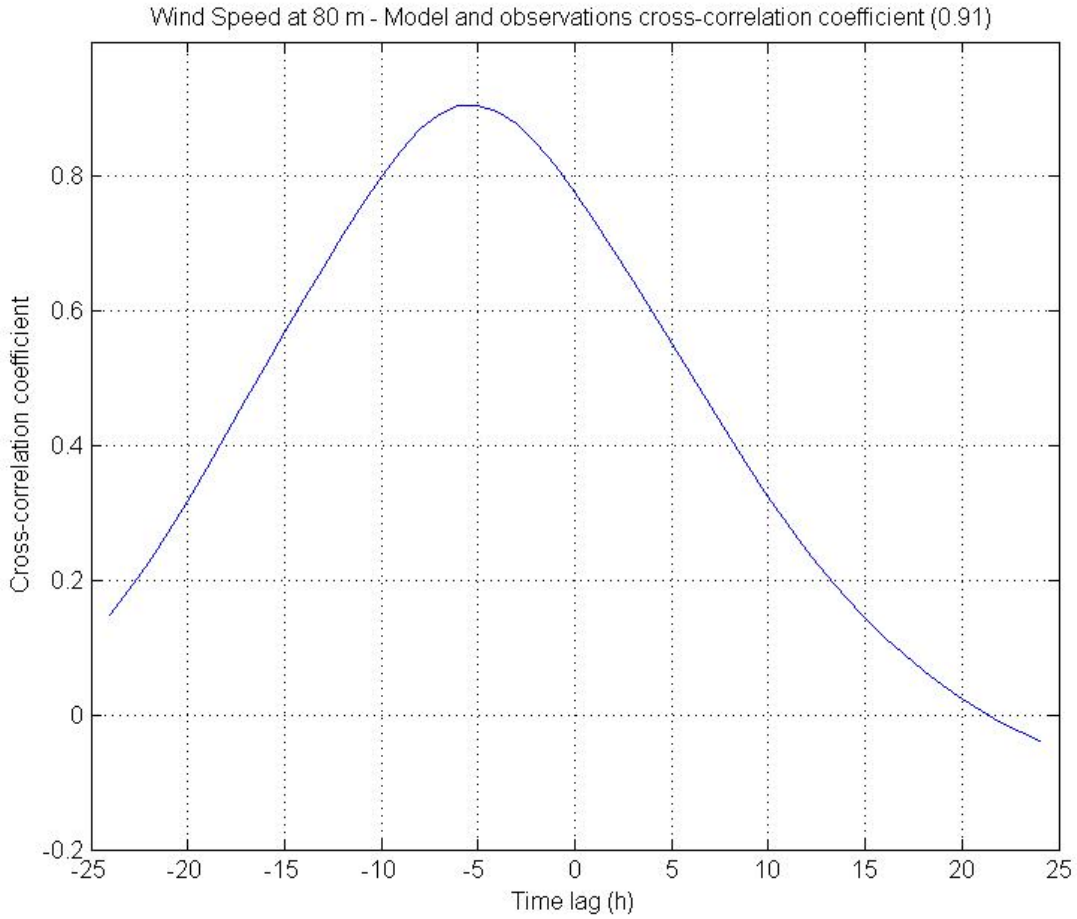

Figure 5:Cross-correlation coefficient for modeled and observed wind speeds at 80 m at Block Island AWS met Tower.

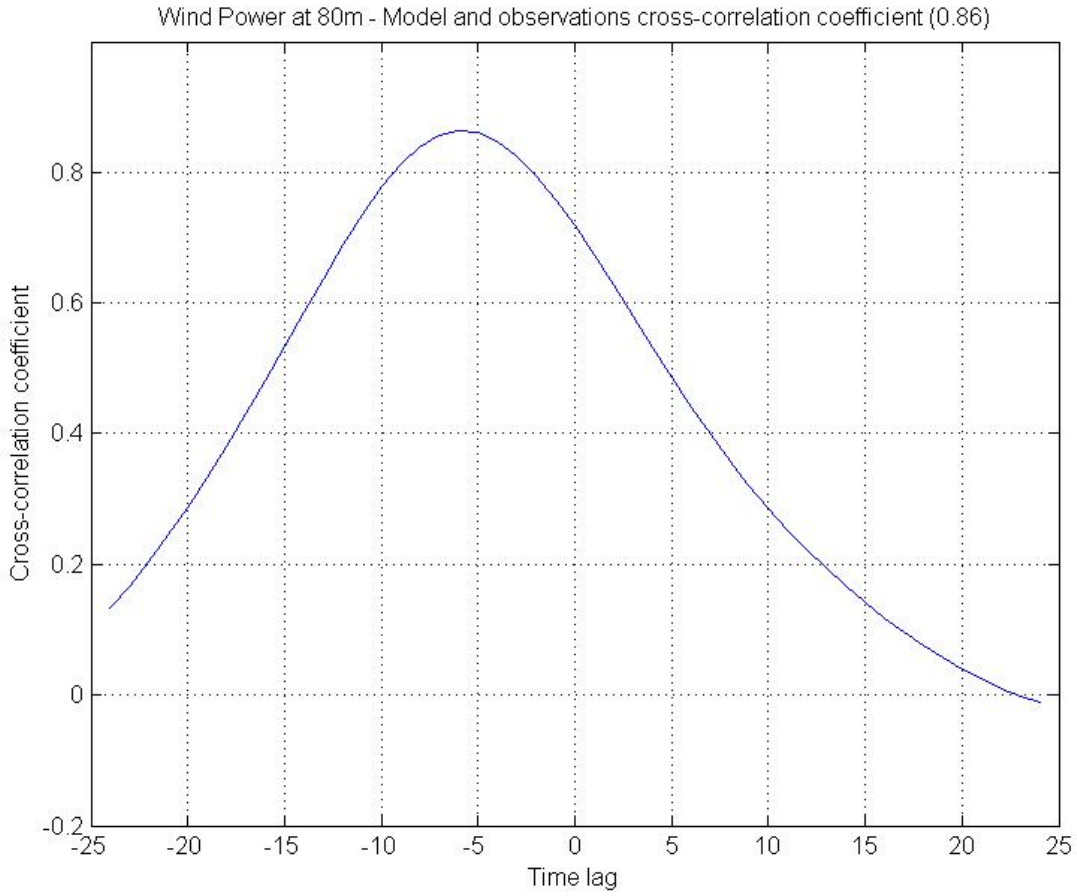

Figure 6:Cross-correlation coefficient for modeled and observed wind powers at 80 m at Block Island AWS met Tower.

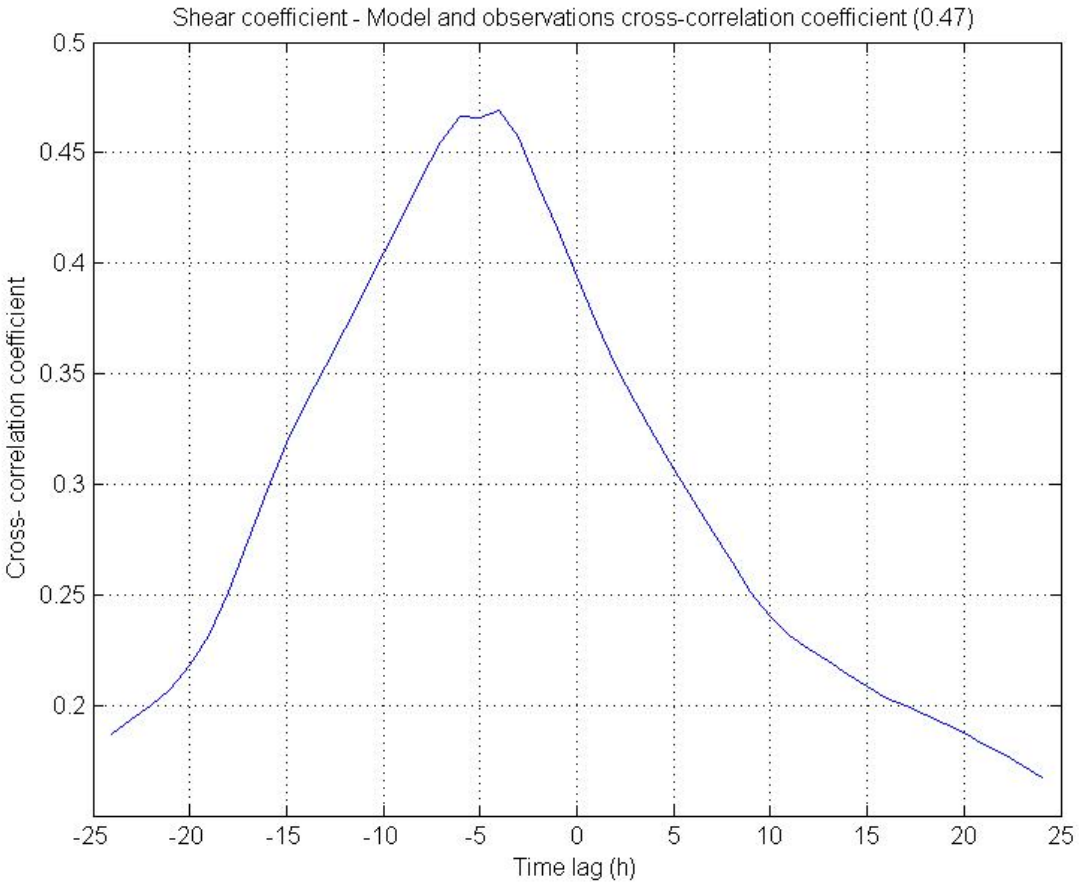

Figure 7:Cross-correlation coefficient for modeled and observed shear coefficients at Block Island AWS met Tower.

3. Spectral density

Spectral density is calculated using the Welch algorithm, using the Hanning window (to taper the time series at the beginning and end to avoid side lobe leakage). Results are shown for 31.2 m observed and simulated wind speed a s well as for power at 80 m, simulated and observed.

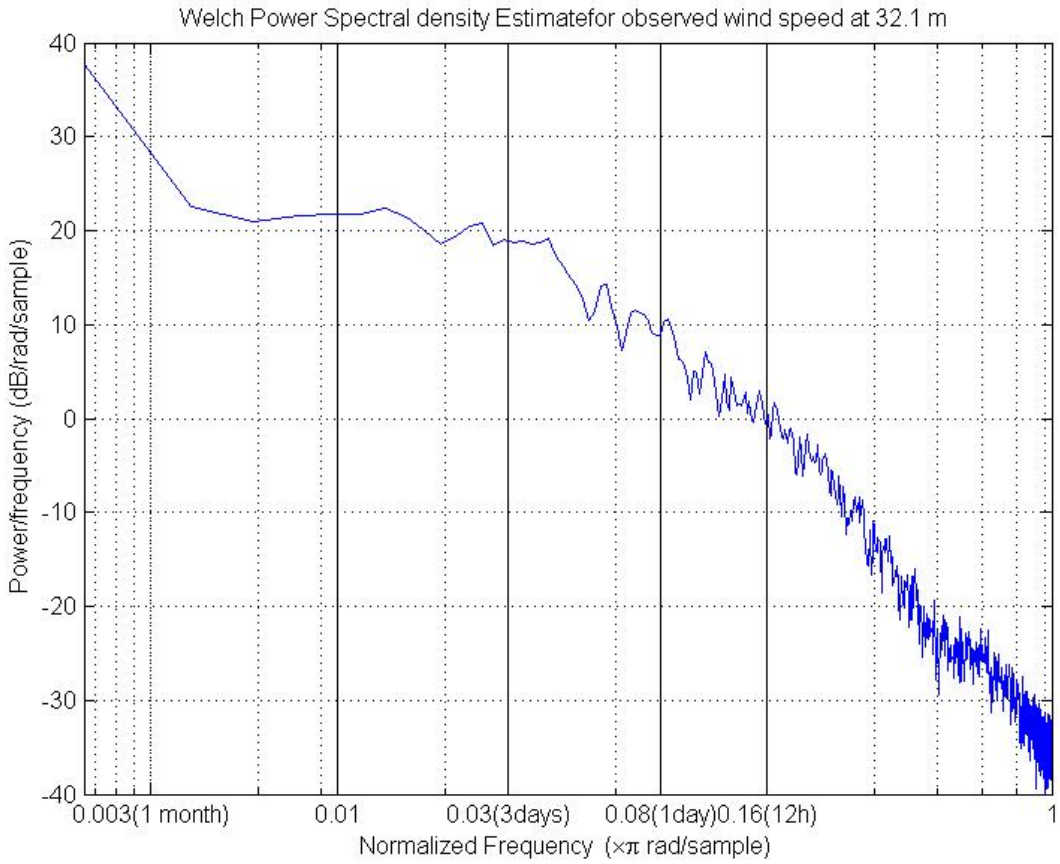

Figure 8:Welch power spectral density estimate for observed wind speeds at 32.1 m at Block Island AWS Met Tower.

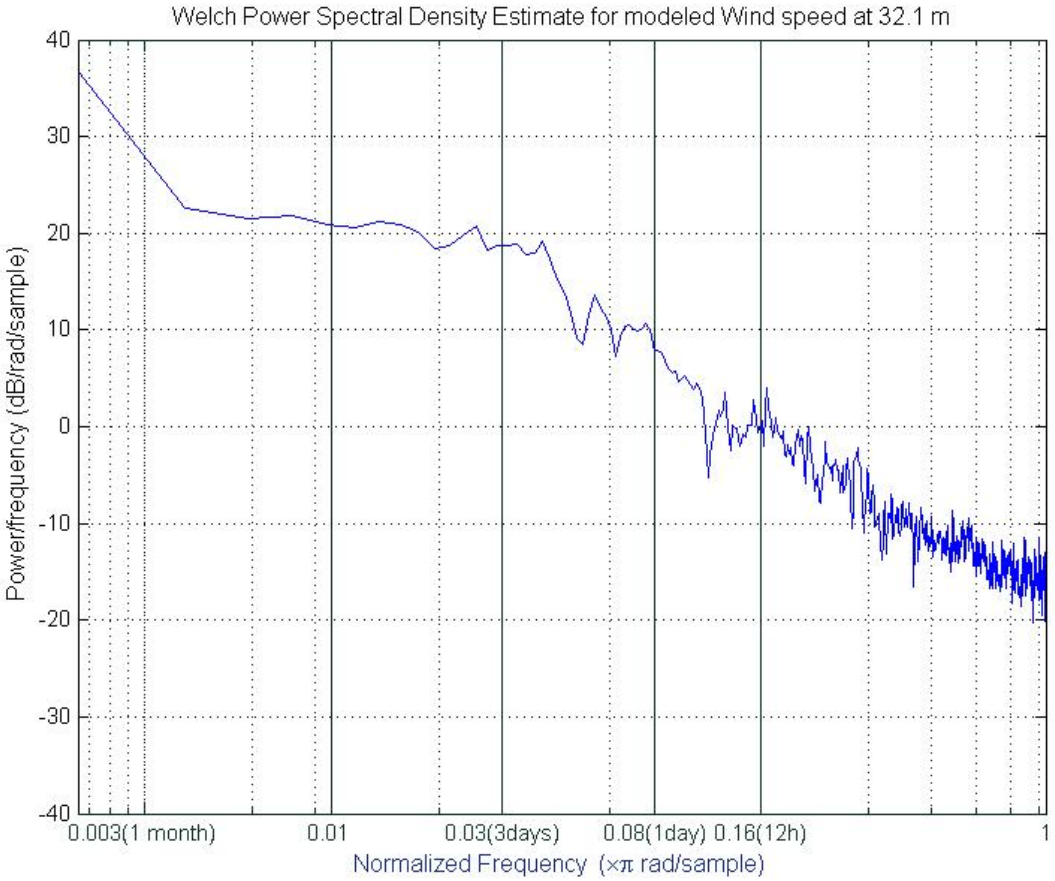

Figure 9:Welch power spectral density estimate for modeled wind speeds at 32.1 m at Block Island AWS Met Tower.

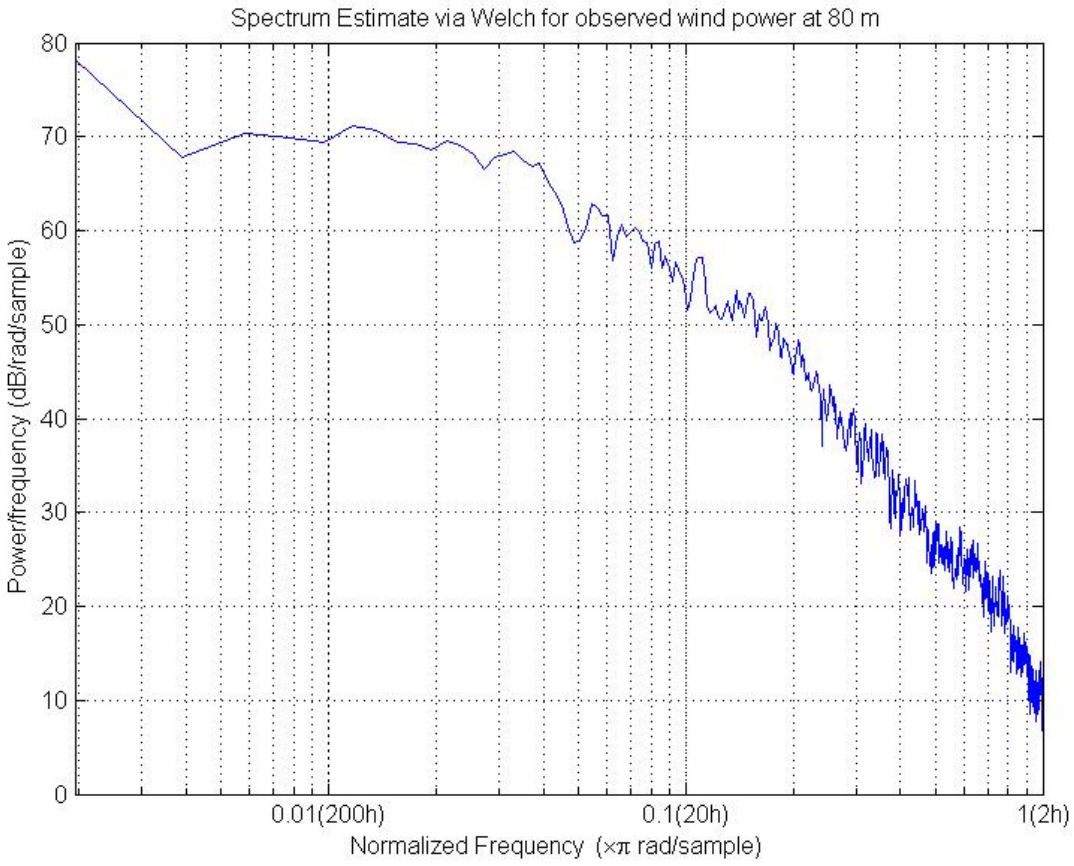

Figure 10: Welch power spectral density estimate for observed wind powers at 80 m at Block Island AWS Met Tower.

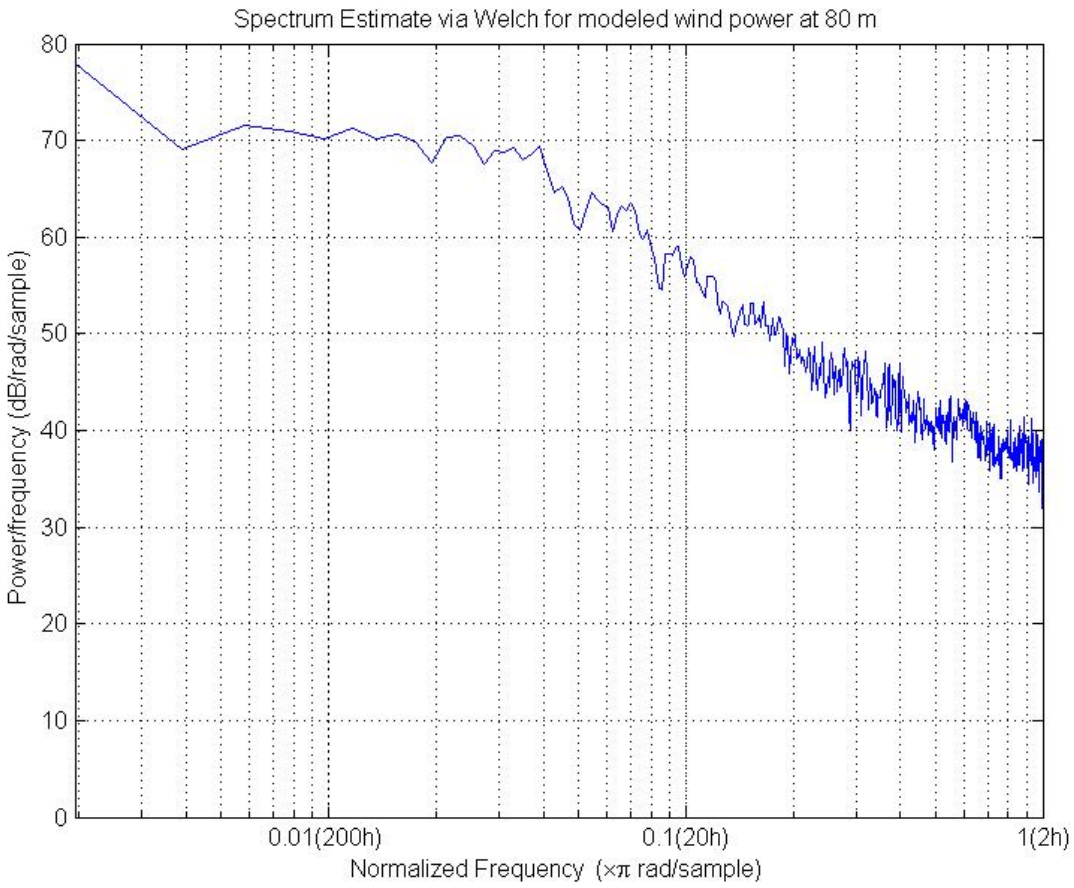

Figure 11: Welch power spectral density estimate for modeled wind powers at 80 m at Block Island AWS Met Tower.

4. Coherence

Definition

The coherence function between two stationary records x(t) and y(t) is defined as:

$$\gamma^2(f) = \frac{|G_{xy}(f)|^2}{G_{xx}(f)G_{yy}(f)}$$

where $G_{xx}(f)$ and $G_{yy}(f)$ are the estimated autospectral density function of x(t) and y(t) respectively, and $G_{xy}(f)$ is the estimated cross-spectral density function between x(t) and y(t).

The coherence function can be interpreted as the fractional portion of the mean square value of record#2 (y=simulations) that is consistent with record#1 (x=observations) at frequency f.

Results are shown for simulations (y) and observations(x) pairs, for wind speed at 32.1 m and power at 80 m in Figure 12 and Figure 13. In both cases a high coherence between observations

and simulations is obtained for low frequencies up to 3 to 2 days. Then the coherence drops to be minimum for frequencies of the order of hours.

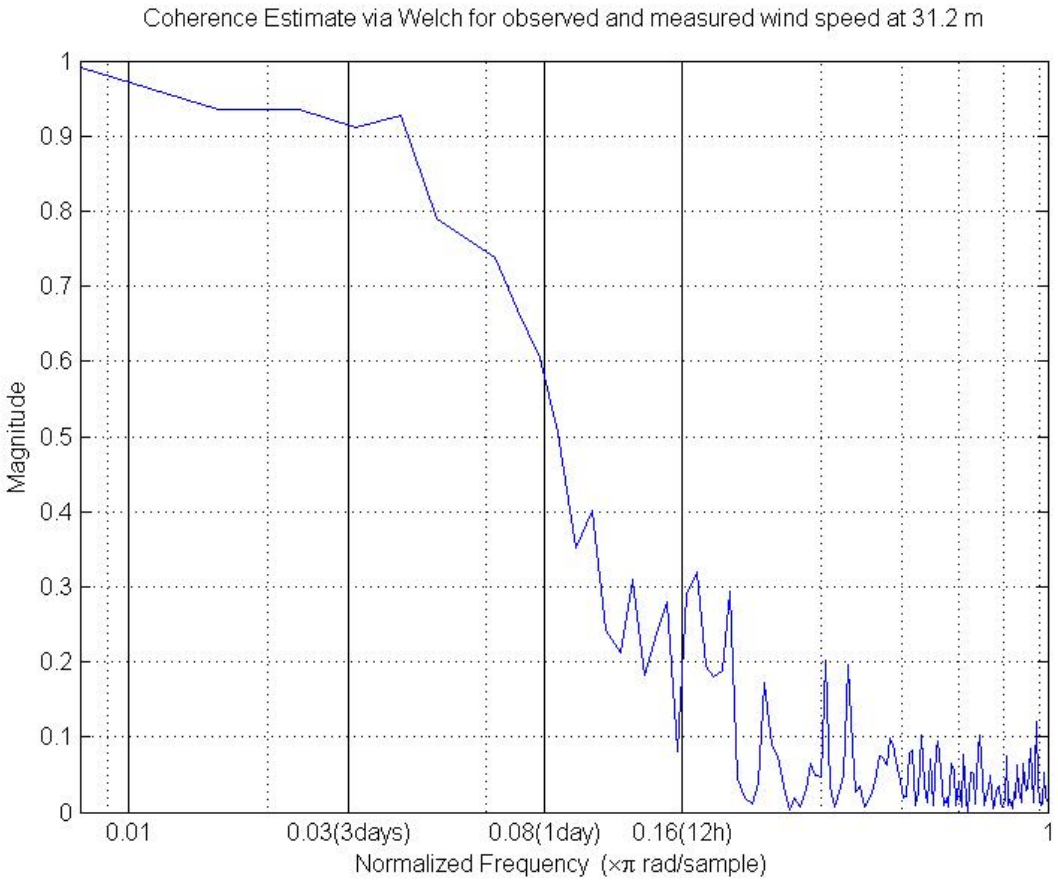

Figure 12 : Coherence estimate via Welch method for observed and measured wind speed at 32.1 m at Block Island AWS Met Tower.

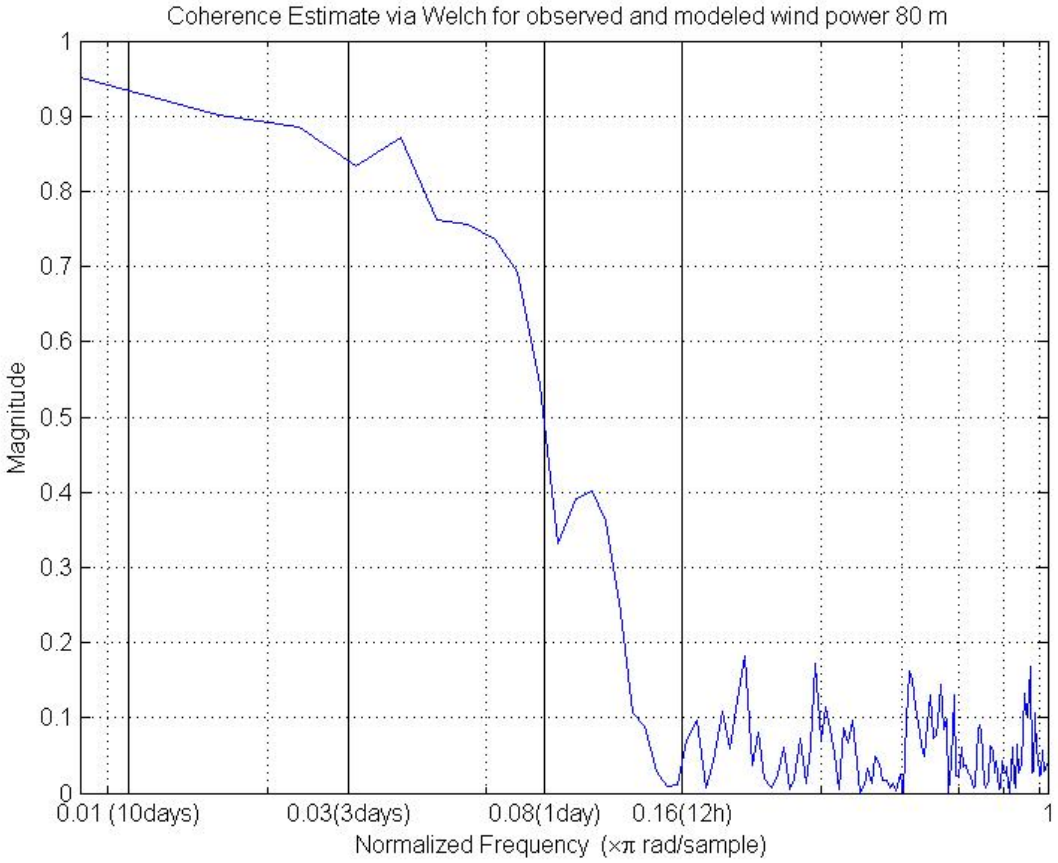

Figure 13: Coherence estimate via Welch method for observed and measured wind power at 80 m at Block Island AWS Met Tower.

5. Weibull

Time series were both fit with a Weibull adjustment (RMSE 0.2% for the modeled time series, 0.5% for the observed time series). Those adjustments are both significantly different in term of scale and shape parameters for observed and modeled time series. Values of those parameters and their confidence interval are indicated on Figure 14 and Figure 15 . However despites those discrepancies both Weibull distributions lead to very similar values of expected average power, 978 W/m^2 versus 929 W/m^2 for the observed and simulated records respectively, which correspond to a power underestimation of the model of 5% versus observations. Let's note that the simulated rose power is similarly noticeably different from the observed rose power, but both again when integrated lead to a similar power: 983 W/m^2 versus 940 W/m^2 for the observed and simulated records respectively, corresponding to a power underestimation of the model of 4% versus observations. Both methods of power estimation are in agreement with a discrepancy of the order of 0.5% for the observed record and of the order of 1% for the simulated record.

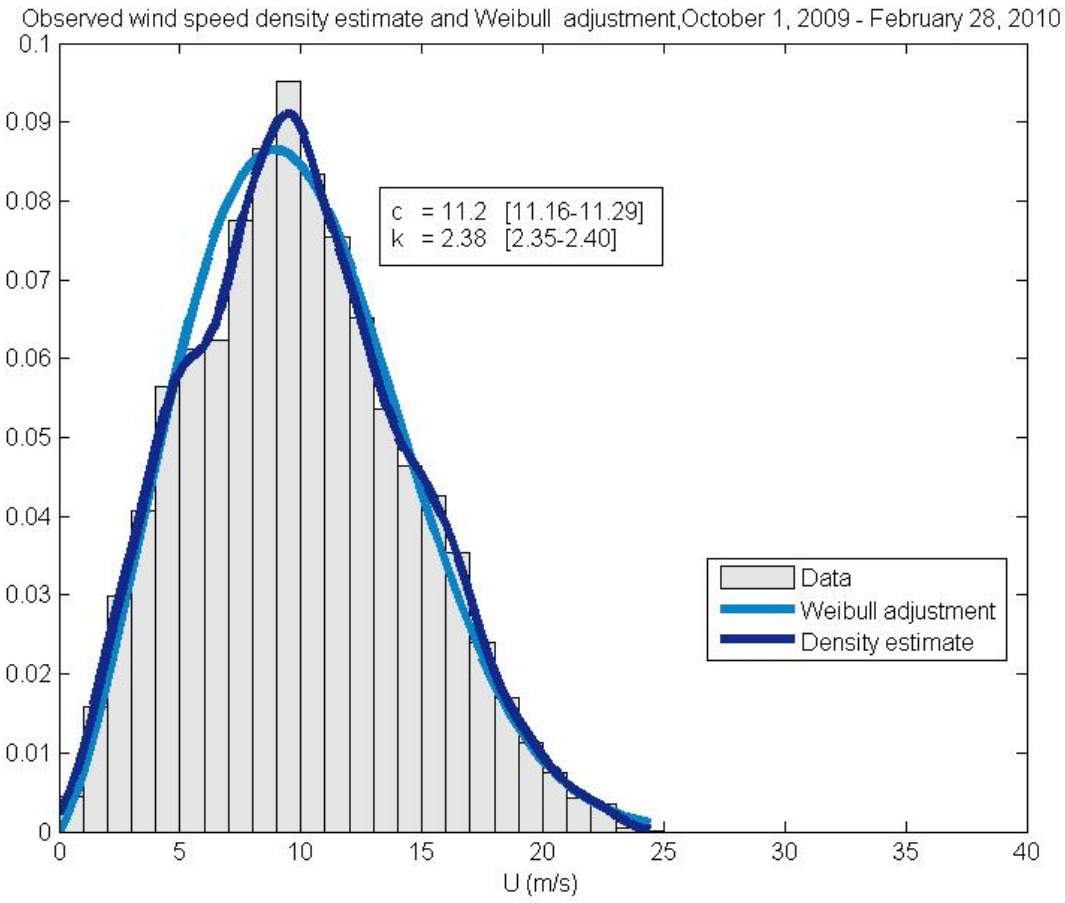

Figure 14: Weibull adjustment of observed wind speeds at 80 m at Block Island AWS Met tower.

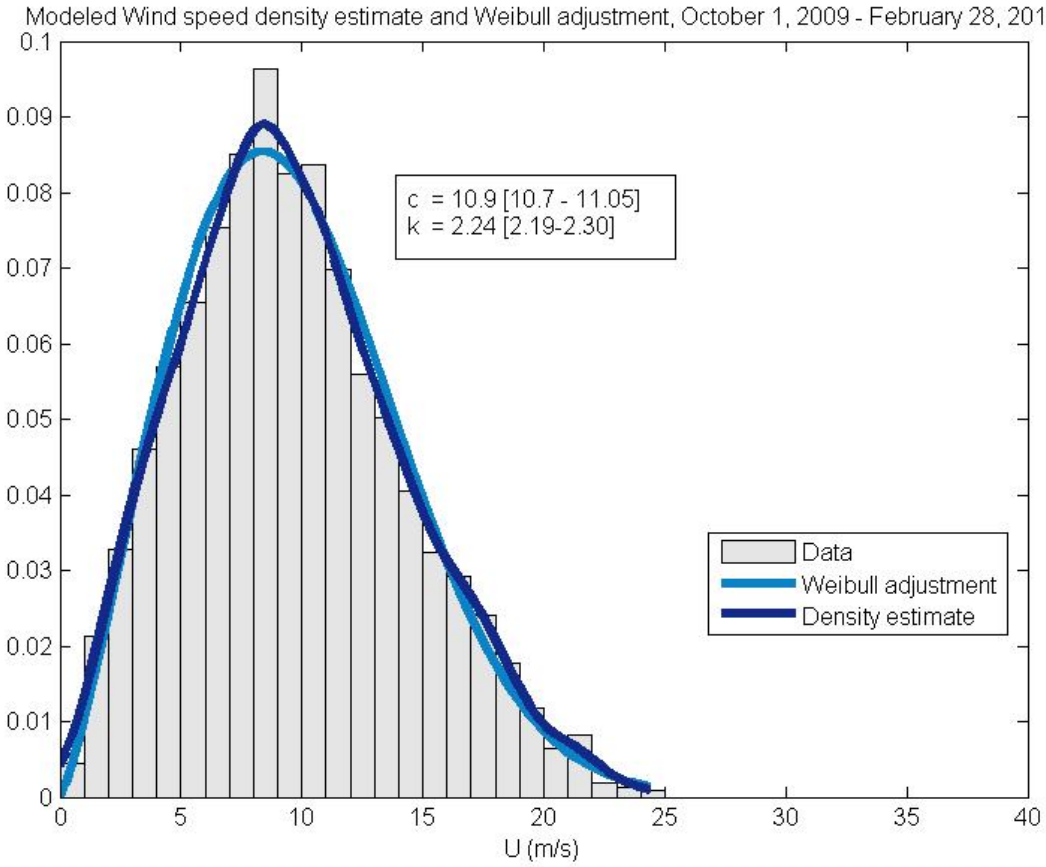

Figure 15: Weibull adjustment of modeled wind speeds at 80 m at Block Island AWS Met tower.

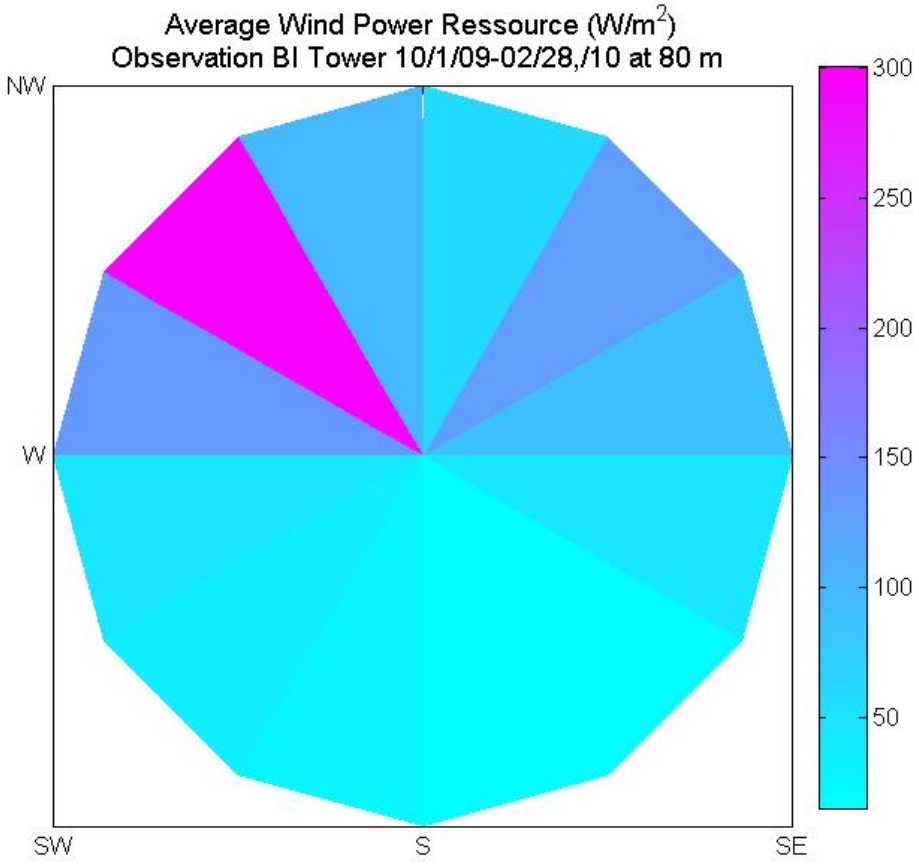

Figure 16: Average wind power resource at 80 m per directional sector estimated from time series of observations at Block island AWS Met Tower between 10/1/09-02/28/10.

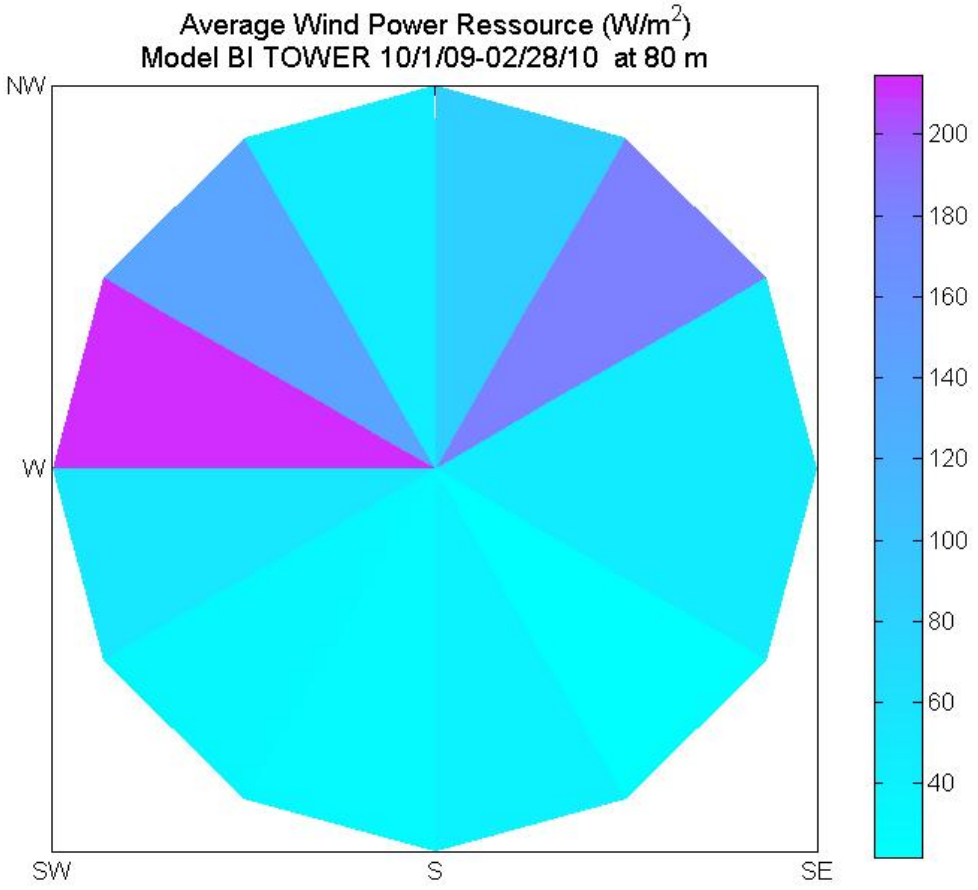

Figure 17:Average wind power resource at 80 m per directional sector estimated from time series of WeatherFlow modeled power at Block island AWS Met Tower between 10/1/09-02/28/10.

22.

Report of the Ocean Special Area Management Plan

STAKEHOLDERS PROCESS

To the

Rhode Island Coastal Resources Management Council

By Ken Payne

June 30, 2010

Overview of the stakeholders process. Stakeholders processes are broadly recognized as vital to effective, legitimate planning. The RI Coastal Resources Management Council (CRMC) has established practice of convening stakeholder groups when developing special area managements plans (SAMPs). Accordingly a stakeholders process was from the outset an integral part of the work program for preparing the Ocean SAMP.

Rhode Island's use of a SAMP for ocean spatial planning is at the very forefront of planning practice. There are not models from elsewhere on which Rhode Island can draw for guidance and insight.

The east coast of the United States has among the best wind resources globally. As renewable energy has become of increasing interest, the potential for off-shore wind has been given higher levels of attention. In Rhode Island, offshore wind has been recognized as the premier opportunity to meet statutory goals, established in 2004, for obtaining energy from renewable resources.

Building a "wind farm" in the waters off Rhode Island would be a major additional use in the marine environment, and as such would require state and Federal approvals. Applications for approval of major new or additional activities in the marine environment can be evaluated on a case-by-case basis, a process which can be expensive and protracted, and they can be evaluated in the context of duly established plans. In the first instance, the project developer has the leading role in making locational decisions; in the latter instance a public process leads and provides a planning context in which developers subsequently act in proposing developments for specific locations. A function of spatial planning is to optimize the location of activities so that adverse impacts and conflicts can be avoided or, if unavoidable but not unacceptable, mitigated.

The Ocean SAMP Stakeholders Process – Three Phases.

Phase I: Establishing the Process: The Ocean SAMP Stakeholders Process was convened under the aegis of the RI Coastal Resources Management Council by the Ocean SAMP management team. The work to get the stakeholders process up and running commenced in August 2008. The management team asked Kenneth F. Payne if he would chair the process in a voluntary capacity, and he agreed to do so. A first task was to assemble a list of persons to be invited to stakeholder meetings—while persons on the list would be deemed "stakeholders," all members of the public could participate in stakeholder meetings with no distinction between their participation and that of formal stakeholders. The list of stakeholders (Attachment A) assured that a comprehensive range of parties with an interest in the Ocean SAMP area, the waters off Rhode Island's shore, would regularly notified of meetings.

The stakeholders process met seventeen (17) times during the twenty (20) month period October 2008 through June 2010. A list of stakeholder meetings is Attachment B.

During the period October 2008 through February 2009, the stakeholders became familiar with the Ocean SAMP and the schedule to produce a draft of the Ocean SAMP for consideration by the RI Coastal Resources Management Council in accordance with the Administrative Procedures Act, concurred in a process for meetings, and received back-ground issues and uses in the Ocean SAMP area.

At the initial meeting of the stakeholders, October 2008, Kenneth Payne stated his position that a basic purpose of the stakeholders process was to bring transparency and fairness to the development of the Ocean SAMP (predominantly a scientific and technical document). The stakeholders process would provide regular, public access to the work being done in the Ocean SAMP and an opportunity to share insights and concerns about what was being done. The stakeholders process would respect the views and concerns of all who participated, recognizing that the presence of conflicting views is reasonable and constructive. It would not be a function of the stakeholders process to subsume minority views in a consensus position on any issue. The process would rather be guided by the principle that all views would be fairly heard and taken into account. The chair of the process would have three functions, first to preside at meetings, second to act as advocate for stakeholders in management committee meetings and with public bodies and other parties, and third to act as an additional point of contact for parties concerned about Ocean SAMP issues.

A general format for meeting was established. Each stakeholders meeting would begin with an update on SAMP activities since the prior meeting, be followed by a presentation on a technical/scientific assessment being undertaken for the Ocean SAMP area, have an open discussion of stakeholder concerns and interests, and conclude with a wrap-up and plan for the next meeting. Stakeholder meetings would routinely be held more or less monthly on Tuesday's beginning at 6 PM and would last between two and three hours; light food would be provided.

A major concern of the participants in the first several meetings was the legitimacy of the stakeholders process. Would it simply be a rubber stamp of positions already taken? The RI Winds stakeholders process convened by the Office of Energy Resources was directed toward recognizing that offshore wind potential is Rhode Island's premier renewable energy resource. Would the Ocean SAMP stakeholders process be different, or was it simply an offshore wind farm siting study?

A second critical concern during the early meetings was whether the stakeholders would be presented the best, most current analyses being done through SAMP studies of the Ocean SAMP area. Would any parties have access to more current analyses than the stakeholders?

These matters were resolved as follows. The Ocean SAMP was an effort in Ocean spatial planning and analyses; it would not be a siting study -- it was understood that the proposal of specific sites for renewable energy facilities would be made by parties seeking to develop such facilities, and that detailed studies would be needed for proposed sites. Neither the Ocean SAMP nor the stakeholders process was directed at a specific outcome. The stakeholders consistent with the principles of transparency and fairness would have the most current analyses as they were available for external presentation and consideration. Ocean SAMP staff made a commitment to post electronically the most current Ocean SAMP documents. The resolution of these matters was achieved by the February 11, 2009, meeting. Afterwards little concern was expressed about the legitimacy of either the stakeholders process itself or the manner in which it was being conducted.

Phase II: Learning about the Ocean SAMP Area. The period from February through October 2009 was one of learning about the Ocean SAMP area: physical conditions; human uses including fishing, marine transportation, naval activity, recreation and tourism; submerged historic sites; and fauna including birds, marine mammals and turtles, and fish stocks.

Phase II provided participants in the stakeholders a fairly comprehensive overview of conditions in the Ocean SAMP area. The meetings had a regular format: a welcome by the chair, a brief orientation to the Ocean SAMP process by Coastal Resources Center (CRC) staff, a summary from Coastal Resources Management Council executive director Grover Fugate on current Ocean SAMP issues, a presentation of a topic area by a scientist or group of scientists (this was the heart of the meeting), and a review of Ocean SAMP related activities during the next by CRC staff, and a wrap-up by the chair.

Phase III: Reviewing draft Ocean SAMP chapters. The Ocean SAMP is both a process and, importantly a document, which has a legal life with its adoption by the Coastal Resources Management Council. Phase III of the Ocean SAMP stakeholders process commenced in October 2009; the Ocean SAMP subcommittee of the CRMC that month approved a nine step public review process for chapters of the Ocean SAMP (Attachment C). After the preliminary steps of the management team agreeing that a

chapter is ready for public review and the integration of comments on the chapter by a chapter-specific technical review committee, draft chapters of the Ocean SAMP would be presented at a stakeholders meeting and posted to the website for public comment. This was step three in the nine step process and the initiation of the public review process of Ocean SAMP chapters. Given its position in the adoption process, the stakeholders process can be understood as a critical portal through which Ocean SAMP chapters passed from being scientific/technical assessments to being components of a public document.

While CRC staff presented a time line of approximately three months for the review of each Ocean SAMP chapter (Attachment D), several stakeholders expressed concern that given the amount of material to be reviewed, the amount of time for review might be insufficient. Others expressed concern that there was insufficient opportunity to review the Ocean SAMP document as a whole. The stakeholders process was a forum for sharing these concerns with public review process of the Ocean SAMP document with the Ocean SAMP management team and CRMC staff and legal counsel.

Presentations of Ocean SAMP chapters were made at monthly stakeholders meetings by CRC staff and Ocean SAMP scientists from November 4, 2009, through June 1, 2010. The presentations were deeply informative but did not give rise to conflict or disagreement among stakeholders at the stakeholders meeting phase of the public review process with regard to the~~ir~~ content or quality of chapters. In sum, stakeholders meetings during Phase III were substantive but not contentious.

Conclusions of the stakeholders process. The absence of contention at stakeholder meetings with regard to the content of the Ocean SAMP chapters gives rise to the reasonable conclusion that the Ocean SAMP is a fair depiction of conditions and activities in the Ocean SAMP area. The notes of the Ocean SAMP stakeholders meetings support this conclusion. Since it was never in the purview of the stakeholders process to formally accept, reject or modified either the Ocean SAMP as a whole or the individual Ocean SAMP chapters; no action for or against the Ocean SAMP was taken. An open and comprehensive stakeholders review was undertaken and completed in the development of an ocean spatial plan.

Beyond providing a public review of the Ocean SAMP as it was being developed, the stakeholders process contributed to resolving how fisheries issues could be handled should there be future development in the ocean area affecting fishing. The Ocean SAMP stakeholders process also provided a means for addressing how the Ocean SAMP would be integrated into the State Guide Plan and made binding for consideration in revisions to local comprehensive plans; essentially it was recognized that the Ocean SAMP and the State Guide Plan would be complementary and would not need to be formally integrated for local planning.

Since people do not occupy the Ocean SAMP area except on a transitory basis for fishing, transportation, and recreation, Ocean SAMP stakeholders participated in the process based on the valuation they placed on activities and conditions, including

ecological conditions, in the Ocean SAMP area. Some of those valuations, especially those of fishers, had the important dimension of a substantial, direct economic interest. What the stakeholders process confirmed is that Rhode Islanders strongly and enduringly value the Ocean SAMP. What takes place in the Ocean SAMP area is important to life in Rhode Island. The Ocean SAMP as a marine spatial plan is a vital expression of those valuations. The Ocean SAMP is more than a scientific and technical document; it is an expression of the interests of the State.

The stakeholders wish to thank the staff of the CRC and the CRMC and the scientists who did the Ocean SAMP analyses for their unstinting contributions to the stakeholders process. These efforts were foundational to the process; the steadiness, the graciousness, and the professionalism of their execution is genuinely appreciated.

This report was presented and discussed at a stakeholders meeting on June 30, 2010. And clarifications to it were made based on that discussion.

The participation in the stakeholders process has been an honor and a privilege; throughout it has been a form of public service. The Rhode Island Coastal Resources Management Council is to be commended for its commitment to having stakeholders processes being an integral part of special area management planning.

Respectfully submitted,

Kenneth F. Payne, Chairperson

CRMC Ocean Special Area Management Plan (SAMP) stakeholder group

Attachment A

Chair: Dr. Kenneth Payne, University of Rhode Island College of the Environment & Life Sciences

Mr. Dan Beardsley	Executive Director, Rhode Island League of Cities and Towns
Mr. Jeff Broadhead	Executive Director, Washington County Regional Planning Council
Mr. Paige Bronk	Director of Planning, City of Newport
Mr. John Brown	Tribal Historic Preservation Officer, Narragansett Indian Tribe
Mr. Chris Brown	President, Rhode Island Commercial Fishermen's Association
Ms. Alison Buckser	Rhode Island Chapter Chair, Sierra Club
Mr. Charlie Cannon	Landscape Architecture Faculty, Rhode Island School of Design
Mr. Jeffry Ceasrine	Town Manager, Town of Narragansett
Capt. Paul Costabile	Captain, Northeast Marine Pilots
Ms. Vicki deAngeli	President, Jamestown Chamber of Commerce
Mr. Lanny Dellinger	President, Rhode Island Lobstermen's Association
Mr. Julio DiGiando	Town Council President, Jamestown Town Council
Mr. Denny Dillon	Rhode Island Party & Charter Boat Association
Ms. Tina Dolen	Executive Director, Aquidneck Island Planning Commission
Ms. Charlene Dunn	Councilor, Charlestown Town Council
Mr. Bernard Fishman	Executive Director, Rhode Island Historical Society
Mr. Richard Fuka	President, Rhode Island Fishermen's Alliance
Ms. Gina Fuller	Appointee representing Westerly Town Council
Ms. Kimberly Gaffett	First Warden, Town of New Shoreham (Block Island)
Ms. Myrna George	President, South County Tourism
Ms.Tricia Jedele	Vice President of RI Advocacy, Conservation Law Foundation
Mr. Doug Harris	Deputy, Narragansett Indian Tribal Historic Preservation Office
Ms. Debbie Kelso	Executive Director, Narragansett Chamber of Commerce
Mr. Michael Keyworth	Director, Rhode Island Marine Trades Association
Mr. John F. Killoy III	Appointee representing Rhode Island AFL-CIO
Ms. Karina Lutz	Director of Development and Advocacy, People's Power & Light
Mr. Mike Marchetti	Eastern New England Scalloper's Association
Ms. Eugenia Marks	Senior Director of Policy, Audubon Society of Rhode Island
Mr. Gregg Mataronas	Sakonnet Point Fishermen's Association
Mr. Steve Medeiros	President, Rhode Island Saltwater Anglers Association
Mr. Robert Mushen	Town Council President, Town of Little Compton
Mr. Ray Nickerson	Principal Planner, Town of South Kingstown
Dr. Eleftherios Pavlides	Director, Professor, Wind Power RI Project, Roger Williams University
Ms. Margaret Petruny-Parker	Executive Director, Commercial Fisheries Research Foundation
Mr. Ted Platz	Fisherman, Rhode Island Monkfishermen's Association
Mr. David Prescott	Chapter Chairman, R.I. Chapter/Surfrider Foundation
Mr. Michael Ryan	President of Rhode Island Distribution, National Grid
Mr. Paul Sanroma	Administrator, Rhode Island Wind Alliance
Mr. Bill Silkes	Ocean State Aquaculture Association
Mr. Evan Smith	President and CEO, Newport County Convention and Visitors Bureau
Mr. David Spencer	Member, Atlantic Offshore Lobster Association
Mr. Keith Stokes	Executive Director, Newport County Chamber of Commerce
Ms. Darlene Towne Evans	President, South Kingstown Chamber of Commerce
Ms. Kathleen Wainwright	Director of Conservation, The Nature Conservancy
Mr. Russell Wallis	President, Ocean State Fishermen's Association
Ms. Wendy Waller	Staff Environmental Attorney, Save the Bay
Ms. Laurie White	President, Greater Providence Chamber of Commerce
Jessica Dugan Willi	Executive Director, Block Island Tourism Council
Mr. Ronald Wolanski	Town Planner, Town of Middletown

ATTACHMENT B

Ocean SAMP Stakeholder Meetings

DATE	TOPIC	PRESENTER
October 29, 2008	Overview of Ocean SAMP	Grover Fugate
December 2, 2008	Climate Change	Pam Rubinoff
January 6, 2009	Ocean Floor	Jon Boothroyd John King
February 10, 2009	TDI Screening Analysis	Malcolm Spaulding
March 19, 2009	Fisheries Mapping	Dave Beutel
April 7, 2009	Acoustics and Electromagnetics	James Miller
June 30, 2009	Marine Mammals and Sea Turtles	Robert Kenney
November 4, 2009	Introduction Recreational and Tourism	Grover Fugate, Jennifer McCann Tiffany Smythe, Michelle Smythe
December 1, 2009	Transportation, Navigation and Infrastructure	Tiffany Smythe, Michelle Armsby
January 5, 2010	Physical Oceanography	Dan Codiga
February 2, 2010	Existing Statutes Air Quality	Brian Goldman John Merrill
March 2, 2010	Renewable Energy	Michelle Armsby
April 6, 2010	Climate Change Other Future Uses	Jim Tobey Barry Costa-Pierce
May 4, 2010	Fisheries Resources and Uses Effects Section of Renewable Energy	Dave Beutel, Tiffany Smythe, Sarah Smith Michelle Armsby, Sarah Smith
June 1, 2010	Cultural and Historical Resources	Teresa Crean, Jon Boothroyd, Rod Mather, Rick Greenwood
June 30, 2010	Reflection on Stakeholder Process	Ken Payne

Attachment C

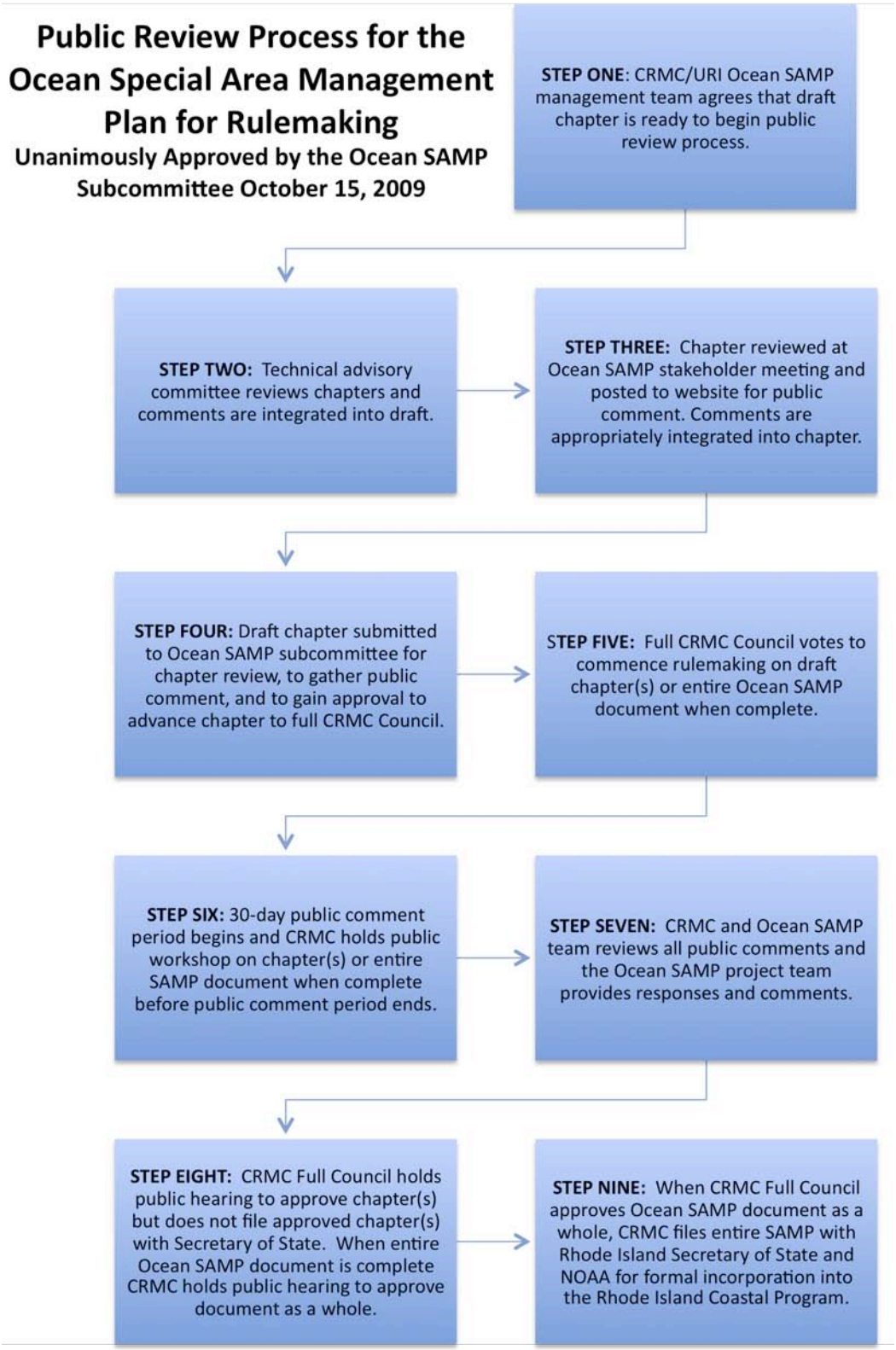

Attachment D

Public Review Process for the Ocean SAMP Rulemaking (Status: 06/02/10)

	Draft Chapters	Step 1: MT Approval	Step 2: TAC Review	Step 3: Informal Public Review	Step 4: CRMC Review	Step 5: CRMC Council Approves Rulemaking	Step 6: Formal Public Review	Step 7: Public Comments Review	Step 8: Public Hearing/Chpt. Adoption
0	Executive Summary*								
100	Introduction*								
200	Ecology								
300	Global Climate Change								
400	Cultural and Historic Resources								
500	Fisheries Resources and Uses								
600	Recreation and Tourism								
700	Marine Trans., Nav., Infrastructure								
800	Renewable Energy								
900	Other Future Uses								
1000	Existing Policies								
1100	Policies of the Ocean SAMP*								

Notes: *: These chapters will be processed with the full document; Dates reflect when the chapters will be presented at public meetings during specific phase.

Step 1: Management Team (MT) Approval
- MT approves draft chapter to proceed to public comment.

Step 2: TAC Review
- Technical Advisory Committee comments on draft chapter.

Step 3: Informal Public Review
- **Draft chapter presented at stakeholder meeting.**
- Informal public comments on draft chapter.

Step 4: CRMC Review
- **Draft chapter submitted to Ocean SAMP Subcommittee.**
- Informal public comments/responses presented at Subcommittee meeting.
- Subcommittee approves draft chapter to advance to full council.

Step 5: Rulemaking
- Full Council votes to commence rulemaking on draft chapters.

Step 6: Formal Public Review
- 30-day comment period takes place.
- Public workshop held.

Step 7: Review
- Public comments reviewed by CRMC and Ocean SAMP team.

Step 8: Public Hearing
- Public hearing for draft chapter.
- Draft Chapter approved by Full Council.

Once all chapters have completed Steps 1 -8, a public hearing will be held for the entire SAMP document prior to Full Council approval (Step 9).

23.

Ecological and Service Valuation, a Principal Component and Cluster Analysis Approach:

An Ecological and Service Typology in the Ocean SAMP Area

by

Annette R. Grilli and Tania Lado

University of Rhode Island, July, 15, 2010

Executive Summary

Assessing the impact of human activities on coastal and offshore environments is an integral part of planning significant developments in these areas, such as the installation of an offshore wind farm. When human impacts are predictable, as in the installation of coastal or offshore structures, the ecological information is essential to managing these environments. Marine Management Tools (MMTs) integrate biological, and other information such as services, typically in the form of synthetic maps. Such MMTs are useful not only for performing environmental impact studies, but also for managing marine sanctuaries and other protected areas. MMTs are emerging from a recent new conceptual approach, the Ecosystem-Based Management approach (EBM), an integrated approach to management that considers the entire ecosystem including humans and seeks an optimal balance between ecology and society. Optimal balance refers to an ecosystem in healthy, productive, and resilient conditions, which can provide the services humans want and need. (Load and Leslie, 2009). These services are defined as: (i) provisioning services (food, fuel, medicines); (ii) regulating services (biological regulation, climate regulation, human disease control, waste processing, flood protection, erosion control); (iii) cultural services (aesthetics, education and research); and (iv) supporting services (biochemical processes, nutrient cycling) (Load and Leslie, 2009).

There is no standard methodology to assess the state of an ecosystem in this extended sense, including humans, although many methods have been proposed. We prepared a literature review of methodologies used in EBM to assess the health of an ecosystem. It will be subsequently included in an appendix, to complement the literature review provided in the companion report of this SAMP sub-project (French et al., 2010).

In the present study, a Principal Component (PCA) and Cluster analysis (CA) approach is selected to extract homogeneous ecological and socio-ecological sub-regions in the SAMP study area. The PCA-CA is a non-value objective way of mapping the attribute data describing an ecosystem. The PCA extracts the natural variance of the primitive variables describing the area, without assigning *a priori* values, scores, or weights. This results in a quantitative ordination or organization of the data in terms of principal components, ultimately leading to a clustering or a grouping of similar areas into homogeneous zones (CA). The resulting map of clustered zones is more an objective typology than a valuation map. Each newly defined zone is described in terms of ecological or socio-ecological assemblages and biodiversity. Once the sub-regions are

objectively delimited this way, these can be interpreted in terms of values relative to the services, as defined above.

The PCA-CA method is applied to seasonal data (Fall) using a first group of variables corresponding to a biodiversity level 1, defined as the minimal level of acceptable ecological diversity in input, including 12 fishes species, whales and dolphins, and to a second group of variables corresponding to a socio-bio diversity level 1, including 14 ecological variables and 2 fisheries and service variables (mobile and fix gear use and recreational use). The application of the method leads to a partitioning of the SAMP area into ecological and socio-ecological sub-regions. In parallel the method is applied to geophysical variables to help with the cluster interpretation in terms of geophysical variables.

Results, presented in terms of ecological groups and biodiversity index, consistently reflect an onshore-offshore gradient and the geological and sedimentological variance. A deeper water group is isolated from a shallow water group. The intermediate and shallow waters are separated into two groups, reflecting both the oceanographic dichotomy between Rhode Island and Block Island Sound, and variance in geological deposits.

Although still at a stage of development, this marine management tool is proving promising for identifying sub-regions. Major expected future developments are:

- Adding ecological and services variables to more accurately represent the ecological and social environment, and therefore better discriminate the space.
- Developing the cluster valuation method:
    - The biodiversity and services indices are a first attempt at valuation and follow up work should include using and comparing the various standard, or newly developed, indices by Shannon (1947) or others (Derous, 2007; Borja et al., 2007; Spellerberg and Fedor, 2003).
    - The concept of valuation should relate the valuation criteria to the different organizational levels of biodiversity, such as: population, community, ecosystem, which means discriminating between migratory species passing though the area and species living in symbiosis with others, or species associated with a particular geomorphologic feature, or related to a particular oceanographic process, such as upwelling (Derous, 2007).
    - The Concept of rarity must be introduced.

- Assessing the uncertainty of the groups isolated by the clusters, due to uncertainty in the data, and discussing the cluster borders in those terms (i.e., rigid or fuzzy borders).

- Addressing the dynamic aspect of the sub-regions, by introducing time series of the variables rather than mean values in input.

Table of Contents

List of Figures

List of Tables

List of Attachments and Appendices

1 Introduction

Assessing the impact of human activities on coastal and offshore environments is an integral part of planning significant developments in these areas, such as the installation of an offshore wind farm. When human impacts are predictable, as in the installation of coastal or offshore structures, the ecological information is essential to managing these environments. Marine Management Tools (MMTs) integrate biological and other information, such as services, typically in the form of synthetic maps. Such MMTs are useful not only for performing environmental impact studies, but also for managing marine sanctuaries and other protected areas. MMTs are emerging from a recent new conceptual approach, the Ecosystem-Based Management approach (EBM), which is an integrated approach to management that considers the entire ecosystem including humans. The EBM's goal is to manage the ecosystem through explicitly integrating the dynamics between ecological and social domains. This approach is relatively new in the sense that the environment—in this specific case the ocean—is no longer considered as this "sacred untouchable place", or this "free open space", which can be used and abused. The interaction between ecological and social domains, inherent to any society, is acknowledged in EBMs and, therefore, an optimal balance is finally sought, which refers to an ecosystem in healthy, productive and resilient conditions, that can provides the services humans want and need (Load and Leslie, 2009; Arkema et al. 2006; Goldman et al. 2008; Lester et al. 2010). Among many published lists of services, we adopted Load and Leslie's definition, whose relevance depends on the specific ecosystem, which includes: (i) provisioning services (food, fuel, medicines); (ii) regulating services (biological regulation, climate regulation, human disease control, waste processing, flood protection, erosion control), (iii) cultural services (aesthetics, education and research); and (iv) supporting services (biochemical processes, nutrient cycling) (Load and Leslie, 2009)

Although there is no standard methodology to assess the state of an ecosystem in this extended sense, including humans, many methods have been proposed. The concept of nature's valuation has been raised, debated, accepted, or refused. It seems that a fundamental step in the concept of nature valuation is the Lauderdale paradigm (1819), which defines public and private wealth and riches as "everything in the world, which is delightful to people, with the additional factor for private riches that it occurs in a certain degree of scarcity". The paradox is that when public wealth becomes relatively scarce, it gains value, but paradoxically falls in the domain of private riches and thus the public wealth decreases (Daly,2007). The ecological valuation process

is entangled in this paradox. It seems that, conceptually, one cannot escape "pricing nature " (Hanley and Barbier, 2009; Wainger and Boyd, 2009; McLeod and Leslie, 2009). There are many methodologies towards this valuation, using or not monetary units, which are more or less complex and more or less complete, but still all of these methods have a common drawback: subjectivity, to a minimal or larger degree, which is inherent to the concept of valuation. A literature review of methodologies used in EBM to assess the health of an ecosystem was prepared and will be subsequently added in an appendix, as a complement to the literature review covered in the companion report of this SAMP sub-project (French et al., 2010).

In the present study a Principal Component (PCA) and Cluster analysis (CA) approach was selected to identify homogeneous ocean areas or sub-regions within the SAMP study area. This method is a non-value and objective way of mapping the attribute data describing an ecosystem (Zuur et al., 2007). The PCA extracts the natural variance of the original variables, which describes the area, without assigning *a priori* values, scores, or weights. This results in a quantitative ordination, or organization of the data (i.e., the principal components), ultimately leading to a clustering or grouping of similar areas into homogeneous zones (i.e., the clusters). The resulting map of clustered zones is more an objective typology than a valuation map. Each newly defined zone is described in terms of original variables and biodiversity (schematic example: deep water, mammals passing through; shallow water, rocky habitat, high biodiversity, bird foraging area). This approach is commonly used in regional geography (Cablk, White, and Kiester, 2002), but less often applied to ocean management, although Jordaan (2010) recently applied a PCA to the Gulf of Main, to extract and interpret the natural geographical structure of the coastal and offshore marine biodiversity. Similarly, Borja et al. (2007) developed a Marine Biotic Index based on a multivariate approach (M-AMBI), to assess the ecological integrity of coastal and estuarine waters, in order to respond to the request of the European Water Framework directive (2000/60/EC). Once the sub-regions are objectively delimited, these can be interpreted in terms of value relative to the service list, as defined above.

It should be pointed out, before we detail our analyses, that the original goal of this study had to be slightly restated, in view of the unavailability of some data and the tight time frame left for the analysis. Specifically, as of July 1st, we were still expecting additional data, but then decided to complete the analysis without it to met the deadline. The present analysis integrates fish data (Collie, 2010) , mammal data (Kinney, 2010), geophysiscal data (Codega and Ullman, 2010), and binary (i.e., use=1; not use=0) fisheries data (Beutel, 2009), representing the services data.

The bird data available at this time was still spatially too sporadic to reliably be included in this analysis. The bird aerial survey currently performed will lead to a denser spatial coverage and will likely be available at the end of the year 2010 (Winarski,2009; Patton,2010). Also, we unfortunately could not have access to benthos data, which should contain the best tracer of ecological health, and the quantitative fisheries data were neither available. In view of additional restrictions on summer and winter fish data, the study will be performed for fall and spring season only . In the current report, only fall season is presented. Spring results will be delivered by the deadline of September 1st.

2 Data source

Data used in the multivariate analysis are grouped into ecological, geophysical, and services variables.

2.1 Ecological data

Seasonal fish biomass by species. Those data were obtained from Jeremy Coolie's team from URI Graduate School of Oceanography (Bohaboy and al., 2010). Data used in the analysis are described in Appendix A of their report. Data are point data in biomass per surface unit (mg/m^2) obtained from 3 sources, Rhode Island Department of Environmental Management (DEM) (monthly,1999 - 2008) , Northeast Area Monitoring and Assessment Program (NEAMAP) (fall 2007, 2008 and spring 2008), National Marine Fisheries Service (NMFS) (spring and fall 1999 – 2008).

Mammals data in sighting-per–unit-effort (SPUE) were obtained from Robert Kenney and Kathleen Vigness-Raposa from URI Graduate School of Oceanography and the Department of Natural resources Science, respectively (Kenney, R.D. and K.J. Vigness-Raposa. 2009).

2.2 Geophysical data

The bathymetry is obtained from NOAA Coastal Relief Model and used to introduce two variables, depth and slope. The depth is the water depth at each grid point (m) and the slope is the maximum slope at each grid cell. It is calculated at each grid cell (200 m by 200 m) as the maximum derivative from the center point of the grid cell to the edge of the grid searching in all direction.

The bottom roughness was provided by John King as the standard deviation of the slope on a radius of 1000 m (J. King, 2010.)

Oceanographic data were obtained from Codega and Ullmann. Variables include in this analysis are sea surface temperature (SST) (deg. C) and stratification (buoyancy frequency squared, 10^{-4} s^{-2}]) (Codega and Ullmann, 2010).

Sediment data includes percentage of clay, silt, sand ,gravel, phi median (Sharma and Baxter, 2010). [The latter parameter is the negative base 2 logarithm of the grain median diameter expressed in mm.]

2.3 Services data

Fisheries data for fixed or mobile gear as well as recreational use data is binary data, reflecting the use or not use of each grid cell (Beutel, 2009). This data is derived from interviews conducted with fishermen.

A detailed description of the data sources can be found in our companion report (French et al., 2010).

3 Methodology

Principal component and cluster analyses are applied to sets of variables to derive typologies. Two ecological typologies are established: (i) a purely ecological typology based on fish and mammals data only; and (ii) an ecological and services typology based on ecological and services variables, including the social and economical domain in the analysis through the fisheries data. Both typologies define homogeneous oceanic ecological or socio-ecological sub-regions. A third geophysical typology defines the area in terms of geophysical sub-regions and is performed to give a physical meaning to the ecological typologies.

Each sub-region is defined by an ecological assemblage of species (or ecological and services group) and can be related to a geophysical sub-region. Let us note that we are using the terminology assemblage in its common definition, referring to a simple group of species, reunited by the clustering analysis, but we do not infer at this point a specific group pertaining to a particular habitat. The ecological assemblages are described in terms of "Biodiversity level 1". We define biodiversity level 1 as the observed diversity in terms of fishes and mammals, as described in the next section. The group of species considered in this study had to be reduced in comparison to the reference list presented in Bohaboy, Malek and Collie's report (Bohaboy et

al., 2010) because of a lack of spatial coverage for many species, and consequently this analysis underestimates fishes that are hard to catch on trawls. A simple ad-hoc biodiversity level 1 index is introduced to describe each sub-region and is presented in the next section. In a subsequent analysis we plan to extend the list of representative individuals in the ecosystem and present a typology of higher levels. For instance, including birds would lead to "Biodiversity level 2", or benthos data to "biodiversity level 3". In a next stage of this study (not presented in the current report), the characterization of each cluster will be refined by comparing various biodiversity indices (Derous, 2007).

The typology methodology is a combination of PCA and CA. The PCA reduces the multi-space into a minimum of independent (principal) components and facilitates the grouping performed with a cluster analysis. The resulting clusters regroup similar assemblages into homogeneous sub-regions.

3.1 Theoretical background

Principal component and cluster analysis can be categorized as Exploratory Data Analysis (EDA) methods. EDA is a means to quantify the inherent structure and variable interactions within a data set, rather than forcing the data to fit a pre-defined model. The fundamental philosophy of EDA is to use as much of the data as possible and extract the structure inherent to the data, free of the traditional assumptions of normality and no-spatial autocorrelation, which are usual obstacles to performing spatial analyses with standard statistical methods (Cablk, et al., 2002). Specifically, PCA and CA are known to be very robust in terms of assumption requirement and "work", even with non-normal distributions and auto-correlated variables, which are inherent to spatial ecological data (Zuur, 2009; Legendre, 1979)

In short, the Principal Component Analysis (PCA) method reduces the multi-space dimension into a minimal number of independent/orthogonal principal components, defined as a linear combination of the original variables. These linear combinations may or may not have physical meaning. The latter does not really matter in our case, since we use the PCA essentially to eliminate the redundancy embedded in the original correlated variables and explains the maximum possible variance with the lesser number of independent variables. This eventually reduces the number of variables or the dimension of the domain, in which we subsequently perform the cluster analysis. Mathematically, the PCA solves an eigenvalue problem on the basis of the covariance matrix of the original variables, transforming it in a diagonal matrix by applying multiple rotations along the principal directions. The principal components are the

"rotated" variables along the principal axes and are independent since they are uncorrelated. Ranking these by decreasing variance, the first principal axis passes through the longest dimension of the "ellipsoid" of the covariance matrix. The next principal axis passes through the next longest directions, respecting the constraint of orthogonality, and so forth for subsequent axes.

The PCA first calculates the dispersion matrix **S**, representing the covariance matrix of all the pairs of N variables y_i ($i = 1, N$), with each other; the matrix is symmetric and the diagonal elements are the variance statistical estimates s_i^2:

$$s_i^2 = \frac{1}{\nu}\sum_{j=1}^{p}\left(y_{ij} - \bar{y}_i\right)^2 \tag{1}$$

for p objects (grid cell), and the off-diagonal are the covariance estimates:

$$s_{ki} = \frac{1}{\nu}\sum_{j=1}^{p}\left(y_{kj} - \bar{y}_k\right)\left(y_{ij} - \bar{y}_i\right) \tag{2}$$

with j the index of the object, i and k the indices of the variables, v (usually $p - 1$) the number of degrees of freedom, and the overbar indicating the mean. We find the principal axes of the dispersion matrix by solving:

$$(\mathbf{S} - \lambda\,\mathbf{I})\mathbf{u} = \mathbf{0} \tag{3}$$

with **I** the identity matrix, λ the eigenvalues, and **u** the eigenvectors. The roots of the characteristic equation yield the eigenvalues, which ensure a non-trivial solution to Eq. (3),

$$|\mathbf{S} - \lambda\,\mathbf{I}| = 0 \tag{4}$$

Substituting these into Eq. (3) allows to calculate the eigenvectors associated with each eigenvalue, which are the principal axes of the dispersion matrix. If the eigenvectors are normalized to have a unit length, one can find the principal components as the coordinates of the original objects in the principal axis. The components of the unit eigenvectors are also the weights of the original variables in the linear combinations, which define the principal components. For instance, the position of a multivariate object j in the first principal axis $k = 1$ is given by the linear combination,

$$f_{1j} = \left(y_{1j} - \bar{y}_1\right)u_{11} + \ldots + \left(y_{jN} - \bar{y}_N\right)u_{1N} \tag{5}$$

of each centered variables y_{ij} describing each object j and their respective weight u_{1i} in the first principal component. The weights of original variables in the principal component allow to gain insight into the physical meaning of each principal component (Jolliffe, 2002).

The Cluster Analysis (CA) calculates the distances between objects in the new multivariate principal components space and regroups similar objects into clusters, based on their proximity in that space. The *k-means* clustering method was selected to perform the partitioning. Each cluster in the partition is defined by its member objects and its centroid. The centroid for each cluster is the point from which the sum of distances from all objects in that cluster is minimum. The method uses an iterative algorithm that minimizes the sum of distances from each object to its cluster centroid, over all clusters. This algorithm moves objects between clusters until the sum cannot be decreased further. The result is a set of clusters that are as compact and well-separated as possible.

3.2 Post clustering data analysis

Physical areas regrouped into a cluster at the end of the PCA-CA analysis, are finally described in terms of the original ecological and services variables characterizing the cluster, as mammals or fish species diversity or abundance; this in turn allows finding an interpretation or meaning for this particular cluster. In order to facilitate this interpretation we developed an ad-hoc biodiversity index combining the relative abundance of a specific species in a cluster, as compared to its general abundance in the entire SAMP area, and the variety or richness of species observed in significant abundance. The abundance is measured in unit of the original variable, e.g., biomass for fishes and view per unit effort for mammals. The relative abundance included in the index is a measure of the mean value of the variable in each cluster, as compared to the general probability distribution of the variable. [Note that these distributions were first normalized for fish biomass, by using the logarithmic transformation of the original variable. Hence, the principal components, which are linear combinations of normal variables, are normal as well. More details are given later on this aspect of data preparation.] In the biodiversity index, if the mean value observed in the cluster pertains to the 1st quartile of the probability distribution, the relative abundance is given a score of 0; if this mean pertains to the 2nd, 3rd, or the 4th quartile the score is 1, 2, or 3, respectively.

Each variable is thus characterized by a standardized score of abundance. The sum of those scores, standardized on a scale of 1 to 10, defines the "Biodiversity index level 1". The group of variables, which have a score of at least 2 (mean cluster value > 50 % of the general population

for this variable) defines a cluster assemblage. We refer to "Biodiversity index level 1" to indicate the level of diversity in species that this index represents. The 14 variables used here are assumed to represent the minimal representative level of diversity. It is hoped that, in the near future, additional data such as birds and benthos will be available, which will allow developing a similar biodiversity index, referred as level 2 and 3. It should be emphasized that we do not propose this index as a new standard of diversity estimation, to replace those already used as standard reference (Shannon, 1947; Derous, 2007; Borja et al., 2008; Spellerberg and Fedor, 2003). Instead, this index should just be viewed as an *ad hoc* local tool, developed to help in identifying the meaning of clusters isolated by the PCA-CA method, considering the specific data used in this analysis. The concept of biodiversity as well as its valuation is discussed in Appendix "More literature and Important definitions" (This appendix will be added by deadline September 1st.)

This biodiversity index is the first step towards valuation. Once the clusters are qualitatively identified, they can be affected a value. In this case the value has only a discriminative role and we do not pretend that it represents an intrinsic value. Future work will focus on valuation, represented here by the biodiversity index, which should be expanded to relate the valuation criteria to the different organizational levels of biodiversity, such as population, community or ecosystem. This will require discriminating migratory species passing through the area from species living in symbiosis with others, or species associated with a particular geomorphologic feature, or related to a particular oceanographic process such as upwelling.

Additionally we introduce a second index, referred to as "services index", complementary to the biodiversity index and based on the same methodology, to assess the relative value in terms of fisheries use of mobile or fixed gears, and recreational variables. This index is used as a proxy for food provision and recreational services, which are combined as a so-called generic "services" index. Goods and Services provided by biodiversity addressed in this study are referred to McLeod and Leslie classification (2007) modified from United Nation Environment Program official classification (2006) (**Table 1**)

Table 1: Goods and Services provided by biodiversity addressed in this study

McLeod and Leslie classification (2007) modified from UNEP 2006	**Sub-Categories addressed in this study**	**Valuation tool introduced in this study**
Provisioning services	Food	Service Index
Cultural services	Recreation	
Regulating services		
Supporting services	Life support Biologically mediated habitat	Biodiversity level 1 index

4 Data preparation

In a preliminary step, prior to performing the PCA-CA analysis, outliers are removed from the data set and, optionally, data is normalized for some variables. Figure 1 shows that the log-transformed biomass distributions, for each of 3 survey agencies, closely match a normal distribution.

For outliers, the probability distribution of each variable is first estimated, and outliers are isolated and removed, when observed to be outside the centered 99% confidence interval of the distribution. Such outlier values are set to the extreme value in the confidence interval at 99%. Data is normalized, when appropriate, for some variables, in order to obtain a multivariate distribution as close to multi-normal as possible (although, normality of the variables is not required by the method). The multivariate data is re-interpolated on a standard grid, here 200 by 200 m, using a krigging interpolation scheme. Seasonal typologies are established for Spring and Fall. Winter and Summer are omitted in the present analysis, for lack of a representative spatial distribution for most data.

The analysis is based on the assumption that we have a complete spatial coverage for each variable. Therefore, all fish data from the 3 sources was combined to have the most extensive possible spatial coverage. Differentiating between sources was not possible since the spatial coverage would have been too sporadic and would have affected the validity of the analysis more significantly than the extra-variance introduced, by causing a potential bias in the survey standardization. Erin Bohaboy, Anna Malek, and Jeremy Collie show in their report (Bohaboy et

al., 2010) that there is a significant variance due to the survey agency. This variance was investigated, but in view of the very little overlapping in location of the three surveys, it was not possible to accurately estimate the part of the variance truly due to survey bias from that due to the location or depth.

From the biomass distributions regrouped by survey agencies, we see in Figure 2 that all data points belong to the same population since their confidence intervals overlap. This is part of the theoretical justification for aggregating the three sources. However there are obviously slight differences between the three surveys. From Figure 1, we see that the DEM and NEAMAP data are indeed extracted from the same population, but show a slight nearly constant bias. This bias can be a bias in the survey standardization or a true difference due to the catching depth, since DEM surveys are systematically done in very shallow water.

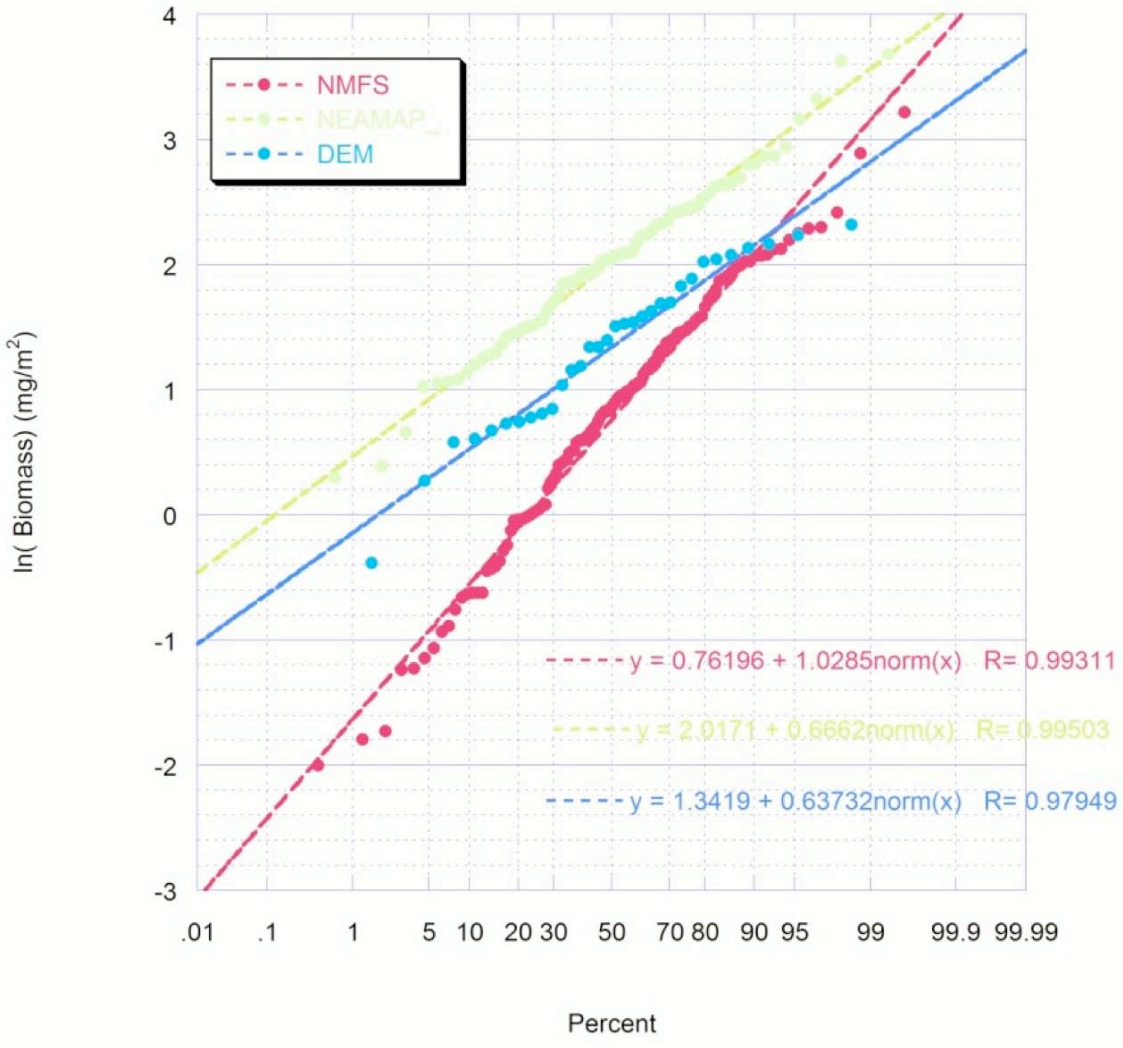

Figure 1:Normality test of the log-transformed Total Biomass [ln(mg/m^2)] for each of the 3 survey

agencies: NEAMAP, DEM, NMFS.

The NMFS population in Figure 1, however, diverges the most from the two others populations, showing a smaller mean value and a larger variance. NMFS survey are the most spread out within the SAMP area, going from shallow onshore waters to deep offshore areas, and therefore are expected to show a larger variance. This divergence could also result from using larger nets (i.e., yielding less small fishes) or different boat speeds in the survey. The sampling period is also significantly different. Those sources of variance could be assessed and accurately addressed, with more overlapping data and a time series analysis. The part of the variance due to the survey bias could be estimated and a corrective term could be applied to standardize the survey. This question could be addressed in an extension of this study, but in the present analysis the aggregation was a necessity, in order to minimize the variance due to under-representation, despite the potential for adding variance due to sampling bias.

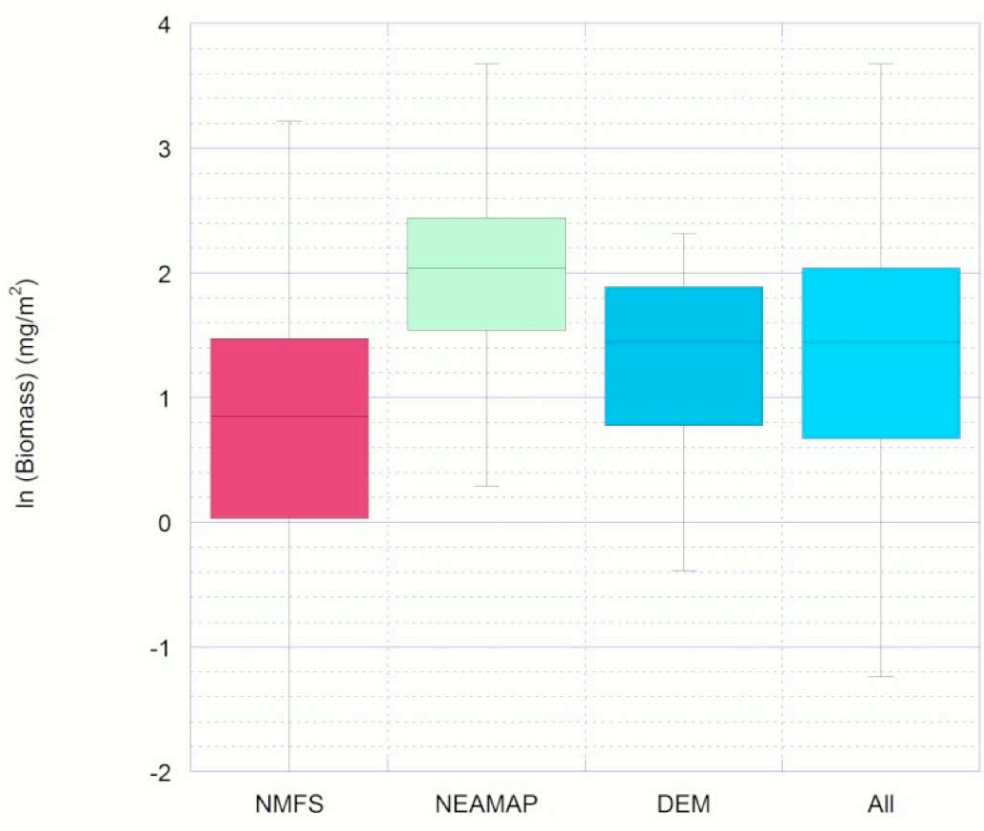

Figure 2: Box plot representation of the samples for the 3 surveys and for all data aggregated together. 25 % to 75% of the population are represented in the boxes. The ”error bars” define the confidence intervals at 95 %.

4.1 Ecological data

Fish variables are assumed to be representative if more than 30 surveys are obtained for the area (in statistical analysis, this number is typically the accepted minimum number of individuals in a sample extracted from a normal distribution, for the sample distribution to behave sufficiently normally). For the Fall, 12 species matched this criterion:

American lobster, *Homarus americanus*

Atlantic sea scallop, *Placopectin magellanicus*

Black sea bass, *Centropristis striata*

Bluefish *Pomatomus saltatrix*

Butterfish ,*Peprilus triacanthus*

Little skate, *Leucoraja erinacea*

Longfin squid, *Loligo peali*

Scup, *Stenotomus chrysops*

Silver hake, *Merluccius bilinearis*

Summer flounder, *Paralichthys dentatus*

Winter flounder, *Pseudopleuronectes americanus*

Winter skate, *Leucoraja ocellata*

Fishes' biomasses are log-normal distributed. Data was normalized for each species, using the natural logarithm transform (see Fig. 1).

Mammals data was regrouped into Whales and Dolphins categories, to obtain a significant spatial coverage, making it possible to have the data included in the analysis. For the Fall, Whale and Dolphin categories regroup the following species:

- Whales: North Atlantic Right Whale; Fin Whale; Common Minke Whale

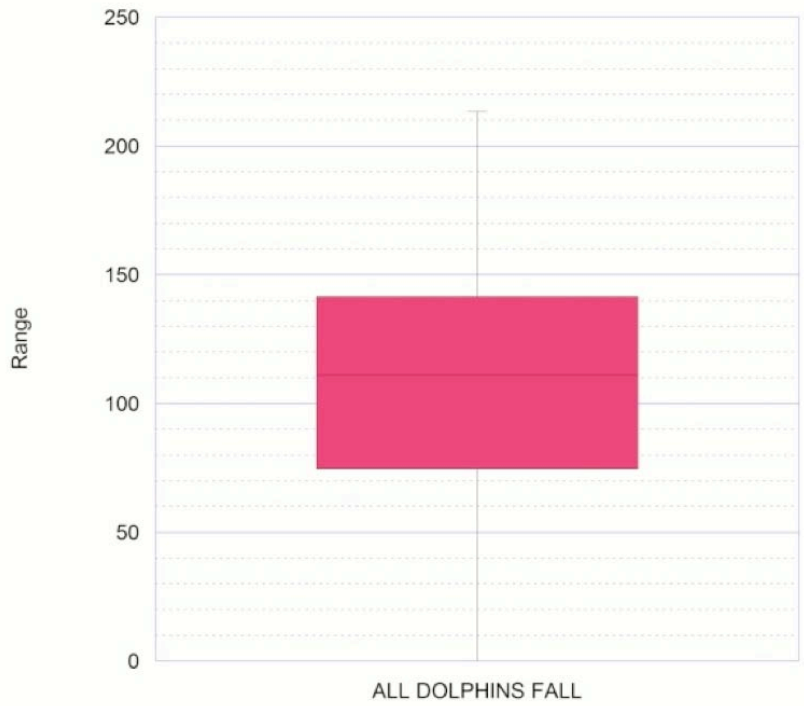

Figure 3: Probability distribution of the entire Fall Dolphin population in the area of occurrence

Figure 4: Probability distribution of the entire Fall Whale population in the area of occurrence

- Dolphins:

Short-beaked common dolphin

Atlantic white-sided dolphin

In the area of occurrence it is found that mammals data, grouped into Whales and Dolphins in view per unit effort, is normally distributed.

The mammals mapping (Appendix A) however shows that there are non-occurrence areas, which biases the normal distribution with a tendency to create a bimodal distribution, with a peak at zero (figure in Appendix B).

When applying the spatial interpolation over the 200 by 200 m grid, the typically 30 to 130 ecological data points are re-interpolated to about 130,000 points covering the entire grid. The first step is to check the validity of such a drastic spatial interpolation. To do so, the probability distributions of the observed data points are compared with the probability distributions of the interpolated data points. Results are shown in Appendix B in the form of cumulative probability distributions for each variable. This comparison shows that both probability distributions for each species are in good agreement. The highest discrepancy occurs in extreme lower values, which are over-represented in the interpolation, reflecting either an under-representation of the data in boundary areas, an inhomogeneous data representation in the sampling, or a true discontinuous spatial representation. Discussing those issues could be done in more depth in a follow-up study, but the outcome of this discussion should not significantly affect the current analysis, since those discrepancies only affect the lower tail of the distributions and concern a small percentage of the SAMP area.

4.2 Services data

Each set of data: mobile gear, fixed gear, or recreational, is provided in a binary format (0=no use; 1=use) this format is transformed into a continuous variable between 0 to 3, by creating a fishing index summing the three use at each grid cell and re-interpolating these on the 200 by 200 m grid.

5 Fall Season Ecological Typology

5.1 Principal component and cluster analysis

The principal component analysis is applied to variables defining the biodiversity of the area: 12 fish species and 2 mammals variables (whales and dolphins). The principal component analysis shows that the first principal components expresses about 23 % of the variance of the original variables, but 8 components are required to express 80 % of the variance (Fig. 5). The cluster analysis is performed in the reduced space of 8 principals components, since 80 % of the variance explained is the usual accepted threshold to select the number of principal components kept in such an analysis (Zuur, 2009). Results are presented for a total of 4 and 5 clusters. Comparisons of the scores of each cluster in the first and second principal component domains and the mapping of each cluster (Figs. 6-8) show that the first component represents the onshore/offshore gradient. This result is consistent with Jordan's results in his work in the Gulf of Main. Comparing the clustering for 4 and 5 clusters shows that one additional cluster better differentiates the intermediate depth clusters into 2 sub-areas, relatively separating Block Island sound from Rhode Island sound.

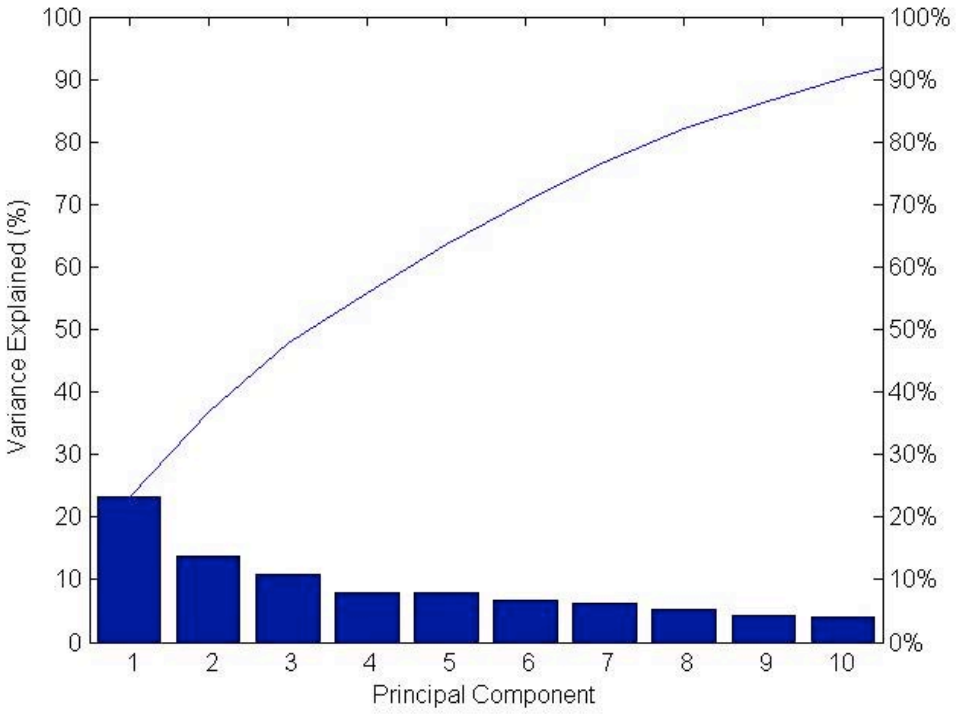

Figure 5:Part of the variance explained by each principal component

It is important to point out that this grouping is based on ecological variables only. No geophysical data are introduced at this stage. Each cluster is defined by a specific ecological assemblage of species used in the analysis. In order to summarize the ecological assemblage of each cluster, as detailed in section 3.2, we developed a simple Biodiversity index combining fish abundance and species diversity. In parallel each cluster is defined with a set of representative geophysical variables. This is discussed in the next section.

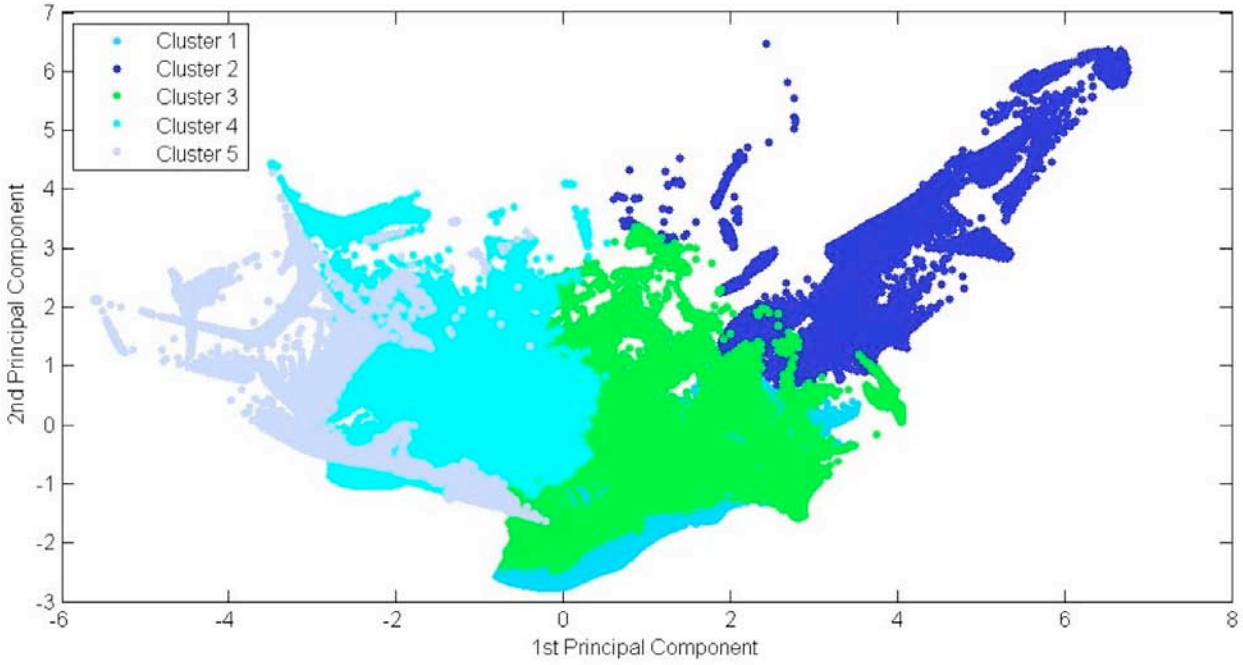

Figure 6 : 5 ecological clusters mapped in the domain of the first and second principal components

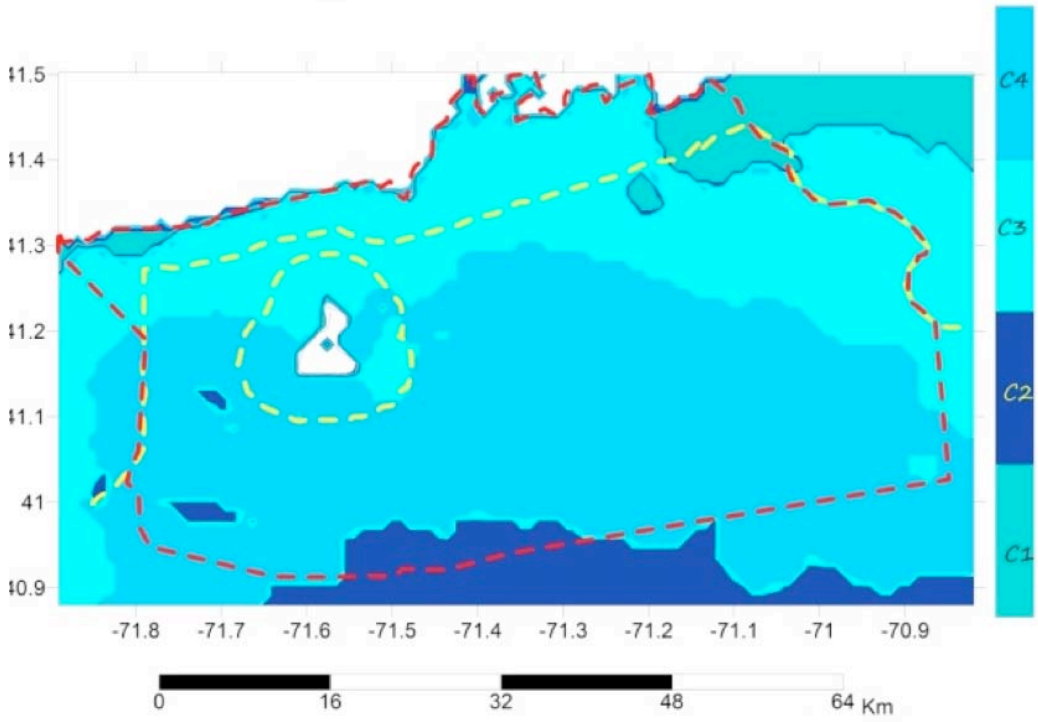

Figure 7 : 4 ecological clusters (biodiversity level 1) mapped in the SAMP area for Fall

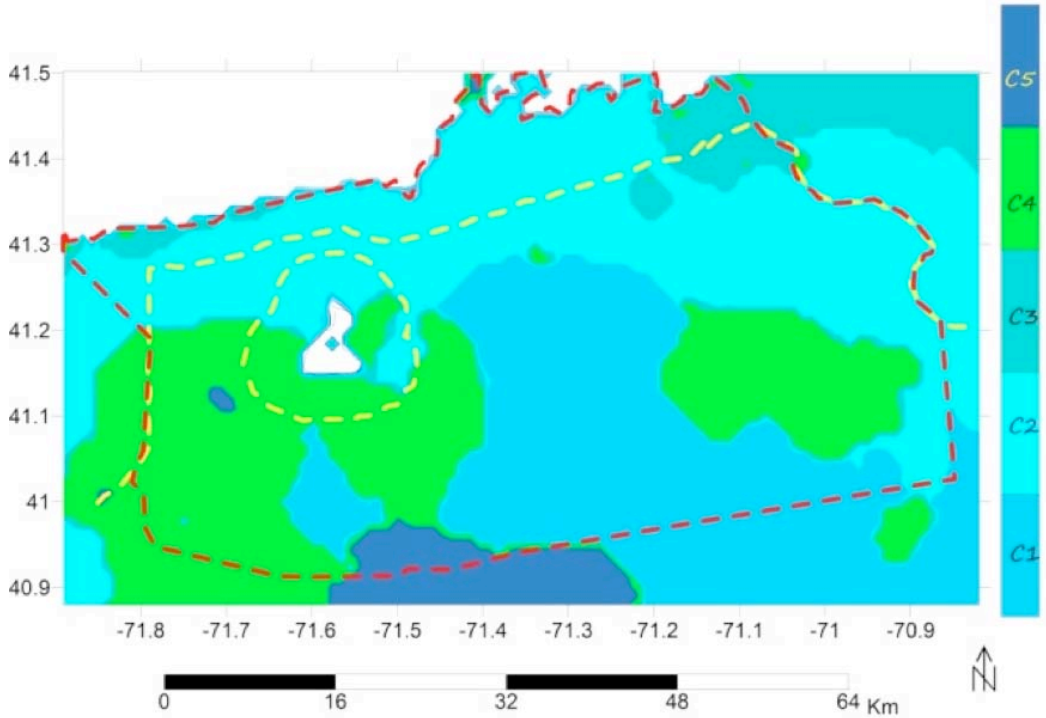

Figure 8 : 5 ecological clusters (biodiversity level 1) mapped in the SAMP area for Fall

Table 2: Ecological Biodiversity --level 1—index for fall season in SAMP area

Ecological Biodiversity Level 1 Index					
Species	Cluster 1	Cluster 2	Cluster 3	Cluster 4	Cluster 5
American Lobster	2	3	0	1	1
Black Sea bass	0	1	2	2	0
Butter fish	0	2	3	0	0
Squid	1	1	3	0	1
Scup	1	2	3	0	0
Summer flounder	1	1	2	2	0
Winter Skate	1	2	2	1	0
Blue fish	2	1	0	2	3
Little Skate	1	2	2	0	0
Scallops	2	1	1	2	2
Silver Hake	3	1	1	1	1
Winter Flounder	2	1	0	1	1
Whale	2	1	1	2	2
Dolphin	2	1	1	1	1
Sum	20	20	21	15	12
Index[1-10]	**9.5**	**9.5**	**10**	**7.1**	**5.7**

5.2 Biodiversity level 1 typology

In order to facilitate the cluster interpretation, scores are calculated based on the relative abundance in each cluster as compared to the general population, as well as a diversity index, combining relative abundance and significant diversity, as defined in section 3.2. The scores and index values are given in

In addition each species considered significant and taken into account in the diversity index (score higher than 1 or mean value larger than 50 % of the global population) is defined as pertaining to the cluster assemblage characterizing the cluster, and is mapped in Figure 9, using various symbols whose size is proportional to this score (score 2 (3^{rd} quartile)=small symbol; score 3 (4^{th} quartile)=large symbol).

The complete score combinations, defining each cluster assemblage, are presented in diagram format in Figure 10.

5.3 Geophysical Interpretation

In order to explore cluster relationships with geophysical conditions, each cluster is related to geophysical variables. These are water depth, bottom slope, bottom roughness, phi median, sea

surface temperature (SST) and stratification, which were described in the data section. As for biodiversity, a score is given to each geophysical variable based on comparing its mean value inside the cluster to its probability distribution in the entire SAMP area (Table 2). The method of scaling is identical but the percentile scale is slightly different, giving a score of 4 for above the 95 % percentile (25%, 50%, 75%, 90%, 95%).

Clusters 1 and 5 are both in deep water where the SST is the highest in the Fall as well as the bottom stratification. Cluster 5 is in flat smooth sandy deep water. Cluster 3 is in homogeneous shallow water, with the highest bottom roughness, slope and clayish sediments, coldest SST and no stratification. Clusters 2 and 4 are both in relatively shallow water, although cluster 4 is relatively further away from the main shore, since mostly around Block Island, and are both in relatively steep, rough bottom geology. Cluster 2 is, however, in a well mixed area with very little stratification, as expected from being close to shore areas. Cluster 4 has some stratification, but far less than for the adjacent Cluster 1. Both Clusters 2 and 4 have low SST, as expected from their closeness to shore. Cluster 4 diverges from the adjacent Cluster 1, as well, regarding those variables, definitely marking the difference in the oceanographic climatology of Rhode Island and Block Island Sound.

Using all those tools and comparing the cluster analysis for 4 and 5 clusters, as well as the results of the PCA, it is clear that the primary variable guiding the sub-regionalization is the depth/distance to shore, subdividing primarily the ecological assemblages into coastal and deep water assemblages; the second factor is a parallel to coast discontinuity related to two processes: (i) primarily a discontinuity in the geology and bottom topography, creating shallower waters with rough habitat, such as in the West of Block Island; and (ii) secondarily the oceanographic discontinuity between Block Island Sound and Rhode Island Sound (Codega and Ullmaan, 2010).

Looking more closely at Figs. 9 and 10 and Table 2, we see that the coastal assemblage is correlated with shallower, well-mixed, and colder waters. In those, were found in great quantity the usual shoreline, shallow water species, such as Summer Flounder, Scup, Little Skate, Lobsters Squid. The coastal assemblage in the north-eastern part of the SAMP area is particularly diverse and more defined by rocky species, such as Sea Bass, Scups, Squids. The offshore assemblage is correlated with deeper, stratified, and colder waters, with smooth sandy bottom. It regroups Whales and Dolphins, Scallops and migratory species such as Bluefish. The partitioning of the intermediate area follows relatively closely the bottom roughness and the

sedimentology. The rocky rough shallow water area of Block Island sound regroups rocky species, such as Sea Bass; migratory species, such as Bluefish are present too, as well as whales. In the relatively smooth sandy/clayish bottom of Rhode Island sound, the semi-pelagic Silver Hake is highly present as well as the Winter flounder.

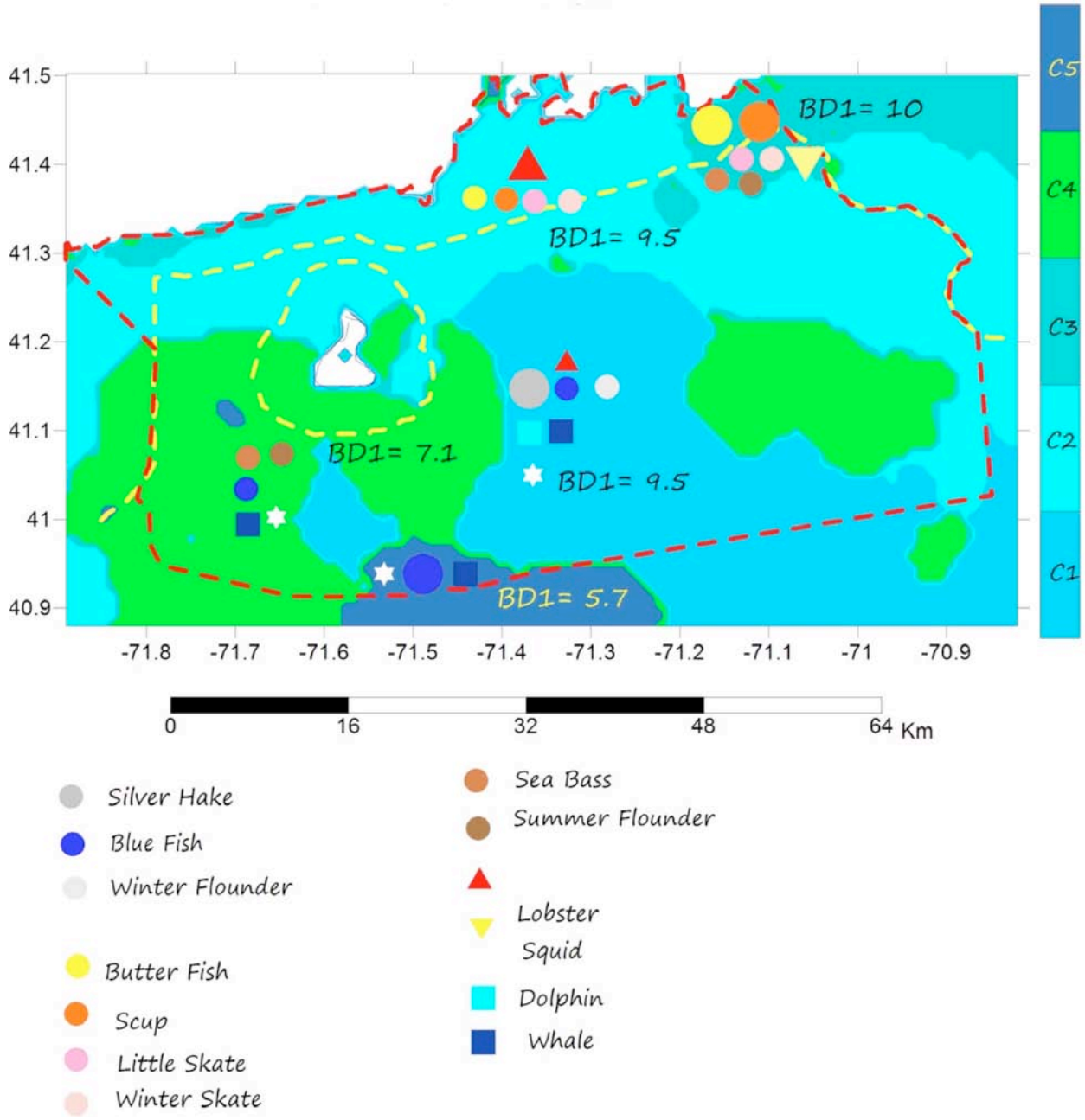

Figure 9: Ecological typology of biodiversity level 1 in SAMP area for Fall based on PCA-CA

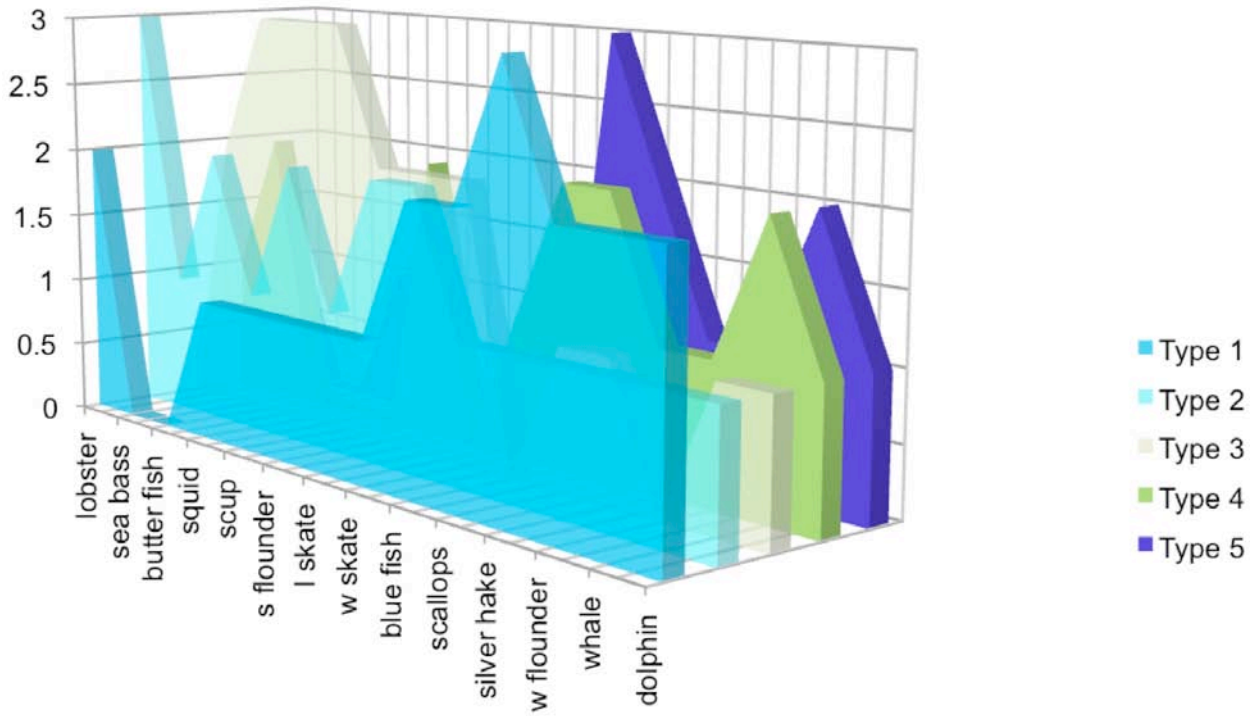

Figure 10: Diagram representing the biodiversity index –level 1—of each cluster (Type 1 to 5) for Fall, in terms of original variables. The index represents the whole area defined by each species sub-index, varying along a discrete scale 0 to 3.

Mammals are present as well, Whales and Dolphins, and the migratory Bluefish. Dolphins have been shown to follow upwellings (Thompsen, 2010). In the present case, they might be used as tracer of the oceanographic limit between Block Island Sound and Rhode Island Sound.

Table 3: Definition of each cluster in terms of geophysical variables. Each geophysical variable is defined by a relative score based on its mean value in the cluster as compared to its global probability distribution. Scale 1 to 4.

Geophysical characteristics of each cluster					
	Cluster 1	Cluster 2	Cluster 3	Cluster 4	Cluster 5
Depth	4	1	0	1	4
Slope	1	2	3	2	0
Roughness	1	3	4	2	0
Phi median	1	2	3	1	2
SST	4	1	0	1	4
Stratification	4	1	0	2	4

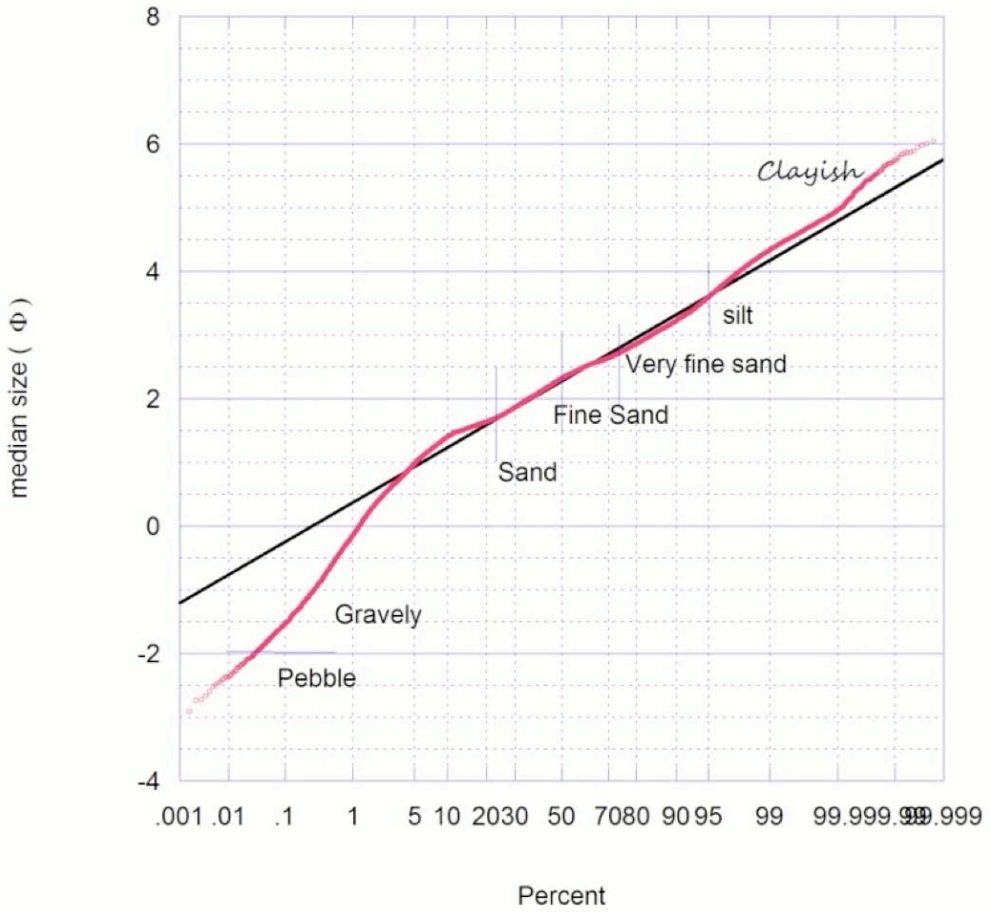

Figure 11: Grain size probability distribution (in phi unit) in the SAMP area.

6 Fall Season Geophysical Typology

In order to have a general overview of the geophysical environment and therefore understand better the relationship between the ecological clusters and the environment, a similar PCA-CA analysis was applied to selected geophysical variables: water depth (m), bottom slope (maximum slope in a 200 by 200 m cell (deg.)), bottom roughness (standard deviation of slope on 1000 m radius (deg.)) , median grain size (phi units) (phi=negative logarithm to the base 2 of the particle diameter in Millimeter), SST at 27 m (deg.), and stratification (buoyancy frequency squared, 10^{-4} s^{-2}]). As before, each of these variables is re-interpolated onto the 200 by 200 m grid and mapped over the SAMP area. These maps are given in Appendix A. The probability distribution of each of these variables is presented hereafter in a cumulative representation, so it is easy to relate each quartile of the distribution to the corresponding value of the variable. For example the median or 50 % of the distribution of the median grain sixe (in phi value) is above 2, defining fine sand. The indexing method defined above, already used to help in the cluster interpretation, is based on comparing the mean cluster value of each variable to that in their general probability

distribution for the entire area, in terms of quartile or percentile. In summary, the indices relate the clusters to the relative value of the distribution, in terms of quartiles or percentiles, and the probability distributions relates the index to the true value of the variables.

Figures 12 to 15 show probability distributions as compared to the expected normal values. We see that grain size in phi unit, depth, and sea surface temperature are fairly normally distributed. Slope and roughness are log-normal and their value is thus log-transformed for the PCA-CA analysis.

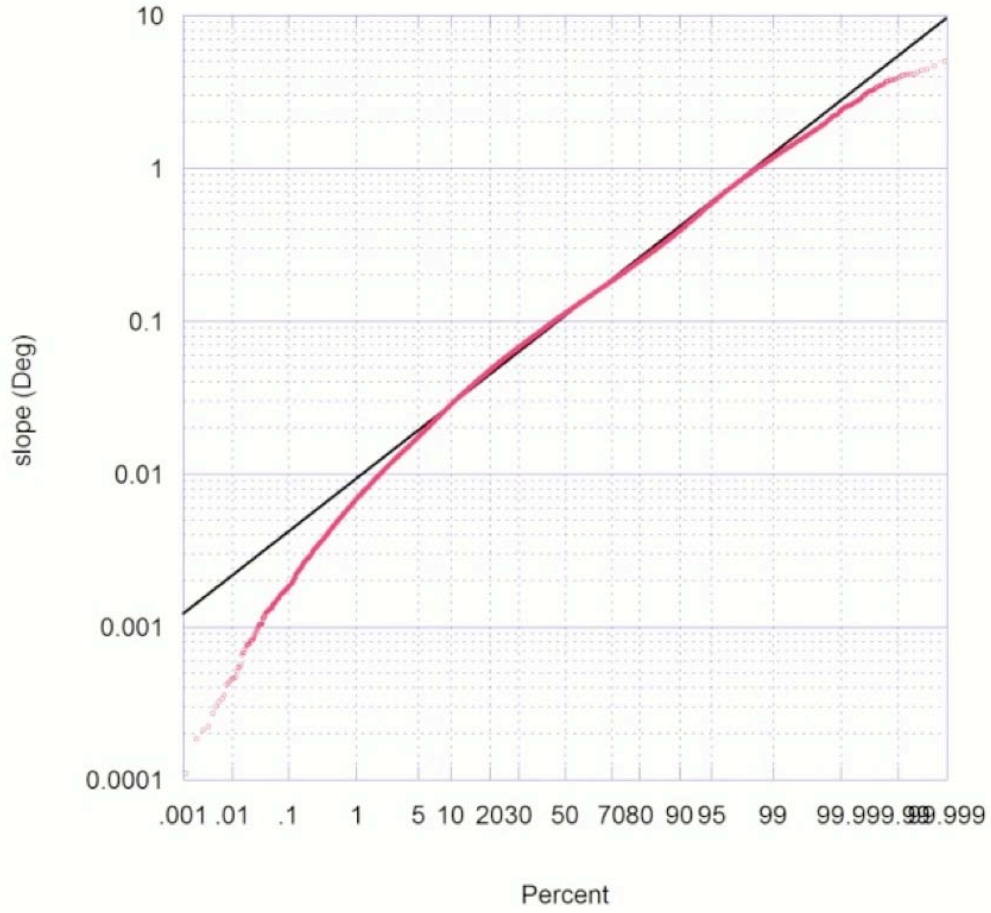

Figure 12: Slope (deg.) probability distribution in the SAMP area (log scale)

As for the ecological analysis, results of the PCA-CA analysis for the geophysical variables in Figure 16 reflect the onshore-offshore gradient, the relative oceanographic dichotomy between Block Island and Rhode Island Sound, and the geological and sedimentological variance. Cluster 4 regroups deeper warm stratified waters over a smooth sandy bottom. It is bordered by Cluster 1, in a Rhode Island Sound intrusion towards the shore, regrouping intermediate waters between the warm stratified offshore waters and the cooler mixed coastal waters, but also corresponding

to the mostly clayish bottom of the area covering the relatively smooth and flat bottom of Rhode Island Sound. Cluster 3 regroups shallower well-mixed cold waters above rough and steep silty bottom. Cluster 2 regroups, shallow to medium depth waters, with mixed waters over a gravely bottom.

Table 4:Geophysical clusters definition in term of original variables scores (scale 1 to 5). Scores are based on the relative value of the cluster mean value of each variable compared to the global probability distribution of each variable.

	c3	c4	c2	c1
Depth	0	5	1	1
Slope	4	1	2	2
Roughness	5	0	2	1
phimedian	3 =silty	1=sand	0 =gravely sand	5 =clayish
SST	0	4	1	1
Statification	0	5	1	1

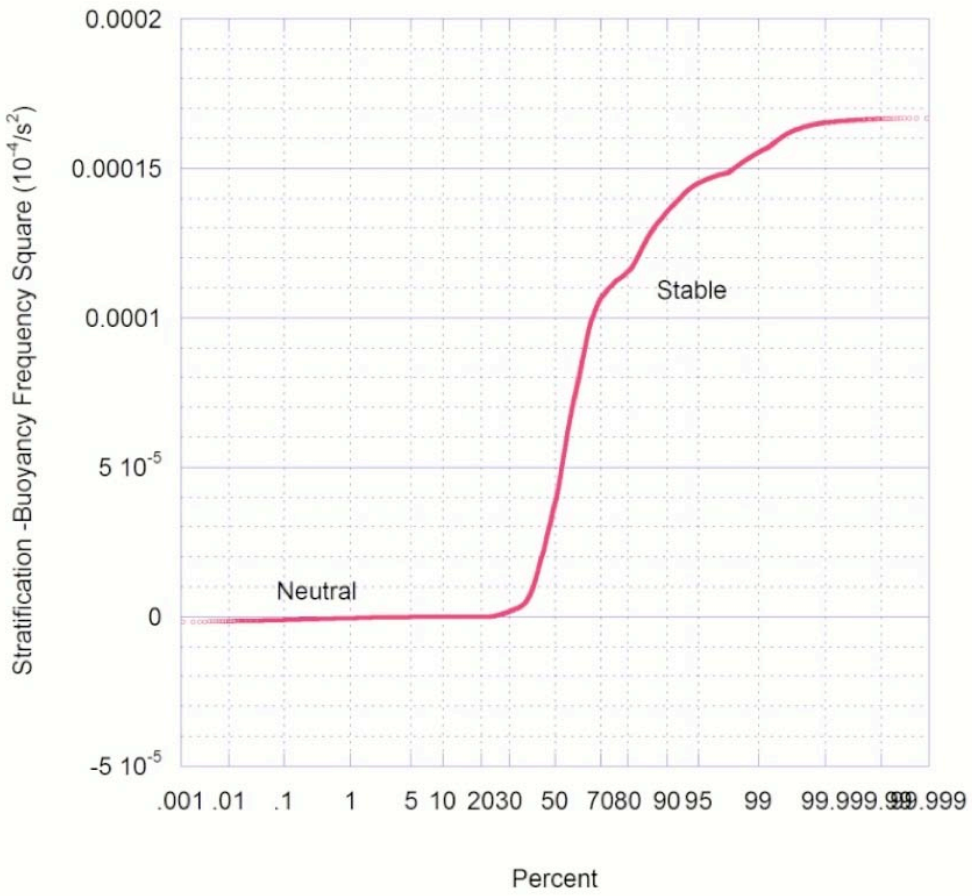

Figure 13: Fall bottom (27 m) stratification (buoyancy frequency fquare (10^{-4} s^{-2})) probability distribution in the SAMP area . Data provided by Codega and Ullmann (2010).

The similar patterns of the geophysical and ecological clusters, which were independently derived, is striking and validates the ecological typology, in the sense that the ecological stuctures correspond to geophysical structures, as could have been expected.

7 Socio-ecological typology for Fall

In a final analysis, we introduce the socio-economic domain by adding the "services" in the analysis: the fisheries use, and mobile, fixed and recreational gears. These are combined into a fishing index (linear sum) quantifying the fisheries use on a scale 1 to 10 (identical method as biodiversity index for scaling).

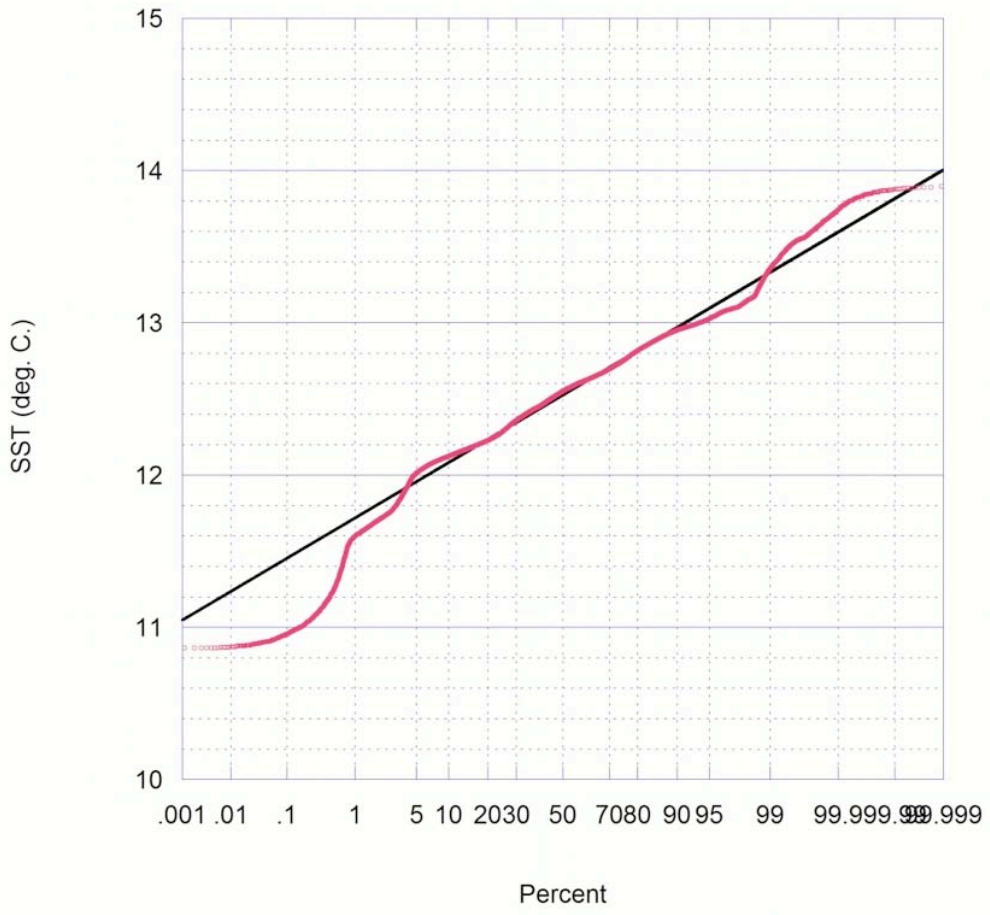

Figure 14: Probability distribution of Fall Sea Surface Temperature (SST) in the SAMP area. Data provided by Codega and Ullman (2010).

Re-doing the ecological analysis when adding the fishing index as a new variable leads to a similar pattern, but two clusters are now dominated by fisheries use, Cluster 3 with a service index of 9, and Cluster 6 with a fishing index of 5, regrouping the areas most intensively used by mobile and fixed gears. Cluster 3 regroups the recreational area in rocky bottom shallow

waters around Block Island and in the center of Rhode Island Sound, around Cox's Ledge. Ironically, Cluster 3 is characterized by a low biodiversity index grouping rocky species such as Sea Bass. It is clear that rocky species are hard to catch and are not correctly statistically represented in the surveys. Striped Bass for example was eliminated from the analysis because it was under-represented (based on our assumed criterion). Clusters 2 and 5 are the shallow water sub-regions, opposing smooth and rocky bottom species. Clusters 4 and 7 are the deep water clusters, differing by their fisheries use. According to our fisheries data, Cluster 7 is fairly used and Cluster 4 is not. This might be due to a lack of data in this area, since most of it is outside the SAMP area. In addition, Cluster 1 regroups an assemblage of high diversity and appears at the eastern border of the area in relatively shallow water, starting at the tip of the southwest shoal and extending northward, but also very punctually at the southeast end of Block Island state Waters. This specific spot corresponds to an area of higher biomass and might reflect the known convergence of currents around the southeast tip of Block Island State Waters. This hypothesis needs to be further investigated.

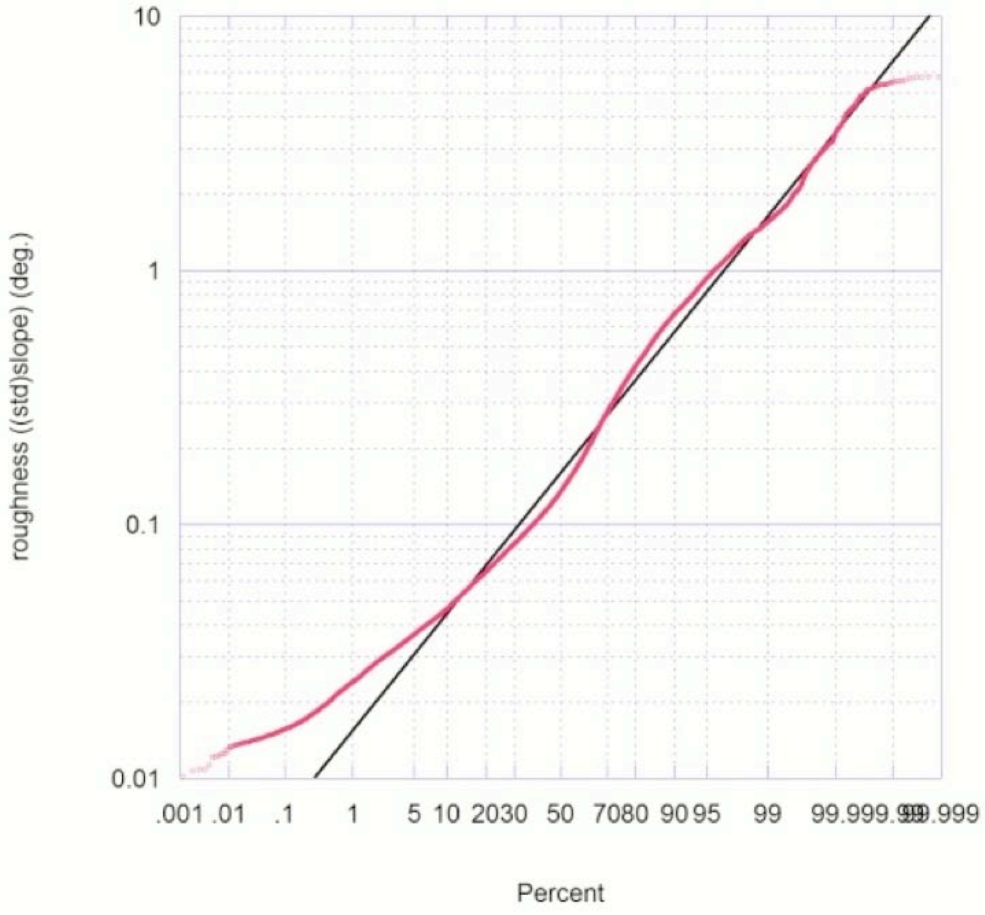

Figure 15:Bottom roughness probability distribution in the SAMP area defined as the standard deviation of the slope in a 1000 m radius (log scale). Data provided by J.King (2010)

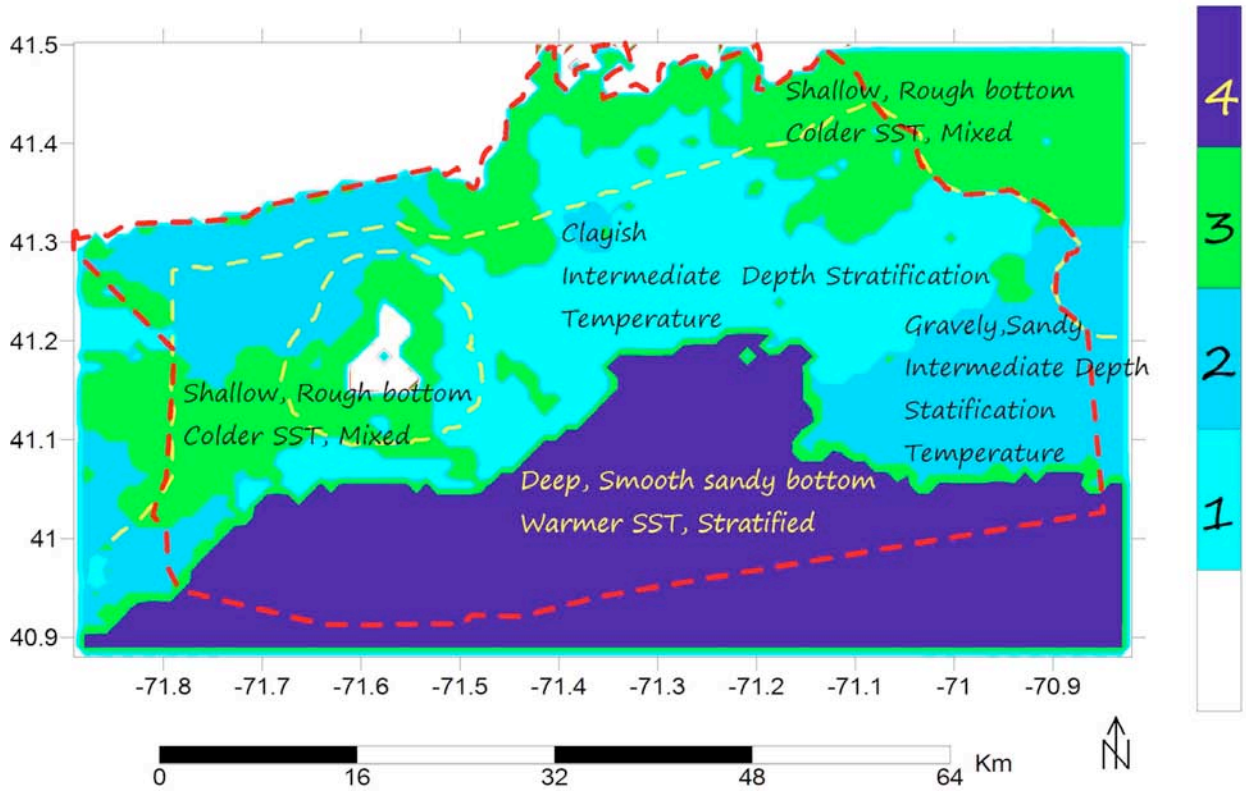

Figure 16 : Seasonal geophysical environment typology for fall season, based on PCA-CA analysis of the 6 geophysical variables in the SAMP area.

8 Conclusions

We applied a PCA-CA analysis method to multivariate ecological/service, and independently geophysical data. As expected from the literature, the method proved to be robust in identifying homogeneous areas among a large set of multivariate spatial data. The comparison of the ecological (clusters) with geophysical sub-regions allows to interpret these sub-regions in terms of habitats, which *a posteriori* justifies the methodology. The additional step of including the socio-economical system through fisheries use data is promising, since it clearly identifies among ecological sub-regions, the recreational, mobile and fixed gear fisherman behaviors.

Results of the PCA-CA analysis, consistently, reflect an onshore-offshore gradient and the geological and sedimentological variance. A deep water assemblage is isolated from a shallow water assemblage. The intermediate and shallow waters are separated into two assemblages, reflecting both the oceanographic dichotomy between Rhode Island and Block Island Sound, and

the variance in geological deposits. The terminal moraine lying intermittently across the Block Island and Rhode Island Sounds, in particular on the southeast of Block Island and at the tip of Sakonnet point, creates area of high bottom rugosity and clayish sediment, favorable to benthic habitats. Those areas are isolated in homogeneous biodiversity cluster representing an homogeneous fish and mammals assemblage.

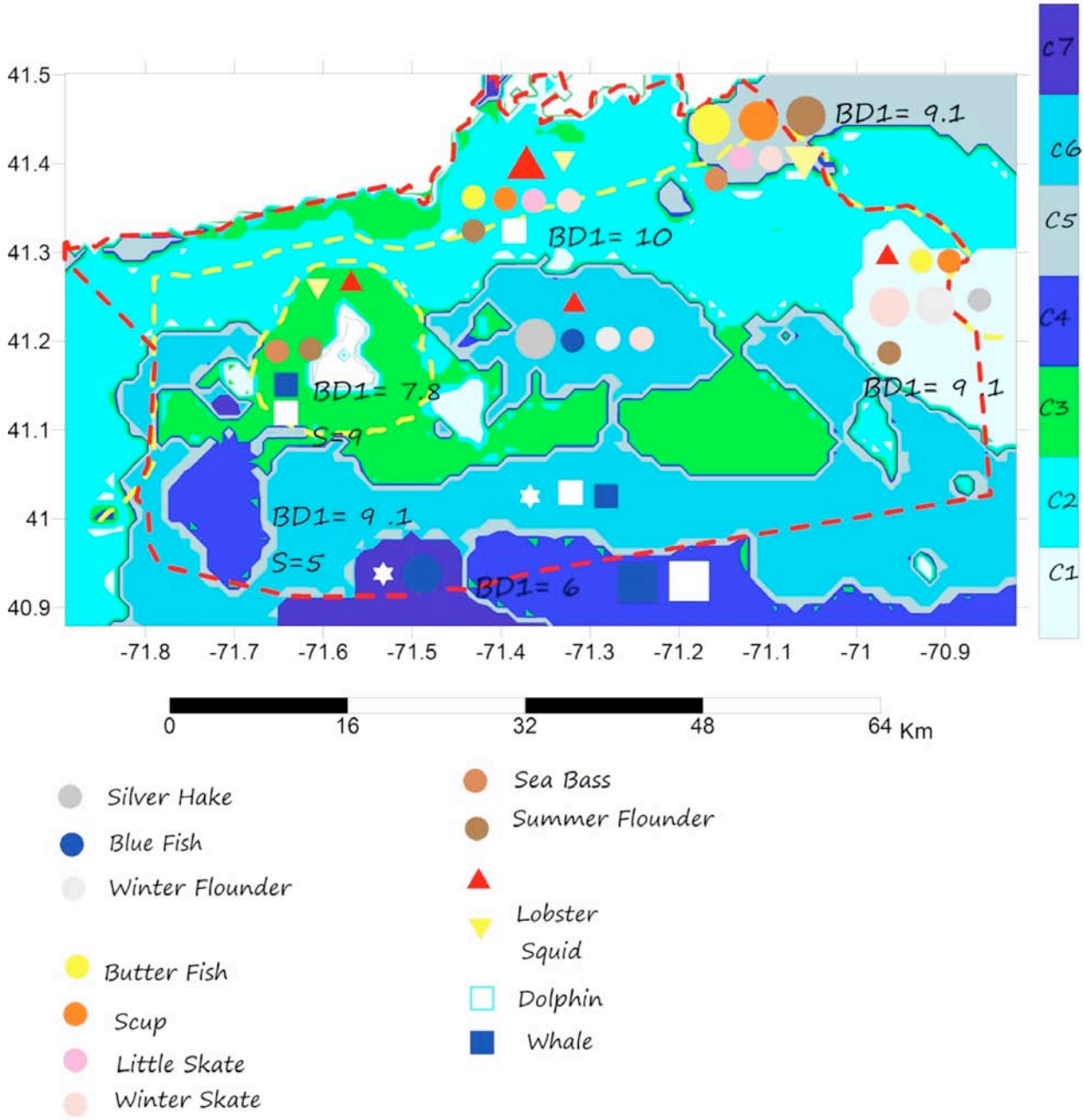

Figure 17: Seasonal ecological and service typology for Fall , based on PCA-CA analysis of the 6 geophysical variables in the SAMP area.

The Biodiversity index is at this point developed for descriptive purpose, and is specific to this area only. However, this step shows that this index is not sufficient to discriminate the area. Identical numbers correspond to different assemblages. Furthermore, the low index value in the high bottom rugosity area defined by Cluster 3 in the Ecological and Services Typology is questionable, since it is antagonistic to the fishermen behaviors. This either reflects an underestimation of the biodiversity in the sampling, or a bias in fisheries data obtained from fishermen, which is possible since those are only binary data.

This PCA-CA based Marine Management Tool developed here proved to be promising in identifying sub-regions, but it is still at a stage of development. Future major stages in furthering the development of this tool are:

- Adding ecological and services variables to represent more accurately the ecological and social environment, and therefore discriminate better the space.
- Developing the method of cluster valuation:
    - The biodiversity and service indices are a first attempt at valuation and follow up work should involve using and comparing the various standards, or newly developed indices (Shannon 1947; Derous, 2007; Borja et al. 2007; Spellerberg and Fedor, 2003).
    - The concept of valuation should relate the valuation criteria to the different organizational levels of biodiversity, such as population, community, ecosystem, which means discriminating migratory species passing though the area, from species living in symbiosis with others, or species associated to a particular geomorphologic feature, or related to a particular oceanographic process, such as upwelling (Derous, 2007).
    - Address the concept of rarity.

- Assess the uncertainty of the groups isolated by the clusters due to the uncertainty in the data and discuss the clusters borders in those terms: rigid or fuzzy borders.
- Address the dynamic aspect of those sub-regions by introducing time series of the variables rather than mean values in input.

Addressing these questions is subject to data availability, but we are hopeful that in a near future we can introduce birds and benthos data in the ecological or Supporting Services category, as well as quantitative fisheries data in the Service Category, or Provisioning Services and Cultural Services Categories, according to the nomenclature of Table 1.

Appendix A : Maps of geophysical/geological and oceanographic data in SAMP area

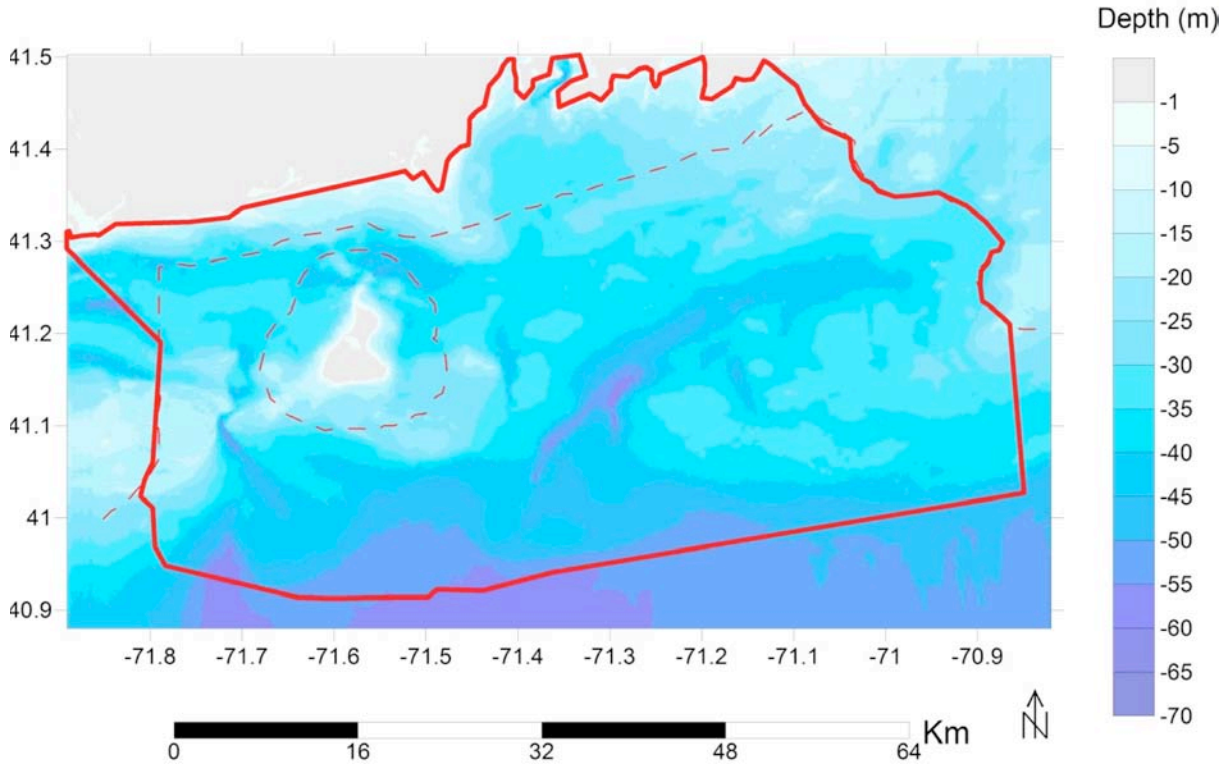

Figure 18: Bathymetry in the SAMP area

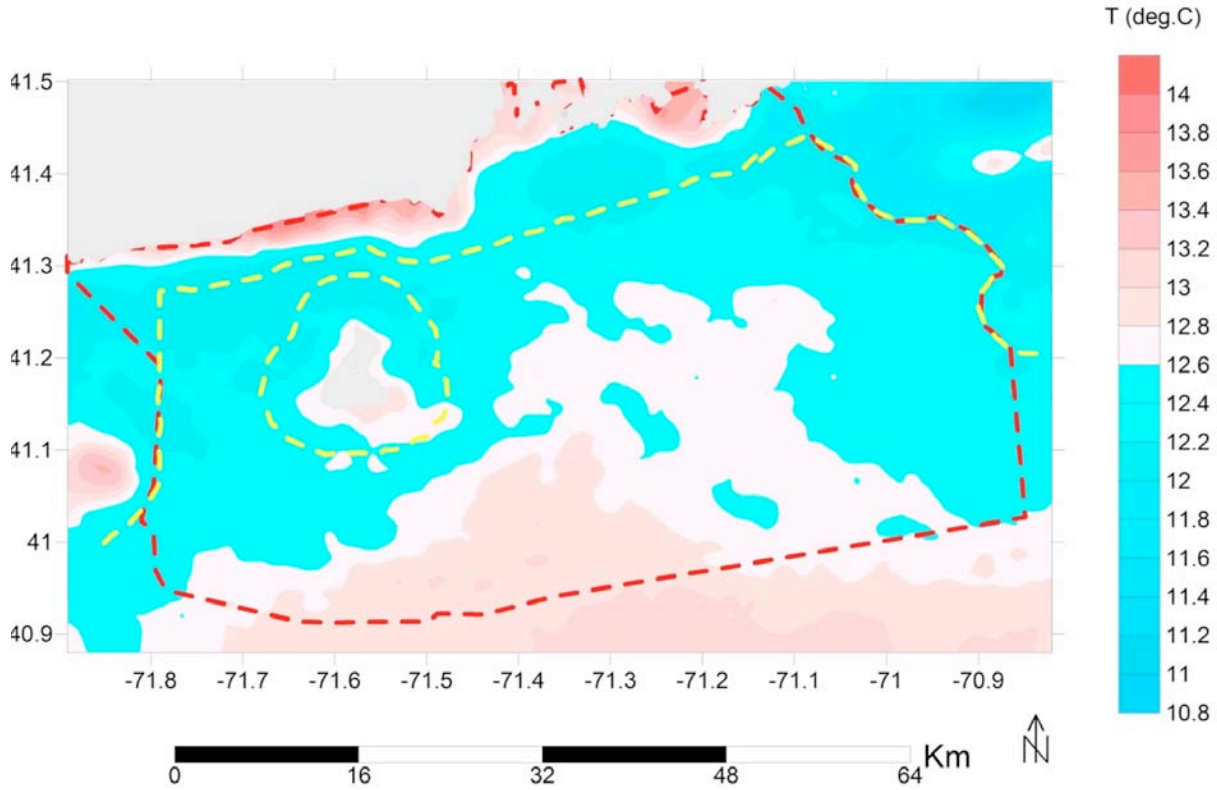

Figure 19 Sea Surface Temperature (SSTD) reinterpolated on a 200 by 200 m grid. Data from Codega and Ullmann (2010)

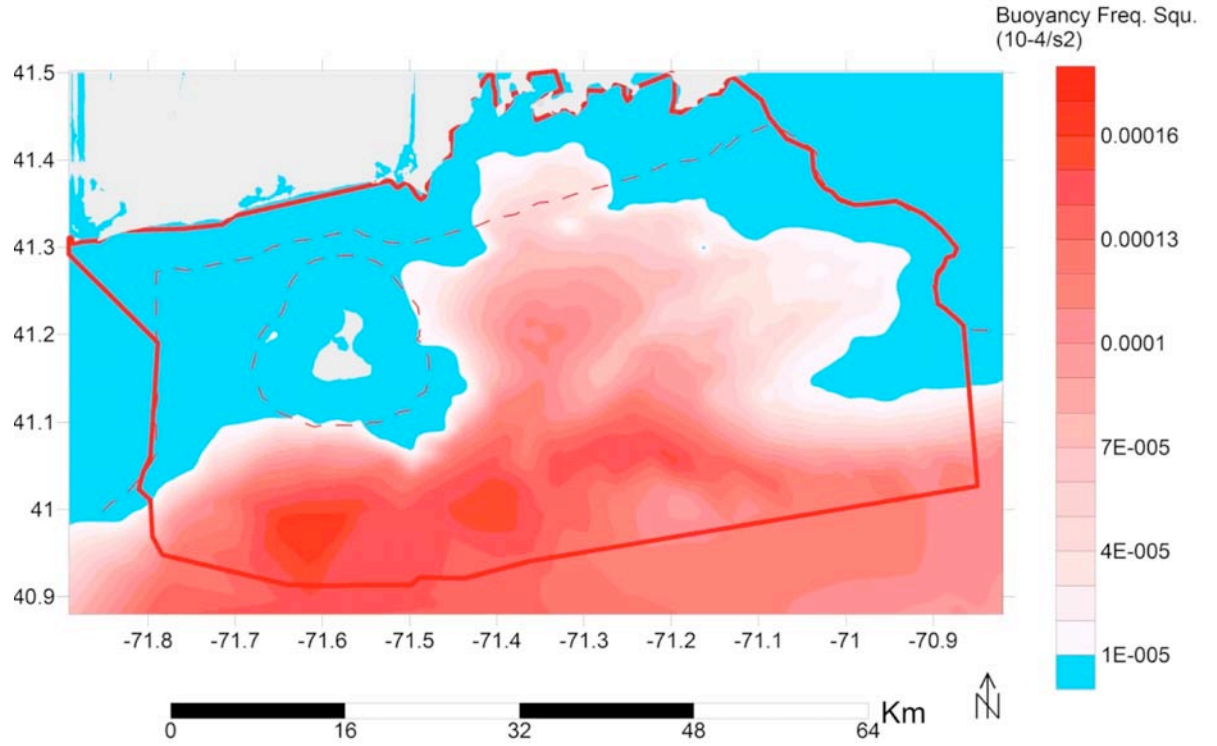

Figure 20: Fall water stratification in buoyancy frequency square ($10^{-4}s^{-2}$). Data obtained from Codega and Ullmann (2010) and reinterpolated on the 200 by 200 m grid

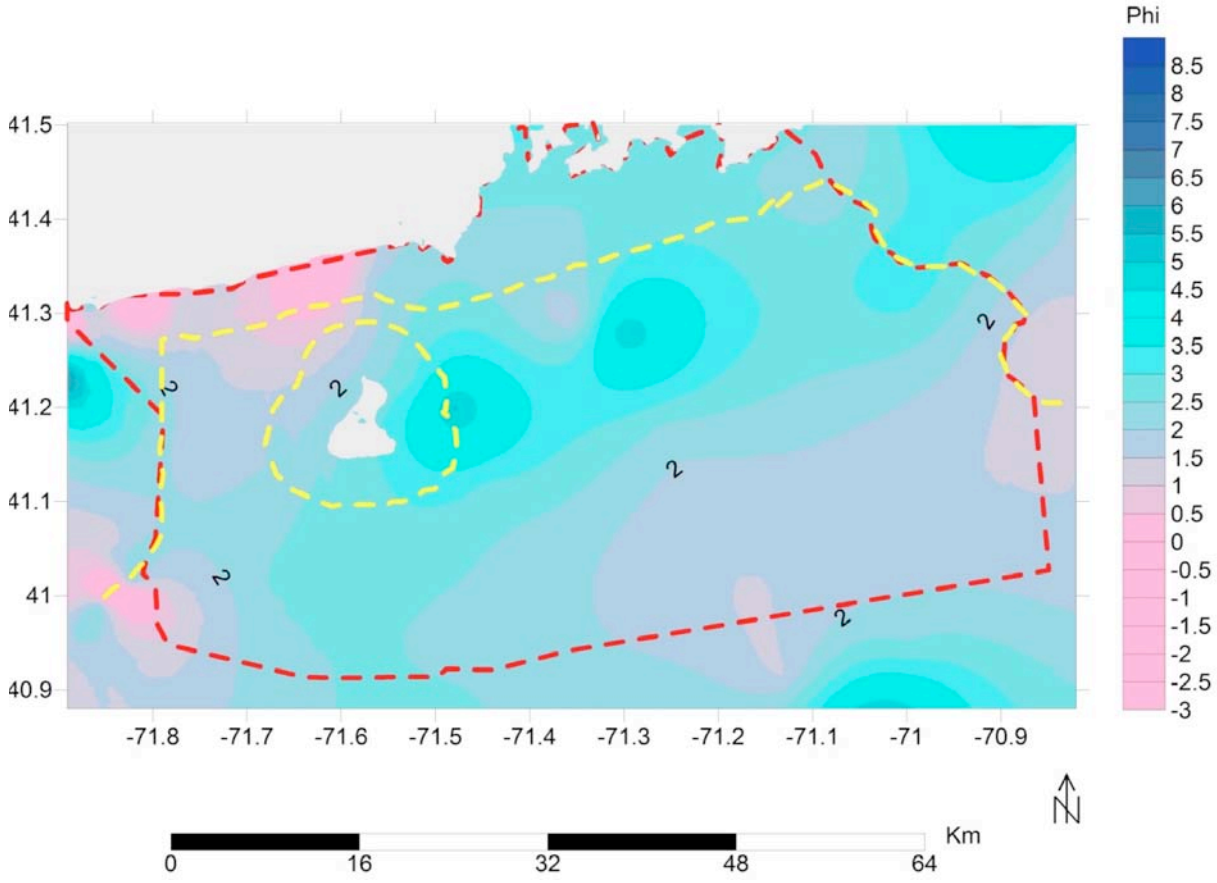

Figure 21: Sediment grain size distribution in phi units

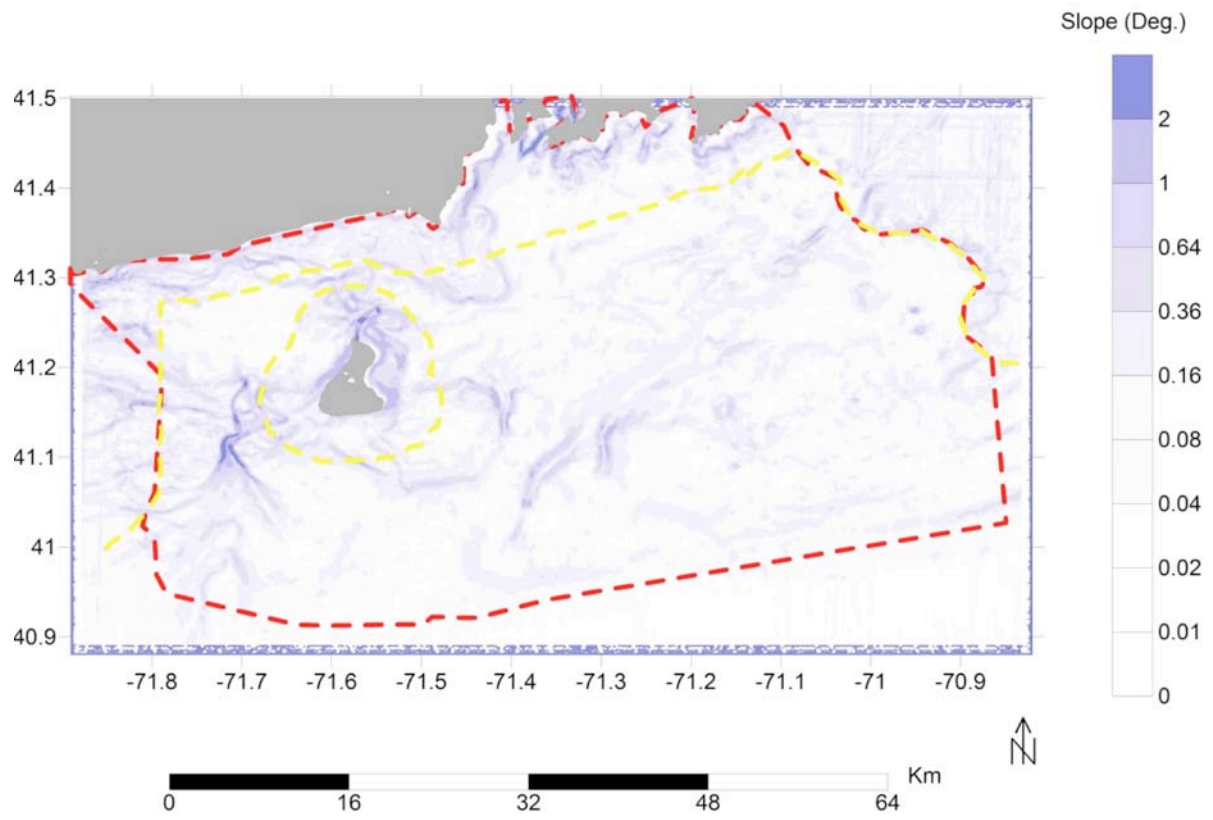

Figure 22 : Maximum slope at each grid cell (deg.)

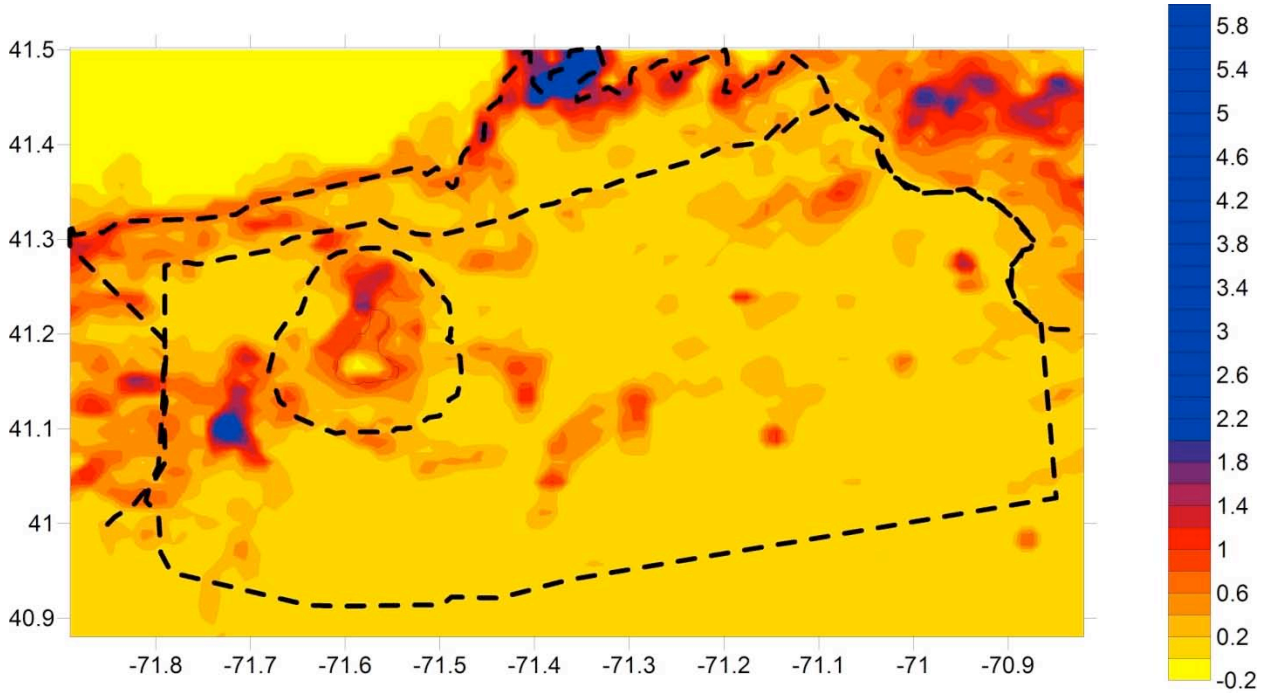

Figure 22: Surface roughness defined as the slope standard deviation on a 1,000 m radius. Data provided by John King (2010)

Appendix B: Statistical distributions of ecological variables

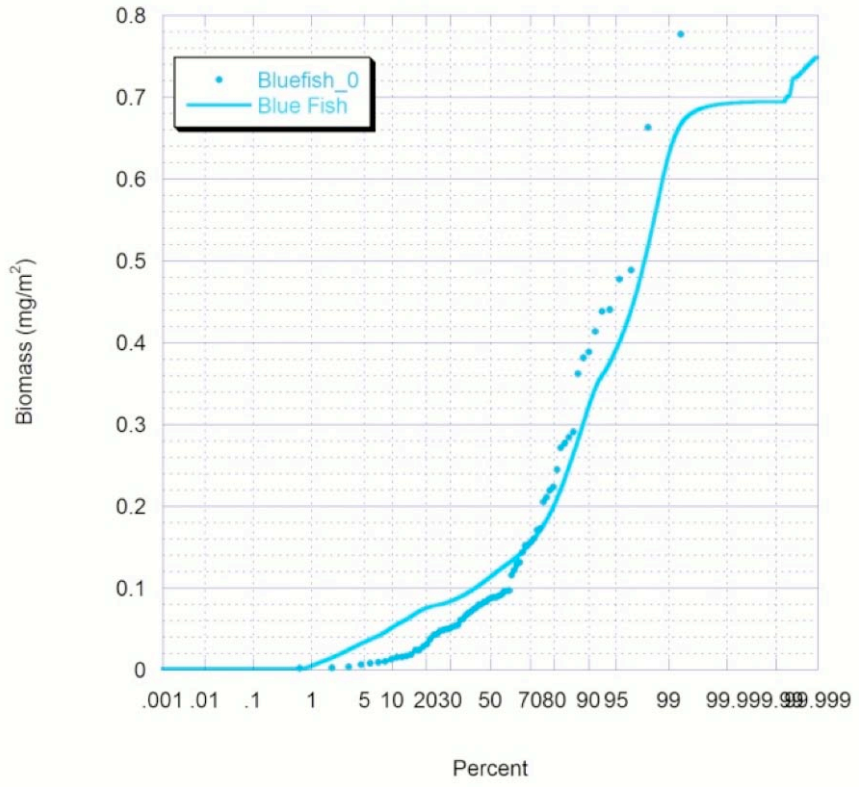

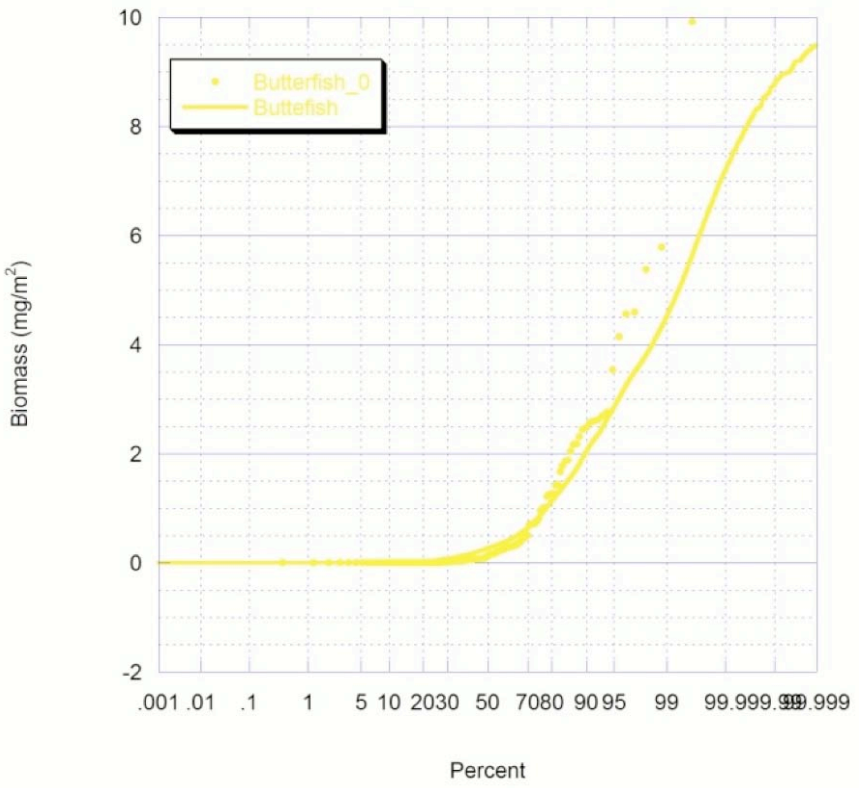

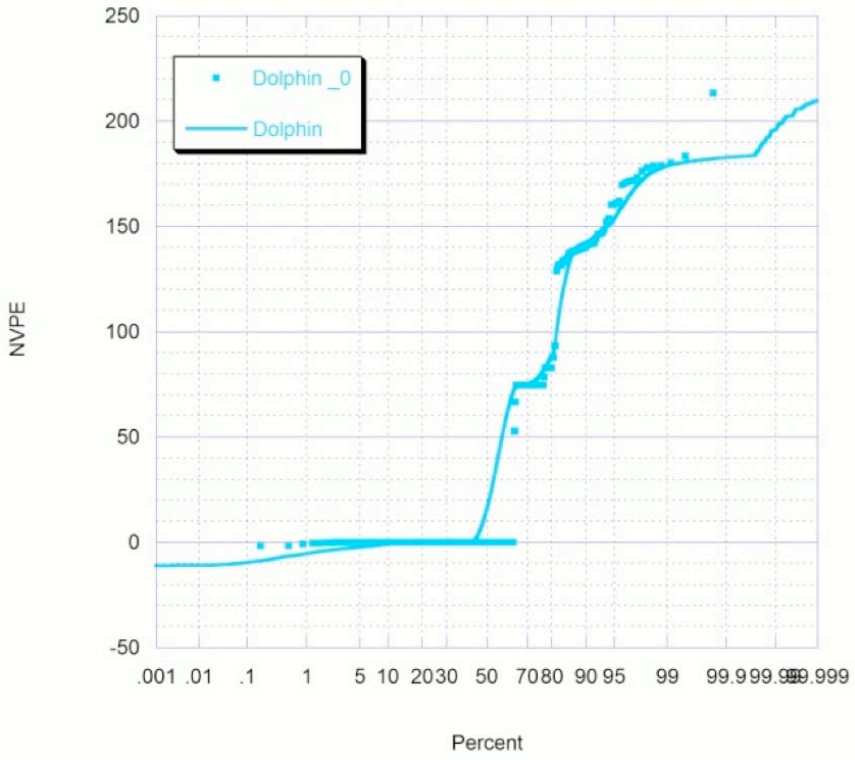
Dolphin _0
Dolphin
NVPE
250
200
150
100
50
0
-50
.001 .01 .1 1 5 10 20 30 50 70 80 90 95 99 99.9 99.99 99.999
Percent

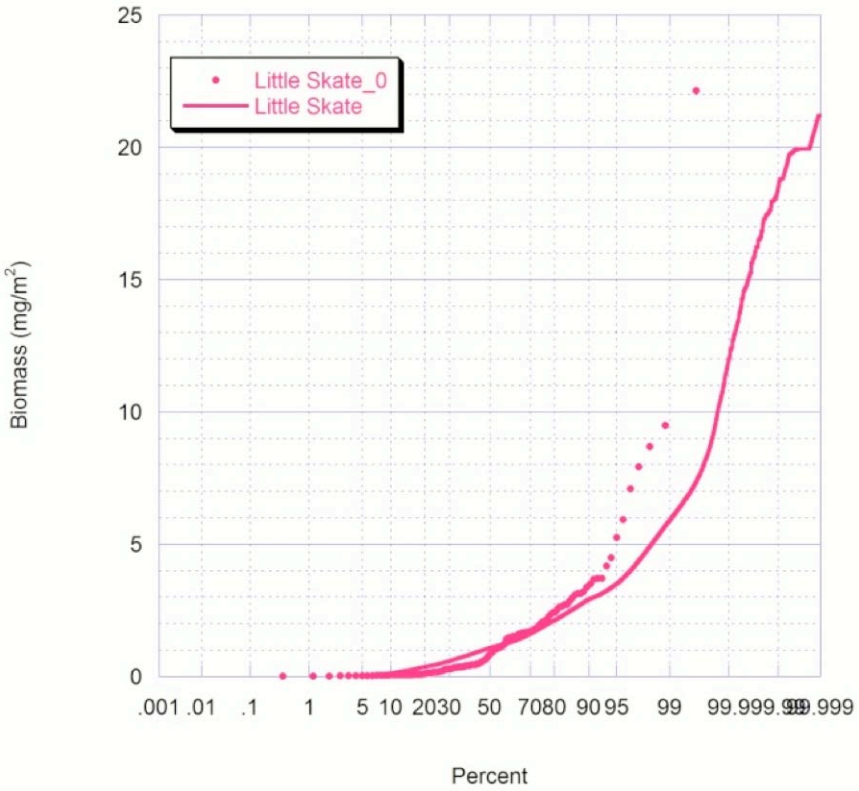
Little Skate_0
Little Skate
Biomass (mg/m2)
25
20
15
10
5
0
.001 .01 .1 1 5 10 20 30 50 70 80 90 95 99 99.9 99.99 99.999
Percent

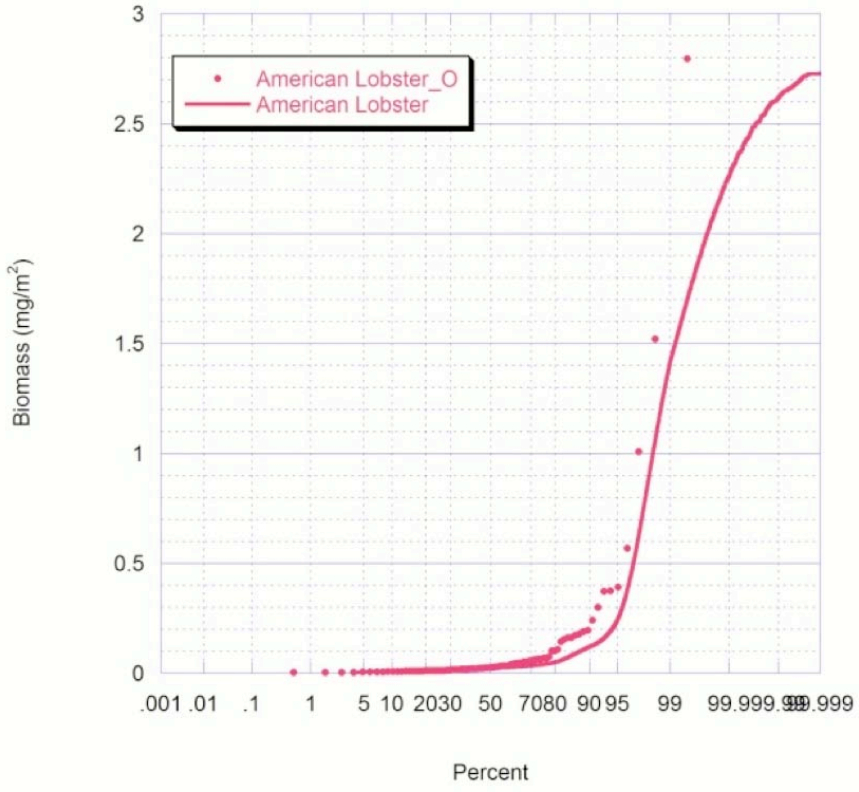
American Lobster_O
American Lobster
Biomass (mg/m2)
3
2.5
2
1.5
1
0.5
0
.001 .01 .1 1 5 10 20 30 50 70 80 90 95 99 99.9 99.99 99.999
Percent

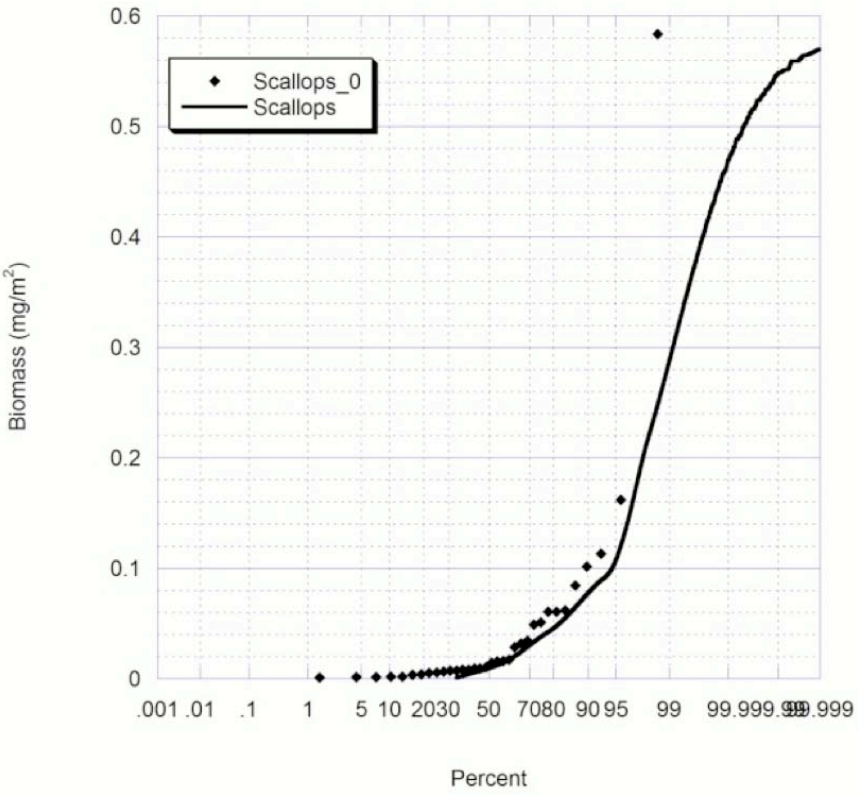
Scallops_0
Scallops
Biomass (mg/m2)
0.6
0.5
0.4
0.3
0.2
0.1
0
.001 .01 .1 1 5 10 20 30 50 70 80 90 95 99 99.9 99.99 99.999
Percent

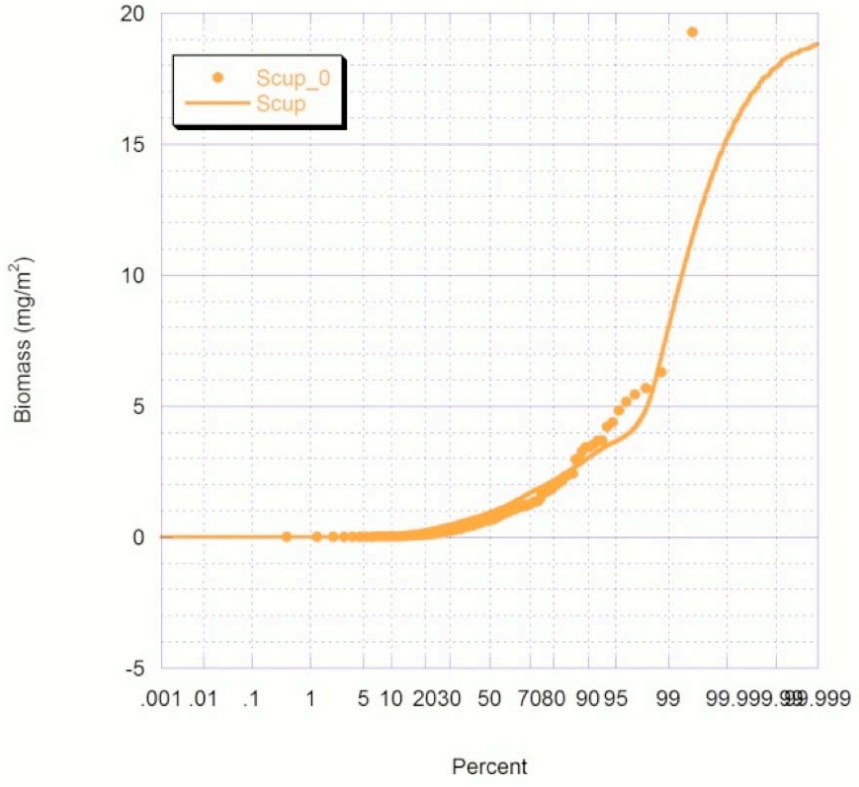
Scup_0
Scup
Biomass (mg/m2)
20
15
10
5
0
-5
.001 .01 .1 1 5 10 20 30 50 70 80 90 95 99 99.9 99.99 99.999
Percent

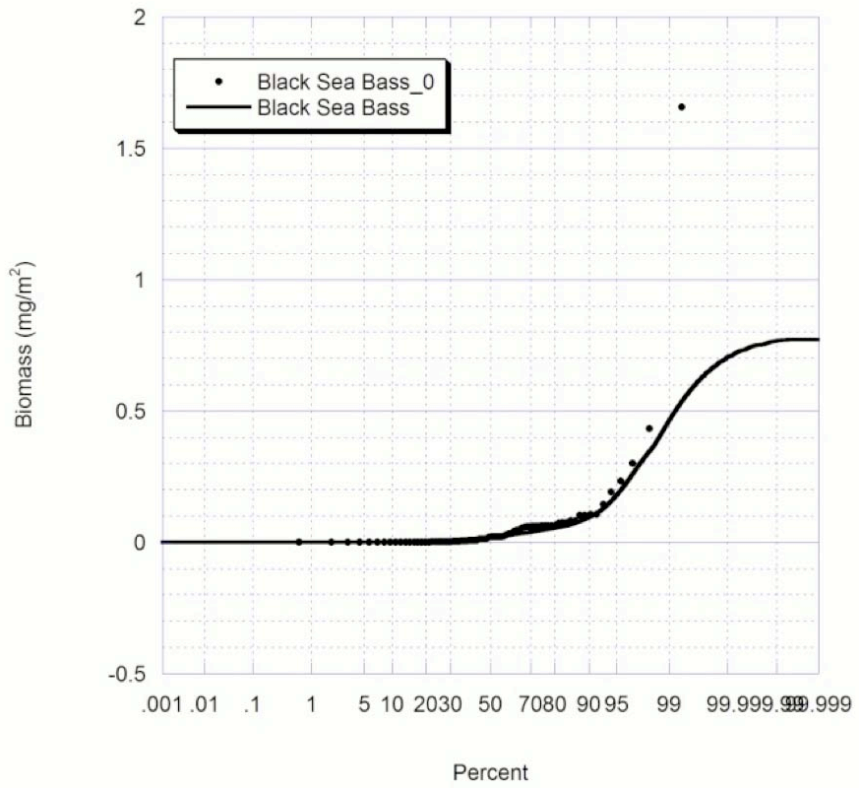
Black Sea Bass_0
Black Sea Bass
Biomass (mg/m2)
2
1.5
1
0.5
0
-0.5
.001 .01 .1 1 5 10 20 30 50 70 80 90 95 99 99.9 99.99 99.999
Percent

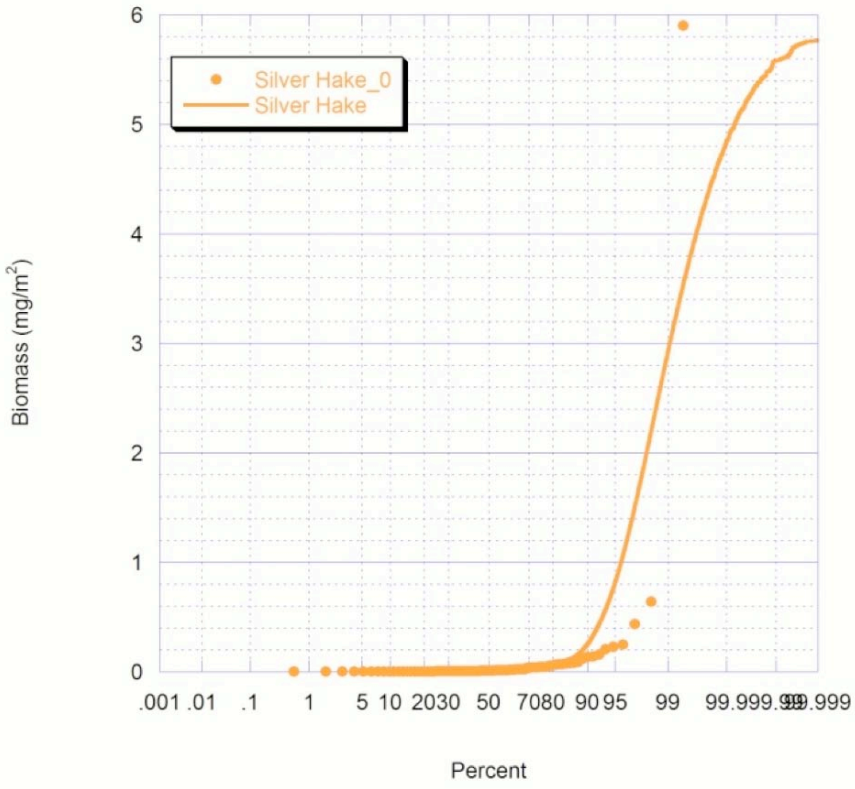
Silver Hake_0
Silver Hake
Biomass (mg/m2)
0
1
2
3
4
5
6
.001 .01 .1 1 5 10 20 30 50 70 80 90 95 99 99.9 99.99 99.999
Percent

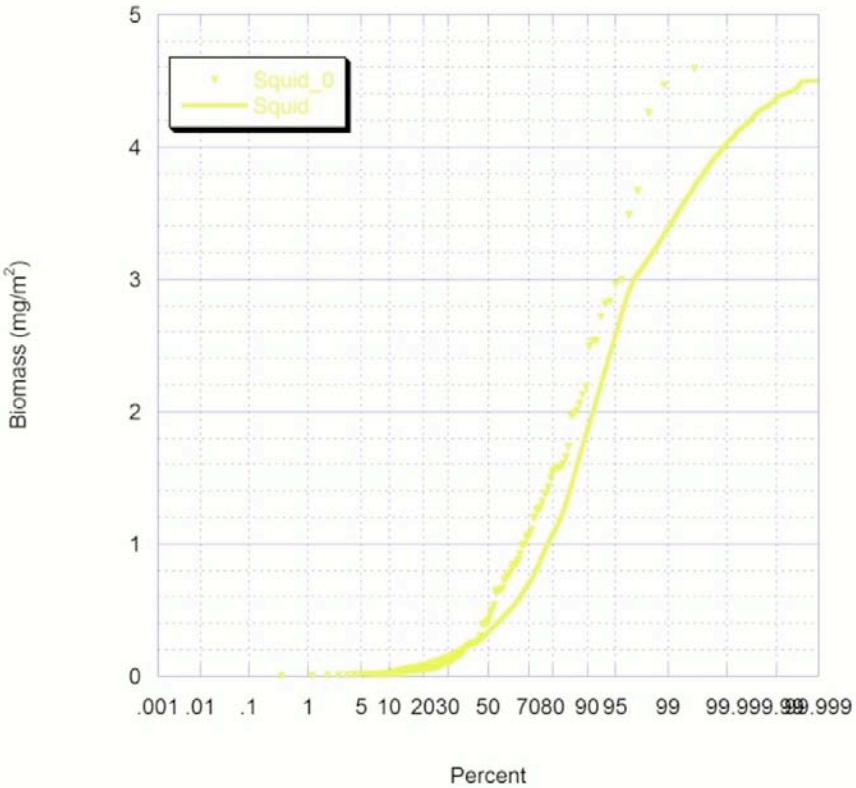
Squid_0
Squid
Biomass (mg/m2)
0
1
2
3
4
5
.001 .01 .1 1 5 10 20 30 50 70 80 90 95 99 99.9 99.99 99.999
Percent

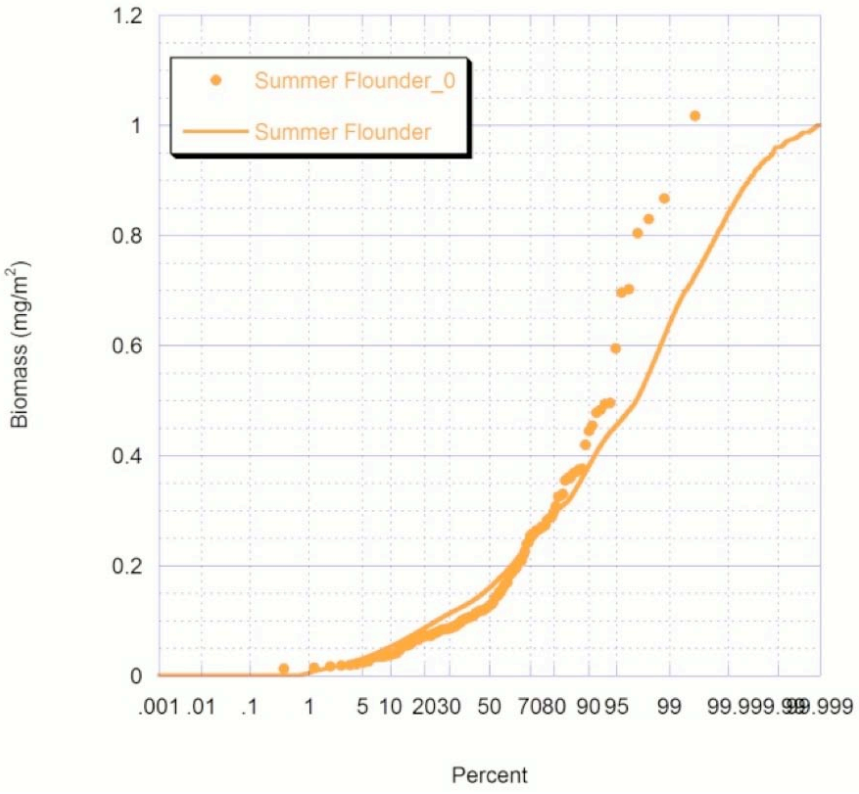
Summer Flounder_0
Summer Flounder
Biomass (mg/m^2)
1.2
1
0.8
0.6
0.4
0.2
0
.001 .01 .1 1 5 10 20 30 50 70 80 90 95 99 99.999 99.999
Percent

Bibliography

Arkema K.K., Abramson S.C. & Dewsbury B.M. 2006. Marine ecosystem-based management: from characterization to implementation. *Frontiers in Ecology and the Environment* 4(10): 525-532.

Borya, A., Dauer, D., Diaz, R., Llanso, R., Muxika, I., Rodriguez, J., et al. 2007. Assessing estuarines benthic quality conditions in Cheasapeake Bay: a comparison of three indices. *Ecological Indicators*.

Apostolakis G. 1990. The Concept of Probability in Safety Assessments of Technological Systems. *Science*, *New Series*, 250(4986): 1359-1364.

Barbier, E.B, and Hanley, N. 2009. *Pricing Nature: Cost-Benefit Analysis and Environmental Policy Making*. Edward Elgard, London.

Bohaboy, E., Malek, A., and Collie, J. 2010. *Ocean Baseline Characterization: Data Sources, Methods, and Results*. Rhode Island Ocean Special Area Management Plan, University of Rhode Island, Kingston, RI.

Beaumont N.J., Austen M.C., Atkins J.P., Burdon D., Degraer S., Dentinho T.P., Derous S., Holm P., Horton T., van Ierland E., Marboe A.H., Starkey D.J., Townsend M. & Zarzycki T. 2007. Identification, definition and quantification of goods and services provided by marine biodiversity: Implications for the ecosystem approach. *Marine Pollution Bulletin* 54: 253-265.

Beutel D., and Damon C. 2009. Fisheries map, Recreational, Mobile and fixed gear. Preapred for the Ocean SAMP.

Borja A., Dauer D., Díaz R., Llansó R.J., Muxika I., Rodríguez J.G., Schaffner L. 2008. Assessing estuarine benthic quality conditions in Chesapeake Bay: A comparison of three indices. *Ecological Indicators* 8(4): 395-403.

Borja A., Franco J. & Pérez V. 2000. A marine biotic index to establish the ecological quality of soft-bottom benthos within European estuarine and coastal environments. *Marine Pollution Bulletin* 40(12): 1100-1114.

Cablk, M.E, D. White, and A.R. Kiester. 2002. Assessment of spatial autocorrelation in empirical models in ecology. In M. Scott, P. Heglund, M. Morrison, M. Rafael, B. Wall, and J.Hoffer, eds. *Predicting Species Occurrences: Issues of Scale and Accuracy*. Island Press.

Codiga, D.L., and Ullman, D.S. 2010. *Characterizing the Physical Oceanography of Coastal Waters off Rhode Island.* Rhode Island Ocean Special Area Management Plan, University of Rhode Island, Kingston, RI.

Commonwealth of Massachusetts. 2009. Ocean Management Plan. Vol. 1 & 2

Constanza R., D'Arge R., de Groot R.S., Farber S., Grasso M., Hannon B., Limburg K., Naeem S., O'Neill R., Paruelo J., Raskin R., Sutton P., van der Belt M. 1997. The values of the world's ecosystem services and natural capital. *Nature* 387: 253-260.

Cooke I.R., Queenborough S.A., Mattison E.H.A., Bailey A.P., Sandars D.L., Graves A.R., Morris J., Atkinson P.W., Trawick P., Freckleton R.P., Watkinson A.R. & Sutherland W.J. 2009. Integrating socio-economics and ecology: a taxonomy of quantitative methods and a review of their use in agro-ecology. *Journal of Applied Ecology* 46: 269-277.

Daly, H. 2007. *Ecological Economics and Sustainable Development: Selected Essays of Herman Daly*. Edward Elgar, MA.

Degraer, S., Verfailie, E., Willems, W., Adriaens, E., Van Lanker, V. and Vincx, M. 2008. Habitat suitability modeling as a mapping tool for macrobenthic communities: an example from the Belgian part of the North Sea. *Continental Shelf Research* 28(3): 369-379.

Derous, S., Agardy, T., Hillewaert, H., Hostens, K., Jamieson, G., Lieberknecht, L., Mees, J., Mouleart, I., Olenin, S., Paelinckx, D., Rabaut, M., Rachor, E., Roff, J., Stienen, E.W.M., Van der Wal, J.T., Van Lancker, V., Verfaillie, E., Vincx, M., Weslawski, J.M., and Degraer, S. 2007a. A concept for biological valuation in the marine environment. *Oceanologia* 49(1): 99-128.

Derous, S., Verfaille, E., Van Lancker, V., Cortens, W., Steinen, E.W.M., Hostens, K., Mouleurt, I., Hillewaert, H., Mees, J., Deneust, K., Deckers, P., Cuvelier, D., Vincx, M., and Degraer, S. 2007b. *A biological valuation map for the Belgian part of the North Sea: BWZee Final Report*. Belgian Science Policy, Brussels, Belgium.

Derous, S., Austen, M., Claus, S., Daan, N., Dauvin, J.C., Deneudt, K., Depestele, J., Desroy, N., Heessen, H., Hostens, K., Husum Marboe, A., Lescrauwaet, A.K., Moreno, M.P., Mouleart, M., Rees, H., Ressurreicao, A., Roff, J., Talhadas Santos, P., Speybroeck, J., Stienen, E.W.M., Tatarek, A., Hofstede, R.T., Vincx, M., Zarzycki, T., and Degraer, S. 2007c. Building on the concept of marine biological valuation with respect to translating it to a practical protocol: Viewpoints derived from a joint ENCORA-MARBEF initiative. *Oceanologia* 49(4): 1-8.

Freeman, A.M., III. 1993. *The measurement of environmental and resource values: Theory and methods*. Resources for the Future, Washington, DC.

French McCay D., Grilli A.R., Schroeder M., Graham E., Rowe J., Reich D., Lado T. 2010. Ecological Value Map (EVM) for the Rhode Island Ocean Special Area Management Plan. Interim Technical Report for the Rhode Island Ocean Special Area Management Plan, University of Rhode Island, Kingston, RI.

Greene, J.K., Anderson, M.G., Odell, J., and Steinberg, N. (eds.). 2010. The Northwest Atlantic Marine Ecoregional Assessment: Species, Habitats and Ecosystems. Phase One. The Nature Conservancy, Eastern U.S. Division, Boston, MA.

Guichard, F. and Peterson, G. 2009. Ecological Cross-Scale Interaction. In: *Ecosystem Based Management for the Ocean*, pp. 74-91. McEleod, K., and Leslie, H., (eds.), Island Press, Washington, DC.

Jolliffe, I.T. 2002. *Principal Component Analysis*. Springer, NY.

Jordan, A. 2010. Fish assemblages spatially structure along a multi-scale wave energy gradient. *Environmental Biology of Fishes* 87:13-24.

Jordan, A., Chen, Y., Townsend, D.W., and Sherman, S. 2010. Identification of ecological structure and species relationships along an oceanographic gradient in the gulf of Maine using multivariate analysis with bootstrapping. *Canadian Journal of Fisheries and Aquatic Sciences* 67:1-19.

Kenney, R.D., and Vigness-Raposa, K.J. 2009. Marine mammals and sea turtles of Narragansett Bay, Block Island Sound, Rhode Island Sound, and nearby waters: an analysis of existing

data for the Rhode Island Ocean Special Area Management Plan. Draft Technical Report, University of Rhode Island, Kingston, RI.

http://seagrant.gso.uri.edu/oceansamp/pdf/research_marine_mammals.pdf).

King, J. 2010. Rugosity map prepared for the Ocean SAMP. School of Oceanography. University of Rhode Island, Kingston, RI.

Lauderdale, J. 1819. *An Inquiry into the Nature and Origin of Public Wealth and into the Means and Causes of its Increase*. Constable, Edinburg.

Leslie, H., and Kinzig, A. 2009. Resilience science. In: *Ecosystem Based Management for the Ocean*, pp. 55-73. McLeod, K., and Leslie, H., (eds.), Island Press, Washington, DC.

Lester S.E., McLeod K.L., Tallis H., Ruckelshaus M., Halpern B.S., Levin P.S., Chavez F.P., Pomeroy C., McCay B.J., Costello C., Gaines S.D., Mace A.J., Barth J.A., Fluharty D.L., & Parrish J.K. 2010. Science in support of ecosystem-based management for the US West Coast and beyond. *Biological Conservation* 143: 576-587.

Levin, S.A., and Lubchenco, J. 2008. Resilience, robustness and marine ecosystem based-management. *Bioscience*, 58(1): 27-32.

McLeod, K., and Leslie, H. 2009. Why ecosystem-based management? In: *Ecosystem-Based Management for the Oceans*, pp. 3-6 McLeod, K., and Leslie, H., (eds.), Island Press, Washington, DC.

Natural Capital Project. 2010. InVEST in Practice: A guidance series on applying InVEST to Policy and Planning. Stanford, CA. www.naturalcapitalproject.org/InVEST.html as of 29 June 2010.

Nijkamp P., Rietveld, P., and Voogd, H. 1990. *Multicriteria evaluation in physical planning*. Holland Publishers, Amsterdam.

NOAA Coastal Relief Model, Volume 1 http://www.narrbay.org/d_projects/oceansamp/gis_bathy.htm

Nunes, P.A.L.D., and van den Bergh, J.C.J.M. 2001. Economic valuation of biodiversity: sense or nonsense ? *Ecological Economics* 39: 203-222.

Owen, S., MacKenzie, R., Bunce, B., Stewart, H., Donovan, R., Stark, G., and Hewitt, C.N. 2006. Urban land classification and its uncertainties using principal components and cluster analyses: a case study for the UK West Midlands. *Landscape and Urban planning* 78: 311-321.

Paton, P., Winiarski, K., Trocki, C., and McWilliams, S. 2010 *Spatial Distribution, Abundance, and Flight Ecology of Birds in Nearshore and Offshore Waters of Rhode Island*. Interim Technical Report for the Rhode Island Ocean Special Area Management Plan, University of Rhode Island, Kingston, RI.

Peeters L. & Chaso-Yrigoyen C. 2006. Ecological inference and spatial heterogeneity: an entropy-based distributionally weighted regression approach. *Papers in Regional Science* 85(2): 257-276.

Peterson, C. 2009. Spatially explicit ecosystem-based management of wind farm development to minimize use conflicts and maximize energy production and ecological synergies: a North Carolina (USA) example for Pamlico and Albemarle Sounds and the coastal ocean. Ronald C. Baird Sea Grant Science Symposium: The Ecology of Marine Wind Farms, Newport, RI, November 2009.

Shannon, C.E. 1948. A mathematical theory of communication. *Bell System Technical Journal* 27:379–423.

Spellerberg I.F. and Fedor P.J. 2003. A tribute to Claude Shannon (1916–2001) and a plea for more rigorous use of species richness, species diversity and the 'Shannon–Wiener' Index. *Global Ecology & Biogeography* 12: 177–179

Skov, H., Thomsen, F., Spanggaard, G., and Jensen, B.S. 2006. *Marine Mammals*. Environmental Impact Assessment, Horns Rev 2 Offshore Wind Farm, Energy E2, Denmark.

Spaulding, M.L., Grilli, A.R., and Damon, C., and Fugate, G. 2010. Application of Technology Development Index and principal component analysis and cluster methods to ocean renewable energy facility siting. *Marine Technology Society Journal* 44(1): 8-23.

Stoms D.M., Davis F.W., Andelman S.J., Carr M.H., Gaines S.D., Halpern B.S., Hoenicke R., Leibowitz S.G., Leydecker A. Madin E.M.P., Tallis H. & Warner R.R. 2005. Integrated coastal reserve planning: making the land-sea connection. *Frontiers in Ecology and the Environment* 3(8): 429-436.

Tallis H.T., Ricketts T., Ennaanay D., Nelson E., Vigerstol K., Mendoza G., Wolny S., Olwero N., Aukema J., Foster J., Forrest J. & Cameron D. 2008. InVEST 1.003 beta User's Guide. The Natural Capital Project, Stanford.

Thomsen, Frank. URI Meeting of March 31, 2010.

Thomsen, F., Lüdemann, K., Kafemann, R., and Piper, W. 2006. Effects of offshore wind farm noise on marine mammals and fish. COWRIE Ltd., Hamburg, Germany.

UNEP(United Nation Environment Program). 2006. Marine and Coastal Ecosystems and human well –being: A synthesis report based on the findings of the Millennium Ecosystem Assessment. Nairobi: UNEP.

Villa, F., Tunesi, L., and Agardy, T. 2002. Zoning marine protected areas through Spatial Multiple-Criteria Analysis: the case of the Asinara Island National Marine Reserve of Italy. *Conservation Biology* 16(2): 515-526.

Wainger, L., and Boyd, J. 2009. Valuing ecosystem services. In: *Ecosystem Based Management for the Ocean*, pp. 92-111. McEleod, K., and Leslie, H., (eds.), Island Press, Washington, DC.

Winarski, K., Paton, P., and McWilliams, S. 2009. *RI Ocean Special Area Management Plan: Preliminary review of the phenology, abundance, spatial distribution and behavior of avian groups common to the Ocean SAMP study area*. University of Rhode Island, Kingston, RI.

Zuur, A.F., Ieno, E.N., Smith, G.M. 2007. *Analyzing Ecological Data*. Springer, NY.

24.

The Northwest Atlantic Marine Ecoregional Assessment: Implications for the Rhode Island Ocean SAMP region

by

Kevin Ruddock

The Nature Conservancy, Rhode Island Chapter, Providence, RI.

July 18, 2010

The following is a first draft of an interpretation of The Nature Conservancy's Identifying Conservation Areas in the Northwest Atlantic Marine Region Final Draft, 06/30/2010. This document intends to illustrate the places in the area of Rhode Island's Ocean SAMP that have been identified as important contributors to biodiversity in the Northwest Atlantic region. Most of this regional analysis was done with data summarized by ten-minute squares and is too coarse at that scale to highlight specific areas within Rhode Island's Ocean SAMP area. With further analysis though, it should be possible to determine some of the features and process that are driving the location of the identified biodiversity hotspots. The purpose of this document is to provide a starting point for deeper investigations into the ecological significance of Rhode Island's marine environment to the larger Northwest Atlantic seascape.

This document is still in development and is currently under review by The Nature Conservancy's Eastern Region and should be considered a draft product.

Please refer to source documents for more details about the data and methods used:

Phase I report:

http://www.nature.org/wherewework/northamerica/states/easternusmarine

Phase II report:

Anderson, M.G, J. Odell, M. Clark, Z. Ferdaña, and J.K. Greene. 2010. The Northwest Atlantic Marine Ecoregional Assessment: Identifying Conservation Areas in the Northwest Atlantic Marine Region. Phase Two. The Nature Conservancy, Eastern U.S. Division, Boston, MA.

The benthic habitat classification described in Phase I of the regional report is used as the base of the following map figures. Each number in the legend refers to following list of benthic habitats in the Southern New England sub-region.

Benthic Habitat Descriptions

Adapted from Chapter 3 of The Nature Conservancy's Northwest Atlantic Marine Ecoregional Assessment, Phase 1 Report. http://www.nature.org/wherewework/northamerica/states/easternusmarine

Shallow

109: Depressions in very shallow water (0 - 23 m) mostly on medium to coarse sand but occasionally on silt.

200: Depressions at very shallow to moderate depths (0 – 44 m) on very fine to medium sand.

25: Flats and side slopes in very shallow to shallow water (0 – 23 m) on fine to coarse sand.

36: Depressions and high flats in very shallow to moderate depths (0 – 75 m) on medium to coarse sand.

390: Depressions in shallow water (23 - 44 m) in very fine to fine sand.

316: Flats in shallow water (8-44 m) on very fine to medium sand.

229: Depressions in shallow depths (8.4 to 44 meter) on very fine sand.

230: Depressions in shallow depths (23 - 44 m) on very fine sand.

873: Flats and side slopes in shallow water (8 - 31 m) on very fine to medium sand.

2537: Depressions and high flats in shallow water (23 - 31 m) on very fine to fine sand.

Moderate Depths

113: Depressions and mid-position flats at moderate depths (23 - 44 m) on very fine sand.

372: Depressions and los slopes at moderate depths (44 – 75 m) on very fine sand.

317: Mid-position flats at moderate depths (31 - 75 m) on fine to medium sand.

223: Mid-position flats and depressions at moderate depths (44 - 75 m) on fine to medium sand.

381: Mid and high position flats in moderate depths (44 - 79 m) on fine to very fine sand.

Moderate to Deep Depths

82: All types of flats in moderately deep water (44 – 139 m) on medium to coarse sand.

949: Mid and low flats in deep water (75-139 m) on medium to fine sand.

3: Flats and slopes at moderate to very deep depths (average 128 m, min 44 m) on fine to very fine sand.

11: High slopes, canyons, flats in deep water (60 – 485 m) on medium to fine sand.

437: High flats and slopes in deep to very deep water (75 - 200 m) on fine sand.

6: High slopes and flats at moderate to deep depths (44 - 139 m) on coarse to fine sand.

1: Variable settings in a wide range of depths on fine to coarse sand. A very mixed set of samples with many un-identified species and few commonalities. Not a benthic habitat type, but listed here for completeness.

Sea Floor Portfolio *Demersal Fish Persistence*

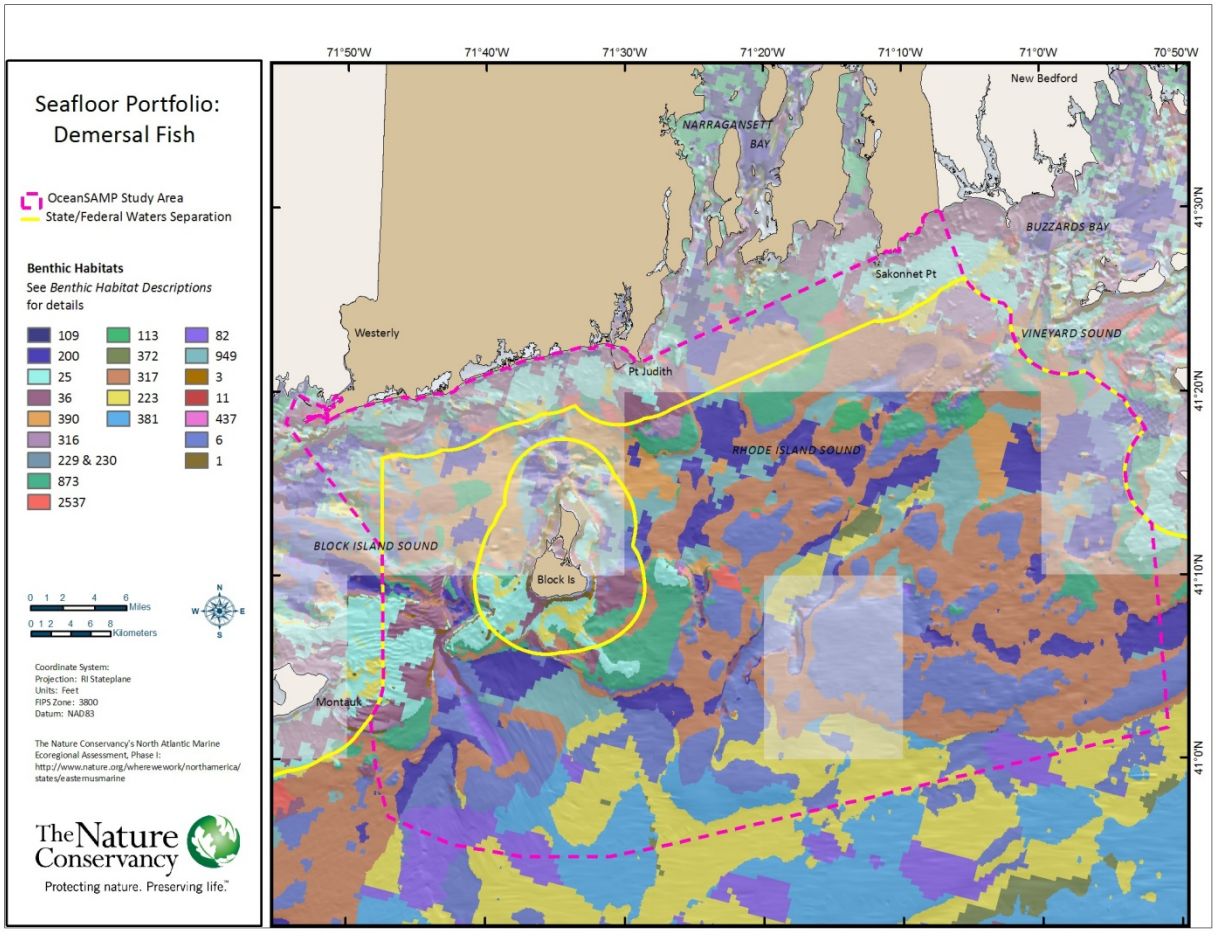

The regional assessment identified the inner shelf south of Long Island and Rhode Island as a hotspot for persistently abundant demersal fish. Since most of the OSAMP is a part of this hotspot and the patterns that are found within this scale could be attributed partly to sampling distribution, it is difficult to highlight particular areas within the OSAMP that merit attention. The regional significance of this area, though, is unquestionable.

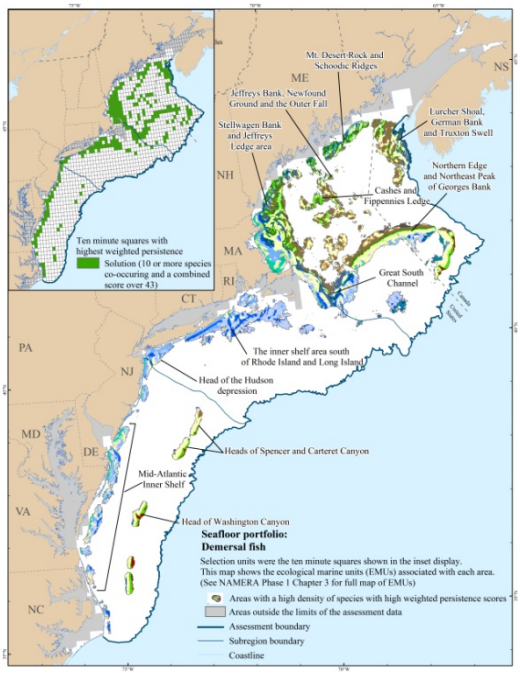

Fish Community Diversity

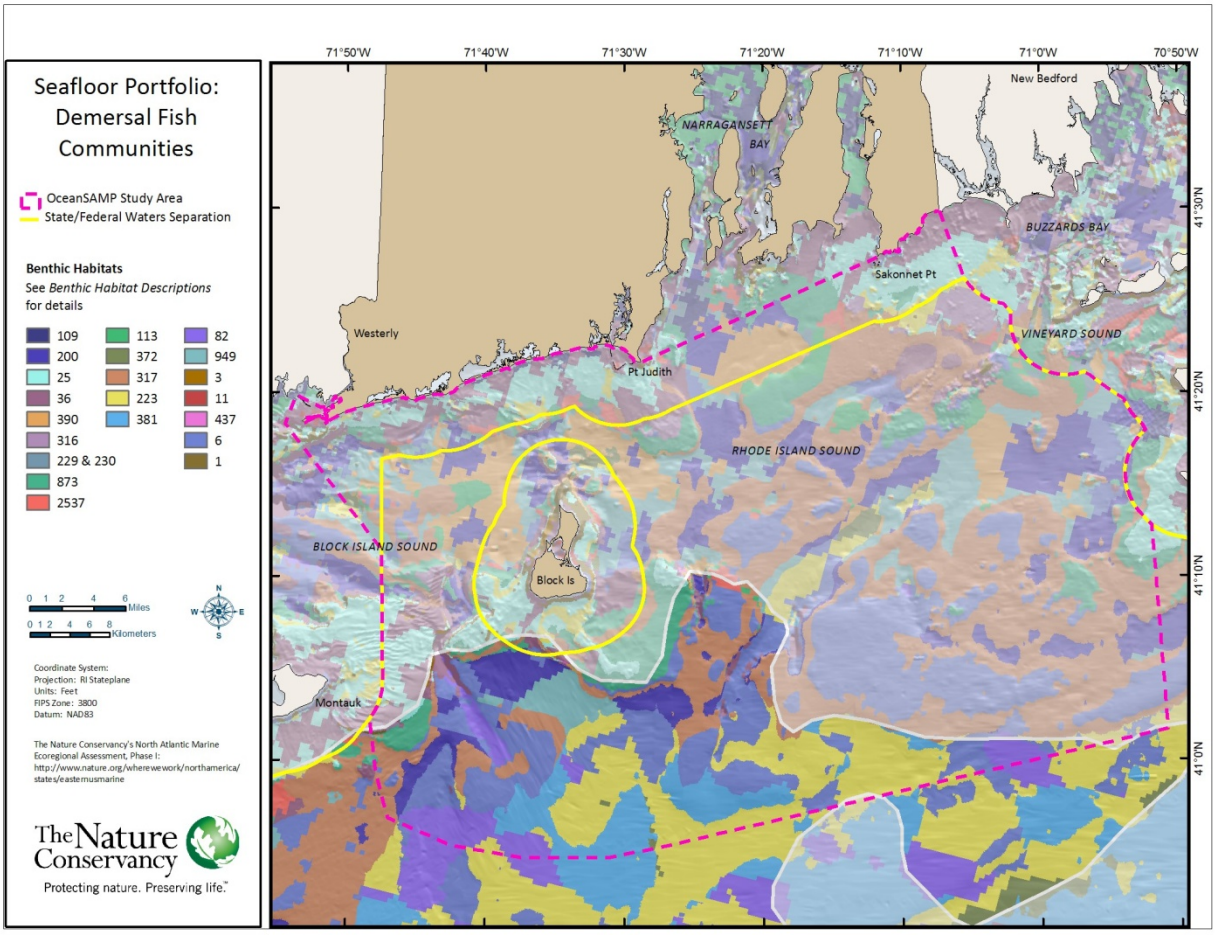

The sandy depressions south of the moraine appear to be an area that supports a high density of multiple fish communities. Further investigation is needed to understand the processes driving this diversity.

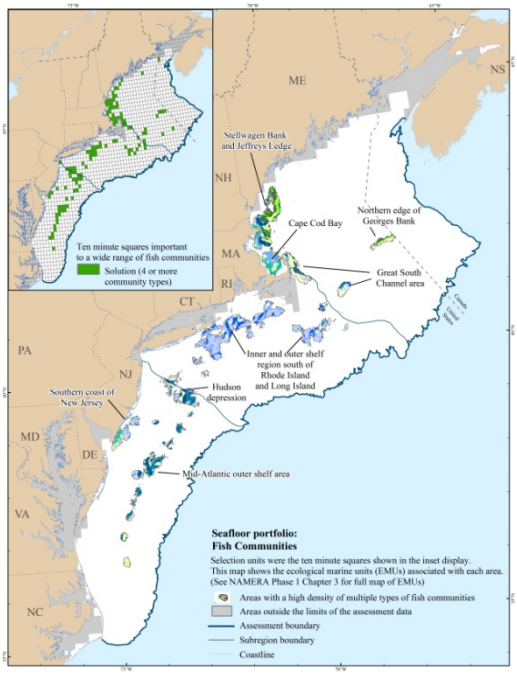

Hard Bottom and Seagrass Habitat

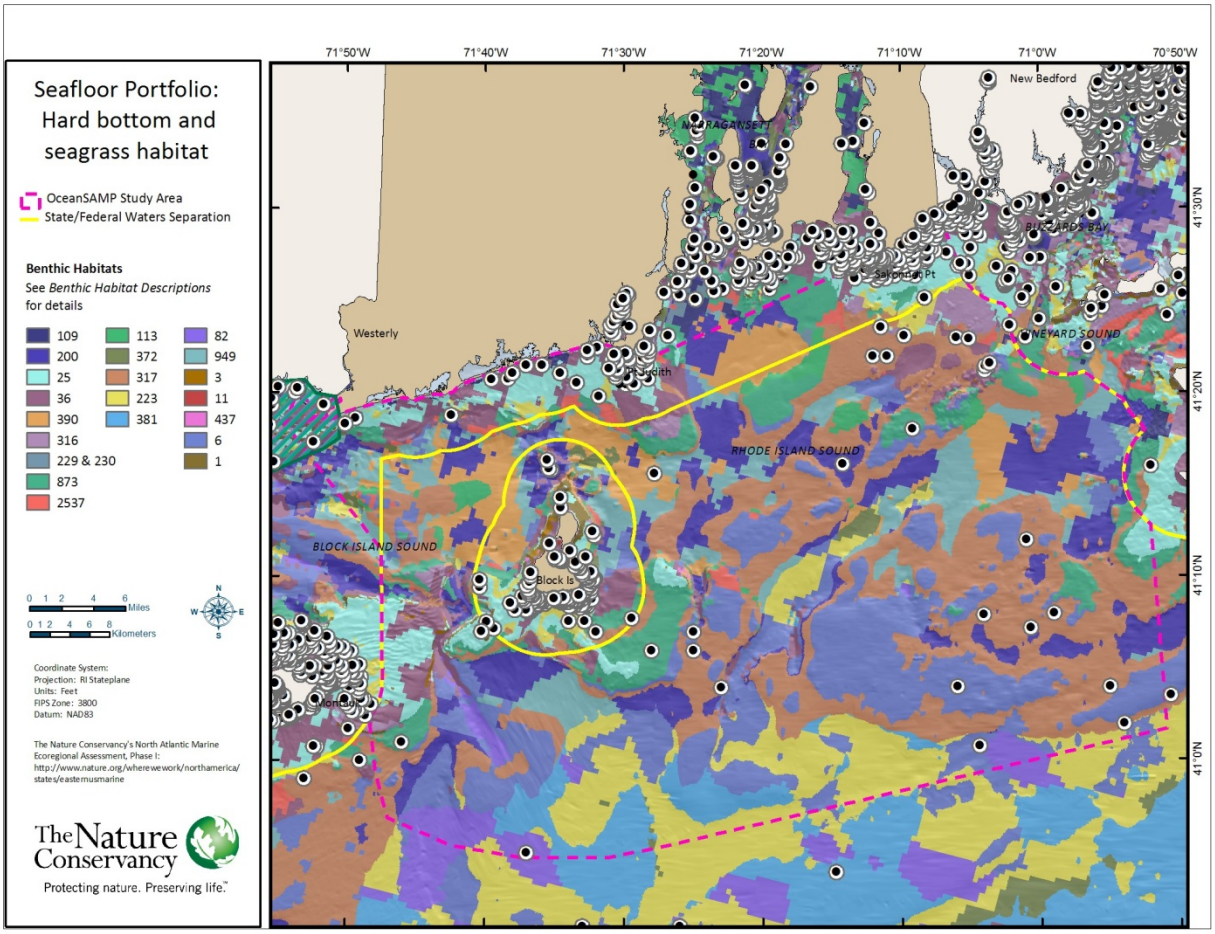

This area has some of the highest concentrations of hard bottom habitat in the Northwest Atlantic.

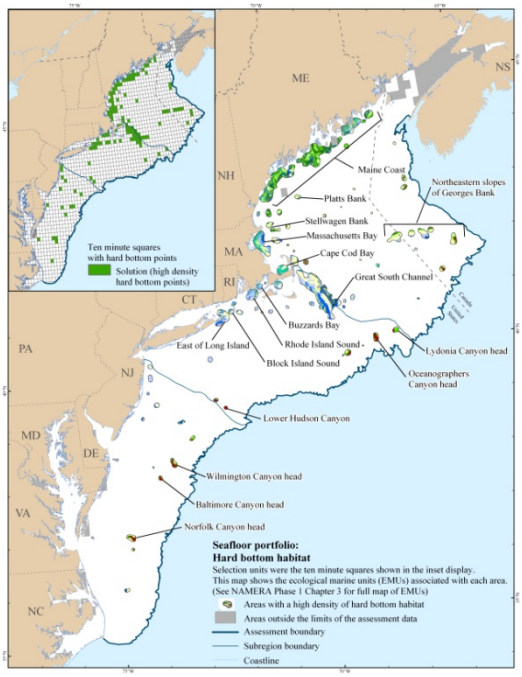

Integrated Seafloor Portfolio

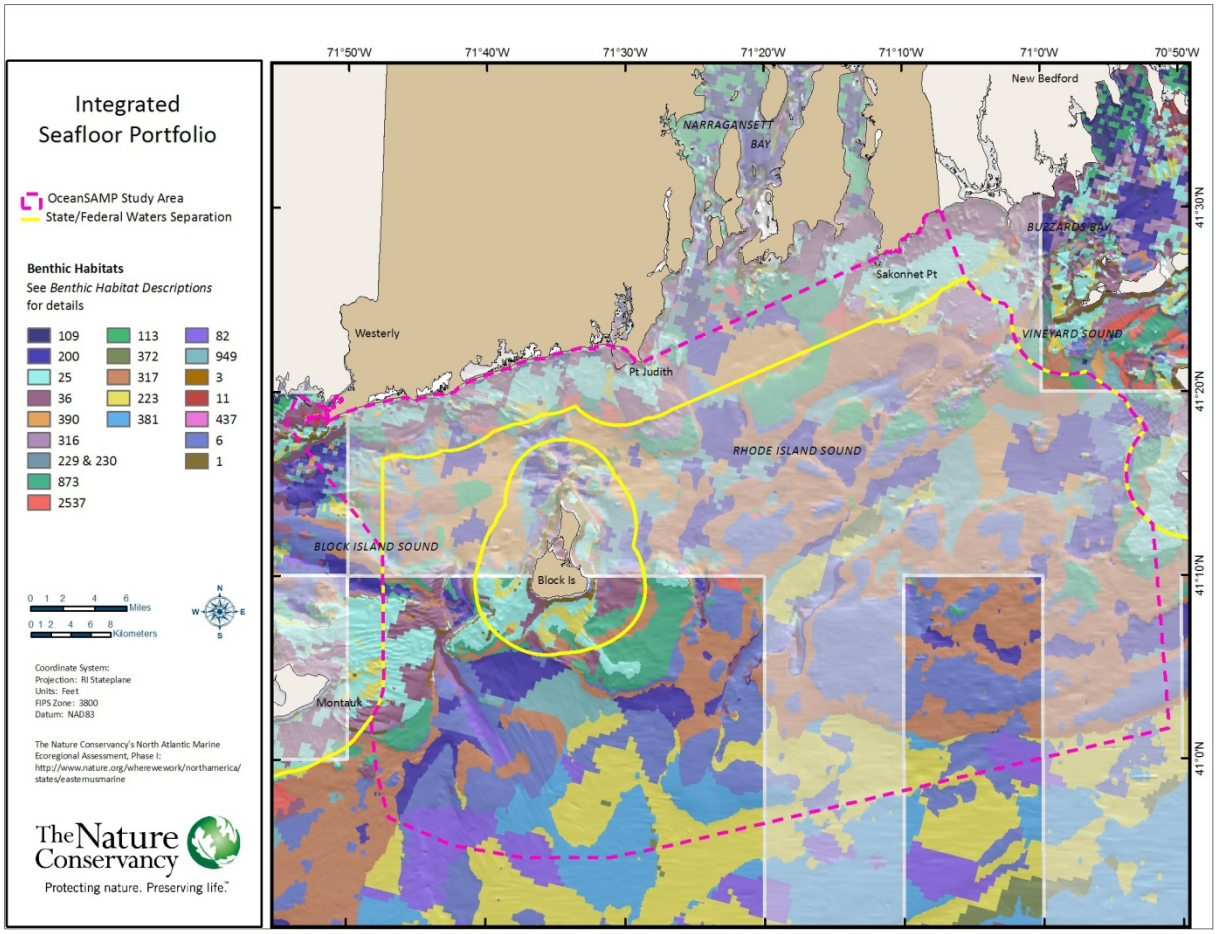

The highlighted areas on the above map shows in a general way the places where there is a coincidence of highly persistent fish, diverse communities, and/or hard bottom habitat. The regional analysis highlights the importance of the area south of the moraine and particularly south of Block Island to demersal fish.

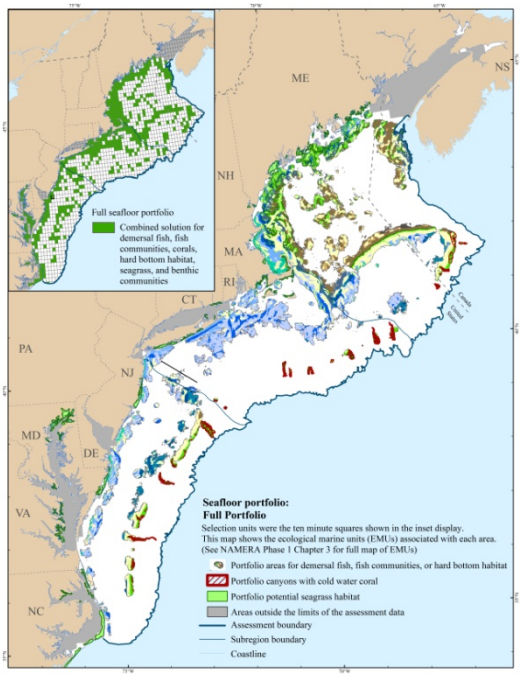

Migratory Portfolio *Large Pelagic Fish*

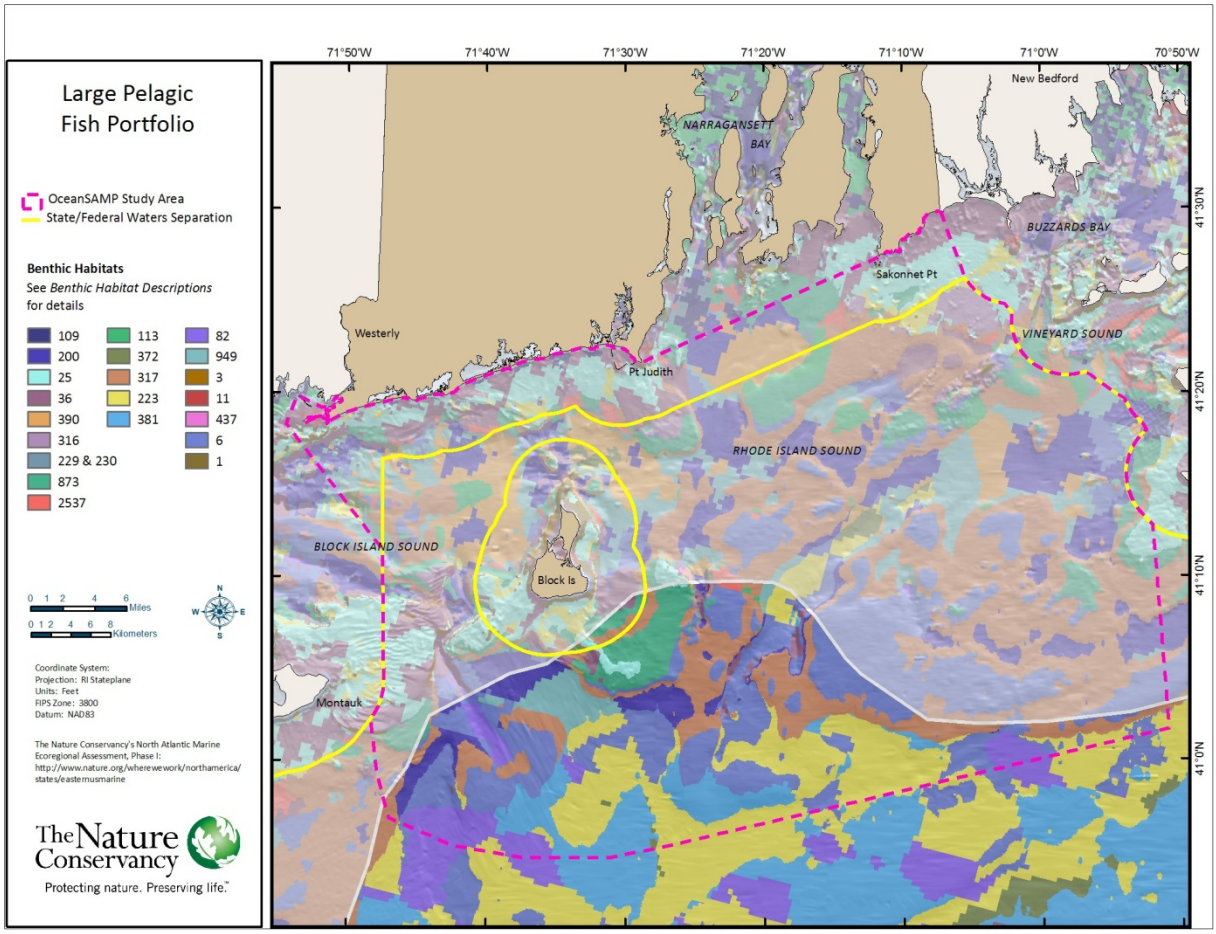

The persistent observations of target large pelagic fish were concentrated in the inner shelf area south of Long Island and Rhode Island as well as the shelf slope break. The highlighted area south of the moraine shows the rough extent of this regionally significant area in relation to the OSAMP.

For the purposes of this draft only the large pelagic fish will be highlighted from the migratory portfolio. This group was the most significant contributor to regional biodiversity of the analyzed migratory species for this area.

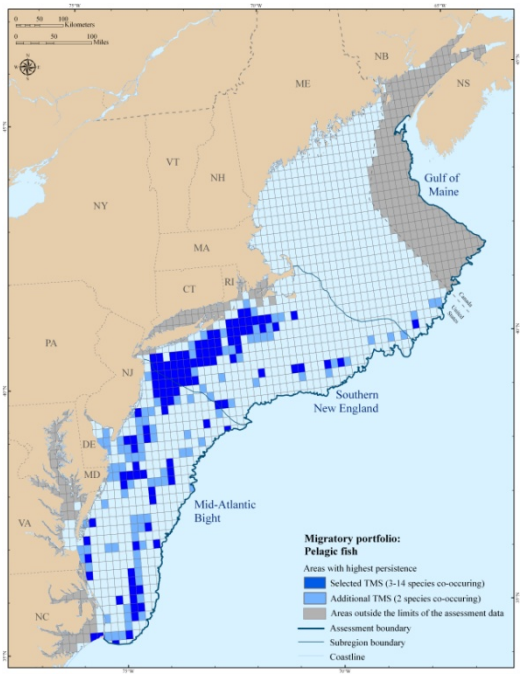

Integrated Portfolio

The Nature Conservancy's assessment looked at the coincidence of ecologically important seafloor, migratory and coastal habitats. Please refer to the original document for text and figures that illustrate this regional perspective in more detail.

Conclusions

Some general observations can be made from this regional analysis. It is clear that the marine environment off of Rhode Island's coast is an important contributor to the biodiversity in the Northwest Atlantic Ocean. The benthic habitats that can be found among the complex structures and hard rocky substrates of the moraine and areas to the north in proximity to the relatively flat sandy depressions to the south contribute to this areas unique role in the Atlantic.

The Rhode Island Chapter of The Nature Conservancy has just begun the interpretation of these data and will continue to refine the content of this document as we get more feedback and continue to analyze more of the source data.